



Moscow International Symposium on Magnetism

1 – 5 July 2017

Book of Abstracts

M.V. Lomonosov Moscow State University, Faculty of Physics

Main Topics

Spintronics and Magnetotransport
Magnetophotonics
High Frequency Properties and Metamaterials
Magnetic Nanostructures and Low Dimensional Magnetism
Soft and Hard Magnetic Materials
Magnetic Shape-memory Alloys and Magnetocaloric Effect
Magnetic Semiconductors and Oxides
Multiferroics
Magnetism and Superconductivity
Magnetic Soft Matter
Magnetism in Biology and Medicine
Study of Magnetism using X-rays and Neutrons
Theory
Scientific equipment
Topological Insulators
Skyrmions
Magnonics
Magnetophotonics and Ultrafast Magnetism
MRAM

Editors: N. Perov
V. Bessalova
A. Kharlamova
L. Makarova
Yu. Alekhina
T. Rusakova

Moscow 2017

C623
УДК 537
ББК 22.334

**Moscow International Symposium on Magnetism
(MISM)**

1 – 5 July 2017, Moscow

Book of Abstracts

The text of abstracts is printed from original contributions.

Faculty of Physics M.V. Lomonosov MSU

Физический факультет МГУ имени М.В. Ломоносова

Contributors to MISM 2017

Moscow International Symposium on Magnetism expresses its warmest appreciation on the following organizations for their generous support



Lomonosov Moscow State University



Russian Foundation for Basic Research



Faculty of Physics

Organizing Committee

Chairmen: A. Vedyayev
A. Granovsky
N. Perov

Secretary: A. Semisalova

International Advisory Committee

Chairman: V. Sadovnichy

S. Bader	<i>Argonne</i>	X. Jin	<i>Shanghai</i>
M. Barandiaran	<i>Bilbao</i>	D. Khmel'nitskii	<i>Cambridge</i>
A. Buzdin	<i>Bordeaux</i>	D. Khomskii	<i>Köln</i>
Ching-Ray Chang	<i>Taipei</i>	C. Lacroix	<i>Grenoble</i>
B. Dieny	<i>Grenoble</i>	S. Maekawa	<i>Tokai</i>
M. Farle	<i>Duisburg</i>	D. Mapps	<i>Plymouth</i>
A. Fert	<i>Orsay</i>	S. Ovchinnikov	<i>Krasnoyarsk</i>
D. Fiorani	<i>Rome</i>	S. Parkin	<i>Halle</i>
D. Givord	<i>Grenoble</i>	Th. Rasing	<i>Nijmegen</i>
J. Gonzalez	<i>San Sebastian</i>	H. Szymczak	<i>Warsaw</i>
B. Heinrich	<i>Burnaby</i>	V. Ustinov	<i>Ekaterinburg</i>
B. Hernando	<i>Oviedo</i>	M. Vazquez	<i>Madrid</i>
M. Inoue	<i>Toyohashi</i>		

National Advisory Committee

Chairman: N. Sysoev

V. Berzhanskii	S. Maleev	V. Shavrov
M. Chetkin	S. Nikitin	A. Sigov
A. Fedyanin	S. Nikitov	A. Vasiliev
D. Khokhlov	R. Pisarev	V. Veselago
N. Kreines	V. Prudnikov	N. Volkov
A. Lagar'kov	A. Saranin	A. Zvezdin

Program Committee

Chairman: A. Granovsky

Secretary: A. Semisalova

M. Acet	<i>Duisburg</i>	A. Michels	<i>Luxembourg</i>
B. Aktas	<i>Gebze</i>	V. Novosad	<i>Argonne</i>
A. Andreev	<i>Prague</i>	Yu. Pastushenkov	<i>Tver</i>
B. Aronzon	<i>Moscow</i>	N. Pugach	<i>Moscow</i>
N. Bebenin	<i>Ekaterinburg</i>	A. Pyatakov	<i>Moscow</i>
D. Berkov	<i>Jena</i>	A. Radkovskaya	<i>Moscow</i>
V. Chernenko	<i>Bilbao</i>	Yu. Raikher	<i>Perm</i>
M. Chshiev	<i>Grenoble</i>	V. Rodionova	<i>Kaliningrad</i>
S. Demokritov	<i>Münster</i>	A. Rogalev	<i>Grenoble</i>
E. Gan'shina	<i>Moscow</i>	K. Rozanov	<i>Moscow</i>
A. Kalashnikova	<i>St. Petersburg</i>	E. Shalygina	<i>Moscow</i>
O. Kazakova	<i>London</i>	E. Shamonina	<i>Erlangen</i>
V. Khovailo	<i>Moscow</i>	A. Smirnov	<i>Moscow</i>
Cheol Gi Kim	<i>Daejon</i>	L. Tagirov	<i>Kazan</i>
A. Kimel	<i>Nijmegen</i>	M. Yamaguchi	<i>Sendai</i>
A. Kirilyuk	<i>Nijmegen</i>	A. Zhukov	<i>San Sebastian</i>
K. Kugel	<i>Moscow</i>	M. Zhuravlev	<i>Moscow</i>
G. Kurlyandskaya	<i>Ekaterinburg</i>	V. Zubov	<i>Moscow</i>
X. Li	<i>Singapore</i>	K. Zvezdin	<i>Moscow</i>

Local Committee

Chairman: N. Perov

N. Abrosimova	Yu. Kurbatova	T. Rusakova
Yu. Alekhina	A. Loseva	N. Ryzhanova
V. Bessalova	L. Makarova	A. Semisalova
S. Granovsky	L. Mironova	T. Shapaeva
E. Gan'shina	S. Norina	N. Strelkov
M. Khairullin	E. Pan'kova	D. Svirin
A. Kharlamova	N. Perova	V. Tyablikov
I. Kovaleva	V. Prudnikov	E. Shalygina
S. Koptsik	M. Prudnikova	V. Zubov
O. Kotel'nikova	A. Radkovskaya	
A. Kudakov	I. Rodionov	

CONTENTS

2 JULY	7
PLENARY LECTURES	7
ORAL SESSION	11
“Spintronics and Magnetotransport”	11
“Magnetism and Superconductivity”	21
“Magnetophotonics (Ultrafast)”	33
“Magnetic Shape Memory and Magnetocaloric Effect”	47
“Soft and Hard Magnetic Materials”	57
“Magnetism in Biology and Medicine”	69
“Diluted Magnetic Semiconductors and Oxides”	79
“High Frequency Properties and Metamaterials”	93
“Study of Magnetism using X-rays and Neutrons”	105
“MRAM”	117
“Theory”	123
POSTER SESSION	131
“Spintronics and Magnetotransport”	131
“Magnetophotonics and Ultrafast Magnetism”	179
“High Frequency Properties and Metamaterials”	203
“Magnetic Nanostructures and Low Dimensional Magnetism”	229
3 JULY	323
PLENARY LECTURES	323
ORAL SESSION	327
“Spintronics and Magnetotransport”	327
“Diluted Magnetic Semiconductors and Oxides”	339
“Magnetism and Superconductivity”	345
“Magnetophotonics and Ultrafast Magnetism”	361
“Multiferroics”	367
“Magnetic Soft Matter (magnetic polymers, fluids and suspensions)”	381
“Study of Magnetism using X-rays and Neutrons”	395
“Magnetism in Biology and Medicine”	407
“Magnetic Nanostructures and Low Dimensional Magnetism”	419
“High Frequency Properties and Metamaterials”	435
“Low Dimensional Magnetism”	443
“Soft and Hard Magnetic Materials”	456
“Magnonics”	467
“Magnetic Shape Memory and Magnetocaloric Effect”	477
POSTER SESSION	487
“Spintronics and Magnetotransport”	487
“Magnetic Soft Matter (magnetic polymers, fluids and suspensions)”	499
“Magnetism in Biology and Medicine”	531
“Magnetism and Superconductivity”	557
“Magnetophotonics and Ultrafast Magnetism”	583
4 JULY	593
PLENARY LECTURES	593
ORAL SESSION	597
“Spintronics and Magnetotransport”	597
“Skyrmions”	619
“Magnetism and Superconductivity”	625
“Topological Insulators”	645
“Multiferroics”	655
“Magnetic Soft Matter (magnetic polymers, fluids and suspensions)”	669
“Scientific equipment”	683
“Magnetism in Biology and Medicine”	689
“Theory”	695
“Magnetic Nanostructures and Low Dimensional Magnetism”	711
“Low Dimensional Magnetism”	729
“Diluted Magnetic Semiconductors and Oxides”	735
“Magnetophotonics and Ultrafast Magnetism”	745

POSTER SESSION.....	755
“Soft and Hard Magnetic Materials”	755
“Magnetic Shape Memory and Magnetocaloric Effect”	829
“Diluted Magnetic Semiconductors and Oxides”	855
“Multiferroics”	903
“Theory”	927
5 JULY.....	947
PLENARY LECTURES	947
ORAL SESSION	953
“Spintronics and Magnetotransport”	953
“Soft and Hard Magnetic Materials”	959
“Magnetophotonics and Ultrafast Magnetism”	965
“Magnetism and Superconductivity”	969
“Skyrmions”	975
“Diluted Magnetic Semiconductors and Oxides”	981
“Magnetic Soft Matter (magnetic polymers, fluids and suspensions)”	987
“Multiferroics”	993
“Magnetic Nanostructures and Low Dimensional Magnetism”	999
“Study of Magnetism using X-rays and Neutrons”	1007
POSTER SESSION	1013
“Magnetic Nanostructures and Low Dimensional Magnetism”	1013
“Study of Magnetism using X-rays and Neutrons”	1029
“Multiferroics”	1045
“High Frequency Properties and Metamaterials”	1059
“Magnetic Shape Memory and Magnetocaloric Effect”	1079
“Magnonics”	1085
“Diluted Magnetic Semiconductors and Oxides”	1091
AUTHOR INDEX.....	1097

2 July

Sunday

10:00-11:30

plenary lectures
2PL-A

2PL-A-1

SPIN ORBITRONICS FOR ADVANCED MAGNETIC MEMORIES*Parkin S.*

Max Planck Institute for Microstructure Physics, Halle (Saale), Germany
Martin Luther University Halle-Wittenberg
office.parkin@mpi-halle.mpg.de

Over the past few years there have been remarkable discoveries in spin-based phenomena that rely on spin-orbit coupling that could spur the development of advanced magnetic memory devices. These include the formation of chiral spin textures in the form of Néel domain walls and topological spin textures, skyrmions, that are stabilized by a Dzyaloshinskii-Moriya exchange interaction. The Dzyaloshinskii-Moriya exchange interaction is derived from broken symmetries and spin-orbit interactions at interfaces or within the bulk of materials. Another important consequence of spin-orbit effects are the unexpectedly high conversion efficiencies of charge current to chiral spin current from topological spin textures and in conventional metals, via the spin Hall effect [1,2]. Such spin currents lead to giant spin-orbit torques that can be used to switch the magnetization in three terminal magnetic tunnel junction memory elements or can be used to move domain walls in Racetrack Memory memory-storage devices. Indeed record-breaking current-induced domain wall speeds exceeding 1,000 m/sec have recently been reported in atomically engineered synthetic antiferromagnetic racetracks in which the domain walls are “invisible” with no net magnetization [3,4]. Non-collinear spin textures including the recent discovery of antiskyrmions [5] promise novel spintronic applications. I will discuss some of these exciting developments in the emerging field of spin orbitronics in my talk.

[1] Zhang, W. et al. *Science Advances*, **2** (2016) e1600759.

[2] Demasius, K.-U. et al. *Nature Communications*, **7** (2016) 10644.

[3] Yang, S.-H., Ryu, K.-S. & Parkin, S. S. P. *Nature Nanotechnology*, **10** (2015) 221-226.

[4] Garg, C., Yang, S.-H., Phung, T., Pushp, A. & S.P.Parkin, S. *Science Advances*, **3** (2017) e1602804.

[5] Nayak, A. K. et al. arXiv:1703.01017, (2017).

2PL-A-2

ALL OPTICAL MAGNETISATION SWITCHING: BASIC PHYSICS AND POTENTIAL FOR NEW RECORDING TECHNOLOGY

Chantrell R.W.

Department of Physics, The University of York, York, YO10 5DD, UK
roy.chantrell@york.ac.uk

Since the pioneering demonstration of ultrafast demagnetization in Ni [1], the field has produced a series of remarkable discoveries, including that of magnetization reversal driven by circularly polarized light [2] giving rise to the intriguing concept of all-optical magnetic recording on the picosecond timescale. Previous experimental studies [3] using large magnetic fields showed that conventional reversal on this timescale was not possible due to a ‘fracturing’ of the magnetization structure. It was shown [4] that all-optical reversal was achieved due to the elevated temperatures achieved in the pulsed laser process, which accessed the so-called ‘linear’ reversal mechanism capable of switching on the sub-picosecond timescale. The talk will firstly outline the physics of these processes, leading to the discovery of Thermally Induced Magnetisation Switching (TIMS) in ferrimagnets, in which magnetization switching occurs in the absence of an externally applied field. This effect is discussed in terms of a 2-magnon bound state, which is responsible for the transfer of angular momentum between sublattices, which drives magnetization reversal. This can be interpreted as arising from a large effective field due to the strong inter-sublattice exchange. In terms of recording technology this field has considerable significance since it has been shown [5] that basic thermodynamic considerations lead to the requirement of fields larger than accessible to conventional inductive switching. The implications of TIMS for future magnetic storage devices is considerable, in terms of the reduction in complexity of write transducers, increased data rate and power reduction. Arguably, a recent paper [6] has brought the technology closer by demonstrating TIMS using ultrafast current pulses, potentially accessible to CMOS technology. We will finally consider potential recording densities and the materials required for their achievement.

- [1] Beaurepaire et.al., *Phys. Rev. Lett.*, **76** (1996) 4250–4253.
- [2] C.D Stanicu et.al., *Phys. Rev. Lett.*, **99** (2007) 217204.
- [3] C.H Back et.al., *Phys Rev. Lett.*, **81** (1998) 3251
- [4] Ostler et.al, *Nat. Commun.*, **3** (2012) 666 doi: 10.1038/ncomms1666.
- [5] RF Evans et. al., *Appl. Phys Lett.*, **100** (2012) 102402 .
- [6] Yang Yang et.al., <https://arxiv.org/abs/1609.06392>.

2 June

Sunday

12:00-13:30

oral session

2TL-A

2OR-A

2RP-A

2OR-P

2RP-P

**“Spintronics and
Magnetotransport”**

2TL-A-1

THE HALL EFFECTS EDWIN HALL NEVER IMAGINED*Jin X.*Department of Physics, Fudan University, Shanghai, China
xfjin@fudan.edu.cn

The anomalous Hall effect (AHE) is one of the oldest and most prominent transport phenomena in magnetic materials. Yet, AHE has remained unresolved for more than a century because its rich phenomenology defies standard classification, prompting conflicting claims of the dominant mechanisms. On the other hand, the more recently discovered spin Hall effect (SHE) has expeditiously attracted a great deal of attention because of its potential applications in spin current devices. Various methods have been developed to generate and detect the SHE, and search for materials with large spin Hall angles. These efforts notwithstanding, reliable and accurate determination of spin Hall angle remains challenging.

In this lecture, I will first give a comprehensive discussion on the basic concepts on AHE and SHE. Exploiting the attributes of epitaxial magnetic thin films, I will then explain how to control independently the different scattering processes through temperature and layer thickness and to identify unambiguously the intrinsic mechanism as well as the extrinsic mechanisms of the AHE. Finally, based on the understanding of the microscopic mechanisms of the AHE, I will describe how we develop a new method using the H-patterns to measure quantities inherent to the SHE.

2TL-A-2

BERRY PHASE EFFECTS ON ORBITAL MAGNETISM*Niu Q.*

Department of Physics, University of Texas, Austin, TX 78712 USA
ICQM & CICQM, Peking University, Beijing 100081, China
niu@physics.utexas.edu

Orbital magnetism is crucial for understanding spin coupling to other degrees of freedom pertaining the orbital motion of electrons, intra atomic or itinerant. Berry curvature gives rise to an important contribution to orbital magnetization [1, 2] and provides a key connection to the anomalous Hall effect [3]. Berry curvature and quantum metric of Bloch states also play important roles in orbital magnetic susceptibility [4]. In materials such as noncolinear antiferromagnets, spontaneous orbital magnetization can exist without net spin magnetization, and can exhibit anomalous Hall effect [5] and magneto-optical Kerr effect [6] as strong as in spin ferromagnets.

- [1] D. Xiao, JR. Shi, Q. Niu, *Physical Review Letters*, **95** (2005) 137204.
- [2] D. Xiao, Yu. Yao, Zh. Fang, Q. Niu, *Physical Review Letters*, **97** (2006) 026603.
- [3] D. Xiao, M.-Ch. Chang, Q. Niu, *Reviews of Modern Physics*, **82** (2010) 1959-2007.
- [4] Y. Gao, Sh. A. Yang, Q. Niu, *Physical Review B*, **91** (2015) 214405.
- [5] H. Chen, Q. Niu, A.H. MacDonald, *Physical Review Letters*, **112** (2014) 017205.
- [6] W. Feng, G.-Yu. Guo, J. Zhou, Yu. Yao, Q. Niu, *Physical Review B*, **92** (2015) 144426.

2TL-A-3

ANOMALOUS TUNNEL HALL EFFECT: ORBITAL CHIRALITY AND GIANT UNIVERSAL ASYMMETRY

*Huong Dang T.¹, Jaffrès H.², Erina E.², Quang T.D.¹, Hoai Nguyen T.L.³, Safarov V.I.⁴,
Drouhin H.-J.¹*

¹ LSI, Ecole Polytechnique, CNRS, and CEA-DSM-IRAMIS, University Paris Saclay, 91128 Palaiseau, France

² UMR CNRS-Thales, University Paris-Sud, University Paris Saclay, 91405 Orsay, France

³ Vietnam Academy of Science and Technology, Institute of Physics, Hanoi, Vietnam

⁴ LPMC, Ecole Polytechnique, CNRS, University Paris Saclay, 91128 Palaiseau, France
henri-jean.drouhin@polytechnique.edu

Recently it was shown that the interplay of spin-orbit coupling (SOC) and exchange interactions at interfaces and tunnel junctions results in spectacular transmission asymmetries, giving rise to an anomalous tunnel Hall effect (ATHE) for electrons *and* holes [1,2]. While they all are related to the SOC anisotropy, ATHE differs from the tunneling Hall effect (THE) [3], anomalous THE and spin Hall effects [4], spin-galvanic effect [5], or tunneling planar Hall conductance in topological insulators [6], by its giant forward asymmetry and chiral nature. A new class of tunneling phenomena can thus be investigated and experimental work is under way. In this talk, theoretical investigations and \mathbf{k} , \mathbf{p} calculations of exchange-split tunnel junctions based on III-V semiconductor compounds, involving SOC, will be presented. A comparison will be made between simple quantum-mechanical calculations, transport perturbative techniques, and spin-orbit-assisted tunneling properties deduced from numerical calculations. It will be shown that, as far as SOC is included in the conduction band of exchange-split semiconductors, the electrons can be differently transmitted with respect to an axis orthogonal to both the axis normal to the interface and the magnetization direction. It is predicted that the transmission asymmetry for opposite incidence angles possibly reaches up to 100% at some points of the Brillouin zone, revealing a totally quenched transmission for given incidence angles. In the case of an exchange step, the universal character of the transmission asymmetry will be established. When valence bands are involved, the ATHE calculations rely on a subtle treatment of the spurious states and an insight into the topology of the complex band structure will be given. The present approach paves the way to a 30-band treatment enabling to address structures based on indirect-bandgap group-IV semiconductors. It will be highlighted how the transmission asymmetry is related to the difference of orbital chirality arising of the mixing of evanescent states with propagative states and to the related branching of the quantum states responsible for the tunneling current. In all cases, the asymmetry appears to be extremely robust.

[1] T.H. Dang et al., *Physical Review B*, **92** (2015) 060403.

[2] A. Matos-Abiague and J. Fabian, *Physical Review Letters*, **115** (2015) 056602.

[3] P.S. Alekseev, *JETP Letters*, **92** (2010) 788.

[4] A. Vedyayev et al., *Physical Review Letters*, **110** (2013) 247204.

[5] S.A. Tarasenko, V.I. Perel, I.N. Yassievich, *Physical Review Letters*, **93** (2004) 056601.

[6] B. Scharf et al., A. arXiv:1601.01009v1 (2016).

2RP-P-1

PECULIARITIES OF THE ELECTRONIC TRANSPORT IN HALF-METALLIC CO-BASED HEUSLER ALLOYS

Marchenkov V.V.^{1,2,3}, Perevozchikova Yu.A.¹, Kourov N.I.¹, Irkhin V.Yu.¹, Eisterer M.⁴, Gao T.⁵

¹ M.N. Mikheev Institute of Metal Physics, UB RAS, Ekaterinburg, Russia

² International Laboratory of High Magnetic Fields and Low Temperatures, Wroclaw, Poland

³ Ural Federal University, Ekaterinburg, Russia

⁴ TU Wien Atominstitut, Vienna, Austria

⁵ Shanghai University of Electric Power, Shanghai, China

march@imp.uran.ru

Heusler alloys X_2YZ (where X and Y are transition 3d-elements and Z is an s- or p-element of the Periodic Table) that exhibit half-metallic ferromagnetism are potential candidates for application in spintronics. The main feature of the electronic structure of half-metallic ferromagnets (HMF) is the presence of an energy gap at the Fermi level in one spin sub-band and a metallic character of the density of states in the other. This can lead to 100% spin polarization of the charge carriers, which can be used for spintronic devices. The depth and the width of the energy gap can vary quite strongly in different HMF. These parameters can be changed by varying the 3d-, s- and p-elements in X_2YZ Heusler alloys, hence, altering the electronic properties. The aim of this work is to study the peculiarities of the electronic transport in Co-based Heusler alloys, namely Co_2YAl , Co_2FeSi and Co_2FeZ , where $Y = \text{Ti, V, Cr, Mn, Fe, Ni}$, and $Z = \text{Al, Si, Ga, Ge, In, Sn, Sb}$ at varying either Y - or Z -components of alloys.

We studied electric resistivity, magnetic and galvanomagnetic properties of bulk Heusler alloys in the temperature range from 4.2 to 800 K and in magnetic fields of up to 10 T. The alloys were prepared by arc and induction melting methods in purified argon atmosphere and annealed at 800 K during 48 h.

It was found that varying Y in Co_2YZ alloys affects strongly the electric resistivity and its temperature dependence, while this effect is not observed upon changing Z . When Y is varied, extrema (maximum or minimum) are observed on $\rho(T)$ near the Curie temperature T_C . At $T \leq T_C$, the $\rho(T)$ behaviour can be ascribed to a changing electronic energy spectrum near the Fermi level E_F .

The coefficients of normal (NHE) R_0 and anomalous Hall Effect (AHE) R_S were determined. Using the NHE data, the type and concentrations of charge carriers and their mobilities were estimated, which are typical for metals. It was shown that the AHE coefficient R_S is related to the residual resistivity ρ_0 by a power law $R_S \approx \lambda_{\text{eff}} \rho_0^k / M_S$, where λ_{eff} is a constant for the spin orbital interaction, k is an exponent whose value depends on the scattering mechanism of the charge carriers, and M_S refers to the spontaneous magnetization. The coefficient k was found to be 1.56 in Co_2FeZ alloys, which is typical for asymmetric scattering mechanisms. In the case of Co_2YAl alloys, $k = 2.9$ indicates an additional contribution to the AHE.

Thus, it was shown that the variation of Y strongly affects the change in number of current carriers and alters the electronic band structure near the Fermi level E_F , and, hence, the electronic properties of Co_2YAl . In case of Co_2FeZ alloys, varying Z does not greatly change the electronic transport properties.

This work was partly supported by the state assignment of FASO of Russia (theme ‘‘Spin’’ No. 01201463330), by the Scientific Program of UB RAS (project No. 15-17-2-12), by the RFBR (grant Nos. 15-02-06686 and 16-32-00072), by the Government of the Russian Federation (state contract No. 02.A03.21.0006), by the National Natural Science Foundation of China (No. 11204171) and by the Shanghai Municipal Natural Science Foundation (No. 16ZR1413600).

2OR-P-2

EFFECT OF LASER FLUENCE ON STRUCTURAL AND MAGNETIC PROPERTIES OF PULSED LASER DEPOSITED $\text{Si}_{1-x}\text{Mn}_x$ ($x \approx 0.5$) FILMS

Pandey P.¹, Drovosekov A.B.², Wang M.¹, Xu C.¹, Nikolaev S.N.³, Chernoglazov K.Yu.³, Savitsky A.O.², Kreines N.M.², Cherebilo E.A.⁴, Mikhalevsky V.A.⁴, Novodvorsky O.A.⁴, Tugushev V.V.³, Rylkov V.V.³, Helm M.¹, Zhou S.¹

¹ HZDR, Institute of Ion Beam Physics and Materials Research, Dresden, Germany

² P.L. Kapitza Institute for Physical Problems RAS, Moscow, Russia

³ NRC ‘‘Kurchatov Institute’’, Moscow, Russia

⁴ Institute on Laser and Information Technologies RAS-Branch of FSRC ‘‘Crystallography and Photonics’’ of RAS, Shatura, Russia

p.pandey@hzdr.de

The development of $\text{Si}_{1-x}\text{Mn}_x$ ($x \approx 0.5$) alloyed films with composition close to the manganese monosilicide MnSi attracts a lot of attention, since these films demonstrate unusual magnetic and transport properties and can be easily incorporated into existing microelectronic technology. The stoichiometric ε -MnSi with B20 structure has the Curie temperature $T_C \approx 29$ K and demonstrates a complex magnetic phase diagram including the region of unusual magnetic states, skyrmions. At the same time, the T_C value of nonstoichiometric $\text{Si}_{1-x}\text{Mn}_x$ alloys slightly enriched in Mn ($x \approx 0.52$) was found to increase by more than an order of magnitude as compared with the stoichiometric ε -MnSi [1]. Our investigations showed that a polycrystalline structure, sizes and shapes of nanocrystallites as well as the tension between the film and substrate arising in the growth process plays an important role in the formation of high-temperature ferromagnetism (HT FM) in nonstoichiometric $\text{Si}_{1-x}\text{Mn}_x$ alloy films [2,3]. Therefore, variation in stoichiometry and crystalline structure of the $\text{Si}_{1-x}\text{Mn}_x$ ($x \approx 0.5$) films controlled by the laser fluence E (i.e. the energy of deposited atoms and their flow) can provide an approach to fabrication of HT FM films.

Here we present the results of magnetization, ferromagnetic resonance (FMR) and transport investigations for the $\text{Si}_{1-x}\text{Mn}_x$ films grown by pulsed laser deposition technique onto $\text{Al}_2\text{O}_3(0001)$ substrates at various laser fluence in the range of $E = (3.8-7.6)$ J/cm² ($\lambda = 532$ nm; $\tau_{imp} = 15$ ns). Rutherford backscattering data on these films revealed that the small laser fluence $E = 3.8$ J/cm² yielded Mn content $x \approx 0.47$, while, the large $E = 7.6$ J/cm² resulted in the Mn content $x \approx 0.54$. The magnetization data of $\text{Si}_{1-x}\text{Mn}_x$ films show the existence of several magnetic phases: HT FM phase with $T_{Ch} = 220-260$ K described by simplified Brillouin function [2] and the low-temperature FM phase (LT FM) with $T_{Cl} \sim 30$ K. The upturn in magnetization below 30 K is more pronounced at $x \approx 0.47 - 0.53$ ($E \leq 4.4$ J/cm²). The FMR and transport measurements confirm the presence of several FM phases in the samples and the amplifying role of LT FM for films grown at $E \leq 4.4$ J/cm². We explain our result by synergy of deposited atoms energy and huge lattice mismatch between the MnSi film and Al_2O_3 substrate ($\approx 10\%$ [2]). At small E the mesoscopic size ε -MnSi crystallites ($T_{Cl} \sim 30$ K) are formed in the $\text{Si}_{1-x}\text{Mn}_x$ matrix yielding to inhomogeneous magnetic phases, while the high E has resulted in homogenization of the HT FM phase due to absence of the large size crystallites [2].

This work was partly supported by the RFBR (grant No. 15-07-01170, 15-07-01160, 15-29-01171). The work at HZDR is financially supported by DFG (ZH 225/6-1).

[1] V. V. Rylkov *et al.*, *Europhys. Lett.*, **103** (2013) 57014-57019.

[2] S.N. Nikolaev *et al.*, *AIP Advances*, **6** (2016) 015020-015033.

[3] A.B. Drovosekov *et al.*, *Europhys. Lett.*, **115** (2016) 37008-37013.

2OR-P-3

TUNNELING MAGNETORESISTANCE WITH ZERO-MOMENT HALF-METALLIC $\text{Mn}_2\text{Ru}_x\text{Ga}$

Titova A.^{1,2}, Fowley C.¹, Borisov K.³, Betto D.³, Lau Y.-C.³, Thiyagarajah N.³, Atcheson G.³, Coey J.M.D.³, Stamenov P.S.³, Rode K.³, Lindner J.¹, Faßbender J.², Deac A.M.¹

¹ Institute of Ion Beam Physics and Materials Research, Helmholtz - Zentrum Dresden - Rossendorf, Dresden, Germany

² Institute for Physics of Solids, Technische Universität Dresden, Dresden, Germany

³ AMBER and School of Physics, Trinity College Dublin, Dublin, Ireland
a.titova@hzdr.de

Intermetallic Heusler compounds can possess high spin polarization, low magnetic moment, low Gilbert damping constant α , and huge uniaxial anisotropy fields, of the order of tens of tesla. Such a wide range of properties, most of them tunable, make these materials very attractive for spin-transfer-torque oscillators in the (sub-) THz range. A particularly suitable candidate is the near-cubic Heusler alloy of Mn, Ru and Ga (MRG) [1]. Here, we show that tunneling magnetoresistance (TMR) of about ten percent can be achieved in MRG-based magnetic tunnel junctions (MTJs), and that the TMR can be improved by integrating different insertion layers acting as diffusion barriers between the half-metallic electrode and the tunnel barrier.

MRG-based stacks were deposited using a “Shamrock” fully automated sputter deposition tool by co-sputtering from a Mn_2Ga and a Ru target. Changing the Ru concentration allows tuning the compensation temperature T_{comp} between 2 and 450 K. The thin-film stacks were subsequently patterned into $20 \times 20 \mu\text{m}^2$ junctions using standard UV lithography, prior to annealing in temperatures ranging from 250 °C to 350 °C. Selected samples were investigated by transmission electron microscopy (TEM).

The magnetic properties of the MTJs were analyzed by magnetotransport measurements as a function of applied bias voltage at room temperature. We found that 0.6 nm of Al acts as good diffusion barrier in $\text{Mn}_2\text{Ru}_x\text{Ga} / \text{MgO} / \text{CoFeB}$ MTJs. Low-temperature measurements on the same device show TMR in excess of 40% close to zero bias [2]. In addition, we demonstrate non-zero TMR while cooling through the compensation temperature (where the magnetic moment is zero), indicating that magnetotransport in MRG is governed by one Mn sublattice only. This hypothesis is further supported by the fact that samples with T_{comp} above room temperature exhibit inverted TMR as compared to samples that compensated below. The precise value of T_{comp} is the result of a delicate balance between the moments carried by Mn ions on the 4c and 4a sites. Upon thermal annealing, this balance is slightly shifted due to partial annihilation of Mn anti-sites, and T_{comp} may pass from above room temperature to below, giving rise to an inverted TMR response. The next step is to fabricate sub- μm devices based on MRG for detecting spin-transfer induced dynamics, which should occur at frequencies of several hundred GHz, given the ultra-high anisotropy of these.

This work is supported by the Helmholtz Young Investigator Initiative Grant No. VH-N6-1048.

[1] Kurt H et al., *Phys. Rev. Lett.*, **112** (2014) 027201.

[2] Borisov K et al., *Appl. Phys. Lett.*, **108** (2016) 192407.

2OR-P-4

MAGNETOTRANSPORT IN HYBRID MAGNETIC NANOWIRES

Andreev S.¹, Hartmann R.¹, Pietsch T.¹

¹ Department of Physics, University of Konstanz, 74464 Konstanz, Germany
Sergej.Andreev@uni-konstanz.de

Ensembles of magnetic nanowires are the core-elements of various applications in nonvolatile memories, microwave devices and communication technologies as well as humidity- and gas sensors. The anodic aluminum oxide masks allow the synthesis of large ensembles of nanowires using electrochemical metal deposition without time consuming electron beam lithography. Moreover, due to their small diameter in the range of few to tens of nanometers, these systems are highly interesting in magnonics and spin-(transfer) electronics, where high spin-current are required.

Here we show how well-defined ensembles of hybrid, magnetic nanowires composed of ferromagnetic and non-magnetic layers can be grown in micro structured arrays and integrated in high-frequency microwave electronic devices.

The static magnetic properties of the nanowire arrays are evaluated via SQUID magnetometry. Furthermore the composed microstructure of the nanowires is correlated with their magnetic properties. Finally, the dynamic magnetic properties are investigated via FMR/EPR measurements of magnetic nanowire arrays integrated in high-frequency device and circuits. We will show that these systems are potential candidates for novel ultra-miniaturized GHz/THz emitters and -detectors.

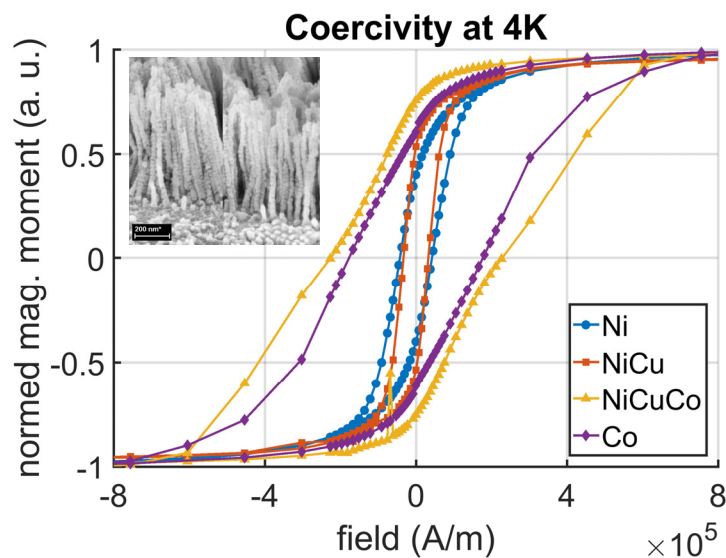


Fig. 1 Coercivity of magnetic nanowire arrays.

2OR-P-5

SYNCHRONIZATION OF SPIN TRANSFER VORTEX-BASED NANO-OSCILLATORS BY AN EXTERNAL HARMONIC EXCITATION

Stremoukhov P.A.¹, Safin A.R.¹, Aleshin K.N.²

¹ Department of Formation and Processing of Radio Signals, National Research University MPEI, Krasnokazarmennaya str.14, 111250, Moscow, Russia

² Lobachevsky State University of Nizhni Novgorod, ave. Gagarina 23, 603022, Nizhny Novgorod, Russia

lopavel1@mail.ru, arsaфин@gmail.com, kirill_al@bk.ru

Magnetic vortices are very interesting nanoscale magnetic states, which have attracted research interest from both fundamental and applied perspectives. Especially interesting are vortices generated in the magnetic nanostructures during the flow of spin-polarized current through them by means of a spin transfer torque.

Based on the magnetization of the vortex dynamics in magnetic nanostructures it is possible to realize a fundamentally new miniature microwave generators widely tunable frequency so-called "Spin-transfer nanooscillators" (STNO). Unlike homogeneous STNO, vortex STNO have considerable advantages: a smaller width of the spectral line (about 1 MHz at frequencies up to 1 GHz), high output power (about 1 μ W), and the absence of an external magnetic field. For practical applications of such generators, it is necessary to reduce the spectral line width of STNO.

One of the methods of reducing the width of the spectral line of oscillations generated by vortex STNO is to use the external synchronization by harmonic high frequency current or a magnetic field. Based on the Thiele equation we obtained truncated equations for slowly varying amplitude and phase of vortex based STNO while it synchronized by external harmonic source. Moreover, not only spin-polarized current may change harmonically, but an external magnetic field may, too.

In this work we find the truncated equations for the slowly varying amplitude and phase difference in the following form:

$$\begin{cases} \dot{\rho} = \rho \cdot (\alpha - \beta \cdot \rho^2) + \frac{1}{2} \sigma \cdot \rho_{ext} \cdot \sin(\theta) \\ \dot{\theta} = \frac{\omega_0 - \omega_{ext}}{\omega_0} + \omega' \cdot \rho^2 + \frac{1}{2} \sigma \cdot \frac{\rho_{ext}}{p} \cdot \cos(\theta) \end{cases}$$

Here α is the stationary amplitude without external force, β is the normalized amplitude of the external force (current or magnetic field), ω_0 is the difference between the external frequency and constant STNO frequency with phases θ and, consequently, ω' and p is the nonisochronous parameter.

Firstly, we find the stationary amplitude and phase difference and then using the small perturbation technic, we find the stability of stationary states on the parameter plane. Secondly, we use the theory of oscillations to find the basic bifurcations of our system and topology of phase plane. Finally, we find the phase-locking bandwidth of the vortex STNO by varying parameters. The case of two coupled STNO is also considered. Our findings are very important for STNO-based microwave oscillator design.

This work is supported by the Russian President grant for young Ph.D. researchers (Grant No. MK-7026.2016.8).

[1] Guru Khalsa, M. D. Stiles, J. Grollier *Appl. Phys. Lett.*, **106** (2015), 242402.

[2] T.J. Silva, W.H. Rippard *Journal of Magnetism and Magnetic Materials*, **320** (2008) 1260–1271.

[3] S. M. Rezende, F. M. de Aguiar, A. Azevedo *Physical Review B*, **73** (2006) 094402.

2OR-P-6

THE DYNAMICS OF REVERSAL MAGNETIZATION IN CoFeB/Ta/CoFeB BILAYER WITH PERPENDICULAR ANISOTROPY

Lvova G.L.^{1,2}, Talantsev A.D.^{1,2}, Morgunov R.B.^{1,2}, Lu Y.³, Lavanant M.³, Petit-Watelot S.³,
Koplak O.^{1,4}, Mangin S.³

¹ Institute of Problems of Chemical Physics, 142432, Chernogolovka, Moscow, Russia

² Tambov State Technical University, 392000, Tambov, Russia

³ Institut Jean Lamour, UMR 7198 CNRS, Nancy, France

⁴ Immanuel Kant Baltic Federal University, 236041, Kaliningrad, Russia

o.koplak@gmail.com

Magnetic relaxation in synthetic CoFeB/Ta/CoFeB antiferromagnet with a strong perpendicular anisotropy has been studied. Magnetic hysteresis contains three hysteresis loops (2 outer loops and 1 inner loop). The time dependences of magnetization of the sample are shown in the Figure 1. Magnetic relaxation was observed in the narrow field range close to coercive fields of the inner and outer hysteresis loops.

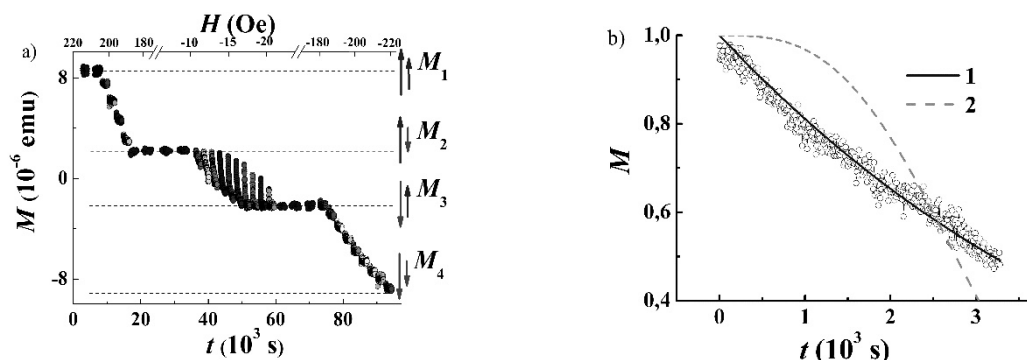


Figure 1. a) Time dependences of the magnetic moment M of the sample. b) Time dependence of magnetization at 300 K and its approximations by Fatuzzo-Labrune model.

Obtained results are in good agreement with the modified Fatuzzo–Labrune model [1, 2]. Approximations of time dependence $M(t)$ for reversal phase nucleation (1) and domain walls (2) are presented on Figure 1. One can see that time dependence obeys exponential law $M(t) = \exp(-\alpha t)$ corresponding to magnetic relaxation by the reversal phase nucleation at 300 K. The critical field of domain wall pinning as well as height of the potential barrier $\Delta E_0 = 0.72$ eV were determined. Competition of the reversal magnetic phase nucleation and DW propagation was revealed at low temperatures below 100 K.

The work was supported by grant 3.1992.2017/ПЧ in the frame of scientific program of Ministry of Education and Science "Scientific projects carrying out by scientific teams of research centers and(or) scientific laboratories of high education organizations"

[1] M. Labrune, S. Andrieu, F. Rio, P. Bernstein, *J. Magn. Magn. Mater.*, **80** (1989) 211.

[2] E. Fatuzzo, *Phys. Rev.*, **127** (1962) 1999.

2 July

Sunday

12:00-13:30

15:00-17:15

oral session

2TL-D

2RP-D

2OR-D

**“Magnetism and
Superconductivity”**

2TL-D-1

SUPERCONDUCTOR-FERROMAGNET DEVICES FOR SUPERSPINTRONICS

Lahabi K.¹, Singh A.^{1,2}, Aarts J.¹

¹ Huygens-Kamerlingh Onnes Laboratory, Leiden University, Leiden, The Netherlands

² QuTech, Delft, The Netherlands
aarts@physics.leidenuniv.nl

Spin-triplet Cooper pairs induced in ferromagnets are the centerpiece of the newly emerging field of superconducting spintronics. Triplets are generated by engineering magnetic inhomogeneities at the S/F interface (S a superconductor, F a ferromagnet) and give rise to long-range supercurrents in the magnet. We show this for the case of CrO₂, which is a ferromagnet with 100% spin polarization. In this system, reliable production of lateral Josephson junctions is challenging due to a poorly controlled interface transparency and an incomplete knowledge of the local magnetization of the CrO₂. These issues can be overcome by growing CrO₂ on pre-patterned TiO₂ substrates via chemical vapor deposition, which results in high-quality, faceted, homogeneous nanowires. With such wires we can produce Josephson junctions with a high interface transparency, leading to very large spin-polarized supercurrents, with critical current densities exceeding 10⁹ A/m² over distances as long as 600 nm [1]. CrO₂ nanowire-based JJs thus provide a realistic route to creating a scalable device platform for dissipationless spintronics.

An equally interesting aspect of the mechanism for triplet generation is that devices can be designed which allow control over the supercurrent distribution. This we demonstrate with a disk-shaped Josephson junction based on Co as the magnet, a Ni-layer to provide magnetic inhomogeneity, and a ferromagnetic weak link which is formed by making a trench in the disk. The weak link contains a magnetic vortex, and micromagnetic simulations (Fig.1) show how this produces *two* distinct supercurrent channels across the junction. This is verified through superconducting quantum interferometry (SQI). With a magnetic field we can change the position of the vortex, and hereby the supercurrent pathways. This device exemplifies a novel platform where adaptable supercurrent paths can be customized for a given application.

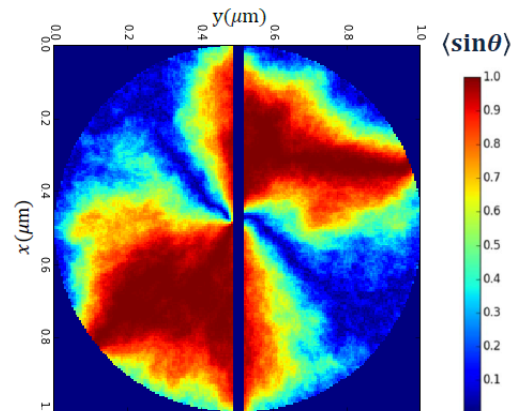


Fig.1. Simulations showing the angle θ between the magnetization vectors in a Co disk with two half-disks of Ni on top. The vortex in the Co aligns both magnetizations in the center.

[1] A. Singh, S. Voltan, K. Lahabi and J. Aarts, Physical Reviews X, **5** (2015) 021019.

2TL-D-2

SPECTROSCOPY OF SPIN POLARIZED CHARGE-LESS BOGOLIUBOV QUASIPARTICLES

Kuzmanovic M.¹, Aprili M.¹, Quay C.H.¹

¹ Laboratoire de Physique des Solides, CNRS, Univ. Paris-Sud, University Paris-Saclay, 91405 Orsay Cedex, France
marco.aprili@u-psud.fr

The excitations in conventional superconductors, Bogoliubov quasiparticles, are spin-1/2 fermions but their charge and group velocity is energy-dependent and, in fact, zero at the gap edge. Therefore, in superconductors (unlike normal metals) the spin and charge degrees of freedom may be spatially separated. I will first present a series of experiments that address spin imbalance [1], magnetization relaxation [2] and spin coherence [3] of the out-of-equilibrium magnetization induced in a mesoscopic superconducting device by spin injection. Then I will focus on a very recent experiment on spectroscopy [4] of this state. I will show that the spins distribution is energy dependent as expected once the quasiparticle velocity taken into account. I will describe such a distribution of charge-less spin polarized quasiparticles using a diffusion equation and I will show that the gap changes follow the self-consistent gap equation. Finally I will address the quasiparticle lifetime and interaction in the situations where either one or both spin species (up and down) are injected.

Support by the ANR, through the project Spinoes is acknowledged.

- [1] C.H.L Quay et al., *Nature Physics*, **9** (2013) 84-88.
- [2] C.H.L Quay et al., *Physical Reviews B*, **93** (2016) 220501 (R).
- [3] C.H.L Quay et al., *Nature Communications*, **6** (2015) 8660.
- [4] M. Kuzmanovic et al. in preparation.

2RP-D-3

PROXIMITY-INDUCED JOSEPHSON EFFECTS IN SUPERCONDUCTING SPIN-VALVES

Rudolf M.¹, Thalmann M.¹, Pietsch T.^{1,2}

¹ Department of Physics, University of Konstanz, Universitätsstrasse 10, D-78464 Konstanz, Germany

² Zukunftskolleg, University of Konstanz, Universitätsstrasse 10, D-78464 Konstanz, Germany
torsten.pietsch@uni-konstanz.de

The interesting notion of superconducting spin-electronics recently attracted a tremendous interest, because this technology promises a new paradigm for quantum information processing. The practical realization of superconducting spintronic devices, however, requires a complete understanding of the transfer and the dynamics of spin and charge currents between superconducting (S) and ferromagnetic (F) circuit elements as well as the coupling between spin and charge degrees of freedom in these systems.

Here we explore both the local and non-local magnetotransport properties of lateral, superconducting FSF spin-valves and ferromagnetic SFS Josephson junctions. Additionally, microwave spectroscopy is used to elucidate fundamental questions related to the complex interplay of competing order parameters and in particular the question of relaxation mechanisms of non-equilibrium distributions with respect to spin, charge and energy.

In non-local transport spectroscopy, we discuss the contributions of crossed Andreev reflection and elastic co-tunnelling as well as spin- and charge accumulation to the non-local voltage signal observed in lateral superconducting spin valves. Moreover, in these systems, the inverse proximity effect induces a series of Josephson weak links in the device, which results in peculiar transport properties. Both the ac and dc Josephson effect are demonstrated in local geometry. However, in such diffusive S/F Josephson junctions, the spin-polarized spacer leads to a non-sinusoidal current-phase relationship, which is investigated via the occurrence of fractional Shapiro steps in the IV characteristics under microwave irradiation depending on the magnetisation state of the F spacer.

Financial Support by Zukunftskolleg and the German Science Foundation (DFG) is acknowledged.

2OR-D-4

SCANNING TUNNELING SPECTROSCOPY TO PROBE ODD-TRIPLET CONTRIBUTIONS TO THE LONG-RANGED PROXIMITY EFFECT IN AL-EuS

Diesch S.¹, Wolz M.¹, Sürgers C.², Beckman D.², Machon P.¹, Belzig W.¹, Scheer E.¹

¹ Universität Konstanz, Konstanz, Germany

² Karlsruhe Institute of Technology, Karlsruhe, Germany

simon.diesch@uni-konstanz.de

In conventional superconductors, electrons are bound in singlet Cooper pairs, i.e. with opposite spin. More recently, experiments on superconductor-ferromagnet systems have shown supercurrents tunneling through ferromagnetic layers, indicating Cooper pairs of equal spin, thus corresponding to a long-range triplet proximity effect [1]. Most experimental evidence for triplet superconductivity comes from observations of the thickness dependence of the Josephson current through a ferromagnetic barrier, and there is now an increasing amount of direct spectroscopic evidence [2] to test the existing theoretical models.

In this talk we present scanning tunneling spectra of thin films of the ferromagnetic insulator europium sulfide on superconducting aluminum measured at 280 mK and in varying magnetic fields. We observe significant broadening of the superconducting energy gap and a variety of sub-gap structures induced by the presence of the ferromagnet. We interpret our findings based on the diffusive theory and a more advanced circuit theory model [3].

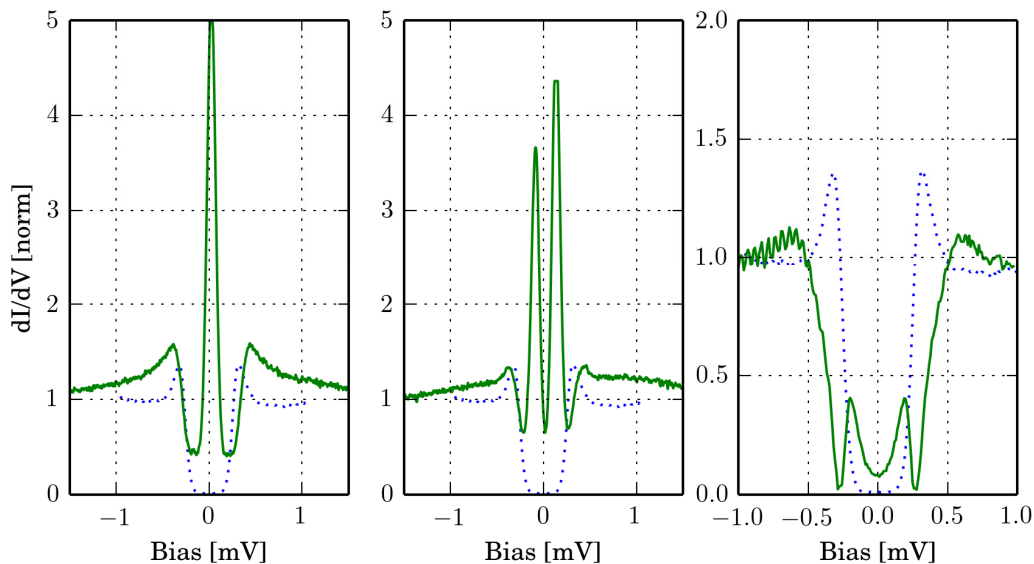


Fig. 1. Experimental observation of the differential conductance at $T = 280$ mK acquired by scanning tunneling spectroscopy in three different locations on an Al/EuS/Ag film sample.

[1] F. S. Bergeret, *Physical Review Letters*, **86** (2011) 4096.

[2] A. Di Bernardo, *Nature Communications*, **6** (2015) 8053.

[3] P. Machon, *Physical Review Letters*, **110** (2013) 047002.

2TL-D-5

STRONGLY SPIN-DEPENDENT EFFECTS AT INTERFACES BETWEEN SUPERCONDUCTORS AND MAGNETIC METALS AND INSULATORS*Machon P.¹, Wolf M.J.², Beckman D.², Belzig W.¹*¹ Department of Physics, University of Konstanz, Konstanz, Germany² Institute for Nanotechnology, Karlsruher Institut für Technologie, Karlsruhe, Germany
Wolfgang.Belzig@uni-konstanz.de

We present a combined experimental and theoretical work that investigates the proximity effect of a ferromagnetic-insulator - superconductor (FI-S) interface. The experimentally found differential conductance of an EuS-Al heterostructure is compared with the theoretical one. The simulation is based on the recent boundary condition, that treats arbitrarily strong spin-dependent effects. With the assumption of a uniform distribution of spin mixing angles that depend on the externally applied field, we already find good agreement between theory and experiment. The theory depends only on very few parameters, mostly specified by the experimental setup. As the main result, we observe that large spin mixing angles are possible, indicated by the highly nonlinear behaviour in dependence on an applied external field. We thus prove that it is not possible to generally assume weak spin-dependence, as it is usually done in theoretical treatments of ferromagnet-superconductor interfaces.

Support by DFG through SPP 1538 SpinCaT is acknowledged.

2TL-D-6

**LONG-RANGE PROXIMITY EFFECT IN NB-BASED
HETEROSTRUCTURES INDUCED BY A MAGNETICALLY
INHOMOGENEOUS PERMALLOY LAYER**

*Cirillo C.¹, Voltan S.², Ilyina E.A.³, Hernandez J.M.⁴, Garcia-Santiago A.⁴,
Aarts J.^{1,2}, Attanasio C.¹*

¹ CNR-SPIN and Dipartimento di Fisica ‘E. R. Caianiello’, Università degli Studi di Salerno,
Fisciano (Sa), Italy

² Kamerlingh Onnes-Huygens Laboratory, Leiden University, Leiden, The Netherlands
³ CERN, Geneva, Switzerland

⁴ Grup de Magnetisme, Departament de Física de la Matèria Condensada, Facultat de Física,
Universitat de Barcelona, Barcelona, Spain
attanasio@sa.infn.it

Superconductivity and ferromagnetism are competing phases whose coexistence is unlikely to occur. Differently from the case of bulk systems, the coexistence between superconductivity and ferromagnetism may be easily achieved in artificial superconductor/ferromagnet (S/F) hybrids. In these systems, the two antagonistic orderings are confined in spatially separated layers interacting via the proximity effect, which arises when a superconductor comes in metallic contact with a ferromagnet. In this case, the spin-singlet Cooper pairs enter the F-layer and magnetic excitations leak into the S-region across the S/F interface. As confirmed by many experiments, the penetration depth of singlets in the F-layer is, in the case of strong ferromagnets, of the order of only few nanometers. However, at the interface between a superconductor and a ferromagnet, conventional singlet Cooper pairs can be converted into equal-spin triplet ones. Since the triplets have their spins equally aligned, they are much less affected by the pair breaking caused by exchange field in F. Thus, once injected in the F-layer, at low temperatures they can survive over distances of the order of hundreds of nanometers, contrary to what happens for the singlets. So far, reproducible long-range effects were observed only in complex layered structures deliberately designed to provide the magnetic inhomogeneity. Here, we report that equal-spin triplet proximity can be induced in simple unstructured Nb/Py/Nb trilayers and Nb/Py bilayers by exploiting the intrinsic magnetic inhomogeneities of Py. In particular, we investigate the temperature dependence of the parallel upper critical field, $H_{c2\text{parallel}}(T)$, of metallic Nb/Py/Nb trilayers and Nb/Py bilayers. The thickness of the Nb layers, d_{Nb} , is kept constant at 25 nm while the thickness of the Py layer, d_{Py} , is varied across different magnetic regimes: homogeneous (H), ESD (emerging stripe-domain) and SD (stripe-domain). For the trilayer with d_{Py} in the ESD regime, namely for $125 \text{ nm} < d_{\text{Py}} < 300 \text{ nm}$, a 2D–3D dimensional crossover (DCO) was observed at T close to $0.9 T_c$, where T_c is the superconducting critical temperature of the system. Moreover, a clear kink is present in the $H_{c2\text{parallel}}(T)$ curves of Nb/Py bilayers when $d_{\text{Py}} = 200 \text{ nm}$. These observations, which we attribute to an increased effective thickness of the superconducting layer, cannot be explained within the spin-singlet proximity effect, because of the short coherence length of Py, estimated to be about 1.9 nm. On the contrary, the results are rather compatible with a long-range spin-triplet proximity effect, induced by the inhomogeneous magnetic configuration of the ESD regime, which seems to provide the optimal degree of inhomogeneous magnetization for the singlet-to-triplet conversion. The interpretation is confirmed by the dependence T_c versus d_{Py} for the trilayers, which shows a strong suppression of T_c in the ESD regime where the leakage of long-range Cooper pairs is maximum.

2TL-D-7

SUPERCONDUCTING SPIN-VALVES*Tagirov L.R.*^{1,2,3}, *Kupriyanov M.Yu.*^{2,4,5}, *Sidorenko A.S.*^{3,6}, *Kushnir V.N.*^{7,8}¹ Zavoisky Physical-Technical Institute of RAS, Kazan 420029, Russia² Institute of Physics, Kazan Federal University, Kazan 420008, Russia³ University of Augsburg, D-86159 Augsburg, Germany⁴ Skobeltsyn Institute of Nuclear Physics, Moscow State University, Moscow 119991, Russia⁵ Moscow Institute of Physics and Technology, Dolgoprudny 141700, Russia⁶ Institute of Electronic Engineering and Nanotechnologies ASM, Kishinev MD-2028, Moldova⁷ Belarus State University, Physics Faculty, 220000 Minsk, Belarus⁸ Belarus State University of Informatics and Radioelectronics, 220013 Minsk, Belarus

ltagirov@mail.ru

A heterostructure comprising several ferromagnetic (F) and superconducting (S) layers acquires functionality of managing the superconducting properties of a system applying external magnetic fields. It is superconducting spin-valve effect. In the talk, several designs of the superconducting spin-valves are considered, the existing experimental data for the weak and strong ferromagnetic materials are analyzed; the role of the domain structure of the ferromagnet and the scattering of electrons with spin flip on the S-F interfaces on the magnitude of the valve effect is described. The effect of the triplet pairing components on the critical temperature of S-F heterostructures is analyzed. The theoretical as well as experimental works in the field are reviewed.

Support by DFG HO 955/9-1 and RFBR (grants No. 16-02-01171-a, 15-32-20362-bel_a_ved) is gratefully acknowledged. L.R.T. thanks the RAS Presidium Programme “Actual problems of low temperature physics” for the partial support.

2OR-D-8

SUPERCONDUCTING SPIN VALVES BASED ON MAGNETIC SPIRAL REORIENTATION

Pugach N.G.^{1,2}, Safonchik M.O.³

¹ Skobeltsyn Institute of Nuclear Physics Lomonosov Moscow State University,
Moscow, Russia

² National Research University Higher School of Economics, Moscow, Russia

³ A. F. Ioffe Physical-Technical Institute, St Petersburg, Russia
pugach@magn.ru

Non-collinear magnetic ordering may convert singlet superconducting correlations into long-range triplet correlations (LRTC) [1-3]. The magnetically controlled appearance of such correlation may be used to change the state of low-temperature spintronics devices. The experimental evidence of such triplet correlations was revealed by the recent observation of long-range Josephson effect [1,2,5,6]. All these LRTC magnetic structures [1,2,4-6] contained from 4 to 9 different layers that demand high requirements to technology and magnetic configuration controlling. Recently also spiral (or conical, like Ho) ferromagnets have been used as elements of complex multilayered magnetic structures [5,7,10], and the corresponding proximity effect was calculated for some configurations [8-11].

We propose to use only one magnetic layer with Dzyaloshinsky-Moriya type interaction and intrinsic non-collinear magnetization to create superconducting LRTC spin valves of a new type. The novel of this proposition is that the spin-valve effect may be realized on only one spiral-magnetic layer. It may be easier fabricated and controlled at contemporary technology.

The calculations are based on Green's functions method within the framework of quasiclassical theory of superconductivity in the "dirty" limit using the Usadel equations. Suitable materials for the realization of the proposed structures may be Nb or Al as a superconductor and MnSi like compounds as magnetic material. These structures are promising for application as elements of magnetic memory for low-temperature electronics. The existence of different magnetic orientations separated by a potential well may help to solve the problem of half-select for the magnetic memory switch [12].

Financial support by CPTGA, the Royal Society RFBR International Exchanges Program, Project T3-89 "Macroscopic quantum phenomena at low and ultralow temperatures" of the National Research University Higher School of Economics, Russia is acknowledged.

- [1] M. G. Blamire and J. W. A. Robinson, *J. Phys.: Condens. Matter*, **26** (2014) 453201.
- [2] J. Linder and J. W. A. Robinson, *Nature Physics*, **11** (2015) 307.
- [3] F. S. Bergeret, A. F. Volkov, and K. B. Efetov, *Rev. Mod. Phys.*, **77** (2005) 1321.
- [4] A. A. Golubov, M. Yu. Kupriyanov, and E. Il'ichev, *Rev. Mod. Phys.*, **76** (2004) 411.
- [5] J. W. A. Robinson, J. D. S. Witt, and M. G. Blamire, *Science*, **329** (2010) 59.
- [6] T. S. Khaire W. P. Pratt, Jr., and N. O. Birge, *Phys. Rev. Lett.*, **104** (2010) 137002.
- [7] I. Sosnin, H. Cho, V. Petrashov, *Phys. Rev. Lett.*, **96** (2006) 157002.
- [8] T. Champel, M. Eschrig, *Phys. Rev. B*, **72** (2005) 054523.
- [9] C. Wu, O. Valls, K. Halterman, *Phys. Rev. B*, **86** (2012) 184517.
- [10] G. Halasz, J. Robinson, M. Blamire, et. al., *Phys. Rev. B*, **79** (2009) 224505, *ibid.* **84** (2011) 024517.
- [11] A. F. Volkov, A. Anishchanka, and K. B. Efetov, *Phys Rev. B*, **73** (2006) 104412.
- [12] T. Larkin, V. Bol'ginov, V. Ryazanov, et. al., *Appl. Phys. Lett.*, **100** (2012) 222601.

2OR-D-9

CRITICAL JOSEPHSON CURRENT CONTROLLED BY SPIRAL RE-ORIENTATION IN MnSi

Heim D.M.¹, Pugach S.², Pugach N.G.^{1,3}

¹ National Research University Higher School of Economics, 101000, Moscow, Russia

² Leibniz Universität Hannover, 30167, Hannover, Germany

³ Skobeltsyn Institute of Nuclear Physics, Moscow State University, 119991, Moscow, Russia
physics@d-heim.de

A new generation of superconductor-based supercomputers is in the focus of current research [1]. Necessary components for their ultralow-power operations are circuit elements based on superconducting/magnetic devices [2]. Similar to [3], we propose a cryogenic memory element by combining superconducting (S) with magnetic material (M) which has a controllable intrinsic non-collinear magnetization. In contrast to [3], we do not consider M in a spin valve with changeable critical temperature T_c , but in a Josephson junction with controllable critical current. We show that the current changes with the spiral vector \mathbf{Q} , which characterizes the magnetic structure of M, see Fig. 1. The vector \mathbf{Q} may be aligned in different directions under the control of a weak magnetic field. Compared to cryogenic memory proposed earlier, our device has the following advantages:

It contains only one magnetic layer, which makes it easier to fabricate and control.

Its ground states are separated by a potential barrier, which prevents uncontrolled switching.

It may be better compatible with discrete and quantum logical elements based on Josephson junctions than the spin valve proposed in [3].

To determine the critical current, we solve the linearized Usadel equations which are valid in the diffusive limit. This is reasonable because low-temperature superconducting nanostructures made by sputtering are usually diffusive. The linearization step is valid close to T_c , where superconducting correlations are weak. As magnetic material, we propose an itinerant cubic helimagnet of the MnSi family, because their magnetic spiral direction may be switched in a few different basic directions [4] in contrast to e.g. the material H_o or E_r .

In conclusion, we calculate the critical current of a Josephson junction involving a spiral magnet which is characterized by a spiral vector \mathbf{Q} . We show that the current changes with the direction of this vector, which may represent basic computational states. This is a promising indicator that our proposed device can be used as a novel superconducting memory element.

Support by Project T3-89 “Macroscopic quantum phenomena at low and ultralow temperatures” of the National Research University Higher School of Economics, Russia, is acknowledged.

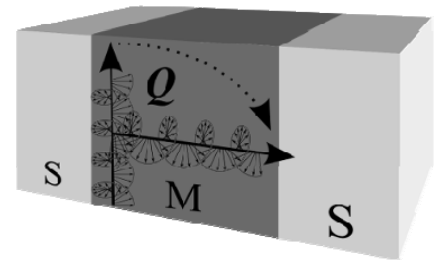


Fig. 1. The Josephson junction configuration we consider. The spiral vector \mathbf{Q} of the magnet M can point in different directions.

[1] J. Linder, J.W.A. Robinson, *Nat. Phys.*, **11** (2015) 307.

[2] M. Manheimer, *IEEE Trans. Appl. Supercond.*, **25** (2015) 1.

[3] N.G. Pugach, M. Safonchik, T. Champel, M.E. Zhitomirsky, E. Lähderanta, M. Eschrig, C. Lacroix, *arXiv:1702.08828v1* (2017).

[4] S.V. Grigoriev, S.V. Maleyev, A.I. Okorokov, Yu.O. Chetverikov, H. Eckerlebe, *Phys. Rev. B*, **73** (2006) 224440.

2OR-D-10

DENSITY OF STATES IN QUASI-ONE-DIMENSIONAL SUPERCONDUCTOR GOVERNED BY QUANTUM FLUCTUATIONS

Arutyunov K.Yu.^{1,2}, *Radkevich A.A.*³, *Semenov A.G.*^{1,3,4}, *Zaikin A.D.*^{4,5}

¹ National Research University Higher School of Economics, Moscow, Russia

² Kapitza Institute for Physical Problems, Moscow, Russia

³ Moscow Physical Technical University, Dolgoprudni, Russia

⁴ Lebedev Physical Institute RAS, Moscow, Russia

⁵ Institute of Nanotechnology, Karlsruhe Institute of Technology, Karlsruhe, Germany
karutyunov@hse.ru

Recently, the subject of quasi-one-dimensional superconductivity has attracted the significant attention [1]. Peculiarity of such systems is the pronounced manifestation of fluctuation effects, which affect both transport [2] and thermodynamic properties [3]. When considering fluctuations of the complex superconducting order parameter $\Delta = |\Delta|e^{i\phi}$, it is necessary to distinguish between fluctuations of phase ϕ and modulus $|\Delta|$. In particular, it has been shown [4] that in thin superconducting channels, phase fluctuations inevitably lead to excitation of charge density waves - the Mooij-Schoen mode [5]. The interaction of charge carriers with such plasmons results in redistribution of electronic states and, in particular, to smearing of gap singularity in density of states (DOS). The objective of the work is the investigation of this intriguing phenomenon.

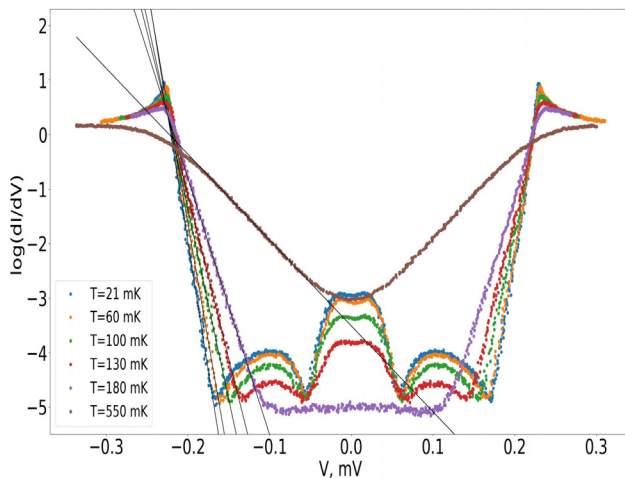


Fig. 1. Differential current-voltage characteristics of S1-I-S2 tunnel structure, where S2 is thin superconducting nanowire governed by quantum fluctuations.

I-V characteristics of tunnel S1-I-S2 junctions, where S1 is massive superconductor and S2 electrode is a thin superconducting nanowire, have been studied. The observed broadening of I-V dependencies at the gap edge is interpreted as manifestation of quantum fluctuations of the order parameter. The model, taking into consideration the modification of DOS by plasmonic modes activated in a quasi-one-dimensional superconductor due to fluctuations, has been suggested [6]. The model provides reasonable qualitative agreement with experiment. The exponential 'penetration' of DOS into the sub-gap region (Fig. 1) is clearly traced, which coincides with prediction of the model [6]. The temperature dependence of the sub-gap DOS 'penetration' well corresponds to the predicted value $k_B/e = 8.6 \cdot 10^{-5}$ V/K.

Presumably better agreement between theory and our experiment can be achieved if an advanced model considers also the 'direct' impact of phase and modulus fluctuations of the superconducting order parameter.

Support by Russian Science Foundation (Grant No. 16-12-10521) is acknowledged.

[1] K.Yu. Arutyunov, D.S. Golubev and A.D. Zaikin, *Phys. Rep.*, **464** (2008) 1.

[2] N.Giordano, *Phys. Rev. Lett.*, **61** (1988) 2137.

[3] K.Yu. Arutyunov et al., *Sci. Rep.*, **2** (2012) 213.

[4] A. van Otterlo, D.S. Golubev, A.D. Zaikin, and G. Blatter, *Eur. Phys. J.*, **10** (1999) 131.

[5] J.E. Mooij and G. Schön, *Phys. Rev. Lett.*, **55** (1985) 114.

[6] A.A. Radkevich, A.G. Semenov and A.D. Zaikin, *Phys. Rev. B*, to be published (2017).

2 July

Sunday

12:00-13:30

15:00-17:15

oral session

2TL-C

2RP-C

2OR-C

**“Magnetophotonics
(Ultrafast)”**

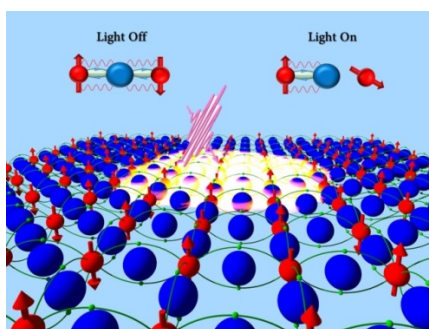
2TL-C-1

MAGNETISM ON THE TIMESCALE OF THE EXCHANGE INTERACTION

Rasing T.

Radboud University, Institute for Molecules and Materials, Nijmegen, the Netherlands
th.rasing@science.ru.nl

From the discovery of sub-picosecond demagnetization over a decade ago to the recent demonstration of magnetization reversal by a single 40 femtosecond laser pulse, the manipulation of spins by ultrashort laser pulses has become a fundamentally challenging topic with a potentially high impact for future spintronics, data storage and manipulation and quantum computation. The realization that femtosecond laser induced all-optical switching (AOS) as observed in ferrimagnets exploits the exchange interaction between their sublattices, opens the way to engineer magnetic materials for AOS. This discovery opens the way to engineer new and rare-earth-free magnetic materials for AOS, such as multilayers containing FePt or Co. Recent results demonstrate that AOS can also be achieved in insulating, magnetic garnets at record low energy, opening new perspectives for highly energy efficient data manipulation.



Support by IEEE, ARC, and ARCNN is acknowledged.

- [1] A. Kirilyuk, et al, *Rev. Mod.Phys.*, **82** (2010) 2731-2784.
- [2] I. Radu et al, *Nature*, **472** (2011) 205.
- [3] J. Mentink et al, *Phys.Rev.Lett.*, **108** (2012) 057202.
- [4] T. Ostler et al, *Nature Comm.*, **3** (2012) 666.
- [5] C. Graves et al, *Nature Materials*, **12** (2013) 293.
- [6] R. Evans et al, *Appl.Phys.Lett.*, **104(8)** (2014) 082410.
- [7] L. LeGuyader et al, *Nature Comm.*, **6** (2015) 5839.
- [8] I. Radu et al, *Spin*, **5** (2015) 550004.
- [9] R. V. Mikhaylovskiy et al, *Nature Comm.*, **6** (2015) 8190.
- [10] Tian-Min Liu et al, *Nano Letters*, **15(10)** (2015) 6862–6868.
- [11] T. J. Huisman, et al, *Nature Nanotechnology*, **11** (2016) 455.
- [12] A. Stupakiewicz et al, *Nature*, **542** (2017) 20807.

2TL-C-2

ULTRAFAST PHOTO-MAGNETIC SWITCHING IN DIELECTRICS

Stupakiewicz A.

Faculty of Physics, University of Białystok, Białystok, Poland
and@uwb.edu.pl

Finding a conceptually new way to switching of the magnetization with the lowest possible production of heat and simultaneously at the fastest possible time-scale is a new challenge in fundamental magnetism [1] as well as an increasingly important issue in modern storage technology. Recent discovery of all-optical switching demonstrates that it is possible to switch magnetization exclusively in metals by femtosecond circularly polarized pulses [2,3]. However, the switching mechanism in these materials are directly related to laser-induced heating close to the Curie temperature. Magnetization switching in optically transparent dielectrics by femtosecond laser pulses can be the way for the ultrafast recording with the lowest heat load, but so far it has remained to be a challenge.

We demonstrate ultrafast nonthermal photo-magnetic switching in magnetic dielectrics using time-resolved magneto-optical imaging tools with Faraday geometry [4]. In ferrimagnetic Co-doped yttrium iron garnet thin film a single linearly polarized femtosecond laser pulse promote switching between two magnetization states at room temperature. Changing the polarization of the laser pulse we deterministically steer the net magnetization in the garnet, write "0" and "1" magnetic bits at will (see Fig. 1). This mechanism allows ever fastest write-read magnetic recording event with about 20 ps accompanied by record low heat load.

The process of recording is based on magnetization precession due to photo-induced magnetic anisotropy in a garnet film. We anticipate that the nonthermal magnetization switching due to the photo-magnetic effect open up a plethora of opportunities for a novel design of all-optical magnetic recording.

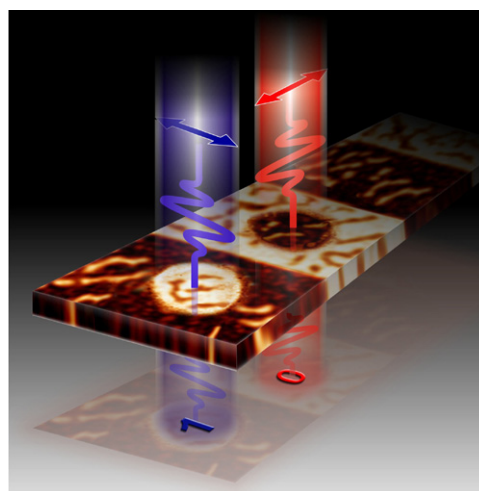


Fig. 1. Schematic visualization of ultrafast nonthermal photo-magnetic recording in Co-doped iron garnet.

Support by the National Science Centre Poland for project DEC-2013/09/B/ST3/02669.

[1] A. Kirilyuk, et al., *Rev. Mod. Phys.*, **82** (2010) 2731.

[2] T. A. Ostler, et al., *Nat. Commun.*, **3** (2012) 666.

[3] S. Mangin, et al., *Nat. Mater.*, **13** (2014) 286.

[4] A. Stupakiewicz, et al., *Nature*, **542** (2017) 71.

2TL-C-3

EXPERIMENTAL OBSERVATION OF DOMAIN WALL MOTION INDUCED BY LASER PUMP-PULSE

Gerasimov M.V.¹, Logunov M.V.^{1,2}, Nikitov S.A.^{2,3}, Nozdrin Yu.N.⁴, Spirin A.V.¹, Tokman I.D.^{4,5}

¹National Research Ogarev Mordovia State University, Saransk, Russia

²Kotel'nikov Institute of Radio Engineering and Electronics of RAS, Moscow, Russia

³Moscow Institute of Physics and Technology, Dolgoprudny, Russia

⁴Institute for Physics of Microstructures of RAS, Nizhny Novgorod, Russia

⁵Lobachevsky State University of Nizhny Novgorod, Nizhny Novgorod, Russia

logunov@cplire.ru

Interest in the study of the interaction of laser pulses with magnetic films is due to the search for ways of ultrafast local switching of the magnetization state [1]. Earlier it was theoretically shown that light pulses can also be used to manipulate the properties of domain walls [2-3]. An infrared-pump-induced change of a spin structure within domain walls on a subpicosecond time scale was observed [4], but the walls remained motionless. In this work, we present an experimental observation of domain wall motion in garnet films induced by circularly polarized laser pump-pulse (the pulse duration is 5 ns; the wavelength is 527 nm). We studied in detail the time evolution of the domain-wall displacement [5]. It was found that photomagnetization signal contains both the part that does not depend on the pump-pulse polarization type, and the part that depends on the circular polarization direction (Fig. 1).

A relationship between this effects, on the one part, and a change in the magnetization and domain widths (i.e. domain-wall motion), on the other part, was demonstrated. The domain-wall motion initiated by the circularly polarized laser pump pulse continues in the same direction for a time more than an order of magnitude exceeding the laser pulse duration. In general, the time evolution of the domain-wall movement occurs in three stages.

Support by RFBR (#15-02-03046, #15-07-08152A) and RSF (#14-19-00760) is acknowledged.

[1] A. Kirilyuk, A.V. Kimel, Th. Rasing, *Rep. Prog. Phys.*, **76** (2013) 026501.

[2] G.M. Genkin, I.D. Tokman, *Sov. Phys. JETP*, **55** (1982) 887-890.

[3] A.F. Kabychenkov, *Sov. Phys. JETP*, **73** (1991) 672-682.

[4] B. Pfau et al., *Nature Comm.*, **3** (2012) 1100.

[5] M.V. Gerasimov et al., *Phys. Rev. B*, **94** (2016) 014434.

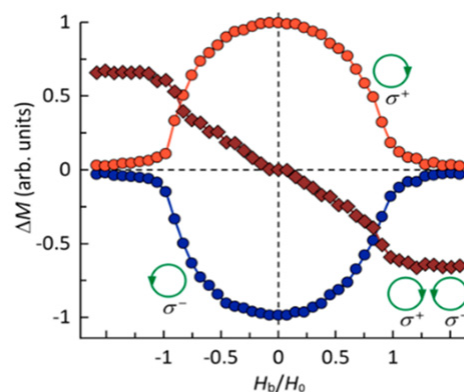


Fig. 1. Normalized field dependences of the photomagnetization pulses amplitudes ΔM caused by the polarization-dependent (red / blue circles for a laser pulse with right / left circular polarizations) and the polarization-independent (diamonds) effects, respectively.

2TL-C-4

MAGNETIC-FIELD-INDUCED OPTICAL HARMONICS GENERATION IN DIAMAGNETIC, DILUTED-MAGNETIC, AND MAGNETICALLY-ORDERED SEMICONDUCTORS

Yakovlev D.R.^{1,2}

¹ Experimentelle Physik 2, Technische Universität Dortmund, D-44227 Dortmund, Germany

² Ioffe Physical-Technical Institute, Russian Academy of Sciences, 194021 St. Petersburg, Russia
dmitri.yakovlev@tu-dortmund.de

Nonlinear optics of semiconductors is an important field of fundamental and applied research, but the role of excitons in the coherent processes leading to optical harmonics generation has remained essentially unexplored. Here we present a survey of our results on experimental and theoretical study of second- and third-harmonic generation (SHG and THG) involving exciton resonances in diamagnetic semiconductors (GaAs, CdTe, ZnO), diluted magnetic semiconductors (CdMnTe) and magnetically-ordered semiconductors (EuTe and EuSe) [1-8]. Additionally to crystallographic signals caused by the symmetry of the crystal lattice and exciton wavefunctions, SHG and THG signals induced by external magnetic and electric fields on the exciton resonances have been found. A microscopic theory of harmonics generation on excitons is developed, which shows that the nonlinear interaction of coherent light with excitons has to be considered beyond the electric-dipole approximation. Depending on the particular symmetry of the exciton states SHG/THG can originate from the electric- and magnetic-field-induced perturbations of the excitons due to the Stark effect, the spin as well as orbital Zeeman effects, or the magneto-Stark effect. The importance of each mechanism is analyzed and discussed by confronting experimental data and theoretical results for the dependences of the SHG signals on photon energy, magnetic field, electric field, crystal temperature, and light polarization. Our recent results show that exciton-polaritons in semiconductors with strong Coulomb interaction like ZnSe can significantly contribute to the optical harmonics generation.

- [1] V.V.Pavlov et al., *Phys. Rev. Lett.*, **94** (2005) 157404.
- [2] I. Sanger et al., *Phys. Rev. Lett.*, **96** (2006) 117211.
- [3] I. Sanger et al., *Phys. Rev. B*, **74** (2006) 235217 .
- [4] B. Kaminski et al., *Phys. Rev. Lett.*, **103** (2009) 057203.
- [5] B. Kaminski et al., *Phys. Rev. B*, **81** (2010) 155201.
- [6] M. Lafrentz et al., *Phys. Rev. Lett.*, **110** (2013) 116402.
- [7] M. Lafrentz et al., *Phys. Rev. B*, **88** (2013) 235207.
- [8] D. Brunne et al., *Phys. Rev. B*, **92** (2015) 085202.

2TL-C-5

MAGNETOPHOTONICS WITH ALL-DIELECTRIC METASURFACES*Barsukova M.G.¹, Shorokhov A.S.¹, Musorin A.I.¹, Neshev D.N.², Kivshar Y.S.², Fedyanin A.A.¹*¹ Faculty of Physics, Lomonosov Moscow State University, Moscow 199991, Russia² Nonlinear Physics Centre, The Australian National University, Canberra, ACT 2601, Australia

fedyanin@nanolab.phys.msu.ru

The concept of metamaterials allows design of artificial subwavelength meta-atoms that support a strong magnetic response, usually termed as optical magnetism, even when they are made of nonmagnetic materials. Recent developments in the nanoscale optical physics gave a birth to a new branch of nanophotonics aiming at the manipulation of optically-induced Mie type resonances in dielectric nanoparticles made of materials with high refractive indices. It has been shown recently that resonant dielectric structures offer unique opportunities for reduced dissipative losses and large resonant enhancement of both electric and magnetic fields. High-index dielectric structures can be employed as new building blocks to realize unique functionalities such as magnetic Fano resonances, highly transmittable metasurfaces, and novel metadevices. Here we extend the concept of high-index resonant nanophotonics to the case of magnetically active materials and study the magneto-optical response of a dielectric metasurface covered with a thin magnetic film. We have reported on the demonstration of the magneto-optical effects enhanced by optically-induced magnetic dipole Mie resonances manifesting a strong interaction of magnetic properties with induced "optical magnetism". We believe our findings will allow novel approaches in a magnetic control of recently reported strong nonlinear effects in nanoparticles as well as in the realization of the time-reversal symmetry breaking at the nanoscale for photonic topological insulators topology. In addition, our results could pave a way towards a new platform for active and nonreciprocal photonic nanostructures and metadevices, which could be tuned by the external magnetic field.

2RP-C-6

PLASMON-ENHANCED MAGNETO-OPTICAL RESPONSE FOR TUNABLE WAVEPLATE

Shaimanov A.N.^{1,2}, Khabarov K.M.^{1,3}, Baryshev A.V.^{1,3}

¹ All-Russia Research Institute of Automatics, 127055 Moscow, Russia

² Moscow State University, Moscow, 119991, Russia

³ Moscow Institute of Physics and Technology, Moscow 141700, Russia

baryshev@vniia.ru

Amplification of the near-field by plasmons is shown to be useful for tailoring properties of magneto-optical (MO) materials comprising various plasmonic subsystems [1]. Fundamental and practical interest to artificial MO structures is to enhance MO responses of existing bulk materials and to control the flow of light by external magnetic fields [2-4].

To demonstrate an enhancement of the MO response of known MO materials due to localized surface plasmon resonance (LSPR), we introduce square two-dimensional (2D) lattices of metal (Au) nanospheres encased in a magnetic host (a layer bismuth-substituted yttrium iron garnet, Bi:YIG). We discuss 2D structures with simple square 2D lattices and discuss LSPRs on single nanospheres and their ensemble. Then, we select one lattice and introduce into it additional nanospheres composing another square lattice, thus forming a nested 2D lattice. Our studies showed that the number and spectral positions of the LSPR bands in spectra of nested gratings are governed by the radius of the additional nanospheres.

All the considered structures had the plasmon-enhanced MO response associated with light propagation damping; the MO response increased as transmission decreased. Experiments aimed at understanding this mechanism illustrated that the studied plasmonic Au-Bi:YIG structures were reciprocal media, since the polarization rotation did not accumulate in multiple-pass regimes in the Faraday geometry. Nature of the enhancement is that coupling to LSPR provides light trapping inside the structure. This trapping can be tuned by magnetic field allowing light to leak from the structure, and the particular design of the 2D structure defines the sign and magnitude of the MO response.

A dependence of LSPR and the MO response on parameters of the lattice and the scatterers in it was demonstrated: we (i) interpreted spectral positions of LSPR bands as a single scatterer- and periodicity-dependent ones, (ii) demonstrated a mechanism of the plasmon-modified enhancement of polarization rotation, and (iii) found that this enhancement can be strongly alternated with the period of the plasmonic 2D lattice and the radius of the nanospheres in it. It is the condition of crossing two LSPRs that attenuates propagation of the incident wave, when strongly localizing light at the Au–Bi:YIG interface, and modifies the initial polarization state. We believe that the current study provides a way for tailoring plasmonic magneto-optical structures for optical applications with requirements for modulating the polarization state on the nanosecond timescale.

[1] M. Inoue, M. Levy, and A. Baryshev, eds., *Magnetophotonics: From Theory to Applications* (Springer, 2013).

[2] V.V. Temnov et al., *Nat. Photonics*, **4**(107) (2010) 404-111.

[3] V.I. Belotelov et al., *Nat. Commun.*, **4** (2013) 2128.

[4] A.V. Baryshev, A.M. Merzlikin, *JOSA B*, **33**(7) (2016) 1399-1405.

2RP-C-7

1D MAGNETO-PHOTONIC CRYSTAL FOR OPTICAL SENSING

Merzlikin A.M.^{1,2}, Kuznetsov E.V.^{1,3}, Baryshev A.V.³

¹ITAE RAS, Moscow, Russia

²MIPT, Moscow, Russia

³FSUE VNIIA, Moscow, Russia

merzlikin_a@mail.ru

Optical sensors where refractive index sensing is achieved by dispersion of surface plasmon resonance are widely applied for detecting tiny variations in biological and chemical analytes [1]. Another effective approach to high-resolution sensing is usage of the s-polarized Bloch surface wave (BSW) resonance [2] excited on a surface of 1D photonic crystals [3]. All those sensors are based on shifting the resonance frequency at variation of analyte refractive index. In order to obtain significant variation in reflectance, this shift should be comparable to the thickness of resonance line. In other words the thinner resonance line the smaller variation of analyte refractive index can be measured. Usually, quality factor for s-polarized BSW resonance is significantly higher than for p-polarized. That is why s-polarized BSW is preferred than p-polarized.

Recently it was shown that magneto-optical effect might be increased at s-polarized BSW resonance [4] and thus it looks reasonable to utilize magneto-optical effects for enhancing sensitivity of such optical sensors. However system with just one s-polarized resonance shows strong anisotropy which may significantly suppress magneto-optical effects [5].

We have considered 1D photonic crystal made of Ta₂O₅/SiO₂ layers (placed on prism) covered by bismuth-doped yttrium-iron-garnet (Bi:YIG) layer. In this way analyte adjoin magneto-optical layer and variance of its refractive index may affect field distribution inside Bi:YIG and thus this variance may affect magneto-optical response.

The structure under consideration provides s- and p-polarized BSWs at zero magnetization of Bi:YIG. Moreover dispersion curves for those waves intersect. Magnetization of Bi:YIG results in hybridization of s- and p- polarized BSWs and rotation of reflected wave polarization. Similar to homogeneous media large rotation angle corresponds to the case when magnetization is parallel to wavevectors of BSWs.

Calculation shows that each BSW resonance results in enhancement of rotation angle; however strong enhancement observed near intersection point of dispersion curves only where both s- and p-polarized BSWs resonance appearance simultaneously. Around this point effective anisotropy (which is proportional to the difference of wavevectors for s- and p- polarized BSWs) is small and magneto-optical activity is not suppressed. Maximum sensitivity at variation of analyte refractive index also corresponds to intersection of dispersion curves and significantly exceeds sensitivity of solitary BSW resonance.

[1] J. Homola, *Surface Plasmon Resonance Based Sensors, Springer Series on Chemical Sensors and Biosensors*, Springer-Verlag, Berlin- Heidelberg-New York, (2006).

[2] P. Yeh, A. Yariv and A.Y. Cho, *Appl. Phys. Lett.*, **32** (1978) 104-115.

[3] E.V. Alieva, V.N. Konopsky, *Sens. Actuators B*, **99** (2004) 90-97.

[4] M.N. Romodina, I.V. Soboleva, A.A. Fedyanin, *JMMM*, **415** (2016) 82-86.

[5] A.M. Merzlikin, A.P. Vinogradov, M. Inoue, A.B. Khanikaev, A.B. Granovsky, *JMMM*, **300** (2006) 108-111.

2RP-C-8

PLASMONIC ARTIFICIAL MAGNETIC LATTICE

Uchida H.¹, Ooki K.², Saito S.², Goto T.^{1,3}, Takagi H.¹, Nakamura Y.¹, Lim P.B.¹, Inoue M.¹

¹ Toyohashi University of Technology, Toyohashi, Japan

² Tohoku University, Sendai, Japan

³ JST PRESTO, Kawaguchi, Japan

uchida@ee.tut.ac.jp

A magnetic material having periodical structure is an artificial magnetic lattice, which can show change of its original property. In a composite structure with Au particles, Faraday rotation is enhanced at a wavelength for exciting surface plasmon resonance [1]. If the Au particles are arranged randomly, a plasmonic wavelength is almost constant like 650 nm. However, the garnet composite with periodically arranged Au particles shows different optical and magneto-optical responses. In this article, we discuss optical and magneto-optical properties obtained by experiments and by using the finite-difference time-domain (FDTD) method.

Fig. 1 shows squarely arranged Au particles that were fabricated by electron beam lithography on a quartz substrate; Bi substituted yttrium iron garnet (Bi:YIG) film was deposited. In transmissivity and rotation spectra, several absorption bands and enhanced Faraday rotation were observed at the same wavelengths. The deepest absorption band shifted to the long wavelength side with increasing periods of Au particles.

In FDTD simulation, similar transmissivity spectra with several absorption bands were also obtained. Fig. 2 shows electric field distributions at (a) 800 nm and (b) 600 nm, which corresponds to the wavelengths at the first absorption band (the deepest band) and the third one. The first and second absorption band shifted to long wavelength side with increasing a diameter, but the third and fourth absorption bands shifted to the short wavelength side. These differences can relate complexity of polarization.

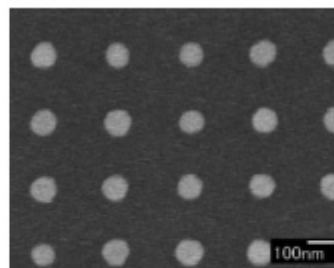


Fig. 1 A SEM image of squarely arranged Au particles. Period: 300nm, diameter: 103nm.

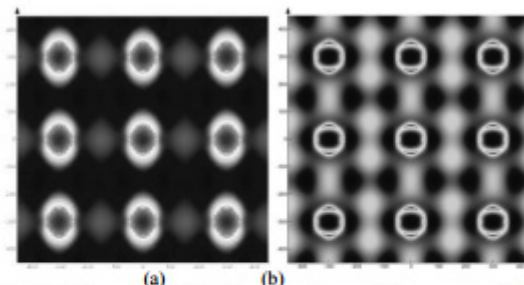


Fig. 2. Electric field distributions of the composite structure obtained by FDTD method. Diameter: 100 nm, period: 300 nm. (a) wavelength: 800 nm, (b) wavelength: 600 nm.

[1] H. Uchida, Y. Mizutani, Y. Nakai, A. A. Fedyanin and M. Inoue, *J. Phys. D: Appl. Phys.*, **44** (2011) 064014.

2RP-C-9

NON-ERROR RECONSTRUCTION OF MAGNETIC HOLOGRAM MEMORY

Nakamura Y.¹, Shirakashi Z.¹, Takagi H.¹, Goto T.^{1,2}, Lim P.B.¹, Uchida H.¹, Inoue M.¹

¹ Toyohashi University of Technology, Toyohashi, Japan

² JST, PRESTO, Kawaguchi, Japan

nakamura@ee.tut.ac.jp

Holographic memory is expected to be a high-capacity data storage exceeding 1 TB/disk with fast data transfer rates [1]. We have developed a collinear holographic system that can write and read data using a single optical axis with a spatial light modulator (SLM). Magnetic volumetric holograms, which are recorded as magnetization directions through thermomagnetic recording using magnetic garnets as recording media, are rewritable holograms with long-term stability. We demonstrated that the magnetic hologram can be recorded and reconstructed from transparent magnetic garnet films of $\text{Bi}_{1.3}\text{Dy}_{0.85}\text{Y}_{0.85}\text{Fe}_{3.8}\text{Al}_{1.2}\text{O}_{12}$ (Bi:RIG) using the collinear holographic system [2]. However, the reconstructed images were not enough clear for the practical recording applications. In this work, we report our recent achievement of magnetic hologram memory including non-error reconstruction of magnetic hologram data using multilayered media with artificial magnetic lattices.

Originally, we used an optical diffuser to suppress excessive energy concentration at focal point in recording process. However, the O to O image through diffuser was not clear, so we modified the recording conditions without diffuser such as recording position from the focal point and the shape of reference beam.

Figure 1(a) shows reconstructed images encoded with 2:4, 3:9, and 3:16 modulation rules, and good reconstructed images could be obtained. From these images, the error ratio defined as the ratio of correctly reconstructed bit number to the number of all bits (48x48) was evaluated for each pattern, and the result is shown in Fig. 1(b). The error ratio decreased as increasing the recording energy. This means that the formation of deep magnetic fringe is important to achieve clear reconstruction images. Especially, applying the 3:16 modulation rule, we could obtain non-error reconstruction at the recording energy higher than 50 $\mu\text{J}/\text{pulse}$. This suggests that the signal pattern and white ratio are important parameters to achieve high quality reconstructed images without error. In conclusion, we succeeded in the error-free reconstruction with the 3:16 modulation rule for signal encoding method. This means that the magnetic hologram has an enough potential for hologram memory. In addition, some recent results such as magnetic assist recording and new media will be also presented in conference.

This work was supported in part by the Grants-in-Aid for Scientific Research (S) 26220902, (A) 15H02240, and No. 26706009. We gratefully acknowledge the works of Mr. Shota Suzuki and Dr. Ryosuke Isogai.

[1] H. Horimai, X. Tan, *Proc. SPIE*, **5939** (2005) 593901(9).

[2] Y. Nakamura, H. Takagi, P. B. Lim, and M. Inoue, *Opt. Express*, **22** (2014) 16439–16444.

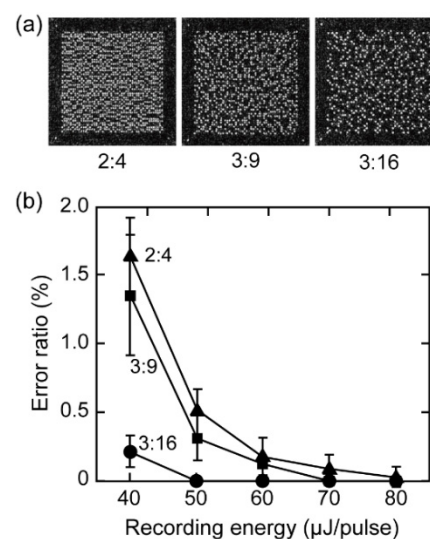


Fig. 1. (a) The reconstructed images and (b) the error ratio encoded with 2:4, 3:9, and 3:16 modulation rules recorded at 80 μJ .

2RP-C-10

BITHMUTH-SUBSTITUTED NEODYMIUM IRON GARNET FILMS FOR MAGNETO-OPTICAL IMAGING

Ishibashi T., Nagakubo Y., Baba and Lou G.

Nagaoka University of Technology, Niigata, Japan

t_bashi@mst.nagaokaut.ac.jp

We developed highly bismuth-substituted iron garnet films, $\text{Nd}_{0.5}\text{Bi}_{2.5}\text{Fe}_5\text{O}_{12}$ (Bi2.5:NIG) that had a large magneto-optical (MO) figure of merit and controllable magnetic anisotropy [1,2]. Consequently, this new material became one of the most promising magneto-optical (MO) material for applications, such as MO imaging plates, optical isolators, MO spatial light modulators, etc. In this paper, we report on magnetic and MO properties of Bi2.5:NIG and new MO imaging techniques using Bi2.5:NIG films [3,4].

Bi2.5:NIG films were prepared on GGG and glass substrates by metal-organic decomposition (MOD) method using metal-organic solutions produced by Kojundo Chemical Laboratory Ltd. MOD process consists of spin coating of MOD solution (3000 rpm, 60 seconds), drying (100°C, 30 minutes), pre-annealing (450°C, 10 minutes), annealing for crystallization (600-700°C, 3 hours).

Figure 1 shows a photo of a $\phi 6$ -inch size Bi2.5:NIG film prepared on a glass substrate. It can be seen that a uniform Bi2.5:NIG film was obtained. Figure 2 shows a photo a MO image of a commercial magnet measured using the Bi2.5:NIG film. Magnetic field distribution was clearly observed. Black and white are representing positive and negative values of perpendicular components of the strayed magnetic fields from the magnet.

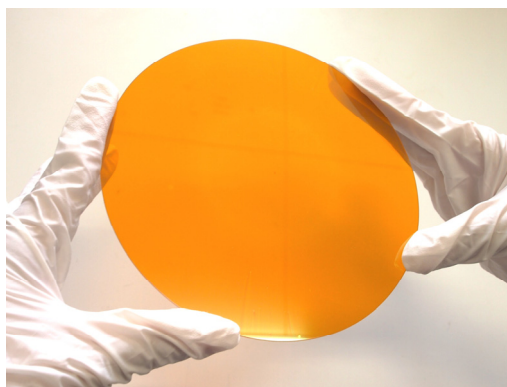


Fig. 1. Bi2.5:NIG film on glass substrate.

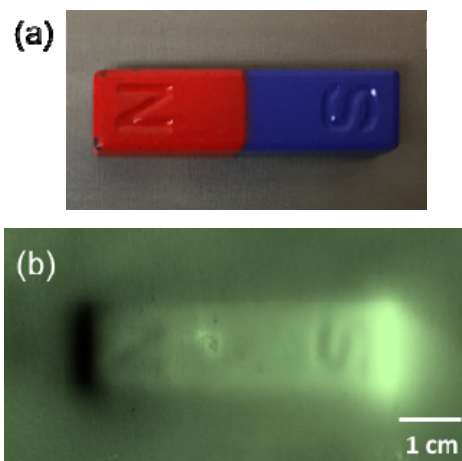


Fig. 2. (a) a photo and (b) a MO image of a commercial magnet.

[1] G. Lou, T. Yoshida, and T. Ishibashi, *J. Appl. Phys.*, **117** (2015) 17A749.

[2] M. Sasaki, G. Lou, Q. Liu, M. Ninomiya, T., Kato, S. Iwata, T. Ishibashi, *Jpn. J. Appl. Phys.*, **55** (2016) 055501.

[3] T. Ishibashi, G. Lou, A. Meguro, T. Hashinaka, M. Sasaki and T. Nishi, *Sensors and Materials*, **27** (2015) 965–970.

[4] Y. Nagakubo, Y. Baba, Q. Liu, G. Lou, T. Ishibashi, *J. Mag. Soc. Jpn.*, **41** (2017) 29-33.

2OR-C-11

OPTIMIZATION OF NONLINEAR MAGNETIC CONTRAST IN KRETSCHMANN MULTILAYER STRUCTURES

Tran N.M.¹, Traum C.², Alekhin A.¹, Juvé V.¹, Vaudel G.¹, Razdolski I.⁴, Makarov D.³, Seletskiy D.², Temnov V.V.¹

¹ Institut des Molécules et Matériaux du Mans (IMMM CNRS 6283), Le Mans, France

² Chair of Ultrafast Phenomena & Photonics, Universität Konstanz, Konstanz, Germany

³ Institute of Ion Beam Physics & Materials Research HZDR, Dresden, Germany

⁴ Fritz-Haber Institute of the Max-Planck Society, Berlin, Germany

ngoc_minh.tran@univ-lemans.fr

Combining the plasmonic field enhancement with nonlinear magneto-optical effects in hybrid silver/cobalt/gold multilayer structures (inset Fig.1) we observe magnetic second harmonic generation (mSHG) with a high magnetic contrast ρ (up to 33%) [1,2]. The mSHG intensity can be controlled by reversing the magnetization in cobalt using a weak (a few mT) external magnetic field. The SHG sources are localized at the interfaces due to the breaking of the spatial inversion symmetry; they are characterized by various components of the nonlinear susceptibility tensor $\chi_{ijk}^{(2)}$, even or odd with respect to magnetization. By a proper selection of (s or p)-polarization of the fundamental radiation at 1250 nm, we have identified the contributions of surface plasmon polaritons (SPP) excitations to the nonlinear magneto-optical response (Fig.1). The mSHG magnetic contrast can be readily optimized by varying the sample thickness (Fig.2).

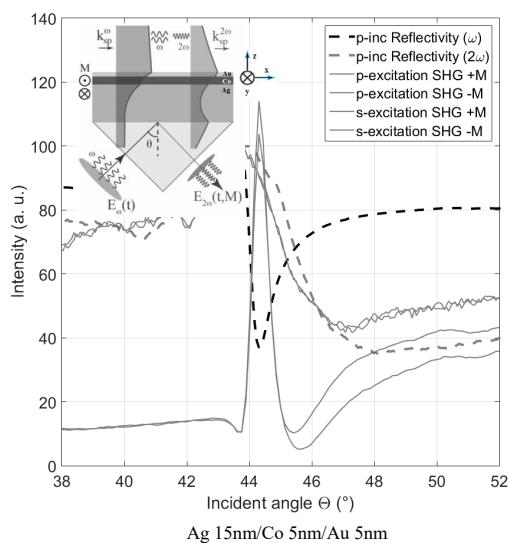


Fig. 1 – Incident light can be coupled to the SPP modes at the air/metal interface in the Kretschmann configuration (inset). The p-polarized light can excite SPP(ω) and SPP(2ω), both of which modify the SHG intensity. In contrast, s-polarized pump can only excite the SPP(2ω)-mode via the nonlinear coupling mechanism.

The support from Stratégie Internationale NNN-Telecom, COST action MP1403 and PRC CNRS-RFBR “Acousto-magneto-plasmonics” are gratefully acknowledged.

[1] I. Razdolski *et al.*, *ACS Photonics*, **3** (2016) 179.

[2] V. V. Temnov *et al.*, *J. Opt.*, **18** (2016) 093002.

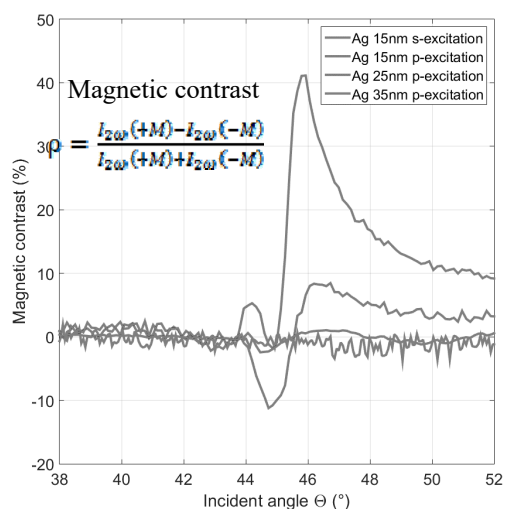


Fig. 2 – For p-excitation, the mSHG magnetic contrast is large and can be tuned by varying the Ag-thickness in a Ag(x nm)/Co(5nm)/Au(5nm) multilayer structure. For s-excitation, the vanishing mSHG contrast indicates the relative ineffectiveness of the purely nonlinear SPP coupling for mSHG.

2RP-C-12

OPTICAL SPECTROSCOPY OF 1D Au/GARNET MAGNETOPLASMONIC CRYSTALS

Chekhov A.L.¹, Naydenov P.N.², Stognij A.I.³, Murzina T.V.¹

¹ Moscow State University, Moscow, Russia

² Moscow Technological University (MIREA), Moscow, Russia

³ Scientific and Practical Materials Center, NAS of Belarus, Minsk, Belarus

murzina@shg.ru

Surface plasmon polaritons (SPPs) propagating in a magnetic medium can substantially increase the efficiency of light-matter coupling and enhance magneto-optical effects. The choice of the magnetic medium is of great importance here. Ferromagnetic metals (Fe, Co, Ni) reveal high magnetic effects, but demonstrate large absorption in the visible range. On the other hand, ferromagnetic dielectrics such as iron garnets have high values of gyration vector and are usually transparent in the visible range. By combining iron garnets with noble metals like Au, one can fabricate new types of structures, which offer an efficient control over the light flow by means of the magnetic field.

We study magneto-optical effects in magnetoplasmonic crystals (MPCs) consisting of bismuth substituted iron garnet covered by a gold grating [1, 2]. The structures are fabricated using combined ion-beam techniques for high-quality gold layer sputtering and etching, which allow us to control the MPC geometry with a high precision. The variety of resonant modes, that are SPPs excited on both sides of the Au film and waveguide (WG) modes in the magnetic slab, offer different types of effects observed in linear and nonlinear responses. Figure 1,a shows a characteristic wavelength-angle transmission spectrum of an MPC. Dashed lines mark the features associated with excitation of different types of SPPs. Sharp features correspond to the excitation of WG modes.

SPPs excitation on Au/garnet interface leads to the enhancement of the linear magneto-optical effect in transmission, which exceeds 1%. Due to high field localization at the interfaces and resonant phase modulation, the second harmonic generation output is strongly modulated by the excitation of various modes. Excitation of Au/Garnet SPPs leads to the enhancement of the nonlinear magneto-optical effect up to 20%.

Finally, we demonstrate a new type of MPC, where the gold grating is placed on epitaxial garnet layer and is coated by a bismuth iron garnet, resulting in formation of symmetrical surrounding of the Au film. This novel type of MPC reveals higher transmission, while keeping the same bunch of the resonant features as is shown in Fig. 1,b.

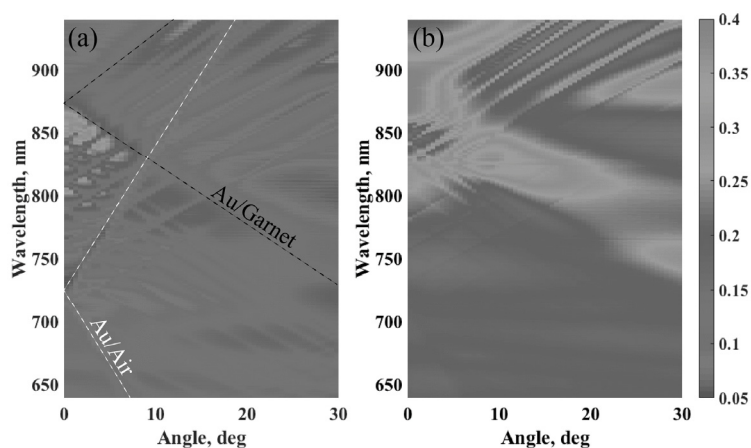


Fig. 1. Wavelength-angle transmission spectra for (a) MPC and (b) capsuled MPC with 700 nm period.

[1] V.I. Belotelov et al., *Nat. Nanotechnol.*, **6** (2011) 370-376.

[2] A.L. Chekhov et al., *Phys. Solid State*, **58** (2016) 2171-2174.

2 July

Sunday

12:00-13:30

15:00-17:00

oral session

2TL-E

2RP-E

2OR-E

**“Magnetic Shape
Memory and
Magnetocaloric Effect”**

2TL-E-1

MEASUREMENT OF THE MAGNETIC AND MAGNETOTHERMAL PROPERTIES OF HEAVY RARE EARTHS*Gimaev R.R.¹, Kopeliovich D.B.¹, Spichkin Y.I.¹, Tishin A.M.^{1,2}*¹ Advanced Magnetic Technologies and Consulting LLC, Troitsk, Moscow, Russia² Faculty of Physics, M.V. Lomonosov Moscow State University, Moscow, Russia

gimaev@amtc.org

Adiabatic temperature change, magnetization, heat capacity and thermal conductivity coefficient of a set of commercial purity heavy rare earth metals have been measured. The temperature and magnetic field dependences of the adiabatic temperature change and magnetization were measured by direct and induction methods, respectively. The temperature dependences of the heat capacity and thermal conductivity coefficient in constant magnetic field were measured by adiabatic calorimetry and steady-state methods.

The obtained experimental results are compared with the literature data on high-purity heavy rare earths magnetothermal properties. The possible effect of the material purity on magnetic refrigerators parameters and ability to use the commercial purity materials in such devices are discussed.

Work at Advanced Magnetic Technologies and Consulting LLC is supported by Skolkovo Foundation, Russia. Authors acknowledge support by the AMT&C Group Ltd., UK.

2TL-E-2

MAGNETOCALORIC MATERIALS: FROM ADVANCED CHARACTERIZATION TO INDUSTRIAL APPLICATION

Skokov K.P., Gutfleisch O.

Institute of Materials Science, FG Functional Materials, TU Darmstadt, Darmstadt, Germany
skokov@fm.tu-darmstadt.de

The technology of magnetic cooling has been successfully used to attain ultra-low temperatures for more than 80 years, however for the last decade it is also regarded as a promising refrigeration technique working at ambient temperatures [1]. From this point of view, magnetic compounds with first-order transition, exhibiting large magnetocaloric effect (MCE) in the temperature range of 270–320K and under magnetic field changes of $\Delta\mu_0H=1-2$ T are attracting much attention due to their potential application in this emerging refrigeration technology.

The main issue related to application of giant MCE materials is the hysteresis of the first-order transition, which is one of the main factors delaying the development of this novel and disruptive cooling technology [2]. The central focus of this talk is the overview of magnetocaloric materials with first order transition, such as FeRh, Gd₅(SiGe)₄, La(FeCoSi)₁₃, La(FeMnSi)₁₃H_x and Heusler alloys. Cyclic measurements of the adiabatic temperature change together with calorimetric data allow us to determine the reversible magnetocaloric effect of these first-order materials with thermal hysteresis [3,4]. This method provides a basis for a comparison of the suitability of different hysteretic magnetocaloric materials for their application in a magnetic refrigerator.

In order to use a magnetocaloric material in a magnetic refrigerator, it should on the one hand be machined into a heat exchanger with a fine porous structure, designed to provide the largest possible contact surface area to the heat transfer liquid. On the other hand, the effective volume of the MCE heat exchanger needs to be maximized for an efficient utilization of the (Nd–Fe–B) permanent magnet field source. In this talk, a method for the production of La(Fe,Mn,Si)₁₃H_x based heat exchangers by using a metal binder will be presented. The magnetocaloric properties, the chemical and mechanical stability of the metal-bonded porous bodies will be compared with polymer-bonded magnetocaloric regenerators, produced from the same La(Fe,Mn,Si)₁₃H_x material [5,6].

- [1] O. Gutfleisch, M. A. Willard, E. Bruck, C. H. Chen, S. G. Sankar, and J. P. Liu, *Advanced Materials*, **23** (2011) 821.
- [2] O. Gutfleisch, T. Gottschall, M. Fries, D. Benke, I. Radulov, K.P. Skokov, H. Wende, M. Gruner, M. Acet, P. Entel, M. Farle, *Philosophical transactions. Series A*, **374** (2016) 2074.
- [3] K.P. Skokov, K.-H. Müller, J.D. Moore, J. Liu, A.Yu. Karpenkov, M. Krautz, O. Gutfleisch *Journal of Alloys and Compounds*, **552** (2013) 310.
- [4] J. Liu, T. Gottschall, K. P. Skokov, J. D. Moore, O. Gutfleisch, *Nature Materials*, **11** (2012) 620.
- [5] K. P. Skokov, D. Yu. Karpenkov, M. D. Kuzmin, I. A. Radulov, T.Gottschall, B. Kaeswurm, M. Fries, and O. Gutfleisch, *Journal of Applied Physics*, **11** (2014) 17A941.
- [6] I.A. Radulov, D. Yu. Karpenkov, K.P. Skokov, A. Yu. Karpenkov, T. Braun, V. Brabänder, T. Gottschall, M. Pabst, B. Stoll, O. Gutfleisch, *Acta Materialia*, **127** (2017) 389.

2TL-E-3

MARTENSITIC AND MAGNETIC TRANSITIONS IN Co-V-Ga ALLOYS

Xu X.^{1,*}, *Nagashima A.*¹, *Miyake A.*², *Nagasako M.*³, *Omori T.*¹, *Tokunaga M.*², *Kanomata T.*^{1,4},
*Kainuma R.*¹

¹ Department of Materials Science, Tohoku University, Sendai, Japan

² The Institute for Solid State Physics, The University of Tokyo, Kashiwa, Japan

³ Institute for Materials Research, Tohoku University, Sendai, Japan

⁴ Research Institute for Engineering and Technology, Tohoku Gakuin University, Tagajo, Japan
 *xu@material.tohoku.ac.jp

The martensitic transformation (MT) behavior has been considered very rare in the Co-based Heusler alloys due to the high stability of the Heusler phase. Recently, MT has been found in the off-stoichiometric quaternary $\text{Co}_2\text{Cr}(\text{Ga},\text{Si})$ Heusler system [1]. Consequently, MT has also been found $\text{Co}_2\text{Cr}(\text{Al},\text{Si})$ [2] and Co-V-Si [3] systems very recently. However, it is not easy to obtain MT near room temperature because of either the limited solubility of the Heusler phase or strong composition dependence of the transformation temperatures in these alloy systems. In this talk, I would like to report the experimental results of the ternary Co-V-Ga system. While the stoichiometric Co_2VGa alloy has been confirmed to be a half-metal, MT behavior was clearly found in off-stoichiometric $\text{Co}_x\text{V}_{(100-x)/2}\text{Ga}_{(100-x)/2}$ (Co_x , $x = 51$ to 63) alloys in this study [4].

By thermoanalysis, Co57 to Co63 samples were found to show clear MT behavior in the temperature range of 250 to 500 K. The Co57 sample was used for TEM observation, since its MT interval covers the room temperature. As shown in Figure (a), Co57 sample almost shows parent phase with Heusler structure at room temperature. After a sub-zero treatment for the TEM sample in liquid nitrogen, an observation on martensite was possible at room temperature, with the results shown in Figure (b). Combined with *in situ* XRD observations, an $\text{L2}_1 \rightarrow \text{D0}_{22}$ martensitic transformation was confirmed in this alloy. Further results, including the magnetic properties as well as the magnetic phase diagrams, will be shown in the presentation.

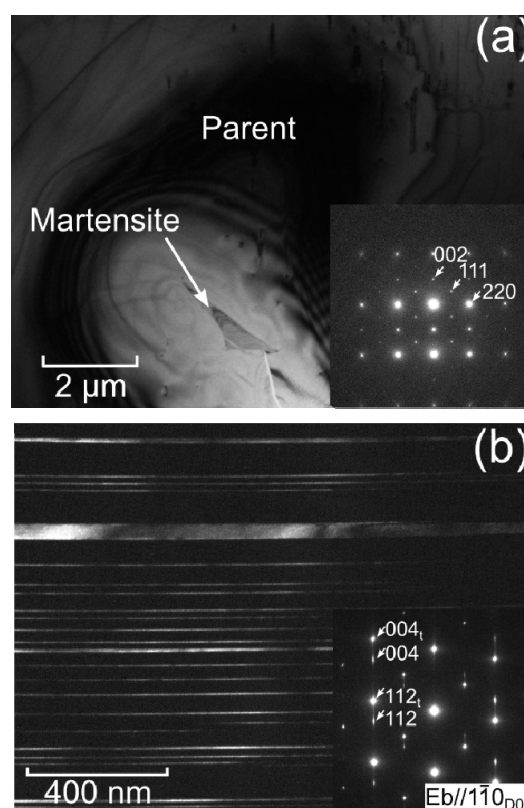


Figure (a) TEM bright-field image and (inset) diffraction pattern for the parent phase for the $\text{Co}_{57.1}\text{V}_{21.6}\text{Ga}_{21.3}$ (Co57) alloy. (b) Dark-field image by 112 spot and (inset) diffraction pattern for the martensite phase from the same sample after sub-zero treatment by liquid nitrogen. Indexes for the other twin variant are shown with subscript 't'.

[1] X. Xu et al., *Applied Physics Letters*, **103** (2013) 164104.

[2] K. Hirata et al., *JALCOM*, **642** (2015) 200-203.

[3] H. Jiang et al., *Materials Science and Engineering: A*, **676** (2016) 191–196.

[4] X. Xu et al., *Applied Physics Letters*, **110** (2017) 121906.

2TL-E-4

INVESTIGATION OF THE MAGNETOCALORIC EFFECT IN Ni-Mn-In-BASED HEUSLER ALLOYS BY A DIRECT METHOD IN HIGH MAGNETIC FIELDS

*Koshkid'ko Yu.¹, Pandey S.², Quetz A.², Aryal A.², Dubenko I.², Cwik J.¹, Dilmieva E.¹,
Granovsky A.³, Lähderanta E.⁴, Zhukov A.⁵, Stadler S.⁶, Ali N.²*

¹ International Laboratory of High Magnetic Fields and Low Temperatures, Wroclaw, Poland

² Department of Physics, Southern Illinois University, Carbondale, USA

³ Faculty of Physics, Lomonosov Moscow State University, Moscow, Russia

⁴ Lappeenranta University of Technology, Lappeenranta, Finland

⁵ Dpto de Fisica de Materiales, Fac. Quimicas, UPV/EHU, San Sebastian, Spain and IKERBASQUE, Basque Foundation for Science, Bilbao, Spain

⁶ Department of Physics & Astronomy, Louisiana State University, Baton Rouge, USA

yuri.koshkidko@ml.pan.wroc.pl

Some of the Ni-Mn-In-based Heusler alloys demonstrate an inverse magnetocaloric effect (MCE) at the of the magnetostructural transition (MST) temperature, T_M . In this case, the values of the total entropy change (ΔS_t) increases with a decrease in the difference between temperatures of the MST and the Curie temperature (T_C) of the austenitic phase (AP) [1, 2]. A study of the adiabatic temperature changes (ΔT_{ad}) demonstrated a similar tendency [see in Ref.2].

In this work we introduce a study of the MCE parameters and their dependence on the difference between the transition temperatures for Ni-Mn-In-based Heusler alloys with different compositions. The magnetic behavior in magnetic fields up to 14 T, “kinetic arrest” of ferromagnetic AP, and the results of the studies of ΔT_{ad} measurements using the direct method and magnetic fields up to 14 T [3] for the series of the Ni-Mn-In-based Heusler alloys are discussed in the current work.

The influence in the rate of change of temperature and magnetic field (kinetic effects) on the ΔT_{ad} of Ni-Mn-In-based Heusler alloys in high magnetic fields are revealed and discussed. We show that differing rates of heating/cooling of the sample before the measurement process can affect the magnitude of ΔT_{ad} , and also result in a change of sign of ΔT_{ad} .

This work was supported by the Office of Basic Energy Sciences, Material Science Division of the U.S. Department of Energy, DOE Grant No. DE-FG02-06ER46291 (SIU) and DE-FG02-13ER46946 (LSU); the grants RFBR No.15-02-01976, 16-32-00905 mol_a; the project No.146-MAGNES of the ERA.Net RUS Plus initiative of the EU 7th Framework Programme; the program NCN SONATA 11 2016/21/D/ST3/03435; RSF project No 14-22-00279.

[1] T. Gottschall et al., *Phys. Rev. B*, **93** (2016) 184431.

[2] Y. Koshkid'ko et al., *J. All. Comp.*, **695** (2017), 3348-3352.

[3] Yu.S. Koshkid'ko et al., *JMMM*, **433** (2017) 234–238.

2OR-E-5

MAGNETOCALORIC EFFECTS OF METAMAGNETIC SHAPE-MEMORY ALLOYS NiCoMnIn and NiCoMnGa IN PULSED-HIGH-MAGNETIC FIELDS UP TO 56 T

Kihara T.¹, Xu X.², Ito W.³, Kainuma R.², Miyake A.⁴, Adachi Y.⁵, Kanomata T.⁶, Tokunaga M.⁴

¹ Institute for Materials Research, Tohoku University, Sendai, Japan

² Department of Materials Science, Tohoku University, Sendai, Japan

³ Materials Science and Engineering, Sendai National College of Technology, Natori, Japan

⁴ The Institute for Solid State Physics, The University of Tokyo, Kashiwa, Japan

⁵ Graduate School of Science and Engineering, Yamagata University, Yonezawa, Japan

⁶ Research Institute for Engineering and Technology, Tohoku Gakuin University, Tagajo, Japan
t_kihara@imr.tohoku.ac.jp

Ni-Mn-Z (Z = Ga, and In) metamagnetic shape memory alloys undergo martensitic transformation (MT) from a high-temperature austenitic phase (A-phase: cubic, ferromagnetic) to a low-temperature martensitic phase of reduced symmetry (M-phase: paramagnetic) at around room temperature [1]. The application of an external magnetic field to the M-phase realizes magnetic-field-induced martensitic transformation (MFIMT) accompanied with significant increase of entropy, whereas the magnetic entropy is reduced due to the forced spin alignment. This unconventional entropy change is called inverse magnetocaloric effect (IMCE). The IMCE appears as a consequence of simultaneous entropy change in different degrees of freedom (spin, lattice and orbital etc.). Therefore, the quantitative evaluations of the electronic, lattice, and magnetic contributions to the total entropy change are important to understand the IMCE in these materials. In addition, direct measurements of MCE not only in the vicinity of the transition temperature, but also in a wide range of temperatures are crucial to provide a greater understanding of this phenomenon.

Recently, we developed a direct measurement system of magnetocaloric effect (MCE) under pulsed magnetic fields [2]. Figures 1 show the representative results of the MCE measurements in the pulsed fields for (a) Ni₄₅Co₅Mn_{36.7}In_{13.3} [3] and (b) Ni₄₁Co₉Mn_{31.5}Ga_{18.5}, respectively. In both materials, the magnetic fields are applied in the M-phase. In Fig. 1(a), the sample temperature steeply decreases (IMCE) at the MFIMT in the field increasing process, and increases in the successive field-decreasing process. The measurements up to 15 T reveal the MCEs not only at the MFIMT, but also in the field induced A-phase, in which the positive slope due to the forced spin alignment can be seen. Ni₄₁Co₉Mn_{31.5}Ga_{18.5} also shows the IMCE at the MFIMT as shown in Fig. 1(b). However, the field dependence of the sample temperature in the field induced A-phase is different from the conventional positive MCE due to spin ordering. To clarify the electronic, lattice, and magnetic contributions to the IMCE in these materials, magnetization, and specific heat measurements were carried out in addition to the MCE measurements. In the presentation, the difference of MCE between Ni₄₅Co₅Mn_{36.7}In_{13.3} and Ni₄₁Co₉Mn_{31.5}Ga_{18.5} will be discussed.

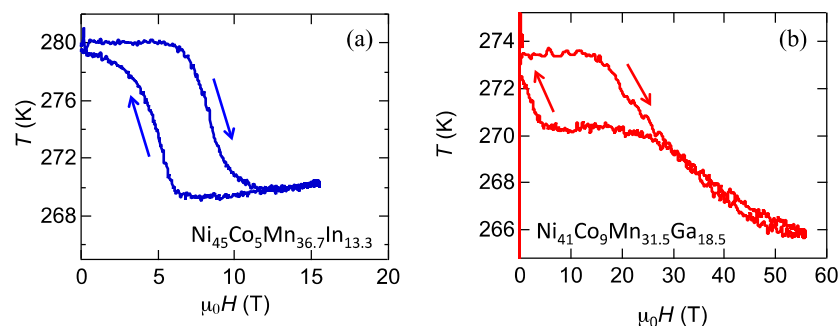


Fig. 1. Adiabatic temperature changes during magnetization and demagnetization processes for (a) Ni₄₅Co₅Mn_{36.7}In_{13.3} and (b) Ni₄₁Co₉Mn_{31.5}Ga_{18.5} measured in pulsed magnetic fields.

[1] A. Planes *et al.*, *J. Phys.: Condens. Mater.*, **21** (2009) 233201.

[2] T. Kihara *et al.*, *Rev. Sci. Instrum.*, **84** (2013) 074901.

[3] T. Kihara *et al.*, *Phys. Rev. B*, **90** (2014) 214409.

2OR-E-6

PHASE FORMATION AND MAGNETOCALORIC EFFECT IN (Pr,Nd)-Fe ALLOYS PREPARED BY RAPIDLY QUENCHED METHOD

Nguyen H.D.^{1,2}, Nguyen H.H.^{2,3}, Nguyen M.A.³, Nguyen H.Y.^{1,2}, Pham T.T.^{1,2}, Kamantsev A.P.⁴, Koledov V.V.⁴, Mashirov A.V.⁴, Tran D.T.^{1,5}, Kieu X.H.⁵, Seong-Cho Y.⁵

¹ Institute of Materials Science, Vietnam Academy of Science and Technology, 18 Hoang Quoc Viet, Ha Noi, Viet Nam.

² Graduate University of Science and Technology, Vietnam Academy of Science and Technology, 18 Hoang Quoc Viet, Ha Noi, Viet Nam.

³ Hong Duc University, 565 Quang Trung, Dong Ve, Thanh Hoa, Viet Nam

⁴ Kotelnikov Institute of Radio-engineering and Electronics of RAS, Moscow, Russia

⁵ Department of Physics, Chungbuk National University, Cheongju 361 - 763, South Korea.
danh@ims.vast.ac.vn

R_2Fe_{17} (R = rare earth) alloys have a potential for magnetic refrigerants at room temperature [1, 2]. However, there are still some problems in fabricating R_2Fe_{17} phase and regulating magnetic phase transition for these alloys. In this work, $Pr_{2-x}Nd_xFe_{17}$ ($x = 0 - 2$) ribbons with thickness of about 15 μm were prepared by melt-spinning method. The alloy ribbons were then annealed at different temperatures (900 - 1100°C) for various time (0.25 - 2 h). The formation of the $(Pr,Nd)_2Fe_{17}$ (2:17) crystalline phase in the alloys strongly depends on the Pr/Nd ratio and annealing conditions. Annealing time for the completed formation of the 2:17 phase in the rapidly quenched ribbons is greatly reduced in comparison with that of bulk alloys. Curie temperature, T_C , of the alloys can be controlled in room temperature region by changing Pr/Nd ratio (Fig. 1). Maximum magnetic entropy change, $|\Delta S_m|_{max}$, of the alloys is quite high ($|\Delta S_m|_{max} > 1.5 J \cdot kg^{-1} K^{-1}$ with $\Delta H = 12$ kOe) in room temperature region (Fig. 2). On the other hand, the full width at half the maximum peak (FWHM) of the magnetic entropy change is quite large (FWHM > 50 K) making it possible for application in magnetic refrigerators at room temperature.

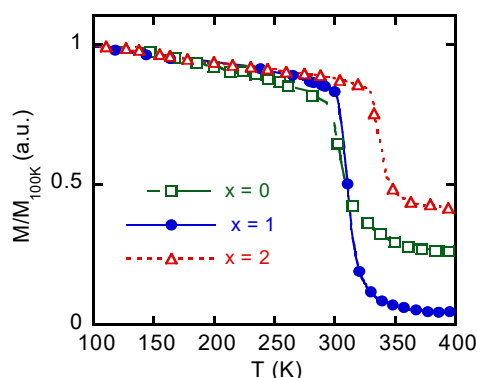


Fig. 1. Reduced thermomagnetization curves of $Pr_{2-x}Nd_xFe_{17}$ ($x = 0 - 2$) ribbons in magnetic field of 100 Oe.

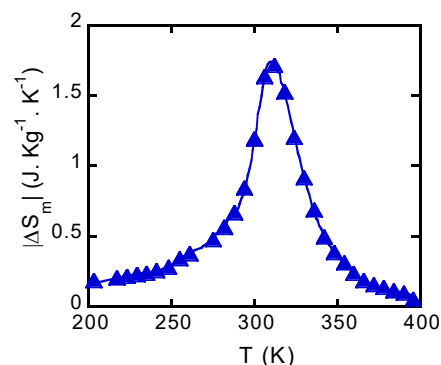


Fig. 2. Temperature dependence of magnetic entropy change (ΔS_m) of $PrNdFe_{17}$ with magnetic field change $\Delta H = 12$ kOe.

Support by Vietnam Academy of Science and Technology (grant No. VAST.HTQT.NGA.05/17-18) and Russian Foundation for Basic Research (grant № 17-58-540002) is acknowledged.

[1] H. Chen et al., *J. Magn. Magn. Mat.*, **320** (2008) 1382.

[2] C. F. Sánchez-Valdés et al., *Appl. Phys. Lett.*, **104** (2014) 212401.

2TL-E-7

MAGNETOCALORIC EFFECT IN CYCLIC MAGNETIC FIELDS*Aliev A.M.¹, Koledov V.V.²*¹ Amirkhanov Institute of Physics of Daghestan Scientific Center RAS,
Makhachkala, Russia² Kotelnikov Institute of Radio Engineering and Electronics RAS, Moscow, Russia
lowtemp@mail.ru

Presently, one of the major requirements for a material to be used as a prospective magnetocaloric material is its capability to exhibit giant magnetocaloric effect (MCE). Because of a refrigerating machine is a device with periodic sweeps of cycles there is a substantial need to study the magnetocaloric properties of materials under frequent cyclic exposures to magnetic fields. Magnetocaloric properties of the materials exposed to alternating and constant magnetic fields can exhibit significantly different behavior for a variety of reasons. Even at low frequencies the field dependence of the magnetocaloric properties of materials may differ significantly from those measured after a single magnetic field applying. First of all, it refers to the first order phase transitions in which the temperature hysteresis can lead to irreversibility of phase transitions induced by an external field in certain temperature ranges. The MCE values on the first and subsequent cycles of the field application in these materials will vary significantly.

This report presents the results of the study of the magnetocaloric properties in various families of promising magnetocaloric materials. In the report the following issues will be discussed:

- Methods of measure of MCEs in alternating (cyclic) magnetic fields,
- Dependence of the MCE values on the frequency of the magnetic field change,
- Temperature and magnetic field ranges of observation of the reversible MCE, and methods for inducing reversible magnetostructural phase transitions in weak magnetic fields,
- Degradation of the magnetocaloric effect in cyclic magnetic fields,
- Methods for estimating the structural and magnetic contributions to the overall magnetocaloric effect,
- Difference of the MCE values in the region of magnetostructural phase transitions in the heating and cooling runs and others.

This work is supported by RFBR, research project № 17-02-01195.

2RP-E-8

PLASTICALLY DEFORMED Gd-X (X=In, Ga, B, Y, Zr) SOLID SOLUTIONS AS A SECOND ORDER MAGNETIC PHASE TRANSITION MATERIALS FOR MAGNETOCALORIC REFRIGERATION

Taskaev S.^{1,2,3}, *Skokov K.*^{1,4}, *Khovaylo V.*^{1,2}, *Karpenkov D.*^{1,2,4}, *Ulyanov M.*¹, *Gunderov D.*⁵, *Aliev A.*⁶, *Gutfleisch O.*⁴

¹ Chelyabinsk State University, Chelyabinsk, Russia

² National University of Science and Technology "MISiS", Moscow, Russia

³ NRU South Ural State University, Chelyabinsk, Russia

⁴ TU Darmstadt, Darmstadt, Germany

⁵ Ufa State Aviation University, Ufa, Russia

⁶ Institute of physics DSC RAS, Mahachkala, Russia

tsv@csu.ru

Nowadays, a bottleneck in designing the effective heat exchanger for magnetic refrigeration devices consist of two problem: from one hand it is the designing magnetocaloric materials exhibiting a good magnetocaloric effect in a wide temperature range, from other hand it is a form factor, e.g. these materials should be produced in the form of thin foils (or other forms with well-developed surface) because the temperature relaxation rate depends on a thickness of magnetocaloric material as a square value. One of the best candidates for this aim is Gd solid solutions in which one can tune Curie temperature T_c by doping solvent element, but with a subsequent decreasing magnetocaloric effect.

Solid solutions of Gd-X (X=In, Ga, B, Y, Zr) treated with the help of cold rolling in severe regime (relative deformation is about 50-70 times) show excellent ductile behavior and unusual magnetic properties initialized by induced magnetic anisotropy. Although magnetization, heat capacity, magnetocaloric effect are depressed, they can be completely restored by a proper thermal treatment of the deformed alloys. It was shown that Gd-Y, Gd-In and Gd-Zr solid solutions have comparable to pure Gd magnetocaloric effect in a wide temperature range up to 37 K, 35 K, and 16 K, respectively, and further they can be useful materials for designing an effective active magnetic regenerator heat exchanger (see Fig. 1). The authors gratefully acknowledge the financial support of Russian Science Foundation (Project № 15-12-10008) for financing all magnetic measurements. The work was partially supported by Act 211 Government of the Russian Federation, contract № 02.A03.21.0011. ST acknowledge to RFBR grant 16-07-00679.

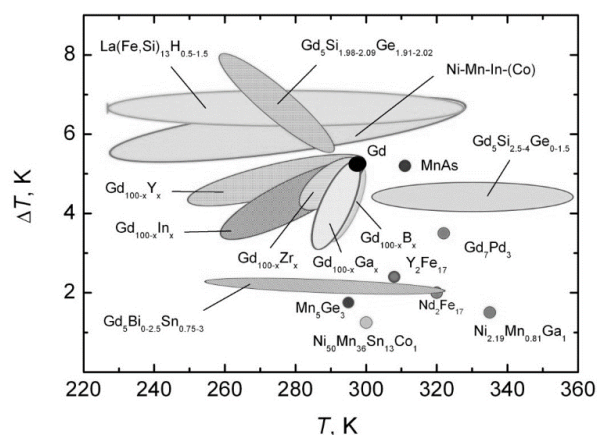


Figure 1. Magnetocaloric effect of Gd based solid solutions and some perspective MCE alloys.

[1] J. Liu, T. Gottschall, K. P. Skokov, J.D. Moore, O. Gutfleisch, *Nat. Mater.*, **11** (2012) 620.

[2] B.Yu, M. Liu, P. W. Egolf, A. Kitanovski, *Int. J. Refrig.*, **33** (2010) 1029.

2RP-E-9

MAGNETOCALORIC EFFECT IN Ni-Co-Mn-(Sn, Al) HEUSLER ALLOYS: THEORETICAL STUDY

Sokolovskiy V.V.^{1,2}, Zagrebin M.A.^{1,3}, Buchelnikov V.D.¹

¹ Chelyabinsk State University, Chelyabinsk, Russia

² National University of Science and Technology «MIS&S», Moscow, Russia

³ National Research South Ural State University, Chelyabinsk, Russia
vsokolovsky84@mail.ru

Nowadays, a new class of ferromagnetic shape-memory alloys (e.g., Co-doped Ni-Mn-(In, Sn, Al)) has received considerable attention due to a variety of magnetic, mechanical and thermal properties which are associated with a coupled magnetostructural first-order phase transition [1-3]. This transition occurs from the magnetically weak martensite to ferromagnetic austenite during heating and can take place near the room temperature region. As a result, the Co-doped NiMn-based Heusler alloys could be promising for prospective applications, such as a magnetic cooling technology and as a magnetic sensor [1-3].

In this work, we present a theoretical study of magnetic and magnetocaloric properties of Co-doped Ni-Mn-(Sn, Al) Heusler alloys by using the microscopical approach consisting of ab initio zero-temperature calculations combined with Monte Carlo finite-temperature simulations. In the first step, we carried out the ab initio supercell calculations of ground state properties (lattice parameters, magnetic order, magnetic moments, exchange coupling constants for austenite and martensite). In the second step, we have done Monte Carlo simulations of temperature dependences of magnetic and magnetocaloric properties for alloys studied by means of Potts-Blume-Emery-Griffiths model [4]. The temperature dependences of magnetization and adiabatic temperature change (ΔT_{ad}) for Ni₄₀Co₁₀Mn₃₆Sn₁₄ compound are shown in Fig. 1. Here, results are presented for both cooling and heating protocols at the magnetic field change of 2 T. In general, the theoretical results are in a good agreement with available experimental data.

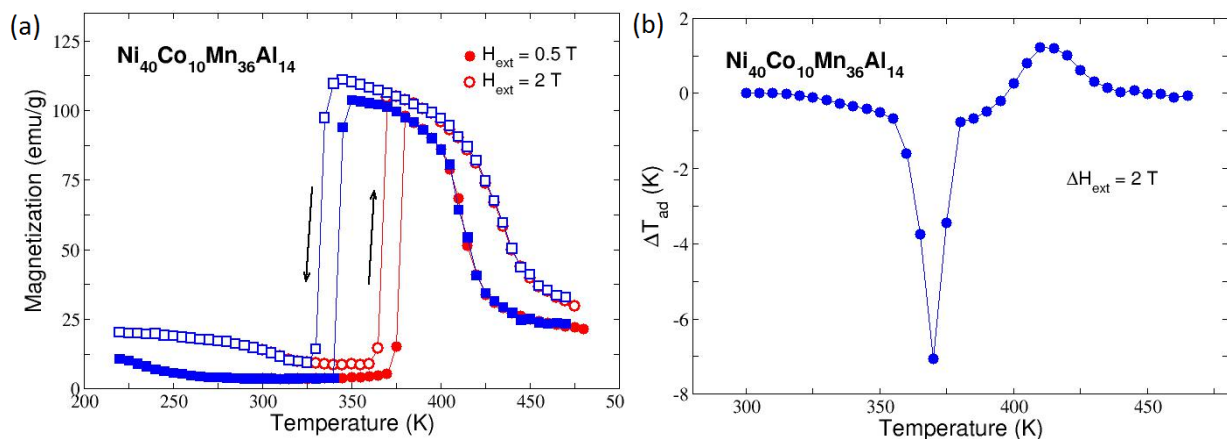


Fig. 1. Theoretical results of (a) magnetization and (b) adiabatic temperature change for Ni₄₀Co₁₀Mn₃₆Sn₁₄ as functions of temperature at the magnetic field change of 2 T.

Supports by Russian Science Fund # 14-12-00570 and President RF Grant MK-8480.2016.2 are acknowledged.

- [1] T. Gottschall et al., *Phys. Rev. B*, **93** (2016) 184431-6.
- [2] L. Huang et al., *Appl. Phys. Lett.*, **104** (2014) 132407-5.
- [3] Y. Kim et al., *J. Alloys Comp.*, **616** (2014) 66-70.
- [4] V. Sokolovskiy et al., *Entropy*, **16** (2014) 4992-5019.

2 July

Sunday

12:00-13:30

15:00-17:00

oral session

2TL-F

2RP-F

2OR-F

**“Soft and Hard
Magnetic Materials”**

2TL-B-1

THE POTENTIAL OF 1:12 ALLOYS FOR THE DEVELOPMENT OF RARE EARTH-LEAN MAGNETS

Hadjipanayis G.C., Gabay A.

University of Delaware Newark, DE 19716 USA

Ferromagnetic tetragonal compounds of the ThMn_{12} type have been around for more than thirty years. Represented by the general formula $\text{R}(\text{Fe},\text{M})_{12}$ where R is a rare earth and M is the stabilizing element, many of these compounds were considered for the development of hard magnetic materials. The compounds with $\text{R} = \text{Sm}$ as well as the metastable nitrides of the compounds with $\text{R} = \text{Nd}, \text{Pr}$ were identified as the most promising based on their fundamental magnetic characteristics. However, the early attempts to develop functional materials did not produce permanent magnets able to compete with the Nd-Fe-B which has been dominating the field of rare-earth magnets since the 1980s. In recent years, interest to the 1:12 has markedly increased owing to two new factors: (i) the nearly full achievement of the theoretical energy density of Nd-Fe-B and (ii) the strong incentive to use less rare earth which had been identified as "critical" elements in several countries. The increasingly popular high-throughput screening (both theoretical and experiment-based) is being actively explored, but the most significant of the recent findings were obtained within more traditional approaches. Superior saturation magnetization values have been reported, the highest – for epitaxially stabilized $\text{NdFe}_{12}\text{N}_x$ films (where the epitaxy made the M element unnecessary)[1]. On the other end, compounds containing less high-demand rare earth are being intensively studied. In this talk, we will briefly review the crystallography, magnetism and history of the of the 1:12 compounds while focusing on the latest developments. Of the latter, our latest mechanochemical synthesis data [2] on the newly discovered rare-earth-free $\text{Zr}(\text{Fe},\text{Si})_{12}$ compounds [3] and our attempts to prepare fully dense 1:12 anisotropic magnet will be discussed in more detail.

[1] Y. Hirayama, Y.K. Takahashi, S. Hirose, K. Hono, *Scripta Materialia*, **95** (2015) 70–72.

[2] A.M. Gabay, G.C. Hadjipanayis, *JMMM*, **422** (2017) 43-48.

[3] A.M. Gabay, G.C. Hadjipanayis, *Journal of Alloys and Compounds*, **657** (2016) 133-137.

2TL-B-2

MAGNETIC DOMAIN STRUCTURE AND LOCAL MAGNETIC PROPERTY OF A Nd-Fe-B SINTERED MAGNET PROBED BY SCANNING XMCD SPECTROMICROSCOPY

Nakamura T.^{1,2}, *Kotani Y.*¹, *Toyoki K.*¹, *Billington D.*¹, *Okazaki H.*¹, *Hirosawa S.*²

¹ JASRI, Sayo, Hyogo, Japan.

² ESICMM/NIMS, Tsukuba, Japan

naka@spring8.or.jp

Nd-Fe-B sintered magnets have the best properties of any permanent magnet to date [1], and are used in a wide variety of applications in energy-saving, (hybrid) electric vehicles, wind power generators, and so on. In these applications, the magnets are used for motors or dynamos which require high coercivities in order to be robust against demagnetization fields. Although the addition of 4-8 at.% Dy to Nd-Fe-B sintered magnets increases the coercivity effectively, improvements in coercivity without the addition of Dy, and without the reduction of magnetization, is crucial because Dy is a critically scarce element. Since it is well-known that the microstructure of permanent magnets is intimately related to the coercivity, controlling the microstructure might bring a solution to the development of high-performance, Dy-free, Nd-Fe-B sintered magnets. In the present study, magnetic domain reversal processes are investigated in order to relate the microstructure to the coercivity through magnetic domain observations via X-ray magnetic circular dichroism (XMCD). In a previous study [2], we showed that the coercivity of the fractured surface closely resembles that of the bulk, in stark contrast to the polished surface in which the coercivity is significantly decreased [3]. The higher coercivity of the fractured surface is attributed to the particular way in which Nd-Fe-B sintered magnets fracture, where the majority of the fractured surface remains covered with a thin layer of the grain boundary phase. Therefore, magnetic domains in the fractured surface may provide more direct information of the bulk magnetic state.

In order to observe the magnetic domain structure in the fractured surface under various magnetic fields, we have developed a new scanning soft X-ray spectromicroscope equipped with a superconducting magnet with a maximum magnetic field of ± 8 T. When used in combination with XMCD and total-electron-yield detection, magnetic domain observations of the fractured surface become possible. Figure 1 shows a demonstrative result obtained using the present technique, where both the microstructure and the magnetic domain contrast in the fractured surface of a $\text{Nd}_{14.0}\text{Fe}_{79.7}\text{Cu}_{0.1}\text{B}_{6.2}$ sintered magnet are clearly observed. Further analysis has allowed us to characterize local magnetic hysteresis loops for areas $\sim 100 \times 100 \text{ nm}^2$.

Support by the ESICMM under the outsourcing project of MEXT is acknowledged. The authors are grateful to T. Nishiuchi of Hitachi Metals, Ltd. for providing the Nd-Fe-B samples.

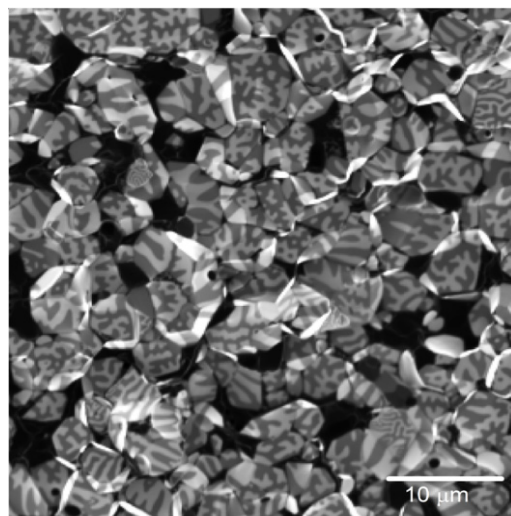


Fig. 1 Intensity map of X-ray absorption at the Fe L_3 -edge in $\text{Nd}_{14.0}\text{Fe}_{79.7}\text{Cu}_{0.1}\text{B}_{6.2}$ sintered magnet.

[1] M. Sagawa *et al.*, *Journal of applied physics*, **55** (1984) 2083.

[2] T. Nakamura *et al.*, *Applied Physics Letters*, **105** (2014) 202404.

[3] K. Kobayashi *et al.*, *Journal of applied physics*, **117** (2015) 173909.

2TL-B-3

OPTIMIZATION OF PERMANENT MAGNET MATERIALS WITH RESPECT TO CRYSTALLITE SHAPE AND EXCHANGE COUPLING

Erokhin S.¹, Berkov D.¹

¹ General Numerics Research Lab, Jena, Germany
d.berkov@general-numerics-rl.de

Our recently proposed new paradigm in micromagnetic modeling of nanocomposites [1] has provided a possibility to optimize nanostructured magnetic materials for permanent magnets before their actual manufacturing. Due to the progress in micromagnetic methodology, we are able to study the dependence of the magnetization reversal process in these materials on their structural and magnetic parameters. High statistical accuracy of our simulation results is achieved by employing simulation 'samples' (Fig. 1) containing a few thousands of grains, each discretized fine enough to analyse the magnetization distribution inside the grain.

This talk covers the results of micromagnetic simulations of ferrite-based nanocomposite materials. High magnetization of the soft phase (Fe or Ni) combined with the strong magnetic anisotropy of the hard phase is supposed to increase the performance of ferrite magnets. We present detailed results on the dependence of hysteresis loops and their most important characteristics (coercivity, remanence, energy product) on various parameters of a nanocomposite.

In contrast to the common belief, we demonstrate that in the system containing hard grains embedded in the soft matrix, the energy product $E_{\text{prod}} = (BH)_{\text{max}}$ is a non-monotonic function of the intergrain exchange coupling [2]: E_{prod} reaches its maximum in a nanocomposite, where the exchange coupling is much less than for the perfect intergrain boundary. This important result concerning the magnetization reversal process should greatly assist in achieving a hysteresis loop with the shape close to rectangular, which is a necessary prerequisite in technological applications of permanent magnet materials. The influence of the magnetodipolar interaction between hard crystallites and the soft phase and the role of the grain shape also will be discussed.

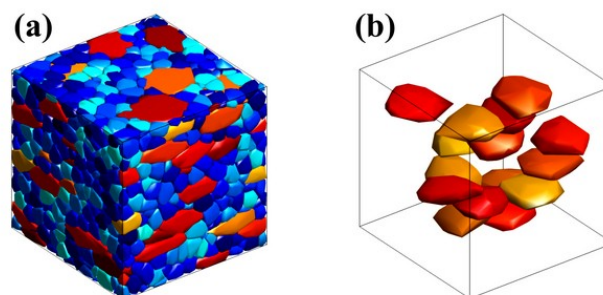


Fig. 1. (a) Example of a microstructure used in micromagnetic simulations; (b) spatial distribution of soft-phase grains (hard-phase crystallites not shown) in modeled microstructure of a ferrite-based nanocomposite.

Support of the EU Horizon-2020 project "AMPHIBIAN" (720853) is greatly acknowledged.

[1] S. Erokhin, D. Berkov, N. Gorn, and A. Michels, *Physical Review B*, **85** (2012) 024410.

[2] S. Erokhin, and D. Berkov, *Physical Review Applied*, **7** (2017) 014011.

2TL-B-4

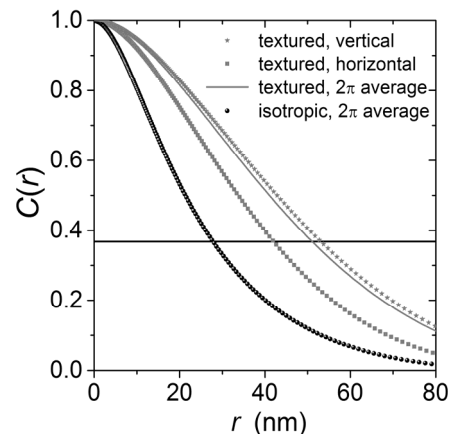
MAGNETIC SANS ON ND-FE-B MAGNETS

Michels A.

Physics and Materials Science Research Unit, University of Luxembourg
andreas.michels@uni.lu

Nd-Fe-B-based permanent magnets have been continuously investigated for the last three decades due to their technological relevance as materials used in energy-related applications (e.g., motors and wind turbines) [1]. A crucial issue is the understanding of the magnetization-reversal process, which eventually may result in the preparation of dysprosium and terbium-free Nd-Fe-B alloys with characteristic magnetic parameters (coercivity, remanence, maximum energy product) that guarantee their performance also at the high operating temperatures of motors (up to ~ 150 °C). In order to achieve this goal, the combination of advanced characterization techniques such as aberration-corrected high-resolution transmission electron microscopy and three-dimensional atom-probe tomography with ab initio calculations and numerical micromagnetic modeling is required. Indeed, recent studies along these lines (e.g., [2-4]) have provided important information regarding the nature (chemical composition, crystalline structure, ferro- or paramagnetic) of the intergranular Nd-rich phases in Nd-Fe-B magnets (including nanocomposites), which decisively determine the coercivity of these materials.

Magnetic neutron scattering, in particular, small-angle neutron scattering (SANS) is another important technique for characterizing the bulk magnetic microstructure of engineering permanent magnets. Magnetic SANS provides information on variations of both the magnitude and orientation of the magnetization on a nanometer length scale (~ 1 -300 nm). However, this method has only recently been employed for studying the spin microstructure of this class of materials (e.g., [5-12]). In this talk, we will discuss SANS data on both isotropic and textured sintered and nanocrystalline Nd-Fe-B magnets; specifically, the field dependence of characteristic magnetic length scales during the magnetization-reversal process is addressed, the exchange-stiffness constant has been determined, the observation of the so-called spike anisotropy in the magnetic SANS cross section has been explained with the formation of flux-closure patterns, the effect of grain-boundary diffusion in isotropic Nd-Fe-B magnets has been studied, and anisotropic spin correlations were detected (see figure below).



Correlation function of an isotropic and textured Nd-Fe-B-based nanocomposite.

- [1] O. Gutfleisch et al., *Advanced Materials*, **23** (2011) 821.
- [2] J. Liu et al., *Acta Materialia*, **61** (2013) 5387.
- [3] H. Sepehri-Amin et al., *Acta Materialia*, **61** (2013) 6622.
- [4] G. Hrkac et al., *Scripta Materialia*, **70** (2014) 35.
- [5] A. Michels et al., *Physical Review Applied*, **7** (2017) 024009.
- [6] E.A. Périgo, E.P. Gilbert, and A. Michels, *Acta Materialia*, **87** (2015) 142-149.
- [7] E.A. Périgo et al., *New Journal of Physics*, **16** (2014) 123031.
- [8] J.-P. Bick et al., *Applied Physics Letters*, **103** (2013) 122402.
- [9] J.-P. Bick et al., *Applied Physics Letters*, **102** (2013) 022415.
- [10] M. Yano et al., *Journal of Applied Physics*, **115** (2014) 17A730.
- [11] K. Saito et al., *Journal of Applied Physics*, **117** (2015) 17B302.
- [12] T. Ueno et al., *Scientific Reports*, **6** (2016) 28167.

2RP-B-5

NANOSTRUCTURE TAILORING OF L1₀-ORDERED EPITAXIAL MAGNETIC THIN FILMS

Futamoto M., Shimizu T., Nakamura M., Ohtake M.

Faculty of Sci. and Eng., Chuo Univ., 1-13-27 Kasuga, Bunkyo-ku, Tokyo 112-8551, Japan
futamoto@elect.chuo-u.ac.jp

$L1_0$ -ordered magnetic thin films (FePt, FePd, CoPt) with K_u values larger than 10^7 erg/cm³ are investigated for BPM and MRAM applications. The films involve disorder ($A1$) to order ($L1_0$) phase transformation [1]. There are more than several requirements for practical applications; high degree of $L1_0$ -ordering, easy magnetization axis (c -axis) alignment perpendicular to the film plane, surface flatness, etc. However, non-negligible surface roughness and unfavorably oriented $L1_0$ -crystal variants are reported in thin films prepared on oxide substrates such as MgO(001) [2, 3]. The problems are associated with the high process temperature (>500 °C) required for $L1_0$ -ordering and the quasi-symmetric structure of $L1_0$ -crystal (tetragonal, $c/a \geq 0.95$). The present paper briefly discusses the fundamental technology in aligning the c -axis perpendicular to the substrate surface and improving the surface flatness with $L1_0$ -ordered magnetic thin films.

Figure 1 compares the structures of FePt thin film of 2 nm average thickness grown on MgO(001) and VN(001). The film is continuous and very smooth ($R_a = 0.1$ nm) on VN (surface energy: 2.8 J/m²) whereas that is consisting of isolated crystals and very rough ($R_a = 4.2$ nm) on MgO underlayer (1.4 J/m²), which indicates that an employment of substrate material with larger surface energy is crucial for the preparation of $L1_0$ -ordered epitaxial thin film with continuous flat surface. Figure 2 shows the atomic-level structure of $L1_0$ -ordered Fe(Pt,Pd)/MgO(001) interface. From a series of structure analysis by TEM, XRD, and RHEED, it has been made clear that the lattice mismatch is playing an important role in enhancing $L1_0$ -ordering, determining the variant structure, and fixing the c -axis perpendicular to the film plane. Control of atomic diffusion and film stress during $L1_0$ -ordering process through modification of magnetic and underlayer material combination as well as process condition are found to be very important in tailoring the film nanostructure to be suitable for magnetic device applications.

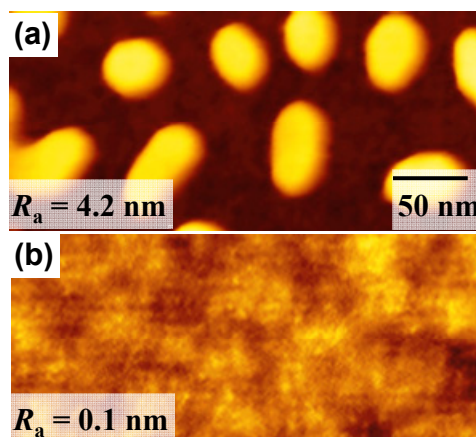


Fig. 1 AFM images of $L1_0$ -ordered FePt films with 2-nm average thickness on (a) MgO and (b) VN.

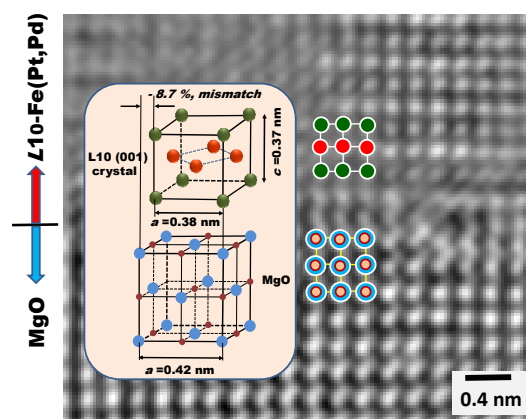


Fig. 2 TEM image of $L1_0$ -Fe(Pt,Pd)/MgO(001) epitaxial interface.

- [1] M. Futamoto, M. Nakamura, M. Ohtake, N. Inaba, T. Shimotsu, *AIP Adv.*, **6** (2016) 085302.
[2] L. S. Huang, J. F. Fu, G. H. Chow, J. S. Chen, *J. Appl. Phys.* **109** (2011) 063910.
[3] H. Ho, J. Zhu, A. Kulovits, D. E. Laughlin, J-G. Zhu, *J. Appl. Phys.* **116** (2014) 193510.

2OR-B-6

STRUCTURE ANALYSIS OF Co-Pt/MgO/Co-Pt TRI-LAYER FILMS GROWN EPITAXIALLY ON Ru(0001) UNDERLAYER

Ohtake M.^{1,2}, Suzuki D.¹, Futamoto M.¹, Kirino F.³, Inaba N.⁴

¹ Faculty of Science and Engineering, Chuo University, Tokyo 112-8551, Japan

² Faculty of Engineering, Kogakuin University, Tokyo 192-0015, Japan

³ Graduate School of Fine Arts, Tokyo University of the Arts, Tokyo 110-8714, Japan

⁴ Faculty of Engineering, Yamagata University, Yamagata 992-8510, Japan
ohtake@futamoto.elect.chuo-u.ac.jp / mitsuru@cc.kogakuin.ac.jp

Tri-layer films consisting of MgO and high K_u magnetic material have been studied for MTJ device applications. FePt and CoPt alloys with fct-based ordered phase of $L1_0$ show K_u greater than 10^7 erg/cm³. However to promote $L1_0$ ordering, it is necessary to process these materials at a high temperature around 600 °C, which enhances the layer interface roughness and the atomic diffusion. On the contrary, CoPt alloy with fcc-based ordered phase of $L1_1$ [1]–[3] and Co₃Pt alloy with hcp-based ordered phase of $D0_{19}$ [3]–[5] show K_u greater than 10^7 erg/cm³ along [111] and [0001], respectively. The Co-Pt films with metastable phases ($L1_1$, $D0_{19}$) have been prepared at a lower temperature around 300 °C. Therefore, the Co-Pt alloys seem suitable as the ferromagnetic electrode material of MTJ. In the present study, Co_xPt_{100-x}(40 nm)/MgO(*t*)/Co_xPt_{100-x}(40 nm) tri-layer films are prepared by sputter deposition on Ru(0001) single-crystal underlayers at 300 °C. The Co contents, *x*, of 50 and 75 at. % are used. The MgO layer thickness, *t*, is varied between 1 and 40 nm. The structure and the magnetic properties are investigated by RHEED, XRD, HR-TEM, AFM, and VSM.

Fully epitaxial Co₅₀Pt₅₀/MgO/Co₅₀Pt₅₀ and Co₇₅Pt₂₅/MgO/Co₇₅Pt₂₅ films are formed on Ru underlayers. Formation of metastable ordered phases are recognized in the Co₅₀Pt₅₀ and the Co₇₅Pt₂₅ lower and upper layers. The Co₅₀Pt₅₀ layers consist of two $L1_1(111)$ variants whose atomic stacking sequences of close-packed plane along the perpendicular direction are ABCABC and ACBACB, whereas the Co₇₅Pt₂₅ layers are $D0_{19}(0001)$ crystal with the stacking sequence of ABAB... Fig. 1(a) shows the HR-TEM image of a Co₅₀Pt₅₀(40 nm)/MgO(2 nm)/Co₅₀Pt₅₀(40 nm) film. Atomically sharp boundaries are formed at the layer interfaces. Figs. 1(b) and (c) show the magnetization curves of Co₅₀Pt₅₀/MgO/Co₅₀Pt₅₀ and Co₇₅Pt₂₅/MgO/Co₇₅Pt₂₅ films. Strong perpendicular magnetic anisotropies are observed. The present study shows that $L1_1$ -CoPt/MgO/ $L1_1$ -CoPt and $D0_{19}$ -Co₃Pt/MgO/ $D0_{19}$ -Co₃Pt films with perpendicular anisotropies can be formed by using a low temperature of 300 °C.

[1] S. Iwata *et al.*, *IEEE Trans. Magn.*, **33** (1997) 3670–3672.

[2] H. Sato *et al.*, *J. Appl. Phys.*, **103**, (2008) 07E114.

[3] M. Ohtake *et al.*, *IEICE Trans. Electron.*, **E96-C** (2013) 1460–1468.

[4] G. R. Harp *et al.*, *Phys. Rev. Lett.*, **71** (1993) 2493–2496.

[5] Y. Yamada *et al.*, *IEEE Trans. Magn.*, **33** (1997) 3622–3624

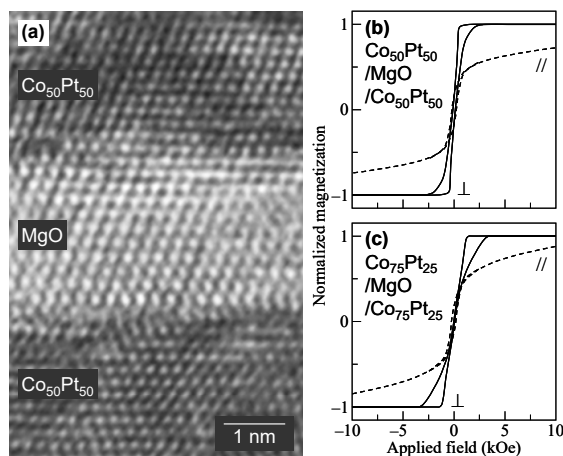


Fig. 1 (a) Cross-sectional HR-TEM image of Co₅₀Pt₅₀(40 nm)/MgO(2 nm)/Co₅₀Pt₅₀(40 nm) film formed on Ru(0001) underlayer. [(b), (c)] Magnetization curves of (b) Co₅₀Pt₅₀(40 nm)/MgO(40 nm)/Co₅₀Pt₅₀(40 nm) and (c) Co₇₅Pt₂₅(40 nm)/MgO(40 nm)/Co₇₅Pt₂₅(40 nm) films.

2OR-B-7

EFFECT OF RARE-EARTH AND TRANSITION METAL ELEMENTS ON COERCIVITY IN ND-FE-B PARTICLES BY REDUCTION-DIFFUSION PROCESS

Kim D.^{1,2}, Galkin V.^{1,3}, Haider K.^{1,4}, Ahn J.^{1,2}

¹Convergence research center for DMR, KIGAM, Daejeon, South Korea

²Powder & Ceramics Division, KIMS, Changwon, South Korea

³Materials Science and Engineering Department, SPbSTU, St. Petersburg, Russia

⁴Department of Chemistry, Sogang Univ., Seoul, South Korea

dskim@kims.re.kr

During the twentieth century, several permanent magnetic materials were discovered. Techniques to effectively manufacture these magnets have been established [1]. It appears that the search for novel hard magnetic compounds with higher remanent magnetization, defined now as the relevant parameter, has somewhat stagnated and no further breakthrough is in sight. On the other hand, only a small number of ternary and quaternary systems have been investigated so far [2]. In view of manufacturing process, main advantages of reduction-diffusion (R-D) process are the use of a relatively inexpensive Nd oxide as raw material and the direct production of alloy powder suitable for further procedures, compared with other methods such as powder metallurgy and rapidly quenching.

In this study, Nd-Fe-B magnetic particles were synthesized by R-D process from oxide precursors. Mixing with Ca as reducing agent and pelletization were performed, followed by R-D process. It was revealed that the amount of Ca played an important role in the formation of Nd₂Fe₁₄B phase, because vigorous H₂ evolution and dissociated hydrogen might be diffused into the lattice of Nd₂Fe₁₄B interstitially to form Nd₂Fe₁₄BH_x (x=1-5) during washing of powders in water in the case of excessive amount of Ca. This is one of the critical reasons for low magnetic property of powders synthesized by R-D process [3]. So, Ca amount was optimized considering stoichiometric ratio from chemical reactions and ball milling in ethanol was carried out before washing with water for efficient removal of impurities preventing oxidation. Nd₂Fe₁₄B powders showed spherical in shape with maximum energy product (BH_{max}) around 15 MGOe. Moreover, rare earth elements and transition metals were added in order to enhance magnetic properties, especially coercivity. Phase, morphology, microstructure, chemical composition and magnetic property were investigated and Nd-Fe-B based particles with additional elements were obtained with Ca content lower than 1.0 wt% and BH_{max} more than 20 MGOe.

Support by the National Research Council of Science & Technology (NST) grant by the Korea government (MSIP) (No.CRC-15-06-KIGAM) is acknowledged.

[1] O. Gutfleisch, *J. Phys. D: Appl. Phys.*, **33** (2000) R157.

[2] J.J. Croat, J.F. Herbst, R.W. Lee and F. E. Pinkerton, *J. Appl. Phys.* **55** (1984) 2078.

[3] C.Q. Chen, D. Kim, C.J. Choi, *JMMM*, **355** (2014) 180.

2OR-B-8

MICROMAGNETIC MODEL OF Nd-Fe-B NANOCOMPOSITE: CORE-SHELL PARTICLES WITH SUPERPARAMAGNETIC INCLUSIONS

Erokhin S.¹, Berkov D.¹, Michels A.²

¹ General Numerics Research Lab, Jena, Germany

² Physics and Materials Science Research Unit, University of Luxembourg, Luxembourg
s.erokhin@general-numerics-rl.de

Nanocrystalline Nd-Fe-B based alloys are one of the most important materials for the production of high-performance permanent magnets which will be used in the new-generation technological applications. Further development of this class of materials requires a clear physical understanding of the relation between their microstructure and the macroscopic magnetic properties. Therefore, the aim of this study is the finding of the most adequate micromagnetic description of this composite based on the comparison of simulation results with experimentally obtained hysteresis loops.

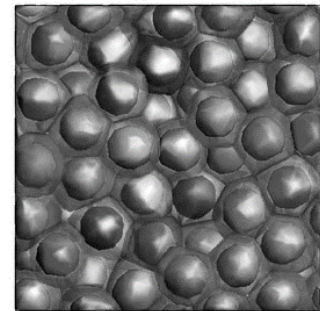
Employing our recently developed micromagnetic approach to the simulation of magnetization behaviour of nanocomposites [1], we are in the position to systematically scan the multidimensional parameter space of proposed models, as it was successfully demonstrated for the example of ferrites [2]. Performing 3D simulations on large volumes of nanocomposites allows us to obtain relevant results on collective remagnetization processes in these materials. This talk is devoted to the study of the following models of a Nd-Fe-B nanocomposite: (i) Stoner-Wohlfarth particles model with and without exchange coupling and interparticle magnetodipolar interaction; (ii) a model where each Nd-Fe-B grain is represented by a core-shell particle (Fig. 1), where reduced magnetic parameters were employed in shell regions; (iii) a core-shell particles model including the superparamagnetic contribution of nanosized iron clusters.

Comparing hysteresis loops obtained in simulations with experimental data, we conclude that only the results of the model with reduced magnetic parameters in the shell region of the grains (unavoidable in the manufacturing process) along with the inclusion of small superparamagnetic clusters (probably present in this material) is able to provide a good agreement with experiment.

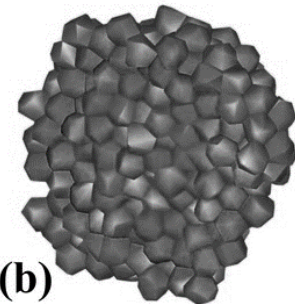
Financial support by the National Research Fund of Luxembourg under the project INTER/DFG/12/07 is gratefully acknowledged.

[1] A. Michels, S. Erokhin, D. Berkov, N. Gorn, *JMMM*, **350** (2014) 55.

[2] S. Erokhin, and D. Berkov, *Phys. Rev. Applied*, **7** (2017) 014011.



(a)



(b)

Fig. 1. (a) 2D cut out of a 3D core-shell microstructure used in the micromagnetic simulations of a Nd-Fe-B nanocomposite; (b) example of a polyhedron mesh element distribution in a grain (blue (yellow) elements correspond to the core (shell), typical mesh size is 2 nm).

2OR-B-9

MAGNETIC HARDNESS IN IRON CHALCOGENIDE COMPOUNDS WITH A LAYERED CRYSTAL STRUCTURE

Baranov N.V.^{1,2}, Selezneva N.V.², Sherokalova E.M.², Gubkin A.F.¹

¹ Institute of Metal Physics, Ural Branch of RAS, Ekaterinburg, Russia

² Institute of Natural Sciences and Mathematics, Ural Federal University, Ekaterinburg, Russia
baranov@imp.uran.ru

In transition metal halcogenides $M_{1-z}X$ ($X = S, Se$) with a layered crystal structure of the NiAs-type, the metal layers are sandwiched between completely filled layers of chalcogen. Because of metal deficiency the cationic layers contain vacancies. The M atoms in $M_{1-z}X$ may be substituted with other 3d metal (M') atoms. The magnetic behavior of compounds $(M, M')_{1-z}X$ is observed to be dependent on the type and concentration of M and M' atoms as well as on the distribution of vacancies between layers. The magnetic structure of iron halcogenides $Fe_{1-z}X$ ($z = 0.125 - 0.25$) consists of ferromagnetic (F) iron layers which are antiferromagnetically (AF) coupled to each other. The presence of vacancies in each second layer leads to a lack of full compensation of magnetic moments and to the existence of the resultant magnetization, i.e. to ferrimagnetism (FI) [1]. In the $Fe_{0.5}TiX_2$ compounds, one cationic layer fully occupied by Ti atoms and the second one is half filled with iron atoms. According to neutron diffraction both the $Fe_{0.5}TiS_2$ and $Fe_{0.5}TiSe_2$ compounds exhibit an AF order with different periodicities below ~ 140 K [2,3]. The $Fe_{0.5}TiS_2$ compounds were observed to undergo the metamagnetic phase transition from AF to a metastable F state below T_N [2].

The present work aims to study the magnetization processes in the layered compounds of the $(Fe, Ti)_{1-z}X$ type with FI and AF magnetic orderings. Some of these compounds are found to exhibit giant values of the coercive field at low temperatures (up to ~ 55 kOe). Fig.1 shows, as an example, the hysteresis loops for the compound $Fe_{0.5}TiS_{1.7}Se_{0.3}$ having an AF ground state.

The magnetic properties of the $(Fe, Ti)_{1-z}X$ compounds are observed to be strongly influenced by substitutions in both the Fe and chalcogen sublattices, by the distribution of Fe and Ti between cation layers. Unusually high values of the coercive field in the $(Fe, Ti)_{1-z}X$ systems may be associated with the presence of an unquenched orbital moment of Fe ions together with coexistence of the AF and F ordered regions in the samples.

This work was supported by the RFBR (project No 16-02-00480), by the program of UB of RAS (project No 15-17-2-22) and by the by the Ministry of Education and Science of Russia (project No 3.2916.2017).

[1] H. Wang, I. Salveson, *Phase transition*, **78** (2005) 547.

[2] N.V. Baranov et al., *J. Physics: Condensed Matter*, **25** (2013) 066004.

[3] A. Gubkin et al., *J. Alloys Compd.*, **616** (2014) 148.

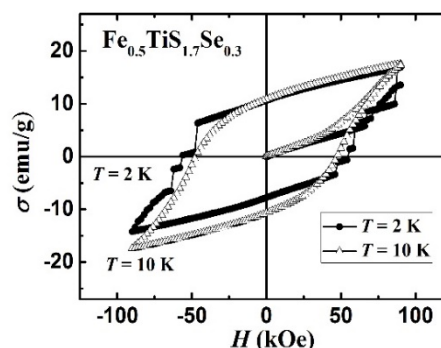


Fig. 1. Field dependences of the magnetization for $Fe_{0.5}TiS_{1.7}Se_{0.3}$ measured at 2 K and 10 K.

2OR-B-10

SPIN STRUCTURE OF ND-FE-B-BASED TEXTURED NANOCOMPOSITES: ROLE OF INTERFACE CHEMISTRY

Titov I.S.¹, Michels A.¹, Barbieri M.¹, Yano M.², Saito K.³, Ono K.³, Kohlbrecher J.⁴

¹FSTC, University of Luxembourg, Luxembourg, Luxembourg

²Advanced Material Engineering Division, Toyota Motor Corporation, Susono, Japan

³Institute of Materials Structure Science, High Energy Accelerator Research Organization, Tsukuba, Japan

⁴Laboratory for Neutron Scattering and Imaging, PSI, Villigen, Switzerland
ivan.titov@uni.lu

Nd-Fe-B-based nanocomposite permanent magnets, which consist of exchange-coupled nanocrystalline hard ($\text{Nd}_2\text{Fe}_{14}\text{B}$) and soft ($\alpha\text{-Fe}$) magnetic phases, are of potential interest for electronic devices due to their preeminent magnetic properties such as high remanence and magnetic energy product [1]. However, a major challenge remains the understanding of how the details of the microstructure (e.g., average particle size and shape, volume fraction of soft phase, texture) correlate with their macroscopic magnetic properties. In this contribution, we report on the effect of interface chemistry (specifically, the amount of Pr-Cu doping) on the magnetic microstructure of textured $\text{Nd}_2\text{Fe}_{14}\text{B}/\alpha\text{-Fe}$ nanocomposites by means of magnetic-field-dependent unpolarized small-angle neutron scattering (SANS).

The unpolarized SANS measurements were carried out starting from the highest available field (9.9 T) down to a 3 T field in the reverse direction for three samples (as-prepared, Pr-Cu 20%, Pr-Cu 40%) at 300 K. The corrected total scattering data were radially averaged and one-dimensional correlation functions were calculated from it, following the analysis reported in Refs. [2,3].

In Fig. 1, the field dependence of the correlation length l_C is displayed for several textured $\text{Nd}_2\text{Fe}_{14}\text{B}/\alpha\text{-Fe}$ nanocomposites as a function of additional Pr-Cu alloying elements. The l_C contain information on the field-dependent size of spin perturbations around microstructural defects, which in the present material system are represented by the intergranular layers (grain boundaries). The l_C at a given field below saturation describes the *magnetic defect size*, while at saturation the l_C approaches to the *structural size of the defect*. It is clearly seen in Fig. 1 that depending on the Pr-Cu content and field the l_C and thus the characteristic size of the spin inhomogeneities varies between about 15 nm up to 40 nm. Qualitatively, the functional behaviors $l_C(H)$ look similar for all three samples with a respective maximum at the coercive field H_c . However, with increasing Pr-Cu content, i.e., with increasing thickness of the intergranular layers, the value of l_C increases. Also, the defect size, which may here be taken as the limiting value of l_C at 9.9 T, increases with Pr-Cu content, from about 15 nm up to 40 nm. These findings together with magnetization and diffraction data provide further insights into the role of Pr-Cu doping on $\text{Nd}_2\text{Fe}_{14}\text{B}$ compounds and they demonstrate the power of the SANS method for analyzing bulk magnetic materials on the nanometer length scale.

[1] O. Gutfleisch, et al., *Adv. Mater.*, **23** (2011) 821.

[2] A. Michels, *J.Phys.: Condens. Matter*, **26** (2014) 383201.

[3] A. Michels, et al.: *Phys. Rev. Applied*, **7** (2017) 024009.

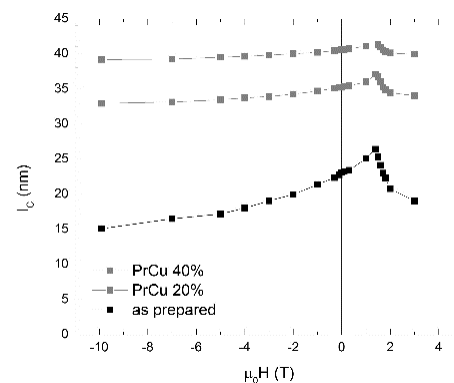


Fig.1: Field-dependent correlation lengths l_C extracted from radially-averaged total SANS cross sections for textured $\text{Nd}_2\text{Fe}_{14}\text{B}/\alpha\text{-Fe}$ nanocomposites containing different amounts of Pr-Cu.

2 July

Sunday

12:00-13:30

15:00-17:00

oral session

2TL-F

2OR-F

**“Magnetism in Biology
and Medicine”**

2TL-F-1

MAGNETIC NANOCHAINS: PROPERTIES, SYNTHESIS APPROACHES AND PROSPECTS

Milosevic I.¹, Motte L.², Li T.³, Ren Y.³, Sun C.³, Russier V.⁴, Saboungi M.-L.^{5,6}

¹ Powder Technology Laboratory, EPFL, CH-1015 Lausanne, Switzerland

² Inserm, U1148, Laboratory for Vascular Translational Science, UFR SMBH, Université Paris 13, Sorbonne Paris Cité, F-93017 Bobigny, France

³ Advanced Photon Source, Argonne National Laboratory, Argonne, IL 60439, USA

⁴ ICMPE, UMR 7182 CNRS and UPEC, F- 94320 Thiais, France

⁵ IMPMC-Université Pierre et Marie Curie F-75252 Paris, France

⁶ FUNSOM, Soochow University, Suzhou 215123, China

marie-louise.saboungi@impmc.upmc.fr

Hierarchical assemblies of magnetic materials arouse considerable interest because of their singular structures, peculiar physical properties and potential technological applications. In particular, one-dimensional (1-D) magnetic nanoparticle (NP) assemblies present a rich research field from both experimental and theoretical viewpoints. In contrast to individual NPs, i.e., 0-D systems, 1-D nanochains (NCs) present enhanced properties because of the many possible alignments and provide surface functionalities that may be suitable to technological applications, especially in the medical and environmental fields.

In this talk I review the state of the art in 1-D assemblies of magnetic NPs, first briefly recalling the properties of individual magnetic NPs with an emphasis on modeling systems of particles with dipolar interactions (DDI). These are responsible for the collective behavior of magnetic NP assemblies because of their long range, making it possible to form chains. Various experimental strategies developed recently to achieve such organization will be discussed. Finally, I present some applications of these NCs, especially in the fields of life sciences and the environment.

[1] H. Khurshid *et al.*, *Scientific Reports*, **5** (2015) 15054.

[2] I. Milosevic *et al.*, *Biochimica & Biophysica Acta*, In Press.

[3] M. Tadic M *et al.*, *Applied Physics Letters*, **106** (2015) 18.

2TL-F-2

FERROGELS WITH EMBEDDED IRON AND IRON OXIDE NANOPARTICLES FOR BIOMEDICAL APPLICATIONS

Safronov A.P.^{1,2}, Shankar A.¹, Mikhnevich E.A.¹, Tyukova I.S.¹, Beketov I.V.^{1,2}

¹ Ural Federal University, Yekaterinburg, Russian Federation

² Institute of Electrophysics UB RAS, Yekaterinburg, Russian Federation

safronov@iep.uran.ru

Ferrogel is a soft material, which incorporates the structural features and the mechanical properties of the polymeric matrix and combines them with the ability to respond to the magnetic field. As the polymers, synthetic and natural, in general, very weakly respond to the applied magnetic field, the only way to provide such ability is to embed dispersed magnetic particles into the polymeric matrix. Thus, ferrogel is by its origin a composite material, which comprises two subsystems: the polymeric gel, which provides the elasticity and softness of the matrix, and the ensemble of magnetic particles, which provides the sensitivity to the applied magnetic field. Both subsystems of ferrogel: polymeric and magnetic, carry on their specific properties. The main structural feature of the polymeric subsystem is that it consists of a cross-linked macromolecular network swollen in liquid. Although it might be any liquid, the focus will be put on water-based gels (hydrogels), which are of special interest for biomedical applications. The properties of hydrogels are governed by the mesh size of their network and by the interaction among macromolecular chains and water. Both parameters are sensitive to a variety of external stimuli, which makes hydrogel an advanced “responsive” material to work as a body in biocompatible actuators, sensors, and transducers [1,2]. The characteristics of the magnetic subsystem of the ferrogel depend on the structural and magnetic properties of the embedded particles and on their alignment in the polymeric matrix.

We report the synthesis and characterization of ferrogels based on iron and iron oxide nanoparticles (MNPs) prepared by the highly productive methods of electric explosion of wire (EEW) and laser target evaporation (LTE). These methods of physical dispersion provide large batches of spherical non-agglomerated nanoparticles with reproducible structural and magnetic properties [3,4]. Ferrogels were synthesized by free-radical polymerization of acrylic monomers with methylene diacrylamide as a cross-linker in water suspensions of MNPs. In case of iron oxide MNPs their de-aggregation and long-term stability of suspensions is provided by the electrostatic dispersants. It makes corresponding ferrogels homogeneous. Synthesis of ferrogels based on iron MNPs is much more challenging due to their strong aggregation, which stems from magnetic interaction between particles. Magnetic forces overwhelm electrostatic repulsion in colloidal suspension and the only way to provide uniformity of ferrogel is to use polymers as steric dispersants.

Ferrogels with embedded iron oxide and iron MNPs show up elasticity under mechanical stress and deformation in the applied magnetic field. The heating of ferrogels in the alternating magnetic field and their detection by the giant magnetic impedance had been demonstrated.

Support by Russian Science Foundation is acknowledged

[1] O.E.Philippova, *Polymer Science C*, **42** (2000) 208-228.

[2] DeRossi D., et al. *Polymer Gels: Fundamentals and Biomedical Applications*. New York: Plenum, 1991.

[3] A. P. Safronov, I. V. Beketov, S. V. Komogortsev, et.al. *AIP ADVANCES*, **3** (2013) 052135.

[4] I.V.Beketov, A.P. Safronov, A.V. Bagazeev, et.al. *JALCOM*, **586** (2014) 483-488.

2TL-F-3

TWO-PHOTON ABSORPTION CROSS SECTION OF MAGNETITE NANOPARTICLES IN MAGNETIC COLLOIDS AND THIN FILMS

Espinosa D., Gonçalves E.S., Figueiredo Neto A.M.

Institute of Physics, University of São Paulo, São Paulo, Brazil
afigueiredo@if.usp.br

Magnetite nanoparticles are present in many biocompatible magnetic fluids used in biomedical applications. Besides imaging, new therapies have been proposed using this type of material in the last years. In this context, the knowledge of the properties of magnetite in nanoscale dimension is essential for the design of new applications of these particles in different branches of interest. The Z-Scan (ZS) experimental technique is usually employed to investigate nonlinear optical properties of materials in the femtoseconds time-scale regime. In this work, ZS measurements of magnetite nanoparticles were performed with the material both in the colloidal suspension and in the thin film form. In our experimental setup, an electro-mechanical shutter was added along the beam path in order to guarantee thermal relaxation of the studied sample and thus investigate only phenomena from the electronic origin (optical Kerr effect in the case of nonlinear refractive index and two-photon absorption in the case of nonlinear absorption). We have shown that in the case of colloidal samples, the amplitude of ZS curves was drastically reduced and asymmetries were corrected when using the shutter. In the case of thin films, on the other hand, the shutter's presence did not alter the results, sustaining the hypothesis of significant contribution from thermal lens formation and even thermodiffusion of nanoparticles in ZS curves obtained without the shutter. Since the nonlinear signal is more intense when increasing the number N of absorbing units (Fe_3O_4), nonlinear parameters n_2 (index of refraction) and β (optical absorption) were studied as a function of N . At low nanoparticles concentrations, magnetite samples presented $n_2 < 0$ and the value similar to that of the liquid carrier. Increasing N , the absolute value of n_2 also increases, staying in the range from about $-10 \times 10^{-14} \text{ cm}^2/\text{W}$ to about $-7 \times 10^{-14} \text{ cm}^2/\text{W}$, and did not show a clear dependence on N . Besides, we have observed a linear dependency of a two-photon absorption coefficient b with the concentration N , as expected, with the proportionality parameter the two-photon absorption cross section σ_{2PA} . Our results have shown that $\sigma_{2PA} = 50(2) \text{ GM}$.

Support by CNPq (Conselho Nacional de Desenvolvimento Científico e Tecnológico), FAPESP (Fundação de Amparo à Pesquisa do Estado de São Paulo), CAPES (Coordenação de Aperfeiçoamento de Pessoal de Nível Superior), INCT-FCx (Instituto Nacional de Ciência e Tecnologia de Fluidos Complexos), and NAP-FCx.

Paper published in: *J. Appl. Phys.* **121** (2017) 043103.

2TL-F-4

MAGNETIC NANOWIRE BIOLABELS USING FORC

Bethanie S.^{1,2}, Sharma A.¹, Shore D.²

¹ University of Minnesota, Electrical & Computer Engineering, Minneapolis, USA

² University of Minnesota, Chemical Engineering & Materials Science, Minneapolis, USA
stadler@umn.edu

Magnetic nanowires [1] have great potential as ‘barcodes’ for cells and other biomarkers, such as exosomes. Ultimately, they promise to allow multiplexed detection by non-optical means for diagnosis of complex medical samples, such as blood or tissue biopsies. Read-out could occur by magnetic measurements, such as hysteresis loops measured using vibrating sample magnetometry (VSM), except that distributions in coercivities make it difficult to distinguish mixed samples. First order reversal curves (FORC), however, provide more information per measurement and also yield a method to quantitatively distinguish multiple coercivities and their distributions.

Here, magnetic nanowires have been synthesized in anodic aluminum oxide (AAO). Barcode nanowires can be designed and synthesized (inset of Fig.1) using magnetic/nonmagnetic segments to produce a large range of intersegment interactions, and therefore a large number of barcode signatures. For this feasibility study, simple Ni nanowires were studied with two different diameters: 18nm (5 μ m long) and 100nm (6 μ m long). Due to differences in magnetic reversal mechanisms, the coercivities of these nanowires by parallel field VSM were 880Oe and 320Oe, respectively. Although these values are quite different, the hysteresis loops were slanted due to interwire interactions, so mixtures of the two samples are very difficult to ‘diagnose’ from simple VSM measurements.

Next FORC measurements were made of the two samples and with mixtures of 23:1 and 115:1 (18nm:100nm), Fig. 1. FORC enables one to separate the effects of interwire interactions from distributions in coercivity. Sample (a) and (b) in Fig. 1 are the 18nm and 100nm diameter samples, resp. The volume of a 100nm diameter nanowire is 9.25 greater than a 18nm diameter nanowire. For two samples of the same materials (eg: Ni), this is also the ratio in masses. Since the moment measured by the VSM scales with volume (mass), mixtures of the two samples will lead to a dominance by the larger biolabel type.

Therefore, the added information obtained by FORC is critical to determining ratios of nanowires present in mixtures. For samples (c) and (d) in Fig1, mixtures with nanowire ratios of $n_a : n_b = 23:1$ and $115:1$ (mass ratios = 0.6 and 3.04, resp.) were measured. Using the distribution in the coercivities of (a) and (b), the mass ratios of the mixtures was determined by statistical analysis to be 0.615 and 2.85; an error of only 2.5% and 6.25% compared to the known mass ratios of mixtures (c) and (d). Barcode samples with less distribution in H_c will allow better multiplexing.

In conclusion, mixtures of nanowires were accurately ‘diagnosed’ using purely magnetic measurements. This technique can be used to measure, for example, the number of tumor cells compared to leukocytes (white blood cells) in either an assay or biopsy if each cell type was labeled with a different nanowire type. Similar nanowires are effective in MRI contrast and hyperthermia [2] for future theranostics.

Support by IEM and NSF is acknowledged.

[1] *Nanotechnology*, **26** (2015) 135102.

[2] *Chemical Communications*, **52** (2016) 12634-7.

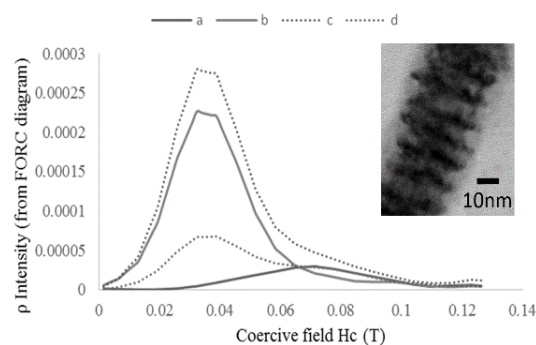


Fig. 1. Distributions of coercivities for samples of Ni nanowires with diameters of 18nm (a), 100nm (b), and mixtures of $n_a : n_b = 23:1$ (c) and $n_a : n_b = 115:1$ (d). Inset shows a ‘barcode’ nanowire.

2TL-F-5

ADVANTAGES OF POLYACRYLAMIDE HYDROGELS FILLED WITH MAGNETIC NANOPARTICLES FOR THE BIOMEDICAL ENGINEERING

*Blyakhman F.A.^{1,2}, Makarova E.B.¹, Makeyev O.G.¹, Melekhin V.V.¹, Safronov A.P.^{1,2},
Sichkar D.A.¹, Shklyar T.F.^{1,2}, Sokolov S.Yu.^{1,2}, Zubarev A.Yu.²*

¹ Ural State Medical University, Yekaterinburg, Russia

² Ural Federal University, Yekaterinburg, Russia

feliks.blyakhman@urfu.ru

The development of biocompatible materials based on the functional properties of gels is promising area of biomedical engineering. In particular, the advantages of polyacrylamide (PAA) gels as the cellular substrates for tissue engineering were reported in a number of investigations. New class of hydrogels filled with the magnetic nanoparticles (MNPs) opens up a potential in the development of magnetically operated materials for the needs of biomedicine. This study was aimed to determine the impact of MNPs on the PAA gel functional properties.

Ferrogels were synthesized by radical polymerization of acrylamide in a stable aqueous suspension of γ -Fe₂O₃ MNPs (d=11 nm) made by laser target evaporation. The gel network density was set to 1:100, the concentration of imbedded MNPs was fixed at 0, 0.25 and 0.75% by weight. Cylindrical gel samples sized in accordance with specific equipment for mechanical, electrical and biological experiments were used.

To determine Young modulus (E) and effective viscosity (η) of gels, the step-wise axial deformations (up to 25% with step size \sim 2.5%) of gel samples were applied by means of the linear electromagnetic motor. The electrical potential of gel (ϕ) was obtained by two identical Ag/AgCl tapered glass microelectrodes (\sim 1 micron in tip diameter) typically used in biophysical studies for intracellular voltage measurement. Cell adhesion to material surfaces as a basic method for the determining of gel samples biocompatibility was studied. Adhesive activities of human dermal fibroblasts (Fig. 1) and human peripheral blood leucocytes were tested. To estimate the impact of MNPs on the cell adhesion quantitatively, the number of cells attached to the ferrogels was normalized to the number of cells adhered to the blank gel.



Fig. 1. Fibroblasts adhered to ferrogel.

We found that the gradual increase of MNPs concentration in the PAA gel network resulted in the significant increase of E, η , ϕ and adhesion index for both the leucocytes (AdL) and the fibroblasts (AdF) cultures. In particular, the following values of E, η , ϕ , AdL and AdF in the blank gel and ferrogel with highest concentration of MNPs (0.75%) were obtained: 26.5 \pm 1.7 and 39.5 \pm 1.5 kPa (n=9, p<0.001); 5.8 \pm 1.2 and 8.6 \pm 1.8 kPa*sec (n=9, p<0.01); -22.5 \pm 3.6 and -62.3 \pm 5.3 mV (n=9, p<0.001); 100 \pm 5 and 181 \pm 13% (n=30, p<0.001); 100 \pm 8 and 116 \pm 3% (n=8, p<0.01), respectively.

The cell adhesion is one of the initial stages of cells monolayer formation, and it characterizes a direct interaction between cells and matrix. In general, the direct and indirect effects of MNPs on the cell adhesion are possible. The impact of MNPs on the stiffness and electrical potential of gels is most likely explanation of obtained results. Thus, from the viewpoint of biomedical engineering applications, the inclusion of MNPs into the polymer network significantly improves the gel properties.

Support by the Russian Scientific Foundation (grant #14-19-00989) is acknowledged.

2TL-F-6

**TOWARD DIGITAL CELLS ON CHIP BASED ON SPINTRONICS:
MANIPULATION AND MONITORING OF PARTICLES AND CELLS VIA
NANO- AND MICRO-SCALE MAGNETOPHORETIC DEVICES**

Byeonghwa L., Torati S.R., Kim K.W., Xinghao H., Reddy V., Kim C.G.

Department of Emerging Materials Science, DGIST, Daegu, 42988, Republic of Korea.
cgkim@dgist.ac.kr

The manipulation of cells has gaining more importance towards gene sequencing, single cell analysis and cell separation technology. Although, several single cell techniques are developed, it is still challenging and complex to collect rare cells and their digital manipulation in large-scale operation. Recently, the flexibility of magnetic transport technology using nano/micro scale magnets for the magnetophoresis has experienced excellent advances and has been used for a wide variety of single cells manipulation tasks with the help of superparamagnetic carriers[1,2]. The magnetic transport technology, which can be integrated within microfluidic channels, relies on both magnetic energy and force tenability, and remote control implemented by micro- and nano-patterned magnetic structures [3-4]. Here, we have demonstrated a class of integrated magnetic track circuits for executing sequential and parallel, timed operations on an ensemble of single particles and cells. The magnetic circuitry tracks are designed by conventional lift-off technology and were used for the passive control of cells/particles similar concept to electrical conductor, diodes and capacitor. When the magnetic tracks are combined into arrays and driven by rotating magnetic field, the single cells are precisely control for multiplexed analysis [5]. The concentric cell transportation and separation were performed by the assembly of this magnetic track into a novel architecture, resembled with spider web network consisted of several radii and spirals, where all the particles/cells are concentrated into one position and then transported to apartments array for the single cell analysis. In addition, a planar Hall resistance (PHR) sensor is integrated with the web networks, and the manipulation and detection are achieved via superparamagnetic particles with dual functions as a biomolecule carrier for transportation and labels for monitoring [6]. This allows the efficient collection of low-density biomolecule carriers to one specific point and monitors the accumulated carriers. Toward cells on chips.

This work was supported by the DGIST R&D Program of the Ministry of Science, ICT and Future Planning (17-BT-02).

- [1] B. Lim, V.Reddy, X.H.Hu, K.W.Kim, M.Jadhav, R.Abedini-Nassab, Y.W. Noh, Y.T.Lim, B. B. Yellen, C. G. Kim, *Nat. Commun.*, **5** (2014) 3846.
- [2] S.Anandakumar, V.Sudha Rani, S.Oh, B.L.Sinha, M.Takahashi, C.G.Kim, *Biosens Bioelectron.*, **26** (2010) 1755.
- [3] B. Lim, P. Vavassori, R. Sooryakumar, C.G.Kim, *J. Phys. D-Appl. Phys.*, **50** (2016) 033002.
- [4] K.W.Kim, V.Reddy, S.R.Torati, X.H. Hu, A.Sandhu, C. G. Kim, *Lab Chip*, **15** (2015) 696-703.
- [5] X. Hu, S.R.Goudu, S.R.Torati, B.Lim, K.Kim, C.Kim, *Lab Chip*, **16**, (2016) 3485-3492
- [6] X. Hu, S.R.Torati, A.I.Shawl, B.Lim, K.Kim, C. Kim. *IEEE Magn. Lett.* **7** (2016) 1508004.

2OR-F-7

RAPID AND ULTRASENSITIVE DETECTION OF SMALL MOLECULES WITH IMMUNOSENSORS BASED ON REGISTRATION OF MAGNETIC NANOLABELS

Guteneva N.V.¹, Znoyko S.L.¹, Nikitin M.P.², Orlov A.V.¹, Nikitin P.I.¹

¹ Prokhorov General Physics Institute, Russian Academy of Sciences, Moscow, Russia

² Moscow Institute of Physics and Technology (State University)

nguteneva@gmail.com

The task of creating simple and rapid test systems for ultrasensitive quantitative detection of small molecules (i.e. toxins, antibiotics, hormones, vitamins) in a small volume of complex biological samples (milk, blood, saliva, etc.) is relevant for such industries as food quality control, in vitro diagnostics, criminalistics, environmental monitoring.

Among the most common approaches used for the detection of biomolecules immunoassays hold a special place. However, quantitative immunoassay (ELISA) is characterized by a long time of obtaining the result (> 2 hours). In connection with this, it is promising to use magnetic particles as detectable labels.

The designed test-system for ultrasensitive detection of small molecules is based on registration of magnetic nanolabels in the competitive immunochromatography which are readout by the magnetic particle quantification (MPQ) method [1-2]. Briefly, the MPQ method employs a nonlinear magnetization of superparamagnetic particles subjected to a magnetic field at frequencies f_1 and f_2 with recording the particle response at a combinatorial frequency that is a linear combination of f_1 and f_2 . The method is insensitive to linear dia- and paramagnetic materials such as glass, water and plastic. In contrast to optical detection methods, the signal is taken from the entire volume of the sample, which significantly increases the sensitivity of the analysis. To optimize the assay, we recorded the magnetic nanolabels distribution along test strip under different conditions by continuous monitoring the magnetic signals while passing the strip through the MPQ reader (Fig. 1).

The test-system for ultrasensitive detection of small molecules was designed based on the described MPQ method. and the IC lateral flow principle [3-4] modified and optimized for using with 200-nm magnetic beads to be quantified by non-linear magnetization. It provides wide linear range and the LOD in blood serum for several substances less than 1 pM. The duration of the analysis does not exceed 30 minutes, including the incubation period. Due to the usage of magnetic particles as detectable labels, this analysis, in contrast to optical detection methods, can be performed in opaque media, for example, in whole blood, milk. Support by RSF and RFBR is acknowledged.

[1] Nikitin, P.I., Vetoshko, P.M., Ksenevich, T.I., *Sens. Lett.*, **5(1)** (2007) 296–299.

[2] Nikitin, P.I., Vetoshko, P.M., Ksenevich, T.I., *JMMM*, **311 (1)** (2007) 445–449.

[3] O'Farrell, B., *Evolution in Lateral Flow-based Immunoassay Systems. Lateral Flow Immunoassay*, Springer, USA, 1–33 (2009).

[4] Posthuma-Trumpie, G. A., Korf, J., van Amerongen, A., *Anal. Bioanal. Chem.*, **393(2)** (2009) 569–582.

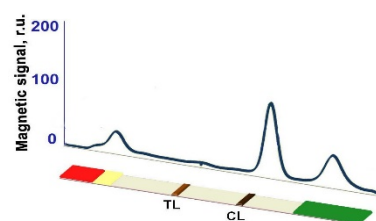


Fig. 1. Signal distribution along the test strips.

2OR-F-8

DETECTION OF CARDIAC BIOMARKERS MYOGLOBIN AND C-REACTIVE PROTEIN BY A GIANT MAGNETOIMPEDANCE-BASED BIOSENSING SYSTEM

Yang Z.^{1,2,3,4}, Dong X.^{1,2}, Guo P.^{1,2}, Yan H.^{1,2}, Lei Ch.³, Wang F.⁴, Luo Y.-S.^{1,2}

¹ School of Physics and Electronic Engineering, Xinyang Normal University, Xinyang 464000, People's Republic of China

² Key Laboratory of Advanced Micro/Nano Functional Materials, Xinyang Normal University, Xinyang 464000, People's Republic of China

³ Key Laboratory for Thin Film and Microfabrication of the Ministry of Education, Department of Micro/Nano Electronics, School of electronic information and electrical engineering, Shanghai Jiao Tong University, Dong Chuan Road 800, Shanghai 200240, People's Republic of China

⁴ Department of Electrical and Electronic Engineering, Southern University of Science and Technology, Shenzhen, China
eyslue@163.com (Y-S Luo)

A novel bio-sensing system based on a multilayered giant magnetoimpedance (GMI) sensor and enclosed microfluidics devices (EMD) was developed for combined detection of cardiac biomarkers myoglobin (Mb) and C-reactive protein (CRP). The NiFe/Cu/NiFe GMI sensors and EMD were fabricated by micro electromechanical system (MEMS) technology. The commercial Dynabeads were used for magnetic labels of Mb and CRP. The classical sandwich assay was used for detection of Mb and CRP targeted with Dynabeads by using antibody-antigen pair combination of biotin-streptavidin. The enclosed microfluidics devices were designed for different detection regions, which were premodified with specific antibody. The GMI ratios of the sensors located under different detection regions with different antigen concentrations were observed. The results showed that the GMI-based bio-sensing system had high selectivity and sensitivity for detection of cardiac biomarkers. Compared with the blank control region, ultrasensitive detection of CRP and Mb was accomplished in the detection region 1 and 2 respectively, the detection limit were 1 pg/ml and 0.1 pg/ml respectively. The linear detection range contained low concentration detection area and high concentration detection area, which were 1 pg/ml-10 ng/ml, 10-100 ng/ml for CRP, and 0.1 pg/ml-1 ng/ml, 1 n/ml-80 ng/ml for Mb. This method in our perception provides a widely applicable basis for multi-target biomolecules rapid diagnostic testing like alpha-fetoprotein (AFP) and carcino embryonic antigen (CEA).

2 July

Sunday

12:00-13:30

15:00-17:00

oral session

2TL-G

2RP-G

2OR-G

**“Diluted Magnetic
Semiconductors and
Oxides”**

2TL-G-1

PROXIMITY EFFECT IN A FERROMAGNET/SEMICONDUCTOR HYBRID STRUCTURE

Korenev V.L.¹, Salewski M.², Akimov I.A.^{1,2}, Sapega V.F.¹, Langer L.², Kalitukha I.V.¹, Debus J.², Dzhioev R.I.¹, Yakovlev D.R.^{1,2}, Müller D.², Schröder C.³, Hövel H.³, Karczewski G.⁴, Wiater M.⁴, Wojtowicz T.⁴, Kusrayev Yu.G.¹, Bayer M.^{1,2}

¹ Ioffe Physical-Technical Institute, Russian Academy of Sciences, 194021 St. Petersburg, Russia

² Experimentelle Physik 2, Technische Universität Dortmund, D-44227 Dortmund, Germany

³ Experimentelle Physik 1, Technische Universität Dortmund, D-44227 Dortmund, Germany

⁴ Institute of Physics, Polish Academy of Sciences, PL-02668 Warsaw, Poland

korenev@orient.ioffe.ru

Exchange interactions are the origin for correlated magnetism in condensed matter such as ferro, antiferro or ferrimagnetism. In magnetic semiconductors (SCs), the exchange occurs between free charge carriers and localized magnetic atoms and is determined by their wavefunction overlap. To assess and control this overlap, hybrid heterostructures consisting of a ferromagnetic (FM) layer and a semiconductor quantum well (QW) are appealing objects because they allow wavefunction engineering. Furthermore, the mobility of QW carriers may not be reduced by inclusion of magnetic ions in the same spatial region. The excellent optical properties of the QW can be preserved as well. More specifically, for a two-dimensional hole gas (2DHG, the p -system) in a QW the overlap of the hole wavefunction with the magnetic atoms in a nearby ferromagnetic layer (the d -system) is believed to result in a p - d exchange interaction. This exchange interaction may cause strong coupling between the SC and FM spin systems, through which the ferromagnetism of the unified system (e.g. magnetic anisotropy) can be tuned. In particular, the 2DHG spin system becomes polarized in the effective magnetic field of the p - d exchange.

Here we consider a FM/QW hybrid consisting of a Co-layer and a CdTe-QW separated by a nanometer-thick non-magnetic barrier (spacer) CdMgTe [1]. This hybrid combination shows ferromagnetic proximity effect due to the effective p - d exchange interaction between Co atoms and CdTe-heavy holes. It manifests itself in the quasi-equilibrium spin polarization of the holes bound to shallow acceptors within the CdTe QW. Surprisingly, however, the ferromagnetic proximity effect is almost constant over large distances up to 14 nm spacer width. In contrast, for conventional p - d exchange via wavefunction overlap an exponential decay with barrier width with a characteristic decay length of about a nanometer would be expected. This novel exchange coupling effect is therefore truly long-range, which is highly advantageous because it is robust with respect to hybrid interface variations. As possible origin of this long-range proximity effect we conjecture an effective p - d exchange interaction mediated by elliptically polarized hybrid phonons in the FM/QW heterostructure.

Support by DFG and RFBR in the frame of the ICRC TRR 160, the Government of Russia via project N14.Z50.31.0021, DEC-2012/06/A/ST3/00247 and DEC-2014/14/M/ST3/00484 is acknowledged.

[1] V.L. Korenev et al., *Nature Physics*, **12** (2016) 85-91.

2RP-G-2

(In,Mn)As QUANTUM DOTS: SYNTHESIS AND PROPERTIES

*Bouravleuv A.D.*¹⁻³, *Nevedomskii V.V.*², *Sapega V.F.*², *Khrebtov A.I.*¹, *Samsonenko Yu.B.*^{1,3},
*Strokov V.N.*⁴, *Cirlin G.E.*¹⁻³

¹ St.Petersburg Academic University RAS, St.Petersburg, Russia

² Ioffe Institute RAS, St.Petersburg, Russia

³ Institute for Analytical Instrumentation RAS, St.Petersburg, Russia

⁴ Paul Scherrer Institute, Villigen-PSI, Switzerland

bour@mail.ioffe.ru

Nanoscale ferromagnetic semiconductor (FS) structures are one of the most promising objects for the control over spin interactions by means of different methods, e.g. electrical or optical, and as a result for the creation of new spintronic devices. Local distribution of spins in such nanostructures seems to be depended not only on their sizes, but also on their shape. This brings up many questions concerning the formation of such nanostructures.

Usually FS layers grow at relatively low temperatures to avoid phase separations, but FS nanostructures can be synthesized at higher temperatures, which correspond to the formation of conventional nanostructures.

We have elaborated the novel techniques for the MBE growth of (In,Mn)As quantum dots (QDs) [1-3] at relatively high growth temperatures. (In,Mn)As QDs have been obtained by molecular beam epitaxy using Mn selective doping of central parts of QDs.

The detailed investigation of the structures obtained demonstrates, that despite relatively high growth temperature, the (In,Mn)As quantum dot structures have a good crystalline quality (see Fig. 1). Moreover, they exhibit interesting magneto-optical properties.

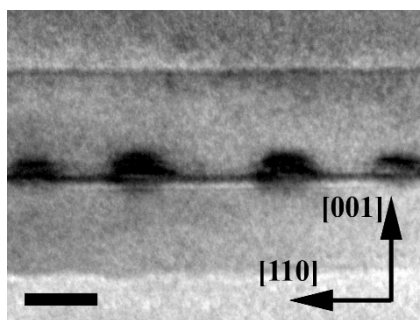


Fig. 1. Dark-field TEM image of the sample with (In,Mn)As QDs.

[1] A. Bouravleuv et al., *Semiconductors*, **47** (2013) 1037-1040.

[2] A. Bouravleuv et al., *Appl. Phys. Lett.*, **105** (2014) 232101.

[3] A. Bouravleuv et al., *Nanotechnology*, **27** (2016) 425706.

2OR-G-3

GIANT MAGNETIC POLARONS INDUCED AND MONITORED BY LIGHT IN EuSe

*Henriques A.B.*¹, *Naupa A.R.*¹, *Usachev P.A.*², *Pavlov V.V.*², *Springholz G.*³

¹Instituto de Física, Universidade de Sao Paulo, 05315-970 Sao Paulo, Brazil

²Ioffe Institute, 194021 St. Petersburg, Russia

³Institut für Halbleiter und Festkörperphysik, Johannes Kepler Universität, A-4040 Linz, Austria
andreh@if.usp.br

Optical manipulation of the magnetic state of matter is a topic of current interest both from the fundamental point of view as well as due to its high relevance in technological applications [1]. One way to magnetize a semiconductor, using light, is by photoexciting an ensemble of coherent magnetic polarons. The magnetic polaron in question consists of a photoexcited conduction band electron, surrounded by a cloud of lattice spins tilted towards the electron's spin. The concept of a magnetic polaron dates back to the sixties [2]. Magnetic polarons have been extensively studied in *dilute* magnetic semiconductors (see for instance Ref. 3). To pick up polaron effects in dilute magnetic semiconductors, photoluminescence (PL) was mostly used, because PL is a technique that is very sensitive to small amounts of impurities. Only very rare polaron investigations based on techniques other than PL, such as SQUID [4] or muon spin rotation [5], have been reported. However, polaron investigations and the optical manipulation of the magnetic state in *intrinsic* magnetic semiconductors have been much less explored. A possible reason for this is that intrinsic magnetic semiconductors do not usually show the near-bandgap PL that is typical of the dilute magnetic material.

Recently, however, our research group demonstrated a new approach for the optical manipulation of magnetic polarons in EuTe, using a two-colour pump-probe Faraday rotation technique [6,7] We found that at 5K light resonant with the EuTe bandgap generates magnetic polarons with a magnetic moment larger than $600 \mu_B$ (Bohr magnetons). This is about an order of magnitude larger than magnetic polarons investigated in diluted magnetic semiconductors.

Here we present new and yet unpublished results obtained by the two-colour pump probe technique for photoinduced magnetic polarons in EuSe. A robust signal associated with photoinduced magnetic polarons was detected. The magnetic polarons observed are described by a magnetic moment that exceeds $1000 \mu_B$ at 5K, which is a new record value, larger than in EuTe by a factor of two. This is explained by the fact that in EuSe the opposition the exchange interaction between lattice spins offers to the exchange magnetic field of the photoexcited electron is smaller than in EuTe. Moreover, our results suggest that the density of magnetic polarons that can be generated in EuSe is orders of magnitude larger than in EuTe, making the EuSe crystal more attractive for practical applications in optomagnetic devices.

This work was supported by FAPESP (Project 2016/24125-5), CNPq (projects 401694/2012-7, 307400/2014-0, and 456188/ 2014-2), RFBR (project 16-02-00377) and RSF (project 17-12-01314).

- [1] A. Kirilyuk, A. V. Kimel, and T. Rasing, *Reviews of Modern Physics*, **82** (2010) 2731.
- [2] P. G. de Gennes. *Physical Review*, **118** (1960) 141.
- [3] J. Kossut and J. A. Gaj, editors. Introduction to the Physics of Diluted Magnetic Semiconductors. Springer Series in Materials Science. Springer, 2010.
- [4] D. D. Awschalom, J. Warnock, and S. von Molnar, *Physical Review Letters*, **58** (1987) 812.
- [5] V. G. Storchak, O. E. Parfenov, J. H. Brewer, et al. *Physical Review B*, **80** (2009) 235203.
- [6] A. B. Henriques, G. D. Galgano, P. H. O. Rappl *et al*, *Physical Review B*, **93** (2016) 201201(R).
- [7] A. B. Henriques et al., *Physical Review B*, **95** (2017) 045205.

2OR-G-4

**THE INFLUENCE OF THE SIZE-FACTOR ON THE
MAGNETOSTRUCTURAL TRANSFORMATION OF MANGANESE
ARSENIDE IN THE COMPOSITE CdGeAs₂-MnAs**

Fedorchenko I.V.¹, Marenkin S.F.¹, Aronov A.N.¹, Ril. A.I.¹, Zheludkevich A.L.²

¹ Kurnakov Institute of General and Inorganic Chemistry RAS, Moscow, Russia

² SSPA "Scientific and Practical Materials Research Center of NAS of Belarus", Minsk, Belarus

irina@igic.ras.ru

An intensive study of the nanoferrromagnetic composites is due to the potential numerous of practice applications. These materials are perspective for magnetic sensors, switches and magnetic refrigerators. One of the promising materials is manganese arsenide (Curie point = 40°C). MnAs has a narrow temperature hysteresis (315-318 at heating and 308 at cooling) in the first-order phase transition zone [1]. The narrow hysteresis loop and anisotropy of the properties lead to the irreversible of the temperature hysteresis. It makes difficult to use the magnetocaloric properties of MnAs. At the same time, wider hysteresis and better cycling was observed in MnAs_{0,99}Sb_{0,01} solid solutions [2] and composite based on MnAs and PVA glue [3].

In this work, we use composite based on semiconductor- ferromagnetic system. CdGeAs₂ was considered as a semiconductor and MnAs as a ferromagnetic. Manganese arsenide is characterized by giant magnetocaloric effect (GME) and the value of cold-storage capacity in MnAs - 442 J/kg, which is much higher than the known magnetocaloric materials, operating at room temperatures, such as Cd with $q = 43.8$ J/kg and Cd₅(SiGe)₄ with $q = 240$ J/kg [1]. In this regard, the nature and mechanism of magnetostructural junction investigation in manganese monoarsenide is given the considerable attention. The narrow range of hysteresis temperature and the presence of anisotropy in the magnetic junction area, leading to irreversible thermal hysteresis loops, create difficulties for devices operating in the "heating-cooling" mode. Therefore, it is seemed interesting to study the magnetic manganese monoarsenide transformation in composite alloys. The phase boundary will reduce the mass transfer possibility, and manganese monoarsenide nanosized clusters of will come to minimizing the anisotropy on the hysteresis loop irreversibility.

By differential scanning calorimetry method (DSC) the structural transformation of MnAs from hexagonal to the orthorhombic modification was studied. It was measured the temperature range and the enthalpy of the thermal effect. The temperature range was 39.5-46 °C, $\Delta H = -5.6$ J/g. In the MnAs-CdGeAs₂ composite due to the phase boundaries, leading to a decrease in mass transfer it was observed a stabilization of monoarsenide magnetostructural transformations cycling in the MnAs-CdGeAs₂ composite alloys. With increasing nanodispersion of the MnAs clusters the change in the nature of the structural transformation from first type to second one was occurred.

The reported study was funded by RFBR according to the research project №17-53-04055.

[1] Mitsiuk V. I., Pankratov N. Yu., Govor G. A. et al, *Physics of Solid State*, **54** №10 (2012).

[2] Pankratov N.Yu. et al., *Solid State Phenomena*, **190** (2012) 343-346.

[3] Patent (Belarus) №19913.

2OR-G-5

COLOSSAL MAGNETORESISTANCE AND ANOMALOUS HALL EFFECT IN NONMAGNETIC SEMICONDUCTORS

Obukhov S.A.¹, Panysheva T.Yu.²

¹ Ioffe PTI of the RAS, St. Petersburg, Russian Federation

² Peter the Great St. Petersburg Polytechnic University, Russian Federation
sobukhov@inbox.ru

Colossal Magnetoresistance (CMR) which features colossal resistivity decrease in external magnetic field and the Anomalous Hall Effect (AHE) described as unusual behavior of the Hall constant in low magnetic field are the major features of Diluted Magnetic Semiconductors (DMS) [1], Magnetic Semiconductors (MS) [2] and Manganite Perovskite [3]. The most cited physical models describing CMR, i.e., Magnetic Polaron and Phase Separation models [2, 3], are based on the suggestion that DMS and MS are the magnetic materials where charge carriers transport is dependent on their interaction with magnetic moments of the host magnetic ions.

However, this approach absolutely ignores the fact that both CMR and AHE have been also experimentally observed in nonmagnetic semiconductors (NMS) – Ge [4,5] and InSb [5,6] where resistivity decrease of $10^2 \div 10^5$ was observed in magnetic field $B \sim 3\text{T}$ and temperature $T \sim 1,5\text{K}$. We stress that these values are comparable with CMR values in DMS and MS like $\text{Hg}_{1-x}\text{Mn}_x\text{Te}$, $\text{Gd}_{1-x}\text{V}_x\text{S}_4$, and etc. at the same B and T.

This similarity in transport properties of DMS, MS and NMS puts forward the idea of CMR and AHE description in magnetic and nonmagnetic materials in the framework of excitonic insulator (EI) model [7]. According to EI model electrons and holes, having significant difference in effective masses (m_h/m_e), form EI phase which, influenced by excitons dissociation in external magnetic field, turns into the phase with metallic conductivity [8]. AHE in the framework of EI model can be explained by different input from electrons and holes with large m_h/m_e ratio into the Hall voltage at high and low magnetic field.

[1] J. K. Furdyna and J. Kossut, *Diluted Magnetic Semiconductors*, **Vol. 25**, Semiconductors and Semimetals (Academic Press, Inc., 1988).

[2] E.L Nagaev. *Colossal Magnetoresistance and Phase Separation in Magnetic Semiconductors* (Imperial College Press, London, 2002).

[3] A. Moreo and E. Dagotto. *Science*, **283** (1999) 2034.

[4] S. D. Ganichev, *et al.*, *Physical Review B*, **63** (2001) 201204.

[5] S. A. Obukhov. *Physica Status Solidi B*, **223** (2001) 535.

[6] S. A. Obukhov. in *Indium: Properties, Technological Applications and Health Issues*, (Novapublisher, New York, 2013).

[7] J. Neueschwander and P. Wachter. *Physical Review B*, **41** (1990) 12693.

[8] S. A. Obukhov, S. W. Tozer and W. A. Coniglio, *Scientific Reports*, **5** (2015) 13451.

2TL-G-6

SPIN-DEPENDENT TUNNELING IN SEMICONDUCTOR HETEROSTRUCTURES WITH A MAGNETIC LAYER

Rozhansky I.V.^{1,2}, Denisov K.S.^{1,2}, Averkiev N.S.¹, Lahderanta E.²

¹ Ioffe Physical Technical Institute, St.Petersburg, Russia

² Lappeenranta University of Technology, Finland

rozhansky@gmail.com

We propose a mechanism for the generation of spin polarization in semiconductor heterostructures with a quantum well (QW) and a magnetic impurity layer spatially separated from the QW. The spin polarization of carriers in a QW originates from spin-dependent tunneling recombination at impurity states in the magnetic layer [1]. An electron is tunneling from the QW into the bound state with a subsequent phonon-assisted non-radiative recombination. Due to an effective exchange field in the paramagnetic layer the bound state is split in the electron spin projection. This results in the different tunneling rates for spin-up and spin-down electrons tunneling from the QW and gives rise to a spin polarizations of the carriers remaining in the QW, which is accompanied by a fast linear increase in the degree of circular polarization of photoluminescence (PL) from the QW.

Two situations are theoretically considered (Fig.1). In the first case, resonant tunneling to the spin-split sublevels of the impurity center occurs and spin polarization is caused by different populations of resonance levels in the QW for opposite spin projections. In the second, non-resonant case, the spin-split impurity level lies above the occupied states of electrons in the QW and plays the role of an intermediate state in the two-stage coherent spin-dependent recombination of an electron from the QW and a hole in the impurity layer [2].

The developed theory allows us to explain both qualitatively and quantitatively the kinetics of photoexcited electrons in experiments with time-resolved PL in Mn-doped InGaAs heterostructures [3]. As our calculations show in these experiments the non-resonant spin-dependent recombination through an interstitial Mn donor state lying close to the conductance band edge is realized. The theory explains quantitatively the experimentally observed PL features, including the PL quenching and linear increase in polarization with a characteristic time shorter than the radiative-recombination time by a few orders of magnitude.

[1] I.V. Rozhansky et al., *Phys. Rev. B*, **92** (2015) 125428.

[2] K.S. Denisov et al., *Semiconductors*, **51** (2017) 43.

[3] I. Akimov et al., *Physica Status Solidi (b)*, **251** (2014) 1663.

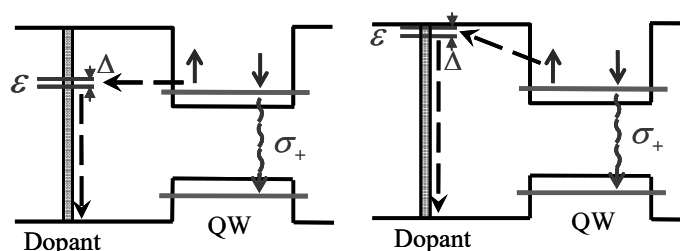


Fig. 1. Resonant (left) and non-resonant (right).spin-dependent tunneling

2RP-G-7

HIGH-FIELD HOPPING MAGNETOTRANSPORT IN KESTERITES

*Lähderanta E.*¹, *Lisunov K.*^{1,2}, *Shakhov M.*^{1,3}, *Guk M.*^{1,2}, *Hajdeu-Chicarosh E.*^{1,2}, *Levcenko S.*^{2,4},
*Zakharchuk I.*¹, *Arushanov E.*²

¹ Lappeenranta University of Technology, Lappeenranta, Finland

² Institute of Applied Physics, Chisinau, Moldova

³ Ioffe Institute, St. Petersburg, Russia

⁴ Helmholtz Zentrum für Materialien und Energie, Berlin, Germany

Erkki.Lahderanta@lut.fi

The Cu based quaternary kesterite-type compounds (briefly, kesterites) $\text{Cu}_2\text{ZnSnS}_4$, $\text{Cu}_2\text{ZnSn}_x\text{Ge}_{1-x}\text{Se}_4$ and $\text{Cu}_2\text{ZnGeS}_4$ were investigated. They belong to a family of I2-II-IV-VI4 quaternary chalcogenide p-type semiconductors. They are among the most promising materials for utilization in photovoltaic conversion, investigated in recent time. Indeed, the efficiency exceeding 11 % for pure $\text{Cu}_2\text{ZnSnS}_4$ based solar cells, and up to 12.6 % for solar cells based on $\text{Cu}_2\text{ZnSn}(\text{S},\text{Se})_4$, have been achieved recently [1]. On the other hand, even a small amount of Ge (less than 10 %) in the solid solution yields a significant increase of the solar cell efficiency [2].

Here, we investigate resistivity, $\rho(T)$, magnetoresistance (MR) and Hall effect of the kesterite single crystals in pulsed magnetic fields up to $B = 20$ T. The purpose is determination of charge transfer mechanisms, microscopic parameters of charge carriers and details of the hole spectrum.

The Mott and the Shklovskii-Efros (SE) variable-range hopping (VRH) conductivities [3] have been found in $\text{Cu}_2\text{ZnSnS}_4$ within different temperature diapasons, lying at T between $\sim 50 - 150$ K and below $T \sim 3 - 4$ K, respectively. Only the positive MR has been observed within the whole interval of B and T . The widths of the acceptor band, W , and of the Coulomb gap, Δ , the values of the density of the localized states (DOS) $g(\mu)$ at the Fermi level μ , and those of the localization radii, a , have been determined. A dramatic increase of the a values in the interval of SE VRH conduction, with respect to those obtained in the Mott VRH interval, has been established. This has been interpreted by influence of the quantum interference effects [4].

The nearest-neighbor hopping (NNH) conduction at higher $T \sim 250 - 320$ K, followed by the Mott VRH conductivity between $T \sim 50 - 250$ K, has been observed in $\text{Cu}_2\text{ZnSn}_x\text{Ge}_{1-x}\text{Se}_4$ single crystals with lowering T . The negative and positive contributions to MR take place, depending on B and T . The hole parameters a , $g(\mu)$, W and the acceptor concentration, NA , have been found exhibiting a non-linear dependence on x .

The Mott VRH conduction has been observed between $T \sim 100 - 200$ K in $\text{Cu}_2\text{ZnGeS}_4$. Outside this interval, $\rho(T)$ is connected to activation of holes into the domain of delocalized states of the acceptor band. MR of $\text{Cu}_2\text{ZnGeS}_4$ contains both the negative and positive contributions, connected to interference effects [4] and shrinkage of the impurity wave functions [3], respectively. The values of a , W , $g(\mu)$ and NA , as well as positions of the mobility edge and the Fermi level in the acceptor band have been determined. The Hall coefficient of $\text{Cu}_2\text{ZnGeS}_4$ is negative, exhibiting an exponential dependence on temperature, which is quite close to that of $\rho(T)$, as typical of the Hall effect in the domain of the VRH charge transfer [5].

[1] W. Wang *et al.*, *Adv. Energy Mater.*, **4** (2014) 1301465.

[2] S. Giraldo *et al.*, *Prog. Photovolt: Res. Appl.*, **24** (2016) 1359-1367.

[3] B. I. Shklovskii and A. L. Efros, *Electronic Properties of Doped Semiconductors* (Springer, Berlin, 1984).

[4] B. I. Shklovskii and B. Z. Spivak, in *Scattering and Interference Effects in Variable Range Hopping Conduction*, edited by M. Pollak and B. Shklovskii (North-Holland, Amsterdam, 1991).

[5] Yu. M. Gal'perin, E. P. German, and V. G. Karpov, *Sov. Phys. JETP*, **72** (1991) 193-200.

2OR-G-8

FERROMAGNETIC (GA,MN)P: MAGNETO-TRANSPORT PROPERTIES AND CO-DOPING EFFECT

Xu Ch.^{1,2}, *Yuan Y.*^{1,2}, *Wang M.*^{1,2}, *Hentschel H.*^{1,2}, *Böttger R.*¹, *Helm M.*^{1,2}, *Zhou Sh.*¹

¹ Helmholtz-Zentrum Dresden Rossendorf, Institute of Ion Beam Physics and Materials Research, Bautzner Landstrasse 400, D-01328 Dresden, Germany

² Technische Universität Dresden, D-01062 Dresden, Germany
c.xu@hzdr.de

The III-Mn-V based diluted magnetic semiconductor offers an opportunity to explore various aspects of carrier transport in the presence of cooperative phenomena [1]. In this work, GaP is chosen as a host semiconductor for magnetic dopants due to its large bandgap (2.2 eV) and short bond length (0.545 nm) with the possibility of obtaining strong p-d hybridization [2]. We have prepared Mn-doped GaP by combining ion implantation and pulsed laser melting and make a systematic investigation on the magnetic and transport properties of (Ga,Mn)P by varying Mn concentration as well as by Zn co-doping. All samples show insulating behavior and different negative magnetic resistance are observed, which indicate that the local moment from Mn 3d electrons have interaction with the holes introduced by Zn co-doping.

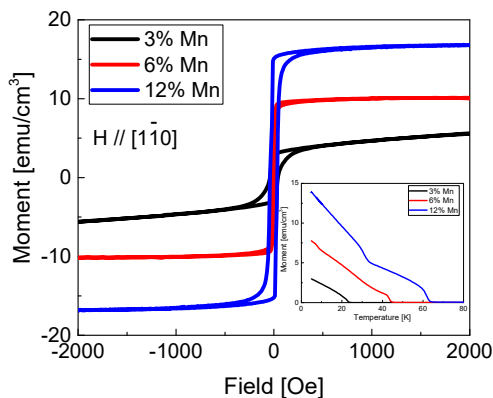


Fig. 1. Ferromagnetism of (Ga, Mn) P.

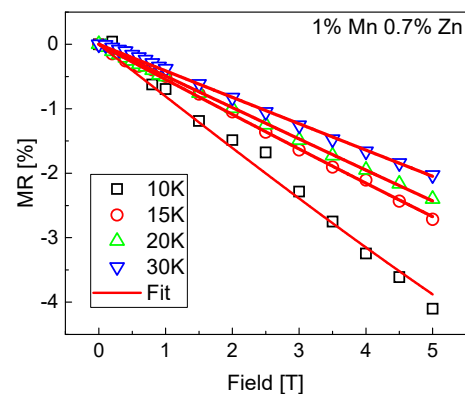


Fig. 2. Magnetoresistance of co-doped sample.

- [1] T. Dietl, *Semicond. Sci. Technol.*, **17** (2002) 377.
- [2] T. Dietl, H. Ohno, and F. Matsukura, *Phys. Rev. B*, **63** (2001) 195205.
- [3] M. Csontos, et al., *Phys. Rev. Lett.*, **95** 227203 (2005).
- [4] S. Kumar, et al., *Nano Lett.* **13** (2013) 5079.

2OR-G-9

MAGNETIC AND TRANSPORT PROPERTIES IN 2D-HETEROSTRUCTURES WITH DIFFERENT CONCENTRATION OF MANGANESE DELTA-LAYER

*Moiseev K.D.¹, Nevedomsky V.N.¹, Lugovikh A.M.², Charikova T.B.², Okulov V.I.²,
Kudriavstev Yu.³, Escobosa A.³, Casallas Y.⁴, Lopez-Lopez M.⁴*

¹ Ioffe Institute, St Petersburg, Russia

² Institute of Metal Physics UB RAS, Ekaterinburg, Russia

³ Dep. Ingenieria Electrica - SEES, Cinvestav- IPN, Mexico

⁴ Dep. Fisica, Cinvestav-IPN, Mexico

mkd@iropt2.ioffe.ru

Heterostructures with GaAs/InGaAs/GaAs quantum wells, doped with Mn-based monatomic layers, were obtained on the GaAs(001) substrate by MBE in the enhanced mode. The proposed growth method allows one to obtain layers based on transition metal compounds within monolayer (ML) concentration that can be located in a distance of several nanometers from another quantum-size object, for example a quantum well. This insertion provides a high doping concentration achieved in a limited space within the width comparable with the lattice constant and the doping profile can be described by Dirac's delta-function. Another GaAs barrier layer was doped with Be to provide a high hole concentration in the quantum well.

Structural quality of the samples under study were examined by means of the combined method using secondary ion mass spectrometry, X-ray diffraction measurement and transmission electron microscopy. The MnAs delta-insertions manifested zinc-blende type of crystal lattice [1].

The temperature and field dependences of the specific magnetization, as well as longitudinal and Hall resistivity in heterostructures with the GaAs:Be/Ga_{0.84}In_{0.16}As/GaAs single quantum well and Mn delta-layer in the concentration range of 0.4-2 ML were investigated and analyzed. Saturation of the magnetization was observed in the magnetic field $B \cong 1$ T at $T=5$ K for samples with a manganese concentration of 1.2 ML and 2 ML with values of $M_{M492} \cong 0.9 \cdot 10^{-4}$ emu/g and $M_{M402} \cong 1.5 \cdot 10^{-4}$ emu/g, respectively. Pronounced magnetization loop with the critical field value up to ~ 0.08 T was observed in the wide temperature range from 4 K to 200 K. Location of delta-layer of a magnetic impurity in the vicinity of 2D-system filled can resonantly induce self-realisation of ferromagnetic order among the Mn spins [2].

This work was done within Federal Program "Electron" with partial support of RFBR (grant N15-02-08909).

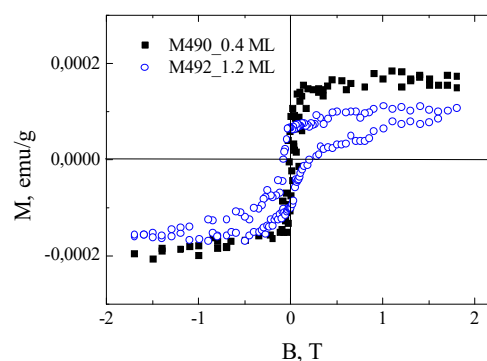


Fig. 1. Magnetic field dependence of the specific magnetization of GaAs:Be/Ga_{0.84}In_{0.16}As/GaAs/ δ -MnAs/GaAs with the different concentration of Mn.

- [1] M. Shirai, T. Ogawa, I. Kitagawa, N. Suzuki, *J. Magn. Magn. Mater.*, **177** (1998) 1383-1387.
[2] A. M. Nazmul, S. Sugahara, M. Tanaka, *Phys. Rev. B*, **67** (2003) 241308R.

2OR-G-10

LASER INDUCED ULTRAFAST MAGNETIZATION DYNAMICS IN MAGNETIC SEMICONDUCTOR CdCr₂Se₄

Pogrebna A.¹, Barsaume S.¹, Telegin A.², Sukhorukov Yu.², Rasing Th.¹, Kimel A.V.¹

¹ Radboud University, Nijmegen, The Netherlands

² M. N. Miheev Institute of metal physics Ural Branch of RAS, 620990, Yekaterinburg, Russia
annapogrebna@gmail.com

The idea to change properties of media with the help of light has been intriguing people for a long time. This research direction became especially appealing after the development of femtosecond laser sources which are able to generate sub-100 fs laser pulses. Such pulses are among the shortest stimuli in contemporary experimental physics and its development has naturally raised the question about the laser-induced magnetization and speed limit of the optical control of magnetism. Seeking to answer these questions led to the discovery of femtosecond inverse Faraday effect in insulating orthoferrites [1] and ultrafast laser-induced magnetization reversal in metallic GdFeCo alloys [2]. Surprisingly, the majority of the experimental studies have been reported for either insulating or metallic media. Magnetic semiconductors have received far less attention [3].

Here we report on investigation of spin dynamics induced in magnetic semiconductor CdCr₂Se₄ by femtosecond circularly polarized laser pulses. CdCr₂Se₄ is a single-sublattice ferromagnetic semiconductor with the Curie temperature $T_C = 130$ K and the band-gap around 1.2 eV at 4 K [4]. Time-resolved measurements of the magneto-optical Faraday rotation with the help of pump-probe technique reveal that sub-100 fs circularly polarized pump pulses are able to trigger oscillations of the signal. The frequency of the oscillations is a linear function of the magnetic field and their phase is defined by the helicity of the pump pulses. This finding reveals that the femtosecond laser pulses act on spins as an effective magnetic field and the direction of the field is controlled by the pump helicity. This field triggers coherent spin precession at the frequency of the ferromagnetic resonance so that the phase of the precession is defined by the field direction. Tuning the photon energy in a wide range from 0.88 to 3 eV shows that the strength of the effective opto-magnetic field has a pronounced spectral dependence with the maximum around 1.2 eV. We further discuss the mechanism of light-spin interaction resulting in the observed helicity dependent spin dynamics by comparing the observed spectrum with those of magnetic circular birefringence and dichroism.

[1] A. V. Kimel et al., *Nature* **435** (2005) 655.

[2] C. D. Stanciu et al., *Physical Review Letters*, **99** (2007) 047601.

[3] A. Kirilyuk, A. V. Kimel, Th. Rasing, *Review of Modern Physics*, **82** (2010) 2731-2784.

[4] G. Harbeke et. al., *Solid State Communications*, **8** (1970).

2OR-G-11

DESIGN OF QUANTUM BITS ON ^{29}Si CRYSTAL SURFACE*Morgunov R.¹, Koplak O.^{1,2}, Yurov A.²*¹ Institute of Problems of Chemical Physics, 142432, Chernogolovka, Moscow, Russia² Immanuel Kant Baltic Federal University, 236041, Kaliningrad, Russia

morgunov2005@yandex.ru

All silicon quantum computing is strategic idea of the nearest steps in information technologies. In purified silicon crystals with low isotope concentration, long coherency time of nuclear spins ^{29}Si (up to ~ 1 min at room temperature) as well as compatibility of silicon q-bits with modern electronics attract efforts of many scientific groups to creation of nanoareas on the Si:B surface convenient to be explored as q-bits [1, 2]. Theoretical basis of spin processing of quantum information [1] as well as concrete scheme of quantum registers containing ^{29}Si chains or layers [2, 3] are well developed. Brief review of these methods and experimental contribution of our group will be proposed.

Particularly, we have found few unexpected effects provided by magnetic isotope in silicon crystals. First of them is effect of external magnetic field [4] and/or hyperfine magnetic field of Si nucleus on oxidation of silicon surface [5]. Hyperfine magnetic field increases oxidation up to 2 times [5]. These data provides possibility to fix image of the q-bit by AFM detected oxidized nano areas of the Si surface [4]. Another significant result is redistribution of the ^{28}Si , ^{29}Si , ^{30}Si isotopes and $^{29}\text{Si}^{16}\text{O}$ complexes in subsurface layers under plastic deformation of Si crystals. The redistributions are selective, i.e. ^{29}Si and $^{29}\text{Si}^{16}\text{O}$ concentrations became rather different with ones correspondent to ^{28}Si , ^{30}Si and $^{29}\text{Si}^{16}\text{O}$, respectively, under plastic deformation. This redistribution can be explored for selection of isotope atoms and isotope distribution control by local stresses under nanoindentation. Thus, mechanical technique of the q-bit formation was proposed.

Measurements of the HR NMR and ESR signals in studied samples provided direct information about nuclear and electron spin subsystems. Analysis of the Pake doublet and its temperature dependence reveals Korringa temperature dependence indicating strong contribution of the heavy and light holes to nuclear spin relaxation. Systematical studying of the spin dynamics in heavy isotope enriched crystals Si:B and Si:P will be presented. Mathematical treatment of the obtained results and consideration of the logic gates correspondent to NMR transitions are proposed.

Authors are grateful to K.Itoh, L.Vlasenko and L.Buchachenko for discussions and organizing help. Support by RFBR is acknowledged. (grants 13-07-12027 and 14-03-31004).

1. F.A. Zwanenburg, A.S. Dzurak, A. Morello et al., *Rev. Mod. Phys.*, **85** (2013) 961.
2. T.D. Ladd, J.R. Goldman, F. Yamaguchi et al., *Phys.Rev. Lett.*, **89** (2002) 017901.
3. Y. Shimizu, Y. Kawamura, M. Uematsu et al., *J. Appl. Phys.*, **106** (2009) 076102.
4. O.V. Koplak, A.I. Ditriev, T. Kakeshita, R.B. Morgunov, *J. Appl. Phys.*, **110** (4) (2011) 044905.
5. O. Koplak, R.Morgunov, A.Buchachenko, *Chemical Physics Letters*, **560** (2013) 29-32.
6. O.V. Koplak, R.B. Morgunov, *Chemical Physics Letters*, **643** (2016) 39-42.

2OR-G-12

SILICON HIGH-TEMPERATURE DIAMONDLIKE FERROMAGNETIC WITH SELFORGANIZED SUPERLATTICE DISTRIBUTION OF MANGANESE IMPURITY

Demidov E.S.¹, Podolskii V.V.², Lesnikov V.P.², Karzanov V.V.¹, Tronov A.A.¹, Budarin L.I.¹

¹ Lobachevsky State University (UNN), Nyzhny Novgorod, Russia

² Physico-Technical Research Institute of UNN, Nyzhny Novgorod, Russia

demidov@phys.unn.ru

The combination of magnetism and semiconductor properties in the diluted magnetic semiconductors (DMS) increases functionality of spintronics. Achievements of laser synthesis of thin 30-110 nm layers of DMS GaSb:Mn and InSb:Mn with Curie temperature T_C above 500 K and Ge:Mn, Si:Mn, Si:Fe with T_C up to 400, 500, 250 K respectively have been shown earlier [1-4]. Variant of DMS on the silicon basis is especially attractive in connection with compatibility of the most widespread silicon microelectronics. Recently [5,6], crystal structure Si:Mn DMS has been investigated by higher resolution electron microscopy HRTEM and LED. The laser technology allows achieve of saturation of solid solution with 15%Mn in silicon DMS Si:Mn (or Si_{2.5}Mn_{0.5}) with high electric and magnetic activity Mn, preservation of diamondlike crystal structure and the epitaxy growth of Si:Mn layers on GaAs with self-organised formation of a superlattice with (110) planes doped by Mn. In the present work the new investigations of properties of Si:Mn DMS layers formed at $T_g=200-400^\circ\text{C}$ on monocrystalline GaAs, Si and on Ge substrates have been presented for the first time. It was possible to grow up ferromagnetic layers in the thickness up to 300 nanometers. The FMR data testify on magnetic uniformity of layers and comparable size of magnetizations on various substrates. The data of influence of chemical processing in acid and alkaline mediums, and also thermal oxidizing annealing on magnetic and transport properties DMS Si:Mn are shown. As well as earlier measurements of FMR, the abnormal Hall effect and magnetizations were made. Comparison of measurements of magnetizations performed by three ways allows to judge about fraction of a magnetic phase. Data of the analysis of angular dependences FMR and their quantitative analysis are presented at temperatures 77-300K. Values of true magnetizations, the contribution of crystal anisotropy and exchange interaction between areas with mutually perpendicular orientations of superlattices are defined. Changes of magnetic and transport properties of Si:Mn DMS connected with weakening of exchange interaction between blocks with various orientation of superlattice modulations. With thermal annealing at temperatures 400-600°C a strengthening of magnetic properties of the Si_{3-x}Mn_x layers is possible. Especially effective this procedure has appeared in case of layers on Ge. Unlike pure silicon DMS Si:Mn well dissolved in fluoric acid HF, especially in case of gallium arsenide substrates. The etching of layers on Si occurs more slowly, the layers on Ge are more resistant. Layers Si:Mn also dissolve in nitric acid HNO₃, but more slowly, than in HF. There is the same tendency in stability of layers depending on material of substrate. The layers Si:Mn are steady against action of alkali KOH, hydrochloric and sulfuric acids.

[1] E.S. Demidov, V.V. Podols'kii, V.P. Lesnikov et al, *JETP Lett.*, **83** (2006) 568–571.

[2] Yu.A. Danilova, E.S. Demidov, Yu.N. Drosdov et al, *JMMM*, **300** (2006) e24–e27.

[3] E.S. Demidov, V.V. Podols'kii, V.P. Lesnikov et al., *JETP*, **106** (2008) 110–116.

[4] E.S. Demidov, B.A. Aronzon, S.N. Gusev et al, *JMMM*, **321** (2009) 690–694.

[5] E.S. Demidov, E.D. Pavlova, A.I. Bobrov, *JETP Lett.*, **96** (2012) 706-709.

[6] E. S. Demidov, V. V. Podol'skii, V. P. Lesnikov et al, *JETP Lett.*, **100** (2014) 719–723.

2 July

Sunday

12:00-13:30

15:00-17:00

oral session

2TL-H

2OR-H

2RP-H

**“High Frequency
Properties and
Metamaterials”**

2TL-H-1

NEAR-FIELD CHIPLESS-RFID TAGS WITH SEQUENTIAL BIT READING IMPLEMENTED IN PLASTIC SUBSTRATES

Herrojo C.¹, Mata-Contreras J.¹, Paredes F.¹, Núñez A.², Ramón E.², Martín F.¹

¹ CIMITEC, Dep. Ingeniería Electrónica, Universitat Autònoma de Barcelona, Bellaterra, Spain

² Institut de Microelectrònica de Barcelona, IMB-CNM (CSIC), Bellaterra, Spain
Ferran.Martin@uab.es

Chipless radiofrequency identification (chipless-RFID) tags based on near-field coupling between the tag and the reader and sequential bit reading are implemented in plastic substrates for the first time. In the proposed chipless-RFID system (first reported in [1] with tags implemented in low-loss microwave substrates) the tag is a set of identical resonant elements (S-shaped split ring resonators, S-SRRs) printed in the plastic substrate forming a chain. The presence or absence of resonant elements at predefined and equidistant positions determines the logic state associated to each resonant element, '1' and '0', respectively. The reader is a coplanar waveguide (CPW) transmission line fed by a harmonic signal tuned to the resonance frequency of the resonant elements of the chain. Tag reading is achieved by displacing the chain of resonant elements above the CPW transmission line, in close proximity to it, so that near-field coupling between the CPW transmission line and the resonant elements of the tag results. By this means, the injected carrier signal is amplitude modulated provided the transmission coefficient of the line varies with the presence or absence of resonant elements in the chain. Therefore, the identification (ID) code is contained in the envelope function, which can be inferred by means of an envelope detector. The illustration of the approach is depicted in Fig. 1(a).

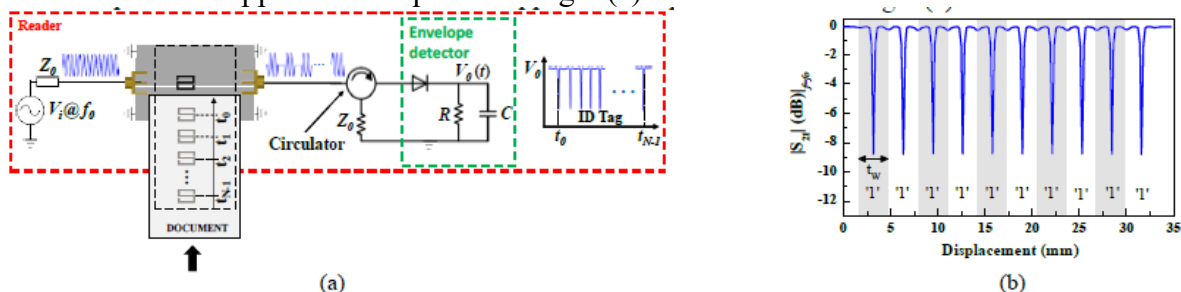


Fig. 1. Illustration of the working principle of the proposed chipless-RFID system (a) and response (simulated) of a chipless-RFID tag (b).

We have characterized several plastic substrates, and we have obtained the dielectric constant and loss tangent by means of a split cylinder resonator. These substrate parameters, as well as conductive ink thickness and conductivity, are essential for tag design. In the present work, we have considered the PEN substrate, with measured dielectric constant of $\epsilon_r = 3.36$ and loss tangent of $\tan\delta = 0.0042$ with thickness $h = 127 \mu\text{m}$, and ink conductivity and thickness of 7 MS/m and $5 \mu\text{m}$, respectively. We have then designed several tags based on the S-SRR, with the aim of obtaining a resonance frequency of 4 GHz. The CPW transmission line (reader) has been implemented in the *Rogers RO3010* substrate with dielectric constant of $\epsilon_r = 10.2$ and loss tangent of $\tan\delta = 0.0022$ with thickness $h = 0.635 \text{ mm}$. The simulated response of one of these tags (with 10 bits and ID code '1111111111') is depicted in Fig. 1(b), demonstrating that the ID of such tag is inferred (experimental results will be provided in the conference presentation).

[1] C. Herrojo, J. Mata-Contreras, F. Paredes, F. Martín, "Near-field chipless RFID encoders with sequential bit reading and high data capacity" *IEEE MTT-S Int. Microw. Symp.*, Honolulu, Hawaii, June 2017.

2TL-H-2

METAMATERIALS FOR ARTIFICIAL MAGNETISM

Lapine M.

School of Mathematical and Physical Sciences, University of Technology Sydney, Australia
mikhail.lapine@uts.edu.au

In this talk, I will review the ways to design artificial magnetic response with metamaterials, and highlight various phenomena which can be observed in magnetic metamaterials.

Specific attention will be offered to effective medium theory of magnetic metamaterials [1], specific properties of finite-size samples [2], and enhanced role of metamaterial boundaries [3]. The latter are also essential in the long-wavelength limit, where magnetoiductive waves [4] are not coming into play, and yet the observed properties deviate significantly from the effective medium predictions and depend on the boundary structure [2-3].

Next, examples will be provided on the implementation of nonlinear response [5] and tunable properties in magnetic metamaterials, as well as novel degrees of freedom in metamaterial design, interlinking physical features of different nature (Fig. 1a). In particular, I will discuss various links between mechanical and magnetic response, emerging in so-called magnetoelastic metamaterials [6] and similar structures (Fig. 1b). I will also address some of the applications of magnetic metamaterials, such as those in magnetic resonance imaging [7], as well as non-resonant designs [8] suitable for strong artificial diamagnetism (Fig. 1c), with a potential for light-weight and reconfigurable magnetic levitation.

Finally, I will discuss the unavoidable scale limitations for artificial magnetism and briefly outline the plausible approaches to implement magnetic metamaterials for radio or microwave frequencies, or THz range, or optics.

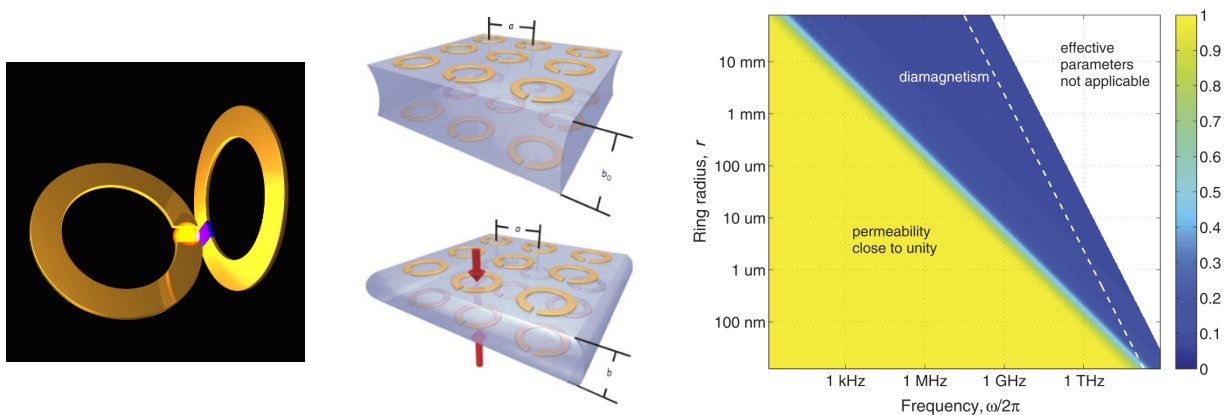


Fig. 1. (a) Optically coupled magnetic meta-atom; (b) Conceptual layout of magnetoelastic metamaterials [6]; (c) Size and frequency limitations for artificial diamagnetism [8].

[1] M. Gorkunov et al., *The European Physical Journal B*, **28** (2002) 263–269.

[2] M. Lapine, R.C. McPhedran, C.G. Poulton, *Physical Review B*, **93** (2016) 235156.

[3] M. Lapine, L. Jelinek, R. Marqués, *Opt. Express* **20** (2012) 18297–18302.

[4] A. Radkovskaya, M. Shamonin, C. J. Stevens, G. Faulkner, D.J. Edwards, E. Shamonina, and L. Solymar, *Journal of Magnetism and Magnetic Materials*, **300** (2006) 29–32.

[5] M. Lapine, I.V. Shadrivov, Y.S. Kivshar, *Rev. Mod. Phys.* **86** (2014) 1093–1123.

[6] M. Lapine, I.V. Shadrivov, D.A. Powell, Y.S. Kivshar, *Nature Materials*, **11** (2012) 30–33.

[7] M. Lapine, L. Jelinek, M. Freire, R. Marqués, *Physical Review B*, **82** (2010) 165124.

[8] M. Lapine et al., *Physical Review B*, **87** (2013) 024408.

2TL-H-3

MAGNETIC METAMATERIALS: COUPLING AND PERMEABILITY

*Radkovskaya A.A., Petrov P.S., Kiriushchikina S.V., Satskiy A.V., Ivanyukovich M.M.,
Vakulenko A.Yu., Prudnikov V.N., Kotelnikova O.A., Korolev A.F., Zakharov P.N.*
Faculty of Physics, M.V.Lomonosov Moscow State University, Moscow, Russia
a_radkovskaya@mail.ru

Since metamaterials – artificial structures with unusual electromagnetic properties - were born at the beginning of Millennium, they attract great attention of researchers all around the world.

Magnetic metamaterials made of conducting resonators – metaatoms - are the essential part of metamaterial world reacting to the ac magnetic field and demonstrating negative permeability [1]. But additive effective media theory can't properly describe the metamaterials' magnetic properties depending as on elements shapes and sizes and also on coupling between them [2].

The coupling leads to the propagation of slow waves of interaction – magnetoinductive (MI) waves [3]. The MI waves pass band is controlled by as the value of interaction as its order [4]. Moreover, the bandwidth of these slow waves depends in different ways on the coupling mechanism - magnetic or electric [5,6], which in turn strongly depends on the operating frequency range [7]. However, even in the MHz range in dense metamaterial (to increase the bandwidth) we should take into account an electrical interaction which significantly influences the dispersion properties of magnetic metamaterials [8]. Therefore, it is important to retrieve separately the coupling coefficients from two interacting metaatoms experimental data [9] to be able to predict MI waves and consequently local currents distributions.

We will show that permeability is not homogeneous along the metasurface and will discuss the peculiarities of slow MI waves and its correlation with the magnetic metamaterials permeability in dependence on coupling mechanisms, metasurfaces symmetry and sizes, and types of the excitation. We also thoroughly analyzed a model of doubly split ring resonators (DSRR) with gaps directed toward each other in the GHz range and confirmed both experimentally and numerically the dominant electric character of coupling in this case. Thus, the use of DSRR makes possible to develop metamaterial which allows the propagation of electroinductive waves.

The understanding of the interaction mechanisms, their impact on the propagation of the slow waves, the ability to determine the coupling coefficients will allow us to predict the magnetic response of metamaterials and create metamaterials with predetermined permeability.

[1] J.B. Pendry et al., *IEEE Transactions on Microwave Theory and Technique*, **47** (1999) 2075–2084.

[2] M. Gorkunov et al., *The European Physical Journal B-Condensed Matter and Complex Systems*, **28** (2002) 253-269.

[3] E. Tatartschuk et al., *Physical Review B*, **81** (2010) 115110-1-115110-10.

[4] R.R.A. Syms et al., *Metamaterials*, **1** (2007) 44-51.

[5] A. Radkovskaya, E. Shamonina, *Advanced Electromagnetic Materials in Microwaves and Optics (METAMATERIALS-2013)* (2013) 79-81.

[6] A. Radkovskaya et al., *Physical Review B*, **84** (2011) 125121-1-6.

[7] E. Tatartschuk et al., *Journal of Applied Physics*, **111** (2012) 094904-1-9.

[8] P. Petrov, A. Radkovskaya, E. Shamonina *Advanced Electromagnetic Materials in Microwaves and Optics (METAMATERIALS-16)*, (2016) 283-285.

[9] P. Petrov, A. Radkovskaya, E. Shamonina, *Advanced Electromagnetic Materials in Microwaves and Optics (METAMATERIALS-15)*, (2015) 259-2616.

2TL-H-4

RF IC CHIP LEVEL NOISE SUPPRESSOR AGAINST POWER ELECTRONIC NOISE INJECTION FOR NEAR-FUTURE TELECOMMUNICATION SYSTEMS

Sai R.¹, Sato M.¹, Shivashankar S.A.², Yamaguchi M.^{1,3}

¹ New Industry Creation Hatchery Center(NICHE), Tohoku University, Sendai, Japan

² Centre for Nano Science and Engineering(CeNSE), Indian Inst. of Science, Bengaluru, India

³ Department of Electrical Engineering, Tohoku University, Sendai, Japan
yamaguti@ecei.tohoku.ac.jp

This work challenges a higher frequency application of soft magnetic materials in UHF to SHF range (300 MHz – 30 GHz), to meet higher carrier-frequency assignment for next generation telecommunication systems. Desensitization of RF receiver chain in mobile handset has been paid attention because of electromagnetic noise injection from electric inverter equipment especially from fast switching SiC or GaN power transistors in electric vehicle or wireless power transmission system [1]. Intra-noise coupling from digital to analogue circuits in an RF IC is another noise coupling new path since RF IC is implemented with millions of RF digital gates after LTE (Long Term Evolution, or 3.9G) era [2]. The 3GPP (Third Generation Partnership Project, mobile communication standard) stipulates that the minimum mean power applied to antenna ports (REFSENS hereafter) at which the throughput shall meet or exceed the minimum receiving sensitivity in the 5 MHz band of popular Band 1 and 19 is -100 dBm / 5 MHz where the throughput shall be $\geq 95\%$ [3].

Firstly, it was clarified for the first time that unnecessary radio wave from a 3 kW-class SiC wireless power transmission (WPT) degraded the REFSENS when the receiver circuit was subjected to the harmonics of the inverter at a distance of 200 mm. which will not meet the 3GPP requirement [1]. Secondary, the FMR losses to dissipate the noise power [2] were studied for sputter-deposited Ni Fe, Co-base amorphous, Co-system granular thin films, Co- and Fe- system amorphous flakes, and hexaferrite [4] powders. The selected candidates to be mixed with epoxy resin on PCB-base IC chip interposer were Sr- and Ba- system M-type hexaferrite polycrystalline powers. Fig. 1 clarifies that the FMR frequency can be tuned in a 2.5 GHz to 20 GHz range for the composite of CoTi substituted Sr-M hexaferrite powder, $\text{SrCo}_x\text{Ti}_x\text{Fe}_{12-2x}\text{O}_{19}$ (x : 1.0 - 1.4). ZFC/FC measurement revealed the absence of inter-particle interactions. Accordingly the relation, $\text{FMR freq} = \gamma H_a$, well explained the experiments. The results outlined the suitability of CoTi-substituted SrM family of hexaferrites for their integration into future high frequency passives.

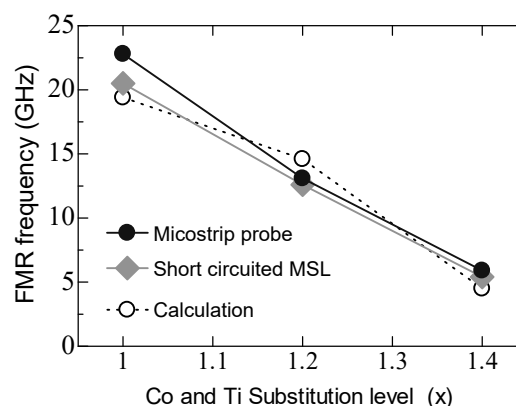


Fig. 1 FMR frequency vs. CoTi substitution level.

Help from S. Tanaka, Y. Miyazawa, A. Takahashi, Y. Endo, H. Aoki, Tohoku Univ., M. Nagata, Kobe Univ., S. Yabukami, Tohoku Gakuin Univ., and S. Takeda, Keycom Corp. are acknowledged. Support by MIC Japan, JSPS-DST, μ SIC Tohoku Univ., RIEC Tohoku Univ. are acknowledged.

[1] Y. Miyazawa et al., *Proc. EMC SI-PI 2017* (2017) in press.

[2] M. Yamaguchi et al., *Proceedings of the 2015 Asia-Pacific International Symposium on Electromagnetic Compatibility (APEMC 2015)*, (2015) 536-539.

[3] 3GPP TS 36.101 version 10.3.0 Release 10, Table 7.3.1-1 Reference sensitivity QPSK REFSENS (2011).

[4] R. Sai, M. Yamaguchi, S. Takeda, S. Yabukami, S. A. Shivashankar, *ICMM-2016*, **A1-05** (2016).

2RP-H-5

TEMPERATURE EFFECTS ON MAGNETIZATION PROCESSES AND MAGNETOIMPEDANCE IN LOW MAGNETOSTRICTIVE AMORPHOUS MICROWIRES

Panina L.V.^{1,2}, Dzhumazoda A.¹, Evstigneeva S.A.¹, Adam A.M.¹, Morchenko A.T.¹, Yudanov N.A.¹, Kostishyn V.G.¹

¹ National University of Science and Technology, MISiS, Moscow 119991, Russia

² Institute for Design Problems in Microelectronics RAS, Moscow 124681, Russia
drlpanina@gmail.com

The investigation into the temperature dependence of magnetoimpedance (MI) response in soft magnetic materials is important for controlling the thermal stability of MI-based sensor devices as well as for developing the miniature temperature-sensing elements. Two different mechanisms of MI temperature effects, namely, the internal stress relaxation upon heating and approaching the Curie temperature T_c are considered. In both cases, sensitive change in impedance for moderate temperature range (<100 °C) can be observed.

The MI sensitivity strongly depends on the effective anisotropy, which is of a magnetoelastic origin in amorphous alloys. In glass coated amorphous microwires the internal stress occurs in the process of rapid solidification and also due to the difference in thermal expansion coefficients of glass and metal. When a microwire is heated, the residual stress is partially released changing the effective anisotropy. In recent works [1-3] it was demonstrated that heating to a moderate temperatures 60-100 oC changes the angle of helical anisotropy in near-zero magnetostrictive wires. Altering the anisotropy inevitably will lead to the temperature dependence of MI. It has been demonstrated that very large change in impedance up to 100% with moderate temperature increase occurs in microwires of Co-rich compositions with high $T_c \sim 300$ °C and very small magnetostriction constant $\sim 10^{-7}$. With increasing the temperature the impedance vs. magnetic field plots can change the shape which indicates the change in the easy anisotropy direction. Such variations in MI with temperature can be stabilized by proper annealing.

MI can be also made highly temperature dependent for moderate temperature regions (20-200 oC) by developing alloys with a reduced Curie temperature. Thus, in alloys of composition CoFeCr(Ni)BSi the Curie temperature T_c is between 20 and 90 oC [4]. When approaching T_c the magnetization m scales as $(1 - T/T_c)^y$, and the magnetostriction scales as m^3 . It will result in the shift of permeability spectra towards lower frequencies when $T \rightarrow T_c$. The drop in the permeability at higher frequencies leads to the decrease in impedance. The modelling results were confirmed by measuring the impedance in microwires with $T_c = 62$ °C. With increasing temperature the impedance vs. field curve preserves its shape so the anisotropy remains axial but the impedance values reduce sharply near T_c . Controlling the value of T_c the impedance temperature dependence can be realized in the desired temperature range. This has potential applications for developing miniature temperature sensor element which may be incorporated in various composite materials for a local temperature monitoring [5].

- [1] M. Kurniawan *et al.*, *J. Appl. Phys.*, **105** (2014) 222407.
- [2] A. Chizhik *et al.*, *J. Magn. Magn. Mat.*, **400** (2016) 356.
- [3] N.A. Yudanov *et al.*, *Physica Status Solidi A*, **213** (2016) 372.
- [4] V. Zhukova *et al.*, *J. Magn. Magn. Mat.*, **300** (2006) 16.
- [5] L.V. Panina *at al.*, *Physica Status Solidi A*, **211** (2014) 1019.

2OR-H-6

ASYMMETRIC MAGNETOIMPEDANCE IN BIMAGNETIC MULTILAYERS*Buznikov N.A.¹, Antonov A.S.²*¹ Scientific & Research Institute of Natural Gases and Gas Technologies – Gazprom VNIIGAZ,
142717 Razvilka, Leninsky District, Moscow Region, Russia² IMPEDANCE JSC, 124527 Zelenograd, Moscow, Russia
n_buznikov@mail.ru

The magnetoimpedance (MI) effect consists in the change of the impedance of a magnetic conductor in the presence of an external magnetic field. The interest in the MI is supported by possible use of the effect for magnetic-field sensor applications. From the point of view of the sensor miniaturization, thin-film structures are one of the most attractive materials for sensitive elements of MI sensors.

The linearity and sensitivity for the external magnetic field are the most important parameters in applications of the MI effect. However, for most of materials, the MI exhibits nonlinear behavior in the vicinity of zero field. To improve the linear features of the MI response, the asymmetric field dependence of the impedance is promising. The asymmetric MI (AMI) may be produced by several methods [1]; one of them consists in the use of materials with asymmetric static magnetic configuration arising from the magnetostatic interactions or exchange bias.

This type of the AMI has been observed in three-layered NiFe/Cu/Co films [2]. It was found that the film structures have biphasic magnetic behaviour, and the origin of the AMI can be ascribed to the magnetostatic coupling between the ferromagnetic layers. It was shown that the linear behavior of the AMI response in the bimagnetic films can be tuned by varying the metallic spacer thickness and current frequency. The field sensitivity of the AMI in the bimagnetic three-layered films is sufficiently low due to small thickness of the film. Recently, the multilayers consisting of a repetition of the base bimagnetic three-layered film structure have been proposed [3]. It was demonstrated that these multilayers exhibit bimagnetic behavior, and the AMI sensitivity increases, which is promising for sensor design.

In this work, a model to describe the AMI in biphasic soft/hard magnetic multilayer is developed. The studied multilayer consists of a repetition of the base three-layered film structure having the soft and hard magnetic layers separated by non-ferromagnetic metallic spacer. The magnetostatic coupling between the hard and soft magnetic layers is described in terms of an effective bias field appearing in soft magnetic layers. The AMI response is found by means of a simultaneous solution of Maxwell equations and Landau–Lifshitz equation. It is shown that the magnetostatic coupling changes the magnetization distribution in soft magnetic layers and leads to asymmetry in the field dependence of the impedance. The influence of the number of layers and the metallic spacer material on the AMI is analyzed. The calculated field and frequency dependences of the impedance describe main features of the experimental study of the AMI effect in biphasic magnetic multilayered films [3]. The applicability of the model proposed for the analysis of the MI effect in different multilayered film structures is discussed. The results obtained may be used in the development of sensors of magnetic field.

[1] M.-H. Phan, H.-X. Peng, *Prog. Mater. Sci.*, **53** (2008) 323.

[2] E.F. Silva et al., *Appl. Phys. Lett.*, **105** (2014) 102409.

[3] E.F. Silva et al., *J. Magn. Magn. Mater.*, **393** (2015) 260.

2RP-H-7

VARIATION OF MICROWAVE MAGNETIC PROPERTIES OF THIN FILMS OF FERROMAGNETIC METALS WITH THE FILM THICKNESS

Bobrovskii S.Y.¹, Iakubov I.T.¹, Lagarkov A.N.¹, Maklakov S.A.¹, Maklakov S.S.¹, Osipov A.V.¹,
 Rozanov K.N.¹, Ryzhikov I.A.¹, Starostenko S.N.¹, Zezyulina P.A.¹

¹ ITAE RAS, Moscow, Russian Federation
 avosipov@mail.ru

Structured magnetic materials based on laminates of thin ferromagnetic films are proposed to obtain uniquely high values of microwave permeability, which is useful for many technical applications [1]. Magnetic properties of these films are known to depend on their thickness: with regard to the microwave properties, growth of the film thickness results a decrease of Acher's coefficient. In turn, Acher's coefficient limits values of the permeability at high frequencies and is considered as a characteristic of microwave performance. For this reason, an investigation of dependence of magnetic properties on thickness of magnetic layers is one of the key points in designing such structured materials.

The study deals with magnetostatic and microwave measurements of single-layer films of ferromagnetic metals (Fe, Fe-N, Co, Ni₈₀Fe₂₀) and is aimed at revealing reasons for deterioration of microwave magnetic performance with increase in film thickness. The films are deposited by magnetron sputtering onto a 12-mcm thick mylar substrate. The microwave permeability is measured at frequencies of 0.1 to 12 GHz by a coaxial technique. The magnetostatic data are obtained with a vibrating sample magnetometer.

A measured microwave permeability for single-layer ferromagnetic films of various thickness are shown in Fig. 1. Two types of variation of microwave permeability with the film thickness are distinguished for the films under study, one exhibiting sharp change and observed, e.g., in Ni₈₀Fe₂₀ (left) and another with gradual worsening of performance, e.g., in Fe (right). In the first case, the permeability decreases abrupt when the film is thicker than 0.2-0.4 mcm, and Acher's coefficient falls drastically, by the factor of ten. In the second case, the microwave performance worsens monotonously, and drop of Acher's coefficient is not so fatal, approximately two fold. The magnetostatic data confirms that the reason is the appearance of perpendicular magnetic anisotropy in the film in the first case and the out-of-plane anisotropy in the second case.

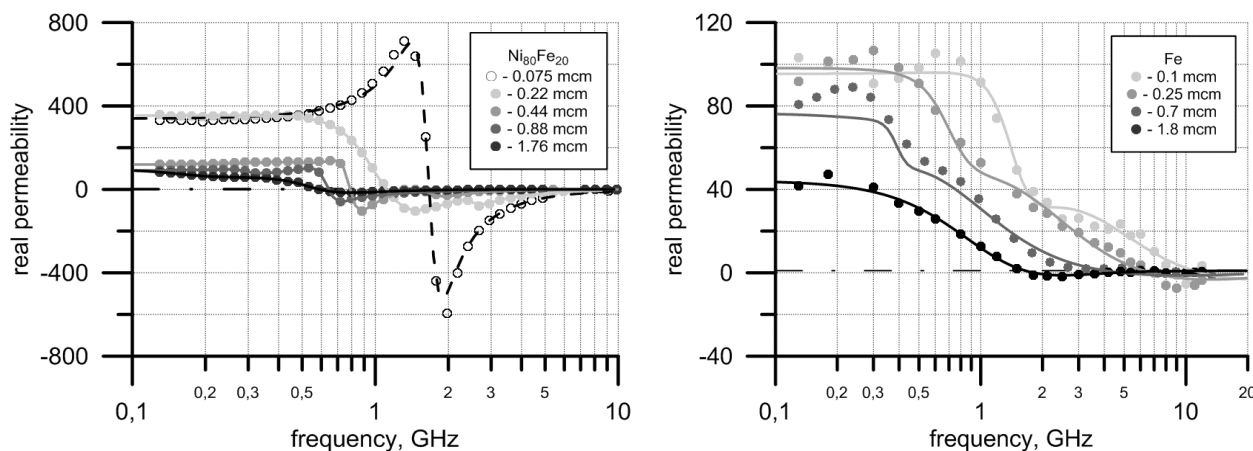


Fig. 1. The measured frequency dependencies of real permeability for ferromagnetic films with various thicknesses: Ni₈₀Fe₂₀ and Fe, dots are measured data, lines are Lorentzian fits

[1] I.T. Iakubov, et al, *AIP Advances*, 4 (2014) 107143.

2RP-H-8

FERROMAGNETIC RESONANCE IN THIN Fe AND Co FILMS

Vyzulin S.A.¹, Rozanov K.N.², Kevraletin A.L.¹, Syr'ev N.E.³, Vyzulin E.S.⁴

¹ Higher Military School named Army General S.M Shtemenko, 350035 Krasnodar, Russia

² Institute for Theoretical and Applied Electromagnetics RAS, 125412 Moscow, Russia

³ Lomonosov Moscow State University, 119991 Moscow, Russia

⁴ Kuban State Technological University, 350072 Krasnodar, Russia

vyzulin@mail.ru

The measured data are presented on the ferromagnetic resonance (FMR) in thin single-layer and multi-layer ferromagnetic films. The films are deposited by the magnetron sputtering onto a flexible polymer substrate. The single-layer films are made of Co (sample 1) and Fe (sample 2) of 160 nm and 270 nm in thickness, respectively. The multi-layer films are made of 140 nm thick Fe layers alternated by 70 nm thick non-magnetic layers, with sample 3 consisting of 16 pairs of magnetic and non-magnetic layers, and sample 4 consisting of 20 pairs of the layers. For samples 1, 2, and 3, the substrate is 12 μm thick mylar film. Sample 4 is deposited on a 20 μm thick polyimide film.

The FMR is measured for a piece of film placed into a resonator at the frequency of 9.14 GHz and at room temperature. The magnetic bias field is swept and the FMR frequency is observed based on a field derivative of microwave absorption. The measured spectra allow the resonance field, H_r , the resonance linewidth, ΔH , and the intensity of the first derivative of the absorbance, J , to be found. The angle between the magnetic bias and the film plane, α , is varied from 0 to 90° with a step of 6°. In the vicinity of $\alpha=0$, the step is decreased to 0.6°, since slight variations of α may result in large shift of the absorption line for these angles.

The FMR spectrum measured with sample 1 comprises a single absorption line. For samples 2, 3, and 4, the spectra contain two absorption lines for any α . Both the lines are observed under magnetic bias that is higher than the saturation field. The low-field line may appear under magnetic bias of 10 to 300 Oe, the high-field line arises under the bias of higher than 600 Oe. The low-field resonance has been observed earlier in nanogranular CoFeB-SiO₂ films [1]. The high-field line corresponds to the uniform FMR.

For all the samples under study, dependences $H_r(\alpha)$, $\Delta H(\alpha)$, and $J(\alpha)$ are symmetrical about $\alpha=0$. For both the low-field and high-field lines, the resonant field is minimal for in-plane bias, $\alpha=0$, and is maximal when the magnetic bias is perpendicular to the film plane, $\alpha=90^\circ$. With a variation of α from 0 to 90°, H_r decreases monotonically.

For the high-field line, H_r is isotropic in the film plane. Dependences $\Delta H(\alpha)$ и $J(\alpha)$ are not monotonic with variation of α from 0 to 90°. Firstly, ΔH increases drastically and J falls. After that, both the values have an extremum at $\alpha \approx 3-6^\circ$, after which ΔH gradually rises and J smoothly decreases. The quality factor of the resonance, $Q=H_r/\Delta H$, is of 1 to 6. The value of Q is the largest in the single-layer films and increases with the number of layers in the multi-layer films.

For the low-field line, H_r is anisotropic in the film plane. The FMR linewidth monotonically decreases with α . Dependences $J(\alpha)$ are not monotonic: the intensity rises with α at small α and falls at higher α . The value of Q is about 0.05 to 0.7.

The measured data allow the saturation magnetization, gyromagnetic ratio, and the damping parameter to be estimated for the films under study.

[1] S. A. Vyzulin et al., *Bull. Russ. Acad. Sci.: Phys.*, **74** (2010) 1652–54.

2RP-H-9

INTRINSIC PERMEABILITY OF COMPOSITES FILLED WITH SENDUST POWDERS

Starostenko S.N.¹, Rozanov K.N.¹, Shiryayev A.O.¹, Shalygin A.N.², Lagarkov A.N.¹

¹ ITAE RAS Moscow, Russia

² MSU Physical department, Moscow, Russia

ssn@itae.ru

The intrinsic permeability spectrum of $Al_{0.054}Si_{0.096}Fe_{0.85}$ alloy is reconstructed from permittivity ϵ and permeability μ measurements of composites filled with sendust flakes or spheres. Diameter of spherical inclusions is about $4\mu m$, flake thickness is about $1\mu m$, the mean diameter of flakes is about $50\mu m$. The shape and size are determined by TEM and by Analysette 22 granulometer. The measurements of ϵ and μ are performed within the frequency band of 0.1 to 20GHz applying the coaxial reflection-transmission technique. The calculations are performed for isotropic mixtures. The effects of filling factor, particle shape and size on parameters of permittivity and permeability spectra are analysed.

The reconstruction of filler permeability is made in frame of generalized Maxwell Garnett (Odelevskiy) theory [1]. The generalization accounts for percolation threshold p_c and may be applied to describe general transfer effects (transfer of charge, mass, polarization, heat, sound, etc.) in binary mixtures. In case of Maxwell Garnett relation $p_c=1$, while in case of Odelevskiy equation (Eq.1) the threshold p_c is the experimentally fitted parameter. Eq.1 describes mixture permittivity ϵ_{mix} dependence on filling factor p , inclusion ϵ_{incl} and host ϵ_h permittivity and inclusion shape. The inclusions are assumed to be identical oblate ellipsoids of rotation, their shape is characterized by depolarization factor N

$$\epsilon_{mix} = \epsilon_h \left[1 + \frac{p}{(1-p/p_c)N + \epsilon_h (\epsilon_{incl} - \epsilon_h)^{-1}} \right] \approx \epsilon_h \left[1 + \frac{p}{(1-p/p_c)N} \right] \quad (1)$$

As metal conductivity is about $108 \text{ Ohm} \times m$, the term $\epsilon_h (\epsilon_{incl} - \epsilon_h)^{-1}$ is small and Eq.1 may be simplified as shown above. The similar relation (Eq.2) describes mixture permeability μ_{mix} , but the term $(\mu_{incl} - 1)^{-1}$ is usually of the magnitude close to $(1-p/p_c)N$.

$$\mu_{mix} = 1 + p / \left[(1-p/p_c)N + (\mu_{incl} - 1)^{-1} \right] \quad (2)$$

This very difference in electric and magnetic susceptibility of metals makes it possible to estimate their intrinsic permeability at microwaves, where the penetration depth is small.

The measured frequency dependence of permeability for mixtures with approximately the same static permittivity filled with flakes and spheres shows that the line shape and the peak frequency of magnetic absorption strongly depend on inclusion shape. The frequency of absorption is lower than that of mixtures with carbonyl iron and the μ_{mix} values measured at 100MHz are far from static ones. For flake-filled mixtures the real part of μ_{mix} steeply grows with frequency decrease below 100MHz, while for sphere-filled μ_{mix} is much closer to saturation.

The measured permittivity and permeability spectra of model composites show that sendust flakes and microspheres both are promising fillers for interference suppressors and UHF-band absorbers. Support by RSF grant No 16-19-10490 is acknowledged.

[1] K.N. Rozanov et al., *JMMM*, **321** (2009) 738–741.

2OR-H-10

DISPERSION OF LINEAR DENSE METAMATERIALS

Petrov P.S.¹, Radkovskaya A.A.¹, Shamonina E.², Kotelnikova O.A.¹

¹ Faculty of Physics, Lomonosov Moscow State University, 119991 Moscow, Russia

² University of Oxford, Department of Engineering Science, Parks Road, Oxford OX1 3PJ, UK
Petrovps01@gmail.com

Magnetic metamaterials consist of meta-atoms such as split-ring resonators (SSRs) reacting to magnetic part of electromagnetic excitation. Inter-element coupling between them is known to give rise to slow magnetoinductive (MI) waves [1], which can be employed for guiding the near field in various devices [2]. The dispersion characteristics of MI waves are tailored by the coupling coefficients that can have a magnetic and/or an electric part (κH and κE) [3].

We have recently proposed a method to retrieve each of these contributions separately by using a modified frequency spectra of two-elements signal representing it in the dependence on the square of normalized reciprocal frequency [4]. Results for various meta-atoms configurations for MHz and GHz frequencies were in good agreement with theory. The existence of non-zero electric coupling κE was shown for small distances between two elements even in MHz.

In this paper we use the values κH and κE obtained by our method to analyze the experimental or simulated MI waves dispersions of dense metamaterials with different geometries of meta-atoms and various distances d between them. In the case of dense metamaterial it is necessary to take into account magnetic coupling not only between nearest neighboring elements, but also the higher order interactions [1]. Furthermore, the influence of electric coupling on MI waves' dispersion becomes essential for smaller separations between meta-atoms. We also improved the experimental results proceedings method, to exclude the contribution of randomly induced signals along the line.

The typical dispersion for axial SSRs structure is presented on Fig. 1. The radius of elements ($r=11.5\text{mm}$) is much larger than $d=1\text{mm}$ and their height $h=5\text{mm}$. Theory without taking into account κE (dashed line) clearly fails to describe the experimental dispersion.

As a result, the method of coupling coefficient retrieval was successfully used for describing the dispersion characteristics of dense linear metamaterials such as the MI waves pass band width and the slope $\omega(k)$ diagram for various configurations of meta-atoms in MHz and GHz frequency ranges.

Results, which may be useful for further construction of metamaterials with predetermined properties, have been obtained.

[1] L. Solymar, E. Shamonina, "Waves in Metamaterials," Oxford Uni. Press, Oxford, 2009.

[2] R.R.A. Syms et al., *J. Appl. Phys.*, **112** (2012) 114911.

[3] F. Hesmer et al., *Phys. Stat. Sol. B*, **244** (2007) 1170.

[4] P. Petrov, A. Radkovskaya, E. Shamonina, *In Proc. 9th Int. Cong. On Advanced Electromagnetic Metamaterials in Microwaves and Optics*, Sept. 7-12, Oxford, UK, 2015.

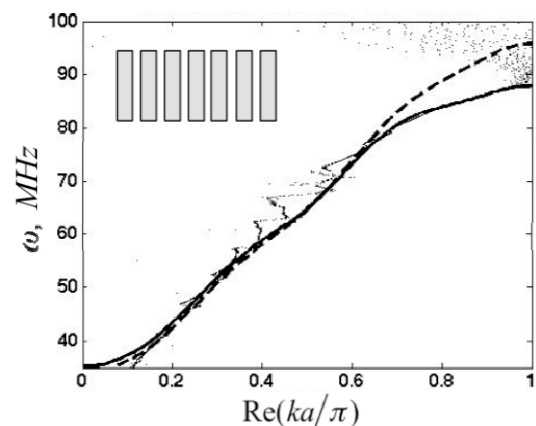


Fig. 1. Dispersion of axial linear dense metamaterial (see insert) with distance between elements $d=1\text{mm}$, size of unit sell along axis $a=6\text{mm}$; resonant frequency $\omega_0 = 52.6\text{MHz}$. Dots – experimental results; solid line – theory with κE , dashed line – without κE .

2 July

Sunday

12:00-13:30

15:00-17:00

oral session

2TL-O

2RP-O

2OR-O

**“Study of Magnetism
using X-rays and
Neutrons”**

2TL-O-1

SPIN WAVES IN FULL-POLARIZED STATE OF DZYALOSHINSKII-MORIYA HELIMAGNETS $\text{Fe}_{1-x}\text{Mn}_x\text{Ge}$: SMALL-ANGLE NEUTRON SCATTERING STUDY

Grigoriev S.V.^{1,2}, *Altynbaev E.V.*^{1,2}, *Siegfried S.-A.*³, *Pschenichnyi K.A.*^{1,2}, *Heinemann A.*³,
*Honnecker D.*⁴, *Tsvyashchenko A.V.*⁵

¹ Petersburg Nuclear Physics Institute, Gatchina, 188300 St-Petersburg, Russia

² Faculty of Physics, Saint-Petersburg State University, 198504 Saint Petersburg, Russia

³ Helmholtz Zentrum Geesthacht, 21502 Geesthacht, Germany

⁴ Institute Laue-Langevin, F-38042 Grenoble Cedex 9, France

⁵ Institute for High Pressure Physics, 142190, Troitsk, Moscow, Russia

grigor@pnpi.spb.ru

Magnetic susceptibility and neutron diffraction measurements have shown that the $\text{Fe}_{1-x}\text{Mn}_x\text{Ge}$ compounds are magnetically ordered in the helical spin structure. The ordering temperature decreases smoothly with concentration x from the maximum ($T_C = 278$ K) for FeGe to $T_C = 180$ K for the compound with $x = 0.5$. The value of the wavevector k changes from 0.09 nm^{-1} for pure FeGe, through its minimum ($|k| \rightarrow 0$) at $x_C = 0.25$, to the value of 0.45 nm^{-1} for $x = 0.5$. The macroscopic magnetic measurements confirm the ferromagnetic nature of the compound with $x = x_C$. The observed transformation of the helix structure to the ferromagnet at $x \rightarrow x_C$, which is explained by different signs of chirality for the compounds with $x > x_C$ and $x < x_C$ [1].

We report on the measurements of the spin-wave stiffness A and its temperature dependence close to T_C for the series of the compounds: FeGe and the solid solution compounds $\text{Fe}_{1-x}\text{Mn}_x\text{Ge}$ with $x = 0.10, 0.20, 0.25$. Recently we develop the technique to study the spin wave dynamics of the full-polarized state of the Dzyaloshinskii-Moriya helimagnets by small-angle neutron scattering [2]. The neutron scattering image displays a circle with a certain radius, which is centered at the momentum transfer corresponding to \mathbf{k}_s , which is oriented along the applied magnetic field \mathbf{H} . The radius of this circle is directly related to the spin-wave stiffness of this system. We have experimentally proven for all compounds that the spin waves dispersion in this state has the anisotropic form: $E_q = A(\bar{q} - \bar{k}_s)^2 + (H - H_{C2})$, where A is the spin-wave stiffness and k_s is the helix wave vector in a helimagnetic phase and H_{C2} is the critical field of the transition from the conical to the fully-polarized state. The spin-wave stiffness A for FeGe-based helimagnets decreases with a temperature but has a finite value at T_C that classifies the order-disorder phase transition in FeGe-based compounds as being the first order one.

[1] S.V. Grigoriev, N.M. Potapova, S.-A. Siegfried, V. A. Dyadkin, E. V. Moskvina, V. Dmitriev, D. Menzel, C. D. Dewhurst, D. Chernyshov, R. A. Sadykov, L. N. Fomicheva, and A. V. Tsvyashchenko, *Phys. Rev. Lett.*, **110** (2013) 207201.

[2] S. V. Grigoriev, A. S. Sukhanov, E. V. Altynbaev, S.-A. Siegfried, A. Heinemann, P. Kizhe, and S. V. Maleyev, *Phys. Rev. B*, **92** (2015) 220415(R).

2TL-O-2

CHIRAL MAGNETS PROBED WITH X-RAYS

Wilhelm F., Rogalev A.

ESRF-The European Synchrotron, Grenoble, France

wilhelm@esrf.fr

Magnetic order breaks time reversal symmetry and in chiral magnetic systems, additionally, space inversion symmetry is broken. Chiral magnets are abundant, existing as metals and molecules, semiconductors and insulators. These symmetry conditions are satisfied in magneto-electric media and multiferroics and also in chiral crystals subjected to a magnetic field. Interestingly, in such systems, in addition to natural and magnetic circular dichroisms, a magneto-chiral dichroism can be observed. It is a non-reciprocal effect featuring an unbalanced absorption of unpolarized light and its sign depends on both the relative orientation of the light propagation direction, the applied magnetic field and the sample chirality. Despite the fundamental interest in a phenomenon breaking both parity and time-reversal symmetries, magneto-chiral dichroism is one of the least investigated aspects of light-matter interaction most likely because of the weakness of the effect. It has been experimentally evidenced only in 1997 [1] in the visible range and a few years later in the X-ray range [2]. A major strength of x-ray magneto-chiral dichroism (XM χ D) is its element specificity and edge selectivity inherent to any x-ray absorption spectroscopy. It is interesting to note that, while X-ray magnetic circular dichroism (XMCD) provides information on the orbital and spin magnetic moment of the absorbing atom, XM χ D gives access to a more elusive quantity: the anapole orbital current or orbital toroidal moment carried by the absorbing atom. Orbital toroidal currents seem to be involved in different phenomena ranging from multiferroicity to superconductivity, and XM χ D offers a unique possibility to its accurate determination. Applications of this new technique to a number of non-centrosymmetric magnetic systems ranging from magnetoelectric crystals [2], multiferroic Ga_{2-x}Fe_xO₃ crystal and chiral single molecule magnets [3] will be presented here.

[1] G. L. J. A. Rikken and E. Raupach, *Nature*, **390** (1997) 493-494.

[2] J. Goulon, A. Rogalev, F. Wilhelm, C. Goulon-Ginet, P. Carra, D. Cabaret and C. Brouder, *Phys. Rev. Lett.*, **88** (2002) 237401.

[3] R. Sessoli, M.-E. Boulon, A. Caneschi, M. Mannini, L. Poggini, F. Wilhelm and A. Rogalev, *Nature Physics*, **11** (2015) 69-74.

2RP-O-3

Ni-Mn-X MAGNETOCALORIC MATERIALS STUDIED BY X-RAY SPECTROSCOPY

Ollefs K.J.^{1,2}, Schöppner C.¹, Gutfleisch O.³, Liu J.³, Meckenstock R.¹, Farle M.¹, Wilhelm F.², Rogalev A.², Acet M.¹, Wende H.¹

¹ University Duisburg-Essen and Cenide, Duisburg, Germany

² European Synchrotron Radiation Facility, Grenoble, France

³ Technical University Darmstadt, Darmstadt, Germany

katharina.ollefs@uni-due.de

Ni-Mn based Heusler alloys belong to an intriguing class of materials exhibiting unusual thermodynamic properties and martensitic transformations, which are first order diffusionless solid-solid phase transitions. In addition to the resulting magnetic shape memory effect, the magnetocaloric properties are currently an interesting and promising field of research for solid state cooling devices [1]. To improve the magnetocaloric properties it is important to understand the relationship between martensitic (thus structural) transition and magnetic properties and possible influencing parameters.

Hard X-ray absorption spectroscopy has been utilized to investigate local atomic structure and magnetism in the Ni, Mn-based Heusler alloys $\text{Ni}_{50}\text{Mn}_{50-x}\text{Sn}_x$ with various Sn concentration ($x=0.13$ and $x=0.15$) and $\text{Ni}_{45}\text{Mn}_{37}\text{In}_{13}\text{Co}_5$. In order to investigate the influence of the martensitic transformation on the electronic structure and magnetic properties of the individual constituents X-ray absorption spectroscopy (XAS) and X-ray Magnetic Circular Dichroism (XMCD) have been used and combined with Ferromagnetic Resonance (FMR).

For $\text{Ni}_{45}\text{Mn}_{37}\text{In}_{13}\text{Co}_5$ we find a mixed antiferromagnetic and ferromagnetic phase for low temperatures up to a critical temperature of about 50 K in the FMR experiment. This is attributed to a spin-glass-like behavior of frustrated magnetic moments of the Mn atoms which is supported by $M(T)$ data. For higher temperatures within the martensite phase, we find weak but clear ferromagnetism from the FMR experiment attributed to Ni (and Co) atoms in the alloy, proven by XMCD measurements [2].

For $\text{Ni}_{50}\text{Mn}_{50-x}\text{Sn}_x$ the structural change between martensite and austenite is reflected in the spectral shape of the XAS (figure1) at the Ni and Mn K-edge. However the change in magnetic interactions is more pronounced for Sn which shows a sizable magnetic polarization at the $L_{2,3}$ -edges.

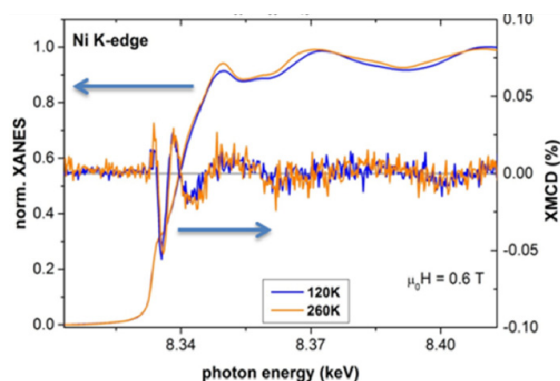


Fig. 1. XANES (left axis) and XMCD (right axis) spectra for the powder sample $\text{Ni}_{50}\text{Mn}_{35}\text{Sn}_{15}$ recorded at the Ni K-edge at 120K (in blue) and 260K (in orange)

This work was supported by Deutsche Forschungsgemeinschaft via priority program SPP1599.

[1] O. Gutfleisch, T. Gottschall, M. Fries, D. Benke, I. Radulov, K. P. Skokov, H. Wende, M. Gruner, M. Acet, P. Entel and M. Farle, *Phil. Trans. R. Soc. A*, **347** (2016) 20150308.

[2] K. Ollefs, Ch. Schöppner, I. Titov, R. Meckenstock, F. Wilhelm, A. Rogalev, J. Liu, O. Gutfleisch, M. Farle, H. Wende and M. Acet, *Phys. Rev. B*, **92** (2015) 224429.

2RP-O-4

SANS STUDY OF INITIAL MAGNETIZATION PROCESS IN Nd-Fe-B hot-DEFORMED MAGNETS

*Saito K.*¹, *Ueno T.*², *Yano M.*³, *Shoji T.*³, *Sakuma N.*³, *Manabe A.*³, *Kato A.*³, *Gilbert E.P.*⁴, *Ono K.*¹

¹ High Energy Accelerator Research Organization, Tsukuba, Japan

² National Institute for Materials Science, Tsukuba, Japan

³ Toyota Motor Corp., Susono, Japan

⁴ Australian Nuclear Science and Technology Organisation, Lucas Heights, Australia
kotaro.saito@kek.jp

Physics inside permanent magnets is very complicated and cannot be explained by simple magnetism due to inhomogeneity and multiscale structures. The coercivity mechanism is a good example. Vast amounts of researches have shown that not only controlling the texture of main-phase grains, but optimizing composition and the texture of grain boundary phases is also critical to achieve high coercivity. Most of permanent magnet researches are based on two major methods: microstructural observation and bulk magnetization measurement. While these methods have made significant contributions for improving permanent magnets, internal magnetic phenomena remain unclear due to intrinsic limitations of these methods. In this report, we present small angle neutron scattering (SANS) results on Nd-Fe-B hot-deformed nanocrystalline magnets providing internal pictures of the initial magnetization process.

We have investigated as-deformed and eutectic-alloy infiltrated samples with different coercivity[1]. Figure 1 shows the magnetic field dependence of SANS intensity for different scattering vector ranges during the initial magnetization process. SANS intensity in the upper figure reflects the number of domain walls inside ferromagnetic grains and that in the lower figure reflects the number of isolated reversed domains. The results show that alloy infiltration affects the domain wall motion and that difference in coercivity is more pronounced in diminution of isolated domains.

This work is supported by the Elements Strategy Initiative Center for Magnetic Materials (ESICMM) under the outsourcing project of the Ministry of Education, Culture, Sports, Science and Technology (MEXT). The sample preparation was performed under the Magnetic Materials for High Efficiency Motors (MagHEM) project.

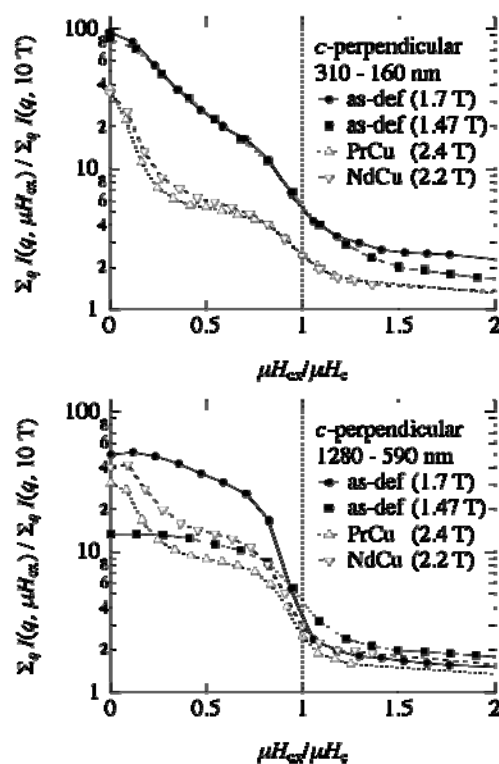


Fig. 1 Magnetic field dependence of SANS intensity for two scattering vector ranges. Numbers in parentheses indicate coercivity fields of the samples. Magnetic field is normalized with coercivity.

[1] H. Sepehri-Amin *et al.*, *Acta Mater.*, **61** (2013) 6622-6634.

2TL-O-5

EXPLORING PROPERTIES OF SINGLE MOLECULE MAGNETS AT THE NANOSCALE USING X-RAY ABSORPTION SPECTROSCOPY

*Mannini M.*¹, *Sainctavit Ph.*²

¹ Department of Chemistry "Ugo Schiff" & INSTM Ru, University of Firenze, Firenze, Italy.

² IMPMC-CNRS, Université Pierre et Marie Curie, Paris, France

matteo.mannini@unifi.it

Due to the wealth and the tuneability of their properties, molecular materials stand out as a possible answer to the needs for innovative technologies. The ensemble of magnetic molecules constitutes a rich playground for chemists and physicists toward the development of novel molecular based devices also because of this possibility to finely tune the device properties through proper design of the molecular structure and the assembling of established building blocks following a rational design. This idea explains the huge efforts of *molecular magnetism*[1] community in the exploration of the use of magnetic molecules for the development of novel devices for the information and computation technologies including spintronics and quantum computation. However a migration from classical materials to future molecular-based devices requires a careful evaluation of the chemical and physical properties of those *fragile* magnetic systems after that nanostructuring processes have been attempted. Soft X-rays absorption-based spectroscopies become fundamental for the verification that chemistry of molecules and their magnetic features survives to the extreme conditions occurring in single-molecule-device-like environments. Going beyond a morphological characterization allowing to “see” isolated molecular objects, intactness of molecules can be evaluated by using surface sensitive techniques that provide a complete overview of the chemical and electronic properties of those systems. In particular X-ray circular magnetic dichroism (XMCD) experiments lead to fundamental steps forward in this demanding exploration by directly accessing to static and dynamic magnetic properties of those systems down to the nanoscale. Here we will present our most recent results achieved at the nanoscale on single molecule magnets (SMMs), a peculiar family of molecules showing slow relaxation of the magnetization and peculiar quantum-based effects [1]. SMMs can be assembled on surfaces by adopting wet-chemistry approaches or sublimating them using high vacuum compatible techniques [2] and the combination of several characterization tools allows to demonstrate that their magnetic behavior can be maintained, lost or enhanced by the interaction with surfaces [3-5].

Support by MIUR (*Futuro in Ricerca* program) is acknowledged.

[1] D. Gatteschi, R. Sessoli, V. Jacques, *Oxford Univ. Press* (2006).

[2] A. Cornia and M. Mannini, “*Single-Molecule Magnets on Surfaces*” in *Molecular Nanomagnets and Related Phenomena*, Springer Berlin Heidelberg (2014) 293–330.

[3] M. Mannini et al., *Nat. Mater.*, **8** (2009) 194.

[4] M. Mannini et al., *Nature*, **468** (2010) 417.

[5] M. Mannini et al., *Nat. Commun.*, **5** (2014) 4582.

2TL-O-6

EUROPEAN XFEL – NOVEL TOOL TO STUDY ULTRAFAST MAGNETIC PHENOMENA

Molodtsov S.L.

European XFEL GmbH, Holzkoppel 4, 22869 Schenefeld, Germany
serguei.molodtsov@xfel.eu

The European X-ray free electron laser (XFEL) is a new international research installation that is currently under construction in the Hamburg area in Germany. The facility will generate new knowledge in almost all the technical and scientific disciplines that are shaping our daily life - including nanotechnology, medicine, pharmaceuticals, chemistry, materials science, power engineering and electronics.

The ultra-high brilliance femtosecond X-ray flashes of coherent radiation will be produced in a 3.4-kilometre long facility. Most of it will be housed in tunnels deep below ground. In its start-up configuration, the European XFEL will comprise 3 self-amplified spontaneous emission (SASE) light sources – undulators operating in energy ranges 3 - 25 keV (SASE 1 and SASE 2) and 0.2 - 3 keV (SASE 3), respectively. The world-unique feature of this free electron laser is the possibility to provide per second up to 27.000 ultra-short (10 - 100 fs), ultra-high brilliance flashes that makes this facility particular suitable for research in the field of ultra-fast magnetic phenomena.

In this presentation, selected examples of experiments will be given and plans for implementation of dedicated instrumentation at the European XFEL will be described.

2OR-O-7

ORBITAL ORDERING AS THE UNIFYING MECHANISM FOR BOTH THE STRUCTURAL AND MAGNETIC TRANSITIONS IN THE Fe-BASED SUPERCONDUCTORS

Bao W.¹

¹ Renmin University of China, Beijing 100872, China
wbao@ruc.edu.cn

We have investigated both the structural and antiferromagnetic transitions in the 1111, 122, 11 and 245 families of the Fe-based superconductors using the capacity of neutron scattering in its simultaneous measurements of the structural and magnetic orders [1-4]. The close relation between the expansion (contraction) of the Fe pair distance with the antiferromagnetic (ferromagnetic) exchange interaction [1-4] is very similar to our previous investigations on classic transition metal oxides, for which such a close relation is shown to be a manifest of an underlying orbital order transition [5,6].

Orbital ordering was initially invoked by Goodenough to explain rich magnetic phases discovered by Wollan and Koehler in their classic neutron scattering study on Manganites [7]. It is an indication of strong coupling between structural, magnetic and orbital degrees of freedom in transition-metal compounds. Our neutron scattering works show that all three types of antiferromagnetic structures

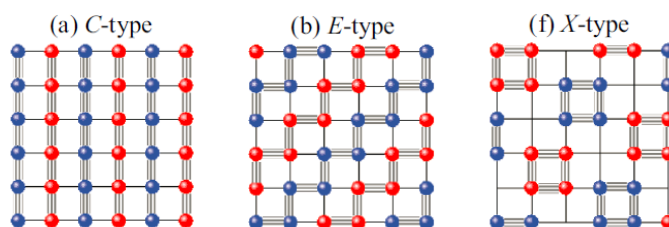


Figure 1: The corresponding ordered pattern of the two types of bonds for the three types of antiferromagnetic and structural orders observed in Fe-based superconductors [1-4,10].

discovered so far in the Fe-based superconductors [1-4] can be attributed to two types of Fe bonds: contracting and ferromagnetic bond, and expanding and antiferromagnetic bond [8,1-4]. We propose that they form with different occupancies of the dxz and dyz orbitals as early as in 2008 [1]. The three orbital ordering schemes in Fig. 1 can consistently explain all occurrences of the structural and magnetic transitions in 1111, 122, 11 and 245 families of Fe-based superconductors [8]. Therefore, the dxz/dyz orbital ordering is the essential physics process in the Fe-based superconductors. Consequently, transport, thermal, and magnetic anisotropy in-plane, namely the so-called nematic properties can be naturally explained [8-10]. And the so-called nematic phase is the critical regime of the orbital transition [11].

Understanding the unconventional Fe-based superconductivity should build on such a normal state physics reality.

[1] Y. Qiu, W. Bao, Q. Huang et al., *Phys. Rev. Lett.*, **101** (2008) 257002.

[2] Q. Huang, Y. Qiu, W. Bao* et al., *Phys. Rev. Lett.*, **101** (2008) 257003.

[3] W. Bao, Y. Qiu, Q. Huang et al., *Phys. Rev. Lett.*, **102** (2009) 247001.

[4] W. Bao et al., *Chinese Phys. Lett.*, **28** (2011) 086104.

[5] W. Bao et al., *Phys. Rev. Lett.*, **78** (1997) 507

[6] W. Bao et al., *Phys. Rev. Lett.*, **78** (1997) 543.

[7] E.O. Wollan, W.C.Koehler, *Phys.Rev.*,**100** (1955) 545; J.B.Goodenough, *ibid.***100**(1955) 564.

[8] W. Bao, *Chinese Phys. B*, **22** (2013) 087405.

[9] W. Lu et al., *Phys. Rev. B*, **84** (2011) 155107.

[10] W. G. Yin et al., *ibid.* **86** (2011) 081106.

[11] J. C. Wang et al., *J. Phys.: Condens. Mater*, **28**.

2RP-O-8

COALESCENCE-DRIVEN, UNCOMPENSATED ANTIFERROMAGNETIC ORDER IN CO DOPED ZnO

Ney V.¹, Henne B.¹, Wilhelm F.², Ollefs K.², Rogalev A.², Ney A.¹

¹ Solid State Physics Division, Johannes Kepler University, Linz, Austria

² ESRF - The European Synchrotron, Grenoble, France

Verena.ney@jku.at

The evolution of the structural and magnetic properties of Co doped ZnO has been investigated over an unprecedented concentration range above the coalescence limit. ZnO films with Co concentrations from 10% to 60% of the cationic sublattice have been grown by reactive magnetron sputtering. Co substitutes predominantly for Zn in the lattice, as measured by x-ray linear dichroism (XLD) - shown in Fig. 1. At low Co concentrations, the films which are devoid of metallic Co precipitations exhibit anisotropic paramagnetism [1]. With increasing Co content, the films become antiferromagnetically ordered with increasing order temperature [2]. Uncompensated spins, coupled to the antiferromagnetic dopant configurations, lead to a vertical exchange-bias-like effect [3], which increases with increasing Co concentration. In parallel, the effective magnetic moment per Co atom and the single-ion anisotropy is gradually reduced [2]. The obtained phase diagram of the magnetic order deviates significantly from theoretical predictions of coalescence-induced magnetic order in Co doped ZnO [4].

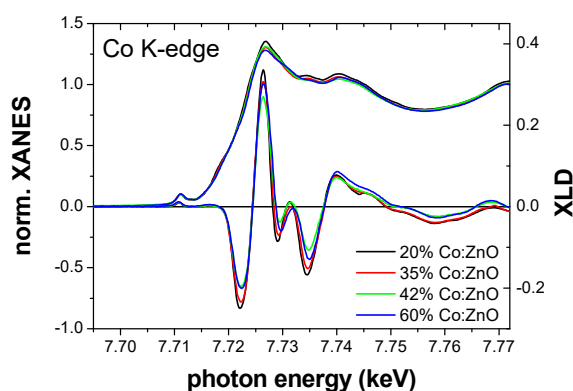


Fig. 1. Co K-edge XANES and XLD of Co:ZnO, with Co concentrations of 20% to 60%.

- [1] A. Ney et al., *Phys. Rev. B*, **81** (2010) 054420.
- [2] V. Ney et al., *Phys. Rev. B*, **94** (2016) 224405.
- [3] B. Henne et al., *Phys. Rev. B*, **93** (2016) 144406.
- [4] S. K. Nayak et al., *J. Phys.: Condens. Matter*, **21** (2009) 064238.

2OR-O-9

PROBING MAGNETIC SUBLATTICES IN $\text{Ho}_{0.5}\text{Nd}_{0.5}\text{Fe}_3(\text{BO}_3)_4$ SINGLE CRYSTAL USING X-RAY MAGNETIC CIRCULAR DICHROISM

Platunov M.S.^{1,2}, Kazak N.V.², Temerov V.L.², Dudnikov V.A.², Wilhelm F.¹, Rogalev A.¹, Ovchinnikov S.G.²

¹ ESRF, 71 Avenue des Martyrs CS40220, F-38043 Grenoble Cedex 9, France

² Kirensky Institute of Physics, Federal Research Center KSC SB RAS, Akademgorodok 50, bld. 38, 660036 Krasnoyarsk, Russia
mikhail.platunov@esrf.fr

Multiferroic $\text{ReFe}_3(\text{BO}_3)_4$ ferroborates have complex magnetic structure. The iron sublattice orders antiferromagnetically below $T_N=38$ and 31 K for Ho and Nd-ferroborates, respectively. Whereas $\text{NdFe}_3(\text{BO}_3)_4$ is an “easy plane” antiferromagnet, $\text{HoFe}_3(\text{BO}_3)_4$ exhibits a spontaneous spin-reorientation transition from the “easy-plane” (ab-plane) to “easy-axis” (c-axis) state at TSR = 5 K [1, 2]. In this study, we focus on $\text{Ho}_{0.5}\text{Nd}_{0.5}\text{Fe}_3(\text{BO}_3)_4$ single crystal, magnetic and magnetoelectric properties of which are drastically different from pure $\text{HoFe}_3(\text{BO}_3)_4$ and $\text{NdFe}_3(\text{BO}_3)_4$ compounds. In this crystal, the spin-reorientation and antiferromagnetic transitions take place at ~ 10 and 32 K, respectively. Macroscopic magnetization measurements indicate two spin-flop transitions at 1 and 3 T. To unravel the role of each magnetic sublattice (Ho, Nd or Fe) in observed magnetic transitions, we have performed an element-specific magnetization measurements using x-ray magnetic circular dichroism (XMCD) at the $L_{2,3}$ -edges of Nd and Ho and at the K-edge of Fe.

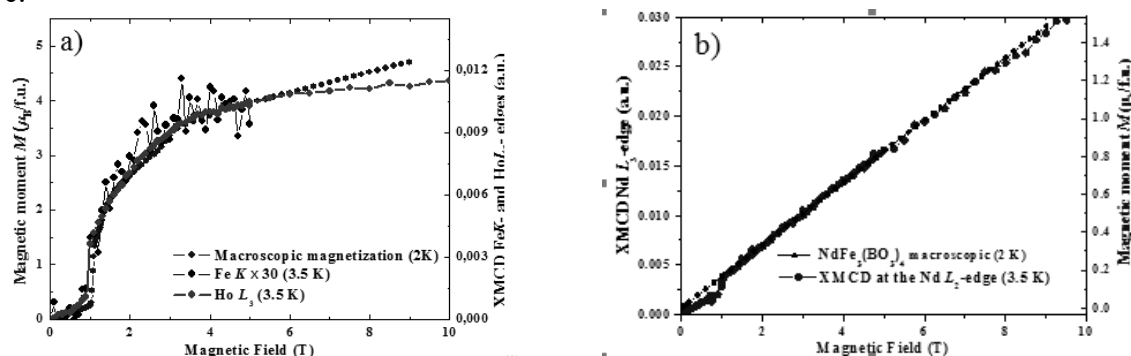


Fig. 1. (a) The element-specific magnetization at the $\text{Ho}L_{3-}$, $\text{Fe}K$ -edges and macroscopic magnetization of $\text{Ho}_{0.5}\text{Nd}_{0.5}\text{Fe}_3(\text{BO}_3)_4$ as a function of applied field; (b) The field dependences of XMCD signal at the Nd L_2 -edge in $\text{Ho}_{0.5}\text{Nd}_{0.5}\text{Fe}_3(\text{BO}_3)_4$ crystal and magnetization curve of $\text{NdFe}_3(\text{BO}_3)_4$ crystal.

The XMCD measurements have been performed at the ESRF beamline ID12 at 3.5 K and magnetic field up to 17 Tesla applied along the c-axis of the crystal. The experimental data confirms that all three magnetic sublattices are strongly coupled and exhibit a spin flop transition at ~ 1 T (fig. 1). Surprisingly, the Nd and Ho magnetization curves are very different whereas the Fe sublattice follows the Ho magnetization. These results shed a new light into complex magnetism of multiferroic rare-earth ferroborates.

This work has been partially financed by the Council for Grants of the President of the Russian Federation (SP-938.2015.5, NSh-7559.2016.2), the Russian Foundation for Basic Research (project nos. 16-32-60049 mol_a_dk, 16-32-00206 mol_a, 17-02-00826_a).

[1] A. Pankrats, et al., *J. Phys.: Condens. Matter*, **21** (2009) 436001.

[2] P. Fischer, et al., *J. Phys.: Condens. Matter*, **18** (2006) 7975.

[3] R. P. Chaudhury, et al., *Physical Review B*, **80**(10) (2009) 104424.

2RP-O-10

ION IRRADIATION INDUCED DISORDER AND MAGNETISM IN Fe₆₀Al₄₀ THIN FILMS PROBED BY X-RAYS

Smekhova A.^{1,2}, *La Torre E.*², *Eggert B.*², *Cöster B.*², *Szyjka Th.*², *Walecki D.*², *Salamon S.*²,
Ollefs K.^{2,3}, *Bali R.*⁴, *Lindner J.*⁴, *Wilhelm F.*³, *Rogalev A.*³, *Weschke E.*⁵, *Banerjee R.*⁶, *Sanyal B.*⁶,
*Schmitz-Antoniak C.*¹, *Wende H.*²

¹ FZ Juelich (PGI-6), Berlin, Germany

² University of Duisburg-Essen and CENIDE, Duisburg, Germany

³ ESRF, Grenoble, France

⁴ HZDR, Dresden, Germany

⁵ HZB (BESSY II), Berlin, Germany

⁶ Uppsala University, Uppsala, Sweden

a.smekhova@fz-juelich.de

The progress in magnetic patterning of Fe₆₀Al₄₀ thin films with ion-irradiation [1, 2] stimulates the structural and magnetic studies of this system on the local scale that could provide more insights on the formation mechanism of a long-range ferromagnetic order induced by ions. In our work the evolution of the local environment and development of Fe magnetic polarizations in thin films of transition metal aluminide Fe₆₀Al₄₀ of 40 nm thickness have been probed by element-specific hard- and soft- X-ray absorption spectroscopy through the order-disorder (B2 → A2) phase transition initiated by 20keV Ne⁺ ion irradiation with low fluences ($\sim 10^{14}$ ions·cm⁻²).

Extended X-ray absorption fine structure (EXAFS) spectra measured at the Fe K edge at room temperature have shown consequential changes in the local environment of Fe absorbers in a course of the transition. The analysis established a number of Fe-Fe nearest-neighbours as 3.47(7) and 5.0(1) for the ordered B2 and the fully disordered A2 state, correspondingly, and $\sim 1\%$ of the unit cell volume expansion [3]. The visualization of the rearrangement of Fe and Al nearest-neighbours was done with wavelet transformations. The observed structural changes were followed by increased net magnetic moments of iron atoms: X-ray magnetic circular dichroism (XMCD) spectra measured either at the Fe K edge or L_{2,3} edges showed a strong rise of Fe 4p orbital and 3d spin net magnetic polarizations with fluence, respectively. The sum rule analysis revealed a characteristic S-shape dependence of iron 3d magnetic moments on fluence as it was previously found by macroscopic magneto-optical Kerr effect (MOKE) measurements [2] in spite of a presence of the top oxide layer. The strength of Fe 4p-3d hybridization for the fully disordered A2 state was found to be the largest among the studied B2 and intermediate A2 states. Self-consistent DFT calculations performed by the VASP program package for relaxed model systems in both phases have shown a clear variation of local configurations and changes in spin-resolved iron DOS. XANES spectra recorded at the Al K edge at low temperature have shown a distinct change in coordination of Al atoms for B2 and A2 phases.

The work was partially funded by Helmholtz Association (Young Investigator's Group "Borderline Magnetism", VH-NG-1031).

[1] J. Fassbender, M. O. Liedke, T. Strache *et al.*, *Phys. Rev. B*, **77** (2008) 174430.

[2] R. Bali, S. Wintz, F. Meutzner *et al.*, *Nanoletters*, **14** (2014) 435-441.

[3] E. La Torre, A. Smekhova, C. Schmitz-Antoniak *et al.*, submitted to *Phys. Rev. B* (2017).

2 July

Sunday

15:00-17:00

oral session

2TL-A

“MRAM”

2TL-A-4

STT-MRAM FOR RFID APPLICATIONS

*Mikhailov A.P.^{1,2}, Belanovsky A.D.^{1,2}, Trofimov A.V.¹, Chauveau A.¹, Aksenova E.¹, Sorokina S.¹,
Smirnov E.¹, Valdez J.¹, Gapihan E.¹, Khvalkovskiy A.V.¹*

¹ Crocus Nanoelectronics LLC, Moscow, Russia

² MIPT, Dolgoprudny, Russia

a.khvalkovskiy@crocusanano.com

STT-MRAM offers unique combination of non-volatility, speed and low-power switching memory comparatively to its semiconductor-based counterparts like Flash [1]. Moreover, comparatively to embedded Flash memory (eFlash) it also offers higher density and reduced complexity of manufacturing. Thus it is a very probable candidate to substitute eFlash in many applications. In this talk we will discuss benefits and challenges of embedded STT-MRAM memory for RFID applications.

[1] Khvalkovskiy, A. V., et al., *Journal of Physics D: Applied Physics*, **46(7)** (2013) 074001.

2TL-A-5

SECOND ORDER ANISOTROPY IN PERPENDICULAR MAGNETIC TUNNEL JUNCTIONS FOR HIGH SPEED SWITCHING MRAM

Timopheev A.¹, Sousa R.C.¹, Chshiev M.^{1,2}, Buda-Prejbeanu L.^{1,2}, Nguyen H.T.¹, Dieny B.¹

¹SPINTEC, CEA-INAC / CNRS / Univ. Grenoble Alpes, Grenoble F-38054, FRANCE

²Univ. Grenoble Alpes, INAC-SP2M, F-38054 Grenoble, France

ricardo.sousa@cea.fr

Magnetic tunnel junctions with perpendicular magnetic anisotropy are particularly attractive to realize devices of reduced lateral dimension due to their large values of perpendicular anisotropy. The writing process is intrinsically stochastic and requires thermal fluctuations to trigger the reversal of the storage layer magnetization. In this study, we have shown that this problem can be circumvented by inducing an easy-cone anisotropy in the storage layer [1]. With this easy cone anisotropy, the storage and reference magnetization layers always keep a relative angle so that upon write, the storage layer magnetization reversal can be triggered at the very onset of the write current pulse. Such easy cone anisotropy has been evidenced at Spintec. It results from higher order anisotropy terms which could be revealed by ferromagnetic resonance experiments. Hard-axis magnetoresistance loops were measured on perpendicular magnetic tunnel junction pillars. By fitting these loops to an analytical model, the effective anisotropy fields in both free and reference layers were derived and their variations in temperature range between 340 K and 5 K were determined. It is found that a second-order anisotropy term must be added to the conventional uniaxial anisotropy to explain the experimental data. This higher order contribution exists both in the free and reference layers. This quadratic anisotropy itself results from spatial fluctuations of uniaxial anisotropy which can be induced during deposition and annealing of the magnetic tunnel junction stacks. With this easy cone anisotropy, the spin transfer torque writing is more reproducible, and can be faster and/or realized at lower write voltage thereby reducing the write energy consumption.

Support by ERC Adv grant MAGICAL n° 669204, CEA-EUROTALENTS fellowship (A.T.) and French National Research Agency (ANR) under project EXCALYB is acknowledged.

[1] A. Timopheev, R. Sousa, M.Chshiev, H.T. Nguyen, B. Dieny, *Scientific Reports.*, **6** (2016) 26877.

2TL-A-6

ORIGIN OF ASYMMETRY IN THERMALLY-DRIVEN MAGNETIZATION REVERSAL FOR PERPENDICULAR STT-MRAM

Apalkov D.¹, Wang S.¹, Schafer S.¹, Nikitin V.¹

¹ New Memory Technology Lab, Samsung Semiconductor Inc., San Jose, CA, USA
d.apalkov@samsung.com

For typical STT-MRAM designs, a synthetic antiferromagnetic (SAF) reference layer is commonly used to cancel the total magnetostatic field acting on the free layer. However, due to the proximity effect, this field is very non-uniform, being negative in the center of the free layer and positive at the edges, as shown on Fig. 1a. For uniform switching (macrospin approximation), this does not create any complications: if the total magnetostatic field is equal to zero, the thermal stability in both P and AP states are equal and the hysteresis loop is fully symmetric, with the coercivities in positive and negative field being equal.

However, for typical device diameters, the switching occurs by domain wall propagation[1]. In this case, there is a very important and unexpected implication of the field non-uniformity. Even though the thermal stability is still symmetric ($\Delta_P = \Delta_{AP}$), the hysteresis loop will be highly asymmetric, having non-zero shift to positive fields [2]. The mechanism behind such asymmetry is in different magnetization state while overcoming energy barrier at $H=0$ and $H=H_c$. Specifically, for $H=0$ case, the energy barrier is determined by a domain wall at the center of the free layer, resulting in a mirror symmetry of magnetization and thus energy change due to non-uniform field from RL with axial symmetry averages out to zero. For $H=H_c$ however, the energy barrier corresponds to having a domain wall close to one of the edges (Fig. 1b), breaking the mirror symmetry and resulting in large (up to 300 Oe) average field from SAF RL, Fig 1b.

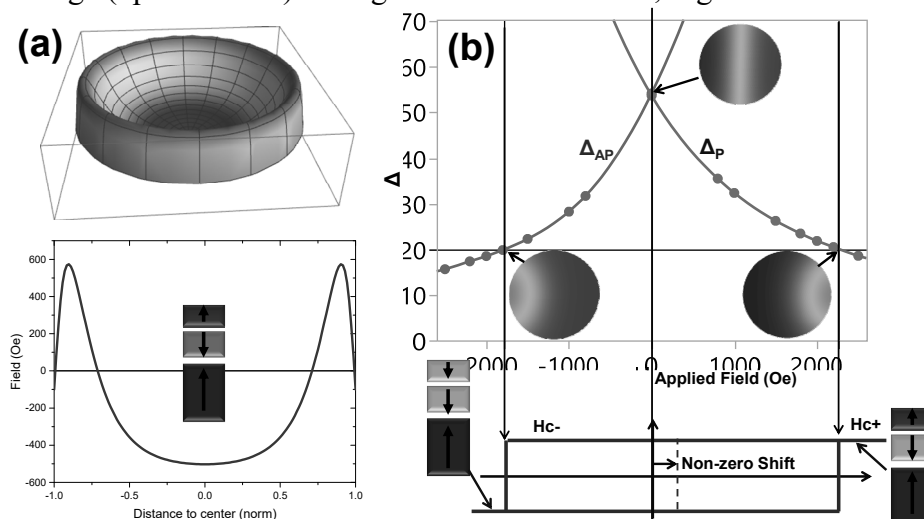


Fig. 1. (a) – Strongly non-uniform field from compensated SAF reference layer (average field is zero). (b) – Effect of this non-uniform field on $\Delta(H)$ dependence for P and AP states and hysteresis loop: even though $\Delta_P = \Delta_{AP}$ at $H=0$, the hysteresis loop is asymmetric.

[1]. D. Apalkov, et al., *12th Joint MMM-Intermag conference*, FF-01 (2013).

[2]. M.P. Lavanant, et al., *61 Annual conference on magnetism and magnetic materials*, BF-09 (2016).

2TL-A-7

UNIQUE SELECTOR DEVELOPMENT FOR 3D CROSS-POINT STT-MRAM*Huai Y.*Avalanche Technology, 46600 Landing Parkway, Fremont CA 94538
yiming@avalanche-technology.com

Spin transfer torque magnetic RAM (STT-MRAM) is one of the best candidates to replace DRAM and may serve as storage class memory (SCM) owing to its superior performance of unlimited endurance ($>10^{16}$) and fast switching speed (<10 ns). For very high density and low cost STT-MRAM, a stackable cross point cell architecture is desired, which requires an adequate individual selector integrated in series with a magnetic tunneling junction (MTJ) memory element to suppress the sneaking current and reduce the power consumption in 3D STT-MRAM array.

We have developed a novel two-terminal bipolar threshold selector device based on doped-HfO_x material and have demonstrated integrated device performance of the selector and the state-of-the-art perpendicular MTJ. The selector shows extremely sharp turn-on slope of around 1.6 mV/dec, which greatly benefits array level operations. The selector device also shows extremely high On/Off ratio (above 10^6), which can greatly suppress the leakage current for the memory array and facilitates high density STT-MRAM array integration. Remarkably, the selector can have very low on-resistance (~ 1 k Ω), 10 pA off-state leakage current, 5 ns turn-on speed and low threshold voltage (0.25 V). The threshold voltage can be tuned by the selector layer film thickness. Furthermore, the selector can still function properly after 400 °C annealing, which is very critical for STT-MRAM integration. The selector works well with pMTJ when it is in either high or low resistance state. The pMTJ devices can be RESET and SET after the selector turns on. This effectual combination of selector and pMTJ provides a novel approach to implement the 3D STT-MRAM array for high density non-volatile memory.

2 July

Sunday

15:00-17:00

oral session

2TL-P

2OR-P

2RP-P

“Theory”

2TL-P-7

QUANTUM RATCHET EFFECT IN A STRONG MAGNETIC FIELD

Ivchenko E.L.

Ioffe Physical-Technical Institute, St. Petersburg, 194021, Russia

ivchenko@coherent.ioffe.ru

Crystals or periodic structures without an inversion center have an inherent fundamental property to induce directed macroscopic fluxes of particles under the action of a variable force with zero average value. If the absence of an inversion center is caused by a microscopic structure of the system, the generation of a dc electric current under homogeneous illumination is called the Photogalvanic Effect. If the 3D, 2D or 1D system is an artificially-prepared non-centrosymmetric object in solid state physics or a natural non-centrosymmetric system in chemistry or biology, the flux generation is called the Ratchet Effect.

The talk concerns the magnetic ratchet effect in a quantum well structure with an asymmetric periodic grating gate subjected to an external magnetic field applied normal to the interface plane [1]. We show that the ratchet photocurrent is caused by a combined action on the 2D electrons of the spatially periodic potential $V(x)$ and spatially modulated near field $E(x)$ of the radiation transmitted through the metallic grating. The photocurrent generation in such a structure is proportional to the asymmetry parameter

$$\Xi_0 = \overline{\frac{dV}{dx} |E(x)|^2},$$

where overline implies averaging over the period.

Mechanisms of the formation of magnetically induced photocurrent are proposed for a structure with a 2D electron gas (quantum well, graphene) with a lateral asymmetric superlattice consisting of metallic stripes on the external surface of the structure. Figure 1 shows both the relative x-component of the Seebeck ratchet photocurrent and the diagonal relative magnetoresistance ρ_{xx}/ρ_0 in the quantum oscillation regime (ρ_0 is the zero-field resistivity). Thus, the theory predicts that (i) the quantum oscillations in the photocurrent are much more pronounced as compared to those of the resistivity, and (ii) the amplitude of oscillations of the ratchet current j_x is by more than two orders of magnitude larger than the photocurrent $\Xi_0 \xi_0 S$ in zero field.

Experimentally, the observation of magnetic quantum ratchet effect has recently been performed on (Cd,Mn)Te- and CdTe-based quantum well structures with an asymmetric lateral dual grating gate superlattice formed by gold stripes [2].

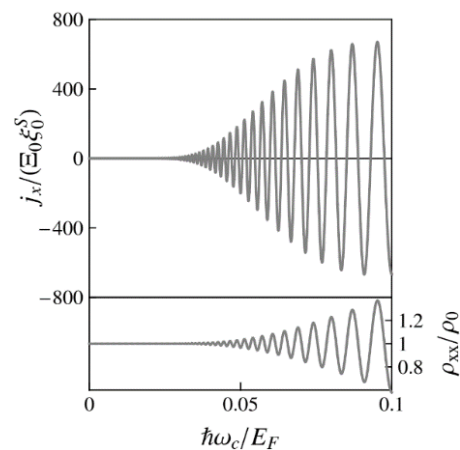


Fig. 1. Calculated quantum magnetic oscillations of the ratchet current and resistivity field. [1]

[1] G.V. Budkin, L.E. Golub, E.L. Ivchenko, S.D. Ganichev, *Pis'ma ZhETF* **104**, 662 (2016) [*JETP Lett.* **104**, 649 (2016)].

[2] P. Faltermeier et al., *Phys. Rev. B*, accepted; arXiv:1702.02819v1.

2OR-P-8

MAGNON ACTIVATION BY HOT ELECTRONS VIA NON-QUASIPARTICLE STATES

Brener S.^{1,2}, Murzaliyev B.², Titov M.², Katsnelson M.I.²

¹ Institute für Theoretischer Physik, Hamburg University, Jungiusstraße 9, D-20355 Hamburg, Germany

² Radboud University, NL-6525 AJ Nijmegen, The Netherlands
sbrener@physnet.uni-hamburg.de

We consider the situation when a femtosecond laser pulse creates a hot electron state in half-metallic ferromagnet (e. g., ferromagnetic semiconductor) on a picosecond timescale but does not act directly on localized spin system. We investigate the energy and magnetic moment transfer from hot itinerant electrons to localized spins. In a half-metal such a transfer is facilitated by the so-called non-quasiparticle states, which are the scattering states of a magnon and spin-majority electron. We predict that in a typical ferromagnetic semiconductor such as EuO magnons remain essentially in non-equilibrium on a scale of the order of microsecond after the laser pulse. In the framework of the s-d exchange model the evolution of the magnon distribution is described by a quantum kinetic equation that we derive using the non-equilibrium Keldysh diagram technique. At short time scales we obtain approximately linear-in-time growth of the number of magnons with a distribution that is, however, essentially different from the Bose-Einstein one. We argue that such a non-equilibrium magnon state must be typical for experiments on ultra-fast magnetization dynamics in many half-metallic materials and magnetic semiconductors.

We make analytical analysis using the hierarchy of energy scales: $\omega_D \ll \varepsilon_F \ll \Delta \ll W$, here ω_D is the magnon band width, W —the electron band width, Δ is the Stoner gap and ε_F is the Fermi energy of the majority spin electrons. In this limit it is possible to solve the non-linear Boltzmann equation analytically. For realistic parameters numerical analysis is necessary.

Within the same approach we consider the role of magnon-magnon interaction and of quasiparticle scattering states. The magnon-magnon contribution turns out to be negligible compared to the non-quasiparticle one, up to times where the approach used is in principle applicable ($N_q \ll 2S$, where N_q is the number of magnons with momentum q , and S is the absolute value of the localized spin system). This is not a priori obvious since these two contributions have formally the same order of magnitude in the collision integral with respect to the only small parameter of the perturbation theory $1/2S$. On the other hand, the quasiparticle scattering, being formally of lower order in $1/2S$ is thermally suppressed as the number of minority spin electrons is proportional to $\exp[-(\Delta - \varepsilon_F)/T]$. But for higher temperatures (for typical values in EuO for $T > 600\text{K}$) it gives rise to a drastic growth of N_q around $q = (2m\Delta)^{1/2}$, where m is effective electron mass.

The authors acknowledge support from the ERC Advanced Grant 338957 FEMTO/NANO, from the Dutch Science Foundation NWO/FOM 13PR3118, from the EU Network FP7-PEOPLE-2013-IRSES Grant No 612624 “InterNoM” and from the NWO via the Spinoza Prize.

2RP-P-9

MAGNETIC PHASE TRANSITIONS AND SPIRAL ORDERING IN INTERACTING SYSTEMS OF LOCALIZED AND ITINERANT ELECTRONS

Igoshev P.A.^{1,3}, Timirgazin M.A.^{1,2}, Arzhnikov A.K.^{1,2}, Irkhin V.Yu.¹

¹ Institute of Metal Physics, Ural Division of RAS, Ekaterinburg 620990, Russia

² Physical-Technical Institute, 426000 Izhevsk, Russia

³ Ural Federal University, 620002, Ekaterinburg, Russia

igoshev_pa@imp.uran.ru

The ground state magnetic phase diagrams of strongly correlated systems are discussed within various many-electron models. The calculations enable one to take into account formation of spiral structures, spin-liquid state, and magnetic phase separation. The limit of strong correlations is considered in detail within the Hubbard and t - J models.

The phase diagram of the infinite- U t - t' Hubbard model calculated within Kotliar-Ruckenstein slave boson approximation [1] for the square lattice in n - t' variables is shown in Fig.1. Phase separation regions found in previous investigation [2] vanish in the vicinity of $n = 1$ electron concentration, but are retained away of half-filling as a result of a first-order phase transition between different types of magnetic orders. The asymptotic solution of the slave boson equations system in the limit of small current carrier number $|1 - n|$ is found. For positive t'/t and $n < 1$ (hole doping) the saturated ferromagnetic state (SFS) is stable for small $1 - n$. On the other hand, already small negative t' values result in an instability of SFS with respect to finite-gap antiferromagnetic (AFM) state, the spin down (in local spin coordinate system) correlation band narrowing factor being proportional to the carrier number and very small. Further increasing $|t'|$ results in a topological transition from gapped AFM state with small number of carriers to gapless AFM state with the asymptotic result $1 - m \sim (1 - n)^{1/2}$ for the relative sublattice magnetization m . At finite U the states with small number of carriers can be unstable with respect to phase separation. We derive analytically physical properties of phase separation states and discuss the conditions where the infinite U limit is applicable to real systems.

For the Anderson lattice and s-d model we present the ground state magnetic phase diagram on the square lattice within the Hartree-Fock approximation and consider the limits of integer and intermediate valence. We find that the presence of local magnetic moments dramatically changes the properties of the phase diagram in the limit of small number of carriers.

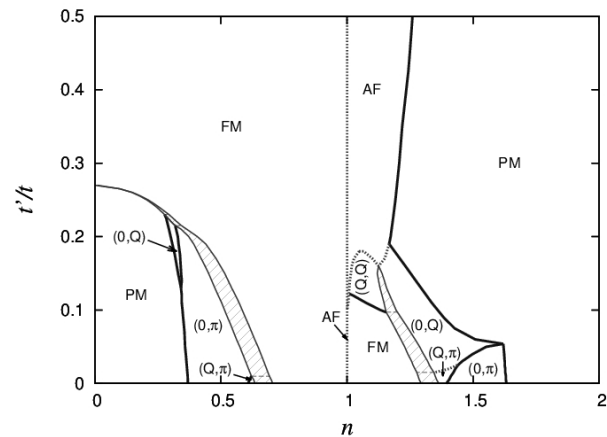


Fig. 1. Ground state magnetic phase diagram of infinite U Hubbard model for the square lattice. Spiral phases are marked by the form of the wave vector. Dashed areas are phase separation regions

[1] R. Fresard and P.Woelfle, *J. Phys.: Cond. Matt.*, **4** (1992) 3625.

[2] P.A. Igoshev et al., *J. Phys.: Condens. Matter*, **27** (2015) 446002.

2OR-P-10

SPIN-DENSITY CORRELATIONS AND SHORT-RANGE ORDER IN METALS ABOVE THE CURIE TEMPERATURE

Melnikov N.B.¹, Reser B.I.², Paradezhenko G.V.¹

¹ Moscow State University, Leninskie Gory, 119991 Moscow, Russia

² Institute of Metal Physics RAS, 18, Kovalevskaya St., 620990 Ekaterinburg, Russia
melnikov@cs.msu.ru

The neutron scattering experiments in the ferromagnetic metals point on the existence of strong short-range order (SRO) above the Curie temperature. However, the estimate 15–20 Å [1] is based on the paramagnetic spin waves assumption, which has been strongly criticized.

In the dynamic spin-fluctuation theory (for a review see [2]), we obtain explicit expressions for the effective and local magnetic moments and spatial spin-density correlator [3, 4]. We show that, at high temperatures, the correlator reduces to the well-known Ornstein–Zernike form, the effective moment $M(q)$ is given by the Lorentzian function, and $M(0)$ tends to the effective moment m_{eff} in the Curie–Wiess law. In the itinerant-electron magnets, we derive relations between effective moment and neutron scattering cross-section.

Our theoretical results are demonstrated by the example of bcc Fe (Fig.1). The effective moment was calculated systematically as a function of wavevector and temperature. The effective moment calculated with an appropriate energy window was found to be in good agreement with the results of polarized neutron scattering experiment over a wide temperature range. The calculated SRO is small (up to 4 Å) and slowly decreases with temperature.

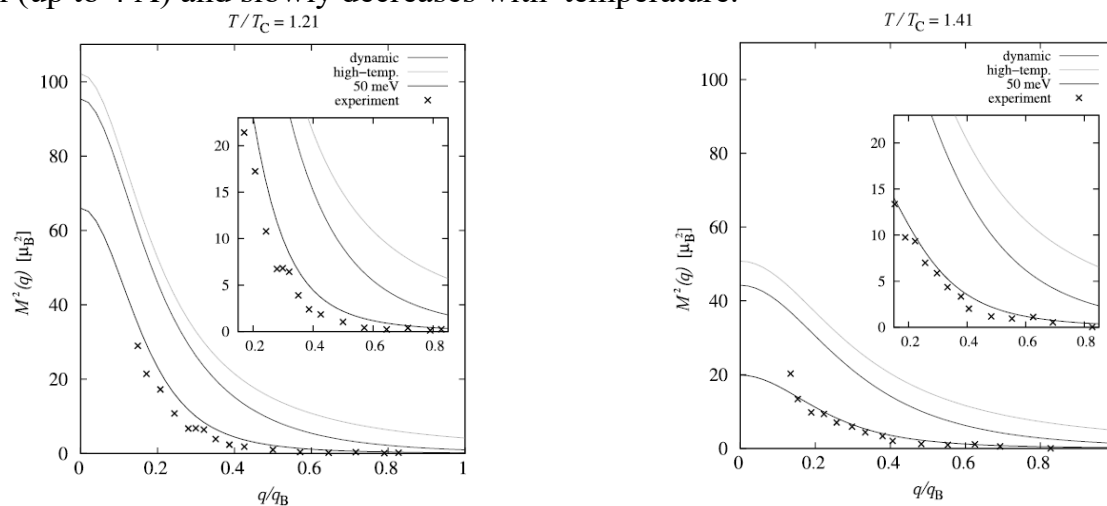


Fig.1. Square of the effective moment for bcc Fe calculated in the dynamic spin fluctuation theory with the use of exact formula, approximate high-temperature formula and formula with the energy cutoff 50 meV compared with the experimental values [1] at different temperatures.

[1] P. Brown et al., *JMMM*, **30** (1982) 243; **30** (1982) 335; **31-34** (1983) 295.

[2] N.B. Melnikov, B.I. Reser, *Phys. Met. Metallogr.*, **117** (2016) 1328-1383.

[3] N.B. Melnikov, B.I. Reser, *J. Magn. Magn. Mater.*, **397** (2016) 347.

[4] N.B. Melnikov, B.I. Reser, G.V. Paradezhenko, *JMMM*, **411** (2016) 133.

2RP-P-11

MULTIPLICITY OF MANY-PARTICLE STATES NEAR THE METAL-INSULATOR TRANSITION IN THE HUBBARD MODEL

Sherman A.

Institute of Physics, University of Tartu, Tartu, Estonia
alekseis@ut.ee

The two-dimensional repulsive one-band Hubbard model at half-filling was investigated using the strong coupling diagram technique. Together with the local terms the lowest-order nonlocal term was included into the irreducible part. The obtained system of equations for the electron Green's function was solved by iteration for moderate Hubbard repulsions U and temperatures T . As the initial Green's function in this procedure we used the result of the Hubbard-I approximation, poles of which were shifted to the lower frequency half-plane to obtain the proper analytic behavior for the retarded function. It was found that obtained solutions are changed with the variation of this shift η . The changes are mainly located in the frequency region near the Fermi level – in insulating solutions the width of the Mott gap is affected, while in metallic solutions the shape of the spectral function is modified. Scenarios of the metal-insulator transition are also changed with η – for its smaller values the transition occurs due to sudden appearance of a narrow band of mobile states in the middle of the Mott gap, while for larger η the transition happens with gradual closure of the gap as the temperature increases. Hence for given values of U and T the derived equations have continua of metallic or insulating solutions. The plurality of the solutions is caused by the nonlocal term – in the similar procedure with the irreducible part constructed from local terms solutions were independent of η . Evidently these solutions correspond to different values of the grand potential, and the continuous variation of their spectral shapes with η implies continuous dependence of the potential on this parameter. In its turn, this suggests the lack of a gap between solutions with the smallest and larger potentials. In spite of the multiplicity of the solutions, they have a common curve separating metallic and insulating states in the U - T phase diagram. This curve separates solutions obtained by iteration from the Hubbard-I Green's function. One can start iteration from one of these solutions and, varying T in iteration, obtain a metallic solution in the insulating region or, conversely, an insulating solution in the metallic region. Thus, not only different metallic or insulating solutions coexist at given U and T , but also distinct types of solutions go together in the vicinity of the separating curve. This result resembles the behavior of solutions near the first-order transition line in DMFT and cluster methods, however in our case, in view of the mentioned continuity, it would be better to say about two competing continua of states rather than two states. Grand potentials of the obtained solutions were not calculated in this work and, therefore, we cannot identify the separation curve with the critical line. However, they can be supposed to be close. In our phase diagram metallic states are located at smaller U and higher T , while insulating states are at higher U and smaller T . This layout is similar to that found in some cluster approaches and in contradiction with DMFT. In accordance with our phase diagram metallic states exist at comparatively large temperatures for moderate U . Therefore, nothing resembling the Fermi liquid behavior is observed in self-energies of these solutions. Spectral functions of both metallic and insulating solutions demonstrate intensity suppressions at frequencies $\omega = \pm U/2$, which were found also in the lower-order approximation and identified with the spectral redistribution due to multiple reabsorption of carriers with the creation of states with double site occupancies. These pseudogaps lead to the distinctive four-band structure of spectral functions, which was noticed earlier in Monte Carlo simulations.

2OR-P-12

LANDAU LEVELS AND QUANTUM OSCILLATIONS IN WEYL SEMIMETALS UNDER CROSSED ELECTRIC AND MAGNETIC FIELDS

Alisultanov Z.Z.^{1,2}, *Demirov N.A.*³

¹ Amirkhanov Institute of Physics RAS, Dagestan Science Centre, Makhachkala, Russia

² Dagestan State University, Makhachkala, Russia

³ Joint Institute for High Temperatures of the RAS, Moscow, Russia
zaur0102@gmail.com

Investigation of Weyl semimetals is one of the most important and hot topics of modern condensed matter physics [1]. These materials exhibit the interesting properties in a magnetic field. In this paper, we investigated the Landau band and quantum oscillations in the Weyl semimetal under crossed magnetic $\mathbf{H} = (0, 0, H)$ and electric $\mathbf{E} = (0, E, 0)$ fields. We obtained an expression for the energy spectrum of such system using three different methods: an algebraic approach, an Lorentz boost approach and quasi-classical approach [2]

$$\varepsilon_{n,p_x,p_z} = \text{sgn}(n) v_F \sqrt{(1-\beta^2)^{3/2} 2\hbar^2 l_H^{-2} n + p_z^2 (1-\beta^2)} + v_0 p_x \quad \text{for } n \neq 0 \quad (1)$$

$$\varepsilon_{0,p_x,p_z} = \pm \sqrt{(1-\beta^2)} v_F p_z + v_0 p_x \quad \text{for } n = 0. \quad (2)$$

where $\beta = v_0/v_F$, $v_0 = cE/H$.

It is interesting that the quasi-classical expression for the energy spectrum completely coincides with the expression obtained in the framework of the microscopic approaches. We have shown that the electric field leads to a cardinal change the Landau bands. In addition, we investigated the classical motion of a three-dimensional Dirac fermions in crossed fields. We have shown that the parallel (with respect to the magnetic field) velocity component (v_z) is an oscillatory function of the magnetic field. When an electric field is equal to $v_F H/c$, the collapse of the Landau levels occurs, and the motion becomes completely linear. But, this linearization occurs in a special way. Under this electric field, the wave function for the bulk states vanishes. The states with $p_z = 0$ only preserved. It will fundamentally change the character of the surface states, called the Fermi arcs. The electric field affects on the character of the quantum oscillations. The density of states has a singularity at $E = v_F H/c$. We have shown that such a result is due to the continuous model. In the lattice model

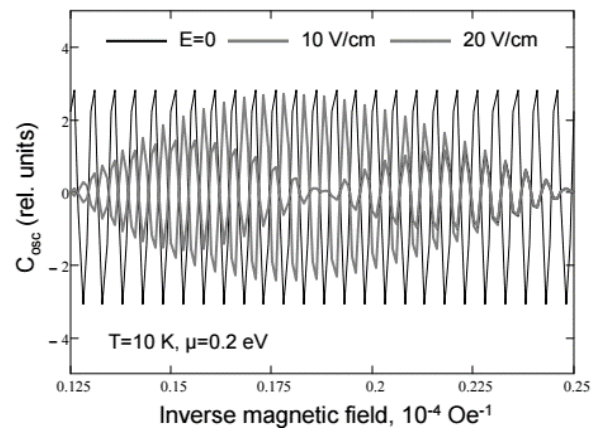


Fig. 1. Quantum capacity oscillations in the case of weak electric field.

this singularity disappears. In case of weak electric field we obtain the modulation of quantum oscillations (fig. 1).

Support by President Grant MK-2130.2017.2, RFBR № 15-02-03311a, Dagestan president grant (2016), Dynasty Foundation is acknowledged

[1] O. Vafeek and A. Vishwanath, *Ann. Rev. of Cond. Matt. Phys.*, **5** (2014) 83-112.

[2] Z.Z. Alisultanov, *Pis'ma v Zh. Eksp. Teor. Fiz.*, **105**(7) (2017) 437-441.

2OR-P-13

LAWS OF VOLUME ELASTICITY IN PHYSICAL PROCESSES AFFECTING LATTICE MODIFICATIONS, PHASE TRANSITIONS, CONDUCTIVITY AND MAGNETISM

Polyakov P.I.

Institute for Physics of Mining Processes, Donetsk
poljakov@mail.fti.ac.donetsk.ua

Analysis of the experimental results [1] allows single out the law of bulk elasticity that implies that the structural binding energy is formed by physical and chemical methods and transformed into elastic stresses that control lattice changes, formation of phase transitions, resistivity and magnetism in the course of physical processes under the effect of parameters.

The laws of volume thermo-, baro- and magnetoelasticity are the determining factors in lattice modifications in the structure sites together with the composition variation. It is the binding energy transformed into the stresses due to thermoelastic compression that redistributes the state of electron-phonon bonds, the volume and the density. Besides, baro- and magnetoelasticity combined with magnetic uncompensation demonstrate “cooling” and “heating” effects due to additional energy of strains that allow redistribution of free and semi-free electrons into a phonon bond and adding to modification of the structure as a whole. The deformation factor accompanied by thermoelastic strains determining phase transitions and magnetic field uncompensation control regularities of conductivity jump in the form of colossal magnetoresistance. X-ray methods provided registered four-fold difference in the pressure effect on the structure compressibility that emphasizes the role of the anisotropy of elasticity [2]. The results of the studies of magnet-containing semiconductors revealed a regularity in the T-H-P effect [3]. It was found that the effect of 6,2K corresponds to that of 2,7 kOe and 1 kbar [4]. Besides, an attention is concentrated on the analysis of the studies of manganite-based polycrystal structures and cuprate-based monocrystals [1]. As examples, the measurements of conductivity [5] are presented; the temperature dependence under the effect of the hydrostatic pressure P and the magnetic field H is separated. As a comparison, in [6] the resistance is modified in the course of varied composition in the structure sites. The introduced energy of the elastic stresses is transformed into the united energy that forms electron and phonon bonds. In the course of the structure formation, the binding energy of the nucleus and the electrons of the closed internal shells is much higher of the binding energy of the stressed shells. These are the energies that play the major role in the formation of the site structure and redistribution of the electron levels in the phonon structure. In the course of gradual filling of the external shells, an additional energy of the elastic stresses related to the binding energy is about 0,1-1 eV. The selected research area including the volume elasticity allows establishing the regularities of the elasticity anisotropy in a magnetodielectric [1]. The temperature of the phase transition at 9,8°K [1] has been demonstrated first. The presented work is aimed at settling the question of the presence of anomalies and regularities in view of the laws of the bulk elasticity.

- [1] P.Polyakov, T. Ryumshina. Magnetism and laws of volume elasticity. Tr.Res.Net. (2009).
- [2] A.A. Galkin, S.V. Ivanova, P.I. Polyakov, V.I. Kamenev, *ФТТ*, **8** (1979) 2580.
- [3] P.I. Polyakov, S.S. Kucherenko, *JMMM*, **248** (2002) 396.
- [4] P.I. Polyakov, S.S. Kucherenko, *Fiz. Nizk.Temp.*, **28** (2002) 1041.
- [5] P.I. Polyakov, S.S. Kucherenko, *JMMM*, **278** (2004) 38.
- [6] L.P.Gor'kov, *Uspekhi Phys. Nauk.*, **168** (1998) 665.

2 July

Sunday

12:00-14:00

poster session

2PO-I

2PO-I1

**“Spintronics and
Magnetotransport”**

2PO-I-1

NON-LOCAL SIGNAL AND NOISE IN LATERAL SPIN-VALVE STRUCTURES

Vedyayev A.^{1,2}, Ryzhanova N.^{1,2}, Strelkov N.^{1,2}, Andrianov T.¹, Lobachev A.¹, Dieny B.²

¹Department of Physics, Moscow Lomonosov State University, Moscow 119991, Russia

²Univ. Grenoble Alpes / CEA-INAC / CNRS, SPINTEC, 38000 Grenoble, France

The influence of the finite width D of the spin current carrying channel on the transport properties of lateral spin-valve (LSV) is theoretically investigated. It is shown that for $D \approx \pi l_{sf}$, where l_{sf} is the spin diffusion length (SDL) in spin current channel the signal substantially changes comparing to the case $D = l_{sf}$. This effect demonstrates the influence of 2D-dimensionality on spin transport in the spin-channel. It is shown that besides drop of voltage along the length of ferromagnetic analyzer it appears noticeable transversal signal, depending on the angle between the direction of the magnetization of the analyzer and the magnetizations of two other magnetic electrodes. It is shown that dependence of the signal on this angle obeys $(1 - \cos\theta)$ law. In addition it was theoretically investigated the noise in LSV due to the fluctuation of the direction of the vector of the spin accumulation within the paramagnetic spacer. The explicit expression for the dependence of the ratio signal/noise on the value SDL in the paramagnetic spacer on its sizes was obtained, and it was shown that this ratio monotonically increases with the value of SDL saturating for its large value.

One of the most effective instruments to generate pure spin current is so called Lateral Spin Valve (LSV) [1,2]. We investigated the distribution of spin accumulation and profile of induced drop of voltage for two-dimensional lateral spin valve in the framework of spin diffusion model

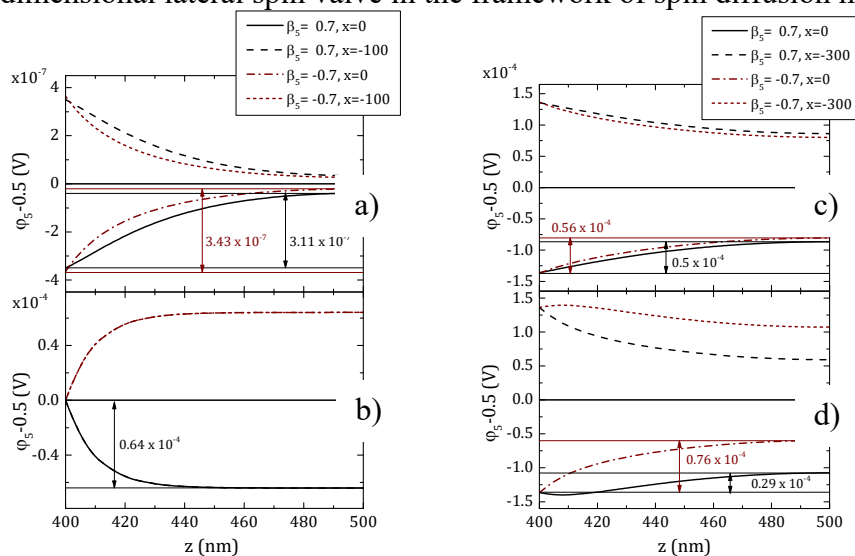


Fig. 1: Potential distribution in thin ($D = 100$ nm) ferromagnetic analyser along both sides in case of $\beta_3 = 0.7$ – “P” state (a) and $\beta_3 = -0.7$ – ”AP” state (b), Potential distribution in thick ($D = 300$ nm) ferromagnetic layer along both sides in case of $\beta_3 = 0.7$ (c) and $\beta_3 = -0.7$ (d).

We also calculated the signal to noise ratio (SNR) in these lateral structures, taking into account the fluctuations of the magnetization direction of ferromagnetic electrodes in the spin-valve.

[1] T. Kimura and Y. Otani, *Phys. Rev. Lett.*, **99** (2007) 196604.

[2] T. Kimura and Y. Otani, *J. Phys.: Cond. Matt.*, **19** (2007) 165216.

2PO-I-2

Sd-ELECTRON SPIN RESONANCE IN FERROMAGNETIC MATERIALS*Nekrasov M.A.¹, Safin A.R.¹, Vilkov E.A.², Chigarev S.G.²*¹ National Research University "MPEI", Moscow, Russia² Kotelnikov Institute of Radio Engineering and Electronics Russian Academy of Sciences,
Fryazino, Russia
juvefan95@yandex.ru

Recently, there has been an increased interest in the generation and detection of electromagnetic waves of the terahertz (THz) frequency range [1, 2]. Promising is the use of spin injection in magnetic transitions, which leads to an inverted population of the spin energy subbands. A number of experimental results were obtained on the generation of THz waves in structures of the "ferro-type or antiferromagnetic-film-metal rod" type [2]. To date, it is important to detect THz waves in such transitions. In this paper, we consider a mathematical model and the conditions for the appearance of a resonance in magnetic transitions due to the sd exchange interaction between the conduction electrons and the magnetic lattice [2, 3].

Let us consider a model in which a plane polarized electromagnetic wave falls on a film of a ferromagnetic material into which spins from an adjacent ferromagnet-injector layer are injected. If the thickness of the film is small, then a uniform alternating magnetic field acts on the conduction electrons. The magnetization of the conduction electrons is described by the precession equation of the following form [2, 3].

A coordinate system is chosen in which the yz plane coincides with the plane of the film, the z axis is parallel to the easy axis of anisotropy and the magnetization direction of the lattice, and the electromagnetic wave falls in the direction of propagation of the conduction electrons (x axis).

If the frequency of the EM wave is comparable with the frequency of the sd exchange, then it is several orders of magnitude greater than the frequency of the ferromagnetic resonance of the film. The magnetization of the lattice does not have time to vary with the frequency of the EM wave and remains in its original position, and the magnetization of the electrons precesses around the magnetization vector of the lattice with the frequency of the EM wave, which leads to a resonance absorption of the EM wave at a frequency close to the frequency of the sd exchange.

The obtained numerical simulation results for typical parameters show the possibility of applying a resonant effect to determine the character of the EM wave polarization. This effect can be used for frequency filtering and detection of THz signals.

The results were obtained in the framework of the state task of the Ministry of Education and Science of the Russian Federation No. 8.8109.2017

[1] A. Kadigrobov, Z. Ivanov, T. Claeson, R. Shekhter, M. Jonson, *Europhys. Lett.*, **67(6)** (2004) 948.

[2] Y.V. Gulyaev, P.E. Zilberman, G.M. Mikhailov, S.G. Chigarev, *Letters to the Journal of Experimental and Theoretical Physics*, **98(11)** (2013) 837-847.

[3] Y.V. Gulyaev, E.A. Vilkov, P.E. Zilberman, A.I. Panas, *Letters to the Journal of Experimental and Theoretical Physics*, **100(3)** (2014) 194-196.

2PO-I-3

ROBUST IMAGE RECONSTRUCTION ALGORITHMS FOR THE MICROWAVE SPINTRONIC HOLOGRAPHIC VISION SYSTEM

Leshchiner D.R.¹, Zvezdin K.A.¹, Popkov A.F.¹, Chepkov G.N.², Perlo P.³

¹ Moscow Institute of Physics and Technology, Moscow Region, Russian Federation

² Higher School of Economics, Moscow, Russian Federation

³ IFEVS & Torino e-District, Torino, Italy

leshchiner@phystech.edu

We discuss image reconstruction algorithms suitable for a spin diode-based holographic vision system. The idea of holographic visualization is to reconstruct the spatial microwave scattering density of an object by detecting an amplitude and phase of a reflected signal by lattice of sensors. That would be a particular case of an inverse scattering problem. A spin diode-based holographic visualization technique in the microwave division (Ku-band) being originally proposed in [1] and a simple image reconstruction algorithm for a model spin diode-based holographic vision system suggested. The technique used there assumed a lattice of microwave emission sources each paired with its own sensor (microwave detector). Our case is more realistic in that there is a lattice of spin-diode based sensors (detectors) and a fixed emission source. Our objective is, by reconstructing the object density, to detect the presence and the nature of road obstacles impeding driving in the near vehicle zone.

We present a robust reconstruction algorithm version suitable for that case, discuss its variants, determine and analyse its resolution limits for various distances, with different number of sensors, for a one-dimensional problem of detecting two walls (or posts) separated by a gap at a fixed distance. As predicted by Kotelnikov–Whittaker–Nyquist–Shannon theorem, the maximal interval between sensors needed for a reliable reconstruction equals approximately Fresnel zone width. We show that object detection threshold (minimal detected object size) achieved by our algorithm with an appropriate number of sensors was about 40% of Fresnel zone width for wall detection and about 30% of zone width for gap detection. That would translate into correspondingly 6 times and 10-12 times gain in detection distance (e.g. the gap 18 cm wide was possible to detect, for 3cm wavelength, at a distance of 6 m instead of at a distance of 52 cm) compared to what it would be if detection threshold would actually equal to Fresnel zone width.

The Russian Science Foundation, project number 16-19-00181, supported the work.

[1] L. Fu et al., *J. Appl. Phys.*, **117** (2015) 213902.

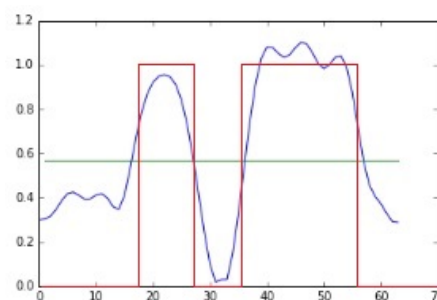


Fig. 1. A reconstruction (in blue), by 32 sensors, of two fixed density walls (in red) 8 wavelengths apart at distance 50. A horizontal line represents a density threshold, obtained by object detection.

2PO-I-4

MAGNETIC AND TRANSPORT PROPERTIES OF Mn₂FEGa MELT-SPUN RIBBONS

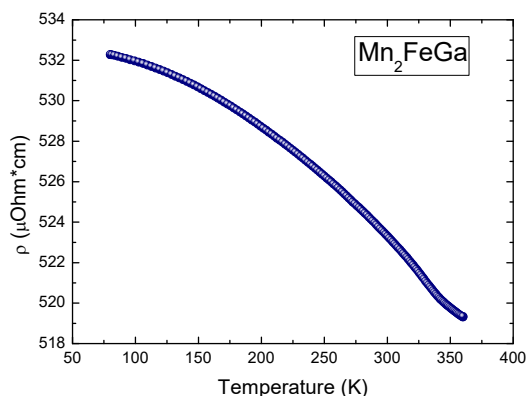
Gavrikov I.S.¹, Seredina M.A.¹, Anikin Yu.A.¹, Arkhipov D.I.¹, Khovaylo V.V.¹

¹National University of Science and Technology “MISiS”, Moscow, Russia
khovaylo@misis.ru

Recently, there has been growing interest in the development of novel materials for spintronic applications. Heusler alloys, specifically so-called inverse Heusler alloys [1] and equiatomic quaternary Heusler alloys [2] have been suggested as a potential candidate in this respect. First principles theoretical calculations have suggested [3] that Mn₂FeZ (Z = Al, Ga, Si, Ge, Sb) Heusler alloys can be of interest for experimental studies due to their half-metallic properties. Experimental studies of the Heusler alloy with Z = Ga, Mn₂FeGa have shown that crystal structure and magnetic properties of Mn₂FeGa strongly depend on annealing temperature. Specifically, it was reported that Mn₂FeGa crystallizes in a tetragonally distorted inverse Heusler structure after annealing at 673 K [4] while the crystal structure of Mn₂FeGa was reported to be hexagonal after annealing at 893 K [5]. Moreover, annealing at 893 K promoted formation of a cubic structure [4]. A large exchange bias was reported for a polycrystalline Mn₂FeGa with hexagonal structure [5], whereas an exchange-spring like magnetic behaviour was reported for a tetragonal modification of Mn₂FeGa.

To further explore physical properties of this alloy, we have prepared Mn₂FeGa by melt spinning technique. The melt-spun ribbons were characterized by X-ray diffraction (XRD), magnetic and transport measurements.

The room-temperature XRD diffraction revealed that as-spun ribbons have a cubic structure with crystal lattice parameter $a = 0.373$ nm. This is in a good agreement with that obtained for polycrystalline Mn₂FeGa annealed at 893 K [4]. However, magnetic properties of the melt-spun ribbons turned out to resemble properties of antiferromagnetic compounds. Measurement of electrical



resistivity revealed that transport properties of melt-spun Mn₂FeGa is abnormal for an intermetallic compound and demonstrate behaviour typical for semiconductors in a temperature interval 80 – 360 K.

Support by Russian Science Foundation (grant No. 16-42-02035) is greatly acknowledged.

- [1] X. Wang, Z. Cheng, J. Wang, X.-L. Wang, G. Liu, *J. Mater. Chem. C*, **4** (2016) 7176-7192.
- [2] L. Bainsla, K.G. Suresh, *Appl. Phys. Rev.*, **3** (2016) 031101.
- [3] H.Z. Luo, H.W. Zhang, Z.Y. Zhu, L. Ma, S.F. Xu, G.H. Wu, X.X. Zhu, C.B. Jiang, H.B. Xu, *J. Appl. Phys.*, **103** (2008) 083908.
- [4] T. Gasi, A.K. Nayak, J. Winterlik, V. Ksenofontov, P. Adler, M. Nicklas, C. Felser, *Appl. Phys. Lett.*, **102** (2013) 202402.
- [5] Z.H. Liu, Y.J. Zhang, H.G. Zhang, X.J. Zhang, X.Q. Ma, *Appl. Phys. Lett.*, **109** (2016) 032408.

2PO-I-5

**THERMODYNAMIC ASPECTS OF DESCRIBING THE SPONTANEOUS
MAGNETISM CONTRIBUTION OF DONOR ELECTRONS OF TRANSITION
ELEMENT IMPURITIES TO THE HALL CONDUCTIVITY OF A
SEMICONDUCTOR**

Okulov V.I.^{1,2}, Pamyatnykh E.A.²,

¹ M.N. Miheev Institute of Metal Physics of Ural Branch of RAS, 620990, Ekaterinburg, Russia

² Ural Federal University, 620083, Ekaterinburg, Russia

Evgeny.Pamyatnykh@urfu.ru

The present report is devoted to stating the problem of originating and justifying the proposed recently section of actively developing now field of studying the manifesting the spontaneous magnetization of electrons in the Hall effect and in all the range of galvanomagnetic phenomena. We show that in mentioned field, which is termed “anomalous Hall effect”, there can be used naturally the methods of describing, characteristic of equilibrium and nonequilibrium thermodynamics. It is the use of these methods that forms contents of research field mentioned above with which we relate the term “thermodynamic anomalous Hall effect”. From the beginning of considering we quote a well known formula for equilibrium magnetization of quantum system of electrons, obtained from thermodynamic potential Ω in variables of temperature, chemical potential ζ and magnetic field strength \mathbf{H} . Taking into account real inhomogeneity of a system, this formula can be transformed to the expression for varying the potential Ω with respect to vector potential of magnetic field $\delta\mathbf{A}(\mathbf{r})$:

$$\delta\Omega = -\frac{1}{c} \int d\mathbf{r} \delta\mathbf{A}(\mathbf{r}) \mathbf{j}_m(\mathbf{r}) = -\frac{1}{c} \int d\mathbf{r} \delta\mathbf{A}(\mathbf{r}) [\mathbf{j}_{eq}(\mathbf{r}) - \mathbf{j}_c(\mathbf{r})] \quad (1)$$

In this equality $\mathbf{j}_m(\mathbf{r}) = c \operatorname{rot} \mathbf{M}$ is the magnetization current density, $\mathbf{j}_{eq}(\mathbf{r}) = c \operatorname{rot} \mathbf{m}$ is the density of mean magnetic moment flux of an electron and we assume that the vectors \mathbf{H} , \mathbf{M} and \mathbf{m} are directed along the symmetry axis. The quantity $\mathbf{j}_c(\mathbf{r})$ is defined by the equality:

$$1/c[\mathbf{j}_c(\mathbf{r}) \times \mathbf{H}] = \operatorname{grad} P, \quad (2)$$

Where $P = -\Omega/V$ is the pressure of electron system. This equality is the condition of equilibrium of the force, with which magnetic field acts the system with current, and the pressure force of the system. It means that the quantity $\mathbf{j}_c(\mathbf{r})$ should be considered as the conduction current density, due to existence of the external force mentioned above. If the system has a spontaneous magnetization M_0 , the pressure in (2) includes the energy $M_0 H$. In homogeneous equilibrium system the currents considered are concentrated at the boundaries. Accordingly the magnitude and distribution of equilibrium conduction currents depends on the structure and shape of the boundaries and one can show that it is they are responsible for the existence of so-called demagnetizing fields.

The ideas presented may be applied in studying the Hall resistance with allowance for the contribution from the local equilibrium current. Local equilibrium in the field with potential $\varphi(\mathbf{r})$ is described by adding the energy $e\varphi(\mathbf{r})$ to chemical potential. Thereby in (2) one has: $\operatorname{grad} P = -en\mathbf{E} - e\mathbf{E}H(\partial M_0/\partial\zeta)$, where \mathbf{E} is the magnetic field strength, n is the electron concentration. It is not difficult to see that after substituting this expression for $\operatorname{grad} P$ into (2) the first term ($en\mathbf{E}$) gives well known simple value of the Hall resistance in high magnetic field. The second term leads to appearing the parameter $\sigma_m = ec(\partial M_0/\partial\zeta)$, characterizing the manifestations of spontaneous magnetism. In the framework of developed theory there has been obtained complete expression for the Hall resistance, describing thermodynamic anomalous Hall effect. Report contains also a number of results of studying concrete specific behaviors of this effect in electron systems of hybridized states of transition element impurities in a semiconductor.

2PO-I-6

DISPERSION OF THE MAGNETOSTATIC VOLUME WAVES IN A MEDIUM WITH DAMPING

Maltceva L.¹, Makarov P.¹, Shcheglov V.²

¹ Pitirim Sorokin Syktyvkar State University, 167001, Syktyvkar, Russia

² Institute of Radio Engineering and Electronics, RAS, 125009, Moscow, Russia
lidija.malceva@rambler.ru

Magnetostatic volume waves (MSVW) in ferrite films is the basic foundation for microwave analog data processors [1]. Minimization of wave losses is a key for its successful work, but the MSVW damping hasn't been studied enough, as the most of the research is performed without consideration of attenuation [2].

The geometry of task is following. The MSVW is propagated in ferrite slab having thickness d magnetized by constant magnetic field H . Oz axis was oriented along the field H . The angle between wave vector and field direction is denoted as φ . Landau-Lifshitz-Gilbert equation was used to describe the motion of the magnetization vector m in a lossy medium. In our task, dispersion equation for MSVW has the form:

$$\operatorname{tg}(kd\mathcal{G}) = \frac{2\mu\mathcal{G}}{\beta-1}, \quad (1)$$

$$\beta = v^2 \cos(\varphi) - \mu^2 \mathcal{G}^2, \quad (2)$$

$$\mathcal{G} = \sqrt{\cos^2(\varphi) + \frac{\sin^2(\varphi)}{\mu}}, \quad (3)$$

μ — the magnetic permeability, v — the magnetic susceptibility of the medium.

Figure 3 shows the dispersion curves for the real and imaginary parts of the wave number for the first four MSVW modes that were obtained by the numerical solution of equation (1).

Thus, in this study dispersion relations for the real and imaginary parts of the wave number were obtained. It was shown that dispersion curves are limited both by the wave number and frequency, and these restrictions tighten with an increase in the damping parameter. With the increase of the angle φ , limitation of dispersion curves is exacerbated, branches of the dispersion curves are shifted toward lower wave numbers and the damping parameter is being bounded below and above.

[1] Ishak, W. S. *Proc. of the IEEE*, **76** (1988) 171-187.

[2] Damon, R. W., Eshbach J. R. *J. Phys. Chem. Solids*, **19** (1961) 308–320.

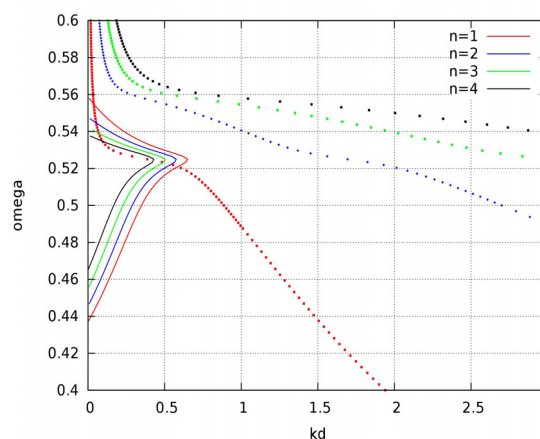


Fig. 1: Imaginary and real parts of the dispersion ratio dependencies on frequency. The intensity of a magnetic field $H = 437.5$ Oe, the magnetization $4\pi M = 1750$ Gs.

2PO-I-7

QUASI-HALL EFFECT AND ANISOTROPIC CONDUCTIVITY OF 2DEG IN AlGaN/AlN/GaN HETEROSTRUCTURES

Chumakov N.K.¹, Mayboroda I.O.¹, Grichuk E.S.¹, Lev L.L.^{1,2}, Valeyev V.G.¹, Zanaveskin M.L.¹, Srtokov V.N.²

¹ NRC «Kurchatov Institute», Moscow, Russia

² Swiss Light Source, Paul Scherrer Institute, Villigen, Switzerland

Chumakov_NK@nrcki.ru

Despite the recent remarkable progress in developing III-nitride functional systems, some of the basic properties of III-nitride semiconductors are still unclear. In particular, the electron effective mass tensor in two-dimensional electron gas (2DEG) of AlGaN/AlN/GaN heterostructures was proved recently to be essentially anisotropic [1].

Here we deliver our results for the conductivity anisotropy and quasi-Hall effect [2] in these structures. The phenomenon, termed the transverse quasi-halvano-anisotropic effect as well, takes place in anisotropic conductive media in the absence of external magnetic field and manifests itself by the occurrence of transverse (quasi-Hall) voltage drop U_{24} in the case when the current I_{13} is not directed along any of the main axes of the system conductivity tensor; $R_{quasi-Hall} = R_{1324} \equiv U_{24} / I_{13} = R_{1243} - R_{2314}$, see Fig. 1. The AlGaN/AlN/GaN structures with barrier layer of 1 nm Al_{0.5}Ga_{0.5}N и 2 nm AlN, deposited on 500 nm thick Ga-polar GaN were grown on c-oriented sapphire substrate. Four probe sheet resistance measurements were carried out in a standard van der Pauw setup. The largest difference of the resistances $R_{1243} = R_{4312}$ and $R_{2314} = R_{1423}$ was detected when the 1-2 current axis is collinear with one of the main crystallographic lattice directions in the 2DEG plane. But the anisotropy definitely vanishes when the 1-3 axis is parallel to the last one. In accordance with the approach [2] we define the anisotropy degree as $\varepsilon \equiv R_{quasi-Hall} / \langle R \rangle = 2(R_{1243} - R_{2314}) / (R_{1243} + R_{2314})$. The parameter ε had been found in the range of 15 ÷ 25 % for various samples. The measurements data mentioned for samples with different carrier density n_s and average mobility $\langle \mu \rangle$ are summarized in Table. 1.

In accordance with the von Neumann principle the latter result may indicate that the system symmetry is lower than that of the bulk GaN hexagonal lattice [3].

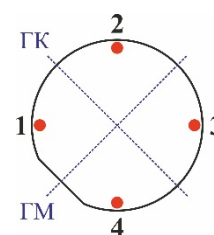


Fig. 1. Scheme of the experiment.

Sample	$n_s, 10^{+12} \text{ cm}^{-2}$	$\langle \mu \rangle, \text{ cm}^2/\text{V}\cdot\text{s}$	$R_{1243}, (\Gamma\text{M}), \Omega$	$R_{2314}, (\Gamma\text{K}), \Omega$	$\varepsilon, \%$
1	7.0	1350	179.0	139.4	24.9
2	8.1	920	160.0	128.0	22.2
3	9.5	1300	123.9	96.6	24.8
4	13.0	620	183.3	157.8	15.5
5	21.0	1320	53.8	45.0	17.8

[1] L.L. Lev et al., *Nature Nanotechnology*, submitted (2017).

[2] N.N. Polyakov, *Soviet Physics Journal*, **32** (1989) 956.

[3] V.V. Filippov et al., *Russian Microelectronics*, **42** (2013) 428.

[4] J.F. Nye. *Physical Properties of Crystals*, Oxford at the Clarendon Press (1964).

2PO-I-8

MAGNETIC-OPTICAL EFFECTS OF CoPt AND CoPd ALLOYS

*Kalentyeva I.L., Danilov Yu.A., Dorokhin M.V., Demina P.B., Vikhrova O.V.,
Zdoroveyshchev A.V., Kudrin A.V.*

Physical–Technical Research Institute, Lobachevsky State University, Nizhny Novgorod, Russia
istry@rambler.ru

In this paper, the magneto-optical properties of CoPt and CoPd alloys are investigated. These materials may have a easy magnetization axis directed perpendicular to the plane of the layers and this fact determines their prospects for the development of spintronics magneto-independent elements, in particular, spin-light-emitting based on InGaAs/GaAs diodes [1].

The CoPt (or CoPd) alloys were formed by electron-beam evaporation in vacuum on GaAs heterostructures over a thin dielectric layer Al_2O_3 (~ 1 nm) pre-deposited in the same technological process [1]. The growth temperature of alloys was 200 or 300°C. The Pt (Pd) layers 0.5 nm thick and the Co layers from 0.1 to 0.3 nm thick were applied alternately for 10-20 cycles. The alloy composition is determined by the ratio of the Co/Pt (Pd) thicknesses. The total thickness of CoPt and CoPd films reached 6-16 nm. The magneto-optical Faraday effect and the transverse Kerr effect in the field range $H = \pm 4000$ Oe at the wavelength of a semiconductor laser of 980 nm and 800 nm, respectively, were studied. The magnetization (M) of the samples was measured on a magnetometer with a variable gradient of the field.

The form of the magnetic field dependence of the Faraday angle ($\Theta_F(H)$) coincides with the $M(H)$ of the 8 nm thick CoPt alloy (fig.1). On both curves there is a hysteresis loop with a coercive field of ~ 160 Oe. The residual magnetization in the zero magnetic field is observed and Θ_F reaches the value $1.5 \cdot 10^6$ deg/cm. With an increase the thickness of the CoPt layer to 16 nm the Θ_F increases to $2 \cdot 10^6$ deg/cm. These values exceed the data for 10-14 nm thick films of the $\text{Co}_{50}\text{Pt}_{50}$ alloy grown on MgO crystals by magnetron sputtering - $\Theta_F = 8 \cdot 10^5$ deg/cm [2]. The absence of the hysteresis loop and the saturation output in the transverse Kerr effect measurements ($\text{TKE}(H)$) confirm the location of the easy magnetization axis perpendicular to the layer plane. The CoPd alloy exhibits similar magnetic properties. However, the achieved values of the Θ_F and saturation magnetization were half that of CoPt films. A changes in the $\Theta_F(H)$ and $\text{TKE}(H)$ form are determined by ratio of the Co/Pt or Co/Pd layer thicknesses. These effects indicate the possibility of controlling the position of easy magnetization axis in CoPt and CoPd layers.

This work was supported by the implementation of the government task (projects № 8.1751.2017/PCh) of the Ministry of Education and Science of Russia under the support of the RFBR (grants 15-02-07824_a, 16-07-01102_a), the scholarship (competition SP-2015) and grant (MK-8221.2016.2) of the president of the Russian Federation.

[1] A.V. Zdoroveyshchev *et al.* // *Physics of the Solid State*, **58** (2016) 2267–2270.

[2] E. M. Artem'ev *et al.* // *Physics of the Solid State*, **52** (2010) 2271–2273.

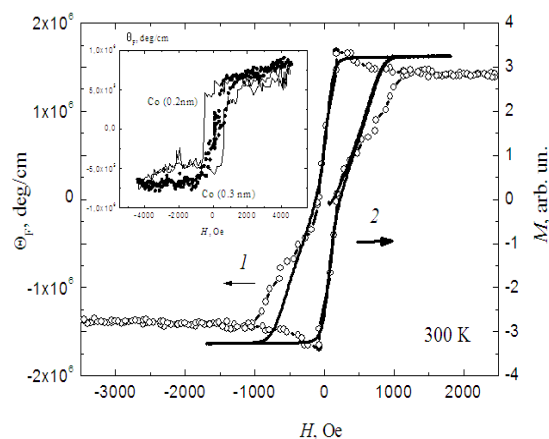


Fig. 1. Magnetic-field dependences of the Faraday angle (1) and magnetization of heterostructure (2) with CoPt (0.3/0.5nm) layer. The inset shows Faraday angle dependence on Co layer thickness for CoPd alloy.

2PO-I-9

INFLUENCE OF MECHANICAL STRESSES ON THE COMPLEX IMPEDANCE OF SOFT MAGNETIC MICROWIRES

Semirov A.V., Kudryavtsev V.O., Moiseev A.A., Vasyukhno N.V.,

Derevyanko M.S., Nemirova V.A.

Irkutsk state university, Irkutsk, Russia

nemirovarvara@mail.ru

The investigations were carried out on $(\text{CoFe})_{74.3}\text{Ni}_1\text{B}_{14.8}\text{Si}_{9.9}$ microwires obtained by the Ulitovsky-Taylor method. The microwires had a small negative magnetostriction constant $|\lambda_s| \sim 10^{-7}$. The diameter of the soft magnetic metal core was 17 μm . The thickness of the glass cover of the microwire was 3,5 μm . Both the original (as cast) samples and the samples with completely removed glass cover were investigated. Before experiment all microwires underwent relaxation annealing at a temperature of 130 $^{\circ}\text{C}$ for 8 hours. The measurements were carried out on automated measuring setup of magnetoimpedance spectroscopy based on the Agilent 4294A impedance analyzer in the frequency range of alternating current from 0.1 MHz to 80 MHz with effective value of AC current of 1 mA. Mechanical stresses were created by the action of an external tensile force applied along the sample codirectional with an AC current. All effects induced by mechanical stresses was reversible.

The method of magnetoimpedance spectroscopy shows a high sensitivity of the complex impedance to a change in the magnetic structure of the material. Earlier it was shown [1] that the use of this method led to a change in the character of the frequency dependence of the imaginary part of the impedance for samples with an inhomogeneous magnetic structure. The frequency dependence of the imaginary part of the impedance Z'' for the microwires with a glass cover (a) and with the removed cover (b) for different values of the tensile force F is shown on Fig.1. The features series of the influence of glass cover on the frequency dependences of the real and imaginary part of impedance under the action of mechanical stresses is detected. The results are explained by the non-uniform magnetic structure of the microwire and its response to the changes of mechanical stresses.

This work was supported by a project part of Government Assignment for Scientific Research from the Ministry of Education and Science, Russia (№ 3.1941.2017)

[1] Semirov, A.V. et al., *Technical Physics.*, **60(5)** (2015) 767-771.

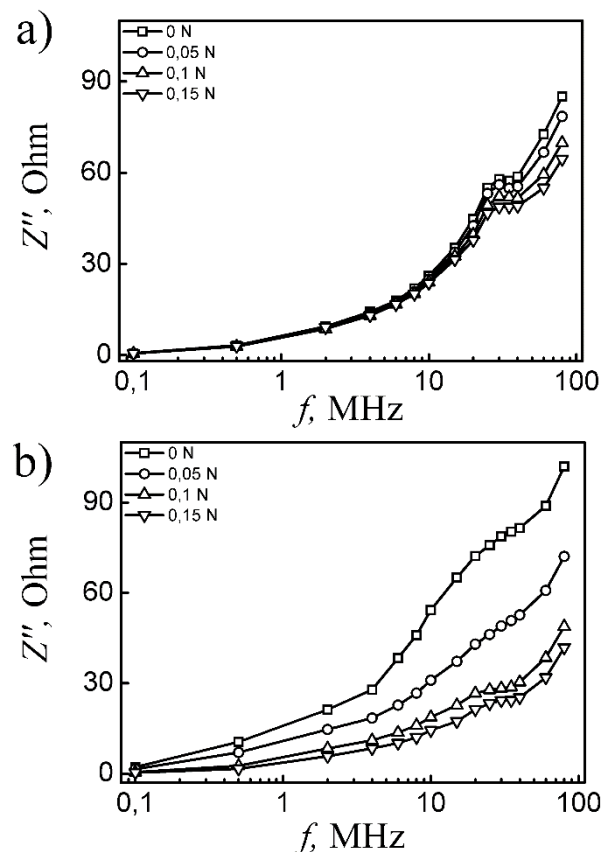


Fig.1 The frequency dependences of the imaginary part of the impedance for an investigated microwires.

2PO-I-10

EFFECTS OF AVERAGE GRAIN SIZE ON THE MAGNETIC PROPERTIES OF PERMALLOY FILMS

Djuzhev N.A.¹, Iurov A.S.¹, Mazurkin N.S.¹, Chinenkov M.Yu.¹, Pushkina M.M.¹

¹ National Research University of Electronic Technology (MIET), 124498, Moscow, Russia
chinenkov@inbox.ru

One of the effects, which provides a promising use of magnetic structures, is the electrical resistance change in the magnetic field, i.e. magnetoresistive effect. It has various applications in the development of sense devices, in particular for use in the magnetic microelectromechanical systems (MEMS) [1]. Permalloy films FeNi and FeNiCo are widely used for anisotropic magnetoresistive transducers (AMR transducers) fabrication. AMR transducers convert magnetic field changing to the electrical signal in the current sensors, angular position sensors, speed sensors and others. It is necessary to maximise the AMR effect and to prevent strong growth of the coercive force and anisotropy field for AMR-transducer output characteristics and sensitivity improvement. These characteristics depend on many parameters, in particular, the value of the average size of the crystallites in the film permalloy. And the crystallites size depends on the parameters of magnetron sputtering. Therefore, the aim of this work is the study of magnetron sputtering parameters influence on the average grain size and their optimal values selection.

It is known the key parameters affecting grain growth in magnetron sputtering process are substrate temperature, deposition rate and the power applied to the magnetron [3]. In this work the functions of the AMR effect value, the coercive field strength and anisotropy in FeNi films of 20:80 and FeNiCo 9:73:18 depending on the film thickness, substrate temperature, magnetron power and gas pressure are obtained. It is shown the variation of power on the magnetron and the pressure of the working gas have little effect on the average grain size and magnetic parameters of the films, while the film thickness changing and substrate temperature can lead to significant changes in the parameters of the film (fig.1).

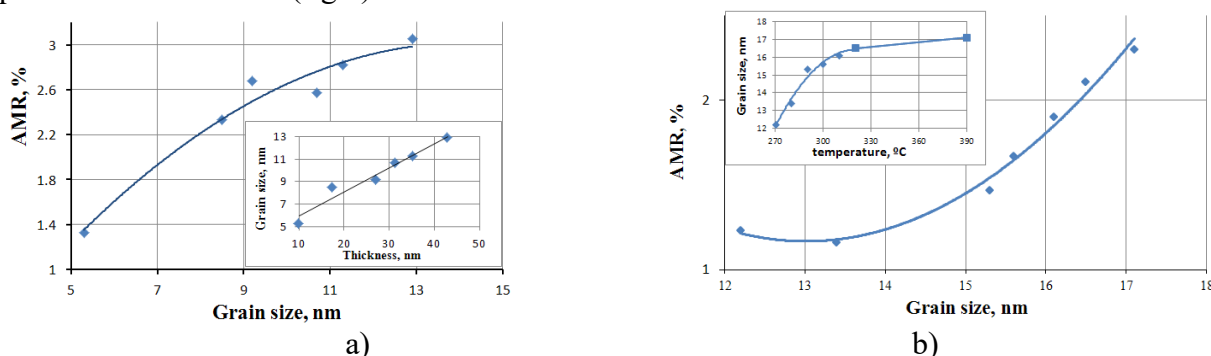


Fig.1 – The dependence of the AMR effect on the average grain size in the film FeNiCo (a) and FeNi (b).

The work was supported by the Minobrnauki RF (GK no. 14.578.21.0188, unique identifier RFMEFI57816X0188) and conducted using the equipment of Multi-access center «Microsystem technics and electronic component base» MIET.

- [1] Tumanski S., Thin Film Magnetoresistive Sensors, *IOP Publishing Ltd*, (2001) 451.
 [2] V. Bespalov, N. Djuzhev, A. Iurov, N. Mazurkin, M. Chinenkov, R. Preobrazhensky, *Solid State Phenomena*, **249** (2016) 124-130.
 [3] Hass G., Thun E., *Physics of thin films* **3** (1966).

2PO-I-11

CREATION OF EXCHANGE BIASED STRUCTURE USING THE PHASE SEPARATION EFFECT

Savin P.A., Svalov A.V., Lepalovskij V.N., Vas'kovskiy V.O.

Ural Federal University, Ekaterinburg, Russia

Peter.Savin@urfu.ru

Magnetic structures with exchange bias are widely used in modern microelectronics. The conventional way of creating such a structure involves the formation of two materials - a ferromagnet and an antiferromagnet. There are various technological ways of creating such a structure, namely:

- 1) Formation of an antiferromagnetic layer by partial oxidation of the ferromagnetic layer [1].
- 2) Formation of an antiferromagnetic layer by thermal diffusion of neighboring FeNi and Mn layers [2].
- 3) The successive deposition of the ferromagnetic and antiferromagnetic layers [3].
- 4) It is possible to form a ferromagnetic phase in antiferromagnetic layer using the phase separation effect [4].

In this study, this effect has been used to obtain exchange-biased structure. The initial antiferromagnetic FeMn films were prepared by ion-plasma sputtering. Samples were annealed in an oxygen-containing gas mixture in the temperature interval of 250-300 °C. The appearance of the α -Fe(Mn) enriched in iron ferromagnetic phase [5] was verified by X-ray diffraction, measurements of the vibration sample magnetometer hysteresis loops and the anisotropic magnetoresistive effect. The amount of the ferromagnetic phase depends on the temperature and time of the annealing. As an example, Fig. 1 shows the $M(H)$ curves for a FeMn film in as deposited state and after heat treatment at the temperature of 300 °C (3 minutes) at the external magnetic field of 1 kOe applied in the film plane. The values of the exchange bias field (H_b) and coercive force (H_c) are indicated in the picture. The maximum value of the magnetoresistive effect for annealed FeMn films was 0.25%, that is equal to one for Fe films.

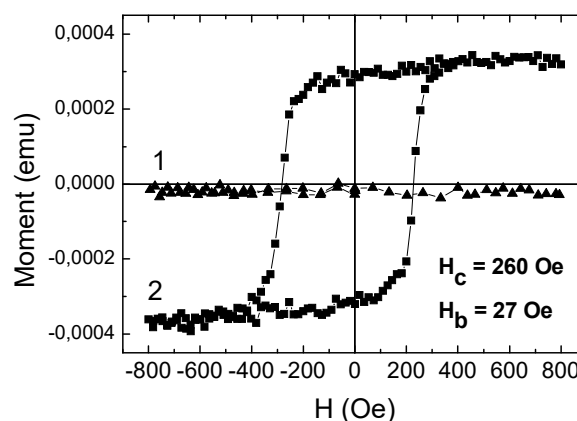


Fig. 1. $M(H)$ curves for a FeMn film: as deposited state (1), after heat treatment at the temperature of 300 °C, 3 minute (2).

The values of the exchange bias field (H_b) and coercive force (H_c) are indicated in the picture. The maximum value of the magnetoresistive effect for annealed FeMn films was 0.25%, that is equal to one for Fe films.

This work was supported by Ministry of Education and Science of the Russian Federation, project 3.6121.2017.

- [1] W.H. Meiklejohn, C.P. Bean, *Phys. Rev.*, **102** (1956) 1413-1414.
- [2] A.A. Glazer, A.P. Potapov, et al., *Phys. Met. Metallography*, **31** (1967) 735-738.
- [3] J. Nogués, I.K. Schuller, *J. Magn. Magn. Mater.*, **192**, (1999) 203-232.
- [4] P.A. Savin, A.V. Svalov, et al., *Phys. Met. Metallography*, **115** (2014) 913-920.
- [5] H. Lefakis, T.C. Huang and P. Alexopoulos, *J. Appl. Phys.*, **64** (1988) 5667-5669.

2PO-I-12

DOMAIN WALL'S STABILITY AND CURRENT-INDUCED DYNAMICS IN NANOWIRE WITH PERPENDICULAR MAGNETIC ANISOTROPY

Tikhomirova K.A.¹, Kindiak I.L.¹, Skirdkov P.N.^{1,2}, Zvezdin K.A.^{1,2}

¹ Moscow Institute of Physics and Technology, Dolgoprudny, Russia

² A.M. Prokhorov General Physics Institute, Russian Academy of Sciences, Moscow, Russia

³ Russian Quantum Center, Novaya St. 100, 143025 Skolkovo, Moscow Region, Russia
ksetikhomirova@gmail.com

The study of domain walls (DW) have attracted great attention in recent few years due to both fundamental and applied interest. DW large resistance [1] and the opportunity to represent a logical unit [2], various manipulations with DW by the current and the external field is the basis phenomena for the most promising spintronics devices. Moreover, the materials with with perpendicular magnetic anisotropy (PMA) are growing interested. Magnetic tunnel junction with the perpendicular magnetic easy axis have the potential to implement in a non-volatile memory and logic devices with high thermal stability and low critical current value for the magnetization switching [3].

It was shown theoretically [4] and experimentally [5] that the CPP (current perpendicular to the plane) configuration can inject DW velocities up to two orders of magnitude larger then in the CIP configuration for equal current densities.

We studied nanostrip system containing the perpendicular magnetized domain wall. The size of nanostrip has been chosen $4000 \times X \times 3$ nm ($X=20:100$ nm). We numerically studied the domain wall (DW) stable states and displacement by spin current injection, we investigate that type of the DW (Bloch or Neel) is stable for different stripe widths (Fig 1). We also show dependence of the DW dynamics on spin-torque configurations and Walker breakdown (Fig 2).

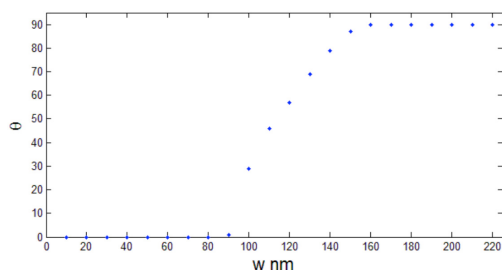


Fig. 1. DW magnetization angle for the stable (0-Neel type, 180-Bloch type)

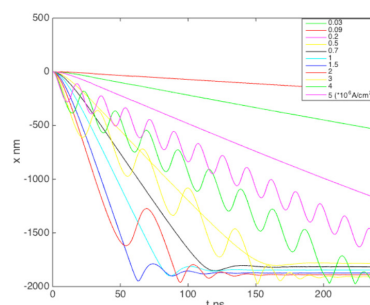


Fig. 2. DW displacement in the nanostrip for the different currents for z polirezer.

- [1] G. G. Cabrera and L. M. Falicov, *Phys. Status Solidi (b)*, **61** (1974) 539, **62** (1974) 217.
 [2] Allwood D.A. et al., *Science*, **309(5741)** (2005) 1688-1692.
 [3] S. Ikeda et al, *Nature Materials*, **9** (2010) 721–724.
 [4] Khvalkovskiy A.V. et al., *Physical review letters*, **102(6)** (2009) 067206.
 [5] A. Chanthbouala et al, *Nature Physics*, **7** (2011) 626–630.

2PO-I-13

PLASMONIC NANOANTENNAS FOR OPTICAL GENERATION OF THE SPIN WAVES IN MAGNETIC DIELECTRIC FILMS

Sylgacheva D.A.^{1,2}, *Kozhaev M.A.*^{2,3}, *Chernov A.I.*^{2,3}, *Kalish A.N.*^{1,2}, *Belotelov V.I.*^{1,2}

¹ Faculty of Physics, M.V. Lomonosov Moscow State University, Moscow, Russia

² Russian Quantum Center, Skolkovo, Moscow Region, Russia

³ Prokhorov General Physics Institute RAS, Moscow, Russia

sylgacheva.darjja@physics.msu.ru

Surface plasmon polaritons provide subdiffraction-limiting localization of light and amplification of electromagnetic fields. Due to this, plasmonics has a huge potential for the development and improvement of the technologies such as solar cells, light generation, microscopy and biosensors. Magnetoplasmonics combines plasmonic and magnetic functionalities and offers unique possibilities for light controlling by magnetic fields. Important research directions in magnetoplasmonics are the enhancement of magneto-optical effects in plasmonic nanostructures, the magnetic fields influence on surface plasmon resonance and its observation in ferromagnets. The interaction between plasmons at the metal / magnetic dielectric interface and electron spins in a ferromagnet is promising part of magnetoplasmonics. However, the integration of plasmonics and spintronics is yet to be realized.

In order to excite coherent spin waves, as a rule, the magnetic field of microwave radiation generated using an antenna in the immediate vicinity of the sample is used [1], but, in a number of important applications it is required to excite spin waves locally and it becomes necessary to create definite distributions of the spin density in space and in time. This can be achieved by means of optical generation of the spin waves in magnetic dielectric films [2] that are coated with plasmonic nanoantennas. The plasmonic nanostructures considered in this work are gratings of slits or holes in gold-layer or Au-nanoparticles deposited on a magnetic dielectric (rare-earth bismuth iron garnet). The parameters of plasmonic structures that are optimal for the effective excitation of magnetostatic spin waves with given parameters are found using rigorous coupled-wave approximation. In small metal particles (nanoparticles) there is manifested a localized surface plasmon. A sufficiently small particle size (particle diameter (~100 nm) less than wavelength of incoming electromagnetic radiation (~500-800 nm)) allows us to consider it as an oscillating dipole. The energy of electromagnetic radiation localized under a nanoparticle is transferred to magnons [3], which leads to increase of inverse Faraday effect as compared to a stand-alone magnetic film of the same thickness and composition. Local excitation of spin waves due to irradiation of plasmonic nanoantennas by femtosecond laser pulses is a very promising direction for developing devices that store and read information and address qubits in quantum technologies.

The work was supported by the Russian Presidential Grant MD-1615.2017.2.

[1] V.E. Demidov et al., *Appl. Phys. Lett.*, **95** (2009) 112509.

[2] C.D. Stanciu et al., *Phys. Rev. Lett.*, **99(4)** (2007) 047601.

[3] K. Uchida et al., *Nature Com.*, **6(5910)** (2015).

2PO-I-14

ZERO-BIAS MAGNETIC FIELD SPIN-TORQUE DIODE FREQUENCY TUNING BY EXCHANGE ANISOTROPY PINNING

Khudorozhkov A.A.^{1,2}, Skirdkov P.N.^{1,2,3}, Zvezdin K.A.^{1,2,3}, Popkov A.F.⁴, Zvezdin A.K.^{1,2,3}

¹ Moscow Institute of Physics and Technology (MIPT), Dolgoprudny, Moscow Region, Russia

² Russian Quantum Center (RQC), Skolkovo, Moscow, Russia

³ A.M. Prokhorov General Physics Institute, Moscow, Russia

⁴ National Research University of Electronic Technology (MIET), Zelenograd, Moscow, Russia
khudorozhkov@phystech.edu

For some applications it is desirable to increase the frequency of the microwave signal. The resonance conditions of the spin-diode are actually determined by the easy-axis and easy-plane anisotropies of magnetostatic origin in the free layer. In our work we consider the possibility of controlling the frequency and the resonant characteristics of the spin-torque diode by the exchange pinning. We propose a magnetic tunneling junction (MTJ) spin-diode structure with both ferromagnetic layers pinned by antiferromagnets with different Neel temperature. To investigate the rectification we have performed a series of simulations using our micromagnetic finite-difference code.

The simulation has been performed for different angles between tilted magnetizations in free and

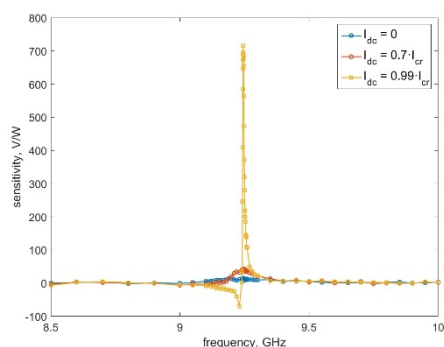


Fig. 1. The dependence of sensitivity on the frequency for different DC bias currents (with the angle between magnetizations equals to 120°)

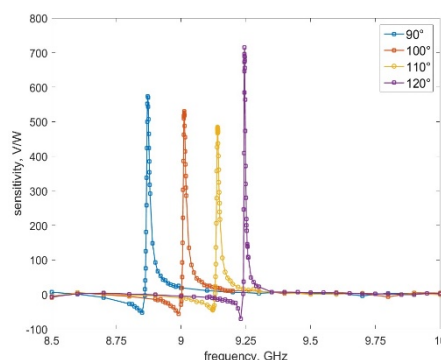


Fig. 2. The dependence of sensitivity on the frequency for different angles between magnetizations (with DC bias current equals to $0.99I_{cr}$)

fixed FM layers. For each option the critical bias current has been found. It has been demonstrated that the maximum sensitivity in such structure is reached at the bias current densities slightly below the critical one (Fig.1). Due to the high values of the exchange pinning fields, the resonance operating frequency of such dual exchange-pinned spin-diode can be significantly higher (up to 10 GHz) than the one of a traditional free layer spin-torque diode. Moreover, the resonance frequency can be tuned by changing the angle between tilted magnetizations in free and fixed ferromagnetic layers (Fig.2).

Our results can be used for the engineering of the MTJ spin-torque diode aiming at maximum sensitivity and the resonance frequency in the range up to 10 GHz and above at zero-bias magnetic field for development of new radiofrequency detectors in a broader frequency range than previous decisions.

The grant RSF No.16-19-00181 is acknowledged.

2PO-I-15

SPIN-TORQUE DIODE SENSITIVITY IN MAGNETIC NANOWIRE WITH A MAGNETIC TUNNEL JUNCTION

Demin G.D.^{1,2}

¹ Moscow Institute of Physics and Technology (MIPT), Moscow region, Dolgoprudny, Russia

² National Research University of Electronic Technology (MIET), Moscow, Russia
gddemin@gmail.com

Nowadays much attention in the field of spintronics is paid to the consideration of so-called spin-torque diodes based on magnetic tunnel junctions (MTJ). Microwave alternating current in such structures generates dc voltage appeared at the resonant frequency of spin oscillations which are induced by the spin-transfer torque effect in the free magnetic layer [1]. The effect of rectification of the microwave signal by the MTJ makes it possible to use it as a highly sensitive microwave detector [2]. In a number of studies it has been shown that in the presence of a bias current, the sensitivity of the spin diode can exceed the sensitivity of a Schottky diode by an order of value [3,4], which makes this detector attractive for practical applications in the microwave vision techniques, for example [5]. On the other hand, the critical value of the current density, in the vicinity of which there is a sharp increase in the sensitivity of the spin diode, is very large and this creates the problem to use MTJ biased by the critical current in practice. In this connection, an alternative way of increasing the sensitivity of a spin diode is of interest by reducing lateral dimensions of the magnetic tunnel structure. In this work we performed an analysis of the microwave sensitivity of the magnetic nanowire with a magnetic tunnel junction as a spin-torque diode depending on the external magnetic field, bias current and the radius of its cross section. We consider also possible effects of quantization of the magnetoresistance and spin torque transfer in the nanowire. Calculations show that a decrease to nm lateral sizes makes it possible to obtain an increase in the microwave sensitivity in the absence of a bias magnetic field and a direct bias current of the spin diode by more than two order of value. The results obtained can be useful for future development of high-sensitivity microwave detectors for microwave imaging and other practical applications.

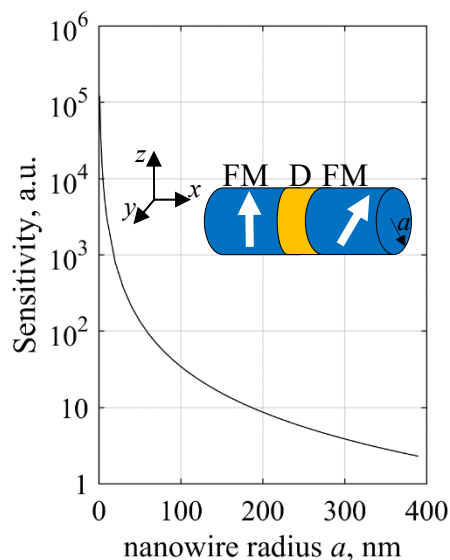


Fig. 1. The microwave sensitivity of a magnetic nanowire vs. its radius.

The work was supported by the Russian Science Foundation (project № 16-19-00181).

[1] S. Miwa et.al., *Nature Materials*, **13** (2014) 50-56.

[2] X. Li, Y. Zhou, P.W.T. Pong, *Journal of Nanotechnology*, **8347280** (2016) 1-11.

[3] S. Miwa et.al., *Nature Communications*, **7** (2016) 11259.

[4] A.F. Popkov, N.E. Kulagin, G.D. Demin, *Solid State Communications*, **248** (2016) 140-143.

[5]] L. Fu, Y. S. Gui, L. H. Bai, H. Guo, H. Abou-Rachid, and C.-M. Hu, *J. Appl. Phys.*, **117** 213902 (2015).

2PO-I-16

MODELING OF MAGNETIC LABEL FIELD SENSING BY GMR STRUCTURE

Bukunov K.A.^{1,2}, Babaizev G.V.^{1,2}, Chechenin N.G.^{1,2}

¹ Skobeltsyn Institute of Nuclear Physics, Lomonosov Moscow State University, Leninskie gory, 1/2, 119991 Moscow, Russia

² Faculty of Physics, Lomonosov Moscow State University, Leninskie Gory, 1/2, 119991 Moscow, Russia

For precise positioning and displacement sensing, using spin valves (SVs), a reliable method of modeling of interaction of the magnetic field, produced by reference labels, with the magnetic layers in the GMR structure, is highly important. In the report, our method of calculation of the space configuration of magnetic field produced by a reference magnetic stripe of different shape is presented. In general, the space components of the magnetic field vector $H(\mathbf{r}) = \{H_x, H_y, H_z\}$ can be written as a gradient of electromagnetic potential ϕ :

$$H_{xi}(x, y, z) = -\frac{\partial \phi(x, y, z)}{\partial xi}, \quad (1)$$

where $xi = \{x, y, z\}$. Using the Ostrogradky-Gauss theorem and taking into account the source of magnetic field is localized within the stripe-label we get

$$\phi(\vec{r}) = -\frac{1}{4\pi} \iiint_{\Omega} (\vec{M}(\vec{r}') \cdot \vec{\nabla}' \frac{1}{|\vec{r} - \vec{r}'|}) dV', \quad (2)$$

where \vec{M} is a local magnetic moment within the label. For the magnetic stripe with magnetic moment M_0 and thickness t , width w and length l , we obtain for the potential at any point (x, y, z) :

$$\phi(x, y, z) = \frac{M_0}{4\pi} \int_{-0.5t}^{0.5t} dx' \int_{-0.5w}^{0.5w} dy' \left(\frac{1}{\sqrt{(x-x')^2 + (y-y')^2 + (z-0.5t)^2}} - \frac{1}{\sqrt{(x-x')^2 + (y-y')^2 + (z+0.5t)^2}} \right) \quad (3)$$

The magnetic field space distribution is used to estimate the effect of the field on the magnetoresistance of the SV structure displaced by a certain distance x_0 from the magnetic stripe. The efficiency of the magnetoresistive sensing effect of the GMR SV structure strongly depends not only from the strength of magnetic field exerted. In a simple approximation, the magnetic field applied at 90° to the uniaxial anisotropy direction in the of the free layer in the SV structure rotates the magnetic moment by the angle

$$\varphi = \arccos(MFHF/2Ku), \quad (4)$$

where MF and HF are magnetic moment and magnetic field acting in the free layer of SV structure. The magnetoresistance of the SV in this case is determined from approximate relation

$$RGMR = RGMR_0(1 - \cos(\varphi))/2. \quad (5)$$

In the report the sensing efficiencies will be considered for a variety of the mutual positioning of the GMR sensor and magnetic label.

The work is supported by Russian Foundation for Basic Research (grant 16-32-50191)

2PO-I-17

EFFECT OF ANNEALING ON HYSTERESIS PROPERTIES AND CRYSTALLINE STRUCTURE OF $\text{Ni}_x\text{Mn}_{100-x}/\text{Fe}_{20}\text{Ni}_{80}$ THIN FILMS

Moskalev M.E.¹, Lepalovskij V.N.¹, Svalov A.V.¹, Larrañaga A.², Vas'kovskiy V.O.^{1,3}

¹ Ural Federal University, Ekaterinburg, Russia

² SGIker, Universidad del País Vasco (UPV/EHU), Bilbao, Spain

³ Institute of Metal Physics, UB RAS, Ekaterinburg, Russia

mikhail.moskalev@urfu.ru

The exchange bias effect, which can be observed in ferromagnet/antiferromagnet thin films, plays an important role in modern magnetic microelectronics. Its practical relevance induces an active search for antiferromagnets whose Néel temperatures significantly exceed room temperature. In this regard, Ni-Mn alloys are high-potential systems. However, to realize the potential of Ni-Mn we have to overcome a number of difficulties. These difficulties are associated with a possible existence of several modifications of sputtered Ni-Mn films [1]. Although several researches have been done, no agreement on annealing parameters and phase transition mechanisms in sputtered Ni-Mn based films has been achieved. To address this ambiguity, we have systematically studied magnetic properties and the crystalline structure of $\text{Ni}_x\text{Mn}_{100-x}/\text{Fe}_{20}\text{Ni}_{80}$ thin films before and after various annealing.

Ta(5 nm)/ $\text{Ni}_x\text{Mn}_{100-x}$ (20 nm)/ $\text{Fe}_{20}\text{Ni}_{80}$ (40 nm)/Ta(5 nm) thin films were deposited on glass substrates by magnetron sputtering in a uniform magnetic field. Ni concentration x was varied from 15 to 75 at.%. The specimens were annealed at various temperatures $T_a=200\div 400$ °C, the time of procedures t was also varied. The values of coercivity H_c and bias field H_{ex} were obtained by means of magneto-optical Kerr effect and a vibrating sample magnetometer. The study of the crystalline structure was performed using X-ray diffraction (XRD) with $\text{CuK}\alpha$ radiation.

Annealing of the specimens has led to a notable change in both H_{ex} and H_c (Fig. 1. (a)). This indicates that a phase transition has occurred in the Ni-Mn layer. The results of X-ray analysis have also confirmed this statement (Fig. 1. (b)).

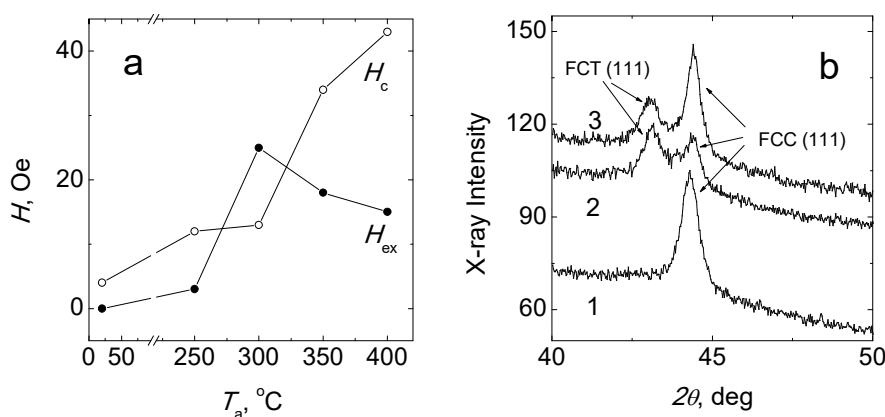


Fig. 1. H_{ex} and H_c dependence on T_a (a) and XRD diffraction spectra (b) for the Ta/ $\text{Ni}_{30}\text{Mn}_{70}$ / $\text{Fe}_{20}\text{Ni}_{80}$ /Ta films: as-deposited (1), annealed at $T_a=300$ °C (2), annealed at $T_a=400$ °C ($t=1$ h). This work was supported by Ministry of Education and Science of the Russian Federation, project No. RFMEFI57815X0125.

[1] M. Huang, P.F. Ladwig, Y.A. Chang, *Thin Solid Films*, **478** (2005) 137-140.

2PO-I-18

SIMULATION OF COUPLED DYNAMICS AND SWITCHING OF THE POLARITY OF VORTICES IN NANOCOLUMNAR CONDUCTING TRIPLEX STRUCTURE

Stepanov S.V.¹, Ekomasov A.E.¹, Zvezdin K.A.², Ekomasov E.G.¹

¹ Bashkir State University, Z. Validy 32, 450076, Ufa, Russia

² General Physics Institute A.M. Prokhorov RAS, Vavilov Str., 38, 119991, Moscow, Russia

The researchers demonstrate great interest in permalloy nanopillars that have two magnetic layers separated by a nonmagnetic interlayer. The magnetic vortex can be realized in them as a basic state. There are many experimental and theoretical papers devoted to the study of the magnetostatically bound magnetic vortices dynamics. For example, the dependence of the magnetic field size, switching all vortices polarities, on the polarized current magnitude for nanodisks of different diameters was experimentally found [1]. It is shown that for a system of two interacting magnetic disks in the vortex state, the magnetic vortices oscillation spectrum can change fundamentally [2]. In this paper, we theoretically investigate the influence of the perpendicular magnetic field, size and degree of current polarization on the bound vortices dynamics in nanodisks.

Considered a nanopillar of circular cross-section with a diameter of 400, 200 and 120 nm. It contains three layers: thick magnetic layer of permalloy (15 nm), an intermediate magnetic layer (10 nm) and a thin magnetic layer of permalloy (4 nm). With the help of SpinPM software package the presence of the current three critical values, separating different vortices motion modes, was found. The possibility of controlling the vortices stationary motion frequency value with an external magnetic field was shown. Using the equation of Thiele for each of the layers the vortices bound dynamics is analytically described. The analytical results comply with the numerically obtained results. Different from the case of medium and large diameter disks, the dynamics of the coupled magnetic vortices is observed in nanostructures of small diameter - 120 nm. It is shown that C-state vortex structures exist (the vortex is partially "squeezed" out of the disk). A steady-state dynamics of bound vortices in the C-state was observed.

By using micromagnetic simulation, the dependence of the magnetic field size, switching the vortex core polarity in thin and thick layers, on current is found. For each field and current value, we calculated the vortex dynamics of the nanopillar. For the case of low currents, the vortex polarity switch in thin and thick layers was observed with a low exit of the vortex from the geometric center. Thus the vortex polarity switching mechanism is similar to «static», but with an excitation of vortex oscillations internal modes and spin waves radiation. For the case of high currents, the «dynamic» mechanism for the vortex core polarity switching¹ was observed only for a vortex in a thick layer.

This study was supported by RFBR, project 16-32-00381.

[1] Locatelli N., Ekomasov A.E., Khvalkovskiy A.V. et. al., *Appl. Phys. Lett.*, **102** (2013) 062401.

[2] Locatelli N., Lebrun R., Naletov V.V. et. al., *IEEE Transactions on Magnetics*, **51(8)** (2015) 4300206.

2PO-I-19

NEW DATA AND DEVELOPING THE IDEAS ABOUT PHYSICAL NATURE OF THE MAGNETIC ORDERING MANIFESTATIONS IN THE HALL EFFECT AND MAGNETORESISTANCE ANOMALIES IN IRON-VANADIUM-ALUMINUM ALLOYS NEAR STOICHIOMETRIC COMPOSITION

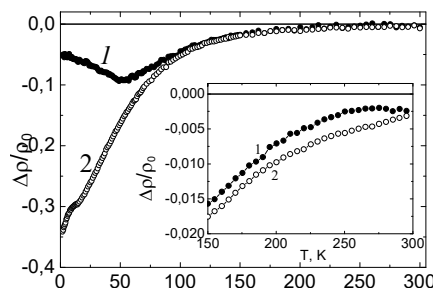
Lonchakov A.T.¹, Marchenkov V.V.^{1,2}, Okulov V.I.^{1,2}, Podgornykh S.M.^{1,2}, Usik A.Yu.¹, Bobin S.B.¹, Deryushkin V.V.¹, Govorkova T.E.¹, Okulova K.A.¹

¹M.N. Miheev Institute of Metal Physics of Ural Branch of RAS 620990 Ekaterinburg, Russia

²Ural Federal State University, 620002, Ekaterinburg, Russia
okulov@imp.uran.ru

Many studies of electronic and magnetic properties of iron-vanadium-aluminum alloys with the compositions near stoichiometric one (Fe_2VAl) have given rise to revealing the unique effects lying, as a rule, in principal change of basic physical parameters and specific behaviors of their variations at small, in essence, modifications of any component content. Work [1] has initiated the study of such effects. The main task of our researches was to make manifest specific features of electron structure, giving rise to the observed anomalies, using the specimens in equilibrium state. One of most interesting late results concerning specific behaviors of magnetic ordering of the alloys enriched with iron has been revealing strong influence of aluminum content on the magnitude and character of manifesting spontaneous magnetization in galvanomagnetic properties [2]. For developing these results with the view of studying the nature of an effect in the present work there has been fulfilled comparative analysis of magnetoresistance and anomalous Hall effect of Fe-V-Al alloys in changing the content near stoichiometric composition both for iron atoms and for aluminum atoms.

Experiments were performed on two alloy samples: sample 1, enriched with iron only (alloy $\text{Fe}_{2.1}\text{V}_{0.91}\text{Al}_{0.99}$) and sample 2, enriched with iron and aluminum (alloy $\text{Fe}_{2.05}\text{V}_{0.91}\text{Al}_{1.04}$). Figure shows the temperature dependence of transverse magnetoresistance, demonstrating considerable difference of negative magnetoresistance of the samples under study in low temperature range but at $T \geq 100\text{K}$ their values are almost coinciding, what is a new



effect of high temperature negative magnetoresistance (Insert). The Hall effect study has shown that additional doping the alloy with Al atoms leads to changing the anomalous contribution sign from negative (sample 1) to positive one (sample 2) above 10 K. Analyzing the correlations of anomalous contribution temperature dependences with transverse magnetoresistance value ρ_{xx} , we have revealed that at $T > 20\text{K}$ the sample 2 has the dependence on ρ_{xx} near linear but the sample 1 near quadratic one. According to the normal Hall resistance measurements the concentration of current carriers (holes) increases weakly in lowering the temperature and becomes constant at $T < 10\text{K}$. Hence the data obtained confirm the existence of sharply changing electron density of states and strong scattering of current carriers by magnetic inhomogeneities near stoichiometric composition of the alloy.

The work was performed as a part of the state task FASO Russia (subject "Electron», № 01201463326) with partial support by the RFBR (project №14-02-01238), Fundamental Research Program of UB RAS 2015-2017 (project № 15-17-2-32)

[1] Y. Nishino, M. Kato, S. Asano, K. Soda, M. Hayasaki, *Phys. Rev. Lett.*, **79** (1997) 1909.

[2] T. E. Govorkova, A. T. Lonchakov et al., *Techn. Phys. Lett.*, **42** (2016) 1122.

2PO-I-20

TUNNEL MAGNETORESISTIVE EFFECT IN NANOSTRUCTURED COMPOSITE SYSTEMS

Stognei O.V., Sitnikov A.V., Kalinin Yu.E.

Voronezh State Technical University, Voronezh, Russia

sto@sci.vrn.ru

An overview of the experimental data on the study of tunnel magnetoresistive effect (TMR) in different type of nanostructure systems (ferromagnetic-dielectric and ferromagnetic–semiconductor nanocomposites) has been made. All mentioned in the overview systems were prepared on the same equipment and obtained under similar conditions.

The influence of material of a ferromagnetic phase (CoFeB, CoNbTa and CoFeZr) on the magnetoresistance has been investigated in composites with amorphous metal granules. At the similar morphology of the composites and absent of a crystalline anisotropy in ferromagnetic granules the TMR values depends on the properties of metal phase. It has been established that maximum values of TMR and saturation magnetostriction of the metallic phase as well as maximum values of the Kerr effect are in composites, containing metal granules which have higher density of electron states at the Fermi level ($g(E_F)$). In studied systems it gives following sequence: CoNbTa \rightarrow CoFeB \rightarrow CoFeZr (fig.1).

In a case of crystalline granules the positive magnetoresistive effect is added to usual negative TMR (see fig.2). The positive effect is observed in Co-Al₂O₃, Co-SiO₂, and Co-MgF₂ composites behind the percolating threshold and is due to complicated morphology of the composites: simultaneous co-existence of relatively large clusters and separated nanogranules having very different anisotropy. The positive magnetoresistance is not observed in every crystalline composite, for example it is not observed in Co-CaF₂ system. According to HRTEM this system has another morphology. One can suppose that the ratio between surface energy of metal and dielectric phases is responsible for morphology of the composites and as a consequence for presence or absence of the positive effect.

In a case of semiconductor matrix the composites also exhibit tunnel magnetoresistivity but the value of the effect is much smaller. Comparison of the TMR values of Fe-Nb₂O_n and Ni-Nb₂O_n composites with Fe-Al₂O_n and Ni-Al₂O_n gives the conclusion: magnetoresistance in composites with semiconductor matrix is one order smaller than in composites with dielectric matrix. On the other hand the current mechanisms in composites with different type matrix are the same: tunneling of electrons between granules and tunneling of electrons via localized states.

The work has been partly supported by the Ministry of Education and Science within project part of the state task (project № 3.1867.2017/ПЧ) and RFBR grant № 15-02-05920_a

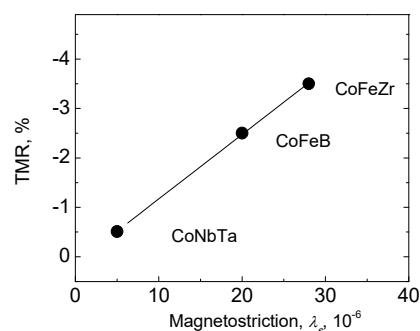


Fig.1. Maximum values of TMR of composites vs maximum values of magnetostriction of the metal phase.

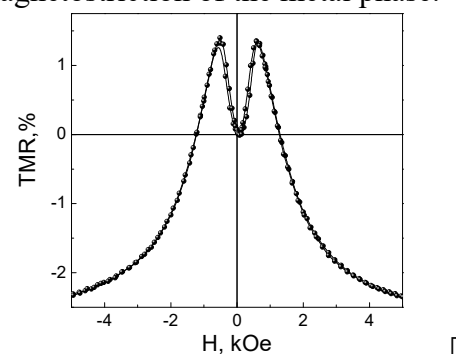


Fig. 2. Example of positive tunnel magnetoresistance observed in Co₆₀(Al₂O₃)₄₀ nanocomposites.

2PO-I-21

NON-UNIFORM FREE LAYER IN PMTJ STACK: IMPACT ON MAGNETIC ANISOTROPY AND STT SWITCHING

Timopheev A.A.¹, Teixeira B.M.S.², Sousa R.C.¹, Auffret S.¹, Nguen T.N.¹, Buda-Prejbeanu L.¹, Chshiev M.¹, Sobolev N.A.^{2,3}, Dieny B.¹

¹ Univ. Grenoble Alpes / INAC-SPINTEC, CEA /CNRS, F-38000 Grenoble, France

² Physics Department & i3N, University of Aveiro, 3810-193 Aveiro, Portugal

³ National University of Science and Technology “MISiS”, 119049 Moscow, Russia
sobolev@ua.pt

Magneto-resistive and magnetoresonance measurements, carried out on patterned perpendicular magnetic tunnel junction (pMTJ) pillars and full-sheet films, reveal magnetic non-uniformity of the Ta/FeCoB/MgO-based free layer. At low FeCoB thicknesses, the magnetic nonuniformity decreases the thermal stability of the free layer due to a granularization of the latter, while for larger thicknesses, when a solidification of the layer occurs, it results in the emergence and further increase of the second-order magnetic anisotropy term ($\sim K_{2\text{eff}} \cos^4\theta$) eventually yielding an easy-cone anisotropy. We show that the static and dynamic magnetic properties of such a free layer can be successfully described by a granular model with three thickness-dependent parameters: mean perpendicular anisotropy of the grains, grain-to-grain anisotropy distribution, and intergrain exchange strength. On the one hand, the easy-cone anisotropy may help to reduce the stochasticity of the spin-transfer torque switching. On the other hand, it appears for intermediate values of the intergrain exchange coupling, for which the multi-macrospin modelling shows that the spin-transfer torque (STT) switching efficiency is degraded. This occurs due to the excitation of exchange modes contributing weakly to the STT switching process while dissipating part of the STT energy.

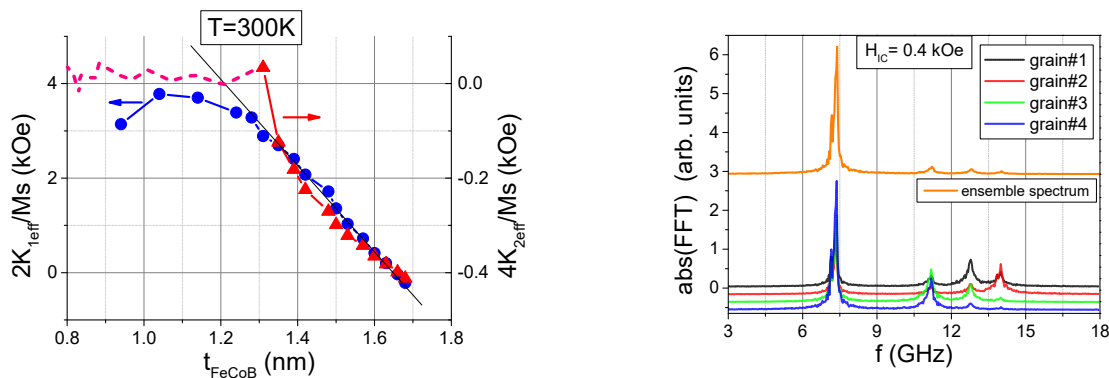


Fig. Left panel: Thickness dependence of the $K_{1\text{eff}}$, $K_{2\text{eff}}$ constants extracted from the angular dependences of ferromagnetic resonance (FMR) field. Right panel: Modeling of four exchange-coupled grains. FFT spectrum of thermally excited FMR in each grain (black, red, green and blue lines) and respective FFT spectrum of the whole ensemble (orange line). Excitation of the exchange modes is observed.

The work was partially supported by Samsung Global MRAM Innovation program, CEA-EUROTALENTS fellowship (A.T.), ERC Adv. grant MAGICAL no 669204, French National Research Agency (ANR) under project EXCALYB. N.A.S. and B.M.S.T. acknowledge financial support of the FCT of Portugal through the project I3N/ FSCOSD (Ref. FCT UID / CTM / 50025 / 2013) and the bursary PD / BD / 113944 / 2015.

[1] A.A. Timopheev, B.M.S. Teixeira, R.C. Sousa et al., *Phys. Rev. B* (submitted).

2PO-I-22

EFFECT OF INTERFACE STATE ON MAGNETORESISTIVE PROPERTIES OF Co/Cu-BASED SUPERLATTICES

Chuprakov S.A.¹, Blinov I.V., Krinitsina T.P., Milyaev M.A., Popov V.V.

M.N. Miheev Institute of Metal Physics, Ekaterinburg, Russian Federation

chuprakov@imp.uran.ru

The state of interlayer boundaries (interfaces) significantly influences the effect of giant magnetoresistance (GMR) of Co/Cu superlattices. To reveal the effect of the state of interfaces on the GMR we have studied the structure of interfaces in Glass//Fe(5nm)/[Co(1.5nm)/Cu(0.9nm)]₁₀/Cr(2nm) samples grown by the DC magnetron sputtering. The interlayer structure was varied by annealing of initially grown samples at different temperatures of 150, 200 and 300°C.

The samples have been studied by the methods of nuclear magnetic resonance (NMR) and X-ray reflectometry. The magnetoresistance properties have been studied as well.

According to the NMR data, the fraction of Co atoms involved in interface formation increases with the increasing annealing temperature (Fig. 1). In other words, the interlayer boundaries get wider and are “smeared”.

The results of the X-ray reflectometry revealed increasing of root mean square roughness (RMS) with the increasing annealing temperature from 0.42 nm to 0.75 nm.

The study of magnetoresistance properties show significant decreasing of GMR with the increasing annealing temperature (Fig. 2): $\Delta R/R_s(20^\circ\text{C}) = 33.87\%$, $\Delta R/R_s(300^\circ\text{C}) = 14.95\%$. This result correlates with the NMR data and X-ray reflectometry which demonstrate interface “smearing” and increasing roughness of interlayer boundaries.

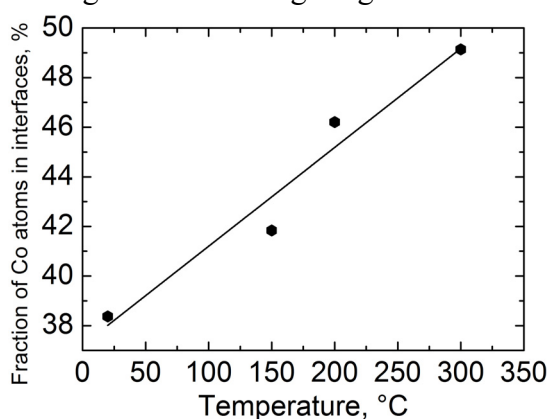


Fig. 1. The fraction of Co atoms involved in interface formation versus the annealing temperature.

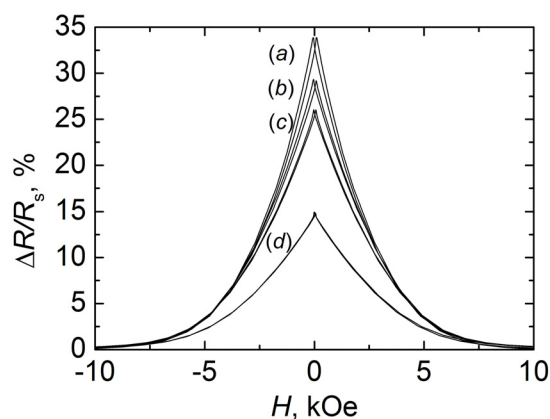


Fig. 2. Dependence of GMR of Glass//Fe(5nm)/[Co(1.5nm)/Cu(0.9nm)]₁₀/Cr(2nm) on temperature: without annealing (a) and annealed at 150°C (b), 200°C (c) and 300°C (d)

The research has been done within the IMP state assignment “Spin”, with partial support by UB RAS (project No. 15-9-2-44) and RFBR (project No. 16-32-00128).

2PO-I1-1

TUNNEL MAGNETORESISTANCE IN HETEROGENEOUS PLANAR SINGLE-BARRIER MAGNETIC TUNNEL JUNCTIONS

Petukhov D.A., Useinov N.Kh.

Kazan Federal University, Kazan, Russia

dapetukhov@mail.ru

Currently, layered magnetic nanostructures FM/I (ferromagnet/insulator) is one of the most exciting and rapidly developing areas of spintronics. Effects of tunneling magnetoresistance and magnetization switching in such structures are used in magnetic field sensors, nonvolatile magnetoresistive memory (MRAM, ST-MRAM), resonant tunneling diodes, spin transistors [1, 2]. In this report, we investigate theoretically the heterogeneous single-barrier magnetic nanostructures $FM^L/I/FM^R$. They consist of two ferromagnetic layers separated by dielectric layer. As the ferromagnetic layers material, Fe, Co, Ni and their alloys (CoFeB, FeNi) are considered. Insulating layers are usually AlO_x or MgO. Magnetization of one of the outer sheets (FM^L , FM^R) are pinned by the exchange bias effect. Magnetization of the other layer can be changed by an external magnetic field.

Here we report on results of investigation of the spin-dependent transport and tunnel magnetoresistance in heterogeneous (asymmetric, $FM^L \neq FM^R$) single-barrier magnetic tunnel junctions. We use free electron model and two parabolic subbands approximation for the conduction band of ferromagnetic layers. Our model of the junction takes into account different effective electron masses in the ferromagnetic metals conduction subbands and the barrier as well, arbitrary widths of the spin-subbands and the barrier heights at the FM-I interface. In every FM layer, we set the orientation of the magnetization with two spherical angles θ , φ . Spin of the electron is conserved during tunneling through the junction.

Analysis of the electron tunneling is based on the model of spin-conduction channels. Current calculation is performed using the quasiclassical theory. The ferromagnetic layers are discussed in the framework of two-band model. Transmission coefficients of the structure are calculated quantum-mechanically in the effective-mass approximation for the conduction electrons. The present model is a modification of the model described in [3] for the case of arbitrary directions of layers magnetizations. This study was partly supported by the Program of the competitive growth of Kazan Federal University.

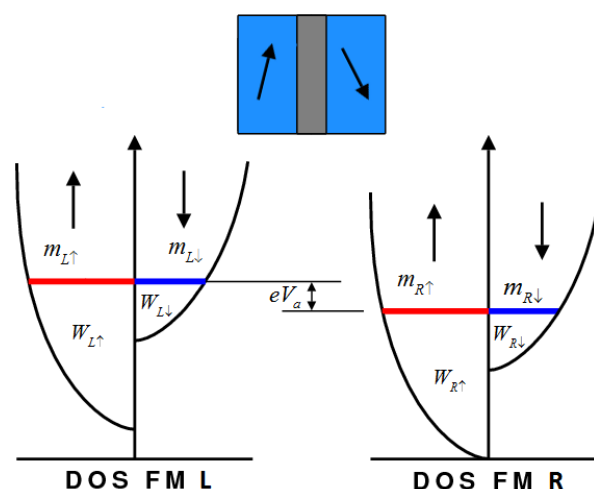


Fig. 1. Schematical view of heterogeneous single-barrier magnetic tunnel junction.

[1] A. Fert, *Thin Solid Films*, **517** (2008) 2-5.

[2] S. Ikeda *et al.*, *IEEE Trans. Electron Devices*, **54** (2007) 991–1002.

[3] D.A. Petukhov, *Physica E*, **80** (2016) 31-35.

2PO-I1-2

MAGNETIC INTERACTION AT THE INTERFACE OF EPITAXIAL MANGANITE FILM AND INTERMETALLIC SUPERLATTICE

Grishin A.S.^{1,2}, *Ovsyannikov G.A.*¹, *Klimov A.A.*^{1,2}, *Demidov V.V.*¹, *Constantinian K.Y.*¹,
*Borisenko I.V.*¹, *Preobrazhensky V.L.*^{3,4}, *Tiercelin N.*⁴, *Pernod P.*⁴

¹ Kotel'nikov Institute of Radio Engineering and Electronics, Russian Academy of Sciences, Moscow, 125009, Russia

² Moscow Technological University, MIREA, Moscow, 119571, Russia

³ The Wave Research Center of Prokhorov General Physics Institute, Moscow, 119991 Russia

⁴ University of Lille, CNRS, Centrale Lille, UMR 8520, IEMN, F-59000 Lille, France
alex1995@hitech.cplire.ru

Hybrid magnetic heterostructures made of epitaxial manganite $\text{La}_{0.7}\text{Sr}_{0.3}\text{MnO}_3$ thin film and intermetallic superlattice $(\text{TeCo}_2/\text{FeCo})_n$ were prepared on orthorhombic NdGaO_3 substrates. It was characterized by means of magneto-optical Kerr effect, magnetoresistance and ferromagnetic resonance.

Fig. 1 shows magnetization hysteresis curves having same two steps that correspond to switch of LSMO/TCFC layers, which represents the soft and hard magnetic layers here, as well as the magnetization directions obtained for the characteristic values of the external field.

From the magnetization distributions that was discussed in [1] it is seen that the switching process proceeds more uniformly in the hard magnetic layer than in the soft one. In the former case, the magnetization undergoes a discontinuous change with its distribution being relatively uniform before the switching. In contrast, the soft magnetic layer is switched very nonuniformly; nonuniformities expand gradually, moving from the edges of the layer to its center. This distinction manifests itself in the fact that on the magnetization curve, the first step is smooth, whereas the second is sharp.

Experimental data show that the features observed in magnetotransport characteristics are caused by the process of magnetization reversal at interface between manganite thin film and intermetallic superlattice [2,3]. Magnetic interaction between $\text{La}_{0.7}\text{Sr}_{0.3}\text{MnO}_3$ and $(\text{TeCo}_2/\text{FeCo})_n$ has antiferromagnetic type of magnetic ordering.

Support by International Associated Laboratory LEMAC-LICS, RFBR 17-02-00145, 16-29-14022 and Scientific school NSh -8168.2016.2 is acknowledged.

The work was performed in the framework of the International Associated Laboratory LEMAC-LICS

[1] K.A. Zvezdin, *J. Physics of the Solid State*, **1** (2000) 120-125.

[2] E. Quandt et al., *J. Appl. Phys.*, **83** (1998) 7267-7269.

[3] J.Q. Xiao, J.S. Jiang, and C.L. Chien, *Phys. Rev. Lett.*, **68** (1992) 3749-3752.

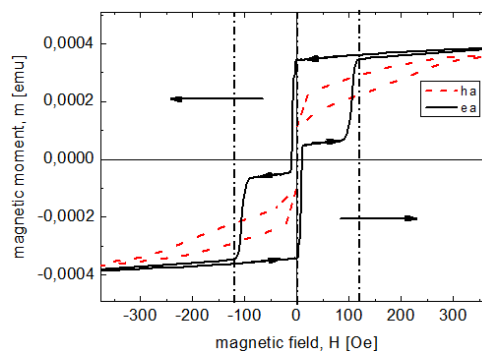


Fig. 1. The magnetization curves for LSMO/TCFC structure. “ha” means that external magnetic field was directed along hard axis, while “ea” means that external magnetic field was directed along easy axis.

2PO-I1-3

MAGNETICALLY INTERCALATED MULTILAYER SILICENE

*Tokmachev A.M.¹, Averyanov D.V.¹, Karateev I.A.¹, Parfenov O.E.¹, Kondratev O.A.¹,
Taldenkov A.N.¹, Storchak V.G.¹*

¹ National Research Center “Kurchatov Institute”, Moscow, Russia
tokm@rambler.ru

Silicene is thought to be a wonder material combining functionalities of graphene and silicon. Similar to graphene, it is expected to host massless Dirac fermions. The band gap in silicene can be tuned by electric fields and chemical functionalization. The recent demonstration of the first field-effect transistor with a silicene channel clearly reflects its potential in electronics. Exotic properties, such as quantum spin Hall effect, quantum anomalous Hall effect, valley polarized quantum Hall effect, chiral superconductivity, are expected as elements of prolific silicene physics. Being coupled with magnetism, it is predicted to be particularly suitable for spintronic applications. However, experimental realization of free-standing silicene and its magnetic derivatives is lacking. Fortunately, magnetism can be induced into silicene layers, in particular, by intercalation.

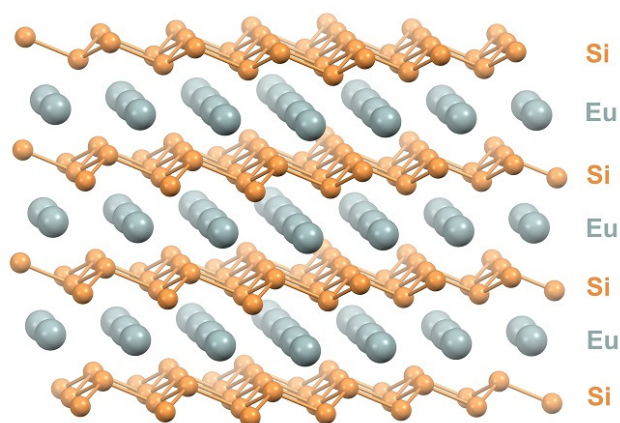


Fig.1. A ball-and-stick model for the atomic structure of Eu-intercalated multilayer silicene

Our aim is to make a system in which silicene sheets are in close proximity to open-shell metal ions – a silicene-based magnetic compound. The requirements of the metal to be inherently magnetic and active (to avoid hybridization) simultaneously leave us no choice but to use europium. We report a successful synthesis of multilayer silicene intercalated by Eu ions (Fig. 1) – a compound expected to exhibit both massless Dirac-cone states, as its Ca analogue, and a nontrivial magnetic structure.

This new polymorph with EuSi_2 stoichiometry is epitaxially stabilized by continual replication of silicene layers employing Sr-intercalated multilayer silicene [1] as a template. The atomic structure of the new compound and its sharp interface with the template are confirmed using electron diffraction, X-ray diffraction, and electron microscopy techniques. Below 80 K, the material demonstrates anisotropic antiferromagnetism coexisting with weak ferromagnetism. The magnetic state is accompanied by an anomalous behaviour of magnetoresistivity [2].

Partial financial support by NRC “Kurchatov Institute”, the Russian Foundation for Basic Research (grants 16-07-00204, 16-29-03027, and 17-07-00170), and the Russian Science Foundation (grant 14-19-00662) is gratefully acknowledged.

[1] A.M. Tokmachev, D.V. Averyanov, I.A. Karateev, O.E. Parfenov, A.L. Vasiliev, S.N. Yakunin, V.G. Storchak, *Nanoscale*, **8** (2016) 16229-16235.

[2] A.M. Tokmachev, D.V. Averyanov, I.A. Karateev, O.E. Parfenov, O.A. Kondratev, A.N. Taldenkov, V.G. Storchak, *Adv. Funct. Mater.*, **27** (2017) 1606603

2PO-I1-4

TRANSPORT PROPERTIES OF $R_x\text{La}_{1-x}\text{B}_6$ SOLID SOLUTIONS

*Anisimov M.A.*¹, *Bogach A.V.*¹, *Glushkov V.V.*^{1,2}, *Samarin N.A.*¹, *Voronov V.V.*¹, *Demishev S.V.*^{1,2},
*Levchenko A.V.*³, *Filipov V.B.*³, *Shitsevalova N.Yu.*³, *Sluchanko N.E.*^{1,2}

¹ Prokhorov General Physics Institute of RAS, Moscow, Russia

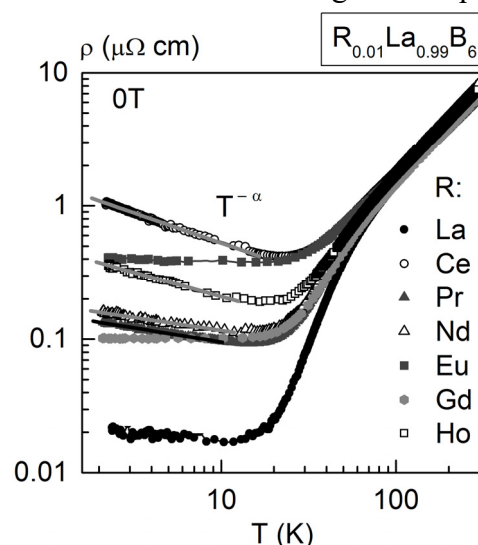
² Moscow Institute of Physics and Technology, Dolgoprudny, Russia

³ Frantsevich Institute for Problems of Materials Science, NASU, Kiev, Ukraine
anisimov.m.a@gmail.com

Unlike the concentrated magnetic hexaborides RB_6 ($\text{R}=\text{Ce}, \text{Pr}, \text{Nd}, \text{Eu}, \text{Gd}, \text{Ho}$) which properties are influenced by complicated interplay of various degrees of freedom the dilute systems $R_x\text{La}_{1-x}\text{B}_6$ ($x \leq 0.1$) are characterized by the reference diamagnetic LaB_6 . The main interest to the $R_x\text{La}_{1-x}\text{B}_6$ investigation attracts the compounds $\text{Ce}_x\text{La}_{1-x}\text{B}_6$, $\text{Nd}_x\text{La}_{1-x}\text{B}_6$ which are attributed as the systems with Kondo impurity [1, 2]. However the using of Kondo paradigm for $R_x\text{La}_{1-x}\text{B}_6$ systems is still the subject of discussion [3, 4]. Thus in order to investigate the influence of magnetic impurity it is of interest to study the whole set of $R_x\text{La}_{1-x}\text{B}_6$ with constant concentration of magnetic impurity $x=0.01$.

In current work we present the transport properties [resistivity and magnetoresistance (MR)] of $R_x\text{La}_{1-x}\text{B}_6$ substitutional solid solutions ($\text{R}=\text{La}, \text{Ce}, \text{Pr}, \text{Nd}, \text{Eu}, \text{Gd}, \text{Ho}$). High quality single crystals were grown by vertical crucible-free inductive floating zone melting in the argon gas atmosphere on a setup described in details in [4]. The EMPA test was used to estimate the real content of magnetic impurity ($x_r \approx 0.007 \div 0.012$). The measurements were performed by a standard four-probe method at temperatures 2–300K in magnetic fields up to 8T.

Taking into account a simple model [5] which treats R ions as independent harmonic (Einstein) oscillators embedded in a Debye framework of boron ions we separated correctly the resistivity contributions. The data obtained allow to estimate (i) the Debye-type term from rigid boron cages [$\Theta_D \approx 1160\text{K}$], (ii) the contribution from quasilocal vibrational mode of La^{3+} ions [$\Theta_E \approx 152 \div 155\text{K}$] and (iii) the residual and magnetic contributions. Indeed, the strong growth of resistivity was detected for compounds with $\text{R}=\text{Ce}, \text{Pr}, \text{Nd}, \text{Ho}$ at low temperatures $T < 20\text{K}$ (Fig.1). It was found that instead of logarithmic behavior $\rho(T) \sim -\ln T$, predicted by Kondo model, the magnetic contribution to resistivity obeys the power law $\sim T^{-\alpha}$, which corresponds to the regime of weak localization of charge carriers [6] with the critical exponent values $\alpha \approx 0.2$ (Pr, Nd), 0.39 (Ho) and 0.5 (Ce).



[1] K. Winzer, *Sol. St. Com.*, **16** (1975) 521.

[2] J. Stankiewicz, M. Evangelisti, Z. Fisk et al., *Phys. Rev. Lett.*, **108** (2012) 257201.

[3] N. Sluchanko et al., *JETP Lett.*, **101** (2015) 36.

[4] G. Friemel et al., *Nature Communications*, **3** (2012) 830.

[5] D. Mandrus et al., *Phys. Rev. B*, **64** (2001) 012302.

[6] W. McMillan, *Phys. Rev. B*, **24** (1981) 2739.

2PO-I1-5

ANALYSIS OF ELECTROMAGNETIC FIELDS GENERATED BY A SPIN-INJECTION THZ SPIN OSCILLATOR

Sherbakov V.A.¹, Shustov V.O.¹, Safin A.R.¹, Vilkov E.A.², Chigarev S.G.²

¹ National Research university "MPEI", Moscow, Russia

² Institute of Radio Engineering and Electronics, Fryazino, Russia
stalker-1994-@mail.ru

Mastering of terahertz waves has been of increased necessity in recent years. Their possible applications include astrophysics and physics of the atmosphere, biology and medicine, safety and search for prohibited materials, nondestructive testing of parameters, communication in space, information technologies, and ultrafast data processing (see, e.g. [1]). New approaches to the design of corresponding devices are sought. In this work, we study results obtained in the THz spin-injection oscillator for its potential application.

Let's consider the structure, which is shown on Fig.1, which consists of ferromagnetic thin-film (work layer) and ferromagnetic rod (polarizer). The feature of the shown magnetic junction is that the point contact is ensured by a thin rod, which is made of a hard ferromagnetic material (hardened steel in our case). Such an electrode is not only a "point" source of current but also an injector of spin-polarized electrons. As a result, it is sufficient to use only one ferromagnetic film. The films used in our experiments had a thickness of 5–10 nm. The diameter of the rod was about 10–50 μm . In this case, current densities above 108 A/cm² could be obtained in the film near the contact with the rod. Current releases heat in a small volume of the metal. Special sources of magnetic field are not required because the rod also serves as a permanent magnet. Such a structure was chosen as the base for experiments on the observation of the current induced generation of terahertz radiation. The electromagnetic fields generated by this spin-injection-based oscillator have been investigated in a specific structure under the macrospin approximation (see for ex. [2]). Particularly our study is focused on characterizing the electromagnetic fields in the near field and far field regimes. In the near field regime, when the distance is much less than the electromagnetic wavelength, the magnetic dipole field of the rotating thin-film layer magnetization is dominant. The E-field strength is detectable in a short distance for an oscillator with reasonable size. The estimate of the magnetic dipole field and the H-field implies alternative methods to detect the free layer magnetization dynamics besides the GMR and TMR signal output from the oscillator. In the far field regime, the E-field and H-field components radiate in the space. Their characteristics are similar to those from an oscillating electric dipole. However, the EM radiation appears to be very weak, considering the relatively small size of the oscillator compared with the electromagnetic wavelength.

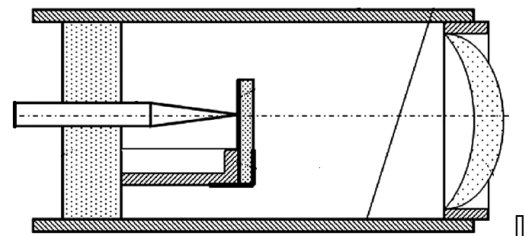


Fig. 1. The point contact spin-injection THz oscillator structure, which consists of ferromagnetic thin-film (work layer) and ferromagnetic rod (polarizer).

This work was supported by the state task of the Ministry of Education and Science of the Russian Federation No. 8.8109.2017/BCh.

- [1] Yu. Gulayev, P. Zilberman, G. Mikhailov, S. Chigarev, *JETP Letters*, **98** (2014) 742-752.
[2] N. Amin, H. Xi, M. Tang, *IEEE Trans. on Magn.*, **45** (2009) 4183-4186.

2PO-I1-6

THE INFLUENCE OF Na SUBSTITUTION ON SPIN-GLASS TO FERROMAGNETIC TRANSITION IN $\text{La}_{0.54}\text{Ho}_{0.11}\text{Ca}_{0.35-x}\text{Na}_x\text{Mn}_{1-y}\text{Cr}_y\text{O}_3$ MANGANITES

Craus M.-L.^{1,2}, Cornei N.³, Mita C.³, Dobrea V.², Erhan R.V.^{1,4}, Turchenko V.¹

¹ JINR, Dubna, Russia

² National Institute of Research and Development for Technical Physics, Iasi, Romania

³ “Al.I.Cuza” University, Iasi, Romania

⁴ Horia Hulubei National Institute for R&D in Physics and Nuclear Engineering

craus_ml@hotmail.com, kraus@nf.jinr.ru

The magnetoresistance of manganites is strongly influenced by the variation of electronic phases concentrations with temperature or with the applied magnetic field intensity. The presence of spin glass like phases besides the ferromagnetic phase could be induced by the local distortion of crystalline lattice and the change of the geometrical features of perovskites structure (ABO_3). Our aim is to determine the influence of Na substitution on A places and Cr substitution of B places in $\text{La}_{0.54}\text{Ho}_{0.11}\text{Ca}_{0.35}\text{MnO}_3$ (LHCMO) manganites.

The samples were synthesized by ceramic technology starting from corresponding mixture of rare earth oxides, calcium carbonate, sodium nitrate and Mn and Cr oxides. The resulted powders were ground and pressed into pellets and presintered at 800°C for 17 hours in air. The presintered samples were again ground and finally sintered at 1200°C for 10 hours in air atmosphere. The samples containing Na were finally sintered at 1100°C in air. Phase composition, structure, lattice constants and volume of the unit cell were determined by X-ray analysis (XRD) (see Fig.1) and neutron diffraction analysis (ND).

The XRD analysis indicate that $\text{La}_{0.54}\text{Ho}_{0.11}\text{Ca}_{0.35-x}\text{Na}_x\text{Mn}_{1-y}\text{Cr}_y\text{O}_3$ (LHCMO) manganites crystallize in SG 62 (Pnma). A small minimum of the unit cell volume was observed for the sample corresponding to $x=0.15$. The variation of magnetization with the temperature and the magnetic field intensity was determined with a Foner type magnetometer. At low temperature a transition from the ferromagnetic state to spin – glass state was observed for all the samples. The observed Curie temperature for the ferromagnetic phase varies in agreement with the Mn-O bond distances and Mn-O-Mn bond angles. The increase of Cr concentration in the samples lead to a decrease of molar magnetization, indicating that the Cr cations have no contribution to the magnetic moment of the samples.

The measurements of resistance in magnetic field were performed by 4-point probes method, on two installations at NIRDTP Iasi Romania and JINR Dubna Russia. The transition from the semiconductor/insulator state to metallic state takes places at temperature much lower that the transition from ferromagnetic to spin-glass state.

We obtained a model with explain the behaviour at low temperatures of magnetoresistance of LHCMO manganites substituted with Na and Cr.

Support by FLNP, JINR, Dubna, Russia and Ministry of Research and Innovation, Romania is acknowledged.

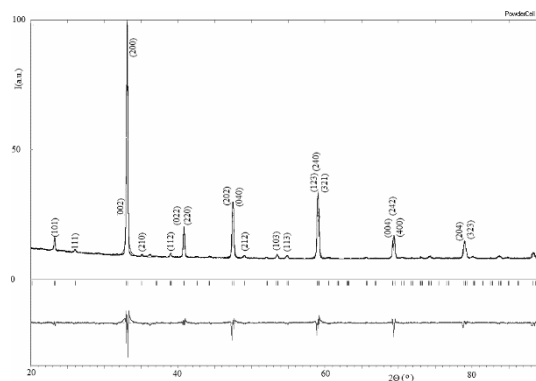


Fig. 1. Observed and calculated diffractograms of $\text{La}_{0.54}\text{Ho}_{0.11}\text{Ca}_{0.35}\text{Mn}_{0.95}\text{Cr}_{0.05}\text{O}_3$. Difference between observed and calculated diffractogram - bellow (PowderCell)

2PO-I1-7

SIZE EFFECT IN THE ELECTRONIC TRANSPORT OF THIN FILMS OF Bi_2Se_3 AND PtSn_4

Marchenkov V.V.^{1,2,3}, Chistyakov V.V.¹, Huang J.C.A.⁴, Naumov S.V.¹, Perevozchikova Y.A.¹,
Marchenkova E.B.¹, Eisterer M.⁵

¹ M.N. Mikheev Institute of Metal Physics, UB RAS, Ekaterinburg, Russia

² Ural Federal University, Ekaterinburg, Russia

³ International Laboratory of High Magnetic Fields and Low Temperatures, Wroclaw, Poland

⁴ National Cheng Kung University, Tainan, Taiwan

⁵ TU Wien Atominstut, Vienna, Austria

wchist@imp.uran.ru

Recently, the new quantum materials with the topologically nontrivial band structure arising due to a strong spin-orbit interaction have been theoretically predicted and discovered experimentally. First of all, they are the topological insulators (TI), whose volume is an insulator and the surface behaves as a topologically protected metal with a linear dispersion law [1], as well as recently discovered topological Weyl semimetals (TWS) with nontrivial charge transfer both in volume and on the surface of such materials [2, 3]. Quasiparticles in TWS are "massless" Weyl fermions with "zero" effective mass, which are also protected topologically. This means that such quasiparticles can be controlled much faster than by conventional charge carriers, and a probability of their scattering is sufficiently small. Therefore, TWS and TI can be used in ultra-fast electronics and spintronics.

Since the electroconductivity in a volume and near surface of such materials can differ substantially, it is of interest to try to "divide" them experimentally. For this, we can use the results of Ref. [4], where we studied the size effect in the conductivity of pure tungsten single crystals under conditions of static skin effect, i.e. a predominant flow of direct electric current near a sample surface. The aim of this paper is to search for and study the size effect in the electronic transport of thin films of TI Bi_2Se_3 and TWS PtSn_4 .

Thin films of Bi_2Se_3 and PtSn_4 were grown by the molecular beam epitaxy method on Al_2O_3 substrates with thickness from 10 to 100 nm. The measurements of the electroresistivity and the galvanomagnetic properties were carried out by the conventional 4-points method at dc-current in the temperature range from 4.2 to 300 K and in magnetic fields of up to 10 T.

It was shown that the size effect, i.e. a dependence of the kinetic coefficients (electro- and magnetoresistance, Hall Effect) on film thickness, is observed in thin films of TI Bi_2Se_3 and TWS PtSn_4 . This allows us to conclude that every of the kinetic coefficients consists two terms - volume contribution and surface one. The value of surface contribution exceeds the bulk one by several orders of magnitude. These results can be used for a "separation" and an estimation of magnitudes for surface and bulk conductivity in such materials.

This work was partly supported by the state assignment of FASO of Russia (theme "Spin" No. 01201463330), by the Scientific Program of UB RAS (project No. 15-17-2-12), by the RFBR (project Nos. 14-02-92012 and 17-52-52008), by the Government of the Russian Federation (state contract No. 02.A03.21.0006).

[1] H. Zhang et al., *Nature Physics*, **5** (2009) 438-442.

[2] S.Y. Xu et al., *Science*, **349** (2015) 613-617.

[3] Z.K. Liu et al., *Nature Materials*, **15** (2016) 27-31.

[4] V.V. Marchenkov et al., *Journal of Low Temperature Physics*, **132** (2003) 132-135.

2PO-I1-8

TWO-MAGNON SCATTERING PROCESSES AND RESISTIVITY OF A HALF-METALLIC FERROMAGNETIC HEUSLER ALLOY Co_2FeSi

Marchenkov V.V.^{1,2}, Irkhin V.Yu.¹, Perevozchikova Yu.A.¹, Kourov N.I.¹, Eisterer M.³

¹ IMP UB RAS, Ekaterinburg, Russia

² UrFU, Ekaterinburg, Russia

³ TU Wien Atominstitut, Vienna, Austria

yu.perevozchikova@imp.uran.ru

The increasing interest in the study of Heusler alloys is largely due to the possibility of their use in spintronics as half-metallic ferromagnets (HMF) [1] with high degree of spin polarization for charge carriers [2]. The main feature of HMF is the presence of a gap in their electronic spectrum at the Fermi level E_F for spin down carriers and its absence for spin up carriers. Depending on the specific conditions and features of the alloy (the size of the gap, the form of the electron spectrum, the Curie temperature T_C , the temperature range, etc.), the gap can manifest itself differently in the electrical resistivity. In the case where the contribution to the resistance and its temperature change is determined by transitions to spin-down states, the resistivity value ρ and the form of its temperature dependences $\rho(T)$ are mainly due to the "gap" features of the electron spectrum near E_F (see, for example, [3]). In the case of the predominant contribution to the resistivity from electron scattering in the spin up subband, two-magnon scattering processes can be important [1], leading to a characteristic dependence $\rho(T) \sim T^n$, $7/2 < n < 9/2$ and negative linear magnetoresistance $\Delta\rho_{xx} \sim H^1$. The Co_2FeSi Heusler alloy is a HMF with large $T_C = 1200$ K. Consequently, at room temperatures and lower, main contribution to the resistivity should be from the scattering of spin up charge carriers. The aim of this paper is to study the role of two-magnon scattering processes in the HMF Heusler alloy Co_2FeSi . To treat this issue, the resistivity and magnetoresistivity for polycrystalline samples were measured in the temperature range from 4.2 to 300 K and in magnetic fields up to 150 kOe.

As a result of the study, it was found that there are three temperature intervals where the resistance depends on temperature and magnetic field in different ways: (a) below 30 K. $\rho(T) \sim T^n$, where $n = 2$, and the magnetoresistance is $\Delta\rho_{xx} > 0$; (b) from 30 to 60 K. $\rho(T) \sim T^n$, where $n \approx 9/2$, and $\Delta\rho_{xx} \sim H^1$; (c) above 60 K. $\rho(T) \sim T^n$, where $n \approx 2$, and $\Delta\rho_{xx} < 0$. The experimental results obtained indicate that in the temperature range $30 \text{ K} < T < 60 \text{ K}$ a power-law temperature dependence of the electrical resistivity with the exponent $n \approx 9/2$ and a linear negative magnetoresistance takes place. This appears to be a manifestation of two-magnon scattering processes as the main mechanism for the scattering of current carriers, which determines the behavior of the resistivity and magnetoresistivity of the Co_2FeSi alloy at temperatures $30 \text{ K} < T < 60 \text{ K}$. At the same time, at higher temperatures one-magnon processes may be included.

This work was partly supported by the state assignment of FASO of Russia (theme "Spin" No. 01201463330), the Scientific Program of UB RAS (project No. 15-17-2-12), RFBR grant (No. 15-02-06686) and RFBR youth grant (No. 16-32-00072).

[1] V.Yu. Irkhin and M.I. Katsnelson, *Eur. Phys. J. B*, **30** (2002) 481.

[2] K. Inomata et al., *Sci. Tech. Adv. Mater.*, **9** (2008) 014101.

[3] N.I. Kourov, V.V. Marchenkov et.al., *J. Exp. Theor. Phys.*, **118** (2014) 426.

2PO-I1-9

OPTICAL PROPERTIES AND ELECTRONIC STRUCTURE OF Co_2TiGe AND Co_2TiSn HEUSLER ALLOYS

Shreder E.I.¹, Makhnev A.A.¹, Lukoyanov A.V.^{1,2}, Suresh K.G.³

¹ Institute of Metal Physics, Kovalevskaya Str. 18, Ekaterinburg 620990, Russia

² Ural Federal University, Mira Str. 19, Ekaterinburg 620002, Russia

³ Department of Physics, Indian Institute of Technology Bombay, Mumbai 400076, India
shreder@imp.uran.ru

The Co_2TiGe and Co_2TiSn Heusler alloys are ferromagnets with Curie temperature (T_C) 384 and 371 K respectively. The current spin polarization (P) value at 4.2 K of 0.63 and 0.64 were deduced for Co_2TiGe and Co_2TiSn respectively [1]. This indicates that the alloys are half-metallic ferromagnets (HMF) and appear to be promising for spintronic devices. Here, we present the results of investigation of optical properties of Co_2TiGe and Co_2TiSn by the ellipsometric Beattie technique in the spectrum range $\lambda = (0.3 - 13) \mu\text{m}$ at room temperature.

The main features of the optical absorption spectra (Fig. 1) are the high level of interband absorption and the absence of the Drude contribution in the whole investigated range, forming complex spectral dependence of $\sigma(\omega)$. The magnitude of the static conductivity at room temperature obtained from the measurements of the electrical resistivity is equal to $\sigma_{\text{cr}} = 22 \cdot 10^{14} \text{ s}^{-1}$ for Co_2TiGe and $19 \cdot 10^{14} \text{ s}^{-1}$ for Co_2TiSn . Therefore, the achievement of these values in the limit $\omega \rightarrow 0$ implies a further reduction of the optical conductivity. The effective concentrations of charge carriers was estimated from infrared data as $N_{\text{eff}} \sim 10^{21} \text{ cm}^{-3}$. As compared to normal metals, these values are lower by one–two orders of magnitude.

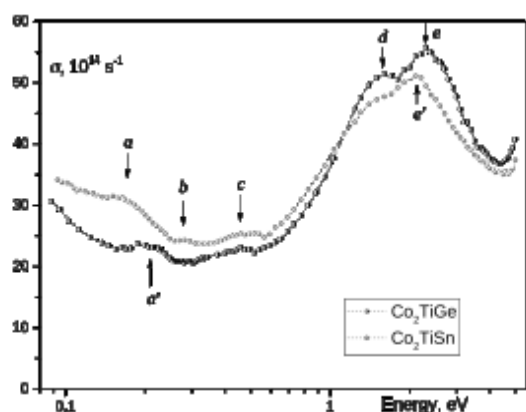


Fig. 1. Optical conductivity $\sigma(\omega)$ of alloys.

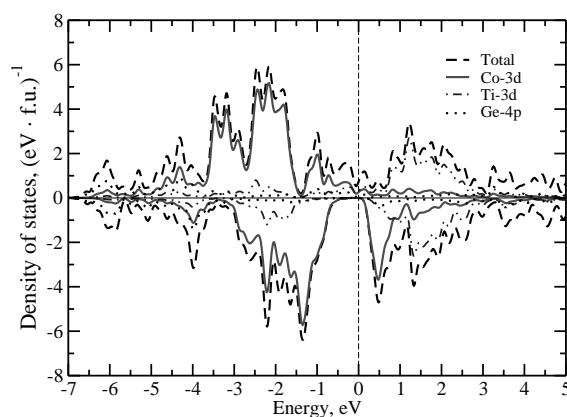


Fig. 2. Density of states $N(E)$ of Co_2TiGe .

To explain the results of the optical research polarization, we used the electronic structure of the calculations were performed employing an exchange approximation (GGA) form in the framework of the electronic structure (Fig. 2) is found to describe the

spin
. The
dient
lated

This work was partly supported by the RFBR (proc.

[1] L. Bainsla, K.G. Suresh. *Current Applied Physics*, **16** (2016) 68–72.

[2] P. Giannozzi, S. Baroni, et.al. *J. Phys.: Condens. Matter*, **21** (2009) 395502.

2PO-I1-10

TEMPERATURE DEPENDENCE OF GILBERT DAMPING IN THIN MANGANITE/NORMAL METAL BILAYERS

Shcaihulov T.A., Demidov V.V., Borisenko I.V., Ovsyannikov G.A.

Kotel'nikov IRE RAS, Moscow, Russia

shcaihulov@hitech.cplire.ru

The temperature dependence of the spin-pumping effect and the Gilbert damping in bilayers based on manganite film grown on neodymium gallate substrate was investigated by measuring the linewidth of ferromagnetic resonance (FMR). Ferromagnetic resonance in thin ferromagnetic manganite ($\text{La}_{0.7}\text{Sr}_{0.3}\text{MnO}_3$ -LSMO) films is used to produce a spin current in a metallic film which cover the ferromagnetic layer. The linewidth of FMR is determined by both internal damping in ferromagnetic layer and leakage of the spin current. The temperature dependence of the FMR spectra, and in particular the resonance linewidth, magnetization, and other parameters in heterostructures Pt/LSMO/NGO, Au/LSMO/NGO and LSMO/NGO heterostructures were measured. Possible source for the additional damping due to the deposition of a Pt or Au layer on the LSMO film is the spin pumping mechanism that relaxes the magnetization precession by producing a flow of angular momentum out of the ferromagnetic film into the normal metal layer[1-3]. Besides the contribution of spin pumping, a number of other processes contribute to the temperature dependence of the damping [4]. The temperature dependence of the FMR linewidth for all three samples given in figure 1. It is seen that with increasing temperature the linewidth decreases in all structures. The increase of linewidth in Au/LSMO/NGO heterostructure at low temperatures can be attributed to decreased Curie temperature on manganite at the Au/LSMO interface which plays the role of a barrier that blocks spin pumping while it is not in the ferromagnetic state.

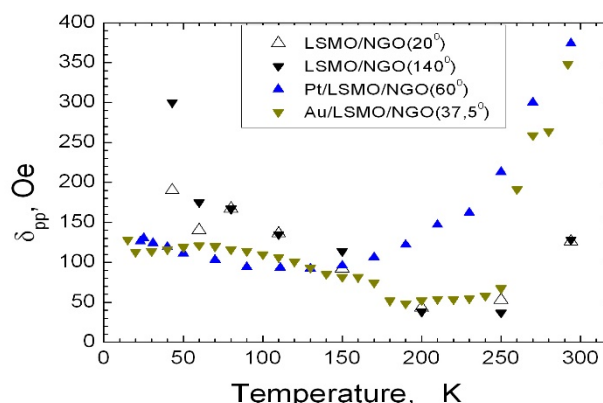


Fig. 1. The temperature dependence of the linewidth of the structures

Support by RFBR 17-02-00145, 16-29-14022 and Scientific school NSh -8168.2016.2.

- [1] O. Mosendz, V. Vlaminc, J. E. Pearson, F. Y. Fradin, G. E. W. Bauer, S. D. Bader, and A. Hoffmann, *Phys. Rev.*, **82** (2010) 214403-1-214403- 10.
- [2] S. M. Rezende, R.L.Rodriguez-Suarez, M. M. Soares, L.H.Vilela-Le, D. Ley Dom_iguez, and A. Azeved, *Appl. Phys. Lett.*, **102** (2013) 012402 -012407.
- [3] Y Tserkovnyak , A.Brataas, Gerrit E.W. Bauer, *Phys. Rev. Lett.*, **88** (2002) 11760-11764.
- [4] T G A Verhagen, H N Tinkey, H C Overweg, M van Son, M Huber, J M van Ruitenbeek and J Aarts, *J. Phys.: Condens. Matter*, **28** (2016) 056004- 056015.

2PO-I1-11

NUMERICAL SIMULATION OF SPIN TRANSPORT IN SYSTEMS WITH COMPLEX GEOMETRY

Andrianov T.¹, Vedyayev A.¹

¹ M.V. Lomonosov Moscow State University, Faculty of Physics, Leninskie Gory 1, 119991, Moscow, Russia

timofey.andrianov@gmail.com

Discovery of the effect of giant magnetoresistance (GMR) was a first step which allowed spintronics to become a very promising field of studies [1]–[3]. One of the most popular theory introduces the concept of spin accumulation and spin diffusion length as key parameters to describe the diffusive transport in CPP metallic multilayers which were generalized for both collinear and non-collinear cases:

$$\vec{j}_e = -\sigma \vec{\nabla} \varphi - \beta \frac{\sigma}{v} (\vec{M}, \vec{\nabla} \vec{m}), \quad (1)$$

$$\vec{j}_m = -\sigma \beta (\vec{M}, \vec{\nabla} \varphi) - \frac{\sigma}{v} \vec{\nabla} \vec{m}, \quad (2)$$

$$\text{div} \vec{j}_e = 0, \quad (3)$$

$$\text{div} \vec{j}_m = -\frac{\sigma}{v l_{sf}^2} \vec{m} - \frac{\sigma}{v l_j^2} [\vec{M}, \vec{m}]. \quad (4)$$

Where φ – electric potential, σ – conductivity, β – parameter of spin asymmetry of conductivity, \vec{M} – unit vector of magnetization; \vec{m} – spin accumulation vector, which has 3 components in spin dimension, l_{sf} – spin diffusion length, l_j – precession length, v – density of states.

In our paper, we numerically investigate structures with complex geometries, using spin transport equations (1)-(4). The structure consists of two large electrodes separated by ferromagnetic pillars. The pillar corresponds to ferromagnetic layers sandwiched by a paramagnetic spacer of the same diameter. The presence of pillars in the system cause non-uniform current flows. Different size or quantity of pillars may lead to the increase of the GMR effect or appearance of the spin current vortices in the system (Fig.1).

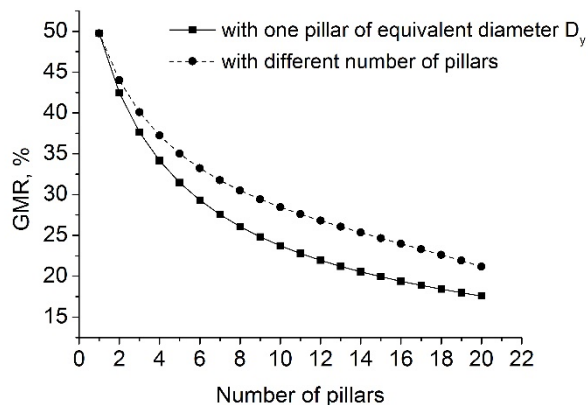


Fig. 1.

Numerical simulation of dependence of the GMR effect in the systems with different number of pillars in comparison with systems with one pillar of equivalent diameter.

[1] M. N. Baibich et al., *Phys. Rev. Lett.*, **61** №21 (1988) 2472–2475.

[2] G. Binasch, P. Grünberg, F. Saurenbach, and W. Zinn, *Phys. Rev. B*, **39** №7 (1989) 4828–4830.

[3] T. Valet and A. Fert, *Phys. Rev. B*, **48** №10 (1993) 7099–7113.

2PO-I1-12

TEMPERATURE INDUCED SWITCHING OF SPIN VALVES WITH A Gd LAYER

*Naumova L.I.¹, Milyaev M.A.¹, Chernyshova T.A.¹, Proglyado V.V.¹, Kamensky I.Y.¹,
Krinitsina T.P.¹, Ryabukhina M.V.¹, Maksimova I.K.¹, Ustinov V.V.¹*

¹ M.N. Miheev Institute of Metal Physics of the Ural Branch of the Russian Academy of Sciences, Ekaterinburg, 620990, Russia
naumova@imp.uran.ru

Realization of new possibilities for spintronic devices by the use of Gd in nano-layered structures is the purpose of intensive investigations. Svalov et. al. [1] created thermally sensitive Gd-Co/Co/Cu/Co “pseudo” spin valve with a ferrimagnetic Gd-Co alloy layer.

In the work presented Ta(50Å)/Gd(t_{Gd})/Co₉₀Fe₁₀(40Å)/Cu(32Å)/Co₉₀Fe₁₀(40Å)/Fe₅₀Mn₅₀(150Å)/Ta(50Å) exchange-biased spin valves with a gadolinium layer have been fabricated by magnetron sputtering. Using the Gd/CoFe as a free layer we get the possibility of changing the magnetic state with temperature. It was revealed that near a compensation temperature of the Gd/CoFe synthetic ferrimagnet the magnetoresistive curve changes drastically from the regular shape to the inverted one. Thus, for an appropriate value of the field, changing the temperature leads switching between the high- and low- resistance states of the spin valves (Fig. 1)

So the spin valves with Gd/CoFe free layer demonstrate temperature-induced changes in the magnetic ordering accompanied with switching between the low- and high-resistance states. The range of temperature at which the switching occurs can be controlled by the thickness of the Gd layer.

The research was carried out within the state assignment of FASO of Russia (“Spin” No. 01201463330, project No. 15-9-2-22), supported in part by RFBR (Project No. 16-02-00061) and Russian Ministry of Education and Science (Contract No. 14.Z50.31.0025).

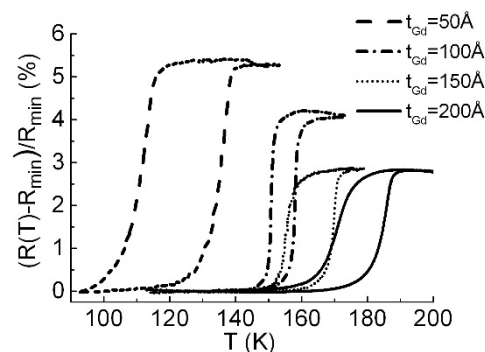


Fig. 1. Temperature dependencies of the relative change of resistance for the spin valves measured in a field of 200 Oe (the conventional resistance-temperature dependency is excluded).

[1] A.V. Svalov, G.V. Kurlyandskaya, and V.O. Vas'kovskiy, *Appl. Phys. Lett.*, **108** (2016) 063504(1 – 4).

2PO-I1-13

WEAK LOCALIZATION IN NANOGETEROGENEOUS SYSTEMS

Sitnikov A.V.¹, Stognei O.V.¹, Grebennikov A.A.², Zhilova O.V.¹, Kalinin Yu.E.¹

¹ Voronezh State Technical University, Voronezh, Russia

² MESCF AF «N.E. Zhukovsky and Y.A. Gagarin Air Force Academy», Voronezh, Russia
anton18885@yandex.ru

It was discovered that resistive and magnetoresistive properties of homogeneous materials such as Cu, Au, In_2O_3 has anomalous behavior at low temperatures. The anomaly is consisted in the TCR sign change on the $R(T)$ dependence during cooling process, as well as a negative magnetoresistance (MR) appearance at low temperatures in non-magnetic samples. Detailed studies conducted on different homogeneous materials has allowed to establish that these anomalies are due

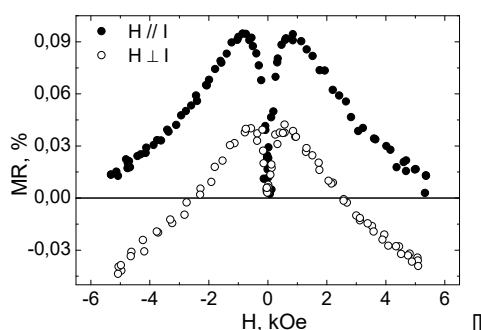


Fig. 1. Magnetoresistance of $\text{Ni}_{27}(\text{MgO})_{73}$ sample after air plasma processing at 77 K

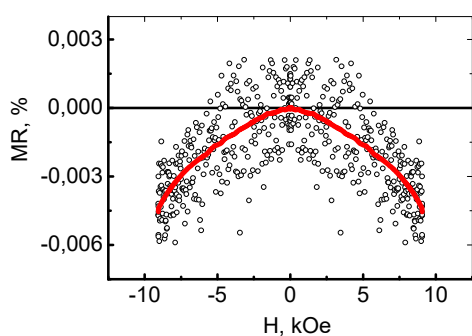


Fig. 2. Magnetoresistance of $(\text{In}_2\text{O}_3/\text{ZnO})_{83}$ multilayer sample (layer thickness is 28 nm) at 77 K.

to the effect of weak localization of electrons [1], which occurs in structures with a strong disorder. In the present work it has been shown that the conditions leading to the effect of weak localization can be obtained in nanoheterogeneous materials. As research objects $\text{Ni}_x(\text{MgO})_{100-x}$ (x : 21-48 at.%) nanocomposites and $(\text{In}_2\text{O}_3/\text{ZnO})_{83}$ (film thickness $h = 0,28 \mu\text{m}$) multilayer system were used.

Samples were obtained by ion-beam sputtering. The $\text{Ni}_x(\text{MgO})_{100-x}$ samples were annealed in vacuum ($\sim 10^{-3}$ Pa) at 500 °C and then were treated by air plasma to create the highly defective structure. The high structure defectiveness in the $(\text{In}_2\text{O}_3/\text{ZnO})_{83}$ samples is due to the small thickness of the layers (~ 1 nm).

It is found that the effect of weak localization significantly affects on the nature of magnetoresistance in $\text{Ni}_x(\text{MgO})_{100-x}$ composites over percolation threshold. In samples that were not treated by the air plasma the weak localization has not been found and as a consequence anisotropic MR was exhibited at 77 K and transverse part of the MR was negative. After plasma processing two positive maxima on the transverse MR appeared and the maximum values of the longitudinal MR increased (fig. 1). Similar dependences are typical for materials in which a strong spin-orbit interaction is realized. A change of TCR sign is observed at 100 K on the $R(T)$ dependence measured in the interval 77 - 280 K.

In a multilayer system $(\text{In}_2\text{O}_3/\text{ZnO})_{83}$ weak localization is manifested in the initial samples. A change of TCR sign is observed at 180 K on the $R(T)$ dependence and the samples show the negative MR at 77 K (fig. 2).

Support by the Minobrnauki of Russia (project № 3.1867.2017/ПЧ) is acknowledged.

[1] G. Bergmann, *Phys. Rep.*, **107** (1984) 58.

2PO-I1-14

SPIN TRANSPORT THROUGH $\text{Co}_{0.9}\text{Fe}_{0.1}/\text{MgO}/\text{InSb}$ TUNNEL JUNCTION*Viglin N.A.¹, Ustinov V.V.¹*

¹ M.N. Miheev Institute of Metal Physics of Ural Branch of RAS, 18 S.Kovalevskaya Str., 620990, Ekaterinburg, Russian Federation
viglin@imp.uran.ru

The goal of many-year research in semiconductor spintronics is to implement the possibility of electrically injecting and detecting spin-polarized electrons in a single device [1]. Use of semiconductors as a medium for spin transport is extremely attractive because of their broad functionality, not implemented in metallic systems. Equilibrium carrier densities can be varied through a wide range by doping. Furthermore, because the typical carrier densities in semiconductors are low compared to metals, electronic properties are easily tunable by gate potentials. However, lower concentration of electrons in semiconductors is the cause of the conductivity mismatch problem, i.e. the efficiency of spin injection into a semiconductor from a ferromagnetic metal dramatically reduces due to a significant difference in conductivity of metals and semiconductors. Theoretically, the mismatch problem can be balanced by creating a tunnel barrier between a metal injector and a semiconductor. This is explained by the fact that the barrier's spin-dependent resistance becomes comparable to the spin-independent resistance of a normal metal. In this case, the spin injection efficiency increases, and the spin polarization of conduction electrons in the semiconductor may be commensurate with the magnitude of the spin polarization of electrons in the ferromagnetic injector. Electrical detection of spin-polarized electrons injected into a semiconductor is a quite difficult task. Recently, it has become possible to detect the spin polarization of the electron gas in a paramagnetic semiconductor/a metal plate (film) with metal ferromagnetic probes, located on the substrate surface. The theory that explains the sensitivity of the ferromagnetic probes to the electron gas magnetization in the paramagnetic near these electrodes has been proposed by Johnson and Silsbee [2]. Over the past few years, several semiconductor spintronic devices with electrical detection of spin-polarized electrons have been designed. Injection and detection have been brought about in a GaAs and a Si semiconductors.

Electric injection and detection of spin-polarized electrons in InSb semiconductors have been implemented in non-local experimental geometry using a device such as an InSb semiconductor-based "lateral spin valve". The valve has contained a semiconductor/an insulator/a ferromagnetic nanoheterojunctions of InSb/MgO/ $\text{Co}_{0.9}\text{Fe}_{0.1}$ composition. Under the Hanle effect conditions, a magnetic field has changed the spin direction in a spin diffusion current. In accordance with the concept of the Johnson-Silsbee spin-charge coupling, ferromagnetic $\text{Co}_{0.9}\text{Fe}_{0.1}$ probes have registered the spin polarization of the electron gas by measuring electrical potentials appearing on them. Once the electrons have been injected from $\text{Co}_{0.9}\text{Fe}_{0.1}$ through an MgO tunnel barrier, the spin relaxation time and spin diffusion length of the conduction electrons, as well as the electron-spin polarization value in InSb have been determined.

The research has been carried out within the state assignment on the theme "Spin", number 01201463330 (project 15-17-2-17) with the support of the Ministry of Education and Science of the Russian Federation (grant 14.Z50.31.0025) and RFBR (grant 16-02-00044).

[1] S. Datta, B. Das, *Appl. Phys. Lett.*, **56** (1990) 665–667.

[2] M. Johnson, R.H. Silsbee, *Phys. Rev. Lett.*, **55** (1985) 1790.

2PO-I1-15

MAGNETIC PROPERTIES OF THREE-LAYER CoNi/Si/FeNi FILMS

*Kobyakov A.V.^{1,2}, Turpanov I.A.^{1,2}, Patrin G.S.^{1,2}, Yushkov V.I.^{1,2}, Patrin K.G.¹,
Yurkin G.Yu.^{1,2}, Zhivaya Ya.A.¹*

¹ Siberian Federal University, pr. Svobodny, 79, Krasnoyarsk, 660041,

² L.V. Kirensky Institute of Physics FRC KSC, Siberian Division, Russian Academy of Science,
Krasnoyarsk, 660036, Russia
nanonauka@mail.ru

Multilayer magnetic film structures consisting of alternative layer of magnetic hard and magnetic soft materials are very suitable objects for employment in spin-electron devices. The interlayer coupling in the described systems is responsible for the formation of the magnetic state and causes some intriguing phenomena. At the conjugation of magnetically soft and magnetically hard FM layers, a new, magnetic spring state occurs, when the magnetization process involves certain stages and the hysteresis loop has a specific shape.

The films of composition CoNi/Si/FeNi were obtained at first. The method was a deposition onto a glass substrate by ion-plasma sputtering at a base pressure of $\sim 10^{-8}$ Torr. The thickness of magnetic hard layer (CoNi) was $t_h = 50$ nm and magnetic soft layer (FeNi) was $t_s = 70$ nm. The thickness of intermediate nonmagnetic semiconducting layer (Si) was variable and it was changed in range $t_{si} = 3 - 15$ nm. Layer thickness was controlled by X-ray spectroscopy with a measurement accuracy of ± 0.5 nm. Surface roughness was controlled on a Veeco MultiMode NanoScope IIIa SPM system. The magnetic properties were investigated on an MPMS-XL magnetic property measurement system and magneto-optical installation NanoMOKE-2. In this layered structure the relation of coersivities separate magnetic hard and magnetic soft layers was more than two orders. Electron microscopy cross-section study was carried out on a JEM-2100 transmission electron microscope and one indicates existence of sharp boundary between silicon and both magnetic layers.

The magnetization curve has form typical for the magnetic exchange-spring (Fig.1). Temperature dependence of coercivity has maximum in range $T \approx 20 - 50$ K and the temperature of that is shifted towards higher temperatures with increasing of nonmagnetic layer thickness. The measurements of magnetic hysteresis loop by magneto-optical Kerr effect on opposite sides layered structure give the partial contributions of different magnetic layers. But an algebraic sum of these curves does not coincide with SQUID-obtained magnetic loops. These data make possible to judge about interlayer coupling in three-layer structure and, changing silicon thickness, to control the behavior of magnetic exchange-spring.

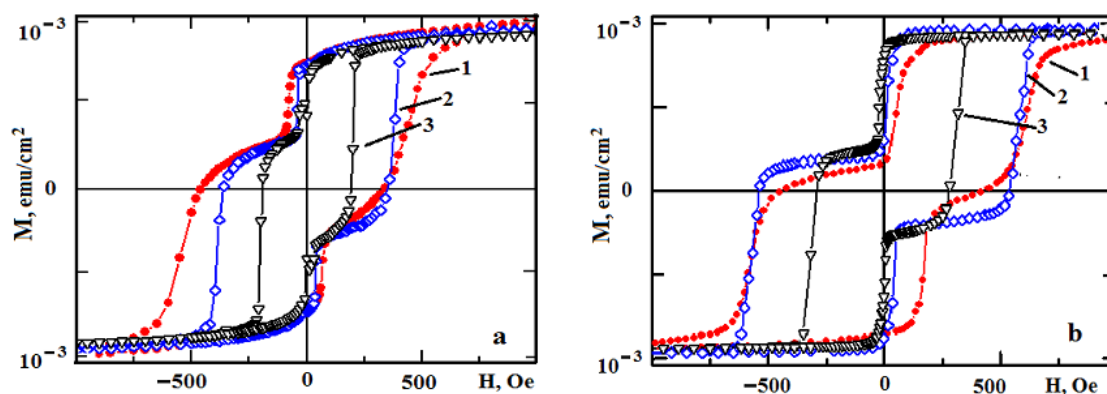


Fig. 1. Magnetization loops for CoNi/Si/FeNi films.. **a**, **b** – $t_{si} = 1.2, 3.5$ nm. 1, 2, 3 – $T = 4.2, 80, 300$ K

2PO-I1-16

MAGNETOSTATIC WAVES IN A MEDIUM WITH DAMPING*Makarov P.A.¹, Shcheglov V.I.², Kotov L.N.¹*¹ Pitirim Sorokin Syktyvkar State University, Syktyvkar, Russia² Institute of Radio Engineering and Electronics, Moscow, Russia
makarovpa@syktsu.ru

The propagating magnetostatic surface and volume waves (MSSW and MSVW) in magnetic films is the basis for variety of microwave analog data devices. Minimization of wave losses is a key for its successful work, but the damping hasn't been studied enough, as the vast majority of the research is performed without consideration of attenuation [1-4].

Let's consider a thin magnetic film deposited on a nonmagnetic dielectric substrate with a constant magnetic field applied in the sample plane. The MSSW and MSVW are propagated along the film plane. The angle between the wave vector k and the field direction is denoted as φ . Landau-Lifshitz-Gilbert equation with the damping parameter α was used to describe the motion of the magnetization vector.

In this study were calculated the dispersion curves for the real and imaginary parts of the wave number that were obtained by the numerical solution of dispersion equation. Also, dispersion relations for the real and imaginary parts of the wave number were studied. It was shown that dispersion curves are limited both by the wave number and frequency spectrum, and these restrictions tighten with an increase in the damping parameter. It was shown that there is a new branch of the backward dissipative surface waves, for which there is a critical value of the damping parameter, beyond which it does not exist. With the increase of the angle φ , limitation of dispersion curves is exacerbated, branches of the dispersion curves are shifted toward lower wave numbers and the damping parameter is being bounded below and above.

This work is supported by Russian Scientific Fund (project № 17-02-01138).

- [1] O. Kolokoltsev et al., *J. Appl. Phys.*, **112** (2012) 013902.
- [2] Y. Kajiwara et al., *Nature*, **464** (2010) 262-266.
- [3] S. Jun et al., *J. Appl. Phys.*, **81** (1997) 1341.
- [4] J.H. Kwon et al., *Appl. Phys. A.*, **111** (2013) 369-378.

2PO-I1-17

ANOMALOUS CYCLOTRON MASS DEPENDENCE ON THE MAGNETIC FIELD AND BERRY'S PHASE IN $(\text{Cd}_{1-x-y}\text{Zn}_x\text{Mn}_y)_3\text{As}_2$ SOLID SOLUTIONS

*Zakhvalinskii V.S.¹, Nikulicheva T.B.¹, Lähderanta E.², Shakhov M.A.³, Nikitovskaia E.A.¹,
Taran S.V.¹*

¹ Belgorod National Research University, 85 Pobedy St, Belgorod, 308015, Russia.

² Department of Mathematics and Physics, Lappeenranta University of Technology, Finland

³ Ioffe Institute, 26 Politechnicheskaya, St Petersburg, 194021, Russia

zakhvalinskii@bsu.edu.ru

There is a great interest connected with study of Dirac semimetal properties during the transition to the other phases under external influences. In single crystals of $(\text{Cd}_{1-x}\text{Zn}_x)_3\text{As}_2$ solid solutions has been experimentally observed phase transition from Dirac semimetal to semiconductor with increasing of Zn concentration above $x = 0.38$ [1]. The symmetry breaking in this 3D Dirac semimetal can turn it into a topological insulator.

Single crystals $(\text{Cd}_{1-x-y}\text{Zn}_x\text{Mn}_y)_3\text{As}_2$ were obtained by the Bridgman method. Shubnikov de Haas (SdH) effect and magnetoresistance measurements of single crystals of diluted II-V magnetic semiconductors $(\text{Cd}_{1-x-y}\text{Zn}_x\text{Mn}_y)_3\text{As}_2$ ($x + y = 0.4$, $y = 0.04$ and 0.08) are investigated in the temperature range $T = 4.2 \div 300$ K and in transverse magnetic field $B = 0 \div 25$ T. The values of the cyclotron mass m_c , the effective g-factor g^* , and the Dingle temperature T_D are defined. In one of the samples ($y = 0.08$) a strong dependence of the cyclotron mass on the magnetic field $m_c(B) = m_c(0) + \alpha B$ is observed. For the samples ($y = 0.04$) it was determined concentration of charge carriers on the 2D-layer surface, $n_{2D} = 5.5 \times 10^{12} \text{ cm}^{-2}$, effective value of 2D-layer: $d_{2D} = n_{2D}/n_{3D} = 16$ nm, wave vector $k_F = 0.16 \text{ nm}^{-1}$, charge carriers relaxation time due to dispersion $\tau_D = 1.9 \times 10^{-13}$ s, velocity of charge carriers on the Fermi surface $v_F = \hbar k_F / m_c = 4.5 \times 10^5$ m/s, mean free path $l_F = v_F \tau_D = 85.5$ nm. It was found the compliance of dependence of cyclotron $m_c(0)/m_0$ from Fermi wave vector k_F for CZMA ($y = 0.04$) theoretical linear dependence, that describes mass-less Dirac fermions.

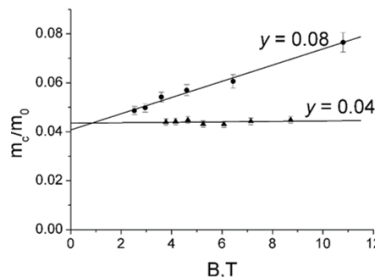


Fig. 1. Field dependence of the cyclotron mass of the samples $(\text{Cd}_{1-x-y}\text{Zn}_x\text{Mn}_y)_3\text{As}_2$ ($x + y = 0.4$) for $y = 0.04$ and $y = 0.08$

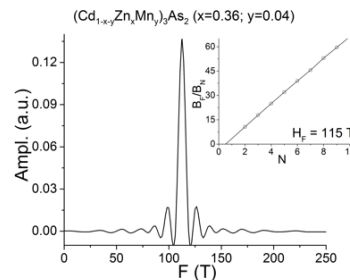


Fig. 2. Results of FFT analysis of SdH oscillations in $(\text{Cd}_{1-x-y}\text{Zn}_x\text{Mn}_y)_3\text{As}_2$ solid solutions for samples ($x = 0.36$, $y = 0.04$). On the interest, it is presented the H_F/H_N dependence from N .

On the inserts in the Fig. 2. it is presented the H_F/H_N dependence from N . It is seen that the results perfectly fit the strict line, that for the sample $y = 0.04$ crosses horizontal axis N in point $\beta \approx 0.54$, which attests the presents of Berry's phase in this sample. It was found that the relation of cyclotron mass $m_c(0)/m_0$ to Fermi wave vector k_F for CZMA ($y = 0.04$) is in a good relation with theoretical linear dependence, that describes mass-less Dirac fermions.

Thus it was found that solid solution of diluted magnetic semiconductor $(\text{Cd}_{1-x-y}\text{Zn}_x\text{Mn}_y)_3\text{As}_2$ ($x + y = 0.4$) demonstrates the properties of topological insulator in case of the concentration of Mn $y = 0.04$ and anomalous dependence of cyclotron mass from the magnetic field in case of the concentration of Mn rises up to $y = 0.08$.

Support by RFBR according to the research Project No. 15-42-03192 is acknowledged.

[1] Hong Lu, Xiao Zhang and Shuang Jia., **arXiv:1507.07169v1** (2015).

[2] S. Borisenko et al., *Phys. Rev. Lett.*, **113** (2014) 027603.

2PO-II-18

GALVANOMAGNETIC EFFECT OF $Gd_xMn_{1-x}Se$ SOLID SOLUTION*Masyugin A.N.¹, Romanova O.B.^{1,2}, Kharkov A.M.¹, Yanushkevich K.I.³*¹ Siberian State Aerospace University M F Reshetnev, Krasnoyarsky Rabochy Av. 31, 660014 Krasnoyarsk, Russia² Kirensky Institute of Physics, Federal Research Center KSC SB RAS, Akademgorodok 50, 660036 Krasnoyarsk, Russia³ Scientific-Practical Materials Research Center NAS, P. Brovski Str.19, 220072 Minsk, Belarus albert.masyugin@mail.ru

The creation of magnetic semiconductors for the element base in microelectronics, and in particular spintronics, capable of operating over a wide range of temperatures, is of interest both from the fundamental and applied point of view. A negative magnetoresistance above the Neel temperature was found in manganese selenide upon anion substitution [1]. The aim of this work is the detection of the magnetoresistive effect and to shed light on the microscopic mechanism of the magnetic-field influence on the transport properties of $Gd_xMn_{1-x}Se$ solid solutions by the comprehensive study of the electrical resistivity and galvanomagnetic properties and the current-voltage characteristics as a function of temperature and magnetic field.

Solid solutions $Gd_xMn_{1-x}Se$ were obtained by solid-phase reaction from powders of starting compounds in vacuumed quartz ampoules in a single-zone resistance furnace. The specific resistivity was measured by a four-probe method in a zero and magnetic field of 13 kOe directed perpendicular to the current. The results of electrical measurements are shown in Fig 1. The activation energy ΔE , which is ~ 0.3 eV, is determined from the slope of the rectilinear part of the $\log(\rho(1/T))$ dependence and does not change in the magnetic field.

The magnetoresistance $\delta = (\rho(H) - \rho(0)) / \rho(0)$ in the Gd-Mn-Se system with concentration $X = 0,2$ changes sign with increasing temperature at $T = 320$ K. A sharp decrease of the Hall constant, a wide hysteresis of the current-voltage characteristic, and a maximum of the thermopower coefficient at some temperature are observed. In the temperature range with a negative magnetoresistance, two types of current carriers were established: electrons and holes. In the temperature range with positive magnetoresistance the electrons prevail. The difference between the signs of the Hall coefficients and the thermoelectric power above room temperature is due to capture of electrons by phonons, as a result of the electron-phonon interaction, was found. The experimental data were explained by the presence of the orbital angular magnetic moment and local electric polarization in the nanoarea, the degeneracy of which are eliminated in electric and magnetic fields. The sharp thermopower maxima induced by splitting of the 4f subband of the gadolinium ions by the crystal field were observed.

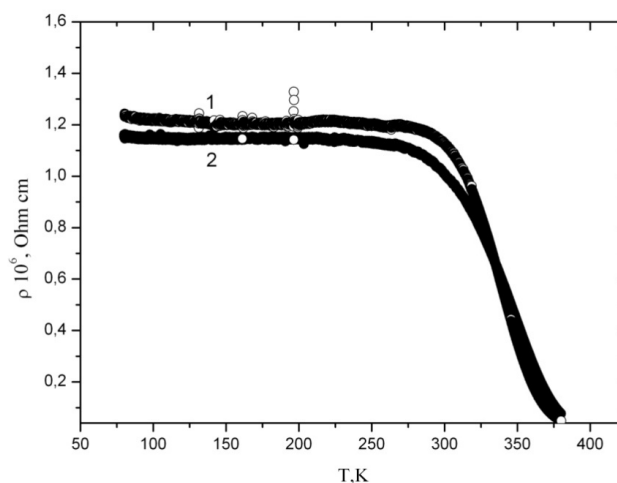


Fig.1 Temperature dependences of electrical resistance in zero magnetic field (1) and field 13 kOe (2) of the system $Gd_xMn_{1-x}Se$ with $X = 0.2$

[1] S.S. Aplesnin, O.B. Romanova, K.I. Yanushkevich. *Phys. Status Solidi (b)*, **252** (2015) 1792.

2PO-I1-19

MULTITERMINAL PLANAR DEVICES BASED ON HYBRID STRUCTURES: FABRICATION AND SPIN-DEPENDENT TRANSPORT

Tarasov A.S.¹, Lukyanenko A.V.^{1,2}, Tarasov I.A.^{1,3}, Rautskii M.V.¹, Bondarev I.A.^{1,2}, Varnakov S.N.^{1,3}, Ovchinnikov S.G.^{1,3}, Patrino G.S.^{1,2}, Volkov N.V.¹

¹ Kirensky Institute of Physics, Federal Research Center KSC SB RAS, Krasnoyarsk, Russia

² Institute of Engineering Physics and Radio Electronics, SFU, Krasnoyarsk, Russia

³ Siberian State Aerospace University, Krasnoyarsk, 660014 Russia

taras@iph.krasn.ru

In recent time, spin-dependent electronic transport in different materials and structures has been intensively studied [1]. This is related, first of all, to the electron spin application perspectives in data storage, transfer, and processing in future spintronic devices and in creation of the spin transistor. The important part of these investigations is synthesis of multilayered ferromagnet/semiconductor structures and creation of micro- and nanoscale devices with a desired layer topology on their basis.

In this work, we present a relatively simple controllable way for fabrication of multiterminal planar devices based on the $\text{Fe}_{1-x}\text{Si}_x$ epitaxial films grown on Si(111) wafers. We demonstrate the spin accumulation effect in the fabricated 4-terminal device.

The $\text{Fe}_{1-x}\text{Si}_x$ films were formed on the *n*-doped Si(111) substrate ($\rho = 7.5 \Omega \cdot \text{cm}$) by molecular beam epitaxy at 400 K under ultrahigh vacuum conditions. X-ray diffraction and transmission electron microscopy studies revealed the single crystallinity and interface abruptness of the thin films. Planar devices were formed by liquid chemical etching in the mixture of hydrofluoric and nitrogen acids ($\text{HF}:\text{HNO}_3:\text{H}_2\text{O} = 1:2:400$). To form a required ferromagnet topology of the multi-terminal planar device, micron resolution photolithography was used. Using atomic force microscopy (Figs. 1a and 1b), we showed that the etching is vertical, which provides high quality of the structures obtained. A "magnetic map" of the device obtained by 3- μm resolution Kerr-effect microscopy (Fig. 1c) shows the surface distribution of the angle of rotation of the reflected light polarization plane in the magnetic field. This experiment showed that in the region uncovered by a mask, Fe_3Si was completely etched away. Study of the Hanle effect in the 3-terminal geometry in a magnetic field applied perpendicular to the sample plane showed that our structures exhibit the spin accumulation effect.

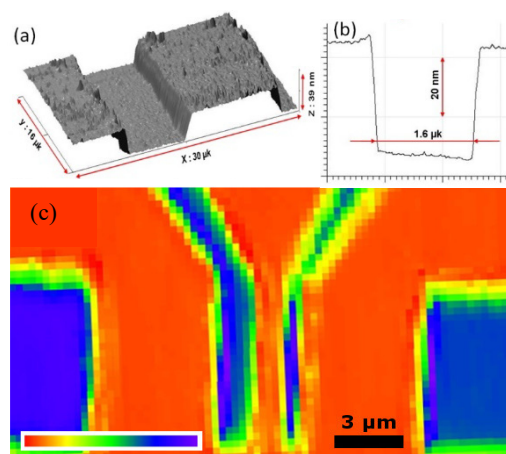


Fig. 1. (a) AFM image and (b) 1D profile of the etched $\text{Fe}_{3+x}\text{Si}_{1-x}/\text{Si}(111)$ device. (c) The Kerr rotation angle distribution over the device surface in the magnetic field.

This study was supported by the Russian Foundation for Basic Research and the Krasnoyarsk Territorial Foundation for Support of Scientific and R&D Activities, projects nos. 16-42-243046 and 16-42-243060.

[1] R. Jansen, *Nature Materials*, **11** (2012) 400–408.

2PO-I1-20

STUDY OF THE LATERAL PHOTOVOLTAIC EFFECT IN THE Fe_3Si/Si HYBRID STRUCTURE

Volkov N.V.¹, Rautskii M.V.¹, Bondarev I.A.^{1,2}, Lukyanenko A.V.^{1,2}, Varnakov S.N.^{1,2,3},
Ovchinnikov S.G.^{1,2}

¹ Kirensky Institute of Physics, FRC KSC RAS, Krasnoyarsk, 660036 Russia

² Siberian Federal University, Krasnoyarsk, 660041 Russia

³ Siberian State Aerospace University, Krasnoyarsk, 660014 Russia

fbi1993@mail.ru

The multilayered FM/I/S and FM/S hybrid nanostructures have been objects of thorough investigation due to the ability of manipulating electron transport via the electron spin state. The iron silicides with the high Curie temperature (~ 840 K), high value of spin polarization ($\sim 43\%$), low magnetocrystalline anisotropy, and high electrical resistance are promising candidates for application as ferromagnets in hybrid structure-based spintronic devices. The lateral photovoltaic effect (LPE) continues attracting a considerable scientific attention due to its application potential, e.g., for creation of the position-sensitive detectors with a possibility to register very small displacements.

In this work, we investigated the lateral photovoltaic effect in the Fe_3Si/Si hybrid structure. The Fe_3Si film was epitaxially grown on an atomically clear boron-doped silicon substrate by thermal evaporation in ultrahigh vacuum [1].

Figure 1 presents the temperature dependences of the magnetophotovoltage (MPV = $[PV(H) - PV(0)]/PV(0) * 100\%$) for the diode geometry at a laser wavelength of $\lambda = 809$ nm and powers of $60 \mu W$ and $1 mW$.

A considerable signal appears at helium temperature. The highest MPV value attaining about 20% is detected at low power. The PV(T) curve (inset to Fig. 1) has a peak with a maximum at about 22 K.

The results obtained have shown that the highest signal appears at the diode geometry and, thus, can be related to spin injection through the interface.

This study is supported by the Krasnoyarsk Territorial Foundation for Support of Scientific and R&D Activities, Travel Grant Competition for Young Scientists (Moscow International Symposium on Magnetism MISM'2017, Moscow, July 1–5, 2017).

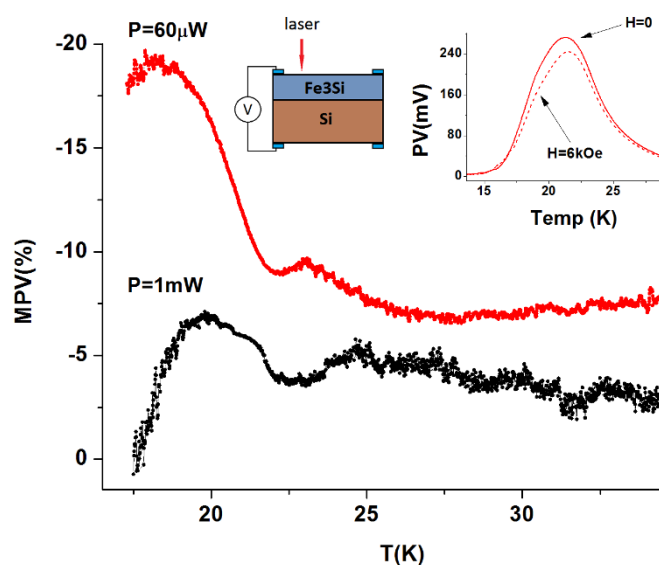


Fig. 1. Temperature dependences of MPV for the Fe_3Si/Si structure. Inset: temperature dependence of PV in fields of $H = 0$ and $H = 6 kOe$.

[1] I. A. Yakovlev, S. N. Varnakov, B. A. Belyaev, et al., *JETP Lett.*, **99** (9) (2014) 527.

2PO-I1-21

VORTEX DYNAMICS IN DISKS WITH TAILORED MAGNETISATIONS

Ramasubramanian L.^{1,2}, Fowley C.¹, Kákay A.¹, Yildirim O.¹, Matthes P.⁴, Lindner J.¹, Fassbender J.³, Gemming S.^{1,2}, Schulz S.E.^{2,4}, Deac A.M.¹

¹ HZDR, Institute of Ion Beam Physics and Materials Research, Dresden, Germany

² Technische Universität Chemnitz, Chemnitz, Germany

³ Institute for Physics of Solids, TU Dresden, Dresden, Germany

⁴ Fraunhofer Institute for Electronic Nano Systems, Chemnitz

l.ramasubramanian@hzdr.de

The fundamental oscillation mode of magnetic vortices in thin-film elements has recently been proposed for designing spin-torque-driven nano-oscillators [1]. Commercial applications require tuning of the output frequency by external parameters, such as applied fields or spin-polarized currents. However, the tunability of vortex-based devices is limited, since the gyrotropic frequency is specific to the individual sample design [2, 3]. Micromagnetic simulations [4] have shown that if regions with different saturation magnetisation can be induced in a magnetic disk, multiple precession frequencies can be generated. Ion implantation is a promising method to fabricate such devices [5].

Disks with different radii- 0.5 μm to 4 μm and thicknesses- 25 nm and 30 nm were prepared using electron beam lithography followed by electron beam evaporation to study the formation of magnetic vortices with respect to size and thickness. The single disks were contacted by gold leads to study the interaction of spin polarized current on the magnetic vortex. The presence of vortex is verified by magneto optic Kerr effect (MOKE) and X-ray magnetic circular dichroism (XMCD).

Magnetotransport measurements on electrically contacted disks (Figure 1 (a)) show the presence of anisotropic magnetoresistance (AMR) in different disks with varying thickness (Figure 1 (b)). The resonance frequencies measured using a lock-in technique on 3 μm and 4 μm radii disks with 25 nm permalloy are 40.9 MHz and 29.5 MHz respectively. Modification of the resonance frequency by ion irradiation will be presented.

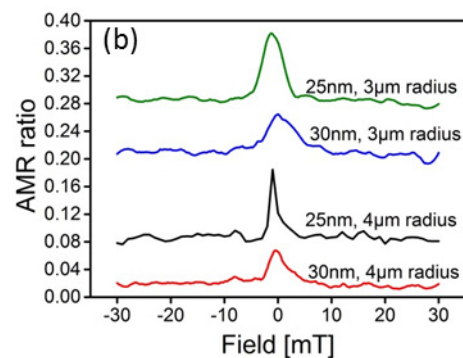
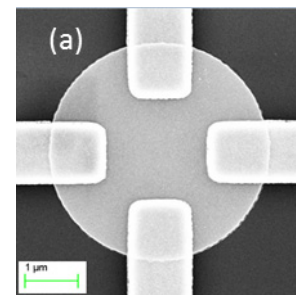


Figure 1(a): Scanning Electron Microscope image of disk with electrical contacts, (b) AMR ratio (change in resistance) versus applied magnetic field for different disks (curves are shifted vertically for clarity with an offset of 8%).

[1] V. S. Pribiag, et al., *Nat. Phys.*, **3** (2007) 498.

[2] V. Sluka, et al., *Nat. Commun.*, **6** (2015) 6409.

[3] S. Gliga, *Forschungszentrum Jülich GmbH* (2009) 978-3-89336-660-6.

[4] A. Kákay, unpublished.

[5] J. Fassbender, et al., *Phys. Rev. B*, **73** (2006) 184410.

2PO-I1-22

TUNNEL MAGNETORESISTANCE AND SPIN TRANSFER TORQUE IN MAGNETIC TUNNEL JUNCTION WITH EMBEDDED NANOPARTICLES

Useinov N.

Institute of Physics, KFU, Kazan, Russia
nuseinov@mail.ru

Currently the magnetic nanostructures (ferromagnet/insulator/metal/ ...) are widely studied in spintronics. The effects of tunnel magnetoresistance and switching of magnetization in such structures find their application in magnetic field sensors, spin current filters, non-volatile magnetoresistive random-access memory (MRAM, STT-MRAM), resonant tunnel diodes, spin transistors (cells and other nanodevices). The conductance of the magnetic nanostructures can be changed by an external magnetic field as well as by a spin-polarized current. The main characteristics of these nanostructures (important for commercial application) are tunnel magnetoresistance (TMR) and spin transfer torque (STT).

In this work a theoretical model of spin-dependent transport in magnetic tunnel junctions (MTJ) containing magnetic or non-magnetic (from a normal metal) nanoparticle is developed. The dependences of the TMR and the in-plane component of the STT on the applied voltage for various sizes of nanoparticles of the order of the mean free path of the conduction electron are calculated. The calculation is performed in the approximation of the ballistic transport of conduction electrons through the insulating layers of the MTJ and the nanoparticles. Note that a single-barrier MTJ with a nanoparticle embedded in the insulator forms a double-barrier MTJ. The spin-polarized current through the nanostructure has been calculated on the basis of the quasi-classical theory. The basic mathematical expressions and calculation details can be found in article [1].

The calculations show that the embedded nanoparticles in the MTJ increase the electron transmission coefficient and create resonance conditions providing a quantization of the conductance in contrast to the MTJ without nanoparticles. It is shown that the value of the in-plane component of the STT in the double-barrier MTJ (i.e., in the MTJ with nanoparticles) for some nanoparticle sizes and nanostructure parameters can be larger than in a single-barrier MTJ for the same thickness of the insulating layer. The simulation includes different nanoparticles distributions by size (with diameter $d = 0.2-3.0$ nm). Figure 1 represents dependence TMR-V simulations: curve 1 shows peak-like TMR for the case of wavenumber $k_n = 0.450 \text{ \AA}^{-1}$ of the nanoparticle, curve 2 shows negative TMR = -8% for $k_n = 0.115 \text{ \AA}^{-1}$. The calculated TMR dependences correspond to experimental data in which peak-like anomalies and suppression of the maximum TMR values at zero voltages are observed [2]. Note that the presented theory does not take into account the models Coulomb blockade and Kondo-assisted tunneling.

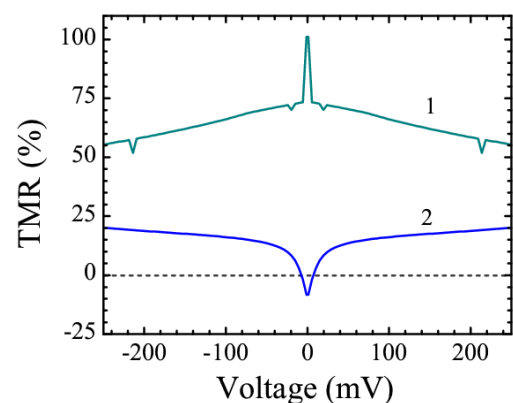


Fig. 1. Bias voltage dependence of TMR for the magnetic tunnel junctions with embedded nanoparticles.

- [1] A. Useinov, L. Ye, N. Useinov, T.H. Wu, C.H. Lai, *Scientific Reports*, **5** (2015) 18026(9).
[2] H. Yang, S.H. Yang, S.S.P. Parkin, *Nano Lett.*, **8** (2008) 340-344.

2PO-I1-23

COMPARISON OF THE CRITICAL SWITCHING CHARACTERISTICS OF MRAM CELLS MADE OF VARIOUS MATERIALS WITH UNIAXIAL ANISOTROPY

Iusipova Iu.A.^{1,2}¹ Institute for Design Problems in Microelectronics RAS (IPPM RAS), Moscow, Russia² National Research University of Electronic Technology (MIET), Moscow, Russia
linda_nike@mail.ru

The work is devoted to the investigation of how magnetic characteristics of the material of spin-valve ferromagnetic layers influence on the magnetization dynamics in the free layer of the valve. The goal of the investigation was to compare the switching characteristics of the MRAM cells manufactured of various ferromagnetic materials with the uniaxial anisotropy and to find the materials with the best switching characteristics. The formulae for switching current estimation have been obtained in many theoretical works previously [1–3].

Using these threshold relations, we analyzed the dependence of the switching current on the material parameters. It was revealed that the annealing alloys of cobalt and iron, such as $\text{Fe}_{60}\text{Co}_{20}\text{B}_{20}$, $\text{Fe}_{40}\text{Co}_{40}\text{B}_{20}$, $\text{Fe}_{70}\text{Co}_{30}$, $\text{Co}_{80}\text{Gd}_{20}$, and $\text{Co}_{93}\text{Gd}_7$, are the perspective materials in this sense.

Figure 1 shows the threshold lines of switching current. Switching of the spin valve is possible only in the region above the line whose equation is has the form (1a), and within elliptical area defined by formula (1b):

$$\frac{\alpha deM_s \mu_0}{\hbar G} H - J + \frac{\alpha de}{\hbar G} \left(\frac{4K + M_s^2 \mu_0^2}{2\mu_0} \right) = 0, \quad (1a)$$

$$\left(\frac{H + \frac{4K + M_s^2 \mu_0^2}{2M_s}}{\frac{M_s}{2}} \right)^2 + \left(\frac{J}{\frac{deM_s^2 \mu_0}{2G\hbar}} \right)^2 - 1 = 0. \quad (1b)$$

The studies of the dynamics of the magnetization vector in the free layer made of these materials allowed us to choose four optimal switching regimes. In the result of calculations of the optimal switching parameters with physical limitations taken into account, it was found that two alloys are the best materials for spin valve manufacturing, namely $\text{Fe}_{40}\text{Co}_{40}\text{B}_{20}$ and $\text{Co}_{80}\text{Gd}_{20}$, annealed at 300°C and 200°C, respectively.

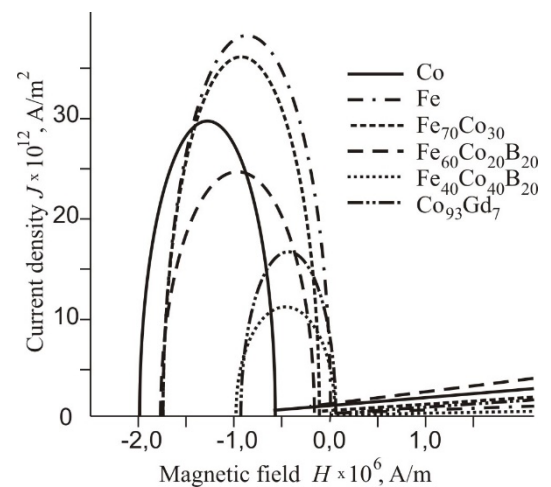


Fig. 1. Threshold lines of switching current.

[1] J.Z. Sun, *Phys. Rev. B*, **62** (2000) 570–578.

[2] J. Grollier, V. Cros, H. Jaffres, A. Hamzic, J.M. George, G. Faini, J.B. Youssef, H. Le Gall, and A. Fert, *Phys. Rev. B*, **67** (2003) 174402–174410.

[3] N.V. Ostrovskaya, V.A. Skidanov, and Iu.A. Iusipova, *Solid State Phenomena*, **233-234** (2015) 431-434.

2PO-I1-24

THE DYNAMICAL REGIMES OF MAGNETIZATION IN MAGNETIC VALVES WITH IN-PLANE AND PERPENDICULAR ANISOTROPY

Ostrovskaya N.¹, Iusipova Iu.², Skidanov V.³, Skvortsov M.⁴

¹ Institute for Design Problems in Microelectronics RAS, Department for Microelectronic Components, Moscow, Russian Federation

² National Research University of Electronic Technology, Department of General Physics, Moscow, Russian Federation

³ Institute for Design Problems in Microelectronics RAS, Department for Microelectronic Components, Moscow, Russian Federation

⁴ National Research University of Electronic Technology, Department of Applied Mathematics, Moscow, Russian Federation
n.ost@ippm.ru

In the approximation of the uniform distribution of the magnetization through the elliptical cross-section of the nano-pillar valve, the dynamical systems for the valves with in-plane and perpendicular anisotropy have been written. The theoretical model is based on the Landau--Lifshits--Gilbert equation with the current term in the Slonczewski--Berger form. The effective magnetic field includes as the easy-axis anisotropy, so and demagnetization contributions. The external field was taken parallel to the easy axis. The spatial dependence of magnetization was ignored. The resulting sets of equations represent nonlinear dynamical systems with right-hand sides being fractionally rational. For each kind of anisotropy, the analysis of bifurcations depending the external magnetic field and injection current and constructed the bifurcation diagrams was performed. This analysis allowed us to classify the dynamical regimes of switching and to find the values of the control parameters, at which the limit cycles of the dynamical systems do exist. The magnetization dynamics for typical values of the field and the current was simulated. The numerical experiments revealed the details of switching process and, for the case of in-plane anisotropy, permitted to find novel regimes of magnetization dynamics, such as incomplete and accidental switching. The estimations of the switching time were performed. It was established that in the case of perpendicular anisotropy the switching current is approximately an order less than in the case of in-plane anisotropy.

2 July

Sunday

12:00-14:00

poster session
2PO-J

**“Magnetophotonics
and Ultrafast
Magnetism”**

2PO-J-1

MOLECULAR AGGREGATES FOR TOPOLOGICALLY PROTECTED EXCITONIC MATERIALS

Shakirov M.A.¹, Saikin S.K.^{1,2}, Proshin Yu.N.¹

¹ Theoretical Physics Department, Kazan Federal University, Kazan, Russian Federation

² Department of Chemistry and Chemical Biology, Harvard University, Cambridge, USA
s.mars-9@mail.ru

Electronic excitations in hybrid structures, which are composed of magneto-optic, plasmonic, and organic layers, can form edge states that are protected from elastic scatterings [1]. Aggregates of pigment molecules that support delocalized Frenkel excitons are one of the most crucial building blocks for the design of just such systems. We explore exciton transport properties of heterotriangulene aggregates that can be used for this purpose. Recent experimental studies of heterotriangulene chains suggested that electronic excitations in these structures can propagate on several micron distances, with a sufficient contribution of a coherent exciton motion [2]. We analyze this possibility theoretically constructing a model that combines electronic structure calculations with microscopic exciton transport.

The inset in Fig. 1 illustrates packing of heterotriangulene molecules in a 1D chain. The electronic transitions in different molecules interact with each other through the Förster interaction, which allows the exciton to delocalize and propagate along the chain. In our model, the intramolecular electronic excitations and intermolecular couplings are computed using time-dependent density functional theory. Then, we build a tight-binding Hamiltonian and propagate electronic excitations in real time using the Haken, Reneiker, and Stroble transport model [3]. The latter model allows us to study effects of different types of disorder on the exciton delocalization. Fig. 1 shows a second moment of an exciton wave function as a function of time. The initial coherent exciton propagation results in a quadratic time dependence of the second moment. At longer times, the exciton transport becomes diffusive with a linear time dependence of the second moment.

We show that for sufficiently large values of structural disorder excitons in heterotriangulene chains are still delocalized over about 10 pigments even at room temperatures. This finding makes the structures promising candidates for the design of topologically protected excitonic materials.

The work is supported by the subsidy allocated to Kazan Federal University for performing the project part of the state assignment in the area of scientific activities (#3.2166.2017). SMA is also thankful to RFBR (#16-02-01016) for a partial financial support.

[1] J. Yuen-Zhou, *et al.*, *Nature Commun.*, **7** (2016) 11783.

[2] A. T. Headler, *et al.*, *Nature*, **523** (2015) 196-199.

[3] S. K. Saikin, *et al.*, *Nanophotonics*, **2** (2013) 21-38.

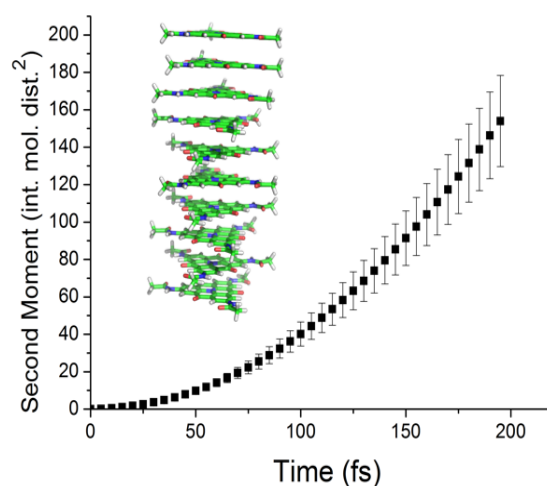


Fig. 1. An exciton second moment (in units of intermolecular distance) as a function of time. Inset: 1D aggregate of heterotriangulene dyes.

2PO-J-2

INVERSE FARADAY EFFECT IN GRAPHENE-DIELECTRIC-METAL STRUCTURE

Tolkachev V.A.¹, Plaksin P.S.¹, Bychkov I.V.^{1,2}, Kuzmin D.A.^{1,2}, Shavrov V.G.³

¹ Chelyabinsk State University, 129 Br.Kashirinykh Str., Chelyabinsk, Russian Federation

² South Ural State University (National Research University), 76 Lenin Prospekt, Chelyabinsk,
Russian Federation

³ Kotelnikov Institute of Radio-engineering and Electronics of RAS, 11/7 Mokhovaya Str.,
Moscow, Russian Federation
tolkachevva91@yandex.ru

Currently, there is strong interest in graphene-based nanostructures. The properties of graphene are very attractive from the point of view of its possible application as an element of nanoelectronic devices for information processing, and as a basis for new nanomaterials with improved electrical [1], thermal and mechanical characteristics [2,3] as well.

We present the results of modeling the inverse Faraday effect (IFE) in the vacuum-graphene-dielectric (SiO₂)-metal (Au) structure. The properties of the structure depend mainly on the dielectric permittivity of the dielectric, its thickness and graphene conductivity. The calculations were performed in the electrodynamics of continuous mediums approximation in the frequency range from 0.3 to 1 THz.

Dispersion equations and conditions of existence of the TM wave of the structure were obtained. Energy and magnetic moment distributions generated by plasmonic modes of the structure (inverse Faraday effect) were obtained. It is shown that the maximum value of the magnetic moment is observed at the boundary vacuum - graphene - dielectric and decreases exponentially to a minimum in the dielectric and vacuum. The dependencies of the magnetic moment on the chemical potential of graphene, the thickness of the dielectric layer, and the frequency were calculated. The behavior of the propagation and attenuation constants for different thicknesses of the dielectric layer and for different chemical potentials of graphene was investigated. Estimations of the change in the magnetic moment (IFE) under effect of the elastic strains were carried out. It was shown that the uniaxial stress of 10⁹ Pa slightly changes the magnetic moment on about 1.5%.

Supported by RFBR (grants ## 16-37-00023, 16-07-00751, 16-29-14045, 17-57-150001), RScF (grant # 14-22-00279), and grant of the President of the Russian Federation MK-1653.2017.2.

[1] TS Sreeprasad, V Berry, *Small*, **9(3)** (2013) 341-350.

[2] K. S. Novoselov, et al., *Nature*, **490** (2012) 192–200.

[3] C Lee, X Wei, JW Kysar, J Hone, *Science*, **321(5887)** (2008) 385-388.

2PO-J-3

TRANSVERSE MAGNETOOPTICAL KERR EFFECT TUNING BY VARIATION OF MAGNETOPLASMONIC CRYSTALS PROFILE

Frolov A.Yu., Novikov I.A., Malyshev V.D., Kiryanov M.A., Popov V.V., Ezhov A.A., Dolgova T.V., Fedyanin A.A.

Lomonosov Moscow State University, Moscow, Russian Federation
frolov@nanolab@phys.msu.ru

Magnetoplasmonic nanostructures are systems combining plasmonic and magneto-optical properties [1]. Magnetoplasmonic nanostructures have gained a lot of attention due to possibility to enhance significantly the magneto optical effects with respect to the ones of bulk ferromagnetics [2,3]. In one or two-dimensional corrugated or perforated metal gratings, called also magnetoplasmonic crystals, surface plasmon-polaritons (SPPs) which are propagating collective oscillations of conducting electrons of metals, are sensitive to the external transverse magnetic field. A lot of attention have been previously mentioned on design of magnetoplasmonic crystals and choosing materials for fabrication to achieve the largest magneto-optical response.

In this work, we investigated transverse magneto-optical Kerr effect (TMOKE) in one-dimensional all-nickel (Ni) magnetoplasmonic crystals, which are corrugated gratings with a different profile. We demonstrated that TMOKE can be adjusted in the visible wavelength range by variation of magnetoplasmonic crystal profile. We demonstrated that both a maximum value and the spectral behaviour of TMOKE are strongly depends on the magnetoplasmonic crystals. TMOKE value is greater in the case of sinusoidal profile grating (Fig.1a) with respect to one with non-sinusoidal profile (Fig.1b) at the same thickness (A) of corrugations.

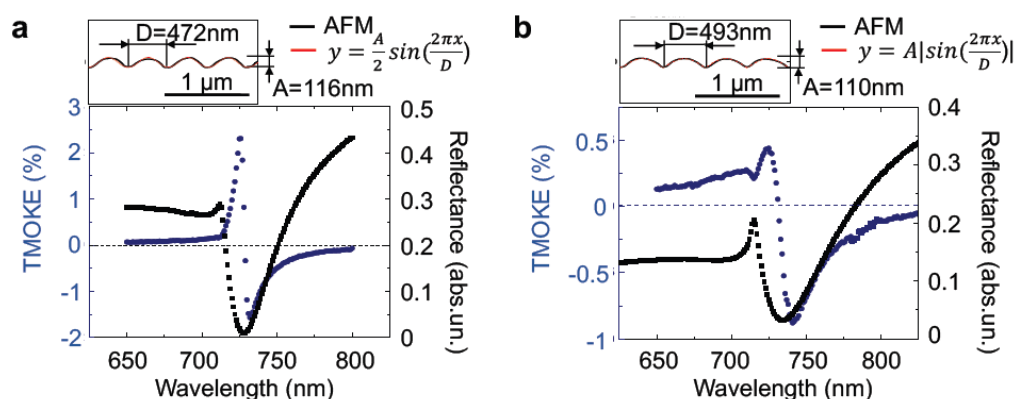


Fig.1. TMOKE and reflectance spectra at 20 degrees angle of incidence. a) grating with sinusoidal spatial profile. b) grating with non-sinusoidal spatial profile.

Support by The Russian Foundation for Basic Research (project no. 16-32-00720).

- [1] G. Armelles et al., *Adv. Opt. Mater.* **1** (2013) 10–35.
- [2] A.V. Chetvertukhin et al., *J. Appl. Phys.*, **111** (2012) 07A946.
- [3] A. A. Grunin et al., *Appl. Phys. Lett.*, **105** (2014) 261908.

2PO-J-4

CRITICAL INFLUENCE OF RHODIUM ON ULTRAFAST DEMAGNETIZATION OF $L1_0$ -Fe(Pt_{1-x}Rh_x) THIN FILMS

Petrov A.V.¹, Yusupov R.V.¹, Nikitin S.I.¹, Valiullin A.A.¹, Kamzin A.S.²

¹ Kazan Federal University, Kazan, Russia

² Ioffe Physical-Technical Institute, St.-Petersburg, Russia
flypetrov@yandex.ru

Thin $L1_0$ -structure FePt films are considered as the materials of a choice for high-capacity magnetic information storage devices. Huge, $K_u \sim 7 \cdot 10^7$ erg/cm³, magnetocrystalline anisotropy, on one hand, allows to decrease strongly a magnetic grain size staying far from the superparamagnetic limit. On the other hand, it demands unrealistic values of the magnetic field for switching of the magnetization. In order to reduce the switching field value the technology of the heat-assisted magnetic recording (HAMR) was proposed with the magnetic grain heating by light prior to the magnetic field application.

One of the ways to control the magnetic properties of FePt-based thin films is a partial substitution of platinum for rhodium. It has been shown recently by Mössbauer spectroscopy and magnetometry that thin films of Fe(Pt_{1-x}Rh_x) reveal ferromagnetism at room temperature in the range of $x < 0.34$. Saturated magnetization and volume fraction of the ferromagnetic phase remains almost unchanged up to $x = 0.20$.

We present an extensive magneto-optical Kerr effect (MOKE) investigation of the FePt and FePt_{0.84}Rh_{0.16} epitaxial thin films, unperturbed and after the femtosecond laser pulse excitation. The films were produced by the magnetron co-sputtering onto a (001)-oriented MgO substrate. Film thickness was 20 nm.

Both the steady-state and time-resolved MOKE results were obtained with the home-built setup with 1 kHz Legend-USP Ti:Sapphire regenerative amplifier used as a source of 800 nm, 35 fs long laser pulses.

Steady-state MOKE hysteresis loops of both films are shown in Fig. 1. While the saturated magnetization of the films remained unchanged, the saturated Kerr rotation angle for FePt_{0.84}Rh_{0.16} sample was reduced more than twice. Coercivity for the FePt_{0.84}Rh_{0.16} film dropped only slightly with respect to FePt and the shape of the loop changed notably.

A striking difference was found in the time-resolved MOKE results between the two studied films. For FePt film the saturated Kerr rotation angle dropped within ~ 0.5 ps by $\sim 65\%$ of its magnitude (8 mJ/cm² at 800 nm) in a nice agreement with the published data. In the identical conditions Kerr angle value for FePt_{0.84}Rh_{0.16} sample could be modified by not more than $\sim 5\%$. This indicates clearly that an admixture of rhodium makes the $L1_0$ -FePt thin films significantly more stable to ultrafast photoexcitation.

MOKE studies were carried out at the PCR Federal Center of Shared Facilities of KFU.

[1] A.A. Valiullin et al., *Bull. of the RAS: Physics*, **79** (2015) 999-1001.

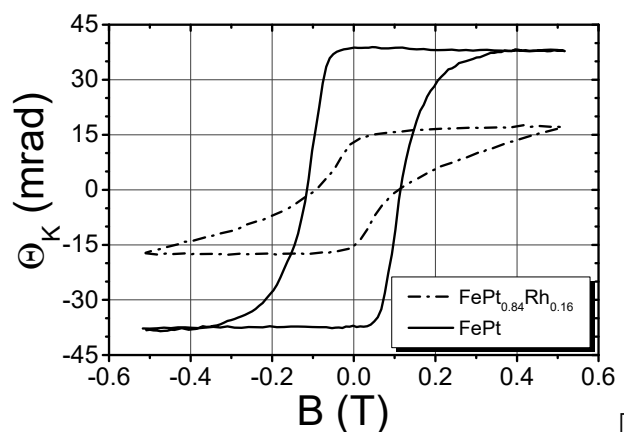


Fig. 1. Room temperature MOKE hysteresis loops of the $L1_0$ FePt and FePt_{0.84}Rh_{0.16} thin films on (001)-MgO substrate.

2PO-J-5

MAGNETOOPTICAL VISUALIZATION OF WELD SEAMS

Berzhansky V.N., Lugovskoy N.V., Filippov D.M., Prokopov A.R., Shuysky A.A.

V.I. Vernadsky Crimean Federal University, 95007, Academician Vernadsky Ave. 4, Simferopol, Russia

lugovskoynv@mail.ru

Magneto-optical (MO) eddy current (EC) defectoscopy is a convenient method for visualization of defects in metal structures. As MOEC sensors are used epitaxial garnet ferrite films. The use of such MO sensors allows to obtain in real time geometric images of micron sizes defects, including subsurface ones. This paper presents the results of visualization of model objects of type «Defect-free weld (DFW)» and "Weld with defects (WWD)". Test objects DFW were welded seams in polished plates of Al alloy and stainless steel. Test objects WWD were welded seams in pipe steel with microcracks. Epitaxial garnet ferrite films of the general formula $(\text{BiSmLu})_3(\text{FeGa})_5\text{O}_{12}$ with magnetic crystallographic anisotropy of the "easy axis" type are used as the MO sensors. The eddy current was excited by an alternating magnetic field of normal or longitudinal configuration. The frequency of the excitation field varied from 8 to 80 kHz, the amplitude was from 20 to 400 Oe, and a constant bias field was also used. The trajectories of eddy currents vary in the vicinity of the defect, what is registered by the MO sensor.

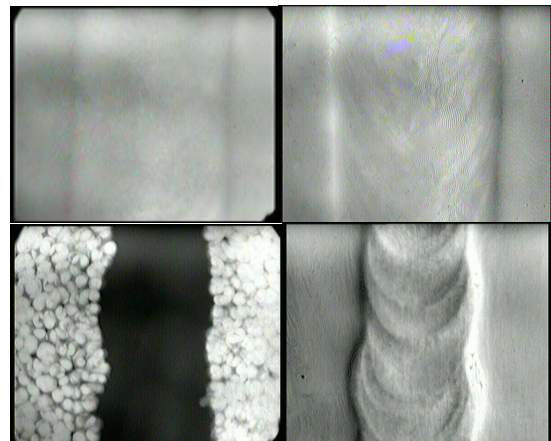


Fig. 1 MO images of welds in samples of aluminium (a, b) and stainless steel (c, d) obtained in normal (a, c) and longitudinal (b, d) fields.

As an example, Fig. 1 shows MO images of defect-free welds in samples from aluminum and stainless steel, measured at a frequency of 25 kHz. Topology and size of the eddy magnetic fields in magnetic and non-magnetic materials is significantly different. The amplitudes of the alternating magnetic field necessary to visualize welds in Al samples are about 3 times larger than for stainless steel samples. It can be seen that the MO images of seams in the case of a normal field have a binary structure, and in the case of a longitudinal field, an analog one. With an analog image, the gradient structure of the seam is visible. Similar effects were observed on weld with defects samples. In addition, images of visually undetectable sub-surface microcracks were obtained. It is also shown that the sensitivity of the MO sensor can be increased by using a weak constant magnetic field.

Calculation of the configuration of the vortex magnetic fields near the defects by solving the corresponding integral equations [1] showed that the amplitude of the total magnetic field and its topology caused by eddy conduction currents and variable magnetization in magnetic materials significantly differ from the magnitude and distribution of induced magnetic fields in nonmagnetic materials, which is well confirmed by experiment.

The work was partially supported by the RF Ministry Education and Science (project no. 3.7126.2017).

[1] V. N. Berzhansky, D. M. Filippov, N.V. Lugovskoy, *Phys. Procedia*, **230** (2016) 273-278.

2PO-J-6

POLARIZATION DEGENERATE PHOTONIC BAND GAPS IN PERIODICALLY MAGNETISED MEDIUM

Karavaeva N.I.^{1,2}, Barabanenkov Y.N.³, Logunov M.V.³, Nikitov S.A.³, Merzlikin A.M.^{1,2}

¹ ITAE RAS, Moscow, Russia

² MIPT (SU), Dolgoprudny, Russia

³ Kotel'nikov IRE RAS, Moscow, Russia

karavaeva@phystech.edu

Recently special interest is attracted to manipulating of light propagation by spatially-periodic media – photonic crystals (PC) that possess photonic band gaps. For PC contained electro-optical and/or magneto-optical components it is possible to manage band structure and control the propagation and polarisation of light by external electric/magnetic fields. In particularly it was shown appearance of new band gap at magnetization of two-dimensional PC [1] and enhancement of Faraday rotation [2]. All these PC can become the key element of fast optical and optoelectronic devices such as spatial modulators (the so-called SLM and MOSLM [2]), switches, splitters and circulators [3].

We have considered the formation of band gaps in homogeneous periodically magnetized (in two dimensions) magneto-optical media (see fig.1). The magnetization is directed along the axe of the crystal. We consider a square cell, which quarter is filled with material that has magnetisation opposite to the magnetisation of the remaining host matrix.

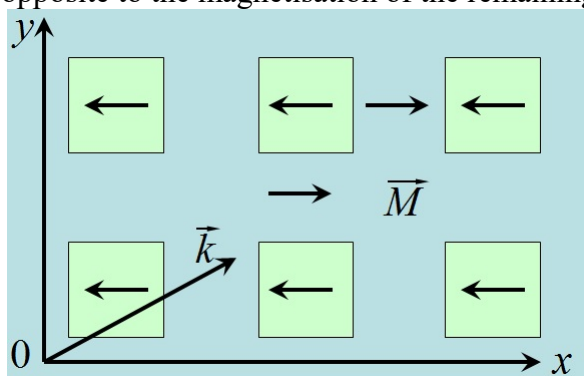


Fig.1. The structure under consideration.

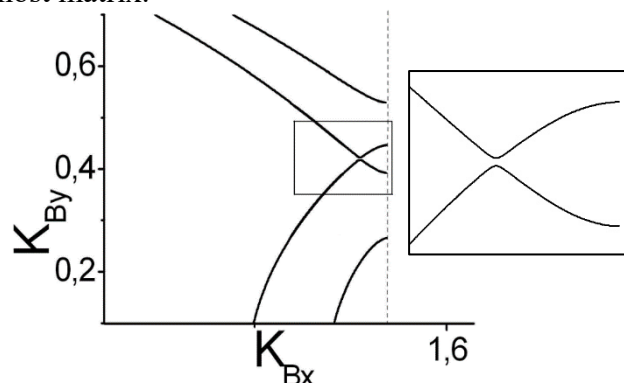


Fig. 2. Isosurface curve, reduced to first Brillouin zone.

The role of magnetization in such spatial structure is dual. Firstly, it leads to spatial periodicity. Secondly, the structure becomes anisotropic. The anisotropy is caused by the geometry, indeed all two-dimensional structure possess anisotropy. We show formation of band gaps and therefore considered structure is a photonic crystal (see fig. 2). Moreover gaps form both at the boundary of Brillouin zone and inside it. The band gap inside Brillouin zone (which is shown at insert on fig. 2) reveals itself as reconnection of isofrequency curves corresponding to different polarization. As a consequence this gap is degenerate with respect to polarization. Such gap is a distinctive feature of two-dimensional periodicity, it cannot be observed in homogeneous structure periodically magnetized along one direction [4].

[1] A.M. Merzlikin, M. Levy, A.A. Jalali, A.P. Vinogradov, *Phys. Rev. B*, **79** (2009) 195103.

[2] S.Mito, H. Takagi, et al., *J. Appl. Phys.*, **109** (2011) 07E313.

[3] Z. Wang, S. Fan, *Optics Letters*., **30** (2005) 1989.

[4] A.M. Merzlikin, M. Levy, et al., *Opt. Commun.*, **283** (2010) 4298–4302.

2PO-J-7

TAMM PLASMON-POLARITONS STRUCTURES WITH BI-SUBSTITUTED GARNET LAYERS

*Mikhailova T.V., Shaposhnikov A.N., Prokopov A.R., Karavainikov A.V., Tomilin S.V.,
Lyashko S.D., Berzhansky V.N.*
V.I. Vernadsky Crimean Federal University, Simferopol, Russia
taciamic@yandex.ru

To construct magneto-optical sensors, elements that allow significant rotation of the polarization plane of the transmitted light are required. The nanostructures of photonic crystals with bismuth-substituted garnet layers can be used as such elements. The amplification of intensity of magneto-optical effects in these structures occurs due to the phenomena of interference and diffraction and, if the structure of a photonic crystal is limited on the one side by a metal, the excitation of optical Tamm states (Tamm plasmon-polaritons – TPP). In this work the TPP structures $[\text{TiO}_2/\text{SiO}_2]^7/\text{M1}/\text{M2}/\text{SiO}_2/\text{Au}$ (No.1) and $[\text{TiO}_2/\text{SiO}_2]^7/\text{M1}/\text{SiO}_2/\text{Au}$ (No.2) with Bi-substituted iron garnets of composition $\text{Bi}_{1,0}\text{Y}_{0,5}\text{Gd}_{1,5}\text{Fe}_{4,2}\text{Al}_{0,8}\text{O}_{12}$ (M1) and $\text{Bi}_{2,5}\text{Gd}_{0,5}\text{Fe}_{3,8}\text{Al}_{1,2}\text{O}_{12}$ (M2) were proposed, synthesized and investigated. To form the structures, the methods of electron-beam evaporation, ion-beam sputtering and thermal evaporation were used. Gold coating was deposited with a gradient of the effective thickness along the selected direction using the procedure outlined in [1]. That made it possible to investigate the features of TPP resonance as a function of the thickness of the metal coating.

Theoretically and experimentally it was shown, that the resonance on TPP has the maximum optical quality factor and transmission at some “optimal” thickness of Au coating (in the range from 30 to 40 nm). The following values of the Faraday rotation were obtained experimentally at gold thickness of 65.2 nm: -12.3 degrees at 645 nm for structure No. 1 and -2.1 degrees at 664 nm for structure No. 2. Spectral dependencies of transmittance and the magneto-optical Faraday effect as a function of the thickness of Au coating for structure No. 1 are shown in Fig. 1.

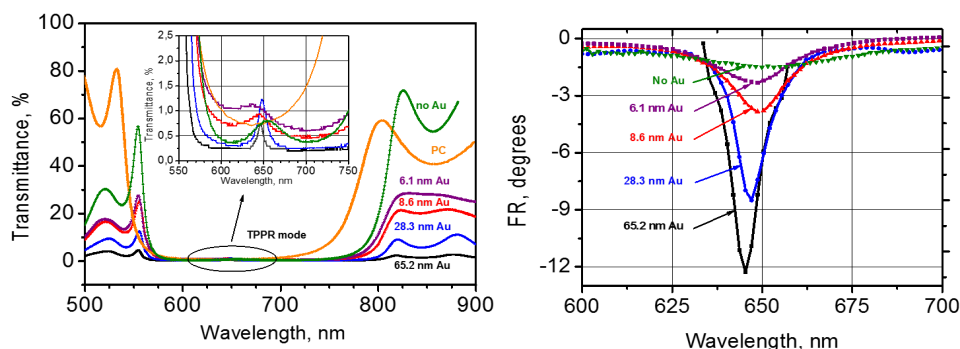


Fig. 1. Spectra of transmittance and Faraday rotation (FR) of structure No.1 as a function of the thickness of Au coating.

This work is support by the RF Ministry of Education and Science (project no. 3.7126.2017).

[1] S.V. Tomilin, V.N. Berzhansky, A.N. Shaposhnikov, A.R. Prokopov, E.T. Milyukova, A.V. Karavaynikov and O.A. Tomilina, *J. Phys.: Conf. Ser.*, **741** (2016) 012113.

2PO-J-8

SHORT-SCALE MAGNETOOPTICAL EFFECTS IN MAGNETIC MEDIA WITH DISORDER

Kozhaev M.A.^{1,2}, Niyazov R.A.³, Belotelov V.I.^{1,4}

¹ Russian Quantum Center, Skolkovo, Moscow, Russia

² Prokhorov General Physics Institute RAS, Moscow, Russia

³ Petersburg Nuclear Physics Institute, Saint-Petersburg, Russia

⁴ Moscow State University, Moscow, Russia

mikhail.kozhaev@gmail.com

Magneto-optical effects provide the ample opportunities for light intensity and polarization manipulation. It is used for a variety of tasks in many fields: information processing, laser measuring techniques, nonreciprocal optics etc. Nanostructured materials are known for their possibility to enhance the light control efficiency. In recent articles on plasmonic and photonic crystals the effects significant increase of magnitude has been demonstrated [1,2]. However, magneto-optical effects in scattering disordered media have not been sufficiently theoretically investigated and described.

In this work we considered infinite magnetic medium with uncorrelated inclusions [3]. Light propagation from infinitely remote dipole source has been examined. The theoretical model we proposed is accurate to the ladder diagram, so only two-particle interactions are considered. To study electromagnetic field correlation between spaced points the spatial field correlation matrix \tilde{W}_{ij} is used. To characterize the field distribution Bethe-Salpeter equation has been solved according to degenerate perturbation theory. Its eigenmodes corresponds to light propagation polarization eigenchannels. The dependence of correlation field matrix on magnetization direction has been studied. A new kind of correlation dependence between perpendicular light polarizations demonstrated (Fig. 1). Such an effect may exist only in magnetic media with light scattering inclusions.

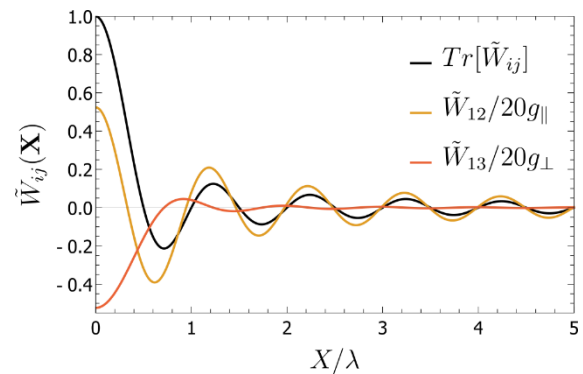


Fig. 1. The correlation of electromagnetic field polarization on the distance between considered points. Here \tilde{W}_{ij} shows the correlation between E_i and E_j components of field. The distance is normalized on wavelength λ . Orange and red lines correspond to magnetization direction parallel and perpendicular to \mathbf{X} , accordingly. Black line shows field intensity correlation.

Support by Russian Foundation for Basic Research (Project No. 16-02-01065) is acknowledged.

[1] V.I. Belotelov et al., *Phys. Rev. B*, **89** (2014) 045118.

[2] N.E. Khokhlov et al., *J. Phys. D*, **48** (2015) 095001.

[3] M.A. Kozhaev, R.A. Niyazov, V.I. Belotelov, *Phys. Rev. A*, **95** (2017) 023819.

2PO-J-9

TUNABILITY OF THE WAVEVECTOR OF SPIN WAVES OPTICALLY GENERATED IN IRON GARNET FILMS

*Savochkin I.V.*¹, *Jäckl M.*², *Belotelov V.I.*^{1,3}, *Akimov I.A.*^{2,4}, *Kozhaev M.A.*^{3,5}, *Sylgacheva D.A.*^{1,3},
Chernov A.I.^{3,5}, *Shaposhnikov A.N.*⁶, *Prokopov A.R.*⁶, *Berzhansky V.N.*⁶, *Yakovlev D.R.*^{2,4},
Zvezdin A.K.^{3,5}, *Bayer M.*^{2,4}

¹ Lomonosov Moscow State University, Moscow, Russia

² Experimentelle Physik 2, TU Dortmund, Dortmund, Germany

³ Russian Quantum Center, Skolkovo, Moscow, Russia

⁴ Ioffe Institute, Russian Academy of Sciences, St. Petersburg, Russia

⁵ Prokhorov General Physics Institute, Russian Academy of Sciences, Moscow, Russia

⁶ Vernadsky Crimean Federal University, Simferopol, Russia

savochkin@physics.msu.ru

Excitation of spin waves (SW) and their detection in magnetic materials can be accomplished all-optically by the fs-laser pulses using the pump-probe technique [1, 2]. However, usually broad spectrum of optically excited magnons hides the microscopic spin dynamics and results in fast decay of the magnetization precession.

In this work we identify a novel feature of the periodic optical excitation of SWs. In particular, we excited magnetization of the sample with a sequence of circularly polarized pulses (Fig 1) at high repetition rate so that interval between pulses was shorter than the decay time of the oscillations, which provides a collective phenomenon. SWs of the frequencies multiple to the laser pulse repetition rate are mostly supported while SWs of the frequencies that are semi-integer multiples to the laser pulse repetition rate become suppressed. As a result, SWs are generated in a specific narrow range of wavenumbers. Furthermore, modifying laser pulse repetition rate or value of the external magnetic field provides significant level of SW wavelength tunability. In our particular case, we have chosen a magnetic film with such magnetic parameters and thickness that allow to change SW wavelength by about 20 times from 15 μm to 290 μm with just tiny modification of the external magnetic field by a few percent.

This work was financially supported by the Russian President Grant (Project No. MD-1615.2017.2).

[1] M. van Kampen et al., *Phys. Rev. Lett.*, **88** (2002) 227201.

[2] T. Satoh et al., *Nature Photon.*, **6** (2012) 662-666.

[3] L.P. Pitaevskii, *J. Exptl. Theoret. Phys.*, **39** (1960) 1450-1458.

[4] J.P. van der Ziel et al., *Phys. Rev. Lett.*, **15** (1965) 190-193.

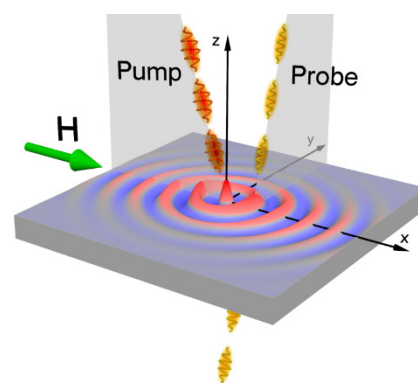


Fig. 1. Scheme of the pump-probe experiment: magnetization dynamics is excited by circularly polarized pump pulses via inverse Faraday effect [3, 4] and is observed by the variation of the Faraday angle of the linearly polarized probe pulses propagating through the sample at some time delay with respect to the pump pulses. The external magnetic field \mathbf{H} is applied in-plane of the sample using electromagnet.

2PO-J-10

LOCAL EXCITATION OF THE ULTRAFAST MAGNETIZATION DYNAMICS IN THE MAGNETOPHOTONIC CRYSTALS BY FS-LASER PULSES

Chernov A.I.^{1,2}, Kozhaev M.A.^{1,2}, Sylgacheva D.A.^{1,3}, Belotelov V.I.^{1,3}

¹ Russian Quantum Center, Skolkovo, Moscow, Russia

² Prokhorov General Physics Institute RAS, Moscow, Russia

³ Moscow State University, Moscow, Russia

ach@rqc.ru

Ultrafast optical excitation is one of few approaches allowing realization of convenient and tunable spin control with high spatial and temporal resolutions. Focused laser pulses induce the effective magnetic field inside the material via inverse Faraday effect (IFE) leading to deviation of the magnetization resulting in the launching of the spin waves. Advantages of the approach are contactless and local excitation [1] within the micron area together with possibility to control the type and parameters of spin waves [2]. Recently it has been demonstrated that micro-structured materials can be used to enhance such phenomena as Faraday effect, transversal magneto optic Kerr effect and others up to the orders of a magnitude [3]. However increase of the inverse magneto optical effects have not been studied.

In this work we used the two-colour pump-probe experimental technique to excite and detect the magnetization dynamics in magnetophotonic crystals (MPCs). The MPC is formed by two Bragg mirrors and a transparent magnetic dielectric sandwiched between them. Magneto optical effects in MPC are governed by the magnetic film layer. The combined theoretical investigation and experimental results demonstrate the possibility to enhance the inverse magneto optical effects. Clear comparison of the MPC and the stand-alone magnetic film of the same thickness and composition give the magnetization precession amplitude enhancement by a factor of 2.5 and the local IFE increase up to 5.6 times. The origin of the enhancement is due to the pronounced concentration of the electromagnetic energy within the magnetic layer gained by the optical confinement. The demonstrated local IFE increase can be used in applications requiring magnetization manipulation in submicron scale.

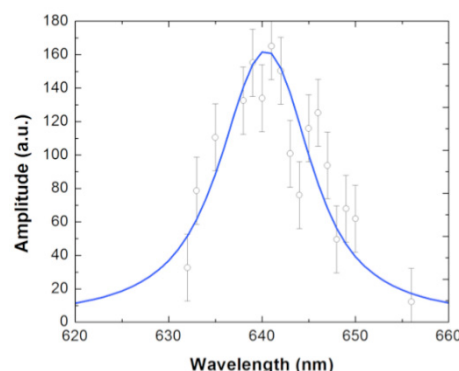


Fig. 1. Optical pumping of the magnetization dynamics in the MPC. Amplitude of the magnetization precession depending on the pump beam wavelength. Points are experimental data, blue solid line – theoretical calculation.

Support by Russian President Grant (Project No. MD-1615.2017.2) is acknowledged.

[1] A.I. Chernov et al., *Phys. Solid State*, **58** (2016) 1128.

[2] A.I. Chernov et al., *Opt. Lett.*, **42** (2017) 279.

[3] V.I. Belotelov et al., *Nature Nanotech.*, **6** (2011) 370.

2PO-J-11

MAGNETO-OPTICAL EFFECTS IN NON-PERIODICAL AND NON-SYMMETRICAL MAGNETO-PLASMONIC STRUCTURES

*Kalish A.N.^{1,2}, Kozhaev M.A.^{1,3}, Komarov R.S.², Achanta V.G.⁴, Agrawal A.⁴, Dagesyan S.A.²,
Khokhlov N.E.^{1,2}, Belotelov V.I.^{1,2}*

¹ Russian Quantum Center, Moscow, Russia

² Faculty of Physics, Lomonosov Moscow State University, Moscow, Russia

³ A.M. Prokhorov General Physics Institute of the Russian Academy of Sciences, Moscow, Russia

⁴ Tata Institute of Fundamental Research, Mumbai, India

kalish@physics.msu.ru

The enhancement of magneto-optical effects in structured media has been a subject of active research during recent years. In particular, magneto-plasmonic crystals have been studied which are periodic structures supporting surface plasmon polaritons and containing magnetic materials. It was demonstrated that the transverse Kerr effect and the Faraday effect are resonantly enhanced in magnetoplasmonic crystals [1], and also novel promising effects arise, namely the longitudinal magneto-photonic intensity effect [2]. These effects are of resonant nature, due to their relation to the excitation of eigenmodes (surface plasmon polaritons or waveguide modes), which leads to narrow spectral range of magneto-optical response.

Plasmonic quasicrystals demonstrate broadband optical response and, moreover, it is polarization-independent for 2D structures [3]. We investigate theoretically and experimentally magneto-optical effects in similar structures formed by a uniform magnetic dielectric film and a quasiperiodic 1D or 2D metallic lattice. Two types of structures are studied: (i) the 1D quasi-periodic grating specially designed for obtaining plasmonic resonances at certain range of frequencies, and (ii) the 2D structure with 10-fold rotational symmetry. Theoretical approach based on modal analysis is developed. The Faraday effect as well as the transverse Kerr effect demonstrate broadband enhancement. We also find the conditions for the enhancement of the longitudinal magneto-photonic intensity effect.

Due to symmetry reasons linear effects associated with in-plane magnetization (such as the transverse Kerr effect) are prohibited at normal incidence. However, for practical reasons it would be useful to observe the transverse Kerr effect at normal incidence. For that reason, the spatial symmetry of the structure should be broken. To achieve that we investigate a plasmonic crystal formed by a uniform magnetic dielectric film and a non-symmetrical 1D metallic lattice. The non-zero transverse Kerr effect was observed at normal incidence, which is consistent with the theoretical considerations.

The work is supported by the Russian Foundation for Basic Research (project 16-52-45061) and the Russian Presidential Grant MK-2047.2017.2.

- [1] V.I. Belotelov et al., *Nature Nanotechn.*, **6** (2011) 370.
- [2] V.I. Belotelov et al., *Nature Comm.*, **4** (2013) 2128.
- [3] S. Kasture, et al., *Sci. Rep.*, **4** (2014) 5257.

2PO-J-12

ENHANCEMENT OF MAGNETO-OPTICAL EFFECTS IN DIELECTRIC METASURFACES WITH MIE-TYPE RESONANCES

*Barsukova M.G.¹, Shorokhov A.S.¹, Musorin A.I.¹, Shcherbakov M.R.¹, Neshev D.N.²,
Kivshar Y.S.², Fedyanin A.A.¹*

¹ Faculty of Physics, Lomonosov Moscow State University, Moscow 119991, Russia

² Nonlinear Physics Centre, Research School of Physics and Engineering, Australian National University, Canberra ACT 2601, Australia
barsukova@nanolab.phys.msu.ru

One of the most powerful method for controlling and modulating light parameters is the use of an external magnetic field. Magneto-optical effects can be notably amplified in nanostructured materials [1, 2]. High-index nanoparticles offer novel opportunities for controlling light at the subwavelength scale based on the strong localization of electric and magnetic fields in the nanoparticles forming Mie-type resonances [3]. This feature makes them similar to plasmonic nanostructures but not suffering from Ohmic losses. In this work, we combine the excellence of all-dielectric resonant nanostructures and magnetic materials for creating active magneto-optical metadevices driven by Mie-type resonances. It is well established that by applying a magnetic field one can control the optical response of various magnetic structures [1, 4].

The samples represent metasurfaces composed of a 5-nm-thick nickel film deposited on top of an array of silicon nanodisks. The shape of the nanodisks is chosen to match the position of the lowest Mie-type resonances [5]. Magnetic dipole resonance of such structures exists in the visible spectral range. Magneto-optical intensity effect is studied in Voigt geometry. The spectrum of the magneto-optical response shows a five-fold resonant enhancement in the spectral vicinity of the magnetic dipole Mie-type resonance compared to the flat nickel film. Thus, the enhancement relates to the magnetic dipole resonances of the silicon nanodisks in the metasurface.

In summary, we have demonstrated experimentally and confirmed numerically the multifold enhancement of magneto-optical response near the magnetic dipole Mie-type resonance of silicon nanoparticles covered with a thin magnetic film. These results establish a novel approach for magnetic-field-controlled devices for silicon nanophotonics.

[1] M. Inoue, et al., *J. Phys. D*, **39** (2006) R151.

[2] L.E. Kreilkamp, et al., *Phys. Rev. X*, **3** (2013) 041019.

[3] A. I. Kuznetsov et al., , *Science*, **354** (2016) aag2472.

[4] M.Inoue et al., *Springer Series in Materials Science (Springer-Verlag, Berlin Heidelberg)*, (2013), Chap. 178

[5] I. Staude et al., *ACS Nano*, **7** (2013) 7824.

2PO-J-13

AC AND DC MAGNETIC FIELD SENSOR BASED ON MAGNETOPLASMONIC CRYSTAL

Belyaev V.¹, Grunin A.², Rodionova V.¹, Fedyanin A.²

¹ STP “Fabrika” & FunMagMa, Immanuel Kant Baltic Federal University, Kaliningrad, Russia

² Lomonosov Moscow State University, Moscow, Russia

v.k.belyaev@gmail.com

One of the modern hot topics nowadays is using magnetic sensors in medicine applications like magnetic cardiography and tomography which requires precision measurements of magnetic field with magnitude of 10 nT for characterizing the stray fields of biological objects. The most reliable techniques which are based on superconductivity, induction or Hall effects have several restrictions connected with decreasing of sensitivity at small volumes and necessity of moving the sensor element for changing the probe position. Alternative variant which allows to avoid these restrictions is using of magneto-optical (MO) effect in reflection geometry. The sensitivity of sensors based on MO effects in reflection geometry is not enough for measuring low magnitudes but it can be increased by excitation of surface plasmon-polaritons (SPPs) on metal-dielectric interface which leads to appearance of resonant MO effects which increase the polarization plane rotation or changing the intensity of reflected light due to maximization of adsorption of light in media [1]. Thereby MO effects can be enhanced by excitation of SPPs in magnetoplasmonic crystals (MPICs) – multilayer structures fabricated of noble and ferromagnetic layers on substrate with 1D diffraction grating which allow designing local and high sensitive AC and DC magnetic field sensor [2].

MPICs were fabricated by ion-beam deposition of metals and dielectrics on a polymer substrate made of commercial digital discs with 1D spatial profile. Fabricated MPICs was attested by atomic force microscopy and stylus profilometry techniques. Magnetic properties of fabricated samples were investigated by vibration sample magnetometer. Optical and MO properties were studied by spectroscopy of reflectivity coefficient technique.

The sensor structure unites the principles of magnetomodulation technique with a possibility of using optical radiation spot as a probe. Using the MPICs allow to enhance transverse magneto-optical Kerr effect by excitation of SPPs. This approach provides high sensitivity at very small volume of media defined by diffraction limit and penetration depth of optical radiation into MPIC. Experimentally measured sensitivity equals 10^{-5} Oe at a spot size of 2 mm^2 .

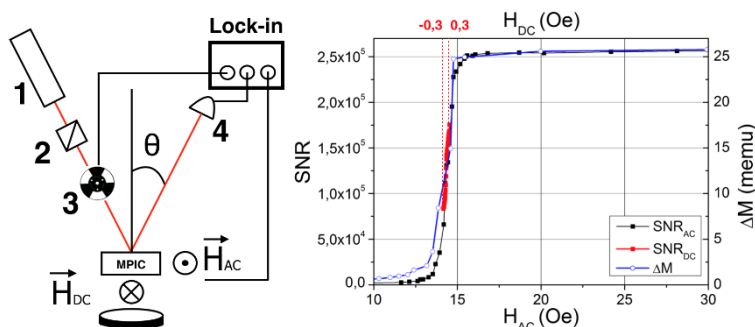


Fig.1. a) principal scheme of sensor setup, where 1 is a light source, 2 - polarizer, 3 - chopper, 4 – PMT, H_{AC} is a modulating field and H_{DC} component is measurable field and b) dependence of MO signal and magnetization curve on magnitude of applied AC and DC fields.

[1] A Grunin, A. Fedyanin, et. al., *Journal of Applied Physics*, (2013) 11317A9462013.

[2] M.Moradi, J. Akerman, et. al., *Electron. Mater. Lett.*, **11(3)** (2015) 440-446.

2PO-J-14

MAGNETIC FIELD SENSOR BASED ON THE MAGNETOPHOTONIC INTENSITY EFFECT

*Belotelov V.I.^{1,2}, Dagesyan S.A.², Kalish A.N.^{1,2}, Kapralov P.O.¹, Knyazev G.A.^{1,2},
Kozhaev M.A.^{1,3}, Vetoshko P.M.¹, Zvezdin A.K.^{1,3}*

¹ Russian Quantum Center, Skolkovo, Moscow Region, Russian Federation

² Faculty of Physics, Lomonosov Moscow State University, Moscow, Russian Federation

³ Prokhorov General Physics Institute of RAS, Moscow, Russian Federation

Corresponding author e-mail address: v.belotelov@rqc.ru

A novel type of magnetic field sensor based on a magnetoplasmonic crystal that consists of ferromagnetic dielectric film covered by gold periodic grating was developed. It is based on the recently discovered longitudinal magnetophotonic intensity effect (LMPIE) that is a resonant change in transmittance or reflectance induced by magnetic field directed in-plane perpendicularly to the grating slits [1].

The LMPIE was used for design of the magnetic field sensor. The in-plane rotating magnetic field was applied as strong as to keep the sample saturated and the intensity of the transmitted light is measured. Due to the LMPIE the second harmonic in signal occurs. The presence of a small additional in-plane constant external magnetic field lead to distortion of the signal. The other harmonics appear, in particular the 1-st and the 3-rd, with their amplitudes being proportional to the constant field. Thus, by observing the quantitative changing of the harmonics amplitudes and phases we determine the values of two planar components of the constant magnetic field.

We designed a sample with rather low saturation magnetization of the dielectric. The samples had different parameters of the gold grating: the period differs from 320 nm to 340 nm and the air slit width differs from 70 nm to 140 nm. The rotating magnetic field was equal 0.7mT. The light was normally incident on the sample. The obtained light modulation in the sample was equal to 2.5%.

On the base of this sample the model of magnetometer with optical measuring of magnetization was designed. To decrease the noise a high rotation frequency of the magnetic field equal to 126 kHz was used. The small continuous or slowly oscillating magnetic field was registered via measuring the value of third harmonic of the photodetector signal. In Fig. 1 a spectrum of measured magnetic field and calibration curve are shown. The spectrum was measured in 1 sec time interval. As follows from the Fig. 1 data the sensitivity value of 20 nT/Hz^{1/2} was obtained. This work was supported by the RFBR grants 16-52-45061 and 16-52-00137.

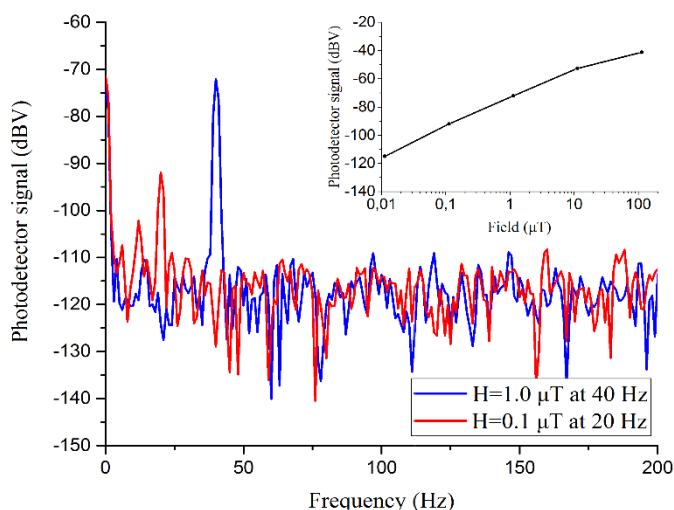


Fig. 1. The spectrum of measured magnetic field oscillating at 20 Hz (red line) and at 40 Hz (blue line).

[1] V.I. Belotelov et al., *Nat. Commun.*, **4** (2013) 2128.

2PO-J-15

TAILORING THE MAGNETO-OPTICAL RESPONSE OF 2D GOLD-GARNET NANOGRATINGS

Shein G.A.¹, Musorin A.I.¹, Chetvertukhin A.V.¹, Dolgova T.V.¹, Uchida H.², Inoue M.², Fedyanin A.A.¹

¹ Faculty of Physics, Lomonosov Moscow State University, 119991 Moscow, Russia

² Toyohashi University of Technology, Hibarigaoka, Tempaku-cho, 441-8580 Toyohashi, Japan
shein@nanolab.phys.msu.ru

Transverse magneto-optical Kerr effect is experimentally studied in two-dimensional magnetoplasmonic crystals. Optical response can be accurately controlled by an azimuthal angle of the sample. Corresponding tuning of the magneto-optical effect is observed.

The use of periodic nanostructured materials allows one to enhance magneto-optical response in various spectral regions due to plasmonic, waveguiding and other resonant effects [1-3]. Excitation and propagation of surface plasmon-polaritons can be implemented by magnetoplasmonic crystals. 1D samples support spectral tuning of the resonance controlled by angle of incidence of radiation while period of the nanostructure is fixed [4]. However, sometimes angle of incidence cannot be changed. In this case 2D magnetoplasmonic crystals can help to solve this issue. They have an additional degree of freedom to control spectral position of the resonance [5]. In this paper a flexible control of the magneto-optical response of 2D gold-garnet nanogratings is demonstrated below the red diffraction limit.

The sample is a 2D square lattice of Au spheres with 100-nm-diameter placed on 1-mm-thick quartz substrate. The periods are 600 nm. The lattice covered by a 95-nm-thick bismuth substituted iron yttrium garnet.

Fig.1 shows experimental spectral dependence of transverse magneto-optical Kerr effect (color bar) for series of azimuthal angle of the sample φ . An azimuthal angle is defined as an angle between a tangential component of wave vector and a vector of reciprocal lattice. If one changes the azimuthal angle, the phase-matching conditions for vectors of diffraction are being changed. This is the reason for the different TMOKE signals: for $\varphi = 0^\circ$ and $\varphi = 45^\circ$. This allows one to guide the light in desired direction and to leave local resonances not disturbed.

The strongest peculiarity of TMOKE is observed in vicinity of wavelength of 650 nm and $\varphi = 45^\circ$. This spectral area corresponds to the localized plasmon excitation. The TMOKE changes a sign over π . If azimuth angle is being detuned from $\varphi = 45^\circ$, magneto-optical response resonantly shifted. By this work, we show that accurate spectral control and reshaping of TMOKE signal can be realized by azimuthal angle rotation of two-dimensional gold-garnet nanogratings.

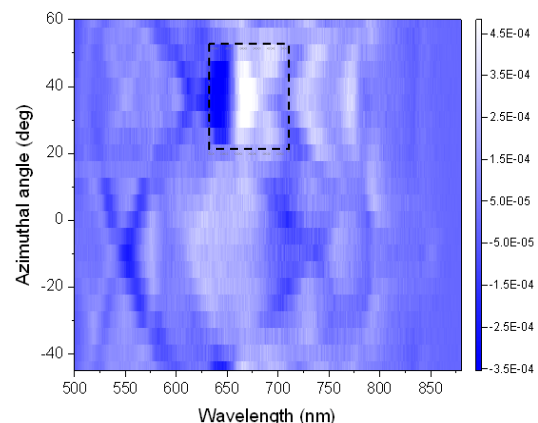


Fig.1 Azimuthal spectral dependence of TMOKE. Black dash-lined square is an area of a strong magneto-optical resonance.

- [1] M. Inoue, et al., *J. Appl. Phys. D*, **39** (2006) 151.
- [2] V.I. Belotelov, et al., *Nature Nanotech.*, **6** (2011) 370.
- [3] Baryshev A.V., et al., *JOSA B*, **30(9)** (2013) 2373.
- [4] A.A. Grunin, et al., *Appl. Phys. Lett.*, **97** (2010) 261908.
- [5] A.V. Chetvertukhin, et al., *J. Appl. Phys.*, (2013) **113** 17A942.

2PO-J-16

CONICAL REFRACTION IN MAGNETO-OPTICAL CRYSTALS

Kuznetsov E.V.^{1,2}, Merzlikin A.M.^{1,2,3}

¹ ITAE RAS, Moscow, Russia

² FSUE VNIIA, Moscow, Russia

³ MIPT, Moscow, Russia

evgenykuznet@gmail.com

Recently a lot of attention attracted to the investigation of light propagation through anisotropic and magneto-optical media or inhomogeneous structures contained anisotropic and magneto-optical components. Particularly, it was shown significant increase of Faraday rotation [1] and formation of a new kind of band gap [2] as a result of combination of anisotropic and magneto-optical properties.

We consider the influence of an external magnetic field on the light propagation through magneto-optical biaxial crystal. The special feature of a biaxial crystal is a presence of a self-intersection point on the isofrequency (the surface of a constant frequency in the space of wave vectors). In this point the wave vectors for two orthogonal polarizations coincide, thus, in this direction light propagation is degenerated in polarization. When a wave vector of incident beam corresponds to this direction, a conical refraction appears – an incident beam splits into a light cone inside the crystal. The magnetic field, as a rule, removes the degeneracy. Therefore, one may expect splitting of isofrequency around the self-intersection point [2, 3], conical refraction disappearance, and, consequently, significant changes in the direction of light propagation. This effect makes it possible to construct an operated element: in the absence of magnetic field the light propagates in the form of a cone, under applied field light propagates rectilinearly.

We show that an external magnetic field results in splitting and reconnection of the isofrequency and consequently it results in disappearance of self-intersection point. In the vicinity of that point the isofrequency splitting is proportional to the first order of off-diagonal elements of dielectric permittivity tensor (that are caused by magnetic field). That is in contrast to the other areas, where isofrequency shift is proportional to the square of off-diagonal element. We have numerically calculated that light propagates in one direction instead of a cone under applied magnetic field [4].

The isofrequency of a hyperbolic biaxial crystal (having one negative component of a dielectric permittivity tensor) intersects itself at much larger angle than the isofrequency of a conventional biaxial crystal. Another remarkable phenomenon is a band gap opening when external magnetic field is applied to hyperbolic crystal.

In practice, not all classes of crystal symmetry possess the necessary magneto-optical activity and are biaxial crystals at the same. These properties can be actualized in a composite material, for example, one representing a periodic layered structure where one layer has anisotropic properties, and the other – magneto-optical properties. In this case, the system will generally behave as a biaxial magneto-optical crystal (anisotropy in the second direction is achieved due to the preferential direction of the photonic crystal).

We have shown that the isofrequency of such photonic crystal has self-intersection points similar to those existing in biaxial crystal. We have calculated light propagation in such a photonic crystal. As in the case of biaxial crystal the conical refraction is observed in the absence of magnetic field, under applied magnetic field straight propagation of light is observed.

[1] M. Inoue and T. Fujii, *J. Appl. Phys.*, **81** (1997) 5659.

[2] A.M. Merzlikin, M. Levy, A.A. Jalali, and A.P. Vinogradov, *Phys. Rev. B*, **79** (2009) 195103.

[3] A.G. Khatkevich and S.N. Kurilkina, *J. Appl. Spectrosc.*, **51** (1989) 1329-1332.

[4] E.V. Kuznetsov and A.M. Merzlikin, *Journal of Optics*, **19** (2017) 055610.

2PO-J-17

MAGNETIC RAMAN SCATTERING IN A LOW-SYMMETRY ANTIFERROMAGNET NiWO_4

Prosnikov M.A.¹, Smirnov A.N.¹, Davydov V.Yu.¹, Volkov M.P.¹, Becker P.², Bohatý L.², Pisarev R.V.¹

¹Ioffe Institute, Russian Academy of Sciences, St. Petersburg, Russia

²University of Cologne, Institute of Geology and Mineralogy, Cologne, Germany
yotungh@gmail.com

The group of magnetic tungstates AWO_4 ($A = \text{Mn, Fe, Co, Ni, Cu}$) possesses interesting physical properties, however up to now their magnetic dynamics remains practically unexplored. A member of this group, NiWO_4 , belongs to the monoclinic crystal system with the space group $P2/c$ (#13, $Z = 2$). Magnetic Ni^{2+} ions ($S=1$) are placed inside the edge-shared oxygen octahedra, forming zig-zag chains along the c axis. Magnetic structure [1] is commensurate, and the propagation vector equals $\mathbf{k} = (1/2, 0, 0)$. In this talk, we present results of the detailed polarized Raman scattering study of NiWO_4 magnetic excitations in both paramagnetic and antiferromagnetic phases.

An intense quasi-elastic scattering due to magnetic fluctuations is observed close to the Néel temperature $T_N=62$ K, which is heavily quenched in the long-range ordered phase (see Fig. 1). Well defined one-magnon excitation (AFMR mode) is observed at 23 cm^{-1} in the $c(aa)c$ and $b(ac)a$ polarizations. Previously, another AFMR mode at 17 cm^{-1} was also observed [2]. For describing their splitting in an applied magnetic field, the symmetric off-diagonal elements were added to the exchange model. These elements can explain deviation of the Ni^{2+} moments from the c axis and their behavior in the magnetic field. For other polarizations, another broad band near 23 cm^{-1} with completely different behavior was found. This band does not soften, it survives even above T_N , and such behavior can be explained by the gapped excitations due to the dimerization. Other types of excitations were also observed in the AFM phase as shown in Fig. 1. Below T_N , noticeable hardening of the most of phonon modes was observed, suggesting magnetostriction mechanism of the spin-lattice coupling. Moreover, the dynamical coupling of the magnetic excitation with the lowest-frequency A_g phonon mode at 99 cm^{-1} was observed. This coupling leads to an asymmetric intense broadening of this mode in the overlapping region. Static magnetic properties of NiWO_4 were measured in the 5-300 K range. Experimental results are supported by magnetic symmetry analysis and numerical calculations within the linear spin wave theory.

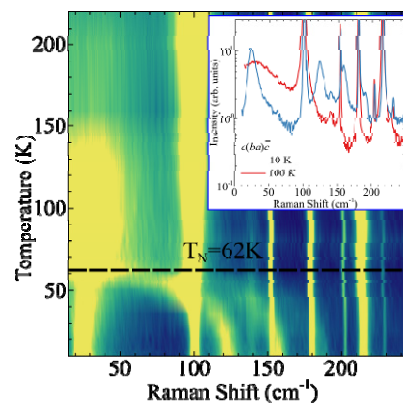


Fig. 1. Temperature dependence of low energy Raman spectra. Two spectra above and below transition in the logarithmic scale are shown as inset.

Support by the Russian Science Foundation grant No. 16-12-10456 and by the Deutsche Forschungsgemeinschaft, SFB 1238 are acknowledged.

[1] C. Wilkinson, M.J. Sprague, *Zeitschrift für Kristallographie*, **145** (1977) 96-107.

[2] V.V. Eremenko et al., *IEEE Trans. Microwave Theory and Techniques*, **12** (1974) 1069-1071.

2PO-J-18

WAVEGUIDE MAGNETOPLASMONIC STRUCTURE BASED ON FERRITE-GARNET FILM

Basiladze G.D.¹, Dolgov A.I.¹, Berzhansky V.N.¹, Karavainikov A.V.¹, Prokopov A.R.¹

¹V.I. Vernadsky Crimean Federal University, Simferopol, Russia

gbasiladze@yandex.ru

The effect of absorption of TM-polarized light in a slab magneto-optical waveguide having a plasmon resonance coating on a surface is demonstrated. The investigated magnetoplasmonic structure is schematically shown in Fig. 1, where a 1 – $\text{Gd}_3\text{Ga}_5\text{O}_{12}/(111)$ (GGG) substrate is 500 μm thick, a 2 – magnetic ferrite-garnet film $(\text{Bi,Lu})_3(\text{Fe,Ga})_5\text{O}_{12}$, 10 μm thick, grown by liquid-phase epitaxy, a 3 – buffer layer of SiO_2 , a 4 – layer of copper (Cu) with a thickness $d_{\text{Cu}} = 30$ nm.

The film of ferrite-garnet had a planar magnetic anisotropy. The input and output ends of the structure are polished along the axis of difficult magnetization. The distance between the polished ends was 4.57 mm, the size along the polished end face was 8 mm.

The SiO_2 and Cu layers are deposited on the surface of the magnetic film by the vacuum deposition method (the size of the sprayed surface is 6.2x3.95 mm). Moreover, to determine the resonance thickness of the buffer, SiO_2 layer is deposited in the form of steps, the thickness (d_{SiO_2}) of which varies along the large side of the sample.

Linearly polarized laser radiation ($\lambda = 1550$ nm) was introduced into the input end face of the magnetic film using a single-mode optical fiber. TM and TE polarization direction was established using a fiber-optic polarizer. The magnetic film was magnetized in the plane by an external magnetic field of intensity > 50 Oe, transverse to the propagation of light. Fig. 2 shows the optical loss in the sample on the coordinate input TM- and TE-polarized light beams into the input end face of the waveguide. Vertical dashed lines indicate the boundaries between longitudinal sections of the structure with different thicknesses of the SiO_2 buffer layer. It can be seen from the figure that the maximum difference between the losses of the TM and TE modes in this sample is achieved when the sections of the heterostructure with the buffer layer thicknesses d_{SiO_2} are 13-18 nm thick.

It is assumed that the optimization of the parameters of the layers of the magnetoplasmonic structure will substantially increase the quenching of the TM modes and the transmission of the TE modes. Such structure can be used to create a magnetically controlled modulator of laser radiation intensity in the infrared range [1].

This work is support by the RF Ministry of Education and Science (project no. 3.7126.2017).

[1] G.D. Basiladze, V.N. Berzhansky, and A.I. Dolgov, *Patent RU 161388* (2016).

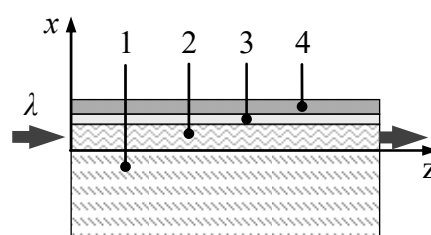


Fig. 1. Magnetoplasmonic structure
1 - GGG substrate, 2 - ferrite-garnet film,
3 - SiO_2 layer, 4 - Cu layer

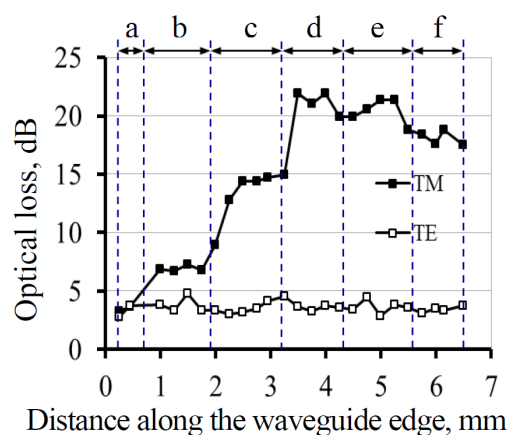


Fig. 2. TM, TE mode loss vs. SiO_2 layer thickness, where $d_{\text{SiO}_2} = 0$ nm (a, b), 8 nm (c), 13 nm (d), 18 nm (e), 23 nm (f); $d_{\text{Cu}} = 0$ nm (a), 30 nm (b-f)

2PO-J-19

**CRYSTAL GROWTH AND SPIN REORIENTATION TRANSITION IN
Sm_{0.4}Er_{0.6}FeO₃ ORTHOFERRITE***Wu A.*Shanghai Institute of Ceramics, CAS, 1295 Dingxi Road, 200050, Shanghai, China
wuanhua@mail.sic.ac.cn

High quality Sm_{0.4}Er_{0.6}FeO₃ single crystal has been successfully grown by the floating zone method. Temperature dependence of the magnetizations of Sm_{0.4}Er_{0.6}FeO₃ under ZFC process is studied in the temperature range of 4–300 K. Spin reorientation transition between Γ_2 (Gz, Fx) and Γ_4 (Gx, Fz) is observed in the temperature range of 170–210 K, which is significantly lower than that of SmFeO₃, while much higher than that of ErFeO₃. A compensation point (35.8 K) corresponding to zero magnetization and a spontaneous magnetization reversal transition at 49.5 K are observed in Sm_{0.4}Er_{0.6}FeO₃. Temperature-induced SRT of Sm_{0.4}Er_{0.6}FeO₃ is systematically studied by Terahertz time-domain spectroscopy (THz-TDS) range from 40 K to 300 K. The temperature dependence of amplitude of AFM mode coincides well with the magnetization measurement which demonstrates that SRT in Sm_{0.4}Er_{0.6}FeO₃ can be studied through the amplitude of AFM mode FID emission. The AF mode frequency is almost invariant, while the F mode frequency significantly decreases with increasing temperature, which could be explained by the temperature dependence of anisotropy energy.

2PO-J-20

MAGNETOPLASMONIC MULTILAYERED HETEROSTRUCTURES WITH GARNET FOR SENSING

*Ignatyeva D.O.^{1,2}, Sekatskii S.K.³, Kapralov P.O.², Knyazev G.A.^{1,2}, Nur-E-Alam M.¹,
Vasiliev M.⁴, Alameh K.⁴, Belotelov V.I.^{1,2}*

¹ Lomonosov Moscow State University, Faculty of Physics, Moscow, Russia

² Russian Quantum Center, Moscow, Russia

³ École Polytechnique Fédérale de Lausanne, IPHYS, Lausanne, Switzerland

⁴ Edith Cowan University, Electron Science Research Institute, Perth, Australia

ignatyeva@physics.msu.ru

The work is devoted to the study of the novel type of the magnetoplasmonic multilayered structures with ultra-high quality factor surface plasmon resonances (SPR). Such structures contain specially designed 1D photonic crystals (PC), covered with the bismuth-substituted iron-garnet layer and thin golden film. Usage of PC allows us to tune the impedance of the heterostructure so that the observed SPR significantly narrows due to the excitation of the long-range propagating modes. Utilization of the magnetic layers in such heterostructure also enhances the quality factor of the magneto-optical resonances and therefore such magnetoplasmonic heterostructure allows for a several orders of magnitude increase of the SPR-sensor sensitivity.

Previously we demonstrated that such structures enhance the sensitivity of the SPR-based sensor [1,2]. We performed the design of the magnetoplasmonic heterostructures and tuned the parameters of the structure in order to enhance the magneto-optical response via excitation of the ultralong-range propagating surface plasmon polariton (SPP) mode at 780 nm wavelength. Fabricated layered heterostructure consists of 1D PC made of alternating SiO₂ and Ta₂O₅ layers 164 nm and 119.4 nm correspondingly, coated with bismuth-substituted iron garnet layer as the ferromagnetic dielectric and 8-nm thick gold film for the excitation of the SPPs. In order to investigate the impact of the garnet layer thickness on the magnetoplasmonic resonance quality factor and magnitude we fabricated the structures with different widths of the garnet layer.

This structure with 125-nm thick garnet has the width of the SPR is 0.13 deg that corresponds to the quality factor of 350 while the resonance of the magneto-optical transversal Kerr effect related to this SPR has the width of 0.06 deg and quality factor 700. As width of the SPR and its position is related to the SPPs propagation constant we can estimate the propagation distance of the magnetoplasmon in this structure which is 42 μm. Switching of the magnetic field direction to the opposite one causes the SPP propagation constant modulation. Such propagation distance is very long compared to other magnetoplasmonic structures (e.g. the SPP propagation distance at the cobalt-air interface is only 4 μm) and is crucial for different applications such as magnetoplasmonic interferometry and signal modulation.

Propagation of the magnetoplasmons in this structure is observed directly via near-field microscopy. We excite SPP waves at the heterostructure surface using the incident laser light diffraction on the specially designed nanorods or gratings deposited on the structure. SiO₂ prism is placed on the other side of the layered heterostructure. In sensing experiments, it is used for the excitation of the SPP waves. In the presented work it is used for visualization of the SPP propagation using the CMOS matrix that detects the leaking SPP radiation.

[1] D.O. Ignatyeva et al., *Scientific Reports*, **6** (2016) 28077.

[2] D.O. Ignatyeva et al., *JETP Letters*, **104** (2016) 689-694.

2PO-J-21

INFLUENCE OF THE DISTRIBUTION ON THE GRANULE SIZE IN NANOCOMPOSITES ON OPTICAL AND MAGNETOOPTICAL SPECTRA

Gan'shina E.A.¹, Yurasov A.N.², Granovsky N.V.², Sokolov A.S.²

¹ Lomonosov Moscow State University, Moscow, Russia

² Moscow Technological University (MIREA), Moscow, Russia

nikita_granovsky@mail.ru

Optical and magneto-optical features in nanocomposites are strictly connected with size effects [1]. So as there is a very important problem to describe optical and magneto-optical spectra of these structures with influence of the distribution on the granule size. We have theoretical investigated the distribution on the granule size in nanocomposites. There is very important to consider the distribution on the granule size in size effect [1]. This fact allows to describe better optical and magneto-optical spectra of nanocomposites especially in near IR that dues intraband electron transitions. It was shown that size effect can changes the amplitude, form and sign of the optical and magneto-optical spectra. We have deduced formulas for size effect and discussed applications the distributions for corrected description optical and magneto-optical properties with regard to the effect of the granule size [2, 3]. The calculations with consideration the distribution on the granule size in size effect allow qualitatively to describe magneto-optical spectra for layerwise sprayed $(\text{Co}_{45}\text{Fe}_{45}\text{Zr}_{10})_z(\text{Al}_2\text{O}_3)_{100-z}$, and $(\text{Co}_{40}\text{Fe}_{40}\text{B}_{20})_z(\text{SiO}_2)_{100-z}$ nanocomposites.

This research was supported by the Russian Foundation for Basic Researches №15-02-02077

[1] A.N. Yurasov, *RTV*, **1(10)** (2016) 25-27.

[2] Niklasson G.A., Granqvist C.G., *J. Appl. Phys.*, **55** (1984) 3382-3410.

[3] Granovsky A.B., Gan'shina E.A., Vinogradov A.N., Rodin I.K., Yurasov A.N., Khan H.R., *Physics of Metals and Metallography*, **91** (2001) 52-56.

2PO-J-22

NEW MECHANISM OF THE ENHANCEMENT OF THE GOOS–HANCHEN EFFECT AT MAGNETIC-NONMAGNETIC INTERFACE

*Dragunov I.E.¹, Savchenko A.S.¹, Sukhorukova O.S.¹, Tarasenko A.S.¹,
Tarasenko S.V.¹, Shavrov V.G.²*

¹ Donetsk Institute for Physics and Engineering named after A.A. Galkin, Donetsk, Ukraine

² Kotelnikov Institute of Radio Engineering and Electronics, RAS, Moscow, Russia

I_dragun60@mail.ru

As is known, the Goos–Hanchen effect is the longitudinal displacement of a beam of bulk waves which is incident on the interface between media from an optically denser medium under the conditions of total internal reflection along the line of the intersection of the sagittal plane with the interface after reflection. The Goos–Hanchen shift increases significantly if the process of energy transfer involves leaky surface polaritons. This was experimentally demonstrated in various optical schemes which allow exciting surface polaritons within the method of violated total internal reflection [1-3]. Photonic crystals in addition to metals are now often used as the optically less dense, surface active, medium [4,5]. However, all these schemes have a restriction significant for this work: an increase in the Goos–Hanchen shift is not due to the excitation of a surface polariton wave immediately at the interface with the optically denser medium.

In this report, using the stationary phase method, we show that the enhancement of the Goos–Hanchen effect for the TM (TE) wave under the condition of total internal reflection can occur even in the case of a single interface between transparent media if the evanescent electromagnetic wave with the same polarization as the incident wave is resonantly excited under the condition that the energy flux through the interface between media is identically zero.

It has been shown for the first time that the enhancement of the Goos–Hanchen effect at the interface between two optically transparent media inside the region of total internal reflection is possible even in the case of a single interface if the frequency and transverse wavenumber of the bulk TM (TE) wave incident on the optically less dense medium are such that the surface impedance (in the case of the TM wave) or the surface wave conductivity (in the case of the TE wave) vanishes, i.e., if the instantaneous energy flux through the interface between the medium owing to the evanescent wave is zero at any time. The gyrotropic or pseudochiral properties of the optically less dense medium are not all possible variants of the implementation of the proposed mechanism of the enhancement of the Goos–Hanchen shift based on the resonance excitation of the evanescent wave.

In particular, according to [6], the condition of zero input wave impedance for the TM wave or zero input wave conductivity for the TE wave (and, thereby, the formation of the proposed mechanism of the enhancement of the Goos–Hanchen effect) can be satisfied if the optically less dense medium is a onedimensional photonic crystal whose unit period is composed of optically isotropic transparent layers.

[1] S.L. Chuang, *J. Opt. Soc. Am.*, **A 3** (1986) 593-599.

[2] C. Bonnet, D. Chanvat, O. Emile, F. Bretenaker, A. le Floch, *Opt. Lett.*, **26** (2001) 666-668.

[3] X.Yin, L. Hesselink, Z.Liu, N. Fang, X.Zhang, *Appl. Phys. Lett.*, **85** (2004) 372-374.

[4] I.V. Shadrivov, A.A. Zharov, Y.S. Kivshar, *Appl. Phys. Lett.*, **83** (2003) 2713-2715.

[5] I.V. Soboleva, V.V. Moskalenko, A.A. Fedyanin, *Phys. Rev. Lett.*, **108** (2012) 123901.

[6] F.G. Bass, A.A. Bulgakov, P.P. Tetervov, *High Frequency Properties of the Semiconductors with Superlattices* (Nauka, Moscow, 1989) [in Russian].

2PO-J-23

Ce:YIG FILM GROWN ON Nd:YAG FOR MICRO LASERS*Morimoto R.¹, Goto T.^{1,2}, Takagi H.¹, Nakamura Y.¹, Uchida H.¹, Inoue M.¹*¹ Toyohashi University of Technology, Toyohashi, Aichi, Japan² JST PRESTO, Kawaguchi, Saitama, Japan

goto@ee.tut.ac.jp

Diode-pumped solid-state micro lasers are compact (~cm), highly stable, and efficient. They are used in various applications, e.g., micromachining, laser radars, and car ignition plugs. Giant pulse power (> MW) was demonstrated via passive Q-switching with saturable absorbers (e.g. Cr⁴⁺:YAG). Especially Cr⁴⁺:YAG could be grown on Nd:YAG crystals using liquid phase epitaxy method because they have the similar crystalline structures and lattice constants, which miniaturize the micro lasers [1]. Recently, we demonstrated a novel active Q-switch [2, 3] using magneto-optical effects based on a 190 μm thick ferrimagnetic rare-earth substituted iron garnet film grown on Gd₃Ga₅O₁₂ substrate by liquid phase epitaxy. Its cavity length was 10³ times smaller than other active Q-switched lasers, showing a large peak power and a small timing jitter. To further miniaturize the cavity length and integrate the Q-switch with lasing materials, magneto-optical film was directly fabricated on Nd:YAG substrates. Ce₁Y₂Fe₅O₁₂ (Ce:YIG) was used as magneto-optical material because of its large Faraday rotation and high transmittance at near-infrared region. A 1.01±0.06 μm thick Ce:YIG film was grown on Nd:YAG substrate. The target used was a one-inch diameter sintered disk with the composition of Ce₁Y_{2.5}Fe₅O_x. A KrF excimer laser producing 25 ns width pulse output at the wavelength of 248 nm was used to ablate the target. The pulse energy was 360 mJ and the repetition rate was 10 Hz throughout the experiment. The deposition was conducted in 2.6 Pa oxygen partial pressure. The substrate temperature was 850°C. The substrate used was (111) oriented Nd:YAG with the doping concentration of 1 at.% and the size of substrate was 5.2 mm × 5.2 mm. Its thickness was 0.5 mm.

The sample showed the Faraday rotation of -0.05 deg/μm at the wavelength of 1064 nm. The easy axis of magnetization was in-plane. Its saturation magnetization was 110±7 emu/cm³. XRD measurement showed that the film was epitaxially grown. This is the first report of the epitaxial growth of Ce:YIG on Nd:YAG substrate.

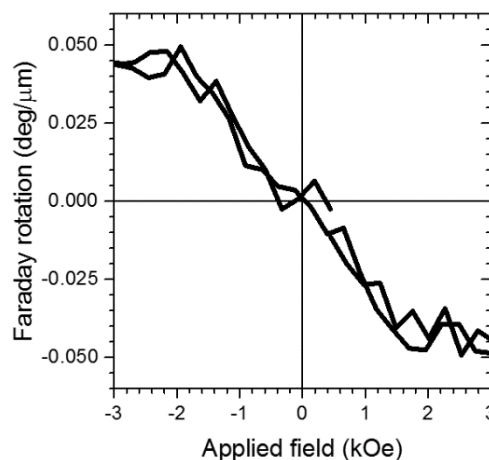


Fig. 1. Faraday rotation loop of Ce:YIG grown on a Nd:YAG substrate. The measured wavelength was 1064 nm.

This research acknowledges support from the JSPS KAKENHI No. 26220902, No. 26706009, No. 15H02240 and JST PRESTO JPMJPR1524.

- [1] B. Ferrand, et al., *Opt. Mater.*, **11** (1999) 101–114.
 [2] T. Goto, et al., *Opt. Express*, **24** (2016) 17635–17643.
 [3] R. Morimoto, et al., *Sci. Rep.*, **6** (2016) 38679.

2 July

Sunday

12:00-14:00

poster session
2PO-K

**“High Frequency
Properties and
Metamaterials”**

2PO-K-1

MANIFESTATIONS OF UNIDIRECTIONAL EXCHANGE ANISOTROPY IN FERRITE-GARNET FILMS WITH A 'WEAK' SUBLATTICE

Poimanov V.¹, Shkar V.², Nepochatykh Yu.², Sampath V.³, Shavrov V.⁴, Koledov V.⁴

¹ Donetsk National University, Universitetskaya 24, Donetsk, Ukraine

² A.A. Galkin Donetsk Institute for Physics and Engineering, 72 R. Luxemburg, Donetsk, Ukraine

³ Indian Institute of Technology Madras, Chennai-600 036, India

⁴ Kotelnikov IRE RAS, Moscow, Russia, 125009, Mokhovaya 11/7

Vladislav.Poymanow@yandex.ru

Gadolinium ferrite-garnet shows the unique characteristic of unidirectional anisotropy of the exchange interaction, which influences the “weak” gadolinium sublattice. The field strength of this anisotropy is in excess of 200 kOe due to a “strong” (“combined”) iron sublattice [1] and it acts in a direction opposite to that of the magnetization of the rare-earth sublattice. This leads to the magnetic compensation appearing at a certain temperature (). The reverse effect of the exchange field from the rare-earth sublattice is very weak. It is therefore called unidirectional exchange anisotropy. The exchange interaction within the gadolinium sublattice is also weak and does not lead to the ordering of the magnetic moments of these cations [1]. These magnetic moments are in paramagnetic state in a negative exchange field iron sublattice which lead to their streamlining, known as paraprocess. With temperature decreasing (below the magnetic compensation point) the exchange interaction within the rare-earth sublattice increases and at a certain temperature, , it becomes ferromagnetic.

For ferrimagnets, which do not have a 'weak' sublattice, in particular for yttrium iron garnet, which is far from the point of magnetic ordering, magnetostriction is a quadratic function of the magnetization. It is shown [1] that the presence of the 'weak' sublattice in rare-earth ferrite-garnets leads to manifestation of abnormal phenomena. In particular, in gadolinium ferrite-garnet a breach of magnetostriction “evenness” and also magnetoresistance and magnetocaloric effect are observed. Magnetostriction shows linear dependence of magnetization due to the influence of unidirectional exchange anisotropy. To the linear magnetostriction is associated a thermodynamically opposite effect, namely piezomagnetism (the occurrence of the magnetization under the action of elastic stresses in the absence of a magnetic field).

The aim of the present study was to detect piezomagnetic and other related effects given rise to by the presence of a 'weak' sublattice in ferrite. Ferromagnetic resonance method was used to study submicron-thick ferrite-garnet film grown by the liquid-phase epitaxy technique on gallium-gadolinium garnet substrate oriented along (111) direction. It has been found that during magnetization in a normal magnetic field an abnormal change in the magnetization of the sample as well as rotation of the magnetic axes occur: i.e., in the straight (one) field direction the magnetization increases and the axis of the magnetic field rotates to align with it; on the other hand, in the opposite external field direction, magnetization decreases and the axis rotates to align with it in the opposite direction. This ferromagnetic behavior in a magnetic field can be explained by the simultaneous manifestation of the linear magnetostriction and the piezomagnetic effect that operate due to the paraprocess in a “weak” magnetic sublattice, which is located in a unidirectional exchange field of the “strong” sublattice [1]. Piezomagnetic effect is observed for the first time in ferrite.

[1] K.P. Belov, *Physics-Uspokhi*, **42** (1999) 711–717.

2PO-K-2

STRUCTURE, CONDUCTION AND HIGH FREQUENCY REFLECTIVE PROPERTIES OF AMORPHOUS NANOGRANULATED COMPOSITES

Antonets I.V.¹, Kotov L.N.¹

¹ Syktyvkar State University, Syktyvkar, Russia
aiv@mail.ru

The micro- and nanostructure of 328–772 nm thick amorphous granulated $(\text{Co}_{45}\text{Fe}_{45}\text{Zr}_{10})_x(\text{ZrO})_{1-x}$ ($0.27 < x < 0.61$) composite films deposited in argon on a lavsan substrate and 2.2–5.8 μm thick amorphous granulated $(\text{Co}_{45}\text{Fe}_{45}\text{Zr}_{10})_x(\text{Al}_2\text{O}_3)_{1-x}$ ($0.30 < x < 0.75$) composite films deposited onto a pyroceramic substrate has been examined using atomic force microscopy, magnetic force microscopy, and scanning electron microscopy. It was found that the mean sizes of the grain and the metallic phase content govern the electrical conductive and high frequency (8-38 GHz) reflective properties of these films [1,2].

Using magnetic force microscopy, we visualized a magnetic domain structure in the films. It was found that with the increase in the content of metals, the character of the behavior of the structure of magnetic domains in films varies significantly. In films with a content of a metallic phase up to 45%, the magnetic structure was not detected. In some films, a uniform regular strip domain structure strongly depending on the film size was discovered. In films where the substrate relief has a considerable influence on the granulated structure, the strip domain structure changes to a low-ordered labyrinth one. Being initially disordered, the surface acquires a strip structure at a metal content above 56 at. % (Fig. 1). With an increase in the thickness of the film and in the metal content, the strip domain structure becomes still more ordered and transforms to subparallel order. Nevertheless, the surface structure of the films directly influences the domain structure, as can be judged by the periodicity disturbance and strip discontinuities, which are topographically related to disturbances in the regular structure.

After high-temperature annealing, the films acquired a distinct granular structure while maintaining the island-bridge microrelief as a whole. Exceptions were films with a total metal content of more than 60–65%, in which a significant part of the islands merged.

According to the results of AFM studies revealed interval content of the metal phase, wherein the observed strong dependence of the grain size and the conductivity. These dependences are the strongest for $Me > 43$ at. %. It was also found that conductivity grows by eight orders of magnitude from 10^{-4} to 10^4 $(\Omega \text{ m})^{-1}$ and high frequency reflection coefficient of the films rises by three orders of magnitude from 4.5×10^{-4} to 7.4×10^{-1} in the range Me up to 60 at. %.

It was shown that the structure of amorphous granulated films influences their conductive and reflective properties and that the dependences of the grain mean size, conductivity, and reflection coefficient on the metal content correlated with each other. The behavior of the reflection coefficient is influenced by the variations in the conductivity of the amorphous films, and the conductivity in turn depends on their structure and composition.

[1] I.V. Antonets, L.N. Kotov et. al., *Technical Physics*, 2, **62**(2017) 261-269.

[2] I.V. Antonets, L.N. Kotov et. al., *Technical Physics*, 3, **61**(2016) 416-423.

2PO-K-3

EFFECTIVE PERMEABILITY OF COMPOSITE FILMS WITH DIFFERENT METALS AND DIELECTRICS

Kotov L.N.¹, Kurdyukova E.G.¹, Kalinin Yu.E.², Sitnikov A.V.²

¹ Radiophysics dept., Syktyvkar State University, Oktyabrsky Pr. 55, 167001, Syktyvkar, Russia

² Voronezh State Technical University, Voronezh, Russia

kurdyukova.kate@gmail.com

The research is devoted to a studying of the spectra effective permeability in composite films with different metals and dielectrics.

We have conducted research of frequency dependences of real and imaginary parts of effective, and loss tangent of composite films for different metals and dielectrics at different ratios of concentrations of metal and dielectric De phases in the composite films. Targets from metallic alloys $Me(\text{Co-Fe-Zr}, \text{Co})$ and dielectrics $De (\text{Al}_2\text{O}_3, \text{SiO}_2, \text{Zr}_2\text{O}_3)$ was used for the production of films^{1,2}. Deposition of films was carried out using ion bombardment of targets on lamsan substrate. The thickness of the films was 0.3-1.5 μm . Measure the actual ϵ' and imaginary ϵ'' component of permittivity were performed on the values of inductance, capacitance and quality factor Q of the serial resonant circuit at room temperature in the frequency range $f = 30\text{-}300$ MHz. Permeability was determined from the ratio of capacitance of the capacitor with a film (magnetic metal-insulator) and without film. The dielectric and magnetic film areas are given deposits in the measured permeability, so it is called the effective permeability. The results the permeability spectra for films for different composition of metals and dielectrics show that they have similar trend of behavior. The weak frequency dependence for the real part ϵ' is observed throughout the frequency range from 30 to 120 MHz. There was a decline for the dependence for higher frequencies. It happened because there is relaxation of the electric polarization vector of inhomogeneous surroundings.

At the same range frequency direct correlation of loss frequency characteristic of the imaginary component ϵ'' . Consider three series of magnetic composite films: $(\text{Co-Fe-Zr})_x+(\text{Zr}_2\text{O}_3)_y$, $(\text{Co-Fe-Zr})_x+(\text{Al}_2\text{O}_3)_y$ and $\text{Co}_x+(\text{SiO}_2)_y$. One of them was cyclotron resonance, which was observed throughout the frequency range from 32 to 35 MHz for all combination of metal phases. Eddy currents determine the basic loss at high frequencies.³

The work performed in part under financial support Ministry of Education and Science of Russian Federation, project №1503.

[1] Antonets I.V., Kotov L.N., Kalinin Yu.E., Sitnikov A.V., Shavrov V.G., Sheglov V.I., *Technical Physics Letters*, **40(7)** (2014) 584-586.

[2] Kotov L.N., Turkov V.K., Vlasov V.S., Kalinin Yu.E., Sitnikov A.V., Asadullin F.F., *JMMM*, **316** (2007) e20-e22.

[3] Lutsev L.V., Kazantseva N.T., Tchmutin I.A., Rynkina N.G., Kalinin Yu.E., Sitnikoff A.V., *J. Physics: Cond. Matter*, **14** (2002) 1-15.

2PO-K-4

MEASUREMENT OF MAGNETIC NOISE IN MAGNETOIMPEDANCE SENSING ELEMENT

Antonov A.S.¹, Sultan-Zade T.T.¹, Buznikov N.A.²

¹ IMPEDANCE JSC, 124527 Zelenograd, Moscow, Russia

² Scientific & Research Institute of Natural Gases and Gas Technologies – Gazprom VNIIGAZ, 142717 Razvilka, Leninsky District, Moscow Region, Russia
asantonov@inbox.ru

The magnetoimpedance (MI) effect is attracted considerable attention due to its potential for magnetic sensing applications. One of the most important features of magnetic sensors is the capability to detect the external field with high accuracy. In this connection, it is of importance to achieve low noise level. The noise performance of the MI-based sensors has been studied previously, and different contributions to the noise have been analyzed [1].

In this work, we present a direct method for the magnetic noise measurement in sensing element. In contrast to previous studies, we investigate the nonlinear off-diagonal MI [2], when the excitation current amplitude is high enough to cause the magnetization reversal in the sensing element. The noise for the second harmonic in the pick-up coil voltage frequency spectrum was analyzed. The sensing element was made of a pick-up coil wound on a glass-coated Co-based amorphous microwire with nearly-zero magnetostriction. The current frequency was about 1MHz. The magnetic noise in the sensing element was measured by means of the frequency demodulation (see Fig. 1).

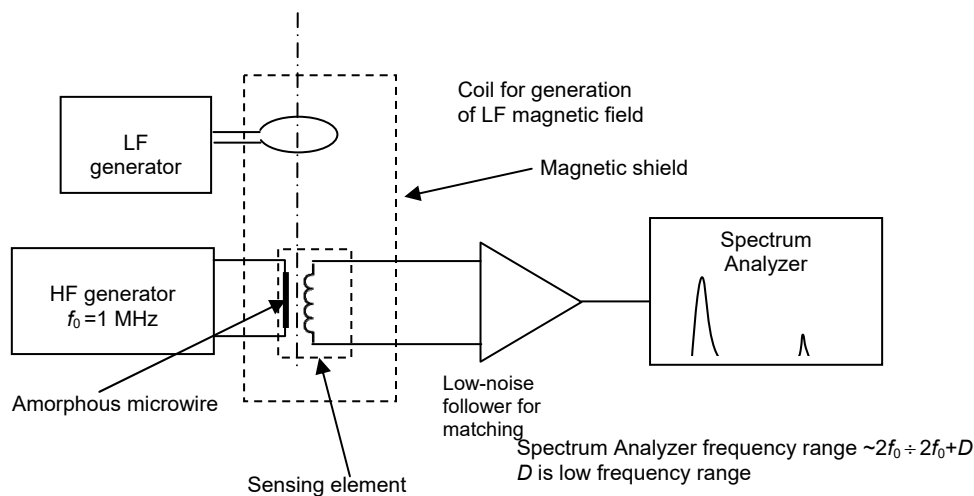


Fig. 1. A schematic of the experimental setup

The advantage of the method is that the signal-to-noise ratio is measured in a single experiment, when the high-frequency generator is turned on and off. In addition, the method allows one to avoid the noise of the electronic circuit forming the detected signal. Results of measurements show that the magnetic noise depends on many parameters such as the excitation conditions, the microwire length, diameter, the magnetic anisotropy, etc. A minimum noise level for the studied sensing elements is about $30\text{pT/Hz}^{1/2}$ in the limit of low frequencies (at 1Hz).

[1] B. Dufay et al., *IEEE Sens. J.*, **13** (2013) 379.

[2] A.S. Antonov et al., *J. Phys. D: Appl. Phys.*, **34** (2001) 752.

2PO-K-5

EXCITATION OF MAGNETOELASTIC OSCILLATIONS IN YIG FILMS BY DOMAIN STRUCTURE

Beznosikov D.S.¹, Osipov S.V.¹, Kotov L.N.¹, Vlasov V.S.¹, Lutsev L.V.²

¹ Pitirim Sorokin Syktyvkar State University, Syktyvkar, Russia

² Ioffe Physical-Technical Institute, RAS, St. Petersburg, Russia

uvn71p3@gmail.com

An experimental investigation of the magnetoelastic oscillations excitation in YIG films with different thicknesses grown on GGG substrates with a thickness of 500 μm was carried out. To excite the magnetoelastic oscillations, the films were placed in a superposition of a constant and an alternating magnetic field. To record elastic oscillations, the film and piezotransducer was glued on a cylindrical quartz delay line with dimensions of 8 mm in diameter and 40 mm in length.

The excitation efficiency as a function of the constant magnetic field magnitude, which varied in the range 8-350 mT, was investigated. The constant magnetic field was applied in the plane of the film, and the alternating field, along the plane normal. To observe the magnetic structure by MFM method, the Integra Prima atomic-force microscope (AFM) (NT-MDT) was used. The cantilevers MFMR (Nanoworld) with a 20-nm thick magnetic CoCr coating and a tip radius about 40 nm were used. A strip domain structure is typical for all films. The number of closed domains increases according to gross of the film thickness. The domain structure period was about 6 μm for all films, the average domain width was 3 μm . With a film thickness more than 10 μm , labyrinth-like domain structures are observed. The obtained dependences of the excited elastic waves amplitudes show that their behavior is determined by the static magnetization and the monodomainization processes.

Two main mechanisms for efficient excitation of elastic oscillations can be identified: these are the processes of the magnetization rotation and synchronous oscillations of the domain structure in a large region of the film. The first mechanism is characterized by the presence of a maximum and decreasing of the elastic oscillations amplitude with increasing of constant field. For the second, the amplitude of the elastic oscillations increases with a further yield in saturation with a constant field increase. There are extrema in the dependencies caused by the rotation processes during the magnetization of the films.

We gratefully acknowledge the financial support from RFBR (grant # 17-02-01138).

2PO-K-6

MODELING OF EXCITATION OF MAGNETOELASTIC OSCILLATIONS IN THE THREE-LAYER STRUCTURE BY RF MAGNETIC FIELD

Dianov M.Yu.¹, Vlasov V.S.¹, Kotov L.N.¹, Shavrov V.G.², Shcheglov V.I.²

¹Syktyvkar State University named after Pitirim Sorokin, Syktyvkar, Russia

²Institute of Radio Engineering and Electronics of RAS, Moscow, Russia

Dianovmy@yandex.ru

The work is devoted to modeling of elastic and magnetic microwave oscillations in a three-layer structure. We consider most general nonlinear case not limit the power of the exciting signal. The method of decomposition into eigenfunctions of the elasticity problem and the method of finite-difference approximation of coordinate derivatives were used in the work.

The geometry of the problem was following. The external dc magnetic field was directed perpendicularly to the plane of multilayer plate and alternating circularly polarized magnetic field was directed in the plane of the plate. For the simplicity of the problem elastic properties and cubic crystallographic symmetry of all the layers were the same. However, the layers have different magnetic properties and thickness. To describe the magnetoelastic oscillations we used Landau-Lifshitz equation in the form of Gilbert and the equations for the elastic displacements.

The method of decomposition into eigenfunctions of the elasticity problem was applied firstly. The solution for elastic displacements was a sum of two terms, of linear function of the coordinate and the deviation from this linear function. The solution was sought in two ways. First, in the form of an expansion in a series of functions that are solutions of the homogeneous equation with homogeneous boundary conditions. Coupling between the layers in our model was carried out by the zero terms Fourier decomposition. For simplicity we consider only the first and zero terms in the decomposition. The system for describing of excitation of magnetoelastic oscillations contains 11 first-order equations for the first and third layer, and 7 first-order equations for second (central nonmagnetic) layer. The resulting system of equations was solved numerically by the 4-5 orders Runge-Kutta method.

Second, Landau-Lifshitz equation and the equations for the elastic displacements were solved by the method of finite-difference approximation of coordinate derivatives.

For calculations the parameters of the yttrium iron garnet were used. The curves of the magnetization components dependence on time were plotted for both methods. At the same time, the parameters of the material were choose as with the absence of magnetoelastic coupling in the case of linear ferromagnetic resonance and the first mode of elastic oscillations eigenfrequencies were equal. Plotted graphs were compared by the two methods, as well as for with the similar cases for a single-layer and double-layer structures. The calculation models for single-layer and double-layer structures were described earlier in works [1, 2]. For the calculations almost the same data for the three-layer and single-layer structure were obtained which means a good agreement with the single-layer and double-layer models. The time dependences of the magnetization and the elastic displacements for various frequencies were plotted. Also the resonance curves were plotted for the cases of linear and nonlinear oscillations.

The support from RFBR (grant # 17-02-01138) are gratefully acknowledged.

[1] V.S. Vlasov et al., *J. Comm. Tech. El.*, **54** (2009) 821-832.

[2] V.S. Vlasov, V.G. Shavrov, V.I. Shcheglov, *J. Comm. Tech. El.*, **59** (2014) 441-455.

2PO-K-7

SURFACE ELECTROMAGNETIC-SPIN COUPLED WAVES IN MAGNETIC SEMICONDUCTOR

Bychkov I.V.¹, Kuzmin D.A.¹, Tolkachev V.A.¹, Plaksin P.S.¹, Shavrov V.G.²

¹ Chelyabinsk State University, 129 Br.Kashirinykh Str., Chelyabinsk, Russian Federation

² Kotelnikov Institute of Radio-engineering and Electronics of RAS, 11/7 Mokhovaya Str.,
Moscow, Russian Federation

bychkov@csu.ru

Surface plasmon-polaritons are usually investigated with the outlook on applications in processing and storing information devices [1]. In our recent works we have considered some graphene-containing structures. Some interesting results on speckle-pattern rotation in graphene-coated optical fibers [2], surface plasmon manipulation by magnetic field in the planar gyrotropic waveguide formed by two graphene layers [3], plasmonically induced magnetic field and Faraday rotation of high order modes in graphene-covered nanowires [4, 5] have been obtained.

In the present work we have theoretically investigated the surface electromagnetic-spin waves in magnetic semiconductor which is placed in the external magnetic field. Semiconductor is described by both frequency-dependent electric and magnetic permittivities. The problem has the following geometry: xz -plane is the surface of the semiconductor ($y > 0$) placed in vacuum ($y < 0$), external magnetic field is pointed along z -axis. Solving the Maxwell's equations with the boundary conditions, dispersion equation of the surface electromagnetic-spin coupled waves has been obtained and the components of electromagnetic field of the surface wave have been calculated.

All calculations have been performed in the framework of phenomenological approach, which is valid while the localization length of the surface wave is much larger than the lattice constant. Electrodynamics of the magnetic semiconductor may be described by tensors of electric and magnetic permittivities.

Dispersion equation allows one to obtain the condition of existence of the surface electromagnetic-spin coupled waves: they may propagate in semiconductor at certain carrier's concentrations and propagation angles. We have calculated the frequency range when these surface electromagnetic-spin waves may be excited. It is shown that under certain conditions the non-reciprocity effect may manifest itself for the surface electromagnetic-spin waves.

This work was supported in part by RFBR (grants ## 16-37-00023, 16-07-00751, 16-29-14045, 17-57-150001), RScF (grant # 14-22-00279) and grant of the President of the Russian Federation MK-1653.2017.2.

- [1] K. S. Novoselov, et al. *Nature*, **490** (2012) 192-200.
- [2] D. A. Kuzminr, et al. *Opt. Lett.*, **40** (2015) 890-893.
- [3] D. A. Kuzminr, et al. *Opt. Lett.*, **40** (2015) 2557-2560.
- [4] D. A. Kuzminr, et al. *Opt. Lett.*, **41** (2016) 396-399.
- [5] D. A. Kuzminr, et al. *Nano Lett.*, **16** (2016) 4391-4395.

2PO-K-8

THE ANALYSIS OF AFM IMAGES OF THE METAL-DIELECTRIC COMPOSITE FILMS

Kotov L.N.¹, Vlasov V.S.¹, Ustyugov V.A.¹, Kalinin Yu.E.², Sitnikov A.V.², Golubev E.A.³

¹ Syktyvkar State University, Syktyvkar, Russia

² Voronezh State Technical University, Voronezh, Russia,

³ Komi Scientific Center of UB RAS, Syktyvkar, Russia

ustyugovva@gmail.com

Nano- and microstructure of $\{(Co_4-Fe_4-Zr_{0.7})_x+(Al_2O_3)_{1-x}\}$ (A1 series) and $\{(Co_1-Nb_{0.2}-Ta_{0.05})_x+(SiO_2)_{1-x}\}$ (A2 series) films was investigated by atomic force microscopy. The chemical composition and thickness of the films were determined using a scanning electron microscope JSM-6400 [4].

Also the surface topology images and density contrast images of the films with different metal/dielectric concentration ratio were obtained. From the topographic image of the films (series A) it can be seen that the films have a strongly inhomogeneous surface structure. At low concentration of metal individual granules on the surface are unselectable, multiple topographical heterogeneities are merged into a single labyrinth-like structure. When the concentration of the metal is above the percolation threshold observed large depressions and elevations. This indicates a more uniform growth of the film by high metal/dielectric concentration ratio.

By analysis of the phase contrast images of films series A different situation is visible. At low concentration of metal phase small metal spherical particles are included in a dielectric matrix. This leads, for example, a broadening of the FMR resonance line due to lack of exchange interaction and particle size variation. By increasing the metal concentration increases the number of fine particles that initially due to surface tension forces uniformly filled with the dielectric matrix. When the concentration of metal exceeds the critical value, particles merge into larger units and by the concentration $x = 58\%$ there is an inversion of the phase structure. This changes also the magnetic structure, which leads to a sharp narrowing of the FMR line.

Support by RFBR (grant number 13-02-01401a).

[1] Kotov L.N. et al., *JMMM*, **316(2)** (2007) 20.

[2] Kotov L.N. et al., *Journal of Nanoscience and Nanotechnology*, **12(2)** (2012) 1696.

[3] Kotov L.N. et al., *Advanced Materials Research*, **47-50 PART 1** (2008) 706-709.

2PO-K-9

ELECTRIC AND MAGNETIC PROPERTIES OF COMPOSITES BASED ON FERROMAGNETICS IN POLYMER FERROELECTRICS

*Shakirzyanov R.I.¹, Astakhov V.A.¹, Morchenko A.T.¹, Kostishyn V.G.¹,
Panina L.V.¹, Trukhanov A.V.¹, Kochervinskii V.V.², Bedin S.A.³, Bessonova N.P.²*

¹ NUST "MISIS", Moscow, Russia

² National Research Physical and Chemical Institute Karpov, Obninsk, Russia

³ Moscow State Pedagogical University, Moscow, Russia

shakirzyaoff.rafael@yandex.ru

Electric and magnetic properties of composites based on magnetic inclusions (Mn-Zn ferrite powders, amorphous ferromagnetic microwires, 3d-metal nano-particles) in matrix of polyvinylidene fluoride P(VDF-TFE) copolymers were investigated with the aim to achieve tunable and broad-band electromagnetic response. These materials have potential for applications in microsystems engineering, radio absorption and shielding, and microwave monitoring systems.

The samples were prepared by two methods, namely, crystallization from solution and hot pressing [1]. The effective permittivity, dielectric loss tangent, AC conductivity and radio absorption characteristics were studied. The structural characteristics were analyzed with the help of differential scanning calorimetry and X-ray diffractometry. The P(VDF-TFE) crystalline phase decreases with increasing the volume concentration of magnetic fillers. The magnetization reversal processes were investigated by vibrating sample magnetometer; the high frequency spectra were measured with the help of vector network analyzer and spectral analyzer.

The X-ray diffraction spectra and permittivity spectra of composites with different Mn-Zn ferrite content are shown in Fig. 1-2.

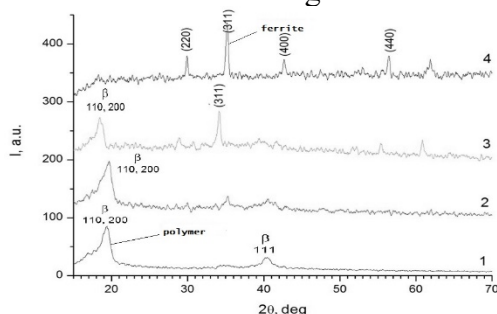


Fig. 1. X-ray diffraction spectra for P(VDF-TFE)/Mn-Zn ferrite composites with different volume concentration of ferrite powder: pure polymer (1), 5% (2), 15% (3), 50% (4)

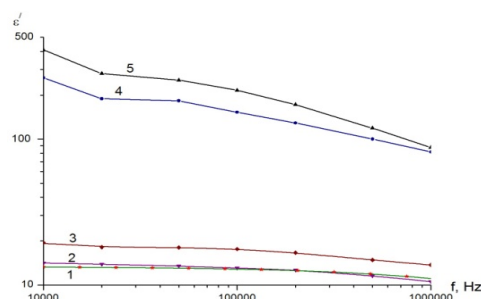


Fig. 2. Spectra of the real part of permittivity of P(VDF-TFE)/Mn-Zn ferrite composites with different volume concentration of ferrite powder: pure polymer (1), 7% (2), 15% (3), 40% (4), 40% of granulated particles (5)

The analysis of permittivity and reflection coefficient of the electromagnetic wave for composites with different contents of magnetic phase was carried out by using modified effective medium approximation [2]. A comparison of experimental and simulated results is presented.

[1] R. I. Shakirzyanov, V.A. Astakhov, A.T. Morchenko, V.V. Kochervinskii, S.A. Bedin, XXIV Int. Conf. Electromagnetic field and materials: Fundamental Physical Research. – Moscow: MPEI, INFRA-M. – 2016 (in Russian).

[2] V.A. Astakhov, R.I. Shakirzyanov, A.T. Morchenko, Z.V. Mingazheva, S.P. Kurochka, *J. Nano-Electron. Phys.* **8** (2016) 03044 (1-3).

2PO-K-10

SELF-GENERATION OF QUASI-PERIODIC SIGNALS IN FERRITE-FILM ACTIVE RING OSCILLATORS

Kondrashov A.V.^{1,2}, Ustinov A.B.^{1,2}, Metelkina K.K.¹, Kalinikos B.A.¹, Lähderanta E.²

¹ St. Petersburg Electrotechnical University, Saint-Petersburg, Russia

² Lappeenranta University of Technology, Lappeenranta, Finland

kondrashov_av@yahoo.com

At present an increased research interest to study microwave stationary and chaotic signal generation in magnetic film active ring oscillators is evident [1,2]. It is well known that a transition from regular dynamical behavior of auto-oscillators to chaotic one takes place through a series of bifurcations [3].

This work reports for the first time a detailed experimental investigation of a transition from the quasi-periodic regime to chaotic regime of the spin-wave self-generation in ferrite-film active-ring oscillator. An unusual peculiarity of this transition was that it was caused not by a chain of modulation instabilities of the initially generated harmonics (like in [4,5]), but due to entering into oscillation the new amplified harmonics of the oscillator. A special attention was given to obtain and study the stationary regimes of self-generation appearing after the third bifurcation. In the experiments, we used a set-up similar to that reported in [5]. The experimental ring system consisted of a spin-wave delay line, a broadband microwave amplifier, and an adjustable attenuator for gain control. The ring signals were measured through a directional coupler, a fast oscilloscope, and a spectrum analyzer.

The experimental investigation was carried out with a gradual increase in the relative ring gain G . We observed three bifurcations in which new sidebands having incommensurate frequencies appeared. The nature of the new sidebands was a four-wave mixing of the initial sidebands with the new single harmonic entering into oscillation. Phase portraits of the observed waveforms were reconstructed on the basis of the measured oscilloscope traces by a method of time delay. Then the values of the fractal dimension D and minimal embedding dimension were calculated using the standard Grassberger-Procaccia method. The results show that D was equaled 1.00 after the first bifurcation that corresponded to the limit cycle in the phase space. After the second and the third bifurcations the values of D were 2.12 and 3.52, respectively. These values allow concluding that the corresponding attractors of the system have a fractal structure in the phase space.

The work supported by the Russian Science Foundation (grant 14-12-01296).

[1] E. Bankowski, et. al., *Appl. Phys. Lett.*, **107** (2015) 122409.

[2] S.V. Grishin et. al. *JETP*, **121** (2015) 623-628.

[3] J. Argyris et al., *An Exploration of Dynamical Systems and Chaos* (Springer-Verlag, Berlin, Heidelberg, 2015).

[4] M. Wu et. al. *Phys. Rev. Lett.*, **102** (2009) 237203.

2PO-K-11

A NOVEL METHOD OF ESR OSCILLATING MAGNETIZATION VALUE DETERMINATION IN STRONGLY CORRELATED METALS

Gilmanov M.I.^{1,2}, Semeno A.V.¹, Samarin A.N.^{1,2}, Demishev S.V.^{1,2,3}

¹ Prokhorov General Physics Institute of RAS, Moscow, Russia

² Moscow Institute of Physics and Technology, Dolgoprudny, Russia

³ National Research University "Higher School of Economics", Moscow, Russia

gilmanov@lt.gpi.ru

All of the electron spin resonance (ESR) line parameters (g -factor, line width and resonance intensity) are substantially informative for the determination of the material magnetic state. However, while g -factor and line width could be directly obtained by the standard ESR experiments, the integral intensity of the resonance line, which is proportional to the static magnetization of oscillating moments M_0 , usually requires non trivial experimental technique to be obtained in absolute values. The value of M_0 allows attaining the concentration of ESR active moments which may differ from the concentration of magnetic moments obtained from static magnetization M_{st} . Here we report a direct experimental method of measurement of the M_0 value in metallic samples, which is based on difference in resonant conditions corresponding to different orientations of the magnetic field (\mathbf{H}) with respect to the wave vector (\mathbf{k}) of high frequency radiation. [1]

In the case of $\mathbf{k} \parallel \mathbf{H}$ microwave absorption is defined by two circularly polarized functions of magnetic permeability $\mu_{\pm} = \mu \pm \mu_a$ where $\mu(\mathbf{H})$ and $\mu_a(\mathbf{H})$ are the diagonal and non-diagonal components of magnetic permeability tensor respectively. Both of them in the ESR have a resonant form that usually corresponds to Landau-Lifshitz or Bloch type of damping. In contrast, the case of the scheme with $\mathbf{k} \perp \mathbf{H}$ may be defined by the expression $\mu = \mu - \mu_a^2/\mu$ [1]. For practical applications one should notice that different settings of experiment in its turn results in different resonance conditions namely $\omega_0 = \gamma(H_1 + 4\pi M_0)$ for $\mathbf{k} \parallel \mathbf{H}$ and $\omega_0^2 = \gamma^2 H_2(H_2 + 4\pi M_0)(1 + a^2)$ for $\mathbf{k} \perp \mathbf{H}$. Here ω_0 denotes frequency, H_1 , H_2 stands for resonance fields, M_0 corresponds to oscillating magnetization and a is a dissipation coefficient. In experiment, the difference in resonance positions for most of metallic systems is strong to make the calculation of oscillating magnetization feasible.

The described technique was applied for two strongly-correlated metallic systems: EuB_6 and CeB_6 . Received values of oscillating magnetization were equal 920Oe for EuB_6 at $T=4.2\text{K}$ and 96Oe for CeB_6 at $T=1.8\text{K}$ which are in a good agreement with quantities obtained by other methods [2, 3].

This work was supported by Programs of RAS "Electron spin resonance, spin-dependent electronic effects and spin technologies", "Electron correlations in strongly interacting systems" and by RFBR grant number 14-02-00800.

[1] J. Young, E. Uehling, *Physical Review*, **94** (1954) 544.

[2] A.V. Semeno et al., *Physical Review B*, **79** (2009) 014423.

[3] S.V. Demishev et al., *Physical Review B*, **80** (2009) 245106.

2PO-K-12

NONLINEAR PHENOMENA IN LAYERED STRUCTURES BASED ON MAGNONIC CRYSTALS

Morozova M.A., Matveev O.V., Romanenko D.V., Sharaevskii Yu.P.

Saratov State University, Saratov, Russia

olvmatveev@gmail.com

Magnonic crystals (MC) – artificial periodic structure based on ferromagnetic films in which magnetostatic waves (MSW) propagate. One of features of periodic structures is Bragg bandgaps for propagating waves. Main nonlinear effects in this structure are frequency shift to low frequencies with increasing power of input signal and formation of Bragg solitons [1].

In coupled homogeneous structures [2] effect of “nonlinear swithing” takes place, which manifests itself in suppression of linear transfer between layers in structure at high power level.

In this paper we study structure of two coupled magnonic crystals (MC-MC) using Brillouin spectroscopy. This structure based on two ferromagnetic iron-yttrium garnet films 12 μm thick. On surface of films were created grooves with period 200 μm , depth of groove 1 μm and width 100 μm . Length of one MC was 7 mm, length of other was 4 mm. Static magnetic field 785 Oe was applied parallel to excitation band, so surface MSW propagated in structure.

Such coupled periodic structure can be placed in the basis of four-port device (see Fig. 1). With help of Brillouin spectroscopy we received patterns of spatial distributions of MSW intensity. Based on this patterns transmission of output ports were constructed. Distance between input port and output ports 2 and 3 was considered equal 3/2 of length of linear transfer which was 0.7 mm. In Fig.2 shows transmissions of output ports 1 and 3 and solutions of mathematical model described in [3]. It can be seen that depending on the input power most of output power of signal is on one of three ports. Low power signals exit from port 1, medium power signals exit from port 2, high power signals exit from port 3. This nonlinear coupling of input signal is due to a combination of two effects - nonlinear shift of the bandgaps in the periodic structure and suppression of linear transfer in coupled homogeneous structure. This work was supported by the Russian Foundation for Basic Research, projects no 15-07-05901-a, no 16-29-03120–ofi-m.

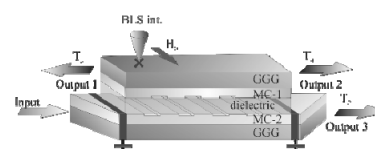


Fig. 1. Scheme of structure

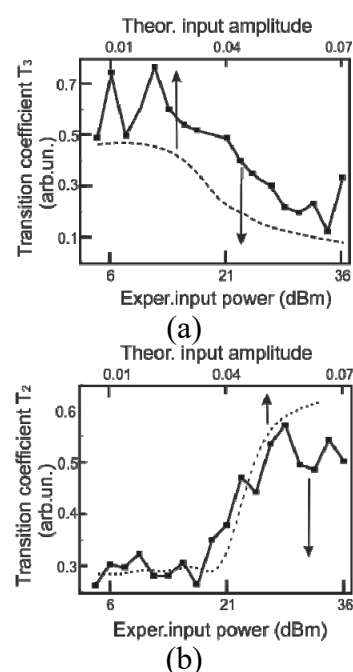


Рис. 2. Экспериментальные (сплошная) и теоретические (пунктирная) передачи выходных портов 1 (а), 3 (б).

[1] A.B. Ustinov, A.V. Drozdovskii, B.A. Kaliniko, *APL*, **96** (2010) 142513.

[2] T. Ueda, M. Tsutsumi, *IEEE Transactions on magnetic*, **38** (2002) 3114-3116.

[3] M.A. Morozova et al., *Physics of the Solid State*, **58** (2016) 1967-1974.

2PO-K-13

TEMPERATURE DEPENDENCE OF IMPEDANCE OF THE PLANAR SOFT MAGNETIC $\text{Fe}_{20}\text{Ni}_{80}/\text{Fe}_3\text{Co}_{67}\text{Cr}_3\text{Si}_{15}\text{B}_{12}/\text{Fe}_{20}\text{Ni}_{80}$ COMPOSITE

Semirov A.V.¹, Derevyanko M.S.¹, Moiseev A.A.¹, Svalov A.V.², Kurlyanskaya G.V.^{2,3}

¹ Irkutsk State University, Irkutsk, Russia

² Ural Federal University, Yekaterinburg, Russia

³ University of the Basque Country UPV-EHU, Leioa, Spain

mr.derevyanko@gmail.com

The temperature dependences of the total impedance, its real and imaginary components were studied in the case of soft magnetic composites $\text{Fe}_{20}\text{Ni}_{80}/\text{Fe}_3\text{Co}_{67}\text{Cr}_3\text{Si}_{15}\text{B}_{12}/\text{Fe}_{20}\text{Ni}_{80}$ derived by sputtering deposition of the $\text{Fe}_{20}\text{Ni}_{80}$ (1 μm thick) covering onto amorphous $\text{Fe}_3\text{Co}_{67}\text{Cr}_3\text{Si}_{15}\text{B}_{12}$ ribbon. The samples geometry was 50 mm \times 2 mm \times 20 μm . Total impedance modulus Z and its components Z' and Z'' were measured on an automated magnetoimpedance spectroscopy complex based on an Agilent 4292A precise impedance analyzer in the temperature range $T = 298 - 443$ (K). Measurements were made at operational value 1 mA of an alternating test current in the frequency range 0.1–70 (MHz).

It was found that contribution of the permalloy layer to the temperature dependences of the impedance mostly pronounced in a Curie temperature region of the amorphous ribbon at the frequencies about 20 MHz and above. So, the impedance demonstrates a change of the temperature behavior at these frequencies near the temperature of 390 K. The main contribution was related to the Z'' component as its temperature dependence at high frequencies was determinative for $Z(T)$ behavior. The temperature dependence of the Z' component is not changed in all frequency range.

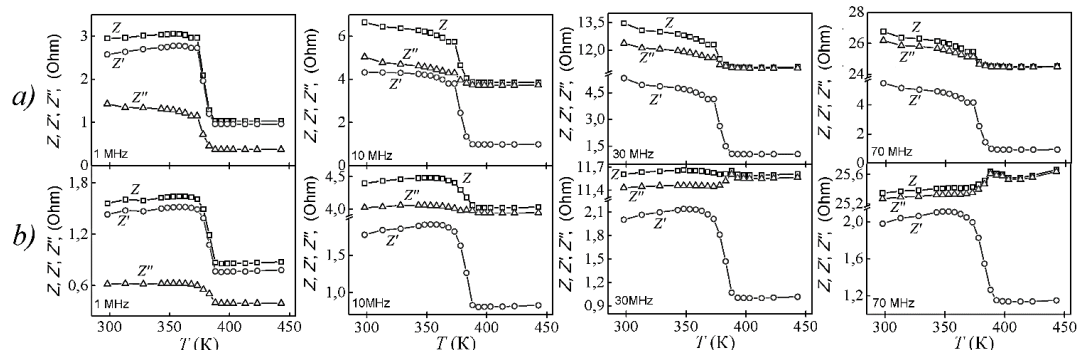


Fig. 1. Temperature dependencies of the impedance and its components of the amorphous ferromagnetic $\text{Fe}_3\text{Co}_{67}\text{Cr}_3\text{Si}_{15}\text{B}_{12}$ ribbons in the initial state (a) and covered by the $\text{Fe}_{20}\text{Ni}_{80}$ layer (b). The dependencies are derived at the alternating current frequencies of 1, 10, 30 and 70 MHz.

The impedance of the ferromagnetic conductor depends on a skin penetration depth. Due to strong skin-effect at frequencies about 30 MHz and above the impedance is conditioned by a primary current features passing in the permalloy layer. Thus, the observed features for $Z(T)$ and $Z''(T)$ dependencies can be explained by the amorphous ribbon transition from ferromagnetic state to the paramagnetic one at the temperature about 390 K. It leads to a change of the $\text{Fe}_{20}\text{Ni}_{80}$ magnetic permeability.

This work was supported by a project part of Government Assignment for Scientific Research from the Ministry of Education and Science, Russia (№ 3.1941.2017) and by the Irkutsk State University, individual research grant № 091-16-213.

2PO-K-14

TUNABLE BAND GAPS IN A LAYERED STRUCTURE BASED ON MAGNONIC CRYSTALS AND FERROELECTRICS

Matveev O.V., Romanenko D.V., Morozova M.A.

Saratov State University, Saratov, Russia

olvmatveev@gmail.com

Composite multiferroic structures (structures of alternating ferromagnetic and ferroelectric layers) are the subject of active research at present [1]. On the basis of such structures, devices in microwave range with electrical and magnetic control can be developed. This effect is based on the phase matching of delayed electromagnetic waves in ferroelectric layer and spin waves in ferromagnetic layer. As a result of synchronism, hybrid electromagnetic-spin waves (HESW) are formed, the properties of which depend both on the applied magnetic field and on the permittivity of the ferroelectric layer [2].

In this paper we study a structure of magnonic crystal with ferroelectric slab (MC-FE). A mathematical model is constructed in the form of the dispersion equation of the HESW, including components of electric and magnetic nonlinearities. In addition to the Bragg bandgaps resulting of the interaction of forward-propagating and backward-propagating spin waves, an additional bandgap (MC-FE bandgap) appears in the spectrum of the HESW in this structure. This bandgap is a result of interaction of backward-propagating spin wave and forward-propagating electromagnetic wave. In Fig. 1 shows the dispersion curves of the HESW in MC-FE, the first Bragg bandgap and MC-FE bandgap are filled.

The structure of ferromagnetic iron-yttrium garnet film with thickness of 12 μm was experimentally studied. On surface of films were created grooves with period 200 μm , depth of groove 1 μm and width 100 μm . Ferroelectric slab of barium-strontium titanate 500 μm thick and permittivity of 4000 was placed on the film. Fig. 2 shows the frequency response of HESW at input power levels -40 dBm and -27 dBm. These plots show the presence of MC-FE bandgap between first and second Bragg bandgaps in spectrum, as well as frequency shift of all bandgaps to low frequency with increasing the

This work was supported by the Russian Foundation for Basic Research, projects no 15-07-05901-a, no16-29-14021-ofi-m.

[1] A. B. Ustinov, B. A. Kalinikos, *Technical Physics Letters*, **40** (2014) 568-570.

[2] V.B.Anfinogenov et al., *Pis'ma v ZhTF*, **12** (1986) 938-943.

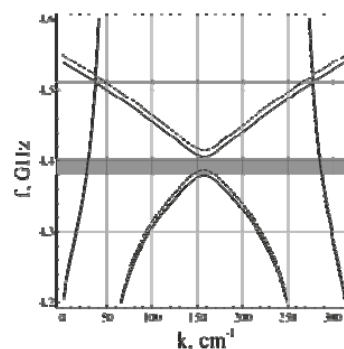


Fig. 1. HESW dispersion at input power u_1 (dashed line) and u_2 (solid line), $u_2 > u_1$.

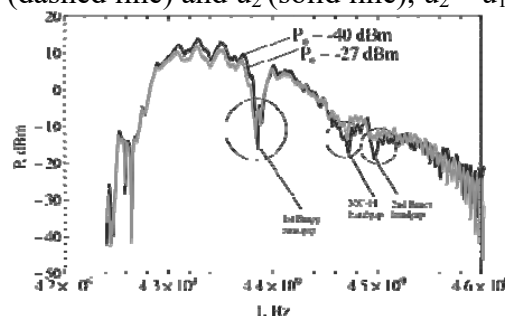


Fig. 2. Frequency response MC-FE at input power -40 dBm (dark curve) and -27 dBm (bright curve).

2PO-K-15

ANOMALOUS SPIN RELAXATION IN $\text{Eu}_{1-x}\text{Gd}_x\text{B}_6$ SOLID SOLUTIONS

*Samarin A.N.*¹, *Glushkov V.V.*^{1,2}, *Gilmanov M.I.*², *Semeno A.V.*^{1,2}, *Bogach A.V.*¹,
*Dukhnenko A.V.*³, *Kuznetsov A.V.*⁴, *Levchenko A.V.*³, *Shitsevalova N.Yu.*³,
*Voronov V.V.*¹, *Sluchanko N.E.*^{1,2}, *Demishev S.V.*^{1,5}

¹ Prokhorov General Physics Institute of RAS, Moscow, Russia

² Moscow Institute of Physics and Technology, Dolgoprudny, Moscow Region, Russia

³ Frantsevich Institute for Problems of Materials Science NAS, Kiev, Ukraine

⁴ National Research Nuclear University “MEPhI”, Moscow, Russia

⁵ National Research University Higher School of Economics, Moscow, Russia

sasha@lt.gpi.ru

We report the study of spin relaxation in the $\text{Eu}_{1-x}\text{Gd}_x\text{B}_6$ ($0 \leq x \leq 0.039$) based on high frequency (60 GHz) electron spin resonance (ESR) measurements. Measurements were performed using original ESR spectrometer based on Agilent PNA network analyzer. High quality single crystal samples were mounted as a part of bottom plate of the cavity [1]. The original technique of absolute calibration of absorption line was applied [2].

Our measurements show that there is single ESR line in the temperature range $1.8 \text{ K} < T < 300 \text{ K}$ [3], which could be fitted by the oscillating localized magnetic moments (LMM) model (fig. 1).

It is found that temperature dependence of ESR line width $W(T)$ in the paramagnetic phase consists of two temperature ranges $T_{min} < T < T_0$ and $T > T_0$. In each case $W(T)$ is linear (fig. 1). We argue that $W(T)$ dependence in the range $T_{min} < T < T_0$ corresponds to the Korringa relaxation mechanism [4]. Using Hall effect measurements we have estimated the effective on-site exchange value J_{sf} , which depends on the Gd concentration and decreases from $J_{sf} \sim 110 \text{ meV}$ for EuB_6 ($T_0 \sim 60 \text{ K}$) down to $J_{sf} \sim 40 \text{ meV}$ for $\text{Eu}_{1-x}\text{Gd}_x\text{B}_6$ ($x = 0.039$, $T_0 \sim 15 \text{ K}$). In the $T > T_0$ range ESR line width slope drastically decreases. This effect could be associated with revealing of the Overhauser relaxation (a.k.a. “bottleneck effect”) [5].

This work was supported by programmes of Russian Academy of Sciences “Electron spin resonance, spin-dependent electronic effects and spin technologies” and “Electron correlations in strongly interacting systems.” The study of parent EuB_6 single crystals was supported by RFBR project 15-02-03166.

[1] A.N. Samarin *et al.*, *Physics Procedia*, **71** (2015) 337.

[2] A.V. Semeno *et al.*, *Phys. Rev. B*, **79** (2009) 014423.

[3] V.V. Glushkov *et al.*, *Phys. Status Solidi B*, (2016), DOI:10.1002/pssb.201600571

[4] S.E. Barnes, *Adv. Phys.*, **30** (1981) 801.

[5] R.H. Taylor, *Adv. Phys.*, **24** (1975) 681.

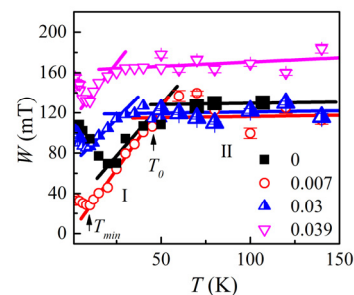


Fig. 1. Temperature dependence of ESR line width $W(T)$ for various Gd concentration. Solid lines denotes linear fits.

2PO-K-16

ASYMMETRIC STOCHASTIC RESONANCE IN FERROMAGNETIC NANOPARTICLES*Isavnin A.G.*Kazan (Volga Region) Federal University, Naberezhnye Chelny, Russian Federation
isavnin@mail.ru

Stochastic resonance is an effect that may be observed in multistable systems. It reveals previous abrupt growth and subsequent gradual decay of response of the system to a weak external periodic signal if intensity of noise in the system goes up evenly. Single-domain ferromagnetic particles with uniaxial anisotropy are bistable elements that have two stable states corresponding to opposite directions of magnetic moment vector of the particle along easy axis. External signal may be weak RF field and internal thermal noise is associated with temperature. Under such conditions dynamic magnetic susceptibility of the particle as an output signal of the system and signal-to-noise ratio display bell-shaped, passing through distinct maximum, dependence on temperature [1].

Here the influence of an auxiliary permanent magnetic field applied at arbitrary angle to the easy axis is considered. Such a field shifts stable orientations of the magnetic moment towards its direction and distorts potential barrier between two minima. That leads to modification of transition rates of the system between stable states and results in change of the dynamic magnetic susceptibility and signal-to-noise ratio. Analytical solutions are obtained within framework of discrete-orientations model based on master equation for transition rates for iron uniaxial nanoparticles in two modes: thermal overbarrier magnetization reversal and underbarrier quantum tunneling of magnetization.

[1] A.G.Isavnin, *Russian Physics Journal*, **49** (2006) 308-313.

2PO-K-17

THE RESONANCE SUSCEPTIBILITY OF TWO-LAYER EXCHANGE-COUPLED FERROMAGNETIC FILM WITH A COMBINED UNIAXIAL AND CUBIC ANISOTROPY IN THE LAYERS

Shul'ga N.V., Doroshenko R.A.

Institute of Molecule and Crystal Physics, Ufa, Russian Federation
shulga@anrb.ru

A numerical investigation of the resonance dynamic susceptibility of ferromagnetic exchange-coupled two-layer films with a combined cubic and uniaxial magnetic anisotropy of the layers has been performed. It has been shown that the value of the amplitudes of the various components of the dynamic susceptibility varies considerably by changing the magnetic field. The presence of cubic anisotropy leads to the fact that the off-diagonal components are essential in addition to the diagonal component of the dynamic susceptibility.

The evolution of the profile of the dynamic susceptibility occurring during the magnetization of the film has been investigated. In the lower fields the dynamic susceptibility distribution maximums are at the outer boundaries of the layers. With increasing of the field there is a shift of the localization of the lower FMR mode to the interlayer boundary. Depending on the direction of the magnetic field and the characteristics of the film, there are three variants of the profile evolution: displacement of the modes between layers, double displacement of the modes between layers and a shift of the localization of the lower FMR mode to the interlayer boundary without displacement of the modes. The latter variant is realized in particular in the case when the field is directed along the axis [011], see Fig. 1. At the saturation point a significant increase of the amplitude is typical for some of the dynamic susceptibility components. After magnetic saturation of the film the dynamic susceptibility distribution maximums are at the outer boundaries of the layers again.

For the lower FMR branch the most significant extremes in the dependencies of integrated dynamic susceptibility components are observed at low fields and at saturation points. Lower extremes can be observed at a shift of the localization of the lower FMR mode toward the interface between the layers. At the same time, there is the closest approach of the FMR branches. A monotonic behavior is typical for the dependencies of integrated dynamic susceptibility components of the upper FMR branches. Usually there is only one distinct extreme.

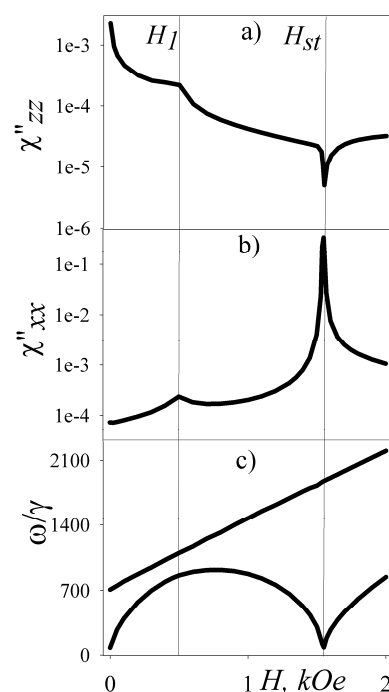


Fig. 1. Dependences of the components of the integrated dynamic susceptibility of the lower FMR mode the FMR frequencies on the external magnetic field. The field is applied along the [011] axis.

2PO-K-18

FORM OF FOCUSING MAGNETOSTATIC WAVE EMITTER MODELED BY MICROMAGNETIC SIMULATIONS

Dudko G.M.¹, Stalmakhov A.V.², Kozhevnikov A.V.¹, Khivintsev Y.V.^{1,2}, Sakharov V.K.¹, Filimonov Y.A.^{1,2}

¹ Kotelnikov SBIRE RAS, Saratov, Russia

² Saratov State University, Saratov, Russia

dugal_2010@hotmail.com

Up-to-date level of magnetostatic waves (MSW) investigations makes it possible to solve wide range of problems associated with MSW focusing in ferrite films [1, 2]. Focusing emitter typically has rather sophisticated form and direct calculation of its properties is difficult enough. The problem can be significantly simplified assuming that the emitting transducer focuses MSW to the point at given magnetizing field and signal frequency. If we interchange the point of focus and the transducer position or, in other words, if we use a point emitter, then we can easily identify the lines of equal phase at any distance from the emitter with the help of micromagnetic calculations performed, for example, in OOMMF [3]. These lines define form and size of focusing emitter at chosen focusing distance.

Fig. 1 shows the result of numerical calculation for propagation of backward volume MSW excited at frequency 4.5 GHz by the point emitter in the yttrium-iron garnet (YIG) film with dimensions 3 mm×3 mm×4 μm that was magnetized by in-plane field $H_0=1000$ Oe. Instantaneous distribution of high-frequency magnetization component m_z at fixed time moment $t=80$ ns is depicted on Fig.1. The position of one of possible focusing antennas is shown on the figure by black solid line.

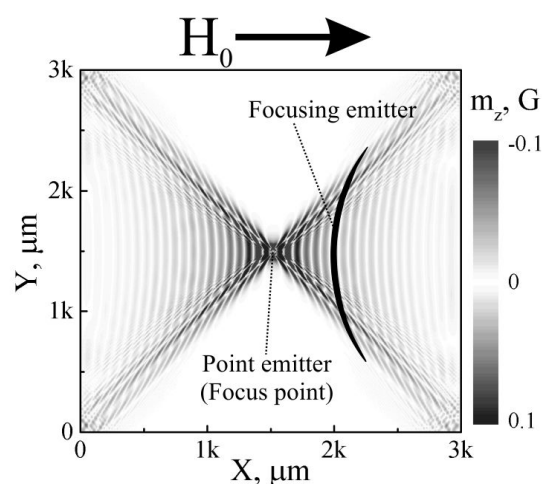


Fig. 1. Distribution of m_z -component in YIG plate from the point emitter and corresponding position of possible focusing antenna for it.

The reported study was funded by RFBR (Research projects Nos.16-07-01092, 17-07-01452).

[1] A. V. Vashkovskii, et al. *Radiotekhnika i Elektronika*, **32** (1987) 1176-1183.

[2] V. Veerakumar and R. E. Camley, *IEEE Transactions on Magnetics*, **42** (2006) 3318-3320.

[3] Donahue M., Porter D (1999), "OOMMF User's Guide, Version 1.0.Ed." In Interagency Report NISTIR 6376. Boulder: Nat. Inst. of Standards and Technology.

2PO-K-19

FERROMAGNETIC RESONANCE AND RANDOM MAGNETIC ANISOTROPY IN NANOCRYSTALLINE Fe-Zr-N FILMS

Sheftel E.N.¹, Harin E.V.¹, Tedzhetov V.A.¹, Koksharov Yu.A.²

¹ A. A. Baikov Institute of Metallurgy and Materials Science, RAS, Moscow, Russia

² Moscow State University, Moscow, Russia

harin-eugene@ya.ru

Nanocrystalline films of quasi-binary Fe-ZrN alloys, which were prepared by magnetron sputtering, are of interest as a new kind of soft magnetic materials characterized by high magnetization and thermal stability [1]. Their soft magnetic state is considered in terms of random anisotropy model [2]. In accordance with the model, the magnetization of individual grains is randomly inhomogeneous and can be described by a magnetization autocorrelation function. A magnetic autocorrelation length R_L , being an important parameter of this function, is the typical magnetic microstructure radius corresponding to relatively uniform magnetization. The model can be applied if $R_L > R_c$, where R_c is the grain radius, and grains are coupled by exchange interaction. In this case, hysteretic properties are determined by magnetic structure parameters, such as R_L , effective anisotropy $\langle K_{eff} \rangle$ on the R_L scale, and effective anisotropy K_{eff} on the R_c scale.

We present results of quantitative evaluation of magnetic structure parameters of *nanocrystalline* Fe-Zr-N films prepared by magnetron sputtering. The structure of the films (phase composition, lattice parameters, and R_c) was characterized by XRD [3]. The saturation magnetization M_s was determined using Akulov's law of approach to saturation. The magnetic structure parameters (K_{eff} , $\langle K_{eff} \rangle$, and R_L) were studied by correlation magnetometry [4]. The ferromagnetic resonance spectra were measured at room temperature and the frequency $f = 9.54$ GHz using a Varian E-4 spectrometer. Resonant condition in the film plane is given by Kittel's law $(f/\gamma)^2 = (H + 4\pi M_s)(H + 2K/M_s)$, where $\gamma = 2.9$ MHz/Oe is the gyromagnetic ratio, K is the FMR-driving magnetic anisotropy, and H is the resonant field.

According to [4], the behavior of dependence of the effective magnetic anisotropy of nanocrystalline ferromagnets on the applied magnetic field varies as the applied magnetic field increases. In particular, the effective magnetic anisotropy of the films under study in external magnetic fields, which are higher than the exchange field H_R [4], is constant and equals K_{eff} within a ferromagnetic grain. In fields below H_R , the effective magnetic anisotropy is $K_H = K_{eff}(R_c/R_H)^{3/2}$, where $R_H = (2A/M_s H)^{1/2}$ is the magnetic autocorrelation radius in field H and A is the exchange stiffness.

By the resonance field value H , the studied films can be divided into two groups: $H \geq H_R$ (group I) and $H < H_R$ (group II). In accordance with the above considerations, $|K| \approx K_{eff}$ for group I and $|K| < K_{eff}$ for group II; the values of K_H and $|K|$ correlate.

This indicates that for a material with a stochastic domain structure the dependence of the resonance field value on the frequency of ferromagnetic resonance makes it possible to estimate the dependence of the stochastic domain effective magnetic anisotropy value on the external magnetic field value.

This study was supported by RFBR (project no. 15-08-02831a).

[1] E.N. Sheftel, *Inorganic Materials: Applied Research*, **1** (2010) 17-24.

[2] G. Herzer, *Acta Materialia*, **61** (2013) 718-734.

[3] E.N. Sheftel, E.V. Harin, V.A. Tedzhetov, *et al.*, *Physica B*, **494** (2016) 13-19.

[4] R.S. Iskhakov, S.V. Komogortsev, *Phys. of Metals and Metallography*, **112** (2011) 666-681.

2PO-K-20

DEVELOPMENT OF THE MAGNETOELASTIC RESONANCE THEORY IN INHOMOGENEOUS MEDIA

Ignatchenko V.A., Polukhin D.S.

Kirensky Institute of Physics, Fed. Research Center KSC SB RAS, 660036 Krasnoyarsk, Russia
polukhin@iph.krasn.ru

The magnetoelastic resonance in a homogeneous medium has been well studied both theoretically and experimentally (see, for example, [1]). The theory of magnetoelastic resonance in an inhomogeneous medium was developed in our works [2] within the framework of the standard self-consistent approximation (SCA). In [3] we derived a new SCA that takes into account both the first and second terms of the vertex function expansion. This paper is a generalization of the new SCA to a system of two interacting wave fields of different physical nature and the development of a more accurate theory of magnetoelastic resonance in inhomogeneous ferromagnets. Diagonal and nondiagonal elements of the matrix Green's function of the coupled spin and elastic waves with a change in the ratio between the mean value ε and the mean square fluctuation $\Delta\varepsilon$ of the coupling parameter from the homogeneous case to the maximum stochastized are calculated. The calculation is carried out for different values of the correlation wave number of inhomogeneities κ_c . An example of a change in the Green's functions of spin waves $G_{mm}''(\omega)$ and elastic waves $G_{uu}''(\omega)$ with increasing $\Delta\varepsilon$ and decreasing ε is shown in Fig. 1. It can be seen that the new SCA corrects all the shortcomings of the standard SCA: dome-shaped resonances and bends on the slopes of resonance peaks. Of particular importance is the confirmation in the new theory of the previously predicted effect [2]: the appearance with a $\Delta\varepsilon$ growth in the crossing resonance point $\omega = \omega_c$ of the fine structure of the spectrum - a narrow minimum (dip) on the Green's function of spin waves and a narrow resonance peak on the Green's function of elastic waves. This phenomenon has not been observed yet experimentally.

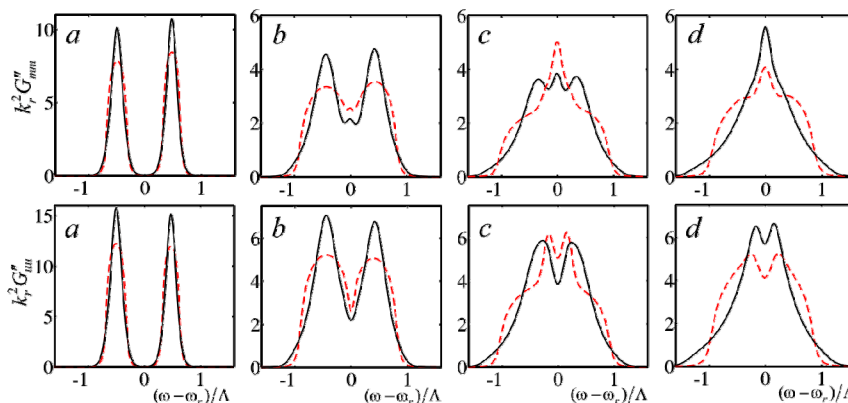


Fig. 1. Imaginary parts of the Green's function of the spin $G_{mm}''(\omega)$ (upper row) and elastic $G_{uu}''(\omega)$ (bottom row) waves in the standard (dashed red curves) and the new SCA (solid black curves) at $\kappa_c = k_c/k_r = 0.01$ and various $(\varepsilon/\varepsilon_0)^2$ and $(\Delta\varepsilon/\varepsilon_0)^2$: $a - 0.95$ and 0.05 , $b - 0.75$ and 0.25 , $c - 0.5$ and 0.5 , $d - 0$ and 1 .

- [1] A.I. Akhiezer, V.G. Bar'yakhtar, S.V. Peletminskii, *Spin Waves* (Nauka, Moscow, 1967).
 [2] V.A. Ignatchenko and D. S. Polukhin, *Zh. Eksp. Teor. Fi,z.*, **143** (2013) 238; **144** (2013) 972.
 [3] V.A. Ignatchenko and D. S. Polukhin, *J. Phys. A: Math. Theor.*, **49** (2016) 095004.

2PO-K-21

DETERMINE OF AMPLITUDES OF MAGNETOELASTIC OSCILLATIONS IN FERRITE PLATE NEAR THE SPIN-REORIENTATION PHASE TRANSITIONS

Kotov L.N., Severin P.A., Vlasov V.S.

Syktyvkar State University named after Pitirim Sorokin, Syktyvkar, Russia
pav9687@yandex.ru

We report the theoretical results on the excitation of magnetoelastic oscillations in ferrite plate by radio frequency magnetic field. The maximum amplitudes of magnetic and elastic oscillations, depending on the material parameters and parameters of external fields [1,2] were obtained. Normally and tangentially magnetized anisotropic magnetic plates were considered. The DC magnetic field was smaller than saturation field. For obtain the maximum amplitudes the method simulated annealing [3] was used.

The plane-parallel plate having magnetic, elastic and magnetoelastic properties was considered. The complete system of differential equations for the problem of excitation of magnetoelastic oscillations by radio frequency magnetic field in the normally and tangentially magnetized ferrite plate [2] were considered. The alternating magnetic field tangential vector is applied along to the surface of the plate. The problem in a Cartesian coordinate system was solved. The initial equations for obtain the system were the Landau-Lifshitz-Gilbert equation and the equations for the elastic displacement vector components. The system of the ordinary differential equations describing the magnetoelastic oscillations are obtained in the paper [3] for normally magnetized ferrite plate. We obtain the similar system of ordinary differential equations for the case of tangentially magnetized ferrite plate.

The systems of the equations were solved numerically by the Runge-Kutta Felberg 7-8 orders method with control the length of the integration step.

Three-dimensional graphics for the amplitudes of elastic displacements and component of the magnetization vector for yttrium iron garnet and manganese-zinc spinel were built over a wide frequency range of 1 MHz to 1 GHz and temperatures 1-600 K. In a narrow range of temperatures in the field of spin-reorientation phase transitions the maximum amplitudes magnetic and elastic oscillations were obtained. The behavior of the magnetic and elastic components of the oscillations in the spin-reorientation phase transitions were considered.

The support from RFBR (grant # 17-02-01138) are gratefully acknowledged.

[1] Ingber L., *Control and Cybernetics*, **25(1)** (1996) 33-54.

[2] Vlasov V.S., Kotov L.N., Asadullin F.F., *Journal of Magnetism and Magnetic Materials*, **300(1)** (2006) 48-51.

[3] Vlasov V.S., Kotov L.N., Shavrov V.G., Shcheglov V.I., *Radio Engineering and Electronics*, **54(7)** (2009), 863-874.

2PO-K-22

MAGNETOELASTIC WAVES IN ION-BEAM SPUTTERED SUBMICRON POLYCRYSTALLINE YIG FILMS ON GGG SUBSTRATES

Sakharov V.K.^{1,2}, Khivintsev Y.V.^{1,2}, Vysotskii S.L.^{1,2}, Stognij A.I.³, Filimonov Y.A.¹

¹ Kotelnikov SBIRE RAS, Saratov, Russia

² Saratov State University, Saratov, Russia

³ Scientific and Practical Materials Research Centre, NASB, Minsk, Belarus

valentin@sakharov.info

Ion-beam evaporation of submicron yttrium iron garnet (YIG) films on semiconductor [1, 2] and dielectric [3] (mainly, gadolinium gallium garnet or GGG) substrates is considered as one of possible technologies that can be used for integration of magnonic devices with semiconductor components. In the present work it is shown that YIG (200 nm)/GGG (600 μm) structure fabricated by the mentioned method can support the propagation of magnetoelastic waves (MEW). For this purpose we experimentally studied propagation of magnetostatic surface waves (MSSW) excited in YIG film by micron-sized coplanar waveguide antennas that were fabricated on its surface by analogy with [3]. A network analyzer and a microwave probe station were used to test the structure.

Excitation of “fast” MEW [4] was detected in the frequency dependence of magnitude of MSSW transmission coefficient $S_{21}(f)$ as a set of equidistant resonances (see Fig. 1) at the cut-off frequencies of transverse elastic waves of the studied YIG/GGG structure. Corresponding oscillations of MSSW phase for wave numbers $k=2000-3000\text{ cm}^{-1}$ were also observed. Those resonances emerged at applied field $H=250-300\text{ Oe}$ when maximum of MSSW transmission zone was at frequencies $f\approx 2-2.5\text{ GHz}$. Further increase of applied field led to the growth of resonances’ depth with maximum observed at $f\approx 5\text{ GHz}$ at which the thickness of YIG film corresponded to the half of wavelength of acoustic wave.

Thus, used ion-beam evaporation technology allows fabrication of magnetostrictive YIG films with good acoustic contact on the border with the GGG substrate.

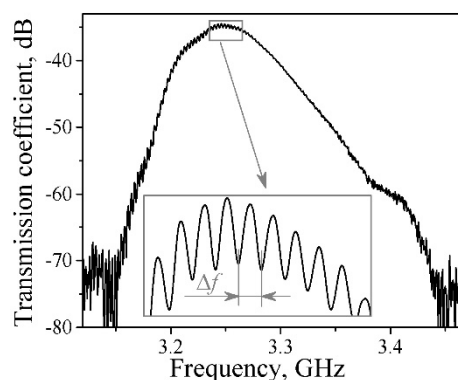


Fig. 1. Magnitude of MSSW transmission coefficient versus frequency at $H=550\text{ Oe}$. Inset – zoomed view to show magnetoelastic resonances.

The reported study was funded by RFBR (Research projects Nos. 16-57-00135, 16-29-14058) and BRFFR (Research project No. F16R-085).

[1] V.K. Sakharov, Y.V. Khivintsev, et al. *IEEE Mag. Let.*, **8** (2017) 3704105.

[2] A.I. Stognij, L.V. Lutsev, et al. *J. Appl. Phys.*, **118** (2015) 023905.

[3] V.K. Sakharov, Y.V. Khivintsev, et al. *Proc. 20th Int. Conf. Mag.*, Barcelona, (2015) 1546.

[4] Y.V. Gulayev, P.E. Zilberman, et al. *JETP Let.*, **34** (1981) 477-481.

2PO-K-23

BRILLOUIN SPECTROSCOPY OF NONLINEAR MAGNETOACOUSTIC RESONANCES IN A LAYERED YIG/GGG STRUCTURE

Tikhonov V.V.¹, Litvinenko A.N.¹, Sadovnikov A.V.¹, Nikitov S.A.²

¹ Saratov State University, Saratov, 410012 Russia

² Kotelnikov Institute of Radio Engineering and Electronics, Russian Academy of Sciences, Moscow, 125009 Russia

tvlad4@yandex.ru

Over the last decade, interest to magneto-elastic excitations has been increased owing to exceptional low damping of acoustic waves [1] and wideband frequency tunability of spinwaves which can be used for advanced signal processing. We have implemented BLS for research of nonlinear magnetoacoustical resonances in a layered YIG/GGG structure.

We studied the effect three-magnon decay on the distribution of intensities of coupled magnetic and elastic waves. Intensity was measured at the main excitation frequency of a magnetoacoustic resonator (MAR) and at its half frequency. The MAR was manufactured from optical polished layered YIG/GGG structures with the thickness of the whole structure 371 μm and thickness of the YIG film 13 μm . The saturated magnetization of the films was 1750 G. In-plane magnetization was used. The MAR was excited by a microstrip transducer at frequency $f_0=2.75$ GHz of the magnetoacoustic resonance. The power was 0 dBm.

In measuring magnetic oscillations, a linearly polarized laser beam was focused on the surface of a YIG film. To eliminate the influence of the elastic oscillations also present in the YIG film, a second light polarizer was inserted in the path of the reflected beam and its axis was oriented orthogonally to the plane of incident beam polarization. It was considered that light scattering on elastic oscillations in crystals with weak anisotropy has virtually no effect on the plane of polarization, while scattering on magnetic oscillations in ferrites is always accompanied by rotation of the plane of polarization. In measuring elastic oscillations, the laser beam was focused on the surface of a GGG substrate. The BLS measurements were made at main frequency f_0 and $f_0/2$ of the magnetoacoustic resonance.

Due to three-magnon decay the YIG-film excited acoustic waves by magnetoelastic coupling at half frequency of external influence and induced a significant differences in distribution pattern (fig.1) of normalized intensities of (a) magnetic and (b) elastic oscillations in the MAR. Distribution pattern of elastic oscillations has two maxima which caused by beating of neighboring frequencies of acoustic modes of the MAR.

The observed effect of nonlinear excitation of hypersound at the half-frequency of magnetoacoustic resonance is of practical interest as a microwave signal frequency divider.

[1] A.N. Litvinenko, A.V. Sadovnikov, et al., *IEEE Magnetics Letters*, **6** (2015) 99-104.

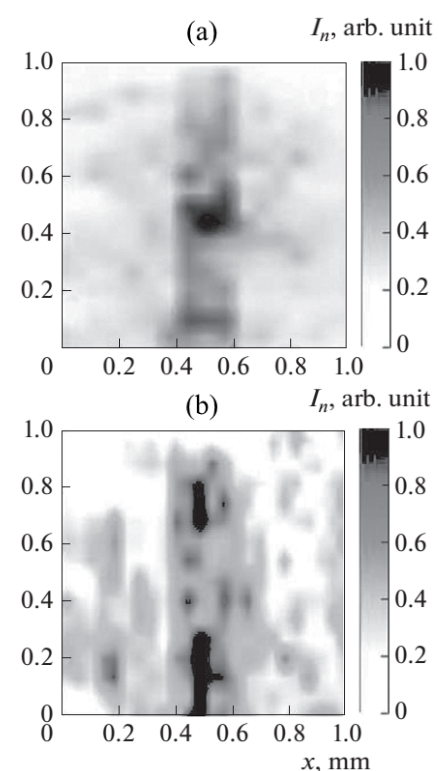


Fig. 1. Distribution pattern of normalized intensities of (a) magnetic and (b) elastic oscillations at $f_0/2$.

2PO-K-24

SPATIAL AND FREQUENCY SELECTIVE YIG WAVEGUIDES CROSSING

Sadovnikov A.V.^{1,2}, Gubanov V.A.¹, Sharaevskii Yu.P.¹, Nikitov S.A.^{1,2}

¹ Saratov State University, Saratov, 410012, Russia

² Kotel'nikov Institute of Radio Engineering and Electronics, RAS, Moscow, 125009, Russia
vladmeen@gmail.com

Recent advances in micro- and nanofabrication allowed development of microscale magnonic logic and memory devices [1,2]. The typical planar topology of the magnonic networks is fabricated by the means of the structured magnetic materials. One of the most prominent magnonic element is the magnetic waveguide crossing, which is widely used as the magnonic interferometric switch for multi-valued logic circuits [3], in magnonic holographic devices [4,5]

The planar yttrium iron garnet (YIG) microstructures open a promising alternative to signal processing by SW in beyond-CMOS computing technology due to the low damping.

We report on the study of the spatial and frequency selective spin wave (SW) propagation in the YIG waveguides crossing. The structure was formed on the Gallium Gadolinium Garnet (GGG) substrate by the microfocused laser ablation technique. The width of the YIG waveguides was 500 μm . Figure 1 shows the sketch of the proposed YIG waveguides crossing. We excite the magnetostatic surface spin wave (MSSW) in the leg P0 (denoted in Fig.1). Then the MSSW propagates and transforms to the backward volume magnetostatic spin wave (BVMSW) propagates along the legs P1 and P3. We use the Brillouin light scattering (BLS) technique to map the SW intensity over the waveguide crossing. We show that using the orientation of the bias magnetic field the control of SW propagation is possible in the proposed topology. By the means of BLS and the micromagnetic simulation we show, that the spin wave transmission varies with the variation of the orientation of the bias magnetic field. We demonstrate that the control over the dispersion of the width modes leads to the spatial filtering of SWs in the proposed structure.

Thus the spatial and frequency selective spin-wave switching is possible in magnonic cross. This leads to the application of the proposed structure as a versatile interconnect in the planar magnonic networks.

Support by RFBR (No. 16-37-00217) and Grant of the President of RF (MK-5837.2016.9, SP-313.2015.5) is acknowledged.

[1] S.A. Nikitov, et. al, *Phys. Usp.*, **58** (2015) 10.

[2] V.E. Demidov, et. al, *Sci. Rep.*, **5** (2015) 8578.

[3] M. Balynsky, et. al., *Journal of Applied Physics*, **121** (2017) 024504.

[4] Yu. Khivintsev, et. al., *Journal of Applied Physics*, **120** (2016) 123901.

[5] F. Gertz, et. al., *IEEE Trans. on Magn.*, **52** (2016) 3401304.

[6] K. Nanayakkara, et. al., *IEEE Trans. on Magn.*, **52** (2016) 3402204.

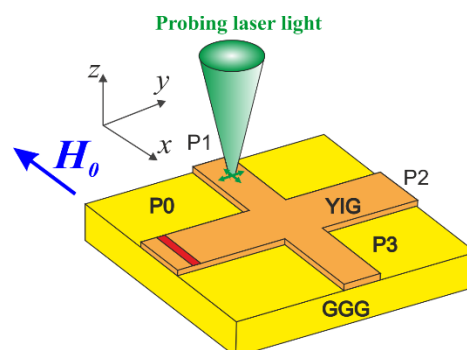


Fig. 1. Sketch of the proposed YIG waveguides crossing

2PO-K-25

FORWARD VOLUME SPIN WAVES PROPAGATING IN THIN YIG FILMS*Yoshimoto T.¹, Goto T.^{1,2}, Shimada K.¹, Sekiguchi K.^{2,3}, Ross C.A.⁴, Takagi H.¹, Nakamura Y.¹, Uchida H.¹, Inoue M.¹*¹ Toyohashi University of Technology, Toyohashi, Japan² JST PRESTO, Kawaguchi, Japan³ Keio University, Yokohama, Japan⁴ MIT, Cambridge, USA

goto@ee.tut.ac.jp

Magnonics is a promising information processing technique with ultra-low power consumption. Recently, we reported a three-port spin wave (SW) interferometer using forward volume (FV) SWs propagating in 10 μm yttrium iron garnet (YIG) [1]. To miniaturize this device, thin YIG film is required because thinner waveguide allows propagation of SW with shorter wavelengths. In this work, thin YIG films were fabricated by pulsed laser deposition (PLD) and the propagation characteristics of FV SW in such thin films were investigated.

A ~ 50 nm thick YIG film was grown on (111) rare-earth substituted gadolinium gallium garnet (SGGG) substrates. A KrF excimer laser ($\lambda = 248$ nm, pulse rate 15 Hz, pulse duration 25 ns, laser energy 360 mJ) was used to deposit the films. During the deposition, a substrate temperature was held at 850°C under 2.6 Pa oxygen partial pressure. The crystalline structure of the fabricated YIG was evaluated by high resolution x-ray diffraction (XRD). A 2θ - ω rocking curve in the vicinity of the YIG (444) and SGGG (444) peaks and a reciprocal space mapping (RSM) around the asymmetric (880) peak was obtained. These results indicated that the YIG film were single crystalline and had compressive strains. After the deposition, YIG film was etched into a $50 \mu\text{m} \times 1 \mu\text{m}$ mesa shape to suppress undesired excitations of SWs at tapered parts of coplanar waveguides (CPW). The two CPWs for excitation and detection of SW were placed on the YIG waveguide.

Fig. 1 shows the transmission spectra of the SWs obtained by vector network analyser. Multimode SW propagation was observed and the peak frequency of the excited SW were shifted with varying the applied field. The wavenumbers k of the SW were fitted to the dispersion curves. Hence, the k of SW were estimated as $0.1 \mu\text{m}^{-1}$, $0.5 \mu\text{m}^{-1}$, and $0.9 \mu\text{m}^{-1}$ respectively. The extinction coefficient at a frequency of 7 GHz was $4.5 \times 10^{-2} \mu\text{m}^{-1}$. At the conference, we will report the detail experimental method of SW propagation analysis and the x-ray reflection properties, magnetic properties and magneto optical properties of the fabricated YIG will also report.

This work was supported in part by the KAKENHI NO. 26706009, 26220902, and JST PRESTO.

[1] N. Kanazawa et al., *Sci. Rep.*, **6** (2016) 30268.

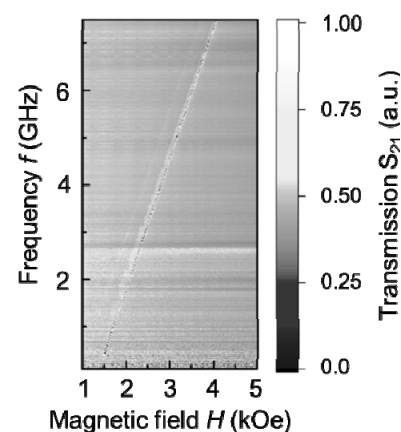


Fig. 1. Transmission spectra of SWs. The YIG thickness was ~ 50 nm. Applied field was varied from 1 kOe to 5 kOe at 20 Oe steps.

2 July

Sunday

17:30-19:30

poster session

2PO-I

2PO-I1

2PO-J

2PO-K

**“Magnetic
Nanostructures and
Low Dimensional
Magnetism”**

2PO-I-23

OPTIMIZATION OF THE GMR-STACK DESIGN IN MAGNETIC FIELD SENSORS BY MICROMAGNETIC SIMULATIONS

Berkov D.¹, Gorn N.¹, Semenova O.¹, Mattheis R.²

¹General Numerics Research Lab, Jena, Germany

²Leibniz-Institut für Photonische Technologien, Jena, GERMANY

e.semenova@general-numeric-rl.de

We report simulation results on the magnetization reversal due to the domain walls (DW) formation in GMR stacks widely used in magnetic field sensors, in which the change of the magnetoresistance due to the motion of DWs is employed for monitoring the external magnetic field.

Especially in so called multiturn sensors the number of turns accomplished by, e.g., a machine wheel, is obtained by measuring the magnetoresistance change due to the motion of DW injected into a GMR stack consisting of multilayered stripes. For this construction it is very important to avoid the spontaneous DW formation in such a stack: undesired domain walls would prevent the normal device functioning. Hence the prediction of the spontaneous domain nucleation field H_{nuc} (where undesired DWs would appear) is crucially important for finding of the upper working field and establishing the optimal layout of such a sensor.

For this purpose we have simulated the GMR stack (IrMn/CoFe/Ru/CoFe/Cu/Py) with the hexagonal lateral shape and the uniform direction of the exchange bias (provided by the IrMn underlayer). In this geometry, for the given external field direction, all possible angles between this field and magnetic stripes are covered in a single simulation run. The DW nucleation occurs in the hexagon region with the smallest value of H_{nuc} . This way we have obtained the dependence of H_{nuc} on the external field direction for various geometries of the GMR stack. The emphasis was put on the dependence of the nucleation field on the thicknesses of AAF layers. We were able to explain variation of H_{nuc} with the external field direction by the strong stray field created by AAF on the Py layer. Basing on this explanation, we suggest the optimal design of the GMR stack, which minimizes the variation of the nucleation field when the external field direction changes.

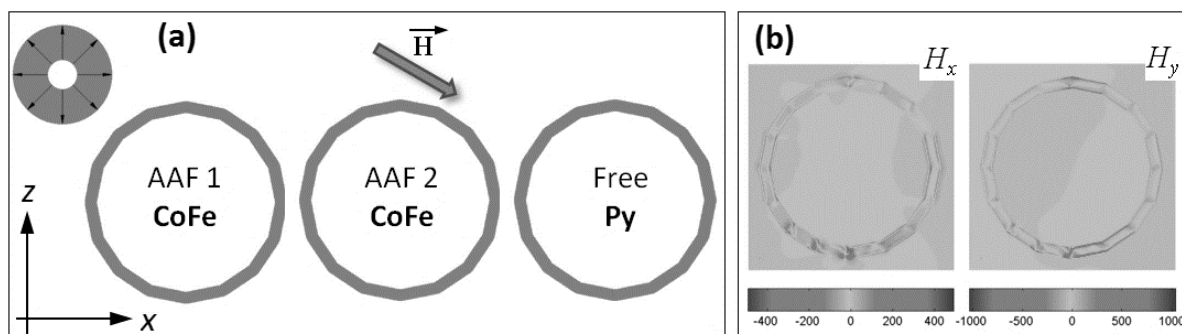


Fig. 1. Magnetization state of both AAF layers and the Py free layer (a) and the stray field from AAF on the Py layer (b) just before the nucleation of two domain walls in the Py layer.

Support of the German Federal Ministry for Economic Affairs and Energy (INNO-KOM project MF 150023 'MAGSIMSENS') is greatly acknowledged.

2PO-I-24

MÖSSBAUER STUDY OF INCOMMENSURATE SPIRAL SPIN STRUCTURES IN SOME ORDERED IRON-BASED ALLOYS

*Voronina E.V.*¹, *Ivanova A.G.*¹, *Arzhnikov A.K.*², *Chumakov A.I.*³, *Chistyakova N.I.*⁴, *Pyataev A.V.*¹,
*Korolyov A.V.*⁵

¹ Institute of Physics, Kazan Federal University, Kazan, Russia

² Physical-Technical Institute UrB RAS, Izhevsk, Russia

³ ESRF, Grenoble, France

⁴ Faculty of Physics, Lomonosov Moscow State University, Moscow, Russia

⁵ M.N. Mikheev Institute of Metal Physics UrB RAS, Ekaterinburg, Russia
evoronina2005@yandex.ru

Non-collinear disordered and ordered structures of magnetic spins remain one of the most intriguing topics of modern solid-state physics [1, 2]. Besides a general need to understand a reason for their existence, they are strongly related to superconductivity [1, 2], appear to be excellent candidates for spintronics [3]. Moreover, even an identification of these structures remains a challenging experimental problem. A number of transition metal systems attributed earlier to spin (or re-entrant spin) glasses in fact seems to be spiral spin structures with phases segregation [4,5]. Neutron diffraction studies of B2-ordered Fe-Al alloys reveal a correlation of magnetic moment in space with a correlation length of about 5 nm [6]. Some theoretical studies also confirm that the spiral spin magnetic structure is the most stable state of these alloys [4, 5].

We present the results of the Mössbauer measurements of the binary alloy and ternary quasicrystalline $\text{Fe}_{65}\text{Al}_{35-x}\text{M}_x$ and $\text{Fe}_{65-y}\text{Al}_{35}\text{M}_y$ alloys (M= Ga, B, V, Mn; x, y = 3, 5, 10 at.%) at variable temperature (3.3 - 80 K) and magnetic field (0 - 7 T). The Mossbauer spectra have a form typical for systems with some degree of chemical disorder inherent in superstructure of non-stoichiometric composition. Analysis of a series of low-temperature in-field Mössbauer spectra clearly showed that the spectra contain components corresponding to the probe atoms whose magnetic moments are ordered ferromagnetically. Comparison of hyperfine magnetic field distributions in spectra, measured without an external magnetic field and in the field, proves that there are also components demonstrating behavior that is out of character for ferromagnetically ordered magnetic moments. From these considerations the model of magnetic microstructure was developed. The Mössbauer spectrum is represented as a superposition of two contributions: from probe atoms whose hyperfine parameters depend on a certain local environment and from the probe atoms whose magnetic moments form a incommensurate spin density wave (SDW). The SDW shape was deduced from experimental spectra. The change of the magnetic sub-systems with temperature increase is discussed.

Support by ESRF is acknowledged. This work was also funded by the subsidy allocated to Kazan Federal University for the state assignment in the sphere of scientific activities.

- [1] S. Mühlbauer, B. Binz, F. Jonietz et al., *Science*, **323** (2009) 915 - 919.
- [2] C. de la Cruz, Q. Huang, J.W. Lynn et al., *Nature*, **453** (2008) 899 - 902.
- [3] A. Manchon, N. Ryzhanova, A. Vedyayev and B. Dieny, *J.Appl.Phys.*, **103** (2008) 07A721-1-3.
- [4] P.A. Igoshev, M.A. Timirgazin, A.A. Katanin et al., *Phys.Rev.B*, **81** (2010) 094407-094407-9.
- [5] A.K. Arzhnikov, L.V. Dobysheva, M.A. Timirgazin, *JMMM*, **320** (2008) 1904-1908.
- [6] D.R. Noakes, A.S. Arrott, M.G. Belk et al, *J. Appl. Phys.*, **95** (2004) 6574 -6579.

2PO-I-25

INHOMOGENEOUS BROADENING OF THE FMR LINE OF FERROMAGNETIC SILICIDE FILMS MADE BY ION-BEAM SYNTHESIS IN EXTERNAL MAGNETIC FIELD

Alekseev A.V.¹, Gumarov G.G.¹, Petukhov V.Yu.^{1,2}, Bakirov M.M.¹

¹Zavoisky Physical -Technical Institute, Kazan, Russia

²Kazan Federal University, Kazan, Russia

alekseevanton@gmail.com

The modification of magnetic properties in thin films by ion irradiation is especially useful as it can be applied to locally alter magnetic properties such as saturation magnetization, magnetic anisotropy etc. Earlier, magnetic-field-assisted ion-beam synthesis used to produce thin ferromagnetic Fe₃Si silicide films in single-crystal silicon substrates [1]. It was shown, that application of the magnetic field during Fe ion implantation led to the pronounced in-plane magnetic anisotropy in the synthesized films. However, the films are magnetically isotropic in the surface plane at doses greater than 2.4×10^{17} cm⁻². The aim of the present work is to investigate the magnetic properties of thin iron silicide films using the method of ferromagnetic resonance.

A typical FMR spectrum for magnetically isotropic samples is shown in Fig. 1. The FMR linewidth rises with temperature decrease for that kind of samples. Such dependence can be explained on the basis of model of magnetic resonance in an ensemble of single-domain anisotropic particles. The approach based on the independent-grain model once proposed for the description of FMR in polycrystals. This behavior is in a good agreement with Raikher model [2]. When the dispersion in the directions of anisotropy axes of the particles is absent the contribution of inhomogeneous broadening to linewidth is negligible at low temperatures.

It should be noted that FMR linewidth for anisotropic samples is nearly constant with temperature variation. When the dispersion in the directions of anisotropy axes of the particles is absent the contribution of inhomogeneous broadening to linewidth is negligible at low temperatures ($\xi_0 > 1$). Superparamagnetic broadening in this region is also insignificant. As a consequence the linewidth is practically temperature independent, at least in scale of relative variations.

Calculations of the FMR spectra on the basis of the Raikher model and comparison with experiment allowed us to estimate the average particle size which is approximately 50 nm and its magnetic moment about 10^{-15} Gs \times cm³. This result agrees with data about mean particle size obtained by X-ray diffraction analysis.

Support by Prog. № 2.3 DNIT RAS and Prog. №24V DPhS RAS is acknowledged.

[1] G.G. Gumarov, etc., *NIMB*, **282** (2012) 92–95.

[2] Yu.L. Raikher, V.I. Stepanov, *JETP*, **101** (1992) 1409–1423.

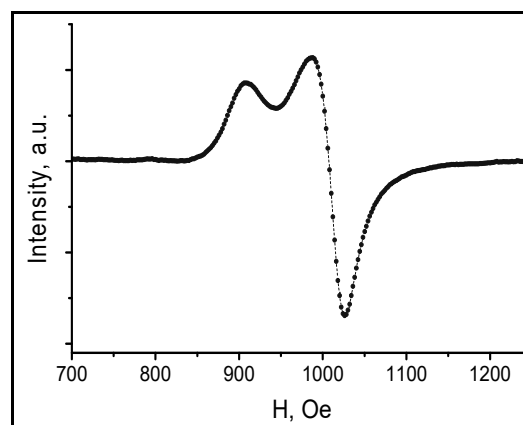


Fig. 1. Experimental FMR line for ferromagnetic silicide films in the in-plane geometry.

2PO-I-26

STRUCTURE OF MAGNETIC REGIONS AND CURRENT LOSS IN COMPOSITE FILMS

*Lasek M.P.¹, Kotov L.N.¹, Kirpicheva O.A.¹, Beznosikov D.S.¹, Golubev E.A.², Kalinin Yu.E.³,
Sitnikov A.V.³*

¹ Syktyvkar State University named after Pitirim Sorokin, Syktyvkar, Russia

² Komi Republican Institute for Educational Development, Syktyvkar, Russia

³ Voronezh State Technical University, Voronezh, Russia

mplasek@yandex.ru

Structures of magnetic regions of composite films constituted by ferromagnetic nanoparticles (Co, Fe) in an insulating amorphous a-SiO₂ and b-Al₂O₃, in relation to the metal concentration were investigated in this work. The thickness of the films was 0.25÷1.2 μm. The investigated films were received by ion beam sputtering method in the argon atmosphere with pressure 0.04 Pa. The chemical composition of the films and the thickness of the films were determined by the scanning electron microscope JSM-6400. High-frequency (HF) and ultrahigh-frequency (UHF) current loss in the composite films were investigated. Electric circuits of the composite films were proposed to describe the current loss in the composite films.

The structures of magnetic regions were obtained by atomic force microscope ARIS-3500. The metal particles in the insulator practically do not have electrical contacts with each other in the films with concentration metal phase before the threshold of percolation. Magnetic labyrinthine structures after percolation threshold were observed in the films with Al₂O₃. The conductive metal channels are elongated and directed along one direction. The length of the channel exceeds the width more than 20 times. The period of the transverse structure of the channels is of the order 0.4 microns. Lattice structures were observed with increasing the metal in the films. Distance between the filaments of the lattice structure is 0.5-0.7 microns. Closed magnetic structures in the composite films were observed with increasing the metal. The structures have almost a zero values of the normal component of the magnetization vector.

The HF and UHF current loss in the composite films were obtained by the spectrum analyzer (INSTEK GSP-7830), sweep-frequency generator and element of coaxial cable [1]. The composite films have the varying conductive properties in the high and ultra high ranges of frequencies, which largely are determined by their nano- and microstructures. The complex structures of the films can be represented as a simplified equivalent electric circuits. The electrical circuits consist resistors, inductors and capacitors that can be connected either in series or in parallel. Parameters of the elements of the circuit are determined by the structure and the concentration of metal in the films. The parameters were determined by using current loss in the composite films. The electrical parameters of the films is an important characteristic of most materials that are used in electronic devices at high and ultrahigh frequencies.

We gratefully acknowledge the financial support from RFBR (grant # 17-02-01138).

[1] L. N. Kotov et al., *Bulletin of Chelyabinsk State University. Phys.*, **21** (2015) 75–82.

2PO-I-27

INFLUENCE OF STATIC CONDUCTIVITY AND STRUCTURE OF COMPOSITE FILMS ON MAGNETIC PROPERTIES

*Kirpicheva O.A.¹, Lasek M.P.¹, Kotov L.N.¹, Beznosikov D.S.¹, Golubev E.A.², Kalinin Yu.E.³,
Sitnikov A.V.³*

¹ Syktyvkar State University named after Pitirim Sorokin, Syktyvkar, Russia

² Komi Republican Institute for Educational Development, Syktyvkar, Russia

³ Voronezh State Technical University, Voronezh, Russia

merlisa@yandex.ru

Recently, attention has been paid to composite metal-dielectric films, which exhibit a giant magnetoresistance and a number of unique structural properties. Nanostructured metal-dielectric films are characterized by two structure distributions: the distribution of metal and dielectric particles is chaotic before the percolation process. After the percolation process, the chaotic nature of the metallic fine granules and particles remains, but at the same time, a strip metal structure arises under the influence of percolation processes. The conductivity jump can be observed somewhere in the region of no more than a half-order. Although it is technologically we can possible to achieve a significant change in conductivity in this area.

Static conductivity, (conductivity measured on a direct current) through thin metal-dielectric composite films (Co + Fe + Zr) / (Al₂O₃) on lavesan and ceramic substrates was experimentally investigated. The thickness of the film on the lavesan substrate was 0.4÷1.2 μm, and on the ceramic substrate, 1÷6 μm. The structures of magnetic regions were obtained by Atomic force microscope ARIS-3500 by the special probe. The probe was made of a silicone thin thread, on which the Co-Cr layer was sprayed. In studies of films, the cantilevers MFMR (Nanoworld) were used with a tip radius of about 40 nm. Radius of the tip rounding determined the resolution, which allowed separately to see similar regions and areas of relief with sizes up to 10÷15 nm. The cantilevers included a silicone probe coated with a magnetic CoCr alloy 20 nm thick. The dependence of the phase difference on the surface coordinates was transformed into an image called the phase contrast, which reflects the dimensions of the similar regions and the shape of the surface relief of the film. To obtain an image of the magnetic regions of the films, the probe was repeatedly inserted along the surface of the films using a program for subtracting the surface relief of the films. Magnet-force microscopy in films with percolation revealed a strip magnetic metal structure with a length of 1÷3 μm and larger, with a period of ~ 200 nm. For films with a less ordered magnetic structure, some disturbance of the strip structure in the form of bifurcation of strips and their curve were developed. Great changes in the granular surface structure of the film conduct to disturbances of the periodicity and to break of strip magnetic metal strips. It is shown that static conductivity does not exhibit a conductivity jump when passing through the concentration at which percolation occurs. This indicates that there is a rather large spread, as well as along the length of the metal lines and the thickness of the dielectric layers between these lines. That is, it is possible to control the conductivity in the percolation areas, using instead of a dielectric, for example, semiconductor media.

We gratefully acknowledge the financial support from RFBR (grant # 17-02-01138).

[1] L. N. Kotov et al., *Bulletin of Chelyabinsk State University. Phys.*, **21** (2015) 75–82.

2PO-I-28

ON-SITE 4F-5D FLUCTUATIONS AND SDW EXCITATIONS AS THE CHARGE CARRIERS SCATTERING CHANNELS IN HoB₁₂

*Khoroshilov A.L.*¹, *Krasnorussky V.N.*², *Bogach A.V.*², *Glushkov V.V.*^{1,2}, *Demishev S.V.*^{1,2}, *Shitsevalova N.Yu.*³, *Levchenko A.*³, *Filipov V.B.*³, *Gabáni S.*⁴, *Flachbart K.*⁴, *Siemensmeyer K.*⁵, *Sluchanko N.*²

¹ Moscow Institute of Physics and Technology, Moscow, Russia

² Prokhorov General Physics Institute, RAS, Moscow, Russia

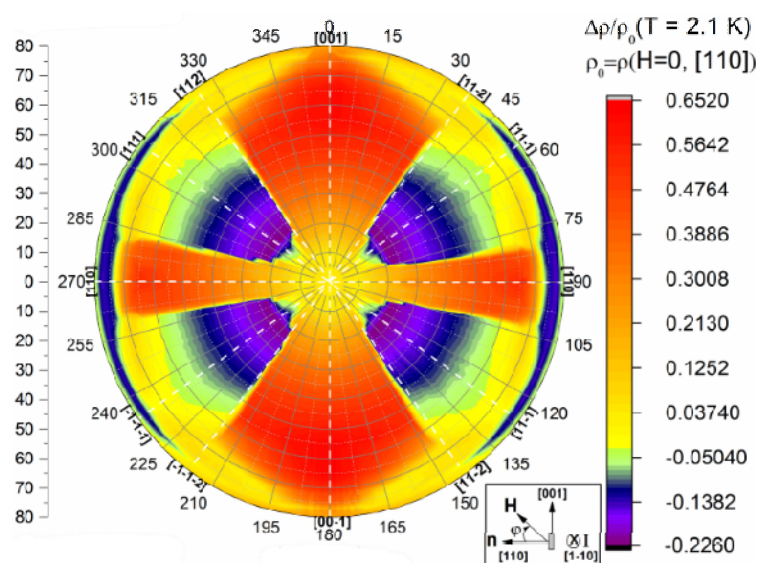
³ Frantsevich Institute for Problems of Materials Science, NASU, Kyiv, Ukraine

⁴ Institute of Experimental Physics SAS, Košice, Slovakia

⁵ Hahn Meitner Institut Berlin, D 14109 Berlin, Germany

poligon-51@yandex.ru

Precise measurements of magnetoresistance (MR) in isotopically pure Ho¹¹B₁₂ have been carried out on the high quality single crystals at temperatures $T < 10$ K and in magnetic fields up to 80 kOe. Measuring current \mathbf{I} was applied along [1-10] direction, an angle φ between the magnetic field \mathbf{H} and normal $\mathbf{n} \parallel (110)$ to the sample surface (see inset in Fig.1) varied in the study to test MR anisotropy. Figure 1 shows MR $\Delta\rho/\rho(\varphi, H)$ dependence at temperature $T = 2.1$ K plotted in polar coordinates (φ, H) , color represents the MR value. Both of the positive MR (pMR, red areas for $\mathbf{H} \parallel [001]$ and $\mathbf{H} \parallel [110]$ on the Fig.1) and the negative MR (nMR, blue areas for $\mathbf{H} \parallel [111]$ on Fig. 1) are clearly detected for Ho¹¹B₁₂. In order to separate between these two contributions into resistivity, we performed analysis in accordance with the approach developed in [1]. The transformation of MR (Fig. 1) discussed in terms of competition between two main mechanisms of charge carriers scattering: (i) on the 4f magnetic moments of Ho³⁺ ions and (ii) on the spin density wave (SDW). Numerical differentiation of MR curves was used to find out phase transitions within the antiferromagnetic phase and to reconstruct the H-T magnetic phase diagram for main crystallographic directions. Calculated parameters of obtained contributions allowed us to estimate drift mobility of charge carriers and effective magnetic moment of AF holmium nanodomains.



[1] N. E. Sluchanko, A. L. Khoroshilov, M. A. Anisimov, A. N. Azarevich, A. V. Bogach, V. V. Glushkov, S. V. Demishev, V. N. Krasnorussky, N. Samarin, S. Gabani, G. Pristas, A. Levchenko, V. Filippov, N. Yu. Shitsevalova and K. Flachbart, *Phys. Rev. B*, **91** (2015) 235104.

2PO-I-29

RELATIONSHIP BETWEEN STRUCTURAL AND MAGNETIC, OPTICAL PROPERTIES OF EPITAXIAL $\text{Fe}_{1-x}\text{Si}_x/\text{Si}(111)$ ALLOY FILMS

Tarasov I.A.¹, Yakovlev I.A.², Volochaev M.N.¹, Zhandun V.S.¹, Velikanov D.A.¹, Kuznetsova T.V.³, Kravtsov E.A.³, Varnakov S.N.¹, Balymov K.G.⁴, Pryahina V.⁴, Kosyrev N.N.¹, Shemukhin A.⁵, Ovchinnikov S.G.¹

¹Kirensky Institute of Physics, Federal Research Center KSC SB RAS, Krasnoyarsk, Russia

²Institute of Chemistry and Chemical Technology, Federal Research Center KSC SB RAS, Krasnoyarsk, Russia

³M.N. Mikheev Institute of Metal Physics, Russian Academy of Sciences, Ural Branch, Ekaterinburg

⁴Ural Federal University Center for shared use, Ural Federal university, Ekaterinburg, Russia

⁵M.V.Lomonosov Moscow State University, Skobeltsyn Institute of Nuclear Physics, Leninskie gory, GSP-1, Moscow 119991, Russia
tia@iph.krasn.ru

The binary Heusler alloy Fe_3Si , which is the potential candidate for spin-injectors, has heavily been investigated over the last decade. However, it has been examined that Fe_3Si has low spin polarisation (P) ($0.15 \leq P \leq 0.45$) and should be improved [1]. One of the ways suggested to increase spin polarisation is to change Si content in the Fe_3Si silicide that could shift unpolarised s-bands of iron either above or below Fermi energy in order to remain only polarised d-bands. Furthermore, controlling chemical and structural order in the $\text{Fe}_{1-x}\text{Si}_x$ thin films grown on Si substrates could also tune the electronic and magnetic properties.

In this work, we investigated the way that the Si content, chemical and structural order affect on optical, electronic and magnetic properties of the epitaxial $\text{Fe}_{1-x}\text{Si}_x$ thin films in composition range $0 \leq x \leq 0.4$.

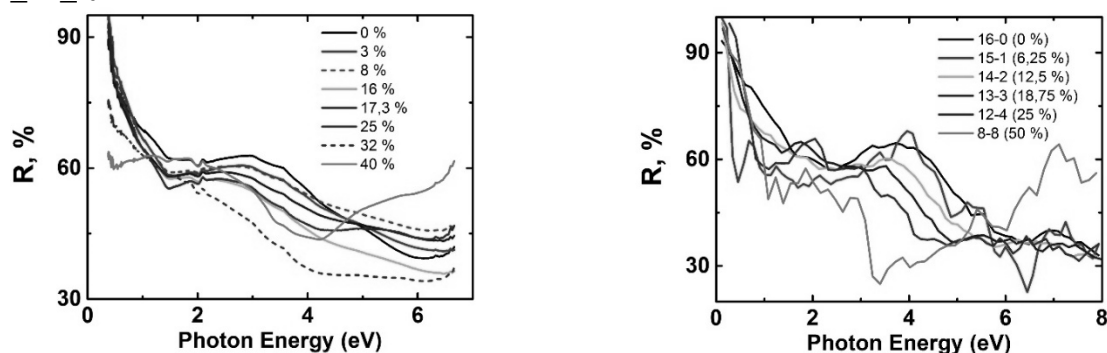


Figure 1. Experimental a) and theoretical b) reflectivity spectra of $\text{Fe}_{1-x}\text{Si}_x$ compounds with different Si content.

Examination of the off-stoichiometric epitaxial $\text{Fe}_{1-x}\text{Si}_x$ thin films obtained was carried out using X-ray diffraction, Rutherford back-scattering, SQUID magnetometry, ferromagnetic resonance, transmission electron microscopy, atomic force microscopy, Kerr effect measurements, spectroscopic ellipsometry and ab initio calculation methods. This work revealed that chemical order is an effective mean to adjust the electronic and magnetic properties of $\text{Fe}_{1-x}\text{Si}_x/\text{Si}(111)$ system.

The work was supported by the Program of the President of the Russian Federation for the support of leading scientific schools (Scientific School 2886.2014.2), RFBR (grants No. 13-02-01265)

[1] Kawano M., Ikawa M., Arima K. et al., *J. Appl. Phys.*, **119** (2016), 045302-1-6.

2PO-I-30

RESEARCHING OF PROPERTIES OF MAGNETIC THIN FILMS FOR STORAGE DEVICES

Valiullin A.A.¹, Kamzin A.S.², Tagirov L.R.¹, Zaripova L.D.¹

¹ Kazan Federal University, Kazan, Russia

² Ioffe Physical–Technical Institute of RAS, St. Petersburg, Russia

fess98@rambler.ru

A great many studies of thin film magnetic materials focus on increasing their magnetic data density. The data density is often raised by minimizing the size of grains (data storage items in a magnetic film) and by switching from longitudinal to transverse recording. However, the minimum possible size of granules is limited by the emergence of the superparamagnetic effect, which prevents the magnetic data density from increasing. The exchange interaction between granules is another limiting factor.

In this report different methods of synthesis of L10 FePt thin films are used to overcome these limitations:

1) Further study indicates that the perpendicular anisotropy in [Fe/Pt]*n* multilayer films has an intimate correlation with the periodicity *n*, and, with the increasing of periodicity *n*, the out-of-plane remanence ratio significantly increases and then decreases slowly. This result suggests that the enhanced perpendicular anisotropy may be caused by the interface anisotropy at the Fe/Pt interfaces in the [Fe/Pt]*n* multilayers.

It has been established that, in multilayer structures based on L10 FePt films obtained by RF magnetron sputtering, the evolution of texture from (111) to (001) can be effectively induced by using multilayer structure. This might be a new method to obtain perpendicular anisotropy and, at same time, to effectively reduce the exchange coupling interaction among grains in FePt films.

2) Bit-patterned media (BPM), which consist of ferromagnetic (FM) nanodots regularly arranged in a nonmagnetic matrix, are a promising candidate to replace continuous film media for ultrahigh density magnetic recording.

It is known that the magnetic properties of FePt films can be tailored by introducing additional elements into them. Adding rhodium (Rh) to the FePt alloy allows us to optimize the magnetic properties of thin films without sacrificing their magnetocrystalline anisotropy energy. FePt_{1-x}Rh_x films with different Rh concentrations ($0 \leq x \leq 0.4$) and a thickness of 20 nm were fabricated by magnetron sputtering. It was found that the film was paramagnetic at room temperature when $x = 0$, and the easy axis of magnetocrystalline anisotropy was perpendicular to the film surface. At rhodium concentrations of $x < 0.32$, the ferromagnetic order was preserved at room temperature in FePt_{1-x}Rh_x, and the high magnetocrystalline anisotropy energy that established the perpendicular magnetization orientation was retained.

3) At the present time, two-layer magnetic films prepared from two materials with different properties extensively studied in connection of their possible applications as magnetic springs or composites that are carriers of superhigh-dense magnetic recording.

Magnetic L10–FePt(10 nm)/Fe(*t*, nm)/Ta(2 nm) (*t* is the Fe film thickness that is varied from 0 to 15 nm) multilayer structures have been prepared by magnetron codeposition. It was stated that the exchange interaction between the FePt and Fe layers was stronger as the soft-magnetic Fe layer thickness was less than 3 nm.

4) The possibility of controlling the properties and orientation of the easy axis of magnetization of the multilayer magnetic structure by means of annealing in an external magnetic field has been investigated. The investigations have been performed on multilayer magnetic structures based on Fe₅₀Pt₅₀ films in the L10 phase.

2PO-I-31

HYSTERESIS PROPERTIES OF FeMn/Gd_xCo_{100-x} FILMS

Vas'kovskiy V.O.^{1,2}, Gorkovenko A.N.¹, Adanakova O.A.¹, Lepalovskij V.N.¹, Svalov A.V.

¹ Ural Federal University, Ekaterinburg, Russia

² Institute of Metal Physics, UB RAS, Ekaterinburg, Russia

olga.adanakova@urfu.ru

The interlayer exchange coupling is an important functional property of the "spin valve" type film media. This fact initiated considerable interest in its investigation for films containing antiferromagnetic or ferrimagnetic "pinning" layers. Recently, it has expanded to the area of structures having "free" ferrimagnetic elements [1, 2]. The presence of Gd sublayers in their composition makes it possible to realize the function of threshold temperature sensitivity in spin valves. This work is devoted to the study of hysteresis properties of exchange-coupled multilayered films with a ferrimagnetic layer based on Gd-Co amorphous system.

The experiment was carried out on Ta(5)/Fe₂₀Ni₈₀(5)/FeMn(20)/Gd_xCo_{100-x}(40)/Ta(5) type samples obtained by magnetron sputtering onto glass substrates in the presence of the uniform magnetic field. The thicknesses of each of the layers are given in nm in the above structural formula parentheses. The relatively complex nature of the layered structure is caused by the presence of several auxiliary layers in it. Ta accessory layer and the permalloy layer deposited on it initiate the formation of fcc structure and, accordingly, antiferromagnetic ordering in the FeMn layer. The outer layer of Ta performs a protective function. The main attention is paid to the hysteretic properties of Gd_xCo_{100-x} ($0 < x < 100$ %) layer and, in particular, to their features, which are due to the exchange coupling between ferrimagnetic and antiferromagnetic layers. They were compared with the properties of Gd-Co single-layer films.

Fig. 1 shows the dependences of coercivity H_c , anisotropy field H_a , and exchange bias field H_{ex} on the composition of Gd-Co layer. They were determined using magneto-optical hysteresis loops measured in the plane of the samples with $x \leq 40$ % at room temperature. For larger x values, the Gd-Co layers do not exhibit magnetic ordering. Characteristic maxima on all dependences indicate the presence of magnetic compensation at $x \sim 20$ %.

The exchange bias analysis performed using the data on concentration and temperature dependences of Gd-Co layers spontaneous magnetization showed that the Co subsystem is responsible for their exchange coupling with the antiferromagnetic layer.

This work has been supported by the Ministry of Education and Science of the Russian Federation, project 3.6121.2017.

[1] A.V. Svalov, G.V. Kurlyandskaya, V.O. Vas'kovskiy, *Appl. Phys. Lett.*, **108** (2016) 063504 (1-4).

[2] M. Milyaev et al., *J. Appl. Phys.*, **121** (2017) 123902 (1-5).

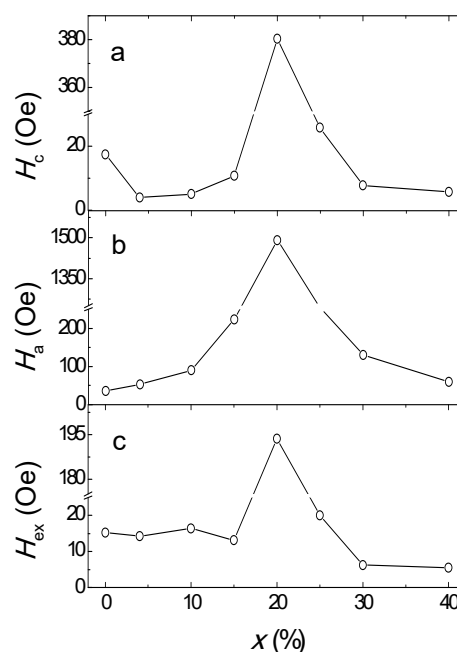


Fig.1. Concentration dependences of the hysteretic properties of the Gd_xCo_{100-x} layers in FeMn/Gd-Co structure.

2PO-I-32

THERMAL-RADIATION MODIFICATION OF NANOSTRUCTURE AND OPTICAL PROPERTIES OF POTASSIUM-ALUMINA-BORON GLASES WITH IRON OXIDES

Ibragimova E.M.¹, Salakhitdinov A.N.², Salakhitdinova M.K.³, Saydirasulov N.², Yusupov A.A.³

¹ Institute of Nuclear Physics Academy of Science Republic of Uzbekistan, Tashkent, Uzbekistan

² Tashkent university of information technology, Samarkand branch; Samarkand, Uzbekistan

³ Samarkand State University, Uzbekistan, Samarkand,

smaysara@yandex.ru

Lately there is increasing interest to magnetic nanosystems due to their prospective applications in magneto-optics and quantum computer technology. Penetrating ionizing irradiation of metal doped glasses at elevated temperatures was shown earlier to influence on the valence and coordination of metals at nano-scale. This work was aimed at studies of optical properties of potassium-aluminum-boron glasses (PAB) consisting of (25K₂O·25Al₂O₃·50B₂O), mol.% with Fe₂O₃ from 0.1 to 3.0 mass.%, which were annealed or irradiated at elevated temperatures. The samples had a shape of polished plates with area 1 cm² and thickness 1±0.05 mm, were irradiated with gamma-quanta of ~1.25 MeV of ⁶⁰Co radioisotope at the facility of INP AS RUz to the dose of 1.7 MR at the dose rate of 236 R/s and selected sample temperatures (323, 423, 473, 523, 573 K), which are well below the temperature of melting at 1603 K and softening at ~1000 K, but close to the temperature of Curie magnetic transition and generation of oxygen defects. Optical absorption spectra were registered at the single-beam spectrophotometer SF-56 within 190 - 1100 nm with an error ± 3 %. Figure 1 shows differential spectra $\Delta D = D_1 - D_{\text{treat}}$, where D_1 - optical density spectrum of a pristine sample, D_{treat} - upon annealing or thermal-radiation treatments.

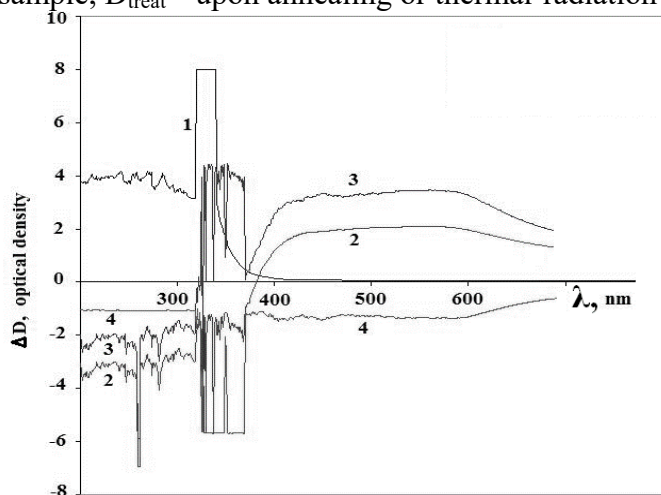


Figure 1. Differential absorption spectra (run at 300 K) of PAB glasses with 2.0 % Fe₂O₃ which were gamma-irradiated at different temperatures :

- 1 – non-irradiated pristine sample;
- 2 and 3 – samples subjected to gamma-irradiation at 423 and 473 K, respectively;
- 4 - differential spectrum between 2 and 3.

It is seen, that the irradiation at 423 and 473 K results in the selecting (320-380 nm) self-transparency of the PAB samples caused by valence-coordination transformations of Fe³⁺ nano-complexes and non-selecting (achromatic) self-transparency (190-700 nm) due to changes of the nanostructure of glass matrix. The valence-coordination transition of iron ions occurs at 327 nm. The obtained results on nano-structure modification of magnetic glasses are useful for magneto-optical and dose-metrical applications.

This research was supported by A-4-9 grant from Ministry of Higher Education Republic of Uzbekistan.

2PO-I-33

WANG-LANDAU SIMULATIONS OF THE ISING MODEL ON THE KAGOME LATTICE

Magomedov M.A.^{1,2}, Murtazaev A.K.^{1,2}

¹ Institute of Physics, Dagestan Scientific Center, RAS, Makhachkala, Russia

² Dagestan State University, Makhachkala, Russia

magomedov_ma@mail.ru

The Ising model on the various low-dimensional lattice (triangular, hexagonal, kagome and other) have extensively investigated by Monte-Carlo methods in last years. The kagome lattice Ising model has been interest in last ears in the role it plays in the high-Tc superconductivity. For example, the structure of the ferrimagnet SrCr₈Ga₄O₁₉, is found to consist of two-dimensional, spinel (kagome) slabs with magnetic spins residing at 1/3 of the lattice sites. Thus it is of interest to consider models with similar structures.

The Hamiltonian of the Ising model on kagome lattice can be written as:

$$H = -J_1 \sum_{\langle i,j \rangle} S_i S_j - J_2 \sum_{\langle\langle i,j \rangle\rangle} S_i S_j \quad (1)$$

where $S = \pm 1$ is the Ising spin. The first term in Eq.(1) makes allowance for the exchange antiferromagnetic interaction of the nearest-neighbors ($J_1 < 0$), and the second one takes account of ferromagnetic interaction for the next-nearest-neighbors ($J_2 > 0$). Each spin on lattice have 4 nearest-neighbors and 4 next-nearest-neighbors, as shown on figure 1. In this work, we focus on a case of $J_1 = -1$ and $J_2 = 1$.

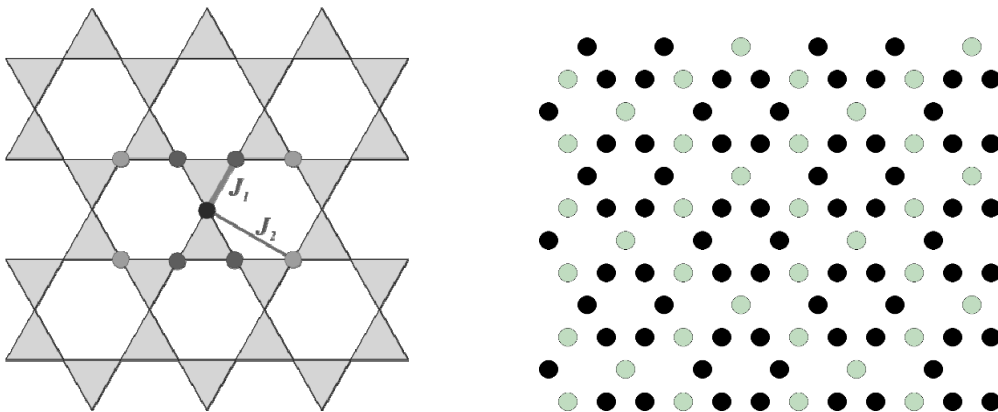


Fig. 1. Ising model on the Kagome lattice and its ground state spin configuration.

The Monte Carlo (MC) algorithms promote the strict and sequential evaluation of such systems based on microscopic Hamiltonians. In the present paper, we use the highly effective MC Wang-Landau algorithm. The Wang-Landau algorithm is the implementation of the entropy modeling method and allows the computation of the system states density function. One of our advantage of algorithm are that we snapshot the spin configuration in ground state and save it in graphic file. Calculations have been carried out for systems with periodic boundary conditions and linear dimensions $L \times L = N$, $L = 12 \div 72$. The example of ground state spins configuration show in figure 1. Dark circle mean spin up and light green circle mean spin down.

The Wang-Landau algorithm rests on that performing random walk in space of energies with probabilities inversely proportional to states density one achieves the uniform energy distribution. So, from the results derived on the system state density the values of thermodynamic observables can be evaluated for any temperatures. We Calculate temperature dependencies of various thermodynamic parameters such as free energy F , the internal energy E , the entropy S and the heat capacity C .

2PO-I-34

NMR ^{59}Co STUDY OF LOCAL MAGNETIC STRUCTURE OF COBALT NANOPARTICLES

Shmyreva A.A.¹, Mazur A.S.¹, De Renzi R.², Allodi G.², Yurkov G.Y.³

¹ Center for Magnetic Resonance, S.-Petersburg University, S.-Petersburg, Russia

² Departments of Physics and Earth Sciences, University of Parma, Parma, Italy

³ Baikov Institute of Metallurgy and Materials Science, Russ.Acad. of Sciences, Moscow, Russia
a.mazur@spbu.ru

Metallic cobalt is one of the materials that are widely used in various spheres of human activity, from metallurgy to medicine. Despite long and thorough studies of various properties of metallic cobalt, many issues still require further attention. One of those challenges is to explain changes in the physico-chemical properties of this material as the linear dimensions of the particles are reduced, which leads to significant changes in their structural, electronic, optical, magnetic, etc. properties.

Decreased value of saturation magnetization compared to its value in bulk samples is one of the aspects of magnetic properties of magnetically-ordered nanoparticles that draw closest attention. There are several approaches to the interpretation of such behavior. Some models assume presence of a "magnetically dead" layer that can be associated with demagnetization of the surface spins, which reduces saturation magnetization due to paramagnetic behavior of these spins. On the other hand, it was suggested for the antiferromagnetic nanoparticles that the decrease in saturation magnetization can be explained by random canting of spins on the surface caused by competing antiferromagnetic exchange interactions.

The spin canting on the surface can be interpreted differently. First, it can be assumed that the inclination of the spins mainly occurs on the particle surface. This assumption is consistent with works, where it was demonstrated that spin canting is caused by surface effects. Second, it is considered that the inclination of spins can result from the finite-size effect, which is uniform throughout volume of the particles.

After careful studies of a large number of nanoscale cobalt particles the existence of noncollinear spins of the metallic ferromagnetic part of nanoparticles was experimentally proved. The data obtained by NMR allow to suggest non-uniform magnetic structure of the metallic part of cobalt nanoparticles for nanocomposites with sizes smaller than the single-domain radius. It was suggested that one of the magnetic phases is presented by nuclei with collinear magnetic structure and is localized in the nanoparticle core. Another magnetic phase has noncollinear magnetic structure and is more likely to be in near-surface layers. It has been demonstrated for the sample with particle size of 5-7 nm that the ratio of nuclei with noncollinear magnetic moments is approximately two times smaller than the ratio of nuclei with collinear magnetic moments. It has been concluded that the presence of matrix does not affect local magnetic structure of investigated nanoparticles. An assumption was made that the canting of spins of the ferromagnetic metallic part of cobalt nanoparticles occurs due to interaction between spins of near-surface cobalt ions with antiferromagnetic oxide CoO on the surface, and that canted spins is not uniform throughout the nanoparticle volume.

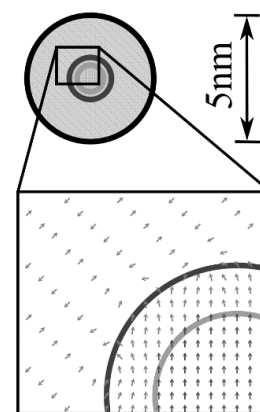


Fig. 1. Model of magnetic moments ordering in a cobalt nanoparticle. There are an AFM shell of CoO, a FM collinearly ordered core and a FM interlayer with canted magnetic moments.

2PO-I-35

ULTRA-THIN Pd_(1-x)Fe_x FILMS SYNTHESIS AND STUDIES OF THEIR COMPOSITION, MORPHOLOGY, STRUCTURAL AND MAGNETIC PROPERTIES

Esmaili A.¹, Vakhitov I.R.¹, Nikitin N.P.¹, Yanilkin I.V.¹, Gumarov A.I.¹, Gabbasov B.F.¹, Rogov A.M.⁴, Aliyev M.N.², Yusupov R.V.¹, Tagirov L.R.^{1,3}

¹ Institute of Physics, Kazan Federal University, Kazan, Russia

² Baku State University, Baku, Azerbaijan

³ Zavoisky Physical-Technical Institute of the Kazan Scientific Center of the Russian Academy of Sciences, Kazan, Russia

⁴ Interdisciplinary Center for Analytical Microscopy, Kazan Federal University, Kazan, Russia
iskvakhitov@gmail.com

Palladium iron (PdFe) alloy is the unique class of ferromagnetic materials. A small, even less than 1 at.%, amount of Fe atoms in palladium matrix induces ferromagnetism (FM) [1]. Iron atoms substituting for palladium in the crystal lattice create strong polarization and produce overlapping polaron clouds of 4d-electrons. Concentration of iron controls principal ferromagnetic properties of these materials. Thin films of Pd_{1-x}Fe_x are attractive for practical applications in cryogenic memory elements.

Ultrathin Pd_{1-x}Fe_x (x=0.01-0.1) films were deposited by molecular beam epitaxy (MBE, SPECS) and magnetron sputtering (MS, BESTEC) techniques under ultra-high vacuum conditions (3×10⁻¹⁰ mbar in the MBE chamber, and 5×10⁻⁹ mbar of the residual gas pressure in the MS chamber). Magnesium oxide (MgO) and silicon single crystals were used as the substrates for MBE and MS depositions, respectively.

SPECS Er-LEED-3000-D setup was used for investigating crystal structures of the substrates and the films. Surface morphology was studied by scanning electron (SEM, Carl Zeiss Merlin) and atomic force (AFM, Bruker Dimension FastScan) microscopies. Elemental composition and atomic concentration of the films were measured by X-Ray photoelectron spectroscopy (XPS, SPECS). Thickness of the deposited films was controlled with the stylus profilometer Dektak XT (Bruker). Magnetic properties were studied by means of the vibrating sample magnetometry technique with Quantum Design PPMS-9. An X-band Bruker ESP300 electron spin resonance spectrometer (ESR) was used for ferromagnetic resonance (FMR) measurements.

Cubic magnetic anisotropy with tetragonal distortion was found for the films with iron concentrations of $x > 0.015$, that were epitaxially grown by MBE. In contrast, films deposited by MS revealed isotropic in-plane magnetic properties. It was found that the magnetization and Curie temperature of the films were growing monotonically while increasing the iron concentration. Coercive fields for the films deposited by MBE were several times smaller compared to the films obtained by MS technique. Magnetic measurements at low temperatures ($T = 5$ K) show coercive field of about 7 Oe for the epitaxial films of Pd_{1-x}Fe_x with $x = 0.01-0.08$.

The Program of Competitive Growth of Kazan Federal University supported by the Russian Government is gratefully acknowledged, as well as partial support from RFBR project No 14-02-00793_a. Synthesis and analysis of the films were carried out at the PCR Federal Center of Shared Facilities of KFU. The SEM and AFM measurements were performed at Interdisciplinary Center for Analytical Microscopy of KFU.

[1] G.J. Nieuwenhuys, *Adv. Phys.*, **24** (1975) 515.

2PO-I-36

CONCENTRATION-DEPENDENT ANTIFERROMAGNETIC CORRELATIONS IN MULTI-SITE $\text{Sr}(\text{Y}_{1-x}\text{Yb}_x)_2\text{O}_4$ OXIDES

Batulin R.G.¹, Gabbasov B.F.¹, Gilmutdinov I.F.¹, Kiiamov A.G.¹, Malkin B.Z.¹, Mumdzhi I.E.¹, Nikitin S.I.¹, Petrenko O.A.², Yusupov R.V.¹, Zverev D.G.¹

¹ Kazan Federal University, Kazan, Russia

² University of Warwick, Coventry, United Kingdom

Roman.Yusupov@kpfu.ru

Nowadays, crystalline compounds with the general formula of SrR_2O_4 , where R is a rare earth (RE) ion, attract an attention of the researchers because of quasi-1D crystal structure, magnetic frustration in zig-zag chains of RE ions and substantially different anisotropic magnetic properties of RE ions at four magnetically nonequivalent sites with the C_s point symmetry. Among the peculiar properties of the up-to-date studied compounds, one can mention a coexistence of a long-range antiferromagnetic and a short-range incommensurate magnetic order in SrEr_2O_4 and SrHo_2O_4 and the absence of the long-range magnetic correlations in SrDy_2O_4 down to the lowest temperatures achieved in the experiments.

Another member of this family, SrYb_2O_4 , undergoes a transition to the non-collinear antiferromagnetic phase at $T_N = 0.9$ K that has been revealed by studies of the inelastic neutron scattering and the heat capacity [1]. These studies, however, didn't provide any information about the electronic structure of Yb^{3+} ions and the nature of interactions which induce the observed magnetic ordering. Some parameters of the magnetic structure should be revised because the values of magnetic moments of the Yb^{3+} ions presented in [1] are not consistent with the measured field dependencies of the magnetization.

We present the results of a systematic investigation of spectral and magnetic properties in the concentration series of $\text{Sr}(\text{Y}_{1-x}\text{Yb}_x)_2\text{O}_4$ single crystals with $x = 10^{-4}$, $5 \cdot 10^{-3}$, $5 \cdot 10^{-2}$, 10^{-1} , $2 \cdot 10^{-1}$, $5 \cdot 10^{-1}$, 1. The samples were grown by the optical floating zone technique from the high-purity initial components. Energies of the crystal-field sublevels of the ground $^2F_{7/2}$ and excited $^2F_{5/2}$ multiplets for the two structurally non-equivalent sites Yb1 and Yb2 were determined by means of the site-selective laser spectroscopy of the strongly diluted ($x = 10^{-4}$) sample. EPR study of the same sample allowed us to characterize the single-ion magnetic anisotropy (principal values and axes of the g -tensors) for the ground states of Yb^{3+} ions at both Yb1 and Yb2 sites.

Crystal-field parameters for Yb^{3+} ions were found from the optimal simultaneous fit of the crystal-field energies and g -tensors for Yb1 and Yb2 sites. These data served as a basis for a description of the magnetization curves in $\text{Sr}(\text{Y}_{1-x}\text{Yb}_x)_2\text{O}_4$ compounds (Fig. 1) with higher Yb-concentrations. A set of exchange interaction parameters were found that allowed us to describe the observed suppression of the magnetization with the Yb-concentration increase. Collected data are used to model the magnetic structure in the SrYb_2O_4 single crystal at $T < T_N$.

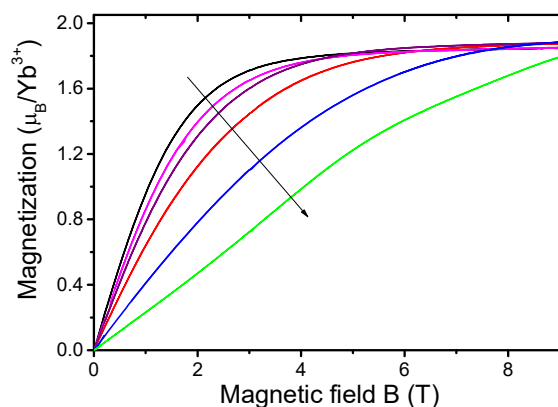


Fig. 1. Magnetization of the $\text{Sr}(\text{Y}_{1-x}\text{Yb}_x)_2\text{O}_4$ series at $T = 2$ K and $\mathbf{B} \parallel c$ (x values along the arrow are 0.005; 0.05; 0.1; 0.2; 0.5; 1).

[1] D.L. Quintero-Castro et al, *Phys. Rev. B*, **86** (2012) 064203.

2PO-I-37

ATOMIC ORDERING AND COERCIVE FORCE OF NANOCRYSTALLINE Fe-Co ALLOY FILMS

Repina N.M.

Krasnoyarsk Institute of Railway Engineering, 89, L.Ketskhoveri St, Krasnoyarsk, 660028, Russia
renomi@yandex.ru

Single (001) films Fe_{0,5}Co_{0,5} и Fe_{0,75}Co_{0,25} were grown by the method of vacuum condensation on the surfaces of the splits of LiF and MgO crystals heating to 150° C. The thickness of research films was laid in the interval 30-50 nm.

Polycrystalline iron-cobalt alloy films received on glass substrates.

As reported in the papers [1, 2], Fe-Co alloy films, under the process conditions are disordering and ordered then at room temperature.

Magnetic anisotropy was measured by the method of the revolving moments.

The coercive force of films was defined from the magnetic–hysteresis loops, with the help of magneto-optical Kerr effect.

Because of the coercive force HC of ferromagnetic being a structurally sensitive characteristic it aroused our interest to trace the changes HC of single crystal films Fe–Co alloys during the time at the room temperature.

The changes of HC were absent during the first three days. After three days of aging the coercive force of film begins to decrease slowly. Between the seventh and tenth days of aging the sharp (approximately 1, 5 times) decrease of HC was observed.

In the course of the investigation of magnetocrystalline anisotropy stoichiometrical compositions the epitaxial films it was discovered that the first constant of this anisotropy changes its value from -5×10^5 to $-0,5 \times 10^5$ erg/sm³. The changes of K₁ are insignificant during three days. The principal changes of K₁ films begin for three days and they finish for nine days. The energy of activation process of the change K₁ process during the natural aging (E=0,25 eV) was measured. The change of K₁ films at natural aging are similar to the change of K₁ at ordering annealing of massive specimens.

The investigations show that process of atomic ordering influences on the coercive force of single crystalline films weakly. The observed sharp decrease of HC on the 7–8 days of aging can be explained by the change of the process magnetization reversal of the film, connected with the decrease of the magnetocrystalline anisotropy. With the high measure K₁ of the film was reversely magnetized by the formation of the wedge manner domains of 90°–neighbouring, orientated along hard magnetic axis and by the removal of domain walls. This magnetization reversal is typical for two–axis films. When the measure $|K_1|$ becomes little, the film is reversed as uniaxial, that is by the formation and growth of the wedges of 180°–neighbouring.

According to the theory of Kondorsky [3] in case of the magnetization reversal with 180° domain–wall movement the coercive force must be 2 times less that under the magnetization reversal 90° domain–wall movement.

The results of above described the conclusion that in film specimens Fe–Co may be received in the disordering condition comparatively easily. This condition of alloy is metastable and at the room temperature it takes place gradually in the atomic ordering condition. These data facilitate the study of atomic ordering influence on the physical properties of alloy.

[1] N.M. Repina, *Izvestiya RAN. Seriya fizicheskaya*, **77(3)** (2013) 373-374.

[2] N.M. Repina, *Bull. R: Phys. Acad. Sci. Physics*, **77(3)** (2013) 337–338.

[3] E.I. Kondorsky, *JETP*, **7** (1937) 1117.

2PO-I-38

MAGNETIC SENSING ENHANCEMENT IN AMORPHOUS MICRO-WIRES VIA FLASH SNNESLING

Adam A.M.^{1,2}, Ahmed M.¹, Panina L.V.^{1,3}, Salem M.M.¹, Dzhumazoda A.¹, Nematov M.G.¹

¹ National University of Science and Technology, MISiS, Moscow 119991, Russia.

² Physics Department, Faculty of Science, Sohag University, Sohag 82524, EGYPT.

³ Institute for Design Problems in Microelectronics RAS, Moscow 124681, Russia

adam_phy@yahoo.com

alaa.adam@misis.ru

Amorphous magnetic wires have long been known as the best candidates for high performance sensors in many sensing applications including security systems. It has been found that physical properties of amorphous ferromagnetic materials such as amorphous microwires can be suitably tailored by means of proper thermal treatments. Fast heating can be explored to produce controlled crystallization of the glassy microwires, including micro- and nanocrystallization. The techniques taking advantage of Joule heat released during the flow of electrical current through a metallic sample are the most widely adopted fast-heating procedures for amorphous materials. Such kind of techniques was first used in amorphous alloys by Jagielinsky [1] who called it ‘flash annealing’ because of a short duration of the current flow and a relatively large magnitude of current. The technique is also known as ‘pulse annealing’ [2]. Flash annealing treatments can be employed to crystallize locally amorphous microwires and then to obtain samples with alternatively soft and hard zones [3-5]. Recently, flash annealed amorphous wires were successfully applied to a torque sensor set on an automobile power steering shaft [6].

In the present work, it was demonstrated that passing a high current pulse through a microwire for short time produces a permanent change in magnetic hysteresis features. We also showed that by passing different controlled current pulses through different sample of the same microwire, different hysteresis loop can be achieved. Due to this permanent change in hysteresis loop, it is possible to store data on microwire with respect to the corresponding hysteresis loop change.

[1] T. Jagielinsky, *IEEE Tram. Magn.*, **19** (1984) 564.

[2] Atalay S, Squire P T and Gibbs M R, *J IEEE Trans. Magn*, **29** (1993) 3412.

[3] C. Morh, C. Aroca, E. Lopez, M. C. Sanchez, and p. Sanchez, *J. Magn. Mugn. Mat.*, **131** (1994) 356-362.

[4] T. Jagielinski, *IEEE Trans. Magn.*, **19** (1983) 1925-1927.

[5] A. I. Taub, *IEEE Trans. Magn.*, (1984) 564-570.

[6] Chang Mei Cai, Kaneo Mohri, Yoshinobu Honkura, and Michiharu Yamamoto, *IEEE Trans. Magn.*, **37** (2001) 4.

2PO-I-39

THE INFLUENCE OF OXYGEN ON QUANTUM MAGNETIC PROPERTIES OF CO NANOWIRES DEPOSITED ON Au AND Pt SURFACES: AB INITIO APPROACH

Koshelev Y.S.¹, Bazhanov D.I.^{1,2}

¹ Moscow State University, physics faculty, Moscow, Russia

² Institution of Russian Academy of Sciences Dorodnicyn Computing Centre of RAS, Moscow, Russia
ys.koshelev@physics.msu.ru

Today the limits of digital memory cell may be estimated as the minimal size of flash memory binary cell, which is about 12 nm [1]. It means that the next principal technological step to increasing recording density will be the step to atomic-size structures. The best structures for nanoscale magnetic memory devices are the systems with large magnetic anisotropy energy (MAE), since they can conserve strong magnetisation under external magnetic fields, electric currents and temperature fluctuations. Strong spin-orbital interaction, large magnetic moment and structural anisotropy are required for obtaining the systems with high magnetic anisotropy energy. In this case the most promising structures for such kind of systems are atomic films, nanowires, chains and clusters of magnetic 3d metals on different noble-metal substrates [2]. At the same time low-dimensional systems may be formed in the atmosphere of different gases such as O, H or N. The presence of this impurities on the surface and their close vicinity to magnetic atoms may lead to the significant magnetic anisotropy energy change [3]. Therefore the influence of gases on magnetic properties of nanostructures nowadays is very important subject to study.

In present work the quantum magnetic properties of Co nanowires were investigated on both clean and oxidized Au and Pt surfaces by means of the first principles calculations based on density functional theory. In the framework of this ab initio approach the influence of oxygen environment on structural and electronic properties of deposited Co nanowires was revealed. The spin-polarised calculations have shown that Co atoms exhibit a large local magnetic moments on clean and oxidized surfaces. Furthermore we found that their magnetic anisotropy energies can be significantly changed by neighbouring oxygen atoms. Besides that we applied the atomistic thermodynamics approach in order to study the stability of all considered structures in wide ranges of temperatures and pressures. The obtained results allowed us to determine these ranges by yielding the corresponding thermodynamical diagrams and comparing them to available experimental data.

- [1] Jim Hutchby and Mike Garner, *Workshop and ERD/ERM Working Group Meeting* (2010).
 [2] S. Blgel and P. H., Dederichs. *Europhys. Lett.*, **9(6)** (1989) 597-602.
 [3] Štěpán Pick and Hugues Dreysse, *Physical Review B*, **63** (2001) 205427.

2PO-I-40

MAGNETOOPTICAL INVESTIGATION OF MAGNETIZATION REVERSAL IN HEXAGONAL ANTIDOT LATTICES

Kulesh N.A.^{1,2}, *Lepalovskij V.N.*¹, *Balymov K.G.*¹, *Palmero E.M.*², *Vas'kovskiy V.O.*¹, *Vázquez M.*^{1,2}

¹ Ural Federal University, Ekaterinburg, Russia

² Institute of Materials Science of Madrid, CSIC, Madrid, Spain

nikita.kulesh@urfu.ru

Array of artificially introduced ordered nanoholes or antidots can be used as a flexible tool for tailoring the magnetic properties of a host material due to the precise control of the nanopores size, shape, and the interpore distance. Antidot lattice leads to the specific microscale magnetization distribution due to the local stray field and contributes to the magnetic anisotropy. In literature micromagnetic structure as well as macroscopic properties were investigated extensively for various antidot systems with in-plane and to less extend with out-of-plane anisotropy [1]. In this study, we investigated mesoscopic magnetization reversal processes using magneto-optic Kerr microscopy, comparing hysteresis loops and domain structure of antidot and continuous films with strong out-of-plane (Tb-Co) and in-plane unidirectional (Fe₂₀Ni₈₀/FeMn) anisotropies.

Samples were synthesized by magnetron sputtering. Thicknesses of Tb₃₀Co₇₀(30nm) and Fe₂₀Ni₈₀(20nm)/FeMn(10nm) films were controlled by the deposition time. For all samples, 3 nm seed and top Ta layers were used to avoid oxidation. For antidot thin films, anodic alumina templates were used as substrates. Two-step anodization process in 0.3M oxalic acid was used with subsequent pore enlargement. The pore diameter of 80 nm was confirmed by scanning electron microscopy. Magnetization processes were analysed by magneto-optical Kerr microscopy.

Typical zigzag domains were observed for Fe₂₀Ni₈₀/FeMn continuous film and torn zigzag-like lower angle domains for the antidot film (see Fig. 1). Despite visible hysteresis on the hysteresis loops measured perpendicular to the anisotropy direction, no magnetic domains were detected in both longitudinal and transversal modes. For Tb-Co samples, maze-like domain structure typical for bubble films was observed. Antidot lattice led to the enhancement of coercivity from 830 Oe to 2400 Oe, shearing of the loop, and decrease of remanence. For antidot film, hysteresis loops had double transition due to the competition between out-of-plane and in-plane magnetic anisotropy.

In conclusion, magnetization processes and magnetic domain structure in continuous and antidot films with in-plane and out-of-plane magnetic anisotropy were investigated by Kerr microscopy. The present study contributes to the understanding of mesoscopic magnetization processes in antidot thin films.

The project was supported by RFFB, grant 16-32-00132 мол_a.

[1] C. Bran, Gawronski P. et al., *J. of Phys. D: Appl. Phys.*, **50** (2017) 065003.

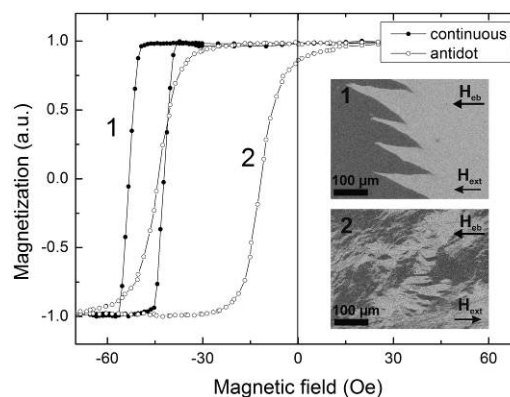


Fig. 1. Hysteresis loops and images of domain structure obtained for continuous (1) and antidot (2) FeNi/FeMn film.

2PO-I-41

MONTE CARLO SIMULATION OF DYNAMIC PHASE TRANSITIONS IN MULTIFERROIC FILMS

Zharmukhametov A.R.¹, Nugumanov A.G.¹, Yuldasheva A. R.¹

¹ Bashkir State University, 450076, Ufa, Russia

aiderfarro@gmail.com

Phase transitions and critical phenomena in bulk and thin film multiferroics became an intense scientific research direction in recent 20 years. Phase transitions in multiferroics from spatially modulated to homogeneous magnetic state are accompanied by a change of electric polarization [1,2]. It was discovered that the electric polarization in multiferroics is coupled with a long range magnetic ordering, one of the effects of which is a generation of polarization induced by an ordering in phase transition [3].

In this work, we consider the multiferroic with strong uniaxial anisotropy, which allows spins on each site to take only two possible values ± 1 and polarization vector can take three values: $-1, 0, +1$. We describe both subsystems with Ising model. Magnetolectric interaction has the form:

$$H_{mf} = -J_{mf} \sum_{i,j,k} S_i S_j P_k - \varepsilon_{mE} \sum_i E_z S_i - \varepsilon_{fH} \sum_i H_z P_i \quad (1)$$

where S_i and P_i are spin and polarization on the i -th site, H_z and E_z - external magnetic and electric fields on the anisotropy axis, ε_{mE} and ε_{fH} are linear magnetolectric susceptibilities for magnetic and ferroelectric subsystems respectively.

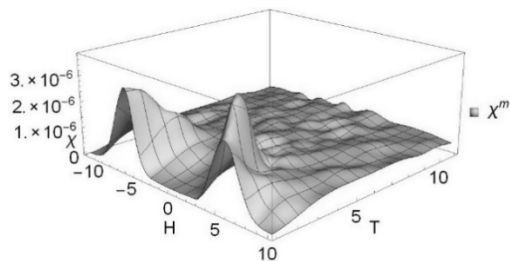


Fig. 1. Magnetic subsystem's susceptibility

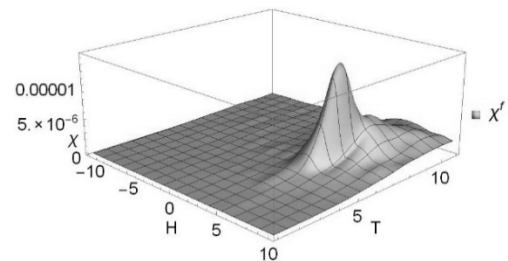


Fig. 2. Ferroelectric susceptibility

We have obtained the dependencies of the magnetic and ferroelectric subsystems on the temperature and external magnetic field (Fig. 1 and Fig. 2). Simulations have been carried over a film with linear sizes $L \times L \times N_z$, $N_z = 4$ is the number of layers, L is the sample width ($L = 16..40$).

The exchange parameters were assumed to have values $J_m = J_f = -1$, $J_{mf} = -3.5..3.5$. All of the macroscopic parameters were averaged over 105 Monte-Carlo iterations. The asymmetry of ferroelectric susceptibility (Fig. 2) over magnetic field we expect to be dependent on the relation between two magnetolectric parameters J_{mf} and ε_{fH} in (1). In addition, the dependences of the ordering parameters on the temperature and magnetic field were obtained, which demonstrate a strong nonlinear dependence on the J_{mf} .

[1] M.K. Kharrasov, I.R. Kyzrygulov, I.F. Sharafullin, *et. al. Bull. Russ. Acad. Sci. Phys.*, **80** (2016) 695

[2] H.T. Diep, V. Bocchetti, D.T. Hoang, V.T. Ngo, *Phys.:Conf. Series*, **537** (2014) 012001

[3] A.P. Pyatakov, A.K. Zvezdin, *Phys.-Usp.*, **55** (2012) 557.

2PO-I-42

INFLUENCE OF INTERFACE ROUGHNESS ON UNIDIRECTIONAL ANISOTROPY IN FeNi/TbCo FILMS

Balymov K.G.¹, Turygin A.P.¹, Adanakova O.A.¹, Kulesh N.A.¹, Svalov A.V.¹, Vas'kovskiy V.O.¹

¹ Ural Federal University, Ekaterinburg, Russia

k.g.balymov@urfu.ru

Presence of the exchange interaction in the interface determines the diversity of heterogeneous films properties. For ferromagnetic/ferrimagnetic layers the interaction leads to the formation of the unidirectional anisotropy [1], which usually manifests itself as a shift of the hysteresis loop of the ferromagnetic layer. The phenomenon of unidirectional anisotropy as well as mechanisms for its tailoring are actively investigated due to the numerous prospective applications. However, there are still limited data on the role of the structural-chemical condition of the interface in the formation of the exchange interaction. The objective of this study is to investigate the influence of the interface roughness on the exchange bias in Fe₁₀Ni₉₀/TbCo films.

Two types of samples were synthesized by high-frequency ion sputtering: Fe₁₀Ni₉₀/TbCo bilayers (series A) and Fe₁₀Ni₉₀ single-layer films (series B).

All samples were deposited onto the Corning cover glass substrates. Thicknesses of Fe₁₀Ni₉₀ and TbCo layers were 50 nm and 110 nm respectively. The roughness of the interface between layers of series A was varied by selective annealing of the Fe₁₀Ni₉₀ layer in a vacuum chamber at temperatures from 100 to 600 °C. The roughness was controlled using NTEGRA Thermo atomic-force microscope (AFM) on the samples of series B, which were annealed in the same conditions.

Data obtained on LakeShore 7407 vibrating sample magnetometer (Fig. 1) demonstrate the crucial role of the roughness in the formation of the unidirectional anisotropy in Fe₁₀Ni₉₀/TbCo films. The increasing temperature of annealing results in the nonmonotonic variation of the exchange bias field. According to the AFM and x-ray diffraction data, it is the consequence of the structural changes induced in the ferromagnetic layer.

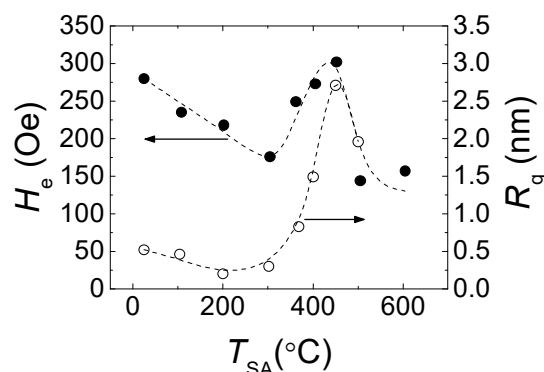


Fig. 1. Dependencies of the exchange bias field H_e of the Fe₁₀Ni₉₀ layer (series A samples) and root-mean-square roughness R_q of the Fe₁₀Ni₉₀ layer's surface (series B samples) on the temperature of annealing.

This work was supported by RFBR, grant № 16-32-00377 мол_a. The equipment of the Ural Center for Shared Use “Modern nanotechnology” UrFU was used.

[1] N. Kulesh, K. Balymov, V. Vas'kovskiy, *Acta Physica Polonica A*, **127** (2015) 525-527.

2PO-I-43

HYSTERESIS PROPERTIES OF $\text{FeMn}/\text{Gd}_x\text{Co}_{100-x}$ FILMS

Vas'kovskiy V.O.^{1,2}, *Gorkovenko A.N.*¹, *Adanakova O.A.*¹, *Lepalovskij V.N.*¹, *Svalov A.V.*¹

¹ Ural Federal University, Ekaterinburg, Russia

² Institute of Metal Physics, UB RAS, Ekaterinburg, Russia

olga.adanakova@urfu.ru

The interlayer exchange coupling is an important functional property of the "spin valve" type film media. This fact initiated considerable interest in its investigation for films containing antiferromagnetic or ferrimagnetic "pinning" layers. Recently, it has expanded to the area of structures having "free" ferrimagnetic elements [1, 2]. The presence of Gd sublayers in their composition makes it possible to realize the function of threshold temperature sensitivity in spin valves. This work is devoted to the study of hysteresis properties of exchange-coupled multilayered films with a ferrimagnetic layer based on Gd-Co amorphous system.

The experiment was carried out on $\text{Ta}(5)/\text{Fe}_{20}\text{Ni}_{80}(5)/\text{FeMn}(20)/\text{Gd}_x\text{Co}_{100-x}(40)/\text{Ta}(5)$ type samples obtained by magnetron sputtering onto glass substrates in the presence of the uniform magnetic field. The thicknesses of each of the layers are given in nm in the above structural formula parentheses. The relatively complex nature of the layered structure is caused by the presence of several auxiliary layers in it. Ta accessory layer and the permalloy layer deposited on it initiate the formation of fcc structure and, accordingly, antiferromagnetic ordering in the FeMn layer. The outer layer of Ta performs a protective function. The main attention is paid to the hysteretic properties of $\text{Gd}_x\text{Co}_{100-x}$ ($0 < x < 100\%$) layer and, in particular, to their features, which are due to the exchange coupling between ferrimagnetic and antiferromagnetic layers. They were compared with the properties of Gd-Co single-layer films.

Fig. 1 shows the dependences of coercivity H_c , anisotropy field H_a , and exchange bias field H_{ex} on the composition of Gd-Co layer. They were determined using magneto-optical hysteresis loops measured in the plane of the samples with $x \leq 40\%$ at room temperature. For larger x values, the Gd-Co layers do not exhibit magnetic ordering. Characteristic maxima on all dependences indicate the presence of magnetic compensation at $x \sim 20\%$.

The exchange bias analysis performed using the data on concentration and temperature dependences of Gd-Co layers spontaneous magnetization showed that the Co subsystem is responsible for their exchange coupling with the antiferromagnetic layer.

This work has been supported by the Ministry of Education and Science of the Russian Federation, project 3.6121.2017.

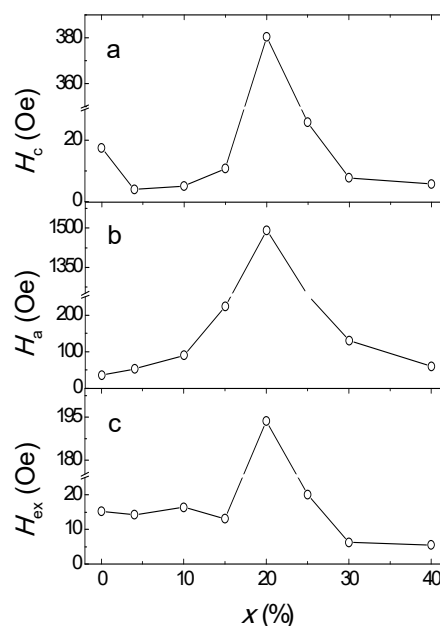


Fig.1. Concentration dependences of the hysteretic properties of the $\text{Gd}_x\text{Co}_{100-x}$ layers in FeMn/Gd-Co structure.

[1] A.V. Svalov et al., *Appl. Phys. Lett.*, **108** (2016) 063504 (1-4).

[2] M. Milyaev et al., *J. Appl. Phys.*, **121** (2017) 123902 (1-5).

2PO-I-44

COMPARATIVE STUDY OF THE MICROSTRUCTURE, MAGNETIC AND MAGNETORESISTIVE PROPERTIES OF Co-Cu AND Co-Al₂O₃ COMPOSITE FILMS

Gorkovenko A.N., Lepalovskij V.N., Adanakova O.A., Kudyukov E.V., Vas'kovskiy V.O.
Ural Federal University, Ekaterinburg, Russia
a.n.gorkovenko@urfu.ru

Recently magnetic heterogeneous structures are the subject of active theoretical research and the basis for a wide range of practical applications. Among these structures, in particular, are granular films in which the granules of magnetic phase embedded in the conductive or dielectric matrix [1, 2].

This work is devoted to the study of the microstructure, magnetic and magnetoresistive and magnetoelastic properties of Co-Cu and Co-Al₂O₃ composite films, which were obtained by magnetron sputtering. The samples with thicknesses of 50 nm were deposited onto the «Corning» glass substrates by cosputtering of Co and Cu (or Al₂O₃) targets. Nominal composition was set by the relative speed of targets sputtering. The content of magnetic metal in the films was varied from 10 to 60 at. % for both types of samples. The structure was analyzed by transmission electron microscopy. Magnetic properties were measured by VSM. The measurements of the magnetoresistance were performed at room temperature by four-point probe method (Co-Cu films) double-point probe method (Co-Al₂O₃ films).

Direct microstructure study showed, that the cobalt in the Co_x(Al₂O₃)_{100-x} films with $x \leq 50\%$ is in a granular state with hcp lattice. The granules have a round shape and their average size is 2-4 nm at the concentration of $x = 40\%$. The crystal lattice of cobalt in the Co_xCu_{100-x} films is fcc which is nonequilibrium at room temperature. Cobalt granules have an irregular shape and exhibit high dispersion of sizes. Average size is 4-10 nm for $x = 40\%$.

Measurements of resistivity in a magnetic field showed, that the investigated Co_x(Al₂O₃)_{100-x} films demonstrate significant negative magnetoresistance, which was observed at the metallic phase concentrations ranging from 30 to 60%. The maximum value of $\Delta R/R$ effect was obtained at $x \sim 50\%$, and was 7.8% at $H = 16$ kOe.

For granular Co_xCu_{100-x} films, in addition to the negative magnetoresistance, the maximum value of which is observed at $x = 30\%$ and amounted $\sim 3\%$, a positive magnetoresistance was found. It was observed for Co concentration from 40 to 50% at magnetic field from 0 to ± 1 kOe. Its magnitude was $\sim 0.2\%$. This fact can be explained by the appearance of anisotropic magnetoresistance effect, which sign depends on the relative orientation of the magnetic field and the current. To check this assumption, additional measurements were accomplished, in which the current flows perpendicular to the applied field. As a result, in this configuration only the decrease of the resistance with the field increasing was observed. This result indicates the integration of the contributions of giant magnetoresistance and anisotropic magnetoresistance.

This work was supported by RFBR (project No. 16-32-00327 mol_a).

[1] A. El Amiri, K. Chafai, H. Lassri, M. Abid, E.K. Hlil, L. Bessais, *Physical and Chemical News*, **71** (2014) 52-55.

[2] M.A.S. Boff, B. Canto, R. Hinrichs, L.G. Pereira, F. Mesquita, J.E. Schmidt, G.L.F. Fraga, *Physica B: Condensed Matter*, **406** (2011) 4304-4306.

2PO-I-45

TEMPERATURE-DEPENDENT FORC PROBING OF MAGNETIC NANOSPRING AND NANOWIRE ARRAYS

Samardak A.Yu.¹, Chebotkevich L.A.¹, Ognev A.V.¹, Samardak A.S.¹, Nam D.Y.², Kim S.H.², Jeon Y.S.², Kim Y.K.²

¹ Far Eastern Federal University, Vladivostok, Russia

² Department of Materials Science and Engineering, Korea University, Seoul, Korea
samardak.aiu@students.dvfu.ru

Recently, nanosprings have been intensely studied because of their unusual helical shape and potential applications under the external magnetic field, such as sensors, motors and locomotion [1]. In the same time, nanowires, due to their remarkable magnetic and structural properties, can be used as elements of computer logic, memory and sensors [2].

Arrays of nanowires and nanosprings, made of Co and CoFe, were fabricated by electrodeposition into an anodized alumina template with the pore diameter of 200 nm. Morphology of nanowires and nanosprings was observed using a field emission scanning electron microscope and a high-resolution transmission electron microscope.

To investigate a magnetic behaviour of CoFe and Co nanospring and nanowire arrays, in addition to ordinary hysteresis methods, the powerful FORC (First Order Reversal Curve) technique has been used and noticeable results have been acquired. Figure 1 shows an example of a FORC diagram of a “stingray” shape measured for CoFe nanospring array. The switching field distribution (SFD) along Hc-axis has a long tail pointing out that nanosprings have different length and, consequently, different coercivity. The wide interaction field distribution (IFD) along Hu-axis indicates the significant dipolar coupling between neighbors. Low temperature (down to 80 K) FORC probing in in-plane and out-of-plane geometries has revealed anisotropic magnetic behaviour of nanosprings, while the hysteresis study demonstrated isotropic loops. At low temperatures the magnetoelastic contribution plays the important role due to the different coefficients of thermal expansion of magnetic elements and alumina templates. Nanowire arrays have strong out-of-plane anisotropy supported by hysteresis measurements at RT and LT. The observed difference of magnetic properties between nanosprings and nanowires originates from the complex shape of nanosprings. Using the approach to magnetic saturation we have defined the dimensionality of stochastic domains and explain magnetic structure of samples within the theory of random local anisotropy.

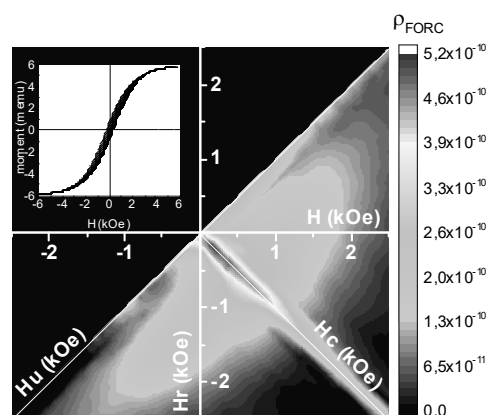


Fig. 1. In-plane FORC distribution of the CoFe nanospring array at RT. The inset contains a family of the seventy FORCs.

Support by RFBR (grant 16-02-01015), the Ministry of Education and Science of Russia (state task 3.5178.2017) and NRF Korea grant (2015R1A2A1A15053002) is acknowledged.

[1] S. Tottori et al. *Adv. Mater.*, **24** (2012) 811-816.

[2] A.S. Samardak et al. *J. Phy.: Conf. Series*, **345** (2012) 012011.

2PO-I-46

MONTE CARLO SIMULATION OF AGING PHENOMENA IN MULTILAYER MAGNETIC STRUCTURES

Purtov A.N.¹, Prudnikov P.V.¹, Prudnikov V.V.¹

¹ Omsk State University, Omsk, Russia
prudnikovpv@omsu.ru

A Monte Carlo simulation of the nonequilibrium behavior of multilayer magnetic structures consisting of alternating magnetic and nonmagnetic nanolayers is realized. The calculated two-time autocorrelation function and the staggered magnetization of the structure at its evolution starting from various initial states are analyzed. The analysis reveals aging effects characterized by a slowing down of the relaxation and correlation characteristics in the system with the waiting time [1]. The dependence of aging characteristics on thickness of ferromagnetic films is investigated. It is shown that, in contrast to bulk magnetic systems, the aging effects in magnetic superstructures arise not only near the ferromagnetic ordering temperature T_c in the films but also within a wide temperature range at $T \leq T_c$. The revealed aging effects in the behavior of the magnetization relaxation for our model multilayer structure are in good agreement with the aging effects observed in experiments for the Co/Cr structure [2].

In investigated magnetic multilayer structures, their nanoscale periodicity gives rise to the mesoscopic effects of the spatial spin correlation with the slow relaxation dynamics of magnetization accompanying the quenching of the system in the nonequilibrium state. In contrast to the bulk magnetic systems, where the slow dynamics and aging effects manifest themselves near the critical point [3], magnetic superstructures with nanoscale periodicity allow increasing the relaxation time owing to the effects related to the larger characteristic spin–spin correlation length. That is why the aging and nonergodicity effects can be observed in the multilayer magnetic structures within a wider temperature range as compared to that for the bulk magnetic systems.

The existence of these nonequilibrium effects should surely be taken into account in any applications of the multilayer magnetic structures for spintronic devices based on the giant magnetoresistance effect.

This work was supported by the grant 17-02-00279 of Russian Foundation of Basic Research and by the grant MD-6024.2016.2 of Russian Federation President. The simulations were carried out on the Supercomputing Center of Lomonosov Moscow State University, Moscow Joint Supercomputer Center and St. Petersburg Supercomputer Center of the Russian Academy of Sciences.

[1] V.V. Prudnikov, P.V. Prudnikov, A.N. Purtov, M.V. Mamonova, *JETP Letters*, **104** (2016) 776.

[2] T. Mukherjee, M. Pleimling, Ch. Binek, *Phys. Rev. B*, **82** (2010) 134425.

[3] P.V. Prudnikov, V.V. Prudnikov, et al. *Prog. Theor. Exp. Phys.*, **2015** (2015) 053A01.

2PO-I1-25

CALCULATION OF CPP- AND CIP-MAGNETORESISTANCE IN MULTILAYER MAGNETIC STRUCTURES

Romanovskiy D.E.¹, Prudnikov P.V.¹, Prudnikov V.V.¹

¹ Omsk State University, Omsk, Russia
prudnikovpv@omsu.ru

We present the Monte Carlo study of trilayer and spin-valve magnetic structures with GMR effects which is carried out with applying an anisotropic Heisenberg model to describe the magnetic properties of the ultrathin ferromagnetic films forming these structures [1]. The temperature and magnetic field dependences of magnetic characteristics are considered for ferromagnetic and antiferromagnetic configurations of these multilayer structures. We developed a new methodology for determination of the magnetoresistance (MR) with the use of the Monte Carlo method both for measurements of the current perpendicular to plane (CPP) - MR [2] and for measurements of the current in plane (CIP) - MR. This methodology permits us to calculate temperature dependence of the CPP- and CIP-MR of multilayer structures for different thicknesses of the ferromagnetic films. We introduce for calculation of the CIP-MR a phenomenological parameter of electron scattering at F/N interfaces, which can be determined from comparison of calculated and experimentally measured CIP-MR values. We demonstrate that the calculated temperature dependence of the CPP- and CIP-MR agrees very well with the experimental results [3] measured for the Fe/Cr(001) and Co/Cu(001) multilayer structures.

Our methodology gives the possibility of predicting maximum values of the magnetoresistance for various temperatures and for room temperature, and also for different multilayer structures with optimum thicknesses of ferromagnetic films. So, we predict that for the Fe/Cr(001) multilayer structure the CPP-MR takes the maximum values for ferromagnetic films with thickness $N=16$.

This work was supported by the grant 17-02-00279 of Russian Foundation of Basic Research and by the grant MD-6024.2016.2 of Russian Federation President. The simulations were carried out on the Supercomputing Center of Lomonosov Moscow State University, Moscow Joint Supercomputer Center and St. Petersburg Supercomputer Center of the Russian Academy of Sciences.

- [1] P.V. Prudnikov, V.V. Prudnikov, M.A. Menshikova, N.I. Piskunova, *J. Magn. Magn. Mater.*, **387** (2015) 77.
- [2] V.V. Prudnikov, P.V. Prudnikov, D.E. Romanovskiy, *J. Phys. D: Appl. Phys.*, **49** (2016) 235002.
- [3] J. Bass, W.P. Pratt, *J. Magn. Magn. Mater.*, **200** (1999) 274.

2PO-I1-26

PROXIMITY EFFECT IN Fe/Fe-V SUPERSTRUCTURES

Mukhamedov B.O.¹, Ponomareva A.V.¹, Palonen H.², Hjörvarsson B.², Abrikosov I.A.³

¹ Materials Modeling and Development Laboratory, National University of Science and Technology 'MISIS', Moscow, Russia

² Department of Physics and Astronomy, Uppsala University, Uppsala, Sweden

³ Department of Physics, Chemistry, and Biology (IFM), Linköpings University, Linköping, Sweden

mbobur991@gmail.ru

Magnetic proximity effect (MPE) is a process of inducing the spin polarization in paramagnetic material close to the interface with magnetically ordered material. MPE is a novel phenomenon which represents a great interest, for instance for spintronic devices. It has been demonstrated that in modulated Fe/Fe_{0.32}V_{0.68} superlattices (where Fe corresponds to ferromagnetic monolayer and Fe_{0.32}V_{0.68} is paramagnetic random alloy with a variable thickness) the range of MPE is quite large; and the interaction between two Fe monolayers extends over more than 30 layers of the Fe_{0.32}V_{0.68} alloy [1]. However, the nature of the MPE in Fe/Fe-V system is still unknown.

We have studied the magnetic proximity effect in modulated Fe/Fe_{0.32}V_{0.68} superstructure from first principles. We have performed electronic structure and total energy calculations in the framework of the density functional theory (DFT) using the exact muffin-tin orbitals (EMTO) method. The chemical disorder of Fe_{0.32}V_{0.68} alloy have been accounted for within the coherent potential approximation. The paramagnetic state has been described within disordered local moment (DLM) approximation. Calculations of magnetic moments, magnetic exchange interactions J_0 and exchange pair interactions J_2 have been performed for ferromagnetic and paramagnetic states.

In Fig. 1 we show values of local magnetic moments at Fe and V atoms in a superlattice. At the interface between Fe monolayer ($N = 1$) and Fe_{0.32}V_{0.68} ($N > 1$) the magnetic moments and magnetic effective exchange interactions J_0 are substantially higher compared to the bulk Fe_{0.32}V_{0.68} alloy. Our theoretical calculations of the pair exchange interactions show strong anisotropy between interlayer and intralayer pair interactions. The calculations for superlattices with different thicknesses of Fe_{0.32}V_{0.68} alloy show that the extent of the MPE depends weakly on the distance between Fe monolayers.

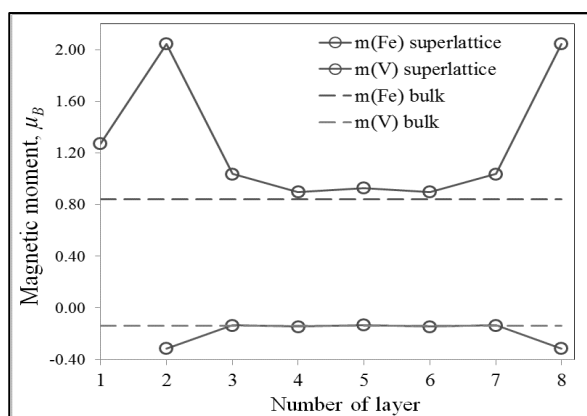


Fig. 1. Magnetic moment of Fe/Fe_{0.32}V_{0.68} superlattice with $N = 8$ layers, where $N = 1$ corresponds to Fe monolayer.

Support by the Ministry of Education and Science of the Russian Federation (Grant No. 14.Y26.31.0005) and the RFBR (Grant No. 16-02-00797) is acknowledged.

[1] H. Palonen, F. Magnus and B. Hjörvarsson, MML (2016) Conference.

2PO-I1-27

MAGNETIC PROPERTIES OF $\text{NiFe}_{0.75}\text{Cr}_{1.25}\text{O}_4$ NANOPARTICLES WITH MAGNETIC COMPENSATION TEMPERATURE

Starchikov S.S.¹, Lyubutin I.S.¹, Gervits N.E.¹, Lin C.-R.², Tseng Y.-T.²

¹ Shubnikov Institute of Crystallography of FSRC “Crystallography and Photonics” RAS, Moscow, 119333 Russia

² Department of Applied Physics, National Pingtung University, Pingtung County, Taiwan
sergey.s.starchikov@gmail.com

Magnetic oxides with a spinel structure are widely applicable in electronic devices. High resistance, the possibility of tuning of magnetic and electric properties, simple and cheap production makes them very useful for magnetic record, ferro-liquids, biosensors and other applications.[1] The valence and location of magnetic ions in octahedral [B] and tetrahedral [A] crystal sites can be varied by introducing different metal ions, size reduction, changing the condition of synthesis. Thus the information of such compounds tends to be vital and highly appreciated for theoretical and practical studies.

A series of nickel-chromium-ferrite $\text{NiFe}_{0.75}\text{Cr}_{1.25}\text{O}_4$ nanoparticles (NPs) with a cubic spinel structure and with size d ranging from 1.6 to 47.7 nm was synthesized by the solution combustion method. In the NPs with $d > 20$ nm, the compensation of the magnetic moments of A- and B-sublattices was revealed at about $T_{\text{com}} = 360\text{-}365$ K. This value significantly exceeds the point T_{com} in bulk ferrites $\text{NiFe}_x\text{Cr}_{2-x}\text{O}_4$ (about 315 K) with the similar Cr concentration.[2] However, in the smaller NPs $\text{NiFe}_{0.75}\text{Cr}_{1.25}\text{O}_4$ with $d \leq 11.7$ nm the compensation effect does not occur. The magnetic anomalies are explained in the term of highly frustrated magnetic ordering in the octahedral B-sites, which appears due to the competition of AFM and FM exchange interactions, and results in a canted magnetic structure in the B sublattice.

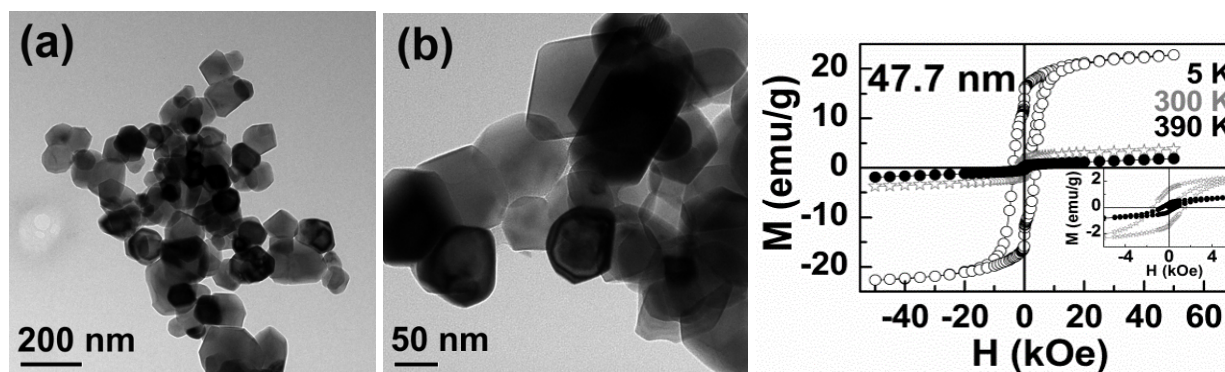


Fig. 1. TEM images of $\text{NiFe}_{0.75}\text{Cr}_{1.25}\text{O}_4$ nanoparticles annealed at 900°C (a, b) and magnetization hysteresis loop (c)

Support by the Russian Scientific Foundation (Project #14-12-00848) is acknowledged.

[1] M. Pardavi-Horvath, *J. Magn. Magn. Mater.*, **215-216** (2000) 171–183.

[2] A. Rais, A. M. Gismelseed and I. A. Al-Omari, *Phys. Stat. Sol. (b)*, **242** (2005) 1497–1503.

2PO-I1-28

QUASI-CLASSICAL LOCALIZED STATES IN THE 2D FERRIMAGNET

Panov Yu.D.¹, Moskvina A.S.¹

¹ Ural Federal University, Ekaterinburg, Russia
yuri.panov@urfu.ru

We consider highly anisotropic 2D quantum $S=1/2$ magnet with a constant total z -component of the magnetic moment. This is equivalent to the frequently used system of charged hard-core bosons on a square lattice [1]. The z -component of pseudospin describes the local density of bosons, so that antiferromagnetic z - z exchange corresponds to the repulsive density-density interaction, while isotropic ferromagnetic planar exchange corresponds to the kinetic energy of bosons. The constant total number of bosons leads to the constraint on total z -component of pseudospin.

We performed numerical minimizing of the ground-state energy in a mean field approximation with the conjugate gradient method on the square lattice 512×512 with periodic boundary conditions. In particular, our numerical calculations indicate the existence of the relatively stable localized excitations with nontrivial topological structure in the ferrimagnetic (FIM) phase. An example of such states is shown in Fig.1.

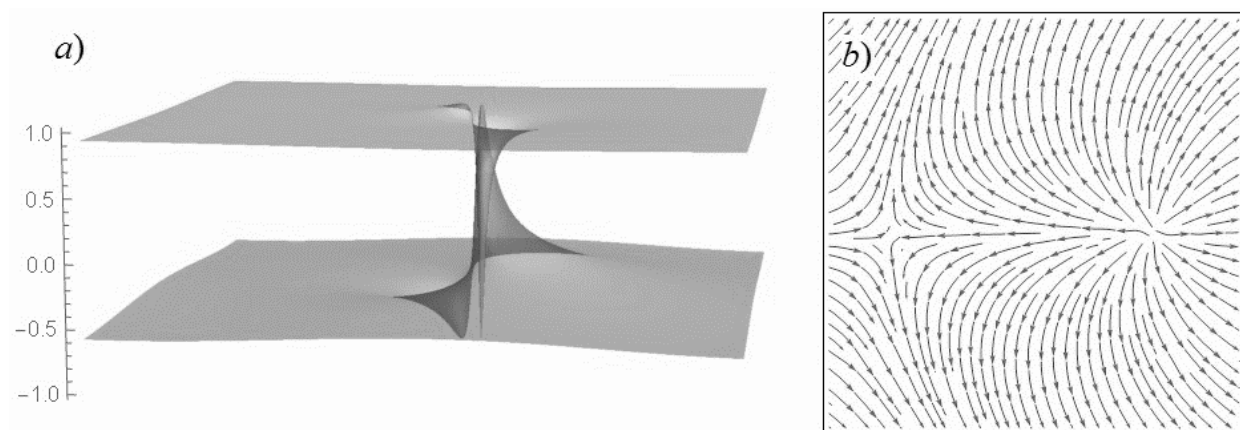


Fig. 1. Inhomogeneous states in FIM phase on the square lattice 512×512 (the results of numerical calculations). a) The z -component of pseudospin demonstrates the separation on two sublattices with checkerboard ordering. b) The phase flow of planar components of the pseudospin reveals the vortex-antivortex pair structure in the core of inhomogeneity (30×30 fragment).

In the continuous quasi-classical two-sublattice approximation, we consider analytically the asymptotic behavior of localized excitations that converge to homogeneous solutions at infinity. In the FIM phase (supersolid phase for hard-core bosons), we find that asymptotic behavior of localized excitations is consistent with skyrmion-like solutions. The asymptotic behavior of localized excitations in ferromagnetic and antiferromagnetic phases are also considered.

The work supported by Act 211 Government of the Russian Federation, agreement № 02.A03.21.0006 and by the Ministry of Education and Science, projects 2277 and 5719.

[1] T. Matsubara, H. Matsuda, *Progr. Theor. Phys.*, **16** (1956) 569-582.

2PO-I1-29

MAGNETIC PROPERTIES OF $Mn_{2-x}Mg_xBO_4$ WARWICKITES

Muftakhutdinov A.R.¹, Eremina R.M.^{1,2}, Mukhamedshin I.R.¹, Matsumoto K.³, Gilmutdinov I.F.¹, Cherosov M.A.¹, Moshkina E.⁴, Bezmaternykh L.⁴

¹ Kazan (Volga region) Federal University, 420008, Kazan, Russia

² Kazan E. K. Zavoisky Physical -Technical Institute, 420029, Kazan, Russia

³ Kanazawa University, 920-1192 Ishikawa Prefecture, Kanazawa, Japan

⁴ L.V. Kirensky Institute of Physics SB RAS, 660036, Krasnoyarsk, Russia
mufta96@mail.ru

$Mn_{2-x}Mg_xBO_4$ is a novel compound of the warwickite family. The homometallic warwickite ($M_{2+} = M_{3+}$) is Mn_2BO_4 compound with the charge ordering (CO). Single crystals of the $Mn_{2-x}Mg_xBO_4$ (the max. size: $1 \times 1 \times 3 \text{ mm}^3$) were synthesized by the flux method. $Mn_{2-x}Mg_xBO_4$ crystallizes within a monoclinic structure (space group $P2_1/n$). The lattice constants at room temperature are given by $a = 9.2934(5) \text{ \AA}$, $b = 9.5413(5) \text{ \AA}$, and $c = 3.2475(2) \text{ \AA}$ and the angles are equal $\alpha = 90.0^\circ$; $\beta = 90.751(1)^\circ$; $\gamma = 90.0^\circ$ [1].

In this work field and temperature dependencies of magnetization of monocrystals $Mn_xMg_yBO_4$ with $y:x=1:1, 1:1.2, 1:1.25, 1:1.5, 1:1.75$ were measured by SQUID detector in 0,02 and 1 T magnetic fields. Temperature dependencies of magnetic susceptibility along c- axes in 200 Oe and 10kOe for $Mn_xMg_yBO_4$ ($x:y=1.2:1$) are presented in Figure 1. Temperature Neel is equal 8K for this crystal. It is smaller than in Mn_2BO_4 with $T_N=26K$. The magnetization dependencies were obtained in FC (cooling the sample at nonzero magnetic field), ZFC (cooling the sample at zero magnetic field) and FH (heating the sample at nonzero magnetic field after FC) regimes.

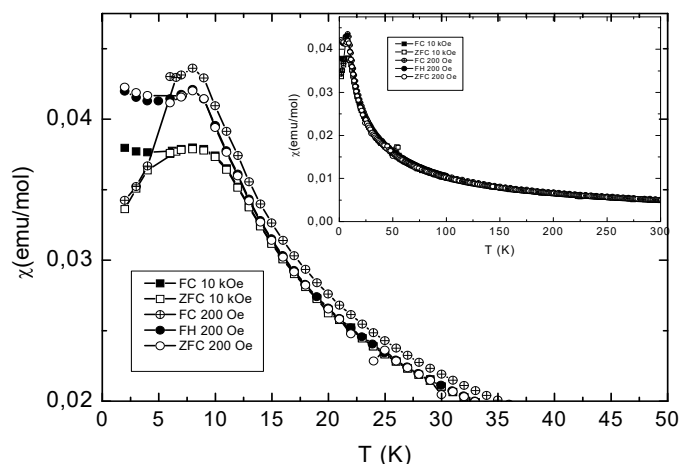


Figure 1. Temperature dependencies of magnetic susceptibility in 200 Oe and 10kOe for $Mn_xMg_yBO_4$ ($x:y=1.2:1$).

This work was supported by JASSO scholarship program.

[1] N.V. Kazak et al., *JMMM*, **393** (2015) 316.

2PO-I1-30

ADSORPTION ENERGY AND SPATIAL DISTRIBUTION OF MAGNETIZATION FOR CO/CU SYSTEM IN DEPENDENCE OF FILM THICKNESS AND GROWTH MODES

Ezhkov P. Yu.¹, Mamonova M. V.¹

¹ Department of Physics, Dostoevsky Omsk State University, Omsk, Russia
ezhkov.pavel@gmail.com

In this work, we investigated multilayer Co/Cu(100) and Co/Cu(111) systems by variational method [1] within of spin density functional theory with taking into account temperature effects and inhomogeneous spatial distribution of relative magnetization in surficial region. We considered different film growth modes and calculated full interface energy, adsorption energy and relative part of adatoms in film in dependence of film thickness up to 10 ML. Effects of intermixing between adatoms and substrate atoms were also taken into consideration.

Inhomogeneous spatial distribution of magnetization was taken proportional to the electron density distribution associated with adsorbate magnetic atoms. In order to calculate the temperature dependence for the relative magnetization $m(T, N)$ we used the following expression:

$$m(T, N) \propto \left[\frac{T_c(N) - T}{T_c(N)} \right]^{\beta(N)}, \quad \beta(N) = \begin{cases} \beta_{2D}, & N \leq N_c; \\ (\beta_{2D} - \beta_{\text{bulk}}) \frac{N_c}{N} + \beta_{\text{bulk}}, & N > N_c; \end{cases}$$

where N – film thickness in monolayers, $T_c(N)$ – thickness-dependent film Curie temperature in molecular field approximation, $\beta(N)$ – system's thickness-dependent critical exponent of the magnetization that reflects the dimensional crossover. For $\beta(N)$ an approximation based on experimental data [2] was used. Parameters β_{2D} , β_{bulk} are critical exponents of the magnetization for ultrathin films (when they can be considered as 2D systems) and for bulk adsorbate material, respectively. The value for β_{2D} had selected between two model values. We used according to [2] for the Co/Cu(111) system $\beta_{2D} = 0.125$ (2D Ising model), for the Co/Cu(100) system $\beta_{2D} = 0.231$ (2D XY model) and $\beta_{\text{bulk}} = 0.42$. The N_c parameter is the critical film thickness above which dimensional crossover occurs and β starts increasing. In our work, we used (for all planes) $N_c = 4$ ML (the smallest reported value among different systems).

Calculations were made in several growth modes: 1) layer by layer growth; 2) island growth; 3) an intermediate mode, in which the coverage of the next to the topmost layer is determined from the minimum of the interfacial energy of the topmost layer.

In fig. 1 we present our results of calculating the spatial distribution of magnetization for 1-, 5-, 9-monolayer-thick films for (100) substrate plane for the case of layer by layer mode.

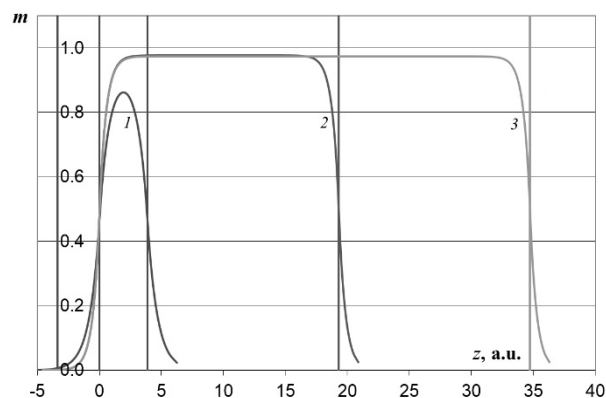


Fig. 1. The spatial distribution of magnetization for Co/Cu(100) system, $T = 100$ K, layer-by-layer mode. Film thickness: 1. 1 ML, 2. 5 ML, 3. 9 ML.

[1] S.P. Klimov, M.V. Mamonova, V.V. Prudnikov, *Solid State Phenomena*, **190** (2012) 27-30.

[2] C.A.F. Vaz, J.A.C. Bland, G. Lauhoff, *Rep. Prog. Phys.*, **71** (2008) 056501.

2PO-I1-31

PHASE DYNAMICS IN ARRAYS OF COUPLED VORTEX SPIN-TORQUE NANO-OSCILLATORS

Katkova O.S., Safin A.R., Kapranov M.V., Udalov N.N.

National Research University "MPEI", Moscow

arnellemorte@gmail.com

Vortex oscillations of magnetization in ferromagnetic nanostructures induced by a spin-polarized current that flows through them are of significant interest [1], [2]. First, and foremost, it is because of its potential telecommunication applications as a microwave master oscillators. Synchronization and addition of capacities vortex STNO is very important problem because of its low output capacity. It is necessary to identify the conditions of phase locking and stability of appropriate stationary state for determination of synchronisms conditions in the array of vortex coupled oscillators. We investigated the phase dynamics in two-dimensional array of STNO.

Mathematic model of coupled vortex STNO is the Thiele equation system [1]-[3] for vortex coordinates vector in the plane of sample \mathbf{X}_i :

$$G \left(\mathbf{e}_z \times \frac{d\mathbf{X}_i}{dt} \right) - k(\mathbf{X}_i) \mathbf{X}_i - D_i \frac{d\mathbf{X}_i}{dt} - \mathbf{F}_{st,i}(\mathbf{X}_i) - \mathbf{F}_{int}(\mathbf{X}_j) \Big|_{j=1..N}^{j \neq i} = 0.$$

Here, G is the gyro constant, D_i are the constants of attenuation, $k(\mathbf{X}_i)$ the non-linear function \mathbf{X}_i that describing energy of vortex [1], $\mathbf{F}_{st,i}$ the forces connected with spin-torque transfer, and \mathbf{F}_{int} the interaction forces of i -vortex with all other elements (amount of elements is N). We cross from Thiele equation system to the phase approximation and expect that each oscillator is in excited state and singing margin is great enough. So the amplitudes of oscillators signals are established faster than phases and one can consider that $|\mathbf{X}_i(t)| = \lim_{t \rightarrow \infty} |\mathbf{X}_i(t)| = X_{0i}$.

Following this approximation for phases θ_i for each vortex STNO is

$$\frac{d\theta_i}{dt} = \omega_i + \sum_{j=1, j \neq i}^N \lambda_{ij} \cdot \sin(\theta_j - \theta_i),$$

where ω_i are eigenfrequencies of oscillator θ_i , λ_{ij} are parameters of connection between θ_i and θ_j , which are θ decreased with increasing of a distance between oscillators, that is $\lambda_{ij} \propto 1/d_{ij}$, where d_{ij} is the distance between vortex STNO.

Analysis of received system of phase equations shows that besides the steady-state regime of equal phases there are also exists complicated chaotic modes and chimera states, where one part of oscillators is phase-synchronizned and another part is in chaotic regime. It is necessary that non-identify of vortex STNO sizes would be least (units of nm when diameter of the sample is hundreds of nm) for capacity addition.

The research was supported by a grant of the President of the Russian Federation for state support of young Russian scientists No.MK-7026.2016.8.

[1] Y. Gaididei, V. Kravchuk, D. Sheka., *Intern. J. Quantum. Chem.*, **110** (2009) 83-97.

[2] P.A.Stremoukhov, A.R.Safin, N.N.Udalov. *Vestnik MPEI*, **6** (2016) 96-100.

[3] V. Flovik, F. Macia, E. Wahlstrom. *Scientific Reports*, **6** (2016) 32528.

2PO-I1-32

FIRST-PRINCIPLE CALCULATIONS OF THE EXCHANGE INTERACTION CHARACTERISTICS FOR MULTILAYER MAGNETIC STRUCTURES

Mamonova M.V.¹, Prudnikov V.V.¹

¹ Omsk State University, Omsk, Russia
MamonovaMV@omsu.ru

Magnetic multilayer structures which consist of the ferromagnetic layers separated by nonmagnetic layers with giant magnetoresistance (GMR) are widely used as spintronic devices and read heads of hard disks. In this work magnetic and exchange interaction characteristics of Co/Cu/Co and Fe/Cr/Fe multilayer structures are studied by using VASP software package [1] within the Projector Augmented Wave (PAW) method with generalized-gradient approximation (GGA PBE) [2].

The exchange interaction parameters for Co and Fe films on Cu and Cr substrates were calculated within a classical Heisenberg model. The energy per unit cell in this model can be written

as $H = -\frac{1}{2n} \sum_{i,j} J_{ij} S_i S_j$, where the summations are over the all sites in the unit cell, where S_i are

quantum spin operators, n is the number of unit cells in the crystal. We introduce the exchange interaction parameters of nearest neighbors J_1 and the next-nearest-neighbors atoms J_2 , which are shown in Fig 1 for some FCC atom configuration. J_1 and J_2 can be obtained from the difference of the total energy for the ferromagnetic and antiferromagnetic spin configurations in the film: $N_{ij} J_j = E_i^{AFM} - E_i^{FM}$, where N_{ij} is a number of antiparallel pairs in one unit cell in the i -th AFM state for nearest neighbors ($j=1$) and the next-nearest neighbors ($j=2$) atoms. The values J_1 and J_2 were calculated for multilayer structures with different thicknesses of ferromagnetic films and nonmagnetic layer.

The total energies of the several collinear spin-configurations, energy of the film formation and atom magnetic moments were calculated for multilayer structures as a function of the convergence parameters with taking into account the relaxation effects. Comparison results of calculation of the atom magnetic moments in different layers allow to conclude that the atoms most distant from the substrate have a greatest magnetic moment.

Using values of the exchange interaction integrals, we calculated the temperature dependence of the magnetoresistance of Fe/Cr(100)/Fe and Co/Cu(100)/Co structures by Monte-Carlo methods [3], which demonstrate a good agreement with experimental data.

Support by RFBR grant № 17-02-00279 is acknowledged.

[1] P. G. Kresse, J. Furthmüller, *Phys. Rev. B*, **54** (1996) 11169.

[2] J. P. Perdew, K. Burke and M. Ernzerhof, *Phys. Rev. Lett.*, **77** (1996) 3865.

[3] M.V. Mamonova, D.E. Romanovskiy, V.V. Prudnikov, P.V. Prudnikov, *Journal of Siberian Federal University. Mathematics & Physics*, **10** (2017) 65–70.

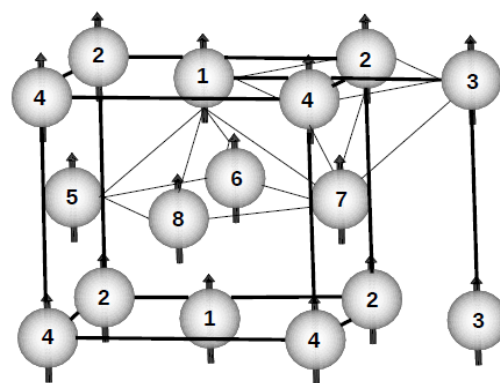


Fig. 1. Atoms configurations in FCC super cell for three monolayers film. The arrows represent magnetic spins directions. The thin and bold lines show connections the nearest and next-nearest neighbors atoms.

2PO-I1-33

THICKNESS IMPACT ON MAGNETIC AND OPTICAL PROPERTIES OF NANOSIZED FILMS WITH FERROMAGNETIC LAYER

Hashim H.¹, Singh S.P.¹, Panina L.V.¹, Pudonin F.A.², Sherstnev I.A.², Podgornaya S.V.¹, Shpetnyy I.³

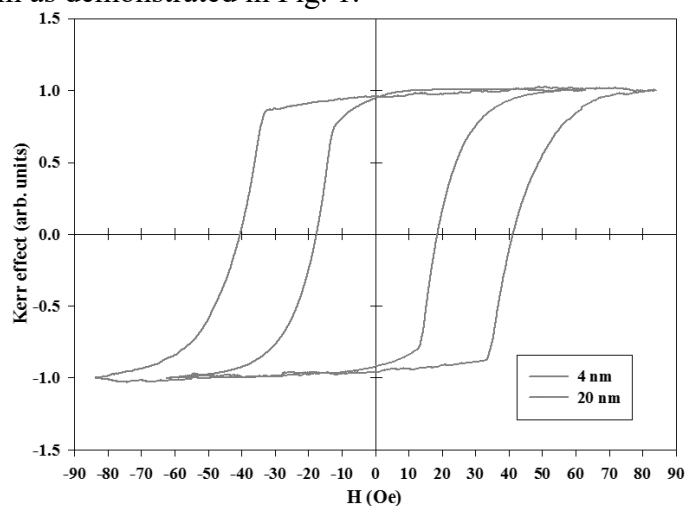
¹ National University of Science and Technology (MISIS), Moscow, 119049, Russia.

² The Lebedev Physical Institute (RAS), Moscow 119991, Russia.

³ Sumy State University, Sumy 40007, Ukraine

hh@science.tanta.edu.eg

Nanosized films with ferromagnetic layers are widely used in nanoelectronics, sensor systems and telecommunication. The physical and magnetic properties of nanolayers may significantly differ from those known for bulk materials due to crystalline structure, influence of interfaces, roughness, and diffusion. In this work, we are employing the methods of spectral ellipsometry, magneto-optical Kerr magnetometry and VSM for the investigation of optical constants and magnetization processes for two and three layer films of the type Al/NiFe, Cr(Al)/Ge/NiFe on sital substrate for different thickness of Cr and Al layers [1-3]. The refractive indexes of two layer films are well resolved by spectral ellipsometry demonstrating their good quality. Modelling data for three layer films show considerable discrepancy with the experiment which can be related with stronger influence of interfaces. The magnetization processes of two-layer films weakly depend on the type and thickness of the upper non-magnetic layers. However, the coercivity of three layer films may significantly change with the thickness of the upper layer: more than twice when the thickness of Al (Cr) layer increases from 4 to 20 nm as demonstrated in Fig. 1.



Fi. 1. Magnetization curves of Al/Ge/NiFe /sital film

[1] S.A. Wolf., *Science*, **294** (2001) 1488.

[2] G. Neuber, R. Rauer, J. Kunze, J. Backstrom, M. Rubhausen., *Thin Solid Films*, **455** (2004) 39.

[3] S. Visnovsky, R. Lopusnik, M. Bauer, J. Bok, J. Fassbender, B. Hillebrands. *Optics express*, **9** (2001) 121.

2PO-I1-34

MAGNETIC Au-Mn NANOWIRES ON COPPER AND SILICON SUBSTRATES

Sitnikov I.I., Tsysar K.M., Smelova E.M., Saletsky A.M.

Lomonosov Moscow State University, Faculty of Physics, (*Lomonosov MSU*), Moscow, Russia
smelova_k_m@mail.ru

The magnetic properties of bimetallic supported Au-Mn nanowires on copper and silicon substrates were studied theoretically. Two types of copper surfaces were used for calculations: Cu(110) and stepped surfaces Cu(111), to find out the influence of substrate geometry on the magnetic properties of the wires. To study the influence of substrate composition on the magnetism of supported nanowires silicon nonmetallic substrate was studied with surface geometry Si(001). As a result of ab initio calculations it was found that Au-Mn nanowires are antiferromagnetic in the ground state for all types of substrates [1]. The strong dependence of magnetic properties of supported Au-Mn nanowires on the substrate geometry and component composition was revealed. Results of our study show the one order decreasing of energy difference ΔE between antiferromagnetic and ferromagnetic states of supported Au-Mn nanowires in compare to freestanding nanowires as the result of “wire-substrate” interaction (see Table 1). The partial density of states (PDOS) was calculated to explain the significant suppressing of magnetic properties in the system. The $s-d_z^2$ - and $d_{xz}-d_{yz}$ - hybridized bands formation was found in PDOS between Au and Mn atoms, similar to the case of freestanding nanowires. However, the DOS of Mn atoms is decreased significantly at the Fermi level due to the strong overlap between orbitals of Mn and Cu atoms [2]. The spin polarization in the system is significantly reduced. Indirect exchange interaction between Au and Mn atoms in nanowire is strongly suppressed by the direct exchange between Mn atoms through the surface Cu atoms. The energy difference between AFM and FM states decreases significantly.

It was found also the strong suppressing of exchange interaction in Au-Mn nanowire on nonmetal silicon substrate in comparison to copper ones. This effect explained by formation of new Si-Mn bonds. Analysis of wire geometry shows that Mn atoms are embedded into the silicon substrate. The study of PDOS revealed the strong hybridization between p -bands of Si and s - and d -bands of Mn atoms. This band hybridization

Table 1. The total energy values, magnetic moments of FM and AFM configurations and energy difference for Au-Mn nanowire deposited on Cu(110), stepped Cu(111) substrates and freestanding Au-Mn nanowire.

	FM	AFM	ΔE
$E_{\text{NW-Cu(110)}}, \text{ eV}$	-171,518	-171,552	0,034
$E_{\text{NW-Cu(111)}}, \text{ eV}$	-205,604	-205,621	0,017
$E_{\text{NW}}, \text{ eV}$	-20,56	-20,582	0,022
$\mu_{\text{NW-Cu(110)}}, \mu_{\text{B}}$	0,06	0,05	-
$\mu_{\text{NW-Cu(111)}}, \mu_{\text{B}}$	0,1	0,05	-
$\mu_{\text{NW}}, \mu_{\text{B}}$	4,35	4,4	-

leads to the redistribution of electronic density of Mn atoms and increasing of PDOS Mn atoms at Fermi level. Our calculations revealed also the strong suppressing of magnetic properties of supported Au-Mn nanowires. The magnetic moments of Mn atoms strongly decrease in supported nanowire in compare to freestanding Au-Mn nanowire due to “wire-substrate” interaction (see Table 1).

[1] J.-T. Wang, Ding-Sheng Wang and Y. Kawazoe, *Appl. Phys. Lett.*, **79** (2001) 1507-1509.

[2] E. M. Smelova, K. M. Tsysar', D. I. Bazhanov and A. M. Saletsky, *JETP Lett.*, **93**(3) (2011) 129-132.

2PO-I1-35

THE STRUCTURAL AND MAGNETIC CHARACTERISTICS OF THE Co/Cu/Co THIN-FILM SYSTEMS

Shalygina E.E.¹, Kharlamova A.M.¹, Makarov A.V.¹, Kurlyandskaya G.V.², Svalov A.V.²

¹ Faculty of Physics, Moscow State University, Moscow, Russia

² Ural Federal University, Ekaterinburg, Russia

shal@magn.ru

Magnetic thin films attract the attention of researchers since the mid of XX century due to their wide use in numerous devices of modern micro- and nanoelectronics. This fact was caused by the discovery of such phenomena as a giant magnetoresistance and an oscillating exchange coupling between ferromagnetic layers. In this work the results on the investigation of the structural and magnetic properties of the Co/Cu/Co thin-film systems are presented.

The Co/Cu/Co samples were grown by magnetron sputtering at room temperature using Co and Cu targets and corning 2845 glass substrates. The Ta seed layers of 5 nm thick were deposited on the glass substrates. The thickness of Co layers, t_{Co} , was equal to 5 nm, and the Cu layer, t_{Cu} , was varied from 0.5 to 4 nm. According to the XRD and AFM data, the Co layers had a nanocrystalline structure with a crystallite size of the order of their thickness, and the average surface roughness, Ra , did not exceed 0.5 nm. The magnetic characteristics of the Co/Cu/Co thin-film systems were measured employing a magneto-optical magnetometer by means of the transverse Kerr effect (TKE) and the vibration sample magnetometer (Lake Shore VSM 7400). The next results had been obtained. The

Co/Cu/Co samples are characterized by in-plane magnetic anisotropy with an easy magnetization axis (EMA) parallel to the direction of magnetic field, applied during the deposition process (Fig. 1a). Some samples are characterized by almost rectangular hysteresis loops (Fig. 1a, b) while others exhibit more complex double-stage loops (Fig. 1c, d). The saturation field, H_S , of Co/Cu/Co samples oscillates in magnitude with increasing t_{Cu} . The maximum values of H_S are observed at $t_{Cu} = 1.4, 2.2$ and 3.2 nm. The hysteresis loops measured for these samples have the two-stage form. The period of these oscillations, Λ , is of the order of 1 nm. The above described data are explained by the presence of exchange coupling between the ferromagnetic layers through a copper spacer and its oscillating behavior with changing t_{Cu} . The value of Λ is consistent with the calculated one, obtained by taking into account of the quantum size effects, which manifest in the change of electronic structure of ultrathin films as compared to the bulk sample [1, 2].

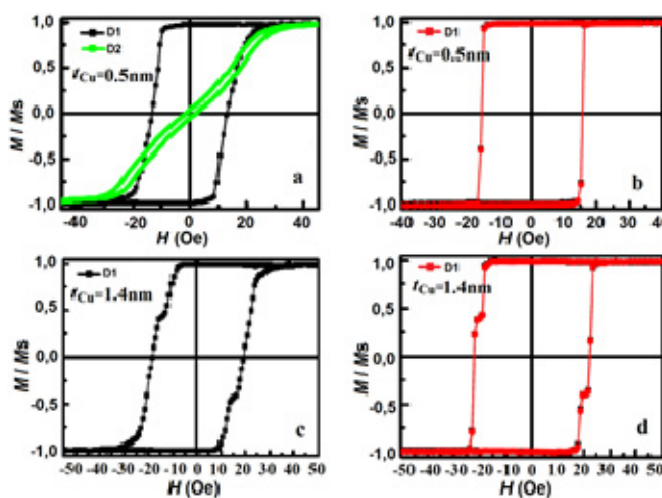


Fig. 1. Hysteresis loops of Co/Cu/Co samples measured employing magneto-optical (a, c) and vibration sample (b, d) magnetometers.

Support by the Russian Foundation of Basic Research, Grants 15-02-02077.

[1] M. D. Stiles, *Phys. Rev. B*, **48** (1993) 7238.

[2] P. Bruno, *Phys. Rev. B*, **52** (1995) 411.

2PO-I1-36

PECULIARITIES OF THE MAGNETIC PROPERTIES OF THIN-FILM THREE-LAYER SYSTEMS Fe /POLY(DIPHENYLENE PHTHALIDE)/Fe

Shalygina E.E.¹, Kharlamova A.M.¹, Makarov A.V.¹, Vorobieva N.V.², Lachinov A.N.²

¹ Faculty of Physics, Moscow State University, Moscow, Russia

² Bashkir State University, Ufa, Bashkortostan, Russia

shal@magn.ru

Electrically conductive polymers, created at the end of XX century, have attracted the attention of researchers due to variety of their mechanical and optical properties, as well as high conductivity. Due to the fact that these polymers can change properties under weak external influences, they have found wide application as functional elements of microelectronic. Moreover, polymers help to understand deeper the nature of high conductivity in non-metallic media. Conductive polymer (polydiphenylene phthalide - PDP) was synthesized in 1983. Studies conducted to date have shown the ability of a polymer to transition from a low-conductivity to a high-conductivity state, caused by various external influences: temperature, electric field, pressure, boundary effects. Its conductivity in highly conducting state is close to metallic and has a strongly marked anisotropy: the conductivity perpendicular to the plane is 14 orders larger than conductivity in the plane. The present work is devoted to the results of investigation of the magnetic properties of Fe / PDP / Fe thin-film systems. The studied samples were obtained by using the centrifugation method. To produce films of various thicknesses the solutions of polymer in cyclohexanone with different concentrations were used. The choice of concentration was determined by the thickness of the formed film. The thickness of Fe and PDP layers were varied from 14 to 50 nm and from 10 to 35 nm, respectively.

The magnetic characteristics of the Fe/PDP/Fe thin-film systems were measured employing the vibration sample magnetometer (Lake Shore VSM 7400). All measurements were carried out in the open air at room temperature. The hysteresis loops were measured in D1 and

D2 directions (D1 is perpendicular to D2) of the external magnetic field, H , applied parallel to the plane of the studied samples. Typical hysteresis loops observed for the studied samples are shown in Fig. 1. An analysis of the experimental data obtained showed that the hysteresis loops measured in a magnetic field applied along the D1 direction have a two-step shape. Herewith, the step size depends on the thickness difference of Fe layers: the more the difference in the thickness of Fe layers, the more strongly marked the two-stage form of the hysteresis loop. These results can be explained if we take into account the data of theoretical work [1], in which it was shown that complex hysteresis loops (up to inverted hysteresis loops) can be observed in thin-film structures due to magnetostatic interactions between magnetic layers. The influence of the exchange interaction between magnetic layers through the polymer layer on the magnetic field behavior of the samples is also possible.

[1] A. Aharoni, *Journal of Applied Physics. B*, **76** 10 (1994) 6977-6979.

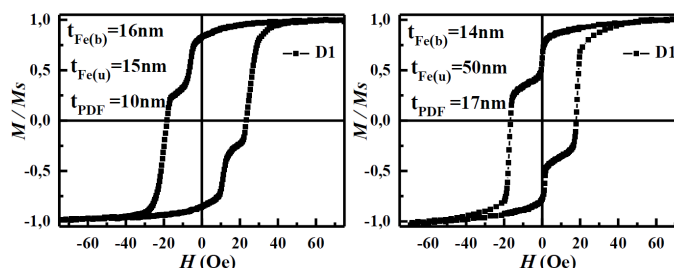


Fig. 1. Hysteresis loops of Fe/PDP/Fe samples measured employing vibration sample magnetometer; Fe(b) and Fe(u) – bottom and upper layers, respectively.

2PO-I1-37

DIPOLAR COUPLING DEPENDENT MAGNETIC DOMAIN STRUCTURE OF EPITAXIAL NANOSTRIP ARRAYS

Kozlov A.G.¹, Pustovalov E.V.¹, Samardak A.S.¹, Chebotkevich L.A.¹

¹Far Eastern Federal University (FEFU), Vladivostok, Russia

kozlov.ag@dvfu.ru

Dipole-dipole interaction in the arrays of closely packed magnetic nanostrips plays an important role in the magnetization reversal processes and significantly affects the critical fields, spin dynamics, and magnetotransport properties [1]. Shape anisotropy in such arrays leads to the closure of the magnetic flux at the poles of adjacent nanostrips. If to induce the magnetic anisotropy oriented across the nanostrip long axis, this will change the micromagnetic configuration of each nanostrip in the array due to the appearance of the domain structure formed by domains with an antiparallel orientation of the magnetization [2].

In this paper, we study the field-dependent behavior of spin vortices in Neel domain walls of the laminar domain structure of the dipolarly coupled epitaxial nanostrip arrays. We investigate the effect of dipole-dipole interaction between nanostrips on the switching fields of magnetization.

The nanostrip arrays were produced by focused ion beam etching of the 15 nm Co films deposited by molecular beam epitaxy on the vicinal Si(111) surface. Magnetic properties were investigated by magneto-optical Kerr effect, magnetic force and Kerr microscopies. Micromagnetic simulations were performed with OOMMF software.

As an example, Figure 1 demonstrates the magnetic force microscopy image of the domain structure of an array consisting of four 1- μm wide nanostrips divided by 80 nm distance, between them. This experimental image is interpreted by the micromagnetic simulation, Fig.1. As seen, dipole-dipole interaction between nanostrips favors the magnetization orientation leading to a closure of the magnetic flux. The magnetization reversal process starts from the shift of vortices along the domain walls. The direction of the propagation depends on the vortex chirality. The movement of the Neel domain walls starts only after the vortices achieve the nanostrip edges.

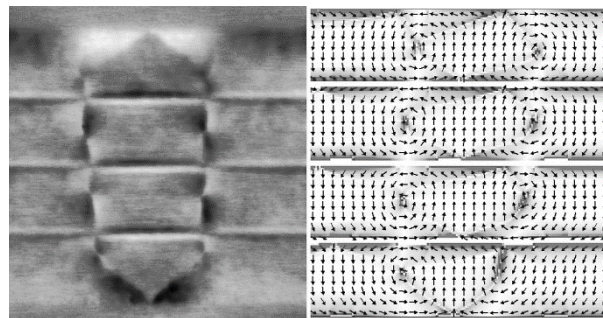


Fig. 1. Domain structure and micromagnetic simulation images of the epitaxial 1- μm wide nanostrips array.

Support by RFBR (grant 16-02-01015) and the state task (3.5178.2017) is acknowledged.

[1] L.C. Sampaio, E.H.C.P. Sinnecker, G.R.C.Cernicchiaro, M.Knobel, M.Vazquez, J.Velazquez, *Phys. Rev. B*, **61** (2000) 8976.

[2] A.G. Kozlov, M.E. Stebliy, A.V. Ognev, A.S. Samardak, A.V. Davydenko, L.A. Chebotkevich, *J. Magn. Magn. Mater.*, **422** (2017) 452-457.

2PO-I1-38

POSITIVE-TO-NEGATIVE REMNANT MAGNETIZATION REVERSAL IN EXCHANGE BIAS TRAINED Ta/NiFe/IrMn/Ta MULTILAYERS

Talantsev A.D.^{1,2}, Elzawawy A.A.¹, Kim Ch.G.¹

¹ Department of Emerging Materials Science, DGIST, Daegu, South Korea

² Institute of problems of chemical physics, Chernogolovka, Russia
adt@dgist.ac.kr

Exchange bias effect is essential for spintronic devices, because it allows setting the definite remnant magnetization direction of the pinned layer. However, multiple periodic changes in magnetic field from positive to negative forward and backward (also called magnetic field training) result in shift of the bias field due to the irreversible magnetic structural changes in the NiFe/IrMn interface. Furthermore, training shift of the exchange bias is almost temperature independent, in comparison with coercive field and initial exchange bias, which are decreasing with temperature [1]. The last may cause domination of the positive trained bias over initial negative bias in the increasing temperature [1]. In this work we have demonstrated directly, that exchange bias training shift can cause positive-to-negative remnant magnetization reversal with increasing temperature.

Firstly we have recorded magnetic hysteresis loop at 300 K before training (figure 1, section A, closed symbols).

The bias field was negative as expected. Then we have cooled down the sample at zero magnetic field and after cooling we have recorded magnetic hysteresis loop at 2 K (figure 1 section B). The -20 Oe – +20 Oe magnetic field range covered saturation field of the sample and was enough to perform magnetic field training [1]. After recording of the magnetic hysteresis loop at 2 K (the last point is $H_{MAX} = 20$ kOe) magnetic field was switched off and recording of the temperature dependence of the remnant magnetization $M_{REM}(T)$ is started (fig.1 section C).

Three temperature regions of the different remnant magnetization behaviour can be distinguished. At $T < 50$ K M_{REM} is positive. That means $|H_{EX.initial}| > |H_{EX.trained}| + |H_C|$ at this temperature range, (H_C – coercive field). At 60 K $< T < 150$ K positive-to-negative magnetization reversal occurs. The crossing point of the graph with zero axis at 90 K corresponds to $|H_{EX.initial}| = |H_{EX.trained}| + |H_C|$ case. Finally, at 160 K $< T < 300$ K remnant magnetization is negative which means training shift of the bias field dominates over initial bias field. After the recording of $M_{REM}(T)$ dependence was finished, magnetic hysteresis loop at 300 K was recorded again. One can see the shift of this loop to the positive magnetic fields due to training, performed at low temperatures (fig.1, section A, open symbols). Thus, training of the exchange biased sample at low temperature resulted in positive-to-negative remnant magnetization switching due to the irreversible shift of the bias during the training.

This work was supported by the DGIST R&D Program of the Ministry of Science, ICT and Future Planning (17-BT-02).

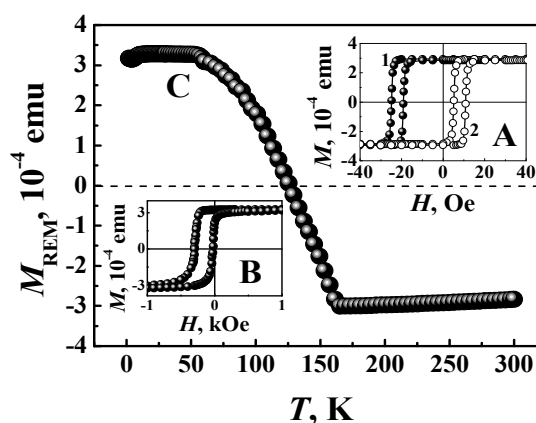


Fig. 1. A – magnetic hysteresis loop at 2 K, B – magnetic hysteresis loops at 300 K before (1) and after (2) magnetic field training. C – temperature dependence of the remnant magnetization.

[1]. S. K. Mishra, F. Radu, H. A. Durr, W. Eberhardt. *Phys. Rev. Lett.*, **102** (2009) 177208.

2PO-I1-39

PECULIARITIES OF MAGNETIZATION OF THIN LAYERS OF MAGNETIC LIQUIDS WITH MAGNETIZED AGGREGATES

Gladkikh D.V.¹, Dikansky Yu.I.¹, Ispiryay A.G.¹

¹ North-Caucasus Federal University, Stavropol, Russian Federation
gladkikhdv@mail.ru

Studies of thin layers and films of magnetic fluid have long attracted the attention of scientists. It is obvious that the kinetics of magnetization of such samples must have significant differences from bulk samples. The presence of a well-developed system of magnetized aggregates in the fluid leads to the appearance of their structural ordering under the influence of external fields [1], which should have a significant effect on the magnetization processes of such systems and its kinetics.

Earlier we began to study thin layers of such magnetic liquids [2]. In this paper, we compare the magnetization kinetics of magnetic colloids with a well-developed system of magnetized aggregates, depending on the shape of the measuring cell. For this purpose, frequency studies of the complex magnetic susceptibility of magnetic colloids with magnetized aggregates in the case of their bulk cylindrical specimens and thin layers have been carried out.

For all the samples (bulk and thin layers) it was found that the frequency dependences of the imaginary part of the complex magnetic susceptibility undergo a maximum at a certain frequency even in the absence of an external magnetic field, which allowed the relaxation time calculating. For bulk samples, it was found that a decrease in the diameter of a tube with a sample for any orientation of the measuring and external constant magnetic fields leads to an increase in the relaxation time. For thin layers of a sample of a magnetic fluid with magnetized aggregates, in general, an analogous picture is found, namely, as the thickness of the layer decreases, the relaxation time increases. However, the nature of this dependence differs for different mutual orientations of the measuring and external fields. In the case when the external magnetic field is directed parallel to the layer, a decrease in the thickness of the layer leads to a monotonic increase in the relaxation time. In the case when the external magnetic field is perpendicular to the plane of the layer and measuring field, a maximum appears on the dependence of the relaxation time on the layer thickness, the position of which does not depend on the magnitude of the external magnetic field (Fig. 1).

It should be noted that for thin layers of a homogeneous sample of a magnetic colloid that does not contain aggregates, the frequency dependences of the complex magnetic susceptibility do not experience a maximum in the whole investigated range of external magnetic fields.

This work was supported by The Ministry of Education and Science of the Russian Federation and Russian Foundation for Basic Research (RFBR) (project No.16-03-00054).

- [1] D.V. Gladkikh et al., *Magnetohydrodynamics*, **52** (2016) 319-332.
[2] Yu.I. Dikansky et al., *Magnetohydrodynamics*, **50** (2014) 27-33.

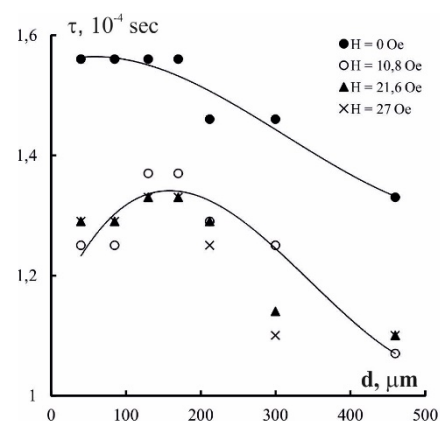


Fig. 1. Relaxation time vs. thickness of layer.

2PO-I1-40

HYSTERESIS LOOP TUNING BY CONFIGURATION OF EXTERNAL MAGNETIC FIELD APPLIED DURING DEPOSITION OF THIN FILMS STRUCTURE COMPOSED OF NiFe AND IrMn LAYERS

Gritsenko Ch.^{1,2}, Rodionova V.^{1,2}, Babaytsev G.³, Dzhun I.³, Chechenin N.³

¹ Center for Functionalized Magnetic Materials, Immanuel Kant Baltic Federal University, 236004, Nevskogo 14, Kaliningrad, Russia

² Laboratory of novel magnetic materials, STP “Fabrika”, Immanuel Kant Baltic Federal University, 236000, Gaidara 6, Kaliningrad, Russia

³ Skobeltsyn Institute of Nuclear Physics, Lomonosov Moscow State University, Leninskie gory 1/2, 119991 Moscow, Russia
christina.byrka@gmail.com

The exchange bias effect is a shifting of hysteresis loop along the field axis. It can be observed below the Neel temperature in a system, which consists of ferromagnetic and antiferromagnetic materials [1]. This phenomenon is very useful for applications of spintronics, magnetic recording, memory devices and others. The shape of hysteresis loop and separation quality of top and bottom hysteresis loops of two- and trilayered systems is important parameters additional to the value of exchange bias itself.

This work is dedicated to investigations of the exchange bias in two- and trilayered thin films structures consist of Ni₄₀Fe₆₀ and Ir₅₀Mn₅₀ layers. The main idea is to follow properties of samples located at different configuration and strength of external magnetic field applied during the deposition of thin films.

The experimental technique is following: samples of mentioned above thin films structures with antiferromagnetic layer thicknesses of 2, 4, 6, 8 nm have been prepared by magnetron sputtering method in presence of external magnetic field, created by two neodymium permanent magnets plates, which were put opposite and parallel to each other. The magnetic field was mapped in each sector of 5x5 mm² in the space between the plates where we placed the substrate. After deposition, we cut the sample into square pieces each of 25 mm² for investigating them by vibrating sample magnetometry. In addition, using COMSOL Multiphysics, calculated the magnetic field configuration created by permanent magnets during deposition.

The advantage of our technique is simultaneous preparation of several samples deposited under different external magnetic field and study its influence on the hysteresis loop. In this sense, our technique can be regarded as so called “combinatorial” approach in modern materials science [2].

In the report, we discuss influence of external magnetic field configuration on exchange bias, coercivity, and hysteresis loop shape. The exchange bias and coercivity dependences on the IrMn layer thickness are presented, as well.

[1] Meiklejohn W. H., Bean C. P., *Phys. Rev.*, **102** (1956) 1413–1414.

[2] Green, Takeuchi, and Hatrick-Simpers, *J. Appl. Phys.*, **113** (2013) 231101.

2PO-I1-41

ON THE NATURE OF INTRODUCED ANISOTROPY OF CoP FILMS RECEIVED BY CHEMICAL DEPOSITION

Chzhan A.V.^{1,2}, *Podorozhnyak S.A.*¹, *Volochaev M.N.*³, *Patrin G.S.*³

¹ Siberian Federal University, the Russian Federation, Krasnoyarsk

² Krasnoyarsk State Agrarian University, the Russian Federation, Krasnoyarsk

³ Kirensky Institute of Physics FIC KNC SB of the RAS, the Russian Federation, Krasnoyarsk
avchz@mail.ru

The nature of artificially induced anisotropy arising during the thermal annealing of ferromagnetics in a magnetic field is not always unambiguous, as is its effect on the magnetic properties of samples. In some cases, induced anisotropy leads to an improvement of the magnetic characteristics, in others, to their deterioration. This is due to the presence of various physical mechanisms of directed ordering, at least three [1], which can lead to its appearance, therefore, to elucidate the nature of the induced anisotropy, detailed investigations are required.

In this paper we present the results of an investigation of the induced anisotropy of Co-P and Co-Ni-P films obtained by chemical deposition, which occurred both during deposition and annealing of a film in a magnetic field.

As it was established earlier [2] in Co-Ni-P films obtained by electrolytically the emergence of induced anisotropy leads to change of the surface topography and phase images of the surface. The magneto-induced modifications in the morphology is explained by the specific local convection of ions at the interface cathode–electrolyte. The electrodeposition process in magnetic field is influenced by additional convection and the grain growth is favourable in the direction of the easiest magnetisation. In Co-P films obtained by chemical deposition appearance of induced anisotropy does not change the shape of the grains and the morphology of the surface. Microstructure of these films is shown in Fig.1.

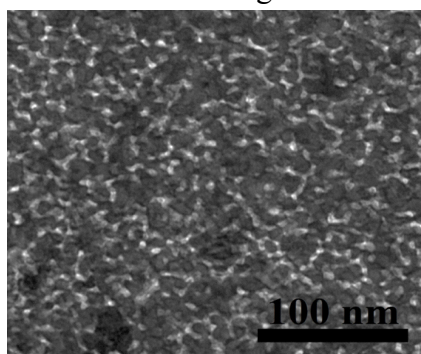


Fig 1. TEM image of Co-P films

This indicates a difference in the mechanisms responsible for the occurrence of induced anisotropy in CoP films obtained by electrolytic and electroless technologies, despite the existing identity in structure and magnetic properties. Investigation of the dynamic changes of the induced anisotropy in Co-P and Co-Ni-P films shows that the Ni addition does not lead to a significant change of K_u , but causes a significant decrease of the relaxation time.

Based on these data, it can be assumed that the most likely cause of induced anisotropy in the studied materials is random magnetic anisotropy [1], which is observed in amorphous alloys.

In this case, for the emergence of uniaxial anisotropy two sorts of atoms are not required that is assumed in pair ordering model. Induced anisotropy associated with local magnetic anisotropy, which contributes to the single-axis anisotropy when vacancies or the impurity atoms were ordering.

[1] J. J. Becker, *IEEE Trans. on Magn.*, **MAG-14** (1978) 938.

[2] V. Georgescu, M. Daub, *Surface Science*, **600** (2006) 4195.

2PO-I1-42

MAGNETIC PROPERTIES OF NANOPARTICLES PREPARED FROM α -FE TARGET BY LASER ABLATION IN LIQUIDS

*Nosan M.M.^{1,2}, Omelyanchik A.S.^{1,2}, Samusev I.G.¹, Myslitskaya N.M.¹, Borkunov R.Y.¹,
Rodionova V.V.^{1,2}*

¹ Immanuel Kant Baltic Federal University, Kaliningrad, Russia

² Center for Functionalized Magnetic Materials, Immanuel Kant Baltic Federal University,
Kaliningrad, Russia
nosanmark@gmail.com

Nowadays magnetic nanoparticles have applications in many different areas such as storage system, catalysis, biomedicine etc. [1]. There are many methods to synth nanoparticles such as co-precipitation, thermal decomposition, solvothermal routs, chemical vapor deposition, arc discharge etc. and all of them fit different applications. One of synthesis method of nanoparticles is laser ablation. Laser ablation is a complex physical and chemical processes – a removal (ablation) of the substance from the surface or volume of the solid target using a laser beam (Fig. 1). In contrast to the chemical ways of synthesis, nanoparticles prepared by laser ablation consist only from the material of target and the liquid (without impurities). Unlike the laser ablation in a vacuum or in a gas, in laser ablation in liquid it is much easier to collect them because nanoparticles remain in the colloid formed instead of being absorbed on the substrate or chamber walls.

In this work, we prepared the magnetic nanoparticles by laser ablation of a α -Fe target in an aqueous medium and in the isopropyl alcohol solution, using two different types of lasers (femtosecond and nanosecond) and power of laser beam (15uJ for ns-laser; 25uJ, 60uJ and 250uJ for fs-laser). Magnetic measurements carried out by vibrating sample magnetometer 7404 System by LakeShore. For analysis of the magnetic properties, the hysteresis loops of each sample at room temperature, the low temperature dependence of magnetization in zero-field cooled and field cooled (ZFC/FC) measurements, and the angle dependence of the magnetization at room temperature and field of 11 kOe were measured. The coercive force of the obtained samples is about 400 Oe, which is greater than value for the bulk material. This indicates, that the synthesized nanoparticles are near a single-domain regime [2]. Peak-like behavior of ZFC magnetization and bifurcation of ZFC and FC curves indicate at the partial existence of superparamagnetic particles around room temperature and broad size distribution. In conclusion, enchanted coercivity, high value of saturation magnetization and small size of synthesized particles are interest for wide range of applications.

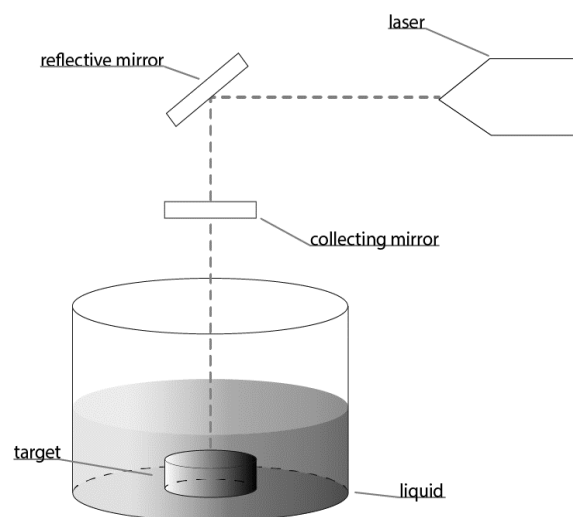


Fig.1 Principal scheme of synthesizing nanoparticles by laser ablation in liquids.

[1] J. Xiao, P. Liu, C.X. Wang, G.W. Yang, *Progress in Materials Science* (2017).

[3] S.P. Gubin, Y.A. Koksharov, G.B. Khomutov, G.Y. Yurkov, *Russ. Chem. Rev.*, **74** (2005) 489.

2PO-I1-43

MAGNETIC PROPERTIES OF Fe-Co AND Fe-Ni NANOWIRES OBTAINED IN PORES OF THE TRACK-ETCHED POLYMER MEMBRANES

Perunov I.^{1,2}, Frolov K.V.¹, Bedin S.A.^{1,3}, Zagorsky D.L.^{1,4}, Lyubutin I.S.¹, Chuev M.A.⁵,
Lomov A.A.⁵, Sulyanov S.N.^{1,6}, Artemov V.V.¹

¹ Shubnikov Institute of Crystallography FSRC "Crystallography and Photonics" RAS, 11933 Moscow, Russia

² Physical Faculty of Physics, Moscow State University. M.V. Lomonosov, 119991 Moscow, Russia

³ Moscow State Pedagogical University, 119991 Moscow, Russia

⁴ Gubkin Russian State University of Oil and Gas. 119991 Moscow, Russia

⁵ Institute of Physics and Technology RAS, 117218 Moscow, Russia

⁶ Research Center "Kurchatov Institute", 123182 Moscow, Russia
qazqwer1@mail.ru

Recently, the interest in synthesis and properties of magnetic nanowires has been significantly increased. Such strongly anisotropic nanoobjects are regarded as promising materials for various magnetic sensors, spintronics devices, biomedical technologies, including antitumor therapy [1,2].

In our work, arrays of iron-cobalt and iron-nickel alloy nanowires were studied at room temperature with ⁵⁷Fe Mossbauer spectroscopy and vibrational magnetometry. Several samples with different parameters of nanowires were obtained by the electrochemical deposition from special electrolytes into pores of the polymer track-etched membranes. It was revealed that all samples of nanowires arrays were magnetically ordered with preferred orientation of the magnetization along the wire length. This effect was formed without application of any external magnetic field. A mechanism for the formation of such a "magnetically textured" state was proposed.

The study was performed with the financial support of the Russian Foundation for Basic Research (project No. 15-08-04949), the Russian Science Foundation (project No. 14-12-00848), and using the equipment of the Centre of collective usage FSRC "Crystallography and Photonics" RAS with the financial support of the Ministry of Education and Science of the Russian Federation.

[1] *Magnetic Nano- and Microwires: Design, Synthesis, Properties and Applications*, ed. by M. Va'zquez, Woodhead Publishing, Elsevier (2015).

[2] W. Hong, S. Lee, H. J. Chang, E. S. Lee, and Y. Cho, *Biomaterials*, **106** (2016) 78.

2PO-I1-44

THERMODYNAMIC PROPERTIES OF $\text{Fe}_7(\text{PO}_4)_6$ AND $\text{Na}_x\text{Fe}_7(\text{PO}_4)_6$

*Kozlyakova E.S.¹, Danilovich I.L.¹, Shvanskaya L.V.¹, Dimitrova O.V.¹, Chareev D.A.²,
Zvereva E.A.¹, Sobolev A.V.¹, Presniakov I.A.¹, Vasiliev A.N.^{1,3,4}, Volkova O.S.^{1,3,4}*

¹ M.V. Lomonosov Moscow State University, 119991 Moscow, Russia

² Institute of Experimental Mineralogy, Russian Academy of Sciences, 142432 Chernogolovka,
Moscow District, Russia

³ National University of Science and Technology MISiS, 119991 Moscow, Russia

⁴ Ural Federal University, 620002 Ekaterinburg, Russia

Evenuel1@gmail.com

The $\text{Fe}_7(\text{PO}_4)_6$ [1] represents a rare case of parent compound of widespread structure type with general formula $\text{Me}_3^{2+}\text{Me}_4^{3+}(\text{XO}_4)_6$ (where Me – first row transition metal, Mg; X – P, V, As, Mo or In) with poorly investigated physical properties. Introduction of transition metals, i.e. manganese, cobalt, nickel and copper into $\text{Fe}_7(\text{PO}_4)_6$ structure results in preferable occupation of iron positions by Me^{2+} ions so that total formula transforms into $\text{Mn}_2^{2+}\text{Fe}^{2+}\text{Fe}_4^{3+}(\text{PO}_4)_6$, $\text{Co}_3^{2+}\text{Fe}_4^{3+}(\text{PO}_4)_6$, $\text{Ni}_3^{2+}\text{Fe}_4^{3+}(\text{PO}_4)_6$ and $\text{Cu}_{3-x}^{2+}\text{Fe}_{4+x}^{3+}(\text{PO}_4)_6$. Available information about their magnetic properties is limited to antiferromagnetic order formation at $T_N = 47$ K in nickel-doped compound. Trivalent positions can be occupied by titanium (Me – Mg, Cr, Mn, Fe, Co, Ni, Cu, Zn), vanadium (Me – Mg, Cr, Mn, Fe, Co, Ni, Zn), chromium (Me – Mg, Cr, Mn, Fe, Co, Cu, Zn) or indium (Me – Mg, Co, Ni, Zn). The magnesium comprising compounds are mostly paramagnets. The combinations of transition metals with vanadium experience antiferromagnetic ordering at low temperatures of about 12 – 15 K. Another route for chemical modifications of $\text{Fe}_7(\text{PO}_4)_6$ structure relates with introduction of alkali metals ions, i.e. Na^+ , into the crystal structure. In our work we focused on parent compound $\text{Fe}_7(\text{PO}_4)_6$, which is isotypic with mineral vanadate howardevansite $\text{NaCuFe}_2(\text{VO}_4)_3$, and its counterpart compound doped with sodium metals ions, $\text{Na}_x\text{Fe}_7(\text{PO}_4)_6$. Here we present basic thermodynamic and magnetic properties of these compounds and their primary characterization.

[1] Yu.A. Gorbunov, B.A. Maksimov, Yu.K. Kabalov, A.N. Ivashchenko, O.K. Mel'nikov; N.V. Belov, *Doklady Akademii Nauk SSSR*, **254** (1980) 873-876.

2PO-I1-45

STUDY THE Ni-Ge INTERFACE EFFECT ON MAGNETIC PROPERTIES OF THE Ni/Ge LAYERED FILMS

Chernichenko A.V.^{1,2}, Samoshkina Yu.E.³

¹ Krasnoyarsk Institute of Railway Transport, Krasnoyarsk, Russia

² School of Engineering Physics and Radio Electronics SibFU, Krasnoyarsk, Russia

³ Kirensky Institute of Physics, Federal Research Center KSC, RAS, Krasnoyarsk, Russia
chernichenko_av@krsk.irkups.ru

Recently, we revealed several peculiarities in the temperature and magnetic field dependences of the layered Ni/Ge films magnetization [1] that were ascribed to the effect of the interface between Ni and Ge layers. The present work is aimed to elucidate the interface structure and the mechanism of its interaction with Ni layers.

Ni/Ge and Ge/Ni/Ge/Ni/Ge films with different thicknesses of the component layers were fabricated with the ion-plasma sputtering technique described in Ref [1]. The X-ray fluorescent analysis (X-ray spectrometer S4 PIONEER, Bruker), EXAFS/XANES spectroscopy and X-ray reflectometry using synchrotron radiation station in the National Research Center «Kurchatov Institute», transmission electron-microscope (JEOL JEM-2100 (LaB6), energy dispersive X-ray spectrometer (Oxford Instruments INCA x-sight), and selected-area electron diffraction (SAED) were used to characterize films. Magnetic properties of the films were studied with a SQUID magnetometer, operating in the 4.2–300 K temperature range.

Structural data have shown that Ni layers were polycrystalline of Fm3m face centered phase, Ge layers were amorphous. Intermediate layers of about 9 nm in thickness were shown to form between Ni and Ge layers. Micro-diffraction images of the layered samples cross-section revealed not only all the reflexes characteristic for Ni but also reflexes, which can be compared with some Ni_xGe_y compounds: Ni₃Ge, Ni₅Ge₂, Ni₅Ge₃. At that, Ni₃Ge and Ni₅Ge₃ are ferromagnetic with different temperature dependences of magnetization. In particular, the Ni₃Ge magnetization increases almost five times in the range 290 - 77 K. The structural data obtained do not allow determining the interface structure unambiguously. However, it is clear that Ni layers are bordered with Ni_xGe_y layers but not with Ge layers. This neighborhood can effect in the layered films magnetic behavior essentially.

One of the most pronounced features of the layered films investigated is the strong low temperature hysteresis loop broadening and its shift along the magnetic field axis. The magnetization loop shift is observed usually in the film structures consisting of a ferromagnetic (FM) and the antiferromagnetic (AFM) layers or including magnetic soft and hard layers and explained by the exchange interaction between these layers. It is possible to expect that the hard FM layer (for example, Ni₃Ge) in the boundary between Ni and Ge layers is responsible for the observed hysteresis loop shift. The processes of Ni layer magnetization in such situation depend on the direction of an external field with respect to the direction of the magnetic moment of the hard FM layer in the interface. When the magnetic moment of this layer and the external magnetic field are oriented in the same direction, the soft magnetic layer Ni magnetized homogeneously in the same direction in relatively low magnetic field. The change of the external magnetic field direction leads to the formation of the helical structure in the soft FM layer similar to the Bloch wall. The helix pitch depends on the thickness of the soft layer and on the magnitude of the exchange interaction between adjacent layers. The increase in thickness of the soft FM reduces a degree of an influence of the hard FM layer on the soft layer magnetic state.

Support by the President of Russia Grant NSh-7559.2016.2 is acknowledged.

[1] I.S. Edelman, D.A. Velikanov, A.V. Chernichenko, et al., *Physica E*, **42** (2010) 2301-2306.

2PO-I1-46

DIPOLAR INTERACTIONS AND MAGNETIC HYSTERESIS IN RANDOM ARRAY OF SINGLE-DOMAIN NANOPARTICLES

Li O.A.¹, Komogortsev S.V.^{2,3}, Fel'k V.A.³

¹ Siberian Federal University, Krasnoyarsk, Russia

² Kirensky Institute of Physics, Federal Research Center KSC SB RAS, Krasnoyarsk, Russia

³ Siberian State Aerospace University, Krasnoyarsk, Russia

Log85@mail.ru

In recent decades, magnetic nanoparticles have been the subject of special interest due to properties suitable for a large variety of biomedical, environmental and technological applications. The intensive development of methods for obtaining and characterizing magnetic nanoparticles led to a huge number of experimental studies of their structure and properties. At present, a significant understanding of the properties of an isolated particle has been achieved. However, in applications and in a majority of experiments, researchers deal with large arrays of particles, for which the effects of interparticle interactions should be taken into account. One of the major interactions in the arrays of magnetic nanoparticles is the magnetic dipole-dipole interaction. Its effect on the magnetization curves of particle arrays at nonzero temperatures, including the problems of thermal stability, is discussed in detail in the literature. The effect of the magnetic dipole-dipole interaction on the magnetization curves in the ground state was studied theoretically and in numerical experiments for small ordered ensembles of particles.

In this paper we numerically investigate the magnetization curves of a positionally disordered ensemble of nanoparticles containing up to $2 \cdot 10^5$ particles. This model corresponds to the conditions realized in standard magnetometric investigations of nanoparticle powders and in a number of applications (particles distributed in nonmagnetic matrices). Thus, the results obtained in this work can be used to interpret the experimental magnetization curves.

We have calculated the magnetization curves in the OOMMF environment for various arrays of single-domain magnetic grains randomly distributed within a square region. The shape of the magnetization curve was found to change significantly when the concentration of particles (c) changes. The magnitude of the coercive force exhibits a strong nonlinear dependence that differs from Neel's prediction $H_c \sim c$, to which some authors refer [1,2]. It turned out that the coercive force and its behavior with a change in the concentration of particles in the ensembles depend on the ratio of the magnetic anisotropy field of the particles (H_a) to their magnetization (M_s). In the case when $H_a > M_s$ the coercive force decreases nonlinearly with increasing c from the value of $H_c = 0.49 \cdot H_a$, predicted in the Stoner–Wohlfarth model for $c = 0$. In the case when $H_a < M_s$ we observe a nonmonotonic $H_c(c)$ dependence with a maximum near $c = 0.3$. The residual magnetization exhibits qualitatively similar behavior in the cases of weak and strong magnetic anisotropy: $M_r/M_s(c)$ is a nonmonotonic dependence with a minimum. The position of the minimum on the $M_r/M_s(c)$ dependence and the minimum value of M_r/M_s itself are sensitive to the H_a/M_s ratio. This can be used to estimate the weight fraction of particles, or the H_a/M_s ratio from the magnetometric measurements.

Support by Russian Foundation for Basic Research, Grant No. 16-03-00969 is acknowledged.

[1] S. Shekhar, E.P. Sajitha, V. Prasad, S. V. Subramanyam, *J. Appl. Phys.*, **104** (2008) 083910.

[2] B. Aslibeiki, P. Kameli, H. Salamati, *J. Appl. Phys.*, **119** (2016) 063901.

2PO-I1-47

FMR STUDY OF THE COMPETITION BETWEEN SHAPE ANISOTROPY AND MAGNETO-CRYSTALLINE ANISOTROPY IN CuCr_2Se_4 THIN FILMS

Rautskii M.V.¹, Ester M.², Johnson D.C.²

¹ Kirensky Institute of Physics FRC KSC RAS, 660036 Krasnoyarsk, Russia

² Department of Chemistry, University of Oregon, Eugene, OR 97402, USA
rmv@iph.krasn.ru

In this work, we investigated the magnetic anisotropy of thin, textured CuCr_2Se_4 films by the ferromagnetic resonance FMR method. Films were synthesized using the Modulated Elemental Reactants (MER) method as outlined in [1], using multi-layer precursors with the sequence Se-Cr-Cu-Cr-Se. The precursors were deposited onto (100)-oriented Si wafers in a custom-built physical vapor deposition chamber with pressures inside the vacuum chamber of less than 5×10^{-7} mbar. Samples were annealed in an evacuated ($p \approx 10^{-5}$ mbar), sealed fused silica tube at 400 °C for 1, 2, and 3 days – samples 1, 2, and 3, respectively. According to the x-ray diffraction and HRTEM data, the films consist of pure CuCr_2Se_4 nanocrystals with the (111) planes oriented parallel to the film surface. The resonance spectra were collected with a Bruker spectrometer (Elexsys E580) operating at X-band (9.7 GHz) using 100 kHz as the modulation frequency in the temperature range 120 – 350 K.

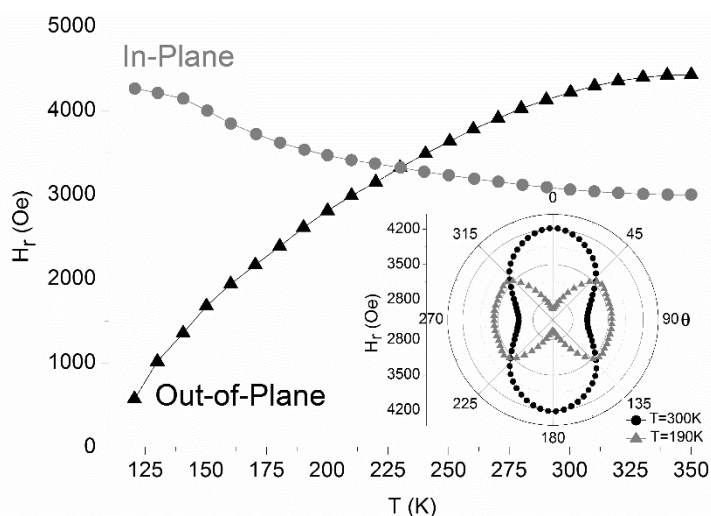


Fig. 1. The H_r temperature dependences for sample 1 with H applied parallel (in-plane) and perpendicular (out-of-plane) to the film plane. (Inset: Polar angle dependence of H_r for sample 1 at 300 K and 190 K. $\theta = 0^\circ$ corresponds to the [111] axis orientation perpendicular to the film plane).

Figure 1 presents the temperature dependences of the resonance field (H_r) for the CuCr_2Se_4 film annealed for 1 days. The crystallographic [111] direction is related to the easy magnetization axis and oriented perpendicular to the film plane. The temperature dependence of H_r may be caused by competition between shape anisotropy and magneto-crystalline anisotropy.

The nearly temperature independent shape anisotropy dominates at high temperatures whereas at lower temperatures, magneto-crystalline anisotropy prevails due to the fast growth of its anisotropy constant [2]. This is confirmed by the change of the shape polar angular dependence of H_r when the temperature is decreasing from 300 to 190 K (inset in Fig.1).

[1] Marco Esters, Andreas Liebig, Jeffrey J. Ditto, Matthias Falmbigl, Manfred Albrecht, David C. Johnson, Synthesis, *J. Alloy Compd.*, **671** (2016) 220.

[2] I. Nakatani, H. Nose, K. Masumoto, *J. Phys. Chem. Solids*, **39** (1978) 743.

2PO-J-24

THE COMPARISON OF MAGNETIC STRUCTURES OF LOW-DIMENSIONAL SPIN FRUSTRATED M^+ABO_6

Kuchugura M.D.^{1,2}, *Kurbakov A.I.*¹, *Senyshyn A.*³, *Nalbandyan V.B.*⁴

¹ Petersburg Nuclear Physics Institute, NRC “Kurchatov institute”, Gatchina, Russia

² St.Petersburg State University, St. Petersburg, Russia

³ Technische Universität München, Munich, Germany

⁴ Southern Federal University, Faculty of Chemistry, Rostov-on-Don, Russia

mariya_kuchugura@mail.ru

In the quasi-two-dimensional magnets with acentric (chiral) crystal structure and a triangular lattice of magnetic atoms in a layer, the competition between exchange interactions, frustrations and anisotropy can revolutionary affect the fundamental mechanisms of ordering and the corresponding phase transitions. Low-dimensional spin frustrated systems assume noncollinear incommensurate spin orderings in order to reduce the degree of their spin frustration. It is inherent in MnSb2O6, a magnet with a chiral crystal (s.g. P321) and a cycloidal magnetic structure, a multiferroic with a unique ferroelectric switching mechanism [1,2].

We have discovered and synthesized a new form of layered MnSb2O6, very different, by the X-ray diffraction pattern, from known and also layered multiferroic form mentioned above [1]. Our MnSb2O6 sample was characterized by Rietveld analysis of the neutron powder diffraction patterns. A new trigonal (s.g. P-31m) form substantially differs from the known form MnSb2O6 (s.g. P321). On the basis of mathematical processing of low-temperature neutron powder diffraction data the model of spin ordering are constructed. Helix magnetic structure is described by the propagation vector $k = (1/3, 1/3, 1/5)$.

Also, we synthesized a new compound MnSnTeO6 (isoelectronic phase with MnSb2O6) with a similar layered trigonal structure P321 (Fig. 1). Unfortunately, the atomic scattering factors Sn and Te are very close not only to X-rays, but also to neutrons, so it is difficult to directly determine their location in the non-equivalent positions. Nevertheless, we managed to do this in terms of the bonds length with oxygen, since they are larger in tin than in tellurium. Finally, the distribution of Mn-Sn-Te cations by four non-equivalent octahedral sites is established.

A model of a magnetic incommensurate spiral structure of MnSnTeO6 ordered along the direction of layers stacking with the vector $k = (0, 0, 0.183)$, which coincides with the accuracy with a vector of MnSb2O6 [1], is constructed. Both MnSnTeO6 and MnSb2O6 magnetic structures refined from neutron diffraction data are different to that of another family of langasites with hereditary cycloidal magnetic chirality with the same crystalline symmetry of P321.

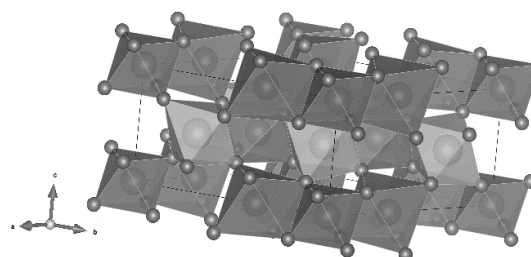


Fig. 1. Three-dimensional projection of the MnSnTeO6 crystal (s.g. P321). The octahedra MnO6, TeO6 and SnO6 are colored violet, blue and gray respectively. Oxygen ions are shown as red spheres.

The reported study was funded by RFBR according to the research project № 16-02-00360-a.

[1] R.D. Johnson et al., *Phys. Rev. Lett.*, **111** (2013) 017202.

[2]. M. Kinoshita et al., *Phys. Rev. Lett.*, **117** (2016) 047201.

2PO-J-25

NOVEL COBALT-BASED SOLID STATE SINGLE-ION MAGNET: DIOXOCOBALTATE (II) IONS IN STRONTIUM APATITE MATRIX

Zykin M.A.¹, Kazin P.E.¹, Vasiliev A.V.¹, Jansen M.²

¹ MSU, Moscow, Russia

² MPI for Chemical Physics of Solids, Dresden, Germany

mzykin@gmail.com

Single-ion magnets (SIMs) are very promising substances for spintronic devices and extra-high density data storage materials. Great efforts are undertaken by scientists testing different d- and f-metals as magnetic centers in SIMs. Along with the sort of a metal center the chemical environment and coordination geometry of magnetic ion are also very important: linear coordination (or highly anisotropic) is preferred. That's why constructing of new SIMs is typically the field of coordination chemistry. However some inorganic matrixes are suitable to isolate highly anisotropic magnetic ions and therefore potentially could be used for synthesis of new completely inorganic SIMs. We have used strontium hydroxyapatite as such inorganic matrix to stabilize highly anisotropic magnetic dioxocobaltate-ions and have obtained a new cobalt-based single-ion magnet with a high relaxation barrier [1].

Strontium hydroxyapatite single-phase polycrystalline samples with general composition $\text{Sr}_5(\text{PO}_4)_3(\text{CoO}_2)_x(\text{OH})_{1-2x}$, where $x = 0.02-0.3$, were synthesized by solid state method and the single crystals were obtained from a solidified melt. The single-crystal X-ray diffraction showed that cobalt is located in linear channels (typically filled by hydroxide ions) and is coordinated by two oxygen atoms forming bent O-Co-O ions. The shortest possible distance between two magnetic cobalt atoms is about 7 Å that allows neglecting interionic magnetic interaction.

ac magnetic measurements showed slow relaxation of magnetization at temperatures below 35 K with narrow distribution of relaxation time (τ) values. By the analysis of the τ temperature dependencies we found two different regimes of slow relaxation (Fig 1). The first is visible below 7 K, is characterized by energy barrier ~ 60 cm⁻¹ ("normal slow relaxation", NSR). The second becomes noticeable at 10 K and above and is characterized by an energy barrier of 200-250 cm⁻¹ ("very slow relaxation", VSR). NSR is present in all samples under a magnetic field whilst VSR is intrinsic to samples with low cobalt concentration and stays alive even in zero magnetic field. VSR fraction increases after a thermal treatment in an oxygen flow.

Support by Russian Science Foundation (RSF) under Grant 16-13-10031 is acknowledged.

[1] P.E. Kazin *et al.*, *Inorg. Chem.*, **56** (2017) 1232-1240.

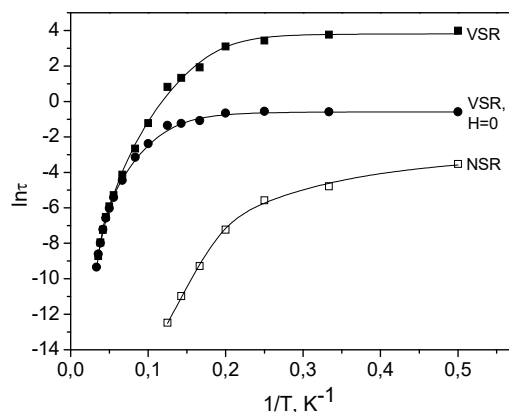


Fig. 1. Temperature dependence of relaxation time: NSR and VSR regimes. VSR stays alive also in zero magnetic field.

2PO-J-26

INFLUENCE OF HYDROGENATION ON MAGNETORESONANCE CHARACTERISTICS OF NANOCOMPOSITE (CoFeB)_mC_{100-m} FILMS

Vyzulin S.A.¹, Kevraletin A.L.¹, Syr'ev N.E.²

¹ Higher Military School named after General of the Army S.M Shtemenko, Krasnodar, Russia

² Faculty of Physics, Lomonosov Moscow State University, Moscow, Russia

vyzulin@mail.ru

The influence of hydrogenation on the magnetoresonance characteristics of nanocomposite films during synthesis is studied by the method of ferromagnetic resonance (FMR). Nanosystems are synthesized via the ion-beam sputtering of amorphous CoFeB with samples of C on to siall substrate. Two series of samples are investigated. The samples of 1 series were sprayed in an argon atmosphere, 2 series – in an atmosphere of argon with added of hydrogen. Magnetic phase concentration m and thickness h were varied along the structure for both series in the same way ($35,3 \leq m \leq 65$ at.%, $1 \leq h \leq 2$ μm).

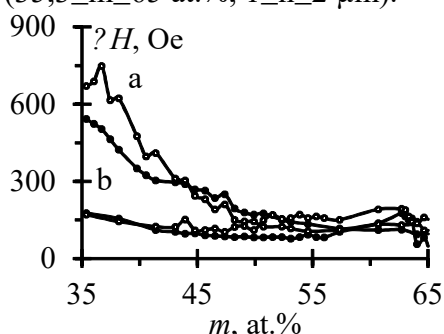


Fig. 1. Dependence ΔH of m :
a – series 1, b – series 2;
● – $\alpha=90^\circ$, ○ – $\alpha=0$.

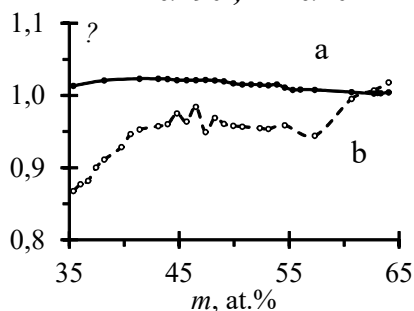


Fig. 2. Dependence δ of m :
a – series 1, b – series 2.

The FMR spectra were recorded at a frequency of $f=9,4$ GHz at a room temperature. The measurements were performed at tangent ($\alpha=90^\circ$) and normal ($\alpha=0$) magnetization of samples (α is the angle between the field of magnetization H and the vector of the normal to the film plane n). The resonance field H_r and absorption line width ΔH were determined. The value of resonance field H_r with $\alpha=90^\circ$ is smaller than with $\alpha=0$ for all samples. While m increasing the value of H_r with $\alpha=90^\circ$ decreases, and increases with $\alpha=0$. At equal m and h the values H_r samples of 1 series with $\alpha=0$ are less, and with $\alpha=90^\circ$ more than of 2 series samples. Fig. 1 shows the dependences $\Delta H(m)$. The absorption line width for samples of 1 series at m variation does not change significantly and has a value of 100-200 Oe. For 2 series if m more 48 at.% the ΔH value is 150-200 Oe. With decreasing m there is a sharp growth of ΔH to values 550 Oe (with $\alpha=90^\circ$) and 750 Oe (with $\alpha=0$). The latter indicates the possibility of transition of the magnetic system at $35 < m < 45$ at.% from ferromagnetic to superparamagnetic state. For series 1 the percolation threshold wasn't observed. For the same system (composition and synthesis condition) of series 1, $48 \leq m \leq 72$ at.%, the percolation threshold was observed at $m \approx 62$ at.% [1]. A possible explanation for the observed discrepancies is the difference in characteristics, on which the phenomenon of percolation is recorded. In [1] it is performed on electrical resistivity along the sample. In our case – on ΔH . Observed differences between magnetoresonance characteristics for series 1 and 2 can be explained by the influence of hydrogenation on the shape of the synthesized magnetic granules. Fig. 2 shows dependence of the aspect ratio $\delta=a/c$ from m , a is the magnetic granules semiaxes length along the normal to the film plane, c – in plane of the film. The values of δ are calculated on experimental values of H_r in the approximation of spheroidal form of the granules (the calculation method described in [2]). It is visible, that for series 1 magnetic granules are extended, and for series 2 – flattened along n . The exceptions are the samples of series 2 with $m > 60$ at.%.

[1] A.A. Abrychkin et al., *Bull. VSTU*, **8** (2012) 71-76.

[2] S.A. Vyzulin et al., *Bull. Russ. Acad. Sci.: Phys.*, **74** (2010) 1687.

2PO-J-27

CALCULATION OF INVERSE OPAL-LIKE STRUCTURE MAGNETIC FORM FACTOR BY MEANS OF MICROMAGNETIC SIMULATION

Dubitskiy I.¹, Syromyatnikov A.^{1,2}, Mistonov A.^{1,2}, Grigoryeva N.², Shishkin I.¹, Grigoriev S.^{1,2}

¹Petersburg Nuclear Physics Institute, Gatchina, Russia

²Faculty of Physics, Saint Petersburg State University, St. Petersburg, Russia

ilya.dubitskiy@mail.ru

Rapid progress in the field of magnetic nanostructures fabrication has led to the possibility of designing nanosystems with predefined geometrical properties. At the same time modern small-angle neutron scattering (SANS) facilities are able to reveal fine details of nanostructures magnetic state. However interpretation of SANS data often is not straightforward due to non-trivial magnetization distribution in studied nanosystems. In order to unambiguously understand results of SANS experiments one has to calculate magnetic form factor defined by the magnetization distribution. Magnetization distribution in turn can be found by solving micromagnetic equations. We have implemented this scheme for inverse opal-like structures (IOLS) made from cobalt. Magnetic IOLS can be considered as 3D network of nanoobjects which connected with each other by thin elongated crosspieces (“legs”) [1].

Co-based IOLS were synthesized by templating technique [2]. At the first step a colloidal crystal was formed from polystyrene microspheres with the mean diameter of about 540 nm by the vertical deposition technique. The microspheres were arranged in the face-centered cubic packing. After that, the electrochemical deposition of the nickel or cobalt into the voids between microspheres was carried out in the three-electrode cell. Finally, we dissolved the polystyrene microspheres in the toluene (fig. 1).

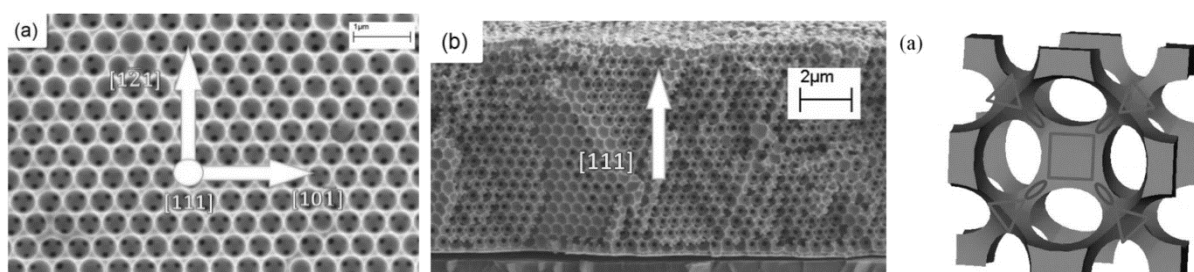


Fig.1: SEM images of top view (a) and side view (b) of IOLS together with unit cell model (c). Arrows indicate main crystallographic directions of IOLS mesostructured

We have found the magnetization distribution in the IOLS unit cell by means of solving Landau-Lifshitz-Gilbert equation. Calculations were carried out in the magnetic field applied along three main crystallographic directions of IOLS mesostructure: [100], [111] и [121]. Then magnetic form factor field dependences were calculated by Fourier transform of the magnetization distribution in the unit cell. Results were compared with the experimental data obtained in SANS experiments. As a result we were able to determine magnetic state of IOLS in a wide range of fields.

[1] A. Mistonov, N. Grigoryeva, A. Chumakova, H. Eckerlebe, N. Sapoletova, K. Napolskii, A. Eliseev, D. Menzrl, and S. Grigoriev, *Physical Review B*, **87** (2013) 220408.

[2] N. Sapoletova, T. Makarevich, K. Napolskii, E. Mishina, A. Eliseev, A. Etteger, T. Rasing, G. Tsirlina, *Physical Chemistry Chemical Physics*, **12** (2010) 15414.

2PO-J-28

INVESTIGATION OF THE HARD/SOFT MAGNETIC BILAYER MODEL BY THE MONTE-CARLO METHOD

Taaev T.A.¹, Khizriev K.Sh.^{1,2}, Murtazaev A.K.^{1,2}

¹ Institute of Physics of Daghestan Scientific Center of Russian Academy of Sciences, Makhachkala, Russian Federation

² Dagestan State University, Makhachkala, Russian Federation
taaev89@mail.ru

The creation of layered nanocomposite materials has opened a new section in the physics of magnetism [1]. The exchange interaction at the interface between layers of different magnetic order forms completely new ground state of a heterophase magnet, radically changes the behavior of spins, and leads to appearing a number of unusual phenomena, such as the formation of an external magnetic field of a one-dimensional heterophase spin spring (exchange-spring behavior).

In the most of hard/soft magnetic bilayers there is strong in-plane anisotropy and magnetic moments lie in plane of bilayers [2]. Therefore, thermodynamic and field properties of magnetic hard/soft bilayer can be estimated using a simple model integrating the standard XY-model [3,4]. The Hamiltonian of the system is written as:

$$H = -\frac{1}{2} \sum_{i,j} J(S_i^x S_j^x + S_i^y S_j^y) - \sum_i K(S_i^x)^2 - g\mu \sum_i \mathbf{H}_0 \mathbf{S}_i \quad (1)$$

where the first sum allows for the exchange interaction of each magnetic atom with nearest neighbors inside layers; the second sum is a contribution of the anisotropy into a system energy; the third sum is a contribution of an external magnetic field into a system energy, $g \approx 2$ is the Lande factor, μ is the Bohr magneton, H_0 is the external magnetic field, $S_i^{x,y}$ are spin projections S_i localized on a site i .

We investigated the temperature dependences of magnetization M , M_{hard} , and M_{soft} , their longitudinal and transverse components, heat capacities C , and magnetic susceptibilities χ , χ_{hard} , and χ_{soft} (subscripts “hard” and “soft” refer to values for the corresponding magnetic hard and soft layers). The results showed that the proposed hard/soft magnetic bilayer model features two phase transitions at different temperatures. The first transition is related to behavior of the hard magnetic layer, while the second transition is related to the soft magnetic layer. Next, we calculated critical exponents of the heat capacity α , the magnetization β , the susceptibility γ , and the correlation radius ν by means of the finite-size scaling theory. The values of the critical exponents are in a good agreement with the theoretical predictions for the XY-model.

We also investigated the processes of magnetization reversal of the hard/soft bilayer model under the action of an external magnetic field: the influence of the soft magnetic phase on the magnetization reversal of the magnetic bilayer. In the course of the numerical experiment, it was also observed the magnetizations of each magnetic monolayer M_j and the rotation angles of the magnetization vectors of monolayers M_j . With the help of these rotation angles, it can be observed a detailed picture of the formation of a one-dimensional heterophase spin spring.

[1] E.F. Kneller, R.Hawig, *IEEE Trans. Magn.*, **27** (1991) 3588-3600.

[2] E.E. Fullerton, J.S. Jiang, et. al., *Phys. Rev. B*, **58** (1998) 12193-12200.

[3] T.A. Taaev, K.Sh. Khizriev, et. al., *J. Alloys and Comp.*, **678** (2016) 167-170.

[4] T.A. Taaev, K.Sh. Khizriev, et. al., *JETP*, **122** (2016) 883-889.

2PO-J-29

MAGNETIC VORTEXES CLUSTERING IN NANOCRYSTALLINE MAGNETIC FILM

Shadrina G.V.³, Felk V.A.¹, Komogortsev S.V.^{1,2}

¹ Siberian State Aerospace University, Krasnoyarsk, Russia

² Kirensky Institute of Physics, Federal Research Center KSC SB RAS, Krasnoyarsk, Russia

³ Siberian Federal University, Krasnoyarsk, Russia

vlaf@sibsau.ru

The vortex distribution of magnetization corresponds to the minimum energy of the magnetic subsystem for soft magnetic particles or magnetic dots with perpendicular anisotropy in the range of sizes between single-domain and multi-domain states. In magnetic films, stable vortex magnetization structures are observed for chiral magnetic materials with the Dzyaloshinsky-Moriya interaction. Magnetic microstructure of the films is an ensemble of vortices observed in the ordered and disordered states. In the magnetic microstructure of thin magnetic films of such traditional materials as 3d metal alloys (permalloy, nickel, iron, cobalt), topological defects of magnetization form as domain walls and at their intersection. For the intersection of the walls, these defects are realized in the form of magnetic vortices. For mono- and polycrystalline films with crystallite size greater than the width of the domain wall, standard ordered domain structures from large Landau-Lifshitz domains are realized. In the case of thin amorphous and nanocrystalline magnetic films, the magnetic microstructure is irregular, the dimensions of the domains are small and comparable to the width of the domain wall and the magnetic correlation size.

Having performed the simulation, we found depending on the ratio of the energy of random magnetic anisotropy and the energy of exchange correlations of magnetization, on the general background of randomly distributed and randomly oriented domains, ordered groups of domains are observed. Vortices of magnetization of the same size with opposite signs of topological charge are located at the intersection of the boundaries of such domains so that the signs of charges alternate in a staggered order (Fig. 1). In general the picture looks like the formation of an ordered cluster of particles in an amorphous matrix. By decreasing the anisotropy constant, we observe a transition to standard ordered domain structures, which can be regarded as a process of crystallization in the initially disordered system of magnetization vortices. Thus vortices are an alternative to the usual domain structure and realize the ground state of small magnetic particles of various shapes.

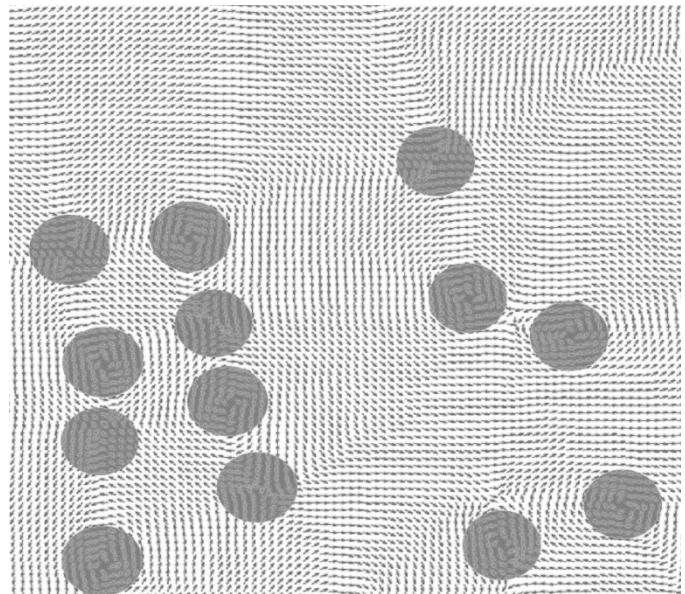


Fig. 1. Vortex clusters in magnetic film.

2PO-J-30

BARKHAUSEN NOISE IN Co/IrMn FILMS WITH UNIDIRECTIONAL ANISOTROPY

Shashkov I.V.¹, Gornakov V.S.¹

¹ Institute of Solid State Physics, Russian Academy of Sciences, 142432 Chernogolovka, Russia
shav@issp.ac.ru

The exchange coupling between ferromagnetic (FM) and antiferromagnetic (AFM) films significantly modifies magnetic properties of ferromagnet material such as shift of hysteresis loop (exchange bias) and coercivity enhancement. The magnetization reversal of ferromagnet in such coupled systems are usually associated with the formation of a partial domain wall (exchange spring) into the AFM layer [1]. The exchange spring leads to asymmetry in domain nucleation and may effect on domain wall mobility during magnetization reversal. The domain wall motions in ferromagnet usually display intermittent scale-free behaviour attributed to avalanche-like processes.

Here we investigate domain wall dynamics during magnetization reversal of polycrystalline Co/IrMn bilayers using Kerr effect magnetometer and magneto-optical indicator film technique. Figure 1 shows hysteresis loop measured by Kerr effect magnetometer. The forward and backward branches of the hysteresis loop usually display series of magnetization jumps that were processed using complementary methods of physics of nonlinear phenomenon such as statistical analysis and multifractal analysis. Effect of roughness of interface between FM and AFM layers on magnetization reversal was studied using OOMMF software.

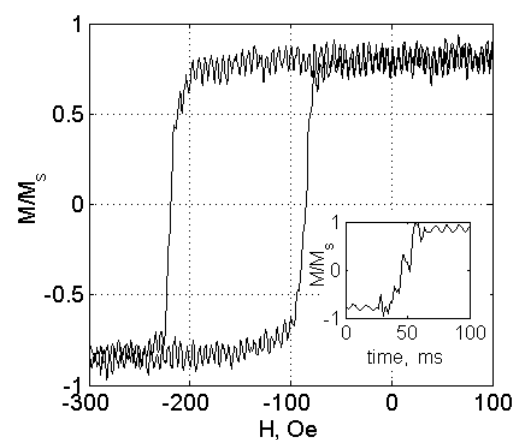


Fig. 1. Kerr hysteresis loop of the Co/IrMn bilayer. Inset shows magnetization jumps on branch of hysteresis loop.

The work was partially supported by RFBR Grant № 16-32-00264.

[1] C.L. Chien, V.S. Gornakov, V. I. Nikitenko et al., *Phys. Rev. B*, **68** (2003) 014418.

2PO-J-31

EXCHANGE PERCOLATION EFFECTS IN MAGNETIZATION CURVES OF GRANULAR NANOLAYER

*Felk V.A.*¹, *Komogortsev S.V.*^{1,2}, *Iskhakov R.S.*², *Shadrina G.V.*³

¹ Siberian State Aerospace University, Krasnoyarsk, Russia

² Kirensky Institute of Physics, Federal Research Center KSC SB RAS, Krasnoyarsk, Russia

³ Siberian Federal University, Krasnoyarsk, Russia

vlaf@sibsau.ru

A granular magnetic film is a composite of magnetic granules dispersed in a nonmagnetic matrix. The granular films with Fe, Co, and their alloy nanoparticles are of interest because of high value of magnetization and high hysteresis properties. Granular magnetic films with the soft magnetic granules and insulating matrix are promising magnetic nanostructures for high-frequency applications [1]. Properties of granular media strongly depend on the volume fraction of magnetic granules and are explained on the basis of percolation theory. If the volume fraction p of magnetic granules is less than percolation threshold p_c , then they become isolated from each other. If the magnetic anisotropy energy is greater than energy of thermal fluctuations, then high values of coercivity are achieved. In the opposite case with magnetic anisotropy energy is less than energy of thermal fluctuations, the granular media below percolation threshold turns to be superparamagnetic. The disappearance of remanence, coercivity, or magnetic susceptibility with the decrease of magnetic granules volume fraction indicates that the percolation threshold is attained [2]. If the film is thicker than the magnetic grain size, then it behaves as 3D granular media and here the percolation point being in the range of 0.3–0.6. In the films with the thickness about magnetic grain size, an increase in percolation point up to 0.6–0.8 is observed.

In literature the emphasis is on transition from the ferromagnetic to the superparamagnetic state below p_c . We draw attention to the fact that transition through the percolation threshold can also be observed in the ground state of nanogranular films. At small p , the hysteresis in the nanogranular medium should reach the maximum value predicted by the Stoner-Wohlfarth model for isolated granules. At p close to unity, the hysteresis of the nanogranulated medium will be sharply reduced in accordance with the predictions of the random magnetic anisotropy model. In this report we focus on the competition of exchange magnetic correlations with random orientation of local easy magnetization axis that takes place in nanogranular magnetic media.

We calculated the magnetization curves for arrays of single-domain magnetic beads (from 102 to $1.764 \cdot 10^5$) randomly distributed within square 420×420 . The axes of easy magnetization of the granules were randomly oriented, and an exchange interaction took place between the contacting granules. We found that in the various ranges of p three different exponential dependencies of the coercive force $H_c(p) \sim \exp(-p/a)$ are realized with different values of the parameter a . We believe that the observed boundaries of these ranges $p_c \approx 0.12$ and $p_c \approx 0.78$ can be considered as an estimate of the percolation thresholds for the exchange correlations of the magnetization in the investigated nanogranular medium in the ground state. The results of these researches can be used for the experimental determination of percolation thresholds in nanogranular films at low temperatures.

[1] C.L. Chien, *J. Appl. Phys.*, **69** (1991) 5267–5272.

[2] J.C. Denardin, A.B. Pakhomov, A.L. Brandl, et.al., *Appl. Phys. Lett.*, **82** (2003) 763–765.

2PO-J-32

MAGNETIC PROPERTIES OF COBALT MICROSPHERES

Novakova A.A., Perov N.S., Levina V.V., Dolzhikova A., Shatrova.N.

Lomonosov Moscow State University, Physical Faculty, Moscow, Russia

Functional Nanosystems&High-temperature Materials Department, NUST MISiS, Moscow, Russia
novakova.alla@gmail.com

Magnetic properties of nanostructured cobalt depend on the particles sizes, morphology, phase structure and chemical composition. Nanostructured magnetic cobalt microspheres were synthesized by two-stage method. First, cobalt oxides Co_3O_4 nanostructured microspheres were synthesized by spray pyrolysis [1]. Second, the obtained powders were reduced to nanostructured metal cobalt microspheres at different temperatures: from 200 up to 350° C in a hydrogen atmosphere.

X-ray diffraction analysis [2] showed that the Co-samples consisted in α -Co with hexagonal close-packed lattice and face-centered cubic β -Co. β -Co content depends on the reduction temperature. We analysed it's impact in the samples on such magnetic properties as coercive force and saturation magnetization. There is a correlation between the saturation magnetization decrease and β -Co content rise in the samples.

[1] N.Shatrova, A.Yudin, V.Levina et al. *Materials Research Bulletin*, **86** (2017) 80-87.

[2] A.Novakova, A.Dolshikova, N.Shatrova, V.Levina, *Moscow University Physics Bulletin*, **72** (2017) 4 in press.

2PO-J-33

SUPERPARAMAGNETIC BEHAVIOR OF TITANIUM NICKELIDE NANOPARTICLES OBTAINED BY LASER ABLATION

*Drozdova A.K.¹, Cherepanov V.N.¹, Svetlichny V.A.¹, Kveglis L.I.², Volochaev M.N.³,
Velikanov D.A.³*

¹ National Research Tomsk State University, Tomsk, Russia

² Siberian Federal University, Krasnoyarsk, Russia

³ Institute of Physics named after L. V. Kirensky FRC KSC Siberian Branch of the Russian Academy of Sciences, Krasnoyarsk, Russia

anna_drozdova709@mail.ru

Magnetic nanoparticles are actively applied in medical and biological researches due to their unique optical, electric and magnetic properties. The particles controlled by magnetic field are used both for targeted drug delivery and for mechanical destruction of target cells. For this reason, the study of structure and magnetic properties of Ni-Ti nanoparticles is perspective (Fig. 1 and Fig. 2).

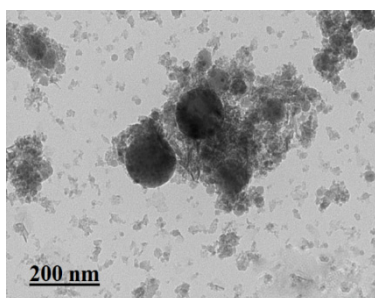


Fig. 1. Transmission electron microscopy images of Ni-Ti nanoparticles.

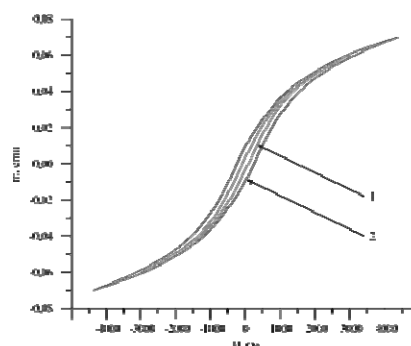


Fig. 2. M-H curves for Ni-Ti nanoparticles: T = 296 K (1); T = 77 K (2).

Magnetic measurements have indicated that nanoparticles behave as a superparamagnetic. Furthermore, the superparamagnetism was demonstrated in bulk samples containing the lenticular crystals [1].

The calculation carried out the method of scattered waves [1] has shown that the undeformed Ni-Ti cluster with the Frank-Kasper structure (FK-16) has a small magnetic moment (the average magnetic moment per atom is $\sim 0.3 \mu\text{B}$). In general, for an alloy, the average magnetic moment is zero because of the chaotic distribution of clusters in the alloy. For clusters elongated by 8% along the selected axis it was shown that the average magnetic moments of any atom of the FK-16 cluster is increased to $\sim 1.2 \mu\text{B}$. This twice exceeds the magnetic moments of Ni atom which is only $0.6 \mu\text{B}$. As a result, both the plastic deformation and laser ablation lead to the increasing the magnetization of the alloy due to rearrangement of the atomic order (see also [2]).

Experimental and theoretical studies carried out this work have shown that the method of pulsed laser ablation allows obtaining the titanium nickelide nanoparticles that have magnetic properties which can be used for production of promising materials to be applied to new nanotechnologies.

[1] F.M. Noskov et al., *Vestnik SibSAU*, **18** (2017) 211-218.

[2] D.I. Khomskii et al., *JETP Lett.*, **122** (2016) 484.

2PO-J-34

THE Ag INCLUSION EFFECT IN MCD AND MAGNETIC PROPERTIES OF Fe_3O_4 NANOPARTICLES SYNTHESIZED WITH CHEMICAL METHOD

*Petrov D.A.*¹, *Ivantsov R.D.*², *Zharkov S.M.*^{1,2}, *Lin C.-R.*³, *Tso C.-T.*³, *Hsu H.-S.*³, *Tseng Y.-T.*³

¹ Kirensky Institute of Physics, Federal Research Center KSC, RAS, Krasnoyarsk, Russia

² Siberian Federal University, Krasnoyarsk, Russia

³ National Pingtung University, Pingtung City, Pingtung County, Taiwan

irbiz@iph.krasn.ru

Magnetite, Fe_3O_4 , nanoparticles (NPs) are currently the key materials for advancements in optoelectronics [1], magnetic storage, and bio-inspired applications [2] because of its excellent chemical stability and the ability to change their properties essentially with including noble metals as Ag and Au. The work is devoted to the effect of Ag inclusion on MCD and magnetic properties of Fe_3O_4 NPs synthesized with chemical method.

Two sets of magnetite (Fe_3O_4) NPs with different type of Ag localization (denoted as AF and H) were synthesized by chemical methods. The NPs were synthesized via thermal decomposition of iron nitrate ($\text{Fe}(\text{NO}_3)_3 \cdot 9\text{H}_2\text{O}$) and silver nitrate (AgNO_3) in the mixture containing paraffin liquid, oleylamine and oleic acid. The atomic molar ratios Ag/Fe of AgNO_3 to $\text{Fe}(\text{NO}_3)_3 \cdot 9\text{H}_2\text{O}$ ranged from 0 to 0.48. Morphology and structure of NPs were investigated with XRD and HR TEM, magnetic properties – with SQUID magnetometer, MCD – with homemade installation in the spectral range 1.2–3.5 eV in the magnetic field 3 kOe at room temperature.

Spherical NPs have Fd-3m structure of magnetite with particle size 4-15 nm. All NPs contain Ag. Probably Ag^{1+} ions create crystalline deficiencies in the shell of NPs [3]. Some samples contain also 30–50 nm faceted fcc-Ag NPs. Magnetic measurements showed no monotonic magnetization decrease with Ag concentration increase.

To measure MCD NPs powder was stirred into the transparent silicon-based glue, placed between two spaced polished glass plates. MCD was measured in the normal geometry: the magnetic vector and the light beam were directed normal to the sample plane. The increase of the Ag concentration effects in the MCD strong changes in the lower energy region while its value at higher energies stays almost unchanged.

The research was carried out with the support of the President of Russia Grant NSh-7559.2016.2 and the regional state autonomous institution “Krasnoyarsk Regional Fund for Support of Scientific and Technical Activity” for participation in the event: “MISM-2017”.

[1] M. Salerno, et al., *Opto-Electron. Rev.*, **10** (2002) 217–224.

[2] A. Jordan, *J. Magnetism. Magn. Mater.*, **194** (1999) 185–196.

[3] B. Aslibeiki, *Current Applied Physics*, **14** (2014) 1659–1664.

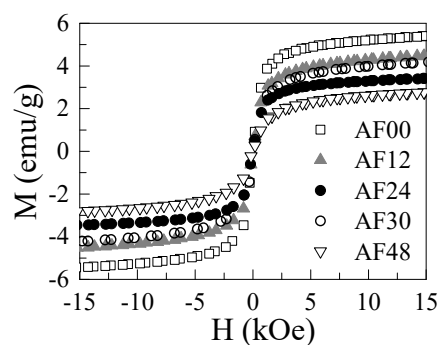


Fig. 1. Magnetization field dependencies at room temperature in dependence on Ag concentration.

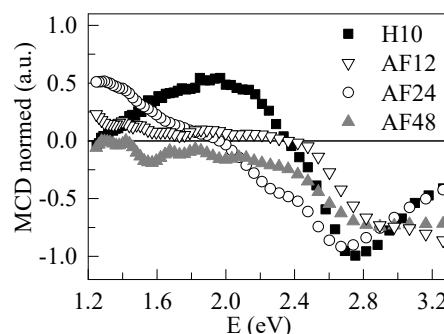


Fig. 2. Magnetic circular dichroism spectra in dependence on Ag concentration at room temperature.

2PO-J-35

MAGNETIC PROPERTIES OF NANOSTRUCTURED (SrFe₁₂O₁₉)_x(CaCu₃Ti₄O₁₂)_{1-x} COMPOSITES

Gavrilova T.^{1,2}, Deeva J.³, Yatsyk I.^{1,2}, Yagfarova A.², Gilmudinov I.², Lyadov N.¹, Chupakhina T.³,
Eremina R.^{1,2}

¹ Kazan E. K. Zavoisky Physical-Technical Institute of the RAS, Kazan, Russia

² Kazan (Volga Region) Federal University, Kazan, Russia

³ Institute of Solid State Chemistry of the RAS (UB), Ekaterinburg, Russia
tatyana.gavrilova@gmail.com

Composite materials attract much attention due to the possibility to create the new structure combining the components with high values of the magnetic susceptibility and dielectric permittivity in different component proportions, because they can be used in variety of applications. Here we present the investigation of core-shell structured two-component composites, which physical properties differ from non-structured composite materials. One of the components of the composite material is CaCu₃Ti₄O₁₂ (CCTO), which dielectric behavior exhibits an extraordinary high dielectric constant and shows good thermal stability in a wide temperature range (100–600K). As the second component of the composite material we chose the strontium hexaferrite SrFe₁₂O₁₉ (SFO) to modulate the magnetic properties of the composite.

SFO_xCCTO_{1-x} composites (x = 0.01, 0.03, 0.07 and 0.1) were prepared by conventional solid-state synthesis route. Strontium hexaferrite was added to the stoichiometric amount of the oxides CaO, CuO and TiO to form the CCTO component around SFO nanoparticles. Depending of the synthesis conditions we can get a simple mixture of the two components or the nanostructured composite, when SFO microinclusions are inside CCTO matrix. In the case of nanostructured composite the ESR spectra consist of one broad line. If the structure of composite is not form the ESR spectra consist of two clearly visible lines from each magnetic component of composite (SFO and CCTO) (Fig. 1a). Based on X-ray diffraction measurements we could find the limit concentration of the formation of a nanostructured sample. We did not observe the SFO reflections in the diffraction patterns of SFO_xCCTO_{1-x} (x = 0.03 and 0.07), therefore, it can be assumed that there was formed a nanostructured composite. SFO reflections in the diffraction patterns of the composite material were observed for x=0.01 and x=0.1. It follows that the concentration x=0.01 is too low and x=0.1 is too high to form the specific microstructure.

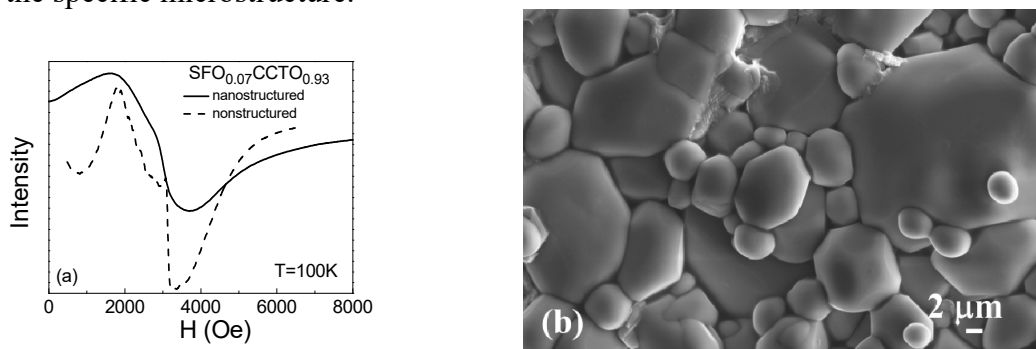


Fig.1. (a) ESR spectra of SFO_{0.07}CCTO_{0.93}: solid line corresponds to the nanostructured composited, dashed line - non-structured composite; (b) SEM images of SFO_{0.03}CCTO_{0.97}.

The reported study was supported by RFBR, research project № 16-32-00660.

2PO-J-36

UNUSUAL MAGNETIC EXCITATIONS IN A WEAKLY ORDERED SPIN-1/2 CHAIN ANTIFERROMAGNET Sr_2CuO_3

Sergeicheva E.G.¹, Sosin S.S.¹, Prozorova L.A.¹, Gu G.D.², Zaliznyak I.A.²

¹P.L. Kapitza Institute for Physical Problems RAS, Moscow, Russia

²CMPMSD, Brookhaven National Laboratory, Upton, New York 11973, USA

sergeicheva.alena@gmail.com

We report on the electron spin resonance (ESR) study of a nearly one-dimensional (1D) antiferromagnet Sr_2CuO_3 . This compound is known as a good realization of an $S=1/2$ Heisenberg chain system with the ratio of an intra- to interchain exchange interactions amounting to $J/J'=105$ ($J \approx 2200$ K) [1]. A long range ordering appears in the system below $T_N=5.4$ K, but the ordered spin component determined from neutron scattering experiments does not exceed the value $0.06\mu_B$ [2]. Because of its nearly disordered ground state the system is expected to combine properties of a classical three-dimensional antiferromagnet and a quantum $S=1/2$ spin chain. It is therefore of interest to compare magnetic excitation spectra at different energy scales. We studied ESR spectra in ordered and paramagnetic phases in the frequency range 9-140 GHz. The measurements were performed on a single crystal sample in magnetic field up to 12 T at temperatures from 0.5 to 50 K.

Frequency-field diagram, measured in three different directions of the applied field at $T < T_N$ is presented in the Fig.1 Except for signals originated from magnetic defects it consists of 2 different types of absorption, which are presented in the Fig.1. AFMR branches can be described by conventional macroscopic theory applied to 2-axes collinear antiferromagnet with $\Delta_1=23.0$ GHz and $\Delta_2=13.3$ GHz as parameters. There are also some discrepancies between the measured spectra and conventional approach: for H directed along the easy axis and $H > H_c$ (after spin-flop transition) the resonance field of the principal line doesn't experience shift below T_N as it is expected. One can consider this as an additional reduction of the order parameter. Secondly, we observe the linear $f(H)$ dependence of the resonance frequency in the vicinity of the gap instead of the expected dependency of a second degree.

The observed lines of the second type are shown with green circles in the Fig.1. These lines are of the same order of intensity as AFMR absorption lines. Their resonance field doesn't experience shift with temperature, and integral intensity of this modes rises gradually when the temperature goes below T_N . The nature of these modes is unclear. We propose, that this new type of absorption lines refers to the modes derived by H.J. Schulz from the mean-field treatment of a weakly ordered $S=1/2$ chain [3].

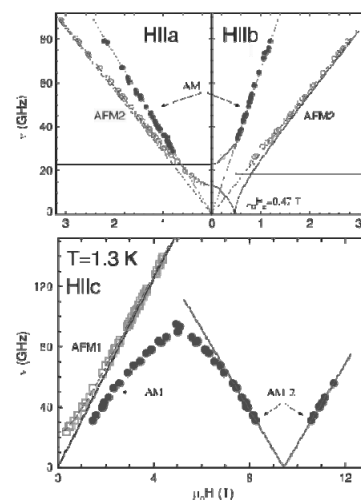


Fig.1. Frequency-field diagrams of the magnetic resonance spectra measured at $T=1.3$ K

[1] M. Motoyama et al., *Phys. Rev. Lett.*, **76** (1996) 3212.

[2] K.M. Kojima et al., *Phys. Rev. Lett.*, **78** (1997) 1787.

[3] H.J. Schulz, *Phys. Rev. Lett.*, **77** (1996) 2790.

2PO-J-37

TRANSITION STRUCTURES ON S-SHAPED DOMAIN WALLS IN IRON AND PERMALLOY FILMS

Baykenov E.Z.¹, Dubovik M.N.^{1,2}, Zverev V.V.¹, Filippov B.N.^{1,2}

¹Ural Federal University, Yekaterinburg, Russia

²Institute of Metal Physics UB RAS, Yekaterinburg, Russia

erlan.baykenov@urfu.ru

We performed the three-dimensional numerical simulations of transition micromagnetic structures emerging at a junction of S-shaped domain wall segments with different orientations. We consider the iron and permalloy films with the easy magnetization axis belonging to the film plane. The computed surface magnetization distributions were in good agreement with the results presented in [1]. Fig. 1 shows an example of such structure section by a plane normal to the magnetization vectors in the domains. We also examined in detail the transition region between segments of the C-shaped domain wall, which contains a short section of the S-shaped wall. Some of the obtained structures contain singular points [2].

The simulations were performed using the MuMax3 software [3] and «Uran» supercomputer at the Institute of Mathematics and Mechanics UB RAS.

The research was carried out within the state assignment of FASO of Russia (theme “Magnet” No. 01201463328).

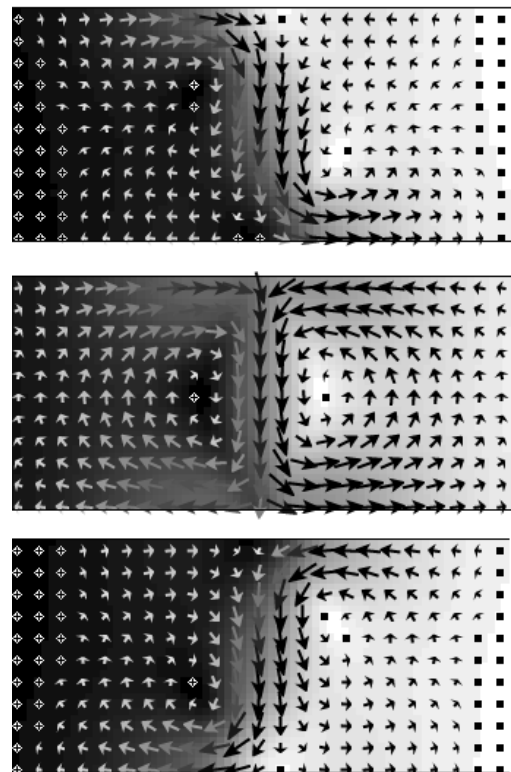


Fig. 1. Transition structure on S-shaped domain wall in a 100 nm permalloy film.

[1] S. Huo, J.E.L. Bishop, *et al*, *J. Magn. Magn. Mater.*, **177-181** (1998) 229-230.

[2] V.V. Zverev, B.N. Filippov, M.N. Dubovik, *Physics of Solid State*, **9** (2014) 1725-1734.

[3] A. Vansteenkiste, J. Leliaert, M. Dvornik, *et al*, *AIP Advances*, **4** (2014) 107133(1-22).

2PO-J-38

INTERFACE EFFECTS IN ULTRA-THIN BI-SUBSTITUTED IRON GARNET FILMS GROWN ON SI SUBSTRATE

Dyuzhev N.A.¹, Kirilenko E.P.¹, Logunov M.V.², Mazurkin N.S.¹, Nikitov S.A.^{2,3}, Stognij A.I.⁴

¹ National Research University of Electronic Technology (MIET), Moscow, Russia

² Kotel'nikov Institute of Radio Engineering and Electronics of RAS, Moscow, Russia

³ Moscow Institute of Physics and Technology, Dolgoprudny, Russia

⁴ Research and Engineering Center for Materials Science of NAS, Minsk, Belarus

logunov@cplire.ru

Bismuth-containing ferrite garnet films are a promising material for magneto-optical devices due to the large Faraday effect [1-3]. In this paper we present the results of properties study of nanometer-thick Bi₃Fe₅O₁₂ films grown on silicon substrates (BiIG/Si). Synthesis of BiIG/Si structures is of interest for ensuring the technological compatibility of magneto-optical devices with silicon electronics devices. The samples under study were films with a thickness of 100-150 nm, which were grown by ion-beam sputtering at room temperature and post growth annealing in a vacuum quartz oven.

For thin films of complex compositions, such as ferrites with a garnet structure, one of the most important issues is the uniformity of the films over the thickness. In this work, craters obtained as a result of Ar⁺ ion sputtering of the sample surface were used to study the dependence of the hysteresis loops on the film thickness. Hysteresis loops were recorded using local Kerr microscopy. With a small diameter of the illuminated film area (<5 μm) and a crater slope extent of ~400 μm (Fig. 1a), the thickness nonuniformity for the film area with the recorded hysteresis loop is ~1 nm.

As a result, the dependence of the shape and parameters of the hysteresis loops on the thickness of the BiIG films was studied (magnetic field H was parallel/perpendicular to the film plane), which made it possible to clarify the influence of interface effects on the properties of nanometer-thick BiIG/Si films with an extremely high bismuth concentration.

Support by RFBR is acknowledged.

[1] Lei Bi et al., *Materials*, **6** (2013) 5094-5117.

[2] R. Gieniusz et al., *Appl. Phys. Lett.*, **104** (2014) 082412.

[3] A. Garzarella, M. A. Shinn, and Dong Ho Wu, *Appl. Phys. Lett.*, **108** (2016) 241101.

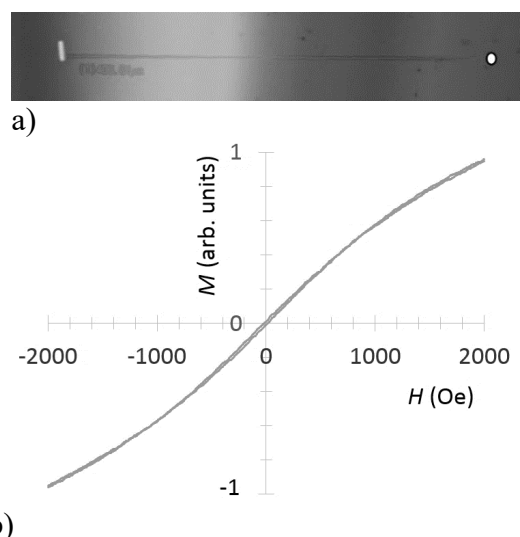


Fig. 1. a). The studied area of the film with a thickness gradient. The boundary of the SiO₂ and BiIG areas in the crater is marked by a risk (left). b). Hysteresis loop of the local film area, marked with a circle (a, right). Magnetic field H is perpendicular to the film plane.

2PO-J-39

MAGNETIC CORRELATIONS IN GRANULAR CO-BAZED NANOCOMPOSITE WITH AMORPHOUS AND CRYSTALLINE MATRIX

Iskhakov R.S.¹, Denisova E.A.¹, Komogortsev S.V.¹, Chekanova L.A.¹, Kalinin Yu.E.², Sitnikov A.V.²

¹L.V. Kirensky Institute of Physics FRC KSC SB RAS, Krasnoyarsk, Russian Federation

²Voronezh State Technical University, Voronezh, Russian Federation

rauf@iph.krasn.ru

The magnetic properties features of two types of granules composite $\text{Co}_X(\text{SiO}_2)_{100-X}$ and $\text{Co}_X(\text{CaF}_2)_{100-X}$ ($34 < X < 70$) produced by the ion-beam sputtering have been investigated. The local magnetic anisotropy field, the magnetic correlation length and the fractal dimensionality of the magnetic correlation volumes have been determined from the magnetization curves near the saturation. Approach magnetization to saturation curves $M(H)$ for granular films are fitted by the expression:

$$M(H) = M_s \cdot \left(1 - 1/15 \cdot H_a^2 \cdot H^{-1/2} \cdot \left(H^{3/2} + H_R^{3/2} \right)^{-1} \right)$$

where $H_a = 2K_g/M_s$ is the local magnetic anisotropy field (magnetic anisotropy of granule) and $H_R = 2A/M_s R_c^2$ is exchange field, where M_s is magnetization and R_c is the granule size. The values of local magnetic anisotropy field H_a are found to decrease with increasing volume fraction of the magnetic phase. The magnetic anisotropy energy constant of granule, K_g , was calculated using fitted parameters H_a and H_R . In this paper, we use grain size dependence of local magnetic anisotropy to separate volume and surface contributions to granule anisotropy. The resulting values are found to be $k_s = 3.4 \text{ erg/cm}^2$ and $K_V \approx 4 \cdot 10^5 \text{ erg/cm}^3$ for Co-SiO₂ films and $k_s = 2.8 \text{ erg/cm}^2$ and $K_V \approx 10^5 \text{ erg/cm}^3$ for Co-CaF₂ films. Figure 1 shows the dependencies of random anisotropy correlation radius R_c and the size of stochastic magnetic domain R_L on magnetic phase content for $\text{Co}_X(\text{SiO}_2)_{100-X}$ films for Co-SiO₂ and Co-CaF₂ films. The extrapolation of these dependences to the low X allows us to estimate the percolation threshold by interparticle exchange as a point of convergence $X_C \approx 30\%$. It is shown that, with respect to the singularities of the magnetization saturation curves, the ferromagnetic region is further subdivided into three regions differing in the character of the spatial propagation of the magnetization ripples or in the magnetic correlation function characteristics for all type of nanocomposite. The fractal dimension of the nanocomposite magnetic microstructure near the percolation threshold is detected.

The spectrum of standing spin-wave has been registered in the perpendicular experiment configuration for all types of films with the metal phase content above 52 vol. %. It is found that the type of the dispersion relation of spin waves in Co-SiO₂ and Co-CaF₂ composite films is affected by the exchange coupling fluctuations.

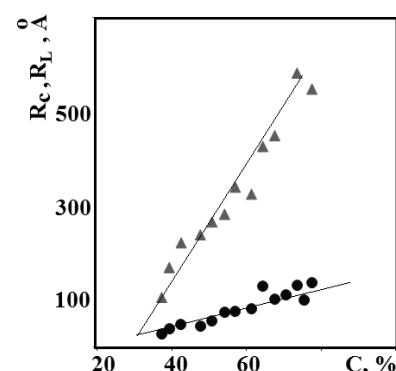


Fig.1. The dependencies of random anisotropy correlation radius R_c (circle) and the size of stochastic magnetic domain R_L (triangle) on magnetic phase content for $\text{Co}_X(\text{SiO}_2)_{100-X}$ films

2PO-J-40

MAGNETISM OF NATURAL COMPOSITES OF HALLOYSITE CLAY NANOTUBES AND AMORPHOUS HEMATITE

Vasiliev A.N.^{1,2,3}, Volkova O.S.^{1,2,3}, Presniakov I.A.¹, Sobolev A.V.¹, Abakumov A.M.,⁴
Koshelev A.V.^{1,3}

¹ Moscow State University, Moscow, Russia

² National University of Science and Technology "MISiS", Moscow, Russia

³ Ural Federal University, Ekaterinburg, Russia

⁴ Skolkovo Institute of Science and Technology, Moscow Region, Russia
anatolkosh@mail.ru

The natural composite of tubular mineral halloysite $\text{Al}_2\text{Si}_2\text{O}_5(\text{OH})_4 \times x\text{H}_2\text{O}$ and nanoparticles of poorly crystallized or amorphous hematite Fe_2O_3 was investigated by means of Mössbauer spectroscopy and characterized in measurements of magnetic susceptibility χ .

The temperature dependence of magnetic susceptibility $\chi = M/B$ taken at cooling in magnetic field $B = 0.5$ T is shown at (Fig 1). The diamagnetic response χ_{dia} of the halloysite nanotubes is superimposed on complex paramagnetic behavior χ_{para} due to the presence of iron impurities in various aggregate forms. The low temperature upturn in $\chi(T)$ dependence is ascribable to isolated Fe^{3+} ions substituting Al^{3+} ions. The ratio of isolated $\text{Fe}^{3+}/\text{Fe}^{2+}$ can be estimated as $n_1/n_2 = 8.9$. The step-like anomaly found in the composite at $T_g \approx 80$ K should be attributed to poorly crystallized or amorphous Fe_2O_3 . Its ordering temperature was defined as 80 K. The weight fraction of Fe_2O_3 can be roughly estimated as 0.012 %.

The ^{57}Fe Mössbauer spectrum of composite was recorded at 300K (Fig 2). Spectrum, can be represented as a superposition of two quadrupole doublets Fe(1) and Fe(2) with significantly different isomer shifts and quadrupole splittings, thus underlying that the ^{57}Fe atoms in two different valence states are located at non-equivalent crystallographic sites, distributed within crystal lattice of halloysite nanotubes. The third subspectrum Fe(3) is Zeeman sextet that corresponds to iron cations in the magnetically ordered state. The analysis of subspectrum showed that for the sextet Fe(3), the values of isomer shift and magnetic hyperfine fields at ^{57}Fe nuclei are close to the published data for hematite. The experimental value H_{hf} , is noticeably lower H_{hf} for large particles for ferric ions, that could be due to the size effects of nanoparticles.

Our measurements of halloysite-based composites extracted from different sources give similar results indicating presence of iron in various aggregate forms. Large part of this iron is randomly distributed in the form of isolated Fe^{3+} and Fe^{2+} ions. Smaller part is assembled as nanoparticles of poorly crystallized or amorphous Fe_2O_3 .

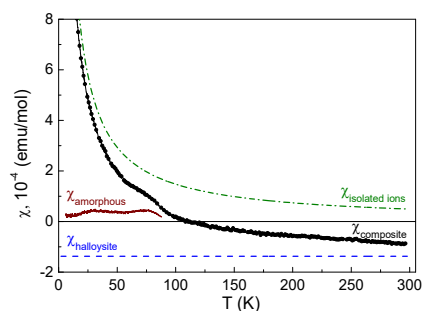


Fig 1. The temperature dependence of magnetic susceptibility of composite sample $\chi_{\text{composite}}$.

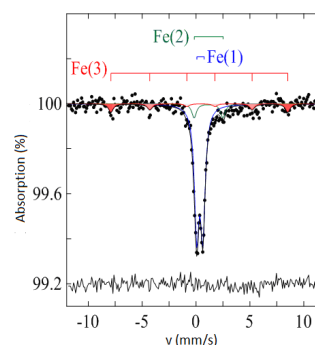


Fig 2. ^{57}Fe Mössbauer spectra recorded at $T = 300$ K. The solid color lines are the result of simulation of the experimental spectrum.

This work was supported by Russian Scientific Foundation (project no. 15-12-20021).

2PO-J-41

PREPARATION AND MAGNETIC PROPERTIES OF IRON-BASED POWDERS

*Chekanova L.A.¹, Stolyar S.V.^{1,2}, Bayukov O.A.¹, Knyazev Yu.V.¹, Iskhakov R.S.¹,
Yaroslavtsev R.N.^{1,2}, Volochaev M.N.¹, Chizhova I.A.¹*

¹ Institute of Physics SB RAS, Krasnoyarsk, Russia

² Siberian Federal University, Krasnoyarsk, Russia

From aqueous solutions of iron salts in the presence of sodium hypophosphite, Trilon B (disodium EDTA), natural arabinogalactan [1], the synthesis of magnetic nanoparticles occurs. Depending on the ratio of reducing agents and complexing agents, it is possible to obtain nanoparticles as bcc-Fe with dimensions of ~ 50 nm with a shell of magnetite of thickness ~ 3 nm (Fig. 1) and lamellar magnetite particles. As can be seen in Figure 2, the prepared magnetite nanoparticles are "square" plates ~ 4 nm thick. The crystal structure of the obtained powders was studied by X-ray diffraction and electron diffraction methods. The electron microscopy examination was carried out at the Center for Collective Use of the Krasnoyarsk Scientific Center of the Siberian Branch of the Russian Academy of Sciences (Krasnoyarsk, Russia) on a Hitachi HT7700 transmission electron microscope operating at an accelerating voltage of 100 kV. The magnetic properties of powders were studied by the Mossbauer spectroscopy method and the ferromagnetic resonance method.

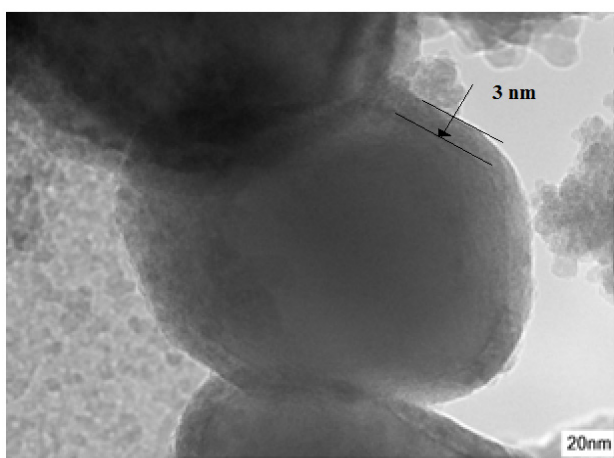


Figure 1 – HRTEM image of bcc-Fe nanoparticles

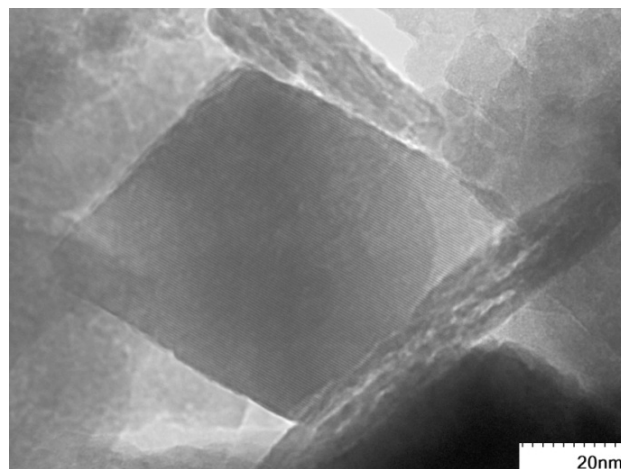


Figure 2 – HRTEM image of magnetite nanoplates

This work was supported by the Russian Foundation for Basic Research, Grants № 16-03-00256, 16-03-00969. Support by the Special Program for Siberian Federal University of the Ministry of Education and Science of the Russian Federation is acknowledged.

[1] G.P. Aleksandrova, L.A. Grischenko et. al., *Physical mesomechanics*, 7 (2004) 139–142.

2PO-J-42

SINGLE-ION MAGNETS BASED ON 3D-ELEMENTS CONFINED IN THE CHANNELS OF APATITE

Kazin P.E.¹, Zykin M.A.¹, Trusov L.A.¹, Gorbachev E.A.², Jansen M.³

¹ Department of Chemistry, Moscow State University, Moscow, Russia

² Department of Material Sciences, Moscow State University, Moscow, Russia

³ Max-Planck Institute for Solid State Research, Stuttgart, Germany

kazin@inorg.chem.msu.ru

Recently defined single-ion magnets (SIM) represent separate paramagnetic ions of d- or f-elements in a highly anisotropic coordination found in metal complex compounds mostly with organic ligands. They exhibit giant magnetic anisotropy, magnetic bi-stability, slow relaxation of magnetization, and may behave like atomic-scale permanent magnets with quantum properties. Here we present a new kind of SIMs which are built inside an extended inorganic diamagnetic and dielectric solid. Our earlier studies have showed that the hydroxyapatite crystal lattice can adopt ions of 3d-elements in the structural channels, the 3d-ions formally substituting protons of OH-groups [1-3]. In the present work we discuss alkaline-earth metal phosphates with apatite structure doped with copper or cobalt oxides and their magnetic properties. The X-ray crystal structure analysis reveals that the 3d-elements form dioxometallate-ions confined in the apatite channels. Copper is initially found as Cu⁺. On the samples' oxygenation, it oxidizes to paramagnetic Cu³⁺ (S = 1) which is included into a linear [OCuO]- ion. A perfectly axial crystal field provides a very high single-ion zero-field splitting (zfs) amounting to several hundreds of cm⁻¹. ac-susceptibility measurements reveal a slow relaxation of magnetization induced by a magnetic field at temperatures below 15 K with a narrow distribution of relaxation time (τ) values. Temperature dependence of τ allows estimating an energy barrier for magnetization reversal (U_{eff}). It varies from few tens to one hundred cm⁻¹ depending on the alkaline-earth metal nature. In contrast to copper, cobalt forms a bent [OCuO]2- ion (d7 configuration, S = 3/2). Its deviation from a linear geometry has no crystallographic reason and may be caused by Renner-Teller effect lifting the orbital degeneracy. The compounds exhibit a slow relaxation of magnetization in a magnetic field below 12 K. Estimated U_{eff} values are of 50 – 60 cm⁻¹ and practically coincide with zfs values determined from dc-magnetization measurements. Theoretical calculations support an observed strong easy-axis magnetic anisotropy and experimental zfs values. Another magnetization relaxation process is found in some of Co-doped apatites, which persists in zero field and is characterized by several times higher U_{eff} . It may be connected to Co-based atomic groups different from the mentioned above dioxocobaltate(II)-ion. Theory predicts that for such two-fold coordination of Co²⁺, zfs and U_{eff} values may reach ca. 500 cm⁻¹ for a linear coordination and maintain a high enough magnitude to fit the experiment even for a substantially bent [OCuO] geometry.

[1] P. E. Kazin et al., *Solid State Sci.*, **9** (2007) 82-87.

[2] P. E. Kazin et al., *Chem. Eur. J.*, **20** (2014) 165-178.

[3] P. E. Kazin et al., *Inorg. Chem.*, **56** (2017) 1232-1240.

2PO-J-43

STUDY OF MAGNETIC BEHAVIOR OF MAGNETITE NANOPARTICLES DISPERSED IN FLUID

Omelyanchik A.^{1,2}, *Laureti S.*³, *Varvaro G.*³, *Rodionova V.*^{1,2}, *Kusigerski V.*⁴, *Knezevic N.*⁴,
*Peddis D.*³, *Illés E.*⁴

¹ Immanuel Kant Baltic Federal University, Kaliningrad, Russian Federation

² Center for Functionalized Magnetic Materials, IKBFU, Kaliningrad, Russian Federation

³ Istituto di Struttura della Materia – CNR, Monterotondo Stazione (Roma), Italy

⁴ Dept. of Theoretical and Condensed Matter Physics, Vinča Institute of Nuclear Sciences,
Belgrade, Serbia

9azazel@gmail.com

Magnetic nanoparticles (MNPs) are studied approximately since the 1950s years and currently are a hot topic in the modern material science, because of their unique physical and chemical properties which make them attractive for many applications, from biomedicine to catalysis, to sensors, etc. Generally, for their application MNPs must be dissolved in a fluid and different strategies can be applied to prepare stable suspension of MNPs: electric double layer, surface modification by organic coating, variety of liquid media [1]. Magnetic characterization of MNPs dispersed in fluids by conventional methods is not trivial, due to the difficulties in handling and installing liquid samples into laboratory instruments. Sample holders in conventional vibrating sample magnetometer (VSM) and superconducting quantum interference device (SQUID) magnetometer are suited for measurements of solid samples in form of thin film or powders, but not enough optimized for installing liquid samples. Moreover, depending on the freezing point of the solvent in which the nanoparticles are dispersed, specific protocols for temperature dependence measurements are needed, due to the different magnetic behavior that the MNPs may show when they are blocked or free to move in a fluid. The additional artifact in measuring of magnetic properties of MNPs occurs due redistribution of a liquid sample in holder, that can lead to center change, and chains or aggregates formations [2].

In this work, a series of procedures for the preparation of liquid samples for SQUID measurements will be presented. In particular, plastic capsules of ferrofluids of magnetite nanoparticles dispersed in a water solution are prepared and tested in different temperature environments in order to check their stability after the thermal stress. Then, the basic magnetic characterization of their magnetic properties in terms of Zero Field Cooling (ZFC) - Field Cooling (FC), and low temperature Isothermal Remanent Magnetization (IRM) and Direct Current Demagnetization (DCD) are carried out with the aim of elucidating the interactions between MNPs, which is expected to be strongly dependent on the solution pH, as previously elucidated by hydrodynamic radius and zeta-potential measurements [3].

[1] A.H. Lu, E.L. Salabas, F. Schüth, *Angew. Chemie - Int. Ed.*, **46** (2007) 1222.

[2] Z. Boekelheide, C.L. Dennis, *AIP Adv.*, **6** (2016).

[3] E. Illés, E. Tombácz, *J. Colloid Interface Sci.*, **295** (2006) 115.

2PO-J-44

STATIC AND DYNAMIC MAGNETIC PROPERTIES OF TRIANGULAR LAYERED OXIDES MSb_2O_6 (M = Mn, Co, Ni, Cu)

Zvereva E.A.¹, Raganyan G.V.¹, Nikulin A.Yu.², Nalbandyan V.B.², Shukaev I.L.², Kurbakov A.I.^{3,4},
Kuchugura M.D.^{3,4}, Vasiliev A.N.¹

¹ Faculty of Physics, Moscow State University, 119991 Moscow, Russia

² Chemistry Faculty, Southern Federal University, 344090 Rostov-on-Don, Russia

³ Petersburg Nuclear Physics Institute – NRC Kurchatov Institute, 188300 Gatchina, Russia

⁴ Faculty of Physics, St. Petersburg State University, 198504 St. Petersburg, Russia

zvereva@mig.phys.msu.ru

We report on the magnetic properties of four new metastable trigonal layered MSb_2O_6 phases (M = Mn, Co, Ni, Cu), which have been prepared by the low-temperature ion-exchange reactions. Except $CuSb_2O_6$, all compounds under study demonstrate a long-range antiferromagnetic order at low temperatures with Neel temperatures ~ 8 K (Mn), ~ 11 K (Co) and ~ 15 K (Ni) respectively. In addition, the magnetization isotherms indicate a magnetic field induced spin-reorientation (spin-flop type) transition below T_N at $BSF \sim 0.8$ T for MSb_2O_6 and $BSF \sim 8$ T for $CoSb_2O_6$ respectively, implying two different spin-configurations in the ordered phases. It is interesting to note that the magnetic properties observed here for these novel compounds possessing the trigonal layered rosielite-type structure are essentially different from those reported for their stable polymorphs MSb_2O_6 (M = Ni, Co, Cu) with tetragonal trirutile-type structure. Magnetic behavior of all trirutile-type compounds MSb_2O_6 (M = Ni, Co, Cu) is quite similar. A characteristic feature is the presence of a wide temperature range where all MSb_2O_6 with trirutile structure exhibit short-range antiferromagnetic order and the temperature dependence of the magnetic susceptibility $\chi(T)$ demonstrates clear low-dimensional broad maximum at T_{max} followed by long-range antiferromagnetic order. Despite the nearly perfect 2D square M^{2+} sublattice the data were well described within the formalism of antiferromagnetic 1D spin chain. In contrast, new metastable MSb_2O_6 phases (M = Mn, Co, Ni, Cu) did not show any sign of low-dimensional behavior and the magnetic susceptibility nicely follows the Curie-Weiss law over the wide temperature range higher T_N . The negative values of Curie-Weiss temperature indicate predominance of the antiferromagnetic interactions and moderate frustration for the 2D triangular M^{2+} magnetic sublattice. The effective magnetic moments calculated from the obtained Curie constants are in excellent agreement with theoretical estimations using the average effective g-factor, which was directly measured by means of electron spin resonance.

2PO-J-45

**MAGNETIC PROPERTIES OF TRIANGULAR LATTICE FRUSTRATED
A₂MnXO₄ (A = Li, Na, Ag; X = Si, Ge)**

Zvereva E.A.¹, Denisov R.S.¹, Nalbandyan V.B.², Shukaev I.L.², Gordon E.³, Politaev V.V.², Whangbo M.-H.³, Petrenko A.A.², Markina M.M.¹, Tzschoppe M.⁴, Klingeler R.⁴, Vasiliev A.N.¹

¹ Faculty of Physics, Moscow State University, 119991 Moscow, Russia

² Chemistry Faculty, Southern Federal University, 344090 Rostov-on-Don, Russia

³ Department of Chemistry, North Carolina State University, Raleigh, NC 27695-8204, USA

⁴ Kirchhoff Institute for Physics, INF 227, Heidelberg University, D-69120 Heidelberg, Germany

zvereva@mig.phys.msu.ru

Static and dynamic magnetic properties of the five members of A₂Mn_XO₄ (A = Li, Na, Ag; X = Si, Ge) family, including four new phases have been comprehensively studied experimentally by magnetization, heat capacity and ESR measurements as well as theoretically by density functional calculations. It was found that the magnetic susceptibility and specific heat data reveal the onset of long-range antiferromagnetic order in all systems of the A₂Mn_XO₄ family under study, except for Ag₂MnSiO₄ which remains in the paramagnetic state down to 2 K. The magnetization isotherms indicate a magnetic field induced spin-reorientation (spin-flop type) transition at T < T_N for all antiferromagnetic systems implying two different spin-configurations in the ordered phases. The spin-flop fields of about 2 T imply small magnetic anisotropy gaps of Δ ≈ 0.23 meV. Summarizing the thermodynamic data in magnetic fields up to 9 T the magnetic phase diagrams of Li₂Mn_XO₄ (X = Si, Ge) and Na₂Mn_XO₄ (X = Si, Ge) have been constructed for the first time. The dynamic magnetic properties obtained from X-band ESR technique corroborate very well the static magnetic data. In addition, the data show an extended temperature range of short-range magnetic correlations which is characteristic of low-dimensional and frustrated materials. The experimental findings are well supported by means of density functional theoretical analysis, which allow to estimate the main exchange parameters and to propose the possible spin-configuration structures for all systems under study.

2PO-K-26

MODIFICATION OF MAGNETIC PROPERTIES OF α -Fe₂O₃ POWDERS AFTER ULTRASONIC TREATMENT

Stolyar S.V.^{1,2}, *Bayukov O.A.*², *Iskhakov R.S.*², *Yaroslavtsev R.N.*^{1,2}, *Ladygina V.P.*³,
*Artemyeva A.S.*¹

¹ Siberian Federal University, Krasnoyarsk, Russia

² Institute of Physics SB RAS, Krasnoyarsk, Russia

³ Presidium of KSC, Federal Research Center KSC SB RAS, Krasnoyarsk, Russia
stol@iph.krasn.ru

Ultrasound is used to obtain noble metal particles from solutions of the corresponding salts. Recovery is due to the sonolysis of water. The reducing agent is the ultrasonically generated H· radicals [1,2]. Reduction of metastable ferrihydrite nanoparticles to metallic iron as a result of ultrasonic treatment in albumin protein solution was discovered in [3]. In this paper, the magnetic properties of hematite powders (d-20 nm) after ultrasound in water and in albumin protein solution are studied. Figure 1 shows the ferromagnetic resonance curves (T = 300 K) of dried powders after ultrasound. Figure 1 shows that powders sonicated in albumin solution are characterized by an additional absorption peak. Figure 2 shows the spectra of Mössbauer spectroscopy (T = 300 K). The interpretation of the spectra indicates that the parameters of the hyperfine structure of the resulting phase after ultrasound in the albumin solution are characteristic for α -Fe.

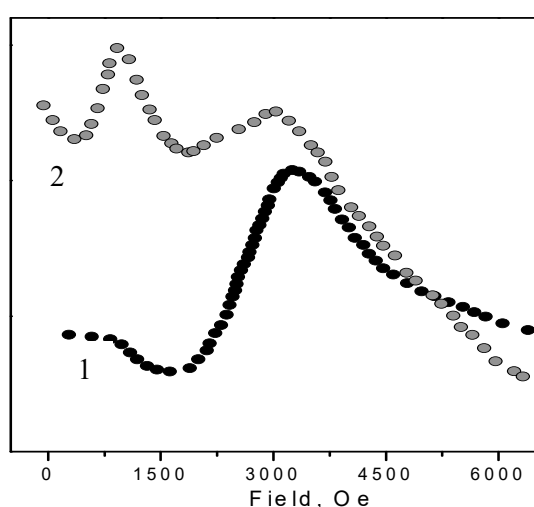


Figure 1 – Ferromagnetic resonance curves of hematite powders after ultrasound in water (1) and in albumin solution (2).

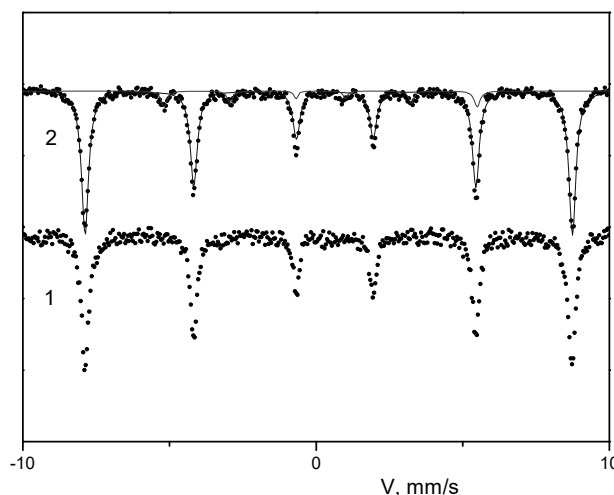


Figure 2 – Mössbauer spectra of hematite powders after ultrasound in water (1) and in albumin solution (2).

This work was supported by the Russian Foundation for Basic Research, Grants № 16-03-00256, 16-03-00969, 17-43-240527. Support by the Special Program for Siberian Federal University of the Ministry of Education and Science of the Russian Federation is acknowledged.

[1] R.A. Caruso, M. Ashokkumar, F. Grieser, *Langmuir*, **18** (2002) 7831–7836.

[2] J.H. Bang and K.S. Suslick, *Adv. Mater.*, **22** (2010) 1039.

[3] S.V. Stolyar, O.A. Bayukov, V.P. Ladygina, R.S. Iskhakov, R.N. Yaroslavtsev, *Bulletin of the Russian Academy of Sciences: Physics*, **5** (2017) 652-655.

2PO-K-27

NOVEL MAGNETICALLY FRUSTRATED MANGANESE PHOSPHATE Mn₂(PO₄)OH WITH TRIPLOIDITE CRYSTAL STRUCTURE

Shvanskaya L.V., Yakubovich O.V., Dimitrova O.V., Volkova O.S., Vasiliev A.N.

M.V. Lomonosov Moscow State University, Moscow, Russia

lshvanskaya@mail.ru

The combination of triangular geometry of magnetic ions with an antiferromagnetic interaction between them may leads to a magnetic frustration. This phenomenon is responsible for novel magnetic ground states of matter, including gapped and gapless spin liquids, spin ices, spin nematics, etc. [1,2]. Here, we report the synthesis, structural and magnetic characterization of Mn₂(PO₄)OH compound which exhibits a novel 1D frustrated lattice based on isolated twisted saw tooth chains from vertex-sharing manganese polyhedra and behaves as a low-temperature antiferromagnet.

According to structural investigation, the title compound belongs to the triplite-triploidite family with the formula Me²⁺(PO₄)(OH, F) and crystallizes in the space group P21c with $a = 12.411(1) \text{ \AA}$, $b = 13.323(1) \text{ \AA}$, $c = 10.014(1) \text{ \AA}$, $\beta = 108.16(1)$, $V = 1573.3 \text{ \AA}^3$, $Z = 8$, $R = 0.0375$. Its crystal structure can be described as a three-dimensional framework of corner and edge-sharing MnO₅ and MnO₆ polyhedra which further straightened by PO₄ tetrahedra. Both magnetization and specific heat data indicate that there is long-range antiferromagnetic order below $T_N = 4.6 \text{ K}$ with the Weiss constant $\Theta = -88 \text{ K}$, derived from the fitting of the magnetization curve. Therefore, the degree of frustration in Mn₂(PO₄)OH is equal to $|\Theta|/T_N \sim 20$. Note, that other members of triplite-triploidite supergroup are characterized by modest frustration strength $|\Theta|/T_N \sim 3$ [3]. The large value of frustration in the title compound is associated with the twisted saw tooth chain geometry of corner sharing triangles of Mn polyhedra, which may be isolated within tubular fragments of triploidite crystal structure (Fig. 1). Topologically this 1D fragment is similar to the distorted chain of triangles cut from the highly frustrated kagomé lattice. The interactions between tubular fragments running along a axes in the Mn₂(PO₄)OH crystal structure are provided by edge-sharing polyhedra, being tentatively ferromagnetic. The cause of different magnetic behaviors of the isostructural triplite-triploidite family members will be discussed.

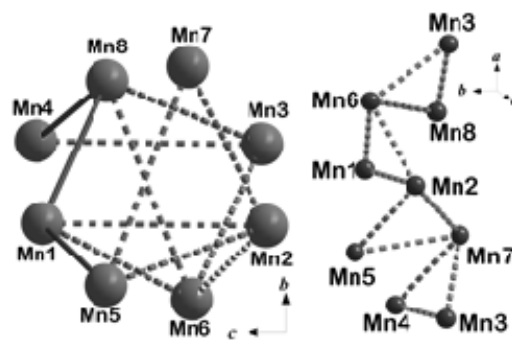


Fig. 1. Tubular structural fragment formed by Mn²⁺ cations shown along the a axis (left); the geometry of corner-sharing twisted saw tooth chain within the tube of Mn atoms (right).

- [1] C. Lacroix, P. Mendels, F. Mila (eds.), *Introduction to Frustrated Magnetism* (2011) Springer Series in Solid-State Sciences.
- [2] H. Liu, L. Yuan, S. Wang, H. Fang, Y. Zhang, C. Hou, S. Feng, *J. Mater. Chem. C*, **4** (2016) 10529-10537.
- [3] M. Leblanc, I. Collin-Fèvre, G. Férey, *J. Magnetism and Magnetic Materials*, **167** (1997) 71-79.

2PO-K-28

NMR STUDY OF THE PARAMAGNETIC STATE OF LOW-DIMENSIONAL MAGNETS LiCu_2O_2 AND NaCu_2O_2

*Sadykov A.F., Piskunov Yu.V., Gerashenko A.P., Ogloblichev V.V., Smolnikov A.G.,
Verkhovskii S.V., Volkova Z.N.*

M.N. Miheev Institute of Metal Physics of Ural Branch of Russian Academy of Sciences,
Yekaterinburg, Russia
sadykov@imp.uran.ru

We have carried out a comprehensive NMR study of the magnetic properties of single crystals LiCu_2O_2 and NaCu_2O_2 in the paramagnetic state. We have obtained the temperature dependence of the spin–lattice relaxation rates and magnetic shifts of NMR lines on different nuclei of LiCu_2O_2 and NaCu_2O_2 , as well as the magnetic susceptibility for various orientations of single crystals in an external magnetic field. The analysis of the orientation dependence of $^{63,65}\text{Cu}$, ^7Li and ^{23}Na NMR spectra has allowed us to determine the components of the electric field gradient tensor at the sites of these nuclei. We have determined the spin and orbital contributions to the NMR shifts and the magnetic susceptibility and evaluated the dipole and transferred hyperfine fields for all the nuclei considered. Quantitative analysis of the anisotropy of the spin-lattice relaxation in LiCu_2O_2 and NaCu_2O_2 made it possible to estimate the contributions from individual neighbouring Cu^{2+} ions to the transferred hyperfine fields on the Li^+ (Na^+) ion nuclei. The analysis of the origin of these fields has allowed us to reveal a sufficiently high degree of covalence between the ions of LiCu_2O_2 and NaCu_2O_2 . Moreover, we have established that “nonmagnetic” ions of $\text{Cu}(1 + \delta)^+$ have nonzero hole population ($\delta \approx 0.2$) and, hence, may have intrinsic magnetic moments. It was found that in the multiferroic LiCu_2O_2 at room temperature the spin fluctuations are isotropic. As the temperature is lowered, a considerable suppression of spin fluctuations in the direction of the *c* axis is observed, which is apparently associated with the development of 2D short-range correlations in planes containing Cu^{2+} moments. The maximum attenuation of such fluctuations is attained at $T \approx 150$ K. The isotropy of fluctuations in the system recovers with further cooling of LiCu_2O_2 to temperature of long-range helicoidal magnetic order. This behaviour indirectly indicates the absence of any crystallographic plane, which would be preferable for the appearance of long-range helicoidal magnetic order in it. In the NaCu_2O_2 cuprate, the spectrum of spin fluctuations remains isotropic over the entire temperature range.

Support by the Russian Science Foundation (project no. 16-12-10514) is acknowledged.

2PO-K-29

THE MEMRISTOR EFFECT IN THE FILM NANOCOMPOSITES

$\text{Co}_x(\text{TiO}_2)_{100-x}$, $(\text{Co}_{41}\text{Fe}_{39}\text{B}_{20})_x(\text{TiO}_2)_{100-x}$

Kalinin Yu.E.¹, Sitnikov A.V.¹, Rylkov V.V.², Korolev K.G.¹, Ryzhkova G.S.¹

¹ Voronezh State Technical University (VSTU), Voronezh, Russia

² National Research Centre "Kurchatov Institute," Moscow, Russia

sitnikov04@mail.ru

The effect of switching the electrical resistance in some materials, consisting in a reversible transition between high and low-resistance states under the action of an electric field and a flowing charge, is called a memorial, and an element with these properties is a memristor (short for "memory resistor" - Resistor with memory). The ion-beam sputtering method was used to synthesize films of nanocomposites $\text{Co}_x(\text{TiO}_2)_{100-x}$ and $(\text{Co}_{41}\text{Fe}_{39}\text{B}_{20})_x(\text{TiO}_2)_{100-x}$ with a thickness of 4-5 microns. Deposition was carried out at room temperature for pyroceramics substrates in an argon atmosphere with the addition of oxygen at a partial pressure of 2.2 %. With the use of shadow masks, metal-nanocomposite-metal structures were formed to study the transport properties of films in strong electric fields (>104 V/cm) in the transverse (vertical) geometry.

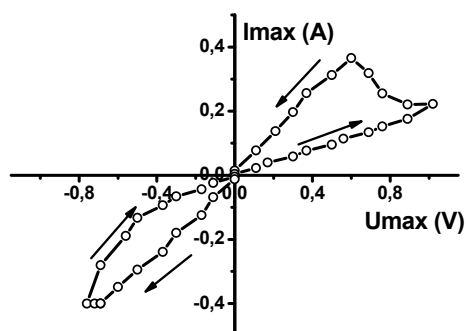


Fig. 2. The volt-ampere characteristics of the composite $\text{Co}_{69,2}(\text{TiO}_2)_{30,8}$ obtained with the addition of oxygen $P_{\text{O}_2}=1,6 \cdot 10^{-5}$ Torr.

A necessary condition for the material to have memorial properties is the detection in it of nonlinear volt-ampere characteristics with hysteresis (Fig. 1).

As a result of the research, it has been established that a reversible change in the electrical resistance of samples under the action of electric fields is observed at a concentration of the metal phase up to the percolation threshold (Fig. 2).

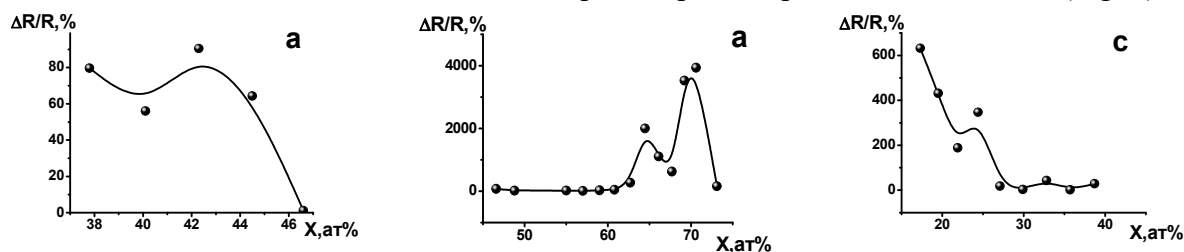


Fig.2. Concentration dependencies of the relative change in electrical resistance after exposure to strong electric fields of composites a – $\text{Co}_x(\text{TiO}_2)_{100-x}$, b - $\text{Co}_x(\text{TiO}_2)_{100-x}+\text{O}_2$, c - $(\text{Co}_{40}\text{Fe}_{40}\text{B}_{20})_x(\text{TiO}_2)_{100-x}$

Introduction of oxygen 2.2% to the pressure of the working gas when the composite film $\text{Co}_x(\text{TiO}_2)_{100-x}$ is sprayed increases the resistive switching effect to 4000% and shifts the concentration of the metal phase corresponding to the maximum response of the system to the region of higher values $x \approx 60 \div 75$ atomic %.

In the $(\text{Co}_{41}\text{Fe}_{39}\text{B}_{20})_x(\text{TiO}_2)_{100-x}$ composite, a more significant change in the electrical resistance of the samples is observed when exposed to a strong electric field than in the $\text{Co}_x(\text{TiO}_2)_{100-x}$ composite, which is obtained under the same conditions.

This work was supported by a grant from the RSF № 16-19-10233.

2PO-K-30

TWO-LATTICE EXCHANGE-ANISOTROPIC NEMATICS WITH $S = 1$ *Kosmachev O.A., Krivtsova A.V., Fridman Yu.A., Vernadsky V.*

Crimean Federal University, 295007, Simferopol, Russia

lkosma@crimea.edu

The main peculiarity of non-Heisenberg spin systems is the quantum reduction of the spin, which is manifested in the existence of such states, in the ground state of which the average spin is zero, the so-called nematics. In the dynamics of such systems, specific modes arise associated with the inclusion of multipole degrees of freedom.

Along with the investigation of the influence of higher invariants on the properties of isotropic spin systems, it is of interest to investigate exchange-anisotropic models. One of the simple models proposed to describe the thermodynamic properties of the He (III) and He (IV) mixtures in the vicinity of the critical point is a generalization of the Ising model with allowance for the biquadratic interaction - the so-called Blum-Emery-Griffiths model [1]. Taking into account the anisotropic exchange interaction has a significant effect on the exchange anisotropy on the dynamics of the system, as well as on the formation of specific phase states.

In the case of negative exchange interactions, various two-sublattice phase states arise: the collinear antiferromagnetic phase and the orthogonal nematic phase [2].

The purpose of this paper is to elucidate the effect of a negative anisotropic exchange interaction on the formation of phase states and the dynamics of a magnet with ion's magnetic spin $S = 1$.

The analysis of the free-energy density made it possible to determine the phase states realized in the case of negative values of the exchange interaction constants. In the case of the prevailing bilinear exchange interaction, depending on the ratios of the anisotropy parameters, axial, planar, and angular antiferromagnetic ordering are realized. The study of the statics and dynamics of the system shows that, depending on whether the angular phase is stable or not, the transition from an axial to a planar antiferromagnet occurs with a continuous change in the direction and modulus of the sublattice magnetizations or abruptly.

In the case of large by modulus biquadratic interaction, the anisotropy of the exchange interaction leads to the realization of several orthogonal nematic phases.

The phase transitions between the orthonormal phases are reorientational. The reorientation is associated with the rotation of the director vector of the sublattice ellipsoid, which is the geometric image of the quadrupole moment tensor.

Transitions from antiferromagnetic to orthonematic phases are the first-order phase transitions, as a result of which the magnetization modulus changes abruptly.

The work is supported by RFBR projects No. 16-02-00069 (YuAF and OAK) and No. 16-42-910441 (OAK), No. 16-32-00098 (AVK)

[1] M. Blume, V. J. Emery, R. B. Griffiths, *Phys. Rev. A*, **10** (1971) 1071.

[2] N. Papanicolaou, *Nuc. Ph. B*, **305** (1988) 367.

2PO-K-31

MAGNETIC RESONANCE OF THE DOPED “TRIANGULAR” ANTIFERROMAGNET $\text{RbFe}(\text{MoO}_4)_2$

Soldatov T.A.^{1,2}, *Smirnov A.I.*¹, *Kida T.*³, *Takata A.*³, *Hagiwara M.*³, *Petrenko O.*⁴, *Zhitomirsky M.*⁵,
*Shapiro A.Ya.*⁶

¹ P.L. Kapitza Institute for Physical Problems RAS, Moscow, Russia

² Moscow Institute for Physics and Technology, Dolgoprudny, Russia

³ AHMF Center, Osaka University, Osaka, Japan

⁴ Warwick University, Coventry, United Kingdom

⁵ CEA-INAC/UJF, Grenoble, France

⁶ A.V. Shubnikov Institute for Crystallography RAS, Moscow, Russia

tim-sold@yandex.ru

The ground state of the two-dimensional Heisenberg antiferromagnet on a triangular lattice (AFMTL) is strongly degenerated in a molecular field approximation. The selection of the ground state is performed by the order-by-disorder mechanism, implying thermal and quantum spin fluctuations, lifting a degeneracy of mean-field ground states [1]. It was theoretically shown that weak chaotic modulation of exchange bonds competes with fluctuation effects and, thus, may be a reason of a striking change of the spin structure of AFMTL [2]. We have checked these theoretical principles in ESR experiments with $S = 5/2$ AFMTL $\text{Rb}_{1-x}\text{K}_x\text{Fe}(\text{MoO}_4)_2$ doped up to 15 % K.

The results of the present ESR study in a frequency range 25 – 150 GHz reveal a significant change of the antiferromagnetic resonance spectrum caused by doping – the descending branch of frequency – magnetic field dependency observed in pure samples completely disappears in a 15 % doped samples, indicating a change of the ground state (see Fig 1). Moreover, the temperature evolution of 27 GHz ESR

records demonstrate that the microwave absorption in the plateau field range is partially restored at heating, showing the appearing of the 1/3-plateau anomaly. These doping-induced changes of magnetic resonance spectra uncover a transformation of the low-field spin structure from “Y-type” to inverted “Y-type” structure as well as a transition from the collinear up-up-down structure, stabilized by fluctuations, to a fan-structure, caused by weak static disorder, according to the theoretical analysis of the spectra. These facts directly demonstrate a competition of structural disorder and fluctuations in formation of the ground state.

Work at the Kapitza Institute is supported by Russian Foundation for Basic Research, grant No. 15-02-05918, and by the Programs of the Presidium of Russian Academy of Sciences.

[1] A.V. Chubukov, D.I. Golosov, *JOP: Condensed Matter*, **3** (1991) 69.

[2] V.S. Maryasin, M.E. Zhitomirsky, *Phys. Rev. Lett.*, **111** (2013) 247201.

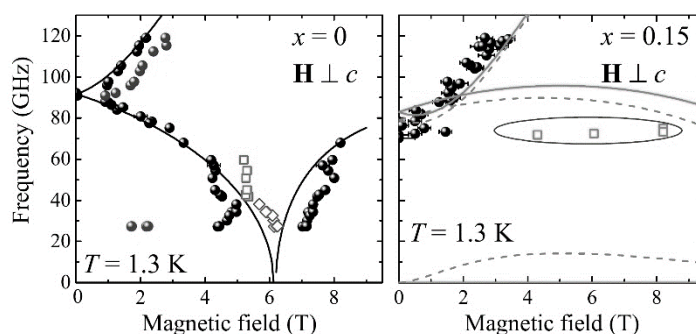


Fig. 1. Frequency – magnetic field diagrams of the $\text{Rb}_{1-x}\text{K}_x\text{Fe}(\text{MoO}_4)_2$ samples.

2PO-K-32

VISUALIZATION OF 3D VORTEX CORE DYNAMICS IN MOVING DOMAIN WALLS (MICROMAGNETIC SIMULATIONS)

Izmozherov I.M.¹, Zverev V.V.¹, Filippov B.N.^{1,2}, Dubovik M.N.^{1,2}

¹Ural Federal University, Yekaterinburg, Russia

²Institute of Metal Physics UB RAS, Yekaterinburg, Russia

vzvzverev49@gmail.com

The processes of creation and annihilation of vortices (antivortices) and singular (Bloch) points (SP) play an important role both in the switching of magnetization in nanodiscs [1] and in the motion of domain walls (DW) in magnetic films [2,3]. Now it became clear that in fairly thick samples the three-dimensionality (3D) in the magnetization dynamics should be taken into account [4]. In this report, we focus on the 3D dynamic transformations of the topological structure of magnetization. We show that ultrafast topological structure transformations give rise to configurations that determine the conditions imposed on spin-wave processes. The irregularity of the dynamics and transformations of the topological structure of the magnetization in a film are explained by instabilities in the DW motion.

The simulations were performed by solving the Landau-Lifshitz-Gilbert equation using MuMax3 solver [5]. We also used visualization programs based on the numerical algorithms for detection of topological charges (rotation and skyrmion numbers) using integration over closed contours and surfaces with variable geometry.

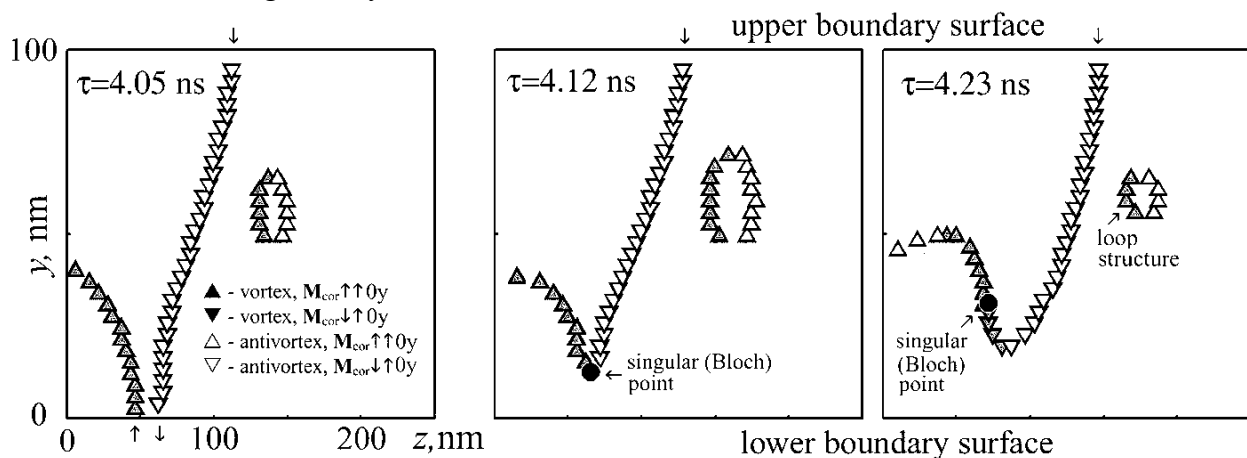


Fig. 1. Snapshots of the projections of the vortex (antivortex) cores and the SPs onto the yz -plane lying along the DW normally to the film boundaries.

In our report, we present the results of numerical simulations for Permalloy films for a wide range of thicknesses and values of the driving magnetic field. We draw attention to qualitative differences in the dynamics of thin (~ 10 nm) and rather thick (~ 20 -100 nm) films and consider the transition from 2D to 3D dynamics.

The research was carried out within the state assignment of FASO of Russia (theme “Magnet” No. 01201463328).

- [1] M. Noske, H. Stoll *et al*, *Phys. Rev. B*, **91** (2015) 014414.
- [2] V.V. Zverev, B.N. Filippov, *Physics of Solid State*, **58** (2016) 473-484.
- [3] V.V. Zverev, B.N. Filippov, M.N. Dubovik, *Physics of Solid State*, **59** (2017) 520-531.
- [4] M. Noske, H. Stoll *et al*, *J. of Appl. Phys.*, **119** (2016) 173901.
- [5] A. Vansteenkiste, J. Leliaert, M. Dvornik, *et al. AIP Advances*, **4** (2014) 107133.

2PO-K-33

CRITICAL PHENOMENA ISING ANTIFERROMAGNETIC WITH NEAREST-NEIGHBOR AND NEXT-NEAREST-NEIGHBOR INTERACTIONS ON A TRIANGULAR LATTICE

Murtazaev A.K.^{1,2}, Ramazanov M.K.¹, Badiev M.K.¹, Kurbanova D.R.¹

¹ Institute of Physics, Dagestan Scientific Center, Russian Academy of sciences, Makhachkala, 367003 Dagestan, Russia

² Daghestan state universities, Makhachkala, 367025 Dagestan, Russia
m_zagir@mail.ru

Ising Model on triangular lattice, as an archetypical example of a frustrated system, was initially studied by Newll [1]. The triangular Ising model has attracted much attention and because of its remarkable properties it has a long history of investigation. No exact solution is available in triangular Ising model. Hence, simulations of the Ising model are essential. Monte Carlo simulation methods have been widely using techniques to update the spins of the system and to study the Ising model on triangular lattice to obtain numerical solutions.

An inclusion of the interaction between the next-to-nearest neighbors results in appearance of frustration that complicates the solution.

In recent years, intensive experimental and theoretical investigations of critical behavior of this model are being carried out. In Refs. [2] investigated Ising model on a stacked triangular lattice, with antiferromagnetic first- and second-neighbor in-plane interactions, are studied by extensive histogram Monte Carlo simulations. The results, in conjunction with the recently determined phase diagram, strongly suggest that the transition from the period-3 ordered state to the paramagnetic phase remains in the XY universality class.

The frustrated Ising model is described by the classical Hamiltonian:

$$H = -J_1 \sum_{\langle ij \rangle} (S_i \cdot S_j) - J_2 \sum_{\langle\langle ij \rangle\rangle} (S_i \cdot S_j)$$

where the summations are over nearest-neighbor (nn) and next nearest-neighbor (nnn) pairs with J_1 and J_2 interactions, respectively. Calculations were carried out for systems with periodic boundary conditions (PBC) and linear dimensions $L \times L \times L = N$, $L=30 - 90$. The ratio of the exchange interaction of the next-to-nearest and nearest neighbors $k=J_2/J_1 = 0.0 \div 1.0$. To bring the system in the state of thermodynamic equilibrium, the segment with the length 2.5×10^5 MC-step/spin (that is several times larger than the nonequilibrium segment) was cut off. The averaging of thermodynamic parameters were made along a Markov chain with the length up to 1.5×10^6 MC-step/spin.

The investigation of the phase transitions of frustrated spin systems by traditional theoretical, experimental, and numerical methods meet some difficulties. The last is due to existence of numerous valleys of local energy minima, which is typical for such systems. The MC algorithms based on microscopic Hamiltonians contribute to strict and sequential evaluation of such systems. May be the most powerful and efficient algorithm tools for phase transitions and critical properties study in frustrated systems is the replica MC algorithms. In the present paper, we use a highly efficient MC replica exchange algorithm.

For calculation of static critical exponents of specific heat α , susceptibility γ , ordering parameter β , and correlation radius ν , we used the relations of the finite-size scaling theory [3].

The work has been supported by the grant of RFBR (project № 16-02-00214; project № 16-32-00105).

[1] G. F. Newell, *Phys. Rev.*, **79**, (1950) 876-882.

[2] H.T. Diep. Et al., *Phys. Rev. B*, **47**, (1993) 14312-14317.

[3] A.K. Murtazaev et al., *Physica B: Condensed Matter*, **476** (2015) 1–5.

2PO-K-34

FEATURES OF THE MAGNETIC STATE OF NIOBIUM DISELENIDE AND NIOBIUM DISELENIDE INTERCALATED WITH GADOLINIUM

Pleshchev V.G., Sherokalova E.M., Selezneva N.V., Simonov M.N.

Institute of Natural Science and Mathematics,
Ural Federal University named after the First President of Russia B. N. Yeltsin,
Ekaterinburg, Russia
v.g.pleshchev@urfu.ru

The intercalated compounds Gd_xNbSe_2 ($0 \leq x \leq 0.33$) with a quasi two-dimensional crystal structure have been synthesized for the first time and their physical properties have been studied. The magnetic properties measurements were executed using the SQUID-magnetometer MPMS-XL-7 at the temperature range 2 -350 K and at the magnetic field range ± 70 kOe. As was reported before [1] an antiferromagnetic order was established with increasing gadolinium content in Gd_xTiSe_2 . A phase transition from an antiferromagnetic to a ferromagnetic order in a magnetic field of about 18 kOe was also observed.

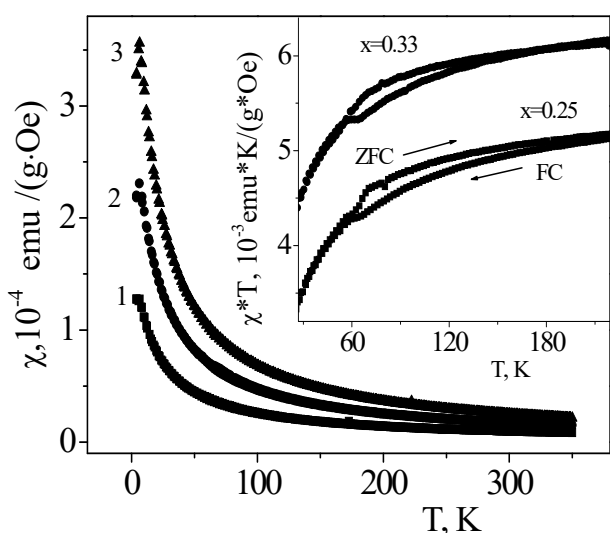


Fig. 1. Temperature dependencies of the magnetic susceptibility for Gd_xNbSe_2 : $x=0.1$ (1); $x=0.25$ (2); $x=0.33$ (3). Inset: $(\chi \cdot T)$ temperature dependencies.

range. For clarity, this is shown in the inset to Fig. 1 in the form of the $\chi \cdot T$ (T) dependencies. The temperature range of the hysteresis corresponds to the range where niobium diselenide magnetic state is changing. The field dependencies of the Gd_xNbSe_2 samples magnetization (M) are nonlinear, and a nonmonotonic dM / dH dependencies was observed.

Niobium diselenide as a matrix for intercalation differs significantly from $TiSe_2$ by the presence of a superconducting transition, the crystal structure modification and the presence of uncompensated magnetic moments in the 4d-shell. The performed studies of $NbSe_2$ demonstrate that the effective magnetic moment on the niobium ion has different values in the temperature range above and below 100K. For the low-temperature interval the value $\mu_{eff} = 0.1 \mu_B$, and for the high-temperature interval $\mu_{eff} = 0.9 \mu_B$. Fig.1 shows the magnetic susceptibility temperature dependencies $\chi(T)$ measured in the ZFC and FC modes for intercalated samples. Their approximation in accordance with the Curie-Weiss law shows the Curie-Weiss temperature negative values, which indicates the existence of antiferromagnetic type interactions in these samples. Hysteresis effects were found on the $\chi(T)$ curves at the intermediate temperature

This work was supported by the Russian Foundation for Basic Research (projects No 16-32-00278).

[1] E.M.Sherokalova, V.G.Pleschov, N.V.Baranov, A.V.Korolev. *Phys.Letters A*, **369** (2007) 236-242.

2PO-K-35

ELECTRICAL PROPERTIES OF FERROMAGNETIC-INSULATOR NANOCOMPOSITES AND MULTILAYER NANOSTRUCTURES BASED ON THEM

Kalinin Yu.E.¹, Makagonov V.A.¹, Sitnikov A.V.¹, Granovsky A.B.²

¹Voronezh State Technical University, Voronezh, Russia

²M.V. Lomonosov Moscow State University, Faculty of Physics, Moscow, Russia
kalinin48@mail.ru

In this paper we present analysis of experimental studying of electrical properties of ferromagnetic-insulator nanocomposites and multilayer nanostructures based on them with conducting interlayers. Various charge carrier transfer mechanisms are realized in ferromagnetic-insulator nanocomposites in pre-percolation region [1].

1. The mechanism of hopping conductivity via localized states near the Fermi level with a variable hopping range (Mott's model). The effective density of electron states at the Fermi level and its derivative with respect to energy estimating from the experimental results showed that the electron density of states at the Fermi level ($g(E_F)$) increases in nanocomposites with replacement of material granules according to the following sequence: $\text{CoNbTa} \rightarrow \text{CoFeB} \rightarrow \text{CoFeZr} \rightarrow \text{Co}$.

2. The inelastic resonant tunneling mechanism of electrons via insulator's localized states between granules. Estimates of average number of localized states within insulator matrix between metal granules, involved into electron transport, made from the experimental results, indicated that it decreases with increasing of heat treatment temperature.

3. The elastic electron tunneling mechanism between granules through a dielectric barrier.

4. The thermally activated hopping conductivity between nearest neighboring states or inelastic resonant tunneling between granules throughout insulator matrix.

In composites beyond the percolation threshold, the electrical resistivity is determined by labyrinth structure of conducting channels between metal granules and can have temperature dependence with a temperature coefficient of electrical resistance close to zero. For systems near the percolation threshold, the logarithmic law $\sigma(T) = A(1 + \alpha \ln T)$ is satisfied for conductivity, where the parameters A and α depend on concentration of conduction phase. This logarithmic dependence, according to the theory of Efetov et al., is associated with features of the Coulomb interaction in nanogranular alloys during intergranular tunneling in transition range of concentrations from metallic conductivity to the dielectric regime [2].

In multilayer structures based on ferromagnetic-insulator composites with different conductivity interlayer's thickness hopping conductivity according to "1/2" Efros-Shklovsky law is observed at wide temperature range (from 80 K to 300 K) [3]. For these systems it is established that there is a critical thickness of a conducting layer at which metal-insulator phase transition is observed and radius of wave function localization depends on thickness and conducting phase structure.

The work was supported by the Ministry of Education and Science within project part of the state task (project № 3.1867.2017/ПЧ).

[1] S.A. Gridnev, Y.E. Kalinin, A.V. Sitnikov, O.V. Stognei, *Non-linear phenomena in nano- and micro-heterogeneous systems*, BINOM. Laboratory of Knowledge, Moscow (2012) (in Russian).

[2] K.B. Efetov, A. Tschersich. *Phys. Rev. B*, **67** (2003) 174 205.

[3] B.I. Shklovskii, A.L. Efros, *Electronic Properties of Doped Semiconductors* (Springer-Verlag, New York, 1984).

2PO-K-36

INFLUENCE OF TECHNOLOGICAL PARAMETERS ON THE MAGNETO-OPTICAL PROPERTIES OF NANOCOMPOSITE-SEMICONDUCTOR MULTILAYERS

Gan`shina E.A.¹, Buravtsova V.E.¹, Kalinin Yu.E.², Sitnikov A.V.²

¹ Moscow State University, Faculty of Physics, Moscow, 119991, Russia

² Voronezh State Technical University, Voronezh, 394026, Russia

v.e.buravtsova@gmail.com

The studies results of magneto-optical (MO) properties variation of nanocomposite/semiconductor multilayers (ML) depending on layer thickness and magnetic phase concentration in the nanocomposite layer are presented in this report.

Either $(\text{Co}_{45}\text{Fe}_{45}\text{Zr}_{10})_Z(\text{SiO}_2)_{100-Z}$ or $(\text{Co}_{40}\text{Fe}_{40}\text{B}_{20})_Z(\text{SiO}_2)_{100-Z}$ composite with magnetic phase concentrations under the percolation threshold was used as a magnetic layer and Si or C as semiconductor layer. Nanomultilayer systems were produced by ion-beam sputtering.

Magneto-optical properties were studied in the energy range of 0.5 - 4.2 eV in the Transversal Kerr Effect (TKE) geometry.

It was found that under certain conditions thin non-magnetic semiconductor layer addition leads to the multilayer MO response increase compared to the bulk nanocomposite one. At the same time, the magnetic properties of ML structure become softer, up to the appearance of FM ordering due to the strengthening of the exchange interaction between the FM granules in the neighboring layers via the semiconductor layer.

The anomalous changes in magnetic and MO properties are well correlated with abrupt changes in the electric properties of all ML structures. This correlation is determined by the peculiarities of «FM-granule – semiconductor» interface forming and the percolation processes in multilayer structures. At the small thicknesses of semiconductor (< 2 nm) and composite (< 3 nm) layers the concentration of FM phase in the "the FM granule - semiconductor" interface layer can reach percolation threshold, which appears as the MO response enhancement.

The decreasing of the nanocomposite layer concentration Z as well as increasing the layer thickness have led to the anomalous MO response reduction in the range of ML structure electric percolation.

The contribution of the new phase considerably decays as C is being replaced with Si, that can be associated to the higher chemical activity of Si compared with C.

Thereby the research indicates the presence of several magnetic phases in ML. The occurrence and dominance of the different phases contribution into ML MO response depends on technological parameters of nanomultilayers films.

This research was supported by the Russian Foundation for Basic Researches №15-02-02077.

2PO-K-37

THERMODYNAMICS OF BIDISPERSE SYSTEM OF DIPOLAR HARD SPHERES

Vtulkina E.D., Elfimova E.A.

Ural Federal University, Ekaterinburg, Russia

katevtulkina@mail.ru

In this study the bidisperse system of dipolar hard spheres (DHSs) is used for describing thermodynamic properties of ferrofluids. Considering bidisperse DHSs, we assume existing of two ferroparticle fractions: small (S) and large (L) particles, which differ in their diameters $d_{S(L)}$ and magnetic moments $m_{S(L)}$. Each fraction has own characteristics: the number of particles $N_{S(L)}$, the volume concentration $\varphi_{S(L)}$ and dipolar coupling constant $\lambda_{SS(LL)}$. The interaction between small and large particles is characterized by additional dipolar coupling constant λ_{SL} . The total volume concentration is defined by $\varphi = \varphi_S + \varphi_L$ and total number of ferroparticles is $N = N_S + N_L$. The theory is based on the transformation of the virial expansion for the Helmholtz free energy into the logarithmic form [1]. In this work, the second and the third virial coefficients are calculated as a series expansion in the dipolar coupling constant λ_y up to the fourth power. The new theory extends the results obtained for the monodisperse DHSs [1, 2]. On Fig. 1 is presented the configurational part of the Helmholtz free energy as the function of volume concentration φ for the bidisperse model where large particle fraction is 10% and 20%. The points are from Monte Carlo simulation [3] and the curves are from present theory. The results for the Helmholtz free energy agree well with computer simulation.

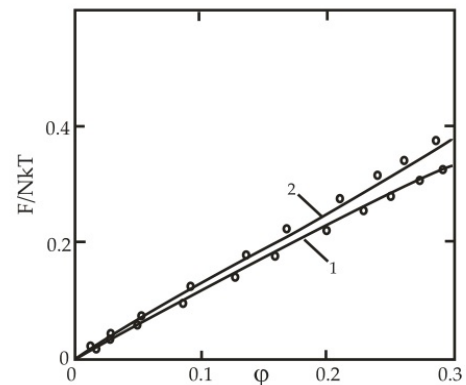


Fig. 1. Configurational part of the Helmholtz free energy for bidisperse DHSs with 20% of large particles (curve 1) and 10% of large particles (curve 2).

In future, we would like to apply our theoretical model to predict critical parameters of bidisperse system and compare these results with monodisperse model to study the influence of polydispersity on phase behavior of ferrofluids.

The authors are grateful to the Ministry of Education and Science of the Russian Federation (Project No. 3.1438.2017/PP).

[1] E.A. Elfimova, A.O. Ivanov, P.J. Camp, *Physical Review E*, **86** (2012) 021126-1-9.

[2] E.D. Vtulkina, E.A. Elfimova, *Fluid Phase Equilibria*, **417** (2016) 109-114.

[3] A.Yu. Solovyuva, E.A. Elfimova, *Magnetohydrodynamics*, **50** (2014) 109-119.

2PO-K-38

SURFACE MAGNETISM AND MORPHOLOGY OF FeBO₃ SINGLE CRYSTALS

Yagupov S.¹, Strugatsky M.¹, Maksimova E.¹, Nauhatsky I.¹, Seleznyova K.¹, Mogilenec Yu.¹, Zubov V.²

¹ Physics and Technology Institute, Crimean Federal University, Simferopol, Russia

² Moscow State University, Moscow, Russia

strugatskymb@cfuv.ru

Surface magnetism is a special magnetic state of the surface caused by lowering of the symmetry in the environment of the surface magnetic ions. Previously, we have studied this effect on the non-basal faces of bulk FeBO₃, synthesized by gas phase technique [1]. These crystals had the faces of the following types: $(10\bar{1}4)$, $(11\bar{2}0)$, $(11\bar{2}3)$, $(01\bar{1}2)$ and (0001) in the hexagonal coordinate system [1]. The maximal value of surface anisotropy has been found for faces of the $(10\bar{1}4)$ type that are parallel to two-fold axis C₂. The surface anisotropy energy for such faces in a dipole-dipole approximation can be expressed as:

$$s = a_s \sin^2 \phi$$

where a_s is the surface anisotropy constant and ϕ is the angle between C₂ and the antiferromagnetic vector in the basal plane.

In the present work, for a more detailed explanation of the relationship between surface magnetism and the type of the face, we have calculated the dependence of a_s on the angle α between the face and the basal plane of the crystal for all possible faces parallel to the C₂ axis, see Fig. 1. As one can see, a_s for different faces considerably changes in magnitude. Moreover, a_s changes the sign depending on the type of the faces from mentioned family. The change of the sign means the changing of equilibrium orientation of antiferromagnetic vector in the basal plane: $a_s > 0$ – easy axis coincides with C₂ ($\phi = 0$); $a_s < 0$ – easy axis is orthogonal to C₂ ($\phi = \pi/2$). Figure 1 shows that the faces of the simple form $(10\bar{1}4)$, studied before on bulk single crystals, possess the maximal a_s value among faces of mentioned series.

The calculation has been carried out for ideal crystal. FeBO₃ single crystals of a high structural perfection can be obtained by solution in the melt technique. In the present work we have synthesized such crystals and have studied them by optical-goniometer technique. It was found that the main type of non-basal faces belong to the $(10\bar{1}4)$ type. Such faces are of optical quality, have a width up to 100 μm and are suitable for magneto-optical studies of surface magnetism. Thus, obtained results open perspective of new, more detailed studies of surface magnetic effects.

[1] V.E. Zubov, G.S. Krinchik, V.N. Seleznyov, M.B. Strugatsky, *JMMM*, **86** (1990) 105-114.

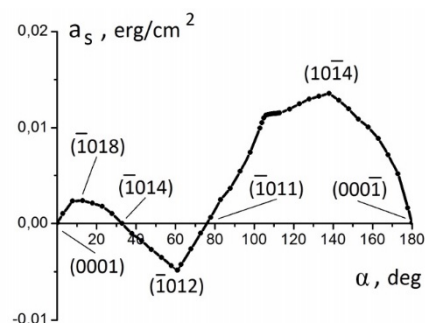


Fig. 1. $a_s(\alpha)$ at room temperature.

2PO-K-39

INTERACTION OF MAGNETIC ELEMENTS IN METALLIC FERROMAGNETIC NANO-FILM

Panaetov V.P.¹

¹High mountainous geophysical institute, Kabardino - Balkar Republic. Nalchik, Russia.
Valen_pvs@rambler.ru

In this paper, a comparative analysis of the distances between magnetic elements is made, under which a noticeable effect arises when they interact. The sides of the domain (domain walls), the terminal part of the domain (the top of the domain), we called magnetic elements. During magnetization, the domain structure is restructured. The distances between the domain walls, between the domain wall and the top of the domain, between the tops of the domains change. When recording information with the help of magnetic moments of electrons, the film will become magnetized. The interaction of domain walls, the interaction of the domain wall and the top of the domain, the interaction of the tops of domains in the design of storage devices must be taken into account. Micro magnetization processes were observed at high magnification in a transmission electron microscope UMV-100K by the method of Lorentz microscopy. The films were obtained by the method described in [1]. The interaction of homogeneous domain walls of the Bloch and the Néel is studied experimentally. The repulsion and attraction of domain walls is associated with their magnetostatic interaction. In the interaction of periodic domain walls, the distances between the walls are measured when the effect of one wall on another manifests itself. We called these distances critical. Walls with cross-links begin to interact with each other at farther distances than homogeneous ones. The distance at which the mutual influence should be taken into account is approximately equal to the length of the transverse coupling. The wall bends, when the top of the domain interacts with the domain wall. The interaction of the tops of domains is investigated, depending on the distance between them. Different types of interaction tops of domains on one another and the effect of this interaction on the magnetic structure are considered. The critical distance was measured at which interaction of the tops of domains begins. It is established that the critical distance (the distance between the domain walls when interaction begins to appear) for homogeneous domain walls in films of thickness 30-40 nm of composition Ni, Co, Ni_{0.90} - Fe_{0.10} is, respectively, ~1000-1200 nm; 2000-2500nm; 1500-1700 nm. For cobalt films, 30 nm thick, the saturation magnetization $I_s = 1.4$ A/m, the critical distance be equal to 1600 nm, for nickel films, 30 nm thick, $I_s = 0.48$ A/m, the distance between the walls is equal to 800 nm. At distance $s > 10$ μ m for films with a thickness of 20 nm, the composition Fe_{0.20}-Ni_{0.80}, the interaction of the tops of domains does not manifest itself. In films with a thickness of more than 50 nm, the interaction between the walls and the tops of the domains is more pronounced. In films with a thickness of 50 nm, the interaction is noticeable even at a distance ~ 20 μ m. The interaction of the tops of domains in the films becomes appreciable at a distance of 100 μ m and exceeds the interaction energy of homogeneous domain walls in magnitude. These results are confirmed by experimental measurements of the distance between the tops of domains in films 50 nm thick with the composition Fe_{0.20}-Ni_{0.80}, $H_k = 250$ A / m.

[1] V.P. Panaetov, *Journal of New Technologies and Materials*, **5(2)** (2015) 1- 4.

2PO-K-40

CRITICAL PROPERTIES OF 2D DISORDERED ANTIFERROMAGNETIC 3-STATE POTTS MODEL ON TRIANGULAR LATTICE

Murtazaev A.K.^{1,2}, Babaev A.B.^{1,3}, Ataeva G.Y.^{1,4}

¹ Institute of Physics, Dagestan Scientific Center, Russian Academy of Sciences,
Makhachkala, 367003 Russia

² Dagestan State University, Makhachkala, 367025 Russia

³ Dagestan State Pedagogical University, Makhachkala, 367003 Russia

⁴ Dagestan State University of National Economy, Makhachkala, 367008 Russia
ataeva20102014@mail.ru

The change in emphasis of the modern condensed matter physics towards microscales provokes the necessity of understanding the phenomena induced by impurities and other structural defects. There are grounds for believing that non-magnetic impurities change the order of the phase transition (PT) in magnetic systems described by the Potts models for which in pure state a first order PT is observed. Such systems are today actively investigated by means of the Monte-Carlo methods [1, 2].

In present work, PT and critical properties of 2D diluted antiferromagnetic (AF) 3-state Potts model on a triangular lattice at impurity concentrations of $p=0.90, 0.80$ are studied. The estimations are performed using the standard Metropolis algorithm along with Monte-Carlo cluster Wolff algorithm. As for the 2D diluted AF 3-state Potts model, there is no a reliable information on the influence of non-magnetic impurities on PT, the dependency of critical exponents on a concentration of non-magnetic impurities, especially in a case of the disorder realized as quenched non-magnetic impurities, and the universality class of the critical behavior is failed to be determined up till now [3]. The only reliably proved fact is that the first-order transition happens in the pure model [4].

The Hamiltonian of the 2D diluted AF Potts model can be written as [4]:

$$H = -\frac{J}{2} \sum_{i,j} \rho_i \rho_j \cos \theta_{i,j}, \quad S_i = 1, 2, 3 \quad (1)$$

where J is the parameter of the exchange antiferromagnetic interaction of nearest neighbors ($J < 0$), $\rho_i = 1$, if the site i is occupied by the magnetic atom, and $\rho_i = 0$, if in i site the non-magnetic impurity presents. The systems with linear sizes of $L \times L = N$, $L = 12 \div 96$ are investigated.

The fourth order Binder cumulant method shows itself to good advantage in such investigations and the analysis of PT character and behavioral features of heat characteristics near the critical point. The use of the Binder cumulants allows also the testing of a phase transition order in the system [5]. For all studied system with a second-order PT the static critical exponents for the heat capacity α , susceptibility γ , magnetization β , and correlation radius ν are computed on the basis of the finite-size scaling theory [6, 7].

[1] R. Folk, Yu. Golovach, and T. Yavorskii, *Phys. Usp.*, **46** (2) (2003) 169.

[2] A.K. Murtazaev et al., *Physics of the Solid State*, **59**(1) (2017) 141-144.

[3] X. Qian, Y. Deng, W. Blöte, J., *Phys. Rev. E*, **72** (2005) 056132-1.

[4] F. Y. Wu, *Rev. Mod. Phys.*, **54** (1982) 235.

[5] K. Eichhorn, and K. Binder, *J. Phys.: Condens. Matter.*, **8** (1996) 5209.

[6] A.E. Ferdinand, M.E. Fisher, *Phys. Rev.*, **185**(2) (1969) 832-846.

[7] M.E. Fisher, M.N. Barber, *Phys. Rev. Lett.*, **28**(23) (1972) 1516-1519.

2PO-K-41

HYDROTHERMAL TREATMENT AND MAGNETIC PROPERTIES OF TiO₂-Fe₃O₄ COMPOSITES

Kharitonskii P.V.^{1,2}, *Gareev K.G.*², *Kirillova S.A.*², *Kosterov A.A.*¹, *Sergienko E.S.*¹

¹ Saint Petersburg State University, Saint Petersburg, Russia

² Saint Petersburg State Electrotechnical University "LETI", Saint Petersburg, Russia
p.kharitonskii@spbu.ru

Composites based on titanium dioxide and magnetite are of interest as a model system in the study of natural titanium-substituted magnetites, as well as hyperthermic therapy and drug delivery systems due to their relatively low toxicity. The complexity of obtaining titanium-substituted magnetites is caused by high temperatures for the realization of solid-phase reactions. An alternative method of synthesis is hydrothermal treatment of a magnetite-silica composite obtained by a sol-gel method.

In the present study, magnetite precipitation was carried out in a suspension of TiO₂ powder by the reaction given in [1]. In 100 ml of distilled water, FeCl₃·6H₂O and FeSO₄·7H₂O were dissolved in a molar ratio of 2:1, further TiO₂ powder was dispersed in the solution. Then, 10 ml of ammonia solution was added to the suspension, the resulting magnetic precipitate was washed using a permanent Nd-Fe-B magnet until pH = 7 and chloride and sulfate ions were removed. The powder was then dried at room temperature. Parameters of hydrothermal treatment were the following: temperature 240 °C, pressure 50 MPa, hydrothermal medium - distilled water, and the duration of isothermal exposure 4 hours.

The analysis of the phase composition of the samples by X-ray diffraction showed the presence of a crystalline phase with a spinel structure, as well as anatase and hematite. The crystal lattice period of the phase with the spinel structure was varying from $a = 0.8362$ to $a = 0.8367$ nm for a titanium dioxide content of 0.5 to 2.0 g, respectively, this value is intermediate between the parameters of the maghemite ($a = 0.8339$ nm) and magnetite ($a = 0.8397$ nm) lattice.

The study of the magnetic properties of the composite before and after hydrothermal treatment (Fig.1) shows that the saturation mass magnetization decreases from 29.1 to 14.3 emu/g, the saturation remanent mass magnetization rises from 0.35 to 1.4 emu/g, and the coercive force increases from 6 to 54 Oe. The result can be explained by the growth of the dimensions of the iron oxide crystallites during the hydrothermal treatment from less than 10 nm [1] to 40 nm (the specific surface area of the powder was reduced from 31 to 12 m²/g), the magnetostatic interaction between the particles [1], and their oxidation to maghemite and hematite.

The development of the synthesis technique was partially supported by RFBR, project No. 16-32-60010.

[1] P.V. Kharitonskii et al, *J. Magn.*, **20** (2015) 221-228.

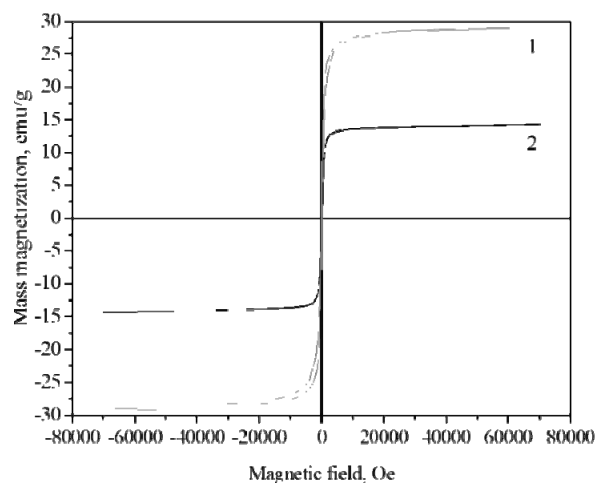


Fig. 1. Magnetization curves of samples:
1 – before hydrothermal treatment,
2 – after hydrothermal treatment.

2PO-K-42

SURFACE MAGNETOCRYSTALLINE ANISOTROPY OF FeBO₃ SINGLE CRYSTALS

Strugatsky M.¹, Seleznyova K.¹, Zubov V.², Kliava J.³

¹ Physics and Technology Institute, Crimean Federal University, Simferopol, Russia

² Moscow State University, Moscow, Russia

³ LOMA, UMR 5798 Université de Bordeaux-CNRS, Talence, France

strugatskymb@cfuv.ru

Single crystals of iron borate FeBO₃, due to particularities of their crystal and magnetic structure, possess surface magnetism – a special magnetic state of the surface. Bulk single crystals of iron borate with large non-basal faces of optical quality have made possible finding the surface magnetism by the magneto-optical Kerr effect [1].

The saturation field of surface magnetization, called the critical field H_c , can be found as

$$H_c = \frac{4a_s^2}{AM} \quad (1)$$

where a_s is the surface magnetocrystalline anisotropy constant, A is the constant of the non-uniform exchange interaction [1] and M is the spontaneous magnetization of the crystal [2]. a_s is expected to include dipole-dipole, $a_{s\text{dip}}$ and crystal field, $a_{s\text{cf}}$ contributions. Previously, a_s has been calculated in the dipole-dipole approximation, neglecting the crystal field contribution [3], in which case the calculated H_c turns out to be much lower than the experimental value $H_c \approx 1.5$ kOe [1].

In order to take into account the crystal field contribution, we have developed a model of structural uniaxial distortions in the

near-surface layer for the $(10\bar{1}4)$ face of FeBO₃. To account for the lowering of symmetry in this layer, the generalized spin Hamiltonian expressed through the tesseral spherical tensor operators has been used [4], and the spin Hamiltonian parameters have been calculated within the superposition model [5]. The crystal field contribution to the surface anisotropy energy at 0 K has been calculated in perturbation theory.

Figure 1 shows the calculated dependence of H_c on relative distortions ε , taking into account both contributions to a_s . One can see that the experimental H_c value is attained at a contraction of ca. 1%. In this case, the crystal-field contribution considerably exceeds the dipole-dipole one.

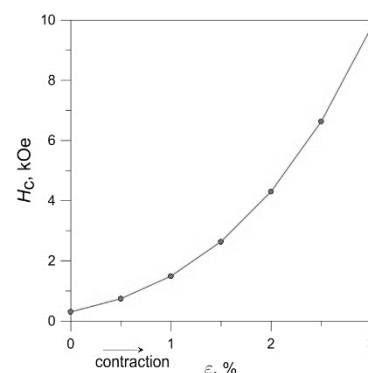


Fig. 1. Calculated $H_c(\varepsilon)$ dependence at 0 K.

[1] V.E. Zubov, G.S. Krinchik, V.N. Seleznyov, M.B. Strugatsky, *JMMM*, **86** (1990) 105-114.

[2] R. Diehl et al., *Current Topics in Materials Science*, Elsevier, New-York, **11** (1984) 241-387.

[3] E.M. Maksimova, I.A. Nauhatsky, M.B. Strugatsky, V.E. Zubov, *JMMM*, **322** (2010) 477-480.

[4] D.G. McGavin, W.C. Tennant, J.A. Weil, *J. Magn. Reson.*, **87** (1990) 92-109.

[5] J. Kliava, R. Berger, *Recent Res. Devel. Non-Cryst. Sol.*, *Transworld Research Network, Kerala*, **3** (2003) 41-84.

2PO-K-43

NUCLEATION MODES OF THIN AMORPHOUS FERROMAGNETIC FILM WITH SURFACE ANISOTROPY

Serebryakova O.N.^{1,2}, Usov N.A.^{1,2}

¹ National University of Science and Technology «MISiS», 119049, Moscow, Russia

² IZMIRAN, Troitsk, Moscow, Russia
silver@izmiran.ru

Thin amorphous ferromagnetic films with perpendicular magnetic anisotropy are promising for creation of high-density data storage devices and spin-transfer torque magnetic random access memory [1]. It is generally accepted [2] that surface anisotropy is responsible for the high perpendicular magnetic anisotropy observed in various ferromagnetic nanostructures. In this report three-dimensional numerical simulation is carried out to study equilibrium micromagnetic configurations and magnetization reversal process in thin amorphous ferromagnetic film with surface anisotropy. The numerical results are obtained in the simplest Néel approximation for surface anisotropy energy, a surface anisotropy constant K_s being a single phenomenological parameter. The calculations are performed for amorphous CoSiB film with thickness $L_z = 4 - 6$ nm, submicron in-plane sizes, saturation magnetization $M_s = 500$ emu/cm³, exchange constant $A = 10^{-6}$ erg/cm, and in-plane induced volume anisotropy constant $K_V = 10^4$ erg/cm³. It is found that for negative values of the surface anisotropy constant the film is perpendicular magnetized for sufficiently small thickness, $L_z < L_{z,min}(|K_s|)$. The critical thickness $L_{z,min}$ depends on the absolute value of the surface anisotropy constant. For thickness $L_z > L_{z,min}$ the spin canted state has the lowest total energy as compared to various multi-domain configurations.

It is shown that the magnetization reversal of the perpendicular magnetized state starts by means of the nucleation of the buckling mode at nucleation field H_n .

However, for the film with $L_z = 6$ nm a nonlinear stabilization of the buckling mode is observed within a relatively small interval of magnetic fields after mode nucleation. The nucleation field of the buckling mode is investigated as a function of the CoSiB film thickness and in-plane aspect ratio.

This work was supported by the Ministry of Education and Science of the Russian Federation in the framework of Increase Competitiveness Program of NUST «MISiS», contract № K2-2015-018.

[1] J. Yoon et al., *J. Appl. Phys.*, **113** (2013) 17A342.

[2] M.T. Johnson et al., *Rep. Prog. Phys.*, **59** (1996) 1409.

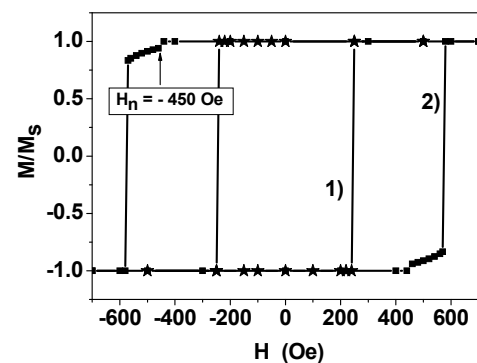


Fig. 1. Perpendicular hysteresis loops of CoSiB amorphous film: 1) $K_s = -0.6$ erg/cm², $L_z = 4$ nm; 2) $K_s = -1.0$ erg/cm², $L_z = 6$ nm

2PO-K-44

SYNTHESIS OF METAL COATINGS USING ARABINO GALACTAN AND THEIR MAGNETIC PROPERTIES

Chekanova L.A.¹, Yaroslavtsev R.N.^{1,2}, Stolyar S.V.^{1,2}, Iskhakov R.S.¹

¹ Institute of Physics SB RAS, Krasnoyarsk, Russia

² Siberian Federal University, Krasnoyarsk, Russia

yar-man@bk.ru

The electroless deposition method as a method of obtaining metallic coatings has been known for quite some time. As a reducing agent, compounds such as hypophosphite, borohydride, hydrazine are commonly used. In this paper, arabinogalactan was used as a reducing agent in the preparation of CoNi metal coatings [1-2]. Arabinogalactan is a natural polysaccharide whose molecule consists of galactose and arabinose units.

Coatings were prepared by precipitation from aqueous solution on a glass and copper substrates. Figure 1 shows the XRD spectrum of CoNi film deposited on a copper substrate. Measurements of ferromagnetic resonance at a frequency of 9.2 GHz at room temperature were performed. Figure 2 shows the dependencies of the FMR resonant field and the linewidth on the angle of rotation of the sample with respect to the external field. The effective magnetization value, calculated from the resonance fields with parallel and perpendicular orientations, was 960 Gs.

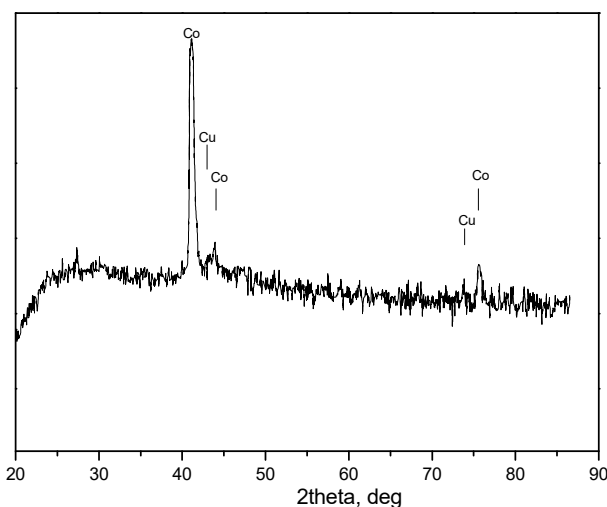


Figure 1 - The XRD spectrum of CoNi film deposited on a copper substrate

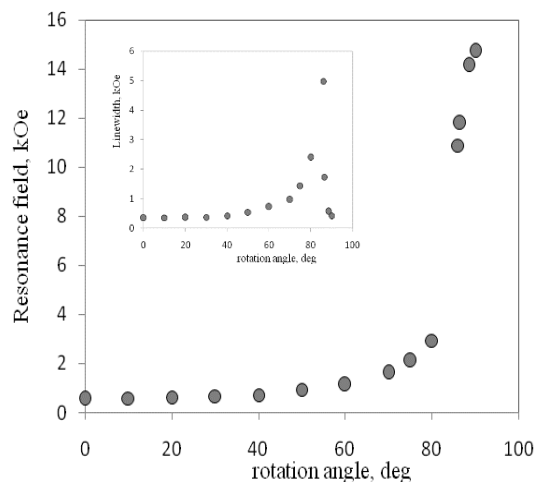


Figure 2 - Angular dependence of the FMR resonance field. On the inset, the angular dependence of the FMR linewidth

The research was carried out with the support of the regional state autonomous institution "Krasnoyarsk Regional Fund for Support of Scientific and Technical Activity" within the framework of participation in the event: Moscow International Symposium on Magnetism. This work was supported by the Russian Foundation for Basic Research, Grants № 16-03-00256, 16-03-00969. Support by the Special Program for Siberian Federal University of the Ministry of Education and Science of the Russian Federation is acknowledged.

[1] Bhamidi S. et al, *Journal of Biological Chemistry*, **19** (2008) 12992–13000.

[2] Aleksandrova G.P., Medvedeva S.A., Grischenko L.A., Dubrovina V.I. RF patent №2194715.

2PO-K-45

MAGNETIC PROPERTIES OF THE NANOCOMPOSITES FABRICATED IN PULSE HIGH-VOLTAGE DISCHARGE PLASMA USING POLYTETRAFLUOROETHYLENE

Kuryavyi V.G.¹, Bouzник V.M.², Tkachenko I.A.¹, Kvach A.A.¹

¹Institute of Chemistry FEBRAS, Vladivostok, Russia

²All Russian Scientific Research Institute of Aviation Materials, Moscow, Russia

kvg@ich.dvo.ru

Nanocomposites containing carbon, fluorocarbon and nanoparticles of fluorides, oxyfluorides or oxides of elements of the electrodes have been fabricated by the combined destruction of electrodes and polytetrafluoroethylene of the grade F-4 in the plasma of pulse high-voltage discharge initiated in air environment [1]. Samples structure have been studied by various physical methods (XRD, TEM, SEM, EDS, IR, Raman, NMR, mass-chromatography). Experimental conditions for regulation of the sizes of particles and for their isolated placement in carbon-fluorocarbon matrix have been picked up. Temperature and field dependencies of a magnetic susceptibility of the received nanocomposites before and after their annealing have been studied with using SQUID magnetometer. Dependencies typical for superparamagnetic states, for states with tunneling of the magnetic moment (an example of fig. 1), for states with interaction between FM and AFM/FerriM components, for the mictomagnetic states (presumably) (fig. 2), for magnetic flip-flop phase transitions, for samples with existence in their volume of the environment of Josephson contacts (at T=300K) [2] (fig. 3) have been received for various samples. Different substances with coercive forces from $H_c = 10$ Oe (soft magnetic) to $H_c = 4400$ Oe (rigid magnetic) have been received. Phase transition of Morin, phase transition of Verway and other magnetic transitions have been found in various samples. Upon the sample annealing, the material containing nanocrystalline hematite, in which the Morin transition is absent, was obtained.

The used synthesis method are promising for obtaining of many various magnetic nanomaterials by way of selection of material of electrodes and of electric conditions of experiment.

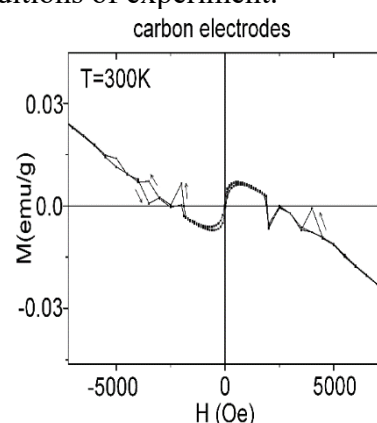
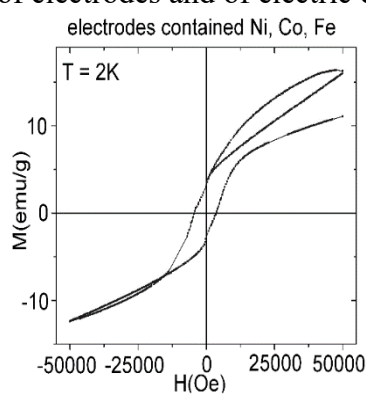
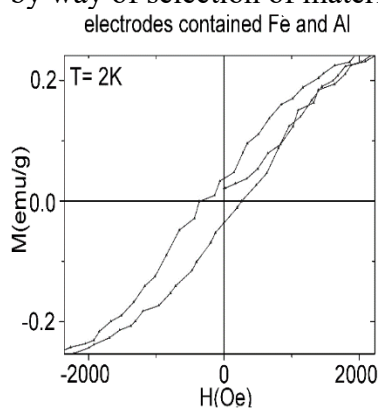


Fig. 1. M(H), example 1

Fig. 2. M(H), example 2

Fig. 3. M(H), example 3

[1] V.G. Kuryavyi, Bouzник V.M. Method for producing nanodispersed fluoroorganic material. Russian Patent №. 341536 (2008).

[2] S.G. Lebedev, *Nucl. Instr. Meth.*, **A521** (2004) 22–29.

2PO-K-46

SPIN-WAVE RESONANCE IN HETEROGENEOUS MAGNETIC Co-Ni FILMS

Vazhenina I.G., Iskhakov R.S., Chekanova L.A.

Kirensky Institute of Physics, Federal Research Center KSC SB RAS (*IPh SB RAS*), Krasnoyarsk, Russia
 irina-vazhenina@mail.ru

The spin-wave resonance (SWR) is traditionally used to determine the fundamental magnetic parameters of the system. The conditions of SWR implementation allow to application of this phenomena as the magnetostructure technique in order to study the magnetic heterogeneities.

The dispersion relationship of spin waves exciting in the homogeneous film is described by the quadratic law in case of pinning the surface spin ($H_n \sim n^2$, H_n – resonance field, n – mode number connected with wave vector $k = \pi n/d$; d – film thickness) [1].

Own of the first theoretical description of spin wave behaviour in heterogeneous film was proposed by the paper [2]. The improved theoretical model which is developed by a group of V. Ignathenko [3] for heterogeneous films with parabolic distribution of magnetization along film thickness demonstrates two event of the magnetic potential realization. It is either potential well or potential hill. According to math simulation [3] the each case is characterized by existing the two ranges in SWR spectrum and certain critical wave vector $k_{critical}$. The dependence of the resonance fields on mode number for the potential well case is described by relations: $H_n \sim n$ ($0 < k < k_{critical}$) or $H_n \sim n^2$ ($k > k_{critical}$). The second case results in the modifications of resonance field positions: $H_n \sim n^{1/2}$ ($0 < k < k_{critical}$) or $H_n \sim n^2$ ($k > k_{critical}$).

The layered magnetic thin films with changing value of the effective magnetization along film thickness were prepared by us to carry out this research. Such modulation of the magnetic parameter in obtained films creates the magnetization profile like parabola (insert of fig.1).

Resonance curves were measured by standard EPR spectrometer (pumping frequency of 9.2GHz) at room temperature. The films were magnetized a parallel and a perpendicular to film plane up to 20 kOe. The $[Co_xNi_{1-x}]N$ films with thick 200-250 nm were obtained by the electroless deposition method, the thickness of individual layers was 18-25 nm.

The recorded SWR spectrums (fig.1) demonstrate exciting the spin waves. The measured system can be described within the bounds of existing potential hill. The critical wave vector $k_{critical}$ is $7.53 \cdot 10^5$ 1/cm.

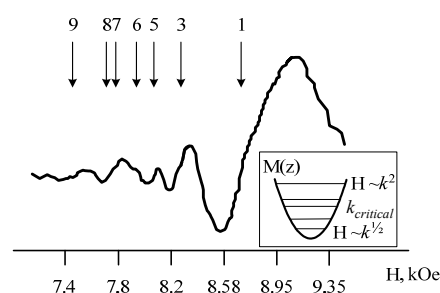


Fig. 1. Example of SWR spectrum

Support by regional start Autonomous institution “Krasnoyarsk regional Fund of support of scientific and scientific technical activity” also Russian Foundation for Basic Research, Grants № 16-03-00256 and № 16-03-00969 is acknowledged.

[1] C. Kittel, *Phys. Rev.*, **110** (1958) 1295-1297.

[2] A.M. Portis, *Appl. Phys.Let.*, **2** (1963) 69-71.

[3] V.A. Ignatchenko, D.S. Tsikalov, *Abstracts of VI Euro-Asian Symposium “Trends in MAGnetism”*, **1** (2016) 264.

2PO-K-47

BIOFUNCTIONALIZED MAGNETIC MICRODISCS APPLIED IN MEDICINE

*Smolyarova T.E.^{1,2}, Lukyanenko A.V.^{1,2}, Tarasov A.S.^{1,2}, Rautskii M.V.², Bondarev I.A.^{1,2},
Ovchinnikov S.G.^{1,2}, Volkov N.V.²*

¹ Institute of Engineering Physics and Radio Electronics, Siberian Federal University, Krasnoyarsk, Russia

² Kirensky Institute of Physics, Federal Research Center KSC SB RAS, Krasnoyarsk, Russia
smol_nano@iph.krasn.ru

Biocompatible magnetic microdiscs can be used in medicine for the treatment of malignant tumors [1]. These microdiscs are coated with gold (Au) and do not have a negative effect on the human body. Without the influence of the magnetic field, magnetic vortex is located in the center of the disc, when magnetic field is applied magnetic vortex shifts toward the increasing magnetization, creating an oscillation, which transmits mechanical force to the cell. Then this mechanical force is efficiently transduced to the membrane and after that to the subcellular components.

The final stage of the destruction of cells is their death. There are two forms of cell death: apoptosis and necrosis. Apoptosis is a genetically programmed active process that is triggered by physiological factors, when necrosis is a passive process that is the effect of the mechanical action on the cell. In apoptosis, the cell shrinks and breaks up into fragments surrounded by a plasma membrane (apoptotic bodies), which are absorbed by neighboring cells. As for necrosis, the cell membrane is destroyed and the contents of the cell pour out into the intercellular fluid, this leads to the development of inflammation and the neighboring cells are damaged.

So as the destruction of a malignant tumor always ends with apoptosis, it is necessary to regulate the magnitude of the frequency of the applied magnetic field.

We used a new approach to fabricate biocompatible microdiscs with a spin-vortex ground state. Dip-Pen Nanolithography (DPN) method is easy-to-use and it is flexible technique for fabrication of magnetic nanostructures. We used Au/Fe₃Si structure grown on Si(111) substrate [2] by molecular beam epitaxy (MBE) in extra-high vacuum on an atomically clean surface. In the experiment, by DPN method the ink (MHA-Acetonitrile) is deposited along the tracing path and diffuses away from the tip. This way we can form desired pattern, on a Fe₃Si/Si(111) substrate coated with Au. SiN probe, coated with ink was used in the experiment. By varying the dwell time, it is possible to create dots of various radii. We used 10 seconds for dwell time. Thus, this way structured array of 0.5- μ m-diameter magnetic microdiscs (dots) was fabricated.

The reported study was funded by Russian Foundation for Basic Research, Government of Krasnoyarsk Territory, Krasnoyarsk Region Science and Technology Support Fund.

[1] D.H. Kim et al., *J. Nature Materials*, **9** (2014) 165-171.

[2] S.W. Chung, A. Mirkin, H. Zhang, *J. Nano Lett*, **3** (2010) 43.

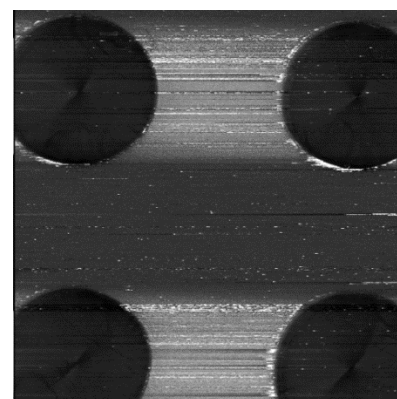


Fig. 1. Au/Fe₃Si magnetic microdiscs fabricated by DPN method.

2PO-K-48

TOPOLOGICALLY NONEQUIVALENT DOMAIN STRUCTURES NEAR MAGNETIC COMPENSATION TEMPERATURE IN IRON GARNET CRYSTALS

Pamyatnykh L.A.¹, Agafonov L.Y.¹, Belskii I.E.¹

¹ Ural Federal University, 51, Lenin Av., Ekaterinburg, Russia
Lev.Agafonov@urfu.ru

The change of the type of ordering of a domain structure (DS) from labyrinth-like to stripe-wise upon variation of the temperature was numerically simulated in [1] and theoretically considered in [2]. In these papers this change of ordering type was considered to be a topological phase transition (TPT).

In this paper, transitions between topologically nonequivalent DSs in thin single crystal layers of iron garnets with a magnetic compensation temperature are being studied experimentally.

The change of ordering of a domain structure from labyrinth-like to stripe-wise upon heating of a sample from a magnetic compensation temperature T_K is revealed. DS of a uniaxial iron garnet plate of composition $(\text{EuTbDy})_3\text{Fe}_5\text{O}_{12}$ (thickness $L = 50 \mu\text{m}$, quality factor $Q > 2$ for the studied temperature range) was revealed by means of a magneto-optical Faraday effect in the temperature range $175\div 300 \text{ K}$. A magnetic compensation is present at $T = 175 \text{ K}$.

Equilibrium DS for $T > T_K$ is shown in Fig 1(a, b). A labyrinth-like DS is observed in the initial demagnetized state at 200 K (Fig 1a). A distribution of local orientation of domain walls (DWs) that was obtained by means of digital processing is shown in the callout. This distribution is close to the isotropic one. The DS becomes more ordered upon increasing the temperature. At $T = 293 \text{ K}$, a regular stripe-wise DS with magnetic dislocations is observed (Fig 1b). In this case, DWs are mostly oriented along one direction (see distribution of DWs orientation in the callout). We interpret the described transformation of a DS from labyrinth-like to stripe-wise upon variation of the temperature as a TPT. The mechanism of this TPT is as follows. In a state of labyrinth-like DS, some number of disclinations are present (Fig 1(c-e)) (ends and branches). Those include both free (Fig 1(c, d)) and bound pairwise into dislocations (Fig 1e). In the temperature range of a TPT, heating shortens the average distance between ends and their nearest branches. Thus, most common type of topological defects in the DS changes from free disclinations to dislocations. A transition between topologically nonequivalent DSs becomes possible through vanishing of single disclinations.

The results of this research were obtained within basic part of the state assignment of the Russian Ministry of Education and Science (project No 3.6121.2017).

- [1] A.D. Stoycheva, S.J. Singer, *Physical Review E*, **65** (2002) 1–15.
[2] P.A. Prudkovskii, *JETP Lett.*, **98** (2013) 115–120.

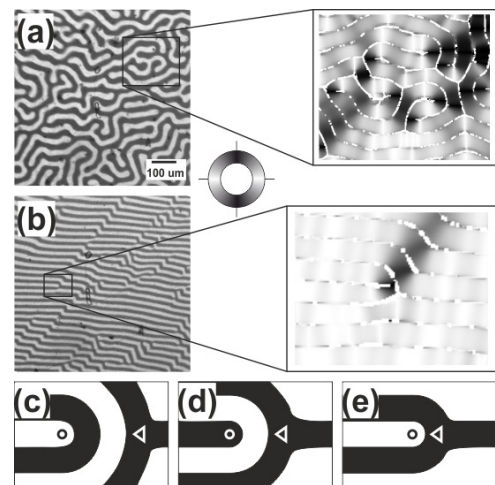


Fig. 1. (a,b) – equilibrium domain structure of an iron garnet crystal sample at temperatures 200 and 293 K, correspondingly, callouts show distributions of orientation of domain walls; (c-e) – a scheme showing how disclinations approach each other and form a dislocation upon increasing the temperature above the compensation point

3 July

Monday

09:30-11:00

plenary lectures
3PL-A

3PL-A-1

MAGNETS AS ENABLERS FOR RENEWABLE ENERGY AND RESOURCE EFFICIENCY

Gutfleisch O.¹

¹ Technische Universität Darmstadt, Darmstadt, 64287, Germany
gutfleisch@fm.tu-darmstadt.de

Magnetic materials are key components in energy related technologies, sensors and information technology. Magnets are inseparable from our everyday life. “Green” energy technologies such as wind turbines, electro-mobility and solid state cooling, heavily rely on high performance magnetic materials which have to be available in bulk quantities, at low-cost and with tailored magnetic hysteresis properties [1].

The realisation of these technologies is closely linked to the sustainable availability of the strategic metals for magnetism such as the group of rare earth elements (REE) namely Nd, Gd, Tb, Dy, transition metals such as Co, Ga, Ge, In, and the platinum group metals. Resource criticality is understood here as a concept to assess potentials and risks in using raw materials for certain technologies, and their functionality in emerging technologies. The concept of criticality of strategic metals is explained by looking at demand, sustainability and the reality of alternatives of rare earth elements [2].

There is an ever-growing demand for the benchmark high performance Nd-Fe-B magnets, most importantly for use in e-motor applications, for example, in all kinds of machinery, automatization and robotics in industry (Industry 4.0). The key question will be whether Nd-Fe-B needs to be and could be substituted substantially in some of the existing and upcoming competing technologies. The arrival of a more widespread use of e-mobility and wind energy and other smart magnet usages has yet to have its impact on this application field in terms of Nd demand. No substitute is at hand for the massive amounts of high-energy density magnet materials needed to run fast moving automated industrial machinery, and the demand is expected to rise for these kinds of applications. The same applies to e-motors in hybrid electric cars, where motor designers find highly limited construction space [2, 3]. There are different concepts for wind turbines, including those that require less or no permanent magnet materials. However, permanent magnet - so-called permanent magnet direct drive wind turbines - are far superior in terms of energy efficiency and maintenance cost and seem to be becoming the dominating type of machinery in Europe and worldwide [4].

Gas-vapour compression technology for refrigeration, heating, ventilation, and air-conditioning has remained unchallenged for more than 150 years. There is a huge demand for a smarter, more flexible and more efficient cooling technology. Magnetic refrigeration could be that alternative working without gas-based refrigerants. Energy spent for domestic cooling is expected to outreach that for heating worldwide over the course of the twenty-first century.

The talk will address these different global trends and will attempt to scale bridge these challenges by discussing the modelling, synthesis, characterization, and property evaluation of novel magnetic materials considering their micromagnetic length scales and phase transition characteristics [5,6].

[1] O. Gutfleisch, et.al., *Advanced Materials*, **23** (2011) 821–842.

[2] R. Gauss, G. Homm, O. Gutfleisch, *J. of Industrial Ecology*, DOI: 10.1111/jiec.12488. (2016).

[3] O. Gutfleisch, M.D. Kuz'min, J. Gassmann, R. Gauss, Int. Workshop on Rare Earth Magnets and their Applications, Annapolis, USA, August 2014.

[4] R. Gauss and O. Gutfleisch, Magnetische Materialien - Schlüsselkomponenten für neue Energietechnologien, in Rohstoffwirtschaft und gesellschaftliche Entwicklung, ed. P. Kausch und J. Matschullat, März 2016, Springer Spektrum Heidelberg, Springer-Verlag GmbH, ISBN 978-3-662-48854-6, pp. 99-118.

[5] K. Loewe, et.al., *Acta Materialia*, **124** (2017) 421-429.

[6] O. Gutfleisch, et.al., *Phil. Trans. R. Soc. A* 374: 20150308. <http://dx.doi.org/10.1098/rsta.2015.0308>. (2016).

3PL-A-2

CONSERVATION OF ANGULAR MOMENTUM AND SPIN CURRENTS IN SYSTEMS WITH SPIN-ORBIT TORQUESS

Demokritov S.O.^{1,2}

¹ Department of Physics, University of Muenster, 48149 Muenster, Germany

² Institute of Metal Physics, Ural Division of RAS, 620041 Yekaterinburg, Russia
demokrit@uni-muenster.de

Spin currents, the flow of angular momentum without the simultaneous transfer of electrical charge, play an enabling role in spintronics and magnonics. Recently a lot of efforts has been made to implement the concept of spin current for description of different dynamic phenomena in magnetic systems, including spin-torque- and spin-Hall nano-oscillators, domain wall motion, and spin wave propagation.

Injection of pure spin currents generated due to the spin Hall effect (SHE) has recently become recognized as an efficient route for the excitation of coherent magnetization auto-oscillations in magnetic nanostructures [1-7]. In contrast to the devices operated by spin-polarized electrical currents, spintronic devices driven by pure spin currents are expected to be less affected by the heating and electromigration effects caused by the charge flow through the active magnetic layer. Separation of charge and spin flows also eliminates a number of constraints on the geometry and thus on the magnetic characteristics of devices.

In addition to the SHE, pure spin currents can be also generated in nonlocal spin valve structures, where charge and spin currents are separated by providing an additional current path that bypasses the active magnetic layer. This approach eliminates the detrimental effects of layers with strong spin-orbital coupling, utilized in the SHE devices, on the dynamic damping in active magnetic layers.

Here we review our recent experiments on the excitation of magnetization auto-oscillations by injection of pure spin currents in SHE-based devices and in nonlocal spin valve structures. We show that nonlocal-spin-injection oscillators exhibit a number of unique features making them significantly more promising in comparison with the spin-Hall oscillators.

Finally, I analyze the flow of the angular momentum between the spin subsystem and the lattice and show that the common definition of the spin current in electrically insulating systems, that takes into account the exchange interaction only, results in qualitatively false statements in some important cases. Moreover, I show that the definition of spin superfluidity based on dissipationless spin currents should be revised. In this connection, I present and discuss a trivial, but pictorial system with a persistent, dissipationless spin current, which has nothing to do with spin superfluidity

- [1] V. E. Demidov, et al., *Phys. Rev. Lett.*, **107** (2011) 107204.
- [2] V. E. Demidov, et al., *Nature Materials*, **11** (2012) 1028.
- [3] V. E. Demidov et al., *Nature Commun.*, **5** (2014) 3179.
- [4] Z. Duan, et al., *Nature Commun.*, **5** (2014) 5616.
- [5] V. E. Demidov et al., *Appl. Phys. Lett.* **105** (2014), 172410.
- [6] V. E. Demidov et al. *Sci. Rep.*, **5** (2015) 8578.
- [7] S. Urazhdin et al. *Appl. Phys. Lett.*, **109** (2016) 162402.

3 July

Monday

11:30-13:00

14:30-17:00

oral session

3TL-A

3RP-A

**“Spintronics and
Magnetotransport”**

3TL-A-1

ENHANCEMENT OF THE EFFICIENCY OF SPIN TRANSFER TORQUE SWITCHING IN A PERPENDICULARLY MAGNETIZED FREE LAYER BY THE SECOND-ORDER UNIAXIAL MAGNETIC ANISOTROPY

Matsumoto R.¹, Arai H.^{1,2}, Yuasa S.¹, Imamura H.¹

¹ AIST, Spintronics Research Center, Tsukuba, Japan

² PRESTO, JST, Kawaguchi, Japan

rie-matsumoto@aist.go.jp

Second-order perpendicular magnetic anisotropy (K_{u2}) has been attracting a great deal of attention because faster spin-transfer-torque (STT) switching with higher STT-switching efficiency (κ) is theoretically expected [1] in the case of a conically magnetized free layer (c-FL) [2] compared with the case of a conventional perpendicularly magnetized free layer (p-FL) without K_{u2} . Here, κ is defined as $\kappa \equiv \Delta_0/I_{sw}$ where Δ_0 is the thermal stability factor and I_{sw} is switching current. In c-FL, the angle (θ) of a magnetization (\mathbf{m}) is tilted from z-direction (see inset in Fig. 1) due to the energetic competition between the first- and second-order magnetic anisotropies ($K_{u1,eff}$ and K_{u2}). κ of c-FL ($\kappa^{(c)}$) can be about 1.3 times larger than that of the conventional p-FL ($\kappa^{(p0)}$).

In this study [3], we theoretically expect the further enhancement of κ in p-FL with finite K_{u2} . The system we consider is illustrated in inset of Fig. 1. The magnetic energy density (g_L) and the effective potential (Φ) of the free layer is given by $g_L = K_{u1,eff} \sin^2 \theta + K_{u2} \sin^4 \theta$, and $\Phi = g_L + M_s (a_J/\alpha) \cos \theta$. Here, $K_{u1,eff}$ and K_{u2} are the first- and second-order magnetic anisotropy constants. In $K_{u1,eff}$, demagnetization energy is subtracted. M_s and α are the saturation magnetization and the Gilbert damping constant of the free layer. (a_J/α) represents the effective field by STT, and a_J is defined as $a_J = hIP/(4\pi eM_sV)$. h is the Planck constant, P is the spin polarization, I is the applied current, e (> 0) is the elementary charge, and V is the volume of the free layer. κ of the free layer can be calculated by analyzing Δ_0 as the energy barrier height in g_L , and by analyzing I_{sw} from the competition between STT and the damping torque with Φ .

The dependence of κ on $K_{u1,eff}$ and K_{u2} is shown in Fig. 1. Here, κ is normalized by $\kappa^{(p0)}$. r_K represents the ratio of K_{u2} to $K_{u1,eff}$, that is $r_K \equiv K_{u2}/K_{u1,eff}$. We assume $K_{u1,eff} \geq 0$. It should be noted that $\kappa/\kappa^{(p0)}$ is larger than unity for a positive r_K and takes a maximum value of $2^{1/2}$ at $r_K = 1$. The switching efficiency is maximized at $K_{u1,eff} = K_{u2}$. $\kappa/\kappa^{(p0)}$ in the p-FL with the positive K_{u2} can be larger than those in the p-FL without K_{u2} and in the c-FL.

This work was partially supported by JSPS KAKENHI Grant Number JP16K17509.

[1] R. Matsumoto et al., *Appl. Phys. Express*, **8** (2015) 063007.

[2] D. Apalkov and W. H. Butler, U.S. Patent No. 8,780,665 (15 July 2014).

[3] R. Matsumoto et al., *Phys. Rev. Applied*, **7** (2017) 044005.

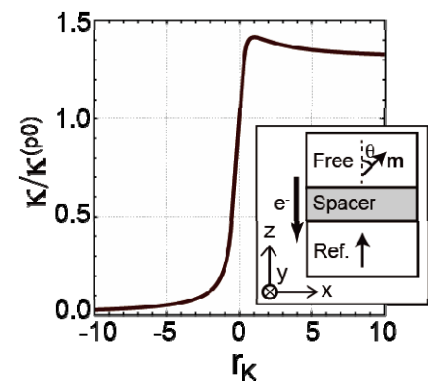


Fig. 1. r_K dependence of the normalized switching efficiency ($\kappa/\kappa^{(p0)}$). Inset: Schematic illustration of the system we considered. The positive I is defined as electrons (e^-) flowing from free layer to reference (Ref.) layer.

3TL-A-2

MAGNETORESISTANCE AND SPIN MANIPULATION FOR DEVICE APPLICATIONS

Yuasa S.¹

¹ National Institute of Advanced Industrial Science and Technology (AIST), Tsukuba, Japan
yuasa-s@aist.go.jp

This paper describes review and future prospects of basic technologies for spintronics and their applications to various electronic devices. As shown in Fig. 1, the giant TMR effect in MgO-based magnetic tunnel junction (MTJ) [1,2] is essential for various device applications today [3]. Concerning spin manipulation, spin-transfer torque (STT) [4-6] is the current main stream for device applications such as STT-MRAM [7,8], spin-torque oscillator (STO) [9,10], spin-torque diode (STD) [11] and physical random number generator (Spin Dice) [12]. Moreover, novel voltage-induced torque [13-15] is expected to be an ultimate technology for spin-manipulation due to its ultra-low power consumption. Perspectives and major challenges for next-generation devices will be discussed. This work was supported by the ImPACT Program of the Council for Science, Technology, and Innovation.

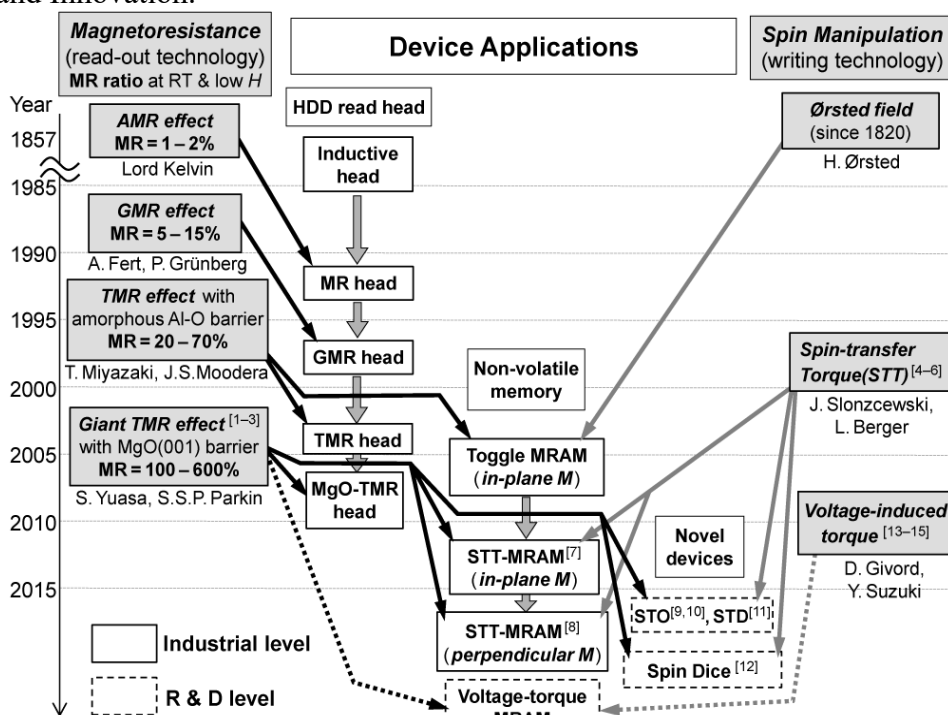


Figure 1. Basic phenomena for spintronics and their device applications.

- [1] S. Yuasa *et al.*, *Nature Mater.* **3**, 868 (2004). [2] S. S. P. Parkin *et al.*, *Nature Mater.* **3**, 862 (2004). [3] D. D. Djayaprawira *et al.*, *Appl. Phys. Lett.* **86**, 092502 (2005). [4] J. Slonczewski, *J. Magn. Magn. Mater.* **159**, L1 (1996). [5] L. Berger, *Phys. Rev. B* **54**, 9353 (1996). [6] J.A. Katine *et al.*, *Phys. Rev. Lett.* **84**, 3149 (2000). [7] M. Hosomi *et al.*, *IEDM Tech. Dig.* 19.1 (2005). [8] T. Kishi *et al.*, *IEDM Tech. Dig.* 12.6 (2008). [9] S. I. Kiselev *et al.*, *Nature* **425**, 380 (2013). [10] A. M. Deac *et al.*, *Nature Phys.* **4**, 803 (2008). [11] A.A. Tulapurkar *et al.*, *Nature* **438**, 339 (2005). [12] A. Fukushima *et al.*, *Appl. Phys. Express* **6**, 083001 (2014). [13] M. Weisheit *et al.*, *Science* **315**, 349 (2007). [14] T. Maruyama *et al.*, *Nat. Nanotech.* **4**, 158 (2009). [15] Y. Shiota *et al.*, *Nature Mater.* **11**, 39 (2012).

3TL-A-3

LATERAL NANO-SPINTRONIC DEVICES

Hirohata A.¹, Samiepour M.¹, Kim J.-Y.¹, Jackson E.¹, Abdullah R.M.¹, Murphy B.A.¹, Vick A.J.¹

¹ University of York, York, United Kingdom
atsufumi.hirohata@york.ac.uk

Recent advancement in nanofabrication and growth allows the utilisation of spin-polarised electrons in transport and dynamics, resulting in the development of spintronic devices [1]. In the spintronic devices, the key technologies are injection, manipulation and detection of spin-polarised electron in a non-magnetic media with high efficiency.

Conventionally such a spin-polarised electron current has been injected into a non-magnetic material by flowing an electrical current through a ferromagnetic layer. However, its spin polarisation is dependent upon the interfacial properties, such as conductance matching, junction resistance and interfacial resonant states. We have been investigated a series of lateral spin-valves to demonstrate their geometrical ratchet effect on spin-current signal amplification [2] and modulation [3].

To characterise their interfacial properties, we have developed a new method using scanning electron microscopy (SEM) [4]. The beam is then decelerated using a negative bias on sample stage so that the beam penetrates only to the depth of an embedded junction. The generated backscattered electrons are selected by an energy filter attached near the detector to map conductance information from the junction. This technique can be used for design and process optimisation of these junctions and can sustain an improvement in the density and functionality. As an example, a lateral spin-valve consisting of NiFe and Cu nanowires has been imaged as shown in Fig. 1(a). The image clearly indicates the presence of defects which are shown as the grey areas in Fig. 1(a). The junction was overloaded with current to create further defects and reimaged [see Fig 1(b)]. Many defects are formed in the damaged junctions. It is also possible that the top Cu wire may be detached from the bottom NiFe wire after junction breakdown. This is supported by the corresponding transport measurements. The black dots observed in the junction are defects which may be formed by means of detached interface.

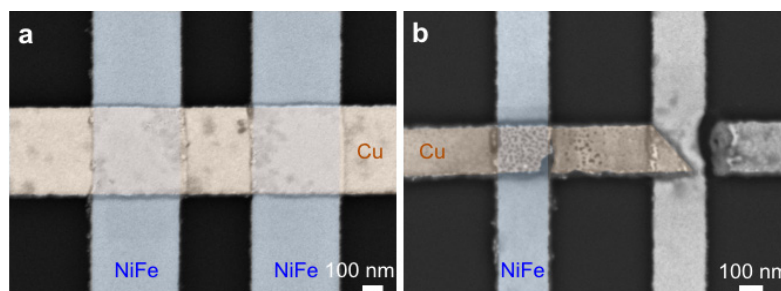


Fig. 1. (a) SEM image of a lateral spin-valve (b) SEM image of a damaged junction.

Support by EPSRC (EP/I000933/1 and EP/M02458X/1), Royal Society Industry Fellowship and JST-PRESTO is acknowledged.

[1] A. Hirohata and K. Takanashi, *J. Phys. D: Appl. Phys.*, **47** (2014) 193001.

[2] R. M. Abdullah *et al.*, *J. Phys. D: Appl. Phys.*, **47** (2014) 482001(FTC).

[3] B. A. Murphy *et al.*, *Sci. Rep.*, **6** (2016) 37398.

[4] A. Hirohata *et al.*, *Nat. Commun.*, **7** (2016) 12701.

3TL-A-4

MOLECULAR SPIN CROSSOVER PHENOMENON AT THE NANOSCALE MOTION AND SPINTRONIC PROPERTIES

Bousseksou A., Molnar G., Salmon L., Nicolazzi W.

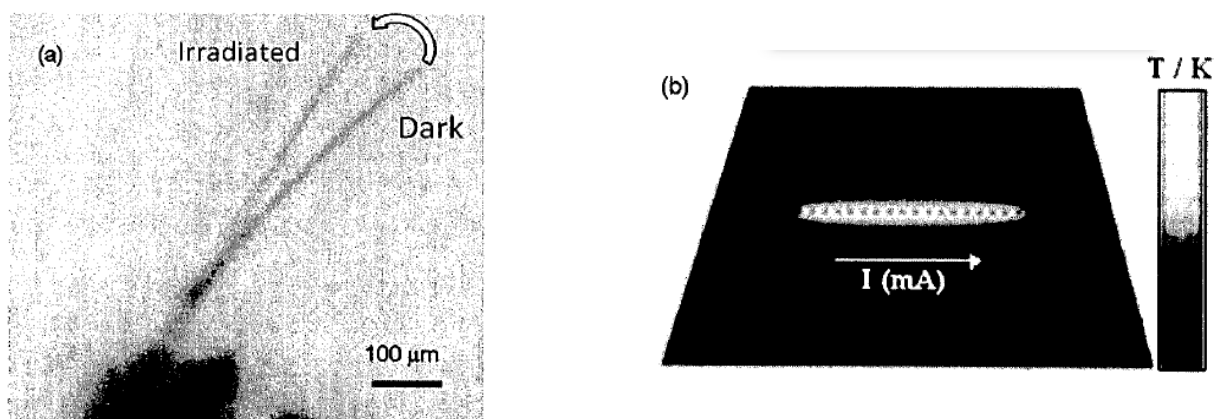
LCC/CNRS, Toulouse, France, boussek@lcc-toulouse.fr. www.lcc-toulouse.fr

azzedine.bousseksou@lcc-toulouse.fr

The spin crossover phenomenon in inorganic materials is one of the most spectacular examples of molecular bistability, which means that these molecules may exist in two different electronic states within a certain range of external perturbations. Most notably, the existence of a thermal hysteresis in certain complexes (in the solid state) confers a memory effect on these systems [1-4] we are particularly interested in the synthetic elaboration of nanometric thin films [5] and nano-sized patterns [6] that we obtain by electron beam lithography and in the application of an external perturbation in the hysteresis loop of spin crossover materials leading to an irreversible switching of their physical properties.⁴

Besides generating new fundamental knowledge on size-reduction effects and the dynamics of the spin crossover phenomenon, this research aims also at the development of practical applications such as sensors, nano- electronic, photonic, motion and nano-mechanical devices [1-12].

In this talk, we will discuss recent work in the field of molecule-based spin crossover materials with a special focus on these emerging issues, including nano-mechanical and spintronic properties.



(a) Comparison of the cantilever bending in the photo-induced high spin (HS) and low spin (LS) states for a $\{\text{Fe}(\text{3-CNpy})[\text{Au}(\text{CN})_2]_2\} \cdot 2/3\text{H}_2\text{O}$ based single crystal actuator [12-13]. (b) Luminescence modulation by high spin, low spin optical absorptions [9].

- [1] Bousseksou A. et al., *Chem. Soc. Rev.*, **40** (2011) 3313.
- [2] Bedoui S. et al., *Phys. Rev. Lett.*, **109** (2012) 135702.
- [4] Bonhommeau S. et al., *Angew. Chem. Int. Ed.*, **44** (2005) 4069-4073.
- [5] Cobo S. et al., *Angew. Chem. Int. Ed.*, **45** (2006) 5786-5789.
- [6] Molnar G. et al., *Adv. Mater.*, **19** (2007) 2163-2167.
- [7] Cobo S. et al., *JACS*, **130** (2008) 9019-9024.
- [8] Mahfoud T. et al., *JACS*, **131** (2009) 15049-15054.
- [9] Cobo S. et al., *J. NanoSci. Nanotech.*, **10** (2010) 5042-5050.
- [10] Lopes M. et al., *Nanoscale*, **5** (2013) 7762-7767.
- [11] Tran Quang Hung et al., *Angew. Chem. Int. Ed.*, **52** (2013) 1185-1188.
- [12] Helena J. Shepherd et al., *Nature Commun.*, **4** (2013) 2607.
- [13] Edna M. Hernández et al., *Adv. Mater.*, **26** (2014) 2889-2893.

3TL-A-5

FLEXIBLE MAGNETIC TUNNEL JUNCTIONS AND SPIN-ORBIT TORQUE DEVICES

Yang H.¹

¹ Department of Electrical and Computer Engineering, National University of Singapore, Singapore
eleyang@nus.edu.sg

The magnetic tunnel junction (MTJ) is a central element for the magnetoresistive random access memory (MRAM). We show that the tunneling magnetoresistance (TMR) of the MTJ is strongly influenced by strain in MTJs [1,2], and demonstrate flexible MTJs on various substrates [3], which can be utilized for future flexible MRAMs.

Current induced spin-orbit torques (SOTs) provide a new way to manipulate the magnetization in MTJs. We examine the role of oxygen bonding in Pt/CoFeB/MgO, and find that a full sign reversal of SOTs occurs as the oxygen bonding level increases, which evidences an interfacial SOT mechanism [4]. We show current induced SOTs from multilayer nanowires such as Co/Pd [5], Co/Tb [6], and Co/Ni [7]. SOTs in a topological insulator Bi₂Se₃ [8,9] as well as an oxide heterostructure LAO/STO [10] show the largest SOTs obtained to date, which may be able to generate strong spin currents to switch the magnetization in SOT-MRAM. Finally, we discuss the role of the Dzyaloshinskii-Moriya interaction [11] for spin orbit torque switching [12,13].

Support by NRF-Singapore is acknowledged.

- [1] A. Sahadevan et al., *Appl. Phys. Lett.*, **101** (2012) 042407.
- [2] L. M. Loong et al., *Sci. Rep.*, **4** (2014) 6505.
- [3] L. M. Loong et al., *Adv. Mat.*, **28** (2016) 4983.
- [4] X. Qiu et al., *Nat. Nanotechnol.*, **10** (2015) 333.
- [5] M. Jamali et al., *Phys. Rev. Lett.*, **111** (2013) 246602.
- [6] D. Bang et al., *Phys. Rev. B*, **93** (2016) 174424.
- [7] J. Yu et al., *Appl. Phys. Lett.*, **109** (2016) 042403.
- [8] P. Deorani et al., *Phys. Rev. B*, **90** (2014) 094403
- [9] Y. Wang et al., *Phys. Rev. Lett.*, **114** (2015) 257202.
- [10] K. Narayanapillai et al., *Appl. Phys. Lett.*, **105** (2014) 162405.
- [11] K. Di et al., *Phys. Rev. Lett.*, **114** (2015) 047201.
- [12] J. Yu et al., *Sci. Rep.*, **6** (2016) 32629.
- [13] W. Legrand et al., *Phys. Rev. Appl.*, **3** (2015) 064012.

3RP-A-6

LARGE SPIN-ORBIT TORQUE EFFICIENCY AT HEAVY METAL/MAGNETIC INSULATOR INTERFACES

Kalitsov A.^{1,2}, Mryasov O.^{1,2}

¹ Western Digital Technologies, Inc., San Jose, CA, 95131, USA

² MINT Center, University of Alabama, Tuscaloosa, AL, 35401, USA

Alan.kalitsov@wdc.com

Spin-orbit torque (SOT) represents a promising way to control the direction of magnetization in ferromagnetic materials. SOT arises at the interfaces between non-magnetic heavy metals (HM) and ferromagnetic metals (FM) when charge current flows parallel to their interfaces. SOT mechanism is generally attributed to spin Hall effect (SHE) that generates pure spin current in HM due to its strong spin-orbit coupling. Spin current from the HM layer penetrates into the FM layer exerting torque on it. To commercialize SOT based magnetic memory it is necessary to reduce switching current density that can be achieved by improving SOT efficiency. Recently it has been demonstrated experimentally that large SOT can be generated at the interface between Pt and BaFe₁₂O₁₉ magnetic insulator (MI) [1].

We develop a theoretical description of SOT in HM/MI bilayers. We identify two mechanisms contributing to SOT in HF/MI structures (i) SHE-associated SOT and (ii) magnetic proximity effect (MPE) associated SOT. Both SHE-associated and MPE-associated torques have same symmetry and the resulting total SOT consists of a damping-like torque (DLT) and a field-like torque (FLT) components. We extract the strength of both SOT components directly from experiment [1]

by comparing current dependent experimental coercivity of MI shown in Fig.1 (a) with its calculated values (Fig.1 (b)) obtained by numerical solution of the LLG equation within the macrospin approximation. Our numerical analyses shows that DLT is responsible for significant variation of current induced coercivity of MI. Moreover, SOT efficiency at HM/MI interface exceeds its values in HM/FM bilayers.

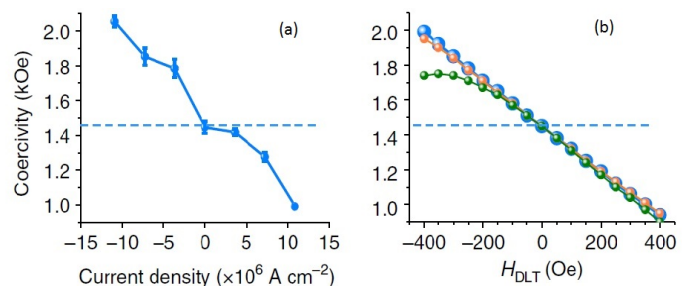


Fig. 1 (a). Experimental coercivity of magnetic insulator versus charge current density. (b) Calculated coercivity versus DLT field for different values of FLT field strength. $H_{FLT} = 0$ (blue), $H_{FLT} = H_{DLT}/2$ (orange), $H_{FLT} = H_{DLT}$ (green).

[1] P. Li, et. al., *Nature Commun.*, DOI: 10.1038/ncomms12688 (2016).

3RP-A-7

SPIN INJECTION IN ANTIFERROMAGNETS*Frangou L.¹, Forestier G.¹, Gladii O.¹, Auffret S.¹, Gambarelli S.², Baltz V.¹*¹ *SPINTEC (Univ. Grenoble Alpes / CNRS / INAC-CEA), F-38000 Grenoble, France*² *SYMMES (Univ. Grenoble Alpes / INAC-CEA), F-38000 Grenoble, France*

Lamprini.frangou@cea.fr and Vincent.baltz@cea.fr

Through spin-pumping experiments we investigated how spin currents can be injected, transmitted and converted in antiferromagnets and what is the influence of the magnetic order [1], [2], [3]. Spin pumping results from the magnetization dynamics of a ferromagnetic spin injector, which pumps a spin current into an adjacent spin sink. This spin sink filters, absorbs and converts the current to an extent which depends on its interface and bulk spin-dependent properties. This can be recorded either through the changes induced in ferromagnetic damping or through direct electrical means by measuring the inverse spin Hall effect. Whether the transport regime is electronic or magnonic depends of the electrical nature of the spin-sink and how strongly injector and sink are coupled. Due to magnetic coupling transfer/sink and propagation of spin angular momentum involves magnons from the oscillating ferromagnet feeding into the antiferromagnet. Measurements of the spin penetration were obtained for several antiferromagnetic metals and insulators. Interestingly, spins propagate more efficiently in layers where the magnetic order is fluctuating rather than static. Magnonic spin transport is also more efficient than its electronic counterpart. The experimental data were compared to some of the recently developed theories.

[1] L. Frangou, S. Oyarzún, S. Auffret, L. Vila, S. Gambarelli, and V. Baltz, *Phys. Rev. Lett.*, **116** (2016) 077203.

[2] L. Frangou, G. Forestier, S. Auffret, S. Gambarelli, and V. Baltz, *Phys. Rev. B*, **95** (2017) 054416.

[3] V. Baltz, A. Manchon, M. Tsoi, T. Moriyama, T. Ono, Y. Tserkovnyak, *arXiv:1606.04284*.

3TL-A-8

ANOMALOUS HALL EFFECT AND QUANTUM CRITICALITY IN $\text{Mn}_{1-x}\text{Fe}_x\text{Si}$ SOLID SOLUTIONS

Demishev S.V.^{1,2,3}, Lobanova I.I.¹, Glushkov V.V.^{1,2,3}

¹ Prokhorov General Physics Institute of RAS, 38 Vavilov str., 119991 Moscow,

² Moscow Institute of Physics and Technology, 9 Institutskiy lane, 141700 Dolgoprudny,
Moscow region, Russia

³ National Research University Higher School of Economics, Myasnitskaya street, 20, 101000
Moscow, Russia
demis@lt.gpi.ru

Studying the Hall effect in the quantum critical (QC) regime constitutes an important direction of research, which allows choosing between various scenarios of non-Fermi liquid behavior in various strongly correlated electron systems [1]. However, in the QC system $\text{Mn}_{1-x}\text{Fe}_x\text{Si}$, where the sequence of two quantum phase transitions at $x^* \sim 0.11$ and $x_c \sim 0.24$ corresponding to suppression of the long-range spiral magnetic order and short-range (spin-liquid like) magnetic order respectively was discovered [2], the realization of the Hall effect measurement and analysis faces immanent difficulties. For example, the recent study of the Hall effect in $\text{Mn}_{1-x}\text{Fe}_x\text{Si}$ has initiated a pessimistic conclusion that any correct Hall constant can hardly be estimated because the ordinary Hall Effect (OHE) in this system is much less than the anomalous Hall effect (AHE) [3]. Moreover the correct separation of the OHE and AHE contributions by application of a strong magnetic field is almost not possible as long as magnetization field dependence in $\text{Mn}_{1-x}\text{Fe}_x\text{Si}$ does not saturate up to 50T [3].

In the present work, the reliable determination of the OHE and AHE is shown to be possible by the implementation of the data analysis technique focused on the low magnetic field region in the paramagnetic (PM) phase of $\text{Mn}_{1-x}\text{Fe}_x\text{Si}$ ($x < 0.3$) [4,5]. Separating between different contributions to Hall effect reveals the skew-scattering dominating in the PM phase of $\text{Mn}_{1-x}\text{Fe}_x\text{Si}$ together with the OHE sign inversion associated with the hidden QC point $x^* \sim 0.11$ and confirms the existence of the crossover between the quantum critical and classical fluctuations in the PM phase as prognosticated earlier [1]. The discovered effective hole doping at intermediate Fe content leads to verifiable predictions in the field of fermiology, magnetic interactions and quantum criticality in $\text{Mn}_{1-x}\text{Fe}_x\text{Si}$ [5]. The change of electron and hole concentrations is considered as a “driving force” for tuning the QC regime in $\text{Mn}_{1-x}\text{Fe}_x\text{Si}$ via modifying of RKKY exchange interaction within the Heisenberg model of magnetism.

Authors are grateful to S.V. Grigoriev, N.M. Chubova and V.M. Dyadkin for providing the high-quality single crystals of $\text{Mn}_{1-x}\text{Fe}_x\text{Si}$. We would like to thank V.Yu. Ivanov for magnetization measurements and V.V. Voronov for X-ray analysis of the studied samples. This work was supported by programmes of Russian Academy of Sciences “Electron spin resonance, spin-dependent electronic effects and spin technologies”, “Electron correlations in strongly interacting systems”.

[1] S.V. Demishev, et al., *JETP Letters*, **98** (2013) 829.

[2] S. Paschen, et al., *Nature*, **432** (2004) 881.

[3] S.V. Demishev et al., *JETP Letters*, **104** (2016) 116.

[4] V.V. Glushkov et al., *JETP Letters*, **101** (2015) 459.

[5] V.V. Glushkov et al., *Phys. Rev. Letters*, **115** (2015) 256601.

3RP-A-9

MULTIPHYSICS AND MULTISCALE MODELING OF MRAM DEVICES USING TEM-MAG CODE

Knizhnik A.A.¹

¹ Kintech Lab Ltd, Moscow, Russia
knizhnik@kintechlab.com

In this work we present a description of a TEM-MAG software package for technology computer-aided design (TCAD) modelling of spintronic devices based on magnetic tunneling junctions (MTJ). Such devices are promising for development of next-generation of non-volatile memory devices with fast switching times and low-energy consumption.

The software package contains the multiphysics and multiscale model for description of magnetic dynamics and calculation of distributions of temperature, electrical current and mechanical stresses in spintronic devices taking into account their mutual interference (see Fig. 1). The model of magnetic dynamics includes a set of methods, starting from coarse-grained macrospin and granular methods and down to micromagnetics method.

We present the examples of application of this software package for solution of basic problems in development of magnetic memory (MRAM) spintronic devices. In particular, we consider a problem of scalability of field-induced switching (FIS-MRAM) and spin-torque switching (STT-MRAM) devices to smaller technology sizes. Moreover, we address the problem of calculation of critical parameters for switching of magnetization in spintronic devices and analysis of reliability of stored information in these devices. We also analyse magnetization switching in MRAM devices with temperature assisted switching (TAS), which use an exchange bias at a AF/FM interface to store information. Finally, we consider an example of interference between thermo-mechanical and magnetic properties of magnetic memory devices due to magnetoelastic coupling.

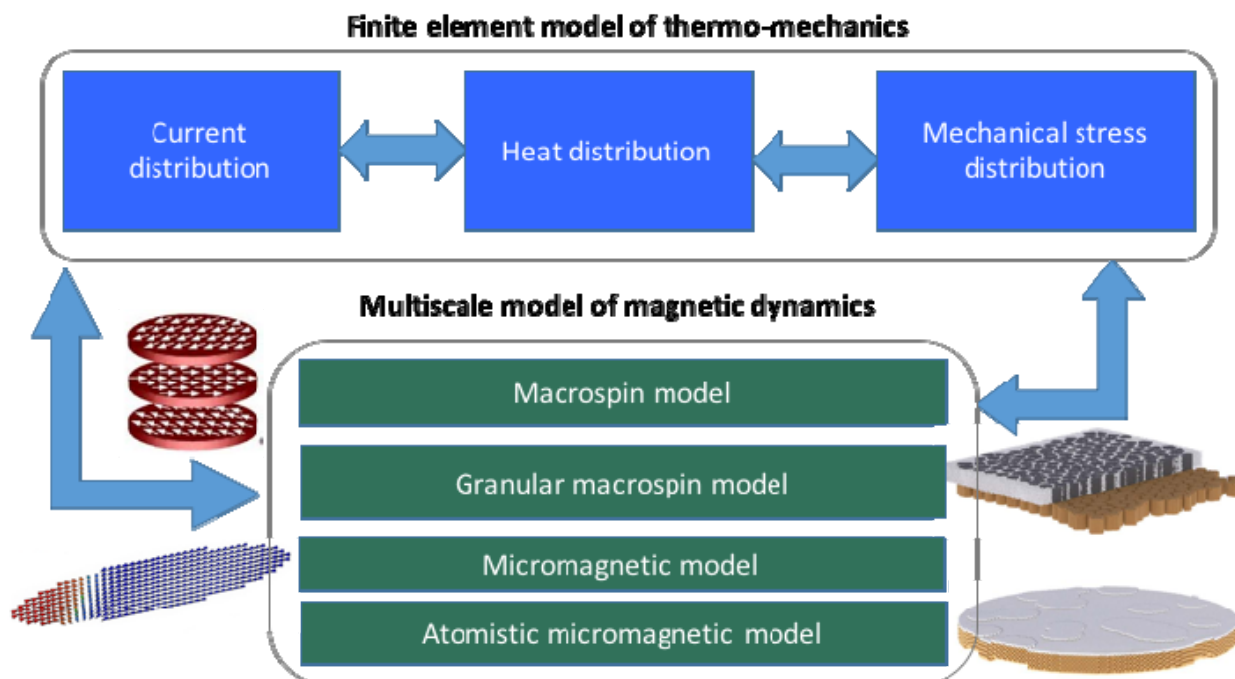


Fig. 1. Multiphysics and multiscale model of an MTJ-based spintronic nanodevice.

3RP-A-10

THE COMPETITION OF ANISOTROPY, EXCHANGE COUPLING, AND ZEEMAN ENERGIES IN PtCo/Ir/PtCo BILAYERS

Lvova G.L.^{1,2}, Talantsev A.D.^{1,2}, Hamadeh A.³, Morgunov R.B.^{1,2}, Dmitreev O.G.², Mangin S.³

¹ Institute of Problems of Chemical Physics, 142432, Chernogolovka, Moscow, Russia

² Tambov State Technical University, 392000, Tambov, Russia

³ Institut Jean Lamour, UMR 7198 CNRS, University de Lorraine, France

gale.l9vova@mail.ru

Exchange coupled ferromagnetic layers are known as synthetic antiferromagnets (SAF) are currently used in technologically relevant systems such as magnetic random access memories (MRAMs) and read heads for magnetic data storage [1]. Magnetic configurations in synthetic ferrimagnet PtCo/Ir/PtCo bilayer with strong perpendicular anisotropy have been systematically studied. Magnetization versus field hysteresis loop has been measured for different temperatures ranging from 5 to 300 K (Fig.1). The competition between anisotropy energies of down $E_{\text{d eff}}$ and upper $E_{\text{u eff}}$ layers, interlayer exchange coupling E_{EX} , and Zeeman energies E_{dZ} and E_{uZ} of the layers provides the sequence of the spin valve switching in external magnetic field. The sequence of the magnetization switching and correspondent shape of the hysteresis loop as well as prohibited and permitted transitions and their threshold magnetic fields controlled by competition of E_{EX} , E_{Z} , $E_{\text{d eff}}$ and $E_{\text{u eff}}$ values has been determined in our work.

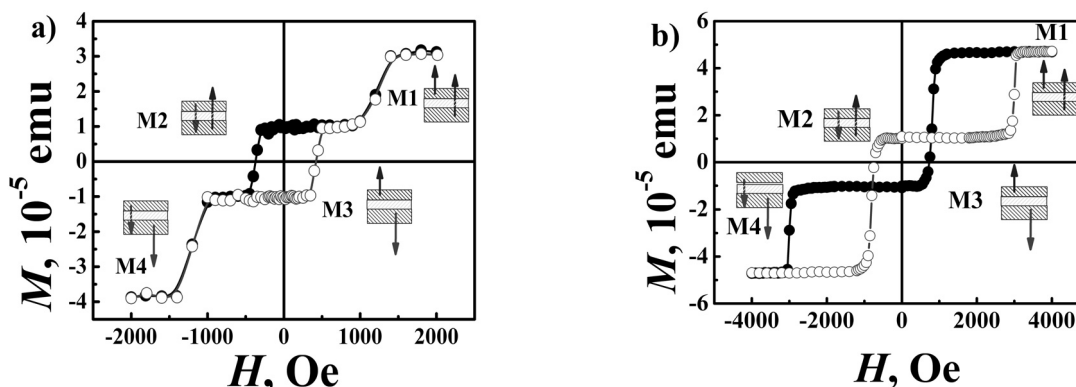


Figure 1. Magnetic hysteresis loops at 300 K (a) and 50 K (b). The arrows correspond to directions of magnetization of each PtCo layer. Black symbols corresponds to “up- down” sweep of the magnetic field, grey symbols corresponds to “down-up” sweep of the magnetic field.

These data allow us to estimate the exchange energy and magnetization reversal barriers at $T = 300$ K: $E_{\text{EX}} / S = 0.075$ erg/cm² (S – the interface area), $E_{\text{d eff}} / S = 3.1 \cdot 10^{-2}$ erg/cm², $E_{\text{u eff}} / S = 1.10^{-3}$ erg/cm². The decrease of temperature results in change of the type of hysteresis loop due to alteration of the energy balance.

The work was supported by grant 3.1992.2017/ПЧ in the frame of scientific program of Ministry of Education and Science "Scientific projects carrying out by scientific teams of research centers and(or) scientific laboratories of high education organizations"

[1] L. Cuchet, B. Rodmacq, S.Auffret, R.C. Sousa, I.L. Prejbeanu and B. Dieny, *Sci. Rep.*, **6** (2016) 21246.

3RP-A-11

MICROSCOPIC ORIGIN OF DZYALOSHINSKII-MORIYA INTERACTION*Ono T.*^{1,2}¹ Institute for Chemical Research, Kyoto University, Gokasho, Uji, Japan² Center for Spintronics Research Network (CSRN), Graduate School of Engineering Science, Osaka University, Japan
ono@scl.kyoto-u.ac.jp

Chiral interaction between two atomic spins with a neighboring atom due to a large spin orbit coupling, which is known as Dzyaloshinskii-Moriya interaction (DMI), has attracted intense interests [1, 2]. In particular, it has been elucidated that DMI at an interface of an ultra-thin ferromagnet/heavy metal bilayer has major role for formation of chiral spin textures such as the skyrmion and homochiral Neel-type domain wall [3-5], which are key phenomena for future information storage technology because of their scalability, thermal stability and efficiency. In spite of recent theoretical progress aiming at understanding the microscopic origin of the DMI [6, 7], an experimental investigation unravelling the physics at stake is still required. Here, we experimentally demonstrate the close correlation of the DMI with the anisotropy of the orbital magnetic moment and with the magnetic dipole moment of the ferromagnetic metal. The density functional theory and the tight-binding model calculations reveal that asymmetric electron occupation in orbitals gives rise to this correlation.

This work was partly supported by JSPS KAKENHI Grant Numbers 15H05702, 26870300, 26870304, 26103002, 25220604, Collaborative Research Program of the Institute for Chemical Research, Kyoto University, R & D project for ICT Key Technology of MEXT from the Japan Society for the Promotion of Science (JSPS), and the Cooperative Research Project Program of the Research Institute of Electrical Communication, Tohoku University. This work has also been performed with the approval of the SPring-8 Program Advisory Committee (Proposal Nos. 2015A0117, 2015A0125).

- [1] I. E. M. Dzyaloshinskii, *Sov. Phys. JETP*, **5** (1957) 1259.
- [2] T. Moriya, *Phys. Rev.*, **120** (1960) 91.
- [3] S. Emori *et al.*, *Nat. Mater.*, **12** (2013) 611.
- [4] K.-S. Ryu, *Nat. Nanotechnol.*, **8** (2013) 527.
- [5] K. Ueda *et al.*, *Appl. Phys. Express*, **7** (2014) 053006.
- [6] V. Kashid *et al.*, *Phys. Rev. B*, **90** (2014) 054412.
- [7] H. Yang *et al.*, *Phys. Rev. Lett.*, **115** (2015) 267210.

3 July

Monday

11:30-13:15

oral session

3TL-B

3OR-B

3RP-B

**“Diluted Magnetic
Semiconductors and
Oxides”**

3TL-B-1

**ORBITAL-SELECTIVE EFFECTS IN TRANSITION METAL COMPOUNDS:
“MOLECULES” IN SOLIDS AGAINST MAGNETISM***Khomsii D.I.*¹¹ II. Physikalisches Institut, Universität zu Köln, 50937 Köln, Germany
khomsii@ph2.uni-koeln.de

Close to Mott transition several novel states can appear. In particular, “molecular clusters” can be formed in the solid, such as dimers, trimers, etc. In my talk, I will illustrate such phenomena, especially dimer formation, on many examples (pyroxenes; $\text{La}_4\text{Ru}_2\text{O}_{10}$; Li_2RuO_3 ; M1 and M2 phases of VO_2 ; V and Cr hollandites). The concept of orbital-selective Peierls transitions will be proposed and justified. In systems containing structural metal dimers there may exist in the presence of different orbitals a special state with partial formation of singlets by electrons on one orbital, while others are effectively decoupled and may give e.g. long-range magnetic order or stay paramagnetic. Similar situation can be realized in dimers spontaneously formed at structural phase transitions, which can be called orbital-selective Peierls transition. This can occur in case of strongly nonuniform hopping integrals for different orbitals and small intra-atomic Hund's rule coupling J_H . Yet another consequence of this picture is that for odd number of electrons per dimer there exist competition between double exchange mechanism of ferromagnetism, and the formation of singlet dimer by electron on one orbital, with remaining electrons giving a net spin of a dimer. The first case is realized for strong Hund's rule coupling, typical for $3d$ compounds, whereas the second is more plausible for $4d$ - $5d$ compounds. We discuss some implications of these phenomena, and consider examples of real systems, in which orbital-selective phase seems to be realized.

[1] S.V. Streltsov, D.I.Khomsii, *PNAS*, **113** (2016) 10491.

3TL-B-2

EXCITONIC INSULATING PHASE IN CORRELATED MAGNETIC OXIDES

Ishihara S.¹, Tatsun T.¹, Nasu J.², Naka M.¹

¹ Department of Physics, Tohoku University, Sendai 980-8578, Japan

² Department of Physics, Tokyo Institute of Technology, Meguro, Tokyo 152- 8551, Japan
ishihara@cmpt.phys.tohoku.ac.jp

Excitonic condensation and excitonic-insulating (EI) state have been studied for a long time since 1960s. When the exciton binding energy exceeds the band-gap energy in semiconductors and semimetals, a macroscopic number of excitations exhibit a condensation. This phenomenon is regarded as a spontaneous quantum mechanical mixing of the conduction band and the valence band, in which one-body electron hoppings are prohibited due to the orbital and lattice symmetries. Recent intensive studies in the layered chalcogenide Ta₂NiSe₅ show that this material is a strong candidate for the EI phase. The perovskite cobalt oxides are another candidate materials for the EI state. A

In this talk, we study the EI system from the orbital physics viewpoint under the strong electron correlation.

(1) We analyse the effective model Hamiltonian derived from the two-orbital Hubbard model with a finite energy difference between the orbitals. The phase diagram at zero temperature is calculated by the mean-field approximation. Two kinds of the EI phases appear between the low-spin and high-spin phases. Magnetic structures are distinguished in the two EI phases: an antiferromagnetic order and a spin nematic order. The collective excitations in each phase are analyzed. The Goldstone modes emerge in the two EI phases. Not only the transverse magnetic modes but also the longitudinal magnetic modes are active in the EI phases.

(2) Magnetic field (H) effects on a correlated electron system with the spin-state degree of freedom are examined. Applying H to the low-spin (LS) phase induces the EI phase, as well as the spin-state ordered phase where the LS and high-spin (HS) states are ordered alternately. A rich variety of the phase diagrams are attributed to the spin-state degree of freedom and their combinations in the wave function as well as in the real-space configuration. Present results provide a possible interpretation for the recent experimental observation under the strong magnetic field in LaCoO₃ [3].

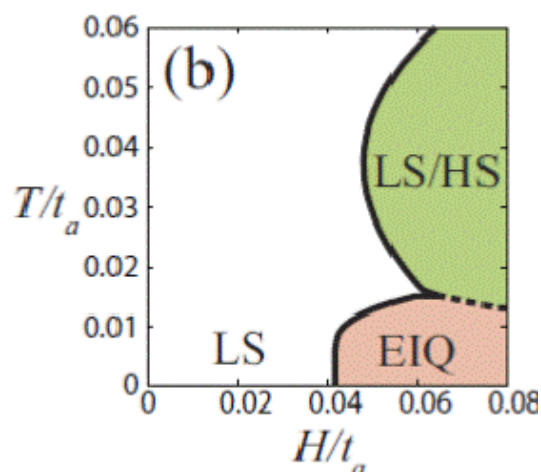


Fig. 1. Finite T phase diagram under H applied to the LS phase. LS/HS and EI represent a LS-HS ordered phase and the excitonic insulating phase, respectively [2].

[1] J. Nasu, T. Watanabe, M. Naka, S. Ishihara, *Phys. Rev. B*, **93** (2016) 205136.

[2] T. Tatsuno, E. Mizoguchi, J. Nasu, M. Nasu, S. Ishihara, *J. Phys. Soc. Jpn.*, **85** (2016) 083706.

[3] A. Ikeda, T. Nomura, S. Takeyama, Y. H. Matsuda, A. Matsuo, K. Kindo, K. Sato, *Phys. Rev. B*, **93** (2016) 220401(R).

3OR-B-3

VIBRONIC INTERACTION AS MAIN REASON OF MAGNETIC ORDERING IN INSULATING MANGANITES $R_{1-x}A_xMnO_3$

Gonchar L.E.^{1,2}, Nikiforov A.E.¹

¹ Ural Federal University, Yekaterinburg, Russia

² Ural State University of Railway Transport, Yekaterinburg, Russia
l.e.gonchar@urfu.ru

The insulating manganites $R_{1-x}A_xMnO_3$ (R^{3+} is a rare earth ion or Bi^{3+} , A^{2+} is alkaline earth ion, $x=0, 0.5, 0.667$) are known as system with strong correlation between crystal, charge, orbital and magnetic subsystems. Within the framework of linear vibronic interaction, the good agreement in description is reached only for pure manganite crystals $RMnO_3$ ($R=La, Pr, Nd$) [1]. This model has clear microscopic support. It could be qualitatively applied for any Jahn-Teller crystal using measured distances between orbitally-degenerated ion and its ligands [1, 2]. After definition of orbital state, the orbitally-dependent superexchange interaction model [1] could be applied to predict or describe the type of magnetic structure. However, in cases of doped manganites or $BiMnO_3$, that model needs further specification and additional terms [3].

The current work proposes semi-phenomenological model of orbital subsystem. The manganese ions in octahedral oxygen neighborhood have 5E -multiplet ground state with $|\theta\rangle, |\varepsilon\rangle$ eigenfunction. The effective e -type orbital operator for each Mn^{3+} ion (i) could be written as:

$$H_{eff}^i = \alpha_1^i X_\theta + \alpha_2^i X_\varepsilon, \quad (1)$$

where operators in matrix form are $X_\theta = \begin{pmatrix} -1 & 0 \\ 0 & 1 \end{pmatrix} \begin{matrix} \theta \\ \varepsilon \end{matrix}$; $X_\varepsilon = \begin{pmatrix} 0 & 1 \\ 1 & 0 \end{pmatrix} \begin{matrix} \theta \\ \varepsilon \end{matrix}$.

This model allows variation of only two parameters α_1^i, α_2^i for each degenerated manganese ion. They include main part – the linear vibronic interaction, and additional parts as long-range Coulomb fields or non-linear vibronic interactions. That is why one could define the orbital structure with respect of magnetic structure without explicit microscopic definition of non-linear and non-local terms.

To describe the experimental magnetic structure and to determine possible types of magnetic orderings, the model of orbitally-dependent exchange interaction is used [1, 3].

Using Eq. (1) Hamiltonian and crystal structure symmetry, the possible orbital structures of compounds $LaMnO_3$, $La_{0.5}Ca_{0.5}MnO_3$, $La_{0.333}Ca_{0.667}MnO_3$, and $BiMnO_3$ are considered. Taking into account the crystal, charge and orbital structures, the diagrams of possible magnetic structures depending on orbital functions mixing are drawn.

Support by Ministry of Education and Science of RF 3.9534.2017 is acknowledged.

[1] L.E. Gontchar, A.E. Nikiforov, *Phys. Rev. B*, **66** (2002) 014437.

[2] M. Snamina, A. Oles, *Phys. Rev. B*, **94** (2016) 214426.

[3] L.E. Gontchar, A.E. Nikiforov, *JMMM*, **300** (2006) e167-e170.

[4] L.E. Gonchar, A.E. Nikiforov, *Phys. Rev. B*, **88** (2013) 094401.

3RP-B-4

ROLE OF LOCAL GEOMETRY IN THE SPIN AND ORBITAL STRUCTURE OF TRANSITION METAL COMPOUNDS

Kugel K.I.^{1,2}, Khomskii D.I.³, Sboychakov A.O.¹, Streltsov S.V.^{4,5}

¹ Institute for Theoretical and Applied Electrodynamics, Russian Academy of Sciences, Moscow, 125412 Russia

² National Research University Higher School of Economics, Moscow, 109028 Russia

³ II. Physikalisches Institut, Universität zu Köln, Köln, 50937 Germany

⁴ Mikheev Institute of Metal Physics, Ural Branch, Russian Academy of Sciences, Ekaterinburg, 620990 Russia

⁵ Ural Federal University, Ekaterinburg, 620002 Russia

kugel@orc.ru

We analyze the role of local geometry in the spin and orbital interaction in transition metal compounds with orbital degeneracy. We stress that the tendency observed for the most studied case (transition metals in O_6 octahedra with one common oxygen – common corner of neighboring octahedra and with $\sim 180^\circ$ metal–oxygen–metal bonds), that ferro-orbital ordering renders antiferro-spin coupling, and, *vice versa*, antiferro-orbitals give ferro-spin ordering, is not valid in general case, in particular for octahedra with common edge and with $\sim 90^\circ$ M–O–M bonds. Special attention is paid to the "third case", neighboring octahedra with common face (three common oxygens) – the case practically not treated until now, although there are many real systems with this geometry. Interestingly enough, the spin–orbital exchange in this case turns out to be simpler and more symmetric than in the first two cases. We also consider which form the effective exchange takes for different geometries in case of strong spin–orbit coupling. Again, the situation for systems with a common face turns out to be simpler also for the strong spin–orbit coupling. Here, the exchange for Kramers doublets $j = 1/2$ has the symmetric Heisenberg-type form, where j corresponds to some entangled state of spin and orbital variables.

[1] K.I. Kugel, D.I. Khomskii, A.O. Sboychakov, S.V. Streltsov, *Phys. Rev. B*, **91** (2015) 155125.

[2] D.I. Khomskii, K.I. Kugel, A.O. Sboychakov, S.V. Streltsov, *Zh. Eksp. Teor. Fiz.*, **149** (2016) 562–577 [*JETP*, **122** (2016) 484–498].

3RP-B-5

LATTICE COMPLEXITY NEAR A LIFSHITZ TRANSITION IN STRONGLY CORRELATED SYSTEMS

Bianconi A.^{1,2,3}, *Campi G.*², *Ivanov V.G.*³, *Ivanov A.A.*³, *Menushenkov A.P.*³

¹ Rome International Center for Materials Science Superstripes (RICMASS), 00185 Rome, Italy

² Institute of Crystallography, CNR, Monterotondo Scalo, 00015 Rome, Italy

³ National Research Nuclear University MEPhI, 115409 Moscow, Russia

antonio.bianconi@ricmass.eu

The physics of complex doped magnetic systems is attracting a wide interest and it is object of active discussions while new functional materials are developed and used in modern nanotechnology. The multiscale lattice and electronic complexity from nanoscale to mesoscale in these systems push the fundamental physics of these systems beyond the physics of twentieth century based on simple models using for example single band and rigid lattice and rigid band approximations. Here, we show that the physics of all known high-temperature superconductors is characterized by a dome of T_c controlled by tuning the chemical potential near the Lifshitz transitions in strongly correlated systems [1-4] by pressure, strain, and charge density [5,6]. A major step in the field has been the prediction of frustrated phase separation occurring at the Lifshitz transitions [1-3], which has been observed by using scanning micro X-ray diffraction in cuprates [7] and using EXAFS method [8] in cuprates [9], iron based superconductors [10], and recently in BaPbBiO systems. Finally, we discuss the emerging role of Fano resonances and complex hyperbolic space for the percolation pathways in this complex scenario for the emergence of quantum coherence at high temperatures.

- [1] K. I. Kugel, A. L. Rakhmanov, A. O. Sboychakov, N. Poccia, and A. Bianconi, *Phys. Rev. B*, **78** (2008) 165124.
- [2] K. I. Kugel, A. L. Rakhmanov, A. O. Sboychakov, F. V. Kusmartsev, N. Poccia, and A. Bianconi, *Supercond. Sci. Techn.*, **22** (2009) 014007.
- [3] A. Bianconi, N. Poccia, A. O. Sboychakov, A. L. Rakhmanov, and K. I. Kugel, *Supercond. Sci. Techn.*, **28** (2015) 024005.
- [4] R. Caivano et al., *Supercond. Sci. Techn.*, **22** (2009) 014004.
- [5] A. Bianconi, *Nature Phys.*, **9** (2013) 536-537.
- [6] M. Fratini et al., *Supercond. Sci. Techn.*, **21** (2008) 092002.
- [7] G. Campi et al., *Nature*, **525** (2015) 359.
- [8] A. Bianconi and R. Z. Bachrach, *Phys. Rev. Lett.*, **42** (1979) 104.
- [9] A. Bianconi, et al., *Phys. Rev. Lett.*, **76** (1996) 3412.
- [10] V. G. Ivanov, A. A. Ivanov, A. P. Menushenkov, B. Joseph, and A. Bianconi, *J. Supercond. Novel Magn.*, **29** (2016) 3035.

3 July

Monday

11:30-13:00

14:30-17:30

oral session

3TL-D

3OR-D

3RP-D

**“Magnetism and
Superconductivity”**

3TL-D-1

SPONTANEOUS SPIN MAGNETIZATION OF TWO-DIMENSIONAL CORRELATED ELECTRON SYSTEM

Pudalov V.M.^{1,2}, Kuntsevich A.Yu.^{1,2}, Morgun L.A.¹, Reznikov M.³

¹ P.N. Lebedev Physical Institute of the RAS, Moscow, Russia

² National Research University Higher School of Economics, Moscow, Russia

³ Solid State Institute, Technion, Haifa, Israel

pudalov@lebedev.ru

An interacting low-density electron system residing in a purely nonmagnetic host lattice has a tendency to magnetic ordering. The latter is determined by the interplay of the Coulomb interaction and Pauli principle. As carrier density n decreases, the ratio r_s between the interaction and kinetic Fermi energies increases pushing the system towards a ferromagnetic instability. Numerical simulations for a clean single-valley 2D electron system (2DES) predict Bloch instability at $r_s \approx 25$ followed by Wigner crystallization at $r_s \approx 37$, whereas a clean two-valley system is believed to be stable against spontaneous spin polarization.

Thus far the ground state spin arrangement of the correlated electron system remained unsettled both for its liquid and solid state. Our spin magnetization [1,2] and transport measurements [3], performed in weak in-plane magnetic field [1,3] $B < k_B T / g \mu_B$, have addressed this issue experimentally.

When magnetic field is applied in the 2D plane, it couples to electron spins solely. We measured the thermodynamic spin magnetization per electron $(\partial M / \partial n) = -(\partial \mu / \partial B)$ from response of the chemical potential μ of the 2D electron layer to weak magnetic field. The main result of the thermodynamic measurements [1] is the observation of “spin- droplets”—spin polarized collective electron states with a total spin of the order of 2. These easily polarized “nanomagnets” exist as a minority phase on the background of the majority Fermi liquid phase even though the density and the dimensionless conductance are high, $k_F l \sim 100 \gg 1$. Note, that the localized electrons in doped semiconductors are known to align spins antiparallel.

The spin droplets contain $N=4$ or more electrons; their average number N (and the droplet size) does not change with density or temperature. What changes is the total amount of the droplets in the 2D system. This causes the spin susceptibility χ to diverge $\propto T^{-2}$ in the $T=0$ limit. With temperature or density increasing, the spin droplets gradually disappear (“melt”). As a result, the derivative $d\chi/dn$ changes sign, showing a critical behavior on the $(T-n)$ plane [1,3]. The density-dependent temperature T^* (where $d\chi/dn$ changes sign) signifies a novel energy scale [3] originating from the phase separation in 2D. T^* is smaller than the Fermi temperature T_F ; obviously, no such large energy scale may exist in the single-phase Fermi liquid. T^* reveals itself [3] (i) in the weak in-plane field magnetotransport, (ii) in the zero field transport, and (iii) in the spin magnetization M . All these features are explained qualitatively in the framework of the two-phase state of the electronic system [3].

Support by RSCF (16-42-01100) is acknowledged.

[1] N.Teneh, A.Yu.Kuntsevich, V.M. Pudalov, M.Reznikov, *Phys.Rev.Lett.*, **109** (2012) 226403.

[2] V.M.Pudalov, A.Yu.Kuntsevich, I.S.Burmistrov, M. Reznikov, *J.Low Temp.Phys.*, **181**(3,4) (2015) 99.

[3] L.A.Morgun, A.Yu.Kuntsevich, V.M.Pudalov, *Phys. Rev. B*, **93** (2016) 235145.

3TL-D-2

SUPERCONDUCTING PROXIMITY EFFECTS IN THE NIOBIUM/ERBIUM SYSTEM

Satchell N.^{1,2}, Witt J.D.S.¹, Flokstra M.G.³, Lee S.L.³, Cooper J.F.K.², Kinane C.J.², Langridge S.², Burnell G.¹

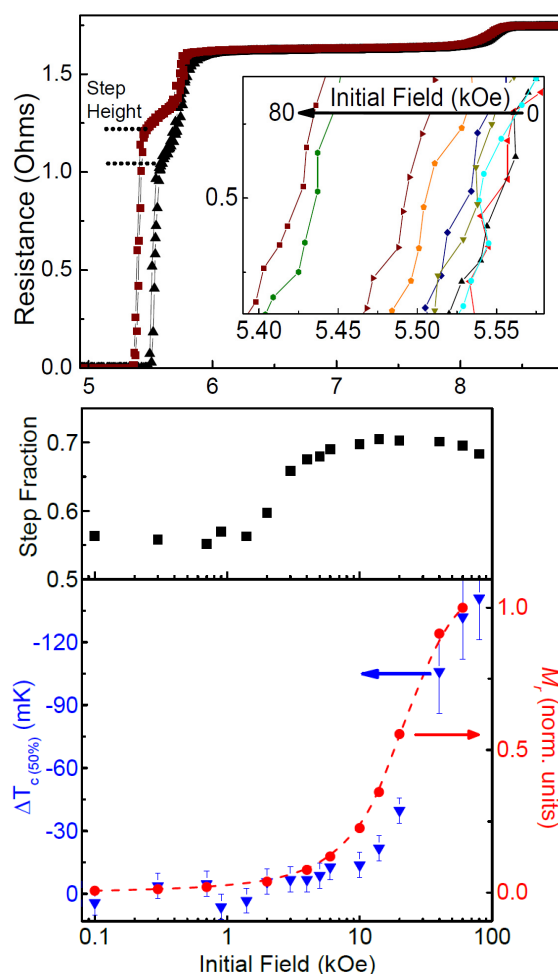
¹ School of Physics and Astronomy, University of Leeds, Leeds, LS2 9JT, United Kingdom

² STFC Rutherford Appleton Labs, Chilton, Didcot, Oxon, OX11 0QX, United Kingdom

³ School of Physics and Astronomy, SUPA, University of St Andrews, St Andrews, KY16 9SS, United Kingdom

G.Burnell@leeds.ac.uk

Hybrid superconductor/ferromagnet (S/F) heterostructures provide an exciting potential new class of device based around superconducting spintronics. The prototypical super-spintronic device is the superconducting spin-valve, where the critical temperature, T_c , of the S-layer can be controlled by the relative orientation of two (or more) F-layers. Such structures have been studied for over 15 years for switching between parallel and anti-parallel magnetic configurations, and for the last 7 years in non-collinear orientations where a spin-triplet, odd frequency state can be generated. Such devices are being actively developed to form cryogenic memory elements as a complement to RSFQ superconducting logic. Notwithstanding this, the changes in critical temperature typically observed are rather small, of the order of 10s mK. Unless high spin-polarised materials are utilised. Here, we show that a similar control is also possible in a simple S/F bilayer where the F layer is an intrinsically non-collinear ferromagnet. Using field history to set the remanent magnetic state of a thin Er layer, we demonstrate for a Nb/Er bilayer a high level of control of both T_c and the shape of the resistive transition, $R(T)$, to zero resistance. We are able to model the origin of the remanent magnetization, treating it as an increase in the effective exchange field of the ferromagnet and link this, using conventional S/F theory, to the suppression of T_c . We observe stepped features in the $R(T)$ which we argue is due to a fundamental interaction of superconductivity with inhomogeneous ferromagnetism, a phenomena currently lacking theoretical description.



Support by the UK EPSRC (grant numbers: EP/J010634/1, EP/J010650/1, EP/J01060X/1 & EP/I031014/1) for their financial support. NS acknowledges JEOL Europe and ISIS neutron and muon source for PhD funding

3TL-D-3

SUPERCONDUCTING NANOWIRES UNDER FERROMAGNETIC PROXIMITY EFFECT

Petrashov V.T.¹, Wren T.¹, Marsh R.¹, Wells J.¹, Shelly C.¹

¹ Royal Holloway, University of London, Egham, Surrey TW20 0EX, UK
v.petrashov@rhul.ac.uk

We report on experimental and theoretical studies of electron transport in hybrids consisting of superconducting nanowires, S, with segments S' where the wires overlay nanoscale ferromagnets electrically contacting them. We find that while the BCS energy gap in the proximity-to-ferromagnets S' segments can be strongly suppressed by the ferromagnetic proximity effect making them normal, the superconductivity can be recovered via coherent Andreev reflections of quasiparticles at the interfaces between proximity S' and plain S segments.

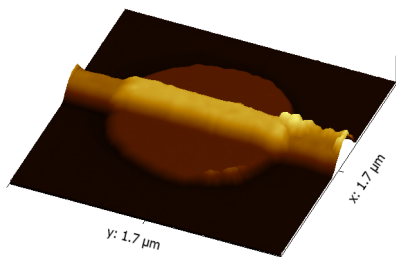


Fig. 1. Superconducting nanowires overlaying ferromagnetic disk

We present a detailed study of critical current-temperature phase diagram of the system at different dimensions and geometries of the nanoscale ferromagnets. The magnetic structure of nanoscale ferromagnets was investigated using Magnetic Force Microscopy. We show that superconductivity in S' depends on the magnetic structure of the nanoscale magnets.

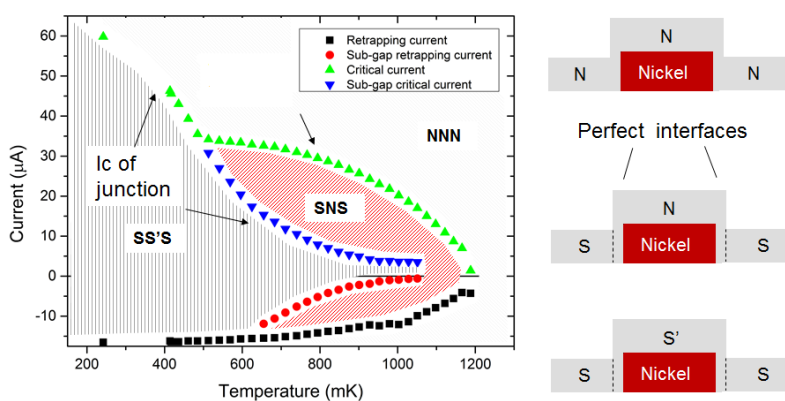


Fig. 2. Phase diagram

We observe strong long range critical current suppression in S when S' segment goes to the resistive state. We explain the suppression as due to the Joule heating of quasiparticles mainly. Based on the study we have developed a novel type of hybrid superconducting quantum interference device (HyQUID) that has great potential as a sensitive vector magnetometer.

3RP-D-4

REVERSING DIRECTION OF SUPERCURRENT CIRCULATION IN SF SANDWICH WITH ABRIKOSOV VORTEX

Bakurskiy S.V.^{1,3,4}, Golubov A.A.^{1,2}, Kupriyanov M.Yu.^{1,3,4}, Khapaev M.M.^{1,5}

¹ Moscow Institute of Physics and Technology, Dolgoprudny, Moscow Region, 141700, Russia

² Faculty of Science and Technology and MESA+ Institute for Nanotechnology, University of Twente, 7500 AE Enschede, The Netherlands

³ Skobeltsyn Institute of Nuclear Physics, Lomonosov Moscow State University, Leninskie gory, Moscow 119991, Russia

⁴ National University of Science and Technology MISIS, 4 Leninsky prosp., Moscow, Russia

⁵ Department of Numerical Methods, Lomonosov Moscow State University, 119992, Leninskie gory, Moscow, Russia
mkupr@pn.sinp.msu.ru

It is well known that the critical temperature, T_C , of superconductor-ferromagnetic (SF) sandwiches and critical current, I_C , of Josephson SFS junctions are nonmonotonic functions of thickness, d_F , of the ferromagnetic layer. It should be noted that these theoretical predictions were obtained in structures, which are homogeneous along SF interfaces. Should we expect similar effects in the two-dimensional case, when the superconducting correlations depend on the spatial coordinates along an SF interface is still an open question.

Abrikosov vortex is one of example providing such an inhomogeneity. We demonstrate that non-monotonic alterations in the structure of Abrikosov vortex in SF sandwich are indeed possible. We show that by varying the exchange energy, E , in an F layer or by varying S/F interface transparency one can achieve vortex current reversal in the F-layer.

We consider SF bilayer in external magnetic field, H , oriented perpendicular to the plane of the bilayer. We assume that the conditions of dirty limit are valid for films and pair potential, Δ , is zero in the F layer, which is supposed to be a single domain ferromagnet with out-of-plane direction of its easy axis. To define the coordinate dependence of the Green's function we replace hexagonal vortex unit cell on a circular one. In the frame of Usadel equations we demonstrate that in the limit of small d_F an increase of E or suppression parameter γ_{BM} results in reversing direction of supercurrent circulation around a vortex core in the F layer compared to that in the S-film. We performed numerical calculations of the supercurrent within the vortex unit cell in the F-layer (see Fig.1) for different values of γ_{BM} , $E/2\pi T_C = 2$, $T/T_C = 0,2$ and $H/H_{C2} = 0,01$. Calculations carried out for finite values of d_F confirm the findings obtained in the limit of small d_F .

The developed numerical algorithms were supported by the Project No. 15-12-30030 from Russian Science Foundation. This work was also supported in part by the Ministry of Education and Science of the Russian Federation in the framework of Increase Competitiveness Program of NUST MISiS (research project 2-2016-051).

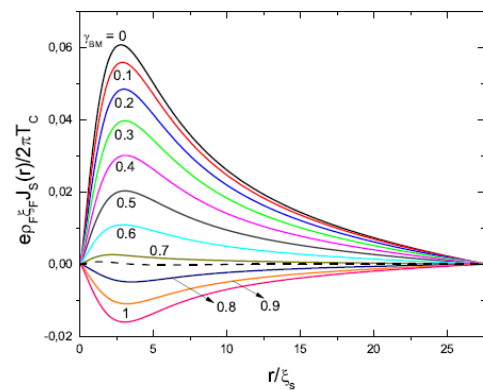


Fig. 1. The spatial distribution of the supercurrent within the vortex unit cell in the F part of SF bilayer for $T = 0.2T_C$, $E = 2\pi T_C$ and for various values of the suppression parameter γ_{BM} . The dashed line corresponds to $\gamma_{BM} \approx 0.73$ □

3OR-D-5

MULTI-VALUED CURRENT PHASE RELATIONS IN JOSEPHSON JUNCTION WITH COMPLEX -ISF- INTERLAYER

*Bakurskiy S.V.^{1,2,4}, Filippov V.I.³, Ruzhickiy V.I.³, Klenov N.V.^{3,1}, Soloviev I.I.^{2,1},
Kupriyanov M.Yu.^{2,1}, Golubov A.A.^{1,5}*

¹ Moscow Institute of Physics and Technology, 141700 Dolgoprudniy, Russia

² Skobeltsyn Institute of Nuclear Physics, Lomonosov MSU, 119991 Moscow, Russia

³ Physics Department, Lomonosov MSU, 119991 Moscow, Russia

⁴ MISIS, 4 Leninsky prosp., Moscow, 119049, Russia

⁵ Faculty of Science and Technology, University of Twente, 7522 NB Enschede, Netherlands
r4zz@mail.ru

Hybrid structures with ferromagnetic F and superconducting S layers are the subjects of intensive research in the recent years. Among them, SIsFS junctions with complex insulator-superconductor-ferromagnetic interlayers belong to most promising structures for implementation in electronic circuits. They provide high performance on the level of tunnel SIS junctions and conserve magnetic features of SFS junctions. However, some unexplored features still remain in SIsFS structures.

Recent theoretical [1] and experimental [2] studies indicated a peculiar behaviour of SIsFS structures in the vicinity of $0-\pi$ transition. The typical dip on $I_C(d_F)$ and $I_C(T)$ dependence disappears at low temperatures and sufficiently large s-layer thickness. We study the reasons of this phenomenon in terms of complicated current-phase relations (CPR).

We consider the CPR in the Josephson junctions in the vicinity of $0-\pi$ transition [3]. We find a strong impact of the second harmonic on CPR of the junctions. It is shown that the critical current can be kept constant in the region of $0-\pi$ transition, while the CPR transforms through multi-valued hysteretic states depending on the relative values of tunnel transparency and magnetic thickness. Moreover, CPR in the transition region has multiple branches with distinct ground states. These states can find practical application during development of Josephson phase memory devices.

This work was supported in part by the Project No. 15-12-30030 from Russian Science Foundation, Ministry of Education and Science of the Russian Federation in the framework of Increase Competitiveness Program of NUST "MISiS" (research project K2-2016-051) and grant number MK-5813.2016.2 and by RFBR grants 17-52 560003Iran-a and 16-29-09515-ofi-m.

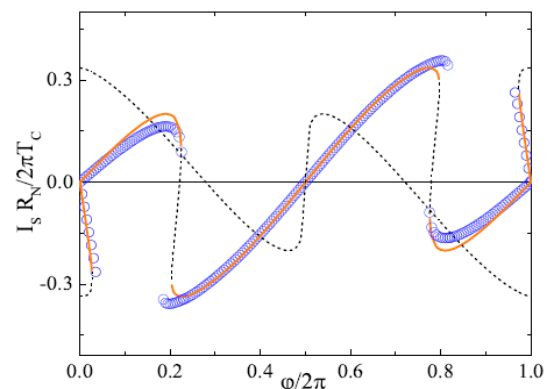


Fig. 1. Current-phase relation of the SIsFS junction in the vicinity of $0-\pi$ transition calculated in the frame of the Usadel equations (open circles) and lumped junctions model (the solid and the dashed lines are stable and unstable parts of solution, respectively).

[1] S. V. Bakurskiy, N. V. Klenov, I. I. Soloviev, M. Yu. Kupriyanov, A. A. Golubov, *Phys. Rev. B*, **88** (2013) 144519.

[2] N. Ruppelt, H. Sickinger, R. Menditto, E. Goldobin, D. Koelle, R. Kleiner, O. Vavra, H. Kohlstedt, *Appl. Phys. Lett.*, **106** (2015) 022602.

[3] S. V. Bakurskiy, V.I. Filippov, V.I. Ruzhickiy, N.V. Klenov, I. I. Soloviev, M.Yu. Kupriyanov, A.A. Golubov, arXiv:1703.04116: (2017).

3OR-D-6

INVERTED ADIABATIC QUANTUM FLUX PARAMETRON SHUNTED BY MAGNETIC JOSEPHSON JUNCTION

Schegolev A.E.^{1,2,4}, Soloviev I.I.³⁻⁵, Klenov N.V.¹⁻⁵, Tereshonok M.V.^{2,4}

¹ Lomonosov Moscow State University, Physics Faculty, Moscow, Russia

² Moscow Technical University of Communications and Informatics (MTUCI), Moscow, Russia

³ Lomonosov Moscow State University Skobeltsyn Institute of Nuclear Physics, Moscow, Russia

⁴ Moscow Technological University (MIREA), Moscow, Russian Federation

⁵ Moscow Institute of Physics and Technology, State University, Dolgoprudniy, Moscow region, Russia

igor.soloviev@gmail.com

In our work we consider modified Adiabatic Quantum Flux Parametron (AQFP) cell shunted by magnetic Josephson junction with additional phase shift equal to π (π -junction with ferromagnetic layer in the weak link area) and with swapped signal and clock generators in superconducting state (Fig. 1). This cell can be also treated as bi-SQUID cell with shunted geometric inductance and parameters, optimized for inclusion in the superconducting adiabatic logic circuits [1-3]. Important characteristic of this cell is a phase gain characteristic which shows output-to-input signals ratio (Fig. 2). Additional contact allows to reach both high output-to-input signals ratio (higher than the one of simple AQFP or bi-SQUID) with wide range of amplification and smooth trajectory of the system evolution which guarantee adiabatically switching (Fig. 3).

This work was supported in part by the Ministry of Education and Science of the Russian Federation, grant number MK-5813.2016.2 and by RFBR grants 17-52 560003Iran-a and 16-29-09515-ofi-m.

[1] N. Takeuchi, Y. Yamanashi; N. Yoshikawa, *Appl. Phys. Lett.*, **102** (2013) 052602.

[2] N. Takeuchi, Y. Yamanashi; N. Yoshikawa, *Appl. Phys. Lett.*, **103** (2013) 062602.

[3] V.K. Semenov, G.V. Danilov, D.V. Averin. *IEEE Trans. Appl. Supercond.*, **13** (2003) 938-943.

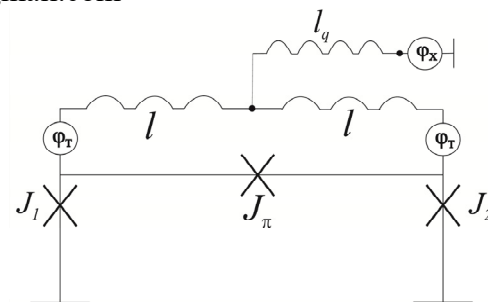


Fig. 1. Inverted AQFP shunted by Josephson π -junction.

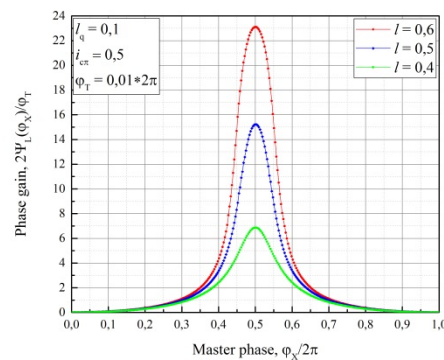


Fig. 2. Phase gain characteristic of Inverted AQFP shunted by Josephson π -junction.

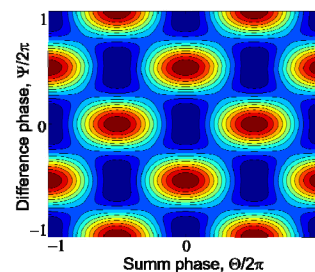


Fig 3. Josephson energy of considered cell.

3TL-D-7

RECENT TOPICS SURFACE ANDREEV BOUND STATESTanaka Y.¹, Bo L.¹, Kobayashi D.¹, Yada K.¹, Yamakage A.¹, Sato M.²¹ Department of Applied Physics, Nagoya University² Yukawa Institute, Kyoto University

ytanaka@nuap.nagoya-u.ac.jp

The study of Surface Andreev bound states (SABS) was activated more than twenty years before in the context of high T_c cuprate [1-3]. We have established a theory of tunneling spectroscopy of unconventional superconductors and clarified that the origin of zero bias conductance peak in high T_c cuprate is this SABS [2-3]. The flat band zero energy state has been recognized as a topological edge state where winding number defined in bulk Hamiltonian is responsible for the generation of SABS [4-5]. Up to now, there have been several types of SABSs stemming from their topological origins in two-dimensional unconventional superconductors [5]. It can be classified into i) dispersionless flat band type realized in cuprate, ii) linear dispersion type realized in chiral superconductor like Sr_2RuO_4 , iii) helical dispersion type realized in non-centrosymmetric superconductor in quasi two-dimensional superconductors.

In three-dimensional superconductor, we can consider chiral superconductor where both line and point nodes exist. Recently, the topological stability of these SABS has been clarified, which behavior is clearly different from high- T_c cuprates and noncentrosymmetric superconductors[6-7].

We have also predicted new types of ABS in doped Topological insulator(TI) and Weyl semimetals. In these materials, there are surface state which can remain even in superconducting state without gap opening due to the strong spin-momentum locking [8]. In the case of superconducting doped TI, SBAS has a so called “caldera type” dispersion. SABSs have a structural transition in the energy dispersions. On the other hand, in superconducting doped Weyl semimetal, crossed flat bands in the superconducting state. We clarify the topological origin of the crossed dispersionless flat bands and the relevant symmetry that stabilizes the cross point [9].

[1] C.R. Hu, *Phys. Rev. Lett.*, **72** (1994) 1526.

[2] Y. Tanaka and S. Kashiwaya, *Phys. Rev. Lett.*, **74** (1995) 3451.

[3] S. Kashiwaya and Y. Tanaka, *Rep. Prog. Phys.*, **63** (2000) 1641.

[4] M.Sato, Y.Tanaka, K.Yada, and T.Yokoyama, *Phys. Rev. B*, **83** (2011) 224511.

[5] Y. Tanaka, M. Sato, and N. Nagaosa, *J. Phys. Soc. Jpn.*, **81** (2012) 011013.

[6] S. Kobayashi, Y. Tanaka and M. Sato, *Phys. Rev. B*, **92** (2015) 214514.

[7] S. Tamura, *Physical Review B*, **95** (2017) 104511.

[7] A. Yamakage, K.Yada, M. Sato and Y. Tanaka, *Phys. Rev. B*, **85** (2012) 180509(R).

[8] B. Lu, K. Yada, M. Sato, and Y. Tanaka, *Phys. Rev. Lett.*, **114** (2015) 096804.

3OR-D-8

MAGNETOELECTRIC EFFECTS IN SPIN-ORBIT COUPLED SUPERCONDUCTORS. ANDREEV INTERFEROMETER WITH TRIPLET COOPER CORRELATIONS

Mal'shukov A.G.¹

¹ Institute of Spectroscopy, Russian Academy of Sciences, Moscow, Troitsk, Russia
malsh@isan.troitsk.ru

An interplay of the spin-orbit coupling (SOC), magnetism and superconductivity leads to electron transport phenomena, which attracted interest in connection with potential spintronic applications. As known, in *s*-wave superconductors the Zeeman interaction and SOC give rise to helix spatial variations of the order parameter [1]. A spontaneous supercurrent appears in this phase when the Zeeman field is spatially inhomogeneous [2]. A major role in this magnetoelectric effect is played by triplet Cooper correlations induced by SOC. The interaction of such an electron pair with the Zeeman field gives rise to an additional phase factor in the pair wave-function. Due to the proximity effect, the triplet correlations also take place in normal metals, which are in a contact with superconductors and have strong SOC. The latter is strong in a two-dimensional electron gas on the surface of a 3D topological insulator, where in low-energy dynamical processes the electron spins are locked to their momenta. In such a system the phase accumulated due to interaction of triplets with a Zeeman field may be observed in Andreev reflection. An interferometer for detection of this effect is shown in Fig.1. Due to a presence of a finite Zeeman field in the upper branch of the topological insulator wire, the phase of triplets is accumulated in this branch. The Zeeman field may be created by the exchange interaction of conduction electrons with electrons in an epitaxial magnetic insulator film, or with magnetic impurities. The interference of reflection amplitudes in the upper and lower branches results in oscillations of the current between the normal (N) and superconducting (S) leads. These oscillations may be observed by varying a direction of the exchange field.

The current was calculated for a dirty wire within the semiclassical theory for electron Green functions.

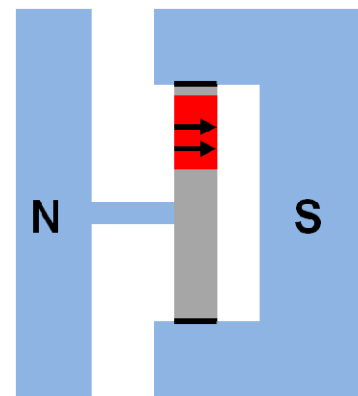


Fig. 1. A phase shift in the Andreev interferometer is provided by a magnetic island (red rectangle) deposited onto a topological insulator wire. Arrows show a magnetization direction.

[1] V.M. Edelstein, *Sov. Phys. JETP*, **68** (1989) 1244.

[2] A.G. Mal'shukov, *Phys. Rev. B*, **93** (2016) 054511.

[3] S.S. Pershoguba, K.Björnson, A.M. Black-Schaffer, A.V. Balatsky, *Phys. Rev. Lett.*, **115** (2015) 116602

[4] K.M.D. Hals, arXiv:1606.08458.

3OR-D-9

**INVESTIGATION OF SUPERCONDUCTING TRIPLET SPIN-VALVE
EFFECTS IN SUPERCONDUCTOR-FERROMAGNET
HETEROSTRUCTURES OF Nb, Co AND CuNi ALLOY**

*Lenk D.¹, Zdravkov V.I.^{1,2}, Widmann S.¹, Khaydukov Yu.³, Morari R.², Ullrich A.¹, Obermeier G.¹,
Müller C.¹, Sidorenko A.S.², Krug von Nidda H.-A.¹, Keimer B.³, Loidl A.¹, Horn S.¹,
Tagirov L.R.^{1,4}, Tidecks R.¹*

¹ Institut für Physik, Universität Augsburg, D-86159 Augsburg, Germany

² D. Ghitsu Institute of Electronic Engineering and Nanotechnologies ASM, Academiei Str. 3/3,
MD-2028 Kishinev, Moldova

³ Max Planck Institut für Festkörperforschung, Heisenbergstr 1, D-70569 Stuttgart, Germany

⁴ E.K. Zavoisky Physical-Technical Institute of RAS, 420029 Kazan, Russia
Daniel.Lenk@physik.uni-augsburg.de

In the present work, we studied the appearance of the superconducting triplet spin-valve effect in different Superconductor-Ferromagnet heterostructures. In this effect, the presence of magnetic moments, which are non-collinear in or between the constituent ferromagnetic layers, leads to the generation of the long-range odd-in-frequency triplet component of superconductivity, yielding a reduction of the singlet component and, thus, of the superconducting transition temperature [1]. In more detail, we investigated the transport properties in the superconducting state and correlated the observed behavior to the magnetic properties obtained by magnetic characterization. Within this study, we also present different ways to induce non-collinear moments into the investigated heterostructures and discuss differences in the obtained results.

This study is supported by the DFG under Grant No. HO 955/9-1 and the TRR-80 Project. The partial support by RFBR (grant No. 16-02-01171-a, L.R.T.), STCU (grant No. 5982, A.S.S. and R.M.) is acknowledged.

[1] Fominov, Y.V., Golubov, A.A., Karminskaya, T.Y. et al. *JETP Lett.*, **91** (2010) 308.

3RP-D-10

MAGNETODIPOLE AND SPIN-MOMENTUM TRANSFER EFFECTS IN THE SF HYBRIDS RESPONSE ON THE MAGNETIC AND ELECTRIC FIELDS*Uspenskaya L.S.¹*¹ ISSP RAS, Chernogolovka, Russia
uspenska@issp.ac.ru

It is well known that the behavior of hybrid S/F structures under the magnetic field or under the electric current flow is determined by various interactions. First of all, these are well-studied proximity effects result in the suppression of superconductivity and of the order parameter near the interface of the superconducting and ferromagnetic layers. Further, there is an interaction through the distortion of the distribution of magnetic stray fields by a superconductor in and around the ferromagnet layer and by ferromagnet in the superconducting layer. These well studied effects lead to an effective change in the anisotropy in the ferromagnet, to a reorientation of the magnetic domain structure, to a change in the type of magnetic domain walls, to the expansion and bias of the hysteresis loops. The "magnetic response" of superconductors is also changed: an additional anisotropy is formed in the penetration of the magnetic flux and in the pinning of the vortices.

The most interesting effects are observed in planar hybrid structures of a ferromagnet-superconductor when the electric current flows along the structure. Thus, in permalloy-niobium structures when a current flows through the superconducting niobium layer, the magnetic domain boundaries in the permalloy layer not only shift, but it shifts with the supersonic velocities. In the ferromagnet dielectric-superconductor structures, the suppression of the superconducting transition temperature T_c as well as the shape of the $R(T)$ depend on the mutual orientation of the electric current flowing through the superconductor and the spontaneous magnetization in the dielectric layer. Moreover, this T_c -suppression turns to be dependent upon the current strength, and under certain conditions the current amplification leads to a decrease of the T_c -suppression.

The review of recent results on spin and spin-momentum transfer in SF structures will be presented.

Support by RFBR under the project # 15-02-06743 is acknowledged.

3RP-D-11

SUPERCONDUCTING SPIN-VALVE EFFECT IN HETEROSTRUCTURE CONTAINING THE HEUSLER ALLOY AS THE FERROMAGNETIC LAYER

Kamashev A.A.¹, Validov A.A.¹, Garifullin I.A.¹, Fominov Ya.V.^{2,3}, Leksin P.V.⁴, Shumann J.⁴, Kataev V.⁴, Büchner B.⁴

¹Zavoisky Physical-Technical Institute, Russian Academy of Sciences, Kazan, Russia

²L.D. Landau Institute for Theoretical Physics, Russian Academy of Sciences, Chernogolovka, Russia

³Moscow Institute of Physics and Technology, 141700 Dolgoprudny, Russia

⁴Leibniz Institute for Solid State and Material Research IFW Dresden, Dresden, Germany
ilgiz0garifullin@gmail.com

The superconducting spin-valve effect attracts considerable interest during the last few decades. Our recent studies [1,2] and the studies of other groups (see, e.g., recent review [3]) show that the usage of elemental superconductors and ferromagnets as construction materials for the superconducting spin valve depleted their functionality with regard to record parameters of the superconducting spin valve. To overcome this problem the use of new unconventional ferromagnetic materials is desirable. At the first step, we decided to concentrate our investigation on the spin-valve construction containing the Heusler alloy $\text{Co}_2\text{Cr}_x\text{Fe}_{1-x}\text{Al}$ which may have 100% spin polarization of the conduction band at the optimal preparation conditions. For our study we prepared the set of samples of the superconducting (SC) spin valve with variation of the Heusler-layer thickness d_{Heusler} in the range between 1 and 8 nm: MgO/CoO_x (3.5nm)/Py(5nm)/Cu(4nm)/Heusler/Cu(2.5nm)/Pb(80nm)/Si3N4(85nm) (where Py = $\text{Ni}_{0.81}\text{Fe}_{0.19}$). The samples were prepared at the substrate temperature $T_{\text{sub}}=300$ K when evaporating the Heusler alloy by sputtering technique. To optimize the growth of the top Cu/Pb fragment after deposition of the Heusler layer we decreased the T_{sub} down to 150 K just as we did in [2]. Our recent investigation (unpublished) of the proximity effect in Heusler/Pb heterostructures showed that the Heusler layer prepared at $T_{\text{sub}}=300$ K manifests behavior which is typical for weak ferromagnets. We have studied the dependence of the SC transition temperature T_c on the angle α between the direction of the cooling field and the external magnetic field both applied in the plane of the sample. For the CoO_x (3.5nm)/Py(5nm)/Cu(4nm)/Heusler(1nm)/Cu(2.5nm)/Pb(80nm) structure we obtained that the T_c does not change monotonically but passes through a minimum. We denote the difference in T_c between 180 and 90 degrees as a triplet spin valve effect. The value of triplet effect was $\Delta T_c^{\text{trip}} = 74$ mK at the width of the T_c of about 38 mK. Thus, the possibility for full switching of the SC current by changing the mutual orientation of magnetizations of Py and Heusler layers from 0^0 to 90^0 was realized. It should be noted that for this sample for the first time it was demonstrated the full switching (on/off) between the SC and normal states due to the triplet spin-valve effect only. Up to now, the switching of the superconducting current was performed by changing the mutual direction of magnetizations of the ferromagnetic layers from antiparallel to parallel orientation or by a combination of classical and triplet SC spin valve effect. Here switching was realized just by the triplet spin valve effect. Our result was obtained for the test samples prepared at $T_{\text{sub}}=300$ K, which provides opportunities for further modifications of the structures by changing the preparation conditions.

This work was partially supported by Russian Foundation for Basic Research (No. 17-02-00229) and the Program of the Russian Academy of Sciences.

[1] I.A. Garifullin *et al.* *J.M.M.M.* **373**, 18 (2015).

[2] P.V. Leksin *et al.* *Phys. Rev. B* **93**, 100502 (2016).

[3] J. Linder and J.W.A. Robinson, *Nat. Phys.* **11**, 307 (2015).

3OR-D-12

THIN FILMS OF Sr₂IrO₄ WITH SPIN-ORBIT INTERACTION*Kislinkii Yu.V.¹, Petrzhik A.M.¹, Andreev N.V.³, Cristiani G.², Diuzhikov I.N.¹,
Logvenov G.², Ovsyannikov G.A.¹*¹ Kotelnikov IRE RAS, Moscow, Russia² Max Plank Institute for Solid State Research, Stuttgart, Germany³ NITU MISiS, Moscow, Russia

yulii@hitech.cplire.ru

Sr₂IrO₄ is a ferromagnetic and dielectric material with strong spin-orbit interaction [1], where a lot of interesting physics is observed. Some properties such as d-wave gap of unknown origin [2], an unique high value of the anisotropic magnetoresistance [3] were observed. Here we report on electrical and infrared properties of Sr₂IrO₄ thin films. Thin films of Sr₂IrO₄ were deposited by laser ablation on SrTiO₃, LaAlO₃, LaAlO₃+Sr₂AlTaO₆ (LSAT) substrates. At high temperatures, resistivity versus temperature, $\rho(T)$ curves were like Mott variable range hopping (VRH) dependences $\rho = \rho_{3D} \cdot \exp[(T_{3D}/T)^{1/4}]$ with experimental constants T_{3D} of 10⁸ K. From experimental VRH dependences we have estimated localization radii of localized carriers a in order of $a \sim 1$ nm and density of states at Fermi level $N_F \sim 10^{18}$ eV⁻¹ cm⁻³. In 100 – 150 K temperature range $\rho(T)$ curves have a semiconductor-like dependence $\rho = \rho_0 \cdot \exp[\Delta E/(2kT)]$ with a slope of $\Delta E \approx 200$ meV. In our samples we have observed 2 times large energy gap ΔE than was reported for Sr₂IrO₄ single crystals [3]. The experimental constants T_{3D} for our samples [4] were large than the constants obtained for Sr₂IrO₄ thin films by other authors [5]. It points on lower density of localized states in our thin films because of the dependency $T_{3D} \sim 1/(a^3 N_F)$. To distinguish between the semiconductor conductivity mechanism and the VRH one a spectral measurements of Sr₂IrO₄ thin films were performed and absorption coefficients were obtained in 12 – 300 THz frequency range. The information about spectroscopic and electron transport properties of strontium iridate thin films is presented.

The work is partially supported by RAS, Scientific School grant NSH-8168.2016.2.

[1] B.J. Kim, H. Ohsumi, et al., *Science*, **323** (2009) 1329-1332.

[2] Y.K. Kim, N.H. Sung, et al., *Nature Phys.*, **12** (2016) 37 – 41.

[3] M. Ge, T.F. Qi, et al., *Physical Rev. B*, **84** (2011) 100402(R) 1-5.

[4] A.M. Petrzhik, et al., *Pis'ma v Zhurnal Tekhnicheskoi Fisiki*, **43** (2017) accepted for publication.

[5] Lu Chengliang, A. Quindeau, et al., *Applied Phys. Lett.*, **105** (2014) 082407 1-5.

3RP-D-13

ULTRAFAST DYNAMICS IN Na-DOPED $K_xFe_{2-y}Se_2$ SUPERCONDUCTORS

Luo C.W.^{1,2}, *Cheng P.C.*¹, *Chu Y.J.*¹, *Tzeng W.Y.*¹, *Lin J.-Y.*³, *Wu K.H.*¹, *Juang J.Y.*¹, *Golovanov A.*⁴,
Chareev D.A.^{5,6}, *Vasiliev A.*^{4,5,7}

¹ Department of Electrophysics, National Chiao Tung University, Hsinchu 300, Taiwan

² Taiwan Consortium of Emergent Crystalline Materials, Ministry of Science and Technology, Taipei 10601, Taiwan

³ Institute of Physics, National Chiao Tung University, Hsinchu 300, Taiwan

⁴ Physics Faculty, Moscow State University, Moscow 119991, Russia

⁵ Institute of Physics and Technology, Ural Federal University, Mira st. 19, 620002 Ekaterinburg, Russia

⁶ Institute of Experimental Mineralogy, Chernogolovka, Moscow Region, 142432, Russia

⁷ National University of Science and Technology "MISiS", Moscow 119049, Russia

cwluo@mail.nctu.edu.tw

The ultrafast dynamics in Na-doped $K_xFe_{2-y}Se_2$ single crystals have been studied by using dual-color pump-probe spectroscopy. The amplitude changes of transient reflectivity change ($\Delta R/R$) below superconducting critical temperature T_c indicate a superconducting gap of 10.8 meV in a $(Na_{0.32}K_{0.68})_{0.95}Fe_{1.75}Se_2$ single crystal as shown in Fig. 1. From the significant variation of electron, spin and acoustic phonon components in $\Delta R/R$ around $T^* \sim 100$ K, the intimate correlation between the metallic and antiferromagnetic (AFM) insulating phases in $(Na_{0.32}K_{0.68})_{0.95}Fe_{1.75}Se_2$ is unambiguously revealed. The results of quasiparticle ultrafast dynamics further imply that the electronic correlation between minority metallic phase and majority AFM insulating phase serve as an energy transfer channel for both separated phases, which plays a key factor for superconductivity and provides a new aspect to clarify pairing mechanism in alkali metal iron selenide superconductors.

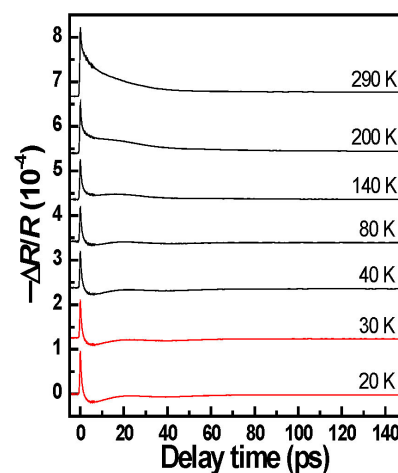


Fig. 1. Typical photoinduced transient reflectivity changes ($\Delta R/R$) transients at various temperatures.

Support by the MOST Taiwan (Grant No. 103-2923-M-009-001-MY3), RFBR (Grant 14-02-92002), the Ministry of Education and Science of the Russian Federation in the framework of Increase Competitiveness Program of NUST «MISiS» (№ K2-2015-075 and K4-2015-020) and Act 211 Government of the Russian Federation (contract № 02.A03.21.0006) is acknowledged.

3OR-D-14

COMPETITION OF D- AND S- WAVE SUPERCONDUCTIVITY INDUCED BY EXCHANGE INTERACTIONS IN THE SPIN-POLARON ENSEMBLE

Val'kov V.V.¹, Dzebisashvili D.M.¹, Korovushkin M.M.¹, Barabanov A.F.²

¹ Kirensky Institute of Physics, Federal Research Center KSC SB RAS, Krasnoyarsk, Russia

² Institute for High Pressure Physics, Moscow, Troitsk, Russia

ddm@iph.krasn.ru

It is known that the spin-fermion interactions are strong in cuprate superconductors. It is due to this interaction the spin-polaron quasiparticles are formed [1]. The ensemble of such quasiparticles exhibits Cooper instability with high critical temperatures [2]. In this case the spin-polarons are coupled via spin-fermion interaction and exchange interaction between localized spins of the copper ions which stands for the coupling constant.

Using the spin-fermion model [3], which follows from the three band p-d-model in the limit of the strong electron correlations, we showed that the Coulomb interaction V between holes on the nearest oxygen ions does not suppress the d-wave superconductivity (as it does in the widely used t-J or Hubbard models). The reason is that when taking into account the real structure of the CuO_2 -plane (specifically spatial separation of the oxygen p_x - and p_y - orbitals and copper $d_{x^2-y^2}$ - orbital in the unit cell) the Fourier transform of the Coulomb interaction V completely disappears from the set of equations for the d-wave superconducting order parameter. At the same time, in the Hubbard or t-J-models on the square lattice the Fourier transform of V preserves and renormalises the coupling constant J additively. Doping dependence of the critical temperature T_c for the d-wave superconducting phase is shown by solid line in figure 1.

Likewise, the possibility of implementation of the s-wave superconducting phase in cuprates was investigated within the same spin-fermion model. It was shown that for the superconducting s-phase the intersite Coulomb interaction suppresses the value of T_c as it is demonstrated in figure 1 by dashed lines. The analysis of these curves shows that it is the intersite Coulomb interaction that leads to the preponderance of the d-wave over the s-wave pairing in the underdoped and optimally doped regime on the phase diagram. Without account for the intersite Coulomb interaction, the superconducting s-phase would be implemented in the optimal doping region.

The work was supported by the Russian Foundation for Basic Research (№ 16-02-00304), Government of Krasnoyarsk Territory, Krasnoyarsk Region Science and Technology Support Fund to the research (№ 16-42-240435, and 16-42-243057) and the grant of the President of the Russian Federation (Project MK-1398.2017.2).

[1] A.F. Barabanov, A.A. Kovalev, O.V. Urazaev, A.M. Belemouk, R. Hayn, *JETP*, **119** (2001) 777.

[2] V.V. Val'kov, D.M. Dzebisashvili, A.F. Barabanov, *Phys.Lett.A*, **379** (2015) 421.

[3] A.F. Barabanov, L.A. Maximov, G.V. Uimin, *JETP Letters*, **47** (1988) 532.

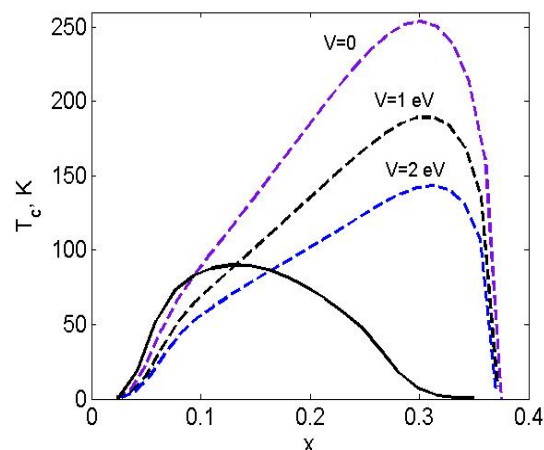


Fig. 1. Doping dependences of T_c at three values of V . Solid line correspond to the d-wave pairing, dashed lines - for the s-wave pairing.

3 July

Monday

11:30-13:15

oral session

3TL-E

3RP-E

3OR-E

**“Magnetophotonics
and Ultrafast
Magnetism”**

3TL-E-1

NONLINEAR AND PARAMETRIC FREQUENCY MIXING IN ACOUSTO-MAGNETO-PLASMONICS

Temnov V.V.¹, Tran N.M.¹, Traum C.², Alekhin A.¹, Juvé V.¹, Vaudel G.¹, Makarov D.³, Seletskiy D.², Razdolski I.⁴, Lomonosov A.¹, Vlasov V.S.¹, Janusonis J.⁵, Chang C.⁵, Tobey R.⁵

¹ Institut des Molécules et Matériaux du Mans (IMMM CNRS 6283), Le Mans, France

² Department of Physics and Center for Applied Photonics, University of Konstanz, Germany

³ Institute of Ion Beam Physics & Materials Research, Helmholtz-Zentrum Dresden-Rossendorf e.V., Dresden, Germany

⁴ Fritz-Haber Institute of the Max-Planck Society, Berlin, Germany

⁵ Zernike Institute for Advanced Materials, University of Groningen, Groningen, Netherlands
vasily.temnov@univ-lemans.fr

In functional magnetic nanostructures the acoustic, magnetic and plasmonic excitations can co-exist and interact on the nanometer spatial and ultrafast time scales. Optical spectroscopy with femtosecond laser pulses highlights a variety of nontrivial spatio-temporal dynamics, which are not only used to monitor individual excitations in real time, but also study interaction mechanisms between them, often observed as frequency mixing phenomena. While the second harmonic generation (SHG), sum- and difference frequency mixing in the optical frequency range originate from the $\chi(2)$ -nonlinearities, in acoustics and magnetism these effects are often dominated by parametric resonances, where system parameters are modulated at frequencies comparable to the natural oscillation frequencies, typically in the MHz-GHz range. Keeping in mind the intrinsic differences in the physical nature and frequency range of these phenomena, here we discuss, in a comparative manner, two examples of frequency mixing in magneto-plasmonics [1,2] and magneto-acoustics [3,4]. The ability to experimentally tune both systems through Surface Plasmon Resonance (SPR) and Ferromagnetic Resonance (FMR) as well as to theoretically describe these resonant interactions within the framework of phenomenological models based on the Lorentz oscillator, represent the key idea behind this presentation.

In nonlinear magneto-plasmonics, the plasmonically assisted SHG is found to strongly depend on the magnetization in a ferromagnetic layer. A simple model utilizing the resonant plasmonic enhancement of the $\chi(2)$ -susceptibility confirms the experimental observation that magnetic effects are most pronounced between the SHG and fundamental SPR resonances [1,2]. In ultrafast transient grating experiments [3,4], the magnetization in a Ni/glass sample is excited by two distinct transient surface acoustic waves (SAW and SSLW). Magnetic tuning of the FMR frequency in resonance to their SHG, sum- and difference frequencies demonstrates the full variety of frequency mixing phenomena. In contrast to nonlinear optics, the frequency mixing is dominated by the parametric effect in the externally driven FMR oscillator, in agreement with an analytical model based on the resonant enhancement of frequency-mixed signals [4].

The support from Strategie Internationale NNN-Telecom, COST action MP1403 and PRC CNRS-RFBR “Acousto-magneto-plasmonics” are gratefully acknowledged.

[1] Razdolski et al., *ACS Photonics*, **3** (2016) 179.

[2] V.V. Temnov et al., *J. Opt.*, **18** (2016) 093002.

[3] J. Janusonis et al., *Phys. Rev. B*, **94** (2016) 024415.

[4] C.L. Chang et al., *Phys. Rev. B*, **95** (2017) 060409(R).

3OR-E-2

PHONON DRIVING MAGNETIZATION PRECESSION IN FERROMAGNETIC NANOGRATINGS

*Salasyuk A.S.¹, Rudkovskaya A.V.¹, Danilov A.P.², Glavin B.A.³, Rushforth A.W.⁴, Sokolov S.V.⁵,
Nekudova P.A.⁵, Elistratov A.A.⁵, Yakovlev D.R.^{1,2}, Akimov A.V.⁴, Bayer M.^{1,2}, Scherbakov A.V.¹*

¹ Ioffe Institute, 194021 Saint Petersburg, Russian Federation

² Experimentelle Physik 2, TU Dortmund, 44227 Dortmund, Germany

³ Lashkaryov Institute of Semiconductor Physics, 03028 Kyiv, Ukraine

⁴ University of Nottingham, NG7 2RD Nottingham, the United Kingdom

⁵ INME of RAS, 119991 Moscow, Russian Federation

salasyuk@mail.ioffe.ru

Femtosecond laser pulse focused on a ferromagnetic metal simultaneously excites both the magnetization precession at the ferromagnetic resonance frequency (FMR), f_{FMR} , and broad spectrum of coherent acoustic phonons. In present work we study the interaction of these excitations lying in GHz range. Periodical spatial profiling of ferromagnet surface can be the reason of lateral localization of certain phonon modes, f_{ph} , which can drive the magnetization precession during their lifetime. We show that this collective behavior can be the source of oscillating magnetic field at GHz frequency with extremely high amplitude and localized at the nanoscale in free space.

In experiment we examine the response of lateral ferromagnetic nanogratings on femtosecond optical excitation. The gratings with size $5 \times 5 \mu\text{m}^2$ are etched by focused ion beam in the 100-nm thick Gallfenol film deposited on (001)-GaAs substrate. Each grating consist of parallel grooves with width of 40 nm etched with

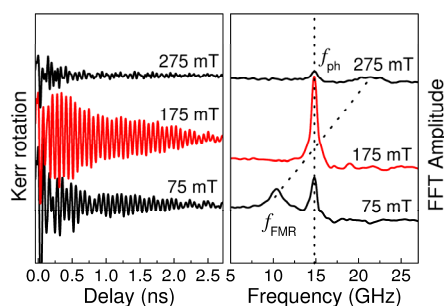


Fig. 1. Pump-probe signals and their FFT spectra

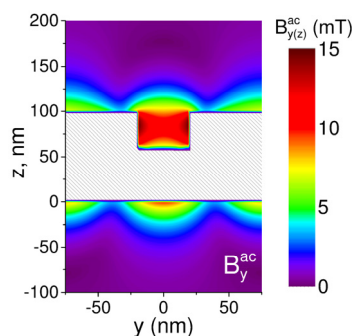


Fig.2 Distribution of ac-magnetic field

unidirectional periodicity of 150 nm. Three nanogratings with different depth and orientation of grooves are studied. We perform conventional magneto-optical pump-probe experiment in magnetic field applied in-plane of the structure. The response of magnetization is detected by magneto-optical Kerr rotation of polarization plane of reflected probe beam. By tuning the FMR frequency to the resonance with the phonon mode, $f_{\text{FMR}} = f_{\text{ph}}$ we achieve maximum efficiency of the phonon driving of the magnetization precession.

The effect of the phonon driving strongly depends on the relative orientation of the grating, crystallographic directions and external magnetic field. The most remarkable result is achieved in the grating with grooves of 40-nm depth oriented along [100]-axis in magnetic field applied at 45° . In this geometry at the resonant conditions the magnetization precession driven by coherent phonons at $f_{\text{ph}} = 15$ GHz lasts longer than 2 ns, and its amplitude exceeds 1% of the saturation magnetization. The respective magnitude of the generated ac-magnetic induction is ~ 10 mT. In Fig. 2 the calculated spatial distribution of in-plane component of ac-magnetic induction is shown. Our experimental observations are in good agreement with theoretical analysis.

We acknowledge the support of the Russian Scientific Foundation by the grant No. 16-12-10485

3TL-E-3

CLOCKED LASER EXCITATION OF SPIN WAVES IN MAGNETIC FILMS

Belotelov V.I.^{1,2}

¹ Lomonosov Moscow State University, Moscow, Russia

² Russian Quantum Center, Skolkovo, Moscow, Russia

belotelov@physics.msu.ru

Optical tools are promising for spin wave generation due to the possibilities of ultrafast manipulation and local excitation. However, a single laser pulse can inject spin waves (SWs) only with a broad frequency spectrum, resulting in short propagation distances and low wave amplitudes. Here we excite a magnetic garnet film by a train of fs-laser pulses with 1 GHz repetition rate (Fig. 1a) so that the pulse separation is shorter than the decay time of magnetic modes which allows us to achieve a collective impact on the magnetization and establish a quasi-stationary source of spin waves, namely a coherent accumulation of magnons (“magnon cloud”). This approach has several appealing features: (i) the magnon source is tunable; (ii) the SW amplitude can be significantly enhanced; (iii) the SW spectrum is quite narrow providing long distance propagation; (iv) the periodic pumping results in an almost constant in time SW amplitude up to 100 μm away from the source; and (v) the SW emission shows pronounced directionality (Fig. 1b) [1]. These results expand the capabilities of ultrafast coherent optical control of magnetization and pave a way for applications in data processing, including the quantum regime. The quasi-stationary magnon accumulation might be also of interest for applying it to magnon Bose-Einstein condensates.

This work was financially supported by the Russian President Grant (Project No. MD-1615.2017.2).

[1] M. Jäckl, V.I. Belotelov, I.A. Akimov, I.V. Savochkin, D.R. Yakovlev, A.K. Zvezdin, M. Bayer, “Magnon accumulation by clocked laser excitation as source of long-range spin waves in transparent magnetic films”, *Physical Review X* (2017) (accepted).

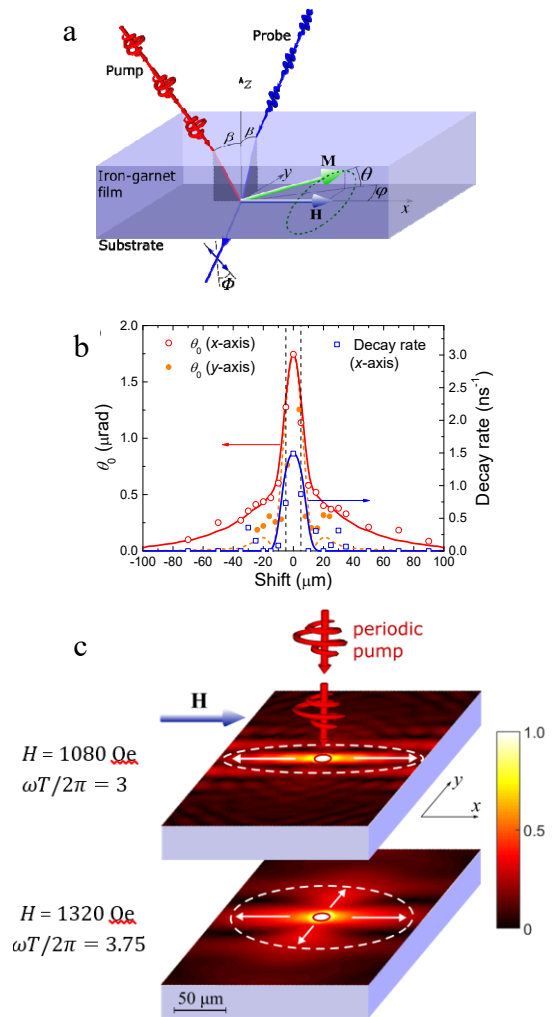


Fig. 1. a) Scheme of the pump-probe experiment. b) Oscillation amplitude (red, orange) and decay rate (blue) at different distances between pump and probe for the probe shifted along the x -axis (open symbols and solid lines) and the y -axis (filled symbols and dashed lines). d, Calculated distribution of m_z in SWs launched at $H = 1060$ Oe ($\omega T/2\pi = 3$), $H = 1320$ Oe ($\omega T/2\pi = 3.75$).

3RP-E-4

TERAHERTZ SPECTROSCOPY AS A PROBE OF ULTRAFAST SPINTRONICS PHENOMENA IN MAGNETIC HETEROSTRUCTURES

Mikhaylovskiy R.V.¹

¹ Radboud University, Nijmegen, Netherlands
R.Mikhaylovskiy@science.ru.nl

Reaching the terahertz (THz) regime has become a key incentive in spintronics. The excitation of magnetic metallic heterostructures with femtosecond laser pulses offers a convenient way to generate equally short spin and charge current pulses. Due to spin-orbit interaction the direction of the current pulses can be controlled by the bias magnetic field and polarization of light [1-2]. These currents can be used to produce ultrabroadband terahertz radiation [3] and serve as a probe of separate magnetic sublattices in transition metal alloys [4].

Despite aforementioned achievements, the spin transport at THz frequencies is poorly understood since directly accessing ultrafast spin-dependent electron motion remains a major experimental challenge. Here, using THz electric fields of freely propagating waves and detecting the magneto-optical response of these waves, we realize contact-free measurements of the anomalous Hall effect in magnetically ordered metallic films (Fig. 1). Next to it, with the help of femtosecond laser pulses we launch sub-100 ps magnetization dynamics, including partial magnetization reversal. By employing a pump-probe approach with a probe at THz frequencies, we reveal ultrafast dynamics of the anomalous Hall effect [5]. In fact, our experiment mimics sub-100 ps operation of a spin transistor, in which the source-drain voltage is applied from a freely propagating THz wave and a femtosecond laser pulse plays the role of the gate by acting on the magnetic ordering. We demonstrate the feasibility to reveal the fundamental and practical limitations on the speed of magnetic control of conductivity and thus to define the ultimate speed for the operation of spintronic devices. The developed experimental scheme allows to study and realize the photoinduced spin-transport properties at THz frequencies in a broad variety of magnetic films and heterostructures.

Support by ERC and NWO is acknowledged.

- [1] T. Kampfrath, et al. *Nature Nanotech.*, **8** (2013) 256–260.
- [2] T. J. Huisman, et al., *Nature Nanotech.*, **11** (2016) 455–458.
- [3] T. Seifert, et al., *Nature Photon.*, **10** (2016) 483–488.
- [4] T. J. Huisman, et al., *Appl. Phys. Lett.*, **110** (2017) 072402.
- [5] T. J. Huisman, et al., *Phys. Rev. B*, **95** (2017) 094418.

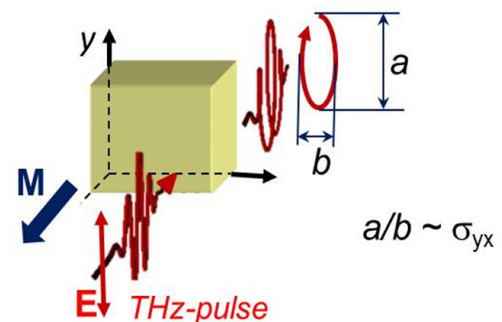


Fig. 1. Anomalous Hall effect seen by THz radiation. The ellipticity/rotation of the transmitted THz pulse is a direct measure of Hall conductivity.

3RP-E-5

DIGITIZATION OF LABYRINTH DOMAIN STRUCTURE IMAGES OBTAINED BY POLARIZED LIGHT MICROSCOPY IN FERRITE-GARNET FILMS

*Ivanov O.V.*¹, *Shalygina E.E.*², *Ignatov M.S.*³, *Magnitskaya M.V.*^{4,1}, *Uspenskii Yu.A.*¹, *Shalygin A.N.*²

¹ Lebedev Physical Institute, RAS, Moscow, Russia

² Faculty of Physics, Lomonosov Moscow State University, Moscow, Russia

³ Main Botanical Garden, RAS, Moscow, Russia

⁴ Institute for High Pressure Physics, RAS, Moscow, Russia

ivanov@td.lpi.ru

Recently, the attention of researchers has been attracted by thin-film systems based on FeN magnetic films which are widely used in various spintronics devices. A peculiarity of FeN films is that the saturation induction of these alloys is higher than in pure iron films (about 2.8 to 3 T instead of 2.2 T), and the addition of nitrogen shifts the ferromagnetic resonance frequency to higher values. The expansion of the functionality of FeN thin-film magnetic systems is largely due to the study of the mechanisms of magnetic field influence on chemical processes occurring on their surface. An analysis of these processes was carried out by means of chemical etching of thin-film systems in a magnetic field, followed by a study of their surface morphology using a well-known method based on the use of a low-coercivity ferrite-garnet film as an indicator of scattering fields.

Here, we present a new method proposed especially for recognition of complex objects, in particular, specific patterns created by the magnetic domain walls on the surface. The method is a generalization of the microstructure digitization technique we developed [1] earlier using simpler objects – the plant cell walls – as an example. It also incorporates the advantages of a new approach proposed in [2] that provides the efficient color-space reduction. Our algorithm takes into consideration special features of the labyrinth domain patterns observed experimentally. This enables us, after digitization, to quantitatively determine the geometric parameters of magnetic domain structures, which is essential for interpretation of data obtained. In this work a number of typical domain structure images are digitized and analyzed. The results demonstrate the wide applicability of our method.

Support by RAS and RFBR is acknowledged.

[1] O.V. Ivanov, M.S. Ignatov, *Cell Tissue Biol.*, **7** (2013) 103-112.

[2] A. Rodriguez, A. Laio, *Science*, **344** (2014) 1492-1496.

3 July

Monday

11:30-13:00

14:30-17:00

oral session

3TL-F

3RP-F

3OR-F

“Multiferroics”

3TL-F-1

QUANTUM CRITICALITY WITHOUT ELECTRONS*Saxena S.S.*¹¹ Quantum Matter Group, Cavendish Laboratory, University of Cambridge, Cambridge, United Kingdom
SSS21@cam.ac.uk

This talk will discuss pressure induced phenomena in the vicinity of ferroelectric and magnetic quantum phase transitions.

Materials tuned to the neighbourhood of a zero temperature phase transition often show the emergence of novel quantum phenomena. Much of the effort to study these new emergent effects, like the breakdown of the conventional Fermi-liquid theory in metals has been focused in narrow band electronic systems. Ferroelectric crystals provide a very different type of quantum criticality that arises purely from the crystalline lattice. In many cases the ferroelectric phase can be tuned to absolute zero using hydrostatic pressure. Close to such a zero temperature phase transition, the dielectric constant and other quantities change into radically unconventional forms due to the fluctuations experienced in this region. The simplest ferroelectrics may form a text-book paradigm of quantum criticality in the solid-state where there are no complicating effects of electron damping of the quantum charge fluctuations. We present low temperature high precision data demonstrating these effects in pure single crystals of SrTiO₃ and KTaO₃. We outline a model for describing the physics of ferroelectrics close to quantum criticality and highlight the expected $1/T^2$ dependence of the dielectric constant measured over a wide temperature range at low temperatures. In the neighbourhood of the quantum critical point we report the emergence of a small frequency independent peak in the dielectric constant at approximately 2K in SrTiO₃ and 3K in KTaO₃. Looking to the future, we imagine that quantum paraelectric fluctuations may lead to new low temperature states and mediate novel interactions in multi-ferroic systems (e.g. EuTiO₃) and ferroelectric crystals supporting itinerant electrons.

3OR-F-2

**ON THE PROBLEM OF STATIC STABILITY
OF A CYLINDRICAL MAGNETIC DOMAIN IN ELECTRIC FIELD.
THE NEW WAY OF MAGNETIC BUBBLE BLOWING**

Pyatakov A.P.¹, Kulikova D.P.¹, Sergeev A.S.¹, Zvezdin A.K.²

¹ Physics Department of M.V. Lomonosov Moscow State University, Moscow, Russia

² A.M. Prokhorov General Physics Institute, Moscow, Russia
pyatakov@physics.msu.ru

From the early 70-th it was believed that the stability of a cylindrical magnetic domain or “bubble” is the balance of three forces: the force associated with Zeeman energy in the external magnetic field, the inward force of domain wall surface tension and the outward demagnetizing force [1]. With the advent of magnetoelectric and multiferroic materials the problem of the bubble stability should be revisited since external electric field or electric polarization in these materials act as an additional effective magnetic field.

The bubble domain nucleation and blowing using tip electrode was observed in a rare earth iron garnet film (fig.1). The theoretical consideration includes classical Thiele theory with the additional term in the force equation proportional to the electric field and spatial derivatives of magnetization (the so called inhomogeneous magnetoelectric or flexomagentoelectric effect). The experimental study and theoretical consideration allow us to formulate the following:

1) The electric field of certain electric polarity (positive in the experiment) serves as a kind of “surfactant” agent lowering the surface tension of a domain wall and facilitating its nucleation.

2) The electric field acts with opposite forces on the opposite sides of the magnetic bubble thus stretching it.

3) The equilibrium size of the bubble domain increases with the electric field.

4) when the electric field is switched off, the bubble detaches from the tip, shrinks to its equilibrium size and remains stable.

This new way of electrical generation of the magnetic topological solitons proposes the viable alternative to the recently reported [2] magnetic bubble and skyrmion blowing by spin polarized current.

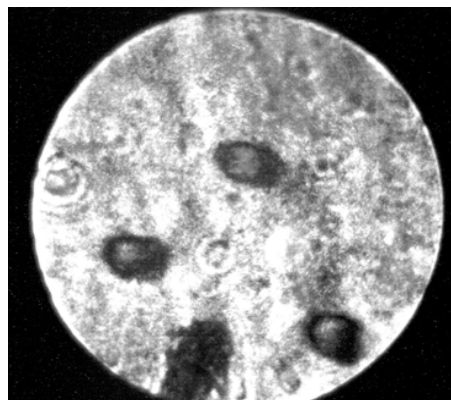


Fig. 1. The magneto-optical image of the series of bubble domains nucleated with the electric tip (the black object at the bottom). The diameter of the microscope field of view is 100 μm)

Support by RFBR grants ##16-02-00494_a, 16-29-14037 ofi_m, and 16-32-00840 mol_a is acknowledged.

[1] A.A. Thiele, *J. Appl. Phys.*, **41** (1970) 1139-1145.

[2] W. Jiang et al, *Science*, **349** (2015) 283–286.

3RP-F-3

MAGNETIC TOPOLOGICAL STRUCTURES IN MULTIFERROICS

Zvezdin A.K.¹, Gareeva Z.V.²

¹ A.M. Prokhorov General Physics Institute, Russian Academy of Sciences, Moscow, Russia

² Institute of Molecule and Crystal Physics, Russian Academy of Sciences, Ufa, Russia
gzv@anrb.ru

Multiferroic materials fascinate scientists by the exciting opportunities given by coexistence of several ferroic properties whose interaction leads to new physical phenomena and opens wide prospects for technological implementations [1].

Nowadays, an accent of multiferroic research is made on nanoscale objects (domains, domain walls, magnetic vortices) that uncovers new physical properties (magnetoelectric pinning, improper ferroelectricity and others) and bears considerable potential for nanoelectronic devices.

In this talk we focus on micromagnetic structures in multiferroics, discuss physical mechanisms of magnetoelectric coupling considering domain walls (DWs), spin spirals and vortices in the high temperature multiferroic bismuth ferrite and rare earth iron garnets whose properties are well established and magnetic topological structures are studied well enough.

We analyze the impacts given by inhomogeneous magnetism to ferroelectricity; consider magnetic DWs, spin cycloids and vortices as the tools to manipulate ferroelectric polarization.

One of the bright examples of DWs tunable ferroelectricity is electric polarization at magnetic DWs in iron garnets. We discuss the complementary physical mechanism responsible for magnetoelectric effect in these materials, inhomogeneous magnetoelectricity and magnetoelectricity arising due to interaction between rare earth and iron sublattices. The example of electric polarization distribution across 71^0 Bloch DW found in the framework of the magnetoelectricity concept by Popov et al [2] is shown in Fig.1.

We consider the structural instabilities in multiferroic bismuth ferrite and demonstrate their close correlation with manifestation of magnetoelectricity (linear magnetoelectric effect, domain wall pinning, phase transitions and other). Ferroic orders couple via magnetic inhomogeneities, that sheds new light on fundamental physics and applications.

Support by the Russian Foundation for Basic Research (Grant No. 16-02-00336 A) is acknowledged.

[1] Fiebig, M. et al., *Nat. Rev. Mater.* **1** (2016) 16046.

[2] Popov, A. I., Gareeva, Z. V., Zvezdin. *Phys. Rev.B* **92** (2015) 144420.

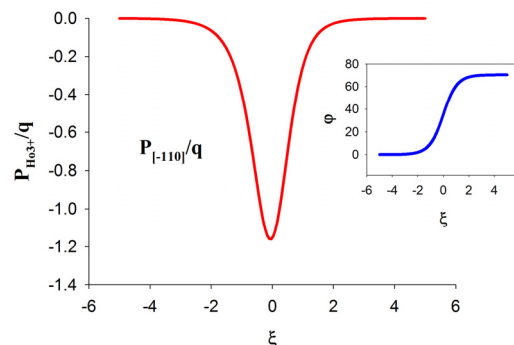


Fig. 1. Distribution of electric polarization in HoIG at the the 71^0 Bloch domain wall,

$$q_{HoIG(T=4K)} \sim 0.2 \cdot 10^{-5} \frac{C}{m^2}$$

3OR-F-4

POLARIZABILITY OF ELECTRICALLY INDUCED MAGNETIC VORTEX “ATOMS”

Karpov P.I.¹, Mukhin S.I.¹

¹ NUST “MISiS”, Moscow, Russia

karpov.petr@gmail.com

Electric field control of magnetic structures, particularly topological defects in magnetoelectric materials, draws a great attention in recent years, which has led to experimental success in creation and manipulation by electric field of single magnetic defects, such as skyrmions [1] and domain walls [2].

In this work we explore a scenario of electric field creation of another type of topological defects – magnetic vortices and antivortices, which are characteristic for materials with easy plane symmetry [3].

Because of interaction of the magnetic and electric subsystems each magnetic vortex (antivortex) in magnetoelectric materials (such as type-II multiferroics) possesses a quantized magnetic and an electric charge [4], where the former is responsible for interaction between vortices and the latter couples the vortices to electric field.

This property of magnetic vortices opens a peculiar possibility of creation of magnetic vortex plasma by non-uniform electric fields. We show that the electric field, created by a cantilever tip (Fig.1a), produces a “magnetic atom” with a localized spatially ordered spot of vortices (“nucleus” of the atom) surrounded by antivortices (“electronic shells”), Fig.1b. Our estimates show that the critical voltage, which is necessary to create first vortex-antivortex pair in big sample ($R \gg r$, Fig.1a) is $\varphi_{\text{crit}} \sim 20\text{V}$ and $\varphi_{\text{crit}} \sim 1\text{V}$ for prototypical type-I and type-II multiferroics BiFeO_3 and TbMnO_3 respectively.

We analytically find the vortex density distribution profile and temperature dependence of polarizability of this structure and confirm it numerically by Monte Carlo simulation. We show that electric polarizability of the “magnetic atom” depends on temperature as $\alpha \sim 1/T^{1-\eta}$ ($\eta > 0$), which is consistent with Euclidean random matrix theory prediction.

We acknowledge discussions with S. Brazovskii, D. Khomskii, and M. Mostovoy.

[1] P.-J. Hsu, A. Kubetzka, A. Finco, N. Romming, K. von Bergmann, and R. Wiesendanger, *Nature Nanotechnology*, **12** (2017) 123-126.

[2] A.P. Pyatakov, D.A. Sechin, A.S. Sergeev, A.V. Nikolaev, E.P. Nikolaeva, A.S. Logginov, and A.K. Zvezdin, *EPL* **93** (2011) 17001.

[3] P.I. Karpov, S.I. Mukhin, arXiv:1701.01842 (2017).

[4] M.V. Mostovoy, *Phys.Rev.Lett.*, **96** (2006) 067601.

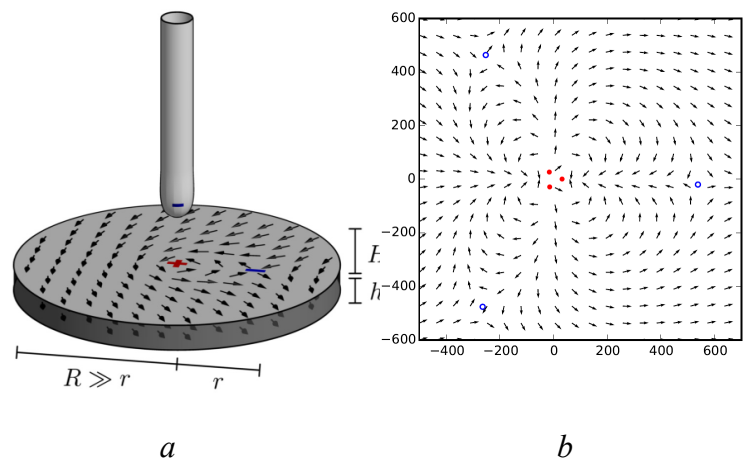


Fig. 1. *a)* For tip’s charge $\varphi_{\text{tip}} = \varphi_{\text{crit}}$ first vortex pair forms. *b)* In-plane view of vortex-antivortex system for $\varphi_{\text{tip}} > \varphi_{\text{crit}}$ vortex cores (filled circles), antivortex cores (open circles), and magnetization (arrows) are shown.

3OR-F-5

THE COULOMB BASED MAGNETO-ELECTRIC COUPLING IN MULTIFERROIC TUNNEL JUNCTIONS

Udalov O.G.^{1,2}, Beloborodov I.S.¹

¹ California State University Northridge, Northridge, CA, USA

² Institute for Physics of Microstructures RAS, Nizhny Novgorod, Russia
oleg.udalov@csun.edu

Magnetic tunnel junctions are of great importance these days because of their promise for next generation memory cells. However, there are several issues to create such memory cells. One of them is control of magnetic state of ferromagnetic leads in magnetic tunnel junctions. This problem requires a fundamental research and understanding of spin currents and interlayer exchange coupling mechanisms in magnetic tunnel junction .

We studied the exchange coupling in magnetic tunnel junction consisting of two ferromagnetic layers separated by the insulating ferroelectric spacer. We calculated the exchange coupling due to many-body effects (the inter-electron Coulomb interaction). The basic idea behind this mechanism is related to the fact that the wave functions of electrons located at different ferromagnetic leads are overlapped inside the insulating layer. In combination with weak screening of electric field inside the insulator these electrons experience the exchange interaction – the spin-dependent part of the Coulomb interaction. This leads to interlayer magnetic coupling. The proposed mechanism is similar to Heitler-London exchange interaction, but extended to the case of two ferromagnetic electrodes. The Coulomb based magnetic coupling complements the known interaction between magnetic layers based on virtual electron hopping considered by Slonczewski. We showed that the Coulomb based interlayer coupling can exceed the hopping based exchange contribution and found that these two mechanisms have essentially different dependence on system parameters.

We found that, in contrast to hopping based exchange, the Coulomb based exchange interaction is inversely proportional to the dielectric constant ϵ of the insulating layer. The dependence of the interlayer magnetic interaction on the dielectric properties of the insulating layer in magnetic tunnel junction is similar to magneto-electric effect where electric and magnetic degrees of freedom are coupled. We calculated the interlayer exchange as a function of temperature and electric field (or voltage) for magnetic tunnel junction with insulating layer made of TTF-CA and HfZrO ferroelectrics. We showed that in the vicinity of the ferroelectric phase transition of TTF-CA the interlayer exchange experiences large variations. We found that even the ferromagnetic-antiferromagnetic transition may occur in magnetic tunnel junction for some system parameters.

We found that exchange interaction between magnetic leads as a function of electric field (or applied voltage) shows strong variations. The electric field can cause the transition from antiferromagnetic to ferromagnetic coupling: for zero field the coupling is antiferromagnetic while for finite field it is ferromagnetic. This effect demonstrates the magneto-electric coupling in the system.

This research was supported by NSF under Cooperative Agreement Award EEC-1160504, the U.S. Civilian Research and Development Foundation (CRDF Global) and NSF PREM Award. O.U. was supported by Russian Science Foundation (Grant 16-12-10340).

3TL-F-6

MAGNON-PHONON/MAGNON COUPLING IN MULTIFERROIC (Y,Lu)MnO₃

Park J.G.^{1,2}

¹ Center for Correlated Electron Systems, Institute for Basic Science (IBS), Seoul 151-747, Korea

² Department of Physics & Astronomy, Seoul National University, Seoul 151-747, Korea
jgpark10@snu.ac.kr

Multiferroic hexagonal manganites are believed to host a generically strong spin-lattice coupling and produce a magnetoelectric coupling [1]. This large spin-lattice coupling has since been observed in many other multiferroic or magnetic materials. However, how this spin-lattice coupling leads to a new form of excitations in its dynamic spectra is unknown. This question is directly related to a rather unusual coupling between magnon and phonon. This coupling is rare in nature and so can be tricky to observe experimentally and analyze theoretically. We have made extensive studies in search for this rare phenomenon in (Y,Lu)MnO₃, where noncollinear antiferromagnetism produces a magnon-phonon coupling. We have now not only demonstrated its existence beyond reasonable doubt but also quantified it [2]. We also found the evidence for a strong magnon-magnon coupling in its spin waves [3]. We will discuss how this rare magnon-phonon coupling can be generalized to other magnetic systems.

- [1] Seongsu Lee, A. Pirogov, Misun Kang, Kwang-Hyun Jang, M. Yonemura, T. Kamiyama, S-W. Cheong, F. Gozzo, Namsu Shin, H. Kimura, Y. Noda, and J.-G. Park, *Nature*, **451** (2008) 805.
- [2] Joosung Oh, Manh Duc Le, Ho-Hyun Nahm, Hasung Sim, Jaehong Jeong, T. G. Perring, Hyungje Woo, Kenji Nakajima, Seiko Ohira-Kawamura, Zahra Yamani, Y. Yoshida, H. Eisaki, S.-W. Cheong, A. L. Chernyshev, and Je-Geun Park, *Nature Communications*, **7** (2016) 13146.
- [3] Joosung Oh, Manh Duc Le, Jaehong Jeong, Jung-hyun Lee, Hyungje Woo, Wan-Young Song, T. G. Perring, W. J. L. Buyers, S-W. Cheong, and Je-Geun Park, *Phys. Rev. Lett.*, **111** (2013) 257202.

3TL-F-7

MAGNETOELECTRICITY AT THE ANTIPEROVSKITE/PEROVSKITE INTERFACE

Shao D.-F.¹, Paudel T.R.¹, Tsymbal E.Y.¹

¹ Department of Physics and Astronomy, University of Nebraska, Lincoln, Nebraska 68588, USA
jgpark10@snu.ac.kr

Complex oxide materials with the perovskite crystal structure (ABO_3) are known for their interesting macroscopic physical properties involving the interplay between magnetism, ferroelectricity, and conductivity. Much less explored are the *antiperovskite* compounds (AXM_3) where the atomic positions of cations and anions are inverted creating unique, wide-ranging properties different from perovskites. For example, it has been demonstrated that antiperovskite materials may exhibit superconductivity, negative thermal expansion, and magnetoresistance. Moreover, theoretical predictions suggest that some of the antiperovskites reveal topologically non-trivial behavior. Due to the structural similarity, interfaces combining perovskite and antiperovskite compounds can be fabricated, forming a new playground for materials design, where the coupling across the interface may lead to new fundamental properties and functional behavior. Here, based on density-functional calculations, we explore the magnetoelectric effect at the (001) interface between antiperovskite $GaN Mn_3$ and perovskite $ATiO_3$ ($A = Sr$ and Ba). Bulk $GaN Mn_3$ is an antiferromagnet with the magnetic moments of the Mn ions lying in the (111) planes, forming non-collinear Γ^{3g} spin configurations with a zero net magnetization ground state. Our calculations predict that different from the Γ^{5g} non-collinear magnetism of the bulk $GaN Mn_3$, strong magnetic moment enhancement and reorientation emerge at the $GaN Mn_3/ATiO_3$ (001) interface, resulting in a sizable net magnetization pointing along the [110] direction. Moreover, we find that switching of the ferroelectric polarization of $BaTiO_3$ drives the reversal of the net magnetization of $GaN Mn_3$. This phenomenon occurs due to the effect of ferroelectric polarization on the magnitude of the antiferromagnetic exchange coupling between the nearest Mn atoms at the interface. Reversal of magnetization by electric means is the holy grail of voltage-controlled spintronics, and thus our results pave a new route to achieve this functionality by exploiting antiperovskite/perovskite interfaces.

3TL-F-8

STRUCTURE AND MAGNETISM OF THE MULTIFERROIC Co/PZT/LSMO INTERFACE

Meyerheim H.L.¹, Ernst A.¹, Mohseni K.¹, Polyakov A.¹, Quindeau A.¹, Antonov V.^{1, 2}, Vasili H.B.³, Crozier E.D.⁴, Xiao Q.F.⁵, Valvidares M.³, Gargiani P.³

¹ MPI für Mikrostrukturphysik, D-06120 Halle, Germany

² Institute for Metal Physics, 36 Vernadsky Street, 03142 Kiev, Ukraine

³ Alba Synchrotron Light Source, 08290 Cerdanyola del Vallès Barcelona, Spain

⁴ Simon Fraser University, Dept. of Physics, Burnaby, Canada

⁵ Canadian Light Source, Saskatoon, SK, Canada

holger.meyerheim@mpi-halle.mpg.de

A ferromagnetic (FM) tunneling junction becomes a multiferroic one if the tunneling barrier is a ferroelectric. Such ferroelectric tunneling junctions (FTJ's) have attracted intense interest, since the polarization switching of the ferroelectric barrier adds another degree of freedom ($P\uparrow$ or $P\downarrow$) in addition to the FM electrodes orientation [1-4]. The FTJ Co/2uc Pb(Ti_{0.8}Zr_{0.2})O₃/ 60uc La_{0.7}Sr_{0.3}MnO₃/SrTiO₃(001) represents one prototype system (uc= layer thickness in unit cells) Using surface x-ray diffraction (SXRD), x-ray absorption fine structure (XAFS) and x-ray circular dichroism (XMCD) experiments we have studied the geometric and magnetic properties of the Co/Pb(Ti_{0.8}Zr_{0.2})O₃ interface after in-situ deposition of sub-monolayer amounts of Co. The SXRD analysis indicates that the Co deposition on the 2 uc thick (Ti, Zr) O₂ terminated Pb(Ti_{0.8}Zr_{0.2})O₃ (PZT) layer leads to the formation of a perovskite (PV) type structure, i.e. the crystal is continued by islands with a CoO₈ like (cubic) environment followed by a layer with a CoO₆ (octahedral) coordination. XAFS experiments above the Co-K-edge support this view by revealing correlations which can be related to a Co-O distances of approximately 2.0 Å (octahedral) and 2.8 Å (cubic) in addition to a metallic Co-Co correlation near 2.4 Å.

In agreement with the structure analysis, XMCD spectra at the Co-L_{2,3} edge reveal three different contributions (see Fig.1). We find two Co-O contributions (A) and (B) related to the octahedral coordination ($m=2.69\mu_B$) and the cubic coordination ($m=2.33\mu_B$). In both cases the easy axis is in the film plane. We find induced moments at the Ti site of the 2 uc thick PZT film, namely $m=-0.005\mu_B$ and $+0.010\mu_B$ for the top and second uc. Our analysis confirms previous studies (e.g. Refs. [2, 4]) suggesting an anti-FM oriented induced moment at the Ti site in the as grown state related to the negative tunneling electro resistance effect. Our study is a direct proof of the "hybridization model" which is valid even in the case of the PV type cobalt oxide structure on the PZT layer being markedly different from theoretically considered site of Co on the O atoms of the PZT layer [1-4]

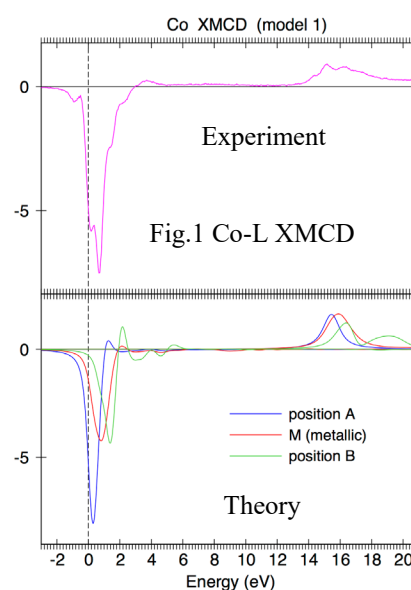
Support by the DFG through SFB 762 is acknowledged.

[1] C.G. Duan, S.S. Jaswal, and E.Y. Tsymlal, *Phys. Rev. Lett.*, **97** (2006) 047201.

[2] M. Fechner, I. V Maznchnko, S. Ostanin et al., *Phys. Rev. B*, **78** (2008) 212406.

[3] V.S. Borisov, S. Ostanin, I.V. Maznchnko et al., *Phys. Rev. B*, **89** (2014) 054436.

[4] D. Pantel, S. Goetze, D. Hesse, and M. Alexe, *Nat. Mat.*, **11** (2012) 289.



3OR-F-9

STRUCTURAL, ELECTRICAL AND MAGNETIC PROPERTIES OF MODIFIED BiFeO₃

Nitin K.¹, Shukla A.¹, Choudhary R.N.P.²

¹ Department of Physics, National Institute of Technology Mizoram, Aizawl-796012, India

² Multifunctional Materials Research Laboratory, Department of Physics, SOA University,
Bhubaneswar-751030, India
aloks.nitmz@gmail.com

Nowadays, much attention is paid on the development of pure as well as mixed metal oxides, to be used for multifunctional applications. The present work mainly reports the studies of electrical and magnetic characteristics of (Ni/Ti) modified BiFeO₃. A polycrystalline multiferroics of lead free compounds (BNT and BFO) in different ratio were synthesized using a standard high temperature solid state reaction technique. The co-substitution of Ni⁺² and Ti⁺⁴ at the Fe⁺³ site of BiFeO₃ enhance its various properties with significant reduction of electrical leakage current. Room temperature surface morphologies and textures of the samples recorded by a field emission scanning electron microscope reveal the uniform distribution of grains on as-prepared samples. Detailed analysis of dielectric and impedance data, collected in a wide range of frequency and temperature has provided many important results on structure-property relation and dielectric relaxation of modified BiFeO₃. The enhanced magnetic parameters will be useful for magnetic field sensor application.

[1]Alok Shukla, Nitin Kumar, C. Behera, R.N.P Choudhary, *J. Mater. Sci. Mater. Electron.*, **27** (2016) 1209–1216.

[2] Alok Shukla, Nitin Kumar, C. Behera, R.N.P Choudhary, *J. Mater. Sci. Mater. Electron.*, **27** (2016) 7115-7123.

[3] Nitin Kumar, Alok Shukla, R.N.P Choudhary, C. Behera, *J. Alloys Comp.*, **688** (2016) 858-869.

3OR-F-10

NEW PEROVSKITES IN R_2O_3 - Mn_2O_3 SYSTEMS ($R =$ RARE-EARTHS)

Zhang L.^{1,2}, Matsushita Y.¹, Katsuya Y.³, Tanaka M.³, Yamaura K.^{1,2}, Belik A.A.¹

¹ National Institute for Materials Science (NIMS), Tsukuba, Japan

² Hokkaido University, Sapporo, Japan

³ Synchrotron X-ray Station at SPring-8, NIMS, Hyogo, Japan

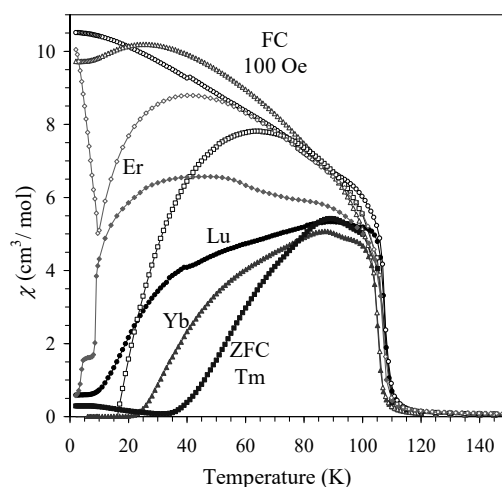
Alexei.Belik@nims.go.jp

Rare earth trivalent manganites, belonging to R_2O_3 - Mn_2O_3 systems with $R =$ rare-earth elements, have been a playground for solid-state and materials chemists and physicists for decades. The most studied compounds have the 1:1 $RMnO_3$ stoichiometry, and two modifications of $RMnO_3$ exist: an orthorhombic perovskite modification with space group $Pnma$ and a non-perovskite hexagonal modification with space group $P6_3cm$. Distortions of $RMnO_3$ perovskites increase with decreasing the size of R^{3+} cations, and it is reflected in the increased magnitude of octahedral tilts, which in turn affect the transition metal-oxygen angles and the ground state magnetic ordering. With small enough tilts spin-driven multiferroic properties appear in $RMnO_3$. The R_2O_3 - Mn_2O_3 systems also have compounds with the 1:7 RMn_7O_{12} stoichiometry, and all manganese cations located at the A site and B site have the oxidation state of +3.

In this work, we report on Mn-self-doping of the 1:1 $RMnO_3$ perovskites with the composition reaching $(R_{0.667}Mn_{0.333})MnO_3$ (or the 1:2 stoichiometry) and discovery of new perovskites with the 1:3 RMn_3O_6 stoichiometry under high-pressure and high-temperature conditions.

Crystal structures were studied by single-crystal X-ray diffraction and synchrotron X-ray powder diffraction. $(R_{0.667}Mn_{0.333})MnO_3$ crystallizes in space group $Pnma$ with $a = 5.50348(2)$ Å, $b = 7.37564(1)$ Å, $c = 5.18686(1)$ Å for $(Lu_{0.667}Mn_{0.333})MnO_3$ at 293 K, and they are isostructural with the parent $RMnO_3$ manganites. Mn enters the A -site in the oxidation state of +2 creating the average oxidation state of +3.333 at the B site. In comparison with $RMnO_3$, $(R_{0.667}Mn_{0.333})MnO_3$ exhibits enhanced Neel temperatures $T_N = 110$ K and canted antiferromagnetic properties (Fig. 1). Compounds with $R =$ Er and Tm show additional magnetic transitions below about 15 K. No multiferroic properties were found in $(R_{0.667}Mn_{0.333})MnO_3$.

The charge distribution in RMn_3O_6 is $[R^{3+}Mn^{2+}_{0.5}Mn^{3+}_{0.5}]_A[Mn^{3+}Mn^{3.5+}]_B O_6$ with unusual five-fold cation ordering, while the average oxidation state of manganese is still +3. They crystallize in space group $Pm\bar{m}n$ with $a = 7.2479(2)$ Å, $b = 7.4525(3)$ Å, and $c = 7.8022(2)$ Å for $DyMn_3O_6$ at 213 K, and they are structurally related with $CaFeTi_2O_6$. RMn_3O_6 compounds show complex magnetic behaviors with several transition temperatures, and magnetic properties are highly sensitive to the non-stoichiometry.



3OR-F-11

PHASE TRANSITIONS AND CRITICAL PHENOMENA IN SUPERLATTICE MULTIFERROIC NANOFILMS

Nugumanov A.G.¹, Sharafullin I.F.^{1,2}, Diep H.T.²

¹ Bashkir State University, Ufa, Russian Federation

² Cergy-Pontoise University, Cergy-Pontoise, France
aidar.nugumanov@gmail.com

Phase transitions and critical phenomena along with surface effects in multilayer multiferroic ultrathin films draw a vast scientific interest due to them having a number of unique properties which can be used for nanoelectronic and spintronic devices as well as for those using a giant magnetoresistance effect [1]. Besides naturally occurring multiferroics (crystals with both magnetic and ferroelectric ordering), such as transition metal oxides with perovskite crystal structure (YMnO₃ etc.), there are a number of options to create crystals with desired properties. One of them is to construct a multiferroic heterostructure (superlattice) – several magnetic ultrathin (<100 atomic layers) magnetic films merged with ultrathin ferroelectric films intersecting them (Fig. 1).

For computation we use Metropolis algorithm of Monte-Carlo methods [2]. We choose the Hamiltonian for the structure as follows:

$$\hat{H} = \hat{H}_m + \hat{H}_f + \hat{H}_{mf} \quad (1)$$

where magnetic part \hat{H}_m is described with Heisenberg model in external magnetic field,

\hat{H}_f – ferroelectric part with continuous Ising model (-1.5..+1.5) in external electric field, and

$$\hat{H}_{mf} = -\frac{1}{2} \sum_{ijk} J_{ijk}^{mf} \vec{S}_i \vec{S}_j P_k \quad (2)$$

– magnetoelectric interaction part (non-zero only for interface sublayers).

Our simulation was held on superlattice with size of 40x40x(4x2) sites. We have obtained phase diagrams in (J^{mf}, T_c) dimensions, as well as temperature dependencies of sublayers' magnetization, polarization, energy and susceptibilities. They show specific behavior and a variety of phase transitions due to the magnetoelectric interaction. The area of parameters $J^{mf} = -0.45..-0.15$ $|\vec{H}| = 0.15$ $|\vec{E}| = 0.15$

and $J^m = J^f$ is of special interest (Fig.2), because in these conditions there exist some frustrated states.

[1] A.P. Pyatakov, A.K. Zvezdin, *Phys.-Usp.*, 55 (2012) 557.

[2] M.Kh. Kharrasov, I.R. Kyzrygulov, I.F. Sharafullin, A.G. Nugumanov, *Solid State Phenom.*, 233-234 (2015) 383-387.

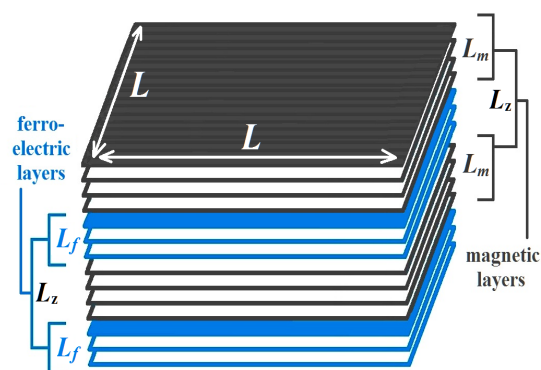


Fig. 1. Multiferroic superlattice nanofilm

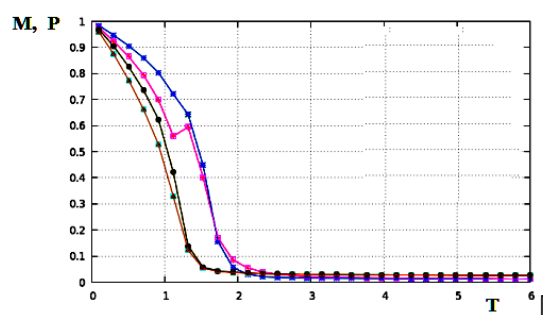


Fig. 2. Temperature dependences of sublayers magnetization and polarization.

3OR-F-12

CRYSTAL STRUCTURE AND MAGNETIC PROPERTIES OF Ca AND Mn Co-DOPED BiFeO₃

Karpinsky D.V.^{1,2}, Troyanchuk I.O.^{1,2}, Silibin M.V.¹, Gavrilov S.A.¹

¹ National Research University of Electronic Technology “MIET”, Zelenograd, Moscow, Russia

² Scientific-Practical Materials Research Centre of NAS of Belarus, 220072 Minsk, Belarus

karpinsky@physics.by

BiFeO₃-based perovskite-like materials have attracted a great attention of the researchers in the field of condensed matter physics [1, 2]. Hence BiFeO₃ has zero remnant magnetization recent investigations testify that BiFeO₃-based compounds with a substitution of Bi- and Fe ions can simultaneously possess polar structure and a weak ferromagnetism. In the current abstract we report on the crystal structure and magnetic properties of Bi_{1-x}Ca_xFe_{1-x}Mn_xO₃ compounds as a function of dopant increase up to $x = 0.3$.

The X-ray and neutron diffraction patterns obtained for the Bi_{1-x}Ca_xFe_{1-x}Mn_xO₃ ceramics have confirmed single-phase rhombohedral crystal structure for the compounds with $x \leq 0.18$. Chemical substitution induces structural phase transition into the orthorhombic phase. The diffraction patterns recorded for the compounds with $x \geq 0.2$ were successfully refined assuming orthorhombic distortion of the unit cell described by centrosymmetric space group *Pnma*. The intermediate region having two structural states is restricted within the concentration range of 1%.

Chemical doping significantly modifies magnetic properties of the compounds. The field dependencies of magnetization testify that the compounds with $x < 0.05$ at room temperature possess antiferromagnetic structure with small remnant magnetization (~ 0.025 emu/g). An increase of the magnetic field up to ~ 5 T triggers the transition into magnetic state with larger magnetization (Fig.1). This transition is associated with a collapse of spatially modulated antiferromagnetic structure and an appearance of homogeneous weak ferromagnetic state. The remnant magnetization gradually increases with dopant concentration. The magnetization data testify that the compounds with $x > 0.2$ are characterized by inhomogeneous magnetic state where relatively small clusters with dominant ferromagnetic interactions coexist along with the long-range antiferromagnetic matrix. It is assumed that ferromagnetic-like clusters are stabilized within Mn-rich regions. The ferromagnetic interactions stabilized within these clusters can be reinforced by strong magnetic field while dominant antiferromagnetic matrix formed by negative interactions between Fe³⁺ - Fe³⁺ remains practically unaffected.

This work was supported by the RSF (project #15-19-20038).

[1] G. Catalan, J.F. Scott, *Adv. Mater.*, **21** (2009) 2463.

[2] M. Fiebig, *J. Phys. D: Appl. Phys.*, **38** (2005) R123.

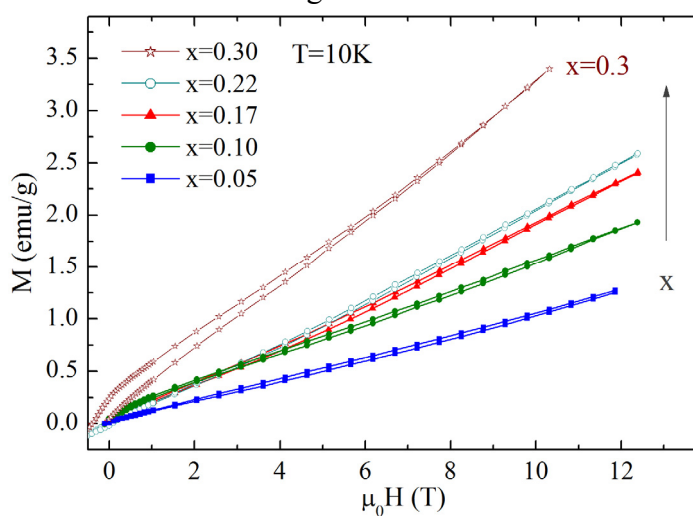


Fig.1 Field dependencies of magnetization obtained at T=10 K.

3 July

Monday

11:30-13:00

14:30-17:00

oral session

3TL-G

3OR-G

**“Magnetic Soft Matter
(magnetic polymers,
fluids and
suspensions)”**

3TL-G-1

INITIAL DYNAMIC SUSCEPTIBILITY OF MAGNETIC FLUIDS: EXPERIMENT, THEORY, AND COMPUTER SIMULATIONS

*Ivanov A.O.¹, Kantorovich S.S.^{1,2}, Elfimova E.A.¹, Zverev V.S.¹, Lebedev A.V.³, Pshenichnikov A.F.³,
Camp P.J.⁴*

¹ Ural Federal University, Ekaterinburg, Russia

² University of Vienna, Vienna, Austria

³ Institute of Continuous Media Mechanics, Perm, Russia

⁴ University of Edinburgh, Edinburgh, Scotland

Alexey.Ivanov@urfu.ru

Here we present a combined experimental and theoretical study [1] aimed at analyzing the dynamic zero-field susceptibility of magnetic nanoparticle suspensions. A specific feature of magnetic nanoparticles suspended in a liquid carrier is that they can exhibit various magnetic relaxations depending on their size. Thus, the polydisperse system is expected to respond to the AC fields in a unique way depending on the particle size distribution. On the other hand, the inherent magnetic interparticle correlations, which change with temperature and nanoparticle concentration, cannot but affect the dynamics of the system and might lead to a qualitative change in the response. In order to carefully separate all these dependencies, we obtained seven samples with an identical particle size distribution different only in the nanoparticle volume fraction by using a basic sample. The particle size distribution was first defined by magneto-granulometry based on static magnetic measurements and then verified comparing a reliable theoretical model to the initial static zero-field susceptibility measured for all the seven samples.

As a next step, we measured dynamic zero-field complex susceptibility at five different temperatures in the range of almost 100 K for all samples. The response we obtained for different nanoparticle concentrations turned out to be qualitatively similar and showed strong temperature dependence. Here, it is worth mentioning that the carrier remained liquid in all the experiments. At high temperatures, the real part of the spectra of the magnetic response remains basically constant, and the imaginary parts show almost no maxima in the investigated frequency range ($10-10^5$ Hz). This clearly changes at lower temperatures, at which the real part shows a rapid decrease at rather low frequencies (10^2 Hz), and the low frequency maximum starts being clearly observable. In order to elucidate the physical origin of this behavior at low concentrations, we applied an earlier developed mean-field approach [2], in which the dipolar correlations are accurately considered. Apart from finding a very good agreement between our theoretical approach and the experimental data for dilute samples, we also managed to show how, in this concentration range, the magnetic correlations determine the dynamic response, which is clearly different from the Debye superposition of individual nanoparticle magnetic relaxations. Beyond the mean-field limit, when the concentrations of magnetic nanoparticles are high and the temperature is low, we perform a thorough analysis of the dynamic spectra, extensively comparing them to the individual particle relaxation times. This allows us to conclude that the slow response cannot be attributed to a very small fraction of large magnetic nanoparticles, but is rather caused by the presence of large particle structures in which magnetic moments are very strongly correlated and cannot react fast enough to the externally applied magnetic field. However, the correlations in this parameter range are dynamic and their signature cannot be found in the static magnetic response.

Support by Russian Science Foundation (Grant No. 15-12-10003) is acknowledged.

[1] A.O. Ivanov, et al., *Phys. Chem. Chem. Phys.*, **18** (2016) 18342-18352.

[2] A.O. Ivanov, V.S. Zverev, S.S. Kantorovich, *Soft Matter*, **12** (2016) 3507-3513.

3TL-G-2

SYNCHRONOUS ROTATION OF MAGNETOTACTIC BACTERIA

Belovs M.¹, Livanovics R.¹, Cebers A.¹
¹ University of Latvia, Riga, Latvia

aceb@tesla.sal.lv

Magnetotactic bacteria in a low frequency rotating field move along circular trajectories. Here we consider the behaviour of an ensemble of these circle swimmers, which shows some interesting features due to their hydrodynamic interactions. Each bacterium is acting on the liquid by a force dipole $Fb\vec{e}_i$ ($i=1,\dots,N$). The equations of motion for the bacteria read (v_b is the self-propulsion velocity of a bacterium)

$$\frac{d\vec{r}_i}{dt} = \pm \frac{Fb}{8\pi\eta} \left(-\frac{\vec{r}_i - \vec{r}_j}{|\vec{r}_i - \vec{r}_j|^3} + \frac{3(\vec{e}_j \cdot (\vec{r}_i - \vec{r}_j))^2 (\vec{r}_i - \vec{r}_j)}{|\vec{r}_i - \vec{r}_j|^5} \right) + v_b \vec{e}_i; \quad \frac{d\vec{e}_i}{dt} = \vec{\omega} \times \vec{e}_i, \quad (1)$$

where the plus sign corresponds to pushers and the minus sign to pullers. In a synchronous regime $\vec{e}_i(t) = (-\sin(t), \cos(t))$. Introducing the position vector of the centers $\vec{R}_i = (X_i, Y_i)$ of the bacterial trajectories according to $\vec{R}_i = \vec{r}_i + (\cos(t), \sin(t))$ and accounting for steric interactions it is possible to derive the following set of equations ($Z_i = X_i + iY_i$)

$$\frac{dz_i}{dt} = \lambda \sum_{j \neq i} \frac{1}{2} \frac{z_i - z_j}{|z_i - z_j|^3} - \frac{3}{4} \frac{e^{2it} (z_i^* - z_j^*)^2 + e^{-2it} (z_i - z_j)^2}{|z_i - z_j|^5} - \frac{z_i - z_j}{|z_i - z_j|^{13}}, \quad (2)$$

where $\lambda = \pm Fb\omega^2 / 8\pi\eta v_b^3$.

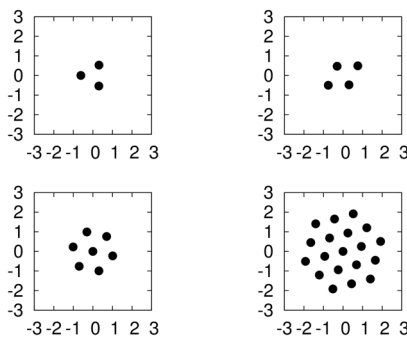


Fig.1

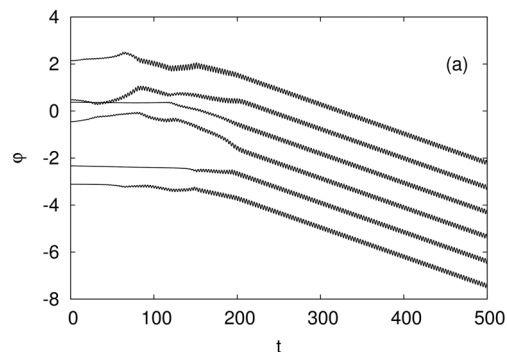


Fig.2

Equations (2) predict the formation of quasi-regular structures in a slow time scale (Fig.1). Simultaneously with the formation of the quasi-regular lattice synchronized rotations of bacteria in the direction opposite to the direction of rotation of the field arise as for the outer boundary of the aggregate in the case $N=7$ is shown in Fig.2. Details of experimental observation of bacteria swarming is given in [1]. The phenomena shown in Figs.1,2 are analysed by a hexatic order parameter calculation, Floquet analysis and stability analysis of different structures.

[1]. K.Bente, G.Kitenbergs, D.Kriman, K.Erglis, M.Belovs, D.Faivre, A.Cebers (to be submitted).

3TL-G-3

DISPERSIONS OF MAGNETIC NANOPARTICLES IN A DEEP EUTECTIC SOLVENT (CHOLINE UREA): MAGNETIC PROPERTIES AND COLLOIDAL STABILITY

Kern C.^{1,2,3}, Gomide G.², Aquino R.^{2,3}, Depeyrot J.², Dubois E.¹, Perzynski R.¹, Peyre V.¹

¹ Sorbonne Universités - UPMC Univ. Paris 6 - CNRS - laboratoire PHENIX, Paris, France

² Complex Fluids Group – Inst. de Física & Inst. de Química – Univ. de Brasília, Brasília, Brazil

³ LNAA – Faculdade UnB Planaltina – Univ. de Brasília, Planaltina (DF), Brazil
regine.perzynski@upmc.fr

Magnetic Fluids (MFs) based on a Deep Eutectic Solvent (DES) are here studied from the point of view of their colloidal and magnetic properties. DES are biodegradable and biocompatible solvents. They present physico-chemical properties similar to those of Ionic Liquids and are a less-expensive alternative to them at room temperature (up to typically 100°C). These DES are mixtures of a quaternary ammonium salt (here Choline chloride) with a hydrogen bond donor (here Urea). The two components, which are solid at room temperature, are here mixed in the proportion 1:2, to form the eutectic ChU 1:2, which is liquid at 300 K [1].

The core-shell $\text{CoFe}_2\text{O}_4@ \gamma\text{-Fe}_2\text{O}_3$ magnetic nanoparticles (NPs) of the MFs are synthesized in water by a co-precipitation method in acid medium [2]. They are then citrate-coated prior to size-sorting thanks to the salt-induced phase-separation method, and transferred in ChU 1:2 following the method described in [3]. The dispersion of three batches of NPs of different median diameter d_0 are here compared in water (pH7) and in ChU 1:2, using different techniques. Fig.1 shows the magnetization of such dispersions in water at a typical volume fraction 1-2% (open symbols) and in ChU 1:2 (full symbols). The direct observation of the corresponding dispersions in ChU 1:2 shows homogeneous samples for (A)- and (B)-NPs, while a macroscopic phase separation is observed with (C)-NPs (top inset of Fig-left). SAXS observations complement the study.

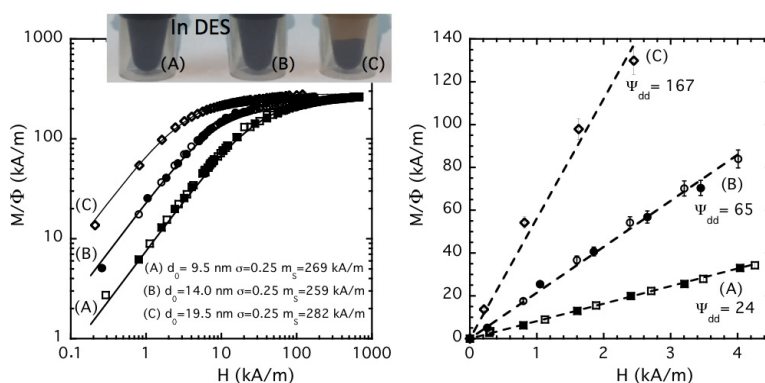


Fig. 1 - (Top left inset) Direct observation of DES dispersions; (Left) Field dependence of the reduced magnetization of the NPs dispersions in water (open symbols) and in ChU 1:2 (closed symbols) with a full field-range adjustment using a lognormal distribution of diameters; (Right) Initial susceptibility adjustment with dipolar magnetic interaction parameter $\Psi_{dd} = \mu_0 m_s^2 V_{NP} / kT$.

Support by ANR-12-PRGE-0011-01(TE-FLIC) and Brazilian Agency CAPES is acknowledged.

[1] A.P. Abbott et al, *Chem. Commun.*, (2003) 70-71.

[2] J. A. Gomes et al *J. Phys. Chem. C*, **112** (2008) 6220-6227.

[3] C. Kern-Barreto, PhD Thesis in Cotutelle between UPMC & UnB - Oct. 27 (2016).

3OR-G-4

THERMOMAGNETIC CONVECTION IN THE CYLINDRICAL ENCLOSURE. 1. ZERO GRAVITY

Krakov M.S.¹, Nikiforov I.V.²

¹ Belarusian National Technical University, 65 Independence Ave., 220013 Minsk, Republic of Belarus

² Belarusian State University, 4 Independence Sq., 220050 Minsk, Republic of Belarus
mskrakov@gmail.com

2D thermomagnetic convection is governed by the system of the equations which are in nondimensional form

$$\operatorname{div} \vec{E} = 0, \operatorname{rot} \vec{H} = 0, \vec{E} = \mu_0(\vec{M} + \vec{H}), \vec{M} = M_s \frac{\chi \vec{H}}{1 + \chi H} (1 - \beta \Delta T), \rho = \rho^*(1 - \beta \Delta T)$$

$$\frac{\partial \omega}{\partial t} + \frac{1}{\operatorname{Pr}} \vec{u} \nabla \omega = \Delta \omega + \operatorname{Ra}_m \left(\frac{\partial \kappa}{\partial x} \frac{\partial \theta}{\partial y} - \frac{\partial \kappa}{\partial y} \frac{\partial \theta}{\partial x} \right), \Delta \psi = -\omega,$$

$$\operatorname{Pr} \frac{\partial \theta}{\partial t} + \vec{u} \nabla \theta = \Delta \theta$$

where $\operatorname{Pr} = \nu/\kappa$, $\operatorname{Ra}_m = \mu_0 M_s^2 \beta \Delta T R^2 / \rho \nu \kappa$, R is the cylinder radius

The cylindrical enclosure filled with the magnetic fluid is surrounded by the solid massive with the constant temperature gradient at the infinity. $\vec{H}_\infty \parallel \nabla T, \vec{H}_\infty = \text{const.}$ The problem was solved numerically for the fluid with the properties: $M_s = 44 \text{ kA/m}$, $\beta = 6.9 \cdot 10^{-4} \text{ K}^{-1}$, $R = 8 \text{ mm}$, $\rho = 1370 \text{ kg/m}^3$, $\nu = 5.0365 \cdot 10^{-5} \text{ m}^2/\text{s}$, $\kappa = 7.1 \cdot 10^{-8} \text{ m}^2/\text{s}$, $\lambda = 0.15 \text{ W}/(\text{m}\cdot\text{K})$, $c = 1547 \text{ J}/(\text{kg}\cdot\text{K})$. For solid massive $\lambda = 0.18 \text{ W}/(\text{m}\cdot\text{K})$, $c = 1270 \text{ J}/(\text{kg}\cdot\text{K})$, $\rho = 1180 \text{ kg/m}^3$.

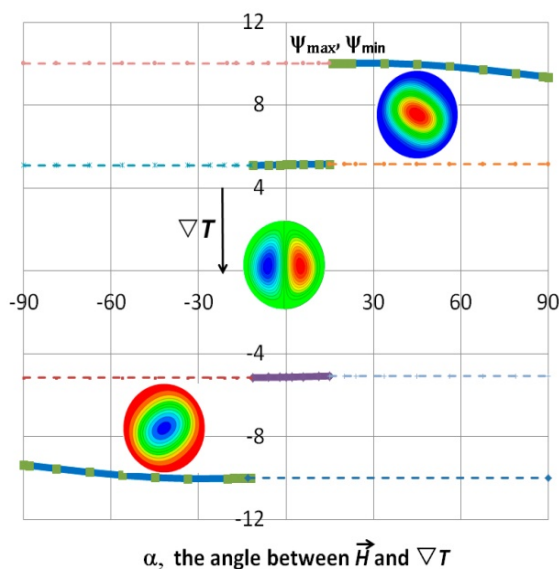


Fig. 1. The maximum (minimum) stream function vs α and the convective structures. Solid lines – structures from the initial zero state, dashed lines – from the neighbor state. $\Delta T = 70 \text{ K}$, $M = 0.95$.

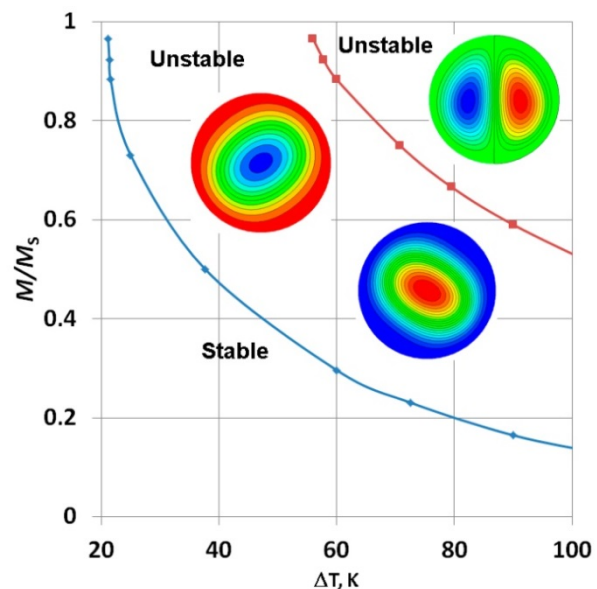


Fig.2. Neutral curves for $\alpha = 0$. The rotation in the case of one cell is arbitrary. The central flow in the two cell case moves in the direction of the temperature gradient.

3OR-G-5

LOW-TEMPERATURE STRUCTURAL PROPERTIES OF THE DIPOLAR HARD SPHERE FLUID

*Ronti M.*¹, *Rovigatti L.*^{2,3}, *Tavares J.M.*⁴, *Ivanov A.O.*⁵, *Sciortino F.*³, *Kantorovich S.S.*^{1,5}

¹ University of Vienna, Vienna, Austria

² University of Oxford, Oxford, United Kingdom

³ University of Rome La Sapienza, Rome, Italy

⁴ University of Lisbon, Lisbon, Portugal

⁵ Ural Federal University, Ekaterinburg, Russian Federation

michela.ronti@univie.ac.at

We investigate the low-temperature behaviour of the dipolar hard sphere (DHS) model. A DHS consists of a point dipole embedded in the centre of a hard sphere, generating long-range anisotropic interactions; at low temperature DHS particles self assemble into complex structures, with primary structures being rings and chains. Despite its simplicity, the DHS model is still the subject of theoretical investigations, aimed at shedding light on the low temperature and low density portion of the phase diagram.

We focus on providing a precise evaluation of the partition functions for the DHS chains and rings. In order to do so, we perform single cluster grand-canonical Monte Carlo (GCMC) simulations. Our approach is much faster than previously used canonical Monte Carlo simulations with large particles ensembles [1]; this advantage in efficiency allows us reaching the part of the DHS phase diagram inaccessible before and observe the precursors of percolation. Secondly, we compare the available analytical expressions of the cluster partition functions [2] against the simulation data and improve them accordingly. In our new theoretical approach we introduce a re-scaling of the temperature to take into account the dipolar interactions between non-nearest neighbours along the cluster backbone [3].

Our results allow us to describe the next hierarchical level of self-assembly in magnetic nano colloids: the aggregation of basic branched clusters into complex networks.

MR acknowledges support from ETN COLLDENSE (H2020-MSCA-ITN-2014, No. 6427774).

[1] L. Rovigatti, J. Russo and F. Sciortino, *Soft Matter*, **8** (2012) 6310-6319.

[2] S.S. Kantorovich, A.O. Ivanov, L. Rovigatti, J.M. Tavares and F. Sciortino, *Phys. Chem. Chem. Phys.*, **139** (2013) 134901-9.

[3] M. Ronti, L. Rovigatti, J.M. Tavares, A.O. Ivanov, S.S. Kantorovich and F. Sciortino, in preparation.

3OR-G-6

DILUTION DEPENDENT MAGNETORHEOLOGICAL EFFECTS OF FLAKE-SHAPED PARTICLE SUSPENSIONS

Siebert E.^{1,2}, Laherisheth Z.², Upadhyay R.V.², Odenbach S.¹

¹ PD PIAS, Charotar University of Science and Technology, Changa, India

² Chair of Magnetofluidynamics, Measuring and Automation Technology, Technische Universität Dresden, Germany
erik.siebert@tu-dresden.de

Magnetorheological (MR)- fluids are suspensions of magnetizable micron-sized particles in non-magnetic carrier liquids, changing their viscous properties in presence of a magnetic field. MR-fluids are part of ongoing developments on innovative technologies such as electronically controlled damping systems, clutches, brakes and artificial joints.

To optimize the performance of MR-fluids it is indispensable to understand how different compositions influence the rheological behaviour. The flake-shaped particles used in this study provide a large relative surface area for interparticle interaction. The dependency of the rheological properties on the particle volume fraction in presence of a magnetic field has been experimentally investigated. Accordingly, the change of viscosity is analyzed, henceforward denoted as the relative viscosity η_r , which is calculated by $\eta_r(\varphi) = (\eta_H - \eta_{H=0}) / \eta_{H=0}$. In consistency the relative yield stress $\tau_{y,r}$ embodies the change of yield stress in dependency of the particle volume portion:

$$\tau_{y,r}(\varphi) = (\tau_{y,H} - \tau_{y,H=0}) / \tau_{y,H=0} \cdot$$

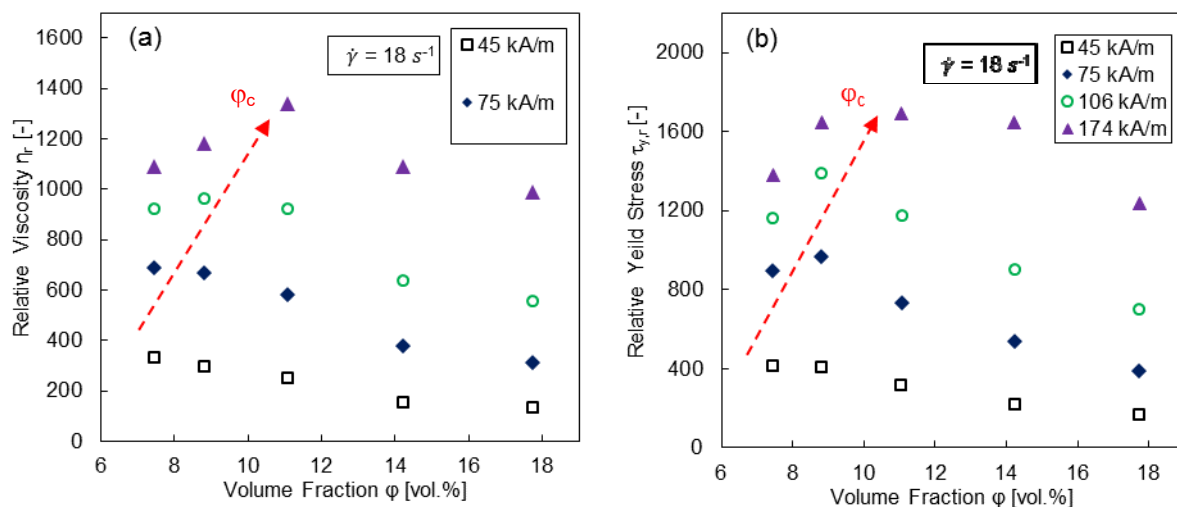


Fig. 1. Relative viscosity (a) and relative yield stress (b) as a function of particle volume fraction under the influence of a magnetic field strength at a constant shear rate of 18 s^{-1} .

As depicted in Fig. 1 (a) the relative viscosity shows a maximum at a critical volume fraction φ_c . The relative viscosity shows a decrement after overcoming this point. The critical volume fraction is dependent on the applied magnetic field strength. The relative yield stress shows qualitatively the same peak shift, as it can be seen in Fig. 1 (b). Concluding, the magnetorheological effect is attenuated by destructive forces due to the presence of a certain amount of particles, which lead to a less efficient microstructure formation [1].

Support by DST-161-G, Government of India, New Delhi.

[1] Siebert et al., *Smart Mater. Struct.* **24** (2015) 075011.

3OR-G-7

ROTATIONAL EFFECT IN SUSPENSIONS OF ANISOTROPIC PIGMENT PARTICLES AND MAGNETIC NANOPARTICLES

Storozhenko A.M.¹, Stannarius R.², Eremin A.², Aref'ev I.M.³

¹ Southwest State University, Kursk, Russia

² Otto von Guericke University, Magdeburg, Germany

³ Ivanovo Power Engineering University, Ivanovo, Russia

Storozhenko_s@mail.ru

The reorientation dynamics of complex liquids in external magnetic fields is important for their potential application in magneto-mechanical and magneto-optical devices, and provides fundamental insights into their structures and internal dynamic mechanisms. The phenomenon that nanostructured magnetic fluids follow a rotating magnetic field is known as the rotational effect [1,2]. We study this effect in binary mixtures of ferrofluids and colloidal suspensions of anisotropic, plate-shaped pigment particles, by exploring its dependence on the concentration of magnetic nanoparticles (MNP) and rheological properties of the carrier fluid.

The detailed description of the setup can be found in Ref. [3]: A spherical glass container completely filled with the liquid sample is fixed to a thin glass fiber and placed in a rotating magnetic field of two pairs of Helmholtz coils. The spherical container geometry provides a uniform demagnetizing field. We determine the magnetic torque density T in dependence on the applied external magnetic field strength B and frequency f from the torsion of the glass string.

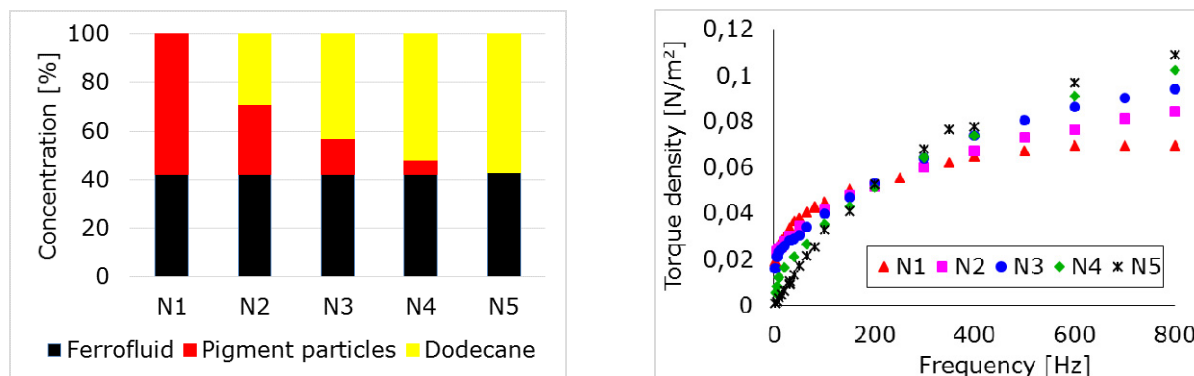


Fig. 1: Compositions (left) and measured torque densities (right) of the investigated samples

We demonstrate that the frequency dependence of the torque strongly depends on the rheological character of the carrier fluid. A monotonic increase of the torque with increasing frequency is found in nearly Newtonian carriers with only small concentrations of the plate-shaped particles (N3-N5). A non-Newtonian character of the fluid (shear-thinning) in suspensions with high concentration of the pigment particles (N1-N2) results in a larger slope of the torque $T(f)$ at low frequencies. The saturation of $T(f)$ shifts to the lower frequency range in samples with higher pigment particles concentrations. This reflects an intricate interaction between the flow induced by the rotating MNPs and the plate-shaped pigments. A detailed theoretical study is required to understand this behavior.

Support by RFBR, Russia within research project No. 16-52-12035/16, and by DFG, Germany within Topical Program SPP 1681, Project STA 425/36, is acknowledged.

[1] A.F. Pshenichnikov, et al., *Magnetohydrodynamics*, **36** (2000) 275-281.

[2] C. Holm, J.-J. Weis, *Current Opinion in Colloid & Interface Science*, **10** (2005) 133.

[3] A.M. Storozhenko, et al., *J. Magn. Magn. Materials*, **431** (2017) 66-69.

3OR-G-8

NONLINEAR RESPONSE OF FERROFLUID TO ALTERNATING MAGNETIC FIELD

Kuznetsov A.A.¹, Pshenichnikov A.F.¹

¹ Institute of Continuous Media Mechanics UB RAS, Perm, Russia
kuznetsov.a@icmm.ru

The dynamic response of magnetic nanoparticle suspension to linearly polarized alternating magnetic field is studied theoretically. Fields of arbitrary amplitude and frequency are considered. Only the Brownian relaxation mechanism of particles' magnetic moments is taken into account. A special emphasis is placed upon the case of a dilute suspension, when interparticle interactions can be neglected. Susceptibilities of the fundamental and high-order magnetization harmonics are calculated via three different equations: Fokker-Planck-Brown equation for the one-particle orientation distribution function, stochastic Langevin equation for the particle rotational movement and Martsenyuk-Raikher-Shliomis macroscopic magnetization equation. Results of the first two approaches coincide in a wide range of frequencies and amplitudes. It is shown that obtaining high-order harmonics via Langevin equation is computationally inefficient at small field amplitudes. Macroscopic equation properly describes the fundamental harmonic, but high-order harmonics deviate from correct values – the error is maximum when the field period is comparable with the Brownian rotational diffusion time. The perspectives of using Langevin equation to study nonlinear dynamic response of concentrated ferrofluids are discussed.

Support by RSF is acknowledged (Grant No. 15-12-10003).

3OR-G-9

MECHANICS OF MAGNETIC FLUID ACTIVE ELEMENT IN STRONG MAGNETIC FIELD

Polunin V.M.¹, Ryapolov P.A.¹, Sheldeshova E.V.¹

¹ Southwest State University, Kursk, Russia
r-piter@yandex.ru

To measure MF-column shear in a strong magnetic field under hydrostatic pressure an experimental setup, the diagram of which is presented in figure 1. In the experiment, we used a laboratory electromagnet FL-1. The transparent tube 1 is fixed between the pole tips. One end of the tube using a silicone tube 3 is connected with the U-shaped tube 4 filled with distilled water. The difference in water levels Δh in the tube elbows is determined using cathetometer.

The diagram of the experimental setup for measuring MF-column oscillation frequency ν is shown in Figure 2. There are some new parts in this setup in comparison with the setup shown in Figure 1. The piston 3 is used to drive oscillations. The signal from the oscillation indicator 4 comes to Selective Nanovoltmeter 5. After amplification, the signal is transmitted oscillograph 6.

From the data of the proposed static experiment (Figure 1) it is possible to estimate magnetostatic saturation magnetization:

$$M_{ss} = \frac{\rho_w g}{2\mu_0} \operatorname{tg} \alpha_s,$$

where $\operatorname{tg} \alpha_s = 2\mu_0 M_x / \rho_w g$.

For a dynamic experiment, we obtain:

$$\pi^3 \nu^2 \rho b d^2 + b d \sqrt{\pi^7 \nu^3 \eta \rho} = \mu_0 \frac{\pi d^2}{2} \left(M_x \frac{\partial H_x}{\partial z} \right)_{z=b/2} \quad \text{The}$$

value of M_x , in the right side of (17) as a result of averaging by approximation represents the saturation magnetization M_{sd} :

$$M_{sd} = \frac{2}{\mu_0 \pi d^2} \operatorname{tg} \alpha_d$$

Let us call the value of M_{sd} , calculated by using this formula magnetodynamic saturation magnetization.

The following results were obtained: the construction and validation of the model theory of elasticity formation of MF in a tube confined by magnetic levitation in a strong magnetic field were carried out, the described technique of complex measuring MF elasticomagnetic parameters in the strong magnetic field is of interest when studying magnetophoresis and aggregation of nanoparticles in magnetic colloids.

The work was support by the project part of the state task of the Ministry of Education and Science of the Russian Federation. Project Code 3.2751.2017 / PP

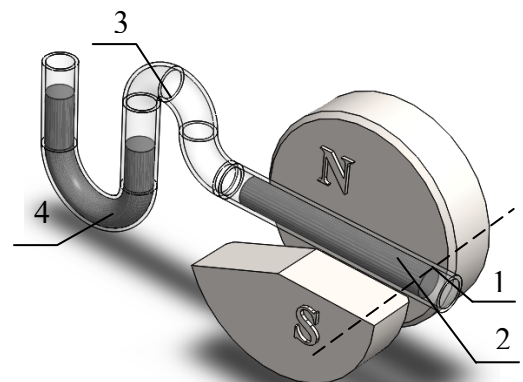


Fig. 1. Static experimental setup diagram

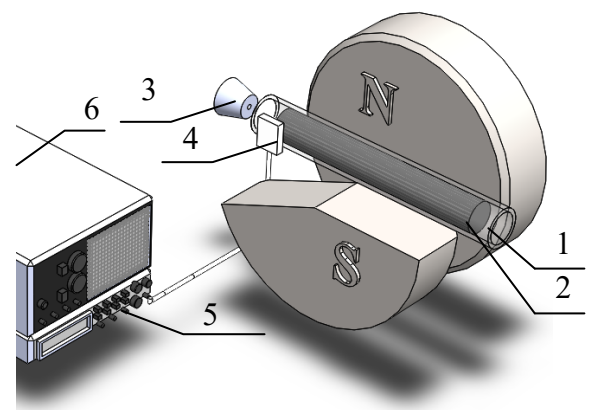


Fig. 2. Dynamic experimental setup diagram

3OR-G-10

ROTATING MAGNETIC MICROPARTICLES IN OPTICAL TRAPS*Romodina M.N.¹, Shchelkunov N.N.¹, Lyubin E.V.¹, Fedyanin A.A.¹*¹ Lomonosov Moscow State University, Moscow, Russia

romodina@nanolab.phys.msu.ru

Magnetic particles actuated by rotating magnetic fields are commonly used as controllable nano- and micromotors and microfluidic mixers. Rotating microparticles are also utilized to twist biological molecules to probe their torsional stiffness as well as to rotate the surrounding fluid to probe the mechanical properties of liquid media [1].

Optical tweezers have emerged as a unique technique allowing for the precise manipulation of the positions of microparticles, thereby making the distance between interacting particles a controllable parameter. Furthermore, optical tweezers are a powerful tool for directly measuring the interaction forces between microparticles and measuring their displacements from the traps and rotation rate [2].

Here we show that rotating magnetic microparticles in optical traps can be used as local microscale heaters and mixers for liquids with volumes on the order of a few picoliters. The temperature of such a trapped microparticle can be controlled with a precision of approximately 1 °C, which may be very useful for studying thermal effects in a variety of biological and chemical microsystems.

Also the determination of the influence of Brownian torque on the rotation of a spherical magnetic microparticle using optical tweezers is reported. The experimental dependences of the microparticle rotation on the external magnetic field strength and the rotational frequency clarify the microparticle dynamics near the transition between the synchronous and asynchronous rotational modes. The results are in agreement with numerical Brownian dynamics simulations of microparticle rotation in the presence of Brownian torques.

The last part of research is devoted to experimental study of the thermophoresis-assisted Magnus force acting on an optically trapped magnetic microparticle rotating in a liquid flow. The results show, that the thermophoretic Magnus force is significant enough to contribute to the motion of the trapped microparticle.

This work was supported by the Russian Foundation of Basic Research (grant #16-32-00100 МОЛ_a).

[1] M.N. Romodina, E.V. Lyubin, A.A. Fedyanin, *Sci. Rep.*, **6** (2016) 21212.

[2] M.N. Romodina, E.V. Lyubin, M.D. Khokhlova, A.A. Fedyanin, *Sci. Rep.*, **5** (2015) 10491.

3OR-G-11

DYNAMICS OF MAGNETIC NANOPARTICLES UNDER ROTATING FIELD WITH ALLOWANCE FOR THE NÉEL AND BROWN RELAXATION MECHANISMS

Stepanov V.I.¹

¹ Institute of Continuous Media Mechanics, Russian Academy of Sciences, Ural Branch, Perm,
614013, Russia
stepanov@icmm.ru

The study of nanoparticles behavior in non-stationary magnetic fields is of a great importance due to direct application of the results to the techniques of biomolecules detection in solution and magnetic hyperthermia. Here we study dynamics of nanoparticles under rotating magnetic field. Two relaxation processes accompany involvement of the particle into rotation. One of them (Brownian) is related to the rotation of the particle in a carrier liquid, thus the corresponding relaxation time τ_B is proportional to the fluid viscosity. The other process (Néel) owes to the magnetization flips from one potential well to another within the particle. Corresponding relaxation time τ_N exponentially depends on the ratio of the barrier height to temperature. An applied magnetic field diminishes the barrier height and thereby τ_N is also diminished. The ratio between τ_B and τ_N determines the coupling of the magnetic and mechanical degrees of freedom. Indeed, in the case $\tau_N \gg \tau_B$ the magnetic moment is "frozen" into the particle body and can rotate only with the particle [1]. In the opposite case ($\tau_N \ll \tau_B$) the magnetic moment is an adiabatic variable that instantly acquires the direction of the effective magnetic field. Then particle's easy axis aligns with it in a time τ_B [2]. Using a general Fokker-Planck equation [3] that takes into account both relaxation processes on equal basis, we study here, besides the mentioned above limits, the crossover case $\tau_N \approx \tau_B$, that was never addressed before.

Support by RFBR grant #14-01-96013 is acknowledged.

[1] Yu.L. Raikher, V.I. Stepanov, *Physical Review E*, **83** (2011) 021401.

[2] J. Cīmurs, A. Cēbers, *Physical Review E*, **88** (2013) 062315.

[3] M.I. Shliomis, V.I. Stepanov, *Advances in Chemical Physics*, **87** (1994) 1-30.

3OR-G-12

COLLOIDAL HEMATITE CUBES: MAGNETIC PROPERTIES AND SELF-ASSEMBLY

Rossi L.¹, Donaldson J.G.², Meijer J.-M.³, Irvine W.T.M.⁴, Petukhov A.V.³, Kantorovich S.S.^{2,5}, Philipse A.P.³, Sacanna S.⁶

¹ Institute of Physics, University of Amsterdam, Amsterdam, the Netherlands

² Faculty of Physics, University of Vienna, Vienna, Austria

³ Debye Institute for Nanomaterials Science, Utrecht University, Utrecht, the Netherlands

⁴ James Franck Institute, Department of Physics, University of Chicago, Chicago, USA

⁵ Ural Federal University, Ekaterinburg, Russian Federation

⁶ Molecular Design Institute, Department of Chemistry, New York University, New York, USA
joe.donaldson@univie.ac.at

Cubic hematite particles carry a unique combination of magnetic, optical and catalytic properties that sets them apart from any other colloidal model systems. Thanks to these distinctive traits, hematite cubes have been vital tools to study the physics of several self-assembling systems [1, 2, 3]. I will present an in-depth study of the magnetic properties of micron-sized hematite cubes. This contribution will focus on the computer simulation portion of the investigation. However, to begin, I will briefly explain how the magnitude and the exact spatial orientation of the particle's magnetic dipole moment was determined experimentally, and provide examples of its impact on the microscopic behaviour observed. I will compare these experimental findings to the computer simulation that were performed, in which various self-assembly scenarios were systematically investigated. These simulations develop upon existing works, already emphasising the importance of dipolar orientation on the resulting self-assembly of cubic magnetic particles [4, 5]. In particular, the simulations discussed here corroborate the conclusions of the experimental studies, providing simultaneously a deeper understanding of the microstructure observed.

[1] J. Palacci *et al.*, *Science*, **339** (2013) 936.

[2] L. Rossi *et al.*, *PNAS*, **112** (2015) 5286.

[3] M. Driscoll *et al.*, *Nat. Phys.*, doi:10.1038/nphys3970.

[4] J.G. Donaldson and S.S. Kantorovich, *Nanoscale*, **7** (2015) 3217.

[5] P. Linse, *Soft Matter*, **11** (2015) 3900.

3OR-G-13

MAGNETIC FLUID BRIDGE BETWEEN TWO CONES AND A CYLINDER IN THE MAGNETIC FIELD OF A CURRENT-CARRYING WIRE

Vinogradova A.S.¹, Turkov V.A.¹, Naletova V.A.¹

¹ Lomonosov Moscow State University, Moscow, Russia
vinogradova.msu@gmail.com

A magnetic fluid (MF) changes its surface shape in the magnetic field of a wire while the current is slowly changing. In [1] the spreading of a MF drop along a wire is studied theoretically and observed in the experiment. A MF drop on a wire with limiting conical surfaces is studied in [2]. In the present paper, we propose to study a MF bridge to open or close the channel of special geometry by imposing the magnetic field of a wire. The use of MF in microvalves is one of actuation methods in microfluidics. In [3] it is shown that a level of pressure in the range of decades of millibar can be expected from a MF. Different magnetic fields could be used to actuate the MF: for example, external magnets [4] and a microcoil [5].

We consider a heavy, incompressible, homogenous, isothermal MF (Fig 1) between two conical surfaces with different apex angles α_1 , α_2 and a cylinder of the radius R_c . There is a wire of the radius r_0 with the current I on the axis of these surfaces. It should be noted that a MF bridge between coaxial cylinders [6] cannot sustain any pressure drop in contrast to this problem where there is the pressure drop $\Delta p = p_1 - p_2$. The MF is immersed in a non-magnetic liquid with the same density. We use the Langevin law to describe a MF magnetization. We get the general analytical solution for any axially symmetric MF surface shape in the magnetic field of a wire from the hydrostatic equation and the boundary condition on the MF surface. Numerical modeling of the MF valve behavior for different values of MF volumes and currents based on this analytical solution is done in the computing environment Maple.

It is shown that the presence of limiting conical surfaces allows the MF to sustain the pressure drop, which is much bigger in case of non-wetting ($90^\circ < \theta_1, \theta_2, \theta_3 \leq 180^\circ$) than in case of wetting ($0^\circ \leq \theta_1, \theta_2, \theta_3 \leq 90^\circ$). In case of wetting the MF cannot sustain any pressure drop for small currents in the wire, but in case of non-wetting the MF bridge can do it even for zero current. Spasmodic and hysteresis phenomena are possible for some values of MF volumes and currents. Presence or absence of these phenomena should be taken into account in the design of microvalves with controlled MF volumes, in which the magnetic field is changed periodically.

Support by the Russian Foundation for Basic Research (project 16-51-12024) is acknowledged.

- [1] J.-C. Bacri et al., *Rev. Phys. Appl.*, **23** (1988) 1017-1022.
 [2] A.S. Vinogradova et al., *Magnetohydrodynamics*, **49** (2013) 350-354.
 [3] R. Pérez-Castillejos et al., *Sensors and Actuators A*, **84** (2000) 176-180.
 [4] H. Hartshorne et al., *Sensors and Actuators B*, **99** (2004) 592-600.
 [5] T.G. Liu et al., *Advanced Materials Research*, **433-440** (2012) 3767-3772.
 [6] V.A. Naletova et al., *Physics Procedia*, **9** (2010) 68-73.

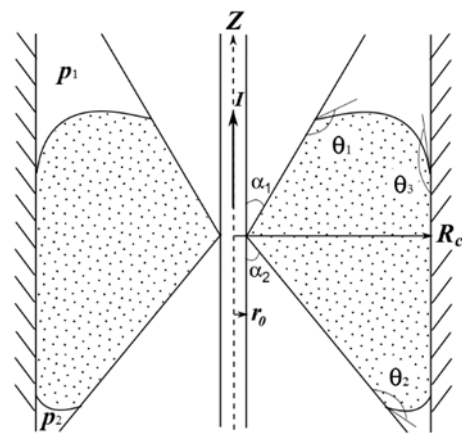


Fig. 1. Magnetic fluid bridge between coaxial conical and cylindrical surfaces in the magnetic field of a wire under a pressure drop in case of non-wetting.

3 July

Monday

11:30-13:00

14:30-17:00

oral session

3TL-H

3OR-H

3RP-H

**“Study of Magnetism
using X-rays and
Neutrons”**

3TL-H-1

STUDIES OF MAGNETISM BY NUCLEAR RESONANCE SCATTERING OF SYNCHROTRON RADIATION

Chumakov A.I.^{1,2}

¹ ESRF-The European Synchrotron, Grenoble, France

² National Research Centre “Kurchatov Institute”, Moscow, Russia

chumakov@esrf.fr

European Synchrotron Radiation Facility (ESRF) offers you to study magnetism by several techniques, in particular – by nuclear resonance scattering of synchrotron radiation. Your access to the facility requires an electronic submission of your proposal for experiment. Once the proposal is approved, all cost for the visit of your team to Grenoble is covered by the ESRF.

The talk reviews the new results obtained by users of the Nuclear Resonance beamline ID18 of the ESRF. They are partly illustrated by the figures below.

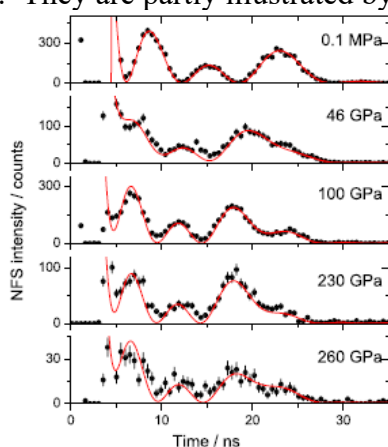


Fig.1. As revealed by quantum beats, Nickel remains magnetic up to 260 GPa. From [1].

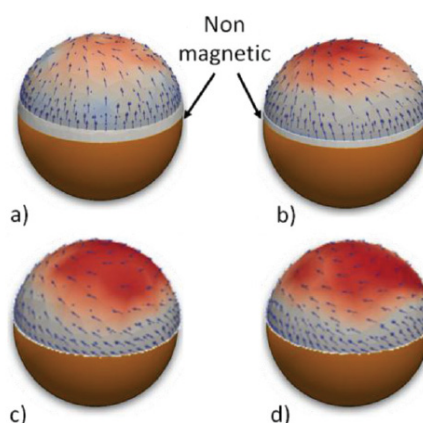


Fig.3. Magnetic structure of iron film on 400 nm nanospheres for film thickness of (a) 28, (b) 38, (c) 42, and (d) 72 Å. From [3].

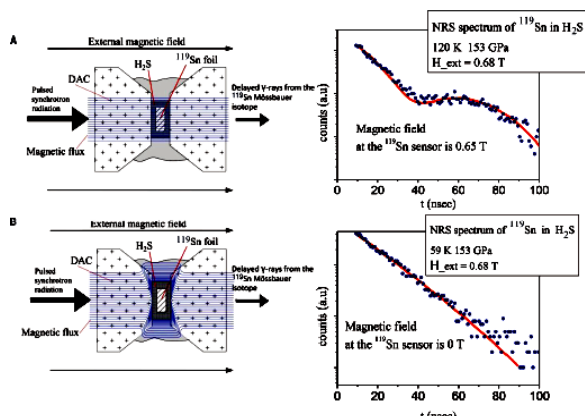


Fig.2. As revealed by nuclear resonance scattering, H₂S at 153 GPa remains in a superconducting state at 120 K. From [2].

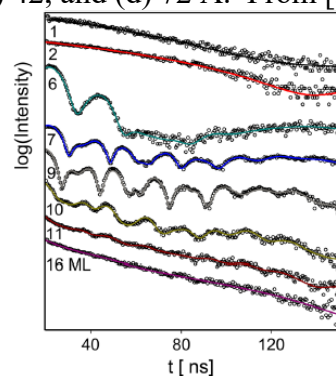


Fig.4. As revealed by quantum beats, 2-Dim. FeO film becomes magnetic for thicknesses between 6 and 9 monolayers. From [4].

[1] I. Sergueev, L. Dubrovinsky, *et al.*, *Physical Review Letters*, **111** (2013) 157601(5).

[2] I. Troyan, A. Gavriluk, R. Ruffer, A. Chumakov, *et al.*, *Science*, **351** (2016) 1303-1306.

[3] D. G. Merkel, D. Bessas, Z. Zolnai, R. Ruffer, *et al.*, *Nanoscale*, **7** (2015) 12878-12887.

[4] N. Spiridis, M. Zajac, P. Piekarczyk, *et al.*, *Physical Review Letters*, **115** (2015) 186102(6).

3TL-H-2

EXCHANGE BIAS IN THIN CO-COO FILMS: INNER SECRETS REVEALED BY POLARIZED NEUTRON REFLECTIVITY

*Temst K.¹, Menendez E.¹, Demeter J.¹, Steitz R.², Wildes A.R.³, Mohd A.S.⁴, Koutsoumpos A.⁴,
Babcock E.⁴, Mattauch S.⁴, Nogués J.⁵, Vantomme A.¹*

¹ Instituut voor Kern- en Stralingsfysica, KU Leuven, Belgium

² Helmholtz-Zentrum Berlin für Materialien und Technologie, Berlin, Germany

³ Institut Laue-Langevin, Grenoble, France

⁴ MLZ, Garching, Germany

⁵ ICN2 and ICREA, Barcelona, Spain

kristiaan.temst@kuleuven.be

Exchange bias (EB) is the interfacial coupling between a ferromagnet (FM) and an antiferromagnet (AFM). It induces a unidirectional magnetic anisotropy in the FM upon cooling in a magnetic field. Since its discovery, this phenomenon has been widely studied in bilayers, core-shell clusters, and patterned films. Polarized neutron reflectivity has played an important role in the study of exchange bias, in particular for the identification of the unusual asymmetry in the magnetization reversal mechanism that is present in e.g. Co/CoO and Fe/FeF₂. Recently we explored a new approach, namely EB systems produced by oxygen ion implantation into Co thin films [1]. The oxygen implantation leads to the local formation of antiferromagnetic CoO buried within the ferromagnetic Co layer, thus creating multiple internal FM/AFM interfaces. Polarized neutron reflectivity allows reconstructing the magnetization depth profile in such an implanted system.

Ferromagnetic Co layers with a thickness of 100 nm were prepared by molecular beam epitaxy. These layers were implanted with oxygen ions using an implantation energy of 60 keV. A strong exchange bias shift is observed once a minimum oxygen fluence has been implanted. We have investigated the correlation between the implantation depth profile and the magnetic depth profile using specular polarized neutron reflectometry (PNR) and found that the local Co magnetization varies in depth as a result of the Gaussian-like implantation profile. PNR experiments also indicated that the implanted exchange bias system does not have the asymmetric magnetization reversal modes typically observed in Co/CoO bilayers.

[1] J. Demeter, J. Meersschaut, F. Almeida, S. Brems, C. Van Haesendonck, A. Teichert, R. Steitz, K. Temst and A. Vantomme, *Appl. Phys. Lett.*, **96** (2010) 132503.

3TL-H-3

MAGNETISM AT EXTREME CONDITIONS: THEORY MEETS X-RAY AND NEUTRONS EXPERIMENTS

Abrikosov I.A.^{1,2}

¹ IFM, Linköping University, Linköping, Sweden

² NUST "MISIS", Moscow, Russia

igor.abrikosov@ifm.liu.se

Theoretical simulations of transition metals and their alloys at extreme conditions of ultra-high pressure and temperature generally rely on a picture of non-magnetic wide-band systems with insignificant local correlations. Upon compression, the overlap between localized states increases and so does the bandwidth W , while the local Coulomb repulsion U between those states is screened more efficiently. The reduction of the U/W ratio is used to rationalize the absence of magnetism and electronic correlations beyond the local or semi-local approximations within the Density Functional Theory (DFT) at high-pressure conditions. We show that this generally accepted picture is incorrect. Carrying out theoretical simulations at the level of Dynamical Mean-Field Theory combined with DFT (DFT+DMFT) coupled to advanced X-rays and neutrons experiments at extreme conditions, we show that magnetic and correlation effects have strong influence on the electronic structure and properties of transition metals, their alloys and compounds. We illustrate this by considering insulator-to-metal transitions (IMT) in transition metal oxides [1,2], and present theoretical and experimental evidences of a novel type of IMT, the site-selective Mott transition in Fe_2O_3 under pressure [3]. Moreover, considering hcp Fe and Os, we show that including correlation effects is necessary for the description of the topological changes of the Fermi surface for valence electrons at high pressure, the so-called electronic topological transition (ETT) [4,5]. Considering Fe at the conditions of the Earth's core, we show that DFT+DMFT calculations allow one for better understanding of the Earth's geodynamo [6,7]. Finally, we illustrate capability of the electronic structure theory to support and interpret neutron powder diffraction measurements of magnetic and structural properties of FeCO_3 at high pressures [8].

- [1] V. Potapkin, L. Dubrovinsky, I. Sergueev, M. Ekholm, I. Kantor, D. Bessas, E. Bykova, V. Prakapenka, R. Hermann, R. Ruffer, V. Cerantola, J. Jönsson, W. Olovsson, S. Mankovsky, H. Ebert, and I. A. Abrikosov, *Phys. Rev. B*, **93** (2016) 201110(R).
- [2] I. Leonov, L. Pourovskii, A. Georges, and I. A. Abrikosov, *Phys. Rev. B*, **94** (2016) 155135.
- [3] E. Greenberg, I. Leonov, S. Layek, Z. Konopkova, M. P. Pasternak, L. Dubrovinsky, R. Jeanloz, I. A. Abrikosov, G. Kh. Rozenberg (submitted).
- [4] K. Glazyrin, L.V. Pourovskii, L. Dubrovinsky, O. Narygina, C. McCammon, B. Hewener, V. Schünemann, J. Wolny, K. Muffler, A. I. Chumakov, W. Crichton, M. Hanfland, V. Prakapenka, F. Tasnádi, M. Ekholm, M. Aichhorn, V. Vildosola, A. V. Ruban, M. I. Katsnelson, I. A. Abrikosov, *Phys. Rev. Lett.* **110** (2013) 117206.
- [5] L. Dubrovinsky, N. Dubrovinskaia, E. Bykova, M. Bykov, V. Prakapenka, C. Prescher, K. Glazyrin, H.-P. Liermann, M. Hanfland, M. Ekholm, Q. Feng, L. V. Pourovskii, M. I. Katsnelson, J.M. Wills, and I. A. Abrikosov, *Nature*, **525** (2015) 226–229.
- [6] L. V. Pourovskii, T. Miyake, S. I. Simak, A. V. Ruban, L. Dubrovinsky, and I. A. Abrikosov, *Phys. Rev. B*, **87** (2013) 115130.
- [7] L. V. Pourovskii, J. Mravlje, A. Georges, S. I. Simak, I. A. Abrikosov, arXiv:1603.02287 [cond-mat.str-el].
- [8] N. O. Golosova, D. P. Kozlenko, L. S. Dubrovinsky, I. A. Abrikosov, A. V. Ponomareva *et al.* (in manuscript).

3RP-H-4

VORTEX MATTER BEYOND SANS: FROM SUPERCONDUCTIVITY TO SKYRMIONS

Muehlbauer S.¹

¹ Heinz Maier-Leibnitz Zentrum (MLZ), Technische Universität München, Garching, Germany
sabrina.disch@uni-koeln.de

Both superconducting vortex [1,2] and skyrmion lattices in chiral magnets [3] can be regarded as macroscopic lattices, formed by topological entities. Analogous to condensed matter, a large variety of phases is also observed for vortex and Skyrmion matter, resembling the particle like character and reflecting the underlying physical properties. Moreover, both vortex and Skyrmion matter represent ideal model systems for questions of general importance as topological stability and decay. As for superconducting vortex matter, Skyrmion melting transitions, Skyrmion liquids and Skyrmion glass phases are expected to exist in various materials. They provide an excellent showcase for the investigation of topological phase conversion [4].

Neutron scattering provides an ideal tool for the investigation of both vortex and Skyrmion matter. We present an overview how to address the static and dynamic properties of superconducting vortex and Skyrmion matter by means of neutron grating interferometry (nGI) [5], time-resolved small angle neutron scattering (TISANE) and neutron resonance spin echo spectroscopy (NRSE). Our study paves the way how to access vortex and Skyrmion lattice melting as well as their current induced motion and dynamic properties in bulk samples.

Work in collaboration with: J. Kindervater, T. Adams, A. Chacon, F. Jonietz, W. Wünzer, R. Georgii, P. Böni, C. Pfleiderer, M. Garst, C. Schütte, J. Waizner, S. Buhandt, A. Rosch, P. Milde, L. Eng, J. Seidel, H. Berger, E. M. Forgan, M. Laver, U. Keiderling, A. Wiedenmann, T. Reimann, M. Schulz.

- [1] S. Mühlbauer et al., *Phys. Rev. Lett.*, **102** (2009) 136408.
- [2] S. Mühlbauer et al., *Phys. Rev. B*, **83** (2011) 184502.
- [3] S. Mühlbauer et al., *Science*, **323** (2009) 915.
- [4] P. Milde et al., *Science*, **340** (2013) 6136.
- [5] T. Reimann et al., *Nature communications*, **6** (2015) article number 8813.

3TL-H-5

CHARACTERIZATION OF MAGNETIC NANOPARTICLES BY SMALL-ANGLE SCATTERING WITHIN THE EUROPEAN FP7 PROJECT NanoMag

Bender P.¹

¹ CITIMAC, Facultad de Ciencias, Universidad de Cantabria, 39005 Santander, Spain
benderpf@unican.es

In recent years, utilization of iron oxide nanoparticles for a wide range of biomedical applications was extensively researched, prompting the need to standardize the characterization of their physical properties. The aim of the EU FP7 project NanoMag (grant no. 604448) is to improve, redefine and ultimately standardize existing analysis methods [1]. For that purpose it is necessary to correlate the macroscopically measured quantities of the ensembles (e.g. magnetization) with the physical properties of the particles on the nanoscale. This is intended within the project by combining the results of various characterization techniques, including small-angle scattering [2].

With small-angle X-ray scattering (SAXS) the purely nuclear scattering cross section is obtained, which enables for example the determination of particle sizes, shape and agglomeration. We apply this technique to reveal the structural composition of complex nanoparticle systems, such as multi-core particles [3,4]. In multi-core systems the small iron oxide nanoparticles (usually in the size range 5-50 nm) are fused together, which modifies their magnetic properties via dipolar interactions [4]. To gain information about magnetic correlations within such interacting nanoparticle ensembles small-angle neutron scattering (SANS) can be used. We will present the results of two polarized SANS experiments performed at the Institut Laue Langevin (ILL, Grenoble, France). In the first experiment we analyzed the spin coupling within multi-core particles and in the second experiment the spin correlations between nanoparticles

(*Inset* of Fig.1) compressed to a dense powder. Fig. 1 shows exemplarily the radially averaged spin flip (sf) cross section $I^{sf}(q)$ of the particle powder detected at 300 K and a field strength of 2 mT. The observed peak at $q = 0.12 \text{ nm}^{-1}$ is a clear sign for antiferromagnetic-like correlations between neighboring particle moments. This is remarkable in a system that macroscopically does not show deviations from superparamagnetic behavior.

To obtain detailed information about the spin correlations we extract the underlying pair distance distribution functions by indirect Fourier transforms of the SANS cross-sections.

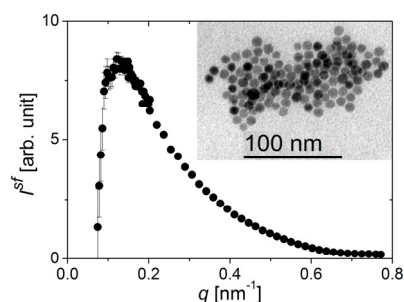


Fig. 1. Radially averaged SANS sf intensity of a dense powder of iron oxide nanoparticles as a function of the scattering vector q detected at 300 K and 2 mT. *Inset*: TEM picture of the nanoparticles.

Funding from the European Union Seventh Framework Programme (FP7/2007–2013) under grant agreement No. 604448 and provision of beamtime at the instrument D33 at the Institut Laue Langevin (ILL, Grenoble, France) are acknowledged.

[1] available online: <http://www.nanomag-project.eu>.

[2] O. Posth et al., In Proceedings of *IMEKO XXI World Congress* (2015) 1362-1367.

[3] W. Szczerba et al., *Journal of Applied Crystallography*, **50** (2017) 481-488.

[4] P. Bender et al., accepted in *Scientific Reports*.

3RP-H-6

AGGREGATE STATE OF FERROFLUIDS BY ANISOTROPY ANALYSIS OF 2D SAXS IN MAGNETIC FIELD

Avdeev M.V.^{1,3}, *Veligzhanin A.A.*², *Shulenina A.V.*^{3,2}, *Gruzinov A.Yu.*⁴, *Zubavichus Y.V.*²

¹ Joint Institute for Nuclear Research, Dubna, Moscow Reg., Russia

² National Research Centre 'Kurchatov Institute', Moscow, Russia

³ Faculty of Physics, Lomonosov Moscow State University, Moscow, Russia

⁴ EMBL, Hamburg, Germany

avd@nf.jinr.ru

The presence of anisotropic aggregates of nanoparticles in ferrofluids can be effectively monitored by small-angle X-ray scattering (SAXS) when the systems are placed in an external magnetic field. In this case, 2D SAXS patterns become anisotropic and can be used to obtain the structural characteristics of the aggregates.

In this paper, a comparative analysis of 2D SAXS patterns for dilute ferrofluids with different degrees of particle interaction is carried out. Experimental data were obtained at SAXS stations of the Kurchatov synchrotron radiation source at NRC "Kurchatov Institute" (Moscow) using a special cell for measurements in external magnetic fields (strength up to 0.2 T). Classical ferrofluids based on organic low-polarity solvents (toluene, decalin) and dispersed nanoparticles of magnetite and cobalt (size ~ 10 nm) coated with oleic acid, are consistent with the aggregation state diagram [1,2] and testify the concept of equilibrium chain-like aggregates. The anisotropy parameter of 2D SAXS patterns follows the Langevin formula and reflects the growth in the preferable orientation of chains along the field. From the analysis of the scattering patterns, we obtain the parameters of magnetic particles (average size and width of the particle size distribution) and characteristics of the aggregates including the fraction of particles forming chains and average chain aggregate number.

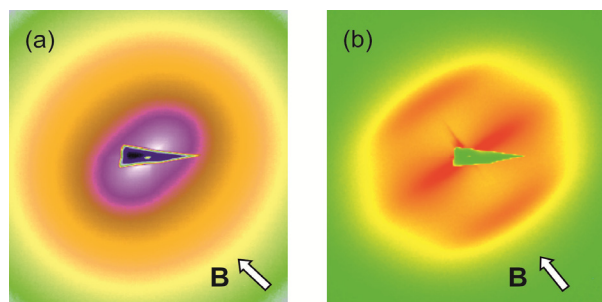


Fig.1. Anisotropic 2D SAXS patterns on the detector (NRC KI) from magnetically saturated $\sim 1\%$ ferrofluids: (a) magnetite in decalin; (b) cobalt in toluene. For cobalt characterized by a considerably larger dipolar coupling parameter as compared to magnetite, pronounced scattering features corresponding to oriented chains are seen.

For water-based ferrofluids where magnetic nanoparticles in aqueous medium are coated with sodium oleate and other agents including surfactant/polymer mixtures, the analysis of 2D SAXS patterns indicates the presence of colloidal (non-equilibrium) aggregates with some shape anisotropy that determines the behavior of scattering by ferrofluids in a magnetic field. Due to a rather large volume of aggregates oriented along the field, the scattering anisotropy tends to saturation at a relatively weak magnetic field strength, also following the Langevin formula. This fact makes it possible to analyze structural characteristics of the aggregates.

Support by RFBR (grant 14-22-01054-ofi_m) is acknowledged.

[1] J.J. Cerdà, E. Elfimova, V. Ballenegger, E. Krutikova, A. Ivanov, Ch. Holm, *Phys. Rev. E*, **81** (2010) 011501.

[2] M.V. Avdeev, *J. Mol. Liq.*, **189** (2014) 68-73.

3RP-H-7

MAGNETIC CORRELATIONS IN ARTIFICIALLY DESIGNED MICRO-DOMAIN PATTERNS INVESTIGATED BY NEUTRON SCATTERING

Saerbeck T.¹, Steinke N.-J.², Huckfeldt H.³, Koch I.³, Ehresmann A.³

¹ Institut Laue-Langevin, Large Scale Structures Group, Grenoble, France

² ISIS, Rutherford Appleton Laboratory, Oxfordshire, UK.

³ University of Kassel, Department of Physics, Kassel, Germany
Saerbeck@ILL.eu

Tailored magnetic domain patterns find applications as magnetic sensors and logic elements in spintronic devices. Artificial stray field landscapes, emerging from the domain boundaries, can further be used as platforms for various lab-on-a-chip applications, for positioning and movement of magnetic micro- and nano-objects in liquid environments [1,2]. We report on a detailed investigation of micrometer sized magnetic stripe domain patterns in a thin film system with a structurally homogeneous surface. A series of stripe domains with different width is created using He-ion bombardment in external magnetic fields of photo-lithographically patterned, exchange biased magnetic thin films [3]. The magnetization of each domain is set perpendicular to the long axis of the stripe and opposite to the neighboring domains.

We will present polarized neutron reflectometry and off-specular scattering (Figure 1a) as an excellent tool to investigate the global magnetic configuration of the domain pattern. Specular reflectivity reveals the laterally averaged, depth resolved structure and magnetism in the thin-film system. Off-specular scattering (Figure 1b) probes the domain correlation lengths and contrast, and the lateral distribution and orientation of magnetic moments. The observed scattering allows conclusions about disordered domains and moments in the lateral directions. Measurements following the magnetic hysteresis reveal domain and disorder evolution and show a persistent domain scattering well beyond apparent saturation.

Due to a quantum-well structure of the layers, enhanced spin-flip and off-specular scattering is observed in a narrow region below the critical edge of total reflection. The analysis of this resonant feature of the neutron evanescent wave provides excellent sensitivity to the layer structure and the magnetic correlations in the lateral dimensions of the sample.

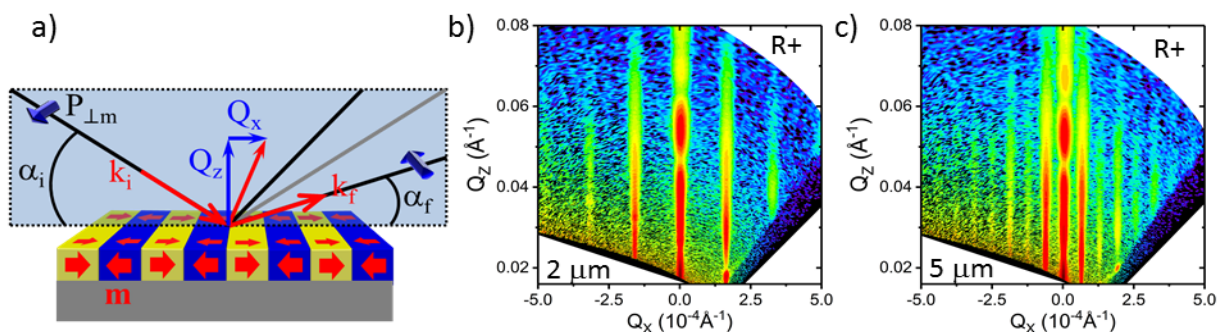


Figure 2: a) Schematic scattering diagram from the magnetic stripe pattern. b), c) Example off-specular scattering contour plots in (Q_x, Q_z) -coordinates obtained from stripe width of $10 \mu\text{m}$ and $5 \mu\text{m}$, respectively.

[1] T.Ueltzhöffer *et al.* *J. Appl. Phys.*, **117** (2015) 123904.

[2] D. Holzinger, *et al.* *J. Appl. Phys.*, **114** (2013) 013908.

[3] F. Ahrend *et al.* *J. Magn. Magn. Mater.*, **381** (2015) 292.

3OR-H-8

SIZE EVOLUTION OF SPIRAL MAGNETIC STRUCTURE IN CoCr_2O_4 NANOPARTICLES

Zákutná D.^{1,2}, Alemayehu A.³, Vlček J.⁴, Nemkovski K.⁵, Nižňanský D.³, Honecker D.¹, Disch S.²

¹ Institut Laue-Langevin, Grenoble, France

² Universität zu Köln, Köln, Germany

³ Charles University in Prague, Prague, Czech Republic

⁴ University of Chemistry and Technology Prague, Prague, Czech Republic

⁵ JCNS at MLZ, Forschungszentrum Jülich GmbH, Garching, Germany

zakutna@ill.fr

Cobalt chromite has attracted great interest due to its multiferroic properties exhibiting spin induced electric polarization locked to the magnetization. The appearance of dielectric polarization in cobalt chromite is associated with a non-collinear arrangement of spins due to the strong near-neighbour exchange interaction [1]. The magnetic phase diagram has been studied for cobalt chromite in single crystal [1,2] and polycrystalline [3,4] form but in-depth structural analysis on nanosized cobalt chromite is scarce up to now, although the magnetic behaviour changes significantly. For example and in contrast to the bulk material, a transition from superparamagnetic to blocked state with ferrimagnetic order is observed at low temperatures. The existence of the spiral magnetic phase in the nanometer regime is an up to now open and discussed question.

In this contribution, the structure, morphology, and magnetic properties of prepared cobalt chromite nanoparticles were investigated by powder X-ray diffraction, transmission electron microscopy and magnetometry, respectively. We have further investigated the evolution of the magnetic phase transitions in cobalt chromite nanoparticles for various particle diameters in the range of 3 – 21 nm by means of neutron diffraction experiments with xyz polarization analysis. The appearance of magnetic satellite reflections, which can only be explained by a transverse conical spiral model [4,5], manifests the presence of spiral magnetic ordering in cobalt chromite nanoparticles. Moreover, a critical coherent domain size for formation of the spiral magnetic structure can be identified together with a shift of the transition temperature of the non-collinear order due to finite size effects.

[1] L. J. Chang *et al.*, *J Phys Condens Matter*, **21** (2009) 456008.

[2] Y. Yamasaki *et al.*, *Phys. Rev. Lett.*, **96** (2006) 204204.

[3] G. Lawes *et al.*, *Phys. Rev. B*, **74** (2006) 024413.

[4] D. H. Lyons *et al.*, *Phys. Rev.*, **126** (1962) 540.

[5] J. M. Hastings, L. M. Corliss, *Phys. Rev.*, **126** (1962) 556.

3OR-H-9

MAGNETIC SMALL-ANGLE NEUTRON SCATTERING ON BULK METALLIC GLASSES

*Mettus D.¹, Honecker D.², Birringer R.³, Leibner A.³, Deckarm M.³, Busch R.³, Stolpe M.³,
Kohlbrecher J.⁴, Hautle P.⁴, Barquín L.F.⁵, Fernández J.R.⁵, Michels A.¹*

¹ University of Luxembourg, Luxembourg, Luxembourg

² Institut Laue-Langevin, Grenoble, France

³ Universität des Saarlandes, Saarbrücken, Germany

⁴ Paul Scherrer Institute, Villigen PSI, Switzerland

⁵ Universidad de Cantabria, Santander, Spain

denis.mettus@uni.lu

Bulk metallic glasses (BMG) are amorphous solids which are well known for their excellent mechanical properties. Although these materials are heavily investigated both experimentally and theoretically, yielding and failure of BMG under external strain is still not fully understood. In particular, the discrete nature of the flow defect in amorphous solids, which enables inelastic deformation before runaway shear bands form leading to catastrophic failure, is still a critical issue [1,2].

In this contribution, we focus on their magnetic behavior and discuss the influence of mechanical deformation on the magnetic microstructure as seen by magnetic-field-dependent small-angle neutron scattering (SANS). We present and compare the results of unpolarized SANS measurements on hard and soft magnetic BMG samples, and analyze the SANS cross sections in real space by computing the correlation function (see Fig. 1).

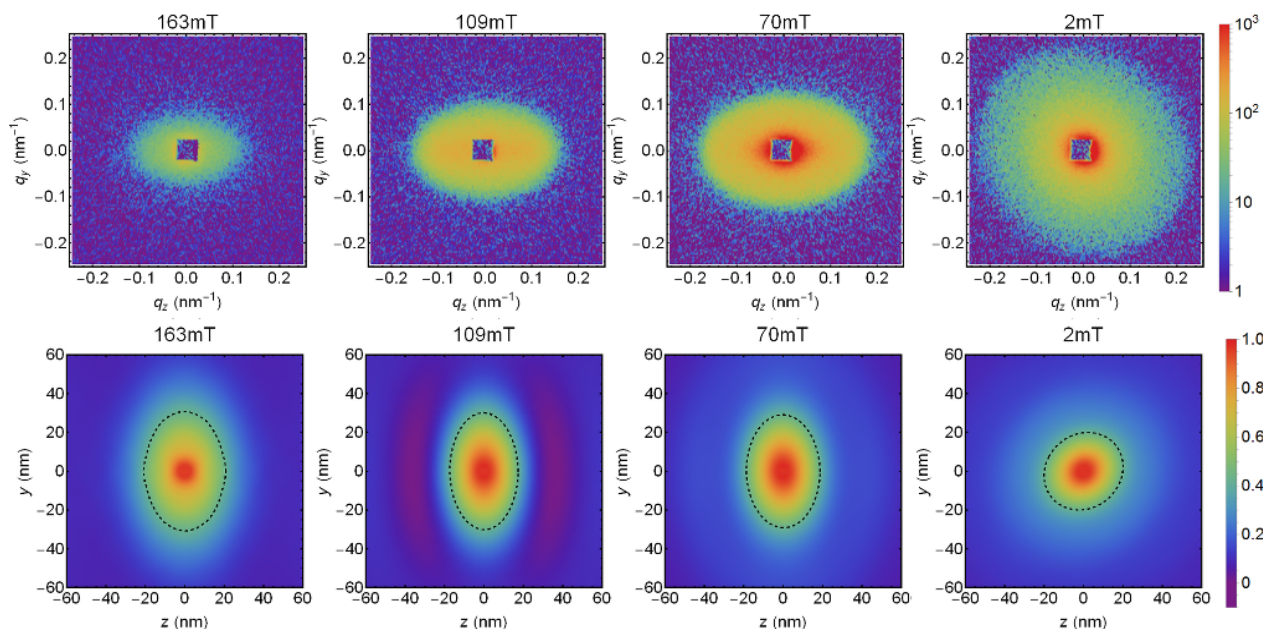


Fig. 1. SANS cross sections (upper row) and corresponding correlation functions (lower row) of aged BMG $\text{Fe}_{70}\text{Mo}_5\text{Ni}_5\text{P}_{12.5}\text{B}_{2.5}\text{C}_5$ at selected applied magnetic fields. \mathbf{H}_0 is horizontal in the plane.

D.M. acknowledges financial support from the FNR (Grant No. INTER/DFG/12/07).

[1] C.A. Schuh, T.C. Hufnagel, and U. Ramamurty, *Acta mater.*, **55** (2007) 4067.

[2] R. Dasgupta, H. G. E. Hentschel, I. Procaccia, *PRL*, **109** (2012) 77777.

3RP-H-10

UNRAVELLING THE COMPLEX MAGNETIC MORPHOLOGY OF MAGNETIC NANOPARTICLES

Zákutná D.^{1,2}, Honecker D.², Disch S.¹

¹ Universität zu Köln, Köln, Germany

² Institut Laue-Langevin, Grenoble, France

sabrina.disch@uni-koeln.de

Magnetic nanoparticles reveal unique magnetic properties which make them relevant for data storage, electronic and mechanical engineering, and biomedical applications [1,2]. With regard to these applications, the main aspects of fundamental interest include magnetic anisotropy and the related magnetization distribution in individual nanoparticles. Reduced magnetization values in nanoparticles as compared to the bulk material and excess susceptibility in high applied fields are commonly attributed to a magnetic dead layer or spin canting at the nanoparticle surface. Polarized small-angle neutron scattering (SANS) gives access to the spatially resolved magnetization distribution and thus allows discriminating between spin disorder contributions in the particle core and at the surface [3].

In this contribution, we will present our latest results on the structural and magnetic morphology of cobalt ferrite nanoparticles. Using a combination of SAXS, polarized SANS, and magnetization measurements, we resolved the core-shell morphology of the as-synthesized nanoparticles in great detail. Due to reducing conditions during synthesis, the obtained particles consist of a weakly magnetic wüstite core surrounded by a spinel shell, a FiM@FiM system that gives rise to exchange bias at low temperatures. A time-dependent evaluation of the magnetization distribution finally enables improvement of the synthesis conditions towards single phase cobalt ferrite nanoparticles.

[1] S. D. Bader, *Rev. Mod. Phys.*, **78** (2006) 1.

[2] Q. A. Pankhurst *et al.*, *J. Phys. D: Appl. Phys.*, **36** (2003) R167.

[3] S. Disch *et al.*, *New J. Phys.*, **14** (2012) 013025.

3OR-H-11

SPIRAL STRUCTURE OF $[^{57}\text{Fe}/\text{Cr}]_N$ MULTILAYERS REVEALED BY NUCLEAR RESONANCE REFLECTIVITY

Andreeva M.A.¹, Baulin R.A.¹, Chumakov A.I.^{2,3}, Ruffer R.², Smirnov G.V.³, Babanov Yu.A.⁴, Devyaterikov D.I.⁴, Milyaev M.A.⁴, Ponomarev D.A.⁴, Romashev L.N.⁴, Ustinov V.V.⁴

¹ Faculty of Physics, MSU, Moscow, Russia

² ESRF-The European Synchrotron, Grenoble, France

³ NRC "Kurchatov Institute", Moscow, Russia

⁴ IMP RAS, Ekaterinburg, Russia

Mandreeva1@yandex.ru

Nuclear resonance reflectivity (NRR) is the very informative method for the depth-resolved magnetization study. Contrary to the polarized neutron reflectivity, giving the magnetization sensitive reflectivity curve, NRR measurements include as well the Mössbauer spectra of reflectivity at different grazing angles (Fig. 1), widening the content of the magnetic information. Nowadays NRR measurements can be done with Synchrotron Mössbauer Source (SMS) implemented at the ID18 beamline [1] of ESRF.

We present the results of NRR investigation of the $[^{57}\text{Fe}(x \text{ nm})/\text{Cr}(y \text{ nm})]_{30}$ multilayers with ultrathin ^{57}Fe layers ($0.08 \text{ nm} < x < 0.8 \text{ nm}$) and different Cr spacers ($y=1.05 \text{ nm}$, 2.0 nm) at varying temperature ($4 - 150 \text{ K}$) and external fields ($H^{\text{ext}}=0 - 4 \text{ T}$) [2,3]. The sample with the $\sim 1 \text{ nm}$ Cr spacer has initially (at $H^{\text{ext}}=0$) the collinear antiferromagnetic interlayer coupling between ^{57}Fe layers. At $H^{\text{ext}}=0.15 \text{ T}$ the spin-flop takes place: the ^{57}Fe layer magnetizations (antiferromagnetically coupled) orientate perpendicular to the H^{ext} . At the H^{ext} increase the ferromagnetic ordering of the ^{57}Fe layers gradually started but at $H^{\text{ext}}=3 \text{ T}$ it is still not complete.

The sample with the $\sim 2 \text{ nm}$ Cr spacer is characterized by the anti-phase spiral antiferromagnetic alignment which contains the spin-flop region at some depth (Fig. 2). The ferromagnetic alignment of the ^{57}Fe layers occurs at the essentially smaller $H^{\text{ext}}=1 \text{ T}$.

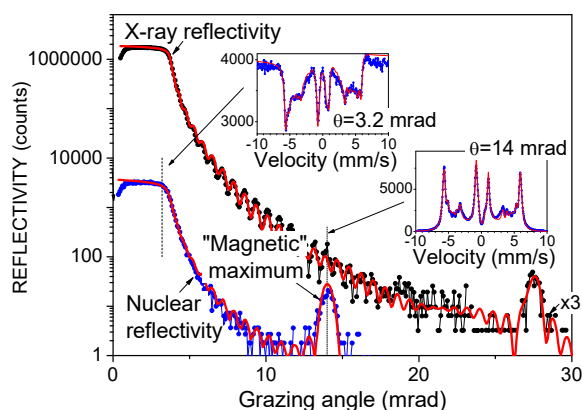


Fig. 1. The example of the NRR data measured for the sample $[^{57}\text{Fe}(0.8 \text{ nm})/\text{Cr}(1.05 \text{ nm})]_{30}$ at zero external field and 4 K .

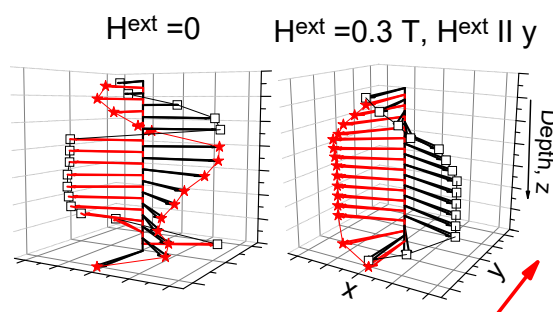


Fig. 2. The obtained hyperfine field orientations in the surface plane for ^{57}Fe layers in the $[^{57}\text{Fe}(0.8 \text{ nm})/\text{Cr}(2.0 \text{ nm})]_{30}$ sample at 4 K .

Support by RFBR (No.15-02-01674-a and 15-02-01502-a) is acknowledged.

[1] V. Potapkin, A.I. Chumakov, G.V. Smirnov, et al., *J. Synch. Rad.*, **19** (2012) 559-569.

[2] M.A. Andreeva, R.A. Baulin, A.I. Chumakov, R. Ruffer, G.V. Smirnov, et al., *JMMM*, (2017), <http://dx.doi.org/10.1016/j.jmmm.2016.12.097>.

[3] M.A. Andreeva, R.A. Baulin, A.I. Chumakov, R. Ruffer, et al., *J. Synch.Rad.* (2017) in press.

3 July

Monday

11:30-13:00

14:30-17:15

oral session

3TL-O

3RP-O

3OR-O

**“Magnetism in Biology
and Medicine”**

3TL-O-1

IN-VITRO AND IN-VIVO SCREENING OF MAGNETIC NANOPARTICLES

Roig A.¹

¹ Nanoparticles and Nanocomposites Group, Institut de Ciència de Materials de Barcelona (ICMAB-CSIC), Campus de la UAB, Bellaterra, E-08193 SPAIN
roig@icmab.es

Superparamagnetic iron oxide nanoparticles (SPIONs) are already demonstrating huge potential in nanomedicine as MRI contrast agents, and for hyperthermia treatments, drug delivery, cell therapies and bio-sensing. Simple biocompatible surface coatings are currently studied to stabilize them in bio-fluids and enhance their therapeutic effect. Albumin is the most abundant protein in serum and has key physiological functions.

I will show that bovine serum albumin (BSA) improves the colloidal stability of SPIONs in biological media [1] and that BSA provides a new bio-identity to the nanoparticle when exposed to biological media, cells and multicellular organisms.

Binding affinity, conformation changes of the protein and its impact on nanoparticles cytotoxicity, cellular uptake and fate will be reported. Experimental evidences will be complemented with molecular simulations [2]. BSA corona lowers unspecific cell uptake and decreases nanoparticle fouling with other proteins.

The albumin coated iron oxide (BSA-SPIONs) bio-composite was also evaluated in *Caenorhabditis elegans*[3,4]. Based on its transparency, short life cycle, differentiated anatomy and ease of cultivation, *C. elegans* is an ideal model organism for *in-vivo* NP evaluation within the synthetic laboratory [5]. Interestingly, all findings indicate the protective effects of the protein both to the nanoparticles and to the worms especially at high concentrations.

Finally, I will show the use of magnetic nanoparticles and nanocapsules for a neurorepair therapy address to promote angiogenesis after stroke [6],[7].



Figure1. Prussian Blue stained *C. elegans*: where SPIONs appear blue.

[1] S. Yu et al. *J. of Nanoparticle Research*, **16** (2014) 2484.

[2] S. Yu et al. *Nanoscale*, **8** (2016) 14393.

[3] L. Gonzalez-Moragas et al. *ACS Biomaterials Science and Engineering*, **1,11** (2015) 1129.

[4] S. Yu, L. Gonzalez-Moragas et al. *Acta Biomaterialia*, **43** (1) (2016) 348.

[5] L. Gonzalez-Moragas, et al. *Advances in Colloid and Interface Science*, **219** (2015) 10.

[6] E. Carenza et al. *Nanomedicine: NBM*, **10** 1 (2014) 225.

[7] E. Carenza et al. *J. Mater. Chem. B*, **2** (2015) 2538.

3TL-O-2

HYSTERESIS LOSSES AND SPECIFIC ABSORPTION RATE MEASUREMENTS IN MAGNETIC NANOPARTICLES FOR HYPERTHERMIA APPLICATIONS

Coisson M.¹, Barrera G.¹, Celegato F.¹, Martino L.¹, Tiberto P.¹

¹ INRIM, Torino, Italy
m.coisson@inrim.it

Magnetic hyperthermia exploiting nanoparticles is currently a significant subject of research in the field of tumour treatment, with many open questions concerning the best choice of material, particles size and dose. A major issue consists in the difficulty of obtaining reproducible measurements of the specific absorption rate, i.e. of the amount of heat that is released by the magnetic nanoparticles submitted to an alternating electromagnetic field usually in the range of a few hundreds of kHz and with amplitudes of a few tens of mT.

To address this open issue, the specific absorption rate (SAR) of different families of particles (including magnetite and other Fe oxides, and ferrites with different substituting elements such as Co, Ni and Zn), prepared with different methods and having different sizes and shapes, has been measured using three approaches: static hysteresis loops areas, dynamic hysteresis loops areas and hyperthermia of a water solution [1]. For dynamic loops and thermometric measurements, specific experimental setups have been developed, that operate at comparable frequencies (~69 kHz and ~100 kHz respectively) and rf magnetic field peak values (up to 100 mT). The hyperthermia setup has been fully modelled to provide a direct measurement of the SAR of the magnetic particles by taking into account the heat exchange with the surrounding environment in non-adiabatic conditions and the parasitic heating of the water due to ionic currents.

Dynamic hysteresis loops are shown to provide an accurate determination of the SAR (see Fig. 1 for an example on a Ni-Zn ferrite) except for superparamagnetic samples, where the boundary with a blocked regime could be crossed in dynamic conditions. Static hysteresis loops consistently underestimate the specific absorption rate but can be used to select the most promising samples.

A means of reliably measuring the SAR of magnetic nanoparticles, within the general subject of metrological traceability in medicine with a specific focus on magnetic hyperthermia, has therefore been developed by exploiting different approaches and by fully modelling the heat exchange processes in a custom-developed hyperthermia setup. The validity of the proposed methods is discussed.

[1] M. Coisson, G. Barrera, F. Celegato, L. Martino, S.N. Kane, S. Raghuvanshi, F. Vinai, P. Tiberto, BBA General Subjects (in press), doi 10.1016/j.bbagen.2016.12.006.

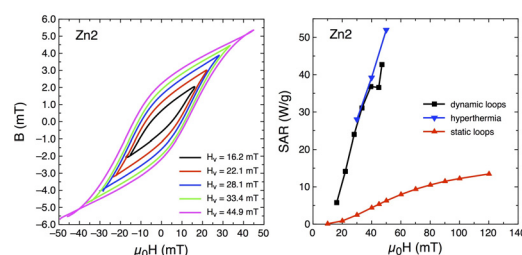


Fig. 1. Dynamic hysteresis loops and specific absorption rate comparisons with three different techniques for a Ni-Zn ferrite sample.

3TL-O-3

NOVEL APPLICATIONS OF MAGNETIC MATERIALS AND TECHNOLOGIES FOR MEDICINE

Tishin A.M.^{1,2}, Zverev V.I.¹, Pyatakov A.P.^{1,2}, Shtil A.A.³

¹ Faculty of Physics, M.V. Lomonosov Moscow State University 119991, Moscow, Russia

² Pharmag LLC 142190, Troitsk, Moscow, Russia

³ Blokhin Cancer Center, 24 Kashirskoye shosse, Moscow 115478, Russia

vi.zverev@physics.msu.ru

The magnetocaloric effect (MCE) can be employed in magnetic refrigeration and hyperthermia technologies [1,2]. Despite the efforts to develop a commercially available prototype of magnetic refrigerators these attempts have not yet led to a wide spread of this technology in real market (mainly due to the cost of the magnetic field source). Currently the ‘boom’ in research activity is directed to biomedical applications of MCE.

Our group has patented the MCE-based composite material for smart coating of implants, which allows to release drugs over time in controlled amounts [3,4]. The material is comprised of two layers: the one manifesting a large MCE and the other made of a temperature-sensitive polymer containing the drug. The latter is released by the polymer if the temperature induced by magnetic field (due to MCE) is changed. The polymer undergoes sharp phase transition in response to the slight temperature drop of ~1-3°C (down to 34-36°C in the body). Local cooling is achieved with FeRh alloy, one of the most perspective MCE materials with the first order phase transition. It is critically important to take into account several peculiarities of phase transition and MCE behavior in these series of alloys [5]. Recent studies on high-purity samples showed an ‘irreversible’ effect of MCE indicating that the temperature of FeRh does not return to its initial value after the full cycle of the magnetic field during dynamic MCE measurements. A theoretical explanation based on *ab initio* calculations has been provided.

Magnetic hyperthermia in oncology is rapidly developing therapeutic modality [6]. Recent experiments have shown that Mn-Zn ferrite emerges as a cost-effective material for this method compared with currently used magnetite nanoparticles. We present our achievements on magnetically guided capsule endoscopy.

Finally, we provide the experimental setup for the computer-controlled system of magnetic field sources that create necessary forces to control the position of the capsule in five degrees of freedom in a given area [7]. The system has the feedback on the position and is designed to monitor the endoscopic capsule during gastrointestinal tract examination.

The work in Pharmag LLC is supported by Skolkovo Foundation, Russia. The authors acknowledge the support by AMT&C Group.

[1] Tishin A.M., Spichkin Y.I., Zverev V.I., Egolf P.W., *Inter. J. Refrig.*, **68** (2016) 177-186.

[2] Tishin A.M. *European patent* 1 897 590 B1 (2016).

[3] Tishin A.M., Rochev Yu A., Gorelov A.V., *US patent* 9,017,713 B2 (2015).

[4] Spichkin Y.I., Pyatakov A.P., Tishin A.M., Zverev V.I., *GB patent* 2520960 (2015).

[5] Zverev V.I., Saletsky A.M., Gimaev R.R., Tishin A.M., Miyanaga T., Staunton J.B., *Applied Physics Letters*, **108** (2016) 192405.

[6] Tishin A., Shtil A.A., Pyatakov A.P., Zverev V.I., *Recent Patents on Anti-Cancer Drug Discovery*, **11** (2016) 360-375.

[7] Shamsudhin N., Zverev V.I., Keller H., Pane S., Egolf P.W., Nelson B.J. and Tishin A.M., *Medical Physics* (2016) in press.

3TL-O-4

INTERFACING MAGNETIC NANOPARTICLES WITH CELLS VIA BIOORTHOGONAL CLICK CHEMISTRY

Idiogo-López F.J.¹, Navascuez M.¹, Moreno Antolín E.¹, Eceiza M.², Aizpurua J.M.²,
Martínez de la Fuente J.¹, Fratila R.M.¹

¹ Institute of Materials Science of Aragón (ICMA – CSIC/University of Zaragoza) and CIBER-BBN, C/ Pedro Cerbuna 12, 50009, Zaragoza, Spain

² José Mari Korta R&D Center, Basque Country University, UPV/EHU, P.O. 20018, Donostia-San Sebastián, Spain
rfratila@unizar.es

Magnetic hyperthermia (MH), based on the ability of some magnetic nanoparticles (MNPs) to generate heat when exposed to alternating magnetic fields (AMF) [1,2] is an extremely active area of research, especially for the development of new therapeutic solutions for cancer treatment. MNPs can be delivered non-invasively and heated using AMFs with frequencies not harmful for healthy tissues. Moreover, MNPs can be decorated with tumour-targeting ligands for selective delivery to malignant tissues, and the use of MNPs as drug carriers and sub-lethal MH for controlled drug release can lead to the development of more efficient multimodal therapeutic agents [3].

Recently, we have initiated a new research line focused on the use of bioorthogonal click chemistry to study magnetic hyperthermia applied using MNPs covalently attached to cell membranes. Our interest lies in the sub-lethal version of magnetic hyperthermia, which we believe is a powerful tool to induce a controlled and localized heating of the cell membrane. This localized heating can produce temporal changes in the membrane biophysical properties, which can be used for enhanced delivery of therapeutics.

We use bioorthogonal strain-promoted “click” [3 + 2] azide-alkyne cycloaddition (SPAAC) [4] as a tool to immobilize magnetic nanoparticles on cell surfaces. Bioorthogonal click chemistry allows for the efficient and selective labelling of biomolecules (in this case cell surface glycans and glycoproteins) in their biological milieu. Herein we report our preliminary results regarding the synthesis of “clickable” magnetic nanoparticles for bioorthogonal click chemistry. The MNPs incorporate in their coating a cyclooctynyl derivative for SPAAC reaction and either a polyethylene glycol or a glucose moiety to ensure stability in biological media. We have tested their reactivity towards azide-functionalized surfaces, demonstrating their potential as bioorthogonal probes [5]. We are currently investigating the incorporation of these MNPs on more complex substrates (azide-modified lipid bilayers as simplified models of animal cell membranes). Studies regarding the cytotoxicity of the MNPs and their covalent attachment on living cell membranes are also underway.

R. M. F. acknowledges financial support from Universidad de Zaragoza (JIUZ-2014-CIE-03) and European Union (Marie Skłodowska-Curie grant agreement No. 657215).

[1] C. S. S. R. Kumar, F. Mohammad, *Adv. Drug Deliv. Rev.*, **63** (2011) 789-808.

[2] Q. A. Pankhurst, N. T. K. Thanh, S. K. Jones, J. Dobson, *J. Phys. D – Appl. Phys.*, **42** (2009) 224001.

[3] A. Hervault, N. T. K. Thanh, *Nanoscale*, **6** (2014) 11553-11573.

[4] J. C. Jewett, C. R. Bertozzi, *Chem. Soc. Rev.*, **39** (2010) 1272-1292.

[5] R. M. Fratila, M. Navascuez, M. Eceiza, J. I. Miranda, J. M. Aizpurua, J. M. de la Fuente, submitted to *Nanoscale Horiz.*

3TL-O-5

QUANTUM EFFECTS AND MAGNETISM IN THE SPATIALLY DISTRIBUTED DNA MOLECULES

Irkhin V.Yu.¹, Nikiforov V.N.²

¹Institute of Metal Physics, Ural Division of RAS, Ekaterinburg 620990, Russia

²Moscow State University, Physics Department, Moscow 119992, Russia

valentin.irkhin@imp.uran.ru

Electronic and magnetic properties of DNA structures doped by simple and transition metal ions (Gd, Cu, Zn, Au) are reviewed. The solid metal-DNA complex Zn-DNA shows characteristics of strongly correlated 1D electron systems with antiferromagnetic spin correlations. High electron density in the conduction band can be essential for future application in nanoelectronics [1].

DNA chains with Gd ions located on the helix spatially ordered phosphate complexes yield a bright example of one-dimensional metal with interacting magnetic moments [2]. This assumption is supported by finite value of paramagnetic Curie temperature. For Gd-DNA, the temperature dependence of magnetic susceptibility indicates the presence of interaction between Gd³⁺ magnetic moments, which is discussed in terms of long-range RKKY-type exchange in one-dimensional metals.

The problem of collective transport (transfer of genetic information during replication and transcription) in biological systems is discussed. In the system of successive codons ATGC, local levels with different depths are formed. Each base modulates a level inside the forbidden band. Tunneling along the chains is possible, depending appreciably on the level positions. The high conductivity in the case of giant tunneling may result in a high rate of information transfer. Since most of mutations in DNA are successfully healed, one may assume the existence of charge transport through delocalized states that are responsible for the transfer of information at long distances [3]. Then the localization length and the conductance of a given segment of the DNA molecule are directly related to the genetic information stored in this segment.

A particular attention is paid to magnetism of Cu-doped DNA systems [4]. Copper ions are nondestructive markers suitable for EPR control. It is known that DNA molecules form a cholesteric phase possessing high conductivity and self-organization. This phase may be the basis for the construction of organometallic complexes. The structure of the liquid crystal complexes formed when introducing Cu ions into DNA is examined. There is also an analogy with organic conductors and copper-oxide perovskites which are strongly correlated electronic systems. The role of chirality and circular dichroism is discussed. The system demonstrates unusual magnetism which cannot be reduced to that of isolated magnetic ions: there occur exotic excitations characteristic of low-dimensional arrays.

[1] A. Omerzu et al, *Phys. Rev. Lett.*, **104** (2010) 156804.

[2] V.N. Nikiforov, V.D. Kuznetsov, Yu.M. Yevdokimov, V.Yu. Irkhin, *JMMM*, **386** (2014) 338.

[3] F.M. Izrailev, A.A. Krokhin, N.M. Makarov, *Physics Reports*, **512** (2012) 125.

[4] Yu. M. Yevdokimov et al, *Int. J. Biol. Macromolecules*, **36** (2005) 103.

3TL-O-6

MAGNETIC PROPERTIES OF “DOPED” DNA*Nikiforov V.N.¹, Koksharov Yu.A.¹, Yevdokimov Yu.M.², Irkhin V.Yu.³*¹ Moscow State University, Physics Department, Moscow 119992, Russia² Engelhardt Institute of Molecular Biology, Moscow 119991, Russia³ Institute of Metal Physics, Ural Division of RAS, Ekaterinburg 620990, Russia

ppnvn@yandex.ru

A series of double-stranded DNA samples, both linear and cholesteric liquid crystal droplets, were investigated. The ring nucleotides were studied too. Binding of DNA molecules with Gd^{3+} , Cu^{2+} , La^{3+} ions was carried out. X-ray, optical, magnetic and EPR studies of DNA samples were performed. It was found that linear and crystal structures differ in their ability to bind ions Gd^{3+} . Namely, linear DNA can bind a large number of ions, because, in addition to phosphates, Gd^{3+} ions can be inserted between the base pairs. Magnetic SQUID magnetometer and ESR research showed that Cu^{2+} and Gd^{3+} ions give main contribution to formation of the total DNA magnetic moment. The temperature behavior of the DNA magnetic susceptibility in all the samples did not depend on the cooling pre-history and coincided both with cooling at zero magnetic field (ZFC) and when finite field was applied (FC). At the same time, DNA gadolinium samples showed a difference of Curie constant C and the paramagnetic Curie temperature in ZFC and FC regimes. Thus a tendency to the spin-glass behavior of these samples is possible. This assumption is confirmed by the study of the EPR spectra of resonance. Only in DNA samples with Gd, an EPR spectrum characteristic for spin glasses was observed. Apart from the main resonance, with g-factor of about 2, an additional pick was detected, probably associated with spin-glass-like Gd clusters.

One of important problems in biomedical applications is to create a magnetic label, which should not have a negative impact on biological objects and molecules. A good example of magnetic marks is copper ions. Unlike the gadolinium ions which are highly toxic, copper ions have no devastating impact. Atomic force microscopy, EPR and SQUID investigations of magnetic properties of liquid crystal Cu^{2+} complexes in DNA cholesteric phase ions were performed. The magnetic moment corresponds to the d^9 configuration. It is shown that copper ions form 6 atom length bridges between adjacent bases of the double helix. Paramagnetic Curie temperature of -1 K (with an accuracy of 0.1 K) shows a marked interaction of magnetic moments.

[1] V.N. Nikiforov, V.D. Kuznetsov, Yu.M. Yevdokimov, V.Yu. Irkhin, *JMMM*, **386** (2014) 338.[2] V. N. Nikiforov et al, *JETP Letters*, **81** (2005) 264.[3] Yu.M. Yevdokimov et al, *Int. J. Biol. Macromolecules*, **36** (2005) 103.

3RP-O-7

HEMOPOIETIC STEM CELLS RESPONSE IN VITRO TO NANOSIZED FERRITES IN A CONSTANT MAGNETIC FIELD

Khlusov I.A.¹⁻³, Slepchenko G.B.³, Feduschak T.A.⁴, Litvinova L.S.¹

¹Immanuel Kant Baltic Federal University, Kaliningrad, Russia

²Siberian State Medical University, Tomsk, Russia

³Tomsk Polytechnic University, Tomsk, Russia

⁴Institute of Oil Chemistry, Siberian Branch of Russian Academy of Sciences, Tomsk, Russia
khlusov63@mail.ru

In vitro effect of ferrimagnetic nanoparticles (FNPs) in a dose of 3 mg/liter (10 maximum permissible concentrations) on colony-forming units of bone marrow granulocytic (CFU-G) and monocytic (CFU-M) unipotent stem cells in a constant magnetic field (CMF) at intensity of 200 Oe was studied. Tested powders were obtained by the methods of electrical explosion of conductors (magnetite Fe₃O₄ and a mixture of hematite α -Fe₂O₃ with magnetite) in the Institute of High-Voltage Electronics (Tomsk, V.S. Sedoi) or by mechanochemical synthesis (cobalt ferrite CoFe₂O₄) in the Department of Structural Macrokinetics of SB RAS (Tomsk, V.I. Itin). According to transmission electron microscopy, mean diameters of FNPs were within 7-40 nm. Magnetic properties were detected by E.P. Naiden in Tomsk State University (Table 1). Stripping voltammetry detected 42-56 μ g/liter Fe³⁺ ions in 3-20-day solutions of nanosized magnetite (initial concentration of Fe³⁺ ions in pure solvent was < 1 μ g/liter). This concentration did not exceed 1.4-1.9% of theoretically possible release of pure iron from the solid phase into the solution. In CMF the 5-day accumulation of iron was 26 μ g/liter unlike 54 μ g/liter expected. Thus, FNPs were weakly soluble materials and did not also induce cell death. Magnetite and hematite added to rat bone marrow cells stimulated themselves the CFU-G yield by 50%. Their influence directly correlated with their mean size growth. The external CMF in the used dose was biologically inert itself and had no effect on the growth of CFU-G and CFU-M. Vice versa, CFU-G growth inhibition caused by CMF was observed in the presence of hematite nanoparticles with minimal magnetic moment (Table 1).

Stromal cells or fibroblast-like elements are essential for hematopoietic progenitor cells [1] and should be also a target of FNPs. At least, similarly to NIH 3T3 fibroblast culture, addition of nanosized magnetite, but not cobalt ferrite to whole bone marrow culture promoted stromal cells adhesion and formation of intercellular contacts along the magnetic field lines.

Table 1. Main characteristics of FNPs at room temperature, X

Index	44 mass. % α -Fe ₂ O ₃ + 56 mass. % Fe ₃ O ₄	CoFe ₂ O ₄	Fe ₃ O ₄
Specific magnetic moment, σ , Gs \times cm ³ /g	2.7	48	71
Residual magnetization (after removal of magnetic field), Gs \times cm ³ /g	0	0	10
Mean diameter of particles, nm	28	7	40

As a result, cobalt ferrite is a promising compound for targeted delivery of drugs and biomolecules due to its magnetic properties, the absence of residual magnetization, and small size of particles (Table 1). Functionally active nanosized magnetite with or without hematite might be applied in cell technologies.

[1] W. Han, Y. Yu, X.Y. Liu, *Cell Research*, **16** (2006) 189-195.

3OR-O-8

MAGNETIC NANOWIRES FOR MRI CONTRAST AND MAGNETIC HYPERTHERMIA

*Shore D.*¹, *Pailloux S.L.*¹, *Zhang J.*¹, *Dragos O.*¹, *Ghemes A.*², *Gage T.*¹, *Flannigan D.J.*¹,
*Garwood M.*¹, *Tabakovic I.*^{1,2}, *Pierre V.C.*¹, *Stadler B.J.H.*¹

¹ University of Minnesota, Minneapolis, USA

² National Institute of R&D for Technical Physics, Iasi, Romania

shore033@umn.edu

Recent data have shown that nanowires have good MRI contrast properties due to their higher surface area and larger magnetic field inhomogeneity compared to spherical nanoparticles [1]. Another recent study showed that magnetic nanowires have large specific absorption rate (SAR) due to their high shape anisotropy [2]. This makes them ideal for magnetic hyperthermia therapy. In this work electrodeposited iron-gold and cobalt-iron-gold magnetic nanowires were investigated for potential applications as MRI contrast and magnetic hyperthermia particles. This is one of the first works examining electrodeposited nanowires for these combined applications.

We characterized the nanowires using SEM, TEM, electron diffraction, dynamic light scatter, and absorbance in the UV-visible range. We highlight the effect of the thiol-linked PEG coating on the gold segments of the nanowires to mitigate magnetic aggregation and sedimentation to increase MRI relaxivity, r_2 , and SAR values.

As Table 1 shows, the r_2 for the nanowires increased with decreasing nanowire length (for 35 nm diameter nanowires) likely because shorter nanowires had less aggregation and sedimentation. Adding Au multilayers to the Fe nanowires and coating the Au with SH-PEG-COOH increased the r_2 values ~10X for Fe-Au 1 nanowires. The Au segments divide the nanowires into smaller magnetic domains and the SH-PEG-COOH helps to mitigate nanowire aggregation and sedimentation. To confirm the effect of the SH-PEG coating we measured light absorbance (300-800 nm wavelengths) of the nanowires, suspended in water, at different time points. We observed a minimal decrease in absorbance up to 25 min. The Au-Fe multilayer nanowires coated with SH-PEG-COOH -remained in suspension especially well.

Preliminary magnetic hyperthermia data show SAR values as high as 1200 W/g Fe for CoFe-Au 1 nanowires. This indicates that these nanowires could be used for hyperthermia therapy or other remote heating applications.

Sample	NW Length (μm)	NW Diameter (nm)	Aspect Ratio	r_2 ($\text{mM}^{-1}\text{s}^{-1}$)
Fe 1	0.5	35	14.3	14.67
Fe 2	1.0	35	28.6	11.8
Fe 3	1.8	35	51.4	6.6
Fe 4	2.3	35	65.7	4.6
Fe 5	1.0	53	18.9	3.14
Fe 6	0.7	111	6.3	4.95
Fe-Au 1	1.0	32.8	30.5	7.93
Fe-Au 1*	1.0	32.8	30.5	77.1*
Fe-Au 2*	2.66	28.8	92.4	39.8*
CoFe-Au 1	2.6	34	76.5	17.8

Fig. 1. Relaxivity of Fe, Fe-Au and CoFe-Au nanowires functionalized with Dop-PEG. *Indicates Au segments were coated with SH-PEG-COOH.

[1] J. Mohapatra, A. Mitra, H. Tyagi, D. Bahadur, and M. Aslam, "Iron oxide nanorods as high-performance magnetic resonance imaging contrast agents," *Nanoscale*, 7(20) (2015) 9174-9184.

[2] J. Alonso *et al.*, "FeCo nanowires with enhanced heating powers and controllable dimensions for magnetic hyperthermia," *J. Appl. Phys.*, 10.1063/1.4908300 **117**(17) (2015) 17D113/1-17D113/4.

3OR-O-9

Fe₃O₄/Ta₂O₅ NANOPARTICLES-BASED MAGNETICALLY CONTROLLED CONTRAST MEDIA

Lukyanenko K.¹, Afremov L.¹, Apanasevich V.²

¹ Far Eastern Federal University, Vladivostok, Russia

² Pacific State Medical University, Vladivostok, Russia
ks.lukyanenko@gmail.com

Last time, the interest to studying the magnetic nanoparticles (NP) for purposes of their use in the cancer diagnostics and treatment has quickened. The important role in the above applications is played by the magnetic core-shell nanoparticles which can be controlled by the external magnetic field. Just control of motion and distribution of the magnetic nanoparticles forms the basis of using them for targeted drug delivery or delivery of magnetic nanoparticles to the cancerous tumors for the purpose of subsequent hyperthermia process or strengthening of the radiological therapy effect due to scattering of radiation by injected particles.

In recent times, a special interest is shown for creation of magnetically controlled nontoxic radiopaque contrast agents such as the core-shell nanoparticles Fe₃O₄/Ta₂O₅.

The aim of the work is to research the increase concentration of NPs at the site of localization of the neoplasm by means of a magnetic field, and the possibility of using core-shell nanoparticles as a radiomodifier in radiation therapy.

We have synthesized the core/shell nanoparticles the cores of which consist of the iron oxide while envelope of the tantalum oxide. The average NP size was 43 nm. The shell of the tantalum oxide is to visualize the core-shell nanoparticles; to increase energy absorption effect during exposing with high-energy gamma rays; not have any toxic effects.

The presence of a magnetic moment in the NP allows with the aid of an inhomogeneous magnetic field, to concentrate core-shell nanoparticles in the tumor region, which substantially increases their radio modulating effect.

The installation was assembled to control the distribution of nanoparticles by the magnetic field, where recording the image brightness was performed using the digital microscope and, afterwards, the mathematical processing of images obtained was accomplished.

In order to check a possibility of controlling the distribution of nanoparticles by the magnetic field, the effect of the field nonuniformity on the nature of nanoparticles distribution in the solution was investigated. With the growth in the magnetic field force, the time of saturation attainment decreases and it was also established that the character of nanoparticles distribution is not practically influenced by their initial concentration. So, the basic parameters of magnetic field are defined with the aim to control of nanoparticles' distribution in volume.

3RP-O-10

BACTERIAL FERRIHYDRITE NANOPARTICLES: PREPARATION, MAGNETIC PROPERTIES, AND APPLICATION IN MEDICINE

Stolyar S.V.^{1,2}, Balaev D.A.^{1,2}, Ladygina V.P.³, Dubrovskiy A.A.², Krasikov A.A.², Popkov S.I.^{1,2}, Bayukov O.A.², Yaroslavtsev R.N.^{1,2}, Volochaev M.N.², Iskhakov R.S.², Dobretsov K.G.⁴, Falaleev O.V.^{2,3}, Chizhova I.A.¹

¹ Siberian Federal University, Krasnoyarsk, Russia

² Kirensky Institute of Physics, Federal Research Center KSC SB RAS, Krasnoyarsk, Russia

³ Presidium of Krasnoyarsk Scientific Center, Federal Research Center KSC SB RAS, Krasnoyarsk, Russia

⁴ Siberian Clinical Center FMBA, Krasnoyarsk, Russia
dabalaev@iph.krasn.ru

In this report we present results of comprehensive study of ferrihydrite nanoparticles produced by *Klebsiella oxitoca* (“biogenic ferrihydrite”) [1]. As prepared samples of different series demonstrate superparamagnetic blocking temperature T_B about 25 K [2-4] and the average size $\langle d \rangle$ of particles obtained from transmission electron microscopy found out to be ~ 3 nm [2,4]. Analysis of magnetization $M(H)$ curves at temperatures above T_B have shown that average magnetic moment of a particle $\langle \mu_p \rangle$ is of order 150-200 Bohr magneton [2-4]. This value is in a good agreement with Neel’s hypothesis [5] concerning the origin of uncompensated magnetic moment of a small antiferromagnetic particle, namely $\mu_p \sim J \cdot N^b$ where N – is the number of magneto-active atoms in particle, J – is the magnetic moment, and $b = 1/2$ for defects in the bulk of a particle. It was found that low temperature heat treatment in air (at 140-200⁰C) results in increase of μ_p and T_B values, as well as in growth of the particle size (the $\langle d \rangle$ value increases from ~ 3 nm to ~ 5 nm after annealing at 24 hours). According to study of a set of annealed samples the values of bulk and surface magnetic anisotropy constants from $\langle T_B \rangle$ vs $\langle V \rangle$ dependence [4] were obtained. Also, detail study of hysteretic $M(H)$ curves at $T < T_B$ under the zero field cooled (ZFC) and FC conditions allowed to conclude that exchange bias (EB) effect takes place in ferrihydrite nanoparticles. The EB in ferrihydrite is stably observed for particles not less than 3 nm in size, and its characteristic value increases with the particle size [6].

The distribution of magnetic nanoparticles in the body of laboratory animals (LA) for various methods of injection was studied using MRI [7]. Toxicity, penetration properties (after exposing in a magnetic field) and ability of ferrihydrite particles to bind an antibiotic were tested in LA (*in vivo*) [8]. Intravenous injection of magnetic nanoparticles into the rat's tail vein did not result in any changes in parenchymatous organs, and the nanoparticles were completely eliminated from the body within 24 hours. Positive results of experimental studies provide a basis for further clinical investigations of these magnetic nanoparticles and their use in otorhinolaryngology [8].

Support by the Special Program for Siberian Federal University of the Ministry of Education and Science of the Russian Federation is acknowledged.

- [1] S.V. Stolyar, O.A. Bayukov, Yu.L. Gurevich, et al, *Inorg. Mater.*, **41** (2007) 638.
- [2] D.A. Balaev, A.A. Dubrovskiy, A.A. Krasikov, et al, *JETP Lett.*, **98** (2013) 139.
- [3] D.A. Balaev, A.A. Krasikov, A.A. Dubrovskiy, et al, *J.Exp.Theor.Phys.*, **119**(2014) 479.
- [4] D.A. Balaev, A.A. Krasikov, A.A. Dubrovskiy, et al, *JMMM*, **410** (2016) 71.
- [5] L. Neel, *C.R. Acad. Sci. Paris*, **252** (1961) 4075.
- [6] D.A. Balaev, A.A. Krasikov, A.A. Dubrovskiy, et al, *J. Appl. Phys.*, **120** (2016) 183903.
- [7] E.V. Inzhevatkin, E.V. Morozov, et al, *Bull. Exp. Biol. Med.*, **158** (2015) 807.
- [8] K. Dobretsov, S.Stolyar, A.Lopatin, *Acta Otorhinolaryngol. Ital.*, **35** (2015) 97–102.

3RP-O-11

SPECIFIC ABSORPTION RATE OF MAGNETIC VORTICES IN IRON AND IRON OXIDE NANOPARTICLES

Usov N.A.^{1,2,3}, Nesmeyanov M.S.³, Bautin V.A.¹

¹ National University of Science and Technology «MISiS», 119049, Moscow, Russia

² IZMIRAN, 108840, Troitsk, Moscow, Russia

³ National Research Nuclear University “MEPhI”, 115409, Moscow, Russia

usov@obninsk.ru

Magnetic nanoparticle hyperthermia [1] is one of the most promising directions in current biomedical research. In most cases, small superparamagnetic iron and iron oxide nanoparticles with typical diameters $d = 15 - 20$ nm are used to generate heat in alternating magnetic field in biological media. In this report we show that magnetic vortices existing in soft magnetic nanoparticles with diameters larger than the single-domain one can be efficient nano-heaters in biomedical applications. Using micromagnetic numerical simulation we prove that in the optimal range of particle diameters, $D = 30 - 42$ nm for spherical iron nanoparticle, and $D = 70 - 100$ nm for magnetite nanoparticle, respectively, the magnetization reversal of the vortex is possible for moderate amplitudes of external alternating magnetic field, $H_0 < 100$ Oe. As an example, Fig. 1 shows the hysteresis loops of spherical iron nanoparticle for various characteristic directions of the external magnetic field, defined by spherical angles ω and ψ , with respect to the particle easy anisotropy axes.

In contrast to the case of superparamagnetic nanoparticles [2], the corresponding hysteresis loop area increases with increase of alternating field frequency, so that enormous values of the specific absorption rate, on the order of 1-2 kW/g, can be obtained at sufficiently high frequencies, $f \sim 1.0$ MHz.

It is important also that the diameter D of a non single-domain particle is several times larger than the diameter d of a superparamagnetic particle. Therefore, the volume of the heat generation turns out to be $(D/d)^3$ times larger.

This work was supported by the Ministry of Education and Science of the Russian Federation in the framework of Increase Competitiveness Program of NUST «MISiS», contract № K2-2015-018.

[1] E.A. Périgo, G. Hemery, O. Sandre, D. Ortega, E. Garaio, F. Plazaola, and F. J. Teran. *Appl. Phys. Rev.*, **2** (2015) 041302.

[2] N.A. Usov, *J. Appl. Phys.*, **107** (2010) 123909.

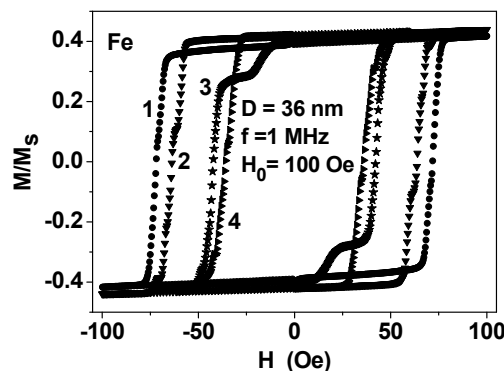


Fig. 1. Hysteresis loops of iron nanoparticle for various characteristic directions of applied magnetic field: 1) $\omega = \psi = 0$; 2) $\omega = 0.9553$, $\psi = \pi/4$; 3) $\omega = \psi = \pi/8$; 4) $\omega = \pi/4$, $\psi = 0$.

3 July

Monday

11:30-13:15

14:30-17:15

oral session

3TL-C

3RP-C

3OR-C

**“Magnetic
Nanostructures and
Low Dimensional
Magnetism”**

3TL-C-1

MAGNETIC NANOWIRES AND NANOTUBES AS BUILDING BLOCKS FOR A 3D RACE-TRACK MEMORY

Staño M.¹, Schaefer S.², Wartelle A.¹, Thirion C.¹, Rioult M.³, Belkhou R.³, Sala A.⁴, Mentş T.O.⁴,
Locatelli A.⁴, Cagnon L.¹, Fernandez-Roldan J. A.⁶, Trapp B.¹, Bochmann S.⁵, Martin S.^{6,1},
Gautier E.⁶, Vazquez M.⁶, Bachmann J.⁵, Gusakova D.⁶, Toussaint J.C.¹, Ensinger W.²,
Fruchart O.^{1,6}

¹ Univ. Grenoble Alpes, CNRS, Institut NEEL, Grenoble, France

² Technische Universität Darmstadt, Darmstadt, Germany

³ Synchrotron SOLEIL, Saint-Aubin, France

⁴ Elettra - Sincrotrone Trieste S.C.p.A., Trieste, Italy

⁵ Friedrich-Alexander University of Erlangen-Nürnberg, Erlangen, Germany

⁶ CSIC, ICMN, Madrid, Spain

⁷ Univ. Grenoble Alpes, CNRS, CEA, SPINTEC, Grenoble, France

olivier.fruchart@cea.fr

The type and motion of magnetic domain walls in cylindrical nanowires has been largely addressed theoretically over the past 15 years, and more recently in nanotubes. While such circular structures may be technologically important as they are the natural geometry for a 3-dimensional race-track memory based on a dense array of vertical 1d magnetic conduits, they also offer a playground for novel synthesis strategies, measurement techniques and physics.

I will present experimental and theoretical work performed in the field. This includes the bottom-up synthesis of various types of structures addressing challenges set by the race-track memory concept; strategies to create and stabilize domain walls in such 1D structures; imaging of domains and domain walls in wires and tubes using shadow XMCD-PEEM, a key technique to unravel three-dimensional magnetization configurations; experimental proof of the existence of the so-called Bloch-point domain wall in wires [1] (a type of wall not found in flat strips); motion of domain walls under application of a magnetic field [2]; a general classification of all possible domain walls in terms of their topology [3]. Some device-oriented issues will be discussed, such as bit coding in a 3D medium and strategies for clocking bits.

This project has received funding from the European Union Seventh Framework Programme (FP7/2007-2013) under grant agreement n° 309589 (M3d).

[1] S. Da Col et al., *Phys. Rev. B*, **89** (R) (2014) 180405.

[2] S. Da Col et al., *Appl. Phys. Lett.*, **109** (6) (2016) 062406.

[3] Head-to-head domain walls in one-dimensional nanostructures: an extended phase diagram ranging from strips to cylindrical wires, S. Jamet et al., in *Magnetic Nano- and Microwires: Design, synthesis, properties and applications*, M. Vázquez Ed., Woodhead (2015).

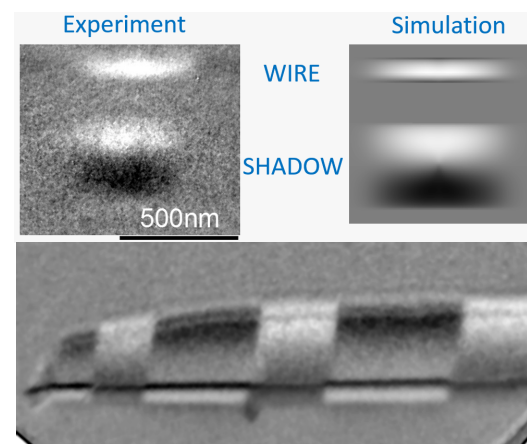


Fig. 1. Shadow XMCD-PEEM images of a Bloch-point domain wall in a wire (top) and orthoradial domains in a nanotube (bottom, FoV 6 microns).

3TL-C-2

NANOMAGNET FABRICATION BY ION BEAMS*Fassbender J.¹*¹ Helmholtz-Zentrum Dresden-Rossendorf, Dresden, D-01328, Germany
j.fassbender@hzdr.de

In recent years the tailoring of magnetic properties by means of ion irradiation and implantation techniques has become fashionable. Early investigations relied on the fact that the perpendicular magnetic anisotropy of Co/Pt multilayers depend sensitively on the interface sharpness [1]. Subsequently also the ion induced modification of exchange bias phenomena as well as interlayer exchange coupling have been investigated [2]. For single magnetic films ion implantation has been used to reduce the Curie temperature and hence the saturation magnetization [3]. Nowadays also the reverse process, i.e. the creation of nanomagnets within special binary alloys is employed [4,5]. In combination with lithography or with focused ion beams a pure magnetic patterning becomes possible [6] leading to hybrid magnetic materials [7] with properties different from both, the ion irradiated as well as the untreated material. Even ion induced chemical reduction can be employed to create a nanomagnetic pattern [8,9].

An overview of the present status in this research field will be given.

- [1] C. Chappert et al., *Science*, **280** (1998) 1919.
- [2] J. Fassbender, D. Ravelosona, Y. Samson, *J. Phys. D*, **37** (2004) R179.
- [3] J. Fassbender, J. McCord, *Appl. Phys. Lett.*, **88** (2006) 252501.
- [4] E. Menendez et al., *Small*, **5** (2009) 229.
- [5] R. Bali et al., *Nano Lett.*, **14** (2014) 435.
- [6] J. Fassbender and J. McCord, *J. Magn. Magn. Mater.*, **320** (2008) 579.
- [7] J. McCord, L. Schultz, J. Fassbender, *Adv. Mater.*, **20** (2008) 2090.
- [8] S. Kim et al., *Nature Nanotechnology*, **7** (2012) 567.
- [9] J. Fassbender, *Nature Nanotechnology*, **7** (2012) 554.

3TL-C-3

INVESTIGATING ENHANCED AND METASTABLE MAGNETISM IN SIZE- AND SHAPE-SELECTED, INDIVIDUAL NANOPARTICLES

Kleibert A.¹

¹ Paul Scherrer Institut, Swiss Light Source, Villigen, CH-5232, Switzerland
armin.kleibert@psi.ch

Magnetic nanoparticles are important building blocks for future technologies ranging from nanomedicine to spintronics [1-3]. Many related applications require nanoparticles with tailored magnetic properties. However, despite significant efforts undertaken towards controlling their magnetism, a broad and poorly-understood dispersion of magnetic properties is reported, even within mono-disperse samples of the canonical ferromagnetic 3d transition metals Fe, Co, and Ni. In this contribution we will show how we address this issue by investigating the magnetism of a large number of size- and shape-selected, individual 3d transition metal nanoparticles using a unique set of complementary characterization techniques [4,5]. Using this approach, we observe that nanoparticles in a size range from 8 to 20 nm can exhibit strikingly high magnetic energy barriers, which are not explained by surface or shape effects [6,7]. Further, we find that in case of Fe and Co these energy barriers can be tuned by thermal treatment. This behavior is assigned to the presence of structural defects, which are expected to significantly impact the magnetism of nanoparticles. Finally, we will present our recent efforts to directly reveal the relation between magnetic properties and atomically resolved microscopic structure of individual nanoparticles.

- [1] A. H. Lu *et al.*, *Angew. Chem. Int. Ed.*, **45** (2007) 1222.
- [2] Q. A. Pankhurst *et al.*, *J. Phys. D: Appl. Phys.*, **42** (2009) 224001.
- [3] Y. Qiang *et al.*, *J. Nanopart. Res.*, **8** (2006) 489.
- [4] A. Fraile Rodríguez *et al.*, *Phys. Rev. Lett.*, **104** (2010) 127201.
- [5] A. Fraile Rodríguez *et al.*, *J. Phys. D: Appl. Phys.*, **43** (2010) 474006.
- [6] A. Balan *et al.*, *Phys. Rev. Lett.*, **112** (2014) 107201.
- [7] A. Kleibert *et al.*, *Phys. Rev. B*, **95** (2017) 195404.

3RP-C-4

SPIN ORDERING IN SEMICONDUCTOR NANOPARTICLES WITHOUT MAGNETIC ELEMENT ATOMS

Uspenskii Yu.A.¹, Baturin V.S.¹, Lepeshkin S.V.¹, Fokina N.A.¹

¹Lebedev Physical Institute of RAS, Moscow
uspenski@lpi.

The unique properties of semiconductor nanoparticles hold great promise for many applications, such as electronics, solar energetics, photocatalysis, biomedicine, etc. A hot avenue is nanomaterials combining semiconducting and magnetic properties which are needed for spintronics, bimodal biosensors and many other applications. One way to develop them is the doping of semiconductor particles by Mn and other magnetic 3d-elements. It replicates the engineering of bulk diluted magnetic semiconductors and shares many of its problems. Another way employs spin polarization existing at the surface of semiconductor nanoparticles. Such spins, in particular, were detected at the surface of CdSe nanocrystals passivated by TOPO (tri-n-octylphosphine oxide) [1]. As was argued later [2], the reordering of spins activates the radiative recombination of dark excitons in CdSe nanocrystals, so photoluminescence is controlled by spin flip-flop processes at the nanocrystal surface. This activation mechanism excellently agrees with the measurements of temperature-dependent recombination rate and light emission however a first-principles support of this model is still absent.

Surface spin polarization was revealed by first-principles calculations in Mg_nO_m [3] and Si_nO_m [4] semiconductor nanoclusters. It was found that in oxygen atmosphere equilibrium Mg_nO_m and Si_nO_m nanoclusters have excessive O atoms, comparing to the stoichiometric MgO and SiO₂ compositions. These are precisely those O atoms, which are responsible for spins at the cluster surface. To understand this effect and study the features of spin ordering, we calculated the atomic structure, electron spectrum and exchange interaction of 30 clusters Si_nO_m with $n \leq 10$ and $2n+1 \leq m \leq 2n+9$, taking into account ferromagnetic, ferrimagnetic and antiferromagnetic spin configurations. It was found that magnetic moments exist only at the specific surface groups of Si and O atoms and all these groups are classified as luminescence centers. This observation strongly supports the assumption [2] about intimate connection between radiative recombination and spin polarization. Calculated energy differences between different magnetic orderings vary widely from 1 meV to 50 meV, depending on distance between spins, cluster geometry and composition, so the room temperature ferromagnetism of semiconductor nanoparticles looks quite possible. Because spins are located only at the cluster surface, magnetic phenomena in clusters have important features distinctive from those in bulk magnets. We believe that these features are typical of oxide nanoparticles and, probably, many semiconductor nanoparticles. Harnessing them can be useful for the construction of magnetically controlled semiconductor nanodevices for miscellaneous applications.

- [1] M.S. Seehra, P. Dutta, S. Neeleshwar, Y.-Y. Chen, C. L. Chen, S. Wei Chou, C.C. Chen, C.-L. Dong, and C.L. Chang, *Adv. Mater.*, **20** (2008) 1656-1660.
 [2] A. Rodina, and A.I. Efros, *Nano Lett.*, **15** (2015) 4214.
 [3] S. Bhattacharya, S.V. Levchenko, L.M. Ghiringhelli, and M. Scheffler, *Phys. Rev. Lett.*, **111** (2013) 135501.
 [4] S. Lepeshkin, V. Baturin, E. Tikhonov, N. Matsko, Yu. Uspenskii, A. Naumova, O. Feya, M.Schoonen and A. Oganov, *Nanoscale*, **8** (2016) 18616-18620.

3OR-C-5

ELECTRONIC STRUCTURE AND MAGNETIC PROPERTIES OF LOW-DIMENSIONAL NONSTOICHIOMETRIC RUTILE

Korotin M.A.¹, Skorikov N.A.¹, Anokhin A.O.¹

¹ M.N. Mikheev Institute of Metal Physics, Yekaterinburg, Russia
michael.korotin@imp.uran.ru

A vast majority of studies devoted to the nature of spontaneous magnetization with a high Curie temperature in TiO₂ and other magnetic semiconductors has been carried out predominantly for the bulk state. At the same time, a sufficient pool of experimental data has by now been accumulated to demonstrate an abnormal magnetic behaviour exhibited by the nonstoichiometric nanocrystalline-state TiO₂-based semiconductors, i.e., when the electronic states of surface atoms make a considerable contribution into the electronic structure. The present talk is aimed at discussion of the surface influence (lowering of the dimensionality down to two) and the effect of weak nonstoichiometry in the oxygen sublattice (TiO_{1.99}) on the electronic structure and magnetic properties of two-dimensional titanium dioxide. This theoretical investigation was done using the coherent potential approximation.

The main results demonstrate that on the (110) surface of rutile the vacancies present in the positions of the surface oxygen atoms provide for the appearance of the spin magnetic moments on the surface titanium atoms, which are surrounded with five rather than six oxygen atoms. The additional vacancies present in the neighbourhood of the magnetic titanium ions increase the value of the spin magnetic moment. The vacancies in other positions of the oxygen sublattice do not make a qualitative change in the semiconductor character of the electronic spectrum and do not result in the magnetism appearance in TiO₂.

The study [1], which is aimed at the experimental investigation of magnetic properties of oxygen-deficient titanium dioxide nanocrystals, has reported that the presence of vacancies in the anion sublattice causes a dominating effect on the formation of magnetic properties of samples under study. New experimental findings were presented to prove that the magnetic moment carriers are localized predominantly in the near-surface regions of nanoparticles. Therefore, the results discussed in the present talk are in full agreement with the experimental results [1].

Support by the grant of the Russian Scientific Foundation (project 16-12-10004) is acknowledged.

[1] A.E. Ermakov, M.A. Uymin, A.V. Korolev, A.S. Volegov, I.V. Byzov, N.N. Schegoleva, A.S.Minin, *Phys. Solid State*, **59** (2017) 469-482.

3OR-C-6

ϵ -Fe₂O₃ NANOPARTICLES IN SILICA MATRIX. SYSTEM WITH UNIQUE MAGNETIC PROPERTIES FOR CATALYSIS

Yakushkin S.S.¹, Balaev D.A.^{2,3}, Shaikhutdinov K.A.², Dubrovskiy A.A.², Bukhtiyarova G.A.¹,
Martyanov O.N.¹

¹ Boreskov Institute of Catalysis, Novosibirsk, Russia

² Kirensky Institute of Physics, Federal Research Center KSC SB RAS, Krasnoyarsk, Russia

³ Siberian Federal University, Krasnoyarsk, Russia

stas-yk@catalysis.ru

The systems based on supported iron-oxide nanoparticles are one of the most available, cheap and nontoxic materials, which can be used in various applications, e.g. magnetic memory, controlled drug delivery, catalysis etc. The systems based on ϵ -Fe₂O₃ nanoparticles among those materials attract particular and growing attention during the last decades. The ϵ -Fe₂O₃ phase, is the intermediate between α - and γ -Fe₂O₃; it was characterized just recently, e.g. in 1998 [1]. ϵ -Fe₂O₃ phase displays high (up to 20 kOe) coercivity at room temperature, and is stable only in the form of nanoparticles, thanks to its low surface energy.

The majority of works on the ϵ -Fe₂O₃ phase is dedicated to the investigation of the magnetic properties of this phase and the search for the routes to synthesize ϵ -Fe₂O₃ in the form of stable and bulk particles (up to 200 nm). Most researches try to study magnetic properties of the ϵ -Fe₂O₃ without taking into account size effects. However in some cases, such as catalysis, studying a few nanometers sized particles can be crucial.

In the Boreskov Institute of Catalysis the ϵ -Fe₂O₃/SiO₂ system based on few nanometers ϵ -Fe₂O₃ supported nanoparticles was created for the first time that has no other detectable iron-oxide polymorphs [2]. It was shown that the system displays superparamagnetic behavior at room temperature [3]. FMR method *in situ* in comparison with HR TEM, XRD, Mossbauer spectroscopy, and magnetization measurements data were applied to investigate the magnetic structure of ϵ -Fe₂O₃/SiO₂ nanoparticles formed [4,5].

The ϵ -Fe₂O₃/SiO₂ system was proved to have some unique chemical properties, i.e. resistance to sulphidation, an important parameter for iron-oxide catalytical systems for selective sulphur dioxide reduction [6]. The results of the FMR *in situ* study of sulphidation process of the ϵ -Fe₂O₃/SiO₂ system are presented.

Support by Russian Science Foundation (Grant No. 17-12-01111).

[1] E. Tronc, C. Chaneac, J.P. Jolivet, *J. Sol. Stat. Chem.*, **139** (1998) 93.

[2] G.A. Bukhtiyarova, M.A. Shuvaeva, O.A. Bujukov, S.S. Yakishkin, O.N. Martyanov, *J. Nanoparticle Res.*, **36** (2011) 5527.

[3] S.S. Yakushkin, A.A. Dubrovskiy, D.A. Balaev, K.A. Shaykhutdinov, G.A. Bukhtiyarova, O.N. Martyanov, *J. Appl. Phys.*, **111** (2012) 044312.

[4] D.A. Balaev, A.A. Dubrovskij, K.A. Shajkhutdinov, O.A. Bayukov, S.S. Yakushkin, G.A. Bukhtiyarova, O.N. Martyanov, *J. Appl. Phys.*, **114** (2013) 163911.

[5] A.A. Dubrovskiy, D.A. Balaev, K.A. Shaykhutdinov, O.A. Bayukov, O.N. Pletnev, S.S. Yakushkin, G.A. Bukhtiyarova, O.N. Martyanov, *J. Appl. Phys.*, **118** (2015) 213901.

[6] M.A. Shuvaeva, I.V. Delii, O.N. Mart'yanov, O.A. Bayukov, E.I. Osetrov, A.A. Saraev, V.V. Kaichev, N.S. Sakaeva, G.A. Bukhtiyarova, *Kinet. Catal.*, **52** (2011) 896.

3RP-C-7

DZYALOSHINSKII-MORIYA INTERACTION DRIVEN BY MODULATED INTERFACES IN 3d-5d(4d) THIN FILMS WITH STRUCTURAL INVERSION ASYMMETRY

Samardak A.S.¹, Pal B.¹, Samardak A.Yu.¹, Davydenko A.V.¹, Ognev A.V.¹, Chebotkevich L.A.¹, Sadovnikov A.V.^{2,3}, Nikitov S.A.^{2,3}, Cha I.H.⁴, Kim Y.K.⁴

¹ School of Natural Sciences, Far Eastern Federal University, Vladivostok Russia

² Laboratory "Metamaterials," Saratov State University, Saratov, Russia

³ Kotel'nikov Institute of Radioengineering and Electronics, Russian Academy of Sciences, Moscow, Russia

⁴ Department of Materials Science and Engineering, Korea University, Seoul, Republic of Korea
samardak.as@dvfu.ru

An interface between 3d transition metal and 5d(4d) heavy metal (HM) is a host of intriguing spin-related effects desirable for spin-orbitronic applications [1]. Chiral interaction between two 3d spins due to a strong spin-orbit coupling (SOC) in an underlying atomic layer of heavy metal is associated with the interfacial Dzyaloshinskii-Moriya interaction (iDMI) [2]. Recently, it has been shown that iDMI depends not only on SOC and the lack of the inversion symmetry, but also on the degree of 3d-5d(4d) orbital hybridization around the Fermi level [3]. Until now the effect of the 3d-5d(4d) interface roughness and intermixing on the iDMI value and on orientation of the iDMI vector is not clear.

We report on results of the investigation of the magnetic anisotropy and interfacial DMI in the magnetic layer sandwiched between two 5d HM (Pt and Ta) or one 5d HM (Pt) from the bottom and 4d HM (Ru) from the top. We have artificially introduced an interface roughness using the atomically smooth Si(111)/Cu surface with the epitaxially grown Pd seed layer of different thickness ranging from 0 to 56 ML (or from 0 to 12.6 nm). In dependence on the thickness, the average roughness of the Pd layer varies from 0.07 to 1.0 nm. The following two series of samples were deposited on the top of the Pd surface by magnetron sputtering: series (i) Pt(2)/CoFeSiB(1.5)/Ta(5) and series (ii) Pt(2)/CoFeSiB(1.5)/Ru(3)/Ta(5), where the layer's thickness is indicated in nm.

The direct measurement of iDMI was performed by Brillouin light scattering (BLS) spectroscopy based on iDMI-driven asymmetric dispersion shift of long-wavelength thermal spin waves in the Damon-Eshbach surface mode. The modulated roughness of the Pd surface leads to the significant changes of iDMI compare to the reference samples. Thus, in series (i) the iDMI value reaches the saturation of 0.54 mJ/m² at 46 ML (10.35 nm) Pd. However, in series (ii) we have found much stronger enhancement of iDMI with increased roughness of the Pd layer. At 5 ML Pd the iDMI value is 0.52 mJ/m² and it increases up to 1.17 mJ/m² at 46 ML Pd thickness. It means that the small variation of the surface roughness (less than 1.0 nm) provides the Pt/CoFeSiB interface modulation at the atomic scale, which is enough for drastic changes in the DMI value. We have revealed that atomic-scale surface engineering enables to precisely control the DMI value and to enhance it up to 2.5 times in case of the 5d-3d-4d system, which opens up a novel route for the design of spintronic devices and development of future information storage technology. Support by RFBR (grant 17-52-50060) and the state task (3.5178.2017) is acknowledged.

[1] A. Soumyanarayanan et al., *Nature*, **539** (7630) (2016) 509.

[2] H. Yang et al., *Physical Review Letters*, **115** (2015) 267210.

[3] A. Belabbes et al., *Physical Review Letters*, **117** (2016) 247202.

3RP-C-8

EFFECT OF Cu, Cu/Ru, OR Ru/Cu SEED-LAYER ON PERPENDICULAR MAGNETIC ANISOTROPY OF Co₈₀Pt₂₀ FILMS

Chen S.C.¹, Jen S.U.², Lu C.F.¹, Chen R.Z.³, Wang C.M.⁴, Kuo P.C.⁴

¹ Department of Materials Engineering and Center for Thin Film Technologies and Applications, Ming Chi University of Technology, Taipei 243, Taiwan.

² Institute of Physics, Academia Sinica, Taipei 11529, Taiwan

³ New Materials R&D Dept., China Steel Corporation, Kaohsiung 812, Taiwan.

⁴ Institute of Materials Science and Engineering, National Taiwan University, Taipei 106, Taiwan.
physjen@gate.sinica.edu.tw

Magnetic anisotropy of the Co₈₀Pt₂₀ films deposited directly on glass substrates (without any seed layer) at room temperature inclines towards random. The perpendicular magnetic anisotropy can be increased slightly by introducing a Cu layer or Cu/Ru bilayers under the Co₈₀Pt₂₀ films [1 – 3]. However, when the Co₈₀Pt₂₀ films are deposited onto a Ru/Cu bilayer, the magnetic anisotropy of the films becomes perpendicular. The magnetic hysteresis curves were measured using a vibrating sample magnetometer (VSM). The phase structure of the films was examined by X-ray diffraction (XRD) using Cu-K α line. The microstructures of the films are investigated by a field emission gun (FEG) transmission electron microscopy (TEM).

From this study, we found that an fcc Cu (111) under-layer can promote the hcp Ru (0002) seed layer, which can, therefore, induce good (0002) texture in the hcp Co₈₀Pt₂₀ magnetic layer. As a result, Co₈₀Pt₂₀/Ru/Cu/glass films display excellent (or improved) perpendicular magnetic anisotropy. In conclusion, our results showed that columnar Co-rich Co-Pt nano-grains with perpendicular coercivity of 4580 Oe and perpendicular squareness of 0.77 can be achieved by depositing Co₈₀Pt₂₀ (50 nm) film onto Ru (30 nm)/Cu (100 nm) bilayer, using a glass substrate, at room temperature.

[1] K.K.M. Pandey, J.S. Chen, B.C. Lim, and G.M. Chow, *J. Appl. Phys.*, **104** (2008) 073904.

[2] K.K.M. Pandey, J.S. Chen, G.M. Chow, and B.C. Lim, *J. Magn. Magn. Mater.*, **321** (2009) 3236-3240.

[3] T. Shimatsu, H. Sato, Y. Okazaki, H. Aoi, H. Muraoka, Y. Nakamura, S. Okamoto, and O. Kitakami, *J. Appl. Phys.*, **99** (2006) 08G908.

3RP-C-9

CYANOMETALLATE BASED LOW-DIMENSIONAL HETEROMETALLIC ASSEMBLIES DISPLAYING SLOW MAGNETIC DYNAMICS

Vostrikova K.E.¹

¹ Nikolaev Institute of Inorganic Chemistry SB RAS, Novosibirsk, Russia
vosk@niic.nsc.ru

During last time interest in discrete 0D/1D polynuclear complexes behaving as single molecule or chain magnets (SMM or SCM) is increased considerably due to their possible application in the high density information storage devices, spintronic and quantum computing [1]. Magnetic compartment of such quantum magnets (QMs) is determined by an energy barrier U that has to be surmount to reverse magnetization. The U height of SMM depends on uniaxial magnetic anisotropy energy and total spin of the molecule. For a chain of ferromagnetically coupled spins, Glauber predicted ability to a slow magnetic dynamics at finite temperatures [2]. Contrary to SMMs, the U of SCMs depends not only on the anisotropy energy but also on the intrachain magnetic interaction [3]; hence, it should be easier to rise U for SCMs compared to SMMs. Thus, for design of the 0D or 1D molecular magnetic materials, a set of key parameters must be considered: high total spin, axial magnetic anisotropy and strong exchange interaction between the magnetic centers. If the first two features concern the height of U separating molecule spin projections, the critical temperature (T_b) depends mostly on the last option. The stronger exchange interactions, the better ground spin state is isolated from excited one.

It was shown that 4d and 5d cyanometalates with a strong spin-orbit coupling are very promising synthons [4] in design of such systems [5] due to an anisotropic exchange interaction between high spin 3d metal complexes and heavier cyanometallates. Namely, this anisotropic interaction is an origin of slow magnetic dynamics [6]. In our report, we present the synthetic approaches for the preparation of 0D and 1D coordination bimetallic assemblies involving cyanide complexes of Fe, Ru, Os and Re and displaying slow magnetic relaxation and hysteresis, Re and Os based chains being the first examples of SCMs. A set of the hysteresis loops for $\text{Mn}^{\text{III}}\text{-Re}^{\text{IV}}$ nanowire is shown in Figure.

Support by RFBR (grant 16-03-00880-a) is acknowledged.

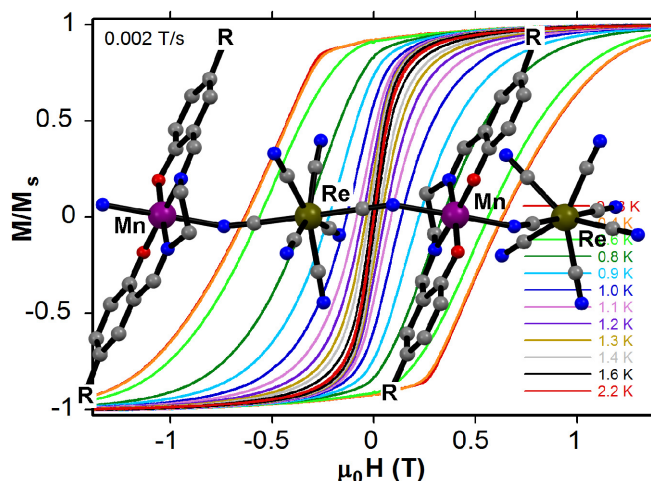


Figure Single crystal hysteresis loops for $[\text{Mn}(\text{SB})\text{Re}(\text{CN})_7]_n$

- [1] D. Gatteschi, R. Sessoli, J. Villain *Molecular Nanomagnets*, Oxford Univ. Press (2006); C. Coulon, H. Miyasaka, R. Clérac in *Structure and Bonding*, R. Winpenney, Springer (2006) 163.
 [2] R. Glauber *J. Math. Phys.*, **4** (1963) 294.
 [3] W.X. Zhang, B. Breedlove, R. Ishikawa, M. Yamashita *RSC Advances*, **3** (2013) 3772.
 [4] V.S. Mironov, *Dokl. Phys. Chem.* 2006, **408**, 130. V. S. Mironov, *Dokl. Phys. Chem.*, **415** (2007) 199.
 [5] X.Y. Wang, C. Avendaño, K.R. Dunbar, *Chem. Soc. Rev.*, **40** (2011) 3213.
 [6] J. Dreiser, K.S. Pedersen et al., *Chem. Eur. J.*, 2013, **19**, 3693; K. Qian, X.C. Huang, C. Zhou, X.Z. You, X.Y. Wang, K.R. Dunbar, *J. Am. Chem. Soc.*, **135** (2013) 13302.

3OR-C-10

DOUBLING OF THE FERROMAGNETIC ENERGY PRODUCT IN NANOWIRES BY TIP-CAPPING WITH AN ANTIFERROMAGNET

Wang F.Z.¹, Salikhov R.¹, Spasova M.¹, Liébana Viñas S.¹, Bran C.²,
Chen Y.S.^{2,3}, Vazquez M.², Farle M.^{1,4}, Wiedwald U.¹

¹ Faculty of Physics and CENIDE, University of Duisburg-Essen, Germany

² Institute of Materials Science of Madrid, CSIC, 28049 Madrid, Spain

³ Department of Chemical Engineering and Materials Science, Yuan-Ze University, Taiwan

⁴ FunMagMa, Immanuel Kant Baltic Federal University, Kaliningrad, Russia
ulf.wiedwald@uni-due.de

3d transition metal-based magnetic nanowires (NW) are currently considered as potential candidates for alternative rare-earth-free permanent magnets, magneto-electric logic elements and memory storage units [1-2]. Exploiting the large shape anisotropy in combination with magnetocrystalline anisotropy of 3d-metal NW yields a large energy product for nanomagnets, i.e. high remanent magnetization (M_R) and large coercive field (H_C) [3]. It has been shown recently that M_R and H_C can be significantly enhanced at low temperatures by oxidizing FeCo NW tips proving that magnetic switching starts at the NWs tips via vortex or domain wall formation [4].

Here we explore the magnetic hardening of $Fe_{30}Co_{70}$ NWs by interfacing their tips with antiferromagnetic (AFM) $Fe_{50}Mn_{50}$ layers. The Néel temperature and the interface exchange energy of $Fe_{50}Mn_{50}$ are expected to bring an enlarged energy product at room temperature. For this purpose, ferromagnetic NWs with diameter of 40 nm and length of 16 μm were grown in Anodic Aluminum Oxide (AAO) nanopores. Both tips of NW's were opened by selective chemical etching of the AAO membrane. Subsequently, the free-standing tips were capped with an AFM $Fe_{50}Mn_{50}$ (~10 nm) by rf-sputtering forming a AFM/FM/AFM sandwich-structure. As a result, the absolute enhancement of the H_C in this sandwich structure is 50 mT, while the relative increase of 50% and 24% for H_C and M_R , respectively, leads to a more than doubled energy product at ambient temperature [5].

The suggested approach is by no means restricted to magnetic properties and can be easily extended to other NW systems. For example, it gets feasible to prepare vertical interconnects between separated functional layers on the nanoscale which are beneficial for further applications such as nanoelectronics, spintronics or plasmonics.

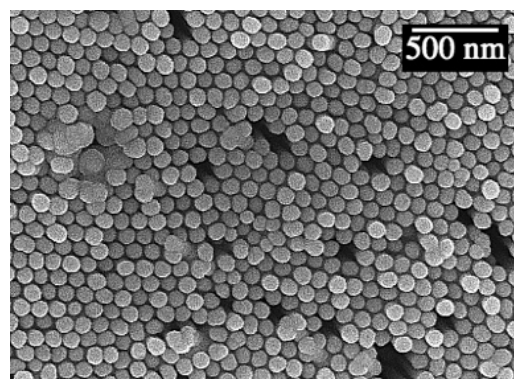


Fig. 1. Top-view scanning electron microscopy image of $Fe_{30}Co_{70}$ NWs in an AAO matrix. The free-standing tips are covered with a nominally 8 nm $Fe_{50}Mn_{50}$ layer.

[1] C. Bran et al., *Journal of Physics D-Applied Physics*, **48** (2015) 145304.

[2] D. Niarchos et al., *Jom*, **67** (2015) 1318.

[3] S. Liébana-Viñas et al., *Chemistry of Materials*, **27** (2015) 4015–4022.

[4] S. Liébana-Viñas et al., *Nanotechnology*, **26** (2015) 415704.

[5] FZ. Wang et al., submitted.

3OR-C-11

UNUSUAL MAGNETIC PROPERTIES OF CARBON BASED NANOCOMPOSITES

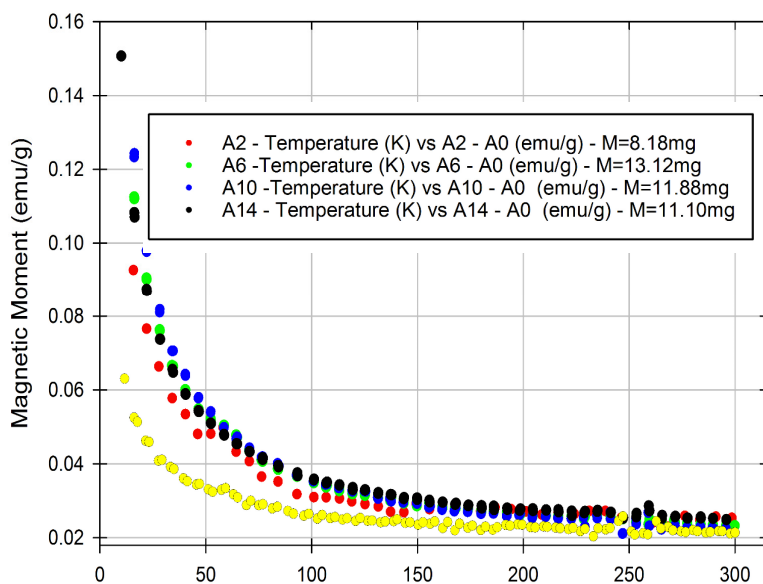
Estipanos M.¹, Sharoyan E.², Manukyan A.², Gyulasaryan H.², Mirzakhanyan A.¹, Bernal O.¹, Kocharian A.¹

¹ California State University, Los Angeles

² Institute for Physical Research, Ashtarak, Armenia

armen.kocharian@calstatela.edu

The novel magnetic nanocomposites of Ni and Cu nanoparticles (NPs) coated by graphite-like shells being a product of pyrolysis (thermal decomposition) of metal (M)-phthalocyanine and metal-free phthalocyanine, $\{(MPC)_x(H_2PC)_{1-x}, 0 < x < 1\}$, were synthesized by controlling the size and



Magnetization vs. temperature at 50 kOe and different concentration of embedded Cu@C

structure of such nanocrystals [1]. The stable ultrasmall (2-30nm) polycrystalline copper and nickel nanoparticles display unusual diamagnetism ferromagnetism and paramagnetism observed in case of ultrafine nickel and copper nanoparticles with the mean size, d , less than 17 nm. Zero-field and field cooled (ZFC-FC) magnetic measurements were carried out by vibrational PPMS magnetometer in the temperature range 5-300 K and broad range of magnetic field (0-50kOe). At low temperatures ($<70K$) a giant paramagnetism was detected due, apparently, to the ballistic conduction electron mean free path (large orbital magnetism). The values of the specific susceptibility at $T = 10K$ is

of the order $\chi_m^{PM} \approx 5 \times 10^{-5} \text{ emu/g} \cdot \text{Oe}$. Magnetic properties of Cu nanoparticles are affected by quantum confinement of the conduction electrons. In contrast to Ni its bulk form Cu is known to be weakly diamagnetic, driven by the Lenz diamagnetic responses from the completely filled ions core and $3d$ -band while the ultra small Cu nanoparticles overcome the diamagnetic responses from the inner core by exhibiting strong paramagnetic and ferromagnetic responses at low temperatures. It is shown that magnetic properties of capped NPs, driven by the dominating exchange interactions between the NPs and the capping carbon, can be very different from their bare form. Magnetization study reveals that at low concentration of Cu nanoparticles leads to the giant enhancement of magnetization and superparamagnetism. The nanoparticle size and concentration dependences of Cu nanoparticles on the magnetic properties of nanoparticles are analyzed.

This work is supported by the RA MES State Committee of Science, in the frames of the research project № 15T-1C249. Work at California State University, Los Angeles, is supported by NSF-PREM Grant No. DMR-1523588.

[1] E. Sharoyan, et. al., *IEEE Transactions on Magnetics*, **52** (2016) 2300803.

3OR-C-12

NON-EQUILIBRIUM CRITICAL DYNAMICS OF LOW-DIMENSIONAL MAGNETICS AND MULTILAYER STRUCTURES

*Prudnikov P.V.*¹

¹ Omsk State University, Omsk, Russia
prudnikp@univer.omsk.su

A significant interest has been recently focused on non-equilibrium processes in magnetic low-dimensional materials. The reduction of the dimension of magnets is accompanied by an increase in fluctuations of the spin density and the manifestation of the effects of critical slowing down and “aging” in the non-equilibrium behavior of low dimensional magnetic systems [1]. Thin films and low-dimensional demonstrates the slow critical evolution from a nonequilibrium initial state. Aging, coarsening and memory effects are nontrivial features in the non-equilibrium behavior of such systems with slow dynamics [2].

The magnetic properties of multilayer magnetic systems have been widely investigated over the past years, since they widely used in magnetic storage devices. Magnetic order in the multilayers is complex due to a strong influence of the shape and the magnetocrystalline anisotropies of the sample. Anisotropy effects leads to dimensionality crossover in Heisenberg films [3]. This study includes the Monte-Carlo simulation of the non-equilibrium critical evolution from different initial states of low-dimensional magnetics [4] and multilayers based on anysotropic Heisenberg films [5, 6].

This work was supported by the grant 17-02-00279 of Russian Foundation of Basic Research and by the grant MD-6024.2016.2 of Russian Federation President. The simulations were carried out on the Supercomputing Center of Lomonosov Moscow State University, Moscow Joint Supercomputer Center and St. Petersburg Supercomputer Center of the Russian Academy of Sciences.

- [1] T. Mukherjee, M. Pleimling, Ch. Binek, *Phys. Rev. B*, **82** (2010) 134425.
- [2] V.V. Prudnikov, P.V. Prudnikov, M.V. Mamonova, *Phys. Usp.*, (2017).
- [3] P.V. Prudnikov, V.V. Prudnikov, M.A. Menshikova, N.I. Piskunova, *J. Magn. Magn. Mater.*, **387** (2015) 77.
- [4] I.S. Popov, P.V. Prudnikov, A.N. Ignatenko, A.A. Katanin, *Phys. Rev. B*, (2017).
- [5] V.V. Prudnikov, P.V. Prudnikov, D.E. Romanovskiy, *J. Phys. D: Appl. Phys.* **49** (2016) 235002.
- [6] V.V. Prudnikov, P.V. Prudnikov, A.N. Purtov, M.V. Mamonova, *JETP Letters*, **104** (2016) 776.

3OR-C-13

QUANTUM-MECHANICAL AND CONTINUAL MODELS OF MAGNETIC DYNAMICS FOR ANTIFERROMAGNETIC PARTICLES AND THEIR APPLICATION TO IDENTIFICATION OF MAGNETIC STRUCTURE OF FERRIC OXIDE NANOPARTICLES BY MÖSSBAUER SPECTROSCOPY

Mischenko I.N.¹, Chuev M.A.¹

¹ Institute of Physics and Technology, Russian Academy of Science, Moscow, Russia
IlyaMischenko@rambler.ru

Among plenty of techniques using for study structural, magnetic and thermodynamic properties of magnetic fine particles Mössbauer spectroscopy is one of the most informative. Often though for the samples of various magnetic structure the temperature evolution of the spectra exhibits the universal form satisfactorily described by many-state relaxation model of the magnetic dynamics for ferromagnetic (FM) particles [1]. On the other hand many experiments with antiferromagnetic (AFM) particles show principally different behavior of their gamma-resonance curves, which main peculiarity is originating and rise with temperature a single peak or quadrupolar doublet of lines in the central part of the spectrum along with the maintenance of the resolved hyperfine structure. Explanation of such behavior within the standard approach is impossible and requires development of specific models of magnetism for AFM particles.

Recently we suggest an approach to the problem on the base of quantum-mechanical description of ideal AFM particles in the limiting case of slowly relaxing macro-spins of magnetic sublattices [2]. This model, even without involving any uncompensated spin, describes principal difference in thermodynamic properties of FM and AFM particles. Moreover, we proved that non-equivalence of the sublattices does not change the qualitative pattern of the description, leading only to slight quantitative modifications in the shape of the absorption curves of AFM particles [3]. Later we developed a continual model of magnetic dynamics for an ensemble of ideal AFM particles based on the classical equations of motion for magnetization vectors of the sublattices [4]. We found that besides four regular modes of uniform precession of sublattices magnetizations around the easy axis, there exists two-parametric multitude of the trajectories with continuous variations of the polar angles of the moments: the nutations of the magnetizations of AFM sublattices, similar to the motions of a heavy gyroscope or a pendulum in the field of gravity [5]. In fact such form of excitation spectrum gives the macroscopic explanation to specific thermodynamics of AFM particles described by the quantum model [2].

The aim of this work is an attempt to use these models in answering the question about magnetic ordering in ferric-oxide nanoparticles. Distinction between ferrimagnetic maghemite $\gamma\text{-Fe}_2\text{O}_3$ and AFM hematite $\alpha\text{-Fe}_2\text{O}_3$ is not an easy task, especially for small particles, when standard X-ray methods fail because of large broadening of the diffraction peaks. At the same time absorption Mössbauer spectroscopy in combination with realistic models of magnetism inherent to the systems under study may become a powerful instrument for analysis in this and similar cases.

Support by RFBR is acknowledged.

[1] D.H. Jones, K.K.P. Srivastava, *Phys. Rev. B*, **34** (1986) 7542–7548.

[2] M.A. Chuev, *JETP Lett.*, **95** (2012) 295–301.

[3] M.A. Chuev, *Doklady Physics*, **57** (2012) 421–426.

[4] M.A. Chuev, *JETP Lett.*, **103** (2016) 175–180.

[5] L.D. Landau, E.M. Lifshitz: *Mechanics*. Pergamon Press, Oxford (1969) Vol. 1 (2nd ed.).

3OR-C-14

NON-MARKOVIAN DYNAMICA IN THE EXTENDED CLUSTER SPIN-1/2 XX CHAIN

Mohammad Ali Zadeh T.¹, MahdaviFar S.¹, Mahmoudi M.¹, Soltani M.R.²

¹ Department of Physics, University of Guilan, 41335-1914, Rasht, Iran

² Department of Physics, Share-rey Branch, Islamic Azad University, Tehran, Iran
t_alizadeh1905@yahoo.com

Recently, the growing interest in the dynamics of open quantum systems was amplified by entanglement sudden death (ESD) phenomenon [1,2], surprising discovery in the dynamical behavior of open systems uncovered theoretically and experimentally. In principle, the interaction between system and environment degrades the quantum correlation in the entangled system and provokes the disappearance of entanglement in a finite time which is in sharp contrast to half-life law. It is worth noticing fact that the dynamics of single-particle is asymptotical which it is not similar to ESD character [3]. The main purpose of this paper is to investigate the effect of the three-spin interaction (TSI) on the dynamics of quantum correlations between the nearest neighbor pair spins in a 1D spin model. The motivation behind this study is the recent progress in the field of quantum magnets. It is known that a wide variety of novel spin-1/2 Hamiltonians can be generated in the different configurations of an optical lattice [4]. We propose the simplest form of the generalized XX models so called the extended XX chain model spin-1/2 with three spin interaction, fully characterized by zig-zag chain. This model is exactly solvable. Using the Jordan-Wigner transformation, spins are mapped onto the one-dimensional non-interacting spinless fermions with creation and annihilation operator. By performing a Fourier transformation into the momentum space, the diagonalized Hamiltonian is derived. The dispersion relation:

$$\varepsilon(k) = \cos(k) + \frac{\alpha}{2} \cos(2k).$$

By selecting the nearest neighbor pair spins as an open quantum system, the others play as an environment. We try to determine the dynamics of the system in the thermodynamic limit of the zigzag chain ($N \rightarrow \infty$). Particularly, we concentrate on the quantum correlations between the nearest neighbor pair spins located at sites m and $m+1$ in the chain system. For this purpose, we consider the initial state in which two sites (m and $m+1$) in the chain system are maximally entangled. By doing so, the rest of the chain (the environment) is disentangled in this configuration. According to results, the dynamics of system is Markovian in the absence of the TSI. However, there is a furthermore subtle point we must consider, in the presence of the TSI, Markovian dynamics remains unchanged up to a critical value where non-Markovian dynamics shows up. To cast more clarification on the offered points, we investigate the propagation of quantum correlations in the environment. Since the dynamics of the system changes from Markovian to the non-Markovian, it is completely natural to search for a critical value in the TSI. To find it, we have calculated the quantum correlation between NN pair spins m and $m+1$ as a function of the time and α . The graphs, in Fig. 1, compare figures for different values of α .

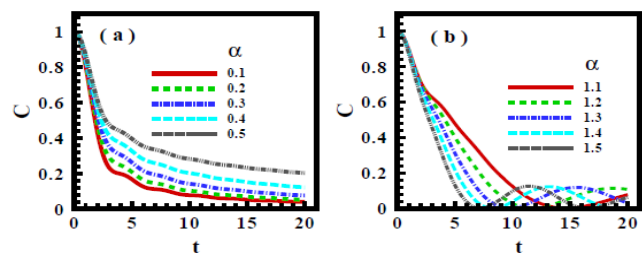


Fig. 1. The time behavior of concurrence in the system, $C_{m,m+1}$, for different values of the TSI interaction.

- [1] T. Yu, J. H. Eberly, *Phys. Rev. Lett.*, **97** (2006) 140403.
- [2] J. H. Eberly and T. Yu, *Science*, **316** (2007) 555.
- [3] T. Yu, J. H. Eberly, *Phys. Rev. Lett.*, **93** (2004) 140404.
- [4] A. B. Kuklov and B. V. Svistunov, *Phys. Rev. Lett.*, **90** (2003) 100401.

3 July

Monday

11:30-13:15

oral session

3OR-P

3RP-P

**“High Frequency
Properties and
Metamaterials”**

3OR-P-1

NONLINEAR INTERACTIONS OF SURFACE ELASTIC WAVES WITH MAGNETIZATION IN METAL FILMS

Vlasov V.S.¹, Lomonosov A.M.², Makarov P.A.¹, Shcheglov V.I.³, Kotov L.N.¹

¹ Syktyvkar State University named after Pitirim Sorokin, Syktyvkar, Russia

² LAUM CNRS 6613, Universite du Maine, Le Mans, France

³ Kotel'nikov Institute of Radio Engineering and Electronics, Moscow, Russia

vlasovv78@mail.ru

The work investigates nonlinear magnetoelastic interactions between surface acoustic waves and magnetic oscillations in thin metal films deposited on dielectric substrates. We consider the case of elastically driven magnetization precession in the limit of large Gilbert damping. But also we show the excitation of the magnetostatic surface spin waves.

Let us consider a thin metal ferromagnetic film deposited on a nonmagnetic dielectric substrate with a DC magnetic field applied in the sample plane. The magnetization dynamics are forced (via inverse magnetostriction) by two surface-confined elastic waves: Rayleigh Surface Acoustic Wave (SAW) and Surface Skimming Longitudinal Wave (SSLW). Excitation of FMR harmonics and frequency-mixing by elastic waves were calculated within the framework of a theoretical model taking into account of Landau-Lifshits-Gilbert (LLG) dynamics, boundary conditions for the magneto-elastic stresses and the equations for the elastic displacements. The effective magnetic field consists of the external DC magnetic field (with an arbitrary in-plane orientation with respect of elastic wave vector), demagnetizing field, and a time-dependent magnetoelastic field. The alternating magnetoelastic field is determined by SAW and SSLW strain components. The equations for the magnetic oscillations subject to the influence of the elastic wave were derived by first and second order perturbation theory. The parametric and nonlinear interaction of the elastic waves with a magnetic oscillator leads to frequency-mixing SAW+SAW, SAW+SSLW and SSLW+SSLW. The magnetic precession amplitude dependences on the DC magnetic field at different angles between the DC magnetic field and the direction of acoustic k-vector were obtained. The minima of the precession amplitude at the some angles were obtained.

Early in the work [1] the surface elastic waves excitation using the all-optical transient grating (TG) geometry was shown. The experimental geometry allowed the simultaneous detection of elastic and magnetic parameters. The measurements were performed on in plane magnetized polycrystalline nickel films, ranging in thickness from 20nm to 80nm, grown on soda lime glass substrates (microscope slides). We compare our theoretical results with the experimental dependencies of the Faraday rotation on the DC magnetic field at different angles between DC magnetic field and propagation direction of the elastic waves obtained in the work [1]. We show excitation of FMR and surface magnetostatic spin waves by the passing elastic waves.

The support from RFBR (grants # 17-57-150001, # 17-02-01138) are gratefully acknowledged.

[1] C.L. Chang et al., *Phys. Rev. B*, **95** (2017) 060409(R).

3OR-P-2

SPIN-WAVE RESONANCE IN GRADIENT THIN FILMS

Ignatchenko V.A.¹, Tsikalov D.S.¹

¹ Kirensky Institute of Physics, Fed. Research Center KSC SB RAS, 660036 Krasnoyarsk, Russia
d_tsikalov@iph.krasn.ru

A phenomenon of smoothly decrease of the magnetization from the film center to its surfaces often occurs spontaneously during deposition of films. It leads to a linear dependence of the spin-wave resonance (SWR) fields H_n on the mode number n instead of the standard quadratic dependence. The SWR theory in such films is well developed [1]. The authors of [2] developed for the first time the technology for creating layered films in which the magnetization of the layers increases from the center of the film to its surfaces according to a predetermined parabolic law and studied the SWR in such gradient samples. In this paper, we investigate theoretically the case, corresponding to the experiments [2]. In contrast to the situation in [1], which leads to the appearance of an energy potential well in the film, the case of [2] corresponds to the appearance of an energy potential barrier (Fig. 1a, red dashed curve). Spin-wave oscillations in the region of action of the inhomogeneous potential occur in this case in two

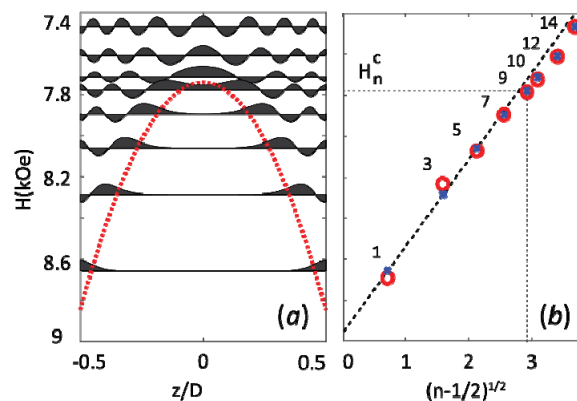


Fig. 1. Calculated form of normalized oscillations for the case of a parabolic potential barrier (a). Dependence of the resonance fields H_n on $(n-1/2)^{1/2}$, calculated theoretically (blue crosses) and obtained experimentally in [2] (red circles) (b).

potential wells between the potential barrier surfaces and the film surfaces (Fig. 1a). At one end of each oscillation, the dynamic pinning condition on the surface of the potential barrier is fulfilled, at the other end the boundary condition on the surface of the film (Fig. 1 corresponds to free boundary conditions). Based on the results of the numerical solution of the problem, we obtained an approximation of the law of the dependence of the positions of the first resonant peaks on the number of the mode n in the form $H_n \sim (n-1/2)^{1/2}$. This dependence corresponds to the energy levels of H_n in Fig. 1a located below the top of the potential barrier $H_n = H_n^c$. The dependence of all calculated H_n on n is shown in Fig. 1b (blue crosses) together with the experimental results of [2] (red circles). The intervals between the peaks of resonance fields H_n first decrease, and then increase with n increasing. The smallest interval corresponds to the vertex of the potential barrier $H_n = H_n^c$. Thus, the character of a smooth change in the magnetization from the center of the film to its surfaces (its decrease or increase) can be determined from the observed experimental dependence of the resonance peaks on the mode number n . The magnitude of the energy potential well or, respectively, the energy potential barrier in the film can also be found from this dependence.

This work was supported in part by the Complex Program No II.2P (0356-2015-0411) of the SB RAS and Krasnoyarsk Regional Fund for support of scientific and technical activity.

[1] A.M. Portis, *Appl. Phys. Lett.*, **2** (1963) 69.

[2] R.S. Iskhakov, L.A. Chekanova, I.G. Vazhenina, *Bulletin of RAS, Physics*, **77** (2013) 1469.

3OR-P-3

NONLINEAR SWITCHING OF SPIN WAVES IN THE SIDE-COUPLED MAGNONIC WAVEGUIDES

Odintsov S.A.¹, Sadovnikov A.V.^{1,2}, Beginin E.N.¹, Sheshukova S.E.¹, Sharaevskii Yu.P.¹,
Nikitov S.A.^{1,2}

¹ Saratov State University, Saratov, 410012, Russia

² Kotel'nikov Institute of Radio Engineering and Electronics, RAS, Moscow, 125009, Russia
 odinoff@gmail.com

In the past decades, patterning of insulating magnetic materials emerges as a promising technology for magnonic integrated circuits [1–3]. The insulating magnetic materials, such as yttrium iron garnet (YIG), possess significantly smaller dynamic magnetic damping compared to the metallic magnetic films (even for the case of the nanometer-thick, YIG). Using of YIG microstructures opens a promising alternative to signal processing by spin waves to provide the basis for beyond-CMOS computing technology with low-level energy consumption. Utilizing the nonlinear effects in YIG opens the possibility to develop nonlinear magnonic devices such as intensity dependent nonlinear phase shifters and filters [4-6], all-magnonic insulator-based switching devices. The width of both stripes was $w = 200 \mu\text{m}$ (Fig.1(a)). The edge-to-edge spacing of waveguides was $40 \mu\text{m}$. The length along the long side was 7 mm for first waveguide and 5 mm for second. The coupling length was 5 mm. The microwave transducer with width of $35 \mu\text{m}$ (along long axis of stripe) was used for spin wave (SW) excitation. Input transducer was attached to the first stripe. The structure was placed into uniform static magnetic field $H_0=1200 \text{ Oe}$ oriented along short axis of each stripe for effective excitation of guided magnetostatic surface wave (MSSW), also referred to as Damon-Eshbach (DE) spin waves. Using the high resolution BLS spectroscopy the two-dimensional map of spin waves propagating in the each stripe was measured (Fig. 1(b)) by the scanning with the probing light spot along the short and long axes with the spatial resolution of $25 \mu\text{m}$ and then integration over the time period of $2 \mu\text{s}$. The spin-wave power transfers from one stripe to the other in a periodic manner with the spatial period equal to the double coupling length $2L$. Increase of the input spin wave power leads to the variation of L . Thus the nonlinear switching is possible in the adjacent magnonic stripes, which can be used in the planar topology of magnonic networks.

Support by RFBR (No. 16-37-00217) and Grant of the President of RF (MK-5837.2016.9, SP-313.2015.5) is acknowledged.

[1] V. V. Kruglyak, et al, *J. Phys. D: Appl. Phys.*, **43** (2010) 264001.

[2] S. A. Nikitov, et al, *Phys. Usp.*, **58** (2015) 1099.

[3] V. E. Demidov, et al, *Sci. Rep.*, **5** (2015) 8578.

[4] A. V. Sadovnikov, et al, *Appl. Phys. Letters*, **107** (2015) 202405.

[5] A. V. Sadovnikov, et al, *Phys. Rev. Appl.*, **7** (2017) 014013.

[6] M. M. Scott, et al, *J. Appl. Phys.*, **95** (2004) 6294–6301.

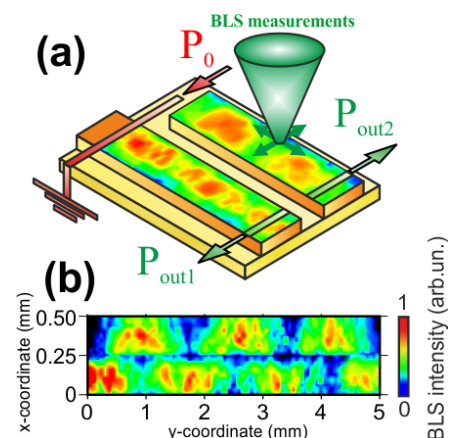


Fig. 1.(a)Schematic view of side-coupled magnonic stripes and BLS experiment. BLS measurement was performed in backscattering configuration. (b) Normalized colour-coded spin-wave intensity map.

3OR-P-4

SPIN WAVES SPECTROSCOPY OF YTTRIUM IRON GARNET FILMS GROWN BY ION BEAM EVAPORATION

Sakharov V.K.¹, Khivintsev Y.V.^{1,2}, Stognij A.I.³, Vysotskii S.L.^{1,2}, Filimonov Y.A.^{1,2}

¹ Kotelnikov SBIRE RAS, Saratov, Russia

² Saratov State University, Saratov, Russia

³ Scientific and Practical Materials Research Centre, NASB, Minsk, Belarus

valentin@sakharov.info

Methods for growth of yttrium-iron garnet (YIG) films on various types of the substrates and compatible with conventional semiconductor technology are of great interest because they can provide opportunities for on-chip integration of the spin waves electronics and other types of the solid state microwave electronics.

In presented work, we study particularities of the spin waves propagation in 0.2-1.2 μm thick YIG films grown on gadolinium-gallium garnet (GGG) and silicon (Si) substrates by ion beam evaporation using two-step deposition technique [1]. Excitation and detection of the waves were performed by coplanar micron-sized antennas fabricated directly on the YIG surface [2]. Microwave measurements were carried out by a vector network analyser along with a microwave probe station. Scattering parameters were measured as a function of the frequency, bias magnetic field and input microwave power for two types of the spin wave: magnetostatic surface wave (MSSW) and magnetostatic backward volume wave (MSBVW).

For the YIG/GGG structures both the MSSW and MSBVW were observed whereas for the YIG/Si – only the MSSW. We associate this feature with the higher perfection of the morphology and microstructure of the YIG/GGG structures that leads to lower spin wave damping.

Experimental dispersion of the MSBVW was in a good agreement with theoretical one. In addition to the lowest MSBVW mode, the modes of higher order were observed as well. The maximum wave numbers achieved in the experiment were around 3.4×10^4 rad/cm.

In the case of the MSSW, we observed dipole-exchange resonances and quite strong nonreciprocity (up to 15-20 dB) which we associate with significant inhomogeneity of the films across the thickness. Moreover, considerable mismatch between experimental dispersion and expected for homogeneous magnetic layer took place. We explain such behaviour on the base of calculations performed for the model of two adjoining magnetic layers taking into account spin pinning on borders, interlayer exchange coupling and damping.

Also, using YIG/Si structures with much higher spin wave damping in comparison with monocrystalline YIG films grown by liquid phase epitaxy we found atypical behavior for the transmission coefficient (S_{21}) versus the input power (P_{in}) – depending on the operating frequency $S_{21}(P_{\text{in}})$ relation could have a region of growth before its typical drop caused by the spin wave instability. This feature is explained by a shift of the MSSW spectrum down in frequency due to dynamic decrease of the effective magnetization and thermal heating which can play a decisive role when damping and respectively the threshold are quite high and P_{in} is lower than the instability threshold.

The reported study was funded by RFBR (Research projects Nos. 16-57-00135, 16-29-14058, 17-07-01452) and BRFFR (Research project No. F16R-085).

[1] A.I. Stognij, L.V.Lutsev, et al. *J. Appl. Phys.*, **118** (2015) 023905.

[2] V.K. Sakharov, Y.V. Khivintsev, et al. *IEEE Mag. Let.*, **8** (2017) 3704105.

3OR-P-5

ELECTRON SPIN RESONANCE ANISOTROPY IN THE ANTIFERROQUADRPOLAR PHASE OF CeB₆

*Semeno A.V.¹, Gilmanov M.I.^{1,2}, Sluchanko N.E.¹, Krasnorussky V.N.¹, Shitsevalova N.Yu.³,
Filipov V.B.³, Demishev S.V.¹*

¹ A.M.Prokhorov General Physics Institute RAS, Moscow, Russia

² Moscow Institute of Physics and Technology, Dolgoprudniy, Russia

³ Institute for Problems of Materials Science of National Academy of Sciences of Ukraine, Kiev,
Ukraine

semeno@lt.gpi.ru

The observation of electron spin resonance (ESR) in heavy fermion compound CeB₆ [1] gives the unique possibility to examine the state of Ce³⁺ ion in antiferroquadrupolar (AFQ) phase of this system. Angular dependencies of ESR line parameters (g -factor and linewidth ΔH) were experimentally explored at frequency $f = 60$ GHz [2]. Strongly anisotropic behavior of g -factor was found (fig.1). Values of the g -factor for [110] and [111] directions are close to each other ($g \approx 1.6$) and remains constant at all temperatures. In contrast, a considerable temperature dependence $g(T)$ was observed for [100] changing from $g \approx 1.7$ at $T = 1.8$ K to $g \approx 1.3$ at $T = 3.2$ K. The obtained angular dependences $g(\Theta)$ at different T were compared with the theoretically predicted g -factor behavior for the Γ_8 state of Ce³⁺ ion in antiferroquadrupolar phase of CeB₆ [3]. It turns out that the experimental g -factor is noticeably smaller at all angles than the theoretically calculated limits ($2 < g < 2.2$) and, moreover, it has a different symmetry. This result together with the strong linewidth anisotropy $\Delta H(\Theta)$ (fig.1) demonstrates that for the relevant description of experimental data the interaction of Ce³⁺ ion with itinerant $5d$ electrons the theoretical models should be taken into account.

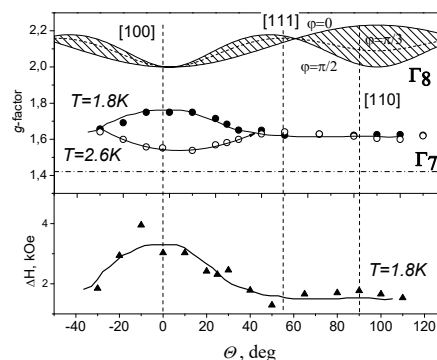


Fig. 1. Experimental angular dependencies of ESR g -factor (circles) and the linewidth (triangles) as well as theoretical simulations of Γ_8 and Γ_7 g -factor dependencies (lines).

Support by programs of Russian Academy of Sciences “Electron spin resonance, spin-dependent electronic effects and spin technologies”, “Electron correlations in strongly interacting systems”.

[1] S. V. Demishev et.al., *Phys. Stat. Sol. B*, **242** (2005) R27-R29.

[2] A.V.Semeno et.al., *Sci. Rep.*, **6** (2016) 39196.

[3] Schlottmann, *Phys. Rev. B*, **79** (2009) 045104.

3OR-P-6

HIGH- T_c SUPERCONDUCTING $\text{Bi}_2\text{Sr}_2\text{CaCu}_2\text{O}_{8+\delta}$ PLASMONIC TERAHERTZ METAMATERIAL

Kalhor S.¹, Ghanaatshoar M.¹, Kashiwagi T.^{2,3}, Kadowaki K.^{2,3}, Delfanazari K.^{4,5}

¹ Laser and Plasma Research Institute, Shahid Beheshti University, G.C., Evin, 1983969411
Tehran, Iran

² Graduate School of Pure and Applied Sciences, University of Tsukuba, 1-1-1 Tennodai, Tsukuba,
Ibaraki, 305-8571, Japan

³ Division of Material Sciences, Faculty of Pure and Applied Sciences, University of Tsukuba, 1-1-1
Tennodai, Tsukuba, Ibaraki, 305-8573, Japan

⁴ Department of Physics, Cavendish Laboratory, University of Cambridge, Cambridge CB3 0HE,
UK

⁵ Centre for Advanced Photonics and Electronics, Electrical Engineering Division, University of
Cambridge, Cambridge CB3 0FA, UK
kd398@cam.ac.uk

The layered high- T_c superconductors are strongly anisotropic systems whose structure is composed of alternating metallic (and superconducting, below T_c) CuO_2 and insulating double layers. They are intrinsically left-handed materials, showing the existence of surface waves and realizing negative refractive index metamaterials. Their electromagnetic response is derived from Cooper pairs that have analogous behaviour to electrons in metals at high frequencies. Among the layered superconductors, $\text{Bi}_2\text{Sr}_2\text{CaCu}_2\text{O}_{8+\delta}$ (Bi-2212) has received particular attention because it can also be a powerful and coherent quantum terahertz (THz) wave source. The THz wave has been found to be necessary for the applications, especially to quantum information and computation.

Here, we report the first demonstration of superconducting Bi-2212 THz metamaterial. We present the temperature and magnetic field induced resonance switching and frequency tuning of subwavelength plasmonic Bi-2212 split-ring resonators (SRR). Figure 1, shows the THz transmission spectra for Bi-2212 SRR metamaterial at various temperatures between 200 K down to 10 K. At temperatures far below T_c ($= 71$ K), e.g., 10 K (plotted in black curve), the metamaterial shows the strongest resonance, as indicated by a sharp dip at 0.52 THz with a minimal of 0.051. As the temperature increases, the resonance strength decreases resulting in broadening and amplitude reduction of the transmission dip. The resonance frequency experiences a redshifting that reaches the lowest value of 0.49 THz below T_c . By further increasing of the temperature, the resonance frequency retunes back to higher frequencies but the resonance strength continues to decrease.

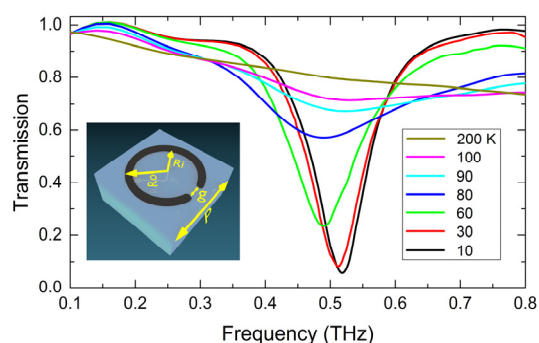


Fig. 1. THz transmission amplitude spectra of the Bi-2212 superconducting THz metamaterial at various temperatures. The inset shows the Bi-2212 SRR unit cell with its structural parameters.

3OR-P-7

EXPERIMENTAL STUDY OF MICROWAVE PROPERTIES OF COMPOSITES FILLED WITH PERMALLOY POWDER

Bobrovskii S.Y.¹, Garanov V.A.¹, Naboko A.S.¹, Osipov A.V.¹, Rozanov K.N.¹

¹Institute for Theoretical and Applied Electromagnetics, Moscow, Russia
sbobrowskiy@yandex.ru

Frequency dependencies of material parameters, permittivity and permeability, of composites filled with permalloy powder with various concentrations and shapes of particles have been measured and discussed. The powder particles of various shapes were obtained by mechanical milling of industrial permalloy powder in organic media. Paraffin wax was used as a matrix for producing the composites. A shape data of the particles was obtained with an electron microscope. The permittivity and permeability were measured by the Nicolson-Ross-Weir technique in a 7/3 coaxial line in the frequency range of 0.13 to 10 GHz.

It is shown that the shape of the particles changes from sphere to platelet with increase of milling time. The change leads to a shift of the ferromagnetic resonance (FMR) frequency and magnetic loss peak. It is shown that larger damping of the FMR is characteristic for the larger particles. With increase of the concentration of the permalloy particles in composite, the magnetic loss peak shifts to lower frequencies. The measured frequency dependencies of the material parameters were discussed in terms of the theory of composites.

Support by RFBR agreement № 15-08-03535 is acknowledged.

3 July

Monday

11:30-13:00

14:30-17:00

oral session

3TL-LT

3OR-LT

**“Low Dimensional
Magnetism”**

3TL-LT-1

**PHASE COEXISTENCE, LATTICE AND MAGNETIC INSTABILITIES IN
Cu₃Bi(SeO₃)₂O₂X (X = Br, Cl)**

*Gnezdilov V.^{1,2}, Pashkevich Yu.³, Lemmens P.¹, Kurnosov V.², Berdonosov P.⁴, Dolgikh V.⁴,
Kuznetsova E.⁴, Pryadun V.⁴, Zakharov K.⁴, Vasiliev A.^{4,5,6}*

¹Institute of Condensed Matter Physics, TU Braunschweig, D-38106 Braunschweig, Germany

²Institute for Low Temperature Physics and Engineering NASU, 61103 Kharkov, Ukraine

³Donetsk Institute for Physics and Engineering NASU, 03680 Kiev, Ukraine

⁴Lomonosov Moscow State University, 119991 Moscow, Russia

⁵National University of Science and Technology "MISiS", 119049 Moscow, Russia

⁶National Research South Ural State University, 454080 Chelyabinsk, Russia

vasil@mig.phys.msu.ru

The specific heat C , dielectric permittivity ε , electric polarization P and Raman scattering measurements are performed on Cu₃Bi(SeO₃)₂O₂X ($X = \text{Br, Cl}$) single crystals. The Cl compound undergoes structural phase transition of second order at about $T^* \sim 120$ K evident in $C(T)$ and $\varepsilon(T)$ dependences and accompanied by appearance of new phonon lines in Raman spectra while no structural changes are detected in Br compound. At $T < T^*$, the polarization loop at $P \parallel c$ axis is seen in Cl compound inherent for a weakly ferroelectric phase. Both compounds order antiferromagnetically at comparable temperatures $T_N \sim 25$ K marked by sharp λ -type singularities. At $T < T_N$, an intensive mode of magnetic origin appears in both compounds. At lowest temperatures, the energy of this mode compares favourably with both magnon excitation observed in infrared spectroscopy and the spin gap found recently in inelastic neutron scattering measurements in Cl compound. The whole of available data points to a coexistence of minor polar with major nonpolar phase at $T < T^*$ in Cu₃Bi(SeO₃)₂O₂Cl.

3TL-LT-2

MAGNETIC STRUCTURE OF QUASI-2D ANTIFERROMAGNET CuCrO_2 IN THE ELECTRIC FIELD

Gotovko S.K.^{1,2}, Svistov L.E.¹, Sakhratov Yu.A.³,

Kuhns P.L.⁴, Reyes A.P.⁴, Kweon J.J.⁴, Choi E.S.⁴, Zhou H.D.⁵

¹ P.L. Kapitza Institute for Physical Problems RAS, 119334 Moscow, Russia

² Moscow Institute of Physics and Technology, 117303, Moscow, Russia

³ Kazan State Power Engineering University, 420066 Kazan, Russia

⁴ National High Magnetic Field Laboratory, Tallahassee, Florida 32310, USA

⁵ Department of Physics and Astronomy, University of Tennessee, Knoxville, Tennessee 37996, USA

svistov@kapitza.ras.ru

CuCrO_2 is an example of quasi-two-dimensional antiferromagnet ($T_c \sim 24$ K) with triangular lattice structure. In this system exotic types of magnetic orderings are expected due to geometrical frustrations of in-plane and inter-planar exchange interactions. We carried out ESR and Cu NMR investigations in the presence of electric field. The ESR study in electric field allows to find the magneto electric constants and examine the nature of electrical polarization in this multiferroic. Electric polarization studies of CuCrO_2 in pulsed magnetic fields up to 92 T [1,2] revealed a number of phase transitions, the nature of which was uncertain. We carried out Cu NMR investigations in magnetic field up to 45 T [3,4]. According to our data the magnetic field destroys inter-plane order and the system goes from three-dimensional (3D) to 2D state. We suppose that this 2D phase is, in fact, a 3D-polar phase with tensor order parameter and can be classified as a p-type nematic phase. To verify this, we carry out control experiments in which Cu NMR spectra are measured after cooling in electric field.

[1] Eundeok Mun, et al., *Phys. Rev. B*, **89** (2014) 054411.

[2] Shi-Zeng Lin, et al., *Phys. Rev. B*, **89** (2014) 220405(R).

[3] Sakhratov, Yu.A., et al., *JETP*, **119** (2014) 880.

[4] Sakhratov, Yu.A., et al., *Phys. Rev. B*, **94** (2016) 094410.

3OR-LT-3

THE ORIGIN OF FINE STRUCTURE IN MAGNETIZATION CURVE OF α -CoV₂O₆

Kudasov Yu.B.^{1,2}, *Kozabaranov R.V.*^{1,2}

¹ Sarov Physics and Technology Institute, NRNU "MEPhI", Sarov, Russia

² National Research Nuclear University "MEPhI", Moscow, Russia

yu_kudasov@yahoo.com

Multiple field-induced plateaus in α -CoV₂O₆ at low temperatures were revealed earlier [1] and carefully investigated recently [2]. Magnetic Co²⁺ ions in this substance are placed in the well separated chains made up of edge-sharing distorted CoO₆ octahedra (see Fig. 1). The chains run along the *b* axis. The lattice of the chains can be considered as a distorted 2D triangular lattice with three AFM coupling constants between the nearest neighboring chains J_1 , J_2 , and J_3 . The values of J_1 , J_3 although are different but comparable, and J_2 is much weaker than the others.

We present a model to describe the four equidistant steps observed in the magnetization curve. The magnetic structure of this substance is formed by highly anisotropic triangular lattice of Ising chains. At the zero magnetic field a stripe structure exists. It transforms to three-sublattice magnetic ordering with increasing the magnetic field. Due to a three-fold degeneracy of the three-sublattice structure, domain boundaries appear [3]. Their transformation under magnetic field variation leads to two additional steps in the 1/3 magnetization plateau and gives rise to complex magnetic behavior observed experimentally.

The domain structure in α -CoV₂O₆ occurs to be strongly anisotropic because a lifetime of the metastable states depends greatly on the configuration orientation.

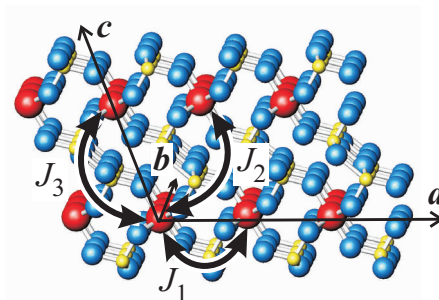


Fig. 1. The crystal structure of α -CoV₂O₆. The large, smaller, and the smallest spheres denote the Co²⁺, O²⁻, and V⁵⁺ ions correspondingly. The arrows show interchain interactions.

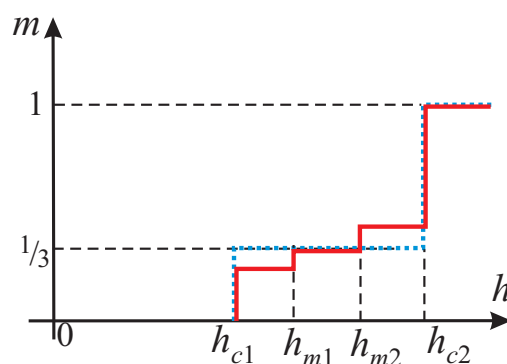


Fig. 2. A schematic view of the magnetization curves of α -CoV₂O₆ in the increasing magnetic field: the dotted and the solid lines correspond to the equilibrium and metastable regimes.

[1] M. Lenertz et al., *J. Phys. Chem. C*, **115** (2011) 17190.

[2] M. Nandi, P. Mandal, *J. Appl. Phys.*, **119** (2016) 133904.

[3] Yu.B.Kudasov et al., *Phys. Usp.*, **55** (2012) 1169.

3OR-LT-4

ORDER BY STRUCTURAL DISORDER IN A DOPED TRIANGULAR ANTIFERROMAGNET $\text{RbFe}(\text{MoO}_4)_2$

Smirnov A.I.¹, Soldatov T.A.¹, Petrenko O.A.², Kida T.³, Takata A.³, Hagiwara M.³,
Shapiro A.Ya.⁴, Zhitomirsky M.E.⁵

¹ P.L.Kapitza Institute for Physical Problems RAS, Moscow, Russia

² University of Warwick, Coventry, United Kingdom

³ Osaka University, AHMF Center, Osaka, Japan

⁴ A.V. Shubnikov Institute for Crystallography RAS, Moscow, Russia

⁵ CEA-INAC/UJF, PHELIQS, Grenoble, France

smirnov@kapitza.ras.ru

The low-temperature spin configuration of a two-dimensional antiferromagnet on a triangular lattice is known to be stabilized from a degenerate manifold of classical ground states by the so-called "order-by-disorder" mechanism. This mechanism of the ground state selection is based on thermal and quantum fluctuations, lifting the degeneracy, because the spectra of excitations of different degenerate states are different (see, e.g., [1]). In particular, the known plateau at 1/3 of the saturation magnetization, corresponding to the "up-up-down" phase has this fluctuation nature [1,2]. The recent theoretical work [3] suggests a method of control of the above mechanism of ground state selection by a weak nonmagnetic doping. It was predicted, that chaotic modulation of exchange bonds will lift degeneracy in another way and, thus, will compete with quantum and thermal fluctuations. It is expected, that instead of a most collinear structure, which is stabilized by fluctuations in the pure triangular antiferromagnet, a most noncollinear structure will arise in a doped sample. We have checked these theoretical predictions for a triangular antiferromagnet $\text{RbFe}(\text{MoO}_4)_2$. The weak chaotic modulation of exchange bonds was performed via substitution of K for Rb. For samples of $\text{Rb}_{1-x}\text{K}_x\text{Fe}(\text{MoO}_4)_2$, $0 < x < 0.15$, in the low-temperature limit, we observe a smearing of the plateau in doped samples and its complete disappearance at $x=0.15$. Besides, the ESR spectra reveal a striking change of the spin structure under a moderate nonmagnetic doping. At the same time, the Néel transition near $T=4$ K remains as sharp as in the pure sample. We believe, that the reason of the observed effects is an effective lifting of degeneracy by a random potential of impurities, which compensates the fluctuation contribution to free energy, in accordance with [3]. These results provide an experimental confirmation of the fluctuation origin of the ground state in a real frustrated system, because the system with a pronounced minimum of the mean-field energy would not be so sensitive to a weak chaotic potential. The change of the ground state to a least collinear spin configuration may be phenomenologically ascribed to an effective positive biquadratic exchange provided by the structural disorder. On heating, doped samples regain the structure of a pure compound demonstrating a competition between thermal and structural disorder. Support by Russian Foundation for Fundamental Research, Programs of the Presidium of RAS, and Russian Science Foundation is acknowledged.

[1] A. V. Chubukov, D. I. Golosov, *Journal of Physics: Condensed Matter*, **3** (1991) 69.

[2] A. I. Smirnov, H. Yashiro, S. Kimura, M. Hagiwara, Y. Narumi, K. Kindo, A. Kikkawa, K. Katsumata, A. Ya. Shapiro, and L. N. Demianets, *Phys. Rev. B*, **75** (2007) 134412.

[3] V. S. Maryasin and M. E. Zhitomirsky, *Phys. Rev. Lett.*, **111** (2013) 247201.

3TL-LT-5

TUNING OF MAGNETIC PROPERTIES IN LOW-DIMENSIONAL OXIDES*Möller A.*¹

¹ Institute of Inorganic Chemistry and Analytical Chemistry, JGU Mainz, Mainz, Germany
angela.moeller@uni-mainz.de

Competing interactions may occur in magnetic materials with geometric frustration and thereby giving rise to non-trivial ground states. The triangular or kagome lattices are examples for such intriguing scenarios. From a chemist's point of view, a welcomed challenge is the development of classes of materials where the magnetic interactions (ferro- or antiferromagnetic) can be tuned by spin, charge, and size degrees of freedom. Moreover, by controlling the structural distortions examples for easy-axis, easy-plane Heisenberg, or collinear antiferromagnets on the triangular lattice can be obtained.^{1,2} Here, we will discuss the structure-property relationships investigated by neutron diffraction, magnetic and spectroscopic studies for a series of model compounds.

[1] N.E. Amuneke, J. Tapp, C. dela Cruz, A. Möller, *Chem. Mater.*, **26** (2014) 5930.

[2] M. Bratsch, A.P. Litvinchuk, J. Tapp, A. Möller; *Inorg. Chem.*, **53** (2014) 4994.

3TL-LT-6

ANISOTROPIC MAGNETISM AND SPIN GAP IN α - RuCl₃*Büchner B.*¹¹ IFW Dresden, Dresden, Germany
b.buechner@ifw-dresden.de

Quantum spin liquids are a central theme in current condensed matter physics as they host emergent topological order and fractionalized excitations. An important example are interacting Kitaev spins on a honeycomb lattice which are theoretically predicted to exhibit topological and quantum spin liquids. Identifying signatures of Kitaevs physics, however, is extremely challenging as real materials, such as the iridates (Na,Li)₂IrO₃, inevitably entail an isotropic Heisenberg and additional spin-exchange interactions, thereby stabilizing a magnetically ordered state. Hexagonal Ru trichloride α -RuCl₃ has been recently reported to be near the Kitaev spin-liquid phase boundary. The layered honeycomb structure of a α -RuCl₃ contains layers weakly coupled by van der Waals interaction, i.e. it is a correlated 2d-materials offering many possibilities for *materials engineering*. We have characterized the electronic and magnetic properties of α -RuCl₃ by a broad spectrum of experimental techniques. From electron spectroscopy basic parameters determining the insulating state of α -RuCl₃ are extracted. Moreover, strongly anisotropic magnetic properties as measured from magnetization, specific heat, thermal conductivity, and NMR measurements will be presented and discussed. Both, the behavior of α - RuCl₃ in the paramagnetic phase as well as the properties of the ordered state strongly differ from that found in conventional two-dimensional magnets. In particular, we find a very unusual field-temperature phase diagram with evidence for a novel quantum critical point.

3OR-LT-7

COEXISTENCE OF MAGNETICALLY ORDERED AND HALDANE STATES IN $(Y_{1-x}Nd_x)_2BaNiO_5$

*Popova E.A.*¹, *Klimin S.A.*², *Popova M.N.*², *Klingeler R.*³, *Büchner B.*⁴, *Vasiliev A.N.*⁵

¹ National Research University Higher School of Economics, Moscow, Russia

² Institute of Spectroscopy RAS, Troitsk, Moscow, Russia

³ Kirchhoff Institute for Physics, University of Heidelberg, Heidelberg, Germany

⁴ Leibniz-Institute for Solid State and Materials Research IFW Dresden, Germany

⁵ Low Temperature Physics Department, Moscow State University, Moscow, Russia

eapopova@hse.ru

In the compounds that contain chains of magnetic ions with $S = 1$ spin, a disordered ground state with a gap in the spectrum of magnetic excitations is realized. The crystal structure of the $(Y_{1-x}Nd_x)_2BaNiO_5$ compounds incorporates Ni^{2+} ($S=1$) chains interconnected by the Nd^{3+}/Y^{3+} and Ba^{2+} ions. Y_2BaNiO_5 is a well-known Haldane system with the spin gap of about 10 meV. R_2BaNiO_5 crystals containing magnetic rare-earth R^{3+} ions order antiferromagnetically, however, the Haldane gap survives in both paramagnetic and ordered states [1].

In the present work, magnetic properties of the mixed-spin $(Y_{1-x}Nd_x)_2BaNiO_5$ powder samples with different neodymium concentration from $x=0.01$ up to $x=1$ (11 compounds) were studied by means of specific heat, magnetic susceptibility, and optical spectroscopy measurements in the temperature range 0.4 – 300 K.

At high temperatures, the contribution of the Nd subsystem into magnetic susceptibility $\chi(T)$ follows the Curie-Weiss law, whereas the Ni subsystem behaves like the Haldane-gap system.

For the compounds with $x>0.05$, a λ -type anomaly in the $C(T)$ dependence points to an antiferromagnetic phase transition. A broad maximum (Schottky anomaly) observed in both the $C(T)$ and $\chi(T)$ dependences originates from the temperature-driven depopulation of the upper component of the Nd^{3+} ground Kramers doublet split in an internal magnetic field that appears in the magnetically ordered state. We estimate a magnetic contribution of the neodymium subsystem into magnetic susceptibility and specific heat using spectroscopic data for every compound studied. The estimated neodymium contribution exceeds experimental data for $x\leq 0.03$, which can be explained by formation of clusters with local magnetic ordering. The Neel temperature gradually decreases with decreasing concentration x in $(Y_{1-x}Nd_x)_2BaNiO_5$.

An anomaly at $T\approx 3$ K in the $\chi(T)$ dependence and spin-glass behavior as well as an anomaly in the $C(T)$ dependence at $T\approx 5$ K, observed after subtracting the magnetic contribution of the Nd subsystem are almost independent of the Nd concentration in the compound. These features are due to both the magnetization of segments of the Ni chain and the ferrons appearing around a hole at the oxygen site inside the Ni chain.

The Schottky anomaly in $C(T)$ dependence shifts to higher temperatures with increasing an external magnetic field for compounds with $x<0.15$, whereas it shifts in the opposite direction for $x\geq 0.15$. It is caused by a competition between the internal and external magnetic fields acting on the Nd subsystem.

Support by the Academic Fund Program at the National Research University Higher School of Economics (HSE) in 2017 (Grant № TZ-89) and by the Russian Academic Excellence Project «5-100» is acknowledged. K.S.A. and P.M.N. acknowledge a support by the Russian Academy of Sciences under the Program “Topical Problems of Low-temperature Physics”.

[1] T. Yokoo, Z. Zheludev, M. Nakamura, and J. Akimitsu, Phys.Rev. B **55** (1997) 11516.

3OR-LT-8

FORMATION OF THE GAPLESS TRIPLET DEGREES OF FREEDOM IN THE BOND-DILUTED SPIN-GAP MAGNET $(\text{C}_4\text{H}_{12}\text{N}_2)(\text{Cu}_2\text{Cl}_6)$

Glazkov V.^{1,2}, *Krasnikova Yu.*^{1,2}, *Hüvonen D.*^{3,4}, *Zheludev A.*⁴

¹ P.Kapitza Institute for Physical Problems RAS, Moscow, Russia

² National Research University Higher School of Economics, Moscow, Russia

³ National Institute of Chemical Physics and Biophysics, Tallinn, Estonia

⁴ Neutron Scattering and Magnetism, Laboratory for Solid State Physics, ETH Zürich, Zürich, Switzerland

glazkov@kapitza.ras.ru

Spin-gap magnets are one of the examples of spin liquids. Due to the particular architecture of the exchange bonds, usually invoking dimer motives, these magnets have a singlet ground state separated from the excited triplets by a gap of exchange origin. As a result, these systems remain in the paramagnetic state down to lowest temperatures despite the strong exchange coupling present. Stability of this singlet state to external effects: applied magnetic field, hydrostatic pressure or controlled introduction of defects is an actively studied problem.

The quasi-two-dimensional magnet $(\text{C}_4\text{H}_{12}\text{N}_2)(\text{Cu}_2\text{Cl}_6)$ (abbreviated PHCC for short) is one of the recently found spin-gap systems [1]. It allows partial substitution of Cl by Br with Br content up to 12% [2]. This *bond-doping* does not deplete magnetic system, but instead introduces random modulation of the exchange coupling constants.

By means of ESR spectroscopy we have found [3] that the low-temperature (below 1K) absorption of the Br-diluted PHCC includes the response of some gapless triplet ($S=1$) objects. I.e., non-magnetic doping of the $S=1/2$ system results in the formation of the triplet degrees of freedom. Coexistence of this new doping-induced triplet degrees of freedom with gapped triplet excitations was observed over the temperature range 1.5-5 K.

We conjecture that these triplet centres are created on double substitution of Cl by Br in a Cu_2Cl_6 dimer, which is a building block of PHCC magnetic system. Such a double substitution results in the effective attracting potential, which traps one of the triplet excitations. This conjecture is supported by the analysis of the ESR intensity, which turns out to be proportional to Br concentration squared.

[1] Stone M. B. et al., *New J. Phys.*, **9** (2007) 31.

[2] Hüvonen D. et al., *Phys. Rev. B*, **85** (2012) 100410; *Phys. Rev. B*, **86** (2012) 214408; *Phys. Rev. B*, **88** (2013) 094402.

[3] Glazkov V. N. et al., *Journ. Phys.:Cond. Matter* **28** (2016) 206003; *Journ. Phys.:Cond. Matter* **26** (2014) 486002.

3OR-LT-9

LOW TEMPERATURE ESR IN SPIN LADDER $(\text{C}_7\text{H}_{10}\text{N}_2)_2\text{Cu}_{(1-x)}\text{Zn}_x\text{Br}_4$

Krasnikova Yu.V.^{1,2}, *Glazkov V.N.*^{1,2}, *Fayzullin M.A.*³, *Schmidiger D.*⁴, *Zheludev A.*⁴,
*Povarov K.Yu.*⁴

¹ P.L.Kapitza Institute for Physical Problems RAS, Moscow, Russia

² National Research University Higher School of Economics, Moscow, Russia

³ Institute for Physics, Kazan Federal University, Kazan, Russia

⁴ Neutron Scattering and Magnetism, Laboratory for Solid State Physics, ETH Zurich, Zurich, Switzerland

krasnikova.mipt@gmail.com

“Spin ladder” is a model low-dimensional spin system. It consists of two coupled chains and can be described by two exchange coupling constants. The spectrum of excitations in such a system has a gap and its ground state is a non magnetic singlet state.

The compound $(\text{C}_7\text{H}_{10}\text{N}_2)_2\text{Cu}_{(1-x)}\text{Zn}_x\text{Br}_4$, DIMPY for short, is an example of the “spin ladder”. The gap and exchange coupling constants for DIMPY are $\Delta=0.33$ meV, $J_{\parallel}=1.42$ meV, $J_{\perp}=0.82$ meV [1].

DIMPY symmetry allows presence of a Dzyaloshinskii-Moriya (DM) interaction. The DM interaction should be uniform along the ladder and has opposite sign on the chains of the ladder. High energy resolution of ESR method gave opportunity to detect this interaction and to prove by analysis of orientation and temperature dependencies of ESR linewidth that uniform Dzyaloshinskii-Moriya interaction ($D\sim 0.3$ K) is the main anisotropic spin-spin interaction in DIMPY [2].

Substitution of Cu by Zn results in the formation of multi-spin defects (“spin islands”) around the impurity [3]. At $x=0.02\dots 0.06$ these defects dominate magnetic response below approx. 4 K, while above 5 K magnetic susceptibility of doped DIMPY is mostly due to copper ions. We have found that ESR linewidth above 5 K systematically decreases with doping. I. e., introduction of random defects suppress spin relaxation mechanisms related to DM interaction.

The work was supported by Russian Foundation for Basic Research Grant No. 15-02-05918.

[1] D. Schmidiger et al. *PRL*, **111** (2013) 107202.

[2] V. N. Glazkov et al. *Phys. Rev. B*, **92** (2015) 184403.

[3] D. Schmidiger et al. *Pys. Rev. Lett.*, **116** (2016) 257203.

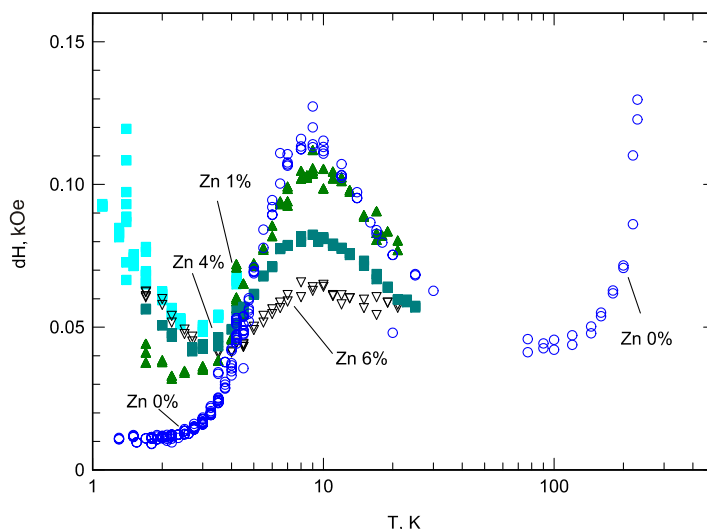


Fig. 1. Linewidth temperature dependence for different Zn concentration in DIMPY.

3OR-LT-10

PHASE TRANSITIONS, RARE-EARTH SINGLE-ION ANISOTROPY, AND POSSIBLE KOSTERLITZ-TOULESS TRANSITION IN $\text{Cu}_3\text{RE}(\text{SeO}_3)_2\text{O}_2\text{Cl}$

Klimin S.A.¹

¹ Institute of Spectroscopy RAS, Troitsk, Moscow, Russia
klimin@isan.troitsk.ru

The family of francisites $\text{Cu}_3M(\text{SeO}_3)_2\text{O}_2X$ ($M = \text{Bi}$ or rare earth (RE), $X = \text{Cl}, \text{Br}, \text{I}$) is a relatively new class of low-dimensional frustrated magnets [1-4] with possible Kosterlitz-Thouless transition from a paramagnetic state to a phase with quasi-long-range spin order [2]. Due to the fact that most of the title compounds are isostructural, they are considered as model systems for studying the influence of atom substitution on their magnetism. Compared to the parent francisite $\text{Cu}_3\text{Bi}(\text{SeO}_3)_2\text{O}_2\text{Cl}$, the magnetic system of which consists of the buckled kagome layers of Cu^{2+} ions, its synthesized RE derivatives $\text{Cu}_3\text{RE}(\text{SeO}_3)_2\text{O}_2\text{Cl}$ [5] have the $4f$ extra magnetic subsystem, which can strongly influence their magnetic and thermodynamic properties. Due to weak interlayer interactions, an antiferromagnetic (AFM) ordering of copper layers in francisites occurs at low temperature ($T_N = 24$ K and for the parent francisite and ~ 35 K for $\text{RE} = \text{Y}$ [3] and Sm [4]); besides, a spin-reorientational transition takes place in the samarium francisite at $T_R = 9$ K [4]. In this study, optical low-temperature measurements of f-f electronic transitions were performed, with the aim to investigate magnetic ordering and RE single-ion anisotropy in compounds with different RE ions.

Transmittance spectra in a wide spectral ($1800 - 12000 \text{ cm}^{-1}$) and temperature ($4 - 300$ K) ranges were registered using a Fourier spectrometer Bruker IFS125HR for the compounds with $\text{RE} = \text{Sm}, \text{Ho}, \text{Yb}, \text{Er}, \text{Nd}, \text{Pr}, \text{Tm}$, and Eu , as well as for $\text{Cu}_3\text{RE}(\text{SeO}_3)_2\text{O}_2\text{Cl}:\text{Er}1\%$ ones, erbium being used as a spectroscopic probe.

The CF energies for RE^{3+} ions were found in the spectral range studied. Spectroscopic data on temperature-dependent low-energy states of RE ions were used to calculate the RE contribution into the magnetic susceptibility and heat capacity. Magnetic ordering was detected spectroscopically in all compounds. In Sm and Yb francisites, spin-reorientational transitions were detected, the reason for which is an energy gain due to a lowering of the ground state of the RE ion (splitting of ground Kramers doublets). It is a single-ion anisotropy of the RE ion that forces copper magnetic moments to rotate. In Yb francisite, presence of exchange magnetic field was found in the temperature range $T < \sim 120$ K which was tentatively assigned to Kosterlitz-Thouless activity.

The author is grateful to P.S. Berdonosov and E.S. Kuznetsova (Lomonosov Moscow State University), who kindly supplied him with the samples.

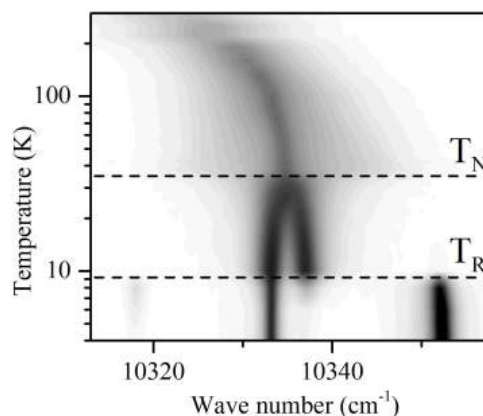


Fig. 1. Temperature behavior of the 0-0 transition of Yb^{3+} ion in $\text{Cu}_3\text{Yb}(\text{SeO}_3)_2\text{O}_2\text{Cl}$ (intensity map).

- [1] A. Pring, B.M. Gatehouse, W.D. Birch, *Amer. Mineral.*, **75** (1990) 1421.
- [2] M. Pregelj, O. Zaharko, A. Günther, et al., *Phys. Rev. B*, **86** (2012) 144409.
- [3] K.V. Zakharov, E.A. Zvereva, P.S. Berdonosov, et al., *Phys. Rev. B*, **90** (2014) 214417.
- [4] K.V. Zakharov, E.A. Zvereva, M.M. Markina, et al., *Phys. Rev. B*, **94** (2016) 054401.
- [5] P.S. Berdonosov, V.A. Dolgikh, *Rus. J. Inorg. Chem.*, **53** (2008) 1353.

3OR-LT-11

TRIMERIZED QUANTUM GROUND STATE IN COPPER POLYANIONIC COMPOUND $\text{Cu}_3(\text{OH})_2\text{F}_4$

Danilovich I.L.¹, Merkulova A.V.¹, Morozov I.V.¹, Ovchenkov Y.A.¹, Zvereva E.A.¹, Volkova O.S.^{1,2,3}, Vasiliev A.N.^{1,2,3}

¹ Moscow State University, Moscow 119991, Russia

² National University of Science and Technology "MISiS", Moscow 119049, Russia

³ Ural Federal University, Ekaterinburg 620002, Russia
danilovichigor@gmail.com

The polyanion compounds of 3d-metals offer vast playground to investigate the relationships between structure and properties in magnetic systems. New copper (II) trifluoride hydroxide $\text{Cu}_3(\text{OH})_2\text{F}_4$ has been synthesized and studied experimentally in measurements of dc- and ac-magnetic susceptibility, static and pulsed field magnetization, specific heat and X-band electron magnetic resonance.

The structure of $\text{Cu}_3(\text{OH})_2\text{F}_4$ is characterized by trimerized chains of edge- and corner-sharing $\text{Cu}(\text{OH})_2\text{F}_4$ polyhedra running along the [011] axis, which are linked to each other via corners to form a three-dimensional framework [1]. The temperature dependences of both real χ' and imaginary χ'' parts of ac-magnetic susceptibility taken at the frequency $f = 10$ Hz in $\text{Cu}_3(\text{OH})_2\text{F}_4$ have very sharp singularities at $T_C = 12.5$ K that show the onset of long range magnetic order. The phase transition is marked by an anomaly on the temperature dependence of the specific heat C_p . The entropy released below T_C equals to 4.2 J/molK being about quarter of total magnetic entropy $S_{\text{magn}} = 3R\ln 2 = 17.3$ J/molK expected for this system.

The temperature dependence of dc-magnetic susceptibility, or reduced magnetization M/B , taken at $B = 0.1$ T is shown in Fig. 1. The sharp increase of magnetization below T_C indicates presence of spontaneous moment in magnetically ordered state of $\text{Cu}_3(\text{OH})_2\text{F}_4$. In paramagnetic state of $\text{Cu}_3(\text{OH})_2\text{F}_4$, the temperature dependence of inverse magnetic susceptibility has been fitted by an expression for isolated magnetic trimers [2]. The fitting with g-factor of Cu^{2+} ions $g = 2.26$ results in exchange interaction parameter within trimer $J_1 = 142$ K (nearest neighbor) and $J_2 = 33$ K (next nearest neighbor), both antiferromagnetic. The value of g-factor used is in good correspondence with the mean value of g-factor as defined from measurements of X-band electron spin resonance. The J_2/J_1 ratio of about quarter puts the magnetic subsystem of $\text{Cu}_3(\text{OH})_2\text{F}_4$ close to quantum critical point separating collinear and non-collinear magnetic structures. At the same time, no indication for 1/3 saturation magnetization plateau which could be expected for trimerized system has been seen in magnetization curve.

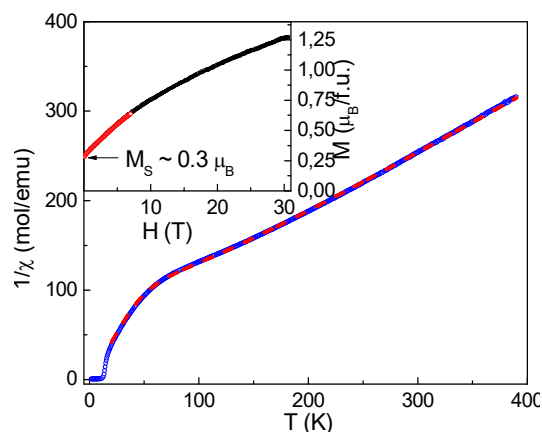


Fig. 1. The temperature dependence of inverse magnetic susceptibility in $\text{Cu}_3(\text{OH})_2\text{F}_4$ fitted (dashed line) by antiferromagnetically coupled trimer model. The inset represents the field dependence of magnetization at 2 K.

Support from Russian Foundation for Basic Research Grants № 16-02-00021 is acknowledged.

[1] G. Giester, E. Libowitzky, *Z. Kristallogr.* **218** (2003) 351.

[2] Y. Yasui, Y. Kawamura, Y. Kobayashi, M. Sato, *J. Appl. Phys.* **115** (2014) 17E125.

3OR-LT-12

THE NICKEL-MANGANESE LUDWIGITE MAGNETIC PROPERTIES STUDY

Nazarenko I.I.¹, Sofronova S.N.¹

¹ Kirensky Institute of Physics, FRC KSC SB RAS, Krasnoyarsk, Russia
ilnz007@live.ru

A new composition of the nickel-manganese ludwigite crystals (Fig. 1) was obtained at the IP of the SB RAS. Its structure was established by X-ray diffraction. The composition of the studied compound was refined by studying the XAS at the K-edge of manganese and nickel ions. The temperature dependences of the magnetization in fields of 1, 5, and 10 kOe were measured in the temperature range 3 ÷ 300 K. The Weiss temperature $\theta = -157$ K was determined, which indicates strong AFM interactions in the crystal.

Exchange interactions for it ($\text{Ni}_{2.14}\text{Mn}_{0.86}\text{BO}_5$) were analyzed in the framework of the Andersen-Zawadzky indirect exchange model [1, 2] in order to understand the possible reasons for the increase in the magnetic ordering temperature, and also to make a comparison with the Ni_2MnBO_5 obtained earlier [3], taking into account that in the studied compound the position 4 is occupied by 0.14 Ni^{2+} , 0.14 Mn^{4+} and 0.72 Mn^{3+} .

When comparing the compound to the Ni_2MnBO_5 , it can be seen that there is no change in the 3-1-3 subsystem, since this system is formed by Ni^{2+} ions, both in one and the other compounds. All changes take place in subsystem 4-2-4. As can be seen from the calculation results, the average interaction of 4-4 is strengthened when 4-3 and 4-1 are weakened.

Ions of tri- and tetravalent manganese, like bivalent nickel, occupy position 4, position 2 is occupied mainly by nickel ions. A disordered arrangement of ions in three-legged ladders was modeled and exchange interactions in this subsystem were considered.

From the results of the calculation, it follows that nickel ions in position 4 have stronger exchange interactions with neighbors, two of which are opposite in sign to the exchanges with manganese ions. Probably, a strong AFM interaction of Ni-Ni (165°) and Ni- Mn^{4+} (90°) stabilize the AFM orientation of the ion moments in positions 4 and 2.

However, the question of the magnetic moments orientation along the c axis remains, the position 2 imposes an FM ordering, the position 4 imposes the AFM. In one and the other case, there are frustrating interactions. It is possible that strong AFM interactions of Ni-Ni (165°) also contribute to the stabilization of the magnetic structure with a cell doubled along the c axis.

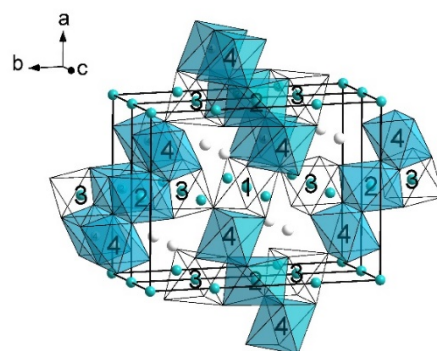


Fig. 1. Ludwigite crystal structure

[1] P. W. Anderson, *Physical Review*, **115** (1) (1959) 2.

[2] G. A. Sawatzky, W. Geertsma and C. Haas, *Journal of Magnetism and Magnetic Materials*, **3** (1-2) (March 1976) 37-45.

[3] E. Moshkina, S. Sofronova, A. Veligzhanin, M. Molokeev, I. Nazarenko, E. Eremin and L. Bezmaternykh, *Journal of Magnetism and Magnetic Materials*, **402** (15 March 2016) 69-75.

3 July

Monday

14:30-17:30

oral session

3TL-B

3RP-B

3OR-B

**“Soft and Hard
Magnetic Materials”**

3TL-B-6

ALLOYING AND PRESSURE EFFECTS ON ITINERANT-ELECTRON METAMAGNETISM OF THE UCoAl-BASED COMPOUNDS

Mushnikov N.V.^{1,2}, *Andreev A.V.*³, *Arnold Z.*³, *Shirasaki K.*⁴, *Yamamura T.*⁴

¹ M.N. Mikheev Institute of Metal Physics UB RAS, Ekaterinburg, Russia

² Institute of Natural Sciences and Mathematics, Ural Federal University, Ekaterinburg, Russia

³ Institute of Physics, Academy of Sciences, Na Slovance 2, 182 21 Prague, Czech Republic

⁴ Institute for Materials Research, Tohoku University, Katahira 2-1-1, 980-8577 Sendai, Japan
mushnikov@imp.uran.ru

UCoAl is a unique itinerant $5f$ electron metamagnet which exhibits a field-induced transition from the paramagnetic to the ferromagnetic state at a critical field 0.7 T and a broad susceptibility maximum at $T_{\max} = 20$ K in magnetic fields applied along the c -axis (Fig. 1). The specific metamagnetic behavior of UCoAl can be easily transformed to ferromagnetism with doping of the Co sublattice by suitable elements [1]. We demonstrate these features in study of the magnetization as a function of magnetic field (0-7 T), temperature (2-40 K) and external pressure (0-0.82 GPa) measured on single crystals of the $\text{UCo}_{1-x}\text{Os}_x\text{Al}$ system (the solubility is found to be up to $x = 0.2$).

All the studied compounds exhibit a huge uniaxial anisotropy with main magnetic response along the c -axis. The Os substitution for Co yields a decrease of the transition field, and already for $x = 0.005$ the ferromagnetic ground state is observed. The metamagnetic and especially the new ferromagnetic state is very sensitive to pressure. The reentrant metamagnetism in $\text{UCo}_{0.995}\text{Os}_{0.005}\text{Al}$ is observed under the pressure (Fig. 2). For higher Os content, ferromagnetism in $\text{UCo}_{1-x}\text{Os}_x\text{Al}$ is much more stable with respect to hydrostatic pressure. Nevertheless, indications of the reentrant metamagnetism are seen under pressure even for $x = 0.02$.

The experimental data for Os-substituted UCoAl have been compared with those for other substituents and analysed with a theory of itinerant electron metamagnetism considering anisotropic thermal fluctuations of magnetic moment. The observed magnetic phase diagrams, pressure dependences of the susceptibility and temperature dependences of the transition field can be explained well with this theory.

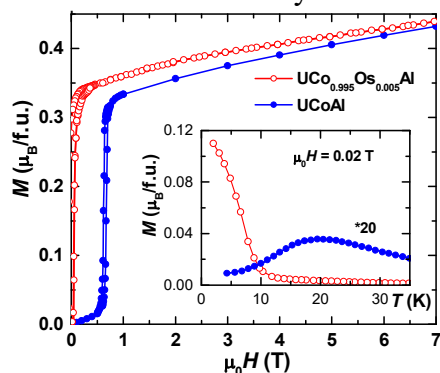


Fig. 1. Magnetization curves of UCoAl and $\text{UCo}_{0.995}\text{Os}_{0.005}\text{Al}$ for $T = 2$ K. Inset: temperature dependences of magnetization in the field 0.02 T.

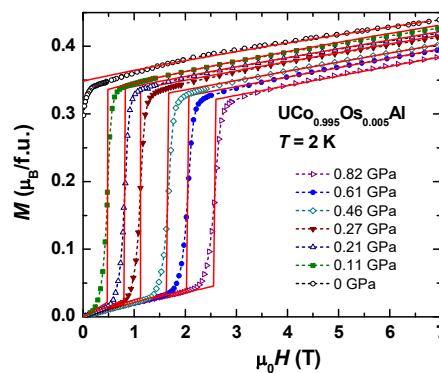


Fig. 2. Magnetization curves of $\text{UCo}_{0.995}\text{Os}_{0.005}\text{Al}$ for different pressures: experimental data (symbols and dashed lines) and calculation (solid lines).

The study was supported by FASO of Russia (theme “Magnet” No. 01201463328), by grant No. 15-02-05681 of RFBR, and by grant 16-03593S of Czech Science Foundation.

[1] A.V. Andreev, H. Aruga Katori, T. Goto, *J. Alloys Comp.*, **224** (1995) 117.

3OR-B-7

STRUCTURAL AND MAGNETIC PROPERTIES OF EXCHANGE-COUPLED MnBi/MnB NANOCOMPOSITE MAGNETS

Simsek T.¹, Ozcan S.¹

¹ Hacettepe University, Physics Eng. Dept., SNTG Lab., 06830 Beytepe, Ankara, Turkey
telem@hacettepe.edu.tr

Exchange-coupled nanocomposite magnets are composed of magnetically hard and soft phases, which interact by magnetic exchange coupling. These magnets have a large potential for advanced permanent magnetic applications, as they have a large energy product $(BH)_{\max}$ when compared to single-phase magnetic materials. The large $(BH)_{\max}$ of the exchange-coupled nanocomposite magnets originates from the combination of permanent magnet field and magnetization[1-4]. In this work, high performance exchange-coupled MnBi/MnB nanocomposite magnet was produced. Firstly, the functionality of the magnetically soft MnB phase was proved by density functional theory (DFT) calculations showing $1.915 \mu_B$ magnetic property per MnB unit that corresponds to 158 emu/g at 0 K. Mn_xB_{100-x} alloys were produced experimentally by arc melting technique[5]. Structural analysis showed that starting melting from $Mn_{55}B_{45}$ composition results single phase orthorhombic MnB structure. The chemical composition of the as-made sample was also confirmed by XPS analysis as $Mn_{48.2}B_{51.8}$. In addition, homogeneity and single phase properties of the as-made sample were also proved by BSE and EDS analyses. Magnetic characterizations showed that MnB alloy has a saturation magnetization of 130 emu/g, anisotropy constant of 517×10^3 erg/g and Curie temperature of 566 K. For exchange-coupling with a hard phase, bulk MnB alloy was milled for controlled durations. Results showed that 7 h of milling reduced the crystallite size to 11.6 nm and saturation magnetization to 85 emu/g. Secondly, the promising hard MnBi alloys were produced by arc melting. For transformation into low temperature phase, samples were annealed for controlled durations at 575 K in a vacuum furnace. Then samples were milled for 10 h. As produced MnBi nanoparticles were found to have 51.7 emu/g saturation magnetization and 12.2 kOe coercivity. This sample was used as the hard phase in MnBi/MnB nanocomposite magnets. In the last part of the study, MnBi/MnB nanocomposite magnets were produced. When MnBi/MnB composite contains 10% MnB in weight, $(BH)_{\max}$ product was increased to 5.74 MGOe. This result shows that addition of 10% soft phase to the MnBi increases the maximum energy product of the magnet by 12%. To sum up, the exchange-coupling of the soft MnB and hard MnBi magnetic phases significantly increases the magnets performance.

[1] H. Zeng, J. Li, J.P. Liu, Z.L. Wang, S. Sun, *Lett. Nat.*, **420** (2002) 395-398.

[2] R. Coehoorn, D.B. Mooji, C. Waard, *J. Magn. Magn. Mat.*, **80** (1989) 101-104.

[3] R. Skomski, J.M.D. Coey, *Phys. Rev. B.*, **48** (1993) 15812-15816.

[4] Z.J. Guo, J.S. Jiang, J.E. Pearson, S.D. Bader, J.P. Liu, *Appl. Phys. Lett.*, **81** (2002) 2029-2031.

[5] T. Simsek, S. Ozcan, *IEEE Trans. Magn.*, **51** (2015) 7-10.

3OR-B-8

TUNING THE MAGNETIC AND STRUCTURAL PROPERTIES OF FE₆₀AL₄₀ THIN FILMS BY ION IRRADIATION

Ehrler J.^{1,2}, Bali R.¹, Böttger R.¹, Semisalova A.¹, Zhou S.¹, Grenzer J.¹, Potzger K.¹

¹ Helmholtz-Zentrum Dresden-Rossendorf, Dresden, Germany

² Dresden University of Technology, Dresden, Germany

j.ehrler@hzdr.de

Magnetic materials are significant for future data storage device and spintronic applications. Recently it has been shown that nano-sized ferromagnetic structures can be generated within non-ferromagnetic B2-Fe₆₀Al₄₀ thin films via local ion-irradiation. Ion-irradiation leads to disordering, forming the ferromagnetic A2 phase. The mechanism of this disorder induced effect has been variously attributed to the increase in the number of Fe-Fe nearest neighbors due to disorder and the corresponding increase of the lattice parameter (a_0) [1,2,3]. Considering a_0 as an indicator for the disorder as the driving parameter for the ferromagnetic order, 250 nm thick B2-Fe₆₀Al₄₀ films irradiated with various ion species, i.e. H⁺, He⁺ and Ne⁺, have been investigated with respect to the correspondence between a_0 and the saturation magnetization (M_S).

The films have been prepared by magnetron sputtering and irradiated at the Ion Beam Center at the Helmholtz-Zentrum Dresden - Rossendorf. The irradiation-induced displacements per atom (dpa) were calculated with the help of the program TRIM [4]. The films have been irradiated at low temperature (LN₂) with an energy of 17 keV and a fluence of 4E17 ions/cm² for H⁺ ions and with 3.52E16 ions/cm² at 27 keV for He⁺. According to TRIM, these implantation parameters induce the same *dpa* for the H⁺ and He⁺ irradiations. M_S was measured by Vibrating sample magnetometry and the order parameter (S) as well as a_0 were derived from X-ray diffraction.

The non-irradiated B2-ordered Fe₆₀Al₄₀ films ($S=1$) possess an M_S of 5 kA/m and a_0 of 2.89 Å. Despite similar ion-induced disorder, films irradiated with H⁺ and He⁺ showed an increased M_S of 314 kA/m and 551 kA/m respectively. This suggests deviations from the TRIM calculations, in particular for the lighter H⁺ ion. Nevertheless, study of a vast number of films irradiated with H⁺, He⁺ as well as Ne⁺ at low and room temperature respectively shows a fundamental correlation between structural and magnetic properties of the Fe₆₀Al₄₀ films, independent of the implanted ion species or temperature treatment (see Figure 1). The films exhibit a sharp transition at $a_0=2.91$ Å, where M_S rapidly increases, tracked exactly by a decrease of S , suggesting that M_S depends on the increase of the Fe-Fe nearest neighbor interactions (as indicated by decreasing S) only being independent on a_0 . DFT calculations will help further understanding of this correlation.

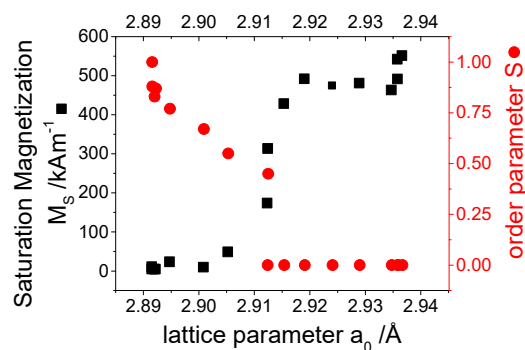


Fig. 1. Variation of the ion irradiation induced saturation magnetization M_S and structural disorder (represented by the order parameter S) with the lattice parameter a_0 .

[1] R. Bali et al., *Nano Lett*, **14** (2014) 435.

[2] L. E. Zamora et al., *Phys. Rev. B*, **79** (2009) 094418.

[3] E. Menéndez et al., *New J. Phys.*, **10** (2008) 103030.

[4] J. F. Ziegler et al., *Nucl. Instrum. Methods B*, **268** (11-12) (2010) 1818.

3TL-B-9

THICKNESS DEPENDENCE OF MAGNETIC PROPERTIES OF THIN AMORPHOUS FERRIMAGNETIC RARE EARTH–TRANSITION METAL MULTILAYERS

Svalov A.V.¹, Adanakova O.A.¹, Vas'kovskiy V.O.¹, Balymov K.G.¹, Kurlyandskaya G.V.^{1,2}

¹ Ural Federal University, Ekaterinburg, Russia

² Universidad del País Vasco (UPV/EHU), Bilbao, Spain

andrey.svalov@urfu.ru

Rare-earth–transition-metal (RE-TM) films are of special interest for their implementation in novel high-density and high-speed magnetic recording technologies [1]. In some cases, the total thickness of RE-TM films is only a few nanometers. It is known, that thickness has an appreciable effect on the magnetic properties of ferromagnetic films in this range of thicknesses. In particular, a thickness-dependent Curie temperature has been observed in various ferromagnetic films [2]. This finite-size effect is caused by the reduced number of atoms in the direction perpendicular to the film plane that leads to a decrease of the total magnetic exchange energy [3]. At the same time, very limited data are available concerning the thickness dependence of magnetic properties for ferrimagnetic RE-TM films [4]. In this work, the influence of the thickness of the ferrimagnetic Gd-Co layers on the magnetic properties of Gd-Co/Ti multilayers was studied.

Gd-Co/Ti multilayers were prepared by magnetron sputtering deposition onto Si and glass substrates. The thickness of the Gd-Co layers was varied in the interval of 250 nm to 0.8 nm. The thickness of Ti spacers was kept constant (2 nm). The compositional ratios of Gd and Co in the Gd-Co layers were determined by energy dispersive X-ray spectroscopy. Low angle X-ray diffraction and high resolution transmission electron microscopy were used in order to determine the quality of the layers. It was found, among the other results that the temperature dependence of magnetization of the samples depends on Gd-Co layer thickness (Fig. 1)

It was shown that the obtained experimental results can be satisfactorily described in the framework of model of the "size factor" and taking into account the possible effect of the electronic structure of Ti on the average magnetic moment of Co atoms, the efficiency of which depends on the thickness of the magnetic layers.

This work was supported by the Russian Foundation of Basic Research, Grant 17-02-00236.

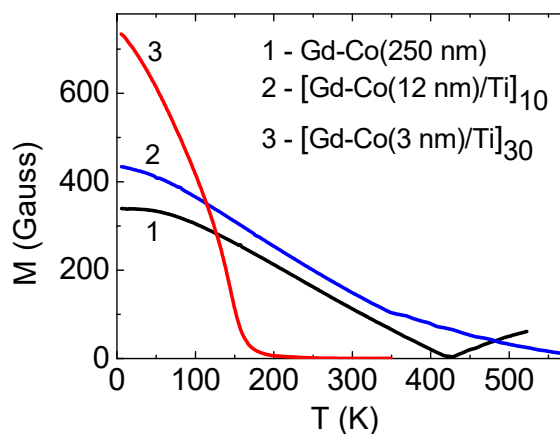


Fig. 1. Temperature dependences of magnetization for the samples with different Gd-Co layer thickness.

[1] A. Kirilyuk, A.V. Kimel, Th. Rasing, *Rev. Mod. Phys.*, **82** (2010) 2731-2784.

[2] F. Huang, G.J. Mankey, M.T. Kief, R.F. Willis, *J. Appl. Phys.*, **73** (1993) 6760-6762.

[3] M.E. Fisher, M.N. Barber, *Phys. Rev. Lett.*, **28** (1972) 1516-1519.

[4] B. Hebler, A. Hassdenteufel, P.Reinhardt, H. Karl, M. Albrecht, *Front. Mater.* **3:8** (2016) 1-8.

3RP-B-10

THE ROLE OF MAGNETISM IN THE FORMATION OF THE ATOMIC STRUCTURE OF SOFT MAGNETIC IRON-BASED ALLOYS

Ershov N.V.¹, Chernenkov Yu.P.², Lukshina V.A.^{1,3}, Gornostyrev Yu.N.^{1,4}, Gorbatov O.I.⁴

¹ Institute of Metal Physics UB RAS, Ekaterinburg, Russian Federation

² PNPI NRC «Kurchatov Institute», Gatchina, Leningrad region, Russian Federation

³ Ural Federal University, Ekaterinburg, Russian Federation

⁴ Institute of Quantum Materials Science, Ekaterinburg, Russian Federation

nershov@imp.uran.ru

Soft magnetic iron based alloys are promising materials for practical application due to the phenomena of induced magnetic anisotropy (in FeSi and FeAl alloys) and high magnetostriction (in FeAl and FeGa) which close connected to features of their atomic structure. Understanding of the relation between short-range order formation and magnetic properties is important for the development of the soft magnetic materials with desirable properties.

The atomic structure of iron-rich Fe-Si, Fe-Al and Fe-Ga alloys was investigated experimentally by X-ray diffraction and NGR spectroscopy and was modelled theoretically by the Monte Carlo method using the effective potentials of interatomic interactions calculated within the density functional theory for the ferromagnetic and paramagnetic states. The features of local ordering of solute atoms in the α -region of the phase diagram after annealing the samples at temperature above T_C (paramagnetic state) followed by quenching into water, and after annealing at temperature below T_C with slow cooling to room temperature in a ferromagnetic state were revealed.

For the first time, nano-sized clusters with $B2$ -type ordering (CsCl structure) were found in all considered alloys after thermal treatment. Each cluster consists of a pair of two $B2$ -cells having a common face surrounded by stretched α -iron cells. $B2$ cluster has the anisotropic form, it is more extended along one of $\langle 100 \rangle$ direction. The appearance of preferential orientation of $B2$ clusters along one of the $\langle 100 \rangle$ axes after the thermomagnetic or thermomechanical treatments, previously predicted in Neel's works, causes the induced axial magnetic anisotropy. When solute concentration increases the small clusters of $D0_3$ phase appear replacing by $B2$. The sizes of regions with $D0_3$ ordering increase after annealing in the ferromagnetic state.

The results of first-principles calculations pointed that in the ferromagnetic state the configurations, in which two solute atoms are in the positions of the 3rd or 4th neighbors, are energetically preferable. And, pairs of solute atoms as 2-nd neighbors can formed, if the alloy is in the magnetically disordered state. Thus, it is shown for the first time that the energy of the effective interaction in bcc iron essentially depends on the magnetic state of the matrix. Therefore, the short-range order of $B2$ type is formed at temperatures above T_C , and is fixed during quenching, while in the ferromagnetic state the short-range order of the $D0_3$ type is the equilibrium. Such a picture is valid for Fe-Si and Fe-Al, while the $B2$ short-range order was found rather weak in Fe-Ga. Rearrangement of the short-range order of $B2 \rightarrow D0_3$ type requires overcoming an essential energy barrier and, consequently, a thermal activation of the diffusion process.

The obtained results reveal the determining role of magnetism in the formation of short-range order in iron-rich Fe-Si, Fe-Al, and Fe-Ga alloys and allow explaining the experimentally observed structural features of the alloy as a function of composition and temperature.

The work was carried out within the framework of the state task of the FASO Russia (theme «Magnet», No 01201463328). Support by UB RAS (project No 15-9-2-33) is acknowledged.

3OR-B-11

119Sn MÖSSBAUER SPECTROSCOPY OF 3d-, 4f-, AND U-BASED INTERMETALLIC COMPOUNDS

*Krylov V.I.*¹

¹ Skobeltsyn Institute of Nuclear Physics, Moscow State University, 119991 Moscow, Russia
vkrylovmag@gmail.com

The results of Mössbauer spectroscopy (MS) investigation of the magnetic hyperfine fields (HFs) on ¹¹⁹Sn probe nuclei for the different groups of 3d-, 4f-elements, and Uranium-based intermetallic compounds are presented in this work. It has been shown that the mechanisms of electron polarization on ¹¹⁹Sn nuclei are significantly different for the following groups of the compounds.

1) The compounds TFe₂ (T=Sc, Ti, Y, Zr, Lu, Hf, and U) with cubic MgCu₂-type and hexagonal MgZn₂-type Laves structures are ferromagnets (FM) except for TiFe₂ that is an antiferromagnetic (AFM). The Fe-Fe magnetic exchange interaction is responsible for magnetic ordering of the TFe₂ compounds. In the FM compounds TFe₂, the HFs for ¹¹⁹Sn atoms localized on T-sites (HF = B₁) are positive and proportional to the Fe magnetic moments: B₁=A₁×μ_{Fe}, where A₁=28 T/μ_B is the hyperfine coupling constant. The HFs for ¹¹⁹Sn atoms localized on Fe-sites (HF = B₂) are negative: B₂=A₂×μ_{Fe}, where A₂=-3.8 T/μ_B.

2) In the magnetically ordered alloys of rare earth metals (RE) with p-metals, the HFs for ¹¹⁹Sn atoms occur due to 4f-4f indirect magnetic interaction and reach the values of 40 T. Systematics of the HFs for ¹¹⁹Sn in the FM and AFM binary Gd - X compounds (X is a p-metal) of different compositions and crystalline structures are presented in this work. The HF values on ¹¹⁹Sn nuclei in REAl₂ и REGa FM compounds are proportional to the spin magnetic moment of RE ions.

3) Huge HFs reaching to 56 T have been found for ¹¹⁹Sn atoms localized on RE-sites of RE-3d compounds (3d are Fe, Co, and Mn atoms with the localized magnetic moments) [1]. This value is the maximum of the known HF values for ¹¹⁹Sn atoms in the metallic magnets. It has been shown that the HFs are created due to two additive contributions of RE- and 3d-magnetic sublattices.

4) The HFs on ¹¹⁹Sn nuclei in UTM (T is a d-metal, M is a p-metal) compounds with ZrNiAl-type crystal structure are proportional to the full magnetic moment of U-ions: B = A × μ_U, where A= 6.5(4) T/μ_B [2]. The HFs are formed by the nearest U-ions and reach of 10 T. The results of ¹¹⁹Sn MS study on UPdSn, UCuSn, UAuSn, UNiSn, UCuGe, UGa₃, UIn₃, UPb₃, UGa₂, UGe₂, USn₂ [3] compounds indicate a strong anisotropy of the magnetic hyperfine interaction and magnetic exchange interaction caused by the significant nonsphericity of 5f-electron shell of uranium ion.

Among the 3d-, 4f-, and U-magnetic moments, the ability to create a spin polarization on the ¹¹⁹Sn nuclei is the largest for 3d-moments (in equivalent of the unit magnetic moment) and this one is the smallest for the unit magnetic moment of RE-ions.

The MS investigations of HFs on the ¹¹⁹Sn probe nuclei in RE- and uranium-based compounds have shown that in the compounds with layered crystal structure the screening effect of the magnetic exchange interaction by layers of p- or s, d-nonmagnetic atoms is observed. In magnetically ordered compounds this effect can lead to the appearance of selected layers, free of magnetic exchange and of transferred (induced by this exchange) electron polarization.

[1] V.I. Krylov, N.N. Delyagin, *J. Magn. Magn. Mater.*, **305** (2006) 1-5.

[2] V.I. Krylov, *J. Appl. Phys.*, **109** (2011) 07E140 (1-3).

[3] V.I. Krylov, N.N. Delyagin S.I. Reiman, et al., *J. Alloys. Comp.*, **343** (2002) 33-37.

3OR-B-12

CARBONYL IRON PARTICLES IN A SiO₂ SHELL: SYNTHESIS, PROPERTIES, MICROWAVE PERMEABILITY AND PERMITTIVITY MEASUREMENTS

Maklakov S.S.¹, Maklakov S.A.¹, Petrov D.A.¹, Rozanov K.N.¹, Adamovich Yu.A.², Polozov V.I.², Talalaev K.A.², Amelichev V.A.³, Bessalova V.V.⁴, Pokholok K.V.⁵, Filimonov D.S.⁵, Ryzhikov I.A.¹, Lagarkov A.N.¹

¹ Institute for Theoretical and Applied Electromagnetics RAS, Moscow, Russia

² Moscow Institute of Physics and Technology (State University), Dolgoprudny, Russia

³ SuperOx, Moscow, Russia

⁴ M.V. Lomonosov Moscow State University, Faculty of Physics, Moscow, Russia

⁵ M.V. Lomonosov Moscow State University, Department of Chemistry, Moscow, Russia
squirrel498@gmail.com

Carbonyl iron (CI) is pure iron powder which often serves as filler in magneto-dielectric composites. These composites are applied as functional materials in electromagnetic interference shielding, microwave absorber designs and for production of inductive electronic components. A disadvantage is that CI easily oxidizes in presence of water and oxygen, or at high temperature. Oxidation strongly reduces area of application because appearance of iron oxide damages structure and destroys assets of such composite. Search for an inhibitor to depress CI corrosion is modern chemical challenge. Promising route is to cover each of CI particles with a shell which shall act as a diffusion barrier between metal and outer media.

We report on a synthesis of a CI-based “Fe@SiO₂” powder which possesses high corrosion resistance to water electrolyte solution, and, in the meantime, show identical magnetic behavior to a pure CI. To deposit 100-nm thick SiO₂ shell, a modified Stöber hydrolysis of tetraethyl orthosilicate was applied [1]. Powder was separated from a solution *via* a magnetic field-assisted sedimentation. Synthesis produces < 5 mass. % of SiO₂, which presents both in the shell form, and as individual spherical particles. According to γ -resonance measurements, lasting contact with water-ethanol solution does not change iron surface.

Fe@SiO₂ powder does not oxidize in NaCl water solution for more than 6 months. It also resists concentrated HCl, although no longer than several hours. SiO₂ shell shifts positions of exothermal peaks in a curve of differential scanning calorimetry by up to 100°C towards higher temperatures.

This powder possesses the same features of microwave permeability in 0.1-10 GHz range as the initial CI does. Microwave permeability and permittivity were measured for a paraffin wax-based composite with the magnetic powder by the Nikolson-Ross-Weir technique in a standard N-type coaxial airline with a vector network analyzer. Prospective effect is that dielectric shell decreases both real and imaginary parts of microwave permittivity. Detailed analysis of quasistatic permeability and permittivity values dependencies on the filler concentration showed that the shell prevents electrical contacts between CI particles and suppresses percolation. Conducted research shows that as-synthesized powder material can be applied in the microwave industry in corrosion resistance is needed.

The work was supported by the Russian Science Foundation (Agreement No. 16-19-10490) and the Russian Foundation for Basic Research (Grant No. 16-33-01089).

[1] S.S. Maklakov, A.N. Lagarkov, S.A. Maklakov, Y.A. Adamovich, D.A. Petrov, K.N. Rozanov, I.A. Ryzhikov, A.Yu. Zarubina, K.V. Pokholok, D.S. Filimonov, *J. Alloys Compounds*. **706** (2017) 267-273.

3OR-B-13

ENGINEERING OF MAGNETIC PROPERTIES, MAGNETIC ANISOTROPY AND GMI EFFECT OF Co- AND Fe- RICH MICROWIRES BY ANNEALING

Zhukov A.^{1,2,3}, Ipatov M.^{1,2}, Blanco J. M.², Churyukanova M.⁴, Zhukova V.^{1,2}

¹ Dept. Phys. Mater., University of Basque Country, UPV/EHU San Sebastián 20018, Spain

² Dpto. de Física Aplicada, EUPDS, UPV/EHU, 20018, San Sebastian, Spain

³ IKERBASQUE, Basque Foundation for Science, 48011 Bilbao, Spain

⁴ National University of Science and Technology «MISIS», Moscow, 119049, Russia

arkadi.joukov@ehu.es

Studies of amorphous magnetic wires attract great attention during last three decades owing to excellent magnetic properties such as magnetic bistability, excellent magnetic, mechanical and corrosion properties, Giant Magnetoimpedance (GMI) effect and fast preparation method [1-2].

Recent tendency in devices miniaturization stimulated development of thin (few micrometers diameters) soft magnetic microwires prepared using Taylor-Ulitovsky method [2]. Excellent soft magnetic properties and GMI effect have been reported for properly prepared and processed Co-rich microwires [2].

Less expensive Fe-rich microwires are preferable for the applications. But amorphous Fe-rich materials exhibit rather high magnetostriction coefficient and consequently present quite low GMI effect [2].

The most common method for magnetic softness optimization is the annealing. Nevertheless, recently the optimization of soft magnetic properties and GMI effect after are reported mostly for brittle devitrified Fe-rich microwires [2].

From previous studies of Co-rich amorphous materials it is known that stress annealing can considerably affect the magnetic properties of amorphous materials [2].

Consequently, we studied the influence of stress- annealing on magnetic properties and GMI effect of Fe- and Fe-Co based glass-coated microwires.

We observed that Fe-rich microwires annealed under stress at appropriate annealing conditions (time and temperature) can present low coercivity, considerable magnetic softening and enhanced GMI effect (see Fig).

For interpretation of observed changes of hysteresis loops after stress annealing we considered internal stresses relaxation and different mechanisms of stress-induced anisotropy.

Observed versatile properties of stress annealed glass-coated microwires with enhanced and tunable soft magnetic properties make them suitable for technological sensing applications.

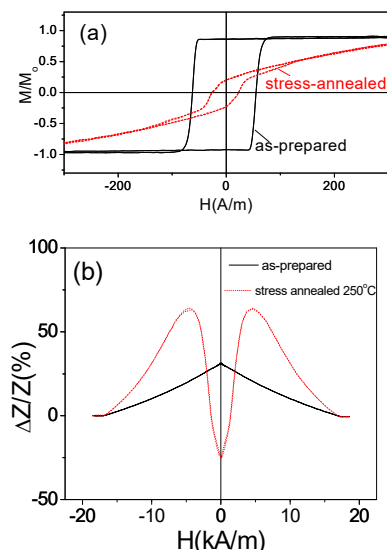


Fig. Effect of stress annealing on hysteresis loops (a) and GMI effect (b) of Fe₇₅B₉Si₁₂C₄ microwires measured at 1GHz.

[1] K. Mohri, T. Uchiyama, L. P. Shen, C. M. Cai, L. V. Panina, *J. Magn. Magn. Mater.*, **249** (2002) 351-356K.

[2] A. Zhukov, M. Ipatov and V. Zhukova, *Advances in Giant Magnetoimpedance of Materials, Handbook of Magnetic Materials*, ed. K.H.J. Buschow, 24: chapter 2 (2015) 139-236.

3RP-B-14

MAGNETIC PROPERTIES OF NANOLAMINATED MAGNETIC MAX PHASES

Novoselova Iu.¹, Salikhov R.¹, Wiedwald U.¹, Spasova M.¹, Rosen J.², Farle M.^{1,3}

¹ Faculty of Physics and CENIDE, University of Duisburg-Essen, Duisburg, Germany

² Thin Film Physics, Department of Physics, Chemistry and Biology (IFM), Linköping University, Linköping, Sweden

³ Center for FunMagMa, Immanuel Kant Baltic Federal University, Kaliningrad, Russia
ruslan.salikhov@uni-due.de

MAX phases are a family of hexagonal compounds with the chemical formula $M_{n+1}AX_n$ ($n = 1-3$) composed of early transition metals M (Ti, V, Cr ...), A -group elements (Al, Ga, Ge ...) and X (C or N) [1]. Due to their atomically laminated structure (Fig. 1) these materials share properties of ceramics such as high structural stiffness and metals such as good electrical and thermal conductivity [1]. The new class of magnetic MAX phases has been recently discovered substituting or composing the M -element by/with Mn in quaternary solid solutions. Also ternary Mn_2GaC magnetic compounds have been synthesized as hetero-epitaxial films containing Mn as the exclusive M -element [1]. Significant interest in these systems is rising due to a recently discovered possibility of delamination of layered MAX phase structures leading to 2D graphene-like transition metal carbides and nitrides $M_{n+1}X_n$, known as MXenes [2]. Mn-based MXenes are predicted theoretically to be intrinsic half-metals with full spin polarization and above room temperature ferromagnetism [3].

We report on magnetic properties of recently synthesized magnetic MAX phases. Magnetometry and ferromagnetic resonance (FMR) reveal ferromagnetic (FM) properties of $(Cr_{0.5}Mn_{0.5})_2GaC$ and $(Mo_{0.5}Mn_{0.5})_2GaC$ at temperatures below 220 K. Both compounds behave as soft magnetic materials possessing small c -axis magnetocrystalline anisotropy energy density (MAE) below 5 kJ/m^3 [4]. Mn_2GaC at room temperature is antiferromagnetic (AFM) with a Néel temperature of approximately 400 K. At $T = 240 \text{ K}$ the system undergoes a phase transition to a canted noncollinear spin state [1]. This state is characterized as a metamagnetic state, in which the magnetic field causes a change of the lattice parameters and FM spin alignment. FM Mn_2GaC has a MAE of $40 \pm 10 \text{ kJ/m}^3$ with the easy axis perpendicular to the c -axis and saturation magnetization of $1.7 \mu_B$ per Mn atom at $T = 5 \text{ K}$.

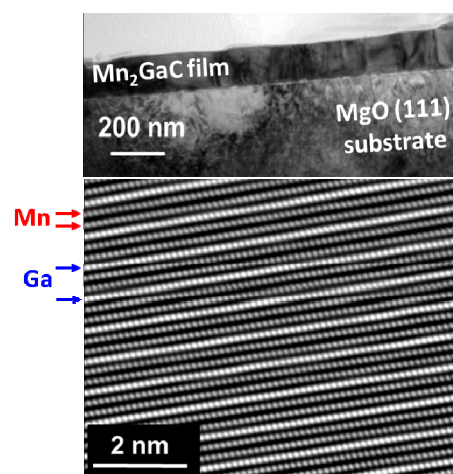


Fig. 1. Cross-sectional TEM image and HAADF/STEM atomic resolution image of the Mn_2GaC .

Support by DFG project SA3095/2-1 and DAAD scholarship 57214224 is acknowledged.

[1] A.S. Ingason, M. Dahlqvist, J. Rosen, *J. Phys.: Condens. Matter*, **28** (2016) 433003 (1-17).

[2] O. Mashtalir, et al., *Nat. Comm.*, **4** (2013) 1716 (1-7).

[3] J. He, P. Lyu, P. Nachtigall, *J. Mater. Chem. C*, **4** (2016) 11143-11149.

[4] R. Salikhov, A.S. Semisalova, A. Petruhins, A.S. Ingason, J. Rosen, U. Wiedwald and M. Farle, *Mater. Res. Lett.*, **3** (2015) 156-160.

3RP-B-15

STRUCTURAL PROPERTIES INFLUENCE ON MAGNETIC CHARACTERISTICS OF GLASS-COATED MICROWIRES

Rodionova V.¹, Baraban I.¹, Chichay K.¹, Shevyrtalov S.¹, Litvinova A.¹, Gorshenkov M.², Perov N.^{1,3}

¹ Immanuel Kant Baltic Federal University, Nevskogo 14, 236004 Kaliningrad, Russia

² National University of Science and Technology MISiS, Moscow 1 19049, Russia

³ Lomonosov Moscow State University, Leninskie Gory 1-2, 119991 Moscow, Russia
rodionova@lnmm.ru

Magnetic amorphous microwires are very sensitive to various influences (stresses, temperature and so on), which make them usable for different types of sensors [1-3]. Microwires magnetic behavior depends on contributions of the magnetoelastic energy components: i) the metallic core composition determining a sign of the magnetostriction constant, ii) the diameters of the metallic core and the total diameter of microwire with the glass shell are determining, in particular, the stresses value and radial distribution. Once the nanocrystalline phase is formed, magnetocrystalline energy should be taken into account and its influence on the magnetic characters should be considered.

The microwires investigated in this work were produced from CoFe alloys by quenching and drawing technique [4] with the parameters d (the diameter of the core) from 10 μm to 25 μm and D (the total diameter) from 24 μm to 33 μm . Due to specific condition of preparation all microwires show biphasic behavior: nanocrystals in an amorphous matrix [6], which was demonstrated using the XRD and DSC investigations. In a classical point of view the stress distribution in the microwire occurs from the center to the edges [5], using the electron microscopy the stresses distribution was visualized. The influence of the partial crystallization of the microwires metallic core on the magnetic characteristics in the temperature range from 300 to 1250 K was studied using the VSM. The contribution of the energy components in the formation of magnetic properties was estimated.

The support is by the Ministry of Education and Science of the Russian Federation in the framework of government assignment (No.3.4168.2017/ПЧ).

- [1] M. Vazquez, *Handbook of Magnetism and Advanced Magnetic Materials*, **4**; H.Kronmuller and S. S. P. Parkin, Eds. Chichester, U.K.: Wiley, (2007) 2193.
- [2] R. Hudak, R. Varga, J. Živcák, J. Hudak, J. Blažek, D. Praslička, *Theory Appl. Topics Intell. Eng. Informat.*, **2** (2013) 413–434.
- [3] D. Praslička et al., *IEEE Trans. Magn.*, **49** (1) (2013) 128–131.
- [4] A. Zhukov, J. González, M. Vázquez, V. Larin, A. Torcunov, *Encyclopedia of Nanoscience and Nanotechnology*, edited by H. S. Nalwa American Scientific, Stevenson Ranch, CA, Chapter 62, **6**, (2004) 365–367.
- [5] A. Zhukov, *Adv. Funct. Mater.*, **16** (5) (2006) 675–680.
- [6] P.Klein, R.Varga, I.Škorvčnek, R.E.Kammouni, M.Vazquez, *IEEE Trans. Magn.*, **50**(11) (2014) 2006303.

3 July

Monday

14:30-17:15

oral session

3TL-E

3RP-E

3OR-E

“Magnonics”

3TL-E-6

EXCITATION AND PROPAGATION OF SPIN WAVES IN GRADED MAGNONIC LANDSCAPES

*Kruglyak V.V.¹, Davies C.S.¹, Au Y.¹, Mushenok F.B.¹, Hrkac G.¹, Whitehead N.J.¹, Horsley S.A.R.¹,
Philbin T.J.¹, Poimanov V.D.², Dost R.³, Allwood D.A.³, Inkson B.J.³, Kuchko A.N.⁴*

¹ University of Exeter, Exeter, United Kingdom

² Donetsk National University, Donetsk, Ukraine

³ University of Sheffield, Sheffield, United Kingdom

⁴ Institute of Magnetism of NASU, Kiev, Ukraine

V.V.Kruglyak@exeter.ac.uk

Even the most general definition of magnonics, as the study of spin waves, leaves a lot of freedom for interpretation and scientific discussion of directions of the field's further development. There is however an aspect of magnonics that has been both ubiquitous and somewhat underrated so far: magnonics is the study not only of spin but also (and most importantly) of waves, which have an extremely rich and peculiar dispersion that is nonlinear, anisotropic and non-reciprocal. The spin wave dispersion is very sensitive to the sample's magnetic properties and micromagnetic state, including both the internal magnetic field and magnetisation, so that spin waves are rarely observed to propagate in uniform media. Inspired by and feeding from other fields of wave physics, such as quantum mechanics, graded-index optics and transformation optics, we have recently tried to formulate the concept of graded-index magnonics as a unifying theme focusing on general aspects of spin wave excitation and propagation in media with continuously non-uniform properties [1,2].

In this talk, we will describe the mechanism of spin-wave excitation enabled by the graded magnonic index and will provide demonstrations of its application to the most recent experiments, in which spin wave emission from effective magnetic field non-uniformities and complex magnetisation textures was observed.

The research leading to these results has received funding from the EPSRC of the UK (Project Nos. EP/L019876/1, EP/L020696 and EP/P505526/1), and from the EU's Horizon 2020 research and innovation program under Marie Skłodowska-Curie Grant Agreement No. 644348 (MagIC).

[1] C.S. Davies and V. V. Kruglyak, *Low Temp. Phys.*, **41** (2015) 976.

[2] C.S. Davies, A. Francis, A.V. Sadovnikov, S.V. Chertopalov, M.T. Bryan, S.V. Grishin, D.A. Allwood, Y.P. Sharaevskii, S.A. Nikitov, V.V. Kruglyak, *Phys. Rev. B*, **92** (2015) 020408.

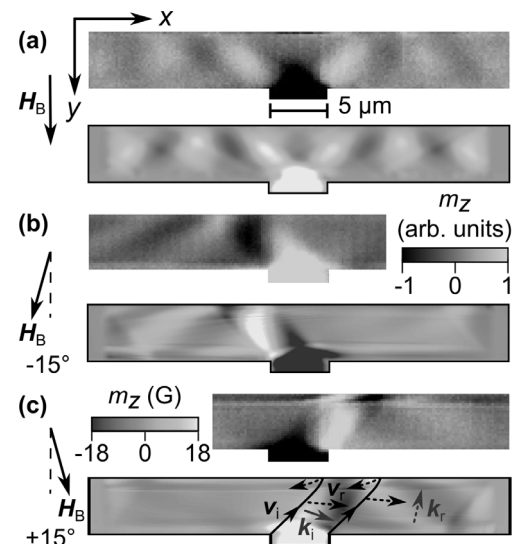


Fig. 1. Snapshots of spin waves excited and propagating in a magnonic T-junction at the bias magnetic field applied (a) parallel to and at angles of (b) -15° and (c) $+15^\circ$ relative to the junction's leg. In each case, the top and bottom panels show results of time resolved Kerr imaging and micromagnetic simulations, respectively [2].

3TL-E-7

SUPERMAGNONICS*Bunkov Yu.M.^{1,2}*¹ Kazan Federal University, Kazan, Russia² MIPT, Dolgoprudnyy, Russia
Yury.bunkov@neel.cnrs.fr

We consider the Bose-Einstein condensation (BEC) of quasi-equilibrium magnons which leads to a spin superfluidity, the coherent quantum transfer of magnetization in magnetic materials. This phenomenon is beyond the classical Landau-Lifshitz-Gilbert paradigm. The critical conditions for excited magnon density in ferro- and antiferromagnets, bulk and thin films, are estimated and discussed.

At certain conditions the RF pumping of excited magnons may lead to a new state, so-called, magnon condensate, in which a macroscopic number of magnons forms a coherent quantum state. This state can significantly change the magnon gas properties, its dynamics and transport.

Particularly, the magnetization precession may live in orders of magnitude longer than the T_2^* time of usual precession, so name long-lived induction decay signal. The spatial gradients of this state exhibit spin superfluidity, the coherent transport of deflected magnetization. The spin superfluidity is an extremely interesting phenomenon both for fundamental and applied studies.

For the first time the existence of quasi-equilibrium Bose condensate was demonstrated in the experiment with nuclear magnons in the superfluid antiferromagnetic liquid crystal $^3\text{He-B}$ in 1984 [1]. The following phenomena were observed later: a) transport of magnetization by spin supercurrent between two cells with magnon BEC; b) phase-slip processes at the critical current; c) spin current Josephson effect; d) spin current vortex formation; e) Goldstone modes of magnon BEC oscillations. The comprehensive reviews of these studies can be found in Ref. [2]. Currently magnon BEC found in different magnetic systems: i) in antiferromagnetic superfluid $^3\text{He-A}$; ii) in in-plane magnetized yttrium iron garnet $\text{Y}_3\text{Fe}_5\text{O}_{12}$ (YIG) film with k about 10^{-5} 1/cm; iii) in antiferromagnetic MnCO_3 and CsMnF_3 with Suhl-Nakamura indirect nuclear spin-spin interaction.

Recently we have found the magnon BEC state and spin supercurrent in YIG film magnetized perpendicularly to the plain. We have observed the BEC state at $k=0$ with the properties very similar to one in $^3\text{He-B}$. This discovery can be applied for number of applications. The results of our current investigations are the main topic of presentation. Particularly we have succeeded to observe the magnetization transport between two BEC states by a thin bridge between them. The stability of this spin supercurrent is protected by energetic gap, similar to one in usual supercurrent. This is why we are able to name this phenomenon "Supermagnonics".

Support by Russian Science Foundation (grant RSF 16-12-10359).

[1] A. S. Borovik-Romanov, Yu. M. Bunkov, V. V. Dmitriev, Yu. M. Mukharskiy, *JETP Lett.* **40** (1984) 1033.

[2] Yu. M. Bunkov, G. E. Volovik, Spin superfluidity and magnon BEC, Chapter IV of the book "Novel Superfluids", eds. K.H.Bennemann and J.B. Ketterson (Oxford, University press, 2013).

3RP-E-8

RE-PROGRAMMABLE DYNAMICS OF COUPLED VORTICES

Lendinez S.¹, Ding J.¹, Jain S.¹, Jungfleisch M.B.¹, Pearson J.¹, Hoffmann A.¹, Novosad V.¹

¹ Materials Science Division, Argonne National Laboratory, Argonne, IL 60439, USA

Novosad@anl.gov

In patterned ferromagnetic elements, the ground state of the static magnetization can be a vortex that consists of a large region of in-plane curling magnetization and a nano-sized core region where the magnetization points out-of-plane. When the vortex core is perturbed from its equilibrium state, it begins a gyrotropic oscillation. The precession frequency does not depend on the vortex core orientation for isolated vortices [1, 2], while for an array of interacting vortices the dynamic dipolar interaction eliminates this degeneracy and results in a variety of collective excitation modes [2-4]. In this work we will discuss a method to control the ground state determined by the relative vortex core polarities and the dynamic excitation mode in a model system of coupled vortex-state magnetic dots. An advantage of the double-dot overlap structure is the strong dynamic interaction between the vortex cores and, consequently, the large difference between the eigenfrequencies of the gyrotropic dynamic modes that correspond to the same and opposite orientations of the interacting cores (Fig. 1).

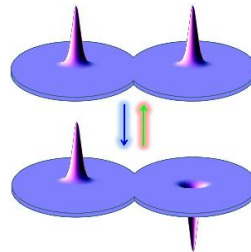


Fig. 1 A spin vortex core typically occupies a very small area ($\sim 10 \times 10 \text{ nm}^2$) in otherwise mesoscopic sample. Dipole-dipole and exchange coupling between the interacting vortices may lead to excitation of collective modes whose frequencies depend on the core polarities.

Our approach involves driving the system by an alternating magnetic field into a quasi-chaotic regime of continuous vortex core reversals. This process is followed by a gradual reduction of the driving field and relaxing of the system to a ground state, which supports the dynamical mode that is non-resonant with the driving frequency and is therefore non-responsive with the driving field. Furthermore, we demonstrate how this technique can be used to induce the dynamic transition of a single vortex into vortex-antivortex-vortex states [3]. The dynamic response of this system is expected to demonstrate a number of collective modes, depending on the combination of the vortex core polarities, and/or the excitation field direction, and, hence, is of interest for future fundamental studies. The proposed technique can be used to dynamically control a variety of physical systems that have multiple stable ground states, as well as in novel device concepts, such as magnonic crystals, spin-torque oscillators, magnetic logics and memories [4, 5].

This work was supported by the U. S. Department of Energy, Office of Science, Office of Basic Energy Sciences, under Contract No. DE-AC02-06CH11357.

- [1] J. Ding, P. Lapa, S. Jain, *et al.*, *Sc. Reports*, **6** (2016) 25196.
- [2] J. Ding, S. Jain, J. E. Pearson, *et al.*, *J. Appl. Phys.*, **117** (2015) 17A707.
- [3] S. Lendinez, S. Jain, V. Novosad *et al.*, *J. Appl. Phys.*, **115** (2014) 17D121.
- [4] S. Jain & V. Novosad, *U.S. Patent*, **8** (2014) 854,871.
- [5] S. Jain, V. Novosad, F. Fradin, *et al.*, *IEEE Trans. Magn.*, **49** (2013) 3081.

3RP-E-9

LOGIC GATES USING FORWARD VOLUME SPIN WAVES BASED ON YTTRIUM IRON GARNETS

Goto T.^{1,2}, Sekiguchi K.^{2,3}, Ross C.A.⁴, Granovsky A.B.⁵, Takagi H.¹, Nakamura Y.¹, Uchida H.¹,
Inoue M.¹

¹ Toyohashi University of Technology, Toyohashi, Japan

² JST PRESTO, Kawaguchi, Japan

³ Keio University, Yokohama, Japan

⁴ MIT, Cambridge, USA

⁵ Moscow State University, Moscow, Russia

goto@ee.tut.ac.jp

Spin wave circuits attract many interests because of its low loss and fruitful wave functionalities. To develop such circuits, yttrium iron garnets (YIG) are widely used because of its low loss, i.e. low damping factor. In addition, a forward volume spin wave is a suitable mode due to its in-plane magnetization uniformity, but the control of this spin wave has been difficult because of the large reflection noise at the boundaries of YIG waveguides. In our previous reports [1,2], the suppression of the reflection of the forward volume spin wave was demonstrated using attenuators comprising gold thin film deposited at the edge of the YIG waveguide. These attenuators for spin waves increased the robustness of the spin wave interference to surrounding noises, e.g. temperature fluctuations. Hence, in this paper, we introduced this attenuation technique into a four terminal logic gate. Fig. 1 shows the top view of our device comprising the Ψ shaped 10 μm thick YIG waveguide placed onto the four microstrip lines. The four YIG terminal's edge were covered by 10 nm thick gold layers. The position of the gold area and the width the YIG waveguide were optimized based on electromagnetic analysis using magnetostatic approximation. At the frequency of 4 GHz, the spin wave interference was demonstrated. Magnetic field of 3095 Oe was applied perpendicular to the waveguide. Due to high robustness, two types of logic gate of AND and OR based on the phase of spin waves were demonstrated. The connecting loss and bending loss of the spin waves at the junction area and its solutions will be discussed.

This work was supported in part by the KAKENHI NO. 26706009, 26220902, and JST PRESTO JPMJPR1524. We acknowledge the works of Dr. Naoki Kanazawa.

[1] N. Kanazawa, T. Goto, K. Sekiguchi, A. B. Granovsky, C. A. Ross, H. Takagi, Y. Nakamura, and M. Inoue, *Sci. Rep.*, **6** (2016) 30268.

[2] N. Kanazawa, T. Goto, K. Sekiguchi, A. B. Granovsky, H. Takagi, Y. Nakamura, and M. Inoue, *AIP Advances*, **6** (2016) 095204.

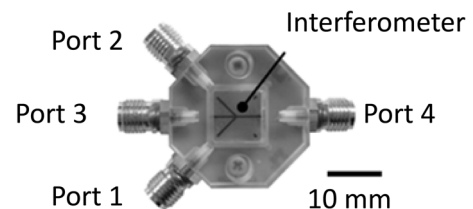


Fig. 1. Overview of the fabricated spin wave interferometer based on 10 μm thick YIG.

3OR-E-10

EXCITATION AND PROPAGATION OF SPIN WAVE PULSES IN A MAGNONIC CRYSTAL

*Ordóñez-Romero C.L.¹, Lazcano-Ortiz Z.¹, Pirruccio G.¹, Viguera-Zúñiga M.O.², Drozdovskii A.²,
Kalinikos B.², Qureshi N.³, Kolokoltsev O.³, Monsivais G.¹*

¹ Instituto de Física, Universidad Nacional Autónoma de México, México, México

² Facultad de Ingeniería, Universidad Veracruzana, Veracruz, México

³ St. Petersburg Electrotechnical University, 197376 St. Petersburg, Russia

⁴ Centro de Ciencias Aplicadas y Desarrollo Tecnológico, UNAM, México, México
cloro@fisica.unam.mx

Magnonic crystals (MCs) have recently demonstrated an outstanding capability to connect fundamental physics with applications at microwave frequencies [1]. Their characteristics have inspired multiple studies where detailed results on the behavior of the frequency-amplitude characteristic as a function of different structural parameters have been demonstrated [2]. However, up to now, all the scientific reports deal exclusively with the resulting spin wave spectrum for the complete MC structure and little has been said about the behavior of the spin wave inside the magnonic crystal. Here, we present a detailed study of the propagation of surface spin waves (MSSW) through a MC, the influence of the pulsed spin wave excitation in the formation and the evolution of frequency bandgaps inside the MC, and the spatial energy distribution as a function of frequency and position. A time and space resolved magneto inductive probing system has been used to map the spin wave propagation in a geometrically structured yttrium iron garnet (YIG) film. The results show that the formation of the bandgaps in the transmitted spin wave spectrum depends not only on the MC structure but also on the duration of the propagating pulse.

This work has been supported by UNAM-DGAPA grant 1N103915.

[1] K. W. Reed, J. M. Owens, and R. L. Carter, *Circuits Syst. Signal Process*, **4** (1985) 157.

[2] A. V. Chumak, A. A. Serga, S. Wolff, B. Hillebrands, and M. P. Kostylev, *J. Appl. Phys.*, **105** (2009) 083906.

3OR-E-11

GENERAL THEORY OF SPIN WAVE PROPAGATION IN CHAINS OF DISCRETE MAGNETIC ELEMENTS

Osokin S.A.^{1,2}, Barabanenkov Y.N.¹, Kalyabin D.V.^{1,2}, Nikitov S.A.^{1,2,3}

¹ Kotel'nikov Institute of Radioengineering and Electronics RAS, Moscow, Russia

² Moscow Institute of Physics and Technology, Dolgoprudny, Russia

³ Laboratory "Metamaterials," Saratov State University, Saratov, Russia

osokinserg@gmail.com

A general theory of the spin wave multiple scattering by a finite 2D ensemble of cylindrical magnetic inclusions in a ferromagnetic film (matrix) is developed. It is predicted that bound spin wave modes are excited around these inclusions. The set of self-consistent equations for spin wave multiple scattering inside the matrix with inclusions is obtained by using an invariant addition theorem for the cylindrical wave functions. We derive simple expressions for eigenmodes (bound modes) in a form of Bloch-like spin waves propagating along the inclusion circular array. The theory is illustrated on practically significant examples: (i) the bound mode excitation by a propagating spin wave, (ii) helix components of the spin wave scattered field around magnetic inclusions, (iii) high quality spin wave resonator based on a small number of magnetic inclusions. We also developed the quantum mechanical type T-scattering operator approach to study the spin wave multiple scattering by a finite ensemble of cylindrical magnetic inclusions in a ferromagnetic film (matrix) metallized from both sides. The approach is applied to the problem of spin wave excitation transfer along linear chain of inclusions. A substantial result consists in deriving an optical theorem for the T-scattering operator and as a consequence deriving a new formula for the collective extinction cross-section of inclusion ensemble, with only the first inclusion of the chain being irradiated by incident narrow spin wave beam. This formula shows that only the directly irradiated inclusion makes contribution in collective extinction cross-section despite the total number of inclusions can be big, that makes the direct summing contribution of all another inclusions in spin wave scattering as were unseen (dark mode). We revealed a regime of distant resonant transfer for the spin wave excitation along a linear chain of big enough but finite inclusions number with dark mode. The revealed regime shows that linear chain of magnetic inclusions at resonant conditions can play a role of a spin wave micro waveguide which transfers distantly an excitation in a form of above mentioned dark mode.

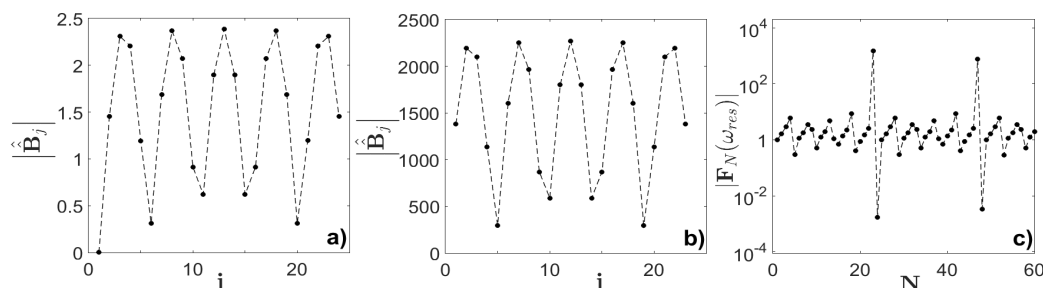


Figure 1. The behavior of scattering amplitudes of inclusions depending on inclusion number j for different number of inclusions $N=24$ (a), $N=23$ (b) and collective extinction factor (c) of a linear chain under condition of dark mode filtering from radiation losses.

[1] Barabanenkov Yu., Osokin S., Kalyabin D., Nikitov S., *Phys. Rev.*, **B 91** (2015) 214419.

[2] Barabanenkov Yu., Osokin S., Kalyabin D., Nikitov S., *Phys. Rev.*, **B 94** (2016) 184409.

3OR-E-12

EXCITATION OF EXCHANGE MAGNONS IN FERROMAGNETIC FILMS BY PICOSECOND ACOUSTIC PULSES

*Alekhin A.¹, Golov A.V.², Vlasov V.S.², Besse V.¹, Melnikov A.³, Makarov D.⁴,
Kotov L.N.², Temnov V.V.¹*

¹ Institut des Molécules et Matériaux du Mans (IMMM CNRS 6283), Le Mans, France

² Syktyvkar State University named after Pitirim Sorokin, Syktyvkar, Russia

³ Martin-Luther-Universität Halle-Wittenberg, Halle, Germany

⁴ Institute of Ion Beam Physics & Materials Research, Dresden, Germany
antogolov@mail.ru

We report the experimental and theoretical results on the excitation of exchange magnons in single ferromagnetic films by laser-induced acoustic pulses. In the theoretical calculations, we use simple model based on the system of ordinary differential equations to describe the excitation of spin waves modes. In order to predict optimum condition for the excitation of ultrashort pulses of exchange magnons, we investigate how sequences of acoustic pulses with different duration and periodicity influence the magnetization dynamics.

In optical pump-probe experiments a permanent magnet is used to tilt the magnetization out of the sample plane. The constant effective magnetic field consisting of the external magnetic field, the field of the magnetocrystalline anisotropy, the demagnetizing field and the exchange field is perturbed by the time-dependent magneto-elastic field propagating at the speed of sound. In the experiment, optical pumping results in the excitation of unipolar or bipolar acoustic pulses which propagate across the sample and drive the precessional motion of the magnetization. In addition to that, laser-induced heating alters the direction of the effective magnetic fields thereby inducing spin waves propagating away from the excited region.

Magnetization dynamics was monitored by the magneto-optical Kerr effect in femtosecond time-resolved pump-probe experiments performed on different ferromagnetic films (Fe, Co, Ni and permalloy). Keeping in mind the possibility to generate trains of acoustic pulses periodic by sequences of fs-pump pulses we have performed theoretical calculations for the acoustically induced magnetization dynamics. Excitation of the homogeneous precession (FMR mode) and standing exchange magnons was calculated within the framework of a theoretical model using Landau-Lifshitz-Gilbert (LLG) equation, free boundary conditions for the magnetization and the equations for the propagated elastic strains pulses. Since the influence of the magnetocrystalline anisotropy is expected to be small in polycrystalline films, we neglected it in our calculations. Neglecting the coupling between exchange magnons, we were able to solve LLG equations separately for each mode. We performed simulations for unipolar and bipolar acoustic pulses, analyzed the spectra of acoustic and magnonic excitations and compared them with experimental results obtained with single acoustic pulses. Experiments with sequences of acoustic pulses are underway.

We gratefully acknowledge the financial support from RFBR (grants # 17-57-150001, # 17-02-01138), PRC CNRS-RFBR “Acousto-magneto-plasmonics” and Strategie Internationale NNN-Telecom de la Region Pays de la Loire.

3OR-E-13

MAGNETOSTATIC SPIN WAVES IN IRREGULAR NARROW FERROMAGNETIC WAVEGUIDES

Kalyabin D.^{1,2}, Beginin E.², Sharaevskii E.³, Sadovnikov A.^{1,3}, Nikitov S.^{1,2,3}

¹ Kotelnikov Institute of Radio Engineering and Electronics, Russian Academy of Sciences, ul. Mokhovaya 11-7, 125009 Moscow, Russian Federation

² Moscow Institute of Physics and Technology (State University), Institutskii per. 9, 141700 Dolgoprudnyi, Moscow region, Russian Federation

³ Chernyshevskii Saratov State University, ul. Astrakhanskaya 83, 410012 Saratov, Russian Federation
dmitry.kalyabin@phystech.edu

Recent results in magnonics demonstrate the possibility of developing magnonic logic circuits – promising counterpart to conventional electron-based logic circuits. The use of magnons instead of electrons provide several advantages (low losses, tunability). Current prototypes of magnonic logic gates are represented by joint of spin wave (SW) interferometers. The interferometers themselves and the connections between them are made of narrow magnetic waveguides. However at the moment there is no rigorous theory describing propagation of SW in such structures especially on nanoscale where the confinement effects reveals.

The aim of the current work is to study magnetostatic surface spin wave propagation (MSSW) in a ferromagnetic films of varied width. We have investigated dynamics of MSSW propagation in such waveguides by theoretical and experimental technique. These waveguides were fabricated from YIG film by laser cutting. Frequency transmission coefficients and spatio-temporal dynamics were measured by Brillouin light scattering technique (BLS). The superposition of different spatial MSSW modes was detected. It was in particular found that magnetization distribution in an irregular waveguide was due to MSSW modes superposition with the specific beating. We have also developed a theoretical method for describing spin wave propagation in such structures based on approach of irregular waveguides. As a result the energy re-distribution between various modes were obtained. Furthermore with specific material and geometrical parameters, external field and excitation frequencies energy re-distribution between modes can lead to dominance of different spatial modes in output signal. It is also important to note that focusing in such the irregular waveguide can compensate losses and even overcome nonlinear threshold. These facts emphasizes the importance of multi-mode approach to irregular narrow waveguides.

The work is supported by Russian Science Foundation (Grant # 14-19-00760), Russian Foundation for Basic Research (Grants # 15-07-08152 A, 16-37-00507 mol_a)

3 July

Monday

14:30-17:15

oral session

3TL-P

3OR-P

3RP-P

**“Magnetic Shape
Memory and
Magnetocaloric Effect”**

3TL-P-8

MAGNETIC STATES OF Ni_2MnX AND Ni_2CrZ ($Z=\text{Ga, Sn, Sb, Ge, In, Si, Al, As, P}$) HEUSLER ALLOYS

Buchelnikov V.D.¹, Zagrebin M.A.¹, Sokolovskiy V.V.¹

¹ Chelyabinsk State University, Chelyabinsk, Russia

buche@csu.ru

The physical effects such as magnetically and thermally induced shape memory effect, large magnetoresistance and giant magnetocaloric effect are promise properties of magnetic Heusler alloys [1]. Ones of the most studied and well-known Heusler alloys are Ni-based materials. The most known from these alloys is Ni_2MnGa . It is ferromagnetic in austenite and martensite states. In the last years it was shown that the properties of ternary Heusler alloys can be enhanced by addition of fourth or fifth element such as Cr, Co, and etc [2]. For optimization, for example, the magnetocaloric effect it was supposed to add to Heusler alloys the chromium atoms. The ab initio and Monte Carlo calculations are shown that the addition of chromium atoms leads in result to large jump of magnetization at magnetostructural transition [2]. It is interesting to investigate how influence Cr atoms on magnetic states in parent ternary Heusler alloys.

In this work we study the magnetic states of ternary Ni_2CrZ ($Z = \text{Ga, Sn, Sb, Ge, In, Si, Al, As, P}$) Heusler alloys in comparison with Ni_2MnZ ones by ab initio methods. For calculation of properties of alloys we used the VASP package [3, 4] and the supercell from 16 atoms.

It was shown that the magnetic order in austenite ($L2_1$ phase) of Ni_2CrZ alloy with $Z = \text{Ga, Sn, Ge, In, Si}$ is fully antiferromagnetic but with $Z = \text{Sb, Al, As, P}$ magnetic order is ferromagnetic. In contrary in all Ni_2MnZ alloys the magnetic order is ferromagnetic except Ni_2MnAl one. It is known that in last alloy the antiferromagnetic or helical magnetic order in B2 phase exists [5]. But we think that in slow-cooling sample we will have ferromagnetic order in $L2_1$ phase (Fig. 1). From Fig. 1 it is seen that ferromagnetic $L2_1$ phase has lower energy. In contrary, for Ni_2CrAl our calculations are shown that in $L2_1$ phase and B2 one the ferromagnetic state is realized.

Thus, in the Ni_2CrZ Heusler alloys with $Z = \text{Ga, Sn, Ge, In, Si}$ the atoms of Cr ordered antiferromagnetically. This properties can be used for optimization of magnetocaloric effects in complex Heusler alloys which contains forth and fifth elements, for example, in Ni-Co-Mn-Cr-(In, Sn) alloys.

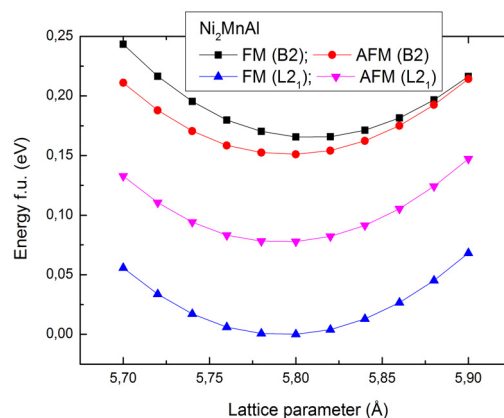


Fig. 1. Dependence of the energy of Ni_2MnAl alloy from the lattice parameter.

Support by RSF 14-12-00570 is acknowledged.

- [1] V.D. Buchelnikov and V.V. Sokolovskiy, 2011 *Phys. Met. Metallogr.*, **112** (2011) 633.
- [2] V.V. Sokolovskiy et al, *Phys. Rev. B*, **91** (2015) 220409(R).
- [3] G. Kresse and J. Furthmuller, *Phys. Rev. B*, **54** (1996) 11 169.
- [4] G. Kresse and D. Joubert, *Phys. Rev. B*, **59** (1999) 1758.
- [5] K.R.A. Ziebeck and P.J. Webster, *J. Phys. F: Metal. Phys.*, **5** (1975) 1756.

3RP-P-9

MAGNETOCALORIC EFFECT IN FERROMAGNET/PARAMAGNET MULTILAYER STRUCTURES

Skorohodov E.V.¹, Vdovichev S.N.¹, Shershevskii I.A.¹, Fraerman A.A.¹, Demidov E.S.², Chang J.³

¹ Institute for physics of microstructures RAS, N.Novgorod, Russia

² Nizhny Novgorod State University, N.Novgorod, Russia

³ Korea Institute of Science and Technology, Seoul, Korea

andr@ipmras.ru

In recent years, multilayers consisting of hard and soft magnetic layers have attracted a great deal of attention due to their potential applications in high density data storage media, permanent magnets, and microelectromechanical systems. We have recently proposed to use a multilayered structure based on exchange coupled soft/hard ferromagnetic layers separated by a paramagnetic layer for magnetocaloric applications [1]. The central point of this idea is to control the distribution of magnetization and the entropy in the paramagnetic interlayer by changing the mutual orientation of the magnetizations in the soft ferromagnetic layer by a weak external magnetic field. In fact, exchange interaction at the interface of paramagnetic and soft ferromagnetic layers leads to a decrease of magnetization when the soft and the hard ferromagnetic layers are coupled antiparallel and, consequently, results in the increase in entropy of the system as compared to the case of parallel orientation. Thus, the switching between states with different entropy could be achieved by switching the direction of magnetization in the soft ferromagnetic layer. Our estimation indicates that it would be possible to overpass a limit of magnetocaloric cooling efficiency of $dT/dH > 20$ deg / Tesla in such hard ferromagnet / paramagnet / soft ferromagnet multilayer [1]. By analogy with the giant magnetoresistance effect, this effect can be called giant magnetocaloric effect. The devices based on this effect can find many applications in electronics, e.g. as thin-film coolers. In addition, the established regularities in behavior of multilayer ferromagnet / paramagnet structures can be useful for description of three-dimensional magneto-heterogeneous materials (magnetic clusters in a paramagnetic matrix). We investigated the temperature dependence of the interlayer interaction in ferromagnet / paramagnet multilayer structures by the ferromagnetic resonance method [2]. Also, the SQUID-magnetometer data was obtained and shown on Figure. These measurements make possible to estimate (volume of the sample $\sim 3 \times 10^{-7}$ cm³, heat capacity $\sim 3,6 \times 10^7$ erg/deg*cm³) the effectiveness of magnetic cooling $dT/dH = 3$ deg/Tesla, which equal to the cooling efficiency for gadolinium.

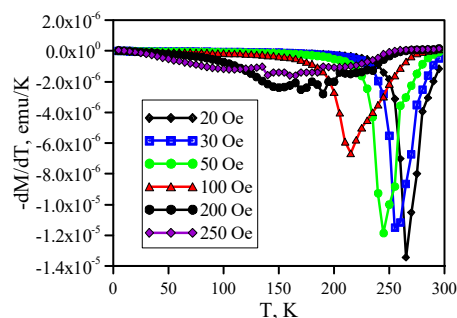


Fig. The dependence of the magnetic moment derivation dM/dT (emu/grad) on the temperature at different values of the external magnetic field for multilayer IrMn (10nm) / CoFe (4nm) / Ni₆₅Cu₃₅ (7nm) / NiFe (11nm)

Support by RFBR (Grant #17-02-00620) is acknowledged.

[1] A. A. Fraerman, I. A. Shereshevskii, *JETP Letters*, **101** (2015) 618.

[2] E.V.Skorohodov, E.S.Demidov, S.N.Vdovichev, A.A. Fraerman, *JETP*, **151**(4) (2017) 724.

3OR-P-10

VISUALIZATION OF MAGNETOSTRUCTURAL TRANSITION IN HEUSLER ALLOYS BY MAGNETIC FORCE MICROSCOPY

Geydt P.¹, Rodionov I.D.², Granovsky A.B.², Lähderanta E.¹

¹ School of Engineering Science, Lappeenranta University of Technology, Lappeenranta, Finland

² Faculty of Physics, Lomonosov Moscow State University, Moscow, Russia

Pavel.Geydt@lut.fi

Ni-Mn-In-based Heusler alloys are promising magnetocaloric and magnetic shape memory materials due to possessing magnetostructural phase transition around room temperature. In spite of numerous studies, the microscopic mechanisms of magnetostructural transition between austenitic and martensitic phases, nucleation and transformation of different phases are far from being well understood. Characteristic temperatures of these transitions are typically evaluated from magnetization-temperature plots in SQUID magnetometry. However, these temperatures are valid solely for bulk material, which do not obligatory resembles the surface [1]. Detailed surface studies are routinely done by Atomic Force Microscopy; although, thorough Magnetic Force Microscopy (MFM) for Heuslers is not adequately reported yet. The stirring interest for surface is related not only with finding the temperature of phase transition T_{SURF} , but also in strive to understand fundamental mechanism of formation of certain magnetic phases. Practically, visualization and dynamics of phase change is likely to answer: which of the questionable mechanisms of phase transition occurs and reveal dimensions of magnetic domains.

We present our recent results on direct visualization of temperature-induced phase transition in $Ni_{48}Mn_{37}In_{13}Cr_2$ Heusler alloy. Registration of transition of magnetic phases on surface was done by MFM in external field ~ 190 Oe. Phase transition temperature appeared shifted by few degrees in comparison to determined by SQUID magnetization-temperature dependence. Magnetic areas with characteristic size about one micrometer were repeatably visible on 100 micron-sized scans.

Explanation for observed phenomenon can be that defects emerged and persisted in surface of samples after polishing. Defects were favorable to release their strained mechanical energy after additional slow heating. It caused easier phase transformation. Surface was expected to have a transition in lower inserted energies, i.e. lower temperatures [1]. Considering that, we could have observed exactly the "colder" phase transition on surface ($T_{BULK} - T_{SURF} > 5$ °C). Mostly, magnetic domains agglomerated in close proximity to deep trenches caused by polishing technique (polishing paste included rigid particles). Above the Curie temperature no MFM contrast was observed, although we might highlight that boundaries of magnetic areas shifted, when cooled sample was scanned again by MFM (Figure 1). Since these magnetic areas are assumed to represent martensitic or austenitic phases, then exactly structural transition was visualized for the first time by MFM. Support by EU project "Horizon2020-MSCA-RISE-691010 Hunter" is greatly acknowledged.

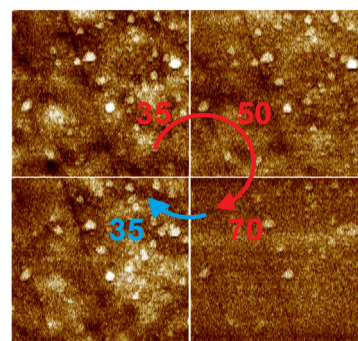


Fig. 1. $7 \times 7 \mu\text{m}^2$ MFM of NiMnInCr surface at (a) 35 °C, (b) 50 °C, (c) 70 °C and cooled down back to (d) 35 °C.

[1] K. Horáková et al., *J. Appl. Phys.*, **120** (2016) 113905.

3OR-P-11

INTENSIFICATION OF THERMAL FLUCTUATIONS OWING TO SPONTANIES TRANSITIONS BETWEEN CLOSED ENERGETIC LEVELS IN HEUSLER ALLOYS

Metlov L.S.^{1,2}, Koledov V.V.³, Shavrov V.G.³

¹ Donetsk Institute for Physics and Engineering (DIPE), Donetsk, Ukraine

² Donetsk National University (DNU), Donetsk, Ukraine

³ Kotelnikov Institute of Radioengineering and Electronics of RAS, Moscow, Russia
lsmet@donfti.ru

Magnetic materials with the shape memory effect (SME) present additional possibilities for control over SME phenomenon with help of magnetic fields. Large effect is especially arisen in a case of coinciding of temperatures for structural martensitic and magnetic transitions, which takes place for Haussler alloys with variable composition. For these alloys from the symmetry analyses the free energy as sum of structural, magnetic and mix contribution was derived [1].

For pure structural part of the problem the free energy has absolutely symmetric disposition of minimums about order parameters (OP) e_2 and e_3 into the critical point T_M of the structural phase transition (PT) (fig 1). The minimum 1 has a zero meaning OP e_2 , and minimums 2 and 3 have non-zero them meaning with opposite signs. Symmetry is obeyed in the critical point only, and below it the minimum 1 is deeper (fundamental), and over it the minimums 2 and 3 are fundamental. At cooling from the austenitic state a system can be go to potential well 2 or 3 (in this moment the potential well 1 is absent). At further cooling to lowest temperatures the potential barriers arrest the system in this state, even though the minimum 1 becomes fundamental. In consequence structural equivalence of minimums 2 and 3 the system forms the set of alternative regions divided by twin boundaries.

Deformation of the system in this state transfers the non-optimal oriented regions into the opposite state with twin boundaries dissipation. The heating of the material into austenite temperatures leads to restore its ideal structure, and as consequence the sample restores its original shape. The repeated cooling into martensitic state region renews twinning structure. Coincide of the critical temperatures of structural and magnetic PT leads to shift of pointed above special features for minimums of free energy that make prerequisites for governing on SME processes with help of a magnetic action. In moment of generation of minimums 2 and 3, when potential barrier between them is enough small, the spontaneous first order PT (jumps) between this minimums as in Ref. [2] initiated by thermal fluctuations are possible.

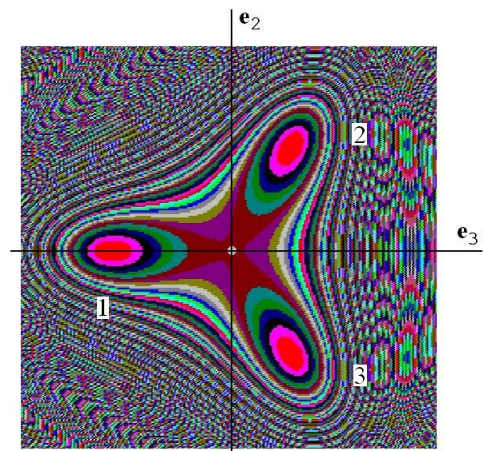


Fig. 1. Put the name and description of figure here.

[1] A.N. Vasil'ev, A.D. Bozhko, V.V. Khovailo, I.E. Dikshtein, V.G. Shavrov, V.D. Buchelnikov, M. Matsumoto, S. Suzuki, T. Takagi, J. Tani, *Phys. Rev. B.*, **59** (2) (1999) 1113-1120.

[2] L.S. Metlov e-print arXiv: cond-mat/1505.03727.

3OR-P-12

IN-SITU RESEARCH OF MARTENSITIC TRANSITION IN POLY- AND SINGLE CRYSTALS HEUSLER ALLOYS UNDER DIFFERENT THERMODYNAMIC CONDITIONS

Dilmeeva E.T.¹, Koshkid'ko Yu.S.², Koledov V.V.¹, Kamantsev A.P.¹, Shavrov V.G.¹, Khovaylo V.V.³

¹ Kotelnikov Institute of Radio Engineering and Electronics of RAS, Moscow, Russia

² International Laboratory of High Magnetic Fields and Low Temperatures, Wroclaw, Poland

³ National University of Science and Technology MISiS, Moscow, Russia

kelvit@mail.ru

In recent years the number of the works devoted to research and use of materials with magnetocaloric effect (MCE) is exponentially grows. At the moment, there are enough a large number of prototypes of refrigerating machines, but none of these systems can't compete with existing by traditional refrigerators based on freon yet. There is a row of basic difficulties of fundamental character on the way of broad use of solid-state magnetic materials with MCE. The basic problem is that the physics of the interaction of a solid body of subsystems in phase transformations in a rather strong magnetic field is poorly studied. In the case of a material with a phase transition and magnetostructural giant MCE (Heusler alloy) is not studied the interaction of martensitic domain walls separating the intermediate state with sharply different phase structure and magnetic properties.

At the moment works on study of martensitic domain structure in impulse magnetic fields are known [1]. But results of observations say that small time of pulse doesn't allow to come to the end completely to process of phase transition in materials. Therefore authors created new original device. Optical microscope allows fixing martensitic domain evolution under the influence of a magnetic field up to 14 T in a temperature range from 77K to 423K under different thermodynamic conditions. Besides, the developed device allows to define a sample temperature in variety point.

Heusler alloys samples which actual as a working body in refrigerators of new generation at the moment were selected. There are a polycrystalline $\text{Ni}_{2.16}\text{Mn}_{0.84}\text{Ga}$ and single crystal $\text{Ni}_{2.19}\text{Mn}_{0.81}\text{Ga}$. In present work the formation of the martensitic structure of the poly- and monocrystals Heusler alloy under the magnetic field up to 14 T in adiabatic and isothermal regimes was studied by using a specially developed optical microscope. Also phase diagram (T-H) of the martensitic phase transition for the Heusler alloy was constructed. It is shown that the dependence of the characteristic temperatures of a 1-st order phase transition on the magnetic field up to 14T has a linear form. The formation of a martensitic structure under isothermal and adiabatic conditions was studied. It is found that under adiabatic conditions a much larger magnetic field is required for a reversible phase transition than in isothermal. A qualitative model is proposed that explains the difference in the course of the magnetically induced phase transition of the 1-st order under different thermodynamic conditions. The difference of formation of domain structure at phase transition in poly-and single crystals is shown outlined.

Support by grant of the RFBR No. 16-32-00905 is acknowledged.

[1] T. Kihara, I.Katakura, M.Tokunaga, A.Matsuo, K.Kawaguchi, A.Kondo, K.Kindo, W.Ito, X. Xu, R.Kainuma. *J. Alloy Compd.*, **577** (2013) 722–S725.

3OR-P-13

APPLICATION OF INFRARED FIBER-OPTICAL TEMPERATURE SENSOR FOR MAGNETOCALORIC MEASUREMENTS IN PULSED MAGNETIC FIELDS

Kamantsev A.P.^{1,2,3}, *Koledov V.V.*^{1,2,3}, *Mashirov A.V.*^{1,2,3}, *Shavrov V.G.*¹, *Yen N.H.*², *Thanh P.T.*²,
*Quang V.M.*², *Dan N.H.*², *Los A.S.*³, *Gilewski A.*³, *Tereshina I.S.*^{3,4}, *Butvina L.N.*⁵

¹ Kotelnikov Institute of Radio-engineering and Electronics of RAS, Moscow, Russia

² Institute of Materials Science of VAST, Hanoi, Vietnam

³ International Laboratory of High Magnetic Fields and Low Temperatures, Wroclaw, Poland

⁴ Lomonosov Moscow State University, Moscow, Russia

⁵ Fiber Optics Research Center of RAS, Moscow, Russia

kama@cplire.ru

The problem of the rate of phase transitions (PT) requires immediate solution because it is crucial for the creation of the new technologies based on “giant” effects in the vicinity of PTs in solid state magnetic functional materials. For example, the magnetocaloric effect (MCE) reaches maximum near the PTs in magnetically ordered solids. The study of PT’s rate is necessary for creation of a new technology of magnetic refrigeration at room temperature with high cooling power of a solid state working body. The rate of PT limits the frequency of thermodynamic cycles. Accordingly, the power of refrigeration will depend on the frequency of cycles, and it is difficult to judge the competitiveness of this machine without determining the fundamental restrictions on the rate of PT in MCE materials. The comparative study of the kinetics of PTs of the prospective magnetic functional materials is very important for creation of the novel devices based on MCE.

We present a new technique for experimental study of kinetics of PTs and direct measurement of the MCE in pulsed magnetic fields by using the fast response temperature probe with infrared fiber optical (IRFO) sensor. As demonstration of the new technique, the results are presented of MCE measurements for Gd near Curie point: $\Delta T_{ad} = 21.3$ K under pulsed magnetic field $\mu_0 H = 12.7$ T (Fig. 1); and inverse MCE for $Fe_{48}Rh_{52}$ sample at initial temperature 305.1 K: $\Delta T_{ad} = -4.5$ K under pulsed magnetic field $\mu_0 H = 8.5$ T. Also, the energy losses on magnetization near the 1st order PT were calculated from the results of direct measurements of magnetization versus time for $Fe_{48}Rh_{52}$ sample: $W = 45$ J/kg [1].

The new system demonstrates the fast response (better than 1 ms) and higher noise immunity than existing systems based on micro-thermocouples and thin film thermoresistors.

Support by RFBR (grant № 17-58-540002) and VAST.HTQT.NGA.05/17-18 is acknowledged.

[1] A.P. Kamantsev, et al. *J. Magn. Magn. Mater.* (2017). DOI: 10.1016/j.jmmm.2016.12.063

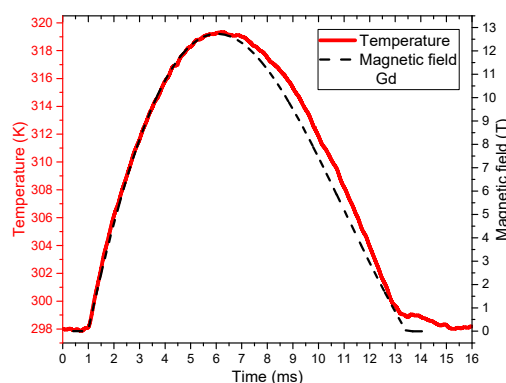


Fig. 1. Measurements of MCE by the IRFO temperature sensor on Gd sample.

3OR-P-14

CLAUSIUS–CLAPEYRON RELATION FOR THE FIRST ORDER PHASE TRANSITION IN NI-MN-IN(CO) HEUSLER ALLOYS

Mashirov A.V.¹, Kamantsev A.P.¹, Koshelev A.V.², Dilmieva E.T.¹, Los A.S.³, Koledov V.V.¹, Shavrov V.G.¹

¹ Kotelnikov Institute of Radio-engineering and Electronics of RAS, Moscow, Russia

² Lomonosov Moscow State University, Moscow, Russia

³ International Laboratory of High Magnetic Fields and Low Temperatures, Wroclaw, Poland
mashirov@cplire.ru

The Clausius–Clapeyron relation is used for describing the shift in the characteristic temperatures of the metamagnetostructural transition, as a special case of the first order phase transition (FOPT) [1]. Researchers apply this relation for thermodynamic treatment of not only the magnetostructural FOPTs, as well as for the martensitic transformation induced by external mechanical stress [2].

The thermodynamic model describing metamagnetostructural the FOPT on the basis of the expansion of the free energy of the austenite and martensite to second-order terms on magnetic field and temperature was proposed to explain the experimental data. The model explains qualitatively the following properties of the metamagneto-structural phase transition in the Ni-Mn-In Heusler alloys: a) decreasing of the phase transition temperature with increasing of magnetic field; b) broadening of the hysteresis loop with increasing of magnetic field; c) a faster shift of the left edge of the hysteresis loop compared to the right edge; d) the possibility of the existence of a critical point on the T-H diagram.

The proposed thermodynamic model for describing the points of stability loss of the FOPT in the second order of the free energy expansion from the magnetic field and temperature changes have qualitative and quantitative agreement with the results of experiments on Heusler alloy samples of Ni-Mn-In(Co) system (fig. 1).

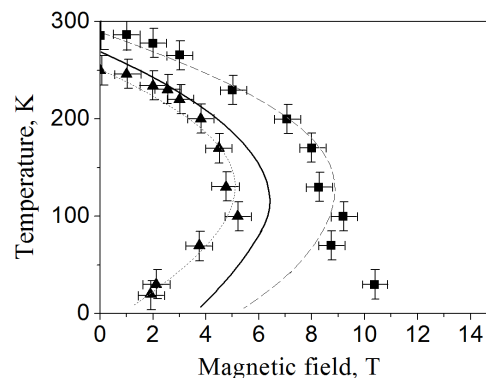


Fig. 1. The temperatures T_{bot} and T_{top} are experimental - triangular and square points, respectively; T_{bot} is calculated - dot line, T_{top} is calculated - dashed line; ΔT is calculated - solid line, depending on the magnetic field (all for the $\text{Ni}_{43}\text{Mn}_{37,65}\text{In}_{12,35}\text{Co}_7$ sample).

Support by Russian Science Foundation, grant No. 14-22-00279.

[1] W. Ito, Y. Imano, R. Kainuma, Y. Sutou, K. Oikawa, K. Ishida, *Metallurgical and Materials Transactions A*, **38A** (2007) 759–765.

[2] X. Xu, W. Ito, R. Umetsu, R. Kainuma, K. Ishida, *Applied Physics Letters*, **95** (2009) 181905.

3OR-P-15

MAGNETIC PROPERTIES OF NANOSTRUCTURED HEUSLER ALLOYS PREPARED BY PULSED LASER DEPOSITION

Checca N.R.¹, Rossi A.², Reis M.S.^{1,3}

¹ Physics Institute, Federal Fluminense University (UFF), Niterói-RJ, Brazil

² Brazilian Center for Research in Physics (CBPF), Rio de Janeiro-RJ, Brazil

³ Physics Department and I3N, Aveiro University, Aveiro, Portugal

marior@if.uff.br

Heusler alloys of the kind X_2YZ (where X and Y are *d* metals and Z is a *sp* metal) have attracted attention of the scientific community due to their notable physical properties, with potential applications on magnetoelectrical and caloric devices, solar cells and much other technologies. Special attention has also been given to the magnetic memory shape functionality, where the system can change its shape due to a variation of temperature and, specially, magnetic field. Within all these useful properties, one deserve special attention: half-metallicity, where the electrons on the conduction band have (almost) hundred percent of spin polarization; and it is due to a gap at the Fermi level on the 'down' sub-band, while the 'up' sub-band behaves like a metal. These half-metals are therefore hybrids in between metals and semi-conductors and can be used in spintronic devices.

In this direction, the present work focuses to produce (half-metal) Heusler alloys with some different number of valence electrons (Fe_2MnAl , Fe_2CrAl , Fe_2MnSi and some other compositions) by PLD technique; and, by this way, observe the influence of the nanostructure and nanomorphology on the physical and magnetic properties of these materials. The samples were produced by laser[1] ablation of the target under Argon atmosphere and then nanoparticles were deposited on a specific substrate.

For all of the produced materials, nanoparticle distribution size (nPDS) were measured by TEM and, due to the asymmetry of the distributions, a log-normal function was considered to be fitted to the data. A successful fitting returned the mean size of the nanoparticles, as well as the mode and standard deviation of the distributions. In what concerns morphology, these NPs present a core-shell structure, with a crystalline core and amorphous shell[2]. A high resolution TEM (HRTEM) was also measured, and we could observe the lattice fringes of the core and the interplanar distance for these materials.

As a consequence of these changes on the morphology, the magnetic properties of the NPs are in fact affected, being completely different from the bulk counterpart. For instance, the Fe_2MnSi system presents a higher Curie temperature in comparison to the bulk material; and a much more pronounced thermal irreversibility. Surprisingly, a Fast Fourier Transform (FFT) on some HRTEM images revealed that the cubic phase of the target changed to a hexagonal phase in these NPs (Fe_2MnSi). This fact is an additional reason for these change on the magnetic behavior of these NPs produced by PLD.

Other compositions without half-metallicity were produced and will also be presented, as, for instance, the Ni_2MnGa magnetic memory shape alloy.

[1] Nd:YAG, 1064 nm, 10 pulses/second, 200 mJ each pulse in 7 ns.

[2] N.R. Checca et al., *Materials Chemistry and Physics* (2017) in press.

3TL-P-16

DIRECT IN SITU STUDY OF MAGNETOCALORIC EFFECT IN HIGH MAGNETIC FIELDS UP TO 14 T

*Shavrov V.G.¹, Ćwik J.², Dilmieva E.T.^{1,2}, Kamantsev A.P.^{1,2}, Khovaylo V.V.³, Koledov V.V.^{1,2},
Koshkid'ko Yu.S.^{1,2}, Mashirov A.V.^{1,2}, Tereshina I.S.^{2,4}*

¹ Kotelnikov Institute of Radio-engineering and Electronics of RAS, Moscow, Russia

² International Laboratory of High Magnetic Fields and Low Temperatures, Wroclaw, Poland

³ National University of Science and Technology MISiS, Moscow, Russia

⁴ Lomonosov Moscow State University, Moscow, Russia

shavrov@cplire.ru

The study of the materials with high magnetocaloric effect (MCE) is of a great interest in view of perspectives of the development of the new solid state technology of magnetic refrigeration. In addition, study of MCE is very attractive for obtaining a new important information about fundamental aspects of magnetic phase transitions and subsystems interaction in magnetically ordered solids. Recently it was proved, that at the first order magnetic phase transition the MCE values measured by indirect methods can differ substantially from the values obtained by the direct method [1]. Therefore, study of MCE by reliable direct method is very actual.

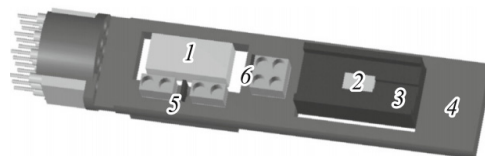


Fig. 1. A 3D model of the Bitter coil magnet insert: (1) sample of the MCE material under the adiabatic conditions, (2) sample of the MCE material under the quasi-isothermal conditions, (3) massive nonmagnetic block, (4) plastic frame holder, (5) “equatorial” and (6) “polar” Hall sensors.

We developed a special insert into the Bitter coil magnet, which made it possible to simultaneously measure the magnetocaloric effect of two samples of magnetic materials, one of which was under adiabatic conditions (ΔT), whereas the other sample was under quasi-isothermal conditions (q), as well as to measure the magnetization of the former sample as a function of the magnetic field. The measurements were performed in the magnetic fields up to 14 T. Fig. 1 shows a three-dimensional model of the insert into a Bitter coil magnet with the samples under investigation.

The insert is placed inside the vacuum chamber in the magnetic field of the Bitter coil magnet. The characteristic time of thermal relaxation of the samples inside the vacuum chamber is approximately 300 sec. A thermal sensor glued to sample (1) is a platinum resistance thermometer measuring a change of the temperature of the sample ΔT . Simultaneously, the magnetization of sample (1) is measured using two Hall sensors located near the “equator” (5) and the “pole” (6) of the sample in the direction perpendicular to the magnetic force lines. The difference between the readings of the two Hall sensors is the useful signal, which is proportional to the magnetization of the sample in the magnetic field [2]. The new vacuum calorimeter was used to simultaneously measure ΔT and q of MCE materials using Bitter coil magnet in the fields up to 14 T. Measurements were performed in $\text{Ni}_{2.18}\text{Mn}_{0.82}\text{Ga}$ Heusler alloy with merged martensitic transition and Curie point. The maximal values of MCE in $\mu_0 H = 14$ T were found to be $\Delta T = 8.4\text{K}$ at initial temperature 340 K and $q = 4,9$ kJ/kg at 343 K.

Support by Russian Science Foundation (project № 14-22-00279) is acknowledged.

[1] V.V. Khovaylo, K.P. Skokov, Yu.S. Koshkid'ko, et al. *Phys. Rev. B*, **78** (2008) 060403.

[2] E.T. Dilmieva, A.P. Kamantsev, V.V. Koledov, et al. *Phys. Solid State*, **58** (2016) 81–85.

3 July

Monday

12:00-14:00

poster session

3PO-I1

**“Spintronics and
Magnetotransport”**

3PO-I1-1

MAGNETORESISTIVE EFFECT IN $\text{Co}_x(\text{MgF}_2)_{100-x}$ OXYGEN-FREE NANOCOMPOSITES

Tregubova T.V.¹, Stognei O.V.¹, Kirpan V.V.¹, Sitnikov A.V.¹
¹Voronezh State Technical University, Voronezh, Russia
 ttv1507@ya.ru

Composite samples $\text{Co}_x(\text{MgF}_2)_{100-x}$ with an oxygen-free dielectric matrix were obtained by ion-beam sputtering of a gradient target. The composition of the obtained samples varies smoothly in a wide range of concentrations ($14 \leq \text{Co, at.\%} \leq 62$). Structure of composites (by x-ray diffraction), electrical (by two-probe potentiometry method) and magnetoresistive properties (in magnetic fields up to 10 kOe) have been investigated.

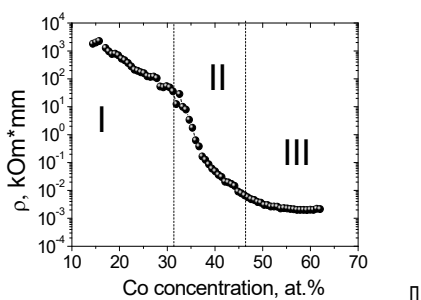


Fig.1. Concentration dependence of the electrical resistivity of $\text{Co}_x(\text{MgF}_2)_{100-x}$ composite samples

Fine-grained MgF_2 phase or nanosized grains of hexagonal cobalt are identified in the composites, located at the edges of the investigated concentration interval. In the middle part of the investigated interval a mixture of these two phases is observed.

Concentration dependence of the resistivity of the $\text{Co}_x(\text{MgF}_2)_{100-x}$ samples (fig. 1) is typical for metal-dielectric composite systems. The sharp decrease of the samples resistivity corresponding to the electrical percolation threshold is observed on the concentration dependence. Estimation of the concentration corresponding to the threshold gives a value of 36 at.% Co.

Negative isotropic tunnel magnetoresistance (MR) is observed in the $\text{Co}_x(\text{MgF}_2)_{100-x}$ composites with the maximum value reaching 7% near the percolation threshold (Fig. 2a). It is assumed that the high values of MR in this system are due to the large width of the bandgap of dielectric magnesium fluoride (12,3 eV) and also the low degree of defectiveness of the dielectric matrix.

In samples with a concentration close to the percolation threshold a positive magnetoresistance is observed in addition to the negative effect (Fig. 2b). Moreover, hysteresis of positive effect due to the formation of ferromagnetic clusters appears on the field dependences of MR with increasing of the cobalt concentration in the composite. The positive effect is related to the complicated morphology of the composites near the percolation threshold and is similar to the effect observed in Co-SiO_2 and $\text{Co-Al}_2\text{O}_3$ composite.

Thermal annealing, carried out in a vacuum at 180 °C, does not affect the magnetoresistive effect and the resistivity. With respect to higher temperature annealing, the granular structure exhibited extreme instability: annealing at 350 °C in a vacuum leads to a radical increase of the composite electrical resistivity, as well as to the disappearance of MR in samples close to the percolation threshold.

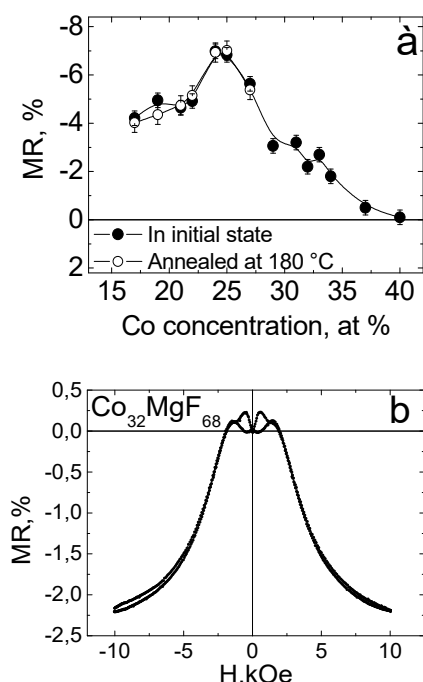


Fig. 2. Magnetoresistive effect of $\text{Co}_x(\text{MgF}_2)_{100-x}$ composites:
 a) concentration dependence;
 b) field dependence

3PO-I1-2

EFFECT OF MAGNETIC-FIELD-INDUCED TUNING OF DISORDER AND BAND STRUCTURE ON THE MAGNETORESISTANCE OF PARAMAGNETIC DILUTE MAGNETIC SEMICONDUCTORS

*Baranovskii S.D.*¹

¹ Department of Physics and Material Sciences Center, Philipps University, Renthof 5, 35032 Marburg, Germany
baranovs@staff.uni-marburg.d

We study theoretically the magnetotransport in p-type wide-gap dilute magnetic semiconductors in the paramagnetic phase. Two models, referred to as mobility model and network model, based on a minimal description of the valence-band structure and the acceptor state of the dilute magnetic semiconductors are discussed. The differences between the two models arise from a different model-specific weighting of disorder and occupation effects.

In both models, band filling effects, magnetic-field splitting of the band states due to the p-d exchange interaction, as well as effects of magnetic-field independent disorder are included whereas carrier—carrier interactions other than those responsible for the local magnetism of the Mn ions are neglected. Despite the exclusion of many-body effects in the bands, positive as well as negative magnetoresistance effects are predicted which show a qualitative agreement with recent experiments on p-type dilute magnetic semiconductors [1-4].

[1] C. Michel, M. T. Elm, B. Goldlücke, S. D. Baranovskii, P. Thomas, W. Heimbrodt, P. J. Klar, *Appl. Phys. Lett.*, **92** (2008) 223119.

[2] C. Michel, S. D. Baranovskii, P. Thomas, W. Heimbrodt, M. T. Elm, P. J. Klar, B. Goldlücke, J. *Appl. Phys.* **102** (2007). 073712.

[3] C. Michel, S.D. Baranovskii, P. Klar, S.D. P. Thomas, B. Goldlücke, *Appl. Phys. Lett.* **89** (2006) 112116.

[4] C. Michel, P. Klar, S.D. Baranovskii, P. Thomas, *Phys. Rev. B* **69** (2004). 165211.

3PO-I1-3

OUTPUT CHARACTERISTICS OF THE NETWORK OF SPIN-TORQUE OSCILLATORS

Safin A.R.^{1,2}, *Udalov N.N.*¹, *Bichurin M.I.*², *Petrov R.V.*², *Tatarenko A.S.*²

¹ National Research university "MPEI", Moscow, Russia

² Novgorod State University, Velikiy Novgorod, Russia
arsafin@gmail.com

Microwave spin transfer torque based self-oscillators, which are called "spin torque nanooscillators" (STNO), are very attractive for potential telecommunication RF-applications. They are highly tunable by bias current and magnetic field, they are the smallest oscillators (more than 50 times smaller than a standard CMOS-oscillators). They can be biased at low currents and voltages. The main drawback of STNOs is its very weak output microwave power (less than 1 μW for a simplest structures). This negative effect creates difficulties for the development of novel spintronic-based devices based on spin-transfer torque [1].

Magnetoresistance of the spin-torque oscillators can be enhanced by employing a ferroelectric material as the barrier layer. Multiferroic materials, which are characterized by two or more ferroic orders (ferroelectric, ferromagnetic, etc) have recently attracted significant interest [2]. Multiferroic tunnel junctions (MFTJ) exploit the possibility to control electron and spin tunnelling by ferromagnetic and ferroelectric polarizations of the sample. A MFTJ is type of magnetic tunnel junctions (MTJ) where a ferroelectric thin film realizes as tunnelling barrier.

A suggested solution of the power problem is to synchronize several STNOs [1,3] and to coherently summarize an output power from each oscillator. Mutual phase locking gives the way to coherent addition of microwave signals from partial nanocontacts to the single load. In this work the phase locking of the microwave oscillators of multilayered oscillators by electrical current, which consists of two nanosized ferromagnetic layers and separated by barrier layer mediated by dc-current, is considered. Our approach is based on the macrospin approximation and spin-wave analysis of the magnetization.

Summary the main result, that we can see in the Fig.1, that the output power of the network of parallel connected spin-torque oscillators is near tens of microwatts, which increases as a number of oscillators. For the impedance matching one need to use the high-Ohm transmission line, which transforms the load resistance (for example 50) onto high-Ohm output optimum resistance of the spin-torque oscillators.

The research was supported by a grant of Russian Science Foundation No.15-19-10036.

[1] A. Slavin, V. Tiberkevich, *IEEE Trans. on Magn.*, **45-4** (2009) 1875-1918.

[2] C. Nan, M. Bichurin, S. Dong, D. Viehland, G. Srinivasan, *J. Appl. Phys.*, **103** (2008) 031101.

[3] A.R. Safin, N.N. Udalov, M.V. Kapranov, *Eur. Phys. J. Appl. Phys.*, **67** (2014) 20601.

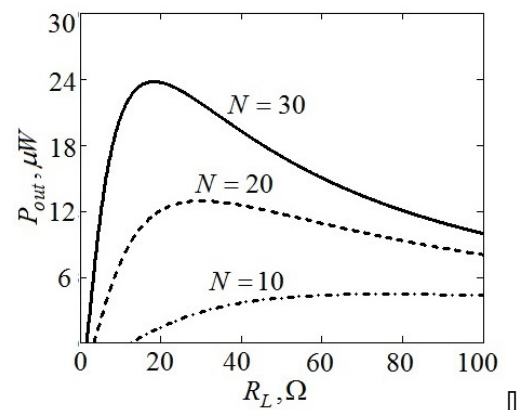


Fig. 1. The output power of the microwave oscillations generated by the network of phase-locked spin-torque oscillators for $N=10,20,30$.

3PO-I1-4

HIGH FIELD MAGNETORESISTANCE OF NANOCOMPOSITES (Co₈₄Nb₁₄Ta₂)_x(Al₂O₃)_{100-x} NEAR THE PERCOLATION THRESHOLD

*Blinov M.I.¹, Zakharchuk I.A.², Lähderanta E.², Sitnikov A.V.³, Prudnikova M.V.¹, Prudnikov V.N.¹,
Rylkov V.V.^{4,5}, Granovsky A.B.^{1,5}*

¹ Faculty of Physics, Lomonosov Moscow State University, 119991 Moscow, Russia

² Lappeenranta University of Technology, 53851 Lappeenranta, Finland

³ Voronezh State Technical University, 394026 Voronezh, Russia

⁴ National Research Centre "Kurchatov Institute", 123182 Moscow, Russia

⁵ Institute of Applied and Theoretical Electrodynamics RAS, 127412 Moscow, Russia

mi.blinov@physics.msu.ru

We present results of experimental studies of structural and magnetic properties, resistivity and magnetoresistance (MR) of (Co₈₄Nb₁₄Ta₂)_x(Al₂O₃)_{100-x} films deposited onto a glass ceramic substrate by the ion-beam sputtering, focusing on MR in high magnetic fields for compositions close to the percolation threshold ($x=47-57$ at.%). The samples consist of Co-Nb-Ta metallic nanogranules with the size 2-5 nm embedded into the non-stoichiometric Al-O matrix. Magnetization was measured by SQUID magnetometer at 4.2-300 K. MR was studied in the pulsed magnetic fields H up to 30 T at 50-300 K in three geometries: magnetic field in plane parallel and perpendicular to current, magnetic field perpendicular to plane. The pulse duration was 11-12 ms.

For the sample with $x=57$ at.% the temperature dependence of conductivity follows the $\ln T$ behavior that matches a strong tunnel coupling between nanogranules [1]. With decreasing metal volume fraction $\ln T$ behavior gradually changes to the $T^{1/2}$ dependence at 47 at.%. For all samples MR is small (<1%), negative and saturates with increasing magnetic field similar to the data reported for Ni_x(SiO₂)_{100-x} [2] and is connected with spin-dependent tunneling. Fig.1 shows the example of such behavior. The positive contribution expected for hopping conductivity or Lorentz term for metallic entities was not found even at $H=20-30$ T. We observed a weak anisotropy of MR at $H<1.0$ T due to planar Hall effect [3] or anisotropic tunnel MR recently considered by Vedyayev et al [4]. Accordingly to structural and magnetic data a large amount of metallic atoms are located between magnetic nanogranules diminishing the tunnel barrier height and making tunnel MR small and weakly dependent on temperature.

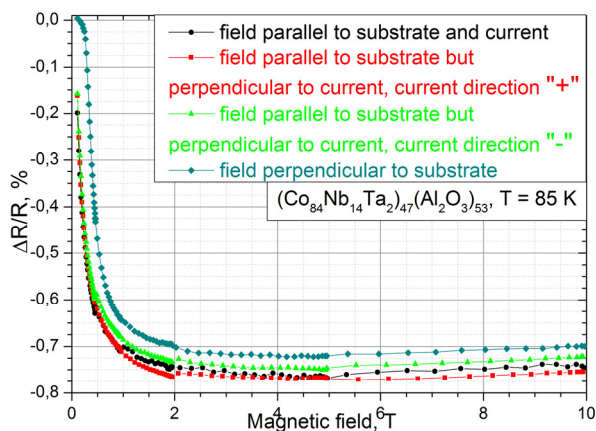


Fig. 1 Field dependence of MR for (Co₈₄Nb₁₄Ta₂)₄₇(Al₂O₃)₅₃

This work was financially supported by Russian Science Foundation, grant No. 16-19-10233.

[1] I.S.Beloborodov, A.V.Lopatin, V.M.Vinokur et al., *Rev. Mod. Phys.*, **79** (2007) 469-518.

[2] A. Milner, A. Gerber, B. Groisman et al., *Phys. Rev. Lett.*, **76** (1996) 475-478.

[3] B.A.Aronzon, A.B.Granovskii, A.B.Davydov et al., *J.Exp.Theor.Phys.*, **103** (2006)110-114.

[4] A. Vedyayev, N. Ryzhanova, N. Strelkov et al., *Phys.Rev. B*, **95** (2017) 064420.

3PO-I1-5

MAGNETIC PROPERTIES OF THE NATURAL AND ISOTOPE-MODIFIED DIAMOND AND SILICON CARBIDE

*Taldenkov A.N.¹, Inyushkin A.V.¹, Chistotina E.A.¹, Ralchenko V.G.²,
Bolshakov A.P.², Mokhov E.N.³*

¹ NRC “Kurchatov Institute”, Moscow, Russia

² A.M. Prokhorov General Physics Institute RAS, Moscow, Russia

³ Ioffe Physico-Technical Institute RAS, St. Petersburg, Russia
box-n3@bk.ru

One of the trends in solid-state electronics is the increasing research activity in the field of wide-gap semiconductors – silicon carbide and diamond. The transport of spin-polarized electrons attracts special attention of theorists and experimenters. The main channel for the relaxation of the electron spin is the scattering on nuclear magnetic moments of the odd isotopes ¹³C and ²⁹Si. This is why, the investigation of isotopically modified crystals is an urgent task.

Diamond is regarded as an ideal material for spin transport and promising "quantum computations". Due to the weak orbital interaction in comparison with other materials, a very long spin diffusion length is expected in it. In isotopically pure diamond, where the content of ¹³C atoms of the isotope is reduced, spin relaxation time may exceed 1ms at room temperature. Despite the great progress in the production of synthetic diamonds, their magnetic properties remain practically unstudied. Nothing like a study of the magnetic properties of natural diamonds [1] was made for synthetic diamonds. Magnetic properties of synthetic diamonds with modified isotopic composition have been also not studied yet.

Investigation of the magnetic properties of SiC became very important after the detection of ferromagnetism in SiC crystals [2] induced by neutron irradiation, neon and xenon ions, protons, and also by doping with aluminium. The combination of ferromagnetism and isotopic modification in one crystal can be promising for the creation of effective spin transport.

We measured the magnetization M(H,T) of several single crystals of synthetic diamond and silicon carbide versus temperature 2K<T<300K and magnetic field H<7 T. We used samples of synthetic diamond grown by high pressure high-temperature process (HPHT) and CVD method. High-purity crystals of Element Six Corp. (USA), New Diamond Technology (Russia), and CVD crystals on a substrate of the company High Optical Technologies (Russia) were investigated. Also, unique diamond crystals with isotope contents of ¹³C of 99.96% and ¹²C of 99.96% obtained by the CVD method were studied. Several SiC crystals produced with various techniques including the crystal of ²⁸SiC with 99.993% of ²⁸Si were measured.

The obtained magnetization data were processed, and three main contributions were identified: diamagnetic, paramagnetic, and ferromagnetic. Traces of the ferromagnetic phase are observed in most of the samples. The temperature dependencies in permanent magnetic field M(T) were fitted with Curie-Weiss function. The low temperature field dependencies M(H) were computed with Brillouin function. The concentration of the paramagnetic centres and effective spin were evaluated. The diamagnetic contribution was calculated with linear approximation of M(H) at high temperature. The obtained results are discussed.

The work is supported by RFBR grants 16-07-00979 and 16-0701188, and the RSF grants 16-42-01098 and No. 14-12-01403.

[1] A. Sigamony, *Indian Acad. of Science, Proc.A*, **19** (1944) 310-314.

[2] Yutian Wang et al., *Scientific Reports*, **5** (2015) 8999.

3PO-I1-6

GIANT MAGNETORESISTANCE OF CoFe/Cu MULTILAYERS WITH THE $(\text{Ni}_{80}\text{Fe}_{20})_{60}\text{Cr}_{40}$ BUFFER LAYER

*Bannikova N.S.¹, Milyaev M.A.¹, Naumova L.I.¹, Krinitsina T.P.¹, Chernyshova T.A.¹,
Proglyado V.V.¹, Ustinov V.V.¹*

¹ M.N. Miheev Institute of Metal Physics UB RAS, S. Kovalevskoy St., 18, 620990 Yekaterinburg, Russian Federation
bannikova@imp.uran.ru

Magnetic metallic multilayers with giant magnetoresistive effect (GMR effect) are artificial nanomaterials and belong to the objects of metallic spintronics. Interest to study of these materials still remains because of two reasons. The first one is the possibility of a controlled change of the physical properties of the multilayer, which are interest to fundamental research. The second reason is the use of the obtained GMR nanostructures in magnetic sensory elements and devices of microelectronics and spintronics.

One of the actively used methods of optimizing the functional characteristics of multilayer is the choice of an effective buffer layer material to form the perfect crystal structure and texture in the subsequent grown layers [1]. In this regard, the problem of finding and using new buffer layers for known types of multilayers with a GMR effect is actual task.

Investigations of the microstructure, magnetoresistive characteristics and surface morphology of the $\text{Co}_{90}\text{Fe}_{10}/\text{Cu}$ multilayers were carried out. The samples were sputtered on glass substrates at room temperature by DC magnetron sputtering from targets of coincident compositions. The paramagnetic alloy $(\text{Ni}_{80}\text{Fe}_{20})_{60}\text{Cr}_{40}$ was used as the buffer layer. The studies of microstructure and texture of the samples were carried out by XRD ($\theta - 2\theta$ and ω - scans). The surface morphology was visualized using atomic force microscopy.

It is shown that the optimized multilayers $\text{Co}_{90}\text{Fe}_{10}/\text{Cu}$ exhibits the GMR effect of 54 % and 27 % with the copper thickness at the first and second antiferromagnetic maximum, respectively.

Hysteresis of the multilayer greatly enhances when the thickness of the NiFeCr buffer increases [1]. It was found that the Ta/NiFeCr composite buffer layer promotes the formation of a strong uniaxial $\langle 111 \rangle$ texture. As the result the hysteresis decreases more than 3 times (Fig. 1) and the magnetoresistive sensitivity increases [2].

Support by the state assignment of FASO of Russia (“Spin” No. 01201463330), RFBR (P. Nos. 16-32-00501, 16-02-00061) and Russian Ministry of Education and Science (Contract No. 14.Z50.31.0025).

[1] N. S. Bannikova, M. A. Milyaev, L. I. Naumova, V. V. Proglyado, T. P. Krinitsina, I. Y. Kamenskii, V. V. Ustinov, *Physics of Metals and Metallography*, **116** (2015) 987-992.

[2] N. S. Bannikova, M. A. Milyaev, L. I. Naumova, T. P. Krinitsina, E. I. Patrakov, V. V. Proglyado, V. V. Ustinov, *Physics of the Solid State*, **58** (2016) 2011-2017.

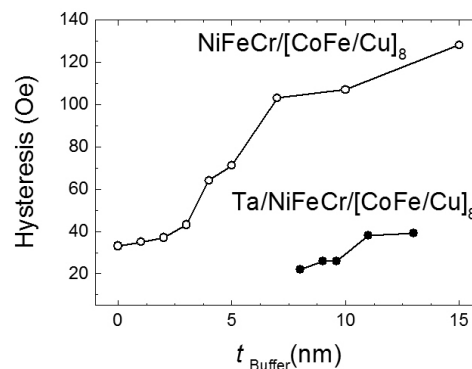


Fig. 1. Hysteresis of multilayers $[\text{Co}_{90}\text{Fe}_{10}(1.6 \text{ nm})/\text{Cu}(2.3 \text{ nm})]_8$ with buffer layers NiFeCr(t_{Buffer}) (white) and Ta(5 nm)/NiFeCr (black).

3PO-I1-7

MAGNETORESISTANCE IN InSb:Mn-InSb p-n JUNCTION AT ROOM TEMPERATURE

Mikhalevsky V.A.¹, Novodvorsky O.A.¹, Parshina L.S.¹, Khramova O.D.¹, Lotin A.A.¹, Cherebylo E.A.¹, Marenkin S.F.², Aronov A.N.², Kochura A.V.³, Aronzon B.A.⁴, Panchenko V.Ya.¹

¹ ILIT RAS – Branch of FSRC “Crystallography and Photonics” of RAS, Shatura, Russia

² Kurnakov Institute of the general and inorganic chemistry of the RAS, Moscow, Russia

³ South – West State University, Kursk, Russia

⁴ National Research Centre «Kurchatov Institute», Moscow, Russia

onov@mail.ru

The investigation of thin films of ferromagnetic semiconductors (AIII-BV): Mn is of great interest in connection with a possibility of their use in the magnetoelectronic and spintronic devices [1]. The diode structures p-(InSb + MnSb) / n-InSb were grown on the single-crystalline n-type InSb substrates from the InSb + MnSb targets using the PLD method. The I-V curves of the p-(96% InSb + 4% MnSb) / n-InSb structure have been investigated at room temperature under the magnetic field of 0.15 T both in the plane of the structure and perpendicular to it.

Figure 1 shows the I-V curves of such a diode structure at room temperature in the absence of the magnetic field and at different orientations of the magnetic field of 0.15 T both in the plane of the structure and perpendicular to it. In the structures p-(InSb:Mn)/n-InSb represented at the inset of Fig. 1 both the electrical contacts are located in the heterostructure plane. As seen from Fig. 1, when the direction of the field H is changed in the film plane, the I-V curves differ, which may be due to the difference in the magnetoresistance of the p-film (96% InSb + 4% MnSb) for different mutual orientations of the electric and magnetic fields. This can be seen from curves 2 and 3 in Fig. 1. The current decreased almost 9 times from 0.35 A to 0.04 A at the voltage of 1 V under the magnetic field of 0.15 T perpendicular to the plane of the diode structure. The results obtained show that in all cases of magnetic field application the phenomenon of giant magnetic resistance (GMR) is observed. The observed crossover of GMR is associated with spin-selective carrier scattering due to the p-d exchange interaction [1].

Thus, we have studied the spin-dependent properties of the p-InMnSb/n-InSb heterojunction where p-InMnSb is a magnetic semiconductor thin film grown by pulsed laser deposition. The measured I-V curves of the diode structure revealed that positive magnetoresistance is observed under direct bias and applying of a magnetic field at 298 K.

The work is supported by RFBR projects No. 15-07-03580, 15-29-01171, 16-29-05385, 16-07-00657, 16-07-00842, pr. of ONIT RAS (code IV.3.3) and Presidium RAS (Code I.III).

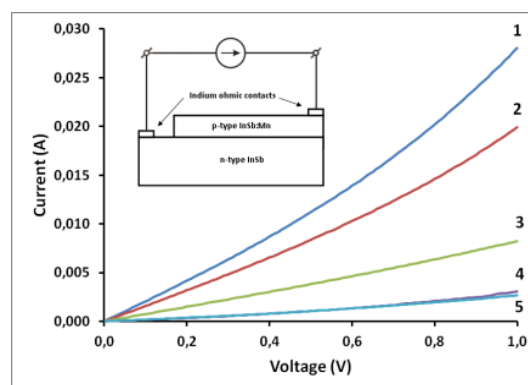


Fig. 1. . The I-V curves of the heterostructure p-(InSb:Mn)/n-InSb with $B = 0,15\text{T}$ (1 – $B = 0$; 2 - $B \uparrow \downarrow E$; 3 - $B \uparrow \uparrow E$) in the plane of the film and $B = 0,15\text{T}$ perpendicularly to the plane of the film 4 – $B (\uparrow)$; 5- $B (\downarrow)$; the inset presents the scheme of the heterostructure.

[1] J.A Peters, N. Rangaraju, C.Feesser, B. W. Wessels, *Appl. Phys. Lett.*, **98** (2010) 193506.

3PO-I1-8

INVESTIGATION OF InSb:Mn THIN FILMS MAGNETORESISTANCE BY I-V CHARACTERISTICS METHOD

Novodvorsky O.A.¹, Mikhalevsky V.A.¹, Parshina L.S.¹, Khramova O.D.¹, Lotin A.A.¹, Cherebylo E.A.¹, Marenkin S.F.², Aronov A.N.², Kochura A.V.³, Panchenko V.Ya.¹

¹ ILIT RAS – Branch of FSRC “Crystallography and Photonics” of RAS, Shatura, Russia

² Kurnakov Institute of the general and inorganic chemistry of the RAS, Moscow, Russia

³ South – West State University, Kursk, Russia

The thin InSb:Mn films were grown on sapphire (0001) substrates by ablation with an excimer KrF laser using the droplet-free pulsed laser deposition (PLD) method [1]. The InSb+MnSb composite alloy target contained up to 20% of MnSb. The investigation of the films with SEM showed the homogeneous distribution of the In, Sb and Mn elements in the surface layer of the film. According to the results of energy-dispersive X-ray spectroscopy, the content of these elements corresponded to the composition of the initial target. The results of the AFM analysis using a magnetic cantilever point to the presence of ferromagnetic clusters of the size of 4 nm. In this paper, we have for the first time investigated the magnetoresistive effect in the thin InSb:Mn films using the I-V curve method. The I-V curve was measured in the range from -10 V to +10 V in steps of 1 mV. The magnetoresistance MR (%) was determined on the basis of I-V curve in the temperature range from 10 K to 300 K using the formula $(R(H) - R(0)) / R(0) * 100\%$.

It was observed that the magnetoresistance of the sample depended on the applied voltage at magnetic field orientation with respect to the current direction at room temperature.

The temperature dependence of the magnetoresistance of p-InSb:Mn films with the MnSb content of 20% was studied in the temperature range from 10 K to 300 K.

The measurements of the I-V curves were performed in the field with permanent magnet and without it. The dependences of the magnetoresistance for a fixed temperature and magnetic field were calculated on the basis of the I-V curve. The results of calculations MR are shown in Fig. 1. Figure 1 shows that the crossover from positive to negative giant magnetoresistance (GMR) is observed at the temperature of 250 K during cooling. As the sample cooled down, the value of GMR increased and reached 800% at 15 K in the magnetic field of 0.15 T directed perpendicular to the plane of the film.

Thus, it has been shown that the magnetoresistance of the InSb:Mn thin films is registered even at room temperature under small magnetic fields, which opens up considerable prospects for using this material to create various spintronic devices.

The work is supported by RFBR projects No. 15-07-03580, 15-29-01171, 16-29-05385, 16-07-00657, 16-07-00842, pr. of ONIT RAS (code IV.3.3) and Presidium RAS (Code I.III).

[1] O. D. Khramova, V.A. Mikhalevsky, L. S. Parshina, O. A. Novodvorsky, S. F. Marenkin, A. A. Lotin, E. A. Cherebylo, B. A. Aronzon, A. N. Aronov, V. Ya. Panchenko, *Optical and Quantum Electronics*, **48**(7) (2016) 1-8.

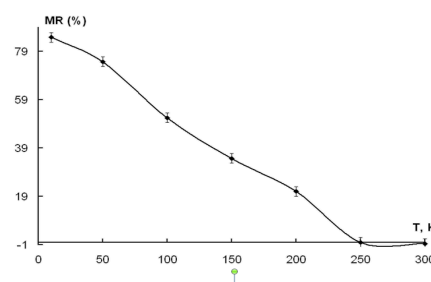


Fig. 1. The dependence of the thin InSb:Mn film magnetoresistance on the temperature at an applied voltage of 10V and under magnetic field of 0.15 T in the plane of the film.

3PO-I1-9

A STUDY OF THE STRUCTURE AND ENERGY OF THE 90° NEEL DOMAIN WALL BY THE NUMERICAL METHOD

Semenov V.S.¹

¹ V.A. Trapeznikov Institute of Control Sciences of Russian Academy of Sciences, Moscow, Russia
vsemsem@mail.ru

Various types of wall structures such as the Bloch wall, the Neel wall, the cross-tie and, lately, two-dimensional walls have been theoretically proposed and also experimentally verified for 180° wall in thin magnetic films. In contrast to the 180° walls, the 90° walls have rarely been studied. Though 90° walls were observed as frequently as 180° walls, no special fine structure has been studied. In present paper, the details of the 90° wall energy and structure have been investigated theoretically by numerical method.

Let us consider thin magnetic films having the thickness $2D$ and easy axis coinciding with z -axis of rectangular coordinate system. x -axis is in the film plane as well, y -axis being perpendicular to the film plane. 180° domain wall (DW) separates two contiguous regions (domains) of opposite magnetisation, so that the directions of wall and domain magnetisation coincide with z -axis. Magnetisation between the domains changes in the plane of the film, in accordance to classical Neel DW model.

With constant external magnetic field H_0 acting in film plane at an angle to easy axis in the positive x -axis direction, magnetization vector of domains changes its direction on the α -angle to easy axis. Equilibrium angle between magnetization vector and easy axis α is determined by the equation: $\sin \alpha = H_0 / H_K$, where $H_K = 2K / M_S$ - anisotropy field, K - anisotropy constant, M_S - saturation magnetization. When external magnetic field reaches the value of $H_0 = H_K \sqrt{2} / 2$, domain wall separates the domains with magnetization directions $\alpha_1 = \pi / 4 (= 45^\circ)$ for left domain and $\alpha_2 = 3\pi / 4 (= 135^\circ)$ for right domain. Magnetization vector of such DW turns on the angle $\alpha_2 - \alpha_1 = \pi / 2 (= 90^\circ)$. Changing magnetization vector in one-dimensional 90° Neel wall through its width $-R \leq x \leq R$ is presented by direction cosines $m_x(x)$ и $m_z(x)$ ($m_y = 0$) $\vec{M} = M_S \vec{m} = M_S (m_x(x)\vec{i} + m_z(x)\vec{k})$ with boundary conditions for direction cosines:

$$m_x(x = \mp R) = \sin \alpha, m_z(x = \mp R) = \pm \cos \alpha, dm_x(x = \mp R) / dx = dm_z(x = \mp R) / dx = 0.$$

We determine 90° wall structure from numerical solution of micromagnetic equation $\vec{m} \times \vec{H}_{eff} = 0$, the components of the effective field \vec{H}_{eff} being determined as derivatives of the whole domain wall energy relative to directing cosines.

The equilibrium state of the DW is determined by the minimum total energy (exchange, anisotropy, magnetostatic, and Zeeman energies). The structure 90° Neel domain walls is described a narrow central region (core) with a width being less than 100 nm and two lateral regions symmetrically located relative to the core, with a width on the order of the hundreds microns.

The calculations were carried out using a supercomputer with the CUDA architecture using the CUDA C programming language.

3PO-I1-10

SPIN POLARIZATION AND MAGNETIC ORDERING OF MAGNETICALLY DOPED TOPOLOGICAL INSULATORS AND MATERIALS WITH GIANT SO INTERACTION

Skirdkov P.N.^{1,2,3}, Zvezdin K.A.^{1,2,3}, Zvezdin A.K.^{1,2,3}, Shikin A.M.⁴, Rybkina A.A.⁴, Klimovskikh I.I.⁴

¹ Moscow Institute of Physics and Technology, 141700 Dolgoprudny, Russia

² Russian Quantum Center, 143025 Skolkovo, Moscow Region, Russia

³ A.M. Prokhorov General Physics Institute, RAS, 119991 Moscow, Russia

⁴ Saint Petersburg State University, 198504 Saint Petersburg, Russia

petr.skirdkov@phystech.edu

Materials with enhanced spin-orbit interaction, such as topological insulators or Rashba systems are of great interest in recent years, owing to a huge potential for novel electronics. Breaking of time reversal symmetry (TRS) in these systems doped by magnetic impurities is predicted to lead to exotic topological quantum effects. In magnetically-doped TIs, spin-orbit interaction is responsible for the Dirac cone-like topological surface states (TSSs) formation at the surface, while the magnetic field induced by magnetic impurities opens an energy gap at the Dirac point due to the TRS breaking and modifies the features of electronic and spins structure [1]. It was demonstrated that at temperatures lower than some critical one spontaneous surface magnetic ordering can appear in case of magnetically doped TI [2]. In systems with trivial topology, spin-orbit interaction at the surface leads to the Rashba splitting of the electronic states. The highest known value of the splitting of 2D electron gas (2DEG) states belongs to BiTeI [3].

We have studied influence of spin-orbit (SO) coupling on electronic structure, spin polarization and magnetic ordering in V-doped BiTeI depending on temperature. The opening of the energy gap and corresponding surface magnetic ordering below Curie temperature were theoretically predicted. The spin polarization, magnetization of dopants and Curie temperature were estimated. The magnetic ordering and energy gap opening by circularly polarized synchrotron radiation were also considered [4]. All the results were compared with experimental measurements done by means of angle- and spin-resolved photoemission spectroscopy carried out at low (15-20 K) and room temperatures with and without synchrotron radiation.

The possibility of the out-of-plane spin polarization of topological surface states induced in magnetically-doped topological insulator $\text{Bi}_{1.37}\text{V}_{0.03}\text{Sb}_{0.6}\text{Te}_2\text{Se}$ by circularly and linear polarized synchrotron radiation at room temperature was demonstrated by means of angle- and spin-resolved photoemission spectroscopy [5]. The qualitative analysis of this phenomenon was conducted. It has been shown that the induced out-of-plane polarization is created due to an “optically”-generated uncompensated spin accumulation with transferring the induced torque to the diluted V 3d ions. In case of the linear polarization the value of the effect is determined by the asymmetry of Dirac cone’s branches. The theoretical estimation of this effect based on experimental asymmetry value was proposed.

The grants RSF No.17-12-01333 and RFBR No. 16-02-00996 are acknowledged.

[1] Y.L. Chen et al., *Science*, **329** (2010) 659-662.

[2] G. Rosenberg and M. Franz, *Physical Review B*, **85** (2012) 195119.

[3] K. Ishizaka et al., *Nature Materials*, **10** (2011) 521–526.

[4] A.M. Shikin et al., *2D Materials*, **4** (2017) 025055.

[5] A.M. Shikin et al., *Applied Physics Letters*, **109** (2016) 222404.

3PO-I1-11

INTRINSIC SPIN HALL CONDUCTIVITY IN THREE-DIMENSIONAL TOPOLOGICAL INSULATOR/NORMAL INSULATOR HETEROSTRUCTURES

Men'shov V.N.^{1,2,3,4}, Shvets I.A.^{3,4}, Tugushev V.V.^{1,2,3}, Chulkov E.V.^{1,4,5}

¹ Donostia International Physics Center (DIPC), 20018 San Sebastián, Basque Country, Spain

² NRC Kurchatov Institute, 123182 Moscow, Russia

³ Tomsk State University, 634050 Tomsk, Russia

⁴ Saint Petersburg State University, 198504 Saint Petersburg, Russia

⁵ Departamento de Física de Materiales UPV/EHU, CFM - MPC UPV/EHU, 20080 San Sebastián/Donostia, Basque Country, Spain

shvets_ia@mail.ru

Here we study how interface and edge perturbations as well as a size effect can be used to manipulate the transport properties in semiconductor heterostructures where a thin film of three-dimensional topological insulator (TI) is sandwiched by normal insulator (NI) slabs. Within the framework of the NI/TI/NI trilayer model based on a continual scheme, we argue that characteristics of electron states in the TI film (energy spectrum, envelope function profile, the Berry curvature etc.) are controlled by the film thickness and TI/NI interface potential whose variation can lead to the modification of topological properties of the system. Calculating a spin Hall response for the NI/TI/NI trilayer infinite in the interface plane, we find that a series of quantum transitions between topological insulating phase and trivial band insulator phase can be induced by tuning both the film thickness and the interface potential. We draw the corresponding phase diagram of the NI/TI/NI trilayer in detail. To quantify the edge effect we formulate a minimal model of the half-infinite in the interface plane NI/TI/NI trilayer, which describes evanescent edge states and provides the necessary conditions under which they exist. It is found that the presence/absence of the in-gap edge states does not connect unambiguously with the interior topological index. Our findings provide a useful guide in choosing the relevant material parameters to facilitate the observation of quantum spin Hall effect in the TI/NI heterostructures.

3 July

Monday

12:00-14:00

poster session

3PO-J

3PO-I3

**“Magnetic Soft Matter
(magnetic polymers,
fluids and
suspensions)”**

3PO-J-1

SELF-ORGANIZATION OF COLLOIDAL HARD MAGNETIC HEXAFERRITE NANOPARTICLES

Eliseev Ar.A.¹, Trusov L.A.¹, Eliseev An.A.¹, Chumakov A.P.², Anokhin E.O.¹, Sleptsova A.E.¹, Kazin P.E.¹

¹ Lomonosov Moscow State University, Moscow, Russian

² ESRF, Grenoble, France

artem.a.eliseev@gmail.com

Magnetic liquids are commonly used in a large number of different technological areas, including magnetorheological fluids, preparation of thin films for magnetic recording media, magnetic seals and numerous biomedical applications. Commonly magnetic fluid consists of small superparamagnetic particles, stabilized either sterically or electrostatically. A number of scientific groups recently tried to obtain stable colloids based on hard-magnetic nanoparticles, which carry large intrinsic magnetic moments. The most successful results were obtained for ϵ -Fe₂O₃ [1], cobalt ferrite [2] and hexaferrite [3] nanoparticles. Such stable colloidal solutions except their unique magnetic properties also possessed a number of optical, piezoelectric and other effects. Due to presence of two counteracting forces: electrostatic or steric repulsion and magnetic attraction, colloid particles should self-organize into various nanostructures. However, in major part of recent papers the internal structures of such colloids were not investigated.

Therefore, the major aim of current work was the study of the externally induced structurization and self-organization of hard-magnetic nanoparticles of hexaferrite based colloids.

Hexaferrite based colloid solutions were prepared via glass-ceramic route reported in [3]. Briefly, nanoparticles were crystallized from quenched amorphous glass of overall composition 4Na₂O-9SrO-5.5Fe₂O₃-4.5Al₂O₃-4B₂O₃ by 2 hour annealing at 700°C. Particle extraction was performed by dissolution of borate matrix in 3% hydrochloric acid; obtained precipitate was then dispersed in distilled water with following colloid solution formation. According to TEM, the obtained colloid particles had platelet shape with mean size of 50 nm × 6 nm. Powder XRD and SAED proved the pure M-type hexaferrite phase of the particles. Magnetic measurements revealed 4 kOe coercive force and 38 emu/g saturation magnetization, while the colloidal solutions showed zero coercivity and saturation magnetization. The estimated concentration of the colloids was 130 mg/l. The SAXS experiment showed that no particular structure was presented in as-obtained colloids, but the magnetic field induced fast particle orientation. Also it was found that long time exposure causes the formation of the structured condensed phase. In that case the concentration of the solution becomes much higher (about 100 times). SAXS spectra showed the presence of thread-like dynamic aggregates with periodic interparticle distance about 20 nm, even in the absence of the external field. It was found, that variation of pH value by addition of base or acid to condensed phase leads to significant change in interparticle distance, particularly compression of thread structure up to few times. Such behavior offers the scope for future development magnetically controlled nanosized structures with easily tunable structure parameters.

This research was funded by Russian Foundation for Basic Research, grant No. 16-03-01052.

[1] S.-I. Ohkoshi, A. Namai, K. Imoto, M. Yoshikiyo, W. Tarora, K. Nakagawa, M. Komine, Y. Miyamoto, T. Nasu, S. Oka, H. Tokoro, *Sci. Rep.*, **5** (2015) 14414.

[2] M. Nabeel Rashin, J. Hemalatha, *Ultrasonics*, **54** (2014) 834–840.

[3] L.A. Trusov, A. V Vasiliev, M.R. Lukatskaya, D.D. Zaytsev, M. Jansen, P.E. Kazin, *Chem. Commun.*, **50** (2014) 14581–14584.

3PO-J-2

SOME CONTRIBUTIONS TO THE STUDY OF METALLIC NANOPARTICLES FOR APPLICATIONS IN LIFE SCIENCES

Creanga D.-E.¹, Andries M.¹, Puscasu E.¹, Popescu L.¹, Oprica L.², Sacarescu L.³, Grigoras M.⁴, Lupu N.⁴, Balasoiu M.^{5,6}

¹ Alexandru Ioan Cuza University, Physics Faculty, Iasi, Romania

² Alexandru Ioan Cuza University, Biology Faculty, Iasi, Romania

³ P. Poni Institute of Macromolecular Chemistry, Iasi, Romania

⁴ National Institute of Research and Development for Technical Physics, Iasi, Romania

⁵ Joint Institute for Nuclear Research, Dubna, Moscow Region, Russian Federation 141980

⁶ Horia Hulubei Institute of Physics and Nuclear Engineering, Bucharest, Romania

mdor@uaic.ro

Metallic nanoparticles with magnetic properties were studied by microstructural methods and magnetometry aiming to reveal physical-chemical properties for further biomedical utilizations. The focus was the surface property changing by silanization since improving of the reactivity at the interface with aqueous media was intended. Magnetic core composition was either magnetite or cobalt ferrite while capping organic layer was citric acid (CA) and sodium oleate (SO) resulting in the samples Fe-CA, Fe-SO, Co-CA and Co-SO. Synthesis method was basically Massart's co-precipitation technology [1] of ferrophase in alkali medium followed by dispersion in aqueous suspensions; silanization by sol-gel technique resulted in the samples Fe-CA-Si, Fe-SO-Si, Co-CA-Si and Co-SO-Si.

Investigation by TEM emphasized nanometric size of quasi-spherical particles, XRD recording evidenced spinel type of crystalline organization while VSM data revealed dominant superparamagnetic properties. In the case of cobalt ferrite samples the contribution of ferromagnetic behaviour was shown related to rare larger particles or particle aggregates. Saturation of specific magnetization was found to be dependent on the capping organic layer since sodium oleate seems to form larger double layer around magnetic cores comparing to citric acid thin monolayer. Also the coating with silica - carried out to enhance surface reactivity due to silanol groups, resulted in noticeable moderation of saturation magnetization in all analysed samples. The behaviour of specific magnetization to the temperature increase was also studied; comparative discussion was carried out regarding possible changing of metallic properties at the interface with coating shell.

The biological impact of magnetic nanoparticles after biomedical use and release in the environment was studied at the level of some beneficial microorganisms such as cellulolytic fungi with important role in degradation of wood wastes of either natural or anthropomorphic origin. Biochemical specific analyses enabled us to suppose that oxidative stress could be induced by low concentrations of magnetic nanoparticles endocytated by fungi cells or attached to cellular wall.

Further study is designed to get deeper insight in the optimization of technology design for the synthesis of metallic nanoparticles suitable for biomedical use and with reduced harmful bioeffects in the environment.

Support by JINR-IUCN Grant 81/04-4-1121/15-17 is acknowledged.

[1] R. Massart, *IEEE Trans. Magn.*, **17** (1981) 1247-1248.

3PO-J-3

COMPLEX REFRACTIVE INDEX OF CONCENTRATED MAGNETIC FLUIDS

Yerin C.V.¹, Lykhmanova V.I.¹, Yerina M.V.¹

¹ North Caucasian Federal University, Stavropol, Russia
exiton@inbox.ru

Complex refractive index is one of the most important characteristics of the condensed materials. Such optical properties of magnetic fluids (MF) as light absorption, effects of a birefringence and light scattering substantially depend on value of a refractive index of magnetic nanoparticles. Results of the ellipsometric measurements of the real and imaginary parts of a complex refractive index of concentrated MF with magnetite nanoparticles in kerosene are presented in this paper.

Measurements of a complex refractive index ($\tilde{n} = n + i \cdot k$) of magnetic fluids were performed on a spectral ellipsometer the Ellipse-1891 in the range of wavelength from 350 to 1050 nanometers on reflex angles of 45 and 60 degrees. Samples of kerosene based magnetic fluid with volume concentrations of a magnetite from 1% to 35% were investigated. All samples were received from one initial MF with magnetite concentration of 14% by dilution and evaporation respectively. Figure 1 presents spectra of the real part $\text{Re}(\tilde{n})$ of a refractive index for samples of MF with concentration of 5%, 21%, 35%. In fig. 2 dependence of $\text{Re}(\tilde{n})$ on the concentration of a magnetite for the wavelength of 633 nanometers is presented.

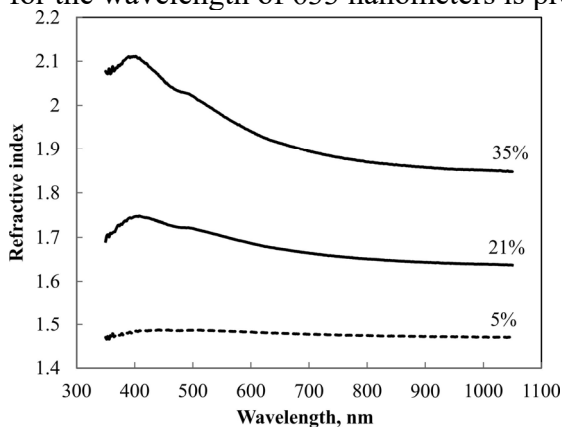


Fig. 1. Spectra of the real part of a complex refractive index for magnetic fluids various concentrations.

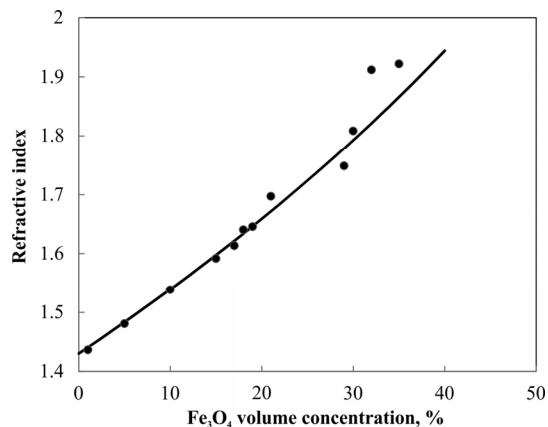


Fig. 2. Dependence of refractive index on the concentration of the magnetite (dots – experimental data; line – Maxwell Garnett effective medium approximation).

The experimental results were compared with calculations of the known Maxwell Garnett equation. Good agreement between the results of calculations and experiment at value of the real part of refractive index of $n(633 \text{ nm}) = 2.28$ was obtained. This result corresponds to the paper [2]. Values of an extinction coefficient in the measured samples ($\text{Im}(\tilde{n}) = 0.01 \div 0.1$) are slightly less values [1,2] and is in a good agreement with the data [3].

Supported by RFBR project No. 16-03-00054a.

[1] M. R. Querry, *Optical Constants*, Aberdeen 1985.

[2] U. Buchenau, I. Muller, *Solid State Comm.*, **11**(9) (1972) 1291 – 1293.

[3] E.Ya. Levitin, N.G. Kokodiy, et al, *Inorganic Materials*, **50**(8) (2014) 817–820.

3PO-J-4

ON THE TEMPERATURE DEPENDENCE OF FERROFLUID SUSCEPTIBILITY

Dikansky Yu.I.¹, Ispiryay A.G.¹, Kunikin S.A.¹

¹ North-Caucasus federal university, Stavropol, Russia
skunikin@yandex.ru

Early models of magnetization processes in ferrofluids were expressed in terms of Langevin theory similar to paramagnetic [1]. An evaluation of magnetic characteristics of homogeneous ferrofluids comes up against the well-known problem of taking into account the interparticle dipole– dipole interaction. The latter is most conspicuous in this systems and controls the correlations in mutual position of nanoparticles and in mutual orientation of their magnetic moments. A number of developed models describe the magnetic properties of ferrofluids in terms of effective magnetic field theory [2,3], and other models [4]. The aim of current study is a research of the temperature dependencies of the initial susceptibility of kerosene based ferrofluid. Study was done on a number of samples with different concentration and mean diameters of magnetic particles. It was found out that in the range of temperature 300-400 K magnetic susceptibility is well described by Curie-Weiss law. This indicates the possibility of the description of interparticle interactions in terms of effective field theory by $H_{\text{eff}} = H + \lambda M$. At the same time, effective field constant λ differs from predicted for dipolar systems value of $1/3$. Moreover value of λ decreases with increasing concentration of magnetic particles. While concentration is less than 7% value of λ reaches greater value than $1/3$. Results of this investigations are presented in fig. 1 for concentrations of disperse media of 14% curve 1, 17% curve 2 and 25% curve 3; while curve presents dependence for powder of ferrofluid particles without a carrier.

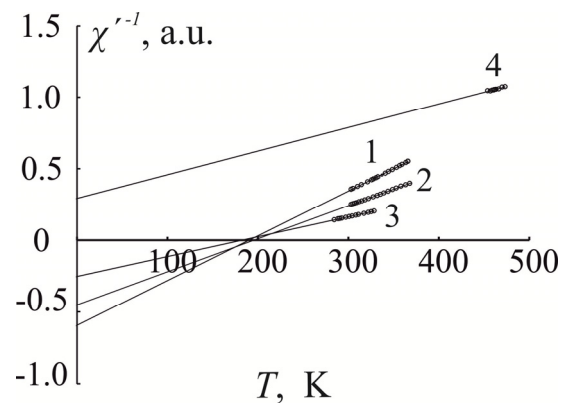


Fig. 1. Temperature dependencies of reverse susceptibility with temperature.

Analysis of results was done by taking into account the local magnetic field generated by adjacent particles. This field plays role of the demagnetizing field which prevents orientation of magnetic moments of magnetic particles along the external magnetic field direction. The magnitude of this local field increases with particle concentration increasing. Moreover increasing of λ by dilution of ferrofluid possibly caused by the formation of clusters of magnetic particles and partial ordering of its magnetic moments.

[1] M.I. Shliomis. *Sov. Phys. Usp.*, **112** (1974) 427–458.

[2] Yu.I. Dikansky *Magnetic Hydrodynamics.*, **3** (1982) 33.

[3] M.Holmes, K.O’Grady, and J. Popplewell. *JMMM.*, **85** (1990) 47.

[4] A. F. Pshenichnikov, A.V. Lebedev. *Colloid Journal.*, **67** (2005) 218–230.

3PO-J-5

THE INFLUENCE OF THE INTERNAL STRUCTURE OF MAGNETIC ELASTOMERS ON THEIR FORC DIAGRAMS

*Dobroserdova A.B.*¹, *Sanchez P.A.*², *Kantorovich S.S.*^{1,2}

¹ Ural Federal University (UrFU), Ekaterinburg, Russia

² University of Vienna (UniVie), Vienna, Austria

alla.dobroserdova@urfu.ru

The first-order reversal curve (FORC) method is a technique of extreme sensitivity for the analysis of experimental and theoretical hysteretic systems [1, 2]. In this contribution we study novel coarse-grained models for magnetic elastomers by performing FORC measurements obtained from computer simulations. The model is aimed at capturing the magnetic response of these materials using a minimal representation. Assuming that the particles in the elastomer are magnetically hard, we model them as soft spheres carrying a permanent magnetic moment in their centres. The elastic effects of the polymer matrix on the magnetic particles are represented by means of finitely extensible elastic springs with different rigidities, κ . These springs connect the particles to fixed points in space, constraining either their translations or both orientations and translations. Our results evidence that these systems have significant hysteretic behaviour, allowing their characterisation with FORC diagrams in order to obtain a comparison with experimental systems. We analyse the dependence of the degree of hysteresis of the system on the rigidity of the springs, which is expected to be non-monotonic.

Support by the projects DFG Ref.No.: OD 18/24-1, RFBR 16-52-12008, FWF START- Projekt Y 627-N27, and the Ministry of Education and Science of the RF (project 3.1438.2017/PCh) is acknowledged.

[1] C.R. Pike, A.P. Roberts, and K.L. Verosub *J. Appl. Phys.*, **85** (1999) 6660-6667.

[2] H.G. Katzgraber, G. Friedman, G.T. Zimanyi *Physica B*, **343** (2004) 10-14.

3PO-J-6

THE DYNAMIC MAGNETIC RESPONSE OF INTERACTING FERROPARTICLES IN MAGNETIC FLUIDS

Batrudinov T.M.¹, Zverev V.S.¹, Elfimova E.A.¹, Ivanov A.O.¹, Camp P.J.²

¹Ural Federal University, Ekaterinburg, Russia

²University of Edinburgh, Edinburgh, Scotland

Ekaterina.Elfimova@urfu.ru

The dynamic magnetic response of ferrofluid in a static magnetic field to a weak, linear polarized, alternating magnetic field is investigated using theory and computer simulations. The ferrofluid is modeled as a monodisperse system of dipolar hard spheres, suspended in a long cylindrical tube whose long axis is parallel to the direction of the static and alternating magnetic fields. It is assumed that the magnetic moments of the particles undergo Brownian relaxation only.

The theory is based on the Fokker-Planck-Brown (FPB) equation formulated for the case when the both static and alternating magnetic fields are applied. Following Ref. [1] an additional term into the FPB equation is included to take into account dipole-dipole interparticle interactions in the form of the first order perturbation. The solution of the FPB equation describing the orientational probability density of a randomly chosen dipolar particle is expressed as a series in terms of the spherical Legendre polynomials. The obtained analytical expression connecting three neighboring coefficients of the series makes possible to determine the probability density with any order of accuracy in terms of the Legendre polynomials. The analytical formula for the probability density truncated at the fifth Legendre polynomial is evaluated and used for the calculation of the dynamic susceptibility spectra. The influence of the static magnetic field on the dynamic susceptibility is analyzed in terms of the low-frequency behavior of the real part and the position of the peak in the imaginary part. It is shown that the real part of the susceptibility in the low-frequency region shift down with increasing the static magnetic field strength. It indicates that the magnetized system reacts less to the alternating magnetic field. The maximum of the imaginary part of the susceptibility decreases and shift to higher frequencies when the static magnetic field increases. The shift of the peak position towards higher frequencies reflects decreasing the characteristic relaxation time. A critical comparison between the theory and computer simulation is performed; the theory correctly predicts the dynamic susceptibility spectra as long as the Langevin susceptibility $\chi_L \ll 1$.

TMB, VSZ, EAE and AOI are grateful to the Russian Science Foundation (Grant No. 15-12-10003)

[1] A.O. Ivanov, V.S. Zverev, S. S. Kantorovich, *Soft Matter*, **15** (2016) 3507–3513.

3PO-J-7

DYNAMIC HYSTERESIS OF INTERACTING FERROPARTICLES IN MAGNETIC FLUIDS UNDER STRONG FIELD

Bushuev A.N.¹, Zverev V.S.¹, Elfimova E.A.¹

¹ Ural Federal University, Ekaterinburg, Russia
vladimir.zverev@urfu.ru

This report is devoted to the investigation dynamic behavior of ferrofluids when an external AC magnetic field is applied. In this investigation interparticle magnetic interaction is taken into account. In this report is assumed that the ferrofluid is the system of spherical particles that are uniformly magnetized and suspended in a liquid filling a long cylinder. An external AC magnetic field H is applied along the symmetry axis of the container.

The probability density of the magnetic moment orientation W of randomly chosen particle is used to describe dynamical characteristics of the ferrofluid. Equation for determination of W is well known Fokker-Planck-Brown equation [1] and can be written in the following form

$$\tau \frac{\partial W}{\partial t} = L(LW + WL(U_{eff})), L = u \times \frac{\partial}{\partial u}$$

Here u is a vector on the three-dimensional unit sphere, L is rotational operator with the gradient on the unit sphere $\partial/\partial u$ and τ is characteristic relaxation time of the particle. Variable U_{eff} plays a role of the energy term. As it suggested in [2], this term includes Zeeman interaction energy and the collective magnetic field produced by all magnetic moments. Former was taken into account by averaging of the pair distribution function over all possible orientations and positions of the randomly chosen particle. Pair distribution function was used in the form that corresponds to the lowest order of the thermodynamic perturbation method.

This equation and its properties were studied numerically and analytically. For small values of the relation between the energy of particle in the magnetic field to its thermal energy α (Langevin parameter), solution of the Fokker-Planck-Brown equation was obtained in [2]. Here we discuss analytical and numerical methods for the case $\alpha \gg 1$. Numerical approach is relied on methods that widely used in the investigation convection-diffusion phenomena. From mathematical point of view, former method has reliable criteria of convergence to the solution. Analytical method is based on expansion to a series of Legendre polynomials, similarly [3]. The solution of the Fokker-Planck equation is used to determine the dynamic magnetic response and behavior of the magnetization loop is analyzed. It was found that area under a magnetization curve is bigger for the case when dipole-dipole interaction was taken into consideration.

Support by Russian Science Foundation (Grant No. 15-12-10003) is acknowledged.

[1] Y L. Raikher, M.I. Shliomis, *Adv. Chem. Phys.*, **87** (1994) 595-751.

[2] A.O. Ivanov, et al., *Phys. Chem. Chem. Phys.*, **18** (2016) 18342-18352.

[3] W.T. Coffey, et al., *Physica A*, **213** (1995) 551-575.

3PO-J-8

CHARACTERIZATION OF MAGNETO-ELASTOMERIC MEMBRANES WITH COBALT FERRITE NANOPARTICLES BY MEANS OF STRUCTURAL METHODS

Balasoiu M.^{1,2}, Bunoiu M.³, Iacobescu G.⁴, Turchenko V.^{1,5}, Soloviov D.^{1,6}, Bica I.³

¹ Joint Institute for Nuclear Research, Dubna, Russia

² Horia Hulubei National Institute for Physics and Nuclear Engineering, Bucharest, Romania

³ West University of Timisoara, Timisoara, Romania

⁴ University of Craiova, Department of Physics, Craiova, Romania

⁵ Donetsk Institute of Physics and Engineering named after O.O. Galkin, Donetsk, Ukraine

⁶ Taras Shevchenko University, Kiev, Ukraine

madalin.bunoiu@e-uvt.ro

New magneto-elastomeric membranes with CoFe₂O₄ nanoparticles were fabricated. In the present paper their microstructure investigation by means of AFM, XRD and SANS is presented.

A comparison with similar magneto-elastomeric membranes with magnetite based ferrofluids is realized. Using these structural methods, the distribution and sizes of the magnetic particles embedded in the elastomeric matrix and the morphological features of the membrane are determined [1, 2].

Support by JINR-Romania Cooperation Programme Projects for 2016-2017 years and Grants of Romanian Governmental Representative to JINR is acknowledged.

[1] M. Balasoiu, V.T. Lebedev, D.N. Orlova, I. Bica, *Crystallography Reports*, **56**(7) (2011) 93-96.

[2] G.E. Iacobescu, M. Balasoiu, I. Bica, *J. Supercond. Nov. Magn.*, **26** (2013) 785-792.

3PO-J-9

COMPUTER MODELING OF HYBRID MAGNETIC ELASTOMERS*Sánchez P.A.¹, Stolbov O.V.², Raikher Yu.L.², Kantorovich S.S.^{1,3}*¹ University of Vienna, Vienna, Austria.² Institute of Continuous Media Mechanics (RAS Ural div.), Perm, Russia.³ Ural Federal University, Ekaterinburg, Russia.

pedro.sanchez@univie.ac.at

Magnetic elastomers are an important type of smart materials characterized by the change of their shape and rheological properties as a response to external magnetic fields [1]. Similarly to magnetic fluids, these are hybrid materials consisting of magnetic nano- or microparticles embedded in a nonmagnetic carrier material. Whereas in magnetic fluids the carrier is a liquid, in magnetic elastomers it is a viscoelastic polymer matrix. This makes them candidate materials for many technological applications, like the creation of artificial muscles, magneto-responsive micromanipulators or tunable vibration absorbers.

Even magnetic elastomers still represent a topic less studied than magnetic fluids, several approaches already exist to provide these materials with the desired properties. In such approaches, different structures and electrical properties of the polymer matrix, as well as diverse concentrations and distributions of the magnetic particles within the matrix, have been explored. Particularly important for the determination of the macroscopic response of the material are the magnetic properties of the particles. In most existing works, magnetically soft particles have been used to create these materials, whereas the choice of magnetically hard particles is more rare. However, the combination of particles of different types and, in particular, with very different magnetic properties, is an approach poorly explored to date.

Here, we study a novel microstructural design for a magnetic elastomer material that has been recently synthesized for the first time [1-2]. This design is based on the presence within the polymer matrix of two types of magnetic particles in different amounts: a low volume fraction of magnetically hard colloidal particles---typically, ferromagnetic particles of 3-5 μm of diameter---and a high volume fraction of smaller, magnetically soft particles---typically, paramagnetic particles with a diameter of around 10nm. We study the properties of this hybrid magnetic material by means of extensive computer simulations and analytical theories. In particular, in this contribution we focus on the computer simulation of this system, based on a bead-spring modeling approach of the material microstructure. Our simulation model takes into account the magnetization of the magnetically soft particles by the presence of the magnetically hard ones, as well as the effect of external magnetic fields on both types of magnetic particles. Extensive computer simulations of a minimal representative volume of the material are performed to characterize its structural and magnetic response depending on the applied field.

Support by DFG, grant Ref. no. OD 18/24-1, is acknowledged.

[1] J.M. Linke, D.Y. Borin, S. Odenbach, *RSC Adv.*, **6** (2016) 100407.

[2] M.V. Vaganov, J. Linke, S. Odenbach, Yu.L.Raikher, *JMMM* (2017).

DOI:10.1016/j.jmmm.2016.08.084.

3PO-J-10

INTERACTION PARAMETERS COMPUTATION FOR A SYSTEM OF PERMANENT MAGNETS AND MAGNETOACTIVE ELASTOMER SAMPLE

*Nadzharyan T.A.¹, Alekhina Yu.A.¹, Makarova L.A.¹, Stepanov G.V.^{1,2}, Perov N.S.¹,
Kramarenko E.Yu.¹*

¹ Lomonosov MSU, Faculty of Physics, 1-2 Leninskie Gory, Moscow, Russian Federation

² SSC RF GNIChTEOS, 38, sh. Entuziastov, Moscow, Russian Federation

nadzharijan.timur@physics.msu.ru

Magnetoactive elastomers (or MAE) are composite polymer materials consisting of relatively soft polymeric matrix and ferromagnetic filler particles of different sizes. Such microstructure allows to control various properties of MAEs, for example their shape and stiffness. Hence the applications include tunable mechanical devices as well as cases where elastic subsystem interaction with an external field is important. One such case involves using MAE as a magnetically controlled retinal seal in eye surgery to treat retinal detachment. This work aims to model and study the interaction between MAE seal and a system of permanent magnets.

The model is created using commercially available software COMSOL Multiphysics to solve partial differential equations with finite element method. Various geometric parameters and their influence on the interaction between magnetic and MAE subsystems were considered. Different magnetization orientations in the magnetic subsystem (parallel and anti-parallel) were used. The dependences of both mechanical and magnetic properties of MAE samples on the external magnetic field were studied. MAE samples were represented by either cuboids or spherical segments to simulate the retinal curvature. Two factors were taken into account during modelling of the magnetic properties of subsystems: inhomogeneous magnetization inside the magnets due to demagnetization and the dependence of the MAE's magnetic permeability on the magnetic field inside the sample (including influence of the sample's shape).

Dependences of the interaction force acting on the MAE sample on the distance between magnetic and elastomeric subsystems as well as other geometric parameters of the problem were obtained. Pressure distributions on sample's surfaces were computed. Tangent forces resulting from the sample's displacement in the direction parallel to the magnetic subsystem were studied. System configurations optimal for practical application in eye surgery were considered. Numerical simulations were supported by real experimental data.

Financial support of the Russian Science Foundation (project 16-15-00208) is acknowledged.

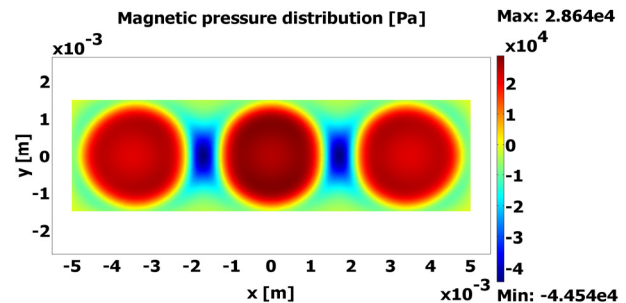


Fig. 1. Magnetic pressure distribution on the MAE sample surface.

3PO-J-11

SILICA COATED STRONTIUM HEXAFERRITE HARD-MAGNETIC COLLOIDAL NANOPARTICLES

Anokhin E.O.¹, Trusov L.A.¹, Sleptsova A.E.¹, Uvarov O.V.², Eliseev A.A.¹, Kazin P.E.¹

¹ Lomonosov Moscow State University, Moscow, Russia

² Prokhorov General Physics Institute, Moscow Russia

anokhin.evgeny@gmail.com

Surface modification of the magnetic particles is an important step towards their further practical application. In the case of hard-magnetic strontium hexaferrite nanoparticles carrying a large permanent magnetic moment, there is a problem of strong aggregation of the particles due to the intense dipole-dipole interactions. One way to reduce the magnetic dipole-dipole attraction, and as a consequence, increase the colloidal stability is to spatially separate the particles by different coatings. Silica coated magnetic particles are perspective for use as magnetic nanocontainers for biomedical *in vitro* applications in the field of diagnostics: due to versatility of silane chemistry, the coupling of bioactive groups like antigens to the particle surface can easily be achieved; by coating magnetic nanoparticles with large non-magnetic shell the polydispersity of a system can be considerably reduced allowing self-organization into highly symmetric mesostructures like magnetically controllable optically active colloidal crystals; also these materials could be used as magnetically controllable sorbents.

Colloids of hard-magnetic strontium hexaferrite nanoparticles were obtained using glass-ceramics method previously reported [1]. Shortly we obtained oxide glasses in the $4\text{Na}_2\text{O}-9\text{SrO}-5.5\text{Fe}_2\text{O}_3-4.5\text{Al}_2\text{O}_3-4\text{B}_2\text{O}_3$ and $13\text{SrO}-6\text{Fe}_2\text{O}_3-6\text{B}_2\text{O}_3$ systems; then heat-treated it at $640-700^\circ\text{C}$ forming glass-ceramics, which were grounded and then treated with 3% HCl at 50°C with simultaneous sonication. The magnetic nanoparticles were magnetically separated from the solution by decantation; finally, water was added to disperse the particles. For obtaining silica coated material we used two different methods based on modified Stöber process and acidic silicate hydrolysis.

According to XRD colloidal particles possess strontium hexaferrite structure; magnetic measurements of dried powders showed that particles exhibit hard-magnetic behaviour with a saturation magnetization of 30–60 emu/g and a coercivity of 3200–4000 Oe. According to TEM colloidal particles are plate-like with mean diameter of the plate 50 and 16 nm and mean thickness 5 and 6 nm for different glass compositions correspondingly.

It was shown that in an aqueous medium colloidal nanoparticles are electrostatically stabilized due to a positive surface charge; colloids are stable in the pH range from 1 to 5 and concentration of a single-charged electrolyte less than 100 mmol/l. We observed condensation of the particles with forming concentrated liquid phase under the influence of gradient magnetic field.

Using two different methods core-shell and plum pudding structures of silica-coated hexaferrite particles were obtained. According to TEM core-shell particles are flattened spheres of silicon dioxide with hexaferrite particle inside (the larger diameter more than 100 nm); plum pudding structures are silica particles gel with randomly dispersed hexaferrite particles inside. According to magnetic measurements of dried powders, these composites consist of more than 80 weight percent of silica.

This research was funded by Russian Foundation for Basic Research, grant No. 16–03–01052.

[1] L. A. Trusov, A. V. Vasiliev, M. R. Lukatskaya, D. D. Zaytsev, M. Jansen, and P. E. Kazin, *Chem. Commun.*, **50**(93) (2014) 14581–14584.

3PO-J-12

DIELECTRIC PROPERTIES INVESTIGATION OF HYBRID MAGNETORHEOLOGICAL ELASTOMERS UNDER A MEDIUM FREQUENCY ELECTROMAGNETIC FIELD

Balasoiu M.^{1,2}, Bica I.³

¹ JINR, Dubna, Russian Federation

² IFIN-HH, Bucharest-Magurele, Romania

³ West University of Timisoara, Timisoara, Romania

ioanbica50@gmail.com; balas@jinr.ru

Magnetorheological elastomers (MREs) belong to the class of smart materials. They are made of an elastic matrix (silicone rubber, natural rubber, etc.) in which a magnetic phase (ferro- and ferromagnetic microparticles) is dispersed orderly or randomly [1]. The MREs modulus of elasticity change drastically in a magnetic field [2].

By filling with additives as titanium dioxide [1], graphite powder [3], and by varying thereof volume fraction in relation to the magnetic phase, the change of MREs electric properties in magnetic field is found. These properties are used to make deformation and mechanical tension sensors [4], Hall sensors [5] etc. Following this research direction, in the paper are presented new hybrid magnetorheological elastomers (hMREs) fabricated from silicone rubber (SR), silicone oil (SO), carbonyl iron (CI) nanoparticles and graphene (nGr), as membranes (Ms), with dimensions: 0.05 m x 0.04 m x 0.0012 m and composition given in table 1.

Table 1 The volume fractions of the hMREs components

Ms	SR(%vol.)	SO(%vol.)	CI(%vol.)	nGr(%vol.)
M ₁	60	20	20	0
M ₂	48	20	20	12
M ₃	40	20	20	20

Using hMREs as dielectric medium, planar capacitors (PCs) are built. The following experiment is accomplished: (i) a magnetic field of variable intensity from 0 to 250 kA/m is applied to planar capacitors with hMRE as dielectric medium; (ii) with the LCR-meter ET-20 (OAO MHIPI, MINSK) the capacitance, C and the dielectric loss angle tangent, D of the planar capacitors is measured for an applied AC electromagnetic field with frequency between 1 kHz to 100 kHz.

Based on the obtained data the dispersion and absorption hMREs characteristics and the Cole-Cole diagrams are plotted. From the obtained plots the conductor-dielectric phase transitions, relaxation time and hMREs dielectric constants are evidenced. It appears that they are dependent on particle volume concentration, Φ of nGr, strength of static magnetic field and frequency, f of the AC electromagnetic field.

Such hMREs can be useful in the realization of hybrid materials for medical and technical purposes.

Support by JINR-Romania Cooperation Programme Projects for 2016-2017 years and Grants of Romanian Governmental Representative to JINR are acknowledged.

[1] M. Balasoiu and I. Bica, *Results in Physics*, **6** (2016) 199-202.

[2] I. Bica, E.M. Anitas, L.M.E. Averis, *J. Ind. Eng. Chem.*, **28** (2015) 86-90.

[3] I. Bica, *Materials Letters*, **63** (2009) 2230-2232.

[4] I. Bica, *J. Ind. Eng. Chem.*, **17** (2011) 83-89.

[5] I. Bica, *Materials Science and Engineering B*, **166** (2010) 94-98.

3PO-J-13

THE RESEARCH OF THE DEFORMATION OF THE THIN BODY WITH A MAGNETIZABLE ELASTOMER IN MAGNETIC FIELDS

Merkulov D.I.¹

¹ Lomonosov Moscow State University, Moscow, Russia
merkulovdima@mail.ru

The deformation of the thin body with the magnetizable elastomer based on silicone in the applied non-uniform axially symmetric magnetic field of the electromagnetic coil was investigated experimentally and theoretically. The existence of two stable equilibrium shapes of the body at certain values of the current in the coil (bi-stability) and hysteresis of a body length during cyclic quasi-static change of the current was observed experimentally (Fig. 1).

The experimental method to determine the elasticity coefficients C_1 and C_2 of for the Mooney - Rivlin model was proposed. A special feature of this methodology is the application of force on the side of the long horizontal sample. When the sample is horizontal, gravity can be neglected and the sample elongates uniformly. Therefore the dependence of value $p_{11n}/(\lambda - \lambda^{-2})$ on λ^{-1} (where λ is the ratio of the deformed length of sample L to its initial length L_0 , p_{11n} is a component of the stress tensor acting on the undeformed body profile S_0) can be used to find the elasticity coefficients. The magnetic permeability of the material was measured by the power method. The dependence of the magnetic field strength on the coordinates was measured by the Hall sensor.

Calculations of the thin body deformation in the magnetic field of the electromagnetic coil were made using the experimentally measured parameters. As a result, the ambiguous dependence L on L_0 for some values of the current in the electromagnetic coil was obtained theoretically: one value L_0 (from a certain range) corresponds to the three values of L (Fig. 2). The following criterion of instability of the equilibrium states was obtained: $dL/dL_0 < 0$. Obviously, that the average values of L are unstable equilibrium states. Thus, the existence of the bi-stability of the thin body deformation in a certain range of currents was shown theoretically.

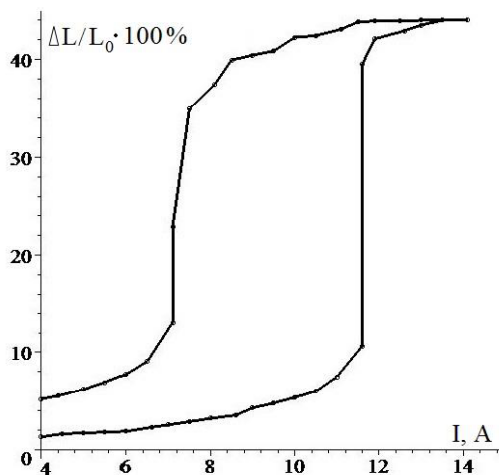


Fig. 1. The experimental dependence of the relative body elongation on the current

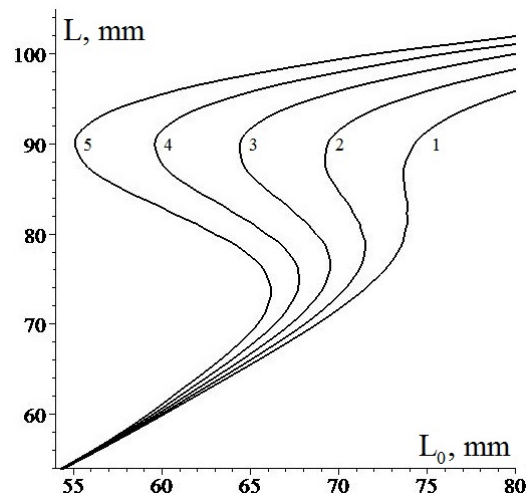


Fig. 2. Theoretical dependence of L on L_0 at currents: 1 - 6A, 2 - 7A, 3 - 8A, 4 - 9A, 5 - 10A

This work was supported by the RFBR grant 16-31-60091, partially supported by RFBR 16-51-12024 and the Russian President grant MK-4541.2016.1.

3PO-J-14

COARSENING DYNAMICS OF FERROMAGNETIC NETWORKS: EXPERIMENTAL RESULTS AND SIMULATIONS

Pyanzina E.¹, Kögel A.², Marezki R.², Sanchez P.³, Kantorovich S.^{1,3}, Richter R.²

¹Ural Federal University, Ekaterinburg, Russia

²University of Bayreuth, Bayreuth, Germany

³University of Vienna, Vienna, Austria

Elena.Pyanzina@urfu.ru

In the last decade, networks that are neither completely regular, nor completely random have attracted a lot of interest [1]. These networks are highly clustered like regular lattices, yet have small characteristic path lengths like random graphs. Examples comprise the connections in-between routers of the internet [1], citation networks [2] or transport networks in plant leaves [3]. These networks may evolve in time, but have no transient nature. In contrast, transient networks emerge during the phase separation of dynamically asymmetric mixtures, like a solution of a polymer in a less viscous solvent [4]. Here, the slow component is the polymer, the fast one is the solvent. For these kinds of dynamically asymmetric mixtures a new type of viscoelastic phase separation has been proposed [5]. Here, we put forward a hypothesis that a dispersion of magnetic particles in a magnetically neutral medium may also be regarded as a dynamically asymmetric mixture. In such a system, the magnetic interactions mediate the elastic forces.

We investigate the phase separation of a shaken mixture of glass and magnetized steel spheres after a sudden quench of the shaker amplitude. After quenching, transient networks of the magnetic dipoles emerge in the experiment. We study the temporal evolution of the mean number of neighbors and of the efficiency of the networks. We observe a sudden increase and then a moderate growth of both order parameters. We use a simple simulation approach to understand the influence of the glass spheres, as well as the magnetization law of the steel spheres, on the transition to compact clusters formed by the latter in quasi two dimensions. Not aiming at describing the experimental results, we rather use the simulation approach to define the key interactions in the experimental system. We discover that along with dipolar and steric interactions, there is a central attraction between the magnetized beads which is responsible for the hydrodynamic regime and the lognormal distribution of clusters [6].

[1] Y. Moreno et al., *Phy. Rep.*, **424** (2006) 175-308.

[2] J. E Hirsch, *Proc. Nat. Acad. Sci.*, USA, **102** (2005) 16569-16572.

[3] E. Katifori et al., *Phys. Rev. Lett.*, **104** (2010) 048704.

[4] H. Tanaka, *Phys. Rev. Lett.*, **71** (1993) 3158-3161.

[5] H. Tanaka, *J. Phys.: Cond. Mat.*, **12** (2000) R207.

[6] A. Kögel, R. Marezki, E. Pyanzina, P. Sanchez, S.R. Kantorovich, R. Richter, (2017) in preparation.

3PO-J-15

SELF-ASSEMBLY AND EQUILIBRIUM PROPERTIES OF MAGNETIC FILAMENT SOLUTIONS

Novak E.¹, Pyanzina E.¹, Rozhkov D.¹, Gudkova A.¹, Sanchez P.², Kantorovich S.²

¹ Ural Federal University, Ekaterinburg, Russia

² University of Vienna, Vienna, Austria

ekaterina.novak@urfu.ru

Systems of permanent semiflexible chains of polymer-crosslinked magnetic colloids, known as magnetic filaments, are the main research subject of our investigation. These systems have many technological applications, like the creation of artificial swimmers [1] or enhanced contrast agents for magnetic resonance measurements in biomedicine [2]. This latter application benefits from the higher magnetic response that dispersions of magnetic filaments show with respect to conventional magnetic fluids. This enhanced magnetorheological response of dispersions of magnetic filaments makes these systems promising candidates to replace conventional magnetic fluids in many applications, as well as to become the main building blocks of sophisticated magnetoresponse materials [3].

This study is devoted to characterize the properties of dispersions of magnetic filaments made out of ferromagnetic nanoparticles with different chain conformations - simple open chains, closed rings and branched structures with “X” and “Y” junctions - inspired by the recent findings on the low temperature self-assembly of dipolar hard spheres [4]. In order to characterize the impact of the different crosslinked configurations on the self-assembly and the equilibrium structural behavior of the filaments, extensive computer simulations have been carried out. A detailed cluster analysis of the equilibrium configurations has been performed to compare the structures formed by these filament solutions to those observed in conventional magnetic fluids containing non-crosslinked nanoparticles. These results will pave the way for the development of analytical models and identify the most interesting building block candidates for the design of novel magnetic fluids and materials with higher resistance to shear stress and sensitivity to external fields.

This research has been partially supported by the RFBR Grant 16-52-12008. Computer simulations were performed at the Ural Federal University Scientific Cluster.

[1] R. Dreyfus et al., *Nature*, **437** (2005) 862-865.

[2] S. A. Corr et al., *J. Am. Chem. Soc.*, **130** (2008) 4214-4215.

[3] P.A.Sánchez et al., *Faraday Discuss.*, **186** (2016) 241-263.

[4] S.S.Kantorovich et al., *PCCP*, **17** (2015) 16601-16608.

3PO-J-16

MICROSTRUCTURE FORMATION AND MACROSCOPIC DYNAMICS OF FERROFLUID EMULSION IN ROTATING MAGNETIC FIELD

Kolesnikova A.A.¹, Zakinyan A.R.¹, Dikansky Yu.I.¹

¹ Department of General and Theoretical Physics, North Caucasus Federal University, Stavropol, Russian Federation
zakinyan.a.r@mail.ru

The ferrofluid emulsion under study has been produced by dispersing a kerosene-based ferrofluid with magnetite nanoparticles in water by means of ultrasonic disperser. Soft soap has been used as emulsifier. The emulsions with various drop sizes from a few micrometers to tens of micrometers can be obtained. The microstructure formation in a flat layer of such emulsions under the action of in-plane rotating magnetic field has been observed and studied. It has been found several microstructure types. At comparatively low magnetic field frequencies and comparatively high magnetic field strengths the chine-like structures has been observed. At higher frequencies and lower magnetic fields the droplet discs are formed in the plane of the field. The frequency of the disc rotation and time evolution of the formation process have been analyzed. The emulsion concentration is also essential factor for the microstructure formation. It has been found that at comparatively high concentrations the mesoscale structures of particle clusters are formed under the action of rotating magnetic field. The inverse system of nonmagnetic water droplets dispersed in a ferrofluid has also been studied. The studied systems have been computationally investigated by molecular dynamics simulations.

The microstructure dynamics in ferrofluid emulsions shows itself in macroscopic mechanical effects. Here we analysed the appearance of macroscopic torque on a ferrofluid emulsion sample in a rotating magnetic field. The internal rotations of formed microstructural elements produce torque acting on a whole emulsion sample due to the viscous coupling. The value of the torque has been measured for the emulsion filled sphere. The results have been analyzed and discussed. The ability of the use of ferrofluid emulsions for actuation properties has been demonstrated. It has been concluded that the ferrofluid emulsions can be regarded as controllable soft magnetic materials.

Support by President of the Russian Federation grant (MK-3169.2017.2) and by Ministry of Education and Science of the Russian Federation (project № 3.5822.2017) is acknowledged.

3PO-J-17

ULTRASOUND VELOCITY ANISOTROPY IN MAGNETIC AND MAGNETOREOLOGICAL FLUIDS

Sokolov V.V.¹, Osipov M.I.¹

¹ Moscow Technological University, Moscow, Russia
vvs1953@rambler.ru

The dynamics of magnetic fluids remains a subject of interest. The previous theories could not describe the propagation of ultrasound wave in magnetic fluid under external magnetic field [1] B.U. Felderhof [2] pointed out that the dynamics of magnetic fluids must be described by different methods in different regimes of density. In this connection, study of the features of propagation of small amplitude ultrasound wave in magnetic fluid occupies a significant place in the development of ferrohydrodynamics, since the results of such studies make it possible now to appraise existing various ferrohydrodynamics equations in a linear approximation, under conditions of reliable experimental data, of course. In our experiment the specifics of a magnetic fluid were accounted for by the fact that the magnetic field was created with permanent magnet, since it had been experimentally established that the holding time of the magnetic fluid in the field, ensuring reproducibility of results, were tens and hundreds of hours [1].

In the report we presented an overview of the main results obtained in the framework of a new approach to the dynamics of magnetic fluids based on the concept of frozen-in magnetization. The discussion the connection the ferrohydrodynamics with frozen-in magnetization with the existing theories is made in [3]. It was shown that the fast and slow magnetosonic waves and Alfvén-type wave are the hydrodynamic modes of the ideal non-conducting magnetic fluid with frozen-in magnetization [1]. We have employed our theory to described the experimental data for the ultrasound velocity anisotropy in magnetic fluids based on the various liquids using theoretical expression for the propagating velocity of fast magnetosonic wave and good quantitative agreement between theory and experiment was demonstrated. Also good quantitative agreement between the theory and experimental data for the ultrasound velocity anisotropy in the water-based magnetic fluid was demonstrated by A. Józefczak et al. [4].

Acoustic metamaterials are being considered for periodic structure where specific microscopic material properties can be tailored to alter macroscopic acoustic field. One type of acoustic meta material being considering is active fluid known as magnetorheological fluids.

The authors of the remarkable experimental work [6] measured ultrasound velocity anisotropy in a hydrocarbon-based magnetic fluid and magnetorheological fluid. The authors of [6] discovered experimentally the propagation of fast and slow waves in a magnetized suspension consisting of glycerin and spherical iron particles. Experimental results [5, 6] are described using the theory of wave propagation in a magnetic fluid with frozen-in magnetization.

The prediction concerning the existence of slow magnetosonic wave and Alfvén -type wave in magnetic and magnetorheological fluids seems very important and requires an experimental verification.

[1] V.V. Sokolov, *Acoustical Physics*, **56** (2010) 972-988.

[2] B.U. Felderhof, *Phys. Rev. E.*, **64** (2001) 063502-11.

[3] B.U. Felderhof, V.V. Sokolov, P.A. Eminov, *J. Chem. Phys.*, **132** (2010) 184907-7.

[4] A. Józefczak *et al.*, *J. Nanopart Res.*, **16** (2014) 2271.

[5] M.A. Bramantya, M. Motozawa, T. Savada, *J. Phys. Cond. Matt.*, **22** (2010) 324102-05.

[6] Y. Nahmad-Molinari, C.A. Arancibia-Bulnes, *Phys. Rev. Lett.*, **82** (1999) 727-730.

3PO-J-18

ON THE STRUCTURE OF WATER BASED FERROFLUIDS WITH COBALT FERRITE PARTICLES

BalasoIU M.^{1,2}, BalasoIU-Gaina A.M.^{1,3,4}, Ivankov O.^{1,5}, Soloviov D.^{1,5}, Stan C.⁶, Lysenko S.⁷,
Lupu N.⁸, Creanga D.⁹

¹ Joint Institute for Nuclear Research, Dubna, Russia

² Horia Hulubei National Institute for Physics and Nuclear Engineering, Bucharest, Romania

³ CMCF, Moscow State University, Moscow, Russia

⁴ West University of Timisoara, Timisoara, Romania

⁵ Taras Shevchenko University, Kiev, Ukraine

⁶ Politehnica University of Bucharest, Faculty of Applied Science, DPI, Bucharest, Romania

⁷ Institute of Technical Chemistry Ural Branch of RAS, Perm, Russia

⁸ National Institute of Research and Development for Technical Physics, Iasi, Romania

⁹ Alexandru Ioan Cuza University, Iasi, Romania

balas@jinr.ru; alexandra@balasoIU.com

Ferrofluids reveal a wide range of applications in many technical and industrial fields, as well as in medicine and biotechnology. Water-based ferrofluids present complex microstructural behaviour and their properties improvement represents an important challenge in this field [1-3].

In the present paper different water based ferrofluid samples with cobalt ferrite particles are investigated by means of small angle neutron scattering (SANS), high resolution transmission electron microscopy (HRTEM), selected area electron diffraction (SAED) and X-ray diffraction [4].

The results are analysed and discussed from the point of view of the influence of particle concentration, temperature, preparation and data modelling methods [5, 6].

Support by JINR-Romania Cooperation Programme Projects for 2016-2017 years and Grants of Romanian Governmental Representative to JINR are acknowledged.

[1] D. Bica, L. Vekas, M.V. Avdeev, O. Marinica, V. Socoliuc, M. BalasoIU, V.M. Garamus *J Magn Magn Mater* **311** (2007)17.

[2] BalasoIU M, Avdeev M V and Aksenov V L 2007 *Crystallography Reports* **52**(3) (2007) 505.

[3] I. Bodale, M. Oprisan, C. Stan, F. Tufescu, M. Racuciu, D. Creanga, M. BalasoIU, *Chapter 3rd International Conference on Nanotechnologies and Biomedical Engineering*, **55** Series IFMBE Proceedings, Springer Singapore, ISBN 978-981-287-735-2, (2016) 153-156.

[4] M. BalasoIU, O. I. Ivankov, D.V. Soloviov, S.N. Lysenko, R.M. Yakushev, A-M. BalasoIU-Gaina, N. Lupu, *J. Optoelectron. Adv. Mater.* **17**(7-8) (2015) 1114-1121.

[5] Cristina Stan, Maria BalasoIU, A. I. Ivankov, C.P. Cristescu, *Romanian Reports in Physics*, **68**(1) (2016) 270–277.

[6] C. Stan, M. BalasoIU, D. Buzatu and C.P. Cristescu, *Journal of Computational and Theoretical Physics*, (2017) (to be published).

3PO-J-19

MAGNETOSTATIC PROPERTIES OF POLYDISPERSE FERROFLUIDS: THEORY AND SIMULATION

Solovyova A.Yu.¹, Elfimova E.A.¹, Ivanov A.O.¹, Camp P.J.²

¹ Ural Federal University, Ekaterinburg, Russia

² University of Edinburgh, Edinburgh, Scotland

anna.soloveva@urfu.ru

The extremely strong magnetic properties of ferrofluid samples are mainly caused by the intensive interparticle dipole-dipole correlations, which appear to be much more pronounced in polydisperse dense ferrofluids containing large-particle fractions. In this work, the effects of particle-size polydispersity on the magnetostatic properties of concentrated ferrofluids are studied using both theory and computer simulation.

A convenient expression for the initial magnetic susceptibility is provided by the well-known second-order modified mean-field (MMF2) theory [1] which approximates the initial magnetic susceptibility as an expansion in the Langevin law $\chi_i = 8\varphi\lambda$ up to the third order, where φ is the volume concentration of ferroparticles, and λ is the dipolar coupling constant. It was found, however, that this simple approach is not able to describe properly the magnetic susceptibility of a polydisperse ferrofluid containing large-particle fractions [2]. In order to improve the theory, additional terms of order $\chi_i^2\lambda^2$ and $\chi_i^3\lambda$ have been calculated in the expansion of the magnetic susceptibility, and the corresponding terms have been added to the expression for the magnetization curve. In the monodisperse case, the expressions are as follows.

$$\chi = \chi_i \left\{ 1 + \chi_i \left(\frac{1}{3} + \frac{\lambda^2}{75} \right) + \chi_i^2 \left[\frac{1}{144} + \lambda \left(\frac{71}{24000} + \frac{3 \ln 2 - 7}{360} \right) \right] \right\} \quad (1)$$

$$M = M_s L(\alpha_s), \quad \alpha_s = \alpha + \chi_i L(\alpha) \left(1 + \frac{\lambda^2}{25} \right) + \chi_i^2 L(\alpha) \left[\frac{1}{16} \frac{dL(\alpha)}{d\alpha} + \lambda \left(\frac{71}{8000} + \frac{3 \ln 2 - 7}{40} \frac{L(\alpha)}{\alpha} \right) \right] \quad (2)$$

Here α is the Langevin parameter, $L(\alpha) = \coth \alpha - 1/\alpha$ is the Langevin function, and M_s is the saturation magnetization. In the polydisperse case, these expressions acquire a more complex form and contain complicated averages over the particle-size distribution [2].

The theoretical predictions for the initial susceptibility and the magnetization curve have been tested rigorously against results from Monte Carlo simulations of monodisperse dipolar hard spheres fluids, and of polydisperse systems with broad particle-size distributions including large-particle fractions. Comparisons have been made between model monodisperse and polydisperse systems with the same Langevin susceptibility ($2 \leq \chi_i \leq 7$) and the same volume fraction concentration. In both cases, the theoretical magnetization curve (2) shows better agreement with simulation data than does the MMF2 theory. As for the magnetic susceptibility, MMF2 theory is most accurate for the monodisperse model, while the polydisperse form of expression (1) works best in the polydisperse case.

The reported study was funded by Russian Foundation for Basic Research according to the research project No. 16-31-00089 mol_a.

[1] A. O. Ivanov, O. B. Kuznetsova, *Phys. Rev. E*, **64** (2001) 41405-1-12.

[2] A. Yu. Solovyova, O. A. Goldina, A. V. Lebedev, A. O. Ivanov, E. A. Elfimova, *J. Chem. Phys.*, **145** (2016) 084909-1-9.

3PO-J-20

LEVITATION AND MOTION OF A MAGNET PARTIALLY IMMERSSED TO A MAGNETIC FLUID

Pelevina D.A.¹, Naletova V.A.¹, Turkov V.A.¹, Kobzev M.M.¹

¹ Lomonosov Moscow State University, Moscow, Russia
pelevna.daria@gmail.com

The interaction of a magnet and a magnetic fluid can be used to construct new types of actuators. The magnetic fluid thin layer between two horizontal planes, when a parallelepiped magnet is located on the upper plate, are analytically investigated in [1, 2], in the case of rest and motion of the lower plane, respectively. In [3,4], the motion of a magnet along a thin layer of a magnetic fluid was experimentally described. Here the levitation and motion of a permanent cylindrical magnet partially immersed in a magnetic fluid on a horizontal plane are studied theoretically and experimentally.

In magnetic fluid volume, a magnet can levitate in equilibrium, like in [5], at a certain distance from the plane (height). The shape of a free surface of a given small magnetic fluid volume near a permanent cylindrical magnet and the height of magnet levitation are found numerically. The magnetic field is simulated using the ANSYS software package. The dependence of the levitation height on the magnetic fluid volume is plotted. The experiments and the theory are compared.

If the cylindrical magnet is immersed in the non-symmetric volume of a magnetic fluid, horizontal force arises. Under the influence of this force, the magnet can move along the plane. The motion of a magnet partially immersed in a magnetic fluid along a thin magnetic fluid layer (see Fig. 1) is investigated experimentally and theoretically. The magnet is placed on the left edge of the magnetic fluid layer. The magnet levitates and moves to the right edge, collecting a magnetic fluid. For some parameters of the experiment, the magnet can move back and return to its initial position. The position and velocity of the magnet, depending on the thickness and length of the magnetic fluid layer, as well as on the amount of magnetic fluid on the magnet are studied.

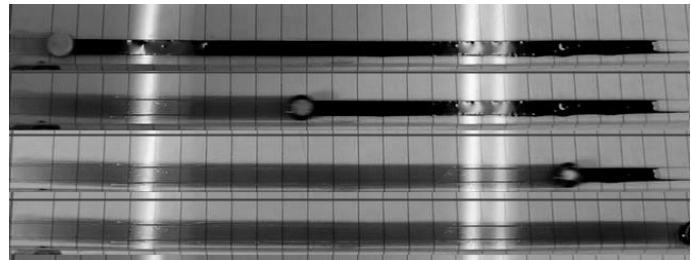


Fig. 1. The magnet motion in a magnetic fluid layer.

This work was supported by the RFBR grant 16-31-60091, partially supported by RFBR 16-91-01224 and the Russian President grant MK-4541.2016.1.

- [1] V. M. Korovin, Yu. L. Raikher, *MHD*, **23** N 1 (1987) 41-44.
- [2] Yu. L. Raikher, P. A. Sosnin, V. M. Korovin, A. F. Pshenichnikov, *MHD*, **28**(4) (1992) 340-345.
- [3] Hartung S., Rehberg I., Rihter R., *Book of Abstracts: 14th German Ferrofluid Workshop*, (2014) 82—83.
- [4] Freundorfer A., Rehberg I., Rihter R., *Book of Abstracts: 15th German Ferrofluid Workshop*, (2015) 74-75.
- [5] R. E. Rosensweig, *Ann. Rev. Fluid Mech.*, **19** (1987) 437-463.

3PO-J-21

EFFECTS OF MAGNETIC FIELDS ON CAPILLARY-GRAVITY WAVES IN THE PRESENCE OF MAGNETIC SURFACTANTS

Zhukov A.V.¹

¹ Institute of Mechanics, Moscow State University, Moscow, Russia
az@imec.msu.ru

Recently, new surfactant molecules with magnetic properties have been synthesized [1]. This makes it possible the magnetic control over liquid surface properties by sufficiently strong (0.4...1 T) external magnetic fields. The surface tension tensor for these media is anisotropic and depends on magnetic field strength. The analogous dependence was found experimentally and explained theoretically for magnetic fluid – water interfaces subjected to moderate-intensity (60...110 G) magnetic fields [2].

To determine the dependence of surface tension on magnetic field strength the structure of the interphase boundary in the presence of magnetic surfactant was studied [3]. This was performed by numerical minimization of the total free energy of the system in external magnetic field. Near the interphase boundary the system was considered as a three-component medium for which the free energy density depends on magnetic field strength, fluids densities, surfactant concentration and their gradients. The surface stress tensor and the surface values of extensive parameters are determined as excess values associated with the Gibbs dividing surface. Constitutive equations, conditions on the interface, and necessary stability conditions are obtained.

For the aforementioned solution of the interphase structure problem the surfactant concentration increases significantly inside the interfacial layer, i.e., the surfactant is significantly adsorbed on the interface, forming the surfactant surface phase. This surfactant surface phase possesses nonzero magnetization proportional to the surfactant concentration. The stability conditions require that the surface phase is paramagnetic in the tangential direction and diamagnetic in the normal direction to the interface.

Using the expression obtained for the surface stress tensor, the problem of gravity-capillary wave motion on horizontal free surface in the presence of magnetic surfactant in external magnetic field is solved. The dispersion equation connecting the frequencies and the wave vectors of surface waves is obtained. The approximate analytic solution of this equation for the case of long wave approximation is found. For any given value of the wave vector the magnetic and gravitational field values determine the frequency, and the viscosity and the surfactant interaction parameters determine the damping decrement of waves.

Support by the Russian Foundation for Basic Research (projects Nos. 16-01-00157 and 17-01-00037) is acknowledged.

[1] P. Brown, T.A. Hatton., J.Eastoe. *Curr. Opinion in Colloid & Interface Sci.* **20** (2015) 140-150.

[2] A.N. Golubyatnikov, G.I. Subhankulov, *Magnetohydrodynamics(Engl.Transl.)*, **22** (1986) 62.

[3] A.V. Zhukov, *Fluid Dynamics*, **51** (2016) 463-468.

3PO-J-22

ON THE STUDY OF MAGNETIC FLUID HYPERTHERMIA IN TUMOR TISSUE: EFFECT OF HEAT EXCHANGE WITH THE SURROUNDING BIOLOGICAL TISSUE

Abu-Bakr A.F.¹, Iskakova L.², Zubarev A.Yu.²

¹ Menoufia University, Shebin El-Koom, Egypt

² Ural Federal University, Ekaterinburg, Russia
alibakrm@yahoo.com

Magnetic hyperthermia is a new type of cancer treatment [1, 2] which allows achieve selective heat up a tumor without damaging the surrounding healthy tissues. The main idea of this method is in embedding of magnetic nanoparticles in a tumor region and heating them with the help of alternating magnetic field. In the temperature corridor 42-50°C the tumor cells undergo the protein destruction and die, whereas the cell of healthy tissue, being more temperature resistant, are not injured.

In physical models of magnetic hyperthermia biological media are usually considered as blood-flooded matrix composed of cells and interstitial space [3, 4]. Tumors with a well defined geometry, typically spherical with radius r , (see Fig. 1) are added to this simple picture that they remain surrounded by a finite, with thickness t , layer of healthy tissue with radius R , or infinite layer of healthy tissue with infinity radius. Specific heat, thermal and electrical conductivities, mass density as well the dielectric constant of the involved biological media - tumors, viscera, muscle, fat, skin, etc - must be included in the model.

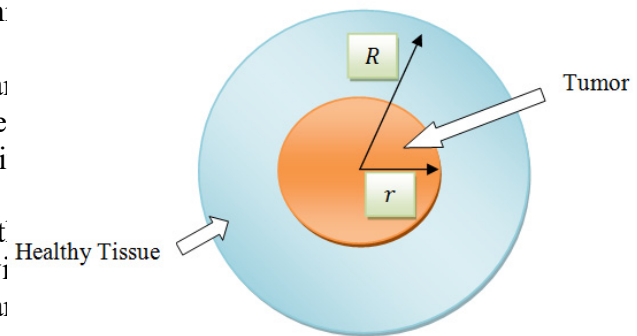


Fig. 1 Typical concentric tumor model,

In this work, we consider spherical region is modeled using the bioheat transfer equation for the thermal interaction between the tissue and the perfused blood. Numerical techniques are used to solve the mathematical model with heat source of constant density power located as distributed in the spherical region. The presented model and obtained results allow predicting the temperature change in tumor as well as in the surrounding tissue depending on intensity of the tumor heating.

[1] A.Yu. Zubarev, L. Iskakova, A.F. Abu-Bakr, *Physica A*, **467** (2017) 59–66.

[2] R. Kappiyoor, M. Liangruksa, R. Ganguly, I.K. Pur., *J. Appl. Phys.*, **108** (2010) 094702.

[3] P.K., Gupta, J. Singh, K.N. Rai, *Mathematical and Computer Modelling*, **57** (2013) 1018-1037.

[4] T. Shih, H. Kou, C.W. Liuh, *J. Biomedical Eng.: Appl., Basis Commun.*, **14** (2002) 86-96.

3PO-J-23

THE DYNAMIC MAGNETIC RESPONSE OF FERROFLUID TO SUPERIMPOSED AC AND DC CROSSED MAGNETIC FIELDS

Nekhoroshkova Yu.E.¹, Paramonov E.I.¹, Zverev V.S.¹, Elfimova E.A.¹

¹ Ural Federal University, Lenin av. 51, Ekaterinburg, 620000, Russia
julia.nekhoroshkova@urfu.ru

The dynamic magnetic response of ferrofluids to a weak linearly polarized AC field is studied in presence of DC magnetic field. In this investigation interparticle interaction is taken into account. The ferrofluid is modeled by the system of uniformly magnetized hard spherical particles, suspended in a long cylindrical tube, whose long axis coincides with Oz coordinate axis. AC magnetic field is perpendicular to the Oz -axis, whereas DC magnetic field is applied along Oz -axis: $\mathbf{H} = (0, \alpha_x e^{i\omega t}, \alpha_z)$ (t denotes time; α_x and α_z are Langevin parameters described the intensity of the dipole-field interactions in DC and AC magnetic fields correspondently; ω is the oscillating frequency). It is assumed that the relaxation of the magnetic moment of the particles occurs according to the Brownian mechanism. The probability density of the orientation of the magnetic moment μ_i of i^{th} randomly chosen particle $W(t, \theta_i, \varphi_i)$ is the solution of the Fokker-Planck equation in which the action of a static field and the interparticle interactions are taken into account with help of the effective energy term U_g :

$$2\tau \frac{\partial W}{\partial t} = \nabla^2 W + \nabla \cdot (W \nabla U_g),$$

where τ is the characteristic relaxation time of the ferroparticle magnetic moment. In Ref. [1] it was shown that the effective interaction U_g between a single particle and the effective AC magnetic field at the first level over concentration n is

$$U_g = U_h + n(U_{dd}(\mathbf{1}, \mathbf{2})\Theta(\mathbf{1}, \mathbf{2})\overline{W}(\mathbf{2}))_2.$$

The second term in U_g is taken into account interparticle correlations and it is weight-averaged dipole-dipole interaction ($U_{dd}(\mathbf{1}, \mathbf{2})$) between particles 1 and 2 over all possible orientations and positions of the randomly chosen particle 2 ($(\dots)_2$); The Heaviside step function $\Theta(\mathbf{1}, \mathbf{2})$ provides the condition of impenetrability of the particles. $\overline{W}(\mathbf{2})$ is one-particle probability density. The first term $U_h = -(\mu_1, \mathbf{H})/kT$ describes the interaction of the randomly chosen first particle with AC and DC fields and has the form of Zeeman energy related to the thermal energy kT .

The solution of the Fokker-Planck equation is expressed as a series in terms of the spherical functions. The analytical solution of the Fokker-Planck equation is used to determine the dynamic susceptibility. The behavior of the real and imaginary parts of the dynamic susceptibility as a function of the intensity of the static magnetic field is analyzed: the real part of the susceptibility in the low-frequency region shift down with increasing of the static magnetic field strength; the maximum of the imaginary part of the susceptibility decreases and shift to higher frequencies when the static magnetic field increases.

The theory is tested against computer simulation results and is found to be robust.

[1] A.O. Ivanov, V.S. Zverev, S. S. Kantorovich, *Soft Matter*, **15** (2016) 3507–3513.

3PO-J-24

DEFORMATION OF A MAGNETIC LIQUID DROP IN AN APPLIED NON-STATIONARY UNIFORM MAGNETIC FIELD

Tyatyushkin A.N.¹

¹ Institute of Mechanics, Moscow State University, Moscow, Russia
tan@imec.msu.ru

Small steady-state deformational oscillations of a drop of magnetic liquid in a non-stationary uniform magnetic field are theoretically investigated. The drop is suspended in another magnetic liquid immiscible with the former. The Reynolds number is so small that the inertia can be neglected. The variation of the magnetic field is so slow that the quasi-stationary approximation for the magnetic field and the quasi-steady approximation for the flow may be used.

The system of equations for the velocity, pressure, and magnetic field intensity consists of the continuity and Navier-Stokes equations for an incompressible fluid in the low Reynolds number and quasi-steady approximations, the Maxwell's equations in the ferrohydrodynamic approximation [1], and the constitutive relation for the magnetic field. The boundary conditions on the interface between the liquids include the impenetrability and no-slip conditions, the conditions for the jumps of the normal and tangential components of the total stress vector, the continuity conditions for the tangential component of the intensity of the magnetic field and for the normal component of the magnetic induction. The boundary conditions at infinity include the conditions for the velocity, pressure, and magnetic field intensity. Besides, the conditions of boundedness for the velocity, pressure, and magnetic field intensity should be fulfilled.

The representation of the magnetic field intensity in the form of the multipole expansion [2] and the general Lamb's solution [3] for the flow written in terms of irreducible tensors are used in solving the problem. Within this approach, the magnetic field intensity, velocity, and pressure are sought for in the form of series with scalar, vector, and tensor coefficients for which some relations are obtained that allow one to determine these coefficients. With the use of these relations, the coefficients are sought for in the form of asymptotic expansions over the parameter $9aH_{am}^2/(32\pi\sigma_s)$, the smallness of which provides the smallness of the deformations of the drop. Here, a is the radius of the undeformed spherical drop, H_{am} is the maximal absolute value of the intensity of the applied field, and σ_s is the surface tension of the interface between the liquids.

With accuracy up to the terms of the first order, in an oscillating applied magnetic field with the intensity $\mathbf{H}_a = H_{am} \cos(\omega t) \mathbf{k}$, the drop is a prolate spheroid, elongated along \mathbf{k} , performing deformational oscillations with the angular frequency 2ω and the phase lag $2\phi = \arctan(2\tau\omega)$, and, in a rotating applied magnetic field with the intensity $\mathbf{H}_a = H_{am} [\cos(\omega t) \mathbf{i} + \sin(\omega t) \mathbf{j}]$, it takes the shape of a tri-axial ellipsoid rotating around its minor axis, directed along $\mathbf{k} = \mathbf{i} \times \mathbf{j}$, with the angular speed ω so that its major axis lags from \mathbf{H}_a by the angle ϕ . Here, t is the time, ω is the angular frequency, \mathbf{i} , \mathbf{j} , and \mathbf{k} form a triple of orthonormal vectors,

$$\tau = \frac{32\eta_e^2 + 119\eta_e\eta_i + 114\eta_i^2}{30(\eta_e + \eta_i)^2} \frac{a(\eta_e + \eta_i)}{4\sigma_s},$$

η_i and η_e are the viscosities of the drop and of the surrounding liquid.

The partial support by RFBR grants 16-01-00157 and 14-01-00056 is acknowledged.

[1] R.E. Rosensweig, *Ferrohydrodynamics* (Cambridge University Press 1985).

[2] L.D. Landau, E.M. Lifshits, *The classical theory of fields* (Pergamon Press 1975).

[3] H. Lamb, *Hydrodynamics* (Cambridge University Press 1932).

3PO-J-25

THE EFFECT OF MAGNETIC NANOPARTICLE CONCENTRATION ON THE STRUCTURE ORGANIZATION OF A MICROFERROGEL

Ryzhkov A.V.^{1,2}, Raikher Yu.L.^{1,2}

¹ Perm National Research Polytechnic University, Perm, Russia

² Institute of Continuous Media Mechanics of UrB of RAS, Perm, Russia

ryzhkovalexandr@gmail.com

Microferrogels (MFGs) are individual soft magnetopolymer objects with typical sizes in the range of 0.1-10 μm . As systems with high sensitivity to magnetic field, they are prospective objects for drug delivery and other biomedical applications. Strong coupling between the magnetic nanoparticles (NPs) and the polymeric mesh, in which the NPs serve as cross-linkers, ensures the dependence of mechanical and structural properties of material on the external magnetic field. Therefore, for MFGs a remote control over their volume and shape is an inherent property. Such a field-tuned behavior is very important, for example, for the drug release. Here we report a molecular dynamics study of magneto-structural and magneto-mechanical responses of a MFG as functions of the NPs concentration.

In Ref. [1] the coarse-grained molecular dynamics was used to explore the structure organization of a MFG with a fixed NP content. In that model, the particles were set in the nodes of a simple cubic lattice constructed of bead-spring polymer chains. Two limiting cases for magnetic NPs were considered. In the first one, the magnetic moment of a NP rotates freely inside its body, i.e., the particle is perfectly magnetically soft (zero magnetic anisotropy). In another one, the magnetic moment is “frozen” inside its body, i.e., the particle is absolutely magnetically hard (infinite magnetic anisotropy). As shown, those models predict rather different types of the particle structuring inside the matrix.

In this work, the coarse-grained approach of Ref. [1] is applied to the case where the magnetic particle content of an MFG is varied as well as the parameter of interparticle dipole-dipole interaction. The simulation results are analyzed to get the degree of aggregation in a microferrogel for the two afore-mentioned types of magnetic anisotropy. The numeric indicator that we monitored, renders the fraction of NPs possessing at least one (q_1), two (q_2) or three (q_3) neighbors whose center-to-center distances are close to the diameter of a NP.

The universal fact is that in all the MFGs the value of q_3 is virtually zero, i.e., there is no ramification, the aggregates are chain-like. The value of q_1 that indicates the presence of any aggregates grows with the increase of the parameter of dipolar interaction λ . Now we are able to evaluate the interval of λ where the transition from non-aggregated to chain-like structured particle arrangement takes place. For the NPs with zero magnetic anisotropy this interval is much smaller compared to that for magnetically hard particles. As found, the greater concentration the smaller the reference value of λ at which the particles aggregate. And this effect is most distinctive in the case of magnetically soft NPs. Notably, at a weak dipolar interaction, the MFGs with magnetically hard particles display a lower degree of aggregation q_1 at a high NP content (about 80% of the lattice nodes occupied) than that at a moderate filling fraction (about 65% of the nodes occupied). It seems that magnetically hard NPs have to overcome the elastic resistance of the mesh with respect to both translational and rotational degrees of freedom, and in this case a larger number of populated nodes enhances this resistance, thus impeding the NPs aggregation.

Support on the part of RFBR-DFG grant 16-51-12001 is gratefully acknowledged.

[1] A.V. Ryzhkov, P.V. Melenev, M. Balasoïu, Yu.L. Raikher *J. Chem. Phys.* **145** (2016) 074905.

3PO-I3-1

DYNAMIC RESPONSE OF A SENSOR ELEMENT MADE OF MAGNETIC HYBRID ELASTOMER WITH CONTROLLABLE PROPERTIES

Becker T.I.¹, Zimmermann K.¹, Borin D.Yu.², Stepanov G.V.³, Storozhenko P.A.³

¹ Technical Mechanics Group, Faculty of Mechanical Engineering, Technische Universität Ilmenau, 98693 Ilmenau, Germany

² Chair of Magnetofluidynamics, Measuring and Automation Technology, TU Dresden, 01062 Dresden, Germany

³ Institute of Chemistry and Technology of Organoelement Compounds, 111123 Moscow, Russia
tatiana.becker@tu-ilmenau.de

At present, the development of modern chemical methods leads to further possibilities for carrying out new materials with exceptional magnetic properties. One special class of such smart materials is magnetic hybrid elastomers (MHEs), which consist of both magnetically hard and soft microparticles embedded into a nonmagnetic elastic matrix. It is known that their properties can be changed sufficiently by means of applied magnetic fields, due to interactions between different types of the magnetic filler and the matrix in the microscopic scale and subsequent structure formation of the particles [1]. Research scientists are interested in the field-dependent properties and behaviour of MHEs, since they can lead to novel opportunities for basic research as well as be suitable for use in applications.

MHE samples were prepared by means of mixing magnetically hard FeNdB and magnetically soft Fe particles with liquid components of SIEL silicone resin, a product of Russian Institute 'GNIChTEOS'. As a result of polymerization, there were obtained composite materials exhibiting a strong capability to interact with magnetic fields. A number of the samples of parallelepiped shape were prepared to be magnetized longitudinally or transversely. The forms of their magnetization curves have rather complex characteristics, which is based on the presence of both magnetically hard and soft components contained in the MHE. The magnetization affects also the viscoelastic properties of the composites.

The use of MHEs with such field-dependent properties offer great potential for designing intelligent technical applications. The concept to design an acceleration sensor system incorporating a sensing element based on the MHE is presented in [2]. According to it, the response of the MHE oscillating unit to external mechanical stimuli of the environment can be identified unambiguously by magnetic field measurements. In this work, we study free bending vibrations shown by macro beam samples made of MHEs in the presence of a uniform magnetic field. It is shown that for the beams magnetized along the length axis, there is a one-to-one correspondence between the displacement and magnetic field distortion measured by means of specially positioned Hall sensor. The sensitivity of the vibrating element can be changed using an external uniform magnetic field of a Helmholtz coil. It is based on the dependencies of the first eigenfrequency on the external applied magnetic field. It is found that for the beams magnetized along their length, these dependencies have almost linearly increasing trend. This is in the contrast to the results presented in [2] for magneto-sensitive elastomers incorporating magnetically soft particles.

Support by the RFBR, project 16-53-12009, and the Deutsche Forschungsgemeinschaft (DFG) within PAK907 under the projects PO 2013/1-1 and BO 3343/1-1 is acknowledged.

[1] D.Yu. Borin, G.V. Stepanov *J. Optoelectron. Adv. M.*, **15** (3-4) (2013) 249-253.

[2] T.I. Volkova, V. Böhm, T. Kaufhold, J. Popp, F. Becker, D.Yu. Borin, G.V. Stepanov, K. Zimmermann *J. Magn. Magn. Mater.*, **431** (2017) 262-265.

3PO-I3-2

MATHEMATICAL MODELING OF AN INVERSE FERROFLUID EMULSION: INFLUENCE OF DROPLET POLYDISPERSITY

*Subbotin I.M.*¹

¹ Ural Federal University, Institute of Natural Sciences and Mathematics, Department of Theoretical and Mathematical Physics, Lenin av. 51. 620000, Ekaterinburg, Russia
Igor.subbotin@urfu.ru

This work is focused on the mathematical modeling of the magnetic properties of an inverse ferroemulsion, which is a system of nonmagnetic fluid micro droplets (radius $\sim 5-10 \mu\text{m}$), suspended in magnetic fluid carrier. Under the action of an external magnetic field these droplets elongate along the applied field direction [1-2]. This behavior is pronounced for emulsions with rather weak values of the interfacial tension ($\sim 10^{-6} \text{ N/m}$) and provides the growth of emulsion magnetic susceptibility in rather weak external magnetic field ($\sim 0 - 0.5 \text{ kA/m}$). The same feature is known for the direct ferrofluid emulsion, in which a ferrofluid is used as the dispersed phase [1-4]. On the other hand, the degree of elongation becomes more significant with droplet's size growth.

In the other words, the size distribution of disperse phase is one of the most important factors, which determines the initial growth of emulsion magnetic susceptibility. In this work we introduce the model that describes the influence of drops polydispersity, which is based on the idea of double statistical averaging of the influence of droplets on the internal field configuration, and, finally, on the magnetic susceptibility of the inverse ferroemulsion. The first one is the averaging over the droplet's position inside the volume of the sample. The second one is the averaging over the size of droplet. The same idea for the direct ferrofluid emulsions is presented in the following paper [4].

In the zero-field limit our model gives a well-known Maxwell-Wagner formula [5] for initial magnetic susceptibility of emulsion:

$$\mu_0 = \mu_f - \mu_f \frac{3(\mu_f - 1)\varphi}{3\mu_f - (\mu_f - 1)(1 - \varphi)},$$

where μ_f stands for the magnetic susceptibility of the ferrofluid, and φ is the volume concentration of disperse phase.

The work is supported by the Ministry of Education and Science of the Russian Federation (Project No. 3.1438.2017/PP).

- [1] Yu.I. Dikanskii, A.R. Zakinyan, N.Yu. Konstantinova. *Technical Physics*, **53** (2008) 19.
- [2] Yu I. Dikansky, A.R. Zakinyan, A.N. Tyatyushkin, *Phys. Rev. E*, **84** (2011) 031402.
- [3] A.O. Ivanov, O.B. Kuznetsova. *Phys. Rev. E*, **85** (2011) 041405.
- [4] A.O. Ivanov, I.M. Subbotin. *Magnetohydrodynamics*, **52** (2016) 269.
- [5] Wagner K.W. ARCHIV FUR ELEKTROTECHNIK, **V. 2-3** (1914), Berlin.

3PO-I3-3

TO THE THEORY OF ELASTIC MODULUS OF MAGNETIC SOFT MATERIALS

Zubarev A.Yu.¹, Chirikov D.N.¹, Dobroserdova A.B.¹

¹ Ural Federal University named after the first President of Russia B.N. Yeltsin, Yekaterinburg, Russia

A.J.Zubarev@urfu.ru, D.N.Chirikov@urfu.ru, alla.dobroserdova@urfu.ru

Magnetic soft materials present new kinds of smart composite materials. Combination of a rich set of properties of polymer and magnetic media provides a new type of the multifunctional smart materials, which find extensive use in industrial and biomedical technologies.

One of the interesting, from the scientific point of view, and valuable, from the viewpoint of practical applications, features of ferrogels is their ability to change mechanical properties and behavior under the action of external magnetic field. Magnetic field induces significantly changes mechanical properties of these systems. These magnetomechanic effects are especially strong in the systems with internal heterogeneous structures (chains, columns, etc.) formed by the particles. Usually these aggregates are created by using magnetic field, at the stage of the polymer matrix curing, when it is liquid. Polymerization of the matrix fixes the internal structures in the composites.

Experiments [1] demonstrate significant increase, under the field action, of the elastic stress σ at a given uniaxial strain ε in magnetic elastomers with the chain-like aggregates, consisting of micron-sized magnetizable particles. The dependence of σ on ε , measured in [1], was nonlinear, with especially fast increase of σ at small ε . Effect of the magnetic field H on the stress in the same systems with homogeneous and isotropic spatial distribution of the particles was rather negligible; in the isotropic composites [1] the stress linearly depended on the strain. It is interesting to note that non monotonic, N -like shape of dependence of the difference $\delta\sigma = \sigma(H) - \sigma(0)$ on the tensile strain ε in the composites with the chains was detected in [1].

We present a microscopic model and results of theoretical study of the stress-strain dependence in magnetic polymers with the chain-like aggregates, consisting of micron-sized magnetizable particles. Both, uniaxial deformation of the sample in the chains direction and its shear deformations are considered. It is supposed that the chains have been created by the application of external magnetic field at the stage of the gel curing. That is why all chains are parallel to the field of polymerization.

Suggested model explains and reproduces experimentally detected [1] features of mechanical behavior of the system in the external field H : nonlinear dependence of the stress σ on the elongation strain ε ; finite (non zero) magnitude of σ at $\varepsilon=0$ in ferrogels placed in the uniform field H ; non monotonic dependence of the stress difference $\sigma(H) - \sigma(0)$ on the strain ε , as well as the N -shaped dependence of σ on ε .

This work has been done under the financial support of the Russian Fund for Basic Research, 16-58-12003, 16-53-12009, 16-32-00019 mol a, of the Program of Russian Ministry of Science and Education, project 3.12.2014/K.

[1] C. Bellan, G. Bossis, *International Journal of Modern Physics B*, **16** (2002) 2447-2453.

3PO-I3-4

MODELLING OF AN ELEMENTARY OF A MAGNETIC COLLOID WITH ACCOUNT FOR HYDRODYNAMIC INTERACTIONS

Melenev P.V.^{1,2}, Raikher Yu.L.², Rusakov V.V.²

¹Ural Federal University, Ekaterinburg, Russia

²Institute of Continuous Media Mechanics, Ural Branch of RAS, Perm, 614013, Russia
melenev@icmm.ru

Applications of nano- and micro-sized magnetic particles in biomedical tasks are developed intensely during the last three decades. The progress of theoretical study of the corresponding problems is restrained by the complex nature of considered phenomena which essential quality is interplay of diverse forces: magnetic, hydrodynamic, biochemical. The hydrodynamic contribution is usually accounted for by introducing Stokes-like friction terms in the equations of motion. However, this is certainly an oversimplification for the case of concentrated suspensions and/or in case of complex shapes of suspended particles like magnetic grains and bioplasts.

Our attempt to pay special attention to the hydrodynamic interactions between colloid particles employs a combination of computation techniques. The flow of the liquid carrier is described by the lattice-Boltzmann (LB) method, while the motion of the suspended particles is modeled in the framework of coarse-grained molecular dynamics (MD) which is bound to the LB system using point-coupling scheme. The actual size and shape of the floating objects are reproduced with the aid of the so-called raspberry (RB) model, which presents a suspended object as a dense and spatially invariant structure of MD-particles. The cooperative motion of these “RB seeds” allows to account for the excluded volume effect and to satisfy the boundary conditions at the object-liquid interface [1]. In the case of magnetic grains, the central seed of the RB entity is furnished with a magnetic dipole moment.

This scheme was successfully applied for the case of rotational diffusion of isolated magnetic particle [2]. Now we consider “cell” models for a concentrated colloidal solution, which contains a mixture of magnetic as well of non-magnetic particles.

The first variant of the problem is aimed at interpretation of microrheology experiments done on complex media. The model system consists of a single-domain spherical magnetic grain (center) surrounded with geometrically the same but non-magnetic objects, placed in the nodes of body-centered cubic or hexagonal crystall lattice cell for which the magnetic grain is the central node. Only rotational motion of the objects is allowed. The dynamic response to the external AC magnetic field is considered and the influence on that of the inter-objects distance and fluid viscosity is evaluated. The second examined case is inspired by the situation where the magnetic nanoparticles are embedded into a living tissue and, thus, interact with the bioplasts, e.g. in the process of magnetic hyperthermia. We assume that spherical single-domain magnetic grains cover a non-magnetic object of larger size and, possibly, non-spherical shape. To obtain a solution, a quasi-2D particle assembly is considered, where the centers of all the RB objects are kept in the same plane. However, the directions of objects and field rotation are not restricted. The magnetic grains sit in the vertexes of regular polygons, and similarly to the previous task, only the rotations of the RB objects is allowed when an external AC magnetic field is applied. The effect of the magnetic moment magnitude on the rotational dynamics of the objects is investigated in addition to the aforementioned factors.

Support by RSF grant 15-12-10003 is gratefully acknowledged.

[1] L.P. Fischer et al, *J. Chem. Phys.*, **143** (2015) 084107.

[2] P.V. Melenev, *J. Magn. Magn. Mater.*, **431** (2017) 145–148.

3PO-I3-5

MAGNETIC AND ACOUSTIC DISTURBANCE OF THE MAGNETIC FLUID COLUMN WITH AIR CAVITY

Polunin V.M.¹, Ryapolov P.A.¹, Ryabtsev K.S.¹

¹ Southwest State University, Kursk, Russia
r-piter@yandex.ru

The setup, designed to investigate the mechanisms of magnetic and acoustic perturbation of a column of magnetic fluid, is shown in Figure 1. Where 1 - moving device, 2 - neodymium magnet, 3 - coil, 4 - piezoelectric cell, 5 - cavity, 6 - tube with magnetic fluid, 7 and 8 - signal amplifiers, 9 - digital oscilloscope. Oscillograms were obtained for signals from an inductor and a piezoelectric plate for processes of air entrapment by a magnetic fluid, as well as for perturbations that occur when air bubbles pass through a bridge from a magnetic fluid.

The frequency of the variable component of the magnetic field within the measurement error corresponds to the expression known in the theory of acoustic cavitation for the frequency ν of the radial oscillations of the air bubble, obtained under the assumption of a spherically symmetric flow of an inviscid fluid:

$$\nu = (2\pi R_0)^{-1} \sqrt{3\gamma(P_0 + 2\sigma / R_0) / \rho},$$

where R_0 is the bubble radius; P_0 – hydrostatic pressure; $\gamma = C_p/C_v$ is the ratio of the specific heats of the gas in the bubble; P is the density of the MF.

The following patterns were revealed for a large number of experiments:

- the volume of the captured cavity is divided into 9-15 bubbles;
- the bubbles that come off the cavity first, have a larger size than the bubbles that come off the cavity last.
- the dependence of the size of the detached bubbles on their ordinal number has been established and presented in Figure 2.

The work was support by the project part of the state task of the Ministry of Education and Science of the Russian Federation. Project Code 3.2751.2017 / PP

[1] V.G.Bashtovoy, V.M.Polunin, M.L. Boev, P.A.Ryapolov // *Nanotechnics.*, **1(33)** (2013) 84-912.

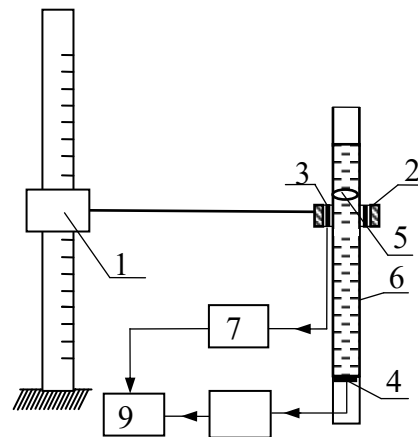


Fig. 1. Block diagram of the experimental setup.

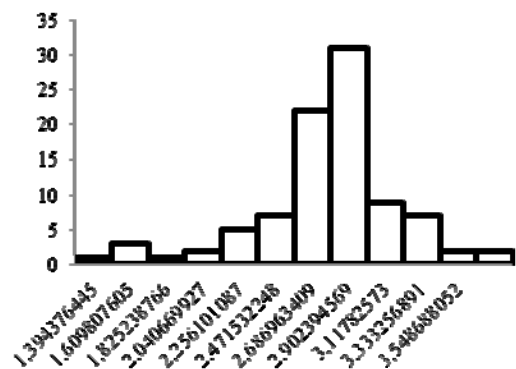


Fig. 2. Bubble size distribution.

3 July

Monday

12:00-14:00

poster session
3PO-K

**“Magnetism in Biology
and Medicine”**

3PO-K-1

POSSIBILITIES OF USING COMBINED MAGNETIC FIELD SENSORS IN MAGNETOCARDIOGRAPHY

Ichkitidze L.P., Telyshev D.V., Selishchev S.V.

National Research University of Electronic Technology, MIET, Zelenograd, Moscow, 124498
Russia
ichkitidze@bms.zone

Usually from living biological objects weak magnetic fields emerge (≤ 1 nT). The tools of their registration allow creating various functional methods of medical diagnostics. In this regard, one of the developing modern methods is magnetocardiography (MCG) [1].

MCG allows to register cardio diseases. High MCG indices are achieved by the use of numerous magnetic field sensors in them with a threshold sensitivity of $\delta B \leq 1$ pT.

The purpose of this paper is to compare the parameters of superconducting quantum interference devices (SQUID) and combined magnetic field sensors (CMFS) with the possibility decrease of their overall dimensions.

The MCG includes several tens or hundreds of SQUIDs with $\delta B \leq 1$ pT, and their dimensions are determined in the sizes of the receiving ring with a diameter of $D \sim 5 \div 10$ mm.

CMFS contains a magnetic field concentrator (MFC) and a structure based on the giant magnetoresistance (GMR) effect as a magnetosensitive element (MSE). Considered CMFS based on MFCs from a superconducting film (niobium, critical current density $\geq 10^{10}$ A/m², London penetration depth 50 nm, thickness 100 nm) and MSE from a GMR resistor with a relative magnetosensitivity of $\sim 10\%/mT$. The MFC had a nanostructured active band, which consisted of alternating parallel superconducting branches and slits with widths of $20 \div 500$ nm. Similar nanostructuring of active bands of CMS was investigated in [2].

The following parameters are obtained. SQUID on the basis of a high-temperature superconductor (HTSC): energy equivalent to noise $E_n \sim 10^{-27}$ J/Hz, magnetic field equivalent to noise $B_n \sim 0.03$ pT/Hz^{1/2}, $D \sim 1$ cm. CMFS consisting of the above parameters: $E_n \sim 10^{-27}$ J/Hz, $B_n \sim 0.1$ pT/Hz^{1/2}, $D \sim 0.2$ cm. These values are an order of magnitude better than those obtained in the CMFS in the composition of an MFC with a non-nanostructured active band, with $D = 2.5$ cm [4]. We assume that for CMFS with $D = 2.5$ cm and with a nanostructured active band, E_n and B_n are comparable in order of magnitude to those for low-temperature SQUIDs [5].

Thus, in the CMFS with nanostructured MFC the parameters close to HTSC SQUIDs are reached, and the dimensions are several times smaller than them. The use of multiple CMFS along with SQUIDs will significantly improve the MCG capabilities in recording the signs of the onset of cardio diseases. These CMFSs have the potential to be used both in the traditional magnetic resonance imaging (MRI, 1.5–4.5 T), so in the new direction of the MRI of a weak magnetic field (≤ 100 mT) [6]. The combination of magnetic systems MCG/MRI can significantly improve the accuracy of the functional state and localization of cardiac diseases, and they will be demand in medical practice.

This work was supported by the Ministry of Education and Science of the Russian Federation, agreement No. 14.581.21.0014 (Project ID RFMEFI58115X0014).

[1] Yu.V. Maslennikov, et al. *Physics Procedia.*, **36** (2012) 88.

[2] L.P. Ichkitidze. *AIP Advances*, **3**(6) (2013) 062125.

[3] M. Pannetier-Lecoecur [et al.]. *Review of scientific instruments*, **84** (2013) 095116.

[4] R.L. Fagaly. *Rev. Sci. Instrum.*, **77** (2006) 101101.

[5] A.N. Matlachov [et al.]. *Proc. of BIOMAG* (Boston), **39** (2004).

3PO-K-2

SELF-ASSEMBLY IN THE SYSTEMS OF MAGNETIC ANISOTROPIC NANOPARTICLES

Gudkova A.¹, Pyanzina E.¹

¹ Ural Federal University, Ekaterinburg, Russia
Elena.Pyanzina@urfu.ru

In the last few years, studying of systems with anisotropic magnetic nanoparticles became an independent fast-emerging branch of dipolar soft matter research. Such particles can be in a shape of spheres, ellipsoids, rods, etc. (for example, see [1,2]) with different orientation of magnetic moments (along/perpendicular to the main axis) placed in the center of their mass. These systems completely correspond to the idea of fine tuning and designing new smart materials with controllable microstructure and as a result various macroproperties via changing the particles shape and structure.

In this work we present a complex investigation influence of self-assembly in the system of magnetic ellipsoids using computer simulations and some theoretical approaches. We use method of molecular dynamics to run computer experiments, calculate initial susceptibility and radial distribution function. Also we performed cluster analysis in order to study type of clusters, their average characteristics and degree of clusterization.

The comparison of our theoretical models and the computer simulations results for a wide range of system parameters demonstrated good quantitative and qualitative agreement. We can conclude that microstructure of the systems significantly change with modifying particles parameters (both the shape and orientation of the magnetic moment) and system characteristics. As a result, macroscopic responses of the system strongly depend on the self-assembly of magnetic particles. That may prove to be very important in various medical applications where strong magnetic response of particles should be united with the absence of strong clustering.

[1] L. A. Trusov et al., *Chem. Commun.*, **50** (2014) 14581.

[2] P. Bender et al., *JMMM*, **372** (2014) 187.

3PO-K-3

STRUCTURE AND MAGNETIC PROPERTIES OF MAGNETITE-GOLD NANODUMBBELLS FOR MAGNETIC RESONANCE IMAGING

*Nalench Y.A.¹, Efremova M.V.², Shchetinin I.V.¹, Abakumov M.A.³, Savchenko A.G.¹,
Majouga A.G.^{1,2}*

¹ National University of Science and Technology "MISiS", Moscow, Russia

² Lomonosov Moscow State University, Moscow, Russia

³ Pirogov Russian National Research Medical University, Moscow, Russia
nalench_yulia@mail.ru

At the present time hybrid magnetite-gold nanoparticles (NPs) are of great interest for biomedical applications due to their unique properties that are different from the properties of individual magnetite and gold NPs [1]. Various types of hybrid NPs structure: core-shell, dumbbell-like NPs (or nanodumbbells), etc., are reported in the literature [2]. Dumbbell-like NPs consist of magnetite and gold NPs that are connected in pairs at the interface boundaries (Fig. 1). The presence of two types of surfaces allows double functionalization of nanodumbbells, for example, covering them with a biocompatible polymer shell and introduction of vector molecules. This feature of dumbbell-like magnetite-gold NPs is an obvious advantage over other types of hybrid NPs and it causes the possibility of their use for hyperthermia, targeted drug delivery and magnetic resonance imaging (MRI) as a contrast agent.

In this study the structure and magnetic properties of dumbbell-like magnetite-gold NPs for MRI diagnostics were investigated. Three samples of dumbbell-like NPs were obtained by thermal decomposition of iron pentacarbonyl in various high-boiling solvents: 1) in diphenyl ether; 2) in benzyl ether; 3) in 1-octadecene. According to the transmission electron microscopy data the magnetite NPs with the size from 10 to 30 nm were obtained. X-ray diffraction analysis, thermogravimetric analysis and measurement of magnetic properties were also carried out for all samples.

All samples were covered with a biocompatible polymer coating (the derivative of polyethylene glycol and phospholipid) transferring them to the aqueous phase before the MRI-relaxivity measurement. The values of the R₂-relaxivity from 200 to 400 mmol⁻¹·s⁻¹ were obtained and exceeded the values of commercial contrast agents (Feridex, Resovist).

Therefore, in this work structure and magnetic properties of magnetite-gold dumbbell-like NPs were investigated. It was also found that they can be potentially used as MRI contrast agents due to their high MRI-relaxivity.

This work was supported by Ministry of Education and Science of the Russian Federation (14.607.21.0132, RFMEFI60715X0132).

[1] C. Wang, C. Xu, H. Zeng, S. Sun, *Adv. Mater.*, **21** (2009) 3045-3052.

[2] K.C.-F. Leung, S. Xuan, X. Zhu, et al, *Chem. Soc. Rev.*, **41** (2012) 1911-1928.

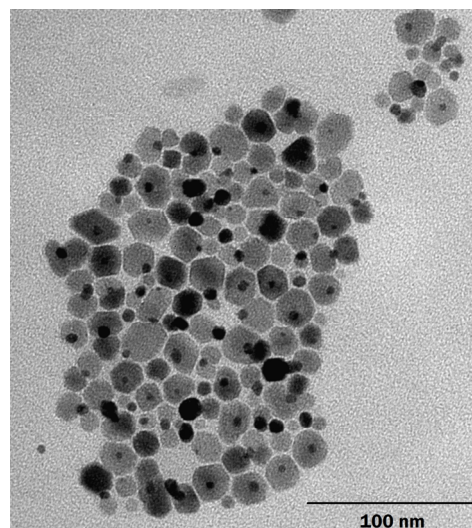


Fig. 1. TEM image of magnetite-gold nanodumbbells obtained in benzyl ether

3PO-K-4

SIZE EFFECTS IN FeGa_2O_4 – FeGaO_3 NANOCOMPOSITES OBSERVED BY MOSSBAUER, RAMAN AND MAGNETIC DATA

Gervits N.E.¹, Lyubutin I.S.¹, Starchikov S.S.¹, Lin C.-R.², Tseng Y.-T.²

¹ Shubnikov Institute of Crystallography of FSRC “Crystallography and Photonics” RAS, Moscow, 119333 Russia

² Department of Applied Physics, National Pingtung University, Pingtung County, Taiwan
ngervits@gmail.com

Magnetic nanoparticles are supposed to find applications in a huge variety of fields, including data record and storage, medical diagnosis and treatment, catalysis of chemical reactions and even magnetic greases. In each field the samples should meet special requirements. For example, the nanoparticles designed for medical purposes have to be biocompatible and their magnetic properties should be tuneable in specific ranges. No wonder the most popular base for design of such samples is biocompatible magnetite Fe_3O_4 . The spinel structure of magnetite itself is very flexible and can absorb a huge variety of ions on two crystal sites octahedral [B] and tetrahedral (A). This makes the search among the magnetite-based spinels very prospective.

In our study we focused on a series of the $\text{Fe}_{1+x}\text{Ga}_{2-x}\text{O}_4$ nanoparticles synthesized by the combustion method. We investigated the structure, magnetic and electronic properties in a wide temperature range of 5 – 300 K

From the comparative analysis by XRD, EDS, Raman and Mössbauer spectroscopy it was established the creation of a new spinel phase $\gamma\text{-FeGaO}_3$ mainly located on the particle surface. As a result, we ascertained that the composition consists of the FeGa_2O_4 core covered by the FeGaO_3 shell.

Different properties of the samples such as particle size, blocking temperature, anisotropy energy, magnetic and electronic state were observed and discussed as dependent of temperatures of annealing. The evolution of Mossbauer spectra in the series of nanocomposites with different particle size helped us to define the composition of the samples and deduce the correlation between annealing temperature and amount of different ions in different sites of the spinel structure [1]. In addition, we synthesized the bulk FeGaO_3 samples and investigated its structure and properties to confirm our statement that the obtained nano-samples consist of the combination of the FeGa_2O_4 and FeGaO_3 phases. Magnetic measurements in combination with Mossbauer data revealed the spin-glass behaviour in nanoparticles, previously observed in bulk samples [2,3].

Support by the Russian Scientific Foundation (Project #14-12-00848) is acknowledged.

[1] J. Ghose, *J. Solid State Chem.*, **79** (1989) 189–193.

[2] J. A. Mydosh, *Taylor & Francis, London, Washington, DC*, (1993).

[3] S. Mørup, M. Bo Madsen and J. Franck, *J. Magn. Magn. Mater.*, **40** (1983) 163–174.

3PO-K-5

STRUCTURAL AND MAGNETIC PROPERTIES OF COPPER SUBSTITUTED Mg-FERRITES FOR MEDIATED HYPERTHERMIA

Kiseleva T.Yu.¹, Kabanov V.M.¹, Ilyushin A.S.^{1,2}, Markov G.P.³, Sangaa D.⁴, Hirazawa H.⁵

¹Moscow M.V.Lomonosov State, Department of Physics, Moscow, Russia

²The Ibragimov Complex Institute, RAS, Grozny, Russia

³The Schmidt Institute of Physics of the Earth RAS, Moscow, Russia

⁴Institute of Physics and Technology, Mongolian Academy of Sciences, Ulan Bator, Mongolia

⁵National Technological Institute, Ehime, Japan

Kiseleva.Tyu@gmail.com

Magnesium ferrite (MgFe_2O_4) is one of the most important ferrites, which finds a number of applications in heterogeneous catalysis, adsorption, sensors, and in magnetic technologies. A modern attractive application of Mg-ferrites is their use in nanosized forms in biomedical technologies as components in systems for magnetically mediated hyperthermia [1]. Specific important magnetic properties of ferrites used for these purposes may be modulated as by type of substituting metals, included in their composition, the cationic distribution and interaction between them, as distributions of particles' sizes [2-3].

In our work, polycrystalline ferrite powders of $\text{Mg}_{1-x}\text{Cu}_x\text{Fe}_2\text{O}_4$ ($x = 0.2, 0.4, 0.6, 0.8, 1$) system obtained by ceramic technology have been investigated. Synthesized samples showed the non-monotonic dependence of heat generation effect in AC magnetic field with increasing concentration of copper. To reveal peculiarities of the structural and magnetic state of the samples and its influence on the heat generation ability we performed complex study, including X-ray diffractometry, Mössbauer spectroscopy, Scanning electron microscopy, measurements of temperature dependences of susceptibility and saturation magnetization, hysteresis parameters.

Typical ferrimagnetic character with small coercivity and saturation magnetization was found. We carried out that anomalous influence of Cu^{2+} ion substitution respectively to the $\text{Mg}_{1-x}\text{Cu}_x\text{Fe}_2\text{O}_4$ ferrite powder manifested in heat generation ability rise up to $x=0.6$ with subsequent sharp reducing of this characteristic was accompanied with the main phase crystal structure distortion followed by phase separation to cubic and tetragonal structure. This was matched by in an increase of ferrite particles crystallite size and size distribution appearance. The saturation magnetization and Curie temperature dependences observed for powders via Cu substitution were explained by phase composition, the cations distributions between ferrite sublattices, modulation of exchange interaction.

[1] T.Maehara, K.Konishi et al. *J. of Materials Science*, **40** (2005) 135-138.

[2] H.Hirazawa, et.al. *J.of Alloys and Compounds*, **461** (2008) 467-471.

[3] H.Hirazawa, Y.Ito, D.Sangaa et al. *AIP Conference Proceed.*, **1763** (2016) 020009.

3PO-K-6

MAGNETIC SEDIMENTATION OF HETEROGENEOUS WATER SUSPENSIONS OF TiO₂ AND Fe₃O₄@SiO₂ NANOPARTICLES

Filinkova M.^{1,2}, Bakhteeva Yu.¹, Byzov I.¹, Medvedeva I.¹

¹ M.N. Mikheev Institute of Metal Physics UB RAS, Ekaterinburg, Russia

² Ural Federal University, Ekaterinburg, Russia

filinkova-ms@yandex.ru

Separation of nanoparticles from liquid solutions is important problem for many processes when nanosorbents are used for water and soils purification from hazardous impurities, for biological cells and organic molecules separation, etc. When the nanoparticles themselves have magnetic core (e.g. iron or magnetic iron oxide) or can be attached to other magnetic particles the particle separation can be strongly enhanced in a gradient magnetic field [1]. In particular, for separation of nonmagnetic TiO₂ nanoparticles from water a magnetic seeding of surface modified magnetite nanoparticles (γ -Fe₃O₄ covered by SiO₂) can be used [2].

Sedimentation of the mixed water suspensions of TiO₂ (15-20 nm) and Fe₃O₄@SiO₂ (30-40 nm) particles was studied in inhomogeneous magnetic field ($B \leq 0.3T$, $dB/dz \leq 0.16$ T/cm). Sedimentation dynamics was monitored by optical method at the nanoparticles concentrations ratio 1:1, 1:0.5 and 1:0.25, at the aqueous medium acidity pH = 4, 5.

Dynamic Light Scattering method was used to determine the aggregates sizes and Zeta potential values. Spectrophotometric and Nuclear magnetic resonance relaxometry methods were used in order to detect the residual nanoparticles concentration in water after magnetic sedimentation. For the spectrophotometric concentration determination of the TiO₂ and Fe₃O₄@SiO₂ separate components a preliminary calibration based on the PLS method has been done.

The aggregates sizes of both initial suspensions were close to 180-200 nm. Zeta potential of the TiO₂ particles changed from 42 ± 2 mV (at pH = 4) to 35 ± 2 mV (at pH = 5) and Zeta potential of the Fe₃O₄@SiO₂ particles was -37 ± 2 mV for both pH values. Prior to the magnetic sedimentation the suspension have been kept without magnetic field for 30 minutes. The average size of the aggregates was dependant on the pH value and on the mass proportions of the nanopowders in water.

The magnetic sedimentation rate depends mainly on the mass ratio of the TiO₂ and Fe₃O₄-SiO₂ nanopowders. The lowest sedimentation rate was observed for the mass ratio 1:0.25, which is accounted for by minimal electrical charge compensation under these conditions. The particles settling dynamics at the ratios 1:0.5 and 1:1 are close because of the features of the aggregates formation. The increase of pH leads to a slowing of the sedimentation process, which reflects the electrostatic interparticle repulsion strengthening. It has been shown that the increase of magnetic sedimentation time over 25 minutes doesn't bring about further nanoparticles concentration reduction in water.

The results obtained can be used for development of water purification technologies by using magnetic separation of nanosized sorbents.

The research was carried out within the state assignment of FASO of Russia (theme "Magnit" No.01201463328), supported in part by the Ural Branch, Russian Academy of Sciences – Russia (project No. 15-9-24-10).

[1] I. Medvedeva, M. Uimin, A. Yermakov, et al, *J. Nanopart. Res.*, **14** (2012) 740.

[2] Iu.Bakhteeva, I. Medvedeva, M. Uimin, et al, *J.Sep. Purif. Technol.*, **159** (2016) 35–42.

3PO-K-7

MAGNETIC NANOPARTICLE BASED STUDY AND TREATMENT OF GLIAL MALIGNANT TUMORS IN RATS

Brusentsov N.A.¹, Polyanskiy V.A.², Pirogov Yu.A.³, Anisimov N.V.³, Gulyaev M.V.³, Nikitin M.P.^{4,5}, Ksevevich T.I.⁵, Nikitin P.I.^{4,6}, Bocharova O.A.¹

¹ Blokhin Russian Cancer Research Center, MHRF, 115478 Moscow, Russia

² Institute of Mechanics, Lomonosov MSU, 119192 Moscow, Russia

³ Faculty of Fundamental Medicine, Lomonosov MSU, 119992 Moscow, Russia

⁴ Prokhorov General Physics Institute, RAS, 119991 Moscow, Russia

⁵ Moscow Institute of Physics and Technology, Dolgoprudny, 141700 Russia

⁶ National Research Nuclear University MEPhI (Moscow Engineering Physics Institute), Russia
brusentsov2005@yandex.ru

A new generation of Magnetic Particle Quantification (MPQ) prototypes, which employ non-linear magnetization of magnetic nanoparticles [1, 2], have been developed for biomedical research in vivo. These room temperature instruments are integrated with a remote inductive probe. By scanning an animal body with the remote probe as shown in Fig. 1, it is possible to record a rough “image” of the MP distribution with high sensitivity. In this work, the MPQ technique was used for metrology of citric-ferrite (CF) nanoparticle doses for contrast-enhanced magnetic resonance imaging (MRI) and combined photodynamic magnetotherapy of glial malignant tumors in rats. For early visualization of proliferation centers of the glial tumors by MRI, a new contrasting method has been developed based on consecutive intravenous injections of CF sol (as a negative contrasting agent) and Magnevist® (a positive agent). This procedure reduces the time before tumor visualization up to 2 - 3 days after inoculation.

As the next step, the CF nanoparticles were used with Radachlorin at light irradiation ($\lambda \sim 650-850$ nm), which induced cell death together with As_2O_3 preparation heated up to 45 °C by CF nanoparticles under effect of an alternating 0.15-kW magnetic field at 0.88 MHz. 24 rats with glioma C6 were divided as follows: group 1 of 12 rats, groups 2 and 3 of 6 rats each. The same was done for 24 rats with glioblastoma 101/8) - groups 1', 2' and 3', respectively. The tumor volumes V were 3 - 4 mm³ in the groups 1-3, and 5 - 7 mm³ in the groups 1'-3'. On the 3rd day, in each rat of groups 1 and 1', solely buffer (0.9 % NaCl) was injected in right and left carotids having a tumor. The chemotherapeutic drug Temodal at the dose of 50 mg/kg was administered to each rat of the groups 2 and 2'. The rats of groups 3 and 3' were treated by a combined therapy: Radachlorin (3 μ l of 0.35% solution) was injected into the tumor through implantation aperture and then irradiated for 30 min by ultra-white LED light as in [3]. After this, CF- As_2O_3 sol (25 μ l of 40%) was injected in the right carotids. Then the rats were maintained for 45 min in a RF magnetic field at 0.88 MHz produced by a localized high-Q-resonator fed with 0.15 kW power.

The combined photodynamic and magneto-thermo-chemo-therapy of tumors were tested for the first time. This treatment of the tumors increased life span of rats with glioma (GC6) up to 190% and at glioblastoma (GB 101/8) up to 96%.

Support by RSF and RFBR is acknowledged.

[1] A.V. Orlov et al. *Analytical Chemistry*, **88** (2016) 10419–10426.

[2] V.O. Shipunova et al.. *Nanoscale*, **8** (2016) 12764-12772.

[3] N.A. Brusentsov, V.A. Polyanskiy et al., *Solid State Phenomena.*, **233-234** (2015) 757-760.



Fig. 1. Experimental setup.

3PO-K-8

RECONFIGURABLE SETUP FOR MAGNETOTHERMAL PROPERTIES MEASUREMENTS OF MAGNETIC FLUIDS AND IMPLANTS

Salakhova R.T.¹, Vylegzhanin A.G.¹, Kritskaya E.A.², Pyatakov A.P.¹, Markov V.K.³,
Malyshev A.Yu.³, Kamilov K.I.¹, Tishin A.M.^{1,3}

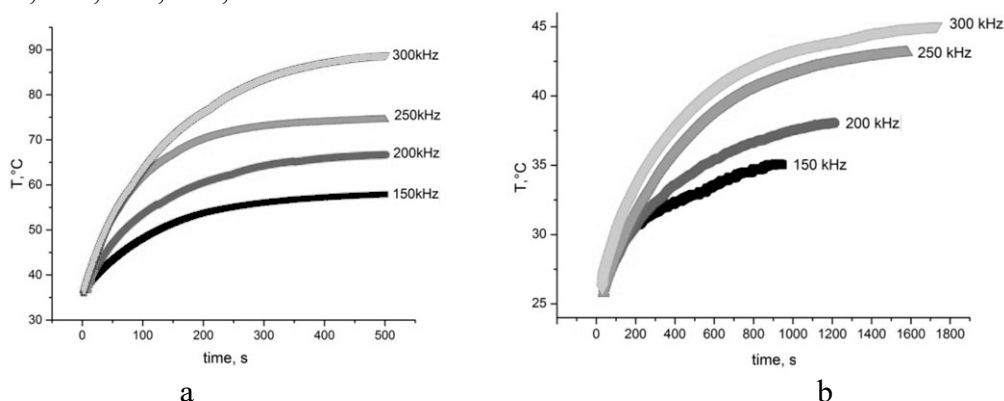
¹ M.V. Lomonosov Moscow State University, Moscow, Russia

² LLC Shell, Moscow, Russia

³ AMT&C Group, Troitsk, Russia
vilegzhanins@yandex.ru

Magnetic nanoparticles (MNp) have attracted attention in modern medicine due to their possibility of injecting and accumulating in the target tissue. Heating of MNp in alternating (AC) magnetic field leads to the therapeutic effect either through direct thermal treatment or due to the release of the drug encapsulated in the nanoparticles [1]. The magnetically functionalized implants, which consist of polymeric matrices and MNp, also can be used in effective non-invasive therapeutic methods. The magnetothermal properties of nanoparticles strongly depend on frequency of AC magnetic field so it is crucial to have the setup with easily changeable frequency range.

The proposed experimental setup for calorimetric measurements comprising an AC magnetic field module (magnetic coil, switched capacitor array, generator) that enables changing the magnetic field amplitude in the range 0-200 Oe and fine tuning of the frequency in the vicinity of the set of values: 100, 150, 200, 250, 300 kHz.



On the figure the two typical cases of heating dynamic dependence on frequency are demonstrated that were obtained with the reconfigurable setup: a) the one is rapidly increasing with frequency for suspension of magnetite nanoparticles (with diameter less than 100nm); b) the another is saturating dependence for large submicron particles (size exceeds 0.5μm) in polymer implant coating. The amplitude of AC magnetic field was 100 Oe.

The support of Foundation for Assistance to Small Innovative Enterprises in Science and Technology (project #C1-21200) is acknowledged.

[1] Ch. S.S.R. Kumar, F. Mohammad, *Advanced Drug Delivery Reviews*, **63** (2011) 789.

3PO-K-9

NOVEL HIGH SENSITIVE METHOD FOR DETECTION OF MAGNETIC NANOPARTICLES IN LIVING CELL AND BIOLOGICAL MEDIA BY NMR RELAXOMETRY

Byzov I.V.¹, Minin A.S.^{1,2}, Uimin M.A.^{1,2}, Yermakov A.E.^{1,2}, Mysik A.A.¹, Zhakov S.V.¹, Ulitko M.V.²

¹ IMP UB RAS, Ekaterinburg, Russian Federation

² UrFU, Ekaterinburg, Russian Federation

ivbyzov@gmail.com

The investigation of the interaction kinetics of magnetic nanoparticles with living cells is important for a wide range of fields in biotechnology, medicine and ecology. Understanding these processes allows us to select the optimal concentrations of magnetic nanoparticles for magnetic hyperthermia, magnetic separation and labeling of cells.

The NMR-relaxometry method permits to determine with high accuracy the concentration of magnetic nanoparticles in biological fluids by measuring the relaxation time T2 on the proton in a liquid [1].

A portable NMR relaxometer with an operating frequency of 4.317 MHz was constructed, which allows to estimate expressively the relaxation time of small volumes (from 10 μ l or more) of liquid. At the same time, the sensitivity in the range of few micrograms of magnetic nanoparticles per milliliter of liquid was achieved. A technique for studying the kinetics of capture of magnetic nanoparticles by HeLa cells has been developed. Using this technique, the interaction of iron-carbon nanocomposites modified with amino- and carboxyl groups with cells at temperatures of 37 and 4 °C was studied (Fig. 1.).

It was shown that the cells absorb only aminated particles at a temperature of 37 °C. The lack of capture at 4 °C indicates that the capture mechanism is active and is not associated with simple sorption of nanoparticles on the surface. The weak capture of carboxylated particles is associated with their negative surface charge, since the surface cell is negatively charged as well.

Thus, by the NMR-relaxation method it is possible to establish the fact of interaction of particles with cells, to estimate them quantitatively and to make an assumption about the capture mechanism.

Support by the state assignment of FASO of Russia (theme "Magnit" No.01201463328) and KCE of URFU are acknowledged.

[1] J.W. Bulte, P.G. Laughlin, E.K. Jordan, V.A. Tran, J. Vymazal, J.A. Frank. *Acad Radiol.* **3** (1996) 301-303.

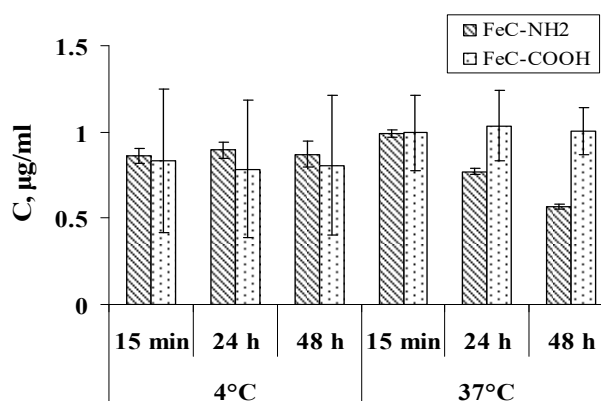


Fig. 1. Temperature and time dependences of magnetic nanoparticle concentration in culture medium.

3PO-K-10

EFFECT OF SYNTHESIS TECHNIQUE ON THE MAGNETIC PROPERTIES OF $\text{Fe}_m\text{O}_n\text{-SiO}_2$ COLLOIDAL PARTICLES

Gareev K.G.¹, Kharitonskii P.V.^{1,2}, Korolev D.V.³, Panov M.F.¹, Pugach V.S.¹, Sergienko E.S.²

¹ Saint Petersburg State Electrotechnical University "LETI", Saint Petersburg, Russia

² Saint Petersburg State University, Saint Petersburg, Russia

³ Federal Almazov North-West Medical Research Centre, Saint Petersburg, Russia

kggareev@yandex.ru

Magnetic nanoparticles based on iron oxide and silica are promising for theranostics since they can be used for targeted drug delivery, hyperthermal therapy and nuclear magnetic resonance imaging. It was previously established that the choice of the method for producing $\text{Fe}_m\text{O}_n\text{-SiO}_2$ particles has a significant effect on their biological properties, and the presence of a SiO_2 shell significantly reduces the toxicity of colloidal particles [1].

In the present study, colloidal iron oxide particles in a silica coating obtained by the sol-gel method in accordance with [1], as well as $\text{Fe}_m\text{O}_n\text{-SiO}_2$ particles modified with the carbohydrate shell via the hydrothermal treatment method were investigated. To do this, D-glucose powder was added to the aqueous solution of $\text{Fe}_m\text{O}_n\text{-SiO}_2$ colloidal particles until a saturated solution was obtained. The treatment was carried out at a temperature of 160 °C for 24 hours. The resulting solution was washed five times with distilled water under the action of a constant magnetic field. The dried powder was examined using scanning and transmission electron microscopy, FTIR spectroscopy, and vibrating sample magnetometry.

It was found that the saturation mass magnetization of particles after hydrothermal treatment increases from 16.0 to 60.0 emu/g and the coercive force decreases from 5 to 2 Oe. Thus, the value of the coercive force corresponds to $\text{Fe}_m\text{O}_n\text{-SiO}_2$ particles with a SiO_2 core [1, 2] that does not have an outer shell but the saturation mass magnetization is 27 times higher (Fig. 1). The magnetic properties of the resulting nanoparticles can be explained by a much lower oxidation of magnetite to maghemite and hematite due to an additional protective shell. Other reasons can be the dimensions of individual grains of magnetite 5–15 nm according to transmission electron microscopy data and weak magnetostatic interaction between grains similar to the colloidal particles with a nucleus of SiO_2 [2].

Measurements of NPs were carried out with the equipment of the Resource Centre "Innovative technologies of composite nanomaterials", Saint-Petersburg State University.

Development of synthesis technique was partially supported by RFBR, project No. 16-32-60010.

[1] Y.G. Toropova et al, *Int. J. Nanomed.*, **12** (2017) 593-603.

[2] P.V. Kharitonskii et al, *Sol. St. Phen.*, **249** (2016) 138-141.

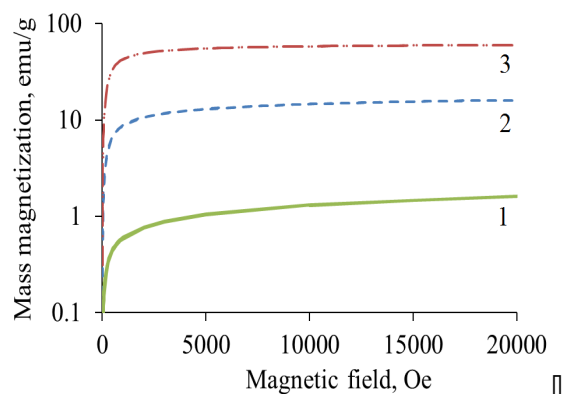


Fig. 1. Magnetization curves of samples: 1 – without shell [2], 2 – with SiO_2 shell, 3 – with SiO_2 and carbohydrate shell.

3PO-K-11

FEM-MODELLING OF THIN FILM MAGNETOIMPEDANCE SENSITIVE ELEMENT DESIGNED FOR BIODETECTION

Volchkov S.O.¹, Chlenova A.A.¹, Lepalovskij V.N.¹

¹ Ural Federal University, Laboratory of Magnetic Sensors, Mira 19, 620002 Ekaterinburg, Russia
stanislav.volchkov@urfu.ru

Magnetic soft matter (ferrofluids or ferrogels) is one of the rapidly growing area of research and applications including magnetic biosensing [1]. Giant magnetoimpedance (GMI) is the effect which with proven capacity to quantify the presence of magnetic nanoparticles in the biological samples. It was used for magnetic label detection in different biological samples from model ferrofluids, ferrogels to *in vitro* grown cell cultures. The aim of this work is to create a universal model to simulate conditions of magnetic biodetection in GMI multilayers. Finite element method (FEM) allows calculations of high-frequency current distribution using the Maxwell's equations taking into account the magnetodynamics of iron oxide water-based ferrofluid in small channels similar to the blood vessels. The modeling was realized with the licensed software Comsol©. The calculations were performed on a specialized engineering server based on four processors Intel Xeon E5 and 124 Gb RAM, adapted for parallel computations. Such hardware is suitable for description of individual layers with nanometer dimensions and the number of elements in the mesh structure more than 10^6 cells. The designed model allows calculations of the current density, the outside magnetic flux, resistivity heating for each one of the created cells and total value by integration of sub-domains. One can quantitatively describe concentration of ferrofluid, velocity and pressure in the blood vessel. These changes affect the magnetoimpedance of the film FeNi-based multilayers.

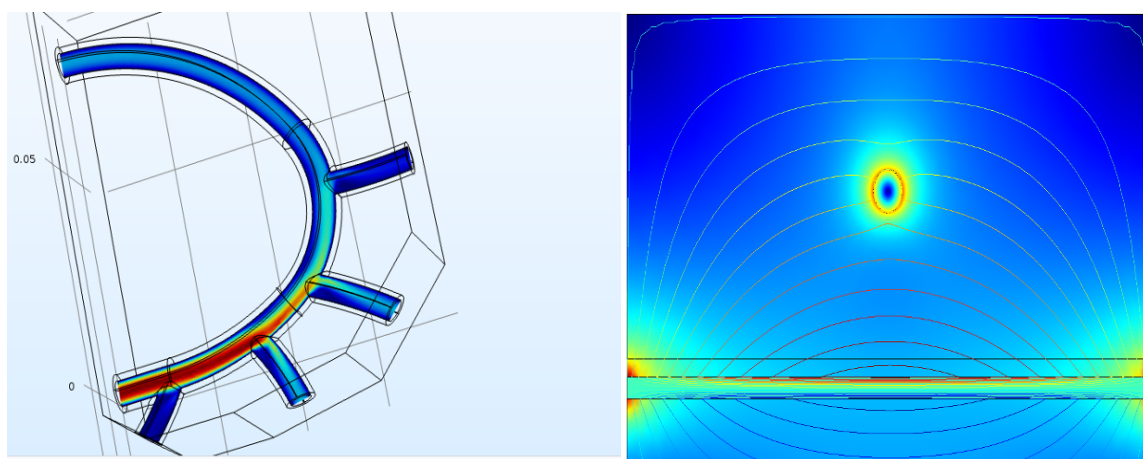


Fig 1. (a) Velocity of Fe_3O_4 nanoparticles in a model of blood vessel with different concentration. (b) Magnetic flux distribution in a model system consisting of a blood vessel and thin film GMI element.

This work was performed under financial support of The Ministry of Education and Science of the Russian Federation, project 3.6121.2017.

[1] V. Fal-Miyar, A. Kumar, Sh. Mohapatra, Sh. Shirley, N.A. Frey, J. M. Barandiarán, G.V. Kurlyandskaya, *AIP Conference Proceedings*, **1025** (2008) 131.

3PO-K-12

BIO-MEDICAL APPLICATIONS OF MAGNETIC DIAMOND NANOPARTICLES

*Karmenyan A.¹, Perevedentseva E.^{1,2}, Lin Y.-C.^{1,3}, Song C.-Y.¹, Lin Z.-R.¹, Liu L.-C.¹,
Chang C.-C.¹, Norina S.⁴, Bessalova V.⁴, Perov N.⁴, Cheng C.-L.¹*

¹ National Dong Hwa University, Hualien, Taiwan

² P. N. Lebedev Physics Institute of Russian Academy of Science, Moscow, Russia

³ Institute of Physics, Academia Sinica, Taipei, Taiwan

⁴ Moscow State University, Moscow, Russia

elena@gms.ndhu.edu.tw

Development of nanoparticles (NP) applications for bio-medical research and theranostic is recently focused on multifunctional NP, with integration of various functionalities. The multifunctional NP are designed to co-deliver multiple components, control the delivery, realizing drug and diagnosis simultaneously. To integrate several functionalities, different methods of surface functionalization and modifying the particles physical properties are developed. Number of NP can reveal wide variability of utilized properties: noble metals NP, carbon- and silicon- based NP of different structure, metal oxides and metal-doped NP, polymer NP, etc., as well as their composites [1].

Among these NP nanodiamond (ND) is promising for development of multifunctional complex due to their widely variable features in sizes, structure, surface chemistry, physical properties and their biocompatibility [2]. Additionally to well-studied structural, surface, electrochemical and photonic properties of ND, strong magnetism can be observed in carbons and nanocarbons. The origin of ferromagnetic and superparamagnetic properties in carbon nanostructures containing intermediate graphite–diamond ordering is studied [3].

In this work we characterise and discuss magnetic-modified ND (Ray Techniques, Israel) [4]. The strong magnetic susceptibility of this ND has been demonstrated. Additionally the ND reveals strong fluorescence at two-photon excitation, and well-detectable signal at fluorescence lifetime analysis. The origins of the magnetism and fluorescence are discussed.

The ND has been characterized, first of all, in terms of its bioapplications. The ND biocompatibility and methods of improving biocompatibility are demonstrated. ND interaction with cells and 3D cellular structures [5] with and without applied magnetic field [6] was observed. The combining fluorescence and magnetic properties of ND with its biocompatibility make it promising for various imaging and delivery bio-applications, e.g. to realize and observe magnetic filtration, magnetic-guided delivery, magnetic-assisted 3D cellular growth.

Support by the Ministry of Science and Technology of Taiwan, Grant No. MOST 103-2112-M-259-001-MY3 is acknowledged. We also are grateful to Dr. O. Levinson (Ray Techniques) for the provided ND samples.

[1] G. Bao et al., *Annu. Rev. Biomed. Eng.*, **15** (2013) 253-282.

[2] E. Perevedentseva, et al., *Future Medicine. Nanomedicine*, **8** (2013) 2041-2060.

[3] O. Levinson et al., *J. Nanoscience & Nanotechnology*, **15** (2015) 1045-1052.

[4] T.L. Makarova, *Semiconductors*, **38** (2004) 615-638.

[5] H.-L. Ma et al., *Molecular Imaging*, **11** (2012) 487-498.

[6] W. M. Guo et al., *Mol. Pharmaceutics*, **11** (2014) 2182-2189.

3PO-K-13

MAGNETOIMPEDANCE EFFECT IN CoFeMoSiB AS-QUENCHED AND SURFACE MODIFIED AMORPHOUS RIBBONS COVERED BY WATER BASED FERROFLUID

Lotfollahi Z.¹, Amirabadizadeh A.¹, Safronov A.P.^{2,3}, Kurlyandskaya G.V.^{2,4}

¹University of Birjand, 97175-615, Birjand, Iran

²Ural Federal University, 620083, Ekaterinburg, Russia

³Institute of Electrophysics UD RAS, 620016, Ekaterinburg, Russia

⁴University of the Basque Country UPV-EHU, 48940, Leioa Spain
lotfollahi@gmail.com

Giant magnetoimpedance (GMI) has been proposed as a powerful technique for biosensing. In GMI biosensors based on the magnetic label detection the change of the impedance of sensitive element under the application of an external magnetic field was analyzed in the presence of magnetic nanoparticles (MNPs) in a test solution [1]. The surface roughness of the ribbon is important in the case of strong skin effect. Naturally formed or artificially designed surface defects are important for control of the sensitivity [2].

In this work, the GMI responses of as-quenched CoFeMoSiB ribbon in initial state and after surface modification were studied in the presence of water based ferrofluid (FF) at different alternating current (AC) frequencies and intensities. Surface modification of the amorphous ribbon was done in an ultrasonic bath with an appropriate H_3PO_3 acid concentration for creation of artificial surface defects. Surface features before and after modifications were studied by the scanning electron microscopy. The geometry of CoFeMoSiB element was 3.5 cm \times 0.7 mm \times 20 μ m. Iron oxide MNPs were synthesized by the laser target evaporation [3]. Electrostatically stabilized FF were prepared by ultrasound treatment using sodium citrate solutions (5 mM) in distilled water. MNPs contained only one crystalline phase of ferrite with a mean crystallite size of 19 ± 2 nm. The lattice parameter a of MNPs $a = 8.375(9)$ Å was lower than the typical for magnetite but higher than the lattice parameter for γ - Fe_2O_3 . For GMI measurements sensitive element was placed into 30 mm long and 1 mm in diameter plastic tube filled with ferrofluid. Magnetic measurements were done by vibrating sample magnetometry. It was observed that after surface modification the coercivity was slightly increased from 0.3 to 0.4 Oe, and saturation of magnetization decreased from 87 to 76 emu/g in a good agreement with the increase of the surface roughness, a decrease of magnetic elements concentrations in the surface layer and formation of a surface protective oxide layer. In a frequency range 0.5-10 MHz the shapes GMI responses of the as-quenched and surface modified ribbons were similar. Covering by FF resulted in a decrease of GMI ratio in comparison with response in absence of MNPs. The GMI difference for as-quenched ribbons in absence and in the presence of FF was more pronounced in comparison with the same measurements for surface modified ribbons. We discuss observed behavior taking into account the effective magnetic anisotropy features and contribution of the stray fields created by superparamagnetic MNPs in the non-zero magnetic field.

This work was supported in part by Spanish MECMAT2014-55049-C2-1-R grant. We thank O.M. Samatov for special support.

[1] Kurlyandskaya G.V., Levit V. *Biosens. Bioelectr.*, **20** (8) (2005) 1611.

[2] Manna S.K., Srinivas V. *J. Magn. Magn. Mater.*, **418** (2016) 62.

[3] Safronov A.P., Beketov I.V., Komogortsev S.V., Kurlyandskaya G.V., Medvedev A.I., Leiman D.V., Larrañaga A., Bhagat S. M. *AIP Adv.* (2016) 052135.

3PO-K-14

CHARACTERIZATION OF MAGNETITE-BASED NANOCOMPOSITE BY NONLINEAR MAGNETIC RESPONSE

Ryzhov V.A.¹, Marchenko Ya.Yu.², Kiselev I.A.¹, Bogachev Yu.V.³, Nicolaev B.P.², Deriglazov V.V.¹

¹NRC "Kurchatov Institute" PNPI, Gatchina, Russia

²Research Institute of Highly Pure Biopreparations, St Petersburg, Russia

³S-Petersburg State Electrotechnical University "LETI", St Petersburg, Russia

deriglaz_vv@pnpi.nrcki.ru

The systems of nanosize iron-oxide particles attract attention as a perspective object for biomedical applications, particularly, in diagnostics and hyperthermal therapy of cancer. They exhibit a strong nonlinear superparamagnetic response at the frequencies ~ 10 MHz and steady magnetic fields ~ 100 Oe what makes this technique perfectly well available for characterizing such systems. In this study, a water suspension of nanosize (~ 10 nm) dextran-coated magnetite particles was studied with the second-harmonic magnetic response (M2) supplemented with transmission electron microscopy (TEM), dynamic light scattering (DLS) and electron paramagnetic resonance (EPR). Using the formalism based on the Fokker-Planck kinetic equation in the treatment of M2 data (Fig.1), a set of geometrical, magnetic and magneto-dynamical parameters completely characterizing the system was extracted from the field dependences of the real and imaginary parts of the response, with the lognormal distribution over volumes verified by TEM and DLS. These are the mean magnetic moment and the distribution width, the damping factor and the Néel relaxation time featuring the magnetic dynamics, the magnetic anisotropy and its direction, the mean magnetic moment per Fe ion, etc. From DLS and TEM, the suspended composite forms a polydisperse system of aggregates containing $\sim 10 - 100$ particles. From M2 measurements, the particles inside an aggregate were shown to be spatially magnetically correlated at a relatively short distance, due to dipole-dipole coupling. However, there is a considerable admixture of magnetic disorder in an aggregate even within the correlation length resulting from anisotropy of the dipolar forces. By simulating the correlations with the cutoff function for the aggregate magnetic moment $F = 1 - \lambda \ln(r/r_c)$, the total magnetite component of the aggregate volume distribution was recovered and the mean dextran shell thickness was determined from comparison with the TEM data. The damping factor $\alpha \sim 0.2$ implies interference of precession and thermal diffusion in dynamics of the aggregate magnetic moments. The moments exhibit the tendency to orient along the field, predominantly by *mechanical* rotation of aggregates driven by their uniaxial magnetic anisotropy. In the EPR signal, two resonance maxima are distinguished, the larger one arising from *uncorrelated* particles. This effect results from breakdown of correlations by EPR Zeeman field exceeding the dipolar forces.

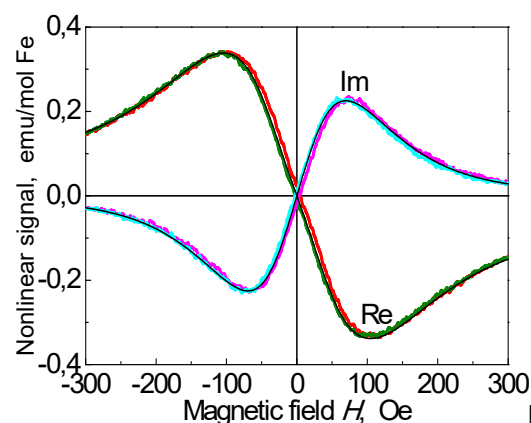


Fig. 1. Real and imaginary parts of 2-nd harmonic magnetic response vs constant magnetic field obtained with exciting field 13.8 Oe and frequency 15.7 MHz (points) and their best fit (solid lines).

3PO-K-15

CONDENSATION OF CARBON IN AROMATIC SOLVENTS AS A FACTOR OF INFLUENCE ON THE MAGNETIC PROPERTIES OF Co-BASED RIBBONS

Golubeva E.V., Chlenova A.A., Stepanova E.A., Volchkov S.O.

Dept. Magnetism and Magnetic Nanomaterials, Ural Federal University, Ekaterinburg, Russia
chlenova.anna@gmail.com

The carbon based functional coating can improve adhesion and antioxidant properties of the surface of the magnetic sensor elements for biomedical applications. The process of low-temperature condensation of carbon [1] in the aromatic solvents is a promising way to create such coatings. Contribution of the surface stresses on the magnetic properties in the case of magnetic ribbons can play a major role. Giant magnetoimpedance (GMI) is an effect of the change of the total impedance of the ferromagnetic conductor when alternating current flows through it and external magnetic field is applied. GMI is very sensitive to changes in the surface properties. Low temperature condensation of carbon was not yet investigated for the case of the amorphous ribbons. In this work magnetic properties, GMI and the surface effects are introduced by carbon coating were investigated for the case of the rapidly quenched amorphous ribbons.

Two alloys were studied: S1 - $\text{Fe}_3\text{Co}_{67}\text{Cr}_3\text{Si}_{15}\text{B}_{15}$ (width 0.8 mm) and S2 - $\text{Fe}_5\text{Co}_{70}\text{Si}_{15}\text{B}_{10}$ (width 1.3 mm) after treatment in an aromatic solvent (toluene) for 1 month (S1-T1m, S2-T1m) and 2 months (S1-T2m, S2-T2m). Samples without treatment (S1-cl and S2-cl) were also studied. The magnetization curves were measured by the magneto-optical Kerr microscope and in the quasi-static regime of magnetization reversal, using the induction-pulse method. GMI was measured using a precision Agilent HP e4991A impedance analyzer in the “microstripe” line for a frequency range of 1–50 MHz. The GMI ratios for the total impedance and its components were defined with respect to the maximum applied field $H_{\text{max}}=100$ Oe as follows $\Delta Z/Z = 100\% \times (Z(H) - Z(H_{\text{max}})) / Z(H_{\text{max}})$.

The deposition of carbon in both S1 and S2 cases leads to the relaxation of the surface layer stresses, which can be confirmed by the magneto-optical Kerr microscopy studies of the domain structure (insert Fig. 1). Also a decrease of the coercive force and an increase of the sensitivity of GMI values were observed that is promising for sensors application. However, those effects are less evident in the case of sample S1, having Cr in the surface layer that prevents the chemical steps of low temperature carbon condensation.

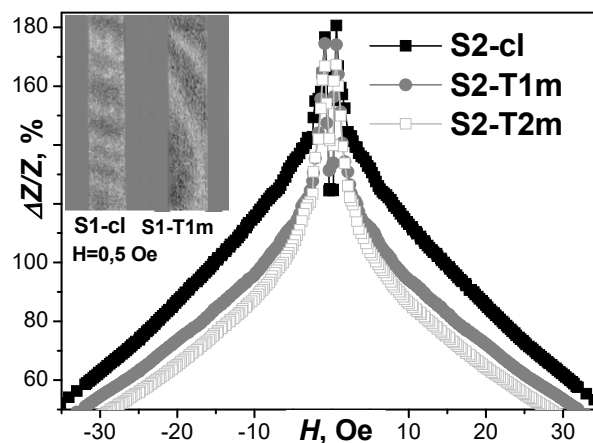


Fig. 1. The dependence of the GMI ratio of S2 from the external field; insert - Magneto-optical images of S1 domain structure.

[1] I.V. Beketov, A.P.Safronov, A.V. Bagazeev, A. Larrañaga, G.V. Kurlyandskaya, A.I. Medvedev, *J. All. Comp.*, **586** (2014) 483–488.

3PO-K-16

METHODOLOGICAL ASPECTS OF SMALL IRON CONCENTRATIONS DETERMINATION IN BLACK YEASTS GROWN IN THE PRESENCE OF IRON OXIDE NANOPARTICLES

Melnikov G.Yu.¹, Denisova T.P.², Safronov A.P.^{1,3}, Samatov O.M.³, Khandukhanov R.T.²,
Kulesh N.A.¹, Andrade R.⁴, Kurlyandskaya G.V.^{1,5}

¹ Ural Federal University, Mira St. 19 Ekaterinburg, 620000, Russia

² Irkutsk State University, Nizhnyaya Embankment St., 6, Irkutsk, 664011, Russia

³ Institute of Electrophysics, Amundsen str., 106, Ekaterinburg, 620016, Russia

⁴ Universidad del País Vasco UPV-EHU, SGIKER, Leioa, Spain

⁵ Universidad del País Vasco UPV-EHU, Depto Electricidad y Electrónica, Leioa, Spain
grisha2207@list.ru

Living systems strongly depend on iron in variety of ways. Therefore, precise determination of a small amount of iron in the biological samples is a challenge. Nonpathogenic *Exophiala nigrum* (*E. nigrum*, black yeast) unicellular organisms of the Baikal Lake [1] were used as a model system for determination of trace concentrations of iron in the samples grown without or with controlled amount of iron in nutrient. Yeast samples were grown in the presence of maghemite Fe₂O₃ nanoparticles (MNPs) produced by laser target evaporation [2]. Structural measurements were performed by transmission electron microscopy (TEM). The crystalline structure of MNPs was determined by X-ray diffraction (XRD) using Bruker D8 X-ray diffractometer. XRD spectra fit gave a mean crystallite size of 19 ± 2 nm. Magnetic measurements were carried out on a MPMS XL-7 SQUID-magnetometer. Electrostatically stabilized suspensions were prepared by ultrasound treatment using sodium citrate solutions (5 mM) in distilled water. Average hydrodynamic diameter of aggregates was tracked by the dynamic light scattering. A Hermle Z383 centrifuge operated at 10.000 rpm for 10 min was used to remove all large aggregates.

Maximum permissive dose of iron in water (MPD) is determined as 0.3 mg/L. For biological experiments Saburo liquid nutrient medium was prepared with following iron concentrations (provided by corresponding amount of MNPs): 0, 100, 10³ or 10⁴ MPD. One ml of *E. nigrum* cell suspension was added to Saburo liquid nutrient for 24 hours exposure. At the end of the exposure period sowing onto a solid agar Saburo was done from which biosamples for TEM, magnetic measurements and total reflection X-ray fluorescence (TRXRF) measurements were collected simultaneously after 30 days colonies grows. For TEM of biosamples cell culture was pre-fixed in 10 ml of 0.5% glutaraldehyde in Sörenson buffer, fixed in 1% Osmium Tetroxide in Sörenson buffer, dehydrated, embedded in Epon Polarbed resin and cut as 70 nm sections for Philips EM208S TEM studies. We were able to comparatively analyze the trace concentrations of iron in the yeast samples measured by TRXRF (Nanohunter spectrometer by Rigaku) and SQUID magnitometry. For example, for yeast biosamples grown with 100 MPD the trace amount of iron calculated from SQUID and TXRF data was 21 and 15 ppm respectively. These values are in a good agreement with TEM observations: few MNPs were observed attached to cell exterior and a very few inside the cell.

The work was supported by the Spanish MEC project MAT2014-55049-C2-1-R and RFFI №16-34-50192 grant. We thank Iu. Novoselova and I.V. Beketov for special support.

[1] I.P. Babieva, I.Yu. Chernov, *Biology of yeasts, M.V. Lomonosov MSU*, (2004) 1-239.

[2] J.P. Novoselova, A.P. Safronov, O.M. Samatov, I.V. Beketov, H. Khurshid, Z. Nemati, H.

Srikanth, T.P. Denisova, R. Andrade, G. Kurlyandskaya, *IEEE Trans. Magn.* **50** (2014) 4600504.

3PO-K-17

SELECTED FEATURES OF MORPHO-FUNCTIONAL REACTIONS OF EUKARYOTIC MICROORGANISMS GROWN IN THE PRESENCE OF MAGHEMITE IRON OXIDE NANOPARTICLES OBTAINED BY LASER TARGET EVAPORATION

Simonova E.V.¹, Denisova T.P.², Khandukhanov R.T.², Melnikov G.Yu.³, Medvedev A.I.^{3,4}, Beketov I.V.^{3,4}, Andrade R.⁵

¹ FSBEI HE ISMU MOH, Red Revolt str., 1, Irkutsk, 664003, Russia

² Irkutsk State University, Nizhnyaya Embankment St., 6, Irkutsk, 664011, Russia

³ Ural Federal University, Mira St. 19 Ekaterinburg, 620000, Russia

⁴ Institute of Electrophysics, Amundsen str., 106, Ekaterinburg, 620016, Russia

⁵ Universidad del País Vasco UPV-EHU, SGIKER, Leioa, 48940, Spain

evsimonova@yandex.ru

Recent focus on wide employment of magnetic nanoparticles (MNPs) in biomedical applications requires the study of the features of their interactions with biocomponents, in particular with eukaryotic organisms. This work is devoted to the studies of the biological activity of iron introduced into nutrient medium as a suspension of iron oxide MNPs synthesized by the laser target evaporation technique [1].

Eukaryotic organisms, melanin-containing microscopic fungi of *Exophiala nigrum* (*E. nigrum*) were grown either in the presence (experimental group) or in absence of MNPs (control). Solutions of de-aggregated suspension of γ -Fe₂O₃ maghemite nanoparticles (a mean crystallite size of 19 ± 2 nm) were prepared on the basis of Saburo liquid nutrient medium in concentrations of 1 to 10⁴ maximum permissive doses (MPD). Maximum permissive dose is determined as 0.3 mg/L of Fe ions in water. Cells in both experimental and control biosamples were exposed for time period of 24 to 96 hours, and then plated onto a solid medium in Petri dishes. The effect of MNPs presents on black yeast fungi was evaluated by the change in the number of cells during exposure. The number and morphology of the colonies grown on solid nutrient substrate were also analyzed.

Yeast, grown in experimental conditions (Fe concentration of 1MPD to 10 MPD) showed characteristics similar to the characteristics of control samples. Suspensions of iron oxide MNPs at 100 or 1000 MPD for 72 hours of exposure and above caused a stimulating effect: the number of cells increases from 3-5 to 30 times in comparison with the control ($P < 0.05$). A pronounced stimulating effect was revealed for a suspension of iron oxide MNPs at a concentration of 10⁴ MPD of iron. A significant excess (52 times) of the number of cells in 1 ml compared with the control was observed for the first day. At exposures of 72 and 96 hours the differences in the number of cells in comparison with the control sample were 11 and 30 times, respectively ($P < 0.05$). A change in the morphology of the colonies was observed in the experiment with a suspension at a concentration of 100 MPD. After 0 to 48 hours exposition of the cells all grown up on a solid medium colonies had a typical morphology for *E. nigrum*. After the yeast exposition with this suspension for 72 hours and longer white colonies appeared on the background of the black ones.

The work was supported by the RFFI №16-34-50192 grant. We thank Iu. P. Novoselova and A.P. Safronov for special support.

[1] J.P. Novoselova, A.P. Safronov, O.M. Samatov, I.V. Beketov, H. Khurshid, Z. Nemati, H. Srikanth, T.P. Denisova, R. Andrade, G. Kurlyandskaya, *IEEE Trans. Magn.*, **50** (2014) 4600504.

3PO-K-18

HETEROGENEITY OF POPULATION OF MICROORGANISMS GROWN IN PRESENCE OF IRON OXIDE MAGHEMITE NANOPARTICLES

Denisova T.P.¹, Simonova E.V.², Kokorina L.A.², Maximova E.N.¹, Samatov O.M.³, Safronov A.P.^{3,4}, Kurlyandskaya G.V.^{4,5}

¹ Irkutsk State University, Nizhnyaya Embankment St., 6, Irkutsk, 664011, Russia

² FSBEI HE ISMU MOH, Red Revolt str., 1, Irkutsk, 664003, Russia

³ Institute of Electrophysics, Amundsen str., 106, Ekaterinburg, 620016, Russia

⁴ Ural Federal University, Mira St. 19 Ekaterinburg, 620000, Russia

⁵ Universidad del País Vasco UPV-EHU, Leioa, 48940 Spain

denis_tp@inbox.ru

Heterogeneity is a universal property of any microbial population showing its adaptive capability. Although some studies of iron oxide nanoparticles (MNPs) had shown their biological activity *E.nigrum* eukaryots case they require further development.

In this work γ -Fe₂O₃ MNPs were obtained laser target evaporation and water based suspensions were prepared. Maximum permissive dose of iron in water (MPD) is 0.3 mg/L. It was found that 100 MPD dose of iron induces formation of non-typical colonies after 72 or 96 hours exposition: against a background of very small black colonies quite large white colonies appeared due to a disruption in tyrosine synthesis. The population grown in above mentioned conditions continued to be cultivated for physiological heterogeneity studies. Control population of *E. nigrum* grown without MNPs was also investigated. The conditions of cultivation and the nutrient medium parameters of the control and experimental groups were identical (except MNPs addition). Multiple re-cloning of the white colonies grown with MNPs using the Saburo nutrient showed that they retained their properties both under standard conditions (temperature of 24° C) and at the temperatures up to 37° C. *E.nigrum* grown with MNPs demonstrated very scant extension of small colonies at the cultivation temperature of 24° C and their growth was completely blocked at 37° C temperature.

We found that the *E. nigrum* test culture in the exponential grows stage can be described as a cell mass with low degree of the morphotype heterogeneity. Significant changes in the structure of the population were noted at 72 and 96 hours exposure. First of all, large cells with pronounced aggregation were observed among the black colonies. These aggregates consisted of large cells connected to each other by matrix. In the white colonies the appearance of very long threadlike cells was evident. The elongated cells were connecting different groups of the cells establishing an intercellular communication. Electron microscopy of cells grown with MNPs confirms the morphological heterogeneity of the population. The observed degree of heterogeneity under experimental conditions is due to the margin of stability, as a result of which physiologically active cells die in adverse environmental conditions, whereas physiologically inactive forms are able to survive. Fe₂O₃ MNPs induce an increase in the heterogeneity of the population, expressed as a change in their morpho-physiological states.

The work was supported by and RFBR №16-34-50192/16 grant. Selected studies were done in SGIKER services of UPV-EHU. We thank R. Andrade and I.V. Beketov for special support.

3PO-K-19

SYNTHESIS AND PHYSICAL INVESTIGATION OF MAGNETITE-GOLD HYBRID NANOPARTICLES FOR THERANOSTIC PURPOSES

Efremova M.V.^{1,2}, Nalench Yu.A.², Blokhina A.D.¹, Garanina A.S.^{1,2}, Abakumov M.A.², Wiedwald U.³, Spasova M.³, Farle M.³, Savchenko A.G.², Klyachko N.L.^{1,2}, Majouga A.G.^{1,2}

¹ Lomonosov Moscow State University, Moscow, Russia

² National University of Science and Technology «MISiS», Moscow, Russia

³ Faculty of Physics and Center for Nanointegration Duisburg-Essen (CENIDE), University of Duisburg-Essen, Duisburg, Germany
efremova33@mail.ru

During last decades magnetite and gold nanoparticles (NPs) attract a deep interest of scientists due to their potential application in therapy and diagnostics. Fe₃O₄ NPs have the ability to enhance T2-contrast in magnetic resonance imaging (MRI) and deliver drugs to certain tissues using an external magnetic field. In turn, Au NPs are characterized by high stability, biocompatibility, and can also be covalently functionalized by a wide spectrum of thiol-containing ligands. The idea of Fe₃O₄-Au hybrid material creation is the combination of magnetite and gold promising properties as well as the presence of two types of surfaces that differ in chemical properties.

Hybrid magnetite-gold NPs were obtained by the decomposition of iron pentacarbonyl on the surface of gold NPs. As a result, so-called dumbbell-like structures were obtained where magnetite with cubic shape and spherical gold NPs were connected together pairwise. The study of structural and magnetic properties revealed a very high quality of Fe₃O₄ NPs with a mean size of 23±2 nm and a saturation magnetization of 86 Am²/kg close to the bulk value of 92 Am²/kg. Further, we obtained an epitaxial relation between Fe₃O₄ and Au NPs. 3D-tomography of such NPs was also performed, revealing only the part of Au NP located on top of Fe₃O₄ NP with being mostly incorporated inside.

The sample was transferred into water with the derivative of phospholipid and polyethylene glycol (DSPE-PEG), and then MRI-characterization was performed. R2-relaxivity rate of 494 mM⁻¹s⁻¹ was obtained; this value is a record one for hybrid Fe₃O₄-Au NPs, which is 2.5 times more than the similar characteristics of commercial contrast agents. When the sample was intravenously administered to Wistar rats at a dose of 7 mg Fe/kg, the accumulation of NPs in the liver was predominant (more than 60% of the input dose) and they effectively increased the contrast of MRI liver images.

The results of 3D-tomography were confirmed by functionalization of Fe₃O₄-Au NPs with two different dyes – fluorescein isothiocyanate, attached to the surface of magnetite, and sulfo-Cyanine 5, which forms the bonds only with gold. Co-localization of these two dyes on the NPs fluorescence images was found – that means so-called double functionality of such materials, e.g., the applicability for simultaneous conjugation with drug and vector molecules, targeting the therapeutic agents to the certain type of cells.

Thereby, in this work magnetite-gold hybrid NPs, which have a strong potential for biomedical application, were synthesized and characterized. That paves the way to the development of a new theranostic approach.

This work was supported by Grant of Russian Scientific Foundation (17-14-01316).

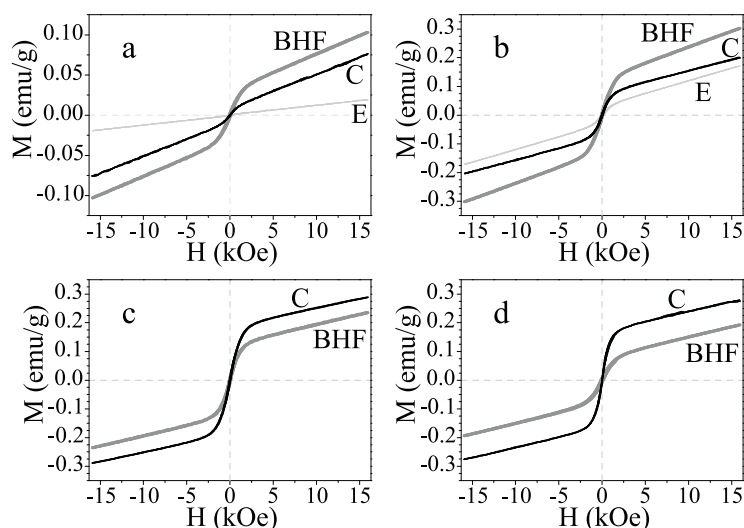
3PO-K-20

SOIL MAGNETIC PROPERTIES IN THE IMPACT ZONE OF “SEVERONIKEL” ENTERPRISES

Danilov G., Koptsik S., Perov N.

Lomonosov Moscow State University, Faculty of Physics, 119991 Moscow, Russia
koptsik@phys.msu.ru

Magnetic properties of soils were studied in the surroundings of the “Severonikel” enterprises (Russia) along a pollution gradient. The soil samples were taken from mineral horizons of podzols under spruce forests at different stages of degradation from the background to the technogenic barrens at intensively studied sites. The soil samples were sieved and homogenized by milling. For magnetic properties investigations we used the vibrating sample magnetometer “LakeShore” (7400). The typical hysteresis curves are shown.



Magnetic hysteresis loops of podzols under unperturbed (a) and dead (b) forests and from technogenic barrens (c, d).

Everything studied magnetic hysteresis loops of the soils under spruce stands (including completely dead stands but still retaining the surface organic layer) fit into the general concept that podzols are formed from the parent bedrock (C-horizons); Al, Fe and organic compounds migrate from the surface soil downwards with the percolating rainwater and precipitate in the illuvial horizon and are enriched with iron compounds that fall onto the soil surface, move and transform in soils. As a result, the illuvial BHF-horizons where iron compounds accumulated are characterized by the maximal ferromagnetic properties (Fig. a, b). The minimal ferromagnetic properties characterize thin upper E-horizons, which lose iron compounds under the impact of weak organic acids formed with decay of the organic layer.

In the very vicinity of the smelter now nothing except the human and soil memory witness about growing up to the last decades of 20-th century spruce forests. Here in some places the inverse magnetic pattern can be observed (Fig. c, d). For the two sites presented both the vegetation and organic layer have gone, the soil erosion processes have started and removed the E-horizons and the upper part of the underlying BHF-horizons thus making their reminders the topsoil. However, their ferromagnetic properties are lower than for the bedrock.

The inversion observed in the succession of the magnetization curves of the illuvial horizon and parent rock reveals the ongoing rapid decrease in ferromagnetic properties of the topsoil in the barren lands. This observation is likely to be connected with direct leaching of stable iron compounds from the topsoil with the acid deposition and the further soil degradation.

3PO-K-21

MAGNETIC AND FLUORESCENT NANOPARTICLES BASED ON IRON-CARBON NANOCOMPOSITES AND CARBON QUANTUM DOTS

Minin A.S.^{1,2}, *Uimin M.A.*¹, *Yermakov A.E.*¹, *Byzov I.V.*¹, *Zubarev I.V.*², *Ulitko M.V.*², *Smoluk L.T.*³,
*Belousova A.V.*³, *Abakumov M.A.*⁴, *Chekhonin V.P.*^{4,5}

¹ IMP UB RAS, Ekaterinburg, Russia

² URFU named after the first President of Russia B.N.Yeltsin, Ekaterinburg, Russia

³ IIP UB RAS, Ekaterinburg, Russia

⁴ RNRMU, Moscow, Russia

⁵ Serbsky National Research Center for Social and Forensic Psychiatry, Moscow, Russia
calamatica@gmail.com

Nanoparticles are used in the field of biology and medicine, e.g. as a contrast agent for various diagnostic studies. The contrasts for MRI based on magnetic nanoparticles are widely known. At present, nanosystems are actively developing, combining several diagnostic modalities. This work describes nanoparticles that combine a fluorescent component that allows to use of various optical techniques and magnetic, suitable for MRI contrast.

As a fluorescent component of bimodal nanoparticles, carbon quantum dots, a promising carbon nanomaterial having low toxicity and fluorescing in a wide range of wavelengths are used [1]. As a magnetic component, magnetic core-shell nanocomposites (an iron core-carbon shell) synthesized by a gas-phase method were used. The iron core provides a high magnetic moment, and the carbon coating gives stability in different environments [2]. As an optically transparent spacer, separating the magnetic nanoparticles from fluorescent CQD, silicon dioxide was used, which avoids the phenomenon of fluorescence quenching.

A high relaxation ability (T2 is about 250 mM-1s-1 relaxivity) of bimodal nanoparticles was shown. Low toxicity was found for cells. Using electron and confocal microscopy (Fig. 1), the intracellular distribution of nanoparticles was studied, it was shown that they accumulate in lysosomes, but are also observed in the cytosol. Using the NMR relaxation method to determine the concentration of magnetic nanoparticles in a medium, the kinetics of absorption of nanoparticles by cells in culture was studied, the predominant accumulation of aminated nanoparticles was shown. The MRI method demonstrated the accumulation of bimodal nanoparticles in the vessels of a tumor in a laboratory animal.

Support by the state assignment of FASO of Russia (theme "Magnit" No.01201463328) and KCE of URFU are acknowledged. This work was performed using the equipment of the Shared Research Center of Scientific Equipment SRC IIP UrB RAS.

[1] M. Tuerhong, Y. XU, and X.-B. YIN, *Chinese J. Anal. Chem.*, **45**, **1** (2017)139–150.

[2] V.A. Tsurin, A.Y. Yermakov, M. A. Uimin, A.A. Mysik, N. N. Shchegoleva, V. S. Gaviko, and V. V. Maikov, *Phys. Solid State*, **56**, **2** (2014) 287–301.

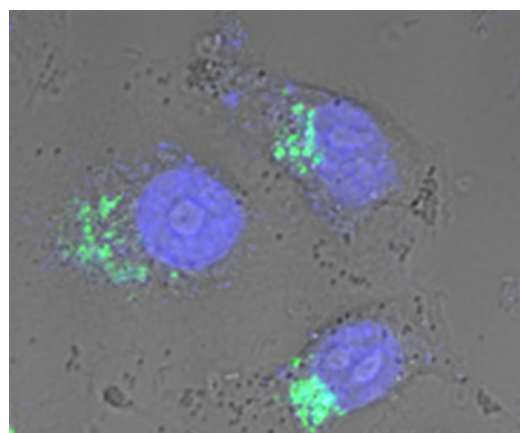


Fig. 1. HeLa culture cells incubated with bimodal NP (green), nuclei stained with Hoechst 33258

3PO-K-22

COMPLEX STUDY OF MULTIFUNCTIONAL MAGNETIC NANOSTRUCTURES FOR THE DEVELOPMENT OF EFFECTIVE THERANOSTIC NANOAGENTS

Shipunova V.O.^{1,2,3}, Deyev S.M.^{1,2}

¹ Shemyakin-Ovchinnikov Institute of Bioorganic chemistry RAS, Moscow, Russia

² National Research Nuclear University "MEPhI", Moscow, Russia

³ Moscow Institute of Physics and Technology, Moscow, Russia

viktoriya.shipunova@phystech.edu

At present, significant attention of researchers in the field of nanomedicine and nanobiotechnology is being directed toward developing effective theranostic nanoagents. A successful theranostic agent must incorporate many functions on a single platform to simultaneously act as an agent both for therapy and for diagnostics. Such multifunctionality is achieved via decoration of an agent by different biomolecules such as toxins, antibodies, different peptides, fluorescent proteins, etc.

The aim of the work was the development of universal ways of simple modification of nano- and microparticles by biomolecules with preservation of the orientation and activity of the molecules being attached, for example, on the basis of specific interactions of peptides that bind the solid phase. It is known that there are peptides that selectively bind a wide range of inorganic materials, and such peptides could potentially mediate the surface modification of nanoparticles by biomolecules without disturbing biomolecules' functional activity. Moreover, since peptides can be genetically fused with other proteins, this opens up wide opportunities for simple and direct modification of nanoparticles without involving additional steps, for example, chemical conjugation. In particular, a high affinity protein pair, barnase*barstar [1] was used as a "molecular glue" for the universal modification of nanoparticles with the required components using the peptide technology. The design of fusion proteins of one component of this pair (for example, barstar) with peptide that binds the surface of nanoparticles as a solid phase and the use of fusion proteins of another component (for example, barnase) with recognizing or fluorescent molecules makes it possible to obtain universal nanostructures with specified characteristics. The effectiveness of this approach was demonstrated both in *in vitro* a cell-free mode and by effective targeted delivery of the obtained multifunctional complexes to cancer cells using the developed by us previously MPQ-cytometry method [2]. The capabilities of the MPQ-cytometry method was also demonstrated by us by quantification of magnetic nanoparticles with transformable architecture possessing biocomputing capabilities [3] bound to cell surface. These particles were shown to implement logic gates and target specific cell surface based on logic-gated analysis of soluble biomolecular inputs thus acting as perspective theranostic nanoagents of new generation.

[1] S.M. Deyev, R. Waibel, E.N. Lebedenko, A.P. Schubiger & A. Plückthun. Design of multivalent complexes using the barnase*barstar module, *Nat. Biotechnol.*, **21** (2003) 1486-1492.

[2] V.O. Shipunova, M.P. Nikitin, P.I. Nikitin, S.M. Deyev. MPQ-cytometry: a magnetism-based method for quantification of nanoparticle-cell interactions, *Nanoscale*, **33** (2016) 133-136.

[3] M.P. Nikitin, V.O. Shipunova, S.M. Deyev & P.I. Nikitin. Biocomputing based on particle disassembly, *Nat. Nanotech.*, **9** (2014) 716-722.

3PO-K-23

POSSIBILITY OF SUPERRADIANT ENHANCEMENT FROM NON-DICKE STATES

Nefedkin N.E.^{1,2}, *Andrianov E.S.*^{1,2}, *Pukhov A.A.*^{1,2,3}, *Vinogradov A.P.*^{1,2,3}

¹ Dukhov Research Institute for Automatics, Moscow, Russia

² Moscow Institute of Physics and Technology, Dolgoprudniy, Russia

³ Institute for Theoretical and Applied Electromagnetics RAS, Moscow, Russia

nefedkin@phystech.edu

Superradiance (SR) is an enhancement of collective spontaneous radiation of an array of emitters interacting with a common light field. For a subwavelength array of quantum emitters, this phenomenon was predicted by Dicke [1]. The Dicke model assumes that identical quantum emitters interact via the common field of their radiative response. Once excited, the emitters form a special Dicke state [2] and radiate a pulse. The dipole moment of a system of N excited identical two-level atoms is zero [3]. The duration of the SR burst is smaller than the radiation time of a single emitter by a factor of $1/N$. The intensity of the radiation is proportional to N^2 and the delay time of the SR peak $\log N/N$.

The Dicke explanation of SR is based on a strong assumption about the time evolution from one Dicke state to another (only in this case can one use the Fermi's golden rule) and on an ability of a quantum system with zero dipole moment to radiate a photon. There is no rigorous proof that these conditions are either necessary or sufficient for SR.

First, a more rigorous description of SR in terms of the master equation

$$\dot{\rho} = \frac{\gamma_0}{2} (2J_- \rho J_+ - J_+ J_- \rho - \rho J_+ J_-) \quad (1)$$

shows that the system evolution does not go through pure Dicke states but rather through mixed states with a density matrix which is a linear combination of density matrices of various pure Dicke states $\rho_{mixed} = \sum_n c_n |\psi_D\rangle \langle \psi_D|$ [2]. These mixed states still have a zero dipole moment. Second, SR

is not the sole prerogative of quantum systems. It can also occur in an ensemble of nonlinear classical oscillators, which surely has a nonzero dipole moment [4]. In such a system, SR results from the constructive interference of long-period envelopes of rapidly oscillating dipoles [4].

We study the possibility of SR in an ensemble of two-level atoms in the general case, in which the system is not initially in a Dicke state, modeling the master equation (1). For a quantum system, there is a unified mechanism of SR for both Dicke states with zero dipole moment and non-Dicke states for which the total dipole moment is not zero. Moreover, there is an analogy between SR in quantum and nonlinear classical systems [4]. This analogy can be recognized by considering SR from non-Dicke states.

To conclude, we have studied the dynamics of quantum emitters interacting via their radiation field. In contrast to the Dicke model, in which all emitters are assumed to be in a state with zero dipole moment, the new SR regime arises in a more realistic system in which the initial state may have a nonzero dipole moment. We demonstrate that the Dicke state is not necessary for SR.

[1] R.H. Dicke, *Phys. Rev.*, **93** (1954) 99-110.

[2] M. Gross, S. Haroche, *Phys. Rep.*, **93** (1982) 301-396.

[3] L. Allen, J. H. Eberly, *Optical Resonance and Two-level Atoms*, N.-Y. (1975).

[4] N.E. Nefedkin, E. S. Andrianov, A. A. Zyablovsky, A. A. Pukhov, A. V. Dorofeenko, A. P. Vinogradov, A. A. Lisyansky, *Opt. Express*, **24** (2016) 3464-3478.

3PO-K-24

APTAMER-FUNCTIONALIZED MAGNETIC NANODEVICES FOR TUMOR CELL MICROSURGERY

Sokolov A.¹, Lukyanenko A.¹, Ivanova O.¹, Zabluda V.¹, Kuzmichenko N.¹, Zamay S.², Zamay T.³, Kolovskaya O.³, Zamay G.³, Svetlichny V.⁴

¹ Kirensky Institute of Physics, Federal Research Center KSC SB RAS, Akademgorodok 50/38, Krasnoyarsk, 660036 Russia

² Federal Research Center KSC SB RAS, Akademgorodok 50, Krasnoyarsk, 660036 Russia

³ Krasnoyarsk State Medical University, Laboratory for Biomolecular and Medical Technologies, ul. P. Zheleznyaka 1, Krasnoyarsk, 660022 Russia

⁴ Tomsk State University, Novosobornaya pl., 1, Tomsk, 634050 Russia
alexey@iph.krasn.ru

Recently, in the field of molecular cell surgery of malignant tumors is increasingly common term theranostics, it combined diagnosis and therapy. For these purposes it is widely used bionanoconjugates consisting of magnetic nanoparticles and DNA- aptamers. For the development of targeted drugs a vital role plays research of properties used bionanoconjugates.

The magnetic core bionanoconjugates provides required magnetic properties for the provision of physical exposure to a low frequency alternating magnetic field. Magnetomechanical cell disruption using nano and micro-sized structures is a promising biomedical technology using for noninvasive elimination of diseased cells. It applies alternating magnetic field for magnetic microdisks making them oscillate and causing cell membrane disruption with following cell death by apoptosis [1,2]. We describe application of gold-coated nickel magnetic microdisks (Au-Ni-Au mMDs) with magnetic moment parallel to its plane in magnetomechanical cancer therapy. It is shown that it is possible to replace microdisks with spherical nanoparticles decorated with gold.

The relationship of shape, size, magnetic properties of bionanoconjugates and the possibility of their use in theranostics is discussed.

Support Grant of the President of the Russian Federation NSh-7559.2016.2 .

[1] Zamay Tatiana, Kolovskaya Olga., Sokolov Alexey, et.al, *Nucleic Acid Therapeutics*. (2016) doi:10.1089/nat.2016.0634.

[2] P.D. Kim, S.S. Zamay, A.E. Sokolov, et.al, *Doklady Biochemistry and Biophysics*, **466** (2016) 66–69.

3PO-K-25

DETECTION OF CARDIAC BIOMARKERS MYOGLOBIN AND C-REACTIVE PROTEIN BY A GIANT MAGNETOIMPEDANCE-BASED BIOSENSING SYSTEM

Yang Z.^{1,2}, Wang H.^{1,2}, Luo Y.-S.^{1,2}

¹ School of Physics and Electronic Engineering, Xinyang Normal University, Xinyang 464000, People's Republic of China

² Key Laboratory of Advanced Micro/Nano Functional Materials, Xinyang Normal University, Xinyang 464000, People's Republic of China
eyslue@163.com (Y-S Luo)

A novel bio-sensing system based on a multilayered giant magnetoimpedance (GMI) sensor and enclosed microfluidics devices (EMD) was developed for combined detection of cardiac biomarkers myoglobin (Mb) and C-reactive protein (CRP). The NiFe/Cu/NiFe GMI sensors and EMD were fabricated by micro electromechanical system (MEMS) technology. The commercial Dynabeads were used for magnetic labels of Mb and CRP. The classical sandwich assay was used for detection of Mb and CRP targeted with Dynabeads by using antibody-antigen pair combination of biotin-streptavidin. The enclosed microfluidics devices were designed for different detection regions, which were premodified with specific antibody. The GMI ratios of the sensors located under different detection regions with different antigen concentrations were observed. The results showed that the GMI-based bio-sensing system had high selectivity and sensitivity for detection of cardiac biomarkers. Compared with the blank control region, ultrasensitive detection of CRP and Mb was accomplished in the detection region 1 and 2 respectively, the detection limit were 1 pg/ml and 0.1 pg/ml respectively. The linear detection range contained low concentration detection area and high concentration detection area, which were 1 pg/ml-10 ng/ml, 10-100 ng/ml for CRP, and 0.1 pg/ml-1 ng/ml, 1 n/ml-80 ng/ml for Mb. This method in our perception provides a widely applicable basis for multi-target biomolecules rapid diagnostic testing like alpha-fetoprotein (AFP) and carcino embryonic antigen (CEA).

[1] W.B. Gibler, C.P. Cannon, A.L. Blomkalns, D.M. Char, B.J. Drew, J.E. Hollander, A.S. Jaffe, R.L. Jesse, L.K. Newby, E.M. Ohman, *Ann. Emerg. Med.*, **46** (2005) 185–197.

[2] S.G. Foy, I. C.S. Kennedy, H. Ikram, C.J.S. Low, T.M. Shirlaw, I.G. Crozier, *Australian and New Zealand Journal of Medicine*, **21** (1991) 335–337.

[3] B.J. Willcox, R.D. Abbott, K. Yano, B.L. Rodriguez, D.C. Willcox, J.D. Curb, *Expert Rev. Neurother*, **4** (2004) 507–518.

3 July

Monday

12:00-14:00

poster session

3PO-I

**“Magnetism and
Superconductivity”**

3PO-I-1

BROKEN SYMMETRY, QUANTUM PROTECTORATE AND EMERGENT BEHAVIOR IN MAGNETIC AND SUPERCONDUCTING SYSTEMS

Kuzemsky A.L.¹

¹ Joint Institute for Nuclear Research, 141980 Dubna, Moscow Reg., Russia
kuzemsky@theor.jinr.ru: <http://theor.jinr.ru/~kuzemsky>

In this report we discuss an approach to analysis of appearance of long-range order in complex substances and artificial materials, where there are various competing interactions. Symmetry and symmetry breaking are the crucial concepts in the theories that describe appearance (emergence) of *ordering* of various types in condensed matter. *Emergence* - macro-level effect from micro-level causes - is an important and profound interdisciplinary notion of modern science. Emergence and complexity refer to the appearance of higher-level properties and behavior of a system that obviously comes from the collective dynamics of that system's components. These properties are not directly deducible from the lower-level motion of that system.

In series of papers [1-7] we analysed these problems from various sides with the aim to establish the specific features and general criteria for emergence of superconducting and magnetically ordered phases. The mechanism of spontaneous symmetry breaking, considered in our study, is usually understood as the mechanism responsible for the occurrence of asymmetric states in quantum systems in the thermodynamic limit [6]. In the context of superconductivity, the masslessness of photon and Goldstone theorem play a crucial role. In particle and condensed matter physics, Goldstone bosons are bosons that appear in models exhibiting spontaneous breakdown of continuous symmetries. Such a particle can be ascribed for each generator of the symmetry that is broken, i.e., that does not preserve the ground state [1-4]. The Nambu-Goldstone mode is a long-wavelength fluctuation of the corresponding order parameter [1].

Some physical implications involved in the concept, termed the "*quantum protectorate*" [1-7], are developed and discussed as well. This is done by considering the idea of quantum protectorate in the context of quantum theory of magnetism. It is suggested that the difficulties in the formulation of quantum theory of magnetism at the microscopic level, that are related to the choice of relevant models, can be understood better in the light of the quantum protectorate concept. We argue that the difficulties in the formulation of adequate microscopic models of electron and magnetic properties of materials are intimately related to dual, itinerant and localized behavior of electrons. We formulate a criterion [1, 3, 5] of what basic picture describes best this dual behaviour. The main suggestion is that quasi-particle excitation spectra might provide distinctive signatures and good criteria for the appropriate choice of the relevant model. By this consideration an attempt was made to link phenomenological and quantum theory of magnetism together more firmly, thus giving a better understanding of the latter.

- [1] A. L. Kuzemsky, *Statistical Mechanics and the Physics of Many-Particle Model Systems*. (World Scientific, Singapore, 2017).
- [2] A.L. Kuzemsky, *Phys. Part. Nucl.*, **40** (2009) 949.
- [3] A.L. Kuzemsky, *Phys. Part. Nucl.*, **41** (2010) 1031.
- [4] A.L. Kuzemsky, *Int. J. Mod. Phys.*, **B24** (2010) 835.
- [5] A.L. Kuzemsky, *Bulletin of PFUR. Ser. Math. Informat. Sci. Phys.*, **1** (2013) 229.
- [6] A.L. Kuzemsky, *Int. J. Mod. Phys.*, **B28** (2014) 1430004.
- [7] A.L. Kuzemsky, *Int. J. Mod. Phys.*, **B29** (2015) 1530010.

3PO-I-2

PROXIMITY EFFECT IN SUPERCONDUCTOR/FERROMAGNET HETEROSTRUCTURES WITH PLANAR DOMAIN STRUCTURE

Tumanov V.A.¹, Proshin Yu.N.¹

Theoretical Physics Department, Kazan Federal University, Kazan, Russia
Yurii.Proshin@kpfu.ru

We study the superconductor/ferromagnet (S/F) heterostructures with the inhomogeneous magnetization in ferromagnetic layer. A model of magnetic superconductor [1], which takes into account the interaction of collectivized electrons with inhomogeneous effective exchange field, is used. Using local unitary rotation in spinor space, we rewrite the Hamiltonian in a new basis where this interaction is diagonal, but effective tensor field appears. In particular, this transformation removes the coordinate dependence from Hamiltonian in the case of helical magnetization. This transformation allows us to simplify boundary value problem for Usadel equations in many cases.

Our work was motivated by experimental results for the superconducting structure consisting of thick vanadium layer and thin layers of iron and chromium, where large amplitude oscillations of the critical temperature were observed under changes of the Cr layer thickness [2,3]. To obtain a theoretical description of this experiment we calculate the critical temperature of the S/F proximity system where the ferromagnet has periodic domain structure with planar domain walls. This simplified model satisfactorily describes a superconducting state in experimental system. We use analytical calculations for model of thin S/F bilayer and numerical calculations for more complex geometry.

Numerically we obtain that the superconducting correlations near domain walls in the ferromagnetic layer are more intensive (see Fig.1). This is in accordance with results [4,5], obtained for other models. To find the system characteristics, which are optimal for spintronic applications, the critical temperature dependence as function of multilayer geometry and domain structure parameters (domain size, domain wall thickness) is also discussed. Note, that obtained results qualitatively agree with experimental data [2,3].

The work is supported by the subsidy allocated to Kazan Federal University for performing the project part of the state assignment in the area of scientific activities. Yu.P. also thanks to the RFBR (#16-02-01016) for partial support

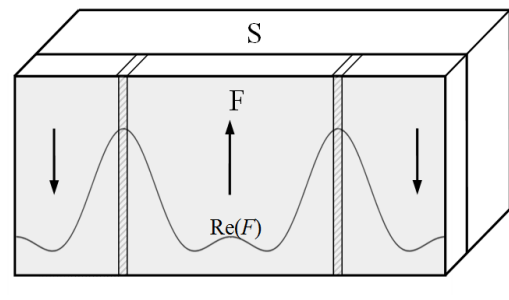


Fig. 1. Geometry of the S/F bilayer with domain structure in plane of boundary. Solid line corresponds to the real part of Usadel function F on the ferromagnetic layer external boundary.

- [1] V.A. Tumanov, Yu.N. Proshin, *J. Low Temp. Phys.*, **185** (2016) 460–466.
- [2] Yu. Goryunov, *11th Internat. Workshop on Low Temp. Electronics (WOLTE 2014)*, (2014), 45-48. doi: [10.1109/WOLTE.2014.6881022](https://doi.org/10.1109/WOLTE.2014.6881022)
- [3] Yu.V. Goryunov, *arXiv:cond-mat* (2003) 0305428.
- [4] M. Houzet, A.I. Buzdin, *Phys. Rev. B*, **74** (2006) 214507.
- [5] Ya.V. Fominov, A.F. Volkov, K.B. Efetov, *Phys. Rev. B*, **75** (2007) 104509.

3PO-I-3

OSCILLATION ELECTRON MODEL OF SYSTEM FeSe—SrTiO₃*Netesova N.P.¹*¹ M.V. Lomonosov Moscow State University, Physics Faculty, Moscow, Russia a
nnp@mig.phys.msu.ru

The parameters FeSe and SrTiO₃ are given in Tables 1-2, where M is the molecular mass, ρ is the density, s is the number of valence electrons, ω_{pv}^2 is the square of the plasma frequency, \hbar is the Planck-Dirac constant, T_c is the temperature of the superconducting phase transition, q is the interaction parameter.

According to our calculations, the FeSe interaction parameter is $q_{ab} = 0.912$, the SrTiO₃ interaction parameter is $q_{ab} = 0.78$. The temperature of the superconducting phase transition FeSe can be increased by introducing a quadratic plasma energy, derived from the strontium titanate energy.

$$q(\text{FeSe}+\text{SrTiO}_3) = 556.96 / (619.2122+713.4546) = 0.418.$$

This corresponds to a superconducting phase transition of 90-100 K.

Superconducting phase transition temperature for bulk iron selenide crystal is 8 K. Superconductivity up to 100 K was manifested in a thin film of iron selenide deposited on a substrate of strontium titanate [1].

Table 1. Parameters of iron selenide				Calculations
	Fe	Se	FeSe	
M (g/mol)	55.845	78.96	134.81	FeSe = 0.5 Fe ₂ + 0.5 Se ₂ , 577.4409 > 468.18,
ρ (g/cm ³)	7.874	4.79	6.7	577.4409 > 151.0322,
s	8	6	14	
$\hbar\omega_{pm}^2$, eV ²	936.36	302.0644	577.4409	577.4409 < 619.2122.
T _c (K)			8	$q_{ab} = 577.4409 / 619.2122 = 0.912$.

Table 2. Parameters of strontium titanate					Calculations
	Sr	Ti	O	SrTiO ₃	
M (g/mol)	87.62	47.88		183.49	SrTiO ₃ =0.5Sr ₂ O ₂ +0.5Ti ₂ +1.5O ₂ , 556.96 > 202.3945
ρ (g/cm ³)	2.63	4.505		5.13	556.96 > 511.06
s	2	4	6	24	
$\hbar\omega_{pm}^2$, eV ²	49.8436	312.2289	354.9456	556.96	556.96 < 713.4546
T _c (K)				0.3	$q_{ab} = 556.9219/713.4546=0.78$

[1]. J. J. Lee et al, « Interfacial mode coupling as the origin of the enhancement of T_c in FeSe films on SrTiO₃», Nature, **515** (2014) 245-256.

3PO-I-4

LOW-TEMPERATURE SPECIFIC HEAT OF HTSC $\text{YBa}_2\text{Cu}_3\text{O}_y$ IN MAGNETIC FIELD: THE NATURE OF THE SCHOTTKY ANOMALY

Mamsurova L.G.¹, Trusevich N.G.¹, Vishnev A.A.¹, Gavrilkin S.Yu.², Mamsurov I.V.^{1,3}, Trakhtenberg L.I.¹

¹ Semenov Institute of Chemical Physics RAS, Moscow, Russia

² Lebedev Physical Institute RAS, Moscow, Russia

³ Moscow State University, Faculty of Physics, Moscow, Russia
mamsurova@chph.ras.ru

We present the measurements of low-temperature specific heat of high temperature superconductor (HTSC) $\text{YBa}_2\text{Cu}_3\text{O}_y$ polycrystals with different oxygen contents ($y=6.63\div 7.00$) in zero magnetic field and $H = 8\text{T}$ at $T = (2\div 10)\text{K}$. The experimental evidence for the existence of different contributions to the specific heat is obtained. Among them, there are contributions arising from the electronic quasiparticle density of states and the lattice phonons. There is also contribution that looks as a Schottky anomaly, which is unusually large and is not typical for other HTSC cuprates. The nature of this contribution can be related to some paramagnetic centers with unpaired spin moments ($s = \pm 1/2$) [1]. However there is no certain opinion in literature about the origin of these paramagnetic centers. It was shown earlier [2] that the existence of broken bond in Cu1-O4 chains leads to the formation of spin paramagnetic moments. Quantity of such moments increases with the number of oxygen vacancies increasing. It is important that the number of Cu^{2+} ions should be odd [3].

To identify the Schottky anomaly we analyzed the various combinations of contributions, such as $[C^{\text{total}}(H) - C^{\text{lattice}}]$, $[C^{\text{total}}(H=0) - C^{\text{lattice}}]$, $[C(H) - C(H=0)]$. The obtained Schottky anomalies at $H=8\text{T}$ are presented in Fig.1 for 3 samples with various values y . It is revealed that the value of the Schottky contribution changes with the oxygen content variation. The decrease of y from 7.00 to 6.63 leads to the doubling of paramagnetic centers quantity n (per unit cell). The obtained experimental data correspond to the conclusions [2]. Thus, the absence of such Schottky contributions in other cuprate HTSC samples is a consequence of the absence of copper-oxygen chains in their structure

Obtaining information about the nature of the Schottky anomaly in $\text{YBa}_2\text{Cu}_3\text{O}_y$ and the method of its extraction from the experimental value of the heat capacity give the possibility to get in pure form other electronic contributions of particular interest, since they present the information on thermally excited quasiparticles in the vicinity of d-wave nodes.

[1] S.C. Riggs, O.Vafek, J.B.Kemper et al., *Nature physics*, **7** (2011) 332-335.

[2] L. Mamsurova, N. Trusevich et al., *Sol.St.Phenomena*, **233-234** (2015) 161-164.

[3] K.A.Shaykhtudinov, S.I.Popkov, A.N.Lavrov et.al., *JETP Lett.*, **92** (2010) 332-337.

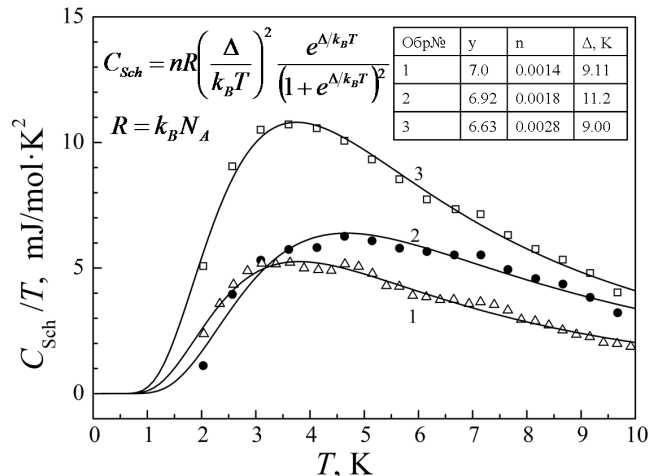


Fig. 1. Shottky-like contributions of $\text{YBa}_2\text{Cu}_3\text{O}_y$ specific heat extracted from the experimental data.

3PO-I-5

UNCONVENTIONAL PHASE TRANSITIONS IN STRONGLY ANISOTROPIC 2D S=1 (PSEUDO) SPIN SYSTEMS

Konev V.V.¹, Vasinovich V.V.¹, Ulitko V.A.¹, Panov Yu.D.¹, Moskvin A.S.¹

¹Ural Federal University, Ekaterinburg, 620083, Russia
KonevVitbka@Yandex.ru

Studying anisotropic S=1 spin and pseudospin systems is of a great importance both for quantum magnets and different bosonic-like systems with the on-site Hilbert space truncated to the three lowest occupation states $n = 0, 1, 2$, in particular, for so-called semi-hard core bosons. Furthermore, the S=1 pseudospin formalism was suggested to describe the charge degree of freedom in a model high- T_c cuprate with the on-site Hilbert space reduced to the only triplet of the three effective valence centers $[\text{CuO}_4]^{7-,6-,5-}$ (nominally $\text{Cu}^{1+;2+;3+}$), where the electronic and lattice degrees of freedom get strongly locked together [1]. Effective S=1 pseudospin Hamiltonian for such a cuprate does incorporate all the on-site and inter-site couplings, three types of correlated one-particle (fermionic) transport and a two-particle (bosonic) charge transfer with a charge density constraint. The Hamiltonian implies possible simplifications, in particular, so-called negative-U model. With the exception of the “three-spin” terms the model becomes equivalent to a generalized strongly anisotropic S=1 quantum magnet in an external magnetic field with a constraint on the magnetization. We have applied several techniques to find the ground state and phase diagrams for the model cuprate starting with a generalized mean-field approach which implies a quantum-mechanical treatment of the S=1 sites in a molecular field. We made use of a special algorithm for CUDA architecture for NVIDIA graphics cards, a nonlinear conjugate-gradient method to minimize energy functional, and Monte-Carlo technique for large square lattices 256×256 and 512×512 to directly observe the forming of the ground state configuration with lowering the temperature and its evolution under deviation from half-filling [2]. The technique allowed us to examine earlier implications and uncover novel features of the phase transitions, in particular, look upon the nucleation of different metastable topological structures, in particular, odd domain structure with emergence of filamentary superconductivity nucleated at the antiphase domain walls in the insulating charge-ordered phase. We made use of two different quantum Monte-Carlo (QMC) methods, the standard stochastic series expansion (SSE) with loop updates and a continuous time world-line QMC, for square lattices 8×8 , 16×16 , and 32×32 to simulate phase diagrams focusing on the role of the on-site correlation and relative role of one- and two-particle transport. All the results are compared with the literature data available and with real phase diagrams for high- T_c cuprates such as $\text{La}_{2-x}\text{Sr}_x\text{CuO}_4$.

The work supported by Act 211 Government of the Russian Federation, agreement № 02.A03.21.0006 and by the Ministry of Education and Science, projects 2277 and 5719.

- [1] A.S. Moskvin, *Low Temp. Phys.* **33** (2007) 234; *Phys. Rev. B* **84** (2011) 075116; *J. Phys.: Condens. Matter* **25** (2013) 085601; *J. Phys.: Conf. Ser.* **592** (2015) 012076; *JETP*, **121** (2015) 477.
[2] A.S. Moskvin, Yu.D. Panov, F.N. Rybakov, A.B. Borisov, *J. Supercond. Nov. Magn.*, **30**(1) (2017) 43.

3PO-I-6

EFFECT OF EXTERNAL MAGNETIC FIELD ON THE JOSEPHSON TRANSPORT IN FERROMAGNETIC NANOWIRE

Avdeev M.V.¹, Proshin Yu.N.¹

¹ Theoretical Physics Department, Kazan Federal University, Kazan, Russia
avdeyev_mv@mail.ru

In superconductor (S) - ferromagnet (F) structures due to the proximity effect [1] the induced singlet superconducting correlations can penetrate into the F region, exponentially decaying and oscillating on the length about few nanometers [2-4]. Nevertheless it is well known that the long-range proximity effect should occur when the magnetizations of the F part is inhomogeneous. In this case, the superconducting triplet correlations appear with total spin projection $S_z = \pm 1$ and therefore they can penetrate at the large distance in F region. Nowadays this triplet long-range proximity effect is well understood [4-6] and clearly seen experimentally [7,8].

In this work we investigate the Josephson transport through single-crystal ferromagnet nanowire sandwiched between superconducting electrodes in accordance with the experimental setup [9] in a presence of external magnetic field (note, that we present the same without magnetic field in another contribution [10]). We stress once more that the most remarkable feature [9] was the first observation of the spin-singlet long-range proximity effect for clean SFS system. Actually the critical current $I_c = 12 \mu\text{A}$ was detected for 40 nm-diameter Co nanowire with wire length $L = 600$ nm.

In our theoretical model, the electron masses of the majority and minority spin band are different that leads to a renormalization of the total momentum of the FFLO-like pair in ferromagnet. Therefore, the effective exchange interaction, entering into the Eilenberger equations, becomes dependent on the quasiparticle momentum. We show that for the single-crystal nanowire, the effective exchange field can be suppressed for crystallographic direction along nanowire axis under certain conditions. We calculate the critical Josephson current I_c , taking into account the external magnetic field H . It is shown, that the behavior of I_c versus H are qualitatively different for both two-dimensional (strip of length L and width d) and three-dimensional wire. This is because the interference from the quasiclassical trajectories in external magnetic field strongly depends on the specific ballistic path along nanowire. Therefore, the magnetoresistance exhibits a nonmonotonic behavior. It is qualitatively fitted to the experimental data [9].

The work is supported by the subsidy allocated to Kazan Federal University for performing the project part of the state assignment in the area of scientific activities (# 3.2166.2017). MVA is also thankful by the RFBR (16-02-01016) for partial support.

- [1] P. G. de Gennes, *Rev. Mod. Phys.*, **36** (1964) 225.
- [2] Y. Izyumov, Y. Proshin, M. Khusainov, *Physics-Uspokhi*, **45** (2002) 109.
- [3] A. I. Buzdin, *Rev. Mod. Phys.*, **77** (2005) 935.
- [4] F. S. Bergeret, A. F. Volkov, K. B. Efetov, *Rev. Mod. Phys.*, **77** (2005) 1321.
- [5] Y. V. Fominov, A. A. Golubov, M. Y. Kupriyanov, *JETP Letters*, **77** (2003) 510.
- [6] Y. V. Fominov, A. A. Golubov, T. Y. Karminskaya, et al. *JETP Letters*, **91**, 308 (2010).
- [7] P. V. Leksin, N. N. Garif'yanov, A. A. Kamashev, et al. *Phys. Rev. B*, **91** (2015) 214508.
- [8] A. Singh, S. Voltan, K. Lahabi, et al. *Phys. Rev. X*, **5** (2015) 021019.
- [9] J. Wang, M. Singh, M. Tian, et al. *Nature Physics*, **6** (2010) 389.
- [10] Yu. N. Proshin, M. V. Avdeev, *MISM-2017. The book of abstracts. -this issue.*

3PO-I-7

ELECTRICAL ANISOTROPY OF GRANULAR HIGH-TC SUPERCONDUCTORS IN APPLIED MAGNETIC FIELD: ESSENTIAL ROLE OF FLUX COMPRESSING IN THE INTERGRAIN MEDIA

Balaev D.A.^{1,2}, Pochekutov M.A.², Semenov S.V.^{1,2}, Velikanov D.A.¹

¹ Kirensky Institute of Physics, Federal Research Center KSC SB RAS, Krasnoyarsk, Russia

² Siberian Federal University, Krasnoyarsk, Russia

bigmike24krsk@gmail.com

It is known that granular high- T_C superconductors (HTSCs) exhibit anisotropy of magnetoresistance $R(H)$ with respect to mutual orientation of magnetic field \mathbf{H} and macroscopic transport current \mathbf{j} . This anisotropy takes place in the ranges of temperature, magnetic field, and transport current where the dissipation (observable magnetoresistance) occurs in the inter-grain media (i.e., subsystem of inter-grain boundaries which behave like Josephson junction network). Daghero et al [1] proposed a model in which the total magnetic field in the inter-grain media is a superposition of external field and field induced by screening currents (due to Meissner effect). This approach can explain the value of anisotropy parameter $R_{H \perp j} / R_{H \parallel j}$ observed in real granular HTSCs [1,2]. In order to advance along this line, we further develop the model of granular HTSC in a magnetic field and determine the effective field in the inter-grain media for various orientations of $\theta = \angle \mathbf{H}, \mathbf{j}$. Within this model in the space between superconducting grains the effective field B_{eff} is much higher than external one due to the flux compressing [3] and it can be derived from magnetization $M(H)$ data:

$$B_{\text{eff}}(H) = H - 4\pi M(H) \cdot \alpha. \quad (1)$$

Here α – is the parameter proportional to the degree of flux compressing [3] and the sign of $M(H)$ dependence is taken into account. Expression (1) explains the hysteretic behaviour of magnetoresistance $R(H)$ of granular superconductor considering that R is a function of effective field ($R \sim f(H) \sim f(B_{\text{eff}})$). To explain the anisotropy of magnetoresistance it is necessary to assume that the trajectories of microscopic current are different for the cases $\mathbf{H} \perp \mathbf{j}$ and $\mathbf{H} \parallel \mathbf{j}$ (microscopic current “choose” the trajectory with lesser flux compressing, therefore with lesser dissipation).

We have measured the $R(H)$ hysteresis dependences of granular $\text{YBa}_2\text{Cu}_3\text{O}_7$ HTSC for various orientations of \mathbf{H} and \mathbf{j} . The field hysteresis widths $\Delta H = H_{\downarrow} - H_{\uparrow}$ at $R(H_{\downarrow}) = R(H_{\uparrow})$ and $B_{\text{eff}}(H_{\downarrow}) = B_{\text{eff}}(H_{\uparrow})$ conditions of $R(H)$ and $B_{\text{eff}}(H)$ dependences [4] were used for analysis. By varying the parameter α in (1) we obtain a good agreement of ΔH values for hysteresis $R(H)$ and $B_{\text{eff}}(H)$ dependences. We found that orientation dependence of $\alpha(\theta)$ behaves as follows: $\alpha(\theta) = \alpha_{(H \parallel j)} + [\alpha_{(H \perp j)} - \alpha_{(H \parallel j)}] \sin\theta$, where $\alpha_{(H \parallel j)} \approx 10$ and $\alpha_{(H \perp j)} \approx 20$. Such a high value of parameter α is a result of flux compressing in the inter-grain media [3]. The proportionality $\alpha(\theta) \sim \sin\theta$ was a hypothesis proposed by Daghero et al [2] and we proved this hypothesis experimentally. Therefore, the flux compressing in the inter-grain media determines experimentally observed anisotropy of magnetoresistance of granular HTSCs ($\alpha_{(H \perp j)} > \alpha_{(H \parallel j)}$).

The reported study was funded by Russian Foundation for Basic Research, Government of Krasnoyarsk Territory, Krasnoyarsk Region Science and Technology Support Fund to the research project № 16-48-243018.

[1] D. Daghero, P. Mazzetti, A. Stepanescu, P. Tura, *Phys. Rev. B*, **66** (2002) 11478.

[2] D.A. Balaev, et al, *Supercond. Sci. Technol.*, **20** (2007) 495.

[3] D.A. Balaev, S.I. Popkov, et al, *J. Appl. Phys.*, **110** (2011) 093918.

[4] S.V. Semenov, D.A. Balaev, et al, *Fizika Tverdogo Tela*, **59**(N7) (2017) 1267.

3PO-I-8

TRANSPORT PROPERTIES OF MAGNESIUM DIBORIDE – MANGANITE NANOCOMPOSITE

Kononenko V.V.¹, Varyukhin V.N.¹

¹ A. Galkin Donetsk Institute for Physics and Engineering, Donetsk, Ukraine
vkkononenko@gmail.com

Progress in the design of computer technology has stimulated the creation of new materials with properties that are absent in the parent components. In work magnesium diboride - manganite $\text{La}_{0.7}\text{Sr}_{0.3}\text{MnO}_3$ nanocomposite with properties that differ from initial components are investigated. They consist of two differing in resistance materials at room and low temperatures. At room temperature, MgB_2 is a normal metal, but in low temperature, it is a superconductor. The manganite is a ferromagnetic metal in a wide range of temperatures. Features of the systems under consideration consist in an essential difference in the sizes of the components and their mutual influence (proximity effect). Namely, the composite consists of microgranules ($\sim 5 \mu\text{m}$) of MgB_2 superconductor and nanogranules ($\sim 15 \text{nm}$) of $\text{La}_{0.7}\text{Sr}_{0.3}\text{MnO}_3$ manganite. The temperature dependence of the resistivity for pure MgB_2 and MgB_2 -LSMO composites (10% and 26% volume content of LSMO) are presented in Fig. 1a. It shows that 10% and 26% LSMO supplements significantly broaden the superconducting $R(T)$ transition of the composite and the resistance of the sample with 26% LSMO concentration is finite over the entire temperature range. The blur of MgB_2 superconducting transition may be due to the influence of the components granules size and of the proximity effect. The current-voltage characteristics of the MgB_2 (the inset of Fig. 1 b) show the behavior characteristic of type-II superconductor. A completely different situation for samples MgB_2 -LSMO (10% and 26% volume content LSMO) (Fig. 1 b). If the 10% LSMO concentration demonstrated critical current, for 26% LSMO concentration the critical current was absent, and the curve has a shape characteristic of a medium of weak contacts with excess current.

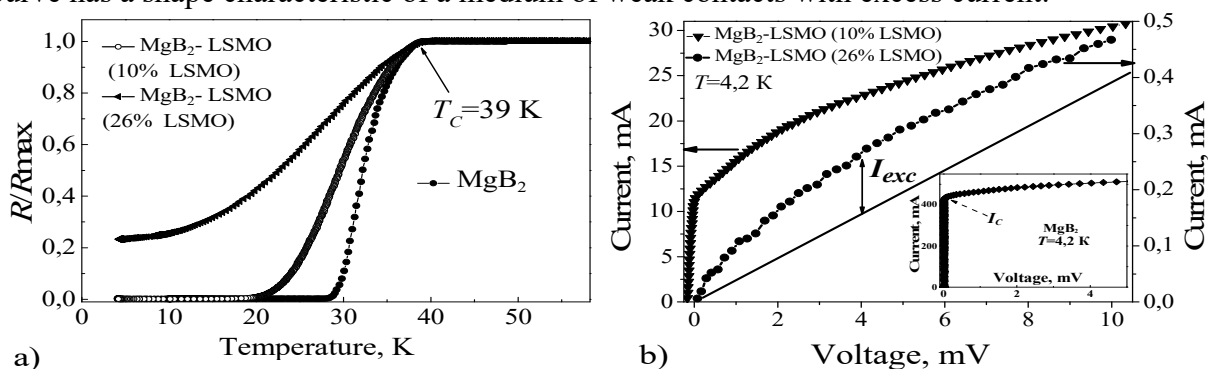


Fig. 1.

- a) The temperature dependence of the resistivity MgB_2 , MgB_2 -LSMO (10% and 26% LSMO);
 b) Current-voltage characteristics of composites MgB_2 -LSMO (10% and 26% LSMO); MgB_2 .

It has been established experimentally that origin of the nanocomposites percolation transition differs above and below superconductor critical temperature (T_C). At $T > T_C$, the main characteristics are determined by the components granules size (geometry). At $T < T_C$, in addition to the components geometry, the proximity effect influences on the superconducting transition temperature, critical current value, the current-voltage dependence. In particularly, superconductor-manganite-superconductor weakly-coupled contacts are formed. As a result, new materials with properties absent in the original components are obtained.

3PO-I-9

ISOLATION OF PROXIMITY-INDUCED TRIPLET PAIRING CHANNEL IN A SUPERCONDUCTOR/FERROMAGNET SPIN VALVE

Kamashev A.A.¹, Validov A.A.¹, Garifyanov N.N.¹, Garifullin I.A.¹, Fominov Ya.V.^{2,3}, Leksin P.V.⁴, Shumann J.⁴, Thomas J.⁴, Kataev V.⁴, Büchner B.⁴

¹Zavoisky Physical-Technical Institute, Russian Academy of Sciences, Kazan, Russia

²L.D. Landau Institute for Theoretical Physics, Russian Academy of Sciences, Chernogolovka, Russia

³Moscow Institute of Physics and Technology, 141700 Dolgoprudny, Russia

⁴Leibniz Institute for Solid State and Material Research IFW Dresden, Dresden, Germany
kamandi@mail.ru

The superconducting spin-valve effect consists of different degree of suppression of superconductivity in the F1/F2/S or F1/S/F2 thin film multilayer constructions at parallel (P) and antiparallel (AP) mutual orientation of magnetizations of the F1 and F2 ferromagnetic layers (here F1 and F2 are two ferromagnetic layers and S is the superconducting layer).

In our previous works on the $\text{CoO}_x/\text{Fe1}/\text{Cu}/\text{Fe2}/\text{In}$ structure we have demonstrated a full switching between the normal (N) and superconducting (SC) states [1] and observed the sign-changing oscillating behavior of the magnitude of the spin valve effect ΔT_c on the thickness of the Fe2 layer [2].

Recent theories predict that at certain conditions a long-range triplet component (LRTC) in the superconducting condensate can arise in the S/F structure. The generation of the LRTC in the F1/F2/S spin-valve structure should manifest itself as a minimum of T_c at noncollinear configuration of magnetizations. We have obtained experimental confirmation of this prediction by studying the $\text{CoO}_x/\text{Fe1}/\text{Cu}/\text{Fe2}/\text{Pb}$ spin valve structure [3]. The observed angular dependence of T_c was caused by a combination of the conventional and triplet components of the condensate. An indication of the triplet contribution to the magnitude of the superconducting spin-valve effect has been also observed.

In the present work we have studied the proximity-induced superconducting triplet pairing in $\text{CoO}_x/\text{Py1}/\text{Cu}/\text{Py2}/\text{Cu}/\text{Pb}$ spin-valve structure (where $\text{Py} = \text{Ni}_{0.81}\text{Fe}_{0.19}$). For $\text{CoO}_x(3\text{nm})/\text{Py}(3\text{nm})/\text{Cu}(4\text{nm})/\text{Py}(0.6\text{nm})/\text{Cu}(2\text{nm})/\text{Pb}(70\text{nm})$ we have studied the dependence of the T_c on the angle α between the direction of the cooling field and the external field both applied in the plane of the sample. We obtained that the T_c does not change monotonically with the angle but passes through a minimum. To observe an “isolated” triplet spin-valve effect we exploited the oscillatory feature of the magnitude of the ordinary spin-valve effect ΔT_c in the dependence of the Py2-layer thickness d_{Py2} . We determined the value of d_{Py2} at which ΔT_c caused by the ordinary spin-valve effect is suppressed. This means that the difference in the T_c between the antiparallel and parallel mutual orientation of magnetizations of the Py1 and Py2 layers is zero. For such a sample a “pure” triplet spin-valve effect which causes the minimum in T_c at the orthogonal configuration of magnetizations has been observed.

This work was partially supported by Russian Foundation for Basic Research (No. 17-02-00229) and the Program of the Russian Academy of Sciences.

[1] P.V. Leksin *et al. Appl. Phys. Lett.*, **97** 102505 (2010).

[2] P.V. Leksin *et al. Phys. Rev. Lett.*, **106** 067005 (2011).

[3] P.V. Leksin *et al. Phys. Rev. Lett.*, **109** 057005 (2012).

3PO-I-10

FEATURES OF MICROSTRUCTURE AND MAGNETIC FLUX DYNAMICS IN SUPERCONDUCTING Nb-Ti TAPES WITH STRONG ANISOTROPIC PINNING

*Shavkin S.V.¹, Guryev V.V.¹, Kruglov V.S.¹, Ovcharov A.V.¹, Likhachev I.A.¹, Vasiliev A.L.¹,
Veligzhanin A.A.¹, Zubavichus Y.V.¹*

¹ NRC “Kurchatov Institute”, Moscow, Russia
shavkin@mail.ru

All practically used low-temperature superconducting materials including them with the cubic lattice structure (Nb-Ti alloy, Nb₃Sn compound, etc.) have pronounced anisotropy of the current-carrying capacity caused by the directional nature of the technological manufacturing processes (rolling, drawing, etc.) which lead to formation of the non-isotropic field of natural or artificial pinning centers. The macroscopic electrodynamics of such a “hard” superconductors with anisotropic (depending on the directions of a magnetic field and Lorentz force) pinning was proposed phenomenologically, on the basis of empirical studying of critical Lorentz forces [1]. Interaction of the vortex structure (magnetic flux) with a anisotropic complex of pinning centers in the superconductor is described by a global potential well which depth depends on the direction of a magnetic induction and described by the tensor field. Force counteraction of system of the pinning centers to driving of a magnetic flux is described by a derivative of this tensor field on coordinates. It is also the tensor field. The proposed macroscopic approach allowed to avoid a problem of summation of the individual pinning forces.

For Nb-50%wt.Ti tapes this formalism allowed to calculate the value of critical Lorentz force for the arbitrary orientation of a magnetic field and transport current, to define the direction of movement of a magnetic flux and the direction of the electric field induced by this driving, as a rule, not coinciding with the direction of the current.

Detailed TEM and SEM investigation of Nb-50%wt.Ti tapes microstructure were done using Titan S-TWIN 80-300 (FEI) microscope with resolution up to 0.08 nm. Detailed phase and texture analysis were carried out on Kurchatov Synchrotron Radiation Source and on high precision X-ray diffractometers.

The main grains sizes in all directions were determined by averaging of statistical data from several dozen of SEM images. Calculated main grains sizes were: 65 nm in the direction of normal to the plane of the tape; 0.4 μm in the transverse direction; and more than 1 μm in the rolling direction. Pronounced grain boundaries were observed only in parallel to the plane. Distribution of Nb-Ti grain sizes was similar in cold-rolled and heat-treated tapes.

Correlations between anisotropic microstructure and flux dynamics in Nb-50%wt.Ti tapes are discussed and summarized.

[1] E.Yu. Klimenko, S.V. Shavkin, P.V. Volkov *Zh.Eksp. Teor. Fiz.*, **112** (1997) 1055-1081.

3PO-I-11

TWO MAGNETIC PHASE TRANSITIONS IN FRANCISITE-TYPE $\text{Cu}_3\text{Yb}(\text{SeO}_3)_2\text{O}_2\text{Cl}$

Zakharov K.V.¹, Markina M.M.¹, Kuznetsova E.S.¹, Berdonosov P.S.¹, Vasiliev A.N.¹

¹ Moscow State University, 119991 Moscow, Russia

zak-konstantin@yandex.ru

The francisite, $\text{Cu}_3\text{Bi}(\text{SeO}_3)_2\text{O}_2\text{Cl}$, is characterized by an unique combination of chemical elements met in this mineral only [1]. The pristine compound, Bi-francisite, experiences long-range magnetic order at $T_N = 24$ K adopting non-collinear antiferromagnetic structure. The rare-earth's anisotropy may influence this complex structure leading to temperature driven spin-reorientation transition.

The ytterbium counterpart of mineral francisite, $\text{Cu}_3\text{Yb}(\text{SeO}_3)_2\text{O}_2\text{Cl}$, is synthesized and studied in measurements of magnetization and specific heat. The polycrystalline sample of $\text{Cu}_3\text{Yb}(\text{SeO}_3)_2\text{O}_2\text{Cl}$ (sp. gr. $Pm\bar{m}n$) have been synthesized from CuO , CuCl_2 , Yb_2O_3 and SeO_2 . The compound reaches antiferromagnetic order at $T_N = 36.7$ K and experiences first-order spin-reorientation transition to ferrimagnetic phase at $T_R = 8.7$ K. The available data suggest that non-collinear antiferromagnetic structure of $\text{Cu}_3\text{Yb}(\text{SeO}_3)_2\text{O}_2\text{Cl}$ at $T_R < T < T_N$ transforms to collinear ferrimagnetic one at $T < T_R$.

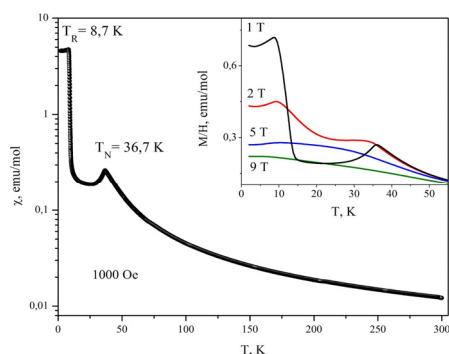


Fig. 1. Temperature dependences of magnetic susceptibility in $\text{Cu}_3\text{Yb}(\text{SeO}_3)_2\text{O}_2\text{Cl}$.

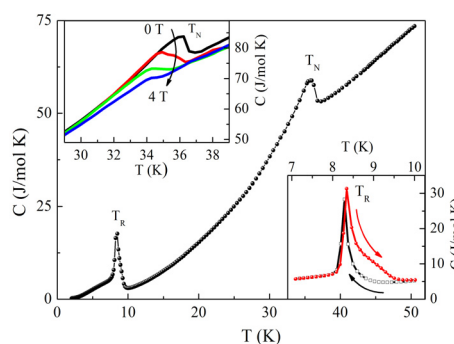


Fig. 2. Temperature dependence of the specific heat in $\text{Cu}_3\text{Yb}(\text{SeO}_3)_2\text{O}_2\text{Cl}$

The temperature dependences of magnetic susceptibility $\chi = M/B$ in $\text{Cu}_3\text{Yb}(\text{SeO}_3)_2\text{O}_2\text{Cl}$ taken at various magnetic fields are shown in Fig. 1. The sharp anomalies at T_N and T_R are seen in low-field measurements. Both anomalies are rapidly suppressed by an external magnetic field. Similar to Sm-francisite [2], it is assumed that the magnetic ordering in Yb-francisite takes place at T_N while the spin-reorientation transition occurs at T_R . Positive $\Theta_{\text{CW}} = 25$ K corresponds to the main ferromagnetic exchange. Further analysis of $\chi(T)$ dependence is complicated by the fact that both Curie-Weiss and van Vleck terms contribute to the magnetic response of this compound. The temperature dependence of the specific heat C_p is shown in Fig. 2. The λ -type anomaly at T_N denote the second order transition, while the sharp spike at T_R indicates the first order transition. Both anomalies are rapidly suppressed by external magnetic field (left Insert). The additional Schottky type anomaly is seen also above T_R when compared are the $C_p(T)$ curves obtained at both cooling and heating (right Insert).

[1] A. Pring, B.M. Gatehouse, W.D. Birch, *Amer. Mineral* **75** (1990) 1421.

[2] K.V. Zakharov et al., *Phys. Rev. B*, **94** (2016) 054401.

3PO-I-12

CALCULATION OF ELECTRONS TRAPS INFLUENCE ON A COLD ELECTRONS BOLOMETER

Balahontsev A.B.¹, Yagovtsev V.O.¹, Levshunov V.V.¹, Pugach N.G.^{1,2}

¹ National Research University Higher School of Economics, Moscow, Russia

² SYN P Lomonosov Moscow State University, Moscow, Russia
voyagovtsev@edu.hse.ru

The concept of Cold-Electron Bolometer (CEB) is based on direct electron cooling of the absorber that serves as negative electrothermal feedback for incoming signal. This feedback is analogous to TES (transition-edge sensor) but additional dc heating is replaced by deep electron cooling to minimum temperature. It could mean a principle breakthrough in realization of supersensitive detectors [1].

In the presented work, the calculation of the influence of a normal layer trap, placed on a top of a superconducting electrode of a cold electron bolometer (CEB) is presented. The behavior of the superconducting layer under the conditions of proximity effect with a normal metal is analyzed. The calculation was done in the frameworks of the Ginzburg-Landau equation [2,3]:

$$\xi^2 \frac{d^2 \psi}{dx^2} + \psi - \psi^3 = 0. \quad (1)$$

For the correct formulation of the mathematical problem, equation (1) must be supplemented by boundary conditions on the boundary of a superconductor with a normal metal:

$$\frac{d\psi}{dx} = \frac{1}{b} \psi, \quad (2)$$

and by the boundary conditions at the boundary of the superconductor with vacuum:

$$\frac{d\psi}{dx} = 0. \quad (3)$$

Also, the phase transition from the superconducting state to the normal state, which is determined by the critical temperature T_c was investigated. T_c is the lowest temperature, which admits only the trivial solution of equation (1) with the boundary conditions (2) and (3). To solve the task, the computer-aided design system Matlab was chosen. Also, an analytic approximate solution was found. A program was written for solving the Ginzburg-Landau equation in a thin superconductor layer under the conditions of proximity effect. Numerical experiments were performed in which the following parameters changed: the value of the parameter b , which describes the proximity effect at the boundary of the superconductor with the normal metal; and the thickness of the superconducting film d_s . The superconducting order parameter over the thickness of the layer, and the dependence of the critical temperature of the superconducting layer on the boundary parameter were investigated. Analysis of the obtained dependences made it possible to draw conclusions about the nature of the phenomenon under study.

[1] Kuzmin L., *International Society for Optics and Photonics*, (2004) 349-361.

[2] Schmidt V. V. *Springer Science & Business Media* (2013).

[3] Abrikosov A. A., *Amsterdam: North-Holland*, (1988).

3PO-I-13

DISTRIBUTION OF PAIRING FUNCTIONS IN SUPERCONDUCTING SPIN-VALVES

*Gaifullin R.R.*¹, *Deminov R.G.*¹, *Tagirov L.R.*^{1,2}, *Kupriyanov M.Yu.*^{1,3,4}, *Golubov A.A.*^{4,5}

¹ Institute of Physics, Kazan Federal University, Kazan, Russia

² Zavoisky Physical-Technical Institute of the Kazan Scientific Center of the Russian Academy of Sciences, Kazan, Russia

³ Skobeltsyn Institute of Nuclear Physics, Moscow State University, Moscow, Russia

⁴ Moscow Institute of Physics and Technology, Dolgoprudny, Russia

⁵ Faculty of Science and Technology and MESA+ Institute of Nanotechnology, University of Twente, Enschede, The Netherlands

gaifullin.rashid@gmail.com

We investigate SF1F2 structures (S is a singlet superconductor, F1 and F2 are ferromagnetic metals, identical in our case), where the long-range triplet superconducting pairing is generated at canted magnetizations of the F layers [1]. An asymptotically exact numerical method [2] is employed here to calculate critical temperature T_c as a function of the trilayer parameters, such as mutual orientation of magnetizations, interfaces transparencies, and the layers thicknesses.

Previously it was demonstrated that transition temperature T_c in semi-infinite SF1F2 structures can be a non-monotonic function of the angle α between magnetizations of the two F layers [3], against the monotonic $T_c(\alpha)$ behavior obtained for the F1SF2 trilayers [4]. It was shown lately [5] the existence of the anomalous dependence of the spin-triplet pairing correlations on the angle α in SF1F2 structures in a limit of thin F layers.

We examine comparatively the spin-singlet and spin-triplet pairing distributions and amplitudes as a function of the layers thicknesses at different values of the angle α in SF1F2 structures to clarify which one of the pairings and how may impact on the superconducting spin-valve switching modes in these heterostructures.

Fig. 1 shows the spin-singlet, the short-range triplet with zero projection and the long-range triplet with ± 1 projections superconducting pairing components in the triplet spin-valve switching mode of the trilayer heterostructure.

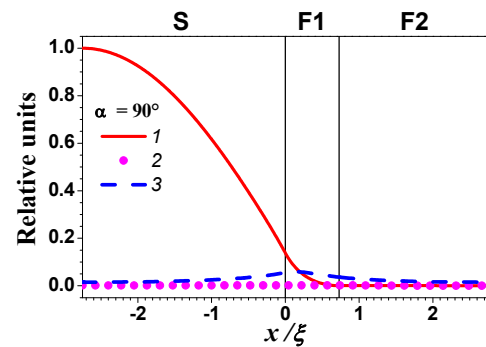


Fig. 1. Distribution spin-singlet (1), triplet with zero projection (2), triplet with ± 1 projections (3) superconducting pairing components at orthogonal orientation of magnetizations.

Support by RFBR (grants No. 16-02-01171-a, 15-32-20362-bel_a_ved), DFG HO 955/9-1 and by the Program of Competitive Growth of Kazan Federal University, funded by the Russian Government is gratefully acknowledged.

[1] F.S. Bergeret, A.F. Volkov, K.B. Efetov, *Rev. Mod. Phys.*, **77** (2005) 1321-1373.

[2] Ya.V. Fominov, N.M. Chtchelkatchev, A.A. Golubov, *Phys. Rev. B*, **66** (2002) 014507(13).

[3] Ya.V. Fominov, A.A. Golubov, T.Yu. Karminskaya, M.Yu. Kupriyanov, R.G. Deminov, L.R. Tagirov, *JETP Lett.*, **91** (2010) 308-313.

[4] Ya.V. Fominov, A.A. Golubov, M.Yu. Kupriyanov, *JETP Lett.*, **77** (2003) 510-515.

[5] T.Yu. Karminskaya, A.A. Golubov, M.Yu. Kupriyanov, *Phys. Rev. B*, **84** (2011) 064531(5).

3PO-I-14

SUPERCONDUCTIVITY AND FERROMAGNETISM IN THE HUBBARD MODEL

Zaitsev R.O.¹

¹ Moscow Institute of Physics and Technology (State University), Institutskii per.9,
Dolgoprudnyi, Moscow region, 141700 Russia
Zaitsev_rogdai@mail.ru

In the framework of Hubbard model at $U > 0$ the phase transition related to the lower underfilled subband are studied. The self-consistent equations determining the superconducting and ferromagnetizing order parameters are derived in the one-loop approximation. The phase boundaries within which ferromagnetic and superconducting phenomena can coexist are discussed.

The simplest paramagnetic Hubbard solution supplemented by the so-called kinematic interaction and devoted the limiting case, where the Hubbard energy is the largest energy parameter. As a result, the temperature and electron density dependences of transition points for both superconducting and ferromagnetic ordering are determined in the one-loop approximation. Under these conditions it is sufficient to consider only the low-energy subband, where transitions occur between empty $|0\rangle$, and one-particle, $|\sigma\rangle$, states. In this case, the following Hamiltonian can be used:

$$\hat{H} = \sum_{\mathbf{r}_1, \mathbf{r}_2, \sigma} \hat{X}_{\mathbf{r}_1}^{\sigma, 0} \hat{X}_{\mathbf{r}_2}^{0, \sigma} t(\mathbf{r}_1 - \mathbf{r}_2) - \mu \sum_{\mathbf{r}, \sigma} \hat{X}_{\mathbf{r}}^{\sigma, \sigma} \quad (1)$$

Here μ is the chemical potential and $\hat{X}^{\sigma, 0}$ and $\hat{X}^{0, \sigma}$ are the one-particle operators.

The calculation of the first Born scattering amplitude using Hamiltonian (1) leads to expression to the expression for the amplitude of the kinematic interaction [1,2]:

$$\Gamma_0(\mathbf{p}_1, \mathbf{p}_2 \| \mathbf{p}_3, \mathbf{p}_4) = -t(\mathbf{p}_3) - t(\mathbf{p}_4). \quad (2)$$

Here and bellow, $t(\mathbf{p})$ is the Fourier transform of the hopping integral involved in the definition of Hamiltonian (1).

To find the superconducting transition temperature, it is necessary to consider the conditions, needing for formation of anomalous self-energy [3], corresponding to the opposite direction of the momentum and to the opposite sign of spin projection change. To study the possibility of the magnetic ordering, it is sufficient to consider the diagrams with zero momentum transfer and with the electron spin flip [4,5].

To study the interplay of superconducting and magnetic phenomena, it is necessary to derive general self-consistent equations. The analysis of these equations indicates that only superconducting pairing at $T = 0$ can exist in the model under consideration. The magnetic solutions exist at finite temperature. The most interesting result of this work is revelation of the coexistence of the superconducting and ferromagnetic phases within limited temperature and electron density ranges [6].

[1] R.O. Zaitsev, *Phys. Lett A*, **134** (1988) 199-201.

[2] R.O. Zaitsev, *Diagrammatics Methods in the Theory Superconducting and Ferromagnetism URSS, Moscow*, (2000).

[3] L.P. Gor'kov, *Sov. Phys. JETP*, **7** (1958) 505-512.

[4] V.P. Silin, *Zh. Eksp. Teor.*, **27** (1954) 269-271.

[5] P.S. Kondratenko, *Sov. Phys. JETP*, **19** (1964) 972-984.

[6] R.O. Zaitsev, *JETP Letters*, **102** (2015) 515-520.

3PO-I-15

SYNTHESIS AND CHARACTERISATION OF SUPERCONDUCTING HETEROSTRUCTURES WITH Sr_2IrO_4 INTERLAYER

Petrzhik A.M.¹, Cristiani G.², Shadrin A.V.¹, Logvenov G.², Ovsyannikov G.A.¹

¹ Kotel'nikov IRE of RAS, Moscow, Russia,

² Max Planck Institute for Solid State Research, Stuttgart, Germany

petrzhik@hitech.cplire.ru

Sr_2IrO_4 is the material with strong spin-orbit interaction [1], where a lot of interesting physics is observed. Some properties were already confirmed experimentally: this is d-wave gap of unknown origin [2], a unique high value of the anisotropic magnetoresistance [3], some data on topological insulator state [4] and so on. But there is one interesting effect predicted only theoretically: as it was shown in [5], Sr_2IrO_4 in system triplet superconductor - iridate - singlet superconductor may work as singlet-triplet converter. To check this possible effect experimentally, the epitaxial heterostructures $\text{YBa}_2\text{Cu}_3\text{O}_7$ (YBCO) - Sr_2IrO_4 was grown in situ for fabrication superconducting mesa structures with Nb as the top electrode. The information about crystal structure and magnetic properties of our heterostructures and some technical parameters of successful synthesis are presented [6]. Also we will present the results of electron transport measurements of fabricated mesa structures.

The work is partially supported by RAS and Scientific School grant NSH-8168.2016.2.

[1] B. J. Kim et al., *Science*, **323** (2009) 1329.

[2] Y. K. Kim et al., *Nature Phys.*, **12** (2016) 37.

[3] M. Ge et al., *Phys. Rev. B*, **84** (2011) 100402(R).

[4] M. Z. Hasan, C. L. Kane, *Rev. of Mod. Phys.*, **82** (2010) 3045.

[5] Mats Horskdal, Giniyat Khaliullin et al., *Phys. Rev. B*, **93** (2016) 20502(R).

[6] A.M. Petrzhik et al., *Pis'ma v Zhurnal Tekhnicheskoi Fiziki*, **43**(12) (2017) 25-33.

3PO-I-16

IRREVERSIBILITY FIELD OF SUPERCONDUCTING Nb-Ti TAPES

Guryev V.V.¹, Shavkin S.V.¹, Kruglov V.S.¹
¹ NRC “Kurchatov institute”, Moscow, Russia
GuryevVV@mail.ru

The magnetizations and the current-voltage characteristics (CVC) of superconducting samples fabricated from cold-rolled and heat-treated tapes of Nb-50%wt.Ti alloy were studied in the range of an external magnetic field close to the upper critical value. In this range of fields, characteristic value of the field exists, at which magnetization change behavior from irreversible (low fields) to reversible (high fields). At the same time, the critical current decrease dramatically, which is often associated with the phase transition of vortex matter.

We have shown that the whole volume of experimental data can be described if we abandon the hypothesis of a phase transition and go over to the hypothesis of macroscopic inhomogeneity [1]. This hypothesis implies a transition from the pinning model to the percolation current path model in the phenomenological description of the superconducting system in fields above the irreversibility field.

[1] E.Yu. Klimenko, S.V. Shavkin, P.V. Volkov *FMM*, **92** (2001) 552-556.

3PO-I-17

THE NON-LINEAR RESPONSE OF A SUPERCONDUCTOR OF THE Bi-Sr-Ca-Cu-O SYSTEM TO AN ALTERNATING MAGNETIC FIELD

Gvozdevskaya V.A.¹, Sergeev A.V.¹, Golev I.M.²

¹ Voronezh State Technical University, Voronezh, Russia

² The Military Educational and Training Center of Air Forces «The Air Force Academy, named after Prof. N.E.Zhukovsky and Y.A.Gagarin», Voronezh, Russia

v-gvozdevskaya@mail.ru

The paper conducts the response measurements of a high-temperature superconductor (HTSC) of the Bi-Sr-Ca-Cu-O system to a low-frequency alternating magnetic field. The specimen, composed of two phases, Bi-2223 (46%) and Bi-2212 (52%) (the dimensions are $3,2 \times 3,2 \times 20 \text{ mm}^3$, the density is $4,1 \text{ g/cm}^3$), was produced by the two-phase ceramic technology.

The measurements of electrical resistance in a specimen have been carried out using the voltmeter-ammeter method. The spectral composition of the HTSC response signal was measured on the basis of the inductive methodology, with the help of a single-layer coil, wound on the specimen. The measurements were conducted in the temperature range of superconducting transition, upon the impact of an alternating magnetic field (the induction $B=10 \text{ Gs}$, the frequency $f=1000 \text{ Hz}$), directed along the principal symmetry axis of the specimen. The harmonics have been isolated from the HTSC response signal using the selective microvoltmeter, as described in [1]. As shown by measurement results (fig.1, 2), in the temperature range $T=100 \div 93 \text{ K}$, the voltages of the 3rd, the 5th and the 7th harmonics have peak values when the superconductor is in the resistive state. With increasing the ordinal number, the harmonic amplitudes fade. No even harmonics were observed during the measurements. The non-linear response occurs in local superconducting zones of the Bi-2223 phase, surrounded by the standard matrix from the Bi-2212 phase, which follows from the analysis of the curve $R(T)$. The induced current in the Bi-2223 phase presumably exceeds the critical current value of the Bi-2223 phase, which results in the emergence of the resistive state in the Bi-2223 phase. The voltage pulses occur, representing the fragments of sinus curves and resulting in emergence of harmonic components. Since, in this case, the HTSC current-voltage characteristics are described by odd functions, the response signal includes the odd harmonics [2, 3].

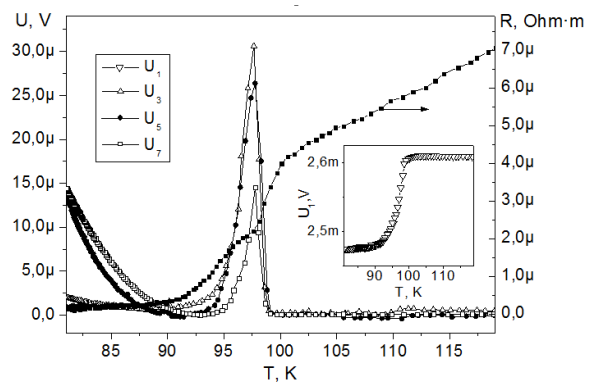


Fig. 1. Temperature dependencies of the 1st, the 3rd, the 5th and the 7th harmonic amplitudes on specific electrical impedance

[1] A.V. Sergeev, I.M.Golev et al. The News of the South-Western State University. The series «Technics and technologies», 3 (2016) 146-153.

[2] I.M.Golev, A.V.Sergeev, O.V. Kalyadin. Solid-State Physics, 1 (2017) 19-22.

[3] Andreev V.S. The theory of non-linear electrical circuits. Radio and communications. Moscow (1982). 280.

3PO-I-18

PECULIAR INTERACTION OF VORTICES WITH MAGNETIC RARE-EARTH IONS IN HTSC $\text{TmBa}_2\text{Cu}_3\text{O}_y$ SINGLE CRYSTAL

*Pigalskiy K.*¹

¹ Semenov Institute of Chemical Physics RAS, Moscow, Russia
pigalskiy@chph.ras.ru

A comparative study of the field dependences of low-frequency complex magnetic permeability μ^* for HTSC YBaCuO and TmBaCuO single crystals have been recently provided [1]. Optimally doped samples ($T_c \approx 88$ K) were in the form of thin plates, the external magnetic field was directed along the plane of the plate, i.e. along the crystallographic *ab*-plane. The two different types of contributions to μ^* were obtained. The first one (μ_v) originates from the reversible vibrational motion of vortices perpendicular to the crystal lattice layers induced by AC component of the external magnetic field. It does not depend on the amplitude of the AC field. The second type of contribution is related to the realization of the critical state along the layers. It was found that, as the temperature approaches T_c , the behavior of the field dependences of μ_v and the critical current J_c was substantially different for the samples under investigation. It was concluded that this effect was related to the manifestation of the unusual mechanism of intrinsic pinning, arising when Y^{3+} is replaced with Tm^{3+} magnetic ion.

In the present work the quantitative information about the interaction of a vortex lattice with the magnetic system of a rare-earth ion is obtained. For this purpose, on the bases of the theoretical approaches developed earlier in [2] for the equilibrium (non-pinned) discrete vortex lattice, the analytical description of the vibrational contribution μ_v to the magnetic permeability are performed taking into account the interaction with pinning centers. The analytical results obtained are compared with the numerical calculations of equilibrium positions and vibration amplitudes for N_r vortex rows ($N_r \leq 50$). In doing so, both the gradient of the vortex density near the surface and the decrease in the amplitude of the reversible oscillations inside the potential pinning well, whose steepness is characterized by the force constant k_p , are taken into account. It is shown that the first mechanism leads to a small hysteresis in the $\mu_v(H)$ dependences while the second one manifests itself in a noticeable decrease in the μ_v value even for moderate values of the critical current density $J_c \sim 10^4$ A/cm².

A comparison of the calculation results with the experimental data for two single-crystal samples TmBaCuO is carried out. Field dependences of the force constant k_p of the interaction between vortex and the layer of magnetic rare-earth ion Tm^{3+} are defined. It is shown that this interaction is induced by the external magnetic field starting from a certain threshold value of $H_{cr} \sim 500$ Oe and practically does not change with temperature when approaching T_c . Also it is obtained that for the sample with larger magnitude of London penetration depth λ the value of k_p is reducing approximately proportionally to $\lambda(T=0)^{-2}$.

The revealed features of the interaction of vortices with a magnetic moment of Tm^{3+} ions indicate that it rather has the unusual magnetic nature than is associated with a change in the condensation energy in the vortex core. One of the proposed mechanisms of this interaction is related to a possible presence of spin in the vortex core, predicted in [3].

The work is supported by RFBR (grant 17-07-00131).

[1] K.S. Pigalskiy, *Phys. Solid State*, **59** (2017) 450.

[2] K.I. Kugel, L.G. Mamsurova, K.S. Pigalskiy, A.L. Rakhmanov. *Physica C*, **300** (1998) 270.

[3] V.N. Muthukumar, Z.Y. Weng, *Phys. Rev. B*, **65** (2002) 174511.

3PO-I-19

TUNING THE PEAK EFFECT BY IN $Y_{1-x}Nd_xBa_2Cu_3O_7$ COMPOUND BY Nd DOPING

Semenov S.V.^{1,2}, Gokhfeld D.M.¹, Balaev D.A.^{1,2}, Yakimov I.S.², Petrov M.I.¹

¹ Kirensky Institute of Physics, Federal Research Center KSC SB RAS, Krasnoyarsk, Russia

² Siberian Federal University, Krasnoyarsk, Russia
svsemenov@iph.krasn.ru

The peak effect on magnetic field dependence of critical current $J_C(H)$ of bulk superconductors reflects enhancement of pinning in a some field range and mainly relates to an Abrikosov vortex lattice transition. This effect reveals as a second peak on magnetization loop $M(H)$ and it is called as “fish-tail peculiarity”. Several approaches are commonly used to induce the peak effect in high- T_C superconductors (HTSCs), and one of them is chemical substitution in rare element subsystem. Here we report on the study of the effect of partial substitution of Yttrium by Neodymium in Y-based HTSC with 1-2-3 structure.

Bulk polycrystalline $Y_{1-x}Nd_xBa_2Cu_3O_7$ samples with $x = 0.02, 0.11, \text{ and } 0.25$ were synthesized by standard solid state reaction technique. X-ray diffraction powder patterns revealed 1-2-3 structure for samples under study. The cell parameters grow linearly with the Nd content. The energy dispersive spectrometry showed homogeneous distribution of Nd both within the grains and different grains. The superconducting transition temperatures lie within 92.5-91.7 K. The magnetization loops were measured by using PPMS-6000 vibrating sample magnetometer.

It was found that $M(H)$ dependences of studied samples exhibit the fish-tail peculiarity, and the position of second magnetization peak depends on Neodymium content in 1-2-3 HTSC. The position H_{peak} of the peak effect on $J_C(H)$ dependences shifts to lesser values of magnetic field as Neodymium concentration increases (see fig.1).

In order to describe the $M(H)$ dependences the extended critical state model [1,2] was used. The peak was accounted by the Boltzmann's function describing the transition between ordered and disordered states. Fitting of the experimental $M(H)$ dependences was performed by this approach [3], also additional paramagnetic contribution from Nd atoms was taken into account.

The field dependences of pinning force $F_P = J_C(H) \cdot H$ are found to scale in coordinates $F_P/F_{P\text{max}}, H/H_{\text{irr}}$, where H_{irr} – the irreversibility field $\{J_C(H \geq H_{\text{irr}}) = 0\}$.

The scaling of $F_P(H)$ curves is an evidence of the vortex lattice transition [4].

Thus, it was found that Nd substitution for Y in 1-2-3 HTSC tunes the peak effect position.

The work was supported by Russian Foundation for Basic Research Grant No. 16-38-00400.

[1] D. M. Gokhfeld, D. A. Balaev, et al, *J. Appl. Phys.*, **109** (2011) 033904.

[2] D. M. Gokhfeld, *Phys. Solid State*, **56** (2014) 2380.

[3] D.M. Gokhfeld, S.V. Semenov, et al, *JMMM*, accepted. DOI: 10.1016/j.jmmm.2016.12.089

[4] M.R. Koblishka, et al, *Phys. Rev.* **B 58** (1998) 2863.

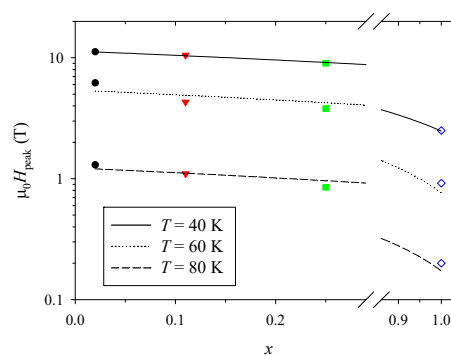


Fig. 1. The peak field at various temperatures as a function of Nd content in $Y_{1-x}Nd_xBa_2Cu_3O_7$.

3PO-I-20

SUPERCONDUCTING-MAGNETIC LAYERED METAMATERIAL*Holder J.S.¹, Pugach N.G.^{2,3}, Bakurskiy S.V.², Kupriyanov M.Yu.², Belzig W.¹*¹ University of Konstanz, Konstanz, Germany² Skobeltsyn Institut of Nuclear Physics Lomonosov Moscow State University, Moscow, Russia³ National Research University Higher School of Economics, Moscow, Russia

jacob.holder@uni-konstanz.de

The idea of a negative refraction index was introduced in 1967 by Veselago [1]. These materials are called metamaterial and have outstanding optical properties. They can be used for example to overcome the diffraction limit of the wave length and for cloaking. The usage of superconductors for metamaterials is discussed in [2].

The Theory of the microwave response of layered superconducting structures containing different magnetic materials: YIG, ferromagnetes and antiferromagnets is developed. These structures may work as a new type of metamaterials having unusual electromagnetic properties in GHz and THz frequency range.

It was shown in the experiment [3] that such hybrid structure may work as a metamaterial with the negative refraction index n , where the negative electric permittivity ε is provided by the superconductor, while the negative magnetic permeability μ is achieved close to the ferromagnetic resonance.

Such metamaterials have some advantages compared to traditional metamaterials, for example: The reduction of the ohmic loses, thanks to the superconductor; the absence of parameter spread of a large number of electromagnetically active elements, like split-rings.

We present the calculation of different optical properties of such hybrids and with different magnetic materials to make its comparison and optimization. Our calculation also clarifies the role of the proximity- and skin-effect in the microwave response of these novel metamaterials.

Financial support by the Project T3-89 “Macroscopic quantum phenomena at low and ultralow temperatures” of the National Research University Higher School of Economics, Russia is acknowledged.

[1] V. G. Veselago, *Soviet Physics Uspekhi*, **10.4** (1968).

[2] S. M. Anlage, *Journal of Optics*, **13.2** (2010).

[3] A. Pimenov et al., *Phys. Rev. Letters*, **95** (2005) 247009.

3PO-I-21

INFLUENCE OF CANTED ANTIFERROMAGNETIC ORDER ON THE ELECTRONIC SPECTRAL FUNCTION IN 2D STRONGLY CORRELATED ELECTRONIC SYSTEMS

Kuz'min V.I.¹, Nikolaev S.V.^{1,2}, Ovchinnikov S.G.^{1,2}

¹ Kirensky Institute of Physics, Federal Research Center KSC SB RAS, 660036 Krasnoyarsk, Russia

² Siberian Federal University, 660041 Krasnoyarsk, Russia
kuz@iph.krasn.ru

One intrinsic property of systems with strong electron correlations is the interdependence of the electronic structure and magnetic or charge order. A magnetic field by acting on the particular spin or charge order can change the electronic structure. This way, the connection between the Fermi surfaces which are obtained from experiments on quantum oscillations in high magnetic fields and the Fermi surfaces seen in angle-resolved photoemission spectroscopy (ARPES) in almost zero magnetic field can be non-trivial for high-temperature superconductors [1].

In this work we investigate the influence of magnetic field on the electronic structure of strongly correlated electron systems by means of the underlying magnetic order, studying the range of p - and n -type doping at which an antiferromagnetic state is essential for cuprates. We apply a slightly modified version of cluster perturbation theory [2] to take into account both long-range canted magnetic order and short-range nearest neighbor correlations and study the t - J model with three-site interactions (t - J^*).

At zero field we obtain the evolution of the electronic structure with doping in agreement with ARPES and quantum oscillations for n -type doping. At non-zero field and small p -type doping we find the sharp changes of the Fermi surface under increasing magnetic field at critical value which depends on the parameters of the model (Figure 1).

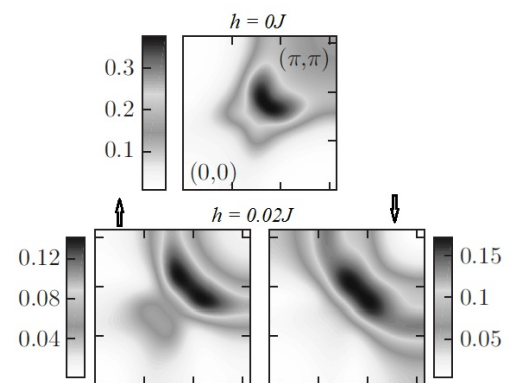


Fig. 1. Field-induced change in the FS obtained in the case of hole doping for parameters from [3]. Up (down) arrows indicate spin projection along (opposite to) the direction of magnetic field.

V.I. Kuz'min is grateful to Krasnoyarsk Regional Fund for Scientific and Technical Development Support, project "Organization of young scientists participation in conferences, scientific events and internships" for financial support.

[1] A. Allais, D. Chowdhury, S. Sachdev, *Nat. Commun.*, **5** (2014) 5771.

[2] D. Sénéchal, D. Perez, M. Pioro-Ladrière, *Phys. Rev. Lett.*, **84** (2000) 522.

[3] V. I. Kuz'min, S. V. Nikolaev, S. G. Ovchinnikov, *JETP*, **123** (2016) 511.

3PO-I-22

THEORETICAL AND EXPERIMENTAL STUDY OF A RhGe HIGH-PRESSURE PHASE WITH ACENTRIC B20 STRUCTURE

Magnitskaya M.V.^{1,2}, *Chtchelkatchev N.M.*^{3,1}, *Lepeshkin S.V.*²,
*Tsvyashchenko A.V.*¹, *Fomicheva L.N.*¹, *Salamatin D.A.*^{1,4},
*Velichkov A.I.*⁴, *Salamatin A.V.*⁴, *Nikolaev A.V.*⁵, *Budzynski M.*⁶

¹Institute for High Pressure Physics, RAS, Moscow, Russia

²Lebedev Physical Institute, RAS, Moscow, Russia

³Landau Institute for Theoretical Physics, RAS, Chernogolovka, Russia

⁴Joint Institute for Nuclear Research, Dubna, Russia

⁵Institute of Nuclear Physics, MSU, Moscow, Russia

⁶Institute of Physics, M. Curie-Sklodowska University, Lublin, Poland

magma@yandex.ru

Single-phase polycrystalline samples of RhGe with a B20-type noncentrosymmetric crystal structure have been synthesized under high pressure $p \sim 8$ GPa [1]. Our measurements of electrical resistivity and magnetic susceptibility demonstrate that this metastable high-pressure phase exhibits the coexistence of weak ferromagnetism ($\sim 0.003 \mu_B/\text{cell}$, $T_m \sim 140$ K) and superconductivity ($T_c \sim 4.3$ K). Our specific heat data confirm the bulk nature of superconductivity in B20 rhodium monogermanide. We also present the results of density-functional-theory calculations performed using the FP-LAPW+lo method (Wien2k package) and pseudopotential method (Quantum Espresso package). The equation of state $p(V)$ is calculated and the pressure range of the B20 phase stability is found. The compressibility, electronic properties, emission spectra and other physical characteristics of RhGe are theoretically studied, including their change upon compression. The results are compared with our experimental data.

Support by RAS and RFBR is acknowledged. The numerical calculations are performed at the Joint Supercomputer Center of RAS and the Supercomputing Center of NRC Kurchatov Institute.

[1] A.V. Tsvyashchenko, V.A. Sidorov, A.E. Petrova, L.N. Fomicheva, I.P. Zibrov, V.E. Dmitrienko, *J. Alloys Compd.*, **686** (2016) 431-437.

3PO-I-23

THE BEHAVIOUR OF THE SECOND HARMONIC OF THE RESPONSE SIGNAL OF BISMUTH HIGH-TEMPERATURE SUPERCONDUCTOR ON APPLIED ALTERNATIVE MAGNETIC FIELD

Barkalova A.S.¹, Sergeev A.V.¹, Golev I.M.²

¹ Voronezh State Technical University, Voronezh, Russia

² The Military Educational and Training Center of Air Forces «The Air Force Academy, named after Prof. N.E. Zhukovsky and Y.A. Gagarin», Voronezh, Russia
anastasiyabarkalova96@mail.ru

The paper conducts the measurements of temperature dependencies of second harmonic voltages of the response signal $U_2(T)$ in a multiphase superconductor, composed of Bi-Sr-Ca-Cu-O (Bi-2223 – 46%; Bi-2212 – 52%) and obtained by the method of solid-phase synthesis, on superposition of low-frequency alternating and direct magnetic fields.

The measurements have been made by the inductive method [1], using the installation described in [2]. It was found that, by contrast with the known literary data the dependence $U_2(T)$ in the resistive state indicates the maximum value. The results of measurements are presented in fig. 1. The fig. 2 represents the dependence of the second harmonic maximum of a response signal upon the magnitude of an induced direct magnetic field. In this case $H_{dc} \gg h_{ac}$, the amplitude of even harmonics tends to zero. Analysing the dependence $R(T)$ and phase composition of the superconductor under consideration, it can be concluded that non-linear response occurs in local superconducting areas (clusters) of the Bi-2223 phase, surrounded by the normal matrix from the Bi-2212 phase. In single-phase superconductors, this effect is described by Kim-Anderson model. In our case, the discovered effect of even harmonics, occurring in a multiphase superconductor in resistive state, is not described by known models and requires further discussion.

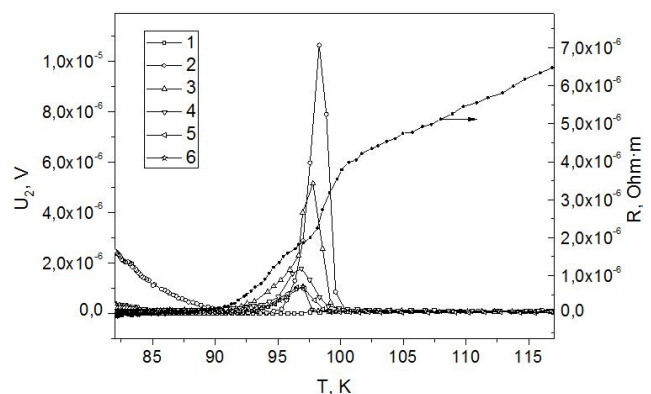


Fig. 1. Temperature dependencies of the second harmonic amplitude $U_2(T)$ for $B_{dc}=0, 1, 2, 5, 7, 10$ Gs (curves 1, 2, 3, 4, 5 and 6, respectively), $f_0=2$ kHz, $B_{ac}=5$ Gs.

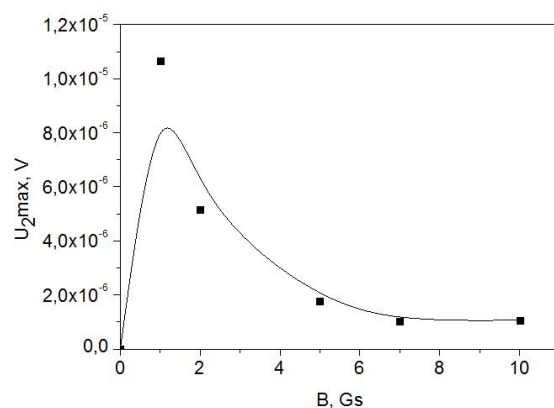


Fig. 2. The maximum amplitude of the second harmonic $U_{2max}(T)$ for $B_{dc}=1, 2, 5, 7, 10$ Gs.

[1] I.M. Golev, A.V. Sergeev, O.V. Kalyadin. *Solid-State Physics* **1** (2017) 19-22.

[2] A.V. Sergeev, I.M. Golev, et al. *The News of the South-Western State University. The Series «Engineering and Technologies»* **3** (2016) 146-153.

3PO-I-24

**NMR STUDIES OF SKUTTERUDITE-RELATED
 $R_3\text{Co}_4\text{Sn}_{13}$ ($R = \text{La, Ce, Pr, Yb}$)**

Lue Ch. Sh.¹, Liu H.F.¹, Kuo Ch.-N.¹, Kuo Y.K.²

¹ Department of Physics, National Cheng Kung University, Tainan 70101, Taiwan

² Department of Physics, National Dong Hwa University, Hualien 97401, Taiwan
 cslue@mail.ncku.edu.tw

We report a systematic study of ternary stannides of $R_3\text{Co}_4\text{Sn}_{13}$ ($R = \text{La, Ce, Pr, Yb}$) by means of the specific heat, ^{59}Co and ^{119}Sn nuclear magnetic resonance (NMR) measurements. Distinctive phenomena associated with the structural phase transition have been identified for $\text{La}_3\text{Co}_4\text{Sn}_{13}$, $\text{Ce}_3\text{Co}_4\text{Sn}_{13}$ and $\text{Pr}_3\text{Co}_4\text{Sn}_{13}$ at $T^* \sim 160$ K, ~ 155 K and ~ 130 K, respectively. For those materials, relative weak ^{59}Co quadrupole splittings are consistently found below T^* , implying that the electrical field gradient (EFG) sensed by the Co site decreases undergoing this phase transition. Such an observation could be attributed to the local distortion of the Sn(2) atom from its initial position below T^* which consequently leads to significant modification of the electronic structures around the Fermi surfaces. We also obtained a resolved ^{119}Sn NMR spectrum on $\text{Ce}_3\text{Co}_4\text{Sn}_{13}$, revealing that the ^{119}Sn NMR line shape of Sn(2) becomes broaden and the peak feature smears below T^* . In addition, the variation of ^{119}Sn NMR Knight shift versus magnetic susceptibility indicates an enhancement on the hyperfine coupling constant on Sn(2) across the phase transition. For $\text{Yb}_3\text{Co}_4\text{Sn}_{13}$, however, the specific heat and NMR results show the absence of the structural-related phase transition. The ^{59}Co NMR Knight shift and spin-lattice relaxation rate $1/T_1$ clearly indicate that $\text{Yb}_3\text{Co}_4\text{Sn}_{13}$ is a Pauli-type paramagnet. From the Korringa relation (constant T_1T), we thus estimated Co $3d$ Fermi-level density of states $N_d(E_F) \sim 3.95$ states/eV f.u. for this compound.

3PO-I-25

PHYSICAL PROPERTIES OF THE TERNARY STANNIDE $\text{Sm}_3\text{Co}_4\text{Sn}_{13}$

Kuo Ch.-N.¹, Wang Ch.-M.¹, Tseng Ch.-W.¹, Lue Ch. Sh.¹

¹Department of Physics, National Cheng Kung University, Tainan 70101, Taiwan
kuochianung@gmail.com

We report the physical properties of the ternary stannide $\text{Sm}_3\text{Co}_4\text{Sn}_{13}$. Single crystals of $\text{Sm}_3\text{Co}_4\text{Sn}_{13}$ were grown using tin flux method [1] and were characterized by x-ray diffraction, resistivity, magnetic susceptibility, and specific heat measurements. The electrical resistivity of $\text{Sm}_3\text{Co}_4\text{Sn}_{13}$ reveals metallic behavior. In contrast with the previous study [2], $\text{Sm}_3\text{Co}_4\text{Sn}_{13}$ exhibits an antiferromagnetic order at $T_N = 7.2$ K with $\theta = -5.3$ K. The obtained effective moment of $0.56 \mu_B$ is smaller than the expected value of $0.86 \mu_B$ for free Sm^{3+} ions. The magnetic entropy at around T_N is about $0.9R \ln 2$. The broad Schottky-type peak can be reproduced with a first excited quadruplet separated from the doublet ground state by approximately 72 K. The value of T_N was found to deviate from the de Gennes scaling, indicative of the important influence from crystal electric field (CEF).

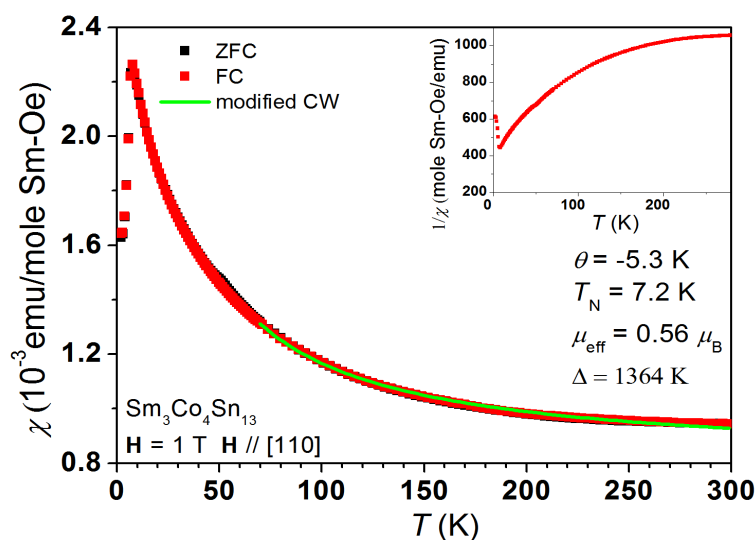


Fig. 1. Temperature dependences of magnetic susceptibility of $\text{Sm}_3\text{Co}_4\text{Sn}_{13}$ for $H // [110]$. The Green line denotes the fit to the modified Curie–Weiss law. Inset: the temperature of the reciprocal magnetic susceptibility.

- [1] G. P. Espinosa, A. S. Cooper and H. Barz, *Mat. Res. Bull.*, **17** (1982) 963.
[2] G. Zhong, X. Lei and J. Mao, *Phys. Rev. B*, **79** (2009) 094424.

3 July

Monday

12:00-14:00

poster session

3PO-I2

**“Magnetophotonics
and Ultrafast
Magnetism”**

3PO-I2-1

APPLICATION OF TOPOLOGICAL METHODS TO THE STUDY OF MAGNETO-OPTICAL IMAGES OF INHOMOGENEOUS MAGNETIC FIELDS

Ivanov V.E.¹, Knyazeva E.A.¹
 UrFU, INS, Ekaterinburg, Russia
 vladimir.ivanov@urfu.ru

Single-crystal films of garnet ferrites have been successfully used to visualize magnetic fluxes of superconductors [1]. In this case, the field component normal to the film plane is recorded. Magnetic metal films with planar anisotropy in the geometry of the meridional Kerr effect reflect the normal and planar component of the field. Observed singular points of magneto-optical images (MOI) corresponding to singular points of the plane component of the field carry information about the global structure of the field [2]. In our work, we studied the features of MOIs, which in our opinion can contribute to the reconstruction of inhomogeneous fields of complex configuration.

As magnetic field sources, magnetic systems composed of magnets of various sizes and shapes were used. The magnetic moments of the magnets are oriented towards each other and perpendicular to the observation plane (Fig. 1a,b).

In the case of a high-symmetry magnetic system consisting of cylindrical magnets with different diameters, a MOI is formed with one singular point and a singular line in the form of a circle. A comparison of this MOI with the calculated vector field makes it possible to formally determine the Poincare index (γ) of this field as a unit, which determines the resulting dipole moment of the magnetic system that is perpendicular to the observation plane [2]. The application of a homogeneous external planar field changes the structure of the vector field and the contrast of the MOI in a singular line. As a result, it is divided into segments containing singular points (one saddle point and one sink). The Poincare index of a vector field, according to the Poincare theorem, becomes zero, which agrees with the behavior of the vector field for a single dipole [2].

The change in the shape of the magnets to the rectangular leads also to the formation of an inhomogeneity in the structure of the singular line and MOI (4 saddle points and 4 sinks, Fig. 1c). An increase in the size of a large magnet (Fig. 1b) changes the topological structure of the singular line (2 saddle-points and two sinks, Fig. 1 d). The Poincare index does not change ($\gamma=1$), which corresponds to the presence of the resulting magnetic moment.

Thus, the topological structure of the MOI and the plane vector field can provide information on the presence of the resulting magnetic moment of the field source.

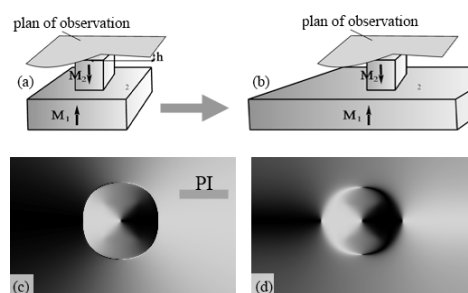


Fig. 1. Magneto-optical images of the planar component of a vector field when its topological properties change. The abbreviation PI shows the orientation of the light beam incidence plane.

[1] L. A. Dorosinskii, M. V. Indenbom, V. I. Nikitenko, Yu. A. Ossip'yan, A. A. Polyanskii, V. K. Vlasko-Vlasov, *Physica C*, **203** (1992) 149-156.

[2] V. E. Ivanov, *Journ. Magn. Magn. Mater.*, **401** (2016) 200-208.

3PO-I2-2

MODULATION OF LIGHT VIA MAGNETOELECTRIC EFFECT ON MAGNETIC DOMAIN WALLS

Khokhlov N.E.^{1,2}, Khramova A.E.^{1,2}, Nikolaeva E.P.¹, Kosykh T.B.¹, Nikolaev A.V.¹, Zvezdin A.K.²,
Pyatakov A.P.¹, Belotelov V.I.^{1,2}

¹ Moscow State University (MSU), Moscow, Russia

² International Center for Quantum Optics, Moscow, Russia

ae.khramova@gmail.com

Nowadays, domain walls has recently attract great interest because on their basis we can create a new devises providing new approaches for light manipulating with consumption of less energy.

We produce and experimental demonstrate a new concept of light modulator via magnetoelectric effect where we apply locally electric field to a magnetic domain wall.

Read more, 15- μm -thick metallic tip generate strong electric field around domain wall in the iron garnet film. The electric field shift domain wall due due to exomagnetoelectric effect. Maximum displacement of domain wall is up to 1/3 of domain width. These parameters allow to create a novel type of the electrically controlled magneto-optical shutter. Polarized laser beam passes through a sample and later through polarizer we can obtain different regimes of the light modulation – linear, nonlinear and tri-stable – for the same domain wall with corresponding controllable displacement features. Such variability to control of domain wall's displacement with spatial scale of about 10 μm makes the proposed concept very promising for nanophotonics and spintronics.

In our experiment we obtained several regimes of the laser modulation for different magnetic and electric field: linear, nonlinear and tri-stable regimes. Maximal shift of domain wall reaches 4 μm .

Main advantages of the this approach for create light modulation :

- 1) possibility for ultra-local magnetization switching
- 2) absence of any electric current flows
- 3) tunability of the modulation regime via constant magnetic field.

[1]Khokhlov N.E., Khramova A.E. et al. Electric-field-driven magnetic domain wall as a microscale magneto-optical shutter. Scientific reports.(7) 2017.

[2] C.D. Eee, F.G. Hhh, *J. Appl. Phys.*, **33** (1999) 133-136

[2]Zhang, X. et al. Magnon dark modes and gradient memory. *Nat. Commun.* **6** (2015) 8914.

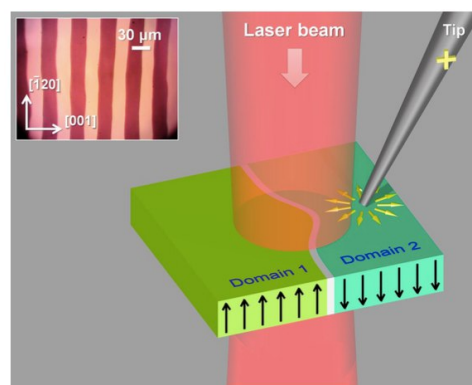


Fig. 1. General scheme of the experiment and configuration of domains.

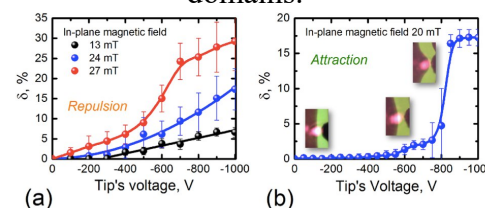


Fig. 2. Laser intensity modulation via tip's voltage for the "large" laser spot, (a) repulsion and (b) attraction.

3PO-I2-3

EXCITONIC ENHANCEMENT OF TMOKE IN THE DILUTED MAGNETIC SEMICONDUCTOR NANOSTRUCTURES

Borovkova O.¹, Spitzer F.², Akimov I.^{2,3}, Belotelov V.^{1,4}, Wiater M.⁵, Wojtowicz T.⁵, Karczewski G.⁵, Yakovlev D.^{2,3}, Bayer M.^{2,3}

¹ Russian Quantum Center, Skolkovo, Russia

² Experimentelle Physik 2, TU Dortmund, Dortmund, Germany

³ Ioffe Institute, Russian Academy of Sciences, St. Petersburg, Russia

⁴ M.V. Lomonosov Moscow State University, Moscow, Russia

⁵ Institute of Physics, Polish Academy of Sciences, Warsaw, Poland

o.borovkova@rqc.ru

Excitons in some semiconductor solid solutions can provide an enhancement of the magneto-optical response of such materials. This effect is well-known, for instance, in CdMnTe. In Ref. [1,2] it has been demonstrated an increase of Faraday effect in CdMnTe due to the giant Zeeman splitting of the excitons.

Here we address a transverse magneto-optical Kerr effect (TMOKE) in the semiconductor nanostructures of CdMnTe and CdMgTe in the spectral region of the excitonic resonances. We report an exciton-assisted enhancement of TMOKE in the bare diluted semiconductor thin films. The reflection and TMOKE spectra of the semiconductor structures are studied theoretically and experimentally. 10 nm CdMnTe quantum well (QW) is sandwiched between non-magnetic CdMgTe barriers. In the QW the energy structure of excitons is defined by the quantization of the carriers in the direction perpendicular to the sample plane [3]. This allows to separate the contributions from light and heavy hole states in the spectral dependence of TMOKE. The concentration of Mn in magnetic layers is about 2-2.5% depending of the sample. The measurements have been performed at the low temperature about 10K.

Two-order enhancement of the TMOKE is observed in the spectral region of the excitonic resonances. In the thin film CdMnTe the TMOKE achieves 3% at the excitonic wavelength, 715nm (applied magnetic field of 570 mT, the incidence angle 20°). Note, that the TMOKE increases linearly with the increase of the incident angle.

The reported study was funded by RFBR, according to the research project no. 16-32-60135 mol_a-dk, and ICRC TRR 160.

[1] A.V. Komarov et al, *Sov. Phys. JETP*, **46** (1977) 318.

[2] J.A. Gaj et al, *Solid State Commun.*, **25** (1978) 193.

[3] J. Kossut, and J.A. Gaj, *Introduction to the Physics of Diluted Magnetic Semiconductors*, Springer, Berlin (2010).

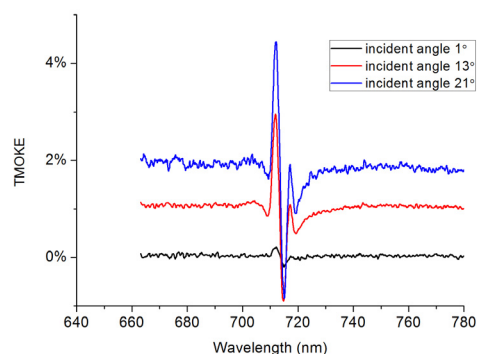


Fig. 1. Exciton-assisted TMOKE enhancement in the CdMnTe thin film for three incident angles.

3PO-I2-4

OPTICAL TM-SURFACE POLARITONS AT THE NONLINEAR SEMICONDUCTOR – LAYERED METAMATERIAL INTERFACE: THE CASE OF A DISSIPATION

Panyaev I.S.¹, Sannikov D.G.¹

¹ Ulyanovsk State University, 432970, L.Tolstoy str., 42, Ulyanovsk, Russia
sannikov-dg@yandex.ru

Nonlinear surface polaritons (SPs) demonstrate a series of remarkable phenomena, which have no analogues in a linear theory. Among them are the existence of TM-type SPs propagating along the interface of the media with dielectric functions of the same signs, nonlinear “bleaching action” of a strong waves which can propagate in an otherwise opaque medium, the ability of creating a channel of propagation for a weak TM-polarized wave by a strong pump wave of TE polarization, the existence of surface magneto-optic solitons [1], etc.

In this communication, we present the theoretical and numerical study of the nonlinear electromagnetic eigenwaves (i.e. SPs) propagating at the semiconductor - layered metamaterial (LM) structure. The electromagnetic wave propagates along the z-axis, the magnetization vector M is transverse to the direction of the wave propagation and is directed along the y-axis (Fig. 1). In contrast to the system discussed in paper [2], the structure under consideration is dissipative and has a different composition of layers.

The analysis of the dispersion relation and the wave field profiles leads to the existence conditions for nonlinear SPs of TE- and TM-polarizations in the structure which are depending on values of the linear dielectric permittivity. The influence of the transverse component of the electric field at the interface on the frequency spectrum is considered. Special attention is paid to the appearance of soliton-like solutions for the longitudinal electric field component. The dispersion spectra for the propagation constant, as well as the field and energetic properties of nonlinear surface polaritons are obtained and analyzed. Features of the dynamics of dispersion spectra for the structure with LM of a different content are also investigated.

Our studies yield a better understanding of the nonlinear SPs control principles in the dissipative optical guiding structures. Also a possible fabrication of highly efficient nonlinear optical devices (microresonators and waveguides) on the basis of a such system operating in near- and mid-infrared frequency-domains are discussed.

The work was partially supported by the Ministry of Education and Science of the Russian Federation (projects No. 14.Z50.31.0015 and No. 3.8154.2017/BP) and the Russian Science Foundation (project 16-42-02012).

- [1] A.D. Boardman, M. Xie and K. Xie *J. Phys. D: Appl. Phys.* **36** (2003) 2211–2217.
[2] I.S. Panyaev, D.G. Sannikov, *JOSA B*, **33** (2016) 220-229.

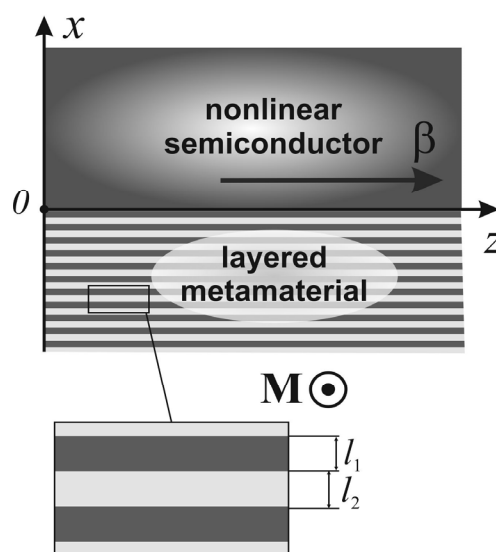


Fig. 1. Geometry of the structure

3PO-I2-5

MAGNETIC CIRCULAR DICHROISM SPECTRA AND ELECTRON STRUCTURE OF $\text{ErAl}_3(\text{BO}_3)_4$ SINGLE CRYSTAL

Sokolov V.V.¹, Malakhovskii A.V.¹, Gudim I.A.¹

¹ Kirensky Institute of Physics, Federal Research Center KSC SB RAS,
Krasnoyarsk, Russian Federation
valer963@iph.krasn.ru

Er^{3+} is a widely-spread active ion used in solid state lasers. In particular, laser generation was obtained in the Er doped $\text{YAl}_3(\text{BO}_3)_4$ crystal. Media with a high concentration of the active rare-earth ions are necessary for miniature solid-state lasers. $\text{ErAl}_3(\text{BO}_3)_4$ crystal has huntite-like structure with the trigonal space group $R\bar{3}2 (D_3^7)$. Er^{3+} ions are in the D_3 local symmetry positions. Earlier we have studied integral paramagnetic magneto-optical activities of transitions between multiplets [1]. Present work is devoted to study of the fine structure of magnetic circular dichroism (MCD) and absorption spectra and, as a consequence, of electron structure of the crystal.

MCD and linearly polarized absorption spectra of the $\text{ErAl}_3(\text{BO}_3)_4$ single crystal were measured at $T=90$ K for 11 $f-f$ absorption bands: $^4I_{15/2} \rightarrow ^4I_{11/2}$, $^4I_{9/2}$, $^4F_{9/2}$, $^4S_{3/2}$, $^2H_{11/2}$, $^4F_{7/2}$, $^4F_{5/2}$, $F_{3/2}$, $^2G_{9/2}$, $^4G_{11/2}$, $^4G_{9/2} + ^2K_{15/2} + ^2G_{7/2}$. Symmetries of the Stark components of the ground and excited $4f$ multiplets were identified, basing on the linearly polarized absorption spectra and selection rules in D_3 local symmetry of the Er^{3+} ion.

MCD spectra permitted us to measure the Zeeman splitting of some transitions and so to determine changes of the Landé factors along the C_3 axis during these transitions. The Landé factors along the C_3 axis and their changes were also found theoretically in the $|J, \pm M_J\rangle$ function approximation. The experimental changes of the Landé factors along the C_3 axis during electron transitions are close in value to the theoretical ones in the majority of cases and are large in all cases in spite of the strong easy plane magnetic anisotropy in the ground electron state. Comparison of the experimental and theoretical values allowed us to identify some states in the $|J, \pm M_J\rangle$ function approximation. In particular, it was shown that the ground state of the Er^{3+} ion in this approximation has $M_J = \pm 13/2$ that corresponds to magnetic moment $m = 7.8 \mu_B$ at $T=0$ K. The latter value is in agreement with the measured magnetic moment of the Er^{3+} ion in $\text{ErFe}_3(\text{BO}_3)_4$ crystal.

The vibrational satellite of one electron transition from the ground state and vibrational satellites of several electron transitions from the upper states of the ground multiplet were revealed. The latter transitions have intensity which is unusually large for the vibronic $f-f$ transitions, but the pure electronic origins of these transitions are not observed. This situation resembles properties of $d-d$ transitions. To the best of our knowledge, such phenomenon in $f-f$ absorption spectra was observed for the first time. Energies of vibrations found from different vibronic transitions are appreciably different since they are local vibrations in different excited states in contrast to collective vibrations in the ground electron state found from the Raman scattering and infrared absorption measurements.

The reported study was funded by Krasnoyarsk Region Science and Technology Support Fund.

[1] A.V. Malakhovskii, A.L. Sukhachev, V.V. Sokolov, T.V. Kutsak, V.S. Bondarev, I.A. Gudim, *Journal of Magnetism and Magnetic Materials*, **384** (2015) 255-265.

3PO-I2-6

FEATURES OF THE MAGNETOREFRACTIVE EFFECT IN METALLIC NANOSTRUCTURES CoFe/Cu

Yurasov A.N.¹, Telegin A.V.², Bannikova N.S.², Milyaev M.A.², Sukhorukov Yu.P.²

¹ Moscow Technological University (MIREA), Moscow, Russia

² M.N. Miheev Institute of Metal Physics, Ural Division of RAS, Ekaterinburg, Russia
alexey_yurasov@mail.ru

Thin film metallic nanostructures with GMR besides spintronic applications are promising magneto-optical materials due to large values of magnetorefractive effect (MRE) in the infrared range. MRE can be considered as a variations of the coefficients of reflection, transmission and absorption of electromagnetic waves of samples with GMR, TMR or CMR effects under magnetization [1-3]. A current actual point of interest is an evaluation of the sample quality and magnitude of GMR effect in metallic nanostructures in accordance with MRE data.

We present the results of theoretical investigations of MRE in metallic nanostructures in such as $\text{Ni}_{48}\text{Fe}_{12}\text{Cr}_{40}(50 \text{ \AA}) / [\text{Co}_{90}\text{Fe}_{10}(14 \text{ \AA})/\text{Cu}(22 \text{ \AA})]_8 / \text{Cr}(20 \text{ \AA})$ involving Fresnel formulas, effective medium approximation and spin-dependent phenomena, according to [1,2,4]. The results of calculations have been analyzed in comparison with experimental data on magnetoreflexion and magnetotransmission of unpolarized light in the IR range. It was shown that the magnitude and frequency dependencies of MRE are very sensitive to the optical properties of the samples involved in simulation, sample thickness and MR values. Changes of the optical constants are strictly connected with the magnetoconductivity (magnetoresistance) of the nanostructures under an applied magnetic field. The possibility of magnifications for MRE has been also discussed. It is interesting that experimental MRE spectra demonstrate a change of sign on reflection and transmission mode. This fact could be satisfactorily explained in frames of the theory of spin-dependence scattering only [4]. Finally, high sensitivity of MRE to an external magnetic field (up to 0.5% per 100 Oe) can be proposed for contactless characterization of metallic structures with GMR and creation magneto-optical IR metallic detectors.

Support by FASO of Russia (“Spin” theme №0120146330), program UB of RAS №15-9-2-4, grant № 14.Z50.31.0025.

[1] A.N. Yurasov, T.N. Bakhvalova, A.V. Telegin, Yu.P. Sukhorukov, *Functional materials*, **2** (2012) 178-181.

[2] A. Granovsky, Yu. Sukhorukov, E. Gan’shina, A. Telegin, in M. Inoue, M. Levy, A.V. Baryshev (Eds.), *Magnetophotonics: From Theory to Applications*, Springer-Verlag Berlin Heidelberg, **178** (2013) 107-133.

[3] A.V. Telegin, Yu.P. Sukhorukov, N.N. Loshkareva, E.V. Mostovshchikova, N.G. Bebenin, E.A. Gan’shina, A.B. Granovsky, *JMMM*, **383** (2015) 104-109.

[4] J.P. Camplin, S.M. Thompson, D.R. Loraine, et al., *J. Appl. Phys.*, **87** (2000) 4846 – 4848.

3PO-I2-7

THE INDUCED BY LASERS OF PUMPING THE ELECTRON-NUCLEAR PARAMAGNETISM IN THE EXCITED ELECTRONIC STATES IN THE SERIES N-,O-,S-HYDROCARBON OF COMPOUNDS, RADICALS, PARAMAGNETIC IONS OF FUELS, AND LUBRICANTS IN CHEMOTOLGY

Obukhov A.E.¹

¹ The FAE "25th State research Institute of chemotology of the Ministry of defense of Russia",
121467, Moscow, Russia
aobukhov@fo.gpi.ru

In this paper we show the results of fundamental research with application of methods of optic and paramagnetic of spin spectroscopy and the main electronic singlet and triplet (doublet and quartet) states: E - and X-ray, Raman, UV and IR, ¹H and ¹³C NMR and EPR, THz, fluorescence and phosphorescence, and laser spectroscopy in the structure of combustive-lubricating materials on the series N-,O-,S-hydrocarbons, ions lanthanides, radicals, and hydrocarbons.

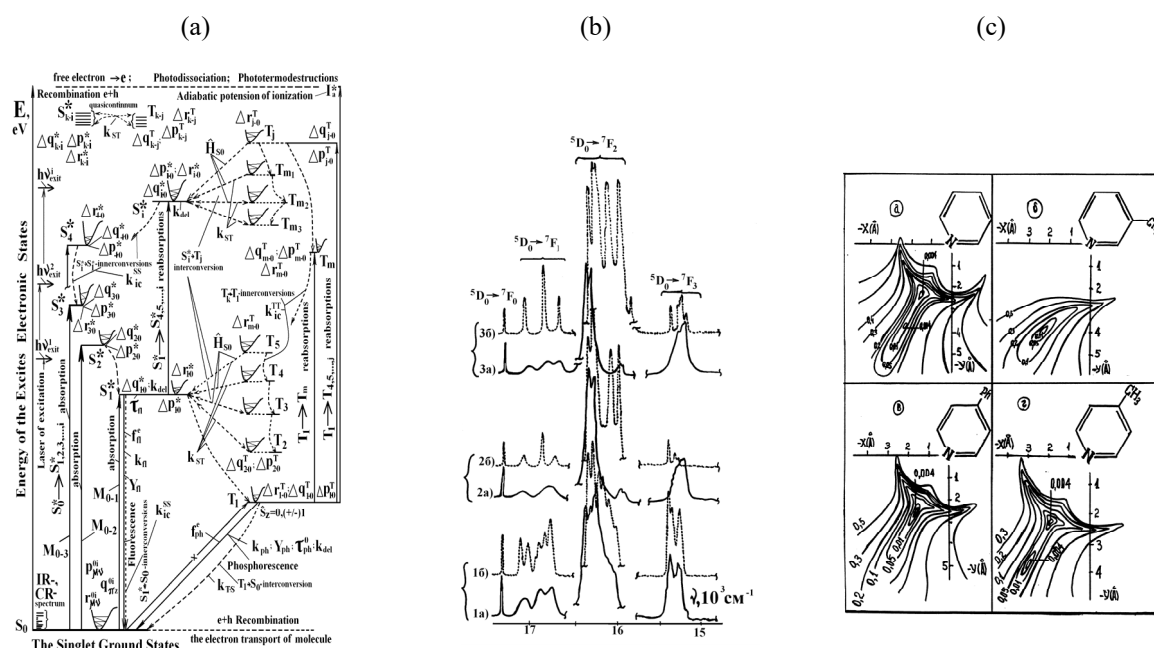


Fig. 1. (a). The full spectra of the optical and nonradiated transition between of the systems of the grounds states and between the singlets ($S^*_{1,\dots,i}$) and triplets ($T_{1,\dots,i}$) of electronic excited states $\sigma\sigma^*$, $\sigma\pi^*$, $\pi\pi^*$, $n\pi^*$ -type (ion is the quartets (Q_n) and duplets D_m) with the LCAO-MO SCF expansion-CI INDO/S methods of calculations. (b) fragments of luminescence spectra of solutions of paramagnetic adducts: (1a and 1b) is $[\text{Eu}(\text{dmp})_3+\text{pyridine}]$, (2a and 2b) is $[\text{Eu}(\text{dmp})_3+2\text{-methylpyridin}]$ and (3a and 3b) is $[\text{Eu}(\text{fod})_3+\text{pyridine}]$ (a is 298K and b is 77K); (c) is contour-cart of the standard deviation of lanthanide ion in the solution of the spatial adduct $\text{Yb}(\text{dpm})_3$: (1): (a) pyridine, (b) α -methylpyridine, (c) is contact shifts, and d is dipole-dipole NMR-shifts) β -phenylpyridine [1].

[1]. Obukhov A.E. Spectroscopy of the ground and excited states of multinuclear compounds in different conditions. 2010 y. Moscow: Publ. Hause "Satellite+" (ISBN 978-5-9973-0657-1) 248.

3PO-I2-8

LANDAU LEVELS IN MAGNETO-TRANSMISSION SPECTRA OF CuInSe_2 THIN FILMS

Yakushev M.V.^{1,2,3,4}, *Rodina A.V.*⁵, *Vaganov S.A.*⁵, *Kitaev Yu.E.*⁵, *Seisyan R.P.*⁵,
*Abdullaev M.A.*⁶, *Kuznetsova T.V.*^{1,3}, *Mudryi A.V.*⁷, *Faugeras C.*⁸, *Martin R.W.*²

¹M. N. Miheev Institute of Metal Physics UB RAS, Ekaterinburg, Russia

²Department of Physics, SUPA, Strathclyde University, Glasgow, UK

³Ural Federal University, Ekaterinburg, Russia

⁴Institute of Solid State Chemistry UB RAS, Ekaterinburg, Russia

⁵A.F. Ioffe Physico-Technical Institute, St. Petersburg, Russia

⁶Institute of Physics of the Russian Academy of Sciences, Makhachkala, Russia

⁷Scientific-Practical Material Research Centre of the National Academy of Sciences of Belarus,
Minsk, Belarus

⁸LNCMI, 25 avenue des Martyrs, BP 166, 38042 Grenoble Cedex 9, France
kuznetsovaups@mail.ru

The direct band gap semiconductor CuInSe_2 is successfully used in absorber layers of thin film solar cells. A conversion efficiency record of 22.6 % for laboratory scale $\text{Cu}(\text{In,Ga})\text{Se}_2$ -based solar cells, and stability place such cells amongst leading thin film photovoltaic(PV) devices. The difference between the achieved efficiency a theoretical limit efficiency of 30% for single junction PV devices suggests however quite a low level of knowledge of the electronic properties of CuInSe_2 .

The electronic structure of CuInSe_2 is studied using magneto-transmission in thin polycrystalline films at magnetic fields up to 29 T. The A and B free excitons are observed resolved at zero field whereas the quantum oscillations due to the recombination of diamagnetic excitons (DX) constituting electrons from the conduction and holes from the valence band quantized by strong magnetic fields, can be seen in Figure for fields over 7 T. Landau level (LL) and DX binding energies, calculated assuming a quasi-cubic approximation of the chalcopyrite lattice and preliminary electronic structure parameters, determined earlier for the C valence sub-band [1], helped to identify the DX lines for the A and B sub-bands in the LL fan. The Luttinger parameters of the CuInSe_2 electronic structure are determined.

[1] M.V. Yakushev, A.V. Rodina et. al., *Appl. Phys. Lett.*, **105** (2014) 142103.
The research was supported by RSF (project No. 17-12-01500).

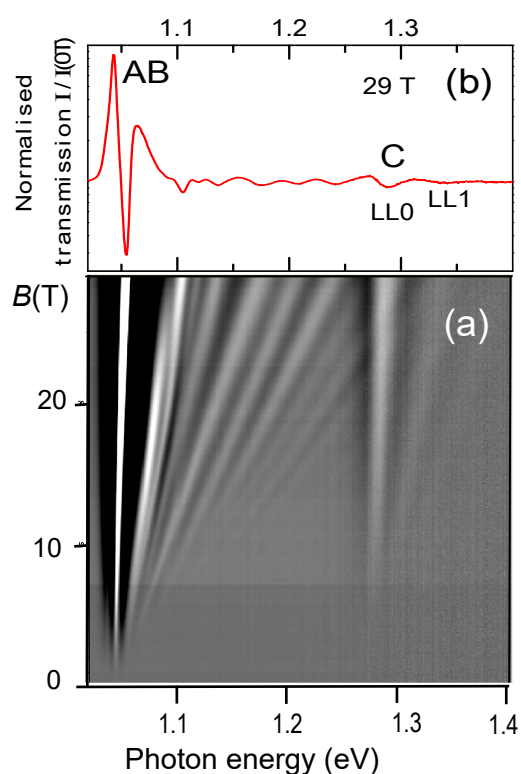


Fig. 1. Evolution of normalised MT spectra for the C exciton and diamagnetic excitons (a), normalised MT spectrum at 29 T (b). AB lines are the Landau fan for the A and B band diamagnetic excitons.

4 July

Tuesday

09:30-11:00

plenary lectures
4PL-A

4PL-A-1

FERROMAGNETIC AND FERROELECTRIC. A WIN-WIN COUPLE*Fontcuberta J.*

Institut de Ciència de Materials de Barcelona (ICMAB-CSIC), Campus UAB, Bellaterra 08153
Catalonia, Spain
fontcuberta@icmab.cat

Multiferroic materials have received much attention in recent years due to the promises of new or improved functionalities that could emerge from a coupling of their ferroic orders. However, single phase materials with simultaneous and coupled ferromagnetic and ferroelectric room-temperature orders have proven to be elusive. In contrast, interface coupling either by exploiting polarization charges and associated field-effect or by strain coupling is achievable and may have far-reaching short implications.

Here we will show examples of ferroelectric tunnel devices that by incorporating layers of magnetic materials which are at the verge of metal-insulator transitions, enhanced electroresistance (ER) is obtained, achieving room-temperature records values above 10⁴% [1,2,3]. In spite of this progress, microscopic understanding of the origin of electroresistance in ferroelectric capacitors is still debated and we will revise this critical issue. We will also review some recent results on strain control of magnetic materials, both ferromagnetic and antiferromagnetic. We will show how stroboscopic X-ray microscopy provides a pathway to the quantitative study of strain waves and magnetization at the nanoscale by simultaneously imaging of the temporal evolution of both strain waves and magnetization dynamics of nanostructures at the picosecond timescale [4]. Magnetoelectric coupling in antiferromagnets will be illustrated by and we will illustrate how strain effects in some martensitic alloys displaying antiferromagnetic-ferromagnetic transitions, allow observing time-dependent magnetoelectric coupling [5, 6].

Support by MINECO (Spain) through the Severo Ochoa Program for Centers of Excellence in R&D (SEV-2015-0496) and MAT2014-56063-C2-1-R and MAT2015-73839-JIN, and the Generalitat de Catalunya (2014-SGR-734) are acknowledged.

- [1] G. Radaelli et al, *Advanced Materials*, **27** (2015) 2602-2607.
- [2] D. Pesquera et al, *Physical Review Applied*, **6** (2016) 034004.
- [3] G. Radaelli et al, *Advanced Electronic Materials*, **2.12** (2016).
- [4] M. Foerster, Ferran Macià et al, submitted (2017).
- [5] X. Marti et al, *Nature Materials*, **13.4** (2014): 367-374.
- [6] I. Fina et al, submitted (2017).

4PL-A-2

MAGNETISM AT ITS SMALLEST LIMIT

Kirilyuk A.

Radboud University, Institute for Molecules and Materials, Nijmegen, Netherlands

A.Kirilyuk@science.ru.nl

Magnetism is a macroscopic phenomenon that at microscopic level occurs due to exchange interactions, whose typical range, or more simply length scale, is determined by the spatial extent of the quantum mechanical wavefunctions. Confinement of these wavefunctions by for example the presence of a surface leads to many unusual magnetic phenomena. A natural question, in light of these considerations, is what happens in a system smaller than the length scale of the bulk exchange field?

Here we follow, both experimentally and theoretically, the development of magnetism in very small particles, or clusters, of various materials, starting from the atomic limit and adding one atom at a time. A wealth of non-intuitive and instructive magnetic phenomena can be found. Thus, in rare-earth clusters the usual bulk RKKY exchange interaction is replaced with an oscillatory ferromagnetic double-exchange and antiferromagnetic superexchange [1], leading to irregular oscillations of magnetic order as a function of the cluster size.

The most unusual is the appearance of magnetism in the normally nonmagnetic materials, such as rhodium [2], or even vanadium and niobium [3]. Particularly striking is Rh, that presents an example of multiferroic behavior in metal clusters. The fact that it is observed in rhodium is even more surprising, since this metal is neither ferromagnetic nor ferroelectric in the bulk. From a broader perspective, the emergence of ferroelectricity in small metal clusters appears to be mediated by very low energy excitations, possibly involving a single vibronic mode that is associated with a broken symmetry ground state [2].

Another intriguing question is how a single dopant atom can modify the properties of a cluster? Thus mixing 3d with 4d or 5d elements combines large magnetic moments of 3d materials with a high spin-orbit coupling of the 4d/5d, giving rise to a material with a large magnetic moment and a strong magnetic anisotropy, ideally suitable in magnetic storage devices. Using X-Ray Magnetic Circular Dichroism (XMCD) at the BESSY II Synchrotron in Berlin we could resolve the spin and orbital contributions to the magnetic moment in Au and Rh-doped Co clusters [4]. Up to 150% increase in the total orbital moment of Co₁₃ cluster is observed by doping it with a single Rh atom. This effect is yet to be understood [5]. Possible mechanisms can be found in hybridization of the 3d Co bands with the dopant 4d/5d bands as well as in the increased magnetic anisotropy at the interface between the Co and Rh/Co atoms.

As a final note, the isolation of the clusters from the environment makes them ideal objects to study a transition between quantum and classical behavior. Kramers degeneracy, onset of Kondo screening, etc, could be studied with exact control of the electronic and geometric structure.

The work was supported by de Nederlandse Organisatie voor Wetenschappelijk Onderzoek (NWO) and the European Research Council.

[1] L. Peters et al., *Sci. Reports*, **6** (2016) 19676.

[2] L. Ma et al., *Phys. Rev. Lett.*, **113** (2014) 157203.

[3] A. Diaz Bachs et al., *to be published*.

[4] D. Dieleman et al., *Phys. Chem. Chem. Phys.*, **17** (2015) 28372.

[5] L. Peters et al., *Phys. Rev. B*, **93** (2016) 224428.

4 July

Tuesday

11:30-13:15

14:30-17:15

oral session

4TL-A

4RP-A

4OR-A

4TL-B

4OR-B

**“Spintronics and
Magnetotransport”**

4TL-A-1

INTERFACE DZIALOSHINSKII-MORIYA INTERACTION, A BRILLOUIN SPECTROSCOPY STUDY

Stashkevich A., Belmeguenai M., Roussigné Y., Chérif M.

LSPM (CNRS-UPR 3407), Université Paris 13, Sorbonne Paris Cité, Villetaneuse, France
stachkevitch@univ-paris13.fr

Manipulating magnetisation in ultra-thin ferromagnetic (FM) structures with current is an extremely appealing prospect for magnetic memory and logic. However the spin arrangement of the magnetostatically favoured Bloch walls in these systems is such that it excludes the possibility of employing spin-orbit torques ensuring high-speed magnetic domain wall dynamics. The latter require a Néel-type domain wall, which can be obtained in the presence of an interfacial Dzyaloshinskii-Moriya interaction (iDMI) across the interface between a ferromagnetic and heavy metal (HM) films. At the same time, iDMI induces a characteristic non-reciprocity of the SW propagation, such that SWs with the same wave-number, but traveling in opposite directions have different frequencies in the so-called Damon-Eshbach geometry. Moreover, this frequency asymmetry scales with the effective iDMI constant D_{eff} and the SW wave-number k_{sw} which makes Brillouin spectroscopy especially effective for its quantification, in which case it is the Stokes/anti-Stokes (S/aS) frequency asymmetry $\Delta F = F_S - F_{AS}$ that is to be directly measured.

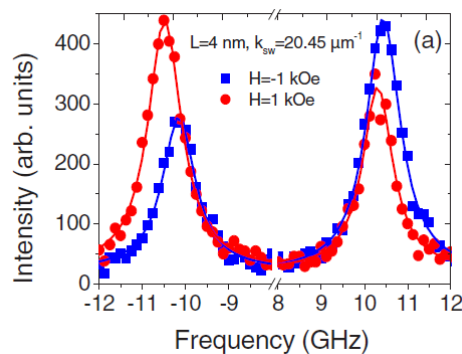


Figure 1.

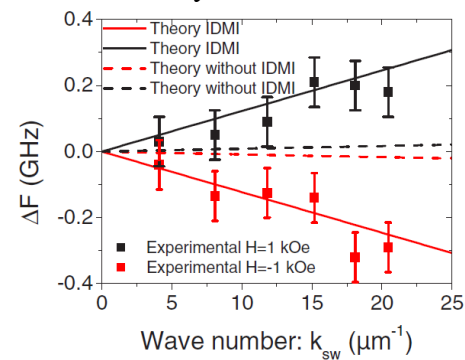


Figure 2.

Importantly, in ultra-thin FM films (under 5 nm) the iDMI contribution can be reliably separated from that induced by conventional asymmetric surface anisotropy [1]. In Fig.1 and Fig.2 are given a typical BLS spectrum of a Py(4nm)/Pt(6nm) bi-layer and ΔF as a function of k_{sw} . Changing magnetic field polarity from a positive (red) to negative (blue) inverts the S/aS pattern. To date the most promising configuration is the Pt/Co (and its alloys) combination [2]. It has proven particularly efficient in stabilising skyrmions at room temperature in a Pt/Co(3ML)/MgO structure [3]. A comparative study of iDMI by similar experimental methods (DW dynamics vs BLS) showed that the measurements obtained from DW dynamics, invariably influenced by a number of other mechanisms, such as static pinning of the domain walls typically underestimate the IDMI strength, from 10 percent up to an order of magnitude with respect to the BLS data [4].

- [1] A. A. Stashkevich et al, *Phys. Rev. B*, **91** (2015) 214409.
- [2] M. Belmeguenai et al, *Phys. Rev. B*, **91**(2015) 180405(R).
- [3] O. Boulle et al, *Nature Nanotechnology*, **11** (2016) 449.
- [4] R. Soucaille et al, *Phys. Rev. B*, **94** (2016) 1044314.

4TL-A-2

SPIN-WAVE EMISSION FROM TOPOLOGICAL SPIN TEXTURES

Sluka V.¹, Schneider T.¹, Kakay A.¹, Weigand M.², Schultheiss K.¹, Warnatz T.¹, Mattheis R.³, Gallardo R.A.⁴, Roldan-Molina A.⁴, Landeros P.⁴, Tiberkevich V.⁵, Slavin A.⁵, Erbe A.¹, Deac A.¹, Lindner J.¹, Fassbender J.¹, Raabe J.⁶, Wintz S.^{1,6}

¹ Helmholtz-Zentrum Dresden-Rossendorf, Dresden, Germany

² Max-Planck-Institut für Intelligente Systeme, Stuttgart, Germany

³ Leibniz Institut für Photonische Technologien, Jena, Germany

⁴ Universidad Técnica Federico Santa María, Valparaíso, Chile

⁵ Oakland University, Rochester, USA

⁶ Paul Scherrer Institut, Villigen PSI, Switzerland

sebastian.wintz@psi.ch

The investigation of propagating spin waves is a key topic of magnetism research [1]. For the excitation of spin waves with short wavelengths, it was typically necessary to either use patterned transducers with sizes on the order of the desired wavelengths (striplines or point-contacts) or to generate such spin waves parametrically by a spatially uniform double-frequency microwave signal [2]. Only recently, we found a novel mechanism for the local excitation of spin waves, which overcomes the lower wavelength limit given by the minimum patterning size. This method utilizes the translation of natural topological magnetic defects, i.e. the gyration of spin vortex cores, to generate isotropically propagating spin waves [3].

Here, we will show that in a stacked vortex pair system in a NiFe/Ru/CoFeB trilayer with uniaxial magnetic anisotropy [Fig. 1(a,b)], directional spin waves of variable dimensionality (2D and 1D) can be excited. The corresponding spin wave dynamics was imaged by means of time-resolved scanning transmission x-ray microscopy (STXM). For excitation frequencies above 500 MHz, circularly spiraling spin waves are generated [3]. At the same time, plane waves are emitted from the anisotropy-induced 180° domain walls in the sample [Fig. 1(c)]. These plane spin waves propagate successively to the edge of the sample. In the vicinity of the cores, even an interference of both distinct 2D spin wave modes (plane and circular) was observed [Fig. 1(d)]. For excitation frequencies below 500 MHz, a transition from the two-dimensional to a one-dimensional spin wave pattern occurs. While the uniform domains remain almost free from detectable magnetic oscillations, high amplitude, propagating spin waves became evident within the sharp 180° domain walls [Fig. 1(e)]. This confinement effect is a consequence of a finite spin wave frequency gap in the domains. We will further show that bend 180° domain walls can be used to efficiently guide one-dimensional spin wave trains along angled tracks.

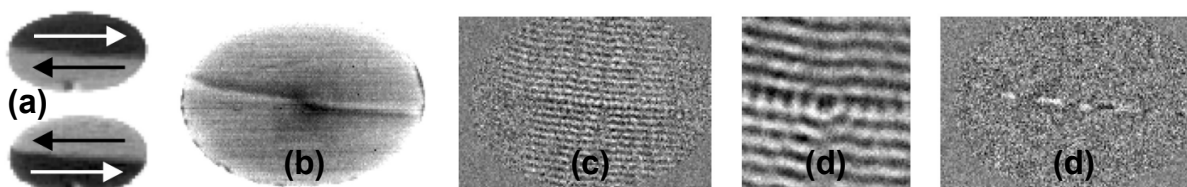


Figure 1. Spin waves in anisotropic vortex pairs [STXM images]. (a) In-plane configuration [bottom: NiFe, top: CoFeB], (b) perpendicular magnetic components, (c) response to $f \sim 1.5$ GHz excitation, (d) spin wave interference, (e) one-dimensional wall mode at $f \sim 250$ MHz excitation.

[1] A.V. Chumak et al., *Nat. Phys.*, **11** (2015) 453.

[2] A.G. Gurevich, G.A. Melkov, *Magnetization Oscillations and Waves*. New York CRC, 1996.

[3] S. Wintz et al., *Nat. Nanotechnol.*, **11** (2016) 948.

4TL-A-3

QUANTUM MAGNETOTRANSPORT IN TOPOLOGICAL SEMIMETALS*Shen Shun-Qing*

Department of Physics, The University of Hong Kong

Weyl semimetals are three-dimensional topological states of matter, in a sense that they host electrons that could mimic massless relativistic particles with linear dispersion in three-dimensional momentum space, i.e, the long-sought Weyl fermions in high energy physics. It inherits many of the properties of Weyl fermions, including the violation of chiral charge conservation or chiral anomaly. Searching for the signature of the violation of chiral charge conservation in solids has inspired a growing passion on the magneto-transport in topological semimetals. One of the open questions is how the conductivity depends on magnetic fields in a semimetal phase. Several recent experiments on both Weyl and Dirac topological semimetals show unconventional behaviors in transport measurement. Here I introduce theories of magnetoconductivity of Weyl and Dirac semimetals in several different regimes, including the weak antilocalization in a weak field, negative magnetoresistance induced by chiral anomaly, and magnetoresistance in a strong field.

This work is supported by the Research Grant Council of Hong Kong under Grant No.:

- [1] H.Z. Lu and S. Q. Shen, *Phys. Rev. B*, **92** (2015) 035203.
- [2] H.Z. Lu, S. B. Zhang, and S. Q. Shen, *Phys. Rev. B*, **92** (2015) 045203.
- [3] S.B. Zhang, H. Z. Lu and S. Q. Shen, *New J. Phys.*, **18** (2016) 053039.
- [4] H.Li et al, *Nat. Commun*, **7** (2016) 10301.
- [5] C.L. Zhang et al, *Nat. Commun.*, **7** (2016) 10735.

4OR-A-4

LONG-LIVED SPIN-VALLEY POLARIZATION IN TRANSITION METAL DICHALCOGENIDE MONOLAYER AND HETEROSTRUCTURES

Hsu Wei-Ting¹, Lu Li-Syuan¹, Chou Yi-Chia¹, Li Lain-Jong², Chang Wen-Hao¹

¹ Department of Electrophysics, National Chiao Tung University, Hsinchu 30010, Taiwan

² Physical Sciences and Engineering, King Abdullah University of Science and Technology, Thuwal, 23955-6900, Kingdom of Saudi Arabia
whchang@mail.nctu.edu.tw

A robust valley polarization is a key prerequisite for exploiting valley pseudospin to carry information in next-generation electronics and optoelectronics. Monolayer transition metal dichalcogenides (TMDs) with inherent spin-valley coupling offer a unique platform to develop such valleytronic devices. However, realization of robust valley polarization at room temperature remains challenging. In this work, I will demonstrate the generation of long-lived valley-polarized holes in monolayer WSe₂ and WSe₂/MoSe₂ heterostructures by optical pumping. Due to the spin-valley locking by the huge spin-orbit coupling in the valance band, valley polarization of holes is indicative of spin polarization. Using time-resolved Kerr rotation spectroscopy [1], we observe a very long-lived spin/valley polarization (~ 1 ns) in monolayer WSe₂ at low temperatures, which is much longer than the trion recombination lifetime (~ 10 -20 ps). The long-lived valley polarization can be attributed to the transfer of valley pseudospin from photocarriers to resident holes in a specific valley. The optically initialized spin and valley polarized holes remains robust even at room temperature, which opens up the possibility to realize room-temperature valleytronics based on TMDs. In WSe₂/MoSe₂ van der Waals heterostructures [2-4], the different stacking configurations combined with the coupled spin-valley physics in monolayer TMDs further enrich the interplay of electron spin, valley pseudospin, and layer pseudospin. We found that the spin-valley polarization in vertical HJs can be further stabilized by interlayer carrier transfer and the formation of interlayer exciton. We show that the stacking symmetry play a critical role in the interlayer spin transfer. The symmetry-dependent spin-valley properties of TMD heterobilayer would shed light on developing future spin and valley based electronic and optoelectronic devices.

This work was supported by the Ministry of Science and Technology of Taiwan (104-2628-M-009-002-MY3, 105-2119-M-009-014-MY3, 103-2923-M-009-002-MY3).

- [1] W.-T. Hsu *et al.*, *Nature Comm.*, **6** (2015) 8963.
 [2] M.-Y. Li *et al.*, *Science*, **349** (2015) 524.
 [3] M.-H. Chiu *et al.*, *ACS Nano*, **8** (2014) 9649.
 [4] W.-T. Hsu *et al.*, *ACS Nano*, **8** (2014) 2951.

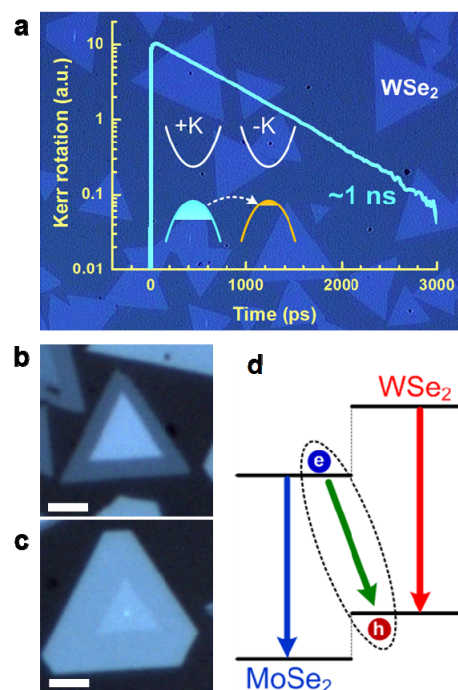


Fig. 1. (a) Kerr rotation of monolayer WSe₂. (b,c) Optical images of WSe₂/MoSe₂ vertical hetero-structures. (c) Type-II band alignment between MoSe₂ and WSe₂.

4TL-A-5

TOWARDS ALL-IN-ONE SPINTRONICS: MANIPULATING ELECTRONIC PHASE SEPARATION IN COMPLEX OXIDES*Shen J.*

Department of Physics, Fudan University, Shanghai, China

In complex oxides systems such as manganites, electronic phase separation (EPS), a consequence of strong electronic correlations, dictates the exotic electrical and magnetic properties of these materials. Investigation of EPS phenomena is not only important for understanding the strong electronic correlations in these materials, but also very useful for tuning their physical properties. Most work in studying EPS has focused on observing EPS and understanding its formation mechanism. The natural appearance of EPS domains, as expected, is totally random in terms of their size and spatial distribution. In order to control the EPS and thus the physical properties of the complex oxides, in recent years we have developed several methods to control the shape, density, location, size, spatial distribution and even the very existence of the EPS domains in manganites. As a result, we are able to order array the EPS domains and finely tune the corresponding physical properties. It is hoped that these abilities will allow us to soon design spintronic devices by patterning EPS domains in one material. These new spintronic devices do not have chemical interfaces and thus are expected to have high spin transport efficiency.

4TL-A-6

SPIN-TRANSFER DRIVEN DYNAMICS IN HYBRID STRUCTURES

Fowley C.¹, Rode K.², Gallardo R.³, Thiyagarajah N.², Lau Yong-Chang², Borisov K.², Betto D.², Atcheson G.², Kampert E.¹, Wang Zh.¹, Lindner J.¹, Coey M.², Stamenov P.S.², Deac A.¹

¹ Helmholtz-Zentrum Dresden-Rossendorf, Dresden, Germany

² Trinity College Dublin, Dublin, Ireland

³ Universidad Técnica Federico Santa María, Valparaíso, Chile
a.deac@hzdr.de

Since the discovery of giant magnetoresistance, metal spintronics has seen unprecedented advances, from the realisation of ultra-high magnetoresistance ratios to substantial output power from both conventional spin transfer torque oscillators as well as spin-torque vortex oscillators [1]. The recently discovered of the fully compensated ferrimagnetic half-metal, manganese ruthenium gallium (MRG), due to its widely tunable magnetic properties [2], could enable spin torque oscillators which work in the range of hundreds of GHz. Being a ferrimagnet, MRG consists of two magnetic sublattices which are coupled antiferromagnetically to each other. It has been shown that in this material the magnetotransport is dominated by one magnetic sublattice whereas the overall magnetisation is determined by both sublattices [3]. This means that MRG behaves magnetically like an antiferromagnet and electrically like a highly spin polarised ferromagnet, implying that spin-transfer torque would act on one sublattice only, enabling efficient current induced excitations. Due to the different temperature dependences of the sublattice magnetisations, MRG displays a compensation temperature at which the total magnetic moment is zero and the magnetic state is impervious to external magnetic fields [4].

Here we conduct high-field magnetotransport measurements [5] on selected films of MRG with differing Ru concentration and, therefore, different compensation temperatures (T_c). Both the transverse Hall resistivity and longitudinal resistivity are recorded in magnetic fields up to 58T. MRG exhibits a large spontaneous Hall angle of $\sim 2\%$, coercivity exceeding 1T at room temperature (and several Teslas close to T_c) and has very low net magnetisation of 25kA/m. Despite having a no net magnetic moment at the compensation temperature the magnitude of the Hall signal does not become zero, further indicating both the half-metallic nature of the material and that the magnetotransport is dominated by one sublattice only. An additional feature is observed in the transport data, which resembles a spin-flop transition. By comparison to analytical and mean-field calculations of the sublattice magnetisation directions we can estimate the both the sublattice anisotropy (H_k) and interlayer exchange coupling (H_{ex}). The out-of-phase and in-phase magnetic resonance modes, therefore, lie in the range of 0.3THz and 4THz, respectively. This makes MRG a uniquely tuneable material as a free layer in spin-transfer oscillator applications [6].

[1] Baibich M.N. et al., *Physical Review B*, **61** (1988) 2472, Ikeda S. et al., *Applied Physics Letters*, **93** 082508 (2008), Tsunegi S. et al., *Applied Physics Letters*, **109** (2016) 252402.

[2] Kurt H. et al., *Physical Review Letters*, **112** (2014) 027201.

[3] Borisov K. et al., *Applied Physics Letters*, **108** (2016) 192407.

[4] Betto D. et al., *AIP Advances*, **6** (2016) 055601.

[5] Fowley C. et al., *Journal of Physics D : Applied Physics*, **48** (2015) 164006.

[6] Awari N. et al., *Applied Physics Letters*, **109** (2016) 032403.

4TL-A-7

MAGNETIC SPIN HALL EFFECTS IN A CHIRAL ANTIFERROMAGNET*Otani Y.*^{1,2,3}, *Kimata M.*¹, *Kondou K.*², *Muduli P.*¹, *Nakatsuji S.*^{1,3}¹ Institute for Solid State Physics, The University of Tokyo, Japan² Center for Emergent Matter Science, RIKEN³ CREST, JST, Japan

yotani@issp.u-tokyo.ac.jp

Spin Hall effects (SHEs) are a collection of relativistic spin-orbit coupling phenomena in which electrical currents can generate transverse spin currents and vice versa. Despite being observed only a decade ago, these effects are already used in spintronics as standard spin-current generators and detectors.

Recently a chiral antiferromagnet Mn_3Sn has been demonstrated to exhibit a large anomalous Hall effect (AHE) at room temperature, the magnitude of which reaches almost the same order of magnitude as in ferromagnetic metals irrespective of a tiny spontaneous magnetization of about 1 mT [1]. The first principle calculation revealed that this large AHE originates from a significantly enhanced Berry curvature associated with the formation of Weyl points near Fermi energy [2,3]. The AHE, as is well known, shares its mechanism with the spin Hall effect. The large AHE therefore implies that a large SHE could take place in the Mn_3Sn .

In this talk we show experimental results of two complementary experiments such as detection of spin accumulation induced by the direct SHE and spin pumping induced inverse SHE in Mn_3Sn . Our experimental results demonstrate that we could observe the spin accumulation associated with the direct SHE and also the signals due to the inverse SHE.

[1] S. Nakatsuji, N. Kiyohara, and T. Higo, *Nature*, **527** (2015) 212–215.

[2] J. Kuebler, and C. Felser, *EPL*, **108** (2014) 67001.

[3] Yang, H. et al. <http://arxiv.org/abs/1608.03404> (2016).

4OR-A-8

THE INFLUENCE OF “INJECTED” AND “THERMAL” MAGNONS ON A SPIN WAVE CURRENT AND DRAG EFFECT IN HYBRID STRUCTURES

Lyapilin I.I.^{1,2}, Okorokov M.S.¹

¹ IMP UB RAS, Ekaterinburg, Russia

² UFSU, Ekaterinburg, Russia

Okorokovmike@gmail.com

Recently, a great deal of attention is devoted to the investigation of thermally excited magnons, particularly in studies of the spin Seebeck effect (SSE) in Pt/YIG/Pt structures. The propagation of magnons in a magnetic insulator is described by two characteristic quantities: mean free path and spin diffusion length that are governed, in turn, by various magnon relaxation mechanisms. For interpreting the experimental results, the works have adopted the hypothesis of the existence of the two magnon subsystems with different energies: “thermal” and “subthermal” magnons in a magnetic insulator. As to the temperature dependence of the Seebeck coefficient, it is non-monotonic and reaches its maximum within the range of 50 - 100K. To explain the low temperature enhancement proposed the phonon-drag SSE scenario. But the phonon contribution to the thermal conductivity reaches its maximum at around 25K which is 50 K lower than the observed peak in the SSE.

We have developed an "enhanced model" of the spin current and drag effect, which is based on the formation of two interacting magnon flows. Indeed, when SSE occurs in such structures, there are two magnon groups with different energies. The first group consists of magnons produced by an inhomogeneous temperature field applied to the magnetic insulator- “thermal” magnons. The energy of the magnons is of the order of a temperature ($k_B T$). Along with them, there are the magnons injected into the magnetic insulator due to inelastic scattering of spin-polarized electrons of the metal by localized spins located in the vicinity of the interface. The energy of the “injected” magnons is of the order of spin accumulation energy of conduction electrons of the metal $\Delta_s \gg k_B T$. Thus, it can be said that the magnetic system of the insulator forms another subsystem of "injected" magnons that are actually responsible for the SSE. As a consequence, in the presence of a non-uniform temperature field, there are three flows inside the magnetic insulator, namely, phonon and two magnon ones. The evolution of the magnon and phonon subsystems to equilibrium occurs due to the relaxation of both their energy and their moment. These subsystems tend to become balanced with different drift velocities. Obviously, the interaction between the flows gives rise to the drag effect.

Here, we study how the formation of two interacting magnon subsystems with distinguished energies influence on the SSE. The analysis of the macroscopic momentum balance equations of the systems for different ratios of the drift velocities of the magnon and phonon currents show that the “injected” magnons relaxation on the “thermal” ones is possible to be dominant over its relaxation on the phonons. This interaction will be the defining in the forming of the temperature dependence of the spin-wave current under SSE conditions, and inelastic part of the magnon-magnon interaction is the dominant spin relaxation mechanism. The existence of the two relaxation channels (magnon-phonon and magnon-magnon) in the case of inelastic scattering of the “injected” magnons on the “thermal” ones may lead to the “warming” of the letter and to Narrow-neck effect.

This study performed on the subject of “Spin” 0120463330, was supported by the Ministry of Education and Science of the Russian Federation (grants nos. 14.Z50.31.0025, 16-02-00044) and project no. 15- 17-2-17).

4OR-A-9

MAGNETIC PROPERTIES OF F/AF(TAF)/F TRILAYERS WITH LOW-NI PERMALLOY FERROMAGNETIC LAYERS

Dzhun I.O.¹, Babaytsev G.V.^{1,2}, Chechenin N.G.^{1,2}, Rodionova V.V.³, Gritsenko Ch.A.³

¹Skobeltsyn Institute of Nuclear Physics, Lomonosov Moscow State University, Leninskie Gory 1/2, 119991 Moscow

²Faculty of Physics, Lomonosov Moscow State University, Leninskie Gory 1/2, 119991 Moscow

³Immanuel Kant Baltic Federal University, Kaliningrad 236004, Russia

For optimized giant magnetoresistance (GMR) based devices, it is important to find a compromise between certain values of magnetization, coercivity, unidirectional and unidirectional anisotropies. In the report, we present the results of our study of magnetic properties of F/AF/F trilayers with low-Ni Permalloy Ni₄₀Fe₆₀ (F-layers) as a function of antiferromagnetic Ir₄₅Mn₅₅ (AF) layer thickness (t_{af}) in the range of 2 to 50 nm and with F-layers thickness of 10 nm. A single peak of ferromagnetic resonance (FMR) was observed showing a close effective magnetization and anisotropies in both bottom (BF) and top (TF) F-layers, in contrast with VSM data where different coercivities, H_c , and exchange bias, H_{eb} , were observed in the BF and TF layers. In particular, TF has higher H_{eb} , compared to BF layers, systematically for all the AF thicknesses. For both, BF and TF layers, $H_{eb}(t_{af})$ has a non-monotonic behavior with a clear peak at small thickness. The dependence of the FMR resonance field (ADFMR) on the angle φ between the direction of the applied field and the magnetic field applied to the sample during the layers deposition (DF), $H_r(\varphi)$, allows to obtain the magnitudes of exchange bias and uniaxial anisotropy fields, as well as the angle

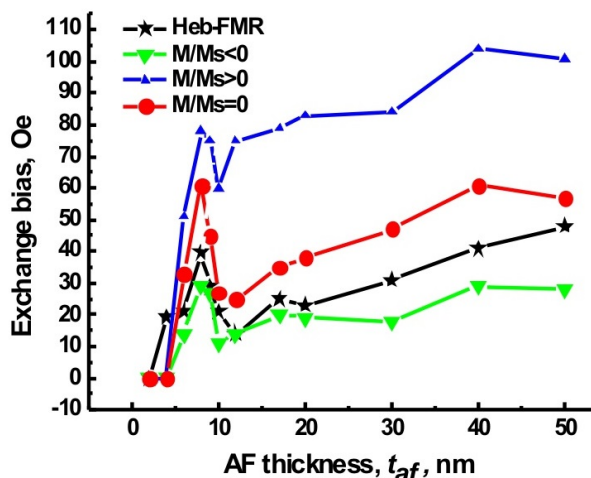


Fig.1. Exchange bias as a function of AF thickness.

of misalignment of AF unidirectional anisotropy with respect to the DF direction. It was found that FMR- $H_{eb}(t_{af})$ has a similar non-monotonic behavior as VSM- $H_{eb}(t_{af})$, being close to the $H_{eb}(t_{af})$ for the bottom F-layer (Fig. 1). The peak at small thickness $t_{af} < 10$ nm was also observed in thickness dependence of the misalignment angle, $\alpha(t_{af})$, between the direction of unidirectional anisotropy and DF direction. The angle-independent isotropic component of the resonance magnetic field $H_{r,0} = (2\pi f / \gamma)^2 / (4\pi M_{eff})$, where f is the FMR frequency, γ is gyromagnetic ratio and $4\pi M_{eff}$ is the effective magnetization, decreases at $t_{af} < 10$ nm, indicating increase of magnetization about 10% at small AF thickness.

The work is supported by Russian Foundation for Basic Research (grant 16-32-50191)

4TL-A-10

MgO, A MAGIC BARRIER FOR SPINTRONICS

Andrieu S.¹, Hauet T.¹, Montaigne F.¹, Le Fèvre P.², Bertran F.²

¹ Institut Jean Lamour, CNRS / Université de Lorraine, Vandoeuvre FRANCE

² SOLEIL Synchrotron, CNRS/CEA, St Aubin, France
stephane.andrieu@univ-lorraine.fr

The MgO insulating material is widely used in spintronic devices. It acts as an insulating barrier in Magnetic Tunnel Junctions (MTJs) constituted by two ferromagnetic layers separated by this barrier layer. The main advantage of using MgO is the very large magnetoresistance effect theoretically predicted in 2001 and demonstrated sometime after [1] on monocrystalline trilayers. These extraordinary tunnel magnetoresistances come from the symmetry filtering of the conduction states of the BCC electrodes (Fe, FeCo) by the MgO barrier.

But other benefits have been found more recently. Indeed, the use of the spin transfer torque allows easy manipulation of the magnetization provided that it has a Perpendicular Magnetic Anisotropy (PMA). Yang et al [2] theoretically predicted a strong Fe/MgO interface anisotropy opening the way to get PMA in MgO-based MTJs. Finally, effects of charge transfers at the Fe / MgO interface under the influence of the enormous electric field in the barrier makes it possible to manipulate the magnetic anisotropy in the iron layer [3], opening the way to devices with very low energy consumption.

We will examine in this talk how MgO epitaxially grows on (001) Fe (elastic and plastic regimes) and show that dislocations in the barrier decrease the magnetoresistance [4], and that the noise in MgO-based magnetic tunnel junctions is intimately linked to the presence of dislocations [5]. We will give a method based on electron diffraction which allows in real time to determine the critical thickness of plastic relaxation [6]. We will also show that the presence of an interface resonant state decreases the magnetoresistance for $\text{Fe}_x\text{Co}_{1-x}(001)$ electrodes with high Co content [7]. Then, we will confirm the predictions in [2] by obtaining perpendicular magnetization layers of Fe/MgO [8] (fig.1). Finally, we will show spectacular effects of the electric field induced in the MgO barrier which make it possible to manipulate the anisotropy of the Fe layers [9].

Supports by the Région Lorraine and ANR are acknowledged.

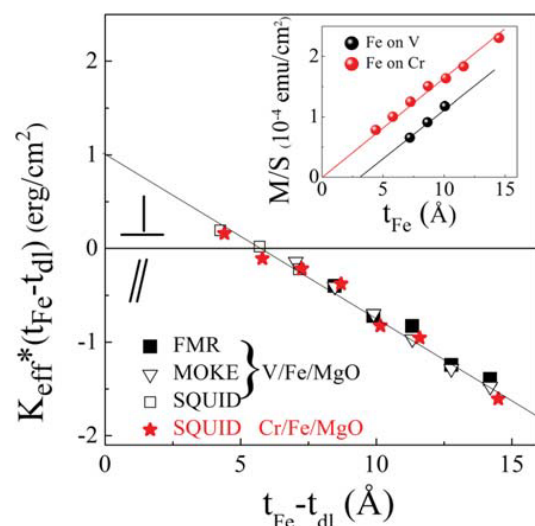


Fig. 1. Effective magnetic anisotropy measured on V/Fe/MgO and Cr/Fe/MgO. From [8]

- [1] For a review see S.Andrieu et al, *Phys. Rev. B*, **90** (2014) 214406.
- [2] H. X. Yang et al, *Phys. Rev. B*, **84** (2011) 054401.
- [3] M. Weisheit et al, *Science*, **315** (2007) 349.
- [4] F. Bonell et al, *Phys. Rev. B*, **82** (2010) 092405.
- [5] D. Herranz et al, *Appl. Phys. Lett.*, **96** (2010) 202501.
- [6] F. Bonell, S. Andrieu, *Surface Science*, **656** (2017) 140–147.
- [7] F. Bonell et al, *Phys. Rev. Lett.*, **108** (2012) 176602.
- [8] C.-H. Lambert et al, *Appl. Phys. Lett.*, **102** (2013) 122410.
- [9] A.Rajanikanth et al, *Appl. Phys. Lett.*, **103** (2013) 062402.

4RP-A-11

**MODELING OF THE SYSTEMS: JJ - NANOMAGNET:
IV-CHARACTERISTICS, MAGNETIC PRECESSION, MAGNETIC MOMENT
REVERSAL**

Shukrinov Yu.M.^{1,2}, Rahmonov I.R.^{1,3}, Buzdin A.⁴, Sengupta K.⁵, Filatrella G.⁶

¹BLTP, JINR, Dubna, Moscow Region, 141980, Russia

²Dubna State University, Dubna, Russian Federation

³Umarov Physical Technical Institute, TAS, Dushanbe, 734063 Tajikistan

⁴University of Bordeaux, LOMA UMR-CNRS 5798, F-33405 Talence Cedex, France

⁵Theoretical Physics Department, Indian Association for the Cultivation of Science, Jadavpur,
Kolkata 700 032, India

⁶Department of Sciences and Technologies and Salerno Unit of CNISM, University of Sannio, Via
Port' Arsa 11, I-82100 Benevento, Italy

shukrinov@theor.jinr.ru

We study the physical phenomena in ϕ_0 -junction with direct coupling between magnetic moment and Josephson current. By using a realistic model of Josephson junction, we simulate the IV-characteristics together with magnetic precession. It is demonstrated that the voltage interval corresponded to the hysteresis region of IV-characteristics is characterized by a cascade of different states of precession. By adding the electric current pulse, we have simulated the dynamics of magnetic moment components and demonstrated the full magnetization reversal [1]. Different protocols of magnetization reversal in ϕ_0 -junction and results at different values of model parameters are presented. The observed features might find an application in different fields of superconducting spintronics.

The reported study was funded by the RFBR research project 16--52—45011_India, 15--29--01217, the DST-RFBR grant INT/RUS/RFBR/P-249, and the French ANR projects

[1] Yu. M. Shukrinov, I. R. Rahmonov, K. Sengupta, A. Buzdin, Cond.-mat. arXiv:1702.08394

4OR-B-5

PATTERN RECOGNITION WITH A NETWORK OF COUPLED SPIN TORQUE OSCILLATORS

Talatchian P.¹, Romera M.¹, Abreu Araujo F.¹, Tsunegi S.², Kubota H.², Yakushiji H.², Fukushima A.², Yuasa S.², Bortolotti P.¹, Cros V.¹, Vodenicarevic D.³, Locatelli N.³, Querlioz D.³, Grollier J.¹

¹ Unité Mixte de Physique CNRS/Thales, Palaiseau, et Université Paris-Sud, Orsay, France

² Spintronics Research Center, AIST, Tsukuba, Japan

³ Centre de Nanosciences et de Nanotechnologies, CNRS, Université Paris-Sud, Orsay, France
philippe.talatchian@gmail.com

Brain-inspired hardware has been anticipated to translate into low-energy, intelligent and highly adaptable computing systems. This requires high density networks of neurons-like complex processing units coupled by tunable connections. Neurons can be modeled as non-linear oscillators coupled through synapses and which are able to synchronize together. Interestingly, spin torque oscillators are non-linear, nano-scale, low power consumption, tunable magnetic microwave oscillators which can synchronize to external stimuli [1] and to other oscillators [2]. Thus they are promising candidates as building blocks for large scale bio-inspired processors. In this work we show the first experimental demonstration of automatic pattern recognition with a network of coupled spin torque oscillators. We use an array of four electrically coupled oscillators, to which we inject two microwave signals encoding information of the spoken vowels. Depending on the input frequencies, one or more oscillators may lock to one of the external signals. Thus, different synchronization patterns arise, giving rise to synchronization maps (Fig. 1). By addressing the synchronization states of the network, we are able to classify 6 spoken vowels with a recognition rate up to 91%. Furthermore, we use the tunability of these oscillators to perform *learning*: an iterative process through which a neural network *adjusts* internal parameters to improve its performance. These results open new paths towards highly energy efficient bio-inspired computing on-chip based on non-linear nano-devices.

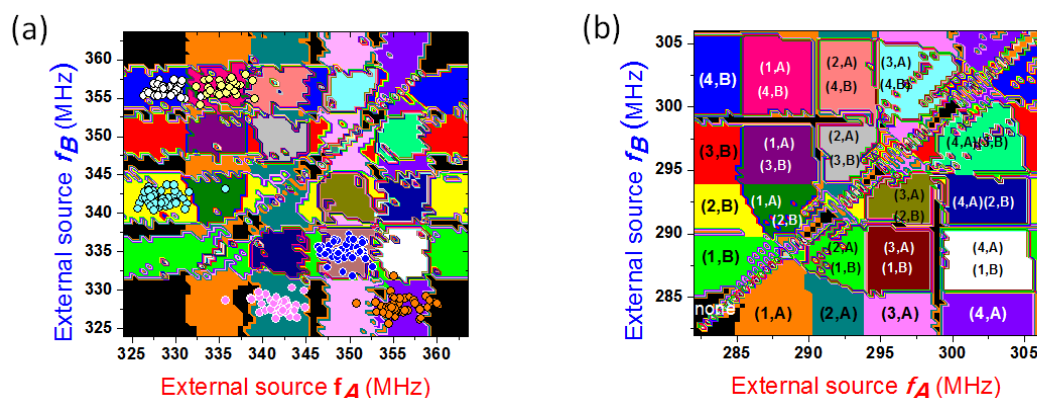


Fig. 1. (a) Experimental synchronization map, as a function of the frequency of the external sources. Each colored pattern represents a different synchronization state. Circular symbols correspond to the six vowels represented in terms of their two characteristic frequencies after transformation. (b) Simulated map using Thiele equations. The labels inside the patterns describe which oscillator is synchronized to which source.

[1] W. H. Rippard et. al. *PRL*, **95** (2005) 067203.

[2] S. Kaka et. al. *Nature*, **437** (2005) 389.

4OR-B-6

INTERACTION BETWEEN SPIN EXCITATIONS AND 2D ELECTRONS IN INTERFACE LAYER IN YIG/GaAs-HETEROSTRUCTURE

Lutsev L.V.¹, Stognij A.I.², Novitskii N.N.²

¹ Ioffe Physical-Technical Institute, St. Petersburg, Russia

² Scientific and Practical Materials Research Centre, Minsk, Belarus

l_lutsev@mail.ru

Nanometer $\text{Y}_3\text{Fe}_5\text{O}_{12}$ (YIG) film / semiconductor heterostructures are perspective materials for spintronics. Recent progress in synthesis of YIG films of high quality on semiconductor substrates [1-3] gives possibility to construct microwave spintronic devices. We describe synthesis of nanosized (40 - 964 nm) YIG films on GaAs substrates by ion-beam sputtering (Fig. 1) and present results of the investigation of ferromagnetic resonance and interaction between spin excitations in YIG film and 2D electrons in the interface layer in GaAs. YIG films were deposited on high-resistance GaAs substrates ($0.9 \cdot 10^5 \Omega \cdot \text{cm}$) with AlO_x (10-20 nm) buffer layers. The difference between magnetization and uniaxial anisotropy field $4\pi M - H_a$ of the sputtered YIG films is in the range of 651-1454 Oe and the minimal value of the FMR linewidth is equal to 73 Oe. Sputtered YIG films contain sublayers (Fig. 2). In order to study interaction between spin excitations in the YIG film and 2D electrons in the interface layer, we measure S -parameters of the interface channel formed in the GaAs between contacts. The channel is exposed by light ($\lambda = 650 \text{ nm}$) with the photon energy greater than the GaAs forbidden energy gap. It is found that at the in-plane magnetic field above the spin-wave instability threshold ($>10 \text{ dBm}$) increase of electrons in the interface induced by light leads to essential changes in the FMR spectrum and in the S_{21} -parameter of the channel (Fig. 3). This instability caused by the three-magnon decay and by light can be used at microwave frequencies as the effective tool of the manipulation of currents flowing in channels of spintronic devices.

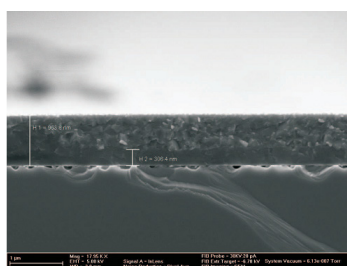


Fig. 1. Cross-section of the YIG film with the thickness of 964 nm ($4\pi M - H_a = 666 \text{ Oe}$) sputtered on GaAs substrate.

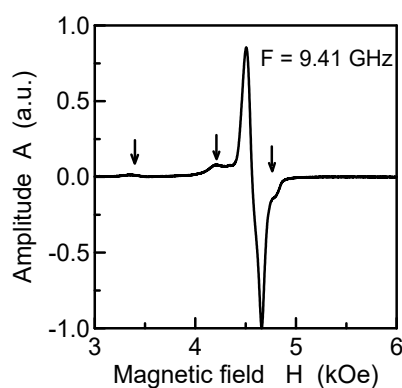


Fig. 2. FMR spectrum of the YIG film (40 nm, $4\pi M - H_a = 1180 \text{ Oe}$) at perpendicular magnetic field. Arrows correspond to FMR peaks of YIG sublayers.

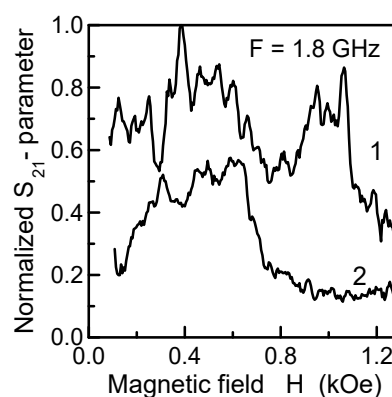


Fig.3. The normalized S_{21} -parameter measured in sample with YIG film (964 nm, 666 Oe) at the microwave power $P = 14 \text{ dBm}$ (1) under the light exposure and (2) without light.

This work was supported by the Government of Russia (project No. 14.Z50.31.0021, leading scientist M. Bayer) and by the Russian Foundation for Basic Research (project 15-02-06208).

[1] A.I. Stognij, L.V. Lutsev, V.E. Bursian, and N.N. Novitskii, *J. Appl. Phys.*, **118** (2015) 023905.

[2] A. Stognij, L. Lutsev, N. Novitskii, et al, *J. Phys. D: Appl. Phys.*, **48** (2015) 485002.

[3] L.V. Lutsev, A. M. Korovin, V.E. Bursian, et al, *Appl. Phys. Lett.*, **108** (2016) 182402.

4TL-B-7

INTERFACIAL DZYALOSHINSKII-MORIYA INTERACTION IN W/CoFeB/MgO FILMS TUNED BY VARIATION OF THE W THICKNESSES AND ANNEALING TEMPERATURES

*Kim G.W.¹, Kim Y.J.¹, Cha I.H.¹, Samardak A.S.², Pal B.², Kolesnikov A.G.², Ognev A.V.²,
Sadovnikov A.V.^{3,4}, Nikitov S.A.^{3,4}, Kim Yo.K.¹*

¹Department of Materials Science and Engineering, Korea University, Seoul 02841, Korea

²School of Natural Sciences, Far Eastern Federal University, Vladivostok 690950, Russia

³Laboratory "Metamaterials," Saratov State University, Saratov, 410012, Russia

⁴Kotel'nikov Institute of Radioengineering and Electronics, Russian Academy of Sciences,
Moscow, 125009, Russia
ykim97@korea.ac.kr

Recently, the interfacial Dzyaloshinskii-Moriya interaction (iDMI) has drawn tremendous attention because it can generate additional exchange energy term and manipulate intra-atomic magnetization dynamics. The prominent effect of iDMI was observed in layered systems with perpendicular magnetic anisotropy (PMA), such as Pt/Co/AlO_x, Pt/CoFeB/AlO_x [1], and Pt/CoFeSiB/MgO [2]. In this study, we investigate the iDMI in perpendicularly magnetized W/CoFeB/MgO trilayers, having different W buffer layer thicknesses. Samples were deposited on thermally oxidized Si wafers. The stacking sequence was Si/SiO₂/W t_w/CoFeB 0.9/MgO 1.0/Ta 2, where t_w = 1-15 nm. All the samples were post-annealed at 300°C (W3) and 400°C (W4) for 1 hr under magnetic field of 6 kOe. The magnetic properties and iDMI were measured using vibrating sample magnetometry and Brillouin light scattering spectroscopy, respectively.

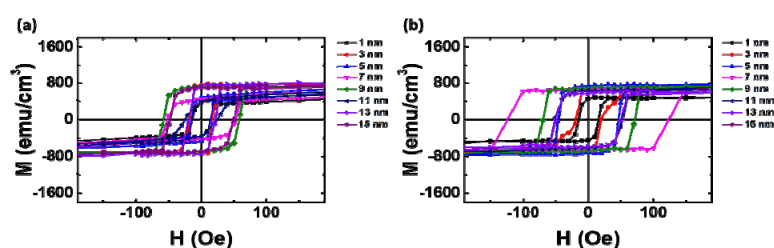


Figure 1. M-H loops for W3 and W4 series.

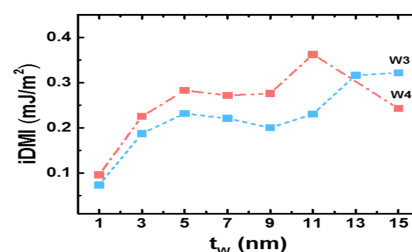


Figure 2. iDMI densities of W3 and W4.

Figure 1(a) and (b) show the out-of-plane hysteresis loops of W/CoFeB/MgO with different thicknesses of the W buffer and post-annealing temperatures. Samples from both series have well-pronounced PMA characteristics. Figure 2 represents the iDMI energy density. We have found that a NM layer thickness can affect to iDMI energy density. In the case of samples which are annealed at 300°C, as the thickness of the W layer becomes thicker, the iDMI energy density increases. However, in 400°C annealed samples, iDMI energy density has peak position (0.36 mJ/m²) at 11 nm of W thickness and decreases when the W buffer is thicker than 11 nm. The presented results enable to the buffer layer thickness-dependent manipulation of iDM for spintronic applications.

Financial support by NRF Korea (grant 2015M3D1A1070465), RFBR (grants 17-52-50060 and 15-02-05302) and the state task (3.5178.2017) is acknowledged.

[1] J. Cho *et al.*, *Nat. Commun.*, **6** (2015) 7635.

[2] I. H. Cha *et al.*, *IEEE Magn. Lett.*, **8** (2017) 3100504.

4OR-B-8

THERMAL STABILITY VS CELL SIZE FOR IP STT-MRAM: THEORY AND EXPERIMENT

Belanovsky A.D.^{1,2}, Mikhailov A.P.^{1,2}, Trofimov A.V.^{1,2}, Gapihan E.¹, Aksenova E.¹, Sorokina S.¹, Lomakin V.³, Khvalkovskiy A.V.^{1,2}

¹ Crocus Nano Electronics, Volgogradskiy prospect 42 build. 5, premise 1, Moscow, 109316, Russia

² Moscow Institute of Physics and Technology (State University), Institutskiy per. 9, 141700 Dolgoprudny, Russia

³ Center for Memories and Recording Research and Dept. of ECE, Univ. of California, San Diego, La Jolla, CA

Spin-Transfer Torque Magnetic Random Access Memory (STT-MRAM) is envisioned as a one of a few candidates for universal memory that can replace conventional dynamic and static RAM in future products. Two main switching performance characteristics of an STT-MRAM cell are the thermal stability factor Δ and the critical current I_{c0} . The thermal stability factor is given by $E_b/k_B T$, where k_B is the Boltzmann constant, T is the absolute temperature, and E_b is the energy barrier between two equilibrium states. The thermal stability factor further defines the retention time, read error rate (RER), and write error rate (WER) [1].

Here, we study the energy barriers as a function of size for in plane (IP) magnetized elliptic STT-MRAM cells using the nudged elastic band approach implemented in the finite element method based micromagnetic simulator FastMag [2]. In addition, by carrying out electrical tests of magnetic tunnel junctions (MTJ) fabricated on silicon wafer, we extract the coercive field from $R(H)$ loops. Using the SEM data for obtaining the cell size, we compare our micromagnetic modelling with the experiment.

Support of the RFBR grants 16-02-01161 A and National Science Foundation (NSF) is gratefully acknowledged

[1] A. V. Khvalkovskiy, D. Apalkov, S. Watts, R. Chepulskii, R. S. Beach, A. Ong, X. Tang, A. Driskill-Smith, W. H. Butler, P. B. Visscher, D. Lottis, E. Chen, V. Nikitin, and M. Krounbi, *J. Phys. D: Appl. Phys.*, **46** 074001 (2013).

[2] FastMag micromagnetic simulator, <http://cem.ucsd.edu/FastMag.html>

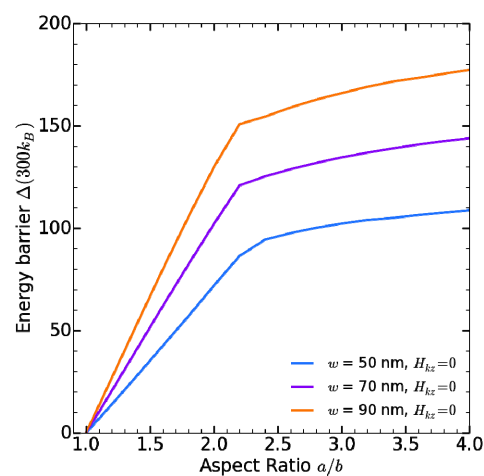


Figure 1. Results of micromagnetic modelling. Energy barrier as function of aspect ratio for different ellipse minor semi-axis. The linear part corresponds to coherent rotation of magnetization while the non-linear part corresponds to domain wall mediated reversal.

4OR-B-9

ELECTRONIC AND MAGNETO-OPTICAL PROPERTIES OF ZnO:Co

Kulatov E.T.^{1,5}, *Novodvorsky O.A.*², *Rylkov V.V.*³, *Gan'shina E.A.*⁴, *Shevyakov D.I.*⁴,
*Tugushev V.V.*³, *Uspenskii Yu.A.*⁵

¹ Prokhorov General Physics Institute RAS, Moscow, Russia

² Institute on Laser and Information Technologies RAS, Shatura, Russia

³ National Research Centre "Kurchatov Institute", Moscow, Russia

⁴ Lomonosov Moscow State University, Moscow, Russia

⁵ Lebedev Physical Institute RAS, Moscow, Russia

kulatov@nsc.gpi.ru

Doping of semiconductors by magnetic metals has been actively proceeded because of their potential applications in the spintronic devices. Main of these efforts is a attempt to control the interactions between induced magnetic properties (via the *d* electrons) and host semiconductor properties (caused by *sp* electrons) at room temperature. Despite the long, intensive efforts, the experimental evidence of thermally robust *sp-d* coupling in a magnetic semiconductor remains scarce and controversial.

Our high-quality ZnO:Co thin films were synthesized on the sapphire (0001) substrates by pulsed laser deposition with high-speed separation of particles. The structural, optical, magnetic and magneto-optical properties of ZnO:Co thin films were studied by experiments and the first-principles density functional theory (DFT). In the DFT study we employed a modified Becke-Johnson theory, which is referred to as the "mimic of exact exchange" and yields electronic properties under our investigation in good agreement with experiment.

X-ray diffraction results reveal that the Zn_{1-x}Co_xO films are all of wurtzite-type crystal structure with $0 < x < 0.35$. The experiments and theory show that ZnO:Co is a semiconductor with a direct band gap up to $x = 0.35$ on growing films conditions under low pressure of buffer oxygen ($\sim 10^{-6}$ Torr) and the substrates temperature of 500° C. The experimental and theoretical data have demonstrated good agreement.

We have computed the electronic structure and magnetic interactions in Co-doped ZnO in the presence and absence of various native defects. Our calculational study focuses on the role of defects in the induced magnetism of Co-doped ZnO, namely, vacancies on Zn and O sublattices, oxygen interstitials. Calculated exchange parameters show that in pure Co-doped ZnO, the interactions between Co spins are antiferromagnetic. In the case of *p*-type acceptor defect—e.g., Zn vacancy—the interactions turn out to be ferromagnetic. This holds true also in the presence of interstitial oxygen, where the defect is of donor type. We identify a crucial role of defects in the observed preparation sensitive ferromagnetism in ZnO:Co and in explaining experimental optical spectra and magneto-optical equatorial Kerr effect.

Support by RFBR No 16-02-00024, 16-02-612, 16-07-00798, 15-02-02077 and the Programs of the Russian Academy of Sciences "Strongly correlated electrons in solids and structures" and "Basic investigations of nanotechnologies and nanomaterials" is acknowledged.

4OR-B-10

TOLERANCE OF IP AND PP MRAM TO EXTERNAL MAGNETIC FIELD

Mikhailov A.P.^{1,2}, Belanovsky A.D.^{1,2}, Leshchiner D.R.², Lomakin V.³, Khvalkovskiy A.V.^{1,2}

¹ Crocus Nanoelectronics LLC, Moscow, Russia

² MIPT, Dolgoprudny, Russia

³ CMRR and Dept. of ECE, UC San Diego, CA, USA

a.mikhaylov@crocusnano.com

Ability of magnetic random access memory (MRAM) to store information is generally described by thermal stability factor Δ [1], which is defined to be the ratio of the energy barrier E_B between two equilibrium states in the free layer and the temperature in k_B units. The lifetime of stored information in one cell is estimated by the Arrhenius-Néel formula $\tau = \tau_0 e^{\Delta}$, where τ_0 is the attempt time.

For both in-plane (IP) and perpendicular-to-plane (PP) cells Δ appears to be sensitive to the external magnetic field H . Moreover, the influence of the external magnetic field has strong dependence of the angle between the field and easy axis of the cell. This dependence is shown in figure 1. These data were obtained by numerical simulation of PP-MRAM cell of 90 nm diameter using the nudged elastic band method implemented in the FastMag micromagnetic simulator [2].

Thermal stability factor in the presence of external magnetic field can be expressed [3] as:

$$\Delta(H) = \Delta_0 \left(1 \pm \frac{H}{H_K(\theta)} \right)^n,$$

where Δ_0 is thermal stability factor without magnetic field, $H_K(\theta)$ is the Stoner-Wohlfarth switching field at an angle θ with respect to the easy axis of the MRAM cell. The \pm sign represents the asymmetry of the minimal energy path (MEP), i.e. different energy barriers when transitioning between the two equilibrium states, which have different energies due to the applied field.

In this work, we show numerically that this formula applies not only to MEP via uniform rotation in MRAM cells, which is considered to be close to Stoner-Wohlfarth particles, but also to MEP via domain wall (DW) switching. We investigate the exponent behavior for IP-MRAM and PP-MRAM cells for both MEP via uniform rotation and DW. We find that for perpendicular external fields, the exponent $n \approx 2$ even for DW MEP. However, for a general external field angle, the exponent is different when the minimal path is via DW.

This work was supported under a joint development program between Crocus Nanoelectronics LLC and MIPT as well as National Science Foundation (NSF). Authors also acknowledge RFBR, project №16-02-01161 A.

[1] Khvalkovskiy, A. V., et al. "Basic principles of STT-MRAM cell operation in memory arrays." *Journal of Physics D: Applied Physics*, **46.7** (2013): 074001.

[2] Chang, R., et al. "FastMag: Fast micromagnetic simulator for complex magnetic structures." *Journal of Applied Physics* **109.7** (2011): 07D358, <http://cem.ucsd.edu/FastMag.html>

[3] Suess, D., et al. "Reliability of Sharrocks equation for exchange spring bilayers." *Physical Review B*, **75.17** (2007): 174430.

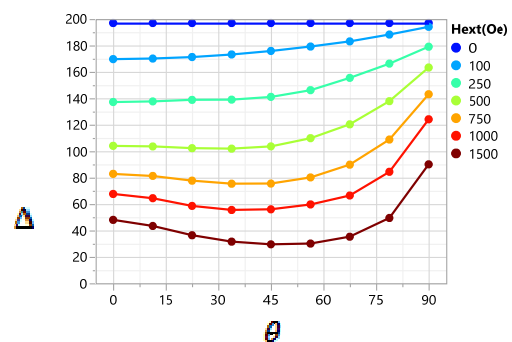


Fig. 1. FastMag simulation thermal stability factor Δ as a function of the applied field angle θ for an PP-MRAM cell of 90 nm diameter with a DW MEP.

4OR-B-11

SPIN-FILTER STATE OF AU-CO NANOWIRES

Smelova E.M.¹, Tsysar K.M.¹, Saletsky A.M.¹

¹ Lomonosov Moscow State University, Faculty of Physics, (*Lomonosov MSU*), Moscow, Russia
smelova_e_m@mail.ru

Our theoretical study reveals the existence of two transmission regime in Au-Co nanowires with low and high conductivity $1G_0$ and $2G_0$ for “zig-zag” and linear nanowire correspondingly. Our calculations revealed the dependence of quantum conductance of Au-Co nanowire on their atomic structure.

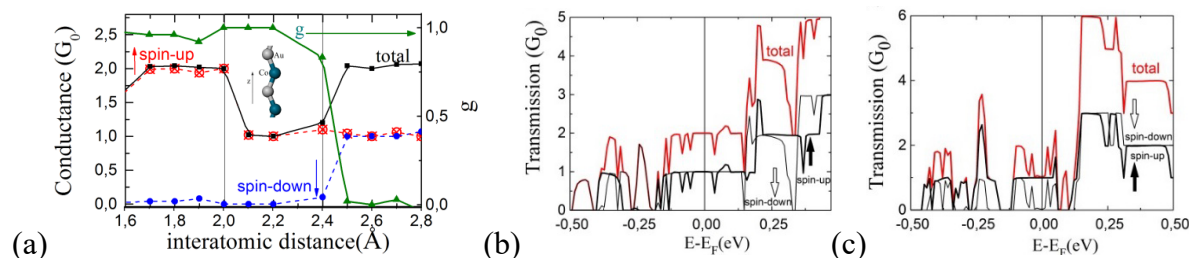


Fig. 1. **a)** Total quantum conductance of Au-Co nanowire (solid black line), spin-polarized conductance of spin-up (dashed red line) and spin-down (dashed blue line) channels and also the degree of spin polarization of quantum electron transport (g) as a function of average interatomic distance (solid green line). Inset figure represent the model of evenly mixed “zig-zag” Au-Co nanowire, **b)** Transmission $T(E)$ through spin-up and spin-down channel and total transmission at zero-bias of linear Au-Co nanowire at average interatomic distance 2.5Å , **c)** Total transmission at zero-bias of zig-zag nanowires at 2.2Å in spin filtering regime. E_F is the Fermi energy of left and right hand side electrodes.

We calculated the conductance of magnetic Au-Co nanowires in the whole range of interatomic distances, corresponding to the area of the wire existence ($1.6\text{Å} - 3.0\text{Å}$) including the region of strongly contracted nanowire ($1.6\text{Å} - 2.0\text{Å}$) degenerated to the state of two interacting one-component Au and Co nanowires. We found the strong dependence of the total conductance of the wire on the “stretching-contraction” deformations emerging during the wire formation (see Fig.1a, solid line). The total conductance of linear stretched nanowires was calculated about $2G_0$ and remains practically unchanged in the range ($2.4\text{Å} - 3.0\text{Å}$) (Fig.1a, solid line). Under contraction wire goes into “zig-zag” configuration at interatomic distance $\sim 2.4\text{Å}$. This structural transition of the wire leads to an abrupt decreasing of conductance to $1G_0$ (Fig.2, solid line). For quantitative estimation of the spin polarization of the electron transport through nanowire, we introduce a term - degree of polarization $g = \frac{g_1 - g_2}{g_1 + g_2}$ [1]. The value of g drastically increases under wire contraction from ~ 0 for linear nanowire up to ~ 1 for “zig-zag” one (see Fig.1a, green line). Thus our conductance calculations revealed the emergence of *spin-filter* state in one-dimensional contracted “zig-zag” Au-Co bimetallic nanowires. Moreover, our study revealed the vanishing of spin-polarization of electron transport in stretched linear bimetallic Au-Co nanowires. We found also the control capability of spin transport regime by changing of bias voltage between bulk electrodes. Figure 1b illustrates the transmission spectra of the linear wire at interatomic distance 2.5Å . Our transmission spectra calculations have shown the absence of spin polarizations of electron transport in linear Au-Co nanowires. The transmission pattern differs greatly for the contracted Au-Co nanowire. We can see that only transmission through spin-up channel is presented at Fermi level ($\sim 1G_0$), the transmission through spin-down channel equals zero (see Fig.1c). Our study of electronic structure of Au-Co nanowire in linear and “zig-zag” configurations has shown that *spin filter* state appears due to quantum interference of electron states of hybridized $s-d_{z^2}$ and $d_{xz}-d_{yz}$ bands, formed between atoms in “zig-zag Au-Co nanowire.

[1] G.A. Nemnes, *Journal of Nanomaterials*, **2013** (2013) 408475.

4OR-B-12

EFFECT OF THE W CAPPING LAYER ON SPIN-ORBIT TORQUES IN Ru/Co/Ru FILMS

Stebliy M.E., Kolesnikov A.G., Ognev A.V., Samardak A.S., Chebotkevich L.A.
Far Eastern Federal University, Vladivostok, 690950, Russian Federation
stebliyme@gmail.com

To observe the spin-orbit torque (SOT) effect, a structure has to consist of a thin ferromagnetic (FM) layer with perpendicular magnetic anisotropy (PMA) and a heavy metal (HM) with strong spin-orbit coupling (SOC). Transverse spin current is generated in HM owing to the spin Hall effect (SHE), and can be used to manipulate the magnetization of FM [1]. In this work we investigated the current-induced reversal of the symmetric Ru/Co/Ru and asymmetric Ru/Co/Ru/W structures. Hall bars with the width of 20 μm were fabricated by means of e-beam lithography and magnetron sputtering. To perform the magnetization switching, a current in the range of $\pm 80\text{mA}$ ($\pm 3 \times 10^{11} \text{A/m}^2$) with a duration of 50 ms in the presence of a co-directional magnetic field of 80 Oe was passed through the Hall bars. The magnetization change was determined as the transverse voltage variation at the applied current. It was found that in the symmetric structure of Ru(100)/Co(9)/Ru(20) (in \AA), the current-induced magnetization reversal reached only 40% of the saturation level. Capping of this structure by W(20) layer enhanced the magnetization switching up

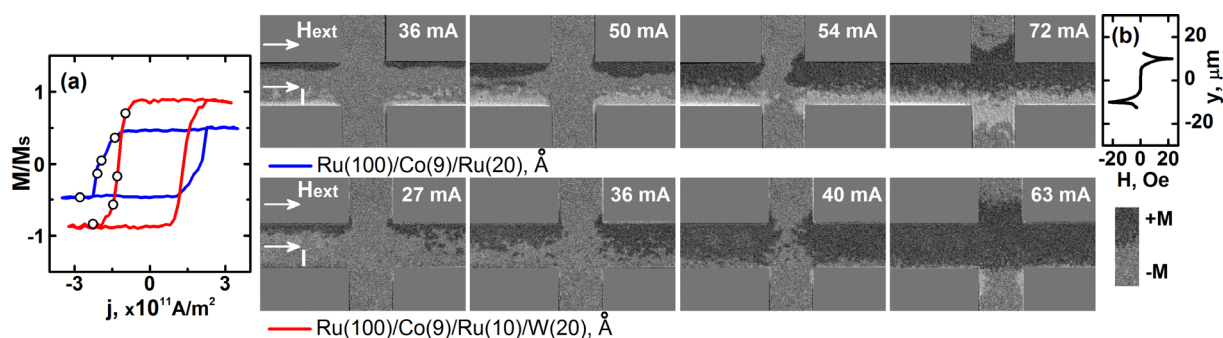


Fig. 1. (a) Current-induced hysteresis loops for the symmetric (blue curve) and asymmetric (red curve) Hall bars. Magnetic states marked by the open circles are visualized by the Kerr microscopy imaging shown on the right for corresponding structures. (b) The transverse profile of the Oersted field at the current of 50 mA.

to 90% of the saturation (Fig.1a).

The Kerr microscopy visualization revealed that for the symmetric structure the current transmission led to a partial magnetization reversal, whereas for the asymmetric one a complete switching was observed. To explain these results, we took into account the fact that the SHE effect occurred in both the lower and upper layers of Ru, which results in the partial compensation of SOT. We considered an impact of the Oersted field on the magnetization switching, which value can be comparable with the coercive force (25 Oe) of FM and in combination with the antiparallel orientation on the edges induced the demagnetization effect, Fig.1b. The asymmetric structure has the different signs of the SHE effect for Ru and W layers causing in increase of the SOT effect and the complete magnetization switching. Using the harmonic measurement technique [2], the value of the effective magnetic field was determined as $8 \times 10^{-11} \text{Oe}/(\text{A/m}^2)$.

Support by the President grant (MK-2643.2017.2), RFBR (grants 17-52-50060 and 15-02-05302) and the state tasks (3.5178.2017 and 3.4956.2017) is acknowledged.

[1] I. M. Miron, *Nature*, **476** (2011) 189.

[2] M. Hayashi, *Phys.Rev. B*, **89** (2014) 144425.

4OR-B-13

HYBRID ANISOTROPY $[\text{Co/Ni}]_{15}/\text{Cu}/[\text{Co/Pt}]_4$ SPIN-VALVES

*Kolesnikov A.G.¹, Steblyy M.E.¹, Ognev A.V.¹, Samardak A.S.¹, Chebotkevich L.A.¹, Hao Wu²,
Xiufeng Han²*

¹ Far Eastern Federal University, Vladivostok, Russia

² State Key Laboratory of Magnetism, Institute of Physics, Chinese Academy of Sciences, Beijing, China
ognev.av@dvfu.ru

Combining of materials in multilayer films and varying of layer parameters, one can fabricate magnetic media with different coercive forces and magnetic anisotropies. Utilization of layers with perpendicular magnetic anisotropy (PMA) enables to increase the switching rate, thermostability, zero-field operation of spin-torque oscillators, but a layer with the in-plane anisotropy, breaking the axial symmetry of layers with PMA, can be both a polarizer and a read-out layer.

We present results of the study of magnetic and magnetoresistance (MR) properties of $[\text{Co/Ni}]_{15}/\text{Cu}/[\text{Co/Pt}]_4$ spin-valves (SVs) with hybrid magnetic anisotropy as a function of the thickness of the nonmagnetic Cu interlayer (t_{Cu}). Series of SVs with the following structure $\text{SiO}_2/\text{Cu}(30)/\text{Ta}(5)/[\text{Co}(0.3)/\text{Ni}(0.37)]_{15}/\text{Co}(0.3)/\text{Cu}(t_{\text{Cu}})/[\text{Co}(0.5)\text{Pt}(2)]_4/\text{Co}(0.5)/\text{Pt}(5)$, where nominal thicknesses are pointed out in nm, and t_{Cu} is varying from 0 to 4 nm with the step 0.5 nm, was prepared using the DC magnetron sputtering. The out-plane magnetic hysteresis loops are shown in Fig.1. MR measurements were done in the “current in to plane” (CIP) geometry, Fig.2. MR curves were modelled by OOMMF.

We found that saturation field depends on the thickness of the copper interlayer (t_{Cu}) and its maximum value was observed at $t_{\text{Cu}} = 2.5$ nm. (Fig.1c). The MR value varied from 1.4 to 0.6% (Fig.2a). Micromagnetic simulations revealed the effect of the indirect exchange coupling on the configuration of magnetic structure. The modelled MR curves showed satisfied matching of the experimental data, Fig.2b.

Support by RFBR (grants 17-52-50060 and 15-02-05302) and under the state tasks (3.5178.2017 and 3.4956.2017) is acknowledged.

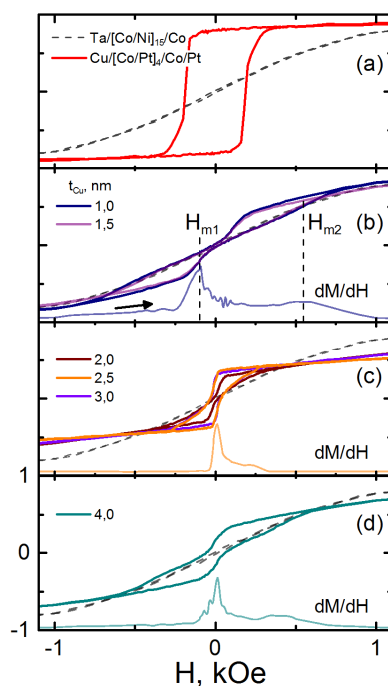


Fig 1. Experimental room temperature M-H loops of Ta/ $[\text{Co/Ni}]_{15}/\text{Co}$ (after etching) and Cu/ $[\text{Co/Pt}]_4/\text{Co/Pt}$ films (a) and $[\text{Co/Ni}]_{15}/\text{Cu}/[\text{Co/Pt}]_4$ spin valves (b-d).

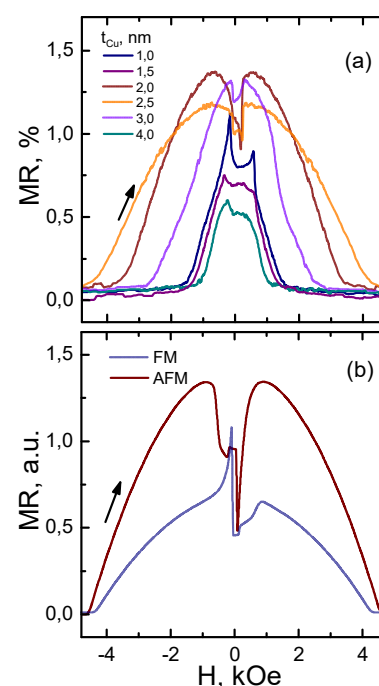


Fig. 2 Experimental room temperature MR loops of $[\text{Co/Ni}]_{15}/\text{Cu}/[\text{Co/Pt}]_4$ (a) and the simulated MR loops with AFM and FM indirect exchange (b).

4 July

Tuesday

11:30-13:30

oral session

4TL-B

“Skymions”

4TL-B-1

SKYRMION HALL EFFECT IN ANTIFERROMAGNETS AND FERROMAGNETS

Tretiakov O.A.^{1,2}

¹ Institute for Materials Research, Tohoku University, Sendai, Japan

² School of Natural Sciences, Far Eastern Federal University, Vladivostok, Russia
olegt@imr.tohoku.ac.jp

Manipulating small spin textures that can serve as bits of information by electric and spin currents is one of the main challenges in the field of spintronics. Ferromagnetic skyrmions attracted a lot of attention because they are small in size and are better than domain walls at avoiding pinning sites while moved by electric current. Moreover, recently in ferromagnet/heavy-metal bilayers they were shown to move very efficiently by the so-called "spin-orbit" torques. We formulate the general theory of these torques including their microscopic treatment in disordered systems [1]. This allows us to calculate the skyrmion Hall angle, which was recently revealed by X-ray microscopy. We show that this angle depends on dynamical deformations of the skyrmion due to spin-orbit torques [1, 2].

Meanwhile, the ferromagnetic skyrmions also have certain disadvantages, such as the presence of stray fields and transverse to current dynamics, making them harder to employ in spintronic devices. To avoid these unwanted effects, we propose a novel topological object: the antiferromagnetic skyrmion [3] and explore its properties using the microscopic analysis, generalized Thiele equation, and micromagnetic simulations. This topological texture has no stray fields and we show that its dynamics are faster compared to its ferromagnetic analogue. More importantly, we show that due to unusual topology the antiferromagnetic skyrmions experience no skyrmion Hall effect (zero velocity component transverse to the current), and thus are better candidates for spintronic memory and logic applications.

[1] I. Ado, O. A. Tretiakov, and M. Titov, *Phys. Rev. B*, **95** (2017) 094401.

[2] K. Litzius, I. Lemesh, B. Kruger, P. Bassirian, L. Caretta, K. Richter, F. Buttner, K. Sato, O. A. Tretiakov, J. Forster, R. M. Reeve, M. Weigand, I. Bykova, H. Stoll, G. Schutz, G. S. D. Beach, and M. Klau, *Nature Physics*, **13** (2017) 170.

[3] J. Barker and O. A. Tretiakov, *Phys. Rev. Lett.*, **116** (2016) 147203.

4TL-B-2

ENERGY SURFACE AND LIFETIME OF MAGNETIC SKYRMIONS

Uzdin V.M.^{1,2}, Potkina M.N.², Lobanov I.S.¹, Jónsson H.³

¹ University ITMO, St.Petersburg, Russia

² SPbGU, St.Petersburg, Russia

³ University of Iceland, Reykjavik, Iceland

v_uzdin@mail.ru

Quantitative measure of the topological protection for skyrmion states is an important fundamental problem connecting topology and physics. The stability of magnetic skyrmions with respect to thermal fluctuations is a principal issue for their application in magnetic memory devices. Stochastic modelling of skyrmion dynamics and stability proves to be a difficult problem due to the large difference in time scales between a typical vibrational period of magnetic moments and the lifetime of a skyrmion state. Nevertheless it is this timescale difference that makes it possible to apply statistical transition state theory (TST) for magnetic degrees of freedom to calculate lifetime of skyrmions as a function of temperature [1]. An Arrhenius law can be obtained for the rates of magnetic transitions and in harmonic TST both the activation energy as well as attempt frequency can be calculated with controlled accuracy.

We consider the multidimensional energy surface of a magnetic system described by a Heisenberg-like Hamiltonian including Dzyaloshinskii-Moriya interaction, anisotropy and external magnetic field as function of angle variables specifying the directions of all magnetic moments. Minima on this surface correspond to the ground and metastable states. Minimum energy paths (MEPs) between them can be calculated using geodesic nudged elastic band method [2]. The maximum energy along an MEP corresponds to a first order saddle point on the energy surface and gives an estimate of the activation energy for magnetic transitions, in particular for creation and annihilation of skyrmions [3]. The attempt frequency can be calculated within harmonic approximation from the shape of the energy surface in the neighbourhood of the saddle point and the minima. It depends on the eigenvalues of the Hessian at those points. Special attention has to be paid to adequate treatment of “zero modes” –degrees of freedom which do not affect the energy of the system. They lead to additional temperature dependence of the attempt frequency.

As an example application of this general theory we have calculated the lifetime of a single skyrmion and a skyrmion in a track of finite width, D , comparable to the size of the skyrmion in a PdFe/Ir(111) system. Various MEPs with annihilation in the middle of the track and via boundary have been considered. The activation energy and attempt frequency have been calculated as a function of D for each mechanism to determine the transition rate as a function of temperature.

The influence of atomic-scale non-magnetic defects on the activation energy for skyrmion creation/annihilation and its lifetime have been calculated. The results help choose optimal parameters for writing and deleting information using skyrmion bits. The pinning of a skyrmion by a non-magnetic impurity makes it possible to direct the skyrmion along a track built from such impurities when the materials are chosen in such a way that the probability of annihilation and unpinning from the impurities is lower than movement along the track.

[1] P. F. Bessarab, V. M. Uzdin, H. Jónsson, *Phys. Rev. B*, **94** (2012) 184409.

[2] P. F. Bessarab, V. M. Uzdin, H. Jónsson, *Comp. Phys. Comm.*, **196** (2015) 335.

[3] I.S. Lobanov, H. Jónsson, V. M. Uzdin, *Phys. Rev. B*, **94** (2016) 174418.

4TL-B-3

ROOM-TEMPERATURE CURRENT-INDUCED GENERATION AND MOTION OF SUB-100NM SKYRMIONS

Legrand W.¹, Maccariello D.¹, Reyren N.¹, Garcia K.¹, Moutafis C.², Moreau-Luchaire C.¹, Collin S.², Bouzheouane K.¹, Cros V.¹, Fert A.¹

¹ Unité Mixte de Physique CNRS Thales, Univ. Paris Sud, Univ. Paris-Saclay, Palaiseau, France

² School of Computer Science, University of Manchester, Manchester, UK

vincent.cros@cnrs-thales.fr

Magnetic skyrmions are nanoscale spin structures that can be stabilized by the Dzyaloshinskii-Moriya interaction (DMI) in magnetic materials which break bulk or interface inversion symmetry. Taking advantage of their reduced dimension and expected low depinning threshold for current-induced motion would be of particular interest in order to allow for magnetic memory applications operating both at low currents and with a high integration density. After the recent observation of sub-100 nm skyrmions stabilized at room temperature by interfacial chiral interaction in magnetic multilayers [1], of skyrmion motion at speeds reaching 100 m.s^{-1} [2,3], of the skyrmion Hall effect [4,5], several questions are still to be solved, notably regarding the means to nucleate individual compact skyrmions and the exact nature of their motion.

In this presentation we will cover our recent experiments of current-induced generation and motion of the skyrmions in Pt/Co/Ir based multilayers, observed by Magnetic Force Microscopy (MFM) at room-temperature [6]. We present a method leading to the formation of a set of magnetic skyrmions in a micrometer-sized track (shown below) using homogeneous current injection, and then discuss the observed spin-orbit-torque-induced motion of the skyrmions in these tracks. With the help of analytical and micromagnetic modeling, we analyze the observed velocities and trajectories. We discuss the influence of the size of the skyrmions on their motion, and link our observation of strong pinning of part of the skyrmions to some magnetic inhomogeneities of the multilayers (see fig. below). We can thus get the critical currents for motion which provide guidelines on the material design of the multilayers.

EU grant MAGicSky No. FET-Open-665095 is acknowledged for financial support.

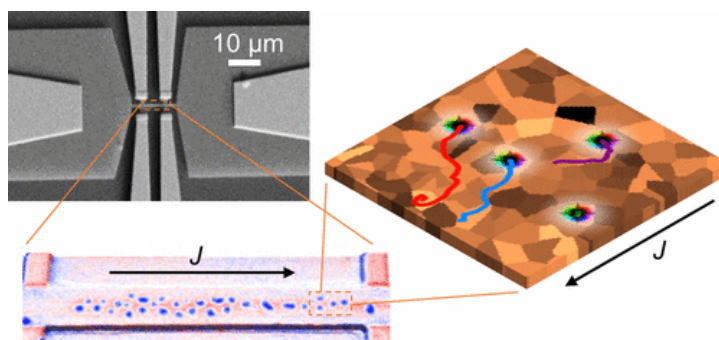


Fig. 1. Upper left: SEM image of the tracks used for the study. Lower left: MFM image of the nanotracks, indicating the magnetic skyrmions in blue and the applied current direction (arrow). Right: Simulation of the skyrmions (black circles) motion with their trajectories (colored lines) in the presence of magnetic inhomogeneities.

[1] C. Moreau-Luchaire et al, *Nature Nanotech.*, **11** (2016) 444-448.

[2] S. Woo et al, *Nature Mater.*, **15** (2016) 501-506.

[3] A. Hrabec et al, arXiv:1611.00647v2.

[4] W. Jiang et al, *Nature Phys.*, **13** (2017) 162-169.

[5] K. Litzius et al, *Nature Phys.*, **13** (2017) 170-175.

[6] W. Legrand et al, *Nano Lett.*, *in press* (2017) DOI:10.1021/acs.nanolett.7b00649.

4TL-B-4

MAGNETIC SKYRMIONS IN CONFINED GEOMETRIES

Farle M.^{1,2}

¹ Faculty of Physics, University Duisburg-Essen, 47057 Duisburg, Germany

² Immanuel Kant Baltic Federal University, Russia

Dzyaloshinskii-Moriya interaction (DMI) in magnetically ordered systems favors a spin canting of otherwise (anti) parallel aligned magnetic moments and thus, e.g., is a source of weak ferromagnetic behavior in an antiferromagnet [1]. Over the last years, the topological nature of spin textures (so called Skyrmions) originating from the existence of DMI at interfaces or in the volume has found a tremendous interest in the magnetism community.

The magnetic textures are the result of a delicate balance between magnetic exchange, DMI, and Zeeman energy. The presence of DMI can be indirectly seen in the chirality of domain walls [2] for example.

For confined geometries it was calculated that the DMI and micromagnetic bound magnetic fields. The color wheel indicates the direction of the in-plane magnetization. Boundary conditions should cause a bending of the magnetization at the edges, which allow for certain geometries the isolation of single skyrmions [3]. Furthermore, spin wave excitations in the presence of DMI show a non-symmetric dispersion relation [4],[5].

Here, I will present the size and shape dependence of skyrmions and skyrmion lattices in geometrically confined FeGe lamellas (Fig. 1).

The electron holography work was performed by Zi-An Li at the FZ Jülich. The work on standing spin wave modes in confined geometries was performed in collaboration with R. Camley, R. Stamps and B. Zingsem. I thank all my collaborators and my team for their contributions to this work.

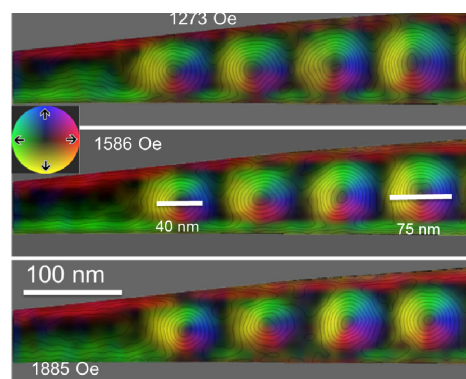


Fig. 1 Electron holography of FeGe lamella. Magnetic contrast images of skyrmions in laterally confined geometry at different magnetic fields. The color wheel indicates the direction of the in-plane magnetization.

- [1] T. Moriya, *Physical Review*, **120** (1960) 91.
- [2] R. Ramchal, A. K. Schmid, M. Farle, and H. Poppa, *Physical Review B* **68** (2003) 054418.
- [3] S. Rohart, and A. Thiaville, *Phys. Rev. B*, **88** (2013) 184422.
- [4] Zakeri, K., et al., *Physical Review Letters*, **104** (2010) 137203.
- [5] Zi-An Li et al., *Nano Lett.*, **17** (2017) 1395.

4 July

Tuesday

11:30-13:00

14:30-17:00

oral session

4TL-D

4RP-D

4OR-D

4TL-LT

4RP-LT

4OR-LT

**“Magnetism and
Superconductivity”**

4TL-D-1

ENHANCEMENT OF THE PAULI LIMIT IN DISORDERED TRANSITION METAL DICHALCOGENIDE MONOLAYERS*Ilic S.¹, Houzet M.¹, Meyer J.S.¹*¹University Grenoble Alpes & CEA, INAC-PHELIQS, F-38000 Grenoble, France
julia.meyer@univ-grenoble-alpes.fr

A new kind of 2D materials have been recently synthesized – monolayers composed of a transition metal and a chalcogenide (TMDC) with a structure similar to graphene, but with two different atoms per unit cell. They exhibit a particularly strong intrinsic spin-orbit coupling, acting as an effective Zeeman field which takes opposite orientations in two different valleys. Intrinsic superconductivity has been experimentally confirmed in several of these compounds.

We calculate the effect of impurities on the superconducting phase diagram of transition metal dichalcogenide monolayers in the presence of an in-plane magnetic field. Due to strong intrinsic spin-orbit coupling, the upper critical field greatly surpasses the usual Pauli limit at low temperatures. We find that it is insensitive to intravalley scattering and, ultimately, limited by intervalley scattering.

Support by the Laboratoire d'excellence LANEF in Grenoble (ANR-10-LABX-51-01) is acknowledged.

4TL-D-2

SUPERCONDUCTING QUANTUM METAMATERIALS: CHAOS AND DISORDER

Kawabata S.¹, Asai H.¹, Savel'ev S.², Zagoskin A.²

¹ National Institute of Advanced Industrial Science and Technology (AIST), Tsukuba, Ibaraki 305-8568, Japan

² Department of Physics, Loughborough University, Loughborough LE11 3TU, UK
s-kawabata@aist.go.jp

Metamaterials are artificial electromagnetic materials consisting of artificial atoms, that is, artificial structures whose sizes are small compared to the wavelength of respective electromagnetic (EM) wave. The effective permittivity and permeability of metamaterials can be controlled at will by changing shapes and arrangements of the artificial atoms. The concept of metamaterial is quite useful for fabricating novel optical devices such as cloaking devices.

Recently, quantum metamaterial (QMM), which utilizes superconducting qubits as artificial atoms, has been theoretically proposed [1] and realized experimentally [2,3]. Unlike conventional metamaterials composed of classical elements, QMMs are expected to show several unique EM responses originating from quantum superposition and entanglement of qubits.

In this talk, we will present our recent theoretical studies on the nonlinear electromagnetic response of a QMM based on superconducting charge qubit arrays in a superconducting transmission line (circuit QED system) [4,5]. Especially, we will discuss on peculiar nonlinear electromagnetic responses, e.g., high-harmonic generation, parametric amplification, and chaotic qubit dynamic in such systems. In addition, we will show nonlinear electromagnetic responses in disordered and dissipative quantum metamaterials.

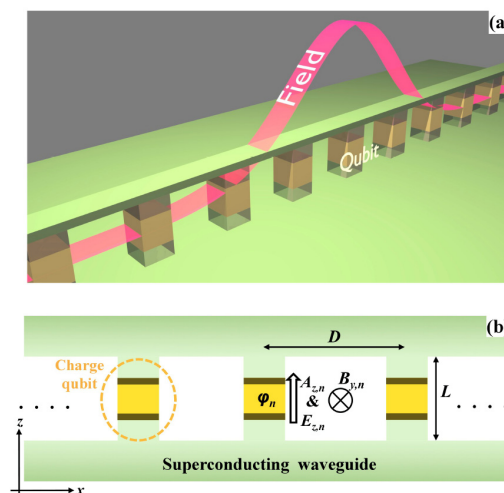


Fig. 1 Schematic of a superconducting quantum metamaterial

- [1] A.L. Rakhmanov, A.M. Zagoskin, S.Savel'ev, F.Nori, *Phys. Rev. B*, **77** (2008) 144507.
- [2] P.Macha, G.Oelsner, J.M.Reiner, M.Marthaler, S.Andre, G.Schon, U.Hubner, H.G.Meyer, E.Il'ichev, A.V.Ustinov, *Nature Comm.*, **5** (2014) 5146.
- [3] K.Kakuyanagi, Y.Matsuzaki, C.Deprez, H.Toida, K.Semba, H.Yamaguchi, W.J.Munro, S.Saito, *Phys. Rev. Lett.*, **117** (2016) 210503.
- [4] H.Asai, S.Savel'ev, S.Kawabata, A.Zagoskin, *Phys. Rev. B*, **91** (2015) 134513.
- [5] H.Asai, S.Kawabata, A.Zagoskin, S.Savel'ev, arXiv:1605.04929.

4RP-D-3

SUBGAP STATES IN DISORDERED SUPERCONDUCTORS WITH STRONG MAGNETIC IMPURITIES

Fominov Ya.^{1,2}, *Skvortsov M.*^{3,1,2}

¹ L.D. Landau Institute for Theoretical Physics RAS, Chernogolovka, Russia

² Moscow Institute of Physics and Technology, Dolgoprudny, Russia

³ Skolkovo Institute of Science and Technology, Skolkovo, Russia

fominov@landau.ac.ru

We study the density of states (DOS) in diffusive superconductors with point-like magnetic impurities of arbitrary strength described by the Poissonian statistics [1]. The mean-field theory predicts a nontrivial structure of the DOS with the continuum of quasiparticle states and (possibly) the impurity band. In this approximation, all the spectral edges are hard, marking distinct boundaries between spectral regions of finite and zero DOS. Considering instantons in the replica sigma-model technique, we calculate the average DOS beyond the mean-field level and determine the smearing of the spectral edges due to the interplay of fluctuations of potential and non-potential disorder. The latter, represented by inhomogeneity in the concentration of magnetic impurities, affects the subgap DOS in two ways: via fluctuations of the pair-breaking strength and via induced fluctuations of the order parameter. In limiting cases, we reproduce previously reported results for the subgap DOS in disordered superconductors with strong magnetic impurities.

Support by RFBR Grant No. 13-02-01389 is acknowledged.

[1] Yakov V. Fominov, Mikhail A. Skvortsov, *Phys. Rev. B*, **93** (2016) 144511.

4RP-D-4

**MAGNETIC DISORDER IN SUPERCONDUCTORS: ENHANCEMENT BY
MESOSCOPIC FLUCTUATIONS***Burmistrov I.S.^{1,2}, Skvortsov M.A.^{2,1}*¹ L.D. Landau Institute for Theoretical Physics, Kosygina street 2, 117940 Moscow, Russia² Skolkovo Institute of Science and Technology, 143026 Moscow, Russia

burmi@itp.ac.ru

We study the density of states (DOS) and the transition temperature in a dirty superconducting film with rare classical magnetic impurities of an arbitrary strength described by the Poissonian statistics. We take into account that the potential disorder is a source for mesoscopic fluctuations of the local DOS, and, consequently, for the effective strength of magnetic impurities. We find that these mesoscopic fluctuations result in a non-zero DOS for all energies in the region of the phase diagram where without this effect the DOS is zero within the standard mean-field theory. This mechanism can be more efficient in filling the mean-field superconducting gap than rare fluctuations of the potential disorder (instantons). Depending on the magnetic impurity strength, the suppression of the transition temperature by spin-flip scattering can be faster or slower than in the standard mean-field theory. The results are published in Ref. [1].

The research was supported by Skoltech NGP Program (Skoltech--MIT joint project).

[1] I.S. Burmistrov, M.A. Skvortsov, *arXiv:1703.02126*.

4TL-D-5

STM INVESTIGATION OF TOPOLOGICAL SUPERCONDUCTIVITY IN SUPERCONDUCTING-FERROMAGNETIC HYBRID SYSTEMS

Cren T.¹, Ménard G.C.¹, Guissart S.², Brun C.¹, Trif M.², Debontridder F.¹, Leriche R.T.¹, Demaille D.¹, Roditchev D.¹, Simon P.²

¹Institut des *NanoSciences* de Paris, CNRS & Sorbonne University

²Laboratoire de *Physique* des Solides, CNRS & Saclay University

tristan.cren@upmc.fr

Majorana fermions are very peculiar quasiparticles that are their own antiparticle. They obey non-abelian statistics: upon exchange, they behave differently from fermions (antisymmetric) and bosons (symmetric). Their unique properties could be used to develop new kind of quantum computing schemes. Majorana states are predicted to appear as edge states of topological superconductors, in a similar way as Dirac surface states appears at the edge of topological insulators. Spectroscopic signatures of Majorana bound states were first observed in one-dimensional (1D) InAs nanowires proximity-coupled to a bulk superconductor. Then Nadj-Perge et al. [1] have realized a chain of Fe adatoms on a Pb(110) that induce locally a 1D topological p-wave superconductivity as demonstrated by the appearance of Majorana bound states at the extremity of the Fe chain. The Majorana states are strongly localized; they appear only on a few atoms at the end of the magnetic chains which inhibits their manipulation.

A different strategy, using sizeable magnetic disks made of Cobalt buried under a superconducting monolayer of Pb/Si(111), allows to generate topological superconductivity in 2D. In this case dispersive edge states crossing the gap appears around the magnetic domains [2]. These spectroscopic features as signatures of a locally induced topological superconductivity in 2D Pb/Co/Si(111). This is at odds with the Fe chains whose edge states are intrinsically 0D and are thus characterized by non-propagative bound states. Indeed, in 2D systems one expects to get some propagative Majorana edge states around the topological domains since the edges have a 1D character. The edge states in 2D topological superconductors are analogous to the edge states in Quantum Spin Hall systems. However, there is a very fundamental difference here as the superconducting topological edge states have the specificity of being Majorana excitations. Superconducting vortices can be generated in topological domains; they support localized Majorana bound states in their core. Such Majorana vortex states have been the focus of numerous theoretical proposals for quantum computing schemes due to their non-Abelian anyonic nature. The manipulation of vortices in such 2D architecture may thus be an efficient way to do braiding experiments with Majorana bound states.

[1] S.Nadj-Perge, I.K.Drozhdov, J.Li, H.Chen, S.Jeon, J.Seo, A.H. MacDonald, B.A.Bernevig, A. Yazdani, *Science*, **346** (2014) 602.

[2] G.C. Ménard, S.Guissart, C.Brun, M.Trif, F.Debontridder, R.T.Leriche, D.Demaille, D.Roditchev, P.Simon, T.Cren, arXiv:1607.06353 (2016).

4RP-D-6

RATCHET BASED ON SIFS JOSEPHSON φ JUNCTION*Goldobin E.¹, Menditto R.¹, Weides M.², Kohlstedt H.³, Koelle D.¹, Kleiner R.¹*¹ University of Tübingen, Tübingen, Germany² Karlsruher Institut für Technologie, Karlsruhe, Germany³ University of Kiel, Kiel, Germany

gold@uni-tuebingen.de

We demonstrate experimentally the operation of a deterministic Josephson ratchet with tunable asymmetry [1]. The ratchet is based on a φ Josephson junction which is fabricated using superconductor-insulator-ferromagnet-superconductor (SIFS) heterostructure with a step-like thickness of the F-layer[2].

We demonstrate not only the idle ratchet effect but also the operation with a load, i.e. in the presence of the additional dc counter current trying to stop the ratchet. Under these conditions the ratchet produces a non-zero output power. We estimate the efficiency of ac current to dc voltage conversion using a general model for Josephson ratchets with hysteresis [3].

Support by Deutsche Forschungsgemeinschaft (DFG) is acknowledged.

[1] R. Menditto, et al. *Phys. Rev. E*, **94** (2016) 042202.

[2] H. Sickinger, et al. *Phys. Rev. Lett.*, **109** (2012) 107002.

[3] E. Goldobin, et al., *Phys. Rev. E*, **94** (2016) 032203.

4OR-D-7

ORIGIN OF THE ROTATIONAL SYMMETRY BREAKING MAGNETIC RESPONSE IN THE TOPOLOGICAL SUPERCONDUCTOR $\text{Cu}_2\text{Bi}_2\text{Se}_3$

Hakioğlu T.^{1,2}, Denizhan E.O.¹, Mehmet G.

¹ QTECH Research - Energy Institute, İstanbul Technical University, İstanbul, Turkey

² Department of Physics, İstanbul Technical University, İstanbul, Turkey

³ Department of Physics, Bilkent University, Ankara, Turkey

hakioğlu@itu.edu.tr

Topological superconductivity (TSC) arose as a field of research where a number of exotic structures that are known in high energy physics are expected to be found. One of the signatures of TSC is the zero energy bound states or the Majorana bound states that exist at the boundaries of the superconducting region, with the latter being a geometric boundary or the core of a spin-1/2 vortex. In this context, the discovery of topological insulators (TIs) has stimulated an intense research in this area. In particular, a three-dimensional strong TI with externally biased surface states separated by excitonic Bohr radius can couple excitonically which can then condense into a Topological Exciton Condensate (TEC). Although TEC has been suggested as a strong candidate for a TSC it has not been observed yet.

Recently number of new superconductors with anomalous properties have been observed by doping the topological insulator Bi_2Se_3 . Here doping is a mean of establishing a Fermi surface, alternative to electrostatically biased states in TEC, as an indispensable background for superconducting pairing. The breaking of the rotational symmetry and the appearance of a magnetic response concurring at the onset of superconductivity have been reported in the Nb, Sr and Cu-doped three dimensional topological insulator Bi_2Se_3 [1]. The breaking of the rotational symmetry is observed as the two and four-fold rotational symmetry of the inplane magnetization upon superconductivity induced by an in-plane external field does not conform with the trigonal point group symmetry of the underlying lattice. Furthermore, unexpected observation of the low-temperature exponential suppression in the specific heat of this strongly spin-orbit coupled system [2] reminds the recently observed BCS-like low temperature anomalies in certain NCSs [3]. There is currently no theoretical explanation about the mechanism(s) leading to these unconventional phenomena.

In this article we provide a theoretical explanation to this phenomena in $\text{M}_x\text{Bi}_2\text{Se}_3$ with $\text{M}=(\text{Cu}, \text{Sr}, \text{Nb})$ by showing that a time reversal symmetry preserving magnetic response is strongly correlated with a real out-of-plane component of the triplet state, hence odd parity is naturally imposed. We compare the effect of the tetragonal and hexagonal/trigonal lattice symmetry and show that while the former breaks the TRS, the latter can accommodate a real TRS preserving triplet producing a rotational symmetry breaking magnetic response.

[1] Tomoya Asaba, et.al., **ArXiv**: 1603.04040 (2016); K. Matano, M.Kriener, K. Segawa, Y. Ando, Guo-qing Zheng, *Nat. Sci.Rep.*, **6** (2016) 28632; L. Fu, *Phys. Rev.*, **B 90** (2014) 100509; Z. Liu, X. Yao, J. Shao, M. Zuo, L. Pi, S. Tan, C. Zhang, *J. Am. Chem. Soc.*, **107** (2015) 10512; Y. Pan, A. M. Nikitin, G. K. Araizi, Y. K. Huang, Y. Matsushita, T. Naka and A. de Visser, *Nature*, **6** (2016) 28632.

[2] Kriener, M., Segawa, K., Ren, Z., Sasaki, S. and Y. Ando, *Phys. Rev. Lett.*, **106** (2011) 127004; N. Levy, T. Zhang, J. Ha, F. Sharifi, A. A. Talin, Y. Kuk, and J.A. Stroscio, *Phys. Rev. Lett.*, **110** (2013) 117001.

[3] Mehmet Gunay, T. Hakioğlu and H.H. Somek, *J. Phys. Soc. Japan*, **86** (2017) 034713.

4RP-D-8

MAJORANA FERMIONS IN THE COEXISTENCE PHASE OF NONCOLLINEAR MAGNETIC ORDERING AND CHIRAL SUPERCONDUCTIVITY

Val'kov V.V., Zlotnikov A.O., Shustin M.S.

Kirensky Institute of Physics, Federal Research Center KSC SB RAS, Krasnoyarsk, Russia
vzv@iph.krasn.ru

It is widely believed that in the presence of the magnetic field Majorana zero modes can be implemented in spin-singlet superconductors due to spin-orbit coupling [1, 2]. The assumption about a new example of systems with the coexistence of the noncollinear magnetic ordering on a triangular lattice and the chiral superconductivity supporting the Majorana fermions has been discussed in paper [3]. It should be noted that the chiral superconducting state is a state with the time-reversal symmetry breaking and nontrivial topology itself [4].

It has been established that in the presence of the stripe spin structure on the triangular lattice the superconducting order parameter does not have the chiral structure [5]. Thus, we describe conditions of appearance of the Majorana zero modes in the coexistence phase of the 120° spin order and the $d_{x^2-y^2} + id_{xy}$ -wave superconductivity preserving the chiral symmetry (see Fig. 1).

In systems with coexisting magnetism and superconductivity, the strong electron correlations may play important role. Therefore, in this work we take into account the strong correlations in the above-mentioned coexistence phase of the triangular lattice. It is shown that the topology of the ground state is described by the topological invariant in terms of the Green functions proposed in Ref. [6]. The existence of the topological transition upon doping in the coexistence phase is found. One of the features is that the topological transition occurs only for the gapless excitations in the coexistence phase with the vanished superconducting order parameter. It is shown that the Majorana fermions may exist in the nontrivial coexistence phase of the 120° noncollinear magnetism and chiral superconductivity of the systems with strong electron correlations.

This study was funded by RFBR, Government of Krasnoyarsk Territory, Krasnoyarsk Science and Technology Support Fund according to the research projects Nos. 16-02-00073-a, 16-42-243069-r-mol-a. A.O.Z. is grateful for support the Council of the President of the Russian Federation (project no. SP-1370.2015.5).

- [1] J.D. Sau, R.M. Lutchyn, S. Tewari, S.D. Sarma *Phys. Rev. Lett.*, **104** (2010) 040502.
- [2] M. Sato, S. Fujimoto *Phys. Rev. Lett.*, **105** (2010) 217001.
- [3] Y.-M Lu, Z. Wang *Phys. Rev. Lett.*, **110** (2013) 096403.
- [4] G.E. Volovik *JETP Letters*, **66** (1997) 522.
- [5] V.V. Val'kov, A.O. Zlotnikov *JETP Letters*, **104** (2016) 483.
- [6] G.E. Volovik, V.M. Yakovenko *J. Phys. Condens. Matter*, **1** (1989) 5263.

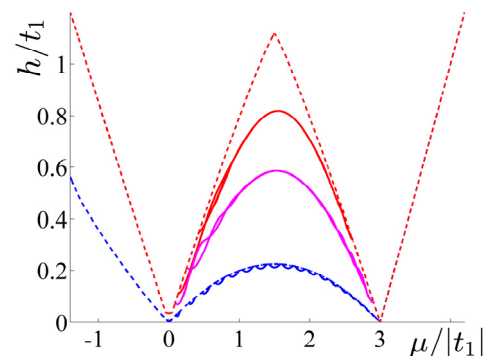


Fig. 1. The parameter lines (solid lines) supporting Majorana fermions on the phase diagram in variables μ (the chemical potential) and h (the exchange field) for different values of the superconducting order parameter.

4RP-D-9

RELATIVISTIC MOTT INSULATOR, SUPERCONDUCTIVITY, AND OTHER EXOTIC STATES IN TRANSITION METAL OXIDES WITH A LARGE SPIN-ORBIT COUPLING

Yunoki S.^{1,2,3}¹ Computational Condensed Matter Physics Laboratory, RIKEN, Wako, Saitama 351-0198, Japan² Computational Quantum Matter Research Team, RIKEN Center for Emergent Matter Science (CEMS), Wako, Saitama 351-0198, Japan³ Computational Materials Science Research Team, RIKEN Advanced Institute for Computational Science (AICS), Kobe, Hyogo 650-0047, Japan
yunoki@riken.jp

Motivated by recent experiments of novel 5d Mott insulators such as Sr_2IrO_4 and Na_2IrO_3 , we have studied theoretically the two-dimensional three-orbital Hubbard model with a strong spin-orbit coupling for $(t_{2g})^5$ local electron configurations on square and honeycomb lattices.

The variational Monte Carlo method and the dynamical mean field theory are used to obtain the ground state phase diagram for $(t_{2g})^5$ local electron configuration on the square lattice with varying a on-site Coulomb interaction U as well as the spin-orbit coupling. It is found that the transition from a paramagnetic metal to an antiferromagnetic (AF) insulator occurs at a finite $U = U_{\text{MI}}$, which is greatly reduced by a large spin-orbit coupling, characteristic of 5d electrons, and leads to the spin-orbit-induced relativistic Mott insulator. It is also found that the Hund's coupling induces the anisotropic spin exchange and stabilizes the in-plane AF order. We have further studied the single-particle excitations using the variational cluster approximation and the dynamical mean field theory, and revealed the internal electronic structure of this novel relativistic Mott insulator, i.e., the effective total angular momentum $J_{\text{eff}}=1/2$ Mott insulator. We have estimated the magnetic exchange coupling and found that it can be as large as 50-100 meV. These findings are in agreement with experimental observations for Sr_2IrO_4 and very similar to mother compounds for high T_c cuprate superconductors except that the latter is spin $S=1/2$ Mott insulator. It is therefore expected that a possibly high T_c superconductivity can be induced once mobile carriers are introduced into the $J_{\text{eff}}=1/2$ Mott insulator. We have considered this possibility using the variational Monte Carlo method as well as RPA and found that indeed the superconductivity with d -wave pairing is most likely induced by electron doping, but not hole doping. We also discuss the similarity in the single-particle excitations between iridates and cuprates, including pseudogap behavior, and other related systems. In addition, we will discuss more interesting exotic ground states such as excitonic insulator and quadrupole order for $(t_{2g})^4$ local electron configuration.

This work has been in collaboration with H. Watanabe, T. Shirakawa, T. Sato, K. Nishiguchi, B. H. Kim, K. Seki, W. Fan, and H. Sakakibara.

- [1] H. Watanabe, T. Shirakawa, and S. Yunoki, *Phys. Rev. Letts.*, **105** (2010) 216410.
- [2] H. Watanabe, T. Shirakawa, and S. Yunoki, *Phys. Rev. Letts.*, **110** (2013) 027002.
- [3] H. Watanabe, T. Shirakawa, and S. Yunoki, *Phys. Rev. B*, **89** (2014) 165115.
- [4] T. Sato, T. Shirakawa, and S. Yunoki, *Phys. Rev. B*, **91** (2015) 125122.
- [5] A. Yamasaki, H. Fujiwara, S. Tachibana, et al., *Phys. Rev. B*, **94** (2016) 115103.
- [6] Q. Cui, J.-G. Cheng, W. Fan, et. al., *Phys. Rev. Letts.*, **117** (2016) 176603.
- [7] B. J. Kim, T. Shirakawa, and S. Yunoki, *Phys. Rev. Letts.*, **117** (2016) 187201.
- [8] T. Sato, T. Shirakawa, and S. Yunoki, arXiv: 1603.02369.

4RP-D-10

QUASICLASSICAL THEORY OF SUPERCONDUCTING HETEROSTRUCTURES WITH STRONG INHOMOGENEOUS FERROMAGNETS

Bobkova I.V.^{1,2}, *Bobkov A.M.*¹, *Silaev M.A.*³

¹ Institute of Solid State Physics, Chernogolovka, Russia

² Moscow Institute of Physics and Technology, Dolgoprudny, Russia

³ Department of Physics and Nanoscience Center, University of Jyväskylä, Finland
bobkova@issp.ac.ru

We develop a theory of the superconducting proximity effect in S/F heterostructures with strongly spin-polarized ferromagnets. So far, proximity and transport calculations in SC/FM hybrids have mostly concentrated on either fully polarized FMs, so called half metals, or on the opposite limit of weakly polarized systems. However, most FMs have an intermediate exchange splitting of the energy bands of the order of 0.2–0.8 times the Fermi energy. The quasiclassical theory for superconducting hybrids with such strongly spin-polarized ferromagnets has already been formulated for the case of homogeneous magnetization of the FM [1]. Here we consider the case of an arbitrary slow magnetic inhomogeneity and formulate the theory in terms of the quasiclassical Eilenberger or Usadel equations supplied by the corresponding boundary conditions at the S/F interface. The boundary conditions are derived microscopically without making use of the phenomenological scattering matrices [1]. The spin-orbit coupling, which can be relevant for the systems with lack of inversion symmetry, is also included into the theory.

On the basis of the developed formalism we consider a number of particular S/F systems. It is demonstrated that in S/F hybrids with inhomogeneous strongly spin-polarized FMs the magneto-electric effects, such as the so-called φ_0 - junctions and spontaneous electric currents, are possible under quite general conditions. For a general case we find a particular component of the magnetic inhomogeneity, which acts as an electromagnetic vector potential. We demonstrate that this effective vector potential is spin-dependent. Due to this reason it causes the spontaneous electric currents only under the condition that the exchange splitting is not much smaller than the Fermi energy. For this reason studies of the diffusive Josephson junctions through various structures, based on inhomogeneous weakly-polarized ferromagnets, including helix, magnetic vortex and skyrmion [2-4], have shown no ground state phase shifts different from 0 and π , and only for the systems with half-metallic elements and in junctions between magnetic superconductors with spin filters a finite anomalous current has been predicted [5-8].

- [1] R. Grein *et al.*, *Phys. Rev. Lett.*, **102** (2009) 227005.
- [2] A. F. Volkov, A. Anishchanka, and K. B. Efetov, *Phys. Rev. B*, **73** (2006) 104412.
- [3] M.S. Kalenkov, A.D. Zaikin, V.T. Petrashov, *Phys. Rev. Lett.*, **107** (2011) 087003.
- [4] T. Yokoyama, J. Linder, *Phys. Rev. B*, **92** (2015) 060503(R).
- [5] V. Braude, Yu.V. Nazarov, *Phys. Rev. Lett.*, **98** (2007) 077003.
- [6] S. Mironov, A. Buzdin, *Phys. Rev. B*, **92** (2015) 184506.
- [7] A. Moor, A. F. Volkov, and K. B. Efetov, *Phys. Rev. B*, **92** (2015) 180506(R); A. Moor, A.F. Volkov, and K. B. Efetov, *Phys. Rev. B*, **92** (2015) 214510.
- [8] M.A. Silaev, I.V. Tokatly, and F.S. Bergeret, arXiv:1702.00056.

4OR-D-11

PROXIMITY EFFECTS IN A HELICAL METAL BASED S/F HETEROSTRUCTURES

Bobkova I.V.^{1,2}, Bobkov A.M.¹

¹ Institute of Solid State Physics, Chernogolovka, Russia

² Moscow Institute of Physics and Technology, Dolgoprudny, Russia
bobkov@issp.ac.ru

We study the effective superconducting order parameter and the condensate wave function, induced in a three-dimensional topological insulator (TI) by proximity to an s-wave superconductor (S) in presence of an external magnetic field or a magnetic moment, when a superconductor/ferromagnet insulator (S/FM) hybrid structure is formed on the TI surface. We perform a symmetry analysis of the induced superconductivity and find that under an applied parallel magnetic field all possible pairings, allowed by the Pauli principle, are present due to the helical nature of the underlying conducting surface state of the TI. It is found that in the presence of the magnetic field the helical nature of the surface states manifests itself not only in the condensate wave function, as it was known previously [1-5], but also in the structure of the effective order parameter, which acquires an odd-frequency component. We discuss possible experimental manifestations of the proximity induced pairing state.

We also analyze the S/F/S Josephson junction formed on the surface of the TI and show that here the helical nature of the conducting surface electrons leads to the strong dependence of the critical current on the direction of the interlayer magnetization, in contrast to the standard S/F/S junction there the value of the critical current is only determined by its magnitude [6].

- [1] J. Linder *et.al*, *Phys. Rev. B*, **81** (2010) 184525.
- [2] M. Snelder *et.al*, *J. Phys.: Condens. Matter*, **27** (2015) 315701.
- [3] M. Snelder *et.al*, *Phys. Rev. B*, **87** (2013) 104507.
- [4] P. Burset *et.al*, *Phys. Rev. B*, **92** (2015) 205424.
- [5] A.S. Vasenko *et.al*, arXiv:1606.00905.
- [6] A. I. Buzdin, *Rev. Mod. Phys.*, **77** (2005) 935.

4RP-D-12

METALLIC FINE CONTAMINANT DETECTION TECHNIQUE USING A SECOND HARMONIC RESPONSE

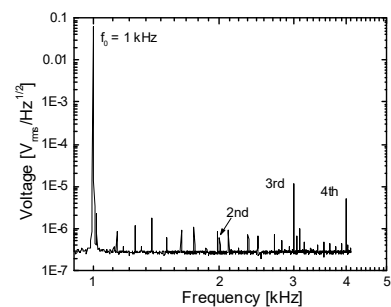
Tanaka S.¹, Ohtani T.¹, Kikuchi M.²

¹ Toyohashi University of Technology, 1-1 Hibarigaoka Tempaku-cho Toyohashi, Aichi 441-8580 Japan

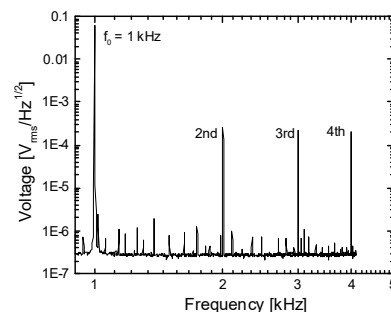
² Nikka Densok Limited, 710 Shimo-akasaka, Kawagoe, Saitama 350-1155 Japan

There is a possibility that small metallic contaminants could be mixed with industrial products made of ceramics or plastic resin. If this event occurs in a battery production line, it may result in a recall because of the possibility of, in the worst case, fire. Consequently, a detection system for fine metallic contaminants is required. Presently, there are conventional methods such as eddy current detection. However, with this method sensitivity is too low for stainless steel because of its low conductivity.

We have developed a fine stainless steel contaminant detection technique for industrial products. An excitation ac magnetic field with a frequency of 1 kHz and a dc bias field were applied [1, 2]. In each of the ac and dc fields a single pair of differential pickup coils was placed [3, 4]. The output signals of the pickup coils were recorded by a spectrum analyzer (Agilent 35670A). A stainless steel (304) wire with dimensions of $\phi 0.2 \times 5$ mm was prepared as a specimen. The signal is highly affected by the $M-H$ characteristics of the specimen. The ac excitation field and the dc bias field were varied and optimized to obtain a larger second harmonic signal. Figure 1 shows spectra of the output signals. In the case of without specimen (a), a small peak of a 2nd harmonic can be seen but not a small peak of the 3rd harmonic. When a specimen was placed in the pickup coil, both the 2nd and 3rd peaks dramatically increased as shown in Fig. 1(b) due to the non-linearity of the $M-H$ characteristics of the specimen. The differential peak signal of the 2nd harmonic is larger than that of the 3rd harmonic. This result demonstrates the advantage of using this technique for stainless steel contaminant detection.



(a) without specimen.



(b) with specimen.

Fig.1. Spectrum of the response. A stainless wire chip was used as a specimen.

[1] B. Gleich and J. Weizenecker, *Nature*, **435** (2005) 1214-1217.

[2] T. Yoshida, K. Ogawa, T. Tsubaki, and N. B. O. a. K. Enpuku, *IEEE Trans. Magn*, **47** (2011) 2863-2866.

[3] Yi Zhang, Hayaki Murata, Yoshimi Hatsukade and Saburo Tanaka, *Review of Scientific Instruments*, **84** (2013) 094702.

[4] Saburo Tanaka, Toshifumi Suzuki, Kazuya Kobayashi, Shu-Hsien Liao, Heng-Er Horng and Hong-Chang Yang, *Journal of Magnetism and Magnetic Materials*, (2017) <http://dx.doi.org/10.1016/j.jmmm.2016.12.067>.

4OR-LT-5

DYNES SUPERCONDUCTORS - GAPLESS ULTRATHIN SUPERCONDUCTING FILMS

*Hašková V.¹, Szabó P.¹, Žemlička M.¹, Samuely T.¹, Kačmarčík J.¹, Lotnyk D.¹, Komanický V.¹,
Grajcar M.², Samuely P.¹*

¹ Centre of Ultra Low Temperature Physics, Institute of Experimental Physics, Slovak Academy of Sciences & P. J. Šafárik University, Košice, Slovakia

² Department of Experimental Physics, Comenius University, Bratislava, Slovakia
samuely@saske.sk

Superconducting films of MoC and MoN are prepared down to the thickness of 3 nm on different substrates. The superconducting transition temperature T_c is decreasing with the film thickness and the thinnest films approach to the superconductor-insulator transition which is characterized by the Ioffe-Regel product $k_F l$ close to unity. By means of a sub-kelvin scanning tunneling microscope we study the spatial homogeneity of the superconducting energy gap Δ with an atomic spatial resolution. The suppression of the both T_c and Δ depends in a particular film also on a used substrate. In the ultrathin samples the in-gap states in the superconducting density of states (DOS) appear [1]. Such DOS can be perfectly described by the Dynes version of the BCS formula with $N(\varepsilon) = N_0 \text{Re}[\varepsilon'^2 / (\varepsilon'^2 - \Delta^2)]$, where $\varepsilon' = \varepsilon + i\Gamma$ is a complex energy and Γ the broadening parameter [2]. The in-gap states are confirmed by significant losses observed in our microwave measurements performed on co-planar waveguide resonators made of the MoC ultrathin films [3]. The origin of the in-gap states is unknown. The theoretical model [4] shows that the phenomenological Dynes formula has been a physical realization of the so called “Dynes superconductors” with a Lorentzian distribution of pair-breaking fields and arbitrary potential disorder. Such pair-breaking fields can be materialized by local magnetic moments/magnetic impurities and/or fluctuating order parameter. Here, we show that the broadening parameter Γ in the tunneling DOS depends not only on the thickness of the superconducting film but also on the substrate. We discuss a possible origin of magnetic moments which can appear at the interface between the superconducting films and the substrate.

Support by APVV-14-0605, VEGA 2/0135/13, VEGA 1/0409/15 is acknowledged.

[1] P. Szabó et al., *Phys. Rev. B.*, **93** (2016) 014505.

[2] R. C. Dynes, V. Narayanamurti, and J. P. Garno, *Phys. Rev. Lett.*, **41** (1978) 1509.

[3] M. Žemlička et al., *Phys. Rev. B.*, **92** (2015) 224506.

[4] F. Hermann and R. Hlubina, *Phys. Rev. B.*, **94** (2016) 144508.

4TL-LT-6

A CONDUCTING FILAMENT NETWORK AS A PRECURSOR TO THE ORIGIN OF SUPERCONDUCTIVITY IN ELECTRON-DOPED COPPER OXIDES

Yu H.¹, He G.¹, Lin Z.², Kusmartseva A.⁴, Yuan J.¹, Zhu B.¹, Yang Yi-feng^{1,3}, Xiang T.^{1,3}, Li L.², Wang J.², Kusmartsev F.V.⁴, Kui Jin^{1,3}

¹ Beijing National Laboratory for Condensed Matter Physics, Institute of Physics, Chinese Academy of Sciences, Beijing 100190, China

² Wuhan National High Magnetic Field Center (WHMFC), Huazhong University of Science and Technology, Wuhan 430074, China

³ Collaborative Innovation Center of Quantum Matter, Beijing, 100190, China

⁴ Department of Physics, Loughborough University, Loughborough LE11 3TU, United Kingdom
F.Kusmartsev@lboro.ac.uk

Emergence of superconductivity at the instabilities of antiferromagnetism (AFM), spin/charge density waves has been widely recognized in unconventional superconductors. In cuprates, spin fluctuations play a predominant role in superconductivity with electron dopants. The existence of an AFM critical endpoint is still in controversy for different probes.] Here, by tuning the oxygen content, a systematic study of the Hall signal and magnetoresistivity up to 58 Tesla on optimally doped $\text{La}_{2-x}\text{Ce}_x\text{CuO}_{4\pm\delta}$ ($x = 0.10$) thin films identifies two characteristic temperatures at 62.5 ± 7.5 K and 25.0 ± 5 K. The former is quite robust, whereas the latter becomes flexible with increasing magnetic field, thereby linking respectively to two- and three- dimensional AFM, evident from the multidimensional phase diagram as a function of oxygen and Ce dopants, Fig. 1. Consequently, the observation of an extended AFM phase in contrast to μSR reports together with the analysis of the presented data suggest the existence of conductive filamentary nanostructures that corroborate elevated critical doping in field. The new findings provide a consistent alternative picture in understanding the interactions between AFM and superconductivity in electron-doped cuprates.

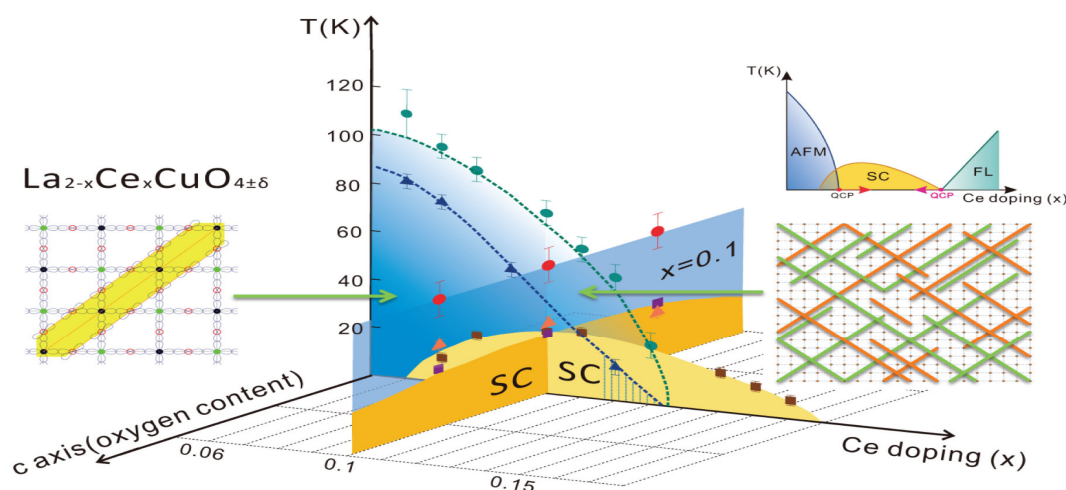


Fig. 1. A multidimensional phase diagram of LCCO as a function of Ce and oxygen content. Along the Ce doping axis, the AFM boundary (blue area) is determined by transport measurement in a magnetic field. Specifically, the border of the two-dimensional AFM regime is established by in-plane angular magnetoresistance measurements (green spheres). This region exhibits strong electron-electron correlations at small doping levels, so that spin-orbital (SO) polarons can arise. A SO polaron is created when a doped electron polarizes free (non-bonded with Cu) p-orbitals of the oxygen atoms nearest to the few copper sites that have the same spin orientation. The polarized orbitals are shown in yellow (the left inset).

4RP-LT-7

THE THEORY OF LONG-RANGE JOSEPHSON CURRENT THROUGH A SINGLE-CRYSTAL FERROMAGNET NANOWIRE

Proshin Yu.N., Avdeev M.V.

Theoretical Physics Department, Kazan Federal University, Kazan, Russia
yurii.proshin@kpfu.ru

It is well known [1-3] that in superconductor - ferromagnet (SF) junctions, the spin-singlet Josephson supercurrent can flow through F weak-link, rapidly decaying within few nanometers. On the other hand, the spin triplet component can penetrate at the large distance in F metal due to the long-range proximity effect. This situation can be realized in multilayered FS structures with inhomogeneous magnetization in F layers [4-7], in the presence of a spin-active interface or domain walls [8,9]. However, an occurrence of the long-range Josephson current through a single-crystal, monodomen ferromagnetic nanowire, is surprisingly reported in experiment [10]. The most striking feature [10] were that the spatial extent of the proximity effect was equal to about 600 nm, and the critical current I_c was 12 μ A at zero magnetic field for 40 nm-diameter Co nanowire. It was the first observation of the spin-singlet long-range proximity effect for clean SFS system. Further, the theoretical model proposed in [11] showed that the long-range spin-singlet superconducting correlations might be due to the spin-orbit interaction in nanowire. In ballistic regime it can result in the long-range contribution to the supercurrent [11], providing that the distances between successive quasiparticle reflections from the nanowire surface should be equal.

We propose different theoretical model of the singlet long-range Josephson transport. Taking into account the anisotropy of the Fermi surface of the hexagonal close-packed Co monocrystal, we show that the mismatch of the electron effective mass of majority and minority spin bands can lead to “effective” renormalized exchange interaction, which becomes dependent on the direction of the quasiparticle momentum in nanowire. Based on the Eilenberger-like equations with a renormalized effective exchange interaction we calculate the critical Josephson current flow through nanowire. It is shown that, the effective exchange field must be completely compensated under certain conditions and, thereby it leads to long-range spatial extent of the supercurrent. Thus, the long-range proximity effect observed in Co single-crystalline nanowire [10] can be quantitatively explained within the proposed theoretical framework.

The work is supported by the subsidy allocated to Kazan Federal University for performing the project part of the state assignment in the area of scientific activities (# 3.2166.2017). YP is also thankful by the RFBR (16-02-01016) for partial support.

- [1] Y. Izyumov, Y. Proshin, M. Khusainov, *Physics-Uspekhi*, **45** (2002) 109.
- [2] A.I. Buzdin, *Rev. Mod. Phys.*, **77** (2005) 935.
- [3] F.S. Bergeret, A.F. Volkov, K.B. Efetov, *Rev. Mod. Phys.*, **77** (2005) 1321.
- [4] Y.V. Fominov, A.A. Golubov, M.Y. Kupriyanov, *JETP Letters*, **77** (2003) 510.
- [5] Y.V. Fominov, A.A. Golubov, T.Y. Karminskaya, *et al.*, *JETP Letters*, **91** (2010) 308.
- [6] P.V. Leksin, N.N. Garif'yanov, A.A. Kamashev, *et al.*, *Phys. Rev. B*, **91** (2015) 214508.
- [7] A. Singh, S. Voltan, K. Lahabi, *et al.*, *Phys. Rev. X*, **5** (2015) 021019.
- [8] J. Linder, M. Cuoco, A. Sudbo, *Phys. Rev. B*, **81** (2010) 174526.
- [9] A.I. Buzdin, A.S. Mel'nikov, N.G. Pugach, *Phys. Rev. B*, **83** (2011) 144515.
- [10] J. Wang, M. Singh, M. Tian, *et al.*, *Nature Physics*, **6** (2010) 389.
- [11] A.S. Mel'nikov, A.V. Samokhvalov, S.M. Kuznetsova, *et al. Phys. Rev. Lett.*, **109** (2012) 237006.

4OR-LT-8

INTERPLAY BETWEEN MAGNETISM AND SUPERCONDUCTIVITY IN METALLIC HYDROGEN AND HYDRIDES AT HIGH PRESSURES

Mazov L.S.¹

¹ Institute for Physics of Microstructures, Russian Academy of Sciences, N.Novgorod, Russia
mazov@ipm.sci-nnov.ru

Recently, it was claimed [1] that metallic hydrogen has been created for the first time. Such result was obtained under ultrahigh pressure of the order of 500 GPa and at helium temperatures. Such conclusion was only made on reflectivity properties of the hydrogen sample, while resistivity measurements were not performed. But as it was studied theoretically before, the metallic state of monoatomic hydrogen at such high pressures should possess by both superconducting (SC) and magnetic properties - on the one hand metallic hydrogen is considered as a potential room-temperature SC but on the other hand it is suspicious for ferromagnetism due to spontaneous magnetization. In addition, as it is followed from theoretical analysis under phase transition from molecular hydrogen phase to monoatomic one the layered structure like graphite is formed in intermediate phase. As it was demonstrated before the conditions for metallic state are essentially easier in hydrides. Such results were obtained for hydrogen sulfides where metallic (linear) behavior of resistivity was observed down to ~ 200 K [2]. The onset of resistive transition below this temperature was treated in [2] as SC in nature. Moreover, this SC was considered as high- T_c conventional one. Here, the detailed analysis of experimental resistive data for hydrogen sulfides is performed on the basis of a Weiss-Marotta approach, characteristic for magnetic metals. The results indicate that the magnetic AF spin-fluctuation (SF) scattering of mobile charge carriers provides a significant part (shaded area in Fig.1), additional to phonon one (Bloch-Gruneisen (BG) curve) in the total normal-state resistivity.

The disappearance of AF SF scattering with decreasing temperature in fact denotes the formation of modulated magnetic (AF SDW-like) structure in the plane of the sample. Such planar character of the effect is supported by recent theoretical models of hydrides [2]. The measurements of magnetization is consistent with resistivity ones for AF ordered metals and compounds. In result, critical temperature of SC transition appears to be essentially lower than 200 K. Anisotropy of NRS spectra of hydrogen sulfide in transverse magnetic field [2] also supports the magnetic nature of resistive transition at ~ 200 K. In conclusion, SC transition in sulfur hydrides can occur only after completion of magnetic (AF SDW) phase transition (cf.[3]).

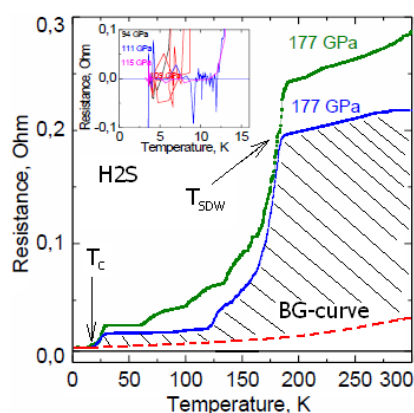


Fig. 1. Magnetic (AF SDW) phase transition and SC one for hydrogen sulfide (see, e.g. [2]). Insert: low-temperature (noise) part of the total resistivity.

[1] R.P.Dias, I.F.Silvera // Science DOI: 10.1126/science.aal1579 (2017).

[2] M.I.Eremets, A.P.Drozdov, *Usp.Fiz.Nauk*, **186** (2016) 1257–1263.

[3] L.S.Mazov, in: *14th Conf. "Strongly correlated electron systems and quantum critical phenomena"* (Inst.for High Press. Phys. RAS, Troitsk-Moscow, 2016), *Abstr.Book*, 17.

4OR-LT-9

INTERPLAY BETWEEN MAGNETIC AND SUPERCONDUCTING ORDERS IN LAYERED HTSC COMPOUNDS

Timirgazin M.A., Gilmutdinov V.F., Arzhnikov A.K.

Physical-Technical Institute of Ural Branch of RAS, Izhevsk, Russia
timirgazin@gmail.com

At the moment, a number of materials has been experimentally discovered in which microscopic coexistence of superconductivity and magnetic ordering or macroscopic phase separation between these states is realized. Despite the obvious importance of this phenomenon for understanding the nature of superconductivity and its relationship with magnetism, there is no theory that would include both the coexistence and the separation of magnetic and superconducting orders with different symmetries.

In this work we consider a single-band model based on the Hubbard Hamiltonian, which also takes into account the superconducting attraction of electrons located at neighboring sites. Mean-field equations are obtained that allow to take into account both the phase separation and the coexistence of the superconducting and magnetic phases. An advantage of our approach is the consideration of the widest possible range of superconducting and magnetic states. We take into account not only the traditional *s*- and *d*-wave symmetries of the superconducting order parameter, but also the mixed *s+id* symmetry, which is proposed in the literature for the interpretation of some experimental data. The magnetic order is considered as an incommensurate spin-spiral structure with an arbitrary wave vector, and the ferro- and antiferromagnetic phases are particular cases of the spiral state.

At the first stage, the superconducting order was studied without taking into account magnetism, and a phase diagram of the ground state of the model was constructed in the variables of the ratio between the next-nearest and nearest neighbors electron transfer integrals t'/t and the electron concentration n . It is shown that besides pure *s*- and *d*-wave solutions, an intermediate *s+id*-wave symmetry is also realized in a wide range of parameters.

At the next stage, magnetism was added to the model and calculations were made for the values of t'/t corresponding to high-temperature cuprate superconductors. It was found that, depending on the parameters of the Hubbard repulsion and the superconducting attraction of electrons, both the separation and coexistence between superconducting and magnetic phases with different symmetries can be realized. For all the parameters studied the microscopic coexistence was obtained to be more energetically favorable than macroscopic phase separation. The interplay between superconductivity and magnetism allows to reproduce the dome-shaped doping dependence of the superconducting order parameter. The boundaries of phase transitions between different phases are calculated, and the experimental data are interpreted.

This work is supported by Ural Branch of RAS in project 15-8-2-12, and by Russian Foundation of Basic Research in projects of 16-02-00995 and 16-42-180516.

4OR-LT-10

SUPERCONDUCTING MESA-STRUCTURES WITH A SPIN FILTERING MANGANITE INTERLAYER

*Constantinian K.Y.¹, Ovsyannikov G.A.¹, Kislinskii Y.V.¹, Demidov V.V.¹, Shadrin A.V.¹,
Petrzhik A.M.¹*

¹ Kotel'nikov Institute of Radio Engineering and Electronics RAS, Moscow, Russia
karen@hitech.cplire.ru

We report on current transport and magnetism in hybrid superconducting mesa-structures prepared from epitaxial thin films of cuprate superconductor $\text{YBa}_2\text{Cu}_3\text{O}_{7-\delta}$ (YBCO) and manganite LaMnO_3 (LMO) grown on the NdGaO_3 substrate. Nb film was used as a top superconducting electrode. Measurements of magnetic resonance in heterostructure Au/LMO/YBCO (without Nb) showed ferromagnetic state at temperature $T=150$ K, as in the case of the autonomous LMO film. The tunneling barrier heights evaluated from conductivity of mesa-structures showed an exponential decrease with increase of manganite thickness (d_M). Temperature dependence of the conductivity in the range $T_c' < T < T_c$ (T_c' and T_c are critical temperatures for Nb and YBCO, correspondingly) could be described taking into account the d-wave nature of superconductivity of YBCO film and a spin filtering affecting the electron transport through the tunneling barrier. Spin filtering is supported also by measurements of tunneling magneto-resistance and a high sensitivity to weak external magnetic field. Mesa-structures did not show superconducting critical current even at reduced temperature $T=300$ mK and the smallest LMO thickness ($d_M=5.6$ nm). Varying the external weak magnetic field $|H| < 10$ Oe and dc bias current, using low noise microwave amplifier, the microwave generation with a linewidth of order 50 MHz was observed in GHz frequency band. Possible physical mechanisms of observed microwave oscillations and the impact of spin filtering of charge current are discussed taking into account the asymmetry of oscillation amplitudes over applied H -field. The frequency of generation could be tuned by biasing current with a rate 10^{13} Hz/A.

Support by RAS, RFBR 16-29-14022, 17-02-00145, and Sci. School 8168.2016.2 is acknowledged.

4OR-LT-11

MAGNETOTRANSPORT PROPERTIES OF FeSe IN FIELDS UP TO 50 T

Ovchikov Y.A.¹, Chareev D.A.², Kulbachinskii V.A.¹, Kytin V.G.¹, Presnov D.E.^{1,3}, Skourski Y.⁴, Volkova O.S.¹, Vasiliev A.N.¹

¹ Faculty of Physics, Moscow State University, Moscow, Russia

² Institute of Experimental Mineralogy, RAS, Chernogolovka, Russia

³ Skobeltsyn Institute of Nuclear Physics, Moscow State University, Moscow, Russia

⁴ Dresden High Magnetic Field Laboratory (HLD-EMFL), HZDR, Dresden, Germany
ovtchenkov@mig.phys.msu.ru

FeSe is a very important and promising superconducting material with unusual electronic and transport properties. We report on the transport properties of a high-quality single crystal studied in a wide temperature range in a pulsed magnetic field up to 50 T.

A picture of the studied crystal is shown in the inset of Fig.1. The calculated ratio of the resistivity at 300 K to the resistivity at 10 K is about 35 which reflects a high quality of the sample. The $R(B)$ dependence measured at 1.5 K (Fig.1) in fields up to 50 T demonstrates a clear superconducting to normal state transition near 8-9 T and a further increase of the resistivity more than 12 times without saturation.

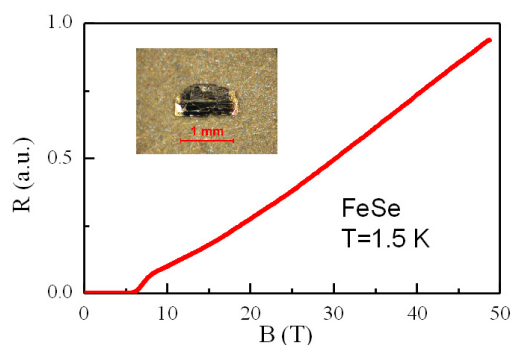


Fig.1 Field dependence of the resistance at 1.5 K. The inset shows a picture of the FeSe crystal studied.

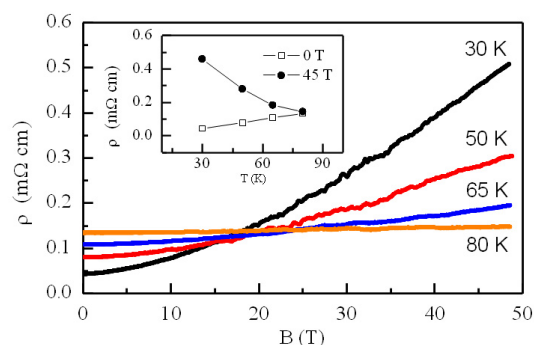


Fig.2 Field dependencies of the resistivity measured at different temperatures. The inset shows the extracted temperature dependencies of the resistivity at zero fields and at 45 T.

Measurements of $R(B)$ in a wide temperature range revealed a crossover from a metallic behavior of resistivity, which is well known for zero magnetic fields, to a semiconductor behavior at high magnetic fields for temperatures below about 80 K. In support, Fig.2 shows $\rho(B)$ measured at temperatures from 30 to 80 K. All curves cross each other in the region 15-20 T and 0.1-0.15 mOhm*cm. The inset of Fig.2 shows the extracted $\rho(T)$ for zero magnetic fields and for 45 T which have opposite slopes. The temperature range of the observed crossover coincides approximately with the range of an orthorhombic state of the FeSe.

We acknowledge the support of HLD at HZDR, a member of the European Magnetic Field Laboratory (EMFL).

4 July

Tuesday

11:30-13:00

14:30-17:00

oral session

4TL-E

4RP-E

4OR-E

**“Topological
Insulators”**

4TL-E-1

QUANTUM SPIN AND ANOMALOUS HALL EFFECTS IN TOPOLOGICAL INSULATOR SYSTEMS: RECENT AB-INITIO AND MODEL RESULTS

Chulkov E.V.^{1,2,3,4}, *Men'shov V.N.*^{5,3,4}, *Otrokov M.M.*^{1,2,3,4}, *Eremeev S.V.*^{6,3,4}, *Menshchikova T.V.*⁴, *Silkin I.M.*⁴, *Shvets I.A.*^{4,3}, *Nechaev I.A.*^{2,3,4}, *Koroteev Y.M.*^{6,3,4}, *Tugushev V.V.*^{5,4}, *Ernst A.*²

¹ Donostia International Physics Center (DIPC), 20018 San Sebastian, Spain

² Departamento de Fisica de Materiales, UPV/EHU, Apdo.1072, 20080 and CFM-MPC, Centro Mixto CSIC-UPV/EHU, 20018 San Sebastian, Spain

³ Saint Petersburg State University, Saint Petersburg 198504, Russian Federation

⁴ Tomsk State University, pr. Lenina 36, 634050 Tomsk, Russian Federation

⁵ National Research Centre Kurchatov Institute, 123182, Moscow, Russian Federation

⁶ Institute of Strength Physics and Materials Science, Tomsk, 634021, Russian Federation

⁷ Max-Planck-Institut für Mikrostrukturphysik, D-06120 Halle Germany

⁸ AInstitut für Theoretische Physik, Johannes Kepler Universität, A 4040 Linz, Austria
evguenivladimirovich.tchoulkov@ehu.eus

Topological insulators (TIs) are narrow-gap semiconductors characterized by Dirac-like surface state and protected by time-reversal symmetry. Magnetic field (external or internal) breaks this symmetry and causes splitting of the topological surface state at the Dirac point thus making the surface insulating. Internal magnetic field in TIs can be create in various ways, in particular, by introducing vacancies or carbon atoms [1], doping with 3d-transition metal atoms [2], displaying magnetic semiconductors or organic overlayers as well as bulk materials on the surface of three- or two-dimensional TIs [3-5]. Magnetic field effect on the TI surface state (SS) can be also realized due to extension of the TI SS into magnetic overlayer [6,7]. Here we present and discuss recent results of the study of two-dimensional topological insulators and the effect of magnetic impurities as well as magnetic proximity effects and extended magnetic effect on electronic and spin structure of TIs and splitting of the topological surface state. We propose a method for engineering of heterostructures that result systematically in a big splitting of the Dirac cone. We also analyze magnetic effects in two-dimensional topological insulators and heterostructures and discuss recent results for quantum spin and anomalous Hall effects [6-9].

[1] S. Roy et al., *Phys. Rev. Lett.*, **113** (2014) 116802.

[2] J. Henk et al., *Phys. Rev. Lett.*, **109** (2012) 076801.

[3] V.N. Men'shov et al. *Phys. Rev. B*, **88** (2013) 224401.

[4] M.M. Otrokov, E.V. Chulkov, A. Arnau, *Phys. Rev. B*, **92** (2015) 165309.

[5] S.V. Eremeev S.V. et al., (2013), *Phys. Rev. B*, **88** (2013) 144430.

[6] M.M. Otrokov et al., *JETP Lett.*, accepted (2017).

[7] M.M. Otrokov et al., *2D Materials*, accepted (2017).

[8] V.N. Men'shov, V.V. Tugushev, E.V. Chulkov, *JETP Lett.*, **102** (2015) 754.

[9] V. N. Men'shov, V.V. Tugushev, E.V. Chulkov, *Europhys. Lett.*, **114** (2016) 37003.

4TL-E-2

**COMPETING ELECTRONIC PHASES IN THE CRYSTALLINE
TOPOLOGICAL INSULATOR $\text{Pb}(x)\text{Sn}(1-x)\text{Te}$** *Kundu S.¹, Tripathi V.¹*

¹ Department of Theoretical Physics, Tata Institute of Fundamental Research, Homi Bhabha Road,
Navy Nagar, Mumbai 400005, India
vtripathi@theory.tifr.res.in

The four topologically protected electron bands on the (001) surface of the crystalline topological insulator $\text{Pb}(x)\text{Sn}(1-x)\text{Te}$ include two containing Type-II van Hove singularities, accessible at relatively small values of doping. Bloch states corresponding to electrons in these bands have nontrivial Berry phases that effectively impart a momentum dependence to the interparticle interactions in a given band. Using a “multipatch” parquet renormalization group scheme, we study the effect of repulsive electron interactions on the competition of different electronic phases on the (001) surface when the chemical potential is tuned to the vicinity of the van Hove singularities. Over a wide region of parameter space of repulsive interactions, we show that a chiral p-wave superconducting phase is favoured. Implications for experiment are discussed.

Support of a DST (India) Swarnajayanti grant is acknowledged.

4TL-E-3

LOCAL MAGNETIC MOMENTS IN THE TOPOLOGICAL INSULATORS

Sakhin V.¹, Kukovitskii E.¹, Garifyanov N.¹, Talanov Yu.¹, Teitel'baum G.¹

¹ Kazan E. K. Zavoisky Physical -Technical Institute of RAS, Kazan, Russia
grteit@kfti.knc.ru

Topological insulators (TIs) belong to a class of quantum materials which are characterized by gapless surface states with Dirac-like dispersion. Their nontrivial topology is protected by time-reversal symmetry (TRS). The breaking of this symmetry gives rise to different topological states corresponding to new quantum materials. One of the most promising ways to study the effects of breaking TRS is the doping of TI with magnetic ions. While at low doping TIs remain stable to such perturbations, at higher doping, a kind of ferromagnetic ordering takes place [1] and the TRS is broken due to the appearance of the spontaneous magnetization. The magnetic ordering of the doped ions is driven by their indirect Ruderman-Kittel-Kasuya-Yosida coupling via the charge carriers. The important consequences of this ordering such as the possibility of different textures and other inhomogeneities together with their characteristic space and time scales are still unknown. The additional circumstance which can give rise to inhomogeneities is the limited solubility of magnetic ions in semiconductors. For elucidations of all these issues, it is helpful that the doped magnetic ions also play a role of the local spin probes which may be used as a sensitive tool for monitoring the space inhomogeneities in a system. This possibility is realized in our work which is focused on the studies of the local properties of Bi₂Te₃ doped by Mn ions using an electron spin resonance (ESR) technique.

Crystals of 3D topological insulators, bismuth telluride Bi₂Te₃, doped with manganese were studied using ESR spectroscopy together with the SQUID magnetometry, transport measurements and X-ray characterization. The obtained ESR data, such as the temperature and the angular dependence of the resonance field, reveal the specific critical behaviour and confirm the ferromagnetic ordering of Mn spins even at modest doping [2]. In addition to the studies of the critical behavior of diluted ferromagnet Bi_{2-x}MnxTe₃, we also discuss the effects of the limited solubility of Mn ions giving rise to microscopic inclusions of the spurious magnetic phases which were revealed using ESR technique.

We address also the problem of another type of the local magnetic moments which originate not from the doped magnetic ions but from the structural imperfections of TI [3, 4]. In the case of basic TI compounds Bi₂Te₃ and Bi₂Se₃ such local moments may be induced due to the anti-site substitutional defects in Se(Te) layer of the typical quintuple structure when some of the Se(Te) atoms are replaced by the Bi atoms. The corresponding local magnetic moment's value is about 0.6μB and it originates from the p-orbital of the guest Bi atom. There is a lack of experimental data concerning such magnetic moments and our work is concentrated on studying their properties in Bi₂Te₂Se by means of magnetic resonance in combination with the other experimental technique.

Support by the RFBR through the Grant No. 15-42-02477 is acknowledged.

- [1] Y.S. Hor, P. Roushan, H. Beidenkopf et al., *Phys. Rev. B*, **81** (2010) 195203.
- [2] V. Sakhin, E. Kukovitskii, N. Garifyanov et al., *J Supercond Nov Magn.*, **30** (2017) 63.
- [3] G. Xiao et al., *Angew. Chem. Int. Ed.*, **53** (2014) 729.
- [4] Li-Xian Wang et al., *Nanoscale*, **7** (2015) 16687.

4TL-E-4

QUANTUM ANOMALOUS HALL CONDUCTIVITY IN 3D MAGNETIC TOPOLOGICAL INSULATOR/NORMAL INSULATOR HETEROSTRUCTURES

Men'shov V.N.^{1,2,3}, Tugushev V.V.^{1,2,3}, Chulkov E.V.^{2,3}

¹ NRC Kurchatov Institute, Kurchatov Sqr. 1, 123182, Moscow, Russia

² Tomsk State University, pr. Lenina 36, 634050, Tomsk, Russia

³ Donostia International Physics Center, 20080 San Sebastián, Basque Country, Spain
tuvictor@yandex.ru

Semiconductor nanostructures comprising three-dimensional (3D) magnetic topological insulator (MTI) thin films interfaced with 3D normal insulator (NI) materials are considered to be highly promising for spintronic device applications [1]. Indeed, an isolated boundary between 3D MTI and 3D NI can host electron states with spin-momentum locking [2]. Here, we consider a more complex object (the NI/MTI/NI trilayer) which can be regarded as fundamental building block and basic model unit for a study of peculiar electronic properties of MTI/NI-type heterostructures. When the thickness of the MTI film is comparable with the penetration length of the interfacial electron state into the film, the boundaries would significantly affect the the 3D MTI film electron structure. This creates opportunities to design desirable magnetic and transport properties in MTI/NI nanostructures.

In this work, in the framework of an effective functional approach [3] based on the 3D **kp** method, we study the combined effect of an interface potential (IP) and a thickness of 3D MTI thin film on the intrinsic anomalous Hall conductivity in layered nanostructures comprising MTI and NI materials. We derive an effective 2D Hamiltonian of a 3D MTI thin film sandwiched by two 3D NI slabs and define the applicability limits of approximations used. The energy gap and mass dispersion of electron states, originated both from the magnetic order inside MTI and hybridization between MTI/NI interfacial bound electron states at the opposite boundaries of a 3D MTI film, are demonstrated to change sign with the MTI film thickness and the IP strength. We obtain a phase diagram of the system and predict a quantization of intrinsic anomalous Hall conductivity at the large region of IP strengths and MTI film thicknesses. The phase diagram contains altered regions of normal and quantum anomalous Hall regime. Comparison with experimental results is also performed.

We demonstrate that the intrinsic anomalous Hall effect in the 3D MTI film sandwiched by 3D NI slabs is more complicated than it was thought before. While our work shed light on the possibility for achieving a control of electron properties in the 3D MTI based nanostructures, profound understanding of the physics in studied nanostructures remains a challenging task.

Support by RFBR grant 16-00042 is acknowledged.

1. D. Pesin and A. H. MacDonald, *Nature Mater.*, **11** (2012) 409; T. Fujita, M. B. A. Jalil, and S. G. Tan, *Applied Physics Express*, **4** (2011) 094201.

2. M. Z. Hasan and C. L. Kane, *Rev. Mod. Phys.*, **82** (2010) 3045; X. L. Qi, S. C. Zhang, *Rev. Mod. Phys.*, **83** (2011) 1057; Y. Ando, *J. Phys. Soc. Jpn.*, **82** (2013) 102001.

3. V.N.Men'shov, V.V.Tugushev, S.V.Eremeev, P.M.Echenique and E.V.Chulkov, *Phys. Rev. B*, **91** (2015) 075307.

4TL-E-5

PHOTO GALVANIC EFFECTS IN TOPOLOGICAL INSULATORS

Tarasenko S.A.

Ioffe Institute, 194021 St. Petersburg, Russia
 tarasenko@coherent.ioffe.ru

Topological insulators have recently emerged as a new class of 3D or 2D semiconductor (gapped) systems with Weyl-like conducting surface or edge states spanning the bulk gap. Strong spin-orbit coupling, giving rise to non-trivial topology of the band structure, locks the orientations of the spin and the momentum of a surface/edge carrier and, therefore, the topologically protected conducting channels are of helical nature.

Here, we discuss the optical and photogalvanic effects in 2D topological insulators based on HgTe/CdHgTe quantum wells associated with the helical edge channels. It is shown that the selective excitation of spin-up and spin-down edge electrons by polarized radiation results in a photocurrent along the sample edge. We present an overview of recent theoretical studies of microscopic mechanisms of the photocurrent generation for different types of optical transitions involving the edge states and compare the results with recent experimental observations. The photogalvanic spectroscopy is shown to be a powerful method to probe surface/edge channels.

The strong natural interface inversion asymmetry of HgTe-based quantum wells mandated by the atomic structure of the interfaces leads to the coupling of the electron-like and hole states [1,2]. Due to the coupling of the states, direct optical transitions between the spin-up and spin-down branches of the edge-state dispersion occur not only in the weak magneto-dipole approximation but also in the much stronger electro-dipole approximation. Moreover, the probability of the absorption of circularly polarized photons is asymmetric in the momentum space, which leads to the emergence of an edge photocurrent whose direction is determined by the radiation helicity. The interference of the electro-dipole and magneto-dipole mechanisms of the light absorption for linearly polarized photons gives rise to the linear photogalvanic effect. Here, the photocurrent direction is determined by the radiation polarization plane with respect to the edge orientation.

For the appropriate position of the Fermi level in the gap and the photon energy, the optical transitions and the associated photocurrent can be dominated by the photoionization of edge channels [3,4]. In this case, the photocurrent is caused by the selective depopulation of spin-up or spin-down branches by polarized radiation and, depending on the radiation helicity, the current circles clockwise and counter-clockwise around the sample edges.

The application of an external magnetic field opens a gap in the spectrum of edge states leading to a peculiarity in the excitation spectrum of the edge photocurrent. The magnetic field also gives rise to additional mechanisms of the current generation.

Support by the Russian Science Foundation (project 17-12-01265) is acknowledged.

- [1] S.A. Tarasenko, M.V. Durnev, M.O. Nestoklon et al., *Phys. Rev. B*, **91** (2015) 081302(R).
- [2] M.V. Durnev and S.A. Tarasenko, *Phys. Rev. B*, **93** (2016) 075434.
- [3] V. Kaladzhyan, P.P. Aseev, and S.N. Artemenko, *Phys. Rev. B*, **92** (2015) 155424.
- [4] K.-M. Dantscher, D.A. Kozlov, M.T. Scherr et al., *arXiv:1612.08854*.

4TL-E-6

MAGNETISM AND MAGNETOTRANSPORT IN TOPOLOGICAL INSULATOR Bi_2Se_3 DOPED WITH Eu

Aronzon B.A.^{1,2}, Oveshnikov L.N.^{1,2}, Prudkoglyad V.A.², Selivanov Yu.G.², Chizhevskii E.G.²

¹ National Research Center “Kurchatov Institute”, Moscow 123182, Russia

² P.N. Lebedev Physical Institute RAS, Moscow 119991, Russia

aronzon@mail.ru

Previously, we have studied magnetoresistance of undoped Bi_2Se_3 thin films of thickness about 25 nm and with 30 nm Se protective cap layer grown on (111)-oriented BaF_2 substrates [1]. Streaky RHEED patterns observed during the growth confirmed the presence of smooth surface and single crystallinity of studied films. It was shown that the observed weak antilocalization and Shubnikov – de Haas oscillations depends on the component of magnetic field perpendicular to the structure plane. Thus, the antilocalization corrections are due to interface states of, presumably, topological nature [1].

In present work we've studied magnetization and magnetotransport in Bi_2Se_3 thin films grown by the same procedure with analogous structure parameters with Eu concentration ranged from 0 to 7 %. Measurements were performed in magnetic fields up to 16 T in temperature range 0.3 – 18 K. The following results were obtained:

1. According to the prediction of theory for topological insulators the antilocalization features are still observed in samples with magnetic impurity (Eu) without any visible signs of consequent weak localization.

2. In samples with Eu the dephasing length saturates with temperature decrease below approximately 2 K, while for undoped samples it follows $T^{-1/2}$ dependence in the whole range of studied temperatures that corresponds to the dominant role of e-e inelastic scattering as a dephasing mechanism.

3. In samples with Eu concentration above 1% the linear magnetoresistance is observed unlike undoped samples where the usual quadratic magnetoresistance takes place. The range of magnetic fields where the magnetoresistance shows linear dependence increase with Eu concentration. dR/dB in linear-in-field region depends on temperature and this dependence looks similar for all samples containing Eu.

4. Magnetization measurements demonstrate the appearance of ferromagnetic behavior in sample with highest Eu concentration (7 %). At saturation $M \approx 3 \cdot 10^{-6}$ emu. This value is in agreement with the assumption of all Eu ions having spin 7/2 (Eu²⁺).

5. The nature of linear magnetoresistance and dephasing length saturation is still not clear and will be discussed.

Support by RSF (grant # 17-12-01345) is acknowledged.

[1] L.N. Oveshnikov et al., *JETP Letter*, **104** (2016) 629.

4TL-E-7

PSEUDOMAGNETIC FIELDS EFFECTS IN DIRAC MATERIALS*Lozovik Yu.E.^{1,2}*¹Institute for Spectroscopy RAS, 142190 Troitsk, Moscow²Moscow Institute of Physics and Technology, Moscow

Influence of giant strain-induced pseudomagnetic fields on new Dirac materials is discussed. A tight-binding model of 8-*Pmmn* borophene, a two-dimensional boron crystal, is developed. We reveal that the crystal hosts massless Dirac fermions and the Dirac points are protected by symmetry. Strain is introduced into the model, and it is shown to induce a pseudomagnetic field vector potential and a scalar potential. The dependence of the potentials on the strain tensor is calculated. The physical effects controlled by pseudomagnetic field are discussed. If the characteristic size of strain inhomogeneity is about tens of nanometers then the pseudomagnetic field can be as large as millions of gauss. Thus it is possible to engineer giant effective pseudomagnetic field via strain to control electric currents in borophene. In particular, since the pseudomagnetic field has different signs for two valleys, that controllable field may be used in valleytronics based on Dirac materials. Another phenomenon that could be observed in strained 8-*Pmmn* borophene is the quantum Hall effect. It would require crossed pseudomagnetic and electric (or pseudo-electric) fields, so because of valley-dependent sign of the pseudomagnetic field and the absence of the external magnetic field we would obtain anomalous quantum valley Hall effect. Pseudomagnetic field in a strained Dirac material provides significant Faraday and Kerr rotation when external field is also present.

4RP-E-8

HIGHLY-ORDERED WIDE BANDGAP MATERIALS FOR QUANTIZED ANOMALOUS HALL AND MAGNETOELECTRIC EFFECTS

Otrokov M.M.^{1,2,3,4}, *Menshchikova T.V.*², *Vergniory M.G.*^{4,5}, *Rusinov I.P.*², *Vyazovskaya A.Yu.*², *Koroteev Yu.M.*^{2,6}, *Bihlmayer G.*⁷, *Ernst A.*^{8,9}, *Echenique P.M.*^{1,4}, *Arnau A.*^{1,4}, *Chulkov E.V.*^{1,2,3,4}

¹ Departamento de Física de Materiales UPV/EHU, Centro de Física de Materiales CFM - MPC and Centro Mixto CSIC-UPV/EHU, San Sebastián/Donostia, Spain

² Tomsk State University, Tomsk, Russia

³ Saint Petersburg State University, Saint Petersburg, Russia

⁴ Donostia International Physics Center (DIPC), San Sebastián/Donostia, Spain

⁵ Department of Applied Physics II, Faculty of Science and Technology, University of the Basque Country UPV/EHU, Bilbao, Spain

⁶ Institute of Strength Physics and Materials Science, Russian Academy of Sciences, Tomsk, Russia

⁷ Institut für Festkörperforschung and Institute for Advanced Simulation, Forschungszentrum Jülich and JARA, Jülich, Germany

⁸ Max-Planck-Institut für Mikrostrukturphysik, Halle, Germany

⁹ Institut für Theoretische Physik, Johannes Kepler Universität, Linz, Austria

mikhail.otrokov@gmail.com

An interplay of spin-orbit coupling and intrinsic magnetism is known to give rise to the quantum anomalous Hall and topological magnetoelectric effects under certain conditions. Their realization could open access to low power consumption electronics as well as many fundamental phenomena like image magnetic monopoles, Majorana fermions and others. Unfortunately, being realized very recently, these effects are only accessible at extremely low temperatures and the lack of appropriate materials that would enable the temperature increase is a most severe challenge. Presented in this talk is a novel material platform with unique combination of properties that is perfectly suitable for the realization of both effects at elevated temperatures. The key element of the computational material design is an extension of a topological insulator surface by a thin film of ferromagnetic insulator, which is both structurally and compositionally compatible with the topological insulator. Following this proposal, we suggest a variety of specific systems and discuss their numerous advantages, in particular wide band gaps with the Fermi level located in the gap.

4OR-E-9

INVERSE SPIN HALL EFFECT IN HETEROSTRUCTURES "NANOSTRUCTURED FERROMAGNET / TOPOLOGICAL INSULATOR"

Petrov P.N.¹, Skirdkov P.N.^{1,2,3}, Zvezdin K.A.^{1,2,3}, Lin J.G.⁴, Huang J.C.A.⁵

¹ Moscow Institute of Physics and Technology, 141700 Dolgoprudny, Russia

² Russian Quantum Center, 143025 Skolkovo, Moscow Region, Russia

³ A.M. Prokhorov General Physics Institute, RAS, 119991 Moscow, Russia

⁴ National Taiwan University, Taipei, 106 Taiwan, Republic of China

⁵ National Cheng Kung University, Tainan 701, Taiwan, Republic of China

petr.petrov@phystech.edu

Interaction between magnetization dynamics and spin polarized electronic transport has been shown and investigated [1]. It has been predicted and later experimentally proven that the spin polarized current can drive magnetization dynamics via a spin torque mechanism, and that in the inverse process, resonant magnetization dynamics can lead to a generation of spin current which is related to the spin pumping mechanism [2]. Inverse spin Hall effect describes the generation of a transverse unpolarized electric charge current by the flow of a spin current. Three-dimensional (3D) topological insulators are known for their strong spin-orbit coupling and the existence of spin-textured topological surface states which could be potentially used for spintronics.

In this work we investigate theoretically and by micromagnetic modeling inverse spin Hall effect in NiFe/Bi₂Se₃ heterostructure. According to spin pumping theory spin current appear in topological insulator as a result of oscillations of chemical potential in ferromagnet [3]. We considered different sizes of ferromagnetic dots with uniform and vortex magnetization distribution. Spin current could be excited in topologic insulator by ferromagnetic resonance and gyrotropic vortex motion induced by external magnetic field. In vortex case we also obtained magnetization dynamic using Thiele equation [4]. Spin current in topological insulator is estimated according to Tserkovnyak model. Taking into account that spin current is converted to charge current due to strong spin orbit coupling, we estimated inverse spin Hall voltage on this structure. The comparison with experimental results of inverse spin Hall voltage measurements was considered.

The grants RSF No.17-12-01333 and RFBR No. 16-02-00996 are acknowledged.

[1] Slonczewski, John C. "Current-driven excitation of magnetic multilayers." *Journal of Magnetism and Magnetic Materials*, **159.1-2** (1996) L1-L7.

[2] Ando, Kazuya, et al. "Inverse spin-Hall effect induced by spin pumping in metallic system." *Journal of applied physics*, **109.10** (2011) 103913.

[3] Tserkovnyak, Yaroslav, Arne Brataas, and Gerrit EW Bauer. "Enhanced Gilbert damping in thin ferromagnetic films." *Physical review letters*, **88.11** (2002) 117601.

[4] Thiele, A. A. "Steady-state motion of magnetic domains." *Physical Review Letters*, **30.6** (1973) 230.

4 July

Tuesday

11:30-13:00

14:30-17:00

oral session

4TL-F

4OR-F

“Multiferroics”

4TL-F-1

DIRECTIONAL ANISOTROPY OF LIGHT IN MULTIFERROICS

Pimenov A.

Vienna University of Technology, Vienna, Austria
andrei.pimenov@tuwien.ac.at

Multiferroics are materials which exhibit electric and magnetic order simultaneously. Due to the coupling of electric and magnetic effects, these materials show a strong potential to control electricity and magnetism and, more generally, the properties and propagation of light. One of the most fascinating and counter-intuitive recent results in multiferroics is directional anisotropy, the asymmetry of light propagation with respect to the direction of propagation. The absorption in the material can be different for forward and backward propagation of light, which in extreme case may lead to complete suppression of absorption in one direction.

Another remarkable effect in multiferroics is directional birefringence, i.e. different velocities of light for different directions of propagation. As an example, in the multiferroic samarium iron-borate giant directional birefringence can be realized. The effect is easily observed for linear polarization of light in the range of millimeter-wavelengths, and survives down to very low frequencies. The dispersion and absorption close to the electromagnon resonance can be controlled and fully suppressed in one direction.

Finally such aspects as controlling of terahertz light propagation by static voltage will be discussed.

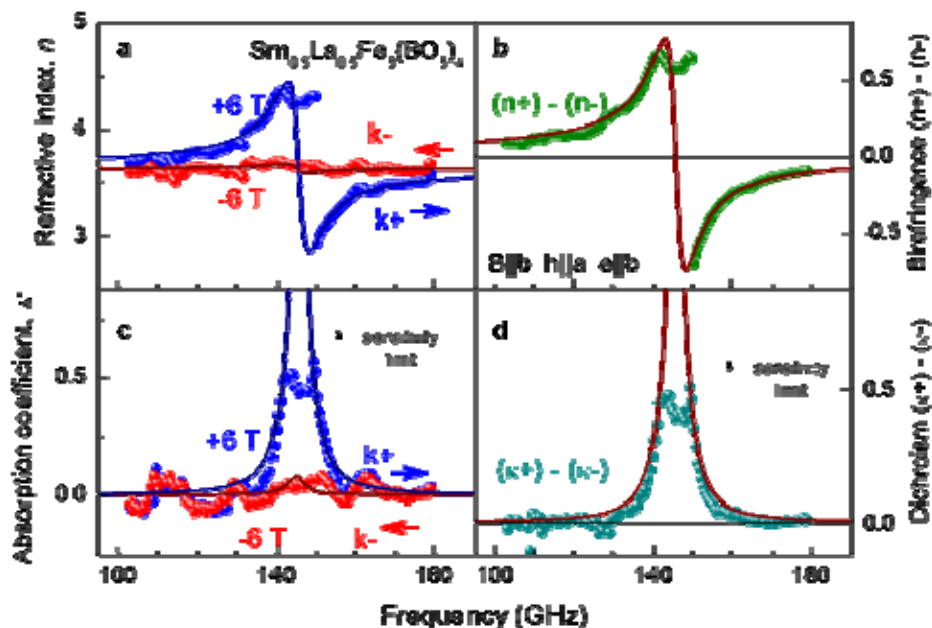


Fig. 1. In multiferroic samarium iron-borate the electromagnon (a magnon with strong electric dipole contribution) reveals strong directional anisotropy.

[1] In collaboration with: A. Shuvaev, W. Dziom, Anna Pimenov, M. Schiebl, A.V. Kuzmenko, V.Yu. Ivanov, A.A. Mukhin, I.A. Gudim and L.N. Bezmaternykh

4OR-F-2

CRYSTAL-FIELD AND EXCHANGE-INTERACTION PARAMETERS FOR MULTIFERROIC $\text{ErFe}_3(\text{BO}_3)_4$

Erofeev D.A.^{1,2}, *Chukalina E.P.*¹, *Yablunovsky A.*², *Popova M.N.*¹, *Malkin B.Z.*³, *Gudim I.A.*⁴

¹ Institute of Spectroscopy Russian Academy of Sciences, Moscow, Troitsk, Russia

² Moscow Institute of Physics and Technology (State University), Dolgoprudny, Russia

³ Kazan (Volga region) Federal University, Kazan, Russia

⁴ Kirensky Institute of Physics, Siberian Branch of RAS, Krasnoyarsk, Russia
erofeev@isan.troitsk.ru

Trigonal borates $R\text{Fe}_3(\text{BO}_3)_4$ ($R = \text{Y}, \text{La} - \text{Er}$) with structure of the natural mineral huntite (space group $R32$) are multiferroics. The research on magnetoelectric (ME) properties of $R\text{Fe}_3(\text{BO}_3)_4$ single crystals has shown that the magnitude of electric polarization induced by a magnetic field of 10 kOe in easy-plane neodymium and samarium compounds reaches values $400 \mu\text{C}/\text{m}^2$ and $500 \mu\text{C}/\text{m}^2$, respectively, which are record values for iron borates. A significant ME effect was expected to occur in easy-plane holmium and erbium iron borates as well. However, the induced electric polarization in $\text{ErFe}_3(\text{BO}_3)_4$ appeared to be extremely small [1]. Two phase transitions were observed in $\text{ErFe}_3(\text{BO}_3)_4$ single crystals, namely, a first-order structural transition from the high-temperature $R32$ phase into a lower-symmetry $P3_121$ phase at $T_S = 431$ K and a second-order transition into an antiferromagnetic easy-plane phase at $T_N = 39$ K. In order to explain magnetic and ME properties of $\text{ErFe}_3(\text{BO}_3)_4$, the crystal-field (CF) and Er-Fe exchange-interaction parameters are required. The parameters can be obtained through an analysis of spectroscopic data. We present the results of spectroscopic research and calculations performed on its basis.

$\text{ErFe}_3(\text{BO}_3)_4$ single crystals were grown by solution-melt technique using bismuth trimolybdate based flux. Polarized broad-band temperature-dependent transmission spectra of oriented $\text{ErFe}_3(\text{BO}_3)_4$ single crystals were registered using a Bruker IFS 125HR Fourier spectrometer. The analysis of the spectra in the region of $f-f$ transitions of the Er^{3+} ion in the paramagnetic phase of the compound allowed us to identify the CF levels of the ground multiplet $^4I_{15/2}$ and nine excited multiplets. The exchange splittings of Kramers doublets of the Er^{3+} ion in $\text{ErFe}_3(\text{BO}_3)_4$ were measured at 5 K. The value of the ground-state exchange splitting was found to be $6.3 \pm 1 \text{ cm}^{-1}$. The CF parameters and the parameters of the Hamiltonian of anisotropic $f-d$ exchange interaction between Er and Fe ions were determined on the basis of analysis of the acquired spectroscopic data. The calculated temperature dependences of the magnetic susceptibility tensor components, field dependences of magnetization and theoretical estimates of ME effects in the erbium iron borate are compared with published experimental data.

This work was supported by the Russian Science Foundation under Grant No. 14-12-01033.

[1] A.M. Kadomtseva, Yu.F. Popov, G.P. Vorob'ev, A.P. Pyatakov, S.S. Krotov et al., *Low Temp. Phys.*, **36** (2010) 511.

4OR-F-3

VOLTAGE TUNABLE MULTIFERROIC MAGNONIC CRYSTALS*Drozdovskii A.V.¹, Vitko V.V.¹, Nikitin A.A.¹, Ustinov A.B., Serga A.A.², Chumak A.V.², Hillebrands B.²*¹ St. Petersburg Electrotechnical University, St. Petersburg, Russia² Technische Universitat Kaiserslautern, Kaiserslautern, Germany
drozdovskyav@gmail.com

At present an increased research interest to study microwave properties of the magnonic crystals (MCs) is evident [1]. It is because that they could be used as a basis for creation new devices for signal processing directly at microwave (MW) frequencies [2]. A main feature of the MCs wave spectrum is presence of the band-gaps that appear due to the Bragg reflection. It is known that the MW properties of the band-gaps can be controlled by both magnetic and electric fields [3].

This work reports for the first time an experimental investigation of a dynamical magnonic crystal (DMC) controlled by voltage. As explained below, such a dynamical crystal enables one to gradually form band-gaps through increasing an applied voltage. The experimental structure consisted of an yttrium iron garnet (YIG) film of thickness 13 μm and a ferroelectric slab of thickness 1 mm attached to each other. In order to provide a demanded periodicity, the thin metal electrodes, namely a continuous and a periodical electrode were fabricated on the different sides of the ferroelectric slab. The slab was placed on the YIG film with the periodical electrode up. The utilized ceramic ferroelectric slab of barium strontium titanate (BST) of the composition $\text{Ba}_{0.5}\text{Sr}_{0.5}\text{TiO}_3$ was in paraelectric phase with a high dielectric constant (about 1200).

A microwave delay-line structure was used for the measurements. Spin waves were excited and received by means of short-circuited input and output microstrip antennas [1]. The experimental DMC was placed between the poles of electric magnet in a uniform magnetic field. The magnetic field was directed in the plane of the dynamical magnonic crystal along the antennas. To create an electric field, voltage was applied to the electrodes. Vector network analyzer was used to carry out the measurements.

The experimental investigation was performed for the different values of the magnetic bias field and voltage. An efficient hybridization between the electromagnetic and spin waves was observed for the magnetic fields H over 2000 Oe. In this case the hybridized spin-electromagnetic waves were propagating in the layered periodic ferrite-ferroelectric structure. It was observed that the dispersion properties of the hybridized waves could be controlled in a wide range. As an example, the voltage of 1800 V at the $H= 2500$ Oe led to the formation of the voltage-tunable band-gaps in the DMC wave-spectrum. A depth of the main band-gap measured against the level of an initially flat amplitude-frequency characteristic was 8 dB.

The work supported by Russian Science Foundation (grant 14-12-01296).

[1] Chumak, A. V., et. al. *Nature communications*, **1** (2010) 141.

[2] Serga A. A., et. al. *J. of Physics D: Appl. Phys.*, **43(26)** (2010) 264002.

[3] Drozdovskii, A. V., et. al. *Tech. Phys.*, **59(7)** (2014) 1032.

4OR-F-4

ULTRAFAST COOLING AND HEATING SCENARIOS FOR THE LASER-INDUCED PHASE TRANSITION IN CUO

*Hellsvik J.*¹, *Mentink J.H.*², *Lorenzana J.*^{3,4}

¹Nordita and Department of Physics, KTH, Stockholm, Sweden

²Radboud University, Nijmegen, The Netherlands

³Istituto dei Sistemi Complessi, Consiglio Nazionale delle Ricerche, Rome, Italy

⁴Universita di Roma "La Sapienza", Rome, Italy

hellsvik@kth.se

We report theoretical modeling of the sub-picosecond magnetic phase transition which recently has been experimentally observed in optically pumped samples of multiferroic CuO [1]. Intriguingly, different excitation mechanisms are found to drive distinct dynamics. Similar as in experiments and independently of the excitation mechanism, our multi-scale modeling [2,3,4] shows that laser excitation of CuO can drive the spin system from the collinear ground state to the incommensurate multiferroic phase on a picosecond time scale. However, depending on the excitation mechanism, the transition proceeds either by heating up the spin system or by cooling it down, where the latter is a manifestation of an ultrafast magneto-caloric effect [4]. In analogue with the ultrafast dynamics observed in ferrimagnetic rare-earth transition metal alloys, it is found that the time-scale of the observed dynamics is determined mainly by the strength of the exchange interactions [5].

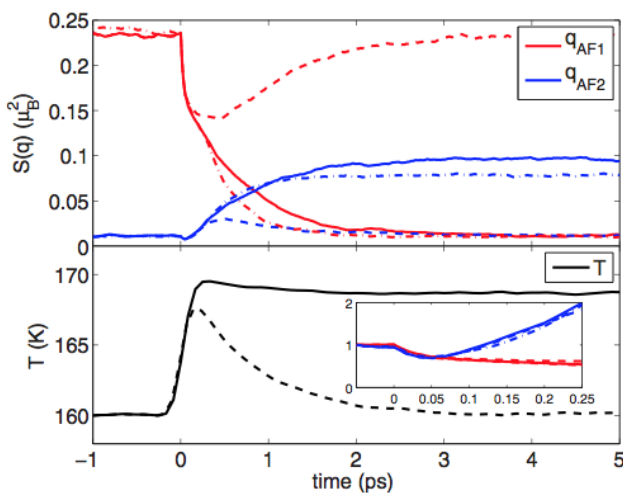


Fig. 1. Dynamics following multimagnon excitation. The upper panel shows the trajectory in time of $S(\mathbf{q}_1, t)$ (red) and $S(\mathbf{q}_2, t)$ (blue), for undamped $\alpha = 0$ (full line) and damped $\alpha = 0.01$ (dashed line) dynamics. $t < 0$ is before pump and $t > 0$ is after pump. The initial temperature is $T = 160$ K, and the initial excitation intensity is $x=0.02$. The lower panel shows the evolution of the temperature of the system. The inset shows the first 250 fs of evolution for the normalised order parameters. The dash-dotted lines are for simulations using the isotropic Hamiltonian H_{iso} .

- [1] S. L. Johnson *et al.*, *Phys. Rev. Lett.*, **108** (2012) 037203.
- [2] O. Eriksson, A. Bergman, L. Bergqvist, and J. Hellsvik, *Oxford University Press* (2017).
- [3] J. Hellsvik *et al.*, *Physical Review B*, **90** (2014) 014437.
- [4] J. Hellsvik, J. H. Mentink, and J. Lorenzana, *Physical Review B*, **94** (2016) 144435.
- [5] J. H. Mentink, J. Hellsvik *et al.*, *Phys. Rev. Lett.*, **108** (2012) 037203.

4OR-F-5

MULTIFERROICITY OF CuCrO_2 TESTED BY ESR

Gotovko S.K.^{1,2}, *Soldatov T.A.*^{1,2}, *Svistov L.E.*², *Zhou H.D.*³

¹ Moscow Institute of Physics and Technology, Moscow, Russia,

² P. L. Kapitza Institute for Physical Problems RAS, Moscow, Russia

³ Department of Physics and Astronomy, University of Tennessee, Knoxville, Tennessee, USA
sofyagotovko@gmail.com

CuCrO_2 is an example of quasi-two-dimensional antiferromagnet ($S = 3/2$) with triangular lattice structure. The neutron scattering experiments detected a three dimensional coplanar magnetic order with incommensurate wave vector $q_{ic} = (0.329, 0.329, 0)$ that slightly differs from the wave vector of a commensurate 120° -structure. According to ESR and NMR investigations the orientation of the spin plane of magnetic structure is defined by strong easy axis anisotropy perpendicular to trigonal plane and weak anisotropy perpendicular to one side of the triangle. The magnetic ordering is

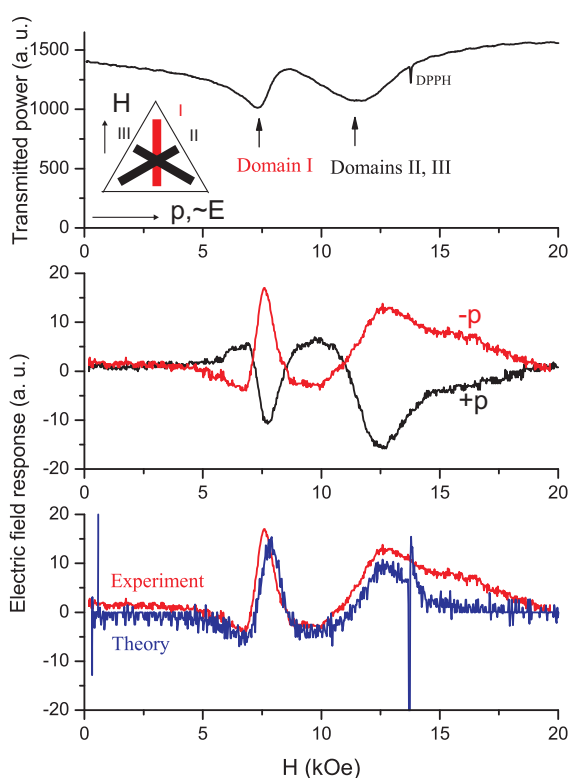


Fig. 1 Upper panel: ESR absorption lines for three domains. Middle panel: The responses of transmitted power on $\sim E$ (red and black lines correspond to different signs of domain polarization) Lower panel: Experimental and theoretical responses on $\sim E$. $T = 4.2$ K, $\nu = 38.5$ GHz

accompanied by the appearance of an electric polarization [1]. The electric polarization is perpendicular to spin plane and is defined by their orientation in space. According to Ref. [2] the main magnetic and multiferroic properties of antiferromagnetic CuCrO_2 have explanation in frame of Dzyaloshinski-Landau theory of magnetic phase transitions. Particularly, the natural frequencies of uniform oscillations of spin plane were found. The oscillation frequencies depend not only on anisotropy constants and applied magnetic field, but on applied static electric field. We report the results of experimental study of ESR experiments on single crystals of CuCrO_2 at the applied electric field. The shift of ESR absorption lines was observed with use of modulation technique. The alternating low frequency electric field $\sim E$ was applied to the sample together with HF magnetic field. The orientations of applied fields H , $\sim E$, polarization P and orientation of spin plane in respect to crystallographic axes are shown in the inset to fig. 1. The field dependency of transmitted through resonator HF power is shown on the upper panel. The response of transmitted power on the alternating electric field is shown on the middle panel. The response on the frequency of applied electric field $\sim E$ is proportional to derivative of absorption line. The change of electric polarization sign leads to change of the response sign (red and black lines). The blue line on the lower panel demonstrates the theoretical expectation what satisfactory agrees with experimental response.

- [1] K.Kimura, H.Nakamura, S.Kimura, M.Hagiwara, T.Kimura, *Phys.Rev.Lett.*, **103** (2009) 107201.
[2] V.I. Marchenko, *JETP* **119** (2014) 1084.

4TL-F-6

MULTIPLE ORDER PARAMETERS AND THEIR CONTROL BY VARIOUS FIELDS IN SPIN-DRIVEN FERROELECTRICS*Kimura T.*^{1,2}¹ Graduate School of Engineering Science, Osaka University, Toyonaka 560-8531, Japan² Department of Advanced Materials Science, University of Tokyo, Kashiwa 277-8561, Japan
kimura@mp.es.osaka-u.ac.jp or tkimura@edu.k.u-tokyo.ac.jp

One of the most important concepts in condensed matter physics is the spontaneous breakdown of symmetry in a solid, which bears the ordered phase and domains in its consequence. In magnetoelectric multiferroics, multiple order parameters coexist in a system, sometimes couple with each other, and exhibit nontrivial crossed phenomena. In this presentation, we deal with magnetoelectric multiferroics in which a symmetry breaking due to the orderings of various order parameters such as electric dipole, magnetic dipole, and magnetic quadrupole moments as well as chirality originating from these multipole moments. We show our recent research activity on exploration for new magnetoelectrics and manipulations of their multiple order parameters as well as domains.

This work has been done in collaboration with T. Honda, J. S. White, M. Kenzelmann, A. B. Harris, K. Kimura, K. Yamauchi, M. Toyoda, P. Babkevich, H. M. Rønnow.

4TL-F-7

STRAIN-MEDIATED MULTIFERROIC MEMORY CELL N*(TbCo₂/FeCo)-PMN-PT

*Preobrazhensky V.^{1,2}, Klimov A.^{2,3,4}, Tiercelin N.², Pernod P.², Dusch Y.², Giordano S.²,
Churbanov A.³, Sigov A.⁴, Nikitov S.³*

Joint International Laboratory LIA LICS:

¹ Wave Research Center, A.M.Prokhorov GPI, RAS, 119991 Moscow, Russia

² University of Lille, CNRS, Centrale Lille, UMR 8520, IEMN, F-59000 Lille, France

³ V. A. Kotel'nikov Inst. of Radioeng. and Electronics, 125009 Moscow, Russia

⁴ Moscow Technological University (MIREA), 119571 Moscow, Russia

The new generation of data storage technology requires high speed, high density, low power and nonvolatile random access memory (RAM). The promising approach for energy efficient RAM is based on magneto-electric interaction in a strain-mediated nano-composite multiferroic structure [1]. Here we demonstrate experimentally not only recording but also reading of stored information using electric field pulses applied to the magneto-electric RAM cell (MELRAM). Fig.1a schematically shows the cell that consists of a uniaxial magnetostrictive nano-structure 25*(TbCo₂ 4nm/ FeCo 4nm) deposited on a 300 μm thick substrate of ferroelectric relaxor PMN-PT <011>. The cell was placed in a magnetic field H normal to the anisotropy easy axis EA and was included in one branch of a Wheatstone Bridge (WB). The magnetic state of the structure was monitored by magneto-optic Kerr effect (MOKE). Fig.1b(1) shows the electric pulse sequence applied to the structure for demonstration of the recording/reading principle. Fig.1b(2) shows the MOKE signal corresponding to switch of magnetization by 90° between the states “0” and “1” for $H=H_A/\sqrt{2}$, where H_A is magnetic anisotropy field. The negative and positive electric pulses record respectively “0” and “1”. The negative reading pulse (RP) does not change the state “0” but the positive RP results in switch from “0” to “1”. Fig.1b(3) shows the electrical response detected across the WB. The response signal indicates the recorded state of magnetization.

Supports by RFBR grant 16-29-14022 and StartAirr program MELRAM are acknowledged.

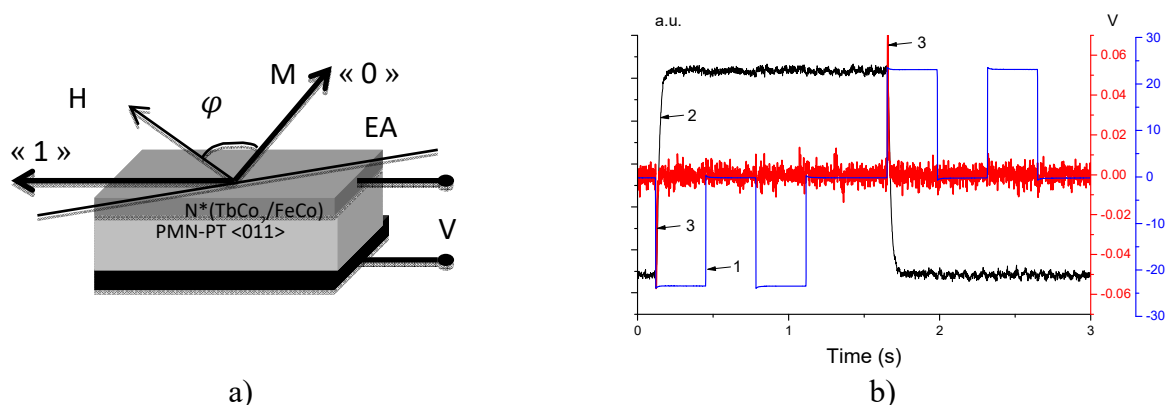


Fig.1 a)-MELRAM cell ; b)- recording/reading (1), MOKE (2) and state indication (3) pulses

[1] N.Tiercelin, Y.Dusch et al., *Nanomagnetic and Spintronic Devices for Energy Efficient Computing*, ed. by S.Bandyopadhyay & J.Atulasimha, Wiley & Sons (2016) 221-257.

4TL-F-8

OBSERVATION OF THE MAGNETIC FIELD INDUCED FERROELECTRICITY IN RARE-EARTH LANGASITES: $\text{Nd}_3\text{Ga}_5\text{SiO}_{14}$

Mukhin A.A.¹, Ivanov V.Yu.¹, Mill B.V.²

¹ Prokhorov General Physics Institute of the Russian Acad. Sci., 119991, Moscow, Russia

² Faculty of Physics, M.V. Lomonosov Moscow State University, 119992 Moscow, Russia
mukhin@ran.gpi.ru

The work reports on the first observation of the magnetic field induced electric polarization in the known compound $\text{Nd}_3\text{Ga}_5\text{SiO}_{14}$ possessing non-centrosymmetrical langasite type crystal structure (space group P321). Due to geometrical frustrations in distorted kagome lattice this compound does not exhibit long-range magnetic order down to the lowest temperatures [1] and shows features of spin liquids [2- 4]. Single crystals of $\text{Nd}_3\text{Ga}_5\text{SiO}_{14}$ were grown by Czochralski method. Electric polarization measurements were performed in magnetic field up to $\mu_0 H = 5\text{T}$ at temperatures 150- 1.9 K. Three components of the polarization ($P_{a,b,c}$) in the basic ab -plane and along third order c -axis were studied including their field and angular dependences. It was established that the polarization along the a - and b -axes is quadratic in H in weak magnetic fields of arbitrary direction and is described by the two quadratic magnetoelectric susceptibilities $\alpha_{1,2}$ in accordance with the trigonal symmetry of the crystal $P_x = \alpha_1 H_y H_z + \alpha_2 (H_x^2 - H_y^2) + \dots$, $P_y = -\alpha_1 H_x H_z - 2\alpha_2 H_x H_y + \dots$, where x, y, z correspond to the crystal axes a, b^*, c , respectively. In strong fields and low temperatures the polarization shows a saturation leading to its deviation from the quadratic dependence and asymmetry for the $P_x(H_x)$ and $P_x(H_y)$ curves. Polarization along the c -axis is also described by the relations obtained from symmetry $P_z = \frac{1}{2}\alpha_3 H_x H_z (H_x^2 - 3H_y^2)$, and is proportional to the $\sim H^4$ in weak fields (Fig.1). At low $T \sim 2\text{K}$ this behavior is violated and the polarization increases almost linearly reaching value $\sim 250 \mu\text{C}/\text{m}^2$ at 5 T (Fig.1) that is comparable to the values of the polarization in the ferro - and alumoborates.

Theory of magnetoelectric effects in $\text{Nd}_3\text{Ga}_5\text{SiO}_{14}$ was developed on the basis of spin-Hamiltonian of the ground doublet of Kramers Nd^{3+} ions occupying local low-symmetry non-centrosymmetrical (C_2) positions. The magnetoelectric interactions allowed by symmetry were included in the spin-Hamiltonian which enabled us to quantitatively describe the observed magnetic field, orientation and temperature dependences of the observed polarization (Fig.1). It was established the important role of the low-symmetry magnetoelectric contribution from the three types of local non-equivalent positions of the Nd^{3+} ions in the formation of abnormally high macroscopic polarization along the trigonal c -axis.

This work was supported by the Russian Scientific Foundation (No. 16-12-10531).

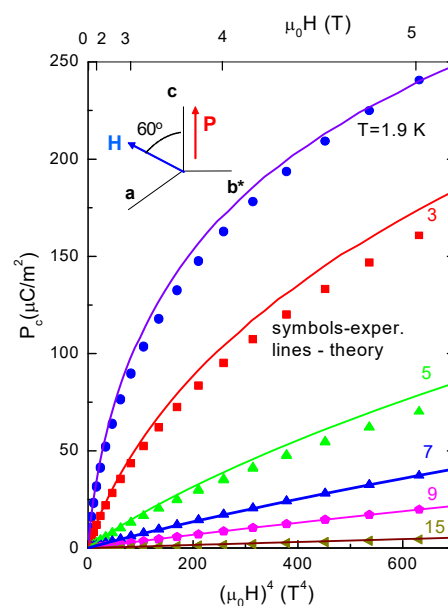


Fig.1 Electric polarization along c -axis versus magnetic field in ac -plane shown in the insert.

- [1] P. Border, I. Gelard, K. Marty, et al., *J. Phys. Condens. Matter*, **18** (2006) 5147.
 [2] J. Robert, V. Simonet, B. Canals, et al., *Phys. Rev. Lett.*, **96** (2006) 197205.
 [3] H. D. Zhou, B.W. Vogt, J. A. Janik, et al., *Phys. Rev. Lett.*, **99** (2007) 236401
 [4] V. Simonet, R. Ballou, J. Robert, B. Canals, et al., *Phys. Rev. Lett.*, **100** (2008) 237204.

4OR-F-9

TEMPERATURE CHARACTERISTICS OF THE NONLINEAR MAGNETOELECTRIC EFFECT

Burdin D.A., Chashin D.V., Ekonomov N.A., Fetisov Y.K.

Moscow Technological University, Moscow, Russia

phantastic@mail.ru

The nonlinear magnetoelectric (ME) effect is of a great interest and a number of high-sensitive magnetic field sensors based on it have been designed during last 2-3 years [1]. It's important to make such devices temperature-stable. In this work temperature characteristics of the nonlinear ME effect have been studied in a rectangle-shaped structures with in-plane dimensions of $5 \times 20 \text{ mm}^2$, containing a $20 \text{ }\mu\text{m}$ thick magnetostrictive amorphous layer and a 0.5 mm thick piezoelectric layer. The sample was placed into magnetic coils, producing dc field $H=0.3 \text{ Oe}$ and ac harmonic field h of 120 Hz frequency. The signal from the piezoelectric layer's electrodes was measured with low frequency spectrum analyzer SR770. Temperature dependences of the first three harmonics $u^{(1)}$, $u^{(2)}$, and $u^{(3)}$ were measured at ac fields 5 Oe and 15 Oe (see Fig.1). One can see that amplitudes of all harmonics change differently with temperature growth from 200 K to 400 K. Thus, $u^{(1)}(T)$ dependence at $h=5 \text{ Oe}$ is nonmonotonic: it rises from 6 mV at $T=150 \text{ K}$ to 8 mV at $T=350 \text{ K}$, $u^{(2)}$ has constant value about 5 mV within the whole temperature range, and $u^{(3)}$ decreases from 5 mV to 1 mV at $T=300 \text{ K}$. Excitation amplitude enlargement up to 15 Oe changes harmonics behavior. The $u^{(1)}$ и $u^{(2)}$ decrease monotonously twice as the temperature changes from 150 K to 350 K, while $u^{(3)}$ demonstrate growth at $T < 200 \text{ K}$. Overall, ME harmonics have different temperature dependences, thereby type of the dependence change with ac field amplitude h . The properties described may be associated with a change of the magnetostriction field dependence. As a result, one can control shape of the temperature dependence for selected harmonic by tuning excitation field amplitude. This technique may be exploited for temperature stability enhancement of the ME composite based devices.

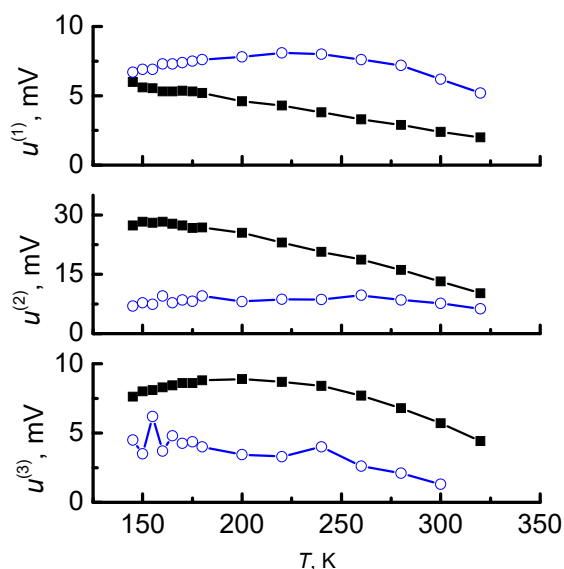


Fig.1. Temperature dependences of ME signal harmonics at $H = 0.3 \text{ Oe}$:
 \circ – $h = 5 \text{ Oe}$; \blacksquare – $h = 15 \text{ Oe}$.

This work was supported by the Russian Foundation for Basic Research, grant 16-32-00417.

[1] D.A. Burdin, D.V. Chashin, N.A. Ekonomov, L.Y. Fetisov et al. *JMMM*, **358-359** (2014) 98-104.

4OR-F-10

INVESTIGATION OF THE MAGNETOELECTRIC AND MAGNETOELASTIC PROPERTIES OF OXIBORATES KHANTITE-TYPE SINGLE CRYSTALS

Dubrovskiy A.A., Freydmann A.L., Balaev A.D., Eremin E.V., Gudim I.A., Temerov V.L.

Kirensky Institute of Physics SB RAS, 660036 Krasnoyarsk, Russia.

Magnetolectric effect, which reflects the interaction between magnetic order, which is due to uncompensated magnetic moment of ions, and electric polarization, which is driven by the ions charges, is well known last decades. However, mechanism, responsible for this effects on the microscopic scale is still unclarified. Materials where the magnetolectric effect occurs show strong dependence of polarization vs. applied magnetic field (direct magnetolectric effect – ME_H), or changing of magnetization vs. applied electric field (so called inverse magnetolectric effect – ME_E).

In the wide row of the materials where this effect can be observed it is possible to emphasize the family of oxiborates $RM_3(BO_3)_4$, where R – rare earth, and M – ion of Al, Fe, Ga, Sc, Cr. These compounds have the space group of $R32$, which is state the absence of inversion centre. As in these crystals the magnetic 3d or 4f ions are presented, it can lead to the magnetic interactions including multiferroism. The crystal structure of this family of crystals is strongly anisotropic. Sublattice of M-ions forms helicoid chain along the c-axis, while the rare earth ions R are isolated from each other, forming the RO_6 -prisms, without the R–O–R interaction.

In the work [1] in $HoAl_3(BO_3)_4$ single crystal the giant direct magnetolectric effect was discovered. It is curiously enough due to the fact this crystal is not multiferroic in general respect as it is not magnetic ordered crystal. Also in this cited work the magnetostriction of this crystal was observed. The authors did not give any explanations of the effects observed.

In the work [2] we bring investigation of the inverse magnetolectric effect and permittivity of the $HoAl_3(BO_3)_4$ single crystal with aim of discovery of the microscopic mechanism responsible for these effects.

With the purpose of the check of this model and to reveal the connection between the 4f and 3d subsystems in this family of single crystals (according to the type of the crystal field splitting the properties of these crystals change) we investigated the direct magnetolectric effect and magnetostriction of the crystals of $RM_3(BO_3)_4$, where R – Sm, La, Ho, Tb, and M – the ion of Al, Fe, Ga.

[1] K.-C. Liang, R. P. Chaudhury, B. Lorenz, et al., *Phys. Rev. B*, **83** (2011) 180417(R).

[2] A. L. Freydmann, A. D. Balaev, A. A. Dubrovskiy, et al., *JAP*, **115** (2014) 174103.

4OR-F-11

MAGNETOCAPACITANCE AND HYSTERESIS OF ELECTRICAL POLARIZATION IN $Gd_xMn_{1-x}Se$

Aplesnin S.S.^{1,2}, Panasevich A.M.³, Sitnikov M.N.², Khar'kov A.M.²

¹ Kirensky Institute of Physics, Federal Research center, 660036 Krasnoyarsk, Russia

² Siberian State Aerospace University, 660014 Krasnoyarsk, Russia

³ GO NPTs Materials Science Center, National Academy of Sciences of Belarus, 220072 Minsk, Belarus

apl@iph.krasn.ru

The study of semiconductors whose dielectric characteristics change in a magnetic field in the absence of a magnetoelectric coupling is of interest from both a fundamental and an applied point of view. It was recently appreciated that the Maxwell-Wagner effect can also yield a magnetocapacitance without multiferroicity. It may be more practical for technological applications. We will show that heterovalent substitution in $Gd_xMn_{1-x}Se$ leads to magnetocapacitance without long range magnetic order.

Real and imaginary parts of the permittivity were measured in the $80\text{ K} < T < 450\text{ K}$ temperature range at frequencies of (1-1000) kHz in magnetic field $H=8\text{ kOe}$ and without of field in dependence on the cooling conditions. Real part of $\epsilon(T)$ sharply increases in the range of temperatures 250 K-350 K and with further heating the permittivity is temperature-independent (Fig.1a) and grows in magnetic field up to concentration $x=0.15$. The imaginary part of the permittivity has the maximum in the range of 250 K -350 K . The temperature of maximum shifts to high temperatures with increasing frequency and magnetic field (Fig.1b). Relative variation of the permittivity $\delta_C = \text{Re}(\epsilon(H) - \epsilon(0)) / \text{Re}(\epsilon(0))$ measured in zero magnetic field and in the $H = 0.8\text{ T}$ attains maxima for $x=0.05$ and disappears at $x=0.2$.

We established the polarization hysteresis upon variation in the external electric field. The remanent polarization dependent on frequency of external electrical field and attains maximum at 100 Hz. At low frequencies (0.1-0.001) Hz polarization hysteresis shifts along polarization axes. The coercive electric field decreases smoothly with increasing frequency. The experimental data have been explained in terms of migration polarization and formation of orbital- charge glass.

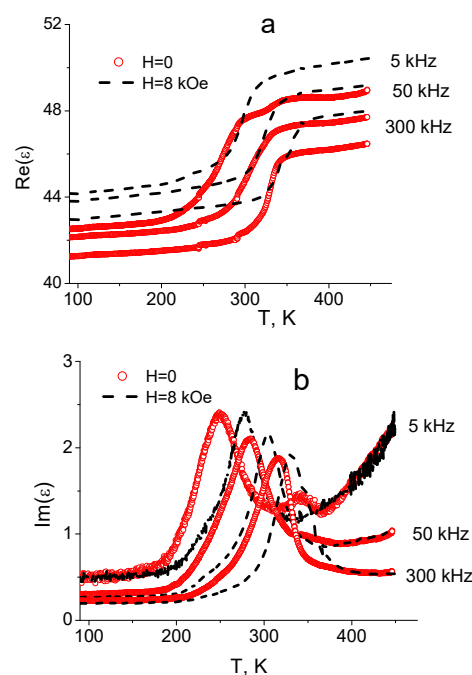


Fig. 1. Real (a) and imaginary (b) parts of the permittivity $Gd_xMn_{1-x}Se$ with $x=0.15$ at frequencies of 5, 50, 300 kHz in magnetic field $H=8\text{ kOe}$ (dotted line) and without of field .

Support by RFBR projects 16-52-00045_Bel_a and №17-42-240079_r_sibir_a.

4OR-F-12

INFLUENCE OF MAGNETIC ORDER PARAMETER SYMMETRY AND SPIN FLUCTUATIONS ON FORMING OF FERROELECTRIC ORDER IN RMn_2O_5 OXIDES

Men'shenin V.V.¹

¹ M.N. Miheev Institute of Mental Physics of Ural Branch of RAS, Yekaterinburg, Russia
menshenin@imp.uran.ru

The materials have been investigated lately in which the long-range magnetic and ferroelectric orders coexist in a certain temperature range. The RMn_2O_5 oxides (R-rare earth element, Bi or Y) in particular are related to these systems. The coupling is strong between the magnetic subsystem and electric polarization in such oxides. It has been found [1] that the ferroelectric long-range order are created in these compounds if only the rare earth element is heavier than neodymium. It has been established experimentally [1] and theoretically [2] that the ferroelectric long-range order emerges in the one spatial direction incommensurate magnetic structure, increases in the commensurate phase and then significantly decreases in the new two directions incommensurate magnetic phase. The phase transition from paramagnetic phase (PMP) to incommensurate magnetic phase in two spatial directions never accompanies the creation of the electric polarization in these oxides [3].

The situation is never simple if the phase transition occurs from the PMP to the commensurate structure. For example, the transitions take place to magnetic phase with the propagation vector $\mathbf{k}=\{1/2, 0, 1/2\}$ in the oxide BiMn_2O_5 and transition happens to phase with $\mathbf{k}=\{1/2, 0, 0\}$ in the oxide PrMn_2O_5 . The electric polarization has been found in the BiMn_2O_5 but it has been absent in the PrMn_2O_5 although the representations of the space group coincide for these propagation vectors. There are two irreducible representations of the space group for these propagation vectors.

Using the projection operate method the irreducible representations was determined which allowed to describe the magnetic phase transitions in the BiMn_2O_5 and PrMn_2O_5 compounds

The magnetic phase transitions were studied in these last compounds on the base of renormalization group approach. It was shown that there is the second order phase transition in the compound PrMn_2O_5 . The spin fluctuations increase the symmetry of the system up to O_2 symmetry in the vicinity of this transition. In this case the invariants vanish in which the electric polarization is contained. Wherefore the ferroelectric long-range order disappears in the PrMn_2O_5 system [4]. The magnetic phase transitions occur for the different representation in the BiMn_2O_5 compared with transition in the PrMn_2O_5 oxide. Where are two transitions from PMS to antiferromagnetic state with close temperatures in the compound contained Bi. It was found [5] that if these transitions occur as second order transitions the electric polarization disappear also. Polarization appears when at least one of these transitions becomes first order transition as a result of spin fluctuations.

This work is partly supported by grant 15-8-2-10 UB RAS.

[1] P.G. Radaelli, L.C. Chapon, *J. Phys. Condens. Matter*, **20** (2008) 434213.

[2] V.V. Men'shenin, *JETP*, **108** (2009) 236-240.

[3] V.V. Men'shenin, *Phys. Solid State*, **55** (2013) 2051-2056.

[4] V.V. Men'shenin, *JETP*, **120**, (2015)1019-1023.

[5] V.V. Men'shenin, *JETP*, **122** (2016) 145-150.

4 July

Tuesday

11:30-13:00

14:30-17:00

oral session

4OR-G

4TL-G

4RP-G

**“Magnetic Soft Matter
(magnetic polymers,
fluids and
suspensions)”**

4TL-G-1

DYNAMICS OF MAGNETO-SENSITIVE ELASTOMERS

Ivaneyko D.¹, Toshchevikov V.¹, Saphiannikova M.^{1,2}

¹ Leibniz-Institute of Polymer Research Dresden, 01069 Dresden, Germany

² Dresden Center for Computational Materials Science, TU Dresden, 01062 Dresden, Germany

³ East Bavarian Centre for Intelligent Materials (EBACIM), Ostbayerische Technische Hochschule Regensburg, Regensburg, Germany
grenzer@ipfdd.de

The low-frequency dynamics of magneto-sensitive elastomers (MSEs) with isotropic, chainlike and plane-like distributions of magnetic particles is studied under a uniform magnetic field \mathbf{H} . A coarse-grained network model is used, in which the magnetic particles are positioned on the sites of a tetragonal lattice [1]. The lattice anisotropy is defined by the ratio a of average distances between neighboring particles along and perpendicular to the symmetry axis of an MSE. In our calculations we take into account the influence of the elastic network and magnetic interactions between the particles under the magnetic field. It is shown that the relaxation spectrum of MSE splits into two branches for the motions of particles parallel and perpendicular to \mathbf{H} and depends on a . The dynamic storage G' and loss G'' moduli are calculated for three different geometries of application of the oscillating shear strain with respect to the symmetry axis of MSE, coinciding with the direction of \mathbf{H} . The application of the magnetic field leads to a strong anisotropy of G' and G'' moduli [1], see Fig. 1. Moreover, G' and G'' can change up to several orders of magnitude in agreement with recent experiments [2]. Financial support of the Russian Science Foundation (project No. 16-15-00208) is gratefully acknowledged.

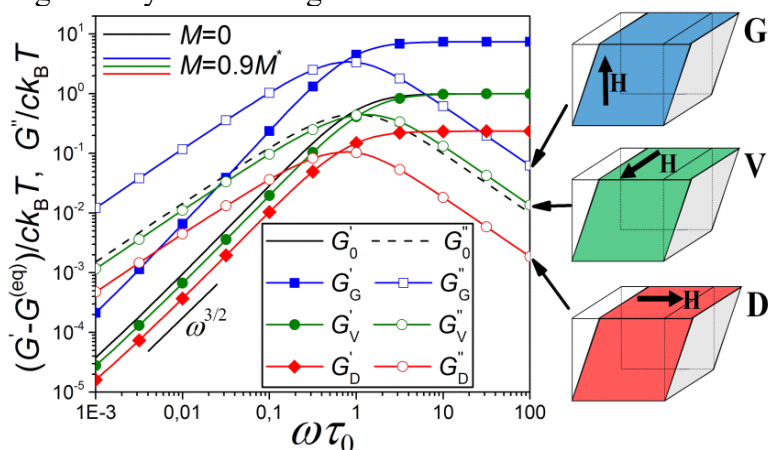


Fig. 1: Both G' and G'' increase if the magnetic field \mathbf{H} is applied along the shear gradient (G-geometry), decrease if it is applied parallel to the shear velocity (D-geometry) and nearly does not change for the V-geometry.

Support by DFG grant GR 3725/6-1 is gratefully acknowledged.

[1] D. Ivaneyko, V. Toshchevikov, M. Saphiannikova, *Soft Matter*, **11** (2015) 7627-7638.

[2] T. Nadzharyan, V. Sorokin, G. Stepanov, A. Bogolyubov, E. Y. Kramarenko, *Polymer*, **92** (2016) 179–188.

4TL-G-2

MAGNETORHEOLOGICAL RESPONSE OF HIGHLY FILLED MAGNETOACTIVE ELASTOMERS FROM PERSPECTIVE OF MECHANICAL ENERGY DENSITY

Sorokin V.V.^{1,2}, Belyaeva I.A.², Shamonin M.², Kramarenko E.Yu.^{1,2}

¹ Faculty of Physics, Lomonosov Moscow State University, Moscow, Russia

² A.N. Nesmeyanov Institute for Organoelement Compounds RAS, Moscow, Russia

³ East Bavarian Centre for Intelligent Materials (EBACIM), Ostbayerische Technische Hochschule Regensburg, Regensburg, Germany
kram@polly.phys.msu.ru

Magnetoactive elastomers (MAEs) comprising soft elastomer matrices filled with μm -sized magnetic particles belong to a class of smart materials due to their ability to change a number of physical properties when an external magnetic field is applied. They are receiving a lot of attention nowadays demonstrating a high potential in various industrial and medical applications.

MAEs also belong to a more general class of filled elastomers. Although the filler particles are much larger than conventional fillers like carbon black and silica, MAEs display similar strain-induced nonlinear phenomena under dynamic mechanical loading conditions like common rubber nanocomposites. In particular, the magnetic field enhanced Payne effect, i.e. a decrease of the storage modulus with increasing strain amplitude, is observed in MAEs [1,2].

In this work we investigate the dynamic shear modulus of magnetoactive elastomers containing 70 and 80 mass% of carbonyl iron microparticles as a function of strain amplitude via dynamic torsion oscillations in various magnetic fields. The results are for the first time presented in terms of the mechanical energy density and considered in the framework of the conventional Kraus model. The form exponent of the Kraus model is further related to a physical model of Huber et al [3] that uses a realistic representation for the cluster network possessing fractal structure. Such an approach suggests that the magnetorheological behavior of these materials depends on the mass fractal dimension of the filler network d_f and the connectivity exponent C of fractal magnetic filler aggregates, where both these parameters can be influenced by external magnetic fields and mechanical loads. Two mechanical loading regimes are identified. At small strain amplitudes the exponent β of the Kraus model changes in an externally applied magnetic field due to rearrangement of ferromagnetic filler particles, while at large strain amplitudes, the exponent β seems to be independent of the magnetic field. The critical mechanical energy characterizing the transition between these two regimes grows with the increasing magnetic field. Similarities between agglomeration/de-agglomeration of magnetic filler under simultaneously applied magnetic field and mechanical shear and the concept of jamming transition are discussed. It is proposed that magnetic field should be considered as an additional parameter to the jamming phase diagram of rubbers filled with magnetic particles.

Abstracts should be prepared as a Rich Text Format (RTF) file and uploaded as an attachment using a link at the end of the Abstract Submission Form.

Financial support of the Russian Science Foundation (project No. 16-15-00208) is gratefully acknowledged.

[1] H. An, S.J. Picken, E. Mendes, *Polymer*, **53** (2012) 4164-4170.

[2] V.V. Sorokin, E. Ecker, G.V. Stepanov, M. Shamonin, G.J. Monkman, E.Y. Kramarenko, A.R. Khokhlov, *Soft Matter*, **10** (2014) 8765-8776.

[3] G. Huber, T.A. Vilgis, G. Heinrich, *J. Phys.: Condens. Matter*, **8** (1996) 409-412.

4TL-G-3

MAGNETO-ELASTIC COUPLING AS A TOOL TO TUNE THE MACROPROPERTIES OF SOFT MATTER

Kantorovich S.S.^{1,2}, Minina E.S.², Sanchez P.A.²

¹ Ural Federal University, Ekaterinburg, Russia

² University of Vienna, Vienna, Austria

sofia.kantorovich@univie.ac.at

Creating functional magnetic soft matter required many years of preliminary work spent on investigating fundamental properties of all its components. The main ingredients of such materials are systems composed of spherical magnetic single-domain nano-sized particles suspended in magneto-passive fluid matrix called magnetic fluid (ferromagnits, ferrofluids, etc.). Over half of the century, scientists from Russia, Europe, Asia, and the USA have actively been investigating these systems both experimentally and theoretically. The second ingredient is the polymer: polymer molecules can be used to stabilise or functionalist magnetic nanoparticles, as well as to cross-link them in various shapes or form gel-like networks.

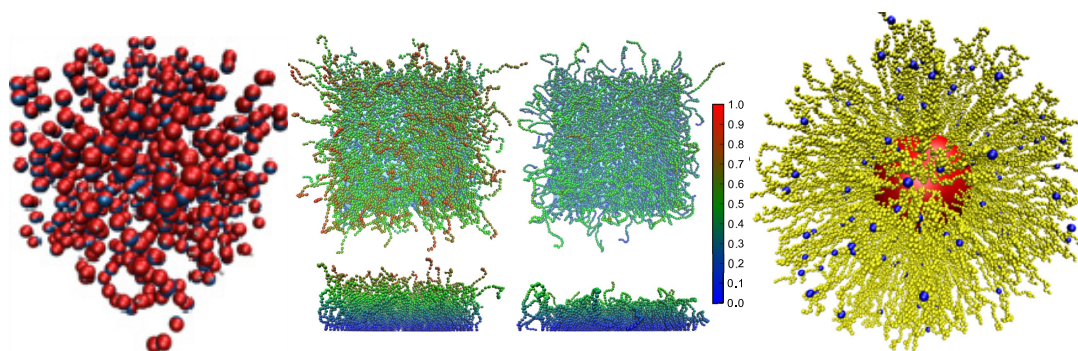


Fig. 1. Simulation representation of magnetic gel (left); filament brush (middle); composite elastomer (right).

In the present contribution we will describe molecular dynamics simulations of magnetic gels, filaments and composite magnetoelastomers (see, Figure 1.). The main idea of this work is to show how using molecular dynamics one can trace back the relationship between the internal structure and the macroscopic magnetic and elastic response of these systems. Along with demonstrating the advantages of our approach and the main results obtained for bottom-up design of magnetic soft matter, we will also discuss the limitations of coarse-grained modelling.

4RP-G-4

VISCOELASTIC RESPONSE OF THE HYBRID MAGNETORHEOLOGICAL ELASTOMERS

Borin D. Yu.¹, Stepanov G.V.², Odenbach S.¹

¹ Chair of Magnetofluidynamics, Measuring and Automation Technology, TU Dresden, Dresden, Germany

² State Research Center GNIICHTEOS, Moscow, Russia
dmitry.borin@tu-dresden.de

Magnetorheological elastomers (MREs) are composites of a rubber or gel-like matrix in which magnetic powder is distributed [1,2]. They belong to the group of controllable materials whose properties can be reversibly changed under the influence of an externally applied magnetic field. One of the most prominent properties of MREs is a field dependent change in viscoelasticity, i.e. an influence of the applied magnetic field on the storage and loss moduli of a specimen at different deformations (ϵ) and loading frequencies (f). In this contribution we report on the effect of the magnetic powder composition and its morphology on the moduli of MREs. Our experimental study is focused on the comparison of MRE samples filled with soft magnetic powder (carbonyl iron powder - CIP), with hard magnetic powder (FeNdB-alloy) and with complex mixtures of both types of powder. Samples with mixed composition (hybrid MREs) as well as specimens containing magnetically hard particles only were magnetized prior to the testing procedure in order to tune their initial state by means of remanence magnetization.

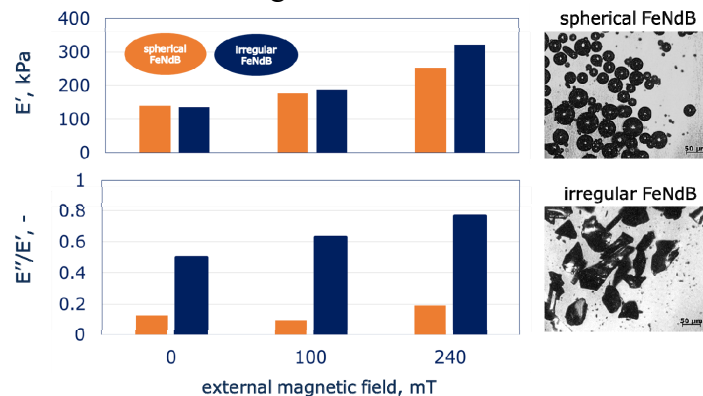


Figure 1. Storage modulus (E') and loss factor (E''/E') of MREs with hybrid particle composition (FeNdB+25% of CIP) in an external magnetic field at $f=0.1\text{Hz}$, $\epsilon\sim 5\%$

Experimental characterization of all samples is performed using dynamic axial loading. The results indicate that different physical processes can be responsible for the obtained material behavior: rotation of particles in the matrix and formation of particle aggregates. Furthermore, a correlation between the powder morphology and viscoelastic response of the MREs is observed.

Financial support by Deutsche Forschungsgemeinschaft (DFG) under Grant Bo 3343/1-1 and Od18/24-1 within PAK 907 providing the basis for our investigations is gratefully acknowledged. G.S. would like to acknowledge the support of RFBR under Grant 16-53-12009.

[1] M. Jolly et al., *J. Intell. Mater. Sys. Struct.* 7 (1996).

[2] M. Kalio, *VTT Publications* (2005).

4RP-G-5

LOW MAGNETIC FIELD RESPONSE OF FERRONEMATICS

*Kopčanský P.¹, Tomašovičová N.¹, Timko M.¹, Gdovinová V.¹, Majorošová J.¹, Jadzyn J.²,
Raikher Y.^{3,4}, Éber N.⁴, Tóth-Katona T.⁵*

¹ Institute of Experimental Physics SAS, Watsonova 47, Košice, Slovakia

² Institute of Molecular Physics, Polish Academy of Sciences, 60179 Poznan, Poland

³ Institute of Continuous Media Mechanics, Russian Academy of Sciences, Ural Branch, Perm, 614013, Russia

⁴ Ural Federal University, Ekaterinburg, 620083, Russia

⁵ Institute for Solid State Physics and Optics, Wigner Research Centre for Physics, Hungarian Academy of Sciences, H-1525 Budapest, Hungary
opcan@saske.sk

The orientational order of liquid crystals (LCs) can be controlled by magnetic or electric fields due to the anisotropy of dielectric permittivity or diamagnetic susceptibility. Very small anisotropy of the diamagnetic susceptibility of LCs causes that they are rather control by electric field in practice than by magnetic field. In order to increase the magnetic susceptibility of LCs Brochard and de Gennes' introduce the great idea of doping them with fine magnetic particles [1]. These colloidal systems are called ferronematics (FNs).

We will demonstrate that even very low magnetic fields ($B < 0.1$ T) may induce a significant magnetic response of suspension of spherical magnetic nanoparticles, single-wall carbon nanotubes (SWCNT), SWCNT functionalized with carboxyl group (SWCNT-COOH), and SWCNT functionalized with Fe_3O_4 nanoparticles [2]. In our previous work [3] we have demonstrated that a small dc magnetic field (of the order of several Oe) applied in the isotropic phase increases the magnetic susceptibility of a FN sample. Driving it through the isotropic-to-nematic phase transition resets the magnetic susceptibility to the value measured prior to the application of the dc bias field. Nematic-isotropic phase transition of these systems in the presence of very small magnetic field opens the doors towards application possibilities such as low magnetic field sensors or basic logical elements for information storage technologies. A new method of detecting low magnetic fields by Whispering gallery mode (WGM) will be also presented. Under the influence of an applied magnetic field the WGM resonances experience spectral shift towards shorter wavelengths. The experimental results demonstrated that the proposed sensor was almost of 3 pm/mT more sensitive for samples infiltrated with rod like and spherical like ferromagnetic suspensions than for undoped liquid crystal sample [4].

FNs can be also realized on the base of lyotropic LCs (biological e.g.) and MNPs. We will present the possible formation of nematic LC phase in solutions containing lysozyme amyloid fibrils (LAF) and MNPs. The adsorption has been studied with the aim to order the fibrils in liquid crystal phase by applying external magnetic field [5]. Ferronematics are materials that may serve as sensor of small magnetic fields. This is the way to obtain magnetovision camera similar like thermovision camera.

This work was supported by project VEGA 2/0016/17, Ministry of Education Agency for Structural Funds of EU in frame of project 26220120033, and the Slovak Research and Development Agency under the contact No. APVV-015-0453.

[1] F. Brochard, P. G. de GENNES, *Journal de Physique*, **31** (1970) 691.

[2] N. Tomasovicova et al. *Phys. Rev E*, **87** (2013) 014501.

[3] N. Tomasovicova et al., *Soft Matter*, **12** (2016) 5780.

[4] A. Mahmood et al., *Optics Express* (2017) in press.

[5] J. Majorosova et al., *Colloids and Surfaces B: Biointerfaces*, **146** (2016) 794.

4OR-G-6

CYCLIC MOTION OF THE PARTICLES INSIDE A MAGNETORHEOLOGICAL ELASTOMER: A STUDY WITH THE TWO- PARTICLE ELEMENT

Biller A.M., Stolbov O.V., Raikher Yu.L.

Institute of Continuous Media Mechanics, UrB RAS, Perm, 614013, Russia
kam@icmm.ru

Technical applications of the magnetorheological elastomers (MRE) are associated with their ability to change a number of properties (mechanical as well as magnetic) under the action of external magnetic field. This feature is entailed by the MRE composition: a soft elastomer matrix within which the micron-size particles of a ferromagnet are dispersed. When the MRE is subjected to a field, the particles magnetize, get into ponderomotive interaction, and begin to move deforming the matrix [1]. Due to the rearrangement of the particles and to the matrix microdeformations caused by each of them, the microscopic properties of the composite change, e.g. its elastic modulus in the direction of the field increases.

Since the magnetization processes inside the particles are very fast, the ponderomotive interaction responds to any re-arrangement in their assembly virtually immediately. However, the mechanical response, even at the mesoscopic (of the order of the interparticle distance) scale takes some time due to the elastoviscous nature of the polymer matrix of an MRE. Therefore, even in the AC fields of low frequency (say, sub-Hz and Hz range), the mechanical reaction of an MRE is retarded. This means that macroscopic mechanic response of an MRE sample should display a notable frequency dispersion and – as the particles are tightly attached to the matrix – the same relates to the magnetic characteristics.

The present work is devoted to the investigation of the influence of the elastomer viscosity on the particle motion inside an MRE. This is done with the aid of the formerly developed structure element model: a pair of magnetically soft (iron) microparticles embedded in a piece of a Mooney-Rivlin medium [2,3]. The issue of most interest is the manifestations of magnetomechanical hysteresis in both the mechanical and magnetic amplitude-frequency characteristics of the element. Indeed, for a particular MRE, there exists a frequency range at the low end of which the response to a cyclically applied field is nearly quasi-static, while at its high end the system is too slow to generate any notable response. Inside that frequency “window” one encounters substantial frequency dispersion of the mechanical and magnetic properties of the structure element and, thus, qualitatively the same reaction should occur in real MRE samples. With the aid of our model, the acceptable range of parameters is determined where the clustering process still exists and, thus, causes the stiffening effect in MREs. Another important characteristic of the dynamic magnetomechanical behavior that our solution enables one to evaluate is the energy dissipation per a cycle of the field.

This work was supported by RFBR projects 16-31-00503, 17-42-590504 and RFBR-DFG project 16-51-12001 (PAK 907).

[1] G.V. Stepanov, D.Yu. Borin, Yu.L. Raikher, P.V. Melenev, N.S. Perov, *J. Phys.: Condensed Matter*, **20** (2008) 204121.

[2] A.M. Biller, O.V. Stolbov, Yu.L. Raikher, *J. Appl. Phys.*, **116** (2014) 114904.

[3] A.M. Biller, O.V. Stolbov, Yu.L. Raikher, *Phys. Rev. E*, **92** (2015) 023202.

4OR-G-7

MICROSTURAL INVESTIGATION OF MAGNETORHEOLOGICAL ELASTOMERS (MRE)

Gundermann Th., Odenbach S.

Chair of Magnetofluidynamics, Measuring and Automation Technology, Technical University of Dresden, Germany

thomas.gundermann@tu-dresden.de

Magnetorheological elastomers are a new kind of smart materials which consists of magnetically controllable particles embedded in an elastic matrix. Thereby a distinction is made into MREs which consist of either magnetically soft or hard particles dispersed in an elastomeric matrix. By using magnetically soft particles, one can obtain an active magnetorheological effect like the change of the elastic modulus in an applied magnetic field. By using magnetically hard particles one can induce passive magnetorheological effects due to the remanent magnetization of the hard particles. By mixing magnetically soft and magnetically hard particles a new kind of magnetic hybrid material can be produced. By preparing hybrid MREs with different mixtures of soft and hard particles, we expect to combine active and passive magnetorheological effects. Furthermore, these hybrid samples display interesting changes in their microstructure.

Fig.1 shows some snapshots of the particle structure inside a magnetized hybrid sample which was polymerised under the influence of a homogeneous magnetic field. It shows a labyrinth like structure caused by the combination of soft and hard particles. By applying a magnetic field after polymerization, the properties of such a material can be changed reversibly due to the interaction of the particles and the elastic restoring forces of the matrix. If strength and direction of the magnetic field are changed a rotation and reorganization of the structure of these particles is induced. An example of reorganization caused by changing the direction of the magnetic field is shown in fig. 2.

By investigation of MRE samples with micro computertomography (X μ -CT) and carrying out an evaluation of the particles using digital image processing one can quantify this particle structuring by measuring the geometrical properties of the particles like centre position, size circularity, eccentricity and their major axes. E.g. the direction of the major axis leads to a statement about the quantity of the particle rotation in relation to the direction of the applied magnetic field. This provides statements about the interaction between particles and matrix.

The financial support by the DFG within SPP1681 under grant no. OD18/21 and PAK 907 under grant no. OD18/24-1 is gratefully acknowledged.

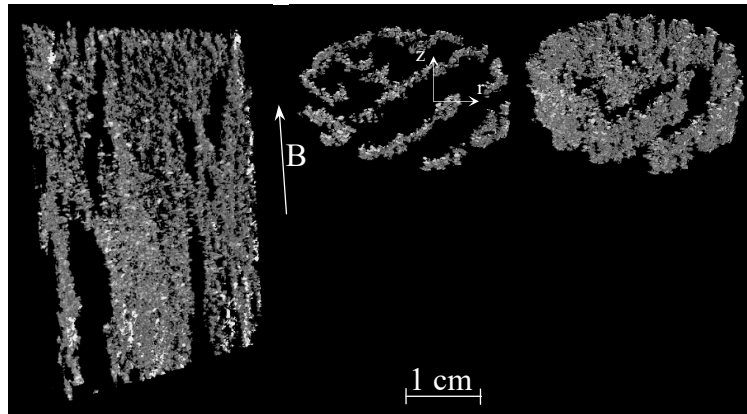


Fig. 1. Snapshots of a tomographic scan of a MRE with a particle content of 5 vol.% of CIP and 5 vol.% of NdFeB particles

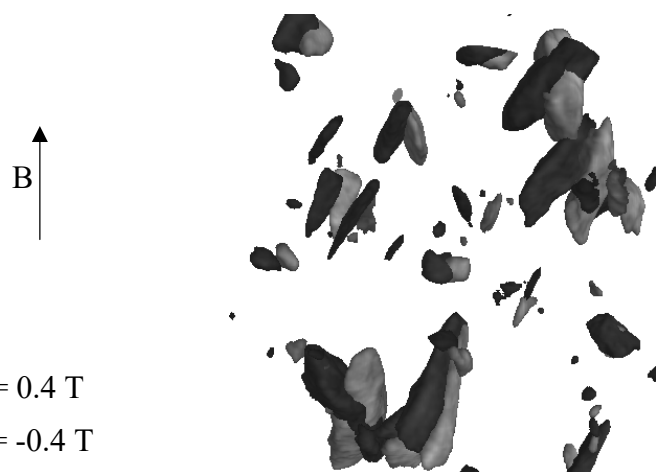


Fig. 2. Rotation of particles in MREs due to changes in the direction of the magnetic field

4RP-G-8

MAGNETIC FLUIDS FOR POWER TRANSFORMER APPLICATIONS*Timko M.¹, Rajnak M.^{1,2}, Tobias T.¹, Kurimsky J.², Dolnik B.², Cimbala R.², Paulovicova K.¹, Kopcansky P.¹*¹ Institute of Experimental Physics SAS, Watsonova 47, 04001 Košice, Slovakia² Faculty of Electrical Engineering and Informatics, Technical University of Košice, Letná 9, 04200 Košice, Slovakia
timko@saske.sk

Magnetic fluids are stable colloidal suspensions of permanently magnetized nanoparticles in a nonmagnetic carrier liquid [1]. As a multifunctional medium, they have found applications in each of its constituent disciplines of chemistry, fluid mechanics, and magnetism. Among the various technical applications [2], there has been increasing interest in the development of magnetic fluids that meet electrical properties and breakdown requirements of high power transformers. For that purpose, magnetic fluids based on transformer oils have been intensively studied [3]. The essential purpose of the development of such a magnetic colloidal medium and its industrial application consists in the service life extension of millions of aging transformers due to the ferrofluid's enhanced cooling and insulating effectiveness. On the other hand, the transformers with magnetic fluids may be smaller, more efficient and possess improved dielectric capabilities.

In this presentation, we focus on recent progress in transformer oil based magnetic fluids research. Besides the basic structural and magnetic properties, we present both thermal and electrical properties of selected magnetic fluids. The cooling effectiveness of the magnetic fluid applied in a model transformer will be shown and compared with that of pure transformer oil. The paper will also demonstrate some peculiar structural behavior of the magnetic fluid exposed to external electric fields. It was found that magnetic nanoparticles in transformer oil can form an electric field driven assembly and patterned structures [4]. The physical conditions allowing the field induced structural changes are therefore discussed too. Finally, we present the electric current-voltage characteristics measured on a transformer oil based magnetic fluid. The recorded hysteresis behavior is analyzed in regard to the structural changes induced by the electric field.

This work was supported by Slovak Academy of Sciences and Ministry of Education: VEGA 2/0016/17, 1/0311/15, 2/0141/16, 1/0377/16, Ministry of Education Agency for structural funds of EU, Project No. 26220120046, 26220120055, 26220120033, and Slovak Research and Development Agency under the contract No. APVV-15-0438, APVV-15-0453.

[1] S. Odenbach, *Ferrofluids: Magnetically Controllable Fluids and Their Applications*. Springer (2008).

[2] W. Yu, H. Xie, W. Yu, and H. Xie, *J. Nanomater.*, **2012** (2011) e435873.

[3] M. Rafiq, Y. Lv, C. Li, M. Rafiq, Y. Lv, and C. Li, *J. Nanomater.*, **2016** (2016) e8371560.

[4] M. Rajnak, V. I. Petrenko, M. V. Avdeev, O. I. Ivankov, A. Feoktystov, B. Dolnik, J. Kurimsky, P. Kopcansky, M. Timko, *Appl. Phys. Lett.*, **107**, 7 (2015) 073108.

4OR-G-9

MAGNETICALLY INDUCED MOVEMENT OF NDFEB PARTICLES IN MAGNETORHEOLOGICAL ELASTOMERS

Schümann M.¹, Odenbach S.¹

¹ Chair of Magnetofluidynamics, Measuring and Automation Technology, TU Dresden, Germany
Malte.Schuemann@tu-dresden.de

In this investigation the effect of external magnetic fields on the inner particle structure of NdFeB-particle loaded magnetorheological elastomers was observed. X-ray micro tomography proved to be a convenient tool for this analysis [1, 2].

40 wt% of highly anisotropically shaped NdFeB particles by Magnequench® ($100 \mu\text{m} < d < 200 \mu\text{m}$) were mixed with Polymer components by Gelest Inc. to produce a soft magnetorheological elastomer. The sample was tomographed without (a), with (b) and again without (c) the presence of a 240 mT magnetic field. Stress-strain tests were performed with a 240 mT field in the same manner. The samples were than magnetised at 2 T for 5 min, thereafter the tomography and the stress-strain testing were repeated.

For every single particle the angle β between its major axis and the magnetic field direction was evaluated from the tomography data. The impact of the magnetic fields on the distribution of β is shown in figure 1. A reversible particle rotation was found for the nonmagnetized state. After magnetization at 2 T the particle structure changed from isotropic to fully formed chains. This is visible as a substantial increase of large particle angles. Here the application of the 240 mT field leads to further rotation, which is not fully reversible. Due to a strong magnetically preferred direction in the NdFeB crystal structure these particles rotate to align perpendicular to the magnetic field direction.

A particle tracking was performed to assign the particles between two data sets [3]. This enables a calculation of the angle individual particles rotate as a reaction on the 240 mT field. A Gaussian distribution of the rotation angles with $\Delta\beta = 9.2^\circ$ and $\sigma_{\Delta\beta} = 9.5^\circ$ was measured for the nonmagnetized sample, $\Delta\beta = 5.1^\circ$ and $\sigma_{\Delta\beta} = 7.2^\circ$ after magnetization at 2 T.

The mechanical testing revealed a magnetorheological effect of $61 \pm 5 \%$ for the magnetized sample and none for the nonmagnetized sample. This effect can be linked to the found change in particle structure. After magnetization the particles are arranged in tight chains and feature a remanent magnetization ($M_R = 52 \text{ kA/m}$ for the whole sample). Both effects lead to enforced particle-particle interaction which induces a magnetorheological effect.

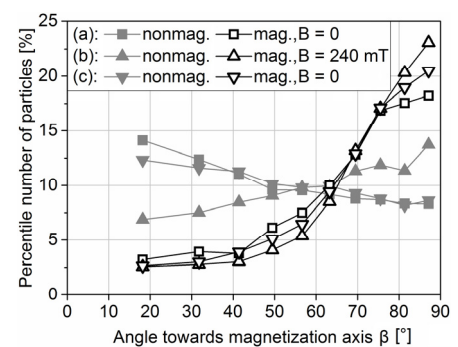


Fig. 1. A rotation of the particles induced by magnetic fields is visible as a change of the distribution of particle angles.

Financial support by DFG (Grant. No. OD18/21) within SPP1681 is gratefully acknowledged.

[1] Borbáth T, Günther S, Borin D Y, Gundermann T, Odenbach S., *Smart Mater. Struct.*, **21(10)** (2012) 105018.

[2] Günther D, Borin D Y, Günther S, Odenbach S., *Smart Mater. Struct.*, **21(1)** (2012) 015005.

[3] Gundermann T, Odenbach S, *Smart Mater. Struct.*, **23(10)** (2014) 1050.

4OR-G-10

MAGNETORHEOLOGICAL EFFECT OF MAGNETOACTIVE ELASTOMER WITH A PERMALLOY FILLER. SYNTHESIS OF THE PERMALLOY FILLER FOR THE MAGNETOACTIVE ELASTOMER

Stepanov G.V.¹, Bakhtiiarov A.V.¹, Borin D.Yu.², Odenbach S.², Storozhenko P.A.¹

¹ State Research Institute for Chemical Technologies of Organoelement Compounds 111123, Moscow, Russia

² Chair of Magnetofluidynamics, Measuring and Automation Technology, TU Dresden, Dresden, Germany

Magnetic or magnetorheological elastomers (MAEs) have been an object of intensive studies since 1996 when Ford Motor Company patented a magnetorheological elastomer and a controllable damping unit on its basis [1]. These investigations have resulted in the discovery and description of more than 10 different field-dependent effects exhibited by these materials. Out of them, however, the magnetorheological effect is paid special attention to. Its detailed study is connected to the good opportunities of its extensive practical applications. Intensification of viscosity growth with the external magnetic field constitutes the principal task of the research.

MAEs are based on two main components, which are a highly elastic polymer matrix and magnetic filler in the form of powder with particle sizes ranging from 1 to 100 μm . For the material of the polymer matrix there are usually selected such elastomers as silicone, urethane, and natural rubber; usage of various gels is also possible. As magnetic fillers, there are used magnetites, ferrites, powder iron and its alloys. The fundamental requirement to the magnetic filler is its magnetization and magnetic susceptibility. The higher magnetization and susceptibility are possessed by the filler, the stronger the magnetorheological effect is exhibited by the magnetic elastomer.

It is a known fact that high values of magnetic susceptibility are demonstrated by permalloys and amorphous magnetically soft alloys. However, these classical magnetic substances also show reduced magnetization. Thus, in order to obtain a filler with a set of desired magnetic properties, there was carried out a mechanochemical synthesis of a permalloy with increased iron concentration. Such a permalloy exhibited increased magnetization, which made it possible to obtain an MAE sample with a high magnetorheological effect. The synthesis was conducted by grinding iron and nickel powders in a planetary mill. The resulting powders had an amorphous structure, which was confirmed by powder XRD-analysis, and increased magnetization as compared to classical permalloys. At the same time, it is important to emphasize that the necessity to grind the permalloy into a powder needed for the synthesis of MAE samples is dictated by the fact that commercially it is available only in the form of sheets and bars. The permalloy obtained with the composition Fe 75 wt.% and Ni 25 wt.% was utilized in the synthesis of MAE.

Studies on the magnetorheological features of such a material showed that the values of its shear modulus in no external field and in a field of 600 mT were 40 kPa and 8 MPa, respectively, which means that the effect of interest defined as the ratio of the final value to the initial value was equal to a factor of 200. An MAE of this type has significant potential in being utilized in controllable damping devices.

Support by the Russian Foundation for Basic Research (RFBR), project 16-53-12009, and the Deutsche Forschungsgemeinschaft (DFG) within PAK907 under the project PO 2013/1-1 and Bo 3343/1-1 is acknowledged.

[1] Ford Motor Company Limited, European Patent 0784163 A1 (1997).

4OR-G-11

STRUCTURING OF MAGNETORHEOLOGICAL ELASTOMERS: FIELD-DEPENDENT MAGNETOSTRICTION EFFECT

Stolbov O.V., Raikher Yu.L.

Institute of Continuous Media Mechanics, Russian Academy of Sciences, Ural Branch, Perm,
614013, Russia
sov@icmm.ru

The ultimate goal of the magnetorheological elastomer (MRE) science is to work out reliable continuum models feasible for being included in engineering design packages. That is why, the problem of advancing from the mesoscopic to macroscopic approaches – analytical as well as numerical – is of paramount importance. The main discussions on the subject turn around the question of how to shape up the “cross-terms” that would correctly couple the cornerstones of the continuum theory: electrodynamics of continuum media and elasticity theory. Several attempts have been undertaken to do that on the basis of the customary set of thermodynamic variables: magnetic induction and magnetization from the one side and stress and strain from the other, maybe adding to that set the filler particle concentration since MRE is an essentially inhomogeneous system.

Those models are constructed by means of power expansions with respect to “mixed” products of the variables from different subsets. The most well-known example is the so-called magnetostriction contribution $-\alpha(\mathbf{H} \cdot \boldsymbol{\varepsilon} \cdot \mathbf{H})$ added to the free energy density of a MRE; here \mathbf{H} is the internal field and $\boldsymbol{\varepsilon}$ the strain tensor [1,2]. The magnetostriction coefficient α (in general case, it is a tensor) is considered to be a material constant.

The afore-mentioned form of the energy term is taken directly from the phenomenology of solid ferromagnets and is responsible for generation of internal deformation under the action of applied uniform field. For the case of small strains, which is always the case for solid ferromagnets, this theoretical description works fairly, as it is established in numerous experiments, see [3], for instance.

It turns out, however, that in MREs the magnetostriction effect is much more complicated, so that the classical contribution, even with added its higher powers, in principle cannot account for the encountered magnetodeformational (for a free sample) and magnetostress (for a confined sample) effects. From our viewpoint, this problem is irresolvable if one deals within the standard set of variables. The modification that we propose is to introduce an additional macroscopic variable that has the meaning of the order parameter and reflects the extent of structuring induced in a MRE by an applied field and/or strain. We show that after including the corresponding terms to the free energy density, the equations, which follow, in a non-contradictive way couple the magnetic and mechanical characteristics of MREs and eliminate the difficulties inherent to the conventional approach.

As an example, we analyze the magnetostriction effect as such – magnetizing of an infinitely long sample (no depolarization) by a uniform field – and show that the classical theory prediction, i.e., proportionality to a field-independent α , is absent or irrelevant. Instead, the theory yields a field-dependent function that modifies both the magnetization curve and the stress-strain ($\sigma - \varepsilon$) dependence of a MRE.

Support by RFBR grant 17-42-590504 is acknowledged.

[1] L. Borcea, O. Bruno, *J. Mech. Phys. Solids*, **49** (2001) 2877–2919.

[2] S.V. Kankanala, N. Triantafyllidis, *J. Mech. Phys. Solids*, **52** (2004) 2869–2908.

[3] S. Chikazumi, *Physics of Ferromagnetism*, Oxford University Press, 2009.

4OR-G-12

MODELING MAGNETO-SENSITIVE ELASTOMERS USING A DIPOLAR MEAN FIELD APPROACH

Romeis D.¹, Saphiannikova M.^{1,2}

¹ Leibniz Institute for Polymer Research Dresden, 01069 Dresden, Germany

² Dresden Center for Computational Materials Science, TU Dresden, 01062 Dresden, Germany
romeis@ipfdd.de

Magneto-sensitive elastomers are composed of magnetizable micro-particles embedded into a soft-elastic polymer network. In the presence of an external magnetic field these composites can change their mechanical properties significantly. The precise relations and conditions responsible for the actual changes are not fully understood, neither experimentally nor theoretically. Recently, we applied a dipolar mean field approach [1] to describe the effective behavior of such composites in the macroscopic limit. We characterize the spatial distribution of magnetizable particles via a continuous dimensionless distribution function $\varphi(\mathbf{r})$ and explicitly calculate a position-dependent magnetization $\mathbf{M}(\mathbf{r})$ as a self-consistent functional of $\varphi(\mathbf{r})$ in presence of an external magnetic field \mathbf{H}_0 . The approach itself provides a very efficient calculation method for various situations and it is partially even analytically solvable. This allows a comprehensive understanding of the mechanisms underlying the behavior of magneto-sensitive elastomers and we are able to predict a phase diagram for the deformation behavior as the external field is switched on, see Fig. 1. The results for the case of a random isotropic distribution of magnetizable particles in the elastomer are in quantitative agreement with a micro-scale continuum model [2,3].

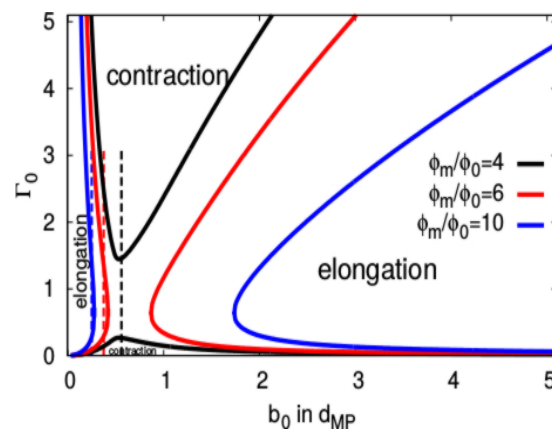


Fig. 1: Prediction of the magnetostrictive effect in samples with columnar-like micro-structures aligned parallel to the external field. Γ_0 denotes the initial (in absence of magnetic fields) aspect ratio of the sample, b_0 is the initial cross-sectional size of the particle columns. Parameter d_{MP} is the size of a micro-particle and Φ_m/Φ_0 characterizes the ratio of particle volume fraction inside the columns and the total particle volume fraction in the sample.

- [1] D. Romeis, V. Toshchevikov, M. Saphiannikova, *Soft Matter*, **12** (2012) 9364-9375.
 [2] D. Romeis, P. Metsch, M. Kästner, M. Saphiannikova *Phys. Rev. E*, **95** (2017) 042501.
 [3] P. Metsch, K.A. Kalina, C. Spieler, M. Kästner, *Comp. Mat. Science*, **124** (2016) 365-374.

4OR-G-13

DETERMINATION OF THE LOCAL ELASTICITY PARAMETERS IN HYBRID MAGNETIC ELASTOMERS USING FORC DIAGRAMS

Vaganov M.V., Raikher Yu.L.

Institute of Continuous Media Mechanics of UrB of RAS, Perm, Russia
mikhail.vaganov.sci@gmail.com

Magnetorheological elastomers (MRE) are a special kind of magnetic field-responsive smart materials, containing magnetic microparticles embedded in a soft elastomer matrix. These composites are of considerable interest due to their possible applications in the field-controlled devices. The subject of this study are MREs of hybrid composition, i.e., those whose magnetic phase consists of magnetically hard (MH) and magnetically soft (MS) particles. The MH fraction provides high coercivity, while the MS part ensures high values of the saturation magnetization.

Magnetomechanical characteristics of MREs depend on the quality of the polymeric matrix and the magnetic properties of the embedded particles. The latter data could be obtained through the FORC (first-order reversal curve) experiments. The FORC diagrams reveal the particles distribution over (1) the intrinsic coercivity and (2) the interaction strength expressed in terms of magnetic field shifts of the hysteresis loops of individual MH particles [1]. As the experiment shows, hybrid MREs possess a highly asymmetrical first magnetization loop. In their FORC diagrams this entails a sharp diagonal ridge absent in the diagrams of rigid materials [2]. Hereby we propose a model enabling one to simulate this unique feature.

As a reference, we use a MRE described in [2]. The sample contains NdFeB particles as the MH filler and carbonyl iron particles as the MS filler. Due to the high magnetic anisotropy of the grains and the softness of the elastomer matrix, a NdFeB particle rotates inside a sample striving to align its magnetic moment with the direction of external field. This behavior could be described with the extended Stoner-Wohlfarth model, where an elastic term is added to the magnetic energy [3]. The magnitude of the latter depends on the structure of the polymer and the quality of its adhesion at the particle surface. Minimization of this energy yields the angle between the magnetic moment of the MH particle and the direction of the applied field.

Due to structural irregularities of the matrix, the elastic resistance to rotation varies from one particle to another. When rotating for the first time, a particle shifts the matrix around it, moving away magnetically soft particles and breaks some part of the chemical bonds at the surface. This impeded motion defines the actual coercivity of the particles and, consequently, that of the whole sample. Because of the irreversible nature of the bond destructions, in all the following cycles of the external field change, the particle rotates more easily. This could be accounted for by ascribing the reduced elastic moduli to the matrix. Moreover, the inhomogeneities of the matrix predetermine that the values of both initial and “trained” elastic moduli are distributed over some interval. As soon as one admits such an assumption, the afore-mentioned diagonal ridge emerges in the model FORC diagram.

In the framework of this concept, the local elasticity of real hybrid MREs could be estimated and analyzed on the basis of their FORC diagrams. In the current study, we step-by-step illustrate this technique.

Support on the part of RFBR-DFG grant 16-51-12001 (PAK907) is gratefully acknowledged.

[1] C.R. Pike, A.R. Roberts, K.L. Verosub, *J. Appl. Phys.*, **85** (1999) 6660-6666.

[2] J.M. Linke, D.Yu. Borin, S. Odenbach, *RSC Adv.*, **6** (2016) 100407-100416.

[3] P. Bender, A. Günter, A. Tschöpe, R. Birringer, *J. Magn. Magn. Mater.*, **323** (2011) 2055-2063.

4 July

Tuesday

11:30-13:00

oral session

4TL-H

4RP-H

4OR-H

“Scientific equipment”

4TL-H-1

CRYOGENIC EQUIPMENT FOR MAGNETIC MEASUREMENTS*Bugoslavsky Yu.*

Cryogenic Ltd, Moscow, Russia

yury@cryogenic.co.uk

We present experimental data from our range of in-house developed measurement modules for investigation of solid state properties, incorporating magnetic, electric and thermal techniques applicable at magnetic fields of up to 18 T and temperatures between 300 mK and 1,000 K. The range includes high sensitivity DC magnetisation and complex AC susceptibility, DC and AC resistivity and Hall effect measurements as well as AC Calorimetry and relaxation heat capacity and thermal transport experiments. We have also developed an extremely reliable method of cryogen free operation for cooling our superconducting magnets and sample spaces to operating temperatures, very useful in a world where liquid helium has become increasingly costly and difficult to obtain.

4RP-H-2

CRYOGENIC EQUIPMENT FOR FULL CYCLE OF LOW TEMPERATURE RESEARCH: CRYOSTATS, CONTROLLERS, MEASUREMENT EQUIPMENT, AMPLIFIERS, ACCESSORIES*Omirov A.*

CTS NAUKA, Moscow, Russia

a.omirov@cts-nauka.ru

Review and comparison of different types of cryostat, its advantages and disadvantages for researches are considered [1]. Much types of complementary equipment (lock-in amplifiers, cryogenic UHF amplifiers, temperature controllers, cryogenic accessories, vacuum equipment) are presented.

[1] <http://scientific-technology.ru/about-us-en>

4OR-H-3

MAGNETIC DOMAIN MICROSCOPE EQUIPPED WITH MEASUREMENT FUNCTION OF LOW NOISE MO KERR LOOP BY LASER

Odagiri Y.¹, Yanagisawa E.¹, Meguro S.¹, Urubkov I.², Saito S.³

¹ Neoark Corporation, Tokyo, Japan

² Tokyo Boeki (Rus) Llc., Moscow, Russia

³ Tohoku University, Miyagi, Japan

odagiri@neoark.co.jp

Studies and developments of spintronics devices such as STT-MRAM are continuously expanding. Investigation of relationship between magnetic domain structure and local magnetization characteristics is essential because magnetic behaviors of local magnetization characteristics significantly influence device's performance. Magneto-optical Kerr effect (MOKE) based microscope is a well-known apparatus to study magnetization behaviors. In most MOKE microscopes, magnetic domain images are obtained by using imaging camera, and magnetization curves are calculated from brightness values of a few pixels of an observed image. However, obtaining low noise magnetization curve by this method contains considerable difficulties due to the limitation of optical detection performance of the imaging camera.

In this study, we report a successful development of a high contrast magnetic domain microscope equipped with low noise magnetization curve measurement system by using focused LASER with the wavelength of 650 nm.

Superimposing an RF signal of 500 MHz on driving current of the LASER was carried out aiming for both speckle noise reduction due to decreasing of coherency [1] and MO signal modulation. A lock-in technique was applied to demodulate the low noise MO signal.

Fig. 1 shows a typical comparison between magnetization curves obtained by brightness of pixels in a domain image and modulated LASER for a thin film. Less noise was observed in the magnetization curve measured by LASER compared with that by brightness. Figs. 2 show (a) magnetic domain image under zero magnetic field and (b)-(c) local magnetization curves in μm area for a NiFe patterned thin film. The pattern showed multi-domain state mainly caused by shape anisotropy. According to the local magnetization curves, different wall-motion and rotational magnetization processes are clearly observed due to low noise MO signal.

In conclusion, low noise magnetization curve combined with changes in domain structure revealed detailed information of magnetization in μm area.

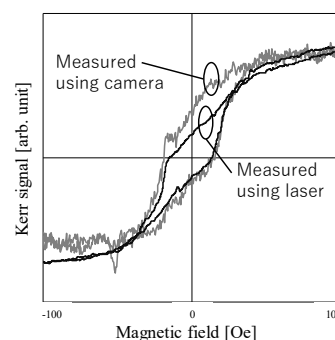


Fig. 1 Comparison of magnetization curves

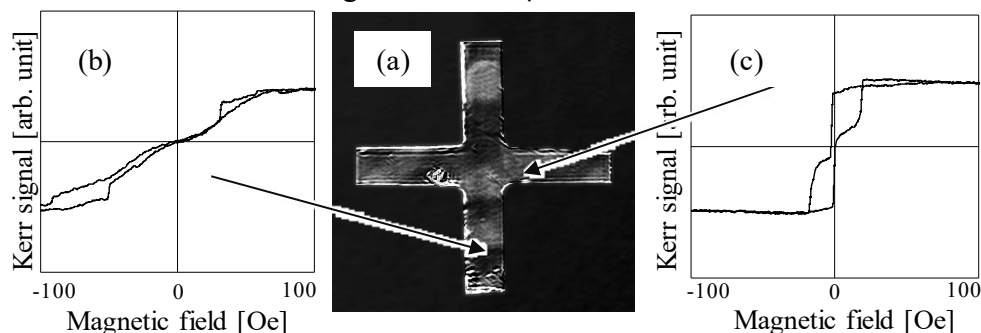


Fig. 2 Magnetic domain image and magnetization curves of the NiFe patterned thin film.

[1] K. Akahane et al., *Magn. Soc. Jpn.*, **28** S1(2004) 122-127.

4OR-H-4

SMALL-ANGLE NEUTRON SCATTERING MACHINE WITH POLARIZED OPTION FOR PIK REACTOR

Shishkin I.S.¹, Moskvina E.V.¹, Eckerlebe H.², Grigoriev S.V.¹

¹ Petersburg Nuclear Physics Institute, National Research Centre “Kurchatov Institute”
(PNPI NRC KI) Gatchina, Russia

² Helmholtz-Zentrum Geesthacht (HZG), Geesthacht, Germany
shishkin_is@pnpi.nrcki.ru

Small-angle diffractometer of polarized neutrons SANS-2 is designed for studies in the fields of materials science (defects, porous), the physics of metals (distinct phases, clusters), technology of nanostructures and nanomaterials (membranes, photonic crystals), physics of the magnetic structures and superconductors (ferromagnetic spirals, spin correlations in the ferromagnetic), physics and chemistry of colloidal particles, microemulsions, colloidal solutions and liquid crystals.

In the framework of the Cooperation agreement between Petersburg Nuclear Physics Institute (Gatchina, Russia) and Helmholtz Zentrum Geesthacht (Geesthacht, Germany) the small-angle neutron diffractometer SANS-2 was transferred from the reactor FRG-1 (shut down in 2010) to the new reactor PIK (to be started in 2018). The reconstruction work to give a new life to SANS-2 at the reactor PIK had started in 2014 within the project “Formation of the Gatchina-Geesthacht platform of neutron stations for research with neutron scattering techniques at the reactor PIK (PIK-GGBase)”.

The main characteristics of the small-angle diffractometer SANS-2 are the following. The monochromaticity of the neutrons beam is provided by the mechanical velocity selector that allows to run the instrument in the wavelength range from 4.5 to 20 Å with a resolution of $\Delta\lambda/\lambda = 0.1$. The collimation of the beam occurs in a collimation tube with a length of 15 m by round and rectangular apertures, with a maximum window size of 30×40 mm². The experiments can be performed with the polarized neutrons. The beam is polarized using a new compact transmission polarizer on silicon wafers with supermirror CoFe/TiZr ($m = 2$) coating. The polarizing efficiency and transmittance of the beam are 0.99 and 0.88, respectively. The adiabatic RF spin-flipper is installed to change the direction of the neutron spins with respect to the magnetic field. The sample unit has the ability to install electromagnets for 1.5 and 2.5 T, linear and rotating tables, closed-cycle refrigerator ($T = 10$ -340 K). The scattered neutrons arrive through the detector tube and are recorded by a two-coordinate position sensitive detector with a size of 55 × 55 cm² with a resolution of 0.7 × 0.7 cm². The sample-detector distance is $1 \leq d \leq 22$ m. The available range for the transmitted pulse is $0.008 \leq q \leq 7$ nm⁻¹.

The assembly and check of the operation of the components and mechanisms of the small-angle diffractometer SANS-2 are currently carried out in the neutron-guide hall of the reactor PIK.

The present work is carried out with the financial support of the Ministry of Education and Science of the Russian Federation, the Agreement on provision of grant No14.616.21.0004 from September 17, 2014, unique identifier of agreement RFMEFI61614X0004.

4OR-H-5

SCIENTIFIC EQUIPMENT FOR LOCAL MAGNETIC PROPERTIES INVESTIGATIONS

Odagiri Y.¹, Wada A.¹, Hatano S.¹, Miyatake Y.², Tatsumi H.³, Kawabe T.⁴, Urubkov I.V.⁴

¹ NEOARK CORPORATION, Tokyo, Japan

² UNISOKU Corporation Ltd., Osaka, Japan

³ JEOL (RUS) LLC., Moscow, Russian Federation

⁴ Tokyo Boeki (RUS) LLC., Moscow, Russian Federation

ilya.urubkov@tokyo-boeki.ru

Local magnetic structure of any material causes properties and thus scope of applications of this material in different machines or devices. The most effective approach of investigating the magnetic structure and properties of a matter is proven to study them at three different levels using three types of instruments: MOKE at micrometer scale, TEM at nanometer scale and SPM at atomic scale.

Modern magneto-optical Kerr effect (MOKE) microscopes are proven to be effective for quick and easy non-destructive studies of magnetic domain behaviour and magnetic properties evolution with a few micrometers resolution at magnetic fields up to 1 Tesla, temperatures from 2 to 500 K, wavelenghtes from 250 to 700 nm. It was developed a benchtop time-resolving magneto-optical Kerr effect microscope (TR-MOKE) which provides very high spatial-temporal resolution (2-3um, 35-50ps) [1]. One of its application examples is shown on Fig. 1. In near future this instrument may be commercialized.

Magnetic domain structures studies at a few nanometers scale became possible with trnsmission electron microscopes equipped with Lorentz TEM option. Usage of cryogenic and nanoindentor built-in TEM holders opens a vast variety of possible studies.

Modern LT SPMs have two directions, one is going to extreme environments, another is going to multifunctionality.

High-field UHV SPMs make it is possible to investigate the atomic and magnetic structures of the samples, their transport and magnetic properties at atomic scale, at temperatures downto 40 mK, magnetic fields up to 15 T and ultrahigh vacuum up to 10^{-8} Pa.

The multi-functional SPMs are widely used for atom manipulations and high-resolution spectroscopy on superconductors. Also these instruments are used for Tip Enhanced Raman Spectroscopy (TERS) studies (Fig. 2).

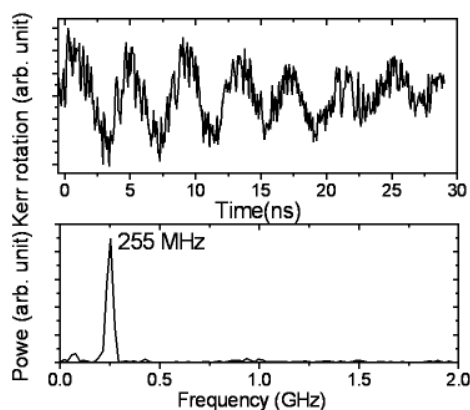


Fig.1. Time-resolved Kerr rotation signal from a permalloy dot (1um diameter, 50nm thick) (top panel) and the corresponding FFT spectrum [1].

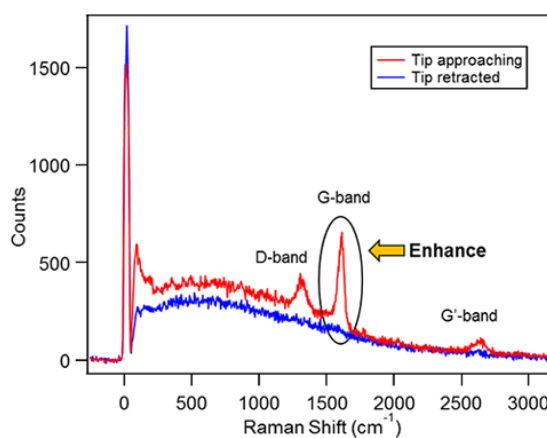


Fig.2. Point TERS spectroscopy on carbon nanotube (temperature 80K, exposure time 0.5s, laser wavelength 633nm).

[1] A. Barman et al., *Rev. Sci. Instrum.*, **79** (2008) 123905.

4 July

Tuesday

11:30-13:00

oral session

4TL-O

4RP-O

**“Magnetism in Biology
and Medicine”**

4TL-O-1

MAGNETIC MICROPARTICLES VIBRATIONS AT LOW FREQUENCY: A NEW APPROACH TO FIGHTING CANCER

Naud C.¹, Joisten H.^{1,2}, Leulmi L.¹, Iss C.¹, Morcrette M.¹, Morel R.¹, Ortiz G.¹, Truong A.¹, Hou Y.³, Livache T.³, Calemczuk R.³, Carriere M.³, Sabon P.¹, Joumard I.¹, Auffret S.¹, Diény B.¹

¹ SPINTEC, Univ. Grenoble Alpes / CEA / CNRS, F-38000 Grenoble, France

² CEA, LETI, MINATEC Campus, F-38000 Grenoble, France

³ SYMMES, Univ. Grenoble Alpes / CEA / CNRS, F-38000 Grenoble, France

helene.joisten@cea.fr

In the field of biotechnology, magnetic nanoparticles are increasingly used for a variety of applications since they allow to exert forces and torques on biological species. Based on top-down approaches (deposition, etching, lift-off), several types of micro/nano particles were prepared for various purposes (see Fig.1 (a-c)). They include synthetic antiferromagnetic particles, vortex microdisks [1], magnetite multidomain particles, magnetic nanoswimmers. A first part of the work has aimed at controlling the agglomeration/dispersion of these particles [2]. To avoid the agglomeration of the particles in solution, these particles are designed to exhibit superparamagnetic-like response and must have a susceptibility below a certain critical threshold to avoid their mutual self-polarization. Thanks to their anisotropic properties, they offer new degrees of freedom in their manipulation when dispersed in solutions [3]. This allows designing ferrofluids with novel properties. In particular interesting optical properties can be obtained [4].

Concerning biomedical applications, a recent approach for cancer cells destruction was proposed, based on the triggering of cancer cell spontaneous death through the mechanical vibration of anisotropic magnetic nanoparticles attached to the cells membrane at low frequencies (20Hz). The induction of cancer cells death was demonstrated in earlier work on glioblastoma cancer cells [5] and in this study with NiFe vortex particles on renal human cancer cells [6] (Fig.1(d)). Statistical analysis of cells death rate was characterized by flow-cytometry and caspases activation studies. The influence of the vibrating/rotating field amplitude was investigated. These results open great perspectives for new cancer treatments with reduced side effects.

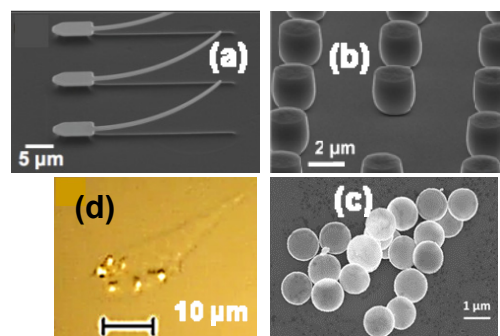


Fig. 1. (a-c) Magnetic particles/swimmers (d) Renal cancer cell + magnetic particles.

This work was funded in part by the H2020 European grant ABIOMATER 665440, in part by ANR grant, P2N NANO-SHARK (ANR-11-NANO-001).

[1] Leulmi S., Joisten H., et al., *Appl.Phys.Lett.*, **13** (2013) 132412.

[2] Joisten H., Courcier T., Balint P., et al., *Appl.Phys.Lett.*, **97** (2010) 253112.

[3] Courcier T., Joisten H., et al., *Appl.Phys.Lett.*, **99** (2011) 093107.

[4] A. Truong, G. Ortiz, M. Morcrette, T. Dietsch, P. Sabon, et al., *Scientific Reports* **6**, Article number: 31634 (2016) 8.

[5] D.H. Kim, E.A. Rozhkova, et al., *Nat. Mater.* **9** (2010) 165–71.

[6] Leulmi S., Chauchet X., et al., *NANOSCALE*, **7** (2015) 15904.

4TL-O-2

MAGNETIC NANOTECHNOLOGY FOR BIOMEDICAL APPLICATIONS

Kosel J., Perez J.E., Alsharif N.A., Martinez Banderas A., Alfadhel A., Yassine O., Contreras M.F.

King Abdullah University of Science and Technology (KAUST), Thuwal, Saudi Arabia
 jurgen.kosel@kaust.edu.sa

Magnetic transducers have played a central role in the areas of sensors and actuators since the discovery of the compass more than 2000 years ago. Continuous developments have always kept this technology at the forefront, and with the advent of new fabrication methods, magnetic transducers at the micro and nano scale became available, exploiting novel properties and providing new features.

While miniaturized magnetic transducers have been central to data storage and sensor devices for some time, magnetic nanotechnology is recently attracting interest in various new areas including life sciences and biomedical applications. The ability to control and manipulate magnetic nanostructures remotely combined with the harmless nature of magnetic fields that penetrate human tissues very efficiently, gives magnetic nanotechnology the edge over many other methods.

Miniaturized magnetic bio devices feature high performance while at the same time hold the potential to reduce the costs associated with healthcare. In this context, magnetic nanobeads have been routinely used for cell separation since many years. In combination with magnetoresistive sensors they can facilitate sensitive diagnostic tools capable of early disease detection and point-of-care diagnostics. Utilizing conducting microstructures, highly integrated microfluidic systems can be implemented in which magnetic nanobeads are moved by electric currents instead of fluid flow. Magnetic nanobeads have also proven to be efficient for cancer treatment via magnetic particle hyperthermia as well as for drug delivery.

Compared to nanobeads, magnetic nanowires offer higher values of magnetization and can be used as nano robots with more degrees of freedom regarding controlling their movement. They can be utilized as extremely efficient nano heaters for magneto-thermoreponsive drug delivery vehicles [1] or as nano permanent magnets in nanocomposites for artificial skins [2]. Nanowires are able to kill cancer cells by a magneto-mechanical effect [3] and, due to their efficient internalization by cells, they can be exploited for drug delivery. Iron nanowires can be easily oxidized by an annealing process, rendering them highly biocompatible. At the same time, an iron core can be maintained and the magnetic properties preserved [4].

This talk covers principles and examples of contemporary magnetic micro and nano devices, with an emphasis on novel magnetic nanowire transducers. The applications range from magnetic nanocomposites, artificial skins, corrosion sensing, energy harvesting and drug delivery to cancer treatment. The magnetic nanowire-based transducers enable both new functionalities as well as a power reduction up to several orders of magnitude compared to similar methods.

Support by King Abdullah University of Science and Technology is acknowledged.

[1] O. Yassine, et al., *Scientific Reports*, **6** (2016) 28539.

[2] A. Alfadhel, J. Kosel, *Advanced Materials*, **27**, 47 (2015) 7888-7892.

[3] M.F. Contreras, et al., *International Journal of Nanomedicine*, **10** (2015) 2141-2153.

[4] Y.P. Ivanov, et al., *Scientific Reports*, **6** (2016) 24189.

4RP-O-3

HIGHLY SENSITIVE MAGNETIC NANOPARTICLE QUANTIFICATION METHOD AND ITS APPLICATION FOR MULTIPLEX BIOSENSING

Nikitin P.I.¹, Orlov A.V.¹, Znoyko S.L.¹, Bragina V.A.¹, Gorshkov B.G.¹, Cherkasov V.R.², Nikitin M.P.²

¹ Prokhorov General Physics Institute, RAS, 119991 Moscow, Russia

² Moscow Institute of Physics and Technology, Dolgoprudny, 141700 Russia

nikitin@kapella.gpi.ru

Magnetic nanoparticles (MP) attract a lot of attention as promising nanolabels for various analytical systems. However, on-site magnetic biosensors that have analytical characteristics comparable to those of laboratory methods are still to be developed. In this work, we developed multiparametric Dry-Reagent ImmunoMagnetic (DRIM) analytical platform and demonstrated its performance for rapid high-precision quantitative *in vitro* diagnostics and food quality control. The platform combines the advantages of simple immunochromatography with highly sensitive magnetic particle quantification (MPQ) from the entire volume of 3D structures by non-linear magnetization [1-3]. A new generation of multichannel MPQ readers has been developed that offer the record limit of detection (LOD) of 0.4 ng or 60 attomoles of MP in 0.2 ml volume within extremely wide 7-order linear dynamic range (Fig. 1). These parameters, to the best of our knowledge, currently have no analogs. The readers also provide the effective means for accurate MP mapping along all 3D components of the test strips for easy optimization of the assays as well as for metrology of MP for a variety of biochemical and medical applications.

The DRIM platform was optimized for multiplex quantitative detection of botulinum neurotoxin (BoNT) types A, B and E in complex matrices such as milk, apple and orange juices. Optimization of MP functionalization and bioassay protocols has been carried out by investigation of affinity constants of antibodies

immobilized on MP based on the spectral correlation interferometry (SPI), which allows recording of thickness changes of a biolayer on a cover slip with a picometer resolution averaged over the sensing area. Besides, the SCI combined with sandwich assay labeled by MP have been used for development of opto-magnetic biosensors based on affordable single-use sensor chips.

For multiplex DRIM concentration measurements of BoNT-A, B and E the LODs were found to be 0.2, 0.12 and 0.35 ng, respectively. The LOD for detection of total prostate specific antigen in human serum was as good as 25 pg/ml. Such LOD permits measurements within the clinically relevant concentration range even when the most sensitive registration is required, e.g., PSA detection after radical prostatectomy.

The developed multiplex DRIM platform is innovative by virtually no sacrifice in performance compared to single-plex assays and by characteristics on the level of complicated laboratory quantitative methods. The platform can be used for simple, rapid and sensitive quantitative detection of bioactive agents for *in vitro* diagnostics, food and safety control, etc.

Support by RSF and RFBR is acknowledged.

[1] P.I. Nikitin, P.M. Vetoshko. *Patents* RU2166751, RU2177611 (2000), EP1262766 (2001).

[2] M.P. Nikitin V.O.Shipunova, S.M.Deyev, P.I.Nikitin, *Nature Nanotech*, **9** (2014) 716–722.

[3] A.V.Orlov, V.A.Bragina, M.P.Nikitin, P.I. Nikitin. *Biosens. Bioelectr.*, **79** (2016) 423–429.

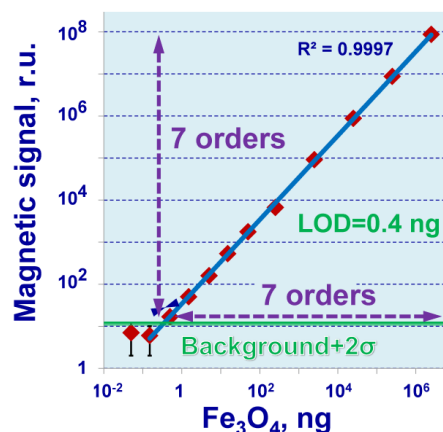


Fig. 1. Calibration curve

4RP-O-4

DESIGN AND STUDY OF CORE-SHELL MAGNETIC NANOPARTICLES*Kamzin A.S.*

Ioffe Physical Technical Institute of RAS, 194021 St. Petersburg, Russia

kamzin@mail.ioffe.ru

The core-shell nanoparticles can be widely defined as comprising a core (inner material) made of a material coated with shell (outer layer) of another material on top of it. These structural features allow the possibility of combining specific properties of varied materials. These core-shell structures have exhibited better physical and chemical properties relative to their single-component counterparts. Thus, the core-shell structures are new important class of nanoparticles made with a core and one or several shell layer(s) and have attracted much attention due to their unique properties that consist of an inner core and an external shell of different chemical compositions.

In the past decade the synthesis and characterization of magnetic nanoparticles of core-shell structures MNPCSS have become a particularly important area of research because they found application in many fields. The core-shell structure provides a stabilized magnetic property and oxidative resistance. The MNPCSS may be with various sizes and various shapes of core and shell thickness with various surface morphology. Whenever the surface of the nanoparticles is coated with a thin layer of other materials, they show improved properties compared to the uncoated particles. MNPCSS have been used in the broad range of various applications. The novel MNPCSS have a particularly interests for different applications such as drug or gene delivery, magnetic resonance image, biomedical diagnosis, catalytic applications, and biomolecule detection. This is the key point for the development of tailored MNPCSS with the appropriate components, spatial arrangement, and interface chemistry significantly enhancing the stability, activity, and biocompatibility.

In this review, the focus was on the recent progress of the synthesis, studying and applications of magnetic nanoparticles of core-shell structure. A summary of the synthetic methods and properties of engineered magnetic core-shell structures presented. The effects of various shells and cores on the physical and chemical properties of the MNPCSS are shown. The applications of the MNPCS in different field as well as for biomedicine are describing.

4 July

Tuesday

11:30-13:00

14:30-17:00

oral session

4TL-P

4RP-P

4OR-P

“Theory”

4TL-P-1

TEMPERATURE DEPENDENT POLARONIC BAND STRUCTURE IN THE 3 BAND P-D MODEL WITH STRONG ELECTRON-PHONON INTERACTION

Makarov I.A.¹, Ovchinnikov S.G.¹, Shneyder E.I.¹

¹ Kirensky Institute of Physics, FRC KSC SB RAS, Krasnoyarsk, Russia
sgo@iph.krasn.ru

The generalized tight binding (GTB) method to calculate the electronic structure of strongly correlated electrons in cuprates is modified to incorporate also strong electron-phonon interaction [1]. By exact diagonalization of the p-d-Holstain model Hamiltonian for a separate CuO₆ unit cell we find the multielectron and multiphonon local eigenstates that are used to construct a set of local Hubbard operators. Then we treat the intercell electron hopping t by the perturbation approach over small ratio t/U , where U is the charge transfer excitation energy. Without electron-phonon interaction we obtain the band of spin polaron and a set of local multiphonon Franck-Condon excitations. The electron-phonon interaction results in the hybridization of spin polaron and Franck-Condon excitations that forms the polaronic band structure with strong temperature dependence. The temperature dependence of the polaronic band structure and Fermi surface is discussed. The peak of a spectral function at the top of the valence band has large width typical to the ARPES data and determined by a large number of the multiphonon excitations.

The temperature dependent spectral function at the top of the valence band is shown in Fig.1. Temperature effected the polaronic band structure via multielectron occupation numbers and nearest neighbour spin correlation functions. The lost of spectral intensity is the largest effect of heating, while the increasing of the line widths also is clear and shown in the inset. Similar increasing has been found in ARPES experiments for undoped cuprates [2] and obtained within the t-J model [3].

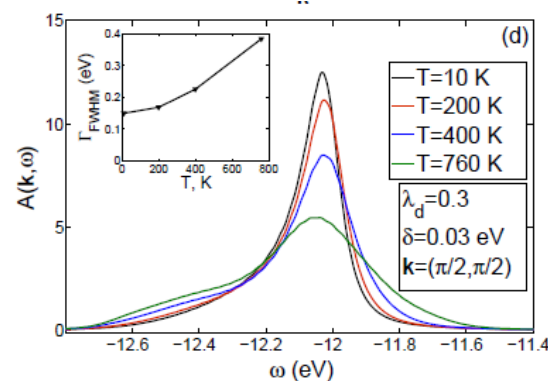


Fig. 1. The spectral function of polaron at the top of the valence band.

Support by RNF 14-12-00061 is acknowledged.

[1] I.A. Makarov, E.I. Shneyder, P.A. Kozlov, S.G. Ovchinnikov *Phys.Rev.B*, **92** (2015) 155143.

[2] K.M. Shen et.al. *Phys. Rev. B*, **75** (2007) 075115.

[3] A.S. Mishchenko, N.Nagaosa, *Phys. Rev. Lett.*, **93** (2004) 036402.

4TL-P-2

MAGNETIC FRICTION: TOWARDS MICROSCOPIC DESCRIPTION INCLUDING THERMAL EFFECTS

Rudoy Yu.G.¹, Kotelnikova O.A.²

¹RUDN, 117198, Moscow, Russia

²M.V. Lomonosov MSU, 119991, Moscow, Russia
rudikar@mail.ru, olga@magn.ru

The problem of magnetic friction stays to be one of the most interesting in nanotechnology in last decades (see, e.g., [1]) due to it's connection with the important problem of magnetic writing and reading. In particular, one may be interested in the dependence of the dissipative friction force upon the velocity of the "tip", which is a probing part of the spin-polarized magnetic force microscopy.

The relevant theoretical calculation in the rather simple setting was undertaken by Fusco et al. [2] and then refined in [3]. These papers were based on the Hamiltonian including the Heisenberg isotropic exchange between linear chain of classic spins and magnetic dipole interaction between tip and spin chain. But the analysis was limited by the semi-phenomenological Landau–Lifshitz–Gilbert equation for the relaxation and dissipation of the bulk magnetic template (see also [4]).

We propose considerably more general setting of the problem as a whole based on the theory of non-equilibrium statistical operator method developed rather long ago by Zubarev, Morozov and Roepke [5], where the dynamics of the combined system tip+template is treated as an interacting classical (tip) and quantum (template) parts.

[1] F.J. Himpsel et al. *Adv. Phys.*, **47** (1998) 511.

[2] C. Fusco, D.E. Wolf, U. Nowak. *Phys. Rev. B*, **77** (2008) 174426.

[3] M.P. Magiera et al. *Europhys. Lett.*, **95** (2011) 17010.

[4] R.F.L. Evans et al. *Phys. Rev. B*, **85** (2012) 014433.

[5] D.N. Zubarev, V.G. Morozov, G. Roepke. *Statistical Mechanics of Nonequilibrium Processes*, Berlin, Akademie Verlag, **1&2** (1996).

4RP-P-3

ITINERANT FERROMAGNETISM IN TWO-COMPONENT ONE-DIMENSIONAL FERMI GASES

Jiang Yu.¹, Kurlov D.V.², Guan Xi-Wen¹, Schreck F.², Shlyapnikov G.V.^{3,4}

¹ Institute of Physics and Mathematics, Chinese Academy of Sciences, Wuhan 430071, China

² University of Amsterdam, Science Park 904, 1098 Amsterdam, The Netherlands

³ Russian Quantum Centre, Novaya Street 100, Skolkovo, Moscow Region 143025, Russia

⁴ LPTMS, CNRS, Univ. Paris Sus, Univ. Paris-Saclay, Orsay 91405, France
shlyapn@lptms.u-psud.fr

Itinerant ferromagnetism of degenerate spin-1/2 fermions is an intriguing problem promoting our understanding of strongly correlated systems. In contrast to ultracold bosons, degenerate fermions try to avoid the ferromagnetic state because it requires them to have a significantly higher kinetic energy than in non-ferromagnetic states. Ultracold gases of atomic fermions which are in two internal states can be mapped onto spin-1/2 fermions treating the internal energy levels as pseudo-spin states. The ferromagnetic phase is the one where all atoms are in the same superposition of the two internal states and one has a system of identical fermions. The kinetic energy is then higher than, for example, in the paramagnetic phase, which represents a statistical mixture of the two spin components.

Itinerant ferromagnetism for fermions is studied since the 1930-ths, when the Stoner criterion for ferromagnetism in a free electron gas was introduced [1,2]. In three dimensions the ground state can be ferromagnetic if there is a strong intercomponent repulsion in the paramagnetic state, which compensates the large difference in the kinetic energies of the ferro- and paramagnetic states. The efforts to stabilize the ferromagnetic state in atomic Fermi gases experimentally did not succeed [3,4]. In three dimensions a large intercomponent repulsion corresponds to a very large and positive s-wave scattering length and there is a weakly bound dimer of two fermions belonging to different internal states. In this situation atom loss by dimer formation is very fast at typical densities.

However, we show that in one dimension (1D) the odd-wave interaction (analog of p-wave in higher dimensions) can drastically change the situation and make the ground state ferromagnetic. This interaction is momentum dependent and does not satisfy the conditions of the Lieb-Mattis theorem [5] which states that in the 1D (two-component) Fermi system the ground state can not be ferromagnetic. To make the odd-wave interaction significant one needs a Feshbach and/or confinement-induced odd-wave resonance. At the same time, another resonance (almost at the same magnetic field) is needed in order to make the even-wave contact interaction strongly repulsive. This is the case for ⁴⁰K atoms, which in this sense provide a "present from nature". Moreover, the reduction of dimensionality to 1D decreases the inelastic decay even not far from the resonances, which is very promising for achieving itinerant ferromagnetism.

[1] E.C. Stoner, *Phil. Mag.*, **15** (1933) 1018.

[2] D.C. Mattis, *The Theory of Ferromagnetism* (Harper & Row, New York, 1965).

[3] G.-B. Jo et al, *Science*, **325** (2009) 1521.

[4] C. Sanner et al, *Phys. Rev. Lett.*, **108** (2012) 240404.

[5] E.H. Lieb and D.C. Mattis, *Phys. Rev.*, **125** (1962) 164.

4RP-P-4

QUANTUM TRANSITIONS FROM ORDERED TO GLASSY PHASES IN MAGNETS WITH QUENCHED DISORDER

Syromyatnikov A.V.

NRC “Kurchatov Institute” Petersburg Nuclear Physics Institute, Gatchina, Russia
asyromyatnikov@yandex.ru

We discuss magnetically ordered (“superfluid”) phases near quantum transitions to the Bose- and Mott-glass phases in simple modeling systems, Heisenberg antiferromagnets with spatial dimension $d > 2$ and with disorder in exchange coupling constants. Our analytical consideration is based on general properties of a system in critical regime, on the assumption that the magnetically ordered part of the system shows fractal properties near the transition, and on a hydrodynamic description of long-wavelength magnons in the magnetically ordered phase.

For the transition to the Bose-glass phase, we demonstrate that the system behaves in full agreement with predictions by Fisher et al. [1] in close vicinity to the quantum critical point (QCP). In particular, we obtain for the dynamical critical exponent $z = d$. We find as an extension to the analysis in [1] that the anomalous dimension $\eta = 2 - d$ and $\beta = vd/2$, where β and v are critical exponents of the order parameter and the correlation length, respectively. The density of states per spin of low-energy localized excitations is found to be independent of d (“superuniversal”). We show that many recent experimental and numerical results obtained in various three-dimensional (3D) systems can be described by our formulas using percolation critical exponents. Then, it is a possibility that a percolation critical regime arises in the ordered phase in some 3D systems not very close to the QCP [2].

For the transition to the Mott-glass phase, we obtain $z = d - \beta/v$. The density of states of localized excitations is found to show a superuniversal behavior [3]. Our results are in agreement with recent numerical findings.

[1] M. P. A. Fisher et al., *Phys. Rev. B*, **40** (1989) 546.

[2] A. V. Syromyatnikov and A. V. Sizanov, *Phys. Rev. B*, **95** (2017) 014206.

[3] A. V. Syromyatnikov, arXiv:1701.08624.

4RP-P-5

PHASE DIAGRAM OF THE $O(n)$ MODEL WITH DEFECTS OF “RANDOM LOCAL ANISOTROPY” TYPE

Berzin A.A.¹, Morosov A.I.², Sigov A.S.¹

¹ Moscow Technological University (MIREA), 78 Vernadskiy Ave., 119454 Moscow, Russian Federation

² Moscow Institute of Physics and Technology (State University), 9 Institutskiy per., 141700 Dolgoprudny, Moscow Region, Russian Federation

It is shown that the Imry-Ma theorem stating that in space dimensions $d < 4$ the introduction of an arbitrarily small concentration of defects of the "random local anisotropy" type in a system with continuous symmetry of the n -component vector order parameter ($O(n)$ model) leads to the long-range order collapse and to occurrence of a disordered state, is not true if an anisotropic distribution of the defect-induced random easy axes directions in the order parameter space creates a global effective anisotropy of the “easy axis” type. For a weakly anisotropic distribution of the easy axes, in space dimensions $2 \leq d < 4$ there exists some critical defect concentration, when exceeded, the inhomogeneous Imry-Ma state can exist as an equilibrium one. At lower defect concentration the long-range order takes place in the system. For a strongly anisotropic distribution of the easy axes, the Imry-Ma state is suppressed completely and the long-range order state takes place at any defect concentration.

An anisotropic distribution of random easy axes of defects induces anisotropy of both “easy axis” and “easy plane” types. The Imry-Ma inhomogeneous state is suppressed only by the “easy axis” type anisotropy [1, 2]. That is why we detail the “easy plane” type anisotropy case. Gaining an answer to the question if there arises in the system the long-range order in the easy plane or the Imry-Ma inhomogeneous state, one should project all random easy axis unit vectors \mathbf{n}_l (l is the defect number) onto the given m -dimensional ($n > m \geq 2$) hyperplane in the order-parameter space and treat the problem at this hyperplane. When the “easy plane” anisotropy arises, the operation should be repeated. As a result we arrive at three possible cases:

(1) projections of random vectors \mathbf{n}_l on the easy plane equal zero. The system behavior therewith is analogous to that of the pure system with the number of the order parameter components corresponding to the hyperplane dimensionality. In any event the Imry-Ma inhomogeneous state does not occur;

(2) the “easy axis” anisotropy takes place in the easy plane itself. Then the problem reduces to that with the given anisotropy, but the number of the order parameter components equals m ;

(3) the distribution of vectors \mathbf{n}_l projections on the easy plane is perfectly isotropic. In this case the Imry-Ma theorem is true.

[1] A.A. Berzin, A.I. Morosov, and A.S. Sigov. *Phys. Solid State*, **58** (2016) 2018.

[2] A.I. Morosov and A.S. Sigov. *JETP Letters*, **90** (2009) 723.

4OR-P-6

FRUSTRATIONS AND PHASE TRANSITIONS IN MAGNETS OF VARIOUS DIMENSIONALITY

Kassan-Ogly F.A., Proshkin A.I.
 IMP UB RAS, Ekaterinburg, Russia
 felix.kassan-ogly@imp.uran.ru

We considered the Ising and Potts models with the nearest-neighbor J , next-nearest-neighbor interactions J' , and external magnetic field on 1D chain, 2D and 3D lattices: square, triangular, kagome, bcc and fcc. For problem solving we mainly calculated the entropy and specific heat using the rigorous analytical solutions for maximum eigenvalue of Kramers-Wannier transfer-matrix and exploiting computer simulation, par excellence, by Wang-Landau algorithm. As a result, many peculiar features concerning magnetic orderings and frustrations were revealed.

The interactions and an external magnetic field may compete between themselves creating either magnetic ordering and phase transitions or frustration points and ranges of frustration.

The interplay of competing interactions results sometime in the partial ordering, as in Ising model on a square and triangular lattice.

An external magnetic field may both favor the ordering of a system or frustrations suppressing ordering.

In some cases the same interactions may be competing and noncompeting. For example, in 4-state Potts model, the antiferromagnetic nearest-neighbor and next-nearest-neighbor interactions on 1D chain compete and lead to frustrations at any values. Quite the contrary, on a triangular lattice these interactions are noncompeting and lead to the phase transitions at any values.

We obtained that magnetic properties of the linear chain with nearest-neighbor and second-neighbor interactions and the 2D square lattice in the Ising model with nearest-neighbor and third-neighbor interactions are alike at almost every aspect if the temperature and magnetic field were rescaled.

In every model on any lattice, in the vicinity of frustration point or frustration field the specific heat splits into a sharp peak and a broad dome-shaped peak, both of which move with the field variation. The splitting and moving of specific heat nearby the frustration field is also observed in the real 3D crystals, for example, in TmTe and in ErBi.

The dependence of the phase-transition point on the ratio $r = J'/J$ may have three different types, some examples of each are shown in Fig.1.

The reported study was carried out within the state assignment of FASO of Russia (theme "Quantum" No. 01201463332).

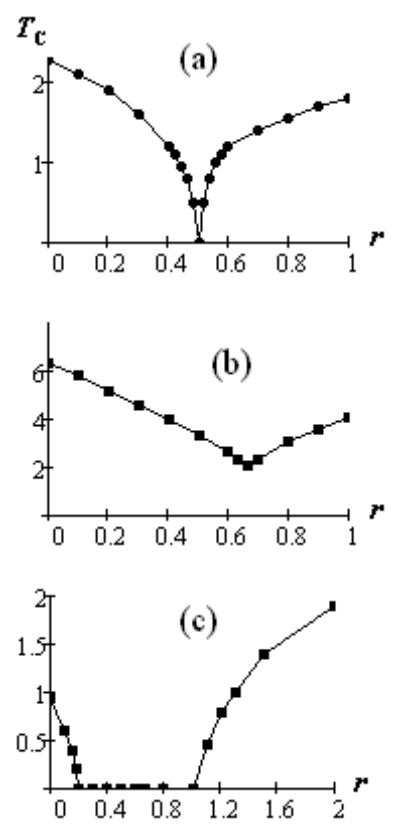


Fig. 1. Ising model on square lattice (a); Ising model on bcc lattice (b); 3-state Potts model on triangular lattice (c);

- [1] A. Kalz, A. Honecker, S. Fuchs, T. Pruschke, *Eur. Phys. J. B*, **65** (2008) 533.
 [2] A.B. Babaev, M.A. Magomedov, et.al., *JETP*, **149** (2016) 310-317.
 [3] A.K. Murtazaev, et.al., *JETP*, **147** (2015) 110–114.

4OR-P-7

MAGNETIC EXCITATIONS OF CARBON NANO-TUBES IN CHIRAL MODEL OF GRAPHENE

*Rybakov Yu.P.*¹

¹ RUDN University, Moscow, Russian Federation
soliton4@mail.ru

The concept behind this research is the following. The carbon atom possesses of four valence electrons in the so-called hybridized sp^2 -states. The one of them is "free" in the honeycomb graphene lattice and all others form the strong covalent bonds with the neighbors. It appears natural to introduce scalar a_0 and 3-vector \vec{a} fields corresponding to the s -orbital and the p -orbital states of the "free" electron respectively. These two fields can be combined into the unitary matrix $U = a_0\tau_0 + i\vec{a}\cdot\vec{\tau}$ considered as the order parameter of the model, the long-wave approximation being adopted, where τ_0 is the unit matrix and $\vec{\tau}$ are the three Pauli matrices, with the condition $a_0^2 + \vec{a}^2 = 1$ being imposed. The model admits the kink-like configuration $U = \exp[i\sigma\Theta(z)]$ of the graphene plane and the hedgehog one of the carbon nano-tube [1]: $U = \exp[i\sigma\Theta(\rho)]$, $\sigma = \tau_1 \cos\phi + \tau_2 \sin\phi$, $\phi = n\varphi$, $n = 1, 2, \dots$, with ρ, φ being polar coordinates. Here n stands for the topological charge of the degree type. For the description of spin and quasi-spin excitations, the latter ones corresponding to the independent excitation modes of the two triangular sub-lattices, we introduce the two Dirac spinors ψ_1, ψ_2 and consider the combined spinor field Ψ as a new order parameter: $\Psi = \xi \otimes (\psi_1 \oplus \psi_2)$, where ξ stands for the first column of the matrix U . The Lagrangian density L of the model

$$L = \frac{I}{2} \overline{D_\mu \Psi} P D^\mu \Psi - \frac{\lambda^2}{2} \vec{a}^2 j_\mu j^\mu + i\mu_0 \vec{a}^2 \overline{\Psi} \sigma_{\mu\nu} F^{\mu\nu} \Psi$$

contains the projector $P = \gamma^v j_v$ on the positive energy states, where $j_\mu = \overline{\Psi} \gamma_\mu \Psi$, $\mu = 0, 1, 2, 3$, designates the Dirac current, $\overline{\Psi} = \Psi^+ \gamma_0$, γ_μ stands for the Dirac matrices, $\sigma_{\mu\nu} = [\gamma_\mu, \gamma_\nu]/4$, $F_{\mu\nu} = \partial_\mu A_\nu - \partial_\nu A_\mu$, and $\mu_0 > 0$ denotes the Bohr magneton per lattice spacing cubed. The model contains the two constant parameters: the exchange energy I per lattice spacing and some characteristic inverse length $\sqrt{\lambda}$. The interaction with the electromagnetic field is realized through the extension of the derivative: $D_\mu = \partial_\mu - ie_0 A_\mu \Gamma_e$, with $e_0 > 0$ being the coupling constant and $\Gamma_e = (1 - \tau_3)/2$ being the charge operator chosen in accordance with the natural boundary condition at infinity: $a_0(\infty) = 1$. However, the additional interaction term of the Pauli type should be added to take into account the proper magnetic moments of the electrons. Within the scope of the graphene chiral model [2], we consider an infinite carbon nano-tube interacting with an external static magnetic field oriented along the tube. The axially-symmetric configuration being studied, we analyze the structure of the corresponding solution in the small field limit via the perturbation method. This method proves to be self-consistent under the supposition that the topological charge of the tube is large. Using the Green's function method, we find the magnetic intensity of the tube and show the field to decrease in the central domain.

[1] Yu.P. Rybakov, *Solid State Phenomena*, **190** (2012) 59-62.

[2] Yu.P. Rybakov, *Solid State Phenomena*, **233-234** (2015) 16-19.

4OR-P-8

NON-MONOTONOUS MAGNETOCONDUCTANCE OF P-N JUNCTIONS IN WEYL SEMIMETALS

Saykin D.R.¹, Tikhonov K.S.², Rodionov Ya.I.³

¹ Moscow Institute of Physics and Technology, Moscow, Russia

² L. D. Landau Institute for Theoretical Physics RAS, Moscow, Russia

³ Institute for Theoretical and Applied Electrodynamics RAS, Moscow, Russia
yaroslav.rodionov@gmail.com

We study the magnetoconductance $G(H)$ of the pn junction realized in ballistic Weyl semimetal with two Dirac cones. We show that unlike the case of a single cone Weyl semimetal, where Klein tunneling manifests itself in positive differential magnetoconductance $dG(H)/dH$, the physically realistic two cone model leads to the non-monotonous behavior of $G(H)$. As a result of the field-induced tunneling between Dirac cones the differential magnetoconductance interpolates between positive values (small fields) to negative ones (large fields).

The magnetoconductance is derived as a function of external magnetic field \mathbf{H} , and orientation of the momentum vector \mathbf{p}_0 connecting two Dirac nodes with respect to the built-in electric field \mathbf{E} of the pn -junction.

The analytical results are obtained in WKB formalism, where the product of magnetic length and \mathbf{p}_0 : $l_H |\mathbf{p}_0| \gg 1$ plays the role of large parameter in the problem.

The effect is the most pronounced when \mathbf{H} is orthogonal to \mathbf{p}_0 and the Hamiltonian of the system is supersymmetric.

The effect observed can be understood from purely qualitative reasons. Indeed, semiconductors have negative differential magnetoconductance. On the other hand, single cone Weyl semimetal has positive magnetoconductance due to Klein tunneling [1]. If the applied field is large enough the particle can tunnel between two Dirac cones due to which the spectrum works in a semiconductor-like way. We used the simplest model of the two-cone Weyl-semimetal Okugawa-Murakami Hamiltonian [2].

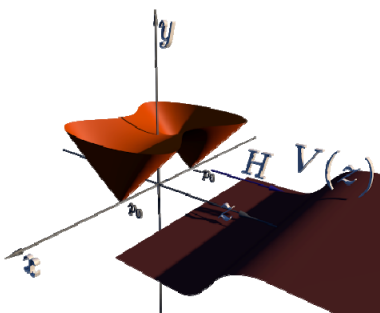


Fig.1. Geometry of pn -junction

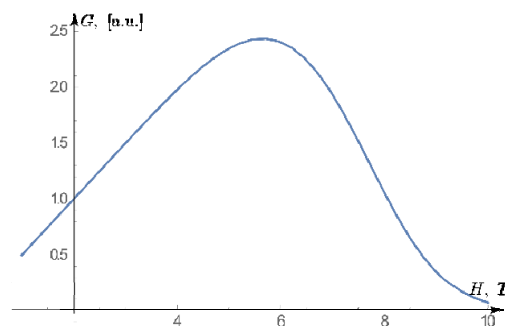


Fig.2. Magnetoconductance as a function of magnetic field

[1] Songci Li, A. V. Andreev, and B. Z. Spivak, *Phys. Rev. B*, **94** (2016) 081408(R).

[2] Ryo Okugawa and Shuichi Murakami, *Phys. Rev. B*, **89** (2014) 235315.

4OR-P-9

AN APPROXIMATE QUANTUM THEORY OF THE ANTIFERROMAGNETIC GROUND STATE

*Orlova N.B.*², *Kurkin M.I.*¹

¹ Novosibirsk State Technical University, Novosibirsk, Russia

² Russia Institute of Metal Physics UB RAS, Ekaterinburg, Russia
orlova.nb@gmail.com

The hypothesis of magnetic sublattices underlies most of the models used to describe the ferri- and antiferromagnetic spin structures ordered by the exchange interaction $V_{\text{ex}} = V(s_z) + V(s_y, s_x)$. The term $V(s_z)$ determines the mutual orientation of the longitudinal components of the spins s_z , therefore it is compatible with the sublattices hypothesis. The term $V(s_y, s_x)$ describes the processes with simultaneous switching of the oppositely directed spins, which is equivalent to their transposition. Such exchange mixing destroys the ferromagnetic order in the sublattices. One of the solutions for the problem of choosing between these two competing mechanisms is proposed by Anderson [1] and Ziman [2]. They associated the destruction of the sublattices with the zero spin-wave oscillations similar to zero phonon oscillations. This mechanism completely destroys the sublattices in one-dimensional and two-dimensional spin structures, but partially keeps them at the three-dimensional antiferromagnetic ordering.

We propose another model, in which the suppression of the sublattices exchange mixture is provided by the magnetic anisotropy. The possibility of such suppression is caused by the degeneracy in the spectrum of the operator V_{ex} by the spin orientations relative to the crystal axes. The magnetic anisotropy V_A removes this degeneracy, which is usually associated with a strong change of the wave functions forms. This effect was demonstrated for the operators U_{ex} and U_A of a special form ensuring the existence of solutions of the equations corresponding to antiferromagnetic ordering.

$$U_{\text{ex}}\Phi_0 = E_{\text{ex}}\Phi_0; \quad (U_{\text{ex}} + U_A)\Phi = E\Phi \quad (1)$$

The wave function Φ_0 provides zero mean value of the spin ($\langle \Phi_0 | s | \Phi_0 \rangle = 0$) corresponding to the absence of spin sublattices. The value of the spin $\langle \Phi | s | \Phi \rangle$ appeared to depend on the number of spins in the sublattice N even for $H_A \ll H_E$ (here H_E is the exchange field, H_A is the magnetic anisotropy field). The condition $N \gg H_E / H_A$ ensures the existence of two sublattices with different values of spins:

$$\langle \Phi | s_1 | \Phi \rangle = -\langle \Phi | s_2 | \Phi \rangle = 1/2 [1 - H_E / (H_A N)] \quad (2)$$

It turned out that the values of (2) correspond to the linear approximation by the small parameter $H_E / (H_A N) \ll 1$ also for the exchange interaction in the nearest-neighbour approximation.

The work was performed as the part of the state task of FASO of Russia (topic №01201463332) and with partial financial support of RFBR (project №17-02-00344).

[1] P.N. Anderson, *Phys.Rev.*, **86** (1954) 694.

[2] J. M. Ziman, *Proc.Phys.Soc.*, **50** (1952) 540.

4OR-P-10

QUANTUM INVERSION DUE TO SUPEROSCILLATING FIELD

Doronin I.V.¹, Pukhov A.A.^{1,2,3}, Andrianov E.S.^{1,2}, Vinogradov A.P.^{1,2,3}, Lisyansky A.A.^{4,5}

¹MIPT, 9 Institutskiy per., Dolgoprudniy 141700, Moscow Reg., Russia

²Dukhov Research Institute for Automatics, 22 Sushchevskaya, Moscow 127055, Russia

³ITAE RAS, 13 Izhorskaya, Moscow 125412, Russia

⁴Department of Physics, Queens College of the City University of New York, Flushing, NY 11367

⁵The Graduate Center of the City University of New York, New York, New York 10016, USA

ildoron2@gmail.com

We consider superoscillations of near field as a possible mechanism, responsible for biophoton emission, first discovered in [1]. Superoscillations are phenomenon, first described in [2], as specific behavior of bandlimited functions, locally oscillating significantly faster than their highest Fourier component. The practical use of superoscillations is hampered by large amplitudes of such functions outside of superoscillating region [3].

We show via numerical simulation, that two-level system with high transition frequency ω_B (HF TLS) can be up-converted due to interaction with a system of lower-frequency $\omega < 0.9\omega_B$ TLSs (basis TLSs), Fig. 1. The effect can be explained in the following way. At special choice of initial conditions the near fields of the basis TLSs form an interval of the superoscillations at frequency $\sim \omega_B$. It causes the Rabi oscillation of HF TLS. This interval should finish right when population inversion of HF TLS reaches its maximum. After that the superoscillations cease, interaction is no longer resonant, which prevents HF TLS from dropping sharply.

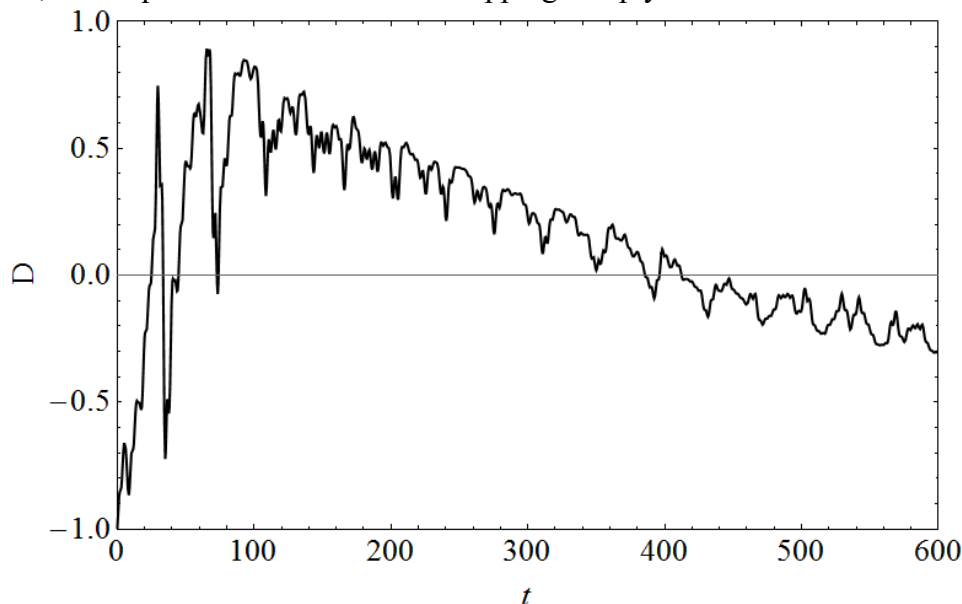


Fig. 1. Time dependence of the population inversion of the HF TLS.

[1] M.V. Berry, *J. Phys. A: Math. Gen.*, **27** (1994) 391-398.

[2] P.J.S.G. Ferreira, A. Kempf., *IEEE Trans. on Signal Process.*, **54** (2006) 3732-3740.

[3] A. Gurwitsch, , *Archiv für Entwicklungsmechanik der Organismen*, **51** (1922) 383-415.

4OR-P-11

ENERGY EXTRACTION FROM RESERVOIR IN OVERHAUSER EFFECT*Shishkov V.Yu.*^{1,2}, *Andrianov E.S.*^{1,2}, *Pukhov A.A.*^{1,2,3}, *Vinogradov A.P.*^{1,2}, *Lisyansky A.A.*^{4,5}¹ Moscow Institute of Physics and Technology (MIPT), Dolgoprudny, Russia² Dukhov Research Institute of Automatics (VNIIA), Moscow, Russia³ Institute for Theoretical and Applied Electromagnetics RAS (ITAE), Moscow, Russia⁴ Queens College of the City University of New York, Department of Physics, New York, USA⁵ The Graduate Center of the City University of New York, New York, USA

vladislavmipt@gmail.com

The nuclear Overhauser effect has been known for more than seven decades [1,2,3]. The effect consists of the transfer of spin polarization from one spin group to another via cross-relaxation [4]. As a consequence, the nuclear magnetic resonance for one spin group is amplified by another. Usually, to explain this phenomenon, one uses the Fermi golden rule and does not consider energy flows between the groups. It seems, however, that the spin polarization transfer should lead to the increase of the energy of the whole system. Thus, the theory appears not self-consistent because the whole system is supposed to be Hermitian.

To solve this paradox, we introduce a reservoir to model spin depolarization and relaxation processes and show that the spin excitation transfer from the nuclei with a low gyromagnetic ratio to the nuclei with a high gyromagnetic ratio [1] is assisted by the energy extraction from the reservoir. During the process of the energy extraction from the reservoir, the entropy increases. This theory self-consistently describes the Overhauser effect [2].

[1] R. R. Ernst, G. Bodenhausen, and A. Wokaun Principles of nuclear magnetic resonance in one and two dimensions. *Oxford, Clarendon Press*, (1990).

[2] I. Solomon, *Phys. Rev.*, **99** (1955) 559.

[3] W. A. Anderson and R. Freeman, *J. Chem. Phys.*, **37** (1962) 85.

[4] S. R. Hartmann and E. L. Hahn, *Phys. Rev.*, **128** (1962) 2042.

4OR-P-12

HALF-METALLIC STATES IN DOPED SPIN-DENSITY WAVE INSULATOR*Rozhkov A.V.^{1,2}, Rakhmanov A.L.^{1,2}, Sboychakov A.O.^{1,2}, Kugel K.I.^{1,2}, Nori F.²*¹ ITAE RAS, Moscow, Russia² RIKEN, Saitama, Japan

arozhkov@gmail.com

For half-metals Fermi surface is completely spin-polarized: electronic states with only one spin projection value reach the Fermi energy. This property is useful for spintronics applications. Usually half-metallicity emerges in electronic systems with strong electron-electron interaction, or when magnetic atoms are present. Here, we demonstrate that doping a spin-density wave insulator in the weak-coupling limit may stabilize new types of half-metallic states, spin-valley half-metal and charge-density wave (CDW) half-metal.

The non-interacting part of the model's hamiltonian consists of two bands, electron band a and hole band b , both with parabolic dispersion and spherical Fermi surface pockets (or valleys). If the Fermi surface valleys nest well (that is, the Fermi momentum of electrons a equals to the Fermi momentum of holes b), repulsive interaction induces the spin-density wave (SDW) state. This state is unique up to symmetry transformations, such as spin rotations.

Introduction of extra charges into such a system makes the situation less clear-cut: it is believed that at finite doping level several states with close energies compete against each other to become true ground state. Various possibilities are discussed in the theoretical literature: incommensurate SDW, electronic phase separation, stripes, etc. We demonstrate that yet another type of many-body state is available. In the doped system two-valley Fermi surface emerges. One valley is electron-like. It composed predominantly of states in band a with spin σ . Another valley is hole-like, composed predominantly of states in band b with spin σ' . These Fermi surface valleys have half-metallic character: states in band a with spin $-\sigma$, as well as states in band b with spin $-\sigma'$, do not reach the Fermi energy.

Depending on parameters, the spin polarizations of the electron-like valley and hole-like valley may be parallel ($\sigma=\sigma'$) or antiparallel ($\sigma=-\sigma'$). The former case is similar to the usual half-metal: quasiparticles at the Fermi surface are completely spin-polarized. In addition, the system exhibits finite CDW order parameter. For this reason we will refer to such a state as CDW half-metal. When $\sigma=-\sigma'$, the total spin polarization averages to zero. It is proven, however, that in this situation the so-called spin-valley polarization is finite. Thus, the state is called the spin-valley half-metal. The properties of these half-metallic states are discussed.

4OR-P-13

TWO ORDER PARAMETERS THEORY OF METAL-INSULATOR PHASE TRANSITION IN MAGNETIC FIELD

Dubovskii L.B.^{1,2}

¹NRC “Kurchatov Institute”, Moscow, Russia

²MFTI Dolgoprudnyi, Moscow, Russia

ldubovskii@mail.ru

Any metal-insulator (MI) phase transition in a crystalline material must be a transition from a situation in which electronic bands overlap to a situation when they do not. Usually, overlapping of the bands occurs as a result of a variation of material density distribution at MI interface. The material density distribution at MI interface exhibits itself as an order parameter of the first order phase transition. In addition, the phase transition is accompanied by appearance of another order parameter which describes distribution of electrons in the system. The new parameter is the second type phase transition order parameter. These two interacting order parameters can be described by self-consistent equations of Ginzburg-Landau type [1].

The magnetic field is involved in the consideration of the system. The magnetic field leads to new singularities of the surface tension at the metal-insulator interface and results in a drastic variation of the phase transition kinetics. A strong singularity in the surface tension results from the Landau diamagnetism and determines anomalous features of the metal-insulator transition kinetics. At low temperature the quantum oscillations of the surface tension in the magnetic field take place [2].

[1] L. Dubovskii, *JETP Letters*, **99** (2014) 22.

[2] L. Dubovskii, *J. Low Temp. Phys.*, **182** (2016) 192.

Support by IEEE, ARC, and ARCNN is acknowledged.

[1] C.D. Ee, F.G. Hhh, *J. Appl. Phys.*, **33** (1999) 133-136.

4OR-P-14

SPIN-DEPENDENT TRANSPORT IN QUADRUPLE QUANTUM-DOT STRUCTURE TAKING INTO ACCOUNT COULOMB CORRELATIONS

Kagan M.Yu.^{1,2}, Val'kov V.V.³, Aksenov S.V.³

¹ P.L. Kapitza Institute for Physical Problems RAS, Moscow, Russia

² National Research University Higher School of Economics, Moscow, Russia

³ Kirensky Institute of Physics, Federal Research Center KSC SB RAS, Krasnoyarsk, Russia
asv86@iph.krasn.ru

Quantum dot (QD) serves as a perfect basic system allowing to study different fundamental processes and interplay between them [1]. Additionally applications ranging from quantum computations to rectifiers, filters, and valves are being considered. In last years due to technological development the arrays of three and more QDs have been attracting attention [2].

Here we present the results of theoretical investigation of a system consisting of four QDs, quadruple QD (QQD) structure (see fig.1). Spectral and transport properties were studied taking into account the intra- and interdot Coulomb correlations as well as the anisotropy of hopping integrals and on-site electron energies. The analysis was based on the nonequilibrium Green's functions, the tight-binding approach and the equation-of-motion method. We demonstrated that the

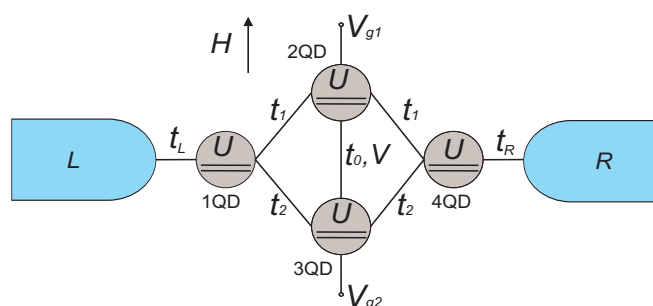


Fig.1. QQD structure between contacts.

conductance of the QQD device as a function of gate voltage has a wide insulating band separating triple-peak structures if the intradot Coulomb interactions are included. The interdot Coulomb correlations between the central QDs result in the broadening of this band and the occurrence of an additional band with low conductance due to the Fano antiresonances. It was shown that in this case the conductance of the anisotropic QQD device can be dramatically changed by tuning the anisotropy of on-site electron energies [3]. In magnetic field the Zeeman splitting of the insulating bands leads to the appearance of so-called spin-polarized windows (SPWs) characterized by the high spin polarization of the current. It's demonstrated that the gate-field controlled switching between the transport channels with opposite spin-polarization of the current can be achieved [4].

Support by the Comprehensive programme SB RAS no. 0358-2015-0007, the Russian Foundation for Basic Research, Government of Krasnoyarsk Territory, Krasnoyarsk Region Science and Technology Support Fund to the research projects nos. 15-02-03082, 16-42-243056, 16-42-242036, 17-42-240441 is acknowledged. M.Yu. K. thanks the Program of Basic Research of the National Research University Higher School of Economics for support.

[1] J. Gores, D. Goldhaber-Gordon, S. Heemeyer, M. A. Kastner, H. Shtrikman, D. Mahalu and U. Meirav, *Phys. Rev. B*, **62** (2000) 2188.

[2] C.-Y. Hsieh, Y.-P. Shim, M. Korkusinski and P. Hawrylak, *Rep. Prog. Phys.*, **75** (2012) 114501.

[3] M. Yu. Kagan, V. V. Val'kov and S. V. Aksenov, *Phys. Rev. B*, **95** (2017) 035411.

[4] M. Yu. Kagan, V. V. Val'kov and S. V. Aksenov, *J. Magn. Magn. Mat.* (2017) <http://dx.doi.org/10.1016/j.jmmm.2016.12.106>.

4 July

Tuesday

11:30-13:00

14:30-17:00

oral session

4RP-C

4OR-C

**“Magnetic
Nanostructures and
Low Dimensional
Magnetism”**

4RP-C-1

PROPERTIES OF MAGNETIC $(\text{Co}_{40}\text{Fe}_{40}\text{B}_{20})_x(\text{Al}_2\text{O}_{3-y})_{100-x}$ AND $(\text{Co}_{40}\text{Fe}_{40}\text{B}_{20})_x(\text{LiNbO}_{3-y})_{100-x}$ NANOCOMPOSITE STRUCTURES

Rylkov V.V.^{1,2,3}, *Sitnikov A.V.*⁴, *Demin V.A.*¹, *Presnyakov M.Yu.*¹, *Vasiliev A.L.*¹,
*Taldenkov A.N.*¹, *Nikolaev S.N.*¹, *Chernoglazov K.Yu.*¹, *Kalinin Yu.E.*⁴, *Bugaev A.S.*^{2,5},
*Tugushev V.V.*¹, *Granovsky A.B.*^{3,6}

¹ NRC "Kurchatov Institute", 123182 Moscow, Russia

² Kotel'nikov Institute of Radio Engineering and Electronics RAS, 141190 Fryazino, Russia

³ Institute of Theoretical and Applied Electromagnetics RAS, 125412 Moscow, Russia

⁴ Voronezh State Technical University, 394026 Voronezh, Russia

⁵ Moscow Institute of Physics and Technology, 141700 Dolgoprudny, Moscow Region, Russia

⁶ Faculty of physics, M.V. Lomonosov MSU, 119991 Moscow, Russia

vvrylkov@mail.ru

Granular systems have unusual transport properties revealed. in particular, in the temperature conductivity dependences: "1/2" law, $\ln\sigma \propto -(T_0/T)^{1/2}$, or logarithmic one: $\sigma(T) \propto \ln T$. The "1/2" law is observed in dielectric samples and is caused by processes of resonance co-tunneling. The logarithmic law is manifested in metal samples near metal insulator transition (MIT) and is caused by features of the Coulomb interaction under strong tunnel coupling between granules [1].

Recently, we have found that the conductivity of $(\text{CoFeB})_x(\text{Al}_2\text{O}_{3-y})_{100-x}$ nanocomposite (NC) follows the $\ln T$ law on the metallic side of MIT in the wide range of ferromagnetic (FM) alloy content variation $x=49-56$ at.%. Furthermore, under these conditions we have observed clearly a manifestation of the tunneling anomalous Hall effect (AHE) [2] recently predicted in [3].

To obtain further insight into previously found phenomena we performed a comparative study of the properties of $(\text{CoFeB})_x(\text{Al}_2\text{O}_{3-y})_{100-x}$ and $(\text{CoFeB})_x(\text{LiNbO}_{3-y})_{100-x}$ NCs with different non-stoichiometric oxides. Both NCs consist of the CoFe nanogranules with the lateral size of 2-4 nm embedded into the oxide matrix with large amount of dispersed Fe or Co atoms. For $(\text{CoFeB})_x(\text{Al}_2\text{O}_{3-y})_{100-x}$ the granules are rounded, but in case of $(\text{CoFeB})_x(\text{LiNbO}_{3-y})_{100-x}$ the granules are strongly extending along the NC growth axis between 5-15 nm. Nevertheless in both cases, the AHE behavior is similar to the one observed in FM films with easy-plane magnetic anisotropy. At $T < 20$ K, in the NC magnetization along the FM direction, additional paramagnetic (PM) component is observed; in case of $(\text{CoFeB})_x(\text{LiNbO}_{3-y})_{100-x}$ it even exceeds FM component in three times. We show that PM component is caused by Fe^{2+} and Co^{2+} ions with the concentration reaching $N_i \approx 3 \cdot 10^{22} \text{ cm}^{-3}$. It is also established that T_0 parameter in the "1/2" law for $(\text{CoFeB})_x(\text{LiNbO}_{3-y})_{100-x}$ is several times less than for $(\text{CoFeB})_x(\text{Al}_2\text{O}_{3-y})_{100-x}$. We explain our results by structure features of NCs as well as essential role of magnetic ions in FM exchange between granules of percolation network.

This work was financially supported by Russian Science Foundation, grant No. 16-19-10233.

[1] I.S. Beloborodov, A.V. Lopatin, V.M. Vinokur, K.B. Efetov. *Rev. Mod. Phys.*, **79** (2007) 469.

[2] V.V. Rylkov, S.N. Nikolaev, K.Yu. Chernoglazov, V.A. Demin, A.V. Sitnikov, M.Yu. Presnyakov, A.L. Vasiliev, N.S. Perov, A.S. Vedenev, Yu.E. Kalinin, V.V. Tugushev, A.B. Granovsky, accepted for publication in *Phys. Rev. B*.

[3] A.V. Vedyayev, N.V. Ryzhanova, N. Strelkov, B. Dieny, *Phys. Rev. Lett.*, **110** (2013) 247204.

4RP-C-2

MAGNETIC PROPERTIES AND ELECTRONIC STRUCTURE OF THE SURFACE ALLOYS OF LANTHANIDES WITH Au AND Ag

Ilyn M.^{1,3}, *Blanco-Rey M.*^{1,2}, *Fernandez L.*³, *Ortega J.E.*^{3,4}, *Schiller F.*³

¹ Donostia International Physics Center (DIPC), Donostia, Spain

² Departamento de Física de Materiales, Universidad del País Vasco, Donostia, Spain

³ Centro de Física de Materiales CSIC-UPV/EHU, Donostia, Spain

⁴ Departamento de Física Aplicada I, Universidad del País Vasco, Donostia, Spain

maxim_ilyn@ehu.es

The progress in the preparation and characterization of the multi-element metallic monolayers (surface alloys) achieved in the field of the heterogeneous catalysis has opened a way to apply the surface science techniques to the investigation of the magnetic properties of the intermetallic compounds. Traditionally, among the most studied materials in the bulk magnetism were intermetallic compounds of the Rare Earth elements whose peculiar magnetic properties stem from the indirect exchange interactions, mediated by the conduction electrons. Preparation of these compounds by means of surface alloying on the single crystal substrates in the ultra-high vacuum environment [1-3] allowed for the determination of the atomic structure employing the scanning tunneling microscopy (STM), measuring the electronic structure by means of the photoelectron spectroscopy with angular resolution (ARPES) and obtaining the element-specific magnetic data with the help of the synchrotron facilities via the X-ray absorption spectroscopy (XMCD).

In this work we present results of investigation of two series of the surface intermetallic compounds REAu₂ and REAg₂ [1-3]. A combination of the advanced experimental surface science techniques and modern methods of ab-initio calculations allowed us to address a number of fascinating effects observed in these materials. For example, we have elucidated that a filling of the hybrid s, p – d band is responsible for the almost four-fold increasing of the Curie temperature in the GdAg₂ (85 K) with respect to the GdAu₂ (19 K) [1] and used calculations of the RE atomic multiplets to explain the anisotropy of the magnetic properties of the SmAu₂ and HoAu₂ observed in the XMCD measurements.

The contribution is intended to give an overview of the results obtained in the investigation of the magnetic properties of the surface intermetallic compounds of lanthanides with Au and Ag and to show the perspective of the future research activity in this particular field of the surface magnetism.

[1] M. Ormaza, L. Fernández, M. Ilyn, A. Magaña, B. Xu, M. J. Verstraete, M. Gastaldo, M.A. Valbuena, P. Gargiani, A. Mugarza, A. Ayuela, L. Vitali, M. Blanco-Rey, F. Schiller, J.E. Ortega, *Nano Lett.*, **16** (2016) 4230–4235.

[2] L. Fernández, M. Blanco-Rey, M. Ilyn, L. Vitali, A. Correa, P. Ohresser, J. E. Ortega, A. Ayuela, F. Schiller, *Nano Lett.*, **14** (2014) 2977–2981.

[3] A. Cavallin, L. Fernández, M. Ilyn, A. Magaña, M. Ormaza, M. Matena, L. Vitali, J.E. Ortega, C. Grazioli, P. Ohresser, S. Rusponi, H. Brune, F. Schiller, *Phys. Rev. B*, **90** (2014) 235419.

4OR-C-3

MAGNETIC PROXIMITY EFFECT IN $(\text{La}_{0.7}\text{Sr}_{0.3}\text{MnO}_3)_x(\text{CaCu}_3\text{T}_4\text{O}_{12})_{1-x}$ NANOSTRUCTURED COMPOSITES

Gavrilova T.P.^{1,2}, *Eremina R.M.*^{1,2}, *Yatsyk I.V.*^{1,2}, *Gilmutdinov I.F.*², *Kiiamov A.G.*²,
*Lyadov N.M.*¹, *Kabirov Yu.V.*³

¹ Kazan Zavoiisky Physical-Technical Institute of RAS, Kazan, Russia

² Kazan Federal University, Kazan, Russia

³ Southern Federal University, Rostov-on-Don, Russia

tatyana.gavrilova@gmail.com

Investigations of composite compounds with high values of magnetic susceptibility and dielectric permittivity are of interest because of they can be used in variety of applications. Here we investigated the materials, which consist of two inorganic phases. One of the components of the composite material is $\text{CaCu}_3\text{T}_4\text{O}_{12}$ (CCTO), which dielectric behavior exhibits an extraordinary high dielectric constant and shows good thermal stability in a wide temperature range (100–600K). As the second component of the composite material we chose the lanthanum-strontium manganite $\text{La}_{0.7}\text{Sr}_{0.3}\text{MnO}_3$ (LSMO), which is ferromagnetic up to $\sim 360\text{--}370$ K and thus can modulate the magnetic properties of the first component.

$\text{LSMO}_x\text{CCTO}_{1-x}$ ($0.01 \leq x \leq 0.3$) nanostructured composites with LSMO microinclusions in CCTO matrix were synthesized using a solid state method. The magnetic susceptibility of investigated samples can be presented as the sum of the paramagnetic contribution from CCTO component and ferromagnetic contribution from LSMO component (see Fig.1). For low concentrations $x=0.01\text{--}0.05$ the Weiss constant and effective magnetic moment for paramagnetic phase are close to same parameters of the bulk CCTO. For high concentrations $x \geq 0.1$ the ferromagnetic contribution

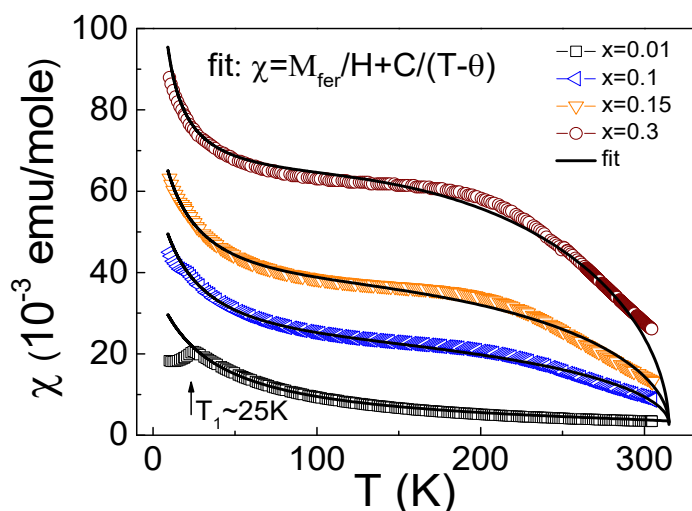


Fig. 1. Temperature dependencies of magnetic susceptibility χ in $\text{LSMO}_x\text{CCTO}_{1-x}$.

predominates and changes linearly with concentration. ESR measurements confirm the concentration dependence of the magnetic properties of $\text{LSMO}_x\text{CCTO}_{1-x}$ composites. The concentration $x=0.1$ is the key point in the changing of the magnetic properties of $\text{LSMO}_x\text{CCTO}_{1-x}$ composites.

The Curie temperature of the ferromagnetic phase $T_C=315$ K is the same for all concentrations, that is less at ~ 50 K than in pure LSMO. The Weiss constant - θ of the paramagnetic phase has the strong concentration dependence. The observed mutual influence on the magnetic properties of both

components can be tentatively attributed to the interface exchange interactions between them, hinting a possible magnetic proximity effect.

The reported study was supported by RFBR, research project № 16-32-00660.

4OR-C-4

MAGNETISM OF THE SPIN-LADDER LUDWIGITES $\text{Co}_{3-x}\text{Fe}_x\text{BO}_5$ *Kazak N.V.¹, Knyazev Yu.V.¹, Platonov M.S.^{1,2}, Bezmaternykh L.N.¹, Rogalev A.², Wilhelm F.²,
Ovchinnikov S.G.¹*¹ Kirensky Institute of Physics, Federal Research Center KSC SB RAS, 660036 Krasnoyarsk,
Russia² ESRF-The European Synchrotron, 71 Avenue des Martyrs CS40220, F-38043 Grenoble Cedex 9,
France
nat@iph.krasn.ru

Transition metal oxyborates with general formula $\text{M}^{2+}_2\text{M}^{3+}\text{BO}_5$ crystallize in the orthorhombic structure (Sp.gr. *Pbam*) and isostructural to the natural ludwigite. These materials have intriguing electronic and magnetic properties. In the past two decades, the investigations have been focused on the atomic instability, low-dimensional crystal and puzzling magnetic structures. The divalent and trivalent ions occupy four crystallographically inequivalent sites 1, 2, 3 and 4. The triads 4-2-4 and 3-1-3 with shortest and longest interionic distances are structurally singled out and are linked in quasi one-dimensional magnetic substructures - three-leg spin ladders (3LL) propagated along the *c*-axis. There are only two homometallic ludwigites Fe_3BO_5 and Co_3BO_5 demonstrating long-range magnetic order [1, 2]. The former undergoes the cascade of magnetic transformations with the temperature decreasing PM-AFM1-F-AFM2 as found from the NPD, Mossbauer Effect (ME), heat capacity and magnetization studies [3]. The antiferromagnetic (AFM1) ordering at $T_{N1}=110$ K and ferrimagnetic (F) one at $T_{N2}=70$ K appear in the 4-2-4 and 3-1-3 spin-ladders, respectively. The 3D antiferromagnetic order (AFM2) is assumed to be set below $T_{N3}=30$ K. The Co_3BO_5 has only one magnetic transition at $T_N=42$ K. The low-spin state of Co^{3+} ion in the metal site 4 is found from recent NPD study [4]. In present study we focus on the $\text{Co}_{3-x}\text{Fe}_x\text{BO}_5$ single crystals with different iron content ($x=0.1, 0.75$ and 1.0). The magnetism of the $\text{Co}_{3-x}\text{Fe}_x\text{BO}_5$ ludwigites has been studied through the combination of the magnetic, the Mossbauer Effect and the X-ray magnetic circular dichroism measurements as well as through the group theoretical analysis and superexchange interactions calculation.

Support by the Council for Grants of the President of the Russian Federation (project nos. SP-938.2015.5, NSh-7559.2016.2) and the Russian Foundation for Basic Research (project nos. 16-32-60049 mol_a_dk, 16-32-00206 mol_a, 17-02-00826-a, 16-32-50058) is acknowledged.

- [1] R.B. Guimarães, M. Mir, J. C. Fernandes, et al., *PRB*, **60**(9) (1999) 6617.
 [2] N.B. Ivanova, A.D. Vasilyev, D.A. Velikanov, et al., *Physics of the Solid State*, **49** (2007) 651.
 [3] J. Bartolomé, A. Arauzo, N.V. Kazak, et al., *PRB*, **83** (14) (2011) 144426 and references therein.
 [4] D.C. Freitas, C.P.C. Medrano, D.R. Sanchez, et al., *PRB*, **94** (17) (2016) 174409.

4OR-C-5

MAGNETIC RESONANCE AND STRUCTURAL INVESTIGATIONS OF PURE AND MIXED CuCr_2S_4 NANOCRYSTALS WITH THE STRONG INTERPARTICLE INTERACTIONS

Pankrats A.^{1,2}, Vorotynov A.¹, Tugarinov V.¹, Zharkov S.^{1,2}, Zeer G.², Gupta A.³, Ramasamy K.³

¹Kirensky Institute of Physics, Federal Research Center KSC SB RAS, Krasnoyarsk, Russia

²Siberian Federal University, Krasnoyarsk, Russia

³MINT Center, University of Alabama, Tuscaloosa, USA

pank@iph.krasn.ru

The chromium-based chalcospinels CuCr_2S_4 , CuCr_2Se_4 , and CuCr_2Te_4 are ferromagnetic metals with high Curie temperatures. Due to their unique magnetotransport and magnetodielectric properties, they are potentially attractive candidates for diverse spin-polarized applications. We studied the resonance and structural properties of the pure CuCr_2S_4 and mixed $\text{CuCr}_2\text{S}_{4-x}\text{Se}_x$ ($x=2; 4$) and $\text{Co}_x\text{Cu}_{1-x}\text{Cr}_2\text{S}_4$ ($x=0.1; 0.2$) nanoparticles (NPs) in the wide frequency (9.5–80 GHz) range and at temperatures down to 4.2 K. The synthesis of the pure and mixed NPs and their magnetic properties are described in [1-3].

SEM and TEM studies. Depending on the technology details, NPs of CuCr_2S_4 were synthesized in two forms: separate cube-shaped nanocrystals and nanoclusters up to 100 nm in sizes composed of smaller particles. All mixed compounds contain both blocks with sizes from 1 to 50 μm consisting of compacted nanosized crystallites and a small amount of free nanoparticles up to 30 nm in size.

Magnetic resonance. Due to the compacted state of the clustered pure and mixed samples, a strong interparticle interaction plays an important role in the formation of the magnetic properties of these samples. There are two main consequences of this interaction in NPs: (i) high values of blocking temperatures T_B , which are caused by freezing of magnetic moments in the characteristic volume which size is determined by the correlation length; (ii) inhomogeneous broadening of the magnetic resonance spectrum and the additional absorption lines (Fig. 1a) appearing in the spectrum below T_B due to the magnetic dipolar field acting in boundary areas of interacting constituent nanocrystals.

Because of the increase in the magnetic anisotropy at low temperatures, a shift of the resonance fields and line broadening (Fig. 1b) occur in all studied compounds below a certain characteristic temperature T_{fr} due to the freezing of the moments in the nanoparticles, in both free and compacted. The shift of the resonance field indicates that the resonance spectrum acquires a gap nature with the energy gap defined by the averaged magnetic anisotropy $\langle H_A \rangle$.

The anionic substitution of sulfur by selenium causes the decreasing of the magnetic anisotropy. In contrast, the anisotropy increases with the cationic substitution of copper ions by cobalt.

[1] A. Pankrats, A. Vorotynov, V. Tugarinov, et al., *J. Appl. Phys.*, **116** (2014) 054302.

[2] K. Ramasamy, H. Sims, S. Keshavarz, et al., *J. Mater. Chem. C*, **4** (2016) 3628-3639.

[3] K. Ramasamy, H. Sims, R. K. Gupta, et al., *Chem. Mater.*, **25** (2013) 4003–4009.

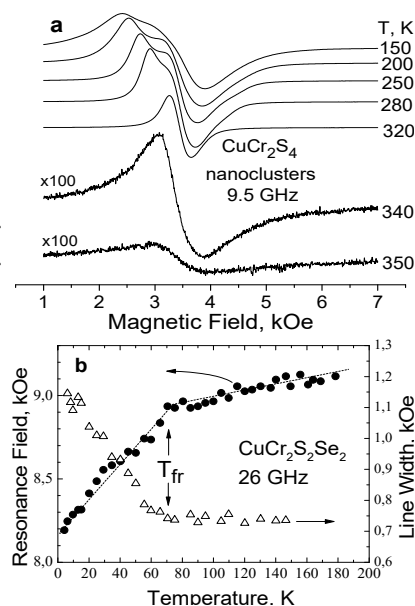


Fig. 1. Temperature dependences of: a - X-band spectra of CuCr_2S_4 nanoclusters; b - resonance field and linewidth for $\text{CuCr}_2\text{S}_2\text{Se}_2$ NPs.

4OR-C-6

MAGNETIC RESONANCE IN $[(\text{CoP})_{\text{soft}}/\text{NiP}/(\text{CoP})_{\text{hard}}/\text{NiP}]_n$ MULTILAYER FILMS

Patrin G.S.^{1,2}, Shiyan Ya.G.^{1,2}, Orlov V.A.^{1,2}, Patrin K.G.¹, Furdyk V.P.¹

¹ Siberian Federal University, pr. Svobodny, 79, Krasnoyarsk, 660041, Russia

² L.V. Kirensky Institute of Physics FRC KSC, Siberian Division, Russian Academy of Science, Krasnoyarsk, 660036, Russia
patrin@iph.krasn.ru

Film system consisting of alternating layers of soft magnetic and hard magnetic materials, are suitable objects for the solution of some problems of spintronics. The interlayer interaction in such systems is responsible for the formation of the magnetic state. In the case when a pair of ferromagnetic and antiferromagnetic layers is conjugated, generally there is realized the effect of exchange bias, and all the observed magnetization process is associated with the behavior of the ferromagnetic layer. When ferromagnetic soft-magnetic and hard magnetic layers are conjugated a new condition arises, such as "magnetic springs". In the case where the interlayer interaction is regulated, there is reason to expect new manifestations that can have practical importance.

It has been shown previously [1], the increase of the number of blocks (n) in the film of ferromagnetic soft magnetic and hard magnetic layers in the $[(\text{CoP})_{\text{soft}}/(\text{CoP})_{\text{hard}}]_n$ structure leads to the strengthening of the influence of soft magnetic layer on the magnetization process of the film structure that effectively manifests itself as a decrease in the volume of the hard magnetic material. The introduction of a non-magnetic layer leads to unusual magnetization process of the film, the oscillations magnitude of the coercive force. And here the nonmagnetic layer affects on the interlayer interaction between the ferromagnetic layers. The aim of this study was to investigate the magnetization processes in multilayer film structures consisting of alternating magnetically soft and magnetically hard layers separated by a nonmagnetic spacer.

$[(\text{CoNiP})_{\text{soft}}/\text{NiP}/(\text{CoP})_{\text{hard}}]_n$ films were formed by chemical deposition. The phosphorous content in all the layers was 8 at.%. In the magnetically hard layer, CoP was in the hexagonal polycrystalline state and in the magnetically soft layer, in the amorphous state with nickel content 30 % at. and cobalt content 70 % at. The intermediate NiP layer was amorphous and nonmagnetic with the thickness $t_{\text{NiP}} = 2$ nm. Such a composition of the layers was chosen because of the absence of sharp structural variations at the interface. The films with the number of blocks $n = 1, 5, 10, 15, 20, 40$ were synthesized. Both ferromagnetic layers had a thickness $t_{\text{F}} = 5$ nm and non-magnetic $t_{\text{NiP}} = 2$ nm. Spectra of magnetic resonance were measured on the spectrometer "Bruker E 500 CW EPR", operating at a frequency of $\omega_{\text{MWF}} = 9.2$ GHz. In the experiment, a constant magnetic field lying in the film plane.

The absence of the microwave signal was observed from a single layer of NiP. In the bilayer structure of the CoP/NiP is observed only one peak of microwave absorption, which speaks about not mixing the layers and the absence of a second magnetic phase of the type of CoNiP alloy. In the film with $n = 1$ the spectrum consists of two lines microwave absorption: one of them belongs to the hard magnetic layer (CoP_{hard}) and another magnetic layer (CoP_{soft}). When the number of blocks (n) is increasing a third peak of microwave absorption arises. The structure of the spectrum is such that the low-field lines have the close values of the resonance field and high field peak has a higher value of the resonant field and has a large line width. Temperature dependences of the resonance field are obtained. The mechanisms of interlayer exchange interactions are proposed. The results are analyzed in the framework of the model of three-sublattice non-collinear structures, where the magnetizations of the soft magnetic layers are skewed.

[1] G.S. Patrin, Ya. Shiyan, K.G. Patrin, G.Yu. Yurkin, *J. Low Temp. Phys.*, **182** (2016) 73.

4OR-C-7

CORRELATION BETWEEN SURFACE MAGNETISM AND IR OPTICAL DATA IN Co-DOPED TiO₂ NANOPOWDERS

Mostovshchikova E.V., Yermakov A.Ye., Uimin M.A., Minin A.S.

M.N. Miheev Institute of Metal Physics of Ural Branch of Russian Academy of Sciences,
Ekaterinburg, Russian Federation
mostovsikova@imp.uran.ru

Titanium dioxide in nanostate is one of the intensively studied materials for nanotechnology applications in photocatalysis and photoelectrochemical solar cells, in sensors, spintronics, and medicine [1]. Various reducing treatments, creation of the oxygen vacancies together with doping by 3d ions modifies the electronic and magnetic properties of nano-TiO₂ and this is the way for improvement of the properties which are important for practice.

Recently it was shown that doping TiO₂ with Co-ions up to 4% and subsequent annealing in vacuum at 1000 K results in appearance of spontaneous magnetization at room temperature that was associated with the increase in the Co atoms content on the surface of nanoparticles [2]. The results were interpreted within the framework of core-shell model. It was assumed that the ferromagnetic ordering is a result of the interaction of delocalized electrons near the vacancies and the nearest neighbour cobalt atoms due to itinerant type interaction.

One of the methods that can answer the question about the existence of the delocalized states in semiconductor is the infrared spectroscopy and study of the absorption spectra in the “transparency window” between the fundamental and phonon absorption where delocalised charge carriers can manifest themselves. In the present work we try to establish the relation between the evolution of the magnetic properties and IR spectra in Co-doped TiO₂ nanopowders under the reducing treatment.

Nanocrystalline TiO₂:Co (Co content is 1.5 at%) were prepared by the hydrothermal method. XRD indicates the formation of anatase structure. The size of the nanoparticles determined by TEM is about 60–80 nm in length and 20–25 nm in width. The reducing annealing was carried out in vacuum of 10⁻⁴ Pa at T~1000 K during 30 minutes. Magnetization at room temperature was measured on the Faraday balance in the fields up to 1.2 T. The absorption spectra were measured in the spectral range 0.9-12.5 μm and in the temperature interval 90-300 K. For the optical measurements nanopowder of TiO₂:Co was mixed with CsI and compacted under 500 MPa.

Magnetic data show that initial TiO₂:Co nanopowder is paramagnetic. After annealing of the nanopowder the behaviour of the magnetization curve changes drastically, and the ferromagnetic contribution is clearly observed. Saturation magnetization at T=300 K is about 1.6 emu/g. Absorption spectrum of the annealed nanopowder also differs significantly in comparison with the spectrum of the initial powder: the short-wave phonon band decreases slightly and near the phonon bands the additional absorption appears. This additional contribution has nonmonotonic character and increases with the wavelength. Such evolution of the IR spectrum may be explained by appearance of the oxygen vacancies and, possibly, delocalised charge carriers.

The research was carried out within the state assignment of FASO of Russia (theme “Spin” No. 01201463330), supported in part by RFBR (project No. 17-02-00093)

[1] X. Chen, *Chin. J. Catal.*, **30** (2009) 839–851.

[2] A.Ye.Yermakov, G.S.Zakharova, M.A.Uimin et al, *J. Phys. Chem. C*, **120** (2016) 28857–28866.

4OR-C-8

MAGNETIC PROPERTIES OF IRON OXIDES IN CORE AND INTERFACE OF THE Fe₃O₄@Au NANOSTRUCTURES

Baskakov A.O.¹, Starchikov S.S.¹, Lyubutin I.S.¹, Solov'eva A.Yu.², Ioni Yu.V.², Khodos I.I.³, Avilov A.S.¹, Gubin S.P.²

¹ FSRC «Crystallography and Photonics» RAS, 119333 Moscow, Russia

² Kurnakov Institute of General and Inorganic Chemistry, RAS, 119991 Moscow, Russia

³ Institute of Technology of Microelectronics and High Purity Materials, RAS, 142432

Chernogolovka, Russia

arseniybaskakov@gmail.com

The «core-shell» nanocomposites, consisting of noble-metal shell and iron-oxide core, have attracted much attention as the materials with unique physical, chemical and biological properties [1]. Size effects stipulate the properties of such nanostructures and they notably differ from their bulk analogues.

In the present study, the «core-shell» Fe₃O₄@Au nanostructures were synthesized with a new technique by HAuCl₄ reduction in the presence of Fe₃O₄ nanoparticles followed further stabilization by polyethylene glycol. These nanostructures were studied with powder X-ray diffraction, electron microscopy and diffraction, optical absorption, Raman and Mössbauer spectroscopy.

The Mössbauer data revealed the difference in magnetic properties of Fe⁺³ ions in the interior areas of Fe₃O₄ nanoparticles and in the surface layer, which makes junction with gold coating.

This can be related to the break of the exchange bonds at the particles surface, which leads to decrease of the effective magnetic moment.

It was observed that the gold coating stabilizes the magnetic properties of the Fe₃O₄ surface layers, approaching them to the properties of magnetite interior areas. The Raman spectroscopy and HRTEM data confirmed the complete gold covering of Fe₃O₄ core in the Fe₃O₄@Au nanocomposites.

This work was supported by the Russian Science Foundation, RSF grant № 14-12-00848.

[1] Y. Hu, et al., *J. Mater. Chem. B*, **3**(47) (2015) 9098.

4OR-C-9

SPIN CURRENT IN NON-COLLINEAR MAGNETIC NANOSTRUCTURES: MAGNETOELECTRIC EFFECT AND SECOND HARMONIC GENERATION

Karashtin E.A.^{1,2}, *Gusev N.S.*¹, *Kolmychek I.A.*³, *Sladkov K.D.*³, *Drovosekov A.B.*⁴, *Savitsky A.O.*⁴,
*Murzina T.V.*³, *Fraerman A.A.*^{1,2}

¹ Institute for Physics of Microstructures RAS, Nizhny Novgorod, Russia

² N.I. Lobachevsky State University of Nizhny Novgorod, Nizhny Novgorod, Russia

³ Department of Physics, Moscow State University, Moscow, Russia

⁴ P.L.Kapitza Institute for Physical Problems RAS, Moscow, Russia

eugenk@ipmras.ru

The non-uniform magnetic media with non-collinear magnetization distribution are known to have the equilibrium spin current. For example in a magnetic helicoid the averaged spin directed along the helix axis flows along the same direction. Similarly, in a double-layer magnetic nanostructure the spin flows from one magnetic layer to the other if the magnetizations of the layers are not parallel. The spin current tensor $\sigma_{ik} \sim [\mathbf{M} \times \nabla_k \mathbf{M}]_i$ (in the exchange approximation) is antisymmetric with respect to the coordinate inversion operation. This can give rise to several effects allowed only in non-centrosymmetric materials with non-collinear magnetization. One of them is the flexo-magnetoelectric (ME) effect that consists in the appearance of the static electric polarization $P_l \sim e_{ikl} \sigma_{ik}$ [1,2] (e_{ikl} is the antisymmetric Levi-Civita tensor). The ME effect is important in the context of manipulating the magnetic moment without application of an external magnetic field. Another effect is the second harmonic generation (SHG). The double-frequency polarization here has the form $P_l^{2\omega} = \beta_{ikml} \sigma_{ik} E_n^\omega E_m^\omega$ [3] (\mathbf{E}^ω is the electric field of light). This effect may be used as an effective tool for the spin current diagnostics. In the present work we investigate the described phenomena both theoretically and experimentally. The SHG effect is observed in a magnetic multilayer with non-collinear ground state (Fig. 1). The ME effect is studied by the excitation of the ferromagnetic resonance (FMR) by the electric microwave field [4] (Fig. 2).

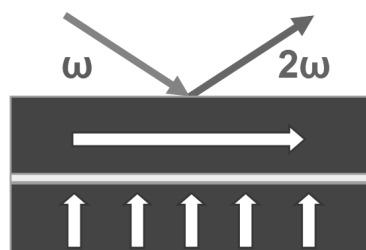


Fig. 1. The scheme of the SHG effect in a non-collinear magnetic structure.

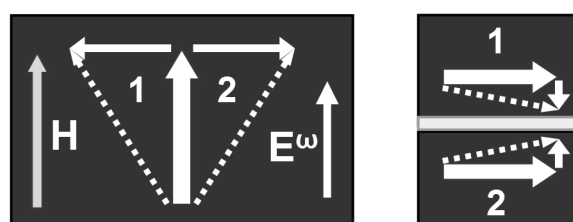


Fig. 2. The scheme of the ME effect through the excitation of FMR by the electric microwave field.

Support by the Russian Science Foundation (Grant No. 16-32-10340) is acknowledged.

[1] H. Katsura, N. Nagaosa, A.V. Balatsky, *Phys. Rev. Lett.*, **95** (2005) 057205.

[2] V.G. Bar'yakhtar, V.A. L'vov, D.A. Yablonskii, *Pis'ma Zh. Exp. Teor. Fiz.*, **37** (1983) 565.

[3] J. Wang, B.-F. Zhu, R.-B. Liu, *Phys. Rev. Lett.*, **104** (2010) 256601.

[4] E.A. Karashtin, A.A. Fraerman, *Phys. Solid State*, **58** (2016) 2228-2232.

4OR-C-10

INFLUENCE OF TUNGSTEN MODIFYING LAYER ON MAGNETIC PROPERTIES AND iDMI OF THE FILMS Ru/Co/W/Ru

*Kolesnikov A.G.¹, Samardak A.S.¹, Ognev A.V.¹, Steblyy M.E.¹, Chebotkevich L.A.¹,
Sadovnikov A.V.², Nikitov S.A.²*

¹ Laboratory of Thin Film Technologies, School of Natural Sciences, FEFU, Vladivostok, Russia

² Laboratory "Metamaterials", Saratov State University, Saratov, Russia

alexanderkolesnickov@yandex.ru

Previous studies of polycrystalline Ru/Co/Ru trilayers with symmetric interfaces have shown that perpendicular magnetic anisotropy (PMA) is observed only when film grows coherently. We have found that the main origin of PMA is magnetoelastic strains due to 8% mismatch between Co and Ru lattice parameters [1]. Here we show transformational effect of ultrathin W interlayer on PMA, coercivity, domain structure and interfacial Dzyaloshinskii-Moriya interaction (iDMI). A batch of experimental samples prepared by magnetron sputtering has the following composition: SiO₂/Ru(10 nm)/Co(*t*_{Co})/W(*t*_W)/Ru(2 nm), where *t*_{Co}=0.7-1.5 nm and *t*_W=0-0.4 nm.

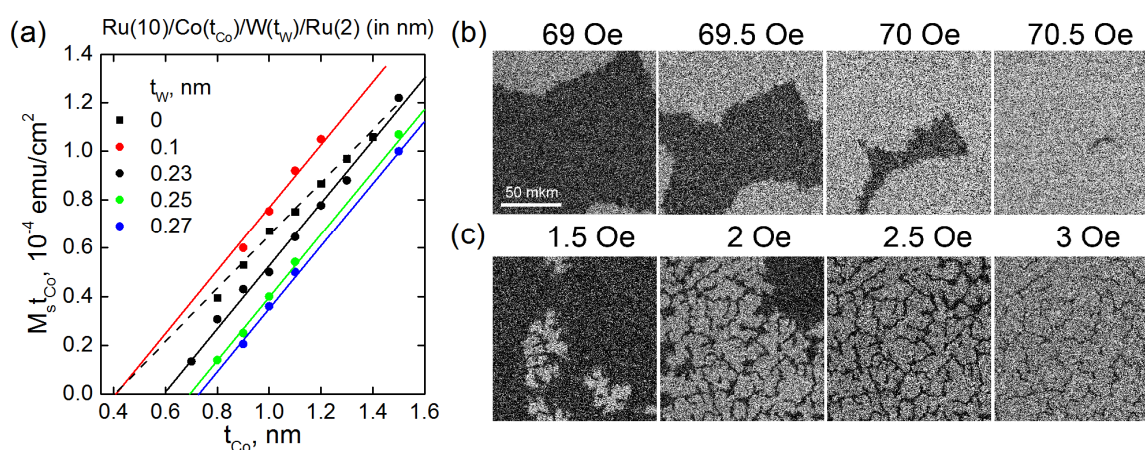


Fig. 1. (a) Dependence of $M_S t_{Co}$ on the thickness of Co layer t_{Co} . PMOKE images during out-of-plane remagnetization of the films $t_{Co}=0.9$ nm (b) $t_W=0$ nm and (c) $t_W=0.25$ nm

Intermixing of W with Co leads to formation of magnetic dead layer on top interface. Using the dependence $M_S t_{Co}=f(t_{Co})$ (Fig. 1a) we defined that thickness of magnetic dead layer on top interface Co/W raises from 0.2 to 0.53 nm when t_W increases from 0.1 to 0.27 nm. We have assumed that the diffusive W atoms form with Co few phases Co₃W and Co₇W₆. Therefore, the lattice mismatch for Co/Co₃W and Co/Co₇W₆ interfaces decreases on 0.53 and 1.2 %, respectively. As a result, the strain relaxation reduces PMA and coercive force linearly decreases from 70 Oe to 2.5 Oe with t_W changing from 0 to 0.25 nm. Moreover we observe dendrite domain structure during out-of-plane remagnetization by polar Kerr microscopy in the film Ru(10 nm)/Co(0.9 nm)/W(0.25 nm)/Ru(2 nm) (Fig. 1b,c). This kind of domain structure indicates the presence of iDMI [2]. Measurements by Brillouin light scattering spectroscopy showed that the film has high value of iDMI 2.82 mJ/m², which is strong enough for skyrmion stabilization.

Support by Russian Foundation for Basic Research (grants 17-52-50060 and 15-02-05302) and the state task (3.5178.2017) is acknowledged.

[1] A.G. Kolesnikov, M.E. Steblyy [et al.] *J. Phys. D: Appl. Phys.*, **49** (2016) № 425302.

[2] M.J. Benitez, *Nature Nanotechnology*, **6** (2015) № 8957.

4OR-C-11

TAILORING OF MAGNETIC PROPERTIES OF DEPOSITED Fe CHAINS BY EXTERNAL ELECTRIC FIELD IN THE PRESENCE OF H

Korobova J.G.¹, Bazhanov D.I.^{1,2}

¹ Lomonosov Moscow State University, Faculty of Physics, Moscow, Russian Federation

² Dorodnicyn Computing Centre of Russian Academy of Sciences, Moscow, Vavilova, 40
korobovajg@gmail.com

Low-dimensional magnetic materials are the backbone of very intense studies now attempting to fulfill both fundamental and technological interests. It is important to provide the easy switching on magnetic states in the system however this switching should not require many resources to be paid. Also the necessary condition is to keep spin locked along its easy axis in spite of thermal fluctuations, i.e. large magnetocrystalline anisotropy (MA) energy. Therefore, development of novel magnetoelectronic and spintronic applications demands the ways to control and to tailor magnetic properties of devices. Transition metals chains are very attractive in this context since their magnetic properties are known to be very sensitive to the local atomic environment of the atoms in the chain. Impurities are considered now as one of the ways to tailor the magnetic properties of nanosystems. F.R. Vukajlović at al. [1] from the first-principles showed that the exchange coupling within monatomic Fe chains deposited in nanostructured ch-Ir(100) surface can be changed by the increase of H impurity coverage, proving the existence of magnetic bistability of Fe chains with almost degenerated AFM and FM states.

In this work we present our *ab initio* DFT study of exchange coupling and MA energy under external electric field in monatomic Fe chain deposited in ch-Ir(100) surface with different H coverage (0.4 ML, 1.3 ML, 1.6 ML), which has strong impact on exchange coupling: AFM state for 0.4 ML, almost degenerated AFM and FM states for 1.3 ML and FM state for 1.6 ML. Electric field was applied perpendicular to the substrate surface and changed in the range from -1 eV/\AA to $+1 \text{ eV/\AA}$. We obtained that for all considered H coverages exchange energy ($\Delta E = E^{\text{AFM}} - E^{\text{FM}}$) value linearly increases as a function of applied field. In the case of 1.3 ML AFM and FM states are still almost degenerated (Fig. 1) under external field. Moreover, we obtained that in this case varying of electric field significantly changes MA energy as a linear function of applied field - around 20% of its value without field (Fig.1), while for other coverages such change is not so significant. This change is caused by the small change of Fe-Fe distance under applied field, which is not observed for the cases of 0.4 ML and 1.6 ML. In all cases we observe the canted spin phase. In our recent work [2] we have shown that spin dynamic in metallic chains depends on MA energy, and for FM chains magnetic field required for magnetization switching is proportional to MA energy. Thus, obtained results open the route to tailor spin dynamic in the system by manipulating the MA energy value of the monatomic deposited Fe chain in presence of H impurities. By changing applied electric field we can low MA energy, providing easy switching between magnetic states in bistable chain, and then stabilise the system by increasing the MA energy.

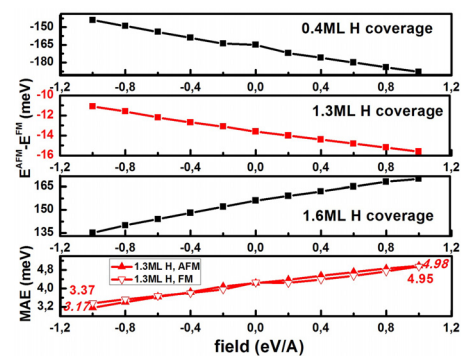


Fig. 1. MA energy and ΔE as a function of electric field for different H coverage

[1] F.R. Vukajlović, Z. S. Popovoć, et al., *Phys. Rev. B*, **81** (2010) 085425.

[2] O. P. Polyakov, J. G. Korobova, et al., *Journal of Applied Physics*, **121** (2017) 014306.

4OR-C-12

CRITICAL PHENOMENA IN 1D ISING MODEL WITH ARBITRARY SPIN

Proshkin A.I.¹, Kassan-Ogly F.A.¹, Zarubin A.V.¹, Ponomareva T.Y.², Menshikh I.A.²

¹ IMP UB RAS, Ekaterinburg, Russia

² UrFU, Ekaterinburg, Russia

proshkin_ai@imp.uran.ru

Due to recent developments in synthesizing low-dimensional systems there is now a great interest devoted to unique properties of these materials. Moreover as was shown previously such real systems as lanthanide and actinide mononictides and monochalcogenides can adequately be described in terms of low-dimensional Ising and Potts models [1, 2]. The aim of this work was to study critical phenomena taking place in the Ising model on linear chain with arbitrary spin values s . The Hamiltonian of the system has the standard form:

$$\mathcal{H} = -J \sum_i S_i S_{i+1} - H \sum_j S_j,$$

where J – exchange interaction value between nearest neighbours, H – applied magnetic field, S in general takes $2s+1$ values $-s, -s+1, \dots, s-1, s$.

It was shown that the antiferromagnetic system ($J < 0$) possesses frustration at low temperatures at frustration field $H_{fr} = -2sJ$. At that field at $T \rightarrow 0$ magnetization has sharp jump from $M=0$ to the asymptotic value $M=s$ and entropy is not equal to zero. The analytical expressions for these functions:

$$M_{fr} = \left(\frac{2s-1}{4} \right) + \left(\frac{2s+1}{4} \right) \frac{1}{\sqrt{1+8s}}, \quad S_{fr} = \ln \left(\frac{1+\sqrt{1+8s}}{2} \right).$$

Additionally the behaviour of Fourier transform of pair spin correlation function was investigated. It was found that the expression for the correlation function of the model in magnetic field consists of several components related to Laue function and diffuse scattering functions. At low temperatures at fields above the frustration field diffuse scattering is absent. At fields below the frustration one correlation function at low temperatures tends to take a form of delta function which means that the system undergoes a phase transition (the temperature of phase transition in one-dimensional systems equals to zero). At frustration field correlation function has smooth maximum and does not take the delta-function form that says about the phase-transition vanishing. The behavior of diffuse scattering function in the case $s=1$ is shown on the Fig. 1.

The reported study was carried out within the state assignment of FASO of Russia (theme “Quantum” No. 01201463332) and was funded by RFBR according to the research project No. 16-32-00032 мол_a.

- [1] A. Proshkin, F. Kassan-Ogly, *Materials Science Forum*, **845** (2016) 93–96.
 [2] F.A. Kassan-Ogly, et al, *J. Magn. Magn. Mat.*, **384** (2015) 247–254.

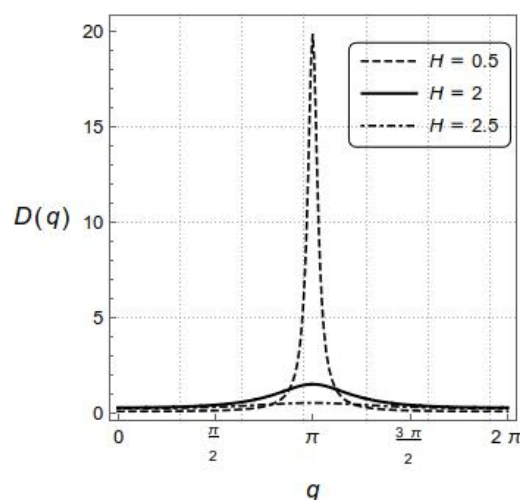


Fig. 1. Diffuse scattering function of the $s=1$ Ising model on linear chain at $T=0.5$

4OR-C-13

FERROMAGNETIC RESONANCE IN A CORE-SHELL NANOPARTICLE: A POLYCRISTALLINE SHELL MODEL

Poperechny I.S.^{1,2}, Raikher Yu.L.^{1,2}

¹ Ural Federal University, Ekaterinburg, 620083, Russia

² Institute of Continuous Media Mechanics, Ural Branch of RAS, Perm, 614013, Russia
ipoperechny@gmail.com

A ubiquitous feature of magnetic core-shell nanoparticles is the presence of texchange anisotropy (EA). It was introduced in 1956 by Meiklejohn and Bean as the reason for the hysteresis loops shift along the field axis in Co / CoO particles [1]. This work entailed the studies of EA in a wide variety of magnetic systems. However, in spite of long and intensive researche, the physical origin of EA is still unclear in many aspects. A simple idea that EA is a result of exchange interaction of spins over the magnet / magnet interface is apparently not comprehensive enough. Indeed, from the phenomenological viewpoint the magnetic order inside a particle cannot change abruptly at the border of two atomic layers abutting on one another. Rather, the core / shell interface is in fact a certain transition layer. Thorough magnetic measurements on layered magnetic films point out to similar conclusions [2]. Another issue that is still much of a “blank spot” is the *dynamic* part of EA – the so-called rotatable anisotropy (RA). Even the symmetry type of RA is not yet fully established up to now.

Among many measurement techniques used to investigate spin-ordered systems, ferromagnetic resonance (FMR) since long ago proves to be one of the most powerful. However, the interpretation of FMR data on nanoparticles needs special attention because the standard athermic FMR theory does not account for the superparamagnetic effect. A kinetic theory of FMR in a single-domain particle with allowance for thermal fluctuations of magnetic moment was developed in [3]. Hereby we extend this approach to the case of nanoparticles with a core-shell structure. A model magnetic energy of a particle comprises three terms: the contributions of the core and shell and that of the interface layer. Experiments on iron and cobalt particles established that the core is a single crystal with virtually uniform magnetization, while the shell consists of numerous randomly oriented crystallites [4,5]. Given that, the energy of the shell is presented as the sum of Zeeman and uniaxial anisotropy terms for each crystallite and the energy of inter-grain interaction, which in a first approximation we neglect. Such a simplification is admissible as long as the magnetization of a crystallite is much smaller than its effective anisotropy field. The energy of the interface layer is taken as a sum of interaction energies between the core and each grain of the shell. Our analysis shows that this interaction effectively leads to redefinition of the anisotropy constant of the core and the onset of exchange and rotatable anisotropies. Both of the latter, expectably, yield a shift of the FMR absorption line. As an illustration, we present the temperature dependence of the resonance field shift caused by RA and show that it consists of two terms. The first one is temperature-independent while the second one goes down with the temperature increase. Therefore, we conclude that a temperature scan of FMR lines of core-shell nanoparticles should render the RA strength as well as its symmetry.

Support by grant 15-12-10003 from Russian Science Foundation is acknowledged.

- [1] W.H. Meiklejohn, C.P. Bean, *Phys. Rev.*, **102** (1956) 1413.
- [2] K. O’Grady et al., *J. Magn. Magn. Mater.*, **322** (2010) 883.
- [3] I.S. Poperechny, Yu.L. Raikher, *Phys. Rev. B*, **93** (2016) 014441.
- [4] H. Khurshid et al., *Appl. Phys. Lett.*, **104** (2014) 072407.
- [5] D. De et al., *Phys. Rev. B*, **94** (2016) 184410.

4OR-C-14

IN SITU MAGNETO-OPTICAL ELLIPSOMETRY STUDY OF FERROMAGNETIC LAYERED NANOSTRUCTURES

Maximova O.A.^{1,2,3}, *Lyaschenko S.A.*^{1,2}, *Kosyrev N.N.*¹

¹ Kirensky Institute of Physics, Federal Research Center KSC SB RAS, Krasnoyarsk, Russia

² Reshetnev Siberian State Aerospace University, Krasnoyarsk, Russia

³ Siberian Federal University, Krasnoyarsk, Russia

maximo.a@mail.ru

Magneto-optical ellipsometry has become one of the powerful techniques for materials properties investigation [1]. Due to being non-destructive, it is especially valuable for *in situ* study of films growth. While optical and structural properties of nanostructures are widely investigated by ellipsometry techniques, magneto-optical properties are typically analysed with the help of extra measurements [2] conducted outside setups for films growth, which is inconvenient and causes technological problems.

That is why in this work we deal with the problem of *in situ* magneto-optical properties analysis of multilayered thin films by means of ellipsometry techniques. The aim is to calculate all components of dielectric permittivity tensor from *in situ* experimental data.

The proposed method of properties analysis is applicable to the isotropic layered media with upper layer being ferromagnetic and other layers being non-magnetic. It involves the analysis of complex reflection coefficients corresponding to in-plane p-polarization and out-of-plane s-polarization. Transverse configuration of magneto-optical Kerr effect, when magnetization is perpendicular to the plane of incidence and parallel to the surface, is considered.

As a result, from conventional ellipsometric spectra (ψ and Δ) we find out information about optical properties such as refractive index and extinction coefficient. In addition, spectra of the magneto-optic coupling parameter Q for ferromagnetic layers in multi-layered thin films are obtained from *in situ* magneto-ellipsometric spectra ($\delta\psi$ and $\delta\Delta$). These parameters completely define dielectric permittivity tensor ϵ .

Thus, the necessary algorithms for measurements data analysis are developed. The approach has been applied to Fe/SiO₂/Si films and Fe silicides of different layer thicknesses. The proposed method is also well applicable to measurements conducted at different temperatures, which enables to obtain correlation of magneto-optic coupling parameter Q spectrum and temperature for ferromagnetic material.

The topicality of the research is highly related to the development of applied sciences, such as electronics, optical technologies, astronautics and spintronics which use above mentioned films to produce high-technology devices for various purposes [3-5].

Support by Russian Foundation for Basic Research, Government of Krasnoyarsk Territory, Krasnoyarsk Region Science and Technology Support Fund to the research project No. 16-42-243058 and Russian Federation President's grant for support of leading scientific schools SS-7559.2016.2 is acknowledged.

[1] S.D. Bader, *J. Magn. Magn. Mater.*, **100** (1991) 440.

[2] K. Mok et al., *Phys. Rev.*, **84** (2011) 094413.

[3] N. V. Volkov et al., *Journal Of Applied Physics.*, **109** (2011) 123924–123924-8.

[4] N. V. Volkov et al., *Journal Of Applied Physics.*, **112** (2012) 123906–123906-10.

[5] N. V. Volkov et al., *Solid State Phenomena.*, **190** (2012) 526–529.

4OR-C-15

MICROWAVE AND MAGNETO-OPTIC PROPERTIES OF ϵ -Fe₂O₃ NANOPARTICLES ARISING IN BORATE GLASSES DOPED WITH Fe AND Gd

Ivanova O.¹, Kliava J.², Edelman I.¹, Ivantsov R.¹, Petrakovskaja E.¹

¹Kirensky Institute of Physics, FRC KSC RAS, Krasnoyarsk, 660036, Russia

²LOMA, UMR 5798 Université Bordeaux 1-CNRS, Talence cedex, 33405, France
osi@iph.krasn.ru

Recently, we have observed the formation of ϵ -Fe₂O₃ nanoparticles in borate glasses co-doped with low concentrations of Fe₂O₃ (3 wt. %) and Gd₂O₃ (0.1, 0.2, 0.3, 0.4, 0.6, 1.0 wt. %) [1]. Here we report a comparative study of these glasses with two experimental techniques – visible magnetic circular dichroism (MCD) and electron magnetic resonance (EMR). MCD is mainly associated with magnetically ordered phases while EMR includes a contribution of diluted paramagnetic ions, as well. The most prominent features of the MCD spectra are: non-linear dependence of intensities of spectral maxima on the Gd concentration and their remarkably strong increase with the decrease of temperature (Fig 1).

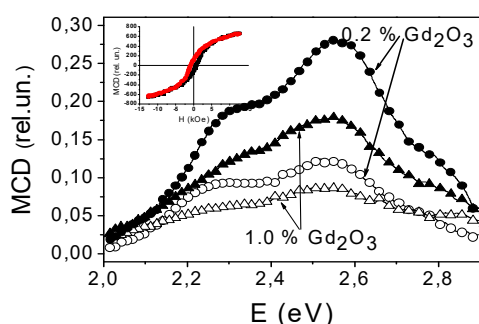


Fig. 1. MCD spectra at 300 and 90 K (resp., empty and full symbols). $H=3.5$ kOe. Inset: MCD hysteresis at 300 K for glass with 0.1 wt % Gd₂O₃.

The EMR spectra in these glasses exhibit two features with $g = 4.3$ and 2.0 due to diluted Fe³⁺ ions. Meanwhile, integrated spectra intensities do not follow the T^{-1} Curie law, see Fig. 2 left, suggesting that a considerable contribution to the resonances arises from magnetically ordered nanoparticles. This assumption is corroborated by computer simulations, carried out using the extended Czjzek-Le Caër model [2], see (Fig 2) right, showing an underlying resonance attributable to magnetic nanoparticles.

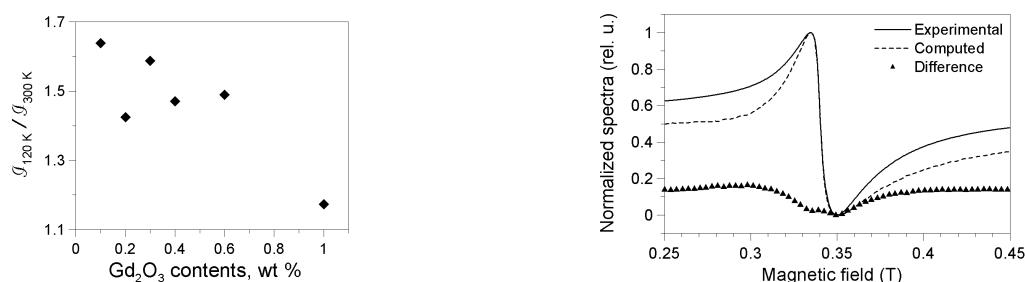


Fig. 2. Left: Ratio of integrated EMR absorptions at 120 and 300 K for glass with 0.2 wt. % Gd₂O₃. Right: Decomposition of the EMR spectrum of this glass at 300 K.

Support by Grant of the President of the Russian Federation NSh-7559.2016.2 is acknowledged.

[1] O.S. Ivanova et al., *J. Magn. Magn. Mater.*, **401** (2016) 880-889.

[2] G. Le Caër, B. Bureau and D. Massiot, *J. Phys.: Condens. Matter*, **22** (2010) 065402, 1-17.

4OR-C-16

EFFECTS OF ELECTRON-ELECTRON INTERACTION IN TWISTED BILAYER GRAPHENE

Sboychakov A.O.^{1,2}, Rozhkov A.V.^{1,2}, Rakhmanov A.L.^{1,2}, Nori F.²

¹ITAE RAS, Moscow, Russia

²RIKEN, Saitama, Japan

sboycha@mail.ru

In twisted bilayer graphene the crystal axes of the layers are not parallel to each other and form a certain angle θ , which may differ significantly for different samples. Rotational misorientation of the layers leads to occurrence of moiré patterns and superstructure, which in turn affects the electronic properties of the bilayer. Analysis in single-electron approximation has shown [1] that there are three areas of twist angles with qualitatively different low-energy physics. At large angles ($\theta > \sim 15^\circ$), the electron spectrum at low energies is different from the Dirac one and it can be characterized by an energy gap whose value is a non-trivial way dependent on the twist angle [2,3]. At smaller angles, the gap is small and electrons have Dirac spectrum. The Fermi velocity, however, monotonically decreases with decreasing θ . Finally, when $\theta < \theta_c \sim 1-2^\circ$, the spectrum at low energies is characterized by flat bands and the density of states has a peak at the Fermi level.

Despite the progress in understanding the electronic properties of twisted bilayer graphene, many issues still remain unclear. First of all this concerns many-body effects, since in the majority of cases, theorists are limited to a single-electron approximation. In our work, we consider the effects of electron-electron interaction in the limit of both large and small twist angles. In the former case, we construct an effective Hamiltonian of the system, valid close to the Dirac point. In the next step, we take into account the Coulomb interaction of electrons. Calculation in the random phase approximation leads to the renormalization of the gap according to the formula

$$\Delta \propto \Delta_0 \ln(E_\Lambda / \Delta_0),$$

where Δ_0 is the bare gap, and E_Λ is the cutoff energy by order of magnitude equal to the bandwidth of the single layer graphene. We also study the possibility of spontaneous exciton gap generation due to the Coulomb interaction of electrons.

The presence of flat bands at the Fermi level at small twist angles makes the system unstable with respect to the spontaneous symmetry breaking and the emergence of some order parameter. We test the spin-density wave as the ground state of the twisted bilayer in this regime. Calculations are performed numerically in the framework of the multiband Hubbard model (the number of bands is equal to twice the number of atoms in superstructure ~ 1000) in the mean-field approximation. We analyze the magnitude and spatial distribution of the order parameter inside the supercell.

[1] A.V. Rozhkov, et al., *Phys. Rep.*, **648** (2016) 1.

[2] A. O. Sboychakov, et al., *Phys. Rev. B*, **92** (2015) 075402.

[3] A.V. Rozhkov et al., *Phys. Rev. B*, **95** (2017) 045119.

4 July

Tuesday

11:30-13:15

oral session

4TL-LT

4OR-LT

**“Low Dimensional
Magnetism”**

4TL-LT-1

ELECTRONIC STRUCTURE OF LOW-DIMENSIONAL SPIN SYSTEMS*Saha-Dasgupta T.*

S.N.Bose National Centre for Basic Sciences, Kolkata, INDIA

t.sahadasgupta@gmail.com

Low-dimensional spin systems, characterized by their unconventional magnetic properties, have attracted much attention. Synthesis of materials appropriate to various classes within these systems has made this field very attractive and a site of many activities. The experimental results like susceptibility data are fitted with the theoretical model to derive the underlying spin Hamiltonian. However, often such a fitting procedure which requires correct guess of the assumed spin Hamiltonian leads to ambiguity in deciding the representative model. In this talk, we will describe how electronic structure calculation within the framework of Nth order muffin-tin orbital (NMTO) based Wannier function technique can be utilized to identify the underlying spin model for a large number of such compounds.[1] In particular, we will discuss two examples, (a) Haldane spin chain compound $\text{SrNi}_2\text{V}_2\text{O}_8$, [2] and (b) Mn^{2+} based vanadate-carbonate compound, $\text{K}_2\text{Mn}_3(\text{VO}_4)_2\text{CO}_3$. [3].

Support by Department of Science and Technology is acknowledged.

[1] T. Saha-Dasgupta, *Journal of Electron Spectroscopy and Related Phenomena*, **208** (2016) 83.

[2] K Samanta, S Kar, T Saha-Dasgupta, *Phys. Rev. B*, **93** (2016) 224404.

[3] K. Samanta and T. Saha-Dasgupta, *Phys. Rev. B*, **90** (2014) 064420.

4TL-LT-2

INTERACTING SPIN ISLANDS IN A DEPLETED SPIN LADDER

*Povarov K. Yu.*¹, *Schmidiger D.*¹, *Galeski S.*¹, *Reynolds N.*¹, *Bewley R.*², *Guidi T.*², *Ollivier J.*³,
*Zheludev A.*¹

¹ Neutron Scattering and Magnetism, Laboratory for Solid State Physics, ETH Zurich, 8093 Zurich, Switzerland

² ISIS Facility, Rutherford Appleton Laboratory, Chilton, Didcot, Oxon OX11 0QX, UK

³ Institut Laue-Langevin, 6 rue Jules Horowitz, 38042 Grenoble, France

povarovk@phys.ethz.ch

Impurities, embedded in a strongly interacting medium, can often give rise to a novel emergent objects with highly non-trivial properties. An illustrative example is a nonmagnetic impurity in a Heisenberg $S=1/2$ spin ladder. Although the ground state of the parent model is a quantum-disordered paramagnet, depletion creates extended clusters of staggered magnetization with total $S=1/2$. They can be treated as localized $S=1/2$ objects, interacting with each other via the distance-dependent Heisenberg sign-alternating exchange. Thus, introducing spinless defects one releases a new strongly interacting spin system “on top” of the spin ladder. We experimentally demonstrate manifestations of this physics in Zn-diluted strong-leg spin ladder $(\text{C}_7\text{H}_{10}\text{N})_2\text{CuBr}_4$ (known as Dimpy) [1]. Magnetization measurements clearly show the presence of spinful objects in depleted Dimpy, with interaction strength between them increasing with the zinc concentration. High resolution time-of-flight neutron spectroscopy also allows us to probe these interactions directly. Figure 1 shows the magnetic excitations in a slightly depleted Dimpy, visualizing the continuum of dynamic spin correlations stemming from nonmagnetic impurities. From the structure factor associated with this continuum we are able to determine the spin island shape in real space. Both static and dynamic properties of Dimpy with non-magnetic defects are in a good agreement with the numerical calculations, based on combination of Density Matrix Renormalization Group for large depleted ladders and the exact diagonalization methods for the effective basis of interacting spin islands [2]. This is a beautiful example of mapping a complex many-body problem in a strongly correlated system to the system of emergent quasiparticles, allowing rigorous tests for corresponding effective theory.

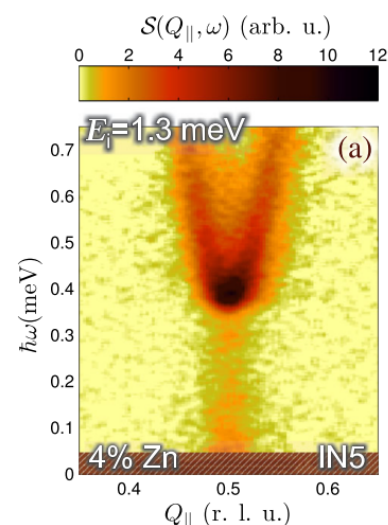


Fig. 1: Neutron spectroscopy in Zn-diluted Dimpy: false color map of scattering intensity as a function of momentum transfer along the ladder Q_{\parallel} and energy transfer $\hbar\omega$. An additional in-gap intensity due to the interacting spin islands is clearly visible [2].

The research was supported by the Swiss National Science Foundation, Division II.

[1] D. Schmidiger, P. Bouillot et al., *Phys. Rev. Lett.*, **108** (2012) 167201.

[2] K. Yu. Povarov, D. Schmidiger et al., *Phys. Rev. Lett.*, **116** (2016) 257203.

4TL-LT-3

EXOTIC PHASE TRANSITIONS IN THE MIXED VALENCE CHROMIUM OXIDES

Isobe M.¹, Etter M.¹, Sakurai H.², Dinnebier R.E.¹, Takagi H.¹

¹ Max Planck Institute for Solid State Research, Stuttgart, Germany

² National Institute for Materials Science (NIMS), Tsukuba, Japan
m.isobe@fkf.mpg.de

The mixed valent oxides have been provided the opportunities to study the competition between electron localization and delocalization. Therefore they often exhibit the metal-insulator transition, which has rich physics because they have strongly coupled to the spin, orbital and lattice degree of the freedom. Here we present two exotic phase transitions in mixed valence chromium oxides. One is the metal-insulator transition without charge ordering. The other is the charge disproportionation triggered by Bi lone-pair.

Hollandite $\text{K}_2\text{Cr}_8\text{O}_{16}$ is a mixed valence oxide with $\text{Cr}^{3.75+}$. $\text{K}_2\text{Cr}_8\text{O}_{16}$ is a ferromagnetic metal with $T_C = 180$ K, which is explained by double exchange mechanism. This ferromagnetic metal phase undergoes a transition to an insulator at $T_{\text{MI}} = 95$ K, retaining ferromagnetism [1]. In the low temperature ferromagnetic insulator phase, there is no evidence of charge separation/order. However, we have observed a slight structural distortion by synchrotron X-ray diffraction. Also detailed electronic structure calculations demonstrate that the metal-insulator transition is caused by a Peierls instability in the quasi-one-dimensional structure made of the four CrO_6 chains [2, 3]. We demonstrated that the uncommon ferromagnetic insulator phase can be realized in $\text{K}_2\text{Cr}_8\text{O}_{16}$ via the metal-insulator transition due to Peierls mechanism in a system of fully spin-polarized electrons.

$\text{BiCu}_3\text{Cr}_4\text{O}_{12}$ has the *A*-site ordered perovskite structure, and also is a mixed valence oxide with $\text{Cr}^{3.75}$. In $\text{BiCu}_3\text{Cr}_4\text{O}_{12}$, ferrimagnetic transition with a structural distortion was observed at around 185K. The resistivity exhibits an anomaly at the transition, but metallic behavior persists even in the magnetic phase. We have revealed a charge disproportionation below the transition from the structural analysis. It is considered that the origin of the transition is the local distortion of the BiO_{12} polyhedron for Bi *6s*-O *2p*-Bi *6p* hybridization. The structural distortion stabilizes the Cr-O hybridization of the Cr^{4+}O_6 octahedra. As the result, the two kinds of $\text{Cr}^{3.5+}\text{O}_6$ and Cr^{4+}O_6 chains ordered in a rocksalt-type substructure in *ac* plane in the low-temperature phase. This is the first observation of Bi lone-pair triggered charge disproportionation transition in mixed valent chromium oxides [4].

[1] K. Hasegawa, M. Isobe, *et al.*, *Phys. Rev. Lett.*, **103** (2009) 146403.

[2] T. Toriyama, *et al.*, *Phys. Rev. Lett.*, **107** (2011) 266402.

[3] P.A. Bhoje, *et al.*, *Phys. Rev. X*, **5** (2015) 041004.

[4] M. Etter, M. Isobe *et al.*, in preparation.

4OR-LT-4

DIFFRACTION STUDIES OF THE LOW-DIMENSIONAL FRUSTRATED MAGNETISM OF LAYERED HONEYCOMB AND TRIANGULAR OXIDES

Kurbakov A.I.^{1,2}, Kuchugura M.D.^{1,2}, Korshunov A.N.^{1,2}, Podchezertsev S.Yu.¹,
Rodriguez-Carvajal J.³, Senyshyn A.⁴, Zvereva E.A.⁵, Nalbandyan V.B.⁶

¹ Petersburg Nuclear Physics Institute, NRC Kurchatov Institute, Gatchina, Russia

² St.Petersburg University, Faculty of Physics, St. Petersburg, Russia

³ Institute Laue Langevin, Grenoble, France

⁴ Technische Universität München, Munich, Germany

⁵ Lomonosov Moscow State University, Faculty of Physics, Moscow, Russia

⁶ Southern Federal University, Faculty of Chemistry, Rostov-on-Don, Russia

kurbakov_ai@pnpi.nrcki.ru

Neutron (NPD) and synchrotron (SPD) powder diffraction studies of the magnetic structures of layered oxides $\text{Na}_3\text{Co}_2\text{SbO}_6$, $\text{Li}_3\text{Ni}_2\text{SbO}_6$ and $\text{Na}_2\text{Ni}_2\text{TeO}_6$ with a honeycomb superstructure of magnetic ions, and MSb_2O_6 ($M = \text{Mn}, \text{Co}, \text{Cu}$) and MnSnTeO_6 with triangular superstructure of magnetic ions within layer are presented. AFM type interaction between nearest, second and third nearest neighbors in honeycomb compounds and triangular structure of layers in MSb_2O_6 and MnSnTeO_6 can lead to frustration in the magnetic subsystem and the emergence of unusual types of magnetic moments ordering.

The crystal structure of $\text{Na}_3\text{Co}_2\text{SbO}_6$ and $\text{Li}_3\text{Ni}_2\text{SbO}_6$ was described as honeycomb-type monoclinic ($C2/m$), whereas crystal structure of $\text{Na}_2\text{Ni}_2\text{TeO}_6$ as honeycomb-type hexagonal ($P6_3/mcm$). However, the structure of M_2SbO_6 and M_2TeO_6 layers containing magnetic ions practically identical and difference consists in the number of alkali metal layers within a unit cell and the packing of honeycomb layers along c-axis. High-resolution SPD has allowed us to define the fine distortions of very rigid hexagons, which are slightly different depending on the type of 3d-ions. There is a delicate balance of competing AFM and FM interactions due to difference in character and sign of exchanges between Co^{2+} (Ni^{2+}) ions within the magnetic layer. It was confirmed by the NPD data according to which the magnetic structures for all studied honeycomb samples can be considered as zigzag FM chains AFM coupled. However, the zigzag type is different for each compound and depends on the type of 3d-ions, character of the layers stacking and the distance between the layers determining the strength of the rather small but sometimes significant interlayer interaction.

Quite recently, MnSb_2O_6 , a magnet with a chiral crystal structure ($P321$), was predicted to be multiferroic with unique ferroelectric switching mechanism. We have discovered and synthesized a new trigonal (s.g. $P-31m$) form of MSb_2O_6 ($M = \text{Mn}, \text{Co}, \text{Cu}$) that is isostructural with MnAs_2O_6 and differs from the known form MnSb_2O_6 (s.g. $P321$). Also we investigated MnSnTeO_6 with a chiral crystal (and magnetic) structure as a certain analog of chiral MnSb_2O_6 . This is strictly isoelectronic phases. Experimental low-temperature NPD patterns for all samples, with honeycomb and triangular superstructures, show additional reflections associated with neutron magnetic scattering AFM nature that appear at temperatures below T_N . Common features of spin ordering are described and the reasons resulting in distinctions between them are analyzed. Discovered that unusual commensurate and incommensurate noncollinear spin arrangements within these systems are lead to a reduction of the degree of their spin frustration.

All neutron results are in perfect agreement with the measurements of temperature dependencies of the magnetic susceptibility and specific heat.

Support by RFBR fund according to the research project № 16-02-00360 is acknowledged.

4 July

Tuesday

14:30-17:30

oral session

4TL-H

4RP-H

4OR-H

**“Diluted Magnetic
Semiconductors and
Oxides”**

4TL-H-6

**TOPOLOGICAL VORTEX DOMAINS AT OXYGEN CAGE TILTING
PLETHORA***Cheong S.-W.*Rutgers Center for Emergent Materials, Rutgers University, Piscataway, New Jersey, USA
sangc@physics.rutgers.edu

Oxygen octahedral cage distortions including tilts/rotations, deformations and off-centering in complex oxides play the key role in their numerous functional properties. Near the polar-centrosymmetric phase boundary in bi-layered perovskite $(\text{RE,Ca,Sr})_3(\text{Ti,Mn,Fe})_2\text{O}_7$ (RE=rare earths), we found the presence of abundant topological eight-state vortex-antivortex pairs, associated with four oxygen octahedral tilts at domains and another four different oxygen octahedral tilts at domain walls. These Z_8 vortex domains will be compared with the Z_6 vortex domains in hexagonal REMnO_3 . The inter-relationship between this unique structural domain topology and magnetic domains with canted magnetic moments will be presented. In addition, we will discuss the general topological classification scheme of the connectivity of structural and magnetic domains and domain walls.

4TL-H-7

SIGNATURES OF THE FIELD-INDUCED SPIN-NEMATIC STATE IN THE FRUSTRATED ANISOTROPIC SPIN-CHAIN COMPOUND LiCuSbO_4

Grafe H.-J.¹, Nishimoto S.¹, Iakovleva M.^{1,2}, Vavilova E.², Spillecke L.¹, Alfonsov A.¹, Sturza M.-I.¹, Wurmehl S.¹, Nojiri H.³, Rosner H.⁴, Richter J.⁵, Rößler U.¹, Drechsler S.-L.¹, Kataev V.¹, Büchner B.¹

¹ Leibniz Institute for Solid State and Materials Research IFW Dresden, D-01069, Dresden, Germany

² Zavoisky Physical Technical Institute, RAS, 420029, Kazan, Russia

³ Institute of Materials Research, Tohoku University, 980-8577, Sendai, Japan

⁴ Max Planck Institute for Chemical Physics of Solids, D-01187 Dresden, Germany

⁵ University of Magdeburg, Institute for Theoretical Physics, D - 39016 Magdeburg, Germany
v.kataev@ifw-dresden.de

Low-dimensional quantum spin systems are predicted to exhibit a variety of novel ground states beyond classical ferro- or antiferromagnetic phases. The quest for experimental realizations of such theoretical models is primarily focused on complex transition metal (TM) oxides where magnetic coupling between the spins of the TM ions can be confined to one or two spatial directions. In this talk, results of high-field NMR and sub-THz ESR studies of the quantum magnet LiCuSbO_4 will be presented [1]. In this material Cu^{2+} ($S = 1/2$) are coupled along the crystallographic a -axis and form weakly interacting but strongly frustrated one-dimensional Heisenberg spin chains as confirmed by our LDA-FPLO band structure calculations. The absence of long-range magnetic order at ambient fields down to sub-Kelvin temperatures is suggestive of the realization of a quantum spin liquid state [2]. Our NMR and ESR data in strong magnetic fields reveal clear indications for the occurrence of a field-induced hidden phase above 13 Tesla which is likely to be of the multipolar character.

To explain these experimental findings an underlying microscopic theoretical scenario based essentially on nearest neighbor XYZ exchange anisotropy within a quantum model for frustrated spin-1/2 chains is developed and investigated by the DMRG technique. The effect of the Dzyaloshinskii-Moriya interaction will be also discussed.

[1] H.-J. Grafe *et al.*, arXiv:1607.05164.

[2] S. E. Dutton *et al.*, *Phys. Rev. Lett.*, **108** (2012) 187206.

4RP-H-8

FRACTIONALIZED EXCITATIONS IN HIGHER DIMENSIONAL KITAEV IRIDATES

Lemmens P.

Inst. Condensed Matter Physics, TU Braunschweig, Braunschweig, Germany and
Lab. for Emerging Nanometrology (LENA), TU Braunschweig, Braunschweig, Germany
p.lemmens@tu-bs.de

Fractionalization of elementary excitations remains an exotic phenomenon usually limited to 1D and 2D systems [1]. In higher dimensional systems topological order becomes relevant [2]. Here we report spectroscopic signatures of fractional excitations in the 3D harmonic-honeycomb iridates beta - and gamma-Li₂IrO₃ [3]. Our experimental evidence is based on Raman spectroscopic investigations of the polarization and temperature dependence of a scattering continuum, a comparison with earlier investigations of alpha-RuCl₃ [4], and a comparison with theoretical modelling of the Kitaev model on different topologies [5,6].

We acknowledge support by KRF 2009-0076079, GIF 1171-486 189.14/2011, NTH-CiN, and DFG-RTG 1952/1.

- [1] R. B. Laughlin, *Phys. Rev. Lett.*, **60** (1988) 2677.
- [2] M. Oshikawa and T. Senthil, *Phys. Rev. Lett.*, **96** (2006) 060601.
- [3] A. Glamazda, P. Lemmens, S.-H. Do, K.-Y. Choi, *Nature Commun.*, **7** (2016) 12286.
- [4] L. J. Sandilands, Y. Tian, K. W. Plumb, Y. -J. Kim, and K. S. Burch, *Phys. Rev. Lett.*, **114** (2015) 147201.
- [5] J. Knolle, G.-W. Chern, D. L. Kovrizhin, R. Moessner, and N. B. Perkins, *Phys. Rev. Lett.*, **113** (2014) 187201.
- [6] B. Perreault, J. Knolle, N. B. Perkins, and F. J. Burnell, *Phys. Rev. B*, **92** (2015) 094439.

4RP-H-9

FIRST OBSERVATION OF MAGNETOOPTICAL RESPONSE ON TUNNEL MAGNETORESISTANCE IN MANGANITE FILMS WITH A VARIANT STRUCTURE

Telegin A.V.¹, Sukhorukov Yu.P.¹, Bessonova V.A.¹, Nosov A.P.¹, Barsaume S.², Gan'shina E.A.³

¹ IMP UB RAS, Yekaterinburg, Russia

² IMM Radboud University, Nijmegen, The Netherlands

³ MSU, Moscow, Russia
telegin@imp.uran.ru

An optical response to the tunnel magnetoresistance (TMR) in the transmission of light through the $\text{La}_{0.67}\text{Ba}_{0.33}\text{MnO}_3$ manganite films with a variant (equivalent) structure [1] was observed. In these doped manganites the mechanism of TMR is a tunneling of spin-polarized electrons through coherent boundaries of structural domains [1]. Theoretically this effect was predicted in [2] for metallic granular systems. The $\text{La}_{0.67}\text{Ba}_{0.33}\text{MnO}_3$ manganite films with the high Curie temperature and thickness of about 100 nm were grown by pulsed laser deposition on $\text{Y}_2\text{O}_3\text{-ZrO}_2$ (YSZ) (the films with variant structure) and SrTiO_3 (the single-crystalline films) substrates. Comparative studies of the optical and electrical properties of films were carried out in the wide IR spectral range ($1 \leq \lambda \leq 22 \mu\text{m}$), at temperatures from 10 to 350 K, and in magnetic fields of up to 15 kOe.

In work the effects of magnetotransmission (MT) of natural light and magnetoresistance were compared for films on different substrates. Contributions from CMR and TMR for various temperatures and applied magnetic fields were identified. In addition to the singularity near the Curie temperature (T_C) associated with CMR, a new mechanism of MT, related to the optical response to TMR, was observed in films on the YSZ substrates. It was shown that this contribution increases with decreasing temperature ($T \ll T_C$) and it can be described within the framework of the theory of magnetorefractive effect developed for granular films. In contrast to the optical response to CMR [4] observed near T_C only, the low-temperature (tunnel) MT related to TMR shows hysteresis behavior with two positive maxima (“butterfly-like”) in relatively small magnetic fields, and negative sign of effects at higher fields (Fig.1).

The results obtained can be useful for further development of theory of the magnetorefractive effect in magnetics and creation novel functional materials for spin-optoelectronics.

The results were obtained within the state assignment of FASO of Russia (“Spin” theme №0120146330), program UB of RAS №15-9-2-4, grant № 14.Z50.31.0025

[1] A.R. Kaul *et al.*, *Russian Chemical Reviews*, **73** (2004) 861-880.

[2] A.B. Granovski *et al.*, *JETP*, **89** (1999) 955-959.

[3] A.V. Telegin *et al.*, *JMMM*, **383** (2015) 104-109.

[4] A.B. Granovskii *et al.*, *JETP*, **112** (2011) 77-86.

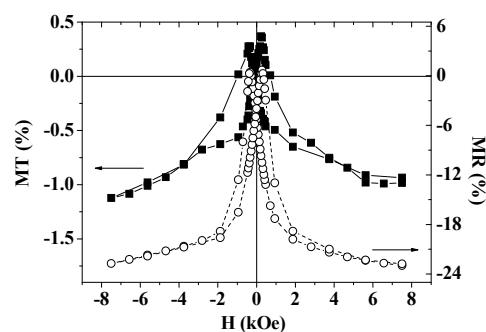


Fig. 1. Magnetic field dependences of MT (solid symbols) and TMR (open symbols) at $T=80$ K and $\lambda=3.4 \mu\text{m}$.

4OR-H-10

SELF-DOPED $\text{Pr}_{1-x}\text{MnO}_{3+\delta}$ MANGANITES: RAMAN VACANCY MODES AND GRIFFITHS-LIKE PHASE

*Ulyanov A.N.*¹, *Savilov S.V.*¹, *Vasiliev A.V.*¹, *Pismenova N.E.*², *Sidorov A.V.*³, *Goodilin E.A.*^{1,3,4}

¹ Faculty of Chemistry, Moscow State University, Moscow, Russia

² Donetsk Physico-Technical Institute, Donetsk, Ukraine

³ Faculty of Materials Science, Moscow State University, Moscow, Russia

⁴ Institute of General and Inorganic Chemistry, Moscow, Russia

a_n_ulyanov@yahoo.com

Complex analysis of the vacancy-doped $\text{Pr}_{1-x}\text{MnO}_{3+\delta}$ manganites ($x=0.0, 0.2$) is performed by X-ray diffraction, Raman and x-ray photoelectron spectroscopy and magnetic measurements to study the features of electron, phonon and magnetic structure of the compounds. The $x=0.0$ and $x=0.2$ oxides belong to orthorhombic $Pnma$ structure and (pseudo) cubic $Pm\bar{3}m$ symmetry, respectively. According to the x-ray photoelectron spectroscopy an average valence of manganese for both samples is found to be ≈ 3.2 due to doping holes localized in the O $2p$ states and the hybridization of Mn $3d$ and O $2p$ states.

For the $x=0.2$ perovskite an intensive Raman mode is observed at 650 cm^{-1} and associated by the high level of vacancies. At the same time, for both the studying oxides the vacancies suppress the Jahn-Teller (JT) (485 cm^{-1}) and charge-transfer $d-d$ (610 cm^{-1}) Raman modes, which are intensive for the parent stoichiometric LaMnO_3 [1], PrMnO_3 [2] perovskites. The later peak is correlated with the optical gap at 2.0 eV [1], which is the result of hopping transition between JT-split e_g levels. Curie temperature of the studied manganites is lower than the Neel temperature of the parent stoichiometric PrMnO_3 oxide.

Downturn anomaly of inverse magnetization in paramagnetic region is observed (Fig. 1). The singularity is associated with the appearance of Griffiths-like phase and supposed to be caused by the vacancies in the A - and B – sites of perovskite ABO_3 cell. The result is in line with those presented in [3,4], where the vacancy doped $\text{La}_{1-x}\text{MnO}_{3+\delta}$ oxides were studied. The role of vacancy and oxygen deficiency for the appearance of Griffiths phase is carefully discussed.

Support by Russian Foundation for Basic Research (projects No. 15-03-09029a and No. 16-03-00888a) is acknowledged.

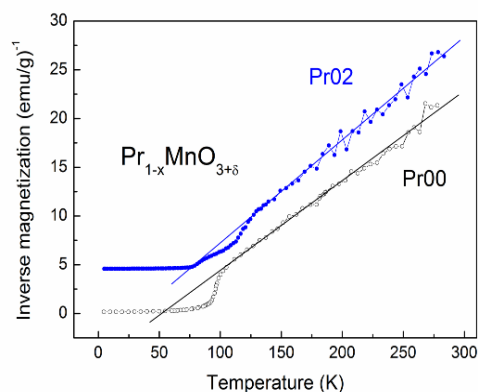


Fig. 1. Temperature dependencies of inverse magnetization of $\text{Pr}_{1-x}\text{MnO}_{3+\delta}$ ($x=0.0, 0.2$) manganites.

- [1] R. Krüger, B. Schulz, S. Naler, R. Rauer, D. Budelmann, J. Bäckström, K. H. Kim, S-W. Cheong, V. Perebeinos, and M. Rübhausen. *Phys. Rev. Lett.*, **92** (2004) 097203.
 [2] L. Martín-Carrón, A. de Andrés. *J. Alloys Compd.*, **323-324** (2001) 417-421.
 [3] A.N. Ulyanov, N.E. Pismenova, D.S. Yang, V.N. Krivoruchko, G.G. Levchenko. *J. Alloys Compd.*, **550** (2013) 124–128.
 [4] A.N. Ulyanov, N.E. Pismenova, D.S. Yang, G.G. Levchenko. *J. Alloys Compd. (letter)*, **618** (2015) 607–608.

4OR-H-11

MAGNETIC-FIELD CONTROL OF SURFACE DOMAINS IN A WEAK FERROMAGNET YFeO_3

Andreeva N.V.^{1,2}, Kalashnikova A.M.², Balbashov A.M.³, Pisarev R.V.¹, Vakhrushev S.B.^{1,2}, Shvartsman V.V.⁴

¹ Peter the Great Polytechnic University, 195251 St. Petersburg, Russia

² Ioffe Institute, 194021 St. Petersburg, Russia

³ Moscow Power Engineering Institute, 111250 Moscow, Russia

⁴ University of Duisburg-Essen, 45141, Essen, Germany
kalashnikova@mail.ioffe.ru

Designing surface and interface properties of magnetic oxides and their control by various external stimuli is nowadays one of the key issues in developing oxide heterostructures, which functionalities address the needs of state-of-the-art spintronics [1,2]. Here we report on observation of room-temperature surface magnetic domains in a model weak ferromagnetic oxide YFeO_3 , and demonstrate their switching by an external magnetic field \mathbf{H} applied *perpendicular* to the magnetization of the domains.

Fig. 1 shows the experimental scheme, where the single-crystalline *a*-plate of the orthoferrites YFeO_3 is placed in the magnetic force microscope (MFM) with a Co-coated tip. The net magnetization \mathbf{M} in the bulk is oriented in the sample plane [4] and its direction can be reversed by changing the sign of the in-plane magnetic field \mathbf{B} .

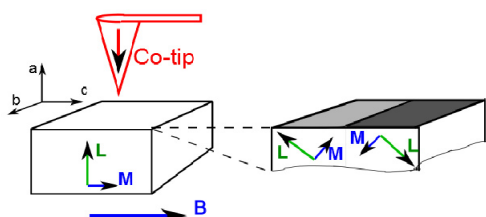


Fig. 1. Geometry of the experiment: magnetization of the MFM tip, direction of the external field \mathbf{B} , and relative orientations of the ferro- (\mathbf{M}) and antiferromagnetic (\mathbf{L}) vectors in the bulk (left) and in the surface layer (right).

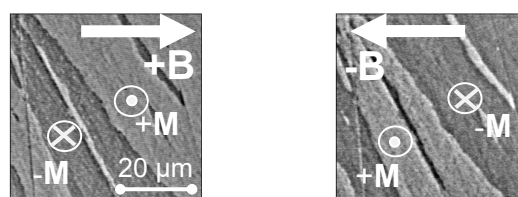


Fig. 2. Magnetic phase contrast in the MFM scans obtained in the in-plane fields of $B = +200$ mT (left) and $B = -200$ mT (right). Reversal of the magnetization \mathbf{M} in the surface magnetic domains is observed.

Fig. 2 shows the magnetic phase contrast of the MFM scan, which clearly reveals the presence of surface domains with the magnetization having significant projection on the sample normal (Fig. 1). We attribute the presence of such surface domains to the change of the magnetic anisotropy in the near-surface region [4], which allows orientation of the magnetization along the crystallographic *a*-axis. We note that the orientation of the bulk magnetization in YFeO_3 along the *a*-axis requires application of large magnetic field of several Tesla along this axis [3].

Finally, we show that the orientation of \mathbf{M} in the surface domains is, nevertheless, coupled to the bulk magnetic structure. As a result, reversal of the magnetization direction in the bulk by a weak in-plane magnetic field of ~ 50 mT switches the local magnetization of the surface domains (Fig. 2). Thus, we demonstrate the control of the surface out-of-plane magnetization of the weak ferromagnet YFeO_3 by weak in-plane external magnetic field.

Support by the Russian Govt. program P220 (grant No.14.B25.31.0025) is acknowledged.

[1] A. Bhattacharya and S. J. May, *Ann. Rev. Mat. Res.*, **44** (2014) 65–90.

[2] X. He, et al., *Nature Materials*, **9** (2010) 579 – 585.

[3] K. P. Belov, et al., *Sov. Phys.—Usp.*, **19** (1976) 574–596.

[4] M. I. Kaganov, *J. Exp. Theor. Phys.*, **35** (1980) 631–633.

4RP-H-12

MAGNETO-ELECTRONIC PHASE SEPARATION ABOVE T_C IN $\text{Sm}_{0.32}\text{Pr}_{0.18}\text{Sr}_{0.5}\text{MnO}_3$ CMR MANGANITE WITH ISOVALENT DOPING

Ryzhov V.A.¹, Kurbakov A.I.¹, Runov V.V.¹, Deriglazov V.V.¹, Martin C.², Maignan A.²

¹ Petersburg Nuclear Physics Institute of NRC ‘Kurchatov Institute’, Gatchina 188300, Russia

² Laboratoire CRISMAT, Université de Caen, Boulevard de Marechal Juin, 14050 Caen, France
 ryzhov@omrb.pnpi.spb.ru

Effect of colossal magnetoresistance (CMR) in hole doped perovskite manganites is observed near paramagnet(P)-ferromagnet(FM) transition, both in compounds with insulator (I) and metallic (M) ground states. Magnetic field can change phase equilibrium or temperature of phase transition. The huge change by field of sample resistance R suggests the presence of conductive M phase in it. Magneto-electronic phase separation (MEPS) provides arising of FM-ordered clusters with M properties above T_C embedded in P-I matrix followed by emergence of heterogeneous magnetic state. Amount of clusters depends strongly on temperature and level of doping, x . At approaching their concentration to percolation limit *I-M phase transition* occurs. So, to insight in physics of manganites one needs to study the details of *MEPS and its connection with P-FM*. The compounds near half doping are of special interest since they exhibit orbital/charge ordering (OO, CO) followed by AFM ordering that can dramatically affect the MEPS. In this study we clarify an affect of additional isovalent doping of $\text{Sm}_{0.5}\text{Sr}_{0.5}\text{MnO}_3$ (SSMO) by Pr on MEPS. The data on its magnetic properties (static magnetization, $M(T)$, second harmonic of nonlinear response in parallel ac and dc (H) magnetic fields, $M_2(H,T)$, neutron depolarization) as well as on resistance are presented here.

Neutron diffraction of $\text{Sm}_{0.32}\text{Pr}_{0.18}\text{Sr}_{0.5}\text{MnO}_3$ (SPSMO) indicates structural transition from orthorhombic ($Pbnm$) phase with small Jahn-Teller (JT) distortions to mixture of initial and monoclinic ($P2_1/m$) phases at $T_{st} \sim 170\text{K}$. The latter exhibits considerable JT compression along apical Mn-O1 bond similar to that in low temperature phase of earlier studied SSMO ($Pbnm$ -I \rightarrow to mixture of two $Pbnm$ at $T_{st} \sim 135\text{K}$ [1]) CMR manganite. In both compounds antiferromagnetic (AF) ordering occurs in low-temperature new phases, two types of order being formed in the SPSMO (AF-A below $T_{AF-A} \sim 170\text{K}$ and pseudo AF-CE at $T_{AF-CE} \sim 125\text{K}$) and one type in the SSMO (AF-A below $T_{AF-A} \sim 135\text{K}$) compounds. Long range FM ordering originates in high-temperature initial phases below $T_C \sim 125\text{K}$ and $\sim 110\text{K}$ respectively. SPSMO keeps insulator behavior in ground state whereas SSMO undergoes I-M transition at $T_{IM} \sim 54\text{K}$. $M_2(H,T)$ measurements evidence a start of MEPS above 310 K in both compounds with FM cluster concentration by two orders of magnitude being larger in SPSMO. This result is in agreement with M data indicating domination of AF correlations in SSMO against FM correlations in SPSMO at high temperatures. Small angle polarized neutron scattering (SAPNS) results indicate the start of neutron depolarization at high temperature $\sim 305\text{K}$ in SPSMO, whereas it begins below $\sim 116\text{K}$ in SSMO, when magnitude of $M_2(H,T)$ response attains the value corresponding to that in the former at 305 K. In SPSMO the characteristic features of $M_2(H,T)$ response at high temperatures correspond to that of ensemble of single-domain magnetic nanoparticles (MNP). Fokker-Planck kinetic equation provides good description of the response with power law distribution of their magnetic moments with exponent $p \sim 2.62 - 2.96$ increasing on cooling, instead of lognormal one found for subsystem of FM clusters in studied earlier $\text{La}_{0.85}\text{Sr}_{0.15}\text{CoO}_3$ cobaltite [2]. This can be attributed to fractal spatial organization of the clusters in the SPSMO which is favorable at combination of charge and isovalent doping.

[1] A.I. Kurbakov, A.V. Lazuta, V.A. Ryzhov et al., *Phys. Phys. B*, **72** (2005) 184432–10.

[2] A.V. Lazuta, V.A. Ryzhov, V.V. Runov et al., *Phys. Phys. B*, **92** (2015) 014404–11.

4OR-H-13

CHARGE AND ORBITAL ORDER IN SODIUM COBALTATES Na_xCoO_2 *Mukhamedshin I.R.^{1,2}, Alloul H.²*¹ Institute of Physics, Kazan Federal University, 420008, Kazan, Russia² Laboratoire de Physique des Solides, Université Paris-Sud, 91405, Orsay, France

Irek.Mukhamedshin@kpfu.ru

The influence of the dopant atoms on the electronic properties of conducting layers has initiated large debates in high temperature superconducting cuprates as well as in other complex layered oxides of transition elements. Whereas in many systems this influence is masked by miscellaneous effects, there are many experimental evidences that in the sodium cobaltates Na_xCoO_2 a large interplay between the Na atomic ordering and the electronic density on the Co sites occurs. The Na_1CoO_2 phase is a band insulator in which the Co sites are in filled-shell nonmagnetic Co^{3+} states. At $x < 1$ the system becomes metallic, but only specific Na compositions can be obtained, which correspond to some Na orderings as observed by diffraction techniques. E.g. for $x=0.5$ the Na atoms are ordered in an orthorhombic superstructure commensurate with the Co lattice and a small charge disproportionation into $\text{Co}^{3.5\pm\epsilon}$ (with $\epsilon < 0.2$) occurs on the two Co sites .

We have synthesized and characterized different stable phases of sodium cobaltates Na_xCoO_2 with sodium content $0.65 < x < 0.80$, including one of the most stable magnetic phases of sodium cobaltates with a well defined Néel temperature of $T_N = 22$ K. We demonstrate that ^{23}Na NMR allows to determine the difference in the susceptibility of the phases and reveals the presence of Na order in each phase. Our detailed NMR /NQR studies allowed us to reveal the peculiarities of the $x=2/3$ phase. We could establish reliably the atomic order of the Na layers and their stacking between the CoO_2 slabs. We found that the Na^+ order stabilizes filled non magnetic Co^{3+} ions on 25% of the cobalt sites Co1 arranged in a triangular sublattice. The transferred holes are delocalized on the 75% complementary cobalt sites Co2 which unexpectedly display a planar cobalt kagomé structure [2].

^{59}Co NMR experiments give clear evidence that such Co charge disproportionation is a dominant feature of Na cobaltates for $0.65 < x < 0.80$ [3]. Only a small fraction ($\approx 25\%$) of cobalts are in a non-magnetic Co^{3+} charge state whereas electrons delocalize on the other cobalts. We found that the magnetic and charge properties of the Co sites are highly correlated with each other as magnetic shift K_{ZZ} scale linearly with quadrupolar frequency ν_Q [2]. Such correlations can be understood as both measured values ν_Q and K_{ZZ} contain terms proportional to the quadrupole moment of the t_{2g} hole density distribution which involves as a coefficient the hole concentration on the Co site. Therefore this correlations reflects the fact that the hole content on the Co orbitals varies from site to site in both phases and the hyperfine coupling (or the local magnetic susceptibility) scales with the on site delocalized charge. Such unusual charge differentiation in sodium cobaltates calls for better theoretical understanding of the incidence of the Na atomic order on the electronic structures of these compounds.

This work was partially funded by the subsidy allocated to Kazan Federal University for the state assignment in the sphere of scientific activities. The crystals growth was carried out at the Federal Center of Shared Facilities of Kazan Federal University. M.I.R. thanks for the support of a visit to Orsay by “Investissements d’Avenir” LabEx PALM (ANR-10-LABX-0039-PALM).

[1] I.R.Mukhamedshin and H. Alloul, *Phys. Rev. B*, **84** (2011) 155112.[2] I.R.Mukhamedshin, A.V.Dooglav, S.A.Krivenko, H.Alloul, *Phys. Rev. B*, **90** (2014) 115151.[3] I.R. Mukhamedshin and H. Alloul, *Physica B*, **460** (2015) 58–63.

4OR-H-14

VALENCE DRIVEN ORDERING AND QUANTUM CRITICALITY IN $\text{Yb}_2\text{Pd}_2(\text{In},\text{Sn})$

Khan T.¹, Michor H.¹, Giovannini M.², Zlatic V.³, Khasanov R.⁴, Yamaoka A.⁵, Bauer E.¹

¹ Institute of Solid State Physics, TU Wien, A-1040 Wien, Austria

² CNR-SPIN, Dipartimento di Chimica e Chimica Industriale, Univ. of Genova, I-16146 Genova

³ Instiute of Physics, Zagreb, Croatia

⁴ Laboratory for Muon-Spin Spectroscopy, PSI, CH-5232 Villigen PSI, Switzerland

⁵ RIKEN SPring-8 Center, RIKEN, 1-1-1 Kouto, Sayo, Hyogo 679-5148, Japan

bauer@ifp.tuwien.ac.at

In this contribution, the observation of *two* pressure driven quantum critical points appearing in ternary $\text{Yb}_2\text{Pd}_2\text{Sn}$ is discussed, where the application of pressure of about 1 GPa establishes long-range antiferromagnetic order, but above an upper bound of about 4 GPa, magnetic order vanishes again, giving rise to two phase transitions at zero temperature. Associated with this quantum criticality in $\text{Yb}_2\text{Pd}_2\text{Sn}$, we observe nFI behaviour from precise resistivity measurements. We argue that this emergent behaviour corresponds to two pressure dependent, mutually competing energy scales exerted to the Yb ions. Electronic properties associated with the paramagnetic state below and above the critical pressures disagree, as evident from a negative and a positive Grüneisen parameter, respectively.

Interestingly, a substitution of Sn/In in this ternary compound mimics the pressure triggered magnetic instabilities in $\text{Yb}_2\text{Pd}_2\text{Sn}$, creating magnetic order within a nonmagnetic periphery.

A complicated balance of mutual interaction mechanisms, among are the Kondo effect, RKKY interaction, crystalline electric field splitting and frustration determines the respective ground states. Very recent pressure dependent spectroscopic studies shed additional light on these materials.

4 July

Tuesday

14:30-17:15

oral session

4TL-O

4OR-O

4RP-O

**“Magnetophotonics
and Ultrafast
Magnetism”**

4TL-O-5

ULTRAFAST EINSTEIN-DE HAAS EFFECT: A NEW LOOK INTO ULTRAFAST DEMAGNETISATION

*Dornes C.¹, Savoini M.¹, Kubli M.¹, Bothschafter E.², Porer M.², Vaz C.A.F.², Zhu D.³, Song S.³,
Glownia J.M.³, Lemke H.⁴, Beaud P.⁴, Staub U.², Acremann Y.⁵, Johnson S.L.¹*

¹ Institute for Quantum Electronics, ETH, Zürich, Switzerland

² Swiss Light Source, Paul Scherrer Institut, Villigen, Switzerland

³ Linac Coherent Light Source, SLAC National Accelerator Laboratory, Menlo Park, USA

⁴ SwissFEL, Paul Scherrer Institut, Villigen, Switzerland

⁵ Institute for Solid State Physics, ETH, Zürich, Switzerland

savoinim@phys.ethz.ch

The interaction of sub-picosecond laser pulses with magnetically ordered materials has developed into a fascinating research topic in modern magnetism. From the discovery of sub-picosecond demagnetisation 20 years ago [1], the manipulation of magnetic order by ultrashort pulses has become a fundamentally challenging topic with a potentially high impact for future spintronics, data storage and manipulation [2]. Despite the ever-increasing number of scientific publications in the field, a general consensus about the origin and properties of the ultrafast demagnetisation process has yet to be reached.

Here we report a recent experiment we have performed using time-resolved X-ray techniques. We exploit the femtosecond resolution of a free electron laser to measure the structural dynamics of a thin film of iron upon laser-induced demagnetisation. The use of this technique enabled us to measure the creation of a magnetisation-dependent strain profile, generated in the sample after laser illumination, within timescales compatible with the demagnetisation process. We interpret this observation in terms of transverse optical phonons induced by the loss of the magnetic moment during the demagnetization step. We thus demonstrate that the lattice is a sufficiently fast recipient of the lost momentum.

[1] E. Beaurepaire, *et al.*, *Phys. Rev. Lett.*, **76** (1996) 4250.

[2] A. Kirilyuk, *et al.*, *Rev. Mod. Phys.*, **82** (2010) 2731.

4TL-O-6

MAGNETISATION MANIPULATION WITH LIGHT AND ELECTRONS FEMTO-SECOND PULSES: TOWARD ULTRAFAST SPINTRONIC

Deb M.¹, Xu Y.¹, El Hadri M.S.¹, Bergeard N.¹, Malinowski G.¹, Hehn M.¹, Mangin S.¹

¹ Institut Jean Lamour, CNRS UMR 7198, Université de Lorraine, 54506 Vandœuvre, France
Stephane.Mangin@univ-lorraine.fr

Since the first observation of ultrafast demagnetization in Ni thin films using femto-second laser by Beaurepaire et al. 20 years ago [1], understanding the mechanism behind ultra-fast magnetization dynamic became a topic of huge interest. The new possibility of using short light or electron pulses to manipulate magnetization attracts a lot of attention also because of the potential application. Indeed in 2007, an intriguing discovery was the observation of all-optical switching of magnetization in ferrimagnetic GdFeCo alloy films using femtosecond laser pulses [2]. Moreover it was shown in 2014 that AOS is a much more general phenomenon with a wide range of choices of materials. [3]. Investigating AOS using spintronic devices, two types mechanism: Single pulse All-Optical Helicity-Independent Switching (AO-HIS) and multiple pulse All Optical Helicity-Dependent Switching (AO-HDS) were clearly distinguished [4]. Moreover optical control of the exchange bias field using polarized femtosecond pulsed laser on IrMn/[Co/Pt]_{xN} antiferromagnetic/ferromagnetic heterostructures was clearly demonstrated [5].

In all the previous reported experiments light is used to manipulate magnetization. However, recently engineered multilayer structures such as Pt/ Cu (t) / [Co/Pt], Pt/ Cu (t) / GdFeCo were used in order to create hot electrons femto second pulses. By shining light on the Pt layer, hot electrons are being created, they travel ballistically into the Cu before interacting with the magnetic layer. It was then demonstrated that hot electrons alone can very efficiently induce ultrafast demagnetization [6] or direct magnetization switching [7] which confirm the work from Wilson et al [8] on magnetization switching of GdFeCo/Au bilayer via hot electrons .

[1] E. Beaurepaire, et al, *Phys. Rev. Lett.*, **76** (1996) 4250.

[2] C. D. Stanciu, et al, *Phys. Rev. Lett.*, **99** (2007) 047601; T. A. Ostler, et. al., *Nat. Commun.*, **3** (2012) 666.

[3] S. Alebrand, et al., *Appl. Phys. Lett.*, **101** (2012) 162408; S. Mangin, et. al., *Nat. Mater.*, **13** (2014) 286; C.-H. Lambert, et al, *Science* (2014) 1253493.

[4] M.S. El Hadri et al, *Appl. Phys. Lett.*, **108** (2016) 092405; M S El Hadri et. Al., *Phys. Rev. B*, **94** (2016) 064412.

[5] P. Vallobra, et al ArXiv 1761494 (2017).

[6] N. Bergeard, et al *Phys. Rev. Lett*, **117** **14** (2016) 147203.

[7] Y. Xu, et al (to be submitted).

[8] R. B. Wilson, et al ArXiv160905155 Cond-Mat (2016).

4OR-O-7

SPATIAL AND TEMPORAL DYNAMICS OF THE LASER-INDUCED MAGNETIZATION REVERSAL IN $Y_3Fe_5O_{12}$

*Prabhakara K.H.¹, Davydova M.D.², Zvezdin K.A.^{2,3}, Shapaeva T.B.⁴, Wang S.⁵, Zvezdin A.K.^{2,6},
Kirilyuk A.¹, Rasing Th.¹, Kimel A.V.^{1,6}*

¹ Radboud University, Institute for Molecules and Materials, Nijmegen, Netherlands

² Moscow Institute of Physics and Technology, Moscow, Russia

³ A. M. Prokhorov General Physics Institute, Moscow, Russia

⁴ Moscow State University, Moscow, Russia

⁵ Jinan University, Guangzhou, China

⁶ Moscow Technological University (MIREA), Moscow, Russia

K.Prabhakara@science.ru.nl

Magnetization reversal by a combined action of an external magnetic field and a laser-induced heat-pulse is the main idea behind Heat-Assisted-Magnetic Recording (HAMR) which promises dramatic improvements in densities of magnetic recording. While this process is extensively studied in metals, its feasibility in magnetic dielectrics is not obvious at all. Here we report an experimental and theoretical study of the laser-assisted magnetization reversal in $Y_3Fe_5O_{12}$.

In the experiment the $Y_3Fe_5O_{12}$ sample with out-of-plane magnetic anisotropy was subjected to a magnetic field with a strong in-plane and a weaker out-of-plane component. To change the orientation of the magnetization, the medium was excited by an intense pump pulse with duration below 100 fs at the central wavelength of 400 nm. To monitor the laser-induced changes we employed the technique of femtosecond single shot imaging in which the out-of-plane component of the magnetization was probed by a time-delayed laser pulse. Imaging is performed in a transmission geometry, with the probe beam normal to the sample surface.

20 μ m

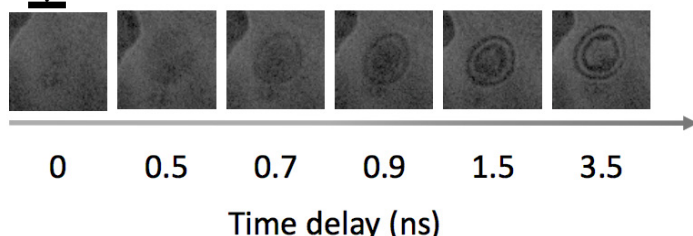


Fig. 1: Dynamics of the laser-induced magnetization reversal in $Y_3Fe_5O_{12}$ measured with the help of femtosecond single-shot magneto-optical imaging.

Typical images obtained in such an experiment are shown in Fig. 1 for several time-delays. The experiment shows that despite a Gaussian distribution of the intensity of the pump pulse, the formed pattern is strongly inhomogeneous. If the intensity of the pump is above 5 mJ/cm^2 , a clear ring structure is formed. The number of the rings increases with the intensity and can be also controlled by the strength of the in-plane magnetic field. Time-resolved measurements revealed that the pattern is formed within less than 1 ns, which indicates that the processes responsible for the formation are not related to domain wall motion and must be assigned to magnetization precession. Theoretical studies of the heat-induced magnetization reversal have been performed, which show that the observed process can be explained in terms of laser-induced changes of magnetic anisotropy and magnetization precession in an effective magnetic field.

The work was supported by de Nederlandse Organisatie voor Wetenschappelijk Onderzoek (NWO) and the Ministry of Education and Science of the Russian Federation (Project No. 14.Z50.31.0034).

4OR-O-8

MECHANISM OF ULTRAFAST ALL-OPTICAL MAGNETIZATION SWITCHING IN IRON GARNETS

Davydova M.D.¹, Zvezdin K.A.^{1,2}, Zvezdin A.K.^{1,2}

¹ Moscow Institute of Physics and Technology, Dolgoprudny, Russia

² A. M. Prokhorov General Physics Institute, Moscow, Russia
davydova @ phystech.edu, konstantin.zvezdin @ gmail.com

Recently, a possibility of ultrafast non-thermal magnetization switching in YIG:Co films was demonstrated experimentally [1]. Although all-optical switching in magnetic dielectrics is an important and broadly discussed subject, no theoretical model has been proposed yet to describe such switching process.

Here we describe ultrafast all-optical photo-magnetic switching in transparent magnetic films with dielectric cobalt-substituted garnet as a particular example. The proposed model is based on nonlinear Landau-Lifshitz-Gilbert equations for a uniformly magnetized [001] iron garnet film. The effect of the laser electric field is taken into account as additional optical spin-torque. In this framework, we simulate the behavior of magnetization under the action of a single ultra-short laser pulse. We investigate the proposed mechanism thoroughly, and obtain different switching patterns. The obtained results are in agreement with the recent experimental work [1]. Thus, by changing the polarization of the laser pulse, the net magnetization in the film may be changed repeatedly, thus storing and conveniently handling information in film. We also find this process to be reversible; the cases of different polarizations of the laser pulse were studied. Different regimes of switching were found and corresponding phase diagrams depending on the parameters of the material and the laser pulse were plotted.

Investigation of energy-efficient ways to control the magnetic state of media and at small timescales is an important task for fundamental magnetism, which will open the way to the broad range of practical applications. This mechanism has already been shown to outperform existing alternatives in terms of the speed and heat efficiency.

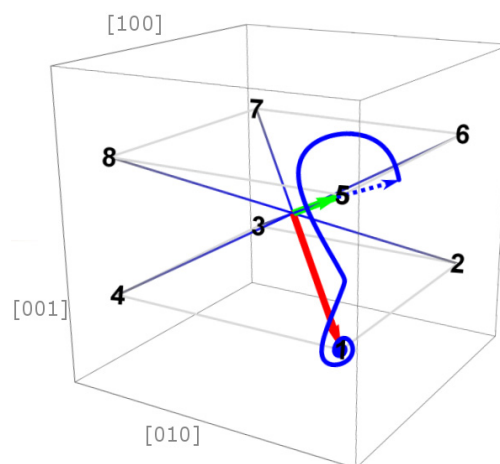


Fig. 1. The simulated dynamics of the magnetization vector in YIG:Co after ultra-short (femtosecond) laser pulse. The directions denoted by numbers '1-8' correspond to equivalent ground states for magnetization vector. At first, the domain has uniform magnetization in the direction '5'. After short-acting laser pulse, the magnetization is diverted due to the optical spin-torque as shown by dashed arrow. The dynamics of the magnetization vector after the pulse is shown by blue curve. The final magnetization in the area is aligned with the direction '1'. Overall timescales of such processes are of the order of 50 ps.

Support by RFBR (grant № 16-29-14005) is acknowledged.

[1] A. Stupakiewicz et al. *Nature*, **542** (2017) 71–74.

4TL-O-9

SPIN EXCITATIONS IN A COMPLEX MULTISUBLATTICE ANTIFERROMAGNET $\text{Ni}_3(\text{BO}_3)_2$

*Pisarev R.V.¹, Prosnikov M.A.¹, Davydov V.Yu.¹, Smirnov A.N.¹, Boldyrev K.N.², Molchanova A.D.²,
Popova M.N.², Kamenskiy D.³, Pashkevich Yu.G.⁴, Zhuravlev A.V.⁴*

¹ Ioffe Physical-Technical Institute, Russian Academy of Sciences, St. Petersburg, Russia

² Institute of Spectroscopy, Russian Academy of Sciences, Moscow, Russia

³ High Magnetic Field Laboratory, Radboud University, Nijmegen, The Netherlands

⁴ O.O. Galkin Donetsk Institute for Physics and Engineering, NAS of Ukraine, Kyiv, Ukraine
pisarev@mail.ioffe.ru

Nickel orthoborate $\text{Ni}_3(\text{BO}_3)_2$ belongs to a family of wide-band gap magnetic insulators with a complex crystal structure, the space group $Pnma$ (#58, $Z=2$) [1]. Magnetic Ni^{2+} ions ($S=1$) occupy two $2a$ and $4f$ distinct crystallographic positions. The 3D antiferromagnetic ordering is observed below $T_N=46$ K [2]. However, up to now the magnetic dynamics of this material remains practically unexplored. In this talk we report on results of comprehensive experimental and theoretical study of magnetic symmetry, spin-wave spectra and spin excitations in $\text{Ni}_3(\text{BO}_3)_2$ obtained with the use of polarized Raman scattering (RS) and infrared (IR) optical spectroscopy. Far infrared studies were also performed in magnetic fields up to 30 T.

Theoretical analysis has shown that magnetic ordering occurs with the doubling of the primitive unit cell and is accompanied by an unusual magnetostriction of exchange origin. The lattice symmetry of the magnetic phase decreases to a monoclinic one. As a consequence, the magnetic frustrations present in the high symmetry phase are fully relaxed.

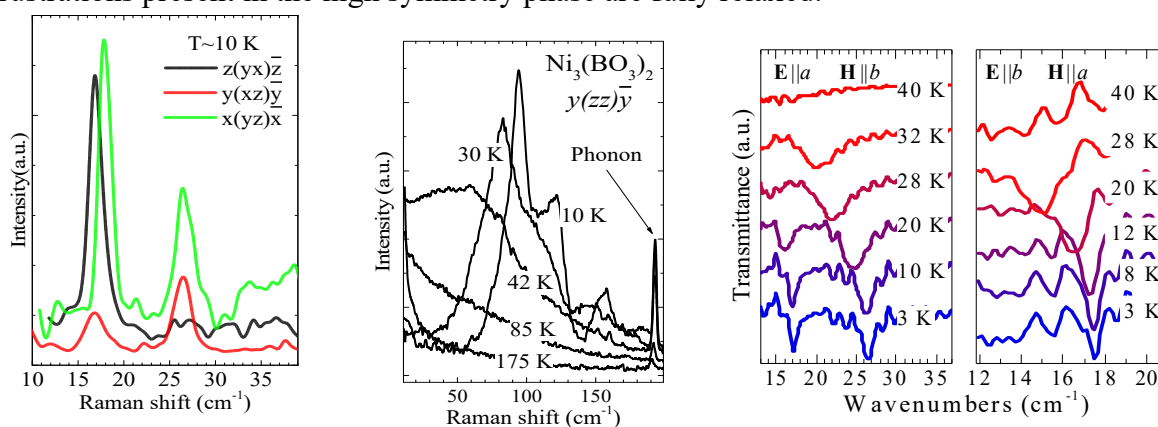


Fig. 1. Low-frequency one-magnon modes in $\text{Ni}_3(\text{BO}_3)_2$ observed in Raman spectra.

Fig. 2. Single-ion excitations as a function of temperature observed in Raman scattering spectra.

Fig. 3. Temperature dependence of the spin-wave modes in far-infrared transmittance spectra for different polarization.

The studies in the broad temperature range below and above $T_N=46$ K allowed us to observe several features in the Raman and IR spectra below 40 cm^{-1} which could be assigned to particular modes of one-magnon excitations (see Figs. 1 and 3). Some of them were reliably attributed to spin modes belonging to twelve modes predicted by theoretical calculations. Besides that, several strong bands with a complex structure were observed in the Raman experiments in the range of 100 - 200 cm^{-1} (see Fig. 2). Their polarization properties and temperature behavior allowed us to assign them to single-ion spin excitations of Ni^{2+} ions. Their frequency values and intensity can be qualitatively explained by the presence of sufficiently large magnetic anisotropy and Dzyaloshinskii-Moriya interactions in $\text{Ni}_3(\text{BO}_3)_2$.

Support by the Russian Science Foundation grant No. 16-12-10456 is acknowledged.

[1] R.V. Pisarev, M.A. Prosnikov, V.Yu. Davydov, *et al*, *Phys. Rev. B*, **93** (2016) 134306.

[2] L.N. Bezmaternykh, S.N. Sofronova, N.V. Volkov, *et al*, *Phys. Stat. Sol. (b)*, **249** (2012) 1628.

4RP-O-10

COUPLED ELECTRON-PHONON MODES IN AN ANTIFERROMAGNET SUBJECTED TO A MAGNETIC FIELD

Boldyrev K.N., Popova M.N.

Institute of Spectroscopy, Russian Academy of Sciences, Troitsk, Moscow, Russia
popova@isan.troitsk.ru

If a phonon and an electronic excitation of a crystal are in resonance, interaction between them leads to formation of coupled electron-phonon modes. This phenomenon is typical of a very broad class of stoichiometric f and d materials and is accompanied by an energy renormalization and redistribution of intensities in the low-frequency part of the spectra. As just this part of the energy spectrum governs thermodynamic and magnetic properties of the compound, it is important to understand physics of coupled electron-phonon modes and of their behavior in external magnetic fields.

In this presentation, we report on a new effect associated with the electron-phonon interaction, namely, appearance of nonzero gap in the spectrum of coupled electron-phonon modes in an antiferromagnetically (AFM) ordered compound subjected to an arbitrarily small external magnetic field. The effect was observed in the far-infrared (terahertz) reflection spectrum of a $\text{PrFe}_3(\text{BO}_3)_4$ single crystal.

The temperature dependence of the spectra in a zero magnetic field, in the region of the lowest-frequency nondegenerate phonon and electronic level of the same symmetry evidences formation of coupled phonon – $4f$ electronic excitations. A successful modeling of this process on the basis of a quadratic equation derived in the frame of the theory of coupled electron-phonon modes results in a value $|W|=14.8 \text{ cm}^{-1}$ for the electron-phonon coupling constant [1]. The behavior of coupled modes in paramagnetic and AFM spin-flop phases in magnetic fields up to 30 T, parallel to the c axis is explained on the same ground [2].

In the case of the easy-axis AFM phase, there are two electronic branches and a phonon, the quadratic equation converts into a cubic one and bifurcations corresponding to an abrupt appearance of the third root are observed. The field behavior of the spectrum of excitations differs qualitatively from the behavior in the absence of electron-phonon coupling, in particular, a nonzero energy gap between two electronic modes exists at an arbitrarily small external magnetic field (see Fig. 1). Again, the field behavior of the coupled modes is successfully simulated using the same set of parameters [2].

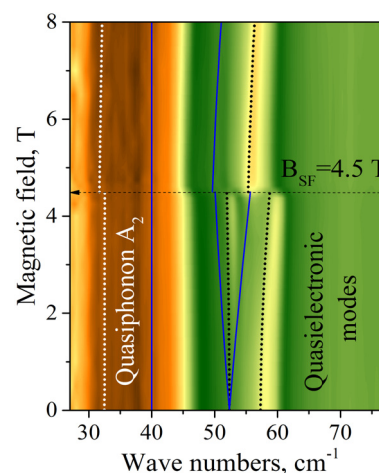


Fig. 1. Intensity maps for the reflection spectra of $\text{PrFe}_3(\text{BO}_3)_4$ in magnetic fields $\mathbf{B}_{\text{ext}} \parallel c$. Calculated frequencies are shown by dotted ($|W|=14.8 \text{ cm}^{-1}$) and solid ($W=0$) lines.

Support by the Russian Science Foundation under Grant No 14-12-01033 is acknowledged.

[1] K.N. Boldyrev, T.N. Stanislavchuk, A.A. Sirenko, L.N. Bezmaternykh, M.N. Popova, *Phys. Rev. B Rapid Comm.*, **90** (2014) 121101(R).

[2] K.N. Boldyrev, T.N. Stanislavchuk, A.A. Sirenko, D. Kamenskyi L.N. Bezmaternykh, M.N. Popova, <http://arxiv.org/abs/1609.02125>; *Phys. Rev. Lett.*, *accepted*.

4OR-O-11

THE ELECTRONIC AND MAGNETIC STRUCTURES OF MANGANESE DOPED COPPER METABORATE $\text{Cu}_{0.98}\text{Mn}_{0.02}\text{B}_2\text{O}_4$

Boldyrev K.N.¹, Molchanova A.D.¹, Moshkina E.M.²

¹ Institute of Spectroscopy, Russian Academy of Sciences, Troitsk, Moscow, Russia

² Kirensky Institute of Physics, Siberian Branch of RAS, Krasnoyarsk, Russia

kn.boldyrev@gmail.com

Magnetic materials with complex crystal and magnetic structure have attracted much attention because of their interesting properties and features. One of the brightest representatives of such compounds is a copper metaborate CuB_2O_4 . The compound demonstrates a unique combination of magnetic, magnetoelectric, linear and nonlinear optical properties.

The copper metaborate CuB_2O_4 has a complex crystal structure (SG *I42d*, $Z=12$). Magnetic Cu^{2+} ions ($S=1/2$) in the unit cell occupy two different crystallographic positions, *4b* and *8d*. In both positions, copper atoms are square-coordinated, the same as in high-temperature superconductors. $\text{Cu}(4b)$ and $\text{Cu}(8d)$ magnetic sublattices order at different temperatures, 21 K and ~ 8 K, respectively. Multiple frustrated and nonfrustrated antisymmetric exchange interactions within and between the *4b* and *8d* magnetic sublattices result in a rich complex magnetic phase diagram.

CuB_2O_4 exhibits unusual optical properties. Recent studies of electronic absorption spectra of CuB_2O_4 revealed narrow zero-phonon lines (ZPL) for all transitions between the crystal-field-split *3d*-states of Cu^{2+} ions [1]. Recently we have found a large sublattice-sensitive optical linear magnetic dichroism (LMD) in the crystallographically isotropic *ab*-plane of copper metaborate. LMD is observed on ZP exciton lines connected with the $\text{Cu}(4b)$ magnetic subsystem, it arises below the temperature of the antiferromagnetic ordering of this subsystem [2]. We elucidated the nature of the LMD attributing it to the magnetic Davydov splitting.

The present work is devoted to the study of magnetic phase transitions in manganese-doped copper metaborate $\text{Cu}_{1-x}\text{Mn}_x\text{B}_2\text{O}_4$ ($x=0.02$). It was expected that a doping with manganese could lead to interesting new magnetic effects. Measurements were carried out both with and without an applied external magnetic field. A study of the absorption spectra allowed us to establish the Neel temperature of the compound ($T_N = 19$ K) and to compare electronic structures of the pure and doped metaborates. Linear antiferromagnetic dichroism associated with the magnetic Davydov splitting has been observed in $\text{Cu}_{0.98}\text{Mn}_{0.02}\text{B}_2\text{O}_4$, the same as in CuB_2O_4 , but the character of the magnetic transitions is different from that for the pure metaborate. The LMD signal of $\text{Cu}_{1-x}\text{Mn}_x\text{B}_2\text{O}_4$ is about ten times weaker than of CuB_2O_4 . The sign of LMD in $\text{Cu}_{0.98}\text{Mn}_{0.02}\text{B}_2\text{O}_4$ changes at the temperature $T^* = 7.0$ K, however, no splitting of the transition at T^* was observed, in contrast to the case of the pure metaborate. Also, the electronic spectra of manganese and copper ions are being discussed.

Support of the Russian Foundation for Basic Research (Grant No 15-02-07451a) and the President of the Russian Federation (Grant MK-3577.2017.2) is acknowledged.

[1] R.V. Pisarev, A.M. Kalashnikova, O. Schöps, L.N. Bezmaternykh, *Phys. Rev. B*, **84** (2011) 075160.

[2] K.N. Boldyrev, R.V. Pisarev, L.N. Bezmaternykh, M.N. Popova, *Phys. Rev. Lett.*, **114** (2015) 247210.

4OR-O-12

NEW MECHANISM OF MAGNETO-OPTIC EFFECT*Vedyayev A.V.¹, Zhuravlev M.Ye.², Lobachev A.V.¹*¹ Faculty of Physics, Lomonosov Moscow State University, 119991 Moscow, Russia² Faculty of Liberal Arts and Sciences, St Petersburg State University, 199034 St. Petersburg, Russia

myezhur@gmail.com

We consider a new magneto-optic effect based upon spin-orbit interaction of the conducting electrons in ferromagnetic metal with the electric field of plane polarized light wave. We calculated off-diagonal components of conductivity tensor for this mechanism of a.c. conductivity, when the direction of the electric field of the wave is perpendicular to the ferromagnetic magnetization. These components determine the current induced by the light wave in the direction perpendicular to the plane of the light polarization. Numerical evaluation shows that the conductivity for this new effect exceeds the off-diagonal components of conductivity tensor for ordinary magneto-optic effect [1]. The components appear to be still considerably smaller than the diagonal elements of the conductivity tensor.

[1] Petros N. Argyres, *Phys. Rev.*, **97** (1955) 334.

4 July

Tuesday

12:00-14:00

poster session

4PO-I

4PO-I1

4PO-J

**“Soft and Hard
Magnetic Materials”**

4PO-I-1

MAGNETIC PROPERTIES OF Fe-Pt AND Fe-Pt- M (M=B, Si) MICROWIRES

Zhukova V.^{1,2}, Ipatov M.^{1,2}, Aronin A.^{3,4}, Abrosimova G.³, del Val J.J.¹, Zhukov A.^{1,2,5}

¹ Dept. Phys. Mater., University of Basque Country, UPV/EHU San Sebastián 20018, Spain

² Dpto. de Física Aplicada, EUPDS, UPV/EHU, 20018, San Sebastian, Spain

³ Inst. Solid State Physics, Russian Academy of Science, Chernogolovka, Moscow region, Russia

⁴ National University of Science and Technology «MISIS», Moscow, 119049, Russia

⁵ IKERBASQUE, Basque Foundation for Science, 48011 Bilbao, Spain

Rapid quenching from the melt has been successfully used during more than 60 years for fast preparation of amorphous, nanocrystalline or metastable crystalline materials with planar (ribbons) or cylindrical (wires) geometry. Most attention has been paid to preparation and studies of amorphous and nanocrystalline rapidly quenched magnetic materials [1]. However, if the quenching rate achieved during the rapidly quenching process is not sufficiently high for preparation of amorphous materials a metastable crystalline materials (i.e. supersaturated solid solutions, nanocrystalline, microcrystalline or granular alloys) can be prepared [1].

It is worth mentioning that even crystalline magnetic wires present a number of interesting and unusual magnetic properties suitable for various applications: propagation of single domain wall along the magnetic wire and giant magnetoimpedance effect (GMI) [1].

In fact rapid solidification and subsequent processing is a well-established route to the formation of hard magnets[1]. Additionally glass-coating can enhance mechanical properties of magnetic microwires. Therefore few attempts have been made to enhance the coercivity on glass-coated microwires [1].

The principal limitation for the preparation of hard magnetic glass-coated microwires containing rare-earth metals using the Taylor-Ulitovsky method is related to the chemical interaction with the glass during the rapid quenching from the melt. This is the limiting factor for rare-earth containing materials. Therefore recently we paid attention on FePt alloys for magnetic microwires preparation [2]. FePt magnetically hard alloys have attracted great attention because of their excellent magnetic and mechanical properties [2]. Thus, Fe-Pt alloys are quite ductile and chemically inert. Elevated coercivity of FePt alloys is usually attributed to high magnetocrystalline anisotropy of the L10 FePt phase. Moreover FePt alloys usually present relatively high Curie temperature ($T_c = 750$ K) and spontaneous magnetization $\mu_0 M_s \approx 1.43$ T.

Consequently we have prepared Fe-Pt and Fe-Pt- M (M=B, Si) microwires using Taylor-Ulitovsky technique and studied their magnetic properties. Magnetic properties considerably depend on the metallic core composition and annealing conditions. As-prepared microwires present either amorphous or mixture of amorphous and nanocrystalline phases with a presence of BCC FePt, FCC PtFe and small amount of tetragonal FePt phase. After annealing at 500 °C Fe₅₀Pt₄₀Si₁₀ microwires we observed a remarkable magnetic hardening related to crystallization of as-prepared amorphous Fe₅₀Pt₄₀Si₁₀ microwires. Coercivity increasing from 5 Oe up to 500 Oe is attributed to the crystallization of amorphous Fe₅₀Pt₄₀Si₁₀ microwires. Annealed Fe₅₀Pt₅₀ sample present coercivity up to 800 Oe at 5K, but the magnetization of FePt is low and rapidly decreases with temperature. We discussed peculiarity of Fe₅₀Pt₅₀ microwires considering the influence of internal stresses on magnetic ordering of Fe-atoms.

[1] Novel Functional Magnetic Materials, Fundamentals and Applications (editor A. Zhukov), *Springer Series in Materials Science*, **231** (2016), ISSN 0933-033X, DOI: 10.1007/978-3-319-26106-5.

[2] V. Zhukova, et.al., *IEEE Magn. Lett.*, **7** (2016) 5200704.

4PO-I-2

THE ORIGIN OF THE MAGNETOCRYSTALLINE ANISOTROPY IN FERRITES

Kotov L.N.¹, Beznosikov D.S.¹

¹ Syktyvkar State University named after Pitirim Sorokin, Syktyvkar, Russia
kotovln@mail.ru

Magnetic phase transitions are usually accompanied by anomalies in the acoustic properties of crystals [1]. In magnetic phase transition a shape of the magnon –phonon spectra changes. The shape of the magnon –phonon spectra is determined by efficiency of magnetoelastic coupling in crystals. The cubic crystals of a nonstoichiometric mangan-zinc spinel $[\text{Mn}_a\text{Zn}_b\text{Fe}_{2+c}\text{O}_4]$ ($a+b+c=1$) are characterized by the existence of a phase temperature interval. In this interval first magnetic anisotropy constant K_1 changes the sign while the second K_2 - negative. When the temperature changes, it occurs in some crystals a change in the magnetization direction from $[100]$ to $[111]$. But not all crystals of similar composition exhibit a change in the sign of $K_1(T)$. Why is this happening? The answer to this question can be received by the nature of the exchange crystallographic anisotropy. For which there is a change in the sign of K_1 , the other does not. Although the behavior of K_2 constants is similar. We have studied these spinels by X-ray diffraction method. The results showed that the crystal structures of the two samples were identical, the lattice parameter calculated by the X-ray data being $a_1=8.40\pm 0.02\text{\AA}$ and $a_2=8.50\pm 0.03\text{\AA}$ for type crystals. However, the crystal (for which $K_1(T)\neq 0$) there is very small deviation from cubic to tetragonal symmetry: $a/c=1.006\pm 0.002$ [1]. We may conclude that the observed difference in magnetic properties in these crystals received due in the lattice configuration. But why does not all the crystals of similar composition exhibit a change in the sign of $K_1(T)$. To elucidate this phenomenon, structural differences between two different crystals of spinel grown were determined. The parameters of elementary cells of crystals and the coordinates of the atom in the cells are found. An analysis of the linear cross section of the electron density distribution indicates that the magnetic phase transition observed in the crystal, the short-range arrangement of the cations. That is, they are characterized by a lower energy of the exchange coupling of two neighboring cations. The influence of a change in the distribution of the electron density of the neighboring cations is observed. In the exchange between neighboring atoms, electrons participate, so we need to talk about an electronic cloud and change the orientation of this cloud.

The authors are grateful to E.A.Golubev, A.P. Petrakov for X-Ray diffraction analysis of samples. We gratefully acknowledge the financial support from RFBR (grant # 17-02-01138).

[1] L. N. Kotov, S.N. Karpachev. *Technics Physical Letters*, **2** (2002) 105-107.

4PO-I-3

INTERACTION OF AMORPHOUS SOFT MAGNETIC ALLOY WITH VAPOR AT HEAT TREATMENT IN AIR

Skulkina N.A., Stepanova E.A., Ivanov O.A., Voronova A.V.
Ural Federal University, 620000, Yekaterinburg, Russia
nadezhda.skulkina@urfu.ru

The ribbon surface interaction with atmospheric vapor at heat treatment (HT) in air is an important process that influence sample's magnetic properties [1, 2]. This interaction leads to the anisotropic hydrogenation and oxidation of its surface. Mostly flat tensile stresses contribute to the decrease the volume of domains with orthogonal magnetization (V_{ort}). This leads to a weakening in the stabilization of domain walls with the planar magnetization and improved magnetic properties. The activity of the ribbon surface interactions with vapor increases with increasing temperature. The influence of this factor on magnetic properties level of amorphous alloy Fe-Ni-Si-B, investigated with increasing concentration of water vapor in the chamber during heat treatment, is represented in this work.

The samples had the form of strips with dimensions 120 x 10 x 0,020 mm. The volume of domains with orthogonal magnetization was determined by the correlation between V_{ort} and the maximum residual induction which was found from Mössbauer studies [3]. Errors in the determination of magnetic permeability and the magnetization distribution were about 3 and 5%.

The main results of heat treatments influence with cooling rate 15 °C/min on μ_{max} and V_{ort} presented in the table. Modes of heat treatment at 410 °C, with the duration of isothermal exposure (τ) for 20 minutes and 420 °C, $\tau = 5$ minutes are optimal. Amorphous-crystalline layer, which formed in these cases on the ribbon surface, has an optimal thickness and we see the same value V_{ort} . Heat treatment with vapor and cooling with vapor contribute to decreasing of V_{ort} and increasing of μ_{max} . This is a consequence of concentration increase of atoms embedded in the ribbon surface and a corresponding increase in the levels mostly flat tensile stresses.

The ribbon state		τ , min	μ_{max}	V_{ort} , %
Heat treatment at 410 °C	HT	20	31000	11,4
	HT+cooling with vapor		91000	7
	HT	5	29700	15
	HT with vapor		29500	16
	HT+cooling with vapor		36400	13
Heat treatment at 420 °C	HT	5	42000	11,7
	HT with vapor		79000	7,4

Support by in part by the Ministry of education and science of the Russian Federation, project 3.6121.2017.

- [1] N.A. Skulkina et al., *The Physics of Metals and Metallography*, **99** (2005) 252-258.
[2] N.A. Skulkina et al., *The Physics of Metals and Metallography*, **115** 6 (2014) 529-537.
[3] N.A. Skulkina et al., *Izvestiya Akademii Nauk. Ser. Fizicheskaya*, **65** 10 (2001) 1483-1486.

4PO-I-4

CA-AL SUBSTITUTED STRONTIUM HEXAFERRITE WITH GIANT COERCIVITY AND EXTREMELY HIGH FMR FREQUENCY

Sleptsova A.E.¹, Trusov L.A.¹, Gorbachev E.A.¹, Mitrofanova E.S.¹, Roslyakov I.V.¹, Lebedev V.A.¹, Vasiliev A.V.¹, Zaytsev D.D.¹, Gorshunov B.P.², Kazin P.E.¹, Dinnebier R.E.³, Jansen M.³

¹ Moscow State University, Moscow, Russia

² Moscow Institute of Physics and Technology, Dolgoprudny, Russia

³ Max Planck Institute for Solid State Research, Stuttgart, Germany

sleptsovaanastasia@gmail.com

Magnetic materials with large coercivity have broad applications ranging from permanent magnets and data storage media to high-frequency electromagnetic wave isolators. The only known ferrite material exhibiting coercivity over 20 kOe (also considered as “giant coercive force”) at room temperatures is ϵ -Fe₂O₃ [1]. Also it shows millimeter wave absorption up to 210 GHz [2-3]. However, ϵ -Fe₂O₃ is a rare iron oxide and its production as pure phase is quite complex. Hard magnetic ferrites (MFe₁₂O₁₉, M = Ba, Sr, Pb) also possess high magnetocrystalline anisotropy but their coercivity is significantly lower and rarely exceeds 6 kOe for pure phase. The doping by aluminum could lead to coercivity rise up to 18 kOe, however the magnetization in this case is significantly lower than of ϵ -Fe₂O₃ [4].

Here we report a simple synthesis of Ca-Al double substituted strontium hexaferrite Sr_{1-x/12}Ca_{x/12}Fe_{12-x}Al_xO₁₉. The rise of the substitution ratio x leads to decrease of magnetization, but significant increase of coercivity. At $x = 4$ the sample coercivity is 21.3 kOe, which is higher than for ϵ -Fe₂O₃ with the same magnetization of 15 emu/g. At $x = 5.5$ the coercivity reaches 36 kOe, which is the highest value known for ferrite materials. The coercivity could be further improved by alignment of the hexaferrite particles dispersed in a polymer by the magnetic field. Such oriented composites possess nearly square hysteresis loops with coercivity up to 40 kOe while magnetized in alignment direction. Also we have studied the millimeter wave absorption properties of the samples. The high anisotropy fields result in very high natural ferromagnetic resonance frequencies. The FMR frequency increases with substitution ratio and reaches the record-high values of 180 – 240 GHz for $x = 4 - 5.5$. Also we have studied the features of the crystalline structure of the samples by high precision synchrotron radiation diffraction and revealed that the presence of calcium results in shrinking of oxygen surroundings in bipyramidal iron position, which could be a reason of the increase of magnetocrystalline anisotropy compared to simple aluminum doping of strontium hexaferrite.

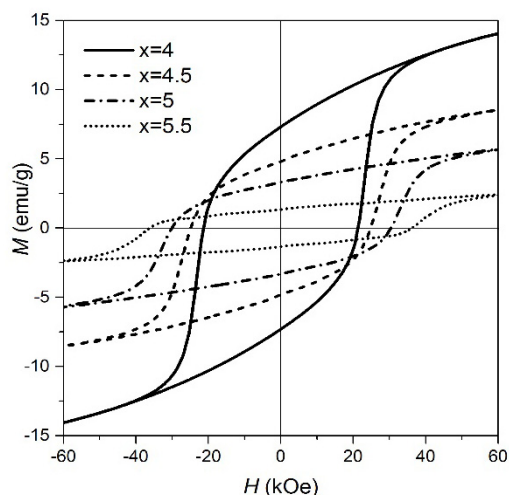


Fig. 1. Hysteresis loops of Sr_{1-x/12}Ca_{x/12}Fe_{12-x}Al_xO₁₉ samples.

Support by RFBR Grant 15-03-04277 is acknowledged.

[1] J. Tuček, R. Zbořil, A. Namai, S. Ohkoshi, *Chem. Mater.*, **22** (2010) 6483.

[2] A. Namai, et. al., *Nat. Commun.*, **3** (2012) 1035.

[3] H. Luo, *J. Magn. Magn. Mater.*, **324** (2012) 2602.

4PO-I-5

STRUCTURE FORMATION AND MAGNETIC PROPERTIES CHANGES OF NANOCOMPOSITE ALLOYS BASED ON Nd-Fe-B SYSTEM WITH Cu ADDITIVES PRODUCED BY MECHANOCHEMICAL SYNTHESIS

*Panov K.¹, Shchetinin I.V.¹, Gudimenko E.S.¹, Gorshenkov M.V.¹, Savchenko E.S.¹,
Menushenkov V.P.¹, Savchenko A.G.¹*

¹ National University of Science and Technology "MISiS", Moscow, Russia
ingvar@misis.ru

Hard magnetic materials are used in almost all fields of science and technology from the production of household appliances to the delivery of drugs in biomedicine. The highest hysteresis properties are obtained in sintered permanent magnets based on $\text{Nd}_2\text{Fe}_{14}\text{B}$ compounds and have practically reached their theoretical limit. The further development of high-energy hard magnetic materials is connected with the discovery of new compounds or with the new approaches to the creation of high-energy hard magnetic materials. Scientific research on nanocomposite hard magnetic materials is currently being considered, for which the theoretical limit of magnetic properties is higher than the same materials in the microcrystalline state. Obtaining such hard magnetic materials associated with the use of extreme methods of producing: quenching from the liquid state, high-energy milling, etc.

The aim of this work was to study the patterns of the formation of the structure and magnetic properties of nanocomposite alloys of the Nd-Fe-B system with the addition of Cu obtained by mechanochemical synthesis.

The $\text{Nd}_9\text{Fe}_{85}\text{B}_6$ and $\text{Nd}_9\text{Fe}_{85}\text{B}_6 + 5\%$ Cu alloys was subjected mechanochemical synthesis in a Retsch PM400 planetary ball mill during 2 hours, in a helium atmosphere. X-ray diffraction analysis of the alloys was carried out on a Rigaku Ultima IV diffractometer. Thermal processing of alloys was carried out in a vacuum furnace in the temperature range 580-680 °C, for 15 minutes. To measure the magnetic properties the VSM 250 vibromagnetometer and the PPMS physical property measuring system in fields up to 90 kOe were used.

Within 2 hours of milling the phase of $\text{Nd}_2\text{Fe}_{14}\text{B}$ is amorphized and, which is accompanied by the release of $\alpha\text{-Fe}$. heat treatment of alloys leads to the crystallization of the amorphous phase and the formation of dispersed mixture of $\text{Nd}_2\text{Fe}_{14}\text{B}$ and $\alpha\text{-Fe}$ phases with grain sizes of 10-30 nm. In the case of Cu addition also formed NdCu_2 phase. The maximum values H_c obtained after annealing at 600 °C: 3.4 kOe for the $\text{Nd}_9\text{Fe}_{85}\text{B}_6$ alloy and 1.5 kOe for $\text{Nd}_9\text{Fe}_{85}\text{B}_6 + 5\%$ Cu (fig. 1). In the both cases, there were no kinks on the hysteresis loops, which may indicate the presence of an exchange-bound state in these alloys.

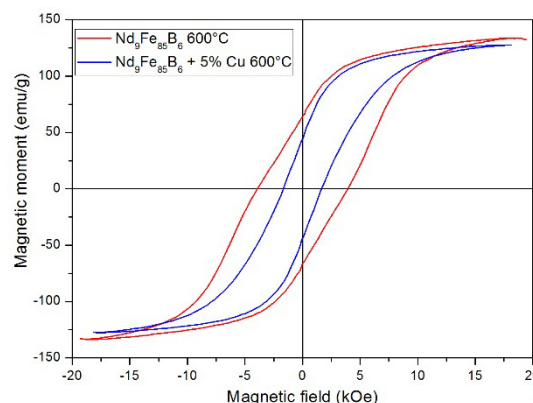


Fig. 1. The hysteresis loops of annealed samples

The work was supported by the Ministry of Science and Education of the Russian Federation under the of the Russian Federation President grants for state support of young Russian scientists, grant №. MK-3616.2017.2.

4PO-I-6

INFLUENCE OF SEVERE PLASTIC DEFORMATION ON FeCo ALLOYS

Shirshikov S.O.¹, Muradimova L.¹, Zadorozhny V.Y.¹, Glezer A.M.¹

¹ National University of Science and Technology «MISiS», Leninsky ave. 4, Moscow, Russia
Keller1250@gmail.com

In this work we study the effects of HPT deformation on long range atomic order, structural and magnetic characteristics of FeCoV_x(x=0-6) alloys.

FeCo-based alloys are well-known for their very good magnetic properties (i.e high saturation magnetization and permeability). Below 730⁰C FeCo alloys have B2 ordered structure. The ordering reaction has significant influence on the mechanical and magnetic characteristics.

FeCo alloys were arc melted under argon atmosphere, then casted into a cylindrical rod. The ingots were then sliced by wire electro-discharge machining (EDM) to prepare HPT discs (10mm in diameter, 0.5mm in thickness). The discs were annealed under argon atmosphere at 1000⁰C for 1 hour and. Annealing was needed to derive high degree of long-range order. After annealing the disks were subjected to HPT deformation. The number of HPT turns N ranged from 0,5 to 4.

Magnetic properties are been investigated by means of Vibrating Sample Magnetometer(VSM) in magnetic fields up to 2T. Structural parameters are been studied with x-ray diffractometry (DRON).

The results of VSM measurements are shown in fig.1. In case of FeCo alloy σ_s grows up to 247 emu/g as the number of HPT increases from 0,5 to 4 turns. However, σ_s of FeCoV₆ alloy seems not to be influenced by HPT. σ_s of FeCoV_{1,5} and FeCoV₃ is in nonlinear dependence with respect to N. Changes in saturation magnetization can be explained by presence of nonmagnetic γ -phase, and its transformation during deformation process. Over and above, HPT deformation leads to changes in degree of long range atomic ordering, and thus lead to shift in σ_s .

X-ray diffraction studies, performed on FeCoV₆ and FeCoV_{4,5} conformed the presence of γ -phase in non-deformed samples. Studies on structure, content of γ -phase before and after deformation, and order-disorder transformations will be continued.

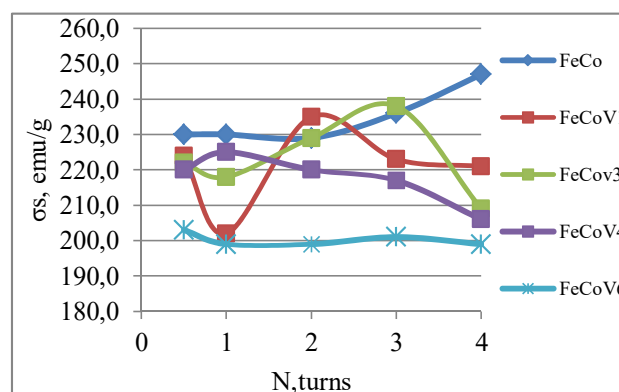


Fig. 1. Saturation magnetization of FeCoV_x(x=0-6) alloys.

[1] Akihide Hosokawa, Hideyuki Ohtsuka, et al., *Materials Transactions.*, **55**, 8 (2014) 1286 -1291.

4PO-I-7

HYSTERESIS PROPERTIES AND STRUCTURE OF Nd₂Fe₁₄B/ α -Fe NANOCOMPOSITES SYNTHESIZED BY A MECHANICAL ALLOYING TECHNIQUE

Rafalskii A.I., Savchenko A.G., Schetinin I.V., Bordyuzhin I.G., Menushenkov V.P., Medvedeva T.M.
 NUST "MISIS", Moscow, Russia
 a.rafalskii@xray.pro

The hard magnetic Nd₂Fe₁₄B/ α -Fe nanocomposites attract much researchers' attention, because of their high energy product (BH)_{max} according to theoretical calculations. A further hysteresis properties increase of hard magnetic materials is possible only with the discovery of new intermetallic compounds with higher fundamental properties. Another way to solve this problem is the implementation of substantially new approaches to the development of high-energy hard magnetic materials.

In this work complex the studies of X-ray diffraction analysis, electron microscopy and hysteresis properties of nanocomposite powders before and after high-energy milling were carried out. Also after heat treatment for a 20 minutes duration in the temperature range 500-600 °C. The method of mixtures in combination with mechanical alloying (MA) seems to be a very promising way of obtaining high-energy hard magnetic materials. In particular, on MA powders C_{0.3} (a mixture of alloy powders of a pre-stoichiometric composition (Nd_{17,0}Pr_{4,5}Fe_{68,4}Co_{4,0}Zr_{5,0}B_{1,1}) with 30% mass. of a Nd-low alloy Nd_{14,5}Fe_{77,1}Co_{5,0}Ti_{1,2}Si_{1,2}B_{1,0}) after annealing at 500 °C for 20 min the following properties were obtained: H_{ci} = 443 kA/m, σ_r = 64 A×m²/kg, $\sigma_s(2T)$ = 125 A×m²/kg and $\sigma_r/\sigma_s > 0.5$. It is obvious that the further annealing and MA conditions optimizing and also the directed alloying of the mixture components would make possible to increase the hysteresis properties of the hard magnetic nanocomposites obtained.

Further development of this work would allow to create techniques for obtaining hard magnetic nanocomposite materials based on R₂Fe₁₄B/ α -Fe and R₂Fe₁₇N_x/ α -Fe systems. Using high-energy exposure for a new generation of permanent magnets creation with effective technical and economic characteristics.

4PO-I-8

THE EFFECTIVENESS OF THE SCREENING CONSTANT MAGNETIC FIELD BY MULTI-LAYERED FILM SYSTEM OF NiFe/Cu

*Muravyev-Smirnov S.S.¹, Vlasik K.F.¹, Grabchikov S.S.², Grachev V.M.¹, Dmitrenko V.V.¹,
Lipatov K.A.¹, Ulin S.E.¹, Uteshev Z.M.¹*

¹ National Research Nuclear University "MEPHI", Moscow, Kashirskoye road, 31

² Scientific-Practical Materials Research Centre of NAS of Belarus, Minsk, P. Brovki Str., 19
SSMuravyevsmirnov@mephi.ru

The results of measuring screening coefficients for multilayer film systems based on NiFe/Cu symmetric and gradient type in permanent magnetic fields of up to 20 Gs are presented. Symmetric film systems are alternating layers of Ni₈₀Fe₂₀/Cu. Gradient film systems are alternating layers of Ni₅₀Fe₅₀/Cu and Ni₈₀Fe₂₀/Cu, which are located in various sequences on different screen samples. Gradient screens have practically the same shielding factor as shields of symmetric type, however the range of magnetic field strengths is much wider than that of symmetrical screens. This makes it possible to successfully apply them to protect electronic equipment in space research, as well as in experimental setups on charged particle accelerators and to solve the problems of electromagnetic compatibility in many cases.

4PO-I-9

STRUCTURAL AND MAGNETIC ANISOTROPY OF DIRECTIONALLY-CRYSTALLIZED FERROMAGNETIC MICROWIRES

Evstigneeva S.A.¹, Volodina N.O.¹, Yudanov N.A.¹, Trukhanov A.V.¹, Morchenko A.T.¹, Panina L.V.¹, Larin V.S.², Salem M.M.¹

¹ NUST "MISIS", Moscow, Russia

² MFTI Ltd, Kishinev, R. Moldova

svetlanaevstigneeva95@mail.ru

Amorphous ferromagnetic microwires have drawn attention primarily due to their soft magnetic properties as the elements of sensors of weak magnetic fields and currents, mechanical stresses and temperatures. It is known that structural and magnetic properties of amorphous alloys strongly depend on the method of their processing. In order to tailoring operational magnetic parameters, the wires are subjected to different thermal treatments [1] including annealing in a magnetic field and/or under stress, current annealing, etc. The transformation from soft to hard magnetic properties was reported for microwires subjected to directional crystallization [2-3]. In the present work, the interplay of structural and magnetic anisotropy in $\text{Fe}_{4.3}\text{Co}_{67.7}\text{Si}_{11}\text{B}_{14}\text{Cr}_3$ wires after directional crystallization is investigated.

XRD analysis of crushed and powered wires identified the formation of the face-centered Co modification as the main phase of directionally crystallized core alloy. A giant increase in coercivity is explained by the formation of cobalt crystallites. Application of a magnetic field during crystallization may orient easy anisotropy axis of crystallites along the wire. To prove this assumption, we checked the effect of the wire orientation relative to the X-rays direction in diffractometer and to the magnetic field in VSM on the measured signal. The results revealed a clear texture towards the axis of the wire (Fig. 1).

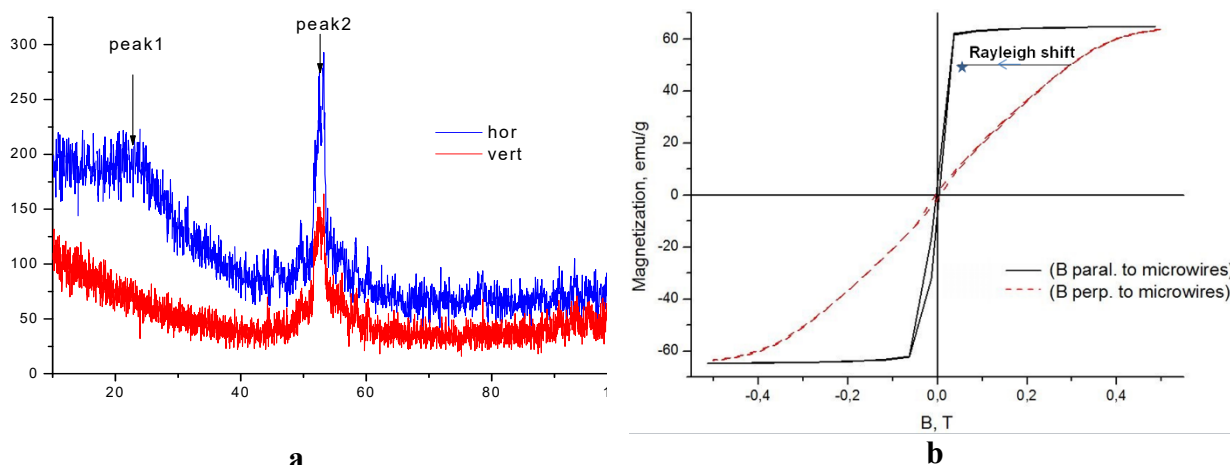


Fig. 1. X-ray diffraction spectra (a) and hysteresis loops (b) of microwire after magnetic-field assistant directional crystallization for various orientations relatively X-ray and coils of VSM.

Obtained result is indirect confirmation that the formation of crystallites in amorphous Co-rich microwires occurs with the predominant direction of the crystallographic axis [111] along the wire axis and direction of magnetic field during directional crystallization process.

[1] A. Zhukov (ed.), *High Performance Soft Magnetic Materials*. – Springer Series in Materials Science, Volume 252. Springer International Publishing AG, 2017.

[2] V. Larin, L.V. Panina, E.A. Patroi et al, *Physica Status Solidi A*, **213** (2016) 384-389.

[3] A.Morchenko, L.Panina, M.Churyukanova, M.Salem, H.Hashim, A.Trukhanov, V.Korovushkin, V. Kostishyn, V. Larin, *Journal of Alloys and Compounds*, **698** (2017).

4PO-I-10

DOMAIN WALLS DRIFT IN PULSED MAGNETIC FIELDS IN IRON GARNET CRYSTAL PLATES

Pamyatnykh L.A.¹, Mekhonoshin D.S.¹, Pamyatnykh S.E.¹, Lysov M.S.¹, Agafonov L.Y.¹, Shmatov G.A.¹

¹ Ural Federal University, Ekaterinburg, Russia
dmitry.mehonoshin@urfu.ru

Results of experimental study and numerical modelling of domain walls (DWs) motion in periodic alternating pulsed magnetic field applied perpendicular to the uniaxial sample plate are reported. Gaussian pulses were applied to a coil with an inductance of 900 μH / 1 kHz, into which iron garnet $(\text{TbErGd})_3(\text{FeAl})_5\text{O}_{12}$ (111) plate was placed. The study was performed for frequency range that includes infrasonic frequencies ($f = 0,15 - 400$ Hz) for amplitudes of pulses up to 350 Oe.

The presence of DWs drift in pulsed magnetic fields in the frequency range that includes infrasonic frequencies was established. Dependences of the DWs drift speed V_{dr} on amplitude of the pulsed field H for a number of frequencies (Fig. 1) and on the frequency of the pulsed field (see inset in Fig.1) were obtained.

DWs displacement in pulsed magnetic field was investigated using stroboscopic technique. It was established that the value of displacement of DWs in the direction of the drift is greater than in the opposite direction. Fig. 2 shows the time dependence of the deviation of the DW under the influence of a pulse of amplitude $H = 270$ Oe, which causes the DW displacement in the direction of the drift (curve 1), and under the influence of backward pulse of the same amplitude (curve 2, the dependence is inverted).

Numerical model takes anisotropy of attenuation parameter into account. Simulations show that anisotropy of attenuation parameter with respect to direction leads to DWs drift in harmonic and pulsed magnetic fields. Calculated DWs displacements are larger in the direction of the drift than in the opposite direction.

The work was performed within the framework of basic parts of the State Task of the Ministry of Education and Science of the Russian Federation (projects № 3.6121.2017, 3.5719.2017).

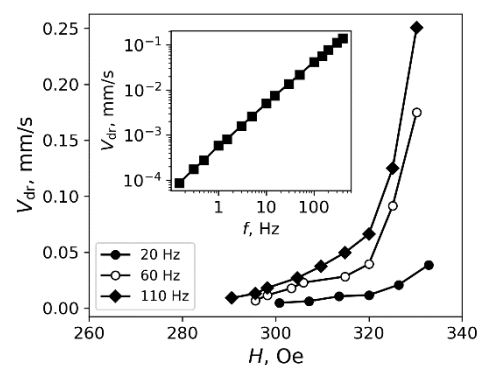


Fig. 1. Dependences of the drift speed V_{dr} on amplitude H of the magnetic field pulse and on the pulse frequency f (inset).

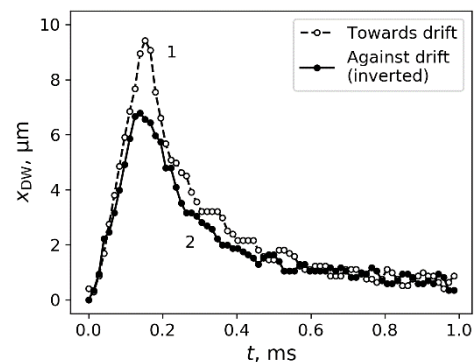


Fig. 2. Time dependence of DW deviation from equilibrium position at magnetic pulse amplitude $H = 270$ Oe and frequency $f = 500$ Hz.

4PO-I-11

AMPLITUDE DEPENDENCES OF MAGNETIC LOSSES IN NANOCRYSTALLINE ALLOYS WITH INDUCED ANISOTROPY

Kataev V.A., Starodubtsev Yu.N., Mikhailitsyna E.A., Bessonova K.O.

Ural Federal University, Ekaterinburg, Russia

vakataev@urfu.ru

A matter of magnetic losses dependence on the amplitude of induction and frequency is one of the most relevant in the area of the soft magnetic materials. There are two reasons for this. On the one hand, presence of corresponding dependence is necessary for selection and rational use of a material. On the other hand, this dependence reflects the change of the magnetization reversal nature with the change of the frequency or amplitude of the magnetic induction, and magnetization reversal mechanisms analysis is demanded [1].

In this paper amplitude dependence of the magnetic losses of $\text{Fe}_{67.5}\text{Co}_5\text{Cu}_1\text{Nb}_2\text{Mo}_{1.5}\text{Si}_{14}\text{B}_9$ nanocrystalline alloy with induced magnetic anisotropy is considered. Under certain conditions, a simple domain structure with 180° domain boundaries can be expected with a high degree of probability. In this case, analysis of the experimental data is carried out by virtue of the theory of 180° domain boundaries and available data [2]. Toroidal samples were annealed in a presence of longitudinal and transverse constant magnetic field to induce anisotropy. The annealing was accompanied by nanocrystallization process. The induced uniaxial anisotropy constant was $K_u = 15 \text{ J/m}^3$. The measurement of the magnetic losses was carried out in the sinusoidal induction mode.

The amplitude dependence of the magnetic losses was plotted in logarithmic coordinates at the frequencies of 50, 500 and 5000 Hz. The presence of the linear sections make easy to determine the corresponding induction ranges and to approximate them by the Steinmetz formula

$$P = \eta B_m^\theta. \quad (1)$$

The attraction of this formula is possibility to identify the nature of the magnetization reversal processes in the samples through the comparison of θ values of the exponent and known magnetization reversal models (displacement of the plane domain walls, rotation of the magnetization) in respect that the data of domain orientation and induced anisotropy constants magnitude is known.

Figure 1 shows the magnetic losses dependence of the samples after transverse (1, 2, 3) and longitudinal (1', 2', 3') annealing. It can be seen that linear sections can be singled out for sufficiently small (up to $B_m \sim 0.1 \text{ T}$) and large values of the induction amplitudes (in the figure the linear approximation is given only for curve 1 corresponding to measurements at 50 Hz of the sample with transverse anisotropy) for all curves. Thus, the values of the coefficients θ in the exponent in (1) for the corresponding linear sections were determined and analyzed.

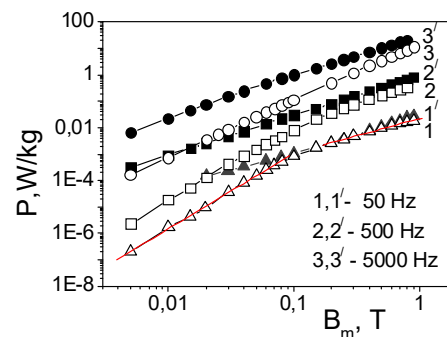


Fig. 1. Magnetic losses as a function of the induction amplitude for nanocrystalline alloy samples.

Support by the project 3.6121.2017 of The Ministry of education and science is acknowledged.

[1] Yu.N. Starodubtsev, V.A. Kataev, *FMM*, **64** (1987) 1076 (in Russian).

[2] S. Flohrer, R. Shafer, J. McCord et al., *Acta Materialia*, **54** (2006) 4693.

4PO-I-12

MAGNETIC SHAPE MEMORY COMPOSITES BASED ON COPOLYURETHANEIMIDES, MODIFIED BY CoFe_2O_4 AND $\text{Al}_3\text{Fe}_5\text{O}_{12}$ NANOPARTICLES

Bugrov A.N.^{1,2}, *Runov V.V.*³, *Kopitsa G.P.*^{3,4}, *Smyslov R.Yu.*^{1,3}, *Kirillova S.A.*²

¹ Institute of Macromolecular Compounds RAS, St. Petersburg, Russia

² Saint Petersburg Electrotechnical University "LETI", St. Petersburg, Russia

³ Petersburg Nuclear Physics Institute, Gatchina, Leningrad region, Russia

⁴ Institute of Silicate Chemistry of RAS, St. Petersburg, Russia

alexander.n.bugrov@gmail.com

Shape-memory polymers are new smart materials capable of taking one or more stable configurations in time and return to the original state under external stimulus such as temperature, light, magnetic field, pH, redox reactions, etc. The magnetically-induced shape memory effect achieved by introducing magnetic nanoparticles into the polymer matrix expands the concept of non-contact mechanisms for removing the temporary fixation of mechanical deformation of composite materials. The particles served as internal mini-antennas to transform the electromagnetic energy to inductive Joule heat, and subsequently to initiate the recovery of shape-memory polymers, which are promising as structures with variable geometry, thermosensitive sensors, actuators and programmable smart implants. In this work, the CoFe_2O_4 nanoparticles with the spinel structure and $\text{Al}_3\text{Fe}_5\text{O}_{12}$ with a garnet structure were synthesized by the glycine-nitrate combustion method. It was confirmed by X-ray diffraction and energy dispersive X-ray microanalysis. According to electron microscopy data, ferrites of cobalt and aluminum were spherical particles with an average size of 60 ± 10 nm and 40 ± 10 nm, respectively. The coercivity $H_c = 880$ Oe, saturation magnetization $M_s = 55$ emu/g, and remanence magnitude $M_r = 31$ emu/g were established for CoFe_2O_4 nanoparticles at 300K, using the SQUID magnetometry. In the case of $\text{Al}_3\text{Fe}_5\text{O}_{12}$, the hysteresis inherent in a superparamagnetic state was observed on the magnetization curves at 300K ($H_c = 47$ Oe, $M_s = 15$ emu/g, $M_r = 5$ emu/g). The Curie temperature (T_c) of the synthesized nanoparticles was evaluated based on analysis of the temperature dependence of the magnetic saturation induction. The obtained T_c estimates for CoFe_2O_4 and $\text{Al}_3\text{Fe}_5\text{O}_{12}$ were 660 and 610K, respectively. The surface functionalization of nanoparticles by NH_2 groups was carried out to prevent aggregation of the

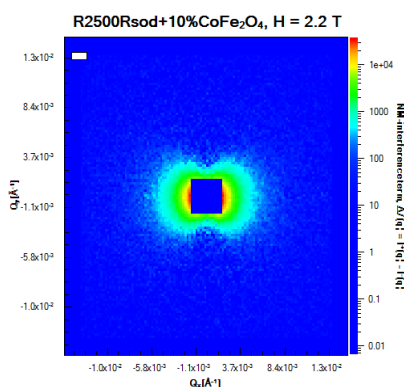


Fig. Nuclear-magnetic interference of copolyurethaneimide with 10wt.% CoFe_2O_4 nanoparticles

inorganic filler in the polymer matrix and to create additional intermolecular chemical cross-links due to ferrites along with a net of physical links. Magnetic hard/soft nanoparticles modified with 3-aminopropyltriethoxysilane in the amount of 1, 4, 7 and 10 wt.% during the in-situ copolycondensation process were introduced into the matrix of segmented copolyurethanamide based on 1,3-bis(3,3',4,4'-dicarboxyphenoxy)benzene, bis[4-(4-aminophenoxy)phenyl] sulfone and poly[di(ethylene glycol) adipate] ($M_n \sim 2,500$), terminated by toluene-2,4-diisocyanate. The structure of the magnetic subsystem in composites based on copolyurethanamides and ferrite nanoparticles was studied by small-angle scattering of polarized neutrons (SASPn). The method has allowed analyzing the different contributions to the scattering: nuclear, magnetic, and the contribution of nuclear magnetic interference scattering by magnetic impurities (Fig.). The form of the correlation function and the values of the characteristic correlation radii of the magnetic impurities in the studied materials were determined from the analysis of the SASPN data.

4PO-I-13

MAGNETIC STRUCTURE EVOLUTION OF THE AMORPHOUS SOFT MAGNETIC WIRE

Moiseev A.A., Kudryavtsev V.O., Derevyanko M.S., Morozova N.V., Gavriilyuk A.A., Semirov A.V.
Irkutsk State University, Irkutsk, Russia
Moiseev.AI.An@Gmail.com

Different treatments influence on electric impedance was investigated for amorphous $\text{Co}_{66}\text{Fe}_4\text{Nb}_{2.5}\text{Si}_{12.5}\text{B}_{15}$ wire. The samples' length and diameter were 30 mm and 180 μm , respectively. Two series of the samples were investigated. The wires of the first series were subjected to a soft heat treatment under temperature 100, 150, and 200 $^{\circ}\text{C}$ during 100 hours. The wires of the second series were treated by Joule heating with current density from 4 MA/m^2 to 33 MA/m^2 during 5 minutes. The all heat treated samples had X-ray amorphous structure. Frequency dependences of the impedance and its components were investigated using automated complex of magnetoimpedance spectroscopy based on Agilent 4294A impedance analyzer in the ac frequency range 0.1 – 80 MHz and root-mean-square value of 1 mA.

It is shown that a section with small slope $dZ''/df \approx 0$ is observed at the frequency dependency of the impedance imaginary component $Z''(f)$ in the frequency range $f = 4 - 10$ MHz for the as-cast samples. The temperature increase of the soft heat treatment leads to the Z'' increase in the whole of frequency range. Besides the $dZ''/df \approx 0$ section is maintained at the $Z''(f)$ dependencies. The Joule heating leads to decrease of the Z'' . At the same time $Z''(f)$ dependence becomes monotone increasing.

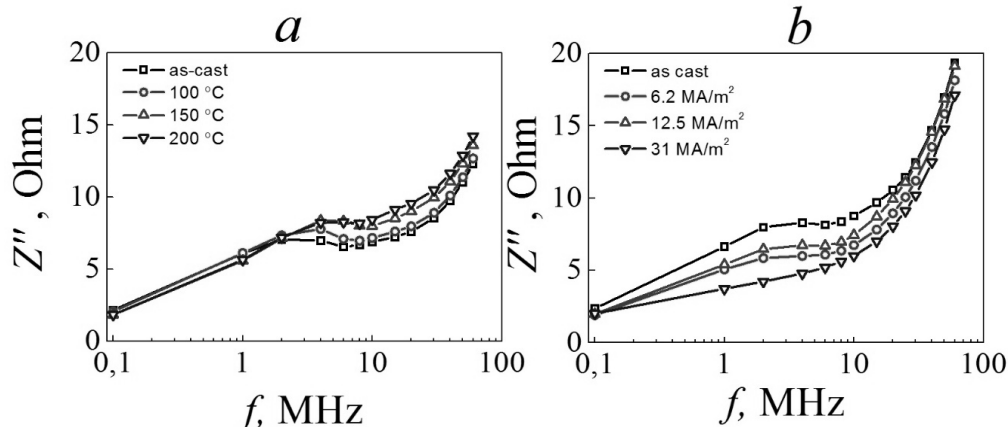


Fig. 1. The frequency dependences of the impedance imaginary component of the $\text{Co}_{66}\text{Fe}_4\text{Nb}_{2.5}\text{Si}_{12.5}\text{B}_{15}$ wire subjected to the soft heat treatment - *a* and Joule heating - *b*.

It was earlier shown [1], that $dZ''/df \approx 0$ section appearance at the $Z''(f)$ dependences could be connected with a change of dominant influence of samples' areas with different easy magnetization axis (EMA) direction on circumferential magnetic permeability. On the basis of this we can suppose that soft heat treatment leads to decrease of magnetoelastic anisotropy without significant change of the EMA direction in the wire volume. In result of the Joule heating the magnetic anisotropy mainly with circumferential direction of the EMA is induced in the all wire volume.

This work was supported by a project part of Government Assignment for Scientific Research from the Ministry of Education and Science, Russia (№ 3.1941.2017)

[1] Semirov A.V., Moiseev A.A., Kudryavtsev V.O. et al., *Technical Physics. The Russian Journal of Applied Physics*, **60** (2015) 767-771.

4PO-I-14

MAGNETIZATION PROCESS IN FERROMAGNETIC AMORPHOUS MICROWIRES FOR STRUCTURAL HEALTH MONITORING

Salem M.M.¹, Nematov M.G.¹, Adam A.M.¹, Dzhumazoda A.¹, Panina L.V.^{1,2}, Morchenko A.T.¹

¹National University of Science and Technology, MISIS, Moscow 119991, Russia

²Institute for Design Problems in Microelectronics RAS, Moscow 124681, Russia
elshshtawy@science.tanta.edu.eg, lpanina@plymouth.ac.uk

The possibility of controlling the electromagnetic properties of composite materials through the external influence such as magnetic field, stress and temperature is of particular interest for various applications including reconfigurable devices and non-destructive tests. Such tunable electromagnetic behavior has been demonstrated in polymer composites with ferromagnetic amorphous microwires with ultra-soft magnetic properties [1-3].

In the present work, we are presenting a new method of monitoring internal stresses. The method can be referred to as embedded sensing technique, where the sensing element is a glass-coated ferromagnetic microwire with a specific magnetic anisotropy. The microwire of composition $\text{Co}_{71}\text{Fe}_5\text{B}_{11}\text{Si}_{10}\text{Cr}_3$ show abrupt transformation of the magnetization process under applied tensile stress owing to stress-dependence of the magnetostriction. Ferromagnetic microwires with positive magnetostriction are characterized by almost rectangular hysteresis loop measured in a magnetic field along the microwire axis. The magnetization takes place by axial domain propagation which generates a sharp voltage signal producing high harmonics. Enhanced stress sensitivity is seen in the case when the magnetostriction constant can change a sign under stress effect. Therefore, these wires can be used as wireless sensors with remote interrogation and can be placed on the surface or inside materials. We demonstrate that the ratio of harmonic amplitude may also sensitively depend on tensile stress which can be used directly for structural health monitoring. The advantage of using magnetic microwires as embedded sensors is related with the tunability of the response, small cost and relatively simple signal processing.

[1] F. Qin, H.X. Peng, *Progress in Materials Science*, **58**, **2** (2013) 183-259.

[2] F.X. Qin, N. Pankratov, H.X. Peng, M.H. Phan, L.V. Panina, M. Ipatov, V. Zhukova, A. Zhukov, J. Gonzalez, *J. Appl. Phys.*, **107** (2010) 09A314.

[3] D.P. Makhnovskiy, L.V. Panina, C. Garcia, A. Zhukov, J. Gonzalez, *Phys. Rev. B.*, **74**, **6** (2006) 064205-064215.

4PO-I-15

STRESS INDUCED MAGNETIC DOMAIN STRUCTURE IN DyFe₁₁Ti COMPOUND

Semenova E.M.¹, Lyakhova M.B.¹, Karpenkov D.Yu.^{1,2}, Kuznetsova Yu.V.¹, Karpenkov A.Yu.^{1,2}, Skokov K.P.^{2,3}

¹ Tver State University, Tver, Russia

² Chelyabinsk State University, Chelyabinsk, Russia

³ Technische Universität Darmstadt, Darmstadt, Germany

Semenova_E_M@mail.ru

In this paper we present the results of the magnetic domain structure (DS) investigation of the single and polycrystalline DyFe₁₁Ti samples. This compound has ThMn₁₂-type tetragonal crystal structure and is characterized with the two spin-reorientation phase transitions (SRPT). SRPT temperatures significantly vary according to the literature data: the SRPT1 is observed in the temperature range of 98-120 K, SRPT2 – 214-250 K [1-6]. The effect of DS relaxation after mechanical impact on the surface is demonstrated. At room temperature the compound has uniaxial magnetic anisotropy. However, after a mechanical impact on the surface observed magnetic DS is typical for compounds with multiaxial magnetic anisotropy (fig. 1a). As shown, over time at room temperature and in the absence of external magnetic field configuration of the domains changes and relaxes to the equilibrium DS typical for uniaxial magnetic materials (fig. 1b, c). The influence of external mechanical stresses on magnetocrystalline anisotropy and magnetic DS together with the mechanism of DS relaxation in DyFe₁₁Ti are discussed.

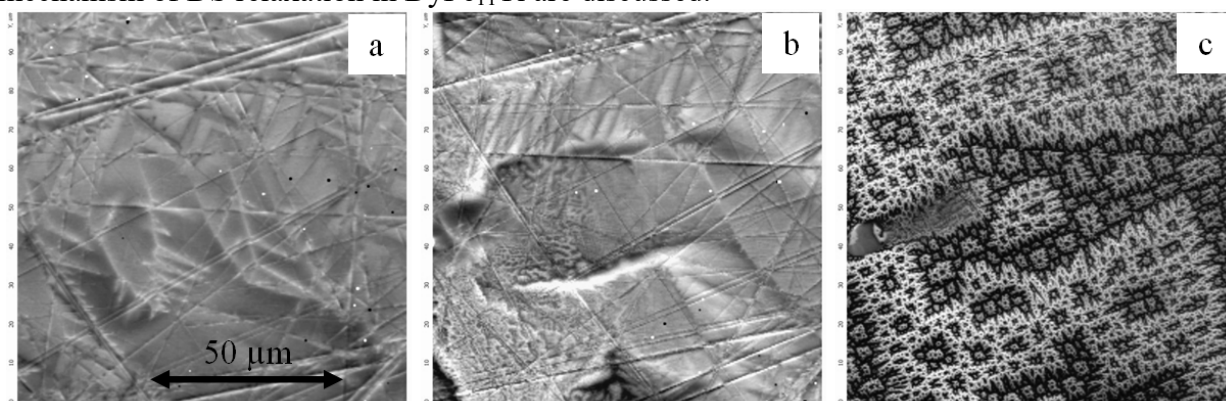


Fig. 1. MFM images of the magnetic domain structure relaxation process on the basal plane of DyFe₁₁Ti single crystal at room temperature: a) immediately after mechanical polishing, b) after 45 h, c) after 300 h.

Support by grant of Ministry of Education and Science of the Russian Federation № 1598 and Russian Science Foundation Grant No. 15-12-10008.

- [1] Bo-Ping Hu, Hong-Shuo Li, Coey J.M.D., Gavigan J.P., *Phys. Rev. B*, **41** (1990) 2221-2228.
- [2] Kou X.C., Zhao T.S., et al., *Phys. Rev. B*, **47** (1993) 3231-3242.
- [3] García L. M. J. A., Ibarra M. R., Kuz'min M. D., *J. Appl. Phys.*, **73** (1993) 5908-5910.
- [4] Guslienko K.Yu., Kou X.C., Grössinger R., *J. of Magn.Magn.Mater.*, **150** (1995) 383-392.
- [5] Nikitin S.A., Tereshina I.S., Pankratov N.Yu., *Phys. Solid State*, **41** (1999) 1508-1510.
- [6] Andreev A.V., Bartashevich M.I., et al., *Physica B: Condensed Matter*, **167** (1990) 139-144.

4PO-I-16

dM PLOTS OF THE EXCHANGE-COUPLED STONER-WOHLFARTH ENSEMBLE

Bolyachkin A.S., Kudrevatykh N.V.

Ural Federal University, Yekaterinburg, Russia
anton.bolyachkin@urfu.ru

Intergrain or interlayer exchange coupling in magnetic materials has a great influence on modern technologies. On the one hand, it can lead to negative effects like reducing of the storage density in recording media. On the other hand, it can improve magnetic properties, as it was shown for nanocrystalline permanent magnets. In both cases, there is a scientific interest to the coupling investigation and to developing and verification of methods of its identification and quantitative estimation.

A numerical study of magnetization processes in the exchange-coupled Stoner-Wohlfarth (SW) ensemble was performed. The space-filling ensemble was corresponded to nanoparticles of the same volume V with the isotropic distribution of easy magnetization axes. For each magnitude of an external magnetic field H the equilibrium configuration of magnetic moments was evaluated from minimum of the following energy:

$$E = \sum_{i=1}^N \left[-KV(\vec{\mu}_i \cdot \vec{n}_i)^2 - M_S V \vec{\mu}_i \cdot (\vec{H} + \vec{H}_{ms}) - \sum_{j \neq i}^{N_{nn}} J_{IEI} S (\vec{\mu}_i \cdot \vec{\mu}_j) \right],$$

where K is a uniaxial magnetic anisotropy constant, $\vec{\mu}_i = \vec{M}_i/M_S$ is a magnetization reduced to the spontaneous magnetization M_S , \vec{n}_i is a unit vector along the easy magnetization axis, H_{ms} is a demagnetizing field calculated within the dipole-dipole approximation, J_{IEI} is an intergrain exchange interaction constant and S is a surface area between neighbouring particles.

The aim of the study was to develop the estimation method of intergrain exchange interaction constant for the isotropic exchange-coupled SW ensemble using dM plots [1]. These plots are based on the comparison of a normalized dc demagnetization remanence $m_d(H)$ dependency on isothermal remnant magnetization $m_r(H)$ with the one for SW ensemble [2]. In the work dM plots were calculated with a systematic variation of the intergrain exchange interaction constant considering different distributions of volumes and magnetic anisotropy constants.

This work was supported by the project No. 3.6121.2017.

[1] A.S. Bolyachkin, A.S. Volegov, N.V. Kudrevatykh. *J. Magn. Magn. Mater.*, **378** (2015) 362.

[2] P.E. Kelly, K. O'Grady et al. *IEEE Trans. Magn.*, **25** (1989) 3881.

4PO-I-17

ELECTROMAGNETIC ABSORPTION OF COMPOSITES BASED ON EPOXY RESIN AND IRON NANOPARTICLES

Krekhno R.V.¹, Safronov A.P.^{1,2}, Beketova A.I.^{1,2}, Beketov I.V.²

¹ Ural Federal University, Yekaterinburg

² Institute of Electrophysics URAN, Ekaterinburg
lipka-lipka-lipka@yandex.ru

Modern polymer composites are multicomponent systems comprising a polymer matrix and particulate filler material that impart various functional properties. The composite materials based on epoxy resins are of particular interest, since this class of composites has a mechanical strength, chemical resistance, high dielectric properties after curing, good adhesion to metals. Epoxy composites are promising materials for use in aviation and space industry, in particular, the metal-filled composites, that have a good radar absorbing ability. Magnet-filled polymer composites containing soft magnetic particles are widely used to produce magnetic screens for the absorption of electromagnetic radiation of various frequencies and coatings to protect instruments and sensors

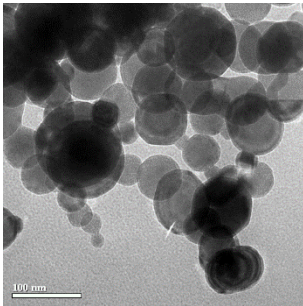


Fig. 1 Ferrum nanoparticles photo

sensitive to electromagnetic radiation. Investigation of the laws of absorption of electromagnetic radiation by magnetically filled polymer composites to improve their operational properties is an actual task and purpose of this work.

Absorption of electromagnetic radiation can be characterized by a thermal effect, the direct measurement of which can be an accurate quantitative estimate of the amount of absorbed radiation. In present work, the properly modified Calvet microcalorimeter was used for direct measurement of thermal power. The solenoids were put inside the measurement cells to bring the electromagnetic field to the samples, which is an innovative method for measuring the intensity of absorbed radiation.

The epoxy resin ED-20 with hardeners PEPA and TEAT was used as the polymer matrix. The nanopowder of metallic iron ($S = 6.06 \text{ m}^2 / \text{g}$), produced in the laboratory of impulse processes of the Institute of Electrophysics of the Ural Branch of the Russian Academy of Sciences by the method of electric wire explosion, was used as the filler. Samples were formed in the cylinders. Electromagnetic absorption was studied in the range from 60 to 200 KHz.

The Calvet microcalorimetry method was used to study the thermal losses for magnetization reversal of magnetically filled polymer composites in homogeneous magnetic fields with an intensity of no more than $1700 \text{ A} / \text{m}$. The heat dissipation power in the $1700 \text{ A} / \text{m}$ magnetization reversal varied from 60 to 400 mW/g , reaching a maximum value of 400 mW/g at a maximum frequency of 214 kHz and with a maximum iron particle concentration of 70%. A linear dependence of the heat power with the concentration of iron and a nonlinear, monotonically increasing frequency dependence was found. It is shown that the largest contribution to the absorption is made by the losses due to hysteresis.

Support by projects of fundamental research of the Ural Branch of the Russian Academy of Sciences is acknowledged.

4PO-I-18

MAGNETIC MICROSTRUCTURE OF Fe-Cu-Nb-Si-B THIN FILMS

Mikhailitsyna E.A.¹, Kataev V.A.¹, Soboleva E.², Geydt P.², Zakharchuk I.², Lähderanta E.²

¹ Ural Federal University, Department of Solid State Magnetism, Yekaterinburg, Russia

² Lappeenranta University of Technology, School of Engineering Science, Lappeenranta, Finland
evgenia.mihalitsyna@urfu.ru

Finemet-type alloys are well known due to their outstanding properties among the soft magnetic materials [1]. Low coercivity together with high saturation magnetization and permeability determines a wide range of their application as magnetic parts of power transformers, microwave devices, magnetic sensors and other [2]. Macroscopic properties of the nanostructured Finemet alloy are closely related to microscopic parameters of the material. This relationship has been successfully described in the framework of random anisotropy model [3].

Thin films were prepared by means of radio frequency ion-plasma sputtering of $\text{Fe}_{73.9}\text{Cu}_1\text{Nb}_3\text{Si}_{13.2}\text{B}_{8.9}$ target onto a glass substrate. The deposition was carried out in the presence of technical magnetic field of 100 Oe oriented parallel to the substrate and under Ar pressure of 10^{-3} Torr. A structural state was controlled by a heat treatment at the temperature of 350, 400 and 450 °C for 30 min. Surface topography and magnetic force microscopy (MFM) were measured using atom force microscopy (AFM) Bruker Multimode 8. Magnetic properties of thin film were measured using SQUID magnetometer.

The MFM images of 200 nm thin films after the heat treatment at 400 and 450 °C are presented in Fig. 1. Presence of magnetic domain microstructure in a form of stripes is clearly seen for the film annealed at 450°C. In comparison to this observation, no magnetic contrast is detected on the surface of the film annealed at 400 °C.

The areas of magnetic contrast could be interpreted as regions of ferromagnetic ordering called stochastic domains. The

stochastic domain size depends on exchange parameter, local anisotropy constant and grain size. Random anisotropy model predicts an increase of the length of ferromagnetic ordering with decreasing correlation length of random perturbations [4].

The structural state of the films according to XRD study can be characterized as amorphous for the film annealed at 400 °C and nanocrystalline for the film annealed at 450°C. Therefore, the crystallization process occurs in this temperature interval. According to the structural state data and prediction of random anisotropy model, the absence of magnetic contrast in fig. 1(a) seems reasonable and can be connected with shorter structural correlation length. The small structural correlation length determines the large length of ferromagnetic correlations, which dimensions exceed the MFM scan size.

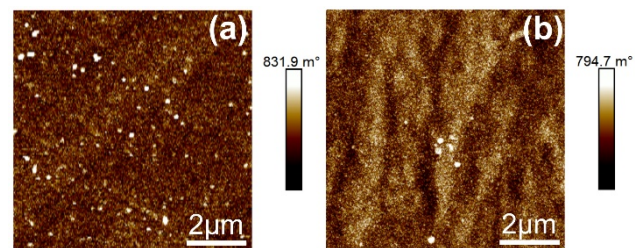


Fig. 1. MFM images of 200 nm thin films of $\text{Fe}_{73.9}\text{Cu}_1\text{Nb}_3\text{Si}_{13.2}\text{B}_{8.9}$ alloy annealed at 400 (a) and 450 °C (b).

Support by the project 3.6121.2017 of The Ministry of education and science is acknowledged.

[1] Y. Yoshizawa *et al.*, *J. Appl. Phys.*, **64** (1988) 6044-6046.

[2] J. Moulin *et al.*, *J. Micromech. Microeng.*, **21** (2011) 074010.

[3] G. Herzer, *Acta Mater.*, **61** (2013) 718-734.

[4] R.S. Iskhakov *et al.*, *The Physics of Metals and Metallography*, **112** (2011) 666-681.

4PO-I-19

STATIC AND HIGH-FREQUENCY MAGNETIC PROPERTIES OF NANOCRYSTALLINE Fe-Zr-N FILMS

Sheftel E.N.¹, Harin E.V.¹, Tedzhetov V.A.¹, Rozanov K.N.², Zezyulina P.A.², Kiryukhantsev-Korneev F.V.³

¹ A.A. Baikov Institute of Metallurgy and Material Science RAS, Moscow, Russia

² Institute for Theoretical and Applied Electromagnetics RAS, Moscow, Russia

³ National University of Science and Technology "MISIS", Moscow, Russia
velmurad@ya.ru

At present, the great attention of researchers is directed to the creation of the soft magnetic films for high-frequency applications. In addition to the high saturation magnetization M_s , such films should have high values of magnetic permeability at high frequencies, up to the GHz interval. In this connection, an important characteristic of soft magnetic films is the magnetic anisotropy field (MAF) in the film plane (H_k). MAF defines the value of the natural ferromagnetic resonance frequency (nFMR) $f_{nFMR} \sim (M_s H_k)^{1/2}$.

The static magnetic properties of nanocrystalline ferromagnets are explained within the framework of the random magnetic anisotropy model [1,2]: when a ferromagnetic grain size ($2R_c$) smaller than the exchange interaction length (R_L), the local (within grain) effective energy of the magnetic anisotropy (K_{eff}) is suppressed, and the magnetic properties in weak magnetic fields are defined by anisotropy of stochastic magnetic domains ($2R_L$). In this connection, the influence of the film stochastic domain structure upon the nFMR phenomenon seems interesting.

The Fe-Zr-N films with different Zr contents were produced by the magnetron sputtering. The targets consist of a Fe disk with uniformly distributed Zr chips. In the magnetron chamber under the action of plasma, surface melting of Fe and Zr were occurred, forming an alloy in the erosion zone. Before each sputtering process the target was overheated above the Curie temperature, which made possible the sputtering process. It was carried out in a gas atmosphere of the Ar, Ar + 5% N₂ or Ar + 15% N₂ composition at a total pressure p_{Ar+N_2} 0,15 Pa. Covering glass plates were used as substrates.

The studied films are XRD amorphous or nanocrystalline, depending on the produce conditions, and contain α -Fe or iron nitride phases with a grain size of 3-6 nm.

From the magnetization curves in strong fields, the parameters of the stochastic domain structure are determined by the method of correlation magnetometry [2]. In accordance with theoretical predictions [2], the value of the coercivity of the films correlates with the magnitude of the mean square fluctuation of the stochastic domain anisotropy field. This means that the magnetic hysteresis is created by the rotation of stochastic domains.

The complex magnetic permeability at frequencies up to 4 GHz was measured by the strip method [3]. The real magnetic permeability of the films remains high value at frequencies up to several hundreds of MHz. The effective MAF, calculated from the nFMR frequency, is 2-5 times less than the film coercivity. This fact means that the nFMR arises due to the oscillations of a magnetic moment of the entire film but not the individual stochastic domains.

Support by RFBR (15-08-02831a) is acknowledged.

[1] G. Herzer, *Acta Materialia*, **61** (2013) 718-734.

[2] R.S. Iskhakov, S.V. Komogortsev, *Phys. of Metals and Metallography*, **112** (2011) 666-681.

[3] S.N. Starostenko, K.N. Rozanov, *J. Commun. Technol. Electron.*, **58** (2013) 1076-1084.

4PO-I-20

EFFECT OF ALLOYING ELEMENTS AND HEAT TREATMENT CONDITIONS ON THE 1:12 PHASE FORMATION IN THE Sm-Zr(Hf)-Fe-Co-Ti ALLOYS

*Urzhumtsev A.N.¹, Anikin M.S.¹, Kudrevatykh N.V.¹, Tarasov E.N.¹, Moskalev V.N.², Zinin A.V.¹,
Cherepkov M.O.¹*

¹ Ural Federal University, Ekaterinburg, Russia

² POZ-Progress Co, Verkhnyaya Pushma, Sverdlovsk region, Russia
andrey707@bk.ru

Rare Earth – 3d-metal intermetallic compounds with the ThMn₁₂ crystal structure are considered as a promising material for a high magnetic energy product permanent magnets due to the proper potential magnetic parameters for several of them [1]. However, the Fe-containing 1-12 phase is formed only with some amount of another 3d-transition metals (Cr, Mo, V, Ti), which prevents to obtain the high magnetization and Curie temperature of this phase [2].

In order to clarify the question on R-Me₁₂ type compounds preparation with maximal Fe and Co content, in this work we studied the three following alloys systems: 1) SmFe_{12-x}Ti_x, x = 0.5, 1.0; 2) (Sm_{0.8}Me_{0.2})(Fe-Co)_{12-x}Ti_x (Me = Zr, Hf); 3) (Sm_{1-x}Zr_x)(Fe-Co)_{11.2+x}Ti_{0.8-x}, x = 0.05 ÷ 0.25.

Initial alloys melting was carried out in an electric arc oven under a helium atmosphere with the addition of 20 % wt. Sm excess. Prepared ingots of No.1 and No.2 systems passed through a homogenizing annealing in an argon atmosphere at 850 °C during 5 hours. Each ingot of No. 3 system was split into two parts, which were sealed in an individual vacuum pumped quartz ampoule, then all ampoules annealed at a temperature of 1050 °C for 8 hours, after which one of the samples was quenched into a water, and the other one slowly cooled to a room temperature in the oven. Magnetic measurements were carried out using a vibrating sample magnetometer in the magnetic fields up to 12 kOe. TMA phase analysis was performed in the temperature range of 25 ÷ 800 °C. It revealed that the all samples of the first and second series contain an α-Fe phase, with the exception of these with Zr and Hf. In the samples of the No.3 series the α-Fe phase do not contribute to their magnetic susceptibility (χ). For the slowly cooled samples with x ≤ 0.15, the χ-peaks from several phases with close Curie temperatures in the range 550-600 °C are observed. For rapidly quenched samples, a only one clear χ-peak corresponding to 1:12 phase is seen with a very minor peaks from the additional phases. It turns out that quenching procedure prevents the α-Fe phase precipitations formation, which is also observed when 20 % of Sm is replaced by Zr or Hf. In addition, the rapid quenching reduces the content of Co-crystals which formed out during the peritectic reaction.

Thus it is established that the most proper metallurgical way for Sm-Zr-Fe-Co-Ti alloy manufacturing, containing basically only the 1:12 phase is its rapid quenching process. It allows to obtain some samples of such material with the largest saturation magnetization and T_c values.

The work was supported by the State contracts No. 3.6121.2017 between UrFU and the Ministry of Education and Science of Russian Federation.

[1] T. Kuno, S. Suzuki, *J. AIP Adv.*, **6** (2016) 025221.

[2] T. Saito, H. Miyoshi, *J. Alloys Compd.*, **519** (2012) 144-148.

4PO-I-21

HEAT TREATMENT OF HARD MAGNETIC Mn-Bi IN A MAGNETIC FIELD*Volkov K.D., Urzhumtcev A.N., Tarasov E.N., Zinin A.V.*

Ural Federal University, Russia, 620002, Ekaterinburg

volkovkd@urfu.ru

It is well known, that Mn-Bi compounds has a large uniaxial magnetocrystallographic anisotropy ($K = 1 \text{ MJ/m}^3$) [1]. As follows from the phase diagram, the Curie temperature of the low-temperature phase (LTP) of MnBi (355 °C) is higher than the temperature of the formation LTP-MnBi structure (262 °C), therefore, it is possible to orient the magnetic moments of the manganese sublattice in a magnetic field.

In [2,3], alloys of the Mn-Bi system obtained by directional crystallization in a magnetic field were studied. The authors noted that after crystallization of the alloys the predominant orientation of the easy magnetization axis in MnBi compound lead along the direction of the magnetic field. In these alloys, observed a pronounced anisotropy of the magnetic propertie.

In [4] it is due to the fact that the ferromagnetic grains of MnBi are magnetized and located along the easy axis-c parallel applied field. After that, it is congregated and grow under the influence of magnetic interaction, aligning and forming the rod-like structure of LTP-MnBi. It is also shown that the orientation of the MnBi grains occurs immediately from a certain critical temperature which is depending on the magnitude of the applied field. The mechanisms of the formation oriented LTP-MnBi structure in alloys obtained under the influence of a magnetic field have not been studied so far.

In the present work, the effect of heat treatment in a constant magnetic field ($H = 6.5 \text{ kOe}$) on the magnetocrystallographic anisotropy was studied. The magnetic-hysteresis properties of the obtained samples were measured by VSM. Using thermomagnetic analysis, the phase composition and the Curie temperature was determined. The structure was studied using an optical microscope.

This work has been supported by the UrFU State contracts № 2582 and № 1362 and grant of Fund of Assistance to Development of Small Enterprises in Science and Technology (contract № 9519GU/2015).

- [1] X. Guo, Z. Altounian, J.O.S. Olsen, *J. Appl. Phys.*, **69(8)** (1991) 6067-6069.
- [2] R.G. Pirich, *IEEE Trans. Magn.*, **16(5)** (1980) 1065-1067.
- [3] R.G. Pirich, *Metall Trans. A*, **15A** (1984) 2139-2145.
- [4] H. Wang, Z. Ren, X. Li, et al., *Trans. Nonferrous Met. Soc.*, **13(6)** (2003) 1405-1409.

4PO-I-22

INTERGRAIN EXCHANGE INTERACTION OF Nd-Fe-Co-B ALLOYS

Alekseev I.V.¹, Andreev S.V.¹, Selezneva N.V.¹, Volegov A.S.¹

¹ Ural Federal University, Yekaterinburg, Russian Federation
supesh@mail.ru

Nd-Fe-B alloys were discovered more than two decades ago, but they still are of interest to investigation. One of the areas is exchange-coupled magnets. In our days materials based on an intergrain exchange interaction can be considered as promising one in a field of high energy magnets [1]. On the other hand, the intergrain exchange interaction can be considered as an unwanted interaction between separated grains in rare-earth reach magnets where the rare-earth element serves as a paramagnetic isolator. Understanding of this phenomenon provides a deep insight on how modern high-energy magnets work.

Curie point grows with the growth of Co content in $\text{Nd}_2(\text{Fe}, \text{Co})_{14}\text{B}$ compounds [2]. It is attributed to the increase of the exchange interaction. It can be assumed that the exchange interaction have to increase also.

In order to verify this, we prepared a series of hypo-stoichiometry $\text{Nd}_9(\text{Fe}_{1-x}\text{Co}_x)_{85}\text{B}_6$ as well as stoichiometry $\text{Nd}_{12}(\text{Fe}_{1-x}\text{Co}_x)_{82}\text{B}_6$ alloys. Melt-spun ribbons were prepared from induction-melt ingots. The ribbons were then sealed in quartz ampoules and annealed at different temperatures to obtain optimal magnetic properties, namely a convex demagnetization curve, the maximum of coercivity and the remanence. Measurements were carried out by vibrating sample magnetometer with magnetic fields H of up to 25 kOe.

Fig. 1 shows the Kelly plot for $\text{Nd}_{12}(\text{Fe}_{1-x}\text{Co}_x)_{82}\text{B}_6$, where $x = 0; 0.2; 0.5$ samples. There are the positive peaks that demonstrate the existence of the intergrain exchange interaction [3]. The further abrupt drops are associated with a collective magnetization reversal of the exchange-coupled magnetic moments. It has been found that the maximums of the Kelly plots reach the peak for $x = 0.2$ and then decrease across the Co content.

This work was supported by The Ministry of Education and Science of the Russian Federation, project 3.6121.2017

[1] R. Skomski, J. M. D. Coey. *Physical Review B*, **48** (1993) 15812 - 15816.

[2] Matsuura Y. et al. *Applied Physics Letters*, **46.3** (1985) 308-310.

[3] I. Panagiotopoulos, L. Withanawasam, G. C. Hadjipanayis. *Journal of magnetism and magnetic materials* **152.3** (1996) 353-358.

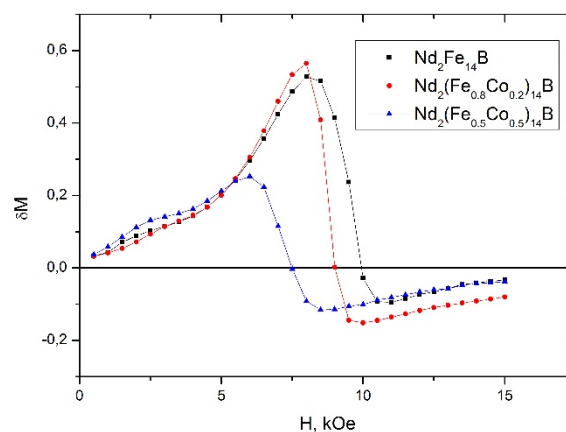


Fig. 1. The Kelly plot for $\text{Nd}_{12}(\text{Fe}_{1-x}\text{Co}_x)_{82}\text{B}_6$, where $x = 0; 0.2; 0.5$.

4PO-I-23

MAGNETIC PROPERTIES OF TEXTURED NiFe(200) AND NiFe(111) PRODUCED BY dc-SPUTTERING

Dzhumaliev A.^{1,2}, *Nikulin Yu.*^{1,2}, *Filimonov Yu.*^{1,2,3}

¹ Kotel'nikov Institute of Radio Engineering and Electronics (Saratov Branch), Russian Academy of Sciences, ul. Zelenaya 38, Saratov, 410019 Russia

² Chernyshevsky Saratov State University, ul. Astrakhanskaya 83, Saratov, 410012 Russia

³ Gagarin State Technical University of Saratov, ul. Politekhnicheskaya 77, Saratov, 410054 Russia
dzhas@yandex.ru

Magnetically soft NiFe films are widely used in magnetoelectronic as magnetic sensitive layers due to the high values of saturation magnetization, magnetic permeability, low magnetostriction and a large value of the anisotropic magnetoresistance [1]. It is known that method, deposition conditions (growth pressure P , substrate temperature T_s and substrate bias U_s), film thickness, substrate material and additional underlayers play a crucial role on microstructure and magnetic properties of the films.

In this work we show that magnetically soft (coercivity $H_c \approx 0.4\text{--}3\text{Oe}$, square hysteresis loops) textured NiFe(200) and NiFe(111) with high effective saturation magnetization $4\pi M \approx 10.5\text{ kG}$, low ferromagnetic resonance linewidth $\Delta H \approx 28\text{--}30\text{ Oe}$ (9.9 GHz) could be obtained on Si/SiO₂ substrate without underlayers [2] by dc-sputtering at a negative U_s (NiFe(111)) or a high T_s (NiFe(200)).

NiFe(111) – fig.1(1,3,4) and NiFe(200) – fig.1 (2) films with $d \approx 20\text{--}530\text{ nm}$ were sputtered at argon pressure $P \approx 0.2\text{ Pa}$: 1 – $U_s = 0$, ambient T_s ; 2 – $U_s = 0$, $T_s \approx 570\text{ K}$; 3 – $U_s = -100\text{ V}$, ambient T_s and $P \approx 0.37\text{ Pa}$ ($U_s = -100\text{ V}$, ambient T_s). Growth rate was in the range $16\text{--}22\text{ nm/min}$.

It is shown that coercivity of NiFe(111) films sputtered at $U_s = 0$ (fig.1 – 1) at a “critical” thickness $d \approx 150\text{ nm}$ increases more than order of magnitude and hysteresis loops are changing from square-shaped (in-plane magnetic anisotropy) to overcritical with low squareness (perpendicular magnetic anisotropy, stripe domain structure). As shows scanning electron microscopy (SEM) cross-section study of the film this change can be attributed to the developing of columnar microstructure after “critical” thickness ($P \approx 0.2\text{ Pa}$), but not to elastic strain of crystalline structure (X-ray diffraction study shows that interplanar spacing doesn't change with thickness).

At a negative U_s (NiFe(111)) or $T_s \approx 570\text{ K}$ (NiFe(200)) (fig.1 – 2,3,4) films demonstrate low $H_c \approx 0.4\text{--}3\text{Oe}$ and high squareness of hysteresis loops at $d \approx 20\text{--}530\text{ nm}$, which can be attributed to the developing of equiaxed grained microstructure of the films (SEM) from early stages of the growth (SEM).

Support by RFBR 16-37-60052.

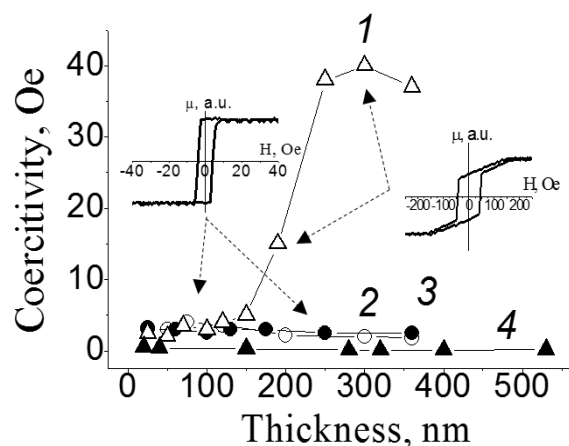


Fig.1. Film thickness dependence of coercivity. Hysteresis loops were obtained by vibrating sample magnetometer technique with magnetic field applied in the film plane.

[1] G. A. Prinz, *J. Magn. Magn. Mater.*, **200** (1999) 57-68.

[2] A. S. Dzhumaliev, et.al., *Physics of the Solid State*, **58** (2016) 1053–1057.

4PO-I-24

MODELING OF THE DYNAMICS AND STRUCTURE OF MAGNETIC 3D-PULSONS AND 3D-SOLITONS IN FERROMAGNETICS WITH DEFECTS

Salimov R.K.¹, Ekomasov E.G.¹

¹ Bashkir State University, 450074, Ufa, Russia
Salems665@yandex.ru

An additional interest in magnetic solitons is currently associated with the emergence of a new experimental technique that allows one to study the processes of formation and propagation of localized magnetization waves of nanometer sizes [1]. Good embryos for the formation of magnetic solitons are defects [2]. As it is usually difficult to make a precise (microscopic) calculation, one is to model the functions, which describe the parameters of a non-homogeneous material [2, 3]. The case is especially interesting, when the size of a magnetic non-homogeneity and the size, describing a non-homogeneity of parameters of a stuff, are of the same order. It results in considerable complication of Landau-Lifshitz equation for the magnetization. Although the task of excitation and distribution of the magnetization waves, under certain conditions, is reduced to the studies of the modified sine-Gordon equation with floating factor [2,4]. The investigation of the big perturbations influence on the solution of the modified sine-Gordon equation in general case can be investigated only with the help of numerical methods. In dynamic, when a temporally or spatial non-homogeneous perturbation acts in the area of such non-homogeneities (or defects), under certain conditions, a strongly non-linear waves of magnetic character can be aroused. Such waves are weakly investigated.

We have investigated for the case of 3D nonhomogeneity of the constant of the magnetic anisotropy (NCMA) of the origin and evolution of the magnetic nonhomogeneities of 3D-pulson and 3D-soliton types, localized in defect region. The description of the program on which the calculations were made is presented in [5]. The dependence of the shape of the localization of the excited magnetic nonhomogeneities from the shape of the defect region was found. The analytical expressions of the soliton type describing the magnetic nonhomogeneities of both types are proposed. The dependences of maximum deflection magnetization in magnetic nonhomogeneities of 3D-pulson and 3D-soliton types on time, nonhomogeneities region characteristics were received. The dependence of the frequency of the 3D-pulson pulsation mode and 3D-soliton from the NCMA parameters was obtained. The possibility of energy expenditure for excitation of localized magnetic inhomogeneities is considered as a new damping channel for the motion of domain walls in ferromagnets with defects.

- [1] R. Kukreja,, S. Bonetti, Z. Chen et. al., *PRL*, **115** (2015) 096601.
- [2] M.A. Shamsutdinov, I.U. Lomakina , V.N. Nazarov et. al. *Nauka, Moscow* (2009).
- [3] Yan Sun, Ruwei Gao. *Solid State Communications*, **149** (2009) 393-395.
- [4] . Ekomasov E.G., Murtazin R.R., Nazarov V.N. // *JMMM*, **385** (2015) 217–221.
- [5] E. G. Ekomasov, R. K. Salimov, *Computational Mathematics and Mathematical Physics*, **56**(9) (2016) 1604-1610.

4PO-I-25

FERROMAGNETIC RESONANCE STUDY OF THE ANTIFERROMAGNETIC-FERROMAGNETIC PHASE TRANSITION IN FeRh

*Semisalova A.^{1,2}, Ehrler J.^{1,3}, Barton C.⁴, Thomson Th.⁴, Lenz K.¹, Fassbender J.^{1,3}, Potzger K.¹,
Lindner J.¹*

¹HZDR, Institute of Ion Beam Physics and Materials Research, Dresden, Germany

²Lomonosov Moscow State University, Faculty of Physics, Moscow, Russia

³Technische Universität Dresden, Dresden, Germany

⁴University of Manchester, School of Computer Science, Manchester, UK

The nearly equiatomic FeRh alloy with the chemically ordered B2 crystal structure demonstrates an unusual first order phase transition from antiferromagnetic (AFM) to ferromagnetic (FM) order at ~ 370 K. This transition can be driven by magnetic field, spin polarized current, as well as tuned by strain, doping and chemical disorder [1-7].

The coexistence of FM and AFM domains within the phase transition makes FeRh an attractive for magnetization dynamics study. Here, we present our first results of FMR study in epitaxial FeRh thin film across the phase transition. The measurements were performed in in-plane geometry, at the frequency range 6-18 GHz. The films were deposited on MgO(001) substrates by means of magnetron sputtering of an alloy FeRh target.

The hysteresis of FMR position and linewidth was observed when the heating and cooling procedure was applied to FeRh sample across the phase transition. The frequency-dependent FMR linewidth was found to be strongly affected by the exchange coupling due to reversible nucleation of AFM and FM domains in FeRh. The decrease of FMR linewidth with frequency was observed at all temperatures up to 490 K which is governed presumably by the co-existence of FMR and AFM phases during the first-order phase transition.

For the ferromagnetic state of FeRh at 500 K we have found the low Gilbert damping $\alpha = 0.0014 \pm 0.0007$ determined from FMR measurements performed in in-plane geometry.

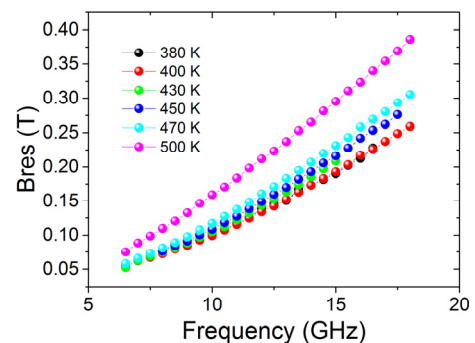


Fig. 1. Frequency dependence of resonance field measured in in-plane geometry during heating from 380 K to 500 K.

- [1] J.-U. Thiele, S. Maat, E.E. Fullerton, *APL*, **82** (2013) 2859.
- [2] X.Marti, I.Fina, C.Frontera, J.Liu, P.Wadley, Q.He, R.J.Paull et al., *Nature Mater.*, **13** (2014) 367.
- [3] E. Mancini, F. Pressacco, M. Haertinger et al. *J. Phys D: Appl. Phys.*, **46** (2013) 245302.
- [4] R.O. Cherifi, V. Ivanovskaya, L.C. Phillips, A. Zobelli, I.C. Infante et al., *Nature Mater.* **13** (2014) 345.
- [5] I. Suzuki, T. Naito, M. Itoh, T. Taniyama, *APL*, **107** (2015) 082408.
- [6] A. Heidarian, R. Bali, J. Grenzer, R.A. Wilhelm et al., *Nucl. Instr. Meth. Phys. Res. Sect. B.*, **358** (2015) 251.
- [7] C.W. Barton, T.A. Ostler, D. Huskisson, C.J. Kinane, S.J. Haigh, G. Hrkac, T. Thomson, *Sci. Rep.*, **7** (2017) 44397.

4PO-I1-1

PECULIARITIES OF THE COERCIVITY KINETICS AND CRYSTAL STRUCTURE OF THE SINTERED $\text{Sm}(\text{Co}_{0.78}\text{Fe}_{0.10}\text{Cu}_{0.10}\text{Zr}_{0.02})_7$ MAGNET ARISING IN THE COURSE OF THE STEP COOLING

Gaviko V.S.^{1,2}, Popov A.G.^{1,2}, Golovnia O.A.^{1,2}, Protasov A.V.^{1,2}

¹ M.N. Miheev Institute of Metal Physics UB RAS, Ekaterinburg, Russia

² Institute of Natural Sciences and Mathematics, Ural Federal University, Ekaterinburg, Russia
gaviko@imp.uran.ru

Precipitation-hardened 2:17-type SmCo permanent magnets have attracted much attention due to their high Curie temperature and excellent magnetic properties at high temperatures. These magnets have a unique cellular microstructure which is formed as a result of the decomposition of the high-temperature solid solution at approximately 850°C. The cellular microstructure is comprised of rhombohedral $\text{Sm}_2(\text{Co,Fe})_{17}$ (2:17) phase cells surrounded by a hexagonal $\text{Sm}(\text{Co,Cu})_5$ (1:5) cell boundary phase with Zr-rich platelets running across cells. In the course of a prolonged slow cooling from 850 to 400 °C, the 1:5 phase becomes enriched with Cu, which has been established by three-dimensional atom probe (3DAP) [1]. The Cu enrichment gives rise to a large domain-wall-energy difference in the $\text{Sm}_2(\text{Co,Fe,Cu,Zr})_{17}$ sintered magnets and increases their coercivity.

In this work, the increase in coercivity of the sintered $\text{Sm}(\text{Co}_{0.78}\text{Fe}_{0.10}\text{Cu}_{0.10}\text{Zr}_{0.02})_7$ magnets in the course of step cooling has been investigated. Upon annealing at 500°C (near the Curie temperature of the $\text{Sm}(\text{Co,Cu})_5$ phase) the coercivity kinetics abruptly accelerates (Fig. 1). This peculiarity correlates with the change in the lattice parameters of the $\text{Sm}(\text{Co,Cu})_5$ phase (Fig. 1). The possible redistribution of chemical elements between the phases of the cellular structure and its effect on the modification of the domain-wall-energy difference and coercivity is discussed.

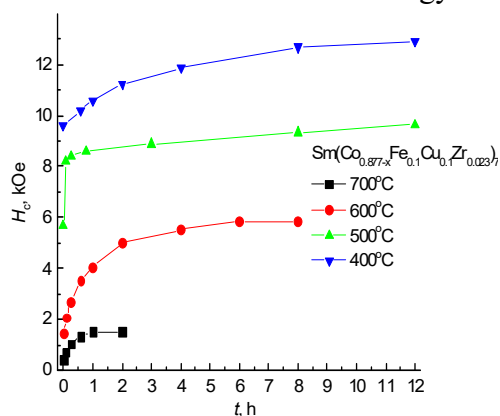


Fig.1 The time dependence of the coercivity of magnets in the course of step ageing

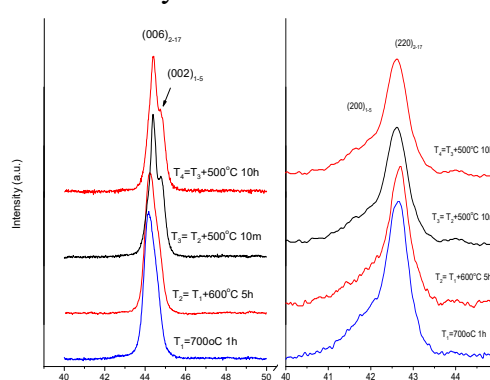


Fig. 2. The dependence of the change in the shape of the spectral lines on time and temperature of the annealing

The research was carried out within the state assignment of FASO of Russia (theme “Magnet” No. 01201463328) and partially supported by the Ural Branch of the RAS (project No. 15-9-2-19). The X-ray investigation and magnetic measurements have been performed in the Collaborative Access Center of IMP UB RAS.

[1] H. Sepehri-Amin, J. Thielsch, J. Fischbacher, T. Ohkubo, T. Schrefl, O. Gutfleisch, K. Hono, *Acta Materialia* **126** (2017) 1-10.

4PO-I1-2

MAGNETIC VISCOSITY IN ND-FE-B RAPIDLY QUENCHED ALLOYS

Volegov A.S.¹, Perepyolkina A.V.¹, Volegova E.A.^{1,2}, Kudrevatykh N.V.¹

¹ Ural Federal University, Yekaterinburg, Russia

² Ural Scientific Research Institute of Metrology, Yekaterinburg, Russia
alexey.volegov@urfu.ru

Magnetic viscosity is the general fundamental property of ferromagnetic materials. In spite of it the magnetic viscosity is not well understood yet. Magnetized permanent magnets are in their own demagnetization field and their magnetization slowly relaxes. In many cases of materials containing ferromagnetic phases, time dependence of the magnetization can be described by

$$M(t) = M(0) - S \ln(1 + t/t_0), \quad (1)$$

where $M(t)$ – magnetization depending on time t , $M(0)$ – magnetization at $t = 0$ after the change of magnetic field, S – the coefficient of magnetic viscosity, t_0 – some reference time depending on the sample and on the detailed measuring procedure.

For many materials, the field dependence of the irreversible part of the magnetic susceptibility, χ_{irr} , and of S are similar, with a maximum close to the coercive field H_c . The phenomenon of magnetic viscosity in terms of fluctuation field (some effective magnetic field with thermal fluctuation nature) described by

$$H_f = S / \chi_{irr}. \quad (2)$$

The aim of this work is to reveal dependencies between fluctuation field and demagnetization field for samples with different distributions of switching fields.

Samples consisting of rapidly quenched Nd-Fe-B-type powders with different coercivities were prepared. Different coercivities were obtained by annealings as is MQP-B+ samples at temperatures 600 °C, 700 °C, 800 °C, 900 °C and 1000 °C. Dependencies H_f vs. H and χ_{irr} vs. H (inset) are presented in Fig. 1. Concentration of powders are 1:1:1:1 for sample 1, 5:4:3:2:1 for sample 2, 1:2:3:4:5 for sample 3.

Experimental dependencies are well fitted with

$$\lg H_f = 0.52 \lg(-H) + c, \quad (3)$$

where c – some constant.

Coefficient 0.52 is two times lower than it in Barbier curve.

Nonadditive character of fluctuation field is shown experimentally.

Results of additional investigation of magnetostatic interaction depend on fluctuation field will be presented in the poster.

The work was supported by 3.6121.2017 Ministry of Education and Science of the Russian Federation project.

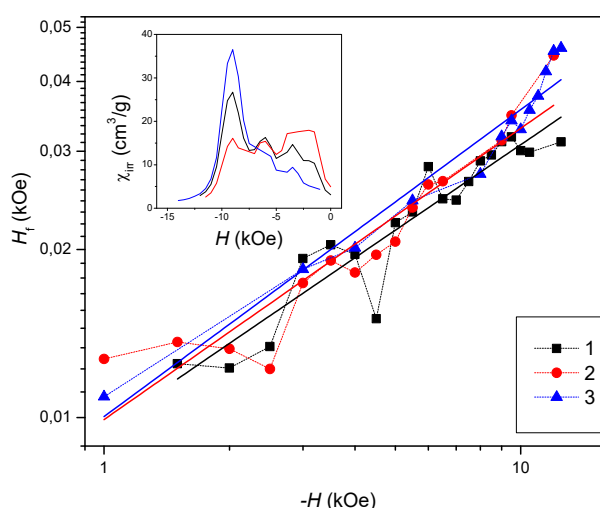


Fig 1. Field dependencies of H_f and χ_{irr} (inset) for investigated samples.

4PO-I1-3

SPONTANEOUS MAGNETIZATION REVERSAL CAUSED BY MAGNETIC NOISE IN ϵ - $\text{In}_{0.24}\text{Fe}_{1.76}\text{O}_3$ NANOPARTICLES

Dmitriev A.¹, Kostyuchenko S.²

¹ IPCP RAS, Chernogolovka, Russia

² MSU, Moscow, Russia

aid@icp.ac.ru

New nanomagnets based on the epsilon phase of iron oxide ϵ - Fe_2O_3 demonstrate giant (up to 2.34 T) coercive field and magnetic anisotropy [1]. In addition, the ϵ - Fe_2O_3 phase exhibits magnetoelectric properties and is known to be a good absorber of millimetre electromagnetic waves. Magnetic properties of ϵ - $\text{In}_{0.24}\text{Fe}_{1.76}\text{O}_3$ nanoparticles ensembles were well studied in paper [2]. The aim of the study is to find the relation between the magnetic viscosity of ϵ - $\text{In}_{0.24}\text{Fe}_{1.76}\text{O}_3$ nanoparticles and magnetic noise caused by the random thermally activated magnetization reversal of single nanoparticle. The physics of magnetic noises is still an intriguing fundamental field of science. In this work, we study the magnetization reversal caused by magnetic noise in ϵ - $\text{In}_{0.24}\text{Fe}_{1.76}\text{O}_3$ nanoparticles with lengths of 80 nm and diameters of 35 nm.

Time dependences $m(t)$ of the magnetic moment in ϵ - $\text{In}_{0.24}\text{Fe}_{1.76}\text{O}_3$ nanoparticles ensembles are measured using a SQUID magnetometer MPMS 5XL Quantum Design (Fig. 1). The sample was first magnetized in magnetic field $H=50$ kOe (exceeding the strength of the saturation field). Following such treatment, the field directed opposite the magnetic moment vector of the sample was switched on.

The $m(t)$ dependences are straightened in semi-logarithmic coordinates $m(\ln t)$. The field dependences of magnetic viscosity $S(H)$ corresponding to the slope of straight lines $m(\ln t)$ are studied.

The logarithmic kinetics of the magnetic viscosity in exotic ϵ - $\text{In}_{0.24}\text{Fe}_{1.76}\text{O}_3$ nanoparticles is determined by the superposition of thermally activated magnetization reversal of single nanoparticle with a wide relaxation time distribution. A relation between the magnetic viscosity and the spectral characteristics of magnetic fluctuations in nanoparticles ensembles was found.

Supported by RFBR, project no. 16-07-00863 a.

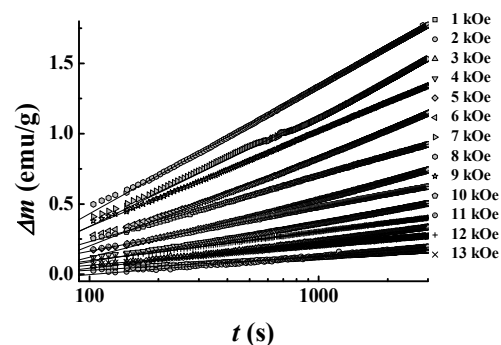


Fig. 1. Time dependences of magnetization $\Delta m(t)$ at $T = 300$ K in different magnetic fields. Approximations are shown by solid lines.

[1] S. Ohkoshi, H. Tokoro, *Bull. Chem. Soc. Jpn.*, **86** (2013) 897-907.

[2] A.I. Dmitriev, R.B. Morgunov, *Low Temp. Phys.*, **41** (2015) 917-921.

4PO-I1-4

INFLUENCE OF ADDITIONAL COMPOUNDS ON COERCIVITY OF SINTERED Nd-Fe-B MAGNETS

Pham Thi Thanh^{1,2}, *Nguyen Van Duong*^{2,3}, *Nguyen Hai Yen*^{1,2}, *Nguyen Mau Lam*³,
*Kamantsev A.P.*⁴, *Koledov V.V.*⁴, *Mashirov A.V.*⁴, *Nguyen Huy Dan*^{1,2}

¹ Institute of Materials Science, Vietnam Academy of Science and Technology, 18 Hoang Quoc Viet, Ha Noi, Viet Nam.

² Graduate University of Science and Technology, Vietnam Academy of Science and Technology, 18 Hoang Quoc Viet, Ha Noi, Viet Nam.

³ Faculty of Physics, Hanoi Pedagogical University 2, 32 Nguyen Van Linh, Vinh Phuc, Vietnam

⁴ Kotelnikov Institute of Radio-engineering and Electronics of RAS, Moscow, Russia
thanhpt@ims.vast.ac.vn

Due to excellent magnetic properties such the high saturation magnetization ($M_s = 16$ kOe) and large magnetocrystalline anisotropy ($K_u = 4.9$ MJ.m⁻³) of the Nd₂Fe₁₄B phase, the sintered Nd-Fe-B magnets are widely applied in practice. An important requirement of the magnets in applications of generators, vehicle motors... is high coercivity. The most common way to enhance coercivity of these magnets is part replacement (up to 40%) of Nd by Dy. However, Dy is much more expensive and scarce in comparison to Nd. Therefore, researching technologies to reduce the Dy content in this kind of permanent magnets is necessary. In this paper, we investigated the influence of the additional compounds of Dy-Nd-Al, Dy-Nd-Cu, Nd-Cu-Al on the coercivity of the sintered Nd_{16.5}Fe₇₇B_{6.5} magnets. The additional compounds were first prepared by arc-melting method and then ground into particles with various size of 0.05 - 5 μm (Fig. 1) using a high-energy ball mill. After that the additional powders were mixed with micrometer Nd_{16.5}Fe₇₇B_{6.5} powder with different ratios before magnetic anisotropic pressing, vacuum sintering, and annealing. The structure of the magnets was thoroughly analyzed using X-ray diffraction and electron microscopy techniques. The magnetic properties of the magnets were investigated on a pulsed field magnetometer. The results show that the coercivity of the sintered Nd-Fe-B magnets can be improved considerably by introducing additional particles to the grain boundaries. The improvement of the coercivity of the magnets is clearly dependent on the composition and particle size of the additional compounds (Fig. 2). The high coercivities ($H_c > 20$ kOe) have been achieved for the magnets with content of the additional compounds less than 2 wt%. The content of Dy in the high-coercivity magnets can be reduced by using this grain boundary-addition method.

Support by Vietnam Academy of Science and Technology (grant No. VAST.03.05/16-17) is acknowledged.

4PO-I1-5

HYSTERESIS PROPERTIES OF AMORPHOUS FERROMAGNETIC RIBBONS

Grebenshchikov Yu.B.^{1,2}, Skomarovsky V.S.³, Lyubimov B.Ya.³, Tarasov V.P.¹, Ignatov A.S.¹, Gudoshnikov S.A.^{1,3}

¹ NUST MISIS, 119049, Moscow, Russia

² FU, 125993, Moscow, Russia

³ IZMIRAN, 108840, Moscow, Russia
vskom@izmiran.ru

Amorphous and nanocrystalline cobalt based alloys fabricated by a melt spinning method have the form of 15 to 30 μm thick ribbons with widths ranging from 2 mm to 50 mm. These materials are characterized by hysteresis properties and a decrease in the magnetic permeability in weak magnetic fields (roughly of 100 nT or less). The paper aims to study the hysteresis properties of amorphous ribbons in weak magnetic fields and under the influence of additional demagnetization fields.

In this study, we used an amorphous ribbon material AMAG-172 [1], 20 μm of thickness and 3 cm of width. Two cylindrical specimens were made from that material. The first cylinder had the diameter $D_1 = 200$ mm, the length $L_1 = 600$ mm and contained one layer of the ribbon magnetic material ($n=1$). The second cylinder was $D_2 = 75$ mm, $L_2 = 400$ mm and was covered with three layers of the ribbon magnetic material ($n=3$).

The dependencies of the residual magnetic field value B_{in} near the internal cylinder surface from the external magnetic field B_{ex} applied in the perpendicular direction to the cylinder axis were measured for both cylindrical specimens. The research showed that the hysteresis loops $B(H)$ of the ribbon material can be determined on the basis of the received dependencies. Fig.1 shows a set of curves $B_{ex}(B_{in})$ for the second cylinder, which demonstrates a transition to a nonhysteresis regime in weak external magnetic fields. Moreover, we found, that a significant hysteresis decrease can be achieved under condition that the material is demagnetized by an alternative reducing field (degaussing). Under these conditions, the value of magnetic permeability may reach the value of $\mu > 10^7$, which was previously shown in [2].

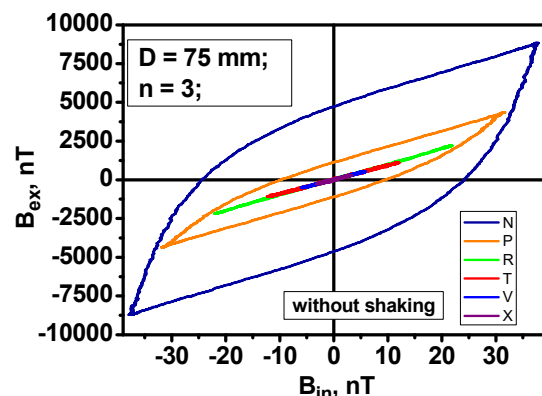


Fig. 1. A set of curves demonstrating a transition to nonhysteresis regime in weak external magnetic fields.

Support by MINOBRNAUKA contract #K2-2015-018 and assignment #3/477.2017/BY is acknowledged.

[1] www.mstator.ru.

[2] Yu.B. Grebenshchikov, S.A.Gudoshnikov, Yu.V. Prokhorova, V.T. Volkov, *Tech. Phys.* **40**, 10 (2014) 869-872.

4PO-I1-6

IN-SITU RESISTANCE MEASUREMENT OF CO-RICH AMORPHOUS FERROMAGNETIC MICROWIRES DURING DC JOULE HEATING

Odintsov V.I.¹, Menshov S.A.^{1,2}, Popova A.V.^{1,2}, Mashera V.S.², Gorelikov E.S.², Gudoshnikov S.A.^{1,2}

¹IZMIRAN, 108840, Moscow, Russia

²NUST MISIS, 119049, Moscow, Russia

menshov-s-a@yandex.ru

In this paper, we present the resistance measurements of the amorphous ferromagnetic microwires (AFM) during Joule annealing heating by direct current. The glass-coated Co-rich AFM had the metallic core with typical diameters from 15 to 30 micrometers. The annealing currents were provided by a programming power supply, which allowed setting up a different heating and cooling regimes. The Wheatstone bridge circuit was used for continuous resistance monitoring during the annealing process.

Fig.1 shows the AFM relative resistance as a function of annealing current during 60 minutes for five AFM samples. First 10 minutes the annealing current linearly increased until the preset value of power supply reached one of the discrete power values: 0,8; 1,3; 1,8; 2,3 or 2,8 W. Next 40 minutes the annealing current kept a constant value for preset power value. Then the annealing current linearly decreased during 10 minutes.

We found that the AFM resistance values increased from 0.15% to 1% of the initial values for a corresponding rising power values. The repeated annealing processes at the same discrete power values resulted in minor increasing in the AFM resistance values and reached a maximum value after long-term annealing. Such fixed values of the AFM resistance acquired were irreversible. The observed dependence of the AFM resistance versus the annealing current will be useful to find interrelation of electric and magnetic AFM properties with the annealing parameters.

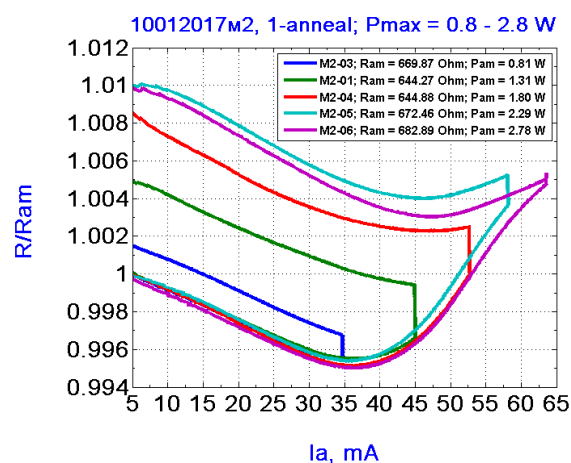


Fig. 1. AFM relative resistance changing as function of current under the DC Joule heating and cooling.

Support by MINOBRNAUKA contract #K2-2015-018 and assignment #3/.477.2017/BY is acknowledged.

4PO-I1-7

PHASE TRANSITIONS IN THE DOMAIN STRUCTURE OF AN UNIAXIAL MAGNETIC FILM

Siryuk Ju.A.¹, Bezus A.V.¹, Bondar E.D.¹, Smirnov V.V.¹

¹ Donetsk National University, 24 Universitetskaya str., Donetsk 83001, Ukraine
juliasiryuk@gmail.com

Phase transitions (PT) in the domain structure (DS) of a ferrite-garnet film were studied. A relationship is shown between the phase transition in the domain boundaries (DB) of the magnetic bubble domain and the phase transition in a rigid CMD lattice with a temperature change (T). The investigations were carried out on a film with a developed surface $\langle 111 \rangle$ grown by liquid-phase epitaxy method on a gadolinium gallium substrate of the composition $(TmBi)_3(FeGa)_5O_{12}$, ($T_N = 437K$, $T_C = 120K$, $h = 8.4 \mu m$) where is the T_N – Neel temperature, T_C – the magnetic compensation temperature, and h – the film thickness. The film at a room temperature has a quality factor $Q > 5$. At such a value of Q in DB, the action of a pulsed magnet field (H_{imp}) is perpendicular to the film plane and creates vertical Bloch lines (VBL) [1]. The amount of VBL in DB depends on the amount of the magnetic film characteristics at a given T: saturation magnetization ($4\pi M_s$), characteristic length (l), and the surface energy density of the domain boundary (σ). The circumference of the CMD is the boundary condition that causes the Bloch lines to approach the interval $s = \pi d / 2N$, where d is the diameter of the CMD, N – the number of spin circulations, and s – the distance between the VBL [1].

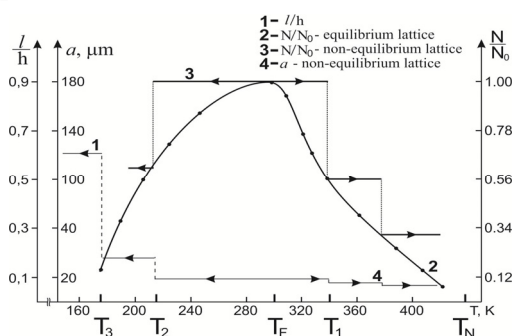


Fig. Temperature dependences of magnetic characteristics of a film.

Because of the complex structure, the domain boundaries are very sensitive to a temperature change in the magnetic film characteristics. In hard domains, the repulsive force of the VBL and the magnetostatic force counterbalance the compressive forces of the surface tension of the Bloch wall. This gives a statically stable domain. The hexagonal lattice of CMD is formed by H_{imp} . Then the field turns off. Such a lattice is equilibrium at T formation. Its order parameter $y = d/a = 0.74$, where a is the lattice period [2]. If the lattice is formed at T_F , and then the T

film changes, then the lattice and the number of VBLs in its DB remain in the interval $T_1 - T_2$ (Fig.), but the DS is non-equilibrium. At T_2 in the CMD lattice, a first-order PT occurs in a two-phase structure with the retaining of the number of domains and the decreasing of parameters [3]. At the same time, a first-order PT occurs in the DB with a decrease in the number of VBLs by the annihilation. At T_2 in the lattice, a first-order phase transition occurs with a decrease in the number of domains and an increase in the parameters. A first-order PT occurs in the domain boundary with a decrease in the number of VBLs by their unwinding. There are several PT in the temperature range of $T_N - T_C$ (Fig.). Near the $T \leq 0.98T_N$, the lattice with a simple Bloch wall is observed. This lattice remains in a wide temperature range ($0.98T_N - T_3$). Thus, it is shown that the phase transitions of the DB cause phase transitions in the CMD lattice. The form of the PT in the DB determines the mechanism of phase transitions in the CMD lattice.

[1] Malozemov A., Slonczewski J. *Mir*, Moscow (1982).

[2] Yu.A. Mamalui, Yu.A. Siryuk, A.V. Bezus, *Fiz. Tverd. Tela*, **45** №9 (2003) 1645.

[3] Yu.A. Siryuk, A.V. Bezus, *Fiz. Tverd. Tela*, **45** №3 (2013) 547.

4PO-I1-8

TUNING LOCAL MAGNETIC ANISOTROPY IN CORE-SHELL Co@Cu PARTICLES BY DYNAMIC COMPACTING AND THE SHELL BUILD-UP

*Kuzovnikova L.A.*¹, *Denisova E.A.*^{2,3}, *Chekanova L.A.*², *Nemtsev I.V.*⁴, *Komogortsev S.V.*²,
*Iskhakov R.S.*²

¹ Krasnoyarsk Institute of Railway Engineering, Irkutsk State Railway Transport Engineering University, Krasnoyarsk, Russia

² Kirensky Institute of Physics, Federal Research Center KSC SB RAS, Krasnoyarsk, Russia

³ Siberian Federal University, Krasnoyarsk, Russia

⁴ Federal Research Center KSC SB RAS, Krasnoyarsk, Russia
lund@mail.ru

Powders of submicron ferromagnetic particles are used in radio-absorbing composite coatings, and as a raw material for powder metallurgy products. Applied characteristics of powders, such as magnetic permeability, the specific absorption rate are largely determined by their local magnetic anisotropy field. However, in a powder, this field can vary within very wide limits due to the no uniform dipole-dipole interaction between neighbouring particles. We use this feature for the tuning the magnitude of the local magnetic anisotropy by controlling fluctuations of dipole-dipole interactions in the powder. We have tested two approaches to controlling this.

The first is to improve the structural homogeneity through dynamic compaction. The second is to reduce the amplitude of the dipole-dipole field fluctuations, due to the gradual build-up of the nonmagnetic shell on the magnetic core particles. The tests have carried out with Co(P)@Cu particles fabricated by electro-less reduction.

The magnetic amorphous Co(P) particles of submicron size have been coated by nonmagnetic copper shell. Bulk samples were formed via dynamic compacting using a flat pressing scheme [1]. According the studies with scanning electron microscopy the particles are characterized by well pronounced core-shell structure both before and after dynamic compacting. Local magnetic anisotropy field have been studied by approach to magnetic saturation curves [2]. Finally we have found that application of these approaches allows several times reduction of the local magnetic anisotropy field to the level of that in magnetic coatings (fig.1). The best result has been obtained by combining the second and the first approaches.

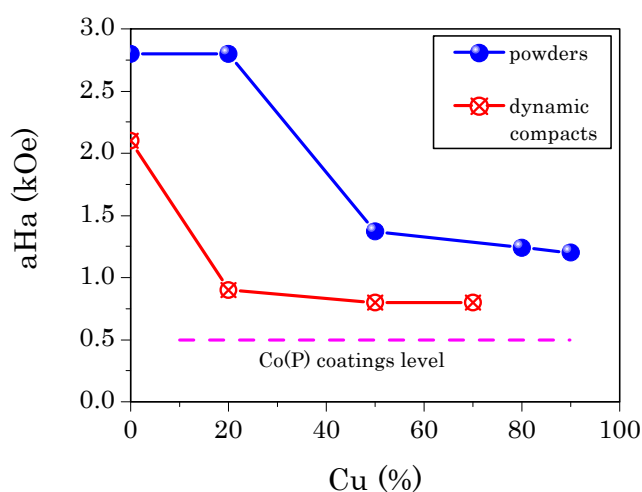


Fig.1. The effect of the shell thickness and dynamic compacting in core-shell Co(P)@Cu particles.

Support by Russian Foundation for Basic Research, Grants No. 16-03-00969 is acknowledged.

[1] L.A. Kuzovnikova, E.A. Denisova, et.al., *Bull. Russ. Acad. Sci. Phys.*, **81** (2017) 295–297.

[2] S.V Komogortsev, R.S. Iskhakov, et.al., *Appl. Phys. Lett.*, **103** (2013) 152404.

4PO-I1-9

STRUCTURAL PHASE TRANSITIONS IN MAGNETIC ELASTOMERS

Farzetdinova R.M., Meilikhov E.Z.

Nat. Res. Centre "Kurchatov Institute", 123182 Moscow, Russia

rimfar@mail.ru

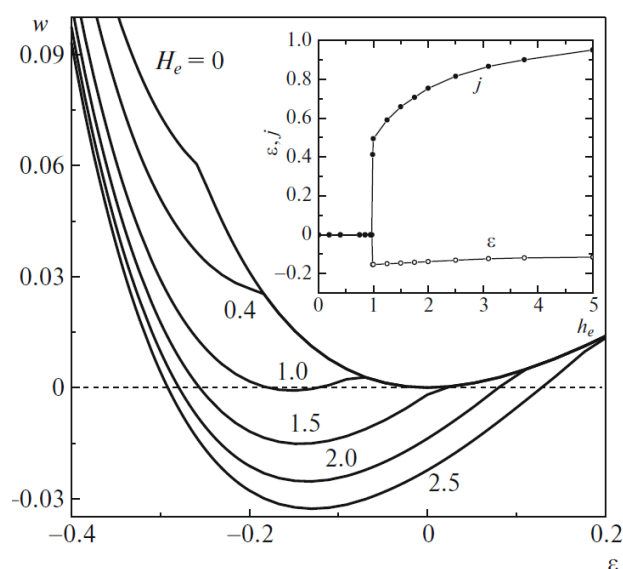
Magnetic elastomers represent a new type of materials that are “soft” rubber-like matrices with “hard” magnetic nano- or microgranules embedded in them. They possess a small elastic modulus (of the order of several tens of kilopascals), so that the elastic forces of the polymer matrix and the magnetic forces acting between magnetic-filler granules turn out to be comparable in magnitude. As a result, these materials acquire a number of new properties. In particular, their mechanical and/or magnetic characteristics can depend strongly on the polymer matrix filling with magnetic particles and can change under the action of an external magnetic field, pressure, and temperature. The softer the polymer matrix, the more pronounced the corresponding effects.

The magnetostrictive effect is the most important (and interesting for applications) among others. We study the elastic properties of magnetic elastomers in the framework of the generalized mean field theory that admits an analytical solution. More specifically, the magnetic granules of the filler are considered as a system of randomly arranged (in space) and interacting single-domain Ising particles (dipoles) with fixed (in magnitude) magnetic moments that can change their orientation. The ground state of the system is ferromagnetic only in the case where the mean distance between magnetic granules is comparable to their diameter. Otherwise (remote dipoles), the system is paramagnetic at any temperature.

The energy of such a system as a function of the number density of filler magnetic granules, temperature, pressure, magnetic field, and sample shape. As the temperature lowers, a spontaneous magnetization of the composite appears abruptly, which is accompanied by an equally abrupt reduction of its length. In fact, this is a structural phase transition. The properties of the composite are also affected significantly by an external magnetic field, which leads to its deformation (compression) and magnetization in a threshold way.

Typical deformation dependences of the system's energy (w) in magnetic field (H_e) are presented in Fig. The inset shows how the system is deformed (ε) and magnetized (j) under the action of a pressure. In this case, we have a material with the shape memory controlled by the temperature.

Within this model, we describe a multitude of deformation, magnetic-field, and temperature effects which are quite accessible to experimental observations.



4PO-I1-10

MAGNETIC PROPERTIES OF THE NON-STOICHIOMETRIC TbCo₂Ni_x ALLOYS

Inishev A.A.^{1,2}, *Gerasimov E.G.*^{1,2}, *Mushnikov N.V.*^{1,2}, *Terentev P.B.*^{1,2}, *Gaviko V.S.*^{1,2}

¹M.N. Miheev Institute of Metal Physics UB RAS, Ekaterinburg, Russia

²Institute of Natural Sciences and Mathematics, Ural Federal University, Ekaterinburg, Russia
inishev@imp.uran.ru

Recently it was shown that the non-stoichiometric ErCo₂Mn_x compounds give new opportunity to gradually modify magnetic properties of the Laves phase compounds by changing in wide range the manganese content [1]. It was found that alloys with $x \leq 0.8$ crystallize in the cubic MgCu₂-type Laves-phase structure, in spite of the 1:3 ratio of the Tb and 3d components. The Curie temperatures (T_C) of the non-stoichiometric ErCo₂Mn_x alloys were found to be considerably higher than that of the parent ErCo₂ compound whereas the spontaneous magnetic moments are smaller than that of the ErCo₂ compound.

In the present work, in order to establish the possibility of the existence of intermetallic Laves-phase compounds RCO_2Ni_x (R - rare earth element) with nickel, we studied structure and magnetic properties of new non-stoichiometric TbCo₂Ni_x alloys.

It was found that single-phase non-stoichiometric compounds with the cubic MgCu₂-type structure are formed for Ni content $x \leq 0.1$. For the alloys with $x \geq 0.1$, in addition to the main MgCu₂-type phase, there appears a rhombohedral phase with the PuNi₃-type structure. Thus, the non-stoichiometric RCO_2M_x alloys with cubic MgCu₂-type Laves-phase structure can be obtained in more narrow concentration range of alloying 3d element in case of $M=Ni$ than $M=Mn$.

In Fig. 1 we summarized the variation of the magnetic properties of the TbCo₂Ni_x alloys with increasing nickel concentration.

The small Ni content ($x \leq 0.025$) causes a sharp increasing of T_C . As x is increased further, the Curie temperature falls off sharply.

Fig. 1 shows also the concentration dependence of the spontaneous magnetic moment μ_s and total magnetic moment of 3d sublattice of TbCo₂Ni_x compounds calculated in assumption of collinear antiparallel alignment of the Tb and Co, Ni magnetic moments. The behavior of concentration changes of magnetic moment of the 3d sublattice in the compounds is similar to those for Curie temperature.

The obtained experimental results on the magnetic properties of the TbCo₂Ni_x alloys are discussed using assumptions about changes in the electron band structure of the compounds.

The research was carried out within the state assignment of FASO of Russia (theme "Magnet" No. 01201463328), supported in part by RFBR (project No. 15-02-05681).

[1] E.G. Gerasimov, N.V. Mushnikov, A.A. Inishev, P.B. Terentev, V.S. Gaviko, *J. Alloy. Compd.*, **680** (2016) 359-365.

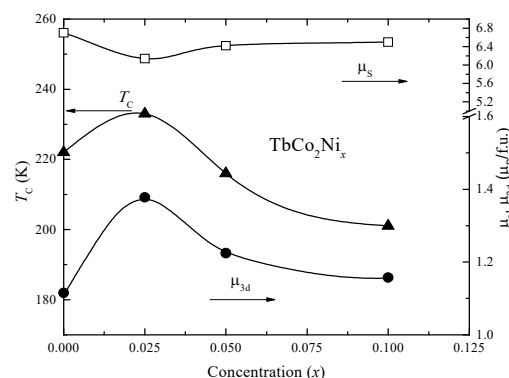


Fig. 1. Concentration dependences of the Curie temperature (\blacktriangle), spontaneous magnetic moment (\square) and magnetic moment of 3d-sublattice (\bullet) for TbCo₂Ni_x alloys.

4PO-II-11

MAGNETIC PROPERTIES OF A $(\text{Nd}_{0.5}\text{Pr}_{0.5})_2\text{Fe}_{14}\text{B}$ SINGLE CRYSTAL

Politova G.A.¹, Tereshina I.S.², Gorbunov D.I.³, Rogacki K.⁴, Volegov A.S.⁵, Kudrevatykh N.V.⁵, Andreev A.V.⁶

¹ Baikov Institute of Metallurgy and Materials Science RAS, Moscow, Russia

² Lomonosov Moscow State University, Faculty of Physics, Moscow, Russia

³ Dresden High Magnetic Field Laboratory (HLD-EMFL), Helmholtz-Zentrum Dresden-Rossendorf, D-01314 Dresden, Germany

⁴ International Laboratory of High Magnetic Fields and Low Temperatures PAS, Wroclaw, Poland

⁵ Institute of Natural Sciences, Ural Federal University, Yekaterinburg, Russia

⁶ Institute of Physics, ASCR, Prague, Czech Republic
gpolitova@gmail.com

In this work the magnetic properties of a $(\text{Nd}_{0.5}\text{Pr}_{0.5})_2\text{Fe}_{14}\text{B}$ single crystal are investigated in a wide range of temperatures and magnetic fields. Temperatures of the magnetic phase transitions are found and the magnitude of the saturation magnetization and the value of the anisotropy field are determined. In the region of the spin-reorientation magnetic phase transition (SRT), the value of the magnetocaloric effect (MCE) as an entropy change - ΔS_m is determined.

Single crystals of $(\text{Nd}_{0.5}\text{Pr}_{0.5})_2\text{Fe}_{14}\text{B}$ were grown by a modified Czochralski method in a tri-arc furnace with W electrodes on a copper water-cooled bottom under an Ar protective atmosphere. The crystal structure was determined by standard X-ray powder diffraction on a piece of the single crystal crushed into fine powder. Back-scattered Laue patterns were used to confirm the single-crystalline state of the ingot and its orientation for magnetization measurements. The later were performed in pulsed magnetic fields up to 580 kOe at 1.8 K (Fig.1) and in steady magnetic fields up to 140 kOe at the 4.2-250 K temperature region. The magnetic field was applied both along and perpendicular to the c ([001]) axis. High-temperature measurements were carried out using PPMS – 9 instrument.

It is established, that the $(\text{Nd}_{0.5}\text{Pr}_{0.5})_2\text{Fe}_{14}\text{B}$ crystal is a ferromagnet below $T_C = 570$ K, having a saturation magnetization of about 198 emu/g at $T = 1.8$ K. This compound demonstrates the SRT at 73 K, where the magnetic anisotropy changes from an “easy axis” to “cone” type. In the SRT area, the MCE was also measured. The ΔS_m maximum value was found to be $2.3 \cdot 10^4$ erg/g·K (140 kOe).

The work is supported by the RFBR according to the research project 16-33-60226 mol_a_dk. and RF MES, pr. 3.6121.2017.

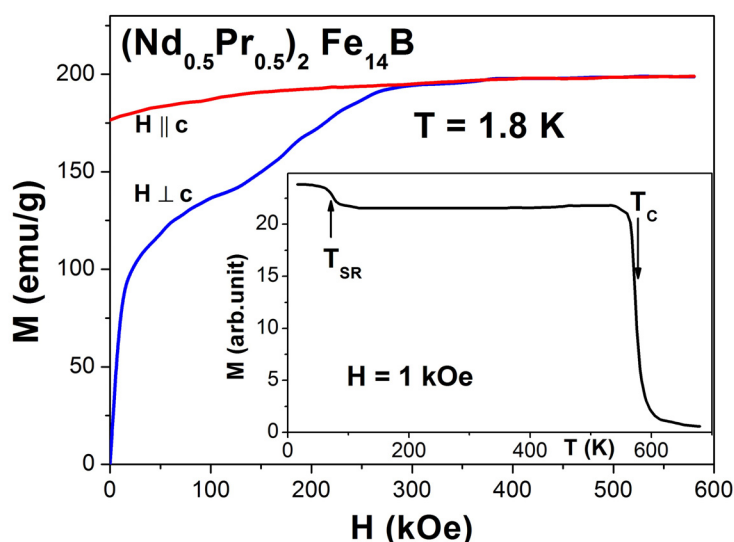


Fig. 1. Magnetization curves of $(\text{Nd}_{0.5}\text{Pr}_{0.5})_2\text{Fe}_{14}\text{B}$ at 1.8 K in fields up to 58 T applied along and perpendicular the easy axis c ([001]). Insert: temperature dependence in 1 kOe.

4PO-II-12

SYNTHESIS OF FeNi TETRATAENITE PHASE BY MEANS OF CHEMICAL PRECIPITATION

Kurichenko V.L.¹, Karpenkov D.Yu.¹, Khovaylo V.V.¹

¹National University of Science and Technology MISIS, Moscow, Russia
vkurichenko@hotmail.com

Recently, the great deal of efforts has been done in order to produce new high-energy permanent magnets because of so-called “rare-earth crisis”. Amongst all rare-earth free systems, FeNi L1₀ has the highest theoretical value of energy product (320 kJ/m³), which is the figure of merit in a hard magnetic material.

The main problem of FeNi tetrataenite phase synthesis is attributed to significantly slow diffusion rate at 320 °C which is the temperature of this phase formation. This is the reason why tetrataenite phase was observed in nature only in meteorites.

To increase the rate of L1₀ phase formation in FeNi alloys by 6-9 order of magnitude, some authors [1] recommend to focus the efforts on two main aspects: i) to increase the driving force for phase transformation, possibly through the addition of ternary alloying elements or additional stimuli that may enhance the stability of the L1₀ phase; ii) to increase the vacancy concentration in order to provide a large reservoir of grain boundaries and to enable atomic rearrangement, possibly through nanostructuring at low temperatures.

In this paper, we used the method proposed by E. Lima et al [2], which includes cyclic oxidation and reduction process at 320 °C. We subjected Fe₅₀Ni₅₀ nanopowder, produced by chemical co-precipitation, to the same heat treatments.

Precursors for chemical precipitation of FeNi were Fe(NO₃)₃·9H₂O and Ni(NO₃)₂·6H₂O. Both solutions of the salts in distilled water were pumped into the reactor, where were mixed with NaOH with ratios that maintained the level of pH at 12. FeNi hydroxide, produced at the end of the reaction, was rinsed in distilled water and dried in air. Resulted sample was then milled and placed in a tube furnace. Reduction of the hydroxide was carried out in H₂ atmosphere at 320 °C.

Obtained powder was subjected to heat treatments, included oxidation for 20 min in N₂/O₂ atmosphere and following reduction in H₂ atmosphere for 40 min. We performed 5 and 10 cycles of treating.

In order to validate the presence of FeNi L1₀ in powders, we used DSC analysis. Recently N. Bordeaux et al [1] reported that chemical disordering process of tetrataenite phase is accompanied with endothermic peak (enthalpy is 4 kJ/mole) in temperature range from 500 °C to 600 °C on DSC curves. Results of DSC analysis for all samples are presented in figure 1.

Obtained data shows endothermic peak at 530 °C for the sample after 10 cycles of oxidation and reduction treatments. The value of enthalpy is in good agreements with the literature data of disordering process of FeNi phase with L1₀ structure.

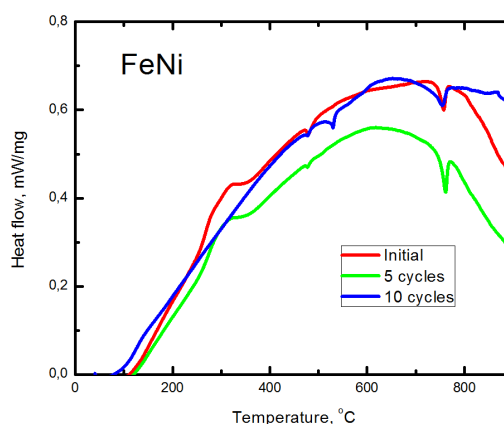


Figure 1. DSC analysis of FeNi powder samples, subjected to 5 and 10 cycles of oxidation and reduction treatment.

[1] N. Bordeaux, A.M. Montes-Arango, *Acta Mater.*, **103** (2016) 608-615.

[2] E. Lima Jr., V. Drago, *Phys. Stat. Sol.*, **187** (2001) 119-124.

4PO-II-13

STUDY OF PHASE TRANSFORMATIONS OF HARD MAGNETIC ALLOYS Fe – Cr – Co

Ostrizhnyaya M.A.¹, Abilov I.¹, Zhukov A.A.¹, Cherdantseva V.V.¹, Perminov A.S.¹, Lileev A.S.¹

¹National University of Science and Technology MISiS, Moscow, Russia
schwepsinka@gmail.com

Many permanent magnets are produced using Fe – Cr – Co alloys. This study was carried out for the research of phase transformations in Fe – Cr – Co alloys. Dilatometric, calorimetric, X-ray diffraction and metallographic methods were used for further results.

Calorimetric analysis on thermo-analyzer Netzsch STA 449 F3 was carried out with heating at a rate of 5 deg / min to a temperature of 1000 °C and subsequent cooling. Dilatometric analysis was carried out on a horizontal differential dilatometer Linseis L75HD1000C. X-ray diffraction studies were performed by the DRON-3, DRON-4 diffractometers. The metallographic analysis was carried out on a Carl Zeiss Axio Scope A1 microscope.

By calorimetric and dilatometric methods, it was established that in all investigated alloys, when the temperature is raised to 1000 °C, three phase transformations occur.

It is assumed that the first phase transformation upon heating is associated with the formation of a modulated nanocrystalline structure upon decay of the quenched α -solid solution.

The X-ray diffraction method has shown that the second and third transformations under heating are associated with the release of γ and σ phases. Similar to the second and third transformations, effects are also observed in the cooling process.

Table 1 provides data for the temperatures of phase transformations in various alloys when heated.

It should be noted that dilatometric method of analysis is more sensitive for detection σ -phase in most cases. X-ray diffraction method is difficult to detect a small amount σ -phase, which locate alongside boundaries of large grains α -phase. Thermal effects of the allocation of the γ - and σ -phases have the same sign, which complicates the identification of those phases in calorimetry. Dilatometrically analysis method is more sensitive, because when heated, the allocation of γ -phase causes compression of the sample, the allocation σ -phase – to extension.

Table 1 – The temperatures of phase transitions (T_{pt})

Composition of alloy (wt, %)	T_{pt} (during heating), °C		
	$\alpha \rightarrow \alpha_1 + \alpha_2$	$\alpha \rightarrow \gamma$	$\alpha \rightarrow \sigma$
Fe – 28 %Cr – 5 %Co	475	585	650
Fe – 30 %Cr – 15 %Co – 3 %Mo	480	625	800
Fe – 25 %Cr – 14 %Co – 3 %Mo – 1 %Ti	480	610	650
Fe – 24 %Cr – 15 %Co – 0,5 %V – 0,5 %Ti	530	620	690

4PO-II-14

STRESS EFFECTS ON MAGNETIC PROPERTIES OF AMORPHOUS MICROWIRES SUBJECTED TO CURRENT ANNEALING

Nematov M.G.¹, Adam A.M.¹, Salem M.M.¹, Yudanov N.A.¹, Yakubtsev R.A.¹, Panina L.V.^{1,2}, Morchenko A.T.¹

¹National University of Science and Technology, MISIS, Moscow 119991, Russia

²Institute for Design Problems in Microelectronics RAS, Moscow 124681, Russia

In the present work, we report on the influence of applied stress on the magnetization processes and magnetoimpedance (MI) in positive magnetostriction glass-coated amorphous microwires previously annealed by a dc current. We have demonstrated that current annealing can produce a controllable change in easy anisotropy direction from almost axial to helical which is especially important for high frequency stress-MI effect [1].

The wires under study are made of cobalt-rich alloys with small addition of iron having the stoichiometric formula of $\text{Co}_{71}\text{Fe}_5\text{B}_{11}\text{Si}_{10}\text{Cr}_3$. The wires are coated with an amorphous glass sheath and synthesized using Taylor-Ulitovsky technique [2-3]. Annealing was done by passing 50 mA dc electric current for specified time (30-120 min) along the sample (wire of 15 cm length and total diameter $29.5\mu\text{m}$). Hysteric properties were investigated before and after applying stresses of 85-340 MPa. As the current annealing led to a substantial change in the direction of magnetic anisotropy, a notable change in the magnetic hysteresis features was detected. After stress employment, the initial hysteresis loop properties of the wires were regained. In other words, the stress application reversed the effect of annealing produced via the electric current. Figure 1 demonstrates the difference in magnetic hysteresis curves of annealed microwires subjected to different stresses. It can be seen that the application of stress increases the remanence magnetization indicating that the anisotropy becomes closer to axial as in the case of as-produced wires.

The experimental results on magnetoimpedance in the range of 1-100 MHz in the annealed wires subjected to external stress were consistent with the anisotropy change. Consequently, a very sensitive stress-MI is realized in the low magnetic field range.

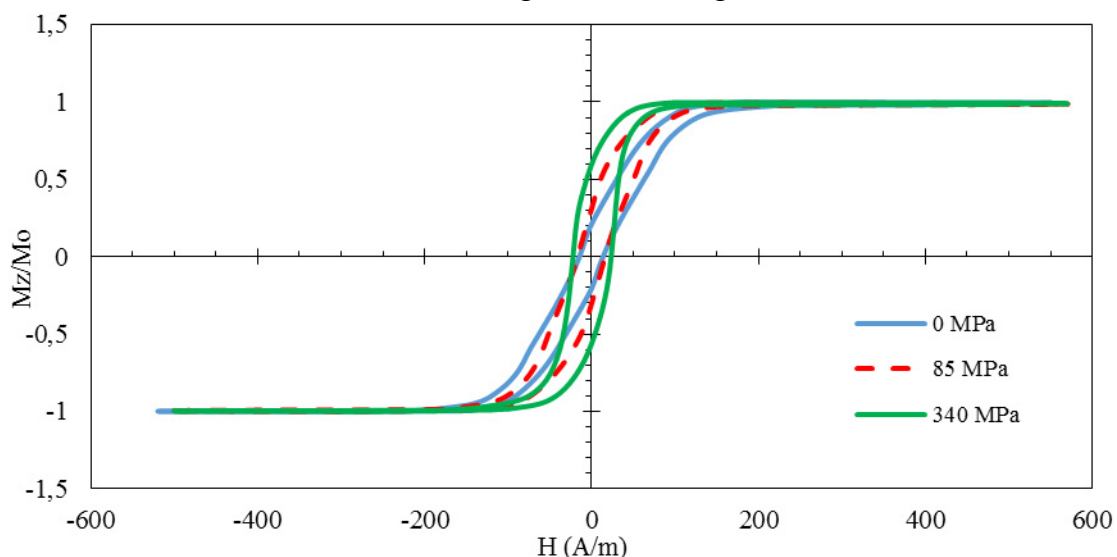


Figure 1: Magnetic hysteresis loops of glass coated $\text{Co}_{71}\text{Fe}_5\text{B}_{11}\text{Si}_{10}\text{Cr}_3$ current annealed microwires at 50 mA for 120 min without and with different stress

[1] D.P. Makhnovskiy, L.V. Panina, et.al., *Phys. Rev B*, **74** (2006) 064205-064215.

[2] A. Zhukov, V. Zhukova, *Nova Science Publishers*, **162** (2009) 11788.

[3] H. Chiriac, S. Corodeanu, et.al., *J. Appl. Phys.*, **107** (2010) 09A301.

4PO-I1-15

A THEORETICAL STUDY OF SPINODAL DECOMPOSITION IN TERNARY Fe-Cr-Co SYSTEM

Mukhamedov B.O.¹, Ponomareva A.V.¹, Abrikosov I.A.^{1,2}

¹ Materials Modeling and Development Laboratory, National University of Science and Technology 'MISIS', Moscow, Russia

² Department of Physics, Chemistry, and Biology (IFM), Linköpings University, Linköping, Sweden

alena.ponomareva@misis.ru

The ternary Fe-Cr-Co alloys have a unique combination of high magnetic properties, including high Curie temperature, residual induction and coercive force, with corrosion stability, ductility and toughness. The high mechanic properties make it possible to subject these alloys to cool and hot mechanic treatment and produce magnets with a different shape and size. At the same time, Fe-Cr-Co alloys demonstrate a high resistance to corrosion, which is beneficial for using these magnets in aggressive surroundings and for medical applications. Also Fe-Cr-Co materials with high Cr concentration ($X_{Cr} \sim 60\%$ wt.) exhibit the effect of giant magnetoresistance. In addition, Fe-Cr-Co alloys present a high thermal and time stability of magnetic properties.

The desired magnetic properties in Fe-Cr-Co alloys can be reached by the formation of the specific microstructure during the spinodal decomposition of metastable bcc solid. In this work [1] using the exact muffin-tin orbitals method (EMTO) in conjunction with the coherent potential approximation (CPA) we have studied the tendency towards spinodal decomposition of solid solution in ternary Fe-Cr-Co system. We predict that an increase Co and Cr content in the ternary Fe-Cr-Co system increases the tendency of the bcc (α)-Fe_xCr_yCo_z alloys towards the spinodal decomposition. Comparison with available experiment confirms that the EMTO-CPA calculations make it possible to predict the most favorable decomposition directions and chemical content of the decomposition products. In addition, we have estimated the Curie temperature of the alloys, and considered the influence of the magnetic state on the decomposition thermodynamics of the ternary alloys. Using the mean field approximation, we have estimated the finite temperature effects on the alloys free energy. On the basis of our simulations, we argue that the high magnetic properties and thermal stability of these properties can be obtained in Fe-Cr-Co alloys with high Co concentration.

Support by the Ministry of Education and Science of the Russian Federation (Grant No. 14.Y26.31.0005) and the Russian Foundation for Basic Researches (Grant No. 16-02-00797) is acknowledged for financial support.

[1] B.O. Mukhamedov, A.V. Ponomareva, I.A. Abrikosov, *Journal of Alloys and Compounds*, **695** (2017) 250-256.

4PO-I1-16

COMPETITION OF EXCHANGE INTERACTIONS IN LAYERED $\text{La}_{1-x}\text{Gd}_x\text{Mn}_2\text{Si}_2$ COMPOUNDS

Terentev P.B.^{1,2}, *Gerasimov E.G.*^{1,2}, *Mushnikov N.V.*^{1,2}, *Gaviko V.S.*^{1,2}, *Yazovskikh K.A.*¹

¹Institute of Metal Physics of UB RAS, Ekaterinburg, Russia

²Yeltsin Ural Federal University, Ekaterinburg, Russia

terentev@imp.uran.ru

The RMn_2X_2 (R is a rare earth element) compounds have tetragonal ThCr_2Si_2 -type layered structure and can be considered as unique sample of natural monoatomic multilayers. They exhibit a unique set of magnetic phase transitions due to an unusual correlation between the intralayer Mn-Mn distance ($d_{\text{Mn-Mn}}$) and interlayer magnetic arrangement of the Mn magnetic moments. In the compounds there exists a critical distance for intralayer Mn atoms, which is considered to be equal to $d_c \approx 0.285\text{-}0.287$ nm at room temperature.

In the present work, we studied magnetic properties of quasi-single crystals of the $\text{La}_{1-x}\text{Gd}_x\text{Mn}_2\text{Si}_2$ ($0 \leq x \leq 1.0$) compounds. In such compounds there is a possibility to gradually change, by increasing Gd content, the intralayer Mn-Mn distances from $d_{\text{Mn-Mn}} > d_c$ (LaMn_2Si_2) to $d_{\text{Mn-Mn}} < d_c$ (GdMn_2Si_2) and the Gd-Mn and Gd-Gd interlayer exchange interactions. We determined the concentration dependencies of the paramagnetic Curie temperatures, type of magnetic anisotropy, effective and spontaneous magnetic moments for the $\text{La}_{1-x}\text{Gd}_x\text{Mn}_2\text{Si}_2$ compounds. The

concentration x - T magnetic phase diagram of $\text{La}_{1-x}\text{Gd}_x\text{Mn}_2\text{Si}_2$ compounds was constructed (Fig.1).

It was shown that in $\text{La}_{1-x}\text{Gd}_x\text{Mn}_2\text{Si}_2$ compounds, the interatomic Mn-Mn distances become less than the critical distance with increasing the Gd concentration up to $x \approx 0.2$. This leads to changing interlayer Mn-Mn magnetic ordering from ferromagnetic to antiferromagnetic ordering.

The competition of negative Gd-Mn, and negative Mn-Mn interlayer exchange interactions and existence of strong easy axis type magnetic anisotropy leads to the appearance of paradoxical magnetic structure (C) in the compounds with $x > 0.2$ at low temperatures (Fig.1). In this structure, the resulting magnetic moment is oriented perpendicular to the easy direction of magnetization.

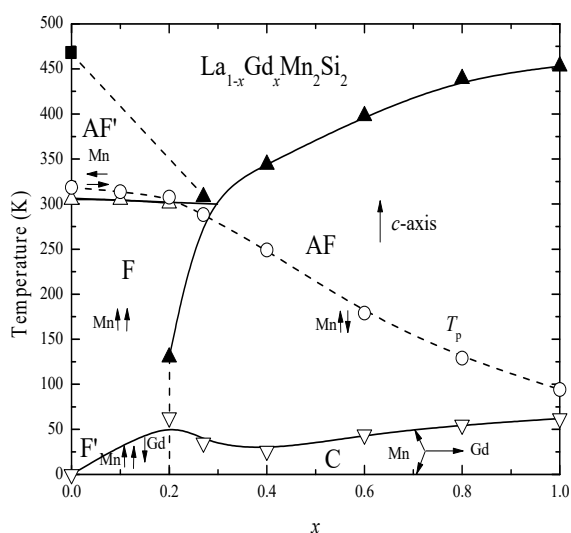


Fig.1. Concentration magnetic phase diagram of $\text{La}_{1-x}\text{Gd}_x\text{Mn}_2\text{Si}_2$ compounds. Arrows schematically show the mutual orientation of the magnetic moments of the Tb layer and Mn layers.

The research was supported by RSF (project No. 15-12-10015).

4PO-II-17

GIANT FORCED MAGNETOSTRICTION IN Tb_{0.2}Gd_{0.8} SINGLE CRYSTAL*Nikitin S.A.¹, Rogacki K.², Zvonov A.I.¹, Ivanova T.I.¹, Koshkid'ko Yu.S.², Cwik J.²*¹ M.V. Lomonosov Moscow State University, Moscow, Russia² International Laboratory of High Magnetic Fields and Low Temperatures, Wroclaw, Poland
zvonov@physics.msu.ru

Giant forced magnetostriction is observed when a strong magnetic field is applied to a ferromagnet. The rare earth metals and their alloys form an important class of materials with giant magnetostriction [1,2]. The forced magnetostriction and volume magnetostriction have not been enough explored in these class of materials yet. The volume magnetostriction values are crucial for determination of exchange interactions dependencies on the unit cell volume and on the interatomic distances. Moreover the volume magnetostriction is very important for practical use in wide range of technical applications.

In this work the magnetostriction of Tb_{0.2}Gd_{0.8} single crystal in strong magnetic fields up to 10 T was investigated. This alloy has a relatively high Curie temperature due to high concentration of Gd and giant values of magnetostriction caused by Tb content, which has high values of single-ion magnetostriction. The combination of strong exchange interactions and high magnetostriction in Tb_xGd_{1-x} alloys makes them interesting objects in terms of theoretical research and practical applications.

We have performed an experimental study of magnetostriction of Tb_{0.2}Gd_{0.8} single crystal in magnetic fields up to 10 T and in temperature range 4.2 K - 300 K. The Tb_{0.2}Gd_{0.8} single crystal has a hexagonal closed packed crystal structure with P6₃/mmc space group. The measurement of magnetostriction was carried out using the SK-06-030 TY-350 type strain gauge. This type of strain gauge allows measuring the deformation of the sample caused by the magnetostriction simultaneously in two mutually perpendicular directions. Magnetostriction measurement was carried out on the Tb_{0.2}Gd_{0.8} single crystal in magnetic field directed along the *c* axis - λ_{cc} , λ_{cb} and directed along the *b* axis - λ_{bb} , λ_{bc} (the first index indicates the direction of the magnetic field, the second - crystallographic direction of magnetostriction measurement).

Temperature dependencies of λ_{cc} and λ_{bc} magnetostrictions in various magnetic fields exhibit maximum near $T_C = 280$ K, the magnetic phase transition temperature of Tb_{0.2}Gd_{0.8} alloy. Similar results were obtained for the temperature dependencies of volume magnetostrictions ω_c and ω_b . The magnetostriction of Tb_{0.2}Gd_{0.8} reach the giant positive values: $\lambda \sim 1 \cdot 10^{-3}$ in magnetic field 10 T and $\lambda \sim 0.3 \cdot 10^{-3}$ in magnetic field 2 T. The experimental magnetic field dependences of λ_{cc} , λ_{bc} , ω_c and ω_b magnetostrictions show an abrupt increase in the area of the magnetic phase transition without saturation. These results suggest that we observe a giant forced magnetostriction. The high values of the volume magnetostriction $\sim 200 \cdot 10^{-6}$ remain also in weak magnetic fields near room temperatures. The results obtained indicate that Tb_{0.2}Gd_{0.8} alloy can be used in new hydraulic devices.

This work is supported by: RFBR grants #16-02-00472 and #16-52-00223; NCN grant, SONATA program (2016/21/D/ST3/03435); ERA.Net RUS Plus project #146 MAGNES.

[1] S.A. Nikitin, Magnetic Properties of Rare Earth Metals and Alloys (Moscow University, Moscow, 1989, in Russian).

[2] K.P. Belov, Magnetostriction Phenomena and Their Technical Applications (Nauka, Moscow, 1987, in Russian).

4PO-I1-18

EFFECT OF AGEING ON THE MAGNETIC PROPERTIES OF RAPIDLY QUENCHED Nd-rich Nd-Fe ALLOYS

Wiafe-Akenteng D.¹, Menushenkov V.P.¹, Shchetinin I.V.¹, Savchenko A.G.¹

¹ National University of Science and Technology «MISiS», Leninskiy pr. 4, Moscow, Russia
nanaortchere1@gmail.com

The interest in the study of the Fe-Nd alloys was renewed during the last decades owing to the important role Nd-rich intergranular phase plays in the formation of high coercivity of sintered Nd-Fe-B-based magnets. High coercivity values of as-cast Nd-rich Fe-Nd alloys were correlated to a metastable eutectic microstructure which includes hard magnetic phase (A_x) with unidentified structure and composition [1]. The formation mechanism of A_x magnetic phase during cooling of the Fe-Nd alloys and its structure-property relationship remain unknown yet. Therefore, the aim of this work was to study the effect of ageing temperature on the magnetic properties of the melt-spun Nd-rich Nd-Fe alloys.

The Fe_xNd_{100-x} alloys ($x = 14, 28$) were prepared by melting pure metals of Nd and Fe in an argon arc furnace. The ingots were quenched by melt-spinning with a copper-wheel at a velocity approximately $40 \text{ m}\cdot\text{s}^{-1}$ to prepare ribbons. Magnetic measurements at temperatures 5 K and 300 K were measured using a PPMS EverCool-II magnetometer in a maximum magnetising field of 9T and 5T respectively. The ageing of the ribbons was performed in a vacuum furnace at temperatures ranging from 300–650°C for 30 min. The hysteresis loops in the magnetisation field of 5T and 9T were studied. The temperature dependence of magnetisation on zero-field cooled and field cooled for the aged ribbons were also measured.

The un-aged sample tested under 300 K-5 T gave H_{ci} of least values of 74 and 4 Oe for the ribbons $x = 14$ and 28, respectively (Fig. 1a). Maximum values of 3.1 kOe and 2.6 kOe were received after ageing at 450°C for 30 minutes for ribbons $x = 14$ and 28, respectively. But ageing at temperatures from 500°C and above decreased the H_{ci} , lower than 200 Oe, for both ribbons. At 5K-9T, coercive forces as high as 8.6 and 11,7 kOe were observed for the initial ribbons with $x = 14$ and 28 respectively (Fig. 1b). However, increasing the ageing temperature from 300 to 575°C resulted in the coercive forces of the ribbon $x = 14$ decreasing monotonically from 6,6 to 0,1 kOe. Also, there was also a drastic decrease in the coercive force, from 10.8 kOe to 1.2 kOe, for the ribbon $x = 28$ between 450 °C and 500°C. Zero-field and field cooling characteristics of aged Fe-Nd ribbons were discussed.

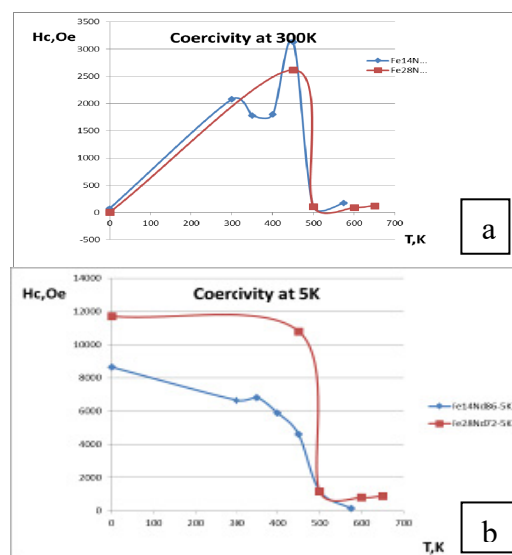


Fig. 1. Coercive force at 300 K (a) and 5K (b) for Fe50Nd50 ribbons vs ageing temperature

This work was supported by the Ministry of Education and Science of the Russian Federation (agreement no. 14.587.21.0028, unique number of project RFMEFI58716X0028).

[1] V.P. Menushenkov, I.V. Shchetinin, M.V. Gorshenkov, A.G. Savchenko, S.V. Ketov, *IEEE Magn. Lett.*, **7** (2016) 5201304.

4PO-II-19

RESONANT INTERACTION OF MAGNETIC BREATHERS AND DOMAIN WALLS IN MULTILAYER FERROMAGNETIC STRUCTURES

Ekomasov E.G., Gumerov A.M., Kudryavtsev R.V., Abakumova N.N.

Department of Theoretical Physics, Physical-Technical Institute, Bashkir State University, 450074,
Ufa, Russia
abakumovan@rambler.ru

Multilayer magnetic structures have been widely studied recently in connection with the opportunity of their practical application. Frequently, these are periodically alternating layers of two materials with different physical properties. The dynamics of spin waves [1] and magnetic inhomogeneities [2] that are extended in such systems in directions perpendicular to the layer interfaces are studied intensely at present. Note that, frequently, the study of one-dimensional models makes it possible to understand the influence of various magnetic parameters. It has been shown [3,4] that the presence of a thin layer with the magnetic anisotropy and exchange parameters, smaller than those in the adjacent layers, can lead to new dynamic effects, e.g., the appearance of a nucleus of a new magnetic phase or the reflection of a moving domain wall (DW) from the attracting potential. In this work, we have studied the effect of spatial modulation of the parameters of magnetic anisotropy, exchange and damping on the nonlinear resonant dynamics of DWs in a three-, five- and N-layered ferromagnetic with allowance for the opportunity of the excitation of localized magnetic inhomogeneities, internal modes of DW oscillations, and the emission of bulk spin waves.

Using as an example the case with two thin layers in a five-layered ferromagnetic we showed that the collective effects of the layers influence on the DW dynamics are largely connected with the resonant energy exchange between the localized waves. The presence of a critical distance is discovered between the thin layers separating the two regions with qualitatively different system behavior. The possibility of the existence of a settings range, in which to pass through both layers of a DW requires significantly less energy, is proved. We demonstrated that damping and external force counteract the onset of the DW resonant reflection from the attracting thin layer, but its initiating cause – resonant energy exchange between the localized waves still takes place. For the experimental observation of the reflections and DW quazitunneling resonance effects in real physical experiments, we suggested a method of measuring the amplitude of the DW center oscillations, and the use of physical systems with sufficiently weak damping.

[1] V.A. Ignatchenko, D.S. Tsikalov, *Solid State Phenomena*, **190** (2012) 71-74.

[2] E.G. Ekomasov, R.R. Murtazin, V.N. Nazarov, *J. Magn. Magn. Mater.*, **385** (2015) 217–221.

[3] E.G. Ekomasov, A.M. Gumerov, R.V. Kudryavtsev, *JETP Letters*, **101**(12) (2015) 835–839.

[4] E.G. Ekomasov, R.R. Murtazin, O.B. Bogomazova, V.N. Nazarov, *Materials Science Forum*, **845** (2016) 195–198.

4PO-I1-20

COMPETING ANISOTROPY IN THE $(\text{Tm}_x\text{Pr}_{1-x})_2\text{Fe}_{17}$ SYSTEM

Platonov S.P.¹, Kuchin A.G.¹, Volegov A.S.², Korolev A.V.¹, Neznakhin D.S.², Voronin V.I.¹, Proskurnina N.V.¹, Kolodkin D.A.¹

¹ M.N. Miheev Institute of Metal Physics UB RAS, Ekaterinburg, Russia

² Institute of Natural Sciences and Mathematics, Ural Federal University, Ekaterinburg, Russia
platonov@imp.uran.ru

The $\text{Pr}_2\text{Fe}_{17}$ and $\text{Tm}_2\text{Fe}_{17}$ compounds exhibit different crystal structures and parallel or antiparallel coupling between the moments of the Pr- or Tm - and the Fe-sublattices, respectively. The $\text{Pr}_2\text{Fe}_{17}$ compound crystallizes in the rhombohedral lattice of the $\text{Th}_2\text{Zn}_{17}$ -type. The $\text{Tm}_2\text{Fe}_{17}$ crystal structure of the $\text{LuFe}_{9.5}$ -type [1] is a disordered variant of ideal hexagonal structure of the $\text{Th}_2\text{Ni}_{17}$ -type and is able to contain more Fe-atoms per R-atom. Ferromagnetic $\text{Pr}_2\text{Fe}_{17}$ is easily magnetized in the basal plane. $\text{Tm}_2\text{Fe}_{17}$ is unique among the R_2Fe_{17} compounds in being an easy-axis ferrimagnet below 77 K; at higher temperatures, the magnetization vector lies in the basal plane, and at 234 K a ferrimagnet transforms to a helimagnet. The temperatures of magnetic ordering equals to 284 K for $\text{Pr}_2\text{Fe}_{17}$ and 274 K for $\text{Tm}_2\text{Fe}_{17}$. So, the properties of the $\text{Pr}_2\text{Fe}_{17}$ and $\text{Tm}_2\text{Fe}_{17}$ binary compounds are rather different, and their solid solution $(\text{Tm}_x\text{Pr}_{1-x})_2\text{Fe}_{17}$ gives a possibility to study change of their magnetic states, magnetic properties, easy-axis orientation and corresponding crystal structures.

It is obtained that the structures of the $\text{Th}_2\text{Zn}_{17}$ -type and of the $\text{Th}_2\text{Ni}_{17}$ -type coexist in the alloys with $x = 0.5-0.75$. The magnetization parallel or perpendicular to the c -axis of the magnetically aligned powder samples was measured at 4 K on SQUID magnetometer. The results for the single-phase compositions of $\text{Th}_2\text{Zn}_{17}$ - or $\text{Th}_2\text{Ni}_{17}$ -type are shown in Fig. 1. Both $\text{Pr}_2\text{Fe}_{17}$ and $\text{Tm}_2\text{Fe}_{17}$ binaries are characterized by FOMP (first order magnetization process) along c -axis and in basal plane, respectively. The FOMP keeps in the neighbors $x=0.2, 0.8$ with somewhat lower critical fields. The magnetization anisotropy in $\text{Tm}_2\text{Fe}_{17}$ decreases when Tm is substituted by Pr. The easy-axis orientation changes in the $(\text{Tm}_x\text{Pr}_{1-x})_2\text{Fe}_{17}$ system with composition variation in accordance with content of $\text{Th}_2\text{Zn}_{17}$ - and $\text{Th}_2\text{Ni}_{17}$ -type lattices in the two-phases compounds.

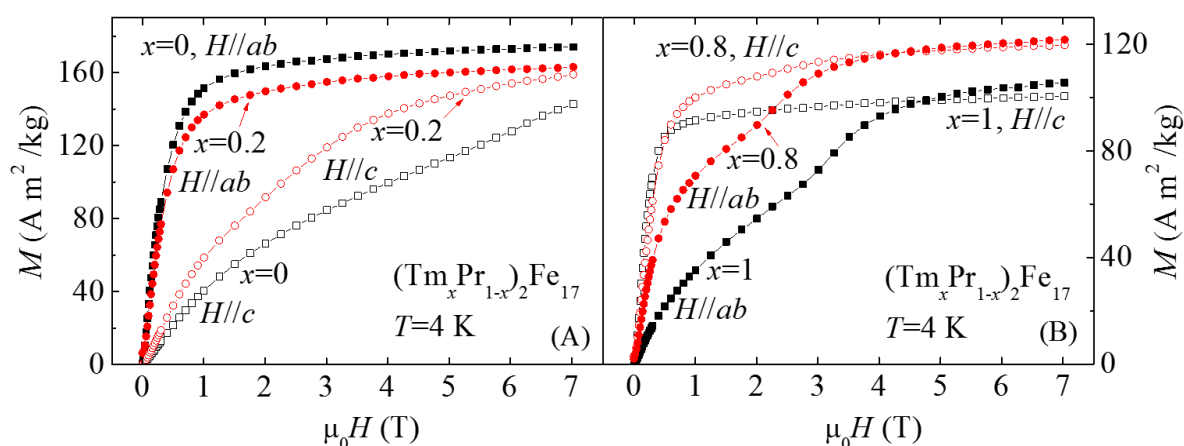


Fig. 1. Magnetization curves of the $(\text{Tm}_x\text{Pr}_{1-x})_2\text{Fe}_{17}$ aligned powder samples, $x=0, 0.2$ (A) and $x=0.8, 1$ (B), measured along the ab -plane and c -axis at $T = 4$ K.

The authors acknowledge a financial support from Project No. 15-12-10015 of RSF.

[1] D. Givord, R. Lemaire et al., *J. Less-Common Met.*, **29** (1972) 361-369.

4PO-I1-21

CRYSTAL STRUCTURE AND MAGNETIC PROPERTIES OF LAYERED COMPOUNDS $\text{Fe}_{2/3}\text{Ti}(\text{S},\text{Se})_2$: INFLUENCE OF THE SELENIUM FOR SULFUR SUBSTITUTION

Selezneva N.V.¹, Sherokalova E.M.¹, Baglaeva J.A.¹, Volegov A.S.¹, Baranov N.V.^{1,2}

¹ Institute of Natural Sciences and Mathematics, Ural Federal University, Ekaterinburg, Russia

² Institute of Metal Physics, Russian Academy of Science, Ekaterinburg, Russia

hope_s@mail.ru

Dichalcogenides of transition metals Fe_yTX_2 ($T = \text{Ti, Nb, Ta}$; $X = \text{S, Se}$) intercalated with Fe atoms exhibit a long-range magnetic order at high Fe concentrations ($y \geq 0.25$) [1]. Occupation of vacant octahedral sites between X-T-X tri-layers upon Fe intercalation results in a large variety of structures ranging between CdI_2 and NiAs structure types. The compounds $\text{Fe}_{0.5}\text{TiS}_2$ and $\text{Fe}_{0.5}\text{TiSe}_2$ have the monoclinic crystal structure ($I12/m$ space group) and show an antiferromagnetic behavior [2]. The substitution of Se for S in $\text{Fe}_{0.5}\text{TiS}_{2-x}\text{Se}_x$ expands the crystal lattice and leads to changes in the periodicity of the arrangement of Fe magnetic moments at low temperatures from quadruplicated (at $x < 0.5$) to doubled (at $x > 0.5$) magnetic unit cell along the a and c axes in respect to the crystal lattice [2].

In the present work, the compounds $\text{Fe}_{2/3}\text{TiS}_{2-x}\text{Se}_x$ ($x = 0 - 2$) have been synthesized and studied by means of X-ray diffraction, magnetic susceptibility, magnetization, electrical resistivity, magnetoresistance measurements in order to reveal the effect of the selenium for sulfur substitution on the crystal structure and magnetic orderings and transport properties of highly intercalated compounds.

The $\text{Fe}_{2/3}\text{TiS}_{2-x}\text{Se}_x$ compounds with Se concentration $x < 0.5$ show a magnetization (see Fig. 1) behavior characteristic for ferromagnetic or ferrimagnetic materials with $T_c \sim 150$ K and with a high magnetocrystalline anisotropy and a large value of the coercive field (H_c up to ~ 25 kOe). The growth of the Se content above $x = 1$ leads to an antiferromagnetic behavior; while, the magnetic state within concentration interval $0.5 < x < 1$ seems to be non-homogeneous. The electrical resistivity shows an anomalous growth with cooling below magnetic ordering temperature.

The results obtained allow us to suggest that the magnetic and transport properties of $\text{Fe}_{2/3}\text{TiS}_{2-x}\text{Se}_x$ compounds are affected by the distribution of Fe atoms and vacancies in the cationic layers together with intercalant concentration and S-Se substitution.

This work was supported by the Ministry of Education and Science of Russia (project No 3.2916.2017).

[1] M. Inoue, H. Hughes, A. Yoffe, *Adv. Phys.*, **38** (1989) 565–604.

[2] A. Gubkin, E. Sherokalova, L. Keller, N. Selezneva, A. Proshkin, E. Proskurina, and N. Baranov, *J. Alloys Compd.*, **616** (2014) 148.

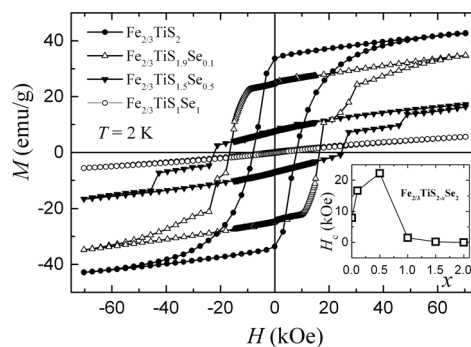


Fig. 1. Field dependences of the magnetization of $\text{Fe}_{2/3}\text{TiS}_{2-x}\text{Se}_x$ measured at $T=2$ K. Insets show the concentration dependence of the coercive field.

4PO-I1-22

MAGNETIC PROPERTIES AND STRUCTURE OF THE MELT SPUN (Sm_{1-x}Zr_x)(Fe_{0.92}Ti_{0.08})₁₀ ALLOYS

Popov A.G.^{1,2}, Protasov A.V.^{1,2}, Gaviko V.S.^{1,2}, Kolodkin D.A.¹, Terentev P.B.^{1,2}

¹ IMP UB RAS, Ekaterinburg, Russian Federation

² UrFU, Ekaterinburg, Russian Federation

protasov@imp.uran.ru

Compounds with R_nFe_m compositions and their nitrides (SmFe₁₁Ti, SmFe₉N_x, NdFe₁₁TiN_x) are interesting possibilities for future permanent magnet materials. Recently was shown that Zr substitution at Sm sites stabilized the ThMn₁₂ structure in (Sm_{0.8}Zr_{0.2})(Fe_{0.75}Co_{0.25})_{11.5}Ti_{0.5} compound [1]. It has saturation magnetization $J_s = 1.63$ T, the Curie temperature $T_C = 880$ K and evaluated anisotropy field $H_a = 5.90$ MA/m. Those values are notably higher than ones for the Nd₂Fe₁₄B compound. To evaluate hysteresis properties of the Zr-substituted alloys with ThMn₁₂ structure we investigated magnetic properties and structure of melt spun Sm-Zr-Fe-Ti and Sm-Zr-Fe-Co-Ti alloys and their hydrides.

Alloys with composition of (Sm_{1-x}Zr_x)(Fe_{0.92}Ti_{0.08})₁₀ (0 ≤ x ≤ 0.3) and (Sm_{0.8}Zr_{0.2})(Fe_{0.75}Co_{0.25})_{11.5}Ti_{0.5} were prepared by induction melting in Ar atmosphere. Melt-spinning was done in argon by ejecting the inductively melted alloys onto a rotating copper wheel at a surface velocity of 30 m/s. The melt-spun “ribbons” were annealed in Ar atmosphere at 700-900 °C for 10 min. Some of the “ribbons” were hydrogenated at 200 °C the same temperature under a hydrogen pressure of 3 × 10⁵ Pa for 2 h. Powder X-ray diffraction (XRD) characterization was performed with a multifunctional Empyrean (PANanalytical) diffractometer using the CuKα radiation. The magnetization measurements were done with a Lake Shore vibrating sample magnetometer (maximum field 17.5 kOe).

As-spun (Sm_{1-x}Zr_x)(Fe_{0.92}Ti_{0.08})₁₀ ribbons were found to consist of a mixture of amorphous and TbCu-type disordered phases at x < 0.2. Only amorphous phase was detected in the ribbons with x ≥ 0.2. After annealing all ribbons were contain the tetragonal ThMn₁₂-type phase and some α-Fe. Figure 1 shows magnetic properties of the (Sm_{1-x}Zr_x)(Fe_{0.92}Ti_{0.08})₁₀ ribbons vs Zr content and annealing temperature. Coercivity decreased, and a specific magnetization σ_{16} , measured in magnetic field 16 kOe, increased with increasing Zr content and decreasing annealing temperature. After hydrogenation the coercivity of all annealed ribbons was increased by 40–60%.

The annealed at 850 °C the ribbons of (Sm_{0.8}Zr_{0.2})(Fe_{0.75}Co_{0.25})_{11.5}Ti_{0.5} alloy have σ_{16} as high as 161 emu/g and only $H_c = 1.1$ kOe.

The research was carried out within the state assignment of FASO of Russia (theme “Magnet” No. 01201463328) and partially supported by the Ural Branch of the RAS (project No. 15-9-2-19).

[1] T. Kuno, S. Suzuki, K. Urushibata, K. Kobayashi, N. Sakuma, M. Yano, A. Kato, A. Manabe, AIP Advances, 6 (2016) 025221.

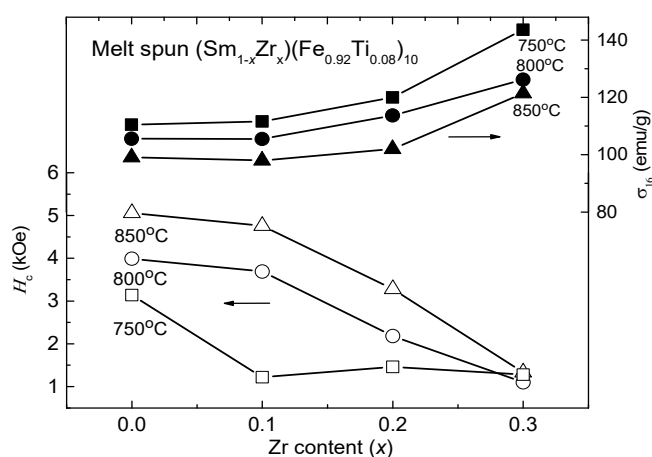


Fig. 1. Magnetic properties of the (Sm_{1-x}Zr_x)(Fe_{0.92}Ti_{0.08})₁₀ ribbons vs Zr content and annealing temperature.

4PO-I1-23

FRUSTRATED STATE OF Tb IN LAYERED $\text{La}_{1-x}\text{Tb}_x\text{Mn}_2\text{Si}_2$ COMPOUNDS

Gerasimov E.G.^{1,2}, *Mushnikov N.V.*^{1,2}, *Pirogov A.N.*^{1,2}, *Yazovskikh K.A.*¹

¹ Institute of Metal Physics UB RAS, Ekaterinburg, Russia

² Ural Federal University, Ekaterinburg, Russia

gerasimov@imp.uran.ru

The compounds RM_2X_2 (R is a rare earth element) for $M = \text{Mn}$ with natural multilayer structure attract the greatest attention since they demonstrate a wide variety of magnetic structures and magnetic phase transitions. One reason of the transitions is existence of a strong unusual dependence of the type of interlayer Mn-Mn ordering on the lattice parameters and on the in-plane Mn-Mn distance. Another reason of the transitions is a competition between the interlayer Mn-Mn, R -Mn and R - R exchange interactions. In the quasi-ternary $\text{La}_{1-x}\text{Tb}_x\text{Mn}_2\text{Si}_2$ compounds, increase of the terbium content leads to a gradual change of the intralayer Mn-Mn distance, and simultaneously enhance both the Tb-Mn and Tb-Tb exchange interactions [1].

In this work we present investigation of magnetic structures and properties of $\text{La}_{1-x}\text{Tb}_x\text{Mn}_2\text{Si}_2$ ($0 \leq x \leq 1$) quasi-single- and polycrystalline samples by magnetic methods and neutron diffraction.

Six various magnetic structures are defined in the $\text{La}_{1-x}\text{Tb}_x\text{Mn}_2\text{Si}_2$ compounds at different concentrations and temperatures. At temperatures above T_R when the rare-earth sublattice is in paramagnetic state, with increasing concentration $x > 0.2$ there appears the change of the type of interlayer Mn-Mn ordering from ferromagnetic (F) to antiferromagnetic (AF) due to the decrease of the in-plane Mn-Mn distance below its critical value. For the low-temperature region below T_R , gradual strengthening of negative Tb-Mn interaction with increasing x provides an indirect positive Mn-Tb-Mn interaction, which leads to the reentrant ferromagnetism in compounds with $x > 0.5$ in the Mn sublattice in spite of the in-plane Mn-Mn distance is below its critical value (Fig.1).

The compounds with $x=0.27$ and 0.4 have the antiferromagnetic ordering of the Mn moments and the Tb moments are in the frustrated magnetic state which result in disappearance of long range magnetic ordering in rare-earth sublattice.

To our knowledge, it is the first direct observation of disappearance of the long-range magnetic ordering in rare-earth sublattice in $\text{La}_{1-x}\text{R}_x\text{Mn}_2\text{Si}_2$ compounds due to the competition of interlayer R -Mn and Mn-Mn exchange interactions.

The study has been supported by Russian Science Foundation (project No. 15-12-10015).

[1] E.G. Gerasimov, N.V. Mushnikov, P.B. Terentev, K.A. Yazovskikh, I.S. Titov, V.S. Gaviko, Rie Y. Umetsu, *J. Magn. Magn. Mater.*, **422** (2017) 237-242.

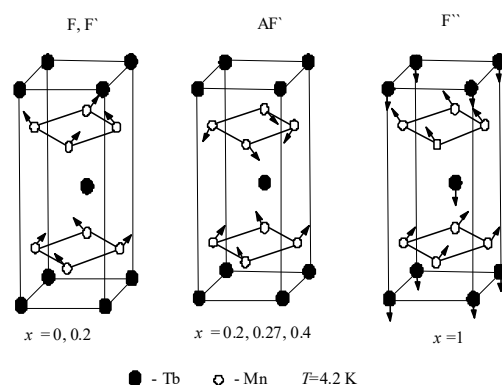


Fig. 1. Magnetic structures of the $\text{La}_{1-x}\text{Tb}_x\text{Mn}_2\text{Si}_2$ compounds at $T=4.2$ K.

4PO-I1-24

CONTROLLED PINNING OF DOMAIN WALLS IN PLANAR FERROMAGNETIC NANOWIRES

Ermolaeva O.L., Mironov V.L.

Institute for physics of microstructures RAS, Nizhny Novgorod, Russian Federation
ermolaeva@ipm.ras.ru

The growing interest to controlled domain wall pinning in ferromagnetic nanowires is stimulated by potential applications of these effects for the development of magnetic logic devices [1,2]. Logic "0" and "1" in such devices are encoded as the magnetization direction of certain parts of the nanowire and logical computation is associated with the processes of motion and pinning/depinning domain wall in an external magnetic field.

Here we present the results of micromagnetic simulations of the domain wall pinning/depinning in two planar ferromagnetic structures. First system contains nanowire and two nanoparticles placed one on either side of the nanowire (fig. 1). The structure consists of two layers of magnetic material separated by nonmagnetic spacer. The second structure consists of multilayer Co/Pt nanowire with perpendicular anisotropy and V-shaped Co nanoparticles with in-plane anisotropy (fig. 2).

The magnetization reversal processes in an external magnetic field were studied by micromagnetic simulation with Object Oriented MicroMagnetic Framework (OOMMF) software [3]. We investigated domain wall pinning/depinning processes in these systems depending on the configuration of magnetic moments in nanoparticle subsystems. Several schemes of magnetic logic cells performing various logic operations in binary and ternary logic are discussed.

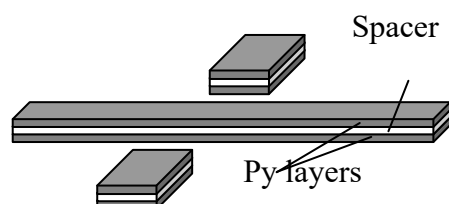


Fig. 1. The multilayer nanowire-nanoparticles system.

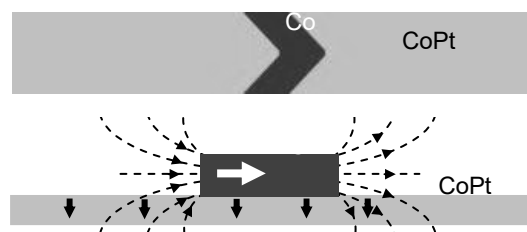


Fig. 2. The system consisting of Co/Pt nanowire and V-shaped Co nanoparticle.

Support by the Russian Foundation for Basic Research (Projects No. 15-02-04462) is acknowledged.

[1] R. A. van Mourik, C. T. Rettner, et al., *J. Appl. Phys.*, **115** (2014) 17D503.

[2] V. L. Mironov, O. L. Ermolaeva, et al., *Phys. Rev. B*, **85** (2012) 144418.

[3] M. J. Donahue and D. G. Porter, "OOMMF User's Guide", Interagency Report NISTIR 6376, (Gaithersburg, MD, 1999) <http://math.nist.gov/oommf>

4PO-J-1

MAGNETIC PROPERTIES OF $\text{Tm}_2\text{Fe}_{16}$ UNDER PRESSURE

Kuchin A.G.¹, Arnold Z.², Kamarád J.², Platonov S.P.¹

¹ M.N. Miheev Institute of Metal Physics UB RAS, Ekaterinburg, Russia

² Institute of Physics AS CR v.v.i., Prague 8, Czech Republic

kuchin@imp.uran.ru

The non-stoichiometric $\text{Tm}_2\text{Fe}_{16}$ compound is a ferrimagnet, whereas the well-known $\text{Tm}_2\text{Fe}_{17}$ compound orders magnetically at the Néel temperature T_N in an incommensurate helimagnetic state and becomes also a ferrimagnet at the transition temperature $\Theta_T < T_N$ [1]. Both these compounds are characterized by spontaneous spin-reorientation transition at $T_{sr} < T_C$ or Θ_T due to the strong competition between the uniaxial magnetic anisotropy of the Tm-subsystem at low T and the planar-type magnetic anisotropy of the Fe-subsystem at high temperatures.

The study of magnetic properties of the $\text{Tm}_2\text{Fe}_{16}$ polycrystalline sample under hydrostatic pressure up to 1 GPa was performed in magnetic fields up to 7 T in the temperature range 5-320 K. The temperature dependences of magnetization $M(T)$ measured in a field of 0.01 T are presented in Fig. 1. The evolutions of T_C , Θ_T , T_N and T_{sr} under pressure determined from the $M(T)$ curves (Fig. 1) are presented in Fig. 2.

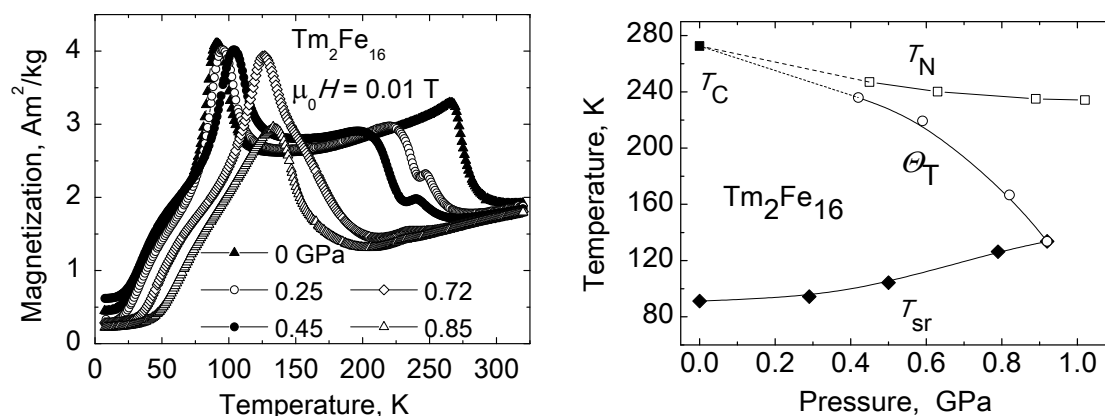


Fig. 1 (on the left). Temperature dependences of magnetization of $\text{Tm}_2\text{Fe}_{16}$ measured in a field of 0.01 T under pressures (right-to-left): 0, 0.25, 0.45, 0.72, 0.85 GPa.

Fig. 2 (on the right). Pressure dependences of T_N (\square), T_C (\blacksquare), Θ_T (\circ), T_{sr} (\blacklozenge) of $\text{Tm}_2\text{Fe}_{16}$.

A transition from paramagnetic to helimagnetic phase at T_N is appeared under pressure 0.25 GPa (Fig. 1). Starting from this pressure, magnetic states in $\text{Tm}_2\text{Fe}_{16}$ becomes the same as in $\text{Tm}_2\text{Fe}_{17}$. An increase of the magnetization at the temperatures below T_N is associated with a transition to a pressure-induced ferrimagnetic phase at Θ_T . In the range $P = 0.25$ - 0.72 GPa, Θ_T characterizes the transition between the pressure-induced high-temperature ferrimagnetic state and the helimagnetic state. Under $P = 0.85$ GPa, the high-temperature ferrimagnetic state disappears, and Θ_T characterizes the transition from the ground ferrimagnetic state easily magnetized along the hexagonal axis to the pressure-induced helimagnet in the basal plane. The ground ferrimagnetic state is preserved under all pressures applied, and T_{sr} grows as pressure increases (Fig. 1) due to the weakening of the planar-type magnetic anisotropy of the Fe-subsystem.

The authors acknowledge support from the Grant Agency of CR (Project No. 15-03777S) for measurements and RSF (Project No. 15-12-10015) for sample preparation and data analysis.

[1] A.G. Kuchin, S.P. Platonov et al., *J. Alloys Compd.*, **599** (2014) 26-31.

4PO-J-2

XMCD CHARACTERIZATION OF MAGNETIC PHASES IN AS-CAST AND RAPIDLY QUENCHED Fe-Nd ALLOYS

Menushenkov V.P.¹, Menushenkov A.P.², Shchetinin I.V.¹, Wilhelm F.³, Ivanov A.A.², Rudnev I.A.², Ivanov V.G.², Rogalev A.³, Savchenko A.G.¹, Zhukov D.G.¹, Rafalskiy A.V.¹, Ketov S.V.⁴

¹ National University of Science and Technology "MISIS", Moscow, RF

² National Research Nuclear University MEPhI, Moscow, RF

³ European Synchrotron Radiation Facility (ESRF), F-38043 Grenoble Cedex 9, France

⁴ WPI-Advanced Institute for Materials Research, Tohoku University, Japan

menushenkov@gmail.com

The large coercivity ($H_{ci} \approx 4200$ kA/m at 20 K) in rapidly quenched Fe-Nd alloys results from different nonequilibrium hard magnetic phases in amorphous or partially crystalline Fe-Nd matrix. The study of magnetization of these alloys is complicated due to the presence of several phases observed by SEM and TEM: primary Nd or Nd_2Fe_{17} phase, Nd and hard A_x phases as part of eutectic structure. X-ray magnetic circular dichroism (XMCD) technique gives possibility to separate the contribution of Nd and Fe-Nd phases in magnetic behavior of the Fe-Nd alloys. The aim of work is to characterize the magnetic phases in Fe-Nd alloys by XMCD and to distinguish their contribution in magnetization process.

The as-cast Fe-Nd alloys were prepared by melting pure metals in an argon-arc furnace. The ingots were quenched by melt-spinning to prepare ribbons. The XMCD studies were performed at the ID12 beamline of the European Synchrotron Radiation Facility (ESRF), Grenoble, France. The XMCD spectra were obtained as a direct difference between consecutive XANES spectra recorded with two opposite helicities of the incoming X-ray beam. The XMCD magnetization loops were measured at 5-350 K in magnetic fields up/down to 17 T. For that, the energy of X-ray monochromator was tuned to the main maxima of XMCD spectra at either K -Fe or L_2 -Nd absorption edges. The element selective magnetization loops were compared with macroscopic ones measured using a PPMS EverCool-II magnetometer.

For the as-cast $Fe_{14}Nd_{86}$ (Fig. 1a) the XMCD loop at K -Fe edge is characterized by low saturation and high $H_{ci} \approx 4,8$ T. This loop describes the magnetization changes of high anisotropic Fe-rich A_x phase at 5 K, which has only $H_{ci} \approx 0,45$ T at 300 K. The narrow XMCD loop at L_2 -Nd edge is not saturated in 17 T. This loop is a sum of contributions of the hard A_x phase and soft Nd (primary and eutectic), which is ferromagnetic lower 35 K.

For the $Fe_{50}Nd_{50}$ ribbon (Fig. 1b) the XMCD loop at K -Fe edge describes the magnetization changes of hard Fe-rich phase with high $H_{ci} \approx 2,4$ T. The XMCD loop at L_2 -Nd edge with $H_{ci} \approx 1,9$ T is the sum of contributions from hard Fe-rich phase ($H_{ci} \approx 2,4$ T) and middle hard Nd-Fe matrix phase ($H_{ci} \approx 1,3$ T). For both samples, the macroscopic loops normalized to the saturation of the XMCD L_2 -Nd loops show the higher H_{ci} in compare with XMCD loops.

This work was supported by the Ministry of Education and Science of the Russian Federation (agreement no. 14.587.21.0028, unique number of project RFMEFI58716X0028).

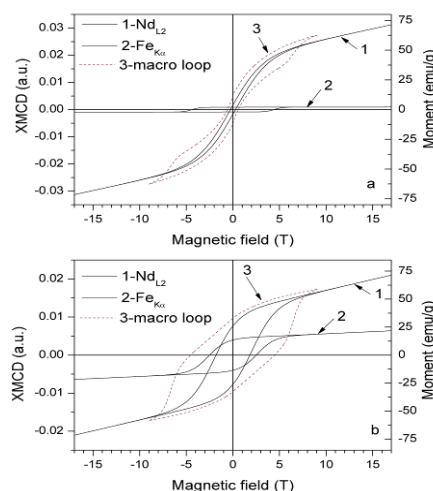


Fig. 1. Hysteresis loops at 5 K for $Fe_{14}Nd_{86}$ and $Fe_{50}Nd_{50}$ ribbon: macroscopic (3), XMCD at L_2 -Nd (1) and K -Fe (2) edges

4PO-J-3

MAGNETIC AND STRUCTURAL PROPERTIES OF Zr-Co THIN GETTER FILMS

Moulin J., Lemettre S., Bosseboeuf A.

C2N, CNRS/Univ. Paris Sud/Univ. Paris Saclay, Orsay, France

johan.moulin@u-psud.fr

Magnetic properties of Co-rich Zr-Co alloys have been extensively studied both for their softness in the amorphous state [1] or their hardness to replace rare-earth permanent magnet [2]. In parallel, Zr-rich Zr-Co are known to present high gettering ability, especially with oxygen, due to the reactivity of zirconium after thermal activation. They present high potentiality as thin getter films for vacuum packaging of MEMS. In this work thin films of Zr-Co have been evaporated in UHV then magnetic and getter properties have been studied and compared to microstructural modifications after annealing.

Results show that as deposited $Zr_{100-x}Co_x$ films become ferromagnetic for $x > 65$ with a magnetization increasing linearly with the Co content. This could be attributed to the appearance of the $ZrCo_2$ cubic Laves phase.

The films have been annealed in primary vacuum to study the gettering of oxygen through the oxidation of the film. The increase of the electrical resistivity with the annealing temperature has been showed to be a consistent criteria for the determination of the activation temperature and the estimation of the activation energy linked to diffusion on oxygen in the film [3]. In this study, we show that the annealing of the films at 300°C (below the activation temperature) does not modify the magnetization of the films. However, above 300°C, the magnetic properties change from ferromagnetic to paramagnetic ($Zr_{22}Co_{78}$) or paramagnetic to ferromagnetic or ferromagnetic ($Zr_{52}Co_{48}$ and $Zr_{73}Co_{27}$).

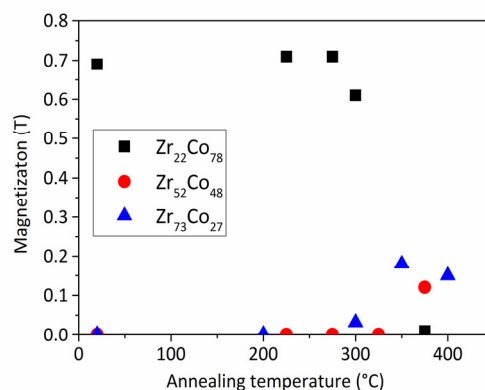


Fig. 1. Magnetization of Zr-Co alloys as a function of the annealing temperature

[1] Y. Shimada and H. Kojima, *J. Appl. Phys.*, **53** (1982) 3156-3160.

[2] G.-T. Lee, K.-W. Moon, K.-W. Jeon and J. Kim, *IEEE Trans. Mag.*, **62(7)** (2016).

[3] M. Wu et al. *Proc. of DTIP of MEMS/MOEMS 2016 conference* (2016).

4PO-J-4

INFLUENCE OF THE STEP ANNEALING ON THE MAGNETIC HYSTERESIS PROPERTIES AND STRUCTURE OF THE $\text{Fe}_{50}\text{Pd}_{50-x}\text{Ni}_x$ ALLOYS ($x = 0, 4, \text{ AND } 8$)

Popov A.G.^{1,2}, Vlasova N.I.¹, Gaviko V.S.^{1,2}, Golovnia O.A.^{1,2}, Tolmachev T.P.

¹ M.N. Miheev Institute of Metal Physics UB RAS, Ekaterinburg, Russia

² Institute of Natural Sciences and Mathematics, Ural Federal University, Ekaterinburg, Russia
golovnya@imp.uran.ru

In our previous work, in order to accelerate the process of ordering, the $\text{Fe}_{50}\text{Pd}_{50-x}\text{Ni}_x$ alloys containing 4 and 8 at % Ni were subjected to deformation by cold rolling and high-pressure torsion with subsequent step annealing in the temperature range from 400 to 500 °C. H_c of the alloys achieved 1191 and 980 Oe, respectively. These values are 1.5 – 2 times higher than the coercivity of the samples not subjected to HPT and exceed the coercivity of the cast alloys by a factor of more than 5. Such investigations have not been carried out for binary alloys. In the work presented the influence of the step annealing on the magnetic hysteresis properties and structure of the $\text{Fe}_{50}\text{Pd}_{50-x}\text{Ni}_x$ alloys ($x = 0, 4, \text{ and } 8$) subjected to HPT is studied.

The $\text{Fe}_{50}\text{Pd}_{50-x}\text{Ni}_x$ ($x = 0 - 8$ at %) alloys were prepared by induction melting. After annealing for disordering at 950°C for 5 h, ingots were subjected to the HPT method at the quasihydrostatic pressure $P = 4 - 6$ GPa and number of revolutions $n = 5 - 10$. To obtain the ordered $L1_0$ structure and high-coercivity state, the samples were annealed stepwise in the temperature range of 400 – 500°C. The crystal structure and phase composition of the deformed and annealed samples were investigated with an Empyrean diffractometer (PANanalytical) using monochromatic Cu $K\alpha$ radiation. The magnetic properties of the samples were investigated using a vibrating sample magnetometer (VSM, Lake Shore). The temperature dependence of the initial ac magnetic susceptibility $\chi(T)$ was measured with a system of compensated pick-up coils in a sinusoidal alternate magnetic field with a frequency of 800 Hz and an amplitude of 10 Oe at a heating rate of 10°C/min. To determine the Curie temperature of the samples the derivatives $d\chi(T)/dT$ were calculated.

Two methods of the heat treatment have been employed. In the first method, we interrupted the isothermal annealing at 500°C at the moment when an increase in coercivity, H_{ci} , slowed. Then the annealing temperature was stepwise decreased to 400°C in increments of 25 °C. In the second method, after isothermal annealing of the samples at an optimal temperature of 450°C, we annealed the samples at 425°C (the second step). The decrease in the annealing temperature substantially increased H_c of the $\text{Fe}_{50}\text{Pd}_{50-x}\text{Ni}_x$ alloys. Relative enhancement of the coercivity $\Delta H_c/H_{ci}$ increases with x . As a result of the step annealing, the H_c values of 1600 Oe, 1600 Oe, and 980 Oe for $x=0, 4, \text{ and } 8$ were achieved. These values exceeded the values of [1].

The research was carried out within the state assignment of FASO of Russia (theme “Magnet” No. 01201463328) and partially supported by the Ural Branch of the RAS (project No. 15-9-2-19). The X-ray investigation and magnetic measurements have been performed in the Collaborative Access Center of IMP UB RAS.

[1] A.G. Popov, N.I. Vlasova, V.S. Gaviko, N.M. Kleinerman, V.V. Serikov, and O.A. Golovnia, *J. Alloys and Compd.*, **701** (2017) 892–900.

4PO-J-5

THE IMPACT OF STRESS ON MAGNETIC PROPERTIES OF FINEMET TYPE AMORPHOUS ALLOYS

Shuvaeva E.¹, Churyukanova M.¹, Hriplevets I.¹, Roy R.K.², Premkumar²

¹ National University of Science and Technology (MISIS), Moscow, Russia

² Insitute of National Metallurgical Laboratory (N.M.L), Jamshedpur, India
shuvea@mail.ru

It is known that magnetic properties of ferromagnetic materials can change under the action of mechanical stresses so greatly that the stress together with magnetic field and temperature should be considered as one of the most important factors influencing on the properties of these materials. The growing attention of investigators to the magnetoelastic properties of amorphous alloys (especially of iron-based) is due to higher values of these properties compared to crystalline alloys. These are caused high values of magnetostriction $\lambda_s (> 10^{-5})$ and high mobility of domain walls [1].

In this paper we investigated the impact of the bending and stretching in the amorphous alloys FineMet type on the level of the magnetic properties.

Bending stresses were induced on circular samples wound on mandrels of different diameters. It was shown that depending on the stress state in the interval of fields from 0 to 500 A/m the investigated alloys are magnetized with different intensities (Fig. 1). Moreover, this effect is observed both under static and dynamic magnetized with the frequency change of the external magnetic fields from 0 to 400 Hz. This effect may be associated with processes underlying the strain-induced magnetization.

Studies of samples of amorphous ribbons and microwires in stretching (from 0 to 1GPa) showed that the magnetization of the sample changes nonlinearly with increasing stress (Fig2).

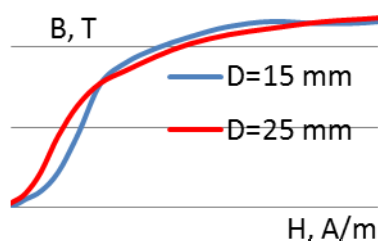


Fig1. The basic curves of magnetization of the glass-coated microwires with FineMet core

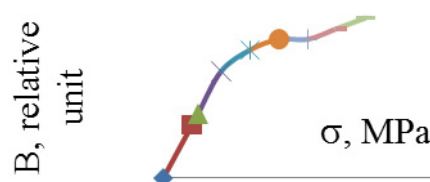


Fig2. Stress dependence of magnetization of amorphous FineMet ribbon

The obtained results partially correlate with the data received in the study of bending stresses. The presence of a difference in changing the level of hysteresis of magnetic properties for different methods of loading due to the fact that a different scheme of the stress state has different influence on the change of the domains structure.

Acknowledgements: Authors acknowledge the Russian Fund for Basic Research (Grant 16-53-48012) for financial support of this work.

[1] Churyukanova M., et. al., *Phys. Status Solidi A*, 2 **213** (2016) 363-367.

4PO-J-6

POLYMER COATING AND MAGNETIC PROPERTIES OF CO-BASED AMORPHOUS ALLOYS

*Skulkina N.A.*¹, *Mazeeva A.K.*², *Ivanov O.A.*¹, *Kuznetsov P.A.*², *Chekis V.I.*¹, *Denisov N.D.*¹

¹ Ural Federal University, 620000, Yekaterinburg, Russia

² FSUE CRISM ‘Prometey’, 191015, St.Petersburg, Russia
nadezhda.skulkina@urfu.ru; nadezhda-skulkina@yandex.ru

Protection of technical and biological objects from the harmful effects of the magnetic and electromagnetic fields is highly relevant. A promising way is to use protective screens made of magnetic amorphous ribbons based on cobalt. For manufacturing magnetic shields a bilateral polymer coating (PC) is used, it also performs a protective function [1]. The polymer coating is formed on the ribbon surface by heating the initial polymer within the temperature range of 90-130 °C in the presence of pressing pressure (PP). Upon cooling of the tape with the polymer coating, shrinkage of the coating occurs, resulting in compressive stresses induced in the plane of the ribbon. Both of these factors (PP and PC) influence the distribution of magnetization and magnetic properties. In the present work the influence of pressing pressure and polymer coating on magnetic properties of Co-Fe-Ni-Cr-Si-B alloy has been investigated. The studies were performed on samples of Co-Fe-Ni-Cr-Si-B alloys with saturation magnetostriction λ_s close to zero. The sample's form was a strip with dimensions 120 x 10 x 0,020 mm. The samples were different from one another by saturation magnetostriction sign. For example after heat treatments (HT) in air at 380 and 370° C for 10 min the state with $\lambda_s < 0$ was formed; and after HT at 380 ° C for 40 min, 360 ° C for 60 min and 350° C for 15 min – $\lambda_s > 0$ [2]. In the as-quenched state is $\lambda_s < 0$. The volume of domains with orthogonal magnetization (V_{ort}) was determined by the correlation between V_{ort} and the maximum residual induction which was found from Mössbauer studies [3]. The analysis of the results showed that the pressing pressure and the polymer coating had opposite effects on the ribbon properties, and the effects of the pressing pressure were partially offset by the coating formation. The influence of the formed polymer coating on the magnetic properties depends on the ribbon state and the saturation magnetostriction sign in this state. Table shows that the pressing pressure leads to an increase in V_{ort} but the formation of the polymer coating contributes to its decline in the state with $\lambda_s < 0$. The stresses induced by the

The ribbon state	V_{ort} , %	The ribbon state	V_{ort} , %
As-quenched			
As-quenched	13,2	PP 90 °C, 7 min	11,4
PP 20 °C, 7 min	15,0	PC 90 °C, 7 min	4,2
HT 370 °C, 10 min			
HT	14,0	PP 90 °C, 7 min	21,5
PP 20 °C, 7 min	18,5	PC 90 °C, 7 min	17,5

polymer coating influence the volume of domains with orthogonal magnetization in the as-quenched state more significantly than in the state after a heat treatment. Amorphous-crystalline layer is formed by the heat treatment on the ribbon surface. The elastic modulus of the surface layer is higher than the one of the amorphous matrix, therefore the ribbon sensitivity to

the surface coating decreases after annealing. The pressing pressure influence on V_{ort} in the ribbon in as-quenched state and after HT is not much different. It is the elasticity modulus of the amorphous matrix which plays the main role in the response of the material to the pressing pressure.

[1] Kuznetsov P.A. et al., Pat. 2274914 Russian Federation MPK G12B 17/02 (2006.01).

[2] N.A. Skulkina et al., *The Physics of Metals and Metallography*, **117** 10 (2016) 982-989.

[3] N.A. Skulkina et al., *Izvestiya Akademii Nauk. Ser. Fizicheskaya*, **65** 10 (2001) 1483-1486.

4PO-J-7

**THE INFLUENCE OF ISOTROPIC COMPOSITIONAL ORDERING ON
HYSTERESIS MAGNETIC PROPERTIES OF Co-BASED AMORPHOUS
ALLOY WITH LOW MAGNETOSTRICTION**

Kekalo I.B., Mogilnikov P.S., Ushakova O.A.

National University of Science and Technology "MISIS", Moscow
pavel_mog@mail.ru

The influences of various types of heat treatment on hysteresis magnetic properties (HMP) of the amorphous alloy $\text{Co}_{69}\text{Fe}_{3.7}\text{Cr}_{3.8}\text{Si}_{12.5}\text{B}_{11}$, after quenching or in preliminary annealed status, were investigated. The formation of HMP plays a major role in the stabilization of domain boundaries (DB) due to the development of the process of directional ordering when the annealing temperature T_a is below the Curie Point T_C (260°C). Preliminary high-temperature annealing at $T_a > T_C$, followed by quenching in water, does not prevent the degradation of the HMP as a result of stabilization of DB (thermally reversible effect). After annealing at $T_a > T_C$, the degradation of the HMP due to the development of clustering process was fixed by the method of Small-angle X-ray scattering. Being irreversible, this type of clustering should not have an effect on the dependence of HMP on T_a when the samples were subjected to preliminary high-temperature treatment. However, the experiments demonstrated that the degradation of the HMP from the temperature of the isochronous annealing at $T_a > T_C$, was distinctly observed like in the original samples before heat treatment. The same degradation is caused by the clustering as a result of the isotropic compositional short-range order, which, by its nature, is a reversible process. This proves that the isotropic composite short-range order can have an effect on the level of HMP of amorphous alloys.

4PO-J-8

MAGNETIC ANISOTROPY OF NANOSTRUCTURED RODS BASED ON ELECTROLESS DEPOSITED 3-d METAL ALLOYS

Denisova E.A.^{1,2}, *Chekanova L.A.*¹, *Komogortsev S.V.*¹, *Nemtsev I.V.*³, *Iskhakov R.S.*¹

¹L.V. Kirensky Institute of Physics FRC KSC SB RAS, Krasnoyarsk, Russian Federation

²Siberian Federal University, Krasnoyarsk, Russian Federation

³Federal Research Center KSC SB RAS, Krasnoyarsk, Russian Federation

len-den@iph.krasn.ru

The current perpendicular to the plane giant magneto-resistance effect makes nano and micro-wires that embedded perpendicular in different porous templates of huge interest as magnetic sensor materials. Magnetic anisotropy determines the frameworks of manipulating the spin-dependent transport in nanowires by the magnetic field. Thus magnetic anisotropy both macroscopic (attributed to whole sample) and microscopic that characterize one crystallite is an important property of template synthesized wires. In this work magnetic anisotropy of the FeNi(P) and Co(P) alloys electroless deposited in the pores of the nuclear track etched polycarbonate membrane (PCTE) has been studied.

The $(\text{Fe}_{100-X}\text{Ni}_X)_{98}(\text{P})_2$ alloy rods with $0 < X < 80$ and the $\text{Co}_{100-Y}(\text{P})_Y$ rods and tubules with $2 < Y < 15$ have been prepared by electroless plating of ferromagnetic metals into linear pores of PCTE membranes with nominal pore sizes 100, 200, and 400 nm. The magnetic and structural properties of the composite materials are characterized by scanning electron microscopy, X-ray diffraction, and vibrating sample magnetometer. Magnetization curves and ferromagnetic resonance spectra are measured as functions of wire material, field orientation, and porous size. Information on local anisotropy field H_a is obtained from investigation of approach magnetization to saturation law. It was found that the local anisotropy field for all Co(P) samples depends on P content. The H_a value increases with a decrease in P content. The increasing of pores size causes a reduction in H_a value. For Co_{92}P_8 rods the local anisotropy field H_a decreases from 2.8 kOe to 1.4 kOe with increasing of nominal pore sizes from 100 nm to 400 nm. The local magnetic anisotropy field of nanocrystalline Fe-Ni(P) rods was evaluated as $1.9 < H_a < 1.2$ kOe. The values of grain size of Fe-Ni(P) alloy only slightly vary with alloy composition (6-8 nm) but crystallite anisotropy is very sensitive to alloy composition.

Magnetization curves of three electroless plated PCTE membrane with the same composition of $\text{Fe}_{90}\text{Ni}_{10}(\text{P})$ alloy but different PCTE membrane pore diameters show different macroscopic magnetic anisotropy. The macroscopic anisotropy is maximal in alloy filled membranes with pore diameter 0.4 μm and its easy magnetization axis is perpendicular to the membrane surface. The energy of macroscopic magnetic anisotropy decreases with decreasing pore diameter. The magnetic anisotropy field for the sample with 0.4 μm pore diameter is close to magnetic shape anisotropy of elongated column πM_s . The easy axis of the Co(P) rods and tubules is along the rods. Hence, the shape anisotropy dominates over the intrinsic magneto crystalline anisotropy.

The FMR spectrum for Co(P) and FeNi(P) rods consists of a single absorption line. It is observed that H_r values for Co(P) rods was determined by phosphorous content and porous size. Resonance field with the applied field along FeNi(P) rods axis is minimal in the sample with 0.4 μm pore diameter and it increases with pore diameter decreasing as it is expected for the above mentioned the macroscopic anisotropy.

Support by by RFBR grants 16-03-00256, 16-03-00969 is acknowledged.

4PO-J-9

DEFORMATION INDUCED MARTENSITE IN DUPLEX STAINLESS STEELS

Ogneva M.S., Rigmant M.B., Davidov D.I., Kazantseva N.V.
 Institute of Metal Physics, Ural Division of RAS, Ekaterinburg, Russia
 ogneva@imp.uran.ru

The properties of the ferrite-austenite materials depend on their structure and phase composition. Percentage of ferritic phase (α -phase) in two-phase, ferritic (α) and austenitic (γ) stainless steel allows us to provide the required level of the exploitation properties. The deformation induced martensite (α' -phase) may form from austenite (γ -phase) under exploitation of the loaded parts of the detail. This additional hard magnetic phase changes all properties of the materials not only magnetic, but electrical and mechanical as well.

The present work aims to trace the association between quantity of the magnetic phase and changing of electric resistivity in the duplex stainless steels.

Seven steel ingots with the different ferrite composition (from 2,8% up to 80%) have been used for study. Samples were prepared by the electrical spark cutting. Measuring of the electric resistivity and magnetic properties was done at room temperature along the rolling direction. Phase composition of the studied samples has been determined by the transmission electron microscope.

Deformation induced martensite (α' -phase) is found after deformation by cold rolling of the pre-hardened in the liquid nitrogen samples. These results are correlated with our previous results [1]. Electric resistivity (ρ) of the initial samples shows the linear dependence on the percentage of the ferritic phase. It is found that the value of the room temperature electrical resistivity increases with the increasing of the quantity of the martensitic phase (Fig.1).

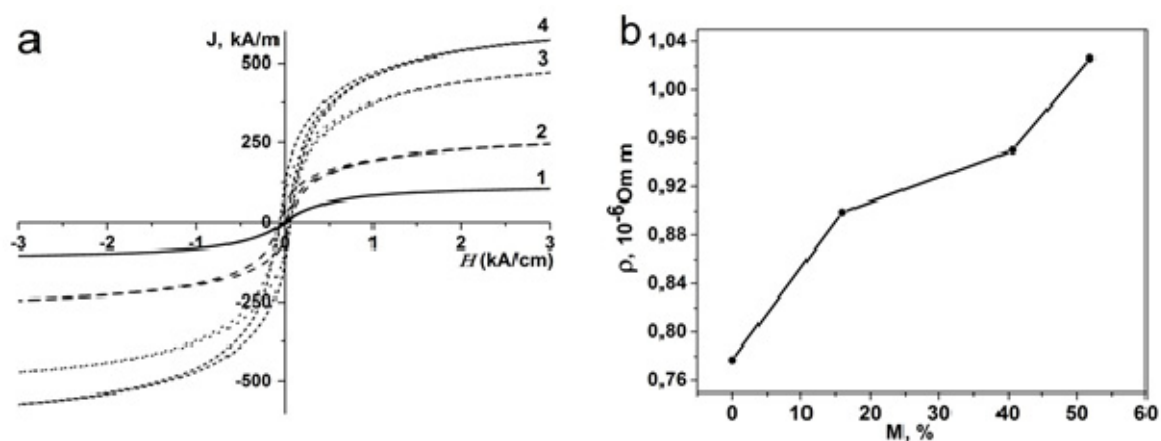


Fig. 1. Results of the magnetic and electric measurements: a – the dependence on the resistivity (ρ) of martensitic content in the sample with 12.1% of ferrite; b – the hysteresis loops of the sample with 12.1% of ferrite after different percent of deformation: 1 – initial, 2 – 10%, 3 – 20%, 4 – 30%.

Research was supported by the Russian Scientific Foundation, project no. 15-12-00001.

[1] M.K. Korkh, Yu.V. Korkh, M.B. Rigmant, N.V. Kazantseva, N.I. Vinogradova, *Russian Journal of Nondestructive Testing*, **52** (2016) 664-672.

4PO-J-10

JUMPWISE DEMAGNETIZATION OF $[\text{Mn(II)(HL)(H}_2\text{O)}][\text{Mn(III)(CN)}_6] \cdot 2\text{H}_2\text{O}$ MOLECULAR FERRIMAGNET

Kirman M.¹, Morgunov R.¹, Vasiliev L.²

¹ ICP RAS, Chernogolovka, Russian Federation

² Lomonosov Moscow State University, Moscow, Russian Federation

kirmanm@yandex.ru

Stochastic magnetization jumps manifested in sweeping and stationary reverse magnetic field were experimentally found in the recent work [1]. Our aim is finding postponed magnetization jumps in molecular ferrimagnet whose structure is similar to the previously studied crystals.

Magnetic jumps were revealed during the magnetization reversal of $[\text{Mn(II)(HL)(H}_2\text{O)}][\text{Mn(III)(CN)}_6] \cdot 2\text{H}_2\text{O}$ molecular ferrimagnet (Fig. 1). Amplitudes of the jumps were 0.01 – 0.1% of the saturation magnetization (M_{SAT}).

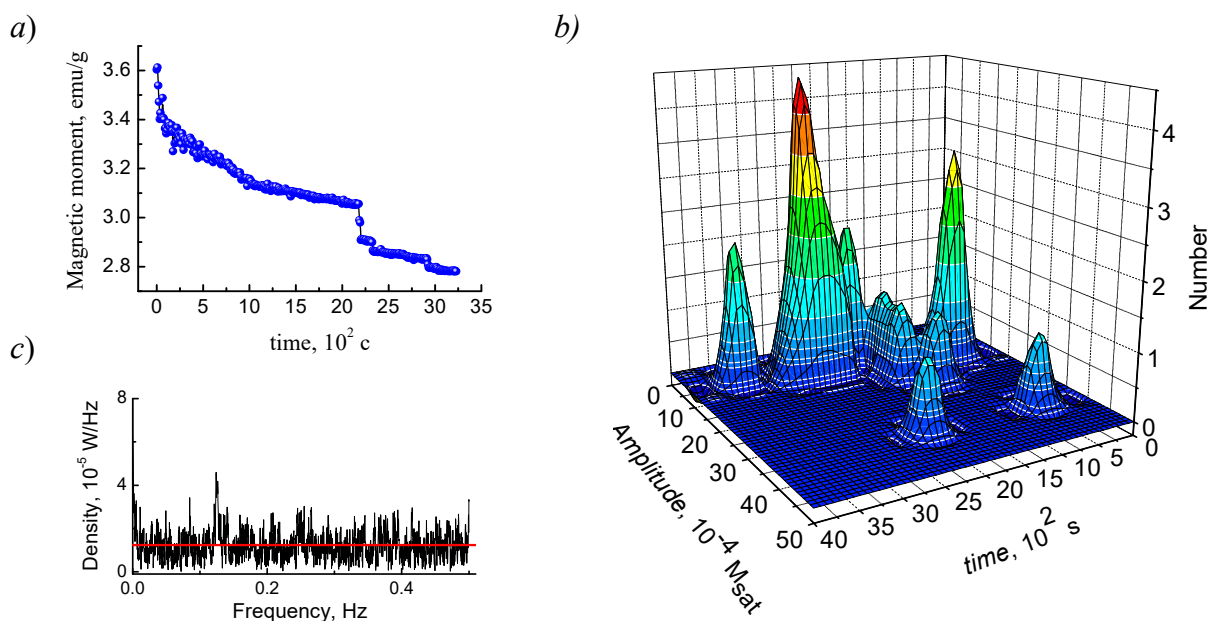


Fig. 1. Time dependence of magnetic moment (a), distribution of amplitude and expectation time of the stochastic magnetization jumps (b), spectral density of the stochastic magnetization jumps (c) in stationary reverse magnetic field $H = -50$ Oe at 10 K. The solid line shows the approximation of spectral density by $(1/f)^\alpha$ function [2], where $\alpha = 0 \pm 0.1$.

Fourier transform of the time series of jumps magnetization indicates, that frequency spectrum is close to the white noise. Amplitude distribution of the jumps versus time reveals domination of the large jumps at the beginning of the demagnetization.

Support by RFBR grant No.15-02-05149-a is acknowledged.

[1] R.B. Morgunov, A.D. Talantsev, *Physical Review B*, **94** (2016) 144421(1-8).

[2] H.D. I. Abarbane, R. Brown, J.J. Sidorowich and L.Sh. Tsimring, *Rev. Mod. Phys.*, **65** (1993) 1331-1392.

4PO-J-11

THE NANOCRYSTALLINE Fe- AND Co-BASED SOFT MAGNETIC ALLOYS WITH REFRACTORY ELEMENTS: PROPERTIES AND THERMAL STABILITY

Lukshina V.A.^{1,2}, Dmitrieva N.V.¹, Filippov B.N.¹, Volkova E.G.¹, Shishkin D.A.^{1,2}, Potapov A.P.¹

¹ Institute of Metal Physics UB RAS, Ekaterinburg, Russia

² Ural Federal University, Ekaterinburg, Russia

lukshina@imp.uran.ru

The soft magnetic alloys (1) - $(\text{Fe}_{0.6}\text{Co}_{0.4})_{86}\text{Hf}_7\text{B}_6\text{Cu}_1$, (2) - $(\text{Fe}_{0.7}\text{Co}_{0.3})_{88}\text{Hf}_7\text{B}_4\text{Cu}_1$, (3) - $(\text{Fe}_{0.7}\text{Co}_{0.3})_{88}\text{Hf}_4\text{Mo}_2\text{Zr}_1\text{B}_4\text{Cu}_1$, (4) - $(\text{Fe}_{0.7}\text{Co}_{0.3})_{88}\text{Hf}_2\text{W}_2\text{Mo}_2\text{Zr}_1\text{B}_4\text{Cu}_1$ with addition of refractory elements were investigated. The alloys were prepared in the form of amorphous ribbons about 20 μm thick and 1 mm wide by melt spinning on a rotating drum. The nanocrystalline state of the alloys samples was created in the course of crystallization in air at different temperatures and holdings in the presence or absence of tensile stresses or alternative magnetic field. Structure, magnetic properties, and thermal stability of the alloys were studied and compared to determine optimal crystallization conditions.

The structure of the alloys was studied by transmission electron microscopy (TEM) using a JEM 200CX electron microscope. The magnetic state of the ribbons was studied via hysteresis loops, which were measured in an open magnetic circuit of a galvanometric compensated microfluxmeter. The hysteresis loops were measured in fields up to 8000 A/m.

It was found that after annealing for nanocrystallization (NA) the Fe-Co-based BCC solid solution and residual amorphous matrix were the main phases in all the alloys.

In alloys (1) and (2) after NA (520-600°C) the average size of grains was 5 nm, which provided the low coercive force $H_c=20$ A/m and $B_r/B_m=0.70-0.75$. In the course of NA at 620°C and higher in the structure of the alloys there appeared oxides Fe_2O_3 and HfO_2 which resulted in the tenfold increase of H_c .

In alloys (3) and (4) the oxides did not form due to presence of Mo. The average size of grain in alloy (3) was 10-11 nm. Addition of W instead of Hf (2%) decreased the average size of grains in alloy (4) up to 4 nm. In both the alloys individual large grains were present which resulted in increase of H_c up to 200-300 A/m and decrease of B_r/B_m up to 0.4-0.2.

For all alloys, it was obtained that due to crystallization in the presence of tensile stresses (stress-annealing, SA, 6-250 MPa) or alternative magnetic field (field-annealing, FA, the amplitude of magnetic field H_{amp} was up to 9 kA/m) the coercive force could decrease several fold, and residual magnetization could noticeably increase.

The thermal stability of the magnetic properties of the samples subjected to NA, SA, or FA was estimated by the change in the magnetic properties after subsequent exposures at 500–600°C without any external action compared to those measured directly after NA, SA, or FA.

It is shown, that magnetic properties of all alloys after SA have the best thermal stability compared to the specimens of all alloys after NA, or FA.

It is obtained that the magnetic properties of alloys (1) and (2) determined at room temperature are not destroyed upon heating up to 500 °C. $T=550$ °C is the temperature of the stability for alloy (3). The composition of alloy (4) provides the stability of its magnetic properties up to 570 °C [1].

Support by FASO of Russia (theme “Magnet” no. 01201463328) and in part by Ural Branch of RAS (project no. 15-9-2-33) is acknowledged.

[1] N.V. Dmitrieva et al, *Physics of Metals and Metallography*, **116**(3) (2015) 248–255.

4PO-J-12

EXCHANGE SPRING MAGNET IN NANOCOMPOSITE OF STRONTIUM FERRITE/NICKEL FERRITE

*Ghasemi A.*¹, *Ashrafi-zadeh A.*²

¹ Department of Materials, Malek Ashtar University of Technology, Shahin Shahr, Iran

² Steel Institute, Isfahan University of Technology, Isfahan, Iran

A series of $\text{SrFe}_{10}\text{Al}_2\text{O}_{19}/\text{NiFe}_2\text{O}_4$ hard/soft nanocomposite ferrites with various weight percent of soft phase have been successfully synthesized via simple one-pot sol gel auto-combustion. XRD patterns confirmed the coexistence of two hard and soft phases together with no detectable unwanted phase. The FE-SEM micrographs of nanocomposites showed homogenous formation of two phases with narrow particle size distribution especially for low fraction of soft phase below 30 wt. % in the composite. Structural analysis showed high level of homogenous mixing of the hard and soft ferrite phase is achievable through one-pot sol gel auto-combustion method due to simultaneously growth of these phases from a single reaction mixture. The magnetic data reveal that existence of exchange coupling between hard and soft phase for nanocomposites synthesized by one-pot method, as they exhibited a single smooth hysteresis loop. However, composites prepared by physical mixing method, showed a typical two loop “bee waist”-type hysteresis loop, suggesting the absence of the exchange couple between the hard and soft phase. A linear increment of M_r/M_s ratio with soft phase content up to 15 wt. % for nanocomposites derived from one-pot method indicating the highest exchange coupling in this sample. But for higher soft phase content and also for composites obtained from physical mixing method, this ratio decreases and show the exchange coupling between hard and soft phase is not fully realized. A continuous reduction of coercivity through soft phase increment was due to dominance of dipolar interaction in soft phase over exchange interaction between hard-soft phases of the nanocomposites. The one-pot sol gel auto-combustion method seems to be a simple but powerful route for fabrication of hard/soft ferrite nanocomposites with good controllable on magnetic properties.

4PO-J-13

MONTE CARLO STUDY OF MAGNETIC STRUCTURES IN RARE-EARTH AMORPHOUS ALLOYS

Bondarev A.V., Bataronov I.L.

Voronezh State Technical University, Voronezh, Russia
bondarev_a_v@mail.ru

Amorphous alloys based on rare-earth metals are of great interest due to their unique magnetic properties. In this work we report on the Monte Carlo simulation of magnetic properties of binary amorphous alloys of rare-earth metals with nonmagnetic 5d-transition metal (rhenium) which are not studied so far.

Using the Monte Carlo method in the frame of the Heisenberg model, the computer simulation of magnetic properties of Re-Tb and Re-Gd amorphous alloys was performed.

For pure amorphous Tb and Re-Tb amorphous alloys, the model Hamiltonian contained two terms responsible for nearest-neighbour exchange interaction between the Tb ions with the mean value J_0 and for random single-ion anisotropy D . For pure amorphous Tb the dependence of the temperature of the spin-glass-like transition T_f on the D/J_0 ratio was calculated. Thus, the magnetic phase diagram for an amorphous magnet with random anisotropy in the $D/J_0 - T$ coordinates was constructed.

In the models of the Re-Tb amorphous alloys, the spin-glass-like phase transition was also observed. With increasing concentration of Tb atoms, the transition temperature linearly increases, which is in a good agreement with the experimental results. The spin-glass transition is observed only above the percolation threshold in this system, i.e. at $x > 13$ at. % Tb.

For pure amorphous Gd and Re-Gd amorphous alloys, the model Hamiltonian contained two terms responsible for ferromagnetic exchange interaction J_1 between the nearest-neighbour Gd ions and for antiferromagnetic exchange interaction J_2 between the Gd ions in the second coordination sphere. For pure amorphous Gd the dependence of the spin-glass transition temperature T_f on the J_1/J_2 ratio was calculated. Thus, the magnetic phase diagram for an amorphous magnet with competition of exchange interactions of different signs in the $J_1/J_2 - T$ coordinates was constructed.

In the models of the Re-Gd amorphous alloys, the spin-glass phase transition was also observed. With increasing concentration of Gd atoms, the spin-glass transition temperature linearly increases, which is in a good agreement with the experimental results.

Magnetic structure of Re-Tb and Re-Gd amorphous alloys was studied on the microscopic level with the use of spin-spin correlation functions and angle spin correlation functions. The difference between magnetic structures of the spin glasses with random anisotropy and with competition of exchange interactions was revealed.

4PO-J-14

FLUX CRYSTAL GROWTH AND THE ELECTRONIC STRUCTURE OF BAFE12O19 HEXAFERRITE

Atuchin V.V.^{1,2}, Vinnik D.A.³, Gavrilova T.A.¹, Gudkova S.A.³, Isaenko L.I.², Jiang X.⁴, Pokrovsky L.D.¹, Prosvirin I.P.⁵, Mashkovtseva L.S.³, Lin Z.⁴

¹ Institute of Semiconductor Physics, SB RAS, Novosibirsk, Russia

² Novosibirsk State University, Novosibirsk, Russia

³ South Ural State University, Chelyabinsk, Russia

⁴ Technical Institute of Physics and Chemistry, Chinese Academy of Sciences, Beijing, China

⁵ Boreskov Institute of Catalysis, SB RAS, Novosibirsk 630090, Russia

Barium hexaferrite, $\text{BaFe}_{12}\text{O}_{19}$, with a magnetoplumbite crystal structure has been actively studied for several decades. Current applications of this magnetic material cover different nanocomposites, a wide range of recording and storing components, as well as inductors and microwave communication devices. The barium hexaferrite microcrystals are obtained by the flux crystal growth method, and the electronic structure is studied complementarily by X-ray photoelectron spectroscopy and first-principles calculation.

Initially, the starting components were treated at 600 °C for 5 h to remove water residuals captured from the air. After that the components were weighed. The optimal batch composition for pure barium hexaferrite growth is Na_2CO_3 – 26.3 at.%, BaCO_3 – 10.53 at.%, Fe_2O_3 – 63.17 at.%. The mixture was gently ground in an agate mortar. Then, it was filled in a 30 ml platinum crucible and placed in a resistive furnace. The furnace was heated from room temperature to 600 °C with the rate of 300 °C/h and from 600 to 1260 °C with the the rate of 100 °C/h. The melted mixture was homogenized in an open crucible at 1260 °C for 4 h in the air. After that, the slow cooling to 900 °C with the rate of 4.5 °C/h was arried out. At 900 °C, the furnace was turned off. The final product of high temperature flux synthesis was black and contained glistening grains.

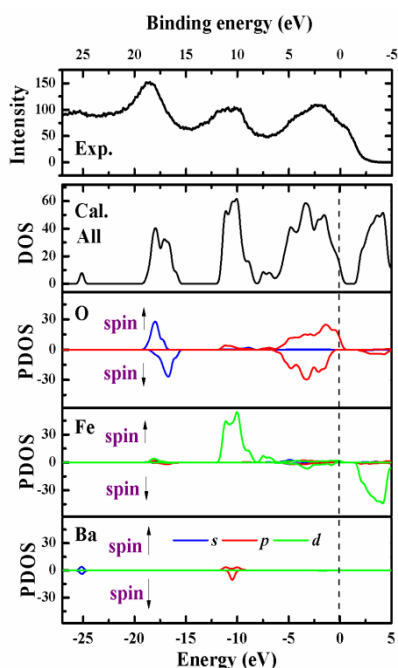


Fig. 1. Comparison of the experimental XPS spectrum and *ab initio* electronic structures.

One of the most widely used methods for the characterization of surface electronic parameters is X-ray photoelectron spectroscopy (XPS), which can be used for quantitative determination of the electron charge transfer induced by the formation of chemical bonds. The spin-polarized first-principles electronic structure calculation of $\text{BaFe}_{12}\text{O}_{19}$ was performed by the plane-wave pseudopotential method implemented by CASTEP based on the density functional theory (DFT).

The calculated electronic partial densities of states (PDOS) projected on the constitutive element in $\text{BaFe}_{12}\text{O}_{19}$ are displayed in Fig.1. Bond characteristics can also be deduced from the PDOS: (i) The Ba 5s and 5p orbitals are strongly localized around -25 eV and -10 eV and hybridize little with the orbitals of other elements, manifesting the strong ionicity of barium. (ii) The O 2s orbitals are also located at the inner energy level around -17 eV, which is relatively difficult to excite. (iii) The electron energy states near the top of the valence bands are mainly composed of Fe 3p 3d and O 2p orbitals, and the strong hybridization in the wide energy range between these orbitals indicates the stronger covalent interaction between iron and oxygen atoms than that between barium and oxygen atoms in $\text{BaFe}_{12}\text{O}_{19}$.

4PO-J-15

MAGNETIC INVESTIGATION OF LOW TEMPERATURE MAGNETIC PHASE TRANSITION IN IRON SELENIDES

Baluyan T.¹, Novakova A.¹, Perov N.¹

¹ Lomonosov Moscow State University, Moscow, Russia

In this work we investigated high purity iron selenide powders, obtained by the solid state reaction method. Two samples were under investigation: Fe₇Se₈ with 3c and 4c superstructure. X-ray diffraction proved the highest purity of the samples. Both samples contain large amounts of ordered vacancies [1], which leads to dramatical changes in magnetic and conductive properties of these samples, that occur when temperature is lowered.

These effects were investigated by means of saturation magnetization and hysteresis loops measurements. Saturation magnetization was measured on a VSM LakeShore 7407 magnetometer in a wide temperature range from 85 to 300K in a 1T magnetic field, hysteresis loops were obtained at 85, 120, 150, 200, 250, 300K. Saturation magnetization values fell sharply in the interval from 110 to 85K for both 3c and 4c samples, but the magnitude of this abrupt change was three times higher for 4c structure. Hysteresis loops for samples were classically shaped for all the temperatures above 85K but their shape was strongly distorted at 85K. All the stated facts confirmed the magnetic phase transition in these structures in a temperature range from 110 to 85K. All the effects are much stronger for 4c-Fe₇Se₈. It occurs because there is an additional atomic layer in 4c structure. As it was shown in [2], this phase transition is associated with the spin transition from ab-plane towards c axis in the selenide structure and leads to a metal-insulator phase transition.

Complex magnetic investigation of given samples helped to find out the influence of ordered vacancies in a magnetic phase transition in the iron selenide samples.

[1] A.F. Andersen, J. Leceiejewicz Le, *Journal De Physique*, **25** (1964) 574-579.

[2] G. Li, B. Zhang, T. Baluyan, et al. *Inorganic Chemistry*, (2016) 12912–12922.

4PO-J-16

TUNING OF THE DOMAIN WALL DYNAMICS BY MAGNETOELASTIC INTERACTION

Chichay K.^{1,2}, Rodionova V.^{1,2}, Zhukova V.³, Perov N.^{1,4}, Zhukov A.^{3,5}

¹ Science and Technology Park “Fabrika”, IKBFU, Kaliningrad, Russia

² Center for Functionalized Magnetic Materials, IKBFU, Kaliningrad, Russia

³ Dpto. Física de Materiales, Fac. Químicas, UPV/EHU, San Sebastian, Spain

⁴ Faculty of physics, Lomonosov Moscow State University, Moscow, Russia

⁵ IKERBASQUE, Basque Foundation for Science, Bilbao, Spain

ks.chichay@gmail.com

Studies of magnetization reversal of low dimensional structures attract increasing interest due to its connection with the development of novel spintronics [1], logic devices [2] and nano-object manipulation [3]. The amorphous magnetically soft glass-coated microwires form part of perspective magnetic materials suitable for the prospective applications related to the coding systems [4], magnetic field and stress sensors [5], and biomedicine [6]. Due to its amorphous structure the formation of the micromagnetic structure and the dominate remagnetization mechanism are defined by the magnetoelastic energy.

In our work we considered the separate and combined influence of the parameters determining the magnetization reversal of amorphous ferromagnetic microwires paying the particular attention to the domain wall dynamics. We investigated the series of Fe- and FeCoNi-based microwires. The magnetic and magnetostrictive properties were investigated for all samples using the fluxmetric and small angle rotation magnetization methods, respectively. The velocity of the domain wall was measured by the Sixtus-Tonks-like technique described elsewhere. To estimate the micromagnetic structure and the reversal magnetization features we investigated an angle dependence of the magnetic properties using the vibrating sample magnetometer and the field dependence of the perpendicular to the magnetic field component of the magnetic moment using the vibrating sample anisometer.

We showed that one of the effective ways to control the magnetic properties and the domain wall dynamics is an annealing. The annealing of Fe-based microwires results in the domain wall velocity increase up to 1.6 times (2400 m/s). The annealing of FeCoNi-based microwires, which had the S-shape hysteresis loop in as-cast state, under applied stresses leads to the drastic changes of the micromagnetic structure and the magnetization reversal process – after annealing the microwires become magnetically bistable. The value of the switching field is strongly depending on the annealing conditions, and hence, can be easily manipulated. Additionally, the domain wall mobility for such microwires is much higher than for the originally bistable microwires. This makes such microwires as promising candidate for the incorporation in novel devices .

[1] S.D. Bader, S.S.P. Parkin, *Annu. Rev. Condens. Matter Phys.*, **1** (2010) 71.

[2] D.A. Allwood, G. Xiong, C.C. Faulkner, D. Atkinson, et.al., *Science*, **309** (2005) 1688.

[3] M. Monticelli, et. al., *Lab Chip*, **16** (2016) 2882.

[4] V. Larin, et.al., Spain Patent №P9601993, (1996).

[5] V. Zhukova, M. Ipatov, A. Zhukov, *Sensors*, **9** (2009) 9216.

[6] A. Talaat, J. Alonso, V. Zhukova, et.al., *Scientific Reports*, **6** (2016) 39300.

4PO-J-17

ORIGIN OF PERPENDICULAR MAGNETIC ANISOTROPY IN EPITAXIAL Pd/Co/Pd TRILAYERS

Davydenko A.V.¹, Kozlov A.G.¹, Ognev A.V.¹, Steblyy M.E.¹, Samardak A.S.¹, Ermakov K.S.¹, Kolesnikov A.G.¹, Chebotkevich L.A.¹

¹ Far Eastern Federal University, Vladivostok, Russia
avdavydenko@gmail.com

Perpendicular magnetic anisotropy in epitaxial Pd/Co/Pd(111) trilayered films grown on Si(111) substrate was investigated. Contributions to perpendicular magnetic anisotropy from the bottom and top Co/Pd interfaces were deduced by replacement of Pd layers by Cu layers and comparative analysis of the magnetic anisotropy in the samples. Model for the numerical calculation of magnetoelastic anisotropy based on the experimentally measured elastic strains in ferromagnetic films using reflection high energy electron diffraction (Fig. 1) was proposed and approved on a Pd/Co/Pd(111) epitaxial system. Perpendicular magnetic anisotropy in Pd/Co/Pd films was induced both by interface electronic effects and by stress caused by lattice mismatch between Pd and Co. Moreover, the results of calculations by proposed model made it possible to quantitatively analyze contributions from strains and interface electronic effects to perpendicular magnetic anisotropy.

Due to asymmetry of the stress in the Co film the contribution to magnetic anisotropy induced by the bottom Co/Pd interface was stronger than that induced by the top Pd/Co interface. The energy of the perpendicular magnetic anisotropy and asymmetrical contributions from the bottom Co/Pd and top Pd/Co interfaces to anisotropy in Pd/Co/Pd trilayers strongly depend on the thickness of the bottom and top Pd layers and may be precisely controlled. The roughness of the interfaces does not have a large influence on the energy of perpendicular magnetic anisotropy in this system.

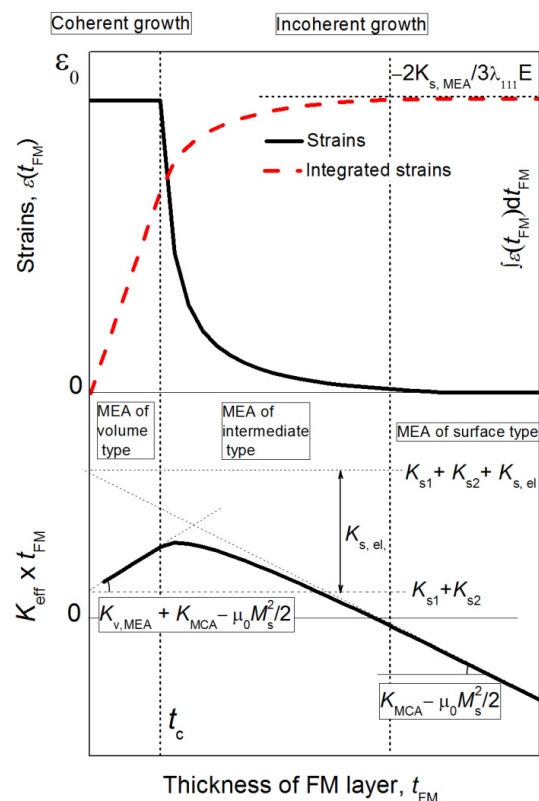


Fig. 1. Scheme of the dependencies of the strains $\varepsilon(t_{FM})$, integrated strains $\int_0^{t_{FM}} \varepsilon(t_{FM}) dt_{FM}$, and $K_{eff} \times t_{FM}(t_{FM})$ on the thickness of the magnetic layer.

Support by the Russian Foundation for Basic Research (grants 17-52-50060 and 15-02-05302) and the state task (3.5178.2017) is acknowledged.

4PO-J-18

HISTERESIS LOOPS OF FILMS WITH PERPENDICULAR MAGNETIC ANISOTROPY AND LOW QUALITY FACTOR. MICROMAGNETIC SIMULATION

Dubovik M.N., Filippov B.N.

Institute of Metal Physics UB RAS, Yekaterinburg, Russia
dubovik@imp.uran.ru

Micromagnetic simulations of domain structure of magnetic films with the easy axis perpendicular to the surface were performed. The magnetic parameters in use corresponded to the Co(0001) and Ni(111) films. The calculated dependence of the stripe domain structure period on the film thickness is in a good agreement with the experimental data [1, 2]. The stripe domain structure is “closed”, with the domain walls and domains widths being comparable. The hysteresis loops for 50 nm Co film and 200 nm Ni film (fig. 1) were obtained and compared with the experimental ones [1, 2]. The stripe domain structure period could be changed while the in-plane external field was applied. The calculated residual magnetization is in a good agreement with the data [1, 2]. This residual magnetization is related to formation of the structure with the domain walls cores polarized in the same direction. The effect is obtained of horizontal Bloch lines formation during the magnetization reversal by the in-plane external field. When the field is applied along the easy axis bubble domains formation occurs.

The simulations were performed using the mumax3 software [3] and «Uran» supercomputer at the Institute of Mathematics and Mechanics UB RAS.

The research was carried out within the state assignment of FASO of Russia (theme “Magnet” No. 01201463328).

- [1] M. Hehn, S. Padovani, K. Ounadjela, J.P. Bucher, *Phys. Rev. B.*, **54** (1996) 3428-3433.
 [2] R. Naik, S. Heemed, P. Talagala, L.E. Wenger, *J. Appl. Phys.*, **91** (2002) 7550-7552.
 [3] A. Vansteenkiste, J. Leliaert, M. Dvornik, et. al., *AIP Advances*, **4** (2014) 107133(1-22).

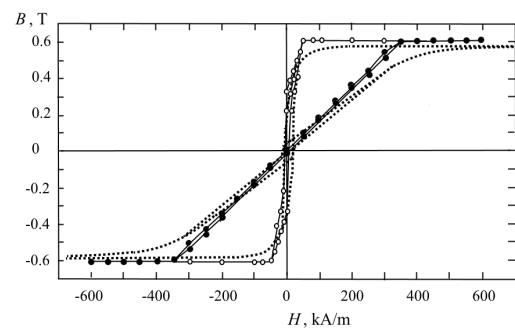


Fig. 1. Hysteresis loops of 200 nm Ni film. Open (solid) circles correspond to the simulation with the in-plane (perpendicular) external field. Dashed lines correspond to the experimental data [2].

4PO-J-19

STUDY OF THE FERROLIQUIDS WITH COBALT FERRITE NANOPARTICLES USING POLARIZED MUONS

Duginov V.N.¹, Andrievskii D.S.², Balasoiu M.^{1,3}, Fluerasu D.³, Getalov A.L.², Gritsaj K.I.¹, Komarov E.N.², Kotov S.A.², Mamedov T.N.¹, Moroslip A.E.², Scherbakov G.V.², Stan C.⁴, Vorob'ev S.I.²

¹ Joint Institute for Nuclear Research, Dubna, Russia

² Petersburg Nuclear Physic Institute, Gatchina, Russia

³ Horia Hulubei National Institute of Physics and Nuclear Engineering, Bucharest, Romania

⁴ Politehnica" University of Bucharest, Department of Physics, Faculty of Applied Sciences, Romania

duginov@jinr.ru

We used polarized positive muons (μ SR[1]) to study the magnetic properties of the ferrofluids. The behaviour of the ferrofluids of the different concentration of the magnetic nanoparticles in H_2O were studied [2]. Main part of muons stops in the medium between the nanoparticles. The frequency of the muon spin precession is proportional to magnetic field value and to the muon's g-factor (~ 13.5 kHz/G).

We studied the difference between the magnetic properties of ferrofluids $CoFe_2O_4$ at the cooling at FC and ZFC conditions. Figure 1 presents the example of obtained data. We analyzed data from the point of view of studying the properties of an ensemble of single-domain magnetic nanoparticles.

The results FC and ZFC measurements evidence that single domain nanoparticles with dimension about 8.5 nm have a high anisotropy coefficient. The mean value of the magnetic field in the colloid created by the randomly distributed $CoFe_2O_4$ nanoparticles was defined. In case of cooling of the fluid with concentration of nanoparticles 3.0% in external magnetic field of 525 Oe, the nanoparticles create in medium an additional magnetic field of 4.7 Oe. Received an indication that the magnetic anisotropy coefficient decreases with decreasing the size of nanoparticle.

The support of the Grants of the Romanian Governmental Plenipotentiary at JINR is acknowledged.

[1] Smilga V.P. and Belousov Yu.M. "The Muon Method in Science." Monograph. Nova Science, NY (1992).

[2] M.Balasoiu, S.G.Barsov, D.Bica et al., *JETP Lett.*, **88(3)** (2008) 210-213.

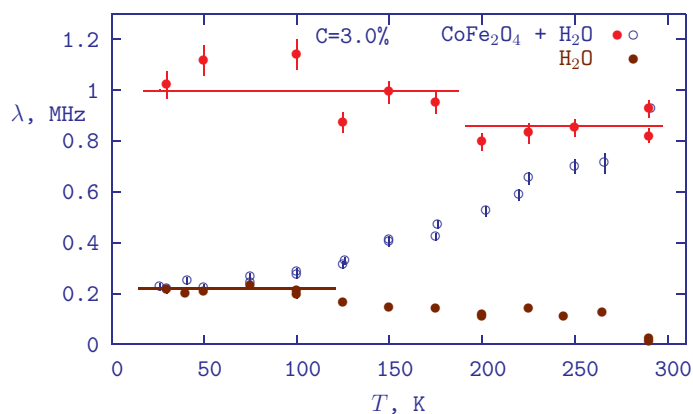


Fig.1 The temperature dependencies of the relaxation rate of the muon spin precessions at ZFC (open circles) and FC (closed points) conditions at 500 G.

4PO-J-20

HIGH-FIELD MAGNETIZATION INVESTIGATIONS OF NdHoFe₁₄B: EXPERIMENT AND THEORY

*Kostyuchenko N.V.*¹, *Tereshina I.S.*², *Gorbunov D.I.*³, *Tereshina E.A.*⁴, *Andreev A.V.*⁴, *Doerr M.*⁵,
*Politova G.A.*⁶, *Zvezdin A.K.*^{1,7}

¹ Moscow Institute of Physics and Technology, Dolgoprudny, Moscow region, 141700, Russia.

² Lomonosov Moscow State University, 119991 Moscow, Russia

³ Dresden High Magnetic Field Laboratory (HLD-EMFL), Helmholtz-Zentrum Dresden-Rossendorf, D-01314 Dresden, Germany

⁴ Institute of Physics, ASCR, Na Slovance 2, 18221 Prague, Czech Republic

⁵ Technische Universität Dresden, D-01062 Dresden, Germany

⁶ Baikov Institute of Metallurgy and Materials Science RAS, 119334 Moscow, Russia

⁷ A. M. Prokhorov General Physics Institute of Russian Academy of Sciences, Moscow
nvkost@gmail.com

For the last decades much attention has been focused on the rare-earth-iron-boron compounds R₂Fe₁₄B which develop very hard magnetic properties such as to be most promising magnet materials [1,2]. The magnetic properties similar to the famous Nd₂Fe₁₄B may be expected to be observed in NdHoFe₁₄B, too, except for the sign of the 3d-4f exchange interaction, because both Nd³⁺ and Ho³⁺ ions in the ground state have the same orbital angular momentum quantum number of L = 6, the smallest negative values of the second order Stevens factor α_J among the light and the heavy rare-earths, respectively, which cooperate with the axial anisotropy of the Fe-sublattice, and the negative fourth order Stevens factor β_J [1,3].

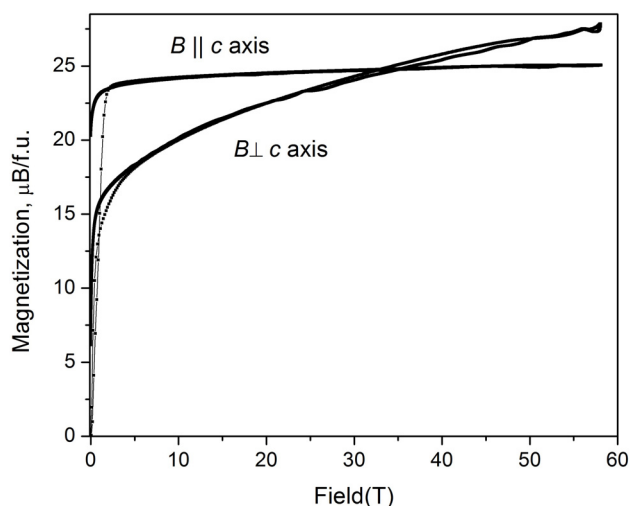
Due to recent major progress in developing methods, experiments in very high (up to 100 T) magnetic fields became feasible. This work reports on the high-field magnetization study of the rare-earth intermetallic NdHoFe₁₄B. The experimental magnetization curves of single crystalline NdHoFe₁₄B were measured along and perpendicular to the *c* axis at 1.8 K in pulsed fields up to 58 T (see Figure 1). To describe the high-field experimental data obtained, we have performed calculations that allowed us to determine the crystal-field and exchange parameters of the compound. Despite the fact that we also do not observe experimentally the full ferromagnetic state in the system in fields up to 58 T, the crystal-electric field and exchange parameters obtained allowed us to calculate the full magnetization process for NdHoFe₁₄B up to 200 T.

The work is supported by RFBR, pr. No. 15-02-08509, 16-03-00612, 16-33-60226-mol_a_dk, the Czech Science Foundation (project 16-03593S) and Czech Research Infrastructures (Project No. LM2011025, MLTL, <http://mltl.eu/>). We acknowledge the support of HLD at HZDR, member of the European Magnetic Field Laboratory (EMFL).

[1] J. Chaboy et al., Phys. Rev. B **76** (2007) 134408.

[2] P. Wolfers et al., J. Alloys Compd. **317-318** (2001) 39-43.

[3] A. Fujita et al., JMMM **69** (1987) 267-275.



Experimental magnetization curves of NdHoFe₁₄B at 1.8 K in fields up to 58 T.

4PO-J-21

"DOMAIN SMILE" IN (Pr,Dy)(Fe,Co)B MAGNET*Kunitsyna E.I., Morgunov R.B., Koplak O.V.*

IPCP RAS, Acad. Semenov av. 1, Chernogolovka, 142432, Russia

kunya_kat@mail.ru

Two processes determine the reversal magnetization in RE-TM-B magnets: the nucleation of the reverse magnetization phase, and the second is the domain walls propagation. The competition between these two mechanisms characterizes the response of the magnetization to external magnetic field. The usual method of study reversal magnetization is measurements and analysis of the time dependences of the magnetization $M(t)$ in magnetic field directed opposite the initial magnetization of the sample. We observed the magnetization jumps in static magnetic field, contrary to the traditional conditions of the sweeping magnetic field necessary on observation of the Barkhausen noise. In this case one can observe only the response of the entire sample to external magnetic field. But it is much more interesting to observe the process of motion of individual domain and nucleation of the reverse magnetization phase. In our work, we observed a change in the distribution of the magnetization of the surface elements of a sample by means FMF in external magnetic field. The data are shown in Fig. 1. We visualized of the domain walls responsible for the demagnetization jumps. The dependence of coercive field on magnetization rate will be analyzed and discussed.

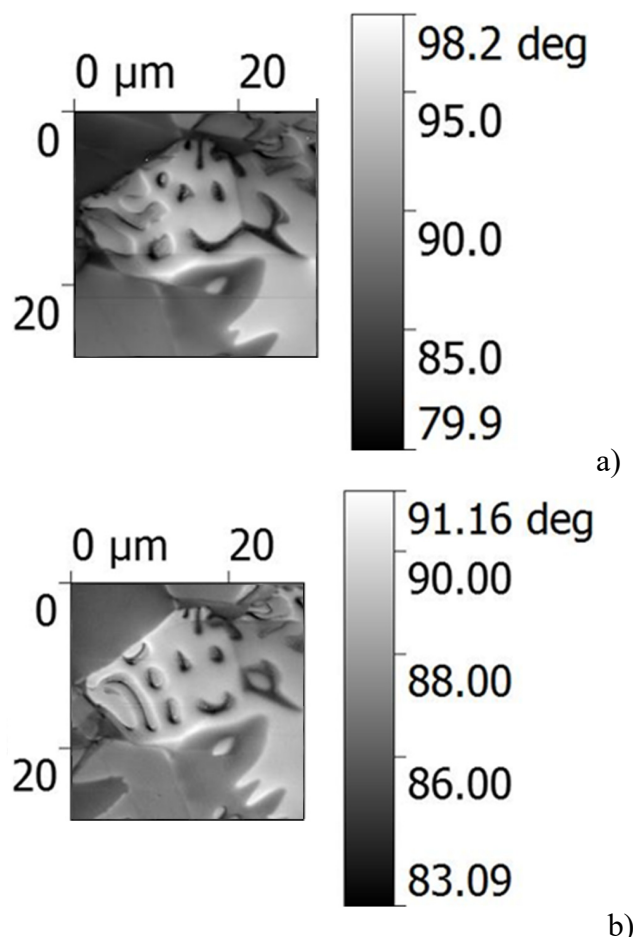


Fig. 1. Distribution of vertical gradient of the magnetic field near sample surface (MFM images): in initial state (a); after magnetization in 100 Oe during 9 min (b).

4PO-J-22

RESEARCH OF REVERSIBILITY OF COERCIVITY UNDER HEAT TREATMENT IN PERMANENT MAGNETS

Lileev A.S., Pinkas V.V., Voronchihina K.V., Gunbin A.V.

NUST "MISIS", Moscow, Russia

pinkasv2014@gmail.com

The aim of the present work was to analyse studies of magnetization reversal processes in real permanent magnets for the possibility of further improvement of technology. In particular, reversible variation of coercivity of the permanent magnets under heat treatments in many cases discovered in current research and previous works remains unclear and is understood ambiguously, and causes many issues of this phenomenon at present. Table presents the coercivity in the initial condition (H_c optimal), after high-temperature heating of the initial state (H_c spoiling) and after the low temperature aging (H_c reconditioning). The modes of obtaining the optimal state and aging correspond to the standard heat treatments of these alloys. Evidently, this phenomenon occurs in almost all alloys for permanent magnets, despite the fundamental differences in the nature of coercivity and magnetization reversal processes. Present work based on studies of changes and the reversibility of magnetic properties under different heat treatments attempted to explain in different alloys for permanent magnets.

Year	Material	H_c optimal (Oe)	H_c spoiling (Oe)	H_c reconditioning (Oe)	Source
1964	Alnico	600	400	600	[1]
1973	Ticonal	1450	450	1450	[2]
1975	SmCo ₅	17500	12000	17500	[3]
1979	Sm-Co-Cu-Fe-Zr	14000	9000	14000	[4]
2014	Sm(Co _{0,65} Fe _{0,26} Cu _{0,07} Zr _{0,02}) ₇	29500	1200	29500	[5]
2014	Nd ₂ Fe ₁₄ B (1050 °C)	19000	11900	19000	[6]
2016	Nd ₂ Fe ₁₄ B (900 °C)	22600	17100	22600	present research
2017	FeCrCo	550	25	550	present research

- [1] A.S. Ermolenko. Diss. candidate of ph. and math. sciences, Institute of metal physics, Sverdlovsk (1964).
- [2] A.S.Lileev, V.P.Menushenkov, V.I. Sumin, *PhMM*, (1973) 183-186.
- [3] B.G. Livshitz, A.S. Lileev, V.P. Menushenkov, *IEEE Trans. Magn.*, (1975) 1673 – 1675.
- [4] V.I.Habarov, T.Z. Puzanova, Ya.S. Shur, *PhMM*, (1979) 921-926.
- [5] A.S. Lileev, O.A. Arinicheva, M. Reissner, F. Kubel, V. A. Sein, *J. MSHT*, (2014) 50-55.
- [6] T.G. Woodcock, F. Bittner, T. Mix, *J. MM*, (2014).

4PO-J-23

NON-BARKHAUSEN JUMPS IN SINTERED (NdDy)(FeCo)B MAGNET

*Kucheryaev V.V.*², *Piskorskii V.P.*², *Morgunov R.B.*^{1,2}

¹ Institute of Problems of Chemical Physics, Russian Academy of Sciences, Chernogolovka, 142432, Russia

² Institute of Aviation Materials, Moscow, 105005, Russia
kudria01@mail.ru

The principal condition of the Barkhausen jumps is non-stationary external magnetic field [1]. In our experiments, sharp jumps appear during continuous relaxation of magnetic moment in stationary magnetic field (fig. 1). Statistically meaningful set of events was received to determine main parameters of jumps, such as average magnetic moment of the jump, its average amplitude, expectation time etc. The time distribution of jump probability was obtained. The main jump flow occurs immediately after magnetic field stabilization and their density decreases decays with time.

Spontaneous emission of stochastic demagnetization jumps was found in static magnetic field opposite to initial magnetization of the specimen. Quantity of the jumps is inversely proportional to their amplitude. Maximal jump probability responds to change of the sample magnetic moment up to 10 % of saturation magnetization.

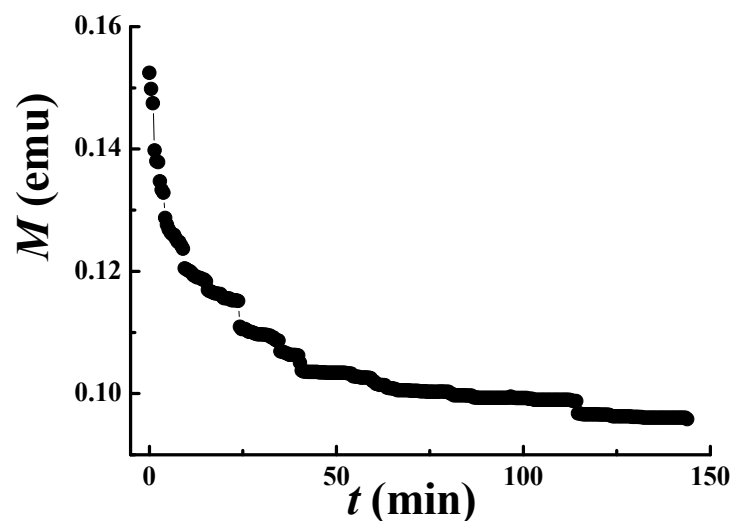


Fig. 1. Time dependence of magnetic moment M after external magnetic field stabilization ($H = -9 \text{ kOe}$, $T = 300 \text{ K}$)

[1] R.B. Morgunov, E.I. Kunitsyna, V.V. Kucheryaev, V.P. Piskorskii, O.G. Ospennikova, E.N. Kablov, *Eur. Phys. J. Plus*, **131** (2016) 344.

[2] E.N. Kablov, O.G. Ospennikova, D.E. Kablov, V.P. Piskorskii, E.I. Kunitsyna, A.I. Dmitriev, R.A. Valeev, D.V. Korolev, I.I. Rezhikova, A.D. Talantsev, R.B. Morgunov, *Journal of Applied Physics*, **117** (2015) 243903.

4PO-J-24

FABRICATION, STRUCTURAL AND MAGNETIC CHARACTERIZATION OF PARTIALLY COVERED MAGNETICALLY BIPHASE MICROWIRES

Baraban I.^{1,2}, Chichay K.^{1,2}, Berganza E.², Perez R.², Rodionova V.^{1,2}, Vazquez M.²

¹ Laboratory of Noval Magnetic Materials, Immanuel Kant Baltic Federal University, 236041, Kaliningrad, Russia

² Center for Functionalized Magnetic Materials (FunMagMa), Immanuel Kant Baltic Federal University, 236041, Kaliningrad, Russia

³ Institute of Materials Science of Madrid, CSIC. 28049 Madrid, Spain
machay@lnmm.ru

Glass-coated ferromagnetic microwires consist of an amorphous ferromagnetic core and a glassy shell, characterized by their cylindrical symmetry and large length to diameter aspect ratio. The modification of the metallic diameter and the glass thickness leads to different properties in microwires for the same ferromagnetic alloy composition [1]. Multilayered microwires with two magnetic phases were recently introduced, where a second magnetic phase was grown by electrodeposition as an additional external shell covering fully the glass-coated microwire [2]. These multilayered magnetic systems present high potential particularly as elements in sensor devices (field, temperature or pressure sensors).

In this work, a new type of multilayered microwires is introduced where the external second magnetic phase, sputtered onto the glassy coat, covers only partly the inner microwire. The particular study has been conducted on microwires consisting of a soft Fe-based core and two different soft FeNi and hard Co external shells. Core and shell were separated by an intermediate insulating Pyrex glass microtube as in case of fully covered microwires. The precursor Fe-based microwire was obtained by quenching and drawing technique [3] with a metallic core diameter of $d = 10.2 \mu\text{m}$, and total $D = 26 \mu\text{m}$. The magnetron sputtered outer shell was up to 300 nm thickness.

Surfaces properties were observed by atomic force microscopy. Manufacturing defects on the glass surface of the precursor glass-coated microwire were identified, and their influence on the final magnetic properties of the microwires was analyzed. The volume magnetic properties of bi-phase microwire were analyzed by vibrating sample magnetometer, while the local surface hysteresis loops of each magnetic phase were determined by magneto-optical Kerr effect. Volume magnetic properties showed a behavior for bi-phase system (i.e., two-stage hysteresis loop). Local surface hysteresis loops allowed us to quantify specific values of coercive force for the soft core and the soft or hard shell. A systematic comparative analysis of the volume and local properties of the microwires has been performed in order to interpret the overall magnetic behavior and to determine the strength of magnetic interactions between the amorphous core and the sputtered shell in case of partially covered microwires.

Support is by the Ministry of Education and Science of the Russian Federation in the framework of government assignment (No.3.4168.2017/ПЧ), and the Regional Government of Madrid under NANOFRONTMAG-CM project (S2013/MIT-2850) are acknowledged.

[1] V. Rodionova, I. Baraban, K. Chichay, A. Litvinova, N. Perov, *JMMM* **422** (2017) 216–220.

[2] J. Torrejón, G. Badini-Confaloni, and M. Vázquez, *JAP* **103** (2008) 07E712.

[3] A. Zhukov, J. González, M. Vázquez, V. Larin, and A. Torcunov, *Encyclopedia of Nanoscience and Nanotechnology*, edited by H. S. Nalwa American Scientific, Stevenson Ranch, CA, Chapter 62, **6** (2004) 365–367.

4 July

Tuesday

12:00-14:00

poster session

4PO-K

**“Magnetic Shape
Memory and
Magnetocaloric Effect”**

4PO-K-1

DOUBLE MAGNETOCALORIC PEAK IN NI-MN-IN BASED HEUSLER ALLOYS

Rodionov I.D.¹, Dubenko I.S.², Prudnikov V.N.¹, Granovsky A.B.¹, Titov I.S.^{1,3}, Saletsky A.M.¹

¹ Faculty of Physics, Lomonosov Moscow State University, Moscow, Russia

² Department of Physics, Southern Illinois University, Carbondale, USA

³ Physics and Materials Science Research Unit, University of Luxembourg, 162a avenue de la Faïencerie, L-1511 Luxembourg, Luxembourg
rodionovID@yandex.ru

The magnetocaloric effect (MCE) is defined as a magnetic-field-induced temperature change in a magnetic material. This effect is widely used in science, cooling devices and medicine [1, 2]. We present our recent results on magnetic and MCE properties of Ni-Mn-In based Heusler compounds, focusing on inverse MCE in $\text{Ni}_{48.5}\text{Mn}_{35}\text{In}_{15}\text{Co}_{1.5}$ and $\text{Ni}_{50}\text{Mn}_{35}\text{In}_{13.5}\text{Al}_{1.5}$ alloys in the vicinity of martensitic transition.

Polycrystalline samples were fabricated using 4N purity metals in argon atmosphere by arc-melting method, and annealed in high vacuum ($\sim 10^{-5}$ Torr) for 24 h at a temperature of 850°C . The crystal structure was determined by powder X-ray diffraction method at room temperature. Chemical composition was found by EDX analysis. Magnetic measurements were carried out with VSM Lake Shore in ZFC and FC regimes. Direct measurements of the adiabatic change of temperature in applied magnetic field were done using an adiabatic magnetocalorimeter (MagEqMMS 801) in a temperature range of 250 K-350 K.

Temperature dependences for Co- and Al-doped alloys in the vicinity of martensitic transition show a step-like behavior, both in case of ZFC and FC measurements (Fig.1a, b). We observed the double-peak structure in (i) the temperature derivative of magnetization (inset in Fig.1a), temperature dependences of (ii) adiabatic temperature change and (iii) isothermal entropy change of inverse MCE. These specific features may be connected with intermartensitic transition or with nonmonotonic behavior of critical field at martensitic transition.

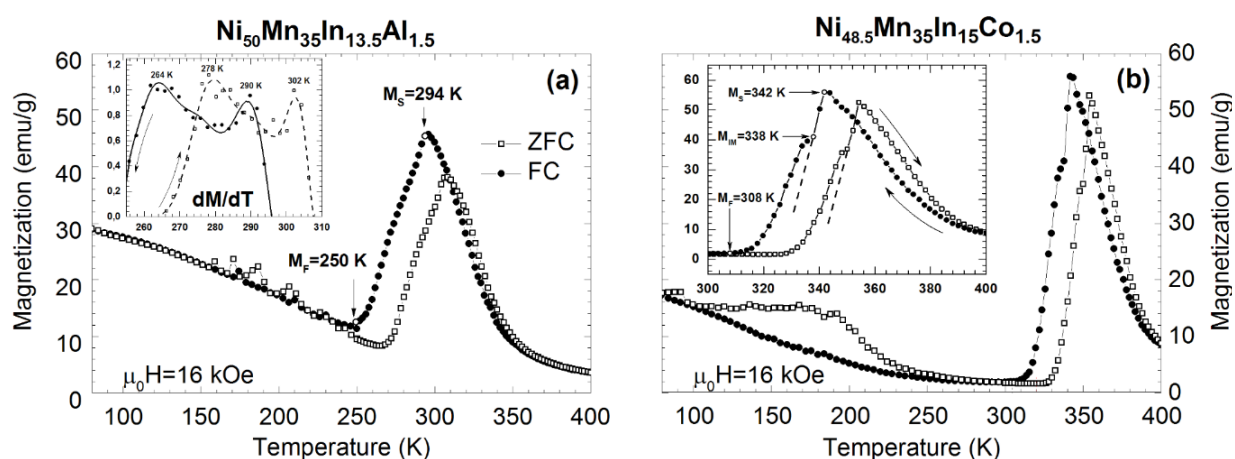


Fig. 1. Temperature dependences of magnetization M for (a) Al and (b) Co-doped Ni-Mn-In Heusler alloys

This work was supported by RFBR (Grants No. 15-02-01976 and No. 16-32-00460).

[1] K. Gschneidner, V. Pecharsky, *International Journal of Refrigeration*, **31** (2008) 945-961.

[2] A. Tishin, Y. Spichkin, et. al., *International Journal of Refrigeration*, **68** (2016) 177-186.

4PO-K-2

MAGNETIC PROPERTIES OF IRON-CONTAINING SUPERELASTIC ALLOYS

Koledov V.V.¹, Kamantsev A.P.¹, Kalashnikov V.S.¹, Koshelev A.V.², Dilmieva E.T.¹, Los A.S.³, Mashirov A.V.¹, Kuchin D.S.¹, Taskaev S.V.⁴, Sampath V.⁵, von Gratowski S.V.¹, Shavrov V.G.¹

¹ Kotelnikov Institute of Radioengineering and Electronics of RAS, Moscow, Russia

² Lomonosov Moscow State University, Moscow, Russia

³ International Laboratory of High Magnetic Fields and Low Temperatures, Wroclaw, Poland

⁴ Chelyabinsk State University, Russia

⁵ Department of Metallurgical and Materials Engineering, Indian Institute of Technology, Chennai, India

victor_koledov@mail.ru

Ferromagnetic alloys with shape memory effect (SME), such as Ni-Mn-Ga-Fe demonstrate the reversible deformations up to 10 %, as a result of thermoelastic martensitic transition induced by magnetic field [1]. The iron-containing, high-strength Fe-Ni-Co (Al-Ta-B) alloy with an superplasticity and reversible deformations of more than 13% with a tensile strength above 1 GPa was presented in [2]. The strength of this alloy is almost twice the maximum result for superelastic deformation in Ni-Ti alloys. In addition, this iron-containing alloy has a high damping capacity and a reversible change in the magnetization value during the loading and unloading process. More recently, other iron-containing alloys with superelasticity have attracted attention [3]. The family of Fe-Ni-Co (Al-Ta-B) alloys demonstrates the unique physical properties: a wide temperature hysteresis of superelasticity, a change in magnetization over a large range of values, and electrical resistance as a result of the load, accompanied by high pseudoplasticity values. In view of these properties, these iron-containing superelastic alloys are expected to be used for a wide range of practical applications, namely, as: damping and functional materials. Significant interest in these alloys is caused by the search for inexpensive structural alloys for the creation of structures, resistant to earthquakes, such as nuclear power plants, high-rise buildings and industrial facilities.

This report will present the results of the development of new Fe-Ni-Co (Al-Ta-B) alloys, experimental study of their structure, phase transitions by temperature change and mechanical stress. Particular attention will be paid to the study of magnetic and functional properties of the alloys under high magnetic fields, in particular, magnetic-field-induced SME, magnetoplasticity, elastocaloric and magnetocaloric effects.

The work is supported by the RFBR grant No. 16-57-45066.

[1] Cherechukin, A. A., et al., *Physics Letters A*, **291**(2) (2001) 175.

[2] Y. Tanaka et al., *Science*, **327** (2010) 1488.

[3] Bhowmick S., Mishra S.K., *Journal of Intelligent Material Systems and Structures*, **27**(15) (2016) 2062.

4PO-K-3

REVERSIBLE-IRREVERSIBLE MAGNETOCALORIC EFFECT IN NI-MN-IN-(CU) HEUSLER ALLOYS

Gamzatov A.G.¹, Aliev A.M.¹, Batdalov A.B.¹, Varzaneh A.G.², Kameli P.², Sarsari I.²

¹ Amirkhanov Institute of Physics, DSC of RAS, 367003, Makhachkala, Russia

² Department of Physics, Isfahan University of Technology, Isfahan, 8415683111, Iran
gamzatov_adler@mail.ru

Magnetic materials exhibiting a large magnetocaloric effect (MCE) have recently gained strong interest due to their potential use in magnetic refrigeration technology. Recently, magnetic shape-memory Ni–Mn–(In, Sn, Sb, Cu)-based Heusler alloys have been proposed as solid-state energy-efficient refrigerants owing to their remarkable first-order transition feature [1-4].

In this paper we present the results of direct measurement of the MCE in Heusler alloys Ni-Mn-In-(Cu:0; 0.5; 1) in a cyclic magnetic field of 1.8 T in heating and cooling runs.

Fig. 1(a) depicts the temperature dependence of MCE in Cu1 and Cu0.5 samples in the magnetic field of 1.8 T in heating and cooling modes. As the concentration of Cu increases, the direct MCE increases from 1.02 K to 1.24 K for Cu0 and Cu0.5 samples, respectively and the temperature of the magnetostructural transition shifts toward high temperatures by about 60 K. But hereby, the width of the hysteresis is practically the same. The inverse MCE accompanied with a wide hysteresis (14-20 K) is observed near the magnetic structural transition. The value of the inverse effect depends on the rate of a sample temperature change (heating or cooling), the higher the rate is, the higher the inverse effect value (see Fig.1(b)). This behavior of MCE is typical for the area of a magnetostructural transitions in Heusler alloys [4]. This behavior of MCE in the region of coexistence of two phases is explained by the gradual increase in the austenite phase due to the martensite-austenite phase transition induced by the magnetic field.

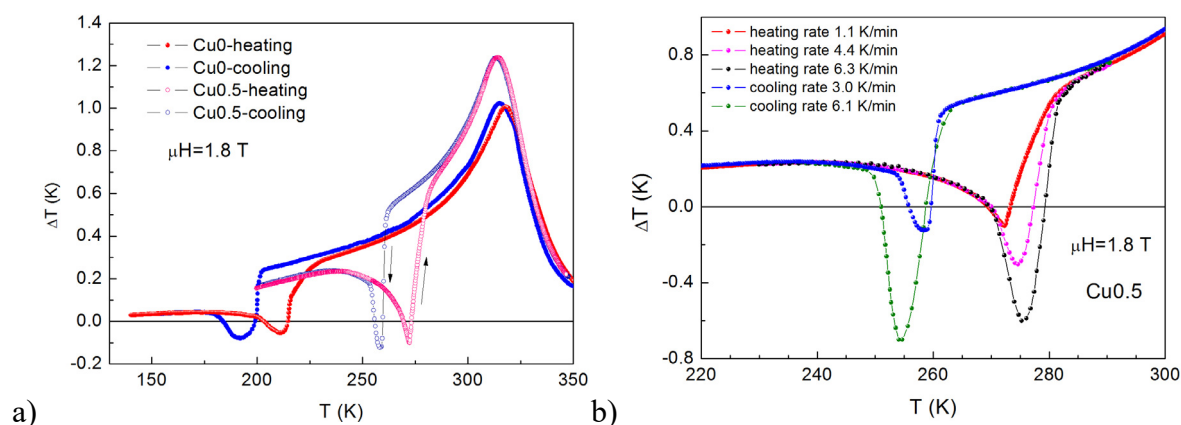


Fig. 1. a) Temperature dependences of MCE for Cu0 and Cu0.5 samples in magnetic field of 1.8 T. b) Dependence of inverse MCE on the rate of a sample temperature change (heating or cooling) for Cu0.5 sample.

This work was partially supported by RFBR, research project № 17-02-01195.

- [1] S. Singh et al. *Advanced Materials*, **28** (2016) 3321-3325.
 [2] J. Liu et al. *Nature materials*, **11** (2012) 620-626.
 [3] V. Basso, et al. *Physical Review B*, **85** (2012) 014430.
 [4] I. Titov, *Journal of Applied Physics*, **112** (2012) 073914.

4PO-K-4

GIANT MAGNETOCALORIC EFFECT IN COMPOSITES BASED ON POLYMERIC MATRIX AND MANGANESE ARSENIDE

Govor G.A.¹, Vetcher A.K.¹, Mitsiuk V.I.¹, Nikitin S.A.², Pankratov N.Yu.², Krokhotin A.I.²

¹ Natl Acad Sci Belarus, Sci. Pract. Mat. Res. Ctr, Minsk 220072, Byelarus

² Lomonosov Moscow State University, Physics faculty, Moscow 119991, Russia
pankratov@phys.msu.ru

The composite material which is made of metallic and polymeric material by certain processes, can retain the advantages of the original components, overcomes some shortcomings and show some new properties. A composite material is a multi-phase system consisted of matrix material and reinforcing material. Matrix material is a continuous phase, and reinforcing material is a dispersed phase, such as fiber, sheet or particle. The composite not only retains the key feature of the original component materials, but also gets the performances that are not depicted by the original components through the combined effects.

Various functional materials can be produced by compounding different materials of function. At present, electromagnetic functional materials develop most rapidly and are used most commonly in the functional composite materials. These composite materials can be processed into magnetic products with the required shape and the certain mechanical properties by the general forming methods (such as compression molding, laminating, etc.) of polymeric materials. In order to obtain a good overall performance, we must increase the amount of filler or enhanced material as much as possible, control the interface of composite materials and make composite materials have better process ability.

It is known, that MnAs is a ferromagnetic, which demonstrates first order phase transition in both magnetic and structural subsystem near room temperature. The temperature dependence of MCE shows a wide hysteresis which blocks of its application. It was shown that both ferro- and paramagnetic metastable phase coexist in MnAs in the region of phase transition, and so the MCE is caused by magnetic phase transition from paramagnetic to ferromagnetic state.

In this work the polymer matrix composites with MnAs powder as reinforcing material were obtained. The aim of this paper is to investigate the influence of both polymeric matrix type and processing methods of composite to the temperature behavior of magnetocaloric effect (MCE) and finding the dependence of MCE and unstable magnetic condition to be produced by thermal and magnetic history of sample. The nanosize particles composites were also investigated.

The composites were prepared from nano- and microcrystalline metallic powder fixed in polymeric matrix; the volume of polymer is less than 8%. There were obtained both textured by magnetic field and isotropic samples fixed by hydrostatic pressure up to 20 kbar.

A bulk MnAs demonstrates a strong temperature and field hysteresis of magnetic properties in magnetic field less than 50 kOe. The maximum value of MCE is $\Delta T = 0.28$ K on heating (at 308 K) and $\Delta T = 0.88$ K on cooling (at $T = 306$ K) for MnAs in magnetic field 10 kOe.

It was shown, that the decreasing of grain size less than 1 μm leads to reduction of the MCE in nanosized composites. It was found, that both the hysteresis and maximum value of MCE are increased in textured composites in compare with bulk MnAs.

It is established that the optimum properties, such as giant MCE and low temperature hysteresis, are found in composite with $\sim 1\mu\text{m}$ particles and polyvinyl acetate matrix hardened at pressure of 10kBar. The maximum of MCE in this composite is $\Delta T \sim 1,3$ K (at 309 K) in 10kOe. These properties are caused by the residual pressure of polymer mold on grains.

The work is supported by RFBR grants #16-52-00223 and #16-02-00472 BRFB grant #T16P-170.

4PO-K-5

THE ORIGIN OF MARTENSITIC TRANSITION IN HEUSLER ALLOY Ni-Mn-In POLYCRUSTALLINE THIN FILMS

Grunin A., Goikhman A., Maksimova K.

REC "Functional Nanomaterials", Immanuel Kant Baltic Federal University, 236041 Kaliningrad,
Russia
agrunin@innopark.kantiana.ru

Over the last decades a lot of attention was devoted to Ni-Mn-In Heusler alloy, because of their intriguing properties important for various applications, such as caloric effects [1], theoretically predicted high spin polarization, magnetic-induced first-order phase transition etc. Many of these properties originates from martensitic transition. Due to the possibility of using this effects for different applications a lot of scientific and technological attention is attracted now to the low-dimensional materials like thin films. Therefore, it's very important to determine structural and magnetic properties changing upon the decreasing z-dimension of the material from bulk to few atomic layers film.

We report the formation of Heusler alloy polycrystalline thin films with $\text{Ni}_{52}\text{Mn}_{48-x}\text{In}_x$ ($12 < x < 16$) composition and thicknesses about 50 nm by pulsed laser deposition. For all samples the presence of martensitic transition was confirmed.

The features of the martensitic transitions were investigated by three different approaches:

1. Structural properties – by laboratory X-Ray diffraction (XRD) at different temperatures.
2. Magnetic properties – by SQUID
3. Electronic properties – by Hard X-ray Photo Electron Spectroscopy (HAXPES) on P09 beamline at PETRA III synchrotron source (DESY, Hamburg, Germany).

It was found, that for this type of samples investigations of electronic and magnetic structures give more accurate information about martensitic transition critical points. Also it was shown that high magnitude of kinetic arrest effect is inherent for all films with transition.

Phase diagrams were plotted for all samples.

[1] T.Krenke, E.Duman, M.Acet, E.F.Wassermann, *Phys. Rev. B*, **75** (2007) 104414.

[2] K. A.Kilian, R. H. Victora *Electronic*, *IEEE MAGN*, **37** (2001) 4, 1976-1978.

4PO-K-6

INFLUENCE OF PLASTIC DEFORMATION ON MICROSTRUCTURE OF HEUSLER ALLOY

Musabirov I.I.¹, Safarov I.M.¹, Galeev R.M.¹, Koledov V.V.², Mulyukov R.R.¹

¹ Institute for Metals Superplasticity Problems of RAS, Ufa, Russia

² Kotelnikov Institute of Radio-engineering and Electronics of RAS, Moscow, Russia

irekmusabirov@mail.ru

Heusler alloys belong to a class of promising functional materials due to the presence of the effects such as the ferromagnetic shape memory effect and the magnetocaloric effect. The main disadvantage of these materials is the susceptibility to damage during cycling through the martensitic transformation, in which region the functional effects are observed. One way of solving this problem is additional thermomechanical processing of polycrystalline alloys after melting. The authors are actively developing the processing method of Heusler alloys by using the multiply isothermal forging (MIF). Through the use of this method it is possible to obtain relatively bulk samples with ultrafine-grained or fine-grained structures. The formation of such structures should contribute to increasing stability of the functional characteristics of a material by repeated cycling through the martensitic transformation temperature.

The paper presents the research results of the influence of plastic deformation by the method of multiply isothermal forging alloy system Ni-Mn-Ga. The microstructural study of the alloy in the initial state shows the presence of an uniaxial grains size of 100-200 microns. As a result of the deformation processing, microstructure of the alloy "necklace" type was obtained, i.e. large grain size of about 200 microns surrounded by chains of small grain size from 10 to 1 μm (fig. 1). It is assumed that the presence of this type of structure can significantly increase the service properties of the Heusler alloys.

The samples for the study of magnetic, electric and dilatometric properties of this alloy in the cast and deformed states are prepared. There are also cut samples for the study of functional properties of the alloy stability.

The reported study was funded by RFBR, according to the research project No. 16-32-60159 mol_a_dk.

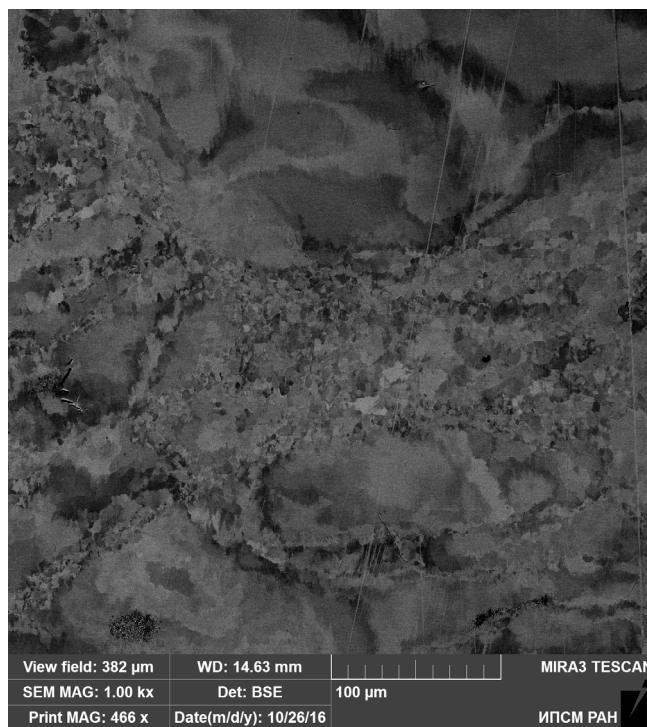


Fig. 1. Microstructure of Ni-Mn-Ga alloy after MIF

4PO-K-7

GIANT MAGNETOCALORIC EFFECT IN Mn(As,P) IN CYCLIC MAGNETIC FIELDS

Aliev A.M.¹, Gamzatov A.G.¹, Batdalov A.B.¹, Mukhuchev A.A.¹, Govor G.A.², Yanushkevich K.I.², Galias A.I.²

¹ Amirkhanov Institute of Physics of Daghestan Scientific Center RAS, Makhachkala, Russia

² Scientific-Practical Materials Research Centre of the National Academy of Sciences of Belarus, Minsk, Republic of Belarus
mukhuch87@mail.ru

First order phase transition materials are considered as the most promising for magnetic refrigeration technology. In these materials both magnetic and lattice subsystems contribute to the overall magnetocaloric effect (MCE) and giant value of MCE can be observed. These materials include MnAs in which one of the highest MCE near room temperature was discovered. In this report we present results of the direct measurements of the adiabatic temperature change in MnAs compound as well as in doped MnAs_xP_{1-x} ($x = 0.02, 0.025, 0.03$) ones in cyclic magnetic fields up to 8 T. The investigations show giant magnetocaloric effect in all studied MnAs_xP_{1-x} compositions and the existence of the critical magnetic field that induces reversible MCE in cyclic magnetic fields (Fig. 1). The substitution of As by P results in a slight shift of the Curie temperature and change in width of the temperature hysteresis and more pronounce change in the MCE value. The maximum value of the MCE is observed in MnAs and reaches a value of 13 K at magnetic field change of 8 T. In the composition with $x = 0.03$, two peaks are observed on the temperature dependence of the MCE, one peak is observed at $T = 312$ K, and the other peak is observed at $T = 272$ K. By measuring the field dependences of the MCE and magnetostriction, the magnetic and lattice contributions to the overall MCE were estimated in the studied materials.

The results of specific heat and thermal expansion studies are reported also.

This work is supported by RFBR, research project № 17-02-01195.

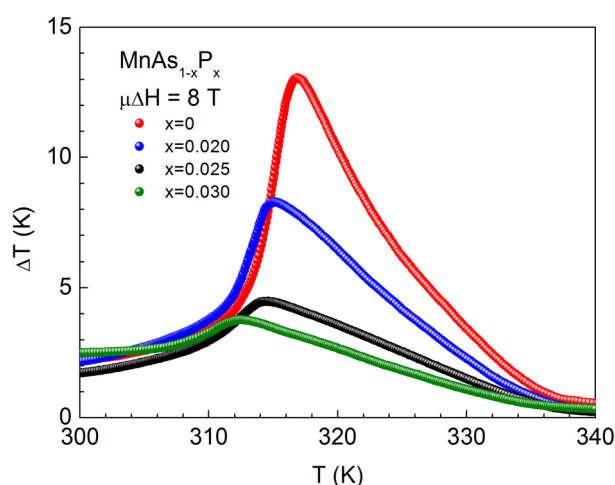


Fig. 1. Adiabatic temperature change in Mn_{1-x}P_x compounds at magnetic field change of 8 T.

4PO-K-8

PECULIARITIES OF THE MAGNETOCALORIC EFFECT IN THE FIRST ORDER PHASE TRANSITIONS MATERIALS IN CYCLIC MAGNETIC FIELDS

*Kurbanova D.R.¹, Aliev A.M.¹, Batdalov A.B.¹, Gamzatov A.G.¹, Khanov L.N.¹, Koledov V.V.²,
Shavrov V.G.²*

¹ Amirkhanov Institute of Physics of Daghestan Scientific Center RAS, Makhachkala, Russia

² Kotelnikov Institute of Radio Engineering and Electronics RAS, Moscow, Russia

d_kurbanova1990@mail.ru

Materials with first order magnetostructural phase transitions (MSPT) are considered as one of the most promising for the magnetic cooling technology. Therefore, studies of the behavior of magnetocaloric effect (MCE) in these materials in cyclic magnetic fields are of particular interest. There are several important problems concerning the behavior of the MCE and related phenomena in MSPT materials, which to date do not have a generally accepted solution. The problems include, in particular, the difference in the MCE values in the heating and cooling modes near the MSPT regions, the dependence of the MCE value on the rate of temperature change, the problem of estimating the contributions of the magnetic and structural subsystems to the overall magnetocaloric effect, etc. The investigation of the MCE in cyclic magnetic fields allows us to find solutions to some of these issues. The investigation of MCE in cyclic magnetic fields is also important from the viewpoint of that in real magnetic refrigeration systems the working body of the refrigerator is exposed to a cyclic magnetic field. In this report we discuss one of the problems, namely, the difference in the values of the MCE in the heating and cooling modes at MSPT, and explain this phenomenon on the basis of MCE, thermal expansion, and magnetostriction in constant and alternating magnetic fields. The results of the MCE investigation in cyclic fields in various MSPT materials, namely, in Heusler alloys Ni-Mn-In, Fe-Rh alloy, $\text{Sm}_{1-x}\text{Sr}_x\text{MnO}_3$ manganites and $\text{MnAs}_x\text{P}_{1-x}$ compounds are reported. In the first two compositions, the inverse MCE takes place in the region of the MSPT, while the direct MCE is observed in the latter two. In all studied materials, there is a difference in the MCE values in the heating and cooling regimes in low magnetic fields. The MCE behavior in various materials is general but there are some differences. The common feature for all compounds is that in low fields the difference in the MCE values in the heating and cooling modes is significant and disappears with the magnetic field increase. The difference in MCE is due to the combination of temperature hysteresis and the difference in the field and temperature history of materials in the region of the MSPT in the heating and cooling modes. The MCE values in the heating and cooling modes are equal to each other when the magnetic field is sufficient to shift the temperature of the MSPT beyond the limits of the temperature hysteresis to zero fields.

This work is supported by RFBR, research project № 17-02-01195.

4PO-K-9

MAGNETIC AND STRUCTURAL CONTRIBUTION TO MAGNETOCALORIC EFFECT

Khanov L.N., Batdalov A.B., Mukhuchev A.A., Aliev A.M.

Amirkhanov Institute of Physics of Daghestan Scientific Center RAS, Makhachkala, Russia
hanov82@mail.ru

In recent times, the materials in which the change of a magnetic state is attended with a change in the structure or volume of a lattice are searched. In some cases, a change in the entropy of lattice and magnetic subsystems is combined and a giant MCE is observed in such materials.

The estimation of contributions of magnetic and lattice subsystems into the general MCE allows goal-directed searches for materials with giant MCE. The synthesis of novel materials based on the already-existing must arrange for the amplification of one contribution without decreasing another.

This abstract presents the experimental results for the MCE and the magnetostriction of some magnetic materials in a region of magnetic structural phase transitions in alternate magnetic fields up to 80 kOe. The temperature and field dependences of the MCE and the magnetostriction obtained under the same conditions allow us to determine the contributions of magnetic and lattice subsystems to the overall magnetocaloric effect. Contributions of magnetic and lattice subsystems are estimated from the suggestion that the magnetic contribution changes according to the law of $\Delta T_m \sim H^{2/3}$ and the lattice contribution is directly proportional to the magnetostriction. In low fields (several kOe), the MCE is caused only by a change in the entropy of the magnetic subsystem. When increasing the magnetic field the structural contribution is also appear in the region of the magnetic structural transition. The estimation of contributions shows a complex character of the dependence of magnetic and structural contributions into the general MCE on the temperature and magnetic field. This may be caused by the non-trivial behavior of the magnetostriction in cyclic magnetic fields: in the lower field (up to 6 kOe) the magnetostriction is observed not only in the region of the magnetic structural transition but in the whole temperature interval from the region of the magnetic structural transition (~ 240 K), gradually decreasing in value, up to the Curie point (~ 320 K). In the stronger field the magnetostriction is observed only in the region of the magnetostructural transition.

Thus, the lattice and magnetic contributions to the overall MCE in materials with magnetostructural phase transitions are estimated basing on the results of measuring the field dependences of MCE and magnetostriction.

The reported study was funded by RFBR according to the research project No. 16-32-00633 mol_a.

4PO-K-10

SPECIFIC HEAT AND MAGNETOCALORIC PROPERTIES OF Cu_2MnBO_5 LUDWIGITE

Gamzatov A.G.¹, Aliev A.M.¹, Moshkina E.², Bezmaternykh L.²

¹ Amirkhanov Institute of Physics, DSC of RAS, 367003, Makhachkala, Russia

² L.V. Kirensky Institute of Physics SB RAS, 660036 Krasnoyarsk, Russia
gamzatov_adler@mail.ru

Ludwigites have a complex crystal structure, which involves quasi-low-dimensional elements (zigzag walls and three-legged ladders) formed by metal-oxygen octahedral. Cu_2MnBO_5 belongs to the family of quasi-two-dimensional oxyborates with the ludwigite structure.

This work presents the results of the study of specific heat and magnetocaloric properties in Cu_2MnBO_5 single crystal ludwigite in the temperature range 60-350 K and in magnetic fields up to 18 kOe. In particular, the anisotropy of the MCE in a magnetic field of 18 kOe and the frequency dependence of the magnetocaloric effect in magnetic field of 6.2 kOe were measured.

The specific heat was measured by the ac-calorimetry. Direct measurements of the adiabatic temperature change ΔT with a change of the external magnetic field were carried out by a modulation method. The MCE was estimated from the specific heat data also.

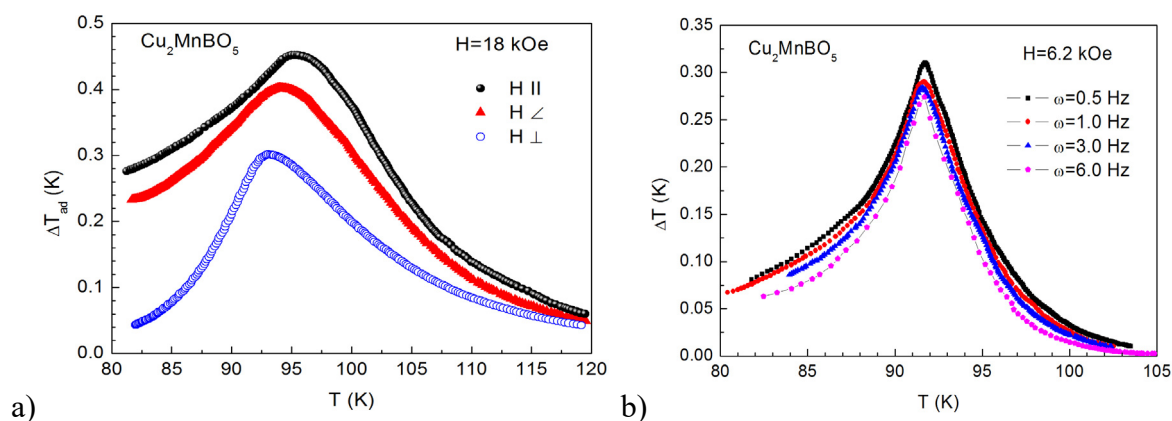


Fig. 1. a) Dependence of MCE on temperature in different orientations of the magnetic field. b) The frequency dependence of the MCE in the magnetic field at 6.2 kOe.

On the temperature dependence of the specific heat at $T = 91$ K a lambda anomaly is observed, which is suppressed in the magnetic field. The maximum value of the MCE according to the direct measurements in a magnetic field of 18 kOe equals to $\Delta T = 0.45$ K. Investigation of the MCE anisotropy shows that its maximum depends on the field direction and decreased by 1.5 times, from $\Delta T = 0.45$ K in a parallel orientation to $\Delta T = 0.3$ K at a perpendicular magnetic field orientation. The change of the magnetic entropy due to the magnetocaloric effect in a magnetic field of 6.2 kOe is equal 1.07 J/kg K. Influence of the frequency of the magnetic field (up to 10 Hz) on the MCE are studied also. There is a weak dependence of the MCE value on the frequency.

4PO-K-11

MAGNETOSTRICTION AND MAGNETOCALORIC EFFECT IN THE Ni₄₆Mn₄₁In₁₃ HEUSLER ALLOY

*Batdalov A.B.*¹, *Aliiev A.M.*¹, *Khanov L.N.*¹, *Koledov V.V.*², *Shavrov V.G.*²

¹ Amirkhanov Institute of Physics of Daghestan Scientific Center RAS, Makhachkala, Russia

² Kotelnikov Institute of Radio Engineering and Electronics RAS, Moscow, Russia
hanov82@mail.ru

This abstract presents the experimental results for the thermal expansion ($\Delta l/l_0$) and the magnetocaloric effect (ΔT_{ad}) in Ni₄₆Mn₄₁In₁₃ alloy which demonstrates magnetic and magnetostructural phase transitions.

When the structural transition is followed by an increase in the volume of a crystal lattice ($\Delta V/V_0 > 0$) under the influence of a magnetic field, the change of the entropy ΔS_{str} under adiabatic conditions will be attended with a cooling of the sample ($\Delta T < 0$), and with heating, if otherwise. The sign of the thermal expansion coefficient indicates whether the structural contribution to the overall entropy change will cause heating or cooling of the sample.

For the purpose of elucidation of this question we measured the dependence of the thermal expansion ($\Delta l/l_0$) and the magnetocaloric effect (ΔT_{ad}) in Ni₄₆Mn₄₁In₁₃ on a temperature and a magnetic field.

The available literature data on the thermal expansion in Ni-Mn-In alloys are contradictory [1, 2]. According to our measurements, presented in Fig. 1, the application of the magnetic field is followed by the sample contraction ($\Delta V/V_0 < 0$) that must result in its heating.

The comparison between the $\Delta V/V_0$ value, estimated from $\Delta l/l_0$ data, the empirical dependency $\Delta S_{str} = f(\Delta V/V_0)$, presented in [3], and the experimental data of $\Delta T_{ad}(T)$ are indicative of insignificant influence of the structural subsystem on the $\Delta T_{ad}(T)$ behavior.

The experimental findings on the temperature and magnetic-field dependence of $\Delta T_{ad}(T)$ near the magnetic and structural phase transition temperatures are reported and discussed.

The reported study was funded by RFBR according to the research project No. 16-32-00633 mol_a.

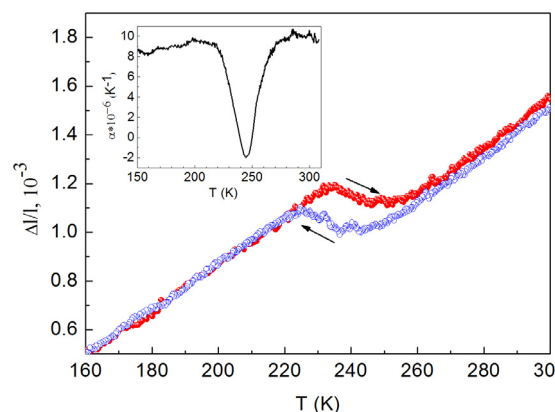


Fig. 1. Temperature dependence of the thermal expansion. Inset shows the thermal expansion coefficient.

[1] V. M. Schastlivtsev, Yu. V. Kaletina et al, *The Physics of Metals and Metallography*, **112** (2011) 61.

[2] A. Pathak, B. Gautam et al., *Journal of Applied Physics*, **103** (2008) 07F315.

[3] K.A. Gschneidner, Jr.Y. Mudryk, V.K. Pecharsky, *Scripta Materialia*, **67** (2012) 572-577.

4PO-K-12

LATTICE DYNAMIC OF ANTIFERRO- AND FERRO-MAGNETIC PHASES OF FeRh

Syzdykova A.B.¹, Belov M.P.¹, Ponomareva A.V.¹, Smirnova E.A.¹, Abrikosov I.A.^{1,2}

¹ Materials Modeling and Development Laboratory, National University of Science and Technology "MISIS" (MISIS), Leninskii Pr 4, Moscow 119049, Russia

² Department of Physics, Chemistry and Biology (IFM), Linköping University, SE-581 83 Linköping, Sweden
aykosy@mail.ru

FeRh undergoes an unusual antiferromagnetic-to-ferromagnetic (AFM-FM) transition just above room temperature. This magnetic transition was discovered for the first time in the late 1930s [1] but the origin of this transition is still a source of active debate. There are basic questions about what drives this transition, and usually the driving force is discussed in terms of magnetic, lattice and electronic entropy differences between the phases. The lattice entropy was extracted from experimental data only at low temperatures [2]. Recent theoretical calculations of the lattice dynamics of both phases have shown that the AFM phase of this compound is dynamically unstable, and the corresponding modulated structure has an energy below the ideal only by 0.125 meV [3]. This small difference in energy can lead to dynamical stabilization of ideal structure due to the zero-point vibrations of the atoms. In this work we have carried out calculations in the framework of Temperature Dependent Effective Potential method (TDEP) [4] based on atomic displacements corresponding to zero-temperature atomic vibrations amplitude and obtained full phonon spectra and corresponding lattice entropies of AFM and FM FeRh in the wide temperature range. In this way we have clarified the effect of lattice entropy difference term.

The support from the Grant of Ministry of Education and Science of the Russian Federation (Grant No. 14.Y26.31.0005) and the Grant of Russian Foundation for Basic Research (No. 16-02-01027) is gratefully acknowledged.

- [1] M. Fallot, *Ann. Phys. Serie*, **11** 18 (1938) 291.
- [2] David W. Cooke and F. Hellman, *Phys.Rev.Lett*, **109** (2012) 255901.
- [3] U. Aschauer et al., *Phys.Rev.B*, **94** (2016) 014109.
- [4] O. Hellman, I.A. Abrikosov, & S.I. Simak, *Phys. Rev. B*, **84** (2011) 180301.

4PO-K-13

MARTENSITIC TRANSFORMATION AND MAGNETIC PROPERTIES IN Ni-Mn-Ga/Al₂O₃ AND FREESTANDING FILMS

Shevyrtalov S.¹, Miki H.², Ohtsuka M.³, Mashirov A.⁴, Grunin A.¹, Lyatun I.¹, Seredina M.⁵, Khovaylo V.⁵, Rodionova V.¹

¹ STP “Fabrika” & FunMagMa, Immanuel Kant Baltic Federal University, Kaliningrad, Russia

² FRIS, Tohoku University, Sendai, Japan

³ IMRAM, Tohoku University, Sendai, Japan

⁴ Kotelnikov IRE RAS, Moscow, Russia

⁵ National University of Science and Technology MISiS, Moscow, Russia
shevyrtalov@gmail.com

Magnetic shape memory alloys (MSMA) based on off-stoichiometric Ni₂MnGa Heusler alloy show a first-order reversible martensitic transformation (MT) from the high temperature cubic L2₁ phase (austenite) to a low temperature phase (martensite) with lower symmetry [1], which can be induced by single or multiple effect of heating, stress or magnetic field.

Here we report an experimental study of Ni-Mn-Ga Heusler alloy film with Ni- and Ga-excess on polycrystalline alumina substrate in comparison with freestanding film (FS). Both obtained films had 2- μ m thickness and martensitic phase transition above the room temperature that is not typical for such composition (Fig. 1a, b). The martensitic phase transition region was found to be wider in the freestanding film. Both the films demonstrate isotropic behavior of magnetic properties for in-plane direction of magnetic field that is related to the presence of (202) fiber texture. Magnetically induced reorientation of variants (MIR) was observed in freestanding film at magnetic field of 0.73 kOe (Fig. 1c). In case of substrate-constrained film MIR process does not occur. Only widening in magnetization loops due to the internal compressive stresses was observed. For the freestanding film, easy magnetization axis orients normally to the film plane, while for the substrate-constrained film it has preferred easy magnetization plane. Both films demonstrate a maze-like surface magnetic domain structure with domain width of about 0.9 μ m.

The differences between the substrate-constrained and the freestanding films were described in terms of compressive stress influence and film growth modes.

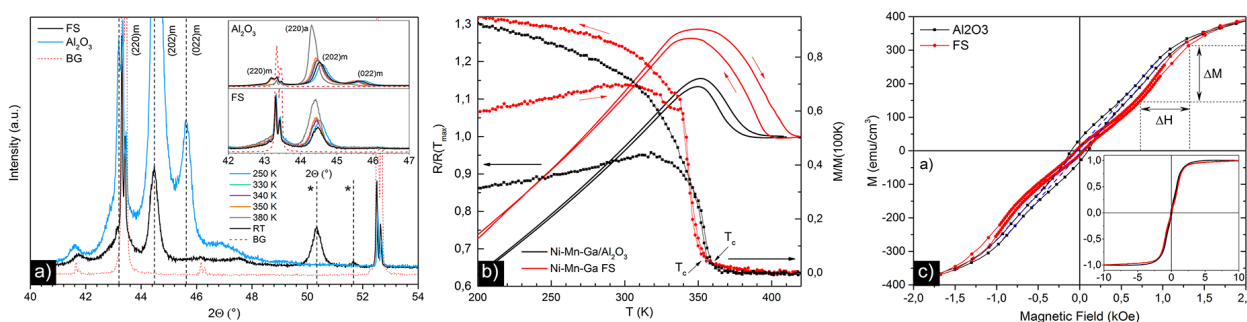


Figure 1. a) XRD pattern made at room temperature. Phase-temperature dependence is shown in the inset; b) Normalized temperature-dependent magnetization curves with applied magnetic field of 0.1 kOe and electrical resistance curves; c) Small field range part of normalized magnetization loops measured in-plane. The inset shows in-plane magnetization loops in field of ± 10 kOe

[1] S. Kaufmann, U.K. Röbler, O. Heczko, M. Wuttig, J. Buschbeck, L. Schultz, S. Fähler, *Physical Review Letters*, **104** (2010)145702.

4PO-K-14

MAGNETOCALORIC EFFECT OF Gd(T-Fe)₂ COMPOUNDS, WERE T = Co, Ni

Anikin M.S., Tarasov E.N., Kudrevatykh N.V., Zinin A.V.

Ural Federal University, Ekaterinburg, Russia

Maksim.Anikin@urfu.ru

RCO₂ or RNi₂ type binary compounds (R are the heavy rare earth elements) possess a high magnetocaloric effect (MCE) at their Curie point (T_c) [1]. The study of the magnetic properties and MCE in the R(T-Fe)₂ (R = Tb, Dy, Ho, Er, T = Ni, Co) systems shown that a partial substitution of T by Fe courses a significant MCE in a wide temperature range below T_c [2].

It is well known that the RFe₂ type compounds having a non-zero R³⁺-ion orbital momentum, possess of enormous magnetocrystalline anisotropy (MCA) at low temperatures originating from crystal field (CF) mechanism [3]. Such MCA mechanism can produce the "umbrella"-like magnetic structure in the R-ions subsystem due to a local MCA fluctuations caused by a random substitution of Me-atoms by Fe ones at the nearest to R-ions positions in R(T-Fe)₂ [2]. In order to find out whether this factor is a key one for the MCE phenomena in R(T-Fe)₂, in this study we examined the magnetic properties and MCE of Gd(T_{1-x}Fe_x)₂ (x ≤ 0.12) compounds. As far as the orbital magnetic moment of the Gd³⁺-ions in pure metal or in compounds with 3d metals is close to zero, the Gd-sublattice does not possess of a high MCA from CF-mechanism [4].

Alloys were melted in an arc furnace with helium protective atmosphere. The techniques of X-ray diffraction analysis, magnetic phase analysis and magnetization curves measurements, magnetic entropy change calculation (ΔS_m) which described in [2] have been used.

The studied alloys show the MCE peak broadening upon the Fe concentration increase. For the Gd(Co-Fe)₂ system this broadening is much less than for the Gd(Ni-Fe)₂ system. Fig. 1 presents the relative ΔS_m temperature dependence of Gd(T_{0.88}Fe_{0.12})₂ samples, where the ΔT_{FWHM} value characterizes the MCE peak width [1]. For comparison of the magnetocaloric materials from the practical applications point of view the refrigerating capacity (q) has been calculated [1]. The grey and shaded areas (Fig. 1) correspond to the region of integration at q calculation. These data are 220 J/kg and 40 J/kg at ΔH = 15 kOe for compounds with Ni and Co respectively. The possible reasons of such MCE temperature dependences are discussed.

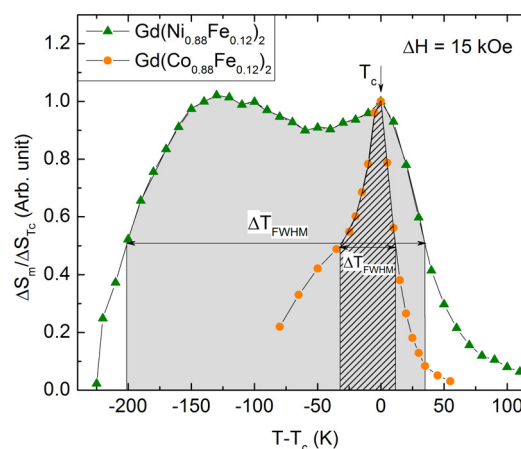


Fig. 1. Relative ΔS_m temperature dependences of Gd(T_{0.88}Fe_{0.12})₂ compounds

The work was supported by the State contract No 3.6121.2017 between UrFU and MES RF and partially by the Fund of assistance to development of small forms enterprises in scientific-technical sphere No. 6576GU/2015.

- [1] K.A. Gschneidner Jr., V.K. Pecharsky, A.O. Tsokol, *Rep. Prog.Phys.*, **68** (2005) 1479–1539.
 [2] M. Anikin, E. Tarasov, et al., *J. Magn. Magn. Mater.*, **418** (2016) 181–187.
 [3] A.M. Van Der Kraan, P. Gubbens, *J. Phys. Colloq.*, **35** (1974) C6-469–C6-472.
 [4] A.E. Baranovskiy, G.E. Grechnev, et al., *J. Magn. Magn. Mater.*, **258–259** (2003) 520–522.

4PO-K-15

EFFECT OF SUBSTITUTION ON MAGNETOCALORIC PROPERTIES OF MELT-SPUN $\text{Gd}_{75}(\text{Fe}_{1-x}\text{M}_x)_{25}$ ($\text{M} = \text{Co}, \text{Ni}$) ALLOYS

Shishkin D.A.^{1,2}, *Gazizov A.I.*², *Volegov A.S.*^{1,2}, *Gaviko V.S.*^{1,2}, *Baranov N.V.*^{1,2}

¹ M.N. Miheev Institute of Metal Physics, Ekaterinburg, Russia

² Ural Federal University, Ekaterinburg, Russia

shishkin@imp.uran.ru

Gadolinium-based materials are prospective for applications in magnetic refrigeration. The amorphization of alloys with different compositions allows varying the magnetic transition temperature. Thus, it's possible to design new composite materials for efficient magnetic cooling in different temperature ranges. The amorphous $\text{Gd}_{75}\text{Co}_{25}$ and $\text{Gd}_{75}\text{Ni}_{25}$ alloys prepared by a melt-spinning technique are found to exhibit a ferromagnetic (F) behavior unlike antiferromagnetic (AF) ordering in the crystalline compounds. The crystalline Gd_3Co and Gd_3Ni compounds have the Neel temperature $T_N = 130$ and 99 K, respectively, and show the AF-F phase transition under application of the magnetic field. [1]. However, a substantial growth of the magnetic ordering temperatures up to 172 K and 118 K has been observed in the melt-spun ribbons, which is associated with the appearance of a magnetic moment on transition metal atoms [2]. The replacement of Fe by Co leads to an increase of the magnetic moment per transition metal atom from $1.1 \mu_B$ for melt-spun $\text{Gd}_{75}\text{Fe}_{25}$ up to $1.6 \mu_B$ for melt-spun $\text{Gd}_{75}\text{Co}_{25}$. A magnetic moment of about $1.2 \mu_B$ per Ni atom is derived from the magnetization measurements for melt-spun $\text{Gd}_{75}\text{Ni}_{25}$. The Fe-containing alloys are observed to exhibit an extended magnetic anomaly around the magnetic ordering temperature.

For amorphous $\text{Gd}_{75}(\text{Fe}_{1-x}\text{M}_x)_{25}$ alloys the maximal values of isothermal magnetic entropy change are observed to increase with replacing Fe by Co from $1.7 \text{ J}/(\text{kg K})$ for $x = 0$ up to $4.9 \text{ J}/(\text{kg K})$ for $x = 1$ under a magnetic field change ΔH of 20 kOe . The substitution of Fe for Ni results in rise of the $-\Delta S_m$ from $1.7 \text{ J}/(\text{kg K})$ for $\text{Gd}_{75}\text{Ni}_{25}$ up to $3.4 \text{ J}/(\text{kg K})$ for $\text{Gd}_{75}\text{Fe}_{25}$ and reduces the Curie temperature.

This work was supported by the Program of Ural Branch of RAS (project No 15-17-2-22) and by FASO Russia (project № 01201463328).

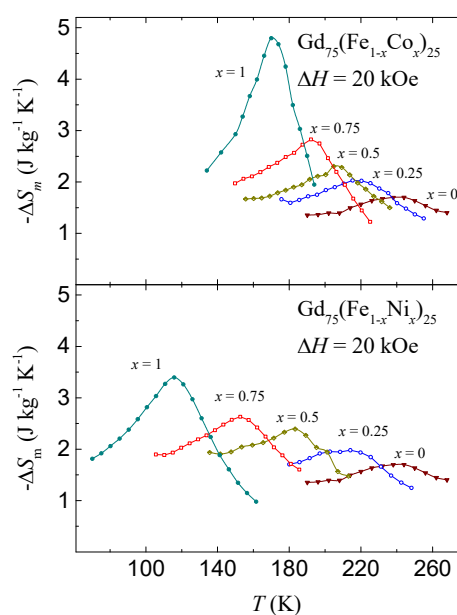


Fig. 1. The $-\Delta S_m$ versus T at a field change of 20 kOe for the melt-spun $\text{Gd}_{75}(\text{Fe}_{1-x}\text{Co}_x)_{25}$ and $\text{Gd}_{75}(\text{Ni}_{1-x}\text{Fe}_x)_{25}$ alloys.

- [1] N.V. Tristan, S.A. Nikitin, T. Palewski, K. Skokov, *J. Magn. Magn. Mater.*, **251** (2002) 148-154.
 [2] D.A. Shishkin, A.S. Volegov, S.V. Andreev, N.V. Baranov, *Phys. Met. Metall.*, **113** (2012) 460-465.

4PO-K-16

BARIC PECULIARITIES OF THE MAGNETIC AND MAGNETOCALORIC PROPERTIES OF THE $Mn_{1-x}Cr_xNiGe$ SYSTEM

Valkov V.I.¹, Gribanov I.F.¹, Golovchan A.V.^{1,2}, Zaporozhets V.D.^{1,2}

¹ State Institution Donetsk Institute for Physics and Engineering named after A.A.Galkin (DonPhTI), Donetsk, Donetsk People's Republic

² State Educational Institution Donetsk National University (DonNU), Donetsk, Donetsk People's Republic
valkov09@gmail.com

Investigations of the germanides of the $Mn_{1-x}Cr_xNiGe$ system [1, 2] made it possible to suggest a fundamental change in the magnetostructural properties and a significant enhancement of the magnetocaloric effect (MCE) under pressure. This report presents the results of measurements of the temperature dependence of the magnetization $M(T)$ under pressure up to 10 kbar and theoretical analysis within the model taking into account the interaction of the magnetic and structural order parameters, and the found baric effects are justified [2].

1. It is shown that the appearance of a ferromagnetic (FM) order (fig.1a) with an orthorhombic crystal structure (orth) as a result of an anhysteric isostructural 2nd order phase transition PM(orth) - FM(orth) is a consequence of the strong interaction of the magnetic and structural order parameters, fig.1b.

2. The change of the PM-FM phase transition order under pressure (fig.1a, b) is due to the combination of magnetic and structural transitions and transformation of the isostructural magnetic transition PM(orth) - FM(orth) (fig.1.b) to a 1st order magnetostructural transition PM(hex) - FM(orth) (fig.1.e).

3. The magnification of the magnetocaloric effect under pressure (fig.1c, f) is predicted due to the combination of magnetic and structural transitions.

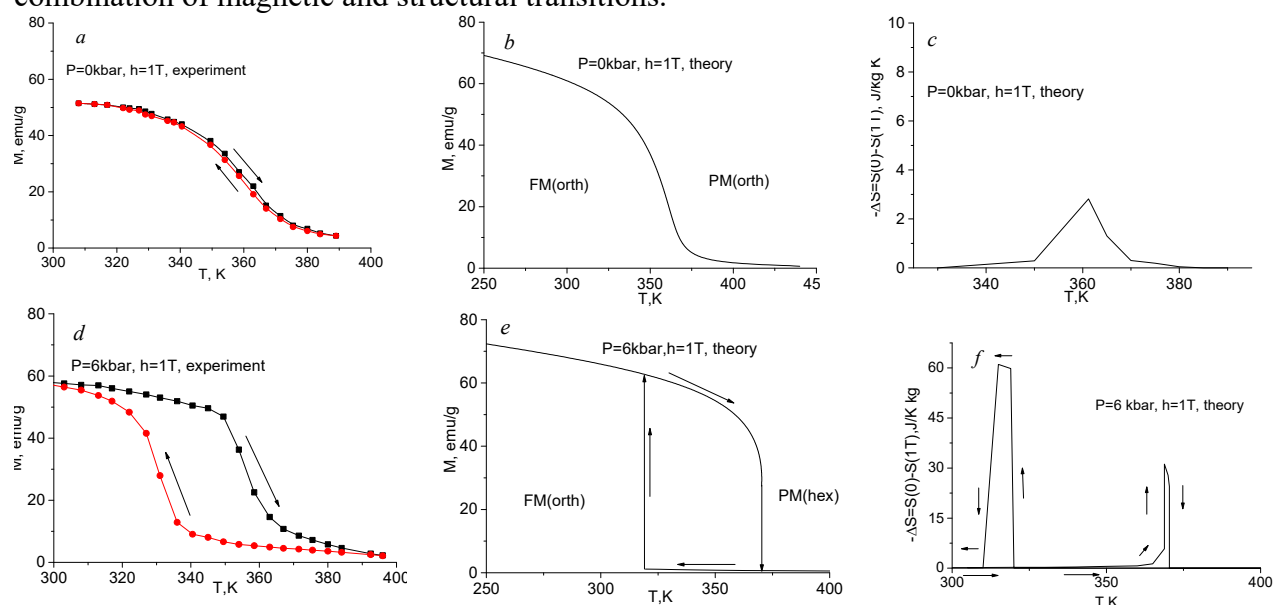


Figure 1. Experimental and theoretic magnetization and entropy changes in $Mn_{0.89}Cr_{0.11}NiGe$.

[1] T. Jaworska-Gołab, S. Baran, R.Duraj et al. *JMMM*, **385** (2015) 1-6.

[2] V.I.Valkov, V.I.Kamenev, V.I.Mitsuk et al. *Fizika Tverdogo Tela*, **59** (2017) 266-274.

4PO-K-17

**MAGNETOCALORIC EFFECT IN FeRhPd ALLOYS IN THE FIRST ORDER
MAGNETIC PHASE TRANSITION TEMPERATURE REGION***Gimaev R.R.¹, Zverev V.I.², Tishin A.M.^{1,2}, Miyanaga T.³*¹ Advanced Magnetic Technologies and Consulting LLC, Troitsk, Moscow, Russia² Faculty of Physics, M.V. Lomonosov Moscow State University, Moscow, Russia³ Department of Mathematics and Physics, Hirosaki University, Hirosaki, Aomori, Japan
gimaev@amtc.org

The large magnetocaloric effect (MCE), which is observed in the whole family of FeRh alloys, has been investigated in Pd-doped samples in slowly cycled magnetic fields of up to 1.8 T in magnitude for a range of temperatures, $250\text{ K} < T < 350\text{ K}$. The shift of the ferromagnetic/antiferromagnetic transition temperature down towards room temperature and the decrease in the MCE have been observed in these alloys in comparison with a quasi-equiatomic FeRh alloy. The measurements have also shown an asymmetric behavior of the first order magnetic phase transition with respect to whether the transition is traversed by heating from lower temperatures or cooling from above. These peculiarities have been explained in the framework of the *ab-initio* density functional theory-based disordered local moment theory of the MCE. The results have been compared with the those for the non-doped FeRh alloy. Thus features of the first order magnetic phase transition that these alloys have in common have been revealed which enable some predictions to be made appropriate for practical applications.

The authors thankful to Prof. Julie B. Staunton for useful discussions. Work at Advanced Magnetic Technologies and Consulting LLC is supported by Skolkovo Foundation, Russia. Authors acknowledge support by the AMT&C Group Ltd., UK.

4PO-K-18

INVESTIGATION OF MAGNETIC PHASE TRANSITION AND MAGNETOCALORIC EFFECT OF (Ni,Co)-Mn-(Sn,Al) MELT-SPUN RIBBONS

Nguyen Hai Yen^{1,2}, *Vu Manh Quang*^{2,3}, *Nguyen Thi Mai*⁴, *Pham Thi Thanh*^{1,2}, *Kamantsev A.P.*⁵,
*Koledov V.V.*⁵, *Mashirov A.V.*⁵, *Tran Dang Thanh*^{1,6}, *Kieu Xuan Hau*⁶, *Yu S.C.*⁶, *Nguyen Huy Dan*^{1,2}

¹ Institute of Materials Science, Vietnam Academy of Science and Technology, Viet Nam

² Graduate University of Science and Technology, Vietnam Academy of Science and Technology,
Viet Nam

³ Faculty of Physics, Hanoi Pedagogical University 2, Viet Nam

⁴ Faculty of Physics, VNU University of Science, Viet Nam

⁵ Kotelnikov Institute of Radio-engineering and Electronics of RAS, Moscow, Russia

⁶ Department of Physics, Chungbuk National University, Cheongju 361 - 763, South Korea.

yennh@ims.vast.ac.vn

The Heusler alloys of Ni-Mn-Z (Z = Ga, In, Sb, Sn, Al) have a lot of interesting features such as half metallic, magnetoresistance, magnetic shape memory effect, magnetocaloric effect... Their structure and properties are very sensitive to composition and fabrication conditions. In this work, we investigate systematically influence of Co-concentration on magnetic phase transition and magnetocaloric effect of (Ni,Co)-Mn-Z (Z = Sn, Al) alloy ribbons prepared by using melt-spinning method. The results show that the Co-concentration strongly influences on magnetic phase transitions of the alloys (Fig. 2). However, the effect of Co on the magnetic phase transitions is greatly different in the two systems with Z = Sn and Al. Amplitude and temperature of Martensitic-Austenitic structure phase transformation of the alloys are also clearly dependent on the Co-concentration. X-ray diffraction patterns manifest multi-crystalline phase behavior of the alloy ribbons including L1₀, B2 and 10M phases. Magnetization measurements exhibit soft magnetic feature with coercive force less than 70 Oe for all the alloy ribbons. Curie temperature of the alloy increases with increasing the Co concentration and decreases with increasing the Al concentration. Magnetic phase transitions in the alloy can be shifted to room temperature region by adjusting Co and Al concentrations. With appropriate compositions, the alloy ribbons possesses both the positive and negative magnetocaloric effects with their maximum magnetic entropy change larger than 0.6 J.kg⁻¹.K⁻¹ in magnetic field change of 12 kOe (Fig. 2). The temperature and magnetic field dependence of these alloys was also investigated.

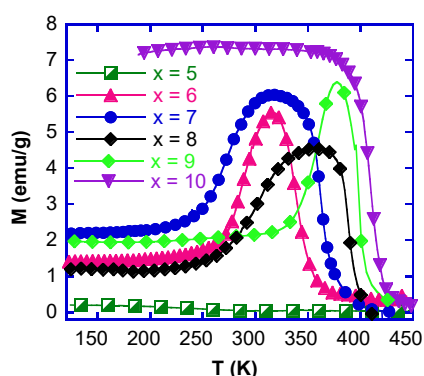


Fig. 1. Thermomagnetization curves in magnetic field of 100 Oe of Ni_{50-x}Co_xMn₃₂Al₁₈ melt-spun ribbons.

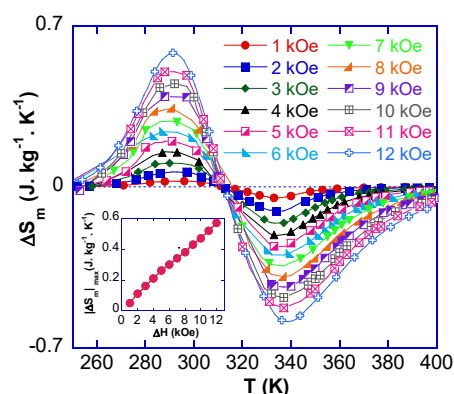


Fig. 2. $\Delta S_m(T)$ curves with various magnetic field change of Ni₄₄Co₆Mn₃₂Al₁₈ ribbon. The inset shows magnetic field dependence of $|\Delta S_m|_{\max}$.

Support by Vietnam Academy of Science and Technology (grant No. VAST.HTQT.NGA.05/17-18) and Russian Foundation for Basic Research (grant № 17-58-540002) is acknowledged.

4PO-K-19

STRUCTURAL, MAGNETIC AND THERMAL PROPERTIES OF HEUSLER ALLOYS Pd₂MnX (X=Ga, Ge, As, In, Sn, Sb, Tl, Pb, Bi): AB INITIO STUDY

Miroshkina O.N.¹, Zagrebin M.A.¹, Sokolovskiy V.V.¹, Buchelnikov V.D.¹

¹Chelyabinsk State University, Chelyabinsk, Russian Federation

miroshkina.on@yandex.ru

Heusler alloys exhibit a number of unique properties such as shape memory effect, effects of superelasticity and superplasticity, giant magnetocaloric effect, giant magnetoresistance and magnetostrain, etc. These effects are associated with martensitic transformations [1-4].

The objective of this work is *ab initio* investigation of the Heusler compounds Pd₂MnX (X=Ga, Ge, As, In, Sn, Sb, Tl, Pb, Bi). All the first-principles calculations on Pd₂MnX are performed based on density functional theory (DFT) as implemented by The Vienna Ab initio simulation package (VASP) [5,6] and Spin Polarized Relativistic Korringa-Kohn-Rostoker (SPR-KKR) [7].

The Heusler compounds Pd₂MnX are L21 type cubic structure with space group Fm-3m (No. 225). The conventional cell consisting of 4 atoms with a cell formula of Pd₂MnX is used for the present calculations. The X atoms locate on the 4a Wyckoff site with fractional coordinates (0, 0, 0), the Pd atoms occupy 8c Wyckoff site with (1/4, 1/4, 1/4), and Mn atom possess 4b Wyckoff site with fractional coordinates (1/2, 1/2, 1/2).

Total energy versus lattice parameter response characteristic for each compound Pd₂MnX was obtained. The equilibrium lattice constant is approximately 6.25 Å for Pd₂Mn(Ga, Ge, As), 6.45 Å for Pd₂Mn(In, Sn, Sb), and 6.57 Å for Pd₂Mn(Tl, Pb, Bi). Found equilibrium lattice constants were used for calculation magnetic exchange interaction and total density of states (DOS).

Analysis of the dependence of energy on tetragonal distortions showed that the energy minimum exists at c/a ratio of 1.3 for alloys Pd₂MnGa, Pd₂MnGe, Pd₂MnAs, Pd₂MnIn, Pd₂MnSn, Pd₂MnSb, and Pd₂MnTl.

- [1] P. Entel, V.D. Buchelnikov, V.V. Khovailo et al, *J. Phys. D: Appl. Phys.*, **39** (2006) 865.
- [2] V.D. Buchelnikov, A.N. Vasiliev, V.V. Koledov et al, *Physics-Uspekhi*, **49** (2006) 871-877.
- [3] P. Entel, M. E. Gruner, A. Dannenberg, *Mat. Sci. Forum*, **635** (2010) 3-12.
- [4] P.J. Webster, K.R.A. Ziebeck, S.L. Town, M.S. Peak, *Philos. Mag. B*, **49** (3) (1984) 295.
- [5] G. Kresse, J. Furthmuller, *Phys. Rev. B*, **54** (1996) 11169.
- [6] G. Kresse and D. Joubert, *Phys. Rev. B*, **59** (1999) 1758.
- [7] H. Ebert, D. Kodderitzsch, J. Minar, *Rep. Prog. Phys.*, **74** (2011) 096501.

4PO-K-20

THE INFLUENCE OF FERRIMAGNETIC STRUCTURE ON MAGNETOCALORIC EFFECT IN $\text{Dy}_2\text{Fe}_{10}\text{Al}_7$ COMPOUND

*Smarzhevskaya A.I.¹, Nikitin S.A.¹, Pankratov N.Yu.¹, Rogacki K.², Koshkid'ko Yu.S.², Cwik J.²,
Karpenkov A.Yu.³, Karpenkov D.Yu.⁴, Pastushenkov Yu.G.³*

¹ M.V. Lomonosov Moscow State University, Moscow, Russia

² ILHMF<, Wroclaw, Poland

³ Tver State University, Tver, Russia

⁴ National University of Science and Technology "MISiS," Moscow, Russia

Smarzhevskaya@physics.msu.ru

The magnetocaloric effect (MCE) has been intensively studied in the ferromagnetic rare-earth compounds. However, the MCE features for the ferrimagnetic materials have not been sufficiently studied.

The ferrimagnetic rare earth compound $\text{Dy}_2\text{Fe}_{10}\text{Al}_7$ was chosen as the object of our investigation. The mentioned compound has two magnetic sublattices: dysprosium and 3d-metal, with antiparallel sublattice magnetisations. Some of $\text{Dy}_2\text{Fe}_{10}\text{Al}_7$ magnetic properties were established earlier [1]. The specific character of ferrimagnetism is most clearly manifested in the range of magnetic compensation temperature T_k . Therefore we carried out a detailed study of the magnetic and magnetothermal properties of $\text{Dy}_2\text{Fe}_{10}\text{Al}_7$ compound in the range of magnetic compensation temperature and Curie temperature.

The $\text{Dy}_2\text{Fe}_{10}\text{Al}_7$ compound was prepared by induction melting method. The crystal structure and phase composition of the powder samples were determined by X-ray diffraction analysis. The diffraction pattern indicates that the $\text{Dy}_2\text{Fe}_{10}\text{Al}_7$ compound has rhombohedral $\text{Th}_2\text{Zn}_{17}$ -type structure (with R3m space group).

The field dependencies of magnetization σ in the 4,2-300K range in magnetic fields up to 100 kOe were investigated. Noteworthy the curves $\sigma(H)$ are not saturated in high fields up to 100kOe both at $T < T_k$ and at $T > T_k$.

The temperature dependencies of MCE were investigated in magnetic fields up to 70kOe. The change in the MCE sign from positive to negative in the region of compensation temperature is observed. The maximum of MCE below T_k shifts to lower temperatures with increasing magnetic field. In the region of Curie temperature $T_C \sim 235\text{K}$ the MCE maximum is also observed.

The molecular field theory for magnetisation and MCE description is used [2]. The estimations of the effective exchange field value near T_k are made on the basis of this theory using the experimental data. The obtained value is in good agreement with that reported earlier [1] for $\text{Dy}_2\text{Fe}_{10}\text{Al}_7$ compound.

The obtained experimental results and theoretical estimations show that the temperature and field dependencies of the MCE in the ferrimagnetic $\text{Dy}_2\text{Fe}_{10}\text{Al}_7$ differ from those in ferromagnetic materials. MCE inversion at T_k is specified by magnetic ordering of rare earth sublattice under applied magnetic field at $T < T_k$ and disordering under applied magnetic field at $T > T_k$.

The work is supported by RFBR grant #16-02-00472.

[1] T.H. Jacobs, K.H.J. Buschow., *Physica B*, **179** (1992) 177-183.

[2] K.P. Belov, S.A. Nikitin., *JETP*, **31** (1970) 505-508.

4PO-K-21

THE MAGNETOCALORIC EFFECT IN SUBSTITUTED RCO_2 COMPOUNDS

Chzhan V.B.¹, Politova G.A.¹, Tereshina I.S.², Cwik J.³

¹ Baikov Institute of Metallurgy and Materials Science RAS, Moscow, Russia

² Lomonosov Moscow State University, Faculty of Physics, Moscow, Russia

³ International Laboratory of High Magnetic Fields and Low Temperatures PAS, Wroclaw, Poland
lemuriform@gmail.com

The cubic Laves phase RCO_2 (R = rare-earth metal) are known as compounds showing both large values of volume magnetostriction and a significant magnetocaloric effect (MCE) near magnetic and/or structural transition temperatures [1]. The present research is focused on analysing magnetocaloric effect of substituted RCO_2 compounds.

The several series of multicomponent alloys have been prepared by arc-melting method of the stoichiometric proportions of constituents under high purity helium atmosphere. The purity of Co and rare-earth metals was 99.99 and 99.9%, respectively. The alloys were remelted three times and annealed (at 900°C for one month) to obtain homogeneous samples. As a result, for further studies, $\text{Tb}_x(\text{Dy}_{0.5}\text{Ho}_{0.5})_{1-x}\text{Co}_2$ ($x = 0, 0.15, 0.3, 0.4, 0.5, 0.6, 1$), $\text{Tb}_x(\text{Dy}_{0.5}\text{Ho}_{0.5})_{1-x}\text{Co}_{1.75}\text{T}_{0.25}$ ($x = 0.3, 0.4, 0.5$, T = Fe, Al) and $\text{Tb}_{0.2}\text{Dy}_{0.8-x}\text{Gd}_x\text{Co}_{2-y}\text{Al}_y$ ($x = 0.3, 0.4, 0.5$, $y = 0, 0.1$) compounds were selected which, according to the results of the X-ray analysis, were single-phase. The magnetization has been measured by using resistivity Bitter-type magnet. The magnetocaloric effect was measured in fields of up to 1.8 T by direct method and indirect method up to 14 T.

The Curie temperature and the type of transition investigated compounds were determined using results of the magnetization measurements. Figure 1 shows the temperature dependences of the maximum adiabatic temperature change, ΔT_{ad} , at 1.8 T obtained from direct measurements.

In the case of some multicomponent compounds it were found that the MCE value remains constant over a wide temperature range. This fact makes such sets of compounds promising for the production of new functional materials based on them.

The work is supported by the RFBR and Moscow city Government according to the research project 15-33-70040 mol_a_mos.

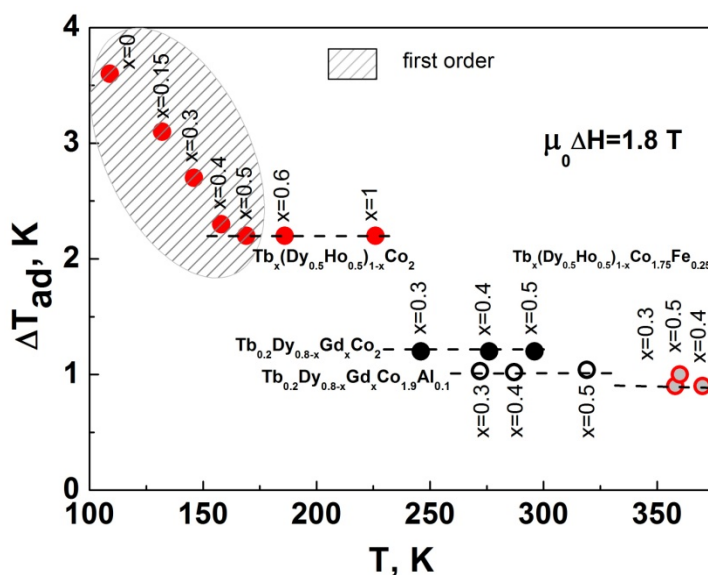


Fig. 1. Temperature dependences of the maximum adiabatic temperature change, ΔT_{ad} , in various substituted RCO_2 compounds obtained by direct method

[1] I.S. Tereshina, J.Cwik, E.A. Tereshina, G.A. Politova et al., *IEEE Trans. Magn.*, **50**, 11 (2014) 2504604.

[2] V.B. Chzhan, E.A. Tereshina, A.B. Mikhailova, G.A. Politova et al., *J. Magn. Magn. Mater.* **432**, 15 (2017) 461-465.

4PO-K-22

TEMPERATURE DEPENDENCE OF $\text{La}(\text{Fe},\text{Si})_{13}$ MAGNETOELASTIC PROPERTIES

Karpenkov A. Yu.^{1,5}, *Karpenkov D. Yu.*^{1,2,3}, *Radulov I.A.*², *Skokov K.P.*², *Gutfleisch O.*²

¹Chelyabinsk State University, Faculty of Physics, 45400 Chelyabinsk, Russia

²Institut für Materialwissenschaft, TU Darmstadt, 64287 Darmstadt, Germany

³NUST MISiS, Leninskiy pr.4, 119991 Moscow, Russia

⁴Fraunhofer ISC, IWKS Group Materials, Recycling and Resource Strategy, 63457 Hanau, Germany

⁵Tver State University, Faculty of Physics, 170002, Tver, Russia

The discovery of the new intermetallic compounds with the first order phase transition, which reveals giant magnetocaloric effect, have become the driving force of progress in alternative solid-state refrigeration technologies. However, wide practical application of such materials is limited by the inadequate intensity of magnetic field in permanent magnets based systems ($\mu_0 H \leq 1\text{T}$), which serves as a magnetic field source in magnetocaloric refrigerators. Consequently, researchers try to find the ways how to enhance cooling power and reduce the negative effect due to thermal and field hysteresis of working bodies. One of the most promising techniques is uniting of magneto-, baro- and elastocaloric effects. To bit hysteresis losses during a process of magnetization and demagnetization in [1, 2] it was proposed to apply the pressure to shift the Curie point down and close the hysteresis loops. To predict the pressure impact a volume dependence of magnetic properties should be investigated.

In this work magnetovolume and magnetocaloric properties were explored for $\text{LaFe}_{11.4}\text{Si}_{1.6}$ undergoing a first-order phase transition. For this purpose the universal insert for PPMS, allowing to simultaneously measure magnetization and magnetostriction, was manufactured. By means of developed setup magnetoelastic quantities of $\text{LaFe}_{11.4}\text{Si}_{1.6}$ including thermal expansion, spontaneous magnetization and magnetostriction, magnetovolume coupling coefficient were investigated.

It was found that the $\text{LaFe}_{11.4}\text{Si}_{1.6}$ magnetovolume coupling coefficient in the ferromagnetic state after the IEM transition is smaller than that in the paramagnetic state: $1.25 \times 10^{-8} \text{Gs}^{-2}$ and $0,6 \times 10^{-8} \text{Gs}^{-2}$ for paramagnetic and ferromagnetic states correspondingly.

To establish the relationship between applied pressure and the Curie temperature shift the Bean Rodbell model was used here to provide a basic starting point. Based on obtained experimental results we calculate the temperature dependence of compressibility (Fig.1). At the Curie point its value is equal to $K=11 \times 10^{-3} \text{GPa}^{-1}$ ($1.1 \times 10^{-12} \text{dyne/cm}^2$). Hence, in order to shift Curie point down by 1 K the pressure of 21 MPa ought to be applied, that is in good agreements with our and previous experimental data [3].

This work was supported by RSF grant N 15-12-10008, RFBR 15-32-70002.

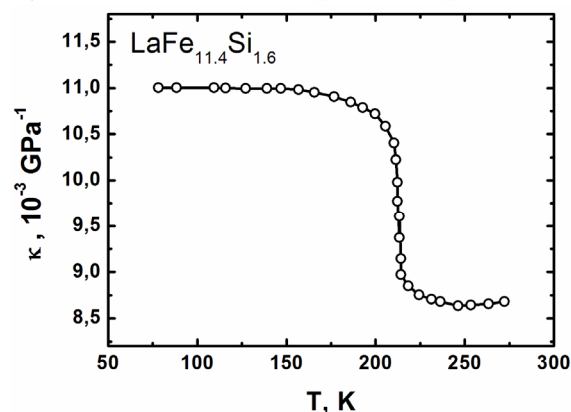


Fig.1. Temperature dependence of compressibility of $\text{LaFe}_{11.4}\text{Si}_{1.6}$ compound

[1] O.Gutfleisch, T.Gottschall, M.Fries, D.Benke, I.Radulov, K.P.Skokov, H.Wende, M.Gruner, M.Acet, P.Entel, M. Farle, *Phil. Trans. R. Soc. A*, **374**: 20150308.

[2] Liu J, Gottschall T, Skokov KP, Moore JD, Gutfleisch O., *Nat. Mater.*, **11**, 620–626.

[3] H Yako, S Fujieda, A Fujita and K Fukamichi, *J. of Phys.: Conf. Ser.*, **266** (2011) 012023.

4PO-K-23

INVESTIGATION OF STRUCTURAL AND MAGNETIC PROPERTIES OF Fe-Rh-(Z) (Z = Co, Pt) ALLOYS BY FIRST PRINCIPLES METHOD

Pavluhina O.O.¹, Buchelnikov V.D.¹, Sokolovskiy V.V.^{1,2}, Zagrebin M.A.¹

¹Chelyabinsk State University, Chelyabinsk, Russia

²National University of Science and Technology, Moscow, Russia

pavluhinaoo@mail.ru

At present, Fe-Rh-based alloys showing a metamagnetic phase transition have attracted a lot of attention because of their possible application in magnetic cooling, thermally assisted magnetic recording and spintronic devices [1-3]. These alloys with nearly equiatomic compositions and body-centered-cubic CsCl structure exhibit a strong competing of ferromagnetic and antiferromagnetic exchange interactions leading to existence of antiferromagnetic - ferromagnetic (metamagnetic) phase transition at room temperature [2].

In the present work we used the density functional theory as implemented in the VASP package. The generalized gradient approximation for the exchange correlation functional in the formulation of Perdew, Burke and Ernzerhof (PBE) was taken into calculations. The energy calculations were performed for L2₁ supercell (Fe₈Rh_{8-x}Z_x). The ab initio calculations have been carried out by using the 16-atom supercell approach with different initial spin configurations.

In the present work we calculated the total energies of the 16-atom supercells for Fe₈Rh_{8-x}Z_x system calculated for different spin configurations as functions of the lattice parameter. For the parent Fe-Rh compound, the antiferromagnetic checkerboard-like spin configuration in a cubic cell is energetically favorable compared to other antiferromagnetic and ferromagnetic configurations. In this case, a total magnetic moment is found to be of 0 μ_B/f.u.

In order to investigate the possibility of martensitic transformation in these alloys in dependence on the third element, we performed total energy calculations for tetragonal distortion of the cubic structure along z axis. To accomplish this, we fixed the volume of a supercell as $V_{\text{cubic}} \approx V_{\text{tetragonal}}$ ($a_0^3 \approx a^2c$). Where a_0 is the parameter for the cubic structure, a and c are the lattice parameters for the tetragonal structure, here c is directed along z axis. The total energy differences between the tetragonal distorted and cubic phases for Fe₈Rh_{8-x}(Co, Pt)_x, ($x = 0 - 3$) compositions with the energetically favorable spin configuration as functions of c/a ratio was found. We note that the calculated optimized lattice parameter for Fe-Rh alloy is in a good agreement with experimental and other theoretical values [1, 2].

Support by Russian Science Fund No. 14-12-00570\14 (VASP calculations), advanced research foundation of the Chelyabinsk State University and President RF Grant MK-8480.2016.2 is acknowledged.

- [1] J.J.M.Ruigrok, R.Coehoorn, S.R.Cumpson, H.W.Kesteren, *J. Appl. Phys.*, **87** (2000) 5398-5403.
 [2] J.U. Thiele, S. Maat, and E. E. Fullerton, *Appl. Phys. Lett.*, **82** (2003) 2859–2861.
 [3] M. Fallot, *Ann. Phys. (Leipzig)*, **10** (1938) 291–332.

4PO-K-24

THE MAGNETOCALORIC EFFECT OF Gd – Co ALLOYS*Drobosyuk M.O.¹, Taskaev S.V.¹, Fayzullin R.R.¹, Buchelnikov V.D.¹, Erager K.R.¹*¹Chelyabinsk State University, Chelyabinsk, Russia

m.syuk@mail.ru

The magnetocaloric effect (MCE) is a phenomenon of adiabatic temperature change ΔT_{ad} of the magnetic material induced by change of the external magnetic field. Materials with high values of the MCE near the room temperature can be used in the magnetic cooling technology [1]. Another important factors for magnetocaloric materials are the relative cooling power (RCP) and the coefficient of performance of the process (COP) of magnetic refrigeration. This coefficient is calculated as the ratio of the quantity of heat transferred from a cold reservoir to the amount of work expended during one thermodynamic cycle [2].

The rare earth (R) and transition metals alloys have been intensively investigated in recent years due to their unique physical properties. R – Co compounds are some of the promising candidates for magnetic refrigeration. For example, the Curie temperature T_C of GdCo₂ is 405 K [3]. In this work we present the MCE of the Gd_{50-x}Co_{50+x} ($x = 0; 2; 5$) alloys measured by the direct method.

Ingots with nominal compositions were prepared by the arc-melting method from pure (99.9 at.%) elements under an argon atmosphere. The composition of alloys was checked by the energy-dispersive X-ray spectroscopy (EDX).

Transition temperatures were determined from magnetization curves measured by an original magnetometer. The magnetocaloric measurements were performed by the setup produced by “AMT&C”. In this setup the adiabatic temperature ΔT_{ad} change measured by the direct method in the magnetic field up to 2 T.

All results including magnetization curves and temperature dependences of the MCE will be shown in the poster during the poster session.

[1] K. Gschneidner, Jr., V.K. Pecharsky, *Int. J. Refrig.*, **31** (2008) 945.

[2] E.T. Dilmieva et al., *Phys. Sol. St.*, **58** (2016) 81.

[3] M. Foldeaki et al., *Adv. Cryog. Eng.*, **43** (1998) 1533.

4PO-K-25

FERH-BASED COMPOSITE MATERIALS FOR ENHANCED MAGNETOCALORIC EFFECT

Amirov A.A.¹, Rodionov V.V.², Rodionova V.V.², Aliev A.A.¹

¹ Institute of Physics, Dagestan Scientific Center of Russian Academy of Sciences, Makhachkala,

² Russia Immanuel Kant Baltic Federal University, Science and technology park “Fabrica”,

Kaliningrad, Russia

amiroff_a@mail.ru

In recent years the magnetic compounds with significant magnetocaloric effect (MCE) near room temperature are intensively studied. On the basis of these studies the possibility of ecological, economically viable solid- state refrigerators is proposed [1]. Recently, among the promising materials for magnetic refrigeration, a considerable interest is attracted to the FeRh alloys in which a giant MCE is found [2, 3].

Fe₄₈Rh₅₂ exhibits a giant negative magnetocaloric effect (MCE) near room temperature, arising from an unusual first-order transition near 320 K between antiferromagnetic (AFM) and ferromagnetic (FM) order, which is accompanied by a unit cell volume expansion. However, the broad hysteresis often associated with the transition, are key drawbacks for applications. The former results in a dramatic degradation of MCE versus refrigeration cycles is observed by recent direct measurements. The irreversibility of the MCE is associated with very broad or incomplete transitions. While the irreversibility and hysteresis losses in other caloric materials with first-order magnetic transitions have been reduced by doping, or introducing porosity, such reductions have remained elusive in the case of FeRh. In paper [4] it is present the results of multicaloric study of layered composite heterostructure and use it to solve a problem, that is, a large hysteresis that impeded reversibility in an otherwise promising magnetocaloric material [4].

For this reason, the simple bilayer multiferroic composite with piezoelectric and magnetostrictive components were prepared. Our sandwich consists of magnetic component of FeRh alloy with formula Fe₄₈Rh₅₂ and piezoelectric PbZr_{0.53}Ti_{0.47}O₃ (PZT) sample with thickness about 0.2 mm of each. The magnetic, magnetocaloric and magnetoelectric properties of FeRh-PZT composite were performed in room temperature. M(H) loops were performed using VSM magnetometer. MCE was measured from direct method, ME effect was studied by measuring a voltage U generating across a sample under both alternating and bias magnetic fields. Anomaly of ME coefficient near temperature of AFM-FM transition was observed and associated with anomaly of magnetostriction of FeRh component near transition point. The MCE and magnetic measurements in FeRh-PZT composite were performed in two regimes: with switching of voltage across the thickness of the sample and when the voltage was switch off. In «switch off» regime the MCE and M(H) loops demonstrate the typical for FeRh alloys behavior. The voltage switching leads to the change of quantity of MCE ΔT and shifting of AFM-FM transition point. M(H) loops also demonstrate the changes in switch on regime and depends from quantity of applying voltage. These results may be used for magnetocaloric control and frozen of the irreversibility of MCE effect in caloric materials.

[1]. M. Tishin and Y. I. Spichkin. 2003, *The Magnetocaloric Effect and its Applications, Inst. of Physics, New York.*

[2]. V. Rodionov, V. Rodionova, M. Annaorazov, *Acta Physica Polonica A*, **127**, **2** (2015) 445.

[3]. S.A. Nikitin, G. Myalikgulyev, A.M. Tishin, M.P. Annaorazov, K.A. Asatryan and A.L. Tyurin, *Physics Letters A* **148** (1990) 363.

[4]. Y.Liu, L.C.Phillips, R.Mattana, M.Bibes, A.Barthe'le'my, B.Dkhil, *Nature Communication* **7** (2016) 1146.

4 July

Tuesday

17:30-19:30

poster session

4PO-I

4PO-I1

**“Diluted Magnetic
Semiconductors and
Oxides”**

4PO-I-26

AB-INITIO STUDY OF ELECTRONIC AND MAGNETO-OPTICAL PROPERTIES OF InAs:Mn

Kulatov E.T.¹, Gan'shina E.A.², Golik L.L.³, Kunkova Z.E.³, Zykov G.S.², Yuan Ye.⁴, Zhou S.⁴

¹ Prokhorov General Physics Institute of RAS, Russia

² Lomonosov Moscow State University, Moscow, Russia

³ Kotel'nikov Institute of Radio engineering and Electronics (Fryazino Branch), RAS,
Fryazino, Russia

⁴ Helmholtz-Zentrum Dresden Rossendorf, Institute of ion-beam science, Dresden, Germany
eagan@mail.ru

Diluted ferromagnetic semiconductors attract considerable attention for semiconductor-based spintronics, as in these devices the spin degree of freedom of carriers can be magnetically and electrically manipulated. The magneto-optical equatorial Kerr (MOEK) spectra and electronic properties of $\text{In}_{1-x}\text{Mn}_x\text{As}$ ($x=6.25\%$) are calculated using the relativistic, full-potential linear augmented plane-wave method as implemented in WIEN2k [1]. Density-functional calculations presented here are performed within a supercell (2x2x2) scheme. All atomic positions in cell are optimized by minimization of the forces acting on atoms. The energy difference between ferromagnetic and antiferromagnetic collinear orderings has been calculated for the uniform, intermediate and dimer Mn-pair geometries in order to find the ground state distribution of the Mn atoms in InAs host. We find the preference of the dimer ferromagnetic configuration of Mn dopants.

Our calculated optical spectra show marked features in the infrared region. The amplitude and energy position of our calculated MOEK resonance in $\text{In}_{1-x}\text{Mn}_x\text{As}$ are found to be in good agreement with our experimental MOEK spectrum at ~ 0.7 eV [2]. Although the MOEK property is a rather complicated function of the on-diagonal and off-diagonal components of the optical conductivity tensor, present calculation provides a clear insight about its origin in this material. The large MOEK effect observed in InAs:Mn can be understood as a combined effect of the on- and off-diagonal components, nearly maximal exchange splitting of Mn 3d states and the large spin-orbit coupling of As. The frequency-dependent optical properties, namely reflectivity, absorption coefficient, refractive index, extinction coefficient and unscreened plasma frequencies are also presented.

Support by Russian Foundation for Basic Research (RFBR No 15-02-02077, 16-02-00024, 16-02-612) and Programs of Russian Academy of Sciences "Strongly correlated electrons in solids and structures" and "Basic investigations of nanotechnologies and nanomaterials" is acknowledged.

[1] P. Blaha, K. Schwarz, G.K.H. Madsen, D. Kvasnicka, and J. Luitz, Wien2k (Karlheinz Schwarz, Techn. Universitat Wien, Austria, 2001).

[2] Elena Gan'shina et al., *Japanese Journal of Applied Physics*, **55** (2016) 07MF02-1-07MF02-5.

4PO-I-27

MAGNETIC PROPERTIES OF $\text{Ln}_6\text{MoO}_{12-\delta}$ (Ln = Lu, Yb)

Denisova K.¹, Volkova O.¹, Vasiliev A.¹, Shlyakhtina A.²

¹Lomonosov Moscow State University, Moscow, Russia

²Semenov Institute of Chemical Physics, RAS, Moscow, Russia

ksdenisova@gmail.com

The compounds with general formula $\text{Ln}_6\text{MoO}_{12-\delta}$ crystallize in two different defect fluorite structures, i.e. cubic $Fm\bar{3}m$ and rhombohedral $R\bar{3}$ ones. The cubic polymorph attracts attention as efficient anion conductor at elevated temperatures. The rare earth molybdenum oxides evidence intense yellow color due to charge transfer transition $\text{O}_{2p} - \text{Mo}_{4d}$ of Mo^{6+} in a fluorite structure.

Despite presence of both transition and rare – earth metals in the structure of these oxides their magnetic properties are not documented. Here, we present the results of magnetic susceptibility measurements of two members of this family $\text{Ln}_6\text{MoO}_{12-\delta}$ (Ln = Yb, Lu) in both structural modifications.

Formally, the non – magnetic $\text{Lu}_6\text{MoO}_{12}$ with Mo^{6+} ions should display the diamagnetic response. However, as shown in Fig. 1, both phases of this compound exhibit paramagnetic behavior which can be attributed to deviation from the oxygen stoichiometry. In cubic $\text{Lu}_6\text{MoO}_{11.5}$ the effective magnetic moment corresponds to Mo^{5+} oxidation state with spin $S = 1/2$. The rhombohedral $\text{Lu}_6\text{MoO}_{11.8}$ contains both Mo^{6+} and Mo^{5+} species. Both compounds are characterized by negative Weiss temperature of about 20 – 30 K.

The magnetic susceptibility of $\text{Yb}_6\text{MoO}_{12}$ largely exceeds that of its lutetium counterpart due to Yb^{3+} magnetic moment. While the chemically disordered cubic phase exhibits purely paramagnetic behavior, the fully chemically ordered rhombohedral phase reaches antiferromagnetic state at $T_N = 3$ K.

Both cubic and rhombohedral $\text{Yb}_6\text{MoO}_{12}$ are characterized by negative Weiss temperature of about 10 K indicating predominance of antiferromagnetic interactions. The insets in both upper and lower panels of Fig.1 reveal the deviation from Curie – Weiss law at low temperature.

This work is supported by RFBR grant No. 17-02-00211.

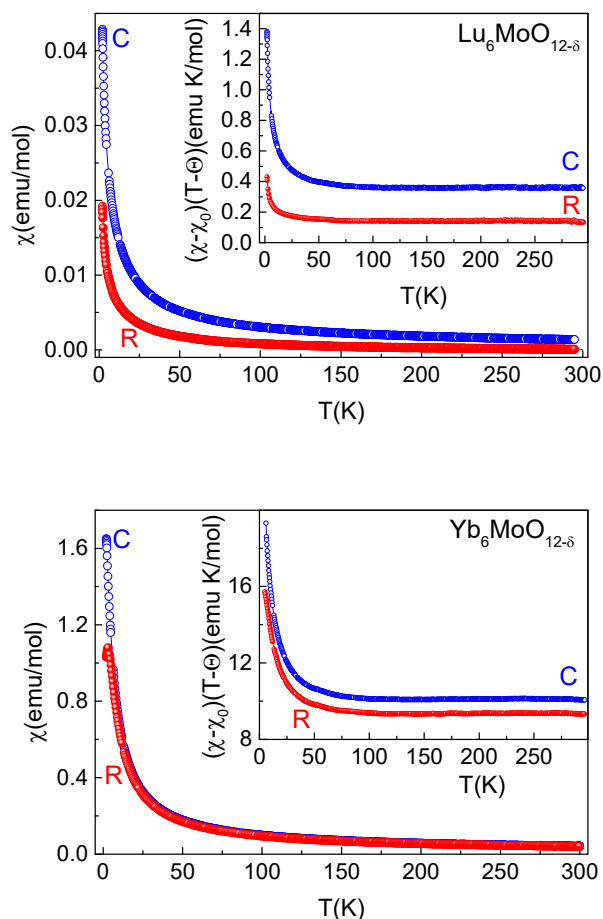


Fig.1. The temperature dependences of magnetic susceptibility χ in cubic (open circles) and rhombohedral (full circles) polymorphs of $\text{Lu}_6\text{MoO}_{12-\delta}$ (upper panel) and $\text{Yb}_6\text{MoO}_{12-\delta}$ (lower panel). The insets represent the temperature dependences of the Curie constant $C = (\chi - \chi_0)(T - \Theta)$ in these compounds.

4PO-I-28

MAGNETIC PROPERTIES OF Co-DOPED ZnO THIN FILMS

Kytin V.G.¹, Maximova O.V.¹, Kulbachinskii V.A.¹, Burova L.I.¹, Kaul A.R.¹, Bandyopadhyay S.², Ahmed A.², Banerjee A.²

¹ M.V. Lomonosov MSU, Moscow, Russia

² University of Calcutta, Calcutta, India

kytin@mig.phys.msu.ru

Diluted magnetic semiconductors such as ZnO doped with transition metal ions attract a considerable interest of scientific society due to their transport and magnetic properties. In particular ZnO:Co materials reveal weak ferromagnetic behavior persisting up to room temperatures, that makes it attractive candidate for applications in spin-based electronics.

In this work we present the results of the investigation of magnetic properties of ZnO thin films (50-590 nm) doped with Co (1.5-7.2 at%). The magnetic properties of ZnO films depend on the concentration of Co and could be modified by varying the Co content.

The magnetization curves of Co-doped ZnO films indicate the ferromagnetic-like signal in temperature range of 4,2 K-300 K (Fig.1). The permanent magnetization and coercive fields of investigated films irregularly depend on the Co content. The saturation magnetic moments of films with 1.5at % and 6.8 at % Co content are $5.3 \mu_B/\text{Co}$ and $0.12 \mu_B/\text{Co}$ correspondingly at 6K.

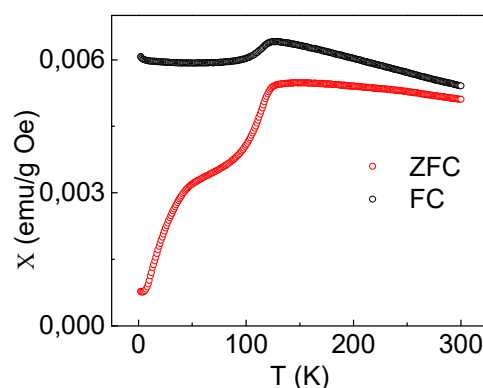
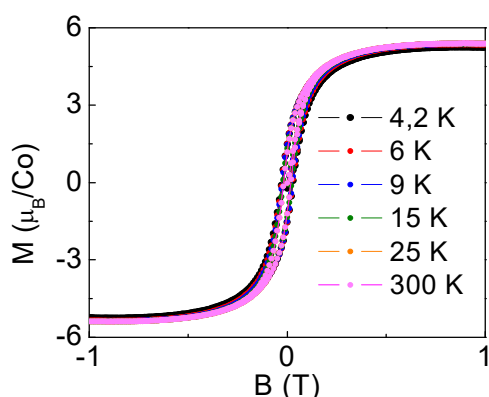


Fig. 1 $M(B)$ for ZnO Co-doped film (1,5 at%) Fig.2 $\chi(T)$ for ZnO Co-doped film (1,5 at%)

The temperature dependence of magnetic susceptibility ($\chi(T)$) investigated in zero field cooling (ZFC) and field cooling (FC) regimes are different for films with different Co content. The behavior of ZFC and FC temperature dependences of magnetic susceptibility of investigated films are typical for disordered magnetic systems and materials incorporating magnetic particles of various sizes [1]. The ZFC and FC temperature dependences of magnetic susceptibility $\chi(T)$ for ZnO film with 1.5 at% Co (Fig.2) do not coincide in temperature range of (5-300K), and the discrepancy between the ZFC and FC $\chi(T)$ increasing below 140K indicating the blocking temperature T_{blocking} for the particles ensemble is about 140K. ZFC and FC $\chi(T)$ dependences of 6.8 at% Co ZnO film are typical for paramagnetic materials containing magnetic nanoclusters [2]. The size of nanoclusters calculated based on $T_{\text{blocking}}=100\text{K}$ is about 5nm.

[1] B. Martínez, et al., *Phys. Rev. B*, **72**, 16 (2005) 165202-1-8.

[2] S. Lee, et al., *RSC Advances*, **5**, 81 (2015) 65840-65846.

4PO-I-29

EFFECT OF Ce-DOPING ON THE MAGNETIC AND STRUCTURE PROPERTIES OF MANGANITE $(\text{Ln}_{1-y}\text{Ce}_y)_{0.67}\text{Sr}_{0.33}\text{MnO}_3$ (Ln=Pr, Nd)

Popov V.V.¹, Melekh B.T.¹

¹ Ioffe Institute, Polytechnicheskaya 26, 194021 St. Petersburg, Russia
13745pop@mail.ru

The conductivity and ferromagnetic properties of manganites with a perovskite structure is based on the replacement of trivalent R^{3+} ions by A^{2+} ions, as a result of which, hole conductivity is formed along the chains $\text{Mn}^{3+}\text{-O-Mn}^{4+}$. Attempts to obtain a similar electronic conductivity, which were made by doping with 4-valence ions (Ce^{4+} , Th^{4+} , Sn^{4+}), did not lead to success. Thus, in the partial replacement of R^{3+} ions by Ce atoms (the valence of which can take values of both 3+ and 4+), an additional phase of fluorite CeO_2 appears, and the oxygen debalance leads to the appearance of hole conductivity in the perovskite phase.

Stabilization of the perovskite phase of manganites with partial replacement of RE atoms by cerium was achieved in the compositions $(\text{Ln}_{1-y}\text{Ce}_y)_{1-x}\text{Sr}_x\text{MnO}_3$ (Ln = La, Pr, Nd) synthesized by high-frequency direct melting method in a cold crucible [1]. The use of the method has allowed to optimize the basic properties of the system, such as significantly reduce the concentration of impurity fluorite phase and to lower the value of the integral valence of cerium.

In this paper we report on the magnetic and crystal properties of $(\text{Ln}_{1-y}\text{Ce}_y)_{0.67}\text{Sr}_{0.33}\text{MnO}_3$ (Ln = Pr, Nd) perovskite manganates with some of trivalent rare-earth ions replaced by Ce ions of varied valency.

The phase diagram of the $(\text{Ln}_{1-y}\text{Ce}_y)_{0.67}\text{Sr}_{0.33}\text{MnO}_3$ (Ln = Pr, Nd) illustrated the increase in temperature of ferromagnetic transition T_C , produces by Ce introduction (fig.1 (a)). With increasing cerium content (y) is also changed structural parameters (Fig.1 (b): crosses - annealed samples, squares-annealed). The results of the experiments show that a considerable part of the cerium ions are in the Ce^{3+} state

The measurements of the magnetic saturation moments was used to calculate the ratio of the cerium valences $\text{Ce}^{3+}/\text{Ce}^{4+}$ in all the compositions studied. A comparison is made with calculations based on the dependence of the Curie temperature on the tolerance factor.

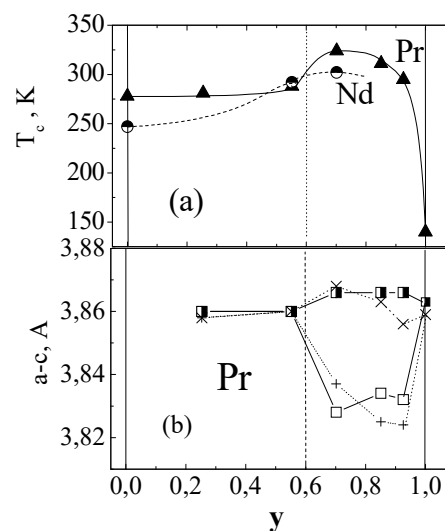


Fig. 1. Curie temperature (a) and Crystal structure parameters (b) versus on the Ce content (y).

[1] B.T. Melekh, Yu.N. Filin, N.F. Kartenko, et al., *Proceedings of the international school-seminar "NMMM-18", Moscow (2002) 587-589.*

4PO-I-30

NMR INVESTIGATION OF THE KAGOME COMPOUND $\text{YBaCo}_3\text{AlO}_7$ *Vavilova E.¹, Iakovleva M.^{1,2}, Grafe H.-J.², Valldor M.², Büchner B.², Kataev V.²*¹ Zavoisky Physical-Technical Institute of the RAS, Kazan, Russia² Leibniz Institute for Solid State and Materials Research IFW Dresden, Dresden, Germany
jenia.vavilova@gmail.com

Here we present a detailed experimental NMR study of the electron spin dynamics in single crystal of the spin-frustrated magnet $\text{YBaCo}_3\text{AlO}_7$ with the layered kagome-type crystal structure. This compound demonstrates strong and frustrated antiferromagnetic interactions between the cobalt spins in the kagome planes. No long-range magnetic order was observed at low temperatures. Instead, a glass-like freezing of the spin lattice was found. It was attributed to the structural disorder due to aluminium-cobalt site inversion and strong magnetic frustration. The use of the local NMR ($^{27}\text{Al}_R$ and $^{27}\text{Al}_D$) spin probes located at the regular and defect positions of the spin lattice has enabled us to disentangle the spin dynamics and magnetic correlations due to the intra-plane and inter-plane magnetic couplings. The development of the 2D correlations in the kagome planes exhibiting an Ising-like critical behavior can be clearly identified over an extended temperature range. The defects in the kagome lattice lead to the magnetic short-range ordering in the planes below 40K. In addition, the development of the 3D inter-plane magnetic correlations, which appear to be more Heisenberg-like and yield a glassy-like static state below 20 K, can be distinguished.

4PO-I-31

INFLUENCE OF HIGH-TEMPERATURE ANNEALS ON MAGNETIC PROPERTIES OF NATURAL TITANOMAGNETITES

Maksimochkin V.I.¹, Tselebrovskiy A.N.¹, Grachev R.A.¹

¹ Lomonosov MSU, Moscow, Russia

tselebr@physics.msu.ru

The effect of annealing at temperatures of 290–530°C in an atmosphere of air and argon on the magnetic properties of natural titanomagnetite contained in the Red Sea basalts is investigated. The concentration of TiO_2 in titanomagnetite was 15–16 wt% [1], the Curie temperature in the natural state, determined from the magnetic susceptibility (Fig. 1, curve 1) is equal to $T_c = 225 \pm 5^\circ C$.

It was found that after annealing for 10 hours at temperatures of 290–460°C, the Curie temperature of formed phase varies from 400°C to 505°C with increasing annealing temperature (Fig. 1, curves 2–4). Thermal magnetic curves also recorded the presence of a low-temperature phase with T_c about 300°C. Annealing at these temperatures led to an increase in saturation magnetization measured at room temperature by (20–50)%, magnetic susceptibility by approximately 50%, and a decrease in the coercive force by (10–20)%. The formation of a new magnetic phase during annealing was monitored by the increase in magnetization in a field of 5 G, whose variation with time could be satisfactorily described by the sum of two functions: exponential and parabolic.

The observed regularities in the variation of the magnetic characteristics after annealing at temperatures of 290–460°C in an air atmosphere, i.e. at a high oxygen partial pressure, can probably be explained by volume mutual diffusion of cations of titanium and iron, characterized as spinodal decomposition, and diffusion of oxygen ions into the titanomagnetite grain with the formation of a cation-deficient spinel along the grain boundaries.

In favor of the decay, the fact that subsequent heating of samples in an argon atmosphere up to 600°C led to homogenization of the solid solution, as evidenced by the $k_\theta(T)$ curves upon cooling of the samples, which show the presence of only one phase with a Curie temperature close to the initial one (Fig. 1, the dotted curves 2–4).

Annealing at 535°C for 10 hours led to the nucleation of the solid solution, since the appearance of magnetic phases with $T_c = 550$ –580°C, close to the Curie temperature of magnetite (Fig. 1, curve 5), was recorded on the thermomagnetic curves $k_\theta(T)$. The coercive force after annealing increased 1.8 times, and the magnetic susceptibility was 10% lower than the initial value. Such changes in magnetic properties are characteristic for the course of heterophase oxidation of titanomagnetite [2,3]. It was found that, unlike the first case, the subsequent heating to 600°C in an argon atmosphere of heterophasically oxidized titanomagnetite does not lead to a restoration of the initial phase (Fig. 1, dotted curve 5).

Support by RFBR, grant 16-05-00144a.

[1] V. I. Maksimochkin, A. N. Tselebrovskiy. *Moscow University Physics Bulletin*, **70** (2015)

[2] V. I. Trukhin, V. I. Maksimochkin. *Fizika Zemli*, **11** (1982) in russian

[3] S. K. Gribov, A. V. Dolotov, V. A. Tselmovich. *Uchenie zapiski Kazanskogo universiteta*, **156** (2014) in russian

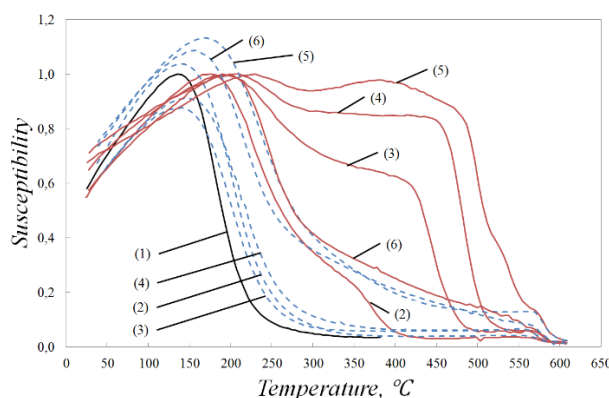


Figure 1

4PO-I-32

STRONG LINEAR AND QUADRATIC MAGNETO-OPTICAL PHENOMENA IN FERROMAGNETIC EPITAXIAL FILMS EuO ON Si AND YSZ

*Nefedov S.G.¹, Kats V.N.¹, Kalashnikova A.M.¹, Usachev P.A.¹, Pavlov V.V.¹, Averyanov D.V.²,
Parfenov O.E.², Taldenkov N.², Tokmachev A.N.², Storchak V.G.²*

¹ Ioffe Institute, 194021, St. Petersburg, Russia

² National Research Center «Kurchatov Institute», 123182, Moscow, Russia
nefedov@mail.ioffe.ru

EuO is an intrinsic Heisenberg ferromagnetic semiconductor with $T_c = 69$ K. EuO and other Eu chalcogenides are considered as most prospective materials for spintronic applications; carrier spin polarization in EuO exceeds 90 % [1]. In particular, Gd-doped EuO is proposed as an efficient spin injector into Si, the workhorse of modern electronics. Silicon has exceptionally long spin coherence lifetime and spin-decoherence transport length [2]. Therefore, optical, magneto-optical, magnetic and transport properties of nanoscale EuO films integrated with Si are of particular interest.

$\text{Eu}_{1-x}\text{Gd}_x\text{O}$ films ($x = 0-0.03$) are formed on Si (001) and yttria-stabilized zirconia (YSZ) substrates by molecular beam epitaxy, and capped by a 20 nm SiO_x protective layer [3]. The thickness of $\text{Eu}_{1-x}\text{Gd}_x\text{O}$ films was in a range of 40-110 nm. All the films had the easy-plane magnetic anisotropy. We have studied magnetic field and temperature dependences of the polar and longitudinal magneto-optical Kerr effects, as well as the Voigt effect in reflection by using a polarimetric setup with a CW laser (1.85 eV) as the light source (see Fig. 1a).

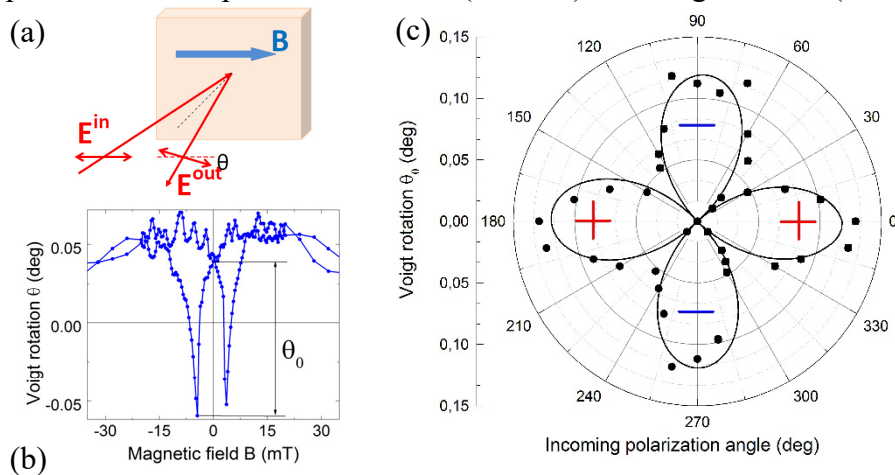


Fig. 1.
(a) Experimental Voigt geometry.
(b) B -field dependence of the Voigt rotation θ in $\text{Eu}_{0.97}\text{Gd}_{0.03}\text{O}/\text{YSZ}$ at $T=20$ K.
(c) The amplitude of the Voigt rotation θ_0 versus the incoming light polarization azimuthal angle.

The light polarization rotation, proportional to the square of the magnetization, was observed in the Voigt geometry below T_c in all studied samples (Fig. 1b). Small quadratic contributions were also observed for the polar magneto-optical Kerr effect due to the Voigt effect. The amplitude of the effect depends on the incident light polarization, and this dependence has a twofold rotational anisotropy (Fig. 1c), thus it revealing pronounced magnetic anisotropy in the sample plane, with the easy axes making an angle of $\pm 45^\circ$ with the field direction. The measurements of the polar and longitudinal magneto-optical Kerr effects and polarization rotation in the Voigt geometry allow for comparison between values of linear and quadratic phenomena in the EuO films.

The work is partially supported by the RSF grants 14-19-00662 and 17-12-01314, RFBR grants 16-02-00377, 16-07-00204, 16-29-03027 and 17-07-00170.

[1] A. Schmehl, *et. al.*, *Nature Mat.*, **6** (2007) 882.

[2] I. Žutic, *et. al.*, *Rev. Mod. Phys.*, **76** (2004) 323.

[3] D.V. Averyanov *et al.*, *Sci. Rep.*, **6** (2016) 22841.

4PO-I-33

MAGNETISM OF AMORPHOUS CARBON

Komlev A.A.^{1,2}, Lahderanta E.¹, Shevchenko E.V.³, Vorob'ev-Desyatovskii N.V.⁴

¹Lappeenranta University of Technology, Lappeenranta, Finland

²ETU "LETI", Saint-Petersburg, Russia

³St.-Petersburg State University, Saint-Petersburg, Russia

⁴JSC Polymetal Engineering, Saint-Petersburg, Russia

KomlevAnton@hotmail.com

Despite the decades of investigations, magnetic properties of carbon allotropes is still a controversial topic. While the defect-induced paramagnetic behaviour is already acknowledged, the problem of possibility of magnetic ordering in carbon materials is not solved yet. Many researches have demonstrated impurity-free carbon materials, where spontaneous magnetization was observed (eg. Ref [1]). However, the question of intrinsic or extrinsic character and the reproducibility of such results exists thus far.

In this work, magnetic behavior of activated carbon coal was investigated. This material, which is also named amorphous carbon, is widely used in practice for extraction of noble metals from ores and filtration processes. Initial coal produced from coconut shell was purified from inorganic contaminants in 1 M solution of HClO₄. The magnetic measurements were done by ESR and SQUID.

SQUID measurements showed anomalous magnetic behavior of pure carbon samples (Fig. 1). Sharp decrease in magnetic susceptibility was observed near 120 K. Such behavior can be explained by antiferromagnetic ordering. In addition, the magnetic susceptibility was positive even at room temperatures. The composition analysis performed by x-ray fluorescence spectroscopy identified down to 20 ppm of Fe and Co atoms. However, this amount is not enough to explain such strong paramagnetic response and the magnitude of the antiferromagnetic transition. Furthermore, antiferromagnetic ordering in the same temperature regions was observed in functionalized graphene samples, where carbon origin of the effect was approved by ESR measurements [2].

The effect of sorbed oxygen, which has antiferromagnetic ordering near 50 K, is also discussed. It was shown, that presence of oxygen can modify the magnetic susceptibility measurements giving a smooth increase to paramagnetic response in 50 – 150 K region. This effect is essential in case of high porous carbon materials. In some investigations [3] the similar behavior of susceptibility of amorphous carbon was observed, while the possible role of oxygen was not discussed at all.

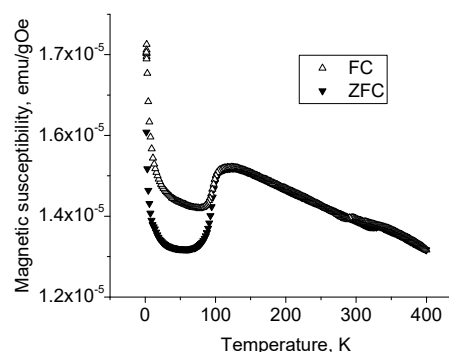


Fig. 1. Magnetic susceptibility of amorphous carbon with antiferromagnetic ordering (measured at 2900 Oe).

[1] J. Červenka, M. I. Katsnelson, and C. F. J. Flipse., *Nature Physics*, **5(11)** (2009) 840-844.

[2] A. A. Komlev, et al., *Journal of Magnetism and Magnetic Materials*, **415** (2016) 45-50.

[3] K. G. Raj, P. A. Joy., *Solid State Communications*, **177** (2014) 89-94.

4PO-I-34

NMR INVESTIGATION OF IR-BASED DOUBLE PEROVSKITES

Iakovleva M.F.^{1,2}, *Vavilova E.L.*², *Grafe H.-J.*¹, *Kataev V.E.*¹, *Kaustuv M.*³, *Vogl M.*¹, *Dey T.*⁴,
*Wurmehl S.*¹, *Büchner B.*¹

¹ IFW Dresden, Dresden, Germany

² KPhTI, Kazan, Russia

³ Max-Planck-Institute for Chemical Physics of Solids, Dresden, Germany

⁴ Universität Augsburg, Augsburg, Germany

y mf.physics@gmail.com

Iridium based double perovskites are unique materials where strong spin-orbit coupling, Coulomb repulsion, exchange interaction and crystal field have comparable energy scales. The interplay between all of these interactions and correlations may lead to the emergence of novel electronic and magnetic states. In the present work we report the ¹³⁹La nuclear magnetic resonance (NMR) results on the double perovskite compounds La₂MIrO₆ with magnetic and nonmagnetic ions at M position (M = Co, Cu, Zn). The magnetic Co (S=3/2) and Cu (S=1/2) spins are strongly coupled to Ir (J_{eff} = 1/2) sublattice and exhibit non-collinear antiferromagnetic phase transitions at 90 K and 74 K, correspondingly [1, 2]. In contrast to this materials the La₂ZnIrO₆ indicates a paramagnetic to ferromagnetic transition at T ~ 10 K [3].

Nuclear relaxation rate T₁⁻¹ measurements in La₂CuIrO₆ shows the peak at T ~ 74K that is the signature of a magnetic transition. Moreover with further decreasing the temperature the T-dependence of T₁⁻¹ shows the shoulder at T ~ 60 K that can be associated with a cooperative ordering of the transverse moments. In case of La₂CoIrO₆ the T₁⁻¹ measurements do not show any anomalies at T below the ordering temperature.

Our investigation has revealed complex magnetic interactions in the compound where strongly spin-orbit coupled 5d transition metal ions coexist with strongly correlated spin-only 3d (Co, Cu) and non-magnetic Zn ions.

[1] Kolchinskaya A., et al.: *Phys. Rev. B* **85**, 224422 (2012).

[2] Kaustuv Manna., et. al.: arXiv:1608.07513 [cond-mat.str-el] 2016.

[3] Zhu W.K., et. al.: *Phys. Rev. B* **91**, 144408 (2015).

4PO-I-35

CRYSTAL GROWTH AND TRANSPORT PROPERTIES OF SODIUM COBALTATES Na_xCoO_2

Gilmutdinov I.F.^{1,2}, Mukhamedshin I.R.^{1,2}, Alloul H.²

¹ Institute of Physics, Kazan Federal University, Kazan, Russia

² Laboratoire de Physique des Solides, Université Paris-Sud, Orsay, France

Ildar.Gilmutdinov@gmail.com

Sodium cobalt oxides attract attention due to enhanced thermoelectric power and existence of magnetically ordered phases [1]. Abundance of interesting physical properties occurs due to complex band structure and strong interplay between Na atomic ordering and the electronic density on the Co sites[2]. Our work devoted to synthesis of Na_xCoO_2 single crystals with different sodium content x and investigation of their transport properties.

The sodium cobaltate crystals Na_xCoO_2 with $x \approx 0.8$ have been grown by optical floating zone technique. The compound in polycrystalline form synthesized from stoichiometric mixture of NaCO_3 and Co_3O_4 by solid state reaction. Stable phases with $x=0.5, 0.67, 0.77$ were obtained by electrochemical deintercalation of sodium [3]. Crystal quality and homogeneity of sodium content was controlled by X-ray diffraction. Resistivity and Hall conductivity measurements were performed using the van der Pauw technique.

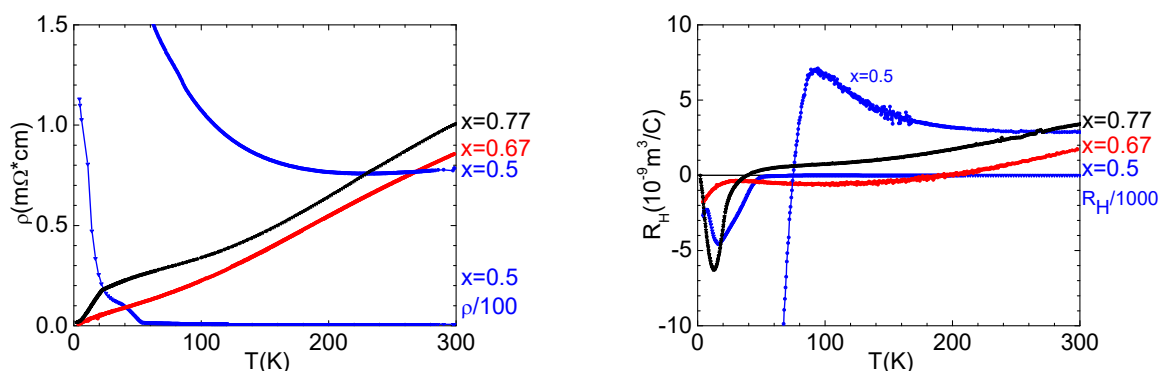


Fig. 1. Temperature dependence of resistivity and Hall conductivity of Na_xCoO_2 .

Temperature dependencies of resistivity and hall conductivity are presented on Fig. 1. Phases with $x = 0.67, 0.77$ show metallic properties, resistivity of $x = 0.5$ phase increases at low temperatures due to metal to insulator transition. All phases have positive Hall coefficient at high temperatures, but negative at low temperatures. The change of Hall coefficient sign is not consistent with single band model. The complex band structure near Fermi level should be accounted or multiband model should be applied.

The crystal growth, XRD, magnetic and transport measurements were carried out at the Federal Center of Shared Facilities of Kazan Federal University. This work was partially funded by the subsidy allocated to Kazan Federal University for the state assignment in the sphere of scientific activities. M.I.R. and G.I.F. thank for the support of a visit to Orsay by “Investissements d’Avenir” LabEx PALM (ANR-10-LABX-0039-PALM).

[1] G. Lang et al., *Phys. Rev. B*, **78** (2008) 155116.

[2] Y.V. Lysogorskiy et al., *Phys. Rev. B*, **94** (2016) 205138.

[3] I.R. Mukhamedshin et al., *JETP Letters*, **99(8)** (2014) 471–475.

4PO-I-36

MAGNETIC FIELD INDUCED GRIFFITHS PHASE IN $\text{Mn}_{1-x}\text{Fe}_x\text{Si}$ SOLID SOLUTIONS

Samarin A.N.¹, Huang J.², Vanacken J.², Demishev S.V.^{1,3,4}, Grigoriev S.V.⁵

¹ Prokhorov General Physics Institute of RAS, Moscow, Russia

² KU Leuven, Department of Physics and Astronomy, Leuven, Belgium

³ Moscow Institute of Physics and Technology, Dolgoprudny, Russia

⁴ National Research University Higher School of Economics, Moscow, Russia

⁵ Petersburg Nuclear Physics Institute, Gatchina, Russia

sasha@lt.gpi.ru

In the present work, we report the results of systematic study of magnetic properties of $\text{Mn}_{1-x}\text{Fe}_x\text{Si}$ solid solutions (iron concentration $x = 0.054, 0.11$ and 0.19) in the high magnetic field (up to 50 T). Pulsed field magnetization measurements were performed in KU Leuven, Belgium [1].

Our low field (up to $B \sim 5.5$ T) MPMS-5 (Quantum Design) measurements show that magnetization $M(B, T)$ of $\text{Mn}_{1-x}\text{Fe}_x\text{Si}$ does not saturate. In our previous work [2] supposed that $M(B)$ may have two contributions: the saturating one provided by spin-polaron subsystem and some additional linear term $M \sim B$. To understand the real magnetization structure it is instructive to perform high field magnetization measurements.

It is found that magnetization of $\text{Mn}_{1-x}\text{Fe}_x\text{Si}$ does not saturate even in the high magnetic field up to 50 T [3]. Analysis of the experimental data shows that in the $B > \sim 10$ T and in the paramagnetic phase magnetization $M(B)$ increases according to the power law $M(B) \sim B^\alpha$ with $\alpha = 0.3-0.5$ (fig. 1).

Power law observed in $M(B)$ dependence is very unusual and may be explained qualitatively by the realization of the quantum critical Griffiths phase in the high field region [3,4]. At the same time, analysis shows that low field magnetization is linear $M(B \rightarrow 0) \sim B$. Full magnetization curve $M(B)$ could be fitted by the interpolating formula $M(B) = C / (T - \theta) \cdot B / (B/B_c + 1)^\xi$, where $\xi = 1 - \alpha$ and B_c is a crossover field (fig. 1). We suggest that high field induced Griffiths phase is formed by spin polarons [5], which may play a role of intrinsic nanoscale magnetic inhomogeneities.

This work was supported by programmes of Russian Academy of Sciences “Electron spin resonance, spin-dependent electron effects and spin technologies” and “Electron correlations in strongly interacting systems”.

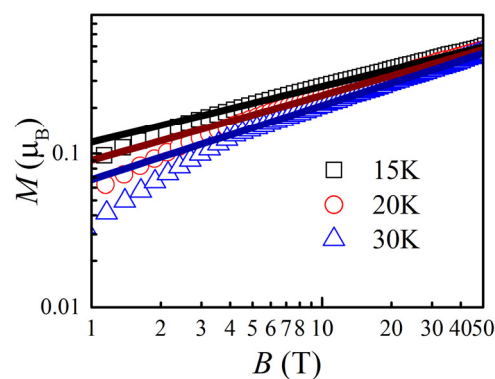


Fig. 1. Experimental $M(B, T)$ data for the sample with iron concentration $x = 0.11$ (points) and high-field power law fits (lines).

[1] J. Vanacken *et al.*, *Journal of Low Temperature Physics*, **170** (2013) 553.

[2] S.V. Demishev *et al.*, arXiv:1403.7332v2 [cond-mat.str-el] (2014).

[3] S.V. Demishev *et al.*, *JETP Letters*, **104** (2016) 116.

[4] D. S. Fisher, *Physical Review B*, **51** (1995) 6411.

[5] S.V. Demishev *et al.*, *Low Temperature Physics*, **41** (2015) 971.

4PO-I-37

CORRELATION BETWEEN THE SPIN-GLASS CONCENTRATION AND MAGNETORESISTANCE IN $\text{La}_{0.54}\text{Ho}_{0.11}\text{Sr}_{0.35}\text{Mn}_{1-x}(\text{Cr/Co})_x\text{O}_3$

Erhan R.V.^{1,2}, Craus M.-L.^{1,3}, Cornei N.⁴, Mita C.⁴, Dobrea V.³, Turchenko V.¹

¹ Frank Laboratory of Neutron Physics, JINR, Dubna, Russia

² Horia Hulubei National Institute for R&D in Physics and Nuclear Engineering, Bucharest-Magurele, Romania

³ National Institute of Research and Development for Technical Physics, Iasi, Romania

⁴ "Al.I.Cuza" University, Iasi, Romania

erhan@tandem.nipne.ro

The spin glass state was very often observed in the manganites. Because the electric properties of ferromagnetic and spin glass state are different, the presence of spin glass strongly influence the magnetoresistance of manganites (ABO_3). We wish to determine the influence of Mn substitution with Co/Cr in $\text{La}_{0.54}\text{Ho}_{0.11}\text{Sr}_{0.35}\text{MnO}_3$ (LHSMO) manganites.

The samples were synthesized by sol gel technology starting from corresponding mixture of rare earth oxides, Sr carbonate, and Mn, Co and Cr acetates. As result we obtained a mixture between a gel and a liquid. After the pour off the remaining liquid the gel was dried and subjected to a thermal treatment. The resulted powders ground and pressed into pellets and presintered at 800°C for 17 hours in air. The presintered samples were again ground and finally sintered at 1200°C for 10 hours in air atmosphere. Phase composition, structure, lattice constants and volume of the unit cell were determined by X-ray analysis (XRD). The samples doped with Cr crystallize in Pnma SG 62 and present a small maximum of the unit cell volume and of the lattice constants with the increase of Cr concentration in the sample. A decrease of unit cell volume with the increase of Co concentration takes places for the $\text{La}_{0.54}\text{Ho}_{0.11}\text{Sr}_{0.35}\text{Mn}_{1-x}\text{Co}_x\text{O}_3$ manganites, because the Co^{3+} radius is smaller than Mn^{3+} radius. An important structural change was observed for $\text{La}_{0.54}\text{Ho}_{0.11}\text{Sr}_{0.35}\text{MnO}_3$.

The substitution of Mn with Cr direct effect is the decrease of molar magnetization and the decrease of Curie temperature (s. Fig.1). For the manganites with $x \in [0.0:0.2]$ the specific magnetization remains constant or exhibits a small decrease with the temperature decrease (s. Fig.1). We interpreted this behavior as a transition from the ferromagnetic state to a spin-glass state, quenched in magnetic field. The decrease of the Curie temperature was attributed to a distortion of the crystalline lattice with increase of Cr concentration. A similar decrease takes places in the $\text{La}_{0.54}\text{Ho}_{0.11}\text{Sr}_{0.35}\text{Mn}_{1-x}\text{Co}_x\text{O}_3$ manganites, but the specific magnetization corresponding to the same concentration as for Cr are smaller. The measurements of resistance in magnetic field were performed by means of four sonde method. The manganites doped with Co have a continuous decrease of transition temperature from insulator to metallic state, while the Cr doped manganites show a strong influence of spin glass state on the magnetoresistance (implicitly on the transition temperature).

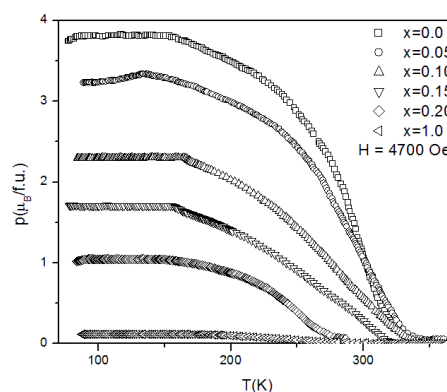


Fig. 1. The variation of specific magnetization with temperature and Cr concentration of $\text{La}_{0.54}\text{Ho}_{0.11}\text{Sr}_{0.35}\text{Mn}_{1-x}\text{Cr}_x\text{O}_3$ manganites

Support by FLNP, JINR, Dubna, Russia and Ministry of Research and Innovation, Romania is acknowledged.

4PO-I-38

ELECTRICAL SPIN INJECTION IN InFeSb/GaAs FERROMAGNETIC HETEROSTRUCTURES

Dorokhin M.V., Lesnikov V.P., Kudrin A.V., Demina P.B., Danilov Yu.A., Ved' M.V., Zdoroveyshchev A.V.

Physical–Technical Research Institute, Lobachevsky State University, Nizhny Novgorod, Russia
dorokhin@nifti.unn.ru

Diluted magnetic semiconductors (DMS), such as (III,Mn)V [1] or (III,Fe)V [2], are considered to be prospective materials for implementation in devices using spin degree of freedom [1]. The use of (III,Mn)V DMS is limited by the hole type conductivity, since short spin relaxation times for holes (as compared to electrons) significantly limit the efficiency of spin transport [1]. Also (III,Mn)V Curie temperature does not exceed 250 K (for (Ga,Mn)As) [1]. In contrast to (III,Mn)V, the (III,Fe)V are n-type semiconductors with the Curie temperature over 300 K [2]. However no devices including (III,Fe)V layers are known up to date. In the present paper we report on the fabrication of spin light-emitting diode (SLED) based on InGaAs/GaAs quantum well (QW) and (In,Fe)Sb ferromagnetic injector. In such structure the (In,Fe)Sb layer was used for the electrical injection of spin-polarized carriers into InGaAs/GaAs quantum well.

The samples were grown on n-GaAs substrate by the combined growth technique of metal-organic chemical vapor deposition (MOCVD) and pulsed laser deposition. The following layers were grown by the MOCVD at 600°C: n-GaAs buffer, In_{0.2}Ga_{0.8}As QW, 90 nm GaAs, $\delta<C>$ -doped layer, 30 nm GaAs. At the next stage the 40 nm In_{0.4}Fe_{0.6}Sb layer was grown at 250°C by laser sputtering of InSb and Fe targets. Final treatment of SLEDs included the deposition of Au contact on (In,Fe)Sb surface and 500 μ m mesa formation by photolithography and etching.

The measurements of electroluminescence (EL) were carried out under the forward bias condition - positive potential to the top contact [3]. The EL circular polarization degree was calculated as

$$P = (I^+ - I^-) / (I^+ + I^-), \quad (1)$$

where I^+ (I^-) are the intensities of left(right) circularly polarized component of the spectrum at the wavelength corresponding to the QW emission.

Fig.1 demonstrates the magnetic field dependence of the EL circular polarization degree. The curve is similar to the magnetic field dependence of the Hall resistance of (In,Fe)Sb layers. We also note that the control sample without (In,Fe)Sb demonstrated $P=0$ in the used magnetic field range. Thus there is a correlation between the EL circular polarization with the injection of spin-polarized carriers from (In,Fe)Sb layer into GaAs followed by the recombination in the QW and circular polarized emission.

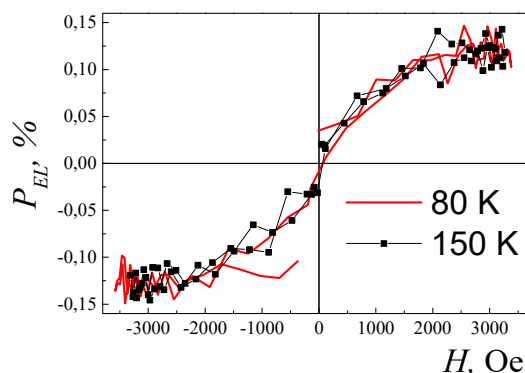


Fig.1. Magnetic field dependencies of P at the diode current $I_d=10$ mA.

This work was supported by the Ministry of Education and Science of Russia (№ 8.1751.2017/PCh), the RFBR (grants 15-02-07824_a, 16-07-01102_a), the grant of the president of the Russian Federation (MK-8221.2016.2).

[1] T. Jungwirth, *et al.*, *Rev. Mod. Phys.*, **78** (2006) 809-864.

[2] N.T. Tu *et al.*, *Phys.Rev. B.*, **92** (2015) 144403.

[3] E.D. Hinkey, *et al.*, *Appl. Phys. Lett.*, **6** (1965) 144-146.

4PO-I-39

THE INVESTIGATION OF CRYSTAL AND MAGNETIC STRUCTURES OF SOLID SOLUTIONS $\text{BaFe}_{12-x}\text{D}_x\text{O}_{19}$ (D= In AND Ga; $x= 0.1 - 1.2$)

Turchenko V.A.^{1,2}, *Trukhanov A.V.*^{3,4}, *Trukhanov S.V.*³, *Kazakevich I.S.*³

¹ Joint Institute for Nuclear Research, 141980 Dubna, Joliot-Curie str., 6, Russia

² Donetsk Institute of Physics and Technology named after A.A. Galkin of the NAS of Ukraine, 46 Nauki Ave, 03680, Kiev, Ukraine

³ SSPA “Scientific and practical materials research centre of NAS of Belarus”, 220072 Minsk, P. Brovki str., 19, Belorussia

⁴ National University of Science and Technology MISiS, 119049, Moscow, Leninsky Prospekt, 4, Russia
turchenko@jinr.ru

The ferroelectric polarization manifested by barium ferrites and their solid solutions at room temperature [1, 2] has not only the scientific but also the practical interest. The magnitude of the ferroelectric polarization is able to reach the value of $11.8 \mu\text{C}/\text{cm}^2$, that is two times higher than observed in the BiFeO_3 multiferroic ($\sim 6.1 \mu\text{C}/\text{cm}^2$) [3]. Taking into account the scanty of practical application of the bulk sample BiFeO_3 as a multiferroic, due to the suppression of its linear magnetoelectric effect because of presence spatially modulated structure in it, the barium ferrite with its unique properties can be considered as a promising material with multiferroic properties. However, the reason for the appearance of ferroelectric polarization in barium ferrites remains controversial. The distortion of oxygen octahedra, previously found in [Ошибка! Залка не определена., 4, 5], is unable to explain the occurrence of ferroelectric polarization in the framework of a centrosymmetric SG $P6_3/mmc$ (No. 194). However, the presence of an order-disorder type structural transition that should manifested itself in a decrease of the spatial symmetry of the SG $P6_3/mmc$ (No. 194), is practically not described in the articles.

The main aim of the work is establishment of the regularities of the influence of partial replacement of iron ions by diamagnetic ions to the features of the crystal and magnetic structures of barium ferrites. The feature of this work is the application of the neutron diffraction method on a High resolution Fourier diffractometer (HRFD) that allowed obtaining information about both the crystalline and magnetic structures and the microstructure of the studied samples. Polycrystalline samples of $\text{BaFe}_{12-x}\text{D}_x\text{O}_{19}$ (D = In and Ga; $x = 0.1 - 1.2$) have been fabricated by solid-phase synthesis at 1200°C (6 h) and annealed at 1300°C (6 h). According to the experimental data, all studied samples are homogeneous with a hexagonal structure. The increase of the concentration of diamagnetic ions leads to decrease of the specific magnetization and the Curie temperature owing to destroying of the magnetic order at lower temperatures that confirms the replacement of magnetoactive iron ions with diamagnetic. The increase of microscopic stresses in a ferrimagnetic crystal is observed. It can be related with uneven distribution of diamagnetic ions in the crystallographic positions.

[1] Guolong Tann, Xiuna Chen, *J. Magn. Magn. Mater.*, **327** (2013) 87.

[2] Xiuna Chen, Guolong Tan, *J. Magn. Magn. Mater.*, **327** (2013) 87.

[3] J.C. Faloh et al., *JMMM*, **222** (2000) 271.

[4] A. S. Mikheykin et al., *Eur. Phys. J. B*, **87** (2014) 232.

[5] J. Rensen, J. van Wieringen, *Solid State Communications*, **7(16)** (1996) 1139.

4PO-I-40

MAGNETOTRANSPORT PROPERTIES OF InSb-MnSb NANOSTRUCTURED FILMS

*Kochura A.V.*¹, *Marenkin S.F.*², *Novodvorsky O.A.*³, *Mikhalevsky V.A.*³, *Shakhov M.A.*⁴,
*Lahderanta E.*⁵, *Zakhvalinskii V.S.*⁶, *Kuzmenko A.P.*¹

¹ South – West State University, Kursk, Russia

² Kurnakov Institute of the general and inorganic chemistry of the RAS, Moscow, Russia

³ ILIT RAS – Branch of FSRC “Crystallography and Photonics” of RAS, Shatura, Russia

⁴ A.F. Ioffe Physico-Technical Institute, St Petersburg, Russia

⁵ Lappeenranta University of Technology, Lappeenranta, Finland

⁶ Belgorod National Research University, Belgorod, Russia

alex_dop@mail.ru

Incorporating of local magnetic moments into semiconductor matrix is one of suitable ways for realization of manipulating by both electron and spin subsystems and can be used for fabricate spintronic devices. To reach the room temperature ferromagnetism it is possible to use hybrid structures. Here ferromagnetic material is inserted to nonmagnetic or diluted magnetic semiconductor. Incorporating Mn into III-Sb compounds layers can substantially alter the observed ferromagnetic characteristics [1]. With relatively high Mn concentration the main contribution to magnetization of samples is by MnSb inclusions [2]. The presence of ferromagnetic micro- and, especially, nanoprecipitates of MnSb (with $T_C \approx 580$ K in bulk samples) embedded in the diluted magnetic semiconductor matrix improves certain device properties of these materials.

Thin hybrid InSb - MnSb films were obtained by pulsed laser deposition using mechanical droplet separation. Films structure was characterized by different methods (electron diffraction, scanning electron microscopy, Raman spectroscopy, atomic and magnetic force microscopy).

The negative magnetoresistance (nMR) takes place below 100 K. This temperature is one order more the temperature at which the nMR is observed in homogeneous $\text{In}_{1-x}\text{Mn}_x\text{Sb}$ samples. At low temperatures prevail the spin-dependent scattering of the holes by the localized Mn^{2+} moment. When the temperature rises the low nMR is observed due to the weak spin-dependent scattering on magnetic inclusions.

Support by The Ministry of Education and Science of the Russian Federation (№ 16.2814.2017/PCh) and RFBR (15-07-06081-a)

[1] S.F. Marenkin et al., *Inorganic Materials*, **50** (2014) 897-902.

[2] A.V. Kochura et al., *J. Appl. Phys.*, **113** (2013) 083905.

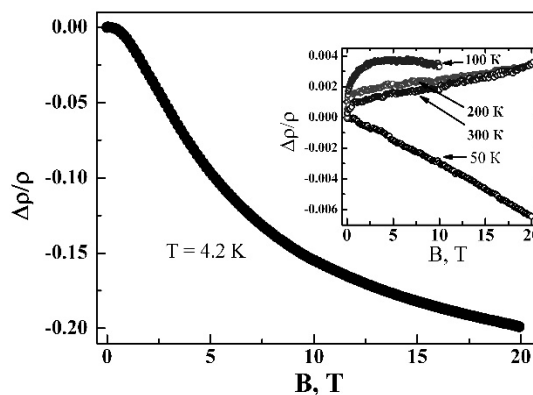


Fig. 1. Magnetic field dependence of magnetoresistance for InSb - MnSb film at different temperatures.

4PO-I-41

NMR AND MÖSSBAUER SPECTROSCOPY STUDY OF BINARY HELIMAGNET FeP

Gippius A.A.^{1,2}, *Zhurenko S.V.*¹, *Sobolev A.V.*³, *Presniakov I.A.*³, *Chernyavskii I.V.*³, *Schaedler M.*⁴,
*Buettgen N.*⁴, *Morozov I.V.*³, *Shevelkov A.V.*³, *Moskvin A.S.*⁵

¹ Faculty of Physics, M.V. Lomonosov Moscow State University, Moscow, Russia

² A.V. Shubnikov Institute of Crystallography, Moscow, Russia

³ Faculty of Chemistry, M.V. Lomonosov Moscow State University, Moscow, Russia

⁴ Experimental Physics V, University of Augsburg, Augsburg, Germany

⁵ Ural Federal University, Ekaterinburg, Russia

gippius@mail.ru

Binary compounds MX (where M is transition metal, X is pnictogen) of the MnP structure type such as MnP, FeP, and CrAs display helimagnetic properties that attract rapt attention [1,2]. Scientific interest to iron phosphide, which seems rather simple at the first glance, is largely associated with intrinsic complexity of its unusual helical magnetic structure, details and generation mechanisms of which are still a matter of discussions.

We report results of ⁵⁷Fe Mössbauer and ³¹P NMR studies of a phosphide FeP powder sample performed in a wide temperature range including the magnetic phase transition point $T_N \approx 120$ K. The ⁵⁷Fe Mössbauer spectra at low temperatures $T < T_N$ present a very complex Zeeman pattern with line broadenings and sizeable spectral asymmetry. It was shown that the change of the observed spectral shape is consistent with the transition into a space-modulated helicoidal magnetic structure. Analysis of the experimental spectra was carried out assuming an anisotropy of the magnetic hyperfine field H_{hf} at the ⁵⁷Fe nuclei when the Fe^{3+} magnetic moment rotates with respect to the principal axis of the electric field gradient (EFG) tensor. The obtained large temperature independent anharmonicity parameter $m \approx 0.96$ of the helicoidal spin structure results from easy-axis anisotropy in the plane of the iron spin rotation. It was assumed that a very low maximal value of $H_{hf}(11\text{ K}) \approx 36$ kOe and its high anisotropy $\Delta H_{anis}(11\text{ K}) \approx 30$ kOe can be attributed to the stabilization of iron cations in the low-spin state with $S = 1/2$.

The ³¹P NMR spectra below T_N demonstrate an extremely broad linewidth reflecting the spatial distribution of the transferred internal magnetic fields of the Fe^{3+} ions onto P sites in the magnetically ordered state (Fig.1).

The obtained results are discussed in terms of anharmonic helical magnetic structure and anisotropic hyperfine interactions.

Partial support by the RFBR Grant № 17-52-80036 is acknowledged.

[1] Z. Gercsi, K.G. Sandeman, *Phys. Rev. B*, **81** (2010) 224426.

[2] Y. Shiomi, S. Iguchi, Y. Tokura, *Phys. Rev. B*, **86** (2012) 180404(R).

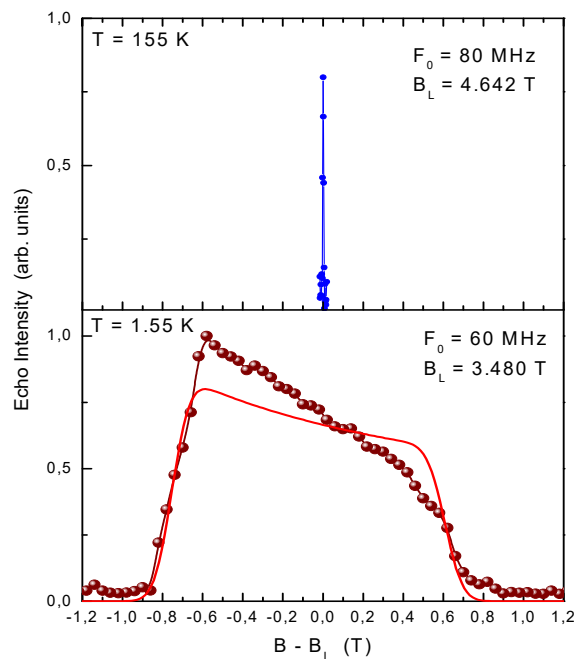


Fig.1. ³¹P NMR spectra of FeP measured at 155 K (upper panel) and at 1.55 K (bottom panel).

4PO-I-42

NMR STUDY OF INHOMOGENEOUS MAGNETIC STATE IN ELECTRON DOPED CUBIC MANGANITES

*Mikhalev K.N.¹, Germov A.Yu.¹, Verkhovskii S.V.¹, Volkova Z.N.¹, Gerashenko A.P.¹, Korolev A.V.¹,
Konstantinova E.I.², Leonidov I.A.², Yakubovskii A.Yu.³, Trokiner A.⁴, Dabrovski B.⁵*

¹ M.N. Miheev Institute of Metal Physics UB RAS, Yekaterinburg, Russia

² Institute of Solid State Chemistry UB RAS, Yekaterinburg, Russia

³ Russian Research Centre Kurchatov Institute, Moscow, Russia

⁴ LPEM, ESPCI Paris, PSL Research University, CNRS, Sorbonne Universites, UPMC University,
Paris, France

⁵ Department of Physics, Northern Illinois University, Illinois, USA

mikhalev@imp.uran.ru

Electron doped manganites with the cubic perovskite structure are ideal objects for studying the double exchange mechanism. Recently, the interest in these oxides increased strongly, since the insulator-metal transition was found in cubic SrMnO₃ at the minimum doping level (1%) owing to the heterovalent substitution of La³⁺(Ce⁴⁺) for Sr²⁺ [1]. The results of magnetic measurements were explained within the de Gennes model: a homogeneous metal state with the canted antiferromagnetic (AF) structure of the magnetic moments of Mn⁴⁺ ions. Investigations with local techniques like NMR should check this exceptional ground state of electron doped magnetic oxide.

We present in this report the ⁵⁵Mn and ¹⁷O NMR study of lightly electron doped cubic polycrystalline samples of Sr_{1-x}La_xMnO₃ (0 < x ≤ 0.04) and SrMnO_{3-y} (y < 0.01). The ⁵⁵Mn NMR lines of Mn ions in different magnetic state are generally well separated [2] so that ⁵⁵Mn NMR is an effective tool to investigate any magnetic heterogeneity existing in the AF lattice. We have shown from the analysis of ⁵⁵Mn NMR spectra that the inhomogeneous magnetic state, where the AF matrix coexists with ferromagnetic (FM) clusters in the region of long-range order, is implemented in electron doped manganites under investigation similar to hole doped manganites [3]. These FM clusters can be considered as small size magnetic polarons (MP). The Curie temperature of the observed FM regions exceeds drastically the Neel point of the AF matrix and their localization begins at temperatures below 77 K.

The low-frequency dynamics of the Mn magnetic moments probed by ¹⁷O spin-echo experiments show a thermal activated hopping of the MP. The observed trend of the energy barrier of hopping to grow with increasing doping indicates that the de Gennes metallic ground state cannot be achieved in oxygen-deficient SrMnO_{3-y}. The random structural defects, i.e., oxygen vacancies destroying the perfectly aligned network of the Mn-O-Mn covalent bonds are probably a major source of adversarial effect on the fast motion of doped electrons at low temperature.

The research was carried out within the state assignment of FASO of Russia (theme “Spin” No. 01201463330), supported in part by UB RAS (project No. 15-9-2-49).

[1] H. Sakai, et. al., *Physical Review B*, **82** (2010) 180409 -180412.

[2] G.Allodi, et al., *Physical Review B*, **56** (1997) 6036-6046.

[3] K.Mikhalev, et al., *The Physics of Metals and Metallography*, **115** (2014) 1139-1159.

4PO-I-43

FERROMAGNETISM OF INDIUM ANTIMONIDE, HIGHLY DOPED BY IRON

Kudrin A.V., Danilov Yu.A., Lesnikov V.P., Vikhrova O.V., Pavlov D.A., Usov Yu.V.,

Pitirimova E.A., Antonov I.N., Krukov R.N.

Lobachevsky State University, Nizhny Novgorod, Russia

danilov@nifti.unn.ru

A search for new ferromagnetic semiconductors is aimed at creating effective spin injectors for spintronic devices, operated at room temperature. In this work we present the results of fabrication and the investigation of InFeSb/GaAs structures with the room temperature ferromagnetism. The ≈ 40 nm-thick InFeSb layers were fabricated on *i*-GaAs substrates by pulsed laser deposition. In the vacuum chamber the solid targets (InSb and Fe) were periodically sputtered by Nd:YAG laser. The ratio of the sputtering times $t_{\text{Fe}}/t_{\text{InSb}}$ was varied in the range of 0.08 – 0.17. The substrate temperature was 30, 150, 200 and 250°C. The Fig. 1 shows the high resolution transmission electron microscopy (HRTEM) image of the cross-section of the InFeSb/GaAs structure with $t_{\text{Fe}}/t_{\text{InSb}} = 0.17$ and a growth temperature (T_g) of 250°C. Due to the large lattice mismatch (14.6 %) between InSb layer and GaAs substrate the large number of stacking faults arise on {111} planes. The stacking faults appear as the net of straight lines at an angle of $\sim 70^\circ$ with respect to each other. The HRTEM images do not reveal the presence of any visible second phase inclusions with a lattice differ from zinc-blende InFeSb matrix. The transmission electron diffraction (TED) pattern obtained from InFeSb/GaAs interface also supports the zinc-blende type lattices (InFeSb and GaAs) only.

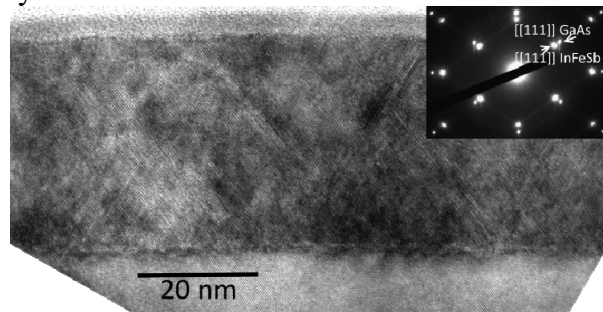


Fig. 1. The HRTEM images of the InFeSb/GaAs structure. The inset shows the TED pattern of the InFeSb/GaAs interface.

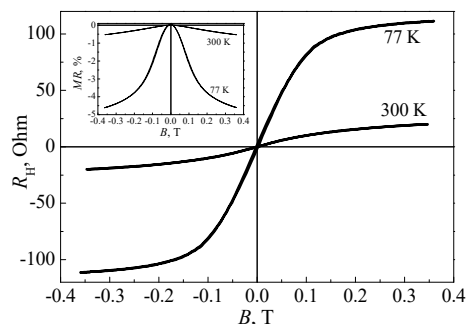


Fig. 2. The $R_H(B)$ dependences of the InFeSb/GaAs structure at 300 and 77 K. The inset shows magnetoresistance dependences on B oriented perpendicularly to the plane.

The Fig. 2 shows the Hall resistance dependences on external magnetic field ($R_H(B)$) at 300 and 77 K for the InFeSb/GaAs structure ($t_{\text{Fe}}/t_{\text{InSb}}=0.17$, $T_g = 250^\circ\text{C}$). The $R_H(B)$ dependences reveal the anomalous Hall effect up to room temperature: the dependences are nonlinear with a saturation at the magnetic fields ≥ 1500 Oe. The negative magnetoresistance with a bend at ~ 1500 Oe also confirms spin-dependent character of the carriers transport in the InFeSb layer. Thus, the obtained InFeSb layers are a single-phase zinc-blende crystal with the room-temperature ferromagnetic properties.

This study was supported by the Grant of President of Russian Federation (MK-8221.2016.2) and by project no. 8.1751.2017/PCh of the Ministry of Education and Science of Russia.

4PO-I-44

MAGNETIC AND MAGNETO-TRANSPORT PROPERTIES OF CRYSTALLOGRAPHICALLY ALIGNED CuCr_2Se_4 THIN FILMS

Edelman I.¹, Esters M.², Ivantsov R.¹, Yurkin G.^{1,3}, Johnson D.C.², Tarasov A.¹

¹Kirensky Institute of Physics, FRC KSC RAS, Krasnoyarsk, 660036, Russia

²Department of Chemistry, University of Oregon, Eugene, OR 97403, USA

³Siberian Federal University, Krasnoyarsk, 660041, Russia

ise@iph.krasn.ru

Crystallographically aligned nanocrystalline films of the ferromagnetic spinel CuCr_2Se_4 were successfully synthesized and their structure and alignment were confirmed by x-ray diffraction and high-resolution transmission electron microscopy. The average size of the crystallites is about 200 - 250 nm, and their (111) crystal planes are oriented parallel to the film plane. The CuCr_2Se_4 films have a negative magneto-crystalline anisotropy with four easy axes along $\langle 111 \rangle$ directions. One of these $\langle 111 \rangle$ axes is oriented perpendicular and the three others are oriented at an angle of 19.5° relative to the (111) crystal plane.

The films exhibit a very strong temperature dependence of the anisotropy constants. The first constant K_1 increases almost one order of magnitude when the temperature is decreased from 300 to 5 K. On the other hand, the films possess in-plane shape anisotropy, so that the films' magnetic properties are determined by the competition between these two types of anisotropy. The shape anisotropy is found to be nearly temperature independent whereas the crystal anisotropy increases with decreasing temperature, resulting in a switch of the easy axis from inside the film plane at room temperature to perpendicular to the film plane as the temperature decreases, which is reflected in changes of the hysteresis loops (Fig.1).

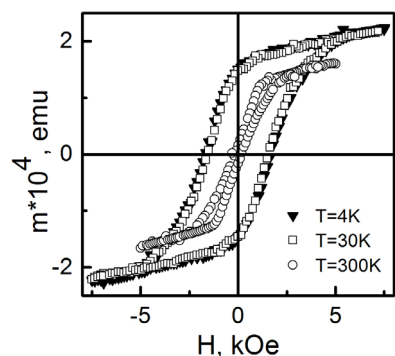


Fig. 1. Magnetization curves of the CuCr_2Se_4 film for out-of-plane geometry at three temperatures.

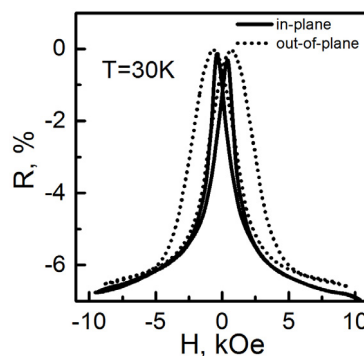


Fig. 2. In-plane and out-of-plane MR as a function of external magnetic field strength H of the CuCr_2Se_4 film at 30 K.

The films exhibit negative magnetoresistance (MR) at low temperatures (Fig.2) with a maximum of -9 % at $T = 4.2$ K. The shape of the MR dependence on the external magnetic field suggests that the MR is mostly due to the film magnetization processes as inferred from the MR hysteresis. Mechanisms that are most likely responsible for MR will be discussed.

Support by Grant of the President of the Russian Federation NSh-7559.2016.2 and the National Science Foundation under grant DMR-1266217 is acknowledged.

4PO-I-45

STATIC AND TIME-RESOLVED MID-INFRARED SPECTROSCOPY OF Hg_{0.95}Cd_{0.05}Cr₂Se₄ SPINEL

*Barsaume S.*¹, *Telegin A.V.*², *Sukhorukov Yu.P.*², *Stavrias N.*¹, *Fedorov V.A.*³, *Menshchikova T.K.*³,
*Kimel A.V.*¹

¹ IMM Radboud University, Nijmegen, The Netherlands

² IMP UB RAS, Yekaterinburg, Russia

³ IGIC RAS, Moscow, Russia

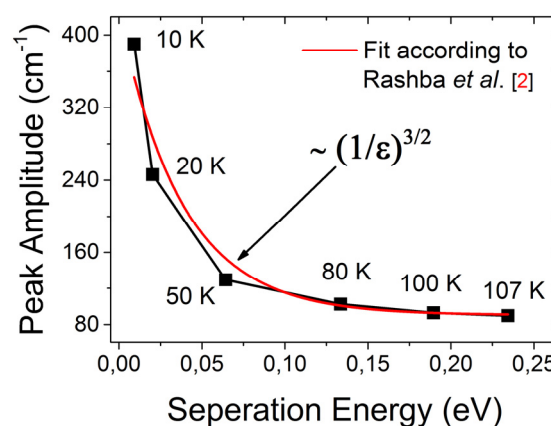
s.barsaume@science.ru.nl

During the last 20 years classical ferromagnetic semiconductors have renewed intense research due to demands of spintronics. The strong correlations between magnetic order and electronic properties is one of the key points of these materials. Spinel (Hg,Cd)Cr₂Se₄ possess high degree of electron spin polarization and giant magneto-optical (MO) effects as well as relatively high Curie temperature ($T_C \sim 106 - 130$ K). The complex electronic structure of spinel are pronounced in non-trivial high frequency transport phenomena, for instance in THz ranges [1]. Here we report mid-infrared static and time-resolved spectroscopy of the ferromagnetic semiconductor Hg_{0.95}Cd_{0.05}Cr₂Se₄ below the absorption edge.

Absorption measurements were performed in the range 4000 – 350 cm⁻¹ with a Bruker Vertex Fourier Transform InfraRed (FTIR) spectrometer. Time-resolved measurements were performed with the help of the Free Electron Laser for Infrared Experiments (FELIX) facility in Nijmegen (The Netherlands). In the pump-probe experiments, we measured the changes in transmissivity of the sample with the pump and probe having the same central photon energy (around 0.236 eV). In all the measurements, the temperature across the sample could be varied from 7 K to 300 K.

A dramatic decrease of the oscillator strength is observed simultaneously with the strong red-shift of the absorption edge in the magnetic semiconductor (see figure 1).

Employing a time-resolved pump-and-probe technique enabled us to determine the lifetime of the electrons in the excited state of this optical transition. In the range from 7 to 80 K, the lifetime changes from 3 to 6 ps. This behavior agrees with the phenomenon of giant oscillator strength described earlier for weakly bound excitons in nonmagnetic semiconductors [2, 3]. Therefore, in this ferromagnetic semiconductor we discover an electronic excitation that has both spectral features of a weakly bound exciton and a coupling to the magnetic order.



This work was supported by the Foundation for Fundamental Research on Matter (FOM), which is part of the Netherlands Organization for Scientific Research (NWO) as well as the Ministry of Education and Science of Russian Federation (grant Nr. 14.Z50.31.0025) and partially by the Russian Federal Agency for Scientific Organizations (project no. 0120146330, “Spin”). We acknowledge that a part of the results was obtained by the FELIX facility in Nijmegen.

[1] Huisman *et al.*, T. J.; *Appl. Phys. Lett.*, **106** (2015) 132411.

[2] Rashba E. I., Gurgenshili, G., *Sov. Phys. – Solid State*, **4** (1962) 759-760.

[3] Minami F. and Era K., *Solid State Comm.* **53**(2), (1985)187-189.

4PO-I-46

THE OSCILLATIONS IN ESR SPECTRA OF $Mn_xHg_{1-x}Te$ IN X- AND Q-BANDS

Shestakov A.V.^{1,2}, Fazlizhanov I.I.^{1,2}, Yatsyk I.V.^{1,2}, Ibragimova M.I.¹, Eremina R.M.^{1,2}

¹ Kazan E.K. Zavoisky Physical-Technical Institute, Kazan, Russia

² Kazan Federal University, Kazan, Russia

Aleksey665@gmail.com

The mercury chalcogenide $Mn_xHg_{1-x}Te$ (MHT) in the zinc-blende structure belongs to a group of unique materials exhibiting the so-called inverted band structure [1] and it is semimagnetic semiconductor ($A^{II}B^{VI}$). Compound $Hg_{1-x}Cd_xTe$ is the most widely used semiconductor with a variable band gap [2]. Solid solution of $Mn_xHg_{1-x}Te$ (MHT) has higher stability of electrophysical properties than in $Hg_xCd_{1-x}Te$ [3]. MHT monocrystal had grown by the Bridgman method, without annealing, $x=0.11$. Electrophysical properties of MHT thin film were investigated by optical absorption method at temperature 80 and 300 K [4] and bulk at 300K [3].

We investigated the crystal MHT by ESR method on spectrometer Varian E12 (at 4.2 K, at the Q-band freq.= 34 GHz) and Bruker EMX+CW (at 5-100 K, at the X-band freq.=9.36GHz). Strong oscillations were observed in the derivative of microwave absorption (DMA) in the magnetic field up to 20 kOe, are known as the De Haas–van Alphen and Shubnikov–de Haas effects. The dependence of the oscillations period of the DMA corresponds to the transverse magnetoresistance and magnetization [1] and is described by formula: $\Delta H = \Delta H_0(1 + \kappa H^2)$, where H - external magnetic field, which connected with resistivity dependencies from magnetic field (Fig. 1).

The carrier concentration n_s has been determined at the magnetic field strength ~ 4 kOe by the formula [5]: $n_s = e / (\pi \hbar \Delta(1/H)) = 2.71 - 2.96 \cdot 10^{21} \text{ cm}^{-2}$. The amplitude of quantum oscillation decreases in 2D gas model from $T_0=6$ to 14 K [6]: $A(T)/A(T_0) = T \cdot \sinh(\alpha \cdot T_0) / T_0 \cdot \sinh(\alpha \cdot T)$, where $\alpha = 0.55 \pm 0.01$ (Fig. 2). The ratio for calculating the effective mass [6]: $m^* = \alpha \cdot e \cdot h \cdot H / (2\pi^2 k_B) = \gamma \cdot m_e$, where k_B - Boltzmann constant, h -Planck's constant. We have obtained $\gamma = 0.09 \pm 0.002$, which connected with result [3].

We determined concentration and effective mass of the charge carriers and we found that the oscillation period in X- and Q-bands depends from angle between directions of external magnetic field and crystal axis.

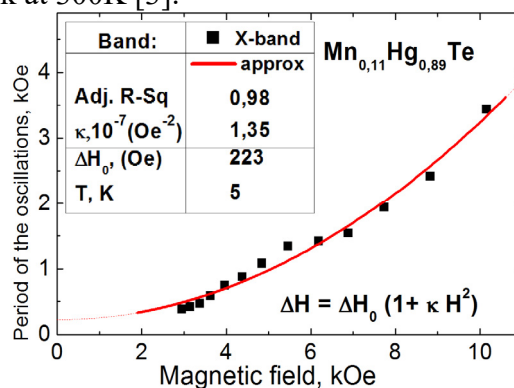


Fig. 1. The dependence of the period of quantum oscillations from the applied magnetic field.

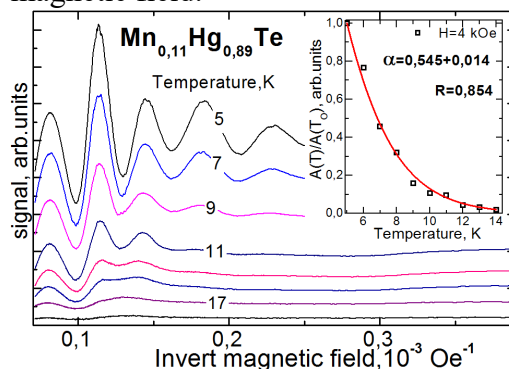


Fig. 2. Temperature evolution of the oscillations period of the DMA, inserted figure: dependence of the quantum oscillations amplitude.

[1] Veynger A. et al , *Phys. and Tech. Semiconductor*, **32** (1998) 557.

[2] Winterfeld L. et al , *Phys. Rev. B*, **87** (2013) 143.

[3] Nesmelova I.M., *Phys. and Tech. Semiconductor*, **37** (2003) 1296.

[4] Nesmelova I.M., Baryshev N.S., Andreev V.A., *Phys. and Tech. Semicond.*, **36** (2002) 49.

[5] Popenko N. et al , *JETF Letters*, **100** (2014) 247.

[6] J. von Bardeleben H. et al , *Applied Physics Letters*, **62** (1993) 90.

4PO-I-47

²⁷Al NMR SPECTROSCOPY STUDY OF FRUSTRATED SPINEL COMPOUND FeAl₂O₄

Gippius A.A.^{1,2}, Harikrishnan S.N.^{3,4}, Strydom A.M.^{2,3}, Baenitz M.²

¹ Faculty of Physics, M.V. Lomonosov Moscow State University, Moscow, Russia

² Max Planck Institute for Chemical Physics of Solids, Dresden, Germany

³ Department of Physics APK, University of Johannesburg, South Africa

⁴ Department of Physics, Colorado State University, Fort Collins, CO 80523, USA
gippius@mail.ru

The spinel structure is composed of a diamond lattice formed by the *A*-site atoms and the pyrochlore network of the *B* site. The ideal diamond lattice with only NN interactions is not geometrically frustrated, in contrast with the pyrochlore lattice, which is inherently geometrically frustrated. In the frustrated *A*-site spinel compound FeAl₂O₄ magnetic Fe²⁺ ions with spin $S = 2$ occupy the tetrahedrally coordinated *A* site. In the *A*-site spinel the frustration effects arise from competing NN and NNN exchange interactions leading to various types of exotic ground states (spin liquid, for instance [1]), and hence these materials are of increased interest in condensed matter physics.

Magnetic susceptibility and polarized neutron diffraction studies of the *A*-site spinels FeAl₂O₄ and MnAl₂O₄ have revealed the presence of significant spin correlations arising purely from frustration effects [2]. Spin-freezing below $T_g \sim 11.4$ K was observed in FeAl₂O₄ [3].

NMR is a sensitive microscopic probe for phase transition and magnetic structure analysis. Here we report the preliminary results on NMR spectroscopy study on frustrated FeAl₂O₄ *A*-spinel compound using ²⁷Al nuclei. NMR experiments were performed using a phase-coherent pulsed Tecmag-Apollo NMR spectrometer. ²⁷Al NMR spectra were measured using a field-sweep point-by-point spin-echo technique at 4.2 K at fixed frequency of 88.2 MHz by integration of the spin-echo envelope in the time domain and averaging over scan accumulation number which depends on the temperature. Fig.1 shows ²⁷Al NMR spectra measured at different temperatures. As clearly seen from this figure, below spin freezing temperature $T_g \sim 11.4$ K [3] the spectra exhibit considerable broadening approximately in one order of magnitude. At the same time, no visible shift of ²⁷Al NMR line was observed in the ordered state. The obtained results are discussed in terms of spin-liquid – spin-glass ground state formation.

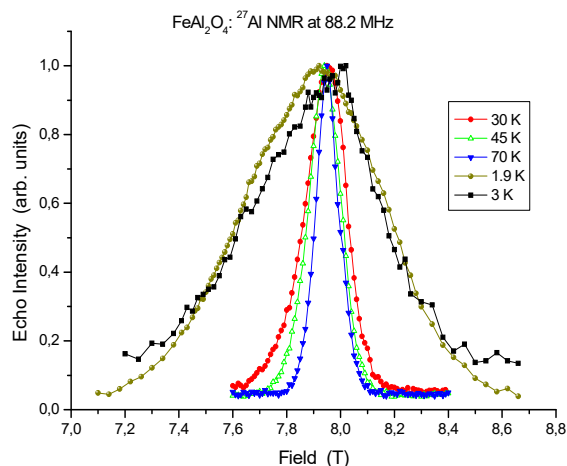


Fig.1. ²⁷Al NMR spectra of FeAl₂O₄ measured at 88.2 MHz at various temperatures.

As clearly seen from this figure, below spin freezing temperature $T_g \sim 11.4$ K [3] the spectra exhibit considerable broadening approximately in one order of magnitude. At the same time, no visible shift of ²⁷Al NMR line was observed in the ordered state. The obtained results are discussed in terms of spin-liquid – spin-glass ground state formation.

Partial support by the RFBR Grant № 17-52-80036 is acknowledged.

[1] J.E. Greedan, *J. Mater. Chem.*, **11** (2001) 37.

[2] R. E. Bailey and J. F. Duncan, *Inorg. Chem.* **6** (1967) 1444.

[3] H.S. Nair et al., *Phys. Rev. B* **91** (2015) 054423.

4PO-I-48

EFFECT OF CATION ORDERING ON A-SITES ON THE PHYSICAL PROPERTIES OF SUBSTITUTED RARE-EARTH COBALTITE OXIDES

$Gd_{1-x}Sr_xCoO_{3-\delta}$

Dudnikov V.A.¹, Orlov Yu.S.¹, Gavrilkin S.Yu.³, Kazak N.V.¹, Platunov M.S.¹, Solovyov L.A.², Vereshchagin S.N.², Velikanov D.A.¹, Ovchinnikov S.G.¹

¹L.V. Kirensky Institute of Physics, FRC “Krasnoyarsk Science Center SB RAS”, Krasnoyarsk, Russia

²Institute of Chemistry and Chemical Technology, FRC “Krasnoyarsk Science Center SB RAS”, Krasnoyarsk, Russia

³Lebedev Physical Institute, Moscow, Russia
slad63@yandex.ru

Substituted rare-earth perovskites $Re_{1-x}M_xCoO_{3-\delta}$ (where Re is the rare-earth element, and M is the alkaline-earth metal) are the promising materials for different technological processes and devices. Also ones belong to the large class of the strongly correlated electron systems with complicated interplay of spin, charge, orbital, and lattice degrees of freedom. Physical and chemical properties strongly depend on the doping level, the oxygen stoichiometry. Most studies are devoted to the compounds with a low content of alkaline earth element. However, compositions with a high content of alkaline earth element also exhibit varied properties. Furthermore, they are characterized by the possibility of obtaining samples with an ordered or disordered cation distribution over perovskite A-positions [1] under certain technological conditions [Fig. 1]. This leads to a difference in the properties of the compounds with the same composition.

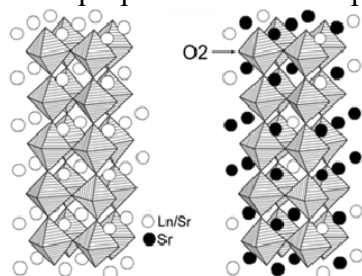


Fig. 1. (a) Cubic structure disordered and (b) structure of the mixed perovskite $Ln_xSr_{1-x}CoO_{3-\delta}$ ($Ln = Sm, Gd, Dy, Y, Ho, Er, Tm, \text{ and } Yb$) ordered with respect to the A positions [1].

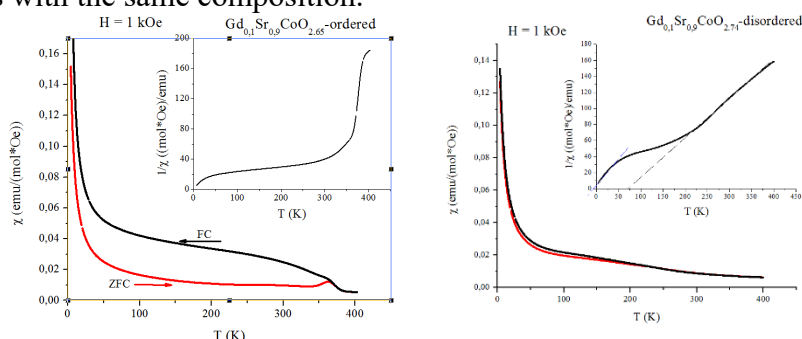


Fig. 2. Temperature dependence of magnetic susceptibility for the GSC-ord and GSC-dis samples measured in FC (red) and ZFC (black) modes in magnetic field $H = 1$ kOe. In the inset, the inverse susceptibility vs temperature is shown.

In our study on example $Gd_{1-x}Sr_xCoO_{3-\delta}$, we show the differences in the physical properties of ordered and disordered samples [Fig. 2].

The reported studies were funded by President of Russia Grant NSh-7559.2016.2; Russian Foundation for Basic Research (RFBR) projects № 16-02-00507, № 17-02-00826, 16-32-60049 mol_a_dk, 16-32-00206 mol_a; RFBR, Government of Krasnoyarsk Territory, Krasnoyarsk Region Science and Technology Support Fund to the research projects № 16-43-240505, 16-42-240413, 17-42-240790, The Council for Grants of the President of the Russian Federation (project SP-938.2015.5).

[1] James, M. et al, *J. Solid State Chem.*, **177** (2004) 1886.

4PO-I-49

EFFECT OF OXYGEN NONSTOICHIOMETRY ON MAGNETIC PHASE TRANSITIONS IN FRUSTRATED COBALTITES

YBaCo₄O_{7+x} (x = 0.0, 0.1, 0.2)

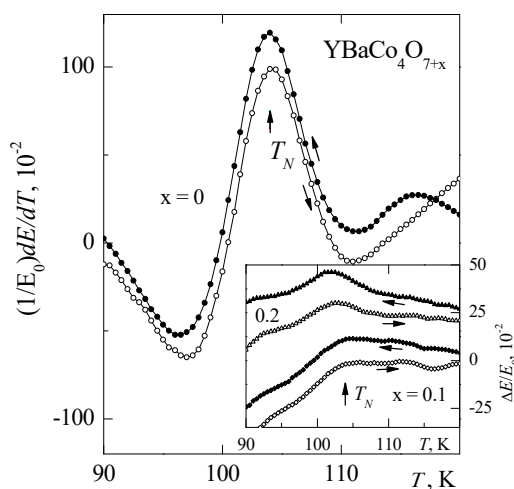
Kazei Z.A., Snegirev V.V., Kozeeva L.P., Kameneva M. Yu., Lavrov A.N.

Moscow State University, 119992 Moscow, Russia

kazei@plms.phys.msu.ru

The family of rare-earth cobaltites RBaCo₄O_{7+x} (R is the RE ion or Y) exhibits an unusual magnetic behavior due to the frustration of exchange interactions and the mixed valence in the 3d-subsystem. Frustrations result in a degenerate ground state and in absence of the long-range magnetic order even at significant constants of exchange interaction. Structure distortion at the phase transition (PT) changes the geometry of exchange bonds and, primarily, lifts their frustration and leads to occurrence of the distinct magnetic order in the Co subsystem. In the present work effect of oxygen nonstoichiometry on structural and elastic characteristics as well as on PT is investigated in cobaltites YBaCo₄O_{7+x} with only one magnetic cobalt subsystem.

Ceramic samples with different synthesis procedure (quenched or annealed on air) were investigated. Samples with controlled oxygen content has been obtained by annealing in vacuum (x = 0.0) or annealing on air (x = 0.10, 0.20); the oxygen content was measured by weight method. Young's modulus $\Delta E/E_0 = [E(T)/E_0(280 \text{ K}) - 1]$ and internal friction coefficient q^{-1} were measured by the composite resonator method at frequency $\sim (110 - 200) \text{ kHz}$ in the temperature range (4.2 - 300) K on polycrystalline samples.



According to FullProf analysis of the full roentgenogram, nonstoichiometric samples possess undistorted hexagonal structure and do not reveal structural transition down to helium temperatures. The structure of stoichiometric samples is characterized by small orthorhombic distortion with value $\varepsilon_o \sim 2 \cdot 10^{-3}$. Distortion of crystal structure results in removal frustration and the occurrence of magnetic order in the cobalt subsystem is expected to be accompanied by sharp anomalies of elastic and magnetic properties at magnetic PT.

For stoichiometric distorted samples, sharp jumps in the $\Delta E/E_0$ curves are observed near $\sim 105 \text{ K}$ caused by magnetic PT of the second order. Values of jumps $\delta E/E_0 \approx 1 \cdot 10^{-2}$ and transition temperature T_N

practically coincide at cooling and heating. The transition temperature T_N corresponds to a jump on the $\Delta E/E_0$ curve or to a maximum of the derivative $(E_0^{-1})(dE/dT)$ (Fig.). Similar anomalies are observed for stoichiometric compounds in the range of the second magnetic PT with $T_{N2} \sim 70 \text{ K}$.

In nonstoichiometric samples with x = 0.1 and 0.2 jumps on the $\Delta E/E_0$ curves at T_N very sharply decrease, smooth and become practically not observable. Their traces can be found out only on the derivative $(E_0^{-1})(dE/dT)$ (insert in fig.). The transition temperature $T_N = 104.0 \text{ K}$ does not vary appreciably at the change of oxygen content. Correlation between oxygen content, structure distortion and character of magnetic PT in Co-subsystem is traced. The reasons for strong effect of the oxygen content on magnetic PT are discussed.

4PO-I1-25

THE CORRELATION OF THE MAGNETIC AND STRUCTURAL PHASES IN $\text{La}_{0.825}\text{Sr}_{0.175}\text{MnO}_3$ MANGANITE

Bulatov A.R., Bogdanova Kh.G.

Kazan E.K.Zavoisky Physical-Technical Institute (KPhTI) of the Kazan Scientific Center of the Russian Academy of Sciences, 420029, Sibirsky Trakt st. 10/7, Kazan
abrphdr.bulatov@yandex.ru

The interrelation between the magnetic and structural order and the role of these interactions in the colossal magnetoresistance (CMR) phenomenon by means of high-frequency ultrasonic waves ($f=700\text{MHz}$) and magnetoresistance measurements was studied. The investigation of the propagation of transverse ultrasonic waves in the $\text{La}_{0.825}\text{Sr}_{0.175}\text{MnO}_3$ crystal revealed sharp variations in the velocity and damping of these waves in three temperature intervals: $T=297\text{-}307$, $280\text{-}285$, and $200\text{-}230\text{K}$. The acoustic anomalies in the region of 283K showed no hysteresis and could be attributed to the phase transition from the paramagnetic (PM) to the ferromagnetic (FM) state, which was confirmed by the results of magnetic measurements performed for the same sample [1]. The changes in the velocity and damping exhibited hysteresises centered at 305 and 220K and, hence, they could be assigned to the first-order phase transitions. We believe that a significant increase in the degree of damping with decreasing in the interval $T=200\text{-}300\text{K}$ is caused by the scattering of ultrasonic waves on the microscopic structural inhomogeneities observed earlier for same sample. Indeed, below 200K , i.e. with the formation of the homogeneous structure, the damping decreases.

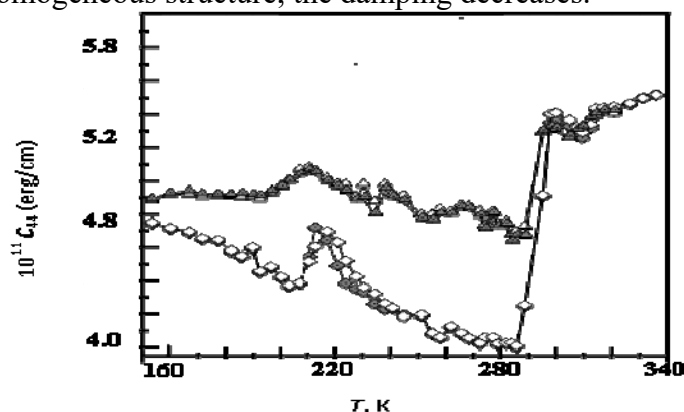


Fig.1. The temperature dependence of the elastic modulus (c_{44}) in $\text{La}_{0.825}\text{Sr}_{0.175}\text{MnO}_3$ manganite. —●— $H=0\text{Oe}$, cooling, —▲— $H=10\text{kOe}$, cooling, △— $H=0\text{Oe}$, heating, ◇— $H=10\text{kOe}$, heating

In the temperature range from 310 to 150K , the velocity and damping of the ultrasonic waves varied in the applied magnetic field. The most pronounced variations of elastic modulus (c_{44}) in the magnetic field were observed in the interval $T=200\text{-}300\text{K}$, where these changes also exhibited hysteresis (Fig.1). The magnetic-field-induced changes were observed even in the fields appreciably lower than 10kOe . The application of a magnetic field also shifted the positions of maxima in the temperature dependences of the ultrasound velocity and damping near 300K to lower temperatures.

Thus, we believe that two structural states, rhombohedral and orthorhombic, coexist in a single crystal of lanthanum strontium manganite $\text{La}_{0.825}\text{Sr}_{0.175}\text{MnO}_3$ over the entire temperature range from 220 to 300K . The rhombohedral state is maintained due to the magnetic ordering of the sample. In turn, the presence of two structural phase states slows down the growth of ferromagnetic ordering in the sample.

[1] A. Asamitsu, Y. Morimoto, R. Kumai, Y. Tomioka, *Phys. Rev.*, **54**, №3 (1996) 1716.

[2] A. Urushibara, Y. Morimoto, T. Arima, A. Asamitsu, G. Kido, Y. Tokura *Phys. Rev.*, **51B** (1995) №20. 14103.

4PO-I1-26

STRUCTURE AND MAGNETIC PROPERTIES OF NI-POLY (P-XYLYLENE) NANOCOMPOSITES

Vdovichenko A.Yu.¹, Oveshnikov L.N.^{1,2}, Orechov A.S.¹, Zavyalov S.A.¹, Chvalun S.N.¹

¹ NRC Kurchatov Institute, Moscow, Russia

² P.N. Lebedev Physical Institute, Moscow, Russia

VdArtem@ya.ru

Thin poly(*p*-xylylene)-nickel nanocomposite films with Ni concentration from 5 to 30 vol.% were prepared by low-temperature vapor deposition polymerization. The relationship between structure, electrical and magnetic properties of this films was studied. Their crystalline structure and surface morphology were studied by X-ray absorption spectroscopy (EXAFS/XANES), transmission electron and scanning probe microscopy. It was found that metal concentration strongly affects morphology of the composites, as well as size and oxidation state of the nanoparticles, and as a consequence determines magnetic properties of nanocomposites, which are shown on Fig. 1.

Based on structural studies one can observe fine-grained morphology of the film with 5 vol.% Ni content, where the inorganic particles of about 4 nm in size are distributed quite homogeneously in the polymer matrix; coarse-grained morphology with 9 vol.% Ni and the Ni nanoparticles are preferably localized on the boundaries of the polymeric grains; and samples with 30 vol.% have Ni fine grain morphology again. Most of the particles in the composite films with low 5 vol.% of Ni are oxidized to NiO, whereas the particles in the PPX-Ni composite with 30 vol.% of Ni are mainly metallic.

Changes in electrical and magnetic behavior of the nanocomposites were observed with the percolation threshold of about 10 vol.%. Such low value of threshold is attributed to the impact of polymer matrix on spatial distribution of metal nanoparticles [1]. Anomalous Hall effect measurements reveal shift of the hysteresis loop toward negative fields, indicating the presence of antiferromagnetic inclusions (NiO). It was demonstrated that the annealing leads to an increase of the magnetoresistance amplitude by more than an order of magnitude and can be used to control magnetic properties of the composites, which is important for potential application of the composites as thin-film flexible magnetic field sensors.

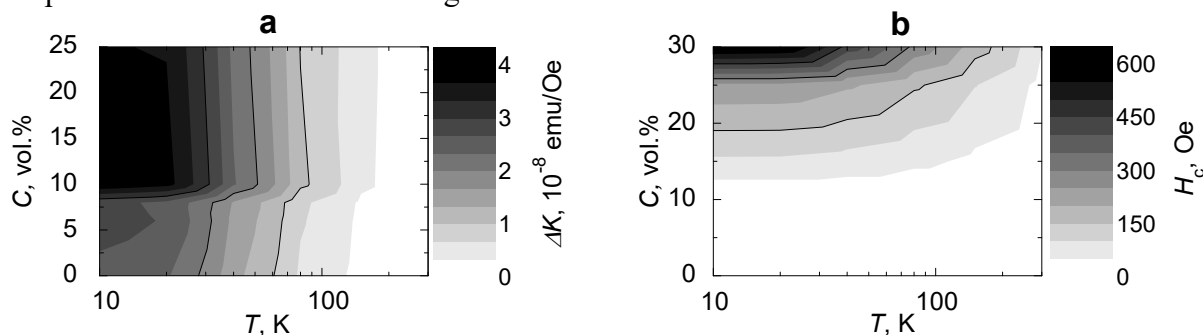


Fig. 1. Temperature-composition diagrams for a) paramagnetic contribution ΔK ; b) coercive force H_c .

This work was partly supported by the Russian Foundation for Basic Research (Grant no. 15-29-01267)

[1] D.R. Streltsov, K.A. Mailyan, A.V. Gusev, et al., *Appl. Phys. A*, **110** (2013) 413-422.

4PO-I1-27

MAGNETIC, DIELECTRIC AND THERMOELECTRIC PROPERTIES OF $\text{Bi}_2\text{Sn}_{1.9}\text{Cr}_{0.1}\text{O}_7$

Udod L.V.^{1,2}, Aplesnin S.S.^{1,2}, Sitnikov M.N.², Molokeev M.N.¹, Yanushkevich K.I.³

¹ Kirensky Institute of Physics, Federal Research Center, KSC SB RAS, Akademgorodok, 50, Krasnoyarsk, 660036 Russia

² Siberian State Aerospace University M. F. Reshetnev, Krasnoyarsky Rabochy Av. 31, 660014 Krasnoyarsk, Russia

³ Scientific and Practical Materials Research Center, National Academy of Sciences of Belarus, P. Brovka Street, 19, Minsk, 220072 Belarus
luba@iph.krasn.ru

Search for compounds with correlation of magnetic and electric effects is relevant problem for use in electronic devices and information storage devices of new generation. The displacement of the bismuth atom and one of oxygen atoms in pyrochlores from the centre of their position in the ideal pyrochlore structure is cause the occurrence of ferroelectricity. The ions of bismuth in $\text{Bi}_2\text{Sn}_2\text{O}_7$ have a lone pair. The absence of the inversion center may lead to spontaneous polarization.

The aim of this study is establishing the effect of doping Cr^{3+} on magnetic properties of $\text{Bi}_2\text{Sn}_2\text{O}_7$ and conditions of occurrence of the pyroelectric effect in $\text{Bi}_2\text{Sn}_{1.9}\text{Cr}_{0.1}\text{O}_7$.

The crystal structure of $\text{Bi}_2\text{Sn}_2\text{O}_7$ at room temperature is a distorted cubic pyrochlore structure and undergoes three polymorphic transition at 360 K is realized the monoclinic α -phase, between 360 and 950 K - a cubic β -phase, above 950 K - face-centered cubic γ -phase. It is known that the $\alpha \rightarrow \beta$ transition is ferroelectric.

The magnetic properties of $\text{Bi}_2\text{Sn}_{1.9}\text{Cr}_{0.1}\text{O}_7$ were investigated using the Faraday method at temperatures up to 1400 K and in magnetic field at 0.86 T. The slope of the temperature dependence of the inverse magnetic susceptibility is changed upon the $\alpha \rightarrow \beta$ transition. The paramagnetic Curie temperature increases three times, $\theta_\alpha=50$ K и $\theta_\beta=150$ K. The temperature dependence of $1/\chi$ reveal a hysteresis in the temperature region 400-900 K corresponding to the existence of the β -phase, the temperature $T=400$ K refers to the $\alpha \rightarrow \beta$ and $T=900$ K $\beta \rightarrow \gamma$ transitions. At heating of the sample, the temperature dependence of the inverse magnetic susceptibility has a broad maximum at $T \sim 714$ K, upon cooling it shifts to $T \sim 681$ K. The formation of hysteresis is associated with the polymorphism, at the cooling of the sample more time is need to complete the $\gamma \rightarrow \beta$ transition.

The temperature dependence of the real and imaginary parts of permittivity have broad maxima in the temperature range 370-500 K, which are shifted in the direction of increasing temperature with increasing frequency. The dipole-charge glass is formed in these temperatures. The electrons are delocalized above 500 K and the growth of current in zero external electric field is observed.

The sign of Seebeck coefficient is changed from positive to negative at $T \sim 400$ K, which corresponds to the $\alpha \rightarrow \beta$ transition and the change of sign of current carriers. The current in zero fields is due to thermoelectric and pyroelectrical current. The prerequisites for the existence of pirocurrent are found.

Support by RFBR №17-42-240079 и 16-52-00045.

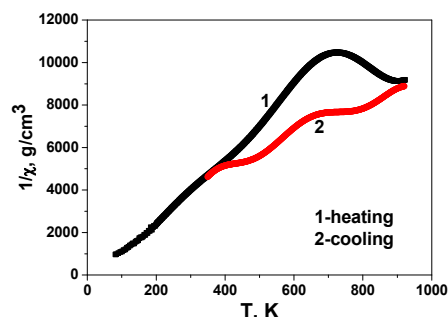


Fig. 1. The temperature dependence of inverse magnetic susceptibility $\text{Bi}_2\text{Sn}_{1.9}\text{Cr}_{0.1}\text{O}_7$

4PO-I1-28

MAGNETIC PROPERTIES OF $\text{Pb}_{1-x-y}\text{Sn}_x\text{V}_y\text{Te}$ ALLOYS

*Skipetrov E.P.*¹, *Konstantinov N.S.*¹, *Skipetrova L.A.*¹, *Knotko A.V.*², *Slynko V.E.*³

¹ Faculty of Physics, M.V. Lomonosov Moscow State University, Moscow, Russia

² Faculty of Chemistry, M.V. Lomonosov Moscow State University, Moscow, Russia

³ I.M. Frantsevich Institute of Materials Science Problems, Chernivtsi, Ukraine

skip@mig.phys.msu.ru

Doping of $\text{Pb}_{1-x}\text{Sn}_x\text{Te}$ alloys with vanadium leads to appearance of a deep impurity level E_V under the bottom of the conduction band ($E_V \approx E_c - 20$ meV in PbTe) [1]. Substituting ions in the metal sublattice, vanadium ions initially exist in the electrically neutral V^{2+} states. However, in the p-type crystals, when the concentration of the impurity increases, the self-ionization of the impurity ions takes place ($V^{2+} \rightarrow V^{3+} + e_{\text{band}}$) due to the flow of electrons from the impurity level to the valence band. Then, after filling the valence band, the Fermi level is stabilized inside the impurity band of vanadium, and the concentrations of filled and empty states in this band should be equal to the concentrations of the impurity ions in two different magnetic states: V^{2+} and V^{3+} , respectively.

In order to determine the concentrations of vanadium ions in different magnetic states and to establish the correlation between magnetic parameters and electronic structure we have studied magnetic properties ($2 \leq T \leq 75$ K, $B \leq 7.5$ T) of $\text{Pb}_{1-x-y}\text{Sn}_x\text{V}_y\text{Te}$ ($x=0.05-0.18$, $y \leq 0.01$).

It is found that the magnetic field and temperature dependences of the magnetization M contain two main contributions: Brillouin-type paramagnetism due to the presence of magnetic V^{2+} and V^{3+} ions and diamagnetism of the host lattice (Fig. 1). An increase of vanadium content along the ingot (from sample 20 to sample 4) leads to the significant increase of the paramagnetic contribution, while the diamagnetic contribution of the lattice remains almost unchanged (see Fig. 1).

Experimental results are discussed in the framework of the model of the electronic structure rearrangement with doping [2], suggesting a change in the ratio of the concentrations of V^{2+} and V^{3+} ions along the ingot. Approximations of $M(B)$ and $M(T)$ dependences by the sum of two modified Brillouin functions corresponding to contributions of vanadium ions in two different magnetic states are performed (see lines in Fig. 1). It was considered that the crystal field causes a quenching of the orbital moments, spins of V^{2+} and V^{3+} ions are $S=3/2$ and $S=1$, g-factor equal to 2. The kinetics of the changes in concentrations of vanadium ions along the ingot is determined. It is shown that the total concentration of the vanadium ions in the samples increases monotonically to about 0.3 mol.%. However, the total concentration of the magnetoactive ions of vanadium in the ingot about an order of magnitude less than the initial concentration of vanadium in the ingot ($y=0.01$).

Support by RFBR (Grant No 16-02-00865) is acknowledged.

[1] A.A. Vinokurov, A.I. Artamkin, S.G. Dorofeev, et al., *Inorg. Mater.*, **44** (2008) 576-581.

[2] E.P. Skipetrov, A.N. Golovanov, E.I. Slynko, et al., *Low Temp. Phys.*, **39** (2013) 76-83.

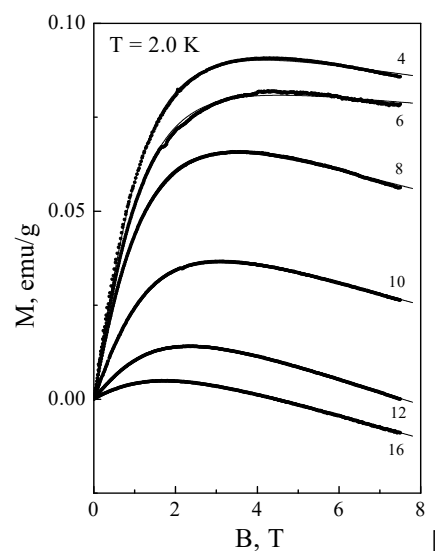


Fig. 1. Magnetic field dependences of magnetization in $\text{Pb}_{1-x-y}\text{Sn}_x\text{V}_y\text{Te}$.

4PO-I1-29

STRAIN EFFECT ON RESISTIVITY OF MANGANITE THIN FILM

*Shaikhulov T.A.¹, Shakhunov V.A.¹, Demidov V.V.¹, Ovsyannikov G.A.¹, Andreev N.V.²,
Pestun A.E.², Sviridova T.A.², Preobrazhensky V.L.³*

¹ Kotel'nikov Institute of Radio Engineering and Electronics, RAS, Moscow, 125009, Russia

² Moscow Technological University, MISIS, Moscow, Russia

³ The Wave Research Center, Prokhorov General Physics Institute RAS, Moscow, 119991, Russia
gena@hitech.cplire.ru

It was demonstrated that using properties of magnates film particular magnetic elastivity [1,2] a memory device with multi level states could be fabricated. A complex study of the dc and magnetic characteristics of epitaxial manganite films $\text{La}_{0.7}\text{Ba}_{0.3}\text{MnO}_3$ (LBMO) was carried out under conditions of the crystal structure tension caused by a mismatch between the parameters of the LBMO crystal and the substrate. The epitaxial thin films with the thickness 40-100 nm were growth by laser ablation at $T=700-800\text{C}$ in pure oxygen pressure 0.3-1 mB[3]. (110)NGO, (001)STO, (001)LAO and (001) LSAT substrate are used. By comparing the lattice parameter of LBMO targets with substrate's one the lattice mismatches was derived. We used substrates in which the lattice parameter was less than LBMO crystal one. It is shown that the temperature dependence of the film resistance in the low-temperature region does not depend on the film strength and is in good agreement with the calculation that takes into account the interaction of carriers with magnetic excitations in the presence of strongly correlated electron states. The study of the lines of ferromagnetic resonance indicated the in homogeneity of the ferromagnetic phase in LBMO films and an increase in the width of the FMR line with decreasing temperature.

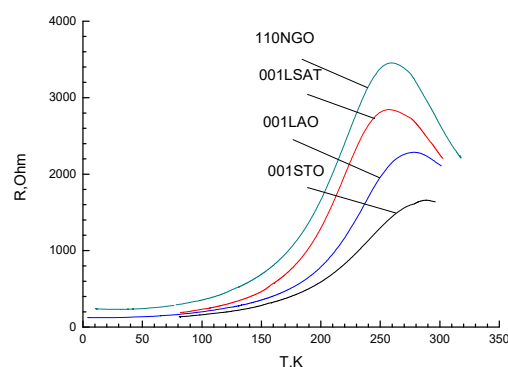


Fig.1. Temperature dependence of LBMO films deposited on the substrates: (001)STO, (110)NGO, (001)LSAT, (001)LAO

Support by International Associated Laboratory LEMAC-LICS, RFBR 17-02-00145, 16-29-14022 and Scientific school NSh -8168.2016.2.

The work was performed in the framework of the International Associated Laboratory LEMAC-LICS

[1] P.B. Demin, L.I. Koroleva, A.Z. Muminov, Ya.M. Mukovski, *Physics of Solid State*, **48** (2006) 322-328.

[2] Weiping Zhou, Yuanqiang Xiong, Zhengming Zhang, et al, *ACS Appl. Mater. Interfaces*, **8** (2016) 5424-5429.

[3] G.A. Ovsyannikov, A.M. Petrzhik, I.V. Borisenko et. al., *J. Exp. Theor. Phys.*, **108** (2009) 48-55.

4PO-I1-30

CONDUCTIVITY, STRUCTURAL AND MAGNETIC PROPERTIES OF MANGANESE CHALCOGENIDE FILMS UNDER ANIONIC SUBSTITUTION BY TELLURIUM

*Romanova O.B.¹, Aplesnin S.S.^{1,2}, Sitnikov M.N.², Kharkov A.M.², Demidenko O.F.³, Galyas A.I.³,
Yanushkevich K.I.³*

¹ Kirensky Institute of Physics, Federal Research center, 660036 Krasnoyarsk, Russia

² Siberian State Aerospace University, 660014 Krasnoyarsk, Russia

³ GO NPTs Materials Science Center, National Academy of Sciences of Belarus, 220072 Minsk,
Belarus

rob@iph.krasn.ru

Manganese chalcogenides have p-type semiconductor conductivity with an energy gap in the spectrum of single-particle electron excitations for MnSe (2.0-2.5eV) and MnTe (0.9-1.3eV) respectively. A magnetoresistive effect $\sim -14\%$ for a single crystal of MnSe was observed in a magnetically ordered cubic phase. In MnTe film magnetoresistive effect reveal at room temperature [1], the effect is absent in bulk samples this system. The transition from bulk samples to thin-film chalcogenides of the Mn-Se-Te system with a growth in anion substitution may lead to an increase in the magnetoresistance in a wide range of temperatures and magnetic fields. In this paper we present the results of an investigation of the structural, magnetic, and electrical properties in the temperature range 80-380 K and magnetic fields up to 13 kOe. Thin-films $\text{MnSe}_{1-X}\text{Te}_X$ compounds with a concentrations $X = 0.3$ and 0.4 were synthesized by thermal evaporation. According to X-ray diffraction analysis, the replacement of selenium by tellurium leads to a decrease in the intensity of the peaks responsible for the cubic structure and the appearance of a wurtzite hexagonal structure. As a result of the investigation of the magnetic properties of thin-film chalcogenides compounds, $\text{MnSe}_{1-X}\text{Te}_X$ ($X = 0.3$ and 0.4), the paramagnetic Curie temperature, the magnetic moment and the Neel temperature were found changing with grow in the substitution concentration in the anion sublattice. From the temperature dependence of the resistivity, a semiconducting character of the conductivity for these compounds was found. Measurements of the I-V characteristics without a field and in a magnetic field showed no dependence on the magnitude of the applied magnetic field. The magnetoresistance effect was not detected. Impedance spectroscopy studies of the $\text{MnSe}_{1-X}\text{Te}_X$ ($X = 0.3$ and 0.4) chalcogenides compounds were performed in magnetic fields of up to 13 kOe at temperatures of 80–400 K in the frequency range of $\omega = 1$ kHz–300 kHz. The magnetoimpedance measurements were carried out using the analyzer components AM-3028. The magnetic field is parallel to capacitor plate. Temperature dependence of the derivative of the impedance dZ/dT reveal two maxima and correlate with the anomalies in $\rho(T)$. The first maximum is found in the magnetic transition region $T \leq 150$ K in the cubic phase (MnSe) and the second maximum is due to the formation of magnetic order in the wurtzite structure (MnTe) and associated with creation of the spin polaron. The frequency dependence of the impedance in a logarithmic scale has a linear form, which indicates the predominance of the capacitive component.

Support by RFBR projects 16-52-00045_Bel_a and №17-42-240079_r_sibir_a.

[1] D.Kriegner, K.Výborný, K.Olejník, H.Reichlová, V.Novák, X.Marti, J.Gazquez, V.Saidl, P.Nêmec, V.V.Volobuev, G.Springholz, V.Holý, T.Jungwirth, *J. Nat. Commun.*, **7** (2016) 11623 (1)-11623(7).

4PO-I1-31

QUANTUM EFFECTS IN MAGNETOTRANSPORT OF InGaAs QUANTUM WELLS WITH REMOTE Mn IMPURITIES

Oveshnikov L.N.^{1,2}, *Morgun L.A.*^{2,3}, *Nekhaeva E.I.*¹, *Kulbachinskii V.A.*¹, *Aronzon B.A.*^{1,2}

¹ National Research Center “Kurchatov Institute”, Moscow 123182, Russia

² P.N. Lebedev Physical Institute RAS, Moscow 119991, Russia

³ Moscow Institute of Physics and Technology, Dolgoprudnyi 141700, Moscow Region, Russia

Oveshln@gmail.com

Two-dimensional (2D) semiconductor structures with magnetic impurities are considered to be one of the most promising candidates as a basic system of next-generation spintronics. Substantial part of related publications are focused primarily on unique effects driven by magnetic subsystem (such as anomalous Hall effect (AHE) [1]), while the impact of magnetic adatoms on more conventional properties of different systems, such as metal-insulator transition and quantum oscillations, is much less discussed in literature.

In present work we've studied heterostructures containing InGaAs quantum wells (QW) with remote Mn impurities (0.3-0.5 monolayers). Spatial separation of magnetic and conducting subsystems allows to maintain high mobility of carriers in QW along with their interaction with Mn atoms. The latter is verified by the observation of the AHE in the investigated structures. The inhomogeneous distribution of Mn impurities gives rise to fluctuation potential (FP) in QW that defines conductivity regime of such systems. Shubnikov – de Haas oscillations observed at low temperatures indicate that FP transforms conducting channel into two-component media with significant difference of carrier mobility values. The effective mass of holes in high-conducting regions is roughly the same as in nonmagnetic heterostructures of same composition. The presence of magnetic impurities highly affects scattering of conducting holes. That fact is confirmed by the observation of resistivity peak, related to magnetic ordering transition at T_c (Fig. 1a), and appearance of negative magnetoresistance (NMR) below 30K. Despite that, the analysis of observed weak localization effect shows that corresponding dephasing length changes along with temperature (Fig. 1b), which contradicts with the assumption of scattering of holes on magnetic impurities being the dominant dephasing mechanism. It is worth to mention, that using standard Hikami-Larkin-Nagaoki (HLN) formula yields an abnormally low prefactor values, which along with abnormally low prefactor of e - e correction (derived from normal Hall effect) indicates the damping of quantum corrections in studied systems. It can be the trace of magnetic impurity impact because theory predicts that quantum interference corrections are absent in ferromagnetic systems and e - e interaction can be drastically modified.

Support by RFBR (grant #16-32-00446) is acknowledged.

[1] L.N. Oveshnikov et al., *Sci. Rep.*, **5** (2015) 17158.

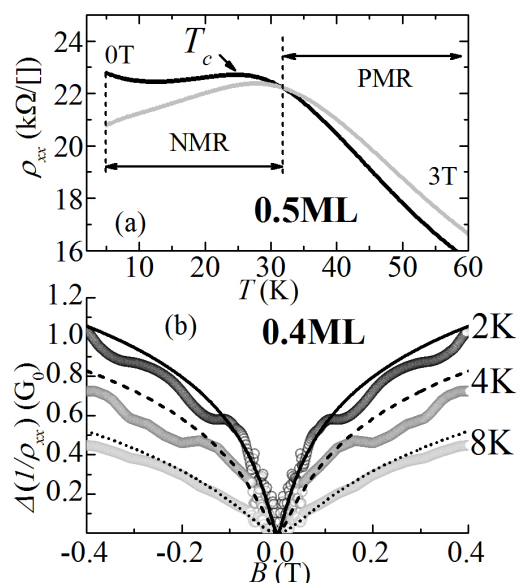


Fig. 1. (a) Temperature dependence of resistivity at 0T and 3T magnetic fields for sample with 0.5ML of Mn; (b) Magnetoconductivity of sample with 0.4ML of Mn and fit by HLN formula

4PO-I1-32

THE COMPLEX NATURE OF THE MAGNETIC STATE OF LANTHANUM MANGANITE UNDER CONDITION OF WEAK DOPING WITH BISMUTH

Tarasenko T.N.¹, Kravchenko Z.F.¹, Burkhovetskiy V.V.¹, Mazur A.S.^{1,2}, Kamenev V.I.¹, Linnik A.I.¹

¹ Donetsk Institute for Physics and Engineering named after A.A. Galkin, Donetsk, Ukraine

² St. Petersburg State University, St. Petersburg, Russia

t.n.tarasenko@mail.ru

The question of the nature of ferromagnetism in Bi-doped lanthanum manganites remains open. For the identical valence of bismuth and lanthanum (+3) and the closeness of their ionic radii ($r(\text{Bi}^{3+}) = 1.24 \text{ \AA}$ and $r(\text{La}^{3+}) = 1.22 \text{ \AA}$), the structure of their external electron shells is significantly different. In contrast to the La^{3+} ion, the Bi^{3+} ion has an isolated pair of $6s^2$ electrons on the outer electron shell, so that when the lanthanum is replaced by bismuth, a shift of the A cations along the $\langle 111 \rangle$ direction of the cubic cell can occur. This will lead to the appearance of three-dimensional static superexchange FM interactions [1].

The aim of this work was to study the structural, magnetic, and resonance properties of solid solutions of the $\text{Bi}_x\text{La}_{1-x}\text{MnO}_3$ system in the weak doping range of $0.0 \leq x \leq 0.1$ [2].

Polycrystalline samples of lanthanum manganite weakly doped with bismuth $\text{Bi}_x\text{La}_{1-x}\text{MnO}_3$ ($x = 0.0; 0.025, 0.05; 0.075$, and 0.1) were synthesized using the sol-gel technique. Compositions with $x = 0.0; 0.05; 0.2$, and 0.6 were obtained via the solid-state reaction in air.

The considerable growth of the grain size that was observed in the samples obtained using the sol-gel technique upon increasing the degree of doping was a consequence of the volume diffusion of Bi^{3+} ions. The NMR spectra of weakly doped $\text{Bi}_x\text{La}_{1-x}\text{MnO}_3$ compositions ($0.0 \leq x \leq 0.05$) prepared via solid-state synthesis were consistent with the rapid exchange between ions $\text{Mn}^{4+} \leftrightarrow \text{Mn}^{3+}$. The intensity of the ^{55}Mn NMR signal of the composition with $x = 0.05$ was ~ 17 times greater than that of the composition with $x = 0$. No NMR signal was observed for concentrations $x \geq 0.2$.

Temperature dependences of the imaginary part of the magnetic susceptibility $\chi''(T)$ was measured in the temperature range of $77 - 300 \text{ K}$. The initial manganite LaMnO_3 obtained via the sol-gel technique had two sharp maxima corresponding to two clearly distinguished FM phases with Curie points at $T_C \sim 113$ and 127 K . Adding bismuth significantly modified the $\chi''(T)$ shape: the maxima of χ'' corresponding to the FM-PM phase transition shifted to the temperature range of $150-170 \text{ K}$.

The presence of Bi in LaMnO_3 alters the magnetic state of lanthanum manganite. Above 130 K , bismuth-containing lanthanum manganite is a slightly inhomogeneous ferromagnetic that consists of several FM phases with Curie points lying in the range of 150 to 170 K (the temperatures of the corresponding maxima of χ''); below 130 K , it transitions to the spin-glass state with temperatures of the freezing of magnetic moments in FM clusters of $T_f \approx 115 \text{ K}$. This follows from the general concepts of spin glass, and from many experimental works that showed the transition to the spin-glass state at falling temperatures is possible not only from the paramagnetic state but also from magnetically ordered states (ferro- or antiferromagnetic) [3].

[1] A. Moreira dos Santos et al., *Phys. Rev. B*, **66** (2002) 064425.

[2] T.N. Tarasenko et al., *Bull. of RAS; Physics*, **81** (2017) 315–319.

[3] I.Ya. Korenblit, E.F. Shender, *Sov. Phys. Usp.*, **32** (1989) 139-162.

4PO-I1-33

BAND STRUCTURE, MAGNETIC AND OPTICAL PROPERTIES OF SEMICONDUCTING $\text{Al}_{0.75}\text{Cr}_{0.25}\text{N}$ SYSTEM: DFT+U MODELING

Shein I.R.¹, Bannikov V.V.¹

¹ Institute of Solid State Chemistry, Ural Branch of RAS, Ekaterinburg, Russia
bannikov@ihim.uran.ru

Within ab initio FLAPW method the band structure, electronic, magnetic and optical properties of $\text{Al}_{0.75}\text{Cr}_{0.25}\text{N}$ solid solution based on meta-stable cubic modification of aluminium nitride have been theoretically modeled for the first time. The role of electron correlation has been taken into account in the frameworks of GGA+*U* approach, the reasonable value of effective repulsion energy for Cr-3*d* states was supposed to be 3.0 eV [1].

It was shown, that Cr ions in $\text{Al}_{0.75}\text{Cr}_{0.25}\text{N}$ system are characterized with local magnetic moments $\sim 2.12 \mu_B$, and that its antiferromagnetic (AFM) state is energetically more favorable than the ferromagnetic (FM) one ($E_{\text{AFM}} - E_{\text{FM}} = -0.06$ eV per one formula unit).

According to the results of FLAPW calculations, the band spectrum of AFM $\text{Al}_{0.75}\text{Cr}_{0.25}\text{N}$ is characterized with gap (see Fig.), minimal width of which is related to indirect $\Delta \rightarrow \Gamma$ electron transition (where Δ is the point between Γ - and X-points of Brillouin zone) and is equal to 2.53 eV (vs 4.30 eV, as compared with pure rock-salt phase of AlN). At the same time, the energy band related to Γ -X direction is of quasi-flat character (as a result, the sharp peak of density of electronic states takes place ~ 0.1 eV below the Fermi level), so the direct Γ - Γ transition is expected to occur for slightly greater $h\nu$ values (by ~ 0.05 eV). Thus, $\text{Al}_{0.75}\text{Cr}_{0.25}\text{N}$ system can be predicted to be an antiferromagnetic semiconductor.

As follows from the results of modeling of frequency-dependent dielectric function (both real and imaginary parts, see Fig.), it is reasonable to expect that intense absorption with maximum at $h\nu \sim 2.55$ eV (blue light) and anomalous character of dispersion should take place in visible region for $\text{Al}_{0.75}\text{Cr}_{0.25}\text{N}$ (as for comparison, pure rock-salt AlN is transparent and exhibits normal dispersion character in whole visible region). The static value of dielectric permittivity for $\text{Al}_{0.75}\text{Cr}_{0.25}\text{N}$ was estimated to equal ~ 7.0 being considerably higher, than that is for pure rock-salt AlN (~ 4.7), and its peak magnitude is ~ 10.4 corresponding to $h\nu \sim 2.38$ eV (green light).

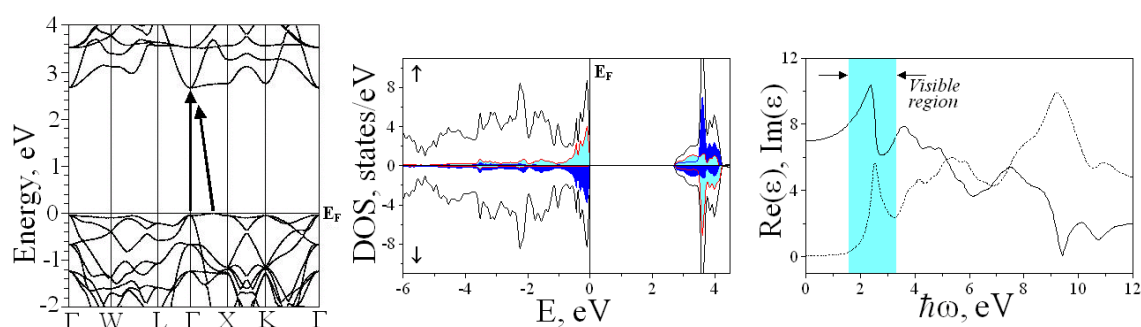


Fig. Band structure $E(k)$, density of states and frequency dependence of real and imaginary parts of dielectric function (solid and dashed lines, respectively) for $\text{Al}_{0.75}\text{Cr}_{0.25}\text{N}$ antiferromagnetic semiconductor.

[1] B. Alling, T.Marten, I.A. Abrikosov, *Phys. Rev. B*, **82** (2010) 184430.

4PO-I1-34

SPIN GLASS MAGNETIC BEHAVIOR IN $\text{GdFeTi}_2\text{O}_7$ COMPOUND

Arauzo A.¹, Bartolomé J.², Drokina T.V.³, Petrakovskii G.A.³, Molokeev M.S.³

¹ Servicio de Medidas Físicas, Universidad de Zaragoza, E-50009 Zaragoza, Spain

² Instituto de Ciencia de Materiales de Aragón (ICMA) and Departamento de Física Condensada, CSIC- Universidad de Zaragoza, 50009 Zaragoza, Spain

³ Kirensky Institute of Physics, Federal Research Center KSC SB RAS, Akademgorodok, 50/38, Krasnoyarsk, 660036, Russia
tvd@iph.krasn.ru

The physics of spin glass systems has been a field of theoretical and experimental interest. There are theoretical predictions and experimental results which give evidence to the magnetic field effect on the freezing temperature [1, 2]. Rare-earth titanates with general chemical formula $\text{R}^{3+}\text{Fe}^{3+}\text{Ti}_2\text{O}_7$ (R-rare earth element) can serve as model materials for the study of disordered systems and spin glass magnetism, since there exists the possibility of cation substitution and of crystal lattice disorder inspection together with the presence of competing magnetic interactions.

Samples of $\text{GdFeTi}_2\text{O}_7$ were prepared by the solid-phase reaction method from a stoichiometric mixture of oxides Fe_2O_3 , TiO_2 , Gd_2O_3 at temperature 1250° C and have been investigated using X-ray powder diffraction, and further characterized by specific heat, magnetization and frequency dependent AC susceptibility measurements.

$\text{GdFeTi}_2\text{O}_7$ is orthorhombic, space group $Pcnc$ at 300 K. The unit cell of the titanate structure is constructed by four-vertex, five-vertex, six-vertex, and eight-vertex oxygen polyhedra; the rare earth cation is arranged in the eight-vertex polyhedron; three nonequivalent octahedral sites ((Fe1-Ti1), (Fe2-Ti2), and (Fe3-Ti3)) are mixed; tetrahedral sites are populated with Fe, and the Fe cations can come out of tetrahedra and populate neighboring sites Fe' and Fe'' with coordination of five. According to the results of the X-ray investigation there are only three positions of iron Fe^{3+} with nonzero population: Fe', Fe'' and the mixed (Fe2-Ti2) position in $\text{GdFeTi}_2\text{O}_7$.

The disorder and the competing magnetic interactions in $\text{GdFeTi}_2\text{O}_7$ lead to the formation of spin glass magnetic state at low temperatures. As one of the illustrations of spin glass behavior, the result of the DC-magnetization measurements both in zero-field-cooled and field-cooled regimes are shown in Fig. 1 (ZFC (open squares) and FC (open circles) curves at external magnetic field $H = 0.05$ kOe and ZFC (solid squares) and FC (solid circles) at $H = 0.5$ kOe). The freezing temperature T_f depends on H ($T_f = 2.6$ K at $H = 0.05$ kOe, $T_f = 4.5$ K at $H = 0.5$ kOe).

Moreover AC susceptibility measurements illustrate that the in-phase and out-of-phase components of the complex AC susceptibility are functions of temperature and frequency of driving field (amplitude of 4 Oe) ($T_f = 5.4$ - 5.8 K in the frequency range $0.01 < f < 1400$ Hz).

Thus, paramagnetic $\text{GdFeTi}_2\text{O}_7$ with the predominantly antiferromagnetic coupling undergoes a spin glass transition at the freezing temperature depending on the value of magnetic field.

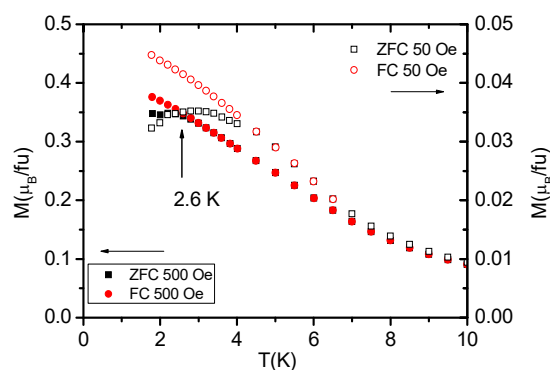


Fig. 1. Temperature dependence of the magnetization in $\text{GdFeTi}_2\text{O}_7$.

[1] L. Leuzzi, G. Parisi, F. Ricci-Tersenghi, J.J. Ruiz-Lorenzo, *Phys. Rev. Lett.*, **103** (2009) 267201(1)-267201(4).

[2] T. Taniguchi, Y. Miyako, *J. Phys. Soc. Jpn.*, **57** (1988) 3520-3531.

4PO-11-35

EFFECT OF AGEING ON MAGNETIC AND ELECTRICAL PROPERTIES OF Ti-SUBSTITUTED La-Sr MANGANITES

Badelin A.G.¹, Datskaya Z.R.¹, Estemirova S.Kh.², Karpasyuk V.K.¹, Merkulov D.I.¹

¹ Astrakhan State University, 414056, Astrakhan, Russia

² Institute for Metallurgy UB RAS, 620016, Yekaterinburg, Russia

alexey_badelin@mail.ru

We have investigated variations of electromagnetic and structural parameters of $\text{La}_{0.8-x}\text{Sr}_{0.2+x}\text{Mn}_{1-x}\text{Ti}_x\text{O}_{3+\gamma}$ ($0.025 \leq x \leq 0.150$) manganites after frequentative thermal cycling in the 300-573 K range, and also during long-continued (up to 50 months) storage at room temperature. Polycrystalline samples were prepared by ceramic processing with final sintering step performed at 1473 K for 10 h. Dc resistance was measured using sputter-deposited copper electrodes.

Changes of magnetization (σ) of all thermal-cycled samples were within the error of measurement, and manganite with $x=0.150$ showed the rise of Curie point (T_c). During the storage period magnetization and Curie point of manganites with relatively low Ti content decreased, while the compositions with high values of "x" exhibited some trend of σ and T_c increase. Temperature dependencies of magnetic permeability (μ) of two samples are cited as an example of these conclusions on Fig.1a).

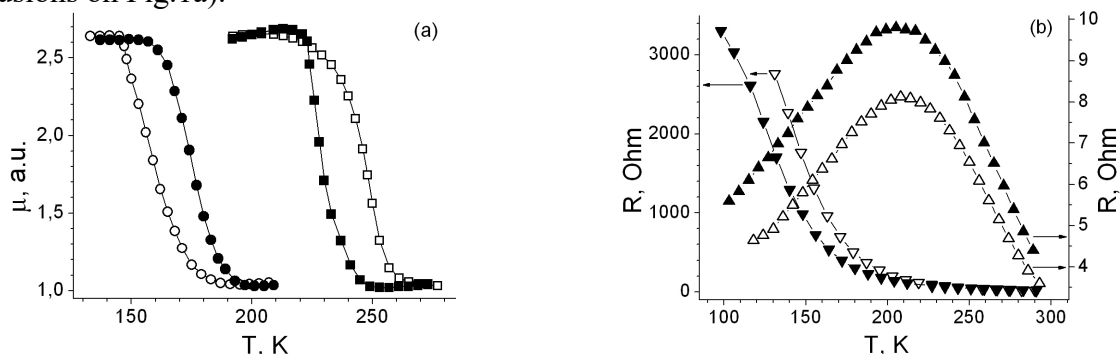


Fig. 1. Temperature dependencies of magnetic permeability (a) and electrical resistance (b) of manganites in initial state (light symbols) and in the end of storage period (black symbols): (\square, \blacksquare) – $x=0.05$; (\circ, \bullet) – $x=0.150$; ($\triangle, \blacktriangle$) – $x=0.025$; ($\nabla, \blacktriangledown$) – $x=0.100$

The resistance of all samples, with the exception of compositions with $x \geq 0.100$, increased during storage period. Fig.1b) illustrates the qualitatively different changes of the resistance of manganites with $x=0.025$ and $x=0.100$.

The unit cell volume (v) of all manganites decreased over time, that indicates an increase in oxygen content. Most considerable decrease of v was observed in the samples with high quantity of titanium, which reduces overstoichiometric oxygen concentration in sintered manganites [1].

From the data obtained it might be inferred that ageing phenomena in Ti-substituted manganites are associated with oxidation processes, the transfer of Ti^{4+} to vacant sites in rare-earth sublattice and relaxation of elastic stresses. Oxidation influences also the properties of the contact zones.

This research was supported by the Ministry of Education and Science of RF (project 334).

[1] D. Merkulov, A. Badelin, S. Estemirova and V. Karpasyuk, *Acta Physica Polonica A.*, **127** (2015) 248-250.

4PO-I1-36

LOW MAGNETIC FIELD INDUCED ANOMALIES IN THE ELASTIC MODULUS OF ZnSe CRYSTALS DOPED BY CHROMIUM IONS

Averkiev N.S.¹, Bersuker I.B.², Gudkov V.V.³, Zhevstovskikh I.V.^{3,4}, Baryshnikov K.A.¹, Sarychev M.N.³, Zherlitsyn S.⁵, Yasin S.^{5,6}, Korostelin Yu.V.⁷

¹Ioffe Institute, 194021, St. Petersburg, Russia

²Institute for Theoretical Chemistry, the University of Texas at Austin, TX 78712, Austin, USA

³Ural Federal University, 620002, Ekaterinburg, Russia

⁴Institute of Metal Physics, Ural Branch RAS, 620137, Ekaterinburg, Russia

⁵Dresden High Magnetic Field Laboratory, Helmholtz-Zentrum Dresden-Rossendorf, D-01314, Dresden, Germany

⁶American University of the Middle East, College of Engineering and Technology, 54200 Egaila, Kuwait

⁷P.N. Lebedev Physical Institute RAS, 119991, Moscow, Russia
zhevstovskikh@imp.uran.ru

In cubic crystals ZnSe:Cr²⁺ the chromium ions substitute the zinc ones, and at the concentration $n_{\text{Cr}} \approx 3.8 \cdot 10^{18} \text{ cm}^{-3}$ they form separate impurity centers with the ground electronic state 5T_2 . For ultrasound waves propagating along [110] with the shear mode polarized along the [1-10] direction (defined by the elastic modulus $(C_{11}-C_{12})/2$) a large temperature peak of attenuation was observed at about 11 K [1]. The peak was attributed to the relaxation transition between the three tetragonal distortions produced by the Jahn-Teller (JT) effect in these centers. Magneto-acoustic study of the ZnSe:Cr²⁺ crystal with $\mathbf{B} \parallel [110]$ in high magnetic fields (up to 14 T) show that the observed anomalies of ultrasound attenuation can be attributed to the same relaxation mechanism [2,3]. In the present work we investigated the magnetic field dependence of the elastic modulus $(C_{11}-C_{12})/2$ at fixed low temperatures (less than 10 K) when condition $\omega\tau > 1$ takes place (ω is the cyclic frequency of the ultrasonic wave, τ is the relaxation time). As apparent from Fig.1, the softening of $(C_{11}-C_{12})/2$ takes place in low magnetic fields (less than 0.2 T). The lattice instability disappears at higher temperatures and in higher magnetic fields. A detailed theoretical evaluation of the magnetic field influence on the elastic modulus of crystals with JT impurity centers like ZnSe:Cr²⁺ in view of these findings seems to be up-to-date.

This research was funded by FASO of Russia (the project Electron 01201463326), and supported in part by RFBR (Project No. 15-02-02750 a), UrFU Center of Excellence Competitiveness Enhancement Program), and the HLD at HZDR, a member of the European Magnetic Field Laboratory (EMFL).

[1] V.V. Gudkov, I.B. Bersuker, I.V. Zhevstovskikh et al. *J. Phys.: Condens. Matter*, **23** (2011) 115401.

[2] N.S. Averkiev, I.B. Bersuker, V.V. Gudkov et al. *Solid State Phen.*, **233-234** (2015) 125-128.

[3] I.V. Zhevstovskikh, V.V. Gudkov, M.N. Sarychev et al. *Appl. Magn. Reson.*, **47** (2016) 685-692.

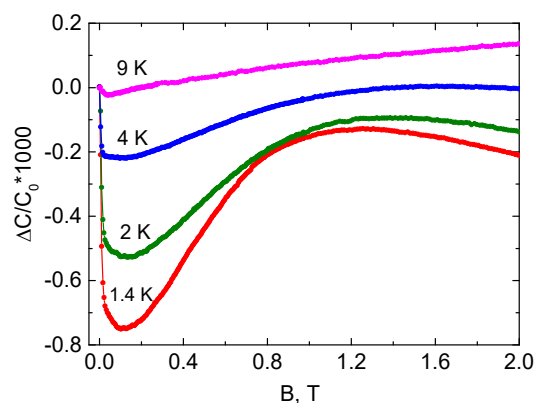


Fig. 1. Magnetic field dependence of the elastic modulus $(C_{11}-C_{12})/2$ at various fixed temperatures, normalized by the values at $B=0$ T, $\omega/2\pi=29.5$ MHz.

4PO-I1-37

DILUTED MAGNETIC SEMICONDUCTORS InFeSb PREPARED BY LASER ABLATION: SPECTROSCOPIC AND MICROSCOPIC INVESTIGATIONS

Gan'shina E.A.¹, Golik L.L.², Kun'kova Z.E.², Zykov G.S.¹, Rukovishnikov A.I.², Temiryazeva M.P.², Lesnikov V.P.³, Markin Yu.V.²

¹ Department of Physics, Lomonosov Moscow State University, Moscow, Russia

² Kotel'nikov Institute of Radioengineering and Electronics (Fryazino Branch), RAS, Fryazino, Russia

³ Lobachevsky Institute of Physics and Technology, Nizhny Novgorod, Russia
eagan@mail.ru

Spintronic devices suggested in theoretical studies may possess characteristics that are unreachable for traditional electronics. However, the implementation of such devices is restrained by the lack of ferromagnetic semiconducting (FMS) thin films, whose Curie temperature (T_c) is above the room temperature. Recently, sets of FMS GaFeSb [1] and InFeSb [2] thin films obtained using molecular beam epitaxy and laser ablation with T_c higher than 300 K have been reported. We study InFeSb thin films, which have been deposited on *i*-GaAs substrate by laser sputtering InSb and Fe targets in vacuum [2], using optical (ellipsometry) and magneto-optical (transversal Kerr effect, TKE) spectroscopy as well as atomic and magnetic force microscopy (AFM and MFM, respectively).

Spectral and temperature ranges of TKE measurements were $E = 0.5 - 4.0$ eV, $T = 20 - 300$ K; H up to 3 kOe. Ellipsometry spectra were measured within the energy range of $E = 1.2 - 4.4$ eV at $T=300$ K. The research was carried out for the layers, whose substrate temperatures (T_g) varied at 20 - 300°C. In according to the calibration curve of the technology process Mn concentration in the layers was estimated of 8 - 17 at.%.

The MFM images obtained at the room temperature have shown that there are high-temperature ferromagnetic particles located on the sample surface. They may include iron, iron oxides and FeSb variations.

Spectral dependences of real, $\langle \varepsilon_1 \rangle(E)$, and imaginary, $\langle \varepsilon_2 \rangle(E)$, parts of pseudo-dielectric function for the layers, which have been calculated using ellipsometry data, confirm that the crystal structure of the investigated layers matches the InSb structure. The spectra also show that another phase contribution is present, which apparently is related to the particles on the surface of the layers.

The study of spectral, temperature and magnetic field TKE dependences has shown that InFeSb/GaAs structures with x above 8 at.%. exhibit ferromagnetic behavior at the room temperature. TKE spectra of these samples have shown a band in the region of E_1 and $E_1 + \Delta_1$ transitions of InSb matrix, which may be caused by the transitions in the InFeSb layers. The TKE spectra of all the samples display a maximum around 1.2 eV, which is apparently associated with contribution of the particles located on the surface of the layers. The presence of a low-temperature ferromagnetic phase was detected in some samples.

This research was supported by the Russian Foundation for Basic Researches №15-02-02077.

[1] N. T. Tu, P. N. Hai, L. D. Anh, and M. Tanaka, *Appl. Phys. Lett.*, **108** (2016) 192401.

[2] A.V. Kudrin, Yu. A. Danilov et al. *Trudy XI Mezhd. Symp. «Nanofizika i Nanoelectronika»*, **1** (2017) 195.

4PO-I1-38

MAGNETIC AND ELASTIC PROPERTIES OF $\text{La}_{0.82}\text{Ca}_{0.18}\text{MnO}_3$ SINGLE CRYSTAL

Zainullina R.I.¹, Bebenin N.G.¹, Ustinov V.V.¹, Shulyatev D.A.²

¹ Institute of Metal Physics UB RAS, Ekaterinburg, Russia

² National University Science and Technology "MISIS", Moscow, Russia

Zainul@imp.uran.ru

The $\text{La}_{1-x}\text{Ca}_x\text{MnO}_3$ system differs from other lanthanum manganites in that the transition from the ferromagnetic to paramagnetic state can be both the first-order and the second-order transition depending on the calcium concentration. [1]. At $x < 0.2$, these manganites undergo structural phase transitions between different modifications of the orthorhombic $Pnma$ structure. One of them (O') is characterized by significant Jahn–Teller distortions of oxygen octahedra. Another phase O^* is called pseudocubic. As a $x < 0.2$ sample is cooled from 400 K, first, the transition from the O^* to Jahn–Teller O' phase takes place; then the magnetic second-order transition from the paramagnetic to ferromagnetic state occurs, and the reverse structural transition from the O' to O^* phase takes place at temperature lightly lower than 100 K. A charge ordering takes place in the low-temperature O^* phase.

The elastic properties of $\text{La}_{1-x}\text{Ca}_x\text{MnO}_3$ single crystals with $x < 0.2$ have not yet been studied up to now; although these properties are known to be sensitive indicators of the structural transitions and structural heterogeneities. In this work, the temperature dependences of the velocity of longitudinal sound waves and the internal friction in a $\text{La}_{0.82}\text{Ca}_{0.18}\text{MnO}_3$ single crystal were studied. The temperature dependences of magnetization M at different magnetic fields were also investigated.

The single crystals of $\text{La}_{0.82}\text{Ca}_{0.18}\text{MnO}_3$ were grown by the floating-zone method. Magnetization was measured using a vibrating sample magnetometer. Temperature dependences of the ultrasound velocity and internal friction were studied by the composite vibrator method. The Curie temperature T_C was found through the extremum of dM/dT .

Dependence $M(T)$ is smooth, and the minimum position in the dM/dT curve is not dependent on magnetic field, which indicates the second order magnetic transition.

The study of the elastic properties of the $\text{La}_{0.82}\text{Ca}_{0.18}\text{MnO}_3$ single crystal (Curie temperature T_C is closed to 181 K) showed that the structural $O^* \rightarrow O'$ phase transition that occurs at $T > T_C$ and the reverse $O' \rightarrow O^*$ phase transition at $T < T_C$ are accompanied by significant changes in the velocity of waves and internal friction. The sound velocity and the internal friction in the Jahn—Teller O' phase are significantly lower than those in the pseudocubic O^* phase. The transitions between the O' and O^* phases are accompanied by much more significant changes in the elastic characteristics than those during transition between the orthorhombic and rhombohedral phases in $\text{La}_{1-x}\text{Sr}_x\text{MnO}_3$ and $\text{La}_{1-x}\text{Ba}_x\text{MnO}_3$ manganites.

This work was performed in the framework of the state task of the Federal Agency for Scientific Organizations of the Russian Federation (theme “Spin,” no. 01201463330) and supported in part by the state task of the Ministry of Education and Science of the Russian Federation (project no. 3.2076.2014/K).

[1] N. G. Bebenin, *Phys. Met. Metallogr.*, **111** (3) (2011) 236.

4PO-I1-39

DEPENDENCE OF THE STRUCTURAL AND MAGNETIC PROPERTIES OF THE LUDWIGITES $\text{Cu}_2\text{Mn}_{1-x}\text{Fe}_x\text{BO}_5$ ON THE IRON CONTENT

Moshkina E.M.^{1,2}, *Platunov M.S.*¹, *Seryotkin Yu.V.*³, *Bovina A.F.*¹, *Eremin E.V.*¹,
*Bezmaternykh L.N.*¹

¹ Kirensky Institute of Physics, Federal Research Center KSC SB RAS, Krasnoyarsk, Russia

² Siberian State Aerospace University, Krasnoyarsk, Russia

³ V.S. Sobolev Institute of Geology and Mineralogy, SB RAS, Novosibirsk, Russia
ekoles@iph.krasn.ru

Magnetic properties of the many ludwigites compounds are very different and strongly affected by the composition [1, 2]. The pair $\text{Cu}_2\text{MnBO}_5 - \text{Cu}_2\text{FeBO}_5$ is a bright example of such behavior. Ludwigite Cu_2FeBO_5 demonstrate three successive magnetic phase transitions at $T_f=63$ K (paramagnetic phase – spin-glass state of Fe-subsystem), $T_N=38$ K (antiferromagnetic ordering of Cu-subsystem), $T_N=20$ K (antiferromagnetic ordering of Fe-subsystem) [2]. Whereas ludwigite Cu_2MnBO_5 demonstrate a single magnetic phase transition at $T=92$ K from paramagnetic to ferrimagnetic phase with weak anisotropy and large magnetic moment [3]. The substitution of the iron ions by the manganese ions fully changes the magnetic behavior of the compound. The objects of the present study are substituted ludwigites $\text{Cu}_2\text{Mn}_{1-x}\text{Fe}_x\text{BO}_5$, where mn and Fe ions are present.

Oxyborates $\text{Cu}_2\text{Mn}_{1-x}\text{Fe}_x\text{BO}_5$ with ludwigite structure have been synthesized by the flux method. The initial flux system for each x is:

$$(100-n)\%mass.(Bi_2Mo_3O_{12}+0,6B_2O_3+0,7Na_2O)+ \\ +n\%mass.\left(2CuO+\frac{(1-x)}{2}Mn_2O_3+\frac{x}{2}Fe_2O_3+\frac{1}{2}B_2O_3\right)$$

Temperature sequences of crystallizing phases have been studied in prepared fluxes. High-temperature crystallizing phase in a wide temperature range was ludwigite $\text{Cu}_2\text{Mn}_{1-x}\text{Fe}_x\text{BO}_5$. Single crystals of $\text{Cu}_2\text{Mn}_{1-x}\text{Fe}_x\text{BO}_5$ with different compositions x were grown at spontaneous nucleation. Size of synthesized single crystals was about $1.5*1.5*5$ mm³.

Structure characterization of the synthesized single crystals has been carried out using X-ray powder method. Homogeneity of the phase composition has been proved, space group and lattice parameters have been determined. As it was expected the synthesized oxyborates $\text{Cu}_2\text{Mn}_{1-x}\text{Fe}_x\text{BO}_5$ posses monoclinically-distorted ludwigite structure with space group $P2_1/c$.

Local structure of the transitional metal ions was studied in crystals $\text{Cu}_2\text{Mn}_{1-x}\text{Fe}_x\text{BO}_5$ ($x=0, 0.2, 0.4, 0.5$) using XANES and EXAFS. The weight composition of the $3d$ ions has been determined by the intensity of the main peaks ratio on K -edge of Fe, Cu and Mn: $\text{Cu}_{1.88}\text{Mn}_{0.74}\text{Fe}_{0.38}\text{BO}_5$ ($x=0.2$), $\text{Cu}_{1.87}\text{Mn}_{0.43}\text{Fe}_{0.7}\text{BO}_5$ ($x=0.4$), $\text{Cu}_{1.83}\text{Mn}_{0.40}\text{Fe}_{0.77}\text{BO}_5$ ($x=0.5$). Refined concentrations are different from the initial concentration “in fluxes” and characterized by the presence in the structure of the Mn^{2+} cations. Temperature dependences of the magnetization of the single crystals $\text{Cu}_2\text{Mn}_{1-x}\text{Fe}_x\text{BO}_5$ ($x=0.2, 0.4, 0.5$) have been obtained in a wide range of the temperature (3-300 K) and magnetic fields (up to 90 T).

The reported study was funded by Russian Foundation for Basic Research (RFBR) and Government of Krasnoyarsk Territory according to the research project No. 16-42-24302 and by Russian Foundation for Basic Research (RFBR) according to the research project No. 16-32-60049.

[1] N. B. Ivanova et. al., *JETP*, **113** (6) (2011) 1015-1024.

[2] M.A. Continentino et. al., *Eur. Phys. J. B*, **9** (1999) 613–618.

[3] S. Sofronova et. al., *Journal of Magnetism and Magnetic Materials*, **420** (2016) 309-316.

4PO-I1-40

STRUCTURAL PHASE TRANSITIONS IN MIXED CHROMIUM SPINELS: LOW TEMPERATURE NEUTRON DIFFRACTION STUDY

Mikheykin A.S.^{1,2}, Torgashev V.I.¹, Razumnaya A.G.¹, Bush A.A.³, Trochenko V.G.¹

¹ Southern federal university, Rostov-on-Don, Russia

² Southern Scientific Center of Russian Academy of Sciences, Rostov-on-Don, Russia

³ Moscow Technological University (MIREA), Moscow, Russia

aleksey.mikheykin@gmail.com

Crystal structure of NiCr_2O_4 and CoCr_2O_4 belongs to normal spinel $AB_2\text{O}_4$ structure type, where A -position and B -position ions have tetrahedral and octahedral coordination by oxygen ions respectively. In the chromium spinels $A\text{Cr}_2\text{O}_4$ the Cr^{3+} ions always occupy octahedral positions due to the much higher crystal field stabilization energy respect to tetrahedral coordination. Consequently, spinels are good model systems for the creation of solid solutions with ions substitution in the tetrahedral positions. If A -cations are Jahn–Teller (JT) ions such as Ni^{2+} in NiCr_2O_4 , as well as their solid solutions, then occurs the orbital degeneracy of electronic states, which can be lifted by cubic-to-tetragonal crystal structure distortions due cooperative Jahn-Teller effect. In case of NiCr_2O_4 critical temperature of first order structural phase transitions is 310 K. Tetragonal phase has lattice parameters ratio more than one, $c/a > 1$. Besides JT effect, there are two magnetic transitions at 75 K and 30 K [1] from paraelectric to complex ferrimagnetic phases. Based on synchrotron powder diffraction data [2,3] another one structural phase transition from tetragonal to orthorhombic phase occurs at 65 K. The close coincidence of structural and magnetic phase transitions is interpreted as evidence of spin-induced symmetry breaking.

Pure cobalt chromium spinel remains cubic down to 5 K [4]. Frustration of the B-cation (pyrochlore) sublattice in these spinels leads to complex non-collinear magnetic structures with three magnetic sublattices: A, Cr_1 and Cr_2 [5]. The collinear ferrimagnetic structure was observed in CoCr_2O_4 below $T_c=93$ K, the spiral component exhibits short-range order below 86 K and the spiral short-range order transforms into long-range order at 31 K [6].

The structural and magnetic phase transitions in a system of NiCr_2O_4 - CoCr_2O_4 solid solutions with the mixed JT (Ni) and non-JT (Co) magnetic ions at tetrahedral A -positions of the normal spinel structure is of interest, because the tuning off JT mechanism of the removing of orbital degeneracy by reducing the concentration of JT ions in solid solution may leads to unexpected states.

Temperature dependent neutron diffraction experiment for $\text{Ni}_{0.5}\text{Co}_{0.5}\text{Cr}_2\text{O}_4$ solid solution from room temperature to 5 K was performed on high resolution powder diffraction station at Swiss spallation neutron source, Villigen, Switzerland. Structural phase transition from cubic to tetragonal phase with ratio of unit cell parameters $c/a < 1$ occurs around 60 K. That directly contradicts to known JT effect: oxygen tetrahedral surrounding of nickel ions should elongate and forms tetragonal phase with $c/a > 1$. Tetragonal-to-orthorhombic structural phase transition takes place at 50 K. Structural phase transformations are accompanied by a magnetic transition to ferrimagnetic conical structure.

Support by grant of Southern federal university № VnGr-07/2017-23.

[1] H. Ishibashi, T. Yasumi, *JMMM*, **310** (2007) e610–e612.

[2] A.S. Mikheykin, et.al., *Journal of Physics and Chemistry of Solids*, **86** (2015) 42–48.

[3] M. R. Suchomel, D. P. Shoemaker, L. Ribaud, M.C. Kemei, R. Seshadri, *Physical review B*, **86** (2012) 054406.

[5] T.A. Kaplan, N. Menyuk, *Philos. Mag.*, **87** (2007) 3711–3785.

[6] K. Tomiyasu, J. Fukunaga, H. Suzuki, *Physical review B*, **70** (2004) 214434.

4PO-I1-41

SPECTRAL AND MAGNETIC PROPERTIES OF Na_2RuO_3 , Na_2RuO_4 AND Na_3RuO_4

Gapontsev V.V.¹, Qamar A.², Moewes A.², Kurmaev E.Z.¹, Sathish C.I.³, Yun S.³, Park J.G.³, Streltsov S.V.¹

¹ M.N. Miheev IMP UB RAS, Yekaterinburg, Russia

² University of Saskatchewan, Saskatoon, Saskatchewan, Canada

³ Center for Correlated Electron Systems, IBS, Seoul, Korea

gapontsev@v.v@gmail.com

Na_2RuO_3 crystallizes in a monoclinic lattice (space group: $C2/m$). It has a quasi-two-dimensional structure with the Ru ions placed in the RuO_6 octahedra, which form a honeycomb lattice (see Fig. 1). The structure is similar to Li_2RuO_3 attracting much attention due to an exotic valence bond liquid state recently found in this compound [2]. While physical properties of Li_2RuO_3 have been extensively studied by means of several experimental and theoretical methods, Na_2RuO_3 stays mostly unexplored: only crystal structure [4], magnetic susceptibility and specific heat data [5] are available.

In the work we present following results for Na_2RuO_3 . (i) The resistivity, susceptibility and heat capacity measurements which gave us no signs of any phase transitions. (ii) The X-ray absorption and emission spectroscopy, which result in determination of band gap width about 0.08 eV. (iii) The density of electronic states calculated using the Wien2k package [6] for O are in good agreement with XES and XAS spectra. The system lowest total energy corresponds to zig-zag antiferromagnetic.

Besides Na_2RuO_3 we provide similar experiment and theoretical investigations for Na_2RuO_4 and Na_3RuO_4 .

The work was supported by the RFBR via grant 16-02-00451, by FASO (themes “ Electron” and “Spin” No. 01201463326 and 01201463330) and by Russian ministry of education and science via contract 02.A03.21.0006.

[1] K. Momma, F. Izumi, *J. Appl. Crystallogr.*, **44** (2011) 1272-1276.

[2] S. A. J. Kimber, I. I. Mazin, J. Shen, H. O. Jeschke, S. V. Streltsov, D. N. Argyriou, R. Valenti, D. I. Khomskii, *Phys. Rev. B*, **89** (2014) 081408-1-081408-5.

[3] Y. Miura, M. Sato, Y. Yamakawa, T. Habaguchi, Y. Ono, *Journal of the Physical Society of Japan*, **78** (2009) 094706-094711.

[4] K. M. Mogare, K. Friese, W. Klein, M. Jansen, *Zeitschrift für anorganische und allgemeine Chemie*, **630** (2004) 547-552.

[5] J. C. Wang, J. Terzic, T. F. Qi, F. Ye, S. J. Yuan, S. Aswartham, S. V. Streltsov, D. I. Khomskii, R. K. Kaul, G. Cao, *Phys. Rev. B*, **90** (2014) 161110-1-161110-6.

[6] P. Blaha, K. Schwarz, G. Madsen, D. Kvasnicka, J. Luitz, *WIEN2k, An Augmented Plane Wave + Local Orbitals Program for Calculating Crystal Properties* (Techn. Universität Wien, Wien, 2001).

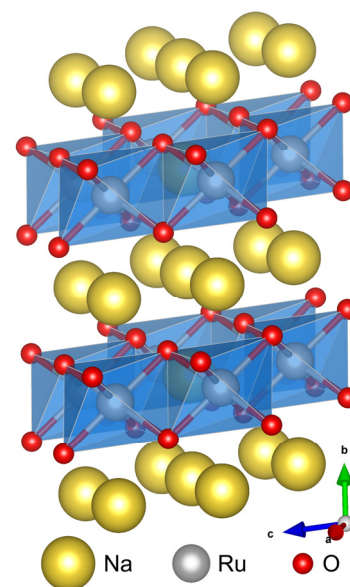


Fig. 1. Crystal structure of Na_2RuO_3 (generated by the Vesta software [1]).

4PO-I1-42

HIGH-TEMPERATURE FERROMAGNETISM OF THIN $Zn_{1-x}Co_xO_y$ FILMS, FABRICATED BY PULSED LASER DEPOSITION

*Lotin A.A.¹, Novodvorsky O.A.¹, Parshina L.S.¹, Khramova O.D.¹, Mikhalevsky V.A.¹,
Cherebilo E.A.¹, Kuz'mina A.S.², Shneider A.G.², Perov N.S.³, Makarova L.A.³*

¹ ILIT RAS - branch of the Federal Scientific Research Center "Crystallography and Photonics"
RAS, Shatura, Russia

² Irkutsk National Research Technical University, Irkutsk, Russia

³ Lomonosov Moscow State University, Moscow, Russia

lotin_82@mail.ru

The features of the structural, magnetic and magneto-optical properties of thin $Zn_{1-x}Co_xO_y$ films ($x=0-0.3$) from 10 to 262 nm thickness, fabricated on *c*-sapphire substrates by the pulsed laser deposition method are studied. It is revealed that all of the synthesized $Zn_{1-x}Co_xO_y$ films possess a wurtzite structure with the lattice parameters $a = 3.2495 \text{ \AA}$, $c = 5.2329-5.2485 \text{ \AA}$. It is established that the ferromagnetic properties of the $Zn_{1-x}Co_xO_y$ films nonmonotonously depend on Co concentration at room temperature. For the $Zn_{0.87}Co_{0.13}O_y$ film, the strongest ferromagnetic signal is observed that is caused by formation of the greatest number of metallic Co clusters. A further increase of doping impurity concentration in the films leads to the oxidation of metallic Co and formation of the paramagnetic Co_3O_4 phase, in consequence of which the ferromagnetic signal subsides. It is defined that the specific magnetic characteristics of the $Zn_{1-x}Co_xO_y$ samples do not depend on the film thickness. The dependence of the equatorial Kerr effect on cobalt concentration and thickness of $Zn_{1-x}Co_xO_y$ films was studied for the first time. The magneto-optical signal amplitude is correlated with the film magnetization value.

The work has been supported by RFBR grants: 15-07-03331, 15-29-01171, 15-38-20369, 15-07-03580, 16-29-05385, 16-07-00842, 16-29-11719.

4PO-I1-43

CORRELATION BETWEEN MAGNETOELASTIC PROPERTIES AND INFRARED MAGNETOREFLECTION IN SPINEL CoFe_2O_4

*Buchkevich A.A., Sukhorukov Yu.P., Telegin A.V., Nosov A.P., Bessonov V.D.,
Mostovshchikova E.V.*

M.N. Miheev Institute of Metal Physics Ural Branch of RAS, Ekaterinburg, Russia
buchkevich@imp.uran.ru

Optics is a local probe that can provide insight into the local crystal structure and the corresponding electronic structure of materials. Spinel ferrites constitute a class of material with significant magneto-optics phenomena potential for application. In particular, CoFe_2O_4 is unique because of its large magnetic anisotropy accompanied by large anisotropic magnetostriction which constants λ_{100} is about 6×10^{-4} at room temperature. This spinel is an insulator with the high Curie temperature ($T_C=812$ K) and interaction of light with free charge carriers is absent in the infrared. Our experimental task was to investigate if there is correlation between magneto-elastic and magneto-optical properties in CoFe_2O_4 crystals in the infrared spectral range 1-30 μm . The single crystals were grown by floating zone melting with radiation heating. Reflectivity of samples was measured with the relative error of 0.2% at angles close to normal incidence of natural light in magnetic fields from 0 to 4 kOe applied in-plane to the sample surface. Magnetoelastic properties $(\Delta l/l)_{100}$ were characterized by the strain gauge technique. The magnetoreflexion effect $(\Delta R/R)$ has been observed in the wide infrared spectral range in CoFe_2O_4 single crystals for the first time [1]. $\Delta R/R$ strictly depends on the orientation of magnetic field and almost vanishes for $\mathbf{H} \parallel [110]$. For $\mathbf{H} \parallel [100]$ magnetoreflexion varies from -1% to +4% in the saturated field of 3.6 kOe depending on the spectral region. Several mechanisms of magnetoreflexion can be separated in CoFe_2O_4 crystals. For example, when $\lambda < 1.5 \mu\text{m}$, positive sign of $\Delta R/R$ indicates that magnetic field gives rise to the shift of the absorption edge. It leads to the increase of $\Delta R/R$. When $1.5 < \lambda < 7 \mu\text{m}$, the $\Delta R/R$ has a peak (up to 4%) near the middle infrared band at $\lambda = 2.96 \mu\text{m}$ connected with the elastic modes in spinel ferrites [1]. For $\lambda > 7 \mu\text{m}$ the spectral dependence of $\Delta R/R$ is characterized by the features associated with the magnetic-field-induced shift of reflection minima near the phonon bands. The clear correlation has been also established for magnetic field dependences of $\Delta R/R$ and $(\Delta l/l)_{100}$. Finally, from Kramers-Kronig relations the clear magnetorefractive effect up to $1.5 \cdot 10^{-3}$ was obtained in the wavelengths range from 3 up to 10 μm . It is in good accordance with theoretical predictions. It was established that magnetic field-induced strains and deformations of lattice can lead to giant changes of reflectivity of magnetostrictive CoFe_2O_4 single crystals in the IR. It paves the way to new branch of straintronics – strain-magneto-optics.

The work was conducted within the state assignment of the Federal Agency for Scientific Organizations of the RF (theme “Spin” No. 0120146330), grant of the Ministry of Education and Science RF (No. 14.Z50.31.0025) and the program of UB RAS (No. 15-9-2-4).

[1] Yu.P. Sukhorukov, A.V. Telegin, A.P. Nosov, V.D. Bessonov, A.A. Buchkevich, *JETP letters*, **104** (2016) 398-401.

4PO-I1-44

SYNTHESIS, CRYSTAL AND ELECTRONIC STRUCTURES, PHYSICAL PROPERTIES AND ^{121}Sb AND ^{151}Eu MÖSSBAUER SPECTROSCOPY OF THE ALUMO-ANTIMONIDE ZINTL PHASE $\text{Eu}_5\text{Al}_2\text{Sb}_6$

Radzieowski M.¹, Block Th.¹, Fickenscher Th.¹, Zhang Yu.², Fokwa B.P.T.², Janka O.¹

¹ Institut für Anorganische und Analytische Chemie, Westfälische Wilhelms-Universität Münster, Corrensstraße 30, 48149 Münster, Germany

² Department of Chemistry, 501 Box Springs Rd, Riverside, CA, 92521, USA
radzieowski@uni-muenster.de

In the ternary system Sr–Al–Sb three compounds ($\text{Sr}_5\text{Al}_2\text{Sb}_6$ [1], $\text{Sr}_{14}\text{AlSb}_{11}$ [2] und Sr_3AlSb_3 [3]) are known. Surprisingly in the system Eu–Al–Sb no compounds have been published in the literature until now. Due to the comparable atomic radii of Eu^{2+} und Sr^{2+} known Sr-compounds offer a suitable basis for the synthesis of isostructural Eu-compounds. $\text{Eu}_5\text{Al}_2\text{Sb}_6$ was synthesized from the elements in niobium ampoules by induction heating. The compound crystallizes in the orthorhombic crystal system ($a = 1200,28(6)$, $b = 1027,55(7)$, $c = 1324,22(7)$ pm) with the space group $Pnma$, isotypic to $\text{Sr}_5\text{Al}_2\text{Sb}_6$ and can be described as a Zintl-phase. The structure contains the polyanion $[\text{Al}_2\text{Sb}_6]^{10-}$, built by corner- and edge-connected $[\text{AlSb}_4]$ -tetrahedrons. At one of the crystallographic independent tetrahedrons a Sb^{3-} -anion is replaced by a covalently connected $[\text{Sb}_2]^{4-}$ -dumbbell. Due to the isotypism to the Sr-compound we assumed divalent Eu-atoms in $\text{Eu}_5\text{Al}_2\text{Sb}_6$ [$\equiv (\text{Eu}^{2+})_5(\text{Al}^{3+})_2(\text{Sb}^{3-})_4(\text{Sb}_2^{4-})$], which is confirmed by magnetic measurements and Mößbauer-spectroscopic investigations. The effective magnetic moment of $\text{Eu}_5\text{Al}_2\text{Sb}_6$ was determined to $\mu_{\text{eff}} = 8.32(1) \mu_{\text{B}}$ which is slightly above the calculated moment for the free Eu^{2+} -ion ($\mu_{\text{calc}} = 7.94 \mu_{\text{B}}$). ZFC-FC measurements show antiferromagnetic ordering at $T_{\text{N}} = 3.5(1)$ K, and additionally a second anomaly at 12.5(1) K (Fig. 1, left). The ^{151}Eu -Mößbauer-spectrum shows three main signals at $\delta = -11.23(6)$, $-11.41(4)$ and $-11.47(4)$ mm s⁻¹ and one at $\delta = -0.2(2)$ mm s⁻¹ due to Eu^{3+} impurities. The observed shifts are in agreement with Eu^{2+} . Remarkably the spectrum at 5 K (Fig. 1, right) indicates only magnetic ordering of the two 8d sites, the third Eu-position (4c) finally orders at 3.5(1) K.

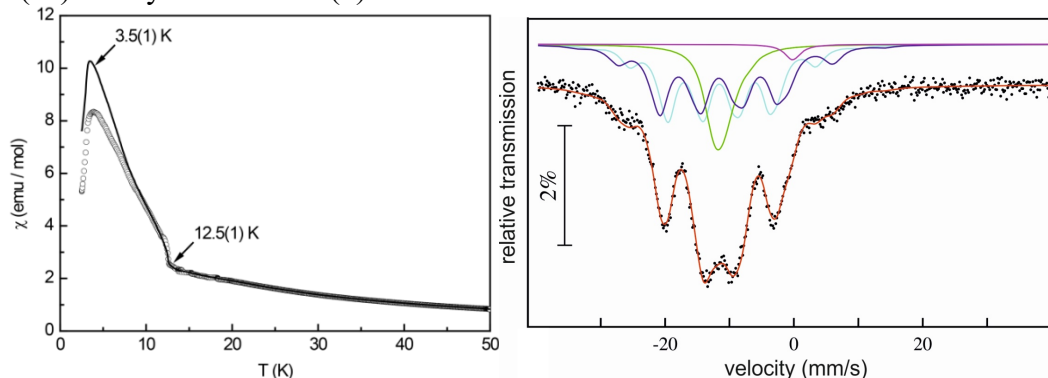


Fig. 1: (left) ZFC-FC susceptibility measurement at 100 Oe of $\text{Eu}_5\text{Al}_2\text{Sb}_6$; (right) ^{151}Eu -Mößbauer-spectrum of $\text{Eu}_5\text{Al}_2\text{Sb}_6$ at 5 K.

- [1] G.Cordier, M.Steher *Z. Naturforsch.*, **43b** (1988) 463-466.
 [2] S.L.Brock, L.J.Weston, M.M.Olmstead, S.M.Kauzlarich, *J.Solid State Chem.*, **107** (1993) 513-523.
 [3] G. Cordier, M. Stelter, H. Schäfer *J. Less-Common Met.*, **98** (1984) 285-290.

4PO-I1-45

MAGNETIC ORDER-DISORDER TRANSITION IN THE FERROMAGNET PbMnBO_4 UNDER THE EXTERNAL MAGNETIC FIELD

Pankrats A.^{1,2}, Kolkov M.^{1,2}, Popkov S.^{1,2}, Sablina K.¹, Balaev A.¹, Miskiv A.¹

¹ Kirensky Institute of Physics, Federal Research Center KSC SB RAS Krasnoyarsk, Russia

² Siberian Federal University, Krasnoyarsk, Russia

maxim_91@mail.ru

The orthoborate PbMnBO_4 single crystals were first grown and their magnetic and resonance properties were studied [1]. The magnetic structure is established to be ferromagnetic below the Curie temperature $T_C=31\text{K}$ [1, 2] and characterized by the strong magnetic anisotropy due to the Jahn-Teller effect associated with the Mn^{3+} cations [1]. The experimental investigations [1] showed that short-range correlations persist significantly above the Curie temperature when the external magnetic field is applied. It results in the non-linear magnetization curves and the temperature dependences of the resonance fields at temperatures up to 70 K. This work is devoted to the investigation of the magnetic order-disorder transition using specific heat study under the external magnetic fields up to 70 kOe.

The temperature dependence of the specific heat measured in zero magnetic field (Fig. 1a) shows the phase transition at $T_C=30.3\text{K}$. The lattice contribution shown here by the solid line was calculated within the framework of the Debye-Einstein model. To determine the magnetic contribution to the specific heat, the lattice one was subtracted from the experimental values measured in different magnetic fields (Fig. 1b). The clearly defined λ -shaped peak of the magnetic specific heat is observed in zero magnetic field. The peak becomes spread and the transition areas are widened with the applying of the external magnetic fields (Fig.1b), the more the stronger magnetic field is used.

Temperature dependences of the magnetic entropy (Fig.1c) are attained a value of $R \cdot \ln(2S+1)$ which confirms that the phase transition is magnetic in nature.

The interpretation of the experimental results on magnetic contribution to the specific heat are carried out within the framework of molecular field approach.

Support by the RFBR, Project No. 16-02-00563.

[1] Pankrats, A., Sablina et al.. *JMMM*, **414** (2016) 82-89.

[2] Park, H. et al. *Chemistry of materials*, **15** (2003) 1703-1712.

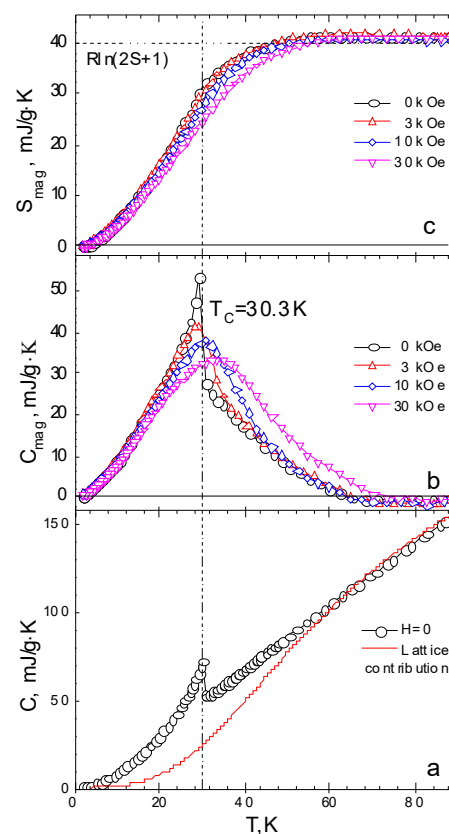


Fig. 1. Temperature dependences of the specific heat (a) and the magnetic contributions to the specific heat (b) and entropy (c).

4PO-I1-46

MAGNETOSTRICTION IN HEXAGONAL HoMnO_3 SINGLE CRYSTAL

Pavlovskiy N., Dubrovskiy A., Shayhutdinov K., Terent'ev K.

Kirensky Institute of Physics Federal Research Center KSC SB RAS, Krasnoyarsk, Russia

mik0la@yandex.ru

Hexagonal manganites RMnO_3 (R - rare earth ion) are promising materials for developing structures on their basis for new functional materials. The typical example of this family is HoMnO_3 , which magnetic phase diagram is well established. Following to [1], at temperature $T_N = 72$ K, HoMnO_3 ordered in noncollinear spin structure with magnetic $\text{P}\bar{6}_3\text{cm}$ group symmetry. At the spin reorientation temperature $T_{\text{off}} = 40$ K, manganese moments rotate in a plane with the changing magnetic $\text{P}\bar{6}_3\text{cm}$ symmetry to $\text{P}\bar{6}_3\text{cm}$, also there is another transition at temperature ~ 4 K associated with rare-earth ordering.

In this study, the single crystal of hexagonal manganite HoMnO_3 was synthesized by optical floating zone melting technique. The effect of magnetostriction was measured in a temperature range of 4.2 to 100 K at applied magnetic fields up to 14 T.

The behavior of the magnetostriction effect showed a large number of features (Fig.1) observed in different temperatures and field configurations, including nonmonotonically striction and change the sign of the effect. Moreover, the behavior of the magnetostriction effect in temperatures below the spin-flip transition of Mn correlates well with the magnetic phase diagram HoMnO_3 .

However, since original compound consists of two magnetic subsystems (4f and 3d elements), it was decided to synthesize a pattern of hexagonal substituted lanthanum manganite with replacement on non-magnetic ion in the rare-earth subsystem in order to determine the impact on the behavior of 4f subsystem magnetostrictive effect.

For this, the sample was synthesized with a nonmagnetic YMnO_3 4f subsystem, on which the measurement of the magnetostriction effect were also been done. Measurement results showed that the value of the magnetostriction decreased by the order and lost all the features typical of HoMnO_3 . It can be concluded that the main role in magnetostriction effect is the role of Ho ions.

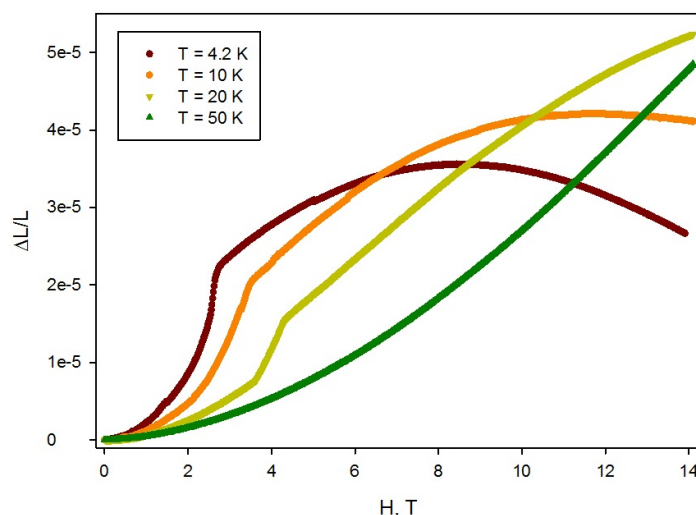


Figure 1. Longitudinal magnetostriction along c -axis of HoMnO_3

[1] F. Yen, C. dela Cruz, B. Lorenz, E. Galstyan, Y.Y. Sun, M. Gospodinov, C.W. Chu, *J. Mater. Res.*, **22** (8) (2007).

4 July

Tuesday

17:30-19:30

poster session

4PO-J

“Multiferroics”

4PO-J-25

PHASE TRANSITIONS AND FEATURES OF SURFACE PROPERTIES IN MULTILAYER MAGNETIC NANOFILMS

Valieva L.R.¹, Sharafullin I.F.¹

¹ Bashkir State University, Ufa, Russian Federation
valieva.post@gmail.com

The study of the kinetics of phase transitions, new physical phenomena occurring in the process of phase transformations in magnetic nanomaterials, and the creation of new functional elements for nanoelectronic devices on their basis are attracted an immense interest [1-3]. In recent years, there has been significant progress in understanding the mechanism of the origin of spontaneous polarization in multiferroics with noncollinear magnetic ordering, but now the microscopic principles of these phenomena are not fully understood. In this direction, good results are shown by the application of the Monte Carlo method.

The aim of this work is to investigate phase transitions and critical phenomena in materials with strongly correlated magnetic, ferroelectric and elastic parts, as well as theoretical studies of the influence of external fields on the dynamics of phase transitions in crystals of the perovskite – type structure. Investigate include the Monte Carlo simulation of the properties of multiferroics on three-dimensional lattices.

We consider the lattice consists of two-dimensional orthorhombic layers folded along the orthogonal axis. In this work the modeling of the properties of the orthorhombic multiferroic is carried out using highly effective techniques, such as histogram technique and the Wang-Landau method. Numerical calculations were carried out for nanofilms of a multiferroic with linear dimensions $N = 100 \times 100 \times (4-16)$. The periodic boundary conditions in the film plane were employed in the system. To achieve a state of thermodynamic equilibrium, we cut off an interval with length $l_0 = 3 \cdot 10^5$ Monte-Carlo steps per spin. The thermodynamic values were averaged over an interval 500 times longer than the above interval. The order parameters of the magnetic and ferroelectric subsystems are determined as follows

$$M_\alpha = \frac{C}{N} \sum_i (-1)^n S_i, M = \frac{1}{2} \sqrt{(M_1 + M_2 - M_3 - M_4)^2 + (M_1 + M_4 - M_3 - M_2)^2} .$$

$$P_\alpha = \frac{C}{N} \sum_i (-1)^n P_i, P = \frac{1}{2} \sqrt{(p_1 + p_2 - p_3 - p_4)^2 + (p_1 + p_4 - p_3 - p_2)^2} ,$$

The results of our work shows that the transition from antiferromagnetic phase to the paramagnetic phase and from antiferroelectric to ferroelectric phases in the magnetic and ferroelectric subsystems of multiferroic, respectively, are second-order transitions. This can be seen also from the histogram of energy near the critical temperature. On this histogram, one maximum is observed, indicating the existence of a second-order phase transition. We have investigated the effect of an applied magnetic field along the axis, perpendicular to the film using Monte – Carlo simulation. We have found that with increasing the temperature and applied magnetic field, the layers with not large spin components, parallel to magnetic fields, undergo a phase transition where the ordering of the transverse spin-components is destroyed. Other layers with large spin component, parallel to magnetic fields, do not make transitions.

- [1] Krotov S.S., Shnaideshtein I.V. // Phenomenology of magnetically induced ferroelectricity. Moscow: Physics Faculty of Moscow State University, 2011, 111 pages.
[2] Diep H. T., *Phys. Rev. B* **91** (2015) 014436.
[3] Sahbi El Hog and H. T. Diep, *Mod. Phys. Lett. B*, **30** (2016) 1650071.

4PO-J-26

MAGNETOELECTRIC EFFECTS IN FERRITE GARNET FILMS

Gareeva Z.V.¹, Mazhitova F.A.², Doroshenko R.A.¹, Popov A.I.³

¹ Institute of Molecule and Crystal Physics, Russian Academy of Sciences, 450075 Ufa, Russia

² Bashkir State University, 450076, Ufa, Russia

³ National Research University of Electronic Technology, 124498, Zelenograd, Moscow, Russia
gzv@anrb.ru

In this report we discuss magnetoelectric effect in iron garnets exemplified on exchanged – coupled iron garnet film. Our research aims to compare the impacts given to garnet magnetoelectricity by different magnetoelectric mechanisms attributed to magnetic inhomogeneity. We address inhomogeneous magnetoelectric mechanism [1] and the mechanism related to rare earth ions occurring in rare earth iron garnets (RIG) [2].

To illustrate manifestations of magnetoelectric effects we consider bi-layered ferrite garnet film. Magnetic inhomogeneity can be created at the interface due to the differences of magnetic anisotropy of the layers. In the case of RIG films the contribution of both mechanisms (flexomagnetolectricity and ferroelectricity of rare-earth origin) are of importance. We consider the rare earth ions in singlet, doublet ground states and strongly anisotropic Ising ions, taking as examples EuIG and HoIG. Distribution of the reduced electric polarization across the film is shown in Fig.1; it is supposed that films have prevailing uniaxial magnetic anisotropy ($K > 0$ at $x < 0$; $K < 0$ at $x > 0$). Curve 1 stands for electric polarization calculated in frame of the concept [1], curves 2,3,4 stand for polarization of EuIG and HoIG ($T \sim 78$ K, $T \sim 4$ K) calculated in frame of the concept [2]. Change of layers thicknesses, magnetic anisotropy, and external magnetic field influence the kind of magnetic inhomogeneity and the polarization profiles.

The distinguished differences in electric polarization, calculated by use of different mechanisms, indicate their importance, and the demand of the electric dipole moments of rare earth ions accounting to forecast electric response.

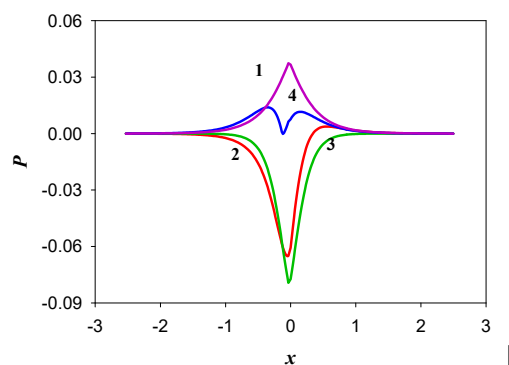


Fig. 1. Distribution of reduced electric polarization across interface in iron garnet bi-layer, $x = \bar{x} / \sqrt{A/K}$, curve 1- $P(x)$ in frame of mechanism [1], curves 2 -4 $P(x)$ in frame of mechanism [2] (2- EuIG, 3 – HoIG at $kT > \mu\text{Hex}$, 4 - HoIG $kT \ll \mu\text{Hex}$) $|K| = 2 \cdot 10^4$ erg/cm³

Support by the Russian Foundation for Basic Research (Grants No. 16-02-00336 A, No.16-29-14005) is kindly acknowledged.

[1] Zvezdin A.K., Pyatakov A.P., *Physics – Uspekhi*, **52** (2009) 845.

[2] Popov, A. I., Gareeva, Z. V., Zvezdin A.K. *Phys. Rev.B*, **92** (2015) 144420.

4PO-J-27

MAGNETIC PROPERTIES OF NdSc₃(BO₃)₄*Gudim I.A., Eremin E.V., Temerov V.L.*Kirensky institute of Physics, Federal Research Center KSC SB RAS, Krasnoyarsk, Russia
irinagudim@mail.ru

The family of RM₃(BO₃)₄ crystals (R=Y or a rare earth, M=Al, Ga, Sc, Cr, Fe) has attracted considerable attention during the last years. These crystals possess the noncentrosymmetric trigonal structural type of the natural mineral huntite CaMg₃(CO₃)₄ that crystallizes in the space group *R*32 of the trigonal system [1]. These borates are prospective materials in the field of nonlinear optics, particularly in the UV region since they are chemically and mechanically very stable, with good transparency down to the deep UV region [2] Among these materials, borate crystals with the huntite structure of the general formula LnM₃(BO₃)₄, where Ln designates a rare-earth element and M = Al, Ga, Fe, Sc, or Cr, are widely known as materials that may exhibit excellent nonlinear optical (NLO) and lasing properties.

Magnetic properties of the huntite family of crystals were reported among others for RA₃(BO₃)₄, [3] RFe₃(BO₃)₄ (R=Y, Nd, La, Tb, Er, Gd), [4] and HoGa₃(BO₃)₄, but no data are available for the scandium huntite crystals. The largest polarization value ($P \approx 4500 \mu\text{C}/\text{m}^2$) was obtained for HoAl₃(BO₃)₄.

In this work, we report the data on the magnetic properties of the NdSc₃(BO₃)₄ single crystal. In this compound, the system of small cations is presented by Sc³⁺ ions with a larger ionic radius as compared with Al³⁺ and different electronic structure. NdSc₃(BO₃)₄ single crystals were grown from bismuth trimolibdate-based fluxes. The crystal growth techniques used were described in detail in [5].

The magnetic and magnetoelectric properties were investigated on a PPMS-9 facility in the temperature range 3–300 K and magnetic fields up to 90 kOe.

The value of the magnetoelectric effect in NdSc₃(BO₃)₄ depends not only on the size and electronic structure of Sc³⁺ ions, but also on the conditions of heat treatment of the grown crystals.

The study was supported by the Russian Foundation for Basic Research, project no. 13-02-12442.

- [1] J. C. Joubert, W. B. White, and R. Roy, *J. Appl. Cryst.*, **1** (1968) 318.
- [2] K. S. Bartwal, R. Bhatt, S. Kar, V. K. Wadhawan, *Mater. Sci. Eng. B*, **85** (2001) 76.
- [3] K.-C. Liang, R. P. Chaudhury, B. Lorenz, et al., *J. Phys.: Conf. Ser.*, (2012) 400. 032046.
- [4] Kadomtseva A.M., Popov Yu.F., Vorob'ev G.P., et al., *Low Temp. Phys.*, **36** (2010) 511.
- [5] I.A. Gudim, E.V. Eremin, and V.L. Temerov, *J. Crystal Growth*, **312** (2010) 2427.

4PO-J-28

MAGNETOELECTRIC EFFECTS IN MULTIFERROICS OF COMPOSITIONALLY-STEPPED LEAD-FREE PIEZOELECTRIC AND MAGNETOSTRICTIVE COMPONENTS

Petrov V.M., Kovalenko D.V., Bichurin M.I.

Novgorod State University, Veliky Novgorod 173003, Russia

vladimir.petrov@novsu.ru

Magnetolectric (ME) effects mediated by mechanical strain are known to be far stronger in composite multiferroics compared to single-phase materials [1]. Using the compositionally-graded piezoelectrics and magnetostrictive components gives rise to an increase in ME coupling strength in piezoelectric-magnetostrictive layered structures [2]. It should be emphasized that the most appropriate piezoelectrics for environmental protection are lead-free ones [3].

The present paper focuses on a theoretical model of ME effect in piezoelectric-magnetostrictive layered structures in the electromechanical resonance region. The piezoelectric and piezomagnetic layers are assumed to be perfectly bonded together so that the piezoelectric layers restrict the deformations of the piezomagnetic layer in an applied magnetic field. Since the shear forces are not applied centrally for asymmetric layered structures, the bending moments are produced in the sample. As a result, a flexural deformation is obtained. The longitudinal axial strains of each layer are assumed to be dependent on the vertical coordinate for taking into account the effect of flexural deformations. The equation of bending motion of bilayer is solved to find the strain and stress components in both phases. We consider boundary conditions for the bilayers that are fixed at one end. We derived the analytical expressions for ME voltage coefficients by substituting the found stress components into open circuit condition. Increase in flexural deformation for bilayer of compositionally-stepped piezoelectric and magnetostrictive component compared to bilayer of homogeneous components leads to an enhanced magnetolectric coupling at bending resonance for specific piezoelectric volume fractions.

As an example, the layered structure based on magnetostrictive permendur, an alloy of Fe-Co-V and lead-free piezoelectric langasite bimorph is considered. We derived the explicit expressions for ME voltage coefficients for bending resonance regions. An increase in ME voltage coefficient by 20 percents was obtained for the structure considered compared to the bilayer of permendur and homogeneous langasite. There is a general agreement between the calculated ME voltage coefficients for the layered structure and measured values. Desired characteristics such as the absence of ferroelectric hysteresis and pyroelectric losses for composites with compositionally-stepped lead-free piezoelectric single crystals facilitate application of these composites in functional devices such as magnetic sensors, energy harvesters etc.

The research was supported by Grant No: 16-12-10158 from the Russian Science Foundation.

[1] M. Bichurin and V. Petrov, Modeling of Magnetolectric Effects in Composites // *Springer Series in Materials Science*, 201 (2014) DOI: 10.1007/978-94-017-9156-4.

[2] Petrov V. M. and Srinivasan G. Enhancement of Magnetolectric Coupling in Functionally Graded Ferroelectric and Ferromagnetic Bilayers, *Phys. Rev. B.*, **78** (2008) 184421.

[3] M. Bichurin, V. Petrov, A. Zakharov, D. Kovalenko, S. Ch. Yang, D. Maurya, V. Bedekar and S. Priya. *Magnetolectric Interactions in Lead-Based and Lead-Free Composites*, *Materials*, **4(4)** (2011) 651-702 doi:10.3390/ma4040651.

4PO-J-29

MAGNETOELECTRIC EFFECT IN THE YIG/PZT FMR RANGE*Lobekin V.N.¹, Petrov V.M.¹, Tatarenko A.S.¹, Bichurin M.I.¹*¹ Novgorod State University, Veliky Novgorod, Russia
slavalobekin@gmail.com

The magnetoelectric (ME) effect in a magnetostrictive-piezoelectric bilayer is known to be a result of mechanical interaction of magnetostrictive and piezoelectric components [1-2]. In an applied magnetic field, magnetostrictive deformation gives rise to induced polarization due to piezoelectric effect. An ac magnetic field δH applied to a magnetically biased sample, gives rise to the induced electric field δE . An electric field E applied to the piezoelectric component produces a mechanical deformation that is transferred to the ferrite, resulting in a shift δH_E in the resonance magnetic field. Observations of shift δH_E as a function of applied electric field E require ferrites with low line width of FMR. A strong ME coupling in bilayers based on YIG/PZT is of importance for a new family of devices.

Effect of excitation of magnetostatic (MS) oscillations in a ferrite resonator by the rf magnetic field was a subject of many publications [3]. In a case of small ferrite disks placed into a region of the *uniform* magnetic field, a long series of oscillating MS modes are excited. It is interesting to note that a layered structure based on a ferrite/piezoelectric resonator possesses double electric and magnetic control. Here we discuss the microwave ME interactions in bilayers based on lead zirconate titanate (PZT) and yttrium iron garnet (YIG) film. Study of the nature of ME interactions at microwave frequencies was recently made for the basic FMR line of ferrite/ferroelectrics [4]. The identification of MS modes for the normally magnetized disk resonator was carried out in the paper [5]. The absorption of microwaves under applied electric and magnetic field in a normally magnetized YIG/PZT disk resonator for the mode (2,2,0) has been measured and analyzed in detail. The effect of magnetic and electric control on the basic FMR mode and a mode (2,2,0) for a layered structure is compared. A conclusion is made about the possible practical application of the microwave ME effect in spectrum of the MS modes.

Support by the Russian Scientific Foundation (project no. 16-12-10158).

- [1] Ce-Wen Nan, M. I. Bichurin, S. Dong, D. Viehland, and G. Srinivasan, *J. Appl. Phys.*, **103** (2008) 031101.
- [2] M.I. Bichurin and V.M. Petrov, *Modeling of Magnetoelectric Effects in Composites*. Springer, Springer Series in Materials Science, Book 201, (2014).
- [3] A.G. Gurevich, G.A. Melkov, *Magnetization Oscillations and Waves*, *CRC Press* (1996) 456.
- [4] S. Shastry, G. Srinivasan, M.I. Bichurin, V.M. Petrov, A.S. Tatarenko, *Phys. Rev. B.*, **70** (2004) 064416.
- [5] Toshinobu Yukawa and Kenji Abe, *J. Appl. Phys.*, **45** (1974) 3146.

4PO-J-30

MAGNETOELECTRIC PHENOMENA IN Fe LANGASITES

Ivanov V.Yu.¹, Mukhin A.A.¹, Kuzmenko A.M.¹, Popov Yu.F.², Vorob'ev G.P.²,
Tikhanovskii A.Yu.^{1,3}, Balbashov A.M.⁴

¹ Prokhorov General Physics Institute of the Russian Acad. Sci., 119991, Moscow, Russia

² Faculty of Physics, M.V. Lomonosov Moscow State University, 119992, Moscow, Russia

³ Moscow Institute of Physics and Technology, 141701, Dolgoprudny, Moscow Region, Russia

⁴ Moscow Power Engineering Institute, 105835, Moscow, Russia

ivanov@ran.gpi.ru

Recently new interesting class of Fe-containing langasite-type multiferroics such as $\text{Ba}_3\text{NbFe}_3\text{Si}_2\text{O}_{14}$ was revealed. They possess noncentrosymmetric crystal structure (group P321) and exhibit a complex helical magnetic order below $T_N \sim 27$ K with a dual chirality for the triangular arranged Fe^{3+} spins [1]. However current studies of the magnetoelectric properties of the Fe langasites are controversial [2-4]. We performed pyroelectric studies of $\text{Ba}_3\text{NbFe}_3\text{Si}_2\text{O}_{14}$, $\text{Ba}_3\text{TaFe}_3\text{Si}_2\text{O}_{14}$ and $\text{Sr}_3\text{TaFe}_3\text{Si}_2\text{O}_{14}$ single crystals grown by floating zone method in static (1.4 T in electromagnet, 5 T in the MPMS Quantum Design and 8 T in the close circle cryocooler) and pulsed (~ 20 T) magnetic fields. We obtained the following main results:

1. No spontaneous polarization in any of the main crystal axes (a , b , c) was observed.

2. Measurements in the electromagnet at 4.2 K while rotating the sample in a particular crystallographic plane around the axis perpendicular to the magnetic field, revealed the following symmetry interrelations for the field-induced polarization (within accuracy of $\sim 0.1 \mu\text{C}/\text{m}^2$): (a) $P_c(H_i) \approx 0$ ($i=a,b$); (b) $P_i(H_c) \approx 0$ ($i=a,b,c$); (c) $P_a \approx 0$ for H in ab - and ac -planes $P_a \sim \sin 2\theta$ for H in bc plane; (d) $P_b \approx 0$ for H in ab and bc - planes, $P_b \sim \sin 2\theta$ for H in ac plane.

3. The polarization in the basis plane $P_a(H_{a,b})$ and $P_b(H_{a,b})$ induced by large static and pulsed fields was observed with a drastic increase in the fields above 3-5 T. It was established, however, a strong sensitivity of the polarization behavior (up to its sign), to the weak c -components of the field resulted from its deviations for few degrees from the basis plane. For the controlled deviations towards the c -axis at angles of $\pm\theta$ in ac plane for the P_b measurements as well as the deviations in bc or $a45^\circ b$ - c - planes for the P_a ones, we obtained well reproducible results. Moreover, the symmetry inter-relation $P(+\theta) = -P(-\theta)$ was approximately fulfilled (Fig.1).

4. The data in pulsed fields at angles of $\pm 45^\circ$ to the c -axis revealed for the P_a and P_b non-monotonic field dependence with a maximum of their absolute values.

Based on a phenomenological symmetry approach we have analyzed possible mechanisms of observed complex behavior of the field induced electric polarization and its relation to changes of the magnetic structure.

This work was supported by the Russian Scientific Foundation (No. 16-12-10531).

[1] K. Marty, et al., *Phys. Rev. Lett.*, **101** (2008) 247201.

[2] H.D. Zhou, et al., *Chem. Mater.*, **21** (2009) 156-159.

[3] N. Lee, J. Choi, S.-W. Cheong, *Appl. Phys. Lett.*, **104** (2014) 072904.

[4] H. Narita, et al., *Phys. Rev. B*, **94** (2016) 094433.

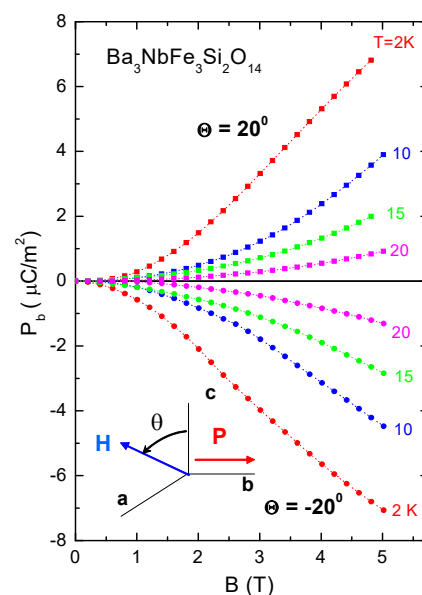


Fig.1 Electric polarization versus magnetic field and its orientation.

4PO-J-31

INFLUENCE OF NON-UNIFORM ELECTRIC FIELD ON THE STRUCTURE AND PROPERTIES OF MAGNETIC INHOMOGENEITIES IN UNIAXIAL MULTIFERROIC FILMS

Vakhitov R.M.¹, Solonetsky R.V.¹, Mazhitova F.A.¹, Gareeva Z.V.²

¹ Institute of Physics and Technology, Bashkir State University, Ufa, Russia,

² IMCP USC, Academy of Sciences, Ufa, Russia

VakhitovRM@Yahoo.com

Magnetolectric materials open new horizons for physics of magnetisms and spintronic technology [1]. The presence of several ferroic orders leads to the series of novel effects related to magnetolectric interactions. Recently magnetolectric properties of magnetic domain walls have been experimentally detected in ferrite garnet films [2]. It has been observed that static electric field leads to the displacement of magnetic domain walls. The presence of garnet magnetolectricity can be explained in the framework of various physical mechanisms (see e.g. Ref. [3]). Herein we consider the mechanism of non – uniform magnetolectricity [2], and the mechanism related to non-uniform electric field acting on the considered magnetic film discussed in Ref. [4]. According to [4] the inhomogeneous electric field results in the defects attributed to ions displacements. Concurrently, very recently it was reported [5] on nucleation of magnetic bubbles under the action of inhomogeneous electric field [5].

In our work we suggest a phenomenological model to explain the discussed phenomena. We consider the uniaxial ferromagnet with non – uniform magnetolectric interaction. It is supposed that electric field applied along the “easy axis” (parallel to OZ axis) is localized in the limited area ($|y| < L/2$), magnetic inhomogeneity develops along OY axis. Numerical analysis of Euler – Lagrange equations shows that soliton –like magnetic inhomogeneities (0° domain walls with quasi Bloch structure) appear due to the action of inhomogeneous electric field (Fig.1). These inhomogeneities are electrically charged, i.e. they are accompanied with electric polarization.

Thus, non – uniform electric field acting in the restricted area can nucleate magnetic bubbles that was experimentally observed in [5].

Support of RFBR grant (№16-02-00336A) is kindly acknowledged.

[1] N.A. Spaldin, S.W. Cheong, R.Ramesh *Phys. Today.*, **10** (2010) 38.

[2] A.S. Loginov et. all. *Appl.Phys. Lett.*, **93** (2008) 182510.

[3] A.I. Popov et al. *J.Phys.: Cond.Matter.*, **28** (2016) 1.

[3] A.A. Arzamastseva et al. *JEPT*, **147** (2015) 793.

[4] D.P. Kulikova et al. *JETP Lett.*, **104** (2016) 196.

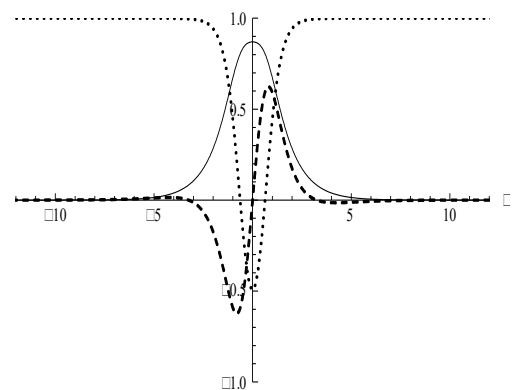


Fig.1. The magnetization components $m_x(\xi)$, $m_y(\xi)$ and $m_z(\xi)$ in the uniaxial crystal at the width $L=5\Delta$, and electric field strength $\varepsilon_1 = \varepsilon_2 = 1.83$. Solid line stands for the dependence $m_x(\xi)$, dash line stands for $m_y(\xi)$, dots stand for $m_z(\xi)$.

4PO-J-32

MAGNETIC FIELD-INDUCED TRANSITIONS AND FULL H-T PHASE DIAGRAMS IN MULTIFERROICS $\text{Mn}_{0.95}\text{Co}_{0.05}\text{WO}_4$ AND $\text{Mn}_{0.8}\text{Co}_{0.2}\text{WO}_4$

Ivanov V.Yu.¹, Mukhin A.A.¹, Popov Yu.F.², Vorob'ev G.P.², Balbashov A.M.³, Skourski Yu.⁴, Wang Zh.⁴, Skumryev V.⁵

¹ Prokhorov General Physics Institute of the Russian Acad. Sci., 119991, Moscow, Russia

² Faculty of Physics, M.V. Lomonosov Moscow State University, 119992 Moscow, Russia

³ Moscow Power Engineering Institute, 105835, Moscow, Russia

⁴ Hochfeld-Magnetlabor Dresden (HLD-EMFL), Helmholtz-Zentrum Dresden-Rossendorf, D-01314 Dresden, Germany

⁵ Institut Català de Recerca i Estudis Avançats (ICREA), Barcelona, Spain; and Departament de Física, Universitat Autònoma de Barcelona, Bellaterra 08193, Spain

ivanov@ran.gpi.ru

The $\text{Mn}_{1-x}\text{Co}_x\text{WO}_4$ system belongs to new type II multiferroics where ferroelectricity is induced by magnetic (spiral) order and a lot of various phase transitions occur both with temperature variations and in magnetic fields [1-3]. In this work we present results of magnetic and magnetoelectric studies of field induced phase transitions in single crystals of $\text{Mn}_{1-x}\text{Co}_x\text{WO}_4$ for $x=0.05$ and 0.2 in static and pulsed magnetic fields up to 60 T which enabled to obtain the full magnetic phase diagrams (i.e. up to spin-flip transitions) for the main crystallographic directions. Their common feature is a presence of transition to the non-polar sinusoidal phases before a spin-flip transition to a pure ferromagnetic (F) state.

In $\text{Mn}_{0.95}\text{Co}_{0.05}\text{WO}_4$ in magnetic field along b axis we observed that the ferroelectric phase AF2 with the spin-cycloid structure in the ab plane and polarization $P||b$ -axis undergoes a continuous transition at 4-7 T to AF2' structure with spins in the $a\omega$ plane and polarization in ac plane (α and ω are, respectively, the easy and the hard magnetic directions in the ac monoclinic plane). Then at ~ 52 T the polarization disappears revealing a transition to the paraelectric AF3 phase and at last at ~ 58 T a spin-flip transition occurs. For $H||\alpha$ AF2 \rightarrow AF2'' phase transition takes place at ~ 10 T accompanying by increase of P_b and the spin-cycloid plane reorientation to the state perpendicular to the field by rotation along b -axis. A further magnetic field increase results in the transition to the paraelectric ($P_b\rightarrow 0$) flopped AF3'' phase at $B\sim 50$ T and then at ~ 58 T – to the spin-flip transition to the ferromagnetic state. At $H||\omega$ there is observed only transition from ferroelectric AF2 to paraelectric AF3 phase which then undergoes to the spin-flip state at ~ 58 T.

In the $\text{Mn}_{0.8}\text{Co}_{0.2}\text{WO}_4$ the ferroelectric ($P||b$) conical spin structure (AF2+AF4) appears at $T < T_{FE}\sim 8.6$ K [4] after collinear antiferromagnetic ordering AF4 at $T_N\sim 20$ K. Moderate magnetic fields ~ 13 -15 T along b - and hard ω - axes suppress the spiral component AF2 of the conical phase and induce new paraelectric phase AF4+AF3 involving AF4 collinear and sinusoidal AF3 components. The AF3 one is suppressed at the fields ~ 52 T and then remaining AF4 phase disappears at the spin flip transition at ~ 55 T. In the field along the easy α -axis the conical AF2+AF4 structure transforms to a pure cycloidal one (AF2') with increased P_b value which undergoes to the AF3 paraelectric phase at ~ 52 T and then –to the spin-flip phase at ~ 55 T.

This work was partially supported by the Russian Scientific Foundation (No. 16-12-10531).

[1] Y.-S. Song, et al., *J. Phys. Soc. Japan*, **82** (2013) 124716.

[2] F. Ye, et al., *Phys. Rev. B*, **86** (2012) 094429.

[3] I. Urcelay-Olabarria, et al., *Phys. Rev. B*, **85** (2012) 094436.

[4] I. Urcelay-Olabarria, et al., *Phys. Rev. B*, **85** (2012) 224419.

4PO-J-33

TERAHERTZ OPTICAL ACTIVITY AT CRYSTAL FIELD TRANSITIONS IN Tm^{3+} IONS IN MAGNETOELECTRIC ALUMOBORATES

*Kuzmenko A.M.*¹, *Mukhin A.A.*¹, *Ivanov V.Yu.*¹, *Shuvaev A.*², *Dziom V.*², *Pimenov A.*²,
*Boldyrev K.N.*³, *Bezmaternykh L.N.*⁴, *Gudim I.A.*⁴

¹ A.M. Prokhorov General Physics Institute of RAS, 119991 Moscow, Russia

² Institute of Solid State Physics, Vienna University of Technology, A-1040 Vienna, Austria

³ Institute of Spectroscopy RAS, 142190 Moscow, Russia

⁴ Institute of Physics SB RAS, 660036 Krasnoyarsk, Russia

krolandin@gmail.com

Rare-earth alumoborates $\text{RAl}_3(\text{BO}_3)_4$ are a new family of magnetoelectrics with noncentrosymmetric trigonal crystal structure (R32) which attracted recently a considerable attention due to interesting magnetoelectric, magnetic, optical etc. properties depending strongly on of the rare-earth (R) ions and their crystal field (CF) states [1]. We studied quasioptical terahertz properties of single crystals of $\text{TmAl}_3(\text{BO}_3)_4$ and diluted $\text{YAl}_3(\text{BO}_3)_4: \text{Tm}^{3+}$ (5%). CF transitions within the ground multiplet 3H_6 of Tm^{3+} ions was observed and they were identified as magnetic-dipole transitions from the ground singlet A_1 to the next excited doublet E of Tm^{3+} ions. Unexpected fine structure of the transitions was detected at low temperatures. The new modes were assigned to local distortions of the sites with D_3 symmetry by internal strains or Bi^{3+} impurities resulted in the splitting of $A_1 \rightarrow E$ transition to two components E^\pm . At least two types of locally distorted sites were observed in concentrated system [2] while only one kind of such sites was revealed in the diluted one (Fig.1). A natural optical activity, i.e. a rotation of the polarization plane, was observed in vicinity of the CF-transitions (Fig.1). This effect is allowed in the studied noncentrosymmetric crystal. The maximum value of the rotation angle of 20-25° was observed in the both types of the crystals in spite of different Tm concentration. It is explained by existence of inversion twins in the pure $\text{TmAl}_3(\text{BO}_3)_4$. We have developed theory of the observed natural optical activity taking into account contribution of the CF transitions to dynamical magnetic, magnetoelectric and electric susceptibilities as well as spatial dispersion of the latter. In order to describe asymmetry of CF lineshape in $\text{YAl}_3(\text{BO}_3)_4: \text{Tm}^{3+}$ we averaged electrodynamic response with respect to a distribution of internal strain distortions according to Ref. [3]. As a result a self consistent description of the both transmission and polarization plane rotation spectra was obtained (Fig.1) and corresponding parameters of the CF transitions were extracted.

This work was supported by the Russian Scientific Foundation (No. 16-12-10531).

[1] R. P. Chaudhury, B. Lorenz, Y. Y. Sun, et al., *Phys. Rev. B*, **81** (2010) 220402(R).

[2] A. M. Kuzmenko, A. A. Mukhin, V. Yu. Ivanov, et al., *Phys. Rev. B*, **94** (2016) 174419.

[3] B. Z. Malkin, D. S. Pytalev, M. N. Popova, et al., *Phys. Rev. B*, **86** (2012) 134110.

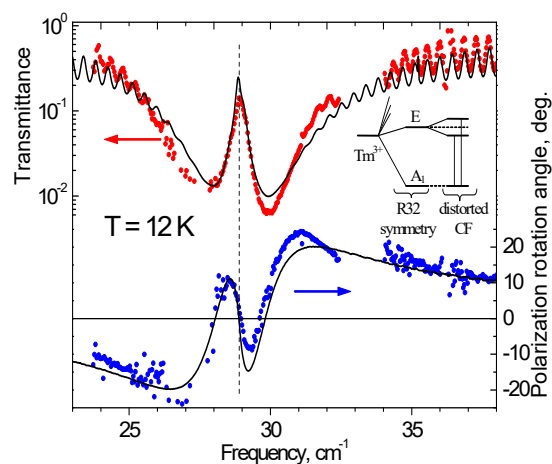


Fig. 1. Transmission spectra of $\text{YAl}_3(\text{BO}_3)_4: \text{Tm}^{3+}$ (5%) c-cut plate near split $A \rightarrow E^\pm$ CF transitions (top) and spectra of polarization plane rotation (bottom). Points-experiment, lines-theory.

4PO-J-34

MÖSSBAUER STUDY OF MULTIFERROICS

$\text{BiFe}_{1-x}\text{Mn}_x\text{O}_3$ ($x = 0.05, 0.10, 0.25$)

*Rusakov V.S.¹, Pokatilov V.S.², Sigov A.S.², Belik A.A.³, Matsnev M.E.¹, Gapochka A.M.¹,
Kulakov K.V.¹*

¹ Lomonosov Moscow State University, Moscow, Russia

² Moscow Technological University (MIREA), Moscow, Russia

³ National Institute for Materials Science, Tsukuba, Japan

rusakov@phys.msu.ru

⁵⁷Fe Mossbauer study of the spatial spin-modulated structure (SSMS) as well as electric and magnetic hyperfine interactions in multiferroics $\text{BiFe}_{1-x}\text{Mn}_x\text{O}_3$ ($x = 0.05, 0.10, 0.25$) with a rhombohedral structure were carried out. The Mossbauer spectra have been analyzed in terms of the incommensurate anharmonic SSMS of cycloid type model.

All substituted ferrites contained the positions of the iron atoms in the first cation coordination sphere of which there are one, two, three, and four atoms of Mn depending on the composition of ferrites. For the studied ferrites it was determined the temperature ranges of existence of incommensurate anharmonic SSMS of the cycloid type in which iron atoms with different cationic environment participated. It was found that with increase temperature from 5.2 K up to ~ 150 K the anharmonicity parameter is almost constant, then it decreases to zero at ~ 350 K, and then it again increases. It is shown that at temperatures below the temperature at which the anharmonicity parameter is zero, a magnetic anisotropy of the "easy axis" type is realized, and above this temperature there is an magnetic anisotropy of the "easy plane" type. An increase of the

anharmonicity parameter was observed for the Mn concentration increasing. A further increase in the concentration leads to the destruction of an anharmonic modulated SSMS and spin structure of the ferrite is transformed into the antiferromagnetic structure of the G-type. Based on the data obtained, a magnetic phase diagram was constructed in the "concentration" – "temperature" axes, indicating the regions of the paramagnetic state (PM), anharmonic SSMS with magnetic anisotropy of the "easy axis" and "easy plane" type, and antiferromagnetic (AFM) ordering (see Fig. 1) as well. In the framework of the model of an

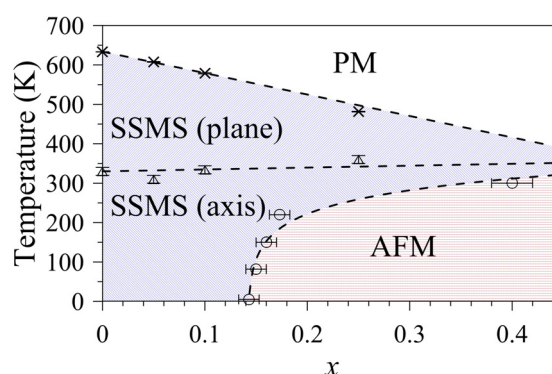


Fig. 1. Magnetic phase diagram of the $\text{BiFe}_{1-x}\text{Mn}_x\text{O}_3$

incommensurate anharmonic SSMS of cycloid type, the temperature dependences of the hyperfine parameters of the ⁵⁷Fe Mossbauer spectrum – the isomer shift, the quadrupole shift of the spectral components, isotropic and anisotropic contributions to the hyperfine magnetic field – were obtained and analyzed. It is established that the anisotropic contributions to the hyperfine magnetic field in the investigated ferrites with increasing temperature firstly (up to ~ 350 K) increase slightly, and then decrease, tending to zero in the temperature range 440-580 K, depending on the degree of substitution. It was also found that the replacement of the Fe atom by the Mn atom in the nearest environment of the Fe atom decreased the isotropic contribution to the hyperfine magnetic field, which increased with increasing temperature. This replacement did not lead to a noticeable change in the anisotropic contribution to the hyperfine magnetic field, quadrupole shift and isomer shift.

This work was supported by RFBR, projects No. 14-02-01109 and the Ministry of education and science of the Russian Federation (state project No. 2017/112, project No. 3.5859.2017/BP).

4PO-J-35

TEMPERATURE MÖSSBAUER STUDY OF THE SPATIAL SPIN-MODULATED STRUCTURE IN THE MULTIFERROIC BiFeO_3

Rusakov V.S.¹, Pokatilov V.S.², Sigov A.S.³, Matsnev M.E.¹, Pyatakov A.P.¹

¹ Lomonosov Moscow State University, Moscow, Russia

² Moscow Technological University (MIREA), Moscow, Russia

rusakov@phys.msu.ru

^{57}Fe Mossbauer detailed study of the spatial spin-modulated structure (SSMS) of the multiferroic BiFeO_3 was carried out in a wide temperature range including the temperature of magnetic phase transition. The Mossbauer spectra have been analyzed by fitting in terms of the anharmonic spin cycloid model [1].

It is established that with the temperature increasing the anharmonicity parameter of the SSMS decreases tending to zero at ~ 330 K and then increases again (see Fig. 1). It is shown that at temperatures below ~ 330 K a magnetic anisotropy of the "easy axis" type is realized and above is the magnetic anisotropy of the "easy plane" type. An explanation for the change in the type of magnetic anisotropy is proposed, based on taking into account the different temperature dependences of the two contributions to the effective uniaxial magnetic anisotropy constant: a crystal anisotropy of net antiferromagnet and a weak ferromagnetism.

In terms of the the cycloid type incommensurate anharmonic SSMS model the temperature dependences of the hyperfine parameters of the Mössbauer spectrum, the shift of the Mossbauer line, quadrupole shift of the spectral components, isotropic and anisotropic hyperfine magnetic field, were obtained and analyzed. The temperature dependence of the isotropic magnetic field at low temperatures has been processed in the spin wave model, at temperatures close to the Neel temperature, within the framework of the similarity theory, and over the entire temperature range, the effective molecular field model. As a result, the parameters and critical indexes of the models are determined. The calculation of the dipole contribution to the hyperfine magnetic field produced by the localized magnetic moments of the surrounding atoms showed that the experimentally observed value of the anisotropic contribution to the hyperfine magnetic field can be explained only when anisotropy of the hyperfine magnetic interaction of the nucleus with the electrons of the own atom is taken into account. It is established that an anisotropic contribution to the hyperfine magnetic field with increasing temperature firstly (up to ~ 330 K) weakly increases, and then decreases, tending to zero in the temperature ~ 600 K. It is shown that the contribution to the tensor of the electric field gradient and, respectively, to the quadrupole shift of the resonance lines, caused by local distortion of the lattice due to the magnetoelectric interaction, is negligibly small. The calculation of the electric field gradient tensor on ^{57}Fe nuclei has shown that the experimentally observed value of the quadrupole shift can be explained only when the dipole contribution from the oxygen anions is taken into account, as well as the electronic contribution due to the covalence effects.

This work was supported by RFBR, projects no. 14-02-01109.

[1] Rusakov V.S., Pokatilov V.S., Sigov A.S., Matsnev M.E., Gubaidulina. // *JETP Letters*, **100**, 7 (2014) 463–469.

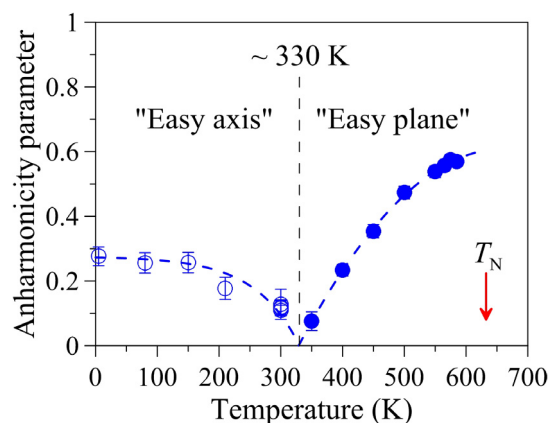


Fig. 1. Temperature dependence of the anharmonicity parameter of the SSMS

4PO-J-36

AN IMMENSE IMPACT OF TENSILE/COMPRESSIVE STRAIN ON THE FUNCTIONAL PROPERTIES OF FERROELECTRIC/FERROMAGNETIC STRUCTURE

Ivanov M.S.¹, Khomchenko V.A.¹, Buryakov A.M.², Mishina E.D.², Paixão J.A.¹

¹CFisUC, Department of Physics, University of Coimbra, 3004-516 Coimbra, Portugal

²Moscow Technological University MIREA, 119454 Moscow, Russian Federation
maxim.ivanov@uc.pt

Multilayered heterostructures (MH) are known as one of the emerging classes of composite materials for the next generation electronics. Since these materials combine a variety of functionalities such as ferroelectric and ferromagnetic behavior, magnetoelectric coupling, nonlinear optical properties etc. [1], the outlook for their application is immense. In the current work we compare the crystallographic, transport and nonlinear optical properties of two bilayer structures (consisting of one ferromagnetic layer – (La,Ca)MnO₃ (LCMO) with a thickness of 12 nm and one ferroelectric layer– BaTiO₃ (BTO) with a thickness of 4 nm) deposited on MgO and SrTiO₃ substrates providing the tensile (~6%) and compressive (~1%) strain tensions, respectively. The thickness of BFO was chosen in agreement with the previous research [2] suggesting that such layer is thin enough for quantum mechanics approach (while it retains the ferroelectric properties). The conductivity vs. temperature measurements show that the LCMO layer-related Ferromagnetic Metal- Paramagnetic Insulator transition is shifted towards low temperatures for STO- ($T_{MI} \sim 160$ K) and towards high temperatures for MgO- ($T_{MI} \sim 210$ K) deposited MH, respectively. The conductivity measurements of the STO-deposited BTO/LCMO structure reveal a large current (and its nonlinear increase) far exceeding that characteristic of the multilayered structure deposited on MgO substrate. The effect of dramatic increase of differential conductivity (dI/dV) was detected only for the STO-deposited BTO/LCMO. Being consistent with the conductivity study, the nonlinear optical measurements reveal the enhancement of polarization for the bilayer structure on STO substrate. Thus, we have shown the great impact of the substrates on MH properties, when the difference in strains causes immense difference in physical and optical properties of the multilayered material.

Supports by Fundação para a Ciência e a Tecnologia (FCT) through the FCT Investigator Programme (project IF/00819/2014), Russian Foundation for Basic Research (projects No. 16-32-60188 mol_a_dk) and by the Ministry of Education and Science of Russian Federation (State task no. 3.7331.2017/II220 and grant № 14.Z50.31.0034) are acknowledged.

[1] M. Fiebig, T. Lottermoser, D. Meier, M. Trassin., *Nature Reviews Materials*, **1** (2016) 16046.

[2] M. S. Ivanov, A. M. Buryakov, V. G. Morozov, E. D. Mishina, A. S. Sigov, *Physics of the Solid State*, **56**, 6 (2014) 1144-1149.

4PO-J-37

DUAL TUNABILITY OF SPIN-ELECTROMAGNETIC WAVES IN ALL-THIN-FILM MULTIFERROIC MULTILAYERS

Vitko V.V.¹, Nikitin Al.A.¹, Nikitin An.A.¹, Kondrashov A.V.^{1,2}, Ustinov A.B.¹, Semenov A.A.¹, Lähderanta E.²

¹ St. Petersburg Electrotechnical University, St. Petersburg, 197376 Russia

² Lappeenranta University of Technology, Lappeenranta, 53850 Finland

Vitaliy.vitko@gmail.com

An increased demand to frequency-agile materials for microwave devices has led to appearance of artificial multiferroics [1]. A distinctive feature of the multiferroics is dual (electric and magnetic) tunability of their electrodynamic properties. The tunability is provided by electrodynamic coupling of the spin waves (SWs) and electromagnetic waves in the ferrite-ferroelectric layered structures [2]. These coupled excitations are called as spin-electromagnetic waves (SEWs). The effective coupling at microwave frequencies is achieved in the structures fabricated with a relatively thick (200-500 μm) ferroelectric layers [3]. Such thicknesses lead to relatively high control voltages (up to 1 kV) for an effective electric tuning of the SEW dispersion.

The purpose of this work is to theoretically report a new mechanism, which provides both an effective electric and magnetic tuning of the SEW dispersion in planar all-thin-film multiferroic structures. This mechanism can be implemented by tunable interaction of the coupled SWs propagating in a heterostructure consisting of two ferrite films separated by a thin ferroelectric film.

The theory is based on an analytical solution of the full set of Maxwell's equations taking into account retardation effects. The theory is used for numerical simulation of the dispersion characteristics of the SEWs propagating in the structure consisting of two ferrite films with different thicknesses and magnetizations separated by the thin ferroelectric. The coupling between the SW in thin and thick ferrites manifests itself as a repulsion of the dispersion branches around the crossing point of the uncoupled SW modes. A dependence of the coupling on the dielectric permittivity of the ferroelectric-film provides a new mechanism for electrical tuning of the SEW dispersion characteristics. For the investigation of dual tunability of SEW the wavenumber variation versus frequency for the different external magnetic field is calculated for investigated structure with the 1- μm -thick ferroelectric film (Fig. 1). The wavenumber variation is induced by the reduction in permittivity by two times. One can see that the change in the external magnetic field by 10 Oe shifts the region of large wavenumber variation on 30 MHz. Therefore, the effective dual tunable phase shifter can be realized on the 1 mm-long structure. The phase shift about 2π can be obtained by the electric tuning in the desirable frequency range from 3 GHz up to 9 GHz by the tuning of magnetic field from 500 up to 2500 Oe.

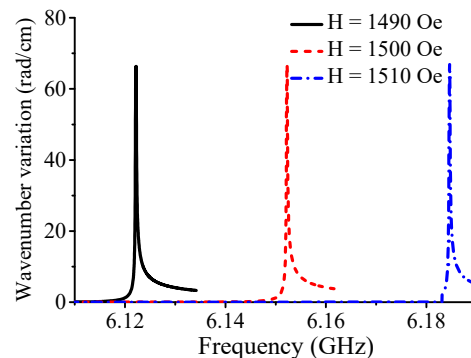


Fig. 1. Wavenumber variation versus frequency.

This work was supported in part by the Russian Science Foundation (Grant# 14-12-01296), the Ministry of Education and Science of Russian Federation (Project "Goszadanie"), and by the Academy of Finland.

[1] M.M. Vopson, *Crit. Rev. in Solid State and Materials Sciences*, **40**(4) (2015) 223-250.

[2] V.E.Demidov, B.A. Kalinikos, P. Edenhofer, *J. Appl. Phys.*, **91** (2002) 10007-10007-10.

[3] V.E.Demidov, B.A. Kalinikos, S.F.Karmanenko, A.Semenov, P.Edenhofer, *Microwave Theory and Techniques, IEEE Transactions on.*, **51**(10) (2003) 2090-2096.

4PO-J-38

SLOT LINE EXCITATION OF SPIN WAVES IN BiFeO₃ MULTIFERROIC FILM

Korneev V.I., Solov'ov S.V.

National Research University of Electronic Technology (MIET), Moscow, Russia
sv.soloviov@yandex.ru

Magnetolectric properties of multiferroics open wide prospects for applications, related with possibility to manipulate magnetic states by electric field. BiFeO₃ multiferroic possessing ferroelectricity and antiferromagnetism on the room temperature is the most studied multiferroic, whose magnetic state can be controlled by electric or magnetic field resulting in the transition from spatially modulated antiferromagnetic state to homogeneous ground state, accompanied by a crucial rearrangement of spin-wave spectrum in the range from 100 to 300 GHz and higher [1]. It seems tempting to master this range for creating delay lines, resonators and phase shifters, controlled by the electric and magnetic fields.

To analyze the magnetolectric impact of electric field on spin dynamics in BiFeO₃ layer we used the Ginzburg-Landau-like thermodynamic potential with order parameters \mathbf{P} , $\mathbf{\Omega}$, \mathbf{L} (electric polarization, antiferrodistortive vector and antiferromagnetic vector, respectively). In a case of high exchange interaction and relatively small magnetic fields the magnetization \mathbf{M} can be eliminated from consideration, supposing that the energy of the crystal depends on antiferromagnetic vector \mathbf{L} . On the basis of the solution of the dynamic equations for antiferromagnetic vector, we performed analysis of the efficiency of magnetolectric excitation of spin waves in BiFeO₃ films for a homogeneous antiferromagnetic state in the presence of a sufficiently large magnetic field as well as for a spatially modulated spin state (SMSS) at zero magnetic field.

It is shown that in the case of a homogeneous antiferromagnetic state the losses on the excitation of spin waves (see Fig. 1) fall off when approaching their frequency gap and become much smaller than in the spatially modulated state. However, in the presence of a cycloidal SMSS, the group and phase velocities of the spin waves coincide in a wide range of frequencies, and propagation loss is less than in a homogeneous antiferromagnet. It is shown that the usage of multiferroics for delay lines in the short-wave frequencies (EHF) range requires a significant reduction in conversion and propagation losses. More promising seems their usage for creating phase shifters.

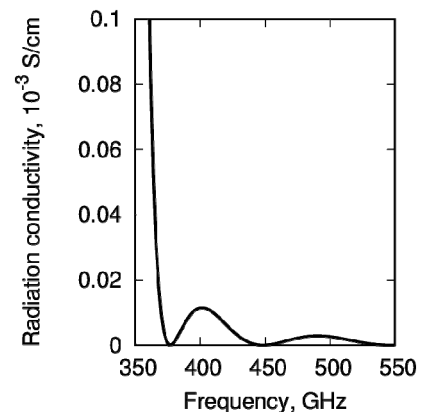


Fig. 1. Frequency dependence of the slot converter conductivity for the BiFeO₃ in homogeneous state.

[1] B. Ruetter, S. Zvyagin, A.P. Pyatakov, et al. *Phys. Rev. B*, **69** (2004) 064114.

4PO-J-39

CONVERSE MAGNETOELECTRIC EFFECT IN METGLAS - PZT LAYERED COMPOSITE STRUCTURES

Fetisov L.Y.¹, Chashin D.V.¹, Saveliev D.V.¹, Plekhanova D.D.¹, Shalygina E.E.², Efremova S.L.²

¹Moscow Technological University, Moscow, Russia

²Moscow State University, Moscow, Russia

fetisovl@yandex.ru

Magnetolectric effects are classified as direct magnetolectric effect (DME) and converse magnetolectric effect (CME). They are observed as electric polarization under the action of a magnetic field and magnetization change caused by an electric field, respectively [1]. To date, most of the papers are devoted to the DME effect due to its applications in sensor technology, microwave devices and energy harvesting [1]. At the same time increasing attention is paid to the investigation of electric field influence on magnetic state. This effect is most often studied in multiferroic heterostructures with the prospects of using in microelectronics and spintronics devices [2, 3].

In this study, we investigate the converse magnetolectric (CME) effect in two-layered composite structures consisting of various Metglas ribbons and Pb (Zr, Ti)O₃ (PZT) plate. The thicknesses of the magnetic and piezoelectric layers were 30 μm and 200 μm , respectively, and the surface area (Metglas) was $10 \times 3 \text{ mm}^2$. The magnetization curves of Metglas ribbons under the application of a constant voltage (up to 200 V) to the PZT substrate were measured employing a magneto-optical magnetometer by means of the transverse Kerr effect. The magnetic field was applied parallel to the long side of the sample along the central line to exclude the effect of edge effects. The values of saturation field, H_S , were defined from magnetization curves as the values of the applied magnetic field, at which the magnetizations reaches more than 98% of their saturation values (M_S).

It was discovered that the constant electric field affects the magnetic characteristics (in particular, the saturation fields) of the Metglas ribbons (for an illustration of this fact, see Fig. 1). Analysis of the data presented in Fig. 1, showed that the value of H_S in the presence of an electrical voltage equal to 200 V, increases by about 18% (from 97 to 115 Oe).

Moreover, it has been found that the value of H_S increases or decreases depending on the value of the magnetostriction of Metglas ribbons.

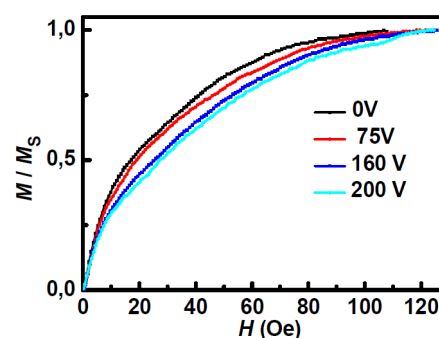


Fig. 1. The magnetization curves, observed for different applied voltage to the PZT substrate at room temperatures. M_S is the saturation magnetization,

The research was supported by the grant of the president of Russian Federation MK-7690.2016.9

[1] C.D. Ee, F.G. Hhh, *J. Appl. Phys.*, **33** (1999) 133-136.

[2] W. Eerenstein, M. Wiora, J.L. Prieto, J.F. Scott, and N.D. Mathur, *Nature Materials*, **6** (2007) 348–351.

[3] S. Fusil, V. Garsia, A. Barthelemy, M. Bibes, *Annu. Rev. Mater. Res.*, **44** (2014) 91-116.

4PO-J-40

MAGNETIC PHASES AND DOMAIN WALLS OF DIFFERENT TOPOLOGY IN THE (210) -ORIENTED FERRITE-GRANATE FILM

Vakhitov R.M.¹, Yumaguzin A.R.¹, Solonetsky R.V.¹, Iskhakova R.R.¹

¹ Institute of Physics and Technology, Bashkir State University, Ufa, Russia
VakhitovRM@Yahoo.com

Films of garnet ferrites with orientation (210) were synthesized about 30 years ago as CMD materials with improved static and dynamic characteristics [1]. However, in the process of studying them, it turned out that they are promising multifunctional materials that can be used as magnetoelectric (ME) materials in various spintronics and nanoelectronic devices [1-3]. However, after detection in these films of a new ME effect, which is contained in the controlled control of the motion of domain walls (DW) under the action of an electric field, interest to them has increased substantially. During the discussion of the nature of the effect, it turned out that (210) -oriented films were practically not studied theoretically [4,5].

To this end, homogeneous and inhomogeneous magnetic states of ferrite-garnet films of the (210) type are investigated in this paper. The analysis shows that the equilibrium directions of the magnetization vector \mathbf{M} , described by the polar (θ) and azimuthal (φ) angles, are determined by the competing influence of the induced uniaxial (decaying into perpendicular (K_w), orthorhombic (K_p) and "oblique" rhombic components [2]) and Cubic (K_1) anisotropy. In particular, this leads to the possibility of the existence of three types of magnetic phases in it, differing in the transformation properties: symmetric ($\mathbf{M} \parallel [001]$), angular ($\mathbf{M} \parallel [uv0]$), and general phase ($\mathbf{M} \parallel [uvw]$). On the phase diagram of the magnet there are a number of features related to the complex nature of the anisotropy in the crystal. In particular, there are a lot of angular phases between which spin-reorientation phase transitions of the first kind, which are called isostructural, are possible [6], since these phases belong to the same symmetry group and differ only in the magnitude of the angle θ . In addition, there is a quinary point on the phase diagram where the stability regions of the five phases converge, and so on. In the region of the existence of the phases found, solutions of the Euler-Lagrange equations for the magnet studied were found, to which magnetic inhomogeneities of the type 180°-DG corresponded. Their characteristic feature is the presence of the Neel component in the DW structure, i.e. there is an output of magnetization \mathbf{M} from the spin rotation plane, which is independent of the anisotropy constants (K_w, K_p, K_1). The latter means that in such DWs, in the presence of a nonuniform ME interaction in the magnet, a polarization \mathbf{P} always arises, which can lead to a wall displacement under the action of the electric field.

This work was supported by a grant from the Russian Foundation for Basic Research (№ 16-02-00336).

[1] A.M. Balbashov, F.V. Lisovskii, E.G. Mansvetova *Preprint IRE AN SSSR*, **25** (1988) 26.

[2] S. Tkachuk et al. *J. of Appl. Phys.*, **105** (2009) 07A524.

[3] A.P. Pyatakov and A.K. Zvezdin, *Phys. Usp.*, **55** (2012) 557.

[4] G.V. Arzamastseva et al. *JETP*, **120** (2015) 687.

[5] A.P. Pyatakov et al. *Phys. Usp.*, **58** (2015) 981.

[6] V.D. Buchel'nikov et al. *The Physics of Metals and Metallography*, **94** (2002) 429.

4PO-J-41

MAGNETIC INHOMOGENEITIES APPEARED ON SECLUDED DEFECTS OF THROUGH TYPE IN MAGNETIC UNIAXIAL FILMS

Vakhitov R.M.¹, Solonetsky R.V.¹, Akhmetova A.A.¹

¹ Institute of Physics and Technology of Bashkir State University, Ufa, Russia,
VakhitovRM@Yahoo.com

The defects of potential well type are of special interest among different type of defects which take place in magnetic materials [1]. This is due to the fact that magnetic inhomogeneities can form on these defects and they adapt to the defect profile and play an important role in the processes of magnetization and magnetization reversal of materials. One of the main mechanisms of the appearance of hysteresis phenomena is connected with them, which appears as kind of delay of the formation and growth of nucleus of magnetic reversal [2]. The researches show, that under definite conditions two types of magnetic inhomogeneities can form on one-dimensional defects of this type, these magnetic inhomogeneities correspond to the 0-degree domain walls, which differ in the parameters of their characteristics: energy, width, and amplitude [1]. However, in the analysis of the experimental data on the scanning of the surface of the investigated films, it was found that the detected in them defects are at least two-dimensional objects [3], on which observed magnetic formations don't fully match to the theoretically predicted magnetic inhomogeneities. For this purpose, in this work we consider micromagnetic structures, which appears in magnetic uniaxial films on the cylindrical shape through type defects. It is assumed that in the defect area ($r < R$, where r is the radial variable of the magnetization vector M , R is the defect radius), the material parameters of the sample change abruptly, and the uniaxial anisotropy constant K_u becomes negative. In this case, micromagnetic inhomogeneities with axial symmetry can nucleate on the defects, which structure is determined from Euler-Lagrange equations for this magnetic material with consideration of the demagnetizing fields of the sample. According to the analysis of the numerical results it follows that two types of vortex-like inhomogeneities that differ in the orientation of the central part of the vortex (the polarity of the core) can arise on defects of the "potential well" type [4]. According to the calculations if the polarity of the core of the vortex coincides with the direction of M in the main part of the magnetic sample (out of defect) then the corresponding vortex-like formation is energetically less favorable than that with the opposite polarity. At the same time, the first type of inhomogeneity is energetically more advantageous than the homogeneous state of the magnet. Moreover phase diagrams of the stable states of both types of vortex-like inhomogeneities in the Q - R variables were constructed (where Q is the a quality factor), from which it follows that these inhomogeneities can become stable structures for $R > R_c$ (R_c is the critical radius) and $Q > Q_c$ ($1,4 < Q_c < 1,8$). Thus it follows from the calculations that vortex-like micromagnetic structures can exist under definite conditions in uniaxial ferromagnetic films on the "potential well" type of a round shape defects (through type). Obviously, their properties have not yet been fully studied and they require further research.

[1] R.M. Vakhitov, E.B. Magadeev. *The Physics of Metals and Metallography*, **115** (2014) 906.

[2] G.S. Kandaurova. *Sorosov. obraz. Journal*, **1** (1997) 100.

[3] R.M. Vakhitov, et.all..*Doklady Physical Chemistry*, **470** (2016) 674.

[4] T. Shinjo et.all. *Science*, **289** (2000) 930.

4PO-J-42

MAGNETIC AND STRUCTURAL PROPERTIES OF THE $\text{NdFe}_3(\text{BO}_3)_4$ AND $\text{SmFe}_3(\text{BO}_3)_4$ MULTIFERROICS STUDIED WITH MÖSSBAUER SPECTROSCOPY

Frolov K.V.¹, Lyubutin I.S.¹, Smirnova E.S.¹, Alekseeva O.A.¹, Bezmaternykh L.N.², Gudim I.A.²

¹ Shubnikov Institute of Crystallography FSRC "Crystallography and Photonics" RAS, Moscow, Russia

² Kirensky Institute of Physics, SB RAS, Krasnoyarsk, Russia
green@crys.ras.ru

Recently, considerable attention has been drawn to multiferroic materials, which demonstrate the coexistence and interrelation of ferroelectric and magnetic ordering [1-5]. One of the actively studied multiferroic systems is the rare-earth ferrobates $R\text{Fe}_3(\text{BO}_3)_4$ ($R = \text{Y}, \text{La-Lu}$). A variety of properties of ferrobates is formed by two magnetic subsystems of iron and rare earth ions. In this case, the nature of the magnetic ordering of both subsystems and the features of the structural and magnetic phase transitions depend on the type of the rare-earth element.

In this work the dynamics of magnetic phase transitions, structural, electronic and spin states of iron ions in the single crystal $\text{NdFe}_3(\text{BO}_3)_4$ and $\text{SmFe}_3(\text{BO}_3)_4$ multiferroics were studied with ^{57}Fe Mössbauer spectroscopy in wide temperature range of 5-295 K. The interaction of the rare-earth and iron magnetic subsystems and its effect on the formation of the multiferroic properties of rare-earth iron borates were discussed.

The study was performed with the financial support of the Russian Foundation for Basic Research (project No 17-02-00766a) and Russian Science Foundation (project No 16-12-10464).

[1] A.M. Kadomtseva, Yu.F. Popov et al., *Low Temp. Phys.*, **36**, 6 (2010) 511.

[2] A.P. Pyatakov and A.K. Zvezdin., *Physics-Uspekhi*, **55**, 6 (2012) 557.

[3] Y. Tokura, S. Seki, N. Nagaosa., *Rep. Prog. Phys.*, **77** (2014) 076501.

[4] S. Dong, J.M. Liu et al., *Adv. in Phys.*, **64**, 5–6 (2015) 519.

[5] M. Fiebig, T. Lottermoser et al., *Nature Rev. Mat.*, **1** (2016) 16046.

4PO-J-43

INVESTIGATION THE MAGNETOELASTIC EFFECT OF PERMALLOY STRUCTURES ON PVDF SUBSTRATE INDUCED BY HEATING

Bukharaev A.A.^{1,2}, Bizyaev D.A.¹, Chirkov V.V.¹, Chuklanov A.P.¹, Khanipov T.F.¹,
Nurgazizov N.I.^{1,2}, Ziganshina S.A.¹

¹ Zavoisky Physical-Technical Institute, 420029 Kazan, Russia

² Kazan Federal University, 420018 Kazan, Russia

achuklanov@kfti.knc.ru

The magnetoelastic effect (or Villari-effect) are promising in patterned magnetic media data recording where an in-plane rotation of magnetization is needed. Polyvinylidene fluoride (PVDF) is the polymer with many interesting properties and one of the most promising is a large negative anisotropic coefficient of thermal expansion [1]. Recently we showed the possibility of inducing a magnetoelastic anisotropy on Py microparticles by applying the mechanical stress [2]. In this work, an attempt to producing magnetoelastic anisotropy of Py microparticles on PVDF by the heating was perform.

The PVDF film was prepared from solvent on glass substrate and mechanically and thermal treated to form a metastable beta-phase of PVDF that have negative anisotropic coefficient of thermal expansion. The presence of beta-phase was proof by X-Ray diffraction and FTIR spectroscopy. The polycrystalline permalloy square particles of size 7x7, 25x25 and 40x40 mkm² Py (Ni75%, Fe25%) were formed by e-beam evaporation through the mask of appropriate size. An average height of particles was from 20 to 30 nm. All samples show initial uniaxial magnetic anisotropy. The samples were investigate by Magneto-Optical Kerr Effect (MOKE) and Ferromagnetic Resonance (FMR) at different temperatures: from room temperature to 80 °C. The selected temperature range is optimal for PVDF thermal expansion response and easily to achieve in MOKE and FMR setups.

Hysteresis loops of Py/PVDF samples were received by MOKE in mutually perpendicular directions under different temperatures. Significant decreasing of coercivity with increasing of temperature was observe in one direction while in another direction the coercivity does not changed (fig. 1a). The data obtained from FMR spectra shows that anisotropy field changes and the easy axis rotates at substrate heating (fig. 1b).

Thus, the obtained results confirm that the heating Py microparticles on PVDF induce the magnetic anisotropy.

Support by Russian Foundation of Basic Research No. 15-02-02728.

[1] Y. Liu, B.Wang, Q.Zhan et al., *Sci. Rep.*, **4** (2014) 6615.

[2] D.A. Bizyaev, A.A. Bukhraev, Yu.E. Kandrashkin et al., *Tech. Phys. Lett.*, **42** No.10 (2016) 1034-1037.

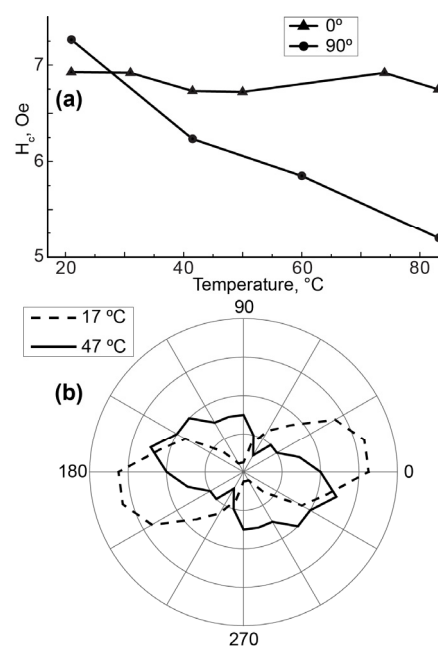


Fig. 1. (a) – the dependence of the Py/PVDF coercivity on temperature of substrate in mutually perpendicular directions; (b) – the angular dependence of resonant field under different temperatures.

4PO-J-44

MAGNETIC PROPERTIES OF SINGLE CRYSTALS $\text{HoFe}_{3-x}\text{Ga}_x(\text{BO}_3)_4$

Eremin E.V., Volkov N.V., Gudim I.A., Temerov V.L.

Kirensky Institute of Physics, Federal Research Center KSC SB RAS, Krasnojarsk, Russia
eev@iph.krasn.ru

In recent years, the multiferroic materials combining the magnetic and electric orderings have been attracting much attention. The interplay of electric and magnetic subsystems in these materials can result in the giant magnetoelectric effect, which is of great importance for application in microelectronics, magnetic memory, and sensor engineering, since the problem of mutual transformation of static magnetic and electric fields must now be solved at a new miniature scale.

Alumoborates hold special place among new multiferroics. It is convenient to use these compounds as model objects for elucidating the contribution of rare-earth ions to the formation of magnetoelectric properties of rare-earth multiferroics. Despite the absence of magnetic ordering, alumoborates exhibit a significant electric polarization in strong magnetic fields. For instance, the magnetic-field-induced polarization of holmium alumoborate is over $5000 \mu\text{C}/\text{m}^2$ in a field of ~ 100 kOe at $T = 4.2$ K [1, 2].

Having investigated the magnetic properties of $\text{HoFe}_{3-x}\text{Ga}_x(\text{BO}_3)_4$, we established that $\text{HoFe}_{1.5}\text{Ga}_{1.5}(\text{BO}_3)_4$ and $\text{HoFe}_1\text{Ga}_2(\text{BO}_3)_4$ are paramagnets. Temperature and field dependences of magnetizations for these compounds are qualitatively similar to those for $\text{HoGa}(\text{BO}_3)_4$. The analysis of field dependences of magnetizations at low temperatures shows that the magnetic susceptibility in strong fields ($H > 1$ T) for $\text{HoFe}_{1.5}\text{Ga}_{1.5}(\text{BO}_3)_4$ and $\text{HoFe}_1\text{Ga}_2(\text{BO}_3)_4$ is almost twice higher than that for $\text{HoGa}(\text{BO}_3)_4$ (fig.1).

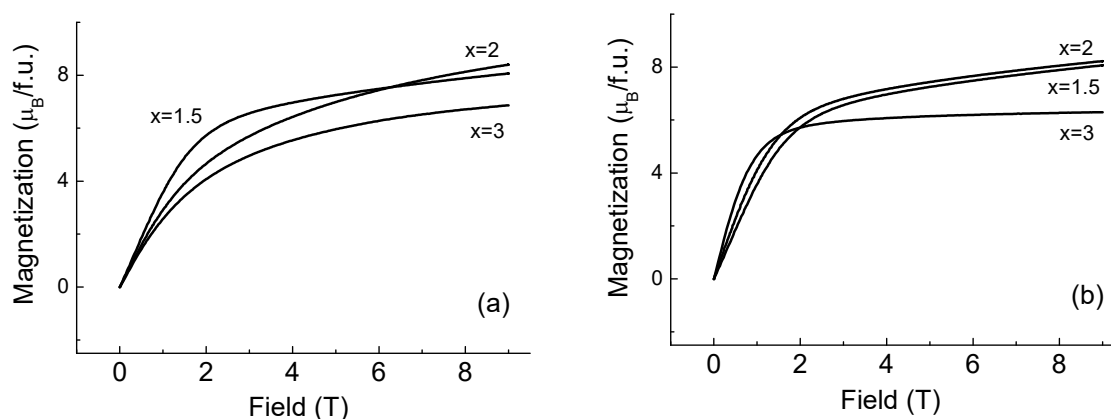


Fig. 1. Field dependences of magnetization for $\text{HoFe}_{3-x}\text{Ga}_x(\text{BO}_3)_4$: a) for $H \perp c$, b) for $H \parallel c$.

[1] Liang K.-C., Chaudhury R. P. et al. *Phys. Rev. B*, **83** (2011) 180417.

[2] Chaudhury R. P., Lorenz B., et al., *Phys. Rev. B*, **81** (2010) 220.

4PO-J-45

CHARGE ORDER AND ELECTRONIC STRUCTURE OF LuFe_2O_4 AT AMBIENT AND HIGH PRESSURE

Maslov D.A.^{1,2,3}, *Kudasov Yu.B.*^{1,2,3}, *Korshunov A.S.*^{1,2}, *Surdin O.M.*^{1,2,3}, *Platonov V.V.*^{1,2,3}

¹ Russian Federal Nuclear Center – VNIIEF, Sarov, Russian Federation

² SarFTI, National Research Nuclear University “MEPhI”, Sarov, Russian Federation

³ National Research Nuclear University “MEPhI”, Moscow, Russian Federation

maslov_dem@mail.ru

Multiferroic LuFe_2O_4 is a hexagonal layered compound with variable valence of iron ions $\text{Fe}^{2+}/\text{Fe}^{3+}$ [1], so a mean valence is +2.5. Due to this feature ferroelectricity of this substance is induced by charge ordering in contrast to common ferroelectrics where lattice distortion takes place. All iron sites are crystallographically equivalent and form triangular bilayers (W layers).

Charge order of stoichiometric and nonstoichiometric substances were investigated theoretically in our previous works [2,3]. It is shown that a high-temperature ordered phase on a triangular bilayer is a dimer partially disordered antiferroelectric (DPDA) state. It is also shown that 3D-CO can be stabilized by interbilayer interaction. Several ferrielectric phases can be realized as low-temperature state and different partial disordered states occur in nonstoichiometric systems.

From the experiment phase transition to high-pressure multiferroic phase (HP) can be observed at 8 GPa [4]. Thermodynamic model described in previous works can be used to estimate influence of pressure in this system (Fig. 1) by varying interlayer distance h in bilayer. Ferroelectric phase should be stabilized when h decreases. But a distortion of crystal lattice occurs due to Yahn-Teller effect. Electronic structure calculations yield to dimerisation in iron ion sublattice [4] with nonsymmetrical dimer formation.

Biased dielectric response in LuFe_2O_4 low-pressure phase can be described in terms of domain wall motion when pinning effect occurs [5]. The weak DC bias applied to the electric domain wall causes its partial detachment from pinning centers.

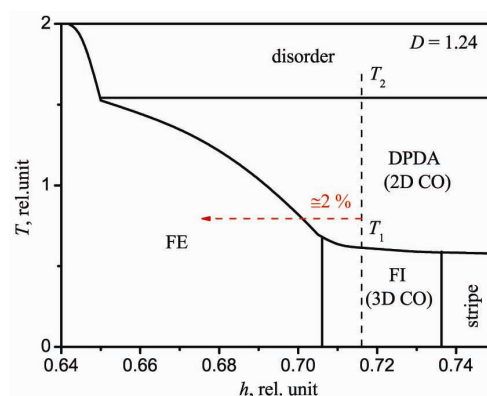


Fig. 1. Phase diagram of LuFe_2O_4 .

The work was supported by the Russian Foundation for Basic Research (Project No. 16-08-00337)

[1] N. Ikeda, H. Ohsumi, K. Ishii et al., *Nature (London)*, **436** (2005) 1136.

[2] Yu.B. Kudasov, D.A. Maslov, *Phys. Rev. B*, **86** (2012) 214427.

[3] D.A. Maslov, Yu.B. Kudasov, *Solid State Phenomena*, **233-234** (2015) 375-378.

[4] G.R. Hearne, E. Carleschi, W.N. Sibanda, P. Musyimi, G. Diguët, Yu.B. Kudasov, D.A. Maslov, A.S. Korshunov, *Phys. Rev. B*, **93** (2016) 105101.

[5] Yu.B. Kudasov, M. Markelova, D.A. Maslov, V.V. Platonov, O.M. Surdin, A. Kaul, *Physics Letters A*, **380** (2016) 3932-3935.

4PO-J-46

MAGNETOPIEZOELECTRIC EFFECTS IN EASY PLANE FERROBORATES

*Bilych I.V.¹, Zhekov K.R.¹, Gaydamak T.N.¹, Burma N.G.¹, Kolodyazhnaya M.P.¹, Zvyagina G. A.¹,
Fil' V.D.¹, Gudim I.A.²*

¹ B.Verkin Institute for Low Temperature Physics and Engineering of the National Academy of Sciences of Ukraine, 47 Nauky Ave., 61103 Kharkov, Ukraine

² L.V. Kirensky Institute for Physics, Siberian Branch of the Russian Academy of Sciences, 660036, Krasnoyarsk, Russia
zvyagina@ilt.kharkov.ua

The rare-earth ferroborates $RFe_3(BO_3)_4$ ($R=Y; La-Nd; Sm-Er$) are of interest during last decade because these crystals combine the properties of magnetically ordered and ferroelectric media. This is why ferroborates belong to the family of multiferroics [1].

Since ferroborates belong to noncentrosymmetric class 32, the direct piezoelectric effect (PE) is allowed in these crystals. We have investigated the piezoelectric properties of $SmFe_3(BO_3)_4$ and $NdFe_3(BO_3)_4$ single crystals using the acoustic method [2, 3]. It was found that in those compounds, the value of the piezoelectric modulus e_{11} in the paraelectric phase ($\approx 1.4 \text{ C/m}^2$) was almost an order of magnitude higher than that of the α -quartz. Therefore, such compounds may be recommended for technical applications.

In addition to the above-mentioned direct PE the indirect piezoelectric effect (IPE) may exist in multiferroics. It consists in the joint action of the magnetoelastic and magnetoelectric mechanisms. Due to magnetoelasticity the deformation changes the state of magnetic variables and through the magnetoelectric coupling excites the electric field (and vice versa). We were the first who discovered this effect [3]: In samarium ferroborate the effective piezo modulus is increased more than twice in the antiferromagnetic phase and it is reduced by a high magnetic field. We have revealed that IPE took place in the $NdFe_3(BO_3)_4$ also [4]. The contribution ratio of rare earth and iron magnetic subsystems into magnetoelectric interaction was estimated [4]. We suppose that the characteristics of this effect are similar for all easy-plane ferroborates.

The effect of the new type - direct renormalization of the piezoelectric interaction in magnetically ordered phase was revealed in $NdFe_3(BO_3)_4$ [4].

We have investigated the occurrence of piezoelectricity in nonpiezoactive (in the paraelectric state) configuration of $SmFe_3(BO_3)_4$. A few channels of the piezoelectric effect occurrence were found. i) IPE appears in monodomenized state of an antiferromagnet. ii) It has been revealed that in the paramagnetic state the piezoelectric response exists too. We relate it with the surface piezoelectricity. Quantitatively, the value of "surface" piezoelectric modulus is not small, and it agrees well with existing theoretical estimates [5].

[1] A. M. Kadomtseva, Yu. F. Popov, G. P. Vorob'ev, et al, *Fiz. Nizk. Temp.* **36** (2010) 640.

[2] Gaydamak T N, Gudim I A, Zvyagina G A, Bilych I V, Burma N G, Zhekov K R, and Fil V D, *Fiz. Nizk. Temp.*, **41** (2015) 792.

[3] Gaydamak T N, Gudim I A, Zvyagina G A, Bilych I V, Burma N G, Zhekov K R, and Fil V D., *Phys. Rev. B*, **92** (2015) 214428-1-7.

[4] Bilych I V, Zhekov K R, Gaydamak T N, Gudim I A, Zvyagina G A, Burma N G, and Fil V D, *Fiz. Nizk. Temp.*, **42** (2016) 1419.

[5] S. Dai, M. Gharbi, P. Sharma, H. S. Park, *J. of Appl. Phys.*, **110** (2011)104305.

4PO-J-47

NMR STUDY OF MULTIFERROIC CuCrO_2

*Smolnikov A.G.¹, Ogloblichev V.V.¹, Verkhovskii S.V.¹, Mikhalev K.N.¹, Sadykov A.F.¹,
Piskunov Yu.V.¹, Gerashenko A.P.¹, Yakubovskii A.Yu.²*

¹ M.N. Mikheev Institute of Metal Physics of the Ural Branch of the Russian Academy of Sciences,
Ekaterinburg 620990, Russia

² National Research Center Kurchatov Institute, Moscow, 123182 Russia
Smolnikov@imp.uran.ru

Nuclear magnetic resonance (NMR) is a local technique sensitive to both magnetic and electrical ordering, which is especially important in the study of multiferroics. NMR complex study of CuCrO_2 carried out on single crystal and powder samples. The measurements were performed in wide range of temperatures ($T = 1.5 - 300$ K) in paramagnetic and magnetic ordered states for the magnetic field $H = 0 - 117$ kOe directed along **a** and **c** axes of the crystal.

Fig.1 shown the ^{53}Cr , $^{63,65}\text{Cu}$, ^{17}O NMR spectra obtained in magnetic ordered phase and their approximation. The shape of the all spectra corresponds to incommensurate magnetic structure with a helicoidal spin ordering in triangular antiferromagnetic lattice (TLA) [1]. The magnetic moment of Cr^{3+} ions $\mu = 2.73(1) \mu_B$ was determined by NMR in local field (Fig.1 a) [2]. The $^{63,65}\text{Cu}$ NMR spectra (Fig.1 b) indicate ferromagnetic correlation of spin helicoids in neighboring TLA. Several lines in NMR spectra (Fig.1 a, b for $H \parallel \mathbf{a}$) are associated with a magnetic domain structure of CuCrO_2 based on hexagonal symmetry of crystal [3].

Spiral magnetic structures arise from the competition of exchange interactions involving exchange through oxygen atoms. Thus, the hyperfine interaction constants and the main parameters of the tensors electric field gradients on each isotopes have been determined. Their evolution with temperature and applied magnetic fields was investigated.

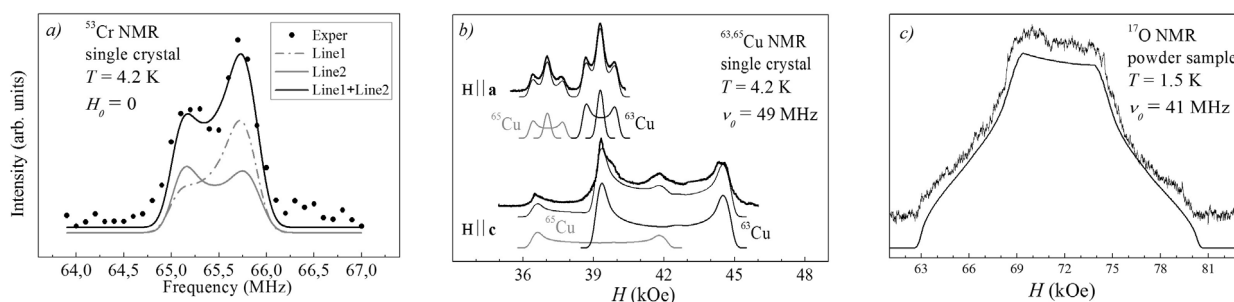


Fig.1 NMR spectra and their approximation by the theoretical line:

- a) ^{53}Cr in single crystal sample at $T = 4.2$ K obtained by frequency sweep ($H_0 = 0$);
- b) $^{63,65}\text{Cu}$ in single crystal sample at $T = 4.2$ K obtained by magnetic field sweep ($\nu_0 = 49$ MHz), magnetic fields applied along **a** and **c** axes of the crystal;
- c) ^{17}O in powder sample at $T = 1.5$ K obtained by magnetic field sweep ($\nu_0 = 41$ MHz)

Support by the Russian Science Foundation (project no. 16-12-10514) is acknowledged.

[1] R. Blinc, *Phys. Rep.*, **79** (1981) 331–398.

[2] A.G. Smol'nikov, V.V. Ogloblichev, et al., *JETP Lett.*, **102** (2015) 674–677.

[3] A.G. Smol'nikov, V.V. Ogloblichev, et al., *FMM*, **108** (2017) 142–150.

4 July

17:30-19:30

Tuesday

poster session
4PO-K

“Theory”

4PO-K-26

PHOSPHORUS-CONTAINING BRIDGING LIGANDS FOR DESIGN OF MOLECULAR MAGNETS

Gavrilova T.P.¹, Gerasimova T.P.², Katsyuba S.A.²

¹ Kazan Zavoisky Physical-Technical Institute of RAS, Kazan, Russia

² A.E. Arbutov Institute of Organic and Physical Chemistry, Kazan Scientific Center, Russian Academy of Sciences, Kazan, Russia
tatyana@gmail.com

In the last decade essential progress is achieved in obtaining and studying new magnetic materials, among them – organic magnets and bistable spin crossover complexes. Bifunctional materials in which magnetism is combined with optical properties or conductivity or porosity attract growing interest. Design of magnetic materials requires considering of two components: spin carriers and bridging ligands between them. For the former component organic radicals or transition metal ions are used. As for the bridging ligands, short or highly conjugated groups such as –OCO-, -CN-, -N3- are popular due to strong magnetic interactions between spin carriers they provide. At the same time including phosphorus atom in the bridging units can lead to wider structural variety and enable bifunctionality of such compounds. However literature examples of phosphorus-containing compounds with magnetic properties are limited by complexes with -OP(R)O- bridging ligands which provide magnetic interaction below 10 cm⁻¹. In this work we quantum-chemically study abilities of different phosphorus-containing bridges for molecular magnets.

We considered a number of model and real binuclear MnM complexes where M is metal center with unpaired electrons, Ni(II), Fe(II), or Mn(II), n is the least number of atoms between metal ions, n=1-3. Constants of exchange coupling, *J*, were calculated using broken symmetry approach. According to our computations, P-containing bridging ligands can form complexes with good exchange interactions between metal ions (up to 100 cm⁻¹). For the complexes under investigation we found magnetostructural correlations that can help in design of materials with desired magnetic properties.

The work was financially supported by the grant of Ministry of Russian Federation (project MK-5149.2014.3).

4PO-K-27

INVESTIGATION OF PHASE TRANSITIONS AND CRITICAL PHENOMENA IN MODELS OF MULTILAYER SYSTEMS

Khizriev K.Sh.^{1,2}

¹ Institute of Physics of Daghestan Scientific Center of Russian Academy of Sciences,
Makhachkala, Russia

² Dagestan State University, Makhachkala, Russia
kamal71@mail.ru

Magnetic Fe/V superlattices with thin alternating layers of magnetic and nonmagnetic materials are convenient objects for the studies of size effects in multilayer structures. The minimum Fe-layer thickness, at which the lattice remains magnetic, is two atomic monolayers; the Curie temperature depends not only on the number of magnetic monolayers but also on the thickness of nonmagnetic vanadium layers. A possible cause of the effect of nonmagnetic layers on the phase-transition temperature is the dependence of the interlayer coupling on the nonmagnetic layer thickness. Another possible cause is related to the mixing effects at the Fe/V interface, which lead to the penetration of iron atoms into vanadium layers.

To investigate the phase transition and the magnetic and thermal properties of nanoscale magnetic superlattices, we proposed a model superlattice Fe₂/V₁₃/Fe₃. The exchange interactions between the nearest neighbors in both the Fe₂ and Fe₃ layers have a ferromagnetic character and are determined by the intralayer exchange parameter J_{\parallel} . In our model, its value was assumed to be constant and equal to unity. There is also interaction J_{\perp} between the atoms of the Fe₂ and Fe₃ layers via the vanadium layer (interlayer coupling). Its value and sign may change, depending on the vanadium layer thickness.

The Hamiltonian of the model can be written as

$$H = -\frac{1}{2} \sum_{i,j} J_{\parallel} (S_i^x S_j^x + S_i^y S_j^y) - \frac{1}{2} \sum_{i,k} J_{\perp} (S_i^x S_k^x + S_i^y S_k^y)$$

where the first sum takes into account the exchange interaction of each magnetic atom with its nearest neighbors in the layer, and the second sum takes into consideration the interaction with the atoms from neighboring layers via the nonmagnetic layer; S_j , are the components of the spin localized at site j . The proposed model takes into account all magnetic and crystallographic features of real magnetic Fe₂/V_n/Fe₃ superlattices [1].

The calculations were performed on the basis of the single-cluster algorithm of the Monte Carlo method for systems with periodic boundary conditions and linear sizes $L \times L \times L$, where $L = 10 \div 40$ is the number of magnetic iron monolayers. For each system, a nonequilibrium segment of the Markov chain with a length up to 5×10^5 MCsteps/spin was cut off; then up to 2×10^6 MCstep/spin were taken; and, finally, the thermodynamic parameters were averaged. Since the Fe₂ and Fe₃ layers are under different conditions and, in general, can be isolated from each other at some value of the interlayer coupling J_{\perp} , these layers may undergo phase transitions at different temperatures.

Distinction in phase transitions temperatures of double and triple layers leads to a variety in behaviour of temperature dependence for spontaneous magnetization of studied model. Probably, that analogous shapes of temperature dependence of magnetizations confirming our calculations, can be observed in laboratory experiments too. However such investigations are not carried out yet.

[1] K.Sh. Khizriev, A.K. Murtazaev, V.M. Uzdin, *J. Magn. Magn. Mater.*, **300** (2006) e546.

4PO-K-28

THE QUANTUM OSCILLATIONS IN SEMICONDUCTORS WITH INVERTED BAND STRUCTURES

Alisultanov Z.Z.^{1,2}, Abdullaev G.O.¹

¹ Amirkhanov Institute of Physics RAS, Dagestan Science Centre, Makhachkala, Russia

² Dagestan State University, Makhachkala, Russia
abd.gm90@yandex.ru

Quantum magnetic oscillations are one of the main tools for studying the electronic spectrum of metals and semiconductors [1]. These oscillations are connected with the quantization of the carrier energy in a magnetic field (Landau quantization). The period of these oscillations is determined from the condition of intersection of two successive Landau levels with the chemical potential:

$$\Delta(1/H) = 2\pi\hbar e/A(\mu)c, \quad (1)$$

where $A(\mu)$ is the area enclosed by line $\varepsilon = \mu$ in momentum space, μ is the chemical potential. Recent studies of quantum oscillations in dielectrics [2] have led to significant progress in understanding the nature of this phenomenon. It was shown [2] that quantum oscillations of the density of states exist in the volume (dielectric phase) of topological dielectrics, which contradicts existing representations. In topological dielectrics, unlike ordinary dielectrics, the intersection of the Landau levels with the chemical potential is achieved due to the inverted band structure of these materials (for details, see [2]).

In the present paper, we investigate quantum oscillations of the density of states in a weakly doped narrow-gap semiconductors with inverted band structure, including bilayer of graphene in the presence of an electrical voltage on the gate. The latter deforms the energy spectrum of the bilayer to the so-called form "mexican hat". This form of the spectrum leads to anomalous oscillations with weak doping. Namely, an additional peaks of oscillations occurs in oscillation spectrum. These peaks are absent in metals and other electronic systems with a direct band structure, including the graphene bilayer without voltage on the gate.

A qualitative description of the effect is shown in [3]. Our results on the density of states are shown in Fig. 1 (see [3]). On fig.1 we used the following denotations: U is the gate potential, Δ is the band gap, Γ is the Dingle parameter.

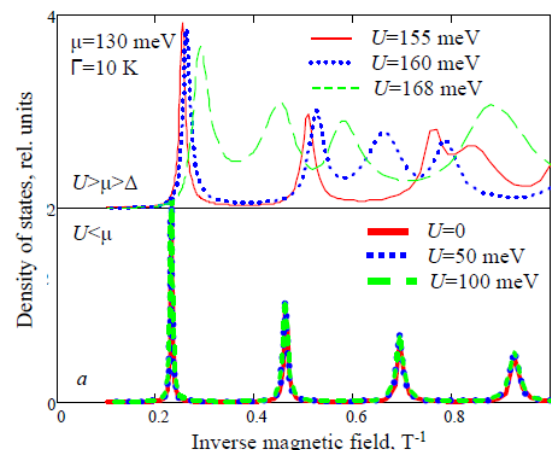


Fig. 1. Quantum oscillations of density of states in doped bilayer graphene.

Support by President Grant MK-2130.2017.2, RFBR № 15-02-03311a, Dagestan president grant (2016), Dynasty Foundation is acknowledged.

[1] D. Shoenberg, *Magnetic oscillations in metals* (Cambridge University Press, 1984)

[2] L. Zhang, X-Y. Song and F. Wang, *Phys. Rev. Lett.*, **116** (2016) 046404.

[3] Z.Z. Alisultanov, *JETP Lett.*, **104**(3) (2016) 188–192.

4PO-K-29

TWO METHODS FOR CONTROLLING PSEUDOMAGNETIZATION IN THE MONTE-CARLO SIMULATION OF SPIN-PSEUDOSPIN SYSTEMS

Chikov A.¹, Panov Yu.¹, Budrin K.¹, Rybakov F.²

¹ Ural Federal University, Ekaterinburg, 620002, Russia

² KTH Royal Institute of Technology, Stockholm, SE-10691, Sweden
alex.chikov@yandex.ru

Spin-pseudospin models is a good tool for studying the thermodynamic properties of systems that demonstrate the coexistence and competition of both the conventional spin subsystem and, for example, the charge subsystem. We address a two-dimensional spin-pseudospin model of a HTSC cuprate, which takes into account both the conventional Heisenberg spin-spin exchange interaction and on-site and inter-site charge correlations [1]. For the system, we have a strictly determined spectrum of the three on-site charge states, that corresponds to a pseudospin $S=1$, and a conventional $s=1/2$ spin subsystem. In this case, the value of the “magnetization” of the pseudospin subsystem, or pseudomagnetization is an external parameter for the thermodynamic calculation, and it should be conserved. There are two ways to control the pseudomagnetization: the formal one implies introducing an effective pseudomagnetic field and allowing fluctuations, while the strict one implies forbidding changes in pseudomagnetization at each step. We investigated the differences in thermodynamic behavior obtained within the framework of two approaches to control the pseudomagnetization, and also discussed the "cost" of introducing a strict control of pseudomagnetization from the viewpoint of computational resources.

[1] Yu. Panov, A. Moskvina, A. Chikov et al, *J. Supercond. Nov. Magn.*, **29** (2016) 1077.

4PO-K-30

MAGNETIC PHASE SEPARATION DEPENDING ON ATOMIC DISORDER IN THE ANDERSON-HUBBARD MODEL

Arzhnikov A.K., Groshev A.G.

Physical-Technical Institute, Kirov Str. 132, Izhevsk 426000, Russia
arzhnikof@bk.ru

The rich magnetic phase diagram of quasi-two-dimensional interacting electronic systems attracts substantial interest. In particular, it is connected with “unconventional” superconductor and with the possibility of creating heterostructures possessing novel properties. Magnetic phase transitions and the nonuniform magnetic states of different types in the considering systems have high sensitivity to external conditions and lead to drastic functionalities of the electric devices [1]. Thus, investigation the influence of different conditions on phase separation both the physical and practical viewpoints is important issue.

Here we study the influence of disorder on the magnetic phase separation between AF and incommensurate spiral (Q,Q) phases [2,3]. The investigations have been made on the basic two dimensional single-band $t-t'$ Hubbard model in the presence of an atomic disorder (Anderson-Hubbard model). We considered binary-alloy disorder where the difference energies between the impurity and host atoms provides a measure of the disorder strength at fixed impurity concentration. The problem was solved within the framework of functional-integral approach using the static approximation with allowance for longitudinal fluctuations of the magnetic moment. The dependence on the temperature and disorder of the magnetic phase separation was obtained. It was shown that, in the case negative of the difference between the impurity and host ionic energies, disorder lead to the quantitative renormalization of the phase separation boundaries. However, in the case positive quantity this difference, the disorder can lead to the qualitative changes the phase separation between AF and incommensurate spiral (Q,Q) phases. The features influence of disorder on the magnetic phase separation of the two dimensional Hubbard model are discussed.

This work was supported in part by the Division of Physical Sciences and Ural Branch, Russian Academy of Sciences (projects no. 15-8-2-12), by the Russian Foundation for Basic Research (projects no. 16-02-00995, 16-42-180516) and Financial Program AAAA-A16-116021010082-8.

[1] N.A. Tulina, *Phys. Usp.*, **50** (2007) 1171.

[2] P.A. Igoshev, M.A. Timirgazin, A.A. Katanin, A.K. Arzhnikov, V.Yu. Irkhin, *Phys. Rev. B*, **81** (2010) 094407.

[3] A.K. Arzhnikov, A.G. Groshev, *Europhys. Lett.*, **102** (2013) 57005.

4PO-K-31

FRUSTRATED HEISENBERG ANTIFERROMAGNETS ON CUBIC LATTICES: MAGNETIC STRUCTURES, EXCHANGE GAPS, AND PHASE TRANSITIONS

Ignatenko A.N., Irkhin V.Yu.

M.N. Miheev Institute of Metal Physics, 620990 Ekaterinburg, Russia
Ignatenko@imp.uran.ru

We consider frustrated Heisenberg antiferromagnets (AF's) on the cubic (simple, bcc, and fcc) Bravais lattices with magnetic correlations described by wave vectors $\mathbf{Q} = \mathbf{R}/2$ equal to halves of reciprocal lattice vectors \mathbf{R} [1]. Provided that \mathbf{Q} is non-invariant under the cubic symmetry group, the corresponding mean-field lowest energy state has an additional degeneracy, as well as an enlarged space of the order parameter. The magnetic structure, being in general non-coplanar, is described by a Neel vector or so-called 4-complex order parameter for AF of type A and B correspondingly [1]. We demonstrate within the spin wave theory (SWT) and large- N expansion (N is the number of spin components) that fluctuations lift degeneracies (the phenomenon known as "order by disorder") and stabilize simple collinear one wave vector states. A satellite of this effect is opening of the exchange gaps at certain wave vectors in the spin wave spectrum (there is an analogous effect in the non-uniform static transverse susceptibility).

The behaviour of exchange gaps with increasing temperature and/or frustration is of considerable interest. At $N \gg 1$ exchange gaps are closing as the temperature approaches Neel point and the system undergoes second-order phase transition [1]. This is consistent with experiments [2]. We have calculated the critical indices η and ν to order of $1/N$ and found that they differ for AF's of types A and B: closing the exchange gaps results in emergence of additional critical modes, which makes the critical behaviour for B-type AF's non-conventional [1].

At the same time, Monte Carlo simulations [3] clearly indicate a first order phase transition. Moreover, the $4 - \epsilon$ renormalization group analysis [4] shows absence of an infrared stable fixed point at $N = 3$, which also implies first-order nature of the phase transition. These results are in apparent contradiction with the scenario of continuously closing exchange gaps.

The contradiction can be related to generation of effective biquadratic (and higher order) exchange interactions by quantum and thermal fluctuations in a purely Heisenberg system [5], which is another manifestation of the "order by disorder" phenomenon. We calculate the effective biquadratic exchange interaction within SWT and study the corresponding effective model by performing large- N expansion, as well as Monte Carlo simulation. A similar phenomenon is also expected in a system with exchange anisotropy: fluctuations will induce exchange anisotropies of higher orders.

The research was carried out within the state assignment of FASO of Russia (theme "Quant" No. 01201463332), supported in part by RFBR (project No. 16-32-00482).

- [1] A.N. Ignatenko, V.Yu. Irkhin, *J. Sib. Fed. Univ. Math. & Phys.*, **9** (2016) 454-458.
- [2] T. Bruckel, B. Dorner, A. Gukasov, and V. Plakhty, *Phys. Lett. A*, **162** (1992) 357.
- [3] C. Pinettes, H.T. Diep, *J. Appl. Phys.*, **83** (1998) 6317; H. T. Diep and H. Kawamura, *Phys. Rev. B*, **40** (1989) 7019.
- [4] P. Bak, S. Krinsky, and D. Mukamel, *Phys. Rev. Lett.*, **36** (1976) 52.
- [5] C. L. Henley, *J. Appl. Phys.* **61** 3962(1987); *Phys. Rev. Lett.*, **62** (1989) 2056.

4PO-K-32

AN ESSENTIALLY GEOMETRICALLY FRUSTRATED MAGNETIC SYSTEM: AN EXACT SOLUTION FOR THE SPIN LIQUID STATE

Andrianov A.VI.¹

¹Moscow State University, Physics Faculty, Moscow, RF 119991
avla@mail.ru

Starting from the archetypical geometrically frustrated magnetic objects - equilateral triangle and tetrahedron - we consider a multidimensional tetrahedron with spins $\frac{1}{2}$ in the each vertex and equal antiferromagnetic Heisenberg exchange along each edge. Many-particle case is obtained by setting dimensionality d to high numbers, hence constituting likely the most geometrically frustrated magnetic system ever possible. This problem has a remarkably easy exact solution for each d . As a result, this imaginary object demonstrates at $d \rightarrow \infty$ all the features characteristic for the geometrically frustrated magnetic systems:

- a) highly degenerate ground state;
- b) absence of the magnetic phase transition down to $T \rightarrow 0$, i.e. frustration factor $f \rightarrow \infty$;
- c) perfect Curie-Weiss behavior well below Curie-Weiss temperature, down to $T \rightarrow 0$;
- d) vanishingly small exchange energy and magnetic entropy per one spin.

Note that this system is not a subject of the Mermin-Wagner theorem, hence all these features are due solely to the geometrical frustration. We conclude that the system at $d \rightarrow \infty$ might represents a quantum spin-liquid state.

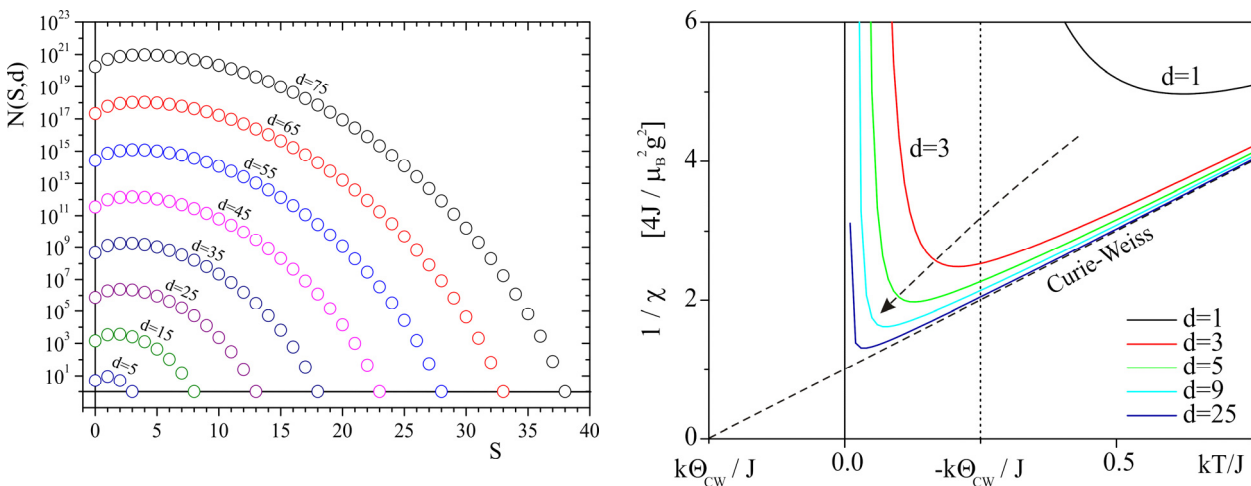


Fig.1. The degeneration of states $N(S,d)$ for different d values, labeled over the d values, dashed line stands for the dependence. Spin $S=0$ corresponds to the ground state.

Fig.2. A set of $1/\chi(T)$ dependences for different d values, dashed line stands for the Curie-Weiss dependences.

Therefore we present an exact solution of a quantum problem with Heisenberg exchange that, while bizarre, may nevertheless be considered as a quantum spin-liquid.

[1] Andrianov A.VI., <https://arxiv.org/abs/1504.05622>.

4PO-K-33

NON-EQUILIBRIUM CRITICAL BEHAVIOR OF HEISENBERG THIN FILMS

*Shlyakhtich M.A.*¹, *Prudnikov P.V.*²

¹ Siberian federal university, Krasnoyarsk, Russia

² Omsk State University, Omsk, Russia

mmed@mail.ru

It is well known now the fundamental role of competing interactions in the emerging features of low-dimensional systems. Among a wide number of numerical and theoretical investigations on equilibrium and dynamical properties of several model Hamiltonian of low-dimensional magnets, Heisenberg-like models are one of the most widely used to approach real magnetic materials. In fact, anisotropic versions of the Heisenberg model describe several compounds as K_2NiF_4 , $BaCo_2(AsO_4)_2$, $CoCl_2$ -GIC and Rb_2CrCl_4 .

In this paper we study the non-equilibrium properties of Heisenberg ferromagnetic films using Monte Carlo simulations by short-time dynamic method. By exploring the short-time scaling dynamics, we have found thickness dependency of critical exponents z , θ' and β/ν for ferromagnetic thin film. For calculating the critical exponents of ferromagnetic films we considered systems with linear size $L = 128$ and layers number $N = 2; 4; 6$. Starting from initial configurations, the system was updated with Metropolis algorithm at the critical temperatures $T_c = 1.03(8)$ for $N = 2$, $T_c = 1.25(5)$ for $N = 4$, $T_c = 1.35(4)$ for $N = 6$ [1, 2]. We have measured the time evolution of the magnetization $m(t)$ (Fig. 1), the second moment $m^{(2)}(t)$ and autocorrelation function $C(t)$ from high-temperature ($m_0 \ll 1$) and low-temperature ($m_0 = 1$) initial states. Critical exponents z , θ' and β/ν have been calculated for different number of layers. Comparing the calculated values $z=2.187(7)$ for $N=2$, $z=2.197(10)$ for $N=4$ with the results for 2D Ising model in various works $z=2.166(7)$ [4], $z=2.0842(39)$ [5], we see the very good agreement among them, i.e. thin ferromagnetic films belong to universality class non-equilibrium behaviour of 2D Ising model. Value of critical exponents $z=2.300(9)$ for $N=6$ demonstrate the dimensional crossover to characteristic values for critical behavior of the 3D model.

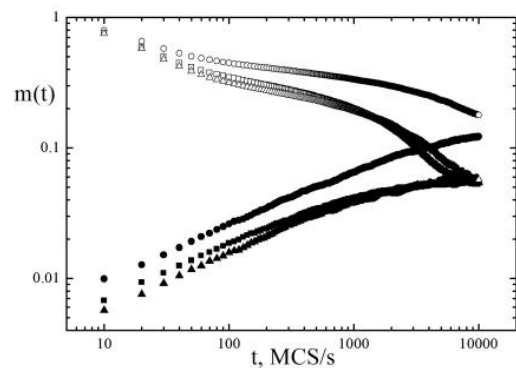


Fig. 1. Time dependencies of magnetization for different $N = 2$ (\circ), 4 (\square), 6 (Δ) and initial state $m_0 \ll 1$ (\bullet), $m_0 = 1$ (\circ).

The work was performed within the project of Russian Fund of Basic Research No. 16-32-00581 mol_a and within the grant No. MD-6024.2016.2 of Russian Federation President. The simulations were supported by the Supercomputing Center of Lomonosov Moscow State University, Moscow Joint Supercomputer Center and St. Petersburg Supercomputer Center of the Russian Academy of Sciences.

[1] P.V. Prudnikov, V.V. Prudnikov, et al., *JMMM*, **387** (2015) 77-82.

[2] P.V. Prudnikov, V.V. Prudnikov, M.A. Medvedeva, *JETP Letters*, **100** (2014) 446-450.

[3] P.V. Prudnikov, M.A. Medvedeva, *Prog. Theor. Phys.*, **127** (2012) 369-382.

[4] F.-G. Wang and C.-K. Hu, *Phys. Rev. E*, **56** (1997) 2310-2313.

[5] A.S. Krinitsyn, V.V. Prudnikov, P.V. Prudnikov, *Theor. Math. Phys.*, **147** (2006) 561-575.

4PO-K-34

CURRENT-DRIVEN QUANTUM DYNAMICS OF TOROIDAL MOMENT IN RARE-EARTH NANOCLUSTERS

Plokhov D.I.¹, Popov A.I.^{1,2}, Zvezdin A.K.^{1,2}

¹ A. M. Prokhorov General Physics Institute, Russian Academy of Sciences, Moscow, Russia

² Moscow Institute of Physics and Technology, Dolgoprudny, Moscow Region, Russia

³ National Research University of Electronic Technology, Zelenograd, Moscow, Russia
dmitry.plokhov@gmail.com

Recently, quite an attention has been drawn to molecular magnets for aims of quantum information processing. Much research has been focused on single-spin manipulation with external fields. It seems that many limitations in molecular magnet quantum computing are rooted in the very idea of spin state control with magnetic fields. Thus, it is highly desirable to control spin for this purpose with an electric current because it is much easier to be localized.

In this context, antiferromagnetic triangular and polygonal molecules, so called spin rings (V15, Cu₃, Dy₃, Dy₄, Dy₆, etc.), are of special interest, because such quantum systems with the ground state of zero magnetic moment are reported to have long decoherence time due to weak inter-cluster dipole interactions.

The rare-earth spin rings might be the best candidates to observe magnetoelectric effect (MEE) connected with spin chirality and toroidal moments. The dysprosium rare-earth spin rings are especially interesting because of the possibility to observe MEE and also other peculiar spin-electric effects due to its spin chiral ground state with long relaxation time. The carrier of these MEEs is an intrinsic toroidal (anapole) magnetic moment, as our subsequent quantum-mechanical analysis reveals. The resulting quantum structure provides new ways to control and manipulate the qubit state in quantum computation.

We study the quantum dynamics of polygonal rare-earth molecular clusters with Ising-type ion magnetization. It is shown that the ground state of such systems is a nonmagnetic quasi-doublet of states with oppositely twisted ion spins. The states differ in the sign of the toroidal moment, a natural physical quantity characterizing the spin chirality of the clusters. The possibility of macroscopic quantum tunneling of the toroidal moment between the states is predicted. The effects of an external current are considered, both in equilibrium and in the framework of the Landau-Zener-Stueckelberg tunneling model. Special treatment is given to the important case of triangular rare-earth clusters.

We show that such rare-earth polygonal molecular clusters meet all the DiVincenzo's criteria, necessary for the implementation of quantum computer. First, we deal with a scalable physical system with well characterized qubits. Second, we describe the way to initialize the state of the qubits to a simple fiducial state. Third, we describe a "universal" set of quantum gates (the most simple set of two-qubit universal quantum gates is the Hadamard gate, the $\pi/4$ phase shift gate, and the controlled NOT gate). All the gates can be performed by a bias current. Fourth, the systems have long relevant decoherence time. Fifth, a qubit read out techniques are described.

Our study suggests that spin chirality and the anapole moment in rare-earth nanoclusters are essential parameters in realizing nanoscale quantum computing device. Although we consider mainly the dysprosium based nanoclusters, many results can be applicable to other Ising-like rare-earth nanoclusters, e.g. based on Tb, Ho, etc.

Support by Russian Foundation for Basic Research (projects 15-02-08509 and 16-29-14005) is acknowledged.

4PO-K-35

AN APPROXIMATE QUANTUM THEORY OF THE ANTIFERROMAGNETIC GROUND STATE

Orlova N.B.², Kurkin M.I.¹

¹ Novosibirsk State Technical University, Novosibirsk, Russia

² Russia Institute of Metal Physics UB RAS, Ekaterinburg, Russia
orlova.nb@gmail.com

The hypothesis of magnetic sublattices underlies most of the models used to describe the ferri- and antiferromagnetic spin structures ordered by the exchange interaction $V_{\text{ex}} = V(s_z) + V(s_y, s_x)$. The term $V(s_z)$ determines the mutual orientation of the longitudinal components of the spins s_z , therefore it is compatible with the sublattices hypothesis. The term $V(s_y, s_x)$ describes the processes with simultaneous switching of the oppositely directed spins, which is equivalent to their transposition. Such exchange mixing destroys the ferromagnetic order in the sublattices. One of the solutions for the problem of choosing between these two competing mechanisms is proposed by Anderson [1] and Ziman [2]. They associated the destruction of the sublattices with the zero spin-wave oscillations similar to zero phonon oscillations. This mechanism completely destroys the sublattices in one-dimensional and two-dimensional spin structures, but partially keeps them at the three-dimensional antiferromagnetic ordering.

We propose another model, in which the suppression of the sublattices exchange mixture is provided by the magnetic anisotropy. The possibility of such suppression is caused by the degeneracy in the spectrum of the operator V_{ex} by the spin orientations relative to the crystal axes. The magnetic anisotropy V_A removes this degeneracy, which is usually associated with a strong change of the wave functions forms. This effect was demonstrated for the operators U_{ex} and U_A of a special form ensuring the existence of solutions of the equations corresponding to antiferromagnetic ordering.

$$U_{\text{ex}}\Phi_0 = E_{\text{ex}}\Phi_0; \quad (U_{\text{ex}} + U_A)\Phi = E\Phi \quad (1)$$

The wave function Φ_0 provides zero mean value of the spin ($\langle \Phi_0 | s | \Phi_0 \rangle = 0$) corresponding to the absence of spin sublattices. The value of the spin $\langle \Phi | s | \Phi \rangle$ appeared to depend on the number of spins in the sublattice N even for $H_A \ll H_E$ (here H_E is the exchange field, H_A is the magnetic anisotropy field). The condition $N \gg H_E / H_A$ ensures the existence of two sublattices with different values of spins:

$$\langle \Phi | s_1 | \Phi \rangle = -\langle \Phi | s_2 | \Phi \rangle = 1/2 [1 - H_E / (H_A N)] \quad (2)$$

It turned out that the values of (2) correspond to the linear approximation by the small parameter $H_E / (H_A N) \ll 1$ also for the exchange interaction in the nearest-neighbour approximation.

The work was performed as the part of the state task of FASO of Russia (topic №01201463332) and with partial financial support of RFBR (project №17-02-00344).

[1] P.N. Anderson, *Phys.Rev.*, **86** (1954) 694.

[2] J. M. Ziman, *Proc.Phys.Soc.*, **50** (1952) 540.

4PO-K-36

SPIN NEMATIC WITH $S = 2$ *Kosmachev O.A.¹, Fridman Yu.A.¹, Ivanov B.A.²*¹ V.I. Vernadsky Crimean Federal University, 295007, Simferopol, Russia² Institute of Magnetism, National Academy of Sciences of Ukraine, Kiev, 03142 Ukraine
yuriifridman@gmail.com

Interest in the study of new phase states of spin systems has been growing for the last three decades. For isotropic magnetics with spin it is possible to realize not only phases with a magnetic order, that is, with a nonzero average value of the spin, but also phases with an average zero spin value, in which the spontaneous breaking of the rotational symmetry is due to the average values of the spin multipoles. Such states of spin systems $S \geq 1$, called nematic systems, are of interest for studying ultracold gases of atoms in optical traps for which the values of the higher exchange integrals are not small [1, 2].

This paper is devoted to the study of phase states for the model of an isotropic magnet with spin $S = 2$ in the mean-field approximation and with the interaction of nearest neighbors on the lattice. The Hamiltonian of an isotropic magnet with $S = 2$ that takes into account the complete set of spin invariants has the form:

$$\hat{H} = -\frac{1}{2} \sum_{n,n'} [J(\mathbf{S}_n \mathbf{S}_{n'}) + K(\mathbf{S}_n \mathbf{S}_{n'})^2 + D(\mathbf{S}_n \mathbf{S}_{n'})^3 + F(\mathbf{S}_n \mathbf{S}_{n'})^4],$$

As shown by the investigation of the static and dynamic properties of an isotropic magnet with $S = 2$, in addition to the dipole phases (ferromagnetic and antiferromagnetic ones), due to the inclusion of exchange integrals in higher spin orders, new stable phase states arise: the nematic and tetragonal phases. The nematic phase is a superposition of the planar and axial nematic state. Analysis of excitation spectra showed that only near the lines of phase instability the nematics becomes either planar or axial. The tetragonal phase is characterized by higher multipole moments, since the average magnetization per node is zero, and the ellipsoid of the quadrupole moment tensor degenerates into a sphere.

The model studied in this work also admits splitting of the magnet into two sublattices. It is shown that there are two-sublattice phases whose phase symmetry is lower than for the phases adjoining them. For these phases (LS phases), the values of both (unsaturated) sublattice spins and correlators of the form $\langle (S_x \cos \chi + S_y \sin \chi)^3 \rangle = C \cos 3\chi$, $|C| < \sqrt{2}$ do not equal to zero. The case of the appearance of nondegenerate phase transitions between phases was first observed: depending on the ratio of the exchange integrals, either a first-order phase transition with a finite region of phase coexistence or two second-order phase transitions via a phase with a low symmetry takes place. We have found the phases for which the symmetry at the site is discrete. This is an orthogonal nematic phase with biaxial symmetry; TH and ATH phases, for which the symmetry at the site is tetrahedral.

The work is partially supported by RFBR projects No. 16-02-00069 (YuAF and OAK) and No. 16-42-910441 (OAK) and the NAS No 1/16-N (BAI) project.

[1] D. M. Stamper-Kurn, M. R. Andrews, A. P. Chikkatur, S. Inouye, H.-J. Miesner, J. Stenger, and W. Ketterle, *Phys. Rev. Lett.*, **80** (1998) 2027.

[2] F. Zhou, *Phys. Rev. Lett.*, **87** (2001) 080401.

4PO-K-37

GROUND STATE OF THE CLASSICAL FRUSTRATED HEISENBERG FERROMAGNET IN A MAGNETIC FIELD

Martynov S.N.

Kirensky Institute of Physics, Federal Research Center KSC SB RAS, 660036, Krasnoyarsk, Russia
 unonav@iph.krasn.ru

A frustrated chain of the classical spins $S=1$ in the presence of an external magnetic field H_0 described by the Hamiltonian

$$H = \sum_i (J_1 \mathbf{S}_i \mathbf{S}_{i+1} + J_2 \mathbf{S}_i \mathbf{S}_{i+2} - H_0 S_i^z),$$

where $J_1 < 0$ and $J_2 > 0$ are the ferromagnetic nearest- and antiferromagnetic next-nearest-neighbor exchange constants, respectively, was considered.

In the continual approach [1] the requirement of the collinearity of the spins and effective fields on the each lattice site (collinearity constraint) [2] leads to an autonomous differential equation. Neglecting the derivatives which are higher than second order and in the linear anharmonicity approximation ($\theta'' \ll 1$) the equation on the angle velocity of the spins in the incommensurate magnetic structure has a form

$$\theta''(\cos\theta' + 4R\cos 2\theta') = 2h\sin\theta, \quad (1)$$

where $R = J_2/J_1$, $h = H_0/J_1$ and the angle of the spin orientation θ is counted from the external field direction. The solution of the equation takes the obvious dependence of the angle velocity from angle and initial velocity at $\theta=0$.

The ground state of the soliton solutions (1) was calculated by a numerical minimization of the energy integral. The phase boundary between the soliton and ferromagnetic phases on the phase $|R|$ - h plane was determined (Fig.1). A phase transition between the phases is a first order one.

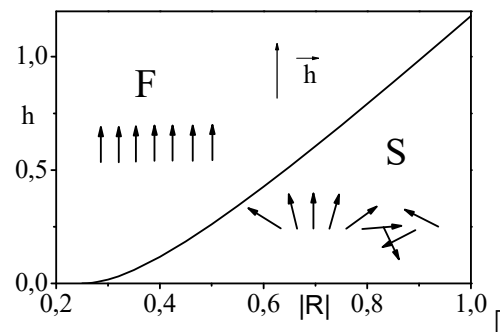


Fig. 1. The phase boundary between the ferromagnetic (F) and soliton (S) phases in external magnetic field (h).

[1] S. N. Martynov, V.I. Tugarinov, A.S. Martynov *JMMM*, DOI 10.1016/j.jmmm.2016.12.086.

[2] S. N. Martynov *JMMM*, **398** (2016) 121-126.

4PO-K-38

RELATIONSHIP BETWEEN SUPERCONDUCTING ORDER PARAMETER SYMMETRY, TEMPERATURE AND NEXT-NEAREST NEIGHBOR HOPPING

Gilmutdinov V.F., Timirgazin M.A., Arzhnikov A.K.

Physical-Technical Institute of Ural Branch of RAS, Izhevsk, Russia
vitaliodestroyer@gmail.com

Since the discovery of high-temperature superconductivity (HTSC) in doped cuprates a huge amount of data is obtained, which are the results of theoretical and experimental studies. Despite some apparent success in high-temperature superconductivity research, still remains an open question about the mechanism of this phenomenon.

An important question in the study of HTSC is the symmetry of the superconducting order parameter. It is generally accepted that cuprate superconductors have $d_{x^2-y^2}$ -wave (further d) symmetry and Fe-based superconductors have s_{\pm} -wave (further s) pairing. However recent Raman spectroscopy and ARPES experiments revealed that the symmetry of the order parameter in copper oxides deviates from the traditional d -wave [1,2]. On the other hand, some calculations based on spin-fluctuation mechanism of superconductivity predict d -wave pairing in iron pnictides [3]. In a number of papers it was proposed that superconducting states in the general case have rather mixed $s+id$ -wave symmetry of the order parameter than pure s - or d -wave [4-6]. It provides a motivation to study the possibility of the transition between s - and d -wave states through the formation of an intermediate phase with mixed $s+id$ -wave pairing.

We consider one-band model on the square lattice within Hartree-Fock approximation to describe the formation of the superconductivity with pure s -, d - and mixed $s+id$ -wave symmetries of the pairing wavefunction. An electron attraction between nearest neighbor sites V is assumed without consideration of its mechanism.

We have constructed the ground state phase diagrams of the model in the variables of the ratio between the next-nearest and nearest neighbors electron transfer integrals t'/t and the electron concentration n for different values of V . It was shown that both the pure superconducting states and the intermediate phase $s+id$ are realized in a wide range of the model parameters. We have defined the boundaries of the second order phase transitions between the superconducting states with different symmetries. It was found that an increase of the attraction parameter V leads to a larger size of the $s+id$ -wave regions.

Furthermore we have studied an evolution of the superconducting order with finite temperature T for certain values of t'/t . It was shown that with increase of temperature the mixed $s+id$ -phase goes to the pure s - or d -wave state which further go to the normal state. No direct transition between $s+id$ -phase and the normal state was found.

This work is supported by Ural Branch of RAS in project 15-8-2-12, and by Russian Foundation of Basic Research in project of 16-42-180516.

- [1] G. Blumberg *et al.*, *Phys. Rev. Lett.*, **88** (2002) 107002.
- [2] K. Terashima *et al.*, *Rev. Lett.*, **99** (2007) 017003.
- [3] S. Maiti *et al.*, *Phys. Rev. Lett.*, **107** (2011) 147002.
- [4] K. Musaelian *et al.*, *Phys. Rev. B*, **53** (1996) 3598.
- [5] C. Platt *et al.*, *Phys. Rev. B*, **85** (2012) 180502(R).
- [6] W.C. Lee *et al.*, **102** (2009) 217002.

4PO-K-39

ELECTRONIC PROPERTIES OF SIMPLE HEXAGONAL GRAPHITE

Mosoyan K.S.¹, Rozhkov A.V.^{1,2}, Sboychakov A.O.², Rakhmanov A.L.^{1,2}

¹ Moscow Institute for Physics and Technology (State University), g. Dolgoprudnyi,
Moscow region, Russia

² Institute for Theoretical and Applied Electrodynamics, Russian Academy of Sciences, Moscow,
Russia
kamosoyan@gmail.com

We investigate electronic properties of AA graphite (simple hexagonal graphite). Due to recent success in the synthesis of the AA graphite [1], such study becomes important. It is well known [2] that the Fermi surface of this material possesses approximate cylindrical symmetry and consists of two fragments resembling two rugby balls (see Fig. 1). We reproduce this result using tight-binding approximation.

It is found that these fragments can be superposed by translation in momentum space (translation vector \mathbf{Q} is shown in Fig.1). Such a feature is known as the ideal nesting. It is a signature of an instability of an electron liquid. In the presence of the electron-electron repulsion the leading instability is the spin density wave (SDW) order.

We investigate SDW phase in the AA graphite electronic subsystem at zero temperature within the framework of the Hubbard model. We use mean-field approximation to describe the transition into low-temperature SDW phase. This approximation is applicable as long as the interaction is not too strong. The values of the SDW gap and the on-site magnetization are estimated. Our mean-field calculations are similar to those performed for the AA stacked bilayer graphene [3].

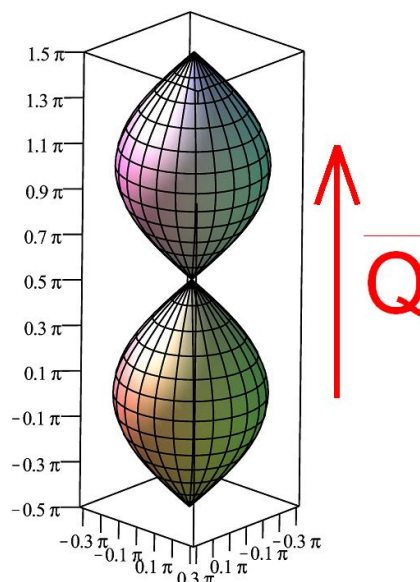


Fig. 1. Fermi surface of simple hexagonal graphite.

[1] J.-K. Lee, et al., *J. Chem. Phys.*, **129** (2008) 234709.

[2] J.-C. Charlier, et al., *Phys. Rev. B*, **44** (1991) 13237.

[3] A. L. Rakhmanov, et al., *Phys. Rev. Lett.*, **109** (2012) 206801.

4PO-K-40

PHASE TRANSITIONS AND CRITICAL PHENOMENA IN FRUSTRATED ISING MODEL ON A CUBIC LATTICE WITH NEXT-NEAREST-NEIGHBOR INTERACTIONS

Murtazaev A.K.^{1,2}, Ramazanov M.K.¹

¹ Institute of Physics, Dagestan Scientific Center, RAS, Makhachkala, Russian Federation

² Dagestan State University, Makhachkala, Russian Federation
sheikh77@mail.ru

The study of phase transitions and critical phenomena in frustrated spin systems is one of the fundamental problems in statistical physics [1]. Recent advances in understanding phase transitions and critical phenomena in frustrated systems have largely been achieved by applying of Monte Carlo methods, because most attempts to calculate the critical exponents and characterize the mechanisms of the critical behavior of such systems by conventional theoretical and experimental methods are confronted by serious difficulties [2-4].

The problem of frustrations and phase transitions in Ising model on a cubic lattice with next-nearest-neighbor intralayer interactions is explored in works [5,6].

In present paper, we investigate critical phenomena and estimate a full set of static critical exponent of the antiferromagnetic Ising model on a cubic lattice with allowance for the next-nearest-neighbor interactions inside layers for $r \in [0.0, 0.5]$ and $r \in [0.9, 1.0]$ with $\Delta r = 0.1$, where the second order PT is observed [5,6] ($r = J_2/J_1 = 1.0$; J_1 and J_2 are the constants of the nearest-neighbor and next-nearest-neighbor interactions, respectively, and r is the magnitude of the next-nearest-neighbor interaction).

The Hamiltonian of the antiferromagnetic Ising model on a cubic lattice can be written as

$$H = -J_1 \sum_{\langle ij \rangle} (S_i \cdot S_j) - J_2 \sum_{\langle ii \rangle} (S_i \cdot S_i), \quad (1)$$

where $S = \pm 1$ is the Ising spin. The lattice consists of two-dimensional square layers packed along the orthogonal axis. The first term in Eq. (1) characterizes an antiferromagnetic interaction of all nearest-neighbors, which is taken to be the same inside and between layers ($J_1 < 0$). The second term describes an antiferromagnetic interaction between next-nearest-neighbors in the same layers ($J_2 < 0$). The Ising model on a cubic lattice becomes frustrated after taking into account the next-nearest-neighbor antiferromagnetic interactions inside layers. Frustrations in the model are caused by a competition between exchange interactions the nearest-neighbors and next-nearest-neighbors.

The static magnetic exponents specific heat α , susceptibility γ , magnetization β , correlation length ν were calculated by using the finite-size scaling theory [2-4]. The system is found to manifest the universal critical behavior within the range of $r \in [0.0, 0.4]$. Show that in the antiferromagnetic Ising model on a cubic lattice with next-nearest-neighbor interactions inside layers another critical behavior takes place in the range of $r \in [0.9, 1.0]$.

The study was supported by grant of RFBR (Project no. 16-02-00214).

- [1] Vik.S. Dotsenko, *Usp. Fiz. Nauk*, **165** (1995) 481.
- [2] A.K. Murtazaev, M.K. Ramazanov, M.K. Badiev, *Low Temp. Phys.* **35** (2009) 521.
- [3] A.K. Murtazaev, M.K. Ramazanov, M.K. Badiev, *JETP*, **115** (2012) 331.
- [4] A.K. Murtazaev, M.K. Ramazanov, F.A. Kassan-Ogly, M.K. Badiev, *JETP*, **117** (2013) 1091
- [5] M.K. Ramazanov, A.K. Murtazaev, *JETP Lett.*, **101** (2015) 714.
- [6] M.K. Ramazanov, A.K. Murtazaev, *JETP Lett.*, **103** (2016) 460.

4PO-K-41

COOPERATIVE PHENOMENA IN SPIN CROSSOVER SYSTEMS*Nesterov A.I.¹, Orlov Yu.S.^{2,3}, Ovchinnikov S.G.^{2,3}, Nikolaev S.V.³*¹ University of Guadalajara, Guadalajara, Mexico² Kirensky Institute of Physics, Krasnoyarsk, Russia³ Siberian Federal University, Krasnoyarsk, Russia

nesterov@cencar.udg.mx

Spin crossover in condensed matter physics is a transformation of a system with one spin S_1 into another state with spin S_2 induced by some external parameter like strong magnetic field, high pressure, light etc. The thermally induced spin crossover transition can be described as the thermal equilibrium between the lowest and excited states. It accompanies by the energy level E_1 and E_2 crossing, where E_α is the local energy of the magnetic ion with spin S_α ($\alpha = 1, 2$). This phenomenon is due to the presence of two low-lying electronic states, resulting from the competition between the ligand (or crystal) field in transition-metal complexes and electronic exchange interaction. We study the spin crossover in magnetic Mott-Hubbard insulators under pressure. The exchange interaction effects near the spin crossover are described by the effective Hamiltonian obtained from a realistic multi-band $p-d$ -model. It is shown that the cooperativity leads to a modification of the quantum phase transition from second- to first-order phase transition near a tricritical point and appearance of metastable states of the system. The pressure-temperature phase diagram are obtained to describe the magnetization and high-spin population near the spin crossover of the Mott's insulators with d^6 -ions.

4PO-K-42

THE MONTE-CARLO INVESTIGATION OF PHASE TRANSITIONS IN THE ANTIFERROMAGNETIC POTTS MODEL ON FCC LATTICE

Babaev A.B.^{1,2}, Murtazaev A.K.^{1,3}

¹ Institute of Physics of Daghestan Scientific Center of Russian Academy of Sciences, Makhachkala, Russia

² Daghestan State Pedagogical Universities, Makhachkala, Russia

³ Daghestan State Universities, Makhachkala, Russia
b_albert78@mail.ru

The phase transitions (PT) in 3D antiferromagnetic (AF) $q=4$ Potts model on the face-centre-cubic (FCC) lattice are studied based on classical Monte-Carlo method. Normile with co-authors [1] showed that the identification of USB neutron diffraction pattern in the 3-k model (Fig. 1a) gives better results than in the collinear model (Fig. 1b). This 3-k structure has no antiparallel directions of magnetic moments and is identical to a 4-state standard Potts model shown in Fig. 1c.

The antiferromagnetic $q=4$ Potts model on FCC lattice with account of the first nearest neighbors (see Fig. 1) is described by microscopic Hamiltonian as follows[2]:

$$H = -\frac{J}{2} \sum_{i,j} \cos \theta_{i,j}, \quad (1)$$

where $J < 0$ takes into account the exchange AF interaction of nearest neighbors, $\theta_{i,j}$ is the angle between interacting spins $S_i - S_j$. The considered model at $J > 0$ were studied in Ref. [3], where it was reported that in the absence of the disorder this model demonstrated a behavior typical for the first order PT in accordance with the predictions of the mean-field theory [2].

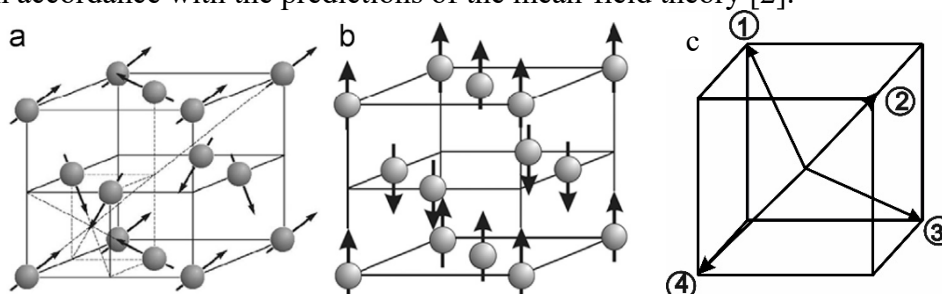


Fig. 1. Identification of the USB diffraction pattern in the collinear one (a) and in the 3-k structure (b). 4-State Potts model (c).

The computations are performed for the systems with periodic boundary conditions and linear sizes $L \times L \times L = N$, $L = 36 \div 72$. The analysis of PT character and the detection of PT temperatures are carried out by means of the fourth order Binder cumulant method [4]. The PTs in studied magnetic systems are discussed using the histogram analysis of data.

This work was supported by the Russian Foundation for Basic Research (project no.16-02-00214)

[1] P.S. Normile, W.G. Stirling, D. Mannix et al., *Phys. Rev. B*, **66** (2002) 014405.

[2] F.Y. Wu, *Rev. Mod. Phys.*, **54** (1982) 235.

[3] A.K. Murtazaev, A.B. Babaev, G.Ya. Aznaurova, *JETP*, **109** (2009) 442.

[4] K. Eichhorn, K. Binder, *J. Phys.: Condens. Matter*, **8** (1996) 5209.

4PO-K-43

UNCONVENTIONAL PHASE SEPARATION IN THE MODEL 2D SPIN-PSEUDOSPIN SYSTEM

Budrin K.S.¹, Panov Yu.D.¹, Moskvina A.S.¹, Chikov A.A.¹

¹ Ural Federal University, Ekaterinburg, Russia
kbudrin@yandex.ru

Competition of charge and spin orders is a challenging problem for high- T_c cuprates. We addressed a simplified static 2D spin-pseudospin model [1] on a square lattice, where the pseudospin $S=1$ describes three valent states on the lattice site. The Hamiltonian includes the on-site and inter-site charge correlations and the Ising spin coupling ($s=1/2$) only for $S_z=0$ states:

$$H = \Delta \sum S_{iz}^2 + V \sum S_{iz} S_{jz} + J \sum P_{0i} S_{iz} S_{jz} P_{0j}.$$

Classical Monte-Carlo calculations for the 256×256 square lattices show that homogeneous ground-state antiferromagnetic solutions found in a mean-field approximation [1] are unstable with respect to phase separation with the charge and spin subsystems behaving like immiscible quantum liquids. In this case, with lowering the

temperature one can observe two sequential phase transitions (the graph for $\Delta = 0.5$ in Fig. 1): first, antiferromagnetic ordering in the spin subsystem diluted by randomly distributed charges, then, the charge condensation in the charge droplets. The inhomogeneous droplet phase reduces the energy of the system and changes the diagram of the ground states.

On the other hand, the ground state energy of charge-ordered state in a mean-field approximation exactly matches the numerical Monte-Carlo calculations. The specific heat for this case (the graph for $\Delta = -1.5$ in Fig. 1) shows with lowering the temperature firstly the cusp due to a freezing of spin subsystem and then the peak that corresponds to the charge ordering. The doped charge in this case (counted out of half filling) is distributed randomly over a system.

Various thermodynamic properties and phase diagram of the 2D spin-pseudospin system are studied by Monte-Carlo simulation.

The work supported by Act 211 Government of the Russian Federation, agreement № 02.A03.21.0006 and by the Ministry of Education and Science, projects 2277 and 5719.

[1] Yu.D. Panov et al., *J. Supercond. Nov. Magn.*, **29** (2016) 1077-1083.

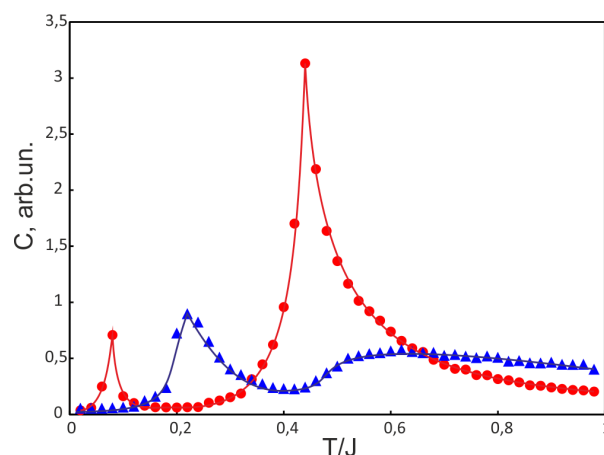


Fig. 1. The temperature dependencies of specific heat in the strong exchange case ($V = 0.1$, $J = 1.0$) for $\Delta = -1.5$ (triangles) and for $\Delta = 0.5$ (circles).

5 July

Wednesday

09:30-11:00

14:30-16:00

plenary lectures

5PL-A

5PL-A-1

MAGNETIC GARNETS FOR SPINTRONIC AND MAGNETOOPTICAL DEVICES

Ross C.A.¹

¹ Massachusetts Institute of Technology, Department of Materials Science and Engineering,
Cambridge MA 02139 USA
caross@mit.edu

Ferromagnetic insulator (FMI) thin films have emerged as an important component of spintronic and magneto-optical devices. Yttrium iron garnet in particular is an excellent insulator with low Gilbert damping and a Néel temperature well above room temperature, and has been incorporated into heterostructures that exhibit a plethora of spintronic phenomena including spin pumping, spin Seebeck and proximity effects. Rare earth garnets can exhibit perpendicular magnetic anisotropy (PMA) by selection of lattice mismatch and magnetostriction constant. We demonstrate robust PMA in films of thulium, europium and terbium iron garnet (TmIG, EuIG and TbIG) with high structural quality down to a thickness of 5.6 nm, about 5 unit cells, which retain a saturation magnetization close to bulk. TmIG/Pt and TbIG/Pt bilayers exhibit a large room temperature anomalous Hall effect which indicates efficient spin transmission across the garnet/Pt interface. Spin Hall magnetoresistance is used to quantify the interfacial spin mixing conductance and the temperature-dependent PMA of the TmIG thin film. Bidirectional switching of the magnetization of TmIG was achieved at room temperature via spin orbit torque by passing a current through an adjacent Pt layer in the presence of a modest fixed inplane field. Additionally, magnetization was induced in a topological insulator (Bi, Sb)₂Te₃ grown onto TmIG. Another important aspect of iron garnets is their magneto-optical activity and high transparency in the infrared, which makes them useful materials at communications wavelengths. We show how Ce- and Bi-substituted YIG can be grown on silicon and incorporated into magneto-optical isolators to control the flow of light in photonic integrated circuits.

5PL-A-2

CURRENT PROGRESSES IN UNDERSTANDINGS OF COERCIVITY FOR DEVELOPING NEXT GENERATION HIGH-PERFORMANCE PERMANENT MAGNETS

Hirosawa S.

Elements Strategy Initiative Center for Magnetic Materials (ECIMM), Research Center for Magnetic and Spintronic Materials, National Institute for Materials Science
1-2-1 Sengen, Tsukuba, Ibaraki, 305-0047, Japan
HIROSAWA.Satoshi@nims.go.jp

Permanent magnets are used in all aspects of our daily life and have become one of the vital key components in modern technologies for renewable energy applications such as EV/HEV driving motors and wind turbine generators. The market-leading permanent magnet materials for these applications today are the Nd-Dy-Fe-B anisotropic magnets. One of the weakness of this class of magnets is their strong temperature dependence of the intrinsic coercivity, H_c , with negative $dH_c(T)/dT$, the origin of which has been the issue to be clarified in order to improve H_c by means of structural manipulations, not by using Dy and Tb, which are a critical element currently used in the magnets to increase H_c . The theory of coercivity for hard magnetic materials has been constructed on the basis of micromagnetic formalism developed on the continuum picture of magnetic materials and has been used successfully applied for description of the microstructure-coercivity relations in many class of permanent magnets. The recent developments of computational micromagnetic simulations have also become powerful aids in deducing guiding concepts to improve the materials and the importance of microstructural manipulations particularly at grain boundaries and interfaces with secondary phases has become evident. However, since the characteristic length scale in these hard magnetic materials are of the order of 1 nm, for further improvements of the materials, the continuum picture is insufficient and atomistic description of the coercivity phenomena has become necessary. Another issue in the coercivity theory is the thermal activation process which has been described with the concept of time-dependence of magnetization process at finite temperatures and the height of energy barrier ($25k_B T$) that can be overcome within a magnetic measurement characteristic time (typically one second). Since the size of activation volume is of the order of magnetic domain wall, atomistic description is required in order to take the effects of local magnetism at surfaces/interfaces into account. The atomistic approach can possibly describe the magnetization reversal phenomena at finite temperature directly if the thermal energy is properly introduced. In ESICMM [1], researchers from plural institutions have constructed an atomistic spin model of Nd₂Fe₁₄B based on the first-principles calculations of atomistic magnetism both in bulk and on surfaces and combined it with stochastic micromagnetic simulations to describe magnetization reversals at elevated temperatures. This talk will give an overview of current progresses in understandings of coercivity at the atomistic level and ongoing efforts at ESICMM to connect the atomistic micromagnetics to the continuum micromagnetics. Experimental investigations toward high-coercivity Dy-free Nd-Fe-B permanent magnets for EV/HEV applications conducted in ESICMM will be also briefly reviewed.

[1] ESICMM is sponsored by MEXT, Japan, under the Elements Strategy Initiative Project and is devoted for development of basic materials science of permanent magnets.
<http://www.nims.go.jp/eng/research/group/ESICMM/index.html>

5PL-A-3

X-RAY MAGNETIC CIRCULAR DICHROISM: UNIQUE PROBE OF MAGNETISM

Rogalev A.

ESRF – The European Synchrotron, Grenoble, France

rogalev@esrf.fr

Discovery of X-ray magnetic circular dichroism (XMCD) more than 25 years ago ushered in a new era of magnetism research with objectives that previously would have been unattainable. The XMCD is obtained as a difference in the x-ray absorption spectra recorded with left and right circularly polarised photons while the sample magnetisation is kept either parallel or antiparallel to the direction of the propagation of the incident x-ray beam. In a way, it may be seen as a high energy counterpart to the magneto-optical effects in the visible discovered by Faraday and Kerr. Because of its inherent element and orbital specificity and ability to probe extremely small sample volumes, XMCD has now become a workhorse technique in magnetism research leading to a deeper understanding of the microscopic origin of magnetic state of matter, as well as to major technological advances. Availability of high fluxes of circularly polarized x-rays at the 3rd generation synchrotron radiation facilities make this technique widely available. Today, more than 50 state-of-the-art beamlines for XMCD are open for users. Sophisticated end stations have facilitated its use, offering a large variety of sample environments, including high static and pulsed magnetic fields, low and ultralow temperatures, high pressure, etc. In this talk, I shall give a current overview of XMCD applications to magnetism research with few examples: the first one deals with studies of paramagnetism in noble metal nanoparticles; the second example concerns magnetic proximity effects at the interfaces of normal metal with ferromagnets and the last one is about measurements on heavy fermion systems under multiple extreme conditions, temperature, magnetic field and pressure.

5PL-A-4

MAGNETISM AT HIGH PRESSURES

Lyubutin I.S.

Shubnikov Institute of Crystallography FSRC "Crystallography and Photonics" RAS, 119333
Moscow, Russia
lyubutinig@mail.ru

High-pressure intensely changes all properties of materials. Pressure-induced magnetic, structural and electronic transitions predicted in strongly correlated electronic systems by many theories, now can be observed experimentally. This becomes to be enabling by the development of the high-pressure diamond-anvil-cell technique and, in particular, due to the synchrotron radiation facilities, which nowadays develop well along with other extreme environments (temperature, applied magnetic fields) [1].

In this report, we are going to sum up the new magnetic effects initiated by pressure and observed experimentally. Inevitable correlations of the magnetic state with the crystal structure, electronic and transport properties will be discussed. The most interesting pressure-effects observed in many crystals were associated with transitions from the magnetic to the nonmagnetic state (magnetic collapse), which were implemented by the spin crossover in $3d$ ions transiting from the high-spin (HS) to the low-spin (LS) state. In many (but not in all) cases the spin HS-LS crossover is accompanied by the structural phase transitions and some crystals transform from the dielectric to the semiconducting or metallic state. For Mott-Hubbard insulators, these effects can be explained by the suppression of strong $d-d$ electronic correlations, in addition, a new mechanism of insulator-metal transition (IMT) has been suggested involving the spin dependence of the effective Hubbard parameter U_{eff} .

In addition to materials science, the high-pressure magnetic properties of iron and minerals are extremely important for the geophysics of the Earth and planetary science. The HS-LS transition can dramatically alter the physical and chemical properties of the minerals most common in the lower mantle of the Earth. For example, the quantum critical point (with a zero value of the HS-LS spin gap) observed at low temperature, and the coexisting HS and LS states at high temperatures result in unexpected new magnetic properties of minerals that occur even in the lower mantle at depths of 1300 - 1900 km and high temperatures of 2000-3600 K. These effects, observed experimentally along with the predicted metallic state arising under these P - T conditions, open up a new concept in the advancement of geophysical science.

Superconductivity and magnetism are considered as mutually competing phenomena, and the recent discovery of iron-based superconductors has accelerated the studies of these materials at high pressures. In this report, several recent results will be given and discussed. Meanwhile, high temperature superconductivity remains one of the main challenges of condensed matter physics and chemistry. Now the main task is to find and explore new HTSCs based on hydride materials, in which the theory predicts very high values of T_C close to room temperature. In addition, new HTSC compounds with unusual stoichiometry, such as CaH_6 , LiH_8 , SiH_8 etc. can be obtained only at high pressures. Recently, a superconducting state with a record onset temperature of about 200 K was discovered in hydrogen sulfide H_2S compressed at pressure of 150 GPa. A new method for study the magnetic parameters of superconducting samples at ultrahigh pressures is suggested.

Supports by RSF grant # 16-12-10464, by RFBR grant #17-02-00766, by Russian Ministry of Science and Education contract # 14.616.21.0068 and by the RAS program "Strongly correlated electron systems" are acknowledged.

[1] G. Shen and H.K. Mao, *Rep. Prog. Phys.* **80** (2017) 016101.

5 July

Wednesday

11:30-13:30

oral session

5OR-A

**“Spintronics and
Magnetotransport”**

5OR-A-1

MICROSCOPIC THEORY OF MAGNETIZATION DYNAMICS IN RASHBA SYSTEMS

Ado I.A.¹, Titov M.^{1,2}

¹ Radboud University, Nijmegen, the Netherlands

² ITMO University, St. Petersburg, Russia

titov@science.ru.nl

Microscopic theory is developed to derive the Landau-Livshitz-Gilbert equation in the presence of electric currents and magnetic textures. The proposed theory completely avoids the concept of spin currents.

We apply the theory to a generic model of two dimensional Rashba ferromagnet and demonstrate that spin-transfer torques and Gilbert damping terms are naturally split into in-plane and out-of-plane components that become essentially different in magnitude when spin-orbit strength is increased (see Fig. 1). Such a splitting leads to different magnetization dynamics for in-the-plane and out-of-the plane magnetic domains.

For a generic Rashba s-d like model we derive the Landau-Livshitz-Gilbert equation on the local magnetization $M = M_{\perp} + M_{\parallel}$ in the following form

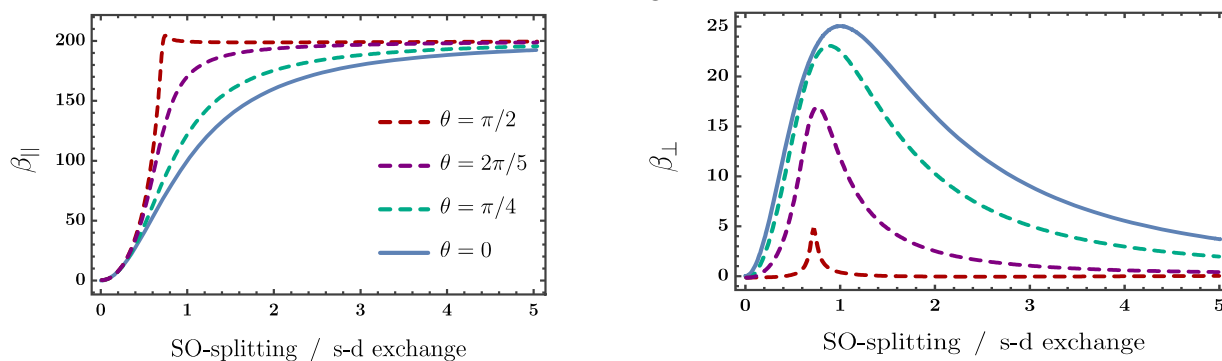
$$\frac{\partial M}{\partial t} = \gamma \mathbf{H}_{eff} \times M + \alpha_{\parallel} M \times \frac{\partial M_{\parallel}}{\partial t} + \alpha_{\perp} M \times \frac{\partial M_{\perp}}{\partial t} + \mathbf{T}_{SOT} + \mathbf{T}_{STT}$$

where the vector M_{\parallel} refers to the in-the-plane component of the magnetization. Our theory predicts that the leading contributions to spin-orbit and spin-transfer torques have the form

$$\mathbf{T}_{STT} = -\beta_{\parallel} M \times (\mathbf{J} \cdot \nabla) M_{\parallel} - \beta_{\perp} M \times (\mathbf{J} \cdot \nabla) M_{\perp} \quad \mathbf{T}_{SOT} = a M \times (z \times \mathbf{J})$$

where \mathbf{J} is the electric current. For a generic Rashba system with electrostatic disorder we find that $\beta_{\perp} \propto \alpha_{\perp}$ and $\beta_{\parallel} \propto \alpha_{\parallel}$ also depend on $(M_{\perp}/M)^2 = \cos^2 \theta$ while the coefficient a is an universal constant. We demonstrate that in-plane and out-of-plane beta torques differ by orders of magnitude for sufficiently strong spin-orbit interaction.

Fig. 1 In-plane and out-of-plane beta torques with increasing spin-orbit strength in 2D Rashba ferromagnet



Finally our theory is applied to derive LLG equation with electric current terms for the ferromagnet/topological insulator heterostructures and for the dynamics of Neel vector in Rashba anti-ferromagnets.

Support by NWO/FOM and ITMO Univeristy is acknowledged.

[1] I.A. Ado, O.A. Tretiakov, M. Titov, *Phys. Rev. B* **95** (2017) 094401.

[2] I.A. Ado, I.A. Dmitriev, P.M. Ostrovsky, M. Titov, *Phys. Rev. Lett.* **117** (2016) 046601.

5OR-A-2

NON-LOCAL GILBERT DAMPING WITHIN THE TORQUE-TORQUE CORRELATION MODEL

Thonig D.¹, Kvashnin Y.¹, Pereiro M.¹, Eriksson O.¹

¹ Department of Physics and Astronomy, Uppsala University, Uppsala, Sweden
danny.thonig@physics.uu.se

An essential property of magnetic devices is the relaxation rate in magnetic switching which depends strongly on the damping in the magnetisation dynamics. It was recently measured that damping depends on the magnetic texture and, consequently, is a non-local quantity [1]. The damping enters the Landau-Lifshitz-Gilbert equation as the phenomenological Gilbert damping parameter α , that doesn't account for non-locality. Efforts were spent recently to obtain Gilbert damping from first principles [2,3] for magnons of wave vector q [4]. But to the best of our knowledge, there is no report about real space non-local Gilbert damping α_{ij} .

We deduce the real space Gilbert damping tensor from the breathing band model [5] and apply it in the framework of a renormalised Green function tight-binding approach. Slater-Koster parameters were obtained by genetic-algorithm optimisation with respect to first-principles results. Magnetic as well as structural disorder are treated by the coherent potential approximation. Our model studies with the tight binding approach are corroborated with first principles simulations based on the full-potential linear muffin-tin orbitals code "RSPT".

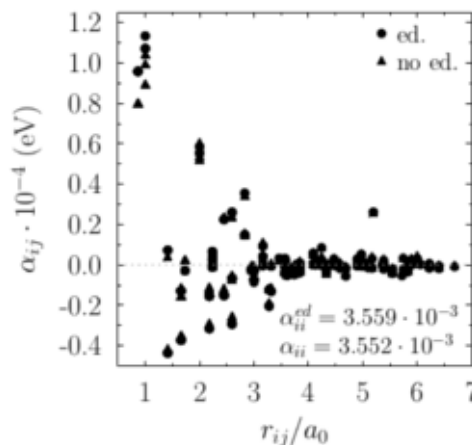


Fig. 1. Non-local real space Gilbert damping in bcc Fe with (circles) and without (triangles) intraband corrections. Lines are edit to guid the eye.

Our approach is applied to the bulk itinerant magnets and predicts negative off-site Gilbert damping contributions. Supported by atomistic magnetisation dynamics simulations we reveal the importance of the non-local Gilbert damping in atomistic magnetisation dynamics. Our model give a deeper understanding in the dynamics of magnetic moments and dissipation processes for magnetic textures.

- [1] T. Weindler, et al., *Phys. Rev. Lett.*, **113** (2014) 237204.
- [2] S. Mankovsky, et al., *Phys. Rev. B*, **87** (2013) 014430.
- [3] D. Thonig, et al., *New Journal of Physics*, **16** (2014) 013032.
- [4] K. Gilmore, et al., *Phys. Rev. B*, **79** (2009) 132407.
- [5] V. Kamborský, *Cz. Journal of Physics B*, **34** (1984) 1111.

5OR-A-3

STABILITY PHASE DIAGRAM OF PERPENDICULAR MAGNETIC TUNNEL JUNCTION IN NON-COLLINEAR GEOMETRY

Strelkov N.^{1,2,3,4}, *Timopheev A.*^{1,2,3}, *Sousa R.C.*^{1,2,3}, *Chshiev M.*^{1,2,3}, *Buda-Prejbeanu L.D.*^{1,2,3},
Dieny B.^{1,2,3}

¹ Univ. Grenoble Alpes, F-38000 Grenoble, France

² CEA, INAC-SPINTEC, F-38000 Grenoble, France

³ CNRS, SPINTEC, F-38000 Grenoble, France

⁴ Department of Physics, Moscow Lomonosov State University, Moscow 119991, Russia
nik@magn.ru

The stability field-voltage diagrams (VH diagrams) are useful tools to study the mechanisms and the properties of STT induced magnetization reversal in magnetic tunnel junctions (MTJ). However, these diagrams are usually measured in a collinear geometry [1, 2]. Non-collinear configuration of magnetic electrodes influences the switching characteristics of the storage layer and its field dependence defines the phase boundaries of the stability diagram.

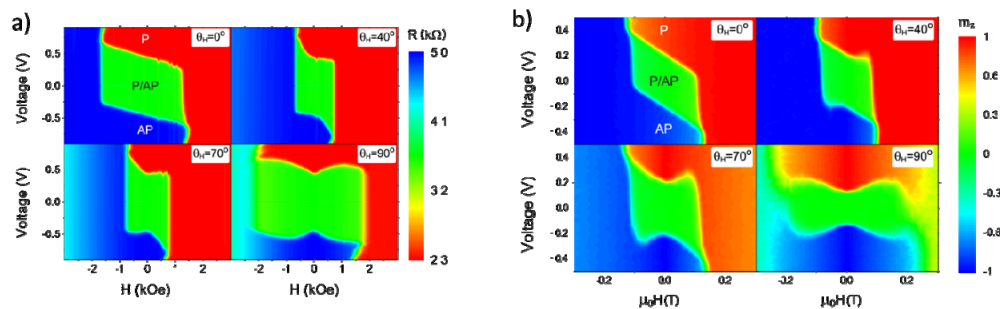


Fig1. a) Experimental stability VH diagrams of 80 nm diameter MTJ at room temperature with the field applied at 0° , 40° , 70° and 90° away from the z-axis. Voltage pulse length was 100 ns. The color scale is related to the resistance of MTJ. (b) Numerical stability diagrams at 300 K of 50 nm diameter dot using 100 events per point. Simulation parameters: $K_1=778$ kJ/m³, $K_2=-150$ kJ/m³, $M_s=10^6$ A/m, $N_{xx}=N_{yy}=0.04$, $N_{zz}=0.92$, $\alpha=0.01$, $\alpha_{||}=6 \cdot 10^{-3}$ T/V, $\alpha_{\perp}=10^{-3}$ T/V².

In this study systematic experimental measurements were performed on MgO-based magnetic tunnel junctions with various diameters ranging from 50 nm to 150 nm. We found that the shape of the stability field-voltage diagrams depends strongly on the direction of the applied field (Fig.1a). A good agreement between experiments and simulations (Fig.1b) is recovered when a second order anisotropy contribution is introduced in the model [3, 4, 5]. Furthermore, performing the stability analysis in linear approximation allowed us to analytically extract the critical switching voltage at zero temperature for in-plane field. This study indicates that in the non-collinear geometry investigations are suitable to detect the presence of second order term in the anisotropy.

[1] A.A. Timopheev, R. Sousa, M. Chshiev, L.D. Buda-Prejbeanu and B. Dieny, *Phys. Rev. B*, **92** (2015) 104430.

[2] L. Cuchet, B. Rodmacq, S. Auffret, R.C. Sousa, I. L. Prejbeanu and B. Dieny, *Scientific Reports*, **6** (2016) 21246.

[3] A.A. Timopheev, R. Sousa, M. Chshiev, H. T. Nguyen and B. Dieny, *Scientific Reports*, **6** (2016) 26877.

[4] J.M. Shaw, H.T. Nembach, M. Weiler, T.J. Silva, M. Schoen, J.Z. Sun and D.C. Worledge, *IEEE Magn. Lett.*, **6** (2015) 1.

[5] J.Z. Sun, *Phys. Rev. B*, **91** (2015) 174429.

5OR-A-4

MICROMAGNETIC DYNAMICS OF VORTEX SPIN-TORQUE DIODE: THE IMPACT OF DC BIAS

Skirdkov P.N.^{1,2,3}, Zvezdin K.A.^{1,2,3}, Zvezdin A.K.^{1,2,3}

¹ Moscow Institute of Physics and Technology, 141700 Dolgoprudny, Russia

² Russian Quantum Center, 143025 Skolkovo, Moscow Region, Russia

³ A.M. Prokhorov General Physics Institute, RAS, 119991 Moscow, Russia

petr.skirdkov@phystech.edu

The three layer magnetic tunnel junction (MTJ) structures attract considerable attention recent times. This is primarily due to the possibility of alternating signal generation under the action of direct current. At the same time there is the opposite effect: the application of radio-frequency (RF) alternating current to the MTJ can lead to appearance of d.c. voltage signal. This phenomenon of rectification of radio-frequency referred to as the spin-torque diode effect was firstly experimentally observed by Tulapurkar et al [1]. However, the RF detection sensitivity in this first work (about 1.4 mV/mW), was more than three orders lower than in case of semiconductor Schottky diode detectors (up to 3800 mV/mW). Later it was shown [2] that the sensitivity can be increased up to 10000 mV/mW through the optimization of tunnel junction. The further researches demonstrate that the application of a DC bias current to a MTJ affords a high RF detection sensitivity of 12000 mV/mW at room temperature [3]. In 2016 work [4], also by using DC bias, declares the highest sensitivity up today 75400 mV/mW. It is important that this result was obtained at room temperature, in the absence of external magnetic field.

The next step in spin-torque diode development is the vortex spin-torque diode in analogy with STNO. In this case the free layer of MTJ has the vortex magnetization distribution. In work [5] it was shown that due to resonant vortex core expulsion from the free layer, caused by simultaneous action of both AC and DC, the sensitivity can be achieved up to 40000 mV/mW. It is worth noting that this sensitivity was obtained for the sample with the value of TMR 8.5 %, while in the papers [3,4] value of TMR was more than 80 %. Since the sensitivity in a first approximation proportional to the TMR, we can say that the vortex spin diode is the best candidate for rectifying the AC signal. Nevertheless, the dynamics of the vortex diode's magnetization and the impact of DC bias on it remain unclear.

In the current work we proposed vortex spin-torque diode represented by MTJ with tilted polarizer and vortex magnetization distribution in the free layer. We analyse vortex dynamics and corresponding spin-torque diode effect using micromagnetic modelling. Also we consider vortex excitation by simultaneous action of RF current and DC bias, which is lower than critical current of vortex excitation. It revealed that, although the used DC current value is not enough for vortex excitation, it can improve the efficiency of RF vortex excitation (and therefore sensitivity) in several times. The analytical description of this phenomenon was proposed. The case of vortex expulsion is also considered.

The grant RSF No.16-19-00181 is acknowledged.

[1] A. Tulapurkar et al., *Nature*, **438** (2005) 339.

[2] C. Wang et al., *Journal of Applied Physics*, **106** (2009) 053905.

[3] S. Miwa et al., *Nature Materials*, **13** (2014), 50.

[4] B. Fang et al., *Nature Communications*, **7** (2016) 11259.

[5] A. Jenkins et al., *Nature Nanotechnology*, **11** (2016) 360-364.

5OR-A-5

SPIN PUMPING VIA BULK ACOUSTIC WAVE MODES IN COMPOSITE RESONATOR WITH YIG/PT BILAYER

Polzikova N.I., Alekseev S.G., Pyataikin I.I., Kotelyanskii I.M., Luzanov V.A., Raevskiy A.O.
Kotel'nikov Institute of Radio Engineering and Electronics of Russian Academy of Sciences,
Moscow, Russia
polz@cplire.ru

Generation of spin currents in a ferromagnet/paramagnet junction caused by acoustically driven magnetization precession, acoustic spin pumping (ASP), was proposed recently. ASP in different spintronic ME structures both under magnetoelastic resonance (MER) and the off-resonance conditions was demonstrated. In particular, considerable attention was drawn to using surface acoustic waves for magnetic dynamics resonance excitation and ASP. More recently, we proposed ASP via MER excitation in a magnetoelectric composite high overtone bulk acoustic wave (BAW) resonator (HBAR) formed by Al-ZnO-Al-GGG-YIG-Pt structure [1].

The schematics of our experimental structure is shown in Fig. 1. Magnetic dynamics excited by transversal BAW modes induces pure spin current j_s from YIG film into a thin Pt layer. It was shown that the dc voltage U_{ISHE} measured on Pt stripe is created by ASP and spin (j_s) - to charge (j_c) current conversion due to inverse spin-Hall effect (ISHE) in platinum.

Here, we present some important features of ASP in such a system. The measured voltage U_{ISHE} and HBAR frequency shift Δf_n dependences on magnetic field H and frequency f have a resonant character and correlate with each other. However, there is some discrepancy between the values of HBAR resonant frequency f_n for a given magnetic field and the frequency at which the maximum dc voltage is observed. We attribute this to the fact that under MER condition, HBAR frequency f_n is determined both by a change in the boundary conditions and by a change in the phase shift (mainly) in the volume of YIG film, while the magnitude of the injected spin current depends on the magnetization precession amplitude at the YIG/Pt interface. The influence of magnetoelastic anisotropy and the mutual orientation of the transverse BAW polarization, the bias magnetic field and the Pt strip axis on the maximal value of HBAR frequency shift Δf_n and ISHE voltage U_{ISHE} is studied in detail. The observed deviation from sinusoidal behavior of $U_{\text{ISHE}}(\theta)$ and $\Delta f_n(\theta)$ is explained in the model taking into account the difference in the efficiency of magnetic precession excitation by BAW with the components of elastic displacement that are in parallel and perpendicular to the bias field. To achieve the maximal value of U_{ISHE} , the piezoelectric axis \bar{c} projection should be oriented perpendicular to the axis of the Pt strip and parallel to the crystallographic axis $\langle 1\bar{1}0 \rangle$ of YIG.

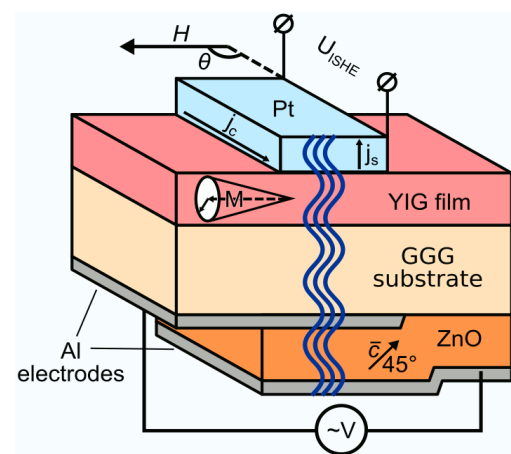


Fig. 1. Schematics of the spintronic composite BAW resonator structure.

Support by RFBR grants 16-07-01210 and 17-07-01498 is acknowledged.

[1] N.I. Polzikova, S.G. Alekseev, I.I. Pyataikin, I.M. Kotelyanskii, V.A. Luzanov, A.P. Orlov, *AIP Adv.* **6** (2016) 56306.

5 July

Wednesday

11:30-13:00

oral session

5TL-B

5RP-B

5OR-B

**“Soft and Hard
Magnetic Materials”**

5TL-B-1

SOFT MAGNETIC MATERIALS FOR SENSOR APPLICATIONS IN A HIGH FREQUENCY RANGE

Kurlyandskaya G.V.^{1,2}, *Shcherbinin S.V.*^{2,3}, *Volchkov S.O.*², *Bhagat S.M.*⁴, *Calle E.*⁵, *Pérez R.*⁵,
Vazquez M.^{2,5}

¹ Universidad del País Vasco UPV-EHU, Depto Electricidad y Electrónica, Leioa, 48940, Spain

² Ural Federal University, Mira 19, Ekaterinburg, 620000, Russia

³ Institute of Electrophysics, Amundsen str., 106, Ekaterinburg, 620016, Russia

⁴ University of Maryland, Dept. of Physics, College Park, MD 20742, USA

⁵ Instituto de Ciencia de Materiales, CSIC, Madrid, 28049, Spain

galina@we.lc.ehu.es

During the past two decades soft magnetic materials for sensor applications have been the subject of an active research. Although their fabrication follows well developed methods there were advances and improvements in the existing techniques [1]. The increase in the number of materials available for research and extending the list of applications requires a parallel optimization of the methods of characterization. Microwave non-resonant absorption in low magnetic fields was proposed for the characterization of the axial magnetization process in amorphous glass covered microwires, ribbons and electroplated wires [2-4]. This regime of absorption for which sample is not saturated is of special interest because it is exactly the region of high GMI effect and promising for technological applications. Similarly to the case of magnetic nanostructures, characterization of the same parameter using different techniques becomes increasingly routine. In this work we describe our experience in the comparative analysis of magnetic properties, ferromagnetic resonance (FMR), non-resonant low field microwave absorption and giant magnetoimpedance (GMI) features of in-water solidified $(\text{Co}_{0.94}\text{Fe}_{0.06})_{72.5}\text{Si}_{12.5}\text{B}_{15}$ amorphous and $\text{CuBe}/\text{Fe}_{19}\text{Co}_{17}\text{Ni}_{64}$ electroplated wires. The longitudinal hysteresis loops for the field applied parallel to the wire axis were measured by vibrating sample magnetometer. Microwave studies were conducted using specially designed installation on the basis of Rohde & Schwarz ZVA-67 Vector Network Analyzer (VNA) with possibility of application of the magnetic field in the -20 to + 20 kOe range (S_{11} reflection coefficient was measured). For VNA measurements test fixtures based on “microstripe” line and SMA-holder were manufactured for 0.1-14 GHz range. FMR was also measured using classic cavity perturbation technique [2]. The analysis of the results allows us to observe evolution of the intensity of two absorption peaks and conclude the corresponding to non-resonant absorption and FMR). The obtained results for the broad band of FMR fields in both cases were in good agreement with Kittel's fit and data measured by the classic cavity perturbation technique.

The Laboratory of Magnetic Sensors acknowledges the support of the Development Program of URFU in creation of microwave measurement installation and licensed COMSOL software cluster for modelization. The work was supported by ELKARTEK KK-2016/00030 of the Basque Government and 3.6121.2017 of Russian Federation grants. We thank E.V. Golubeva and A. A. Chlenova for special support.

[1] F. E. Atalay, H. Kaya, S. Atalay, *Physica B: Cond. Matter.*, **371** (2006) 327.

[2] H. Garcia-Miquel, S.M. Bhagat, S.E. Lofland et. al., *J. Appl. Phys.* **94** (2003) 1868.

[3] S. E. Lofland, S. M. Bhagat, M. Domínguez, et al., *J. Appl. Phys.* **85** (1999) 4442.

[4] S. E. Lofland, H. García-Miquel, M. Vazquez, S. M. Bhagat, *J. Appl. Phys.* **92** (2002) 2058.

5OR-B-2

INFLUENCE OF REVERSIBLE ADSORPTION ON MAGNETIC SUSCEPTIBILITY OF IRON BORATE

Zubov V.E.¹, Kudakov A.D.¹, Levshin N.L.¹, Belov I.A.¹, Strugatsky M.B.²

¹ Department of Physics, Lomonosov Moscow State University, GSP-1, Leninskie Gory, Moscow, 119991, Russian Federation

² Physico - technical Institute V.I. Vernadsky Crimean Federal University, 4 Vernadskogo Prospekt, Simferopol, 295007, Republic of Crimea, Russian Federation
zubov@magn.ru

The adsorption of water molecules occurs according to the mechanism of hydrogen bond formation and the magnitude of the binding energy with the surface of solids refers to an intermediate type between chemical and very weak physical adsorption. At room temperature, the adsorption of water molecules is reversible. Earlier, we discovered the effect of reversible adsorption of water molecules on the dynamics of domain walls on the surface of filamentary single crystals of iron. The effect of weak adsorption on the initial magnetic susceptibility of an amorphous ferromagnetics due to the displacement of domain walls was observed. The effect of reversible adsorption on the domain structure of ferrite garnet was found. In this paper we investigate the effect of the adsorption of water molecules on the magnetic properties of one more class of magnetic materials, antiferromagnetics with weak ferromagnetism. Iron borate (FeBO_3) was chosen as a representative of weak ferromagnetics.

The magnetic properties of iron borate were studied at room temperature using the Faraday effect. The samples were thin hexahedral plates of iron borate parallel to the basal plane of the crystal. The thickness of the plates is $\sim 30 \mu\text{m}$, the linear dimensions are several millimetres. Since in the iron borate the magnetization lies in the basal plane of the samples, to observe the Faraday effect, the angle of incidence of light on the sample must be nonzero. In our case, it was 45° . Observations of the domain structure with a microscope showed that some domain walls intersected and moved independently of each other. This concludes that such walls are perpendicular to the basal plane and are located in different layers. On the surface of the sample under dark-field illumination, parallel growth bands were observed, located at a distance of $10\text{-}20 \mu\text{m}$ from each other. When studying domain walls oscillations in an alternating magnetic field, the sample was placed in an optical vacuum cell and illuminated by a parallel beam of light. We measured the change in the magnitude of the Faraday effect in an alternating magnetic field applied to the sample. Faraday effect is proportional to the projection of the magnetization of the sample on the direction of light propagation. A reversible change in the quasistatic magnetic susceptibility of the samples during the adsorption of water molecules was observed. The change in the magnetic susceptibility in saturated water vapour was about 30%. The observed effect is reversible. The effect is explained by the appearance of uniaxial surface magnetic anisotropy in the basal plane induced by the adsorption of water molecules.

Adsorption, proceeding along the mechanism of the formation of hydrogen bonds, leads to the appearance of a compressive stress of the surface. Since iron borate crystals are characterized by considerable magnetoelastic energy, the compression stress leads to the appearance of induced magnetic anisotropy. The orientation of the easy axis of magnetic anisotropy, induced by the adsorption, is related to the orientation of the growth bands on the surface of the crystal. Adsorption occurs mainly on surface defects, which are growth bands.

5RP-B-3

Co₃(Al,W) INTERMETALLIC COMPOUND: FROM SOFT TO HARD FERROMAGNETS

Kazantseva N.¹, Davidov D.¹, Shishkin D.¹, Terentev P.¹, Vinogradova N.¹, Kabanov Yu.²

¹ Institute of Metal Physics Ural Division of RAS, Ekaterinburg, Russia

² Institute of Solid State Physics, RAS, Chernogolovka, Russia

kazantseva-11@mail.ru

Crystal structure and magnetic properties of Co_{75+x}Al_yW_x alloys, where x was changed from 4.6 to 12.6 and y was between 8 and 9, were investigated. The phase and chemical compositions were determined by energy dispersive X-ray analysis and by the transmission electron microscope. A vibrating sample magnetometer and the SQUID magnetometer were used for the magnetic studies.

The Co_{75+x}Al_yW_x alloys are found to be heat-resistant ferromagnetic composite materials that consist of cobalt solid solution matrix and Co₃(Al,W) intermetallic compound with cubic L12 structure. The Curie temperature T_C , which was determined through ac susceptibility, also depends on tungsten content and increases from 1178 to 1184 K. The coercive force H_c of the Co_{75+x}Al_yW_x is found to increase from 1 Oe to 500 Oe with the increase in tungsten content from 4.6 to 12.6, respectively while saturation magnetization falls down from 86 to 12 emu/g (Fig.1). Ferromagnetic Co_{78.4}Al₉W_{12.6} was found to have a stripe magnetic domain structure with the domain thickness of 5-7 μm . The effect of deformation on magnetic properties of the materials under study was also investigated.

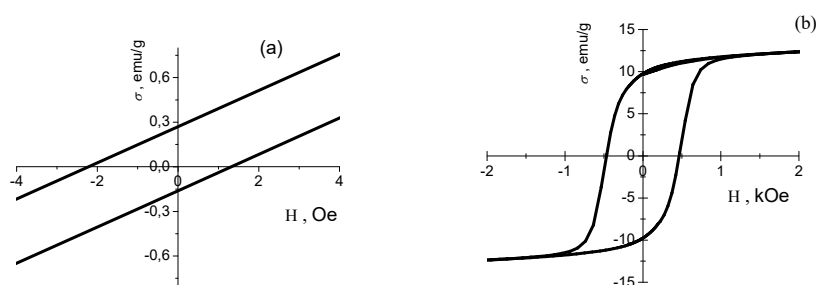


Fig.1. Room-temperature hysteresis loops for the ferromagnetic materials:
a- Co_{86.4}Al₉W_{4.5}; b- Co_{79.2}Al_{8.2}W_{12.6}

This work was supported by the Russian Scientific Foundation, project no. 15-12-00001.

5OR-B-4

MAGNETIC PHASE DIAGRAMS OF Gd-H, Tb-H, Dy-H SYSTEMS

Chzhan V.B.¹, Tereshina I.S.², Burkhanov G.S.¹, Politova G.A.¹, Drulis H.³

¹ Baikov Institute of Metallurgy and Materials Science RAS, Moscow, Russia

² Lomonosov Moscow State University, Faculty of Physics, Moscow, Russia

³ Institute of Low Temperature and Structural Research, Wroclaw, Poland

Irina_tereshina@mail.ru

The aim of this work is to study the impact of structural inhomogeneities and gaseous impurities on the temperature of magnetic phase transitions of high purity rare-earth metals Gd, Tb and Dy. On the base of the obtained results the magnetic phases diagrams have been constructed.

Commercial Gd, Tb and Dy were purified by vacuum distillation. High purity rare earth metals contain low concentrations of gaseous elements (10^{-2} - 10^{-3} wt %). The metal purity was 99.96 wt %. To obtain a hydrogen solid-solution phase in a metal sample the Sieverts-type apparatus was used, and pure (impurities content $< 10^{-3}$ - 10^{-4} vol. %) hydrogen gas under pressures up to 0.1 MPa. Magnetic properties were studied over wide temperature range with SQUID magnetometr. Thermomagnetic analysis was carried out in a magnetic field of 0.02 T.

X-ray diffraction analysis shows that Gd, Tb and Dy metals, as well as the prepared hydrogen solid solutions α -RH_x (x = 0.1, 0.2) were a single-phase samples with hexagonal close-packed crystal structure (space group P6₃ / mcc). The introduction of hydrogen into the metal leads to an increase of the crystal lattice parameters and the unit cell volume (about ~ 1% for the α -GdH_{0.2} solid solution, for instance) [1]. However, the α -GdH_x sample with x=0.22 already contains an admixture of the GdH₂ phase. For hydrogen content higher than x > 0.2 the obtained samples are two phases. In addition to the main α -RH_x solid solution phase a cubic structure phase of β -RH₂ is observed. It was found that an increase of the hydrogen concentration up to x = 0.5-0.6 in TbH_x and DyH_x samples leads to an increase of the unit cell volume by ~ 0.2%. For higher hydrogen concentration the cell volume remains practically unchanged.

It has been found that various magnetic phase transitions: "ferromagnet-paramagnet" (FM-PM), "ferromagnet-antiferromagnet" (FM-AFM), "antiferromagnet-paramagnet" (AFM-PM) take place. It was established that the type of transitions does not change during hydrogenation. However, the temperature of the magnetic phase transitions exhibits different dependences versus the hydrogen content in the samples. Magnetic phase diagrams for all the studied samples were constructed and are illustrated in Fig.1.

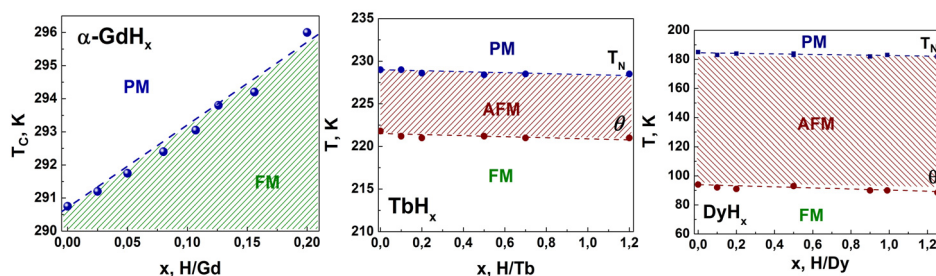


Fig. 1. Magnetic phase diagrams of Gd-H, Tb-H, Dy-H systems

The work is supported by RFBR within the research project 16-03-00612-a.

[1] G.S. Burkhanov, N.B. Kolchugina, E.A. Tereshina, I.S. Tereshina at al. *J. Appl. Phys. Lett.*, **104** (2014) 242402.

5OR-B-5

MAGNETIC DOMAIN STRUCTURE OF RE-3D INTERMETALLICS WITH EASY PLANE AND EASY CONE ANISOTROPY

Pastushenkov Yu.G.¹, Skokov K.P.², Lahova M.B.¹, Semenova E.M.¹, Denisov F.O.¹

¹Tver State University, 170100, Tver, Russia

²TU Darmstadt, 64287, Darmstadt, Germany

pastushenkov.yg@tversu.ru

The magnetic domain structure (DS) of intermetallic compounds RCO_5 , $\text{R}_2\text{Fe}_{14}\text{B}$, RFe_{11}Ti and some others (with R being a rare-earth metal) has been thoroughly investigated with regards to the anisotropy type easy axis as these materials are used as the basis for permanent magnets [1]. On the other hand, orientation phase transitions have been found in these compounds, which means that the anisotropy type in this region changes from the easy axis to the easy cone and easy plane. In recent years, there have been a lot of research on low-temperature permanent magnets and magnetocaloric materials. However, this requires a more detailed understanding of the DS transformation processes in the region of orientation phase transitions, and, thus, in the region corresponding to the anisotropy types easy cone and easy plane.

Despite growing research on easy-axial magnetics, less is known about the domain structure of magnetics with the easy cone and easy plane anisotropy types. Therefore, the goal of this study is to investigate the magnetic domain structure of intermetallic compounds of 4f-3d metals in the region corresponding to the anisotropy types easy cone and easy axis.

The DS investigation in the temperature region $10 < T < 300$ K was carried out using the magneto-optic Kerr effect and the methods described in [2]. The DS investigation in the temperature region $290 < T < 450$ K was carried out using the magnetic force microscopy method.

The DS in the MCA easy axis region was investigated in $\text{R}_2\text{Fe}_{14}\text{B}$, RFe_{11}Ti and RCO_5 compounds. The DS in the MCA easy plane region was investigated in $\text{R}_2\text{Fe}_{14}\text{B}$, RFe_{11}Ti and R_2Fe_{17} compounds. Furthermore, the domain structure transformation of a powder permanent magnet $\text{Nd}_{15}\text{Fe}_{77}\text{B}_8$ in the spin reorientation region was investigated.

Figure 1 shows the DS of a $\text{Nd}_2\text{Fe}_{14}\text{B}$ single crystal with the anisotropy type easy cone.

The new data received during the experiment on the magnetic domain structure of magnetics with the anisotropy types easy cone and easy plane helps to clarify the distribution of magnetization in these magnetics and better understand the magnetization processes in these compounds.

Support by the Ministry of Education and Science of Russian Federation is acknowledged.

[1] A. Hubert, R. Schäfer, *Springer*, (1998) 696.

[2] Yu.G.Pastushenkov, A.Forkl, H.Kronmueller, *J. Magn. Magn. Mater.*, **174** (1997) 278-288.

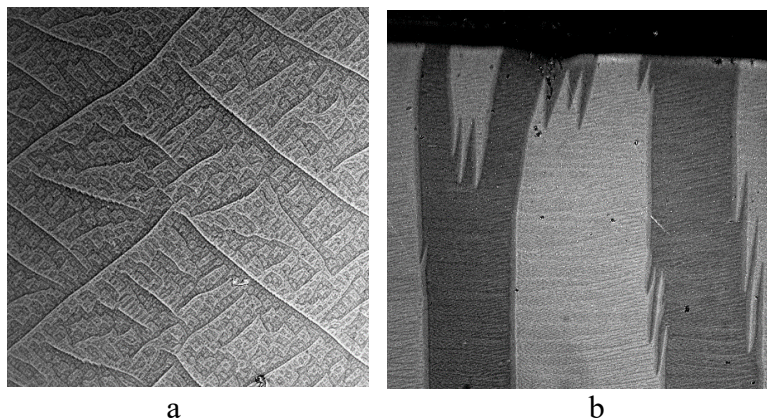


Fig. 1. Domain structure of the $\text{Nd}_2\text{Fe}_{14}\text{B}$ single crystal on the planes (001) (a) and (273) (b) in the MCA easy cone region. $T = 65$ K. 150 μm .

5 July

Wednesday

11:30-13:30

oral session

5TL-C

**“Magnetophotonics
and Ultrafast
Magnetism”**

5TL-C-1

ULTRAFAST MAGNETISM AND THZ SPINTRONICS

Münzenberg M.

Institute of Physics, Ernst-Moritz-Arndt-University Greifswald, Greifswald, Germany
muenzenberg@physik.uni-greifswald.de

Magnetization manipulation is an indispensable tool for both basic and applied research. I will discuss some of the knobs to tune dynamics at ultrafast time scales. I will show in my presentation an actual overview over actual achievements in the developing field of ultrafast magnetism and THz spintronics, with focus on those in which we were directly involved.

The dynamics of the spin response depends on the energy transfer from the laser excited electrons to the spins within the first femtoseconds. This determines the speed of the ultrafast demagnetization: if the electrons are driven to a strong excitation density, a second slower process is found, a signature of the intrinsic ferromagnetic electron correlations in a ferromagnet. A special material of interest for magnetic storage development is FePt. The electron temperature shoots to higher values above the Curie temperature, a precondition for all-optical writing using magnetic quenching [1,2]. Not only magnetic nanoparticles can be reversibly written. Also vortex, antivortex networks can be written in standard thin Fe films [3].

On the other side, due to the non-equilibrium electron distribution in layered nanoscale spintronic devices, also ultrafast spin currents are generated and contribute to the laser driven spin dynamics. Layers of a noble metals like Pt, Au or transition metals like W, Ta, Ru can convert ultrafast laser-driven spin currents via the ultrafast spin-Hall effect into a charge current burst [4]. This opens a way towards novel THz spintronic devices: optimizing thicknesses and layers, we can realize efficient metallic THz spintronic emitters of ultra-broadband terahertz radiation that can even compete with state-of-art photo-conductive switches THz emitters that are currently used for airport security [5]. In addition, spintronic THz emitters own a very broad frequency spectrum from 0.5-30 THz (Fig. 1). This sets the stage of first applications in the field of ultrafast magnetism.

[1] J. Mendil, P.C. Nieves, O. Chubykalo-Fesenko, J. Walowski, M. Münzenberg, T. Santos, S. Pisana, *Sci. Rep.* **4** (2014) 3980, R. John, et al. *arXiv:1606.08723*.

[2] J. Walowski and M. Münzenberg, *J. Appl. Phys.*, **120** (2016) 140901.

[3] T. Eggebrecht, M. Möller, J.G. Gatzmann, N. Rubiano da Silva, A. Feist, U. Martens, H. Ulrichs, M. Münzenberg, C. Ropers, S. Schäfer, *Phys. Rev. Lett.*, **118** (2017) 097203.

[4] T. Kampfrath, M. Battiato, P. Maldonado, G. Eilers, J. Nötzold, S. Mährlein, V. Zbarsky, F. Freimuth, Y. Mokrousov, S. Blügel, M. Wolf, I. Radu, P.M. Oppeneer, M. Münzenberg, *Nature Nanotech.*, **8** (2013) 256.

[5] T. Seifert, S. Jaiswal, U. Martens, J. Hannegan, L. Braun, P. Maldonado, F. Freimuth, A. Kronenberg, J. Henrizi, I. Radu, E. Beaurepaire, Y. Mokrousov, P.M. Oppeneer, M. Jourdan, G. Jakob, D. Turchinovich, L.M. Hayden, M. Wolf, M. Münzenberg, M. Kläui, T. Kampfrath, *Nature Photonics*, **10** (2016) 483–488.

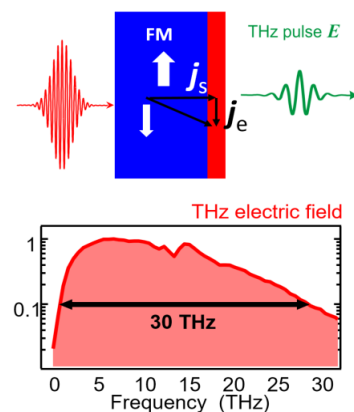


Fig. 1. Spintronic THz emitter based on ultrafast laser excited spin current bunches, driving the inverse spin Hall effect (ISHE) and subsequent THz emission.

5TL-C-2

MULTISCALE DYNAMICS OF HELICITY-DEPENDENT ALL-OPTICAL SWITCHING IN FERROMAGNETIC NANOSTRUCTURES

Medapalli R.¹, Afanasiev D.², Kim D.K.¹, Quessab Y.¹, Manna S.¹, Montoya S.A.¹, Kirilyuk A.², Rasing Th.², Kimel A.V.², Fullerton E.E.¹

¹CMRR, UCSD, La Jolla, CA92093-0401, USA

²Radboud University, IMM, Heyendaalseweg 135, 6525AJ Nijmegen, The Netherlands
rmedapalli@ucsd.edu

Understanding the helicity dependent all-optical switching (HD-AOS) [1-3] in high anisotropy magnetic systems is of fundamental interest for the optical manipulation of spins, especially, in ferromagnetic nanostructures [4]. The most important stages in a magnetic first order phase transition, e.g., magnetization reversal by an external stimulus, are the nucleation and growth processes of a reversed magnetic domain. Using time-resolved magneto-optical imaging we demonstrate the ability to trigger and control these stages, in a ferromagnetic multilayer, with a sequence of circularly polarized ultrashort laser pulses and reveal the mechanism of deterministic optical manipulation of spins. Our results show that the only degree of freedom to nucleate reversed magnetic domains is the energy per optical pulse, whereas the growth and the size of the reversed domain are precisely controllable by the helicity and the number of pump laser pulses, respectively, when the pulse width is optimized. Here, our results demonstrate a novel mechanism of helicity dependent all-optical switching (HD-AOS) in a ferromagnetic Co/Pt multilayer achieved by driving the domain wall displacement in the direction defined by the helicity of the pump light (see Fig.1).

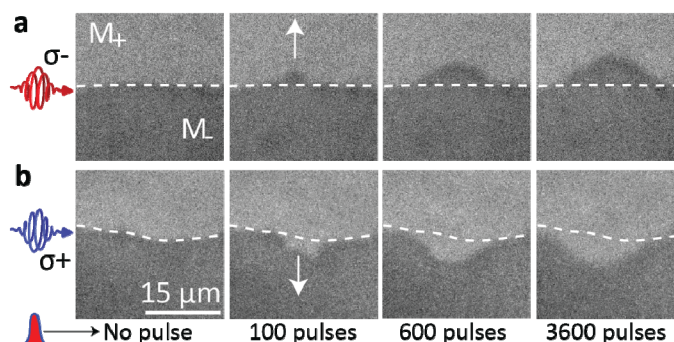


Fig.1 Magneto-optical images of laser-induced domain wall displacement at the region separating magnetization up (bright) and down (dark) domains, when subjected to the repetitive action of the left circularly polarized (σ^-) pump pulses. The repetition rate is 1 Hz. (b) Same as (a) but for the case of right circularly polarized (σ^+) pump pulse pulses.

[1] C.D. Stanciu *et al.*, *Physical Review Letters*, **99** (2007) 047601.

[2] A. Kirilyuk, A. V. Kimel, and Th. Rasing, *Rev. Mod. Phys.*, **82** (2010) 2731-2784.

[3] Mangin *et al.*, *Nat. Mater.*, **13** (2014) 286.

[4] Lambert *et al.*, *Science*, **345** (2014) 1337.

[5] R. Medapalli *et al.*, submitted.

5TL-C-3

MANIPULATING MAGNETIZATION WITH PULSES OF LIGHT*Eisebitt S.¹*¹ Max-Born-Institute, Berlin, Germany
eisebitt@mbi-berlin.de

Demagnetization and switching of suitable, magnetically ordered materials can be triggered with femtosecond light pulses. X-ray magnetic circular dichroism employed as a spectroscopy, or as a contrast mechanism in spatially resolving experiments in either reciprocal or real space can shed light on the underlying mechanisms in pump-probe experiments. I will introduce pump-probe x-ray holography as a technique allowing to follow magnetization dynamics on the <50 nm nanometer spatial scale with femtosecond resolution.[1] Results on demagnetization experiments where a lateral evolution of the magnetization can be observed in real time down to the femtosecond time scale will be presented. Near field localization, shaping and enhancement of infrared pump radiation is used to test the predictions of the concept of superdiffusive spin currents in the demagnetization process. [2,3,4] Optically induced switching is investigated in ferrimagnetic iron garnets, where we see evidence for a long-lived transient ferromagnetic state and start to obtain a picture of the switching dynamics in this superexchange-coupled system.

- [1] F. Büttner et al., *Nature Physics*, **11** (2015) 225.
- [2] B. Pfau et al., *Nature Comm.*, **3** (2012) 1100.
- [3] C. von Korff Schmising et al., *PRL*, **112** (2014) 217203.
- [4] D. Weder et al. (unpublished).
- [5] I. Radu et al. (unpublished).

5 July

Wednesday

11:30-13:00

oral session

5TL-D

5RP-D

**“Magnetism and
Superconductivity”**

5TL-D-1

SPECTROSCOPY OF CORRELATED ELECTRONIC STATES IN SINGLE CRYSTALS OF Cu_xTiSe_2

Karapetrov G.¹, Lioi D.B.¹, Schaller R.D.², Gosztola D.J.², Wiederrecht G.P.²

¹Department of Physics, Drexel University, Philadelphia, PA 19104, USA

²Center for Nanoscale Materials, Argonne National Laboratory, Argonne, Illinois 60439, US
goran@drexel.edu

TiSe_2 is a member of transition metal dichalcogenide family of layered van der Waals materials that has attracted significant interest due to the intricate mechanism that drives its transition from a semiconducting to a charge density wave (CDW) phase in the presence of excitonic condensate. Intercalation of TiSe_2 with copper donates electrons to the conduction band near the Fermi surface, producing a metallic phase at room temperature and a superconducting phase at low temperatures with highest superconducting critical temperature of 4.15K. The relationships between these phases are nontrivial, especially considering that both the CDW and superconducting phases rely on specific electronic and electron-phonon interactions.

We investigate the transient optical response of electronic states in Cu_xTiSe_2 as a function of temperature and copper doping from $x=0$ (semimetal and commensurate charge density wave phases) to $x=0.08$ (metallic and superconducting phases). We find that the cooperative driving mechanisms for the CDW, the excitonic insulator mechanism and the soft L_1^- phonon mode, decouple at $x=0.04$, where fluctuations of a quantum critical point were observed in the folded Se-4p band. We also demonstrate a loss of coherence in the A_{1g} phonon signal with increased copper intercalation of the parent lattice, indicating a loss of long-range lattice order. These findings provide compelling evidence that TiSe_2 undergoes a quantum phase transition upon Cu intercalation from a state of commensurate charge order without superconductivity to a state with a different symmetry in which new charge order coexists with the superconducting phase.

Superconductivity in TiSe_2 is very intriguing by itself as it appears with copper or palladium intercalation or under pressure in the intrinsic system. We will discuss the results obtained in Cu_xTiSe_2 system and the conclusions drawn from complex set of STM/STS and thermodynamic bulk measurements on single crystals.

We would like to acknowledge the support by the National Science Foundation under Grant No. ECCS-1408151. D.B.L. acknowledges support by Drexel Areas of Research Excellence (DARE) initiative. The use of the Center for Nanoscale Materials, an Office of Science user facility, was supported by the U.S. Department of Energy, Office of Science, Office of Basic Energy Sciences, under Contract No. DE-AC02-06CH11357.

[1] Lioi, D. B., Gosztola, D. J., Wiederrecht, G. P., & Karapetrov, G. "Photon-induced selenium migration in TiSe_2 " *App. Phys. Lett.* **110** (2017) 08190.

[2] Lioi, D. B., R. D. Schaller, G. P. Wiederrecht, and G. Karapetrov. "Ultrafast Dynamics of the Charge Density Wave State in Layered Cu_xTiSe_2 ", arXiv:1612.01838

5TL-D-2

**SCANNING TUNNELING SPECTROSCOPY AS A PROBE OF MULTI-Q
MAGNETIC STATES OF ITINERANT MAGNETS***Eremin I.¹, Gastiasoro M.N.², Fernandes R.M.³, Andersen B.M.²*¹ Institut für Theoretische Physik III, Ruhr-Universität Bochum, 44801 Bochum, Germany² Niels Bohr Institute, University of Copenhagen, Universitetsparken 5, DK-2100 Copenhagen, Denmark³ School of Physics and Astronomy, University of Minnesota, Minneapolis, Minnesota 55455, USA
Ilya.Eremin@rub.de

The combination of electronic correlations and Fermi surfaces with multiple nesting vectors can lead to the appearance of complex multi-Q magnetic ground states, hosting unusual states such as chiral density waves and quantum Hall insulators. Distinguishing single-Q and multi-Q magnetic phases is however a notoriously difficult experimental problem. Here we propose theoretically that the local density of states (LDOS) near a magnetic impurity, whose orientation may be controlled by an external magnetic field, can be used to map out the detailed magnetic configuration of an itinerant system and distinguish unambiguously between single-Q and multi-Q phases. We demonstrate this concept by computing and contrasting the LDOS near a magnetic impurity embedded in three different magnetic ground states relevant to iron-based superconductors—one single-Q and two double-Q phases. Our results open a promising avenue to investigate the complex magnetic configurations in itinerant systems via standard scanning tunnelling spectroscopy, without requiring spin-resolved capability.

[1] Maria N. Gastiasoro, Ilya Eremin, Rafael M. Fernandes, Brian M. Andersen, *Nature Commun.*, **8** (2017) 14317.

[2] P.J. Hirschfeld, D. Altenfeld, I. Eremin, I.I. Mazin, *Phys. Rev. B*, **92** (2015) 184513 [Editor's suggestion].

5RP-D-3

HARD SUPERCONDUCTING GAP in INDIUM GALLIUM ARSENIDE QUANTUM WELLS

Delfanazari K.^{1,2}, Puddy R.K.¹, Ma P.¹, Yi T.¹, Cao M.¹, Gul Y.³, Farrer I.^{1,4}, Ritchie D.A.¹, Joyce H.J.², Kelly M.J.¹, Smith C.G.¹

¹ Department of Physics, Cavendish Laboratory, University of Cambridge, Cambridge CB3 0HE, UK

² Centre for Advanced Photonics and Electronics, Electrical Engineering Division, University of Cambridge, Cambridge CB3 0FA, UK

³ Department of Electronic and Electrical Engineering, University College London, London WC1E 7JE, UK

⁴ Department of Electronic and Electrical Engineering, University of Sheffield, Mappin Street, Sheffield, S1 3JD, UK

kd398@cam.ac.uk

A superconducting hardgap in hybrid superconductor-semiconductor devices has been found to be necessary in order to access topological superconductivity that hosts Majorana modes (non-Abelian excitation). This requires the formation of homogeneous and barrier-free interfaces between the superconductor and semiconductor which is very challenging to achieve for most material systems. The earlier reports on measurements of a hard gap in such systems are mostly based on indium arsenide (InAs) in a two-dimensional electron gas (2DEG) formed in a quantum well in a heterostructure or in a one-dimensional nanowire. This involved the in situ deposition of Al on InAs in an MBE chamber after the semiconductor growth has been completed.

Here, we report a new platform for topological superconductivity based on hybrid Nb-In_{0.75}Ga_{0.25}As/ In_{0.75}Al_{0.25}As/ GaAs-Nb that results in hard superconducting gap detection in symmetric, planar and ballistic Josephson junctions. We show that with careful etching, sputtered Nb films can make high-quality and transparent contacts to an In_{0.75}Ga_{0.25}As quantum well and we discuss the cryogenic measurements of these Andreev devices as a function of temperature and magnetic field. We demonstrate that proximity induced superconductivity in the In_{0.75}Ga_{0.25}As quantum well 2DEG results in detection of a hard gap in 75% of our devices with critical current values of up to 0.2 μ A and transmission probabilities of 0.96. Our results together with the large g -factor and Rashba spin-orbit coupling in In_{0.75}Ga_{0.25}As quantum wells, which indeed can be tuned by the indium composition, suggest that the Nb-In_{0.75}Ga_{0.25}As/ In_{0.75}Al_{0.25}As/ GaAs-Nb system could be an excellent candidate to achieve topological phase and to realise hybrid topological superconducting devices.

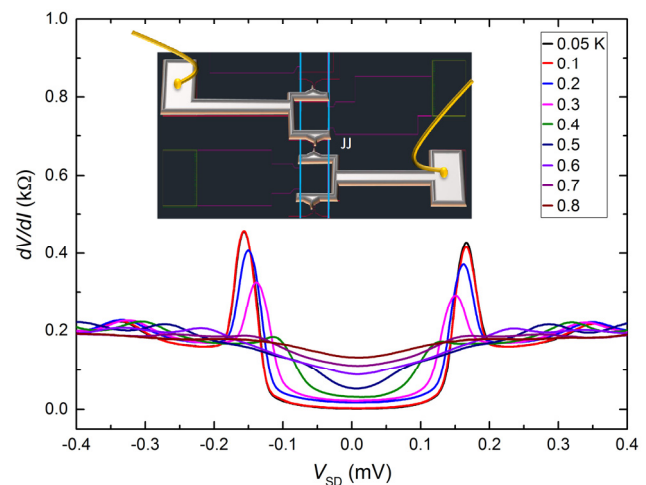


Fig. 1. Differential resistance dV/dI versus source-drain voltage (V_{SD}) for a junction at temperatures between 50 and 800 mK. The inset is a schematic view of a planar and ballistic Josephson junction. The active channel (mesa) underneath the junctions is shown in blue.

5RP-D-4

FLUCTUATIONS OF NEMATICITY AND THE SPIN SUBSYSTEM IN FeSe AND FeSeS

*Lin J.-Y.¹, Luo C.W.^{2,3}, Cheng P.C.², Wang S.-H.¹, Yao S.-Yu¹, Chiang J.-C.¹, Wu K.-H.²,
Juang J.-Y.², Chareev D.A.^{4,6}, Volkova O.S.^{5,6,7}, Vasiliev A.N.^{5,6,7}*

¹ Institute of Physics, National Chiao Tung University, Hsinchu 30010, Taiwan

² Department of Electrophysics, National Chiao Tung University, Hsinchu 30010, Taiwan

³ Taiwan Consortium of Emergent Crystalline Materials, Ministry of Science and Technology,
Taipei 10601, Taiwan

⁴ Institute of Experimental Mineralogy, Russian Academy of Sciences, 142432, Chernogolovka,
Moscow District, Russia

⁵ Physics Faculty, Moscow State University, Moscow 119991, Russia

⁶ Institute of Physics and Technology, Ural Federal University, Mira st. 19, 620002 Ekaterinburg,
Russia

⁷ National University of Science and Technology "MISiS", Moscow 119049, Russia

The nematic order (nematicity) is considered one of the essential ingredients to understand the mechanism of Fe-based superconductivity. In most Fe-based superconductors (pnictides), nematic order is reasonably close to the antiferromagnetic order. In FeSe and FeSeS, in contrast, a nematic order emerges below the structure phase transition at $T_s = 90$ K (70 K for FeSeS) with no magnetic order. The case of FeSe is of paramount importance to a universal picture of Fe-based superconductors. The polarized ultrafast spectroscopy provides a tool to probe simultaneously the electronic structure and the magnetic interactions through quasiparticle dynamics. Here we show that this novel approach reveals both the electronic and magnetic nematicity below and, surprisingly, far above T_s to at least 200 K. The quantitative pump-probe data clearly identify a correlation between the topology of the Fermi surface (FS) and the magnetism in all temperature regimes, thus providing profound insight into the driving factors of nematicity in both FeSe and FeSeS and the origin of its uniqueness.

Support by Most of Taiwan is acknowledged.

5 July

Wednesday

11:30-13:00

oral session

5TL-E

5RP-E

5OR-E

“Skymions”

5TL-E-1

ULTRAFAST MAGNETIZATION DYNAMICS IN SKYRMIONIC MATTER

Versteeg R.¹, Padmanabhan P.¹, Boguschewski C.¹, Slivina E.¹, Bordács S.², Kézsmárki I.²,
Becker P.³, Aqeel A.⁴, Palstra T.T.M.⁴, Grüninger M.¹, van Loosdrecht P.H.M.¹

¹ II. Physikalisches Institut, Universität zu Köln, 50937 Köln, Germany.

² Department of Physics, Budapest University of Technology and Economics and MTA-BME
Lendület Magneto-Optical Spectroscopy Research Group, Budapest 1111, Hungary.

³ Institut für Geologie und Mineralogie, Universität zu Köln, 50939 Köln, Germany.

⁴ Zernike Institute for Advanced Materials, University of Groningen, 9747 AG Groningen, The
Netherlands

pvl@ph2.uni_koeln.de

Materials lacking both time-reversal and space-inversion symmetry show a variety of intriguing phenomena, including magneto-electric and multiferroic behaviour, the occurrence of toroidal phases, and the formation of magnetic chiral and skyrmionic ground states. Skyrmionic phases arise in chiral magnetic materials due to a delicate interplay between Heisenberg interactions, Dzyaloshinskii-Moriya interaction, and uniaxial anisotropy. In this contribution we will review some of our recent time resolved Raman and magneto-optical experiments on the dynamical and non-equilibrium properties of the insulating chiral magnet Cu_2OSeO_3 as well as on the polar chiral magnet GaV_4S_8 .

Our results on the static optical properties of Cu_2OSeO_3 [1] show the presence of an important magneto-elastic coupling which leads to a marked increase of the optical activity of this material when entering the magnetically ordered phases. They also show the presence of a very large Faraday effect in the helical and conical phases, which originates from the ease of magnetic domain reorientation by the external magnetic field. The Faraday effect can conveniently be used to study the magnetic phase diagram, but also, for instance, the magnetic fluctuations near the first order helimagnetic-paramagnetic phase transition. We have furthermore used ultrafast pump-probe spectroscopy experiments (unpublished) to coherently excite collective magnetic modes in the GHz range in the chiral and skyrmion phases of both Cu_2OSeO_3 and GaV_4S_8 and to study their dynamics. Finally, we present a time resolved Raman study of higher energy magnetic excitations in Cu_2OSeO_3 , leading to further insight in the nature of these excitations and yielding important information on the spin-lattice coupling in this system.

Part of this work was financially supported the Deutsche Forschungsgemeinschaft (DFG) through the Collaborative Research Center SFB 1238, projects B02 and B05.

[1] R.B. Versteeg, I. Vergara, S.D. Schäfer, D. Bischoff, A. Aqeel, T.T.M. Palstra, M. Grüninger, and P.H.M. van Loosdrecht, *Phys. Rev. B*, **94** (2016) 094409.

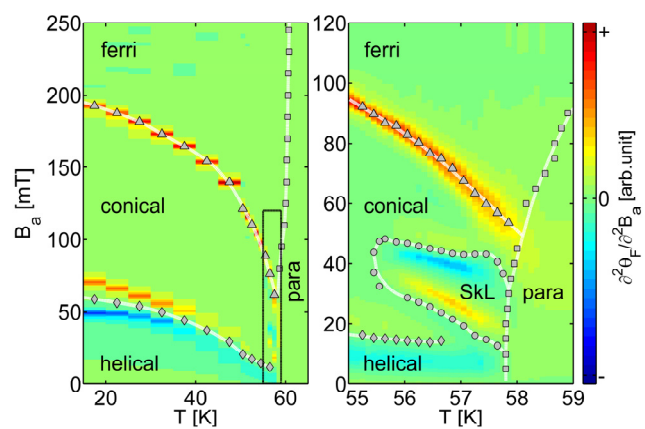


Figure 1: Magnetic phase diagram of Cu_2OSeO_3 determined using magneto-optical spectroscopy [1]

5RP-E-2

MAGNETIC SKYRMIONS IN NANOSTRUCTURES

Sapozhnikov M.V.¹, Vdovichev S.N.¹, Ermolaeva O.L.¹, Gusev N.S.¹, Fraerman A.A.¹, Gusev S.A.¹, Petrov Yu.V.²

¹ Institute for Physics of Microstructures RAS, Nizhny Novgorod, Russia

² Saint Petersburg state University, St.Petersburg, Universitetskaya nab. 7/9, 199034, Russia
msap@ipmras.ru

In the report we summarise our efforts of the last few years in theoretical and experimental study of the possibility of magnetic skyrmion stabilization in a magnetic film in the absence of Dzyaloshinskii-Moriya interaction. Usually the skyrmion exhibits collapse or runout leading to formation of a labyrinth domain structure in this case. The type of the instability is caused by interplay between its domain wall and magnetostatic energies. The main idea on which we based our research is that it is possible to stabilize skyrmion in the film with perpendicular anisotropy if create the area with the locally decreased domain wall energy. In this case the local potential well for skyrmion will be there which will prevent its runout. Such potential wells in common ferromagnetic films with perpendicular anisotropy (CoPt, FePt, FePd) can be manufactured by means of proper nanostructurisation.

The first way is to geometrically modulate the film thickness and to create the regular array of blind holes or stubs, for example. Micromagnetic simulations demonstrate that the skyrmion lattice can be formed in the simple process of the magnetization of such system in the uniform external field [1]. The skyrmion charge density can be more than $100 \mu\text{m}^{-2}$ in such system. The second way is to locally change the value of the perpendicular anisotropy of the film. We analytically calculate the skyrmion stability conditions in such situation [2].

Both ideas are verified experimentally. We used Co/Pt multilayered film as the template for both types nanopatterning. The regular array of the stubs is formed by electron beam lithography while the local decrease of the anisotropy is reached by the focused He ion beams. The irradiated spots are arranged in the square lattice with 200 nm period in last case. We experimentally observed the formation of the dense skyrmion lattice (Fig.1). The magnetic force microscopy (MFM) investigations are supported by Hall effect loop measurements.

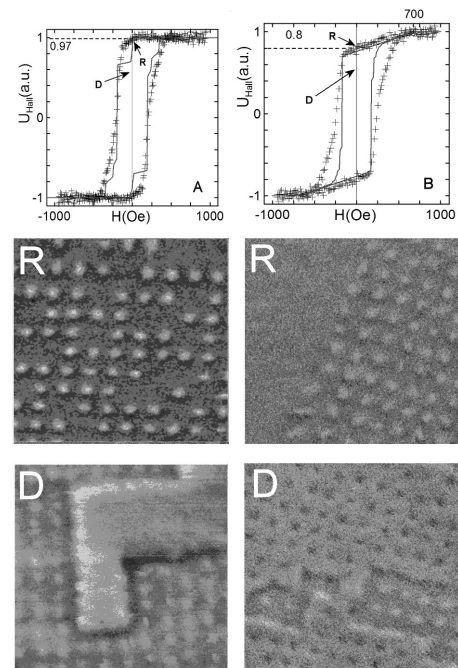


Fig. 1. The left column: the data for the sample with low dose irradiation (2×10^{15} ions/cm²), the right - for a higher dose (3×10^{15} ions/cm²). From top to bottom: the hysteresis of the Hall effect (the crosses are for experimental data, the line is for calculation), (R) MFM images of the remanent state of the sample and for demagnetized state (D). The scan size is $2 \mu\text{m} \times 2 \mu\text{m}$.

[1] M.V. Sapozhnikov and O.L. Ermolaeva, *Phys. Rev. B*, **91** (2015) 024418.

[2] M.V. Sapozhnikov, *J. Magn. Magn. Mat.*, **396** (2015) 338.

[3] M.V. Sapozhnikov *et.al*, *Appl. Phys. Lett.*, **109** (2016) 042406.

5OR-E-3

CHIRAL HALL EFFECT IN VARIOUS REGIMES

Denisov K.S.^{1,2}, Rozhansky I.V.^{1,2}, Averkiev N.S.¹, Lahderanta E.²

¹ Ioffe Institute, Saint-Petersburg, Russia

² LUT, Lappeenranta, Finland

denisokonstantin@gmail.com

In this work we develop the theory of Chiral Hall effect (also known as Topological Hall effect) in two-dimensional magnetic systems with metallic type of conductivity. Chiral Hall effect (CHE) is the appearance of additional transverse electric response in systems having swirling and chiral textures of magnetization. Unlike other mechanisms of Anomalous Hall effect (AHE), CHE is not based on spin-orbit splitting of free carrier band states; it arises instead due to exchange interaction of carriers with chiral magnetic configurations (magnetic vortices, skyrmions).

We theoretically revealed the existence of different regimes in CHE [1]. In case of not fully spin polarized carriers there are two limiting regimes with qualitatively different behaviour. For large exchange splitting and large skyrmion sizes there is very pronounced transverse spin current, so the appearance of charged Hall effect is only due to nonzero carrier spin polarization (similar to others mechanisms of AHE). In the opposite case of weak exchange interaction and small skyrmion sizes the transverse charge current dominates over spin Hall effect. In the intermediate region the system undergoes the transition. We hence manifest the existence of the nontrivial crossover in CHE.

Our consideration is based on a computation of an electron elastic scattering cross-section on a single chiral magnetic centre, e.g. magnetic skyrmion, in case when both electron spin subbands are activated (the Fermi level is greater than an exchange splitting of spin states). The generation of transverse response within this model is due to the asymmetric term in cross-section, which appears within all scattering channels (two spin-conserving and two spin flip processes). We found out that in the weak coupling regime the scattering asymmetry doesn't depend on incident electron spin state: both spin-up and down electrons are preferably scattered in the very same half-plane (spin-flip processes are also activated), so the pure charged transverse current is generated, without being accompanied by spin Hall effect [2]. Based on the perturbation expansion for the scattering amplitude we've shown that the minimal configuration of magnetization leading to the transverse scattering is coupled to the spin chirality $\mathbf{M}_1 [\mathbf{M}_2 \times \mathbf{M}_3]$. (\mathbf{M}_i - $i=1,2,3$ are three non-collinear vectors of magnetization). From the symmetry consideration the latter behaves as z-component of a magnetic field, which causes the transverse current disregard to an electron spin state. In the opposite adiabatic regime (spin flip channels are suppressed) spin-up and down electrons are mostly scattered in different half-planes, which generates transverse spin current. This is in agreement with previous theories [3] treating the chiral magnetic texture by means of an effective magnetic field acting on orbital motion of electron and having opposite sign for spin-up and down electron states. The crossover in the intermediate region has a nontrivial character: both charge and spin transverse currents coexist exhibiting irregular and oscillating behaviour.

We applied our microscopic model to describe the behaviour of CHE in two-dimensional disordered magnetic systems. We calculated the Hall coefficient in case when system contains randomly distributed non-magnetic scatterers and magnetic skyrmions. The existence of crossover in carrier scattering on a skyrmion leads to a non-monotonic dependence of Hall resistance on the Fermi level position.

[1] K.S. Denisov, I.V. Rozhansky, N.S. Averkiev, et al., *arXiv*: 1702.0485 (2017).

[2] K.S. Denisov, I.V. Rozhansky, N.S. Averkiev, et al., *PRL*, **117** (2016) 027202.

[3] P. Bruno, V.K. Dugaev, M. Taillefumier, *PRL*, **93** (2004) 096806.

5RP-E-4

TWO STATES OF SKYRMION LATTICE IN CHIRAL MAGNET MnSi*Glushkov V.V.*^{1,2,3}, *Lobanova I.I.*^{1,2}, *Sluchanko N.E.*¹, *Demishev S.V.*^{1,2,3}¹ Prokhorov General Physics Institute of RAS, Moscow, Russia² Moscow Institute of Physics and Technology, Dolgoprudny, Moscow region, Russia³ National Research University Higher School of Economics, Moscow, Russia

glushkov@lt.gpi.ru

Identifying of universal features in cooperative phenomena induced in quantized vortex matter stays a real challenge for physical community. An archetypal example of these systems is chiral magnet MnSi, where skyrmions exist as topologically stable knots in the vector field of non-uniform magnetization distribution [1]. While long range (18 nm pitch) magnetic helices appear in MnSi due to competition between isotropic ferromagnetic exchange ($J \sim 2.5$ meV) and asymmetric Dzyaloshinskii-Moriya (DM) interaction $D \sim 0.4$ meV [2,3], the skyrmion lattice (SL) is hosted only by a small pocket (A -phase) on the magnetic phase diagram, which exists in the vicinity of T_C at moderate magnetic fields [4-6]. However, there is no unique understanding of whether SL in MnSi is constructed from individual magnetic vortices [1] or the A -phase corresponds to a complicated triple- k spin structure stabilized by Gaussian thermal fluctuations under magnetic field [5].

Here we present the results of the experimental study of the angular dependences of magnetoresistance (MR) and Hall effect (HE) inside and near this skyrmion state (A -phase domain) in the bulk MnSi single crystals [7]. Our precise measurements of MR and HE carried out in the B - T range corresponding to the SL state discover new macroscopic feature of SL, which appears as isotropic MR in the A -phase in addition to topological HE reported earlier in [6]. The analysis of the MR data allow concluding that the A -phase in the bulk MnSi (a) is not metastable and (b) includes the region, where the SL state is decoupled from the crystalline magnetic anisotropy [7]. We argue that this region on the magnetic phase diagram represents the inhomogeneous state constructed of individual skyrmions in a way similar to Abrikosov-type magnetic vortexes in superconductors [7]. The results obtained are shown to provide a new look on the problems of skyrmion stability in the 3D case and melting of the skyrmion lattice.

Support by RAS programs “Electron spin resonance, spin-dependent electronic effects and spin technologies” and “Strongly correlated electrons” is acknowledged.

- [1] C. Pfleiderer, A. Rosch, *Nature*, **465** (2010) 880-881.
- [2] Y. Ishikawa et al., *Solid State Commun.*, **19** (1976) 525-528.
- [3] S. V. Grigoriev et al., *Phys. Rev. B*, **79** (2009) 144417.
- [4] K. Kadowaki et al., *J. Phys. Soc. Jpn.*, **51** (1982) 2433-2438.
- [5] S. Mühlbauer et al., *Science*, **323** (2009) 915-919.
- [6] A. Neubauer et al., *Phys. Rev. Lett.*, **102** (2009) 186602.
- [7] I. Lobanova et al., *Sci. Rep.*, **6** (2016) 22101.

5OR-E-5

DYNAMICAL AND REVERSIBLE CONTROL OF TOPOLOGICAL SPIN TEXTURES

Stepanov E.A.¹, Dutreix C.^{1,2}, Katsnelson M.I.¹

¹Radboud University, Institute for Molecules and Materials, Nijmegen, Netherlands

²Univ Lyon, Ens de Lyon, Univ Claude Bernard, CNRS, Laboratoire de Physique, Lyon, France
e.stepanov@science.ru.nl

Recent observations of topological spin textures brought spintronics one step closer to new magnetic memories. Nevertheless, the existence of skyrmions – a robust magnetic textures that were proposed as an attractive candidates for a data storing in magnetic memories, as well as their stabilization, require very specific intrinsic magnetic properties which are usually fixed in magnets.

Here we address the possibility to dynamically control their intrinsic magnetic interactions by varying the strength of a high-frequency laser field [1]. It is shown that drastic changes can be induced in the antiferromagnetic exchange interactions and the latter can even be reversed to become ferromagnetic, provided the direct exchange is already non-negligible in equilibrium as predicted, for example, in Si doped with C, Sn or Pb adatoms. In the presence of Dzyaloshinskii-Moriya interactions, this enables to manipulate some of the skyrmionic features such as their shape and characteristic size. Importantly, the later can be drastically reduced, which makes the stabilization of these magnetic textures easier and looks rather promising for storing more information in magnetic memories. Alternatively, such topological spin textures can occur in frustrated triangular lattices. Then, we demonstrate that a high-frequency laser field can induce dynamical frustration in antiferromagnets, where the degree of frustration can subsequently be tuned suitably to drive the material toward a skyrmionic phase.

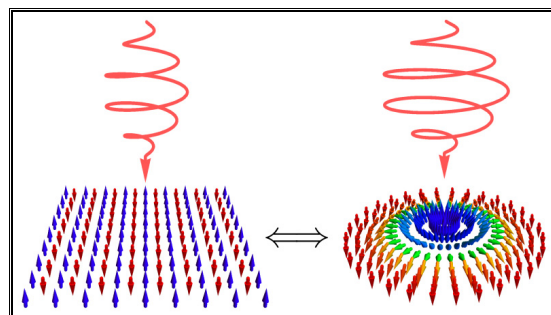


Fig. 1. Reversible manipulation of magnetism under light irradiation (red helicoid) from an antiferromagnetic order (left) toward a Skyrmionic structure (right) and vice versa. Small arrows depict the magnetization of lattice sites.

Support by NWO via Spinoza Prize, ERC Advanced Grant 338957 FEMTO/NANO, and the Stichting voor Fundamenteel Onderzoek der Materie (FOM), which is financially supported by the Nederlandse Organisatie voor Wetenschappelijk Onderzoek (NWO) is acknowledged.

[1] E.A. Stepanov, C. Dutreix, M.I. Katsnelson, accepted for *Phys. Rev. Lett.* (2017) // arXiv:1611.05075[cond-mat.mes-hall];

5 July

Wednesday

11:30-13:00

oral session

5TL-F

5RP-F

5OR-F

**“Diluted Magnetic
Semiconductors and
Oxides”**

5TL-F-1

FeO₂: POSSIBLE NOVEL MAGNETIC CONSTITUENT OF EARTH'S LOWER MANTLE*Streltsov S.V.¹, Shorikov A.O.¹, Skorniyakov S.L.¹, Poteryaev A.I.¹, Khomskii D.I.²*¹ Institute of Metal Physics, Ekaterinburg, Russia² Universitat zu Koeln, Cologne, Germany

streltsov.s@gmail.com

The recent discovery [1] of FeO₂, which may be an important ingredient of the Earth's lower mantle and which in particular may serve as a source of oxygen and water at the Earth's surface and atmosphere, opens new perspectives for geophysics and geochemistry, but this is also an extremely interesting material from physical point of view.

We found that in contrast to naive expectations, its electronic structure and physical properties are very different from the well-known pyrite FeS₂. FeO₂ turned out to be metallic with Fe ions nearly 3+, while FeS₂ is an insulator with Fe ions having 2+ oxidation state. Moreover, while FeS₂ is diamagnetic, FeO₂ is magnetic, with nontrivial temperature dependence of the magnetic susceptibility.

It is found that magnetic response of FeO₂ is strongly enhanced by doping, which can be important for the Earth's magnetism. The fact that FeO₂ lies "in between" the usual dioxides and peroxides makes it also an extremely interesting material for physics and solid state chemistry.

This work was supported by the Russian ministry of education and science via act 11 contract 02.A03.21.000, Russian President council via project MD-916.2017.2 and by the Deutsche Forschungsgemeinschaft through SFB 1238 and by the Koeln University via German Excellence Initiative.

[1] Q. Hu, D. Y. Kim, W. Yang, L. Yang, Y. Meng, L. Zhang, and H. Mao, *Nature* **534** (2016) 241.

5OR-F-2

NON-EQUILIBRIUM THERMODYNAMICS OF MAGNETIC SEMICONDUCTOR

Bebenin N.G., Lyapilin I.I.

Institute of Metal Physics UB RAS, Ekaterinburg, Russia
bebenin@imp.uran.ru

Spin electronics (spintronics) is a dynamic and perspective part of the solid state physics. The spin transport is usually considered in terms of kinetic equations for spin-up and spin-down distribution functions. If charge carriers move in inhomogeneous field this language is inconvenient to use and a general approach of non-equilibrium thermodynamics can be more appropriate. In our report, we consider the carriers that move in the effective field \mathbf{H}_{eff} created by localized magnetic moments. It is assumed that the number N of the carriers is so small that \mathbf{H}_{eff} is independent of N . The chemical potential μ is a function of N and magnetization \mathbf{m} of the charge carriers. The electric current and the magnetization current are defined as $j_{\alpha} = eNV_{\alpha}$ and $J_{\alpha\beta} = V_{\beta}m_{\beta}$ where \mathbf{V} stands for the charge carriers velocity. The local conservation laws are formulated and the expression for the entropy production is obtained.

Taking linear relations between thermodynamic forces and currents we consider transport properties of a ferromagnetic semiconductor near Curie point and the polarization of current that flows in a crystal with helical magnetic ordering.

This work was performed in the framework of the state task of the Federal Agency for Scientific Organizations of the Russian Federation (theme "Spin," no. 01201463330) and supported in part by RFBR grant 16-02-00044.

5RP-F-3

EFFECT OF MAGNETIC FIELD ON THE SYSTEMS WITH IMPERFECT NESTING

Rakhmanov A.L.^{1,2}, Kugel K.I.^{1,2}, Rozhkov A.V.^{1,2}, Sboychakov A.O.^{1,2}, Nori F.²

¹ITAE RAS, Moscow, Russia

²RIKEN, Saitama, Japan

alrakhmanov@mail.ru

The existence of fragments of the Fermi surface, which can be matched upon translation by a nesting vector, entails an instability of a Fermi-liquid state. A superstructure or additional order parameter related to nesting vector is generated due to this instability. The nesting is widely invoked for the analysis of charge and spin density waves (SDW), mechanisms of high- T_c superconductivity, fluctuating charge/orbital modulation in magnetic oxides, chromium and its alloys, etc. The nesting may be imperfect, i.e., the Fermi surface fragments can only match approximately. It was demonstrated that the imperfect-nesting mechanism can be responsible for the nanoscale phase separation in quasi-one-dimensional metals, chromium alloys, iron-based superconductors, and in doped bilayer graphene.

We investigated the effect of magnetic B field on weakly correlated electron systems with imperfect nesting [1]. Such study may be relevant for experiments on doped rare-earth borides [2]. We found that, when the cyclotron frequency ω_α is comparable to the electron energy gap, Δ , the magnetic field effects must be taken into account. The magnetic field enters the model Hamiltonian via two channels: (i) the Zeeman term, and (ii) orbital (or, diamagnetic) contribution. We investigated the combined effects of both terms in the limit of ideal electron-hole symmetry. Our study demonstrated that in the presence of the Zeeman term, the number of possible homogeneous magnetically ordered phases increases, compared to the case of $B = 0$. We defined nine possible states with different symmetries. If necessary, this list may be increased by taking into account incommensurate SDW phases and phases with “stripes”. Of this abundance, only two ordered homogeneous phases could serve as a ground state of our model.

When inhomogeneous states are included into consideration, even the zero-temperature phase diagram becomes quite complex. The phase separation is a very robust phenomenon. Its generality goes beyond the weak-coupling nesting instabilities of a Fermi surface: the phase separation is found in multiband Hubbard and Hubbard-like models, where the nesting is not crucial. However, phase separation is not universal: the long-range Coulomb interaction, lattice effects, disorder, etc, can restore the stability of homogeneous states. Therefore, in experiments the inhomogeneous states may occupy fairly modest part of the phase diagram. The final location of the segregated region at the phase diagram is affected by the Zeeman energy, as our calculations demonstrated.

The orbital contribution to the Hamiltonian leads to the Landau quantization of the single-particle orbits. As a result, the order parameters and the Néel temperature T_N oscillate as the magnetic field changes. This behavior is associated with the oscillatory part of the single-particle density of states, which emerges due to the Landau quantization. Yet another related phenomenon, the so-called field-induced SDW, is known to occur in quasi-one-dimensional materials. Pronounced oscillations of both Δ and T_N develop at large magnetic fields. However, if the electron-hole symmetry is broken, the magnetic field may destroy the SDW.

[1] A. O. Sboychakov, et al., *Phys. Rev. B*, **95** (2017) 014203.

[2] N. E. Sluchanko et al., *Phys. Rev. B*, **91** (2015) 235104.

5OR-F-4

MAGNETO-OPTICAL SPECTROSCOPY OF DILUTED MAGNETIC SEMICONDUCTORS GaMnAs PREPARED BY ION IMPLANTATION AND FURTHER PULSE LASER ANNEALING

Gan'shina E.A.¹, Golik L.L.², Kun'kova Z.E.², Zykov G.S.¹, Bykov I.V.³, Rukovichnikov A.I.², Yuan Ye.⁴, Zhou S.⁴

¹ Department of Physics, Lomonosov Moscow State University, Moscow, Russia

² Kotelnikov Institute of Radioengineering and Electronics (Fryazino Branch), RAS, Fryazino, Russia

³ Institute for Theoretical and Applied Electromagnetics, RAS, Moscow, Russia

⁴ Helmholtz-Zentrum Dresden Rossendorf, Institute of ion-beam science, Dresden, Germany
eagan@mail.ru

Building of diluted magnetic semiconductors (DMS) with Curie temperature above the ambient temperature may influence significantly on the development of modern technologies as spintronic and magnetophotonic. Nevertheless, there are still a lot of fabrication difficulties due to different cluster formation that prevents the achievement of the required intrinsic ferromagnetism in DMS.

Magneto-optical spectra studies allow us to distinguish the spectral features related to the magnetic cluster formation (MnAs or Mn clusters, etc.) and those caused by the spin-dependent transitions between valence and conduction bands of a semiconductor matrix as well as by the transitions from the Mn impurity band, since these contributions are visible at distinct energies.

In our report the results of magneto-optical (MO) and optical studies of Ga_{1-x}Mn_xAs DMS prepared with Mn concentrations 1% < x < 8% by ion-implantation with further pulse laser annealing [1] are presented. For all samples spectral-, field- and temperature dependences of the transversal Kerr effect (TKE) in the energy range of 0.5 - 4.0 eV, fields up to 3.0 kOe and temperatures of 15 – 300 K have been measured. Spectra of ellipsometry parameters were recorded in the range of 0.55 – 6.5 eV at room temperature (RT). Using them, we have calculated the spectra of pseudo-dielectric function, $\langle \varepsilon_1 \rangle(E)$ and $\langle \varepsilon_2 \rangle(E)$, of the studied layers. Peaks corresponding to the optical transitions near the L and X critical points of the Brillouin zone of GaAs are present in the $\langle \varepsilon_2 \rangle(E)$ spectra and there is noticeable interference component below 2.5 eV.

All studied samples revealed a strong magneto-optical response at low temperatures with a dependence of an effective Curie temperature (at which TKE appears) on the Mn concentration. The MO spectra differ significantly from ones of GaMnAs system prepared by laser ablation. The latter materials have the Curie temperature around RT and their magnetism is caused by the presence of MnAs clusters as shown in [2]. We compared the position of spectral features in the TKE spectra of the studied Ga_{1-x}Mn_xAs system with the energies of transitions in the critical points of the GaAs band structure as well as analyzed the TKE spectra shape taking into account both magneto-optical and optical (interference) contributions.

The conclusion about the intrinsic nature of the observed ferromagnetism in the Ga_{1-x}Mn_xAs layers prepared by ion-implantation with further impulse laser annealing was formulated.

The work has been supported by RFBR grant #15-02-02077 and by Helmholtz Association VH-NG-713.

[1] S. Zhou *J. Phys. D: Appl. Phys.*, **48** (2015) 263001.

[2] E. A. Gan'shina, L.L. Golik, V.I. Kovalev *et al. Solid State Phenomena*, **168-169** (2011) 35.

5RP-F-5

ATOMIC-SCALE ENGINEERING OF THE FERROMAGNETIC SEMICONDUCTOR/SILICON INTERFACE

Averyanov D.V.¹, Karateev I.A.¹, Tokmachev A.M.¹, Storchak V.G.¹

¹ National Research Center “Kurchatov Institute”, Moscow, Russia
musr@triumf.ca

Semiconductor spintronics provides a framework for hybrid devices combining logic, communication and storage. Enormous efforts are invested worldwide into the development of spintronics based on Si, the mainstream semiconductor platform. However, Si spintronics still experiences a technological bottleneck – creation of significant spin polarization in nonmagnetic Si. An emerging approach based on direct electrical spin injection from a ferromagnetic semiconductor – EuO being the prime choice – is a key to this novel technology. It is contingent on our ability to engineer flawless interfaces of Si with a spin injector to prevent spin-flip scattering.

Here we report a novel technology for integration of functional oxides with silicon [1]. The proposed approach solves the long-standing problem of direct epitaxial integration of functional oxides with Si. In particular, we demonstrate epitaxial growth of the EuO/Si structure [2]. Transmission electron microscopy displays an atomically abrupt EuO/Si interface (Fig.1) [3]. Magnetic properties of the EuO films rival those of the bulk [2]. We employ a soft-X-ray ARPES technique, using synchrotron radiation with photon energies around 1 keV, to probe the electronic structure of the buried EuO/Si interface. The band structure reveals a conduction band offset of 1.0 eV attesting the technological potential of the EuO/Si system [4]. These developments open a new avenue for semiconductor spintronics and may have general implications for the growth of functional oxides on silicon.

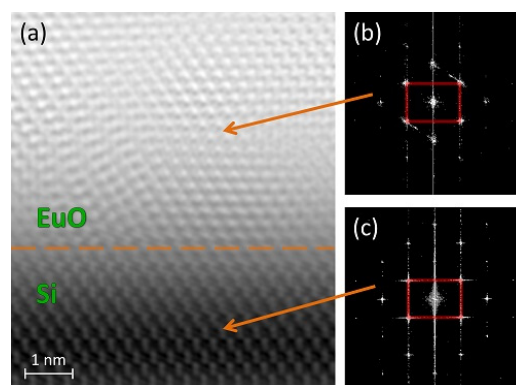


Fig. 1. An atomic-resolution structure of the EuO/Si interface.

a) High-resolution cross-sectional STEM image of EuO on Si.

b) and c) Two-dimensional Fourier spectra for the EuO and Si regions.

This work is partially supported by NRC “Kurchatov Institute”, the Russian Foundation for Basic Research (grants 16-07-00204, 16-29-03027 and 17-07-00170), and the Russian Science Foundation (grant 14-19-00662).

[1] D.V. Averyanov, C.G. Karateeva, I.A. Karateev, A.M. Tokmachev, A.L. Vasiliev, M.V. Kuzmin, P. Laukkanen, V.G. Storchak, *Materials and Design*, **116** (2017) 616-621.

[2] D.V. Averyanov, Yu.G. Sadofyev, A.M. Tokmachev, A.E. Primenko, I.A. Likhachev, Karateev, V.G. Storchak, *ACS Applied Materials & Interfaces* **7** (2015) 6146-6152.

[3] D.V. Averyanov, C.G. Karateeva, I.A. Karateev, A.M. Tokmachev, A.L. Vasiliev, S.I. Zolotarev, I.A. Likhachev, V.G. Storchak, *Scientific Reports*, **6** (2016) 22841(9).

[4] L.L. Lev, D.V. Averyanov, A.M. Tokmachev, F. Bisti, V.A. Rogalev, V.N. Strocov, V.G. Storchak, *J. Materials Chemistry C*, **5** (2017) 192-200.

5 July

Wednesday

11:30-13:00

oral session

5TL-G

5OR-G

**“Magnetic Soft Matter
(magnetic polymers,
fluids and
suspensions)”**

5TL-G-1

CAPTURE OF MAGNETIC NANOPARTICLES ON ORDERED MAGNETIZABLE ARRAYS: A PARAMETRIC STUDY

Ezzaier H.^{1,2}, Alves Marins J.¹, Schaub S.³, Amara B.H.², Kuzhir P.¹

¹ University of Côte d'Azur, CNRS U.M.R. 7010 INΦNI, Parc Valrose, 06108, Nice, France

² Laboratory of Physics of Lamellar Materials and Hybrid Nano-Materials, Faculty of Sciences of Bizerte, University of Carthage, 7021 Zarzouna, Tunisia

³ University of Côte d'Azur, CNRS, INSERM, iBV – UMR 7277, UMR-S 1091, Parc Valrose, 06100 Nice, France

kuzhir@unice.fr

The present work is focused on experimental study of magnetic separation of magnetic nanoparticles of a size range of 20-100 nm on ordered arrays of nickel micro-pillars when a dilute suspension of nanoparticles (ferrofluid) flows through a flat narrow channel with micro-pillars spanning the channel width and magnetized by an external magnetic field oriented at different angles with respect to the main flow. In a typical experiment, a part of suspended nanoparticles is captured by micro-pillars forming deposits whose size and shape depend on the flow speed, magnetic field intensity, field orientation, etc., while the rest of the particles escape from the micro-pillar array if the applied magnetic field is not strong enough. On the contrary, a relatively strong magnetic field induces a phase separation of nanoparticles manifested by appearance of bulk needle-like aggregates extended along the field. Such particle aggregation enhances significantly the efficiency of particle capture described by the steady-state volume V of deposits and the parameter $\Lambda = \ln(\phi_{in}/\phi_{out})$, appearing in the filtration equation, where ϕ_{in} and ϕ_{out} are particle concentrations at the channel inlet and outlet, respectively. The effects of different dimensionless parameters governing the physics of nanoparticle capture (Mason number, dipolar coupling parameter, particle concentration, angle between the field and the flow, geometry – square or hexagonal arrays) are studied in details and the optimal set of parameters ensuring the maximum capture efficiency is found. A theoretical model based on the particle trajectory analysis is developed and confirms the main experimental findings on strongly decreasing capture efficiency as function of Mason number and dipolar coupling parameter.

5TL-G-2

MAGNETIC RESPONSE OF A JEFFREYS FERROSUSPENSION

Rusakov V.V.¹, Raikher Yu.L.^{1,2}

¹ Institute of Continuous Media Mechanics, Russian Academy of Sciences, Ural Branch, Perm, 614013, Russia

² Ural Federal University, Ekaterinburg, 620083, Russia
raikher@icmm.ru

The Jeffreys scheme (JS) of classical rheology that comprises two dashpots and a spring is the most simple way to describe the mechanical response of a complex medium whose type might vary from a Newton fluid (linear viscosity, no equilibrium elasticity) via a viscoelastic medium (Jeffreys fluid proper) to an elastoviscous Kelvin gel (finite equilibrium elasticity). A sketch of a solid particle capable of orientational motion inside a JS medium is shown in Fig. 1. As seen, the said tuning is done by changing the viscosity coefficient η_M from zero to infinity. This makes a JS-based ferrosuspension a very useful theoretical model for soft magnetic matter studies.

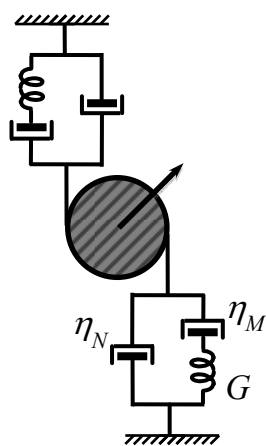


Figure 1

The case of nanoscale, i.e., single-domain, ferroparticles embedded in a complex fluid and subjected to a uniform magnetic field requires considering the particle magnetodynamics and mechanics, which evolve on the background of rather intense Brownian motion. Provided such a model exists, with its aid the magnetic susceptibility of the system could be presented in a unified form for all the range of η_M . The appropriate model has been developed in [1] and there applied to the viscoelastic situation. Hereby we recall those results presenting alongside them the opposite limit, that of very high, virtually infinite, η_M , i.e., explore the case of a ferrogel.

Note that the dynamic magnetic susceptibility of a complex magnetic fluid (any η_M) is an issue of interest in two aspects. As such, it is the source of information on the local rheology parameters, i.e., the tool for micro- or nanorheology. On the other hand, its out-of phase component multiplied by frequency is proportional to the rate of the applied AC field

energy dissipation and, thus, renders the major characteristic of magnetic hyperthermia, viz. the specific loss power.

In the present work the kinetic equation describing rotary motion of a magnetically hard nanoparticle (permanent magnetic moment) in a Jeffreys matrix is considered with allowance for the full orientational freedom and not in the planar motion approximation, as it is often done. We show that similarity between our results and those of the preceding planar models is rather remote. Moreover, with respect to the absorption spectra this difference is qualitative: while the planar approach predicts a well-resolved doublet, the complete solution renders a wide trapezium-like line. When applied to magnetic relaxometry – measurement of the response to a step-wise field change – the time dependence given by our theory at $\eta_M \rightarrow \infty$ yields the results, which fairly well resemble the experimental evidence obtained on cobalt-ferrite ferrogels [2].

Support by RSF grant 15-12-10003 is gratefully acknowledged.

[1] V.V. Rusakov, Yu.L. Raikher, R. Perzynski, *Mathematical Modelling in Natural Phenomena*, **10** (2015) 1-43.

[2] H. Remmer, J. Dieckhoff, A. Tschöpe, E. Roeben, A. Schmidt, F. Ludwig, *Physics Procedia*, **75** (2015) 1150-1154.

5OR-G-3

MAGNETIC MICROGELS IN COMPUTER SIMULATIONS*Minina E.S.^{1,2}, Likos C.¹, Kantorovich S.S.^{1,2}*¹ University of Vienna, Vienna, Austria² Ural Federal University, Ekaterinburg, Russia
elena.minina@univie.ac.at

Microgels, colloidal particles consisting of cross-linked polymers, are able to swell or shrink as a response to their external environment [1]. The fact that the swelling can be controlled makes microgels promising materials for many applications. However, embedding magnetic particles into such systems has to change their behaviour dramatically and, therefore, offers an additional mechanism to control microgel properties. For example, elastic and magnetic response of soft materials to the surrounding environment can change as it has been demonstrated in the recent works on the novel magnetic dipolar materials like magnetic gels and filaments [2-4].

In this work, we study the behavior of magnetic microgels and their elastic properties by means of molecular dynamic computer simulations. Initially, we construct a microgel as a non-magnetic polymer network of spherical shape which has been cross-linked randomly. Then, randomly embedding magnetic particles into such reference systems, we obtain magnetic microgels with different volume fraction of magnetic particles that varies from 0.5 to 10 per cent of the total volume fraction of particles comprising the polymer network of the microgel. Studying such systems at different strength of dipole-dipole interactions and solvent, we estimate the change of magnetic microgel in size and its conformations comparing to its reference non-magnetic counterpart. In order to investigate elastic properties, we place the microgel particles between two planar walls. Squeezing the gel between the walls consequently and measuring the elastic properties without magnetic field as well as in a magnetic field applied perpendicular to the walls with different strength, we observe that the contribution of magnetic dipolar interactions and the magnetic field play a significant role in controlling elastic properties and therefore in manipulation of such material.

[1] A. Fernandez-Nieves, H. M. Wyss, J. Mattsson, and D. A. Weitz. *Microgel Suspensions: Fundamentals and Applications*, 2011.

[2] R. Weeber, S. Kantorovich, and C. Holm, *J. Chem. Phys.*, **143** (15) (2016).

[3] P.A. Sanchez, E.S. Pyanzina, E.V. Novak, J.J. Cerda, T. Sintes and S.S. Kantorovich, *Faraday Discuss.*, **186** (2016) 241.

[4] P.A. Sanchez, E.S. Pyanzina, E.V. Novak, J.J. Cerda, T. Sintes and S.S. Kantorovich, *Macromolecules*, **48** (20) (2015) 7658.

5OR-G-4

ON THE ELASTIC PROPERTIES OF MAGNETIC ELASTOMERS BY MEANS OF STRUCTURAL METHODS

*Balasoiu M.^{1,2}, Rogachev A.V.^{1,3}, Iacobescu G.⁴, Turchenko V.^{1,5}, Ivankov O.^{1,6}, Soloviov D.^{1,6},
Bunoiu M.⁷, Bica I.⁷, Raikher Yu.L.⁸*

¹ Joint Institute for Nuclear Research, Dubna, Russia

² Horia Hulubei National Institute for Physics and Nuclear Engineering, Bucharest, Romania

³ Moscow Institute of Physics and Technology, Dolgoprudniy, Russia

⁴ University of Craiova, Department of Physics, Craiova, Romania

⁵ Donetsk Institute of Physics and Engineering named after O.O. Galkin, Donetsk, Ukraine

⁶ Taras Shevchenko University, Kiev, Ukraine

⁷ West University of Timisoara, Timisoara, Romania

⁸ Institute of Continuous Media Mechanics, RAS, Ural Branch, Perm, Russia

balas@jinr.ru

Magnetorheological elastomers (MREs) have mechanical, viscoelastic and “magnetostrictive” properties which make them attractive for various applications as electric current passive and active elements, adaptive tuned vibration absorbers, resonator absorber, seismic protection devices and, as shown recently, for electric capacitors.

In the present work the microstructure and elastic properties of several types of MREs investigated by means of AFM, XRD and SANS is presented.

Using these methods, the dispersion of the magnetic particles embedded in the elasomeric matrix can be detected, the diameters of the magnetic particles measured, the morphological features as interdomains of soft and hard segments observed, the mapping of regions with different hardness accomplished and adhesion forces measured [1-6].

Support by JINR-Romania Cooperation Programme Projects for 2016-2017 years and Grants of Romanian Governmental Representative to JINR is acknowledged.

[1] M. Balasoiu, M.L. Craus, E.M. Anitas, I. Bica, J. Plestil, A.I. Kuklin, *Phys. Solid State*, **52**(5) (2010) 917–921.

[2] M. Balasoiu, V.T. Lebedev, D.N.Orlova, I.Bica, *Crystallography Reports*, **56**(7) (2011) 93-96.

[3] I. Bica, M. Balasoiu, A.I. Kuklin, *Solid State Phenomena*, **190** (2012) 645-648.

[4] I. Bica I., Y.D. Liu, H.J. Choi, *Colloid. Polym. Sci.*, **290** (12) (2012) 1115–1122.

[5] G.E. Iacobescu, M. Balasoiu, I. Bica, *J. Supercond. Nov. Magn.*, **26** (2013) 785-792.

[6] M. Balasoiu, V.T. Lebedev, Yu. L. Raikher, I. Bica, M. Bunoiu, *J Magn Magn Mater*, **431** (2016) 126-129.

5 July

Wednesday

11:30-13:00

oral session

5TL-H

5OR-H

“Multiferroics”

5TL-H-1

ELECTRIC-FIELD CONTROL OF MAGNETISM IN MULTIFERROIC HETEROSTRUCTURES

van Dijken S.

NanoSpin, Department of Applied Physics, Aalto University School of Science, P.O. Box 15100,
FI-00076 Aalto, Finland
sebastiaan.van.dijken@aalto.fi

Spintronic devices currently rely on magnetic switching or controlled motion of magnetic domain walls by an external magnetic field or electric current. Achieving the same degree of magnetic controllability using an electric field has potential advantages including low power consumption. Here, an approach to electrically control local magnetic properties will be discussed [1-4]. The method is based on recurrent strain transfer from regular ferroelastic stripe domains in a ferroelectric BaTiO₃ substrate to magnetostrictive films (e.g. CoFe, CoFeB, and Fe). Dominance of the strain-induced magnetoelastic anisotropy in these heterostructures causes full imprinting of ferroelectric domain patterns into ferromagnetic films and strong pinning of magnetic domain walls onto ferroelectric boundaries [1,2]. Optical polarization microscopy measurements of the ferromagnetic and ferroelectric domain structures indicate that domain correlations and strong inter-ferroic domain wall pinning are maintained in an applied electric field. As a result, deterministic electric-field control over the formation and erasure of ferromagnetic domains [3,4] and reversible motion of magnetic domain walls [5] are obtained. In addition, regular modulations of magnetic anisotropy in strain-coupled multiferroic heterostructures provide a versatile platform for the excitation and manipulation of spin waves [6]. These findings open up new routes towards electric-field driven spintronics and magnonics.

- [1] T.H.E. Lahtinen et al., *Adv. Mater.*, **23** (2011) 3187.
- [2] K. J. A. Franke et al., *Phys. Rev. B*, **85** (2012) 094423.
- [3] T.H.E. Lahtinen et al., *Sci. Rep.*, **2** (2012) 258.
- [4] Y. Shirahata et al., *NPG Asia Mater.*, **7** (2015) e198.
- [5] K. J. A. Franke et al., *Phys. Rev. X*, **5** (2015) 011010.
- [6] B. Van de Wiele et al., *Sci. Rep.*, **6** (2016) 21330.

5OR-H-2

INVERSE EFFECT OF MAGNETOSTRICTION IN MAGNETOELECTRIC LAYERED STRUCTURES

Zadov B.¹, Liverts E.², Auslender M.¹

¹ Department of Electrical and Computer Engineering, BGU of the Negev, Beersheba Israel

² Department of Mechanical Engineering, BGU of the Negev, Beersheba Israel
marka@bgu.ac.il

The structures comprising intermittently bonded (laminated or deposited) magnetostrictive and piezoelectric layers attract a keen interest in sensor applications since they exhibit strong strain-mediated magnetolectric (ME) coupling. The bonding compliance exerts hidden stresses on the structure's layers that causes changes in their properties at *no* mechanical load, which we termed *inverse effect of magnetostriction* (IEM) for the ME structures. The term was borrowed from the case of ferromagnetic magnetostrictive materials [1], where IEM means change in the magnetic anisotropy and, as a result, the magnetization curve under external stresses.

We studied theoretically and experimentally IEM for laterally wide bi/tri-layer ME structures. Our theory is based on minimization of the energy including bare magnetic anisotropy, elastic and magneto-elastic energies under conditions of the strains matching and zero mean traction at the layers' interfaces and facets, respectively. Unlike the previous theories [2, 3], our theory involves also the shear strain and traction. For the ME structures, IEM manifests itself in: (i) a latent-stress induced magnetic anisotropy unnoted previously [2,3]; (ii) a decrease of the ME coupling coefficient [2, 3] below the value obtained previously [2], which may make a slipping correction factor [3] redundant; (iii) a decrease of the permittivity of the piezoelectric layer(s) larger than in the previous theories [2,3].

The type (i) IEM is clearly seen in Fig.1 showing the magnetization curves of a standalone Ni layer and Ni/PZT laminate that contains the similar layer. A notable decrease of the initial susceptibility and magnetic saturation lag in the laminate compared to the bare Ni layer. The above noted predictions of our theory agree well with the experimental data also semi-quantitatively.

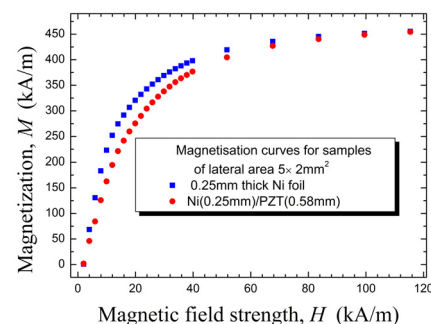


Fig. 1. Magnetization curves of Ni/PZT laminate and standalone Ni layer, see a description in the text

[1] S. Chikazumi, *Physics of Ferromagnetism*, Oxford University Press Inc., NY 1997.

[2] G.Harshe, J.O. Dougherty, R.E.Newnham, *Int. J. Appl. Electromagn. Mater.*, **4** (1993) 145-159.

[3] M.I. Bichurin, V.M. Petrov, G. Srinivasan, *J. Appl. Phys.*, **92** (2002) 7681-7683

5OR-H-3

SUPPRESSION OF THE NONLINEAR MAGNETOELECTRIC EFFECT HYSTERESIS IN A LAYERED FERROMAGNETIC-PIEZOELECTRIC COMPOSITE

Burdin D.A., Chashin D.V., Ekonomov N.A., Fetisov L.Y., Fetisov Y.K.
Moscow Technological University, Moscow, Russia
fetisov@mirea.ru

The nonlinear magnetoelectric (ME) effect in planar composites consisting of ferromagnetic (FM) and piezoelectric (PE) layers manifests itself as generation of electrical voltage harmonics $u(f)$ under simultaneous action of dc bias magnetic field H and ac pumping magnetic field $h(f)$ [1]. The effect arises due combination of the FM layer magnetostriction and the PE layer piezoelectricity and nonlinear dependence of the magnetostriction λ on H . It was shown, that for small $h \ll H$, the hysteresis of the magnetostriction $\lambda(H)$ leads to a hysteretic type $u(H)$ dependence [2]. This ambiguity reduces absolute accuracy of the ME field sensors and complicates their design. This paper shows a possibility to suppress hysteresis in the ME voltage u vs H dependence by increasing the amplitude of the pumping field h .

The planar structure comprising a magnetostrictive Ni layer ($5 \times 15 \times 0.2 \text{ mm}^3$) and a PE lead zirconate titanate layer (PZT) ($15 \times 5 \times 0.5 \text{ mm}^3$), connected with an epoxy glue, was used in measurements. The dc bias field $H=0-500 \text{ Oe}$ and ac pumping field $h \cos(2\pi ft)$ with frequency $f=120 \text{ Hz}$ and amplitude $h=1-100 \text{ Oe}$ were produced by the Helmholtz coils and applied along the long axis of the structure. Under the pumping field the structure generated voltage harmonics with amplitudes $u_1(f)$, $u_2(2f)$, and $u_3(3f)$. Figure 1 shows dependence $u_1(H)$ for $h=13 \text{ Oe}$. It is seen that the dependence is ambiguous, the coercive field is $H_C \approx 8 \text{ Oe}$. The coercive field decreases from $\sim 22 \text{ Oe}$ to $\sim 0.3 \text{ Oe}$ as the pumping field growths from 1 Oe to 100 Oe . The 1st harmonic amplitude u_1 growths linearly and then saturates at the level of $u_1 \approx 12 \text{ mV}$. The decrease in the coercive field H_C was observed for the 3^d harmonic u_3 as well. It was shown by numerical modeling that observed suppression of the hysteresis in the ME voltage is due to saturation of the magnetostriction in high pumping fields. Similar effect takes place in the fluxgate magnetometers due to saturation of the FM layer magnetization. The results obtained demonstrate a possibility to increase the accuracy of ME magnetic field sensors by ~ 2 orders in magnitude.

The research was supported by the RFBR and Ministry of Education and Science of Russia.

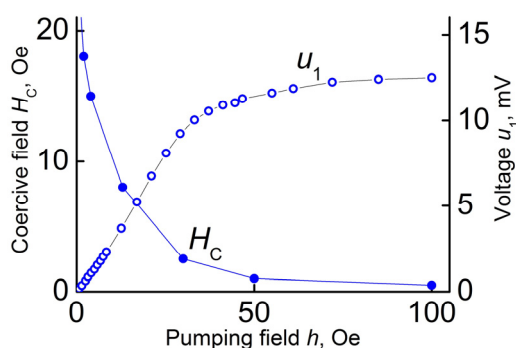


Fig. 2 Coercive field H_C and ME voltage u_1 as functions of the pumping field h .

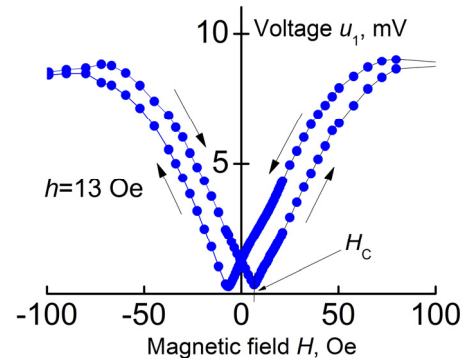


Fig 1 Magnetolectric voltage u_1 vs dc bias magnetic field H hysteresis curve.

[1] D.A. Burdin, D.V. Chashin, N.A. Ekonomov et al, *JMMM*, **258-359** (2014) 98-104.

[2] Y.K. Fetisov, D.V. Chashin, N.A. Ekonomov et al, *IEEE Trans. Mag.*, **51** (2015) 7120129.

5OR-H-4

MAGNETOELECTRIC EFFECT IN FERROMAGNETIC-SEMICONDUCTOR LAYERED COMPOSITE STRUCTURES

Fetisov L.Y.¹, Chashin D.V.¹, Saveliev D.V.¹, Plekhanova D.D.¹, Stognij A.I.²

¹Moscow Technological University, Moscow, Russia

² Scientific and Practical Materials Research Centre of NAS of Belarus, Minsk, Belarus

fetisovl@yandex.ru

Layered composite structures consisting of mechanically coupled ferromagnetic (FM) and piezoelectric (PE) layers exhibit magnetoelectric (ME) effect due to combination of magnetostriction and piezoelectricity [1]. Such structures usually use FM materials of large magnetostriction λ (Ni, Co, alloys FeCo, FeGa, terfenol, FeSiCB etc) and PE materials of high piezomodule d_{31} (PZT, PMN-PT, langatate, piezopolymers etc). In order to incorporate ME devices with modern electronics, it is of considerable interest to investigate ME effects in composite structures comprising semiconductor layers those also posses piezoelectric effect, for example, GaAs [2,3].

In the present work ME effect was measured in two different structures based on GaAs substrates: Ni-GaAs and Metglas-GaAs. The substrates had dimensions of 13.5x5x0.4 mm³ and 1 μ m thick Au/Cr electrodes on both sides. The first structure with 1.4 μ m thick Ni layer was fabricated by the ion-beam scattering method. The second one contained 30 μ m thick Metglas layer and GaAs substrate glued to each other with epoxy resin.

The frequency and field dependencies of linear ME effect in the structures were measured under simultaneous action of dc bias field H and ac excitation field $h\cos(2\pi ft)$, both directed along the long side of the structure. Figure 1 shows typical dependences of generated ME voltage u as function of ac field frequency f . The resonances correspond to excitation of longitudinal acoustic resonances in the samples. The monolithic Ni-GaAs sample demonstrated the highest ever observed for ME structures quality factor $Q \approx 29278$ at 155.178 kHz frequency and had ME coefficient of $\alpha_1 \approx 49$ V/(Oe·cm). The combined Metglas-GaAs sample had an order of magnitude smaller $Q_2 \approx 3113$ at $f_2 = 174.336$ kHz and ME coefficient of $\alpha_2 \approx 18$ V/(Oe·cm). Amplitudes of ME voltage for the samples at resonance reached maxima at bias fields, corresponding to maxima of piezomagnetic moduli $q = \partial\lambda/\partial H$ for Ni and Metglas, respectively.

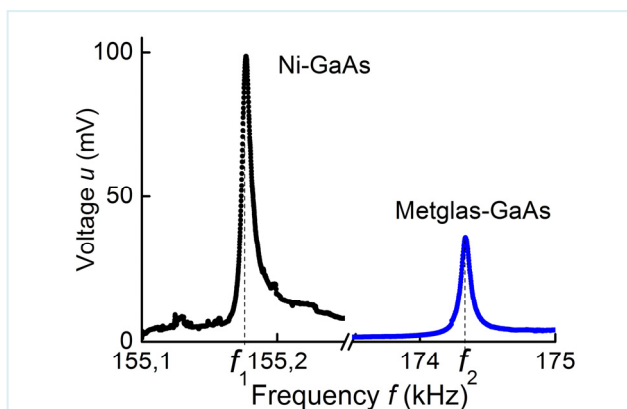


Fig. 1 Frequency dependence of ME voltage generated by Ni-GaAs and Metglas-GaAs structures at $h = 0.05$ Oe and $H = 17$ Oe.

The results obtained demonstrate high efficiency of ME interaction in composite structures with semiconductor GaAs layers and prospects of their usage in frequency selective ME devices, for example, in narrow-band ac magnetic field sensors or energy harvesting systems.

The research was supported by the RFBR and Ministry of Education and Science of Russia.

[1] C.-W. Nan, M.I. Bichurin, S. Dong, D. et al, *J. of Appl. Phys.*, **103** (2011) 031101.

[2] N.N. Paddubnaya, V.M. Laletsin, A.I. Stognij, N.N. Novitskii, *JTP Letters*, **40** (2014) 71–77.

[3] N.N. Paddubnaya, V.M. Laletsin, A.I. Stognij et al, *Functional materials*, **17** (2010) 329-333.

5OR-H-5

NEW COMPOSITE MULTIFERROIC MATERIALS CONSISTED OF FERROMAGNETIC AND FERROELECTRIC PARTICLES EMBEDDED IN ELASTIC MATRIX

*Makarova L.A.¹, Alekhina Yu.A.¹, Kramarenko E.Yu.¹, Omelyanchik A.S.², Rodionova V.V.²,
Perov N.S.^{1,2}, Malyshkina O.V.³*

¹ Lomonosov Moscow State University, 119991, Leninskie gory 1, Moscow, Russia

² Immanuel Kant Baltic Federal University, 236004, Nevskogo 14, Kaliningrad, Russia

³ Tver State University, 170100, Tver, Russia

la.loginova@physics.msu.ru

Smart magnetorheological materials are widely explored. Deformational properties of magnetorheological elastomers (MREs), viscous properties of magnetorheological fluids (MRFs), damping properties of magnetorheological foams attract great attention due to their wide range of application. Magneto-deformation and magneto-dielectric effects, which have already been observed in MREs, allow to classify these materials to multiferroic materials. Additive ferroelectric particles in polymer medium allow us to investigate the influence of electric fields to magnetic properties.

It was prepared and investigated 9 samples, based on polymer Wacker Silicone (WaSi) and SIEL. The volume ratio between WaSi and SIEL was 2:1 and was selected so that polymerization process occurred at the temperature 100 C during 1 hour. The total volume concentrations of filling powder varied from 20% to 40%. The types of filling particles were magnetic hard NdFeB particles (sizes varied from 5 to 30 μm) and ferroelectric particles PZT-26 (size was about 5 μm). The amount of each type of powder was calculated from mass concentrations and densities of each material. The volume ratios between NdFeB and PZT particles were 1:1, 2:1, 1:3 and 1:6, respectively. Also the elastomer with 40 vol% of NdFeB particles (this volume concentration corresponds to 82% mass concentration) and the elastomer with 20 vol% of PZT particles were prepared. Separately the two-layer sample consisted of two elastomers was prepared: firstly the elastomer with 20vol% of PZT particles was prepared and it was used as a substrate to polymerization of the next elastomer with 20 vol% of NdFeB particles.

Magnetic properties of prepared composite samples were investigated by Vibration Sample Magnetometer (VSM) Lake Shore 7400 in the field range ± 16 kOe in the temperature range from 100 K to 300 K. To carry out the measurements, the flat square shape (3×3 mm²) sample with thickness about 1 mm was cut from elastomer material. To investigate the influence of electric fields to the magnetic properties, the sample was previously placed between conducting plates (the sizes of plates were 4×4 mm²), connected to the high voltage source. The plane of the sample was parallel or perpendicular to the direction of external magnetic field. So the mutual orientation between magnetic and electric fields was parallel or perpendicular. It was found that in the external electric field (up to 5 kV) the magnetic properties of the samples with both ferroelectric and ferromagnetic particles changed compared with those in the absence of electric field.

This magnetoelectric effect was also detected by researching of the electric properties of the composites in the external magnetic fields. The electrical properties were investigated with immitance meter Aktakom 3016 (electrical capacitances were investigated). Also electric hysteresis loops of the samples were researched by Sawyer-Tower method.

The influence of PZT particles to the Young's modulus of elastomers and the influence of external magnetic fields to the elastic properties of composited were investigated with rheometer Anton Paar model MCR 301.

5 July

Wednesday

11:30-13:00

oral session

5RP-O

5OR-O

**“Magnetic
Nanostructures and
Low Dimensional
Magnetism”**

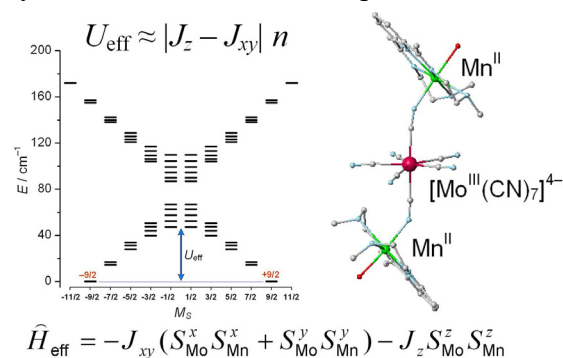
5RP-O-1

TOWARD HIGH-TEMPERATURE SINGLE-MOLECULE MAGNETS: PRINCIPLES AND APPROACHES

*Mironov V.S.*¹

¹ Shubnikov Institute of Crystallography of Federal Scientific Research Centre “Crystallography and Photonics” RAS, Leninsky prospect 59, 119333 Moscow, Russian Federation
mirsa@list.ru

This contribution discusses modern trends in the development of advanced single-molecule magnets (SMMs), which are high-spin molecules exhibiting slow magnetic relaxation and magnetic hysteresis of purely molecular origin below characteristic blocking temperature T_B . Since the discovery of SMMs in the 1990s, they attract extensive interest as promising materials for high-density information storage, quantum computing and molecular spintronics [1]. SMM behavior originates from a combined effect of negative uniaxial magnetic anisotropy D and large ground-state spin S resulting in an energy barrier $U_{\text{eff}} = |D|S^2$ between the two lowest degenerate $|+S\rangle$ and $|−S\rangle$ quantum spin states. However, the blocking temperature T_B is still too low for practical applications of SMMs ($T_B < 5$ K in most cases). Early efforts toward higher U_{eff} and T_B values were focused on maximizing the total spin S . Nowadays, it has been commonly recognized that high magnetic anisotropy D can only be produced by metal ions with unquenched orbital momentum [1,2]. Particularly, lanthanide Ln^{3+} ions exhibit exceptionally strong magnetic anisotropy stemming from large orbital momentum and strong spin-orbit coupling. In recent years, reports for lanthanide SMMs are increasing rapidly, and considerable progress has been achieved [2]. Thus, Ln-based SMMs display the record barrier ($U_{\text{eff}} = 1815$ K) and blocking temperature ($T_B = 20$ K), which are far superior to those of 3d-based SMMs ($U_{\text{eff}} = 90$ K and $T_B = 4.5$ K). However, further progress is difficult since these advances exploit single-ion magnetic anisotropy, which is already close to the physical limits for 4f and 3d ions. Alternative approaches toward high- T_B SMMs are discussed with a special emphasis on pair-ion magnetic anisotropy resulting from anisotropic spin coupling. In this respect, especially promising are orbitally-degenerate pentagonal-bipyramidal 4d and 5d complexes (such as $[\text{Mo}^{\text{III}}(\text{CN})_7]^{4-}$) which provide highly anisotropic (Ising-type) spin coupling with attached high-spin 3d ions, such as $-J_z S_{5d}^z S_{3d}^z - J_{xy}(S_{5d}^x S_{3d}^x + S_{5d}^y S_{3d}^y)$ with $|J_z| > |J_{xy}|$. In this case, the barrier U_{eff} is controlled by exchange parameters: namely, U_{eff} is directly proportional to $|J_z - J_{xy}|$ and to the number n of exchange-coupled 5d–3d pairs in a SMM (Figure) [3]. This provides a very efficient straightforward strategy for scaling U_{eff} and T_B values by means of enhancing exchange parameters J_z , J_{xy} and increasing the number of pentagonal 5d complexes in a SMM molecule [3]. New molecular 5d-based building blocks for development of high- T_B SMMs are presented. General principles of engineering of large U_{eff} barriers are formulated and some specific 5d-3d based molecules with expected high- T_B SMM behavior are discussed. Support by the Russian Foundation for Basic Research is acknowledged (grant 15-03-07904a).



- [1] S. Gao, *Molecular Nanomagnets and Related Phenomena*, Springer: Berlin, 2015.
 [2] J. Tang, P. Zhang, *Lanthanide Single-Molecule Magnets*, Springer: Berlin, 2015.
 [3] V.S. Mironov, *Inorg. Chem.*, **54** (2015) 11339-11355.

5OR-O-2

MAGNETIC PHASE CHANGE MEMORY BY LASER HEATING

Bali R.¹, Polushkin N.I.², Ehrler J.¹, Wintz S.^{1,3}, Liersch V.¹, Cornelius S.¹, Potzger K.¹, Lindner J.¹, Fassbender J.¹, Ünal A.⁴, Valencia S.⁴, Kronast F.⁴, Shugaev M.V.⁵, He M.⁵, Zhigilei L.V.^{5,6}

¹ Helmholtz-Zentrum Dresden-Rossendorf, D-01328 Dresden, Germany

² Institute for Physics of Microstructures of RAS, 603950 GSP-105 Nizhny Novgorod, Russia

³ Paul Scherrer Institute, 5232 Villigen, Switzerland

⁴ Helmholtz-Zentrum Berlin, D-12489 Berlin, Germany

⁵ MSE, University of Virginia, Charlottesville, 22904-4745 Virginia, United States

⁶ ITMO University, 197101 St. Petersburg, Russia

nip@ipmras.ru

It is well established [1] that laser pulses are able to reversibly transform so-called phase-change alloys [2] between states with different structural order, thereby altering their electrical resistivity and/or optical reflectivity. We demonstrate that short-pulsed lasers induce a local reversible transition in the thin-film (~ 40 nm) $\text{Fe}_{60}\text{Al}_{40}$ alloyed system from its non(ferro)magnetic to ferromagnetic state. We argue that the observed phenomenon can be explained in terms of the chemical order (B2) – disorder (A2) transformation. A high-intensity pulse causes superheating and rapid melting at ~ 1700 K of the initially nonmagnetic, structurally ordered, material and its disordering. Upon cooling, the molten region can be undercooled down to a sufficiently low temperature (~ 1100 K) to ensure that the resolidified alloy does not recover the chemically ordered state and appears to be ferromagnetic after cooling down.

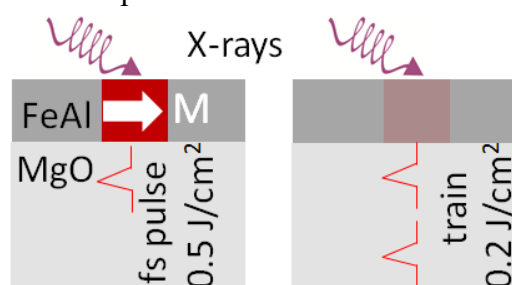


Fig.1. Experimental scheme for laser writing (left) and erasing (right) of a ferromagnetic region having magnetization \mathbf{M} in an $\text{Fe}_{60}\text{Al}_{40}$ film on MgO substrate. In these experiments, the ferromagnetism is generated by irradiation of the $\text{Fe}_{60}\text{Al}_{40}$ film by a high-intensity (~ 0.5 J/cm²) femtosecond (fs) pulse, while a train of lower-intensity (~ 0.2 J/cm²) fs pulses provides its erasing. The outer $\text{Fe}_{60}\text{Al}_{40}$ surface is probed by X-rays for detecting the magnetic state with X-ray magnetic circular dichroism.

However, a subsequent irradiation by low-intensity (below melting) pulse restores the order and nonmagnetic state. Such cycling of the ferromagnetism by laser, shown schematically in Fig.1, can be considered as an alternative [3, 4] to conventional magnetic recording. We believe that the approach proposed here (and previously in Refs. [3, 4]) has a potential in view of beating a limitation for magnetic storage data density because of thermal fluctuations of magnetization.

Support by DFG is acknowledged.

[1] M. Wuttig, N. Yamada, *Nature Mater.*, **6** (2007) 824-832.

[2] G. W. Burr *et al.*, *J. Vac. Sci. & Tech. B*, **28** (2010) 223-262.

[3] J. Timmerwilke *et al.*, *J. Phys. D: Appl. Phys.*, **49** (2016) 165005.

[4] T. Takayama, H. Takagi, *Appl. Phys. Lett.*, **88** (2006) 012512.

5OR-O-3

MAGNETIC TWIST STATES AND INHOMOGENEOUS RESONANCE MODES IN FE/GD AND FE/CR/GD LAYERED STRUCTURES

Drovosekov A.B.¹, Kholin D.I.¹, Kreines N.M.¹, Savitsky A.O.¹, Kravtsov E.A.^{2,3}, Ryabukhina M.V.², Proglyado V.V.², Ustinov V.V.²

¹ P.L.Kapitza Institute for Physical Problems RAS, Moscow, Russia

² M.N.Mikheev Institute of Metal Physics UB RAS, Ekaterinburg, Russia

³ Ural Federal University, Ekaterinburg, Russia

sao1992@mail.ru

Recently, studies of magnetization dynamics in rare-earth/transition-metal multilayers attract a lot of attention since these materials are considered as candidates for realization of ultrafast magnetic switching, promising for potential applications in magnetic storage devices [1]. An Fe/Gd layered structure is a possible system of this sort. The Fe/Gd multilayer is a model ferrimagnet system demonstrating a rich magnetic phase diagram [2]. Due to a large antiferromagnetic (AFM) coupling at the Fe-Gd interface and relatively weak ferromagnetic (FM) exchange in gadolinium, a sufficiently strong external magnetic field can initiate essentially non-uniform distribution of magnetization inside Gd layers (“twisted state”). Introduction of a spacer between Fe and Gd layers can change both the absolute value and the sign of the interfacial coupling, leading to modification of the magnetic state in the superlattice.

In this work we studied $[\text{Fe}(35\text{\AA})/\text{Gd}(50\text{\AA})]_{12}$ and $[\text{Fe}(35\text{\AA})/\text{Cr}(6\text{\AA})/\text{Gd}(50\text{\AA})/\text{Cr}(6\text{\AA})]_{12}$ multilayers prepared by magnetron sputtering technique on glass substrates. The quality of the samples was verified by X-ray diffraction studies. Static magnetization, magneto-optical Kerr effect (MOKE) and ferromagnetic resonance (FMR) measurements were performed in a wide temperature range $T = 4 - 300$ K. The experimental data were analysed theoretically in frame of the effective field model [2,3].

Static magnetization and MOKE studies showed that the investigated Fe/Gd superlattice has a compensation point at $T_{\text{comp}} \approx 90$ K. In weak fields, a collinear magnetic phase is preferable with Fe magnetisation aligned either in the field direction ($T > T_{\text{comp}}$) or opposite to it ($T < T_{\text{comp}}$). An increase of the magnetic field leads first to distortion of the collinear state near the superlattice surface (“surface twist state”). At higher fields the “bulk” twisted state is realized. FMR studies demonstrated the presence of two absorption lines. Comparison of the experimental and simulated spectra shows that the high-frequency spectral branch corresponds to essentially non-uniform precession mode within Gd layers. To describe the experimental results better, we consider a diffusion-type term in Landau-Lifshitz equations associated with dissipative spin currents in the superlattice.

Introduction of a 6Å thick Cr spacer between Fe and Gd layers reduces the interlayer coupling significantly while its sign does not change. The observed exchange between Fe and Gd layers is probably caused by pin-holes in the spacer due to interfacial roughness. In spite of relatively weak interlayer interaction in the Fe/Cr/Gd superlattice comparing to the Fe/Gd structure, we demonstrated that the magnetization twist effect in Gd layers must also be taken into account to describe the magnetic properties of the system. At the same time, the reduction of the interlayer coupling leads to a decrease of the non-uniform resonance mode frequency.

The work was partially supported by RFBR (grant No. 15-07-01170, 16-02-00061) and by the Ministry of Education and Science of the Russian Federation (grant No. 14.Z.50.31.0025).

[1] S. Mangin et al, *Nat. Mater.*, **13** (2014) 286.

[2] R.E. Camley, *Handbook of Surface Science*, **5** (2015) 243–295.

[3] A.B. Drovosekov et al, *J. Phys.: Condens. Matter*, **29** (2017) 115802.

5OR-O-4

FRACTAL CLUSTER OF MAGNETIC NANOPARTICLES: DIMENSIONALITY EFFECT TO MAGNETIZATION CURVES

Komogortsev S.V.¹, Felk V.A.², Iskhakov R.S.^{1,2}

¹ Kirensky Institute of Physics, Federal Research Center KSC SB RAS, Krasnoyarsk, Russia

² Siberian State Aerospace University, Krasnoyarsk, Russia

komogor@iph.krasn.ru

Random distribution of local easy magnetization axis in the clusters of nanoparticles results in the destruction of the ferromagnetic order but exchange interaction restores it on the scale of magnetic correlations inside stochastic magnetic domains. The macroscopic magnetic characteristics of nanomagnets are directly correlated with magnetic correlation length and the magnetic anisotropy of stochastic domains.

One can determine the magnetic correlation length, the magnetic anisotropy in stochastic magnetic domain, the nanoparticle size and its local magnetic anisotropy, as well as the spatial dimensionality of the system of exchange-coupled ferromagnetic nanoparticles from approach magnetization to saturation. Analytical theory exists for the one-, two- and three dimensional cases only.

The effect of the fractal dimension of exchange-coupled clusters of magnetic nanoparticles on their magnetization curves is predicted by simple scaling estimates. These predictions provide the basis for a technique for the experimental determination of the fractal dimension of nanoparticle clusters from analysis their magnetization curves.

We have tested such technique carefully by means of micromagnetic modeling using package OOMMF. Flat fractal clusters in the form of Brownian trees or dendrite structures obtained in the process known as diffusion-limited aggregation of nanoparticles are investigated. These trees are known as natural fractals. As a separate control cases we simulate film pattern in the form of Sierpinski carpet and continuous thin film composed of magnetic nanoparticles. In micromagnetic problem the easy magnetization axis of single-domain nanoparticles were oriented randomly, but the adjacent nanoparticles were exchange coupled. Exchange constant and uniaxial magnetic anisotropy constants were set on the levels needed to provide the spread of magnetic correlations over numerous nanoparticles. So we expect that stochastic magnetic domain in our clusters will be fractal also. Dimensionality of Brownian trees was determined by box counting. Magnetization curves were calculated for the number of fractal clusters with different dimensionalities. Then dimensionality estimations were made from the magnetization curves using two different approaches. The first one uses scaling prediction for the allometric dependence of coercive force on the grain size with the exponent closely connected with dimensionality value [1]. The second uses analysis of approach to magnetic saturation [1].

It has been shown that the effective dimensionality of the magnetic correlation volumes estimated from the analysis of the dependence of the coercive force on the particle size, agrees with the dimensionality of the fractal clusters. The effective dimensionality of the magnetic correlation volumes determined from the analysis of the approach to magnetic saturation is close to the cluster dimensionality (D) in the region D from 1.8 to 2 and deviates to the smaller values for the clusters with D about 1.5.

Support by Russian Foundation for Basic Research, Grants No. 16-03-00256 is acknowledged.

[1] R.S. Iskhakov, S.V Komogortsev, *Phys. Met. Metallogr.*, **112** (2011) 666–681.

5OR-O-5

NOVEL MAGNETIC NANOSTRUCTURES: IRON-CONTAINING DENDRIMERS WITH THERMO- AND PHOTOCONTROLLED MAGNETIC PROPERTIES

Domracheva N.E.¹, Vorobeva V.E.^{1,2}, Pyataev A.V.², Gruzdev M.S.³

¹ Zavoisky Kazan Physical-Technical Institute, Kazan, Russia

² Kazan Federal University, Kazan, Russia

³ G.A. Krestov Institute of Solution Chemistry, Ivanovo, Russia
ndomracheva@gmail.com

The creation of nanostructures with multifunctional properties is the most important and rapidly developing area of materials science. Dendronization is a useful synthetic strategy for obtaining multifunctional materials. The association of self-assembling properties of dendritic molecules with magnetic/semiconductor properties of nanoparticles (NPs) leads to new and interesting compounds with special tailored properties. The main goal of our research is the creation of new magnetic nanostructures based on iron oxide dendrimeric nanocomposites, which combine two (or more) physical properties that can be controlled under the influence of each other.

We present here the results of a study of superparamagnetic/semiconductor γ -Fe₂O₃ nanoparticles (NPs) encapsulated in a second-generation liquid crystalline poly(propylene imine) (PPI) dendrimer which were obtained by means of electron magnetic resonance (EMR), SQUID magnetometry, Mössbauer and optical spectroscopy [1, 2, 3].

The EMR and Mössbauer investigations showed that the ferrimagnetic NPs in the dendrimeric nanocomposite have an average diameter of ~ 2.5 nm, they possess uniaxial magnetic anisotropy, an increased value of the effective magnetic anisotropy constant with respect to the bulk material, and have a "core(α -Fe)/shell(γ -Fe₂O₃)" structure [1]. A temperature-driven transition from superparamagnetic to ferrimagnetic state has been observed for the sample with blocking temperature 18 K. The Mössbauer studies also showed the manifestation of low-spin properties in the surface monoatomic layer of a high-spin NPs shell bound to the dendrimer [2].

The optical absorption investigations of semiconductor γ -Fe₂O₃ NPs in dendrimer nanocomposite revealed a direct allowed transition with the band gap width (4.5 eV), which is blue shifted with respect to the value of the bulk material (2.2 eV). This blue shift has been explained by quantum size effects [3].

The influence of pulsed laser irradiation on the superparamagnetic properties of γ -Fe₂O₃ NPs was studied by EPR spectroscopy. It has been shown that irradiation of the sample held in vacuo and cooled in zero magnetic field to 6.9 K leads to the appearance of a new EPR signal, which decays immediately after the irradiation is stopped. The appearance and disappearance of this new signal can be repeated many times at 6.9 K when we turn on/turn off the laser. We suppose that the generation of conduction band electrons by irradiation into the band gap of the γ -Fe₂O₃ changes the magnetic anisotropy and superparamagnetic properties of NPs [3].

We gratefully acknowledge the financial support by RAS Presidium program No. 24.

[1] N. Domracheva, A. Pyataev, R. Manapov, M. Gruzdev, *ChemPhysChem*, **12** (2011) 3009- 3019.

[2] A.F. Abdullin, A.V. Pyataev, N.E. Domracheva, M.S. Gruzdev, *J. Surf. Invest.: X-Ray, Synchrotron Neutron Tech.*, **10** (2016) 35-38.

[3] N. Domracheva, V. Vorobeva, M. Gruzdev, A. Pyataev, *J. Nanopart.Res.*, **17** (2015) 83.

5OR-O-6

EFFECT OF MAGNETIC STRUCTURE OF MAGNETIC NANOPARTICLES AND ITS DIPOLAR INTERACTION ON NONLINEAR MAGNETISATION DYNAMICS

Eberbeck D.¹¹ Physikalisch-Technische Bundesanstalt Braunschweig und Berlin, Berlin, Germany
dietmar.eberbeck@ptb.de

To contribute to the quantitative description of the signals in Magnetic Particle Imaging (MPI) and magnetic Hyperthermia (promising methods for diagnostics and e.g. cancer therapy in medicine, respectively, employing magnetic nanoparticles (MNP)) on the base of the distribution of the magnetic moments, $f(\mu)$, and anisotropy constant, K , of MNP as well as its dipolar interaction, λ_d , the link between these structure parameters and MPS-signal (MPS: Magnetic Particle Spectroscopy = zero dimensional MPI) was investigated. The values of $f(\mu)$, K , λ_d for different samples were obtained from $M(H)$ and Magnetorelaxometry (MRX) data. Utilizing these parameters the MP-spectra were calculated solving the Landau-Lifshitz-Gilbert (LLG) equation numerically. The LLG-model describes the measured data for non-interacting size-distributed MNP well. Depending on the matrix the MNP were immobilised in, the MPS signal may change strongly (Fig. 1). This is attributed to an aggregation which switches on the dipole-dipole-interaction (DDI) between the MNP. Applying the interaction parameter of close packed MNP, here $\lambda_d=6.6$, the LLG-model describes the data quite well, at least the amplitudes of 3rd and 5th harmonics (Fig. 1) which contain the overwhelming part of the total signal.

Interestingly, the interaction effect increases with decreasing MNP-concentration and also develop systematically special characteristics like the kink within the spectrum (Fig. 1). Furthermore, amplitude and phase spectra of dried MNP (Fig. 1) and highly concentrated dispersions reveal features of a coherent movement of the individual moments, here $\phi(k) \propto k$ (Fig. 1 Inset) and the occurrence of an oscillatory part within the spectrum, respectively. Thus, thanks its highly sensitive measurement of higher harmonics MPS provides a powerful tool for the detailed analysis of the magnetic structure of MNP and its collective dynamic behaviour as well as that of other magnetic materials.

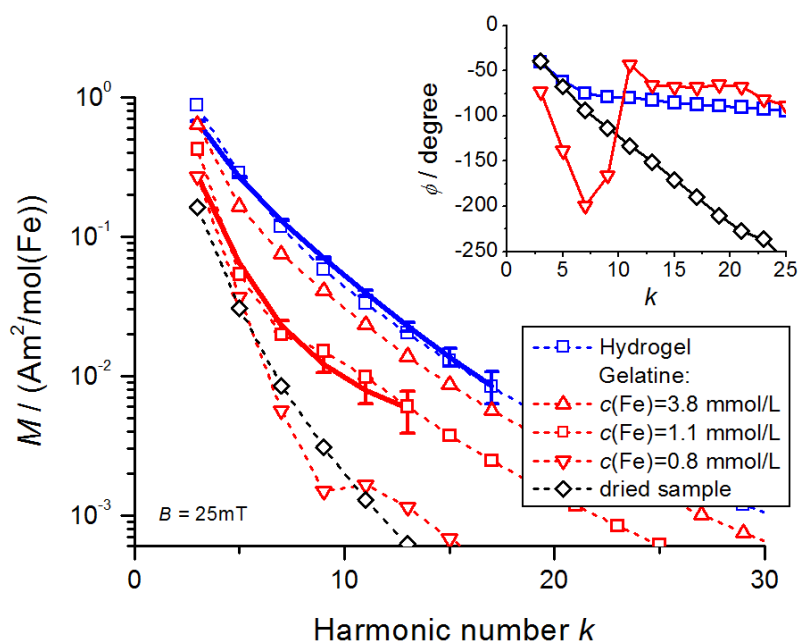


Fig. 1. Measured MP-spectra (symbols with dashed lines as guide to the eyes) and related LLG-model (full lines, not fitted) of MNP immobilised within indicated matrices.

Interestingly, the interaction effect increases with decreasing MNP-concentration and also develop systematically special characteristics like the kink within the spectrum (Fig. 1). Furthermore, amplitude and phase spectra of dried MNP (Fig. 1) and highly concentrated dispersions reveal features of a coherent movement of the individual moments, here $\phi(k) \propto k$ (Fig. 1 Inset) and the occurrence of an oscillatory part within the spectrum, respectively. Thus, thanks its highly sensitive measurement of higher harmonics MPS provides a powerful tool for the detailed analysis of the magnetic structure of MNP and its collective dynamic behaviour as well as that of other magnetic materials.

Support by the DFG priority program SPP 1681 (TR408/8-2) is acknowledged.

5 July

Wednesday

11:30-13:00

oral session

5TL-P

5RP-P

5OR-P

**“Study of Magnetism
using X-rays and
Neutrons”**

5TL-P-1

POLARIZED NEUTRONS FOR THE INVESTIGATIONS OF MAGNETIC NANOSTRUCTURES

Kozhevnikov S.V.

Frank Laboratory of Neutron Physics, Joint Institute for Nuclear Research, Dubna, Russia
kozhevni@nf.jinr.ru

Neutron scattering is the powerful tool for the investigations of biological objects, polymers and magnetism due to isotope sensitivity, high penetration ability and magnetic moment of neutrons. Polarized neutron reflectometry is the conventional method for the investigations of thin magnetic films and multilayers. But there are some significant restrictions of this method. First, the accessible thickness of the films is less than 200 nm. Second, reflectometry is not a direct method. We have to extract parameters of the investigated system from fitting the calculated reflectivity to the experimental data. Third, in polarized neutron reflectometry the useful signal is extracted from the raw data containing the background from imperfect polarizing efficiencies of polarizer and analyzer.

We review the new developed methods for the direct investigations of magnetic nanostructures. Larmor precession technique is used for the direct determination of magnetic induction value and direction in thick magnetic films of the thickness about 20 μm [1].

Zeeman spatial beam-splitting takes place on the boundary of two magnetically non-collinear media. By Zeeman beam-splitting it is possible to extract directly the magnetic induction value near the separate boundary in the thick film [1,2], in the magnetic domains [2] or in magnetic nanoclusters [3].

Neutron magnetic resonance [1,4] takes place in the magnetic film placed in crossed permanent and oscillating magnetic field. By this method it is possible to define the value of magnetic induction in the individual domain even in the macroscopic non-saturated magnetic state of the film.

The width of the conventional neutron beam used in experiment is about 0.1-10 mm. To investigate local nanostructures with high spatial resolution, the narrow microbeam is required. The neutron planar waveguides transform the initial neutron macrobeam into a narrow microbeam of submicron width of 0.1-10 μm . We used the polarized neutron microbeam of 2.6 μm width for the spatial scan of the magnetic amorphous wire of 190 μm in diameter with "core-shell" magnetic domain structures [5].

The planar waveguide is a tri-layer film with the neutron optical potential like as potential well. In the middle layer, the neutron wave propagates along the interfaces and goes out as a neutron microbeam. The neutron wave is resonantly enhanced inside the waveguide. We developed the polarized neutron channeling method for the direct determination of low magnetization of TbCo_5 middle layer of the order of 10 G [6]. Such materials containing rare-earth elements are widely used for the development of new methods of magnetic recording and switching.

[1] S.V. Kozhevnikov, F. Ott, F. Radu, *JMMM*, **402** (2016) 83-93.

[2] S.V. Kozhevnikov, F. Ott, F. Radu, *J. Appl. Crystallography*, **45** (2012) 814–825.

[3] S.V. Kozhevnikov, F. Ott, E.M. Semenova, *Physica B*, **508** (2017) 12-21.

[4] S.V. Kozhevnikov, V.K. Ignatovich, Yu.V. Nikitenko, F. Ott, F. Radu, A. Rühm, J. Major, *Journal of Physics: Conference Series*, **340** (2012) 012084.

[5] F. Ott, S. Kozhevnikov, A. Thiaville, J. Torrejon, M. Vazquez, *NIM A*, **788** (2015) 29-34.

[6] S.V. Kozhevnikov, Yu.N. Khaydukov, T. Keller, F. Ott, F. Radu, *JETP Lett.*, **103** (2016) 36-40.

5RP-P-2

SPIN-WAVE DYNAMIC AND EXCHANGE INTERACTIONS IN MULTIFERROIC $\text{NdFe}_3(\text{BO}_3)_4$ EXPLORED BY INELASTIC NEUTRON SCATTERING

*Golosovsky I.V.¹, Ovsyanikov A.K.¹, Aristov D.N.¹, Matveeva P.G.¹, Mukhin A.A.², Boehm M.³,
Regnault L.-P.³, Bezmaternykh L.N.⁴*

¹ NRC "Kurchatov Institute", B.P. Konstantinov Petersburg Nuclear Physics Institute, 188300,
Gatchina, Russia

² Prokhorov General Physics Institute, RAS, 119991, Moscow, Russia

³ Institut Laue Langevin, 6 rue Jules Horowitz, BP 156, F-38042 Grenoble, France

⁴ Kirenskii Institute of Physics, Siberian Division, RAS, 660038, Krasnoyarsk, Russia
golosovsky_iv@pnpi.nrcki.ru

The inelastic neutron scattering experiments were performed to reveal the magnetic excitations and to obtain the exchange parameters in phase with collinear antiferromagnetic structure.

Rich picture of spin excitations and strong hybridization and anticrossing of Fe and Nd-subsystems were observed. The experimental spectra were analyzed in a frame of spin-wave theory. The model, which includes the exchange interactions up to 8 coordination spheres, satisfactorily describes the observed dispersion curves up to ~ 5.5 meV. It was shown that the spin-wave dynamic is defined by the strongest antiferromagnetic intra-chain interaction along the Fe chains and three nearly inter-chain interactions. Other interactions, including ferromagnetic exchange, appeared to be insignificant. The overall energy balance of the three antiferromagnetic inter-chain exchange parameters, which couple moments from the adjacent ferromagnetic layers, stabilizes parallel moments in the layer. It demonstrates that the pathway geometry plays a crucial role in the forming of the magnetic structure [1].

Support of grants RFBR 16-02-00058, RFBR 15-02-07647 and RG14.B25.31.0025 is acknowledged.

[1] I.V. Golosovsky, A.K. Ovsyanikov, D.N. Aristov, P.G. Matveeva, A.A. Mukhin, M. Boehm, L.-P. Regnault, and L. N. Bezmaternykh, Submitted to PRB, 2017.

5OR-P-3

STRUCTURAL AND MAGNETIC PROPERTIES OF THE TRIRUTILE-TYPE 1D HEISENBERG ANTIFERROMAGNET CuTa_2O_6

*Golubev A.*¹, *Dinnebier R.E.*¹, *Schulz A.*¹, *Kremer R.K.*¹, *Langbein H.*², *Senyshyn A.*³, *Law J.M.*⁴,
*Hansen T.*⁵, *Koo H.-J.*⁶, *Whangbo M.-H.*⁷

¹ Max Planck Institute for Solid State Research, Stuttgart, Germany

² Institut für Anorganische Chemie der Technischen Universität Dresden, Dresden, Germany

³ Forschungsneutronenquelle Heinz Maier-Leibnitz (FRM II), Garching, Germany

⁴ Dresden High Magnetic Field Laboratory (HLD), Dresden, Germany

⁵ Institut Laue-Langevin, Grenoble, France

⁶ Kyung Hee University, Seoul, Republic of Korea

⁷ North Carolina State University, North Carolina, USA

A.golubev@fkf.mpg.de

Polycrystalline samples of CuTa_2O_6 prepared by low-temperature decomposition of Cu-Ta-oxalate precursors at room temperature crystallize with a monoclinically distorted trirutile structure type. By detailed high temperature X-ray and neutron powder diffraction studies we detected a structural phase transition to the tetragonal trirutile structure-type at 503(3) K. The structural phase transition was ascertained by Raman scattering. GGA+*U* density functional calculations of the spin exchange parameters, magnetic susceptibility and isothermal magnetization measurements constitute CuTa_2O_6 as new 1D Heisenberg chain with predominant antiferromagnetic nearest neighbor exchange interaction $J_{\text{nn}} \approx 50$ K. Heat capacity and low temperature high intensity neutron powder diffraction studies could not find long range order down to 0.4K.

5OR-P-4

HOW TO EXPLORE MAGNETIC STRUCTURE OF THREE-DIMENSIONAL ARTIFICIAL SPIN ICE?

Mistonov A.A.^{1,2}, *Dubitskiy I.S.*², *Shishkin I.S.*², *Grigoryeva N.A.*¹, *Grigoriev S.V.*^{1,2}

¹ Saint Petersburg State University, Saint Petersburg, Russia

² Petersburg Nuclear Physics Institute, Gatchina, Russia

a.mistonov@spbu.ru

At present time, there are a lot of techniques allowing to determine magnetic structure of different complexity, while for three-dimensional (3D) mesoscale (hundreds of nanometers) systems this task is still challenging. Herewith revealing of 3D magnetic structure of so-called cluster lattices becomes very important, since the amount of them increasing drastically and application fields become wider.

As an example of cluster lattice one can consider inverse opal-like structure (IOLS). We have suggested phenomenological model of the IOLS magnetizing based on the analogue of the “ice-rule” for nanosystems taking IOLS as a 3D artificial spin-ice [1]. There are 4 magnetic subsystems, each of them directed along the one of the $\langle 111 \rangle$ fcc axis. These subsystems, consisting of the Ising-like magnetization vectors localized in “legs”-connectors between cubes and tetrahedra, constituting the IOLS. The “ice-rule” in this case stands, that amounts of magnetizations of the “legs” going in and out of each tetrahedron or cube should be equal.

Magnetic structure of the IOLS is strongly determined by interplay between external magnetic field \mathbf{H} and the “ice-rule”. There are three types of the interplay: “competition”, when the energy minimum of the “ice-rule” does not coincide with the one of Zeeman energy; “independence”, when the field cannot affect on perpendicular to it subsystem, but the “ice-rule” determines behaviour of the subsystem; “cooperation”, when the “ice-rule” and field tend to lead the system to the same state. These situations almost totally cover all possible sceneries of the IOLS magnetic structure evolution. Phenomenological approach allows to assume the states, which the sample should goes through, while magnetizing, however the total picture of the magnetizing process is hard to reveal.

Small-angle diffraction of neutrons is very powerful instrument for the mesoscopic magnetic structure studies [2,3], but experimental data interpretation is tricky and can be unclear. Thus, some other techniques should be also involved. The problem is, that other methods either two-dimensional (magnetic force microscopy or Lorenz microscopy) or integral (PPMS, SQUID-magnetometry) and cannot give enough information about three-dimensional magnetic structure.

We propose to calculate magnetic form factor defined by the magnetization distribution in the sample in order to unambiguously understand results of SANS experiments. The most rigorous and straightforward way to determine magnetization distribution is to solve micromagnetic equations [4]. Clear advantage of the micromagnetic framework is that no adjustable parameters have to be used. Magnetization distribution depends on well known parameters of the material and its geometric shape only.

We have used this approach for three types of the field and the “ice-rule” interplay mentioned above and obtained good agreement between calculated and experimental data.

Authors acknowledge the help of Andre Heinemann (Meier-Leibnitz Zentrum) in carrying out of SANS experiments and RFBR for financial support (pr. № ofi_m 14-22-01113).

[1] A.A. Mistonov et al., *Phys. Rev. B*, **87** (2013) 220408.

[2] E.G. Iashina et al., *J. Synch. Investig.*, **9** (2015) 655.

[3] E. Altynbaev et al., *Phys. Rev. B*, **94** (2016) 174403.

[4] A. Aharoni, Introduction to the Theory of Ferromagnetism, *Clarendon Press*, **109** (2000).

5OR-P-5

SPIRAL-LIKE MAGNETIC STATE IN EXCHANGE BIASED CoO/Co STRUCTURES SEEN BY WAVEGUIDE-ENHANCED PNR

Khaydukov Yu.^{1,2,3}, Zdravkov V.^{4,5}, Lenk D.⁴, Morari R.⁵, Ullrich A.⁴, Obermeier G.⁴, Müller C.⁴, Sidorenko A.S.⁵, Krug von Nidda H.-A.⁴, Keller T.^{1,2}, Horn S.⁴, Tagirov L.R.^{4,6}, Tidecks R.⁴, Keimer B.¹

¹ Max-Planck-Institut für Festkörperforschung, D-70569 Stuttgart, Germany

² Max Planck Society Outstation at the MLZ, D-85748 Garching, Germany

³ Skobeltsyn Institute of Nuclear Physics of Moscow State University, 119991 Moscow, Russia

⁴ Institut für Physik, Universität Augsburg, D-86158 Augsburg, Germany

⁵ Institute of Electronic Engineering and Nanotechnologies ASM, MD2028 Kishinev, Moldova

⁶ E.K. Zavoisky Physical-Technical Institute of RAS, 420029 Kazan, Russia

y.khaydukov@fkf.mpg.de

Exchange bias phenomenon was intensively investigated and actively utilized in spintronics applications [1]. Perhaps, the archetypical CoO/Co structure is the most studied object by various methods, including neutron scattering [2-3]. Due to well studied properties, CoO/Co-based systems are used in many studies, including triplet spin valve effects in hybrid superconductor/ferromagnet heterostructures [4].

In this report we present results of polarized neutron reflectometry (PNR) of exchange biased CoO(20nm)/Co(1÷20nm) structures. In order to enhance sensitivity of neutron scattering to the magnetic state of the cobalt layer we have used special design of the structure, known as neutron waveguide. In the waveguide, the investigated magnetic layer is placed between the highly reflecting layer of CoO and the sapphire substrate. The Nb layer is used as a spacer for formation of neutron standing wave and also can be used for the study of the triplet spin valve effect [4]. The waveguide enhancement allowed us to measure neutron intensity of specular and off-specular scattering in four spin states. At low temperature, in certain region of magnetic fields, we have observed strong difference in reflectivities of two spin-flip channels in the waveguide mode (Fig. 1). Such a difference is typical for neutron scattering from non-complanar magnetic structures, like helicoids [5] or skyrmion [6]. The PNR measurements are complemented with transport and SQUID data. Possible explanation of the magnetic arrangement is discussed. We acknowledge the financial support of DFG (projects TRR 80 and HO 955/9-1).

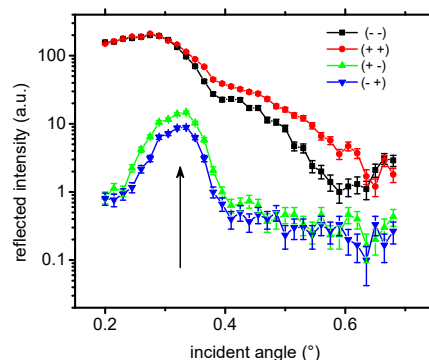


Fig. 1. Spin-polarized neutron reflectivity curves measured on sample CoO(20nm)/Co(4nm)/Nb(20nm)/Al₂O₃. Position of the waveguide mode is shown by vertical arrow.

[1] F. Radu and H. Zabel, *STMP*, **227** (2007) 97–184.

[2] F. Radu et al, *Phys. Rev. B*, **67** (2003) 134409.

[3] A. Paul et al, *J. Phys. Condens Matter.*, **19** (2007) 086229.

[4] V. Zdravkov et al, *Phys. Rev. B*, **87** (2013).

[5] S. Grigoriev et al, *Phys. Rev. Lett.*, **100** (2008) 197203.

[6] S. Mühlbauer et al, *Science.*, **323** (2009) 915.

5 July

Wednesday

12:00-14:00

poster session
5PO-I

**“Magnetic
Nanostructures and
Low Dimensional
Magnetism”**

5PO-I-1

CRITICAL PHENOMENA IN THE ANTIFERROMAGNETIC ISING MODEL ON A BODY-CENTERED CUBIC LATTICE WITH NEXT-NEAREST- NEIGHBOR INTERACTIONS

Murtazaev A.K.^{1,2}, Ramazanov M.K.¹, Kurbanova D.R.¹, Badiev M.K.¹, Murtazaev K.Sh.²

¹ Institute of Physics, Dagestan Scientific Center, RAS, Makhachkala, Russian Federation

² Dagestan State University, Makhachkala, Russian Federation

sheikh77@mail.ru

The quantitative description of phase transitions and critical phenomena in the contemporary physics of condensed states is based on various lattice models. [1]. Recent advances in understanding phase transitions and critical phenomena in frustrated systems have largely been achieved by applying of Monte Carlo methods [2-4].

In present paper, we investigate critical phenomena and estimate a full set of static critical exponent of the antiferromagnetic Ising model on a body-centered cubic lattice with allowance for the next-nearest-neighbor interactions. Numerical simulation by the Monte Carlo method for the Ising model on a body-centered cubic lattice were performed in [5,6].

The Hamiltonian of the antiferromagnetic Ising model on a body-centered cubic lattice can be written as

$$H = J_1 \sum_{\langle ij \rangle} (S_i \cdot S_j) + J_2 \sum_{\langle il \rangle} (S_i \cdot S_l), \quad (1)$$

where $S = \pm 1$ is the Ising spin. The first term in expression (1) takes into account the exchange antiferromagnetic interaction of nearest-neighbors of intensity $J_1 > 0$, the second terms describes an antiferromagnetic interaction between next-nearest-neighbors $J_2 > 0$ ($k = J_2/J_1 = 1.0$; J_1 and J_2 are the constants of the nearest-neighbor and next-nearest-neighbor interactions, respectively, and r is the magnitude of the next-nearest-neighbor interaction). Frustrations in the model are caused by a competition between exchange interactions the nearest-neighbors and next-nearest-neighbors.

The static magnetic exponents specific heat α , susceptibility γ , magnetization β , correlation length ν were calculated by using the finite-size scaling theory [2-4].

Research conducted for the ratio of the exchange interactions and the next-nearest neighbors $k=J_2/J_1$ in increments $\Delta k=0.1$ range of values $k \in [0.0, 1.0]$. Within the framework of the theory of finite-size scaling calculated static critical exponents of the heat capacity of α , susceptibility γ , the order parameter β , correlation radius ν , as well as the Fisher index η . It is shown that the universality class of the critical behavior of the model is maintained in the range of $k \in [0.0, 0.6]$. It was found that a non-universal critical behavior is observed in the range of $k \in [0.8, 1.0]$.

The work was supported by the Russian Foundation for Basic Research (project no. 16-02-00214 and project no. 16-32-00105).

[1] Vik.S. Dotsenko, *Usp. Fiz. Nauk*, **165** (1995) 481.

[2] A.K. Murtazaev, M.K. Ramazanov, M.K. Badiev, *Low Temp. Phys.*, **35** (2009) 521.

[3] A.K. Murtazaev, M.K. Ramazanov, M.K. Badiev, *JETP*, **115** (2012) 331.

[4] A.K. Murtazaev, M.K. Ramazanov, F.A. Kassan-Ogly, M.K. Badiev, *JETP*, **117** (2013) 1091.

[5] P.H. Lundow, K. Markstrom, A. Rosengren, *Philos. Mag.*, **89** (2009) 2042.

[6] A.K. Murtazaev, M.K. Ramazanov, F.A. Kassan-Ogly, D.R. Kurbanova, *JETP*, **120** (2015) 110.

5PO-I-2

INFLUENCE OF STRUCTURAL DISORDER ON MAGNETIC STRUCTURE OF $\text{Cr}_{1/3}\text{NbS}_2$ AND $\text{Mn}_{1/3}\text{NbS}_2$ HELICAL MAGNETS: ^{55}Mn AND ^{53}Cr NMR STUDY

Ogloblichev V.V.¹, Piskunov Y.V.¹, Mushenok F.B.^{2,3}

¹ M.N. Miheev Institute of Metal Physics UB RAS, Yekaterinburg, Russia

² Institute of Problems of Chemical Physics, Chernogolovka, Russia

³ University of Exeter, Stocker road, Exeter, EX4 4QL, United Kingdom
ogloblichev@imp.uran.ru

Peculiarities of magnetic ordering of helical magnet $\text{Cr}_{1/3}\text{NbS}_2$ have been investigated by nuclear magnetic resonance (NMR) method at zero magnetic field in a broad temperature range $T = 4.4 - 77$ K. NMR signal was observed in two different frequency ranges (64 – 68) MHz and (49 – 51) MHz ($T = 4.2\text{K}$). Components of electric field gradients, hyperfine fields and magnetic moments of chromium ions were estimated and analyzed. It was concluded that structural disorder induces at least two valence states of chromium ions - Cr^{4+} and Cr^{3+} . Magnetic moments of Cr^{3+} ions lie in basal ab plane due to magnetocrystalline “easy-plane” anisotropy and form two different types of magnetic structure: commensurate structure and incommensurate magnetic soliton lattice.

Question of the valence state of manganese in such compounds Mn_xNbS_2 is extremely relevant [1]. According to the literature data [2], the effective magnetic moments of the manganese ions in $\text{Mn}_{1/3}\text{NbS}_2$ and $\text{Mn}_{1/4}\text{NbS}_2$ are $(5.2-5.6)\mu_B$ and $(5.2-5.4)\mu_B$ respectively. It turned out that the total spin quantum number of manganese ions is close to the value of $S=5/2$ ($\mu_{\text{eff}}=g(S(S+1))^{0.5} \approx 5.9\mu_B$), and manganese valence state is, hence, Mn^{2+} . According to other experimental data [3], the effective magnetic moment of manganese these compounds is $(4.6-5.1)\mu_B$, which gives the total spin number $S=2$ and valence state of Mn^{3+} ($\mu_{\text{eff}}=4.9\mu_B$).

As a result of NMR studies the local magnetic hyperfine field and the values of the effective magnetic moments of the manganese ions in $\text{Mn}_{1/4}\text{NbS}_2$ and $\text{Mn}_{1/3}\text{NbS}_2$ has been obtained as $h_{\text{st}} = 422\text{kOe}$, $\mu_{\text{eff}} = 4.3\mu_B$ and $h_{\text{st}} = 446\text{kOe}$, $\mu_{\text{eff}} = 4.5\mu_B$ respectively. These values clearly indicate that the manganese ions in the tested niobium dichalcogenides are Mn^{3+} .

Measurements of spin-spin relaxation clearly indicate about the existence of two positions of Mn atoms in these compounds. The first position corresponds to the manganese atoms, forming a “homogeneous” helical structure, the second position corresponds to the manganese atoms in the areas with impaired helical magnetic structure.

The research was carried out within the state assignment of FASO of Russia (theme “Spin” No. 01201463330), supported in part by RFBR (project No. 15-02-02000).

[1] Y. Kousaka, et. al., *Nuclear Instruments and Methods in Physics Research Section A*, **600** (2009) 250-253.

[2] S. S. P. Parkin and R. H. Friend, *Philosophical magazine*, **41** (1980) 65-93.

[3] K. Anzenhofer, et. al., *Journal of Physics and Chemistry of Solids*, **31** (1970) 1057–1067.

5PO-I-3

DIP PEN NANOLITHOGRAPHY USING MHA-ACETONITRILE AND ODT-ACETONITRILE FOR HIGH-RESOLUTION STRUCTURES

*Lukyanenko A.V.^{1,2}, Smolyarova T.E.^{1,2}, Tarasov A.S.^{1,2}, Rautskii M.V.², Bondarev I.A.^{1,2},
Ovchinnikov S.G.^{1,2}, Volkov N.V.²*

¹ Institute of Engineering Physics and Radio Electronics, Siberian Federal University, Krasnoyarsk, Russia

² Kirensky Institute of Physics, Federal Research Center KSC SB RAS, Krasnoyarsk, Russia
lav@iph.krasn.ru

Atomic force microscopy-based nanotechnological tool, dip-pen nanolithography (DPN) has provided an ideal direct-write lithographic tool that allows materials to be patterned from DPN tips onto a surface with high resolution. [1]

In DPN, the tip of an atomic force microscope (AFM) probe is coated with “ink” and traced across a target surface. As the probe traverses the surface, the ink is deposited along the tracing path and diffuses away from the tip. By varying the tip speed and/or dwell time, it is possible to create lines of various widths and/or dots of various radii, and the lines and dots can be combined to create complex patterns.

This method allows to work with a wide variety of inks — such as DNA, polymers, and proteins — and can create patterns on many different kinds of materials, including silicon, metal, and glass. It also works with a large selection of probe types — from single-cantilever probes to active-pen arrays to multi-pen arrays with 55,000 probes on a single chip. It can also be used for a variety of non-fabrication tasks, including additive repair on electronic devices and photomasks.

DPN experimentation was automated by NanoInk’s InkCAD software. InkCAD controls when the MHA-coated tip is in contact with the surface, and how long it dwells (creating dots).

In the experiment we used structure Au/Fe₃Si grown on Si(111) by molecular beam epitaxy(MBE) [2]. In DPN method the ink (MHA-Acetonitrile) is deposited along the tracing path and diffuses away from the tip. This way we can form desired pattern, on a Fe₃Si/Si(111) substrate coated with Au (18 nm). In the experiment was used a SiN probe, coated with two different “inks”.

The substrate patterned with MHA-polymer for 20 minutes in the wet-etching of 1:1:1:1 (v/v/v/v) aqueous mixture of 0.1M Na₂S₂O₃, 1.0M KOH, 0.01M K₃Fe(CN)₆, и 0.001M K₄Fe(CN)₆ [3] with constant stirring to completely remove Au from areas not covered with ink-polymer.

The reported study was funded by Government of Krasnoyarsk Territory, Russian Foundation for Basic Research, Krasnoyarsk Region Science and Technology Support Fund

[1] J. Zhong, G. Sun, D. He, *Nanoscale*, **6** (2014) 12217.

[2] I.A. Yakovlev, S.N. Varnakov, B.A. Belyaev, S.M. Zharkov, M.S. Molokeev, I.A. Tarasov, S.G. Ovchinnikov, *J. JETP Letters*, **99** (2014) 572.

[3] J.C. Hulteen, R.P. Van Duyne, *J. Vac. Sci. Technol.*, **13** (1995) 153-158.

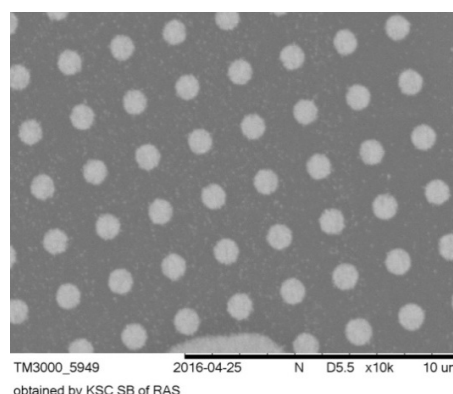


Fig. 1. An array of disks with a diameter of 700 nm obtained by DPN.

5PO-I-4

THE MONTE-CARLO INVESTIGATION OF 2D ANNNI-MODEL

Murtazaev A.K.^{1,2}, Ibaev Zh.G.^{1,2}

¹ Institute of Physics DSC RAS, Makhachkala, Yaragского 94, Russia

² Dagestan State University, Makhachkala, Gadjieva 43a, Russia

ibaev77@mail.ru

The progress in the study of quasi-one-dimensional and quasi-two-dimensional transition-metal-based magnets is largely conditioned by the application of simplified many-electron approaches with the use of Heisenberg and Ising models [1]. Hamiltonians of these models have a rather simple algebraic structure.

The Ising model with competing ferromagnetic and antiferromagnetic interactions on a cubic lattice (so called ANNNI-model) was introduced to describe ordered magnetic phases in CeSb crystals. An identical model is successfully used for the description of the thermodynamics of oil microemulsions named the Vidom-model. In the present work, we investigate a two-dimensional analog of such model using the standard Metropolis algorithm of the Monte-Carlo method (Fig.1)

The Hamiltonian of the model is:
$$H_{ANNI} = -J \sum_{i,j} s_i s_j - J_1 \sum_i s_i s_{i+2}, \quad (1)$$

$s_i = \pm 1$, $J > 0$ is the parameter of the exchange interactions of neighboring spin pairs, $J_1 < 0$ is the parameter of the antiferromagnetic interaction of next-nearest neighbors along the Y axis.

The investigations are performed using the cubic systems with periodic boundary conditions and sizes $L \times L$; $L = 26, 28, 32$. The number of spins in simulated system is $N_{eff} = 676, 784, \text{ and } 1024$. The Markov chains of $\tau = 1000\tau_0$ in length ($\tau_0 = 10^4$ MC steps per spin is the length of the non-equilibrium section) are generated on the computer. The thermodynamic parameters of the system are computed by averaging along this chain. Additionally, the averaging is carried out along thousand different initial configurations.

The temperature dependences of thermodynamic parameters such as internal energy, order parameter, heat capacity, and susceptibility are obtained from investigation results. Also modulated structures are obtained at different temperatures and values of parameters of the competing interaction. The investigation results demonstrate the occurrence of several phases and transitions between them in the ANNNI-model as well. The values of phase transition temperatures are computed using the Binder cumulant method and the Fourier analysis methods. Based on these results, the phase diagram of 2D anisotropic Ising model with competing interactions is plotted.

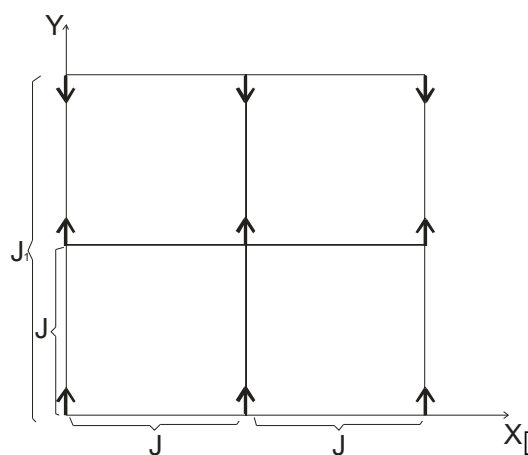


Fig. 1. 2D ANNNI-model.

[1] A.A. Ovchinnikov, I.I. Ukrainskii, G.V. Kventsel', *Physics-Uspehi*, **15** (1973) 575–591.

5PO-I-5

TOP AND BOTTOM SPIN VALVES WITH Ni-Fe-Mn ANTIFERROMAGNETIC LAYER

Blinov I.V., Krinitsina T.P., Milyaev M.A., Popov V.V., Ustinov V.V.

M.N. Miheev Institute of Metal Physics, Ekaterinburg, Russian Federation

¹ blinov@imp.uran.ru

Bilayers permalloy/antiferromagnetic triple Ni-Fe-Mn alloy have been studied, as well as magnetic and magnetoresistive properties of spin valves (SVs) with Ni-Fe-Mn antiferromagnet (AF) as a pinning layer. A technique of fabrication of bottom spin valves with an enhanced thermal stability and improved hysteretic characteristics has been elaborated.

According to the results of the studies carried out, the bilayers with antiferromagnetic triple layer $\text{Ni}_{14}\text{Fe}_6\text{Mn}_{80}$ are characterized by moderate energy of exchange interaction $J_{\text{ex}} = 0.05 \text{ erg/cm}^2$ and medium blocking temperature $T_b \cong 150^\circ\text{C}$. Higher $T_b \cong 270^\circ\text{C}$ and $J_{\text{ex}} = 0.27 \text{ erg/cm}^2$ were obtained for the annealed bilayers manganese/permalloy. In this case an ordered AF phase Ni-Fe-Mn is formed. The ordered AF phase formation is testified by an appearance of super-structural Debye rings (100), (110), (210), (211) in electron diffraction patterns of sample $\text{Al}_2\text{O}_3/\text{Mn}(50\text{nm})/\text{Ni}_{77}\text{Fe}_{23}(30\text{nm})/\text{Ta}(5\text{nm})$ after its annealing in the magnetic field at $T_{\text{ann}} = 260^\circ\text{C}$ for 4 h. In this case in the electron-microscope images one can see columnar structure, and an intermediate layer between manganese and permalloy layers is absent. To fabricate a bottom SV with the ordered AF phase Ni-Fe-Mn a technological cycle has been worked out, including the following operations: 1) Formation of the ordered AF phase Ni-Fe-Mn in a sample

$\text{Al}_2\text{O}_3/\text{Ni}_{77}\text{Fe}_{23}(5\text{nm})/\text{Mn}(50\text{nm})/\text{Ni}_{77}\text{Fe}_{23}(30\text{nm})/\text{Ta}(5\text{nm})$ by the thermal-magnetic treatment at 260°C for 4 h. 2) Ion etching for 20 min of the annealed sample for the surface layer removing. The ion etching duration was chosen to assure the removal of the contaminated surface layer and retaining the ferromagnetic area together with the ordered AF phase required for the formation of the unidirectional anisotropy in the FM layer sputtered on the sample after etching. 3) Magnetron sputtering of the layered structure consisting of ferromagnetic $\text{Co}_{90}\text{Fe}_{10}$ layers separated by Cu on the as-prepared sample $\text{Al}_2\text{O}_3/\text{Ni-Fe-Mn}$. 4) Annealing of the as-prepared structure in a magnetic field at $T_{\text{ann}} = 300^\circ\text{C}$ for 15 min.

The magnetoresistance of the as-fabricated spin valve $\text{Al}_2\text{O}_3/\text{Ni-Fe-Mn}/\text{Co}_{90}\text{Fe}_{10}(5.5\text{nm})/\text{Cu}(3.6\text{nm})/\text{Co}_{90}\text{Fe}_{10}(5.5\text{nm})/\text{Ta}(5\text{nm})$ is $\Delta R/R_s = 3.8 \%$ (Fig. 1).

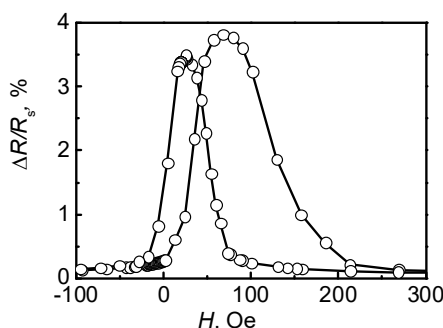


Fig. 1 – Field dependence of the magnetoresistance of bottom spin valve $\text{Al}_2\text{O}_3/\text{Ni-Fe-Mn}/\text{Co}_{90}\text{Fe}_{10}(5.5\text{nm})/\text{Cu}(3.6\text{nm})/\text{Co}_{90}\text{Fe}_{10}(5.5\text{nm})/\text{Ta}(5\text{nm})$

The research has been done within the IMP state assignment “Spin”, with partial support by UB RAS (project No. 15-9-2-44) and RFBR (project No. 16-32-00128).

5PO-I-6

SPIN CLUSTERS IN WARWICKITE SINGLE CRYSTALS

*Knyazev Yu.V.¹, Bayukov O.A.¹, Kazak N.V.¹, Bezmaternykh L.N.¹, Platonov M.S.¹,
Ovchinnikov S.G.¹*

¹ Kirensky Institute of Physics, Federal Research Center KSC SB RAS, Krasnoyarsk, Russia
yuvknyazev@mail.ru

We have synthesized high-quality single crystals CoFeBO_4 and $\text{Mn}_{1.3}\text{Fe}_{0.7}\text{BO}_4$ with a warwickite structure. The crystal structure of warwickites was thoroughly solved [1].

According to our magnetic measurements samples CoFeBO_4 and $\text{Mn}_{1.3}\text{Fe}_{0.7}\text{BO}_4$ show transition to a spin glass state at temperature (T_{SG}) of 22 K and 17 K, respectively. The deviation from the Curie-Weiss law occurs at higher temperatures (150 K) and indicates the spin correlations between nearest magnetic neighbors.

Due to the very small time scale of Mössbauer spectroscopy ($10^{-8} - 10^{-12}$ s) we have observed the dipole-dipole interactions, which leads to the magnetic correlations at temperature (T_M) for our samples CoFeBO_4 (33 K) and $\text{Mn}_{1.3}\text{Fe}_{0.7}\text{BO}_4$ (20 K). Relaxation Mössbauer spectra clearly demonstrated the spin-glass state transition. Our spectra are typical for a frustrated state of magnetic moments of iron [2]. The equal value for hyperfine field (H_{hf}) of the CoFeBO_4 and $\text{Mn}_{1.3}\text{Fe}_{0.7}\text{BO}_4$ samples at 4 K indicates the formation of iron spin clusters in warwickite structure (Table 1).

These clusters are connecting to each other by the strong frustrated indirect exchange interactions (Fig.1), which leads to the spin-glass state. Thus, the T_M/T_{SG} relation for the samples CoFeBO_4 and $\text{Mn}_{1.3}\text{Fe}_{0.7}\text{BO}_4$ amounts to 1.5 and 1.3, respectively. According to Ref. [3] we can conclude that the average size of the iron spin clusters is about 80 Å.

Support by RFBR №№16-32-60049 mol_a_dk,
16-32-00206 mol_a, 17-02-00826_a

Table 1. Hyperfine parameters obtained from the low-temperature (4 K) Mossbauer spectra of $\text{Mn}_{1.3}\text{Fe}_{0.7}\text{BO}_4$ and CoFeBO_4 .

	H_{hf} , (± 0.05 T)	IS, (± 0.01 mm/s)	QS, (± 0.01 mm/s)	Γ , (± 0.05 mm/s)	S, (± 1.5 %)
CoFeBO₄					
1	47.6	0.50	-0.06	0.78	41.6
2	40.9	0.50	-0.06	0.68	35.7
3	36.5	0.48	-0.06	0.78	22.7
Mn_{1.3}Fe_{0.7}BO₄					
1	46.7	0.54	0.12	0.55	44.8
2	43.8	0.54	-0.06	0.61	42.9
3	40.8	0.56	-0.02	0.52	12.3

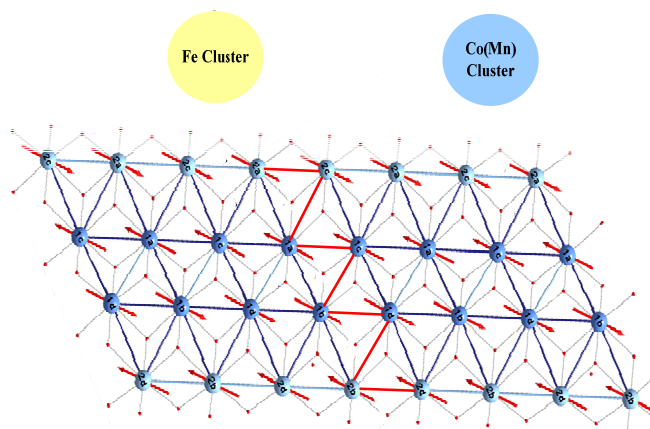


Fig.1 Representation of spin clusters in warwickite single crystals. Red bonds indicates frustrated indirect interactions in magnetic structure

[1] A. Arauzo et al., *J. Magn. Magn. Mater.*, **392** (2015) 114–125.

[2] A. Wiedenmann et al., *J. Magn. Magn. Mater.*, **15-18** (1980) 216-218.

[3] Mørup, S., Tronc, E.: *Phys. Rev. Lett.*, **72** (1994) 3278.

5PO-I-7

MAGNETIZATION CURVES AND HYSTERESIS LOOPS OF NANOSTRUCTURED RARE EARTH TITANATES

Rinkevich A.B.¹, Korolev A.V.¹, Samoilovich M.I.², Demokritov S.O.^{1,3}, Perov D.V.¹

¹ Institute of Metal Physics, Ekaterinburg, Russia

² Central Research Technological Institute "TECHNOMASH", Moscow, Russia

³ Institute for Applied Physics and Center for Nonlinear Science, University of Muenster, Muenster, Germany
peroff@imp.uran.ru

Magnetic properties of nanocomposite materials containing particles of rare earth titanates of $R_2Ti_2O_7$ type, including "spin ice" materials are investigated. Major and minor magnetic-hysteresis loops of nanocomposite materials containing particles of rare earth titanates Nd^{3+} , Pr^{3+} , Sm^{3+} , Dy^{3+} , Er^{3+} , Yb^{3+} , La^{3+} of $R_2Ti_2O_7$ type have been investigated in temperature range from 2K to 50K. The choice of materials allows for investigation of nanocomposite pyrochlore titanates both belonging and not belonging to spin ice materials, as well as comparison of the magnetic properties of titanates with different values of magnetic moment of R^{3+} ions, and with Kramers and non-Kramers ions. The nanocomposite materials based on opal matrices under investigation comprise the rare earth titanates placed in inter-spherical volumes of spherical particles. The size of the particles varied from 5 to 60 nm. Embedded particles are placed approximately periodically with the distance between the particles located in neighboring inter-sphere voids being about 250-300 nm.

Two reasons for the presence of hysteresis loop are considered: 1. Influence of admixture of 3d elements leading to magnetic polarization and magnetic ordering of the nanocomposite. 2. Intrinsic magnetic polarization due to nano-size of titanate particles. For several nanocomposites we observed an interesting experimental feature: several demagnetization curves e.g. descending branches of the hysteresis loop measured at different temperatures cross at one point of the magnetization M – magnetic field H plane. This fact means that there is a temperature interval within which magnetization only weakly depends on temperature. This fact has been established for nanocomposite titanates with $Yb_2Ti_2O_7$, $Dy_2Ti_2O_7$, $Er_2Ti_2O_7$ particles. For nanocomposite with $Sm_2Ti_2O_7$ particles the area has been defined where these dependences intersect. The hysteresis loop is lacking for the nanocomposites with $La_2Ti_2O_7$, $Pr_2Ti_2O_7$ and $Nd_2Ti_2O_7$ particles.

Temperature dependences of coercive field and remanent magnetization for all samples indicate that values of coercive force for samples of various composition differ, at least, by one order of the magnitude. The shapes of temperature dependences for different nanocomposites are also different. No specific features was disclosed for the nanocomposites containing of Kramers-type (Nd^{3+} , Sm^{3+} , Dy^{3+} , Er^{3+} , Yb^{3+}) and non-Kramers-type (Pr^{3+}) ions. It should be pointed out that the points of intersection and high values of H_c and M_r are specific for the nanocomposites which possess high value of magnetic moment e.g. Dy^{3+} and Yb^{3+} . These are exactly the titanates that are related to classical spin ice ($Dy_2Ti_2O_7$) and quantum spin ice ($Yb_2Ti_2O_7$) systems. Crossing of the demagnetization curves takes place, however, at temperatures much higher than the spin ice state occurs.

The work is carried out within the RAS plan (theme "Spin" No. 01.2.006 01201463330), with partial support of grant from Russian Ministry of Education and Science No. 14.Z50.31.0025 and RFBR grant No. 17-02-00029.

5PO-I-8

HIGH ROTATABLE MAGNETIC ANISOTROPY IN $L1_0$ FePt AND $L1_0$ CoPt THIN FILMS

Myagkov V.G., Bykova L.E., Zhigalov V.S.

Kirensky Institute of Physics, Federal Research Center KSC SB RAS, Krasnoyarsk, Russia
miagkov@iph.krasn.ru

The manipulation of the magnetic anisotropy by electric field, via spin-orbit coupling, by strains is of great interest because it can potentially lead to extend the functional capabilities of the thin ferromagnetic films. The control of perpendicular magnetic anisotropy (PMA) including the $L1_0$ -ordered CoPt and FePt film alloys also has been studied intensively because it is important for technological applications. However, the manipulation of the PMA by the rotation of the easy magnetization axis to perpendicular film plane remains unnoticed. The first investigations of the magnetic properties of thin films the new type of magnetic anisotropy was discovered in which easy axis can be rotated by applying a in-plane magnetic field and now it known as rotatable magnetic anisotropy (RMA). Recently, we show that large RMA, overcoming the shape in-plane magnetic anisotropy, was obtained in epitaxial $L1_0$ CoPt(111) [1] and polycrystalline δ -Mn_{0.6}Ga_{0.4} thin films after the solid-state reactions in Co/Pt(111) and Ga/Mn bilayers, respectively. In these films the easy axis can be arrange by magnetic field in any (in-plane and out-of-plane) direction and this proves that large PMA can be achieved by magnetic field tuning in RMA films (Fig.1).

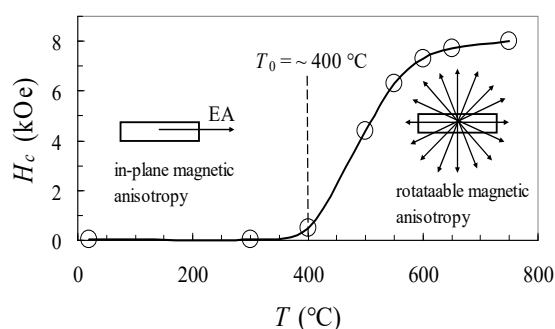


Fig. 1. Coercivity H_C Co/Pt(111) of the film system versus the annealing temperature T . The vertical dashed line shows the temperature of the initiation of the solid-state synthesis of the $L1_0$ CoPt(111) phase ($T_0 \sim 400^\circ\text{C}$) in Co/Pt(111)films.

High RMA was also obtained in the $L1_0$ -FePt(001) films above $T_0 \sim 400^\circ\text{C}$ by the solid-state reaction of the Pt(001)/Fe(001) bilayers. Although RMA origin still remains unknown, among possible explanations is the existence of epitaxial intergrown $L1_0$ and $L1_2$ phases, inducing large magnetostriction and magnetic-field-induced strain, creating uniaxial anisotropy with an easy axis along the direction of the magnetic field. Based on a literature review and our investigations, we believe that high RMA, overcoming the shape in-plane magnetic anisotropy, is a widespread phenomenon the thin-film magnetism.

This study was supported by by the RFBR (grants # 15-02-00948, 16-03-00069).

[1] V.G. Myagkov, V.S. Zhigalov, L.E. Bykova, G.N. Bondarenko, A.N. Rybakova, A.A. Matsynin, I.A. Tambasov, M.N. Volochaev, D.A. Velikanov, *JETP Letters*, **102** (2015) 355-360.

5PO-I-9

HIGH ROTATABLE MAGNETIC ANISOTROPY IN MnBi ALLOYS, OBTAINED BY SOLID STATE REACTIONS IN Mn/Bi/Mn FILMS

Bykova L.E.¹, Myagkov V.G.¹, Yakovchuk V.Yu.¹, Patrin G.S.^{1,2}, Bondarenko G.N.³

¹ Kirensky Institute of Physics, Federal Research Center KSC SB RAS, Krasnoyarsk, Russia

² Siberian Federal University, Krasnoyarsk, Russia

³ Institute of Chemistry and Chemical Technology, Federal Research Center KSC SB RAS, Krasnoyarsk, Russia
lebyk@iph.krasn.ru

Rotatable magnetic anisotropy (RMA) was discovered in the first studies of thin-film magnetism. RMA is characterized by an easy axis of magnetic anisotropy, which can be rotated by a magnetic field that exceeds the coercive force H_C . Unlike other kinds of anisotropies, RMA is not described by a sinusoidal law and therefore has no unambiguous characteristic. The difference $H_{rot} = H_k^{dyn} - H_k^{stat}$ between the dynamic field of the magnetic anisotropy, measured by ferromagnetic resonance, and the static field of the magnetic anisotropy is used to characterize the RMA. In torque measurements, RMA can be characterized by the average torque value L_{rot} at large rotational angles of the magnetic field [1]. The intermetallic compound MnBi has many unique magnetic and structural properties and is seen as a possible replacement for expensive rare-earth magnets. We present the first observations of high RMA in hard magnetic MnBi polycrystalline films, obtained by a solid state reaction in Mn/Bi/Mn films. After annealing at 270°C, the samples contained nanoclusters with the dominating α -MnBi phase epitaxially intergrown with the $Mn_{1.08}Bi$ phase. A high RMA, whose easy axis can be rotated in fields exceeding the coercivity in the plane (Fig.1) and perpendicular (Fig.2) to the sample plane, was found in the prepared samples. Although the detailed mechanism of high RMA remains unclear, we suppose that high RMA is a result of the epitaxial intergrowth of the hard magnetic α -MnBi phase with the $Mn_{1.08}Bi$ phase.

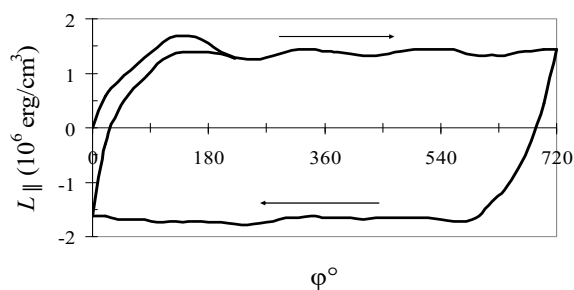


Fig.1

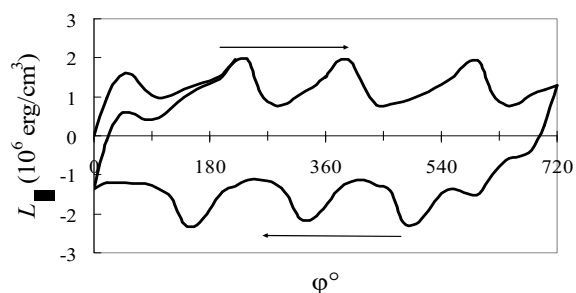


Fig.2

This study was supported by the RFBR (grants ## 15-02-00948, 16-03-00069).

[1] V.G.Myagkov, V.S.Zhigalov, L.E.Bykova, G.N.Bondarenko, A.N.Rybakova, A.A.Matsynin, I.A.Tambasov, M.N.Volochaev, D.A.Velikanov, *JETP Letters* **102** (2015) 355-360.

5PO-I-10

ROLE OF ANTIFERROMAGNETIC SPACER LAYER IN FORMING MAGNETIC ORDER IN Fe/Cr/Gd SUPERLATTICES

Ryabukhina M.V.¹, Kravtsov E.A.¹, Khaydukov Yu.², Proglyado V.V.¹, Ustinov V.V.¹

¹ Institute of Metal Physics, Ural Branch, Russian Academy of Sciences, Ekaterinburg, Russia

² Max Planck Institute for Solid State Research, Stuttgart, Germany

ryabukhina@imp.uran.ru

Fe/Cr/Gd multilayers, where Fe-Gd interlayer exchange is mediated by antiferromagnetic Cr, display novel magnetic phases in applied magnetic fields and temperature, including possible switching an otherwise antiferromagnetic interlayer coupling to ferromagnetic or non-collinear one. Including Cr spacer may also affect Fe-Gd magnetic proximity effects and lead to structural transitions inside Fe and Gd layers.

Here we report on structural and magnetic studies of a series of multilayers [Fe(35Å)/Cr(t Å)/Gd(50 Å) /Cr(t Å)]₁₂ (t=0 -60 Å) grown with an UHV sputtering onto Si (001) substrates. Structural investigation done with high-resolution X-ray reflectometry and glancing angle X-ray diffraction has confirmed that the multilayers have a well-defined layered structure with rms interface roughness of ca. 3–5 Å. The multilayers were found to be polycrystalline, with Gd/Fe multilayer containing Gd hcp and Fe bcc phases, in Fe/Cr/Gd an extra fcc Gd phase appearing. As Cr spacer becomes thicker fcc Gd phase becomes stronger.

The depth-resolved magnetic structure of the multilayers was determined by complementary application of SQUID magnetometry and polarized neutron reflectometry (PNR). We found that insertion of Cr spacer and further increase in its thickness leads to switching Fe-Gd interlayer magnetic ordering from antiferromagnetic to non-collinear one, for thick enough Cr spacers Fe and Gd being uncoupled. The saturated Gd magnetic moment decreases as Cr thickens, which we explain by nucleation of fcc Gd crystallographic phase with lower magnetic moment. PNR measurements have revealed the existence of an Fe-Gd proximity effect when there is an enhancement Gd magnetic moment at ca 2-3 monolayers near the interfaces and decrease in the core of Gd layers. The enhanced Gd magnetic moment is temperature independent, it is the strongest one in Fe/Gd and decreases as Cr spacer becomes thicker.

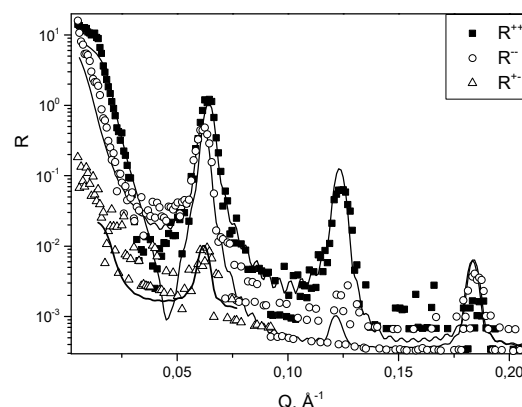


Figure 1. Experimental (symbols) and calculated (lines) PNR spectra from the Fe/Cr(10 Å)/Gd sample measured at $T = 15$ K in field $H = 500$ Oe

This research was carried out within the state assignment of FASO of Russia (theme “Spin” No. 01201463330), supported in part by RFBR (project No. 14-22-01063).

5PO-I-11

SPIN-CHAIN BEHAVIOR IN $\text{La}_3\text{CrGe}_3\text{Be}_2\text{O}_{14}$ COMPOUND FROM THE LANGASITE FAMILY

*Markina M.M.*¹, *Mill B.V.*¹, *Kazei Z.A.*¹, *Granovsky S.A.*^{1,2}

¹ Faculty of Physics, M.V. Lomonosov Moscow State University, Moscow, Russia

² Institut for Solid State Physics, TU Dresden, Dresden, Germany
markina@lt.phys.msu.ru

Recently, Be substituted compounds of langasite family with $\text{Ca}_3\text{Ga}_2\text{Ge}_4\text{O}_{14}$ crystal structure (sp. gr. $P321$) containing magnetic $4f$ ions were discovered and investigated [1,2]. In our work we present the investigation of $\text{La}_3\text{CrGe}_3\text{Be}_2\text{O}_{14}$, the new member of langasite family, combining $3d$ and $4f$ ions in the lattice. In this compound, Cr^{3+} ($S = 3/2$) ions occupy octahedral position $1a$ in the structure and organize one-dimensional magnetic chains along c direction with the distances $\sim 5 \text{ \AA}$ between nearest Cr^{3+} ions in chain and $\sim 8 \text{ \AA}$ between the chains. We investigated the magnetic susceptibility and specific heat of $\text{La}_3\text{CrGe}_3\text{Be}_2\text{O}_{14}$ in the range 1.8–320 K using Quantum Design PPMS. Temperature dependence of the magnetic susceptibility $\chi(T)$ is shown in Fig. 1. It follows the Curie-Weiss law in the range 50–320 K. The value of the effective magnetic moment is $3.8\mu_B$ for Cr^{3+} . Antiferromagnetic $\theta_{\text{CW}} = -23 \text{ K}$ allows to estimate roughly the magnetic exchange in 1D-chain as $J \sim 5 \text{ K}$. The broad maximum at 16.5 K is a typical feature for the low-dimensional magnetism and the $\chi(T)$ behavior can be successfully modelled by the Fisher's expression for Heisenberg $S = 3/2$ spin-chain with $J = 7.6 \text{ K}$ [3].

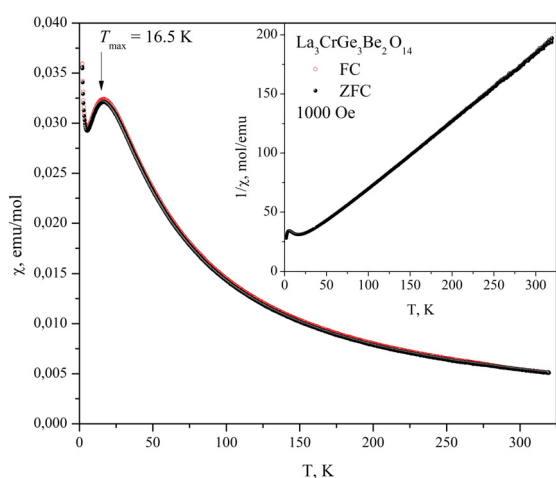


Fig. 1. Magnetic susceptibility of $\text{La}_3\text{CrGe}_3\text{Be}_2\text{O}_{14}$. Inset: $1/\chi$ curve

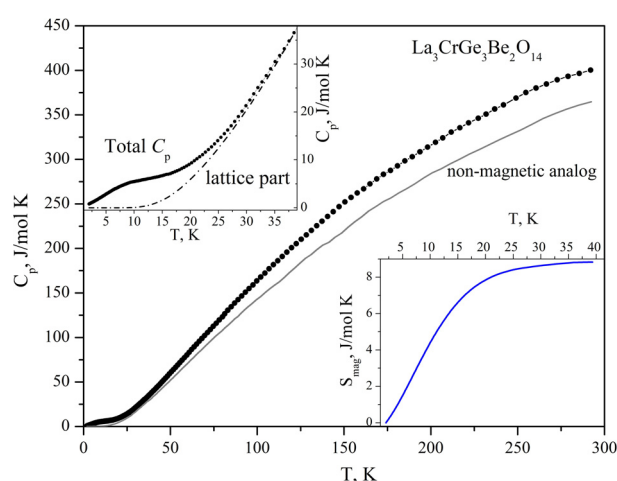


Fig. 2. Specific heat of $\text{La}_3\text{CrGe}_3\text{Be}_2\text{O}_{14}$. Insets: calculated lattice part (left); magnetic entropy (right).

On the specific heat temperature dependence $C(T)$ shown in Fig. 2 we found the broad maximum at $\sim 7 \text{ K}$ which is shown in details on the left inset to Fig. 2. The scaling procedure using the $C(T)$ data of nonmagnetic analog $\text{La}_3\text{AlGe}_3\text{BeO}_{14}$ gave the magnetic entropy $S_{\text{mag}} = 8.8 \text{ J/mol K}$ (right inset to Fig. 2) for $\text{La}_3\text{CrGe}_3\text{Be}_2\text{O}_{14}$ that agrees with theoretical estimation $R \ln 4 = 11.5 \text{ J/mol K}$. We do not see the long-range magnetic order formation and suppose that the magnetic structure in $\text{La}_3\text{CrGe}_3\text{Be}_2\text{O}_{14}$ is 1D spin-chains by Cr^{3+} ions ($S = 3/2$) elongated along the c direction.

[1] Mill B.V., *Russ. J. Inorg. Chem.*, **47** (2002) 721–723.

[2] A.Z. Sharma et al., *J. Sol. St. Chem.*, **233** (2016) 14–22.

[3] M.E. Fisher, *Am. J. Phys.*, **32** (1964) 343–346.

5PO-I-12

CRYSTAL STRUCTURE AND SPIN ORDERING OF A LAYERED HONEYCOMB-TYPE $\text{Li}_3\text{Ni}_2\text{SbO}_6$ ANTIMONATE

Podchezertsev S.Yu.¹, Korshunov A.N.^{1,2}, Malyshev A.L.¹, Kurbakov A.I.^{1,2}

¹ Petersburg Nuclear Physics Institute, NRC «Kurchatov Institute», Gatchina, Russia

² St.Petersburg University, Faculty of Physics, St. Petersburg, Russia
stpcz@mail.ru

Due to an interest to low-dimensional magnetism aroused in past years researches are in search of physical realizations of systems in which already existing theoretical models could be implemented. One of the examples of such systems is a novel family of a quasi-two-dimensional mixed oxides with chemical formula $\text{A}_3\text{M}_2\text{XO}_6$ where A – alkali metal or some 3d-metals cations, M – 3d- metal cations and X – Sb. These compounds are characterized by layered structure within which alkali metal layers are separated by honeycomb ordered M_2XO_6 layers. It was predicted that due to frustrated interactions between first, second and third neighboring magnetic cations such hexagonal ordering gives rise to a complicated magnetic phase diagram [1]. However, currently there are only few works devoted to experimental studies of magnetic structures of honeycomb systems. Another important feature of honeycomb layered oxides is the crystal structure itself. Layered structure of these compounds allows certain shifts between adjacent layers that may lead to different types of superstructure ordering as well as stacking faults presence, thereby complicating structure determination.

So the main aims of a present works were to determine the real symmetry of the crystal structure and its fine details and the magnetic structure of a layered honeycomb $\text{Li}_3\text{Ni}_2\text{SbO}_6$ antimonate by the means of high resolution synchrotron (SPD) and neutron (NPD) powder diffraction.

SPD studies revealed diffraction peaks splitting that allow defining unambiguously the crystal symmetry to be monoclinic ($C2/m$). At the same time, peak shape analysis revealed significant strains along crystallographic c -axis indirectly indicating a presence of stacking faults in studied compound. Monoclinic symmetry in these systems allows local surroundings of Ni and Sb ions to be distorted, however our structural analysis didn't revealed any significant difference in Ni-O or Sb-O bond distance pairs in NiO_6 and SbO_6 octahedra. Close to 90° (91.63° and 90.31° for different oxygen positions) values of Ni-O-Ni bond angles indicates the superexchange interaction within honeycomb layer via half-occupied e_g orbitals to be ferromagnetic. It should be also noted that in comparison to related compounds containing other alkali metals, small ionic radius of lithium led interlayer Ni-Ni distances to be slightly shorter than distances between second neighboring nickel ions within honeycomb layer.

At the same time low-temperature NPD revealed emergence of a set of additional Bragg peaks associated with long-range AFM ordering at temperatures below 15 K. Magnetic diffraction peaks were indexed with a commensurate propagation vector $\mathbf{k}=(1/2 \ 1/2 \ 0)$. Low temperature NPD analysis based on a representation analysis and value of a \mathbf{k} -vector determined the spin configuration to be so-called zigzag FM chains coupled AFM within honeycomb layer, while interlayer interactions have ferromagnetic nature. Temperature evolution of a magnetic scattering showed that the spins undergo a tilt with temperature decreasing: just below the T_N magnetic moments directed straight along c -axis, but upon cooling spins incline and finally stabilize perpendicular to (001) plane with a total tilt angle of 15.6° . The obtained value of a magnetic moment is $1.62(2) \mu_B/\text{Ni}$ which is smaller than theoretically predicted value of $\sim 2.0 \mu_B/\text{Ni}$ for Ni^{2+} in the high spin state ($S = 1$) with $g=2.15$. Such reduced value can be caused by frustrations of long-range magnetic interactions as well as glassy-like behavior caused by stacking faults.

[1] Li, P. H. Y., et al., *Physical Review B*, **86.14** (2012) 144404.

5PO-I-13

UNUSUAL SEMICONDUCTING AND TRANSPORT BEHAVIOR IN CLUSTER-BASED Fe/Mo MAGNETIC SYSTEMS

Antipov S.D., Goryunov G.E., Kornilov A.A., Senina V.A., Avksentev Y.I.

Faculty of Physics, M.V.Lomonosov Moscow State University, Leninskie Gory, Moscow, 119991, Russia
Vera_sen@mail.ru

The cluster-based metallic nanostructures have unusual magnetic and transport properties.

Earlier it was reported on the magnetic properties of Fe/Mo magnetic superlattices (MSL) [1] and Mo/Fe/Co MSL [2]. The spontaneous magnetization of the samples $[\text{Fe}(10 \text{ \AA})/\text{Mo}(t_{\text{Mo}})] \times 100$ ($t_{\text{Mo}} = 6,8 \div 22 \text{ \AA}$) has an oscillatory dependence on the Mo thickness with period 8 \AA and its value exceeds 1700Gs at the thickness of the Mo layers 10 \AA [1]. The Mo/Fe/Co MSL dc resistance has the semiconducting behavior in the temperature range $10\text{K} \div 250\text{K}$, with the maximum magnetoresistance value being 0.04% [2]. The theoretical description of the structure and magnetic properties of the $\text{Mo}_{4-x}\text{Fe}_x$ ($x=1 \div 3$) clusters have been suggested in [3]. These binary clusters are of a particular interest since Mo_4 is a 1D cluster, and Fe_4 is a 3D cluster and one can expect that the $\text{Mo}_{4-x}\text{Fe}_x$ clusters will have a 1D-3D transition with X increasing that changes both structure and magnetic properties.

We have deposited the nanosize cluster superlattices $[\text{Fe}(10 \text{ \AA})/\text{Mo}(t_{\text{Mo}})] \times 100$, $t_{\text{Mo}} = 4 \div 19 \text{ \AA}$, and cluster-based films $[\text{Fe}(0,6 \text{ \AA})/\text{Mo}(0,5 \text{ \AA})] \times 2346$, $[\text{Fe}(1,2 \text{ \AA})/\text{Mo}(0,4 \text{ \AA})] \times 1200$ and $[\text{Fe}(0,8 \text{ \AA})/\text{Mo}(1,2 \text{ \AA})] \times 1750$. The samples were prepared by the cathode sputtering with oscillating electrons at the next conditions: the pressure of the working gas Kr ($P=10^{-5}$ Topp), the anode voltage $U=2\text{kV}$, the magnetic field $H=320 \text{ Oe}$. The mica and monocrystalline Si were used as a substrate.

The X-ray diffraction studies were performed on the diffractometer “Stoe Study P” and did not reveal the presence of the coherent reflections.

In our report we present the experimental investigation results both the magnetic and transport properties of the above samples in a wide range of temperatures ($10\text{K} \div 290\text{K}$) and magnetic fields ($\pm 15 \text{ kOe}$).

The samples magnetization was superparamagnetic at room temperature. The resistivity semiconducting behavior was found in $[\text{Fe}(1,2 \text{ \AA})/\text{Mo}(0,4 \text{ \AA})] \times 1200$ and the resistivity change $\Delta R/R = [R(10\text{K}) - R(290\text{K})]/R(290\text{K}) \cong 10^3$ was in $[\text{Fe}(10 \text{ \AA})/\text{Mo}(19 \text{ \AA})] \times 100$.

The transition “insulator-metal” was observed in cluster superlattices $[\text{Fe}(10 \text{ \AA})/\text{Mo}(19 \text{ \AA})] \times 100$ at 460 K.

[1]. S.D. Antipov, G.E. Goryunov, G.V. Smirnikskaja, P.N. Stetsenko. *J. Magn. Magn. Mater.*, **258-259** (2003) 594-596.

[2]. S.D. Antipov, G.E. Goryunov, T.P. Kaminskaya, A.A. Kornilov, I.M. Novikov, M.A. Pivkina, V.A. Senina and G.V. Smirnikskaja. *Phys. Status. Solidi C*, **11** (2014) 1097-1101.

[3]. A. Garcia-Fuente, A. Vega, F. Aguilera-Granja, L.J. Galledo. *Phys. Rev. B.*, **79** (18) (2009) 4403.

5PO-I-14

COMBINING X-PEEM WITH HR-STEM FOR CORRELATING MAGNETISM AND STRUCTURE OF INDIVIDUAL COBALT NANOPARTICLES

Savchenko T.M.¹, Béch e A.², Timm M.¹, Bracher D.M.¹, Khadra G.³, Tamion A.³, Tournus F.³, Albin C.³, Dupuis V.³, Verbeeck J.², Nolting F.¹, Kleibert A.¹

¹ Swiss Light Source, Paul Scherrer Institut, CH-5232 Villigen, Switzerland

² Electron Microscopy for Material Science, University of Antwerp, Belgium

³ Institut Lumi re Mati re, UMR5306 Universit  Lyon 1-CNRS, Universit  de Lyon, 69622

Villeurbanne cedex, France

tatiana.savchenko@psi.ch

Unique size effects occurring in magnetic nanoparticles such as single domain states or superparamagnetism are of great interest for applications in medicine and spintronics [1]. However, despite significant experimental and theoretical efforts in the last decades a solid understanding of nanoparticles magnetism is still lacking, even for the canonical 3d transition metals such as Fe, Co, and Ni. For instance, it was recently demonstrated experimentally that apart from expected superparamagnetic state, Fe and Co nanoparticles can also exist in magnetically blocked state associated with a strongly enhanced magnetic anisotropy, which has been attributed to the presence of lattice defects in the core of the nanoparticles [2,3]. However, a direct correlation of magnetism and structural defects was not achieved in these works. In this contribution we tackle this issue by combining X-ray photo-emission electron microscopy (X-PEEM) with high-angle annular dark-field scanning transmission electron microscopy (HAADF-STEM) for correlating magnetism and microstructure of individual cobalt nanoparticles. Our findings suggest that a competition between various anisotropy contributions, such as shape, surface and magnetocrystalline magnetic anisotropies result in a complex behavior which can easily mask the commonly expected size dependence of properties such as magnetic energy barriers.

[1] S. Majetich et al, *MRS Bulletin*, **38** (2013) 11 899-903.

[2] A. Balan et al., *Phys. Rev. Lett.*, **112** (2014) 107201.

[3] A. Kleibert et al., *Phys. Rev. B*, **95** (2017) 195404.

5PO-I-15

FORMATION OF THE GAPLESS TRIPLET DEGREES OF FREEDOM IN THE BOND-DILUTED SPIN-GAP MAGNET $(\text{C}_4\text{H}_{12}\text{N}_2)(\text{Cu}_2\text{Cl}_6)$

Glazkov V.^{1,2}, *Krasnikova Yu.*^{1,2}, *Hüvonen D.*^{3,4}, *Zheludev A.*⁴

¹ P.Kapitza Institute for Physical Problems RAS, Moscow, Russia

² National Research University Higher School of Economics, Moscow, Russia

³ National Institute of Chemical Physics and Biophysics, Tallinn, Estonia

⁴ Neutron Scattering and Magnetism, Laboratory for Solid State Physics, ETH Zürich, Zürich, Switzerland

glazkov@kapitza.ras.ru

Spin-gap magnets are one of the examples of spin liquids. Due to the particular architecture of the exchange bonds, usually invoking dimer motives, these magnets have a singlet ground state separated from the excited triplets by a gap of exchange origin. As a result, these systems remain in the paramagnetic state down to lowest temperatures despite the strong exchange coupling present. Stability of this singlet state to external effects: applied magnetic field, hydrostatic pressure or controlled introduction of defects is an actively studied problem.

The quasi-two-dimensional magnet $(\text{C}_4\text{H}_{12}\text{N}_2)(\text{Cu}_2\text{Cl}_6)$ (abbreviated PHCC for short) is one of the recently found spin-gap systems [1]. It allows partial substitution of Cl by Br with Br content up to 12% [2]. This *bond-doping* does not deplete magnetic system, but instead introduces random modulation of the exchange coupling constants.

By means of ESR spectroscopy we have found [3] that the low-temperature (below 1K) absorption of the Br-diluted PHCC includes the response of some gapless triplet ($S=1$) objects. I.e., non-magnetic doping of the $S=1/2$ system results in the formation of the triplet degrees of freedom. Coexistence of this new doping-induced triplet degrees of freedom with gapped triplet excitations was observed over the temperature range 1.5-5 K.

We conjecture that these triplet centres are created on double substitution of Cl by Br in a Cu_2Cl_6 dimer, which is a building block of PHCC magnetic system. Such a double substitution results in the effective attracting potential, which traps one of the triplet excitations. This conjecture is supported by the analysis of the ESR intensity, which turns out to be proportional to Br concentration squared.

[1] Stone M. B. et al., *New J. Phys.*, **9** (2007) 31.

[2] Hüvonen D. et al., *Phys. Rev. B*, **85** (2012) 100410; *Phys. Rev. B*, **86** (2012) 214408; *Phys. Rev. B*, **88** (2013) 094402.

[3] Glazkov V. N. et al., *Journ. Phys.:Cond. Matter*, **28** (2016) 206003; *Journ. Phys.:Cond. Matter*, **26** (2014) 486002.

5 July

Wednesday

12:00-14:00

poster session
5PO-I1

**“Study of Magnetism
using X-rays and
Neutrons”**

5PO-II-1

MAGNETIC HYPERFINE FIELDS FOR ^{111}Cd PROBE NUCLEI IN FeRh AND Fe_3X (X=C, Ge, and Ga) ALLOS

Krylov V.I.^{1,2}, Bosch-Santos B.¹, Cabrera-Pasca G.A.¹, Carbonari A.W.¹

¹ Instituto de Pesquisas Energéticas e Nucleares, IPEN, São Paulo, SP, Brazil

² Skobeltsyn Institute of Nuclear Physics, Moscow State University, Moscow, Russia
vkrylovmag@rambler.ru

FeRh ordered alloy crystallizes in the bcc B2 structure [1], presents first order phase transition from antiferromagnetic (AFM) ordering at low temperature to ferromagnetic (FM) state above 350 K [2], and shows significant magnetocaloric effect near RT [3]. In recent years, Fe_3X (X = C, Ga, and Ge) alloys are actively investigated experimental and theoretical methods due to their potential practical use as invar, magnetostrictive materials, and multi-layered ferromagnetic film [4, 5]. The Fe_3C alloy was studied by nuclear resonant scattering on ^{57}Fe and by x-ray emission spectroscopy at high pressure up to 50 GPa because this substance could be the major Earth's inner core component [6].

1) The magnetic hyperfine fields (B_{hf}) at ^{111}Cd probe nuclei located in Fe sites of two ordered FeRh alloys with bcc B2 structure were investigated by perturbed γ - γ angular correlation (PAC) spectroscopy in the range from 40 K to a temperature above T_C . $\text{Fe}_{0.48}\text{Rh}_{0.52}$ alloy (A_1) is AFM at low temperatures. At temperature increasing, the first order phase AFM-FM transition is observed at $T_m=345$ K, then A_1 alloy remains ferromagnetic (FM) up to $T_C = 685$ K. $\text{Fe}_{0.52}\text{Rh}_{0.48}$ alloy (A_2) is ordered FM below $T_C = 800$ K. The B_{hf} values at ^{111}Cd nuclei extrapolated to 0 K are equal to $B_{\text{AFM}}(0) = 8.70(5)$ T and $B_{\text{FM}}(0) = 5.53(5)$ T in AFM and FM phases of A_1 and A_2 alloys, respectively. The phase AFM-FM transition is accompanied by an abrupt drop of the B_{hf} due to a competition of Rh and Fe magnetic moment contributions to the B_{hf} .

2) In this work we found huge negative B_{hf} reaching a magnitude of $B_{\text{hf}} = -46\text{T}$ on ^{111}Cd probe nuclei in FM Fe_3X (X = C, Ga, and Ge) alloys by PAC spectroscopy. These values are the highest known HFs on ^{111}Cd nuclei in metallic magnets. It was established that in Fe_3C crystallizing in the orthorhombic DO_{11} structure (Pnma space group) ^{111}Cd probes are placed in Fe_g sites with 11Fe atoms as nearest neighbours (n.n.). For Fe_g positions, the n.n. arrangement is similar to normal hexagonal close packing. The HF value for ^{111}Cd atoms in Fe_3C is equal to $B_{\text{hf}} = -38.0(1)$ T at 77K. In tetragonal DO_3 crystal structure of Fe_3Ga ^{111}Cd probes are placed in both Ga sites (12 n.n. Fe) and in Fe_{II} (8n.n.Fe). The HFs for ^{111}Cd atoms in Fe_3Ga are equal to $B_{\text{hf}} = -39.8(1)$ T and $B_{\text{hf}} = -24.2(3)$ T at 77K for Ga and Fe_{II} sites of ^{111}Cd localization. In hexagonal DO_{19} crystal structure of Fe_3Ge ^{111}Cd probes are placed in Ge sites (12 n.n.). The HF value for ^{111}Cd probes in Fe_3Ge is equal to $B_{\text{hf}} = -46.0(1)$ T at 40K. There are no any anomalies of the B_{hf} (T) on ^{111}Cd nuclei in the spin reorientation region of Fe_3Ge .

The results of this work are analyzed with the previously obtained HF's values on ^{111}Cd nuclei in 3d metals and their alloys including Heusler alloys.

[1] M. Fallot, *Ann. Phys. (Paris)*, **10** (1938) 291-332.

[2] G. Shirane, C. W. Chen, P. A. Flinn, R. Nathan, *Phys. Rev.*, **133** (1963) 183-190.

[3] M. P. Annaorazov, S. A. Nikitin, A. L. Tyurin, K. A. Asatryan, A. Kh. Dovletov, *J. Appl. Phys.*, **79** (1996) 1689 -1695.

[4] I. G. Wood, L. Vocadlo, K. S. Knight, D. P. Dobson, W. G. Marshall, G. D. Price, John Brodholt, *J. Appl. Cryst.*, **37** (2004) 82-90.

[5] R. Wu, *J. Appl. Phys.*, **91** (2002) 7358 -7360.

[6] J. F. Lin, V. V. Struzhkin, H.K. Mao, R. J. Hemley, P. Chow, M. Y. Hu, J. Li, *Phys. Rev. B*, **70** (2004) 212405-4.

5PO-I1-2

INVESTIGATION OF THE MESOSTRUCTURE OF TRANSITION METALS MONOGERMANIDES

Safiulina I.A.^{1,2}, *Grigoriev S.V.*^{1,2}, *Altynbaev E.V.*^{1,2}

¹ Saint Petersburg State University, Saint Petersburg, Russia

² NRC Kurchatov institute «Petersburg Nuclear Physics Institute», Gatchina, Russia
ira93@inbox.ru

The magnetic properties of the transition metal monogermanides (MeGe, where Me = Fe, Mn, Co) are determined by an interplay of various interactions. The complex magnetic structure is based on the competition of the strong isotropic ferromagnetic exchange interaction and the Dzyaloshinskii-Moria (DM) interaction breaking the spin symmetry [1, 2]. Their magnetic properties have been heavily studied during recent years (see, for example, [3]). The newly synthesized samples [4] were repeatedly proven by X-ray powder diffraction to possess the B20 structure. Indeed, the B20 structure lacking the symmetry center results in appearance of the DM interaction and therefore in the helical magnetic structure.

Nevertheless, the mesostructure of these compounds synthesized under high pressure had not been studied yet. Preliminary SANS experiments demonstrated the power-law dependence of the neutron scattering intensity versus the scattering vector $I \sim Q^{-n}$. This exponent $n = 3$ corresponds to the logarithmic spatial pair correlation function $\xi(r) \sim \ln(\xi/r)$ and to unusual scaling law. The correlation function increases with an additive rather than multiplicative constant, upon reducing the scale length by a fixed rescaling factor. This leads to a logarithmic law instead of the usual power law for fractals. There are numerous examples of objects in nature [5-7], which give the power law $I \sim Q^{-3}$ in SANS experiment.

Support by Russian Foundation of Basic Research (Grant 14-22-01073) is acknowledged.

[1] I.E. Dzyaloshinsky, *Sov. Phys. JETP*, **19** (1964) 960. [*Zh. Eksp. Teor. Fiz.*, **46** (1964) 1420].

[2] P. Bak and M.H. Jensen, *J.Phys.C: Solid St.Phys.*, **13**(31) (1980) L881-L885.

[3] S.V. Grigoriev et al., *Phys.Rev.Lett.*, **110** (2013) 207201.

[4] A.V. Tsvyashchenko, *J. Less-Common Met.*, **99** (1984), L9.

[5] D.V. Lebedev, M.V. Filatov, A.I. Kuklin, A.Kh. Islamov et al., *FEBS Letters.*, **579** (2005) 1465-1468.

[6] D.V. Lebedev, M.V. Filatov, A.I. Kuklin, A.Kh. Islamov, J. Stellbrink, *Cryst.Rep.*, **53,1** (2008) 110-115

[7] Fedotov G.N., Tret'yakov Yu.D., Pakhomov E.I., Kuklin A.I., *Doklady. Chemical technology*, **405** (2005) 3.

5PO-I1-3

PHASE DIAGRAMS OF (Tb,Y)Mn₂Ge₂ AND (Gd,Y)Mn₂Ge₂ STUDIED BY NEUTRON POWDER DIFFRACTION

*Gaidukova I.Yu.*¹, *Granovsky S.A.*^{1,2}, *Ritter C.*³

¹ Faculty of Physics, M.V. Lomonosov Moscow State University, Moscow, Russia

² IFP, TU Dresden, Dresden, Germany

³ Institut Laue-Langevin, Grenoble, France

ser@plms.ru

Among the large variety of intermetallic compounds the RMe₂X₂ series (tetragonal *I4/mmm*, R= rare earth and Y, Me = transition metal, X= Ge or Si) attract an interest because of "natural layered" crystal structure with two-dimensional *3d*-atom arrangements. The interplay between different types of magnetic exchange interactions, intra- and interlayer Mn couplings gives rise to a number of interesting phenomena, such as re-entrant ferromagnetism, separate ordering of magnetic sublattices, temperature-, field-, pressure-induced phase transitions and anomalous transport properties.

The aim of the current work was to probe and refine magnetic structures in pseudo-ternary systems (Tb_{1-x}Y_x)Mn₂Ge₂ and (Gd_{1-x}Y_x)Mn₂Ge₂, where changes of low-temperature magnetic phase were expected. The hot neutron source ($\lambda = 0.4972 \text{ \AA}$) was used to probe the magnetic structures of Gd-contained materials, others were studied by conventional technique (ILL D1B, D1A diffractometers).

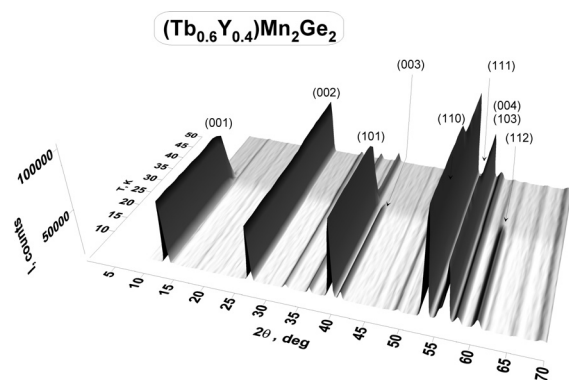


Fig.1. 2 θ –temperature–intensity plot for (Tb_{0.6}Y_{0.4})Mn₂Ge₂.

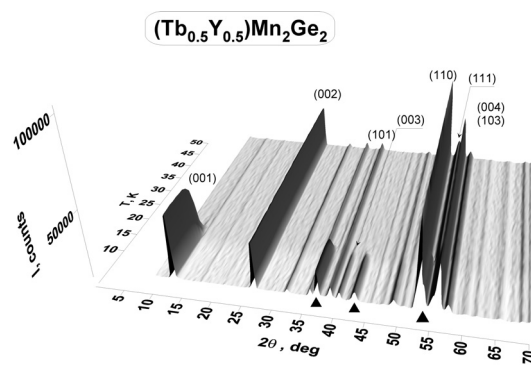


Fig.2. 2 θ –temperature–intensity plot for (Tb_{0.5}Y_{0.5})Mn₂Ge₂.

The magnetic transition temperatures were found in a good agreement with results of our magnetisation, resistivity and ac-susceptibility measurements. The high-temperature magnetic phase for all compounds studied confirmed to be *AFil*. Canted *Fmc* and specific triple low temperature phases were observed in diluted (Tb_{1-x}Y_x)Mn₂Ge₂. Contrary to expectations, Gd-based diluted compounds show only the collinear low-temperature magnetic phase.

5PO-I1-4

SOFT X-RAY ABSORPTION SPECTROSCOPY OF COBALT-DOPED ANATASE TiO₂ NANOPOWDERS

Mesilov V.V.¹, Galakhov V.R.¹, Udintseva M.S.², Yermakov A.E.¹, Uimin M.A.¹, Gubkin A.F.¹, Sherstobitova E.A.³

¹ M.N. Miheev Institute of Metal Physics, Ural Branch of the Russian Academy of Sciences, Yekaterinburg, Russia

² Ural State University of Railway Transport, Yekaterinburg, Russia

³ Institute of High-Temperature Electrochemistry, Ural Branch of the Russian Academy of Sciences, Yekaterinburg, Russia
mesilov@imp.uran.ru

Co-doped TiO₂ is one of the most extensively studied oxides for applying as dilute magnetic semiconductors. There are at least two points of view on the origin of ferromagnetism in this material: (i) ferromagnetism in TiO₂:Co originates from the presence of Co clusters, (ii) ferromagnetism is intrinsic nature. Therefore, oxidation state of cobalt is of particular interest in such materials.

Anatase Ti_{1-x}Co_xO₂ ($x=0.02, 0.12$) nanopowders were obtained by hydrothermal method. The samples were annealed in vacuum and in hydrogen at 700 K for 2 h. The size of coherent scattering region estimated from the X-ray diffraction data was about 10 nm. Ti $L_{2,3}$ and Co $L_{2,3}$ X-ray absorption spectra were measured at Russian-German beamline at BESSY-II (Berlin) in the total photoelectron yield mode (see Fig. 1).

We have found that in Ti_{0.98}Co_{0.02}O₂, Co²⁺ ions are coordinated tetrahedrally and octahedrally. Number of tetrahedrally coordinated ions increase after heating of the sample in vacuum. According to the Ti $L_{2,3}$ X-ray absorption spectra, all the samples before the thermal treatment contain an amorphous phase of titanium dioxide on the surface. After annealing in vacuum or hydrogen anatase structure of Ti_{0.98}Co_{0.02}O₂ remains and the amorphous phase disappears. In the sample with 12 at. % of Co, the amorphous phase persists after the annealing. Annealing of Ti_{0.88}Co_{0.12}O₂ in the hydrogen atmosphere leads to the appearance of metallic cobalt.

The work was supported by the Russian Scientific Foundation, Grant No. 16-12-10004. X-ray absorption measurements were carried out according to the bilateral Program "Russian-German Laboratory at BESSY". X-ray diffraction studies were performed using facilities of the shared access center "Composition of compounds" IHTE, UB RAS.

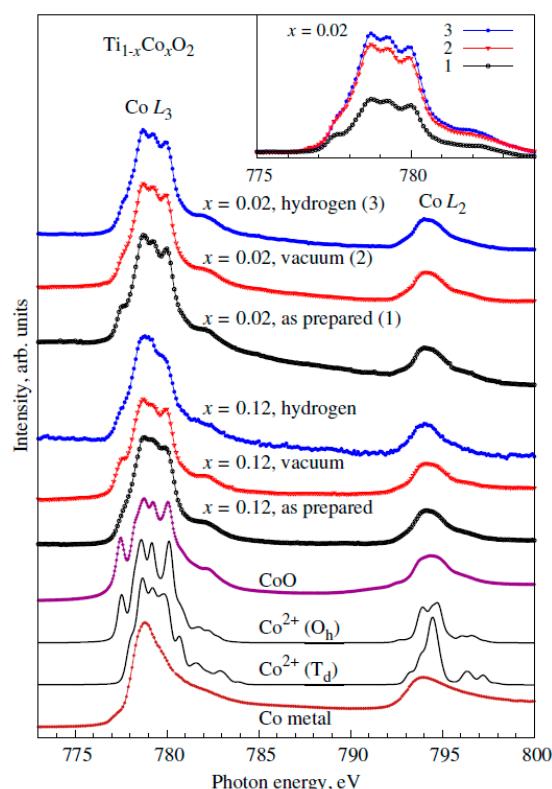


Fig. 1. Co $L_{2,3}$ of TiO₂:Co nanopowders after annealing in vacuum and hydrogen. For comparison, results of crystal-field multiplet calculations are given. In the insert, the Co L_3 spectra are normalized to the intensities of Ti L_3 lines of corresponded sample.

5PO-I1-5

SYMMETRY DEPENDENT MAGNETISM OF PALLADIUM IONS IN POLYOXOPALLADATES

Svechkina N.¹, Izarova N.¹, Schmitz D.², Smekhova A.¹, Schmitz-Antoniak C.¹

¹Forschungszentrum Jülich (PGI-6), Jülich, Germany

²Helmholtz-Zentrum-Berlin, Berlin, Germany

n.svechkina@fz-juelich.de

It is well-known that bulk palladium is paramagnetic, but it is also theoretically predicted that palladium can change its magnetic state under structural transformations. Recent studies have shown that palladium magnetism can be observed in Pd films, nanoparticles and nanowires [1]. Here, we investigated palladium in polyoxopalladates (POPs) nanoclusters. POPs form a new class of nanoscale materials with unique physical and chemical properties. These properties give them high potential for applications in catalysis and nanotechnology.

POPs are polyatomic anionic clusters consisting of Pd(II) ions which are linked together by shared oxygen ions and RXO_3^{n-} groups. An example of this class presented in the current study is $[\text{Pd}^{II}_{13}\text{As}^{\text{V}}_8\text{O}_{34}(\text{OH})_6]^{8-}$ palladate, denoted as Pd-Pd₁₂. In this species the central Pd ion is surrounded by eight oxygens. The twelve palladium(II) ions in the outer shell are coordinated by four oxygen ions in a square planar geometry.

Replacing the central palladium(II) ion by iron(III) (see in Fig. 1) or cobalt(II) ions while maintaining the symmetry and number of the palladium(II) ions in the outer shell gave us the possibility to distinguish the contributions from the central and outer shell palladium ions. This has been done by element- and in principle site-specific soft x-ray magnetic circular dichroism (XMCD) technique at the palladium $M_{3,2}$ absorption edges and iron and cobalt $L_{3,2}$ absorption edges as well.

Particular features of XMCD and XANES spectra of palladium ions in different local environments were explained through comparison with results of multiplet calculations performed by the CTM4XAS program [3]. The crystal field parameters and the valence state of the central ion were quantified.

In addition the influence of a soft hydrogen plasma treatment on the palladium magnetism was investigated.

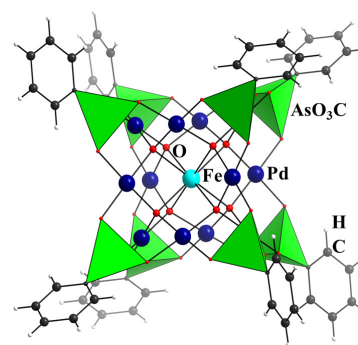


Fig. 1: Crystal structure of Fe-Pd₁₂ polyoxopalladate [2].

The work was funded by Helmholtz Association (Young Investigator's group "Borderline Magnetism", VH-NG-1031).

[1] A. Delin, E. Tosatti, R. Weht, *Phys. Rev. Lett.*, **92** (2004) 057201.

[2] M. Barsukova-Stuckart, N.V. Izarova et al, *Inorg. Chem.*, **18** (2012) 6167-6171.

[3] E. Stavitski, F.M.F. de Groot, *Micron*, **41** (2010) 687-694.

5PO-I1-6

**CRYSTAL STRUCTURE, CHARGE, SPIN STATES OF Co IONS IN
Tb_{1-y}Ba_{1+y}Co_{2-x}O_{5.5-δ}: NEUTRON-DIFFRACTION AND X-RAY
SPECTROSCOPY STUDIES**

*Naumov S.V.¹, Voronin V.I.¹, Telegin S.V.^{1,2}, Galakhov V.R.¹, Mesilov V.V.¹, Udintseva M.S.³,
Patrakov E.I.¹, Gaviko V.S.^{1,2}, Gizhevskii B.A.¹*

¹ M.N. Miheev Institute of Metal Physics, Ural Branch of the Russian Academy of Sciences,
Yekaterinburg, Russia

² Institute of Natural Sciences, Ural Federal University, Yekaterinburg, Russia

³ Ural State University of Railway Transport, Yekaterinburg, Russia
naumov@imp.uran.ru

Crystal structure, charge and spin states of cobalt ions in Tb_{1-y}Ba_{1+y}Co_{2-x}O_{5.5-δ} compounds were studied by means of neutron diffraction and soft X-ray absorption spectroscopy.

The following single-phase samples were synthesized: TbBaCo₂O_{5.36}, TbBaCo_{1.95}O_{5.29}, TbBaCo_{1.9}O_{5.22}, and Tb_{0.95}Ba_{1.05}Co_{1.9}O_{5.19}. Elemental EDX analysis was carried out on a scanning electron microscope Inspect F (FEI). The oxygen content was determined by reduction of the samples in hydrogen. Neutron-diffraction studies were done on a stationary research nuclear reactor (IMP, Zarechnyi). X-ray diffraction structure and phase analyses were carried out on an X-ray diffractometer PANalytical Empyrean. Full-profile Rietveld analysis was applied for refinement of structural parameters. It was established that all the samples are characterized by orthorhombic structure (space group *Pmmm*, no. 47). Tb *M*_{4,5}, Ba *M*_{4,5}, Co *L*_{2,3} and O *K* X-ray absorption spectra were measured at Russian-German beamline at BESSY-II (Berlin) in the total photoelectron-yield mode. Using the neutron-diffraction data, lattice parameters, atomic coordinates, positions of atoms and the populations of these positions, interatomic distances, and distortion degrees of polyhedrons were determined. According to the measurements of X-ray absorption spectra, the most of Co ions in these Tb_{1-y}Ba_{1+y}Co_{2-x}O_{5.5-δ} cobaltites at room temperature are in the high-spin 3+ state ($3d_{\uparrow}^5 3d_{\downarrow}^1$).

The following scenarios of the influence of distortion of atomic composition on the spin states of cobalt ions are considered: (i) spin states of cobalt ions are changes due to the forming of oxygen vacancies in equatorial and apical positions which are connected with cobalt vacancies; (ii) exchange interactions $\text{Co}^{3+} - \text{O} - \text{Co}^{2+}$; (iii) charge disproportionation $\text{Co}^{3+}(3d^6) \rightarrow \text{Co}^{2+}(3d^7) + \text{Co}^{4+}(3d^6)$; (iv) local heterogeneity of composition. Features of the TbBaCo₂O_{5.5-δ} system in comparison with the GdBaCo₂O_{5.5-δ} and EuBaCo₂O_{5.5-δ} systems are discussed.

Supporting by the FASO of the Russian Federation (theme “Spin”, no. 01201463330), RFBR 16-02-00577, and UB RAS (project no. 15-9-2-4) are acknowledged.

5PO-I1-7

DEBYE-WALLER FACTOR IN THE POLARIZED NEUTRON SCATTERING BY FERROMAGNETIC METALS

Paradezhenko G.V.¹, Melnikov N.B.¹, Reser B.I.²

¹ Moscow State University, Leninskie Gory, 119991 Moscow, Russia

² Institute of Metal Physics RAS, 18, Kovalevskaya St., 620990 Ekaterinburg, Russia
gparadezhenko@cs.msu.su

The correction to the neutron scattering cross-section from the lattice vibrations is mainly determined by the elastic phonon processes. The correction coefficient, called the Debye-Waller factor (DWF), leads to a reduction of about 10% at $T = 0$, which increases substantially with temperature. However, theoretical estimates are available only at specific temperatures and experimental measurements of the DWF are missing in the literature.

We calculate the DWF for the ferromagnetic metals above the Curie temperature as a function of temperature T and scattering vector κ in the same range of κ from zero to 4 \AA^{-1} as in the polarized magnetic neutron scattering experiment [1]. As can be seen from Fig. 1, in this range the DWF can give a sizable correction to experiment of up to 20-30%.

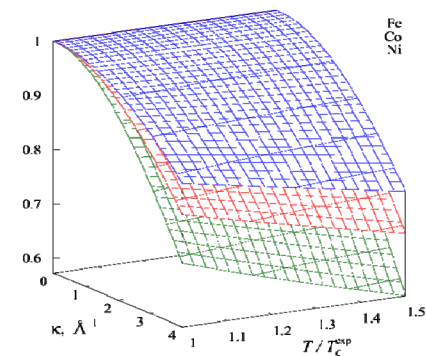


Fig. 1. The Debye-Waller factor for the ferromagnetic metals above the Curie temperature.

For values of κ within the Brillouin zone, the phonon contribution to the temperature dependence of magnetic characteristics such as the local magnetic moment, local

susceptibility, etc. is small and the temperature dependence is mainly determined by the spin fluctuations. We illustrate this by the calculation of the local magnetic moment for bcc Fe. The square of the local magnetic moment is calculated by the formula $m_L^2 \propto \int_0^{q_B} q^2 M^2(q) dq$, where $M(q)$ is the effective moment and $q_B = 1.7 \text{ \AA}^{-1}$ is the Brillouin zone radius. Fig. 2 shows $q^2 M^2(q)$ calculated in the Gaussian approximation (GA) of the dynamic spin-fluctuation theory (DSFT) [2] with the energy cutoff of 50 and 200 meV and by the exact formula. The DWF correction is within 4%, and the calculated magnetic moment is in good agreement with experiment (for details, see [3,4]).

The research was carried out within the state assignment of FASO of Russia (program 'Electron' No. 01201463326) and was supported in part by the Program of Ural Branch of Russian Academy of Sciences (Project No. 15-8-2-10).

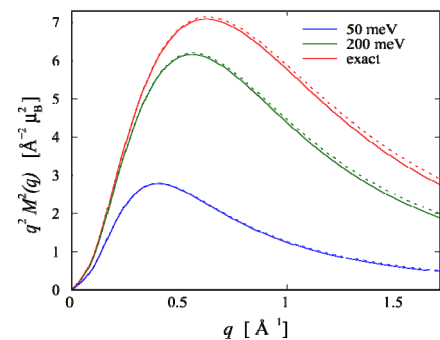


Fig. 2. $q^2 M^2(q)$ calculated for bcc Fe at $T/T_C^{cal} = 1.21$ in the GA of the DSFT (dotted line) with the energy cutoff of 50 and 200 meV and by the exact formula. The solid lines show the same quantities multiplied by the Debye-Waller factor.

- [1] P. Brown, H. Capellmann, J. Deportes, D. Givord, K.R.A. Ziebeck, *JMMM*, **30** (1983) 335.
 [2] N.B. Melnikov, B.I. Reser, V.I. Grebennikov, *J. Phys.: Condens. Matter*, **23** (2011) 276003.
 [3] N.B. Melnikov, G.V. Paradezhenko, B.I. Reser, *Theor. Math. Phys.* **191** (2017) 600.
 [4] N.B. Melnikov, B.I. Reser, G.V. Paradezhenko, *J. Magn. Magn. Mater.*, **411** (2016) 133.

5PO-I1-8

INFLUENCE OF SEVERE PLASTIC DEFORMATION ON SPIN AND VALENCE STATES OF COBALT IONS IN $\text{EuBaCo}_2\text{O}_{5.5}$ STUDIED BY MEANS OF X-RAY ABSORPTION SPECTROSCOPY

Mesilov V.V.¹, Galakhov V.R.¹, Udintseva M.S.², Gizhevskii B.A.¹, Naumov S.V.¹

¹ M.N. Miheev Institute of Metal Physics, Ural Branch of the Russian Academy of Sciences, Yekaterinburg, Russia

² Ural State University of Railway Transport, Yekaterinburg, Russia
mesilov@imp.uran.ru

Layered cobaltites $\text{EuBaCo}_2\text{O}_{5.5-\delta}$ are considered important potential materials for spintronics, solid-oxide fuel cells and thermoelectricity. Of special interest are spin and valence states of Co ions, which determine magnetic and electrical properties of these compounds.

Severe plastic deformation was carried out by milling of initial coarse-grained samples in a vibration mill with Al_2O_3 balls. Time of milling was varied from 1 to 9 h and determined size of particles. The size of coherent scattering region estimated from the line broadening of the diffraction lines was about 140 nm for the samples subjected milling for 9 hours. No second phases were observed. The lattice parameters of cobaltites after milling are close to those of the initial sample. X-ray absorption spectra (XAS) were measured at Russian-German beamline at BESSY-II (Berlin) in the total photoelectron yield mode.

On the base of our measurements of Co $L_{2,3}$ absorption spectra (see Fig. 1), Eu $M_{4,5}$ X-ray absorption spectra, and crystal field multiplet calculations, we have found that Co and Eu ions in $\text{EuBaCo}_2\text{O}_{5.5-\delta}$ are in the 3+ valence states. O K X-ray absorption spectra (see Fig.1) are sensitive to the populations of the t_{2g} and e_g levels and, therefore, allowed to determine the spin state of Co ions. It was established that in $\text{EuBaCo}_2\text{O}_{5.5-\delta}$, Co ions are both in the high-spin ($3d_{\uparrow}^5 3d_{\downarrow}^1$) and low-spin ($3d_{\uparrow}^3 3d_{\downarrow}^3$) states. The high and low spin states are found to be at the almost equal ratio in the Co^{3+} ions in the initial sample. Severe plastic deformation leads to a change in the shape of the O K spectrum of $\text{EuBaCo}_2\text{O}_{5.5-\delta}$. It means that the predominant state of cobalt 3+ ions in the $\text{EuBaCo}_2\text{O}_{5.5-\delta}$ cobaltites subjected to the milling is the low-spin state.

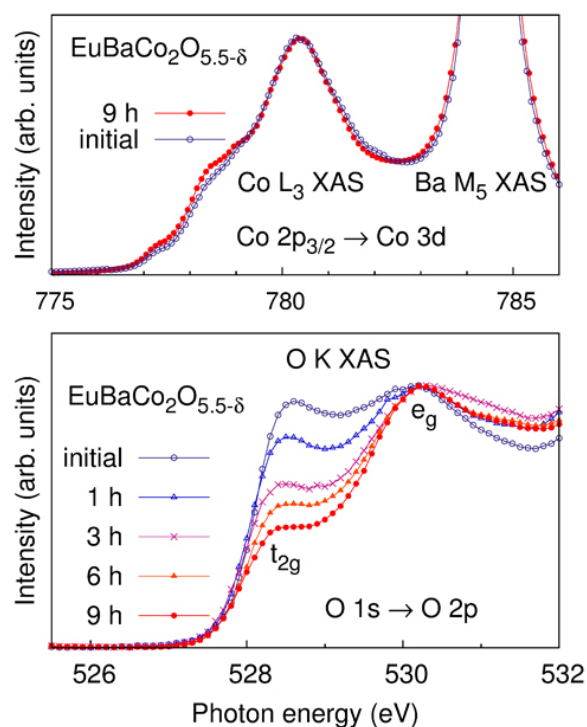


Fig. 1. Co L_3 , Ba M_5 and O K X-ray absorption spectra (XAS) of $\text{EuBaCo}_2\text{O}_{5.5}$ after milling for 1, 3, 6 and 9 hours.

The research was carried out within the state assignment of FASO of Russia (theme “Spin” No. 01201463330), supported in part by RFBR (projects No. 16-02-00577), UB RAS (project No. 15-9-2-4) and by the bilateral Program “Russian–German Laboratory at BESSY”.

5PO-I1-9

MAGNETIC ORDERING IN $\text{Fe}_x\text{Mn}_{1-x}\text{S}$ UNDER PRESSURE INVESTIGATED BY NEUTRON DIFFRACTION

*Abramova G.¹, Boehm M.², Schefer J.³, Piovano A.³, Zeer G.⁴, Zharkov S.^{1,4}, Mita Y.⁵,
Vorotynov A.¹, Sokolov V.⁶*

¹ Kirensky Institute of Physics, Federal Research Center KSC SB RAS, Akademgorodok,
Krasnoyarsk, 660036 Russia

² Institute Max von Laue - Paul Langevin, Grenoble Cedex 9, France

³ Paul Scherrer Institut, Laboratory for Neutron Scattering and Imaging (LNS), CH-5232 Villigen
PSI, Switzerland

⁴ Siberian Federal University, 79 Svobodny pr., Krasnoyarsk, 660041, Russia

⁵ Materials Physics, Engineering Science, Osaka University Toyonaka, Osaka 560-8531, Japan

⁶ Institute of Inorganic Chemistry SB RAS, Novosibirsk, 630090, Russia
agm@iph.krasn.ru

$\text{Fe}_x\text{Mn}_{1-x}\text{S}$ belongs to the strong electron correlations compounds of MnO. We present here experimental results for the antiferromagnetic iron-manganese sulfide system, based on X-ray and neutron diffraction studies. The magnetic investigations are carried out at ambient pressure and hydrostatic pressure up to 4.2 GPa in the range of 65-300 K. We followed the powder line for the magnetic (1/2,1/2,1/2) reflection line for $\text{Fe}_{0.27}\text{Mn}_{0.73}\text{S}$ to establish a magnetic phase diagram. The measuring time was adjusted to get reasonable statistics within the accepted temperature intervals available for one measurement. Simple Gaussian function fitting was used for evaluating the magnetic peaks as a function of temperature. For the analysis of the data, for every pressure P the fitting parameters (background, the center of the peak, width FWHM and maximum intensity) were iteratively adjusted and fixed for the complete set. The intensities were normalized to a neutron monitor value of 15000 corresponding to the counting time of around 1 minute per temperature. Our results indicate that the Néel temperature of MnS increases up to room temperature by applying chemical ($0 < x < 0.29$) or weak hydrostatic pressure. A shift of T_N was observed, due to chemical pressure x at $P=0$ from 150K ($x=0$) to $207 \pm 2\text{K}$ ($x=0.29$) with $dT_N/dX = 1,96 \text{ K/at.\%Fe}$ and due to external pressure at 100 K from 205K to 280 K for $x=0.27$ with $dT_N/dP = 17,9 \text{ K/GPa}$. The magnetization of the sublattice decreases with increasing the hydrostatic pressure (Fig1.). The mechanism of the increasing Néel temperature can be associated with the lattice compression and the increase of the exchange integral. The increases of the octahedral coordination distortion with pressure may lead to a spin crossover and transition of the magnetic Fe^{2+} and Mn^{2+} ions from the high spin (HS) to the low-spin (LS) state.

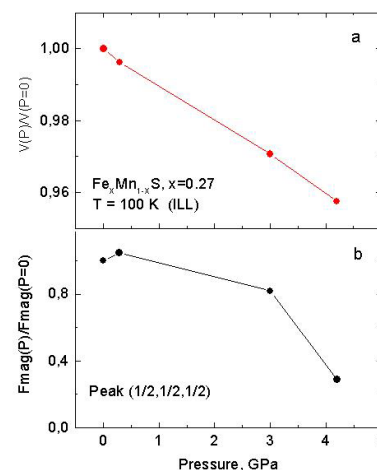


Fig. 1. Change of normalized lattice volume (a) and magnetization (b) for $\text{Fe}_{0.27}\text{Mn}_{0.73}\text{S}$ under pressure.

5PO-I1-10

EFFECTS OF SPIN POLARIZATION ON XMCD AND RESONANT PHOTOEMISSION FROM D, F- STATES IN TbNi₂Mn_x COMPOUNDS

Grebennikov V.I., Kuznetsova T.V.

M.N. Miheev Institute of Metal Physics UB RAS, 620099, Ekaterinburg, Russia
vgrebennikov@list.ru

The electronic magnetic structure of TbNi₂Mn_x and features of the interaction of *d*- and *f*- shells are studied using the techniques of the circular magnetic circular dichroism (XMCD) [1] in the soft x-ray range and the resonant x-ray photoemission spectroscopy (RXPS). The RXPS method takes an advantage of a variation in the photoionization cross-section of a specific atom when the photon energy is tuned across a certain core-level excitation thresholds. The observations of RXPS from valence band at Tb M₅ and N_{4,5} edges and Mn and Ni L₃ edges are reported. We study the basic scenarios of valence electron photoemission (PE) [2]: (i) Interference between a direct PE channel with an indirect PE channel that opens after excitation a core-level electron to an intermediate state followed by autoionization of a valence band (VB) electron, (ii) the inelastic Auger decay of the core-level hole accompanied by the electron emission and the formation of two holes in the valence band and (iii) other inelastic losses.

In the 4*d* → *εf* transition region of the Tb shape (or giant) resonance (about 150 eV), the VB photoemission increases up to 6 times from the entire valence band. Dependence of the PE intensity on the photon energy is described by the Fano-like profile. It should be the case if the 4*d*-electrons goes into a virtual *εf*-state and then returns back to its initial state. The impact on terbium electrons is larger (the Tb signal amplification is 14 times) than for electrons localized near other components. On the Tb M₅ edge (1240 eV), the terbium VB resonates stronger (20-fold increase) with an absolute interference of direct VB PE channel and indirect resonant PE channel opened by the 3*d*_{5/2} electron excitation into an intermediate 4*f*-states.

When the photon energy was tuned to the 2*p* → 3*d* transition region of the Mn (640 eV), a 13-fold enhancement PE observed from the VB states with a binding energy of 5 eV and only 2-fold increase from the terbium VB states of 8 eV. The degree of interference of the elastic channels in the system TbNi₂Mn_x is 0.9 for *x* = 1 and weakened to 0.2 for *x* = 0.25 due to the relative increase in the nickel states contribution. A totally different situation arises for the same 2*p* → 3*d* resonance on nickel atoms. The relaxation of the excited state occurs through the generation of a high power LVV Auger line with the constant electron kinetic energy. This means that, unlike manganese, nickel has no trap for an electron excited in 3*d* states.

The atomic magnetic moments determine the magnitude and width of the resonance spectra. For example, if all five 3*d*-states with spin up are filled (like in Mn), only a 2*p*-level hole with spin down occurs when photon is absorbed. The photo hole can be filled only by means of the reverse transition of the excited electron accompanied by autoionization of a VB electron, since transitions of the valence electrons are forbidden because of the conservation of the spin projection [3]. If the valence band contains electrons with the same spin projection as a hole (like in Ni), the competing inelastic channel of the LVV Auger decay appears. So, the higher the atomic spin, the smaller the number of the final states and the greater and sharper resonance.

The research was carried out within the state assignment of FASO of Russia (theme “Quant” No. 01201463332).

[1] T.V. Kuznetsova, *J. Magn. Magn. Mat.*, <http://dx.doi.org/10.1016/j.jmmm.2016.12.083>.

[2] V.I. Grebennikov, A. Buling, M. Neumann, et al, *J. Struct. Chem.*, **56** (2015) 511-516.

[3] V.I. Grebennikov, T.V. Kuznetsova, A.G. Kuchin, *Bull. RAS Phys.*, **79** (2015) 134-138.

5PO-II-11

NANOPARTICLES OF COBALT FERRITE IN SiO₂-MATRIX: SYNTHESIS, STRUCTURE AND MAGNETIC PROPERTIES

Khamova T.V.¹, Kopitsa G.P.^{1,2}, Shilova O.A.¹, Sokolov A.E.², Baranchikov A.E.³

¹ Grebenshchikov Institute of Silicate Chemistry, Russian Academy of Sciences, St.Petersburg, Russia

² Konstantinov Petersburg Nuclear Physics Institute NRC KI, Gatchina, Leningrad district, Russia, 188300

³ Kurnakov Institute of General and Inorganic Chemistry of the Russian Academy of Sciences, Moscow, Russia

kopitsa@lns.pmpi.spb.ru

In the present work, the structural and magnetic properties of CoFe₂O₄ xerogels in SiO₂-matrix have been performed using small-angle X-ray scattering (SAXS), small-angle polarized neutron scattering (SAPNS), powder neutron diffraction, scanning electron microscopy and low-temperature nitrogen adsorption.

Samples were prepared by sol-gel method using sol of tetraethoxysilane (TEOS) hydrolyzed in aqueous-alcoholic acidic media in the presence of modifying inorganic substances Fe(NO₃)₃·9H₂O and Co(NO₃)₂·6H₂O. The basis of preparation of silica sol was lying two-step method of acid hydrolysis of TEOS. At the 1st stage of hydrolysis of the starting components Si(OEt)₄, EtOH, H₂O and HNO₃ successively mixed at a molar ratio of 1: 1.6: 2.5: 0.001, respectively. The resulting silica sol obtained in the 1st stage of hydrolysis, was placed in a closed vessel and kept at 5 ° C during the day. Preparation of silica sol containing modifying components of iron and cobalt nitrates (2nd hydrolysis stage) was carried out as follows. First, Fe(NO₃)₃·9H₂O and Co(NO₃)₂·6H₂O were dissolved in distilled water. The resulting solution was added with vigorous stirring to the silica sol obtained in the 1st stage of the hydrolysis, at room temperature. As a result, the transparent modified silica sol maroon color was obtained. Concentration of modifying agents has been selected based receiving material of the following composition: 23CoO·31Fe₂O₃·46SiO₂ wt.%.

A modified silica sol was to grow old in a closed vessel to transition into a gel at room temperature. The obtained gel was dried at 100°C in air before the formation of the xerogel. The xerogel was subjected to heat treatment at 800, 900 and 1000°C for 2 hours in air. As a result, the sample of cobalt ferrite in SiO₂ matrix was obtained.

From the analysis of the experimental scattering cross-sections $d\Sigma(q)/d\Omega$ of polarized neutrons the type of magnetic correlator and the magnetic-nuclear cross-correlator, and estimates of the characteristic radii of the magnetic R_m and magnetic-nuclear R_m correlations were obtained. The results of SAPNS measurements were compared with SAXS, powder neutron diffraction and low temperature nitrogen adsorption data.

The work was supported by the Fundamental Research Program of RAS No. 1 'Nanostructures: Physics, Chemistry, Biology, technology basics'.

5PO-I1-12

MAGNETIC PROPERTIES AND SPIN STRUCTURE OF HONEYCOMB LAYERED Na₂Ni₂TeO₆ TELLURATE

Korshunov A.N.^{1,2}, Kurbakov A.I.^{1,2}, Malyshev A.L.¹, Podchezertsev S.Yu.¹

¹Petersburg Nuclear Physics Institute, Gatchina, Russian Federation

²Saint Petersburg University, Saint Petersburg, Russian Federation

korshunov_an@pnpi.nrcki.ru

Layered oxides of alkali and transition metals are presently investigated due to the different reasons: (i) possibility of their use as electrode materials for lithium-ion or sodium-ion batteries and (ii) rich variety of magnetic and electronic phenomena such as, for example, quasi-two-dimensional magnetism with different types of spin ordering [1]. Magnetic properties of these compounds are closely related to their crystal structures therefore crystal and spin structure of Na₂Ni₂TeO₆ have been studied in the present work.

The crystal structure of the Na₂Ni₂TeO₆ can be described in frame of P63/mcm (193) space group. It represents the ordered hexagonal layers consisting of magnetic Ni²⁺ and nonmagnetic Te⁶⁺ cations inside oxygen octahedra alternating with Na layers. Initially the magnetic susceptibility and specific heat were measured for the studied compound, where clear anomalies due to the antiferromagnetic transition were found in the temperature dependences of these quantities at $T_N = 27$ K [2]. The experimental low-temperature data of neutron measurements (G4.1, LLB, Saclay, France; $\lambda = 2.428$ Å) have shown additional reflections associated with the neutron magnetic scattering, that appear at temperatures below T_N . It should be emphasized that the magnetic susceptibility and neutron scattering data slightly above the critical point indicates the presence of strong 2D AF short-range correlations in studied system that precede the establishment of a long-range magnetic ordering.

In the ordered phase all the magnetic Bragg peaks at 1.7 K can be indexed with a commensurate propagation vector $k = (1/2 \ 0 \ 0)$. Possible irreducible representations were tested by refining the differential powder diffraction pattern (1.7-30 K) using the scaling factor and the peak shape parameters determined from the crystal structure refinement. During the analysis, we have found that the magnetic moment of nickel atoms preferably directed along the c-axis with z-component equals to $M_z = 1.68(1) \mu_B$, but y-component has also nonzero value equal to $M_y = 0.39(2) \mu_B$. Without y-component of magnetic moment, the obtained structure can be considered as known zigzag ferromagnetic chains coupled antiferromagnetically in *ab*-plane [1]. In this case the interlayer interactions along the c-direction are significant and they have antiferromagnetic nature. The presence of y-component leads to a slight ferromagnetic interaction along the c-direction according to symmetry transformations of irreducible representation.

This work was supported by the RFBR (project 16-02-00360).

[1] P.H.Y. Li, R.F. Bishop, D.J.J. Farnell, C.E. Campbell, *Phys. Rev. B*, **86** (2012) 144404.

[2] R. Sankar, I. P. Muthuselvam, G. J. Shu, W. T. Chen, S. K. Karna, R. Jayavel, and F. C. Chou, *CrystEngComm*, **16** (2014) 10791.

5PO-II-13

INCOMMENSURATE ANTIFERROMAGNETISM IN THE CENTROSYMMETRIC CUBIC PHASES OF $\text{REGe}_{2.85}$ (RE = Tb, Dy)

Salamatin D.A.^{1,2,6}, *Tsvyashchenko A.V.*^{1,3}, *Sidorov V.A.*¹, *Petrova A.E.*¹, *Fomicheva L.N.*¹,
*Kichanov S.E.*², *Salamatin A.V.*², *Velichkov A.*^{2,7}, *Kozlenko D.P.*², *Nikolaev A.N.*^{3,6}, *Ryasny G.K.*³,
*Makarova O.L.*⁴, *Budzynski M.*⁵

¹ Vereshchagin Institute for High Pressure Physics, RAS, 142190, Moscow, Troitsk, Russia

² Joint Institute for Nuclear Research, P.O. Box 79, Moscow, Russia

³ Skobeltsyn Institute of Nuclear Physics, MSU, Vorob'evy Gory 1/2, 119991 Moscow, Russia

⁴ National Research Center "Kurchatov Institute," 123182 Moscow, Russia

⁵ Institute of Physics, M. Curie-Sklodowska University, 20-031 Lublin, Poland

⁶ Moscow Institute of Physics and Technology, SU, 141700 Dolgoprudny, Russia

⁷ Institute for Nuclear Research and Nuclear Energy, 1784 Sofia, Bulgaria

dasalam@gmail.com

Polycrystalline samples of $\text{TbGe}_{2.85}$ and $\text{DyGe}_{2.85}$ were synthesized at a pressure of 8 GPa. They both have AuCu_3 -type cubic structure with space group $Pm-3m$ and lattice constants $a = 4.287(5)$ Å and $4.286(4)$ Å, respectively [1].

The charge density wave (CDW) is formed in $\text{TbGe}_{2.85}$ below $T_{CDW} = 145$ K at ambient pressure. This was shown by electrical resistivity, heat capacity and magnetic susceptibility measurements. The nuclear method of time dependent perturbed angular $\gamma\gamma$ -correlations (TDPAC) revealed the commensurability of CDW modulation at low temperatures.

$\text{TbGe}_{2.85}$ compound becomes antiferromagnetic below $T_N = 19$ K. The magnetic diffraction peaks in the neutron powder diffraction experiment have been indexed with a propagation vector $\mathbf{k}_{ic} = 2\pi/a(1/2, 0, 0.165)$ indicating an incommensurate antiferromagnetic helimagnetic structure.

It was supposed that this magnetic ordering closely related with CDW modulation because CDW also becomes incommensurate below the Néel temperature [2]. The similar magnetic structure was observed in a $\text{DyGe}_{2.85}$ compound in which the CDW is formed below 82 K. The Néel temperature for $\text{DyGe}_{2.85}$ is $T_N = 22$ K.

In addition, the neutron powder diffraction experiment at high pressure on $\text{TbGe}_{2.85}$ compound was performed. The results of this experiment demonstrates that above $P = 1.2$ GPa the second magnetic commensurate phase with wave vector $\mathbf{k}_c = 2\pi/a(1/2, 0, 0)$ is formed [3].

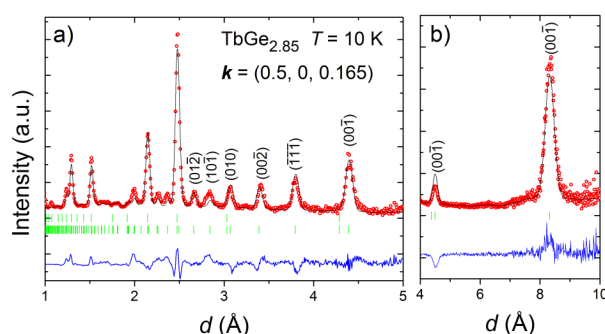


Fig. 1. Refined neutron powder diffraction pattern of $\text{TbGe}_{2.85}$ obtained at $T = 10$ K and $P = \text{atm.}$ in the magnetically ordered state.

[1] A. V. Tsvyashchenko, A. I. Velichkov, et al., *JALCOM*, **552** (2013) 190.

[2] A. V. Tsvyashchenko, D. A. Salamatin, et al., *Phys. Rev. B*, **92** (2015) 104426.

[3] D.A. Salamatin, V. A. Sidorov, et al., *Phys. Rev. B*, **94** (2016) 214435.

5PO-I1-14

MAGNETIC RELAXATION OF Dy IN [Dy/Gd]*20 MULTILAYER DETECTED BY NUCLEAR RESONANCE REFLECTIVITY

Andreeva M.A.¹, Antropov N.O.², Baulin R.A.¹, Kravtsov E.A.², Proglyado V.V.², Ryabukhina M.V.², Chumakov A.I.^{3,4}, Ruffer R.³, Ustinov V.V.²

¹ M.V. Lomonosov Moscow State University Faculty of Physics, Moscow, Russia

² M.N. Mikheev Institute of Metal Physics RAS, Ekaterinburg, Russia

³ ESRF-The European Synchrotron, Grenoble, France

⁴ National Research Centre "Kurchatov Institute", Moscow, Russia

romanbaulin17@gmail.com

Dy-based superlattices exhibit peculiar magnetic behavior. Magnetic order in Dy/Gd was usually probed with polarized neutron diffraction. We present the results of the nuclear resonance reflectivity investigation for $\text{Al}_2\text{O}_3/\text{Nb}(1000\text{\AA})/\text{Y}(100\text{\AA})/[\text{Dy}(60\text{\AA})/\text{Gd}(60\text{\AA})]_{20}\text{Al}(100\text{\AA})$ multilayer (the details of preparation are in [1]) at the Nuclear Resonance beamline ID18 [2] of the ESRF. Natural Dy layers contain 18.9% of ^{161}Dy isotope, so the 25.6 keV ($7/2 \rightarrow 5/2$) resonant transition was used in the experiment. Mössbauer spectra of reflectivity were measured in the time domain.

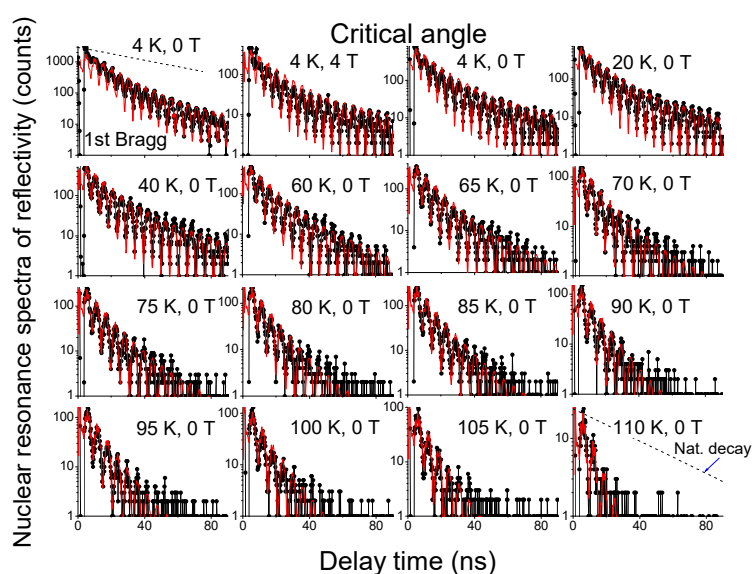


Fig. 1.

The enhanced relaxation at 110 K indicates the onset of the magnetic phase transition. It significantly diminishes the count rate and limits the measurements to 110 K.

The measured angular dependences of the nuclear resonance reflectivity testified to the rather complicated magnetic alignment of the Dy layers.

Supported by the Ministry of Education and Science of the Russian Federation (project RFMEFI61616X0067).

[1] M.A. Andreeva, N.O. Antropov, R.A. Baulin, E.A. Kravtsov, et al., *The Physics of Metals and Metallography*, **117**(12) (2016) 1201–1209.

[2] R. Ruffer., A.I. Chumakov, *Hyperfine Interactions*, **97/98** (1996) 589-604.

The quantum beats in the time spectrum of reflectivity (for more details see [1]) and the decay speed (Fig. 1) allow us to obtain the magnetic hyperfine field and the relaxation time dependence in the 4 - 110 K temperature range (Fig. 2).

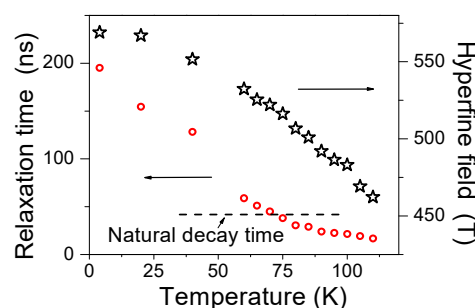


Fig.2.

5 July

Wednesday

12:00-14:00

poster session
5PO-I2

“Multiferroics”

5PO-I2-1

PHASE SEPARATION OF MANGANITES-MULTIFERROICS

$\text{Yb}_{1-x}\text{Sr}_x\text{MnO}_3$

Bykov E.O.^{1,2}, *Kurbakov A.I.*^{2,1}, *Malyshev A.L.*², *Eremina R.M.*³

¹ Saint Petersburg University, St. Petersburg, Russia

² Petersburg Nuclear Physics Institute, NRC Kurchatov Institute, Gatchina, Russia

³ E.K. Zavoisky Physical-Technical Institute, Kazan, Russia

mcgector@yandex.ru

The manganites of rare-earth elements with general formula RMnO_3 (R for rare-earth) are interesting as perspective materials with magnetic and electric order. In the some compounds different mechanisms of electrical ordering are realized depending on the crystal structure. For R with large ionic radius from Ho (Tb, Gd, Eu...) the structure is a perovskite-like, and ferroelectricity is the result of magnetic ordering: polarization is induced by displacement of oxygen in Mn-O-Mn bonds because of magnetic ordering. For ionic radii less then Dy (Y, Er, Yb...) there is a hexagonal structure, electric and magnetic orders are independent, ferroelectricity due to the "geometric" mechanism which consists in the distortion of the Mn environment.

Some mixed-valence compounds $\text{R}_{1-x}\text{A}_x\text{MnO}_3$ which doped by divalent element A (Ca, Sr, Ba...), like manganites with colossal magnetoresistance effect, are very interesting multiferroics. It becomes possible to smoothly control its structure and properties by concentration x of A elements. In this research we investigate $\text{Yb}_{1-x}\text{Sr}_x\text{MnO}_3$ composition ($x = 0, 0.18, 0.4$) by neutron powder diffraction. The main result is the observation of phase separation and the coexistence of two structures ($Pbnm$ and $P6_3cm$) in compounds doped by Sr. The experiment was carried out over a wide temperature range to observe magnetic transitions for each phase. We also calculated from crystal structure displacement maps for finding electric polarization. Finally, we modeled magnetic structures for both phases.

Supported by RFBR project № 16-02-00360.

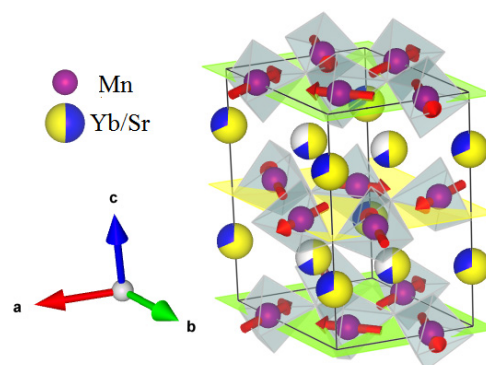


Fig. 1. Crystal and magnetic (red vectors) structures of $h\text{-Yb}_{1-x}\text{Sr}_x\text{MnO}_3$, space group $P6_3cm$. Oxygens are located at the vertices of blue bipyramids.

5PO-I2-2

CAPACITANCE DILATOMETER FOR SMALL DEFORMATIONS MEASUREMENTS CAUSED BY EXTERNAL MAGNETIC AND ELECTRIC FIELDS AND TEMPERATURE

Freydman A.L., Popkov S.I., Krasikov A.A., Mihashenok N.V.

Kirensky Institute of Physics, Federal Research Center KSC SB RAS, Krasnoyarsk, Russia
dir@iph.krasn.ru

Deformation of solids reflects many processes in crystal lattice. For example, it is complicated to determine fine displacements in unit cell by direct methods (X-ray, elastic neutrons and etc) at phase transition, but it results in deformation of whole sample, which can be measured by dilatometry methods. For this reason new publication about dilatometer measurement setup is appeared time and again.

Multiferroics is very interesting compounds due to relation between various elastic interaction. For magnetoelectric materials it is interesting to investigate more than magnetostriction, but also piezoelectric effect, piezoelectric effect in magnetic field and magnetostriction in electric field. But any publication about such experimental setup is not occurrence.

This work is devoted to develop of capacitance dilatometer for measurements of small deformations due to thermal expansion, influence of magnetic (magnetostriction and piezomagnetic effect) and electric fields (piezoelectric effect and electrostriction). The Physical Property Measurement System PPMS QD is very appropriate to this method because of ability of creating of high magnetic field and temperature stabilization in wide region. The measurement puck for its cryostat was developed and shown in figure 1.

Almost all elements of measurement cell is produced from copper, because of its high thermo- and electro- conductive properties, simplicity of machining and well known thermal-expansion coefficient. The cell is equipped with electrical cutoff point, which is proper to PPMS and groove for mounting and dismantling by standard holder. It enables measurement in high vacuum.

The calibration measurements were carried out on several samples of pure silver, copper and aluminium. On figure 2 the temperature dependence of capacitance is present for aluminium sample AB000 10 millimeters in height.

The work was supported by Russian Foundation for Basic Research, Government of Krasnoyarsk Territory, Krasnoyarsk Region Science and Technology Support Fund according to the research project №16-48-243040.



Fig. 1. Measurement cell for thermal expansion, magnetostriction and piezoelectric effect measure.

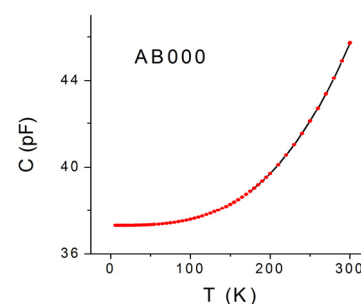


Fig. 2. The temperature dependence of measurement capacitor capacitance on sample AB000.

5PO-I2-3

TRANSFORMATION OF DOMAIN STRUCTURE OF PERMALLOY MICROPARTICLES UNDER MECHANICAL TENSION

*Bizyaev D.A.¹, Bukharaev A.A.^{1,2}, Chuklanov A.P.¹, Khanipov T.F.¹, Nurgazizov N.I.^{1,2},
*Russkikh I.V.¹, Sadchikov Yu.V.¹**

¹ Kazan E. K. Zavoisky Physical-Technical Institute, Kazan, Russia

² Kazan Federal University, Kazan, Russia

niazn@mail.ru

Recently the scientists are intensively investigated of the using of Villari effect (changing of magnetic properties of a solid under mechanical tension) for magnetic reversal processes of micro and nanostructures. It is caused by a possibility to significantly reduce of energy for rewriting of one bit of magnetic information by simultaneous using of magnetic field and mechanical tension. Also the Villari effect can be used for detecting of a mechanical tension in ferromagnetic solids with high spatial resolution. In this work a change of magnetic properties of the permalloy (Py) particles under mechanical compression was investigated.

Researches were carried out on samples consisting of the array of the planar Py (Ni75%, Fe25%) particles (size $25 \times 25 \times 0.02$ mkm³) located on a silicon substrate. Particles have been fabricated by electron beam evaporation through a metal grid in the ultrahigh vacuum conditions. For creation of a tension in particles the substrate was elastically bend by fastening in the holder before carrying out evaporation and after unbending of the substrate the particles have been compressed. Using of various holders has allowed to make samples with equally compressed particles, and samples with different value of particles compression along one of axes.

MFM was used for visualization of particles domain structure. Area for MFM scanning of a surface was set with a fixed step along a long axis of a sample (parallel axis to a particles compression). The obtained MFM images were compared with results of computer modeling of a particle magnetic structure. Its calculations were carried out by the OOMMF [1] and "Virtual MFM" [2] software. The size and the form of particles obtained by MFM were used for modeling. The coefficient of magnetoelastic anisotropy is being varied under calculations until the modeling MFM image was coincided with the experimental image. Obtained value of the coefficient was used for estimation of the effective anisotropy field of a particle. A modeling of distribution of a tension tensor in a substrate surface depending on its bend was carried out. It was shown that the distribution of values of the tension tensor along a substrate surface corresponds to the distribution of values of the anisotropy effective field of particles.

It has been shown that uncompressed particles have classical four-domain structure, with domains equal by the sizes. At one axe compression of particles is resulted to an increasing of the sizes of domains with direction of magnetization perpendicular to a compression. For non-uniformly curved samples has been estimated the increasing of the effective anisotropy field from 2,32 mT on the edge of a sample (the most poorly compressed particles) up to 4,65 mT in the center (the most strongly compressed particles). It has been estimated that for non-uniformly curved samples there is an increase in the anisotropy effective field of from 2,32 mT on the edge of a sample (the weakly compressed particles), to 4,65 mT in the center (the most strongly compressed particles).

Support by RFBR 17-08-00915.

[1] M.J. Donahue, D.G. Porter: (<http://math.nist.gov/oommf/>).

[2] D.V. Ovchinnikov, A.A. Bukharaev, *Technical Physics*, **46** (2001) 1014–1019.

5PO-I2-4

SPIN-FLOP DRIVEN MAGNETO-DIELECTRIC EFFECT IN SINGLE CRYSTALS $\text{Cu}_3\text{B}_2\text{O}_6$ AND $\text{Pb}_2\text{Fe}_2\text{Ge}_2\text{O}_9$.

Balaev D.A.^{1,2}, Freydmann A.L.¹, Krasikov A.A.¹, Balaev A.D.¹, Pankrats A.I.^{1,2}, Popkov S.I.^{1,2}, Kolkov M.I.^{1,2}, Sablina K.A.¹, Bovina A.F.¹

¹ Kirensky Institute of Physics, Federal Research Center KSC SB RAS, Krasnoyarsk, Russia

² Siberian Federal University, Krasnoyarsk, Russia

kaa3000@yandex.ru

We report the study of magneto-dielectric (MD) effect (i.e., the dependence of permittivity ε as a function of and magnetic field H) in the crystals $\text{Cu}_3\text{B}_2\text{O}_6$ and $\text{Pb}_2\text{Fe}_2\text{Ge}_2\text{O}_9$. These crystals have complex antiferromagnetic ordering with the Néel temperatures about ≈ 10 K ($\text{Cu}_3\text{B}_2\text{O}_6$ [1]) and ≈ 46 K ($\text{Pb}_2\text{Fe}_2\text{Ge}_2\text{O}_9$ [2]). The single crystals were grown by flux technique. To measure the permittivity, conductive plates were applied to the crystal bases.

$\text{Cu}_3\text{B}_2\text{O}_6$ has a layered structure (the space group is PI , $a = 3.344$ Å, $b = 19.757$ Å, $c = 19.587$ Å, $\alpha = 88.91^\circ$, $\beta = 70.05^\circ$, $\gamma = 69.93^\circ$) in which layers correspond to bc -planes spaced by 2.90 Å. For this crystal the permittivity ε was measured in case when electric field $\mathbf{E} \perp bc$ -planes (at a frequency of 10 kHz). It was found that MD effect ($\approx 0.1\%$ at $H = 60$ kOe) is observed only for one direction of magnetic field \mathbf{H} with respect to crystallographic axes of a crystal, namely for $\mathbf{H} \parallel b$. From the other hand, the magnetization curve for this direction exhibit portion with positive curvature, which reflects “sequential spin-flop transitions” between various magnetic structures. Therefore, the existence of the MD effect in $\text{Cu}_3\text{B}_2\text{O}_6$ correlates with the anisotropic behavior of magnetic properties [3].

$\text{Pb}_2\text{Fe}_2\text{Ge}_2\text{O}_9$ possess the orthorhombic crystal structure (the space group is $Pbcn$) with the cell parameters $a=7.149$ Å, $b=11.177$ Å, $c=10.144$ Å. We measured the MD effect for $\mathbf{E} \parallel a$ and $\mathbf{E} \parallel c$ directions (at a frequency of 100 kHz). It was found that $\varepsilon(H)$ curves demonstrate pronounced anomalies for the case $\mathbf{H} \parallel c$, see the fig.1. Additionally, a sharp spin-flop transition at $H \approx 40$ kOe (for $T = 4.2$ K) takes place for this field direction [2]. Strong correlation of spin-flop transition with the behavior of MD effect is obvious. This, probably, indicate that spin rearrangement, induced by spin-flop transition, results in change of electronic polarization. Also, magnetic structure of $\text{Pb}_2\text{Fe}_2\text{Ge}_2\text{O}_9$ is discussed in the view of new experimental results on heat capacity and MD effect.

Thus, the crystals $\text{Cu}_3\text{B}_2\text{O}_6$ and $\text{Pb}_2\text{Fe}_2\text{Ge}_2\text{O}_9$ reveal strong correlation between MD effect and spin-flop transitions.

Support by RFBR No. 16-02-00563 is acknowledged.

[1] G.A. Petrakovskii, K.A. Sablina, et al, *Phys. Solid State*, **41** (1999) 610.

[2] G.A. Petrakovskii, M.A. Popov, A.D. Balaev, et al, *Phys. Solid State*, **51** (1999) 1853.

[3] D.A. Balaev, K.A. Sablina, A.L. Freydmann, et al, *Phys. Solid State*, **58**(N2), (2016) 284.

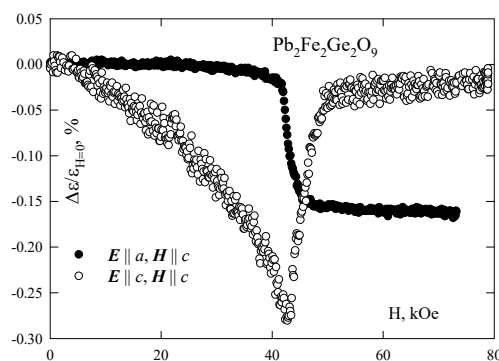


Fig. 1. MD effect at 4.2 K for $\text{Pb}_2\text{Fe}_2\text{Ge}_2\text{O}_9$ single crystal.

5PO-I2-5

COMPARATIVE STUDY OF MAGNETOELECTRIC EFFECT IN $\text{HoAl}_3(\text{BO}_3)_4$ AND $\text{HoGa}_3(\text{BO}_3)_4$ SINGLE CRYSTALS

Freydman A.L., Balaev A.D., Dubrovskiy A.A., Temerov V.L., Gudim I.A.

Kirensky Institute of Physics, Federal Research Center KSC SB RAS, Krasnoyarsk, Russia
fss4@yandex.ru

In recent years materials, which simultaneously possess (anti) ferromagnetism and (anti) ferroelectricity, called multiferroics, were the subject of intensive research. In these materials there is strong correlation between the magnetic and ferroelectric subsystems, and they are promising in spintronic applications. Rare earth ferrobates with general formula $\text{RFe}_3(\text{BO}_3)_4$ are the class of the crystals which belongs to the multiferroic family. A substitution of Fe^{3+} ions to nonmagnetic ions (for example, Ga^{3+} or Al^{3+}) results in paramagnetic behavior, therefore, a compound no more belongs to multiferroics. Nevertheless, paramagnetic oxi-borates are known to exhibit magnetoelectric properties.

In our previous work [1] the magnetoelectric ME_E -effect in $\text{HoAl}_3(\text{BO}_3)_4$ was measured and the qualitative microscopic model was proposed. The model is based on nonspherical distribution of electron charge density of 4f-subshells of Ho^{3+} ions. When the sample magnetization is raised a shell overlap of holmium and oxygen ions is changed and additional electrostatic force is appeared. This results in magnetostriction and magnetoelectric effects, which originate from elastic interaction (magnetoelastic effect and piezoelectricity).

The aim of present work is to find out the influence of a nonmagnetic aluminium subsystem on magnetoelectric effect. With this aim in mind, comparison of magnetoelectric properties of $\text{HoAl}_3(\text{BO}_3)_4$ and $\text{HoGa}_3(\text{BO}_3)_4$ crystals was carried out.

The single crystals of $\text{HoGa}_3(\text{BO}_3)_4$ were grown from the flux. The experimental investigation of magnetization, ME_E - and ME_H -effect, piezoelectric effect, magnetostriction and magnetodielectric effect was realized.

On figure 1 the susceptibilities of magnetoelectric ME_E -effect as function of magnetic field and temperature of $\text{HoAl}_3(\text{BO}_3)_4$ (a) and $\text{HoGa}_3(\text{BO}_3)_4$ (b) single crystals are shown. One can see that the behavior of $\beta(H,T)$ is similar for both compounds, but the absolute value is slightly higher for the aluminium borate. It means that the rare-earth subsystem plays the main role in formation of magnetoelectric effect.

The work was supported by Russian Foundation for Basic Research, the project №16-38-00245 and by Russian Foundation for Basic Research, Government of Krasnoyarsk Territory, Krasnoyarsk Region Science and Technology Support Fund according to the research project №16-48-243040.

[1] A.L. Freydmán, A.D. Balaev, A.A. Dubrovskiy et. al. *J. Appl. Phys.*, **115** (2014) 174103.

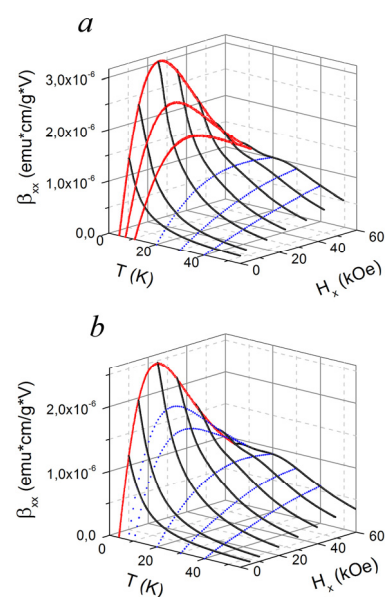


Fig. 1. Susceptibility of magnetoelectric ME_E -effect in $\text{HoAl}_3(\text{BO}_3)_4$ (a) and $\text{HoGa}_3(\text{BO}_3)_4$ (b).

5PO-I2-6

A NEW CLASS OF THE HYBRID DIPOLE SPIN WAVES

Savchenko A.S.¹, Sukhorukova O.S.¹, Tarasenko A.S.¹, Tarasenko S.V.¹, Shavrov V.G.²

¹ Donetsk Institute for Physics and Engineering named after A.A. Galkin, Donetsk, Ukraine

² Kotelnikov Institute of Radio Engineering and Electronics, RAS, Moscow, Russia
s.v.tarasenko@mail.ru

In recent years, the physics of electromagnetic metamaterials has been actively studied. In the framework of the effective medium theory, the coupling equations describing such composite structure can be represented in the form

$$\mathbf{B} = \overline{\overline{\mu}} \mathbf{H} + \overline{\overline{A}}^* \mathbf{E}, \quad \mathbf{D} = \overline{\overline{\varepsilon}} \mathbf{E} + \overline{\overline{A}}^T \mathbf{H}, \quad \overline{\overline{\mu}}^T = \overline{\overline{\mu}}^*, \quad \overline{\overline{\varepsilon}}^T = \overline{\overline{\varepsilon}}^* \quad (1)$$

Here, \mathbf{B} and \mathbf{D} are the magnetic flux density and electric displacement, respectively, and \mathbf{H} and \mathbf{E} are the magnetic and electric fields, respectively. Superscripts * and T correspond to complex conjugation and transposition, respectively. Some nonzero tensor components in Eqs. (1) can exhibit resonance features as functions of the frequency ω . In magnonics (one of the most dynamically progressing fields of the modern physics of magnetic phenomena), the creation of controllable magnetic metamaterials is based on implementing a system of locally resonating and electromagnetically coupled structural elements (spins). Up to now, the main attention in the field of the slow electromagnetic waves has traditionally been focused on the usage of potentialities provided by the magneto- or electro dipole types of spin waves. In the Coulomb limit, using the Maxwell type intralayer and/or interlayer (in particular, surface) boundary conditions, we can describe the dispersion characteristics of these slow electromagnetic waves using the set of magnetostatic equations and electrostatic equations. But the studies of the dispersion characteristics of the hybrid EMW (resulting from the interaction of TM and TE types of the waves) in finite-size magnetically ordered materials are of no doubt interesting for developing electromagnetic metamaterials controlled by the applied electric and magnetic fields.

In this report the necessary condition of existence for the new type dipole hybrid magnons are discussed. Let us consider the sagittal plane with the normal given by the vector \mathbf{a} ($\mathbf{a} \perp \mathbf{q}$, \mathbf{q} is the normal to the surface of layer of an easy-axis antiferromagnet with antisymmetry center) and let the magnetic permeability and permittivity tensors in (1) have the structure

$$\begin{aligned} \overline{\overline{\mu}} &= \mu_1 (\mathbf{b} \otimes \mathbf{b} + \mathbf{q} \otimes \mathbf{q}) + \mu_2 (\mathbf{b} \otimes \mathbf{q} - \mathbf{q} \otimes \mathbf{b}) + \mu_3 \mathbf{a} \otimes \mathbf{a}, \\ \overline{\overline{\varepsilon}} &= \varepsilon_1 (\mathbf{b} \otimes \mathbf{b} + \mathbf{q} \otimes \mathbf{q}) + \varepsilon_2 (\mathbf{b} \otimes \mathbf{q} - \mathbf{q} \otimes \mathbf{b}) + \varepsilon_3 \mathbf{a} \otimes \mathbf{a} \end{aligned} \quad (2)$$

where $\overline{\overline{I}}$ is the unit tensor, $\mathbf{q} = [\mathbf{ab}]$, $\mu_{1,2} = \mu_{1,2}(\omega)$, $\varepsilon_{1,2} = \varepsilon_{1,2}(\omega)$, $\mu_3, \varepsilon_3 - constant$. The calculation shows that the for case

$$\overline{\overline{A}} \equiv \frac{tr \overline{\overline{A}}}{3} \overline{\overline{I}} + \overline{\overline{P}} + \overline{\overline{Q}}, \quad \overline{\overline{P}} \equiv \left(\frac{\overline{\overline{M}} + \overline{\overline{M}}^T}{2} \right), \quad \overline{\overline{Q}} \equiv \left(\frac{\overline{\overline{M}} - \overline{\overline{M}}^T}{2} \right), \quad \overline{\overline{M}} \equiv \overline{\overline{A}} - \left(\frac{tr \overline{\overline{A}}}{3} \right) \overline{\overline{I}} \quad (3)$$

$$\overline{\overline{P}} = p_1 (\mathbf{b} \otimes \mathbf{b} - \mathbf{q} \otimes \mathbf{q}) + p_2 (\mathbf{b} \otimes \mathbf{q} + \mathbf{q} \otimes \mathbf{b})$$

where $p_{1,2}$ are some scalar parameters ($|p_1| + |p_2| \neq 0$) the combination of magneto- and electric-dipole mechanisms of the indirect spin-spin interactions gives rise to the previously unknown class of propagating hybrid dipole bulk spin waves in magnetic film

The work was supported by the Russian Foundation for Basic Research (project no. 14-02-90416).

5PO-I2-7

NONLINEAR CONVERSION OF MAGNETIC NOISE IN MAGNETOELECTRIC COMPOSITES

Burdin D.A., Chashin D.V., Ekonomov N.A., Fetisov Y.K.

Moscow Technological University, Moscow, Russia

ekonomov@mirea.ru

Nonlinear magnetoelectric (ME) effects in layered ferromagnetic-piezoelectric (FM-PE) composites are considered as promising basis to design new type magnetic field sensors. The up-frequency conversion of harmonic magnetic field via ME magnetic fields mixing significantly enhanced the sensitivity and decreased the noise level of the sensors [1]. Therefore, it is important to study nonlinear conversion of magnetic noise in the ME composites, that is a goal of the present research.

This work describes ME effect in a bilayer composite being excited via noise-like and harmonic magnetic fields simultaneously. The sample of rectangular shape with in-plane dimensions of 25x5 mm² contained a 0.5 mm thick single-crystal langatate layer and a 20 μm thick amorphous alloy Metglas layer, glued to each other. Excitation magnetic fields were created by two coaxial coils and dc bias field H was produced by Helmholtz coils. The white-noise voltage with center frequency $f_n=10$ kHz and bandwidth $\Delta f_n \approx 4$ kHz from the Agilent 33210a generator followed by the band-pass programmable filter SR650 was applied to the first coil. The harmonic ac voltage with frequency $f_p=10-70$ kHz from another function generator was applied to the second coil. Frequency spectrum of the ME signal was registered with the spectral analyzer SR770.

Figure 1a shows that magnetic noise excites a noise-like ME voltage and two high Q peaks at frequencies of bending $f_1=17$ kHz and longitudinal $f_2=85$ kHz acoustic resonances of the sample. Addition of harmonic pumping magnetic field of frequency $f_p=50$ kHz (Fig.1b) results in effective nonlinear transfer of the low-frequency noise spectrum to the higher frequency region. Amplitudes of the peaks at $f_p \pm f_n$ undergo resonance enhancement when their frequencies coincide with f_1 and f_2 . The amplitudes are proportional to the nonlinear piezomagnetic coefficient of the Metglas layer and gradually go down with an increase in the bias field H , in accordance with the theory [2].

The results obtained should be taken into account when considering noise characteristics of magnetic field sensors based on nonlinear ME effects.

The research was supported by Ministry of Education and Science of Russia, project 8.1183.2017.

[1] S.M. Gillette, A.L. Geiler, D. Gray et al, *IEEE Magnetic Lett.*, **2** (2011) 2500104.

[2] D.V. Chashin, N.A. Ekonomov, L.Y. Fetisov et al. *JMMM*, **358-359** (2014) 98-104.

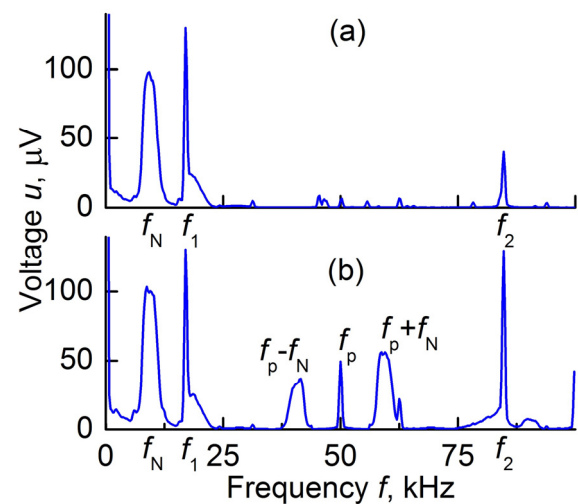


Fig.1 ME signal spectra under: (a) noise-like field excitation and (b) simultaneous noise-like and harmonic field excitation at $H=0.1$ Oe.

5PO-I2-8

INVESTIGATIONS OF THE SPIN-WAVE RESONANCE SPECTRA IN MULTILAYER FERRITE-GARNET FILMS WITH ASYMMETRIC BOUNDARY CONDITIONS

Bazhanov A.G., Trofimov N.O.

Mordovian State University, Saransk, Russia
bajanovag@mail.ru

In the present work experimental studies and a theoretical calculation of the temperature and angular dependence of the resonance fields in two-layer films with a mixed spin-fixing mechanism in the presence of near-surface anisotropy in the excitation layer are carried out. In this case, the fixation of the spins in the excitation layer of the spin waves is asymmetric.

Experimental studies have shown that in the spectrum of such films intermediate spin-wave modes are observed even under the initial conditions: at room temperature and at a perpendicular orientation of the external magnetic field relative to the film plane [1]. The peculiarity of the intermediate spin-wave modes is that they have an intensity an order of magnitude smaller than the intensity of the main spin-wave modes.

As a result of solving the magnetization motion equations written for each of the layers of a two-layer magnetic film, and also taking into account the boundary conditions at the outer boundaries of the film and at the interlayer boundary, the distributions of the variable magnetization in these layers were found. According to [2], the width of the absorption line of each (spin-wave) SW-mode $2\Delta H_n$ can be expressed in terms of the effective damping parameter and the effective gyromagnetic ratio of the n -th spin-wave mode.

The calculation showed that the decrease in the slope of the dispersion dependences with increasing angle θ_H is due to the fact that when the homogeneous resonance fields approach each other, the degree of fixation of the spins at the interlayer boundary decreases. As a result, the depth of penetration of the spin wave into the fixing layer increases, and, consequently, the wave number $k_1 = (n + 1/2)\pi/h$ decreases and the slope of the dispersion curve $H_0 - H_n = f((n + 1/2)^2)$ decreases. When $\theta_H \geq 65^\circ$ the resonance field of the second layer exceeds the resonance field of the first layer, and the anchoring layer becomes a dispersive medium for spin waves, i.e. there is a fixation, but less than at corners $\theta_H \leq 65^\circ$. The depth of penetration of the spin wave again decreases and the tangent of the slope of the dispersion curve increases.

As a result of temperature studies, a monotonous decrease in the resonance fields of the spin-wave modes was observed, which is associated with a decrease in the magnetization of the substance with increasing temperature in accordance with the Bloch law. It should be noted that the magnetization also enters into the term $(2A/M)k^2$ in the dispersion relations. However, as it was established earlier, with an increase in temperature the value of the exchange constant decreases monotonically and as a whole the ratio $(2A/M)k^2$ with the temperature increase practically does not change. Thus, the main contribution to the decrease of the resonance fields with increasing temperature is associated with a decrease in the magnetization of matter

[1] A.M. Zyuzin, A.G. Bazhanov, *Bul. of Russian Academician. Phys. series*, **77** (2013) 1533-1538.

[2] A.M. Zyuzin, A.G. Bazhanov, *Solid State Physics*, **42** (2000) 1279-1283.

5PO-I2-9

INFLUENCE NEUTRON IRRADIATION ON THE STRUCTURAL AND MAGNETIC STRUCTURES OF THE $\text{Bi}_{0.85}\text{La}_{0.15}\text{FeO}_3$ MULTIFERROIC

Semkin M.A.^{1,2}, *Teplykh A.E.*², *Parkhomenko V.D.*², *Bogdanov S.G.*², *Karpinsky D.V.*³,
Kholkin A.L.^{1,4}, *Pirogov A.N.*^{1,2}

¹ Institute of Natural Sciences and Mathematics, Ural Federal University, Ekaterinburg, Russia

² M.N. Mikheev Institute of Metal Physics of Ural Division of RAS, Ekaterinburg, Russia

³ Scientific-Practical Materials Research Centre of NAS of Belarus, Minsk, Belarus

⁴ Department of Physics, CICECO-Aveiro Institute of Materials, University of Aveiro, Portugal

m.a.semkin@urfu.ru

To study an interplay between the crystal and magnetic structure of the polycrystalline $\text{Bi}_{0.85}\text{La}_{0.15}\text{FeO}_3$ multiferroic we irradiated the sample with fast ($E_{\text{eff}} \geq 1$ MeV) neutrons up to fluence $F = 5 \cdot 10^{20}$ n/cm². The $\text{Bi}_{0.85}\text{La}_{0.15}\text{FeO}_3$ powder was synthesized by the solid-state reaction method. High resolution X-ray powder diffraction (XRD) patterns were recorded at room temperature (RT) using Bruker D8 diffractometer with Cu K_{α} radiation (wave length $\lambda = 1.54056$ Å). Patterns were obtained in the range scattering of $10^{\circ} \leq 2\theta \leq 100^{\circ}$ with the step $\Delta 2\theta = 0.0195^{\circ}$. Neutron powder diffraction (NPD) patterns have been recorded at 293 K using the D2 diffractometer installed on a horizontal channel of the RWW-2M reactor (Zarechny, Russia). The used neutron length was $\lambda = 1.805$ Å. The analysis of all XRD and NPD patterns was performed using the software package “Fullprof” [1].

Fig. 1 shows NDP patterns of the pristine (not irradiated) $\text{Bi}_{0.85}\text{La}_{0.15}\text{FeO}_3$ ($F = 0$) multiferroic at 293 K. The crystal structure of this multiferroic belongs to rhombohedral $R3c$ space group. The La-ions are placed in the Bi-sublattice of the BiFeO_3 structure. To refine a magnetic structure of the $\text{Bi}_{0.85}\text{La}_{0.15}\text{FeO}_3$ we used $k = 0$. The magnetic structure is described as the cycloidal spiral. The Fe-ion moments are oriented ferromagnetically in planes perpendicular to the [111] direction and antiferromagnetically in adjacent planes. Calculation of neutron powder diffraction patterns of irradiated $\text{Bi}_{0.85}\text{La}_{0.15}\text{FeO}_3$ samples has shown that lattice parameters increased with increasing fluence, pointing to an accumulation of irradiated defects in the samples. Lattice parameters increase from $V = 369.14(3)$ Å by 1.1%. The value of the Fe-ion moment is $3.74(5) \mu_B$ for $F = 0$ and at least the same, $3.71(9) \mu_B$, after neutron fluence $F = 5 \cdot 10^{20}$ n/cm². Irradiation stimulates an increase of the concentration of impurity phases less 10% (Fe_3O_4 , Bi_2O_3) in comparison with that in the initial sample.

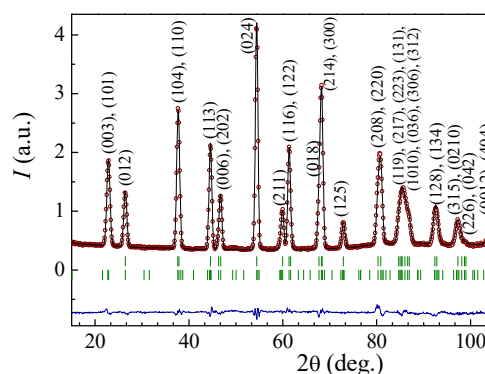


Fig. 1. Observed (points), calculated (line), and differential NDP of $\text{Bi}_{0.85}\text{La}_{0.15}\text{FeO}_3$ at 293 K (neutron length was $\lambda = 1.805$ Å). Bars show angle position of the nuclear and magnetic reflections.

The research was supported partially at IMP Neutron Material Science Complex within the state assignment of FASO of Russia (theme “Flux” No. 01201463334), supported in part by grant 15-8-2-2 of the Program of Fundamental Researches of UB RAS and by the State contract (No. 3.6121.2017) between UrFU and the Ministry of Education and Science of Russian Federation. [1] J. Rodriguez-Corvajal, *Phys. B.* **192** (1993) 55-69.

5PO-I2-10

FERROMAGNETIC RESONANCE BROADENING IN FERRITE/PIEZOELECTRIC LAYERED STRUCTURE

Petrov V.M., Saplev A.F., Tatarenko A.S., Bichurin M.I.
Novgorod State University, Veliky Novgorod 173003, Russia
nightroud1991@yandex.ru

The aim of this work is the theoretical modeling of ferromagnetic resonance (FMR) in the laminate composite of ferrite, piezoelectric bimorph, and buffer layers. It is shown that an external electric field induces an uniaxial magnetic anisotropy that is inhomogeneous in thickness. As a result, FRM line is shifted and broadened.

In layered magnetostrictive-piezoelectric structures, the applied electric field produces the strains that induce a uniaxial magnetic anisotropy. As a result, one obtains a shift of the FMR line [1]. Our findings suggest that the thickness-dependent strains contribute to the flexural deformations of magnetic layer. Thus FMR line appears to be shifted and inhomogeneously broadened due to flexure. For symmetric laminate which includes the ferrite layer between two piezoelectric layers with opposite poling direction, the average shift of resonance field vanishes and we obtain the pure broadening of the FMR line. Using the buffer layers between the ferrite and piezoelectric layers enables one to reduce influence of high-permittivity piezoelectric on microwave circuit.

For theoretical modeling of the electric field induced magnetic anisotropy, we solve the equation of motion of magnetization, $\frac{\partial M}{\partial t} = -\gamma[M, H_{eff}]$, where the effective field is determined

by $H_{eff} = -\frac{\partial^m W}{\partial M}$ with ${}^m W$ and M denoting the free energy density for the ferrite and magnetization.

The free energy density of a single crystal ferrite includes the magnetic crystallographic anisotropy energy, shape anisotropy, and magnetoelastic energy. The stress components that enter into the expression for the magnetoelastic energy are produced by the applied electric field. In order to find these components, the elasticity equations for ferrite and piezoelectric layers must be solved taking into account the material equations. Note that the total longitudinal strain is thickness-dependent and includes the axial strain and flexural deformation. Estimates have been obtained for yttrium iron garnet (YIG) layer placed between the two lead zirconate titanate (PZT) layers with opposite poling directions. The peak broadening of the FMR line equals 7 Oe at 9.3 GHz for $E=10$ kV/cm. For specific ferrite to piezoelectric layer thickness ratios, the buffer layer thickness dependence of FMR line broadening shows a maximum. This is accounted for by redistribution of axial deformations due to buffer layer.

The study described here can be used in microwave signal processing devices such as FMR-based filters with controlled bandwidth. The mode of operation of such devices includes the electric field control.

The research is supported by Grant No: 16-12-10158 from the Russian Science Foundation.

- [1] M. Bichurin and V. Petrov, *Springer Series in Materials Science*, **201** (2014) DOI:10.1007/978-94-017-9156-4.
- [2] M.I. Bichurin, I. A. Kornev, V. M. Petrov, A. S. Tatarenko, Yu. V. Kiliba, and G. Srinivasan, *Phys. Rev. B*, **64** (2001) 094409.

5PO-I2-11

MAGNETOELECTRIC EFFECT IN TWO-LAYERED SELF-BIASED COMPOSITES $\text{Tb}_{0.12}\text{Dy}_{0.2}\text{Fe}_{0.68} - \text{PbZr}_{0.53}\text{Ti}_{0.47}\text{O}_3$

Kalgin A.V., Gridnev S.A., Poryadsky A.A.

Voronezh State Technical University, Voronezh, 394026, Russia

kalgin_alexandr@mail.ru

Layered magnetoelectric (ME) composites thanks to the opportunity to mutually transform magnetic and electric fields (ME effect) are attractive materials for basic researches and practical developments of new-generation devices.

To obtain maximal ME responses in such composites, researchers use a permanent magnet or an electromagnet, which create the external magnetic field providing the condition of the maximal piezomagnetic coefficient. However, the use of the external magnetic field sources leads to large sizes of devices that limits their practical application.

In order to solve this problem, in our opinion, it is necessary to get rid of sources of the external magnetic field and to create layered ME composites with the significant magnetization gradient as such composites have large internal (self-biased) magnetic fields and, as a consequence, large ME responses.

Therefore, this paper is devoted to the study of the ME effect in layered self-biased composites at various frequencies of the alternating magnetic field, magnetostrictive layer thicknesses, and strengths of the internal magnetic field.

The ME effect under the alternating magnetic field with the strength of 5 Oe and frequencies of 100 – 300 kHz, in the absence of the bias magnetic field, and at 20 °C has been studied in two-layered composites $\text{Tb}_{0.12}\text{Dy}_{0.2}\text{Fe}_{0.68} - \text{PbZr}_{0.53}\text{Ti}_{0.47}\text{O}_3$ (TDF – PZT) with magnetostrictive layers of the epoxy both with randomly and with gradiently distributed $\text{Tb}_{0.12}\text{Dy}_{0.2}\text{Fe}_{0.68}$ (TDF) granules in it and thickness-polarized piezoelectric layers of ceramics PZT. Magnetostrictive layers were $6 \times 6 \times a \text{ mm}^3$ ($a = 0.3 - 1.5 \text{ mm}$) in sizes, and piezoelectric layers had sizes of $8 \times 6 \times 0.7 \text{ mm}^3$. The most transverse ME voltage coefficient $\alpha_{31} = 8.8 - 14 \text{ mV}/(\text{cm} \cdot \text{Oe})$ was observed at resonant frequencies of the first harmonic longitudinal oscillations along the sample width of 205.6-214.8 kHz and increased up to 17.1 – 24.2 mV/(cm·Oe) for composites with the gradient distribution of TDF granules in magnetostrictive layers. Magnetoelectric coefficients are found to be larger for composites with the concentration gradient of granules in magnetostrictive layers along the length and not along the thickness of samples. Dependences of α_{31} on the average granule size varying over the interval of 40-200 μm and α_{31} on the magnetostrictive layer thickness taking values from 0.3 to 1.5 mm pass through maxima corresponding to 71 μm and 0.9 mm, respectively. Dependences of α_{31} on the internal magnetic field strength for composites TDF – PZT with the gradient distribution of TDF granules in magnetostrictive layers similarly to dependences α_{31} on the external magnetic field strength for composites TDF – PZT with the random distribution of TDF granules in magnetostrictive layers have the maximum falling on 720 Oe.

The results are discussed using the model of effective parameters of a heterogeneous medium.

The work was executed with the financial support of RFBR (grant no. 16-02-00072 and grant no. 16-42-360412).

5PO-I2-12

STRUCTURAL AND MAGNETIC PROPERTIES OF THE LiMPO_4 ($M = \text{Ni, Co, Mn}$) SINGLE CRYSTALS

Semkin M.A.¹, Urusova N.V.¹, Choi K.-Y.², Sim H.², Barykina Yu.A.^{1,3}, Kellerman D.G.³,
Park J.G.², Kratochvilova M.², Pirogov A.N.^{1,4}

¹ Ural Federal University, Ekaterinburg, Russia

² Seoul National University, Seoul, Korea

³ Institute of Solid State Chemistry of the Ural Branch of the RAS, Ekaterinburg, Russia

⁴ Institute of Metal Physics of the Ural Branch of the RAS, Ekaterinburg, Russia

Natalia.urusova@mail.ru

Lithium-transition metal orthophosphates LiMPO_4 ($M = \text{Ni, Co, Mn}$) are multiferroics in which at least two of three order parameters exist simultaneously: ferro (or anti)-ferromagnetic, ferroelectric and ferroelastic ordering at the same time. They possess the olivine-type orthorhombic crystallographic crystal structure (space group $Pnma$) and an antiferromagnetic (AFM) ordering at low-temperatures [1]. These materials have recently attracted the interest of scientists for possible applications as cathode materials for power batteries in electric devices [2].

The aims of this work are to study the crystal structure and the temperature evolution of magnetic ordering in LiMPO_4 , with $M = \text{Ni, Co, Mn}$ in order to find correlation between magnetic structure and the type of $3d$ -transition, and detected physical properties for these materials in order to explain the nature of a very strong interaction between ferroelectric and magnetic subsystems in multiferroics.

Single crystals were synthesized by the standard flux growth method. The orientation of the single crystal was determined by the X-ray Laue back-scattering method, which was performed at an Imaging Plate XRD Laue Camera (IP-XRD). Magnetic measurements were recorded with MPMS-3 EverCool (Seoul, Korea) with a primary converter based on SQUID up to 7 T, along the a - and c -axes. X-ray measurements were carried out at Single Crystal X-ray Diffractometer Rigaku Model: XtaLAB P200 (Seoul, Korea).

Fig. 1 shows single crystal X-ray pattern at room temperature (RT) of the $\text{LiNi}_{0.9}\text{Co}_{0.1}\text{PO}_4$. As shown in the fig. 1, the sample possesses good quality with a mosaic of not more than 1 deg. The information of the lattice parameters for this sample are $a = 4.6999 \text{ \AA}$, $b = 5.8733 \text{ \AA}$, $c = 10.0573 \text{ \AA}$. $\text{LiNi}_{0.9}\text{Co}_{0.1}\text{PO}_4$ has a first-order transition from a commensurate antiferromagnetic (AFM) phase to an incommensurate (IC) AFM phase at 20.4 K. As the temperature increases further, a second-order phase transition occurs from the long-range IC magnetic order to a paramagnetic state at 21.1 K. At these transition temperatures we detected anomalies on the temperature dependence of the magnetic susceptibility of the $\text{LiNi}_{0.9}\text{Co}_{0.1}\text{PO}_4$ single crystal. The temperature dependences of the magnetic susceptibility of a LiNiPO_4 and $\text{LiNi}_{0.9}\text{Mn}_{0.1}\text{PO}_4$ have similar anomalies that are described for the previous sample [1].

The research was supported by the State contract (No. 3.6121.2017) between UrFU and the Ministry of Education and Science of Russian Federation.

[1] M. Semkin, and et. al, *AIP Conf. Proc.*, **1767** (2016) 020035-8.

[2] R.P. Santoro, and et. al, *Phys. Chern. Solids*, **27** (1966) 1192-1193.

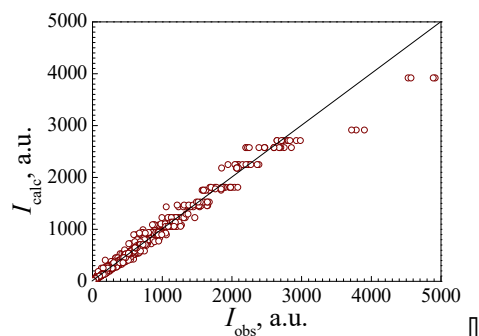


Fig. 1. Single crystal X-ray pattern at RT of the $\text{LiNi}_{0.9}\text{Co}_{0.1}\text{PO}_4$.

5PO-I2-13

ELECTROINDUCED MAGNETIC BUBBLE DOMAIN NUCLEATION

Kulikova D.P., Gareev T.T., Nikolaeva E.P., Pyatakov A.P.

M.V. Lomonosov Moscow State University, Physics Department, Moscow, Russia
dp.kulikova@physics.msu.ru

Since the beginning of this century, there is an increasing interest in magnetoelectric materials and multiferroics. It was experimentally shown that magnetic domain walls in iron garnet films can be displaced under the action of non-uniform electric field of tip electrode [1]. This phenomenon has a magnetoelectric nature with the magnetic domain wall considered as electrically polarized objects. Later the possibility of the enhancement of this magnetoelectric effect by an in-plane magnetic field was demonstrated [2]. In [3] the possibility of the local nucleation of magnetic bubble domains from a single-domain state of an iron garnet film by means of an electrically charged tip electrode has been experimentally demonstrated.

In this work we continue investigations started in [3] with studying the nucleation conditions of bubble domain and dynamics of the electrically induced bubble domain motion. Experiments were carried out with external magnetic fields applied in plane (H_{\parallel}) and perpendicular (H_{\perp}) to an iron garnet film. The sample used was $(\text{BiLu})_3(\text{FeGa})_5\text{O}_{12}$ garnet film grown by liquid-phase epitaxy on (210) $\text{Gd}_3\text{Ga}_5\text{O}_{12}$ substrate. Non-uniform high strength electric field an order of 1 MV/cm is induced by the voltage applied to the sharpened molybdenum tip touching the sample. Visualization of the micromagnetic structure was realized by Faraday magneto-optical effect. To study the dynamics the electric signal in the form of 1 μs rectangular pulse was used. By varying the delay of the illuminating laser pulses with respect to the electric field pulse we are able to observe instant positions of the domain structure.

The nucleation of magnetic bubble domain was observed when the voltage of the electrode was positive. With increasing voltage of the electrode, the magnetic bubble domains nucleation take place in a bias magnetic field with lower intensity (the H_{\perp} was codirectional with the vertical component of magnetization in bubble). The established dependence of the critical voltage on the electrode, at which the nucleating occurs, on the strength of the magnetic bias field is shown in the Fig 1. The experimental results were obtained with a temperature control ($T= 320$ K). The surface charge density of the domain wall estimated from Fig.1 is not exceeding $0.1\mu\text{C}/\text{m}^2$. The collapse of the bubble domain under the action of negative electric field pulse was observed. The domain wall velocity of electrically induced motion is nearly 50 m/s.

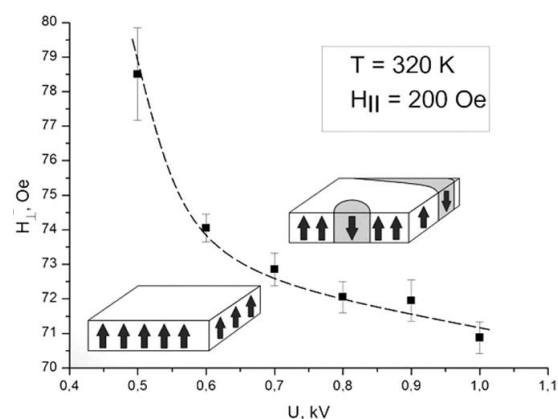


Fig. 1. Dependence of the critical voltage on the electrode on the strength of perpendicular component of the bias field.

Work was supported by RFBR grants ## 16-02-00494, and 16-29-14037_ofi_m.

[1] A.S. Logginov, G.A. Meshkov, A.V. Nikolaev, A.P. Pyatakov, *JETP Lett.*, **86** (2007) 115.

[2] A.P. Pyatakov, A.S. Sergeev, E.P. Nikolaeva *et al Phys. Usp.*, **58** (2015) 981.

[3] D.P. Kulikova, A.P. Pyatakov, E.P. Nikolaeva, A.S. Sergeeva, T.B. Kosykh, Z.A. Pyatakova, A.V. Nikolaeva, A.K. Zvezdin, *JETP Lett.*, **104** (2016) 197.

5 July

Wednesday

12:00-14:00

poster session
5PO-J

**“High Frequency
Properties and
Metamaterials”**

5PO-J-1

EXCITATION OF THE MAGNETIC BREATHER IN THREE-LAYERED FERROMAGNETIC STRUCTURE IN AUTORESONANCE MODE

Nazarov V.N.¹, Murtazin R.R.², Ekomasov E.G.²

¹ Institute of Molecule and Crystal Physics Ufa Research Centre of Russian Academy of Sciences,
Ufa, Russia

² Bashkir State University, Ufa, Russia
NazarovVN@gmail.com

At present sandwich-like magnetic structures are investigated extensively because of expected practical applications. Often they represent periodically alternating layers of two materials with different physical properties. For such new magnetic materials and processes occurring in them, the investigation of dynamics of magnetization reversal, generation of homogeneous and heterogeneous structure of dynamical status under the action of high-frequency field seems to be relevant [1]. From a mathematical point of view the problem reduces to a modified sine-Gordon equation in a model with impurities. Of special interest is the study of controlled dynamic conditions, in which high angles of precession of the magnetization may be attained by application of fields of sufficiently small amplitude [2, 3].

This work describes autoresonance parametric excitation of magnetic breather in three-layered ferromagnet with reduced value of the anisotropy in a thin layer by fields of variable frequency and small amplitude of a special form. As it was shown previously [4], the nucleus with the subcritical amplitude weakly responds to the defect size and disappears by transforming into a damping breather. In the case of an alternating external field, a probability exists for appearance of resonance effects that lead to more significant change of amplitude of breather. With variable frequency of pump field, the time evolution of the square of the amplitude is determined from the resonance conditions. Such conditions are interpreted as capturing the system by parametric resonance and make possible to obtain approximate solution for the amplitude at long period of time. Starting point is chosen near the boundary layer, where the approximate solution is determined by the differential equations obtained by averaging. The analysis of these equations shows the existence of solutions with a growing and reduced amplitudes. Also, possibility is shown for generation of magnetic breather with increasing amplitude in the field of thin layer from the equations of motion formulated as sine-Gordon equation in a model with inclusion of impurities [5] and solved with the help of numerical methods [6].

[1] D.I. Sementsov and A.M. Shutyi, *Physics–Uspekhi*, **50** (2007) 793–818.

[2] M.A. Shamsutdinov, I.Yu. Lomakina, V.N. Nazarov and et. el., *Ferro- and Antiferromagnetodynamics. Nonlinear Oscillations, Waves, and Solitons*, Nauka, Moscow, 2009.

[3] L.A. Kalyakin, M.A. Shamsutdinov, R.N. Garifullin and R.K. Salimov, *Physics of Metals and Metallography*, **104** (2007) 107–120.

[4] V.N. Nazarov, R.R. Shafeev, M.A. Shamsutdinov and I.Yu. Lomakina, *Physics of the Solid State*, **54** (2012) 298–304.

[5] E.G. Ekomasov, A.M. Gumerov, and R.R. Murtazin, *Math. Meth. Appl. Sci.* (DOI: 10.1002/mma.3908) (2016).

[6] E.G. Ekomasov, A.M. Gumerov, R.V. Kudryavtsev, *Journal of Computational and Applied Mathematics*, **312** (2017) 198–208.

5PO-J-2

STUDY OF TORQUE ACTING ON MAGNETIZATION DURING 180° PULSED REVERSAL PROCESS IN FERRITE-GARNET FILMS WITH BIAXIAL ANISOTROPY

Kolotov O.S.¹, Matyunin A.V.¹, Nikoladze G.M.¹, Polyakov P.A.¹

¹ MSU, Faculty of Physics, 1-2 Leninskiye Gory, GSP-1, Moscow, 119991, Russia
physphak@mail.ru

To calculate the torque acting on the magnetization during the 180° pulsed reversal process in real ferrite-garnet films, in which besides in-plane anisotropy biaxial anisotropy is present, the method based on the analysis of the trajectory of an operating point is used [2]. As the coordinates of the operating point the azimuthal angle φ and the torque component T_p caused by the switching field H_p are used. Fig.1 illustrates this statement. Solid thick line corresponds to the braking torque $\tau_{an} = T_{an}/(M_S \cdot H_{K2})$ (here we use the normalized value of the torque) caused by the uniaxial H_{K1} and biaxial H_{K2} anisotropy and setup field H_0 . Other lines correspond to the different values of accelerating torque $\tau_p = T_p/(M_S \cdot H_{K2})$ and applied switching field H_p ($= 30$ Oe): thin solid line corresponds to the H_p field pulse with rise time of 0.3 ns, dashed line – 0.9 ns, dotted line – 1.5 ns, dash-dotted line – 3.5 ns, dash-dot-dotted line – 6.5 ns. The

behaviour of the magnetization vector in this regime is similar to the process of 90° pulsed magnetization of such ferrite-garnet films, which was investigated earlier [1]. Thus it has been shown that the «effect of delayed acceleration of the transient process» also takes place during this regime. Meanwhile an additional maximum on the resulting torque $\tau_\varphi = \tau_p - \tau_{an}$ is observed (Fig.2). It appears at the moment of excitation of nonlinear magnetization oscillations [1], when magnetization reaches easy axis. Its influence is not significant and can be explained by the magnetization's inertia.

[1] O.S. Kolotov, A.V. Matyunin, G.M. Nikoladze, P.A. Polyakov, *Phys. Solid State*, **54** N 12 (2012) 2380–2386.

[2] O.S. Kolotov, A.V. Matyunin, G.M. Nikoladze, P.A. Polyakov, *Sol. State Phenomena*, **233** (2015) 490–493.

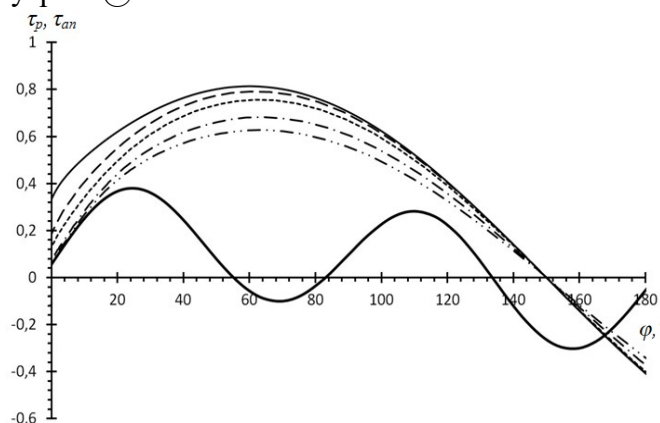


Fig.1. The normalized components of the torque τ_φ acting on the magnetization vector as a function of the angle φ .

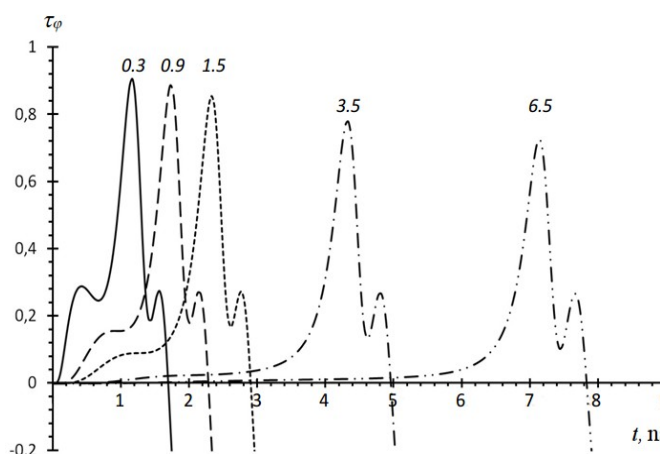


Fig.2. The time dependences of the torque τ_φ . The numbers above the dependences represent the corresponding front duration values.

5PO-J-3

PLASMONS IN CHAINS OF NANOPARTICLES OF COMPLEX SHAPE

Pikalov A.M.^{1,2}, *Dorofeenko A.V.*^{2,3,4}, *Granovsky A.B.*^{1,2}

¹ MSU, Physical department, Moscow, Russia

² ITAE RAS, Moscow, Russia

³ Dukhov Research Institute of Automatics, Moscow, Russia

⁴ MIPT, Dolgoprudniy, Russia

Wild.Voltmeter@yandex.ru

A method of plasmon dispersion calculation in chains of complex-shaped plasmonic particles is suggested. The method is a generalization of a technique developed previously for spherical nanoparticle chains [1]. An advantage of this approach is the possibility to take into account interaction of chain elements at arbitrarily long distances (higher-order interactions).

As an example an axial chain of split-ring resonators is considered. Inter-element interaction is calculated using a formalism given in [2].

The method involves approximation of distance dependence of inter-element interaction function with an inverse-power series (Fig. 1). The obtained approximant is used for building a sequence of dispersion curves corresponding to different numbers of the approximation series terms (N) using the method described in [1] (Fig. 2). One can see that with N increasing the dispersion converges to some limit state, which therefore can be considered as a true dispersion. This method can be applied to find plasmon dispersion in chain of particles of any arbitrary shape.

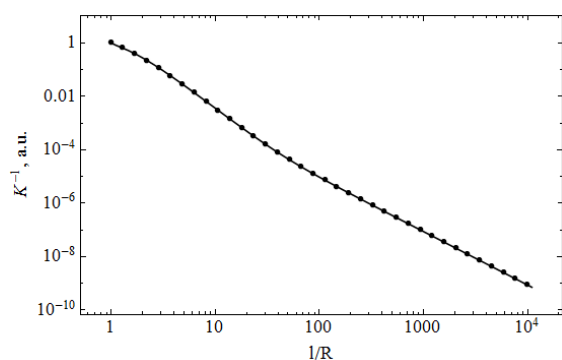


Fig. 1. Numerically calculated values of reverse mutual capacitance K^{-1} (points) and result of approximation with inverse-power series using terms number $N=6$ vs the inter-element distance l normalized by the SRR radius R .

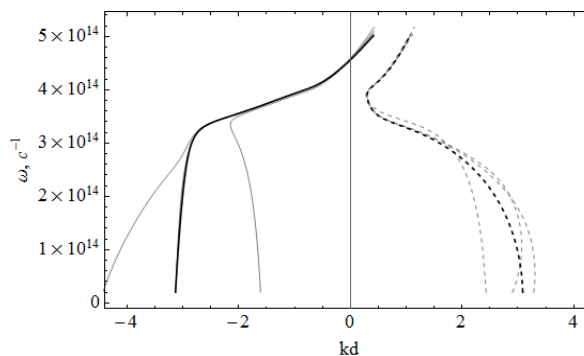


Fig. 2. A family of dispersion plots converging to a limit state (thick black curves) with N increasing from 4 to 7. Solid and dashed curves represent real and imaginary parts of the wavenumber k , respectively. d is chain period.

[1] A.F. Koenderink, A. Polman, *Physical Review B*, **74** (2006) 033402.

[2] E. Tatartschuk, et al. *J. App. Phys.*, **111** (2012) 094904.

5PO-J-4

MEASUREMENTS OF FREQUENCY DEPENDENCE OF MICROWAVE COMPLEX PERMEABILITY UNDER MAGNETIC BIAS

Shiryayev A.O., Bobrovskii S.Y., Osipov A.V., Petrov D.A., Rozanov K.N., Starostenko S.N.

ITAE RAS, Moscow, Russian Federation

artemshiryayev@mail.ru

For the characterization of microwave permeability of magnetic materials, ferromagnetic resonance measurements with fixed frequency and swept magnetic bias is frequently used. The main problem in performing such measurements is poor matching of the microwave feeding line. This leads to decrease in accuracy of measurement of the resonant frequency and resonant linewidth. Also, for a fixed frequency, it is possible that the sample is not saturated. However, the geometry of the measurement provides an opportunity to change shape, size and orientation of the measured sample.

An alternative way of microwave measurement of magnetic materials is a measurement of frequency dependence of complex permeability μ under external magnetic field. The permeability is conventionally measured with high accuracy in a coaxial line in the frequency range of 0.1 to 20 GHz. This measurement geometry allows for achieving larger fields and makes the sample closer to the saturation. However, the samples of coaxial shape are nonuniformly magnetized. The demagnetization factors in the direction along coaxial axis are calculated in [1].

The measured frequency dependence of the real permeability for different values of external magnetic field and thickness of samples is shown at Fig. 1. The sample is a roll made of a thin Fe-N film deposited on a flexible mylar substrate. The demagnetization leads to difference in resonant frequencies for samples of different thickness. This difference decreases with increasing external magnetic field. Measurement results agree with calculated values.

Also, the frequency dependence of permeability of composite materials containing sendust powder is measured in external magnetic field, see Fig. 2. The effect of filler concentration and particle shape on the microwave magnetic properties of the composites is studied. The field inside the composite sample is calculated with account for the demagnetization coefficient and the magnetic susceptibility of the sample. The anisotropy field and magnetization of saturation of sendust particles are calculated.

[1] M. Beleggia et al, *J. Magn. Magn. Mater.*, **321**, 9 (2009) 1306–1315.

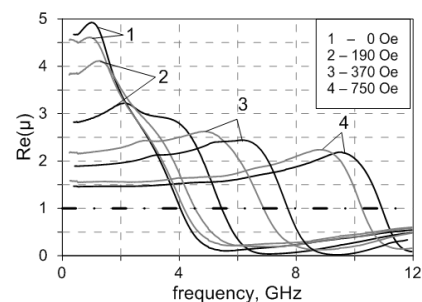


Fig. 1. The measured real part of permeability of thick Fe-N film in external magnetic field (black lines correspond to 5.4 mm sample thick, gray lines to 2.5 mm)

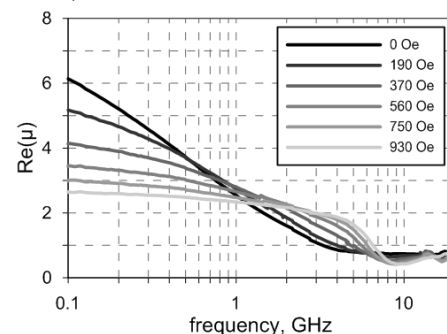


Fig. 2. The measured real part of permeability of composite material filled with sendust powder in external magnetic field

5PO-J-5

CONDITIONS FOR DIVISION AND MULTIPLICATION OF FREQUENCIES IN FERRITE

Pleshev D.A.^{1,2,a}, *Vlasov V.S.*^{2,b}, *Asadullin F.F.*^{1,2}, *Kotov L.N.*², *Poleshchikov S.M.*¹, *Shavrov V.G.*³,
*Shcheglov V.I.*³

¹ Saint-Petersburg state forest technical university named after S.M. Kirov, St-Petersburg, Russia

² Pitirim Sorokin Syktyvkar State University, Syktyvkar, Russia

³ Institute of Radioengineering and Electronics of the Russian Academy of Sciences, Moscow,
Russia

^a dpleshev@gmail.com, ^b vlasovv78@mail.ru

The paper is dealing with coupled oscillations of magnetization and elastic displacement in the normally magnetized single-layer and multilayered ferrite plates that have magnetoelastic properties. The coupled oscillations excited by the alternating magnetic field when the parametric excitation of spin waves is blocked [1-2]. The excitation of elastic oscillations on frequency of elastic resonance is possible in case when frequency of elastic subsystem resonance composes multiple part of the magnetic subsystem frequency in a single-layer ferrite plate [3] and in case of a multilayered ferrite plate with different saturation magnetisation. The excitation of magnetic oscillations on the frequency of elastic resonance takes place in the latter case.

The system of ordinary differential equations is described in the paper [1]. Home-made computer programs based on method of finite-difference approximation of coordinate derivatives and method of lines were used in calculations. The systems of ordinary differential equations were solved numerically by the Runge-Kutta 7-8 orders method with control of the integration at every step.

Time evolution of magnetic and elastic oscillations caused by the alternating field was analysed in case of frequency multiplication and frequency division. Frequency multiplication and frequency division are considered both by the integer case and by the fractional case.

Conditions of both processes of frequency division and multiplication in the single-layer and multilayered ferrite plate is considered in the paper. The paper describes dependences of magnetoelastic oscillation relaxation time on magnitudes of dc and alternating magnetic fields, layers properties, saturation magnetization, the magnetoelasticity constant, magnetic and elastic relaxation parameters. Diagrams of time dependences, phase portraits and spectrums of the excited magnetic and elastic fluctuations in layers with identical and distinct properties are made.

Mechanism of the shock-excitation of elastic oscillations is offered for interpretation of the presented effects.

Support by Russian Foundation for Basic Research (grant № 17-02-01138-a).

[1] D.A. Pleshev, F.F. Asadullin, S.M. Poleshchikov, L.N. Kotov, V.S. Vlasov, V.G. Shavrov, V.I. Shcheglov. *Solid State Phenomena*, **233-234** (2015) 471-475.

[2] V.S. Vlasov, L.N. Kotov, V.G. Shavrov, V.I. Shcheglov, *J. Comm. Tech. El.*, **54** (2009) 821-832.

[3] D.A. Pleshev, F.F. Asadullin, S.M. Poleshchikov, L.N. Kotov, V.S. Vlasov, V.G. Shavrov, V.I. Shcheglov. *Journal of Siberian Federal University. Mathematics & Physics*, **10(1)** (2017) 36-39.

5PO-J-6

HYPERMAGNETIC EXCITATION OF MAGNETIZATION AND ELASTIC DISPLACEMENT IN CASE OF MAGNETIZATION REVERSAL

Asadullin F.F.^{1,2,a}, *Pleshev D.A.*^{1,2}, *Vlasov V.S.*^{2,b}, *Kotov L.N.*², *Poleshchikov S.M.*¹, *Shavrov V.G.*³,
*Shcheglov V.I.*³

¹ Saint-Petersburg state forest technical university named after S.M. Kirov, St-Petersburg, Russia

² Pitirim Sorokin Syktyvkar State University, Syktyvkar, Russia

³ Institute of Radioengineering and Electronics of the Russian Academy of Sciences, Moscow,
Russia

^a aff@sfi.komi.com, ^b vlasovv78@mail.ru

The paper is dealing with excitation of coupled oscillations of magnetization and elastic displacement in the normally magnetized single-layer and multilayered ferrite plates that have magnetoelastic properties in case of magnetization reversal.

The system of ordinary differential equations described in the paper [1] is dealing with the electromagnetic excitation of nonlinear magnetoelastic oscillations in the single-layer and multilayered ferrite plates when the parametric excitation of spin waves is blocked [2].

Home-made computer programs based on the method of finite-difference approximation of coordinate derivatives and the method of lines were used in calculations [3]. Systems of ordinary differential equations were solved numerically by the Runge-Kutta 7-8 orders method with control of the integration at every step.

The paper describes magnetoelastic oscillations dependences on magnitude of dc field, anisotropy constants, saturation magnetization, the magnetoelasticity constant, magnetic and elastic relaxation parameters in every layer. Crystal anisotropy influence on processes of coupled oscillations excitation in the single-layer and multilayered ferrite plate is considered in the paper. The time dependences, phase portraits and spectrums of the excited magnetic and elastic oscillations in layers with identical and distinct properties are made.

Time evolution of the process of development of magnetic and elastic oscillations caused by impulse magnetization reversal were revealed. Efficient excitation of magnetic and elastic oscillations relation to the parameters of the magnetic and elastic damping and structure of multilayered ferrite plate were defined.

Support by Russian Foundation for Basic Research (grant № 17-02-01138-a).

[1] D.A. Pleshev, F.F. Asadullin, S.M. Poleshchikov, L.N. Kotov, V.S. Vlasov, V.G. Shavrov, V.I. Shcheglov. *Solid State Phenomena*, **233-234** (2015) 471-475.

[2] V.S. Vlasov, L.N. Kotov, V.G. Shavrov, V.I. Shcheglov, *J. Comm. Tech. El.*, **54** (2009) 821-832.

[3] D.A. Pleshev, F.F. Asadullin, S.M. Poleshchikov, L.N. Kotov, V.S. Vlasov, V.G. Shavrov, V.I. Shcheglov, *Journal of Siberian Federal University. Mathematics & Physics*, **10(1)** (2017) 36–39.

5PO-J-7

ROTATIONAL REMAGNETIZATION AND ORIENTATIONAL TRANSITIONS IN SUBMICRON FILMS OF YIG

Poimanov V.¹, Shkar V.², Nepochatykh Yu.², Shavrov V.³, Koledov V.³

¹Donetsk National University, Universitetskaya 24, Donetsk, Ukraine

²Donetsk Institute for Physics and Engineering named after A.A. Galkin, R. Luxemburg str. 72,
Donetsk, Ukraine

³Kotelnikov IRE RAS, Moscow, Russia, 125009, Mokhovaya 11/7
Vladislav.Poymanow@yandex.ru

Despite the fact that the magnetic properties of ferrite garnet films have been studied for a long time, their potential has not yet been fully revealed. This concerns both the detection of new effects in them and their practical application [1]. In particular, as it turns out, submicron YIG films (about 0.1 μm) can be used as both high frequency field generators and switching devices. These films were obtained by liquid-phase epitaxial technique on a substrates of gadolinium- gallium garnet and subsequent partial etching of the magnetic film [2-3].

A number of unusual effects appearing in such films was indicated in [2]. In particular, it was shown that for the direct and inverse magnetization the frequency field dependencies diverge with the increase of the applied field. It should be noted that this effect is not manifested in the zero field. This is due to the fact that the resulting unidirectional anisotropy is not an ordinary magnetic anisotropy, but an exchange anisotropy [1]. The latter is due to the existence of a weak magnetic sublattice of gadolinium in the film that leads to the appearance of a linear magnetostriction and piezomagnetism. We draw attention to the fact that in [2-3] this effect was attributed to a possible vortical structure.

The present work is devoted to the features of remagnetization of ferrite-garnet films by a quasinormal field. In a real experiment, it is quite difficult to achieve the condition that the external field is applied strictly perpendicular to the film. This also concerns the orientation of the light axes of cubic symmetry – the film growth can occur not strictly along any axis of symmetry. Due to asymmetry in the plane of the film this leads to a number of interesting effects. In particular, there appears a nonreciprocity of the direct and reverse remagnetization in both angular dependences and in the frequency field dependencies.

It is shown that the presence of a disorientation angle of the applied field from the perpendicular to the film [111] leads to the appearance of the orientational transitions of two types. The first of them occurs in a field of the order of cubic anisotropy, the second – in a field of the order of saturation magnetization. The presence of unidirectional anisotropy, in addition to the shift of the frequency field dependencies, leads to an additional asymmetry in the FMR spectrum – the sizes of the gaps for direct and reverse magnetization turn out to be different.

[1] K.P. Belov, *Physics-Uspeski*, **42** (1999) 711–717.

[2] V.F.Shkar', V.N.Varyukhin, *JETP Letters*, **88** (2008) 271-274.

[3] V.F.Shkar', V.N.Varyukhin, *JETP Letters*, **92** (2010) 338-342.

5PO-J-8

**MAGNETOOPTICAL AND MAGNETIC RESONANCE PROPERTIES OF
NANO-SCALED GRANULAR FILMS (CoFeB)_x(SiO₂)_{100-x} AND
(CoFeB)_xC_{100-x}**

Vyzulin S.A.¹, Gan'shina E.A.², Garshin V.V.², Kirov S.A.², Perova N.N.², Syr'ev N.E.²

¹Army General S.M Shtemenko Higher Military School, 350035, Krasnodar, Russia

²M.V. Lomonosov Moscow state University, Physics faculty, 119991, Moscow, Russia

We present experimental results on magneto-optical and magnetic resonance properties of nano-scaled granular structures with CoFeB magnetic granules imbedded in the non-magnetic SiO₂ matrix (system 1) and in the carbon matrix (system 2). The nano-samples were prepared by ion-beam sputtering.

Thin films with thickness h and magnetic phase concentration x both varying along the length of the samples have been prepared using successive sputtering without interlayers. For the system 1 these parameters varied from 210 to 420 nm and from 10 to 40 at% correspondingly (thickness of one composite layer varied from 4,6 to 8 nm). For the system 2 the intervals were $50 \text{ nm} < h < 250 \text{ nm}$ and $17 \text{ at}\% < x < 56 \text{ at}\%$ (thickness of one layer varied from 1,0 to 4.9 nm).

Magneto-optical properties were studied in the energy range 0.5 – 4.2 eV in the Transversal Kerr Effect (TKE) geometry and magnetic field up to 3 kOe. The FMR spectra were measured with highly sensitive EPR spectrometer JEOL FA-300. For each sample the spectra were measured at various orientations of the magnetization DC field H respective the film surface, from $\alpha = 0$ ($H \parallel n$) to $\alpha = 90^\circ$ ($H \perp n$), n being the normal to the film plane. Resonance fields H_r were obtained from the spectra.

It was found that the TKE spectra of the system 1 are similar to the spectra of the bulk composites (CoFeB)_x(SiO₂)_{100-x} (as sputtered on a fixed substrate) with concentrations below percolation threshold $x \leq x_{\text{per}} \approx 43\text{-}47 \text{ at}\%$ [1]. The TKE magnetic field dependence exhibits a linear (superparamagnetic) behavior at $x \leq 30,8 \text{ at}\%$ and a non-linear one in the $30,8 \text{ at}\% \leq x \leq 40,7 \text{ at}\%$ region. The TKE spectra of the system 2 differ essentially from the ones of the system 1. The TKE showed a non-linear magnetic field dependence starting with the first sample with $x = 17,3 \text{ at}\%$, that is system 2 demonstrated a ferromagnetic ordering through the whole concentration range investigated.

For all the samples, the magnitudes of H_r monotonously decreased with α varying from 0 to 90°. The curves $H_r(\alpha)$ were virtually symmetric about the axis $\alpha = 0$.

In the samples of the system 1 for $\alpha \in [0, 90^\circ]$ only one FMR mode was observed. In the spectra of the system 2 samples there were, as a rule, several absorption lines. For $\alpha = 0$ and x varying from 56 to 17 at% the number of the observed modes decreased from 8 to 3, and for $\alpha = 90^\circ$ the number of modes dropped from 3 to 1. There was found an in-plane anisotropy of H_r .

A comparative analysis of the experimental TKE and FMR spectra of the (CoFeB)_x(SiO₂)_{100-x} and (CoFeB)_xC_{100-x} systems suggests that preparation of the system 2 could involve plasma-chemical processes – chemical reactions of carbon with metals. This results in formation of new, originally absent, compounds (possibly, Co₃C, Co₂C, Fe₃C). The nanoparticles formed demonstrate magnetic properties. The multimode FMR spectra of the system 2 may be attributed to different compositions of the particles. With increase of the metallic phase concentration x the shape of the granules approaches the spheroidal one (irrespective of composition).

5PO-J-9

DEFECT MODES COUPLING IN SPIN-WAVE MAGNONIC CRYSTALS

Sharaevskaia A.Yu.^{1,2}, Beginin E.N.¹

¹ Laboratory "Metamaterials," Saratov State University, Saratov, Russia

² Kotelnikov Institute of Radioengineering and Electronics, Russian Academy of Sciences, Moscow, Russia
annasharik2@gmail.com

Periodic magnetic structures have been extensively studied in the past decades. Periodicity can be created by e.g. periodically varying the thickness or width of planar spin wave (SW) waveguides. Such artificially fabricated magnonic crystals (MC) [1] demonstrate formation of magnonic band gaps (frequency regions, in which the SWs exponentially decay due to the Bragg reflections). Fabrication of MCs based on yttrium-iron-garnet (YIG) ferrite films leads to the extension of the application area of magnetic thin films in the perspective direction of magnonic and spintronic. Properties of magnonic crystals, in the form of periodic stripes can also be controlled or enhanced by the presence of defects [2]. For instance, a structural or compositional defect could be a stripe element, of a different width or material, in an otherwise perfect periodic multi-component array of stripes. Defect modes can also be used for an increase or improvement in quality of nonlinear effects for microwave generators and signal filtering.

In present work we consider two coupled adjacent MCs with broken translational symmetry (see Fig.1(a)). In such waveguides propagates surface magnetostatic waves (MSSW). We constructed transfer matrix T of 4x4 size (using transfer matrix method) for propagating waves for two MCs and studied dependence of the reflection and transmission coefficients by changing coupling parameters and geometric size of defects.

Figure 1(b) shows transmission coefficients T_2 , T_4 depending in different MCs. Applying static magnetic field is $H_0=1000$ Oe, thickness of magnonic layers are 13 and 15 μm , periodic sequences of the grooves with the period of 100 μm , length of defects is 200 μm . Thus, we demonstrate two picks on transmission dependences (Figure 1(b), f_1 , f_2 - green dashed line), this fact confirms the existence of defects modes.

The model describing the features of formation defects modes in planar structure, which consists of two side-coupled MCs was introduced. Also, we shown the possibility of control defect modes position in spin wave spectra by changing coupling between structures. It should be pointed, that the results can be used for creating controlled devices for planar magnonic and elements of the spin-wave logic.

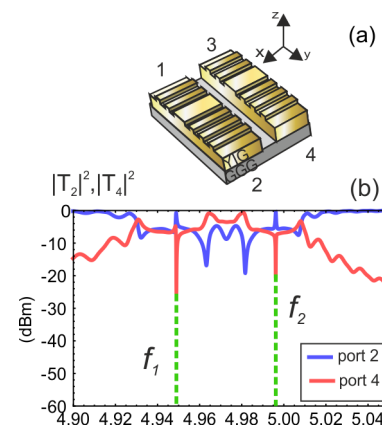


Fig. 1. (a) Scheme of side-coupled magnonic crystals, (b) transmission coefficients in quad magnonic structure (blue and red curves for different ports).

Supported by the Grant from Russian Science Foundation (Project # 16-19-10283).

[1] Nikitov S.A., Tailhadesand Ph., Tsai C.S., *Journal of Magnetism and Magnetic Materials*, **236** (2001) 320–330.

[2] Beginin E.N., Filimonov Yu.A., Pavlov E.S., Vysotskii S.L., and Nikitov S.A., *Appl. Phys. Lett.* **100** (2012) 252412.

5PO-J-10

MULTIMODE MAGNETIC RESONANCE IN HEUSLER ALLOY**Ni₅₀Mn₃₅In_{14,9}Ag_{0,1}***Vyzulin S.A.¹, Kevraletina A.L.¹, Syr'ev N.E.², Pasternak D.G.², Dubenko I.S.³, Granovsky A.B.²*¹Higher Military School named after General of the Army S.M Shtemenko, Krasnodar, Russia²Faculty of Physics, Lomonosov Moscow State University, Moscow, Russia³Department of Physics, Southern Illinois University, Carbondale, USA

vyzulin@mail.ru

Magnetic resonance in bulk polycrystalline Heusler alloy Ni₅₀Mn₃₅In_{14,9}Ag_{0,1} was investigated in the temperature range T=100-470 K with JEOL JES FA-300 electron spin resonance spectrometer. Modulation technique was used at the frequency 9.14 GHz. We determined the resonance field H_r and the width of absorption line ΔH for all observed resonances. High frequency magnetic field was applied in the sample plane. Two series of measurements were carried out. In the first one we fixed the temperature and change orientation of constant magnetizing field H with respect to the sample plane from normal ($\alpha=0^\circ$) to tangential ($\alpha=90^\circ$) directions. In the second one the temperature dependences of spectra were studied at the fixed orientation ($\alpha=\text{const}$) of magnetizing field H . Magnetic measurements showed that the sample exhibits martensitic transition at T=200-320 K, the Curie temperature of austenitic phase is about $T_C^A=340$ K and of martensitic phase is $T_C^M \approx 170-180$ K, that is in a good agreement with recently reported data [1].

We observed three different absorption lines and corresponding modes A, B, C in high magnetic fields. The modes A, B and C were detected at T=140-470 K, 100-300 K and 100-200 K, respectively. The modes A and B were registered at all orientations of magnetic field H , but the mode C only in relatively narrow ranges of α close to $\alpha \approx 27, 80$ и 159° . Perhaps, it is the reason why the mode C was not detected in Ni-Mn-In-Si alloy [2].

With increasing temperature up to T>340 K the only mode A survived and in this case the dependence $H_r(\alpha)$ is symmetrical in the respect of $\alpha=0$ и 90° directions. Both the resonance field H_r and the width of absorption line ΔH for this mode depend on temperature. Below 340 K the curve $H_r(\alpha)$ is asymmetrical for all three modes and the dependences of the resonance field H_r and the width of absorption line ΔH on orientation of magnetizing field H and temperature become very complicated that indicate on coexistence of several magnetic phases in the whole studied temperature range. For example, there are one, two and three maximums in the dependences of $H_r(\alpha)$ for modes A, B and C, respectively.

The obtained experimental data clearly show that at each temperature in martensitic state there are at least two different magnetic phases which weakly connected with each other. We discuss the dependences of the resonance field H_r and the width of absorption line ΔH on orientation of magnetization field and temperature for all three modes.

This work was supported by RFBR (Grants No. 15-02-01976 and No. 16-32-00460)

[1] S. Pandey et al., *AIP Advances*, **6** (2016) 056213-7.

[2] Y.S. Chen et al., *JMMM*, **407** (2016) 365–368.

5PO-J-11

MAGNETODYNAMIC PROPERTIES OF A COMPOSITE ($\text{Co}_{40}\text{Fe}_{40}\text{B}_{20}$) $_{65}$ (SiO_2) $_{35}$ DEPOSITED ON GLASS CLOTH

Kalinin Yu.E.¹, Sitnikov A.V.¹, Tarasova O.S.¹, Philoppov V.V.¹
¹ Voronezh State Technical University (VSTU), Voronezh, Russia
 oksanchik2603@mail.ru

Metal-insulator nanocomposites are promising materials for use in the high frequencies and the superhigh frequencies regions of electromagnetic radiation. The main disadvantages of these materials is the low electrical resistivity and as a result, high reflectivity homogeneous film coating.

In this paper, we use glass fiber cloth as a substrate, which, on the one hand, allows us to fragment the film coating in 3d space, and on the other hand, to combine structural materials with functional properties. Nanostructured films were obtained by ion-beam sputtering of the composite target of

the $\text{Co}_{40}\text{Fe}_{40}\text{B}_{20}$ alloy with SiO_2 samples both in the argon medium and during the cyclic addition of oxygen to the working gas with different partial pressure.

Magnetostatic studies have shown that the magnetization curves depend on the direction of the external field relative to the glass fibers (Fig 1. a), (Fig 1. b) curve 1 glass fiber measured along the field, the glass-fiber curve 2 measured across the field.

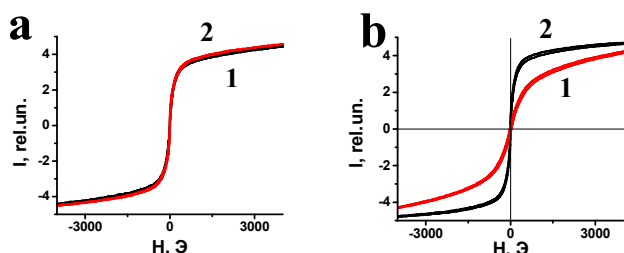


Fig. 1. The magnetization curves of the glass-textolite with the film of the nanocomposite ($\text{Co}_{40}\text{Fe}_{40}\text{B}_{20}$) $_{65}$ (SiO_2) $_{35}$ measured along (curve 1) and across (curve 2) fields on the glass fabric (a) and on the glass nitrides (b).

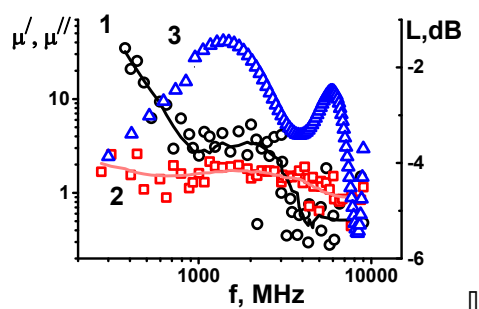


Fig. 2. The frequency dependence of the real (curve 1) and imaginary (curve 2) magnetic permeability and absorption coefficient (curve 3) of the glass-textolite with a nanocomposite film ($\text{Co}_{40}\text{Fe}_{40}\text{B}_{20}$) $_{65}$ (SiO_2) $_{35}$

Since we have several fields of anisotropy in measuring the length and breadth of the fibers, this can lead to the appearance of two resonant frequencies. An estimate was made of the frequencies of the natural ferromagnetic resonance for the samples under study.

The measurement of the complex magnetic permeability of the samples also revealed several frequencies of natural ferromagnetic resonance (Fig 2 (curve 1,2)).

Measurement of the absorption by the horn method revealed several frequency bands with maximum absorption, which correlate with the values of the frequencies of the natural ferromagnetic resonance of the samples under study.

This work was supported by RFBR grant № 16-45-360483 p_a and the Ministry of Education and Science in the framework of the project part of the state task.

5PO-J-12

MAGNETIC PROPERTIES OF THIN YIG FILMS PREPARED BY PULSED LASER DEPOSITION

Nosov A., Dubinin S., Kravtsov E., Ryabukhina M., Antropov N., Starichenko D., Ivanov D., Bessonov V., Kobelev A.

M.N.Miheev Institute of Metal Physics of Ural Branch of the Russian Academy of Sciences,
Yekaterinburg, Russia
nossov@imp.uran.ru

Numerous spin-dependent phenomena are intensively investigated during last decade in the nanostructures of the type nonmagnetic metal/insulating ferromagnet [1, 2] including such effects as direct and inverse spin-Hall effects, thermally driven spin caloritronics, spin injection, and others. Special attention is paid to magnetization dynamics including ferromagnetic resonance spin pumping, modulation of damping, and spin-transfer torque [3]. In most of such experiments the $\text{Y}_3\text{Fe}_5\text{O}_{12}$ (YIG) iron garnet is used as the insulating ferromagnet owing to its uniquely low magnetic damping which is two orders of magnitude smaller than that of ferromagnetic metals [4]. Potential applications of such effects and devices utilizing them require novel techniques for growth of very thin YIG films (in the nanometer thickness range) while preserving low damping. Traditionally liquid phase epitaxy was used for fabrication of the YIG films with micrometer thicknesses. In this work we report the properties of nanometer-thick YIG films prepared by pulsed laser deposition.

Thin epitaxial YIG films on the $\text{Gd}_3\text{Ga}_5\text{O}_{12}$ substrates with orientation (111) were prepared by pulsed laser deposition using the excimer KrF laser with the wavelength of 248 nm. The films had the thicknesses in range from 96 to 333 nm. Structural properties were characterized using the PANalytical X'Pert diffractometer. Static (*dc* hysteresis loops) and dynamic (in the frequency range from 5.4 to 9.86 GHz) magnetic properties were investigated.

The deposition conditions permitted to obtain thin epitaxial films with excellent structural quality, see Fig.1. Evolution of magnetic properties with the thickness of films was analyzed. The observe dependences are interpreted within the framework of the model [5, 6] implying distribution of Fe vacancies over octahedral and tetrahedral positions of the YIG lattice.

The results obtained can be useful for development of novel spintronic nanostructures using low damping YIG layers with nanometer thickness.

The results were obtained within the state assignment of FASO of Russia ("Spin" theme №0120146330), program UB of RAS №15-9-2-30, and the grant No.14.Z50.31.0025.

- [1] A. J. Sinova, *et al.*, *Rev.Mod.Phys.*, **87** (2015) 1213-1259.
- [2] J. Niimi, *et al.*, *Rep.Progr.Phys.*, **75** (2015) 124501 (19 pp.).
- [3] K. Ando, *Semicond.Sci.Technol.*, **29** (2014) 043002 (13 pp.).
- [4] A. A. Serga, *et al.*, *J.Phys.D*, **43** (2010) 264002 (16 pp.).
- [5] S. A. Manuilov, *et al.*, *JAP*, **106** (2009) 123907 (11 pp).
- [6] S. A. Manuilov, *et al.*, *JAP*, **105** (2009) 033917 (9 pp).

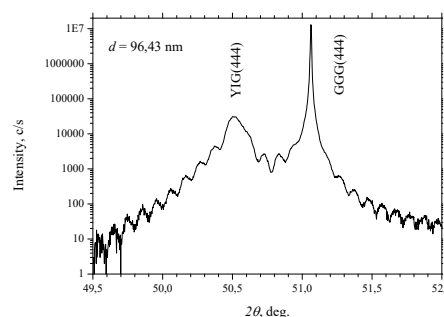


Fig. 1. X-ray diffraction pattern in the vicinity of the (444) peak for the film with the thickness of 96.43 nm recorded at room temperature.

5PO-J-13

BRILLOUIN LIGHT SCATTERING STUDY OF YIG-GALLIUM ARSENIDE

Sadovnikov A.V.^{1,2}, Beginin E.N.¹, Stognij A.I.³, Sharaevskii Yu.P.¹, Nikitov S.A.^{1,2}

¹ Laboratory "Metamaterials," Saratov State University, Saratov, Russia

² Kotel'nikov Institute of Radioengineering and Electronics, RAS, Moscow, Russia

³ Scientific-Practical Materials Research Center, NASB, Minsk, Belarus

sadovnikovav@gmail.com

Recently, it was shown that the extreme low-damping yttrium iron garnet ($Y_3Fe_5O_{12}$, YIG) materials is appropriate for emerging technologies, such as spintronics and magnonics due to excitation of magnetization dynamics by pure spin currents and spin-transfer torque [1-5]. The integration of magnonic functional structures in the semiconductor-based electronics faces a problem of incompatible substrates, which are typically used in YIG magnonics and conventional CMOS-based electronics. The former concept uses the gadolinium gallium garnet (GGG) substrate to solid phase epitaxial growth, radio frequency magnetron sputtering or pulsed laser deposition (PLD) technique, whereas the gallium arsenide (GaAs) substrate is predominantly utilized in the latter concept. The straightforward advantages of YIG on GaAs substrate over YIG on GGG substrate are integration capability of magnonic and spintronic elements in the semiconductor architecture. This is the prominent step in the beyond CMOS computing and CMOS-compatible spintronic devices.

The amorphous $Y_3Fe_5O_x$ layers are deposited at the room temperature on GaAs (100) substrates by double ion-beam sputter-deposition method. Then samples are annealed for 5 min in the quartz vacuum oven at 22% O_2 +78% N_2 gas input, at 10 Tor, at 620° C. We use the Brillouin Light Scattering (BLS) technique to demonstrate the spin-wave modes in fabricated samples. The BLS spectra (Fig. 1) demonstrates the three well-pronounced peaks, which are corresponded to the Damon-Eshbach modes at $f_{sDE}=7.2$ GHz and two first bulk spin-wave modes at $f_{sb1}=10$ GHz and $f_{sb2}=20$ GHz (in wavenumber range of $k \sim 0 \div 3 \mu m^{-1}$). The frequencies of the $f_{sb1,2}$ can be determined by the spin-wave dispersion of the magnetic film of the thickness d and saturation magnetization M_0 with free spins[6]:

$$f_{nk} = \frac{\gamma}{2\pi} \left(H_0 + \frac{2A_{ex}}{M_0} \left[k^2 + \left(\frac{n\pi}{d} \right)^2 \right] \right), \quad n=1,2,$$

where $H_0=2$ kOe is bias in-plane magnetic field, $A_{ex}=3.614 \cdot 10^{-7}$ Erg/cm, is the exchange constant, γ is the gyromagnetic ratio. The fitting parameters of YIG film were $d=78$ nm, $M_0=107$ G. Support by RFBR (No. 16-29-03120) is acknowledged.

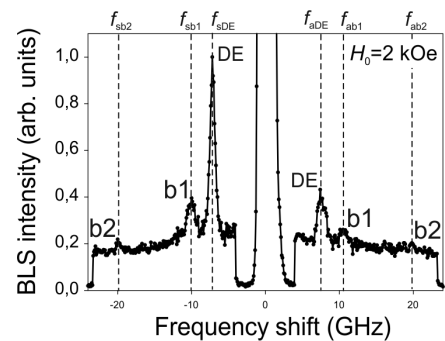


Fig. 1. BLS spectrum of YIG/GaAs in a field of 2 kOe showing spin-wave modes.

- [1] Y. Kajiwara et al., *Nature*, **464** (2010) 262-266.
- [2] H. Kurebayashi et al., *Nat. Mater.*, **10** (2011) 660.
- [3] H. Nakayama, *Phys. Rev. Lett.*, **110** (2013) 206601.
- [4] M. Collet et. al., *Nature Comm.*, **7** (2016) 10377.
- [5] V.E. Demidov et.al., *Scientific Reports*, **6** (2016) 32781.
- [6] R. E. De Wames and T. Wolfram, *Journal of Applied Physics*, **41** (1970) 987.

5PO-J-14

NON-UNIFORMITY OF THE DEMAGNETIZING FIELD AS A BROADBAND SOURCE OF SPIN WAVES

Mushenok F.B.¹, Dost R.², Davies C.S.¹, Allwood D.A.², Inkson B.J.², Kruglyak V.V.¹

¹University of Exeter, Stocker road, Exeter, United Kingdom

²University of Sheffield, Sheffield, S1 3JD, United Kingdom

F.Mushenok@exeter.ac.uk

Magnonics is attracting a remarkable amount of research attention due to the prospects of using magnonic devices for high-speed data and analogue signal processing. The operational principles of many magnonic (and more generally, wave-based) logic devices are based on the interference of multiple spin waves. The ability to excite multiple coherent spin waves is therefore crucial for the perceived magnonic technology. Here, we use time resolved scanning Kerr microscopy (TRSKM) and micromagnetic simulations to demonstrate that the magnetisation aligned along the edges of patterned magnetic structures can serve as a source of propagating magnetostatic spin waves.

Specifically, we consider a transversely-magnetised Permalloy stripe excited by a spatially-uniform microwave magnetic field at frequencies above that of the uniform ferromagnetic resonance (FMR). Spin waves at the frequency of excitation are observed in both experiments and simulations to propagate from the edges of the stripe (Fig. 1). The excitation mechanism arises from the spatial variation of the dynamic demagnetising field intrinsic to the magnetic structure, rather than by spatial inhomogeneity of the excitation field. The dynamic demagnetising field increases locally the frequency of FMR, thereby enabling the global microwave magnetic field h to efficiently couple to specific regions of magnetisation. Our findings demonstrate an alternative approach devoid of the restrictions associated with nanoscale electrical circuitry by which magnonic technology could be realised.

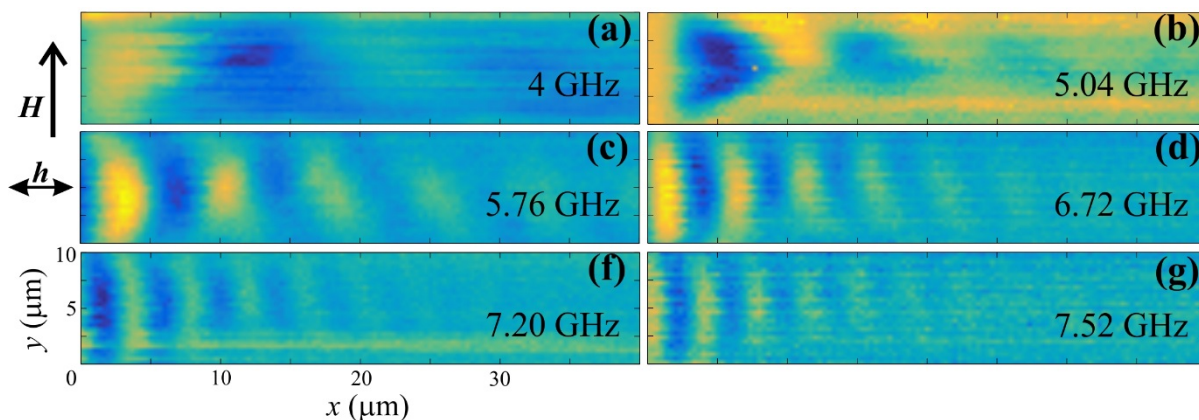


Fig. 1. Kerr images are shown for the magnetic stripe driven at a frequency of 4 GHz, 5.04 GHz, 5.76 GHz, 6.72 GHz, 7.20 GHz, and 7.52 GHz, respectively. Bias magnetic field H has value of 200 Oe.

The research leading to these results has received funding from the Engineering and Physical Sciences Research Council (EPSRC) of the United Kingdom (Project Nos. EP/L019876/1, EP/L020696 and EP/P505526/1).

5PO-J-15

THE FERROMAGNETIC RESONANCE IN CONDITIONS OF ORIENTATION TRANSITION IN MAGNETIC FILMS WITH COMPLEX CHARACTER OF ANISOTROPY

Shavrov V.G., Shcheglov V.I.

IRE RAS, Moscow, Russia

vshcheg@mail.cplire.ru

The ferromagnetic resonance in anisotropic magnetic films is investigated. As a model of our investigation it is taken the uniaxial magnetic anisotropy having the easy magnetization axis oriented in arbitrary direction relatively to the film plane and cubic anisotropy having orientation (111) relatively to same plane. By the established method (iteration method) we found the equilibrium orientation of magnetization vector and revealed its multi-position character which is determined by the relative values of anisotropy constants and axis orientations. We have found the typical values and admissible range of external magnetic field which are necessary to the orientation transition realization. It is investigated the equilibrium orientation of magnetization vector in large interval of magnetic field variation using the spherical coordinate system. The most attention is paid to two cases: when external field is oriented in plane passing through the normal to film plane parallel and perpendicular to projection of anisotropy axis onto film plane. In both of these cases it was calculated the field of ferromagnetic resonance in wide interval of fields and film parameters. It was shown that in the first case the equilibrium magnetization vector position is always oriented in magnetic field variation plane and polar angle of magnetization vector is always equal to right angle. In this case the azimuth dependence of resonance field has the view of regular sinusoid which amplitude is constant and phase is behind on some value from external field direction. In the second case both azimuth and polar angles of magnetization vector equilibrium position are modified. In this case both azimuth and polar dependencies of resonance field have sinusoid character and their reciprocal amplitudes are defined by anisotropy constant and film demagnetizing factor and also the inclination of anisotropy axis direction from the normal to film plane. It is found the dynamic magnetic susceptibility tensor. It is shown that in common case this tensor contains of as symmetrical, so anti-symmetrical components whose role in formation of orientation transition character is defined by axis orientation and mutual correlation between uniaxial and cubic anisotropy constants and also the demagnetization field of magnetic film. The nonlinear equations of magnetization motion are derived which are able to investigate the orientation transition dynamics. It is investigated the nonlinear reorientation of magnetization vector and the relaxation time is found. It is investigated the ferromagnetic resonance excitation in linear and nonlinear regimes. It is shown that in nonlinear conditions the nonlinear ferromagnetic resonance may be accompanied by orientation transitions having hysteresis character. The received results are applied to the investigation of composition medium containing from arbitrary oriented ferrite particles. By means of averaging over all possible directions of anisotropy axis orientation it is found the magnetic susceptibility tensor of medium as a whole. It is noted that presented in previous papers conclusion about a great extent of supplementary non-diagonal components of this tensor is not whole correct because it is related to media with limited quantity of particles. It is investigated the application of received susceptibility tensor to the question about reflection and propagation electromagnetic waves through multilayer anisotropic ferrite medium. It was found the field dependence of reflection and propagation coefficients and their hysteresis character brought about orientation transitions in layers. It was carried the comparison of received results with experiments and took some recommendations for further investigations.

This work is supported by Russian Scientific Fund (project № 14-22-00279).

[1] V.I.Zubkov, V.I.Shcheglov, *J. Comm. Tech. Electron.* **58** (2013) 143-148.

5PO-J-16

MILLIMETER-WAVE CHARACTERIZATION OF FLUX GROWN $\text{Ba}_{0.8}\text{Pb}_{0.2}\text{Fe}_{10}\text{Al}_2\text{O}_{19}$ SINGLE CRYSTALS

*Vinnik D.A.*¹, *Ustinov A.B.*², *Ustinova I.A.*², *Gudkova S.A.*^{1,3}, *Zherebtsov D.A.*¹

¹ South Ural State University, Chelyabinsk, Russia

² St. Petersburg Electrotechnical University, St. Petersburg, Russia

³ Moscow Institute of Physics and Technology (State University), Dolgoprudny, Russia
 vinnikda@susu.ru

Hexagonal ferrites having large uniaxial magnetocrystalline anisotropy may find a variety of applications in mm-wave and in sub-terahertz ranges of electromagnetic wave spectrum [1-2]. Purpose of the present work is to investigate an aluminum substituted Ba-Pb-ferrite having a chemical formula $\text{Ba}_{0.8}\text{Pb}_{0.2}\text{Fe}_{10}\text{Al}_2\text{O}_{19}$.

Lead, aluminum and iron oxides (PbO , Fe_2O_3 , Al_2O_3) and barium carbonate were used as starting materials. The mixture was ground in an agate mortar and filled in a 30 ml platinum crucible. The crucible was placed in an oven equipped with a resistive heater. To homogenize the components, the furnace was maintained at 1260 °C for 3 h. After that the Pt-rod was placed in the crucible. After 140 h. the rod with crystallized solution was pulled out. The crystals were separated from the solidified flux by leaching in hot nitric acid.

Millimeter-wave characterization was carried out for substituted well faceted single crystals in the frequency range of 75-100 GHz. The vector network analyzer Rohde&Schwarz ZVA40 with millimeter-wave converters ZVA-Z110 was used. Typical thickness of the slabs was about 100 μm . The slabs had no specific shape in their plane. Typical in-plane sizes of the slabs were of approximately 2 mm^2 . The easy axis of the magnetocrystalline anisotropy (c-axis) was orientated perpendicular to the slab plane. For characterization each sample was positioned on the short load attached to the end of the 90 degree bend of the WR-10 waveguide section. The bend was placed between the poles of electromagnet. The magnetic sample was magnetized with uniform magnetic field directed perpendicular to the sample plane. The bias field was varied in the range of 0-0.6 T.

Typical absorption curves of barium hexaferrite resonator structure measured under the influence of an external magnetic field with values greater than the saturation magnetization (Fig. 1), demonstrate two distinct resonant peaks corresponding to the lower ferromagnetic modes. A linear increase in the frequency of these peaks with increasing bias field

took place with a slope close to a value of gyromagnetic ratio. It confirms the ferromagnetic nature of the measured resonant peaks. A similar frequency responses were observed for the other magnetic samples. The obtained results show that the aluminum substituted flux grown hexaferrites looks favorable for fabrication of mm-wave devices (see e.g. [3]).

The work was supported by Government of the Russian Federation (Act 211, contract № 02.A03.21.0011) and by the RFBR (№ 16-08-01043). Additionally the work was partially supported by the Ministry of ESRF (№ 4.1346.2017/PP).

[1] M. Popov, I. Zavislyak, A. Ustinov, G. Srinivasan. *IEEE Trans. Mag.*, **47** (2011) 289–294.

[2] V.G. Harris. *IEEE Trans. Mag.*, **48** (2012) 1075–1104.

[3] D.A.Vinnik, A.B.Ustinov, D.A.Zherebtsov, V.V.Vitko, S.A.Gudkova, I.Zakharchuk, E.Lähderanta, R.Niewa. *Ceram. Int.*, **41** (2015) 12728–127337.

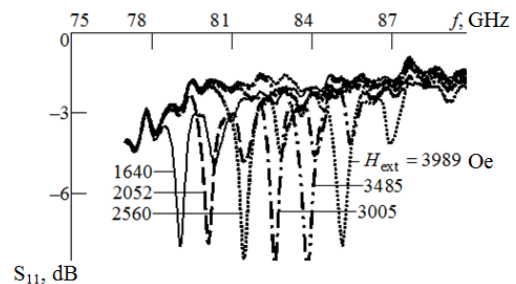


Fig. 1. Absorption curves of barium hexaferrite resonator

5PO-J-17

HIGH FREQUENCY PROPERTIES OF THE SUBSTITUTED M-TYPE HEXAFERRITES

Trukhanov A.V.^{1,2}, Panina L.V.¹, Trukhanov S.V.^{1,2}, Yakovenko O.S.³, Turchenko V.A.⁴

¹ NUST MISiS, Moscow, Russia

² S&P materials research centre of the NAS of Belarus, Minsk, Belarus

³ Taras Shevchenko National University of Kyiv, Kiev, Ukraine

⁴ JINR, Dubna, Russia

truhanov86@mail.ru

As a rule HF (hexaferrites) are widely used as permanent magnets and in magnetic storage with high density information. But there are a lot of publications in present time concern with effective EMR (electromagnetic radiation) absorption by these materials in microwave range [1-3]. Anomalous microwave properties of the doped M-type HF and possibility of their changes (by substitution or under magnetic field) let us to say that these compounds are perspective for practical applications for electromagnetic absorption. The $\text{BaFe}_{12-x}\text{D}_x\text{O}_{19}$ ($\text{D}=\text{Al}^{3+}, \text{In}^{3+}$ $x = 0.1-1.2$) ceramics were obtained via solid state reactions. All studied HF correspond to single-phase samples with SG:*P63/mmc*. Microwave properties were investigated in the 25.8-78.3 GHz range. The k_{tr} transmission and k_{ref} reflection coefficients are defined as :

$$k_{\text{tr}} = 10 * \lg\left(\frac{P_{\text{tr}}}{P_{\text{inc}}}\right); \quad k_{\text{ref}} = 10 * \lg\left(\frac{P_{\text{ref}}}{P_{\text{inc}}}\right);$$

Where P_{inc} —incident, P_{tr} — transmitted and P_{ref} — reflected EMR power. The k_{abs} EMR absorption coefficient can be calculated from the k_{tr} and k_{ref} coefficients by formula:

$$k_{\text{abs}} = 10 * \lg(1 - 10^{0.1*k_{\text{tr}}} - 10^{0.1*k_{\text{ref}}})$$

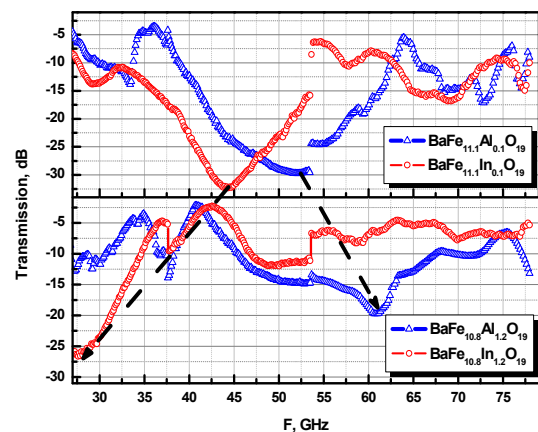
The range of NFR for pure Ba-HF is 47-50 GHz and critically depends on internal magnetic anisotropy field value (H_a): $\omega = \gamma H_a$ (ω —NFR frequency, γ —gyromagnetic ratio). The absorption range in HF can be changed by changing the H_a value (by diamagnetic substitution or under external magnetic field): $f = \gamma(H_0 + H_a - 4\pi M_s)$. The k_{tr} transmission (see Fig.) and k_{ref} reflection coefficients are negative that indicates reduction of the transmitted and reflected EMR power in relation to the incident EMR. It means that these compounds are effective as absorbing materials. It has been shown that increasing of Al-content from $x=0.1$ to 1.2 leads to broadening of the absorption band with decrease of the intensity (from -29.4 dB to -19.3 dB). NFR peak is shifted to the higher frequencies. Increasing of the In-content from $x=0.1$ to 1.2 leads to intensity decrease (from -32.3 dB to -26.7 dB). NFR peak is shifted to the lower frequencies. Magnetic field for both cases (Al and In-doping) linearly shifts the NFR peak to the higher frequencies. Anomalous microwave properties (broadening of the absorption band) allow using these solid solutions for practical applications as control elements in microwave circuits and as effective absorbing shields. An external magnetic field allows not only expand the NFR area, but also to make the necessary settings to the operating frequency.

Present work is financing by the Ministry of Education and Science of the Russian Federation on the program of Increase of Competitiveness of NUST "MISIS" among the leading world scientific and educational centers (grants No. K4-2015-040, and No. K3-2016-019).

[1] V.G. Harris et al, *JMMM*, **321** (2009) 2035-2041.

[2] V.G. Harris, *IEEE Trans. Magn.*, **48** (2012) 1075-1082.

[3] L. Liet al *J. Alloys Compd.*, **557** (2013) 11-17.



5PO-J-18

THE PARTICIPATION OF ELASTIC DISSIPATION IN CREATION OF MAGNETIC DISSIPATION IN MAGNETOELASTIC MEDIUM

Vetoshko P.M., Shavrov V.G., Shcheglov V.I.

IRE RAS, Moscow, Russia

vshcheg@mail.cplire.ru

The precession of magnetization vector in magnetoelastic medium is investigated in supposition that magnetic and elastic systems have dissipation properties. It is investigated the free vibration process establishment of magnetization after its initial deflection from equilibrium position when magnetic dissipation is absent. It is shown that the time of magnetic vibrations establishment is in a great extent depended on elastic system dissipation. On the dependence of time establishment from value of elastic dissipation parameter it is found the pronounced minimum. It is investigated the critical correlation between elastic dissipation parameter and magnetoelastic constant which correspond to this minimum. It is shown that the critical value of dissipation parameter and magnetoelastic constant are the directly proportional quantities. In this case the corresponding to critical value established time is inversely proportional to value of magnetoelastic constant. It is found that in the course of establishment process both the magnetic and elastic vibrations are decreased in time according to exponential law and the time establishing constant for both vibrations is equal. When parameter of dissipation is less than critical value the establishment of vibrations takes place with beatings. The period of these beatings is inversely proportional to value of magnetoelastic constant and during the approach to critical value is increased. When parameter of dissipation is more than critical value the beatings are absent. It is investigated the dependence of effective magnetic dissipation parameter from dissipation parameter of elastic vibrations. It is found that this dependence has bell-formed character and its maximum corresponds to critical value of elastic dissipation parameter. For the interpretation of observed phenomena it is proposed the model consisted of two oscillators – magnetic and elastic connected by magnetoelastic interaction. In the free vibration regime it is found the whole quality correspondence proposed model with observed phenomena picture, in the first turn – the formation magnetic oscillator dissipation at elastic oscillator dissipation expense, and also the existence of critical elastic dissipation value both higher and lower that is the influence of elastic dissipation to magnetic dissipation is decreased. In the case when dissipation of first oscillator is absent and dissipation of second oscillator is very large the analytical solution is found. It is found that by increasing of second oscillator dissipation its influence to first oscillator dissipation is decreased. On the base of numerical calculation of whole model system for two oscillators it is found four different regimes of vibrations establishment: weak dissipation with beatings, strong dissipation without beatings, weak dissipation without beatings and super-critical exponential growth. It is shown that first three of these regimes correspond to magnetic vibrations establishment which are described by solution of whole magnetoelastic equations system and the fourth correspond to reorientation of magnetization vector from one equilibrium position to other. From the obtained results it is made the conclusion about high efficiency of model system for real forming of magnetic dissipation at elastic dissipation expense in establishment regime. For the illustration of observed phenomena the mechanical model is discussed. It is proposed some recommendations for observation described phenomenon in experiments and also point at the possibility of effective guiding of magnetic system dissipation by elastic dissipation changing.

This work is supported by Russian Scientific Fund (project № 14-22-00279).

5PO-J-19

FERROMAGNETIC RESONANCE OF NONHOMOGENEOUS STATES IN MAGNETIC NANOSTRUCTURES

Mironov V.L., Gorev R.V., Sapozhnikov M.V., Skorohodov E.V.

Institute for physics of microstructures RAS, Nizhny Novgorod, Russian Federation
mironov@ipmras.ru

We report the results of micromagnetic modeling for ferromagnetic resonance (FMR) of localized nonuniform states in different thin film ferromagnetic nanostructures. The FMR frequency spectra and spatial distributions of the magnetization oscillations were calculated by numerical solution of Landau-Lifshitz-Gilbert equation using standard Object Oriented MicroMagnetic Framework (OOMMF) software. The algorithm of simulations was approved on the test system of Permalloy microstripe array [1]. Here we present the modeling of localized FMR for domain wall in planar nanowire-nanoparticle (NW-NP) system [2] and for skyrmion state in thin film multilayer structure Co/Pt with spatially modified perpendicular anisotropy [3].

The transverse domain wall (DW) in NiFe NW was stabilized by stray field generated by NP located close to NW and elongated perpendicular NW axis. The DW nucleation was initiated by an external magnetic field directed perpendicular to NW. The magnetizing along the NW leads to the DW removal. The FMR spectra of NW for states with DW and without DW are presented in Fig. 1. The strong resonance at 0.76 GHz is due to the localized DW resonant oscillations. The intensity and position of this DW resonant peak can be varied in a wide range by changing the gap between NP and NW.

Another type of DW can be realized in magnetic films with locally modified perpendicular anisotropy [3]. We simulated the FMR in Co/Pt multilayer containing cylindrical areas with reduced anisotropy. The skyrmion state in this system can be created by remagnetization in reverse external magnetic field. The FMR spectra for quasi-uniform state (US) and skyrmion state (SS) are presented in Fig. 2. The strong peak in US corresponds to uniform resonance localized in modified area. In SS case the resonant peaks correspond to the rotating spin waves [4]. The positions of these peaks can be tuned in a wide range by changing of geometric parameters and anisotropy constant.

In conclusion, the transitions between states with and without DW in planar NW as well as the transitions between US and SS in modified Co/Pt multilayer enable the creation of switchable elements for high frequency nanoelectronics based on coplanar waveguides.

The investigations are supported by Russian Science Foundation (Grant No. 16-12-10254).

[1] E.V. Skorohodov, R.V. Gorev, R.R. Yakubov, et al., *JMMM*, **424** (2017) 118-121.

[2] R.V. Gorev, V.L. Mironov, *Technical Physics Letters*, **43**(3) (2017) 254-257.

[3] M.V. Sapozhnikov, S.N. Vdovichev, et al., *Appl. Phys. Lett.*, **109** (2016) 042406.

[4] M.V. Sapozhnikov, R.V. Gorev, E.V. Skorohodov, V.L. Mironov, submitted to *JMMM*.

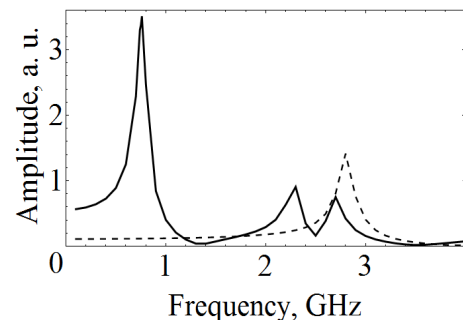


Fig. 1. FMR spectra of NW-NP with DW (solid) and without DW (dashed).

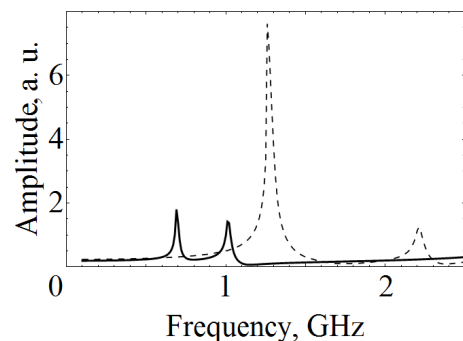


Fig. 2. FMR spectra of US (solid) and SS (dashed) in modified Co/Pt.

5 July

Wednesday

12:00-14:00

poster session
5PO-K1

**“Magnetic Shape
Memory and
Magnetocaloric Effect”**

5PO-K1-1

AB INITIO STUDY OF GROUND STATE AND MAGNETIC PROPERTIES OF Fe-Ga ALLOYS

Matyunina M.V.¹, Zagrebin M.A.¹, Sokolovskiy V.V.^{1,2}, Buchelnikov V.D.¹

¹ Chelyabinsk State University, Chelyabinsk, Russia

² National University of Science and Technology 'MIS&S', Moscow, Russia
matunins.fam@mal.ru

The huge interest to theoretical and experimental studies of the Fe-Ga alloys (Galfenol) is due to a giant magnetostriction observed at room temperature in low magnetic fields [1]. The theoretical investigations of the effect of a phase consisting on the properties of magnetostrictive alloys noted that areas of maximum magnetostriction in $\text{Fe}_{1-x}\text{Ga}_x$ alloys were discovered at $x = 0.18-0.19$ [1] and $x = 0.25-0.27$ [1, 2]. A study of phase transitions in Fe-Ga alloys shows that a large influence on the magnetic properties is exerted by the technological process of fabrication [3]. Moreover, as it was shown in Ref. [1] the magnetostriction coefficient and its sign can be sufficiently affected by the different atomic arrangements in the A2, B2, and D0₃, L1₂ structures.

In this study we investigate the structural and magnetic properties of $\text{Fe}_{1-x}\text{Ga}_x$ alloys ($x = 0.0-0.3$) possessing the A2, D0₃, and L1₂ structures by means of the density functional theory, delayed in the first principle package of spin-polarized relativistic Korringa-Kohn-Rostoker (SPR-KKR) [4]. Structural optimization was performed using the exchange-correlation potential in the approximation of the generalized gradient (GGA) and in the approximation of local electron density (LDA).

The calculations of optimized lattice parameters for A2, D0₃, L1₂ phases were carried for compositions with $x = 0$ up to 0.3. The obtained equilibrium lattice parameters were further used to calculate the magnetocrystalline anisotropy. In this case, we considered that the volume of crystal lattice does not change due to tetragonal distortions (c/a) along z axis.

For the optimized lattice parameter, the exchange interaction parameters were calculated using a spin-polarized scalar-relativistic Hamiltonian (SP-SREL) [4]. The Heisenberg exchange interaction parameters J_{ij} were calculated using the expression proposed by Liechtenstein et al. [5].

As the result, the optimized lattice parameters a_0 , total magnetic moments M_0 , and equilibrium ground state energies E_0 were calculated in dependence on the Ga excess in $\text{Fe}_{1-x}\text{Ga}_x$ ($x = 0.0 - 0.30$) for A2, D0₃, and L1₂ crystal structures. It was shown that the lattice parameter increases linearly, while the total magnetic moment decreases linearly for all phases studied with increasing Ga content. The obtained values of the equilibrium parameter taking into account the exchange correlation of energy in the GGA approximation are closer to the experimental values [1] than the results obtained in the LDA approximation.

By using the optimized lattice parameters, we calculated the magneto-crystalline anisotropy energies ($E_{MCA} = E_{111} - E_{001}$) for a series compositions with D0₃ and L1₂ phases. The negative slope of E_{MCA} (c/a) curves was found for both phases. These results are in good agreement with theoretical results, obtained by using FLAPW method [2].

Support by Advanced research foundation of the Chelyabinsk State University is acknowledged.

[1] I.S. Golovin, *Mater. Design.*, **88** (2015) 577.

[2] R. Wu, *J. Appl. Phys.*, **91** (2002) 7358.

[3] I.S. Golovin et al., *J. Alloy. Compd.*, **675** (2016) 393.

[4] H. Ebert et al., *Rep. Prog. Phys.*, **74** (2011) 096501

[5] A.I. Liechtenstein et al., *J. Magn. Magn. Mater.*, **67** (1987) 65.

5PO-K1-2

TERNARY PHASE DIAGRAM OF Ni-Mn-Ga: INSIGHTS FROM AB INITIO CALCULATIONS

*Sokolovskaya Y.A.*¹, *Zagrebin M.A.*^{1,2}, *Sokolovskiy V.V.*^{1,3}, *Buchelnikov V.D.*¹, *Zayak A.T.*⁴

¹ Chelyabinsk State University, Chelyabinsk, Russia

² National Research South Ural State University, Chelyabinsk, Russia

³ National University of Science and Technology "MIS&S", Moscow, Russia

⁴ Bowling Green State University, Bowling Green, USA

miczag@mail.ru

Heusler alloys represent a large family of ternary metallic compounds that became known at first as magnetic shape-memory effect materials. At sometime later, more Heusler alloys became known as half-metals, promising for realizing spintronic technologies. Another subgroup of Heusler alloys is explored with respect to the magnetocaloric effect (magnetic refrigeration). The large number of members of Heusler family and the richness of properties exhibited by them make this class of materials highly suitable for emerging materials-dependent technologies [1-3]. At present, among many ferromagnetic (FM) shape memory alloys, Ni-Mn-Ga Heusler systems are the most studied. Such high interest is related to the unique properties exhibited by the prototypical stoichiometric shape-memory compound Ni₂MnGa [1-3]. A variety of different off-stoichiometric Ni-Mn-Ga compositions, which have been synthesized and characterized in the past twenty years are mapped on the ternary diagram. However the most popular compositions are localized in the middle part of a ternary diagram, close to the stoichiometric system. The majority of well-studied compounds belong to the families of Ni_{2+x}Mn_{1-x}Ga ($x = 0.0-0.39$) and Ni₂Mn_{1+x}Ga_{1-x} ($x = 0.0-0.40$), showing a strong coupling between the magnetic and structural subsystems [4].

In this work we perform a wide-range systematic study of the family off-stoichiometric Ni-Mn-Ga alloys by using the supercell approach in the framework of DFT. Our goal is to explore the compositional variations of the structural stability and magnetic properties of Ni-Mn-Ga compositions, especially focusing on the areas that have not been covered by the experimental research. In order to investigate the magnetic and structural ground state properties of Ni-Mn-Ga Heusler alloys, we used the projector augmented wave method as implemented in VASP (Vienna *ab initio* simulation program) [5, 6]. The optimization for the geometrical structure of the austenite phase was carried out using the VASP package in combination with the 16-atom supercell approach. As a result equilibrium lattice parameters, bulk moduli, total magnetic moments, and formation energies of a wide range of Heusler alloys have been mapped on compositional ternary diagrams.

Support by Advanced research foundation of the Chelyabinsk State University and President RF Grant MK-8480.2016.2 is acknowledged.

- [1] P. Entel, M.E. Gruner, A. Dannenberg et al., *Mat. Sci. Forum* **635** (2010) 3.
- [2] V.D. Buchelnikov, V.V. Sokolovskiy, *Phys. Met. Metallogr.*, **112** (2011) 633.
- [3] V.V. Sokolovskiy, M.A. Zagrebin, V.D. Buchelnikov, *Mat. Sci. Foundations*, **81** (2015) 38.
- [4] P. Entel, V.D. Buchelnikov, V.V. Khovailo et al. *J. Phys. D: Appl. Phys.* **39** (2006) 865.
- [5] G. Kresse and J. Furthmuller, *Phys. Rev. B*, **54** (1996) 11169.
- [6] G. Kresse and D. Joubert, *Phys. Rev. B*, **59** (1999) 1758.

5PO-K1-3

THE TRANSFORMATION OF THE MAGNETOSTRUCTURAL PHASE TRANSITION WITH TI ADDITION IN $Gd_5Si_2Ge_2$

Nikitin S.A.¹, Smirnov A.V.¹, Bogdanov A.E.¹, Ovchenkova I.A.¹, Ovchenkov E.A.¹, Morozkin A.V.¹
¹Lomonosov Moscow State University, Moscow, Russia
 andrey07_91@mail.ru

The $Gd_5Si_2Ge_2$ compound have attracted the considerable attention since it exhibits the giant magnetocaloric effect (MCE) [1]. For this compound the large magnetic and temperature hysteresis associated with the magnetostructural phase transition is also observed, which is the substantial lack from the point of view of its practical application [2]. Therefore it is actual to search the optimal substitution in p- or 4f-sublattice for reduction of hysteresis with preserving of the large magnitude of MCE. In this work the complex investigations including the magnetic, magnetocaloric, thermal expansion, magnetostriction and heat capacity measurements of $Gd_{5-x}Ti_xSi_2Ge_2$ compounds have been carried out in wide range of fields and temperatures.

The $Gd_{5-x}Ti_xSi_2Ge_2$ ($x=0, 0.05, 0.1$) samples were prepared by arc-melting. The ingots were remelted three times followed by annealing at 970 K for 300 h. X-ray diffraction and electron microprobe analysis revealed that the dominate phase in $Gd_5Si_2Ge_2$ is monoclinic $Gd_5Si_2Ge_2$ -type whereas in $Gd_{4.9}Ti_{0.1}Si_2Ge_2$ it is orthorhombic Gd_5Si_4 -type. $Gd_{4.95}Ti_{0.05}Si_2Ge_2$ contains both $Gd_5Si_2Ge_2$ -type and Gd_5Si_4 -type phases.

Magnetization measurements revealed that $Gd_{5-x}Ti_xSi_2Ge_2$ compounds demonstrate typical ferromagnetic behavior. The Ti substitution raises the Curie temperature T_C from 271 K for basic compound to 292 K for $Gd_{4.9}Ti_{0.1}Si_2Ge_2$ and 296 K for $Gd_{4.95}Ti_{0.05}Si_2Ge_2$. At the same time the temperature hysteresis significantly decreases. The Belov-Arrott plots (H/σ vs. σ^2) are linear near T_C for Ti substituted compounds and nonlinear for $Gd_5Si_2Ge_2$. It indicates that the phase transition is second order for substituted compounds and it is first order for $Gd_5Si_2Ge_2$. The different shape of the peak on the temperature dependence of heat capacity for $Gd_5Si_2Ge_2$ and substituted compounds also confirms the change of the order of phase transition with Ti addition.

Direct MCE measurements in the fields up to 13.5 kOe revealed that for Ti substituted compounds the temperature dependencies of MCE upon cooling and upon heating are almost the same, while the large hysteresis is observed for $Gd_5Si_2Ge_2$. The maximum MCE value increases from 1.5 K for $Gd_5Si_2Ge_2$ to 1.64 K for $Gd_{4.9}Ti_{0.1}Si_2Ge_2$ for a field change of 13.5 kOe.

The thermal expansion measurements showed the presence of the anomaly on the $\Delta l/l(T)$ associated with the structural phase transition for $Gd_5Si_2Ge_2$, which is absent for $Gd_{4.9}Ti_{0.1}Si_2Ge_2$. The volume magnetostriction ω is large and positive for $Gd_5Si_2Ge_2$. The Ti addition leads to the considerable reduction of ω magnitude with changing of its sign.

The small Ti addition in $Gd_5Si_2Ge_2$ compound leads to the disappearance of the structural transformation and thus changes the order of the phase transition. However it preserves the MCE value making substituted compounds more efficient for practical use than $Gd_5Si_2Ge_2$.

The work has been supported by RFBR grant N 16-02-00472 A.

- [1] V.K. Pecharsky, K.A. Gschneidner Jr., *Physical Review Letters*, **78** (1997) 4494–4497.
 [2] V. Provenzano, A.J. Shapiro, R.D. Shull, *Nature*, **429** (2004) 853–857.

5PO-K1-4

MAGNETOCALORIC EFFECT IN Ni-Mn-Sn-BASED HEUSLER ALLOYS DOPING BY Si AND Ge

Marchenkov V.V.^{1,2,3}, Emelyanova S.M.¹, Marchenkova E.B.¹, Dyakina V.P.¹, Koshkid'ko Yu.S.³,
Ćwik J.³, Dilmieva E.T.³, Wang R.L.⁴, Yang C.P.⁴, Sauerzopf F.⁵, Frischauf K.⁵, Belozerova K.A.¹

¹ M.N. Mikheev Institute of Metal Physics, 620990 Ekaterinburg, Russia

² Ural Federal University, 620002 Ekaterinburg, Russia

³ International Laboratory of High Magnetic Fields and Low Temperatures, 53-421 Wroclaw,
Poland

⁴ Hubei University, 430062 Wuhan, China

⁵ TU Wien Atominstitut, 1020 Vienna, Austria
emelyanova@imp.uran.ru

The search for and study of new materials with a high magnetocaloric effect (MCE) are of great interest, especially because they can be used for creating new types of magnetic refrigerators. In addition, a study of the MCE provides new and important information about magnetic phase transitions and many other physical phenomena. Heusler alloys based on Ni-Mn-X (X = Ga, In, Sb, Sn) are promising candidates for these aims due to their first order phase (martensitic) transition, where the MCE is realized with a maximal value. It takes place in a wide temperature range depending on the Heusler alloy composition. In order to regulate and change the martensitic transition temperature and, hence, to control the MCE, there are two possibilities at least: (1) to change a ratio of magnetic atoms Ni/Mn [1]; and (2) to replace a fraction of the non-magnetic atoms Z by doping (see, e.g., Refs [2, 3]). The purpose of the present work is to study the effect of Al and Si doping on the MCE in Heusler compound $\text{Ni}_{43}\text{Mn}_{46}\text{Sn}_{11-x}\text{Z}_x$ (Z = Ge, Si; x = 0, 1, 2).

Heusler alloys were prepared in an induction furnace in an inert atmosphere. The melted ingots were annealed at 1123 K for 24 hours followed by furnace cooling. Elemental analysis, which was carried out using a scanning electron microscope (Inspect F, FEI Company) equipped with an EDAX spectrometer demonstrated that the alloys indeed correspond to their nominal composition. XRD investigations confirmed the presence of the L_{21} -structure in all samples. Magnetization measurements were carried out in a SQUID-magnetometer (MPMS XL, Quantum Design) at temperatures from 4.2 to 350 K in the magnetic fields of up to 7 T. The magnetic entropy change ΔS_M was calculated from the magnetization $M(T)$ data using the Maxwell relation.

The characteristic temperatures of the phase transitions, the martensitic and the austenitic start and finish temperatures, M_s , M_f , A_s and A_f , were determined from the temperature dependence of the magnetization for all investigated alloys. It was demonstrated that the substitution of Sn atoms by Ge changes the MCE and shifts its maximum to higher temperatures. On the contrary, when the Sn atoms are replaced by Si atoms, the temperature maximum is shifted to lower temperatures.

This work was partly supported by the state assignment of FASO of Russia (theme "Spin" No. 01201463330), by the Scientific Program of UB RAS (project No. 15-17-2-12), by the RFBR (grant Nos. 15-02-06686 and 16-32-00072), by the Government of the Russian Federation (state contract No. 02.A03.21.0006), and by the NCBR (Poland) within the project "ERA.Net RUS Plus: No. 146-MAGNES" financed by the EU 7th FP, grant No. 609556.

[1] H.C. Xuan, Y.Q. Zhang et al., *Phys. Status Solidi A*, **212**, 3 (2014) 680-685.

[2] D.H. Wang, C.L. Zhang et al., *Journal of Applied Physics*, **102** (2007) 013909(1-4).

[3] S.C. Ma, H.C. Xuan et al., *Applied Physics Letters*, **97** (2010) 052506(1-3).

5PO-K1-5

COUPLE CALORIC EFFECTS IN MULTIFERROIC COMPOSITES*Aliev A.A.¹, Sokolovskiy V.V.³, Chichay K.A.², Rodionova V.V.², Amirov A.A.¹, Abdulkadirova N.Z.¹*¹ Institute of Physics, Dagestan Scientific Center of Russian Academy of Sciences, Makhachkala, Russia² Immanuel Kant Baltic Federal University, Science and technology park “Fabrica”, Kaliningrad, Russia³ Department of Physics, Chelyabinsk State University, Chelyabinsk, Russia
amiroff_a@mail.ru

In recent years, multiferroics are considered as a perspective materials for solid-state refrigerators, due to the coexisting of the magnetocaloric (MCE), electrocaloric (ECE) and elastocaloric (BCE) effects. Multiferroics with a two or more caloric effect called multicalorics and observation in them caloric effects named multicaloric effect. In particular, in multicalorics due to the interaction of the electric and magnetic subsystems increased the caloric effects near the phase transition temperatures. In this regard, recently search for multicalorics with room temperatures of magnetic and ferroelectric transitions.

Thus, the measurements of the direct and indirect MCE were performed on the multiferroic composites consisting of the modified PMN-PT relaxor-type ferroelectric ceramics with formula $Pb_{(1-z)}Ba_z(Mg_{1/3}Nb_{2/3})_m(Zn_{1/3}Nb_{2/3})_y(Ni_{1/3}Nb_{2/3})_nTi_xO_3$ ($z=0.10$, $m = 0.4541$, $y= 0.0982$, $n = 0.1477$, $x=0.3$) and ferromagnetic compound of MnAs. Both components have the ferroelectric (FE) and magnetic (FM) ordering around 315 K. MnAs is a ferromagnet with its Curie temperature $T_c = 317$ K. The ferromagnetic–paramagnetic transition is of first-order, which is accompanied by a structural transition from hexagonal type to orthorhombic type. The composites (x)MnAs-(1-x)PMN-PT ($x=0,2; 0,3$) were synthesized by a cold pressing method of powders of PMN-PT and MnAs under hydrostatic pressure with value 3GPa at room temperature, which previously were milled and mixed in different proportions. The microstructure of the composite was studied using X-ray powder diffractometer and scanning electronic microscope.

Differences on values of entropy (ΔS) and temperature (ΔT) changes between pure MnAs and composites were observed from direct and undirect magnetocaloric measurements. If the peak of ΔS for pure MnAs has only magnetic field induced origin, anomaly of ΔS for composites (x)MnAs-(1-x)PMN-PT may be observed due to stress of the FE phase on magnetic component, where FE phase has anomalous increasing of the thermal expansion near 315 K. Strong correlation between caloric effects confirms the multicaloric nature of the samples.

5 July

Wednesday

12:00-14:00

poster session
5PO-K2

“Magnonics”

5PO-K2-1

SPIN WAVE CONTROLLER

Khivintsev Y.V.^{1,2}, Sakharov V.K.¹, Kozhevnikov A.V.¹

¹ Saratov Branch of Kotelnikov Institute of Radioengineering and Electronics of Russian Academy of Sciences, Saratov, Russia

² Chernyshevsky Saratov State University, Saratov, Russia
khivintsev@gmail.com

In this work, we introduce and test an idea of the spin wave controller – device that allows programming and tuning properties of the spin wave and, thus, can be used as a microwave device with programmable transmission characteristics.

Sketch of the device is shown in Fig. 1. It consists of magnetic film – a waveguide for the spin wave, two antennas for excitation and detection of the spin wave and array of the electrodes in the form of the stripes placed on the top of the film between the antennas to control the spin wave propagation characteristics by applying the electrical current through them.

Principle of the control is based on dependence of the spin wave characteristics on the bias magnetic field. The electrical current in the single electrode locally changes the bias field in the film and affect on the spin wave. Distribution of the current between multiple electrodes produces certain bias field distribution in the film and this way programs the total (antenna-to-antenna) transmission characteristics. For example, using such system with large numbers of the electrodes and periodical distribution of the current one can realize so called dynamic magnonic crystal [1] and easily tune properties of the Bragg band gaps (position, depth, formation of the defect modes in it) by changing the currents code. Another possible way to affect on the spin wave using such structure is through the wavelength conversation mechanism in the spatially non-uniform bias field [2] that allows tuning the group velocity and delay.

Experimentally, the idea of such spin wave controller was tested using 12.3 μm thick Ga, Sc - substituted yttrium iron garnet (YIG) film with the magnetization of 370 G. The antennas and 80 control electrodes between them were fabricated on alumina plate. The YIG film was placed on the top of this plate and transmission characteristics were measured using a vector network analyser for various distributions of the currents between the electrodes. The possibility to realize the Bragg band gaps for the magnetostatic surface wave, the possibility to change its position and to form the defect mode in it were demonstrated. Micromagnetic simulation of the studied structure performed using OOMMF software [3] showed qualitative agreement with the experimental results.

Support by Russian Foundation for Basic Research (project # 16-07-00988) is acknowledged.

[1] A.V. Chumak, et al, *J. Phys. D: Appl. Phys.*, **42** (2009) 205005.

[2] J.R. Eshbach, *J. Appl. Phys.*, **34** (1963) 1298.

[3] <http://math.nist.gov/oommf/>

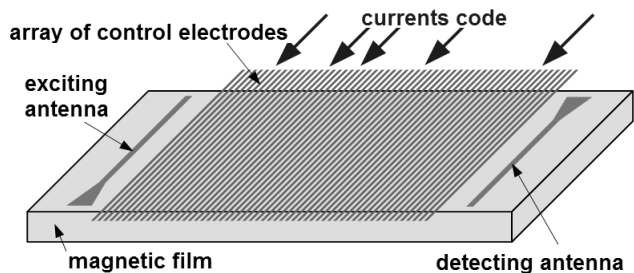


Fig. 1. Sketch of the spin wave controller.

5PO-K2-2

MICROMAGNETIC SIMULATION OF MSSW PROPAGATION IN THE SUBWAVELENGTH MAGNONIC STRUCTURE

Dudko G.M.¹, Vysotskii S.L.^{1,2}, Khivintsev Y.V.^{1,2}, Filimonov Y.A.^{1,2}, Sakharov V.K.¹,
Novitskii N.N.³, Stognij A.I.³

¹ Kotelnikov SBIRE RAS, Saratov, Russia

² Saratov State University, Saratov, Russia

³ Scientific and Practical Materials Research Centre, NASB, Minsk, Belarus
vysotsl@gmail.com

Magnetic periodic structures - magnonic crystals (MCs) - attract scientific attention due to many promising applications for future devices in information technology [1]. The main feature of MC is formation of forbidden band gaps in the spectra of spin wave's (SW) propagating therein. The gaps appear at Bragg resonance's frequencies f_B corresponding to the condition $\lambda(f_B) = 2\Lambda/n$, where Λ is the period of the structure, n is integer, λ is the SW's wavelength. Magnetostatic waves (MSW) propagation in MCs based on yttrium-iron garnet (YIG) films is usually studied using microstrip antennas. In these experiments the width w of microstrip antennas defines the short wavelength limit λ_{\min} of effective excitation and receiving of MSW ($\lambda_{\min} \approx 2w \approx 50 \mu\text{m}$ typically). That is why experiments using microstrip technique deal with MC having $\Lambda > w$ where w usually equals to several tens of microns. The structures having $\Lambda \ll \lambda_{\min}$ that we would call subwavelength magnonic structure (SMS) were poorly theoretically studied. Experimental features of surface MSW (MSSW) propagation in 2D MCs having $\Lambda \approx \lambda_{\min}$ were studied in [2] but they were not considered as a result of quasi-subwavelength regime of propagation in a part of the studied MSSW spectrum. To our knowledge the structures clearly announced as SMS ones were experimentally investigated in the single work [2] for the case of MSSW propagation in the YIG films with etched grooves in the form of 1D periodic lattice having the period $\Lambda < 10 \mu\text{m}$. The rejection bands in frequency dependence of MSSW transmission characteristic not observed earlier for ferrite MC were found. The number and bandwidth of these resonance-like features depended on the angle between directions of the bias magnetic field and the grooves.

To explain the formation of the features of MSSW propagation in the SMS [3] we performed its micromagnetic simulations using OOMMF [4]. The distribution of microwave components of effective magnetic field inside the sample was studied. Calculations were performed for wave vector of the 1D surface structures directed both perpendicular to and along the bias magnetic field. It was found that in the first case propagation of dipole (long wavelength) MSSW was accompanied by generation of short wavelength SW that could be localized inside the crests of the surface structure or could have the form of caustic beams emitted from the areas of the surface close to the grooves' corners. In the second case, the generation of short wavelength SW in the regions of the surface structure under the grooves was found. Thus, the results of the simulation allow explaining the experimental data as a formation of Fano-like resonances.

Support by RFBR (16-57-00153, 17-07-01452) and BRFFR (F16R-086) is acknowledged.

[1] A. V. Chumak, A. A. Serga, and B. Hillebrands, arXiv:1702.06701, **22** (2017).

[2] S. L. Vysotskii, S. A. Nikitov, and Yu. A. Filimonov, *JETP*, **101** (2005) 547.

[3] S.L. Vysotskii, Y. V. Khivintsev, V.K. Sakharov, G.M. Dudko, A.V. Kozhevnikov, S.A. Nikitov, N.N. Novitskii, A.I. Stognij, Y.A. Filimonov, "Magnetostatic surface wave dispersion and losses in subwavelength periodic structure", *IEEE Magnetic Letters*, in press.

[4] Donahue M., Porter D (1999), "OOMMF User's Guide, Version 1.0.Ed." In Interagency Report NISTIR 6376. Boulder: Nat. Inst. of Standards and Technology.

5PO-K2-3

MULTI-CHANNEL STRAIN-TUNED LATERAL MAGNONIC COUPLER

*Grachev A.A.¹, Sadovnikov A.V.^{1,2}, Beginin E.N.¹, Serdobintsev A.A.¹, Mitin D.M.¹,
Sharaevskii Yu.P.¹ and Nikitov S.A.^{1,2}*

¹ Saratov State University, Saratov, 410012, Russia

² Kotel'nikov Institute of Radio Engineering and Electronics, RAS, Moscow, 125009, Russia
andrew.a.grachev@gmail.com

The recent development of magnon-based electronics and spintronics shows, that spin wave (SW) can be used as a signal carrier in the waveguiding structures operating in the GHz and THz frequency range [1-3]. The planar yttrium iron garnet (YIG) microstructures open a promising alternative to signal processing by SW in beyond-CMOS computing technology, based on magnonic networks with low-level energy consumption. The magnetic field tunability of magnonic devices is inherently slow and needs a large power consumption. In contrast, the electrical tuning is potentially much faster and more relevant to energy-consumption-based applications [4,5].

We report on the study of the spin wave propagation in the multi-channel magnonic coupler which consists of three lateral magnetic stripes (MSs) and piezoelectric layer (PZT). MSs of 200 μm -width and $d=40\ \mu\text{m}$ edge to edge spacing were fabricated from 10 μm -thick monocrystalline ferrimagnetic YIG film with a saturation magnetization of $M_0=139\ \text{G}$. 50-nm-thick Nickel (Ni) electrodes deposited to the surface of PZT plate of dimensions of $680\times 3000\times 100\ \mu\text{m}^3$ on each YIG magnetic stripes (at the side which are strain coupled with YIG). Onto the top of PZT a 250-nm-thick Ni electrode was placed. The electric voltage V_c in the range of 0–250 V is applied to Ni electrodes. The electric field in PZT varies within the range of $E=0\dots 12.5\ \text{kV/cm}$. The distribution of stress tensor component S_z is depicted in Fig. 1(a), where the lateral contraction and an axial extension of PZT layer are shown for the electric field of $E=12.5\ \text{kV/cm}$. The scale factor for the geometry transformation is 100 to improve the visualization of the calculated data. Figure 1 (b) shows the internal magnetic field profile in the case of positive (red dashed curve) and zero electric field values. The lateral confinement of magnonic stripes in x -direction leads to a reduction of the internal magnetic field H_{int} . Thus the spin-wave switching is possible between the adjacent magnonic channels. This leads to the application of the proposed coupler in the critical energy-consumption devices.

Support by RFBR (No. 16-29-14021) and Grant of the President of RF (MK-5837.2016.9, SP-313.2015.5) is acknowledged.

[1] S.A. Nikitov, et. al, *Phys. Usp.*, **58** (2015) 10.

[2] V.E. Demidov, et. al, *Sci. Rep.*, **5** (2015) 8578.

[3] A.V. Chumak, et al, *Nature Physics*, **11** (2015).

[4] M. Bichurin and D. Viehland, *Pan Stanford Publishing, Singapore*, (2012).

[5] G. Srinivasan, and Y.K. Fetisov, *Ferroelectrics*, **342** (2006) 65-71.

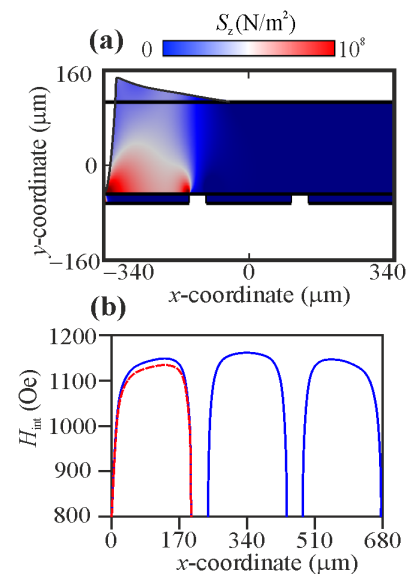


Fig. 1. (a) Distribution of stress tensor component S_z . (b) Internal magnetic field profile transformation as a result of the variation of the static electric field

5PO-K2-4

SUPERDIRECTED BEAM OF THE BACKWARD VOLUME SPIN WAVE

Annenkov A.Yu., Gerus S.V., Lock E.H.

Kotel'nikov Institute of Radio Engineering and Electronics of RAS (Fryazino branch), Fryazino, Moscow region, Russia
edwin@ms.ire.rssi.ru

Superdirected (nonexpanding) beam of the backward volume spin wave (BVSW) was observed experimentally in tangentially magnetized ferrite film (Fig. 1). The angular width of this beam was about zero so the smearing of the beam energy along the film surface was minimal and the length of the beam trajectory was maximal (~ 50 mm). The possibility of observing such superdirected beams was predicted in the theory [1], where it is deduced the common analytical formula describing angular beamwidth of the wave with noncollinear wave vector \mathbf{k} and group velocity vector \mathbf{V} for the case when the wave exciter length D is much larger than the wave length λ . Basing on the theory [1], the angular beam width of BWSW was calculated in [2].

The amplitude distribution of BWSW beam in the plane of the yttrium iron garnet film is studied experimentally by the special probing method, that was used earlier in [3, 4]. Recently this method was improved cardinally [5] and now it is possible to visualise amplitude (or phase) distribution of spin wave along the film surface by means of microwave signal processing in computer. Calculations and experiments are carried out for the film with thickness $s = 48.5 \mu\text{m}$ and magnetization $4\pi M_0 = 1800 \text{Gs}$. The uniform applied field H_0 was 500Oe . Exciting transducer represented the gold-plated tungsten wire of $12 \mu\text{m}$ thick had a length of $D = 5$ mm. The orientation φ of wave vector \mathbf{k}_0 was about -17° with respect to the z axis. Spin wave frequency was about 2800 MHz , $k_0 = 118 \text{ cm}^{-1}$, $\lambda_0 = 532 \mu\text{m}$ and $\lambda_0/D = 0.106$. The change of colors in Fig.1 corresponds to the amplitude change of 3 dB. It should be noted, that in isotropic media such beam (with ratio $\lambda_0/D = 0.106$) would have angular width about 6.1° whereas in Fig.1 spin wave beam has angular width about 0.5° !

The comparison between calculated and measured angular beam widths both for BVSW and for surface spin waves (see [6]) demonstrates good agreement. Thus it is shown experimentally that such phenomenon as "superdirected propagation of the wave" exists in the nature.

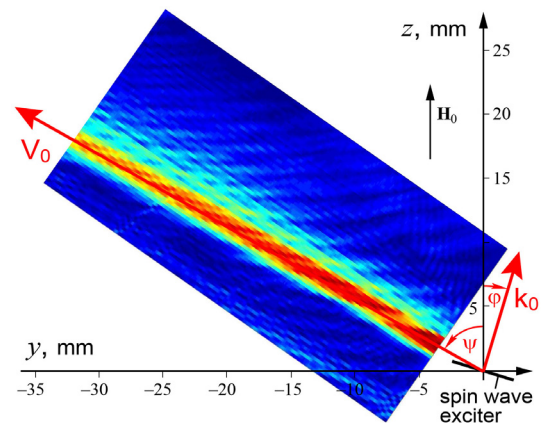


Fig. 1. Amplitude distribution of superdirected beam of BVSW along ferrite film surface (experiment).

The work is supported by Russian Foundation for Basic Research (project No. 17-07-00016).

- [1] E.H. Lock, *Physics-Uspekhi.*, **55** (2012) 1239.
 [2] E.G. Loka, *Journ. of Communications Techn. Electron.*, **60** (2015) 97.
 [3] A.V. Vashkovsky, V.I. Zubkov, E.H. Lock et al. *IEEE Trans. on Magn.*, **26** (1990) 1480.
 [4] A.Yu. Annenkov, I.V. Vasil'ev, S.V. Gerus, S.I. Kovalev. *Tech. Phys.*, **40** (1995) 330.
 [5] A.Yu. Annenkov, S.V. Gerus, *Journ. of Communications Techn. Electron.*, **57** (2012) 519.
 [6] A.Yu. Annenkov, S.V. Gerus, E.H. Lock. *Cornell University Library*, <http://arxiv.org/abs/1611.09595>

5PO-K2-5

DAMPING PROCESS OF NON-REFLECTION SPIN WAVE IN YTTRIUM IRON GARNET FILM

Bessonov V.D.¹, Telegin A.V.¹, Sukhorukov Yu.P.¹, Gieniusz R.², Guzowska U.², Maziewski A.², Stognij A.I.³

¹ M.N. Miheev Institute of Metal Physics of Ural Branch of Russian Academy of Sciences, Yekaterinburg, Russian Affiliation

² Faculty of Physics, University of Bialystok, Bialystok, Poland

³ Scientific-Practical Materials Research Center at National Academy of Sciences of Belarus, Minsk, Belarus

bessonov@imp.uran.ru

The short propagation length of magnetostatic spin waves (MSW) due to strong, exponential damping in magnetic medium is a main problem in creation real magnonic application [1]. Numerous attempts to compensate the damping of magnetic system as well frequency restrictions by the spin-torque effect could not solve the problems [2]. The researchers were forced to create complex waveguide structures [4] in which there are significant energy losses due to inherent multiple reflection of MSW [5]. Recently, the effect of formation a non-reflection spin waves was detected [6]. Non-reflection spin waves can propagate at distances significantly exceeding the MSW decay length in a magnetized medium (e.g. YIG film). The process of attenuation of a non-reflected spin wave cannot be explained by the magnons lifetime and activation mechanisms and is being left unclear yet.

In this work, we determine the damping length of the non-reflection MSW, as well as the physical mechanisms of the damping of MSW in an artificial magnon crystal based on patterned YIG films. The results have been compared with the excitation of MSW from an antenna in an unbounded film and caustic waves created by a single artificial defect. The YIG films with thickness of 4.5 μm were grown by liquid-phase epitaxy method on a GGG (111) substrate. Samples were patterned in the form of line of square antidotes with a side of 67 μm and period of 104 μm made by chemical etching on surface of the film. The dynamics of magnetization was studied by the Brillouin light scattering using a six-pass Fabry-Perot interferometer and a single-mode solid-state laser with a wavelength of 532 nm.

It was established that the mean free path of the non-reflected MSW is an order of magnitude (1 \sim 5 mm) exceeds one of the surface MSW in the absence of antidotes (1 \sim 0.5 mm), at the same parameters. The decay law has a smoothed maximum near the edge of the antidotes and can be explained by the contributions of the MSW scattering on each antidote and the exponential decay of the non-reflected wave in film far from the antidotes. A few intensive maxima detected in the non-reflected wave are probably associated with the formation of standing waves or interference of the non-reflected wave in the surface layer of the film.

The results are promising towards effective control of propagation of MSW and creation real magnonic analogous structures.

Support by IREE, ARC, and ARCNN is acknowledged, and by the Ministry of Education and Science of Russian Federation (grant Nr. 14.Z50.31.0025) and partially by the Russian Federal Agency for Scientific Organizations (project no. 0120146330, "Spin").

- [1] A.V. Chumak *et. al.*, *Nature Physics*, **11** (2015) 453-461.
- [2] V.E. Demidov *et. al.*, *Nature Materials*, **9** (2010) 984-988.
- [3] V.E. Demidov *et. al.*, *Appl. Phys. Lett.*, **104** (2014) 152402.
- [4] C.S. Davies *et. al.* *Phys Rev B*, **95** (2017) 019901(E).
- [5] R. Gieniusz *et. al.* *Appl. Phys. Lett.*, **104** (2014) 082412.

5 July

Wednesday

12:00-14:00

poster session
5PO-K3

**“Diluted Magnetic
Semiconductors and
Oxides”**

5PO-K3-1

CONNECTION OF THERMOPOWER, MAGNETOTHERMOPOWER WITH RESESTIVITY AND MAGNETORESESTIVITY IN MANGANITES WITH Nd AND Sm

Koroleva L.I.¹, Batashev I.K.¹, Morozov A.S.¹, Balbashov A.V.², Szymczak H.³, Slawska-Waniewska A.³

¹ Moscow State University, Moscow, Russia

² Moscow State Power Engineering Institute, Moscow, Russia

³ Institute of Physics Polish Academy of Sciences, Warsaw, Poland
koroleva@phys.msu.ru

In this work thermopower S , magnetothermopower $\Delta S/S$, electrical resistivity ρ and magnetoresistance $\Delta\rho/\rho$ were studied in single-crystals $\text{Sm}_{(1-x)}\text{Sr}_x\text{MnO}_3$ ($x = 0.15, 0.2, 0.25, 0.3$) and $\text{Nd}_{(1-x)}\text{Sr}_x\text{MnO}_3$ ($x = 0.15, 0.2, 0.3$). The study of the magnetic properties of these compounds showed that they consist of ferromagnetic clusters located in A-type antiferromagnetic matrix. Giant negative magnetoresistance, which was observed in these compounds, indicates that these ferromagnetic clusters belong to ferron type. A sharp increase of S and absolute value of negative $\Delta S/S$ were discovered near Curie temperature T_C , where $|\Delta S/S|$ reach giant values, up to $|\Delta S/S| = 94.5\%$ in magnetic field of 13.2 kOe. This means that thermopower is caused by presence of ferrons, as the value of the thermopower slumps with the destruction of ferrons caused by magnetic field or heating of sample over T_C . Therefore, thermopower in doped magnetic semiconductors is determined by the doping level and volume of the sample. So, after dividing the sample in two parts thermopower of each part decreased proportionally the volume of the sample. Thus, in doped magnetic semiconductors the value of thermopower can be considerably increased by enlarging the volume of sample, the level of doping and furthermore, can be controlled by magnetic field.

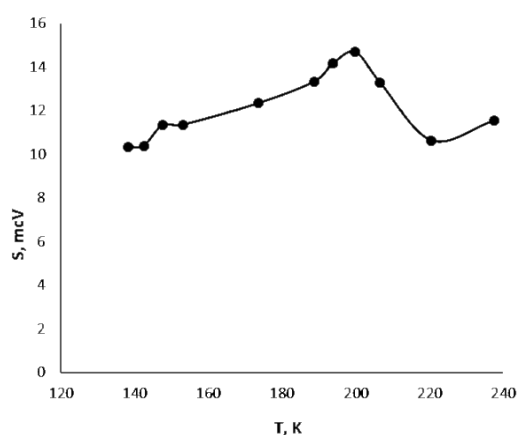


Fig. 1. Temperature dependency of thermopower of $\text{Nd}_{0.7}\text{Sr}_{0.3}\text{MnO}_3$

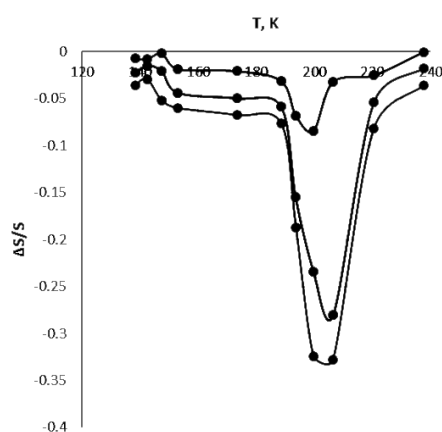


Fig. 2. Temperature dependency of magnetothermopower of $\text{Nd}_{0.7}\text{Sr}_{0.3}\text{MnO}_3$

5PO-K3-2

FEATURES OF THE MAGNETO-OPTICAL RESPONSE IN MANGANITE FILMS

Samoshkina Yu.E.¹, Edelman I.S.¹, Sokolov A.E.¹, Molokeev M.S.¹, Maximova O.A.¹, Andreev N.V.², Chichkov V.I.²

¹ Kirensky Institute of Physics, Federal Research Center KSC SB RAS, Krasnoyarsk, Russia

² National University of Science and Technology "MISIS", Moscow, Russia
uliag@iph.krasn.ru

In this work, we investigated the temperature behavior of the magneto-optical response of doped manganite films. Polycrystalline samples $\text{La}_{0.7}\text{Sr}_{0.3}\text{MnO}_3$, $\text{Pr}_{0.8}\text{Sr}_{0.2}\text{MnO}_3$ and $\text{Pr}_{0.6}\text{Sr}_{0.4}\text{MnO}_3$ from 20 nm to 150 nm in thickness were prepared by dc magnetron sputtering. Single-crystal zirconium oxide stabilized by yttrium (YSZ) was used as the substrates. Magneto-optical (MO) properties of the films were studied with the magnetic circular and linear dichroism spectroscopy (MCD and MLD, correspondingly) in the range 1-4 eV at temperatures 90-300 K.

Temperature behavior of the MCD and MLD spectra was compared with the temperature behavior of the magnetization and electric resistance of the samples. A correlation was revealed between some features in the MO spectra and the conductivity of the films. The maximum in the range 2- 2.5 eV was observed in the spectra of the semiconductor $\text{Pr}_{0.6}\text{Sr}_{0.4}\text{MnO}_3$ and $\text{La}_{0.7}\text{Sr}_{0.3}\text{MnO}_3$ samples (Fig. 1: top), which appears at temperatures coinciding with the temperature of the «semiconductor-insulator» transition. At the same time, this maximum was absent in the spectra of the insulator $\text{Pr}_{0.8}\text{Sr}_{0.2}\text{MnO}_3$ films. Experimental MCD and MLD spectra were decomposed to several MO bands, and different temperature dependences of their intensity were revealed for the semiconductor samples (Fig. 1: middle and bottom). In the case of insulating $\text{Pr}_{0.8}\text{Sr}_{0.2}\text{MnO}_3$, the intensity temperature course was identical for all revealed bands and corresponded to the temperature dependence of the films magnetization. The nature of the MO bands as well as the effect of the crystallites size and the films structure on their magnetic and magneto-optical behavior are discussed. The work was supported by the Russian Foundation for Basic Researches, Grant No. 16-32-00209 mol_a, and the Grant of the President of the Russian Federation no. NSH- 7559.2016.2.

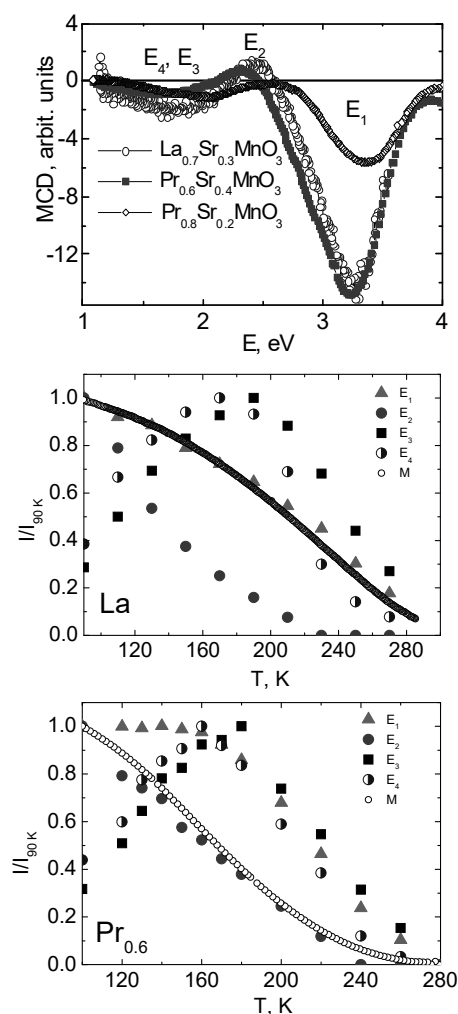


Fig. 1. Top – MCD spectra of the films at $T = 90$ K, middle and bottom - temperature dependences of intensity of the revealed in the MCD spectra MO bands in comparison with the samples magnetization (M). Magnetic field $H = 3$ kOe.

5PO-K3-3

**COMPETING INTERACTIONS, AND MAGNETIZATION DYNAMICS IN
DOPED RARE-EARTH MANGANITES NANOSTRUCTURAL SYSTEM***Shah W.H.*Department of Physics, Faculty of Basic and Applied Sciences, Islamic International University,
Islamabad, Pakistan

The Structural, magnetic and transport behavior of $\text{La}_{1-x}\text{Ca}_x\text{MnO}_{3+\delta}$ ($x=0.48, 0.50, 0.52$ and 0.55 and $\delta=0.015$) compositions close to charge ordering, was studied through XRD, resistivity, DC magnetization and AC susceptibility measurements. With time and thermal cycling ($T < 300$ K) there is an *irreversible* transformation of the low-temperature phase from a partially ferromagnetic and metallic to one that is less ferromagnetic and highly resistive. For instance, an increase of resistivity can be observed by thermal cycling, where no effect is obtained for lower Ca concentration. The time changes in the magnetization are logarithmic in general and activation energies are consistent with those expected for electron transfer between Mn ions. The data suggest that oxygen non-stoichiometry results in mechanical strains in this two-phase system, leading to the development of *irreversible* metastable states, which relax towards the more stable charge-ordered and antiferromagnetic microdomains at the nano-meter size. This behavior is interpreted in terms of strains induced charge localization at the interface between FM/AFM domains in the antiferromagnetic matrix. Charge, orbital ordering and phase separation play a prominent role in the appearance of such properties, since they can be modified in a spectacular manner by external factor, making the different physical properties metastable. Here we describe two factors that deeply modify those properties, viz. the doping concentration and the thermal cycling. The metastable state is recovered by the high temperature annealing. We also measure the magnetic relaxation in the metastable state and also the revival of the metastable state (in a relaxed sample) due to high temperature ($800\text{ }^\circ\text{C}$) thermal treatment.

5PO-K3-4

PROPERTIES OF POROUS SILICON PRECIPITATED WITH NI*Soboleva E.A.¹, Geydt P.¹, Zakharchuk I.¹, Spivak Y.M.², Moshnikov V.A.², Lahderanta E.¹*¹Lappeenranta University of Technology, Lappeenranta, Finland²Saint-Petersburg Electrotechnical University "LETI", Saint-Petersburg, Russia

Ekaterina.Soboleva@lut.fi

Cheap and reliable sensors for determination of alcohol vapours and ketones are of interest for road safety and toxic safety instances, e.g. in chemical plants and nearby livelihoods, during large volume carriage on vessels, by sea and via railway transport systems. Our main motivation was to design a sensor with potential to work in variable conditions and possible to be fabricated on large scales.

Samples were based on boron-doped n-silicon and were prepared by electrochemical etching. Two different current densities of the anodizing were used to mesoporous silicon and microporous silicon. Moreover, two methods of surface modification were used: electrochemical deposition of nickel with bias voltage $U = 2V$ and Ni precipitation from $NiCl_2 \cdot H_2O$ isopropanol solution. The variable parameter for both methods was duration of Ni treatment. Totally 15 different samples were made.

The samples surface morphology was analysed using Bruker Multimode 8 Atomic Force Microscope. Topography investigation was done in PeakForce mode. Peculiarities of surface morphology were proven to depend from the conditions of Si etching and Ni deposition. The surface roughness increased substantially during etching, while the size of assumed Ni clusters increased with duration of deposition. Surface magnetism studied by Magnetic Force Microscopy allowed visualization of magnetic centres where Ni particles were deposited in surface trenches.

The bulk samples' electrical properties were studied by impedance spectroscopy. Sensitivity to isopropanol vapour was observed. Equivalent electrical circuits for each sample were matched, calculated and analysed. This allowed to understand why the samples based on mesoporous Si were the most promising for sensing.

Magnetic properties of the porous silicon (PS) precipitated with Ni were investigated by means of SQUID magnetometer in the 2 – 400 K temperature range at various magnetic fields. Magnetization had paramagnetic temperature dependences with pronounced irreversibility between zero-field-cooled and field-cooled curves in the measured temperature range. Origin of the irreversibility was attributed to the ferromagnetic Ni particles. The magnetic field dependences were nonlinear with small saturation magnetization and coercivity up to 500 Oe, confirming presence of the ferromagnetic particles in the material. It was found that samples based on mesoporous Si were more intensively precipitated with Ni under the same conditions.

Scanning Electron Microscopy and RAMAN spectroscopy were used as additional investigation methods. They allowed visualization of spectral characteristics and elemental mapping approving the location of Ni centres and their phase composition.

The conclusion is that mesoporous Si precipitated with Ni was optimal for preparation of sensors with remarkable gas sensitivity. This was determined from the imaginary part of the complex impedance 0.7–2. Moreover, increasing of the precipitation time improved the gas sensitivity by 4 orders of magnitude.

5PO-K3-5

MAGNETIC PROPERTIES OF COBALTITES DOPED BY Cr, Ga, Ti, Fe

Troyanchuk I.O.^{1,2}, Karpinsky D.V.^{1,2}, Silibin M.V.¹, Gavrilov S.A.¹

¹ National Research University of Electronic Technology “MIET”, Zelenograd, Moscow, Russia

² Scientific-Practical Materials Research Centre of NAS of Belarus, 220072 Minsk, Belarus
karpinsky@physics.by

Perovskite oxides of transition metal elements are of particular interest due to unusual magnetic and magnetotransport properties. Cobaltites of $R\text{CoO}_3$ systems (R – rare earth ion) have attracted special attention because of additional degree of freedom associated with different spin configurations of Co ions [1]. However the origin of the ferromagnetism in the metallic cobaltites remains the subject of discussions for a long time. In the current abstract we declare effects caused by a substitution of cobalt ions by Cr, Ga, Ti and Fe ones in $\text{La}_{0.5}\text{Sr}_{0.5}\text{Co}_{1-x}\text{Me}_x\text{O}_3$ system with dopants concentrations up to $x \leq 0.25$.

Magnetic and magnetotransport properties of stoichiometric cobaltites $\text{La}_{0.5}\text{Sr}_{0.5}\text{Co}_{1-x}\text{Me}_x\text{O}_3$ have been investigated by neutron powder diffraction, magnetization and electrical measurements in fields up to 14T. The results of neutron diffraction measurements indicate that all the studied samples are characterized by single phase rhombohedral perovskite structure (space group $R\bar{3}c$).

Magnetization and electrical measurement is shown that the substitution with Fe ions up to the concentration $x=0.2$ does not strongly affect spontaneous magnetization and the Curie point (Fig. 1). In contrast, chromium substitution leads to dramatic decrease of magnetization and the Curie point, associated coherent magnetic contribution in NPD patterns quickly decreases with doping and becomes nearly negligible for $x=0.2$ compound. The substitution with diamagnetic Ga and Ti ions decreases the magnetization to a lesser extent than in the chromium doped compound (Fig. 1). The Cr, Ti and Ga substitution leads to a strong increase in magnetoresistance at low temperature as compared with undoped

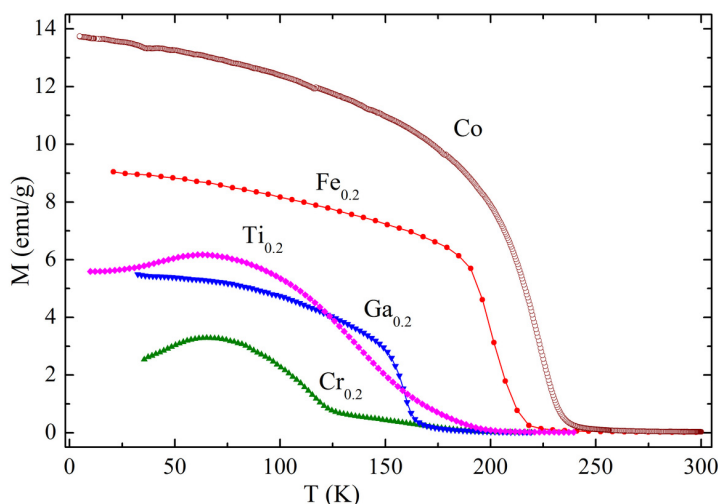


Fig.1 Field-cooled magnetization of the $\text{La}_{0.5}\text{Sr}_{0.5}\text{CoO}_3$ and $\text{La}_{0.5}\text{Sr}_{0.5}\text{Co}_{0.8}\text{Me}_{0.2}\text{O}_3$ compounds ($\text{Me} = \text{Cr, Ga, Ti, Fe}$) recorded in magnetic field of 0.01 T.

cobaltite and causes a metal-insulator transition whereas Fe-doped cobaltite remains predominantly metallic. Drastic increase of magnetoresistance is caused by local antiferromagnet-ferromagnet transition driven by strong magnetic field. The obtained results indicate that the magnetic interactions between Co and Fe are positive whereas those between Co and Cr ions are negative. Enhancement of magnetoresistance is attributed to the magnetic field induced transition from local antiferromagnetic order to ferromagnetic one.

This work was supported by the RSF (project #15-19-20038).

[1] B. Raveau, M.M. Seikh, Cobalt Oxides: From Crystal Chemistry to Physics, Wiley-VCH Verlag GmbH & Co. KGaA, Weinheim, 2012.

Author Index

A

Aarts J.	22, 27	Alekseev A.V.	232
Abakumov A.M.	293	Alekseev I.V.	777
Abakumov M.A.	534, 550, 552	Alekseev S.G.	958
Abakumova N.N.	799	Alekseeva O.A.	921
Abdulkadirova N.Z.	1084	Alemayehu A.	403
Abdullaev G.O.	930	Aleshin K.N.	19
Abdullaev M.A.	591	Alfadhel A.	691
Abdullah R.M.	330	Alfonsov A.	737
Abilov I.	793	Ali N.	51
Abramova G.	1038	Aliev A.A.	854, 1084
Abreu Araujo F.	609	Aliev A.M.	54, 55, 832, 836, 837, 838, 839, 840
Abrikosov I.A.	255, 398, 795, 841	Alisultanov Z.Z.	129, 930
Abrosimova G.	756	Aliyev M.N.	242
Abu-Bakr A.F.	521	Allodi G.	241
Acet M.	108	Alloul H.	743, 865
Achantá V.G.	190	Allwood D.A.	468, 1073
Acremann Y.	746	Alsharif N.A.	691
Adachi Y.	52	Altynbaev E.V.	106, 1031
Adam A.M.	98, 245, 769, 794	Alves Marins J.	988
Adamovich Yu.A.	463	Amara B.H.	988
Adanakova O.A.	238, 249, 250, 251, 460	Amelichev V.A.	463
Ado I.A.	954	Amirabadizadeh A.	544
Afanasiev D.	967	Amirov A.A.	854, 1084
Afremov L.	416	Andersen B.M.	971
Agafonov L.Y.	321, 765	Andrade R.	547, 548
Agrawal A.	190	Andreev A.V.	457, 791, 824
Ahmed A.	858	Andreev N.V.	357, 884, 1093
Ahmed M.	245	Andreev S.	18
Ahn J.	64	Andreev S.V.	777
Aizpurua J.M.	411	Andreeva M.A.	406, 1043
Akhmetova A.A.	920	Andreeva N.V.	741
Akimov A.V.	363	Andrianov A.VI.	934
Akimov I.A.	80, 188, 586	Andrianov E.S.	554, 705, 706
Aksenov S.V.	709	Andrianov T.	132, 164
Aksenova E.	118, 612	Andries M.	501
Alameh K.	199	Andrieu S.	607
Albin C.	1027	Andrievskii D.S.	823
Alekhin A.	44, 362, 474	Anikin M.S.	775, 843
Alekhina Yu.A.	509, 998	Anikin Yu.A.	135
		Anisimov M.A.	157
		Anisimov N.V.	538
		Annenkov A.Yu.	1089

Anokhin A.O.	424
Anokhin E.O.	500, 510
Antipov S.D.	1026
Antonets I.V.	205
Antonov A.S.	99, 207
Antonov I.N.	873
Antonov V.	375
Antropov N.O.	1043, 1071
Apalkov D.	120
Apanasevich V.	416
Aplesnin S.S.	666, 882, 885
Aprili M.	23
Aqeel A.	976
Aquino R.	384
Arai H.	328
Arauzo A.	889
Aref'ev I.M.	388
Aristov D.N.	1009
Arkipov D.I.	135
Arnau A.	653
Arnold Z.	457, 805
Aronin A.	756
Aronov A.N.	83, 494, 495
Aronzon B.A.	494, 651, 886
Artemov V.V.	272
Artemyeva A.S.	299
Arushanov E.	86
Arutyunov K. Yu.	31
Aryal A.	51
Arzhnikov A.K.	126, 231, 642, 932, 940
Asadullin F.F.	1064, 1065
Asai H.	627
Ashrafizadeh A.	816
Astakhov V.A.	212
Ataeva G.Y.	313
Atcheson G.	17, 603
Attanasio C.	27
Atuchin V.V.	818
Au Y.	468
Auffret S.	152, 334, 690
Auslender M.	995
Avdeev M.V.	401, 563, 640
Averkiev N.S.	85, 891, 978
Averyanov D.V.	156, 862, 986
Avilov A.S.	719
Avksentev Y.I.	1026

B

Baba and Lou G.	43
Babaev A.B.	313, 944

Babaizev G.V.	147
Babanov Yu.A.	406
Babaytsev G.V.	269, 606
Babcock E.	397
Bachmann J.	420
Badelin A.G.	890, 891
Badiev M.K.	306, 1014
Baenitz M.	877
Baglaeva J.A.	801
Bakhteeva Yu.	537
Bakhtiarov A.V.	679
Bakirov M.M.	232
Bakurskiy S.V.	349, 350, 577
Balaev A.D.	665, 900, 1049, 1050
Balaev D.A.	417, 425, 564, 576, 1049
Balahontsev A.B.	569
Balasoiu M.	501, 507, 511, 517, 823, 991
Balasoiu-Gaina A.M.	517
Balbashov A.M.	741, 909, 911
Balbashov A.V.	1092
Bali R.	115, 459, 1001
Baltz V.	334
Baluyan T.	819
Balymov K.G.	236, 247, 249, 460
Bandyopadhyay S.	858
Banerjee A.	858
Banerjee R.	115
Bannikov V.V.	888
Bannikova N.S.	493, 589
Bao W.	112
Baraban I.	466, 828
Barabanenkov Y.N.	185, 473
Barabanov A.F.	359
Baranchikov A.E.	1040
Baranov N.V.	66, 801, 844
Baranovskii S.D.	489
Barbieri M.	67
Barkalova A.S.	580
Barquín L.F.	404
Barrera G.	409
Barsaume S.	89, 739, 875
Barsukova M.G.	38, 191
Bartolomé J.	889
Barton C.	780
Barykina Yu.A.	1057
Baryshev A.V.	39, 40
Baryshnikov K.A.	891
Basiladze G.D.	197
Baskakov A.O.	719
Bataronov I.L.	817
Batashev I.K.	1092
Batdalov A.B.	832, 836, 837, 838, 840

Batrudinov T.M.	505	Bessonova N.P.	212
Batulín R.G.	243	Bessonova V.A.	739
Baturin V.S.	423	Bethanie S.	73
Bauer E.	744	Betto D.	17, 603
Baulin R.A.	406, 1043	Bewley R.	731
Bautin V.A.	418	Bezmaternykh L.N.	258, 715, 839, 894, 912, 921, 1009, 1019
Bayer M.	80, 188, 363, 586	Beznosikov D.S.	208, 233, 234, 757
Baykenov E.Z.	290	Bezus A.V.	787
Bayukov O.A.	294, 299, 417, 1019	Bhagat S.M.	960
Bazhanov A.G.	1053	Bianconi A.	344
Bazhanov D.I.	246, 722	Bica I.	507, 511, 991
Beaud P.	746	Bichurin M.I.	490, 907, 908, 1055
Bebenin N.G.	893, 983	Bihlmayer G.	653
Béché A.	1027	Biller A.M.	675
Becker P.	196, 976	Billington D.	59
Becker T.I.	525	Bilych I.V.	925
Beckman D.	25, 26	Birringer R.	404
Bedin S.A.	212, 272	Bizyaev D.A.	922, 1048
Beginin E.	475	Blanco J.M.	464
Beginin E.N.	438, 1068, 1072, 1088	Blanco-Rey M.	713
Beketov I.V.	71, 548, 772	Blinov I.V.	153, 1018
Beketova A.I.	772	Blinov M.I.	491
Belanovsky A.D.	118, 612, 614	Block Th.	899
Belik A.A.	377, 913	Blokhina A.D.	550
Belkhou R.	420	Blyakhman F.A.	74
Belmeguenai M.	598	Bo L.	352
Beloborodov I.S.	372	Bobin S.B.	150
Belotelov V.I.	144, 187, 188, 189, 190, 193, 199, 364, 585, 586	Bobkov A.M.	635, 636
Belousova A.V.	552	Bobkova I.V.	635, 636
Belov I.A.	961	Bobrovskii S.Y.	100, 442, 1063
Belov M.P.	841	Bocharova O.A.	538
Belovs M.	383	Bochmann S.	420
Belozerova K.A.	1083	Boehm M.	1009, 1038
Belskii I.E.	321	Bogach A.V.	157, 218, 235
Belyaev V.	192	Bogachev Yu.V.	545
Belyaeva I.A.	671	Bogdanov A.E.	1082
Belzig W.	25, 26, 577	Bogdanov S.G.	1054
Bender P.	400	Bogdanova Kh.G.	880
Berdonosov P.	444, 568	Boguschewski C.	976
Berganza E.	828	Bohatý L.	196
Bergeard N.	747	Boldyrev K.N.	750, 751, 752, 912
Berkov D.	60, 65, 230	Bolshakov A.P.	492
Bernal O.	430	Bolyachkin A.S.	771
Bersuker I.B.	891	Bondar E.D.	787
Bertran F.	607	Bondarenko G.N.	1022
Berzhansky V.N.	184, 186, 188, 197	Bondarev A.V.	817
Berzin A.A.	700	Bondarev I.A.	172, 173, 320, 1016
Bessalova V.V.	463, 543	Bordács S.	976
Besse V.	474	Bordyuzhin I.G.	762
Bessonov V.D.	898, 1071, 1090	Borin D.Yu.	525, 673, 679
Bessonova K.O.	766	Borisenko I.V.	155, 163

Borisov K.	17, 603
Borkunov R.Y.	271
Borovkova O.	586
Bortolotti P.	609
Bosch-Santos B.	1030
Bosseboeuf A.	807
Bothschafter E.	746
Böttger R.	87, 459
Bouravleuv A.D.	81
Bousseksou A.	331
Bouzehouane K.	622
Bouznik V.M.	318
Bovina A.F.	894, 1049
Bracher D.M.	1027
Bragina V.A.	692
Bran C.	429
Brener S.	125
Brun C.	630
Brusentsov N.A.	538
Buchelnikov V.D.	56, 478, 848, 852, 853, 1080, 1081
Buchkevich A.A.	898
Büchner B.	356, 449, 450, 566, 737, 860, 864
Buda-Prejbeanu L.	119, 152, 956
Budarin L.I.	91
Budrin K.S.	931, 945
Budzynski M.	579, 1042
Buettgen N.	871
Bugaev A.S.	712
Bugoslavsky Yu.	684
Bugrov A.N.	767
Bukharaev A.A.	922, 1048
Bukhtiyarova G.A.	425
Bukunov K.A.	147
Bulatov A.R.	880
Bunkov Yu.M.	469
Bunoiu M.	507, 991
Buravtsova V.E.	309
Burdin D.A.	664, 996, 1052
Burkhanov G.S.	963
Burkhovetskiy V.V.	887
Burma N.G.	925
Burmistrov I.S.	629
Burnell G.	347
Burova L.I.	858
Buryakov A.M.	915
Busch R.	404
Bush A.A.	895
Bushuev A.N.	506
Butvina L.N.	483
Buzdin A.	608
Buznikov N.A.	99, 207

Bychkov I.V.	181, 210
Byeonghwa L.	75
Bykov E.O.	1046
Bykov I.V.	985
Bykova L.E.	1021, 1022
Byzov I.V.	537, 540, 552

C

Cabrera-Pasca G.A.	1030
Cagnon L.	420
Calemczuk R.	690
Calle E.	960
Camp P.J.	382, 505, 518
Campi G.	344
Cao M.	972
Carbonari A.W.	1030
Carriere M.	690
Casallas Y.	88
Cebers A.	383
Celegato F.	409
Cha I.H.	426, 611
Chang C.	362
Chang C.-C.	543
Chang J.	479
Chang Wen-Hao	601
Chantrell R.W.	9
Chareev D.A.	273, 358, 644, 973
Charikova T.B.	88
Chashin D.V.	664, 918, 996, 997, 1052
Chauveau A.	118
Chebotkevich L.A.	252, 266, 426, 616, 617, 721, 821
Cecca N.R.	485
Chechenin N.G.	147, 269, 606
Chekanova L.A.	292, 294, 317, 319, 788, 812
Cekhonorin V.P.	552
Chekhov A.L.	45
Chekis V.I.	810
Chen R.Z.	427
Chen S.C.	427
Chen Y.S.	429
Cheng C.-L.	543
Cheng P.C.	358, 973
Cheong S.-W.	736
Chepkov G.N.	134
Cherdantseva V.V.	793
Cherebilo E.A.	16, 897
Cherebylo E.A.	494, 495
Cherepanov V.N.	286
Cherepkov M.O.	775

- Chérif M.....598
Cherkasov V.R.....692
Chernenkov Yu.P.....461
Chernichenko A.V.....274
Chernoglazov K.Yu.....16, 712
Chernov A.I.....144, 188, 189
Chernyavskii I.V.....871
Chernyshova T.A.....165, 493
Cherosov M.A.....258
Chetvertukhin A.V.....194
Chiang J.-C.....973
Chichay K.A.....466, 820, 828, 1084
Chichkov V.I.....1093
Chigarev S.G.....133, 158
Chikov A.A.....931, 945
Chinenkov M.Yu.....141
Chirikov D.N.....527
Chirkov V.V.....922
Chistotina E.A.....492
Chistyakov V.V.....160
Chistyakova N.I.....231
Chizhevskii E.G.....651
Chizhova I.A.....294, 417
Chlenova A.A.....542, 546
Choi E.S.....445
Choi K.-Y.....1057
Chou Yi-Chia.....601
Choudhary R.N.P.....376
Chshiev M.....119, 152, 956
Chtchelkatchev N.M.....579
Chu Y.J.....358
Chuev M.A.....272, 432
Chukalina E.P.....657
Chuklanov A.P.....922, 1048
Chulkov E.V.....498, 646, 649, 653
Chumak A.V.....658
Chumakov A.I.....231, 396, 406, 1043
Chumakov A.P.....500
Chumakov N.K.....138
Chupakhina T.....288
Chuprakov S.A.....153
Churbanov A.....662
Churyukanova M.....464, 809
Chvalun S.N.....881
Chzhan A.V.....270
Chzhan V.B.....850, 963
Cimbala R.....677
Cirillo C.....27
Cirlin G.E.....81
Coey J.M.D.....17, 603
Coisson M.....409
Collin S.....622
Constantinian K.Y.....155, 643
Contreras M.F.....691
Cooper J.F.K.....347
Cornei N.....159, 867
Cornelius S.....1001
Cöster B.....115
Craus M.-L.....159, 867
Creanga D.-E.....501, 517
Cren T.....630
Cristiani G.....357, 572
Cros V.....609, 622
Crozier E.D.....375
Cwik J.....51, 486, 797, 849, 850, 1083
-
- D**
- Dabrovski B.....872
Dagesyan S.A.....190, 193
Dan N.H.....483
Danilov A.P.....363
Danilov G.....551
Danilov Yu.A.....139, 868, 873
Danilovich I.L.....273, 454
Datskaya Z.R.....890
Davidov D.....813, 962
Davies C.S.....468, 1073
Davydenko A.V.....426, 821
Davydov V.Yu.....196, 750
Davydova M.D.....748
De Renzi R.....241
Deac A.M.....17, 174, 599, 603
Deb M.....747
Debontridder F.....630
Debus J.....80
Deckarm M.....404
Deeva J.....288
del Val J.J.....756
Delfanazari K.....441, 972
Demaille D.....630
Demeter J.....397
Demidenko O.F.....885
Demidov E.S.....91, 479
Demidov V.V.....155, 163, 643, 884
Demin G.D.....146
Demin V.A.....712
Demina P.B.....139, 868
Deminov R.G.....570
Demirov N.A.....129
Demishev S.V... 157, 214, 218, 235, 335, 440,
866, 979
Demokritov S.O.....325, 1020

Elfimova E.A.	310, 382, 505, 506, 518, 522
Eliseev A.A.	510
Eliseev An.A.	500
Eliseev Ar.A.	500
Elistratov A.A.	363
Elzawawy A.A.	267
Emelyanova S.M.	1083
Ensinger W.	420
Erager K.R.	853
Erbe A.	599
Eremeev S.V.	646
Eremin A.	388
Eremin E.V.	665, 894, 906, 923
Eremin I.	971
Eremina R.M.	258, 288, 714, 876, 1046
Erhan R.V.	159, 867
Eriksson O.	955
Erina E.	14
Ermakov K.S.	821
Ermolaeva O.L.	804, 977
Ernst A.	375, 646, 653
Erofeev D.A.	657
Erokhin S.	60, 65
Ershov N.V.	461
Escobosa A.	88
Esmaeili A.	242
Espinosa D.	72
Estemirova S.Kh.	890
Ester M.	276
Esters M.	874
Estipanos M.	430
Etter M.	732
Evstigneeva S.A.	98, 764
Ezhkov P.Yu.	259
Ezhov A.A.	182
Ezzaier H.	988

F

Falaleev O.V.	417
Farle M.	108, 429, 465, 550, 623
Farrer I.	972
Farzetdinova R.M.	789
Fassbender J.	17, 174, 421, 599, 780, 1001
Faugeras C.	591
Fayzullin M.A.	452
Fayzullin R.R.	853
Fazlizhanov I.I.	876
Fedorchenko I.V.	83
Fedorov V.A.	875
Feduschak T.A.	414

Fedyanin A.A.	38, 182, 191, 192, 194, 391
Felk V.A.	275, 282, 284, 1003
Fernandes R.M.	971
Fernández J.R.	404
Fernandez L.	713
Fernandez-Roldan J.A.	420
Fert A.	622
Fetisov L.Y.	918, 996, 997
Fetisov Y.K.	664, 996, 1052
Fickenscher Th.	899
Figueiredo Neto A.M.	72
Fil' V.D.	925
Filatrella G.	608
Filimonov D.S.	463
Filimonov Y.A.	221, 225, 439, 778, 1087
Filinkova M.	537
Filipov V.B.	157, 235, 440
Filippov B.N.	290, 305, 815, 822
Filippov D.M.	184
Filippov V.I.	350
Flachbart K.	235
Flannigan D.J.	415
Flokstra M.G.	347
Fluerasu D.	823
Fokina N.A.	423
Fokwa B.P.T.	899
Fomicheva L.N.	579, 1042
Fominov Ya.V.	356, 566, 628
Fontcuberta J.	594
Forestier G.	334
Fowley C.	17, 174, 603
Fraerman A.A.	479, 720, 977
Frangou L.	334
Fratila R.M.	411
Freydman A.L.	665, 1047, 1049, 1050
Fridman Yu.A.	303, 938
Frischauf K.	1083
Frolov A.Yu.	182
Frolov K.V.	272, 921
Fruchart O.	420
Fukushima A.	609
Fullerton E.E.	967
Furdyk V.P.	717
Futamato M.	62, 63

G

Gabáni S.	235
Gabay A.	58
Gabbasov B.F.	242, 243
Gage T.	415

Gaidukova I.Yu.	1032	Ghanaatshoar M.	441
Gaifullin R.R.	570	Ghasemi A.	816
Galakhov V.R.	1033, 1035, 1037	Ghemes A.	415
Galeev R.M.	835	Gieniuzs R.	1090
Galeski S.	731	Gilbert E.P.	109
Galias A.I.	836	Gilewski A.	483
Galkin V.	64	Gilmanov M.I.	214, 218, 440
Gallardo R.A.	599, 603	Gilmutdinov I.F.	243, 258, 288, 714, 865
Galyas A.I.	885	Gilmutdinov V.F.	642, 940
Gambarelli S.	334	Gimaev R.R.	48, 846
Gamzatov A.G.	832, 836, 837, 839	Giordano S.	662
Gan'shina E.A.	200, 309, 613, 739, 856, 892, 985, 1067	Giovannini M.	744
Gao T.	15	Gippius A.A.	871, 877
Gapihan E.	118, 612	Gizhevskii B.A.	1035, 1037
Gapochka A.M.	913	Gladii O.	334
Gapontsev V.V.	896	Gladkikh D.V.	268
Garanina A.S.	550	Glavin B.A.	363
Garanov V.A.	442	Glazkov V.	451, 452, 1028
Garcia K.	622	Glezer A.M.	761
Garcia-Santiago A.	27	Glownia J.M.	746
Gareev K.G.	314, 541	Glushkov V.V.	157, 218, 235, 335, 979
Gareev T.T.	1058	Gnezdilov V.	444
Gareeva Z.V.	370, 905, 910	Goikhman A.	834
Gargiani P.	375	Gokhfeld D.M.	576
Garifullin I.A.	356, 566	Goldobin E.	631
Garifyanov N.	566, 648	Golev I.M.	574, 580
Garshin V.V.	1067	Golik L.L.	856, 892, 985
Garwood M.	415	Golosovsky I.V.	1009
Gastiasoro M.N.	971	Golov A.V.	474
Gautier E.	420	Golovanov A.	358
Gaviko V.S.	781, 790, 796, 802, 808, 844, 1035	Golovchan A.V.	845
Gavrikov I.S.	135	Golovnia O.A.	781, 808
Gavrilkin S.Yu.	561, 878	Golubev A.	1010
Gavrilov S.A.	379, 1096	Golubev E.A.	211, 233, 234
Gavrilova T.A.	818	Golubeva E.V.	546
Gavrilova T.P.	288, 714, 928	Golubov A.A.	349, 350, 570
Gavrilyuk A.A.	768	Gomide G.	384
Gaydamak T.N.	925	Gonçalves E.S.	72
Gazizov A.I.	844	Gonchar L.E.	342
Gdovinová V.	674	Goodilin E.A.	740
Gemming S.	174	Gorbachev E.A.	295, 759
Gerashenko A.P.	301, 872, 926	Gorbatov O.I.	461
Gerasimov E.G.	790, 796, 803	Gorbunov D.I.	791, 824
Gerasimov M.V.	36	Gordon E.	298
Gerasimova T.P.	928	Gorelikov E.S.	786
Germov A.Yu.	872	Gorev R.V.	1078
Gerus S.V.	1089	Gorkovenko A.N.	238, 250, 251
Gervits N.E.	256, 535	Gorn N.	230
Getalov A.L.	823	Gornakov V.S.	283
Geydt P.	480, 773, 1095	Gornostyrev Yu.N.	461
		Gorshenkov M.V.	466, 760
		Gorshkov B.G.	692

Gorshunov B.P.	759	Gul Y.	972
Goryunov G.E.	1026	Gulyaev M.V.	538
Gosztola D.J.	970	Gumarov A.I.	242
Goto T.	41, 42, 202, 228, 471	Gumarov G.G.	232
Gotovko S.K.	445, 660	Gumerov A.M.	799
Govor G.A.	833, 836	Gunbin A.V.	826
Govorkova T.E.	150	Gundermann Th.	676
Grabchikov S.S.	763	Gunderov D.	55
Grachev A.A.	1088	Guo P.	77
Grachev R.A.	861	Gupta A.	716
Grachev V.M.	763	Guryev V.V.	567, 573
Grafe H.-J.	737, 860, 864	Gusakova D.	420
Grajcar M.	638	Gusev N.S.	720, 977
Granovsky A.B.	51, 308, 471, 480, 491, 712, 830, 1062, 1069	Gusev S.A.	977
Granovsky N.V.	200	Guteneva N.V.	76
Granovsky S.A.	1024, 1032	Gutfleisch O.	49, 55, 108, 324, 851
Grebennikov A.A.	166	Guzowska U.	1090
Grebennikov V.I.	1039	Gvozdevskaya V.A.	574
Grebenshchikov Yu.B.	785	Gyulasaryan H.	430
Grenzer J.	459		
Gribanov I.F.	845	H	
Grichuk E.S.	138	Hadjipanayis G.C.	58
Gridnev S.A.	1056	Hagiwara M.	304, 447
Grigoras M.	501	Haider K.	64
Grigoriev S.V.	106, 280, 686, 866, 1011, 1031	Hajdeu-Chicarosh E.	86
Grigoryeva N.A.	280, 1011	Hakioğlu T.	632
Grishin A.S.	155	Hamadeh A.	337
Gritsaj K.I.	823	Hansen T.	1010
Gritsenko Ch.A.	269, 606	Hao Wu	617
Grollier J.	609	Harikrishnan S.N.	877
Groshev A.G.	932	Harin E.V.	222, 774
Grunin A.	192, 834, 842	Hartmann R.	18
Grüninger M.	976	Hashim H.	262
Gruzdev M.S.	1004	Hašková V.	638
Gruzinov A.Yu.	401	Hatano S.	687
Gu G.D.	289	Hauet T.	607
Guan Xi-Wen	698	Hautle P.	404
Gubanov V.A.	227	He G.	639
Gubin S.P.	719	He M.	1001
Gubkin A.F.	66, 1033	Hehn M.	747
Gudim I.A.	657, 665, 906, 912, 921, 923, 925, 1050	Heim D.M.	30
Gudimenko E.S.	760	Heinemann A.	106
Gudim I.A.	588	Hellsvik J.	659
Gudkov V.V.	891	Helm M.	16, 87
Gudkova A.	514, 533	Henne B.	113
Gudkova S.A.	818, 1075	Henriques A.B.	82
Gudoshnikov S.A.	785, 786	Hentschel H.	87
Guidi T.	731	Hernandez J.M.	27
Guissart S.	630	Herrojo C.	94
Guk M.	86	Hillebrands B.	658

Hirazawa H.	536
Hirohata A.	330
Hirosawa S.	59, 949
Hjörvarsson B.	255
Hoai Nguyen T. L.	14
Hoffmann A.	470
Holder J.S.	577
Honecker D.	403, 404, 405
Honnecker D.	106
Horn S.	354, 1012
Horsley S.A.R.	468
Hou Y.	690
Houzet M.	626
Hövel H.	80
Hriplevets I.	809
Hrkac G.	468
Hsu H.-S.	287
Hsu W.-T.	601
Huai Y.	121
Huang J.	866
Huang J.C.A.	160, 654
Huckfeldt H.	402
Huong Dang T.	14
Hüvonen D.	451, 1028

I

Iacobescu G.	507, 991
Iakovleva M.	737, 860, 864
Iakubov I.T.	100
Ibaev Zh.G.	1017
Ibragimova E.M.	239
Ibragimova M.I.	876
Ichkitidze L.P.	532
Idiago-López F.J.	411
Ignatchenko V.A.	223, 437
Ignatenko A.N.	933
Ignatov A.S.	785
Ignatov M.S.	366
Ignatyeva D.O.	199
Igoshev P.A.	126
Ilic S.	626
Illés E.	296
Ilyina E.A.	27
Ilyn M.	713
Ilyushin A.S.	536
Imamura H.	328
Inaba N.	63
Inishev A.A.	790
Inkson B.J.	468, 1073
Inoue M.	41, 42, 194, 202, 228, 471

Inyushkin A.V.	492
Ioni Yu.V.	719
Ipatov M.	464, 756
Irkhin V.Yu.	15, 126, 161, 412, 413, 933
Irvine W.T.M.	393
Isaenko L.I.	818
Isavnin A.G.	219
Ishibashi T.	43
Ishihara S.	341
Iskakova L.	521
Iskhakov R.S.	284, 292, 294, 299, 317, 319, 417, 788, 812, 1003
Iskhakova R.R.	919
Isobe M.	732
Ispiryay A.G.	268, 503
Iss C.	690
Ito W.	52
Iurov A.S.	141
Iusipova Iu.A.	176, 177
Ivaneyko D.	670
Ivankov O.	517, 991
Ivanov A.A.	344, 806
Ivanov A.O.	382, 386, 505, 518
Ivanov B.A.	938
Ivanov D.	1071
Ivanov M.S.	915
Ivanov O.A.	758, 810
Ivanov O.V.	366
Ivanov V.E.	584
Ivanov V.G.	344, 806
Ivanov V.Yu.	663, 909, 911, 912
Ivanova A.G.	231
Ivanova O.	555, 726
Ivanova T.I.	797
Ivantsov R.	726, 874
Ivantsov R.D.	287
Ivanyukovich M.M.	96
Ivchenko E.L.	124
Izarova N.	1034
Izmozherov I.M.	305

J

Jäckl M.	188
Jackson E.	330
Jadzyn J.	674
Jaffrès H.	14
Jain S.	470
Janka O.	899
Jansen M.	278, 295, 759
Janusonis J.	362

Jen S.U.	427
Jeon Y.S.	252
Jiang X.	818
Jiang Yu.	698
Jin X.	12
Johnson D.C.	276, 874
Johnson S.L.	746
Joisten H.	690
Jónsson H.	621
Joumard I.	690
Joyce H.J.	972
Juang J.-Y.	358, 973
Jungfleisch M.B.	470
Juvé V.	44, 362

K

Kabanov V.M.	536
Kabanov Yu.	962
Kabirov Yu.V.	714
Kačmarčík J.	638
Kadowaki K.	441
Kagan M. Yu.	709
Kainuma R.	50, 52
Kakay A.	174, 599
Kalashnikov V.S.	831
Kalashnikova A.M.	741, 862
Kalentyeva I.L.	139
Kalgin A.V.	1056
Kalhor S.	441
Kalinikos B.	213, 472
Kalinin Yu.E.	151, 166, 206, 211, 233, 234, 292, 302, 308, 309, 712, 1070
Kalish A.N.	144, 190, 193
Kalitsov A.	333
Kalitikha I.V.	80
Kalyabin D.V.	473, 475
Kamantsev A.P.	53, 482, 483, 484, 486, 784, 831, 847
Kamarád J.	805
Kamashev A.A.	356, 566
Kameli P.	832
Kamenev V.I.	887
Kameneva M. Yu.	879
Kamensky I.Y.	165
Kamenskyi D.	750
Kamilov K.I.	539
Kampert E.	603
Kamzin A.S.	183, 237, 693
Kanomata T.	50, 52
Kantorovich S.S.	382, 386, 393, 504, 508, 513, 514, 672, 990
Kapralov P.O.	193, 199
Kapranov M.V.	260
Karapetrov G.	970
Karashtin E.A.	720
Karateev I.A.	156, 986
Karavaeva N.I.	185
Karavainikov A.V.	186, 197
Karczewski G.	80, 586
Karmenyan A.	543
Karpasyuk V.K.	890
Karpenkov A. Yu.	770, 849, 851
Karpenkov D. Yu.	55, 770, 792, 849, 851
Karpenkov M.	55
Karpinsky D.V.	379, 1054, 1096
Karpov P.I.	371
Karzanov V.V.	91
Kashiwagi T.	441
Kassan-Ogly F.A.	701, 723
Kataev V.A.	766, 773
Kataev V.E.	356, 566, 737, 860, 864
Katkova O.S.	260
Kato A.	109
Katsnelson M.I.	125, 980
Katsuya Y.	377
Katsyuba S.A.	928
Kaul A.R.	858
Kaustuv M.	864
Kawabata S.	627
Kawabe T.	687
Kazak N.V.	114, 715, 878, 1019
Kazakevich I.S.	869
Kazantseva N.V.	813, 962
Kazei Z.A.	879, 1024
Kazin P.E.	278, 295, 500, 510, 759
Keimer B.	354, 1012
Kekalo I.B.	811
Keller T.	1012
Kellerman D.G.	1057
Kelly M.J.	972
Kern C.	384
Ketov S.V.	806
Kevraletin A.L.	101, 279, 1069
Kézsmárki I.	976
Khabarov K.M.	39
Khadra G.	1027
Khamova T.V.	1040
Khan T.	744
Khandukhanov R.T.	547, 548
Khanipov T.F.	922, 1048
Khanov L.N.	837, 838, 840

Khapaev M.M.	349	Kirpicheva O.A.	233, 234
Khar'kov A.M.	666	Kiryakov M.A.	182
Kharitonskii P.V.	314, 541	Kiryukhantsev-Korneev F.V.	774
Kharkov A.M.	171, 885	Kiselev I.A.	545
Kharlamova A.M.	264, 265	Kiseleva T.Yu.	536
Khasanov R.	744	Kislinkii Yu.V.	357
Khaydukov Yu.	354, 1012, 1023	Kislinskii Yu.V.	643
Khivintsev Y.V.	221, 225, 439, 1086, 1087	Kitaev Yu.E.	591
Khizriev K.Sh.	281, 929	Kivshar Y.S.	38, 191
Khlusov I.A.	414	Kleibert A.	422, 1027
Khodos I.I.	719	Kleiner R.	631
Khokhlov N.E.	190, 585	Klenov N.V.	350, 351
Kholin D.I.	1002	Kliava J.	315, 726
Kholkin A.L.	1054	Klimin S.A.	450, 453
Khomchenko V.A.	915	Klimov A.A.	155, 662
Khomskii D.I.	340, 343, 982	Klimovskikh I.I.	497
Khoroshilov A.L.	235	Klingeler R.	298, 450
Khovaylo V.V.	55, 135, 482, 486, 792, 842	Klyachko N.L.	550
Khramova A.E.	585	Knezevic N.	296
Khramova O.D.	494, 495, 897	Knizhnik A.A.	336
Khrebtov A.I.	81	Knotko A.V.	883
Khudorozhkov A.A.	145	Knyazev G.A.	193, 199
Khvalkovskiy A.V.	118, 612, 614	Knyazev Yu.V.	294, 715, 1019
Kichanov S.E.	1042	Knyazeva E.A.	584
Kida T.	304, 447	Kobayashi D.	352
Kieu X.H.	53, 847	Kobelev A.	1071
Kihara T.	52	Kobyakov A.V.	168
Kiiamov A.G.	243, 714	Kobzev M.M.	519
Kikuchi M.	637	Koch I.	402
Kim C.G.	75	Kocharian A.	430
Kim Ch.G.	267	Kochervinskii V.V.	212
Kim D.	64	Kochura A.V.	494, 495, 870
Kim D.K.	967	Koelle D.	631
Kim G.W.	611	Kögel A.	513
Kim J.-Y.	330	Kohlbrecher J.	67, 404
Kim K.W.	75	Kohlstedt H.	631
Kim S.H.	252	Kokorina L.A.	549
Kim Y.J.	611	Koksharov Yu.A.	222, 413
Kim Yo.K.	252, 426, 611	Koledov V.V.	53, 54, 204, 481, 482, 483, 484, 486, 784, 831, 835, 837, 840, 847, 1066
Kimata M.	604	Kolesnikov A.G.	611, 616, 617, 721, 821
Kimel A.V.	89, 748, 875, 967	Kolesnikova A.A.	515
Kimura T.	661	Kolkov M.I.	900, 1049
Kinane C.J.	347	Kolmychek I.A.	720
Kindiak I.L.	143	Kolodkin D.A.	800, 802
Kirilenko E.P.	291	Kolodyazhnaya M.P.	925
Kirillova S.A.	314, 767	Kolokoltsev O.	472
Kirilyuk A.	595, 748, 967	Kolotov O.S.	1061
Kirino F.	63	Kolovskaya O.	555
Kirushechkina S.V.	96	Komanický V.	638
Kirman M.	814	Komarov E.N.	823
Kirov S.A.	1067	Komarov R.S.	190
Kirpan V.V.	488		

Komlev A.A.	863	Koutsiumaps A.	397
Komogortsev S.V.	275, 282, 284, 292, 788, 812, 1003	Kovalenko D.V.	907
Kondou K.	604	Kozabaranov R.V.	446
Kondrashov A.V.	213, 916	Kozeeva L.P.	879
Kondratev O.A.	156	Kozhaev M.A.	144, 187, 188, 189, 190, 193
Konev V.V.	562	Kozhevnikov A.V.	221, 1086
Kononenko V.V.	565	Kozhevnikov S.V.	1008
Konstantinov N.S.	883	Kozlenko D.P.	1042
Konstantinova E.I.	872	Kozlov A.G.	266, 821
Koo H.-J.	1010	Kozlyakova E.S.	273
Kopcansky P.	674, 677	Krakov M.S.	385
Kopeliovich D.B.	48	Kramarenko E.Yu.	509, 671, 998
Kopitsa G.P.	767, 1040	Krasikov A.A.	417, 1047, 1049
Koplak O.	20, 90	Krasnikova Yu.	1028
Koplak O.V.	825	Krasnikova Yu.V.	451, 452
Koptsik S.	551	Krasnorussky V.N.	235, 440
Korenev V.L.	80	Kratochvilova M.	1057
Korneev V.I.	917	Kravchenko Z.F.	887
Kornilov A.A.	1026	Kravtsov E.A.	236, 1002, 1023, 1043, 1071
Korobova J.G.	722	Kreines N.M.	16, 1002
Korolev A.F.	96	Krekhno R.V.	772
Korolev A.V.	800, 872, 1020	Kremer R.K.	1010
Korolev D.V.	541	Krinitsina T.P.	153, 165, 493, 1018
Korolev K.G.	302	Kritskaya E.A.	539
Koroleva L.I.	1092	Krivtsova A.V.	303
Korolyov A.V.	231	Krokhotin A.I.	833
Korostelin Yu.V.	891	Kronast F.	1001
Koroteev Yu.M.	646, 653	Krug von Nidda H.-A.	1012
Korotin M.A.	424	Kruglov V.S.	567, 573
Korovushkin M.M.	359	Kruglyak V.V.	468, 1073
Korshunov A.N.	733, 1025, 1041	KrugvonNidda H.-A.	354
Korshunov A.S.	924	Krukov R.N.	873
Kosel J.	691	Krylov V.I.	462, 1030
Koshelev A.V.	293, 484, 831	Ksevevich T.I.	538
Koshelev Y.S.	246	Kubli M.	746
Koshkid'ko Yu.S.	51, 482, 486, 797, 849, 1083	Kubota H.	609
Kosmachev O.A.	303, 938	Kucheryaev V.V.	827
Kosterov A.A.	314	Kuchin A.G.	800, 805
Kostishyn V.G.	98, 212	Kuchin D.S.	831
Kostyuchenko N.V.	824	Kuchko A.N.	468
Kostyuchenko S.	783	Kuchugura M.D.	277, 297, 733
Kosykh T.B.	585	Kudakov A.D.	961
Kosyrev N.N.	236, 725	Kudasov Yu.B.	446, 924
Kotani Y.	59	Kudrevatykh N.V.	771, 775, 782, 791, 843
Kotelnikova O.A.	96, 103, 697	Kudriavstev Yu.	88
Kotelyanskii I.M.	958	Kudrin A.V.	139, 868, 873
Kotov L.N. 169, 205, 206, 208, 209, 211, 224, 233, 234, 436, 474, 757, 1064, 1065		Kudryavtsev R.V.	799, 800
Kotov S.A.	823	Kudryavtsev V.O.	140, 768
Kourov N.I.	15, 161	Kudyukov E.V.	251
		Kugel K.I.	343, 707, 984
		Kuhns P.L.	445
		Kui Jin.	639

Makagonov V.A.	308	Martynov S.N.	939
Makarov A.V.	264, 265	Mashera V.S.	786
Makarov D.	44, 362, 474	Mashirov A.V.	53, 483, 484, 486, 784, 831, 842, 847
Makarov I.A.	696	Mashkovtseva L.S.	818
Makarov P.A.	137, 169, 436	Maslov D.A.	924
Makarova E.B.	74	Masyugin A.N.	171
Makarova L.A.	509, 897, 998	Mata-Contreras J.	94
Makarova O.L.	1042	Matsnev M.E.	913, 914
Makeyev O.G.	74	Matsumoto K.	258
Makhnev A.A.	162	Matsumoto R.	328
Maklakov S.A.	100, 463	Matsushita Y.	377
Maklakov S.S.	100, 463	Mattauch S.	397
Maksimochkin V.I.	861, 862	Mattheis R.	230, 599
Maksimova E.	311	Matthes P.	174
Maksimova I.K.	165	Matveev O.V.	215, 217
Maksimova K.	834	Matveeva P.G.	1009
Mal'shukov A.G.	353	Matyunin A.V.	1061
Malakhovskii A.V.	588	Matyunina M.V.	1080
Malinowski G.	747	Maximova E.N.	549
Malkin B.Z.	243, 657	Maximova O.A.	725, 1093
Maltceva L.	137	Maximova O.V.	858
Malyshev A.L.	1025, 1041, 1046	Mayboroda I.O.	138
Malyshev A.Yu.	539	Mazeeva A.K.	810
Malyshev V.D.	182	Mazhitova F.A.	905, 910
Malyshkina O.V.	998	Maziewski A.	1090
Mamedov T.N.	823	Mazov L.S.	641
Mamonova M.V.	259, 261	Mazur A.S.	241, 887
Mamsurov I.V.	561	Mazurkin N.S.	141, 291
Mamsurova L.G.	561	Meckenstock R.	108
Manabe A.	109	Medapalli R.	967
Mangin S.	20, 337, 747	Medvedev A.I.	548
Manna S.	967	Medvedeva I.	537
Mannini M.	110	Medvedeva T.M.	762
Manukyan A.	430	Meguro S.	685
Marchenko Ya.Yu.	545	Mehmet G.	632
Marchenkov V.V.	15, 150, 160, 161, 1083	Meijer J.-M.	393
Marchenkova E.B.	160, 1083	Meilikhov E.Z.	789
Marenkin S.F.	83, 494, 495, 870	Mekhonoshin D.S.	765
Maretzki R.	513	Melekh B.T.	859
Markin Yu.V.	892	Melekhin V.V.	74
Markina M.M.	298, 568, 1024	Melenev P.V.	528
Markov G.P.	536	Melnikov A.	474
Markov V.K.	539	Melnikov G.Yu.	547, 548
Marsh R.	348	Melnikov N.B.	127, 1036
Martin C.	742	Men'shenin V.V.	667
Martín F.	94	Men'shov V.N.	498, 649
Martin R.W.	591	Ménard G.C.	630
Martin S.	420	Menditto R.	631
Martinez Banderas A.	691	Menendez E.	397
Martínez de la Fuente J.	411	Menshchikova T.K.	875
Martino L.	409	Menshchikova T.V.	646, 653
Martyanov O.N.	425		

Menshikh I.A.	723	Mohammad Ali Zadeh T.....	433
Menshov S.A.....	786	Mohd A.S.....	397
Men'shov V.N.	646	Mohseni K.....	375
Menteş T.O.....	420	Moiseev A.A.	140, 216, 768
Mentink J.H.....	659	Moiseev K.D.....	88
Menushenkov A.P.....	344, 806	Mokhov E.N.....	492
Menushenkov V.P.....	760, 762, 798, 806	Molchanova A.D.....	750, 752
Merkulov D.I.....	512, 890	Möller A.....	448
Merkulova A.V.	454	Molnar G.....	331
Merzlikin A.M.	40, 185, 195	Molodtsov S.L.	111
Mesilov V.V.....	1033, 1035, 1037	Molokeev M.N.....	882
Metelkina K.K.....	213	Molokeev M.S.	889, 1093
Metlov L.S.	481	Monsivais G.....	472
Mettus D.....	404	Montaigne F.....	607
Meyer J.S.	626	Montoya S.A.	967
Meyerheim H.L.....	375	Morari R.....	354, 1012
Michels A.....	61, 65, 67, 404	Morchenko A.T.....	98, 212, 764, 769, 794
Michor H.....	744	Morcrette M.....	690
Mihashenok N.V.....	1047	Moreau-Luchaire C.....	622
Mikhailov A.P.....	118, 612, 614	Morel R.	690
Mikhailova T.V.....	186	Moreno Antolín E.	411
Mikhalev K.N.....	872, 926	Morgun L.A.	346, 886
Mikhalevsky V.A.....	16, 494, 495, 870, 897	Morgunov R.B.	20, 90, 337, 814, 825, 827
Mikhalitsyna E.A.	766, 773	Morimoto R.....	202
Mikhaylovskiy R.V.....	365	Moroslip A.E.	823
Mikheykin A.S.....	895	Morosov A.I.....	700
Mikhnevich E.A.....	71	Morozkin A.V.....	1082
Miki H.	842	Morozov A.S.....	1092
Mill B.V.	663, 1024	Morozov I.V.....	454, 871
Milosevic I.	70	Morozova M.A.....	215, 217
Milyaev M.A....	153, 165, 406, 493, 589, 1018	Morozova N.V.	768
Minin A.S.....	540, 552, 718	Moshkina E.M.	258, 752, 839, 894
Minina E.S.	672, 990	Moshnikov V.A.	1095
Mironov V.L.	804, 1078	Moskalev M.E.....	148
Mironov V.S.....	1000	Moskalev V.N.....	775
Miroshkina O.N.	848	Moskvin A.S.	257, 562, 871, 945
Mirzakhanyan A.....	430	Moskvin E.V.....	686
Mischenko I.N.....	432	Mosoyan K.S.	941
Mishina E.D.	915	Mostovshchikova E.V.....	718, 898
Miskiv A.	900	Motte L.	70
Mistonov A.A.....	280, 1011	Moulin J.	807
Mita C.	159, 867	Moutafis C.	622
Mita Y.	1038	Mryasov O.	333
Mitin D.M.	1088	Mudryi A.V.....	591
Mitrofanova E.S.....	759	Muduli P.	604
Mitsiuk V.I.....	833	Muehlbauer S.....	399
Miyake A.....	50, 52	Muftakhutdinov A.R.....	258
Miyanaga T.	846	Mukhamedov B.O.....	255, 795
Miyatake Y.....	687	Mukhamedshin I.R.	258, 743, 865
Moewes A.	896	Mukhin A.A.....	663, 909, 911, 912, 1009
Mogilenec Yu.....	311	Mukhin S.I.	371
Mogilnikov P.S.	811	Mukhuchev A.A.....	836, 838

Müller C.....	354, 1012
Müller D.....	80
Mulyukov R.R.....	835
Mumdzhi I.E.....	243
Münzenberg M.....	966
Muradimova L.....	761
Muravyev-Smirnov S.S.....	763
Murphy B.A.....	330
Murtazaev A.K. 240, 281, 306, 313, 942, 944, 1014, 1017	
Murtazaev K.Sh.....	1014
Murtazin R.R.....	1060
Murzaliev B.....	125
Murzina T.V.....	45, 720
Musabirov I.I.....	835
Mushenok F.B.....	468, 1015, 1073
Mushnikov N.V.....	457, 790, 796, 803
Musorin A.I.....	38, 191, 194
Myagkov V.G.....	1021, 1022
Mysik A.A.....	540
Myslitskaya N.M.....	271

N

Naboko A.S.....	442
Nadzhyryan T.A.....	509
Nagakubo Y.....	43
Nagasako M.....	50
Nagashima A.....	50
Naka M.....	341
Nakamura M.....	62
Nakamura T.....	59
Nakamura Y.....	41, 42, 202, 228, 471
Nakatsuji S.....	604
Nalbandyan V.B.....	277, 297, 298, 733
Nalench Y.A.....	534
Nalench Yu.A.....	550
Naletova V.A.....	394, 519
Nam D.Y.....	252
Nasu J.....	341
Naud C.....	690
Nauhatsky I.....	311
Naumov S.V.....	160, 1035, 1037
Naumova L.I.....	165, 493
Naupa A.R.....	82
Navascuez M.....	411
Naydenov P.N.....	45
Nazarenko I.I.....	455
Nazarov V.N.....	1060
Nechaev I.A.....	646
Nefedkin N.E.....	554

Nefedov S.G.....	862
Nekhaeva E.I.....	886
Nekhoroshkova Yu.E.....	522
Nekludova P.A.....	363
Nekrasov M.A.....	133
Nematov M.G.....	245, 769, 794
Nemirova V.A.....	140
Nemkovski K.....	403
Nemtsev I.V.....	788, 812
Nepochatykh Yu.....	204, 1066
Neshev D.N.....	38, 191
Nesmeyanov M.S.....	418
Nesterov A.I.....	943
Netesova N.P.....	560
Nevedomskii V.V.....	81
Nevedomsky V.N.....	88
Ney A.....	113
Ney V.....	113
Neznakhin D.S.....	800
Nguyen T.N.....	152
Nguyen H.H.....	53
Nguyen H.T.....	119
Nguyen Hai Yen.....	53, 784, 847
Nguyen Huy Dan.....	53, 784, 847
Nguyen M.A.....	53
Nguyen Mau Lam.....	784
Nguyen Thi Mai.....	847
Nguyen Van Duong.....	784
Nicolaev B.P.....	545
Nicolazzi W.....	331
Nikiforov A.E.....	342
Nikiforov I.V.....	385
Nikiforov V.N.....	412, 413
Nikitin A.A.....	658
Nikitin A.I.A.....	916
Nikitin An.A.....	916
Nikitin M.P.....	76, 538, 692
Nikitin N.P.....	242
Nikitin P.I.....	76, 538, 692
Nikitin S.A.....	797, 833, 849, 1082
Nikitin S.I.....	183, 243
Nikitin V.....	120
Nikitov S.A. 36, 185, 226, 227, 291, 426, 438, 473, 475, 611, 662, 721, 1072, 1088	
Nikitovskaia E.A.....	170
Nikoladze G.M.....	1061
Nikolaev A.N.....	1042
Nikolaev A.V.....	579, 585
Nikolaev S.N.....	16, 712
Nikolaev S.V.....	578, 943
Nikolaeva E.P.....	585, 1058
Nikulicheva T.B.....	170

Nikulin A.Yu.....	297
Nikulin Yu.	778
Nishimoto S.	737
Nitin K.	376
Niu Q.....	13
Niyazov R.A.....	187
Nižňanský D.....	403
Nogués J.....	397
Nojiri H.	737
Nolting F.	1027
Nori F.	707, 727, 984
Norina S.	543
Nosan M.M.	271
Nosov A.P.	739, 898, 1071
Novak E.....	514
Novakova A.A.	285, 819
Novikov I.A.	182
Novitskii N.N.....	610, 1087
Novodvorsky O.A.	16, 494, 495, 613, 870, 897
Novosad V.....	470
Novoselova Iu.	465
Nozdrin Yu.N.....	36
Nugumanov A.G.....	248, 378
Núñez A.	94
Nur-E-Alam M.....	199
Nurgazizov N.I.....	922, 1048

O

Obermeier G.....	354, 1012
Obukhov A.E.	590
Obukhov S.A.....	84
Odagiri Y.....	685, 687
Odenbach S.	387, 673, 676, 678, 679
Odintsov S.A.....	438
Odintsov V.I.....	786
Ogloblichev V.V.....	301, 926, 1015
Ognev A.V. 252, 426, 611, 616, 617, 721, 821	
Ogneva M.S.	813
Ohtake M.....	62, 63
Ohtani T.	637
Ohtsuka M.....	842
Okazaki H.	59
Okorokov M.S.....	605
Okulov V.I.	88, 136, 150
Okulova K.A.	150
Ollefs K.....	108, 113, 115
Ollivier J.....	731
Omelyanchik A.S.....	271, 296, 998
Omirov A.	684

Omori T.....	50
Ono K.....	67, 109
Ono T.	383
Ooki K.....	41
Oprica L.	501
Ordóñez-Romero C.L.	472
Orechov A.S.....	881
Orlov A.V.	76, 692
Orlov V.A.	717
Orlov Yu.S.....	878, 943
Orlova N.B.....	704, 937
Ortega J.E.....	713
Ortiz G.....	690
Osipov A.V.	100, 442, 1063
Osipov M.I.....	516
Osipov S.V.....	208
Osokin S.A.....	473
Ostrizhnyaya M.A.....	793
Ostrovskaya N.....	177
Otani Y.....	604
Otrokov M.M.....	646, 653
Ovcharov A.V.....	567
Ovchenkov E.A.....	1082
Ovchenkov Y.A.	454, 644
Ovchenkova I.A.....	1082
Ovchinnikov S.G.	114, 172, 173, 236, 320, 578, 696, 715, 878, 943, 1016, 1019
Oveshnikov L.N.....	651, 881, 886
Ovsyanikov A.K.	1009
Ovsyannikov G.A.	155, 163, 357, 572, 643, 884
Ozcan S.	458

P

Padmanabhan P.....	976
Pailoux S.L.	415
Paixão J.A.	915
Pal B.....	426, 611
Palmero E.M.	247
Palonen H.....	255
Palstra T.T.M.	976
Pamyatnykh E.A.	136
Pamyatnykh L.A.	321, 765
Pamyatnykh S.E.....	765
Panaetov V.P.....	312
Panasevich A.M.....	666
Panchenko V.Ya.	494, 495
Pandey P.	16
Pandey S.	51

Panina L.V. .98, 212, 245, 262, 764, 769, 794, 1076	Petrashov V.T. 348
Pankratov N.Yu. 833, 849	Petrenko A.A. 298
Pankrats A. 716	Petrenko O.A. 243, 304, 447
Pankrats A.I. 900, 1049	Petrov A.V. 183
Panov K. 760	Petrov D.A. 287, 463, 1063
Panov M.F. 541	Petrov M.I. 576
Panov Yu.D. 257, 562, 931, 945	Petrov P.N. 654
Panyaev I.S. 587	Petrov P.S. 96, 103
Panysheva T.Yu. 84	Petrov R.V. 490
Paradezhenko G.V. 127, 1036	Petrov V.M. 907, 908, 1055
Paramonov E.I. 522	Petrov Yu.V. 977
Paredes F. 94	Petrova A.E. 1042
Parfenov O.E. 156, 862	Petrzhik A.M. 357, 572, 643
Park J.G. 373, 896, 1057	Petukhov A.V. 393
Parkhomenko V.D. 1054	Petukhov D.A. 154
Parkin S. 8	Petukhov V.Yu. 232
Parshina L.S. 494, 495, 897	Peyre V. 384
Pashkevich Yu. 444, 750	Pham Thi Thanh. 53, 784, 847
Pasternak D.G. 1069	Philbin T.J. 468
Pastushenkov Yu.G. 849, 964	Philipse A.P. 393
Patrakov E.I. 1035	Philopov V.V. 1070
Patrin G.S. 168, 172, 270, 717, 1022	Pierre V.C. 415
Patrin K.G. 168, 717	Pietsch T. 18, 24
Paudel T.R. 374	Pigalskiy K. 575
Paulovicova K. 677	Pikalov A.M. 1062
Pavlov D.A. 873	Pimenov A. 656, 912
Pavlov V.V. 82, 862	Pinkas V.V. 826
Pavlovskiy N. 901	Piovano A. 1038
Pavlukhina O.O. 852	Pirogov A.N. 803, 1054, 1057
Pearson J. 470	Pirogov Yu.A. 538
Peddis D. 296	Pirruccio G. 472
Pelevina D.A. 519	Pisarev R.V. 196, 741, 750
Pereiro M. 955	Piskorskii V.P. 827
Perepyolkina A.V. 782	Piskunov Yu.V. 301, 926, 1015
Perevedentseva E. 543	Pismenova N.E. 740
Perevozchikova Yu.A. 15, 160, 161	Pitimova E.A. 873
Perez J.E. 691	Plaksin P.S. 181, 210
Perez R. 828, 960	Platonov S.P. 800, 805
Perlo P. 134	Platonov V.V. 924
Perminov A.S. 793	Platunov M.S. 114, 715, 878, 894, 1019
Pernod P. 155, 662	Plekhanova D.D. 918, 997
Perov D.V. 1020	Pleshchev V.G. 307
Perov N.S. .285, 466, 509, 543, 551, 819, 820, 897, 998	Pleshev D.A. 1064, 1065
Perova N.N. 1067	Plokhov D.I. 936
Perunov I. 272	Pochekutov M.A. 564
Perzynski R. 384	Podchezertsev S.Yu. 733, 1025, 1041
Pestun A.E. 884	Podgornaya S.V. 262
Petit-Watelot S. 20	Podgornykh S.M. 150
Petrakovskaja E. 726	Podolskii V.V. 91
Petrakovskii G.A. 889	Podorozhnyak S.A. 270
	Pogrebna A. 89
	Poimanov V.D. 204, 468, 1066

Pokatilov V.S.	913, 914
Pokholok K.V.	463
Pokrovsky L.D.	818
Poleshchikov S.M.	1064, 1065
Politaev V.V.	298
Politova G.A.	791, 824, 850, 963
Polozov V.I.	463
Polukhin D.S.	223
Polunin V.M.	390, 529
Polushkin N.I.	1001
Polyakov A.	375
Polyakov P.A.	1061
Polyakov P.I.	130
Polyanskiy V.A.	538
Polzikova N.I.	958
Ponomarev D.A.	406
Ponomareva A.V.	255, 795, 841
Ponomareva T.Y.	723
Poperechny I.S.	724
Popescu L.	501
Popkov A.F.	134, 145
Popkov S.	900
Popkov S.I.	417, 1047, 1049
Popov A.G.	781, 802, 808
Popov A.I.	905, 936
Popov V.V.	153, 182, 859, 1018
Popov Yu.F.	909, 911
Popova A.V.	786
Popova E.A.	450
Popova M.N.	450, 657, 750, 751
Porer M.	746
Poryadsky A.A.	1056
Potapov A.P.	815
Poteryaev A.I.	982
Potkina M.N.	621
Potzger K.	459, 780, 1001
Povarov K.Yu.	452, 731
Prabhakara K.H.	748, 749
Premkumar	809
Preobrazhensky V.L.	155, 662, 884
Presniakov I.A.	273, 293, 871
Presnov D.E.	644
Presnyakov M.Yu.	712
Proglyado V.V.	165, 493, 1002, 1023, 1043
Prokopov A.R.	184, 186, 188, 197
Proshin Yu.N.	180, 559, 563, 640
Proshkin A.I.	701, 723
Proskurnina N.V.	800
Prosnikov M.A.	196, 750
Prosvirin I.P.	818
Protasov A.V.	781, 802
Prozorova L.A.	289

Prudkoglyad V.A.	651
Prudnikov P.V.	253, 254, 431, 935
Prudnikov V.N.	96, 491, 830
Prudnikov V.V.	253, 254, 261
Prudnikova M.V.	491
Pryadun V.	444
Pryahina V.	236
Pschenichnyi K.A.	106
Pshenichnikov A.F.	382, 389
Pudalov V.M.	346
Puddy R.K.	972
Pudonin F.A.	262
Pugach N.G.	29, 30, 569, 577
Pugach S.	30
Pugach V.S.	541
Pukhov A.A.	554, 705, 706
Purtov A.N.	253
Puscasu E.	501
Pushkina M.M.	141
Pustovalov E.V.	266
Pyanzina E.	513, 514, 533
Pyataev A.V.	231, 1004
Pyataikin I.I.	958
Pyatakov A.P.	369, 410, 539, 585, 914, 1058

Q

Qamar A.	896
Quang T.D.	14
Quang V.M.	483
Quay C.H.	23
Querlioz D.	609
Quessab Y.	967
Quetz A.	51
Quindeau A.	375
Qureshi N.	472

R

Raabe J.	599
Radkevich A.A.	31
Radkovskaya A.A.	96, 103
Radulov I.A.	851
Radzieowski M.	899
Raevskiy A.O.	958
Rafalskii A.I.	762
Rafalskiy A.V.	806
Raganyan G.V.	297
Rahmonov I.R.	608

Raikher Yu.L.....	508, 524, 528, 674, 675, 680, 682, 724, 989, 991
Rajnak M.....	677
Rakhmanov A.L.....	707, 727, 941, 984
Ralchenko V.G.....	492
Ramasamy K.....	716
Ramasubramanian L.....	174
Ramazanov M.K.....	306, 942, 1014
Ramón E.....	94
Rasing T.....	34
Rasing Th.....	89, 748, 967
Rautskii M.V.....	172, 173, 276, 320, 1016
Razdolski I.....	44, 362
Razumnaya A.G.....	895
Reddy V.....	75
Regnault L.-P.....	1009
Reis M.S.....	485
Ren Y.....	70
Repina N.M.....	244
Reser B.I.....	127, 1036
Reyes A.P.....	445
Reynolds N.....	731
Reyren N.....	622
Reznikov M.....	346
Richter J.....	737
Richter R.....	513
Rigmant M.B.....	813
Ril. A.I.....	83
Rinkevich A.B.....	1020
Riout M.....	420
Ritchie D.A.....	972
Ritter C.....	1032
Rode K.....	17, 603
Rodina A.V.....	591
Rodionov I.D.....	480, 830
Rodionov V.V.....	854
Rodionov Ya.I.....	703
Rodionova V.V.....	192, 269, 271, 296, 466, 606, 820, 828, 842, 854, 998, 1084
Roditchev D.....	630
Rodriguez-Carvajal J.....	733
Rogachev A.V.....	991
Rogacki K.....	791, 797, 849
Rogalev A.....	107, 108, 113, 114, 115, 715, 806, 950
Rogov A.M.....	242
Roig A.....	408
Roldan-Molina A.....	599
Romanenko D.V.....	215, 217
Romanova O.B.....	171, 885
Romanovskiy D.E.....	254
Romashev L.N.....	406
Romeis D.....	681
Romera M.....	609
Romodina M.N.....	391
Ronti M.....	386
Rosen J.....	465
Roslyakov I.V.....	759
Rosner H.....	737
Ross C.A.....	228, 471, 948
Rossi A.....	485
Rossi L.....	393
Rößler U.....	737
Roussigné Y.....	598
Rovigatti L.....	386
Roy R.K.....	809
Roazanov K.N.....	100, 101, 102, 442, 463, 774, 1063
Rozhansky I.V.....	85, 978
Rozhkov A.V.....	707, 727, 941, 984
Rozhkov D.....	514
Rudkovskaya A.V.....	363
Rudnev I.A.....	806
Rudolf M.....	24
Rudoy Yu.G.....	697
Rüffer R.....	406, 1043
Rukovishnikov A.I.....	892, 985
Runov V.V.....	742, 767
Rusakov V.S.....	913, 914
Rusakov V.V.....	528, 989
Rushforth A.W.....	363
Rusinov I.P.....	653
Russier V.....	70
Russkikh I.V.....	1048
Ruzhickiy V.I.....	350
Ryabtsev K.S.....	529
Ryabukhina M.V.....	165, 1002, 1023, 1043, 1071
Ryapolov P.A.....	390, 529
Ryasny G.K.....	1042
Rybakov F.....	931
Rybakov Yu.P.....	702
Rybkina A.A.....	497
Rylkov V.V.....	16, 302, 491, 613, 712
Ryzhanova N.....	132
Ryzhikov I.A.....	100, 463
Ryzhkov A.V.....	524
Ryzhkova G.S.....	302
Ryzhov V.A.....	545, 742
<hr/>	
S	
Sablina K.....	900

Sablina K.A.	1049	Samuely P.	638
Sabon P.	690	Samuely T.	638
Saboungi M.-L.	70	Samusev I.G.	271
Sacanna S.	393	Sanchez P.A.	504, 508, 513, 514, 672
Sacarescu L.	501	Sangaa D.	536
Sadchikov Yu.V.	1048	Sannikov D.G.	587
Sadovnikov A.V.	226, 227, 426, 438, 475, 611, 721, 1072, 1088	Sanyal B.	115
Sadykov A.F.	301, 926	Sapega V.F.	80, 81
Saerbeck T.	402	Saphiannikova M.	670, 681
Safarov I.M.	835	Saplev A.F.	1055
Safarov V.I.	14	Sapozhnikov M.V.	977, 1078
Safin A.R.	19, 133, 158, 260, 490	Sarsari I.	832
Safiulina I.A.	1031	Sarychev M.N.	891
Safonchik M.O.	29	Satchell N.	347
Safronov A.P.	71, 74, 544, 547, 549, 772	Sathish C.I.	896
Saha-Dasgupta T.	730	Sato M.	97, 352
Sai R.	97	Satskiy A.V.	96
Saikin S.K.	180	Sauerzopf F.	1083
Sainctavit Ph.	110	Savchenko A.G.	534, 550, 760, 762, 798, 806
Saito K.	67, 109	Savchenko A.S.	201, 1051
Saito S.	41, 685	Savchenko E.S.	760
Sakharov V.K.	221, 225, 439, 1086, 1087	Savchenko T.M.	1027
Sakhin V.	648	Savel'ev S.	627
Sakhratov Yu.A.	445	Saveliev D.V.	918, 997
Sakuma N.	109	Savilov S.V.	740
Sakurai H.	732	Savin P.A.	142
Sala A.	420	Savitsky A.O.	16, 720, 1002
Salakhitdinov A.N.	239	Savochkin I.V.	188
Salakhitdinova M.K.	239	Savoini M.	746
Salakhova R.T.	539	Saxena S.S.	368
Salamatin A.V.	579, 1042	Saydirasulov N.	239
Salamatin D.A.	579, 1042	Saykin D.R.	703
Salamon S.	115	Sboychakov A.O.	343, 707, 727, 941, 984
Salasyuk A.S.	363	Schaedler M.	871
Salem M.M.	245, 764, 769, 794	Schaefer S.	420
Saletsky A.M.	263, 615, 830	Schafer S.	120
Salewski M.	80	Schaller R.D.	970
Salikhov R.	429, 465	Schaub S.	988
Salimov R.K.	779	Scheer E.	25
Salmon L.	331	Schefer J.	1038
Samardak A.S.	252, 266, 426, 611, 616, 617, 721, 821	Schegolev A.E.	351
Samardak A.Yu.	252, 426	Scherbakov A.V.	363
Samarin A.N.	214, 218, 866	Scherbakov G.V.	823
Samarin N.A.	157	Schetinin I.V.	762
Samatov O.M.	547, 549	Schiller F.	713
Samiepour M.	330	Schmidiger D.	452, 731
Samoilovich M.I.	1020	Schmitz D.	1034
Samoshkina Yu.E.	274, 1093	Schmitz-Antoniak C.	115, 1034
Sampath V.	204, 831	Schneider T.	599
Samsonenko Yu.B.	81	Schöppner C.	108
		Schreck F.	698
		Schröder C.	80

Schultheiss K.....	599	Shankar A.	71
Schulz A.	1010	Shao D.-F.	374
Schulz S.E.	174	Shapaeva T.B.	748
Schümann M.	678	Shapiro A.Ya.	304, 447
Sciortino F.	386	Shaposhnikov A.N.	186, 188
Seisyan R.P.	591	Sharaevskaia A.Yu.	1068
Sekatskii S.K.	199	Sharaevskii E.	475
Sekiguchi K.	228, 471	Sharaevskii Yu.P.	215, 227, 438, 1072, 1088
Seletskiy D.	44, 362	Sharafullin I.F.	378, 904
Selezneva N.V.	66, 307, 777, 801	Sharma A.	73
Seleznyova K.	311, 315	Sharoyan E.	430
Selishchev S.V.	532	Shashkov I.V.	283
Selivanov Yu.G.	651	Shatrova N.	285
Semeno A.V.	214, 218, 440	Shavkin S.V.	567, 573
Semenov A.A.	916	Shavrov V.G.	181, 201, 204, 209, 210, 481, 482, 483, 484, 486, 831, 837, 840, 1051, 1064, 1065, 1066, 1074, 1077
Semenov A.G.	31	Shayhutdinov K.	901
Semenov S.V.	564, 576	Shcaihulov T.A.	163
Semenov V.S.	496	Shcheglov V.I.	137, 169, 209, 436, 1064, 1065, 1074, 1077
Semenova E.M.	770, 964	Shchelkunov N.N.	391
Semenova O.	230	Shcherbakov M.R.	191
Semensmeyer K.	235	Shcherbinin S.V.	960
Semirov A.V.	140, 216, 768	Shchetinin I.V.	534, 760, 798, 806
Semisalova A.S.	459, 780	Sheftel E.N.	222, 774
Semkin M.A.	1054, 1057	Shein G.A.	194
Sengupta K.	608	Shein I.R.	888
Senina V.A.	1026	Sheldeshova E.V.	390
Senyshyn A.	277, 733, 1010	Shelly C.	348
Seong-Cho Y.	53	Shemukhin A.	236
Serdobintsev A.A.	1088	Shen J.	602
Serebryakova O.N.	316	Shen S.-Q.	600
Seredina M.A.	135, 842	Sherbakov V.A.	158
Serga A.A.	658	Sherman A.	128
Sergeev A.S.	369	Sherokalova E.M.	66, 307, 801
Sergeev A.V.	574, 580	Shershevskii I.A.	479
Sergeicheva E.G.	289	Sherstnev I.A.	262
Sergienko E.S.	314, 541	Sherstobitova E.A.	1033
Seryotkin Yu.V.	894	Sheshukova S.E.	438
Severin P.A.	224	Shestakov A.V.	876
Shadrin A.V.	572, 643	Shevchenko E.V.	863
Shadrina G.V.	282, 284	Shevelkov A.V.	871
Shah W.H.	1094	Shevyakov D.I.	613
Shaikhulov T.A.	884	Shevyrtalov S.	466, 842
Shaikhutdinov K.A.	425	Shikin A.M.	497
Shaimanov A.N.	39	Shilova O.A.	1040
Shakhov M.A.	86, 170, 870	Shimada K.	228
Shakhunov V.A.	884	Shimizu T.	62
Shakirov M.A.	180	Shipunova V.O.	553
Shakirzyanov R.I.	212	Shirakashi Z.	42
Shalygin A.N.	102, 366	Shirasaki K.	457
Shalygina E.E.	264, 265, 366, 918		
Shamonin M.	671		
Shamonina E.	103		

Shirshikov S.O.	761	Simonov M.N.	307
Shiryayev A.O.	102, 1063	Simonova E.V.	548, 549
Shishkin D.A.	815, 844, 962	Simsek T.	458
Shishkin I.S.	280, 686, 1011	Singh A.	22
Shishkov V. Yu.	706	Singh S.P.	262
Shitsevalova N. Yu.	157, 218, 235, 440	Siryuk Ju.A.	787
Shivashankar S.A.	97	Sitnikov A.V.	151, 166, 206, 211, 233, 234, 292, 302, 308, 309, 488, 491, 712, 1070
Shiyani Ya.G.	717	Sitnikov I.I.	263
Shkar V.	204, 1066	Sitnikov M.N.	666, 882, 885
Shklyar T.F.	74	Skidanov V.	177
Shlyakhtich M.A.	935	Skipetrov E.P.	883
Shlyakhtina A.	857	Skipetrova L.A.	883
Shlyapnikov G.V.	698	Skirdkov P.N.	143, 145, 497, 654, 957
Shmatov G.A.	765	Skokov K.P.	49, 55, 770, 851, 964
Shmyreva A.A.	241	Skomarovsky V.S.	785
Shneider A.G.	897	Skorikov N.A.	424
Shneyder E.I.	696	Skornyakov S.L.	982
Shoji T.	109	Skorohodov E.V.	479, 1078
Shore D.	73, 415	Skourski Y.	644
Shorikov A.O.	982	Skourski Yu.	911
Shorokhov A.S.	38, 191	Skulkina N.A.	758, 810
Shpetnyy I.	262	Skumryev V.	911
Shreder E.I.	162	Skvortsov M.	177, 628, 629
Shtil A.A.	410	Sladkov K.D.	720
Shugaev M.V.	1001	Slavin A.	599
Shukaev I.L.	297, 298	Slawska-Waniewska A.	1092
Shukla A.	376	Slepchenko G.B.	414
Shukrinov Yu.M.	608	Sleptsova A.E.	500, 510, 759
Shul'ga N.V.	220	Slivina E.	976
Shulenina A.V.	401	Sluchanko N.E.	157, 218, 235, 440, 979
Shulyatev D.A.	893	Sluka V.	599
Shumann J.	356, 566	Slynko V.E.	883
Shustin M.S.	633	Smarzhevskaya A.I.	849
Shustov V.O.	158	Smekhova A.	115, 1034
Shuvaev A.	912	Smelova E.M.	263, 615
Shuvaeva E.	809	Smirnov A.I.	304, 447
Shuyskyy A.A.	184	Smirnov A.N.	196, 750
Shvanskaya L.V.	273, 300	Smirnov A.V.	1082
Shvartsman V.V.	741	Smirnov E.	118
Shvets I.A.	498, 646	Smirnov G.V.	406
Sichkar D.A.	74	Smirnov V.V.	787
Sidorenko A.S.	28, 354, 1012	Smirnova E.A.	841
Sidorov A.V.	740	Smirnova E.S.	921
Sidorov V.A.	1042	Smith C.G.	972
Siebert E.	387	Smolnikov A.G.	301, 926
Siegfried S.-A.	106	Smoluk L.T.	552
Sigov A.S.	662, 700, 913, 914	Smolyarova T.E.	320, 1016
Silaev M.A.	635	Smyslov R. Yu.	767
Silibin M.V.	379, 1096	Snegirev V.V.	879
Silkin I.M.	646	Sobolev A.V.	273, 293, 871
Sim H.	1057	Sobolev N.A.	152
Simon P.	630		

Tagirov L.R.	28, 237, 242, 354, 570, 1012
Takagi H.	41, 42, 202, 228, 471, 732
Takata A.	304, 447
Talalaev K.A.	463
Talanov Yu.	648
Talantsev A.D.	20, 267, 337
Talatchian P.	609
Taldenkov A.N.	156, 492, 712
Taldenkov N.	862
Tamion A.	1027
Tanaka M.	377
Tanaka S.	637
Tanaka Y.	352
Taran S.V.	170
Tarassenko A.S.	201, 1051
Tarassenko S.A.	650
Tarassenko S.V.	201, 1051
Tarassenko T.N.	887
Tarasov A.S.	172, 320, 874, 1016
Tarasov E.N.	775, 776, 843
Tarasov I.A.	172, 236
Tarasov V.P.	785
Tarasova O.S.	1070
Taskaev S.	55, 831
Taskaev S.V.	853
Tatarenko A.S.	490, 908, 1055
Tatsumi H.	687
Tatsun T.	341
Tavares J.M.	386
Tedzhetov V.A.	222, 774
Teitel'baum G.	648
Teixeira B.M.S.	152
Telegin A.V.	89, 589, 739, 875, 898, 1090
Telegin S.V.	1035
Telyshev D.V.	532
Temerov V.L.	114, 665, 906, 923, 1050
Temiryazeva M.P.	892
Temnov V.V.	44, 362, 474
Temst K.	397
Teplykh A.E.	1054
Terent'ev K.	901
Terentev P.	962
Terentev P.B.	790, 796, 802
Tereshina E.A.	824
Tereshina I.S.	483, 486, 791, 824, 850, 963
Tereshonok M.V.	351
Thalmann M.	24
Thanh P.T.	483
Thirion C.	420
Thiyagarajah N.	17, 603
Thomas J.	566
Thomson Th.	780
Thonig D.	955
Tiberkevich V.	599
Tiberto P.	409
Tidecks R.	354, 1012
Tiercelin N.	155, 662
Tikhanovskii A.Yu.	909
Tikhomirova K.A.	143
Tikhonov K.S.	703
Tikhonov V.V.	226
Timirgazin M.A.	126, 642, 940
Timko M.	674, 677
Timm M.	1027
Timopheev A.	119, 152, 956
Tishin A.M.	48, 410, 539, 846
Titov I.S.	67, 830
Titov M.	125, 954
Titova A.	17
Tkachenko I.A.	318
Tobey R.	362
Tobias T.	677
Tokmachev A.M.	156, 157, 986
Tokmachev A.N.	862
Tokman I.D.	36
Tokunaga M.	50, 52
Tolkachev V.A.	181, 210
Tolmachev T.P.	808
Tomašovičová N.	674
Tomilin S.V.	186
Torati S.R.	75
Torgashev V.I.	895
Toshchevnikov V.	670
Tóth-Katona T.	674
Tournus F.	1027
Toussaint J.C.	420
Toyoki K.	59
Trakhtenberg L.I.	561
Tran D.T.	53, 847
Tran N.M.	44, 362
Trapp B.	420
Traum C.	44, 362
Tregubova T.V.	488
Tretiakov O.A.	620
Trif M.	630
Tripathi V.	647
Trochenco V.G.	895
Trofimov A.V.	118, 612
Trofimov N.O.	1053
Trokiner A.	872
Tronov A.A.	91
Troyanchuk I.O.	379, 1096
Trukhanov A.V.	212, 764, 869, 1076
Trukhanov S.V.	869, 1076

Truong A.	690
Trusevich N.G.	561
Trusov L.A.	295, 500, 510, 759
Tselebrovskiy A.N.	861
Tseng Ch.-W.	582
Tseng Y.-T.	256, 287, 535
Tsikalov D.S.	437
Tso C.-T.	287
Tsunegi S.	609
Tsvyashchenko A.V.	106, 579, 1042
Tsymbal E.Y.	374
Tsysar K.M.	263, 615
Tugarinov V.	716
Tugushev V.V.	16, 498, 613, 646, 649, 712
Tumanov V.A.	559
Turchenko V. ...	159, 507, 867, 869, 991, 1076
Turkov V.A.	394, 519
Turpanov I.A.	168
Turygin A.P.	249
Tyatyushkin A.N.	523
Tyukova I.S.	71
Tzeng W.Y.	358
Tzschope M.	298

U

Uchida H.	41, 42, 194, 202, 228, 471
Udalov N.N.	260, 490
Udalov O.G.	372
Udintseva M.S.	1033, 1035, 1037
Udod L.V.	882
Ueno T.	109
Uimin M.A.	540, 552, 718, 1033
Ulin S.E.	763
Ulitzko M.V.	540, 552
Ulitzko V.A.	562
Ullrich A.	354, 1012
Ulyanov A.N.	740
Ünal A.	1001
Upadhyay R.V.	387
Urubkov I.V.	685, 687
Urusova N.V.	1057
Urzhumtcev A.N.	776
Urzhumtsev A.N.	775
Usachev P.A.	82, 862
Useinov N.Kh.	154, 175
Ushakova O.A.	811
Usik A.Yu.	150
Usov N.A.	316, 418
Usov Yu.V.	873
Uspenskaya L.S.	355

Uspenskii Yu.A.	366, 423, 613
Ustinov A.B.	213, 658, 916, 1075
Ustinov V.V.	165, 167, 406, 493, 893, 1002, 1018, 1023, 1043
Ustinova I.A.	1075
Ustyugov V.A.	211
Uteshev Z.M.	763
Uvarov O.V.	510
Uzdin V.M.	621

V

Vaganov M.V.	682
Vaganov S.A.	591
Vakhitov I.R.	242
Vakhitov R.M.	910, 919, 920
Vakhrushev S.B.	741
Vakulenko A.Yu.	96
Valdez J.	118
Valencia S.	1001
Valeyev V.G.	138
Validov A.A.	356, 566
Valieva L.R.	904
Valiullin A.A.	183, 237
Valkov V.I.	845
Val'kov V.V.	359, 633, 709
Valldor M.	860
Valvidares M.	375
van Dijken S.	994
van Loosdrecht P.H.M.	976
Vanacken J.	866
Vantomme A.	397
Varnakov S.N.	172, 173, 236
Varvaro G.	296
Varyukhin V.N.	565
Varzaneh A.G.	832
Vas'kovskiy V.O.	142, 148, 238, 247, 249, 250, 251, 460
Vasili H.B.	375
Vasiliev A.	444
Vasiliev A.L.	567, 712
Vasiliev A.N.	273, 293, 297, 298, 300, 358, 450, 454, 568, 644, 857, 973
Vasiliev A.V.	278, 740, 759
Vasiliev L.	814
Vasiliev M.	199
Vasinovich V.V.	562
Vasyukhno N.V.	140
Vaudel G.	44, 362
Vavilova E.	737, 860, 864

Wintz S.....	599, 1001
Witt J.D.S.....	347
Wojtowicz T.....	80, 586
Wolf M.J.	26
Wolz M.	25
Wren T.	348
Wu A.....	198
Wu K.H.	358, 973
Wurmehl S.	737, 864

X

Xiang T.	639
Xiao Q.F.....	375
Xinghao H.....	75
Xiufeng Han.....	617
Xu Ch.	16, 87
Xu X.	50, 52
Xu Y.	747

Y

Yablunovsky A.	657
Yada K.	352
Yagfarova A.	288
Yagovtsev V.O.....	569
Yagupov S.....	311
Yakimov I.S.	576
Yakovchuk V.Yu.	1022
Yakovenko O.S.	1076
Yakovlev D.R.....	37, 80, 188, 363, 586
Yakovlev I.A.....	236
Yakubovich O.V.	300
Yakubovskii A.Yu.	872, 926
Yakubtsev R.A.	794
Yakushev M.V.	591
Yakushiji H.	609
Yakushkin S.S.....	425
Yamaguchi M.....	97
Yamakage A.....	352
Yamamura T.	457
Yamaoka A.	744
Yamaura K.	377
Yan H.	77
Yanagisawa E.....	685
Yang C.P.	1083
Yang H.	332
Yang Yi-feng.....	639
Yang Z.....	77, 556
Yanilkin I.V.	242

Yano M.	67, 109
Yanushkevich K.I.	171, 836, 882, 885
Yao S.-Yu	973
Yaroslavtsev R.N.....	294, 299, 317, 417
Yasin S.	891
Yassine O.....	691
Yatsyk I.V.....	288, 714, 876
Yazovskikh K.A.....	796, 803
Yen N.H.	483
Yerin C.V.....	502
Yerina M.V.	502
Yermakov A.E.	540, 552, 1033
Yermakov A.Ye.....	718
Yevdokimov Yu.M.	413
Yi T.	972
Yildirim O.....	174
Yoshimoto T.	228
Yu H.....	639
Yu S.C.....	847
Yuan J.	639
Yuan Ye.	87, 856, 985
Yuasa S.	328, 329, 609
Yudanov N.A.	98, 764, 794
Yuldasheva A.R.....	248
Yumaguzin A.R.	919
Yun S.	896
Yunoki S.	634
Yurasov A.N.	200, 589
Yurkin G.Yu.	168, 874
Yurkov G.Y.	241
Yurov A.	90
Yushkov V.I.....	168
Yusupov A.A.	239
Yusupov R.V.	183, 242, 243

Z

Zabluda V.	555
Zadorozhny V.Y.	761
Zadov B.....	995
Zagorsky D.L.....	272
Zagoskin A.....	627
Zagrebin M.A... 56, 478, 848, 852, 1080, 1081	
Zaikin A.D.	31
Zainullina R.I.	893
Zaitsev R.O.	571
Zakharchuk I.	86, 491, 773, 1095
Zakharov K.	444
Zakharov K.V.	568
Zakharov P.N.....	96
Zakhvalinskii V.S.	170, 870

Zakinyan A.R.	515	Zlotnikov A.O.	633
Zácutná D.	403, 405	Znoyko S.L.	76, 692
Zaliznyak I.A.	289	Zubarev A.Yu.	74, 521, 527
Zamay G.	555	Zubarev I.V.	552
Zamay S.	555	Zubavichus Y.V.	401, 567
Zamay T.	555	Zubov V.E.	311, 315, 961
Zanaveskin M.L.	138	Zverev D.G.	243
Zaporozhets V.D.	845	Zverev V.I.	410, 846
Zaripova L.D.	237	Zverev V.S.	382, 505, 506, 522
Zarubin A.V.	723	Zverev V.V.	290, 305
Zavyalov S.A.	881	Zvereva E.A.	273, 297, 298, 454, 733
Zayak A.T.	1081	Zvezdin A.K.	145, 188, 193, 369, 370, 497, 585, 748, 749, 824, 936, 957
Zaytsev D.D.	759	Zvezdin K.A.	134, 143, 145, 149, 497, 654, 748, 749, 957
Zdoroveyshchev A.V.	139, 868	Zvonov A.I.	797
Zdravkov V.I.	354, 1012	Zvyagina G.A.	925
Zeer G.	716, 1038	Zykin M.A.	278, 295
Žemlička M.	638	Zykov G.S.	856, 892, 985
Zezyulina P.A.	100, 774		
Zhakov S.V.	540		
Zhang J.	415		
Zhang L.	377		
Zhang Yu.	899		
Zharkov S.	716		
Zharkov S.M.	287, 1038		
Zharmukhametov A.R.	248		
Zhekov K.R.	925		
Zheludev A.	451, 452, 731, 1028		
Zheludkevich A.L.	83		
Zherebtsov D.A.	1075		
Zhevstovskikh I.V.	891		
Zhigalov V.S.	1021		
Zhigilei L.V.	1001		
Zhilova O.V.	166		
Zhitomirsky M.	304, 447		
Zhivaya Ya.A.	168		
Zhou H.D.	445, 660		
Zhou S.	16, 87, 459, 856, 985		
Zhu B.	639		
Zhu D.	746		
Zhukov A.	51, 464, 756, 820		
Zhukov A.A.	793		
Zhukov A.V.	520		
Zhukov D.G.	806		
Zhukova V.	464, 756, 820		
Zhuravlev A.V.	750		
Zhuravlev M.Ye.	753		
Zhurenko S.V.	871		
Zhandun V.S.	236		
Ziganshina S.A.	922		
Zimmermann K.	525		
Zinin A.V.	775, 776, 843		
Zlatic V.	744		

<http://www.amtc.org>

<http://www.amtc.ru>

e-mail: kopel@amtc.org

tel/fax: +7 (495) 777 72 26

MAGNETIC FIELD SYSTEMS

AMT&C, LLC offers a wide range of services in designing and manufacturing PM assemblies and electromagnets with customer-specified magnetic field geometry. You are welcome to order:

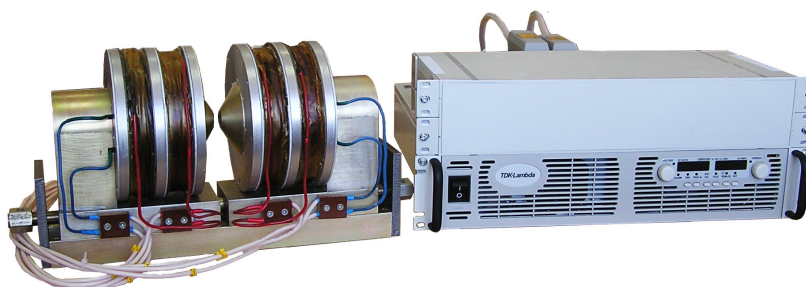
- **magnetic flux density up to 3 Tesla with the permanent magnet systems;**
- **magnetic field uniformity up to 10^{-5} ;**
- **magnetic systems under customized requirements;**
- **computer controlled PM systems with variable field.**



ADJUSTABLE PM SYSTEMS – the powerful instrument for scientific research. Their principal advantages are:

- highly intensive field – up to ± 2 T in the bore ~ 40 mm;
- high field changing rate – up to 10 Tesla/sec;
- compact design, in comparison with electromagnets;
- low power consumption.

CUSTOMIZED ELECTROMAGNETS are provided with a computer controlled supply unit, including polarity reversal.





<http://www.amtc.org>

<http://www.amtc.ru>

e-mail: kopel@amtc.org

tel/fax: +7 (495) 777 72 26

AUTOMATED MEASURING SYSTEMS

AMT&C LLC offers automated system intended for measuring magneto-thermal and other magnetic parameters and including:

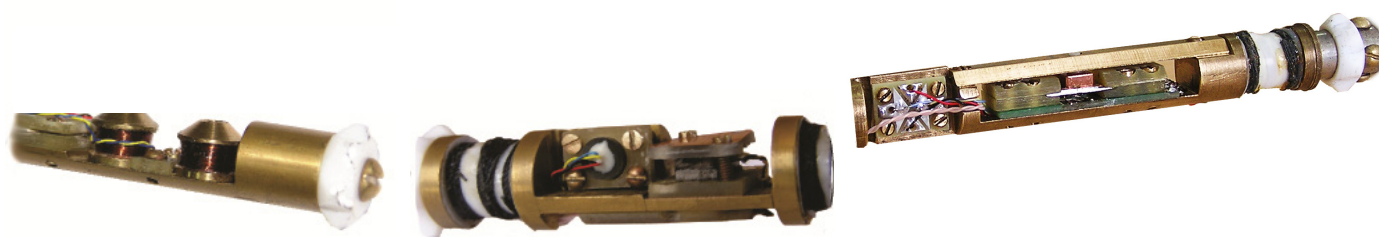
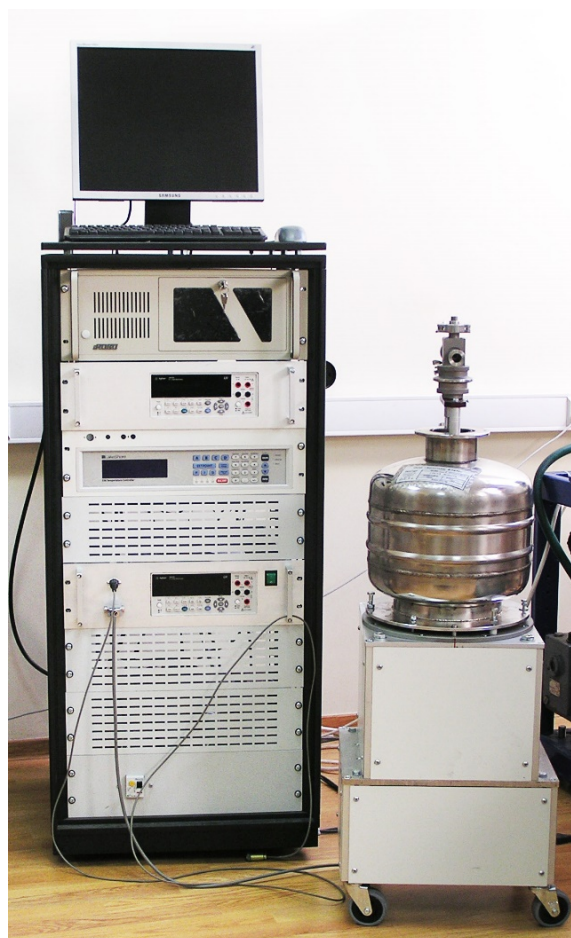
- PC controlled magnetic field source,
- liquid nitrogen cryostat,
- data acquisition system,
- measuring inserts.

The setup has the following working parameters:

- variable magnetic field strength
 - in limits ± 1.85 T,
- magnetic field changing rate
 - from 0.05 to 6 T/s,
- operating volume (heterogeneity $\sim 0.5\%$)
 - $\varnothing 20 \times 20$ mm,
- operating temperature range
 - $80 \div 365$ K,
- automatic and manual measuring modes.

The set of measuring inserts is intended for measurement of field and/or temperature dependences of:

- the magnetocaloric effect by a direct method,
- magnetization by induction method,
- heat capacity by the adiabatic method,
- thermal conductivity by a stationary method.



Notes

Notes

Notes

Notes

Notes

Notes

PRINT LETO
КНИЖНАЯ ТИПОГРАФИЯ

ISBN 978-5-9500168-2-0



9 785950 016820

Изготовлено PrintLETO.ru
г. Москва, Нижняя Сыромятническая д. 10/4, этаж 1
Тел. + 7(495) 728-09-42, Офис +7(495) 995-09-39
Тираж 300 экз.